Tue. May 28, 2019

[J] Oral | U (Union)：Union

9:00 AM - 10:30 AM JST | 12:00 AM - 1:30 AM UTC | 101 1F

[U-03] Future of Scientific Publishing in Geosciences

convener:Hodaka Kawahata(Atmosphere Ocean Research Institute, the University of Tokyo), Hirokuni Oda(Institute of Geology and Geoinformation, Geological Survey of Japan, AIST), Chairperson:Hirokuni Oda, Hodaka Kawahata

9:00 AM - 9:30 AM JST | 12:00 AM - 12:30 AM UTC

[U03-01] Game-change of scholarly communication based on papers and the role of learned society and peer-review

★Invited Papers

*Kazuhiro Hayashi[1] (1.National Institute of Science and Technology Policy)

9:30 AM - 10:00 AM JST | 12:30 AM - 1:00 AM UTC

[U03-02] The future of the journal metrics and new trend of the scholarly publishing

★Invited Papers

*Yoshiko Tanahashi[1] (1.Clarivate Analytics)

10:00 AM - 10:30 AM JST | 1:00 AM - 1:30 AM UTC

[U03-03] Underlying Issues and Problems in Publishing International Scientific Journals in Japan. “DNA Research” As A Case Study.

★Invited Papers

*Michio Oishi[1] (1.Kazusa DNA Research Institute)

[J] Oral | U (Union)：Union

10:45 AM - 12:15 PM JST | 1:45 AM - 3:15 AM UTC | 101 1F

[U-03] Future of Scientific Publishing in Geosciences

convener:Hodaka Kawahata(Atmosphere Ocean Research Institute, the University of Tokyo), Hirokuni Oda(Institute of Geology and Geoinformation, Geological Survey of Japan, AIST), Chairperson:Hirokuni Oda, Hodaka Kawahata

10:45 AM - 11:05 AM JST | 1:45 AM - 2:05 AM UTC

[U03-04] Review of editorial work for PEPS in 2018-2019 and new strategy for 2019–2020

★Invited Papers

*Yasufumi Iryu[1] (1.Institute of Geology and Paleontology Graduate School of Science Tohoku University)

11:05 AM - 11:25 AM JST | 2:05 AM - 2:25 AM UTC

[U03-05] "Earth, Planets and Space" An Open Access Journal: Past, Present and and Future

★Invited Papers

*Yasuo Ogawa[1], Kiyoshi Baba[2] (1.Volcanic Fluid Research Center, School of Science, Tokyo Institute of Technology, 2.Earthquake Research Institute, University of Tokyo)

11:25 AM - 11:55 AM JST | 2:25 AM - 2:55 AM UTC

[U03-06] Scientific Research Output and Publication: research article, data, and digital transformation

★Invited Papers

*Yasuhiro Murayama[1] (1.Strategic Program Produce Office, National Institute of Information and Communications Technology)

11:55 AM - 12:15 PM JST | 2:55 AM - 3:15 AM UTC

[U03-07] **Enhancing dissemination of research activities to international communities by Japanese Geoscience Union**

★Invited Papers

*Hodaka Kawahata[1] (1.Atmosphere Ocean Research Institute, the University of Tokyo)

[E] Oral | P (Space and Planetary Sciences)：P-PS Planetary Sciences

9:00 AM - 10:30 AM JST | 12:00 AM - 1:30 AM UTC | A03 TOKYO BAY MAKUHARI HALL

[P-PS01] Outer Solar System Exploration Today, and Tomorrow

convener:Jun Kimura(Osaka University), Yasumasa Kasaba(Planetary Plasma and Atmospheric Research Center, Tohoku University), Kunio M. Sayanagi(Hampton University), Chairperson:Kunio Sayanagi(Hampton University), Takeshi Kuroda

9:00 AM - 9:15 AM JST | 12:00 AM - 12:15 AM UTC

[PPS01-06] Radiative transfer simulation including a non-LTE model for terahertz observations of Ganymede's atmosphere

*Takayoshi Yamada[1], Ladislav Rezac[2], Richard Larsson[2], Paul Hartogh[2], Naohiro Yoshida[3], Yasuko Kasai[1,3] (1.National Institute of Information and Communications Technology, 2.Max Planck Institute for Solar System Research, 3.Tokyo Institute of Technology)

9:15 AM - 9:30 AM JST | 12:15 AM - 12:30 AM UTC

[PPS01-07] Vertical Mass Flux by the 2010-2011 Great Storm of Saturn

*Kunio M. Sayanagi[1], Jacob L. Gunnarson[1], John J. Blalock[1], Richard K. Achterberg[2], F. Michael Flasar[2], Andrew P. Ingersoll.[3], Shawn P. Ewald[3], Ulyana A. Dyudina[3] (1.Hampton University, 2.NASA Goddard Space Flight Center, 3.California Institute of Technology)

9:30 AM - 9:48 AM JST | 12:30 AM - 12:48 AM UTC

[PPS01-08] Microwave observations of the giant planets - Cassini/Radar and Juno/MWR

★Invited Papers

*Cheng Li[1], Virgil Adumitroaie[2], John Arballo[2], Sushil K Atreya[3], Scott J Bolton[4], Andrew Ingersoll[1], Michael Janssen[2], Steven Levin[2], Jonathan Lunine[5], Glenn Orton[2], Paul Steffes[6], Hunter Waite[4] (1.California Institute of Technology, 2.Jet Propulsion Laboratory, 3.University of Michigan Ann Arbor, 4.Southwest Research Institute, 5.Cornell University, 6.Georgia Institute of Technology)

9:48 AM - 10:06 AM JST | 12:48 AM - 1:06 AM UTC

[PPS01-09] Tracing Formation and Evolution of Outer Solar System Bodies through Stable Isotopes and Noble Gas Abundances

★Invited Papers

*Kathleen Mandt[1] (1.Johns Hopkins University Applied Physics Laboratory)

10:06 AM - 10:24 AM JST | 1:06 AM - 1:24 AM UTC

[PPS01-10] Icy Giant Planet Exploration

★Invited Papers

*Sushil K Atreya[1], Mark D. Hofstadter[2], Amy Simon[3], Kim R. Reh[2], Olivier Mousis[4], Krista Soderlund[5] (1.University of Michigan Ann Arbor, 2.Jet Propulsion Laboratory, 3.Goddard Space Flight Center, 4.Laboratoire d'Astrophysique de Marseille, 5.University of Texas at Austin)

[E] Oral | P (Space and Planetary Sciences)：P-PS Planetary Sciences

10:45 AM - 12:15 PM JST | 1:45 AM - 3:15 AM UTC | A03 TOKYO BAY MAKUHARI HALL

[P-PS01] Outer Solar System Exploration Today, and Tomorrow

convener:Jun Kimura(Osaka University), Yasumasa Kasaba(Planetary Plasma and Atmospheric Research Center, Tohoku University), Kunio M. Sayanagi(Hampton University), Chairperson:Jun Kimura(Osaka University), 鎌田 俊一(北海道大学創成研究機構)

10:45 AM - 11:03 AM JST | 1:45 AM - 2:03 AM UTC

[PPS01-11] Saturn's ring rain and Enceladus' subsurface ocean as seen by the Cassini Cosmic Dust Analyser

★Invited Papers

*Sean Hsu[1], Sascha Kempf[1], Mihaly Horanyi[1], Ralf Srama[2], James O'Donoghue[3] (1.LASP, University of Colorado, Boulder, CO, USA, 2.IRS, University of Stuttgart, Stuttgart, Germany, 3.NASA Goddard Space Flight Center, Greenbelt, Maryland, USA)

11:03 AM - 11:18 AM JST | 2:03 AM - 2:18 AM UTC

[PPS01-12] Titan Trek: A New Online NASA Visualization and Analysis Portal for Saturn’s Largest Moon

*Emily Law[1], Brian Hamilton Day[2] (1.NASA Jet Propulsion Laboratory, 2.NASA Ames Research Center)

11:18 AM - 11:36 AM JST | 2:18 AM - 2:36 AM UTC

[PPS01-13] Internal structure of icy moons: ice-ocean systems as commonly seen in the outer solar system

★Invited Papers

*Hauke Hussmann[1] (1.DLR Institute of Planetary Research)

11:36 AM - 11:51 AM JST | 2:36 AM - 2:51 AM UTC

[PPS01-14] Callisto as a keystone to reproduce the formation process of the Jovian system

*Yasuhito Sekine[1], Shunichi Kamata[2], Yuhiko Aoyama[3], Masahiro Ikoma[3], Takayuki Tanigawa[4] (1.Earth-Life Science Insitute, Tokyo Institute of Technology, 2.Creative Res. Institution, Hokkaido Univerisity, 3.Dept of Earth and Planetary Sci., University of Tokyo, 4.Nat'l Inst. Tech., Ichinoseki Col.)

11:51 AM - 12:09 PM JST | 2:51 AM - 3:09 AM UTC

[PPS01-15] Origin of Jupiter Trojan asteroids: To be explored by OKEANOS

★Invited Papers

*Yoko Kebukawa[1], Tatsuaki Okada[2], Motoo Ito[3], Jun Aoki[4], Yosuke Kawai[4], Jun Matsumoto[2], Noel Grand[5], Arnaud Buch[6], Michisato Toyoda[4], Hervé Cottin[5], Hisayoshi Yurimoto[7,2], Hajime Yano[2], Takahiro Iwata[2], Osamu Mori[2] (1.Yokohama National University, 2.Japan Aerospace Exploration Agency, 3.Kochi Institute for Core Sample Research JAMSTEC, 4.Osaka University, 5.LISA, Université Paris-Est Créteil, 6.Ecole Centrale Paris, 7.Hokkaido University)

[E] Poster | P (Space and Planetary Sciences)：P-PS Planetary Sciences

3:30 PM - 5:00 PM JST | 6:30 AM - 8:00 AM UTC | Poster Hall International Exhibition Hall8, Makuhari Messe_1

[P-PS01] Outer Solar System Exploration Today, and Tomorrow

convener:Jun Kimura(Osaka University), Yasumasa Kasaba(Planetary Plasma and Atmospheric Research Center, Tohoku University), Kunio M. Sayanagi(Hampton University)

[PPS01-P01] Critical Role of Entry Probes in Giant Planet Exploration

*Sushil K Atreya[1], Olivier Mousis[2] (1.University of Michigan Ann Arbor, 2.Laboratoire d'Astrophysique de Marseille)

[PPS01-P02] OKEANOS – Jupiter Trojan Asteroid Rendezvous and Landing Experiments Using a Solar Power Sail

*Tatsuaki Okada[1,2], Takahiro Iwata[1], Yoko Kebukawa[3], Motoo Ito[4], Jun Aoki[5], Yosuke Kawai[5], Shoichiro Yokota[5], Yoshifumi Saito[1], Kentaro Terada[5], Michisato Toyoda[5], Hikaru Yabuta[6], Hisayoshi Yurimoto[1,7], Shuji Matsuura[8], Kohji Tsumura[9], Daisuke Yonetoku[10], Tatehiro Mihara[11], Ayako Matsuoka[1], Reiko Nomura[12], Hajime Yano[1], Takayuki Hirai[13], Atsushi Kumamoto[9], Ryosuke Nakamura[14], Stephan Ulamec[15], Ralf Jaumann[15], Jean-Pierre Bibring[16], Noel Grand[17], Cyril Szopa[18], Ernesto Palomba[19], Jorn Helbert[15], Alain Herique[20], Matthias Grott[15], Hans-Ulrich Auster[21], Goester Klingelhoefer[22], Fumi Yoshida[13], Makoto Yoshikawa[1], Jun Matsumoto[1], Toshihiro Chujo[1], Masanori Matsushita[1], Takanao Saiki[1], Hideki Kato[1], Osamu Mori[1], Junichiro Kawaguchi[1] (1.Japan Aerospace Exploration Agency, 2.University of Tokyo, 3.Yokohama National University, 4.Japan Agency for Marine-Earth Science and Technology, 5.Osaka University, 6.Hiroshima University, 7.Hokkaido University, 8.Kwansei Gakuin University, 9.Tohoku University, 10.Kanazawa University, 11.RIKEN, 12.National Astronomical Observatory of Japan, 13.Chiba Institute of Technology, 14.National Institute of Advanced Industrial Science and Technology, 15.German Aerospace Center, 16.Institut d'Astrophysique Spatiale, 17.LISA, 18.LATMOS, 19.INAF-IAPS, 20.IPAG, 21.TU Braunschweig, 22.Leibniz Universität Hannover)

[PPS01-P03] Magnetic field model of Jovian magnetosphere

*Naoya Momoki[1], Hiroaki TOH[1] (1.Division of Earth and Planetary Sciences, Graduate School of Science, Kyoto University)

[PPS01-P04] Enhancement of the Jovian thermospheric temperature above the Great Red Spot based on the infrared spectroscopic data obtained with IRTF/iSHELL

*Ayumu Kambara[1], Hajime Kita[2], Takeshi Sakanoi[1], Yasumasa Kasaba[1], Masato Kagitani[1], Haruna Watanabe[1] (1.Planetary Plasma and Atmospheric Research Center, Graduate School of Science, Tohoku University, 2.Institute of Space and Astronautical Science, Japan Aerospace Exploration Agency)

[PPS01-P05] Pulsation-like variation of Jovian infrared polar emission observed by Subaru 8-m: H3+ and methane emissions

*Yasumasa Kasaba[1], Haruna Watanabe[1], Hajime Kita[2], Chihiro Tao[3], Takeshi Sakanoi[1], Masato Kagitani[1], Orton Glenn[1,4], James Sinclair[4] (1.Planetary Plasma and Atmospheric Research Center, 2.ISAS/JAXA, 3.NICT, 4.NASA/JPL)

[PPS01-P06] Structure of Io plasma torus observed with the Tohoku 60-cm telescope

*Masato Kagitani[1], Fuminori Tsuchiya[1], Kazuo Yoshioka[2], Go Murakami[3], Tomoki Kimura[1], Ryoichi Koga[1], Reina Hikida[4], Takeshi Sakanoi[1] (1.Graduate School of Science, Tohoku University, 2.Graduate School of frontier Science, The University of Tokyo, 3.Institute of Space and Astronautical Science, Japan Aerospace Exploration Agency, 4.Department of Earth and Planetary Science, Graduate School of Science, Tokyo University)

[PPS01-P07] Ion Scale Height Variability in Hisaki Io Torus Observations

*Nicholas McCord Schneider[1], Carl Schmidt[2], Masato Kagitani[3], Yasumasa Kasaba[3], Tomoki Kimura[3], Go Murakami[4], Fuminori Tsuchiya[3], Hajime Kita[3], Reina Hikida[5], Ichiro Yoshikawa[5], Kazuo Yoshioka[5] (1.LASP, University of Colorado Boulder, 2.Boston University, 3.Tohoku University, 4.ISAS/JAXA, 5.University of Tokyo)

[PPS01-P08] Size of the Smallest Particles in Saturn's Rings

*Keiji Ohtsuki[1], Hiroshi Kawamura[1], Naoyuki Hirata[1], Hiroshi Daisaka[2], Hiroshi Kimura[3] (1.Graduate School of Science, Kobe University, 2.Graduate School of Commerce and Management, Hitotsubashi University, 3.Planetary Exploration Research Center, Chiba Institute of Technology)

[PPS01-P09] The Radio & Plasma Wave Investigation (RPWI) for JUICE for the investigation of Jupiter and Icy Moons System: Contributions from Japan

*Yasumasa Kasaba[1], Hiroaki Misawa[1], Fuminori Tsuchiya[1], Atsushi Kumamoto[2], Yuto Katoh[2], Tomoki Kimura[2], Hajime Kita[3], J.-E. Wahlund[4] (1.Planetary Plasma and Atmospheric Research Center, Tohoku University, 2.Department of Geophysics, Tohoku University, 3.ISAS/JAXA, 4.IRF Uppsala, Sweden)

[PPS01-P10] Magnetic field experiment at Jupiter icy moons (JUICE J-MAG) and in-flight alignment calibration

*Ayako Matsuoka[1], Michele Karen Dougherty[2], Patrick Brown[2], Futoshi Takahashi[3], Hisayoshi Shimizu[4], Masaki Matsushima[5] (1.Research Division for Space Plasma, Institute of Space and Astronautical Science, Japan Aerospace Exploration Agency, 2.Imperial College London, 3.Kyushu University, 4.University of Tokyo, 5.Tokyo Institute of Technology)

[PPS01-P11] Science targets of the GAnymede Laser Altimeter (GALA) for the JUICE mission

*Jun Kimura[1], Shunichi Kamata[2], Koji Matsumoto[3], Noriyuki Namiki[3], Keigo Enya[4], Masanori Kobayashi[5], Hiroshi Araki[3], Hirotomo Noda[3], Ko Ishibashi[5], Hauke Hussmann[6], Kay Lingenauber[6] (1.Osaka University, 2.Hokkaido University, 3.National Astronomical Observatory Japan, 4.ISAS/JAXA, 5.Chiba Institute of Technology, 6.German Aerospace Center (DLR), Berlin)

[PPS01-P12] Current status of the antenna developments, the data processing, scientific target for JUICE/SWI JAPAN.

*YASUKO KASAI[1], JUICE SWI Japanese Team (1.National Institute of Information and Communications Technology (NICT))

[E] Poster | P (Space and Planetary Sciences)：P-PS Planetary Sciences

5:15 PM - 6:30 PM JST | 8:15 AM - 9:30 AM UTC | Poster Hall International Exhibition Hall8, Makuhari Messe_1

[P-PS01] Outer Solar System Exploration Today, and Tomorrow

convener:Jun Kimura(Osaka University), Yasumasa Kasaba(Planetary Plasma and Atmospheric Research Center, Tohoku University), Kunio M. Sayanagi(Hampton University)

[PPS01-P01] Critical Role of Entry Probes in Giant Planet Exploration

*Sushil K Atreya[1], Olivier Mousis[2] (1.University of Michigan Ann Arbor, 2.Laboratoire d'Astrophysique de Marseille)

[PPS01-P02] OKEANOS – Jupiter Trojan Asteroid Rendezvous and Landing Experiments Using a Solar Power Sail

*Tatsuaki Okada[1,2], Takahiro Iwata[1], Yoko Kebukawa[3], Motoo Ito[4], Jun Aoki[5], Yosuke Kawai[5], Shoichiro Yokota[5], Yoshifumi Saito[1], Kentaro Terada[5], Michisato Toyoda[5], Hikaru Yabuta[6], Hisayoshi Yurimoto[1,7], Shuji Matsuura[8], Kohji Tsumura[9], Daisuke Yonetoku[10], Tatehiro Mihara[11], Ayako Matsuoka[1], Reiko Nomura[12], Hajime Yano[1], Takayuki Hirai[13], Atsushi Kumamoto[9], Ryosuke Nakamura[14], Stephan Ulamec[15], Ralf Jaumann[15], Jean-Pierre Bibring[16], Noel Grand[17], Cyril Szopa[18], Ernesto Palomba[19], Jorn Helbert[15], Alain Herique[20], Matthias Grott[15], Hans-Ulrich Auster[21], Goester Klingelhoefer[22], Fumi Yoshida[13], Makoto Yoshikawa[1], Jun Matsumoto[1], Toshihiro Chujo[1], Masanori Matsushita[1], Takanao Saiki[1], Hideki Kato[1], Osamu Mori[1], Junichiro Kawaguchi[1] (1.Japan Aerospace Exploration Agency, 2.University of Tokyo, 3.Yokohama National University, 4.Japan Agency for Marine-Earth Science and Technology, 5.Osaka University, 6.Hiroshima University, 7.Hokkaido University, 8.Kwansei Gakuin University, 9.Tohoku University, 10.Kanazawa University, 11.RIKEN, 12.National Astronomical Observatory of Japan, 13.Chiba Institute of Technology, 14.National Institute of Advanced Industrial Science and Technology, 15.German Aerospace Center, 16.Institut d'Astrophysique Spatiale, 17.LISA, 18.LATMOS, 19.INAF-IAPS, 20.IPAG, 21.TU Braunschweig, 22.Leibniz Universität Hannover)

[PPS01-P03] Magnetic field model of Jovian magnetosphere

*Naoya Momoki[1], Hiroaki TOH[1] (1.Division of Earth and Planetary Sciences, Graduate School of Science, Kyoto University)

[PPS01-P04] Enhancement of the Jovian thermospheric temperature above the Great Red Spot based on the infrared spectroscopic data obtained with IRTF/iSHELL

*Ayumu Kambara[1], Hajime Kita[2], Takeshi Sakanoi[1], Yasumasa Kasaba[1], Masato Kagitani[1], Haruna Watanabe[1] (1.Planetary Plasma and Atmospheric Research Center, Graduate School of Science, Tohoku University, 2.Institute of Space and Astronautical Science, Japan Aerospace Exploration Agency)

[PPS01-P05] Pulsation-like variation of Jovian infrared polar emission observed by Subaru 8-m: H3+ and methane emissions

*Yasumasa Kasaba[1], Haruna Watanabe[1], Hajime Kita[2], Chihiro Tao[3], Takeshi Sakanoi[1], Masato Kagitani[1], Orton Glenn[1,4], James Sinclair[4] (1.Planetary Plasma and Atmospheric Research Center, 2.ISAS/JAXA, 3.NICT, 4.NASA/JPL)

[PPS01-P06] Structure of Io plasma torus observed with the Tohoku 60-cm telescope

*Masato Kagitani[1], Fuminori Tsuchiya[1], Kazuo Yoshioka[2], Go Murakami[3], Tomoki Kimura[1], Ryoichi Koga[1], Reina Hikida[4], Takeshi Sakanoi[1] (1.Graduate School of Science, Tohoku University, 2.Graduate School of frontier Science, The University of Tokyo, 3.Institute of Space and Astronautical Science, Japan Aerospace Exploration Agency, 4.Department of Earth and Planetary Science, Graduate School of Science, Tokyo University)

[PPS01-P07] Ion Scale Height Variability in Hisaki Io Torus Observations

*Nicholas McCord Schneider[1], Carl Schmidt[2], Masato Kagitani[3], Yasumasa Kasaba[3], Tomoki Kimura[3], Go Murakami[4], Fuminori Tsuchiya[3], Hajime Kita[3], Reina Hikida[5], Ichiro Yoshikawa[5], Kazuo Yoshioka[5] (1.LASP, University of Colorado Boulder, 2.Boston University, 3.Tohoku University, 4.ISAS/JAXA, 5.University of Tokyo)

[PPS01-P08] Size of the Smallest Particles in Saturn's Rings

*Keiji Ohtsuki[1], Hiroshi Kawamura[1], Naoyuki Hirata[1], Hiroshi Daisaka[2], Hiroshi Kimura[3] (1.Graduate School of Science, Kobe University, 2.Graduate School of Commerce and Management, Hitotsubashi University, 3.Planetary Exploration Research Center, Chiba Institute of Technology)

[PPS01-P09] The Radio & Plasma Wave Investigation (RPWI) for JUICE for the investigation of Jupiter and Icy Moons System: Contributions from Japan

*Yasumasa Kasaba[1], Hiroaki Misawa[1], Fuminori Tsuchiya[1], Atsushi Kumamoto[2], Yuto Katoh[2], Tomoki Kimura[2], Hajime Kita[3], J.-E. Wahlund[4] (1.Planetary Plasma and Atmospheric Research Center, Tohoku University, 2.Department of Geophysics, Tohoku University, 3.ISAS/JAXA, 4.IRF Uppsala, Sweden)

[PPS01-P10] Magnetic field experiment at Jupiter icy moons (JUICE J-MAG) and in-flight alignment calibration

*Ayako Matsuoka[1], Michele Karen Dougherty[2], Patrick Brown[2], Futoshi Takahashi[3], Hisayoshi Shimizu[4], Masaki Matsushima[5] (1.Research Division for Space Plasma, Institute of Space and Astronautical Science, Japan Aerospace Exploration Agency, 2.Imperial College London, 3.Kyushu University, 4.University of Tokyo, 5.Tokyo Institute of Technology)

[PPS01-P11] Science targets of the GAnymede Laser Altimeter (GALA) for the JUICE mission

*Jun Kimura[1], Shunichi Kamata[2], Koji Matsumoto[3], Noriyuki Namiki[3], Keigo Enya[4], Masanori Kobayashi[5], Hiroshi Araki[3], Hirotomo Noda[3], Ko Ishibashi[5], Hauke Hussmann[6], Kay Lingenauber[6] (1.Osaka University, 2.Hokkaido University, 3.National Astronomical Observatory Japan, 4.ISAS/JAXA, 5.Chiba Institute of Technology, 6.German Aerospace Center (DLR), Berlin)

[PPS01-P12] Current status of the antenna developments, the data processing, scientific target for JUICE/SWI JAPAN.

*YASUKO KASAI[1], JUICE SWI Japanese Team (1.National Institute of Information and Communications Technology (NICT))

[E] Oral | P (Space and Planetary Sciences)：P-PS Planetary Sciences

10:45 AM - 12:15 PM JST | 1:45 AM - 3:15 AM UTC | A01 TOKYO BAY MAKUHARI HALL

[P-PS03] Solar System Small Bodies: A New Frontier Arising Hayabusa 2, OSIRIS-REx and Other Projects

convener:Masateru Ishiguro(Department of Physics and Astronomy, Seoul National University), Taishi Nakamoto(Tokyo Institute of Technology), Masanao Abe(Institute of Space and Astronautical Science, Japan Aerospace Exploration Agency), Olivier S Barnouin(Johns Hopkins University Applied Physics Laboratory), Chairperson:Masateru Ishiguro(Seoul National University)

10:45 AM - 11:00 AM JST | 1:45 AM - 2:00 AM UTC

[PPS03-01] The shape and origin of the rubble-pile asteroid Ryugu

★Invited Papers

*Sei-ichiro WATANABE[1,5], Masatoshi Hirabayashi[2], Naru Hirata[3], Naoyuki Hirata[4], Rina Noguchi[5], Yuri Shimaki[5], Hitoshi Ikeda[6], Eri Tatsumi[7], Makoto Yoshikawa[5], Shota Kikuchi[5], Hikaru Yabuta[8], Tomoki Nakamura[9], Shogo Tachibana[7,5], Yoshiaki Ishihara[10], Tomokatsu Morota[1], Kohei Kitazato[3], Naoya Sakatani[5], Koji Matsumoto[11,12], Koji Wada[13], Hiroki Senshu[13], Chikatoshi Honda[3], Tatsuhiro Michikami[14], Hiroshi Takeuchi[5], Toru Kouyama[15], Rie Honda[16], Robert Gaskell[17], Eric Palmer[17], Olivier S. Barnouin[18], Patrick Michel[19], Paul Abell[20], Yukio Yamamoto[5], Satoshi Tanaka[5], Kei Shirai[5], Moe Matsuoka[5], Seiji Sugita[5,7], Tatsuaki Okada[5], Noriyuki Namiki[11], Masahiko Arakawa[4], Masateru Ishiguro[21], Kazunori Ogawa[4], Fuyuto Terui[5], Takanao Saiki[5], Satoru Nakazawa[5], Yuichi Tsuda[5], Hayabusa2 Science Team (1.Division of Earth and Planetary Sciences, Graduate School of Science, Nagoya University, 2.Auburn University, 3.University of Aizu, 4.Kobe University, 5.ISAS, JAXA, 6.Research and Development Directorate, JAXA, 7.University of Tokyo, 8.Hiroshima University, 9.Tohoku University, 10.National Institute for Environmental Studies, 11.National Astronomical Observatory of Japan, 12.SOKENDAI, 13.Chiba Institute of Technology, 14.Kindai University, 15.National Institute of Advanced Industrial Science and Technology, 16.Kochi University, 17.Planetary Science Institute, 18.John Hopkins University, 19.Universite Cote d'Azur, Observatorie de la Cote d'Azur, 20.NASA, Johnson Space Center, 21.Seoul National University)

11:00 AM - 11:15 AM JST | 2:00 AM - 2:15 AM UTC

[PPS03-02] Results of Hayabusa2 Near Infrared Spectroscopy at Asteroid Ryugu

*Takahiro Iwata[1], Kohei Kitazato[2], Masanao Abe[1], Makiko Ohtake[1], Yusuke Nakauchi[1], Moe Matsuoka[1], KOHJI TSUMURA[3], Shuji Matsuura[4], Lucie Riu[1], NIRS3 Team (1.Institute of Space and Astronautical Science, Japan Aerospace Exploration Agency, 2.The University of Aizu, 3.Tohoku University, 4.Kwansei Gakuin University)

11:15 AM - 11:30 AM JST | 2:15 AM - 2:30 AM UTC

[PPS03-03] Impact experiment on asteroid Ryugu by Small-Carry on impactor of Hayabusa-2 and observation of the impact ejecta by a Deployable CAMera-3

★Invited Papers

*Masahiko Arakawa[1], Takanao Saiki[2], Toshihiko Kadono[3], Yasuhiko Takagi[4], Koji Wada[5], Yu-ichi Iijima[2], Hiroshi Imamura[2], Chisato Okamoto[1], Yuri Shimaki[2], Kei Shirai[2], Satoru Nakazawa[2], Masahiko Hayakawa[2], Naru Hirata[6], Hajime Yano[2], Hirotaka Sawada[2], Kazunori Ogawa[1], Ko Ishibashi[5], Hiroshi Kimura[5], Masanori Kobayashi[5], Naoya Sakatani[2], Hajime Hayakawa[2], Rie Honda[7], Seiji Sugita[8], Tomokatsu Morota[9], Shingo Kameda[10], ERI TATSUMI[8], Chikatoshi Honda[6], yokota yasuhiro[2], Toru Kouyama[11], Manabu Yamada[5], Hidehiko Suzuki[12], Kazuo Yoshioka[13], Yuichiro Cho[8], Moe Matsuoka[2] (1.Graduate School of Science, Kobe University, 2.Institute of Space and Astronautical Science, Japan Aerospace Exploration Agency, 3.University of Occupational and Environmental Health, 4.Aichi Toho University, 5.Planetary Exploration Research Center, Chiba Institute of Technology, 6.Dep. of Computer Science and Engineering, Univ. of Aizu, 7.Department of Science and Technology, System of Natual Science, Kochi University, 8.Department of Earth and Planetary Science, Graduate School of Science Sciece, The University of Tokyo, 9.Graduate School of Environmental Studies, Nagoya University, 10.School of Science, Rikkyo University, 11.National Institute of Advanced Industrial Science and Technology, 12.Department of physics, Meiji university, 13.Graduate School of frontier Science, The University of Tokyo)

11:30 AM - 11:45 AM JST | 2:30 AM - 2:45 AM UTC

[PPS03-04] Impact cratering experiments on glass beads with bead size frequency distribution: Implications for cratering process on asteroid Ryugu

*Minami Yasui[1], Masahiko Arakawa[1], Sunao Hasegawa[2], Yuya Yamamoto[1], Ryo Sugimura[1] (1.Graduate School of Science, Kobe University, 2.ISAS, JAXA)

11:45 AM - 12:00 PM JST | 2:45 AM - 3:00 AM UTC

[PPS03-05] Enhancement of impact heating in strength-supported media

*Kosuke Kurosawa[1], Hidenori Genda[2], Shigeru Wakita[2], Thomas M Davison[3], Ryuki Hyodo[2], Tomoki Nakamura[4] (1.Planetary Exploration Research Center, Chiba Institute of Technology, 2.Earth-Life Science Institute, Tokyo Institute of Technology, 3.Department of Earth Science & Engineering, Imperial College London, 4.Department of Earth Science, Tohoku University)

12:00 PM - 12:15 PM JST | 3:00 AM - 3:15 AM UTC

[PPS03-06] Global Thermal Inertia and Surface Roughness of Asteroid 162173 Ryugu by TIR on Hayabusa2

*Yuri Shimaki[1], Hiroki Senshu[2], Naoya Sakatani[1], Tatsuaki Okada[1,3], Tetsuya Fukuhara[4], Satoshi Tanaka[1], Makoto Taguchi[4], Takehiko Arai[5], Hirohide Demura[6], Yoshiko Ogawa[6], Kentaro Suko[6], Tomohiko Sekiguchi[7], Toru Kouyama[8], Jun Takita[9], Tsuneo Matsunaga[10], Takeshi Imamura[3], Takehiko Wada[1], Sunao Hasegawa[1] (1.Institute of Space and Astronautical Science, Japan Aerospace Exploration Agency, 2.Chiba Institute of Technology, 3.University of Tokyo, 4.Rikkyo University, 5.Ashikaga University, 6.University of Aizu, 7.Hokkaido University of Education, 8.National Institute of Advanced Industrial Science and Technology, 9.Hokkaido Kitami Hokuto High School, 10.National Institute for Environmental Studies)

[E] Oral | P (Space and Planetary Sciences)：P-PS Planetary Sciences

1:45 PM - 3:15 PM JST | 4:45 AM - 6:15 AM UTC | A01 TOKYO BAY MAKUHARI HALL

[P-PS03] Solar System Small Bodies: A New Frontier Arising Hayabusa 2, OSIRIS-REx and Other Projects

convener:Masateru Ishiguro(Department of Physics and Astronomy, Seoul National University), Taishi Nakamoto(Tokyo Institute of Technology), Masanao Abe(Institute of Space and Astronautical Science, Japan Aerospace Exploration Agency), Olivier S Barnouin(Johns Hopkins University Applied Physics Laboratory), Chairperson:Olivier Barnouin(Johns Hopkins University Applied Physics Laboratory)

1:45 PM - 2:00 PM JST | 4:45 AM - 5:00 AM UTC

[PPS03-07] Asteroid Ryugu's parent body and its properties inferred from Haybusa2 multi-band imaging observations

★Invited Papers

*Seiji Sugita[1,6], Rie Honda[2], Tomokatsu Morota[3], Shingo Kameda[4], ERI TATSUMI[1], Chikatoshi Honda[7], yokota yasuhiro[2,5], Toru Kouyama[8], Naoya Sakatani[5], Manabu Yamada[6], Hidehiko Suzuki[10], Kazuo Yoshioka[1], Yuichiro Cho[1], Moe Matsuoka[5], Kazunori Ogawa[9], Deborah Domingue[11], Hideaki Miyamoto[1], Olivier Barnouin[12], Patrick Michel[13], Carolyn Ernst[12], Sei-ichiro WATANABE[3], Yuichi Tsuda[5] (1.University of Tokyo, 2.Kochi University, 3.Nagoya University, 4.Rikkyo University, 5.JAXA/ISAS, 6.Chiba Institute of Technology, PERC, 7.University of Aizu, 8.National Institute of Advanced Industrial Science and Technology, 9.Kobe University, 10.Meiji University, 11.Planetary Science Institute, 12.Johns Hopkins University/Applied Physics Laboratory, 13.Observatoire de la Coˆte d'Azur)

2:00 PM - 2:15 PM JST | 5:00 AM - 5:15 AM UTC

[PPS03-08] REDDENING PROCESS OF THE RYUGU SURFACE BASED ON THE CRATER SIZE-FREQUENCY DISTRIBUTION

*Tomokatsu Morota[1], Yuichiro Cho[2], Masanori Kanamaru[3], Rie Honda[4], Shingo Kameda[5], ERI TATSUMI[2], yokota yasuhiro[6], Toru Kouyama[7], Hidehiko Suzuki[8], Manabu Yamada[9], Naoya Sakatani[6], Chikatoshi Honda[10], Masahiko Hayakawa[6], Kazuo Yoshioka[2], Moe Matsuoka[6], Tatsuhiro Michikami[11], Hideaki Miyamoto[2], Hiroshi Kikuchi[2], Ryodo Hemmi[2], Masatoshi Hirabayashi[12], Naoyuki Hirata[13], Naru Hirata[10], Carolyn Ernst[14], Olivier Barnouin[14], Hirotake Sawada[6], Seiji Sugita[2] (1.Nagoya University, 2.The University of Tokyo, 3.Osaka University, 4.Kochi University, 5.Rikky University, 6.JAXA, 7.AIST, 8.Meiji University, 9.Chiba Institute of Technology, 10.The University of Aizu, 11.Kindai University, 12.Auburn University, 13.Kobe University, 14.Johns Hopkins University/Applied Physics Laboratory)

2:15 PM - 2:30 PM JST | 5:15 AM - 5:30 AM UTC

[PPS03-09] Preliminary report on global distribution visible spectra of asteroid Ryugu based on clustering

*Rie Honda[1], Yasuhiro Yokota[1,2], Eri Tatsumi[3], Antonella Barucci[12], Davide Perna[13], Moe Matsuoka[2], Deborah Domingue[14], Tomokatsu Morota[4], Shingo Kameda[5], Toru Kouyama[15], Hidehiko Suzuki[6], Manabu Yamada[10], Naoya Sakatani[2], Chikatoshi Honda[7], Lucille LeCorre[14], Masahiko Hayakawa[2], Kazuo Yoshioka[3], Yuichiro Cho[3], Yukio Yamamoto[2], Naru Hirata[7], Naoyuki Hirata[8], Tomoki Nakamura[9], Takahiro Hiroi[11], Hirotaka Sawada[2], Yuki Fujii[1], Seiji Sugita[3], Ryo Hayashi[1] (1.Kochi University, 2.ISAS/JAXA, 3.University of Tokyo, 4.Nagoya University, 5.Rikkyo University, 6.Meiji University, 7.Aizu University, 8.Kobe University, 9.Tohoku University, 10.Chiba Institute of Technology, 11.Brown University, 12.Paris Observatory, 13.INAF, 14.Planetary Science Institute, 15.National Institute of Advanced Industrial Science and Technology)

2:30 PM - 2:45 PM JST | 5:30 AM - 5:45 AM UTC

[PPS03-10] Visible spectra of small bright spots on asteroid 162173 Ryugu

*Chiho Sugimoto[1], Eri Tatsumi[1], Yuichiro Cho[1], Kazuo Yoshioka[1], Hirotaka Sawada[2], Yasuhiro Yokota[2], Naoya Sakatani[2], Masahiko Hayakawa[2], Moe Matsuoka[2], Rie Honda[3], Tomokatsu Morota[4], Shingo Kameda[5], Manabu Yamada[6], Toru Kouyama[7], Hidehiko Suzuki[8], Chikatoshi Honda[9], Kazunori Ogawa[10], Deborah Domingue[11], Patrick Michel[12], Seiji Sugita[1] (1.University of Tokyo, 2.JAXA/ISAS, 3.Kochi University, 4.Nagoya University, 5.Rikkyo University, 6.Chiba Institute of Technology, 7.AIST, 8.Meiji University, 9.University of Aizu, 10.Kobe University, 11.Planetary Science Institute, 12.Nice Observatory)

2:45 PM - 3:00 PM JST | 5:45 AM - 6:00 AM UTC

[PPS03-11] Geomorphological characteristics of asteroid Ryugu: implications to its evolutional history

*Hideaki Miyamoto[1], Ryodo Hemmi[1], Hiroshi Kikuchi[1], Goro Komatsu[2], Chikatoshi Honda[3], Tatsuhiro Michikami[4], Tomokatsu Morota[5], Yuichiro Cho[1], Olivier S Barnouin[6], Sho Sasaki[7], Naru Hirata[3], Naoyuki Hirata[8], Rie Honda[10], Shingo Kameda[11], ERI TATSUMI[1], Yasuhiro Yokota[12], Toru Kouyama[13], Hidehiko Suzuki[14], Manabu Yamada[15], Naoya

Sakatani[12], Masahiko Hayakawa[12], Kazuo Yoshioka[1], Moe Matsuoka[12], Masatoshi Hirabayashi[9], Hirotaka Sawada[12], Seiji Sugita[1] (1.University of Tokyo, 2.D'Annunzio University, 3.Aizu University, 4.Kinki University, 5.Nagoya University, 6.Johns Hopkins University, 7.Osaka University, 8.Kobe University, 9.Auburn University, 10.Kouchi University, 11.Rikkyo University, 12.ISAS/JAXA, 13.AIST, 14.Meiji University, 15.Chiba Inst Tech)

3:00 PM - 3:15 PM JST | 6:00 AM - 6:15 AM UTC

[PPS03-12] Global distribution of sub-meter boulders measured with texture analysis of Ryugu images

*Naoya Tanabe[1], Yuichiro Cho[1], ERI TATSUMI[1], Tomokatsu Morota[4], Chikatoshi Honda[9], Tatsuhiro Michikami[11], Patrick Michel[12], Carolyn Ernst[13], Olivier S Barnouin[13], Kazuo Yoshioka[1], Sawada Hirotaka[2], yokota yasuhiro[2,3], Naoya Sakatani[2], Masahiko Hayakawa[2], Moe Matsuoka[2], Rie Honda[3], Shingo Kameda[5], Manabu Yamada[6], Toru Kouyama[7], Hidehiko Suzuki[8], Kazunori Ogawa[10], Seiji Sugita[1] (1.University of Tokyo, 2.JAXA/ISAS, 3.Kochi University, 4.Nagoya University, 5.Rikkyo University, 6.Chiba Inst. Tech., PERC, 7.AIST, 8.Meiji University, 9.University of Aizu, 10.Kobe University, 11.Kindai University, 12.Observatoire de la Côte d'Azur, 13.Johns Hopkins University APL)

[E] Oral | P (Space and Planetary Sciences)：P-PS Planetary Sciences

3:30 PM - 5:00 PM JST | 6:30 AM - 8:00 AM UTC | A01 TOKYO BAY MAKUHARI HALL

[P-PS03] Solar System Small Bodies: A New Frontier Arising Hayabusa 2, OSIRIS-REx and Other Projects

convener:Masateru Ishiguro(Department of Physics and Astronomy, Seoul National University), Taishi Nakamoto(Tokyo Institute of Technology), Masanao Abe(Institute of Space and Astronautical Science, Japan Aerospace Exploration Agency), Olivier S Barnouin(Johns Hopkins University Applied Physics Laboratory), Chairperson:Masanao Abe(Institute of Space and Astronautical Science, JAXA)

3:30 PM - 3:45 PM JST | 6:30 AM - 6:45 AM UTC

[PPS03-13] Brightness and morphology variations on surface boulders of 162173 Ryugu: Space Weathering, Breccia, and Thermal Cracks

*Sho Sasaki[1], Seiji Sugita[2], Eri Tatsumi[2], Hideaki Miyamoto[3], Chikatoshi Honda[4], Tomokatsu Morota[5], Masatoshi Hirabayashi[6], Shiho Kanda[1], Naru Hirata[4], Takahiro Hiroi[7], Tomoki Nakamura[8], Takaaki Noguchi[9], Rie Honda[10], Tatsuhiro Michikami[11], Sei-ichiro Watanabe[5], Noriyuki Namiki[12], Patrick Michel[13], Shingo Kameda[14], Toru Kouyama[15], Hidehiko Suzuki[16], Manabu Yamada[17], Hiroshi Kikuchi[3], Yuichiro Cho[2], Kazuo Yoshioka[18], Masahiko Hayakawa[19], Moe Matsuoka[19], Rina Noguchi[19], Naoya Sakatani[19], Hirotaka Sawada[19], yokota yasuhiro[19,10], Makoto Yoshikawa[19] (1.Department of Earth and Space Science, School of Science, Osaka University, 2.Department of Earth and Planetary Science, School of Science, University of Tokyo, 3.Department of Systems Innovation, School of Engineering, University of Tokyo, 4.University of Aizu, 5.Graduate School of Environmental Studies, Nagoya University, 6.Auburn University, 7.Brown University, 8.Department of Earth and Planetary Materials Sciences, Faculty of Science, Tohoku University, 9.Department of Arts and Science, Kyushu University, 10.Department of Science and Technology, System of Natural Science, Kochi University, 11.Faculty of Engineering, Kinki University, 12.RISE Project, National Astronomical Observatory of Japan, 13.Observatoire de la Cote d'Azur, 14.School of Science, Rikkyo University, 15.National Institute of Advanced Industrial Science and Technology, 16.Department of physics, Meiji university, 17.Planetary Exploration Research Center, Chiba Institute of Technology, 18.School of frontier Science, University of Tokyo, 19.Institute of Space and Astronautical Science, Japan Aerospace Exploration Agency)

3:45 PM - 4:00 PM JST | 6:45 AM - 7:00 AM UTC

[PPS03-14] Topography of large craters and equatorial bulge of 162173 Ryugu

*Noriyuki Namiki[1,2], Takahide Mizuno[3], Hiroki Senshu[4], Hirotomo Noda[1,2], Koji Matsumoto[1,2], Naru Hirata[5], Ryuhei Yamada[5], Yoshiaki Ishihara[6], HItoshi Ikeda[3], Hiroshi Araki[1,2], Keiko Yamamoto[1,2], Shinsuke Abe[7], Fumi Yoshida[4], Arika Higuchi[1], Sho Sasaki[10], Shoko Oshigami[1], Seiitsu Tsuruta[1], Kazuyoshi Asari[1], Seiichi Tazawa[1], Makoto Shizugami[1], Hideaki Miyamoto[8], Hirohide Demura[5], Jun Kimura[10], Toshimichi Otsubo[9] (1.National Astronomical Observatory of Japan, 2.SOKENDAI (The Graduate University for Advanced Studies), 3.Japan Aerospace Exploration Agency, Institute of Space and Astronautical Science, 4.Chiba Institute of Technology, 5.The University of Aizu, 6.National Institute of Advanced Industrial Science and Technology, 7.Nihon University,8Osaka University, 8.The University of Tokyo, 9.Hitotsubashi University, 10.Osaka University)

4:00 PM - 4:15 PM JST | 7:00 AM - 7:15 AM UTC

[PPS03-15] Observation of 1064 nm normal albedo around equator of the Ryugu using the Hayabusa2 LIDAR

*Ryuhei Yamada[1], Keiko Yamamoto[2], Hiroshi Araki[2], Hirotomo Noda[2], Hiroki Senshu[3], Noriyuki Namiki[2], Koji Matsumoto[2], Fumi Yoshida[3], Shinsuke Abe[4], Naru Hirata[1] (1.The University of Aizu, Department of Computer Science and Engineering, 2.National Astronomical Observatory of Japan, 3.Chiba Institute of Technology, 4.Nihon University)

4:15 PM - 4:30 PM JST | 7:15 AM - 7:30 AM UTC

[PPS03-16] Improved Trajectory of Hayabusa2 by Combining LIDAR Data and a Shape Model

*Koji Matsumoto[1], Hirotomo Noda[1], Yoshiaki Ishihara[2], Hiroki Senshu[3], Keiko Yamamoto[1], Naru Hirata[4], Naoyuki Hirata[5], Noriyuki Namiki[1], Toshimichi Otsubo[6], Sei-ichiro WATANABE[7], Takahide Mizuno[8], Yukio Yamamoto[8], Hitoshi Ikeda[8], Naoko Ogawa[8], Shota Kikuchi[8], Takanao Saiki[8], Yuichi Tsuda[8] (1.RISE Project, National Astronomical Observatory of Japan, 2.National Institute for Environmental Studie, 3.Chiba Institute of Technology, 4.The University of Aizu, 5.Kobe University, 6.Hitotsubashi University, 7.Nagoya University, 8.JAXA)

4:30 PM - 4:45 PM JST | 7:30 AM - 7:45 AM UTC

[PPS03-17] Present status of preparation for the Ryugu sample curation returned by the Hayabusa2

*Toru Yada[1], Masanao Abe[1], Aiko Nakato[1], Kasumi Yogata[1], Kanako Sakamoto[1], Masahiro Nishimura[1], Tatsuaki Okada[1], Yuki Nakano[2], Miwa Yoshitake[1], Kazuya Kumagai[3], Ayako Iwamae[3], Shizuho Furuya[1], Shogo Tachibana[4,1],

Hisayoshi Yurimoto[1,2] (1.Japan Aerospace Exploration Agency, 2.Hokkaido University, 3.Marine Works Japan Ltd., 4.University of Tokyo)

4:45 PM - 5:00 PM JST | 7:45 AM - 8:00 AM UTC

[PPS03-18] Analysis of the grain from the asteroid Ryugu proposed by the Phase 2 curation “Team KOCHI”

*Motoo Ito[1], Naotaka Tomioka[1], Masayuki Uesugi[2], Kentaro Uesugi[2], Ohigashi Takuji[3], Akira Yamaguchi[4], Naoya Imae[4], Yuzuru Karouji[5], Naoki Shirai[6], Toru Yada[5], Masanao Abe[5] (1.Kochi Institute for Core Sample Research, JAMSTEC, 2.JASRI, 3.UVSOR Synchrotron Facility, Institute for Molecular Science, 4.National Institute Polar Research, 5.JAXA, 6.Tokyo Metropolitan University)

[J] Oral | P (Space and Planetary Sciences)：P-PS Planetary Sciences

9:00 AM - 10:30 AM JST | 12:00 AM - 1:30 AM UTC | A01 TOKYO BAY MAKUHARI HALL

[P-PS06] Planetary Sciences

convener:Kenji Kurosaki(Department of Physics, Nagoya University), Yusuke Nakauchi(Japan Aerospace Exploration Agency), Chairperson:Ryo Suetsugu(University of Occupational and Environmental Health, Japan), Keisuke Sugiura(Nagoya University)

9:00 AM - 9:15 AM JST | 12:00 AM - 12:15 AM UTC

[PPS06-25] Tensile Strength of Porous Dust Aggregates Measured with Dust N-body Simulations

*Misako Tatsuuma[1,2], Akimasa Kataoka[2], Hidekazu Tanaka[3] (1.The University of Tokyo, 2.National Astronomical Observatory of Japan, 3.Tohoku University)

9:15 AM - 9:30 AM JST | 12:15 AM - 12:30 AM UTC

[PPS06-26] **Filling factor dependence of the thermal conductivity understood from the graph structure of dust aggregates**

*Sota ARAKAWA[1], Masaki TAKEMOTO[1], Taishi NAKAMOTO[1] (1.Tokyo Institute of Technology)

9:30 AM - 9:45 AM JST | 12:30 AM - 12:45 AM UTC

[PPS06-27] Collisional disruption of planetesimals: dependence of material strength

*Ryo Suetsugu[1], Hidekazu Tanaka[2], Hiroshi Kobayashi[3], Hidenori Genda[4] (1.University of Occupational and Environmental Health, 2.Tohoku University, 3.Nagoya University, 4.Tokyo Institute of Technology)

9:45 AM - 10:00 AM JST | 12:45 AM - 1:00 AM UTC

[PPS06-28] Size and cooling rate of chondrules formed thorough collision between planetesimals containing volatile materials

*Sin-iti Sirono[1] (1.Department of Earth and Planetary Sciences, Nagoya University)

10:00 AM - 10:15 AM JST | 1:00 AM - 1:15 AM UTC

[PPS06-29] From Dust to Planet via collisional growth

*Hiroshi Kobayashi[1], Hidekazu Tanaka[2] (1.Department of Physics, Nagoya University, 2.Tohoku University)

10:15 AM - 10:30 AM JST | 1:15 AM - 1:30 AM UTC

[PPS06-30] Impact Conditions for the Formation of the Extremely Elongated Shape of 1I/’Oumuamua

*Keisuke Sugiura[1], Hiroshi Kobayashi[1], Shu-ichiro Inutsuka[1] (1.NAGOYA UNIVERSITY Graduate School of Science)

[J] Poster | P (Space and Planetary Sciences)：P-PS Planetary Sciences

3:30 PM - 5:00 PM JST | 6:30 AM - 8:00 AM UTC | Poster Hall International Exhibition Hall8, Makuhari Messe_2

[P-PS06] Planetary Sciences

convener:Kenji Kurosaki(Department of Physics, Nagoya University), Yusuke Nakauchi(Japan Aerospace Exploration Agency)

[PPS06-P01] The Study of Using SLR and GPS Observation Data to Estimate Geocenter Motion.

*Yih Jack Cheng[1], Fang-shii Ning[1] (1.National Chengchi University)

[PPS06-P02] Evolution of Pluto's surface albedo due to sublimation and condensation of ice

*Hisashi Matsui[1], Jun Kimura[1] (1.Osaka University)

[PPS06-P03] ***Origin of the moon*, Reason why Moon is always facing to Earth, Origin of Moon Sea, reasons why there is no Ocean behind Moon**

*Akira Taneko[1] (1.SEED SCIENCE Lab.)

[PPS06-P04] ***Proposed the Good model*** to verify**Origins of Solar System (Planet, Asteroid belt, Earth, Moon)**
*with "Multi Impact Hypothesis ",***from 16' results of one time Evolution *by Abduction.***
cf. Simulation is an example by Abduction from 1.

*Akira Taneko[1] (1.SEED SCIENCE Lab.)

[PPS06-P05] Quantitative evaluation of the cumulus convection schemes for the implementation into the Paleo Martian Global Climate Model

*Katsushige Toriumi[1], Arihiro Kamada[1], Takeshi Kuroda[1,2], Naoki Terada[1], Yasumasa Kasaba[3], Isao Murata[1], Hiromu Nakagawa[1] (1.Tohoku university, Geophysics, Planetary Atmospheric Physics, 2.NICT, 3.Tohoku university, Geophysics, Planetary Plasma and Atmosperic Research Center)

[PPS06-P06] Forced libration of Ganymede including the visco-elastic tidal deformation

*shinichiro kojima[1], Jun Kimura[1], Shunichi Kamata[2] (1.Department of Earth and Space Science, Graduate School of Science, Osaka University, 2.Creative Research Institution, Hokkaido University)

[PPS06-P07] Experimental study on collision destruction simulating the primitive meteorite parent body

*Horikawa Kazuhiro[1], Masahiko Arakawa[1], Minami Yasui[1], Ryo Sugimura[1] (1.Kobe University Faculty of Science)

[PPS06-P08] Evolution of atmospheric composition in the early Martian atmosphere

*Ryosuke Yagi[1], Naoki Terada[1] (1.Planetary Atmospheric Physics Group, Tohoku University, Japan)

[PPS06-P09] Observation of catastrophic destruction of two different targets using X Ray photography

*Takumi Nagano[1], Masahiko Arakawa[1], Minami Yasui[1], masato nakamura[1], Fumiya Nagatomo[1] (1.Faculty of Science Kobe University)

[PPS06-P10] Charge transport between granular particles in an ejecta curtain produced by hypervelocity impacts

*Kosuke Kurosawa[1], Takanori Iwasawa[2], Satoshi Okuzumi[2], Sunao Hasegawa[3], Takayuki Muranushi[4] (1.Planetary Exploration Research Center, Chiba Institute of Technology, 2.Department of Earth and Planetary Sciences, Tokyo Institute of Technology, 3.ISAS, JAXA, 4.AICS, RIKEN)

[PPS06-P11] Nonlinear outcome of gravitational instability in irradiated protoplanetary disks

*Shigenobu Hirose[1], Jiming Shi[2] (1.Japan Agency for Marine-Earth Science and Technology, 2.Spotify USA Inc)

[PPS06-P12] Rheology of clay paste and application to the investigation of formation process of surface topography on the Mars

*Chihiro Uemura[1], Takahiro Iwata[1,2], Akio Nakahara[3], Yosuke Matsuo[3], Tomohiro Usui[2], Rina Noguchi[2] (1.SOKENDAI, 2.ISAS/JAXA, 3.Nihon Univ.)

[PPS06-P13] An Explanation for Physical Mechanism of the Streaming Instability

*Hiroaki Kaneko[1] (1.Tokyo Institude of Technology)

[PPS06-P14] Spatial motion of the Earth-Moon system and Earth pole oscillatory process

*Alexandra Sergeevna Filippova[1], Vadim Vladimirovich Perepelkin[1], Wai Yan Soe[1] (1.Moscow Aviation Institute)

[PPS06-P15] Chondrule formation model by lightning in high dust density regions

*Chihiro Ikeda[1], Taishi Nakamoto[1] (1.Tokyo Institute of Technology)

[PPS06-P16] The transition to superrotation in stratospheric atmospheres

*Motoki Sumi[1] (1.Tokyo Institute of Technology)

[PPS06-P17] **ExPRES: a Tool to Simulate Exoplanetary and Planetary Radio Emissions**

*Corentin LOUIS[1,2,3], Sebastien L. Hess[4], Baptiste Cecconi[2,3], Philippe Zarka[2,3], Laurent Lamy[2,3], Stéphane Aicardi[5], Alan Loh[2] (1.IRAP, Toulouse, 2.LESIA - Observatoire de Paris, 3.USN, Observatoire de Paris, 4.ONERA-The French Aerospace Lab, FR-31055 Toulouse, France, 5.DIO, Observatoire de Paris, PSL Research University, CNRS, Paris, France)

[PPS06-P18] Crustal structures of major mercurian basins

*Qingyun Deng[1], Fei Li[1], Jianguo Yan[1], Zhiyong Xiao[2] (1.State Key Laboratory of Information Engineering in Surveying, Mapping and Remote Sensing, Wuhan University, 2.Planetary Science Institute, China University of Geoscience)

[PPS06-P19] Application of LiDAR Technique for the 3D Digital Documentation of Cultural Heritage Sites

*Sachchidanand [1], Mayank Sharma[1], Rahul Dev Garg[1] (1.Indian Institute of Technology Roorkee)

[PPS06-P20] Tidal Interaction in the Earth-Moon System Treated as a Double Planet

*Aleksandr Aphanasievich Zlenko[1], Irina Michailovna Ryabikova[2] (1.Department of high mathematics, Moscow automobile and road construction state technical university, 2.Department of descriptive geometry, Moscow automobile and road construction state technical university)

[PPS06-P21] **The consequences of Saturn's "ring rain"**

*James O Donoghue[1,2], Luke Moore[3], Jack Connerney[4,1], Henrik Melin[5], Tom Stallard[5], Sean Hsu[6], Steve Miller[7], Kevin Baines[8] (1.NASA Goddard Space Flight Center, USA, 2.Institute of Space and Astronautical Science, Japan Aerospace Exploration Agency (ISAS; JAXA), Japan, 3.Boston University, USA, 4.Space Research Corporation, Maryland, USA, 5.University of Leicester, UK, 6.Laboratory for Atmospheric and Space Physics, University of Colorado–Boulder, CO, USA, 7.University College London, UK, 8.NASA Jet Propulsion Laboratory, California, USA)

[PPS06-P22] **Calculation of kinetic rate constants using high-level *ab initio* quantum chemical methods for planetary sciences and astrochemistry**

*Shiblee Ratan Barua[1,2], Paul Romani[1] (1.NASA Goddard Space Flight Center, Greenbelt MD USA, 2.Universities Space Research Association (USRA), Columbia MD USA)

[PPS06-P23] How many conditions must be satisfied to produce a habitable planet?

*Shigenori Maruyama[1], Soichi Omori[2] (1.Earth-Life Science Institute, Tokyo Institute of Technology, 2.The Faculty of Liberal Arts, The Open University of Japan)

[PPS06-P24] Quantitative Evaluations for Meteorite Impact Tsunami

*Naotaka YAMAMOTO CHIKASADA[1], Tetsuharu Fuse[2], Toshitaka Baba[3] (1.NIED, 2.NICT, 3.Tokushima University)

[J] Poster | P (Space and Planetary Sciences)：P-PS Planetary Sciences

5:15 PM - 6:30 PM JST | 8:15 AM - 9:30 AM UTC | Poster Hall International Exhibition Hall8, Makuhari Messe_2

[P-PS06] Planetary Sciences

convener:Kenji Kurosaki(Department of Physics, Nagoya University), Yusuke Nakauchi(Japan Aerospace Exploration Agency)

[PPS06-P01] The Study of Using SLR and GPS Observation Data to Estimate Geocenter Motion.

*Yih Jack Cheng[1], Fang-shii Ning[1] (1.National Chengchi University)

[PPS06-P02] Evolution of Pluto's surface albedo due to sublimation and condensation of ice

*Hisashi Matsui[1], Jun Kimura[1] (1.Osaka University)

[PPS06-P03] ***Origin of the moon*, Reason why Moon is always facing to Earth, Origin of Moon Sea, reasons why there is no Ocean behind Moon**

*Akira Taneko[1] (1.SEED SCIENCE Lab.)

[PPS06-P04] ***Proposed the Good model*** to verify**Origins of Solar System (Planet, Asteroid belt, Earth, Moon)**
with "Multi Impact Hypothesis ";**from 16' results of one time Evolution *by Abduction.***
cf. Simulation is an example by Abduction from 1.

*Akira Taneko[1] (1.SEED SCIENCE Lab.)

[PPS06-P05] Quantitative evaluation of the cumulus convection schemes for the implementation into the Paleo Martian Global Climate Model

*Katsushige Toriumi[1], Arihiro Kamada[1], Takeshi Kuroda[1,2], Naoki Terada[1], Yasumasa Kasaba[3], Isao Murata[1], Hiromu Nakagawa[1] (1.Tohoku university, Geophysics, Planetary Atmospheric Physics, 2.NICT, 3.Tohoku university, Geophysics, Planetary Plasma and Atmosperic Research Center)

[PPS06-P06] Forced libration of Ganymede including the visco-elastic tidal deformation

*shinichiro kojima[1], Jun Kimura[1], Shunichi Kamata[2] (1.Department of Earth and Space Science, Graduate School of Science, Osaka University, 2.Creative Research Institution, Hokkaido University)

[PPS06-P07] Experimental study on collision destruction simulating the primitive meteorite parent body

*Horikawa Kazuhiro[1], Masahiko Arakawa[1], Minami Yasui[1], Ryo Sugimura[1] (1.Kobe University Faculty of Science)

[PPS06-P08] Evolution of atmospheric composition in the early Martian atmosphere

*Ryosuke Yagi[1], Naoki Terada[1] (1.Planetary Atmospheric Physics Group, Tohoku University, Japan)

[PPS06-P09] Observation of catastrophic destruction of two different targets using X Ray photography

*Takumi Nagano[1], Masahiko Arakawa[1], Minami Yasui[1], masato nakamura[1], Fumiya Nagatomo[1] (1.Faculty of Science Kobe University)

[PPS06-P10] Charge transport between granular particles in an ejecta curtain produced by hypervelocity impacts

*Kosuke Kurosawa[1], Takanori Iwasawa[2], Satoshi Okuzumi[2], Sunao Hasegawa[3], Takayuki Muranushi[4] (1.Planetary Exploration Research Center, Chiba Institute of Technology, 2.Department of Earth and Planetary Sciences, Tokyo Institute of Technology, 3.ISAS, JAXA, 4.AICS, RIKEN)

[PPS06-P11] Nonlinear outcome of gravitational instability in irradiated protoplanetary disks

*Shigenobu Hirose[1], Jiming Shi[2] (1.Japan Agency for Marine-Earth Science and Technology, 2.Spotify USA Inc)

[PPS06-P12] Rheology of clay paste and application to the investigation of formation process of surface topography on the Mars

*Chihiro Uemura[1], Takahiro Iwata[1,2], Akio Nakahara[3], Yosuke Matsuo[3], Tomohiro Usui[2], Rina Noguchi[2] (1.SOKENDAI, 2.ISAS/JAXA, 3.Nihon Univ.)

[PPS06-P13] An Explanation for Physical Mechanism of the Streaming Instability

*Hiroaki Kaneko[1] (1.Tokyo Institude of Technology)

[PPS06-P14] Spatial motion of the Earth-Moon system and Earth pole oscillatory process

*Alexandra Sergeevna Filippova[1], Vadim Vladimirovich Perepelkin[1], Wai Yan Soe[1] (1.Moscow Aviation Institute)

[PPS06-P15] Chondrule formation model by lightning in high dust density regions

*Chihiro Ikeda[1], Taishi Nakamoto[1] (1.Tokyo Institute of Technology)

[PPS06-P16] The transition to superrotation in stratospheric atmospheres

*Motoki Sumi[1] (1.Tokyo Institute of Technology)

[PPS06-P17] **ExPRES: a Tool to Simulate Exoplanetary and Planetary Radio Emissions**

*Corentin LOUIS[1,2,3], Sebastien L. Hess[4], Baptiste Cecconi[2,3], Philippe Zarka[2,3], Laurent Lamy[2,3], Stéphane Aicardi[5], Alan Loh[2] (1.IRAP, Toulouse, 2.LESIA - Observatoire de Paris, 3.USN, Observatoire de Paris, 4.ONERA-The French Aerospace Lab, FR-31055 Toulouse, France, 5.DIO, Observatoire de Paris, PSL Research University, CNRS, Paris, France)

[PPS06-P18] Crustal structures of major mercurian basins

*Qingyun Deng[1], Fei Li[1], Jianguo Yan[1], Zhiyong Xiao[2] (1.State Key Laboratory of Information Engineering in Surveying, Mapping and Remote Sensing, Wuhan University, 2.Planetary Science Institute, China University of Geoscience)

[PPS06-P19] Application of LiDAR Technique for the 3D Digital Documentation of Cultural Heritage Sites

*Sachchidanand [1], Mayank Sharma[1], Rahul Dev Garg[1] (1.Indian Institute of Technology Roorkee)

[PPS06-P20] Tidal Interaction in the Earth-Moon System Treated as a Double Planet

*Aleksandr Aphanasievich Zlenko[1], Irina Michailovna Ryabikova[2] (1.Department of high mathematics, Moscow automobile and road construction state technical university, 2.Department of descriptive geometry, Moscow automobile and road construction state technical university)

[PPS06-P21] **The consequences of Saturn's "ring rain"**

*James O Donoghue[1,2], Luke Moore[3], Jack Connerney[4,1], Henrik Melin[5], Tom Stallard[5], Sean Hsu[6], Steve Miller[7], Kevin Baines[8] (1.NASA Goddard Space Flight Center, USA, 2.Institute of Space and Astronautical Science, Japan Aerospace Exploration Agency (ISAS; JAXA), Japan, 3.Boston University, USA, 4.Space Research Corporation, Maryland, USA, 5.University of Leicester, UK, 6.Laboratory for Atmospheric and Space Physics, University of Colorado–Boulder, CO, USA, 7.University College London, UK, 8.NASA Jet Propulsion Laboratory, California, USA)

[PPS06-P22] **Calculation of kinetic rate constants using high-level *ab initio* quantum chemical methods for planetary sciences and astrochemistry**

*Shiblee Ratan Barua[1,2], Paul Romani[1] (1.NASA Goddard Space Flight Center, Greenbelt MD USA, 2.Universities Space Research Association (USRA), Columbia MD USA)

[PPS06-P23] How many conditions must be satisfied to produce a habitable planet?

*Shigenori Maruyama[1], Soichi Omori[2] (1.Earth-Life Science Institute, Tokyo Institute of Technology, 2.The Faculty of Liberal Arts, The Open University of Japan)

[PPS06-P24] Quantitative Evaluations for Meteorite Impact Tsunami

*Naotaka YAMAMOTO CHIKASADA[1], Tetsuharu Fuse[2], Toshitaka Baba[3] (1.NIED, 2.NICT, 3.Tokushima University)

[E] Oral | P (Space and Planetary Sciences)：P-EM Solar-Terrestrial Sciences, Space Electromagnetism & Space Environment

9:00 AM - 10:30 AM JST | 12:00 AM - 1:30 AM UTC | A04 TOKYO BAY MAKUHARI HALL

[P-EM12] Space Weather and Space Climate

convener:Ryuho Kataoka(National Institute of Polar Research), Antti A Pulkkinen(NASA Goddard Space Flight Center), Kanya Kusano(Institute for Space-Earth Environmental Research, Nagoya University), Kaori Sakaguchi(National Institute of Information and Communications Technology), Chairperson:Ryuho Kataoka(National Institute of Polar Research)

9:00 AM - 9:15 AM JST | 12:00 AM - 12:15 AM UTC

[PEM12-25] Variation of carbon-14 in tree rings around the onset of the Spoerer Minimum

★Invited Papers

*Hiroko Miyahara[1], Fuyuki Tokanai[2], Toru Moriya[2], Motonari Ohyama[3], Masataka Hakozaki[4], Mirei Takeyama[2], Hirohisa Sakurai[2] (1.Musashino Art University, 2.Yamagata University, 3.Tohoku University, 4.Nagoya University)

9:15 AM - 9:30 AM JST | 12:15 AM - 12:30 AM UTC

[PEM12-26] Current Status of WASAVIES: Warning System for Aviation Exposure to Solar Energetic Particles

★Invited Papers

*Tatsuhiko Sato[1], Ryuho Kataoka[2,3], Daikou Shiota[4,5], Yuki Kubo[4], Mamoru Ishii[4], Hiroshi Yasuda[6], Shoko Miyake[7], InChun Park[5], Yoshizumi Miyoshi[5] (1.Japan Atomic Energy Agency, 2.National Institute of Polar Research, 3.SOKENDAI, 4.National Institute of Information and Communications Technology, 5.Nagoya University, 6.Hiroshima University, 7.National Institute of Technology, Ibaraki College)

9:30 AM - 9:45 AM JST | 12:30 AM - 12:45 AM UTC

[PEM12-27] Statistical analysis of solar energetic particle events

*Kosuke Kihara[1], Yuwei Huang[2], Nobuhiko Nishimura[3], Seiji Yashiro[4], Nariaki Nitta[5], Kiyoshi Ichimoto[2], Ayumi Asai[2] (1.Department of Astronomy, Kyoto University, 2.Astronomical Observatory, Kyoto University, 3.Institute for Space Earth Environmental Research, Nagoya University, 4.The Catholic University of America, 5.Lockheed Martin Advanced Technology Center)

9:45 AM - 10:00 AM JST | 12:45 AM - 1:00 AM UTC

[PEM12-28] Long-term variation of galactic cosmic ray intensity observed with the Nagoya multidirectional muon detector

*Kazuoki Munakata[1], Rafael Mendonca[2], Chihiro Kato[1], Munetoshi Tokumaru[3] (1.Department of Physics, Faculty of Science, Shinshu University, 2.INPE, Brazil, 3.ISEE, Nagoya University)

10:00 AM - 10:15 AM JST | 1:00 AM - 1:15 AM UTC

[PEM12-29] Solar modulation of galactic cosmic rays during grand minima: A hybrid simulation

*Shoko Miyake[1], Tomoaki Matsumoto[2,3], Ryuho Kataoka[4,5], Tatsuhiko Sato[6], Daikou Shiota[7], Hiroko Miyahara[8], Shinsuke Imada[9], Haruka Ueno[10] (1.NIT, Ibaraki College, 2.Hosei Univ., 3.Princeton Univ., 4.NIPR, 5.SOKENDAI, 6.JAEA, 7.NICT, 8.Musashino Art Univ., 9.Nagoya Univ., 10.JAXA)

10:15 AM - 10:30 AM JST | 1:15 AM - 1:30 AM UTC

[PEM12-30] Overview of radio propagation project

*Kornyanat Hozumi[1], Hiroyuki Nakata[2], Susumu Saito[3], Takumi Kondo[1], Ryo Nakao[2], Takashi Maruyama[1], Takuya Tsugawa[1], Mamoru Ishii[1] (1.National Institute of Information and Communications Technology, 2.Graduate School of Engineering, Chiba University, Chiba, Japan, 3.National Institute of Maritime, Port and Aviation Technology, Electronic Navigation Research Institute (ENRI), Tokyo, Japan)

[E] Oral | P (Space and Planetary Sciences)：P-EM Solar-Terrestrial Sciences, Space Electromagnetism & Space Environment

10:45 AM - 12:15 PM JST | 1:45 AM - 3:15 AM UTC | A04 TOKYO BAY MAKUHARI HALL

[P-EM12] Space Weather and Space Climate

convener:Ryuho Kataoka(National Institute of Polar Research), Antti A Pulkkinen(NASA Goddard Space Flight Center), Kanya Kusano(Institute for Space-Earth Environmental Research, Nagoya University), Kaori Sakaguchi(National Institute of Information and Communications Technology), Chairperson:Kaori Sakaguchi

10:45 AM - 11:00 AM JST | 1:45 AM - 2:00 AM UTC

[PEM12-31] Dynamic Spectral Characteristics of Equatorial Plasma Bubbles

★Invited Papers

*Tatsuhiro Yokoyama[1], Charles L Rino[2], Charles S Carrano[2] (1.Kyoto University, 2.Boston College)

11:00 AM - 11:15 AM JST | 2:00 AM - 2:15 AM UTC

[PEM12-32] Recent advances in space weather monitoring using the Super Dual Auroral Radar Network

★Invited Papers

*Evan G Thomas[1], Simon G Shepherd[1] (1.Dartmouth College)

11:15 AM - 11:30 AM JST | 2:15 AM - 2:30 AM UTC

[PEM12-33] **A Study of Solar Flare Effects on Radio Wave Propagation using SuperDARN & riometer**

*Shibaji Chakraborty[1], Joseph Baker[1], John Michael Ruohoniemi[1], Nozomu Nishitani[2] (1.Virginia Tech, 2.Institute for Space-Earth Environmental Research, Nagoya University)

11:30 AM - 11:45 AM JST | 2:30 AM - 2:45 AM UTC

[PEM12-34] Exploring the use of cell phone GNSS receivers for global monitoring of the ionosphere

*Dawn Kellogg Merriman[1], Omar A Nava[1], Jennifer L Meehan[2], Hsien-Liang R Tseng[1] (1.AFIT, 2.NOAA)

11:45 AM - 12:00 PM JST | 2:45 AM - 3:00 AM UTC

[PEM12-35] Large enhancements of global GPS total electron content during a magnetic storm on 7-8 November 2004

*Sori Takuya[1], Yuichi Otsuka[1], Atsuki Shinbori[1], Takuya Tsugawa[2], Michi Nishioka[2] (1.Institute for Space-Earth Environmental Research, Nagoya University, 2.National Institute of Information and Communications Technology)

12:00 PM - 12:15 PM JST | 3:00 AM - 3:15 AM UTC

[PEM12-36] Large scale traveling ionospheric disturbances origin and propagation

*Iurii Cherniak[1,2], Irina Zakharenkova[2,5], Paul Prikryl[3,4], William Schreiner[1] (1.COSMIC Program Office, University Corporation for Atmospheric Research, 2.University of Warmia and Mazury in Olsztyn, 3.Physics Department, University of New Brunswick, 4.Geomagnetic Laboratory, Natural Resources Canada, 5.West Department of IZMIRAN)

[E] Poster | P (Space and Planetary Sciences)：P-EM Solar-Terrestrial Sciences, Space Electromagnetism & Space Environment

3:30 PM - 5:00 PM JST | 6:30 AM - 8:00 AM UTC | Poster Hall International Exhibition Hall8, Makuhari Messe_3

[P-EM12] Space Weather and Space Climate

convener:Ryuho Kataoka(National Institute of Polar Research), Antti A Pulkkinen(NASA Goddard Space Flight Center), Kanya Kusano(Institute for Space-Earth Environmental Research, Nagoya University), Kaori Sakaguchi(National Institute of Information and Communications Technology)

[PEM12-P01] Reconnection signatures in solar magnetograms during the solar storms of 4-10 September 2017

*Robert Dean Loper[1,2] (1.Air Force Institute of Technology, Department of Engineering Physics, 2.National Center for Atmospheric Research, High Altitude Observatory)

[PEM12-P02] Statistical Relation between Solar Flares and Coronal Mass Ejections with Respect to Sigmoidal Structures in Active Regions

*Yusuke Kawabata[1,2], Yusuke Iida[3], Takafumi Doi, Sachiko Akiyama[4], Seiji Yashiro[4], Toshifumi Shimizu[2] (1.Earth and Planetary Science, The University of Tokyo, 2.Institute of Space and Astronautical Science, JAXA, 3.Kwansei Gakuin University, 4.The Catholic University of America)

[PEM12-P03] Multi-wavelength Observations of Pre-flare Quasi-periodic Pulsation in the C2.2 Flare on 2012 October 15

*Yung-Chi Yang[1], Ya-Hui Yang[1], Baolin Tan[2], Chengming Tan[2], Y.H. Yan[2] (1.Graduate Institute of Space Science National Central University, 2.Key Laboratory of Solar Activities, National Astronomical Observatories)

[PEM12-P04] Investigation of pre-flare type III solar radio bursts and their potential solar origins

*Shao-Fu Hsieh[1], Ya-Hui Yang[1], Baolin Tan[2], Chengming Tan[2], Y.H. Yan[2] (1.Graduate Institute of Space Science National Central University, 2.Key Laboratory of Solar Activities, National Astronomical Observatories, Chinese Academy of Sciences)

[PEM12-P05] Statistical and observational research of solar flare for constructing total emission spectra prediction model

*Shohei Nishimoto[1], kyoko Watanabe[1], Shinsuke Imada[2], Tomoko Kawate[3], Kyoung-Sun Lee[4] (1.National Defense Academy, 2.Institute for Space-Earth Environmental Research, Nagoya University, 3.Institute Of Space And Astronautical Science, Japan Aerospace Exploration Agency, 4.National Astronomical Observatory of Japan)

[PEM12-P06] Modeling of solar active regions using local linear force-free fields to estimate magnetic twist

*Kento Nakatani[1], Kanya Kusano[1], Sung-Hong Park[1], Leka KD[2] (1.Institute for space-Earth Environmental Research, Nagoya University, 2.North West Reserch Associates)

[PEM12-P07] **Magnetohydrodynamic Simulation of an Erupting Magnetic Flux Rope on February 13 2009: Journey to Coronal Mass Ejection**

*Satoshi Inoue[1], Antonia Savcheva[2] (1.Institute for Space-Earth Environmental Research, Nagoya University, 2.Harvard-Smithsonian Center for Astrophysics)

[PEM12-P08] Investigation of flow structures in the solar interior through the surface magnetic elements' tracking

*Yusuke Iida[1] (1.Kwansei Gakuin University)

[PEM12-P09] High-precision measurement of carbon-14 in tree rings around the onset of the Maunder Minimum

*Hiroko Miyahara[1], Fuyuki Tokanai[2], Toru Moriya[2], Hideyuki Hotta[3] (1.Musashino Art University, 2.Yamagata University, 3.Chiba University)

[PEM12-P10] Examination of ^{10}Be in travertine sediment as a possible tool to reconstruct past solar activity

*Hongyang Xu[1,2], Hiroko Miyahara[2], Kazuho Horiuchi[3], Hiroyuki Matsuzaki[4], Hailong Sun[5], Weijun Luo[5], Xiangmin Zheng[1], Yusuke Suganuma[6,7], Shijie Wang[5], Limin Zhou[1] (1.East China Normal University, 2.Musashino Art University,

3.Hirosaki University, 4.University of Tokyo, 5.Chinese Academy of Sciences, 6.National Institute of Polar Research, 7.The Graduate University for Advanced Studies (SOKENDAI))

[PEM12-P11] Examination of ^{10}Be in travertine sediment as a possible tool to reconstruct past solar activity II

*Hongyang Xu[1,2], Hiroko Miyahara[2], Kazuho Horiuchi[3], Hiroyuki Matsuzaki[4], Hailong Sun[5], Weijun Luo[5], Xiangmin Zheng[1], Yusuke Suganuma[6,7], Shijie Wang[5], Limin Zhou[1] (1.East China Normal University, 2.Musashino Art University, 3.Hirosaki University, 4.University of Tokyo, 5.Chinese Academy of Sciences, 6.National Institute of Polar Research, 7.The Graduate University for Advanced Studies (SOKENDAI))

[PEM12-P12] 1 year of CR observation at Syowa Station in the Antarctic.

*Chihiro Kato[1], Kazuoki Munakata[1], Akira Kadokura[2], Ryuho Kataoka[2], Paul Evenson[3] (1.Shinshu University, 2.National Institute of Polar Research, 3.University of Delaware)

[PEM12-P13] Space weather forecast archives at NICT: handwritten solar activity charts

*Kaori Sakaguchi[1], Daikou Shiota[1], Kaori Fukunaga[1], Katsuhide Marubashi[1], Hiromitsu Ishibashi[1], Yuki Kubo[1], Mamoru Ishii[1] (1.National Institute of Information and Communications Technology)

[PEM12-P14] IMF dependence on solar wind parameters

*Tohru Araki, Yuki Harada[1] (1.Kyoto University)

[PEM12-P15] **Dipole Tilt Effect of Geomagnetic Activity from Low- to High-latitudes**

*Nowada Motoharu[1] (1.Shandong University at Weihai)

[PEM12-P16] A New Prediction Model for Solar Wind-Triggered Magnetospheric Disturbances Based on Potential Learning (Neural Network)

*Ryozo Kitajima[1], Motoharu Nowada[2], Ryotaro Kamimura[3] (1.Seikei University, 2.Shandong University at Weihai, 3.Tokai University)

[PEM12-P17] Real-time magnetosphere simulator for space weather using REProduce Plasma Universe code

*Yasubumi Kubota[1], Aoi Nakamizo[1], Kaori Sakaguchi[1], Mitsue Den[1], Yuki Kubo[1], Tsutomu Nagatsuma[1], Takashi Tanaka[1,2] (1.National Institute of Information and Communications Technology, 2.Kyushu University)

[PEM12-P18] **Simulation of GIC flowing through the power transmission network (187 kV-500 kV) in Japan**

*Nishida Yuichiro[1,6], Yusuke Ebihara[1], Satoko Nakamura[1], Shinichi Watari[2], Kumiko Hashimoto[3], Kentaro Kitamura[4], Takashi Kikuchi[5] (1.Kyoto University Reserch Institute for Sustainable Humanosphere, 2.National Institute of Information and Communications Technology, 3.Kibi International University, 4.National Insutitute of Technology, Tokuyama College, 5.Nagoya University, 6.Kyoto University Department of Electrical Engineering)

[PEM12-P19] Climatological features of the upper atmosphere reproduced by a revised version of a whole atmosphere-ionosphere coupled model GAIA

*Hidekatsu Jin[1], Yasunobu Miyoshi[2], Chihiro Tao[1], Hiroyuki Shinagawa[1], Hitoshi Fujiwara[3] (1.National Institude of Information and Communications Technology, 2.Kyushu University, 3.Seikei University)

[PEM12-P20] Investigation of the thermospheric mass density variations below 200 km

*Hitoshi Fujiwara[1], Yasunobu Miyoshi[2], Masayoshi Utashima[1], Huixin Liu[2] (1.Faculty of Science and Technology, Seikei University, 2.Department of Earth and Planetary Sciences, Faculty of Sciences, Kyushu University)

[PEM12-P21] Low-latitude HF Doppler observations of magnetospheric electric fields during space weather disturbances

*Kumiko K. Hashimoto[1], Takashi Kikuchi[2], Ichiro Tomizawa[3], Keisuke Hosokawa[3], Jaroslav Chum[4] (1.Kibi International University, 2.Nagoya University, 3.University of Electro-Commnunications, 4.Institute of Atmospheric Physics, Prague)

[PEM12-P22] Stratospheric ionization during magnetic storms

*Ryuho Kataoka[1] (1.National Institute of Polar Research)

[PEM12-P23] Calculating propagation time of HF radio wave using ray-tracing method and simple comparison with the observation.

*Ryo Nakao[1], Hiroyuki Nakata[1], Hiroyo Ohya[1], Toshiaki Takano[1], Kornyanat Hozumi[2], Takuya Tsugawa[2], Susumu Saito[3], Mamoru Ishii[2] (1.Graduate School of Engineering, Chiba University, 2.National Institute of imformation and Communications Technology, 3.Electronic Navigation Research Institute)

[PEM12-P24] Why do some probabilistic forecasts lack reliability?

*Yuki Kubo[1] (1.National Institute of Information and Communications Technology)

[PEM12-P25] An estimation method of GEO spacecraft surface charging for a real-time spacecraft risk assessment

*Masao Nakamura[1], Ryota Kawachi[1], Go Takahashi[1], Tsutomu Nagatsuma[2], Mamoru Ishii[2] (1.Osaka Prefecture University, 2.NICT)

[PEM12-P26] A network of HF Doppler sounding systems in Japan

*Keisuke Hosokawa[1], Hiroyuki Nakata[2], Kumiko K. Hashimoto[3], Ichiro Tomizawa[1], Jun Sakai[1], Takashi Kikuchi[4] (1.University of Electro-Communications, 2.Chiba University, 3.Kibi International University, 4.ISEE, Nagoya University)

[E] Poster | P (Space and Planetary Sciences)：P-EM Solar-Terrestrial Sciences, Space Electromagnetism & Space Environment

5:15 PM - 6:30 PM JST | 8:15 AM - 9:30 AM UTC | Poster Hall International Exhibition Hall8, Makuhari Messe_3

[P-EM12] Space Weather and Space Climate

convener:Ryuho Kataoka(National Institute of Polar Research), Antti A Pulkkinen(NASA Goddard Space Flight Center), Kanya Kusano(Institute for Space-Earth Environmental Research, Nagoya University), Kaori Sakaguchi(National Institute of Information and Communications Technology)

[PEM12-P01] Reconnection signatures in solar magnetograms during the solar storms of 4-10 September 2017

*Robert Dean Loper[1,2] (1.Air Force Institute of Technology, Department of Engineering Physics, 2.National Center for Atmospheric Research, High Altitude Observatory)

[PEM12-P02] Statistical Relation between Solar Flares and Coronal Mass Ejections with Respect to Sigmoidal Structures in Active Regions

*Yusuke Kawabata[1,2], Yusuke Iida[3], Takafumi Doi, Sachiko Akiyama[4], Seiji Yashiro[4], Toshifumi Shimizu[2] (1.Earth and Planetary Science, The University of Tokyo, 2.Institute of Space and Astronautical Science, JAXA, 3.Kwansei Gakuin University, 4.The Catholic University of America)

[PEM12-P03] Multi-wavelength Observations of Pre-flare Quasi-periodic Pulsation in the C2.2 Flare on 2012 October 15

*Yung-Chi Yang[1], Ya-Hui Yang[1], Baolin Tan[2], Chengming Tan[2], Y.H. Yan[2] (1.Graduate Institute of Space Science National Central University, 2.Key Laboratory of Solar Activities, National Astronomical Observatories)

[PEM12-P04] Investigation of pre-flare type III solar radio bursts and their potential solar origins

*Shao-Fu Hsieh[1], Ya-Hui Yang[1], Baolin Tan[2], Chengming Tan[2], Y.H. Yan[2] (1.Graduate Institute of Space Science National Central University, 2.Key Laboratory of Solar Activities, National Astronomical Observatories, Chinese Academy of Sciences)

[PEM12-P05] Statistical and observational research of solar flare for constructing total emission spectra prediction model

*Shohei Nishimoto[1], kyoko Watanabe[1], Shinsuke Imada[2], Tomoko Kawate[3], Kyoung-Sun Lee[4] (1.National Defense Academy, 2.Institute for Space-Earth Environmental Research, Nagoya University, 3.Institute Of Space And Astronautical Science, Japan Aerospace Exploration Agency, 4.National Astronomical Observatory of Japan)

[PEM12-P06] Modeling of solar active regions using local linear force-free fields to estimate magnetic twist

*Kento Nakatani[1], Kanya Kusano[1], Sung-Hong Park[1], Leka KD[2] (1.Institute for space-Earth Environmental Research, Nagoya University, 2.North West Reserch Associates)

[PEM12-P07] **Magnetohydrodynamic Simulation of an Erupting Magnetic Flux Rope on February 13 2009: Journey to Coronal Mass Ejection**

*Satoshi Inoue[1], Antonia Savcheva[2] (1.Institute for Space-Earth Environmental Research, Nagoya University, 2.Harvard-Smithsonian Center for Astrophysics)

[PEM12-P08] Investigation of flow structures in the solar interior through the surface magnetic elements' tracking

*Yusuke Iida[1] (1.Kwansei Gakuin University)

[PEM12-P09] High-precision measurement of carbon-14 in tree rings around the onset of the Maunder Minimum

*Hiroko Miyahara[1], Fuyuki Tokanai[2], Toru Moriya[2], Hideyuki Hotta[3] (1.Musashino Art University, 2.Yamagata University, 3.Chiba University)

[PEM12-P10] Examination of ^{10}Be in travertine sediment as a possible tool to reconstruct past solar activity

*Hongyang Xu[1,2], Hiroko Miyahara[2], Kazuho Horiuchi[3], Hiroyuki Matsuzaki[4], Hailong Sun[5], Weijun Luo[5], Xiangmin Zheng[1], Yusuke Suganuma[6,7], Shijie Wang[5], Limin Zhou[1] (1.East China Normal University, 2.Musashino Art University,

3.Hirosaki University, 4.University of Tokyo, 5.Chinese Academy of Sciences, 6.National Institute of Polar Research, 7.The Graduate University for Advanced Studies (SOKENDAI))

[PEM12-P11] Examination of ^{10}Be in travertine sediment as a possible tool to reconstruct past solar activity II

*Hongyang Xu[1,2], Hiroko Miyahara[2], Kazuho Horiuchi[3], Hiroyuki Matsuzaki[4], Hailong Sun[5], Weijun Luo[5], Xiangmin Zheng[1], Yusuke Suganuma[6,7], Shijie Wang[5], Limin Zhou[1] (1.East China Normal University, 2.Musashino Art University, 3.Hirosaki University, 4.University of Tokyo, 5.Chinese Academy of Sciences, 6.National Institute of Polar Research, 7.The Graduate University for Advanced Studies (SOKENDAI))

[PEM12-P12] 1 year of CR observation at Syowa Station in the Antarctic.

*Chihiro Kato[1], Kazuoki Munakata[1], Akira Kadokura[2], Ryuho Kataoka[2], Paul Evenson[3] (1.Shinshu University, 2.National Institute of Polar Research, 3.University of Delaware)

[PEM12-P13] Space weather forecast archives at NICT: handwritten solar activity charts

*Kaori Sakaguchi[1], Daikou Shiota[1], Kaori Fukunaga[1], Katsuhide Marubashi[1], Hiromitsu Ishibashi[1], Yuki Kubo[1], Mamoru Ishii[1] (1.National Institute of Information and Communications Technology)

[PEM12-P14] IMF dependence on solar wind parameters

*Tohru Araki, Yuki Harada[1] (1.Kyoto University)

[PEM12-P15] **Dipole Tilt Effect of Geomagnetic Activity from Low- to High-latitudes**

*Nowada Motoharu[1] (1.Shandong University at Weihai)

[PEM12-P16] A New Prediction Model for Solar Wind-Triggered Magnetospheric Disturbances Based on Potential Learning (Neural Network)

*Ryozo Kitajima[1], Motoharu Nowada[2], Ryotaro Kamimura[3] (1.Seikei University, 2.Shandong University at Weihai, 3.Tokai University)

[PEM12-P17] Real-time magnetosphere simulator for space weather using REProduce Plasma Universe code

*Yasubumi Kubota[1], Aoi Nakamizo[1], Kaori Sakaguchi[1], Mitsue Den[1], Yuki Kubo[1], Tsutomu Nagatsuma[1], Takashi Tanaka[1,2] (1.National Institute of Information and Communications Technology, 2.Kyushu University)

[PEM12-P18] **Simulation of GIC flowing through the power transmission network (187 kV-500 kV) in Japan**

*Nishida Yuichiro[1,6], Yusuke Ebihara[1], Satoko Nakamura[1], Shinichi Watari[2], Kumiko Hashimoto[3], Kentaro Kitamura[4], Takashi Kikuchi[5] (1.Kyoto University Reserch Institute for Sustainable Humanosphere, 2.National Institute of Information and Communications Technology, 3.Kibi International University, 4.National Insutitute of Technology, Tokuyama College, 5.Nagoya University, 6.Kyoto University Department of Electrical Engineering)

[PEM12-P19] Climatological features of the upper atmosphere reproduced by a revised version of a whole atmosphere-ionosphere coupled model GAIA

*Hidekatsu Jin[1], Yasunobu Miyoshi[2], Chihiro Tao[1], Hiroyuki Shinagawa[1], Hitoshi Fujiwara[3] (1.National Institude of Information and Communications Technology, 2.Kyushu University, 3.Seikei University)

[PEM12-P20] Investigation of the thermospheric mass density variations below 200 km

*Hitoshi Fujiwara[1], Yasunobu Miyoshi[2], Masayoshi Utashima[1], Huixin Liu[2] (1.Faculty of Science and Technology, Seikei University, 2.Department of Earth and Planetary Sciences, Faculty of Sciences, Kyushu University)

[PEM12-P21] Low-latitude HF Doppler observations of magnetospheric electric fields during space weather disturbances

*Kumiko K. Hashimoto[1], Takashi Kikuchi[2], Ichiro Tomizawa[3], Keisuke Hosokawa[3], Jaroslav Chum[4] (1.Kibi International University, 2.Nagoya University, 3.University of Electro-Commnunications, 4.Institute of Atmospheric Physics, Prague)

[PEM12-P22] Stratospheric ionization during magnetic storms

*Ryuho Kataoka[1] (1.National Institute of Polar Research)

[PEM12-P23] Calculating propagation time of HF radio wave using ray-tracing method and simple comparison with the observation.

*Ryo Nakao[1], Hiroyuki Nakata[1], Hiroyo Ohya[1], Toshiaki Takano[1], Kornyanat Hozumi[2], Takuya Tsugawa[2], Susumu Saito[3], Mamoru Ishii[2] (1.Graduate School of Engineering, Chiba University, 2.National Institute of imformation and Communications Technology, 3.Electronic Navigation Research Institute)

[PEM12-P24] Why do some probabilistic forecasts lack reliability?

*Yuki Kubo[1] (1.National Institute of Information and Communications Technology)

[PEM12-P25] An estimation method of GEO spacecraft surface charging for a real-time spacecraft risk assessment

*Masao Nakamura[1], Ryota Kawachi[1], Go Takahashi[1], Tsutomu Nagatsuma[2], Mamoru Ishii[2] (1.Osaka Prefecture University, 2.NICT)

[PEM12-P26] A network of HF Doppler sounding systems in Japan

*Keisuke Hosokawa[1], Hiroyuki Nakata[2], Kumiko K. Hashimoto[3], Ichiro Tomizawa[1], Jun Sakai[1], Takashi Kikuchi[4] (1.University of Electro-Communications, 2.Chiba University, 3.Kibi International University, 4.ISEE, Nagoya University)

[E] Oral | P (Space and Planetary Sciences)：P-EM Solar-Terrestrial Sciences, Space Electromagnetism & Space Environment

1:45 PM - 3:15 PM JST | 4:45 AM - 6:15 AM UTC | A04 TOKYO BAY MAKUHARI HALL

[P-EM13] Inner magnetosphere: Recent understanding and new insights

convener:Yusuke Ebihara(Research Institute for Sustainable Humanosphere, Kyoto University), Danny Summers(Memorial University of Newfoundland), Yoshizumi Miyoshi(Institute for Space-Earth Environmental Research, Nagoya University), Shinji Saito(Graduate School of Science, Nagoya University), Chairperson:Danny Summers, Yoshizumi Miyoshi(ISEE, Nagoya University)

1:45 PM - 2:05 PM JST | 4:45 AM - 5:05 AM UTC

[PEM13-01] Developing an improved understanding of Earth's outer radiation belt electrons with combined observations from Van Allen Probes, MMS, and Arase

★Invited Papers

*Drew L Turner[1], Ian Cohen[2], Alexander Boyd[1,3], Joseph Fennell[1], Geoff Reeves[3], Yoshizumi Miyoshi[4] (1.Aerospace Corporation El Segundo, 2.Johns Hopkins University Applied Physics Lab, 3.Los Alamos National Laboratory, 4.Nagoya University)

2:05 PM - 2:25 PM JST | 5:05 AM - 5:25 AM UTC

[PEM13-02] Recent results from Van Allen Probes and future prospects from the CeREs Cubesat

★Invited Papers

*Shrikanth G Kanekal[1], Daniel N Baker[2], Ashley Greeley[1], Lauren Blum[1], Quintin Schiller[1], David G Sibeck[1], Hong Zhao[2], Xinlin Li[2], Allison Jaynes[3] (1.NASA Goddard Space Flight Center, 2.LASP, University of Colorado, Boulder, 3.Univeristy of Iowa)

2:25 PM - 2:40 PM JST | 5:25 AM - 5:40 AM UTC

[PEM13-03] **Optimal Use of Time Lags Between MMS Spacecraft : Application to the Estimation of Wave-Vectors**

*Gerard Marcel CHANTEUR[1,2,3], Drew L. Turner, Olivier Le Contel[1,2,3], Alessandro Retino[1,2,3], Laurent Mirioni[1,2,3] (1.CNRS, 2.SORBONNE UNIVERSITE, 3.ECOLE POLYTECHNIQUE)

2:40 PM - 2:55 PM JST | 5:40 AM - 5:55 AM UTC

[PEM13-04] Conjugate observation of EMIC waves by Arase and RBSP with associated POES and AARDDVARK detected electron precipitation

*Aaron T. Hendry[1], Ondrej Santolik[1,2], Yoshizumi Miyoshi[3], Yoshiya Kasahara[4], Yasumasa Kasaba[5], Ayako Matsuoka[6], Craig J Rodger[7], Mark Clilverd[8], Masafumi Shoji[3], Shoya Matsuda[6], Craig Kletzing[9], Iku Shinohara[6] (1.Dept. of Space Physics, Inst. of Atmospheric Physics, Czech Acad. of Science, 2.Fac. of Mathematics and Physics, Charles Univ., 3.Inst. for Space Earth Environmental Research, Nagoya Univ., 4.Graduate School of Natural Science and Technology, Kanazawa Univ., 5.Planetary Plasma and Atmospheric Research Center, Tohoku Univ., 6.Inst. of Space and Astronautical Science, Japan Aerospace Exploration Agency, 7.Dept. of Physics, Univ. of Otago, 8.British Antarctic Survey (NERC), 9.Dept. of Physics and Astronomy, Univ. of Iowa)

2:55 PM - 3:10 PM JST | 5:55 AM - 6:10 AM UTC

[PEM13-05] Over-darkening pulsating aurora: simultaneous observations with Arase and an all-sky camera in Scandinavia

*Keisuke Hosokawa[1], Yoshizumi Miyoshi[2], Shin-ichiro Oyama[2], Yasunobu Ogawa[3], Satoshi Kurita[2], Yoshiya Kasahara[4], Mitsunori Ozaki[4], Yasumasa Kasaba[5], Satoshi Yagitani[4], Shoya Matsuda[6], Fuminori Tsuchiya[5], Atsushi Kumamoto[5], Iku Shinohara[6], Ryoichi Fujii[7] (1.Department of Communication Engineering and Informatics, University of Electro-Communications, 2.ISEE, Nagoya University, 3.National Institute of Polar Research, 4.Kanazawa University, 5.Tohoku University, 6.ISAS/JAXA, 7.Research Organization of Information and Systems)

[E] Oral | P (Space and Planetary Sciences)：P-EM Solar-Terrestrial Sciences, Space Electromagnetism & Space Environment

3:30 PM - 5:00 PM JST | 6:30 AM - 8:00 AM UTC | A04 TOKYO BAY MAKUHARI HALL

[P-EM13] Inner magnetosphere: Recent understanding and new insights

convener:Yusuke Ebihara(Research Institute for Sustainable Humanosphere, Kyoto University), Danny Summers(Memorial University of Newfoundland), Yoshizumi Miyoshi(Institute for Space-Earth Environmental Research, Nagoya University), Shinji Saito(Graduate School of Science, Nagoya University), Chairperson:Yoshizumi Miyoshi(ISEE, Nagoya University), Danny Summers

3:30 PM - 3:50 PM JST | 6:30 AM - 6:50 AM UTC

[PEM13-06] Deformation of electron pitch angle distributions caused by chorus waves observed by the Arase satellite

★Invited Papers

*Satoshi Kurita[1], Yoshizumi Miyoshi[1], Satoshi Kasahara[2], Shoichiro Yokota[3], Yoshiya Kasahara[4], Shoya Matsuda[5], Ayako Matsuoka[5], Iku Shinohara[5] (1.Institute for Space-Earth Environmental Research, Nagoya University, 2.The University of Tokyo, 3.Graduate School of Science, Osaka University, 4.Information Media Center, Kanazawa University, 5.ISAS/JAXA)

3:50 PM - 4:10 PM JST | 6:50 AM - 7:10 AM UTC

[PEM13-07] Electron scattering by isolated chorus elements observed near the magnetospheric equator

★Invited Papers

*Satoshi Kasahara[1], Yoshizumi Miyoshi[2], Shoichiro Yokota[3], Yoshiya Kasahara[4], Shoya Matsuda[5], Ayako Matsuoka[5], Kunihiro Keika[1], Tomoaki Hori[2], Iku Shinohara[5] (1.The university of Tokyo, 2.Nagoya University, 3.Osaka University, 4.Kanazawa University, 5.Institute of Space and Astronautical Science)

4:10 PM - 4:25 PM JST | 7:10 AM - 7:25 AM UTC

[PEM13-08] Continuous precipitation of low-energy electrons associated with pulsating aurora obtained by the Reimei satellite

*Takeshi Sakanoi[1], Fukizawa Mizuki[1], Yoshizumi Miyoshi[2], Yusuke Ebihara[3], Kazushi Asamura[4], Masafumi Hirahara[2] (1.Planetary Plasma and Atmospheric Research Center, Graduate School of Science, Tohoku University, 2.ISEE, Nagoya University, 3.RISH, Kyoto University, 4.ISAS/JAXA)

4:25 PM - 4:40 PM JST | 7:25 AM - 7:40 AM UTC

[PEM13-09] Origin of energetic electron precipitation with fast fluctuation: Data-driven simulations using the ERG plasma wave observations

*Shinji Saito[1], Yoshizumi Miyoshi[2], Shoya Matsuda[3], Satoshi Kurita[2], Yoshiya Kasahara[4], Atsushi Kumamoto[5], Fuminori Tsuchiya[5], Ayako Matsuoka[3] (1.Graduate School of Science, Nagoya University, 2.ISEE, Nagoya University , 3.ISAS/JAXA, 4.Kanazawa University, 5.Tohoku University)

4:40 PM - 4:55 PM JST | 7:40 AM - 7:55 AM UTC

[PEM13-10] Conjugated quasi-periodic ELF/VLF emissions between the Arase satellite and both Van Allen Probes

*Claudia Martinez Calderon[1,2], Frantisek Nemec[3], Kazuo Shiokawa[2], Yuto Katoh[1], Yoshiya Kasahara[4], Shoya Matsuda[2], Fuminori Tsuchiya[1], Atsushi Kumamoto[1], Mariko Teramoto[2], Ayako Matsuoka[5], Yoshizumi Miyoshi[2], Ondrej Santolik[6,3], George Hospodarksy[7] (1.Dept. Geophys., Grad. Sch. Sci., Tohoku University, 2.Instute for Space-Earth Environmental Research, Nagoya University, 3.Faculty of Mathematics and Physics, Charles University, Prague, Czech Republic, 4.Kanazawa University, 5.Japan Aerospace Exploration Agency, 6.Institute of Atmospheric Physics, Prague, Czech Republic, 7.Department of Physics and Astronomy, University of Iowa, USA)

[E] Poster | P (Space and Planetary Sciences)：P-CG Complex & General

10:45 AM - 12:15 PM JST | 1:45 AM - 3:15 AM UTC | Poster Hall International Exhibition Hall8, Makuhari Messe_1

[P-CG22] Shock responses of planetary materials elucidated from meteorites and dynamic compression experiments

convener:Toshimori Sekine(Center for High Pressure Science and Technology Advanced Research), Takuo Okuchi(Institute for Planetary Materials, Okayama University)

[PCG22-P01] discussion

*Takuo Okuchi[1], Toshimori Sekine[2] (1.Institute for Planetary Materials, Okayama University, 2.Center for High Pressure Science and Technology Advanced Research)

[PCG22-P02] Shock-compressed behavior of quartz by XFEL

*Tomoko Sato[1], Yoshinori Tange[2], Yusuke Seto[3], Toshimori Sekine[4,5], Norimasa Ozaki[4], Toyohito Nishikawa[4], Kohei Miyanishi[4], Kensuke Matsuoka[4], Ryosuke Kodama[4], Tadashi Togashi[2], Yuichi Inubushi[2], Toshinori Yabuuchi[6], Makina Yabashi[6] (1.Hiroshima University, 2.Japan Synchrotron Radiation Research Institute, 3.Kobe University, 4.Osaka University, 5.Center for High Pressure Science &Technology Advanced Research, 6.RIKEN)

[PCG22-P04] **Laser-shock experiments of dense polymorphs of Mg_2SiO_4: technical developments using synthetic single crystals**

*Narangoo Purevjav[1], Takuo Okuchi[1], Norimasa Ozaki[2], Takayoshi Sano[3], Yuhei Umeda[2], Shintaro Morioka[2], Nobuki Kamimura[2] (1.Institute for Planetary Materials, Okayama University, 2.Graduate School of Engineering, Osaka University, 3.Institute of Laser Engineering, Osaka University)

[PCG22-P05] Richtmyer-Meshkov instability in inhomogeneous density materials and its application to planetary science

*Takayoshi Sano[1] (1.Institute of Laser Engineering, Osaka University)

[PCG22-P06] Impact-induced dehydration reactions of Fe- and Al-hydrates as potential storage, carrier and source of water

*Tsubasa Tobase[1], Toshimori Sekine[1], Ginga Kitahara[2], Makoto Tokuda[2], Akira Yoshiasa[2], Makoto Takafuji[2], Tsutomu Mashimo[2], Nobuaki Kawai[2] (1.HPSTAR, 2.Graduate School of Science and Technology, Kumamoto University)

[PCG22-P07] Crystallization of amorphous $MgSiO_3$ by shock compression

*Akane Arasuna[1], Masayuki Okuno[1], Nobuaki Kawai[2] (1.Kanazawa University, 2.Kumamoto University)

[PCG22-P08] First-principle study of the structural and electronic properties of N-doped $MgAl_2O_4$ spinel

*Chi Pui Tang[1], Pak Kin Leong[1], Toshimori Sekine[2,3] (1.State Key Laboratory of Lunar and Planetary Sciences, Macau University of Science and Technology, 2.Center for High Pressure Science and Technology Advanced Research (HPSTAR) Shanghai Laboratory of HPSTAR, Shanghai, P.R. China, 3.Graduate School of Engineering, Osaka University)

[PCG22-P09] Transparency of shock-compressed single crystal diamond

*Kento Katagiri[1], Norimasa Ozaki[1,2], Kohei Miyanishi[2], Yuhei Umeda[1], Shintaro Morioka[1], Takayoshi Sano[2], Ryosuke Kodama[1,2] (1.Osaka University, 2.Institute of Laser Engineering, Osaka Unversity)

[PCG22-P10] Pb-Pb dating of the NWA 7203 angrite and relationship to its shock metamorphism

*Hideyuki Hayashi[1], Takashi Mikouchi[1], Yuji Sano[1], Martin Bizzarro[2] (1.The university of Tokyo, 2.University of Copenhagen)

[PCG22-P11] Shock recovery of high-pressure phase of SiO_2 using high-power laser

*Tadashi Kondo[1], Hiromoto Kengo[1], Tatsuhiro Sakaiya[1], Hidenori Terasaki[1], Keisuke Shigemori[2], Youichiro Hironaka[2] (1.Department of Earth and Space Science, Graduate School of Science Osaka University, 2.Institute of Laser Engineering, Osaka University)

[PCG22-P12] Hugoniot measurement of calcite under meteorite collision condition

*Fukui Keiya[1], Norimasa Ozaki[1,2], Yuhei Umeda[1], Kohei Miyanishi[3], Kento Katagiri[1], Shintaro Morioka[1], Takayoshi Sano[3], Ryosuke Kodama[1,2,3] (1.Graduate School of Engineering,Osaka univ., 2.PPC, Osaka Univ., 3.ILE, Osaka Univ.)

[PCG22-P13] Direct observation of the transformation toughening of tetragonal stabilized zirconia under shock deformation condition by ns time-resolved XRD.

*Sota Takagi[1,2], Kouhei Ichiyanagi[2,3], Nobuaki Kawai[4], Ryo Fukaya[2], Shunsuke Nozawa[2], Atsushi Kyono[1], Nobumasa Funamori[2], Shin-ichi Adachi[2] (1.University of Tsukuba, 2.KEK PF, 3.Jichi Medical University, 4.Kumamoto University)

[E] Poster | P (Space and Planetary Sciences)：P-CG Complex & General

5:15 PM - 6:30 PM JST | 8:15 AM - 9:30 AM UTC | Poster Hall International Exhibition Hall8, Makuhari Messe_4

[P-CG22] Shock responses of planetary materials elucidated from meteorites and dynamic compression experiments

convener:Toshimori Sekine(Center for High Pressure Science and Technology Advanced Research), Takuo Okuchi(Institute for Planetary Materials, Okayama University)

[PCG22-P01] discussion

*Takuo Okuchi[1], Toshimori Sekine[2] (1.Institute for Planetary Materials, Okayama University, 2.Center for High Pressure Science and Technology Advanced Research)

[PCG22-P02] Shock-compressed behavior of quartz by XFEL

*Tomoko Sato[1], Yoshinori Tange[2], Yusuke Seto[3], Toshimori Sekine[4,5], Norimasa Ozaki[4], Toyohito Nishikawa[4], Kohei Miyanishi[4], Kensuke Matsuoka[4], Ryosuke Kodama[4], Tadashi Togashi[2], Yuichi Inubushi[2], Toshinori Yabuuchi[6], Makina Yabashi[6] (1.Hiroshima University, 2.Japan Synchrotron Radiation Research Institute, 3.Kobe University, 4.Osaka University, 5.Center for High Pressure Science &Technology Advanced Research, 6.RIKEN)

[PCG22-P04] Laser-shock experiments of dense polymorphs of Mg_2SiO_4: technical developments using synthetic single crystals

*Narangoo Purevjav[1], Takuo Okuchi[1], Norimasa Ozaki[2], Takayoshi Sano[3], Yuhei Umeda[2], Shintaro Morioka[2], Nobuki Kamimura[2] (1.Institute for Planetary Materials, Okayama University, 2.Graduate School of Engineering, Osaka University, 3.Institute of Laser Engineering, Osaka University)

[PCG22-P05] Richtmyer-Meshkov instability in inhomogeneous density materials and its application to planetary science

*Takayoshi Sano[1] (1.Institute of Laser Engineering, Osaka University)

[PCG22-P06] Impact-induced dehydration reactions of Fe- and Al-hydrates as potential storage, carrier and source of water

*Tsubasa Tobase[1], Toshimori Sekine[1], Ginga Kitahara[2], Makoto Tokuda[2], Akira Yoshiasa[2], Makoto Takafuji[2], Tsutomu Mashimo[2], Nobuaki Kawai[2] (1.HPSTAR, 2.Graduate School of Science and Technology, Kumamoto University)

[PCG22-P07] Crystallization of amorphous $MgSiO_3$ by shock compression

*Akane Arasuna[1], Masayuki Okuno[1], Nobuaki Kawai[2] (1.Kanazawa University, 2.Kumamoto University)

[PCG22-P08] First-principle study of the structural and electronic properties of N-doped $MgAl_2O_4$ spinel

*Chi Pui Tang[1], Pak Kin Leong[1], Toshimori Sekine[2,3] (1.State Key Laboratory of Lunar and Planetary Sciences, Macau University of Science and Technology, 2.Center for High Pressure Science and Technology Advanced Research (HPSTAR) Shanghai Laboratory of HPSTAR, Shanghai, P.R. China, 3.Graduate School of Engineering, Osaka University)

[PCG22-P09] Transparency of shock-compressed single crystal diamond

*Kento Katagiri[1], Norimasa Ozaki[1,2], Kohei Miyanishi[2], Yuhei Umeda[1], Shintaro Morioka[1], Takayoshi Sano[2], Ryosuke Kodama[1,2] (1.Osaka University, 2.Institute of Laser Engineering, Osaka Unversity)

[PCG22-P10] Pb-Pb dating of the NWA 7203 angrite and relationship to its shock metamorphism

*Hideyuki Hayashi[1], Takashi Mikouchi[1], Yuji Sano[1], Martin Bizzarro[2] (1.The university of Tokyo, 2.University of Copenhagen)

[PCG22-P11] Shock recovery of high-pressure phase of SiO_2 using high-power laser

*Tadashi Kondo[1], Hiromoto Kengo[1], Tatsuhiro Sakaiya[1], Hidenori Terasaki[1], Keisuke Shigemori[2], Youichiro Hironaka[2] (1.Department of Earth and Space Science, Graduate School of Science Osaka University, 2.Institute of Laser Engineering, Osaka University)

[PCG22-P12] Hugoniot measurement of calcite under meteorite collision condition

*Fukui Keiya[1], Norimasa Ozaki[1,2], Yuhei Umeda[1], Kohei Miyanishi[3], Kento Katagiri[1], Shintaro Morioka[1], Takayoshi Sano[3], Ryosuke Kodama[1,2,3] (1.Graduate School of Engineering,Osaka univ., 2.PPC, Osaka Univ., 3.ILE, Osaka Univ.)

[PCG22-P13] Direct observation of the transformation toughening of tetragonal stabilized zirconia under shock deformation condition by ns time-resolved XRD.

*Sota Takagi[1,2], Kouhei Ichiyanagi[2,3], Nobuaki Kawai[4], Ryo Fukaya[2], Shunsuke Nozawa[2], Atsushi Kyono[1], Nobumasa Funamori[2], Shin-ichi Adachi[2] (1.University of Tsukuba, 2.KEK PF, 3.Jichi Medical University, 4.Kumamoto University)

[E] Oral | P (Space and Planetary Sciences)：P-CG Complex & General

1:45 PM - 3:15 PM JST | 4:45 AM - 6:15 AM UTC | A03 TOKYO BAY MAKUHARI HALL

[P-CG22] Shock responses of planetary materials elucidated from meteorites and dynamic compression experiments

convener:Toshimori Sekine(Center for High Pressure Science and Technology Advanced Research), Takuo Okuchi(Institute for Planetary Materials, Okayama University), Chairperson:Toshimori Sekine(HPSTAR & Osaka University), Ai-Cheng Zhang(Nanjing University)

1:45 PM - 2:00 PM JST | 4:45 AM - 5:00 AM UTC

[PCG22-01] Shock-induced phase transformation in howardite-eucrite-diogenite meteorites

★Invited Papers

*Ai-Cheng Zhang[1,2], De-Liang Chen[1], Run-Lian Pang[1] (1.School of Earth Sciences and Engineering, Nanjing University, China, 2.CAS Center for Excellence in Comparative Planetary, China)

2:00 PM - 2:15 PM JST | 5:00 AM - 5:15 AM UTC

[PCG22-02] Lattice-shear-induced metastable formation of high-pressure silicates in shocked meteorites

★Invited Papers

*Naotaka Tomioka[1], Takuo Okuchi[2], Masaaki Miyahara[3] (1.Kochi Institute for Core Sample Research, Japan Agency for Marine-Earth Science and Technology, 2.Institute for Planetary Materials, Okayama University, 3.Department of Earth and Planetary Systems Science, Hiroshima University)

2:15 PM - 2:30 PM JST | 5:15 AM - 5:30 AM UTC

[PCG22-03] Can high-pressure polymorphs clarify an ordinary chondrite parent-body breakup?

*Masaaki Miyahara[1], Akira Yamaguchi[2], Masato Saitoh[1], Kanta Fukimoto[1], Takeshi Sakai[3], Hiroaki Ohfuji[3], Naotaka Tomioka[4], Yu Kodama[5], Eiji Ohtani[6] (1.Department of Earth and Planetary Systems Science, Graduate School of Science, Hiroshima University, 2.National Institute of Polar Research, 3.Geodynamics Research Center, Ehime University, 4.Kochi Institute for Core Sample Research, Japan Agency for Marine-Earth Science and Technology, 5.Marine Works Japan, 6.Department of Earth Sciences, Graduate School of Science, Tohoku University)

2:30 PM - 2:45 PM JST | 5:30 AM - 5:45 AM UTC

[PCG22-04] Linking occurrence and texture of dense silicate minerals in shocked meteorites with laser-shock experimental results of Mg_2SiO_4 analyzed by XFEL probe

*Takuo Okuchi[1], Narangoo Purevjav[1], Norimasa Ozaki[2], Takeshi Matsuoka[2], Yusuke Seto[3], Yoshinori Tange[4], Toshinori Yabuuchi[5], Naotaka Tomioka[6], Toshimori Sekine[7], Ryosuke Kodama[2] (1.Institute for Planetary Materials, Okayama University, 2.Graduate School of Engineering, Osaka University, 3.Graduate School of Science, Kobe University, 4.Japan Synchrotron Radiation Research Institute, 5.RIKEN Harima Branch, 6.Kochi Institute for Core Sample Research, Japan Agency for Marine-Earth Science and Technology, 7.Center for High Pressure Science and Technology Advanced Research)

2:45 PM - 3:00 PM JST | 5:45 AM - 6:00 AM UTC

[PCG22-05] **Laser-shock evolution of organic molecules in carbonaceous meteorite**

*Hikaru Yabuta[1], Hikaru Fujioka[2], Tatsuhiro Sakaiya[2], Tadashi Kondo[2], Sohsuke Ohno[3], Kosuke Kurosawa[3], Toshihiko Kadono[4], Keisuke Shigemori[5], Yoichiro Hironaka[5], Takamitsu Yamanaka[6] (1.Hiroshima University, Department of Earth and Planetary Systems Science, 2.Osaka University, Department of Earth and Space Science, 3.Chiba Institute of Technology, Planetary Exploration Research Center (PERC), 4.University of Occupational and Environmental Health, 5.Osaka University, Institute of Laser Engineering, 6.Center for High Pressure Science & Technology Advanced Research, Shanghai, China)

3:00 PM - 3:15 PM JST | 6:00 AM - 6:15 AM UTC

[PCG22-06] Shock barometer using cathodoluminescence and synchrotron angle-dispersive x-ray diffraction analyses of minerals

★Invited Papers

*Masahiro KAYAMA[1] (1.Tohoku University)

[E] Oral | P (Space and Planetary Sciences)：P-CG Complex & General

3:30 PM - 5:00 PM JST | 6:30 AM - 8:00 AM UTC | A03 TOKYO BAY MAKUHARI HALL

[P-CG22] Shock responses of planetary materials elucidated from meteorites and dynamic compression experiments

convener:Toshimori Sekine(Center for High Pressure Science and Technology Advanced Research), Takuo Okuchi(Institute for Planetary Materials, Okayama University), Chairperson:Takuo Okuchi(Okayama University), Yongjae Lee(Yonsei University)

3:30 PM - 3:45 PM JST | 6:30 AM - 6:45 AM UTC

[PCG22-07] Dynamic Compression at Pohang X-ray Free Electron Laser Facility (PAL-XFEL)

★Invited Papers

*Yongjae Lee[1] (1.Yonsei University, Seoul, Korea)

3:45 PM - 4:00 PM JST | 6:45 AM - 7:00 AM UTC

[PCG22-08] Exploration of extreme melt states of silicate usign high-power laser and XFEL

★Invited Papers

*Norimasa Ozaki[1] (1.Osaka University)

4:00 PM - 4:15 PM JST | 7:00 AM - 7:15 AM UTC

[PCG22-09] Hugoniot measurements for silicate: Understanding silicate magma under the planetary impacts

*Yuhei Umeda[1], Norimasa Ozaki[1], Toshimori Sekine[2], Bruno Albertazzi[3], Alessandra Benuzzi-Mounaix[3], Riccardo Bolis[3], Marco Guaruaglini[3], Kento Katagiri[1], Kodama Ryosuke[1], Michel Koeing[3], Kohei Miyanishi[4], Shintaro Morioka[1], Toyohito Nishikawa[1], Syugo Ohi[5], Alessandra Ravasio[3], Yoichi Sakawa[4], Takayoshi Sano[4], Tomoko Sato[6] (1.Graduate School of Engineering, Osaka Univ., 2.Center for High Pressure Science & Technology Advanced Research, 3.Ecole Polytechnique, 4.Institute of Laser Engineering, Osaka University, 5.Shiga Univ., 6.Graduate School of Science, Hiroshima University)

4:15 PM - 4:30 PM JST | 7:15 AM - 7:30 AM UTC

[PCG22-10] **An experimental design to determine iron melting at the Earth's core conditions via in-situ X-ray diffraction technique at high power laser facility**

★Invited Papers

*Hao Liu[1] (1.Laser fusion research center)

4:30 PM - 4:45 PM JST | 7:30 AM - 7:45 AM UTC

[PCG22-11] **Study on transport properties of liquid iron and iron alloy under high temperature and high pressure using the laser shock technique**

*Kohei Miyanishi[1], Norimasa Ozaki[2], Satoshi Ohmura[3], Marion Harmand[4], Andy Krygier[5], Toyohito Nishikawa[2], Yuhei Umeda[2], Shigemori Keisuke[1], Youichi Sakawa[1], Takayoshi Sano[1], Ryosuke Kodama[1,2] (1.Institute for Laser Engineering, Osaka University, 2.Graduate school of engineering, Osaka University, 3.Faculty of Engineering, Hiroshima Institute of Technology, 4.IMPMC, Sorbonne Université, 5.LLNL)

4:45 PM - 5:00 PM JST | 7:45 AM - 8:00 AM UTC

[PCG22-12] **Laser shock compression in LFRC**

*Liang Sun[1] (1.Laser Fusion Research Center, CAEP)

[J] Oral | P (Space and Planetary Sciences)：P-CG Complex & General

9:00 AM - 10:30 AM JST | 12:00 AM - 1:30 AM UTC | A05 TOKYO BAY MAKUHARI HALL

[P-CG25] Planetary Magnetosphere, Ionosphere, and Atmosphere

convener:Kanako Seki(Graduate School of Science, University of Tokyo), Takeshi Imamura(Graduate School of Frontier Sciences, The University of Tokyo), Hiroyuki Maezawa(Department of Physical Science Osaka Prefecture University), Naoki Terada(Graduate School of Science, Tohoku University), Chairperson:Masaki Nishino(名古屋大学宇宙地球環境研究所), Hiroyuki Maezawa(大阪府立大学大学院理学系研究科)

9:30 AM - 9:45 AM JST | 12:30 AM - 12:45 AM UTC

[PCG25-01] On the observational constraint on time and spatial variation of Titan's atmospheric trace gases driven with the ALMA solar system big-data

*Takahiro IINO[1,2], Hideo Sagawa[3], Takashi Tsukagoshi[4] (1.The University of Tokyo, 2.Tokyo Univ. of Agr. and Tech., 3.Kyoto Sangyo University, 4.NAOJ)

9:45 AM - 10:00 AM JST | 12:45 AM - 1:00 AM UTC

[PCG25-02] Transport and energization of planetary ions in the magnetospheric flanks of Mercury

*Sae Aizawa[1], Dominique Delcourt[2], Naoki Terada[1] (1.Graduate School of Science,Tohoku University, 2.LPC2E, CNRS)

10:00 AM - 10:15 AM JST | 1:00 AM - 1:15 AM UTC

[PCG25-03] Exploring the real-time prediction of Mercury's magnetosphere

*Manabu Yagi[1], Kanako Seki[2], Yosuke Matsumoto[3], Dominique C. Delcourt[4], Francois Leblanc[4] (1.RIKEN Center for Computational Science, 2.Graduate School of Science, University of Tokyo, 3.Graduate School of Science, Chiba University, 4.The National Center for Scientific Research)

10:15 AM - 10:30 AM JST | 1:15 AM - 1:30 AM UTC

[PCG25-04] Model study on the contribution of various physical processes for generation and dissipation of Mercury's exosphere

*Yudai Suzuki[1], Kazuo Yoshioka[1] (1.University of Tokyo)

[J] Oral | P (Space and Planetary Sciences)：P-CG Complex & General

10:45 AM - 12:15 PM JST | 1:45 AM - 3:15 AM UTC | A05 TOKYO BAY MAKUHARI HALL

[P-CG25] Planetary Magnetosphere, Ionosphere, and Atmosphere

convener:Kanako Seki(Graduate School of Science, University of Tokyo), Takeshi Imamura(Graduate School of Frontier Sciences, The University of Tokyo), Hiroyuki Maezawa(Department of Physical Science Osaka Prefecture University), Naoki Terada(Graduate School of Science, Tohoku University), Chairperson:Hiromu Nakagawa(Planetary Atmosphere Physics Laboratory, Department of Geophysics, Graduate School of Science, Tohoku University), Kanako Seki(Department of Earth and Planetary Science, Graduate School of Science, University of Tokyo,)

10:45 AM - 11:00 AM JST | 1:45 AM - 2:00 AM UTC

[PCG25-05] Updated status and science goals of the BepiColombo mission

*Go Murakami[1], Hajime Hayakawa[1], Masaki Fujimoto[1], BepiColombo Project Team (1.Institute of Space and Astronautical Science, Japan Aerospace Exploration Agency)

11:00 AM - 11:15 AM JST | 2:00 AM - 2:15 AM UTC

[PCG25-06] A Novel High-Moment Multifluid Model for Mercury: From the Planetary Conducting Core to the Dynamic Magnetosphere

*Chuanfei Dong[1], Liang Wang[1], Ammar Hakim[1], Amitava Bhattacharjee[1], James A Slavin[2], Gina A DiBraccio[3], Kai Germaschewski[4] (1.Princeton University, 2.University of Michigan, Ann Arbor, 3.NASA Goddard Space Flight Center, 4.University of New Hampshire)

11:15 AM - 11:30 AM JST | 2:15 AM - 2:30 AM UTC

[PCG25-07] DSMC simulation of slow hydrodynamic escape from terrestrial planets

Kaori Terada[1], *Naoki Terada[1], Hitoshi Fujiwara[2] (1.Graduate School of Science, Tohoku University, 2.Faculty of Science and Technology, Seikei University)

11:30 AM - 11:45 AM JST | 2:30 AM - 2:45 AM UTC

[PCG25-08] The influence of Martian crustal magnetic fields on atmospheric escape

*Dave A Brain[1,2], Robin Ramstad[1], Yaxue Dong[1], Tristan Weber[1], Shogo Inui[2], Kanako Seki[2], Andrew Poppe[3], Riku Jarvinen[4], Jim McFadden[3], Jasper Halekas[5], Jared Espley[6], David Mitchell[3], Laila Andersson[1], Bruce Jakosky[1] (1.University of Colorado, 2.University of Tokyo, 3.University of California Berkeley, 4.Finnish Meteorological Institute, 5.University of Iowa, 6.NASA Goddard Space Flight Center)

11:45 AM - 12:00 PM JST | 2:45 AM - 3:00 AM UTC

[PCG25-09] Effects of the IMF direction on atmospheric escape under a weak intrinsic magnetic field at Mars

*Shotaro Sakai[1], Kanako Seki[1], Naoki Terada[2], Hiroyuki Shinagawa[3], Ryoya Sakata[1], Takashi Tanaka[3,4], Yusuke Ebihara[5] (1.Graduate School of Science, The University of Tokyo, 2.Graduate School of Science, Tohoku University, 3.National Institute of Information and Communications Technology, 4.International Center for Space Weather Science and Education, Kyushu University, 5.Research Institute for Sustainable Humanosphere, Kyoto University)

12:00 PM - 12:15 PM JST | 3:00 AM - 3:15 AM UTC

[PCG25-10] Simulating solar energetic electron precipitation and drift at Mars

*Rebecca Jolitz[1], Chuanfei Dong[2], Dave A Brain[1], Steve Bougher[3], Christina Lee[4], Rob Lillis[4], Shannon Curry[4], Bruce Jakosky[1] (1.Univ. of Colorado Boulder, 2.Princeton Univ., 3.Univ. of Michigan, 4.Univ. of California Berkeley)

[J] Oral | P (Space and Planetary Sciences)：P-CG Complex & General

1:45 PM - 3:15 PM JST | 4:45 AM - 6:15 AM UTC | A05 TOKYO BAY MAKUHARI HALL

[P-CG25] Planetary Magnetosphere, Ionosphere, and Atmosphere

convener:Kanako Seki(Graduate School of Science, University of Tokyo), Takeshi Imamura(Graduate School of Frontier Sciences, The University of Tokyo), Hiroyuki Maezawa(Department of Physical Science Osaka Prefecture University), Naoki Terada(Graduate School of Science, Tohoku University), Chairperson:Takeshi Imamura(Graduate School of Frontier Sciences, University of Tokyo), Naoki Terada(School of Science, Tohoku University)

1:45 PM - 2:00 PM JST | 4:45 AM - 5:00 AM UTC

[PCG25-11] Effects of the intrinsic magnetic field on the ion loss from ancient Mars

*Ryoya Sakata[1], Kanako Seki[1], Shotaro Sakai[1], Naoki Terada[2], Hiroyuki Shinagawa[3], Takashi Tanaka[3,4] (1.Department of Earth and Planetary Science, Graduate School of Science, The University of Tokyo, 2.Graduate School of Science, Tohoku University, 3.National Institute of Information and Communications Technology, 4.International Center for Space Weather Science and Education, Kyushu University)

2:00 PM - 2:15 PM JST | 5:00 AM - 5:15 AM UTC

[PCG25-12] Global characterization of wave perturbations in the middle atmosphere on Mars

*Hiromu Nakagawa[1], Naoki Terada[1], Hannes Groller[7], Roger Yelle[7], Montmessin Franck[8], Schneider M Nicholas[4], England Scott[5], Kanako Seki[6], Takeshi Kuroda[3], Hitoshi Fujiwara[2], Takeshi Imamura[6], Kaori Terada[1], Nao Yoshida[1], Justin I Deighan[4], Sonal K Jain[4], Bruce M Jakosky[4] (1.Planetary Atmosphere Physics Laboratory, Department of Geophysics, Graduate School of Science, Tohoku University, 2.Seikei University, 3.National Institute of Information and Communications Technology, 4.Laboratory for Atmospheric and Space Physics, University of Colorado, 5.Aerospace and Ocean Engineering, Virginia Tech, 6.Department of Earth and Planetary Science, University of Tokyo, 7.Lunar and Planetary Laboratory Science, University of Arizona, 8.LATMOS, UVSQ/CNES/IPSL)

2:15 PM - 2:30 PM JST | 5:15 AM - 5:30 AM UTC

[PCG25-13] Seasonal variation of the dayside N_2/CO_2 at 140 km altitude derived from MAVEN/IUVS

*Nao Yoshida[1], Hiromu Nakagawa[1], Naoki Terada[1], Nicholas Schnider[2], Scott Evans[3], Sonal Jain[2], Hitoshi Fujiwara[4], Takeshi Imamura[5], Justin Deighan[2], Ian Stewart[2], Michael Stivens[6], Roger Yelle[7] (1.Dep. Geophysics Graduate School of Science Tohoku University, 2.Laboratory for Atmospheric and Space Physics, Boulder, USA, 3.Computational Physics, Inc., Springfield, Virginia, USA, 4.Faculty of Science and Technology, Seikei University, 5.Department of Complexity Science and Engineering, Graduate School of Frontier Sciences, The University of Tokyo, 6.Naval Research Laboratory, Washington, USA, 7.Department of Planetary Sciences, University of Arizona)

2:30 PM - 2:45 PM JST | 5:30 AM - 5:45 AM UTC

[PCG25-14] Automated segmentation of Martian dust storms in MGS/MOC images using a deep learning technique

*Kazunori Ogohara[1], Ryusei Gichu[2] (1.School of Engineering, University of Shiga Prefecture, 2.Graduate School of Engineering, University of Shiga Prefecture)

2:45 PM - 3:00 PM JST | 5:45 AM - 6:00 AM UTC

[PCG25-15] Investigation of variation mechanisms of the Jovian radiation belt using ALMA

*Hajime Kita[1], Hideo Sagawa[2], Takahiro Iino[3], Chihiro Tao[4], Takeshi Kuroda[4], Fuminori Tsuchiya[5], Hiroaki Misawa[5], Yasumasa Kasaba[5], Masaki Fujimoto[1] (1.Institute of Space and Astronautical Science, Japan Aerospace Exploration Agency , 2.Faculty of Science, Kyoto Sangyo University, 3.Nature and Science Museum, Tokyo University of Agriculture and Technology, 4.National Institute of Information and Communications Technology, 5.Tohoku University)

3:00 PM - 3:15 PM JST | 6:00 AM - 6:15 AM UTC

[PCG25-16] Jupiter's radio Riddle arcs observed by LWA and Juno

*Kazumasa Imai[1], Charles A. Higgins[2], Masafumi Imai[3], Tracy Clarke[4] (1.Department of Social Design Engineering, National Institute of Technology, Kochi College, 2.Middle Tennessee State University, 3.University of Iowa, 4.Naval Research Laboratory)

[J] Poster | P (Space and Planetary Sciences)：P-CG Complex & General

3:30 PM - 5:00 PM JST | 6:30 AM - 8:00 AM UTC | Poster Hall International Exhibition Hall8, Makuhari Messe_4

[P-CG25] Planetary Magnetosphere, Ionosphere, and Atmosphere

convener:Kanako Seki(Graduate School of Science, University of Tokyo), Takeshi Imamura(Graduate School of Frontier Sciences, The University of Tokyo), Hiroyuki Maezawa(Department of Physical Science Osaka Prefecture University), Naoki Terada(Graduate School of Science, Tohoku University)

[PCG25-P01] Particle-in-cell simulation on the dayside magnetopause in a small-scale magnetosphere

*Hideyuki Usui[1], Satoki oki[1], Yohei Miyake[1], Naoki Terada[2], Kanako Seki[3], Yuto Katoh[2], Manabu Yagi[4] (1.Graduate school of system informatics Kobe University, 2.Graduate school of science, Tohoku University, 3.Graduate school of science, University of Tokyo, 4.Riken R-CCS)

[PCG25-P02] Developments and performance evaluations of 0.48 THz band heterodyne receivers for the future Mars terahertz sensor missions with micro-satellites

*Ayaka Tomihara[1], Satoshi Matsumoto[1], Hiroyuki Maezawa[1], Yasuko Kasai[2], Shigeru Yamada[2], Takeshi Kuroda[2], Takayoshi Yamada[2], Toshiyuki Nishibori[3], Yutaka Hasegawa[3], Yasumasa Kasaba[4], Richard Larsson[5], Shinichi Nakasuka[6] (1.Osaka Prefecture University, Osaka, Japan, 2.National Institute of Information and Communications Technology (NICT), Tokyo, Japan, 3.Japan Aerospace Exploration Agency, 4.Tohoku University, Tohoku, Japan, 5.Max planck Institute Solar System Research, Göttingen Germany, 6.Tokyo University, Tokyo, Japan)

[PCG25-P03] Time response of the self-regulation of H and O escapes from Mars

*Shungo Koyama[1], Naoki Terada[1], Hiromu Nakagawa[1], Takeshi Kuroda[2] (1.Graduate School of Science, Tohoku University, 2.National Institute of Information and Communications Technology)

[PCG25-P04] Study of ion composition in the polar plume from Mars based on MAVEN observations

*Sakakura Kotaro[1], Kanako Seki[1], Shogo Inui[1], Shotaro Sakai[1], David A Brain[2], James P McFadden[3], Jasper S Halekas[4], Gina A Dibraccio[5], Bruce Jakosky[2] (1.Department of Earth and Planetary Science, Graduate School of Science, University of Tokyo, Tokyo, Japan., 2.Laboratory for Atmospheric and Space Physics, University of Colorado Boulder, Boulder, Colorado, USA., 3.Space Sciences Laboratory, University of California, Berkeley, California, USA., 4.Department of Physics and Astronomy, University of Iowa, Iowa City, Iowa, USA., 5.Solar System Exploration Division, NASA Goddard Space Flight Center, Greenbelt, MD, USA.)

[PCG25-P05] Automated detection of Martian dust devils in multiframe images observed by the MER/Spirit rover.

*Kazuki Yajima[1], Kazunori Ogohara[2] (1.Graduate School of Engineering, The University of Shiga Prefecture, 2.School of Engineering, The University of Shiga Prefecture)

[PCG25-P06] Temperature change during the global dust storm period obtained by ground observation of the Martian mesosphere by infrared heterodyne spectroscopy

*Akiho Miyamoto[1], Hiromu Nakagawa[1], Kosuke Takami[1], Takeshi Kuroda[1,3], Isao Murata[2], Naoki Terada[1], Nao Yoshida[1], Katsushige Toriumi[1], Shohei Aoki[4], Yasumasa Kasaba[1] (1.Graduate School of Sciences in Tohoku University, 2.Graduate School of Environmental Sciences, 3. National Institute of Information and Communications Technology, 4.Royal Belgian Institute for Space Aeronomy(IASB-BIRA))

[PCG25-P07] Observation of Neptune's storms with Pirka telescope

*Yuuki Sato[1], Yukihiro Takahashi[1], Seiko Takagi[1], Mitsuteru Sato[1], Ono Tatsuharu[1] (1.Graduate School of Science, Hokkaido University)

[PCG25-P08] The study of Jupiter's zonal wind formation mechanism based on cumulonimbus observation

*Tatsuharu Ono[1], Yukihiro Takahashi[1], Shigeto Watanabe[1], Seiko Takagi[1] (1.Department of Cosmosciences, Graduate School of Science, Hokkaido University)

[PCG25-P09] Development of a radial diffusion model of Jovian inner magnetospheric plasma aimed at comparison with HISAKI satellite observation

*Kazuki Yamaguchi[1], Takeshi Sakanoi[1], Fuminori Tsuchiya[1], Masato Kagitani[1], Ryoichi Koga[1], Tomoki Kimura[2] (1.Planetary Plasma and Atmospheric Research Center, Graduate School of Science, Tohoku University, 2.Frontier Research Institute for Interdisciplinary Sciences, Tohoku University)

[PCG25-P10] Pitch angle scattering due to elastic collisions between magnetospheric 500eV-50keV electrons and neutral H_2O originated from Enceladus: Test particle simulation

*Hiroyasu Tadokoro[1], Yuto Katoh[2] (1.Musashino University, 2.Tohoku University)

[PCG25-P11] Study of Jovian atmosphere dynamics by a multi-band imaging observation

Hayate Ito[1], Sumito Hirota[2], Isshi Tabe[3], *Hidehiko Suzuki[1] (1.Meiji university, 2.Kawasaki municipal science museum, 3.Association of Lunar and Planetary Observers in Japan)

[PCG25-P12] Examination of the relation between Jupiter's inner magnetosphere and magnetic reconfiguration events

*Hiroaki Misawa[1] (1.Planetary Plasma and Atmospheric Research Center, Graduate School of Science, Tohoku University)

[PCG25-P13] Effects of the charged particles of solar wind on planetary atmospheres

*Shinji Karasawa[1] (1.Miyagi National College of Technology Professor emeritus)

[J] Poster | P (Space and Planetary Sciences)：P-CG Complex & General

5:15 PM - 6:30 PM JST | 8:15 AM - 9:30 AM UTC | Poster Hall International Exhibition Hall8, Makuhari Messe_5

[P-CG25] Planetary Magnetosphere, Ionosphere, and Atmosphere

convener:Kanako Seki(Graduate School of Science, University of Tokyo), Takeshi Imamura(Graduate School of Frontier Sciences, The University of Tokyo), Hiroyuki Maezawa(Department of Physical Science Osaka Prefecture University), Naoki Terada(Graduate School of Science, Tohoku University)

[PCG25-P01] Particle-in-cell simulation on the dayside magnetopause in a small-scale magnetosphere

*Hideyuki Usui[1], Satoki oki[1], Yohei Miyake[1], Naoki Terada[2], Kanako Seki[3], Yuto Katoh[2], Manabu Yagi[4] (1.Graduate school of system informatics Kobe University, 2.Graduate school of science, Tohoku University, 3.Graduate school of science, University of Tokyo, 4.Riken R-CCS)

[PCG25-P02] Developments and performance evaluations of 0.48 THz band heterodyne receivers for the future Mars terahertz sensor missions with micro-satellites

*Ayaka Tomihara[1], Satoshi Matsumoto[1], Hiroyuki Maezawa[1], Yasuko Kasai[2], Shigeru Yamada[2], Takeshi Kuroda[2], Takayoshi Yamada[2], Toshiyuki Nishibori[3], Yutaka Hasegawa[3], Yasumasa Kasaba[4], Richard Larsson[5], Shinichi Nakasuka[6] (1.Osaka Prefecture University, Osaka, Japan, 2.National Institute of Information and Communications Technology (NICT), Tokyo, Japan, 3.Japan Aerospace Exploration Agency, 4.Tohoku University, Tohoku, Japan, 5.Max planck Institute Solar System Research, Göttingen Germany, 6.Tokyo University, Tokyo, Japan)

[PCG25-P03] Time response of the self-regulation of H and O escapes from Mars

*Shungo Koyama[1], Naoki Terada[1], Hiromu Nakagawa[1], Takeshi Kuroda[2] (1.Graduate School of Science, Tohoku University, 2.National Institute of Information and Communications Technology)

[PCG25-P04] Study of ion composition in the polar plume from Mars based on MAVEN observations

*Sakakura Kotaro[1], Kanako Seki[1], Shogo Inui[1], Shotaro Sakai[1], David A Brain[2], James P McFadden[3], Jasper S Halekas[4], Gina A Dibraccio[5], Bruce Jakosky[2] (1.Department of Earth and Planetary Science, Graduate School of Science, University of Tokyo, Tokyo, Japan., 2.Laboratory for Atmospheric and Space Physics, University of Colorado Boulder, Boulder, Colorado, USA., 3.Space Sciences Laboratory, University of California, Berkeley, California, USA., 4.Department of Physics and Astronomy, University of Iowa, Iowa City, Iowa, USA., 5.Solar System Exploration Division, NASA Goddard Space Flight Center, Greenbelt, MD, USA.)

[PCG25-P05] Automated detection of Martian dust devils in multiframe images observed by the MER/Spirit rover.

*Kazuki Yajima[1], Kazunori Ogohara[2] (1.Graduate School of Engineering, The University of Shiga Prefecture, 2.School of Engineering, The University of Shiga Prefecture)

[PCG25-P06] Temperature change during the global dust storm period obtained by ground observation of the Martian mesosphere by infrared heterodyne spectroscopy

*Akiho Miyamoto[1], Hiromu Nakagawa[1], Kosuke Takami[1], Takeshi Kuroda[1,3], Isao Murata[2], Naoki Terada[1], Nao Yoshida[1], Katsushige Toriumi[1], Shohei Aoki[4], Yasumasa Kasaba[1] (1.Graduate School of Sciences in Tohoku University, 2.Graduate School of Environmental Sciences, 3. National Institute of Information and Communications Technology, 4.Royal Belgian Institute for Space Aeronomy(IASB-BIRA))

[PCG25-P07] Observation of Neptune's storms with Pirka telescope

*Yuuki Sato[1], Yukihiro Takahashi[1], Seiko Takagi[1], Mitsuteru Sato[1], Ono Tatsuharu[1] (1.Graduate School of Science, Hokkaido University)

[PCG25-P08] The study of Jupiter's zonal wind formation mechanism based on cumulonimbus observation

*Tatsuharu Ono[1], Yukihiro Takahashi[1], Shigeto Watanabe[1], Seiko Takagi[1] (1.Department of Cosmosciences, Graduate School of Science, Hokkaido University)

[PCG25-P09] Development of a radial diffusion model of Jovian inner magnetospheric plasma aimed at comparison with HISAKI satellite observation

*Kazuki Yamaguchi[1], Takeshi Sakanoi[1], Fuminori Tsuchiya[1], Masato Kagitani[1], Ryoichi Koga[1], Tomoki Kimura[2] (1.Planetary Plasma and Atmospheric Research Center, Graduate School of Science, Tohoku University, 2.Frontier Research Institute for Interdisciplinary Sciences, Tohoku University)

[PCG25-P10] Pitch angle scattering due to elastic collisions between magnetospheric 500eV-50keV electrons and neutral H_2O originated from Enceladus: Test particle simulation

*Hiroyasu Tadokoro[1], Yuto Katoh[2] (1.Musashino University, 2.Tohoku University)

[PCG25-P11] Study of Jovian atmosphere dynamics by a multi-band imaging observation

Hayate Ito[1], Sumito Hirota[2], Isshi Tabe[3], *Hidehiko Suzuki[1] (1.Meiji university, 2.Kawasaki municipal science museum, 3.Association of Lunar and Planetary Observers in Japan)

[PCG25-P12] Examination of the relation between Jupiter's inner magnetosphere and magnetic reconfiguration events

*Hiroaki Misawa[1] (1.Planetary Plasma and Atmospheric Research Center, Graduate School of Science, Tohoku University)

[PCG25-P13] Effects of the charged particles of solar wind on planetary atmospheres

*Shinji Karasawa[1] (1.Miyagi National College of Technology Professor emeritus)

[E] Poster | A (Atmospheric and Hydrospheric Sciences)：A-AS Atmospheric Sciences, Meteorology & Atmospheric Environment

10:45 AM - 12:15 PM JST | 1:45 AM - 3:15 AM UTC | Poster Hall International Exhibition Hall8, Makuhari Messe_2

[A-AS03] Large-scale moisture and organized cloud systems

convener:Hiroaki Miura(The University of Tokyo), Atsushi Hamada(University of Toyama), Satoru Yokoi(Japan Agency for Marine-Earth Science and Technology), Masaki Satoh(Atmosphere and Ocean Research Institute, The University of Tokyo)

[AAS03-P01] Numerical investigation on the shape, terminal velocity, and drag coefficient of a small raindrop by the improved immersed boundary method

*Ong Chia Rui[1], Hiroaki Miura[1] (1.The University of Tokyo)

[AAS03-P02] **A diagnostic study of water vapor during an extreme precipitation event in Yili river valleyA diagnostic study of water vapor during an extreme precipitation event in Yili river valley**

*Jing LiU[1], Yushu Zhou[2], Lianmei Yang[1] (1.Institute of Desert Meteorology,CMA, 2.Institute of Atmospheric Physics,CAS)

[AAS03-P03] **The Study on the Characteristics of Weather and Cloud Types in the Summer and Winter Seasons of the South China Sea**

*Jou Ping Hou[1], Bo-Shiou Wei[1], Li-Zhen Su[1] (1.Chung Cheng Institute of Technology)

[AAS03-P04] **Linkages between the South and East Asian Monsoon water vapor transport during boreal summer**

*Yong Liu[1] (1.Institute of Atmospheric Physics, Beijing , China)

[AAS03-P05] Interannual Modulation of the Local Hadley Circulation on Clouds, Radiation and Diagnostic Fields over the Western North Pacific

*Xinyue Wang[1], Hironobu Iwabuchi[1] (1.Tohoku Univ.)

[AAS03-P06] Seasonal and Regional Variation of Diurnal Cycle of Rainfall over Java Island and the Surrounding Area

*Madam Taqiyya Maulana[1], Takeshi Yamazaki[1] (1.Tohoku University)

[AAS03-P07] **Study on atmospheric circulation characteristics of precipitation anomalies in arid region of Central Asia**

*Lianmei Yang[1], Xuefeng Guan[1] (1.Institute of Desert Meteorology, China Meteorological Administration,)

[AAS03-P08] Mechanisms for northward propagation of boreal summer intraseasonal oscillation

*Kanta Nakae[1], Masaki Satoh[1], Daisuke Takasuka[1] (1.Atmosphere and Ocean Research Institute, The University of Tokyo)

[AAS03-P09] Fractality in the perimeter of tropical clouds observed by Himawari-8 or simulated by a high-resolution model

*Takuya Jinno[1] (1.Graduate School of Science, The University of Tokyo)

[AAS03-P10] **Large-scale deformation of tropical cloud band in the ITCZ detected in NICAM simulations**

*Noriyuki Nishi[1], Atsushi Hamada[4], Yohei Yamada[2], Tomoe Nasuno[2], Reona Satoh[5], Masaki Satoh[3] (1.Faculty of Science, Fukuoka Universtiy, 2.JAMSTEC, 3.AORI, University of Tokyo, 4.Graduate School of Science and Engineering for Education, University of Toyama, 5.Graduate School of Science, Fukuoka University)

[AAS03-P11] **Improvement of single-moment bulk microphysics for super-cooled water clouds over the Southern Ocean in NICAM using Joint simulator and double-moment microphysics**

*Woosub Roh[1], Tatsuya Seiki[2], Masaki Satoh[1], Tempei Hashino[3] (1.AORI, the university of Tokyo, 2.JAMSTEC, 3.Kochi university of technology)

[AAS03-P12] High-cloud property responses to SST change: sensitivity study using a global nonhydrostatic model

*Tomoki Ohno[1], Masaki Satoh[2] (1.Japan Agency for Marine-Earth Science and Technology, 2.Atmosphere and Ocean Research Institute, The University of Tokyo)

[AAS03-P13] Effects of different cloud overlapping parameters on simulated total cloud fraction over the globe and East Asian region

*bo hai Wang[1], hua Zhang[2] (1.Institute of Atmospheric Physics, Chinese Academy of Sciences, 2.State Key Laboratory of Severe Weather, Chinese Academy of Meteorological Sciences)

[E] Poster | A (Atmospheric and Hydrospheric Sciences)：A-AS Atmospheric Sciences, Meteorology & Atmospheric Environment

5:15 PM - 6:30 PM JST | 8:15 AM - 9:30 AM UTC | Poster Hall International Exhibition Hall8, Makuhari Messe_6

[A-AS03] Large-scale moisture and organized cloud systems

convener:Hiroaki Miura(The University of Tokyo), Atsushi Hamada(University of Toyama), Satoru Yokoi(Japan Agency for Marine-Earth Science and Technology), Masaki Satoh(Atmosphere and Ocean Research Institute, The University of Tokyo)

[AAS03-P01] Numerical investigation on the shape, terminal velocity, and drag coefficient of a small raindrop by the improved immersed boundary method

*Ong Chia Rui[1], Hiroaki Miura[1] (1.The University of Tokyo)

[AAS03-P02] **A diagnostic study of water vapor during an extreme precipitation event in Yili river valleyA diagnostic study of water vapor during an extreme precipitation event in Yili river valley**

*Jing LiU[1], Yushu Zhou[2], Lianmei Yang[1] (1.Institute of Desert Meteorology,CMA, 2.Institute of Atmospheric Physics,CAS)

[AAS03-P03] **The Study on the Characteristics of Weather and Cloud Types in the Summer and Winter Seasons of the South China Sea**

*Jou Ping Hou[1], Bo-Shiou Wei[1], Li-Zhen Su[1] (1.Chung Cheng Institute of Technology)

[AAS03-P04] **Linkages between the South and East Asian Monsoon water vapor transport during boreal summer**

*Yong Liu[1] (1.Institute of Atmospheric Physics, Beijing , China)

[AAS03-P05] Interannual Modulation of the Local Hadley Circulation on Clouds, Radiation and Diagnostic Fields over the Western North Pacific

*Xinyue Wang[1], Hironobu Iwabuchi[1] (1.Tohoku Univ.)

[AAS03-P06] Seasonal and Regional Variation of Diurnal Cycle of Rainfall over Java Island and the Surrounding Area

*Madam Taqiyya Maulana[1], Takeshi Yamazaki[1] (1.Tohoku University)

[AAS03-P07] **Study on atmospheric circulation characteristics of precipitation anomalies in arid region of Central Asia**

*Lianmei Yang[1], Xuefeng Guan[1] (1.Institute of Desert Meteorology, China Meteorological Administration,)

[AAS03-P08] Mechanisms for northward propagation of boreal summer intraseasonal oscillation

*Kanta Nakae[1], Masaki Satoh[1], Daisuke Takasuka[1] (1.Atmosphere and Ocean Research Institute, The University of Tokyo)

[AAS03-P09] Fractality in the perimeter of tropical clouds observed by Himawari-8 or simulated by a high-resolution model

*Takuya Jinno[1] (1.Graduate School of Science, The University of Tokyo)

[AAS03-P10] **Large-scale deformation of tropical cloud band in the ITCZ detected in NICAM simulations**

*Noriyuki Nishi[1], Atsushi Hamada[4], Yohei Yamada[2], Tomoe Nasuno[2], Reona Satoh[5], Masaki Satoh[3] (1.Faculty of Science, Fukuoka Universtiy, 2.JAMSTEC, 3.AORI, University of Tokyo, 4.Graduate School of Science and Engineering for Education, University of Toyama, 5.Graduate School of Science, Fukuoka University)

[AAS03-P11] **Improvement of single-moment bulk microphysics for super-cooled water clouds over the Southern Ocean in NICAM using Joint simulator and double-moment microphysics**

*Woosub Roh[1], Tatsuya Seiki[2], Masaki Satoh[1], Tempei Hashino[3] (1.AORI, the university of Tokyo, 2.JAMSTEC, 3.Kochi university of technology)

[AAS03-P12] High-cloud property responses to SST change: sensitivity study using a global nonhydrostatic model

*Tomoki Ohno[1], Masaki Satoh[2] (1.Japan Agency for Marine-Earth Science and Technology, 2.Atmosphere and Ocean Research Institute, The University of Tokyo)

[AAS03-P13] Effects of different cloud overlapping parameters on simulated total cloud fraction over the globe and East Asian region

*bo hai Wang[1], hua Zhang[2] (1.Institute of Atmospheric Physics, Chinese Academy of Sciences, 2.State Key Laboratory of Severe Weather, Chinese Academy of Meteorological Sciences)

[E] Oral | A (Atmospheric and Hydrospheric Sciences)：A-AS Atmospheric Sciences, Meteorology & Atmospheric Environment

1:45 PM - 3:15 PM JST | 4:45 AM - 6:15 AM UTC | 104 1F

[A-AS03] Large-scale moisture and organized cloud systems

convener:Hiroaki Miura(The University of Tokyo), Atsushi Hamada(University of Toyama), Satoru Yokoi(Japan Agency for Marine-Earth Science and Technology), Masaki Satoh(Atmosphere and Ocean Research Institute, The University of Tokyo), Chairperson:Hiroaki Miura

1:45 PM - 2:00 PM JST | 4:45 AM - 5:00 AM UTC

[AAS03-01] Boundary-Layer Control on Convective Self-Aggregation

★Invited Papers

*Da YANG[1,2] (1.University of California, Davis, 2.Lawrence Berkeley National Laboratory)

2:00 PM - 2:15 PM JST | 5:00 AM - 5:15 AM UTC

[AAS03-02] Statistical Properties of Cumulus Ensembles in High-Resolution Radiative-Convective Equilibrium Simulations

*Tomoro Yanase[1,2], Tetsuya Takemi[2] (1.Graduate School of Science, Kyoto University, 2.Disaster Prevention Research Institute, Kyoto University)

2:15 PM - 2:30 PM JST | 5:15 AM - 5:30 AM UTC

[AAS03-03] **The role of interactive SST in the cloud-resolving simulations of aggregated convection**

★Invited Papers

*Chien-Ming Wu[1], Yan-Ting Chen[1] (1.National Taiwan University)

2:30 PM - 2:45 PM JST | 5:30 AM - 5:45 AM UTC

[AAS03-04] **Role of coastal convection to moisture buildup during the South China Sea summer monsoon onset**

*Wei-Ting Chen[1], Wei-Ming Tsai[1,2], Chien-Ming Wu[1], Peng-Jen Chen[1] (1.National Taiwan University, 2.University of Miami)

2:45 PM - 3:00 PM JST | 5:45 AM - 6:00 AM UTC

[AAS03-05] Resolution dependencies of tropical convection in a global cloud/cloud-system resolving model

★Invited Papers

*Tomoki Miyakawa[1], Hiroaki Miura[2] (1.Atmosphere and Ocean Research Institute, The University of Tokyo, 2.Graduate School of Science, The University of Tokyo)

3:00 PM - 3:15 PM JST | 6:00 AM - 6:15 AM UTC

[AAS03-06] Effects of the local convection over the western Maritime Continent on the large-scale: numerical study during the YMC Sumatra campaigns

*Tomoe Nasuno[1] (1.Japan Agency for Marine-Earth Science and Technology)

[E] Oral | A (Atmospheric and Hydrospheric Sciences)：A-AS Atmospheric Sciences, Meteorology & Atmospheric Environment

3:30 PM - 5:00 PM JST | 6:30 AM - 8:00 AM UTC | 104 1F

[A-AS03] Large-scale moisture and organized cloud systems

convener:Hiroaki Miura(The University of Tokyo), Atsushi Hamada(University of Toyama), Satoru Yokoi(Japan Agency for Marine-Earth Science and Technology), Masaki Satoh(Atmosphere and Ocean Research Institute, The University of Tokyo), Chairperson:Satoru Yokoi

3:30 PM - 3:45 PM JST | 6:30 AM - 6:45 AM UTC

[AAS03-07] A Mechanism for the Maintenance of Sharp Tropical Margins

★Invited Papers

*Hirohiko Masunaga[1], Brian Earle Mapes[2] (1.Nagoya University, 2.University of Miami)

3:45 PM - 4:00 PM JST | 6:45 AM - 7:00 AM UTC

[AAS03-08] Observational Evidence of Mixed Rossby-Gravity Waves as a Driving Force for the MJO Convective Initiation and Propagation

*Daisuke Takasuka[1,2], Masaki Satoh[1], Satoru Yokoi[2] (1.Atmosphere and Ocean Research Institute, The University of Tokyo, 2.Japan Agency for Marine-Earth Science and Technology)

4:00 PM - 4:15 PM JST | 7:00 AM - 7:15 AM UTC

[AAS03-09] A characteristic of the MJO as a part of enhanced large-scale zonal circulation

*Tamaki Suematsu[1], Hiroaki Miura[2] (1.Atmosphere and Ocean Reaserch Institute, The University of Tokyo, 2.School of Science, The University of Tokyo)

4:15 PM - 4:30 PM JST | 7:15 AM - 7:30 AM UTC

[AAS03-10] **The role of the moisture on the occurrences and distribution of the Amazonian mesoscale convective systems**

*Amanda Rehbein[1,2], Masaki Satoh[2], Tercio Ambrizzi[1] (1.Univ. of Sao Paulo, 2.Univ. of Tokyo)

4:30 PM - 4:45 PM JST | 7:30 AM - 7:45 AM UTC

[AAS03-11] Interdecadal Change of the Impact of Eurasian Snow on Spring Precipitation Over Southern China

*Dingrui Cao[1] (1.Zhejiang University)

4:45 PM - 5:00 PM JST | 7:45 AM - 8:00 AM UTC

[AAS03-12] Atmospheric Rivers and related atmospheric circulations associated with Japanese disastrous precipitation in warm season

Naho Suetou[1], *Akiyo Yatagai[1], Yukari Takayabu[2] (1.Graduate School of Science and Technology/Hirosaki University, 2.Atmosphere and Ocean Research Institute/The University of Tokyo)

[J] Oral | A (Atmospheric and Hydrospheric Sciences)：A-OS Ocean Sciences & Ocean Environment

10:45 AM - 12:15 PM JST | 1:45 AM - 3:15 AM UTC | 106 1F

[A-OS17] Kuroshio Large Meander

convener:Toru Miyama(Japan Agency for Marine-Earth Science and Technology, Application Laboratory), Norihisa Usui(Meteorological Research Institute), Takashi Setou(National Research Institute of Fisheries Science, Fisheries Research and Education Agency), Chairperson:Toru Miyama, Takashi Setou, Norihisa Usui

10:45 AM - 11:00 AM JST | 1:45 AM - 2:00 AM UTC

[AOS17-01] The progress of the Kuroshio large meander in and after 2017

★Invited Papers

*Toshiyuki Sakurai[1], Mikitoshi Hirabara[1], Yoshikazu Fukuda[1], Mika Kimura[1], Kotaro Mine[1], Masaomi Takahashi[1], Kensaku Kobayashi[1], Yuka Okunaka[1], Hiromu Kobayashi[1] (1.Japan Meteorological Agency)

11:00 AM - 11:15 AM JST | 2:00 AM - 2:15 AM UTC

[AOS17-02] Influences of the Kuroshio path variation south of Honshu on summer surface air temperature in Kanto district, Japan

*Shusaku Sugimoto[1] (1.Graduate School of Science, Tohoku University)

11:15 AM - 11:30 AM JST | 2:15 AM - 2:30 AM UTC

[AOS17-03] Bio-chemilcal difference between the large meander and the non case of the Kuroshio current

*Takashi Setou[1], Tuneo Ono[2], Kiyotaka Hidaka[1], Yugo Shimizu[1], Atsushi Nishimoto[1], Sayaka Sogawa[1], Akira Kusaka[1], Daisuke Ambe[1], Daiki Itoh[1], Takashiko Kameda[1], Yutaka Hiroe[3] (1.National Research Institute of Fisheries Science, Fisheries Research and Education Agency , 2.National Research Institute of Far Seas Fisheires,Fisheries Research and Education Agency , 3.National Research Institute of Far Seas Fisheires,Seikai National Fisheries Research Institute)

11:30 AM - 11:45 AM JST | 2:30 AM - 2:45 AM UTC

[AOS17-04] The late arrival of 2017-18 Japanese eel recruitment and its links to ocean circulation

*Yu-Lin Eda Chang[1], Yasumasa Miyazawa[1], Michael Miller[2], Katsumi Tsukamoto[2] (1.Application Laboratory, Japan Agency for Marine-Earth Science and Technology, 2.Department of Aquatic Bioscience, The University of Tokyo)

11:45 AM - 12:00 PM JST | 2:45 AM - 3:00 AM UTC

[AOS17-05] A probabilistic forecast of the Kuroshio current path variability using an 80-member ensemble simulation.

*Kunihiro Aoki[1], Yasumasa Miyazawa[1], Tsutomu Hihara[1] (1.JAMSTEC)

12:00 PM - 12:15 PM JST | 3:00 AM - 3:15 AM UTC

[AOS17-06] Long-term forecast of the Kuroshio large meander in 2017

*Norihisa Usui[1], Nariaki Hirose[1], Kei Sakamoto[1], Yosuke Fujii[1], Nadao Kohno[1] (1.Meteorological Research Institute)

[J] Poster | A (Atmospheric and Hydrospheric Sciences)：A-OS Ocean Sciences & Ocean Environment

3:30 PM - 5:00 PM JST | 6:30 AM - 8:00 AM UTC | Poster Hall International Exhibition Hall8, Makuhari Messe_5

[A-OS17] Kuroshio Large Meander

convener:Toru Miyama(Japan Agency for Marine-Earth Science and Technology, Application Laboratory), Norihisa Usui(Meteorological Research Institute), Takashi Setou(National Research Institute of Fisheries Science, Fisheries Research and Education Agency)

[AOS17-P01] Temporal and spacial changes in relative vorticity along the Kuroshio axis

*Yuya Hirano[1], Kazuyuki Uehara[1] (1.The Graduate School of Geo-environmental Science, Tokai University)

[AOS17-P02] The Kuroshio large meander in 2017 and its coastal impact reproduced by a 2-km resolution assimilation model

*Nariaki Hirose[1], Norihisa Usui[1], Kei Sakamoto[1], Goro Yamanaka[1], Nadao Kohno[1] (1.Meteorological Research Institute, Japan Meteorological Agency)

[AOS17-P03] Reintesification of the Kuroshio Large Meander in Summer 2018

*Toru Miyama[1], Yasumasa Miyazawa[1] (1.Japan Agency for Marine-Earth Science and Technology, Application Laboratory)

[J] Poster | A (Atmospheric and Hydrospheric Sciences)：A-OS Ocean Sciences & Ocean Environment

5:15 PM - 6:30 PM JST | 8:15 AM - 9:30 AM UTC | Poster Hall International Exhibition Hall8, Makuhari Messe_7

[A-OS17] Kuroshio Large Meander

convener:Toru Miyama(Japan Agency for Marine-Earth Science and Technology, Application Laboratory), Norihisa Usui(Meteorological Research Institute), Takashi Setou(National Research Institute of Fisheries Science, Fisheries Research and Education Agency)

[AOS17-P01] Temporal and spacial changes in relative vorticity along the Kuroshio axis

*Yuya Hirano[1], Kazuyuki Uehara[1] (1.The Graduate School of Geo-environmental Science, Tokai University)

[AOS17-P02] The Kuroshio large meander in 2017 and its coastal impact reproduced by a 2-km resolution assimilation model

*Nariaki Hirose[1], Norihisa Usui[1], Kei Sakamoto[1], Goro Yamanaka[1], Nadao Kohno[1] (1.Meteorological Research Institute, Japan Meteorological Agency)

[AOS17-P03] Reintesification of the Kuroshio Large Meander in Summer 2018

*Toru Miyama[1], Yasumasa Miyazawa[1] (1.Japan Agency for Marine-Earth Science and Technology, Application Laboratory)

[J] Oral | A (Atmospheric and Hydrospheric Sciences)：A-OS Ocean Sciences & Ocean Environment

1:45 PM - 3:15 PM JST | 4:45 AM - 6:15 AM UTC | 106 1F

[A-OS18] Physical Oceanography (General)

convener:Yoshimi Kawai(Research and Development Center for Global Change, Japan Agency for Marine-Earth Science and Technology), Tomoki Tozuka(Department of Earth and Planetary Science, Graduate School of Science, The University of Tokyo), Kitade Yujiro(Tokyo University of Marine Science and Technology), Chairperson:Yoshimi Kawai(Japan Agency for Marine-Earth Science and Technology), Tomoki Tozuka(The University of Tokyo)

1:50 PM - 2:05 PM JST | 4:50 AM - 5:05 AM UTC

[AOS18-01] **Real-Time Subsurface Moorings as a Promising Component of Global Ocean Monitoring System**

*Jianing Wang[1], Fan Wang[1] (1.Institute of Oceanology, Chinese Academy of Sciences)

2:05 PM - 2:20 PM JST | 5:05 AM - 5:20 AM UTC

[AOS18-02] Seasonal Variation of the Mixed Layer Depth at 60°S and its governing dynamics

*Matheus Ferreira Azevedo[1], Yujiro Kitade[1], Shigeru Aoki[2] (1.Tokyo University of Marine Science and Technology, 2.Institute of Low Temperature Science, Hokkaido University)

2:20 PM - 2:40 PM JST | 5:20 AM - 5:40 AM UTC

[AOS18-03] **21st-Century Flood Hazards along the U.S. Atlantic Coast: Impacts of Sea Level Rise and Tropical Cyclone Climatology Change**

★Invited Papers

*Reza Marsooli[1], Ning Lin[2], Kerry Emanuel[3] (1.Stevens Institute of Technology, 2.Princeton University, 3.Massachusetts Institute of Technology)

2:40 PM - 3:00 PM JST | 5:40 AM - 6:00 AM UTC

[AOS18-04] **The Effect of Ocean Waves on an Explosive Cyclone Development: Investigation with a Coupled Model**

★Invited Papers

*Yuki Kita[1], Takuji Waseda[1] (1.University of Tokyo)

[J] Poster | A (Atmospheric and Hydrospheric Sciences)：A-OS Ocean Sciences & Ocean Environment

5:15 PM - 6:30 PM JST | 8:15 AM - 9:30 AM UTC | Poster Hall International Exhibition Hall8, Makuhari Messe_8

[A-OS18] Physical Oceanography (General)

convener:Yoshimi Kawai(Research and Development Center for Global Change, Japan Agency for Marine-Earth Science and Technology), Tomoki Tozuka(Department of Earth and Planetary Science, Graduate School of Science, The University of Tokyo), Kitade Yujiro(Tokyo University of Marine Science and Technology)

[AOS18-P01] Mathematical modeling for initial profile of tsunami by instantaneous- or slow-faulting

*Chi-Min Liu[1] (1.Chienkuo Technology University)

[AOS18-P02] Geoid height and sea surface changes due to the 2004 Sumatra-Andaman earthquake and the 2012 Indian-Ocean earthquake from satellite gravimetry and satellite altimetry

★Invited Papers

*Yusaku Tanaka[1] (1.Earthquake Research Institute)

[AOS18-P03] An irregularly shaped warm eddy observed by Chinese underwater gliders

*Huabin MAO[1] (1.South China Sea Institute of Oceanology)

[AOS18-P04] sea surface cooling in the northern South China Sea observed using Chinese underwater glider

*Chunhua Qiu[1] (1.Sun Yat-sen University)

[AOS18-P05] Airborne SAR observation of dependence of ocean surface backscattering on wind direction

*Akitsugu Nadai[1] (1.NICT National Institute of Information and Communications Technology)

[J] Oral | A (Atmospheric and Hydrospheric Sciences)：A-OS Ocean Sciences & Ocean Environment

9:00 AM - 10:30 AM JST | 12:00 AM - 1:30 AM UTC | 106 1F

[A-OS20] Global ocean observing systems, obtained results and system optimization: toward OceanObs19

convener:Shigeki Hosoda(Japan Marine-Earth Science and Technology), Shuhei Masuda(Japan Agency for Marine-Earth Science and Technology), Yosuke Fujii(Meteorological Research Institute, Japan Meteorological Agency), Fujiki Tetsuichi(Japan Agency for Marine-Earth Science and Technology), Chairperson:Shigeki Hosoda(Japan Agency for Marine-Earth Science and Technology)

9:00 AM - 9:15 AM JST | 12:00 AM - 12:15 AM UTC

[AOS20-01] Global Ocean Observing System: The Past, the Present and the Future

★Invited Papers

*Toshio Suga[1,2] (1.Graduate School of Science, Tohoku University, 2.JAMSTEC)

9:15 AM - 9:30 AM JST | 12:15 AM - 12:30 AM UTC

[AOS20-02] Observed long-term change and variability in the global upper-ocean stratification

*Ryohei Yamaguchi[1], Toshio Suga[1,2] (1.Graduate School of Science, Tohoku University, 2.Japan Agency for Marine-Earth Science and Technology)

9:30 AM - 9:45 AM JST | 12:30 AM - 12:45 AM UTC

[AOS20-03] Estimation of changes in salinity and dissolved oxygen based on observational networks

★Invited Papers

*Shinya Kouketsu[1] (1.JAMSTEC Japan Agency for Marine-Earth Science and Technology)

9:45 AM - 10:00 AM JST | 12:45 AM - 1:00 AM UTC

[AOS20-04] Remotely forced decadal physical and biogeochemical variability of North Pacific Subtropical Mode Water over the last 40 years

*Daisuke Sasano[1], Eitarou Oka[2], Yudai Yamada[2], Enyo Kazutaka[1], Toshiya Nakano[1], Masao Ishii[3] (1.Japan Meteorological Agency, 2.Atmosphere and Ocean Research Institute, The University of Tokyo, 3.Meteorological Research Institute)

10:00 AM - 10:15 AM JST | 1:00 AM - 1:15 AM UTC

[AOS20-05] Asessing the impact of the global ocean observing system using ocean data assimilation systems

*Yosuke Fujii[1] (1.Meteorological Research Institute, Japan Meteorological Agency)

10:15 AM - 10:30 AM JST | 1:15 AM - 1:30 AM UTC

[AOS20-06] **Global ocean state estimation with new float observations**

*Shuhei Masuda[1], Satoshi Osafune[1], Tadashi Hemmi[1] (1.Japan Agency for Marine-Earth Science and Technology)

[J] Poster | A (Atmospheric and Hydrospheric Sciences)：A-OS Ocean Sciences & Ocean Environment

3:30 PM - 5:00 PM JST | 6:30 AM - 8:00 AM UTC | Poster Hall International Exhibition Hall8, Makuhari Messe_6

[A-OS20] Global ocean observing systems, obtained results and system optimization: toward OceanObs19

convener:Shigeki Hosoda(Japan Marine-Earth Science and Technology), Shuhei Masuda(Japan Agency for Marine-Earth Science and Technology), Yosuke Fujii(Meteorological Research Institute, Japan Meteorological Agency), Fujiki Tetsuichi(Japan Agency for Marine-Earth Science and Technology)

[AOS20-P01] Fresh bias with pressure dependency at the measurements of SBE 41CP for deep float

*Taiyo Kobayashi[1] (1.Japan Agency for Marine-Earth Science and Technology)

[AOS20-P02] Long-term thermohaline variations in the North Pacific subtropical gyre observed by repeat hydrography along the 165°E meridian

*Yuma Kawakami[1,2], Yoshiteru Kitamura[1], Toshiya Nakano[1,2] (1.Japan Meteorological Agency, 2.Meteorological Research Institute)

[AOS20-P03] First detection of chlorofluorocarbons into bottom layer in the Melanesian Basin of the North Pacific

*Toshiya NAKANO[1], Kazutaka ENYO[1], Daisuke SASANO[1], Shogo URAKAWA[2], Hiroyuki TSUJINO[2], Hideyuki NAKANO[2], Masao ISHII[2] (1.Japan Meteorological Agency, 2.Meteorological Research Institute)

[AOS20-P04] **Global grid mapping of temperature and salinity based on Argo float data**

*Shigeki Hosoda[1] (1.Japan Marine-Earth Science and Technology)

[AOS20-P05] **Evolutions of water mass anomalies in the upper North Pacific based on Argo data, in STMW, ESTMW, and CMW.**

*Tong Wang[1], Toshio Suga[1,2], Shinya Kouketsu[2] (1.Graduate School of Science, Tohoku University, 2.Research and Development Center for Global Change, JAMSTEC)

[AOS20-P06] Impacts of temperature measurements from sea turtles on seasonal prediction around the Arafura Sea

*Takeshi Doi[1], Andrea Storto[2], Takuya Fukuoka[3], Hiroyuki Suganuma[4], Katsufumi Sato[3] (1.JAMSTEC, 2.CMRE, 3.The University of Tokyo, 4.ELNA)

[AOS20-P07] Physical and biogeochemical processes from winter to spring in the south of the Kuroshio Extension

*Chiho Sukigara[1], Ryuichiro Inoue[2], Takeyoshi Nagai[1], Andrea J Fassbender[3], Yuichiro Takeshita[3], Stuart P Bishop[4], Eitarou Oka[5] (1.Tokyo University of Marine Science and Technology, 2.Japan Agency for Marine-Earth Science and Technology, 3.Monterey Bay Aquarium Research Institute, 4.North Carolina State University, 5.The University of Tokyo)

[J] Poster | A (Atmospheric and Hydrospheric Sciences)：A-OS Ocean Sciences & Ocean Environment

5:15 PM - 6:30 PM JST | 8:15 AM - 9:30 AM UTC | Poster Hall International Exhibition Hall8, Makuhari Messe_9

[A-OS20] Global ocean observing systems, obtained results and system optimization: toward OceanObs19

convener:Shigeki Hosoda(Japan Marine-Earth Science and Technology), Shuhei Masuda(Japan Agency for Marine-Earth Science and Technology), Yosuke Fujii(Meteorological Research Institute, Japan Meteorological Agency), Fujiki Tetsuichi(Japan Agency for Marine-Earth Science and Technology)

[AOS20-P01] Fresh bias with pressure dependency at the measurements of SBE 41CP for deep float

*Taiyo Kobayashi[1] (1.Japan Agency for Marine-Earth Science and Technology)

[AOS20-P02] Long-term thermohaline variations in the North Pacific subtropical gyre observed by repeat hydrography along the 165°E meridian

*Yuma Kawakami[1,2], Yoshiteru Kitamura[1], Toshiya Nakano[1,2] (1.Japan Meteorological Agency, 2.Meteorological Research Institute)

[AOS20-P03] First detection of chlorofluorocarbons into bottom layer in the Melanesian Basin of the North Pacific

*Toshiya NAKANO[1], Kazutaka ENYO[1], Daisuke SASANO[1], Shogo URAKAWA[2], Hiroyuki TSUJINO[2], Hideyuki NAKANO[2], Masao ISHII[2] (1.Japan Meteorological Agency, 2.Meteorological Research Institute)

[AOS20-P04] **Global grid mapping of temperature and salinity based on Argo float data**

*Shigeki Hosoda[1] (1.Japan Marine-Earth Science and Technology)

[AOS20-P05] **Evolutions of water mass anomalies in the upper North Pacific based on Argo data, in STMW, ESTMW, and CMW.**

*Tong Wang[1], Toshio Suga[1,2], Shinya Kouketsu[2] (1.Graduate School of Science, Tohoku University, 2.Research and Development Center for Global Change, JAMSTEC)

[AOS20-P06] Impacts of temperature measurements from sea turtles on seasonal prediction around the Arafura Sea

*Takeshi Doi[1], Andrea Storto[2], Takuya Fukuoka[3], Hiroyuki Suganuma[4], Katsufumi Sato[3] (1.JAMSTEC, 2.CMRE, 3.The University of Tokyo, 4.ELNA)

[AOS20-P07] Physical and biogeochemical processes from winter to spring in the south of the Kuroshio Extension

*Chiho Sukigara[1], Ryuichiro Inoue[2], Takeyoshi Nagai[1], Andrea J Fassbender[3], Yuichiro Takeshita[3], Stuart P Bishop[4], Eitarou Oka[5] (1.Tokyo University of Marine Science and Technology, 2.Japan Agency for Marine-Earth Science and Technology, 3.Monterey Bay Aquarium Research Institute, 4.North Carolina State University, 5.The University of Tokyo)

[E] Oral | A (Atmospheric and Hydrospheric Sciences)：A-HW Hydrology & Water Environment

1:45 PM - 3:15 PM JST | 4:45 AM - 6:15 AM UTC | 103 1F

[A-HW23] Hydrology & Water Environment

convener:Isao Machida(Geological Survey of Japan), Dai Yamazaki(Institute of Industrial Sciences, The University of Tokyo), Takeshi Hayashi(Faculty of Education and Human Studies, Akita University), Keisuke Fukushi(Institute of Nature & Environmental Technology, Kanazawa University), Chairperson:Isao Machida(Geological Survey of Japan, AIST)

1:45 PM - 2:00 PM JST | 4:45 AM - 5:00 AM UTC

[AHW23-01] Method for measuring the pore air pressure in the mountainous slope for rainfall-runoff processes research

★Invited Papers

*Sho Iwagami[1], Shoji Noguchi[1], Takanori Shimizu[1], Tayoko Kubota[1], Shin'ichi Iida[1], Makoto Araki[1] (1.Forestry and Forest Products Research Institute, Forest Research and Management Organization, National Research and Development Agency)

2:00 PM - 2:15 PM JST | 5:00 AM - 5:15 AM UTC

[AHW23-02] **A method to quantify the influence of total water storage change on climate elasticity of streamflow**

*Yin Tang[1] (1.Institute of Geographic Sciences and Natural Resources Research, Chinese Academy of Science)

2:15 PM - 2:30 PM JST | 5:15 AM - 5:30 AM UTC

[AHW23-03] **Trade-off analysis of discharge-desiltation-turbidity and sediment simulation of a combined reservoir–river system under multi-phase and multi-layer conjunctive releasing operation**

*Chien-Lin Huang[1], Nien-Sheng Hsu[1], Gene Jiing-Yun You[1] (1.National Taiwan University, Taiwan)

2:30 PM - 2:45 PM JST | 5:30 AM - 5:45 AM UTC

[AHW23-04] Gradient change of soil moisture effect on next-day precipitation identified via a Random Forest-Granger causality model

*Lu Li[1], Wei ShangGuan[1], Shu Peng Zhang[1], Jin Jing Pan[1], Nan Wei[1], Yong Jiu Dai[1] (1.Guangdong Province Key Laboratory for Climate Change and Natural Disaster Studies, School of Atmospheric Sciences, Sun Yat-sen University)

2:45 PM - 3:00 PM JST | 5:45 AM - 6:00 AM UTC

[AHW23-05] **Using data-driven methods to explore the predictability of surface soil moisture with FLUXNET site data**

*jinjing Pan[1] (1.Guangdong Province Key Laboratory for Climate Change and Natural Disaster Studies, School of Atmospheric Sciences, Sun Yat-sen University.)

3:00 PM - 3:15 PM JST | 6:00 AM - 6:15 AM UTC

[AHW23-23] Global Analyis of the Hydrological Sensitivity to Climate Variability

*Marisol Dominguez[1], Hugo Alberto Gutierrez-Jurado[1] (1.University of Texas at El Paso)

[E] Oral | A (Atmospheric and Hydrospheric Sciences)：A-HW Hydrology & Water Environment

3:30 PM - 5:00 PM JST | 6:30 AM - 8:00 AM UTC | 103 1F

[A-HW23] Hydrology & Water Environment

convener:Isao Machida(Geological Survey of Japan), Dai Yamazaki(Institute of Industrial Sciences, The University of Tokyo), Takeshi Hayashi(Faculty of Education and Human Studies, Akita University), Keisuke Fukushi(Institute of Nature & Environmental Technology, Kanazawa University), Chairperson:Megumi Watanabe

3:30 PM - 3:45 PM JST | 6:30 AM - 6:45 AM UTC

[AHW23-06] **A review on the global soil property maps for Earth system model**

Yongjiu Dai[1], *Wei Shangguan[1], Dagang Wang[2], Nan Wei[1], Qinchuan Xin[2], Hua Yuan[1], Shupeng Zhang[1], Shaofeng Liu[1], Fapeng Yan[3], Xingji Lu[1] (1. Guangdong Province Key Laboratory for Climate Change and Natural Disaster Studies, School of Atmospheric Sciences, Sun Yat-sen University, 2.School of Geography and Planning, Sun Yat-sen University, 3.College of Global Change and Earth System Science, Beijing Normal University)

3:45 PM - 4:00 PM JST | 6:45 AM - 7:00 AM UTC

[AHW23-07] **Estimating near surface soil moisture at a high spatial resolution using an in-situ data based model**

*Indishe Prabath Senanayake[1], In-Young Yeo[1,2], Natthachet Tangdamrongsub[3,4], Garry R Willgoose[1], Gregory R Hancock[5], Tony Wells[1], Bin Fang[6], Venkataraman Lakshmi[6], Jeffrey P Walker[7] (1.School of Engineering, Faculty of Engineering and Built Environment, The University of Newcastle, Callaghan, NSW 2308, Australia., 2.Department of Geographical Sciences, University of Maryland, College Park, MD 20742, USA., 3.Earth System Science Interdisciplinary Center, University of Maryland, College Park, Maryland, USA., 4.Hydrological Sciences Laboratory, NASA Goddard Space Flight Center, Greenbelt, Maryland, USA., 5.School of Environmental and Life Sciences, Faculty of Science, The University of Newcastle, Callaghan, NSW 2308, Australia., 6.School of Earth Ocean and Environment, University of South Carolina, Columbia, SC 29223, United States., 7.Department of Civil Engineering, Monash University, Clayton, Victoria 3800, Australia.)

4:00 PM - 4:15 PM JST | 7:00 AM - 7:15 AM UTC

[AHW23-08] Representation of dams in global flood inundation simulations by coupling the global hydrological model H08 and the global hydrodynamic model CaMa-Flood

*Julien Eric Boulange[1], Naota Hanasaki[1] (1.National Institute for Environmental Studies)

4:15 PM - 4:30 PM JST | 7:15 AM - 7:30 AM UTC

[AHW23-09] An investigation into a potential long subglacial river beneath the Greenland ice sheet using SICOPOLIS simulations.

*Christopher Chambers[1], Ralf Greve[1], Bas Altena[2], Pierre-Marie Lefeuvre[2] (1.Hokkaido University, 2.University of Oslo)

4:30 PM - 4:45 PM JST | 7:30 AM - 7:45 AM UTC

[AHW23-10] **Changes in Annual Rainfall patterns in the Democratic Republic of Congo: Congo river basin**

*Chetan Sharma[1], Chandra Shekhar Prasad Ojha[1] (1.Indian Institute of Technology Roorkee)

4:45 PM - 5:00 PM JST | 7:45 AM - 8:00 AM UTC

[AHW23-11] Seasonality in the extreme precipitation events linked to temperature over Japan

*Sridhara Nayak[1], Tetsuya Takemi[1] (1.Disaster Prevention Research Institute, Kyoto University)

[J] Oral | A (Atmospheric and Hydrospheric Sciences)：A-CC Cryospheric Sciences & Cold District Environment

9:00 AM - 10:30 AM JST | 12:00 AM - 1:30 AM UTC | 201B 2F

[A-CC26] Ice cores and paleoenvironmental modeling

convener:Ryu Uemura(University of the Ryukyus), Kenji Kawamura(National Institute of Polar Research, Research Organization of Information and Systems), Ayako Abe-Ouchi(Atmosphere and Ocean Research Institute, The University of Tokyo), Nozomu Takeuchi(Chiba University), Chairperson:Ryu Uemura(University of the Ryukyus), Ikumi Oyabu(National Institute of Polar Research)

9:00 AM - 9:15 AM JST | 12:00 AM - 12:15 AM UTC

[ACC26-01] Aerosols and climate change in the Arctic in the historical experiments using the MRI Earth System Model

★Invited Papers

*Naga Oshima[1], Taichu Y Tanaka[1], Tsuyoshi Koshiro[1], Makoto Deushi[1], Takuro Aizawa[1], Masahiro Hosaka[1], Hideaki Kawai[1], Seiji Yukimoto[1], Iizuka Yoshinori[2], Kumiko Goto-Azuma[3], Teruo Aoki[4] (1.Meteorological Research Institute, 2.Institute of Low Temperature Science, Hokkaido University, 3.National Institute of Polar Research, 4.Okayama University)

9:15 AM - 9:30 AM JST | 12:15 AM - 12:30 AM UTC

[ACC26-02] Particles in ice layers of SIGMA-A ice core, northwestern Greenland

*Kaoru Kawakami[1,2], Yoshinori Iizuka[2], Sumito Matoba[2], Teruo Aoki[3], Shin Sugiyama[2], Takuto Ando[4] (1.Graduate School of Environmental Science, Hokkaido University, 2.Institute of Low Temperature Science, Hokkaido University, 3.Graduate School of Natural Science and Technology, Okayama University, 4.Arctic Research Center, Hokkaido University)

9:30 AM - 9:45 AM JST | 12:30 AM - 12:45 AM UTC

[ACC26-03] Snow modification due to climate change in southeastern high-accumulation area of Greenland over the last 60 years evaluated by physical properties of firn core.

*Takuto Ando[1], Iizuka Yoshinori[2,3], Mai Shibata[2,3], Sumito Matoba[2,3], Shin Sugiyama[2,3], Satoru Adachi[4], Satoru Yamaguchi[4], Koji Fujita[5], Akira Hori[6], Teruo Aoki[7], Shuji Fujita[8] (1.Arctic Research Center, Hokkaido University, 2.Institute of Low Temperature Science, Hokkaido University, 3.Graduate School of Environmental Science, Hokkaido University, 4.National Research Institute for Earth Science and Disaster Resilience, 5.Graduate School of Environmental Studies, Nagoya University, 6.Department of Civil and Environmental Engineering, Kitami Institute of Technology, 7.Graduate School of Natural Science and Technology, Okayama University, 8. National Institute of Polar Research)

9:45 AM - 10:00 AM JST | 12:45 AM - 1:00 AM UTC

[ACC26-04] **Temporal variations of concentrations, size distributions, and seasonal variations of anthropogenic and natural black carbon in Greenland**

*Kumiko Goto-Azuma[1,2], Yoshimi Ogawa-Tsukagawa[1], Yutaka Kondo[1], Remi Dallmayr[1,10], Motohiro Hirabayashi[1], Jun Ogata[1], Kyotaro Kitamura[1], Kenji Kawamura[1,2], Hideaki Motoyama[1,2], Sumito Matoba[3], Teruo Aoki[4], Nobuhiro Moteki[5], Sho Ohata[5], Tatsuhiro Mori[6], Makoto Koike[5], Yuki Komuro[7], Akane Tsushima[8,9], Naoko Nagatsuka[1], Wataru Shigeyama[1,2], Koji Fujita[9] (1.National Institute of Polar Research, 2.SOKENDAI, 3.Hokkaido University, 4.Okayama University, 5.University of Tokyo, 6.University of Science, 7.Yamagata University, 8.Research Institute for Humanity and Nature, 9.Nagoya University, 10.AWI)

10:00 AM - 10:15 AM JST | 1:00 AM - 1:15 AM UTC

[ACC26-05] Mineral composition of dust layers in a shallow ice core drilled in Pamir Alay Mountains of Central Asia

*Shunsuke Takeuchi[1], Nozomu Takeuchi[1], Koji Fujita[2], Kenji Kawamura[3], Akane Tsushima[2], Vladimir Aizen[4] (1.Chiba University, 2.Nagoya University, 3.National Institute of Polar Research, 4.Idaho University)

10:15 AM - 10:30 AM JST | 1:15 AM - 1:30 AM UTC

[ACC26-06] Estimation of snow surface patterns from the coast to the inland, Dome-Fuji Station, of Antarctica, using camera images

*Konosuke Sugiura[1], Kengo Watanabe[1], Naohiko Hirasawa[2], Kenji Kawamura[2], Fumio Nakazawa[2], Hiroshi Ohno[3], Shuji Fujita[2], Ikumi Oyabu[2], Takashi Yamanouchi[2], Hideaki Motoyama[2] (1.University of Toyama, 2.National Institute of Polar Research, 3.Kitami Institute of Technology)

[J] Oral | A (Atmospheric and Hydrospheric Sciences)：A-CC Cryospheric Sciences & Cold District Environment

10:45 AM - 12:15 PM JST | 1:45 AM - 3:15 AM UTC | 201B 2F

[A-CC26] Ice cores and paleoenvironmental modeling

convener:Ryu Uemura(University of the Ryukyus), Kenji Kawamura(National Institute of Polar Research, Research Organization of Information and Systems), Ayako Abe-Ouchi(Atmosphere and Ocean Research Institute, The University of Tokyo), Nozomu Takeuchi(Chiba University), Chairperson:Nozomu Takeuchi(千葉大学), Kenji Kawamura(国立極地研究所)

10:45 AM - 11:00 AM JST | 1:45 AM - 2:00 AM UTC

[ACC26-07] Isolation of living fungi from Antarctic ice cores

★Invited Papers

*Masaharu Tsuji[1] (1.National Institute of Polar Research)

11:00 AM - 11:15 AM JST | 2:00 AM - 2:15 AM UTC

[ACC26-08] **Study of ancient fungi resting in the polar ice cores and its future prospects**

*Fumio Nakazawa[1,2], Masaharu Tsuji[1], Satoshi Imura[1,2] (1.National Institute of Polar Research, 2.SOKENDAI (The Graduate University of Advanced Studies))

11:15 AM - 11:30 AM JST | 2:15 AM - 2:30 AM UTC

[ACC26-09] **Flux, provenance and modification of terrestrial dust and sea salt in the Dome C and Dome Fuji ice cores from Last Glacial Maximum to early Holocene by ice-sublimation and single-particle measurement of soluble and insoluble particles**

*Ikumi Oyabu[1,2], Iizuka Yoshinori[3], Kenji Kawamura[1,4,5], Eric Wolff[6], Mirko Severi[7], Margareta Hansson[8] (1.National Institute of Polar Research, Research Organization of Information and Systems, 2.Japan Society for the Promotion of Science, 3.Institute of Low Temperature Science, Hokkaido University, 4.SOKENDAI (The Graduate University of Advanced Studies), 5.Japan Agency for Marine Science and Technology (JAMSTEC), 6.Department of Earth Sciences, University of Cambridge, 7.Department of Chemistry “Ugo Schiff”, University of Florence, 8.Department of Physical Geography, Stockholm University)

11:30 AM - 11:45 AM JST | 2:30 AM - 2:45 AM UTC

[ACC26-10] Spatial variation of surface mass balance over the last few millennia in the Dome Fuji area from the analyses of shallow ice cores

*Kenji Kawamura[1], Ikumi Oyabu[1], Fumio Nakazawa[1,2], Shuji Fujita[1,2], Kyohei Yamada[1], Naoyuki Kurita[4], Shun Tsutaki[5], Hiroshi Ohno[6], Konosuke Sugiura[7], Kumiko Goto-Azuma[1,2], Hideaki Motoyama[1,2], Ayako Abe-Ouchi[5,3] (1.National Institute of Polar Research, Research Organization of Information and Systems, 2.SOKENDAI (The Graduate University of Advanced Studies), 3.JAMSTEC, 4.Nagoya University, 5.University of Tokyo, 6.Kitami Institute of Technology, 7.University of Toyama)

11:45 AM - 12:00 PM JST | 2:45 AM - 3:00 AM UTC

[ACC26-11] Sensitivity of global nonhydrostatic atmospheric model to changes in orbital forcing for the early Holocene

*Minoru Chikira[1], Ayako Abe-Ouchi[1], Masaki Satoh[1] (1.Atmosphere and Ocean Research Institute, The University of Tokyo)

12:00 PM - 12:15 PM JST | 3:00 AM - 3:15 AM UTC

[ACC26-12] **Roles of sea ice–surface wind feedback in maintaining contrasting modes of glacial Atlantic meridional overturning circulation and climate**

*Sam Sherriff-Tadano[1], Ayako Abe-Ouchi[1] (1.Atmosphere and Ocean Research Institute, the University of Tokyo)

[J] Oral | A (Atmospheric and Hydrospheric Sciences)：A-CC Cryospheric Sciences & Cold District Environment

1:45 PM - 3:15 PM JST | 4:45 AM - 6:15 AM UTC | 201B 2F

[A-CC26] Ice cores and paleoenvironmental modeling

convener:Ryu Uemura(University of the Ryukyus), Kenji Kawamura(National Institute of Polar Research, Research Organization of Information and Systems), Ayako Abe-Ouchi(Atmosphere and Ocean Research Institute, The University of Tokyo), Nozomu Takeuchi(Chiba University), Chairperson:Ayako Abe-Ouchi(東京大学大気海洋研究所), Sam Sherriff-Tadano(University of Tokyo)

1:45 PM - 2:00 PM JST | 4:45 AM - 5:00 AM UTC

[ACC26-13] Simulated Dansgaard-Oeschger like oscillations and abrupt climate changes

*Ayako Abe-Ouchi[1,2,3], Wing-Le Chan[1], Sam Sherriff-Tadano[1], Takashi Obase[1], Masakazu Yoshimori[1], Akira Oka[1], Kenji Kawamura[3], Rumi Ohgaito[2] (1.Atmosphere and Ocean Research Institute, The University of Tokyo, 2.JAMSTEC, 3.National Institute of Polar Research)

2:00 PM - 2:15 PM JST | 5:00 AM - 5:15 AM UTC

[ACC26-14] **Reproduction of the increasing amplitude and period in the glacial cycles using a model incorporating diatomaceous activity.**

*Tasuku Akagi[1], Takahiro Hasegawa[2] (1.Department of Earth and Planetary Sciences, Faculty of Science, Kyushu University, 2.Graduate School of Science, Kyushu University)

2:15 PM - 2:30 PM JST | 5:15 AM - 5:30 AM UTC

[ACC26-15] Development of an Ice Sheet Model coupled General Circulation Model and application of Energy Balance Model on the estimation of Ice Sheet mass balance

*Ryouta O'ishi[1], Ayako Abe-Ouchi[2,1], Fuyuki SAITO[2], Takashi Obase[1] (1.Atmosphere and Ocean Research Institute, the Universitoy of Tokyo, 2.JAMSTEC)

2:30 PM - 2:45 PM JST | 5:30 AM - 5:45 AM UTC

[ACC26-16] An ice-flow modeling study for evaluation of sites for and oldest ice core around Dome Fuji, Antarctica

★Invited Papers

*Takashi Obase[1], Ayako Abe-Ouchi[1,2], Fuyuki SAITO[2], Shun Tsutaki[1], Shuji Fujita[3], Kenny Matsuoka[4], Kenji Kawamura[3,5,2], Ralf Greve[6] (1.Atmosphere and Ocean Research Institute, the University of Tokyo, 2.Japan Agency for Marine-Earth Science and Technology, 3.National Institute of Polar Research, Research Organization of Information and Systems, 4.Norwegian Polar Institute, 5.SOKENDAI (The Graduate University of Advanced Studies), 6.Institute of Low Temperature Science, Hokkaido University)

2:45 PM - 3:00 PM JST | 5:45 AM - 6:00 AM UTC

[ACC26-17] International studies of ice sheet and bedrock at Dome Fuji, East Antarctica

*Shuji Fujita[1,2], Kenji Kawamura[1,2,10], Prasad Gogineni[3], Ayako Abe-Ouchi[4], David Braaten[5], Jean-Charles Gallet[6], Elisabeth Isaksson[6], Brice van Liefferinge[6], Kenny Matsuoka[6], Charles O'Neill[3], John Paden[5], Fernando Rodriguez-Morales[5], Ryan A. Taylor[3], Shun Tsutaki[4], Jie-Bang Yan[3], Kumiko Goto-Azuma[1,2], Ralf Greve[7], Stephen Hudson[6], Jack Kohler[6], Shriniwas Kolpuke[3], Linfeng Li[3], Geir Moholdt[6], Hideaki Motoyama[1,2], Fumio Nakazawa[1], Takashi Obase[4], Hiroshi Ohno[8], Ikumi Oyabu[9,1], Fuyuki Saito[10], Konosuke Sugiura[11] (1.National Institute of Polar Research, Research Organization of Information and Systems(ROIS), 2.Department of Polar Science, The Graduate University for Advanced Studies (SOKENDAI), Japan, 3.The University of Alabama, USA, 4.Atmosphere and Ocean Research Institute, The University of Tokyo, Japan, 5.CReSIS, University of Kansas, USA, 6.Norwegian Polar Institute, Norway, 7.Institute of Low Temperature Science, Hokkaido University, Japan, 8.Kitami Institute of Technology, Japan, 9.JSPS, Japan, 10.Japan Agency for Marine-Earth Science and Technology (JAMSTEC), Japan, 11.University of Toyama, Japan)

3:00 PM - 3:15 PM JST | 6:00 AM - 6:15 AM UTC

[ACC26-18] Possible cause for rapid deformation of ice from glacial periods, investigated from laboratory-based deformation experiments and microstructural observations

*Tomotaka Saruya[1], Morimasa Takata[1], Tomoyuki Homma[1], Nobuhiko Azuma[1], Kumiko Goto-Azuma[2,3] (1.Nagaoka University of Technology, 2.National Institute of Polar Research, 3.SOKENDAI (The Graduate University for Advaced Research))

[J] Poster | A (Atmospheric and Hydrospheric Sciences)：A-CC Cryospheric Sciences & Cold District Environment

3:30 PM - 5:00 PM JST | 6:30 AM - 8:00 AM UTC | Poster Hall International Exhibition Hall8, Makuhari Messe_7

[A-CC26] Ice cores and paleoenvironmental modeling

convener:Ryu Uemura(University of the Ryukyus), Kenji Kawamura(National Institute of Polar Research, Research Organization of Information and Systems), Ayako Abe-Ouchi(Atmosphere and Ocean Research Institute, The University of Tokyo), Nozomu Takeuchi(Chiba University)

[ACC26-P01] Pollen analysis of ice cores drilled in the Pamir-Arai Mountains, central Asia

*Haruka Ogaya[1], Nozomu Takeuchi[1], Koji Fujita[2], Kenji Kawamura[3], Akane Tsushima[4], Vladimir Aizen[5], Azamat Osmonov[6] (1.Chiba University, 2.Nagoya University, 3.National Institute of Polar Research, 4.Research Institute for Humanity and Nature, 5.University of Idaho, 6.Central Asian Institute of Applied Geo-Science)

[ACC26-P02] Variations in mineralogy of dust in the Greenland SIGMA-D ice core over the past 100 years using SEM

*Naoko Nagatsuka[1], Kumiko Goto-Azuma[1,2], Akane Tsushima, Hideaki Motoyama[1,2], Sumito Matoba[3], Koji Fujita[4], Tetsuhide Yamasaki[5], Yukihiko Onuma[6], Masahiro Minowa[7], Teruo Aoki[8], Motohiro Hirabayashi[1] (1.National Institute of Polar Research, 2.SOKENDAI, 3.Institute of Low Temperature Science, Hokkaido University, 4.Graduate School of Environmental Studies, Nagoya University, 5.Avangnaq Arctic Project Corp., 6.Institute of Industrial Science, University of Tokyo, 7.Universidad Austral de Chile, 8.Graduate School of Natural Science and Technology, Okayama University)

[ACC26-P03] Size and shape of solid particles in a Greenland ice core

*Wataru Shigeyama[1,2], Kumiko Goto-Azuma[2,1], Kaori Fukuda[2], Fumio Nakazawa[2,1], Morimasa Takata[3], Tomoyuki Homma[3], Nobuhiko Azuma[3], Dorthe Dahl-Jensen[4] (1.The Graduate University for Advanced Studies (SOKENDAI), School of Multidisciplinary Sciences, Department of Polar Science, 2.National Institute of Polar Research, 3.Nagaoka University of Technology, 4.University of Copenhagen)

[ACC26-P04] Methane concentration measurements of the Dome Fuji ice core using Continuous Flow Analysis system

Ikumi Oyabu[1], Miho Arai[1,4,5], *Kenji Kawamura[1,2,3], Kyotaro Kitamura[1], Jun Ogata[1], Kumiko Goto-Azuma[1,2] (1.National Institute of Polar Research, Research Organization of Information and Systems, 2.SOKENDAI (The Graduate University of Advanced Studies), 3.JAMSTEC, 4.Yamagata University, 5.Weathernews Inc.)

[ACC26-P05] A basal topographic map in the Dome Fuji region constructed from the ground-based radar survey in the JARE 59

*Shun Tsutaki[1], Takashi Obase[1], Shuji Fujita[2,3], Ayako Abe-Ouchi[1,4], Kenji Kawamura[2,3,4], Kenichi Matsuoka[5], Hiroshi Ohno[6], Ikumi Oyabu[2,7], Fumio Nakazawa[2], Konosuke Sugiura[8] (1.The University of Tokyo, 2.National Institute of Polar Research, 3.The Graduate University for Advanced Studies, 4.Japan Agency for Marine-Earth Science and Technology, 5.Norwegian Polar Institute, 6.Kitami Institute of Technology, 7.Japan Society for the Promotion of Science, 8.University of Toyama)

[ACC26-P06] Performance of RCIP scheme on 1-d age computation of ice sheet.

*Fuyuki SAITO[1], Takashi Obase[2], Ayako Abe-Ouchi[2,1] (1.Japan Agency for Marine-Earth Science and Technology, 2.Atmosphere and Ocean Research Institute, University of Tokyo)

[ACC26-P07] Climate changes of the last deglaciation simulated by MIROC AOGCM

*Takashi Obase[1], Ayako Abe-Ouchi[1,2], Sam Sherriff-Tadano[1] (1.Atmosphere and Ocean Research Institute, the University of Tokyo, 2.Japan Agency for Marine-Earth Science and Technology)

[ACC26-P08] A Last Glacial Maximum experiment using MIROC-ES2L earth system model in comparison with ice core and the other paleo-proxy data

*Rumi Ohgaito[1], Tomohiro Hajima[1], Akitomo Yamamoto[1], Hiroaki Tatebe[1], Michio Kawamiya[1], Ayako Abe-Ouchi[2,1] (1.Japan Agency for Marine-Earth Science and Technology, 2.AORI, Univ. Tokyo)

[ACC26-P09] On the possible bifurcation mechanisms and associated dynamical properties of Dansgaard-Oeschger oscillations

*Takahito Mitsui[1], Ayako Abe-Ouchi[1], Wing-Le Chan[1], Sam Sherriff-Tadano[1] (1.The University of Tokyo)

[ACC26-P10] The role of climate-vegetation feedback in climate changes driven by orbital parameter changes: the Arctic land surfaces and seasonality

*Kanon Kino[1], Ayako Abe-Ouchi[1,2], Ryouta O'ishi[1], Fuyuki SAITO[2], Masakazu Yoshimori[1] (1.Atmosphere and Ocean Research Institute, the University of Tokyo, 2.Japan Agency for Marine-Earth Science and Technology)

[J] Poster | A (Atmospheric and Hydrospheric Sciences)：A-CC Cryospheric Sciences & Cold District Environment

5:15 PM - 6:30 PM JST | 8:15 AM - 9:30 AM UTC | Poster Hall International Exhibition Hall8, Makuhari Messe_10

[A-CC26] Ice cores and paleoenvironmental modeling

convener:Ryu Uemura(University of the Ryukyus), Kenji Kawamura(National Institute of Polar Research, Research Organization of Information and Systems), Ayako Abe-Ouchi(Atmosphere and Ocean Research Institute, The University of Tokyo), Nozomu Takeuchi(Chiba University)

[ACC26-P01] Pollen analysis of ice cores drilled in the Pamir-Arai Mountains, central Asia

*Haruka Ogaya[1], Nozomu Takeuchi[1], Koji Fujita[2], Kenji Kawamura[3], Akane Tsushima[4], Vladimir Aizen[5], Azamat Osmonov[6] (1.Chiba University, 2.Nagoya University, 3.National Institute of Polar Research, 4.Research Institute for Humanity and Nature, 5.University of Idaho, 6.Central Asian Institute of Applied Geo-Science)

[ACC26-P02] Variations in mineralogy of dust in the Greenland SIGMA-D ice core over the past 100 years using SEM

*Naoko Nagatsuka[1], Kumiko Goto-Azuma[1,2], Akane Tsushima, Hideaki Motoyama[1,2], Sumito Matoba[3], Koji Fujita[4], Tetsuhide Yamasaki[5], Yukihiko Onuma[6], Masahiro Minowa[7], Teruo Aoki[8], Motohiro Hirabayashi[1] (1.National Institute of Polar Research, 2.SOKENDAI, 3.Institute of Low Temperature Science, Hokkaido University, 4.Graduate School of Environmental Studies, Nagoya University, 5.Avangnaq Arctic Project Corp., 6.Institute of Industrial Science, University of Tokyo, 7.Universidad Austral de Chile, 8.Graduate School of Natural Science and Technology, Okayama University)

[ACC26-P03] Size and shape of solid particles in a Greenland ice core

*Wataru Shigeyama[1,2], Kumiko Goto-Azuma[2,1], Kaori Fukuda[2], Fumio Nakazawa[2,1], Morimasa Takata[3], Tomoyuki Homma[3], Nobuhiko Azuma[3], Dorthe Dahl-Jensen[4] (1.The Graduate University for Advanced Studies (SOKENDAI), School of Multidisciplinary Sciences, Department of Polar Science, 2.National Institute of Polar Research, 3.Nagaoka University of Technology, 4.University of Copenhagen)

[ACC26-P04] Methane concentration measurements of the Dome Fuji ice core using Continuous Flow Analysis system

Ikumi Oyabu[1], Miho Arai[1,4,5], *Kenji Kawamura[1,2,3], Kyotaro Kitamura[1], Jun Ogata[1], Kumiko Goto-Azuma[1,2] (1.National Institute of Polar Research, Research Organization of Information and Systems, 2.SOKENDAI (The Graduate University of Advanced Studies), 3.JAMSTEC, 4.Yamagata University, 5.Weathernews Inc.)

[ACC26-P05] A basal topographic map in the Dome Fuji region constructed from the ground-based radar survey in the JARE 59

*Shun Tsutaki[1], Takashi Obase[1], Shuji Fujita[2,3], Ayako Abe-Ouchi[1,4], Kenji Kawamura[2,3,4], Kenichi Matsuoka[5], Hiroshi Ohno[6], Ikumi Oyabu[2,7], Fumio Nakazawa[2], Konosuke Sugiura[8] (1.The University of Tokyo, 2.National Institute of Polar Research, 3.The Graduate University for Advanced Studies, 4.Japan Agency for Marine-Earth Science and Technology, 5.Norwegian Polar Institute, 6.Kitami Institute of Technology, 7.Japan Society for the Promotion of Science, 8.University of Toyama)

[ACC26-P06] Performance of RCIP scheme on 1-d age computation of ice sheet.

*Fuyuki SAITO[1], Takashi Obase[2], Ayako Abe-Ouchi[2,1] (1.Japan Agency for Marine-Earth Science and Technology, 2.Atmosphere and Ocean Research Institute, University of Tokyo)

[ACC26-P07] Climate changes of the last deglaciation simulated by MIROC AOGCM

*Takashi Obase[1], Ayako Abe-Ouchi[1,2], Sam Sherriff-Tadano[1] (1.Atmosphere and Ocean Research Institute, the University of Tokyo, 2.Japan Agency for Marine-Earth Science and Technology)

[ACC26-P08] A Last Glacial Maximum experiment using MIROC-ES2L earth system model in comparison with ice core and the other paleo-proxy data

*Rumi Ohgaito[1], Tomohiro Hajima[1], Akitomo Yamamoto[1], Hiroaki Tatebe[1], Michio Kawamiya[1], Ayako Abe-Ouchi[2,1] (1.Japan Agency for Marine-Earth Science and Technology, 2.AORI, Univ. Tokyo)

[ACC26-P09] On the possible bifurcation mechanisms and associated dynamical properties of Dansgaard-Oeschger oscillations

*Takahito Mitsui[1], Ayako Abe-Ouchi[1], Wing-Le Chan[1], Sam Sherriff-Tadano[1] (1.The University of Tokyo)

[ACC26-P10] The role of climate-vegetation feedback in climate changes driven by orbital parameter changes: the Arctic land surfaces and seasonality

*Kanon Kino[1], Ayako Abe-Ouchi[1,2], Ryouta O'ishi[1], Fuyuki SAITO[2], Masakazu Yoshimori[1] (1.Atmosphere and Ocean Research Institute, the University of Tokyo, 2.Japan Agency for Marine-Earth Science and Technology)

[J] Oral | A (Atmospheric and Hydrospheric Sciences)：A-GE Geological & Soil Environment

1:45 PM - 3:15 PM JST | 4:45 AM - 6:15 AM UTC | 202 2F

[A-GE30] Conservation and Restoration of Soil Environment at Terrestrial Surface

convener:Yasushi Mori(Graduate School of Environmental and Life Science, Okayama University), Chairperson:Yasushi Mori(Okayama University)

1:50 PM - 2:05 PM JST | 4:50 AM - 5:05 AM UTC

[AGE30-01] Soil Organic Cabon Contents Estimation using Neural Network System

Ikumi Kaida[1], *Yasushi Mori[1], Takayuki Shuku[1] (1.Graduate School of Environmental and Life Science, Okayama University)

2:05 PM - 2:25 PM JST | 5:05 AM - 5:25 AM UTC

[AGE30-02] Methane emission from rice paddies and its response to climate change

★Invited Papers

*Takeshi Tokida[1] (1.Institute for Agro-Environmental Sciences, National Agriculture and Food Research Organization)

2:25 PM - 2:40 PM JST | 5:25 AM - 5:40 AM UTC

[AGE30-03] **Relationship between degradation of rice grain quality due to chalky kernels and available nutrients in soil**

*Shingo Matsumoto[1], Junko Kasuga[1] (1.Shimane University)

2:40 PM - 2:55 PM JST | 5:40 AM - 5:55 AM UTC

[AGE30-04] The effects of trenching and insertion of crop residue on infiltration and soil erosion in a farmland

*Kazutoshi Osawa[1], Yasushi Mori[2], Akira Hoshikawa (1.Utsunomiya University, 2.Graduate school of Environmental and Life Science, Okayama University)

2:55 PM - 3:15 PM JST | 5:55 AM - 6:15 AM UTC

[AGE30-05] Measuring wide-range soil water content using GPS signals

★Invited Papers

*Kosuke Noborio[1], Natsumi Naganuma[1] (1.Meiji University)

[J] Poster | A (Atmospheric and Hydrospheric Sciences)：A-GE Geological & Soil Environment

3:30 PM - 5:00 PM JST | 6:30 AM - 8:00 AM UTC | Poster Hall International Exhibition Hall8, Makuhari Messe_8

[A-GE30] Conservation and Restoration of Soil Environment at Terrestrial Surface

convener:Yasushi Mori(Graduate School of Environmental and Life Science, Okayama University)

[AGE30-P01] Analysis of soil erosion on cropland considering future climate change in Okinawa

*Gen Machida[1], Kazutoshi Osawa[1], Hiroyuki Matsui[1] (1.Utsunomiya University)

[AGE30-P02] Linear Macro pore Installation to Reduce Surface Flow

*Masaki Kiyohiro[1], Yasushi Mori[1], Kazutoshi Osawa[2], Akira Hosihkawa[3] (1.Okayama University Graduate school of Environmental and Life Science, 2.Utsunomiya University Faculty of Agriculture, 3.Fund of Coral reef in Sekisei Lagoon)

[AGE30-P03] Conservation of the Rice Terraces of the Philippine Cordilleras Based on the Soil Environmental Factors.

*Tomoyo Kurozumi[1], Yasushi Mori[2], Hiroaki Somura[2], Milagros Ong How[3] (1.Faculty of Environmental Science and Technology, Okayama University, 2.Graduate School of Environmental and Life Science, Okayama University, 3.Universal Harvester Incorporated)

[AGE30-P04] A preliminary study for water and substances simulation modeling in Cordilleras terraced paddy fields, Philippines

*Hiroaki Somura[1], Yasushi Mori[1], Tomoyo Kurozumi[2], Milagros Ong How[3] (1.Graduate School of Environmental and Life Science, Okayama University, 2.Faculty of Environmental Science and Technology, Okayama University, 3.Universal Harvester Incorporated)

[J] Poster | A (Atmospheric and Hydrospheric Sciences)：A-GE Geological & Soil Environment

5:15 PM - 6:30 PM JST | 8:15 AM - 9:30 AM UTC | Poster Hall International Exhibition Hall8, Makuhari Messe_11

[A-GE30] Conservation and Restoration of Soil Environment at Terrestrial Surface

convener:Yasushi Mori(Graduate School of Environmental and Life Science, Okayama University)

[AGE30-P01] Analysis of soil erosion on cropland considering future climate change in Okinawa

*Gen Machida[1], Kazutoshi Osawa[1], Hiroyuki Matsui[1] (1.Utsunomiya University)

[AGE30-P02] Linear Macro pore Installation to Reduce Surface Flow

*Masaki Kiyohiro[1], Yasushi Mori[1], Kazutoshi Osawa[2], Akira Hosihkawa[3] (1.Okayama University Graduate school of Environmental and Life Science, 2.Utsunomiya University Faculty of Agriculture, 3.Fund of Coral reef in Sekisei Lagoon)

[AGE30-P03] Conservation of the Rice Terraces of the Philippine Cordilleras Based on the Soil Environmental Factors.

*Tomoyo Kurozumi[1], Yasushi Mori[2], Hiroaki Somura[2], Milagros Ong How[3] (1.Faculty of Environmental Science and Technology, Okayama University, 2.Graduate School of Environmental and Life Science, Okayama University, 3.Universal Harvester Incorporated)

[AGE30-P04] A preliminary study for water and substances simulation modeling in Cordilleras terraced paddy fields, Philippines

*Hiroaki Somura[1], Yasushi Mori[1], Tomoyo Kurozumi[2], Milagros Ong How[3] (1.Graduate School of Environmental and Life Science, Okayama University, 2.Faculty of Environmental Science and Technology, Okayama University, 3.Universal Harvester Incorporated)

[J] Oral | A (Atmospheric and Hydrospheric Sciences)：A-GE Geological & Soil Environment

3:30 PM - 5:00 PM JST | 6:30 AM - 8:00 AM UTC | 202 2F

[A-GE31] New Roles of Soil Science for Extraterrestrials

convener:Kosuke Noborio(Meiji University), Masaru Mizoguchi(Graduate school of Agricultural and Life Sciences, The University of Tokyo), Chairperson:Naoto Sato

3:30 PM - 4:00 PM JST | 6:30 AM - 7:00 AM UTC

[AGE31-01] Life search on Mars by Life Detection Microscope (LDM)

★Invited Papers

*Yoshitaka Yoshimura[1] (1.College of Agriculture, Tamagawa University)

4:00 PM - 4:15 PM JST | 7:00 AM - 7:15 AM UTC

[AGE31-02] **Moisture movement in sand during evaporation under reduced pressure**

*Masaru Mizoguchi[1] (1.Graduate school of Agricultural and Life Sciences, The University of Tokyo)

4:15 PM - 4:30 PM JST | 7:15 AM - 7:30 AM UTC

[AGE31-03] Gravity effects on liquid behavior in porous media of uniform glass beads.

*Naoto Sato[1], Natsumi Naganuma[2], Kento Nogawa[2], Yuichi Maruo[2], Kosuke Noborio[1] (1.School of Agriculture, Meiji University, 2.Graduate School of Agriculture, Meiji University)

4:30 PM - 4:45 PM JST | 7:30 AM - 7:45 AM UTC

[AGE31-04] Effects of changes in viscosity under low gravity on infiltration rate

*Kento Nogawa[1], Naoto Sato[2], Yuichi Maruo[1], Natsumi Naganuma[1], Kosuke Noborio[2] (1.Graduate School of Agriculture, Meiji University, 2.School of Agriculture, Meiji University)

4:45 PM - 5:00 PM JST | 7:45 AM - 8:00 AM UTC

[AGE31-05] Differences in infiltration process on the planets under different gravity.

*Yasushi Mori[1] (1.Graduate School of Environmental and Life Science, Okayama University)

[J] Poster | A (Atmospheric and Hydrospheric Sciences)：A-GE Geological & Soil Environment

1:45 PM - 3:15 PM JST | 4:45 AM - 6:15 AM UTC | Poster Hall International Exhibition Hall8, Makuhari Messe_1

[A-GE31] New Roles of Soil Science for Extraterrestrials

convener:Kosuke Noborio(Meiji University), Masaru Mizoguchi(Graduate school of Agricultural and Life Sciences, The University of Tokyo)

[AGE31-P01] Roles of soil science in ectraterestrial space

*Kosuke Noborio[1] (1.Meiji University)

[AGE31-P02] **Characterization of Soil Organic Matter using Fourier Transform Infrared Spectrometer**

*Iwasaki Masayoshi[1], Yasushi Mori[1] (1.okayama university graduate school environmental and life science)

[AGE31-P03] The slowing down of water movement in capillary tubes under microgravity.

*Yuichi Maruo[1], Naoto Sato[1], Natsumi Naganuma[1], Kento Nogawa[1], Kosuke Noborio[2] (1.Graduate school of Agriculture, Meiji University, 2.Meiji University)

[AGE31-P04] Challenges to measuring of the contact angle and the surface tension of water under reduced gravity

*Natsumi Naganuma[1], Naoto Sato[1], Kento Nogawa[1], Yuichi Maruo[1], Kosuke Noborio[2] (1.Graduate School of Agriculture, Meiji University, 2.School of Agriculture, Meiji University)

[J] Poster | A (Atmospheric and Hydrospheric Sciences)：A-GE Geological & Soil Environment

5:15 PM - 6:30 PM JST | 8:15 AM - 9:30 AM UTC | Poster Hall International Exhibition Hall8, Makuhari Messe_12

[A-GE31] New Roles of Soil Science for Extraterrestrials

convener:Kosuke Noborio(Meiji University), Masaru Mizoguchi(Graduate school of Agricultural and Life Sciences, The University of Tokyo)

[AGE31-P01] Roles of soil science in ectraterestrial space

*Kosuke Noborio[1] (1.Meiji University)

[AGE31-P02] **Characterization of Soil Organic Matter using Fourier Transform Infrared Spectrometer**

*Iwasaki Masayoshi[1], Yasushi Mori[1] (1.okayama university graduate school environmental and life science)

[AGE31-P03] The slowing down of water movement in capillary tubes under microgravity.

*Yuichi Maruo[1], Naoto Sato[1], Natsumi Naganuma[1], Kento Nogawa[1], Kosuke Noborio[2] (1.Graduate school of Agriculture, Meiji University, 2.Meiji University)

[AGE31-P04] Challenges to measuring of the contact angle and the surface tension of water under reduced gravity

*Natsumi Naganuma[1], Naoto Sato[1], Kento Nogawa[1], Yuichi Maruo[1], Kosuke Noborio[2] (1.Graduate School of Agriculture, Meiji University, 2.School of Agriculture, Meiji University)

[E] Poster | A (Atmospheric and Hydrospheric Sciences)：A-CG Complex & General

10:45 AM - 12:15 PM JST | 1:45 AM - 3:15 AM UTC | Poster Hall International Exhibition Hall8, Makuhari Messe_3

[A-CG32] Global Carbon Cycle Observation and Analysis

convener:Kazuhito Ichii(Chiba University), Prabir Patra(Research Institute for Global Change, JAMSTEC), Forrest M. Hoffman(Oak Ridge National Laboratory), Makoto Saito(National Institute of Environmental Studies)

[ACG32-P01] Regional budgets of 3 major greenhouse gases using inverse modelling of atmospheric data

*Prabir Patra[1], Naveen Chandra[1], Jagat Bisht[1] (1.Japan Agency for Marine-Earth Science and Technology (JAMSTEC))

[ACG32-P02] Analysis of hot summer in 2018

*Kazutaka Murakami[1], Kazuhito Ichii[1,2], Yukio Yoshida[1], Haruki Oshio[1], Makoto Saito[1] (1.National Institute for Environmental Studies, 2.Chiba University)

[ACG32-P03] Updated Data-Driven GPP and NEE Estimation Using Machine Learning Algorithms with Remote Sensing and Flux Data

*Zhiyan Liu[1], Kazuhito Ichii[1], Yusuke Hayasi[1], Riku Kawase[1], Masahito Ueyama[2], Yuji Kominami[3] (1.Chiba University, 2.Osaka Prefecture University, 3.Forest Research and Management Organization)

[ACG32-P04] **Response of a Bornean Rainforest to the Climatic Changes imposed by ENSO during 2009-2016**

*Julie Karine Michelon[1], Tomo'omi Kumagai[2,3], Tetsuya Hiyama[3], Hatsuki Fujinami[3], Kazuho Matsumoto[4], Tomonori Kume[5], Takami Saito[6] (1.Graduate School of Environmental Studies, Nagoya University, 2.Graduate School of Agricultural and Life Sciences, The University of Tokyo, 3.Institute for Space-Earth Environmental Research, Nagoya University, 4.Faculty of Agriculture, University of the Ryukyus, 5.Faculty of Agriculture, Kyushu University, 6.Forest Research and Management Organization)

[ACG32-P05] **Monitoring and Evaluating CO2 Flux in the Grassland Areas of Mongolia**

*Qinxue Wang[1], Tomohiro Okadera[1], Deni Eer[1], Masataka Watanabe[2], Tomohiro Shishime[2], Akihiro Oba[2], Ochirbat Batkhishig[3] (1.National Institute for Environmental Studies, 2.Research and Development Initiative, Chuo University, 3.Institute of Geography and Geoecology, Mongolian Academy of Sciences)

[ACG32-P06] Data-driven monitoring of terrestrial carbon cycle in Mongolia

*ZAYA MART[1], Zhiyan Liu[1], Riku Kawase[1], Kazuhito Ichii[1] (1.Chiba University)

[E] Poster | A (Atmospheric and Hydrospheric Sciences)：A-CG Complex & General

5:15 PM - 6:30 PM JST | 8:15 AM - 9:30 AM UTC | Poster Hall International Exhibition Hall8, Makuhari Messe_13

[A-CG32] Global Carbon Cycle Observation and Analysis

convener:Kazuhito Ichii(Chiba University), Prabir Patra(Research Institute for Global Change, JAMSTEC), Forrest M. Hoffman(Oak Ridge National Laboratory), Makoto Saito(National Institute of Environmental Studies)

[ACG32-P01] Regional budgets of 3 major greenhouse gases using inverse modelling of atmospheric data

*Prabir Patra[1], Naveen Chandra[1], Jagat Bisht[1] (1.Japan Agency for Marine-Earth Science and Technology (JAMSTEC))

[ACG32-P02] Analysis of hot summer in 2018

*Kazutaka Murakami[1], Kazuhito Ichii[1,2], Yukio Yoshida[1], Haruki Oshio[1], Makoto Saito[1] (1.National Institute for Environmental Studies, 2.Chiba University)

[ACG32-P03] Updated Data-Driven GPP and NEE Estimation Using Machine Learning Algorithms with Remote Sensing and Flux Data

*Zhiyan Liu[1], Kazuhito Ichii[1], Yusuke Hayasi[1], Riku Kawase[1], Masahito Ueyama[2], Yuji Kominami[3] (1.Chiba University, 2.Osaka Prefecture University, 3.Forest Research and Management Organization)

[ACG32-P04] **Response of a Bornean Rainforest to the Climatic Changes imposed by ENSO during 2009-2016**

*Julie Karine Michelon[1], Tomo'omi Kumagai[2,3], Tetsuya Hiyama[3], Hatsuki Fujinami[3], Kazuho Matsumoto[4], Tomonori Kume[5], Takami Saito[6] (1.Graduate School of Environmental Studies, Nagoya University, 2.Graduate School of Agricultural and Life Sciences, The University of Tokyo, 3.Institute for Space-Earth Environmental Research, Nagoya University, 4.Faculty of Agriculture, University of the Ryukyus, 5.Faculty of Agriculture, Kyushu University, 6.Forest Research and Management Organization)

[ACG32-P05] **Monitoring and Evaluating CO2 Flux in the Grassland Areas of Mongolia**

*Qinxue Wang[1], Tomohiro Okadera[1], Deni Eer[1], Masataka Watanabe[2], Tomohiro Shishime[2], Akihiro Oba[2], Ochirbat Batkhishig[3] (1.National Institute for Environmental Studies, 2.Research and Development Initiative, Chuo University, 3.Institute of Geography and Geoecology, Mongolian Academy of Sciences)

[ACG32-P06] Data-driven monitoring of terrestrial carbon cycle in Mongolia

*ZAYA MART[1], Zhiyan Liu[1], Riku Kawase[1], Kazuhito Ichii[1] (1.Chiba University)

[E] Oral | A (Atmospheric and Hydrospheric Sciences)：A-CG Complex & General

1:45 PM - 3:15 PM JST | 4:45 AM - 6:15 AM UTC | 301A 3F

[A-CG32] Global Carbon Cycle Observation and Analysis

convener:Kazuhito Ichii(Chiba University), Prabir Patra(Research Institute for Global Change, JAMSTEC), Forrest M. Hoffman(Oak Ridge National Laboratory), Makoto Saito(National Institute of Environmental Studies), Chairperson:Kazuhito Ichii

1:45 PM - 2:00 PM JST | 4:45 AM - 5:00 AM UTC

[ACG32-01] A high-resolution fossil fuel CO2 emission gridded dataset for tracer transport simulations and flux inversions: An overview, evaluations, applications and future perspectives

★Invited Papers

*Tomohiro Oda[1,2], Shamil Maksyutov [3], Miguel O. Roman [2,4], Zhousen Wang [4], Thomas Lauvaux[6,5], Sha Feng [5], Rostyslav Bun [7,8], James Wang [2,1], Randy Kawa [1], Lesley Ott[1], Steven Pawson[1] (1.NASA Goddard Space Flight Center, Greenbelt, MD, USA , 2.Universities Space Research Association, Columbia, MD, USA , 3.Center for Global Environmental Research, National Institute for Environmental Studies, Tsukuba, Ibaraki, Japan , 4.Terrestrial Information Systems Laboratory, NASA Goddard Space Flight Center, Greenbelt, MD, USA , 5.Department of Meteorology and Atmospheric Science, Penn. State University, State College, PA, USA , 6.Laboratoire des sciences du climat et de l'environnement, Gif sur Yvette, France, 7.Lviv Polytechnic National University, Lviv, Ukraine , 8.University of Dąbrowa Górnicza, Górnicza, Poland)

2:00 PM - 2:15 PM JST | 5:00 AM - 5:15 AM UTC

[ACG32-02] **Towards Decreasing the Uncertainty in Global Carbon Dioxide Emission Inventory**

*Richao Cong[1], Makoto Saito[1], Ryuichi Hirata[1], Akihiko Ito[1] (1.Center for Global Environmental Research, National Institute for Environmental Studies)

2:15 PM - 2:30 PM JST | 5:15 AM - 5:30 AM UTC

[ACG32-03] Evaluation of MIROC4-ACTM reanalysis of GHGs concentrations using aircraft

*Jagat Bisht[1], Prabir Patra[1], Naveen Chandra[1], Sergey Gromov[2], Taku Umezawa[3], Andreas Zahn[4], cARL A. M. Brenninkmeijer[5] (1.Japan Agency for Marine-Earth Science and Technology (JAMSTEC), Yokohama, Japan, 2.Max Planck Institute for Chemistry, Mainz, Germany, 3.National Institute for Environmental Studies, Tsukuba, Japan, 4.Karlsruhe Institute of Technology (KIT), Institute for Meteorology and Climate Research, Karlsruhe, Germany, 5.Max Planck Institute for Chemistry, Air Chemistry Division, Mainz, Germany)

2:30 PM - 2:45 PM JST | 5:30 AM - 5:45 AM UTC

[ACG32-04] **Carbon flux estimation using NICAM-TM 4D-Var and GOSAT data towards GOSAT-2 Level 4 product**

*Tazu Saeki[1], Yosuke Niwa[1], Makoto Saito[1] (1.National Institute for Environmental Studies)

2:45 PM - 3:00 PM JST | 5:45 AM - 6:00 AM UTC

[ACG32-05] **Attribution of the ambiguity in methane's growth rate shifts during 1988-2016.**

*Naveen Chandra[1], Prabir Patra[1] (1.Japan Agency for Marine Earth Science and Technology)

3:00 PM - 3:15 PM JST | 6:00 AM - 6:15 AM UTC

[ACG32-06] **Ocean uptake and land use change emissions suppressed atmospheric CO_2 growth in the 2015/16 El Niño**

*Masayuki Kondo[1], Peter Landschützer[2], Yousuke Iida[3], Richard Houghton[4], Stephen Sitch[5] (1. Center for Environmental Remote Sensing, Chiba University, 2.Max Planck Institute for Meteorology, 3.Global Environment and Marine Department, Japan Meteorological Agency, 4.Woods Hole Research Center, 5.University of Exeter)

[E] Oral | A (Atmospheric and Hydrospheric Sciences)：A-CG Complex & General

3:30 PM - 5:00 PM JST | 6:30 AM - 8:00 AM UTC | 301A 3F

[A-CG32] Global Carbon Cycle Observation and Analysis

convener:Kazuhito Ichii(Chiba University), Prabir Patra(Research Institute for Global Change, JAMSTEC), Forrest M. Hoffman(Oak Ridge National Laboratory), Makoto Saito(National Institute of Environmental Studies), Chairperson:Prabir Patra

3:30 PM - 3:45 PM JST | 6:30 AM - 6:45 AM UTC

[ACG32-07] Observing vegetation seasonal dynamics in Japan with Himawari-8 hypertemporal data

*Tomoaki Miura[1,2], Shin Nagai[2], Kazuhito Ichii[3], Hiroki Yoshioka[4] (1.University of Hawaii at Manoa, 2.Japan Agency for Marine-Earth Science and Technology, 3.Center for Environmental Remote Sensing, Chiba University, 4.Aichi Prefectural University)

3:45 PM - 4:00 PM JST | 6:45 AM - 7:00 AM UTC

[ACG32-08] Carbon and Water Fluxes at High spatial Resolutions through Down-Scaling

*Jiquan Chen[1], Pietro Sciusco[1], Ranjeet John[1], Zutao Ouyang[1] (1.Michigan State University)

4:00 PM - 4:15 PM JST | 7:00 AM - 7:15 AM UTC

[ACG32-09] **Connecting Satellite Based Spectral Modelling Approach and Forest Inventory to Model Biomass and Carbon Stocks in Natural and Planted Forest over part of Semi-arid zone, India**

*SWATI UNIYAL[1], Siti Raju Rao (1.Andhra University)

4:15 PM - 4:30 PM JST | 7:15 AM - 7:30 AM UTC

[ACG32-10] **Allocation of forest net primary production varies by forest age and air temperature**

*Xiang Song[1], Xiaodong Zeng[1], Dongxiao Tian[2] (1.IAP, CAS, 2.Beijing Meteorological Information Center)

4:30 PM - 4:45 PM JST | 7:30 AM - 7:45 AM UTC

[ACG32-11] Analyzing Model Biases in Terrestrial Carbon Cycle Submodels in Earth System Models and Offline Models

*Kazuhito Ichii[1], Kazutaka Murakami[2], Hiroaki Takayama[3], Tomohiro Hajima[3], Kaoru Tachiiri[3] (1.Chiba University, 2.National Institute for Environmental Studies, 3.Japan Agency for Marine-Earth Science and Technology)

4:45 PM - 5:00 PM JST | 7:45 AM - 8:00 AM UTC

[ACG32-12] Assessing terrestrial biogeochemical feedbacks in a strategically geoengineered climate

*Forrest M. Hoffman[1,2], Cheng-En Yang[2,1], Joshua S. Fu[2,1], Simone Tilmes[3], Lili Xia[4], Douglas G. MacMartin[5], Jadwiga H. Richter[3], Michael Mills[3], Ben Kravitz[6] (1.Oak Ridge National Laboratory, 2.University of Tennessee, 3.National Center for Atmospheric Research, 4.Rutgers University, 5.Cornell University, 6.Pacific Northwest National Laboratory)

[J] Oral | A (Atmospheric and Hydrospheric Sciences)：A-CG Complex & General

9:00 AM - 10:30 AM JST | 12:00 AM - 1:30 AM UTC | 104 1F

[A-CG38] Multi-scale ocean-atmosphere interaction in the tropical Indo-Pacific region

convener:Ayako Seiki(Japan Agency for Marine-Earth Science and Technology), Tomoki Tozuka(Department of Earth and Planetary Science, Graduate School of Science, The University of Tokyo), Motoki Nagura(Japan Agency for Marine-Earth Science and Technology), Youichi Kamae(Faculty of Life and Environmental Sciences, University of Tsukuba), Chairperson:Ayako Seiki(Japan Agency for Marine-Earth Science and Technology), Motoki Nagura(Japan Agency for Marine-Earth Science and Technology)

9:00 AM - 9:15 AM JST | 12:00 AM - 12:15 AM UTC

[ACG38-01] Various aspects of climate system variability associated with ENSO

★Invited Papers

*Shuhei Maeda[1] (1.Climate Prediction Division, Japan Meteorological Agency)

9:15 AM - 9:30 AM JST | 12:15 AM - 12:30 AM UTC

[ACG38-02] Influence and mechanism of the tropical Pacific variability on the Arctic and its seasonality

*Tsubasa Takigawa[1], Yu Kosaka[1], Bunmei Taguchi[1], Lea Svendsen[2] (1.Research Center for Advanced Science and Technology, University of Tokyo, 2.Bjerknes Centre for Climate Research, University of Bergen)

9:30 AM - 9:45 AM JST | 12:30 AM - 12:45 AM UTC

[ACG38-03] Subsurface nonlinear dynamical heating and ENSO asymmetry in CMIP5: Implications for anthropogenic tropical-warming uncertainties

★Invited Papers

*Michiya Hayashi[1], Fei-Fei Jin[1] (1.Department of Atmospheric Sciences, University of Hawaii at Manoa)

9:45 AM - 10:00 AM JST | 12:45 AM - 1:00 AM UTC

[ACG38-04] **Uncertainty in the projections of ENSO amplitude change under global warming: Role of the response of atmospheric circulation to SST anomalies**

*Jun Ying[1] (1.Second institute of Oceanography, Ministry of Natural Resources)

10:00 AM - 10:15 AM JST | 1:00 AM - 1:15 AM UTC

[ACG38-05] Impact of atmospheric variability on Indian Ocean Dipole mode

*Yuya Baba[1] (1.JAMSTEC Japan Agency for Marine-Earth Science and Technology)

10:15 AM - 10:30 AM JST | 1:15 AM - 1:30 AM UTC

[ACG38-06] Do salinity anomalies matter for the evolution of the IOD? –Experimental assessments using a regional ocean model-

*Shoichiro Kido[1], Tomoki Tozuka[1], Weiqing Han[2] (1.Graduate School of Science, The University of Tokyo, 2.Department of Atmospheric and Oceanic Sciences, University of Colorado Boulder)

[J] Oral | A (Atmospheric and Hydrospheric Sciences)：A-CG Complex & General

10:45 AM - 12:15 PM JST | 1:45 AM - 3:15 AM UTC | 104 1F

[A-CG38] Multi-scale ocean-atmosphere interaction in the tropical Indo-Pacific region

convener:Ayako Seiki(Japan Agency for Marine-Earth Science and Technology), Tomoki Tozuka(Department of Earth and Planetary Science, Graduate School of Science, The University of Tokyo), Motoki Nagura(Japan Agency for Marine-Earth Science and Technology), Youichi Kamae(Faculty of Life and Environmental Sciences, University of Tsukuba), Chairperson:Tomoki Tozuka(The University of Tokyo), Youichi Kamae(University of Tsukuba)

10:45 AM - 11:00 AM JST | 1:45 AM - 2:00 AM UTC

[ACG38-07] Mechanisms of future changes in equatorial upwelling: CMIP5 inter-model analysis

★Invited Papers

*Shoshiro Minobe[1,2], Mio Terada[2], Curtis Deutsch[3] (1.Earth and Planetary Sciences, Faculty of Science, Hokkaido University, 2.Graduate School of Science, Hokkaido University, 3.School of Oceanography, University of Washington)

11:00 AM - 11:15 AM JST | 2:00 AM - 2:15 AM UTC

[ACG38-08] The Indo-Pacific cross-basin interaction of the decadal climate variability under the progress of the global warming

*Yuma Miyaji[1], Youichi Tanimoto[2] (1.Hokkaido University, Graduate School of Environmental Science, 2.Hokkaido University, Faculty of Environmental Earth Science)

11:15 AM - 11:30 AM JST | 2:15 AM - 2:30 AM UTC

[ACG38-09] Air-sea flux observation by unmanned autonomous sea surface vehicle in the Tropics - Application of the Wave Glider -

★Invited Papers

*Iwao Ueki[1] (1.JAMSTEC Japan Agency for Marine-Earth Science and Technology)

11:30 AM - 11:45 AM JST | 2:30 AM - 2:45 AM UTC

[ACG38-10] **Radar-derived Fresh water flux and its possible impact to the oceanic stratification observed during the Years of the Maritime Continent (YMC)**

*Masaki Katsumata[1], Biao Geng[1], Satoru Yokoi[1], Shuichi Mori[1], Iwao Ueki[1] (1.Japan Agency for Marine-Earth Science and Technology)

11:45 AM - 12:00 PM JST | 2:45 AM - 3:00 AM UTC

[ACG38-11] **Driving Mechanism of Inter-Annual Precipitation Variability during Monsoon Season over the Northern Part of Sumatra Island, Indonesia**

*Yahya Darmawan[1,2,3], Huang-Hsiung Hsu[2] (1.Taiwan International Graduation Program, Academia Sinica, 2.Research Center for Environmental Changes, Academia Sinica, 3.Indonesian Agency for Meteorology, Climatology and Geophysics (BMKG))

12:00 PM - 12:15 PM JST | 3:00 AM - 3:15 AM UTC

[ACG38-12] The impact of diurnal precipitation over the maritime continent on synoptic disturbances and its relation to the MJO

*Ayako Seiki[1], Satoru Yokoi[1], Masaki Katsumata[1], Kunio Yoneyama[1] (1.Japan Agency for Marine-Earth Science and Technology)

[J] Poster | A (Atmospheric and Hydrospheric Sciences)：A-CG Complex & General

3:30 PM - 5:00 PM JST | 6:30 AM - 8:00 AM UTC | Poster Hall International Exhibition Hall8, Makuhari Messe_9

[A-CG38] Multi-scale ocean-atmosphere interaction in the tropical Indo-Pacific region

convener:Ayako Seiki(Japan Agency for Marine-Earth Science and Technology), Tomoki Tozuka(Department of Earth and Planetary Science, Graduate School of Science, The University of Tokyo), Motoki Nagura(Japan Agency for Marine-Earth Science and Technology), Youichi Kamae(Faculty of Life and Environmental Sciences, University of Tsukuba)

[ACG38-P01] Impacts of seasonal transitions of ENSO on frequency of atmospheric rivers over East Asia

*Youichi Kamae[1], Moeka Naoi[2], Hiroaki Ueda[1] (1.Faculty of Life and Environmental Sciences, University of Tsukuba, 2.Graduate School of Life and Environmental Sciences, University of Tsukuba)

[ACG38-P02] Impact of tropical Pacific sea surface temperature on the regional heavy rainfall events in Japan

*Yukiko Imada[1], Hiroaki Kawase[1], Masahiro Watanabe[2], Izuru Takayabu[1] (1.Meteorological Research Institute, Japan Meteorological Agency, 2.Atmosphere and Ocean Research Institute, the University of Tokyo)

[ACG38-P03] The North Pacific pacemaker effect on historical ENSO and its mechanisms

*Yu Kosaka[1], Dillon J. Amaya[2], Wenyu Zhou[2], Yu Zhang[2], Shang-Ping Xie[2], Arthur J. Miller[2] (1.Research Center for Advanced Science and Technology, University of Tokyo, 2.Scripps Institution of Oceanography, University of California San Diego)

[ACG38-P04] **Detection of the dry intrusions from the mid-latitudes to the Equator and their association with MJO**

*Saki Yanagisawa[1], Akiyo Yatagai[1] (1.Hirosaki Univercity)

[ACG38-P05] **Relationship between oceanic and atmospheric variations in the Philippine Sea and modulation of El Nino events**

*Takuya Hasegawa[1], Akira Nagano[2], Iwao Ueki[2], Kentaro Ando[2] (1.Tohoku University, 2.JAMSTEC)

[ACG38-P06] Contribution of oceanic wave propagation from the tropical Pacific to asymmetry of the Ningaloo Nino/Nina

*Hidehiro Kusunoki[1], Shoichiro Kido[1], Tomoki Tozuka[1] (1.Department of Earth and Planetary Science, Graduate School of Science, The University of Tokyo)

[ACG38-P07] The life-cycle of annual waves in the Indian Ocean as identified by a seamless diagnosis for the energy flux

*Zimeng Li[1], Hidenori Aiki[2] (1.Graduate school of environmental studies, Nagoya university, 2.Institute for space-earth environmental research, Nagoya university)

[J] Poster | A (Atmospheric and Hydrospheric Sciences)：A-CG Complex & General

5:15 PM - 6:30 PM JST | 8:15 AM - 9:30 AM UTC | Poster Hall International Exhibition Hall8, Makuhari Messe_14

[A-CG38] Multi-scale ocean-atmosphere interaction in the tropical Indo-Pacific region

convener:Ayako Seiki(Japan Agency for Marine-Earth Science and Technology), Tomoki Tozuka(Department of Earth and Planetary Science, Graduate School of Science, The University of Tokyo), Motoki Nagura(Japan Agency for Marine-Earth Science and Technology), Youichi Kamae(Faculty of Life and Environmental Sciences, University of Tsukuba)

[ACG38-P01] Impacts of seasonal transitions of ENSO on frequency of atmospheric rivers over East Asia

*Youichi Kamae[1], Moeka Naoi[2], Hiroaki Ueda[1] (1.Faculty of Life and Environmental Sciences, University of Tsukuba, 2.Graduate School of Life and Environmental Sciences, University of Tsukuba)

[ACG38-P02] Impact of tropical Pacific sea surface temperature on the regional heavy rainfall events in Japan

*Yukiko Imada[1], Hiroaki Kawase[1], Masahiro Watanabe[2], Izuru Takayabu[1] (1.Meteorological Research Institute, Japan Meteorological Agency, 2.Atmosphere and Ocean Research Institute, the University of Tokyo)

[ACG38-P03] The North Pacific pacemaker effect on historical ENSO and its mechanisms

*Yu Kosaka[1], Dillon J. Amaya[2], Wenyu Zhou[2], Yu Zhang[2], Shang-Ping Xie[2], Arthur J. Miller[2] (1.Research Center for Advanced Science and Technology, University of Tokyo, 2.Scripps Institution of Oceanography, University of California San Diego)

[ACG38-P04] **Detection of the dry intrusions from the mid-latitudes to the Equator and their association with MJO**

*Saki Yanagisawa[1], Akiyo Yatagai[1] (1.Hirosaki Univercity)

[ACG38-P05] **Relationship between oceanic and atmospheric variations in the Philippine Sea and modulation of El Nino events**

*Takuya Hasegawa[1], Akira Nagano[2], Iwao Ueki[2], Kentaro Ando[2] (1.Tohoku University, 2.JAMSTEC)

[ACG38-P06] Contribution of oceanic wave propagation from the tropical Pacific to asymmetry of the Ningaloo Nino/Nina

*Hidehiro Kusunoki[1], Shoichiro Kido[1], Tomoki Tozuka[1] (1.Department of Earth and Planetary Science, Graduate School of Science, The University of Tokyo)

[ACG38-P07] The life-cycle of annual waves in the Indian Ocean as identified by a seamless diagnosis for the energy flux

*Zimeng Li[1], Hidenori Aiki[2] (1.Graduate school of environmental studies, Nagoya university, 2.Institute for space-earth environmental research, Nagoya university)

[J] Oral | A (Atmospheric and Hydrospheric Sciences)：A-CG Complex & General

9:00 AM - 10:30 AM JST | 12:00 AM - 1:30 AM UTC | 301A 3F

[A-CG39] Biogeochemical cycles in Land Ecosystem

convener:Tomomichi Kato(Research Faculty of Agriculture, Hokkaido University), Kazuhito Ichii(Chiba University), Takeshi Ise(FSERC, Kyoto University), Munemasa Teramoto(National Institute for Environmental Studies), Chairperson:Tomomichi Kato(Hokkaido University)

9:00 AM - 9:15 AM JST | 12:00 AM - 12:15 AM UTC

[ACG39-01] Laboratory examination of combined effects of temperature rising and increased water fluctuation on CO_2 release from volcanic ash soils

*Hirohiko Nagano[1], Mariko Atarashi-Andoh[1], Jun Koarashi[1] (1.Japan Atomic Energy Agency)

9:15 AM - 9:30 AM JST | 12:15 AM - 12:30 AM UTC

[ACG39-02] Field observation of GHGs emission from pome palm oil mill effluent (POME) treatment ponds in an oil palm plantation in tropical peatland.

*Yoshiyuki Takahashi[1], Takashi Onodera[2], Ryuichi Hirata[1], Kazuya Nishina[2], Joseph Wenceslaus Waili[3], Kevin Kemudang Musin[3], Edward Baran Aeries[3], Frankie Kiew[3], Guan Xhuan Wong[3], Zufaqar Sa'adi[3], Lulie Melling[3] (1.Center for Global Environmental Research, National Institute for Environmental Studies, 2.Center for Regional Environmental Research, National Institute for Environmental Studies, 3.Sarawak Tropical Peat Research Institute)

9:30 AM - 9:45 AM JST | 12:30 AM - 12:45 AM UTC

[ACG39-03] Soil CO_2 efflux dynamics with land-use changes in Southeast Asia

*HAJIME TOMIMATSU[1], NAISHEN LIANG[1], MUNEMASA TERAMOTO[1], JIYE ZENG[1], ZHAO XIN[1] (1.National Institute for Environmental Studies)

9:45 AM - 10:00 AM JST | 12:45 AM - 1:00 AM UTC

[ACG39-04] Individual-based analyses of the carry-over effects from recent climatic conditions on the interannual variability of LAI of an evergreen conifer stand

*Akihiro Sumida[1], Tsutomu Watanabe[1], Tomiyasu Miyaura[2] (1.Institute of Low Temperature Science, Hokkaido University, 2.Faculty of Science and Technology, Ryukoku University)

10:00 AM - 10:15 AM JST | 1:00 AM - 1:15 AM UTC

[ACG39-05] Carbon dioxide balance of an oil palm plantation on tropical peat

*Takashi Hirano[1], Frankie Kiew[2], Ryuichi Hirata[3], Guan Xhuan Wong[2], Edward Baran Aries[2], Kevin Kemudang[2], Joseph Wenceslaus[2], Lo Kim San[2], Lulie Melling[2] (1.Research Faculty of Agriculture, Hokkaido University, 2.Sarawak Tropical Peat Research Institute, 3.CGER, National Institute for Environmental Studies)

10:15 AM - 10:30 AM JST | 1:15 AM - 1:30 AM UTC

[ACG39-06] The effect of heat wave in the summer of 2018 on carbon and water fluxes in an open black spruce forest in an interior Alaska

*Hideki Kobayashi[1], Robert Busey[2], Yongwon Kim[2], Sigrid Dengel[3], Stephen Chan[3] (1.Japan Agency for Marine-Earch Science and Technology, 2.International Arctic Research Center, University of Alaska, Fairbanks, 3.Lawrence Berkeley National Laboratory)

[J] Oral | A (Atmospheric and Hydrospheric Sciences)：A-CG Complex & General

10:45 AM - 12:15 PM JST | 1:45 AM - 3:15 AM UTC | 301A 3F

[A-CG39] Biogeochemical cycles in Land Ecosystem

convener:Tomomichi Kato(Research Faculty of Agriculture, Hokkaido University), Kazuhito Ichii(Chiba University), Takeshi Ise(FSERC, Kyoto University), Munemasa Teramoto(National Institute for Environmental Studies), Chairperson:Tomomichi Kato(Hokkaido University)

10:45 AM - 11:00 AM JST | 1:45 AM - 2:00 AM UTC

[ACG39-07] Evaluation of feasibility of continental vegetation monitoring using Himawari-8.

*Kodai Hayashi[1], Kazuhito Ichii[1], Hiroki Yoshioka[2], Kazutaka Murakami[3], Reiko Ide[3], Kenlo Nasahara[4], Tomoko Akitsu[4], Tomoaki Miura[5] (1.Chiba Univ., 2.Aichi Prefectural Univ., 3.NIES, 4.Tsukuba Univ., 5.Univ. Hawaii)

11:00 AM - 11:15 AM JST | 2:00 AM - 2:15 AM UTC

[ACG39-08] Estimation of global carbon dioxide emissions by fires

*Tomohiro Shiraishi[1], Ryuichi Hirata[1] (1.National Institute for Environmental Studies)

11:15 AM - 11:30 AM JST | 2:15 AM - 2:30 AM UTC

[ACG39-09] Interactions between topography, permafrost, and vegetation in Siberian larch forest: a simulation study

*Hisashi Sato[1] (1.Institute of Arctic Climate and Environment Research, Japan Agency for Marine-Earth Science and Technology (JAMSTEC))

11:30 AM - 11:45 AM JST | 2:30 AM - 2:45 AM UTC

[ACG39-10] Data assimilation experiments with MODIS LAI observation and the dynamic global vegetation model SEIB-DGVM in Japan

*Hazuki Arakida[1], Shunji Kotsuki[1], Shigenori Otsuka[1], Takemasa Miyoshi[1] (1.RIKEN Center for Computational Science)

11:45 AM - 12:15 PM JST | 2:45 AM - 3:15 AM UTC

[ACG39-11] Studying ecosystem dynamics with deep neural networks

★Invited Papers

*Takeshi Ise[1], Masanori Onishi[2] (1.FSERC, Kyoto University, 2.Grad. School of Agriculture, Kyoto University)

[J] Poster | A (Atmospheric and Hydrospheric Sciences)：A-CG Complex & General

1:45 PM - 3:15 PM JST | 4:45 AM - 6:15 AM UTC | Poster Hall International Exhibition Hall8, Makuhari Messe_2

[A-CG39] Biogeochemical cycles in Land Ecosystem

convener:Tomomichi Kato(Research Faculty of Agriculture, Hokkaido University), Kazuhito Ichii(Chiba University), Takeshi Ise(FSERC, Kyoto University), Munemasa Teramoto(National Institute for Environmental Studies)

[ACG39-P01] Long-term warming effect on heterotrophic respiration in a beech forest on Mount Naeba

*Munemasa Teramoto[1], Naishen Liang[1], Masaaki Naramoto[2], Jiye Zeng[1], Zhao Xin[1], Hajime Tomimastu[1] (1.Center for Global Environmental Research, National Institute for Environmental Studies, 2.Faculty of Agriculture, Shizuoka University)

[ACG39-P02] Simple approach to predict flowering and full blooming dates by bi-directional Self Organizing Maps

*Shin Nagai[1], Hiroshi Morimoto[2], Taku M Saitoh[3] (1.Research and Development Center for Global Change, Japan Agency for Marine-Earth Science and Technology, 2.Nagoya University, 3.River Basin Research Center, Gifu University)

[ACG39-P03] Effects of undergrowth mowing on understory carbon balance in a deciduous broadleaf forest of an urban park in central Japan

Guochao Wang[2], *Tomotsugu Yazaki[1], Toshio Kume[1], Takamitsu Kai[3] (1.School of Agriculture, Meiji University, 2.Graduate School of Agriculture, Meiji University, 3.Kurokawa Field Science Center, Meiji University)

[ACG39-P04] Solar-induced chlorophyll fluorescence for detecting ecosystem photosynthetic activity by high-resolution spectrum measurement in a paddy field in Japan

*KANOKRAT BUAREAL[1], Tomomichi Kato[2], Keisuke Ono[3] (1.Graduate School of Global Food Resources, Hokkaido University, Sapporo, Japan, 2.Research Faculty of Agriculture, Hokkaido University, Sapporo, Japan, 3.National Institute for Agro-Environmental Sciences, Tsukuba, Ibaraki, Japan)

[ACG39-P05] Environmental controls on anomalous variation in solar-induced fluorescence during the last 10 years

*Tomomichi Kato[1], Kazuki Mizuno[2] (1.Research Faculty of Agriculture, Hokkaido University, 2.Graduate School of Agriculture, Hokkaido University)

[ACG39-P06] Estimation of terrestrial carbon cycle in Asia using a machine learning and satellite data

*Riku Kawase[1], Kazuhito Ichii[2], Yusuke hayashi[1], Zhiyan Liu[1], Masahito Ueyama[3], Yuji Kominami[4] (1.Chiba University, 2.Center for Environmental Remote Sensing, Chiba University, 3.Osaka Prefecture University, 4.Forest Research and Management Organization)

[ACG39-P07] Estimation of global solar-induced chlorophyll fluorescence (SIF) by terrestrial ecosystem model VISIT and comparison with SIF observed by GOSAT

*Tatsuya Miyauchi[1], Makoto Saito[1], Hibiki M Noda[1], Yukio Yoshida[1], Haruki Oshio[1], Akihiko Ito[1] (1.National Institute for Environmental Studies)

[ACG39-P08] Automatic vegetation identification in the satellite image using a convolutional neural network

*Watanabe Shuntaro[1], Kazuaki Sumi[2], Takeshi Ise[1,3] (1.Field Science Education and Research Center, Kyoto University, 2.Graduate School of Agriculture, Kyoto University, 3.PRESTO, Japan Science and Technology Agency)

[J] Poster | A (Atmospheric and Hydrospheric Sciences)：A-CG Complex & General

5:15 PM - 6:30 PM JST | 8:15 AM - 9:30 AM UTC | Poster Hall International Exhibition Hall8, Makuhari Messe_15

[A-CG39] Biogeochemical cycles in Land Ecosystem

convener:Tomomichi Kato(Research Faculty of Agriculture, Hokkaido University), Kazuhito Ichii(Chiba University), Takeshi Ise(FSERC, Kyoto University), Munemasa Teramoto(National Institute for Environmental Studies)

[ACG39-P01] Long-term warming effect on heterotrophic respiration in a beech forest on Mount Naeba

*Munemasa Teramoto[1], Naishen Liang[1], Masaaki Naramoto[2], Jiye Zeng[1], Zhao Xin[1], Hajime Tomimastu[1] (1.Center for Global Environmental Research, National Institute for Environmental Studies, 2.Faculty of Agriculture, Shizuoka University)

[ACG39-P02] Simple approach to predict flowering and full blooming dates by bi-directional Self Organizing Maps

*Shin Nagai[1], Hiroshi Morimoto[2], Taku M Saitoh[3] (1.Research and Development Center for Global Change, Japan Agency for Marine-Earth Science and Technology, 2.Nagoya University, 3.River Basin Research Center, Gifu University)

[ACG39-P03] Effects of undergrowth mowing on understory carbon balance in a deciduous broadleaf forest of an urban park in central Japan

Guochao Wang[2], *Tomotsugu Yazaki[1], Toshio Kume[1], Takamitsu Kai[3] (1.School of Agriculture, Meiji University, 2.Graduate School of Agriculture, Meiji University, 3.Kurokawa Field Science Center, Meiji University)

[ACG39-P04] Solar-induced chlorophyll fluorescence for detecting ecosystem photosynthetic activity by high-resolution spectrum measurement in a paddy field in Japan

*KANOKRAT BUAREAL[1], Tomomichi Kato[2], Keisuke Ono[3] (1.Graduate School of Global Food Resources, Hokkaido University, Sapporo, Japan, 2.Research Faculty of Agriculture, Hokkaido University, Sapporo, Japan, 3.National Institute for Agro-Environmental Sciences, Tsukuba, Ibaraki, Japan)

[ACG39-P05] Environmental controls on anomalous variation in solar-induced fluorescence during the last 10 years

*Tomomichi Kato[1], Kazuki Mizuno[2] (1.Research Faculty of Agriculture, Hokkaido University, 2.Graduate School of Agriculture, Hokkaido University)

[ACG39-P06] Estimation of terrestrial carbon cycle in Asia using a machine learning and satellite data

*Riku Kawase[1], Kazuhito Ichii[2], Yusuke hayashi[1], Zhiyan Liu[1], Masahito Ueyama[3], Yuji Kominami[4] (1.Chiba University, 2.Center for Environmental Remote Sensing, Chiba University, 3.Osaka Prefecture University, 4.Forest Research and Management Organization)

[ACG39-P07] Estimation of global solar-induced chlorophyll fluorescence (SIF) by terrestrial ecosystem model VISIT and comparison with SIF observed by GOSAT

*Tatsuya Miyauchi[1], Makoto Saito[1], Hibiki M Noda[1], Yukio Yoshida[1], Haruki Oshio[1], Akihiko Ito[1] (1.National Institute for Environmental Studies)

[ACG39-P08] Automatic vegetation identification in the satellite image using a convolutional neural network

*Watanabe Shuntaro[1], Kazuaki Sumi[2], Takeshi Ise[1,3] (1.Field Science Education and Research Center, Kyoto University, 2.Graduate School of Agriculture, Kyoto University, 3.PRESTO, Japan Science and Technology Agency)

[J] Oral | A (Atmospheric and Hydrospheric Sciences)：A-CG Complex & General

9:00 AM - 10:30 AM JST | 12:00 AM - 1:30 AM UTC | 102 1F

[A-CG40] Coastal Ecosystems - 1. Water Cycle and Land-Ocean Interactions

convener:Masahiko Fujii(Faculty of Environmental Earth Science), Makoto Yamada(Faculty of Economics, Ryukoku University), Jun Shoji(The University of Tokyo), Ryo Sugimoto(Faculty of Marine Biosciences, Fukui Prefectural University), Chairperson:Masahiko Fujii, Makoto Yamada

9:05 AM - 9:20 AM JST | 12:05 AM - 12:20 AM UTC

[ACG40-01] Submarine groundwater discharge from Mt. Fuji in Suruga Bay(VI)

*Yasuhide Muranaka[1], Takafumi Kamitani[1], Noriaki Fushimi[1], Tomoya Oka[1], Masahiko Ono[2], Atsunao Marui[2] (1.Shizuoka Institute of Environment and Hygiene, 2.National Institute of Advanced Industrial Science and Technology)

9:20 AM - 9:35 AM JST | 12:20 AM - 12:35 AM UTC

[ACG40-02] Relationship between the distribution of freshwater groundwater under the seabed at Obama Bay and the surrounding terrain of the land

*Makoto Yamada[1], Ryo Sugimoto[2], Toshimi Nakajima[3] (1.Faculty of Economics, Ryukoku University, 2.Fuculty of Marine Biosciences, Fukui Prefectural University, 3.Fukui Prefectural University)

9:35 AM - 9:50 AM JST | 12:35 AM - 12:50 AM UTC

[ACG40-03] Influence of recirculated submarine groundwater discharge on phytoplankton dynamics in Moune Bay, Kesennuma

*Toshimi Nakajima[1], Takahiro Kusunoki[1], Yoshitake Takao[1], Ryo Sugimoto[1] (1.Fukui Prefectural University)

9:50 AM - 10:05 AM JST | 12:50 AM - 1:05 AM UTC

[ACG40-04] Estimation of contribution rate of Submarine Groundwater Discharge to *Ulva pertusa* using nitrogen stable isotope ratio analysis

*Tatsuhiro Ishida[1], Masaru Takeuchi[1], Toshimi Nakajima[1], Ryo Sugimoto[1], Shiho Kobayashi[2], Keisuke Koba[3], Keitaro Fukushima[3], Osamu Tominaga[1] (1.Fukui Prefectural University, 2.Kyoto University, 3.Center for Ecological Research,Kyoto Univrsity)

10:05 AM - 10:20 AM JST | 1:05 AM - 1:20 AM UTC

[ACG40-05] Evaluation of the environmental condition of Submarine Groundwater Discharge (SGD) using carbon and oxygen stable isotope ratio of the sessile bivalve *Crassostrea nippona* shell

*Osamu Tominaga[1], Takeuchi Masaru[1], Ryo Sugimoto[1], Ishida Tatsuhiro[1], Takeru Hirai[1], Toshimi Nakajima[1], Jun Shoji[2], Hisami Honda[4], Makoto Taniguchi[3] (1.Fukui Prefectural University, 2.Tokyo Univ. AORI, 3.RIHN, 4.Fukui Pref Gov)

[J] Oral | A (Atmospheric and Hydrospheric Sciences)：A-CG Complex & General

10:45 AM - 12:15 PM JST | 1:45 AM - 3:15 AM UTC | 102 1F

[A-CG40] Coastal Ecosystems - 1. Water Cycle and Land-Ocean Interactions

convener:Masahiko Fujii(Faculty of Environmental Earth Science), Makoto Yamada(Faculty of Economics, Ryukoku University), Jun Shoji(The University of Tokyo), Ryo Sugimoto(Faculty of Marine Biosciences, Fukui Prefectural University), Chairperson:Masahiko Fujii, Makoto Yamada

10:45 AM - 11:00 AM JST | 1:45 AM - 2:00 AM UTC

[ACG40-06] Influence of climate change on river and submarine groundwater discharge for three decades and the change of nutrient fluxes from the land to the coastal area

*Saki KATAZAKAI[1], Jing ZHANG[2], Kota NOJIMA[3] (1.Graduate School of Science and Engineer, University of Toyama, 2.Graduate School of Science and Engineering for Science, University of Toyama, 3.University of Toyama)

11:00 AM - 11:15 AM JST | 2:00 AM - 2:15 AM UTC

[ACG40-07] The assessment of human impacts on the distribution patterns of mangroves: a comparative study between the Rewa and Ba delta, Fiji

*Masahiko Fujii[1], Jone Ravuci Sassen[2] (1.Faculty of Environmental Earth Science, 2.Graduate School of Environmental Science)

11:15 AM - 11:30 AM JST | 2:15 AM - 2:30 AM UTC

[ACG40-08] Landscape factors affect persistence and accumulation of organic carbon in sediment of secondary mangrove forests: A preliminary study

*Toshihiro Miyajima[1], Rempei Suwa[2], Keith Limuel C. Bejasa[3], Rene N. Rollon[3], Maria Lourdes San Diego-McGlone[3], Caroline M.B. Jaraula[3], Fernando P. Siringan[3], Kenji Ono[4], Yasmin H. Primavera Tirol[5], Yosuke Miyairi[1], Yusuke Yokoyama[1] (1.Atmosphere and Ocean Research Institute, The University of Tokyo, 2.Japan International Research Center for Agricultural Sciences, 3.Marine Science Institute, University of the Philippines, 4.Forestry and Forest Products Research Institute, 5.Aklan State University)

11:30 AM - 11:45 AM JST | 2:30 AM - 2:45 AM UTC

[ACG40-09] Multiple benefits of blue carbon ecosystems in promoting blue economy and reinforcing resilience in coastal communities

*Atsushi Watanabe[1] (1.The ocean policy research institute, The Sasakawa peace foundation)

11:45 AM - 12:05 PM JST | 2:45 AM - 3:05 AM UTC

[ACG40-10] Significant storage of organic carbon in mineral matrix in both land and ocean and the role of Fe

★Invited Papers

*Rota Wagai[1] (1.NARO, Institute for Agro-Environmental Sciences)

[J] Poster | A (Atmospheric and Hydrospheric Sciences)：A-CG Complex & General

3:30 PM - 5:00 PM JST | 6:30 AM - 8:00 AM UTC | Poster Hall International Exhibition Hall8, Makuhari Messe_10

[A-CG40] Coastal Ecosystems - 1. Water Cycle and Land-Ocean Interactions

convener:Masahiko Fujii(Faculty of Environmental Earth Science), Makoto Yamada(Faculty of Economics, Ryukoku University), Jun Shoji(The University of Tokyo), Ryo Sugimoto(Faculty of Marine Biosciences, Fukui Prefectural University)

[ACG40-P01] Submarine groundwater discharge and dissolved material fluxes quantified by radium isotopes in sandy beach, central Wakasa Bay

*Toshimi Nakajima[1], Ryo Sugimoto[1], Yuta Sumino[1], Makoto Taniguchi[2], Osamu Tominaga[1] (1.Fukui Prefectural University, 2.Research Institute for Humanity and Nature)

[ACG40-P02] Influence of difference in river shape on heat supply to coastal area by hot spring drainage river

*Makoto Yamada[1], Taketoshi Mishima[2], Shinji Ohsawa[2] (1.Faculty of Economics, Ryukoku University, 2.Institute for Geothermal Sciences, Graduate School of Sciences, Kyoto University)

[ACG40-P03] Construction of an artificial outlet channel affects organic carbon accumulation in a coastal lagoon

*Kenta Watanabe[1], Tomohiro Kuwae[1] (1.Port and Airport Research Institute)

[ACG40-P04] Evaluation of the influence of swans, *Cygnus cygnus* on the distribution of seagrass, *Zostera japonica*

*Yoshiyuki TANAKA[1], Fumiyuki SATO[1] (1.Hachinohe Institute of Technology, Department of Life and Environmental Science)

[ACG40-P05] Assessment and future projection of variational characteristics of ocean warming and acidification proxies in Oshoro Bay, Japan

*Masahiko Fujii[1], Takuto Yamaka[2], Shintaro Takao[3] (1.Faculty of Environmental Earth Science, 2.Graduate School of Environmental Science, 3.National Institute of Polar Research)

[J] Poster | A (Atmospheric and Hydrospheric Sciences)：A-CG Complex & General

5:15 PM - 6:30 PM JST | 8:15 AM - 9:30 AM UTC | Poster Hall International Exhibition Hall8, Makuhari Messe_16

[A-CG40] Coastal Ecosystems - 1. Water Cycle and Land-Ocean Interactions

convener:Masahiko Fujii(Faculty of Environmental Earth Science), Makoto Yamada(Faculty of Economics, Ryukoku University), Jun Shoji(The University of Tokyo), Ryo Sugimoto(Faculty of Marine Biosciences, Fukui Prefectural University)

[ACG40-P01] Submarine groundwater discharge and dissolved material fluxes quantified by radium isotopes in sandy beach, central Wakasa Bay

*Toshimi Nakajima[1], Ryo Sugimoto[1], Yuta Sumino[1], Makoto Taniguchi[2], Osamu Tominaga[1] (1.Fukui Prefectural University, 2.Research Institute for Humanity and Nature)

[ACG40-P02] Influence of difference in river shape on heat supply to coastal area by hot spring drainage river

*Makoto Yamada[1], Taketoshi Mishima[2], Shinji Ohsawa[2] (1.Faculty of Economics, Ryukoku University, 2.Institute for Geothermal Sciences, Graduate School of Sciences, Kyoto University)

[ACG40-P03] Construction of an artificial outlet channel affects organic carbon accumulation in a coastal lagoon

*Kenta Watanabe[1], Tomohiro Kuwae[1] (1.Port and Airport Research Institute)

[ACG40-P04] Evaluation of the influence of swans, *Cygnus cygnus* on the distribution of seagrass, *Zostera japonica*

*Yoshiyuki TANAKA[1], Fumiyuki SATO[1] (1.Hachinohe Institute of Technology, Department of Life and Environmental Science)

[ACG40-P05] Assessment and future projection of variational characteristics of ocean warming and acidification proxies in Oshoro Bay, Japan

*Masahiko Fujii[1], Takuto Yamaka[2], Shintaro Takao[3] (1.Faculty of Environmental Earth Science, 2.Graduate School of Environmental Science, 3.National Institute of Polar Research)

[J] Poster | A (Atmospheric and Hydrospheric Sciences)：A-CG Complex & General

1:45 PM - 3:15 PM JST | 4:45 AM - 6:15 AM UTC | Poster Hall International Exhibition Hall8, Makuhari Messe_3

[A-CG41] Promotion of Application and Utilization of Aircrafts for Earth sciences

convener:Nobuhiro Takahashi(Institute for Space-Earth Environmental Research, Nagoya University), Makoto Koike(Department of Earth and Planetary Science, Graduate School of Science, The University of Tokyo), Toshinobu Machida(National Institute for Environmental Studies), Taro Shinoda(Institute for Space-Earth Environmental Research, Nagoya University)

[ACG41-P01] In situ measurements of aerosol and cloud microphysical properties and cloud seeding experiments over the UAE

*Narihiro Orikasa[1], Masataka Murakami[2,1], Takuya Tajiri[1], Yuji Zaizen[1], Taro Shinoda[2] (1.Meteorological Research Institute, 2.Nagoya Univ., ISEE)

[ACG41-P02] Analysis and Forecast Using Dropsonde Data from the Inner-Core Region of Tropical Cyclone Lan (2017) Obtained during the First Aircraft Missions of T-PARCII

*Kosuke Ito[1], Hiroyuki Yamada[1], Munehiko Yamaguchi[2], Tetsuo Nakazawa[2], Norio Nagahama[3], Kensaku Shimizu[3], Tadayasu Ohigashi[4], Taro Shinoda[5], Kazuhisa Tsuboki[5] (1.University of the Ryukyus, 2.Meteorological Research Institute, 3.Meisei Electric Co. LTD., 4.National Research Institute for Earth Science and Disaster Resilience, 5.Nagoya University)

[ACG41-P03] On the Spatial Distribution of Freezing height of Typhoon Trami

*Nobuhiro Takahashi[1], Yuki Kaneko[2], Kazuhisa Tsuboki[1] (1.Institute for Space-Earth Environmental Research, Nagoya University, 2.Japan Aerospace Exploration Agency)

[ACG41-P04] Revision of Research Plan on “Promotion of Climate and Earth System Science Research by Aircraft Observation”

*Nobuhiro Takahashi[1], Makoto Koike[2] (1.Institute for Space-Earth Environmental Research, Nagoya University, 2.School of Science, The University of Tokyo)

[J] Poster | A (Atmospheric and Hydrospheric Sciences)：A-CG Complex & General

5:15 PM - 6:30 PM JST | 8:15 AM - 9:30 AM UTC | Poster Hall International Exhibition Hall8, Makuhari Messe_17

[A-CG41] Promotion of Application and Utilization of Aircrafts for Earth sciences

convener:Nobuhiro Takahashi(Institute for Space-Earth Environmental Research, Nagoya University), Makoto Koike(Department of Earth and Planetary Science, Graduate School of Science, The University of Tokyo), Toshinobu Machida(National Institute for Environmental Studies), Taro Shinoda(Institute for Space-Earth Environmental Research, Nagoya University)

[ACG41-P01] In situ measurements of aerosol and cloud microphysical properties and cloud seeding experiments over the UAE

*Narihiro Orikasa[1], Masataka Murakami[2,1], Takuya Tajiri[1], Yuji Zaizen[1], Taro Shinoda[2] (1.Meteorological Research Institute, 2.Nagoya Univ., ISEE)

[ACG41-P02] Analysis and Forecast Using Dropsonde Data from the Inner-Core Region of Tropical Cyclone Lan (2017) Obtained during the First Aircraft Missions of T-PARCII

*Kosuke Ito[1], Hiroyuki Yamada[1], Munehiko Yamaguchi[2], Tetsuo Nakazawa[2], Norio Nagahama[3], Kensaku Shimizu[3], Tadayasu Ohigashi[4], Taro Shinoda[5], Kazuhisa Tsuboki[5] (1.University of the Ryukyus, 2.Meteorological Research Institute, 3.Meisei Electric Co. LTD., 4.National Research Institute for Earth Science and Disaster Resilience, 5.Nagoya University)

[ACG41-P03] On the Spatial Distribution of Freezing height of Typhoon Trami

*Nobuhiro Takahashi[1], Yuki Kaneko[2], Kazuhisa Tsuboki[1] (1.Institute for Space-Earth Environmental Research, Nagoya University, 2.Japan Aerospace Exploration Agency)

[ACG41-P04] Revision of Research Plan on “Promotion of Climate and Earth System Science Research by Aircraft Observation”

*Nobuhiro Takahashi[1], Makoto Koike[2] (1.Institute for Space-Earth Environmental Research, Nagoya University, 2.School of Science, The University of Tokyo)

[J] Oral | A (Atmospheric and Hydrospheric Sciences)：A-CG Complex & General

3:30 PM - 5:00 PM JST | 6:30 AM - 8:00 AM UTC | 201B 2F

[A-CG41] Promotion of Application and Utilization of Aircrafts for Earth sciences

convener:Nobuhiro Takahashi(Institute for Space-Earth Environmental Research, Nagoya University), Makoto Koike(Department of Earth and Planetary Science, Graduate School of Science, The University of Tokyo), Toshinobu Machida(National Institute for Environmental Studies), Taro Shinoda(Institute for Space-Earth Environmental Research, Nagoya University), Chairperson:Nobuhiro Takahashi(Institute for Space-Earth Environmental Research, Nagoya University)

3:30 PM - 3:45 PM JST | 6:30 AM - 6:45 AM UTC

[ACG41-01] In situ observation of typhoon central pressure using dropsondes

*Kazuhisa Tsuboki[1], Hiroyuki Yamada[2], Yukihiro Takahashi[3], Taro Shinoda[1], Tadayasu Ohigashi[4], Munehiko Yamaguchi[5], Hisayuki Kubota[3], Tetsuo Nakazawa[5], Norio Nagahama[6], Kensaku Shimizu[6], Masaya Kato[1], Sachie Kanada[1], Mayumi Yoshioka[1], Nobuhiro Takahashi[1] (1. Institute for Space-Earth Environmental Research, Nagoya University, 2.University of the Ryukyus, 3.Hokkaido University, 4.National Research Institute for Earth Science and Disaster Resilience, 5.Meteorological Research Institute, Japan Meteorological Agency, 6.Meisei Electric Co. Ltd.)

3:45 PM - 4:00 PM JST | 6:45 AM - 7:00 AM UTC

[ACG41-02] New observation strategies for typhoon intensity over the western North Pacific

*Hiroyuki Yamada[1], Kazuhisa Tsuboki[2], Taro Shinoda[2], Hisayuki Kubota[3], Yukihiro Takahashi[3], Norio Nagahama[4], Kensaku Shimizu[4], Tadayasu Ohigashi[5], Kosuke Ito[1], Munehiko Yamaguchi[6], Tetsuo Nakazawa[6] (1.University of the Ryukyus, 2.Nagoya University, 3.Hokkaido University, 4.Meisei Electric, 5.National Research Institute for Earth Science and Disaster Resilience, 6.Meteorological Research Institute, Japan Meteorological Agency)

4:00 PM - 4:15 PM JST | 7:00 AM - 7:15 AM UTC

[ACG41-03] Observing System Experiment for Typhoon Trami (2018) using T-PARCII dropsondes and JMA Global Forecasting System

*Munehiko Yamaguchi[1], Toshiyuki Ishibashi[1], Tetsuo Nakazawa[1], Kosuke Ito[2], Hiroyuki Yamada[2], Tadayasu Ohigashi[3], Norio Nagahama[4], Kensaku Shimizu[4], Hisayuki Kubota[5], Yukihiro Takahashi[5], Masaya Kato[6], Sachie Kanada[6], Mayumi Yoshioka[6], Taro Shinoda[6], Nobuhiro Takahashi[6], Kazuhisa Tsuboki[6] (1.Meteorological Research Institute, Japan Meteorological Agency, 2.Faculty of Science, University of the Ryukyus, 3.National Research Institute for Earth Science and Disaster Resilience, 4.Meisei Electric, 5.Graduate School of Science, Hokkaido University, 6.Institute for Space-Earth Environmental Research, Nagoya University)

4:15 PM - 4:30 PM JST | 7:15 AM - 7:30 AM UTC

[ACG41-04] Fundamental characteristics of black carbon and iron oxide aerosols in the troposphere revealed from the aircraft measurements

*Nobuhiro Moteki[1], Makoto Koike[1], Sho Ohata[2], Yutaka Kondo[3], Nobuyuki Takegawa[5], Kouji Adachi[4], Naga Oshima[4], Hitoshi Matsui[2], Kazuyuki Kita[6], Tatsuhiro Mori[7], Atsushi Yoshida[1] (1.The Univerisity of Tokyo, 2.Nagoya University, 3.National Institute for Polar Research, 4.Meteorological Research Institute, 5.Tokyo Metropolitan University, 6.Ibaraki University, 7.Tokyo University of Science)

4:30 PM - 4:45 PM JST | 7:30 AM - 7:45 AM UTC

[ACG41-05] Aerosol measurements around the ridge of East Antarctica using a Rogallo wing UAV

*Ryohei Haraguchi[1], Masahiko Hayashi[1], Keiichiro Hara[1], Naohiko Hirasawa[2], Koki Nakata[3], Kei-ichi Ozuka[4,1] (1.Fukuoka University, 2.National Institute of Polar Research, 3.kkt Inovate Co., Ltd, 4.Nippon Tungsten Co., Ltd)

4:45 PM - 5:00 PM JST | 7:45 AM - 8:00 AM UTC

[ACG41-06] Wind Mesurements Based on In-situ Data -Direct Vector Calculation and Hodograph Analyses-

*Masahiko Hayashi[1], Tomoyuki Onohara[1], Ryohei Haraguchi[1,3], Kei-ichi Ozuka[2,4], Kazuo Okabe[3] (1.Faculty of Science, Fukuoka University, 2.Nippon Tungsten Co.,Ltd, 3.SkyRemote Co.,Ltd, 4.FIT-EH, Fukuoka University)

[J] Poster | A (Atmospheric and Hydrospheric Sciences)：A-CG Complex & General

10:45 AM - 12:15 PM JST | 1:45 AM - 3:15 AM UTC | Poster Hall International Exhibition Hall8, Makuhari Messe_4

[A-CG44] Coastal Ecosystems 2 Coral reefs, seagrass and macroalgal beds, and mangrove

convener:Yu Umezawa(Tokyo University of Agriculture and Technology), Toshihiro Miyajima(Marine Biogeochemistry Group, Division of Ocean-Earth System Science, Atmosphere and Ocean Research Institute, The University of Tokyo), Atsushi Watanabe(The ocean policy research institute, The Sasakawa peace foundation), Tomihiko Higuchi(Atmosphere and Ocean Research Institute, The University of Tokyo)

[ACG44-P01] Characteristics of organic carbon in coastal carbonate sediment accompanied by seagrass meadows

*Toshihiro Miyajima[1] (1.Marine Biogeochemistry Group, Division of Ocean-Earth System Science, Atmosphere and Ocean Research Institute, The University of Tokyo)

[ACG44-P02] **Perceptions of Coastal Communities on Blue Carbon Ecosystems Services at the Municipalities of Eastern Samar and Western Visayas, Philippines**

*Jay Mar Dioquito Quevedo[1], Yuta Uchiyama[1], Kaoru Kakinuma[1], Ryo Kohsaka[1] (1.Tohoku University)

[ACG44-P03] Numerical simulation of typhoon events in Sekisei Lagoon, Okinawa, Japan using a coupled ocean-wave model

*Lawrence Patrick Cases Bernardo[1], Takashi Nakamura[1], Kazuo Nadoka[1] (1.Department of Transdisciplinary Science and Engineering, Tokyo Institute of Technology)

[ACG44-P04] Study of macrobenthic community structure at mesophotic depths in the South Ryukyus based on ROV and AUV seafloor imaging

*Marc Humblet[1], Toshihiro Maki[2], Yasuo Furushima[3], Yukiyasu Noguchi[2], Hiroumi Horimoto[2], Hiroya Yatagai[2], Takashi Sakamaki[2], Shohei Ito[4], Sadao Suzuki[5] (1.Department of Earth and Planetary Sciences, Nagoya University, 2.Institute of Industrial Science, The University of Tokyo, 3.JAMSTEC, 4.FullDepth Co., Ltd., 5.ORE)

[ACG44-P05] Enhancement of antioxidant activity of scleractinian coral *Galaxea Fascicularis* by feeding treatment.

*Hiroyuki Fujimura[1], Sayaka Higa[1], Toshihiro Miyajima[2], Tomihiko Higuchi[2], Sylvain Agostini[3], Ikuko Yuyama[3], Takashi Nakamura[4] (1.University of the Ryukyus, 2.The University of Tokyo, 3.Tsukuba University, 4.Tokyo Institute of Technology)

[ACG44-P06] Effects of environmental stresses on coral bleaching

*Tomihiko Higuchi[1] (1.Atmosphere and Ocean Research Institute, The University of Tokyo)

[J] Poster | A (Atmospheric and Hydrospheric Sciences)：A-CG Complex & General

5:15 PM - 6:30 PM JST | 8:15 AM - 9:30 AM UTC | Poster Hall International Exhibition Hall8, Makuhari Messe_18

[A-CG44] Coastal Ecosystems 2 Coral reefs, seagrass and macroalgal beds, and mangrove

convener:Yu Umezawa(Tokyo University of Agriculture and Technology), Toshihiro Miyajima(Marine Biogeochemistry Group, Division of Ocean-Earth System Science, Atmosphere and Ocean Research Institute, The University of Tokyo), Atsushi Watanabe(The ocean policy research institute, The Sasakawa peace foundation), Tomihiko Higuchi(Atmosphere and Ocean Research Institute, The University of Tokyo)

[ACG44-P01] Characteristics of organic carbon in coastal carbonate sediment accompanied by seagrass meadows

*Toshihiro Miyajima[1] (1.Marine Biogeochemistry Group, Division of Ocean-Earth System Science, Atmosphere and Ocean Research Institute, The University of Tokyo)

[ACG44-P02] **Perceptions of Coastal Communities on Blue Carbon Ecosystems Services at the Municipalities of Eastern Samar and Western Visayas, Philippines**

*Jay Mar Dioquito Quevedo[1], Yuta Uchiyama[1], Kaoru Kakinuma[1], Ryo Kohsaka[1] (1.Tohoku University)

[ACG44-P03] Numerical simulation of typhoon events in Sekisei Lagoon, Okinawa, Japan using a coupled ocean-wave model

*Lawrence Patrick Cases Bernardo[1], Takashi Nakamura[1], Kazuo Nadoka[1] (1.Department of Transdisciplinary Science and Engineering, Tokyo Institute of Technology)

[ACG44-P04] Study of macrobenthic community structure at mesophotic depths in the South Ryukyus based on ROV and AUV seafloor imaging

*Marc Humblet[1], Toshihiro Maki[2], Yasuo Furushima[3], Yukiyasu Noguchi[2], Hiroumi Horimoto[2], Hiroya Yatagai[2], Takashi Sakamaki[2], Shohei Ito[4], Sadao Suzuki[5] (1.Department of Earth and Planetary Sciences, Nagoya University, 2.Institute of Industrial Science, The University of Tokyo, 3.JAMSTEC, 4.FullDepth Co., Ltd., 5.ORE)

[ACG44-P05] Enhancement of antioxidant activity of scleractinian coral *Galaxea Fascicularis* by feeding treatment.

*Hiroyuki Fujimura[1], Sayaka Higa[1], Toshihiro Miyajima[2], Tomihiko Higuchi[2], Sylvain Agostini[3], Ikuko Yuyama[3], Takashi Nakamura[4] (1.University of the Ryukyus, 2.The University of Tokyo, 3.Tsukuba University, 4.Tokyo Institute of Technology)

[ACG44-P06] Effects of environmental stresses on coral bleaching

*Tomihiko Higuchi[1] (1.Atmosphere and Ocean Research Institute, The University of Tokyo)

[J] Oral | A (Atmospheric and Hydrospheric Sciences)：A-CG Complex & General

1:45 PM - 3:15 PM JST | 4:45 AM - 6:15 AM UTC | 102 1F

[A-CG44] Coastal Ecosystems 2 Coral reefs, seagrass and macroalgal beds, and mangrove

convener:Yu Umezawa(Tokyo University of Agriculture and Technology), Toshihiro Miyajima(Marine Biogeochemistry Group, Division of Ocean-Earth System Science, Atmosphere and Ocean Research Institute, The University of Tokyo), Atsushi Watanabe(The ocean policy research institute, The Sasakawa peace foundation), Tomihiko Higuchi(Atmosphere and Ocean Research Institute, The University of Tokyo), Chairperson:Yu Umezawa(Tokyo University of Agriculture and Technology), Toshihiro Miyajima(The University of Tokyo), Tomihiko Higuchi(Atmosphere and Ocean Research Institute, The University of Tokyo), Atsushi Watanabe(Tokyo Institute of Technology)

1:50 PM - 2:10 PM JST | 4:50 AM - 5:10 AM UTC

[ACG44-01] Evaluation of mangrove ecosystems as a dissolved iron supplying system to tropical coastal waters

★Invited Papers

*Yasuhiro Nakanishi[1], Ko Hinokidani[1] (1.Tokyo University of Agriculture)

2:10 PM - 2:25 PM JST | 5:10 AM - 5:25 AM UTC

[ACG44-02] Dissolved organic carbon and optical properties in tropical and subtropical mangrove environments

*Raghab Ray[1], Toshihiro Miyajima[1], Charissa M Ferrera[2], Chia-Jung Lu[1], M.L San Diego-McGlone[2], Hiroshi Ogawa[1], Kazuo Nadaoka[3] (1.Atmosphere and Ocean Research Institute, The University of Tokyo, 2.Marine Science Institute, University of the Philippines, Diliman, 3.School of Environment and Society, Tokyo Institute of Technology)

2:25 PM - 2:45 PM JST | 5:25 AM - 5:45 AM UTC

[ACG44-03] Modeling coral polyp-scale bleaching phenomenon and upscaling to reef-scale

★Invited Papers

*Takashi Nakamura[1], Tomihiko Higuchi[2], Toshihiro Miyajima[2], Lawrence Patrick Cases Bernardo[1], Kazuo Nadaoka[1], Atsushi Watanabe[1,3], Hiroyuki Fujimura[4] (1.School of Environment and Society, Tokyo Institute of Technology, 2.AORI, The University of Tokyo, 3.The ocean policy research institute, The Sasakawa peace foundation, 4.University of the Ryukyus)

2:45 PM - 3:00 PM JST | 5:45 AM - 6:00 AM UTC

[ACG44-04] Reversal of surface ocean acidification and recovery potential of calcification: ecology of proton concentration control

*Kazuhiko Ichikawa[1] (1.(post) Graduate School of Environmental Earth Science, Hokkaido University)

3:00 PM - 3:15 PM JST | 6:00 AM - 6:15 AM UTC

[ACG44-05] Revisit of massive *Porites* coral growth under the outbreak of crown-of-thorns starfish and thermal stress in Sekisei Lagoon, Japan

*Kohki Sowa[1] (1.Japan Agency for Marine-Earth Science and Technology)

[J] Oral | A (Atmospheric and Hydrospheric Sciences)：A-CG Complex & General

3:30 PM - 5:00 PM JST | 6:30 AM - 8:00 AM UTC | 102 1F

[A-CG44] Coastal Ecosystems 2 Coral reefs, seagrass and macroalgal beds, and mangrove

convener:Yu Umezawa(Tokyo University of Agriculture and Technology), Toshihiro Miyajima(Marine Biogeochemistry Group, Division of Ocean-Earth System Science, Atmosphere and Ocean Research Institute, The University of Tokyo), Atsushi Watanabe(The ocean policy research institute, The Sasakawa peace foundation), Tomihiko Higuchi(Atmosphere and Ocean Research Institute, The University of Tokyo), Chairperson:Yu Umezawa(Tokyo University of Agriculture and Technology), Toshihiro Miyajima(The University of Tokyo), Atsushi Watanabe(Tokyo Institute of Technology), Tomihiko Higuchi(Atmosphere and Ocean Research Institute, The University of Tokyo)

3:30 PM - 3:45 PM JST | 6:30 AM - 6:45 AM UTC

[ACG44-06] Reconstructing sedimentation process of lagoon sediment in the Eastern Kume Island, Ryukyus

*Wataru Sano[1], Shoko Hirabayashi[2], Yusuke Yokoyama[3], Yosuke Miyairi[3], Kazuhiko Fujita[4], Hironobu Kan[2], Lauren T. Toth[5], Richard B. Aronson[6] (1.Graduate School of Integrated Sciences for Global Society, Kyushu University, 2.Graduate School of Social and Cultural Studies, Kyushu University, 3.Atmosphere and Ocean Research Institute, University of Tokyo, 4.Department of Physics and Earth Sciences, University of the Ryukyus, 5.United States Geological Survey, 6.Florida Institute of Technology)

3:45 PM - 4:00 PM JST | 6:45 AM - 7:00 AM UTC

[ACG44-07] Addressing challenges in long-term coral reef monitoring: Statistical tools to address the effect of new methods

*Iwao Fujii[1,2], Jennifer Selgrath[3,2], Amanda Vincent[2] (1.The Ocean Policy Research Institute of the Sasakawa Peace Foundation, 2.Project Seahorse, Institute of the Oceans and Fisheries, The University of British Columbia, 3.Hopkins Marine Station, Stanford University)

4:00 PM - 4:20 PM JST | 7:00 AM - 7:20 AM UTC

[ACG44-08] Ocean currents and herbivory drive macroalgae-to-coral community shift under climate warming

★Invited Papers

*Naoki H. Kumagai[1], Jorge García Molinos[2], Hiroya Yamano[1], Shintaro Takao[1], Masahiko Fujii[2], Yasuhiro Yamanaka[2] (1.National Institute for Environmental Studies, 2.Hokkaido University)

4:20 PM - 4:35 PM JST | 7:20 AM - 7:35 AM UTC

[ACG44-09] Estimation of temperature of seaweed bed vegetation boundary in the Western Seto Inland Sea using satellite SST

*Naoki Yoshie[1], Anri Kabe[1], Hiromori Shimabukuro[2], Goro Yoshida[2] (1.Center for Marine Environmental Studies, Ehime University, 2.Japan Fisheries Research and Education Agency)

4:35 PM - 4:55 PM JST | 7:35 AM - 7:55 AM UTC

[ACG44-10] Fate of macroalgal organic matter and its effects on in and outside of algal bed

★Invited Papers

*Shigeki Wada[1], Yuko Omori[1], Takeo Hama[1,2] (1.University of Tsukuba, 2.Dokkyo University)

[J] Oral | A (Atmospheric and Hydrospheric Sciences)：A-CG Complex & General

9:00 AM - 10:30 AM JST | 12:00 AM - 1:30 AM UTC | 103 1F

[A-CG45] Visible Remote Sensing of Hydrospheric Science and Its Application

convener:Joji Ishizaka(Institute for Space-Earth Environmental Research, Nagoya University), Mitsuhiro Toratani(School of Engineering, Tokai University), Yuji Sakuno(Graduate School of Engineering, Hiroshima University), Toru Hirawake(Faculty of Fisheries Sciences, Hokkaido University), Chairperson:Yuji Sakuno(広島大学大学院工学研究科)

9:00 AM - 9:15 AM JST | 12:00 AM - 12:15 AM UTC

[ACG45-01] Further information in the coastal areas from 250-m resolution multiple bands of GCOM-C “SHIKISAI”

★Invited Papers

*Hiroshi Murakami[1], Manabu Shimizu[2], Goh Onizuka[3] (1.Earth Observation Research Center, Japan Aerospace Exploration Agency, 2.Japan Fisheries Research and Education Agency, 3.National Research Institute of Fisheries and Environment of Inland Sea, Japan Fisheries Research and Education Agency)

9:15 AM - 9:30 AM JST | 12:15 AM - 12:30 AM UTC

[ACG45-02] Features of GCOM-C/SGLI standard atmospheric correction scheme and its processing results

*Mitsuhiro Toratani[1], Kazunori Ogata[2], Hajime Fukushima[3] (1.School of Engineering, Tokai University, 2.Japan Aerospace Exploration Agency/Earth Observation Research Center, 3.Tokai University)

9:30 AM - 9:45 AM JST | 12:30 AM - 12:45 AM UTC

[ACG45-03] Verification of GCOM-C/SGLI-derived chlorophyll *a* data in the western North Pacific during May 2018 aboard the R/V *Shinsei Maru*

*Koji Suzuki[1], Stanford B. Hooker[2], Tomonori Isada[1], Kazunori Ogata[3], Mitsuhiro Toratani[4], Hiroshi Murakami[3] (1.Hokkaido University, 2.NASA, 3.JAXA, 4.Tokai University)

9:45 AM - 10:00 AM JST | 12:45 AM - 1:00 AM UTC

[ACG45-04] **Toward a global retrieval of in-water optical properties using Deep Neural Network**

*Salem Ibrahim Salem[1], Hiroto Higa[2], Kazuo Oki[1], Taikan Oki[1] (1.The University of Tokyo, 2.Yokohama National University)

10:00 AM - 10:15 AM JST | 1:00 AM - 1:15 AM UTC

[ACG45-05] Development of atmosphere and in-water combining algorithm using GCOM-C/SGLI in Tokyo Bay

*Taiga Nakayama[1], HIROTO HIGA[1], Kazuki Ogata[2] (1.Yokohama National University, 2.Japan Aerospace eXploration Agency)

10:15 AM - 10:30 AM JST | 1:15 AM - 1:30 AM UTC

[ACG45-06] Analysis of the uncertainty of backscattering coefficient by radiative transfer simulation in coastal areas and lakes

*Hidehito Taki[1], Hiroto Higa[1], Yoshiyuki Nakamura[1], Takayuki Suzuki[1] (1.Graduate School of Urban Innovation, Yokohama National University)

[J] Oral | A (Atmospheric and Hydrospheric Sciences)：A-CG Complex & General

10:45 AM - 12:15 PM JST | 1:45 AM - 3:15 AM UTC | 103 1F

[A-CG45] Visible Remote Sensing of Hydrospheric Science and Its Application

convener:Joji Ishizaka(Institute for Space-Earth Environmental Research, Nagoya University), Mitsuhiro Toratani(School of Engineering, Tokai University), Yuji Sakuno(Graduate School of Engineering, Hiroshima University), Toru Hirawake(Faculty of Fisheries Sciences, Hokkaido University), Chairperson:Joji Ishizaka(名古屋大学宇宙地球環境研究所)

10:45 AM - 11:00 AM JST | 1:45 AM - 2:00 AM UTC

[ACG45-07] Development of a blue tide estimation method based on the optical properties of sulfur colloid particles by geostationary ocean color satellite

*HIROTO HIGA[1], WATARU NAKAMURA[1] (1.Yokohama National University)

11:00 AM - 11:15 AM JST | 2:00 AM - 2:15 AM UTC

[ACG45-08] Characteristics of water quality and red tide distribution in the Seto Inland Sea immediately after heavy rain in the western Japan by GCOM-C SGLI data

*Yuji Sakuno[1], Hiroto Higa[2], Hiroshi Kobayashi[3], Mitsuhiro Toratani[4] (1.Hiroshima University, 2.Yokohama National University, 3.Yamanashi University, 4.Tokai University)

11:15 AM - 11:30 AM JST | 2:15 AM - 2:30 AM UTC

[ACG45-09] Application of Satellite Remote Sensing to Monitor Eutrophication Status of Inland Lakes

*Wei Yang[1], Bunkei Matsushita[2] (1.Chiba University, 2.University of Tsukuba)

11:30 AM - 11:45 AM JST | 2:30 AM - 2:45 AM UTC

[ACG45-10] **Exploring the Potentials of Google Earth Engine for Global Assessment of Coastal Eutrophication Based on Chlorophyll-*a* concentration**

*Eligio de Raus Maure[1], Genki Terauchi[1], Joji Ishizaka[2] (1.Northwest Pacific Region Environmental Cooperation Center, 2.Institute for Space-Earth Environmental Research, Nagoya University)

11:45 AM - 12:00 PM JST | 2:45 AM - 3:00 AM UTC

[ACG45-11] Seasonal and interannual variability of seagrass distribution detected by Landsat TM, ETM+ and OLI images in western Nanao Bay

*Genki Terauchi[1] (1.Northwest Pacific Region Environmental Cooperation Center)

[J] Poster | A (Atmospheric and Hydrospheric Sciences)：A-CG Complex & General

3:30 PM - 5:00 PM JST | 6:30 AM - 8:00 AM UTC | Poster Hall International Exhibition Hall8, Makuhari Messe_11

[A-CG45] Visible Remote Sensing of Hydrospheric Science and Its Application

convener:Joji Ishizaka(Institute for Space-Earth Environmental Research, Nagoya University), Mitsuhiro Toratani(School of Engineering, Tokai University), Yuji Sakuno(Graduate School of Engineering, Hiroshima University), Toru Hirawake(Faculty of Fisheries Sciences, Hokkaido University)

[ACG45-P01] About GCOM-C/SGLI Ocean Standard Products

*Kazunori Ogata[1] (1.Japan Aerospace Exploration Agency)

[ACG45-P02] Verification of GCOM-C/SGLI product in coastal area

*Joji Ishizaka[1] (1.Institute for Space-Earth Environmental Research, Nagoya University)

[ACG45-P03] Hyperspectral Radiometry towards Classification of Marine Phytoplankton Groups

*Takafumi Hirata[1], Robert J.W. Brewin[2], Girgio Dall'Olmo[2], Mariana Altenburg Soppa[3], Astrid Bracher[3] (1.Faculty of Environmental Earth Science, Hokkaido University, 2.Plymouth Marine Laboratory, 3.Alfred-Wegener Institute for Polar and Marine Research)

[ACG45-P04] Improvement of absorption-based primary production model for SGLI/GCOM-C

*Toru Hirawake[1], Takuhei Shiozaki[2], Hisatomo Waga[1], Koji Suzuki[1] (1.Hokkaido University, 2.JAMSTEC)

[ACG45-P05] Attempt to distinguish river water influencing concentration of chlorophyll *a* off Miho Peninsula

*Akihiko Tanaka[1], Kyoko Takashima[2], Gen Fukuda[2], Takaaki Katsumata[1], Hiroyuki Tan[1], Masato Niki[2], Daisuke Takahashi[2] (1.Liberal Arts Education Center, Shimizu Campus, Tokai University, 2.School of Marine Science and Technology, Tokai University)

[ACG45-P06] **Estimation of chlorophyll-a from RGB digital camera data collected in Ise-Mikawa Bay**

*Akiko N. Mizuno[1], Joji Ishizaka[1] (1.Institute for Space-Earth Environmental Research, Nagoya University)

[ACG45-P07] **Seasonal variability of MODIS chlorophyll-a and total suspended matter in the spring-neap tidal cycle in the Ariake Bay, Japan**

*Mengmeng Yang[1], Joji Ishizaka[2], Joaquim I. Goes[3], Hongzhen Tian[4], Elígio R. Maúre[5], Masataka Hayashi[6] (1.Graduate School of Environmental Studies, Nagoya University, Furo-cho, Chikusa-ku, Nagoya, Aichi, Japan., 2.Institute for Space-Earth Environmental Research (ISEE) Nagoya University Furo-cho, Chikusa-ku, Nagoya, Aichi, Japan., 3.Lamont-Doherty Earth Observatory, Marine Biology and Paleo Environment, Columbia University, 61 Route 9W - PO Box 1000, Palisades, NY 10964-8000, US., 4.School of Management and Economy, Tianjin Polytechnic University, Tianjin 300387, China., 5.Dept. of Research and Study, Northwest Pacific Region Environmental Cooperation Center, Toyama, Japan., 6.Science and Technology co., Ltd., 3-9-2, Koubai-cho, Showa, Nagoya, Aichi 466-0031, Japan.)

[ACG45-P08] **Discrimination of green *Noctiluca scintillans* in the upper Gulf of Thailand using remote sensing techniques**

*Jutarak Luang-on[1], Joji Ishizaka[2], Anukul Buranapratheprat[3], Jitraporn Phaksopa[4] (1.Graduate School of Environmental Studies, Nagoya University, 2.Institute for Space-Earth Environmental Research, Nagoya University, Japan, 3.Department of Aquatic Science, Faculty of Science, Burapha University, Thailand, 4.Department of Marine Science, Faculty of Fisheries, Kasetsart University, Thailand)

[ACG45-P09] **Monthly variability of Chlorophyll-a distribution in the Gulf of Thailand**

*Dudsadee Leenawarat[1], Anukul Buranapratheprat[2], Joji Ishizaka[3] (1.Graduate School of Environmental Studies, Nagoya University, Japan, 2.Department of Aquatic Science, Faculty of Science, Burapha University, Thailand, 3.Institute for Space-Earth Environmental Research, Nagoya University, Japan)

[ACG45-P10] AERONET-Ocean Color time series in Ariake Bay.

*yifei wu[1], Joji Ishizaka[2], Mengmeng Yang[1], Naoki Fujii[3], Masahiro Hori[4] (1. Graduate School of Environmental Studies, Nagoya University, 2. Institute for Space-Earth Environmental Research, Nagoya University, 3. Graduate School of Agriculture, Saga University, 4.EORC, JAXA)

[J] Poster | A (Atmospheric and Hydrospheric Sciences)：A-CG Complex & General

5:15 PM - 6:30 PM JST | 8:15 AM - 9:30 AM UTC | Poster Hall International Exhibition Hall8, Makuhari Messe_19

[A-CG45] Visible Remote Sensing of Hydrospheric Science and Its Application

convener:Joji Ishizaka(Institute for Space-Earth Environmental Research, Nagoya University), Mitsuhiro Toratani(School of Engineering, Tokai University), Yuji Sakuno(Graduate School of Engineering, Hiroshima University), Toru Hirawake(Faculty of Fisheries Sciences, Hokkaido University)

[ACG45-P01] About GCOM-C/SGLI Ocean Standard Products

*Kazunori Ogata[1] (1.Japan Aerospace Exploration Agency)

[ACG45-P02] Verification of GCOM-C/SGLI product in coastal area

*Joji Ishizaka[1] (1.Institute for Space-Earth Environmental Research, Nagoya University)

[ACG45-P03] Hyperspectral Radiometry towards Classification of Marine Phytoplankton Groups

*Takafumi Hirata[1], Robert J.W. Brewin[2], Girgio Dall'Olmo[2], Mariana Altenburg Soppa[3], Astrid Bracher[3] (1.Faculty of Environmental Earth Science, Hokkaido University, 2.Plymouth Marine Laboratory, 3.Alfred-Wegener Institute for Polar and Marine Research)

[ACG45-P04] Improvement of absorption-based primary production model for SGLI/GCOM-C

*Toru Hirawake[1], Takuhei Shiozaki[2], Hisatomo Waga[1], Koji Suzuki[1] (1.Hokkaido University, 2.JAMSTEC)

[ACG45-P05] Attempt to distinguish river water influencing concentration of chlorophyll *a* off Miho Peninsula

*Akihiko Tanaka[1], Kyoko Takashima[2], Gen Fukuda[2], Takaaki Katsumata[1], Hiroyuki Tan[1], Masato Niki[2], Daisuke Takahashi[2] (1.Liberal Arts Education Center, Shimizu Campus, Tokai University, 2.School of Marine Science and Technology, Tokai University)

[ACG45-P06] **Estimation of chlorophyll-a from RGB digital camera data collected in Ise-Mikawa Bay**

*Akiko N. Mizuno[1], Joji Ishizaka[1] (1.Institute for Space-Earth Environmental Research, Nagoya University)

[ACG45-P07] **Seasonal variability of MODIS chlorophyll-a and total suspended matter in the spring-neap tidal cycle in the Ariake Bay, Japan**

*Mengmeng Yang[1], Joji Ishizaka[2], Joaquim I. Goes[3], Hongzhen Tian[4], Elígio R. Maúre[5], Masataka Hayashi[6] (1.Graduate School of Environmental Studies, Nagoya University, Furo-cho, Chikusa-ku, Nagoya, Aichi, Japan., 2.Institute for Space-Earth Environmental Research (ISEE) Nagoya University Furo-cho, Chikusa-ku, Nagoya, Aichi, Japan., 3.Lamont-Doherty Earth Observatory, Marine Biology and Paleo Environment, Columbia University, 61 Route 9W - PO Box 1000, Palisades, NY 10964-8000, US., 4.School of Management and Economy, Tianjin Polytechnic University, Tianjin 300387, China., 5.Dept. of Research and Study, Northwest Pacific Region Environmental Cooperation Center, Toyama, Japan., 6.Science and Technology co., Ltd., 3-9-2, Koubai-cho, Showa, Nagoya, Aichi 466-0031, Japan.)

[ACG45-P08] **Discrimination of green *Noctiluca scintillans* in the upper Gulf of Thailand using remote sensing techniques**

*Jutarak Luang-on[1], Joji Ishizaka[2], Anukul Buranapratheprat[3], Jitraporn Phaksopa[4] (1.Graduate School of Environmental Studies, Nagoya University, 2.Institute for Space-Earth Environmental Research, Nagoya University, Japan, 3.Department of Aquatic Science, Faculty of Science, Burapha University, Thailand, 4.Department of Marine Science, Faculty of Fisheries, Kasetsart University, Thailand)

[ACG45-P09] **Monthly variability of Chlorophyll-a distribution in the Gulf of Thailand**

*Dudsadee Leenawarat[1], Anukul Buranapratheprat[2], Joji Ishizaka[3] (1.Graduate School of Environmental Studies, Nagoya University, Japan, 2.Department of Aquatic Science, Faculty of Science, Burapha University, Thailand, 3.Institute for Space-Earth Environmental Research, Nagoya University, Japan)

[ACG45-P10] AERONET-Ocean Color time series in Ariake Bay.

*yifei wu[1], Joji Ishizaka[2], Mengmeng Yang[1], Naoki Fujii[3], Masahiro Hori[4] (1. Graduate School of Environmental Studies, Nagoya University, 2. Institute for Space-Earth Environmental Research, Nagoya University, 3. Graduate School of Agriculture, Saga University, 4.EORC, JAXA)

[E] Oral | H (Human Geosciences)：H-DS Disaster geosciences

9:00 AM - 10:30 AM JST | 12:00 AM - 1:30 AM UTC | 304 3F

[H-DS09] Landslides and related phenomena

convener:Masahiro Chigira(Disaster Prevention Research Institute, Kyoto University), Gonghui Wang(Disaster Prevention Research Institute, Kyoto University), Fumitoshi Imaizumi(Faculty of Agriculture, Shizuoka University), Chairperson:Fumitoshi Imaizumi

9:00 AM - 9:15 AM JST | 12:00 AM - 12:15 AM UTC

[HDS09-01] Mechanical behavior modulated by shear surface morphology of simulated shear zone

*Yao Jiang[1], Gonghui Wang[2], Toshitaka Kamai[2] (1.Institute of Mountain Hazards and Environment, Chinese Academy of Sciences, China, 2.Research Center on Landslide, Disaster Prevention Research Institute, Kyoto University, Japan)

9:15 AM - 9:30 AM JST | 12:15 AM - 12:30 AM UTC

[HDS09-02] On the Pre-failure Shear Behavior of Clayey Soil

*Chengrui Chang[1], Gonghui Wang[1] (1.Disaster Prevention Research Institute, Kyoto University)

9:30 AM - 9:45 AM JST | 12:30 AM - 12:45 AM UTC

[HDS09-03] **GeoGuard: low-cost GNSS sensors for the continuous monitoring of landslides and structures**

*Andrea Gatti[1], Giulio Tagliaferro[1], Eugenio Realini[1], Stefano Caldera[1] (1.Geomatics Research & Development srl)

9:45 AM - 10:00 AM JST | 12:45 AM - 1:00 AM UTC

[HDS09-04] **Landslide Susceptibility Analysis in the Chenyulan River Watershed, Taiwan**

*Po-Tsun Yeh[1], Kuang-Tsung Chang[1] (1.National Chung Hsing University, Taiwan)

10:00 AM - 10:15 AM JST | 1:00 AM - 1:15 AM UTC

[HDS09-05] Investigating the Relationship Between Tree Height and Landslide Occurrence in the Ikawa Catchment, Central Japan

*Jamie Rhys Evans[1], Fumitoshi Imaizumi [1] (1.Faculty of Agriculture, Shizuoka University)

10:15 AM - 10:30 AM JST | 1:15 AM - 1:30 AM UTC

[HDS09-06] Landslides induced by the knickpoint migration in the southern and the eastern margins of the Tibetan Plateau.

*Masahiro Chigira[1], Ching-Ying Tsou[2], Siyuan Zhao[4], Xiong Wu[3] (1.Disaster Prevention Research Institute, Kyoto University, 2.Hirosaki University, 3.Souithwest Jiaotong University, 4.Graduate School of Science, Kyoto University)

[E] Oral | H (Human Geosciences)：H-DS Disaster geosciences

10:45 AM - 12:15 PM JST | 1:45 AM - 3:15 AM UTC | 304 3F

[H-DS09] Landslides and related phenomena

convener:Masahiro Chigira(Disaster Prevention Research Institute, Kyoto University), Gonghui Wang(Disaster Prevention Research Institute, Kyoto University), Fumitoshi Imaizumi(Faculty of Agriculture, Shizuoka University), Chairperson:Wang Gonghui, Issei Doi

10:45 AM - 11:15 AM JST | 1:45 AM - 2:15 AM UTC

[HDS09-07] Landslides caused by the 2018 Hokkaido Eastern Iburi Earthquake

★Invited Papers

*Shin-ichiro Hayashi[1], Nobutomo Osanai[1], Takashi Yamada[1], Shin'ya Katsura[1], Takahisa Furuichi[1], Seiji Yanai[2], Yasuharo Murakami[3], Tomoyoshi Miyazaki[4], Yuichiro Tanioka[1], Shigetaka Takiguchi[5], Mayumi Miyazaki[6] (1.Hokkaido University, 2.Ishikawa Prefectural University, 3.Civil Engineering Research Institute for Cold Region, PWRI, 4.Shin Engineering Consultant, Co., Ltd., 5.Ministry of Land, Infrastructure, Transport and Tourism, 6.Pasco Corporation)

11:15 AM - 11:45 AM JST | 2:15 AM - 2:45 AM UTC

[HDS09-08] On the coseismic landslides occurring on tephra slopes during the 2018 Hokkaido Eastern Iburi Earthquake

★Invited Papers

*Gonghui Wang[1], Gen Furuya[2] (1.Disaster Prevention Research Institute, Kyoto University, 2.Toyama Prefectural University)

11:45 AM - 12:00 PM JST | 2:45 AM - 3:00 AM UTC

[HDS09-09] Seismological and geotechnical surveys on the landslides induced by the 2018 Hokkaido Eastern Iburi earthquake

*Issei Doi[1], Hikaru Osawa[2], Sumio Matsuura[1] (1.Disaster Prevention Research Institute, Kyoto University, 2.Mountain Science Center, University of Tsukuba)

[E] Oral | H (Human Geosciences)：H-DS Disaster geosciences

1:45 PM - 3:15 PM JST | 4:45 AM - 6:15 AM UTC | 304 3F

[H-DS09] Landslides and related phenomena

convener:Masahiro Chigira(Disaster Prevention Research Institute, Kyoto University), Gonghui Wang(Disaster Prevention Research Institute, Kyoto University), Fumitoshi Imaizumi(Faculty of Agriculture, Shizuoka University), Chairperson:Fumitoshi Imaizumi, Chigira Masahiro

1:45 PM - 2:15 PM JST | 4:45 AM - 5:15 AM UTC

[HDS09-10] Initiation conditions of debris flows in Ohsawa landslide, Mt. Fuji

★Invited Papers

*Fumitoshi Imaizumi[1], Kazuki Yamamoto[1], Atsushi Ikeda[4], Okihiro Ohsaka[1], Hiroyuki Sugimoto[2], Satoru Suzuki[2], Shinichi Sato[2], Yoshiaki Kashiwabara[3], Naoki Nishimura[3] (1.Faculty of Agriculture, Shizuoka University, 2.Fuji Sabo Office, Ministry of Land, Infrastructure and Transport, 3.Asia Air Survey Co., Ltd., 4.Faculty of Life and Environmental Sciences, Tsukuba University)

2:15 PM - 2:30 PM JST | 5:15 AM - 5:30 AM UTC

[HDS09-11] The role of thrust faults with incohesive clayey fault materials to generate deep-seated gravitational slope deformations and catastrophic landslides in the Shimanto accretionary complex

*Noriyuki Arai[1], Masahiro Chigira[1] (1.Disaster Prevention Research Institute,Kyoto University)

2:30 PM - 2:45 PM JST | 5:30 AM - 5:45 AM UTC

[HDS09-12] Control effect of huge faults on the structure of surrounding regional rock mass in the whole mountain: implications for the distribution pattern of coseismic landslides

*Chao HUANG[1,2], Yusheng LI[1], Chunhao WU[3], Shujian YI[1,3], Kai LIU[1,4], Gonghui WANG[2] (1.State Key Laboratory of Geohazard Prevention and Geoenvironment Protection, Chengdu University of Technology, China, 2.Disaster Prevention Research Institute, Kyoto University, Japan, 3.Institute of Mountain Hazards and Environment, Chinese Academy of Sciences, China, 4.China Railway Eryuan Engineering Group CO. LTD, China)

[E] Poster | H (Human Geosciences)：H-DS Disaster geosciences

3:30 PM - 5:00 PM JST | 6:30 AM - 8:00 AM UTC | Poster Hall International Exhibition Hall8, Makuhari Messe_12

[H-DS09] Landslides and related phenomena

convener:Masahiro Chigira(Disaster Prevention Research Institute, Kyoto University), Gonghui Wang(Disaster Prevention Research Institute, Kyoto University), Fumitoshi Imaizumi(Faculty of Agriculture, Shizuoka University)

[HDS09-P01] **Fluidized landslides triggered by the liquefaction of subsurface volcanic deposits during the 2018 Iburi–Tobu earthquake, Hokkaido**

*Jun Kameda[1], Hiro Kamiya[2], Hirokazu Masumoto[1], Tomonori Morisaki[1], Toru Hiratsuka[2], Chisaki Inaoi (1.Department of Natural History Sciences, Graduate School of Science, Hokkaido University, 2.Department of Earth and Planetary Sciences, School of Science, Hokkaido University)

[HDS09-P02] A comparison between the acoustic signals and seismic signals generated during a dam-break test

★Invited Papers

*Zheng-yi Feng[1], Hao-yang Huang[1], Chia-Ming Chuang[1] (1.Department of Soil and Water Conservation, National Chung Hsing University, Taichung, Taiwan)

[HDS09-P03] Evaluation of factors of safety and landslide risk for a watershed by Scoops3D

*Zheng-yi Feng[1], Chia-Ming Chuang[1], Hao-yang Huang[1] (1.Department of Soil and Water Conservation, National Chung Hsing University, Taichung, Taiwan)

[HDS09-P04] **Fuzzy Clustering Algorithms for Establishing Landslide Susceptibility Map**

*Pei-hsun Tsai[1], Syuan-yi Wang[1], Jie-shin Cheng[1] (1.Chaoyang University of Technology)

[HDS09-P05] **A Study on Landslides and Debris Flows Susceptibility Mapping Using Unmanned Aerial Vehicles**

*Sheng-Jia Liu[1] (1.qwepoi13@gmail.com)

[HDS09-P06] Largescale landslide induced by AD1586 Tensho-Earthquake in Gifu Prefecture, central Japan

*Takahiro Kurimoto[1], Yoshihiko Kariya[2], Kuniyasu Mokudai[3], Ryuji Yamada[4], Takashi Kimura[4] (1.Undergraduate Senshu University, 2.Department of Geography, Senshu University, 3.Japan Geoservice Incorporated, 4.National Research Institute for Earth Science and Disaster Resilience)

[HDS09-P07] Failure Probability of Lushan Landslide, Taiwan

*Wei-Ting Lin[1], Kuang-Tsung Chang[1] (1.National Chung Hsing University)

[HDS09-P08] Interpretation of landslide surface deformation in Kali Gandaki River watershed, Nepal using ALOS-2/PALSAR-2 InSAR image

*Hiroshi, P. Sato[1] (1.College of Humanities and Sciences, Nihon University)

[HDS09-P09] A depth-integrated model for granular flows on the transition of different bed conditions

*Ling-Yi Hsu[1], Chi-Yao Hung[1] (1.National Chung Hsing University)

[HDS09-P10] A viscous granular flow experiment with new refractive index matching material

*Tsai-Jung Lin[1], Chi-Yao Hung[1] (1.National Chung Hsing University)

[HDS09-P11] Sandbox experiments of submarine landslide caused by water film in low permeability layer

*Shogo Kawakita[1], Daisuke Asahina[2], Keiji Kitajima[3], Mitsukazu Nakanishi[3] (1.Graduate School of Science & Technology, Nihon Univ., 2.National Institute of Advanced Industrial Science and Technology, 3.College of Science & Technology, Nihon Univ.)

[HDS09-P12] **Study on Creep Properties of Sand and Cemented Sand**

*JIN-YI YU[1], KUANG-TSUNG CHANG[1] (1.National Chung Hsing University)

[HDS09-P13] The effects of seepage force and the Poisson’s ratio on slope stability

*Hirokazu Fukui[1], Tomomi Terajima[2] (1.Graduate school of Science, Kyoto University, 2.Disaster Prevention Research Institute, Kyoto University)

[HDS09-P14] Study on the factors of seepage erosion

*Szu-Wei Fu[1], Kuang-Tsung Chang[1] (1.National Chung Hsing University)

[HDS09-P15] Deformation of slope models with different orientations of weak planes

*taeyuan tseng[1], Kuang-Tsung Chang[1] (1.National Chung Hsing University)

[E] Poster | H (Human Geosciences)：H-DS Disaster geosciences

5:15 PM - 6:30 PM JST | 8:15 AM - 9:30 AM UTC | Poster Hall International Exhibition Hall8, Makuhari Messe_20

[H-DS09] Landslides and related phenomena

convener:Masahiro Chigira(Disaster Prevention Research Institute, Kyoto University), Gonghui Wang(Disaster Prevention Research Institute, Kyoto University), Fumitoshi Imaizumi(Faculty of Agriculture, Shizuoka University)

[HDS09-P01] **Fluidized landslides triggered by the liquefaction of subsurface volcanic deposits during the 2018 Iburi–Tobu earthquake, Hokkaido**

*Jun Kameda[1], Hiro Kamiya[2], Hirokazu Masumoto[1], Tomonori Morisaki[1], Toru Hiratsuka[2], Chisaki Inaoi (1.Department of Natural History Sciences, Graduate School of Science, Hokkaido University, 2.Department of Earth and Planetary Sciences, School of Science, Hokkaido University)

[HDS09-P02] A comparison between the acoustic signals and seismic signals generated during a dam-break test

★Invited Papers

*Zheng-yi Feng[1], Hao-yang Huang[1], Chia-Ming Chuang[1] (1.Department of Soil and Water Conservation, National Chung Hsing University, Taichung, Taiwan)

[HDS09-P03] Evaluation of factors of safety and landslide risk for a watershed by Scoops3D

*Zheng-yi Feng[1], Chia-Ming Chuang[1], Hao-yang Huang[1] (1.Department of Soil and Water Conservation, National Chung Hsing University, Taichung, Taiwan)

[HDS09-P04] **Fuzzy Clustering Algorithms for Establishing Landslide Susceptibility Map**

*Pei-hsun Tsai[1], Syuan-yi Wang[1], Jie-shin Cheng[1] (1.Chaoyang University of Technology)

[HDS09-P05] **A Study on Landslides and Debris Flows Susceptibility Mapping Using Unmanned Aerial Vehicles**

*Sheng-Jia Liu[1] (1.qwepoi13@gmail.com)

[HDS09-P06] Largescale landslide induced by AD1586 Tensho-Earthquake in Gifu Prefecture, central Japan

*Takahiro Kurimoto[1], Yoshihiko Kariya[2], Kuniyasu Mokudai[3], Ryuji Yamada[4], Takashi Kimura[4] (1.Undergraduate Senshu University, 2.Department of Geography, Senshu University, 3.Japan Geoservice Incorporated, 4.National Research Institute for Earth Science and Disaster Resilience)

[HDS09-P07] Failure Probability of Lushan Landslide, Taiwan

*Wei-Ting Lin[1], Kuang-Tsung Chang[1] (1.National Chung Hsing University)

[HDS09-P08] Interpretation of landslide surface deformation in Kali Gandaki River watershed, Nepal using ALOS-2/PALSAR-2 InSAR image

*Hiroshi, P. Sato[1] (1.College of Humanities and Sciences, Nihon University)

[HDS09-P09] A depth-integrated model for granular flows on the transition of different bed conditions

*Ling-Yi Hsu[1], Chi-Yao Hung[1] (1.National Chung Hsing University)

[HDS09-P10] A viscous granular flow experiment with new refractive index matching material

*Tsai-Jung Lin[1], Chi-Yao Hung[1] (1.National Chung Hsing University)

[HDS09-P11] Sandbox experiments of submarine landslide caused by water film in low permeability layer

*Shogo Kawakita[1], Daisuke Asahina[2], Keiji Kitajima[3], Mitsukazu Nakanishi[3] (1.Graduate School of Science & Technology, Nihon Univ., 2.National Institute of Advanced Industrial Science and Technology, 3.College of Science & Technology, Nihon Univ.)

[HDS09-P12] **Study on Creep Properties of Sand and Cemented Sand**

*JIN-YI YU[1], KUANG-TSUNG CHANG[1] (1.National Chung Hsing University)

[HDS09-P13] The effects of seepage force and the Poisson’s ratio on slope stability

*Hirokazu Fukui[1], Tomomi Terajima[2] (1.Graduate school of Science, Kyoto University, 2.Disaster Prevention Research Institute, Kyoto University)

[HDS09-P14] Study on the factors of seepage erosion

*Szu-Wei Fu[1], Kuang-Tsung Chang[1] (1.National Chung Hsing University)

[HDS09-P15] Deformation of slope models with different orientations of weak planes

*taeyuan tseng[1], Kuang-Tsung Chang[1] (1.National Chung Hsing University)

[J] Poster | H (Human Geosciences)：H-DS Disaster geosciences

1:45 PM - 3:15 PM JST | 4:45 AM - 6:15 AM UTC | Poster Hall International Exhibition Hall8, Makuhari Messe_4

[H-DS13] Tsunami and Tsunami Forecast

convener:Naotaka YAMAMOTO CHIKASADA(National Research Institute for Earth Science and Disaster Resilience), Hiroaki Tsushima(Japan Meteorological Agency), Tatsuya Kubota(National Research Institute for Earth Science and Disaster Resilience)

[HDS13-P01] Possible submarine landslides as sources of the 2018 Sulawesi tsunami

*Kenji Nakata[1], Akio Katsumata[1], Abdul Muhari[2] (1.Meteorological Research Institute, Japan Meteorological Agency, 2.Ministry of Marine Affairs and Fisheries, Indonesia)

[HDS13-P02] Tsunami Data Assimilation of the 2015 Torishima Earthquake

*Yuchen Wang[1], Kenji Satake[1], Osamu Sandanbata[1], Takuto Maeda[2] (1.Earthquake Research Institute, University of Tokyo, 2.Graduate School of Science and Technology, Hirosaki University)

[HDS13-P03] Method for real-time estimation of tsunami sources using a network of dense ocean bottom pressure sensors

*Mayu Inoue[1], Yuichiro Tanioka[1], Yusuke Yamanaka[2] (1.Hokkaido University, 2.The University of Tokyo)

[HDS13-P04] Application of AI Technology for Tsunami Prediction by Oceanographic Radar

*hiromu yokosu[1], Yoshihito - Tanaka[1], Kenji - hayashi[2], Kentarou - Uehara[2] (1.Chubu Electric Power Co., Inc., 2.Japan Weather Association)

[HDS13-P05] Development of the Tsunami Prediction System using fault plane solution of W-phase inversion

*Seolhan You[1], Mikyung Choi[1], Sun-Cheon Park[1], Hye-Won Lee[1], Duk Kee Lee[1] (1.Korea Meteorological Administration)

[HDS13-P06] Can we detect tsunami magnetic signals at on-land observatories prior to tsunami arrivals? : From the perspective of numerical experiments

*Takuto Minami[1], Tungcheng Ho[1], Zhiheng Lin[2], Hiroaki TOH[2] (1.Earthquake Research Institute,The University of Tokyo, 2.Graduate School of Science, Kyoto University)

[HDS13-P07] Probability of Tsunami Inundation Estimated from Tsunami Database and G-R law

*Toru Takeda[1], Toshitaka Baba[1], Tsuneo Ohsumi[2], Hiroyuki Fujiwara[2] (1.Tokushima Univ, 2.NIED)

[HDS13-P08] The Detection of Tsunami Propagation Path by Using Sensitivity Kernel Distribution

*Norihiko Hashimoto[1], Kyosuke Okamoto[2], Seiji Tsuno[3] (1.ITOCHU Techno-Solutions Corporation, 2.National Institute of Advanced Industrial Science and Technology, 3.Railway Technical Research Institute)

[HDS13-P09] Estimation of local seismic waves and rapid magnitudes for ‘slow tsunami earthquakes’ based on moment rate spectrum

*Takahito Nishimiya[1], Akio Katsumata[1] (1.Meteorological Research Institute, Japan Meteorological Agency)

[HDS13-P10] Development of tsunami simulator TNS and release of version 1.0

*Takayuki Miyoshi[1], Wataru Suzuki[1], Naotaka YAMAMOTO CHIKASADA[1], Shin Aoi[1], Sho Akagi[2], Toshihiko Hayakawa[2] (1.National Research Institute for Earth Science and Disaster Resilience, 2.Mitsubishi Space Software Co.,Ltd.)

[HDS13-P11] A Study on Tsunami Inundation Simulation for the Nankai Trough Earthquake for Osaka City

*Kaoru Kawaji[1], Seiji Tsuno[2] (1.ITOCHU Techno-Solutions Corporation, 2.Railway Technical Research Institute)

[HDS13-P12] Database construction of Tsunami inundation simulation for large subduction earthquakes

*Mariko Korenaga[1], Seiji Tsuno[2], Kaoru Kawaji[1] (1.ITOCHU Techno-Solutions Corporation, 2.Railway Technical Research Institute)

[HDS13-P13] Sediment Transport Modeling due to Tsunamis caused by the Nankai great earthquakes

*Takuya Saito[1], Kei Yamashita[2], Toshitaka Baba[1] (1.Tokushima Univ., 2.Tohoku Univ.)

[HDS13-P14] Tsunami model of the 2011 Tohoku Earthquake reproducing the wave gauge record offshore the Fukushima Daiichi NPP

*Toshimichi Kaneto[1], Ayumi Nishi[2], Tadashi Annaka[2] (1.Tokyo Electric Power Company Holdings,Inc, 2.Tokyo Electric Power Services Co,Ltd)

[HDS13-P15] Development of tsunami fragility curves on railway structures based on the 2011 off the Pacific coast of Tohoku earthquake

*Teppei Ono[1], Seiji Tsuno[2], Yuko Sato[2], Marioko Korenaga[1] (1.ITOCHU Techno-Solutions Corporation, 2.Railway Technical Research Institute)

[HDS13-P16] The characteristic of the cause of death in each city in Miyagi prefecture during the Great East Japan Earthquake

*Shuji SETO[1], Fumihiko IMAMURA[1] (1.IRIDeS, Tohoku University)

[HDS13-P17] The reflective south going current, accompanied by the third wave of Tsunammi at Iioka , Asahi City , Chiba Prefecture in 2011.

*Mitsuo Harukawa[1], Noboru Hashimoto[1], Fumio Ooshima[1] (1.The Group of Recording for Tsunami Damage of Asahi City in 2011)

[J] Poster | H (Human Geosciences)：H-DS Disaster geosciences

5:15 PM - 6:30 PM JST | 8:15 AM - 9:30 AM UTC | Poster Hall International Exhibition Hall8, Makuhari Messe_21

[H-DS13] Tsunami and Tsunami Forecast

convener:Naotaka YAMAMOTO CHIKASADA(National Research Institute for Earth Science and Disaster Resilience), Hiroaki Tsushima(Japan Meteorological Agency), Tatsuya Kubota(National Research Institute for Earth Science and Disaster Resilience)

[HDS13-P01] Possible submarine landslides as sources of the 2018 Sulawesi tsunami

*Kenji Nakata[1], Akio Katsumata[1], Abdul Muhari[2] (1.Meteorological Research Institute, Japan Meteorological Agency, 2.Ministry of Marine Affairs and Fisheries, Indonesia)

[HDS13-P02] Tsunami Data Assimilation of the 2015 Torishima Earthquake

*Yuchen Wang[1], Kenji Satake[1], Osamu Sandanbata[1], Takuto Maeda[2] (1.Earthquake Research Institute, University of Tokyo, 2.Graduate School of Science and Technology, Hirosaki University)

[HDS13-P03] Method for real-time estimation of tsunami sources using a network of dense ocean bottom pressure sensors

*Mayu Inoue[1], Yuichiro Tanioka[1], Yusuke Yamanaka[2] (1.Hokkaido University, 2.The University of Tokyo)

[HDS13-P04] Application of AI Technology for Tsunami Prediction by Oceanographic Radar

*hiromu yokosu[1], Yoshihito - Tanaka[1], Kenji - hayashi[2], Kentarou - Uehara[2] (1.Chubu Electric Power Co., Inc., 2.Japan Weather Association)

[HDS13-P05] Development of the Tsunami Prediction System using fault plane solution of W-phase inversion

*Seolhan You[1], Mikyung Choi[1], Sun-Cheon Park[1], Hye-Won Lee[1], Duk Kee Lee[1] (1.Korea Meteorological Administration)

[HDS13-P06] Can we detect tsunami magnetic signals at on-land observatories prior to tsunami arrivals? : From the perspective of numerical experiments

*Takuto Minami[1], Tungcheng Ho[1], Zhiheng Lin[2], Hiroaki TOH[2] (1.Earthquake Research Institute,The University of Tokyo, 2.Graduate School of Science, Kyoto University)

[HDS13-P07] Probability of Tsunami Inundation Estimated from Tsunami Database and G-R law

*Toru Takeda[1], Toshitaka Baba[1], Tsuneo Ohsumi[2], Hiroyuki Fujiwara[2] (1.Tokushima Univ, 2.NIED)

[HDS13-P08] The Detection of Tsunami Propagation Path by Using Sensitivity Kernel Distribution

*Norihiko Hashimoto[1], Kyosuke Okamoto[2], Seiji Tsuno[3] (1.ITOCHU Techno-Solutions Corporation, 2.National Institute of Advanced Industrial Science and Technology, 3.Railway Technical Research Institute)

[HDS13-P09] Estimation of local seismic waves and rapid magnitudes for ‘slow tsunami earthquakes’ based on moment rate spectrum

*Takahito Nishimiya[1], Akio Katsumata[1] (1.Meteorological Research Institute, Japan Meteorological Agency)

[HDS13-P10] Development of tsunami simulator TNS and release of version 1.0

*Takayuki Miyoshi[1], Wataru Suzuki[1], Naotaka YAMAMOTO CHIKASADA[1], Shin Aoi[1], Sho Akagi[2], Toshihiko Hayakawa[2] (1.National Research Institute for Earth Science and Disaster Resilience, 2.Mitsubishi Space Software Co.,Ltd.)

[HDS13-P11] A Study on Tsunami Inundation Simulation for the Nankai Trough Earthquake for Osaka City

*Kaoru Kawaji[1], Seiji Tsuno[2] (1.ITOCHU Techno-Solutions Corporation, 2.Railway Technical Research Institute)

[HDS13-P12] Database construction of Tsunami inundation simulation for large subduction earthquakes

*Mariko Korenaga[1], Seiji Tsuno[2], Kaoru Kawaji[1] (1.ITOCHU Techno-Solutions Corporation, 2.Railway Technical Research Institute)

[HDS13-P13] Sediment Transport Modeling due to Tsunamis caused by the Nankai great earthquakes

*Takuya Saito[1], Kei Yamashita[2], Toshitaka Baba[1] (1.Tokushima Univ., 2.Tohoku Univ.)

[HDS13-P14] Tsunami model of the 2011 Tohoku Earthquake reproducing the wave gauge record offshore the Fukushima Daiichi NPP

*Toshimichi Kaneto[1], Ayumi Nishi[2], Tadashi Annaka[2] (1.Tokyo Electric Power Company Holdings,Inc, 2.Tokyo Electric Power Services Co,Ltd)

[HDS13-P15] Development of tsunami fragility curves on railway structures based on the 2011 off the Pacific coast of Tohoku earthquake

*Teppei Ono[1], Seiji Tsuno[2], Yuko Sato[2], Marioko Korenaga[1] (1.ITOCHU Techno-Solutions Corporation, 2.Railway Technical Research Institute)

[HDS13-P16] The characteristic of the cause of death in each city in Miyagi prefecture during the Great East Japan Earthquake

*Shuji SETO[1], Fumihiko IMAMURA[1] (1.IRIDeS, Tohoku University)

[HDS13-P17] The reflective south going current, accompanied by the third wave of Tsunammi at Iioka , Asahi City , Chiba Prefecture in 2011.

*Mitsuo Harukawa[1], Noboru Hashimoto[1], Fumio Ooshima[1] (1.The Group of Recording for Tsunami Damage of Asahi City in 2011)

[J] Oral | H (Human Geosciences)：H-DS Disaster geosciences

3:30 PM - 5:00 PM JST | 6:30 AM - 8:00 AM UTC | Convention Hall B 2F

[H-DS13] Tsunami and Tsunami Forecast

convener:Naotaka YAMAMOTO CHIKASADA(National Research Institute for Earth Science and Disaster Resilience), Hiroaki Tsushima(Japan Meteorological Agency), Tatsuya Kubota(National Research Institute for Earth Science and Disaster Resilience), Chairperson:Osamu Sandanbata, Tatsuya Kubota

3:30 PM - 3:45 PM JST | 6:30 AM - 6:45 AM UTC

[HDS13-01] Sensibility analysis for the inundation tsunami height due to 2018 Sulawesi earthquake and tsunami

★Invited Papers

*Taro Arikawa[1], Abdul Muhari[3], Shota Takeda[1], Anawat Suppasri[2], Fumihiko Imamura[2] (1.Chuo University, 2.IRIDES, Tohoku University, 3.Ministry of Marine Affairs and Fisheries, Indonesia)

3:45 PM - 4:00 PM JST | 6:45 AM - 7:00 AM UTC

[HDS13-02] Tsunami Source of the 2018 Sulawesi Earthquake Estimated from Tsunami and InSAR Data

*Tungcheng Ho[1], Kenji Satake[1], Shingo Watada[1], Ray Y Chuang[2], Chih-Heng Lu[2] (1.Earthquake Research Institute,The University of Tokyo, 2.Department of Geography, National Taiwan University)

4:00 PM - 4:15 PM JST | 7:00 AM - 7:15 AM UTC

[HDS13-03] **Source Models of the Two September and December 2018 Indonesia Tsunamis Based on Spectral Analyses and Numerical Modeling**

*Mohammad Heidarzadeh[1], Abdul Muhari[2], Tomoya HARADA[3], Takeo Ishibe[4], Antonius Wijanarto[5] (1.Brunel University London, 2.Ministry of Marine Affairs and Fisheries, Jakarta 10110, Indonesia, 3.Earthquake Research Institute, The University of Tokyo, Japan, 4.Association for the Development of Earthquake Prediction, Tokyo, 101-0064, Japan, 5.Badan Informasi Geospasial, Cibinong, Indonesia)

4:15 PM - 4:30 PM JST | 7:15 AM - 7:30 AM UTC

[HDS13-04] Abrupt Large Uplift Caused by Volcanic Tsunami Earthquakes near the Kermadec Islands, New Zealand

*Osamu Sandanbata[1], Shingo Watada[1], Kenji Satake[1] (1.Earthquake Research Institute, the University of Tokyo)

4:30 PM - 4:45 PM JST | 7:30 AM - 7:45 AM UTC

[HDS13-05] **Adaptive tsunami waveform inversion for estimating coseismic vertical displacements and slip distribution**

*Iyan E. Mulia[1], Aditya Riadi Gusman[2], M. Jakir Hossen[3], Kenji Satake[1] (1.Earthquake Research Institute, The University of Tokyo, 2.GNS Science, 3.BRAC University)

4:45 PM - 5:00 PM JST | 7:45 AM - 8:00 AM UTC

[HDS13-06] Real-time tsunami prediction in a coastal zone, using a superposition of Green’s function

*Seiji Tsuno[1], Norihiko Hashimoto[2] (1.Railway Technical Research Institute, 2.ITOCHU Techno-Solutions Corporation)

[J] Poster | H (Human Geosciences)：H-RE Resource and Engineering Geology

1:45 PM - 3:15 PM JST | 4:45 AM - 6:15 AM UTC | Poster Hall International Exhibition Hall8, Makuhari Messe_5

[H-RE17] Application of earth science data towards the renewable energy field

convener:Hideaki Ohtake(National Institute of Advanced Industrial Science and Technology), Fumichika Uno(National Institute of Advanced Industrial Science and Technology), Teruhisa Shimada(Graduate School of Science and Technology, Hirosaki University), Daisuke Nohara(Central Research Institute of Electric Power Industry)

[HRE17-P01] Evaluation of spring, groundwater and stream water quality for use as a cooling heat source at Iwaki volcano

*Seiichiro Ioka[1], Kazuyoshi Asai[2], Kazumi Asai[2] (1.Institute of Regional Innovation, Hirosaki University, 2.Geo Science Laboratory)

[HRE17-P02] Characteristics of the confined groundwater based on the monitoring results in the western part of Osaka area: For thermal utilization of groundwater

*Hiroko Ito[1], Naoko Kitada[1], Tomoo Echigo[1], Teruyuki Fujiwara[1] (1.Geo-Research Institute)

[HRE17-P03] Predictability of Wind Power Ramp Events based on Dynamical and Statistical Ensemble Prediction

*Daisuke Nohara[1], Takeshi Watanabe[1], Masamichi Ohba[1], Shinji Kadokura[1] (1.Central Research Institute of Electric Power Industry)

[HRE17-P04] Offshore wind resource in the vicinity of Cape Erimo

*Teruhisa Shimada[1] (1.Graduate School of Science and Technology, Hirosaki University)

[HRE17-P05] An Efficient Method for Estimating the Surface Solar Irradiance Based on Satellite-Observed Scattered Solar Radiation

*Keiichi Nishizawa[1] (1.Central Research Institute of Electric Power Industry)

[HRE17-P06] Advance detection method of large forecast error on surface solar radiation considering atmospheric circulation patterns

*Fumichika Uno[1,3], Mio Matsueda[2], Takashi oozeki[1], Hideaki Ohtake[1,3], Yoshinori Yamada[3] (1.National Institute of Advanced Industrial Science and Technology, 2.University of Tsukuba, 3.Meteorological Research Institute)

[J] Poster | H (Human Geosciences)：H-RE Resource and Engineering Geology

5:15 PM - 6:30 PM JST | 8:15 AM - 9:30 AM UTC | Poster Hall International Exhibition Hall8, Makuhari Messe_22

[H-RE17] Application of earth science data towards the renewable energy field

convener:Hideaki Ohtake(National Institute of Advanced Industrial Science and Technology), Fumichika Uno(National Institute of Advanced Industrial Science and Technology), Teruhisa Shimada(Graduate School of Science and Technology, Hirosaki University), Daisuke Nohara(Central Research Institute of Electric Power Industry)

[HRE17-P01] Evaluation of spring, groundwater and stream water quality for use as a cooling heat source at Iwaki volcano

*Seiichiro Ioka[1], Kazuyoshi Asai[2], Kazumi Asai[2] (1.Institute of Regional Innovation, Hirosaki University, 2.Geo Science Laboratory)

[HRE17-P02] Characteristics of the confined groundwater based on the monitoring results in the western part of Osaka area: For thermal utilization of groundwater

*Hiroko Ito[1], Naoko Kitada[1], Tomoo Echigo[1], Teruyuki Fujiwara[1] (1.Geo-Research Institute)

[HRE17-P03] Predictability of Wind Power Ramp Events based on Dynamical and Statistical Ensemble Prediction

*Daisuke Nohara[1], Takeshi Watanabe[1], Masamichi Ohba[1], Shinji Kadokura[1] (1.Central Research Institute of Electric Power Industry)

[HRE17-P04] Offshore wind resource in the vicinity of Cape Erimo

*Teruhisa Shimada[1] (1.Graduate School of Science and Technology, Hirosaki University)

[HRE17-P05] An Efficient Method for Estimating the Surface Solar Irradiance Based on Satellite-Observed Scattered Solar Radiation

*Keiichi Nishizawa[1] (1.Central Research Institute of Electric Power Industry)

[HRE17-P06] Advance detection method of large forecast error on surface solar radiation considering atmospheric circulation patterns

*Fumichika Uno[1,3], Mio Matsueda[2], Takashi oozeki[1], Hideaki Ohtake[1,3], Yoshinori Yamada[3] (1.National Institute of Advanced Industrial Science and Technology, 2.University of Tsukuba, 3.Meteorological Research Institute)

[J] Oral | H (Human Geosciences)：H-RE Resource and Engineering Geology

3:30 PM - 5:00 PM JST | 6:30 AM - 8:00 AM UTC | 301B 3F

[H-RE17] Application of earth science data towards the renewable energy field

convener:Hideaki Ohtake(National Institute of Advanced Industrial Science and Technology), Fumichika Uno(National Institute of Advanced Industrial Science and Technology), Teruhisa Shimada(Graduate School of Science and Technology, Hirosaki University), Daisuke Nohara(Central Research Institute of Electric Power Industry), Chairperson:Hideaki Ohtake(National Institute of Advanced Industrial Science and Technology (AIST))

3:30 PM - 3:55 PM JST | 6:30 AM - 6:55 AM UTC

[HRE17-01] Application of geological dara to ground source heat pump systems with special reference to thermal conductivity of geological materials

★Invited Papers

*Masakatsu SASADA[1] (1.Geo-Heat Promotion Association of Japan)

3:55 PM - 4:10 PM JST | 6:55 AM - 7:10 AM UTC

[HRE17-02] Use of groundwater in the Nishi-Osaka Area and its activities.

*Naoko Kitada[1], Hiroko Ito[1], Tomoo Echigo[1], Teruyuki Fujiwara[1], Makoto Nishigaki[2] (1.Geo-Research Institute, 2.Okayama University)

4:10 PM - 4:25 PM JST | 7:10 AM - 7:25 AM UTC

[HRE17-03] Improvement of prediction of wind power ramp by using monitoring data

*Shinji Kadokura[1], Daisuke Nohara[1], Masamichi Ohba[1], Atsushi Hashimoto[1], Keisuke Nakao[1], Yasuo Hattori[1], Takeshi Watanabe[1], Hiromaru Hirakuchi[1] (1.Central Research Institute of Electric Power Industry)

4:25 PM - 4:40 PM JST | 7:25 AM - 7:40 AM UTC

[HRE17-04] A study of the use of meteorological data for energy management

*Hideaki Ohtake[1], Takashi Oozeki[1], Junichi Imura[2] (1.National Institute of Advanced Industrial Science and Technology, 2.Tokyo institute of technology)

[E] Oral | H (Human Geosciences)：H-TT Technology & Techniques

9:00 AM - 10:30 AM JST | 12:00 AM - 1:30 AM UTC | 302 3F

[H-TT18] Development and application of environmental traceability methods

convener:Ichiro Tayasu(Research Institute for Humanity and Nature), Nobuhito Ohte(Department of Social Informatics, Graduate School of Informatics, Kyoto University), Gabriel J Bowen(University of Utah), Chairperson:Nobuhito Ohte(Kyoto University)

9:00 AM - 9:15 AM JST | 12:00 AM - 12:15 AM UTC

[HTT18-01] Environmental traceability methodology by multi-isoscapes

*Ichiro Tayasu[1], Lei Fujiyoshi[1], Shiho Yabusaki[1], Ki-Cheol Shin[1], Takanori Nakano[1], Makoto Taniguchi[1] (1.Research Institute for Humanity and Nature)

9:15 AM - 9:45 AM JST | 12:15 AM - 12:45 AM UTC

[HTT18-02] Exploring physical and biological connections using isoscapes

★Invited Papers

*Gabriel J Bowen[1] (1.University of Utah)

9:45 AM - 10:00 AM JST | 12:45 AM - 1:00 AM UTC

[HTT18-03] Spatial and temporal variations in stable isotopes and soluble ions on high mountain snow surface of Mt. Tateyama, Toyama Prefecture, Japan

*Nozomu Takeuchi[1], Ryo Sugiyama[1] (1.Chiba University)

10:00 AM - 10:15 AM JST | 1:00 AM - 1:15 AM UTC

[HTT18-04] Using Sr isotopes to determine the contribution of volcanic ash to Sr and Ca in stream waters in a chert watershed.

*Masami Koshikawa[1], Mirai Watanabe[1], Tomoyoshi Murata[1], Takejiro Takamatsu[1], Shingo Miura[1], Ki-Cheol Shin[2], Takanori Nakano[2] (1.National Institute for Environmental Studies, 2.Research Institute for Humanity and Nature)

10:15 AM - 10:30 AM JST | 1:15 AM - 1:30 AM UTC

[HTT18-05] Influences of soil dust, sea salt and anthropogenic activities on ionic and Sr isotopic compositions of wet deposition in Iran

*Yoriko Yokoo[1], Kosuke Asai[1], Sae Horii[1], Ryo Anma[2], Shiva Mehrabani[3], KiCheol Shin[4] (1.Faculty of Science and Engineering, Doshisha University, 2.Tokushima University, 3.Kurdistan University, 4.RIHN)

[E] Oral | H (Human Geosciences)：H-TT Technology & Techniques

10:45 AM - 12:15 PM JST | 1:45 AM - 3:15 AM UTC | 302 3F

[H-TT18] Development and application of environmental traceability methods

convener:Ichiro Tayasu(Research Institute for Humanity and Nature), Nobuhito Ohte(Department of Social Informatics, Graduate School of Informatics, Kyoto University), Gabriel J Bowen(University of Utah), Chairperson:Gabriel Bowen(The University of Utah)

10:45 AM - 11:00 AM JST | 1:45 AM - 2:00 AM UTC

[HTT18-06] Long-term increasing trend of line-conditioned excess in groundwater

*Masanori Katsuyama[1] (1.Graduate School of Agriculture, Kyoto University)

11:00 AM - 11:15 AM JST | 2:00 AM - 2:15 AM UTC

[HTT18-07] Geochemistry of river water in the Okayama and Tottori Prefectures, Japan

*Katsuyuki Yamashita[1], Takahiro Kamei[1], Yuga Kishimoto[1], Masahiko Mori[1], Aya Ooi[2], Ayaka Onishi[2], Yoko Kurihara[2], Hitoshi CHIBA[1], Takanori Nakano[3], Ki-Cheol Shin[4] (1.Graduate School of Natural Science and Technology, Okayama University, 2.Faculty of Science, Okayama University, 3.Ono City, 4.Research Institute for Humanity and Nature)

11:15 AM - 11:30 AM JST | 2:15 AM - 2:30 AM UTC

[HTT18-08] Study on groundwater flow system at Oshino Village in Yamanashi Prefecture – Report 5. Estimation of the residence time in spring water and groundwater at Oshino Village.

*Shiho Yabusaki[1], Makoto Taniguchi[1], Ichiro Tayasu[1], Tomoya Akimichi[1], Noboru Ohomori[2], Ken Gotou[2], Souichirou Watanabe[2], Hitoshi Watanabe[2] (1.Research Institute for Humanity and Nature, 2.Oshino Village)

11:30 AM - 11:45 AM JST | 2:30 AM - 2:45 AM UTC

[HTT18-09] The hydrogen and oxygen isotopic compositions of water in the Chikusa River

*Ken'ichi Ohkushi[1], Shiho Yabusaki[2], Ichiro Tayasu[2], Lei Fujiyoshi[2], Takanori Nakano[2], Ki-Cheol Shin[2], Tadashi Yokoyama[3], Hiromune Mitsuhashi[4], Masayuki Itoh[1], Kazuki Yasugi[1] (1.Kobe University, 2.The Research Institute for Humanity and Nature, 3.Ako School for Students with Special Ne, 4.University of Hyogo)

11:45 AM - 12:00 PM JST | 2:45 AM - 3:00 AM UTC

[HTT18-10] Dynamics of sulfate and nitrate inferred from stable isotope techniques in Chikusa river watershed, Hyogo Prefecture

*Lei Fujiyoshi[1], Ichiro Tayasu[1], Shiho Yabusaki[1], Takashi F Haraguchi[1], Chikage Yoshimizu[1], Ken'ichi Ohkushi[2], Fumiko Furukawa[2], Masayuki Itoh[2], Yudai Yamamoto[3], Tadashi Yokoyama[4], Hiromune Mitsuhashi[5] (1.The Research Institute for Humanity and Nature, 2.Kobe University, 3.Nagoya University, 4.Hyogo prefectural Ako School for Students with Special Needs, 5.University of Hyogo)

12:00 PM - 12:15 PM JST | 3:00 AM - 3:15 AM UTC

[HTT18-11] Chemistry and sulfur and oxygen isotope ratios of sulfate ion of water soluble component of suspended particulate matter at Okayama city.

*Hitoshi CHIBA[1], Tsubasa Yamamoto[1] (1.Graduate School of Natural Science and Technology, Okayama University)

[E] Oral | H (Human Geosciences)：H-TT Technology & Techniques

1:45 PM - 3:15 PM JST | 4:45 AM - 6:15 AM UTC | 302 3F

[H-TT18] Development and application of environmental traceability methods

convener:Ichiro Tayasu(Research Institute for Humanity and Nature), Nobuhito Ohte(Department of Social Informatics, Graduate School of Informatics, Kyoto University), Gabriel J Bowen(University of Utah), Chairperson:Ichiro Tayasu(Research Institute for Humanity and Nature)

1:45 PM - 2:00 PM JST | 4:45 AM - 5:00 AM UTC

[HTT18-12] **Do mountain-climbing mammals protect plants from global warming by their vertical seed dispersal?**

*Shoji NAOE[1], Ichiro Tayasu[2] (1.Forestry and Forest Products Research Institute, Forest Research and Management Organization, 2.Research Institute for Humanity and Nature)

2:00 PM - 2:15 PM JST | 5:00 AM - 5:15 AM UTC

[HTT18-13] Spatial distribution of nitrogen stable isotope ratio in deer feces in an agro-environment, Osaka

*Takashi F Haraguchi[1], Ryosuke Koda[2], Ichiro Tayasu[1] (1.Research Institute for Humanity and Nature, 2.RIEAF, Osaka)

2:15 PM - 2:30 PM JST | 5:15 AM - 5:30 AM UTC

[HTT18-14] Nutrient supply from forest to river in eastern Toyama: carbon and nitrogen isotopic composition of Epilithic Organic Matter

*JING ZHANG[1], Ryosuke Masuda[1], SAKI KATAZAKAI[1], Tamihisa Ohta[1], OSAMU INAMURA[2], Fumiko Nakagawa[3] (1.University of Toyama, 2.Uozu Aquarium, 3.Nagoya University)

2:30 PM - 2:45 PM JST | 5:30 AM - 5:45 AM UTC

[HTT18-15] Investigation on the possibility of the identification of air pollutant sources using stable isotope ratios of lead and strontium

*Shinji Sakurai[1], Takao Nakagiri[1], Kosuke Tanaka[1], Haruhiko Horino[1], Ki-Cheol Shin[2], Ichiro Tayasu[2], Shiho Yabusaki[2] (1.Osaka Prefecture University, 2.Research Institute for Humanity and Nature)

2:45 PM - 3:00 PM JST | 5:45 AM - 6:00 AM UTC

[HTT18-16] **Magnesium and zinc stable isotopes in stream ecology**

*Kai Nils Nitzsche[1], Yoshikazu Kato[1], Ki-Cheol Shin[1], Hiromitsu Kamauchi[1], Ichiro Tayasu[1] (1.Research Institute for Humanity and Nature)

3:00 PM - 3:15 PM JST | 6:00 AM - 6:15 AM UTC

[HTT18-17] A mechanitic metabolic model of nitrogen stable isotope dynamics in trophic processes

*Reiichiro Ishii[1], Maki Noguchi Aita[2], Eitaro Wada (1.Research Institute for Humanity and Nature, 2.Japan Agency for Marine-Earth Science and Technology)

[E] Poster | H (Human Geosciences)：H-TT Technology & Techniques

3:30 PM - 5:00 PM JST | 6:30 AM - 8:00 AM UTC | Poster Hall International Exhibition Hall8, Makuhari Messe_13

[H-TT18] Development and application of environmental traceability methods

convener:Ichiro Tayasu(Research Institute for Humanity and Nature), Nobuhito Ohte(Department of Social Informatics, Graduate School of Informatics, Kyoto University), Gabriel J Bowen(University of Utah)

[HTT18-P01] Isotopic study on seasonal nitrogen dynamics at Lake Biwa

*Takaaki Ishibashi[1], Ken'ichi Osaka[1], Keisuke Koba[2], Takashi Nakamura[3], Kei Nishida[3] (1.Department of ecosystem study, University of Shiga Prefecture, 2.Center for Ecological Research, Kyoto University, 3.International Research Center for River Basin Environment, University of YAMANASHI)

[HTT18-P02] Relationship between residence time, water quality, and stable isotopes of spring water and groundwater in coastal area of Fukushima prefecture

*Shiho Yabusaki[1], Kazuyoshi Asai[2] (1. Research Institute for Humanity and Nature・Faculty of Symbiotic Systems Science, Fukushima University, 2.Geo Science Laboratory)

[HTT18-P03] Applicability evaluation of CIA due to river and lake

*yusuke hataya[1], SEIKI KAWAGOE[1], Shiho Yabusaki[2], KEN Suzuki[1] (1.fukushima university, 2.Research Institute for Humanity and Nature)

[HTT18-P04] Chemical property analysis of short time scale to determine snowfall source

*Suzuki hiromichi[1], SEIKI KAWAGOE[1], SHO ADACHI[1], Shiho Yabusaki[2] (1.Fukushima University, 2.Research Institute for Humanity and Nature)

[HTT18-P05] Analyzing the origin of surface water in the Saijo Plain, Japan, based on the antimony concentration in the water

*Minoru TOKUMASU[1,2], Ki-Cheol SHIN[3], Yoshihiro YAMADA[4] (1.The United Graduate School of Agricultural Sciences, Ehime University, 2.Saijo City, 3.The Research Institute for Humanity and Nature (RIHN) , 4.Kagawa University, Faculty of Agriculture)

[HTT18-P06] Basic kinetic study on stable isotope ratios of nitrogen compounds: a case study for groundwater in the Kathmandu Valley, Nepal

*Ken Yokozawa[1,2], Kei Nishida[1,3], Takashi Nakamura[1,3], Ken'ichi Osaka[4] (1.University of Yamanashi, 2.Special Graduate Program on River Basin Environmental Science,, 3.ICRE, 4.Department of ecosystem study Univercity of Shiga prefecture)

[HTT18-P07] Usefulness of strontium isotope composition for determining the geographical origin of wasabi and potato

*Takafumi Kamitani[1], Ki-Cheol Shin[2], Sachiko Nakamura[1], Rika Koda[1], Tomoya Oka[1], Noriaki Fushimi[1], Yasuhide Muranaka[1] (1.Shizuoka Institute of Environment and Hygiene, 2.Research Institute for Humanity and Nature)

[HTT18-P08] Reconstruction of sea surface temperature and salinity for the Medieval Climatic Anomaly using a long-lived fossil coral collected at Ishigaki Island, southwestern Japan

*Osamu Abe[1], Maki Morimoto[2], Ryuji Asami[3], Takeshi Nakatsuka[1,4] (1.Graduate School of Environmental Studies, Nagoya University, 2.School of Education, Gifu University, 3.Graduate School of Science, Tohoku University, 4.Research Institute for Humanity and Nature)

[HTT18-P09] Development of the analytical method for sulfur isotope in SO_2 gas

*Masaaki Takahashi[1], Hiroyuki Sase[1], Tsuyoshi Ohizumi[1] (1.Asia Center for Air Pollution Research)

[HTT18-P10] Zinc isotope analysis on human tooth enamel samples to reconstruct diet of the Jomon period.

*Soichiro Kusaka[1], Ki-Cheol Shin[2] (1.Tokai Univ., 2.Research Institute for Humanity and Nature)

[HTT18-P11] Zinc stable isotope analysis of environmental reference materials

*Ki-Cheol Shin[1] (1.Research Institute for Humanity and Nature)

[E] Poster | H (Human Geosciences)：H-TT Technology & Techniques

5:15 PM - 6:30 PM JST | 8:15 AM - 9:30 AM UTC | Poster Hall International Exhibition Hall8, Makuhari Messe_23

[H-TT18] Development and application of environmental traceability methods

convener:Ichiro Tayasu(Research Institute for Humanity and Nature), Nobuhito Ohte(Department of Social Informatics, Graduate School of Informatics, Kyoto University), Gabriel J Bowen(University of Utah)

[HTT18-P01] Isotopic study on seasonal nitrogen dynamics at Lake Biwa

*Takaaki Ishibashi[1], Ken'ichi Osaka[1], Keisuke Koba[2], Takashi Nakamura[3], Kei Nishida[3] (1.Department of ecosystem study, University of Shiga Prefecture, 2.Center for Ecological Research, Kyoto University, 3.International Research Center for River Basin Environment, University of YAMANASHI)

[HTT18-P02] Relationship between residence time, water quality, and stable isotopes of spring water and groundwater in coastal area of Fukushima prefecture

*Shiho Yabusaki[1], Kazuyoshi Asai[2] (1. Research Institute for Humanity and Nature・Faculty of Symbiotic Systems Science, Fukushima University, 2.Geo Science Laboratory)

[HTT18-P03] Applicability evaluation of CIA due to river and lake

*yusuke hataya[1], SEIKI KAWAGOE[1], Shiho Yabusaki[2], KEN Suzuki[1] (1.fukushima university, 2.Research Institute for Humanity and Nature)

[HTT18-P04] Chemical property analysis of short time scale to determine snowfall source

*Suzuki hiromichi[1], SEIKI KAWAGOE[1], SHO ADACHI[1], Shiho Yabusaki[2] (1.Fukushima University, 2.Research Institute for Humanity and Nature)

[HTT18-P05] Analyzing the origin of surface water in the Saijo Plain, Japan, based on the antimony concentration in the water

*Minoru TOKUMASU[1,2], Ki-Cheol SHIN[3], Yoshihiro YAMADA[4] (1.The United Graduate School of Agricultural Sciences, Ehime University, 2.Saijo City, 3.The Research Institute for Humanity and Nature (RIHN) , 4.Kagawa University, Faculty of Agriculture)

[HTT18-P06] Basic kinetic study on stable isotope ratios of nitrogen compounds: a case study for groundwater in the Kathmandu Valley, Nepal

*Ken Yokozawa[1,2], Kei Nishida[1,3], Takashi Nakamura[1,3], Ken'ichi Osaka[4] (1.University of Yamanashi, 2.Special Graduate Program on River Basin Environmental Science,, 3.ICRE, 4.Department of ecosystem study Univercity of Shiga prefecture)

[HTT18-P07] Usefulness of strontium isotope composition for determining the geographical origin of wasabi and potato

*Takafumi Kamitani[1], Ki-Cheol Shin[2], Sachiko Nakamura[1], Rika Koda[1], Tomoya Oka[1], Noriaki Fushimi[1], Yasuhide Muranaka[1] (1.Shizuoka Institute of Environment and Hygiene, 2.Research Institute for Humanity and Nature)

[HTT18-P08] Reconstruction of sea surface temperature and salinity for the Medieval Climatic Anomaly using a long-lived fossil coral collected at Ishigaki Island, southwestern Japan

*Osamu Abe[1], Maki Morimoto[2], Ryuji Asami[3], Takeshi Nakatsuka[1,4] (1.Graduate School of Environmental Studies, Nagoya University, 2.School of Education, Gifu University, 3.Graduate School of Science, Tohoku University, 4.Research Institute for Humanity and Nature)

[HTT18-P09] Development of the analytical method for sulfur isotope in SO_2 gas

*Masaaki Takahashi[1], Hiroyuki Sase[1], Tsuyoshi Ohizumi[1] (1.Asia Center for Air Pollution Research)

[HTT18-P10] Zinc isotope analysis on human tooth enamel samples to reconstruct diet of the Jomon period.

*Soichiro Kusaka[1], Ki-Cheol Shin[2] (1.Tokai Univ., 2.Research Institute for Humanity and Nature)

[HTT18-P11] Zinc stable isotope analysis of environmental reference materials

*Ki-Cheol Shin[1] (1.Research Institute for Humanity and Nature)

[J] Oral | H (Human Geosciences)：H-TT Technology & Techniques

9:00 AM - 10:30 AM JST | 12:00 AM - 1:30 AM UTC | 301B 3F

[H-TT22] New Developments in Shallow Geophysics

convener:Kyosuke Onishi(Public Works Research Institute), Kunio Aoike(Oyo corporation), Keisuke Inoue(National Agriculture and Food Research Organization), Tishiyuki Yokota(National Institute of Advanced Industrial Science and Technology), Chairperson:Toshiyuki Yokota, Keisuke Inoue

9:00 AM - 9:15 AM JST | 12:00 AM - 12:15 AM UTC

[HTT22-01] High-frequency seismic reflection measurements for imaging internal structure of a sabo dam damaged by a huge debris flow

*Tomio INAZAKI[1], Hiroshi Kisanuki[2], Takanori Ogahara[1], Takeshi Shimizu[1], Naoki Fujimura[1] (1.Public Works Research Institute, Tsukuba Central Institute, 2.PWRI (Present address: OYO Corporation))

9:15 AM - 9:30 AM JST | 12:15 AM - 12:30 AM UTC

[HTT22-02] Development and applications of 3D ambient noise tomography

*Chisato Konishi[1], Koichi Hayashi[1] (1.OYO Corporation)

9:30 AM - 9:45 AM JST | 12:30 AM - 12:45 AM UTC

[HTT22-03] An Attempt to Estimate the Level of Non-confind Groundwater by Earthing Resistance (I) - Outline of Theory -

*Kunihiro Ryoki[1] (1.Polytechnic University)

9:45 AM - 10:00 AM JST | 12:45 AM - 1:00 AM UTC

[HTT22-04] Experimental and Theoretical Studies for Seafloor Survey by Ground Penetrating Radar

*Jun Sonoda[1], Tomoyuki Kimoto[2] (1.National Institute of Technology, Sendai College, 2.National Institute of Technology, Oita College)

10:00 AM - 10:15 AM JST | 1:00 AM - 1:15 AM UTC

[HTT22-05] Evaluation of the 3-D Distribution of Fractures in a Rock Mass using Directional Borehole Radar Data from a Horizontal Borehole

*Kazuhiko Masumoto[1], Tomoaki Matsushita[2], Suguru Shirasagi[1], Takashi Ueki[3], Shinsuke Karasawa[3], Daiki Makino[3], Kazushige Wada[4] (1.Kajima Technical Research Institute, 2.Kajima Corporation, 3.Matsunaga Geo-Survey Co., Ltd., 4.Mitsui Mineral Development Engineering Co., Ltd.)

10:15 AM - 10:30 AM JST | 1:15 AM - 1:30 AM UTC

[HTT22-06] Automatic Detection of Deteriorated Concrete Bridge Deck using 2 GHz Horn Antennae

*Kunio Aoike[1], Shogo Tanaka[2], Naoto Takase[1], Akio Matsuyama[1], Masaya Yamauchi[1], Yoshinori Uno[1] (1.OYO Corporation, 2.Professor Emeritus of Yamaguchi Univ.)

[J] Poster | H (Human Geosciences)：H-TT Technology & Techniques

3:30 PM - 5:00 PM JST | 6:30 AM - 8:00 AM UTC | Poster Hall International Exhibition Hall8, Makuhari Messe_14

[H-TT22] New Developments in Shallow Geophysics

convener:Kyosuke Onishi(Public Works Research Institute), Kunio Aoike(Oyo corporation), Keisuke Inoue(National Agriculture and Food Research Organization), Tishiyuki Yokota(National Institute of Advanced Industrial Science and Technology)

[HTT22-P01] The shallow structure imaging of integrated geophysical surveying of GPR and ERT at Oyunuma in the Goshougake geothermal area, northeast of Japan

*Inoue Yusuke[1], Tomoki Tsutsui[1], Shinya Sakanaka[1] (1.Graduate School of International Resource Sciences in Akita University)

[HTT22-P02] The P and S wave velocity and geological conditions of shallow surrounding tunnel ground by velocity logging on tunnel side wall

*Kenji OKAZAKI[1], Toshiyuki KURAHASHI[1], Hiroumi NIWA[2] (1.Civil Engineering Research Institute for cold region, Public Works Research Institute, 2.FUJITA corporation)

[HTT22-P03] Rock physical interpretation of the relationship between S-wave velocity and fluid saturation in rocks

*Toru Takahashi[1] (1.Fukada Geological Institute)

[HTT22-P04] Estimation of Rayleigh wave group velocities in Zushi City using seismic interferometry in the short period range

*jun ueno[1], Yoshiya - Oda[1] (1.Tokyo Metropolitan University)

[HTT22-P05] Acquiring distributions of phase velocity for wave frequency to use DAS for surface wave method

*Kyosuke Onishi[1], Kobayashi Takayuki[1], Takanori Ogahara[1], Tomio INAZAKI[1] (1.Public Works Research Institute)

[HTT22-P06] Imaging of deteriorated floor slabs using a test model by ground-penetrating radar

*Kyosuke Onishi[1] (1.Public Works Research Institute)

[J] Poster | H (Human Geosciences)：H-TT Technology & Techniques

5:15 PM - 6:30 PM JST | 8:15 AM - 9:30 AM UTC | Poster Hall International Exhibition Hall8, Makuhari Messe_24

[H-TT22] New Developments in Shallow Geophysics

convener:Kyosuke Onishi(Public Works Research Institute), Kunio Aoike(Oyo corporation), Keisuke Inoue(National Agriculture and Food Research Organization), Tishiyuki Yokota(National Institute of Advanced Industrial Science and Technology)

[HTT22-P01] The shallow structure imaging of integrated geophysical surveying of GPR and ERT at Oyunuma in the Goshougake geothermal area, northeast of Japan

*Inoue Yusuke[1], Tomoki Tsutsui[1], Shinya Sakanaka[1] (1.Graduate School of International Resource Sciences in Akita University)

[HTT22-P02] The P and S wave velocity and geological conditions of shallow surrounding tunnel ground by velocity logging on tunnel side wall

*Kenji OKAZAKI[1], Toshiyuki KURAHASHI[1], Hiroumi NIWA[2] (1.Civil Engineering Research Institute for cold region, Public Works Research Institute, 2.FUJITA corporation)

[HTT22-P03] Rock physical interpretation of the relationship between S-wave velocity and fluid saturation in rocks

*Toru Takahashi[1] (1.Fukada Geological Institute)

[HTT22-P04] Estimation of Rayleigh wave group velocities in Zushi City using seismic interferometry in the short period range

*jun ueno[1], Yoshiya - Oda[1] (1.Tokyo Metropolitan University)

[HTT22-P05] Acquiring distributions of phase velocity for wave frequency to use DAS for surface wave method

*Kyosuke Onishi[1], Kobayashi Takayuki[1], Takanori Ogahara[1], Tomio INAZAKI[1] (1.Public Works Research Institute)

[HTT22-P06] Imaging of deteriorated floor slabs using a test model by ground-penetrating radar

*Kyosuke Onishi[1] (1.Public Works Research Institute)

[E] Poster | H (Human Geosciences)：H-CG Complex & General

1:45 PM - 3:15 PM JST | 4:45 AM - 6:15 AM UTC | Poster Hall International Exhibition Hall8, Makuhari Messe_6

[H-CG28] Implementing Integrated Research for Sustainable Future

convener:Yukio Himiyama(Emeritus Professor, Hokkaido University of Education), Akihiko Kondoh(Center for Environmental Remote Sensing, Chiba University), Takeshi Sakurai(Graduate School of Agricultural and Life Sciences, The University of Tokyo), Kenichi Abe(Research Institute for Humanity and Nature)

[HCG28-P01] **Ground Motion Instrumentation Network and Earthquake Early Warning System for Uttarakhand**

*Pankaj Kumar[1,2], Ashok - Kumar[1,2], Ajay - Gairola[1,2] (1.Indian Institute of Technology Roorkee, India, 2.Earthquake Early Warning Laboratory, Centre of Excellence in Disaster Mitigation & Management, IIT Roorkee)

[HCG28-P02] Linking Socioeconomic and Geographical Model to Analyze Land Use Changes in the Jakarta - Bandung Mega Urban Regions

*Didit Okta Pribadi[1,2] (1.Center for Regional Systems Analysis, Planning and Development (CrestPent) - IPB University, 2.Research Center for Plant Conservation and Botanic Gardens - Indonesian Institute of Sciences)

[HCG28-P03] **Development of an Integrated Model for Evaluation of Pasture Carrying Capacity and its Vulnerability based on Water Resources in Arid and Semi-arid Regions- - - - -A Case Study in Mongolia**

★Invited Papers

*Qinxue Wang[1], Tomohiro Okadera[1], Tadanobu Nakayama[1], Deni Eer[1], Ochirbat Batkhishig[2], Dorjgotov Battogtokh[2], Uudus Bayasaikhan[3] (1.National Institute for Environmental Studies, 2.Institute of Geography and Geoecology, Mongolian Academy of Sciences, 3.School of Arts and Sciences, National University of Mongolia)

[HCG28-P04] Influence of land use histories on vegetation and ecosystem services of restored wetlands in Tumen River basin, China

*CAO GUANGLAN[1], Kazuaki Tsuchiya[1], Weihong Zhu[2], OKURO TOSHIYA[1] (1.The University of Tokyo, 2.Yanbian University)

[HCG28-P05] The spatial flow of freshwater ecosystem services: A case study of Tumen River watershed

*JIAN ZHANG[1], Shizuka hashimoto[1], Kazuaki Tsuchiya[1], Weihong Zhu[2], OKURO TOSHIYA[1] (1.The University of Tokyo, 2.Yanbian University)

[E] Poster | H (Human Geosciences)：H-CG Complex & General

5:15 PM - 6:30 PM JST | 8:15 AM - 9:30 AM UTC | Poster Hall International Exhibition Hall8, Makuhari Messe_25

[H-CG28] Implementing Integrated Research for Sustainable Future

convener:Yukio Himiyama(Emeritus Professor, Hokkaido University of Education), Akihiko Kondoh(Center for Environmental Remote Sensing, Chiba University), Takeshi Sakurai(Graduate School of Agricultural and Life Sciences, The University of Tokyo), Kenichi Abe(Research Institute for Humanity and Nature)

[HCG28-P01] Ground Motion Instrumentation Network and Earthquake Early Warning System for Uttarakhand

*Pankaj Kumar[1,2], Ashok - Kumar[1,2], Ajay - Gairola[1,2] (1.Indian Institute of Technology Roorkee, India, 2.Earthquake Early Warning Laboratory, Centre of Excellence in Disaster Mitigation & Management, IIT Roorkee)

[HCG28-P02] Linking Socioeconomic and Geographical Model to Analyze Land Use Changes in the Jakarta - Bandung Mega Urban Regions

*Didit Okta Pribadi[1,2] (1.Center for Regional Systems Analysis, Planning and Development (CrestPent) - IPB University, 2.Research Center for Plant Conservation and Botanic Gardens - Indonesian Institute of Sciences)

[HCG28-P03] Development of an Integrated Model for Evaluation of Pasture Carrying Capacity and its Vulnerability based on Water Resources in Arid and Semi-arid Regions- - - - -A Case Study in Mongolia

★Invited Papers

*Qinxue Wang[1], Tomohiro Okadera[1], Tadanobu Nakayama[1], Deni Eer[1], Ochirbat Batkhishig[2], Dorjgotov Battogtokh[2], Uudus Bayasaikhan[3] (1.National Institute for Environmental Studies, 2.Institute of Geography and Geoecology, Mongolian Academy of Sciences, 3.School of Arts and Sciences, National University of Mongolia)

[HCG28-P04] Influence of land use histories on vegetation and ecosystem services of restored wetlands in Tumen River basin, China

*CAO GUANGLAN[1], Kazuaki Tsuchiya[1], Weihong Zhu[2], OKURO TOSHIYA[1] (1.The University of Tokyo, 2.Yanbian University)

[HCG28-P05] The spatial flow of freshwater ecosystem services: A case study of Tumen River watershed

*JIAN ZHANG[1], Shizuka hashimoto[1], Kazuaki Tsuchiya[1], Weihong Zhu[2], OKURO TOSHIYA[1] (1.The University of Tokyo, 2.Yanbian University)

[E] Oral | H (Human Geosciences)：H-CG Complex & General

3:30 PM - 5:00 PM JST | 6:30 AM - 8:00 AM UTC | 302 3F

[H-CG28] Implementing Integrated Research for Sustainable Future

convener:Yukio Himiyama(Emeritus Professor, Hokkaido University of Education), Akihiko Kondoh(Center for Environmental Remote Sensing, Chiba University), Takeshi Sakurai(Graduate School of Agricultural and Life Sciences, The University of Tokyo), Kenichi Abe(Research Institute for Humanity and Nature), Chairperson:Ernan Rustiadi(Bogor Agricultural University), Qinxue Wang(National Institute for environmental Studies), takeshi sakurai

3:30 PM - 3:45 PM JST | 6:30 AM - 6:45 AM UTC

[HCG28-01] Implementing Integrated Research for Sustainable Future - a human geoscience perspective

*Yukio Himiyama[1] (1.Emeritus Professor, Hokkaido University of Education)

3:45 PM - 4:00 PM JST | 6:45 AM - 7:00 AM UTC

[HCG28-02] **Application of environmental carrying capacity analysis and land cover change scenarios in collaborative spatial planning process: The Jakarta Megacity Case**

★Invited Papers

*ERNAN RUSTIADI[1], Andrea Emma Pravitasari[2], Diar Shiddiq[1], Laode Syamsul Iman[1], Setyardi Pratika Mulya[2], Mia Ermyanila[1], Nur Etika Karyati[1] (1.Center for Regional System Analysis, Planning and Development, Bogor Agricultural University , 2.Department of Soil Science and Land Resource, Faculty of Agriculture, Bogor Agricultural University)

4:00 PM - 4:15 PM JST | 7:00 AM - 7:15 AM UTC

[HCG28-03] Does the Market Economy Save the Local Natural Resources While Improving Human Welfare? The Case of 101 Natural Forests in the Middle Hills of Nepal

*Takeshi Sakurai[1], Towa Tachibana[2], Santosh Rayamajhi [3] (1.The University of Tokyo, 2.Chiba University , 3.Tribhuvan University)

4:15 PM - 4:30 PM JST | 7:15 AM - 7:30 AM UTC

[HCG28-04] Academic-public-private partnerships for sustainable herding under increasing frequency of climate hazards

*Masato Shinoda[1] (1.Graduate School of Environmental Studies Nagoya University)

4:30 PM - 4:45 PM JST | 7:30 AM - 7:45 AM UTC

[HCG28-05] Land use after death and funeral of citizen mainly based on public cemeteries in modern Beijing city

*Haruhiro Doi[1], Yanwei Chai[2], Peiwei Xu[3] (1.Faculty of Education, Oita University, 2.Peking University, 3.Beijing Normal University)

4:45 PM - 5:00 PM JST | 7:45 AM - 8:00 AM UTC

[HCG28-06] Restoration and sustainable land management of degraded landscapes in Asia and Africa

★Invited Papers

*OKURO TOSHIYA[1] (1.Graduate School of Agricultural and Life Sciences, The University of Tokyo)

[J] Poster | S (Solid Earth Sciences)：S-GD Geodesy

10:45 AM - 12:15 PM JST | 1:45 AM - 3:15 AM UTC | Poster Hall International Exhibition Hall8, Makuhari Messe_5

[S-GD01] Gravity and Geoid

convener:Tokuro Kodama(Geospatial Information Authority of Japan), Daisuke Oka(Geological Survey of Hokkaido, Environmental and Geological Research Department, Local Independent Administrative Agency, Hokkaido Research Organization)

[SGD01-P01] An Improved GRACE time-varying gravity field model and its application in China and Antarctica

*Yunlong Wu[1], Yi Zhang[1], Zhengbo Zou[1], Minzhang Hu[1] (1.Institute of Seismology, China Earthquake Administration)

[SGD01-P02] Numerical modeling of crustal deformation and gravity change caused by glacier melting in Southeast Alaska

*Kazuhiro Naganawa[1], Takahito Kazama[1] (1.Graduate School of Science, Kyoto University)

[SGD01-P03] Gravity gradient variations considered to have occured 3 months before the Tohoku-Oki earthquake

*Naoki Hasumi[1], Kosuke Heki[1] (1.Hokkaido University Graduate School of Science)

[SGD01-P04] Density structure inferred from gravity and airborne gravity gradiometry data in the northwestern part of Kuju volcano, Oita prefecture

*Jun Nishijima[1], Yasuhiro Fujimitsu[1] (1.Department of Earth Resources Engineering, Graduate School of Engineering, Kyushu University)

[SGD01-P05] On the effect of higher-order terms in the gravity sensor of the superconducting gravimeter

*Yuichi Imanishi[1], Kazunari Nawa[2], Yoshiaki Tamura[3], Hiroshi Ikeda[4] (1.Earthquake Research Institute, The University of Tokyo, 2.AIST, 3.NAOJ, 4.University of Tsukuba)

[SGD01-P06] **Gravity Effect of Local Snow Accumulation obtained from Superconducting Gravimeter and UAV survey at Syowa Station**

*Akihisa Hattori[1], Yuichi Aoyama[1,2], Koichiro Doi[1,2], Hajime Oishi[3], Jun Nishijima[4], Hiroshi Ikeda[5] (1.SOKENDAI (The Graduate University of Advanced Studies), 2.National Institute of Polar Research, 3.NEC Networks & System Integration Corporation, 4.Kyushu University, 5.University of Tsukuba)

[J] Poster | S (Solid Earth Sciences)：S-GD Geodesy

5:15 PM - 6:30 PM JST | 8:15 AM - 9:30 AM UTC | Poster Hall International Exhibition Hall8, Makuhari Messe_26

[S-GD01] Gravity and Geoid

convener:Tokuro Kodama(Geospatial Information Authority of Japan), Daisuke Oka(Geological Survey of Hokkaido, Environmental and Geological Research Department, Local Independent Administrative Agency, Hokkaido Research Organization)

[SGD01-P01] An Improved GRACE time-varying gravity field model and its application in China and Antarctica

*Yunlong Wu[1], Yi Zhang[1], Zhengbo Zou[1], Minzhang Hu[1] (1.Institute of Seismology, China Earthquake Administration)

[SGD01-P02] Numerical modeling of crustal deformation and gravity change caused by glacier melting in Southeast Alaska

*Kazuhiro Naganawa[1], Takahito Kazama[1] (1.Graduate School of Science, Kyoto University)

[SGD01-P03] Gravity gradient variations considered to have occured 3 months before the Tohoku-Oki earthquake

*Naoki Hasumi[1], Kosuke Heki[1] (1.Hokkaido University Graduate School of Science)

[SGD01-P04] Density structure inferred from gravity and airborne gravity gradiometry data in the northwestern part of Kuju volcano, Oita prefecture

*Jun Nishijima[1], Yasuhiro Fujimitsu[1] (1.Department of Earth Resources Engineering, Graduate School of Engineering, Kyushu University)

[SGD01-P05] On the effect of higher-order terms in the gravity sensor of the superconducting gravimeter

*Yuichi Imanishi[1], Kazunari Nawa[2], Yoshiaki Tamura[3], Hiroshi Ikeda[4] (1.Earthquake Research Institute, The University of Tokyo, 2.AIST, 3.NAOJ, 4.University of Tsukuba)

[SGD01-P06] **Gravity Effect of Local Snow Accumulation obtained from Superconducting Gravimeter and UAV survey at Syowa Station**

*Akihisa Hattori[1], Yuichi Aoyama[1,2], Koichiro Doi[1,2], Hajime Oishi[3], Jun Nishijima[4], Hiroshi Ikeda[5] (1.SOKENDAI (The Graduate University of Advanced Studies), 2.National Institute of Polar Research, 3.NEC Networks & System Integration Corporation, 4.Kyushu University, 5.University of Tsukuba)

[J] Oral | S (Solid Earth Sciences)：S-GD Geodesy

1:45 PM - 3:15 PM JST | 4:45 AM - 6:15 AM UTC | 303 3F

[S-GD01] Gravity and Geoid

convener:Tokuro Kodama(Geospatial Information Authority of Japan), Daisuke Oka(Geological Survey of Hokkaido, Environmental and Geological Research Department, Local Independent Administrative Agency, Hokkaido Research Organization), Chairperson:Toshiyuki Tanaka, Takahito Kazama

1:45 PM - 2:00 PM JST | 4:45 AM - 5:00 AM UTC

[SGD01-01] Seasonal variation of gravity values at the Ishioka Geodetic Observing Station

*Akira Tomiyama[1], Tokuro Kodama[1], Shuichi Oomori[1], Yoshifumi Hiraoka[1], Toshihiro Yahagi[1] (1.GSI of Japan)

2:00 PM - 2:15 PM JST | 5:00 AM - 5:15 AM UTC

[SGD01-02] Installation of the First Gravity Station in the Mount Fuji Research Institute, and the Phase-Free gravity measurement

*Ryo Honda[1], Yuichi Imanishi[2], Kazunari Nawa[3], Toshiyuki Tanaka[4], Tokuro Kodama[5], Akira Tomiyama[5] (1.MFRI, Yamanashi Prefectural Government, 2.ERI, University of Tokyo, 3.GSJ, AIST, 4.TRIES, ADEP, 5.GSI)

2:15 PM - 2:30 PM JST | 5:15 AM - 5:30 AM UTC

[SGD01-03] Absolute gravity and GNSS measurements on bedrock outcrops in Dronning Maud Land, East Antarctica

*Takahito Kazama[1], Yuichi Aoyama[2], Yoichi Fukuda[1], Koichiro Doi[2] (1.Graduate School of Science, Kyoto University, 2.National Institute of Polar Research)

2:30 PM - 2:45 PM JST | 5:30 AM - 5:45 AM UTC

[SGD01-04] **Capability of ICA Method for separating GIA and Ice Mass Signals in Antarctica**

*SHI TIANYAN[1], Yoichi Fukuda[1] (1.Graduate School of Science, Kyoto University)

2:45 PM - 3:00 PM JST | 5:45 AM - 6:00 AM UTC

[SGD01-05] Preliminary result of continuous observation with an iGrav superconducting gravimeter at the Teshikaga observatory, eastern Hokkaido, Japan

*Kazunari Nawa[1], Hiroaki Takahashi[2], Mako Ohzono[2], Kazumi Okada[2], Teruhiro Yamaguchi[2], Daisuke Oka[3], Noritoshi Okazaki[3], Ryo Honda[4], Hiroshi Ikeda[5] (1.National Institute of Advanced Industrial Science and Technology, 2.Hokkaido University, 3.Geological Survey of Hokkaido, 4.Mount Fuji Research Institute, 5.University of Tsukuba)

3:00 PM - 3:15 PM JST | 6:00 AM - 6:15 AM UTC

[SGD01-06] On the anomalous temporal gravity change between VERA and F-net stations at Ishigakijima, Japan

*Kazunari Nawa[1], Yuichi Imanishi[2], Yoshiaki Tamura[3], Hiroshi Ikeda[4], Takeshi Kimura[5] (1.National Institute of Advanced Industrial Science and Technology, 2.Earthquake Research Institute, The University of Tokyo, 3.National Astronomical Observatory of Japan, 4.University of Tsukuba, 5.National Research Institute for Earth Science and Disaster Resilience)

[J] Oral | S (Solid Earth Sciences)：S-GD Geodesy

3:30 PM - 5:00 PM JST | 6:30 AM - 8:00 AM UTC | 303 3F

[S-GD01] Gravity and Geoid

convener:Tokuro Kodama(Geospatial Information Authority of Japan), Daisuke Oka(Geological Survey of Hokkaido, Environmental and Geological Research Department, Local Independent Administrative Agency, Hokkaido Research Organization), Chairperson:Kazunari Nawa, Ryo Honda(山梨県富士山科学研究所)

3:30 PM - 3:45 PM JST | 6:30 AM - 6:45 AM UTC

[SGD01-07] **Absolute gravity signals at the Sakurajima volcano since 2009 through 2018**

*Shuhei Okubo[1], Keigo Yamamoto[2], Masato Iguchi[2], Yoshiyuki Tanaka[3], Yuichi Imanishi[1], Ryuichi Nishiyama[1], Miwako Ando[1], Atsushi Watanabe[1] (1.Earthquake Research Institute, The University of Tokyo, 2.Disaster Prevention Research Institute, Kyoto University, 3.Graduate School of Science, The University of Tokyo)

3:45 PM - 4:00 PM JST | 6:45 AM - 7:00 AM UTC

[SGD01-08] Detection of Earthquake-induced Prompt Gravity Signals in Multi-channel Data

*Masaya Kimura[1], Nobuki Kame[1], Shingo Watada[1], Makiko Ohtani[2], Akito Araya[1], Yuichi Imanishi[1], Masaki Ando[3], Takashi Kunugi[4] (1.Earthquake Research Institute,The University of Tokyo, 2.National Institute of Advanced Industrial Science and Technology, 3.Department of Physics, The University of Tokyo, 4.National Research Institute for Earth Science and Disaster Resilience)

4:00 PM - 4:15 PM JST | 7:00 AM - 7:15 AM UTC

[SGD01-09] Evaluation of atmospheric attraction effect using local-scale objective analysis (LANAL)

*Toshiyuki Tanaka[1] (1.Tono Research Institute of Earthquake Science, Association for the Development of Earthquake Prediction)

4:15 PM - 4:30 PM JST | 7:15 AM - 7:30 AM UTC

[SGD01-10] Airborne gravity survey for establishment of a new precise gravimetric geoid model

*Tokuro Kodama[1], Akira Tomiyama[1], Shuichi Oomori[1], Erika Wada[1], Toshihiro Yahagi[1], Yoshifumi Hiraoka[1], Hiroshi Kawawa[1] (1.GSI of Japan)

4:30 PM - 4:45 PM JST | 7:30 AM - 7:45 AM UTC

[SGD01-11] Gravimetric geoid modeling using airborne gravity data : a case study in Colorado, U.S.A.

*Koji Matsuo[1], Rene Forsberg[2] (1.GSI of Japan, 2.Denmark Technical University)

[J] Oral | S (Solid Earth Sciences)：S-GD Geodesy

9:00 AM - 10:30 AM JST | 12:00 AM - 1:30 AM UTC | 105 1F

[S-GD02] Engineering Application of Space Geodesy

convener:Seiichi Shimada(Graduate School of Frontier Sciences, University of Tokyo Nippo Co. Ltd.), Shuichi Rokugawa(The University of Tokyo), Basara Miyahara(GSI of Japan), Toshiaki Tsujii(Department of Aerospace Engineering, Osaka Prefecture University), Chairperson:Masaatsu Aichi, Kazuki Sakai

9:00 AM - 9:15 AM JST | 12:00 AM - 12:15 AM UTC

[SGD02-01] Future vision of the society for utilizing highly precise three dimensional positioning data by applying crustal deformation and precise gravimetric geoid model

*Toshihiro Yahagi[1], Kensuke Kokado[1], Kenji Yoshida[1], Takashi Toyofuku[1], Masao Iwata[1], Basara Miyahara[1] (1.GSI of Japan)

9:15 AM - 9:30 AM JST | 12:15 AM - 12:30 AM UTC

[SGD02-02] Preliminary study on the application of satelite-based monitoring for land surface displacement to inverse analyses of groundater flow/land subsidence modeling

*Masaatsu Aichi[1] (1.Graduate School of Frontier Sciences, The University of Tokyo)

9:30 AM - 9:45 AM JST | 12:30 AM - 12:45 AM UTC

[SGD02-03] Monitoring of ground deformation all over Japan by InSAR and utilizing 2.5-D analysis

*Kazuki Sakai[1], Kyonosuke Hayahsi[1], Masaki Kuwahara[1], Tatsuya Yamashita[1], Masaki Honda[1], Hiroshi Munekane[1] (1.GSI of Japan)

9:45 AM - 10:00 AM JST | 12:45 AM - 1:00 AM UTC

[SGD02-04] Resource Exploration using Interferometric Synthetic Aperture Radar Measurement Technology

*Shuichi Rokugawa[1], Takako Nakamura[1] (1.The University of Tokyo)

10:00 AM - 10:15 AM JST | 1:00 AM - 1:15 AM UTC

[SGD02-05] The application example of GNSS for natural gas development together with PDCA Management Method

★Invited Papers

*Yoshiyuki Muramoto[1], Susumu Hayatsu[1], Michiharu Hiyama[1], Daisuke Murai[1], Shoji Kunisue[1] (1.KANTO NATURAL GAS DEVELOPMENT CO., LTD)

10:15 AM - 10:30 AM JST | 1:15 AM - 1:30 AM UTC

[SGD02-06] New threats and countermeasures in the aviation field where the use of GNSS satellite navigation expands

★Invited Papers

*Takeshi Fujiwara[1], Toshiaki Tsujii[2] (1.Japan Aerospace Exploration Agency, 2.Osaka Prefecture University)

[J] Poster | S (Solid Earth Sciences)：S-GD Geodesy

3:30 PM - 5:00 PM JST | 6:30 AM - 8:00 AM UTC | Poster Hall International Exhibition Hall8, Makuhari Messe_15

[S-GD02] Engineering Application of Space Geodesy

convener:Seiichi Shimada(Graduate School of Frontier Sciences, University of Tokyo Nippo Co. Ltd.), Shuichi Rokugawa(The University of Tokyo), Basara Miyahara(GSI of Japan), Toshiaki Tsujii(Department of Aerospace Engineering, Osaka Prefecture University)

[SGD02-P01] Dynamic map for engineering use of GNSS positioning

*Mikio Satomura[1], Seiichi Shimada[1,2], Hirokazu Ito[1], UKEI KAZUYUKI[1], Mikio Sueno[1,3], Shigeru Nakao[4] (1.Nippo Company, Limited, 2.Graduate School of Frontier Sciences, University of Tokyo, 3.Calsystem Company, Limited, 4.Graduate School of Scienece and Engineering, Kagoshima Univeresity)

[SGD02-P02] Utilization of Interferometric Synthetic Aperture Radar Time Series Analysis Technology for Disaster Prevention

*Takako Nakamura[1], Shuichi Rokugawa[1] (1.The University of Tokyo)

[SGD02-P03] The annual and secular movements of vertical component in GEONET sites caused by groundwater usages

*Seiichi Shimada[1], Masaatsu Aichi[1] (1.Graduate School of Frontier Sciences, University of Tokyo)

[J] Poster | S (Solid Earth Sciences)：S-GD Geodesy

5:15 PM - 6:30 PM JST | 8:15 AM - 9:30 AM UTC | Poster Hall International Exhibition Hall8, Makuhari Messe_27

[S-GD02] Engineering Application of Space Geodesy

convener:Seiichi Shimada(Graduate School of Frontier Sciences, University of Tokyo Nippo Co. Ltd.), Shuichi Rokugawa(The University of Tokyo), Basara Miyahara(GSI of Japan), Toshiaki Tsujii(Department of Aerospace Engineering, Osaka Prefecture University)

[SGD02-P01] Dynamic map for engineering use of GNSS positioning

*Mikio Satomura[1], Seiichi Shimada[1,2], Hirokazu Ito[1], UKEI KAZUYUKI[1], Mikio Sueno[1,3], Shigeru Nakao[4] (1.Nippo Company, Limited, 2.Graduate School of Frontier Sciences, University of Tokyo, 3.Calsystem Company, Limited, 4.Graduate School of Scienece and Engineering, Kagoshima Univeresity)

[SGD02-P02] Utilization of Interferometric Synthetic Aperture Radar Time Series Analysis Technology for Disaster Prevention

*Takako Nakamura[1], Shuichi Rokugawa[1] (1.The University of Tokyo)

[SGD02-P03] The annual and secular movements of vertical component in GEONET sites caused by groundwater usages

*Seiichi Shimada[1], Masaatsu Aichi[1] (1.Graduate School of Frontier Sciences, University of Tokyo)

[E] Oral | S (Solid Earth Sciences)：S-SS Seismology

1:45 PM - 3:15 PM JST | 4:45 AM - 6:15 AM UTC | Convention Hall B 2F

[S-SS06] Nankai Trough Seismogenic Zone Experiment: Logging and sampling the seismogenic megathrust

convener:Kyuichi Kanagawa(Graduate School of Science, Chiba University), Demian M Saffer(Pennsylvania State University), Masataka Kinoshita(Earthquake Research Institute, University of Tokyo), Chairperson:Kyuichi Kanagawa(Graduate School of Science, Chiba University), Demian Saffer(Department of Geosciences, Pennsylvania State University), Masataka Kinoshita(Earthquake Research Institute, the University of Tokyo)

1:45 PM - 2:00 PM JST | 4:45 AM - 5:00 AM UTC

[SSS06-01] Geoscientific information about plate boundary along the Nankai Trough provided by the GNSS-A

★Invited Papers

*Yusuke Yokota[1], Tadashi Ishikawa[2] (1.Institute of Industrial Science, The University of Tokyo, 2.Hydrographic and Oceanographic department, Japan Coast Guard)

2:00 PM - 2:15 PM JST | 5:00 AM - 5:15 AM UTC

[SSS06-02] Deep Drilling at the Nankai Trough: IODP NanTroSEIZE Expedition 358 Summary and First Results

★Invited Papers

*Harold Tobin[1], Takehiro Hirose[7], Matt Ikari[5], Kyuichi Kanagawa[10], Gaku Kimura[3], Masataka Kinoshita[8], Hiroko Kitajima[6], Demian M Saffer[4], Asuka Yamaguchi[9], Lena Maeda[2], Nobu Eguchi[2], Sean Toczko[2] (1.Department of Earth and Space Sciences, University of Washington, 2.JAMSTEC-CDEX, 3.Tokyo Un. of Marine Science-Technology, 4.Penn State University, 5.MARUM Un. of Bremen, 6.Texas A&M University, 7.JAMSTEC-KCC, 8.Un. of Tokyo Earthquake Research Institute, 9.Un. of Tokyo AORI, 10.Chiba University)

2:15 PM - 2:30 PM JST | 5:15 AM - 5:30 AM UTC

[SSS06-03] Coexistence of soft and hard sediments at deep Nankai accretionary prism, NanTro SEIZE Project, IODP Exp.358

*Arito Sakaguchi[1,2], Michael Strasser[3], Mari Hamahashi[4,5], Takehiro Hirose[2], Hiroko Kitajima[6], Expedition 358 Scientists IODP (1.Yamaguchi Univ., 2.JAMSTEC, 3.University of Innsbruck, 4.University of Tokyo, 5.Nanyang Technological University, 6.Texas A&M University)

2:30 PM - 2:45 PM JST | 5:30 AM - 5:45 AM UTC

[SSS06-04] Active and passive seismic experiment during the IODP Exp. 358 deep riser drilling in the Nankai Trough, Japan

*Toshinori Kimura[1], Takashi Tonegawa[1], Kazuya Shiraishi[1], Eiichiro Araki[1], Yasuyuki Nakamura[1], Yuka Kaiho[1], Gou Fujie[1], Seiichi Miura[1], Shuichi Kodaira[1], Noriaki Sakurai[1], Yoshinori Sanada[1], Yukari Kido[1], Masataka Kinoshita[2], Narumi Takahashi[3,1], Yuya Machida[1], Shuhei Nishida[1] (1.Japan Agency for Marine-Earth Science and Technology, 2.Earthquake Research Institute, The University of Tokyo, 3.National Research Institute for Earth Science and Disaster Resilience)

2:45 PM - 3:00 PM JST | 5:45 AM - 6:00 AM UTC

[SSS06-05] Microfabric analysis of damaged zone of principal shear zone in the frontal megathrust in the Nankai Trough

*Gaku Kimura[1], Asuka Yamaguchi[2], Yohei Hamada[3], Suguru Yabe[4] (1.Tokyo University of Marine Science and Technology, 2.Atomosphere and Ocean Research Institute, The University of Tokyo, 3.Kochi Institute for Core Sample Research, Japan Agency for Marine-Earth Science and Technology, 4.Japan Agency for Marine-Earth Science and Technology)

3:00 PM - 3:15 PM JST | 6:00 AM - 6:15 AM UTC

[SSS06-06] Seismic Imaging of Mud Diapirs in Northern Kumano Basin, Nankai Trough

*Gregory F Moore[1], Miho Asada[2], Shuichi Kodaira[2], Achim Kopf[3] (1.University of Hawaii at Manoa, 2.JAMSTEC, 3.MARUM)

[E] Poster | S (Solid Earth Sciences)：S-SS Seismology

3:30 PM - 5:00 PM JST | 6:30 AM - 8:00 AM UTC | Poster Hall International Exhibition Hall8, Makuhari Messe_16

[S-SS06] Nankai Trough Seismogenic Zone Experiment: Logging and sampling the seismogenic megathrust

convener:Kyuichi Kanagawa(Graduate School of Science, Chiba University), Demian M Saffer(Pennsylvania State University), Masataka Kinoshita(Earthquake Research Institute, University of Tokyo)

[SSS06-P01] Crustal structure in the Nankai Trough seismogenic zone based on renewed depth images and seismic attribute analysis

*Kazuya Shiraishi[1], Yasuhiro Yamada[1], Masataka Kinoshita[2], Gaku Kimura[3] (1.Japan Agency for Marine-Earth Science and Technology, 2.Earthquake Research Institute, The University of Tokyo, 3.Tokyo University of Marine Science and Technology)

[SSS06-P02] Along-strike variations in protothrust zone characteristics at the Nankai Trough subduction margin

*Hannah Tilley[1], Gregory F Moore[1], Mikiya Yamashita[2], Shuichi Kodaira[2] (1.University of Hawaii at Manoa, 2.JAMSTEC)

[SSS06-P03] Temporal change in seismic velocity in the Nankai subduction zone from cross-correlation analysis of ambient noise

*Tatsunori Ikeda[1], Takeshi Tsuji[1] (1.Kyushu University)

[SSS06-P04] Strength profile of the Nankai accretionary prism evaluated from drilling parameters

★Invited Papers

*Yohei Hamada[1], Manami Kitamura[2], Takehiro Hirose[1], Yasuhiro Yamada[1], Yoshinori Sanada[1], Takamitsu Sugihara[1], Saneatsu Saito[1], KYAW MOE[1] (1.Japan Agency for Marine-Earth Science and Technology, 2.National Institute of Advanced Industrial Science andTechnology)

[SSS06-P05] Paleotemperature anomalies deduced from thermal-maturity parameters within the décollement, off Cape of Muroto, Japan

*Nana Kamiya[1,2], Takehiro Hirose[2], Yuzuru Yamamoto[2], Yohei Hamada[2], Stephen A Bowden[3], Man-Yin Tsang[4], Kiho Yang[5], Satoshi Tonai[6], Weiren Lin[1,2] (1.Graduate School of Engineering, Kyoto University, 2.JAMSTEC, 3.University of Aberdeen, 4.University of Toronto, 5.Yonsei University, 6.Kochi University)

[SSS06-P06] Modelling thermal maturity of an accretionary wedge

Utsav Mannu[2], *Masataka Kinoshita[1], Taras Gerya[3] (1.Earthquake Research Institute, University of Tokyo, 2.Department of Earth and Climate Science, IISER Pune, 3.Institute of Geophysics, ETH Zürich)

[E] Poster | S (Solid Earth Sciences)：S-SS Seismology

5:15 PM - 6:30 PM JST | 8:15 AM - 9:30 AM UTC | Poster Hall International Exhibition Hall8, Makuhari Messe_28

[S-SS06] Nankai Trough Seismogenic Zone Experiment: Logging and sampling the seismogenic megathrust

convener:Kyuichi Kanagawa(Graduate School of Science, Chiba University), Demian M Saffer(Pennsylvania State University), Masataka Kinoshita(Earthquake Research Institute, University of Tokyo)

[SSS06-P01] Crustal structure in the Nankai Trough seismogenic zone based on renewed depth images and seismic attribute analysis

*Kazuya Shiraishi[1], Yasuhiro Yamada[1], Masataka Kinoshita[2], Gaku Kimura[3] (1.Japan Agency for Marine-Earth Science and Technology, 2.Earthquake Research Institute, The University of Tokyo, 3.Tokyo University of Marine Science and Technology)

[SSS06-P02] Along-strike variations in protothrust zone characteristics at the Nankai Trough subduction margin

*Hannah Tilley[1], Gregory F Moore[1], Mikiya Yamashita[2], Shuichi Kodaira[2] (1.University of Hawaii at Manoa, 2.JAMSTEC)

[SSS06-P03] Temporal change in seismic velocity in the Nankai subduction zone from cross-correlation analysis of ambient noise

*Tatsunori Ikeda[1], Takeshi Tsuji[1] (1.Kyushu University)

[SSS06-P04] Strength profile of the Nankai accretionary prism evaluated from drilling parameters

★Invited Papers

*Yohei Hamada[1], Manami Kitamura[2], Takehiro Hirose[1], Yasuhiro Yamada[1], Yoshinori Sanada[1], Takamitsu Sugihara[1], Saneatsu Saito[1], KYAW MOE[1] (1.Japan Agency for Marine-Earth Science and Technology, 2.National Institute of Advanced Industrial Science andTechnology)

[SSS06-P05] Paleotemperature anomalies deduced from thermal-maturity parameters within the décollement, off Cape of Muroto, Japan

*Nana Kamiya[1,2], Takehiro Hirose[2], Yuzuru Yamamoto[2], Yohei Hamada[2], Stephen A Bowden[3], Man-Yin Tsang[4], Kiho Yang[5], Satoshi Tonai[6], Weiren Lin[1,2] (1.Graduate School of Engineering, Kyoto University, 2.JAMSTEC, 3.University of Aberdeen, 4.University of Toronto, 5.Yonsei University, 6.Kochi University)

[SSS06-P06] Modelling thermal maturity of an accretionary wedge

Utsav Mannu[2], *Masataka Kinoshita[1], Taras Gerya[3] (1.Earthquake Research Institute, University of Tokyo, 2.Department of Earth and Climate Science, IISER Pune, 3.Institute of Geophysics, ETH Zürich)

[J] Poster | S (Solid Earth Sciences)：S-SS Seismology

10:45 AM - 12:15 PM JST | 1:45 AM - 3:15 AM UTC | Poster Hall International Exhibition Hall8, Makuhari Messe_6

[S-SS10] Seismicity

convener:Kei Katsumata(Institute of Seismology and Volcanology, Hokkaido University)

[SSS10-P01] Spatial-temporal and seismogram characteristics of foreshock and aftershock activities for tsunami earthquakes

*Yifeng Liu[1], Yoshihiro Ito[2], Kazuaki Ohta[2], Satoshi Katakami[1] (1.Division of Earth and Planetary Sciences, Graduate School of Science, Kyoto University, 2.Disaster Prevention Research Institude, Kyoto University)

[SSS10-P02] Successively occurring large earthquakes in the world – comparison of real cases with expectations by the space-time ETAS

*Tetsuo Hashimoto[1], Takashi YOKOTA[2] (1.Seismology and Tsunami Research Department, Meteorological Reaserch Institute, 2.Aichi Institue Technology)

[SSS10-P03] Seismicity beneath stable oceanic plate

*Yasushi Ishihara[1] (1.R&D Center for Earthquake and Tsunami, JAMSTEC)

[SSS10-P04] Relation between long-term slow slip events and correlation between tidal triggering effect and deep low-frequency earthquakes in Bungo Channel: Part 2

*Fuyuki Hirose[1], Akio Kobayashi[1], Kenji Maeda[2] (1.Seismology and Tsunami Research Department, Meteorological Research Institute, 2.Seismology and Volcanology Department, Japan Meteorological Agency)

[SSS10-P05] Arrival-time and hypocenter determination using S-net

*Tomomi Okada[1], Ryota Takagi[1], Takashi NAKAYAMA[1], Syuichi Suzuki[1], Ryosuke Azuma[1], Genti Toyokuni[1], Keisuke Yoshida[1], Naoki Uchida[1], Ryota Hino[1] (1.Research Center for Prediction of Earthquakes and Volcanic Eruptions, Graduate School of Science, Tohoku University)

[SSS10-P06] Focal mechanisms of the double seismic zone in the Pacific plate, off Boso: Temporal change after the 2011 Tohoku EQ

*Guanyu Chen[1], Toshinori Sato[2], Tomoharu Sato[1], Asami Terada, Masanao Shinohara[3], Kimihiro Mochizuki[3], Tomoaki Yamada[3], Kenji Uehira[4], Takashi Shimbo[5], Shuichi Kodaira[5], Yuya Machida[5], Ryota Hino[6], Ryosuke Azuma[6], Yoshio Murai[7], Yoshihiro Ito[8], Hiroshi Yakiwara[9], Kenji Hirata[4], Akinori Hashima[3], Andrew M. Freed[10] (1.Faculty of Science, Chiba University, 2.Graduate School of Science, Chiba University, 3.Earthquake Research Institute, University of Tokyo, 4.National Research Institute for Earth Science and Disaster Resilience, 5.Japan Agency for Marine-Earth Science and Technology, 6.Graduate School of Science, Tohoku University, 7.Institute of Seismology and Volcanology, Faculty of Science, Hokkaido University, 8.Disaster Prevention Research Institute, Kyoto University, 9.Nansei-toko Observatory for Earthquakes and Volcanoes, Kagoshima University, 10.Purdue University)

[SSS10-P07] Ocean bottom seismographic observation and similar earthquake detection in the northern part of the Nansei Islands

*Yukihiro Nakatani[1], Hiroshi Yakiwara[1], Shuichiro Hirano[1], Reiji Kobayashi[2], Hiroki Miyamachi[2], Shigeru Nakao[2], Kazunari Uchida[3], Takeshi Matsushima[3], Hiroshi Shimizu[3], Kazuo Nakahigashi[4], Yusuke Yamashita[5], Hideji Abe[6], Tomoaki Yamada[6], Masanao Shinohara[6] (1.Nansei-Toko Observatory for Earthquakes and Volcanoes, Kagoshima University, 2.Graduate School of Science and Engineering, Kagoshima University, 3.Institute of Seismology and Volcanology, Faculty of Science, Kyushu University, 4.Tokyo University of Marine Science and Technology, 5.Disaster Prevention Research Institute, Kyoto University, 6.Earthquake Research Institute, the University of Tokyo)

[SSS10-P08] Seismicity and crustal structure in the Okinawa Trough

*Azusa Nishizawa[1], Takeshi Kimura[1], Kentaro Kaneda[2] (1.National Research Institute for Earth Science and Disaster Resilience, 2.Japan Coast Guard)

[SSS10-P09] Time series analyses of the seismic activities in southwestern Japanese Island to southeastern Korean Peninsula excited by the deep fluid heat flow

*Takayuki Kawabe[1] (1.Faculty of Education, Arts and Sciences, Yamagata University)

[SSS10-P10] Integrated monitoring of seismicity in and around the Suruga Bay using Ocean Bottom Seismometers and inland stations.

*Yannis Panayotopoulos[1], Hisatoshi Baba[2], Takahito Nishimiya[3], Taiyo Sotani[4], Nakao Nagisa[4] (1.Association for the Development of Earthquake Prediction, 2.Department of Marine and Earth Science, Tokai University, 3.Meteorological Research Institute, Japan Meteorological Agency, 4.Tokai University)

[SSS10-P11] Linear distribution of the intraslab earthquakes in Tokai

*Sadaomi Suzuki[1] (1.Tono Research Institute of Earthquake Science, Association for the Development of Earthquake Prediction)

[SSS10-P12] The stress change of Chubu region before and after the 2011 Tohoku-oki Earthquake(Mw9.0)

*Yuki Susukida[1], Kei Katsumata[1] (1.Institute of Seismology and Volcanology, Hokkaido University)

[SSS10-P13] Repeating earthquake activity off Miyagi Prefecture triggered by the 2011 Tohoku-oki earthquake

*Kenshiro Tsumura[1] (1.Association for Developement of Earthquake Prediction)

[SSS10-P14] Seismic Moments of Inland Small Earthquakes in Japan: Spectral Analyses Using the Hi-net

*Tomotake Ueno[1], Tatsuhiko Saito[1] (1.National Research Institute for Earth Science and Disaster Resilience)

[SSS10-P15] Spatiotemporal variations of stress field in the 2016 Kumamoto earthquake (M 7.3) area

*Dapeng Zhao[1], Zhiteng Yu[2], Jiabiao Li[2], Zhouchuan Huang[3] (1.Department of Geophysics, Tohoku University, 2.State Oceanic Administration, 3.School of Earth Sciences and Engineering, Nanjing University)

[SSS10-P16] Seismicity and crustal deformation following the 2016 Kumamoto earthquakes

*Kazuyoshi Nanjo[1], Jun Izutsu[2], Yoshiaki Orihara[3], Masashi Kamogawa[4], Toshiyasu Nagao[3] (1.University of Shizuoka, 2.Chubu University, 3.Tokai University, 4.Tokyo Gakugei University)

[SSS10-P17] The unique characters of intensity distribution of the 2018 Sep. 6 Mw6.6 Earthquake of Iburi region in Hokkaido, Japan

*Ritsuko S. Matsu'ura[1], Hiroto Tanaka[2], Mitsuko Furumura[1], Tsutomu Takahama[2] (1.Earthquake Research Center, Association for the Development of Earthquake Prediction, 2.Kozo Keikaku Engineering Inc.)

[SSS10-P18] **Determination of Hypocenter Location in Sumani and Sianok Fault Segments, West Sumatra region Using Oct-Tree Importance Sampling Method**

*Ade Surya Putra[1], Nanang Tyasbudi Puspito[2], Andri Dian Nugraha[2], Pepen Supendi[3,1] (1.Geophysical Engineering, Faculty of Mining and Petroleoum Engineering, Institute of Technology Bandung, 2.Global Geophysics Research Group, Faculty of Mining and Petroleoum Engineering, Institute of Technology Bandung, 3.Agency of Meteorology, Climatology and Geohysics (BMKG), Indonesia, Bandung, Indonesia)

[SSS10-P19] **1D Seismic Velocity Modelling and Hypocenter Relocation around Central and East Java Region: Preliminary Result**

*Faiz Muttaqy[1], Andri Dian Nugraha[2], Nanang Tyasbudi Puspito[2] (1.Geophysical Engineering Study Program, Faculty of Mining and Petroleum Engineering, Institut Teknologi Bandung, 2.Global Geophysics Research Group, Faculty of Mining and Petroleum Engineering, Institut Teknologi Bandung)

[SSS10-P20] ***Seismicity and Tectonics of the Bingöl Area: Eastern Anatolia***

*Dogan Kalafat[1] (1.Bogazici University Kandilli Observatory and Earthquake Research Institute Cengelkoy, Istanbul Turkey)

[SSS10-P21] Seismicity along the North Anatolian Fault beneath the Marmara Sea, deduced from long-term ocean bottom seismographic observations

*Yojiro Yamamoto[1], Narumi Takahashi[2,1], Dogan Kalafat[3], Ali Pinar[3], Remzi Polat[3], Zeynep Coskun[3], Haluk Ozener[3], Yoshiyuki Kaneda[4] (1.Japan Agency for Marine-Earth Science and Technology (JAMSTEC), 2.NIED, 3.KOERI, Bogaziti University, 4.Kagawa University)

[SSS10-P22] **Microseismic Monitoring of the Sultandagi Fault Zone: Western Turkey**

*Dogan Kalafat[1], Yavuz Gunes[1], Mehmet Kara[1], Kivanc Kekovali[1] (1.Bogazici University Kandilli Observatory and Earthquake Research Institute Cengelkoy, Istanbul Turkey)

[SSS10-P23] Analysis of radiated seismic energy distributing in aftershock sequences at the Guerrero, Mexico subduction zone.

*Raymundo Omar Plata Martinez[1], Xyoli Pérez Campos[2], Krishna Shri Singh[2] (1.Kyoto University, 2.Geophysics Institute, UNAM)

[J] Poster | S (Solid Earth Sciences)：S-SS Seismology

5:15 PM - 6:30 PM JST | 8:15 AM - 9:30 AM UTC | Poster Hall International Exhibition Hall8, Makuhari Messe_29

[S-SS10] Seismicity

convener:Kei Katsumata(Institute of Seismology and Volcanology, Hokkaido University)

[SSS10-P01] Spatial-temporal and seismogram characteristics of foreshock and aftershock activities for tsunami earthquakes

*Yifeng Liu[1], Yoshihiro Ito[2], Kazuaki Ohta[2], Satoshi Katakami[1] (1.Division of Earth and Planetary Sciences, Graduate School of Science, Kyoto University, 2.Disaster Prevention Research Institude, Kyoto University)

[SSS10-P02] Successively occurring large earthquakes in the world – comparison of real cases with expectations by the space-time ETAS

*Tetsuo Hashimoto[1], Takashi YOKOTA[2] (1.Seismology and Tsunami Research Department, Meteorological Reaserch Institute, 2.Aichi Institue Technology)

[SSS10-P03] Seismicity beneath stable oceanic plate

*Yasushi Ishihara[1] (1.R&D Center for Earthquake and Tsunami, JAMSTEC)

[SSS10-P04] Relation between long-term slow slip events and correlation between tidal triggering effect and deep low-frequency earthquakes in Bungo Channel: Part 2

*Fuyuki Hirose[1], Akio Kobayashi[1], Kenji Maeda[2] (1.Seismology and Tsunami Research Department, Meteorological Research Institute, 2.Seismology and Volcanology Department, Japan Meteorological Agency)

[SSS10-P05] Arrival-time and hypocenter determination using S-net

*Tomomi Okada[1], Ryota Takagi[1], Takashi NAKAYAMA[1], Syuichi Suzuki[1], Ryosuke Azuma[1], Genti Toyokuni[1], Keisuke Yoshida[1], Naoki Uchida[1], Ryota Hino[1] (1.Research Center for Prediction of Earthquakes and Volcanic Eruptions, Graduate School of Science, Tohoku University)

[SSS10-P06] Focal mechanisms of the double seismic zone in the Pacific plate, off Boso: Temporal change after the 2011 Tohoku EQ

*Guanyu Chen[1], Toshinori Sato[2], Tomoharu Sato[1], Asami Terada, Masanao Shinohara[3], Kimihiro Mochizuki[3], Tomoaki Yamada[3], Kenji Uehira[4], Takashi Shimbo[5], Shuichi Kodaira[5], Yuya Machida[5], Ryota Hino[6], Ryosuke Azuma[6], Yoshio Murai[7], Yoshihiro Ito[8], Hiroshi Yakiwara[9], Kenji Hirata[4], Akinori Hashima[3], Andrew M. Freed[10] (1.Faculty of Science, Chiba University, 2.Graduate School of Science, Chiba University, 3.Earthquake Research Institute, University of Tokyo, 4.National Research Institute for Earth Science and Disaster Resilience, 5.Japan Agency for Marine-Earth Science and Technology, 6.Graduate School of Science, Tohoku University, 7.Institute of Seismology and Volcanology, Faculty of Science, Hokkaido University, 8.Disaster Prevention Research Institute, Kyoto University, 9.Nansei-toko Observatory for Earthquakes and Volcanoes, Kagoshima University, 10.Purdue University)

[SSS10-P07] Ocean bottom seismographic observation and similar earthquake detection in the northern part of the Nansei Islands

*Yukihiro Nakatani[1], Hiroshi Yakiwara[1], Shuichiro Hirano[1], Reiji Kobayashi[2], Hiroki Miyamachi[2], Shigeru Nakao[2], Kazunari Uchida[3], Takeshi Matsushima[3], Hiroshi Shimizu[3], Kazuo Nakahigashi[4], Yusuke Yamashita[5], Hideji Abe[6], Tomoaki Yamada[6], Masanao Shinohara[6] (1.Nansei-Toko Observatory for Earthquakes and Volcanoes, Kagoshima University, 2.Graduate School of Science and Engineering, Kagoshima University, 3.Institute of Seismology and Volcanology, Faculty of Science, Kyushu University, 4.Tokyo University of Marine Science and Technology, 5.Disaster Prevention Research Institute, Kyoto University, 6.Earthquake Research Institute, the University of Tokyo)

[SSS10-P08] Seismicity and crustal structure in the Okinawa Trough

*Azusa Nishizawa[1], Takeshi Kimura[1], Kentaro Kaneda[2] (1.National Research Institute for Earth Science and Disaster Resilience, 2.Japan Coast Guard)

[SSS10-P09] Time series analyses of the seismic activities in southwestern Japanese Island to southeastern Korean Peninsula excited by the deep fluid heat flow

*Takayuki Kawabe[1] (1.Faculty of Education, Arts and Sciences, Yamagata University)

[SSS10-P10] Integrated monitoring of seismicity in and around the Suruga Bay using Ocean Bottom Seismometers and inland stations.

*Yannis Panayotopoulos[1], Hisatoshi Baba[2], Takahito Nishimiya[3], Taiyo Sotani[4], Nakao Nagisa[4] (1.Association for the Development of Earthquake Prediction, 2.Department of Marine and Earth Science, Tokai University, 3.Meteorological Research Institute, Japan Meteorological Agency, 4.Tokai University)

[SSS10-P11] Linear distribution of the intraslab earthquakes in Tokai

*Sadaomi Suzuki[1] (1.Tono Research Institute of Earthquake Science, Association for the Development of Earthquake Prediction)

[SSS10-P12] The stress change of Chubu region before and after the 2011 Tohoku-oki Earthquake(Mw9.0)

*Yuki Susukida[1], Kei Katsumata[1] (1.Institute of Seismology and Volcanology, Hokkaido University)

[SSS10-P13] Repeating earthquake activity off Miyagi Prefecture triggered by the 2011 Tohoku-oki earthquake

*Kenshiro Tsumura[1] (1.Association for Developement of Earthquake Prediction)

[SSS10-P14] Seismic Moments of Inland Small Earthquakes in Japan: Spectral Analyses Using the Hi-net

*Tomotake Ueno[1], Tatsuhiko Saito[1] (1.National Research Institute for Earth Science and Disaster Resilience)

[SSS10-P15] Spatiotemporal variations of stress field in the 2016 Kumamoto earthquake (M 7.3) area

*Dapeng Zhao[1], Zhiteng Yu[2], Jiabiao Li[2], Zhouchuan Huang[3] (1.Department of Geophysics, Tohoku University, 2.State Oceanic Administration, 3.School of Earth Sciences and Engineering, Nanjing University)

[SSS10-P16] Seismicity and crustal deformation following the 2016 Kumamoto earthquakes

*Kazuyoshi Nanjo[1], Jun Izutsu[2], Yoshiaki Orihara[3], Masashi Kamogawa[4], Toshiyasu Nagao[3] (1.University of Shizuoka, 2.Chubu University, 3.Tokai University, 4.Tokyo Gakugei University)

[SSS10-P17] The unique characters of intensity distribution of the 2018 Sep. 6 Mw6.6 Earthquake of Iburi region in Hokkaido, Japan

*Ritsuko S. Matsu'ura[1], Hiroto Tanaka[2], Mitsuko Furumura[1], Tsutomu Takahama[2] (1.Earthquake Research Center, Association for the Development of Earthquake Prediction, 2.Kozo Keikaku Engineering Inc.)

[SSS10-P18] **Determination of Hypocenter Location in Sumani and Sianok Fault Segments, West Sumatra region Using Oct-Tree Importance Sampling Method**

*Ade Surya Putra[1], Nanang Tyasbudi Puspito[2], Andri Dian Nugraha[2], Pepen Supendi[3,1] (1.Geophysical Engineering, Faculty of Mining and Petroleoum Engineering, Institute of Technology Bandung, 2.Global Geophysics Research Group, Faculty of Mining and Petroleoum Engineering, Institute of Technology Bandung, 3.Agency of Meteorology, Climatology and Geohysics (BMKG), Indonesia, Bandung, Indonesia)

[SSS10-P19] **1D Seismic Velocity Modelling and Hypocenter Relocation around Central and East Java Region: Preliminary Result**

*Faiz Muttaqy[1], Andri Dian Nugraha[2], Nanang Tyasbudi Puspito[2] (1.Geophysical Engineering Study Program, Faculty of Mining and Petroleum Engineering, Institut Teknologi Bandung, 2.Global Geophysics Research Group, Faculty of Mining and Petroleum Engineering, Institut Teknologi Bandung)

[SSS10-P20] ***Seismicity and Tectonics of the Bingöl Area: Eastern Anatolia***

*Dogan Kalafat[1] (1.Bogazici University Kandilli Observatory and Earthquake Research Institute Cengelkoy, Istanbul Turkey)

[SSS10-P21] Seismicity along the North Anatolian Fault beneath the Marmara Sea, deduced from long-term ocean bottom seismographic observations

*Yojiro Yamamoto[1], Narumi Takahashi[2,1], Dogan Kalafat[3], Ali Pinar[3], Remzi Polat[3], Zeynep Coskun[3], Haluk Ozener[3], Yoshiyuki Kaneda[4] (1.Japan Agency for Marine-Earth Science and Technology (JAMSTEC), 2.NIED, 3.KOERI, Bogaziti University, 4.Kagawa University)

[SSS10-P22] **Microseismic Monitoring of the Sultandagi Fault Zone: Western Turkey**

*Dogan Kalafat[1], Yavuz Gunes[1], Mehmet Kara[1], Kivanc Kekovali[1] (1.Bogazici University Kandilli Observatory and Earthquake Research Institute Cengelkoy, Istanbul Turkey)

[SSS10-P23] Analysis of radiated seismic energy distributing in aftershock sequences at the Guerrero, Mexico subduction zone.

*Raymundo Omar Plata Martinez[1], Xyoli Pérez Campos[2], Krishna Shri Singh[2] (1.Kyoto University, 2.Geophysics Institute, UNAM)

[J] Oral | S (Solid Earth Sciences)：S-SS Seismology

1:45 PM - 3:15 PM JST | 4:45 AM - 6:15 AM UTC | A10 TOKYO BAY MAKUHARI HALL

[S-SS10] Seismicity

convener:Kei Katsumata(Institute of Seismology and Volcanology, Hokkaido University), Chairperson:Aitaro Kato(Earthquake Research Institute, University of Tokyo), Shinji Toda(東北大学)

1:45 PM - 2:00 PM JST | 4:45 AM - 5:00 AM UTC

[SSS10-01] Seasonal variations in crustal seismicity in San-in district, southwest Japan

*Taku Ueda[1], Aitaro Kato[1] (1.Earthquake Research Institute, the University of Tokyo)

2:00 PM - 2:15 PM JST | 5:00 AM - 5:15 AM UTC

[SSS10-02] **Source fault model of the 2018 M_W 5.6 northern Osaka earthquake, Japan, inferred from the aftershock sequence**

*Aitaro Kato[1], Taku Ueda[1] (1.Earthquake Research Institute, the University of Tokyo)

2:15 PM - 2:30 PM JST | 5:15 AM - 5:30 AM UTC

[SSS10-03] The 2018 Hokkaido Eastern Iburi earthquake (M_{JMA} = 6.7) was triggered by a strike-slip faulting in a stepover segment: Insights from the aftershock distribution and the focal mechanism solution of the mainshock

*Kei Katsumata[1], Mako Ohzono[1], Hiroshi Aoyama[1], Ryo Tanaka[1], Masamitsu Takada[1], Masayoshi Ichiyanagi[1], Teruhiro Yamaguchi[1], Kazumi Okada[1], Hiroaki Takahashi[1], Shin'ichi Sakai[2], Satoshi Matsumoto[3], Tomomi Okada[4], Toru Matsuzawa[4], Shuichiro Hirano[5], Toshiko Terakawa[6], Shinichiro Horikawa[6], Masahiro Kosuga[7], Hiroshi Katao[8], Yoshihisa Iio[8], Airi Nagaoka[8], Noriko Tsumura[9], Tomotake Ueno[10], the Group for the Aftershock Observations of the 2018 Hokkaido Eastern Iburi Earthquake (1.Institute of Seismology and Volcanology, Faculty of Science, Hokkaido University, 2.Earthquake Research Institute, University of Tokyo, 3.Institute of Seismology and Volcanology, Faculty of Science, Kyushu University, 4.Research Center for Prediction of Earthquakes and Volcanic Eruptions, Graduate School of Science, Tohoku University, 5.Nansei-Toko Observatory for Earthquakes and Volcanoes, Graduate School of Science and Engineering, Kagoshima University, 6.Earthquake and Volcano Research Center, Graduate School of Environmental Studies, Nagoya University, 7.Graduate School of Science and Technology, Hirosaki University, 8.Research Center for Earthquake Prediction, Disaster Prevention Research Institute, Kyoto University, 9.Graduate School of Science, Chiba University, 10.National Research Institute for Earth Science and Disaster Prevention)

2:30 PM - 2:45 PM JST | 5:30 AM - 5:45 AM UTC

[SSS10-04] Layered structure of the upper mantle and the crust revealed in the time series analyses of the aftershocks of the 2018 Hokkaido Eastern Iburi Earthquake

*Takayuki Kawabe[1] (1.Faculty of Education, Arts and Sciences, Yamagata University)

2:45 PM - 3:00 PM JST | 5:45 AM - 6:00 AM UTC

[SSS10-05] Aftershock sequence of the 1847 Zenkoji earthquake: Temporal decay presented in four historical materials and best fit values of paramaters for Omori-Utsu law

*Kentaro Hattori[1], Ichiro Nakanishi[1] (1.Kyoto Univ.)

3:00 PM - 3:15 PM JST | 6:00 AM - 6:15 AM UTC

[SSS10-06] The aseismic islands, Amakusa-Kamishima and Shimoshima, Kumamoto Prefecture, southwest Japan: What persistently shuts off regional seismicity

*Shinji Toda[1] (1.International Research Institute of Disaster Science, Tohoku University)

[J] Oral | S (Solid Earth Sciences)：S-SS Seismology

3:30 PM - 5:00 PM JST | 6:30 AM - 8:00 AM UTC | A10 TOKYO BAY MAKUHARI HALL

[S-SS10] Seismicity

convener:Kei Katsumata(Institute of Seismology and Volcanology, Hokkaido University), Chairperson:Akio Katsumata(気象研究所地震津波研究部第一研究室), Yasushi Harada(東海大学)

3:30 PM - 3:45 PM JST | 6:30 AM - 6:45 AM UTC

[SSS10-07] Seismicity in the matle wedge around Ogasawara Islands and Lesser Antilles

*Akio Katsumata[1], Kenji Nakata[1], Akio Kobayashi[1], Fuyuki Hirose[1], Takahito Nishimiya[1] (1.Meteorological Research Institute, Japan Meteorological Agency)

3:45 PM - 4:00 PM JST | 6:45 AM - 7:00 AM UTC

[SSS10-08] Improvement of the accuracy of the unified Japan Earthquake Catalog using ocean bottom seismographs

*Hiroshi UENO[1], Mitsuharu Ueda[1], Hiromi Misu[1], Hirofumi Yokoyama[1], Yuriko Iwasaki[1], Iwakiri Kazuhiro[1] (1.Seismology and Volcanology Department, Japan Meteorological Agency)

4:00 PM - 4:15 PM JST | 7:00 AM - 7:15 AM UTC

[SSS10-09] Spatial distribution of seismic activity and stress field in the source region after the 2011 Tohoku-Oki earthquake

Tomoya Nishimori[1], *Ryota Hino[1], Masanao Shinohara[2] (1.Graduate School of Science, Tohoku University, 2.Earthquake Research Institute, The University of Tokyo)

4:15 PM - 4:30 PM JST | 7:15 AM - 7:30 AM UTC

[SSS10-10] Assessment for a large earthquake occurrence on the northern side of the focal region of the 2011 off-Tohoku mega-thrust earthquake

*Kazuyoshi Nanjo[1], Kazuki Miyaoka[2], Akio Yoshida[3] (1.University of Shizuoka, 2.Japan Meteorological Agency, 3.Shizuoka University)

4:30 PM - 4:45 PM JST | 7:30 AM - 7:45 AM UTC

[SSS10-11] Spatial and temporal distributions of *b*-values related to long-term slow-slip and low-frequency earthquakes in the Bungo Channel and Hyuga-nada regions, Japan

*Keita Chiba[1] (1.Institute of Seismology and Volcanology, Faculty of Science, Kyushu University)

4:45 PM - 5:00 PM JST | 7:45 AM - 8:00 AM UTC

[SSS10-12] 4D b-Value Mapping for Japan

*Yasushi Harada[1], Yuichi Akamine[1], Masayoshi Anzai[1] (1.School of Marine Science and Technology, Tokai University)

[J] Oral | S (Solid Earth Sciences)：S-SS Seismology

9:00 AM - 10:30 AM JST | 12:00 AM - 1:30 AM UTC | A09 TOKYO BAY MAKUHARI HALL

[S-SS11] Seismic wave propagation: Theory and Application

convener:Kiwamu Nishida(Earthquake Research Institute, University of Tokyo), Kazuya Shiraishi(Japan Agency for Marine-Earth Science and Technology), Takao Nibe(JAPEX), Kaoru Sawazaki(National Research Institute for Earth Science and Disaster Resilience), Chairperson:Shunsuke Takemura(防災科研)

9:01 AM - 9:23 AM JST | 12:01 AM - 12:23 AM UTC

[SSS11-13] Fluid flows inferred from microseismic events associated with injection test in Okuaizu Geothermal Field

★Invited Papers

*Kyosuke Okamoto[1], Li Yi[2], Hiroshi Asanuma[1], Takashi Okabe[3], Yasuyuki Abe[4], Masatoshi Tsuzuki[5] (1.National Institute of Advanced Industrial Science and Technology, 2.Osaka University, 3.Geothermal Energy Research and Development Co., Ltd., 4.Okuaizu Geothermal Co., Ltd., 5.Japan Oil, Gas and Metals National Corporation)

9:23 AM - 9:45 AM JST | 12:23 AM - 12:45 AM UTC

[SSS11-14] 3D distribution of intrinsic attenuation factors and random velocity fluctuations in southwestern Japan inferred from seismogram envelopes

★Invited Papers

*Masashi Ogiso[1] (1.Meteorological Research Institute, Japan Meteorological Agency)

9:45 AM - 10:00 AM JST | 12:45 AM - 1:00 AM UTC

[SSS11-15] Regional to teleseismic strong ground motions from a 610 km deep 24 May 2013 Sea of Okhotsk earthquake

*Takashi Furumura[1], Brian LN Kennett[2] (1.Earthquake Research Institute The University of Tokyo, 2.Research School of Earth Sciences, The Australian National University)

10:00 AM - 10:15 AM JST | 1:00 AM - 1:15 AM UTC

[SSS11-16] Trial estimation of eclogitization depths within subducting oceanic crust of the Philippine Sea slab inferred from head wave propagating along the oceanic Moho

*Shunsuke Takemura[1], Takashi Tonegawa[2], Junichi Nakajima[3], Katsuhiko Shiomi[1] (1.National Research Institute for Earth Science and Disaster Resilience, 2.Japan Agency for Marine-Earth Science and Technology , 3.Tokyo Institute of Technology)

10:15 AM - 10:30 AM JST | 1:15 AM - 1:30 AM UTC

[SSS11-17] **Transient gravity perturbations due to a buried gravitational source in a homogeneous elastic half space**

*Aditya Nitin Deshmukh[1], Pratik Laxman Borate[1], Abhishek Venkatesh Chitgopkar[1], Nobuki Kame[2], Ranjith Kunnath[1] (1.Mahindra Ecole Centrale, Hyderabad, India , 2.Division of Theoretical Geoscience, Earthquake Research Institute, University of Tokyo, Japan)

[J] Poster | S (Solid Earth Sciences)：S-SS Seismology

3:30 PM - 5:00 PM JST | 6:30 AM - 8:00 AM UTC | Poster Hall International Exhibition Hall8, Makuhari Messe_17

[S-SS11] Seismic wave propagation: Theory and Application

convener:Kiwamu Nishida(Earthquake Research Institute, University of Tokyo), Kazuya Shiraishi(Japan Agency for Marine-Earth Science and Technology), Takao Nibe(JAPEX), Kaoru Sawazaki(National Research Institute for Earth Science and Disaster Resilience)

[SSS11-P01] Estimation of Love wave phase velocity based on array analysis in the northern Tokyo bay area : Numerical experiments using synthetic seismograms

*Kaori Shimazu[1], Kazuo Yoshimoto[1], Shunsuke Takemura[2] (1.Graduate School of Nanobioscience, Yokohama City University, 2.National Research Institute for Earth Science and Disaster Resilience)

[SSS11-P02] Similutanious estimation of amplitude and travel time variation in the transfer function with ACROSS

*Shuhei Tsuji[1], Koshun Yamaoka[1], Takahiro Kunitomo[1], Toshiki Watanabe[1], Ikuta Ryoya[2] (1.Graduate School of Environmental Studies, Nagoya University, 2.Faculty of Science, Shizuoka University)

[SSS11-P03] Temporal variation in travel time of P and S-waves using ACROSS

*rina suzuki[1], Koshun Yamaoka[2] (1.Graduate School of Environmental Studies, Nagoya University, 2.Earthquake and Volcano Research Center,Graduate School of Environmental Studies,Nagoya University)

[SSS11-P04] Inversion analysis of S coda wave envelope based on radiation transfer theory - Estimation of heterogeneous structure of Izu Oshima volcano -

*Takahiro Ueda[1] (1.Department of Geophysics, Graduate School of Science, Tohoku University)

[SSS11-P05] Strong motion characteristics at Nagomi-machi, Eta, during the northern Kumamoto pref. earthquake of Jan. 3rd, 2019

*Tomotaka Iwata[1], Kimiyuki Asano[1], Masayuki Yoshimi[2], Takeshi Sugiyama (1.Disaster Prevention Research Institute, Kyoto University, 2.Geological Survey of Japan, AIST)

[SSS11-P06] **Effects of the heterogeneous crustal structure on the amplitude fluctuation of high-frequency seismic waves**

*Kazuo Yoshimoto[1], Shunsuke Takemura[2] (1.Graduate School of Nanobioscience, Yokohama City University, 2.National Research Institute for Earth Science and Disaster Resilience)

[SSS11-P07] Long-duration long-period ground motion in Hokkaido during off-Tohoku earthquakes (2) Roles of crust and Pacific slab

*Shinako Noguchi[1], Takuto Maeda[2], Takashi Furumura[3] (1.Association for the Development of Earthquake Prediction, 2.Faculty of Science and Technology, Hirosaki University, 3.Earthquake Research Institute, The University of Tokyo)

[SSS11-P08] Measuring the NCF dispersion without the long inter-station distance limitation – a new method based on hybrid peak time matching

*Ying-Nien Chen[1], Yuancheng Gung[2], Ling-Yun Chiao[3] (1.Institute of Seismology, National Chung Cheng University, Taiwan., 2.Department of Geosciences, National Taiwan University, Taipei, Taiwan., 3.Institute of Oceanography, National Taiwan University, Taipei, Taiwan.)

[SSS11-P09] Dynamic Triggering Earthquakes Exploration by Sonification of Seismograms

*Takahiko Uchide[1], Yota Morimoto[2], Masaki Matsubara[3] (1.Research Institute of Earthquake and Volcano Geology, Geological Survey of Japan, National Institute of Advanced Industrial Science and Technology (AIST), 2.Institute of Sonology, Royal Conservatory of the Hague, 3.University of Tsukuba)

[SSS11-P10] The effect of P-wave velocity on the ellipticity of Rayleigh waves in a transversely isotropic medium

*Shun Fukushima[1], Kiyoshi Yomogida[1] (1.Hokkaido University,Graduate school of Science,Department of Natural History Sciences,Seismology Laboratory)

[SSS11-P11] Time series analyses of amplitude of the Earth’s background free oscillations

*Ryuichi Kunugi[1], Naoki Suda[1] (1.Hiroshima University)

[SSS11-P12] Regional shear waves from an unusually deep earthquake beneath Ogasawara Islands: 660 km discontinuity and anisotropy

*Keiko Kuge[1] (1.Department of Geophysics, Graduate School of Science, Kyoto University)

[SSS11-P13] On the estimation of G discontinuity in the oceanic upper mantle using ScS reverberations

*Jumpei Maruyama[1], Hitoshi Kawakatsu[1], Nozomu Takeuchi[1] (1.University of Tokyo, Earthquake Research Institute)

[SSS11-P14] Short-period body wave (1-3 Hz) extraction from ambient noise records observed at seafloor and borehole in the Nankai subduction zone

*Takashi Tonegawa[1], Toshinori Kimura[1] (1.Research and Development center for Earthquake and Tsunami, Japan Agency for Marine-Earth Science and Technology)

[SSS11-P15] Characteristics of T-wave envelopes observed by S-net

*Kentaro Emoto[1], Hisashi Nakahara[1] (1.Graduate School of Science, Tohokuk University)

[SSS11-P16] Reverse time reflection imaging of active and passive seismic data with ocean-bottom seismographs

*Kazuya Shiraishi[1], Takao Nibe[2], Yasuhiro Yamada[1] (1.Japan Agency for Marine-Earth Science and Technology, 2.Japan Petroleum Exploration Co. Ltd.)

[J] Poster | S (Solid Earth Sciences)：S-SS Seismology

5:15 PM - 6:30 PM JST | 8:15 AM - 9:30 AM UTC | Poster Hall International Exhibition Hall8, Makuhari Messe_30

[S-SS11] Seismic wave propagation: Theory and Application

convener:Kiwamu Nishida(Earthquake Research Institute, University of Tokyo), Kazuya Shiraishi(Japan Agency for Marine-Earth Science and Technology), Takao Nibe(JAPEX), Kaoru Sawazaki(National Research Institute for Earth Science and Disaster Resilience)

[SSS11-P01] Estimation of Love wave phase velocity based on array analysis in the northern Tokyo bay area : Numerical experiments using synthetic seismograms

*Kaori Shimazu[1], Kazuo Yoshimoto[1], Shunsuke Takemura[2] (1.Graduate School of Nanobioscience, Yokohama City University, 2.National Research Institute for Earth Science and Disaster Resilience)

[SSS11-P02] Similutanious estimation of amplitude and travel time variation in the transfer function with ACROSS

*Shuhei Tsuji[1], Koshun Yamaoka[1], Takahiro Kunitomo[1], Toshiki Watanabe[1], Ikuta Ryoya[2] (1.Graduate School of Environmental Studies, Nagoya University, 2.Faculty of Science, Shizuoka University)

[SSS11-P03] Temporal variation in travel time of P and S-waves using ACROSS

*rina suzuki[1], Koshun Yamaoka[2] (1.Graduate School of Environmental Studies, Nagoya University, 2.Earthquake and Volcano Research Center,Graduate School of Environmental Studies,Nagoya University)

[SSS11-P04] Inversion analysis of S coda wave envelope based on radiation transfer theory - Estimation of heterogeneous structure of Izu Oshima volcano -

*Takahiro Ueda[1] (1.Department of Geophysics, Graduate School of Science, Tohoku University)

[SSS11-P05] Strong motion characteristics at Nagomi-machi, Eta, during the northern Kumamoto pref. earthquake of Jan. 3rd, 2019

*Tomotaka Iwata[1], Kimiyuki Asano[1], Masayuki Yoshimi[2], Takeshi Sugiyama (1.Disaster Prevention Research Institute, Kyoto University, 2.Geological Survey of Japan, AIST)

[SSS11-P06] **Effects of the heterogeneous crustal structure on the amplitude fluctuation of high-frequency seismic waves**

*Kazuo Yoshimoto[1], Shunsuke Takemura[2] (1.Graduate School of Nanobioscience, Yokohama City University, 2.National Research Institute for Earth Science and Disaster Resilience)

[SSS11-P07] Long-duration long-period ground motion in Hokkaido during off-Tohoku earthquakes (2) Roles of crust and Pacific slab

*Shinako Noguchi[1], Takuto Maeda[2], Takashi Furumura[3] (1.Association for the Development of Earthquake Prediction, 2.Faculty of Science and Technology, Hirosaki University, 3.Earthquake Research Institute, The University of Tokyo)

[SSS11-P08] Measuring the NCF dispersion without the long inter-station distance limitation – a new method based on hybrid peak time matching

*Ying-Nien Chen[1], Yuancheng Gung[2], Ling-Yun Chiao[3] (1.Institute of Seismology, National Chung Cheng University, Taiwan., 2.Department of Geosciences, National Taiwan University, Taipei, Taiwan., 3.Institute of Oceanography, National Taiwan University, Taipei, Taiwan.)

[SSS11-P09] Dynamic Triggering Earthquakes Exploration by Sonification of Seismograms

*Takahiko Uchide[1], Yota Morimoto[2], Masaki Matsubara[3] (1.Research Institute of Earthquake and Volcano Geology, Geological Survey of Japan, National Institute of Advanced Industrial Science and Technology (AIST), 2.Institute of Sonology, Royal Conservatory of the Hague, 3.University of Tsukuba)

[SSS11-P10] The effect of P-wave velocity on the ellipticity of Rayleigh waves in a transversely isotropic medium

*Shun Fukushima[1], Kiyoshi Yomogida[1] (1.Hokkaido University,Graduate school of Science,Department of Natural History Sciences,Seismology Laboratory)

[SSS11-P11] Time series analyses of amplitude of the Earth's background free oscillations

*Ryuichi Kunugi[1], Naoki Suda[1] (1.Hiroshima University)

[SSS11-P12] Regional shear waves from an unusually deep earthquake beneath Ogasawara Islands: 660 km discontinuity and anisotropy

*Keiko Kuge[1] (1.Department of Geophysics, Graduate School of Science, Kyoto University)

[SSS11-P13] On the estimation of G discontinuity in the oceanic upper mantle using ScS reverberations

*Jumpei Maruyama[1], Hitoshi Kawakatsu[1], Nozomu Takeuchi[1] (1.University of Tokyo, Earthquake Research Institute)

[SSS11-P14] Short-period body wave (1-3 Hz) extraction from ambient noise records observed at seafloor and borehole in the Nankai subduction zone

*Takashi Tonegawa[1], Toshinori Kimura[1] (1.Research and Development center for Earthquake and Tsunami, Japan Agency for Marine-Earth Science and Technology)

[SSS11-P15] Characteristics of T-wave envelopes observed by S-net

*Kentaro Emoto[1], Hisashi Nakahara[1] (1.Graduate School of Science, Tohokuk University)

[SSS11-P16] Reverse time reflection imaging of active and passive seismic data with ocean-bottom seismographs

*Kazuya Shiraishi[1], Takao Nibe[2], Yasuhiro Yamada[1] (1.Japan Agency for Marine-Earth Science and Technology, 2.Japan Petroleum Exploration Co. Ltd.)

[J] Oral | S (Solid Earth Sciences)：S-SS Seismology

3:30 PM - 5:00 PM JST | 6:30 AM - 8:00 AM UTC | A05 TOKYO BAY MAKUHARI HALL

[S-SS14] Fault Rheology and Earthquake Physics

convener:Keishi Okazaki(Japan Agency for Marine-Earth Science and Technology), Hideki Mukoyoshi(Department of Geoscience Interdisciplinary Graduate School of Science and Engineering, Shimane University), Hiroyuki Noda(Kyoto University, Disaster Prevention Research Institute), Keisuke Yoshida(Tohoku University), Chairperson:Keisuke Yoshida(東北大学大学院理学研究科 地球物理学専攻), Keishi Okazaki(JAMSTEC)

3:30 PM - 3:45 PM JST | 6:30 AM - 6:45 AM UTC

[SSS14-01] **Spatio-temporal Evolution of Micro-Earthquakes illuminated by “0.1 manten” Hyper Dense Seismic Observation: Implication of Fault Growth**

*Aitaro Kato[1], Shin'ichi Sakai[1], Satoshi Matsumoto[2], Yoshihisa Iio[3] (1.Earthquake Research Institute, the University of Tokyo, 2.Kyushu University, 3.Kyoto University)

3:45 PM - 4:00 PM JST | 6:45 AM - 7:00 AM UTC

[SSS14-02] Estimation of fault model of the 2017 Pohang, South Korea earthquake using seismic and geodetic analyses

*Sun-Cheon Park[1], Won-Jin Lee[2], Geunyoung Song[1], Duk Kee Lee[1] (1.Korea Meteorological Administration, 2.National Institute of Environmental Research)

4:00 PM - 4:15 PM JST | 7:00 AM - 7:15 AM UTC

[SSS14-03] Estimation of rupture directivity, fault plane, and stress drop of small earthquakes in inland areas of Japan

*Keisuke Yoshida[1], Tatsuhiko Saito[2], Kentaro Emoto[1], Yumi Urata[2] (1.Tohoku University, 2.NIED)

4:15 PM - 4:30 PM JST | 7:15 AM - 7:30 AM UTC

[SSS14-04] **Possible aseismic phenomena causing the hypocenter migration in the precursory activity and aftershocks of the 2017 M 5.3 Kagoshima Bay earthquake, Kyusyu, SW Japan**

*Yoshiaki Matsumoto[1], Keisuke Yoshida[1], Toru Matsuzawa[1], Akira Hasegawa[1] (1.Research Center for Prediction of Earthquakes and Volcanic Eruptions, Tohoku University)

4:30 PM - 4:45 PM JST | 7:30 AM - 7:45 AM UTC

[SSS14-05] Stress and pore fluid pressure changes in fault zone preceding the earthquake occurrence

*Teruo Yamashita

4:45 PM - 5:00 PM JST | 7:45 AM - 8:00 AM UTC

[SSS14-06] Micromechanical model of fluid-induced seismicity to reproduce observed spatiotemporal changes in source parameters and on-fault fluid diffusion

*Daisuke Sato[1], Keisuke Yoshida[2] (1.Disaster Prevention Research Institute, Kyoto University, 2.Tohoku University)

[J] Poster | S (Solid Earth Sciences)：S-SS Seismology

1:45 PM - 3:15 PM JST | 4:45 AM - 6:15 AM UTC | Poster Hall International Exhibition Hall8, Makuhari Messe_7

[S-SS15] Active faults and paleoseismology

convener:Mamoru Koarai(Earth Science course, College of Science, Ibaraki University), Takashi OGAMI(National Institute of Advanced Industrial Science and Technology), Ryosuke Doke(Hot Springs Research Institute of Kanagawa Prefecture), Hisao Kondo(Geological Survey of Japan, National Institute of Advanced Industrial Science and Technology)

[SSS15-P01] Paleoseismicity of Atsuma Town , Hokkaido: Evidence from landslide deposits

*Jun Tajika[1], Tetsuya Inui[2] (1.Docon Co.,Ltd., 2.Board of Education, Atsuma Town)

[SSS15-P02] Gravity survey and subsurface structure across the Aomoriwan-Seigan Fault Zone, Northeast Japan(part 2; estimation of the subsurface structure using the density of rock samples)

*Shinsuke Okada[1], Hideki Kosaka[2], Kyoko Kagohara[3], Toshifumi Imaizumi[4], Kohei Abe[5], Susumu Sakashita[5], Atsushi Miwa[5], Kouta Koshika[5], Yusuke Oda[5], Yuki tsukamoto[6], Takahiro Miyauchi[7], Tomoo Echigo[8] (1.International Research Institute of Disaster Science, Tohoku University, 2.Kankyo Chishitsu, Co. Ltd., 3.Faculty of Education, Yamaguchi University, 4.Emeritus professor of Tohoku University, 5.OYO Corporation, 6.Graduate School of Science, Tohoku University, 7.Department of Earth Sciences, Graduate School and Faculty of Science, Chiba University, 8.Geo-Research Institute)

[SSS15-P03] Was the 1611 Keicho earthquake a giant interplate event like the 2011 Tohoku earthquake?

*Tomoya Harada[1], Akihito Nishiyama[1], Kenji Satake[1], Takashi Furumura[1] (1.Earthquake Research Institute, The University of Tokyo)

[SSS15-P04] **Neotectonic characteristics along both flanks of the Ou Backbone Range, Tohoku Region, Japan, from fluvial geomorphic analyses**

*Jhih Hao Liao[1], J Bruce H Shyu[1], Yasufumi Iryu[2], Hiroyuki Tsutsumi[3], Chia-Yu Chen[1] (1.Department of Geosciences, National Taiwan University, Taipei, Taiwan, 2.Graduate School of Science, Tohoku University, Sendai, Japan, 3.Department of Environmental Systems Science, Doshisha University, Kyotanabe, Japan)

[SSS15-P05] Tsunami record of the last 700 years in bottom sediment of lake Kasumi-ga-ura, southeastern part of Ibaragi Prefecture

*Yoshio Inouchi[1] (1.Faculty of Human Sciences, Waseda University)

[SSS15-P06] Detecting concealed fault by microtremor H/V study in Miura Peninsula

*Kazuzi Ogawa[1], Yasuyuki Iwase[1], Takumi Murakoshi[1], Toshihisa Itano[1] (1.National Defense Academy)

[SSS15-P07] Distribution, geometry and slip rates of branch faults around the Kita-Izu fault zone

*Ryuhei Oda[1], Daisuke Ishimura[1], Takehiko Suzuki[1] (1.Tokyo Metropolitan University)

[SSS15-P08] Paleoseismology of the southern part of Kamishiro fault, ISTL active fault zone, central Japan

*Kotaro Mizutani[1], Daisuke Hirouchi[1], Nobuhisa Matsuta[2], Tatsuya Ishiyama[3], Nobuhiko Sugito[4], Ken-ichi Yasue[5], Yoshihiro Takeshita[1], Natsuko Fujita[6], Hiroshi Sawa[7], Ryosuke Doke[8], Haruo Maruyama[9], Kazutaka Ikeda[10], Kamishiro Fault (1.Shinshu University, 2.Okayama University, 3.ERI, University of Tokyo, 4.Hosei University, 5.Toyama University, 6.JAEA, 7.Tsuruoka Nat.Col.Tech., 8. Hot Springs Research Institute of Kanagawa Pref., 9.Kisoseiho High school, 10.Mochiduki Elementary School)

[SSS15-P09] **Geotectonic history of the Inadani fault zone in southern part of Nagano prefecture, central Japan**

*Shuuhei Tsukui[1], Kenta Kobayashi[1] (1.Department of Geology, Faculty of Science, Niigata University)

[SSS15-P10] Characteristics of the fault zone with only the recent slips in the Atera Fault

Atsushi Nishida[1], *Tomoyuki Ohtani[1], Takuya Niimi[1], Jun'ichi Tsubaki[1], Keiichi Ueta[2] (1.Department of Civil Engineering, Gifu University, 2.CRIEPI)

[SSS15-P11] Identification of active fault location using real-time ground measurements of atmospheric methane concentration by portable Cavity Ring-down Spectroscopy system: Case study at the Atera fault

*Michito Shimo[1], Masakazu Niwa[2], Kenji Amano[2], Tomochika Tokunaga[3], Kenichi Tonokura[3], Toshifumi Matsuoka[1], Sebastien Biraud[4] (1.Fukada Geological Institute, 2.Japan Atomic Energy Agency, 3.Department of Environment Systems, University of Tokyo, 4.Lawrence Berkeley National Laboratory, USA)

[SSS15-P12] Geomorphological evudence of a newly found active fault along the Shirakawa fault in western part Gifu Prefecture

*Yorihide Kohriya[1], Masashi Omata[1], Hiroshi Yokota[1] (1.PASCO CORPORATION)

[SSS15-P13] Active faults around the Niu Mountains, northern part of Fukui Prefecture, Japan

*Masayoshi Tajikara[1], Takashi Nakata[2], Hiroyuki Tsutsumi[3], Hideaki Goto[2] (1.Association for the Development of Earthquake Prediction, 2.Hiroshima University, 3.Doshisha University)

[SSS15-P14] Gifu-Ichinomiya Fault shown from the characteristics of the damage of the Nobi earthquake

*Nobuhisa Matsuta[1,2], Fumiaki KIMATA[2] (1.Okayama University Graduate School of Education, 2.Tono Research Institute of Earthquake Science)

[SSS15-P15] Electrical resistivity structure from the surface to the seismogenic zone below the Gomura fault zone, Kyoto, Southwest Japan

*Satoru Yamaguchi[1], Akira Mimura[1], Kazuki Fukue[1], Shigehiro Katoh[2], Hideki Murakami[3], Makoto Uyeshima[4] (1.Department of Geosciences, Graduate School of Science, Osaka City University, 2.The Museum of Nature and Human Activities, Hyogo, 3.Science and Technology Unit, Research and Education Faculty, Kochi University, 4.Earthquake Research Institute, The University of Tokyo)

[SSS15-P16] Re-analysis and re-interpretation of the very shallow land seismic reflection survey data across the Naruto-South fault, north side of Tokushima Plain.

*Kobayashi Takayuki[1], Dai Nobuoka[2], Tomio Inazaki[1] (1.Public Works Research Institute Japan, 2.OYO Corporation)

[SSS15-P17] Bathymetric mapping and seafloor imaging for finding historical records of Nankai earthquakes at Nomi bay in Susaki city, Kochi Prefecture, Japan

*Wataru Tanikawa[1], Masafumi MURAYAMA[2], Hidekazu Tokuyama[3], Kouki Tanaka[4], Akira Ijiri[1], Tatsuhiko Hoshino[1], Takehiro Hirose[1], Kazuya Kitada[5], Toshiya Fujiwara[5] (1.Japan Agency for Marine-Earth Science and Technology, Kochi Instutute for Core Sample Research, 2.Kochi Univerisity, Faculty of Agriculture and Marine Science, 3.Kochi Univerisity, Center for Advanced Marine Core Research , 4.Kochi Univerisity, 5.Japan Agency for Marine-Earth Science and Technology)

[SSS15-P18] Tectonic geomorphological and paleoseismological study in the Anoriguchi Canyon: Foraminiferal analysis and ^{14}C dating

*Nobuhiko Sugito[1], Masao Iwai[2], Hitomi Wakaki-Uchimura[2], Hiroki Matsui[2], Yasuhiro Suzuki[3] (1.Faculty of Sustainability Studies, Hosei University, 2.Center for Advanced Marine Core Research, Kochi University, 3.Disaster Mitigation Research Center, Nagoya University)

[SSS15-P19] Subsurface survey around the Matoishi-bokujo 1 Fault in the northwest of the outer rim of the Aso caldera, southwestern Japan

*Takayuki Nakano[1], Hiroshi Une[1], Hiroshi, P. Sato[2], Keitaro Komura[3] (1.GSI of Japan, 2.Nihon Univ., 3.CRIEPI)

[SSS15-P20] Past activity of 'triggered fault' in the northwest of outer rim of Aso caldera estimated from the results of excurvation survey and displacement topography

*Hiroshi Une[1], Takayuki Nakano[1], Hiroshi, P. Sato[2], Hiroshi YAGI[3], Keitaro Komura[4] (1.Geospatial Information Authority of Japan, 2.Nihon University, 3.Yamagata University, 4.Central Research Institute of Electric Power Industry)

[SSS15-P21] Visualization of three-dimensional SAR analysis data by stereo isogram map: Precise detection of surface ruptures of the 2016 Kumamoto earthquake sequence

*Yasuo Awata[1] (1.Institute of Earthquake and Volcano Geology, Geological Survey of Japan, National Institute of Advanced Industrial Science and Technology)

[SSS15-P22] Preliminary active fault mapping of Mongolia by interpretation of ALOS 30 DEM image

*Takashi Nakata[1], Yasuhiro Suzuki[2], Mitsuhisa Watanabe[3] (1.Hiroshima University, 2.Nagoya University, 3.Toyo University)

[SSS15-P23] Ground penetrating radar profiling across the Sanchiao fault in northeast Taiwan

*Mamoru Nakamura[1], How-wei Chen[2] (1.Faculty of Science, University of the Ryukyus, 2.National Central University, Taiwan)

[SSS15-P24] Paleo-earthquake records of the Hengchun offshore structure, southern Taiwan

*Sze-Chieh Liu[1], J Bruce H Shyu[1], Yuan-Lu Tsai[1], Chuan-Chou Shen[1] (1.National Taiwan University)

[SSS15-P25] LC-InSAR analysis of the Sulawesi earthquake in Indonesia

*Jun Sugimoto[1], Masashi Omata[1], Yoshiteru Akiyama[1], Yutaka Horaku[1] (1.PASCO CORPORATION)

[SSS15-P26] **Risk evaluation and disaster education around the coastal areas of Sea of Marmara, Turkey through the fault model construction of the North Anatolian Fault**

*Yoshiyuki Kaneda[1,2,3], Haluk Ozener[4], Nurcan Meral Ozel[4,5], Dogan Kalafat[4], Seckin Ozgur Citak , Narumi Takashi[2,3], Takane Hori[2], Muneo Hori[2,6], Mayumi Sakamoto[10,7], Ali Pinar[4], Asim Oguz Ozel[11], Ahmet Cevdet Yalciner[8], Gulum Tanircan[4], Ahmet Demirtas[9] (1.Kagawa University, 2.JAMSTEC, 3.NIED, 4.Bogazici University, 5.CTBTO, 6.ERI, 7.Nagoya University, 8.Middle East Technical University, 9.AFAD, 10. University of Hyogo, 11.Istanbul University)

[SSS15-P27] Estimation of fault activity by multivariate analysis using chemical composition of fault gouge

*Ryo Tateishi[1], Koji Shimada[2], Tadamasa Ueki[2], Mayuko Shimizu[2], Tetsuya Komatsu[2], Shigeru Sueoka[2], Masakazu Niwa[2], Ken-ichi Yasue[1], Tsuneari Ishimaru[2] (1.University of Toyama, 2.Japan Atomic Energy Agency)

[SSS15-P28] Bayesian optimization of fault-shape parameters using finite element analysis: parameter sets for strong slip partitioning

*Hidetaka Saomoto[1] (1.National Institute of Advanced Industrial Science and Technology)

[J] Poster | S (Solid Earth Sciences)：S-SS Seismology

5:15 PM - 6:30 PM JST | 8:15 AM - 9:30 AM UTC | Poster Hall International Exhibition Hall8, Makuhari Messe_31

[S-SS15] Active faults and paleoseismology

convener:Mamoru Koarai(Earth Science course, College of Science, Ibaraki University), Takashi OGAMI(National Institute of Advanced Industrial Science and Technology), Ryosuke Doke(Hot Springs Research Institute of Kanagawa Prefecture), Hisao Kondo(Geological Survey of Japan, National Institute of Advanced Industrial Science and Technology)

[SSS15-P01] Paleoseismicity of Atsuma Town , Hokkaido: Evidence from landslide deposits

*Jun Tajika[1], Tetsuya Inui[2] (1.Docon Co.,Ltd., 2.Board of Education, Atsuma Town)

[SSS15-P02] Gravity survey and subsurface structure across the Aomoriwan-Seigan Fault Zone, Northeast Japan(part 2; estimation of the subsurface structure using the density of rock samples)

*Shinsuke Okada[1], Hideki Kosaka[2], Kyoko Kagohara[3], Toshifumi Imaizumi[4], Kohei Abe[5], Susumu Sakashita[5], Atsushi Miwa[5], Kouta Koshika[5], Yusuke Oda[5], Yuki tsukamoto[6], Takahiro Miyauchi[7], Tomoo Echigo[8] (1.International Research Institute of Disaster Science, Tohoku University, 2.Kankyo Chishitsu, Co. Ltd., 3.Faculty of Education, Yamaguchi University, 4.Emeritus professor of Tohoku University, 5.OYO Corporation, 6.Graduate School of Science, Tohoku University, 7.Department of Earth Sciences, Graduate School and Faculty of Science, Chiba University, 8.Geo-Research Institute)

[SSS15-P03] Was the 1611 Keicho earthquake a giant interplate event like the 2011 Tohoku earthquake?

*Tomoya Harada[1], Akihito Nishiyama[1], Kenji Satake[1], Takashi Furumura[1] (1.Earthquake Research Institute, The University of Tokyo)

[SSS15-P04] **Neotectonic characteristics along both flanks of the Ou Backbone Range, Tohoku Region, Japan, from fluvial geomorphic analyses**

*Jhih Hao Liao[1], J Bruce H Shyu[1], Yasufumi Iryu[2], Hiroyuki Tsutsumi[3], Chia-Yu Chen[1] (1.Department of Geosciences, National Taiwan University, Taipei, Taiwan, 2.Graduate School of Science, Tohoku University, Sendai, Japan, 3.Department of Environmental Systems Science, Doshisha University, Kyotanabe, Japan)

[SSS15-P05] Tsunami record of the last 700 years in bottom sediment of lake Kasumi-ga-ura, southeastern part of Ibaragi Prefecture

*Yoshio Inouchi[1] (1.Faculty of Human Sciences, Waseda University)

[SSS15-P06] Detecting concealed fault by microtremor H/V study in Miura Peninsula

*Kazuzi Ogawa[1], Yasuyuki Iwase[1], Takumi Murakoshi[1], Toshihisa Itano[1] (1.National Defense Academy)

[SSS15-P07] Distribution, geometry and slip rates of branch faults around the Kita-Izu fault zone

*Ryuhei Oda[1], Daisuke Ishimura[1], Takehiko Suzuki[1] (1.Tokyo Metropolitan University)

[SSS15-P08] Paleoseismology of the southern part of Kamishiro fault, ISTL active fault zone, central Japan

*Kotaro Mizutani[1], Daisuke Hirouchi[1], Nobuhisa Matsuta[2], Tatsuya Ishiyama[3], Nobuhiko Sugito[4], Ken-ichi Yasue[5], Yoshihiro Takeshita[1], Natsuko Fujita[6], Hiroshi Sawa[7], Ryosuke Doke[8], Haruo Maruyama[9], Kazutaka Ikeda[10], Kamishiro Fault (1.Shinshu University, 2.Okayama University, 3.ERI, University of Tokyo, 4.Hosei University, 5.Toyama University, 6.JAEA, 7.Tsuruoka Nat.Col.Tech., 8. Hot Springs Research Institute of Kanagawa Pref., 9.Kisoseiho High school, 10.Mochiduki Elementary School)

[SSS15-P09] **Geotectonic history of the Inadani fault zone in southern part of Nagano prefecture, central Japan**

*Shuuhei Tsukui[1], Kenta Kobayashi[1] (1.Department of Geology, Faculty of Science, Niigata University)

[SSS15-P10] Characteristics of the fault zone with only the recent slips in the Atera Fault

Atsushi Nishida[1], *Tomoyuki Ohtani[1], Takuya Niimi[1], Jun'ichi Tsubaki[1], Keiichi Ueta[2] (1.Department of Civil Engineering, Gifu University, 2.CRIEPI)

[SSS15-P11] Identification of active fault location using real-time ground measurements of atmospheric methane concentration by portable Cavity Ring-down Spectroscopy system: Case study at the Atera fault

*Michito Shimo[1], Masakazu Niwa[2], Kenji Amano[2], Tomochika Tokunaga[3], Kenichi Tonokura[3], Toshifumi Matsuoka[1], Sebastien Biraud[4] (1.Fukada Geological Institute, 2.Japan Atomic Energy Agency, 3.Department of Environment Systems, University of Tokyo, 4.Lawrence Berkeley National Laboratory, USA)

[SSS15-P12] Geomorphological evudence of a newly found active fault along the Shirakawa fault in western part Gifu Prefecture

*Yorihide Kohriya[1], Masashi Omata[1], Hiroshi Yokota[1] (1.PASCO CORPORATION)

[SSS15-P13] Active faults around the Niu Mountains, northern part of Fukui Prefecture, Japan

*Masayoshi Tajikara[1], Takashi Nakata[2], Hiroyuki Tsutsumi[3], Hideaki Goto[2] (1.Association for the Development of Earthquake Prediction, 2.Hiroshima University, 3.Doshisha University)

[SSS15-P14] Gifu-Ichinomiya Fault shown from the characteristics of the damage of the Nobi earthquake

*Nobuhisa Matsuta[1,2], Fumiaki KIMATA[2] (1.Okayama University Graduate School of Education, 2.Tono Research Institute of Earthquake Science)

[SSS15-P15] Electrical resistivity structure from the surface to the seismogenic zone below the Gomura fault zone, Kyoto, Southwest Japan

*Satoru Yamaguchi[1], Akira Mimura[1], Kazuki Fukue[1], Shigehiro Katoh[2], Hideki Murakami[3], Makoto Uyeshima[4] (1.Department of Geosciences, Graduate School of Science, Osaka City University, 2.The Museum of Nature and Human Activities, Hyogo, 3.Science and Technology Unit, Research and Education Faculty, Kochi University, 4.Earthquake Research Institute, The University of Tokyo)

[SSS15-P16] Re-analysis and re-interpretation of the very shallow land seismic reflection survey data across the Naruto-South fault, north side of Tokushima Plain.

*Kobayashi Takayuki[1], Dai Nobuoka[2], Tomio Inazaki[1] (1.Public Works Research Institute Japan, 2.OYO Corporation)

[SSS15-P17] Bathymetric mapping and seafloor imaging for finding historical records of Nankai earthquakes at Nomi bay in Susaki city, Kochi Prefecture, Japan

*Wataru Tanikawa[1], Masafumi MURAYAMA[2], Hidekazu Tokuyama[3], Kouki Tanaka[4], Akira Ijiri[1], Tatsuhiko Hoshino[1], Takehiro Hirose[1], Kazuya Kitada[5], Toshiya Fujiwara[5] (1.Japan Agency for Marine-Earth Science and Technology, Kochi Instutute for Core Sample Research, 2.Kochi Univerisity, Faculty of Agriculture and Marine Science, 3.Kochi Univerisity, Center for Advanced Marine Core Research , 4.Kochi Univerisity, 5.Japan Agency for Marine-Earth Science and Technology)

[SSS15-P18] Tectonic geomorphological and paleoseismological study in the Anoriguchi Canyon: Foraminiferal analysis and ^{14}C dating

*Nobuhiko Sugito[1], Masao Iwai[2], Hitomi Wakaki-Uchimura[2], Hiroki Matsui[2], Yasuhiro Suzuki[3] (1.Faculty of Sustainability Studies, Hosei University, 2.Center for Advanced Marine Core Research, Kochi University, 3.Disaster Mitigation Research Center, Nagoya University)

[SSS15-P19] Subsurface survey around the Matoishi-bokujo 1 Fault in the northwest of the outer rim of the Aso caldera, southwestern Japan

*Takayuki Nakano[1], Hiroshi Une[1], Hiroshi, P. Sato[2], Keitaro Komura[3] (1.GSI of Japan, 2.Nihon Univ., 3.CRIEPI)

[SSS15-P20] Past activity of 'triggered fault' in the northwest of outer rim of Aso caldera estimated from the results of excurvation survey and displacement topography

*Hiroshi Une[1], Takayuki Nakano[1], Hiroshi, P. Sato[2], Hiroshi YAGI[3], Keitaro Komura[4] (1.Geospatial Information Authority of Japan, 2.Nihon University, 3.Yamagata University, 4.Central Research Institute of Electric Power Industry)

[SSS15-P21] Visualization of three-dimensional SAR analysis data by stereo isogram map: Precise detection of surface ruptures of the 2016 Kumamoto earthquake sequence

*Yasuo Awata[1] (1.Institute of Earthquake and Volcano Geology, Geological Survey of Japan, National Institute of Advanced Industrial Science and Technology)

[SSS15-P22] Preliminary active fault mapping of Mongolia by interpretation of ALOS 30 DEM image

*Takashi Nakata[1], Yasuhiro Suzuki[2], Mitsuhisa Watanabe[3] (1.Hiroshima University, 2.Nagoya University, 3.Toyo University)

[SSS15-P23] Ground penetrating radar profiling across the Sanchiao fault in northeast Taiwan

*Mamoru Nakamura[1], How-wei Chen[2] (1.Faculty of Science, University of the Ryukyus, 2.National Central University, Taiwan)

[SSS15-P24] Paleo-earthquake records of the Hengchun offshore structure, southern Taiwan

*Sze-Chieh Liu[1], J Bruce H Shyu[1], Yuan-Lu Tsai[1], Chuan-Chou Shen[1] (1.National Taiwan University)

[SSS15-P25] LC-InSAR analysis of the Sulawesi earthquake in Indonesia

*Jun Sugimoto[1], Masashi Omata[1], Yoshiteru Akiyama[1], Yutaka Horaku[1] (1.PASCO CORPORATION)

[SSS15-P26] **Risk evaluation and disaster education around the coastal areas of Sea of Marmara, Turkey through the fault model construction of the North Anatolian Fault**

*Yoshiyuki Kaneda[1,2,3], Haluk Ozener[4], Nurcan Meral Ozel[4,5], Dogan Kalafat[4], Seckin Ozgur Citak , Narumi Takashi[2,3], Takane Hori[2], Muneo Hori[2,6], Mayumi Sakamoto[10,7], Ali Pinar[4], Asim Oguz Ozel[11], Ahmet Cevdet Yalciner[8], Gulum Tanircan[4], Ahmet Demirtas[9] (1.Kagawa University, 2.JAMSTEC, 3.NIED, 4.Bogazici University, 5.CTBTO, 6.ERI, 7.Nagoya University, 8.Middle East Technical University, 9.AFAD, 10. University of Hyogo, 11.Istanbul University)

[SSS15-P27] Estimation of fault activity by multivariate analysis using chemical composition of fault gouge

*Ryo Tateishi[1], Koji Shimada[2], Tadamasa Ueki[2], Mayuko Shimizu[2], Tetsuya Komatsu[2], Shigeru Sueoka[2], Masakazu Niwa[2], Ken-ichi Yasue[1], Tsuneari Ishimaru[2] (1.University of Toyama, 2.Japan Atomic Energy Agency)

[SSS15-P28] Bayesian optimization of fault-shape parameters using finite element analysis: parameter sets for strong slip partitioning

*Hidetaka Saomoto[1] (1.National Institute of Advanced Industrial Science and Technology)

[J] Oral | S (Solid Earth Sciences)：S-SS Seismology

3:30 PM - 5:00 PM JST | 6:30 AM - 8:00 AM UTC | A02 TOKYO BAY MAKUHARI HALL

[S-SS15] Active faults and paleoseismology

convener:Mamoru Koarai(Earth Science course, College of Science, Ibaraki University), Takashi OGAMI(National Institute of Advanced Industrial Science and Technology), Ryosuke Doke(Hot Springs Research Institute of Kanagawa Prefecture), Hisao Kondo(Geological Survey of Japan, National Institute of Advanced Industrial Science and Technology), Chairperson:Mamoru KOARAI(Ibaraki University), Taku Komatsubara(産業技術総合研究所)

3:30 PM - 4:00 PM JST | 6:30 AM - 7:00 AM UTC

[SSS15-01] Historical documents and oral transmissions on historical tsunamis in the Paciffic coast of Tohoku

★Invited Papers

*ebina yuichi[1] (1.International Research Institute of Disaster Science)

4:00 PM - 4:15 PM JST | 7:00 AM - 7:15 AM UTC

[SSS15-02] Co-seismic crustal movements along reverse faults which subsidence component is larger than uplifting component

*Taku Komatsubara[1] (1.Institute of Geology and Geoinformation, Advanced Industrial Science and Technology)

4:15 PM - 4:30 PM JST | 7:15 AM - 7:30 AM UTC

[SSS15-03] The Iyo-Bungo, southwest Japan, earthquake on September 1st, 1596 as deduced from contemporary historical records

*Katsuhiko Ishibashi[1] (1.Emeritus Professor, Kobe University)

4:30 PM - 4:45 PM JST | 7:30 AM - 7:45 AM UTC

[SSS15-04] Geologically recorded historical and prehistoric tsunamis in the Tonankai region

*Shigehiro Fujino[1], Haruo Kimura[2], Junko Komatsubara[3], Dan Matsumoto[3], Yuichi Namegaya[3], Yuki Sawai[3], Masanobu Shishikura[3] (1.Faculty of Life and Environmental Sciences, University of Tsukuba, 2.Civil Engineering Research Laboratory, Central Research Institute of Electric Power Industry, 3.Geological Survey of Japan, National Institute of Advanced Industrial Science and Technology (AIST))

[E] Oral | S (Solid Earth Sciences)：S-IT Science of the Earth's Interior & Techtonophysics

9:00 AM - 10:30 AM JST | 12:00 AM - 1:30 AM UTC | A10 TOKYO BAY MAKUHARI HALL

[S-IT21] Interaction and Coevolution of the Core and Mantle in the Earth and Planets

convener:Kenji Kawai(Department of Earth and Planetary Science, School of Science, University of Tokyo), Tsuyoshi Iizuka(University of Tokyo), Kenji Ohta(Department of Earth and Planetary Sciences, Tokyo Institute of Technology), Taku Tsuchiya(Geodynamics Research Center, Ehime University), Chairperson:Kenji Kawai, Sebastian Ritterbex

9:00 AM - 9:15 AM JST | 12:00 AM - 12:15 AM UTC

[SIT21-19] Seismological Explorations of Earth's Outer Core: Normal Mode and Body Wave Analyses

★Invited Papers

*Jessica C E Irving[1], Sanne Cottaar[2], Vedran Lekic[3], Wenbo Wu[4] (1.Princeton University, 2.University of Cambridge, 3.University of Maryland, College Park, 4.California Institute of Technology)

9:15 AM - 9:30 AM JST | 12:15 AM - 12:30 AM UTC

[SIT21-20] Discussion

*Kenji Kawai[1] (1.University of Tokyo)

9:30 AM - 9:45 AM JST | 12:30 AM - 12:45 AM UTC

[SIT21-21] On the 1-D radial convective structure of the Earth’s core inferred from a coupled core-mantle evolution model

*Takashi Nakagawa[1] (1.Department of Earth Sciences, The University of Hong Kong)

9:45 AM - 10:00 AM JST | 12:45 AM - 1:00 AM UTC

[SIT21-22] Structural and transport properties of liquid iron-light-element mixtures under outer core conditions

*Satoshi Ohmura[1], Taku Tsuchiya[2] (1.Hiroshima Inst. of Tech., 2.Ehime Univ.)

10:00 AM - 10:15 AM JST | 1:00 AM - 1:15 AM UTC

[SIT21-23] Development of New Technology for Geoneutrino Directional Measurement

*Hiroko Watanabe[1] (1.Research Center for Neutrino Science, Tohoku University)

10:15 AM - 10:30 AM JST | 1:15 AM - 1:30 AM UTC

[SIT21-24] Investigation of multi light elements in iron-silicate-water system using high pressure and temperature neutron experiments: Implications for the Earth's evolution

★Invited Papers

*Riko Iizuka-Oku[1], Hirotada Gotou[2], Ko Fukuyama[1], Hiroyuki Kagi[1] (1.Geochemical Research Center, Graduate School of Science, The University of Tokyo, 2.The Institute for Solid State Physics, The University of Tokyo)

[E] Oral | S (Solid Earth Sciences)：S-IT Science of the Earth's Interior & Techtonophysics

10:45 AM - 12:15 PM JST | 1:45 AM - 3:15 AM UTC | A10 TOKYO BAY MAKUHARI HALL

[S-IT21] Interaction and Coevolution of the Core and Mantle in the Earth and Planets

convener:Kenji Kawai(Department of Earth and Planetary Science, School of Science, University of Tokyo), Tsuyoshi Iizuka(University of Tokyo), Kenji Ohta(Department of Earth and Planetary Sciences, Tokyo Institute of Technology), Taku Tsuchiya(Geodynamics Research Center, Ehime University), Chairperson:Noriyoshi Tsujino, Kenta Ueki

10:45 AM - 11:00 AM JST | 1:45 AM - 2:00 AM UTC

[SIT21-25] Low hydrogen contents in the cores of terrestrial planets

★Invited Papers

*Vincent Clesi[1], Mohamed Ali Bouhifd[2], Nathalie Bolfan-Casanova[2], Geeth Manthilake[2], Federica Schiavi[2], Caroline Raepsaet[3], Hélène Bureau[4], Hicham Khodja[3], Denis Andrault[2] (1.Laboratoire de Geologie de Lyon - Terre, Planètes, Environnement, Université Claude Bernard Lyon 1, CNRS, ENS-Lyon, 69622 Villeurbanne, France., 2.Laboratoire Magmas et Volcans, Université Clermont Auvergne, CNRS UMR 6524, OPGC–IRD, Campus Universitaire des Cézeaux, 6 Avenue Blaise Pascal, 63178 Aubière Cedex, France., 3.Laboratoire d'Etude des Eléments Légers, NIMBE, CEA, CNRS, Université Paris-Saclay, CEA Saclay, 91191 Gif sur Yvette Cedex, France., 4.Institut de Minéralogie et de Physique de la Matière et de Cosmochimie, Sorbonne Universités, UMR CNRS-UPMC 7590, 4 place Jussieu, 75252 Paris, France.)

11:00 AM - 11:15 AM JST | 2:00 AM - 2:15 AM UTC

[SIT21-26] Discussion

*Taku Tsuchiya[1] (1.Geodynamics Research Center, Ehime University)

11:15 AM - 11:30 AM JST | 2:15 AM - 2:30 AM UTC

[SIT21-27] Fe_2S: the most iron-rich Fe-S compound at pressures of the inner core

*Shigehiko Tateno[1,2], Haruka Ozawa[2,3], Kei Hirose[1,4], Toshihiro Suzuki[5] (1.Earth-Life Science Institute, Tokyo Institute of Technology, 2.Institute for Planetary Materials, Okayama University, 3.Nuclear Science and Engineering Center, Japan Atomic Energy Agency, 4.Department of Earth and Planetart Science, The University of Tokyo, 5.Geochemical Research Center, The University of Tokyo)

11:30 AM - 11:45 AM JST | 2:30 AM - 2:45 AM UTC

[SIT21-28] First-principles Investigation of Iron Diffusion Properties with Implications to Inner Core Plasticity

★Invited Papers

*Sebastian Ritterbex[1], Taku Tsuchiya[1] (1.GRC Ehime University)

11:45 AM - 12:00 PM JST | 2:45 AM - 3:00 AM UTC

[SIT21-29] Dependence of the dipole component dominancy on the Rayleigh number and inner core size in geodynamo simulations

*Yuki Nishida[1], Yuto Katoh[1], Hiroaki Matsui[2], Masaki Matsushima[3], Atsushi Kumamoto[1] (1.Department of Geophysics, Graduate School of Science, Tohoku University, 2.Dept. of Earth and Planetary Sciences, University of California, Davis, 3.Department of Earth and Planetary Sciences, School of Science, Tokyo Institute of Technology)

12:00 PM - 12:15 PM JST | 3:00 AM - 3:15 AM UTC

[SIT21-30] Elasticity of Fe-Si Alloy

*Taku Tsuchiya[1], Yu Fukunaga[1] (1.Geodynamics Research Center, Ehime University)

[E] Poster | S (Solid Earth Sciences)：S-MP Mineralogy & Petrology

10:45 AM - 12:15 PM JST | 1:45 AM - 3:15 AM UTC | Poster Hall International Exhibition Hall8, Makuhari Messe_7

[S-MP29] Oceanic and Continental Subduction Processes

convener:REHMAN Ur Hafiz(Department of Earth and Environmental Sciences, Graduate School of Science and Engineering, Kagoshima University), Tatsuki Tsujimori(Tohoku University), Chin-Ho Tsai(Department of Natural Resources and Environmental Studies, National Dong Hwa University), Kazuaki Okamoto(Faculty of Education, Saitama University)

[SMP29-P01] Zircon U-Pb ages of metasedimentary rocks in the Hakogase (Hida Marginal) area, Fukui Prefecture.

*Atsushi MIYASHITA[1], Tatsuki Tsujimori[2], Daniel Pastor-Galán[3], Yi Keewook[4] (1.Seikei University, 2.Tohoku University, 3.Salamanca University, 4.Korea Basic Science Institue)

[SMP29-P02] Late Permian to Early Triassic back-arc type volcanism in the southern Mongolia volcano-plutonic belt of the Central Asian Orogenic Belt: Implication for timing of the final closure of the Palaeo-Asian Ocean

*Takeshi Imayama[1], Yoichiro Koh[2], Kazumasa Aoki[3], Mototaka Saneyoshi[4], Koshi Yagi[5], Shogo Aoki[4], Yoshihiro Sawada[6], Chiaki Ikawa[5], Tomoya Terada[4], Shinobu Ishigaki[4], Shin Toyoda[3], Khishigjav Tsogtbaatar[7], Buuvei Mainbayar[7] (1.Research Institute of Natural Sciences, Okayama University of Science, 2.Graduate School of Environmental Science, Hokkaido University, 3.Faculty of Science, Okayama University of Science, 4.Faculty of Biosphere - Geosphere Science, Okayama University of Science, 5.Hiruzen Institute for Geology and Chronology, 6.Emeritus Professor of Shimane University, 7.Institute of Paleontology and Geology, Mongolian Academy of Sciences)

[SMP29-P03] Mantle dynamics of slab breakoff constrained from the temporal change of the melting depth estimated from the Cumulate Member of the Ordovician Hayachine-Miyamori Ophiolite

*Takafumi Kimura[1], Kazuhito Ozawa[1] (1.Department of Earth and Planetary Science, The University of Tokyo)

[SMP29-P04] **Evidence of HIMU seamount on the Farallon Plate: Application of *in-situ* Sr-Pb isotope analysis to Franciscan lawsonite-bearing metagreywacke**

*Tomomi Hara[1], Tatsuki Tsujimori[1], Jun-Ichi Kimura[2] (1.Tohoku University, 2.Japan Agency for Marine-Earth Science and Technology)

[SMP29-P05] Boron isotope variations of antigorite serpentinites associated with high-pressure metamorphic rocks: A case study in the Itoigawa–Omi area of the Hida-Gaien Belt, Japan

*Chinatsu Yamada[1], Tatsuki Tsujimori[1], King Chang[2], Jun-Ichi Kimura[2] (1.Tohoku University, 2.Japan Aegency for Marine-Earth Science and Technology)

[SMP29-P06] **Study of zircons structures from the Miocene Shibi-san Granodiorite, Kagoshima Prefecture, Japan**

*Nakabayashi Marimo[1], REHMAN Ur Hafiz[1] (1.Kagoshima University)

[SMP29-P07] **Experimental modeling of eclogite and C-O-H fluid interaction in the subduction zones**

*Nadezda Chertkova[1], Shigeru Yamashita[2], Hiroaki Ohfuji[1], Tetsuo Irifune[1], Hirokazu Kadobayashi[1], Yoshitaka Yamamoto[3] (1.Ehime University, Geodynamics Research Center, 2.Okayama University, Institute for Planetary Materials, 3.National Institute of Advanced Industrial Science and Technology)

[SMP29-P08] Microfabrics of omphacite and garnet in eclogite from the Lanterman Range, northern Victoria Land, Antarctica

*Daeyeong Kim[1], Taehwan Kim[2], Jungmin Kim[3] (1.Division of Polar-Earth Sciences, Korea Polar Research Institute, 2.School of Earth and Environmental Sciences, Seoul National University, 3.Earth and Environmental Sciences, Korea University)

[SMP29-P09] Primordial Apatite from Ophiolite in Taiwan

*Nobuaki Niitsuma[1], Reishi Takashima[2], Yuan Hsi Lee[3] (1.Institute of Geosciences,Shizuoka University, 2.Tohoku University Museum, 3.National Chung-Cheng University, Taiwan)

[SMP29-P10] The evolution of the Cretaceous Jinan Basin in South Korea and the age and tectonic setting for the volcanic rocks in it

*Seung Hwan LEE[1], Chang Whan Oh[1] (1.Department of earth and environmental sciences Chonbuk national university)

[SMP29-P11] GEOCHORONOLOGY AND PETROCHEMISTREY OF LATE PALEOZOIC MAGMATIC ROCKS OF THE MANDAKH AREA, SOUTHEAST MONGOLIA

*Undarmaa Batsaikhan[1], Noriyoshi Tsuchiya[1], Masaoki Uno[1], Yukio Isozaki[2], Uyanga Bold[2], Hikaru Sawada[2] (1.Graduate School of Environmental Studies, Tohoku University, 2.Graduate School of Arts and Sciences The University of Tokyo)

[SMP29-P12] Feedbacks Offshore the Cascadia Margin

*Joan S Gomberg[1] (1.USGS Earthquake Science Center)

[E] Poster | S (Solid Earth Sciences)：S-MP Mineralogy & Petrology

5:15 PM - 6:30 PM JST | 8:15 AM - 9:30 AM UTC | Poster Hall International Exhibition Hall8, Makuhari Messe_32

[S-MP29] Oceanic and Continental Subduction Processes

convener:REHMAN Ur Hafiz(Department of Earth and Environmental Sciences, Graduate School of Science and Engineering, Kagoshima University), Tatsuki Tsujimori(Tohoku University), Chin-Ho Tsai(Department of Natural Resources and Environmental Studies, National Dong Hwa University), Kazuaki Okamoto(Faculty of Education, Saitama University)

[SMP29-P01] Zircon U-Pb ages of metasedimentary rocks in the Hakogase (Hida Marginal) area, Fukui Prefecture.

*Atsushi MIYASHITA[1], Tatsuki Tsujimori[2], Daniel Pastor-Galán[3], Yi Keewook[4] (1.Seikei University, 2.Tohoku University, 3.Salamanca University, 4.Korea Basic Science Institue)

[SMP29-P02] Late Permian to Early Triassic back-arc type volcanism in the southern Mongolia volcano-plutonic belt of the Central Asian Orogenic Belt: Implication for timing of the final closure of the Palaeo-Asian Ocean

*Takeshi Imayama[1], Yoichiro Koh[2], Kazumasa Aoki[3], Mototaka Saneyoshi[4], Koshi Yagi[5], Shogo Aoki[4], Yoshihiro Sawada[6], Chiaki Ikawa[5], Tomoya Terada[4], Shinobu Ishigaki[4], Shin Toyoda[3], Khishigjav Tsogtbaatar[7], Buuvei Mainbayar[7] (1.Research Institute of Natural Sciences, Okayama University of Science, 2.Graduate School of Environmental Science, Hokkaido University, 3.Faculty of Science, Okayama University of Science, 4.Faculty of Biosphere - Geosphere Science, Okayama University of Science, 5.Hiruzen Institute for Geology and Chronology, 6.Emeritus Professor of Shimane University, 7.Institute of Paleontology and Geology, Mongolian Academy of Sciences)

[SMP29-P03] Mantle dynamics of slab breakoff constrained from the temporal change of the melting depth estimated from the Cumulate Member of the Ordovician Hayachine-Miyamori Ophiolite

*Takafumi Kimura[1], Kazuhito Ozawa[1] (1.Department of Earth and Planetary Science, The University of Tokyo)

[SMP29-P04] **Evidence of HIMU seamount on the Farallon Plate: Application of *in-situ* Sr-Pb isotope analysis to Franciscan lawsonite-bearing metagreywacke**

*Tomomi Hara[1], Tatsuki Tsujimori[1], Jun-Ichi Kimura[2] (1.Tohoku University, 2.Japan Agency for Marine-Earth Science and Technology)

[SMP29-P05] Boron isotope variations of antigorite serpentinites associated with high-pressure metamorphic rocks: A case study in the Itoigawa–Omi area of the Hida-Gaien Belt, Japan

*Chinatsu Yamada[1], Tatsuki Tsujimori[1], King Chang[2], Jun-Ichi Kimura[2] (1.Tohoku University, 2.Japan Aegency for Marine-Earth Science and Technology)

[SMP29-P06] **Study of zircons structures from the Miocene Shibi-san Granodiorite, Kagoshima Prefecture, Japan**

*Nakabayashi Marimo[1], REHMAN Ur Hafiz[1] (1.Kagoshima University)

[SMP29-P07] **Experimental modeling of eclogite and C-O-H fluid interaction in the subduction zones**

*Nadezda Chertkova[1], Shigeru Yamashita[2], Hiroaki Ohfuji[1], Tetsuo Irifune[1], Hirokazu Kadobayashi[1], Yoshitaka Yamamoto[3] (1.Ehime University, Geodynamics Research Center, 2.Okayama University, Institute for Planetary Materials, 3.National Institute of Advanced Industrial Science and Technology)

[SMP29-P08] Microfabrics of omphacite and garnet in eclogite from the Lanterman Range, northern Victoria Land, Antarctica

*Daeyeong Kim[1], Taehwan Kim[2], Jungmin Kim[3] (1.Division of Polar-Earth Sciences, Korea Polar Research Institute, 2.School of Earth and Environmental Sciences, Seoul National University, 3.Earth and Environmental Sciences, Korea University)

[SMP29-P09] Primordial Apatite from Ophiolite in Taiwan

*Nobuaki Niitsuma[1], Reishi Takashima[2], Yuan Hsi Lee[3] (1.Institute of Geosciences,Shizuoka University, 2.Tohoku University Museum, 3.National Chung-Cheng University, Taiwan)

[SMP29-P10] The evolution of the Cretaceous Jinan Basin in South Korea and the age and tectonic setting for the volcanic rocks in it

*Seung Hwan LEE[1], Chang Whan Oh[1] (1.Department of earth and environmental sciences Chonbuk national university)

[SMP29-P11] GEOCHORONOLOGY AND PETROCHEMISTREY OF LATE PALEOZOIC MAGMATIC ROCKS OF THE MANDAKH AREA, SOUTHEAST MONGOLIA

*Undarmaa Batsaikhan[1], Noriyoshi Tsuchiya[1], Masaoki Uno[1], Yukio Isozaki[2], Uyanga Bold[2], Hikaru Sawada[2] (1.Graduate School of Environmental Studies, Tohoku University, 2.Graduate School of Arts and Sciences The University of Tokyo)

[SMP29-P12] Feedbacks Offshore the Cascadia Margin

*Joan S Gomberg[1] (1.USGS Earthquake Science Center)

[E] Oral | S (Solid Earth Sciences)：S-MP Mineralogy & Petrology

1:45 PM - 3:15 PM JST | 4:45 AM - 6:15 AM UTC | A08 TOKYO BAY MAKUHARI HALL

[S-MP29] Oceanic and Continental Subduction Processes

convener:REHMAN Ur Hafiz(Department of Earth and Environmental Sciences, Graduate School of Science and Engineering, Kagoshima University), Tatsuki Tsujimori(Tohoku University), Chin-Ho Tsai(Department of Natural Resources and Environmental Studies, National Dong Hwa University), Kazuaki Okamoto(Faculty of Education, Saitama University), Chairperson:Hafiz REHMAN(Kagoshima University), Tatsuki Tsujimori

1:45 PM - 2:00 PM JST | 4:45 AM - 5:00 AM UTC

[SMP29-01] Pb-isotope of Fe-Ni alloy associated with serpentinite: Geochemical constraints on the fluid-mediated hyper-reducing environment in mantle wedge

★Invited Papers

*Mayu Kakefuda[1], Tatsuki Tsujimori[1], Katsuyuki Yamashita[2], Yoshiyuki Iizuka[3] (1.Tohoku University, 2.Graduate School of Natural Science and Technology, Okayama University, 3.Institute of Earth Sciences, Academia Sinica)

2:00 PM - 2:15 PM JST | 5:00 AM - 5:15 AM UTC

[SMP29-02] PETROCHEMISTRY AND AGE DETERMINATION OF THE NEWLY DISCOVERED ECLOGITE IN THE WESTERN MONGOLIA

*Kosuke Naemura[1], Erdenjargal Choindonjamts[4], Takenori Kato[5], Otgonkhuu Javkhlan[3], Katsuyoshi Michibayashi[2] (1.Nagoya University Museum, 2.Nagoya University Graduate school of environmental studies, 3.Chinese Academy of Geological Sciences, 4.Mongolian Academy of Sciences, 5.Nagoya University Space-Earth Environmental Research)

2:15 PM - 2:45 PM JST | 5:15 AM - 5:45 AM UTC

[SMP29-03] **Continental subduction, "*Intraslab UHP Metasomatism*", and the formation of metamorphic diamond**

★Invited Papers

*Yoshihide Ogasawara[1] (1.Department of Earth Sciences, Waseda University)

2:45 PM - 3:00 PM JST | 5:45 AM - 6:00 AM UTC

[SMP29-04] Ultrahigh-pressure pseudotachylyte in a marble

★Invited Papers

*Tadao Nishiyama[1], Tomoya Fujimoto[1] (1.Department of Earth and Environmental Sciences, School of Science, Graduate School of Science and Technology, Kumamoto University)

3:00 PM - 3:15 PM JST | 6:00 AM - 6:15 AM UTC

[SMP29-05] Dehydration and Deformation process of subducted large Oceanic Pleateau -case study of the Mikabu blueschist-

*Kazuaki Okamoto[1] (1.Faculty of Education, Saitama University)

[E] Oral | S (Solid Earth Sciences)：S-MP Mineralogy & Petrology

3:30 PM - 5:00 PM JST | 6:30 AM - 8:00 AM UTC | A08 TOKYO BAY MAKUHARI HALL

[S-MP29] Oceanic and Continental Subduction Processes

convener:REHMAN Ur Hafiz(Department of Earth and Environmental Sciences, Graduate School of Science and Engineering, Kagoshima University), Tatsuki Tsujimori(Tohoku University), Chin-Ho Tsai(Department of Natural Resources and Environmental Studies, National Dong Hwa University), Kazuaki Okamoto(Faculty of Education, Saitama University), Chairperson:Tsai Chin-HO(National Dong Hwa University), Hafiz REHMAN(Kagoshima University)

3:30 PM - 3:45 PM JST | 6:30 AM - 6:45 AM UTC

[SMP29-06] Unusually high Nb/Ta ratio of fluid-precipitated jadeites from New Idria serpentinite body, California: Implications for extreme fractionation in slab fluids

*Naoko Takahashi[1], Tatsuki Tsujimori[2], Qing Chang[3], Jun-Ichi Kimura[3] (1.Graduate School of Science, Tohoku Univ., 2.CNEAS, Tohoku Univ., 3.Department of Solid Earth Geochemistry, JAMSTEC)

3:45 PM - 4:00 PM JST | 6:45 AM - 7:00 AM UTC

[SMP29-07] The collision process interpreted using the systematic change of metamorphic pattern along theQinling–Dabie–Odesan collisional belt between the North and South Korea-China Cratons

★Invited Papers

*Chang Whan Oh[1,2] (1.Department of Earth and Environmental Sciences, Chonbuk National University, Jeonju, Republic of Korea, 2.Environmental Science System Research Center, Chonbuk National University,Jeonju, Republic of Korea)

4:00 PM - 4:15 PM JST | 7:00 AM - 7:15 AM UTC

[SMP29-08] Contrasting collision processes between northwest and central Himalaya: examination from the "Lesser Himalayan granites” in Pakistan

*Masatsugu Ogasawara[1], Mayuko Fukuyama[2], Rehanul H Siddiqui[3] (1.Institute of Geology and Geoinformation, Geological Survey of Japan, National Institute of Advanced Industrial Science and Technology, 2.Graduate School of Engineering Science, Akita University, 3.Balochistan University of Information Technology, Engineering and Management Sciences)

4:15 PM - 4:30 PM JST | 7:15 AM - 7:30 AM UTC

[SMP29-09] New petrologic indications of subduction metamorphism in the Yuli belt, eastern Taiwan

*Chin-Ho Tsai[1], Chih-Ying Yeh[1], Dominikus Deka Dewangga[1], Yui Kouketsu[2], Masaki Enami[3] (1.Department of Natural Resources & Environmental Studies, National Dong Hwa Univ., 2.Department of Earth & Planetary Sciences, Nagoya Univ., 3.Institute for Space-Earth Environmental Research, Nagoya Univ.)

4:30 PM - 4:45 PM JST | 7:30 AM - 7:45 AM UTC

[SMP29-10] **The importance of Mn-nodules on the sea floor during subduction for the formation of ophiolitic diamond**

*Richard Wirth[1] (1.Helmholtz Centre Potsdam GFZ German Research Centre for Geosciences 3.5 Surface Geochemistry)

4:45 PM - 5:00 PM JST | 7:45 AM - 8:00 AM UTC

[SMP29-11] **Along-strike variability of primitive magmas inferred from olivine-hosted melt inclusions, southernmost Andean Southern Volcanic Zone, Chile**

*Derek Weller[1,2], Charles R Stern[2] (1.Earthquake Research Institute, 2.University of Colorado)

[E] Poster | S (Solid Earth Sciences)：S-MP Mineralogy & Petrology

10:45 AM - 12:15 PM JST | 1:45 AM - 3:15 AM UTC | Poster Hall International Exhibition Hall8, Makuhari Messe_8

[S-MP30] Crust-Mantle Connections

convener:Yoshihiko Tamura(Research Institute for Marine Geodynamics, Japan Agency for Maine-Earth Science and Technology), Osamu Ishizuka(Geological Survey of Japan, AIST), Chris Conway(Geological Survey of Japan)

[SMP30-P01] Secular evolution of proto-Izu-Bonin-Mariana arc volcanism: Constraints from statistical analysis of melt inclusion compositions

*Morihisa Hamada[1], Hikaru Iwamori[1,2], Philipp A. Brandl[3], Takayuki Ushikubo[4], Kenji Shimizu[4], Motoo Ito[4], He Li[5], Ivan P. Savov[6] (1.Department of Solid Earth Geochemistry, Japan Agency for Marine-Earth Science and Technology, 2.Earthquake Research Institute, University of Tokyo, 3.GEOMAR Helmholtz Centre for Ocean Research Kiel, 4.Kochi Institute for Core Sample Research, Japan Agency for Marine-Earth Science and Technology, 5.Institute of Oceanology, Chinese Academy of Sciences, 6.School of Earth and Environment, University of Leeds)

[SMP30-P02] The Jurassic magmatism of protoliths of Mikabu greenstones in SW Japan: zircon U-Pb dating and trace element analysis

*Hikaru Sawada[1], Yukio Isozaki[1], Shogo Aoki[3], Shuhei Sakata[2], Ryo Hasegawa[1], Yasuo Nakamura[1] (1.Department of General Systems Studies, the University of Tokyo, 2.Department of Chemistry, Gakushuin Universtiy, 3.Department of Applied Science, Okayama University of Science)

[SMP30-P03] **Origin of variable CaO/Al_2O_3 in olivine-hosted melt inclusions from Kibblewhite Volcano, Kermadec Arc**

*Yasuhiro Hirai[1], Yoshihiko Tamura[2], Kaj Hoernle[3], Christian Timm[4], Folkmar Hauff[3], Reinhard Werner[3], Takeshi Hanyu[2], Bogdan Vaglarov[2], Qing Chang[2], Takashi Miyazaki[2], Jun-Ichi Kimura[2] (1.Graduate School of Natural Science and Technology, Kanazawa University, Japan, 2.Japan Agency for Marine-Earth Science and Technology (JAMSTEC), Yokosuka, Kanagawa, Japan, 3.GEOMAR Helmholtz Centre for Ocean Research, Kiel, Germany, 4.GNS Science, Lower Hutt, New Zealand)

[SMP30-P04] Ankaramite from Doyo seamount in the Izu-Ogasawara arc: A precursor of continents?

*Yoshihiko Tamura[1], Tomoki Sato[1], Osamu Ishizuka[1,2], Takashi Miyazaki[1], Yasuhiro Hirai[1,3], Mami Takehara[4], Eri Sakamoto[5] (1.JAMSTEC, 2.AIST, 3.Kanazawa Univ., 4.NIPR, 5.NME)

[SMP30-P05] Different Moho reflections adjacent to Minami-Tori Shima and their petrologic origins

*Yoshihiko Tamura[1], Kentaro Kaneda[2], Gou Fujie[1], Akane Ohira[1], Eiichi TAKAZAWA[3], Georges Ceuleneer[4], Katsuyoshi Michibayashi[5], Tomoki Sato[1], Shuichi Kodaira[1], Seiichi Miura[1] (1.Japan Agency for Maine-Earth Science and Technology, 2.Japan Coast Guard, 3.Niigata University, 4.Universite de Toulouse, 5.Nagoya University)

[SMP30-P06] **Melt-rock interaction in plagioclase peridotites from the southern Palawan Ophiolite, Philippines**

*FLORENCE ANNETTE CRUSPERO LABIS[1], BETCHAIDA D PAYOT[1], GABRIEL THEOPHILUS V VALERA[1], JULIUS A PASCO[1], JESLEY MEI A DYCOCO[1] (1.UNIVERSITY OF THE PHILIPPINES)

[SMP30-P07] Intra-oceanic arc magma genesis: a case study from Havre volcano, Kermadec arc

*Chris Conway[1], Kenichiro Tani[2] (1.Geological Survey of Japan, 2.National Museum of Nature and Science)

[E] Poster | S (Solid Earth Sciences)：S-MP Mineralogy & Petrology

5:15 PM - 6:30 PM JST | 8:15 AM - 9:30 AM UTC | Poster Hall International Exhibition Hall8, Makuhari Messe_33

[S-MP30] Crust-Mantle Connections

convener:Yoshihiko Tamura(Research Institute for Marine Geodynamics, Japan Agency for Maine-Earth Science and Technology), Osamu Ishizuka(Geological Survey of Japan, AIST), Chris Conway(Geological Survey of Japan)

[SMP30-P01] Secular evolution of proto-Izu-Bonin-Mariana arc volcanism: Constraints from statistical analysis of melt inclusion compositions

*Morihisa Hamada[1], Hikaru Iwamori[1,2], Philipp A. Brandl[3], Takayuki Ushikubo[4], Kenji Shimizu[4], Motoo Ito[4], He Li[5], Ivan P. Savov[6] (1.Department of Solid Earth Geochemistry, Japan Agency for Marine-Earth Science and Technology, 2.Earthquake Research Institute, University of Tokyo, 3.GEOMAR Helmholtz Centre for Ocean Research Kiel, 4.Kochi Institute for Core Sample Research, Japan Agency for Marine-Earth Science and Technology, 5.Institute of Oceanology, Chinese Academy of Sciences, 6.School of Earth and Environment, University of Leeds)

[SMP30-P02] The Jurassic magmatism of protoliths of Mikabu greenstones in SW Japan: zircon U-Pb dating and trace element analysis

*Hikaru Sawada[1], Yukio Isozaki[1], Shogo Aoki[3], Shuhei Sakata[2], Ryo Hasegawa[1], Yasuo Nakamura[1] (1.Department of General Systems Studies, the University of Tokyo, 2.Department of Chemistry, Gakushuin Universtiy, 3.Department of Applied Science, Okayama University of Science)

[SMP30-P03] Origin of variable CaO/Al_2O_3 in olivine-hosted melt inclusions from Kibblewhite Volcano, Kermadec Arc

*Yasuhiro Hirai[1], Yoshihiko Tamura[2], Kaj Hoernle[3], Christian Timm[4], Folkmar Hauff[3], Reinhard Werner[3], Takeshi Hanyu[2], Bogdan Vaglarov[2], Qing Chang[2], Takashi Miyazaki[2], Jun-Ichi Kimura[2] (1.Graduate School of Natural Science and Technology, Kanazawa University, Japan, 2.Japan Agency for Marine-Earth Science and Technology (JAMSTEC), Yokosuka, Kanagawa, Japan, 3.GEOMAR Helmholtz Centre for Ocean Research, Kiel, Germany, 4.GNS Science, Lower Hutt, New Zealand)

[SMP30-P04] Ankaramite from Doyo seamount in the Izu-Ogasawara arc: A precursor of continents?

*Yoshihiko Tamura[1], Tomoki Sato[1], Osamu Ishizuka[1,2], Takashi Miyazaki[1], Yasuhiro Hirai[1,3], Mami Takehara[4], Eri Sakamoto[5] (1.JAMSTEC, 2.AIST, 3.Kanazawa Univ., 4.NIPR, 5.NME)

[SMP30-P05] Different Moho reflections adjacent to Minami-Tori Shima and their petrologic origins

*Yoshihiko Tamura[1], Kentaro Kaneda[2], Gou Fujie[1], Akane Ohira[1], Eiichi TAKAZAWA[3], Georges Ceuleneer[4], Katsuyoshi Michibayashi[5], Tomoki Sato[1], Shuichi Kodaira[1], Seiichi Miura[1] (1.Japan Agency for Maine-Earth Science and Technology, 2.Japan Coast Guard, 3.Niigata University, 4.Universite de Toulouse, 5.Nagoya University)

[SMP30-P06] Melt-rock interaction in plagioclase peridotites from the southern Palawan Ophiolite, Philippines

*FLORENCE ANNETTE CRUSPERO LABIS[1], BETCHAIDA D PAYOT[1], GABRIEL THEOPHILUS V VALERA[1], JULIUS A PASCO[1], JESLEY MEI A DYCOCO[1] (1.UNIVERSITY OF THE PHILIPPINES)

[SMP30-P07] Intra-oceanic arc magma genesis: a case study from Havre volcano, Kermadec arc

*Chris Conway[1], Kenichiro Tani[2] (1.Geological Survey of Japan, 2.National Museum of Nature and Science)

[E] Oral | S (Solid Earth Sciences)：S-MP Mineralogy & Petrology

1:45 PM - 3:15 PM JST | 4:45 AM - 6:15 AM UTC | A07 TOKYO BAY MAKUHARI HALL

[S-MP30] Crust-Mantle Connections

convener:Yoshihiko Tamura(Research Institute for Marine Geodynamics, Japan Agency for Maine-Earth Science and Technology), Osamu Ishizuka(Geological Survey of Japan, AIST), Chris Conway(Geological Survey of Japan), Chairperson:Yoshihiko Tamura(JAMSTEC), Chris Conway, Tomoaki Morishita(Kanazawa University)

1:45 PM - 2:00 PM JST | 4:45 AM - 5:00 AM UTC

[SMP30-01] **Noble gas and carbon isotopic compositions of petit-spot lavas from southeast of Marcus Island**

★Invited Papers

*Junji Yamamoto[1], Tetsuma Kawano[2], Naoto Takahata[3], Yuji Sano[3] (1.Hokkaido University Museum, 2.Graduate School of Science, Hokkaido University, 3.Atmosphere and Ocean Research Institute)

2:00 PM - 2:15 PM JST | 5:00 AM - 5:15 AM UTC

[SMP30-02] A series of cummingtonite-bearing rhyolites in Niijima, Izu-Bonin arc, Japan: petrological and geochemical constraints

★Invited Papers

*Yoji Arakawa[1], Daisuke Endo[2], Junya Oshika[3], Taro Shinmura[4], Kei Ikehata[1] (1.Earth Evolution Sciences, Faculty of Life and Environmental Sciences, University of Tsukuba, 2.Shimane Prefectural Sanbe Nature Museum Sahimeru (Shimane) , 3.Earth Resoueces Faculty, China University of Geosciences, 4.Faculty of Economics, Kumanoto-Gakuen University)

2:15 PM - 2:30 PM JST | 5:15 AM - 5:30 AM UTC

[SMP30-03] **Generation of primary andesitic magma in oceanic arcs: Evidence from Kibblewhite Volcano, Kermadec Arc**

★Invited Papers

*Yasuhiro Hirai[1,2], Yoshihiko Tamura[2], Kaj Hoernle[3], Christian Timm[4], Folkmar Hauff[3], Reinhard Werner[3], Bogdan Vaglarov[2], Qing Chang[2], Takashi Miyazaki[2], Jun-Ichi Kimura[2] (1.Graduate School of Natural Science and Technology, Kanazawa University, Japan, 2.Japan Agency for Marine-Earth Science and Technology (JAMSTEC), Yokosuka, Kanagawa, Japan, 3.GEOMAR Helmholtz Centre for Ocean Research, Kiel, Germany, 4.GNS Science, Lower Hutt, New Zealand)

2:30 PM - 2:45 PM JST | 5:30 AM - 5:45 AM UTC

[SMP30-04] Petrogenesis of high-Mg# andesite lavas from Ruapehu volcano, New Zealand

*Chris Conway[1], Katy Chamberlain[2], Yumiko Harigane[1], Daniel Morgan[3] (1.Geological Survey of Japan, 2.Univ. Derby, 3.Univ. Leeds)

2:45 PM - 3:00 PM JST | 5:45 AM - 6:00 AM UTC

[SMP30-05] Hydrous felsic magma generated by unmixing of slab-derived supercritical liquid: evidence from Rishiri Volcano, Kuril Arc

★Invited Papers

*Hajime Taniuchi[1], Takeshi Kuritani[2,3], Tetsuya Yokoyama[4,3], Eizo Nakamura[3], Mitsuhiro Nakagawa[2] (1.Department of Natural History Science, Graduate School of Science, Hokkaido University, 2.Department of Earth and Planetary Science, Faculty of Science, Hokkaido University, 3.Institute for Planetary Materials, Okayama University, 4.Department of Earth and Planetary Sciences, Tokyo Institute of Technology)

3:00 PM - 3:15 PM JST | 6:00 AM - 6:15 AM UTC

[SMP30-06] Genesis of recent mafic volcanism in the Taupo Volcanic Zone, New Zealand: insights into the birth and death of cataclysmic caldera-forming systems?

*Georg F Zellmer[1], Jun-Ichi Kimura[2], Claudine Stirling[3], Gert Lube[1], Phil A Shane[4] (1.Volcanic Risk Solutions, Massey University, Tennent Drive, Palmerston North 4410, New Zealand, 2.Department of Solid Earth Geochemistry, Japan Agency for Marine-Earth Science and Technology [JAMSTEC], Natsushima-cho 2-15, Yokosuka 237-0061, Japan, 3.Department of Chemistry, University of Otago, Dunedin 9054, New Zealand, 4.School of Environment, University of Auckland, Auckland 1142, New Zealand)

[E] Oral | S (Solid Earth Sciences)：S-MP Mineralogy & Petrology

3:30 PM - 5:00 PM JST | 6:30 AM - 8:00 AM UTC | A07 TOKYO BAY MAKUHARI HALL

[S-MP30] Crust-Mantle Connections

convener:Yoshihiko Tamura(Research Institute for Marine Geodynamics, Japan Agency for Maine-Earth Science and Technology), Osamu Ishizuka(Geological Survey of Japan, AIST), Chris Conway(Geological Survey of Japan), Chairperson:Chris Conway, Yoshihiko Tamura(JAMSTEC)

3:30 PM - 3:45 PM JST | 6:30 AM - 6:45 AM UTC

[SMP30-07] **Introducing an oceanic core complex in the Shikoku Basin: Mado Megamullion**

★Invited Papers

*Yasuhiko Ohara[1,2], Kyoko Okino[3], Norikatsu Akizawa[3], Masakazu Fujii[4], Yumiko Harigane[5], Naoto Hirano[6], Ken-ichi Hirauchi[7], Osamu Ishizuka[5], Shiki Machida[8], Katsuyoshi Michibayashi[9], Alessio Sanfilippo[10], Jonathan E. Snow[11], Hiroyuki Yamashita[12] (1.Hydrographic and Oceanographic Department of Japan, 2.Japan Agency for Marine-Earth Science and Technology, 3.Atmosphere and Ocean Research Institute, University of Tokyo, 4.National Institute of Polar Research, 5.Geological Survey of Japan/AIST, 6.Tohoku University, 7.Shizuoka University, 8.Chiba Institute of Technology, 9.Nagoya University, 10.University of Pavia, 11.University of Houston, 12.Kanagawa Prefectural Museum of Natural History)

3:45 PM - 4:00 PM JST | 6:45 AM - 7:00 AM UTC

[SMP30-08] Spatial variation of petrological and geochemical characteristics of mantle peridotites in Mado Megamullion, Shikoku Basin

*Norikatsu Akizawa[1], Shiki Machida[2], Kyoko Okino[1], Yasuhiko Ohara[3] (1.Atmosphere and Ocean Research Institute, The University of Tokyo, 2.Ocean Resources Research Center for Next Generation, Chiba Institute of Technology, 3.Hydrographic and Oceanographic Department of Japan)

4:00 PM - 4:15 PM JST | 7:00 AM - 7:15 AM UTC

[SMP30-09] **Magmatism-hydrothermalism interaction along the crust-mantle transition below oceanic spreading centres**

★Invited Papers

*Mathieu Rospabe[1,2], Mathieu Benoit[1], Georges Ceuleneer[1] (1.GET, OMP, Univ. of Toulouse, CNRS, IRD, F-31400 Toulouse, France, 2.JAMSTEC, Yokosuka 237-0061, Japan.)

4:15 PM - 4:30 PM JST | 7:15 AM - 7:30 AM UTC

[SMP30-10] **Serpentinization and carbonation of dunites in the western part of the Isua Supracrustal Belt, Southwestern Greenland**

*Juan Miguel Ramirez Guotana[1], Tomoaki Morishita[1], Akihiro Tamura[1], Ikuya Nishio[1], Kenichiro Tani[2], Yumiko Harigane[3], Kristoffer Szilas[4], D. Graham Pearson[5] (1.Kanazawa University, 2.National Museum of Nature and Science, Japan, 3.Institute of Geology and Geoinformation Geological Survey of Japan/AIST, 4.University of Copenhagen, 5.University of Alberta)

4:30 PM - 4:45 PM JST | 7:30 AM - 7:45 AM UTC

[SMP30-11] **Petrogenesis of fertile abyssal peridotites of the Pujada Ophiolite, SE Mindanao, Philippines**

*Valerie Shayne Vargas Olfindo[1], Betchaida Duetes Payot[1], Gabriel Theophilus Valera[1], Shoji Arai[2], Tomoyuki Shibata[4], Masako Yoshikawa[3] (1.Rushurgent Working Group, National Institute of Geological Sciences, University of the Philippines, 2.Department of Earth Sciences, Kanazawa University, Kakuma, Kanazawa, Ishikawa 920-1192, Japan, 3.Institute for Geothermal Sciences, Graduate School of Science, Kyoto University, Beppu 874-0903, Japan, 4.Department of Earth and Planetary Systems Science, Hiroshima University, Hiroshima 739-8526, Japan)

4:45 PM - 5:00 PM JST | 7:45 AM - 8:00 AM UTC

[SMP30-12] Ultramafic rock in the Hida metamorphic belt: an example of arc plutons

Yohei Ogusu[1], *Tomoaki Morishita[1], Akihiro Tamura[1] (1.Kanazawa University)

[E] Oral | S (Solid Earth Sciences)：S-MP Mineralogy & Petrology

10:45 AM - 12:15 PM JST | 1:45 AM - 3:15 AM UTC | A08 TOKYO BAY MAKUHARI HALL

[S-MP31] Supercontinents and Crustal Evolution

convener:Madhusoodhan Satish-Kumar(Department of Geology, Faculty of Science, Niigata University), Tomokazu Hokada(National Institute of Polar Research), Krishnan Sajeev(Centre for Earth Sciences, Indian Institute of Science), Yasuhito Osanai(Division of Evolution of Earth Environments, Faculty of Social and Cultural Studies, Kyushu University), Chairperson:M. Satish-Kumar(Niigata University), Tomokazu Hokada(National Institute of Polar Research)

10:45 AM - 11:00 AM JST | 1:45 AM - 2:00 AM UTC

[SMP31-01] Tectonic development of the East Indian cratonic margin and its status in Columbia Supercontinent

★Invited Papers

*Kaushik Das[1] (1.Hiroshima University)

11:00 AM - 11:15 AM JST | 2:00 AM - 2:15 AM UTC

[SMP31-02] **Continental crust formation and metamorphism during the Neoarchean–Paleoproterozoic: an example from the Nilgiri Block, southern India**

★Invited Papers

*VINOD O SAMUEL[1] (1.Yonsei University)

11:15 AM - 11:30 AM JST | 2:15 AM - 2:30 AM UTC

[SMP31-03] Preliminary paleomagnetic studies on the mafic dykes in Western Dharwar craton, South India.

*Silpa Ammini Sasidharan[1], Madhusoodhan Satish-Kumar[2], Naoto Ishikawa[3], Krishnan Sajeev[4] (1.Graduate School of Science and Technology, Niigata University, 2.Department of Geology, Faculty of Science, Niigata University, 3.Graduate School of Human and Environmental Studies, Kyoto University, Kyoto, Japan, 4.Centre for Earth Sciences, Indian Institute of Science, Bangalore, India)

11:30 AM - 11:45 AM JST | 2:30 AM - 2:45 AM UTC

[SMP31-04] Syn-metamorphic boron-bearing fluid infiltrations deduced from tourmaline in the Main Central Thrust zone, eastern Nepal Himalayas

★Invited Papers

*Tetsuo Kawakami[1], Harutaka Sakai[1], Katsushi Sato[1] (1.Graduate School of Science, Kyoto University)

11:45 AM - 12:00 PM JST | 2:45 AM - 3:00 AM UTC

[SMP31-05] **Geochemical characteristics of mafic and felsic igneous rocks (1.9-1.75 Ga) in the Lesser Himalaya: Regional variation and its implications for tectonic setting**

*Ryuichi Shinjo[1], Tomoki Amuro[1], Kohei Oura[1], Kazuya Oshiro[1], Shiro Tahara[1], Harutaka Sakai[2] (1.Department of Physics and Earth Sciences, University of the Ryukyus, 2.Faculty of Science, Kyoto University)

12:00 PM - 12:15 PM JST | 3:00 AM - 3:15 AM UTC

[SMP31-06] Petrogenesis and tectonic implications of orbicular granodiorite from Yangtze cratonic nucleus

*Yihe Li[1] (1.China University of Geosciences Wuhan)

[E] Poster | S (Solid Earth Sciences)：S-MP Mineralogy & Petrology

3:30 PM - 5:00 PM JST | 6:30 AM - 8:00 AM UTC | Poster Hall International Exhibition Hall8, Makuhari Messe_18

[S-MP31] Supercontinents and Crustal Evolution

convener:Madhusoodhan Satish-Kumar(Department of Geology, Faculty of Science, Niigata University), Tomokazu Hokada(National Institute of Polar Research), Krishnan Sajeev(Centre for Earth Sciences, Indian Institute of Science), Yasuhito Osanai(Division of Evolution of Earth Environments, Faculty of Social and Cultural Studies, Kyushu University)

[SMP31-P01] Re-examination of metamorphic and geochronologic events in Rayner Complex and Western Rayner Complex in Antarctica

*Tomokazu Hokada[1,2], Sotaro Baba[3], Atsushi Kamei[4], Ippei Kitano[5], Kenji Horie[1,2], Yoshikuni Hiroi[1,6], Yoichi Motoyoshi[1,2], Mami Takehara[1], Kazuyuki Shiraishi[1] (1.National Institute of Polar Research, 2.The Graduate University for Advanced Studies (SOKENDAI), 3.University of the Ryukyus, 4.Shimane University, 5.Kyushu University, 6.Chiba University)

[SMP31-P02] Composition of constituent minerals in corona-bearing and -free mafic gneisses from the Lützow-Holm Complex at Skallen, East Antarctica

*Yuki Mori[1], Takeshi Ikeda[2] (1.Department of Earth and Planetary Sciences, Graduate School of Sciences, Kyushu University, 2.Department of Earth and Planetary Sciences, Faculty of Sciences, Kyushu University)

[SMP31-P03] “Pseudo-concordance” of U-Pb system in zircon at Harvey Nunatak, Napier Complex, East Antarctica

*Mami Takehara[1] (1.National Institute of Polar Research)

[SMP31-P04] Rapid UHT metamorphism and exhumation of the Lützow-Holm Complex in Antarctica

*Yoshikuni Hiroi[1], Tomokazu Hokada[2], Tatsuro Adachi[3], Yasuhito Osanai[3], Yoichi Motoyoshi[2], Kazuyuki Shiraishi[2] (1.Chiba Univ, 2.National Institute of Polar Research, 3.Kyushu University)

[SMP31-P05] Tectonic History of Hiroo Complex and its implication inpaleo-Kuril Arc evolution

*Sreehari Lakshmanan[1], Tsuyoshi Toyoshima[2], Futoshi Nanayama[3] (1.Graduate School of Science and Technology, Niigata University, Niigata, Japan, 2.Department of Geology, Faculty of Science, Niigata Univ. , 3.Geological Survey of Japan, AIST)

[SMP31-P06] Behaviour of C, O, Sr, Nd and Pb isotopes in high-grade metacarbonate rocks

*Madhusoodhan Satish-Kumar[1], Akari Imura[1], Momoko Shirakawa[2], Gen Shimoda[3], Kosuke T. Goto[3], M A Sanjeewa P K Malaviarachchi[4] (1.Department of Geology, Faculty of Science, Niigata University, 2.Graduate School of Science and Technology, Niigata University, 3.Geological Survey of Japan, 4.University of Peradeniya, Sri Lanka)

[E] Poster | S (Solid Earth Sciences)：S-MP Mineralogy & Petrology

5:15 PM - 6:30 PM JST | 8:15 AM - 9:30 AM UTC | Poster Hall International Exhibition Hall8, Makuhari Messe_34

[S-MP31] Supercontinents and Crustal Evolution

convener:Madhusoodhan Satish-Kumar(Department of Geology, Faculty of Science, Niigata University), Tomokazu Hokada(National Institute of Polar Research), Krishnan Sajeev(Centre for Earth Sciences, Indian Institute of Science), Yasuhito Osanai(Division of Evolution of Earth Environments, Faculty of Social and Cultural Studies, Kyushu University)

[SMP31-P01] Re-examination of metamorphic and geochronologic events in Rayner Complex and Western Rayner Complex in Antarctica

*Tomokazu Hokada[1,2], Sotaro Baba[3], Atsushi Kamei[4], Ippei Kitano[5], Kenji Horie[1,2], Yoshikuni Hiroi[1,6], Yoichi Motoyoshi[1,2], Mami Takehara[1], Kazuyuki Shiraishi[1] (1.National Institute of Polar Research, 2.The Graduate University for Advanced Studies (SOKENDAI), 3.University of the Ryukyus, 4.Shimane University, 5.Kyushu University, 6.Chiba University)

[SMP31-P02] Composition of constituent minerals in corona-bearing and -free mafic gneisses from the Lützow-Holm Complex at Skallen, East Antarctica

*Yuki Mori[1], Takeshi Ikeda[2] (1.Department of Earth and Planetary Sciences, Graduate School of Sciences, Kyushu University, 2.Department of Earth and Planetary Sciences, Faculty of Sciences, Kyushu University)

[SMP31-P03] “Pseudo-concordance” of U-Pb system in zircon at Harvey Nunatak, Napier Complex, East Antarctica

*Mami Takehara[1] (1.National Institute of Polar Research)

[SMP31-P04] Rapid UHT metamorphism and exhumation of the Lützow-Holm Complex in Antarctica

*Yoshikuni Hiroi[1], Tomokazu Hokada[2], Tatsuro Adachi[3], Yasuhito Osanai[3], Yoichi Motoyoshi[2], Kazuyuki Shiraishi[2] (1.Chiba Univ, 2.National Institute of Polar Research, 3.Kyushu University)

[SMP31-P05] Tectonic History of Hiroo Complex and its implication inpaleo-Kuril Arc evolution

*Sreehari Lakshmanan[1], Tsuyoshi Toyoshima[2], Futoshi Nanayama[3] (1.Graduate School of Science and Technology, Niigata University, Niigata, Japan, 2.Department of Geology, Faculty of Science, Niigata Univ. , 3.Geological Survey of Japan, AIST)

[SMP31-P06] Behaviour of C, O, Sr, Nd and Pb isotopes in high-grade metacarbonate rocks

*Madhusoodhan Satish-Kumar[1], Akari Imura[1], Momoko Shirakawa[2], Gen Shimoda[3], Kosuke T. Goto[3], M A Sanjeewa P K Malaviarachchi[4] (1.Department of Geology, Faculty of Science, Niigata University, 2.Graduate School of Science and Technology, Niigata University, 3.Geological Survey of Japan, 4.University of Peradeniya, Sri Lanka)

[J] Oral | S (Solid Earth Sciences)：S-VC Volcanology

9:00 AM - 10:30 AM JST | 12:00 AM - 1:30 AM UTC | IC 2F

[S-VC38] Active Volcanism

convener:Yuta Maeda(Nagoya University), Takahiro Miwa(National research institute for earth science and disaster prevention), Takeshi Nishimura(Department of Geophysics, Graduate School of Science, Tohoku University), Chairperson:Fukashi Maeno, Yosuke Aoki

9:00 AM - 9:15 AM JST | 12:00 AM - 12:15 AM UTC

[SVC38-06] A sequence of volcanic flank collapse and tsunami event on 22 December 2018 at Anak Krakatau volcano, Indonesia

*Fukashi Maeno[1], Takayuki Kaneko[1] (1.Earthquake Research Institute, University of Tokyo)

9:15 AM - 9:30 AM JST | 12:15 AM - 12:30 AM UTC

[SVC38-07] The 2018 eddifice collapse event of Anak Krakatau, Indonesia: Telseismic waveform analysis and tsunami simulation

*Shingo Watada[1], Iyan E. Mulia[1], Masumi Yamada[2], Dimas Sianipar[3] (1.Earthquake Research Institute, University of Tokyo, 2.Disaster Prevention Research Institute, Kyoto University, 3.TIGP-ESS Academia Sinica, National Central University, Taiwan)

9:30 AM - 9:45 AM JST | 12:30 AM - 12:45 AM UTC

[SVC38-08] The 2018 edifice collapse event of Anak Krakatau, Indonesia: Landslide movement history estimated from seismic waveforms

*Masumi Yamada[1], Shingo Watada[2], Haruhisa Nakamichi[1], Iyan Mulia[2], Karyono Dr.[3] (1.Disaster Prevention Research Institute, Kyoto University, 2.Earthquake Research Institute, University of Tokyo, 3.Center for Earthquake and Tsunami, BMKG)

9:45 AM - 10:00 AM JST | 12:45 AM - 1:00 AM UTC

[SVC38-09] Intense Swarm Activity in the Vicinity of Yake-dake Volcano, Central Japan, Started in November 2018

*Shiro Ohmi[1] (1.Earthquake Hazards Division, Disaster Prevention Research Institute, Kyoto University)

10:00 AM - 10:15 AM JST | 1:00 AM - 1:15 AM UTC

[SVC38-10] Change of the volcanic activity at Kuju volcano.

*Mori Takehiko[1], Muga Yaguchi[1], Yasushi Kawamura[2], Hideyuki Hiramatsu[3], Keiji Ikeda[2], Sugai Akira[2], Michitomo Sugahara[2], Kenichi Takata[2], Kyo Matsumoto[2], Fukuoka Regional Headquarters Japan Meteorological Agency, Oita Meteorological Office Japan Meteorological Agency (1. Meteorological Research Institute, Japan Meteorological Agency, 2.Fukuoka Regional Headquarters, Japan Meteorological Agency, 3.Oita Meteorological Office, Japan Meteorological Agency)

10:15 AM - 10:30 AM JST | 1:15 AM - 1:30 AM UTC

[SVC38-11] Posteruptive Thermoelastic Deflation of Intruded Magma in Usu Volcano, Japan, 1992–2017

*Yosuke Aoki[1], Xiaowen Wang[1] (1.Earthquake Research Institute, University of Tokyo)

[J] Oral | S (Solid Earth Sciences)：S-VC Volcanology

10:45 AM - 12:15 PM JST | 1:45 AM - 3:15 AM UTC | IC 2F

[S-VC38] Active Volcanism

convener:Yuta Maeda(Nagoya University), Takahiro Miwa(National research institute for earth science and disaster prevention), Takeshi Nishimura(Department of Geophysics, Graduate School of Science, Tohoku University), Chairperson:Jun Oikawa, Takeshi Tameguri

10:45 AM - 11:00 AM JST | 1:45 AM - 2:00 AM UTC

[SVC38-12] Volcanic tremors and ash fall volumes associated with the 2018 vulcanian eruptions of Shinmoe-dake

*Jun Oikawa[1], Yasuhisa Tajima[2] (1.Earthquake Research Institute, University of Tokyo, 2.NIPPON KOEI CO.,LTD.)

11:00 AM - 11:15 AM JST | 2:00 AM - 2:15 AM UTC

[SVC38-13] Crustal deformation around the Kirishima Volcano Group detected by GNSS and SAR observation after 2018 eruption.

*Hiroshi Yarai[1], Tomokazu Kobayashi[1], Satoshi Fujiwara[1], Tomokazu Kobayashi[1], Hiroshi Munekane[1], Masaki Honda[1], Kyonosuke Hayahsi[1], Satoshi Kawamoto[1], Atsuko Oowaki[1] (1.GSI of Japan)

11:15 AM - 11:30 AM JST | 2:15 AM - 2:30 AM UTC

[SVC38-14] Harmonic tremor during 2011 eruption at Shinmoedake, Japan

*Minoru Takeo[1] (1.Earthquake Research Institute, University of Tokyo)

11:30 AM - 11:45 AM JST | 2:30 AM - 2:45 AM UTC

[SVC38-15] Forecasting Volcanic Eruption of Sakurajima Volcano Based on Magma Intrusion Rate

*Masato Iguchi[1], Takeshi Tameguri[1], Jun-ichi Hirabayashi, Haruhisa Nakamichi[1] (1.Sakurajima Volcano Research Center, Disaster Prevention Research Institute, Kyoto University)

11:45 AM - 12:00 PM JST | 2:45 AM - 3:00 AM UTC

[SVC38-16] Tilt and strain change before and after the explosion at Minami-dake, Sakurajima, in 2017

*Kohei Hotta[1], Masato Iguchi[2] (1.University of Toyama, 2.Disaster Prevention Research Institute, Kyoto University)

12:00 PM - 12:15 PM JST | 3:00 AM - 3:15 AM UTC

[SVC38-17] Pyroclastic Flow Accompanied with an Eruption on June 16, 2018 at Sakurajima Volcano

*Takeshi Tameguri[1], Masato Iguchi[1], Masayuki Maki[2], Haruhisa Nakamichi[1], Daisuke Miki[1] (1.Sakurajima Volcano Research Center,Disaster Prevention Research Institute, Kyoto University, 2.Research Field in Integrated Studies,Kagoshima University)

[J] Oral | S (Solid Earth Sciences)：S-VC Volcanology

1:45 PM - 3:15 PM JST | 4:45 AM - 6:15 AM UTC | IC 2F

[S-VC38] Active Volcanism

convener:Yuta Maeda(Nagoya University), Takahiro Miwa(National research institute for earth science and disaster prevention), Takeshi Nishimura(Department of Geophysics, Graduate School of Science, Tohoku University), Chairperson:Hiroshi Aoyama, Satoshi Miura

1:45 PM - 2:00 PM JST | 4:45 AM - 5:00 AM UTC

[SVC38-18] Ground deformation observed at the crater area of Tokachidake volcano

*Hiroshi Aoyama[1], Takeshi Hashimoto[1], Ryo Tanaka[1], Hiromitsu Oshima[1], Koichiro Saito[2], Tsuyoshi Michishita[2], Satoshi Okuyama[2], Volcanic Observation and Warning Center Sapporo Regional Headquarters[2] (1.Institute of Seismology and Volcanology, Faculty of Science, Hokkaido University, 2.Japan Meteorological Agency)

2:00 PM - 2:15 PM JST | 5:00 AM - 5:15 AM UTC

[SVC38-19] Moment tensor inversion of very-long-period seismicity at Stromboli volcano based on a very-near-field observation

*Shunsuke Sugimura[1,2], Maurizio Ripepe[2], Giorgio Lacanna[2], Denis Legrand[3], Sébastien Valade[4], Takeshi Nishimura[1] (1.Department of Geophysics, Graduate School of Science, Tohoku University, 2.Department of Earth Sciences, University of Florence, Italy, 3.UNAM University, Mexico, 4.GFZ-German Research Centre for Geosciences, Potsdam, Germany)

2:15 PM - 2:30 PM JST | 5:15 AM - 5:30 AM UTC

[SVC38-20] Pressure source estimation of tilt changes associated with small explosions at Stromboli volcano

*Ayumu Ishikawa[1], Takeshi Nishimura[1], Hiroshi Aoyama[2], Ryohei Kawaguchi[3], Eisuke Fujita[4], Takahiro Miwa[4], Taishi Yamada[4], Maurizio Ripepe[5], Riccardo Genco[5] (1.Graduate school of science, Tohoku university, 2.Faculty of science, Hokkaido university, 3.Meteorological Research Institute, 4.National Research Institute for Earth Science and Disaster Resilience, 5.University of Florence)

2:30 PM - 2:45 PM JST | 5:30 AM - 5:45 AM UTC

[SVC38-21] Seismic and acoustic waves excited by volcanic explosion: analyses of energy ratio and source spectra

*Mohammad Hasib[1], Takeshi Nishimura[1], Hisashi Nakahara[1] (1.Department of Geophysics, Graduate School of Science, Tohoku University)

2:45 PM - 3:00 PM JST | 5:45 AM - 6:00 AM UTC

[SVC38-22] Field survey report on Zao Volcano (2012–2018)

*Akio Goto[1], Noriyoshi Tsuchiya[2], Nobuo Hirano[2], Miwa Kuri[3], Tetsuya Matsunaka[4], Kengo Sawayama[2] (1.Center for Northeast Asian Studies, Tohoku University, 2.Graduate School of Environmental Studies, Tohoku University, 3.International Research Institute of Disaster Science, Tohoku University, 4.Institute of Nature and Environmental Technology, Kanazawa University)

3:00 PM - 3:15 PM JST | 6:00 AM - 6:15 AM UTC

[SVC38-23] **Inflation Event of Zao Volcano in 2015**

*Satoshi Miura[1], Mare Yamamoto[1], Masahiro Ichiki[1], Tomotsugu Demachi[1] (1.Graduate School of Science, Tohoku University)

[J] Oral | S (Solid Earth Sciences)：S-VC Volcanology

3:30 PM - 5:00 PM JST | 6:30 AM - 8:00 AM UTC | IC 2F

[S-VC38] Active Volcanism

convener:Yuta Maeda(Nagoya University), Takahiro Miwa(National research institute for earth science and disaster prevention), Takeshi Nishimura(Department of Geophysics, Graduate School of Science, Tohoku University), Chairperson:Mare Yamamoto, Yuta Maeda(Nagoya University)

3:30 PM - 3:45 PM JST | 6:30 AM - 6:45 AM UTC

[SVC38-24] A machine-learning-based estimation of large amplitude regions for monitoring volcano seismicity

*Yuta Maeda[1] (1.Nagoya University)

3:45 PM - 4:00 PM JST | 6:45 AM - 7:00 AM UTC

[SVC38-25] Development of a technique for automatic determination of volcanic earthquakes with unclear onsets - Application to Mt. Asama -

*Takao Ohminato[1], Shigeki Horiuchi[2] (1.Earthquake Research Institute, Tokyo University, 2.Home Seismometer Corporation)

4:00 PM - 4:15 PM JST | 7:00 AM - 7:15 AM UTC

[SVC38-26] Amplitude source location method with depth-dependent scattering and attenuation structures for volcano-seismic signals

*Hiroyuki Kumagai[1], John Makario Lonodno[2], Alvaro Esteban Acevedo Rivas[2], Yuta Maeda[1] (1.Graduate School of Environmental Studies, Nagoya University, 2.Colombian Geological Survey)

4:15 PM - 4:30 PM JST | 7:15 AM - 7:30 AM UTC

[SVC38-27] Seismic interferometry at active volcanoes in Japan: Analyses of seismic records of JMA for the period from 2012 to 2018

*Takeshi Nishimura[1], Tomoya Takano[1], Takashi Hirose[1], Hisashi Nakahara[1] (1.Department of Geophysics, Graduate School of Science, Tohoku University)

4:30 PM - 4:45 PM JST | 7:30 AM - 7:45 AM UTC

[SVC38-28] Empirical relation for *Q* factors of crack resonances and its use to estimate source properties of volcanic LP events

*Kimiko Taguchi[1], Hiroyuki Kumagai[1], Yuta Maeda[1], Roberto Torres[2] (1.Nagoya University Environmental Studies, 2.Colombian Geological Survey)

4:45 PM - 5:00 PM JST | 7:45 AM - 8:00 AM UTC

[SVC38-29] A study on the radiation pattern for resonating fluid-filled crack

*Mare Yamamoto[1] (1.Research Center for Prediction of Earthquakes and Volcanic Eruptions, Graduate School of Science, Tohoku University)

[E] Oral | S (Solid Earth Sciences)：S-CG Complex & General

9:00 AM - 10:30 AM JST | 12:00 AM - 1:30 AM UTC | A07 TOKYO BAY MAKUHARI HALL

[S-CG49] Hard-Rock Drilling Science: From Continental to Deep Sea Drilling, and Oman Project

convener:Katsuyoshi Michibayashi(Department of Earth and Planetary Sciences, Nagoya University), Eiichi TAKAZAWA(Department of Geology, Faculty of Science, Niigata University), Norikatsu Akizawa(Department of Ocean Floor Geoscience, Atmosphere and Ocean Research Institute, The University of Tokyo), Chairperson:Eiichi Takazawa(Niigata University), Norikatsu Akizawa(AORI The University of Tokyo)

9:00 AM - 9:15 AM JST | 12:00 AM - 12:15 AM UTC

[SCG49-06] Melt transport and compositional heterogeneity of the mantle: a case study of peridotite, dunite, and wehrlite from Atlantis Massif

*Norikatsu Akizawa[1], Gretchen L. Früh-Green[2], Akihiro Tamura[3], Chiori Tamura[1], Tomoaki Morishita[3] (1.Atmosphere and Ocean Research Institute, The University of Tokyo, 2.Department of Earth Sciences, Eidgenössische Technische Hochschule-Zürich, 3.Institute of Science and Engineering, Kanazawa University)

9:15 AM - 9:30 AM JST | 12:15 AM - 12:30 AM UTC

[SCG49-07] Lower crustal accretion processes revealed from the study of gabbroic cores in Holes GT1A and GT2A, the ICDP Oman Drilling Project

*Sayantani Chatterjee[1], Eiichi TAKAZAWA[1], Katsuyoshi Michibayashi[2], Peter B Kelemen[3], Damon A.H. Teagle[4], Oman Drilling Project Phase I Science Party (1.Department of Geology, Faculty of Sciences, Niigata University, Japan, 2.Department of Earth and Environmental Sciences, Nagoya University, Japan, 3.Lamont Doherty Earth Observatory, Columbia University, USA, 4.Southampton Marine and Maritime Institute, University of Southampton, United Kingdom)

9:30 AM - 9:45 AM JST | 12:30 AM - 12:45 AM UTC

[SCG49-08] Petrology of Oman listvenite : Implications for carbon cycle in the subduction zone

*Toma Takahashi[1], Tomoaki Morishita[2], Hiroki Sato[3], Juan Miguel Guotana[2], Tatsuhiko Kawamoto[4], Peter B Kelemen[5], Jude Ann Coggon[6], Michelle Harris[7], Juerg Michael Matter[6], Katsuyoshi Michibayashi[8], Eiichi TAKAZAWA[9], Damon A H Teagle[6], The Oman Drilling Project Phase 1 science Party (1.Faculty of Geosciences and Civil Engineering, Kanazawa university, 2.Division of Natural Sciences, Graduate School of Natural Science and Technology, Kanazawa university, 3.Faculty of Science, Kyoto university, 4.Department of Geoscience, Faculty of Science, Shizuoka university, 5.Lamont-Doherty Earth Observatory, Columbia university, 6.School of Ocean and Earth Science, National Oceanography Center Southampton, University of Southampton, 7.School of Geography, Earth and Environmental Sciences, Plymouth University, 8.Department of Earth Planetary Sciences, Graduate School of Environmental Studies, Nagoya university, 9.Institute of Science and Technology, Niigata university)

9:45 AM - 10:00 AM JST | 12:45 AM - 1:00 AM UTC

[SCG49-09] PGE and Os isotope variation in the gabbros and peridotites from the Oman DP drilling cores in the Samail ophiolite, Oman

*Ryoko Senda[1,2], Katsuhiko Suzuki[2], Tomoaki Morishita[3], Eiichi TAKAZAWA[4], Katsuyoshi Michibayashi[5], Peter B Kelemen[6], Damon AH Teagle[7], Jude Ann Coggon[7], Marguerite Godard[8], The Oman DP Science Party (1.Faculty of Social and Cultural Studies, Kyushu University, 2.Research and Development Center for Submarine Resources, JAMSTEC, 3.School of Natural System, Colleage of Science and Technology, Kanazawa University, 4.SDepartment of Geology, Faculty of Science, Niigata University, 5.Department of Earth and Planetary Sciences, Nagoya University, 6.Columbia University, 7.University of Southampton, 8.Géosciences Montpellier)

10:00 AM - 10:15 AM JST | 1:00 AM - 1:15 AM UTC

[SCG49-10] Overview of drilling of crust-mantle boundary at CM1&2 sites of Wadi Tayin massif of Oman ophiolite: the ICDP Oman Drilling Project

*Eiichi TAKAZAWA[1], Damon A H Teagle[2], Katsuyoshi Michibayashi[3], Yoshihiko Tamura[4], Jude Ann Coggon[2], Juerg Matter[2], Peter B Kelemen[5], Oman Drilling Project Phase 2 Science Party (1.Department of Geology, Faculty of Science, Niigata University, 2.University of Southampton, 3.Nagoya University, 4.JAMSTEC, 5.Columbia University)

10:15 AM - 10:30 AM JST | 1:15 AM - 1:30 AM UTC

[SCG49-11] Petrological observation of core samples drilled from a mantle section of the Oman ophiolite: A preliminary report of the Oman Drilling Project Phase 2

*Yuji Ichiyama[1], Oman Drilling Project Phase 2 Scientific Party (1.Chiba University)

[E] Oral | S (Solid Earth Sciences)：S-CG Complex & General

10:45 AM - 12:15 PM JST | 1:45 AM - 3:15 AM UTC | A07 TOKYO BAY MAKUHARI HALL

[S-CG49] Hard-Rock Drilling Science: From Continental to Deep Sea Drilling, and Oman Project

convener:Katsuyoshi Michibayashi(Department of Earth and Planetary Sciences, Nagoya University), Eiichi TAKAZAWA(Department of Geology, Faculty of Science, Niigata University), Norikatsu Akizawa(Department of Ocean Floor Geoscience, Atmosphere and Ocean Research Institute, The University of Tokyo), Chairperson:Tomoaki Morishita(Kanazawa University), Katsuyoshi Michibayashi

10:45 AM - 11:00 AM JST | 1:45 AM - 2:00 AM UTC

[SCG49-12] Structural analyses of ultramafic rocks used by X-ray CT core imaging (Oman Drilling Project Phase 2, D/V CHIKYU)

*Katsuyoshi Michibayashi[1], Yuki Kakihata[1], Ikuo Katayama[2], Atsushi Okamoto[3], Keishi Okazaki[4], Peter B Kelemen[5], Eiichi TAKAZAWA[6], Damon A H Teagle[7], Oman Drilling Project Phase 2 Science Party[8] (1.Department of Earth and Planetary Sciences, Graduate School of Environmental Studies, Nagoya University, 2.Hiroshima University, 3.Tohoku University, 4.KCC, JAMSTEC, 5.Columbia University of New York, 6.Niigata University, 7.Southampton University, 8.ICDP)

11:00 AM - 11:15 AM JST | 2:00 AM - 2:15 AM UTC

[SCG49-13] Petrophysical characteristics of serpentinized peridotites of Hole BA1B, BA3A and BA4A

*Kakihata Yuki[1], Katsuyoshi Michibayashi[2], Laura Crispini[3], Bjorn Jamtveit[4], Samuel Barbier[5], Joe Aslin[6], Manuel Menzel[7], Marguerite Godard[8] (1.Graduate School of Science, Shizuoka University, 2.Graduate School of Environmental Studies, Nagoya University, 3.University of Genova, 4.University of Oslo, 5.Claude Bernard University Lyon 1, 6.University of Liverpool, 7.Andalusian Earth Science Institute, 8.Géosciences Montpellier, CNRS, Univ. Montpellier)

11:15 AM - 11:30 AM JST | 2:15 AM - 2:30 AM UTC

[SCG49-14] Physical properties of the Moho TZ: Implications from ICDP Oman Drilling Project Phase I & II on-board measurements

*Natsue Abe[1,12], Keishi Okazaki[1], Ikuo Katayama[2], Kohei Hatakeyama[2], Yuya Akamatsu[2], Benoit Ildefonse[3], Ulven Ivar Ole[4], Gilvert Hong[5], Wenlu Zhu[6], Benoit Cordonnier[4], Katsuyoshi Michibayashi[7], Eiichi TAKAZAWA[8], Michell Harris[10], Damon Teagle[11], Peter Kelemen[9], Marguerite Godard[3], Jurg Matter[11], Jude Coggon[11], Oman Drilling Project Scientific Party (1.Japan Agency for Marine-Earth Science and Technology, 2.Hiroshima University, 3.Universitè de Montpellier, 4.University of Oslo, 5.Seoul National University, 6.University of Maryland, 7.Nagoya University, 8.Niigata University, 9.Columbia University, 10.Polymouth University, 11.University of Southampton, 12.Kanazawa University)

11:30 AM - 11:45 AM JST | 2:30 AM - 2:45 AM UTC

[SCG49-15] Seismic anisotropy under high pressure conditions of harzburgite collected from Oman Drilling Project Phase II

*Kohei Hatakeyama[1], Ikuo Katayama[1], Natsue Abe[2], The Oman Drilling Project Phase II Science Party (1.Department of earth and planetary systems science, Hiroshima University , 2.JAMSTEC)

11:45 AM - 12:00 PM JST | 2:45 AM - 3:00 AM UTC

[SCG49-16] Understanding of the mode of seafloor spreading and the architecture of upper oceanic crust by oceanfloor drilling at off-Hawaii MoHole candidate site

*Susumu Umino[1], Tomoaki Morishita[1], Mikiya Yamashita[2], Osamu Ishizuka[3] (1.Department of Earth Sciences, Kanazawa University, 2.Japan Agency for Marine-Earth Science and Technology, 3.Geological Survey of Japan, AIST)

[E] Poster | S (Solid Earth Sciences)：S-CG Complex & General

3:30 PM - 5:00 PM JST | 6:30 AM - 8:00 AM UTC | Poster Hall International Exhibition Hall8, Makuhari Messe_19

[S-CG49] Hard-Rock Drilling Science: From Continental to Deep Sea Drilling, and Oman Project

convener:Katsuyoshi Michibayashi(Department of Earth and Planetary Sciences, Nagoya University), Eiichi TAKAZAWA(Department of Geology, Faculty of Science, Niigata University), Norikatsu Akizawa(Department of Ocean Floor Geoscience, Atmosphere and Ocean Research Institute, The University of Tokyo)

[SCG49-P01] **Permeability profile in the Oman Drilling Project inferred from resistivity measurements**

*Ikuo Katayama[1], Keishi Okazaki[2], Natsue Abe[2], Ole Ivar Ulven[3], Gilbert Hong[4], Wenlu Zhu[5], Benoit Cordonnier[3], Kohei Hatakeyama[1], Yuya Akamatsu[1], Katsuyoshi Michibayashi[6], Marguerite Godard[7], Peter Kelemen[8], Science Party The Oman Drilling Project Phase 2 (1.Hiroshima University, 2.JAMSTEC, 3.University of Oslo, 4.Seoul National University, 5.University of Maryland, 6.Nagoya University, 7.Universitè Montpellier, 8.Columbia University)

[SCG49-P02] Relationship between alteration intensity and elastic wave velocity of gabbroic rocks from ICDP Hole CM1A, Oman Drilling Project Phase II

*Kosuke Kimura[1], Ikuo Katayama[1], Kohei Hatakeyama[1], Yuya Akamatsu[1], Natsue Abe[2], Keishi Okazaki[2], The Oman Drilling Project Phase II Science Party (1.Hiroshima University, 2.JAMSTEC)

[SCG49-P03] Physical property of the fossilized crust-mantle transition zone from ICDP Oman Drilling Project Hole CM1A and CM2B measured onboard D/V Chikyu

*Keishi Okazaki[1], Natsue Abe[1], Kohei Hatakeyama[2], Yuya Akamatsu[2], Ikuo Katayama[2], Eiichi TAKAZAWA[3], Damon A H Teagle[4], Peter B Kelemen[5], Jude Coggon[4], The Oman Drilling Project Phase 2 Science Party (1.Japan Agency for Marine-Earth Science and Technology, 2.Hiroshima University, 3.Niigata University, 4.University of Southampton, 5.Columbia University)

[SCG49-P04] Microstructures of lower crust gabbros from the Oman Ophiolite: Analyses of the drilled cores of the Oman Drilling Project

*Koki Iida[1], Takahiro Fudai[1], Susumu Umino[1], Yuki Kusano[2] (1.Kanazawa University, 2.Geological Survey of Japan)

[SCG49-P05] Olivine fabric and mineral compositions in the Maqsad area of the Samail massif, the southern Oman ophiolite

*Kaho Takahashi[1], Eiichi TAKAZAWA[2,3], Katsuyoshi Michibayashi[4], Kakihata Yuki[4], Ryoko Senda[5] (1.Graduate School of Science and Technology, Niigata University, 2.Department of Geology, Faculty of Science, Niigata University, 3.JAMSTEC, 4.Nagoya University, 5.Kyushu University)

[SCG49-P06] The evolution of melt inclusions in podiform chromitite in Oman

*Yuan YAO[1], Eiichi TAKAZAWA[2,3], Oman Drilling Project Phase 2 Science Party (1.Graduate School of Sciences& Technology, Niigata University, Japan, 2.Department of Geology, Faculty of Science, Niigata University, Japan, 3.Research and Development Center for Ocean Drilling Science, JAMSTEC, Japan)

[SCG49-P07] Melt/fluid - rock reaction inferred from the Wadi Tayin mantle section in the southern Oman ophiolite

*Keisuke ISHII[1], Eiichi TAKAZAWA[2], Akihiro kuriyama[2], Kyouka Someya[2], Yoshihiko Tamura[3] (1.Graduate School of Science and Technology, Niigata University, 2.Department of Geology, Faculty of Science, Niigata University , 3.R&D Center for Ocean Drilling Science, Japan Agency for Marine-Earth Science and Technology)

[SCG49-P08] Numerical simulations for reaction-induced fracture formation of layered gabbro during hydration process

*Kazuki Yoshida[1], Hiroyuki Shimizu[2], Noriyoshi Tsuchiya[1], Atsushi Okamoto[1], Phase 2 Science Party Oman Drilling Project[3] (1.Tohoku university, 2.Geotechnical Analysis Group, Advanced Analysis Department, Civil Engineering Design Division, Kajima Corporation, 3.Oman Drilling Project Phase 2 Science Party)

[SCG49-P09] X-ray CT images of oceanic lithologies obtained on Oman Drilling Project drillcores during ChikyuOman 2017 and 2018

*Katsuyoshi Michibayashi[1], Peter B Kelemen[2], Margurette Godard[3], Eiichi TAKAZAWA[4], Damon A H Teagle[5], The Oman Drilling Project Science Party[6] (1.Department of Earth and Planetary Sciences, Nagoya University, 2.Columbia University, 3.Université Montpellier, 4.Niigata University, 5.Southampton University, 6.ICDP)

[SCG49-P10] Re-examination of the crystallization process of clinopyroxene oikocrysts in layered gabbros at Hess Deep Rift, EPR

*Akane Yasui[1], Takashi Hoshide[1] (1.Graduate School of International Resource Sciences, Akita University)

[SCG49-P11] Structural petrology of peridotites from the Kalaymyo ophiolite

*Kouhei Asano[1,2], Katsuyoshi Michibayashi[1], Jung-Woo Park[3] (1.Graduate School of Environmental Studies, Nagoya University, 2.Shizuoka University, 3.Seoul National University)

[SCG49-P12] Reevaluation of the origin of mafic layers in the Upper Zone of the Horoman Peridotite

*Yumeto KOGURE[1], Eiichi TAKAZAWA[1] (1.Department of Geology, Faculty of Science, Niigata University)

[SCG49-P13] A structural and petrological study of "Shibukawa ultramafic body" in the Sanbagawa belt, western Shizuoka, Japan

*Hikaru Shioya[1,2], Katsuyoshi Michibayashi[1], Ken-ichi Hirauchi[2] (1.Graduate School of Environmental Studies, Nagoya University, 2.Institute of Geosciences, Shizuoka University)

[E] Poster | S (Solid Earth Sciences)：S-CG Complex & General

5:15 PM - 6:30 PM JST | 8:15 AM - 9:30 AM UTC | Poster Hall International Exhibition Hall8, Makuhari Messe_35

[S-CG49] Hard-Rock Drilling Science: From Continental to Deep Sea Drilling, and Oman Project

convener:Katsuyoshi Michibayashi(Department of Earth and Planetary Sciences, Nagoya University), Eiichi TAKAZAWA(Department of Geology, Faculty of Science, Niigata University), Norikatsu Akizawa(Department of Ocean Floor Geoscience, Atmosphere and Ocean Research Institute, The University of Tokyo)

[SCG49-P01] **Permeability profile in the Oman Drilling Project inferred from resistivity measurements**

*Ikuo Katayama[1], Keishi Okazaki[2], Natsue Abe[2], Ole Ivar Ulven[3], Gilbert Hong[4], Wenlu Zhu[5], Benoit Cordonnier[3], Kohei Hatakeyama[1], Yuya Akamatsu[1], Katsuyoshi Michibayashi[6], Marguerite Godard[7], Peter Kelemen[8], Science Party The Oman Drilling Project Phase 2 (1.Hiroshima University, 2.JAMSTEC, 3.University of Oslo, 4.Seoul National University, 5.University of Maryland, 6.Nagoya University, 7.Universitè Montpellier, 8.Columbia University)

[SCG49-P02] Relationship between alteration intensity and elastic wave velocity of gabbroic rocks from ICDP Hole CM1A, Oman Drilling Project Phase II

*Kosuke Kimura[1], Ikuo Katayama[1], Kohei Hatakeyama[1], Yuya Akamatsu[1], Natsue Abe[2], Keishi Okazaki[2], The Oman Drilling Project Phase II Science Party (1.Hiroshima University, 2.JAMSTEC)

[SCG49-P03] Physical property of the fossilized crust-mantle transition zone from ICDP Oman Drilling Project Hole CM1A and CM2B measured onboard D/V Chikyu

*Keishi Okazaki[1], Natsue Abe[1], Kohei Hatakeyama[2], Yuya Akamatsu[2], Ikuo Katayama[2], Eiichi TAKAZAWA[3], Damon A H Teagle[4], Peter B Kelemen[5], Jude Coggon[4], The Oman Drilling Project Phase 2 Science Party (1.Japan Agency for Marine-Earth Science and Technology, 2.Hiroshima University, 3.Niigata University, 4.University of Southampton, 5.Columbia University)

[SCG49-P04] Microstructures of lower crust gabbros from the Oman Ophiolite: Analyses of the drilled cores of the Oman Drilling Project

*Koki Iida[1], Takahiro Fudai[1], Susumu Umino[1], Yuki Kusano[2] (1.Kanazawa University, 2.Geological Survey of Japan)

[SCG49-P05] Olivine fabric and mineral compositions in the Maqsad area of the Samail massif, the southern Oman ophiolite

*Kaho Takahashi[1], Eiichi TAKAZAWA[2,3], Katsuyoshi Michibayashi[4], Kakihata Yuki[4], Ryoko Senda[5] (1.Graduate School of Science and Technology, Niigata University, 2.Department of Geology, Faculty of Science, Niigata University, 3.JAMSTEC, 4.Nagoya University, 5.Kyushu University)

[SCG49-P06] The evolution of melt inclusions in podiform chromitite in Oman

*Yuan YAO[1], Eiichi TAKAZAWA[2,3], Oman Drilling Project Phase 2 Science Party (1.Graduate School of Sciences& Technology, Niigata University, Japan, 2.Department of Geology, Faculty of Science, Niigata University, Japan, 3.Research and Development Center for Ocean Drilling Science, JAMSTEC, Japan)

[SCG49-P07] Melt/fluid - rock reaction inferred from the Wadi Tayin mantle section in the southern Oman ophiolite

*Keisuke ISHII[1], Eiichi TAKAZAWA[2], Akihiro kuriyama[2], Kyouka Someya[2], Yoshihiko Tamura[3] (1.Graduate School of Science and Technology, Niigata University, 2.Department of Geology, Faculty of Science, Niigata University , 3.R&D Center for Ocean Drilling Science, Japan Agency for Marine-Earth Science and Technology)

[SCG49-P08] Numerical simulations for reaction-induced fracture formation of layered gabbro during hydration process

*Kazuki Yoshida[1], Hiroyuki Shimizu[2], Noriyoshi Tsuchiya[1], Atsushi Okamoto[1], Phase 2 Science Party Oman Drilling Project[3] (1.Tohoku university, 2.Geotechnical Analysis Group, Advanced Analysis Department, Civil Engineering Design Division, Kajima Corporation, 3.Oman Drilling Project Phase 2 Science Party)

[SCG49-P09] X-ray CT images of oceanic lithologies obtained on Oman Drilling Project drillcores during ChikyuOman 2017 and 2018

*Katsuyoshi Michibayashi[1], Peter B Kelemen[2], Margurette Godard[3], Eiichi TAKAZAWA[4], Damon A H Teagle[5], The Oman Drilling Project Science Party[6] (1.Department of Earth and Planetary Sciences, Nagoya University, 2.Columbia University, 3.Université Montpellier, 4.Niigata University, 5.Southampton University, 6.ICDP)

[SCG49-P10] Re-examination of the crystallization process of clinopyroxene oikocrysts in layered gabbros at Hess Deep Rift, EPR

*Akane Yasui[1], Takashi Hoshide[1] (1.Graduate School of International Resource Sciences, Akita University)

[SCG49-P11] Structural petrology of peridotites from the Kalaymyo ophiolite

*Kouhei Asano[1,2], Katsuyoshi Michibayashi[1], Jung-Woo Park[3] (1.Graduate School of Environmental Studies, Nagoya University, 2.Shizuoka University, 3.Seoul National University)

[SCG49-P12] Reevaluation of the origin of mafic layers in the Upper Zone of the Horoman Peridotite

*Yumeto KOGURE[1], Eiichi TAKAZAWA[1] (1.Department of Geology, Faculty of Science, Niigata University)

[SCG49-P13] A structural and petrological study of "Shibukawa ultramafic body" in the Sanbagawa belt, western Shizuoka, Japan

*Hikaru Shioya[1,2], Katsuyoshi Michibayashi[1], Ken-ichi Hirauchi[2] (1.Graduate School of Environmental Studies, Nagoya University, 2.Institute of Geosciences, Shizuoka University)

[J] Oral | S (Solid Earth Sciences)：S-CG Complex & General

10:45 AM - 12:15 PM JST | 1:45 AM - 3:15 AM UTC | A09 TOKYO BAY MAKUHARI HALL

[S-CG54] Rheology, fracture and friction in Earth and planetary sciences

convener:Miki Tasaka(Shimane University), Osamu Kuwano(Japan Agency for Marine-Earth Science and Technology), Ichiko Shimizu(Division of Earth and Planetary Sciences, Graduate School of Science, Kyoto University), Hidemi Ishibashi(Faculty of Science, Shizuoka University), Chairperson:Osamu Kuwano(Japan Agency for Marine-Earth Science and Technology (JAMSTEC)), Ichiko Shimizu

10:45 AM - 11:00 AM JST | 1:45 AM - 2:00 AM UTC

[SCG54-01] Rheology of granular materials near the jamming transition under oscillatory shear

★Invited Papers

*Michio Otsuki[1], Hisao Hayakawa[2] (1.Graduate School of Engineering Science, Osaka University, 2.Yukawa Institute for Theoretical Physics, Kyoto University)

11:00 AM - 11:15 AM JST | 2:00 AM - 2:15 AM UTC

[SCG54-02] The real-scale numerical sandbox experiments for understanding stress state in accretionary prisms

*Mikito Furuichi[1], Arthur Bauville[1], Daisuke Nishiura[1], Takane Hori[1], Osamu Kuwano[1] (1.Japan Agency for Marine-Earth Science and Technology)

11:15 AM - 11:30 AM JST | 2:15 AM - 2:30 AM UTC

[SCG54-03] Numerical analysis on the fracture of Maxwell fluid by phase field models

*Masaharu Kameda[1], Keita Yamanishi[1], Akinori Yamanaka[1], Mie Ichihara[2] (1.Department of Mechanical Systems Engineering, Tokyo University of Agriculture and Technology, 2.Earthquake Research Institute, The University of Tokyo)

11:30 AM - 11:45 AM JST | 2:30 AM - 2:45 AM UTC

[SCG54-04] Diagenesis- and earthquake-driven transformations of carbonaceous materials and their implication for frictional strength and earthquake rupture dynamics in carbon-bearing plate-subduction faults

*Shunya Kaneki[1], Tetsuro Hirono[1] (1.Graduate School of Science, Osaka University)

11:45 AM - 12:00 PM JST | 2:45 AM - 3:00 AM UTC

[SCG54-05] Viscous behavior of chert during frictional melting

*Ginta Motohashi[1], Kiyokazu Oohashi[2], Kohtaro Ujiie[1] (1.University of Tsukuba, 2.Yamaguchi University)

12:00 PM - 12:15 PM JST | 3:00 AM - 3:15 AM UTC

[SCG54-06] Effect of friction and comminution on the optically-stimulated luminescence of quartz grains

*Kiyokazu Oohashi[1], Koji Akasegawa[2], Yuki Minomo[1], Noriko Hasebe[3], Kazumasa Miura[4] (1.Graduate School of Sciences and Technology for Innovation, Yamaguchi University, 2.Daiwa Exploration & Consulting Co., Ltd., 3.Institute of Nature and Environmental Technology, Kanazawa University, 4.Graduate School of Natural Science & Technology, Kanazawa University)

[J] Oral | S (Solid Earth Sciences)：S-CG Complex & General

1:45 PM - 3:15 PM JST | 4:45 AM - 6:15 AM UTC | A09 TOKYO BAY MAKUHARI HALL

[S-CG54] Rheology, fracture and friction in Earth and planetary sciences

convener:Miki Tasaka(Shimane University), Osamu Kuwano(Japan Agency for Marine-Earth Science and Technology), Ichiko Shimizu(Division of Earth and Planetary Sciences, Graduate School of Science, Kyoto University), Hidemi Ishibashi(Faculty of Science, Shizuoka University), Chairperson:Miki Tasaka(島根大学), Hidemi Ishibashi(Shizuoka University)

1:45 PM - 2:00 PM JST | 4:45 AM - 5:00 AM UTC

[SCG54-07] Frictional behaviors of smectite clay: constraints for the mobility of slow-moving landslides in the cold season

★Invited Papers

*Tatsuya Shibasaki[1], Sumio Matsuura[2] (1.Japan Conservation Engineers and Co., Ltd, 2.DPRI, Kyoto University)

2:00 PM - 2:15 PM JST | 5:00 AM - 5:15 AM UTC

[SCG54-08] Strength of a deep fault zone along the Median Tectonic Line: Influence of chrolite friction

*Ichiko Shimizu[1], Ayumi S. Okamoto, Andre R. Niemeijer[2], Christopher J. Spiers[2], Shun Arai[3], Toru Takeshita[4] (1.Division of Earth and Planetary Sciences, Graduate School of Science, Kyoto University, 2.Faculty of Geosciences, Utrecht University, 3.Tohoku University, 4.Hokkaido University)

2:15 PM - 2:30 PM JST | 5:15 AM - 5:30 AM UTC

[SCG54-09] Changes in seismic wave velocity during brittle deformation of gabbro and peridotite

*Yuya Akamatsu[1], Ikuo Katayama[1] (1.Hiroshima University)

2:30 PM - 2:45 PM JST | 5:30 AM - 5:45 AM UTC

[SCG54-10] Dislocation textures in shock-compressed MgO and their formation mechanisms

*Kiyoshi Fujino[1], Xun Liu[2], Tsutomu Mashimo[2] (1.Geodynamics Research Center, Ehime University, 2.Institute of Pulsed Power Science, Kumamoto University)

2:45 PM - 3:00 PM JST | 5:45 AM - 6:00 AM UTC

[SCG54-11] Development of rotational diamond anvil cell and large strain deformation experiments of lower-mantle materials

★Invited Papers

*Shintaro Azuma[1,2], Ryuichi Nomura[3,4], Kentaro Uesugi[5], Yu Nishihara[4], Doi Shunta[4], Takeshi Arimoto[4], Tetsuo Irifune[4] (1.Tokyo Tech., 2.Kyushu Univ., 3.Kyoto Univ., 4.Ehime Univ., 5.Japan Synchrotron Radiation Research Institute (JASRI))

3:00 PM - 3:15 PM JST | 6:00 AM - 6:15 AM UTC

[SCG54-12] Rheology of hcp-iron

*Yu Nishihara[1], Doi Shunta[1], Noriyoshi Tsujino[2], Daisuke Yamazaki[2], Yuji Higo[3] (1.Geodynamics Research Center, Ehime University, 2.Institute of Planetary Materials, Okayama University, 3.Japan Synchrotron Radiation Research Institute)

[J] Poster | S (Solid Earth Sciences)：S-CG Complex & General

3:30 PM - 5:00 PM JST | 6:30 AM - 8:00 AM UTC | Poster Hall International Exhibition Hall8, Makuhari Messe_20

[S-CG54] Rheology, fracture and friction in Earth and planetary sciences

convener:Miki Tasaka(Shimane University), Osamu Kuwano(Japan Agency for Marine-Earth Science and Technology), Ichiko Shimizu(Division of Earth and Planetary Sciences, Graduate School of Science, Kyoto University), Hidemi Ishibashi(Faculty of Science, Shizuoka University)

[SCG54-P01] First-principles study on frictional characteristics of gibbsite

*Hanaya Okuda[1], Kenji Kawai[1], Hiroshi Sakuma[2] (1.Department of Earth and Planetary Science, School of Science, University of Tokyo, 2.Research Center for Functional Materials, National Institute for Materials Science)

[SCG54-P02] Feasibility Study of Morphological Characterization to Comminuted Particles by A Particle Characterization Approach (4)

*Daisuke Sasakura[1], Osamu Kuwano[2] (1.MalvernPanalytical Japan ,Div of Spectris Co.Ltd,., 2.JAMSTEC)

[SCG54-P03] Rheological property of basaltic lava at rigid-deformable transition

*Akio Goto[1] (1.Center for Northeast Asian Studies, Tohoku University)

[SCG54-P04] Cataclasitic texture in gabbroic xenoliths of the Fuji 1707 eruption, Japan

*Hidemi Ishibashi[1], Yumiko Harigane[2], ATSUSHI YASUDA[3], Natsumi Hokanishi[3] (1.Faculty of Science, Shizuoka University, 2.Geological Survey of Japan, AIST, 3.Earthquake Research Institute, University of Tokyo)

[SCG54-P05] Heterogeneous deformation and intragranular recrystallization in experimentally deformed fossil-bearing limestone

*Nahyeon Kim[1], Miki Takahashi[2], Jin-Han Ree[1], Haemyeong Jung[3] (1.Korea University, 2.Geological Survey of Japan, AIST, 3.Seoul National University)

[SCG54-P06] Development of the geobarometer using size and mineral species dependence of residual pressure of fluid inclusions

*Yuuki Hagiwara[1], Junji Yamamoto[1] (1.Hokkaido University)

[SCG54-P07] Microstructures and misorientation analysis of quartz in the Sanbagawa metamorphic belt, Shikoku, Japan

*Tadamasa Ueda[1], Ichiko Shimizu[1] (1.Division of Earth and Planetary Sciences, Graduate School of Science, Kyoto University)

[SCG54-P08] Microstructural & petrological analysis of peridotite xenolith in Noyama-dake, Shimane prefecture ~ implication of plastic deformation during Japan sea opening

*Miki Tasaka[1], Shunsuke Inagawa[1] (1.Shimane University)

[SCG54-P09] Thermodynamic approach to grain boundary premelting in a binary eutectic system

*Akihiro Tsunoda[1], Yasuko Takei[1], Hatsuki Yamauchi[1] (1.Earthquake Research Institute, The University of Tokyo)

[SCG54-P10] Size effects on hardness and fracture toughness of olivine

*Sanae Koizumi[1], Tohru S Suzuki[2], Takehiko Hiraga[1] (1.Earthquake Research Institute,The University of Tokyo, 2.National Institute for Materials Science)

[SCG54-P11] Dislocation creep of dry orthoenstatite aggregates under high *P-T* conditions

*Yumiko Tsubokawa[1], Tomohiro Ohuchi[1], Yuji Higo[2], Yoshinori Tange[2], Tetsuo Irifune[1] (1.Ehime University Geodynamics Research Center, 2.Japan Synchrotron Radiation Research Institute)

[J] Poster | S (Solid Earth Sciences)：S-CG Complex & General

5:15 PM - 6:30 PM JST | 8:15 AM - 9:30 AM UTC | Poster Hall International Exhibition Hall8, Makuhari Messe_36

[S-CG54] Rheology, fracture and friction in Earth and planetary sciences

convener:Miki Tasaka(Shimane University), Osamu Kuwano(Japan Agency for Marine-Earth Science and Technology), Ichiko Shimizu(Division of Earth and Planetary Sciences, Graduate School of Science, Kyoto University), Hidemi Ishibashi(Faculty of Science, Shizuoka University)

[SCG54-P01] First-principles study on frictional characteristics of gibbsite

*Hanaya Okuda[1], Kenji Kawai[1], Hiroshi Sakuma[2] (1.Department of Earth and Planetary Science, School of Science, University of Tokyo, 2.Research Center for Functional Materials, National Institute for Materials Science)

[SCG54-P02] Feasibility Study of Morphological Characterization to Comminuted Particles by A Particle Characterization Approach (4)

*Daisuke Sasakura[1], Osamu Kuwano[2] (1.MalvernPanalytical Japan ,Div of Spectris Co.Ltd,., 2.JAMSTEC)

[SCG54-P03] Rheological property of basaltic lava at rigid-deformable transition

*Akio Goto[1] (1.Center for Northeast Asian Studies, Tohoku University)

[SCG54-P04] Cataclasitic texture in gabbroic xenoliths of the Fuji 1707 eruption, Japan

*Hidemi Ishibashi[1], Yumiko Harigane[2], ATSUSHI YASUDA[3], Natsumi Hokanishi[3] (1.Faculty of Science, Shizuoka University, 2.Geological Survey of Japan, AIST, 3.Earthquake Research Institute, University of Tokyo)

[SCG54-P05] Heterogeneous deformation and intragranular recrystallization in experimentally deformed fossil-bearing limestone

*Nahyeon Kim[1], Miki Takahashi[2], Jin-Han Ree[1], Haemyeong Jung[3] (1.Korea University, 2.Geological Survey of Japan, AIST, 3.Seoul National University)

[SCG54-P06] Development of the geobarometer using size and mineral species dependence of residual pressure of fluid inclusions

*Yuuki Hagiwara[1], Junji Yamamoto[1] (1.Hokkaido University)

[SCG54-P07] Microstructures and misorientation analysis of quartz in the Sanbagawa metamorphic belt, Shikoku, Japan

*Tadamasa Ueda[1], Ichiko Shimizu[1] (1.Division of Earth and Planetary Sciences, Graduate School of Science, Kyoto University)

[SCG54-P08] Microstructural & petrological analysis of peridotite xenolith in Noyama-dake, Shimane prefecture ~ implication of plastic deformation during Japan sea opening

*Miki Tasaka[1], Shunsuke Inagawa[1] (1.Shimane University)

[SCG54-P09] Thermodynamic approach to grain boundary premelting in a binary eutectic system

*Akihiro Tsunoda[1], Yasuko Takei[1], Hatsuki Yamauchi[1] (1.Earthquake Research Institute, The University of Tokyo)

[SCG54-P10] Size effects on hardness and fracture toughness of olivine

*Sanae Koizumi[1], Tohru S Suzuki[2], Takehiko Hiraga[1] (1.Earthquake Research Institute,The University of Tokyo, 2.National Institute for Materials Science)

[SCG54-P11] Dislocation creep of dry orthoenstatite aggregates under high *P-T* conditions

*Yumiko Tsubokawa[1], Tomohiro Ohuchi[1], Yuji Higo[2], Yoshinori Tange[2], Tetsuo Irifune[1] (1.Ehime University Geodynamics Research Center, 2.Japan Synchrotron Radiation Research Institute)

[J] Oral | S (Solid Earth Sciences)：S-CG Complex & General

9:00 AM - 10:30 AM JST | 12:00 AM - 1:30 AM UTC | Convention Hall A 2F

[S-CG61] Dynamics in mobile belts

convener:Yukitoshi Fukahata(Disaster Prevention Research Institute, Kyoto University), Toru Takeshita(Department of Natural History Sciences, Graduate School of Science, Hokkaido University), Hikaru Iwamori(Geochemical Evolution Research Program, Japan Agency for Marine-Earth Science and Technology), Chairperson:Keisuke Yoshida(東北大学大学院理学研究科 地球物理学専攻), Masaoki Uno(東北大学)

9:00 AM - 9:15 AM JST | 12:00 AM - 12:15 AM UTC

[SCG61-13] Deciphering dynamics of thermal events at lithosphere-asthenosphere boundary from peridotite xenoliths of Ichinomegata maar, NE Japan

*Yuto Sato[1], Kazuhito Ozawa[1] (1.Department of Earth and Planetary Science, Graduate School of Science, The University of Tokyo)

9:15 AM - 9:30 AM JST | 12:15 AM - 12:30 AM UTC

[SCG61-14] **Experimental investigation of reaction-induced stress and permeability evolution in MgO–H_2O system**

*Masaoki Uno[1], Hisamu Kasahara[1], Atsushi Okamoto[1], Noriyoshi Tsuchiya[1] (1.Graduate School of Environmental Studies, Tohoku University)

9:30 AM - 9:45 AM JST | 12:30 AM - 12:45 AM UTC

[SCG61-15] Fluid-Flow, Resistivity and Elastic Wave Velocity Simulation of Digital Rock Fracture and Comparison with Experimental Data

*Kazuki Sawayama[1], Fei Jiang[2], Takuya ISHIBASHI[3], Takeshi Tsuji[4], Yasuhiro Fujimitsu[4] (1.Department of Earth Resources Engineering, Graduate school of engineering, Kyushu University, 2.Department of Mechanical Engineering, Faculty of Engineering, Yamaguchi University, 3.Fukushima Renewable Energy Institute, National Institute of Advanced Industrial Science and Technology, 4.Department of Earth Resources Engineering, Faculty of engineering, Kyushu University)

9:45 AM - 10:00 AM JST | 12:45 AM - 1:00 AM UTC

[SCG61-16] Fluid distribution in the crust – inference from seismic velocity and electrical conductivity

*Tohru Watanabe[1], Kenta Yoshida[2] (1.Gradudate School of Science and Engineering, University of Toyama, 2.Research and Development Center for Ocean Drilling Science, Japan Agency for Marine-earth Science and Technology)

10:00 AM - 10:15 AM JST | 1:00 AM - 1:15 AM UTC

[SCG61-17] The seismological structure about fault zone extending to the lower crust in the northern Kinki district, southwestern Japan

*Shinya Kato[1], Yoshihisa Iio[1], Takuo Shibutani[1], Hiroshi Katao[1], Masayo Sawada[1], Kazuhide Tomisaka[1] (1.Disater Prevention Research Institute, Kyoto University)

10:15 AM - 10:30 AM JST | 1:15 AM - 1:30 AM UTC

[SCG61-18] Inland repeating earthquakes in the vicinity of low frequency earthquakes around Hakodate, Hokkaido

*Keisuke Yoshida[1], Akira Hasegawa[1], Shinako Noguchi[2], Keiji Kasahara[2] (1.Tohoku University, 2. Association for the Development of Earthquake Prediction)

[J] Oral | S (Solid Earth Sciences)：S-CG Complex & General

10:45 AM - 12:15 PM JST | 1:45 AM - 3:15 AM UTC | Convention Hall A 2F

[S-CG61] Dynamics in mobile belts

convener:Yukitoshi Fukahata(Disaster Prevention Research Institute, Kyoto University), Toru Takeshita(Department of Natural History Sciences, Graduate School of Science, Hokkaido University), Hikaru Iwamori(Geochemical Evolution Research Program, Japan Agency for Marine-Earth Science and Technology), Chairperson:Bunichiro Shibazaki, Daisuke Sato

10:45 AM - 11:00 AM JST | 1:45 AM - 2:00 AM UTC

[SCG61-19] Modeling strain concentration and mountain building processes in central Japan considering heterogeneous rheological structure

*Bunichiro Shibazaki[1] (1.International Institute of Seismology and Earthquake Engineering, Building Research Institute)

11:00 AM - 11:15 AM JST | 2:00 AM - 2:15 AM UTC

[SCG61-20] Inelastic strain rate and deviatoric stress field of the seismic gap in west part of Kyushu, Japan, estimated from seismic and geodetic data

*Yuhei Yuasa[1], Satoshi Matsumoto[2], Shigeru Nakao[3], Takeshi Matsushima[2], Takahiro Ohkura[4] (1.Department of Earth and Planetary Sciences, Graduate School of Science, Kyushu University, 2.Institute of Seismology and Volcanology, Faculty of Sciences, Kyushu University, 3.Department of Earth and Environmental Sciences, Graduate School of Science and Engineering, Kagoshima University, 4.Aso Volcanological Laboratory, Institute for Geothermal Sciences, Graduate School of Science, Kyoto University)

11:15 AM - 11:30 AM JST | 2:15 AM - 2:30 AM UTC

[SCG61-21] Persistent and time-dependent crustal deformation in northern Fossa Magna and its tectonic implications

*Takeshi Sagiya[1], Koki Kumagai[2], Angela Meneses-Gutierrez[3], Nobuhisa Matsuta[4], Daisuke Hirouchi[5], Kenjiro Matsuhiro[2], Takashi OKUDA[2] (1.Disaster Mitigation Research Center, Nagoya University, 2.Graduate School of Environmental Studies, Nagoya University, 3.Disaster Prevention Research Institute, Kyoto University, 4.Graduate School of Education, Okayama University, 5.Faculty of Education, Shinshu University)

11:30 AM - 11:45 AM JST | 2:30 AM - 2:45 AM UTC

[SCG61-22] Unexpected relationship between ΔCFF and the strain-rate paradox: separation of plastic strain from inelastic strain

*Yukitoshi Fukahata[1], Angela Meneses-Gutierrez[1], Takeshi Sagiya[2] (1.Disaster Prevention Research Institute, Kyoto University, 2.Disaster Mitigation Research Center, Nagoya University)

11:45 AM - 12:00 PM JST | 2:45 AM - 3:00 AM UTC

[SCG61-23] Active period of inland earthquakes based on numerical simulation of megathrust earthquake cycle incorporating viscoelasticity

*Tsukasa MITOGAWA[1], Takuya NISHIMURA[2] (1.Graduate School of Science, Kyoto University, 2.Disaster Prevention Research Institute, Kyoto University)

12:00 PM - 12:15 PM JST | 3:00 AM - 3:15 AM UTC

[SCG61-24] Influence of viscoelastic relaxation on estimated interplate coupling along the Nankai Trough, southwest Japan

*Takuya NISHIMURA[1], Fred F Pollitz[2] (1.Disaster Prevention Research Institute, Kyoto University, 2.U.S. Geological Survey)

[J] Oral | S (Solid Earth Sciences)：S-CG Complex & General

1:45 PM - 3:15 PM JST | 4:45 AM - 6:15 AM UTC | Convention Hall A 2F

[S-CG61] Dynamics in mobile belts

convener:Yukitoshi Fukahata(Disaster Prevention Research Institute, Kyoto University), Toru Takeshita(Department of Natural History Sciences, Graduate School of Science, Hokkaido University), Hikaru Iwamori(Geochemical Evolution Research Program, Japan Agency for Marine-Earth Science and Technology), Chairperson:Naoki Uchida, Takeshi Iinuma

1:45 PM - 2:00 PM JST | 4:45 AM - 5:00 AM UTC

[SCG61-25] Revisiting the Forearc Sliver Scenario Along the Southern Kurile Trench to Reconcile Interdisciplinary Observations

*Yuji ITOH[1], Kelin WANG[2], Takuya NISHIMURA[3] (1.Graduate School of Science, Kyoto University, 2.Pacific Geoscience Centre, Geological Survey of Canada, 3.Disaster Prevention Research Institute, Kyoto University)

2:00 PM - 2:15 PM JST | 5:00 AM - 5:15 AM UTC

[SCG61-26] Segmentation of crustal deformation area within the Sanriku coast, northeast Japan, on the basis of spatial distribution of millennial-scale crustal movements

*Yuichi Niwa[1] (1.Faculty of Science and Engineering, Chuo University)

2:15 PM - 2:30 PM JST | 5:15 AM - 5:30 AM UTC

[SCG61-27] Shear wave splitting east off NE Japan based on the S-net data

*Naoki Uchida[1], Junichi Nakajima[2], Ryota Takagi[1], Keisuke Yoshida[1], Takashi NAKAYAMA[1], Ryota Hino[1], Tomomi Okada[1], Youichi Asano[3], Sachiko Tanaka[3] (1.Research Center for Prediction of Earthquakes and Volcanic Eruptions Graduate School of Science, Tohoku University, 2.Department of Earth and Planetary Sciences, Graduate School of Science and Engineering, Tokyo Institute of Technology, Tokyo, 3.National Research Institute for Earth Science and Disaster Resilience)

2:30 PM - 2:45 PM JST | 5:30 AM - 5:45 AM UTC

[SCG61-28] Gravity anomaly due to active faults and crustal rheology in the northeastern Japan arc inferred by fault dislocation model

*Mitsuhiro Hirano[1], Hiroyuki Nagahama[1], Jun Muto[1] (1.tohoku university)

2:45 PM - 3:00 PM JST | 5:45 AM - 6:00 AM UTC

[SCG61-29] On the temporal decay of the localized strain rate in the Tohoku region after the Tohoku-Oki earthquake

*Youichiro Takada[1], Tomomi Inamatsu[2] (1.Faculty of Science, Hokkaido University, 2.Dept. Natural History Sciences, Hokkaido University)

3:00 PM - 3:15 PM JST | 6:00 AM - 6:15 AM UTC

[SCG61-30] Revisiting the Coseismic Slip Distribution of the 2011 Tohoku-oki Earthquake Considering Early Postseismic Deformation, Non-linear Viscoelasticity, and Heterogeneous Structure

*Takeshi Iinuma[1], Ryoichiro Agata[1], Yusaku Ohta[2], Ryota Hino[2], Takane Hori[1] (1.Japan Agency for Marine-Earth Science and Technology (JAMSTEC), 2.Graduate School of Science, Tohoku University)

[J] Poster | S (Solid Earth Sciences)：S-CG Complex & General

3:30 PM - 5:00 PM JST | 6:30 AM - 8:00 AM UTC | Poster Hall International Exhibition Hall8, Makuhari Messe_21

[S-CG61] Dynamics in mobile belts

convener:Yukitoshi Fukahata(Disaster Prevention Research Institute, Kyoto University), Toru Takeshita(Department of Natural History Sciences, Graduate School of Science, Hokkaido University), Hikaru Iwamori(Geochemical Evolution Research Program, Japan Agency for Marine-Earth Science and Technology)

[SCG61-P01] Three-dimensional imaging of geo-fluid distribution at NE-Japan forearc using wideband magnetotelluric measurements

*Masato Fukai[1], Yasuo Ogawa[1], Kuo Hsuan Tseng[1], Masahiro Ichiki[2], Shinichi Takakura[3] (1.Tokyo Institute of Technology, 2.Tohoku University, 3.National Institute of Advanced Industrial Science and Technology)

[SCG61-P02] **Elastic wave velocity and electrical conductivity in brine-saturated rocks and microstructure of pores**

*Arina Tomioka[1], Tohru Watanabe[1] (1.University of Toyama)

[SCG61-P03] Influence of grain shape and grain size distribution on connectivity of pores in granular materials.

*Katazakai Haruka[1], Tohru Watanabe[1] (1.Toyama University)

[SCG61-P04] Change of pore connectivity in granular materials under axial compression

*MAREMICHI ABE[1], Tohru Watanabe[1] (1.Toyama University)

[SCG61-P05] **Estimation of crustal strength using residual strain of quartz in deformed conglomerate and inhomogenous strain of conglomerate layer -As an example of multiple collision zone of Izu-Bonin arc, Fujikawa valley, Central Japan-**

*Shun Suzuki[1], Kenta Kobayashi[1] (1.Graduate School of Science and Technology, Niigata University)

[SCG61-P06] **An Introduction to Ryoke Cataclastic Rocks in Tsukide, Mie Prefecture, Japan: An Approach Using 3D Reconstructions From Thin Sections**

*Thomas Jing Yi Yeo[1], Toru Takeshita[1] (1.Department of Natural History Sciences, Graduate School of Science, Hokkaido University)

[SCG61-P07] Relationships between spacing and growth or linkage of normal faults in the Miyako Island, South Ryukyu arc, Japan

*Sumire Maeda[1], Makoto Otsubo[1], Daisuke Asahina[1], Yuki Furuno [1] (1.Research Institute of Earthquake and Volcano Geology, Geological Survey of Japan/AIST)

[SCG61-P08] **3D fault architecture along the Median Tectonic Line, eastern Kii Peninsula, SW Japan**

*Norio Shigematsu[1], Takuma Katori[1,2], Jun Kameda[3], Ayumu Miyakawa[4] (1.Research Institute of Earthquake and Volcano Geology, Geological Survey of Japan, National Institute of Advanced Industrial Science and Technology, 2.Graduate School of Science and Technology, Niigata University, 3.Department of Natural History and Sciences, Hokkaido University, 4.Research Institute of Geology and Geoinformation, Geological Survey of Japan, National Institute of Advanced Industrial Science and Technology)

[SCG61-P09] Significant of thrust zone at Fuji river basin in the South Fossa Magna, Southern Yamanashi Prefecture, Central Japan
-Study of Structural geology of Minobu and Neguma fault-

*Minami Madoka[1], Kenta Kobayashi[1] (1. Niigata university department of geology science)

[SCG61-P10] Mineralogical characteristics of fault rocks in the aftershock regions of the 2000 Western Tottori earthquake and its spatial distribution

*Shunya Kaneki[1], Tetsuro Hirono[1], Hideki Mukoyoshi[2], Kenta Kobayashi[3], Toru Takeshita[4] (1.Graduate School of Science, Osaka University, 2.Graduate School of Science and Engineering, Shimane University, 3.Graduate School of Science and Technology, Niigata University, 4.Graduate School of Science, Hokkaido University)

[SCG61-P11] Relationship between seismicity of the 2016 the Central Tottori Earthquake and fault distribution in the aftershock area

*Masayuki Ichimura[1], Hideki Mukoyoshi[2] (1.Graduate School of Natural Science and Technology, Shimane University, 2.Department of Earth Science, Shimane University)

[SCG61-P12] History of fault activity considered from the brittle shear zone and the geological structure near the Cape Otachi, Kumamoto Prefecture

*Keiji Ogashiwa[1], Kenta Kobayashi[1] (1.Niigata University)

[SCG61-P13] Study on fault activity evaluation method (A new attempt to understand fault activities) No.1 - Overall plan and current situation at Shionohira Fault -

*Kazuhiro Aoki[1], Takahiro Watanabe[1], Yukumo Tanaka[1], Kazuyoshi Seshimo[1] (1.Japan Atomic Energy Agency)

[SCG61-P14] Study on fault activity evaluation method (A new attempt to understand fault activities) No.2
- Injection experiment using a SIMFIP probe at Shionohira Fault and southern fault-

*Takahiro Watanabe[1], Yukumo Tanaka[1], Kazuhiro Aoki[1], Yves Guglielmi[2], Paul Cook[2], Florian Soom[2], Wakahama Hiroshi[3], Noujou Haruka[3], Etsuo Iwasaki[3], Masao Kametaka[3], Kazuyoshi Seshimo[1] (1.Japan Atomic Energy Agency, 2.Laurence Berkley National Laboratory, 3.DIA CONSULTANTS)

[SCG61-P15] Dynamic rupture simulation of 2018, Hokkaido Eastern Iburi earthquake: Role of non-planar fault geometry

*Tatsuya Hisakawa[1], Ryosuke Ando[1] (1.The University of Tokyo)

[SCG61-P16] A New Fully-Dynamic Earthquake Cycle Simulator Applicable to Arbitrary Nonplanar Fault Geometries - A Benchmark Test

*Daisuke Sato[1], Nadia Lapusta[2], Hiroyuki Noda[1] (1.Disaster Prevention Research Institute, Kyoto University, 2.California Institute of Technology)

[SCG61-P17] Stress and displacement Green's functions to treat volumetric inelastic strain and elastic inhomogeneity in boundary integral equation method

*Daisuke Sato[1] (1.Disaster Prevention Research Institute, Kyoto University)

[SCG61-P18] Frictional properties of dolerite and granite at intermediate slip rates and controlled ambient temperatures

*Michiyo Sawai[1], Yuuki Yokoyama[1], Kyuichi Kanagawa[1] (1.Chiba University)

[SCG61-P19] Extraction of features of strata using borehole data of geothermal area by multivariate analysis

*Ojima Hiroki[1], Kazuya Ishitsuka[2], Toru Mogi[3], Tatsuya Kajiwara[4], Takeshi Sugimoto[4], Hiroshi Asanuma[5] (1.Department of Socio-Environmental Engineering Hokkaido University, 2.Division of Urban Management, Graduate School of Engineering, Kyoto University, 3.Division of sustainable Resources Engineering, Faculty of Enginieering, Hokkaido University, 4.Geothermal Engineering Co. Ltd, 5.Fukushima Renewable Energy Institute, AIST)

[SCG61-P20] Low-temperature thermochronology of Cretaceous granitoids from the northern Northeast Japan Arc: Towards reconstructing arc-parallel thermal/denudation histories

*Shoma Fukuda[1], Shigeru Sueoka[2], Barry Paul Kohn[3], Noriko Hasebe[4], Akihiro Tamura[5], Tomoaki Morishita[5], Takahiro Tagami[1] (1.Graduate School of Science, Kyoto University , 2.Japan Atomic Energy Agency, 3.School of Earth Sciences, The University of Melbourne, 4.Institute of Nature and Environmental Technology, Kanazawa University, 5.Department of Earth Sciences, Kanazawa University)

[SCG61-P21] Uplift and denudation history of the South Fossa Magna region using low-temperature thermochronometric methods

*Yumi Kobayashi[1], Shigeru Sueoka[2], Shoma Fukuda[1], Barry P. Kohn[3], Tatsunori Yokoyama[2], Noriko Hasebe[4], Akihiro Tamura[5], Tomoaki Morishita[5], Takahiro Tagami[1] (1.Graduate School of Science, Kyoto University, 2.Tono Geoscience Center, Japan Atomic Energy Agency, 3.University of Melbourne, 4.Institute of Nature of Environmental Technology, Kanazawa University, 5.Department of Earth Sciences, Kanazawa University)

[SCG61-P22] Correlation between residual uplift and recurrence interval of the Kanto earthquake based on developmental process of coastal lowland

*Haeng-Yoong Kim[1] (1.Osaka City University, Graduate School of Science, Division of Biology &Geosciences)

[SCG61-P23] Mechanics preserving co-seismic uplift and marine terraces: dissymmetric patterns of co-seismic and inter-seismic deformation

*Kyohei Suzuki[1], Junki Komori[1], Ryosuke Ando[1] (1.Graduate School of Science, University of Tokyo)

[SCG61-P24] Enhanced resolution of stress tensor inversion by using fault instability analysis

★Invited Papers

*Katsushi Sato[1] (1.Division of Earth and Planetary Sciences, Graduate School of Science, Kyoto University)

[SCG61-P25] Focal mechanisms of the aftershocks of the 2000 Western Tottori Earthquake inferred from P wave first-motion data and spatial stress pattern

*Takaki Iwata[1] (1.Tokiwa University)

[SCG61-P26] Stress tensor inversion in focal area of the 2016 Mw7.8 Kaikoura earthquake, New Zealand

*Miu Matsuno[1], Tomomi Okada[1], Satoshi Matsumoto[2], Yuta Kawamura[2], Yoshihisa Iio[3], Tadashi Sato[1], Stephen C Bannister[4], John Ristau[4], Martha K Savage[5], John Townend[5], Jarg Pettinga[6], Francesca Ghisetti[7], Richard H Sibson[8] (1.Research Center for Prediction of Earthquakes and Volcanic Eruptions Graduate School of Science, Tohoku University, 2.Institute of Seismology and Volcanology, Faculty of Sciences, Kyushu University, 3.Disater Prevention Research Institute, Kyoto University, 4.GNS Science, New Zealand, 5.Victoria University of Wellington, Wellington, New Zealand, 6.University of Canterbury, Christchurch, New Zealand, 7.TerraGeologica, Ruby Bay, New Zealand, 8.University of Otago, Dunedin, New Zealand)

[SCG61-P27] Precise hypocenter distribution in the focal area of the 2016 Mw7.8 Kaikorua Earthquake, New Zealand

*Yuta Kawamura[1], Satoshi Matsumoto[1], Tomomi Okada[2], Miu Matsuno[2], Yoshihisa Iio[3], Tadashi Sato[2], Stephen C Bannister[4], John Ristau[4], Martha K Savage[5], John Twonend[5], Jarg Pettinga[6], Francesca Ghisetti[7], Richard H Sibson[8] (1.Kyushu University, Shimabara, Japan, 2.Tohoku University, Sendai, Japan, 3.Kyoto University, Uji, Japan, 4.GNS Science, Lower Hutt, New Zealand, 5.Victoria University of Wellington, Wellington, New Zealand, 6.University of Canterbury, Christchurch, New Zealand, 7.TerraGeologica, Ruby Bay, New Zealand, 8.University of Otago, Dunedin, New Zealand)

[SCG61-P28] **3-dimensional GPS velocities in Colombia and their implications for interplate coupling**

*Sindy Carolina Lizarazo[1], Takeshi Sagiya[2], Hector Mora-Paez[3] (1.Graduate School of Environmental Studies, Nagoya University, 2.Disaster Mitigation Research Center, Nagoya University, 3.Geological Survey of Colombia)

[J] Poster | S (Solid Earth Sciences)：S-CG Complex & General

5:15 PM - 6:30 PM JST | 8:15 AM - 9:30 AM UTC | Poster Hall International Exhibition Hall8, Makuhari Messe_37

[S-CG61] Dynamics in mobile belts

convener:Yukitoshi Fukahata(Disaster Prevention Research Institute, Kyoto University), Toru Takeshita(Department of Natural History Sciences, Graduate School of Science, Hokkaido University), Hikaru Iwamori(Geochemical Evolution Research Program, Japan Agency for Marine-Earth Science and Technology)

[SCG61-P01] Three-dimensional imaging of geo-fluid distribution at NE-Japan forearc using wideband magnetotelluric measurements

*Masato Fukai[1], Yasuo Ogawa[1], Kuo Hsuan Tseng[1], Masahiro Ichiki[2], Shinichi Takakura[3] (1.Tokyo Institute of Technology, 2.Tohoku University, 3.National Institute of Advanced Industrial Science and Technology)

[SCG61-P02] **Elastic wave velocity and electrical conductivity in brine-saturated rocks and microstructure of pores**

*Arina Tomioka[1], Tohru Watanabe[1] (1.University of Toyama)

[SCG61-P03] Influence of grain shape and grain size distribution on connectivity of pores in granular materials.

*Katazakai Haruka[1], Tohru Watanabe[1] (1.Toyama University)

[SCG61-P04] Change of pore connectivity in granular materials under axial compression

*MAREMICHI ABE[1], Tohru Watanabe[1] (1.Toyama University)

[SCG61-P05] **Estimation of crustal strength using residual strain of quartz in deformed conglomerate and inhomogenous strain of conglomerate layer -As an example of multiple collision zone of Izu-Bonin arc, Fujikawa valley, Central Japan-**

*Shun Suzuki[1], Kenta Kobayashi[1] (1.Graduate School of Science and Technology, Niigata University)

[SCG61-P06] **An Introduction to Ryoke Cataclastic Rocks in Tsukide, Mie Prefecture, Japan: An Approach Using 3D Reconstructions From Thin Sections**

*Thomas Jing Yi Yeo[1], Toru Takeshita[1] (1.Department of Natural History Sciences, Graduate School of Science, Hokkaido University)

[SCG61-P07] Relationships between spacing and growth or linkage of normal faults in the Miyako Island, South Ryukyu arc, Japan

*Sumire Maeda[1], Makoto Otsubo[1], Daisuke Asahina[1], Yuki Furuno [1] (1.Research Institute of Earthquake and Volcano Geology, Geological Survey of Japan/AIST)

[SCG61-P08] **3D fault architecture along the Median Tectonic Line, eastern Kii Peninsula, SW Japan**

*Norio Shigematsu[1], Takuma Katori[1,2], Jun Kameda[3], Ayumu Miyakawa[4] (1.Research Institute of Earthquake and Volcano Geology, Geological Survey of Japan, National Institute of Advanced Industrial Science and Technology, 2.Graduate School of Science and Technology, Niigata University, 3.Department of Natural History and Sciences, Hokkaido University, 4.Research Institute of Geology and Geoinformation, Geological Survey of Japan, National Institute of Advanced Industrial Science and Technology)

[SCG61-P09] Significant of thrust zone at Fuji river basin in the South Fossa Magna, Southern Yamanashi Prefecture, Central Japan
-Study of Structural geology of Minobu and Neguma fault-

*Minami Madoka[1], Kenta Kobayashi[1] (1. Niigata university department of geology science)

[SCG61-P10] Mineralogical characteristics of fault rocks in the aftershock regions of the 2000 Western Tottori earthquake and its spatial distribution

*Shunya Kaneki[1], Tetsuro Hirono[1], Hideki Mukoyoshi[2], Kenta Kobayashi[3], Toru Takeshita[4] (1.Graduate School of Science, Osaka University, 2.Graduate School of Science and Engineering, Shimane University, 3.Graduate School of Science and Technology, Niigata University, 4.Graduate School of Science, Hokkaido University)

[SCG61-P11] Relationship between seismicity of the 2016 the Central Tottori Earthquake and fault distribution in the aftershock area

*Masayuki Ichimura[1], Hideki Mukoyoshi[2] (1.Graduate School of Natural Science and Technology, Shimane University, 2.Department of Earth Science, Shimane University)

[SCG61-P12] History of fault activity considered from the brittle shear zone and the geological structure near the Cape Otachi, Kumamoto Prefecture

*Keiji Ogashiwa[1], Kenta Kobayashi[1] (1.Niigata University)

[SCG61-P13] Study on fault activity evaluation method (A new attempt to understand fault activities) No.1 - Overall plan and current situation at Shionohira Fault -

*Kazuhiro Aoki[1], Takahiro Watanabe[1], Yukumo Tanaka[1], Kazuyoshi Seshimo[1] (1.Japan Atomic Energy Agency)

[SCG61-P14] Study on fault activity evaluation method (A new attempt to understand fault activities) No.2
- Injection experiment using a SIMFIP probe at Shionohira Fault and southern fault-

*Takahiro Watanabe[1], Yukumo Tanaka[1], Kazuhiro Aoki[1], Yves Guglielmi[2], Paul Cook[2], Florian Soom[2], Wakahama Hiroshi[3], Noujou Haruka[3], Etsuo Iwasaki[3], Masao Kametaka[3], Kazuyoshi Seshimo[1] (1.Japan Atomic Energy Agency, 2.Laurence Berkley National Laboratory, 3.DIA CONSULTANTS)

[SCG61-P15] Dynamic rupture simulation of 2018, Hokkaido Eastern Iburi earthquake: Role of non-planar fault geometry

*Tatsuya Hisakawa[1], Ryosuke Ando[1] (1.The University of Tokyo)

[SCG61-P16] A New Fully-Dynamic Earthquake Cycle Simulator Applicable to Arbitrary Nonplanar Fault Geometries - A Benchmark Test

*Daisuke Sato[1], Nadia Lapusta[2], Hiroyuki Noda[1] (1.Disaster Prevention Research Institute, Kyoto University, 2.California Institute of Technology)

[SCG61-P17] Stress and displacement Green's functions to treat volumetric inelastic strain and elastic inhomogeneity in boundary integral equation method

*Daisuke Sato[1] (1.Disaster Prevention Research Institute, Kyoto University)

[SCG61-P18] Frictional properties of dolerite and granite at intermediate slip rates and controlled ambient temperatures

*Michiyo Sawai[1], Yuuki Yokoyama[1], Kyuichi Kanagawa[1] (1.Chiba University)

[SCG61-P19] Extraction of features of strata using borehole data of geothermal area by multivariate analysis

*Ojima Hiroki[1], Kazuya Ishitsuka[2], Toru Mogi[3], Tatsuya Kajiwara[4], Takeshi Sugimoto[4], Hiroshi Asanuma[5] (1.Department of Socio-Environmental Engineering Hokkaido University, 2.Division of Urban Management, Graduate School of Engineering, Kyoto University, 3.Division of sustainable Resources Engineering, Faculty of Enginieering, Hokkaido University, 4.Geothermal Engineering Co. Ltd, 5.Fukushima Renewable Energy Institute, AIST)

[SCG61-P20] Low-temperature thermochronology of Cretaceous granitoids from the northern Northeast Japan Arc: Towards reconstructing arc-parallel thermal/denudation histories

*Shoma Fukuda[1], Shigeru Sueoka[2], Barry Paul Kohn[3], Noriko Hasebe[4], Akihiro Tamura[5], Tomoaki Morishita[5], Takahiro Tagami[1] (1.Graduate School of Science, Kyoto University , 2.Japan Atomic Energy Agency, 3.School of Earth Sciences, The University of Melbourne, 4.Institute of Nature and Environmental Technology, Kanazawa University, 5.Department of Earth Sciences, Kanazawa University)

[SCG61-P21] Uplift and denudation history of the South Fossa Magna region using low-temperature thermochronometric methods

*Yumi Kobayashi[1], Shigeru Sueoka[2], Shoma Fukuda[1], Barry P. Kohn[3], Tatsunori Yokoyama[2], Noriko Hasebe[4], Akihiro Tamura[5], Tomoaki Morishita[5], Takahiro Tagami[1] (1.Graduate School of Science, Kyoto University, 2.Tono Geoscience Center, Japan Atomic Energy Agency, 3.University of Melbourne, 4.Institute of Nature of Environmental Technology, Kanazawa University, 5.Department of Earth Sciences, Kanazawa University)

[SCG61-P22] Correlation between residual uplift and recurrence interval of the Kanto earthquake based on developmental process of coastal lowland

*Haeng-Yoong Kim[1] (1.Osaka City University, Graduate School of Science, Division of Biology &Geosciences)

[SCG61-P23] Mechanics preserving co-seismic uplift and marine terraces: dissymmetric patterns of co-seismic and inter-seismic deformation

*Kyohei Suzuki[1], Junki Komori[1], Ryosuke Ando[1] (1.Graduate School of Science, University of Tokyo)

[SCG61-P24] Enhanced resolution of stress tensor inversion by using fault instability analysis
★Invited Papers

*Katsushi Sato[1] (1.Division of Earth and Planetary Sciences, Graduate School of Science, Kyoto University)

[SCG61-P25] Focal mechanisms of the aftershocks of the 2000 Western Tottori Earthquake inferred from P wave first-motion data and spatial stress pattern

*Takaki Iwata[1] (1.Tokiwa University)

[SCG61-P26] Stress tensor inversion in focal area of the 2016 Mw7.8 Kaikoura earthquake, New Zealand

*Miu Matsuno[1], Tomomi Okada[1], Satoshi Matsumoto[2], Yuta Kawamura[2], Yoshihisa Iio[3], Tadashi Sato[1], Stephen C Bannister[4], John Ristau[4], Martha K Savage[5], John Townend[5], Jarg Pettinga[6], Francesca Ghisetti[7], Richard H Sibson[8] (1.Research Center for Prediction of Earthquakes and Volcanic Eruptions Graduate School of Science, Tohoku University, 2.Institute of Seismology and Volcanology, Faculty of Sciences, Kyushu University, 3.Disater Prevention Research Institute, Kyoto University, 4.GNS Science, New Zealand, 5.Victoria University of Wellington, Wellington, New Zealand, 6.University of Canterbury, Christchurch, New Zealand, 7.TerraGeologica, Ruby Bay, New Zealand, 8.University of Otago, Dunedin, New Zealand)

[SCG61-P27] Precise hypocenter distribution in the focal area of the 2016 Mw7.8 Kaikorua Earthquake, New Zealand

*Yuta Kawamura[1], Satoshi Matsumoto[1], Tomomi Okada[2], Miu Matsuno[2], Yoshihisa Iio[3], Tadashi Sato[2], Stephen C Bannister[4], John Ristau[4], Martha K Savage[5], John Twonend[5], Jarg Pettinga[6], Francesca Ghisetti[7], Richard H Sibson[8] (1.Kyushu University, Shimabara, Japan, 2.Tohoku University, Sendai, Japan, 3.Kyoto University, Uji, Japan, 4.GNS Science, Lower Hutt, New Zealand, 5.Victoria University of Wellington, Wellington, New Zealand, 6.University of Canterbury, Christchurch, New Zealand, 7.TerraGeologica, Ruby Bay, New Zealand, 8.University of Otago, Dunedin, New Zealand)

[SCG61-P28] **3-dimensional GPS velocities in Colombia and their implications for interplate coupling**

*Sindy Carolina Lizarazo[1], Takeshi Sagiya[2], Hector Mora-Paez[3] (1.Graduate School of Environmental Studies, Nagoya University, 2.Disaster Mitigation Research Center, Nagoya University, 3.Geological Survey of Colombia)

[J] Poster | B (Biogeosciences)：B-BG Biogeosciences & Geosphere-Biosphere Interactions

1:45 PM - 3:15 PM JST | 4:45 AM - 6:15 AM UTC | Poster Hall International Exhibition Hall8, Makuhari Messe_8

[B-BG02] Microbial ecology in earth and planetary sciences

convener:Michinari Sunamura(University of Tokyo Dept. of Earth & Planetary Science), Yuki Morono(Kochi Institute for Core Sample Research, Japan Agency for Marine-Earth Science and Technology), Natsuko Hamamura(Kyushu University)

[BBG02-P01] Density separation of magnetotactic bacteria *Magnetospirillum magnetotacticum* MS-1

*Kohei Masaoka[1], Yuki Morono[2], Naotaka Tomioka[2], Go-Ichiro Uramoto[1], Yuhji Yamamoto[1] (1.Kochi University, 2.Kochi Institute for Core Sample Research, Japan Agency for Marine-Earth Science and Technology)

[BBG02-P02] Exploring biogeographic patterns of marine planktonic cyanobacteria in coastal habitats-integrating uncultured and cultured approaches

*Punyasloke Bhadury[1] (1.Integrative Taxonomy and Microbial Ecology Research Group, Centre for Climate and Environmental Studies, Indian Institute of Science Education and Research Kolkata)

[BBG02-P03] The precise structure of “unsaturated” archaeol derivatives in the halophilic archaea lipid-core

*Noriaki YAMAUCHI[1] (1.Department of Earth and Planetary Sciences, Faculty of Sciences, Kyushu University)

[BBG02-P04] Estimation of microbial chemosynthesis efficiency in deep sea hydrothermal plume

*Michinari Sunamura[1] (1.University of Tokyo Dept. of Earth & Planetary Science)

[J] Poster | B (Biogeosciences)：B-BG Biogeosciences & Geosphere-Biosphere Interactions

5:15 PM - 6:30 PM JST | 8:15 AM - 9:30 AM UTC | Poster Hall International Exhibition Hall8, Makuhari Messe_38

[B-BG02] Microbial ecology in earth and planetary sciences

convener:Michinari Sunamura(University of Tokyo Dept. of Earth & Planetary Science), Yuki Morono(Kochi Institute for Core Sample Research, Japan Agency for Marine-Earth Science and Technology), Natsuko Hamamura(Kyushu University)

[BBG02-P01] Density separation of magnetotactic bacteria *Magnetospirillum magnetotacticum* MS-1

*Kohei Masaoka[1], Yuki Morono[2], Naotaka Tomioka[2], Go-Ichiro Uramoto[1], Yuhji Yamamoto[1] (1.Kochi University, 2.Kochi Institute for Core Sample Research, Japan Agency for Marine-Earth Science and Technology)

[BBG02-P02] Exploring biogeographic patterns of marine planktonic cyanobacteria in coastal habitats-integrating uncultured and cultured approaches

*Punyasloke Bhadury[1] (1.Integrative Taxonomy and Microbial Ecology Research Group, Centre for Climate and Environmental Studies, Indian Institute of Science Education and Research Kolkata)

[BBG02-P03] The precise structure of “unsaturated” archaeol derivatives in the halophilic archaea lipid-core

*Noriaki YAMAUCHI[1] (1.Department of Earth and Planetary Sciences, Faculty of Sciences, Kyushu University)

[BBG02-P04] Estimation of microbial chemosynthesis efficiency in deep sea hydrothermal plume

*Michinari Sunamura[1] (1.University of Tokyo Dept. of Earth & Planetary Science)

[J] Poster | B (Biogeosciences)：B-BC Biogeochemistry

10:45 AM - 12:15 PM JST | 1:45 AM - 3:15 AM UTC | Poster Hall International Exhibition Hall8, Makuhari Messe_9

[B-BC03] Interrelation between Life, Water, Mineral, and Atmosphere

convener:Takeshi Kakegawa(Graduate School of Science, Tohoku University), Tadashi Yokoyama(Graduate School of Integrated Arts and Sciences, Hiroshima University), Keisuke Fukushi(Institute of Nature & Environmental Technology, Kanazawa University), Fumito Shiraishi(Department of Earth and Planetary Systems Science, Graduate School of Science, Hiroshima University)

[BBC03-P01] Geochemical studies for seawater/rock interaction recorded on the submarine lava flows of 12 Ma in the *Hokuroku* district in Akita, Japan and their implication to phosphorus cycle on the modern ocean floor

*Tsukasa Sai[1], Takeshi Kakegawa[1] (1.Graduate School of Science, Tohoku University)

[BBC03-P02] Detection of methylphosphonate and phosphite contained in suspended particles in spring water

*Kazuma Tsuji[1], Masahiro Maruo[3], Hajime Obata[2] (1.Graduate School of Environmental Science, The University of Shiga Prefecture, 2.Atmosphere and Ocean Research Institute, The University of Tokyo, 3.School of Environmental Science, The University of Shiga Prefecture)

[BBC03-P03] **The Influence of Aerosol Optical Thickness and Mesoscale Eddies on Chlorophyll-a**

*xiangguang zhang[1], Yongsheng Xu[1], Ichio Asanuma[2] (1.Institute of Oceanology, Chinese Academy of Sciences, 2.Tokyo University of Information Sciences)

[BBC03-P04] Glyoxylate from CO atmosphere via UV photochemistry

*Kenta Isoda[1], Xiaofeng Zang[1], Yuichiro Ueno[1,2] (1.Department of Earth and Planetary Sciences, Tokyo Institute of Technology, 2.Earth Life-Science Institute, Tokyo Institute of Technology)

[BBC03-P05] Carbon reservoir perturbations in the Indian subcontinent induced by the Deccan volcanism in marine and terrestrial realm

*Sohom Roy[1], Prasanta Sanyal[1], Sambit Ghosh[1] (1.Indian Institute of Science Education and Research Kolkata)

[BBC03-P06] Organic matter around Miocene Kuroko ore deposits: Implications to Archean submarine hydrothermal microbial community

*Takeshi Kakegawa[1] (1.Graduate School of Science, Tohoku University)

[BBC03-P07] Formation and solubility of hydrous carbonates formed in alkaline lakes under freezing condition

*TAKUMA KITAJIMA[1], Haruna Matsumiya[1], Keisuke Fukushi[1] (1.kanazawa university)

[BBC03-P08] Effect of difference in mineral wettability on water-mineral reaction in rock pores

*Tadashi Yokoyama[1], Naoki Nishiyama[2] (1.Graduate School of Integrated Arts and Sciences, Hiroshima University, 2.Graduate School of Life and Environmental Sciences, University of Tsukuba)

[J] Poster | B (Biogeosciences)：B-BC Biogeochemistry

5:15 PM - 6:30 PM JST | 8:15 AM - 9:30 AM UTC | Poster Hall International Exhibition Hall8, Makuhari Messe_39

[B-BC03] Interrelation between Life, Water, Mineral, and Atmosphere

convener:Takeshi Kakegawa(Graduate School of Science, Tohoku University), Tadashi Yokoyama(Graduate School of Integrated Arts and Sciences, Hiroshima University), Keisuke Fukushi(Institute of Nature & Environmental Technology, Kanazawa University), Fumito Shiraishi(Department of Earth and Planetary Systems Science, Graduate School of Science, Hiroshima University)

[BBC03-P01] Geochemical studies for seawater/rock interaction recorded on the submarine lava flows of 12 Ma in the *Hokuroku* district in Akita, Japan and their implication to phosphorus cycle on the modern ocean floor

*Tsukasa Sai[1], Takeshi Kakegawa[1] (1.Graduate School of Science, Tohoku University)

[BBC03-P02] Detection of methylphosphonate and phosphite contained in suspended particles in spring water

*Kazuma Tsuji[1], Masahiro Maruo[3], Hajime Obata[2] (1.Graduate School of Environmental Science, The University of Shiga Prefecture, 2.Atmosphere and Ocean Research Institute, The University of Tokyo, 3.School of Environmental Science, The University of Shiga Prefecture)

[BBC03-P03] **The Influence of Aerosol Optical Thickness and Mesoscale Eddies on Chlorophyll-a**

*xiangguang zhang[1], Yongsheng Xu[1], Ichio Asanuma[2] (1.Institute of Oceanology, Chinese Academy of Sciences, 2.Tokyo University of Information Sciences)

[BBC03-P04] Glyoxylate from CO atmosphere via UV photochemistry

*Kenta Isoda[1], Xiaofeng Zang[1], Yuichiro Ueno[1,2] (1.Department of Earth and Planetary Sciences, Tokyo Institute of Technology, 2.Earth Life-Science Institute, Tokyo Institute of Technology)

[BBC03-P05] Carbon reservoir perturbations in the Indian subcontinent induced by the Deccan volcanism in marine and terrestrial realm

*Sohom Roy[1], Prasanta Sanyal[1], Sambit Ghosh[1] (1.Indian Institute of Science Education and Research Kolkata)

[BBC03-P06] Organic matter around Miocene Kuroko ore deposits: Implications to Archean submarine hydrothermal microbial community

*Takeshi Kakegawa[1] (1.Graduate School of Science, Tohoku University)

[BBC03-P07] Formation and solubility of hydrous carbonates formed in alkaline lakes under freezing condition

*TAKUMA KITAJIMA[1], Haruna Matsumiya[1], Keisuke Fukushi[1] (1.kanazawa university)

[BBC03-P08] Effect of difference in mineral wettability on water-mineral reaction in rock pores

*Tadashi Yokoyama[1], Naoki Nishiyama[2] (1.Graduate School of Integrated Arts and Sciences, Hiroshima University, 2.Graduate School of Life and Environmental Sciences, University of Tsukuba)

[J] Oral | B (Biogeosciences) : B-BC Biogeochemistry

1:45 PM - 3:15 PM JST | 4:45 AM - 6:15 AM UTC | 201A 2F

[B-BC03] Interrelation between Life, Water, Mineral, and Atmosphere

convener:Takeshi Kakegawa(Graduate School of Science, Tohoku University), Tadashi Yokoyama(Graduate School of Integrated Arts and Sciences, Hiroshima University), Keisuke Fukushi(Institute of Nature & Environmental Technology, Kanazawa University), Fumito Shiraishi(Department of Earth and Planetary Systems Science, Graduate School of Science, Hiroshima University), Chairperson:Tadashi Yokoyama, Keisuke Fukushi

1:45 PM - 2:00 PM JST | 4:45 AM - 5:00 AM UTC

[BBC03-01] Chemical speciation analysis of the brown and black precipitates observed in the gill chamber of the vent shrimp *Rimicaris kairei*

*Masanari Hikosaka[1], Yoshio Takahashi[2], Chong Chen[3], Robert Jenkins[1] (1.Kanazawa University, 2.Tokyo University, 3.Japan Agency for Marine-Earth Science and Technology)

2:00 PM - 2:15 PM JST | 5:00 AM - 5:15 AM UTC

[BBC03-02] Experimental study on hydrogen generation during low temperature serpentinization by using natural samples

*Shunta Higashino[1], Ryohei Kawakita[1], Tsubasa Otake[2], Tsutomu Sato[2] (1.Graduate School of Engineering, Hokkaido University, 2.Faculty of Engineering, Hokkaido University)

2:15 PM - 2:30 PM JST | 5:15 AM - 5:30 AM UTC

[BBC03-03] **Constraint on the origin of methane from Hakuba Happo serpentinite-hosted hot spring by using $^{14}CH_4$ and noble gas isotope**

*Konomi Suda[1], Takahiro AZE[2], Yosuke Miyairi[2], Yusuke Yokoyama[2], Yohei Matsui[3,2], Hisahiro Ueda[3], Takuya Saito[3], Tomohiko Sato[4], Yusuke Sawaki[2], Ryosuke Nakai[1], Hideyuki Tamaki[1], Hiroshi A Takahashi[1], Noritoshi Morikawa[1] (1.National Institute of Advanced Industrial Science and Technology, 2.The University of Tokyo, 3.Japan Agency for Marine-Earth Science and Technology, 4.Tokyo Institute of Technology)

2:30 PM - 2:45 PM JST | 5:30 AM - 5:45 AM UTC

[BBC03-04] Inhibition of calcium silicate hydrate formation by lignosulfonate and lignin

*Kanako Toda[1], Tsubasa Otake[1], Tsutomu Sato[1] (1.Laboratory of Environmental Geology, Faculty of Engineering, Hokkaido University)

2:45 PM - 3:00 PM JST | 5:45 AM - 6:00 AM UTC

[BBC03-05] Calcium carbonate formation processes on cyanobacterial surface

*Fumito Shiraishi[1], Takeru Omori[1], Naotaka Tomioka[2], Satoko Motai[2], Hiroki Suga[3], Yoshio Takahashi[3] (1.Hiroshima University, 2.JAMSTEC, 3.The University of Tokyo)

3:00 PM - 3:15 PM JST | 6:00 AM - 6:15 AM UTC

[BBC03-06] Mineralogical and geochemical study on sedimentary rock containing microfossils from 1.9 billion years ago(Ga) Gunflint Formation, Canada

*kouhei Sasaki[1], Akizumi Ishida[1], Takeshi Kakegawa[1] (1.Graduate School of Science, Tohoku University)

[J] Oral | B (Biogeosciences) : B-BC Biogeochemistry

3:30 PM - 5:00 PM JST | 6:30 AM - 8:00 AM UTC | 201A 2F

[B-BC03] Interrelation between Life, Water, Mineral, and Atmosphere

convener:Takeshi Kakegawa(Graduate School of Science, Tohoku University), Tadashi Yokoyama(Graduate School of Integrated Arts and Sciences, Hiroshima University), Keisuke Fukushi(Institute of Nature & Environmental Technology, Kanazawa University), Fumito Shiraishi(Department of Earth and Planetary Systems Science, Graduate School of Science, Hiroshima University), Chairperson:Takeshi Kakegawa, Fumito Shiraishi(Hiroshima Univ.)

3:30 PM - 3:45 PM JST | 6:30 AM - 6:45 AM UTC

[BBC03-07] Secular variation of multiple sulfur isotopic compositions of sulfate and sulfide during long term incubation of *Desulfovibrio desulfuricans*

*Fumihiro Matsuura[1], Hiroko Makita[2], Ken Takai[3], Yuichiro Ueno[1,3] (1.Tokyo Institute of Technology, 2.Tokyo University of Marine Science and Technology, 3.Japan Agency for Marine-Earth Science & Technology (JAMSTEC))

3:45 PM - 4:00 PM JST | 6:45 AM - 7:00 AM UTC

[BBC03-08] **Origins of volcanic SO_2 on Earth**

*Hiroshi Ohmoto[1] (1.The Pennsylvania State University)

4:00 PM - 4:15 PM JST | 7:00 AM - 7:15 AM UTC

[BBC03-09] **Volcanism, sedimentation, and development of life in a Mesoarchaean intracratonic setting: the Dominion Group, South Africa**

*Andrea Agangi[1,2], Axel Hofmann[2], Dora Paprika[2], Andrey Bekker[2,3], Frantz Ossa-Ossa[2,4] (1.Akita University, 2.University of Johannesburg, 3.University of California, 4.University of Tuebingen)

4:15 PM - 4:30 PM JST | 7:15 AM - 7:30 AM UTC

[BBC03-10] New microbial ecology results from genome centered metagenomics studies of iron carbonate and sulfidic hot springs

*Shawn E McGlynn[1], Lewis Ward[2], Takeshi Kakegawa[3], Yuichiro Ueno[1], Mayuko Nakagawa[1] (1.Earth-Life Science Institute, Tokyo Institute of Technology, 2.Harvard University, 3.Tohoku University)

4:30 PM - 4:45 PM JST | 7:30 AM - 7:45 AM UTC

[BBC03-11] Superhabitability in ultradeep rocky environments

*Yohey Suzuki[1] (1.Graduate School of Science, The University of Tokyo)

4:45 PM - 5:00 PM JST | 7:45 AM - 8:00 AM UTC

[BBC03-12] Exploring planetary habitability beneath the oceans

★Invited Papers

*Fumio Inagaki[1] (1.Japan Agency for Marine-Earth Science and Technology)

[E] Oral | B (Biogeosciences)：B-CG Complex & General

9:00 AM - 10:30 AM JST | 12:00 AM - 1:30 AM UTC | 201A 2F

[B-CG06] Earth and Planetary Science Frontiers for Life and Global Environment

convener:Yoshinori Takano(Japan Agency for Marine-Earth Science and Technology (JAMSTEC)), Yohey Suzuki(Graduate School of Science, The University of Tokyo), Shingo Kato(RIKEN), Keisuke Fukushi(Institute of Nature & Environmental Technology, Kanazawa University), Chairperson:Yuki Morono(JAMSTEC), Masanori Kaneko(AIST/GSJ), Shingo Kato(RIKEN)

9:00 AM - 9:15 AM JST | 12:00 AM - 12:15 AM UTC

[BCG06-01] Earth as an open system to the Universe, and five multi-layered spheres to produce a habitable planet

*Shigenori Maruyama[1] (1.Earth-Life Science Institute, Tokyo Institute of Technology)

9:15 AM - 9:30 AM JST | 12:15 AM - 12:30 AM UTC

[BCG06-02] Holocene Antarctic subglacial weathering and ice-sheet history reconstructed using the $^{10}Be/^{9}Be$ ratios of lake Maruwan Oike sediments

*Adam David Sproson[1], Yusuke Yokoyama[1,2], Yoshinori Takano[2], Yosuke Miyairi[1], Takahiro AZE[1] (1.Atmosphere and Ocean Research Institute, The University of Tokyo, 2.Department of Biogeochemistry, Japan Agency for Marine Science and Technology)

9:30 AM - 9:45 AM JST | 12:30 AM - 12:45 AM UTC

[BCG06-03] Chemical speciation and solubility of heavy elements (lead, zinc, copper, arsenic and cadmium) in contaminated soil from Kamegai mine tailing, Toyama, Japan

*Baasansuren Gankhurel[1], Keisuke Fukushi[2], Akitoshi Akehi[1], Yoshio Takahashi[3], Kazuo Kawasaki[4] (1.Graduate School of Natural Science and Technology, Kanazawa University, 2.Instutute of Nature and Environmental Technology, Kanazawa University, 3.Department of Earth and Planetary Science, The University of Tokyo, 4.Graduate School of Science and Engineering for Research, Toyama University)

9:45 AM - 10:00 AM JST | 12:45 AM - 1:00 AM UTC

[BCG06-04] High-mass resolution molecular imaging of organic compounds on the Murchison meteorite.

★Invited Papers

*Minako Hashiguchi[1], Hiroshi Naraoka[1,2] (1.Research Center for Planetary Trace Organic Compounds, Kyushu University, 2.Department of Earth and Planetary Sciences, Kyushu University)

10:00 AM - 10:15 AM JST | 1:00 AM - 1:15 AM UTC

[BCG06-05] Fe(II) oxidation processes at the surface of bacterially colonized iron deposits

★Invited Papers

*Fumito Shiraishi[1], Kohei Nakao[1], Chizuru Takashima[2], Akihiro Kano[3], TAKAAKI ITAI[3] (1.Hiroshima University, 2.Saga University, 3.The University of Tokyo)

10:15 AM - 10:30 AM JST | 1:15 AM - 1:30 AM UTC

[BCG06-06] Heme: The distribution and dynamics of a ubiquitous iron-tetrapyrrole molecule

*Yuta Isaji[1], Yoshinori Takano[1], Nanako O. Ogawa[1], Naohiko Ohkouchi[1] (1.Japan Agency for Marine-Earth Science and Technology)

[E] Oral | B (Biogeosciences) : B-CG Complex & General

10:45 AM - 12:15 PM JST | 1:45 AM - 3:15 AM UTC | 201A 2F

[B-CG06] Earth and Planetary Science Frontiers for Life and Global Environment

convener:Yoshinori Takano(Japan Agency for Marine-Earth Science and Technology (JAMSTEC)), Yohey Suzuki(Graduate School of Science, The University of Tokyo), Shingo Kato(RIKEN), Keisuke Fukushi(Institute of Nature & Environmental Technology, Kanazawa University), Chairperson:Yoshinori Takano(JAMSTEC), Keisuke Fukushi, Yohey Suzuki(Univ. Tokyo)

10:45 AM - 11:00 AM JST | 1:45 AM - 2:00 AM UTC

[BCG06-07] Diversity and evolution of biosynthetic enzymes for chlorophyll pigments

★Invited Papers

*Yusuke Tsukatani[1] (1.Japan Agency for Marine-Earth Science and Technology (JAMSTEC))

11:00 AM - 11:20 AM JST | 2:00 AM - 2:20 AM UTC

[BCG06-08] **Microdolomites are not MDACs: microbially-derived carbon source for microcrystalline dolomite found within massive gas hydrates and implications for the shallow marine carbon cycle**

★Invited Papers

*Glen Snyder[1], Ryo Matsumoto[1], Naizhong Zhang[1], Yoshihiro Kakizaki[2], Yohey Suzuki[2], Yuji Sano[3], Naoto Takahata[3], Kentaro Tanaka[3], Takumi Imajo[5], Stephen Bowden[4] (1.Gas Hydrate Research Laboratory, Meiji University, 2.University of Tokyo, 3.AORI, University of Tokyo, 4.University of Aberdeen, Scotland, 5.Tokyo University of Marine Science and Technology)

11:20 AM - 11:35 AM JST | 2:20 AM - 2:35 AM UTC

[BCG06-09] **Discriminative biogeochemical signatures of methanotrophs inhabiting different chemosynthetic fields in an active mud volcano of the Canadian Beaufort Sea**

*Dong-Hun Lee[1], Yung Mi Lee[2], Jung-Hyun Kim[2], Young Keun Jin[2], Charles Paull[3], Helge Niemann[4,5], Ji-Hoon Kim[6], Kyung-Hoon Shin[1] (1.Hanyang Univ., 2.KOPRI, 3.MBARI, 4.NIOZ and Utrecht Univ., 5.CAGE, UiT , 6.KIGAM)

11:35 AM - 11:50 AM JST | 2:35 AM - 2:50 AM UTC

[BCG06-10] Determination of the absolute stereochemistry of the hydroxyl group in 2-hydroxyarchaeol, the main lipid core of methanogenic and methanotrophic archaea

*Noriaki YAMAUCHI[1], Masanori Kaneko[2] (1.Department of Earth and Planetary Sciences, Faculty of Sciences, Kyushu University, 2.National Institute of Advanced Industrial Science and Technology)

11:50 AM - 12:10 PM JST | 2:50 AM - 3:10 AM UTC

[BCG06-11] Mineral-Microbe interaction – Identification of extracellular electron transfer mechanisms by using MetaOmics approach

★Invited Papers

*Shunichi Ishii[1], Shino Suzuki[1], Kenneth H Nealson[2] (1.Japan Agency for Marine-Earth Science and Technology (JAMSTEC), 2.University of Southern California)

12:10 PM - 12:15 PM JST | 3:10 AM - 3:15 AM UTC

[BCG06-12] Interactive discussion with the invited speakers

*Yoshinori Takano[1] (1.Japan Agency for Marine-Earth Science and Technology (JAMSTEC))

[E] Poster | B (Biogeosciences)：B-CG Complex & General

3:30 PM - 5:00 PM JST | 6:30 AM - 8:00 AM UTC | Poster Hall International Exhibition Hall8, Makuhari Messe_22

[B-CG06] Earth and Planetary Science Frontiers for Life and Global Environment

convener:Yoshinori Takano(Japan Agency for Marine-Earth Science and Technology (JAMSTEC)), Yohey Suzuki(Graduate School of Science, The University of Tokyo), Shingo Kato(RIKEN), Keisuke Fukushi(Institute of Nature & Environmental Technology, Kanazawa University)

[BCG06-P01] Dynamisms and characteristics of dissolved organic matter (DOM) in deep aquifer: A scope for deep biosphere

*Atsushi Urai[1,2], Yoshinori Takano[2], Naohiko Ohkouchi[2] (1.Department of Science and Technology, Graduate School of Medicine, Science and Technology, Shinshu University, 2.Department of Biogeochemistry, Japan Agency for Marine-Earth Science and Technology)

[BCG06-P02] Correlations of magnetosome-related genes in Nitrospirae genomes to magnetosome geometry and redox stratification in deep-sea environments

*Shinsaku Nakano[1], Shingo Kato[2], Mariko Kouduka[1], Toshitsugu Yamazaki[3], Yohey Suzuki[1] (1.Graduate School of Science, The University of Tokyo, 2.RIKEN, 3.Atmosphere and Ocean Research Institute, The University of Tokyo)

[BCG06-P03] Reconstruction of key ecological responses leading to the most recent dead zone formations in Japan Sea through ancient DNA metabarcodring

*Mariko Kouduka[1], Yohey Suzuki[1] (1.Department of Earth and Planetary Science, The University of Tokyo, 7-3-1 Hongo, Bunkyo-ku, Tokyo, Japan.)

[BCG06-P04] Search for microbial CH_4 production processes in lake sediments and surface water associated with cyanobacterial bloom

*Makoto Matsushita[1], Yoshinori Takano[1], Hiroyuki Imachi[1], Atsushi Urai[2], Ho-Dong Park[3], Hiroki Iwata[3], Naohiko Ohkouchi[1] (1.Japan Agency for Marine-Earth Science and Technology, 2.Department of Science and Technology, Graduate School of Medicine, Science and Technology, Shinshu University, 3.Department of Environmental Sciences, Faculty of Science, Shinshu University)

[BCG06-P05] Did life emerge in a deep-sea metal sulfide chimney? New insights from an archaeal genome and a nanoscale microbe-silicate assemblage

*Hinako Takamiya[1], Hiroki Mukai[2], Mariko Kouduka[1], Shingo Kato[4], Motoo Ito[3], Yohey Suzuki[1] (1.Earth and Planetary Science Graduate School of Science, The University of Tokyo , 2.National Institute of Advanced Industrial Science and Technology, 3.Kochi Institute for Core Sample Research JAMSTEC, 4.RIKEN)

[BCG06-P06] X-ray computed nano-tomography for visualizing microbial cells and their surrounding environments

*Yuki Morono[1], Go-Ichiro Uramoto[2,1], Kentaro Uesugi[3], Nobuhisa Takeuchi[3], Masayuki Uesugi[3], Kengo Kubota[4], Tatsuhiko Hoshino[1], Fumio Inagaki[1] (1.Japan Agency for Marine-Earth Science and Technology, 2.Kochi University, 3.Japan Synchrotron Radiation Research Institute, 4.Tohoku University)

[BCG06-P07] Carbon signatures in amino acids during deep-sea anoxic methanotrophy

*Yoshinori Takano[1] (1.Japan Agency for Marine-Earth Science and Technology (JAMSTEC))

[E] Poster | B (Biogeosciences)：B-CG Complex & General

5:15 PM - 6:30 PM JST | 8:15 AM - 9:30 AM UTC | Poster Hall International Exhibition Hall8, Makuhari Messe_40

[B-CG06] Earth and Planetary Science Frontiers for Life and Global Environment

convener:Yoshinori Takano(Japan Agency for Marine-Earth Science and Technology (JAMSTEC)), Yohey Suzuki(Graduate School of Science, The University of Tokyo), Shingo Kato(RIKEN), Keisuke Fukushi(Institute of Nature & Environmental Technology, Kanazawa University)

[BCG06-P01] Dynamisms and characteristics of dissolved organic matter (DOM) in deep aquifer: A scope for deep biosphere

*Atsushi Urai[1,2], Yoshinori Takano[2], Naohiko Ohkouchi[2] (1.Department of Science and Technology, Graduate School of Medicine, Science and Technology, Shinshu University, 2.Department of Biogeochemistry, Japan Agency for Marine-Earth Science and Technology)

[BCG06-P02] Correlations of magnetosome-related genes in Nitrospirae genomes to magnetosome geometry and redox stratification in deep-sea environments

*Shinsaku Nakano[1], Shingo Kato[2], Mariko Kouduka[1], Toshitsugu Yamazaki[3], Yohey Suzuki[1] (1.Graduate School of Science, The University of Tokyo, 2.RIKEN, 3.Atmosphere and Ocean Research Institute, The University of Tokyo)

[BCG06-P03] Reconstruction of key ecological responses leading to the most recent dead zone formations in Japan Sea through ancient DNA metabarcodring

*Mariko Kouduka[1], Yohey Suzuki[1] (1.Department of Earth and Planetary Science, The University of Tokyo, 7-3-1 Hongo, Bunkyo-ku, Tokyo, Japan.)

[BCG06-P04] Search for microbial CH_4 production processes in lake sediments and surface water associated with cyanobacterial bloom

*Makoto Matsushita[1], Yoshinori Takano[1], Hiroyuki Imachi[1], Atsushi Urai[2], Ho-Dong Park[3], Hiroki Iwata[3], Naohiko Ohkouchi[1] (1.Japan Agency for Marine-Earth Science and Technology, 2.Department of Science and Technology, Graduate School of Medicine, Science and Technology, Shinshu University, 3.Department of Environmental Sciences, Faculty of Science, Shinshu University)

[BCG06-P05] Did life emerge in a deep-sea metal sulfide chimney? New insights from an archaeal genome and a nanoscale microbe-silicate assemblage

*Hinako Takamiya[1], Hiroki Mukai[2], Mariko Kouduka[1], Shingo Kato[4], Motoo Ito[3], Yohey Suzuki[1] (1.Earth and Planetary Science Graduate School of Science, The University of Tokyo , 2.National Institute of Advanced Industrial Science and Technology, 3.Kochi Institute for Core Sample Research JAMSTEC, 4.RIKEN)

[BCG06-P06] X-ray computed nano-tomography for visualizing microbial cells and their surrounding environments

*Yuki Morono[1], Go-Ichiro Uramoto[2,1], Kentaro Uesugi[3], Nobuhisa Takeuchi[3], Masayuki Uesugi[3], Kengo Kubota[4], Tatsuhiko Hoshino[1], Fumio Inagaki[1] (1.Japan Agency for Marine-Earth Science and Technology, 2.Kochi University, 3.Japan Synchrotron Radiation Research Institute, 4.Tohoku University)

[BCG06-P07] Carbon signatures in amino acids during deep-sea anoxic methanotrophy

*Yoshinori Takano[1] (1.Japan Agency for Marine-Earth Science and Technology (JAMSTEC))

[J] Oral | B (Biogeosciences)：B-CG Complex & General

10:45 AM - 12:15 PM JST | 1:45 AM - 3:15 AM UTC | 105 1F

[B-CG08] Phanerozoic biodiversity change: Extinction and diversification

convener:Yukio Isozaki(Department of Earth Science and Astronomy, Multi-disciplinary Sciences - General Systems Studies, Graduate School of Arts and Sciences, The University of Tokyo), Yusuke Sawaki(The University of Tokyo), Chairperson:Yukio Isozaki(Department of Earth Science and Astronomy, The University of Tokyo), Yusuke Sawaki(The University of Tokyo)

10:50 AM - 11:10 AM JST | 1:50 AM - 2:10 AM UTC

[BCG08-01] **The Ediacaran-Cambrian transition of North China**

★Invited Papers

*Xingliang Zhang[1] (1.State Key Laboratory of Continental Dynamics, Shaanxi Key Laboratory of Early Life and Environments, and Department of Geology, Northwest University)

11:10 AM - 11:30 AM JST | 2:10 AM - 2:30 AM UTC

[BCG08-02] The Qingjiang biota – An extraordinary new Burgess Shale-type fossil Lagerstätte from the early Cambrian of South China

★Invited Papers

*Dongjing Fu[1], Xingliang Zhang[1], Robert R. Gains[2] (1.State Key Laboratory of the Continental Dynamics, Shaanxi Key Laboratory of Early Life and Environment, Department of Geology, Northwest University, Xi'an 710069, PR China, 2.Department of Geology, Pomona College, Claremont, CA 91711, USA)

11:30 AM - 11:50 AM JST | 2:30 AM - 2:50 AM UTC

[BCG08-03] Enhanced flux of extraterrestrial ^{3}He across the Permian–Triassic boundary

★Invited Papers

*Tetsuji Onoue[1], Naoto Takahata[2], Honami Sato[4], Akira Ishikawa[3], Katsuhito Soda[1], Yuji Sano[2], Yukio Isozaki[2] (1.Kumamoto Univ., 2.Univ. Tokyo, 3.Tokyo Inst. Tech., 4.Chiba Inst. Tech.)

11:50 AM - 12:10 PM JST | 2:50 AM - 3:10 AM UTC

[BCG08-04] **End-Triassic Mass Extinction: Causes and Consequences**

★Invited Papers

*Wataru Fujisaki[1] (1.Japan Agency for Marine-Earth Science and Technology)

[J] Oral | B (Biogeosciences) : B-CG Complex & General

1:45 PM - 3:15 PM JST | 4:45 AM - 6:15 AM UTC | 105 1F

[B-CG08] Phanerozoic biodiversity change: Extinction and diversification

convener:Yukio Isozaki(Department of Earth Science and Astronomy, Multi-disciplinary Sciences - General Systems Studies, Graduate School of Arts and Sciences, The University of Tokyo), Yusuke Sawaki(The University of Tokyo), Chairperson:Wataru Fujisaki(Japan Agency for Marine-Earth Science and Technology)

1:45 PM - 2:00 PM JST | 4:45 AM - 5:00 AM UTC

[BCG08-05] Transition of biodiversity in mobile populations and the small world in local subpopulations

*Kota Imaoka[1], Kazuhito Yamasaki[1] (1.Kobe University Graduate school of Science)

2:00 PM - 2:15 PM JST | 5:00 AM - 5:15 AM UTC

[BCG08-06] Rivision of the lowermost Cambrian SSF stratigraphy

*KONO SENA[1], Yukio Isozaki[1], Tomohiko Sato[2], Xingliang Zhang[3], Wei Liu[3] (1.The University of Tokyo School of Arts &Sciences, 2.Earth-Life Science Institute, Tokyo Institute of Technology, 3.Northwest university, China)

2:15 PM - 2:30 PM JST | 5:15 AM - 5:30 AM UTC

[BCG08-07] δ^{88}Sr and^{87}Sr/^{86}Srrecords of the Middle-Late Permian seawater: mass extinction-relevant change in ocean Sr budget

*Tomomi Kani[1], Yukio Isozaki[2], Keiji Misawa[3], Akira Ishikawa[4], Shigekazu Yoneda[5] (1.Kumamoto University, 2.The University of Tokyo, 3.National Institute of Polar Research, 4.Tokyo Tech, School of Science, 5.National Museum of Nature and Science)

2:30 PM - 2:45 PM JST | 5:30 AM - 5:45 AM UTC

[BCG08-08] Formation of stratiform manganese deposits during the Carnian (Late Triassic) “pluvial event” in the pelagic Panthalassa

*Yuki Tomimatsu[1], Tetsuji Onoue[2], Daisuke Yamashita[3], Tatsuo Nozaki[4,5,6,7], Yutaro Takaya[8] (1.Graduate school of Science and Technology, Kumamoto University, 2.Faculty of Advanced Science and Technology, Kumamoto University , 3.Satsumasendai City Office, 4.Research and Development Center for Submarine Resources, Japan Agency for Marine-Earth Science and Technology, 5.Frontier Research Center for Energy and Resources (FRC- ER), Graduate School of Engineering, Tokyo University, 6.Department of Planetology, Graduate School of Science, Kobe University, 7.Ocean Resources Research Center for Next Generation, Chiba Institute of Technology, 8.Department of Resources and Environmental Engineering School of Creative Science and Enginerring, Waseda University)

2:45 PM - 3:00 PM JST | 5:45 AM - 6:00 AM UTC

[BCG08-09] Enrichment of chalcophile elements in Cretaceous–Paleogene boundary clays

*Teruyuki Maruoka[1], Yoshiro Nishio[2] (1.Faculty of Life and Environmental Sciences, University of Tsukuba, 2.Research and Education Faculty, Kochi University)

3:00 PM - 3:15 PM JST | 6:00 AM - 6:15 AM UTC

[BCG08-10] Mass extinctions: hierarchy of causes and cosmoclimatological perspective

*Yukio Isozaki[1] (1.Department of Earth Science and Astronomy, Multi-disciplinary Sciences - General Systems Studies, Graduate School of Arts and Sciences, The University of Tokyo)

[J] Poster | B (Biogeosciences)：B-CG Complex & General

3:30 PM - 5:00 PM JST | 6:30 AM - 8:00 AM UTC | Poster Hall International Exhibition Hall8, Makuhari Messe_23

[B-CG08] Phanerozoic biodiversity change: Extinction and diversification

convener:Yukio Isozaki(Department of Earth Science and Astronomy, Multi-disciplinary Sciences - General Systems Studies, Graduate School of Arts and Sciences, The University of Tokyo), Yusuke Sawaki(The University of Tokyo)

[BCG08-P01] Marine Osmium isotope record across the Aptian/Albian boundary to elucidate the relationship between the Oceanic Anoxic Event 1b and massive volcanic activities at the Southern Kerguelen Plateau

*Hironao Matsumoto[1], Junichiro Kuroda[1], Rodolfo Coccioni[2], Naohiko Ohkouchi[3], Nanako O. Ogawa[3], Saburo Sakai[3], Katsuhiko Suzuki[3], Fabrizio Frontalini[2], Andrea Mazzoli[2] (1.Department of Earth and Planetary Science, The University of Tokyo, 2.DiSPeA, University of Urbino, 3.Japan Agency for Marine-Earth Science and Technology)

[BCG08-P02] Rhaetian (Late Triassic) conodont biostratigraphy of the Panthalassa Ocean and the final extinction of conodonts at the end of the Triassic

*Kanna Yamasaki[1], Daisuke Yamashita[2], Tetsuji Onoue[1] (1.Kumamoto University, 2.Satsumasendai City Office)

[BCG08-P03] Paleoenvironmental changes across the Permian/Triassic boundary sections in the Mino Belt, central Japan

*Shinya Uemura[1], Tetsuji Onoue[1] (1.Kumamoto University)

[BCG08-P04] Geotectonic history of Mona Complex in Anglesey-Lleyn, Wales

*HISASHI ASANUMA[1], Yusuke Sawaki[1], Shigenori Maruyama[2] (1.The University of Tokyo, 2.Earth-Life Science Institute, Tokyo Institute of Technology)

[BCG08-P05] Radiogenic Sr isotope chemostratigraphy of the Ediacaran Doushantuo Formation in the Yangtze Craton, South China

*Yusuke Sawaki[1] (1.The University of Tokyo)

[J] Poster | B (Biogeosciences)：B-CG Complex & General

5:15 PM - 6:30 PM JST | 8:15 AM - 9:30 AM UTC | Poster Hall International Exhibition Hall8, Makuhari Messe_41

[B-CG08] Phanerozoic biodiversity change: Extinction and diversification

convener:Yukio Isozaki(Department of Earth Science and Astronomy, Multi-disciplinary Sciences - General Systems Studies, Graduate School of Arts and Sciences, The University of Tokyo), Yusuke Sawaki(The University of Tokyo)

[BCG08-P01] Marine Osmium isotope record across the Aptian/Albian boundary to elucidate the relationship between the Oceanic Anoxic Event 1b and massive volcanic activities at the Southern Kerguelen Plateau

*Hironao Matsumoto[1], Junichiro Kuroda[1], Rodolfo Coccioni[2], Naohiko Ohkouchi[3], Nanako O. Ogawa[3], Saburo Sakai[3], Katsuhiko Suzuki[3], Fabrizio Frontalini[2], Andrea Mazzoli[2] (1.Department of Earth and Planetary Science, The University of Tokyo, 2.DiSPeA, University of Urbino, 3.Japan Agency for Marine-Earth Science and Technology)

[BCG08-P02] Rhaetian (Late Triassic) conodont biostratigraphy of the Panthalassa Ocean and the final extinction of conodonts at the end of the Triassic

*Kanna Yamasaki[1], Daisuke Yamashita[2], Tetsuji Onoue[1] (1.Kumamoto University, 2.Satsumasendai City Office)

[BCG08-P03] Paleoenvironmental changes across the Permian/Triassic boundary sections in the Mino Belt, central Japan

*Shinya Uemura[1], Tetsuji Onoue[1] (1.Kumamoto University)

[BCG08-P04] Geotectonic history of Mona Complex in Anglesey-Lleyn, Wales

*HISASHI ASANUMA[1], Yusuke Sawaki[1], Shigenori Maruyama[2] (1.The University of Tokyo, 2.Earth-Life Science Institute, Tokyo Institute of Technology)

[BCG08-P05] Radiogenic Sr isotope chemostratigraphy of the Ediacaran Doushantuo Formation in the Yangtze Craton, South China

*Yusuke Sawaki[1] (1.The University of Tokyo)

[E] Poster | M (Multidisciplinary and Interdisciplinary)：M-IS Intersection

10:45 AM - 12:15 PM JST | 1:45 AM - 3:15 AM UTC | Poster Hall International Exhibition Hall8, Makuhari Messe_10

[M-IS05] New technologies to monitor thunderstorm and severe weather activities

convener:Mitsuteru Sato(Department of Cosmoscience, Hokkaido University), Yukihiro Takahashi(Department of Cosmosciences, Graduate School of Science, Hokkaido University), Hisayuki Kubota(Hokkaido University), Kozo Yamashita(Ashikaga University, Department of Engineering.)

[MIS05-P01] Study on monitoring of thunderstorm activity based on multiple electrostatic measurement

*Kozo Yamashita[1], Kakeru Kanno[1], Mitsuteru Sato[2], Yukihiro Takahashi[2] (1.Ashikaga Univ., 2.Hokkaido Univ.)

[MIS05-P02] **Contribution of Rainfall and Lightning Activities to the Fair Weather Electric Field Evaluated by 3D GEC Model**

*Kittanapat Bandholnopparat[1], Mitsuteru Sato[2], Yukihiro Takahashi[2], Toru Adachi[3], Masashi Kamogawa[5], Yasuhiro Minamoto[5], Akira Kadokura[6], Tomoo Ushio[4] (1.Department of Cosmosciences, Hokkaido University, Sapporo, Japan, 2.Faculty of Science, Hokkaido University, Sapporo, Japan, 3.Meteorological Research Institute, Tsukuba, Japan, 4.Department of Aerospace Engineering, Tokyo Metropolitan University, Hino, Japan, 5.Tokyo Gakugei University, Tokyo, Japan, 6.National Institute of Polar Research, Tokyo, Japan)

[MIS05-P03] A method for locating lightning discharges using tweek atmospherics

*Masafumi Kanno[1], Hiroyo Ohya[2], Kazuo Shiokawa[3], Hiroyuki Nakata[2], Toshiaki Takano[2] (1.Graduate School of Science and Engineering, Chiba University, 2.Graduate School of Engineering, Chiba University, 3.Institute for Space-Earth Environmental Research, Nagoya University)

[MIS05-P04] Monitoring for lightning activities and thunder cloud development over the Tokyo metropolitan area during the 2018 summer

*Jun-Ichi Hamada[1], Jun Matsumoto[1], Kozo Yamashita[2], Masashi Kamogawa[3], Yukihiro Takahashi[4] (1.Faculty of Urban Environmental Sciences, Tokyo Metropolitan University, 2.Department of Engineering, Ashikaga University, 3.Department of Physics, Tokyo Gakugei University, 4.Department of Cosmosciences, Graduate School of Science, Hokkaido University)

[E] Poster | M (Multidisciplinary and Interdisciplinary)：M-IS Intersection

5:15 PM - 6:30 PM JST | 8:15 AM - 9:30 AM UTC | Poster Hall International Exhibition Hall8, Makuhari Messe_42

[M-IS05] New technologies to monitor thunderstorm and severe weather activities

convener:Mitsuteru Sato(Department of Cosmoscience, Hokkaido University), Yukihiro Takahashi(Department of Cosmosciences, Graduate School of Science, Hokkaido University), Hisayuki Kubota(Hokkaido University), Kozo Yamashita(Ashikaga University, Department of Engineering.)

[MIS05-P01] Study on monitoring of thunderstorm activity based on multiple electrostatic measurement

*Kozo Yamashita[1], Kakeru Kanno[1], Mitsuteru Sato[2], Yukihiro Takahashi[2] (1.Ashikaga Univ., 2.Hokkaido Univ.)

[MIS05-P02] **Contribution of Rainfall and Lightning Activities to the Fair Weather Electric Field Evaluated by 3D GEC Model**

*Kittanapat Bandholnopparat[1], Mitsuteru Sato[2], Yukihiro Takahashi[2], Toru Adachi[3], Masashi Kamogawa[5], Yasuhiro Minamoto[5], Akira Kadokura[6], Tomoo Ushio[4] (1.Department of Cosmosciences, Hokkaido University, Sapporo, Japan, 2.Faculty of Science, Hokkaido University, Sapporo, Japan, 3.Meteorological Research Institute, Tsukuba, Japan, 4.Department of Aerospace Engineering, Tokyo Metropolitan University, Hino, Japan, 5.Tokyo Gakugei University, Tokyo, Japan, 6.National Institute of Polar Research, Tokyo, Japan)

[MIS05-P03] A method for locating lightning discharges using tweek atmospherics

*Masafumi Kanno[1], Hiroyo Ohya[2], Kazuo Shiokawa[3], Hiroyuki Nakata[2], Toshiaki Takano[2] (1.Graduate School of Science and Engineering, Chiba University, 2.Graduate School of Engineering, Chiba University, 3.Institute for Space-Earth Environmental Research, Nagoya University)

[MIS05-P04] Monitoring for lightning activities and thunder cloud development over the Tokyo metropolitan area during the 2018 summer

*Jun-Ichi Hamada[1], Jun Matsumoto[1], Kozo Yamashita[2], Masashi Kamogawa[3], Yukihiro Takahashi[4] (1.Faculty of Urban Environmental Sciences, Tokyo Metropolitan University, 2.Department of Engineering, Ashikaga University, 3.Department of Physics, Tokyo Gakugei University, 4.Department of Cosmosciences, Graduate School of Science, Hokkaido University)

[E] Oral | M (Multidisciplinary and Interdisciplinary) : M-IS Intersection

1:45 PM - 3:15 PM JST | 4:45 AM - 6:15 AM UTC | 101 1F

[M-IS05] New technologies to monitor thunderstorm and severe weather activities

convener:Mitsuteru Sato(Department of Cosmoscience, Hokkaido University), Yukihiro Takahashi(Department of Cosmosciences, Graduate School of Science, Hokkaido University), Hisayuki Kubota(Hokkaido University), Kozo Yamashita(Ashikaga University, Department of Engineering.), Chairperson:Mitsuteru Sato(Faculty of Science, Hokkaido University), Kozo Yamashita(Department of Technology, Ashikaga Institute of Technology)

1:45 PM - 2:00 PM JST | 4:45 AM - 5:00 AM UTC

[MIS05-01] Quasi real-time observation of typhoon and thunderstorms by the system of micro-satellites and ground-based lightning sensors

*Yukihiro Takahashi[4,1], Mitsuteru Sato[1,4], Hisayuki Kubota[4], Kozo Yamashita[2], Tetsuro Ishida[4], Ellison Caparas Castro[3], Purwadi Purwadi[1], Kazuhisa Tsuboki[5], Hiroyuki Yamada[6], Taro Shinoda[5], Loren Joy De Vera Estrebillo[1], Doreena Karmina Abril Pulutan[1] (1.Graduate School of Science, Hokkaido University, 2.Department of Engineering, Ashikaga University, 3.University of the Philippines, Diliman, 4.Faculty of Science, Hokkaido University, 5.Institute for Space-Earth Environmental Research (ISEE), Nagoya University, 6.University of the Ryukyus)

2:00 PM - 2:15 PM JST | 5:00 AM - 5:15 AM UTC

[MIS05-02] **Towards the Implementation of the Understanding Lightning and Thunderstorms for Extreme Weather Monitoring and Information Sharing in the Philippines (ULAT) Project**

★Invited Papers

*Glenn Vincent C. Lopez[1] (1.Advanced Science and Technology Institute)

2:15 PM - 2:30 PM JST | 5:15 AM - 5:30 AM UTC

[MIS05-03] **Airborne observation of Super Typhoon Trami in 2018 for understanding the intensity of tropical cyclone in the Philippine Sea**

★Invited Papers

*Hisayuki Kubota[1], Kazuhisa Tsuboki[2], Hiroyuki Yamada[3], Yukihiro Takahashi[1], Taro Shinoda[2], Tadayasu Ohigashi[4], Munehiko Yamaguchi[5], Kosuke Ito[3], Tetsuo Nakazawa[5], Norio Nagahama[6], Kensaku Shimizu[6], Mitsuteru Sato[1] (1.Hokkaido University, 2.Nagoya University, 3.University of the Ryukyus, 4.National Research Institute for Earth Science and Disaster Resilience, 5.Meteorological Research Institute, 6.Meisei Electronic)

2:30 PM - 2:45 PM JST | 5:30 AM - 5:45 AM UTC

[MIS05-04] Relation between Lightning and Typhoon Activities (Typhoon LAN) in the Western Pacific Region

*Mitsuteru Sato[1], Yukihiro Takahashi[1], Hisayuki Kubota[1], Kozo Yamashita[2], Jun-Ichi Hamada[3], Joel J. Marciano[4] (1.Department of Cosmoscience, Hokkaido University, 2.Department of Engineering, Ashikaga University, 3.Graduate School of Urban Environmental Sciences, Tokyo Metropolitan University, 4.ASTI, DOST)

2:45 PM - 3:00 PM JST | 5:45 AM - 6:00 AM UTC

[MIS05-05] Infrasound multi-site observation of thunders 3: preparation process for SATREPS

★Invited Papers

*Masa-yuki Yamamoto[1] (1.Department of systems engineering, Kochi University of Technology)

3:00 PM - 3:15 PM JST | 6:00 AM - 6:15 AM UTC

[MIS05-06] Data Acquisition System for an Infrasound Network for Thunderstorm Monitoring

*Doreena Karmina Abril Pulutan[1], Yukihiro Takahashi[1], Mitsuteru Sato[1], Hisayuki Kubota[1], Kozo Yamashita[2], Masa-yuki Yamamoto[3] (1.Department of Cosmosciences, Hokkaido University, 2.Department of Engineering, Ashikaga University, 3.Department of Systems Engineering, Kochi University of Technology)

[E] Oral | M (Multidisciplinary and Interdisciplinary) : M-IS Intersection

3:30 PM - 5:00 PM JST | 6:30 AM - 8:00 AM UTC | 101 1F

[M-IS05] New technologies to monitor thunderstorm and severe weather activities

convener:Mitsuteru Sato(Department of Cosmoscience, Hokkaido University), Yukihiro Takahashi(Department of Cosmosciences, Graduate School of Science, Hokkaido University), Hisayuki Kubota(Hokkaido University), Kozo Yamashita(Ashikaga University, Department of Engineering.), Chairperson:Yukihiro Takahashi(Hokkaido University), Hisayuki Kubota(Department of Cosmoscience, Hokkaido University)

3:30 PM - 3:45 PM JST | 6:30 AM - 6:45 AM UTC

[MIS05-07] Estimation of Lightning Location Using V-POTEKA Lightning Observation Network

*Loren Joy De Vera Estrebillo[1], Mitsuteru Sato[2], Yukihiro Takahashi[2], Hisayuki Kubota[2], Kozo Yamashita[3], Junichi Hamada[4], Joel Marciano[5] (1.Department of Cosmosciences, Hokkaido University, 2.Faculty of Science, Hokkaido University, 3.Faculty of Engineering, Ashikaga University, 4.Graduate School of Urban Environmental Sciences, Tokyo Metropolitan University, 5.ASTI/DOST)

3:45 PM - 4:00 PM JST | 6:45 AM - 7:00 AM UTC

[MIS05-08] **Observation system for thunderstorm development using ground lightning detection network and thermal infrared camera onboard satellite LAPAN-A4 in Indonesia**

*Purwadi Purwadi[1,2], Yukihiro Takahashi[1], Mitsuteru Sato[1], Kozo Yamashita[3], M. Arif Saifudin[4] (1.Department of Cosmosciences, Hokkaido University, Sapporo 0600810, Japan, 2.Agency for Assessment and Application of Technology (BPPT), Jakarta 10340, Indonesia, 3.Department of Technology, Ashikaga Institute of Technology, Tochigi 3268558, Japan, 4.Indonesian National Institute of Aeronautics and Space (LAPAN), Jawa Barat 16310, Indonesia)

4:00 PM - 4:15 PM JST | 7:00 AM - 7:15 AM UTC

[MIS05-09] Remote Sensing Water Quality Determination using Multi-spectral Analysis

*Ahmad Shaqeer Mohamed Thaheer[1], Yukihiro Takahashi[1] (1.Hokkaido University)

4:15 PM - 4:30 PM JST | 7:15 AM - 7:30 AM UTC

[MIS05-10] Study of cloud effects on atmospheric electric field during lightning activities and snowfall using the 95-GHz cloud radar FALCON-I

★Invited Papers

*Hiroyo Ohya[1], Kota Nakamori[1], Masashi Kamogawa[2], Tomoyuki Suzuki[2], Toshiaki Takano[1], Kazuomi Morotomi[3], Hiroyuki Nakata[1], Kazuo Shiokawa[4] (1.Graduate School of Engineering, Chiba University, 2.Tokyo Gakugei University, 3.Japan Radio Co. Ltd., 4.Nagoya University)

4:30 PM - 4:45 PM JST | 7:30 AM - 7:45 AM UTC

[MIS05-11] Preferred environmental conditions of precipitation systems in and around Bangladesh observed by ground-based radars

★Invited Papers

*Fumie Murata[1], Shuhei Azuma[2], Toru Terao[3], Quamrul S.M. Hassan[4] (1.Faculty of Science and Technology, Kochi University, 2.Faculty of Science, Kochi University, 3.Faculty of Education, Kagawa University, 4.Bangladesh Meteorological Department)

4:45 PM - 5:00 PM JST | 7:45 AM - 8:00 AM UTC

[MIS05-12] Thundercloud gamma-ray observations at Kashiwazaki aiming at source altitude and beaming measurements and a new trial at Tokyo Skytree in FY2018

★Invited Papers

*Kazuhiro Nakazawa[1], Takahiro Matsumoto[2], Yuuki Wada[2], Alexia Fabiani[1], Teruaki Enoto[3], Kazufumi Okuda[2], Yoshihiro Furuta[4], Yuki Aizawa[2], Takayuki Yuasa[5], Harufumi Tsuchiya[4], Mitsuteru Sato[6], Kazuo Makishima[7] (1.Nagoya University, 2.University of Tokyo, 3.Kyoto University, 4.JAEA, 5.RIKEN, 6.Hokkaido University, 7.Kalvi IPMU, University of Tokyo)

[J] Oral | M (Multidisciplinary and Interdisciplinary)：M-IS Intersection

9:00 AM - 10:30 AM JST | 12:00 AM - 1:30 AM UTC | 303 3F

[M-IS10] Interface- and nano-phenomena on crystal growth and dissolution

convener:Yuki Kimura(Institute of Low Temperature Science, Hokkaido University), Hitoshi Miura(Graduate School of Natural Sciences, Department of Information and Basic Science, Nagoya City University), Hisao Satoh(Naka Energy Research Laboratory, Mitsubishi Materials Corporation), Katsuo Tsukamoto(Graduate School of Engineering, Osaka University), Chairperson:Yuki Kimura (Institute of Low Temperature Science, Hokkaido University)

9:00 AM - 9:15 AM JST | 12:00 AM - 12:15 AM UTC

[MIS10-01] Fabrication of octacalcium phosphate block through a dissolutionprecipitation reaction and its biological evaluation

*Yuki Sugiura[1], Munar L Melvin[2], Kunio Ishikawa[2] (1.National Institute of Advanced Industrial Science and Technology, 2.Kyushu University)

9:15 AM - 9:30 AM JST | 12:15 AM - 12:30 AM UTC

[MIS10-02] Development of optimized incineration process of fisheries waste for synthesizing a functional heat storage material

*Hidekazu Kobatake[1], SHinji Kirihara[1] (1.Hirosaki University Institute of Regional Innovation)

9:30 AM - 9:45 AM JST | 12:30 AM - 12:45 AM UTC

[MIS10-03] “Manipulated” Organic Crystallization and Two-step Dissolution Process Attained by Plasmonic Optical Tweezers

*Hiromasa Niinomi[1], Teruki Sugiyama[2,3,4], Miho Tagawa[5], Toru Ujihara[5], Katsuhiko Miyamoto[6,7], Takashige Omatsu[6,7], Jun Nozawa[1], Junpei Okada[1], Satoshi Uda[1] (1.Institute for Materials Research, Tohoku University, 2.Department of Applied Chemistry, National Chiao Tung University, 3.Center for Emergent Functional Matter Science, National Chiao Tung University, 4.Division of Materials Science, Nara Institute of Science and Technology, 5.Institute of Materials and Systems for Sustainability (IMaSS), Nagoya University, 6.Molecular Chirality Research Center (MCRC), Chiba University, 7.Graduate School of Engineering, Chiba University)

9:45 AM - 10:00 AM JST | 12:45 AM - 1:00 AM UTC

[MIS10-04] Investigation of liquid cell transmission electron microscopy combined with antisolvent crystallization

*Tomoya Yamazaki[1], Yuki Kimura[1] (1.Institute of Low Temperature Science Hokkkaido University)

10:00 AM - 10:30 AM JST | 1:00 AM - 1:30 AM UTC

[MIS10-05] DNA-guided crystallization of nanoparticles: optimization of crystallization conditions and structure analysis

★Invited Papers

*Miho Tagawa[1], Shoko Kojima[1], Hayato Sumi[1], Arisa Nishibu[1], Takumi Isogai[1], Maasa Yokomori[2], Shunta Harada[1], Toru Ujihara[1], Katsuo Tsukamoto[1] (1.Nagoya University, 2.The University of Tokyo)

[J] Oral | M (Multidisciplinary and Interdisciplinary)：M-IS Intersection

10:45 AM - 12:15 PM JST | 1:45 AM - 3:15 AM UTC | 303 3F

[M-IS10] Interface- and nano-phenomena on crystal growth and dissolution

convener:Yuki Kimura(Institute of Low Temperature Science, Hokkaido University), Hitoshi Miura(Graduate School of Natural Sciences, Department of Information and Basic Science, Nagoya City University), Hisao Satoh(Naka Energy Research Laboratory, Mitsubishi Materials Corporation), Katsuo Tsukamoto(Graduate School of Engineering, Osaka University), Chairperson:Hisao Satoh

10:45 AM - 11:00 AM JST | 1:45 AM - 2:00 AM UTC

[MIS10-06] Growth mechanism of binary colloidal crystals

*Jun Nozawa[1], Suxia Guo[1], Hiromasa Niinomi[1], Junpei Okada[1], Satoshi Uda[1] (1.Tohoku University)

11:00 AM - 11:15 AM JST | 2:00 AM - 2:15 AM UTC

[MIS10-07] Solution-Mediated-Transformation Kinetics of Norsethite

*Harutoshi Asakawa[1], Hiroshi Uneda[1], Itaru Echigo[1], Ryuichi Komatsu[1] (1.Graduate School of Sciences and Technology for Innovation Yamaguchi University)

11:15 AM - 11:30 AM JST | 2:15 AM - 2:30 AM UTC

[MIS10-08] Formation of low-crystalline magnesium silicate in natural alkaline environment and flow-through experiments

*Yuto Nishiki[1], Misato Shimbashi[1], Tsutomu Sato[2], Tsubasa Otake[2] (1.Graduate School of Engineering, Hokkaido University, 2.Faculty of Engineering, Hokkaido University)

11:30 AM - 11:45 AM JST | 2:30 AM - 2:45 AM UTC

[MIS10-09] Homogeneous Nucleation from Vapor in Al-O Binary System

*Shinnosuke Ishizuka[1], Jun Kawano[2], Tomoya Yamazaki[3], Tetsuya Hama[3], Yuki Kimura[3] (1.National Institute for Environmental Studies, 2.Faculty of Science, Hokkaido University, 3.Institute of Low Temperature Science, Hokkaido University)

11:45 AM - 12:00 PM JST | 2:45 AM - 3:00 AM UTC

[MIS10-10] Crystal growth hysteresis in birth-and-spread mechanism

*Hitoshi Miura[1] (1.Graduate School of Natural Sciences, Department of Information and Basic Science, Nagoya City University)

[J] Poster | M (Multidisciplinary and Interdisciplinary)：M-IS Intersection

3:30 PM - 5:00 PM JST | 6:30 AM - 8:00 AM UTC | Poster Hall International Exhibition Hall8, Makuhari Messe_24

[M-IS10] Interface- and nano-phenomena on crystal growth and dissolution

convener:Yuki Kimura(Institute of Low Temperature Science, Hokkaido University), Hitoshi Miura(Graduate School of Natural Sciences, Department of Information and Basic Science, Nagoya City University), Hisao Satoh(Naka Energy Research Laboratory, Mitsubishi Materials Corporation), Katsuo Tsukamoto(Graduate School of Engineering, Osaka University)

[MIS10-P01] Theoretical Model of Crystallization through Homogeneous Nucleation in Water Droplets

*Kyoko Kitakami Tanaka[1], Yuki Kimura[2] (1.Tohoku University, 2.Hokkaido University, Institute of Low Temperature Science)

[MIS10-P02] Mean Height of the Self-Assembled Faceted Macrosteps: Steady Crystal Growth/Dissolution in a Reaction- (Interface-) Limited Process

*Noriko Akutsu[1] (1.Faculty of Engineering, Osaka Electro-Communication University)

[MIS10-P03] In-situ observation of natural snow crystals by optical techniques

*Yuki Kimura[1], Tomoya Yamazaki[1], Takao Maki, Yoshinori Furukawa[1] (1.Institute of Low Temperature Science, Hokkaido University)

[MIS10-P04] Visualization of local environment around forming/dissolving carbonate minerals with the fluorescent probe

*Jun Kawano[1], Kotaro Osawa[2], Takashi Toyofuku[3,4], Yukiko Nagai[4,5], Jun-ya Tanaka[6], Takaya Nagai[1] (1.Faculty of Science, Hokkaido University, 2.School of Science, Hokkaido University, 3.JAMSTEC, 4.Tokyo University of Marine Science and Technology, 5.National Museum of Nature and Science of Tokyo, 6.Graduate School of Science, Hokkaido University)

[MIS10-P05] Influence of Ammonium Nitrate on Crystallization of Norsethite from Aqueous Solution

*Itaru Echigo[1], Harutoshi Asakawa[1], Hiroshi Uneda, Ryuichi Komatsu[1] (1.Graduate School of Science and Technology for Innovation Yamaguchi University)

[MIS10-P06] Direct observation of zeolite nucleation from compacted bentonite under hyperalkaline condition

*Hisao Satoh[1], Mayumi Takazawa[2], Daisuke Hayashi[3], Masaya Ida[3] (1.Naka Energy Research Laboratory, Mitsubishi Materials Corporation, 2.Mitsubishi Materials Corporation, 3.Radioactive Waste Management Funding and Research Center)

[J] Poster | M (Multidisciplinary and Interdisciplinary)：M-IS Intersection

5:15 PM - 6:30 PM JST | 8:15 AM - 9:30 AM UTC | Poster Hall International Exhibition Hall8, Makuhari Messe_43

[M-IS10] Interface- and nano-phenomena on crystal growth and dissolution

convener:Yuki Kimura(Institute of Low Temperature Science, Hokkaido University), Hitoshi Miura(Graduate School of Natural Sciences, Department of Information and Basic Science, Nagoya City University), Hisao Satoh(Naka Energy Research Laboratory, Mitsubishi Materials Corporation), Katsuo Tsukamoto(Graduate School of Engineering, Osaka University)

[MIS10-P01] Theoretical Model of Crystallization through Homogeneous Nucleation in Water Droplets

*Kyoko Kitakami Tanaka[1], Yuki Kimura[2] (1.Tohoku University, 2.Hokkaido University, Institute of Low Temperature Science)

[MIS10-P02] Mean Height of the Self-Assembled Faceted Macrosteps: Steady Crystal Growth/Dissolution in a Reaction- (Interface-) Limited Process

*Noriko Akutsu[1] (1.Faculty of Engineering, Osaka Electro-Communication University)

[MIS10-P03] In-situ observation of natural snow crystals by optical techniques

*Yuki Kimura[1], Tomoya Yamazaki[1], Takao Maki, Yoshinori Furukawa[1] (1.Institute of Low Temperature Science, Hokkaido University)

[MIS10-P04] Visualization of local environment around forming/dissolving carbonate minerals with the fluorescent probe

*Jun Kawano[1], Kotaro Osawa[2], Takashi Toyofuku[3,4], Yukiko Nagai[4,5], Jun-ya Tanaka[6], Takaya Nagai[1] (1.Faculty of Science, Hokkaido University, 2.School of Science, Hokkaido University, 3.JAMSTEC, 4.Tokyo University of Marine Science and Technology, 5.National Museum of Nature and Science of Tokyo, 6.Graduate School of Science, Hokkaido University)

[MIS10-P05] Influence of Ammonium Nitrate on Crystallization of Norsethite from Aqueous Solution

*Itaru Echigo[1], Harutoshi Asakawa[1], Hiroshi Uneda, Ryuichi Komatsu[1] (1.Graduate School of Science and Technology for Innovation Yamaguchi University)

[MIS10-P06] Direct observation of zeolite nucleation from compacted bentonite under hyperalkaline condition

*Hisao Satoh[1], Mayumi Takazawa[2], Daisuke Hayashi[3], Masaya Ida[3] (1.Naka Energy Research Laboratory, Mitsubishi Materials Corporation, 2.Mitsubishi Materials Corporation, 3.Radioactive Waste Management Funding and Research Center)

[J] Oral | M (Multidisciplinary and Interdisciplinary)：M-IS Intersection

9:00 AM - 10:30 AM JST | 12:00 AM - 1:30 AM UTC | A02 TOKYO BAY MAKUHARI HALL

[M-IS11] Aqua planetology

convener:Yasuhito Sekine(Earth-Life Science Insitute, Tokyo Institute of Technology), Tomohiro Usui(Earth-Life Science Institute, Tokyo Institute of Technology), Keisuke Fukushi(Institute of Nature & Environmental Technology, Kanazawa University), Takazo Shibuya(Japan Agency for Marine-Earth Science and Technology), Chairperson:Yasuhito Sekine(Dept. Earth & Planetary Sci., University of Tokyo), Takazo Shibuya(JAMSTEC), Tomohiro Usui

9:00 AM - 9:15 AM JST | 12:00 AM - 12:15 AM UTC

[MIS11-13] A forward modeling of infrared reflectance spectra of asteroids

*Hiroyuki Kurokawa[1], Takazo Shibuya[2], Yasuhito Sekine[1], Bethany L Ehlmann[3,4] (1.ELSI, Tokyo Tech, 2.JAMSTEC, 3.Caltech, 4.JPL)

9:15 AM - 9:30 AM JST | 12:15 AM - 12:30 AM UTC

[MIS11-14] Estimation of formation mechanism and morphological condition in calcite concretion

*Takayuki Ihara[1], Sin-iti Sirono[1] (1.Nagoya University)

9:30 AM - 9:45 AM JST | 12:30 AM - 12:45 AM UTC

[MIS11-15] Reconstructing groundwater hydrology and water-rock reactions around Gale Crater on early Mars

*Natsumi Noda[1,2], Yasuhito Sekine[1], Shuya Tan[1,2], Takazo Shibuya[3], Hidenori Genda[1] (1.Earth-Life Science Institute, Tokyo Institute of Technology, 2.Department of Earth and Planetary Science, Graduate School of Science, The University of Tokyo, 3.Department of Subsurface Geobiological Analysis and Research, Japan Agency for Marine-Earth Science and Technology)

9:45 AM - 10:00 AM JST | 12:45 AM - 1:00 AM UTC

[MIS11-16] Habitable zone for a land planet

*Takanori Kodama[1], Hidenori Genda[2], Ryouta O'ishi[3], Ayako Abe-Ouchi[3] (1.University of Bordeaux, 2.Earth-Life Science Institute, Tokyo Institute of Technology, 3.Atmosphere and Ocean Research Institute, University of Tokyo)

10:00 AM - 10:15 AM JST | 1:00 AM - 1:15 AM UTC

[MIS11-17] A study on the dependence of ocean planet climate on solar constant: influence of oceanic heat transport in the case of large absorption coefficients of gray atmosphere

*Yuta Kawai[1,2], Yoshiyuki O. Takahashi[1], Masaki Ishiwatari[5], Kensuke Nakajima[3], Shin-ichi Takehiro[4], Hiroki Kashimura[1,6], Seiya Nishizawa[2], Hirofumi Tomita[2], Yoshi-Yuki Hayashi[1,6] (1.Kobe University, 2.RIKEN Center for Computational Science, 3.Kyusyu University, 4.Kyoto University , 5.Hokkaido University, 6.Center for Planetary Science)

10:15 AM - 10:30 AM JST | 1:15 AM - 1:30 AM UTC

[MIS11-18] Water cycle and its evolution: High-speed H_2O transport to upper atmosphere on Mars

★Invited Papers

*Hiromu Nakagawa[1], Shohei Aoki[1], Nao Yoshida[1], Naoki Terada[1], Takeshi Imamura[2], Kazunori Ogohara[3], Toru Kouyama[4], Hiroki Ando[6], Katsuyuki Noguchi[5], Akiho Miyamoto[1], Kosuke Takami[1], Isao Murata[1], Yasumasa Kasaba[1], IUVS team MAVEN (1.Planetary Atmosphere Physics Laboratory, Department of Geophysics, Graduate School of Science, Tohoku University, 2.Graduate school of Frontier sciences, University of Tokyo, 3.University of Shiga prefecture, 4.The National Institute of Advanced Industrial Science and Technology, 5.Nara Women's university, 6.Kyoto Sangyo university)

[J] Poster | M (Multidisciplinary and Interdisciplinary)：M-IS Intersection

3:30 PM - 5:00 PM JST | 6:30 AM - 8:00 AM UTC | Poster Hall International Exhibition Hall8, Makuhari Messe_25

[M-IS11] Aqua planetology

convener:Yasuhito Sekine(Earth-Life Science Insitute, Tokyo Institute of Technology), Tomohiro Usui(Earth-Life Science Institute, Tokyo Institute of Technology), Keisuke Fukushi(Institute of Nature & Environmental Technology, Kanazawa University), Takazo Shibuya(Japan Agency for Marine-Earth Science and Technology)

[MIS11-P01] Three-dimensional simulations of methane-based hydrological cycles in north-pole regions of Titan

*Takufumi Chida[1,2], Yasuhito Sekine[1], Hidenori Genda[1] (1.Earth-Life Science Institute, Tokyo Institute of Technology, 2.Department of Earth and Planetary Science, University of Tokyo)

[MIS11-P02] Inclusion of brine into icy shell of Enceladus

*Ryusuke Nishitani[1], Atsushi Tani[2], Sho Sasaki[1], Jun Kimura[1] (1.Department of Earth and Space Sciences, School of Science, Osaka University, 2.Graduate School Human Development and Environment, Kobe University)

[MIS11-P03] Electron irradiations onto ice-salt mixtures at low temperatures: Implications for chemical evolution and oxidant formation on Europa

*Shuya Tan[2,1], Yasuhito Sekine[2], Tetsuya Hama[3] (1.Department of Earth and Planetary Science, Graduate School of Science, the University of Tokyo, 2.Earth-Life Science Institute, Tokyo Institute of Technology, 3.Institute of Low Temperature Science, Hokkaido University)

[MIS11-P04] Water-rock reactions in the parent body of Ryugu

*Takazo Shibuya[1], Yasuhito Sekine[2], Sakiko Kikuchi[1], Keisuke Fukushi[3], Tomoki Nakamura[4], Sei-ichiro WATANABE[5] (1.Japan Agency for Marine-Earth Science and Technology, 2.Tokyo Institute of Technology, 3.Kanazawa University, 4.Tohoku University, 5.Nagoya University)

[MIS11-P05] Investigation of the organic matter in ALH 77307 by STXM

*Hiroki Suga[1], Motoo Ito[2], Yoko Kebukawa[3], Matthew A Marcus[4], Takuji Ohigashi[5], Yoshio Takahashi[1] (1.Graduate School of Science, The University of Tokyo, 2.Kochi Institute for Core Sample Research JAMSTEC, 3.Faculty of Engineering, Yokohama National University, 4.Advanced Light Source, Lawrence Berkeley National Laboratory, 5.UVSOR Synchrotron Facility, Institute for Molecular Science)

[MIS11-P06] The development of UV spectrometer and preliminary measurement of carbonaceous chondrites

*Akira Igarashi[1], Tomoki Nakamura[1], Shingo Kameda[2], Keiichi Moroi[2] (1.Department of Earth and Planetary Materials Sciences, Faculty of Science, Tohoku University, 2.Department of Physics, Faculty of Science, Rikkyo University)

[MIS11-P07] A coupled experimental and thermodynamic study of chondrite-water interaction under anoxic condition

*Sakiko Kikuchi[1], Takazo Shibuya[1] (1.Japan Agency for Marine-Earth Science and Technology)

[MIS11-P08] Two-dimensional numerical experiments on subduction initiation in oceanic lithosphere: Effects of rheological properties of hydrous minerals

*Miki Izumi[1], Masaki Yoshida[2], Ken-ichi Hirauchi[1] (1.Department of Geosciences, Faculty of Science, Shizuoka University, 2.Department of Deep Earth Structure and Dynamics research, Japan Agency for Marine–Earth Science and Technology –JAMSTEC–)

[MIS11-P09] Electrical energy generation at hydrothermal environments in the Solar System estimated by fuel cell model experimentations

*Hiroyuki Kashima[1], Masahiro Yamamoto[1], Ken Takai[1] (1.Japan Agency for Marine-Earth Science and Technology)

[MIS11-P10] Experimental study of abiotic nitrate reduction at a high temperature and high-pressure condition and implication for nitrogen chemistry in Hadean hydrothermal environments

*Manabu Nishizawa[1], Takuya Saito[1], Akiko Makabe[1], Takazo Shibuya[1], Ken Takai[1] (1.Japan Agency for Marine-Earth Science and Technology)

[MIS11-P11] Interaction experiments between eucritic glass and 0.1 M NaCl aqueous solution at 300-500°C and 1.5 kbar: Suggestions on water-rock interactions at the bottom of Europa's subsurface ocean

*Makoto Nagasawa[1,2], Yutaro Takaya[1] (1.Department of Resources and Environmental Engineering, School of Creative Science and Engineering, Waseda University, 2.Department of Earth and Planetary Science, Graduate School of Science, The University of Tokyo)

[MIS11-P12] **Relationship between tellurium in the Fe-Mn oxides in the ocean and ambient seawater**

*Yusuke Fukami[1], Teruhiko Kashiwabara[1], Hiroshi Amakawa[1], Takazo Shibuya[1], Akira Usui[2], Katsuhiko Suzuki[1] (1.Japan Agency for Marine-Earth Science and Technology, 2.Kochi University)

[MIS11-P13] Laboratory reproduction of earthquake faulting beneath the internal ocean of Enceladus

*Takehiro Hirose[1], Takazo Shibuya[2] (1.Kochi Institute for Core Sample Research, Japan Agency for Marine-Earth Science and Technology, 2.Japan Agency for Marine-Earth Science and Technology)

[MIS11-P14] Why does Titan have an atmosphere, and why not Ganymede?—The origin of Titan-Ganymede dichotomy

*Yasuhito Sekine[1], Yuhiko Aoyama[2], Masahiro Ikoma[2], Takayuki Tanigawa[3] (1.Earth-Life Science Insitute, Tokyo Institute of Technology, 2.Dept. of Earth and Planetary Sci., University of Tokyo, 3.Section of Liberal Arts and Sciences, National Inst. of Tech., Ichinoseki College)

[MIS11-P15] Development of observation system of gas hydrate forming in the environment simulated near the bottom of icy shell in icy bodies (2)

*Atsushi Tani[1], Kenshiro Moriyama[1] (1.Graduate School of Human Development and Environment, Kobe University)

[MIS11-P16] Rheology of non-water ices inferred from diffusion coefficients: A compilation study

*Naoki Noguchi[1] (1.Graduate School of Technology, Industrial and Social Sciences, Tokushima University)

[MIS11-P17] Swelling behavior of magnesium saturated smectites

Morida Koki, Keisuke Fukushi, Hiroshi Sakuma

*Koki Morida[1] (1.Kanazawa University)

[MIS11-P18] Possibility of hydrogen peroxide as a warming agent on early Mars with oxidized condition

*Yuichi Ito[1], George HASHIMOTO[2], Yoshiyuki O. Takahashi[3], Masaki Ishiwatari[1], Kiyoshi Kuramoto[1] (1.Department of Cosmosciences, Graduate school of Science, Hokkaido University, 2.Department of Earth Sciences, Okayama University, 3.Graduate School of Science, Kobe University)

[J] Poster | M (Multidisciplinary and Interdisciplinary)：M-IS Intersection

5:15 PM - 6:30 PM JST | 8:15 AM - 9:30 AM UTC | Poster Hall International Exhibition Hall8, Makuhari Messe_44

[M-IS11] Aqua planetology

convener:Yasuhito Sekine(Earth-Life Science Insitute, Tokyo Institute of Technology), Tomohiro Usui(Earth-Life Science Institute, Tokyo Institute of Technology), Keisuke Fukushi(Institute of Nature & Environmental Technology, Kanazawa University), Takazo Shibuya(Japan Agency for Marine-Earth Science and Technology)

[MIS11-P01] Three-dimensional simulations of methane-based hydrological cycles in north-pole regions of Titan

*Takufumi Chida[1,2], Yasuhito Sekine[1], Hidenori Genda[1] (1.Earth-Life Science Institute, Tokyo Institute of Technology, 2.Department of Earth and Planetary Science, University of Tokyo)

[MIS11-P02] Inclusion of brine into icy shell of Enceladus

*Ryusuke Nishitani[1], Atsushi Tani[2], Sho Sasaki[1], Jun Kimura[1] (1.Department of Earth and Space Sciences, School of Science, Osaka University, 2.Graduate School Human Development and Environment, Kobe University)

[MIS11-P03] Electron irradiations onto ice-salt mixtures at low temperatures: Implications for chemical evolution and oxidant formation on Europa

*Shuya Tan[2,1], Yasuhito Sekine[2], Tetsuya Hama[3] (1.Department of Earth and Planetary Science, Graduate School of Science, the University of Tokyo, 2.Earth-Life Science Institute, Tokyo Institute of Technology, 3.Institute of Low Temperature Science, Hokkaido University)

[MIS11-P04] Water-rock reactions in the parent body of Ryugu

*Takazo Shibuya[1], Yasuhito Sekine[2], Sakiko Kikuchi[1], Keisuke Fukushi[3], Tomoki Nakamura[4], Sei-ichiro WATANABE[5] (1.Japan Agency for Marine-Earth Science and Technology, 2.Tokyo Institute of Technology, 3.Kanazawa University, 4.Tohoku University, 5.Nagoya University)

[MIS11-P05] Investigation of the organic matter in ALH 77307 by STXM

*Hiroki Suga[1], Motoo Ito[2], Yoko Kebukawa[3], Matthew A Marcus[4], Takuji Ohigashi[5], Yoshio Takahashi[1] (1.Graduate School of Science, The University of Tokyo, 2.Kochi Institute for Core Sample Research JAMSTEC, 3.Faculty of Engineering, Yokohama National University, 4.Advanced Light Source, Lawrence Berkeley National Laboratory, 5.UVSOR Synchrotron Facility, Institute for Molecular Science)

[MIS11-P06] The development of UV spectrometer and preliminary measurement of carbonaceous chondrites

*Akira Igarashi[1], Tomoki Nakamura[1], Shingo Kameda[2], Keiichi Moroi[2] (1.Department of Earth and Planetary Materials Sciences, Faculty of Science, Tohoku University, 2.Department of Physics, Faculty of Science, Rikkyo University)

[MIS11-P07] A coupled experimental and thermodynamic study of chondrite-water interaction under anoxic condition

*Sakiko Kikuchi[1], Takazo Shibuya[1] (1.Japan Agency for Marine-Earth Science and Technology)

[MIS11-P08] Two-dimensional numerical experiments on subduction initiation in oceanic lithosphere: Effects of rheological properties of hydrous minerals

*Miki Izumi[1], Masaki Yoshida[2], Ken-ichi Hirauchi[1] (1.Department of Geosciences, Faculty of Science, Shizuoka University, 2.Department of Deep Earth Structure and Dynamics research, Japan Agency for Marine–Earth Science and Technology –JAMSTEC–)

[MIS11-P09] Electrical energy generation at hydrothermal environments in the Solar System estimated by fuel cell model experimentations

*Hiroyuki Kashima[1], Masahiro Yamamoto[1], Ken Takai[1] (1.Japan Agency for Marine-Earth Science and Technology)

[MIS11-P10] Experimental study of abiotic nitrate reduction at a high temperature and high-pressure condition and implication for nitrogen chemistry in Hadean hydrothermal environments

*Manabu Nishizawa[1], Takuya Saito[1], Akiko Makabe[1], Takazo Shibuya[1], Ken Takai[1] (1.Japan Agency for Marine-Earth Science and Technology)

[MIS11-P11] Interaction experiments between eucritic glass and 0.1 M NaCl aqueous solution at 300-500°C and 1.5 kbar: Suggestions on water-rock interactions at the bottom of Europa's subsurface ocean

*Makoto Nagasawa[1,2], Yutaro Takaya[1] (1.Department of Resources and Environmental Engineering, School of Creative Science and Engineering, Waseda University, 2.Department of Earth and Planetary Science, Graduate School of Science, The University of Tokyo)

[MIS11-P12] **Relationship between tellurium in the Fe-Mn oxides in the ocean and ambient seawater**

*Yusuke Fukami[1], Teruhiko Kashiwabara[1], Hiroshi Amakawa[1], Takazo Shibuya[1], Akira Usui[2], Katsuhiko Suzuki[1] (1.Japan Agency for Marine-Earth Science and Technology, 2.Kochi University)

[MIS11-P13] Laboratory reproduction of earthquake faulting beneath the internal ocean of Enceladus

*Takehiro Hirose[1], Takazo Shibuya[2] (1.Kochi Institute for Core Sample Research, Japan Agency for Marine-Earth Science and Technology, 2.Japan Agency for Marine-Earth Science and Technology)

[MIS11-P14] Why does Titan have an atmosphere, and why not Ganymede?—The origin of Titan-Ganymede dichotomy

*Yasuhito Sekine[1], Yuhiko Aoyama[2], Masahiro Ikoma[2], Takayuki Tanigawa[3] (1.Earth-Life Science Insitute, Tokyo Institute of Technology, 2.Dept. of Earth and Planetary Sci., University of Tokyo, 3.Section of Liberal Arts and Sciences, National Inst. of Tech., Ichinoseki College)

[MIS11-P15] Development of observation system of gas hydrate forming in the environment simulated near the bottom of icy shell in icy bodies (2)

*Atsushi Tani[1], Kenshiro Moriyama[1] (1.Graduate School of Human Development and Environment, Kobe University)

[MIS11-P16] Rheology of non-water ices inferred from diffusion coefficients: A compilation study

*Naoki Noguchi[1] (1.Graduate School of Technology, Industrial and Social Sciences, Tokushima University)

[MIS11-P17] Swelling behavior of magnesium saturated smectites

Morida Koki, Keisuke Fukushi, Hiroshi Sakuma

*Koki Morida[1] (1.Kanazawa University)

[MIS11-P18] Possibility of hydrogen peroxide as a warming agent on early Mars with oxidized condition

*Yuichi Ito[1], George HASHIMOTO[2], Yoshiyuki O. Takahashi[3], Masaki Ishiwatari[1], Kiyoshi Kuramoto[1] (1.Department of Cosmosciences, Graduate school of Science, Hokkaido University, 2.Department of Earth Sciences, Okayama University, 3.Graduate School of Science, Kobe University)

[J] Oral | M (Multidisciplinary and Interdisciplinary)：M-IS Intersection

10:45 AM - 12:15 PM JST | 1:45 AM - 3:15 AM UTC | A02 TOKYO BAY MAKUHARI HALL

[M-IS21] Gas hydrate in environmental-resource sciences

convener:Hitoshi Tomaru(Department of Earth Sciences, Chiba University), Akihiro Hachikubo(Kitami Institute of Technology), Atsushi Tani(Graduate School of Human Development and Environment, Kobe University), Shusaku Goto(Institute for Geo-Resources and Environment National Institute of Advanced Industrial Science and Technology), Chairperson:Naoto Ishida, 戸丸 仁

10:45 AM - 11:00 AM JST | 1:45 AM - 2:00 AM UTC

[MIS21-01] Equilibrium pressure of clathrate hydrates encaged $^{13}CH_4$

*Yuki Kikuchi[1], Akihiro Hachikubo[1], Takahiro Ozeki[1], Satoshi Takeya[2] (1.Kitami Institute of Technology, 2.National Institute of Advanced Industrial Science and Technology (AIST))

11:00 AM - 11:15 AM JST | 2:00 AM - 2:15 AM UTC

[MIS21-02] Hydrogen isotopic fractionation of ethane encaged in different crystallographic structure

*Jumpei Matsuda[1], Akihiro Hachikubo[1], Satoshi Takeya[2] (1.Kitami Institute of Technology, 2.National Institute of Advanced Industrial Science and Technology (AIST))

11:15 AM - 11:30 AM JST | 2:15 AM - 2:30 AM UTC

[MIS21-03] Trend of effect of temperature on C–H symmetric stretching vibrational frequencies of hydrocarbon molecules in 12, 14 and 16-hedra cages of gas hydrates

*Go Fuseya[1], Satoshi Takeya[2], Akihiro Hachikubo[1] (1.Kitami Institute of Technology, 2.National Institute of Advanced Industrial Science and Technology (AIST))

11:30 AM - 11:45 AM JST | 2:30 AM - 2:45 AM UTC

[MIS21-04] The study on relations of the methane plume and atmospheric methane concentration

*Chiharu Aoyama[1] (1.Tokyo University of Marine Science and Technology)

11:45 AM - 12:00 PM JST | 2:45 AM - 3:00 AM UTC

[MIS21-05] Sampling of Methane Bubble Plumes and Solid Gas Hydrate on the Cascadia Margin, Pacific Northwest

*John E Lupton[1], Tamara Baumberger[1], Robert W. Embley[1], Susan G. Merle[1], Camilla Wilkinson[1], Conrad Young[2] (1.NOAA Pacific Marine Environmental Laboratory, Newport, Oregon, USA, 2.Young Engineering, Ramona, CA. USA)

[J] Oral | M (Multidisciplinary and Interdisciplinary)：M-IS Intersection

1:45 PM - 3:15 PM JST | 4:45 AM - 6:15 AM UTC | A02 TOKYO BAY MAKUHARI HALL

[M-IS21] Gas hydrate in environmental-resource sciences

convener:Hitoshi Tomaru(Department of Earth Sciences, Chiba University), Akihiro Hachikubo(Kitami Institute of Technology), Atsushi Tani(Graduate School of Human Development and Environment, Kobe University), Shusaku Goto(Institute for Geo-Resources and Environment National Institute of Advanced Industrial Science and Technology), Chairperson:八久保 晶弘(北見工業大学), 戸丸 仁

1:45 PM - 2:00 PM JST | 4:45 AM - 5:00 AM UTC

[MIS21-06] The distribution of atmospheric CH_4 concentration and gas plume location in the sea around Japanese islands.

*Shinsuke Aoki[1], Shujiro Komiya[2], Kosuke Noborio[3], Ryo Matsumoto[4] (1.Graduate School of Agriculture, Meiji Universiy, 2.Max Planck Institute, 3.School of Agriculture, Meiji Universiy, 4.Gas Hydrate Laboratory - Meiji University Organization for the Strategic Coordination of Research and Intellectual Property)

2:00 PM - 2:15 PM JST | 5:00 AM - 5:15 AM UTC

[MIS21-07] Reaction/fixation/migration of methane within the gas chimney on the Umitaka Spur, eastern margin of the Japan Sea

*Hitoshi Tomaru[1], Ryo Matsumoto[2] (1.Department of Earth Sciences, Chiba University, 2.Gas Hydrate Research Laboratory, Meiji University)

2:15 PM - 2:30 PM JST | 5:15 AM - 5:30 AM UTC

[MIS21-08] Slope failures induced by methane hydrate dissociation: a case of submarine slide in the southwestern Oki Trough, Japan Sea

*Naoto Ishida[1], Shota Morihita[2], Takao Ebinuma[1], Hitoshi Tomaru[3], Ryo Matsumoto[4] (1.Social Systems and Civil Engineering, Graduate School of Engineering, Tottori University, 2.Department of Social Systems and Civil Engineering, Faculty of Engineering, Tottori University, 3.Department of Earth Sciences, Faculty of Science, Chiba University, 4.Gas Hydrate Research Laboratory, Organization for the Strategic Coordination of Research and Intellectual Properties, Meiji University)

2:30 PM - 2:45 PM JST | 5:30 AM - 5:45 AM UTC

[MIS21-09] Origin and evolution of H_2S-bearing methane hydrate in the Sea of Japan

*Ryo Matsumoto[1], Tomoko Fukazawa[2], Akihiro Hiruta[1], Glen Snyder[1] (1.Organization for the Strategic Laboratory of Research and Intellectual Properties, Meiji University, 2.Department of Applied Chemistry, School of Science and Technoloty, Meiji University)

2:45 PM - 3:00 PM JST | 5:45 AM - 6:00 AM UTC

[MIS21-10] Discovery of gas hydrate at the new point off Abashiri, the Sea of Okhotsk

*Akihiro Hachikubo[1], Jumpei Matsuda[1], Satoshi Yamashita[1], Hirotoshi Sakagami[1], Masaaki Konishi[1], Hirotsugu Minami[1], Kenji Nishina[2], Kenji Sakaguchi[3] (1.Kitami Institute of Technology, 2.Geological Survey of Hokkaido, Hokkaido Research Organization, 3.Kushiro Fisheries Research Institute, Hokkaido Research Organization)

3:00 PM - 3:15 PM JST | 6:00 AM - 6:15 AM UTC

[MIS21-11] All about gas hydrates and heat flow offshore Chile

*LUCIA ALEJANDRA VILLAR MUNOZ[1], IVAN VARGAS-CORDERO[2], JOAQUIM P. BENTO[3], JAN BEHRMANN[1], UMBERTA TINIVELLA[4], MICHELA GIUSTINIANI[4] (1.Helmholtz Centre for Ocean Research, 2.Universidad Andres Bello , 3.Pontificia Universidad Catolica de Valparaiso, 4.Istituto Nazionale di Oceanografia e di Geofisica Sperimentale)

[J] Poster | M (Multidisciplinary and Interdisciplinary)：M-IS Intersection

3:30 PM - 5:00 PM JST | 6:30 AM - 8:00 AM UTC | Poster Hall International Exhibition Hall8, Makuhari Messe_26

[M-IS21] Gas hydrate in environmental-resource sciences

convener:Hitoshi Tomaru(Department of Earth Sciences, Chiba University), Akihiro Hachikubo(Kitami Institute of Technology), Atsushi Tani(Graduate School of Human Development and Environment, Kobe University), Shusaku Goto(Institute for Geo-Resources and Environment National Institute of Advanced Industrial Science and Technology)

[MIS21-P01] Raman spectroscopic analysis of isotopologue methane hydrates

*Yuki Kikuchi[1], Jumpei Matsuda[1], Akihiro Hachikubo[1], Satoshi Takeya[2] (1.Kitami Institute of Technology, 2.National Institute of Advanced Industrial Science and Technology (AIST))

[MIS21-P02] Gas origin of hydrate-bound gas in Lake Baikal

*Jumpei Matsuda[1], Yuki Kikuchi[1], Akihiro Hachikubo[1], Oleg Khlystov[2], Gennadiy Kalmychkov[3], Marc De Batist[4], Hirotoshi Sakagami[1], Hirotsugu Minami[1], Satoshi Yamashita[1] (1.Kitami Institute of Technology, 2.Limnological Institute, SB RAS, 3.Vinogradov Institute of Geochemistry, SB RAS, 4.Ghent University)

[MIS21-P03] Validation of self-preservation effect of methane and ethane mixed-gas hydrate by Raman spectroscopy

*Yunosuke Hase[1], Jumpei Matsuda[1], Akihiro Hachikubo[1], Satoshi Takeya[2] (1.Kitami Institute of Technology, 2.National Institute of Advanced Industrial Science and Technology (AIST))

[MIS21-P04] Experimental study on the phase equilibrium condition of CO_2 hydrate with marine sediment

*Daisuke Maki[1], Hitoshi Tomaru[1] (1.Graduate School of Science and Engineering, Chiba University)

[MIS21-P05] Raman spectroscopic analysis of structure H gas hydrates encapsulating cyclic hydrocarbons

*Go Fuseya[1], Satoshi Takeya[2], Akihiro Hachikubo[1] (1.Kitami Institute of Technology, 2.National Institute of Advanced Industrial Science and Technology (AIST))

[MIS21-P06] Investigation of self-preservation of argon hydrate by measuring specific surface area

*Yuki Ikeura[1], Daisuke Yahagi[1], Akihiro Hachikubo[1], Satoshi Takeya[2] (1.Kitami institute of technology, 2.National Institute of Advanced Industrial Science and Technology (AIST))

[MIS21-P07] Carbon isotope fractionation of CO_2 during the formation of clathrate hydrate

*Hiromi Kimura[1], Jumpei Matsuda[1], Yuki Kikuchi[1], Akihiro Hachikubo[1], Satoshi Takeya[2] (1.Kitami Institute of Technology, 2.National Institute of Advanced Industrial Science and Technology)

[MIS21-P08] Gas hydrate survey off Tokachi (the Pacific Ocean) in the framework of practical education of Kitami Institute of Technology

*Yunosuke Hase[1], Jumpei Matsuda[1], Yuki Ikeura[1], Akihiro Hachikubo[1], Masaaki Konishi[1], Hirotoshi Sakagami[1], Hirotsugu Minami[1], Satoshi Yamashita[1] (1.Kitami Institute of Technology)

[MIS21-P09] Geochemistry of pore water and gas in shallow sediments from offshore Primorsky Krai, Russia

*Musashi Yokoyama[1], Hitoshi Tomaru[1], Ryo Matsumoto[2], Glen Snyder[2], A.V. Yatsuk[3], D.A Shvalov[3] (1.Department Earth Sciences, Chiba University, 2.Gas Hydrate Research Laboratory, Meiji University, 3.Gas Geochemistry Laboratory, V.I.Ilichev Pacific Oceanological Institute)

[MIS21-P10] Late Quaternary Total Organic Carbon fluctuation in the eastern Japan Sea and offshore of the Russian maritime provinces

*Yuta Hirano[1], Kyousuke Sakamoto[1], Naoto Ishida[2], Takao Ebinuma[2], Koji Seto[3], Ryo Matsumoto[4] (1.Graduate School of Sustainability Science Methane Hydrate Course ,Tottori University, 2.Tottori Univ., 3.Shimane Univ., 4.Meiji Univ.)

[MIS21-P11] Geochemical behavior of carbon in shallow sediment within the gas chimney in Hidaka Trough, offshore Hokkaido

Tsuyoshi Mamata[1], *Hitoshi Tomaru[1], Ryo Matsumoto[2] (1.Department of Earth Sciences, Chiba University, 2.Gas Hydrate Research Laboratory, Meiji University)

[J] Poster | M (Multidisciplinary and Interdisciplinary)：M-IS Intersection

5:15 PM - 6:30 PM JST | 8:15 AM - 9:30 AM UTC | Poster Hall International Exhibition Hall8, Makuhari Messe_45

[M-IS21] Gas hydrate in environmental-resource sciences

convener:Hitoshi Tomaru(Department of Earth Sciences, Chiba University), Akihiro Hachikubo(Kitami Institute of Technology), Atsushi Tani(Graduate School of Human Development and Environment, Kobe University), Shusaku Goto(Institute for Geo-Resources and Environment National Institute of Advanced Industrial Science and Technology)

[MIS21-P01] Raman spectroscopic analysis of isotopologue methane hydrates

*Yuki Kikuchi[1], Jumpei Matsuda[1], Akihiro Hachikubo[1], Satoshi Takeya[2] (1.Kitami Institute of Technology, 2.National Institute of Advanced Industrial Science and Technology (AIST))

[MIS21-P02] Gas origin of hydrate-bound gas in Lake Baikal

*Jumpei Matsuda[1], Yuki Kikuchi[1], Akihiro Hachikubo[1], Oleg Khlystov[2], Gennadiy Kalmychkov[3], Marc De Batist[4], Hirotoshi Sakagami[1], Hirotsugu Minami[1], Satoshi Yamashita[1] (1.Kitami Institute of Technology, 2.Limnological Institute, SB RAS, 3.Vinogradov Institute of Geochemistry, SB RAS, 4.Ghent University)

[MIS21-P03] Validation of self-preservation effect of methane and ethane mixed-gas hydrate by Raman spectroscopy

*Yunosuke Hase[1], Jumpei Matsuda[1], Akihiro Hachikubo[1], Satoshi Takeya[2] (1.Kitami Institute of Technology, 2.National Institute of Advanced Industrial Science and Technology (AIST))

[MIS21-P04] Experimental study on the phase equilibrium condition of CO_2 hydrate with marine sediment

*Daisuke Maki[1], Hitoshi Tomaru[1] (1.Graduate School of Science and Engineering, Chiba University)

[MIS21-P05] Raman spectroscopic analysis of structure H gas hydrates encapsulating cyclic hydrocarbons

*Go Fuseya[1], Satoshi Takeya[2], Akihiro Hachikubo[1] (1.Kitami Institute of Technology, 2.National Institute of Advanced Industrial Science and Technology (AIST))

[MIS21-P06] Investigation of self-preservation of argon hydrate by measuring specific surface area

*Yuki Ikeura[1], Daisuke Yahagi[1], Akihiro Hachikubo[1], Satoshi Takeya[2] (1.Kitami institute of technology, 2.National Institute of Advanced Industrial Science and Technology (AIST))

[MIS21-P07] Carbon isotope fractionation of CO_2 during the formation of clathrate hydrate

*Hiromi Kimura[1], Jumpei Matsuda[1], Yuki Kikuchi[1], Akihiro Hachikubo[1], Satoshi Takeya[2] (1.Kitami Institute of Technology, 2.National Institute of Advanced Industrial Science and Technology)

[MIS21-P08] Gas hydrate survey off Tokachi (the Pacific Ocean) in the framework of practical education of Kitami Institute of Technology

*Yunosuke Hase[1], Jumpei Matsuda[1], Yuki Ikeura[1], Akihiro Hachikubo[1], Masaaki Konishi[1], Hirotoshi Sakagami[1], Hirotsugu Minami[1], Satoshi Yamashita[1] (1.Kitami Institute of Technology)

[MIS21-P09] Geochemistry of pore water and gas in shallow sediments from offshore Primorsky Krai, Russia

*Musashi Yokoyama[1], Hitoshi Tomaru[1], Ryo Matsumoto[2], Glen Snyder[2], A.V. Yatsuk[3], D.A Shvalov[3] (1.Department Earth Sciences, Chiba University, 2.Gas Hydrate Research Laboratory, Meiji University, 3.Gas Geochemistry Laboratory, V.I.Ilichev Pacific Oceanological Institute)

[MIS21-P10] Late Quaternary Total Organic Carbon fluctuation in the eastern Japan Sea and offshore of the Russian maritime provinces

*Yuta Hirano[1], Kyousuke Sakamoto[1], Naoto Ishida[2], Takao Ebinuma[2], Koji Seto[3], Ryo Matsumoto[4] (1.Graduate School of Sustainability Science Methane Hydrate Course ,Tottori University, 2.Tottori Univ., 3.Shimane Univ., 4.Meiji Univ.)

[MIS21-P11] Geochemical behavior of carbon in shallow sediment within the gas chimney in Hidaka Trough, offshore Hokkaido

Tsuyoshi Mamata[1], *Hitoshi Tomaru[1], Ryo Matsumoto[2] (1.Department of Earth Sciences, Chiba University, 2.Gas Hydrate Research Laboratory, Meiji University)

[J] Oral | M (Multidisciplinary and Interdisciplinary)：M-IS Intersection

9:00 AM - 10:30 AM JST | 12:00 AM - 1:30 AM UTC | 202 2F

[M-IS27] Atmospheric electricity: Applications toward natural disaster mitigation

convener:Yasuhide Hobara(Graduate School of Information and Engineering Department of Communication Engineering and Informatics, The University of Electro-Communications), Masashi Kamogawa(Department of Physics, Tokyo Gakugei University), Chairperson:Takeshi Morimoto

9:00 AM - 9:15 AM JST | 12:00 AM - 12:15 AM UTC

[MIS27-01] Advantage and Disadvantage of the Phased Array Weather Radar

*Tomoo Ushio[1], Tomoaki Mega[1], Hiroshi Kikuchi[2], Eiichi Yoshikawa[3] (1.Tokyo Metropolitan University, 2.University of Electro-Communications, 3.JAXA)

9:15 AM - 9:30 AM JST | 12:15 AM - 12:30 AM UTC

[MIS27-02] Initial Observations with X-band Dual Polarimetric Phased Array Weather Radar in Tokyo

*Hiroshi Kikuchi[1], Taku Suezawa[2], Yasuhide Hobara[1], Tomoo Ushio[2] (1.The University of Electro-Communications, 2.Tokyo Metropolitan University)

9:30 AM - 9:45 AM JST | 12:30 AM - 12:45 AM UTC

[MIS27-03] Three-dimensional total lightning characteristics of convective cells observed by the Tokyo LMA in the summer season in Tokyo Metropolitan area

*Namiko Sakurai[1], Paul R. Krehbiel[2], William Rison[2], Ronald J. Thomas[2], Daniel Rodeheffer[2], Shingo Shimizu[1], Koyuru Iwanami[1], Takeshi Maesaka[1], Kaori Kieda[1], Yasushi Uji[1] (1.National Research Institute For Earth Science and Disaster Resilience, 2.New Mexico Tech.)

9:45 AM - 10:00 AM JST | 12:45 AM - 1:00 AM UTC

[MIS27-04] Estimating rainfall in heavy rain events using lightning data in Japan

*Ogawa Tetsuya[1], Yasuhide Hobara[1], Hiroyuki IWASAKI[2], Stan Heckman[3], Michael Stock[3] (1.University of Electro-Communications, 2.Gunma University, 3.EarthNetworks)

10:00 AM - 10:15 AM JST | 1:00 AM - 1:15 AM UTC

[MIS27-05] The Effect of Lightning Phenomena on Lightning Protection for Objects on the Ground

★Invited Papers

*Yokoyama Shigeru[1] (1.Shizuoka University)

10:15 AM - 10:30 AM JST | 1:15 AM - 1:30 AM UTC

[MIS27-06] Lightning charge moment changes deduced from highly sensitive ELF magnetic field observations in Southeast Asia

*Yasuhide Hobara[1], Amir Izzani Mohamed[2], Chandima Gomes[3], Wan Ismail Bin Ibrahim[2], Zulkurnain Abdul-Malek[4], Syahrun Nizam[5], Michael Stock[6], Kazuo Shiokawa[7], Hiroshi Kikuchi[1], Takuo T. Tsuda[1] (1.Graduate School of Information and Engineering Department of Communication Engineering and Informatics, The University of Electro-Communications, 2.University of Malaysia Pahang Pekan, Malaysia, 3.University of the Witwatersrand Johannesburg, South Africa, 4.Universiti Teknologi Malaysia Johor Bahru, Malaysia, 5.University Malaysia Perlis Perlis, Malaysia, 6.EarthNetworks, Inc. Germantown, USA, 7.Nagoya University, Nagoya, Japan)

[J] Oral | M (Multidisciplinary and Interdisciplinary)：M-IS Intersection

10:45 AM - 12:15 PM JST | 1:45 AM - 3:15 AM UTC | 202 2F

[M-IS27] Atmospheric electricity: Applications toward natural disaster mitigation

convener:Yasuhide Hobara(Graduate School of Information and Engineering Department of Communication Engineering and Informatics, The University of Electro-Communications), Masashi Kamogawa(Department of Physics, Tokyo Gakugei University), Chairperson:Yasuhide Hobara

10:45 AM - 11:00 AM JST | 1:45 AM - 2:00 AM UTC

[MIS27-07] Earthquake precursory electromagnetic phenoma : Summary and prospective

★Invited Papers

*Masashi Hayakawa[1] (1.Hayakawa Institute of Seismo Electromagnetics.Co. LTD. University of Electro-Communications venture company)

11:00 AM - 11:15 AM JST | 2:00 AM - 2:15 AM UTC

[MIS27-08] Detection of lower ionospheric anomaly preceding earthquake using nonlinear autoregressive neural network

*Kakeru Matsuki[1], Hayato Iibuchi[1], Hendy Santosa[3], Yasuhide Hobara[1], Michael A Balikhin[2] (1.The University of Electro-Communications , 2.University of Sheffield, 3.University of Bengkulu)

11:15 AM - 11:30 AM JST | 2:15 AM - 2:30 AM UTC

[MIS27-09] Analysis of multipoint measurements of plasma turbulence

*Michael A Balikhin[1], Simon N Walker[1] (1.University of Sheffield)

11:30 AM - 11:45 AM JST | 2:30 AM - 2:45 AM UTC

[MIS27-10] Progress of Observation Project for High-energy Phenomena in Winter Thunderstorms

*Yuuki Wada[1,2], Teruaki Enoto[3], Takahiro Matsumoto[1], Kazuhiro Nakazawa[4], Yoshihiro Furuta[5], Takayuki Yuasa, Harufumi Tsuchiya[5], Daisuke Yonetoku[6], Tatsuya Sawano[6], Kazuo Makishima[1,2], Masashi Kamogawa[7], Yoshitaka Nakamura[8], Takeshi Morimoto[9], Mitsuteru Sato[10], Hideo Sakai[11], Hidehito Nanto[12], Tomoo Ushio[13] (1.The University of Tokyo, 2.RIKEN, 3.Kyoto University, 4.Nagoya University, 5.Japan Atomic Energy Agency, 6.Kanazawa University, 7.Tokyo Gakugei University, 8.Kobe City College of Technology, 9.Kindai University, 10.Hokkaido University, 11.University of Toyama, 12.Kanazawa Institute of Technology, 13.Tokyo Metropolitan University)

11:45 AM - 12:00 PM JST | 2:45 AM - 3:00 AM UTC

[MIS27-11] Electromagnetic and stroke current observations on rocket-triggered lightning

*Takeshi Morimoto[1], Shinya Kurokawa[1], Yoshitaka Nakamura[2], Kazuo Yamamoto[3] (1.Kindai University, 2.Kobe City College of Technology, 3.Chubu University)

[J] Poster | M (Multidisciplinary and Interdisciplinary)：M-IS Intersection

3:30 PM - 5:00 PM JST | 6:30 AM - 8:00 AM UTC | Poster Hall International Exhibition Hall8, Makuhari Messe_27

[M-IS27] Atmospheric electricity: Applications toward natural disaster mitigation

convener:Yasuhide Hobara(Graduate School of Information and Engineering Department of Communication Engineering and Informatics, The University of Electro-Communications), Masashi Kamogawa(Department of Physics, Tokyo Gakugei University)

[MIS27-P01] Design of C-band polarimetric phased array weather radar

★Invited Papers

*Kento Nakamura[1], Hiroshi Kikuchi[2], Tomoaki Mega[1], Tomoo Ushio[1] (1.Tokyo metropolitan university, 2.The University of Electro-Communications)

[MIS27-P02] Examination of Improving the Precision of Ionospheric F-Layer Electron Density Estimation Using Thunder-origin Whistler Wave

*Shu Hirai[1], Shogo Kanazawa[1], Yasuhide Hobara[1], Jean-Louis Pincon[2] (1.The University of Electro-Communications, 2.LPC2E/CNRS)

[MIS27-P03] Rn flux anomaly and local seiemicity around Asahi station,Boso,Japan

*Haruna Kojima[1], Katsumi Hattori[2], Chie Yoshino[2], Michikuni Shimo[3], Toshiharu Konishi[4], Ryuichi Furuya[5] (1.Graduate School of Science and Engineering,Chiba University, 2.Department of Earth Sciences,Graduate School of Scince, 3.Fujita Health University, 4.OHYO KOKEN KOGYO Co.,Ltd, 5.COM SYSTEM Inc.)

[MIS27-P04] Study on electric energy derivation of lightning using optical observation of lightning from TRMM tropical rainfall observation satellite

*Hirata Kodai[1], Yasuhide Hobara[1], Hiroshi Kikuchi[1] (1.The University of Electro-Communications)

[J] Poster | M (Multidisciplinary and Interdisciplinary)：M-IS Intersection

5:15 PM - 6:30 PM JST | 8:15 AM - 9:30 AM UTC | Poster Hall International Exhibition Hall8, Makuhari Messe_46

[M-IS27] Atmospheric electricity: Applications toward natural disaster mitigation

convener:Yasuhide Hobara(Graduate School of Information and Engineering Department of Communication Engineering and Informatics, The University of Electro-Communications), Masashi Kamogawa(Department of Physics, Tokyo Gakugei University)

[MIS27-P01] Design of C-band polarimetric phased array weather radar

★Invited Papers

*Kento Nakamura[1], Hiroshi Kikuchi[2], Tomoaki Mega[1], Tomoo Ushio[1] (1.Tokyo metropolitan university, 2.The University of Electro-Communications)

[MIS27-P02] Examination of Improving the Precision of Ionospheric F-Layer Electron Density Estimation Using Thunder-origin Whistler Wave

*Shu Hirai[1], Shogo Kanazawa[1], Yasuhide Hobara[1], Jean-Louis Pincon[2] (1.The University of Electro-Communications, 2.LPC2E/CNRS)

[MIS27-P03] Rn flux anomaly and local seiemicity around Asahi station,Boso,Japan

*Haruna Kojima[1], Katsumi Hattori[2], Chie Yoshino[2], Michikuni Shimo[3], Toshiharu Konishi[4], Ryuichi Furuya[5] (1.Graduate School of Science and Engineering,Chiba University, 2.Department of Earth Sciences,Graduate School of Scince, 3.Fujita Health University, 4.OHYO KOKEN KOGYO Co.,Ltd, 5.COM SYSTEM Inc.)

[MIS27-P04] Study on electric energy derivation of lightning using optical observation of lightning from TRMM tropical rainfall observation satellite

*Hirata Kodai[1], Yasuhide Hobara[1], Hiroshi Kikuchi[1] (1.The University of Electro-Communications)

[E] Oral | M (Multidisciplinary and Interdisciplinary)：M-GI General Geosciences, Information Geosciences & Simulations

10:45 AM - 12:15 PM JST | 1:45 AM - 3:15 AM UTC | 301B 3F

[M-GI29] Near Surface Investigation and Modeling for Groundwater Resources Assessment and Conservation

convener:Jui-Pin Tsai(National Cheng Kung University, Taiwan), Hwa-Lung Yu(National Taiwan University), Ching-Chung Cheng(National Chiao Tung University Taiwan), Jing-Sen Cai(China University of Geosciences), Chairperson:Jui-Pin Tsai(National Cheng Kung University, Taiwan), Hwa-Lung Yu(National Taiwan University, Taiwan)

10:45 AM - 11:00 AM JST | 1:45 AM - 2:00 AM UTC

[MGI29-01] Groundwater management for global sustainability

★Invited Papers

*Makoto Taniguchi[1] (1.Research Institute for Humanity and Nature)

11:00 AM - 11:15 AM JST | 2:00 AM - 2:15 AM UTC

[MGI29-02] **Building the large-scale specific yields over the Zhuoshui river alluvial fan and Minzhu basin with gravimetric technique**

*Ren-Jhih Yang[1], Shen Yu Hsiao[1], Yan-Jyun Lin[1], Zhen-Yu Wu[1] (1.National Chung Hsing University)

11:15 AM - 11:30 AM JST | 2:15 AM - 2:30 AM UTC

[MGI29-03] **Poro-elastic Deformation of a Heterogenous Geologic Medium due to Groundwater Withdrawal**

*Ajit Joshi[1], Masaatsu Aichi[1] (1.Department of Environment Systems, Graduate School of Frontier Sciences, The University of Tokyo)

11:30 AM - 11:45 AM JST | 2:30 AM - 2:45 AM UTC

[MGI29-04] **Analytical Solution of a Ditch Drainage System for the restoration of waterlogged site considering a Subsurface Source/Sink**

*SHUBHAM TIWARI[1], BRIJESH KUMAR YADAV[1], RATAN SARMAH[2] (1.Indian Institute of Technology Roorkee, 2.Indian Institute of Technology Ropar)

11:45 AM - 12:00 PM JST | 2:45 AM - 3:00 AM UTC

[MGI29-05] **Variable-density flow and mass transport in unsaturated-saturated aquifers under horizontal groundwater flow conditions**

*Jiaqi Liu[1], Tomochika Tokunaga[1] (1.The University of Tokyo)

12:00 PM - 12:15 PM JST | 3:00 AM - 3:15 AM UTC

[MGI29-06] A practical approach to evaluating water inflow for underground water-sealed storage cavern

*Jing-Sen Cai[1] (1.China University of Geosciences)

[E] Poster | M (Multidisciplinary and Interdisciplinary)：M-GI General Geosciences, Information Geosciences & Simulations

3:30 PM - 5:00 PM JST | 6:30 AM - 8:00 AM UTC | Poster Hall International Exhibition Hall8, Makuhari Messe_28

[M-GI29] Near Surface Investigation and Modeling for Groundwater Resources Assessment and Conservation

convener:Jui-Pin Tsai(National Cheng Kung University, Taiwan), Hwa-Lung Yu(National Taiwan University), Ching-Chung Cheng(National Chiao Tung University Taiwan), Jing-Sen Cai(China University of Geosciences)

[MGI29-P01] Modelling of self-potential signals associated with groundwater flows

*ayaka ishikawa[1], Katsumi Hattori[1] (1.chiba university)

[MGI29-P02] Estimating the Hydraulic Conductivity and Heat Capacity of the Aquifer between the River and Well Site Using Joint Inversion Approach

*Jui-Pin Tsai[1], Chin-Tsai Hsiao[4], Liang-Cheng Chang[2], You-Cheng Chen[2], Chun-Hung Chen[3], Yun-Ta Cheng[3], Jen-Hung Yu[3] (1.National Cheng Kung University, Taiwan , 2.National Chiao Tung University, Taiwan , 3.Water Resources Planning Institute, Water Resources Agency, Taiwan, 4.Department of Information Management, Chung Chou University of Science and Technology)

[MGI29-P03] Evaluation on Soil Permeability Using Electrical Resistant Tomography

*CHIHPING KUO[1], BONIAN SHEN[1], CHIHWEI HUANG[1], YUCHIAO LEE[1], SHENXIANG HUANG[1], YENLIN CHEN[1] (1.Department and Institute of Civil Engineering and Environmental Informatics, Minghsin University of Science and Technology)

[MGI29-P04] The Potential Study of Open Loop System Geothermal Heat Pump in Gifu City, Japan

*Randa Permanda[1], Tomoyuki Ohtani[2] (1.Department of Civil and Environmental Engineering, Gifu University, 2.Department of Civil Engineering, Gifu University)

[MGI29-P05] Application of TL-CHERT Smart Characterization Method to Investigate a Groundwater Contaminated Site

*Tzu-Pin Wang[1,2,5], Yao-Tsung Chen[3], Tien-Hsing Tung[3], Chih-Hung Cheng[2], Jie Wang[4] (1.NCU TW, 2.Geophysical Technology and Engineering Co.,Ltd. R.O.C, 3.Apollo Technology Co.,Ltd. R.O.C., 4.Department of Civil Engineering, Chien Hsin University of Science and Technology, Taoyuan City, Taiwan, 5.Disaster Reduction Research Center, Chien Hsin University of Science and Technology, Taoyuan City, Taiwan)

[MGI29-P06] Data Assimilation in Hydraulic Conductivity Identification using Bayesian Statistical Method

*Shih-Yang Cheng[1], Kuo-Chin Hsu[1] (1.National Cheng Kung Univ.)

[MGI29-P07] Groundwater recharge estimation by using empirical orthogonal function method

Hua-Ting Zeng [1], *Hwa-Lung Yu[1] (1. National Taiwan University)

[MGI29-P08] The Application of Drought Early Warning Index for Regional Hydrological Circumstance Analysis

*Chih Chao Ho[1], Ta Wei Chen[2] (1.Construction and Disaster Prevention Research Center, Feng Chia Univ., 2.Taiwan Hsin-Chu Irrigation Association)

[E] Poster | M (Multidisciplinary and Interdisciplinary)：M-GI General Geosciences, Information Geosciences & Simulations

5:15 PM - 6:30 PM JST | 8:15 AM - 9:30 AM UTC | Poster Hall International Exhibition Hall8, Makuhari Messe_47

[M-GI29] Near Surface Investigation and Modeling for Groundwater Resources Assessment and Conservation

convener:Jui-Pin Tsai(National Cheng Kung University, Taiwan), Hwa-Lung Yu(National Taiwan University), Ching-Chung Cheng(National Chiao Tung University Taiwan), Jing-Sen Cai(China University of Geosciences)

[MGI29-P01] Modelling of self-potential signals associated with groundwater flows

*ayaka ishikawa[1], Katsumi Hattori[1] (1.chiba university)

[MGI29-P02] Estimating the Hydraulic Conductivity and Heat Capacity of the Aquifer between the River and Well Site Using Joint Inversion Approach

*Jui-Pin Tsai[1], Chin-Tsai Hsiao[4], Liang-Cheng Chang[2], You-Cheng Chen[2], Chun-Hung Chen[3], Yun-Ta Cheng[3], Jen-Hung Yu[3] (1.National Cheng Kung University, Taiwan , 2.National Chiao Tung University, Taiwan , 3.Water Resources Planning Institute, Water Resources Agency, Taiwan, 4.Department of Information Management, Chung Chou University of Science and Technology)

[MGI29-P03] Evaluation on Soil Permeability Using Electrical Resistant Tomography

*CHIHPING KUO[1], BONIAN SHEN[1], CHIHWEI HUANG[1], YUCHIAO LEE[1], SHENXIANG HUANG[1], YENLIN CHEN[1] (1.Department and Institute of Civil Engineering and Environmental Informatics, Minghsin University of Science and Technology)

[MGI29-P04] The Potential Study of Open Loop System Geothermal Heat Pump in Gifu City, Japan

*Randa Permanda[1], Tomoyuki Ohtani[2] (1.Department of Civil and Environmental Engineering, Gifu University, 2.Department of Civil Engineering, Gifu University)

[MGI29-P05] Application of TL-CHERT Smart Characterization Method to Investigate a Groundwater Contaminated Site

*Tzu-Pin Wang[1,2,5], Yao-Tsung Chen[3], Tien-Hsing Tung[3], Chih-Hung Cheng[2], Jie Wang[4] (1.NCU TW, 2.Geophysical Technology and Engineering Co.,Ltd. R.O.C, 3.Apollo Technology Co.,Ltd. R.O.C., 4.Department of Civil Engineering, Chien Hsin University of Science and Technology, Taoyuan City, Taiwan, 5.Disaster Reduction Research Center, Chien Hsin University of Science and Technology, Taoyuan City, Taiwan)

[MGI29-P06] Data Assimilation in Hydraulic Conductivity Identification using Bayesian Statistical Method

*Shih-Yang Cheng[1], Kuo-Chin Hsu[1] (1.National Cheng Kung Univ.)

[MGI29-P07] Groundwater recharge estimation by using empirical orthogonal function method

Hua-Ting Zeng [1], *Hwa-Lung Yu[1] (1. National Taiwan University)

[MGI29-P08] The Application of Drought Early Warning Index for Regional Hydrological Circumstance Analysis

*Chih Chao Ho[1], Ta Wei Chen[2] (1.Construction and Disaster Prevention Research Center, Feng Chia Univ., 2.Taiwan Hsin-Chu Irrigation Association)

[J] Poster | M (Multidisciplinary and Interdisciplinary)：M-GI General Geosciences, Information Geosciences & Simulations

1:45 PM - 3:15 PM JST | 4:45 AM - 6:15 AM UTC | Poster Hall International Exhibition Hall8, Makuhari Messe_9

[M-GI34] Marine Manganese Minerals

convener:Akira Usui(Marine Core Research Center, Kochi University), Yoshio Takahashi(Department of Earth and Planetary Science, Graduate School of Science, The University of Tokyo), Katsuhiko Suzuki(Research and Development Center for Submarine Resources, Japan Agency for Marine-Earth Science and Technology), Takashi Ito(Faculty of Education, Ibaraki University)

[MGI34-P01] Microstratigraphy of hydrogenetic ferromanganese crusts in the Takuyo-Daisan and -Daigo seamounts

*Akira Usui[1], An-na Nagaoka[2], Michiko Kawamura[1] (1.Marine Core Research Center, Kochi University, 2.Graduate School of Science, Kochi University)

[MGI34-P02] Manganese Crusts with Super Smooth Surface (3S Manganese Crusts) observed at Takuyo No.3 Seamount, Northwest Pacific

*Masaki Saito[1], Takashi Ito[2] (1.Graduate School of Education,Ibaraki University, 2.Department of Education,Ibaraki University)

[MGI34-P03] **Geochemical characteristics of the nuclei of ferromanganese nodules in the Minamitorishima EEZ**

*Daiki Terauchi[1], Kentaro Nakamura[1], Ryo Shimomura[1], Koichi Horinouchi[1], Kazutaka Yasukawa[1,2], Shiki Machida[2,1], Yasuhiro Kato[1,2,3] (1.Department of Systems Innovation, School of Engineering, University of Tokyo, 2.Ocean Resources Research Center for Next Generation, Chiba Institute of Technology, 3.Frontier Research Center for Energy and Resources, School of Engineering, The University of Tokyo)

[MGI34-P04] **Micro X-ray fluorescence mapping for the whole cross-section of ferromanganese nodules in the western North Pacific**

*Shiki Machida[1,2], Ryo Shimomura[2], Koichi Horinouchi[2], Kentaro Nakamura[2], Tetsu Kogiso[3], Yasuhiro Kato[2,1] (1.Ocean Resources Research Center for Next Generation, Chiba Institute of Technology, 2.University of Tokyo, 3.Kyoto University)

[J] Poster | M (Multidisciplinary and Interdisciplinary)：M-GI General Geosciences, Information Geosciences & Simulations

5:15 PM - 6:30 PM JST | 8:15 AM - 9:30 AM UTC | Poster Hall International Exhibition Hall8, Makuhari Messe_48

[M-GI34] Marine Manganese Minerals

convener:Akira Usui(Marine Core Research Center, Kochi University), Yoshio Takahashi(Department of Earth and Planetary Science, Graduate School of Science, The University of Tokyo), Katsuhiko Suzuki(Research and Development Center for Submarine Resources, Japan Agency for Marine-Earth Science and Technology), Takashi Ito(Faculty of Education, Ibaraki University)

[MGI34-P01] Microstratigraphy of hydrogenetic ferromanganese crusts in the Takuyo-Daisan and -Daigo seamounts

*Akira Usui[1], An-na Nagaoka[2], Michiko Kawamura[1] (1.Marine Core Research Center, Kochi University, 2.Graduate School of Science, Kochi University)

[MGI34-P02] Manganese Crusts with Super Smooth Surface (3S Manganese Crusts) observed at Takuyo No.3 Seamount, Northwest Pacific

*Masaki Saito[1], Takashi Ito[2] (1.Graduate School of Education,Ibaraki University, 2.Department of Education,Ibaraki University)

[MGI34-P03] **Geochemical characteristics of the nuclei of ferromanganese nodules in the Minamitorishima EEZ**

*Daiki Terauchi[1], Kentaro Nakamura[1], Ryo Shimomura[1], Koichi Horinouchi[1], Kazutaka Yasukawa[1,2], Shiki Machida[2,1], Yasuhiro Kato[1,2,3] (1.Department of Systems Innovation, School of Engineering, University of Tokyo, 2.Ocean Resources Research Center for Next Generation, Chiba Institute of Technology, 3.Frontier Research Center for Energy and Resources, School of Engineering, The University of Tokyo)

[MGI34-P04] **Micro X-ray fluorescence mapping for the whole cross-section of ferromanganese nodules in the western North Pacific**

*Shiki Machida[1,2], Ryo Shimomura[2], Koichi Horinouchi[2], Kentaro Nakamura[2], Tetsu Kogiso[3], Yasuhiro Kato[2,1] (1.Ocean Resources Research Center for Next Generation, Chiba Institute of Technology, 2.University of Tokyo, 3.Kyoto University)

[J] Oral | M (Multidisciplinary and Interdisciplinary)：M-GI General Geosciences, Information Geosciences & Simulations

3:30 PM - 5:00 PM JST | 6:30 AM - 8:00 AM UTC | A09 TOKYO BAY MAKUHARI HALL

[M-GI34] Marine Manganese Minerals

convener:Akira Usui(Marine Core Research Center, Kochi University), Yoshio Takahashi(Department of Earth and Planetary Science, Graduate School of Science, The University of Tokyo), Katsuhiko Suzuki(Research and Development Center for Submarine Resources, Japan Agency for Marine-Earth Science and Technology), Takashi Ito(Faculty of Education, Ibaraki University), Chairperson:takashi ito(Ibaraki Univ.), Yoshio Takahashi(東京大学), Katsuhiko Suzuki(JAMSTEC)

3:30 PM - 3:45 PM JST | 6:30 AM - 6:45 AM UTC

[MGI34-01] Challenges in microstratigraphy on the hydrogenetic ferromanganese crusts: Depositional processes and environments recorded as secular variations in microstructure, chemical and mineralogical compositions.

*Akira Usui[1], Anna Nagaoka[2], Go-Ichiro Uramoto[1], Masafumi MURAYAMA[3] (1.Marine Core Research Center, Kochi University, 2.Graduate School of Science, Kochi University, 3.Fac. Agriculture and Marine Sciences, Kochi University)

3:45 PM - 4:00 PM JST | 6:45 AM - 7:00 AM UTC

[MGI34-02] Abundant ferromanganese microparticles in oxic pelagic sediments

*Go-Ichiro Uramoto[1,2], Yuki Morono[2], Naotaka Tomioka[2], Shigeyuki Wakaki[2], Ryoichi Nakada[2], Rota Wagai[3], Kentaro Uesugi[4], Akihisa Takeuchi[4], Masato Hoshino[4], Yoshio Suzuki[4,5], Satoshi Mitsunobu[6], Fumito Shiraishi[7], Hiroki Suga[5], Yasuo Takeichi[8], Yoshio Takahashi[5], Fumio Inagaki[2] (1.Kochi University, 2.Japan Agency for Marine-Earth Science and Technology, 3.National Agriculture and Food Research Organization, 4.Japan Synchrotron Radiation Research Institute, 5.University of Tokyo, 6.Ehime University, 7.Hiroshima University, 8.High Energy Accelerator Research Organization)

4:00 PM - 4:15 PM JST | 7:00 AM - 7:15 AM UTC

[MGI34-03] Fractionation of Zirconium-Hafnium in ferromanganese crusts

*Aya Sakaguchi[1], Junpei Inagaki[1], Minami Inoue[2], Akira Usui[3], Hiromitsu Haba[4], Masashi Kaneko[5], Shinya Yamasaki[1], Keisuke Sueki[1], Yoshio Takahashi[6] (1.Faculty of Pure and Applied Science, 2.Graduate School of Science, Hiroshima University, 3.Center for Advanced Marine Core Research , Kochi University, 4.Nishina Center, Riken, 5.Nuclear Science and Engineering Center, Japan Atomic Energy Agency, 6.Graduate School of Science, The University of Tokyo)

4:15 PM - 4:30 PM JST | 7:15 AM - 7:30 AM UTC

[MGI34-04] Isotope fractionation of Mo-like elements during adsorption to ferromanganese oxides

*Masato Tanaka[1], Yoshio Takahashi[1] (1.Graduate School of Science, The University of Tokyo)

4:30 PM - 4:45 PM JST | 7:30 AM - 7:45 AM UTC

[MGI34-05] **Distinct distribution trends of arsenate and molybdate in marine ferromanganese nodules**

*Shitong Yang[1], Soichiro Uesugi[1], Haibo Qin[1], Akira Usui[2], Yoshio Takahashi[1] (1.Department of Earth and Planetary Science, Graduate School of Science, The University of Tokyo, 2.Geology Department, Kochi University)

4:45 PM - 5:00 PM JST | 7:45 AM - 8:00 AM UTC

[MGI34-06] Mineralogical and geochemical characteristics of ferromanganese nodules in the Minamitorishima EEZ

*Kentaro Nakamura[1], Koichi Horinouchi[1], Ryo Shimomura[1], Shiki Machida[2], Kazutaka Yasukawa[1,2], Koichiro Fujinaga[1,2], Yasuhiro Kato[1,2] (1.Department of Systems Innovation, School of Engineering, University of Tokyo, 2.ORCeNG, Chiba Institute of Technology)

[J] Oral | M (Multidisciplinary and Interdisciplinary)：M-GI General Geosciences, Information Geosciences & Simulations

1:45 PM - 3:15 PM JST | 4:45 AM - 6:15 AM UTC | 301B 3F

[M-GI35] Development of computational sciences on planetary formation, evolution and surface environment

convener:Yoshi-Yuki Hayashi(Department of Planetology/CPS, Graduate School of Science, Kobe University), Masaki Ogawa(Division of General Systems Studies, Graduate School of Arts and Sciences, University of Tokyo), Shigeru Ida(Earth-Life Science Institute, Tokyo Institute of Technology), Kanya Kusano(Institute for Space-Earth Environmental Research, Nagoya University), Chairperson:Hiroki Kashimura

1:45 PM - 2:00 PM JST | 4:45 AM - 5:00 AM UTC

[MGI35-01] Simulation Studies of Solar Activities as a Cause of Solar-Terrestrial Environment Variation

*Kanya Kusano[1], Hideyuki Hotta[2] (1.Institute for Space-Earth Environmental Research, Nagoya University, 2.Faculty of Science and Engineering, Chiba University)

2:00 PM - 2:15 PM JST | 5:00 AM - 5:15 AM UTC

[MGI35-02] Development of a global non-hydrostatic Martian atmospheric model and its high-resolution simulation

*Hiroki Kashimura[1], Hisashi Yashiro[2], Seiya Nishizawa[2], Hirofumi Tomita[2], Kensuke Nakajima[3], Masaki Ishiwatari[4], Yoshiyuki O. Takahashi[1], Yoshi-Yuki Hayashi[1] (1.Kobe University/Center for Planetary Science, 2.RIKEN Center for Computational Science, 3.Kyushu University, 4.Hokkaido University)

2:15 PM - 2:30 PM JST | 5:15 AM - 5:30 AM UTC

[MGI35-03] Numerical simulations on the collision, adhesion, and growth of dust particles in turbulent gas in a protoplanetary disk

*Takashi Ishihara[1], Kohei Hamabata[2], Yoshiki Sakurai[2], Masayuki Umemura[3] (1.Graduate School of Environmental and Life Science, Okayama University, 2.Graduate School of Engineering, Nagoya University, 3.Center for Computational Sciences, University of Tsukuba)

2:30 PM - 2:45 PM JST | 5:30 AM - 5:45 AM UTC

[MGI35-04] Development of N-body Simulation Code for Planetary System Formation With Particle-Particle Particle-Tree Scheme

*Yota Ishigaki[1,4], Junko Kominami[2], Junichiro Makino[3], Masaki Fujimoto[4] (1.University of Tokyo, 2.Tokyo Institute of Technology, 3.RIKEN AICS, 4.Institite of Space and Astronautical Science, Japan Aerospace Exploration Agency)

2:45 PM - 3:00 PM JST | 5:45 AM - 6:00 AM UTC

[MGI35-05] Current status of post-K Exploratory Challenge, computational planetary science

*Junichiro Makino[1,2] (1.Kobe Univ, 2. RIKEN R-CCS)

[J] Poster | M (Multidisciplinary and Interdisciplinary)：M-GI General Geosciences, Information Geosciences & Simulations

3:30 PM - 5:00 PM JST | 6:30 AM - 8:00 AM UTC | Poster Hall International Exhibition Hall8, Makuhari Messe_29

[M-GI35] Development of computational sciences on planetary formation, evolution and surface environment

convener:Yoshi-Yuki Hayashi(Department of Planetology/CPS, Graduate School of Science, Kobe University), Masaki Ogawa(Division of General Systems Studies, Graduate School of Arts and Sciences, University of Tokyo), Shigeru Ida(Earth-Life Science Institute, Tokyo Institute of Technology), Kanya Kusano(Institute for Space-Earth Environmental Research, Nagoya University)

[MGI35-P01] Global N-body Simulation from Inner Region to Outer Region

*Junko Kominami[1], Shigeru Ida[1], Junichiro Makino[2], Yota Ishigaki[5], Hiroshi Daisaka[3], Masaki Fujimoto[4] (1.Tokyo Institute of Technology, 2.Kobe University, 3.Hitotsubashi University, 4.JAXA, 5.Tokyo University)

[MGI35-P02] Attempts at numerical modeling of 3-D mantle convection with magmatism and plate tectonics

*Masanori Kameyama[1,2], Masaki Ogawa[3,2], Takehiro Miyagoshi[2], Takatoshi Yanagisawa[2] (1.Geodynamics Research Center, Ehime University, 2.Japan Agency for Marine-Earth Science and Technology, 3.University of Tokyo at Komaba)

[MGI35-P03] Surface zonal flows induced by anelastic thermal convection in a rapidly rotating spherical shell

*Youhei SASAKI[1], Shin-ichi Takehiro[2], Keiichi ISHIOKA[3], Takeshi Enomoto[4] (1.Department of Mathematics, Kyoto University, 2.Research Institute for Mathematical Sciences, Kyoto University, 3.Department of Earth and Planetary Sciences, Kyoto University, 4.Disaster Prevention Research Institute, Kyoto University)

[MGI35-P04] Protostellar flares driven by accretion in protoplanetary disks

*Shinsuke Takasao[1], Kengo Tomida[2], Shinsuke Takasao[2], Takeru Suzuki[3] (1.Nagoya University, 2.Osaka University, 3.University of Tokyo)

[MGI35-P05] Cross-reference simulations by scalable communication library for the study of wave-particle interactions in planetary magnetospheres

*Yuto Katoh[1], Keiichiro Fukazawa[2], Takeshi Nanri[3], Yohei Miyake[4] (1.Department of Geophysics, Graduate School of Science, Tohoku University, 2.Academic Center for Computing and Media Studies, Kyoto University, 3.Research Institute for Information Technology, Kyushu University, 4.Graduate School of System Informatics, Kobe University)

[MGI35-P06] Radiative transfer calculation for various planetary atmospheres: Application to a general circulation model

*Yoshi-Yuki Hayashi[1], George HASHIMOTO[2], Kiyoshi Kuramoto[3], Masaki Ishiwatari[3], Yoshiyuki O. Takahashi[1] (1.Department of Planetology/CPS, Graduate School of Science, Kobe University, 2.Department of Earth Sciences, Okayama University, 3.Department of Cosmosciences, Graduate School of Sciences, Hokkaido University)

[MGI35-P07] Effect of the compressibility of turbulent flows on dust particle collision statistics in a protoplanetary disk

*Yoshiki Sakurai[1], Hitomi Furuya[2], Naoki Kobayashi[1], Takashi Ishihara[3], Naoya Okamoto[4], Kenji Shiraishi[5], Masayuki Umemura[6] (1.Graduate School of Engineering, Nagoya University, 2.Doctoral and Master's Programs in Physics, Graduate School of Pure and Applied Sciences, University of Tsukuba, 3.Graduate School of Environmental and Life Science, Okayama University, 4.Center for Computational Science, Graduate School of Engineering, Nagoya University, 5.Institute of Materials and Systems for Sustainability, Nagoya University, 6.Center for Computational Science, University of Tsukuba)

[MGI35-P08] Algorithms to use accelerators effectively with FDPS and performance of applications

*Daisuke Namekata[1], Masaki Iwasawa[1], Keigo Nitadori[1], Kentaro Nomura[1], Long Wang[3,1], Miyuki Tsubouchi[1], Junichiro Makino[2,1,4] (1.RIKEN Center for Computational Science, 2.Department of Planetology, Graduate School of Science, Kobe University, 3.Helmholtz Institut fur Strahlen und Kernphysik, 4.Earth-Life Science Institute, Tokyo Institute of Technology)

[J] Poster | M (Multidisciplinary and Interdisciplinary)：M-GI General Geosciences, Information Geosciences & Simulations

5:15 PM - 6:30 PM JST | 8:15 AM - 9:30 AM UTC | Poster Hall International Exhibition Hall8, Makuhari Messe_49

[M-GI35] Development of computational sciences on planetary formation, evolution and surface environment

convener:Yoshi-Yuki Hayashi(Department of Planetology/CPS, Graduate School of Science, Kobe University), Masaki Ogawa(Division of General Systems Studies, Graduate School of Arts and Sciences, University of Tokyo), Shigeru Ida(Earth-Life Science Institute, Tokyo Institute of Technology), Kanya Kusano(Institute for Space-Earth Environmental Research, Nagoya University)

[MGI35-P01] Global N-body Simulation from Inner Region to Outer Region

*Junko Kominami[1], Shigeru Ida[1], Junichiro Makino[2], Yota Ishigaki[5], Hiroshi Daisaka[3], Masaki Fujimoto[4] (1.Tokyo Institute of Technology, 2.Kobe University, 3.Hitotsubashi University, 4.JAXA, 5.Tokyo University)

[MGI35-P02] Attempts at numerical modeling of 3-D mantle convection with magmatism and plate tectonics

*Masanori Kameyama[1,2], Masaki Ogawa[3,2], Takehiro Miyagoshi[2], Takatoshi Yanagisawa[2] (1.Geodynamics Research Center, Ehime University, 2.Japan Agency for Marine-Earth Science and Technology, 3.University of Tokyo at Komaba)

[MGI35-P03] Surface zonal flows induced by anelastic thermal convection in a rapidly rotating spherical shell

*Youhei SASAKI[1], Shin-ichi Takehiro[2], Keiichi ISHIOKA[3], Takeshi Enomoto[4] (1.Department of Mathematics, Kyoto University, 2.Research Institute for Mathematical Sciences, Kyoto University, 3.Department of Earth and Planetary Sciences, Kyoto University, 4.Disaster Prevention Research Institute, Kyoto University)

[MGI35-P04] Protostellar flares driven by accretion in protoplanetary disks

*Shinsuke Takasao[1], Kengo Tomida[2], Shinsuke Takasao[2], Takeru Suzuki[3] (1.Nagoya University, 2.Osaka University, 3.University of Tokyo)

[MGI35-P05] Cross-reference simulations by scalable communication library for the study of wave-particle interactions in planetary magnetospheres

*Yuto Katoh[1], Keiichiro Fukazawa[2], Takeshi Nanri[3], Yohei Miyake[4] (1.Department of Geophysics, Graduate School of Science, Tohoku University, 2.Academic Center for Computing and Media Studies, Kyoto University, 3.Research Institute for Information Technology, Kyushu University, 4.Graduate School of System Informatics, Kobe University)

[MGI35-P06] Radiative transfer calculation for various planetary atmospheres: Application to a general circulation model

*Yoshi-Yuki Hayashi[1], George HASHIMOTO[2], Kiyoshi Kuramoto[3], Masaki Ishiwatari[3], Yoshiyuki O. Takahashi[1] (1.Department of Planetology/CPS, Graduate School of Science, Kobe University, 2.Department of Earth Sciences, Okayama University, 3.Department of Cosmosciences, Graduate School of Sciences, Hokkaido University)

[MGI35-P07] Effect of the compressibility of turbulent flows on dust particle collision statistics in a protoplanetary disk

*Yoshiki Sakurai[1], Hitomi Furuya[2], Naoki Kobayashi[1], Takashi Ishihara[3], Naoya Okamoto[4], Kenji Shiraishi[5], Masayuki Umemura[6] (1.Graduate School of Engineering, Nagoya University, 2.Doctoral and Master's Programs in Physics, Graduate School of Pure and Applied Sciences, University of Tsukuba, 3.Graduate School of Environmental and Life Science, Okayama University, 4.Center for Computational Science, Graduate School of Engineering, Nagoya University, 5.Institute of Materials and Systems for Sustainability, Nagoya University, 6.Center for Computational Science, University of Tsukuba)

[MGI35-P08] Algorithms to use accelerators effectively with FDPS and performance of applications

*Daisuke Namekata[1], Masaki Iwasawa[1], Keigo Nitadori[1], Kentaro Nomura[1], Long Wang[3,1], Miyuki Tsubouchi[1], Junichiro Makino[2,1,4] (1.RIKEN Center for Computational Science, 2.Department of Planetology, Graduate School of Science, Kobe University, 3.Helmholtz Institut fur Strahlen und Kernphysik, 4.Earth-Life Science Institute, Tokyo Institute of Technology)

[E] Poster | M (Multidisciplinary and Interdisciplinary)：M-ZZ Others

1:45 PM - 3:15 PM JST | 4:45 AM - 6:15 AM UTC | Poster Hall International Exhibition Hall8, Makuhari Messe_10

[M-ZZ50] Governance for Trans-boundary Volcanic Disaster

convener:Mayumi Sakamoto(Graduate School of Disaster Resilience and Governance, University of Hyogo), Haruhisa Nakamichi(Sakurajima Volcano Research Center, Disaster Prevention Research Institute, Kyoto University), MASARU ARAKIDA(Asian Disaster Reduction Center)

[MZZ50-P01] Governance for Trans-boundary Volcanic Disaster -a case of 2010 Eyjafjallajökull Eruption-

*Mayumi Sakamoto[1] (1.Graduate School of Disaster Resilience and Governance, University of Hyogo)

[MZZ50-P02] Regional Cooperation against Cross-border Disasters

*MASARU ARAKIDA[1] (1.Asian Disaster Reduction Center)

[MZZ50-P03] Issues of Japan's volcanic disaster prevention system as viewed from overseas alert systems

*Erika Ishimizu[1], Mayumi Sakamoto[1] (1.Graduate School of Disaster Resilience and Governance University of Hyogo)

[E] Poster | M (Multidisciplinary and Interdisciplinary)：M-ZZ Others

5:15 PM - 6:30 PM JST | 8:15 AM - 9:30 AM UTC | Poster Hall International Exhibition Hall8, Makuhari Messe_50

[M-ZZ50] Governance for Trans-boundary Volcanic Disaster

convener:Mayumi Sakamoto(Graduate School of Disaster Resilience and Governance, University of Hyogo), Haruhisa Nakamichi(Sakurajima Volcano Research Center, Disaster Prevention Research Institute, Kyoto University), MASARU ARAKIDA(Asian Disaster Reduction Center)

[MZZ50-P01] Governance for Trans-boundary Volcanic Disaster -a case of 2010 Eyjafjallajökull Eruption-

*Mayumi Sakamoto[1] (1.Graduate School of Disaster Resilience and Governance, University of Hyogo)

[MZZ50-P02] Regional Cooperation against Cross-border Disasters

*MASARU ARAKIDA[1] (1.Asian Disaster Reduction Center)

[MZZ50-P03] Issues of Japan's volcanic disaster prevention system as viewed from overseas alert systems

*Erika Ishimizu[1], Mayumi Sakamoto[1] (1.Graduate School of Disaster Resilience and Governance University of Hyogo)

[E] Oral | M (Multidisciplinary and Interdisciplinary)：M-ZZ Others

3:30 PM - 5:00 PM JST | 6:30 AM - 8:00 AM UTC | 304 3F

[M-ZZ50] Governance for Trans-boundary Volcanic Disaster

convener:Mayumi Sakamoto(Graduate School of Disaster Resilience and Governance, University of Hyogo), Haruhisa Nakamichi(Sakurajima Volcano Research Center, Disaster Prevention Research Institute, Kyoto University), MASARU ARAKIDA(Asian Disaster Reduction Center), Chairperson:Mayumi Sakamoto(兵庫県立大学大学院減災復興政策研究科), Haruhisa Nakamichi(京都大学防災研究所), Masaru Arakida(アジア防災センター)

3:35 PM - 3:50 PM JST | 6:35 AM - 6:50 AM UTC

[MZZ50-01] The development of the European collaborative mechanism of volcanic monitoring systems after 2010 Eyjafjallajokull eruption - from the perspective of European Union law -

*Chizu Arashima[1] (1.KOBE GAKUIN UNIVERSITY)

3:50 PM - 4:05 PM JST | 6:50 AM - 7:05 AM UTC

[MZZ50-02] Preparing for volcanic disasters: Risk communication issues when dealing with international tourists.

★Invited Papers

*Ana Maria Cruz Naranjo[1], Giuseppe Aliperti[1] (1.Kyoto University Disaster Prevention Research Institute)

4:05 PM - 4:20 PM JST | 7:05 AM - 7:20 AM UTC

[MZZ50-03] Mitigation of volcanic hazard in Sakurajima, Japan, through the coordinating committee and through communication with the public

*Haruhisa Nakamichi[1] (1.Sakurajima Volcano Research Center, Disaster Prevention Research Institute, Kyoto University)

4:20 PM - 4:35 PM JST | 7:20 AM - 7:35 AM UTC

[MZZ50-04] An experimental forecasting technique for the ash hazard from Sakurajima volcano, Japan

*Alexandros Panagiotis Poulidis[1], Tetsuya Takemi[1], Masato Iguchi[1] (1.Disaster Prevention Research Institute, Kyoto University)

4:35 PM - 4:50 PM JST | 7:35 AM - 7:50 AM UTC

[MZZ50-05] Utilization of Space Technology for Early Warning and Efficiently Response Against Transboundary Disaster

★Invited Papers

*Koji Suzuki[1] (1.Asian Disaster Reduction Center, Research Center for Urban Safety and Security Kobe University)

4:50 PM - 5:00 PM JST | 7:50 AM - 8:00 AM UTC

[MZZ50-06] Discussion -Research Framework for Trans-boudary Disaster

*Mayumi Sakamoto[1] (1.Graduate School of Disaster Resilience and Governance, University of Hyogo)

[J] Oral | U (Union)：Union

Tue. May 28, 2019 9:00 AM - 10:30 AM JST | Tue. May 28, 2019 12:00 AM - 1:30 AM UTC | 101 1F

[U-03] Future of Scientific Publishing in Geosciences

convener:Hodaka Kawahata(Atmosphere Ocean Research Institute, the University of Tokyo), Hirokuni Oda(Institute of Geology and Geoinformation, Geological Survey of Japan, AIST), Chairperson:Hirokuni Oda, Hodaka Kawahata

JpGU has launched a new open journal "Progress in Earth and Planetary Science" (PEPS) in 2014 and Impact Factor has been given in 2018. Support from JSPS and MEXT for the promotion of open access journals are fundamental for the development of PEPS. In addition to PEPS, academic societies supporting JPGU also promote academic publishing. This session will discuss future of scientific publishing in Geosciences, specially focused on open access e-journal, data publishing and relationships with author ID etc. Keynote speakers will be invited.

9:00 AM - 9:30 AM JST | 12:00 AM - 12:30 AM UTC

[U03-01] Game-change of scholarly communication based on papers and the role of learned society and peer-review

★Invited Papers

*Kazuhiro Hayashi[1] (1.National Institute of Science and Technology Policy)

9:30 AM - 10:00 AM JST | 12:30 AM - 1:00 AM UTC

[U03-02] The future of the journal metrics and new trend of the scholarly publishing

★Invited Papers

*Yoshiko Tanahashi[1] (1.Clarivate Analytics)

10:00 AM - 10:30 AM JST | 1:00 AM - 1:30 AM UTC

[U03-03] Underlying Issues and Problems in Publishing International Scientific Journals in Japan. “DNA Research” As A Case Study.

★Invited Papers

*Michio Oishi[1] (1.Kazusa DNA Research Institute)

Game-change of scholarly communication based on papers and the role of learned society and peer-review

*Kazuhiro Hayashi[1]

1. National Institute of Science and Technology Policy

Author reviews current topics of game-changing in scholarly communication base on papers and discuss the significance of learned society and peer review. Both couldn't stay as they are, but still have potential to keep scholarly communication healthier, resulting in transformation of scholarly society to the new research paradigm.

Keywords: Open Science, Open Access, Research Platform, Peer review

©2019. Japan Geoscience Union. All Right Reserved.

The future of the journal metrics and new trend of the scholarly publishing

*Yoshiko Tanahashi[1]

1. Clarivate Analytics

The future of the journal metrics and new trend of the scholarly publishing will be discussed.Clarivate Analytics has consistent selection criteria from the 1970s to the present as carefully selecting journals to be included in Web of Science. By looking at the selection criteria, I would like to consider a viewpoint for becoming a globally distinctive journal, managing journals from a global perspective, and seeing the journals originating from Japan to face the global research community with strategy. Furthermore, we summarize statistical data of Web of Science into journals related to JpGU, and present the benchmark which is the basis of grasping the current situation of the journal. I summarize the current status of OA journals, Japan's journal, China's journals on Web of Science as statistics and look at recent trends in the field related to JpGU, and a useful point for strategy formulation to raise the presence of the journal.

©2019. Japan Geoscience Union. All Right Reserved.

Underlying Issues and Problems in Publishing International Scientific Journals in Japan. “DNA Research” As A Case Study.

*Michio Oishi[1]

1. Kazusa DNA Research Institute

In this presentation, I would like to discuss certain issues and problems in regards to publishing scientific journals in Japan. My talk is a reflection of my experience as the Editor-in-Chief of the journal “DNA Research” which was launched at the inauguration of the Kazusa DNA Research Institute in 1994.

Firstly, I would like to introduce the current status of DNA Research, an open access journal, regarding the editorial policy and processes, the scope, the publisher, the geographical distribution of the submitted and published papers, the acceptance rate, the impact factor (IF) and some other aspects.

Secondly, I would like to discuss some of the issues and problems in publishing scientific journals in Japan. One important issue is how to ensure objectivity in reviewing manuscripts; a problem often stemming from the unique cultural, social and academic environment of Japan. Another important issue is how to maintain a consistent editorial policy over the long term, ideally by the same Editor-in-Chief, Executive Editor and majority of associated editors. This may be difficult for some journals of academic societies in which editors selected from their members undergo turnover of their duties every few years. Furthermore, since any of these editorial jobs is quite demanding, few scientists active in research are willing to accept or assume these positions. Regarding the financing of scientific journals, we, DNA Research, decided not to seek financial support from outside; the reason will be presented.

Thirdly, I would like to list our efforts to improve the IF of our journal which now stands at between 5 and 6. Most researchers agree that it may not be correct to evaluate scientific journals by IF alone, but it is also true that there is no other reliable way to evaluate scientific journals objectively and quantitatively. In fact, the IF is now also being utilized for the evaluation of researchers themselves for the purposes of their promotion, job accession and others by taking into consideration the IF of the journals where their papers have appeared. These developments have prompted us to take steps to strive for a higher IF for our journal.

Fourthly, I would like to mention the challenge of dealing with online-publication (e-publication) and open access of scientific journals. Online-publication has virtually eliminated costs for the printing and delivery of journals, thus paving a way to publishing papers at lower cost which benefits scientific journals like ours without outside financial support. The open access movement, which was originally conceived as the result of the demand from the general public and research funders in US and EU countries, has become a mainstream trend in the publication of scientific journals. In an open access world, revenues come from the article processing charge (APC) rather than subscription charges, providing a new incentive for higher IF journals, since the level of APC often reflects the IF of the journal. Because of these trends, the number of journals which employ online only publication and/or open access is rapidly increasing, thus creating more competitions among scientific journals which are vying for higher-grade (IF) rankings.
Finally, I would like to discuss the need and possibility of creating a journal such as Nature or Science in Japan which focuses specifically on emerging research in the natural sciences in Asia.

©2019. Japan Geoscience Union. All Right Reserved.

©2019. Japan Geoscience Union. All Right Reserved.

[J] Oral | U (Union)：Union

Tue. May 28, 2019 10:45 AM - 12:15 PM JST | Tue. May 28, 2019 1:45 AM - 3:15 AM UTC | 101 1F

[U-03] Future of Scientific Publishing in Geosciences

convener:Hodaka Kawahata(Atmosphere Ocean Research Institute, the University of Tokyo), Hirokuni Oda(Institute of Geology and Geoinformation, Geological Survey of Japan, AIST), Chairperson:Hirokuni Oda, Hodaka Kawahata

JpGU has launched a new open journal "Progress in Earth and Planetary Science" (PEPS) in 2014 and Impact Factor has been given in 2018. Support from JSPS and MEXT for the promotion of open access journals are fundamental for the development of PEPS. In addition to PEPS, academic societies supporting JPGU also promote academic publishing. This session will discuss future of scientific publishing in Geosciences, specially focused on open access e-journal, data publishing and relationships with author ID etc. Keynote speakers will be invited.

10:45 AM - 11:05 AM JST | 1:45 AM - 2:05 AM UTC

[U03-04] Review of editorial work for PEPS in 2018-2019 and new strategy for 2019–2020

★Invited Papers

*Yasufumi Iryu[1] (1.Institute of Geology and Paleontology Graduate School of Science Tohoku University)

11:05 AM - 11:25 AM JST | 2:05 AM - 2:25 AM UTC

[U03-05] "Earth, Planets and Space" An Open Access Journal: Past, Present and and Future

★Invited Papers

*Yasuo Ogawa[1], Kiyoshi Baba[2] (1.Volcanic Fluid Research Center, School of Science, Tokyo Institute of Technology, 2.Earthquake Research Institute, University of Tokyo)

11:25 AM - 11:55 AM JST | 2:25 AM - 2:55 AM UTC

[U03-06] Scientific Research Output and Publication: research article, data, and digital transformation

★Invited Papers

*Yasuhiro Murayama[1] (1.Strategic Program Produce Office, National Institute of Information and Communications Technology)

11:55 AM - 12:15 PM JST | 2:55 AM - 3:15 AM UTC

[U03-07] **Enhancing dissemination of research activities to international communities by Japanese Geoscience Union**

★Invited Papers

*Hodaka Kawahata[1] (1.Atmosphere Ocean Research Institute, the University of Tokyo)

Review of editorial work for PEPS in 2018-2019 and new strategy for 2019–2020

*Yasufumi Iryu[1]

1. Institute of Geology and Paleontology Graduate School of Science Tohoku University

Progress in Earth and Planetary Science (PEPS) is a peer-reviewed, open-access electric journal published by the Japan Geoscience Union in partnership with Springer. PEPS received its first manuscript at the end of 2013 and we published our first papers in April 2014. By the end of the year 2018 we had published 244 scientific articles. In the first half of the year 2018 PEPS received good news. PEPS received its first Impact Factor of 2.481, which was announced in the June 2018 edition of Clarivate Analytics Journal Citation Reports. PEPS currently ranks 66/189 in the category ‘Geosciences, Multidisciplinary’. Whilst this does not yet make us a Q1 journal we are close.

In addition to being funded by the JpGU, PEPS received a grant-in-aid for scientific research from the Japan Society for the Promotion of Science. As the period covered by this five year grant-in-aid drew to an end we applied for funds for the next five fiscal years (2018-2012). Unfortunately our application has been rejected. Due to this, we were forced to raise article processing charges (APC). Since its inception we have always planned for PEPS to become entirely supported by APCs and therefore completely self financing and we have done some analysis and planning towards this goal. Our analysis shows that the most important thing is that we all focus on maintaining and increasing PEPS’ status as one of the leading journals in our field because this is the surest way of increasing our APC income.

New strategy for 2019-2020 is in preparation and will be introduced in the JpGU meeting 2019.

Keywords: Earth and planetary science, Progress in Earth and Planetary Science, Open access e-journal, Japan Geoscience Union

©2019. Japan Geoscience Union. All Right Reserved.

"Earth, Planets and Space" An Open Access Journal: Past, Present and and Future

*Yasuo Ogawa[1], Kiyoshi Baba[2]

1. Volcanic Fluid Research Center, School of Science, Tokyo Institute of Technology, 2. Earthquake Research Institute, University of Tokyo

EPS (Earth, Planets and Space) is a peer-reviewed open access journal published on behalf of the following five societies; The Society of Geomagnetism and Earth, Planetary and Space Sciences, The Seismological Society of Japan, The Volcanological Society of Japan, The Geodetic Society of Japan, The Japanese Society for Planetary Sciences. These five societies are all society members of the Japan Geoscience Union.

EPS was established in 1998 as a continuation of the two journals, the Journal of Geomagnetism and Geoelectricity (1949 to 1997) and the Journal of Physics of the Earth (1952 to 1997). In 2014 we started open access publication under the SpringerOpen platform. Open Access publication successfully shortened the publication time, increased visibility of the journal and widened its international readership. We publish average of 190 papers per year and half of the authors are from overseas. One of the qualification indices of the journal, impact factor (IF), is continuously increasing from 1.328 (2014) to 2.773 (2017) and it will also go over 2.6 in 2018. The increasing IF is supported both by increase of highly cited papers and by decrease of uncited papers, suggesting the success of quality control by the editorial board and possibly increasing of the visibility via open access.

The scope of EPS covers Earth and Planetary Sciences, particularly geomagnetism, aeronomy, space science, seismology, volcanology, geodesy, and planetary science. The EPS share common scopes as well as a common journal platform with PEPS (Progress in Earth and Planetary Science). In contrast to PEPS, which emphasizes review papers, EPS is characterized by the following article types: (1) “Express Letter” which aims at fast publications, (2) “Technical reports “, which describe technical developments for scientific researches and (3) “Frontier Letters” for leading edge researches only with the invitation from the editor in chief. EPS promotes topical article collections (what we call special issues) on the first results of geoscientific events (earthquakes and volcanic eruptions) and scientific missions (satellite missions). EPS has been recently successful in attractive special issues.

Aiming at fast and qualified review system, we have expanded editorial board members internationally since 2017. Now we have currently 50 regular editors (including 22 oversea editors). The oversea editors are 10 from Europe, 3 from North America, 5 from Asia, and 3 from Oceania.

As part of the promotion of the journal we have four annual awards to recognize authors and reviewers: (1) EPS Excellent paper awards, (2) EPS Young researcher award, (3) Highlighted Paper Awards and (4) Excellent Paper Awards.

From 2018, EPS has strengthened ties with JpGU. EPS has started collaborative advertisement activities at major domestic and international academic meetings, like JpGU, AGU, EGU and AOGS. EPS has updated the APC (Article Processing Charge) in September 2018 for sustainable operations of the journal.

©2019. Japan Geoscience Union. All Right Reserved.

Keywords: open access journal, Earth and Planetary sciences

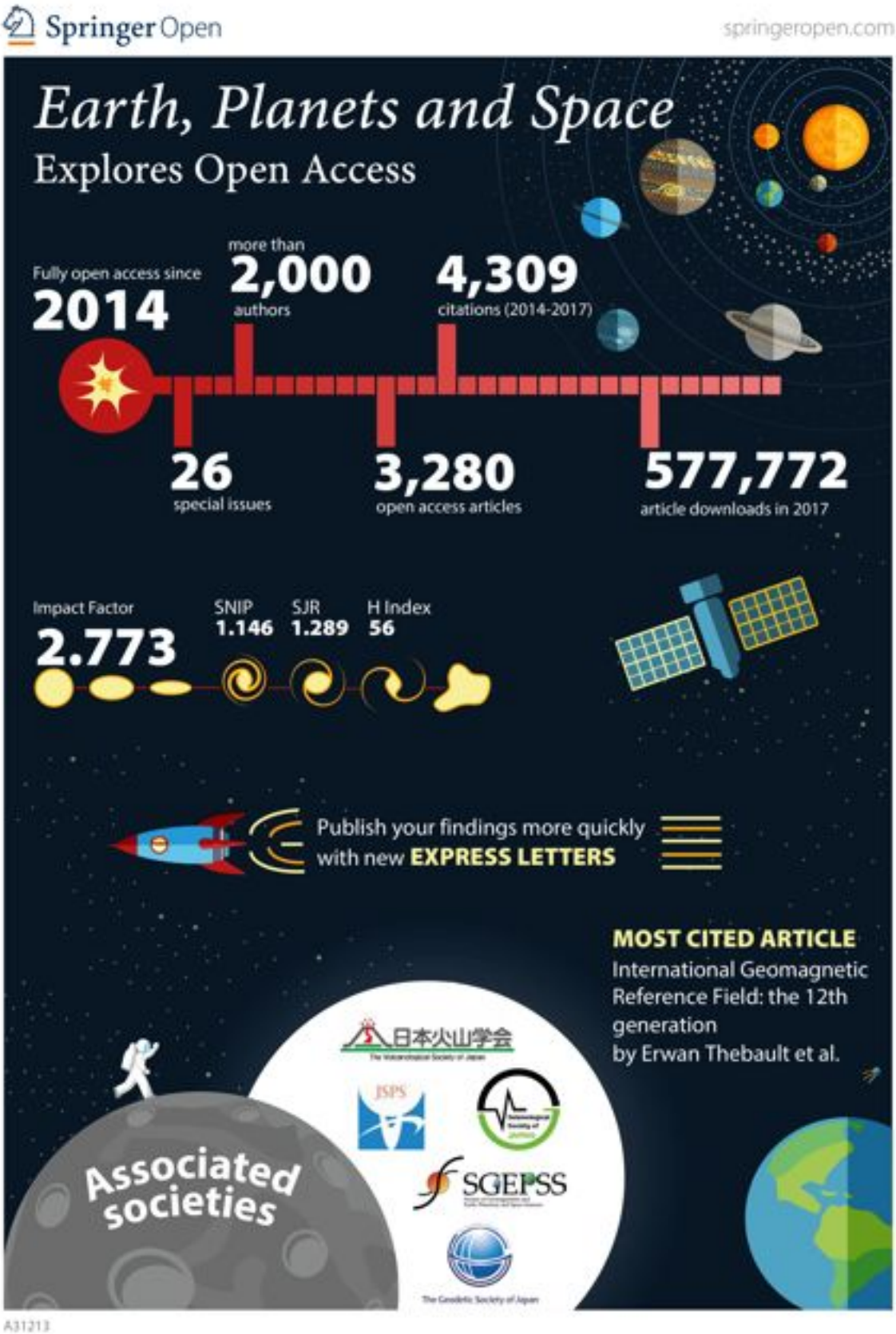

©2019. Japan Geoscience Union. All Right Reserved.

Scientific Research Output and Publication: research article, data, and digital transformation

*Yasuhiro Murayama[1]

1. Strategic Program Produce Office, National Institute of Information and Communications Technology

Scientific Research Output and Publication will be argued in terms of original research paper, research data, and digital transformation of the society, which is expected to contribute to the better conduct of science and better contribution to the society and tax payers for a longer term with sustaianble ecocycle of scientific results, scientific data, scientists and scientific research invenstiment. This paper attempts to discuss the points.

Keywords: open access, research data, digital transformation

©2019. Japan Geoscience Union. All Right Reserved.

Enhancing dissemination of research activities to international communities by Japanese Geoscience Union

*Hodaka Kawahata[1]

1. Atmosphere Ocean Research Institute, the University of Tokyo

Progress in Earth and Planetary Science (PEPS) is our official scientific journal established in April 2014 with 51 society members by partnership with Springer. 5 years have passed. This is an English-language peer-reviewed open access e-journal under a collaboration with Springer-Nature. The journal is to be devoted to original articles and reviews (>20%) in the research fields of space and planetary sciences; atmospheric and hydrospheric sciences; human geosciences; solid earth sciences; and bio-geosciences.

In June, 2018, PEPS got the first Impact factor of around 2.48. Now we are taking effective steps (measures) and then hope to get higher IF, around 3, in 2019, hopefully.

JpGU will make an effort to promote the journals which have been published by Japanese Geoscience Societies, taking part in JpGU, including EPS.

Keywords: open access, e-journal , Progress in Earth and Planetary Science

©2019. Japan Geoscience Union. All Right Reserved.

[E] Oral | P (Space and Planetary Sciences)：P-PS Planetary Sciences

Tue. May 28, 2019 9:00 AM - 10:30 AM JST | Tue. May 28, 2019 12:00 AM - 1:30 AM UTC | A03 TOKYO BAY MAKUHARI HALL

[P-PS01] Outer Solar System Exploration Today, and Tomorrow

convener:Jun Kimura(Osaka University), Yasumasa Kasaba(Planetary Plasma and Atmospheric Research Center, Tohoku University), Kunio M. Sayanagi(Hampton University), Chairperson:Kunio Sayanagi(Hampton University), Takeshi Kuroda

The giant planets provide many keys to understanding planetary processes. They play an important role in shaping our solar system, and the physical and chemical processes they harbor also provide a unique opportunity to study the phenomena relevant for studying Earth and other planets, including exoplanetary systems. In this session, we discuss a wide range of topics encompassing the giant planets and their moons, including their origins, interiors, atmospheres, compositions, surface features, and electromagnetic fields. To advocate for current and future outer planets exploration (Cassini, Juno, New Horizons, JUICE, and beyond), we also call for discussions on future missions to explore giant planet systems, including how to develop better international cooperation. Discussion in this latter category will include progress in developing a solar sail mission concept for observing the Jupiter system and its trojan asteroids.

9:00 AM - 9:15 AM JST | 12:00 AM - 12:15 AM UTC

[PPS01-06] Radiative transfer simulation including a non-LTE model for terahertz observations of Ganymede's atmosphere

*Takayoshi Yamada[1], Ladislav Rezac[2], Richard Larsson[2], Paul Hartogh[2], Naohiro Yoshida[3], Yasuko Kasai[1,3] (1.National Institute of Information and Communications Technology, 2.Max Planck Institute for Solar System Research, 3.Tokyo Institute of Technology)

9:15 AM - 9:30 AM JST | 12:15 AM - 12:30 AM UTC

[PPS01-07] Vertical Mass Flux by the 2010-2011 Great Storm of Saturn

*Kunio M. Sayanagi[1], Jacob L. Gunnarson[1], John J. Blalock[1], Richard K. Achterberg[2], F. Michael Flasar[2], Andrew P. Ingersoll.[3], Shawn P. Ewald[3], Ulyana A. Dyudina[3] (1.Hampton University, 2.NASA Goddard Space Flight Center, 3.California Institute of Technology)

9:30 AM - 9:48 AM JST | 12:30 AM - 12:48 AM UTC

[PPS01-08] Microwave observations of the giant planets - Cassini/Radar and Juno/MWR

★Invited Papers

*Cheng Li[1], Virgil Adumitroaie[2], John Arballo[2], Sushil K Atreya[3], Scott J Bolton[4], Andrew Ingersoll[1], Michael Janssen[2], Steven Levin[2], Jonathan Lunine[5], Glenn Orton[2], Paul Steffes[6], Hunter Waite[4] (1.California Institute of Technology, 2.Jet Propulsion Laboratory, 3.University of Michigan Ann Arbor, 4.Southwest Research Institute, 5.Cornell University, 6.Georgia Institute of Technology)

9:48 AM - 10:06 AM JST | 12:48 AM - 1:06 AM UTC

[PPS01-09] Tracing Formation and Evolution of Outer Solar System Bodies through Stable Isotopes and Noble Gas Abundances

★Invited Papers

*Kathleen Mandt[1] (1.Johns Hopkins University Applied Physics Laboratory)

10:06 AM - 10:24 AM JST | 1:06 AM - 1:24 AM UTC

[PPS01-10] Icy Giant Planet Exploration

★Invited Papers

*Sushil K Atreya[1], Mark D. Hofstadter[2], Amy Simon[3], Kim R. Reh[2], Olivier Mousis[4], Krista Soderlund[5] (1.University of Michigan Ann Arbor, 2.Jet Propulsion Laboratory, 3.Goddard Space Flight Center, 4.Laboratoire d'Astrophysique de Marseille, 5.University of Texas at Austin)

10:24 AM - 10:30 AM JST | 1:24 AM - 1:30 AM UTC

Discussion

Radiative transfer simulation including a non-LTE model for terahertz observations of Ganymede's atmosphere

*Takayoshi Yamada[1], Ladislav Rezac[2], Richard Larsson[2], Paul Hartogh[2], Naohiro Yoshida[3], Yasuko Kasai[1,3]

1. National Institute of Information and Communications Technology, 2. Max Planck Institute for Solar System Research, 3. Tokyo Institute of Technology

We are developing a teraherz radiative transfer code, named Atmospheric Teraherz Radiation Simulator (ATRASU), for simulations of sub-millimeter observations of planetary atmospheres.
Because of the tenuous Ganymede atmosphere we need to include non-local thermodynamic equilibrium (non-LTE) conditions of H_2O rotational levels to simulate observations by the Submillimeter Wave Instrument (SWI) on the JUpiter ICy moon Explorer (JUICE). The frequency windows of the JUICE/SWI are 530 to 625 GHz and 1080 to 1275 GHz with 100 kHz spectral resolution.
We developed a deterministic non-LTE solution based on the multilevel Gauss–Seidel method. The simulated energy level populations of H_2O for SWI observations start to deviate from LTE at 100 to 200 km altitude around sub-solar latitudes of 10 degrees. At sub-solar latitudes around 60 degrees the populations are in non-LTE over the entire range, starting from the surface. The difference of the simulated spectra between LTE and non-LTE conditions, and their sensitivity to various parameters, such as collisional rates for H_2O, will be presented.

Keywords: THz, Radiative trasfer

©2019. Japan Geoscience Union. All Right Reserved.

Vertical Mass Flux by the 2010-2011 Great Storm of Saturn

*Kunio M. Sayanagi[1], Jacob L. Gunnarson[1], John J. Blalock[1], Richard K. Achterberg[2], F. Michael Flasar[2], Andrew P. Ingersoll.[3], Shawn P. Ewald[3], Ulyana A. Dyudina[3]

1. Hampton University, 2. NASA Goddard Space Flight Center, 3. California Institute of Technology

We present a re-analysis of Cassini Composite Infrared Spectrometer (CIRS) data captured during the 2010-2011 Great Storm of Saturn to calculate the vertical mass flux caused by the storm. The intense cumulus outburst started on December 5, 2010 at 33ºN planetocentric latitude, and the clouds that emanated from the storm engulfed the entire latitude band over the subsequent months. The CIRS observation captured the storm's impact on the tropospheric thermal structure (Achterberg et al. 2014). The change in the thermal structure detected by Achterberg et al. (2014) is caused by the vertical uplifting of mass by the cumulus convection in the storm. We re-analyze the CIRS data processed by Achterberg et al. (2014) to determine the vertical mass flux. Images captured by the Imaging Science Subsystem (ISS) camera showed that active convective phase of the storm lasted until August 2011 (Sayanagi et al. 2013). Our preliminary analysis of CIRS data shows that, by August 2011, between 15ºN and 45ºN latitudes, the storm lifted about 1.65×10^{19} kg of mass to levels above the 700-mbar pressure altitude from levels below.

Analyzing images captured by ISS using the CB2 (750 nm) filter and Cassini Visible and Infrared Mapping Spectrometer (VIMS)'s 5-micron channel reveals that, after August 2011, cumulus activities ceased in the storm's latitudes, and a vast cloudless area grew until it encircled the entire band between 30ºN and 40ºN latitude by January 2012. The cloudless region further grew to the south and reached 20ºN by December 2012. Interestingly, analysis of the CIRS data indicates that the vertical mass flux continued as the clouds cleared after the storm. Our preliminary analysis shows that, between August 2011 and August 2012, 1.9×10^{18} kg more mass was lifted to altitudes above the ~700-mbar level. We hypothesize that the vertical mass flux during the cloud clearing was caused when the tropospheric air parcels became buoyant when they were relieved from the mass loading of the storm clouds.

We note that measuring vertical mass flux caused by a cumulus storm is extremely difficult for storms on Earth because the mass uplifted by the storms is rapidly dispersed and diluted by the storm's environment. In comparison, Saturn's Great Storm of 2010-2011 completely filled the latitude zone between 20˚N and 40˚N; thus, the storm was essentially contained in a closed box, and allowed us to measure the storm's vertical mass flux.

References:

Achterberg, R. K., Gierasch, P. J., Conrath, B. J., Fletcher, L. N., Hesman, B. E., Bjoraker, G. L., Flasar, F. M., 2014. Changes to Saturn's Zonal-mean Tropospheric Thermal Structure after the 2010-2011 Northern Hemisphere Storm. Astrophysical Journal 786, 92.

Sayanagi, K. M., Dyudina, U. A., Ewald, S. P., Fischer, G., Ingersoll, A. P., Kurth, W. S., Muro, G. D., Porco, C. C., West, R. A., 2013. Dynamics of Saturn's great storm of 2010-2011 from Cassini ISS and RPWS. Icarus 223, 460-478.

©2019. Japan Geoscience Union. All Right Reserved.

Keywords: Saturn, Planetary Atmospheres, Cassini Mission

©2019. Japan Geoscience Union. All Right Reserved.

Microwave observations of the giant planets - Cassini/Radar and Juno/MWR

*Cheng Li[1], Virgil Adumitroaie[2], John Arballo[2], Sushil K Atreya[3], Scott J Bolton[4], Andrew Ingersoll[1], Michael Janssen[2], Steven Levin[2], Jonathan Lunine[5], Glenn Orton[2], Paul Steffes[6], Hunter Waite[4]

1. California Institute of Technology, 2. Jet Propulsion Laboratory, 3. University of Michigan Ann Arbor, 4. Southwest Research Institute, 5. Cornell University, 6. Georgia Institute of Technology

The thermal emission of a giant planet's atmosphere in the microwave region reveals the thermal structure and composition of the atmosphere below the clouds. During the last decade, the Cassini/Radar instrument mapped Saturn's global thermal radiation at 2.2 cm wavelength. Particularly, in the year 2010, the planet-encircling giant storm on Saturn appeared 16 K brighter than average, revealing desiccation of ammonia gas due to convection and atmospheric dynamics. More recently at Jupiter, the Juno spacecraft has completed a dozen orbits around the planet, making detailed observations of Jupiter's troposphere from north to south and down to pressures of about 200 bars. The results are both astonishing and stimulating. Jupiter's equatorial zone appears cold in all six channels of Juno/MWR, which range from 1.2 –50 cm, whereas the other latitudes are significantly warmer than what was predicted by an adiabatic model. The internal structure of the GRS has also been mapped during orbit 7th close approach. Yet, the interpretation is partly confounded by the inhomogeneous distribution of ammonia gas. We will give an overview of the previous findings, current challenges, and future opportunities of microwave sounding of the giant planets.

Keywords: Jupiter, Saturn, Cassini, Juno, microwave, composition

©2019. Japan Geoscience Union. All Right Reserved.

Tracing Formation and Evolution of Outer Solar System Bodies through Stable Isotopes and Noble Gas Abundances

*Kathleen Mandt[1]

1. Johns Hopkins University Applied Physics Laboratory

Comparative planetology using isotope geochemistry has played a critical role in understanding processes at work in and the history of outer Solar System bodies [see 1, and references therein]. The $^{12}C/^{13}C$ measured in methane on Titan has enabled us to determine the maximum length of time that methane has been present in the atmosphere [2,3], showing that methane has not been present in Titan's atmosphere throughout the history of the solar system and is limited to no more than 1 billion years (Gyr) [3]. We have also determined how much methane has been converted to organics over that were then deposited on the surface [3] and find agreement with estimates of surface inventories [4]. Observations of $^{14}N/^{15}N$ in HCN and N_2 in the atmosphere of Titan provides direct evidence of how photochemistry influences stable isotopes [5,6]. We have used these observations to determine that Titan's nitrogen originated as NH_3 in the protosolar nebula [7]. All of this work relies on spacecraft-based observations made at Titan. Ground-based observations combined with spacecraft observations are also of high value. The lower limit observed for $^{14}N/^{15}N$ in HCN in Pluto's atmosphere by ALMA [8] combined with New Horizons observations of the atmospheric composition [9] provides a valuable tool for determining the origin of nitrogen for Pluto if the influences of condensation and aerosol trapping on isotopes can be constrained [10] for which work is ongoing. All of this work is relevant to a future Ice Giants mission to Neptune, where the same methods could be applied to Triton and combined with ALMA observations. Furthermore, a mission to Io that makes in situ observations of the isotopic composition of the atmosphere could provide important information about volatile loss and interior processes at Io, assuming production and loss processes can be well constrained. Finally, noble gas abundances have been an important tool for understanding the origin and evolution of volatiles in the terrestrial planet atmospheres [see review in 1]. The recent measurement of cometary noble gas abundances [11] provides important information on the composition of the icy bodies that contributed to the formation of the gas giants, providing constraints for future in situ measurements that should be made with an atmospheric probe [12].

[1] Mandt K. E. et al. (2015a) *SSRv, 197,* 297–342. [2] Mandt K. E. et al., (2009) *PSS, 57,* 1917–1930. [3] Mandt K. E. et al., (2012) *ApJ, 749,* 160. [4] Lorenz, R. D. et al. (2008). *GRL*, *35*(2), L02206. [5] Liang et al. (2007) *ApJL, 664*, L115-L118. [6] Mandt et al. (2012b) *JGR, 117*, E10006. [7] Mandt K. E. et al., (2014) *ApJL, 788,* L24. [8] Lellouch et al. (2017) *Icarus, 286*, 289-307. [9] Young et al. (2017). [10] Mandt et al. (2017) *MNRAS*, *472*, 118-128. [11] Rubin et al. (2017) *Sci Adv*, *4*(7), eaar6297. [12] Mandt et al., in preparation.

Keywords: Titan, Pluto, Triton, Ice Giants, Stable Isotopes, Noble Gases

©2019. Japan Geoscience Union. All Right Reserved.

Icy Giant Planet Exploration

*Sushil K Atreya[1], Mark D. Hofstadter[2], Amy Simon[3], Kim R. Reh[2], Olivier Mousis[4], Krista Soderlund[5]

1. University of Michigan Ann Arbor, 2. Jet Propulsion Laboratory, 3. Goddard Space Flight Center, 4. Laboratoire d'Astrophysique de Marseille, 5. University of Texas at Austin

Giant planets hold the secrets of solar system formation, and there is much interest in their exploration. They also serve as analogs for the giant planets in extrasolar systems. While Saturn-Jupiter sized exoplanets number about 500, mini-Neptune and Neptune sized objects (2-5 times Earth) comprise nearly half of approximately 4000 confirmed exoplanets to date. Since the early 1970’s, spacecraft have explored the gas giants, Jupiter and Saturn, extensively using flybys, orbiters and an entry probe (at Jupiter). Voyager 2 is the only spacecraft ever to visit the two icy giants, with a flyby of Uranus in 1986 and Neptune in 1989. Though the Voyager instruments were optimized for observations of Jupiter and Saturn, tantalizing data were collected at Uranus and Neptune as well. Those data have raised such fundamental questions as: did Uranus and Neptune form in the same manner as the gas giants, did they form at their present orbital locations or not, what role did migration play in their formation and evolution, why (and how) does Neptune generate internal heat, whereas Uranus does not, what is responsible for their intrinsic magnetic fields in the absence of a metallic hydrogen phase, why are the rings of Uranus different from Neptune’s rings and what’s maintaining them, why does Neptune’s moon Triton possess an atmosphere of nitrogen and methane, etc. To address these questions and others requires a comprehensive exploration of the icy giant planet systems by an orbiter-probe spacecraft at Uranus or Neptune or both [1], like the Galileo orbiter-probe mission at Jupiter. International partnership is most desirable for maximizing the science return of such a mission. [1] M. Hofstadter, A. Simon, K. Reh, J. Elliott, and the NASA Ice Giants Science Definition Team, Ice Giants Pre-Decadal Survey Report (2017) NASA-JPL-ID-100520, https://www.lpi.usra.edu/icegiants/mission_study/Full-Report.pdf

Keywords: Giant Planets, Origin and Evolution, Uranus and Neptune Missions, Extrasolar Planets, International Partnerships

©2019. Japan Geoscience Union. All Right Reserved.

[E] Oral | P (Space and Planetary Sciences)：P-PS Planetary Sciences

Tue. May 28, 2019 10:45 AM - 12:15 PM JST | Tue. May 28, 2019 1:45 AM - 3:15 AM UTC | A03 TOKYO BAY MAKUHARI HALL

[P-PS01] Outer Solar System Exploration Today, and Tomorrow

convener:Jun Kimura(Osaka University), Yasumasa Kasaba(Planetary Plasma and Atmospheric Research Center, Tohoku University), Kunio M. Sayanagi(Hampton University), Chairperson:Jun Kimura(Osaka University), 鎌田 俊一(北海道大学創成研究機構)

The giant planets provide many keys to understanding planetary processes. They play an important role in shaping our solar system, and the physical and chemical processes they harbor also provide a unique opportunity to study the phenomena relevant for studying Earth and other planets, including exoplanetary systems. In this session, we discuss a wide range of topics encompassing the giant planets and their moons, including their origins, interiors, atmospheres, compositions, surface features, and electromagnetic fields. To advocate for current and future outer planets exploration (Cassini, Juno, New Horizons, JUICE, and beyond), we also call for discussions on future missions to explore giant planet systems, including how to develop better international cooperation. Discussion in this latter category will include progress in developing a solar sail mission concept for observing the Jupiter system and its trojan asteroids.

10:45 AM - 11:03 AM JST | 1:45 AM - 2:03 AM UTC

[PPS01-11] Saturn's ring rain and Enceladus' subsurface ocean as seen by the Cassini Cosmic Dust Analyser

★Invited Papers

*Sean Hsu[1], Sascha Kempf[1], Mihaly Horanyi[1], Ralf Srama[2], James O'Donoghue[3] (1.LASP, University of Colorado, Boulder, CO, USA, 2.IRS, University of Stuttgart, Stuttgart, Germany, 3.NASA Goddard Space Flight Center, Greenbelt, Maryland, USA)

11:03 AM - 11:18 AM JST | 2:03 AM - 2:18 AM UTC

[PPS01-12] **Titan Trek: A New Online NASA Visualization and Analysis Portal for Saturn's Largest Moon**

*Emily Law[1], Brian Hamilton Day[2] (1.NASA Jet Propulsion Laboratory, 2.NASA Ames Research Center)

11:18 AM - 11:36 AM JST | 2:18 AM - 2:36 AM UTC

[PPS01-13] Internal structure of icy moons: ice-ocean systems as commonly seen in the outer solar system

★Invited Papers

*Hauke Hussmann[1] (1.DLR Institute of Planetary Research)

11:36 AM - 11:51 AM JST | 2:36 AM - 2:51 AM UTC

[PPS01-14] Callisto as a keystone to reproduce the formation process of the Jovian system

*Yasuhito Sekine[1], Shunichi Kamata[2], Yuhiko Aoyama[3], Masahiro Ikoma[3], Takayuki Tanigawa[4] (1.Earth-Life Science Insitute, Tokyo Institute of Technology, 2.Creative Res. Institution, Hokkaido Univerisity, 3.Dept of Earth and Planetary Sci., University of Tokyo, 4.Nat'l Inst. Tech., Ichinoseki Col.)

11:51 AM - 12:09 PM JST | 2:51 AM - 3:09 AM UTC

[PPS01-15] Origin of Jupiter Trojan asteroids: To be explored by OKEANOS

★Invited Papers

*Yoko Kebukawa[1], Tatsuaki Okada[2], Motoo Ito[3], Jun Aoki[4], Yosuke Kawai[4], Jun Matsumoto[2], Noel Grand[5], Arnaud Buch[6], Michisato Toyoda[4], Hervé Cottin[5], Hisayoshi Yurimoto[7,2], Hajime Yano[2], Takahiro Iwata[2], Osamu Mori[2] (1.Yokohama National University, 2.Japan Aerospace Exploration Agency, 3.Kochi Institute for Core Sample Research JAMSTEC, 4.Osaka University, 5.LISA, Université Paris-Est Créteil, 6.Ecole Centrale Paris, 7.Hokkaido University)

12:09 PM - 12:15 PM JST | 3:09 AM - 3:15 AM UTC

Discussion

Saturn's ring rain and Enceladus' subsurface ocean as seen by the Cassini Cosmic Dust Analyser

*Sean Hsu[1], Sascha Kempf[1], Mihaly Horanyi[1], Ralf Srama[2], James O'Donoghue[3]

1. LASP, University of Colorado, Boulder, CO, USA, 2. IRS, University of Stuttgart, Stuttgart, Germany, 3. NASA Goddard Space Flight Center, Greenbelt, Maryland, USA

Dust particles serve as microscopic messengers carrying information from sources inaccessible by space probes. The compositional and dynamical information of various dust populations provided by the Cosmic Dust Analyser offer a unique perspective to examine the rings, moons, and their interactions in the Saturnian system. In this talk I will focus on the latest results from the Cassini Grand Finale mission about Saturn's ring rain, i.e., the ring-planet interactions driven by the infall of ring material to Saturn's atmosphere, and its implications about Saturn and its magnificent ring system. I will also provide a brief summary of other major findings by the Cassini Cosmic Dust Analyser, including the discovery of the subsurface ocean and hydrothermal activities within the geologically active moon Enceladus, the composition of interstellar grains, Saturn's diffuse rings, and the electromagnetic interactions of charged nanodust particles with the magnetosphere and the solar wind.

Keywords: Saturn, Dust, Planetary Rings

©2019. Japan Geoscience Union. All Right Reserved.

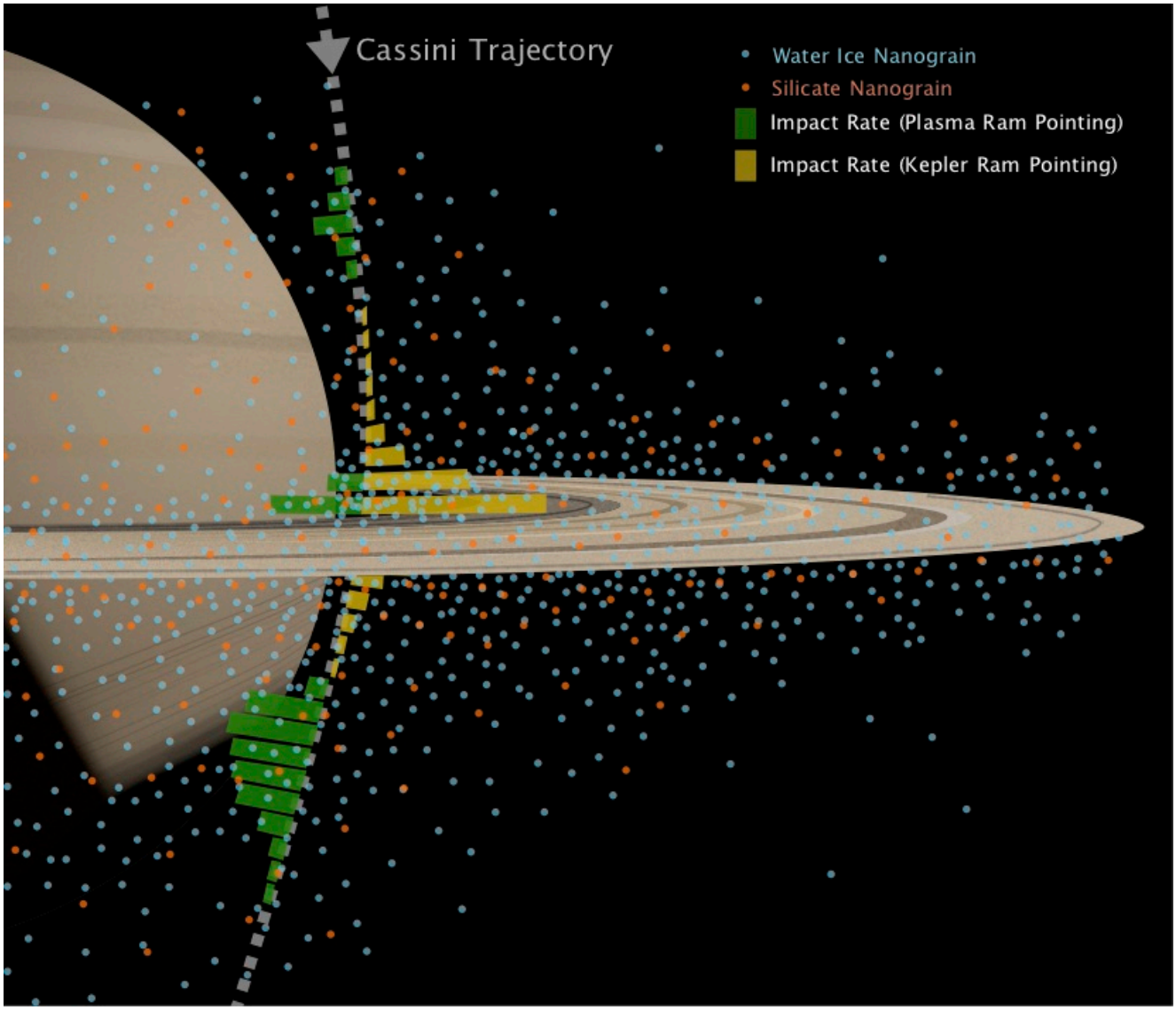

©2019. Japan Geoscience Union. All Right Reserved.

Titan Trek: A New Online NASA Visualization and Analysis Portal for Saturn's Largest Moon

*Emily Law[1], Brian Hamilton Day[2]

1. NASA Jet Propulsion Laboratory, 2. NASA Ames Research Center

In its investigations of Saturn's moons, NASA's Cassini mission and ESA's Huygens lander have returned an immense amount of data detailing the dynamic surface of Saturn's largest moon, Titan. In order to greatly facilitate dissemination, visualization, and analysis of this data, the Cassini mission has partnered with NASA's Solar System Treks Project (SSTP). SSTP has recently released a new online portal (https://trek.nasa.gov/titan/), Titan Trek, that enables mission planners, planetary scientists, engineers, students, and the general public to interactively access, visualize, and analyze Cassini's mapped data products of Saturn's largest moon.

The initial release of Titan Trek provides a suite of interactive tools and incorporates over 130,000 data products from the range of Cassini encounters with Titan, creating a comprehensive Titan research and educational web portal. Titan Trek data products include: Global Radar mosaic, Radar SAR BIDR BIFQI swaths, Global VIMS mosaics, Global ISS mosaic, Vector data (geological units of Afekan region, material flux based on dune orientation, fluvial networks), Nomenclature, ISS footprints, VIMS footprints, and Global radar topography.

We intend to continue to enhance the new Titan Trek portal with new data products as they are released by the Cassini mission including Huygens DISR, Global radiometry, scatterometry, VIMS, ISS, UVIS, CIRS, and other topography products.

Titan Trek is the latest addition to the NASA Solar System Treks Project (SSTP), available at https://trek.nasa.gov. NASA's Solar System Trek online portals provide web-based suites of interactive data visualization and analysis tools providing access to mapped data products from past and current missions for the Moon, Mars, Vesta, etc. As web-based toolsets, the portals do not require users to purchase or install any software beyond current web browsers. These portals are being used for site selection and analysis by NASA and a number of its international partners, supporting upcoming missions.

Keywords: Titan, Cassini, Visualization, Analysis

©2019. Japan Geoscience Union. All Right Reserved.

Internal structure of icy moons: ice-ocean systems as commonly seen in the outer solar system

*Hauke Hussmann[1]

1. DLR Institute of Planetary Research

Among the icy satellites in the outer solar system, several objects have been identified that may contain substantial amounts of liquid water in their interiors. In particular the large satellites, e.g., Europa, Ganymede, Callisto, and Titan may contain subsurface oceans until the present day. However, the example of Enceladus shows that also smaller satellites can have sufficient internal heat sources to maintain liquid water layers. Also Pluto and Triton are potential ocean candidates. The available heat sources differ considerably among the icy moons depending on their initial composition, and thus the amount of radiogenic heating, the tidal interaction with the primary planet, their rheological states and -in some cases- their interaction with other satellites due to orbital resonances. In this talk the current knowledge on the ice-ocean systems in the outer solar system will be summarized. Prospects for their investigation with future planetary missions will be discussed.

Keywords: solar system, icy satellites, oceans

©2019. Japan Geoscience Union. All Right Reserved.

Callisto as a keystone to reproduce the formation process of the Jovian system

*Yasuhito Sekine[1], Shunichi Kamata[2], Yuhiko Aoyama[3], Masahiro Ikoma[3], Takayuki Tanigawa[4]

1. Earth-Life Science Insitute, Tokyo Institute of Technology, 2. Creative Res. Institution, Hokkaido Univerisity, 3. Dept of Earth and Planetary Sci., University of Tokyo, 4. Nat'l Inst. Tech., Ichinoseki Col.

Callisto is the outermost Galilean satellite, with 2410 km of radius and 1.83 g/cc of density. The size and mass are comparable to those of another Jovian moon, Ganymede and the largest moon of Saturn, Titan. Unlike Ganymede and Titan, however, heavily-cratered Callisto may have experienced only limited geological activities since its formation. Owing to the low geological activities, Callisto may serve as a “fossil” of the Jovian system formation in the early Solar System. Volatile and isotope compositions of ice materials on Callisto would reflect ice compositions of the building materials of the Jovian satellites, which is critical to constrain the disk temperature of the formation region of proto-Jupiter as well as both shock heating and size of infalling materials onto proto-Jupiter. The interior structure, namely degree of differentiation, of Callisto is essential to constrain the inflow rate of the building materials from the protoplanetary disk. In this talk, we discuss the key observations, e.g., surface materials and interior structure of Callisto, in future missions to constrain the formation process of the Jovian system.

Keywords: icy satellite, Solar System exploration, planetary formation

©2019. Japan Geoscience Union. All Right Reserved.

Origin of Jupiter Trojan asteroids: To be explored by OKEANOS

*Yoko Kebukawa[1], Tatsuaki Okada[2], Motoo Ito[3], Jun Aoki[4], Yosuke Kawai[4], Jun Matsumoto[2], Noel Grand[5], Arnaud Buch[6], Michisato Toyoda[4], Hervé Cottin[5], Hisayoshi Yurimoto[7,2], Hajime Yano[2], Takahiro Iwata[2], Osamu Mori[2]

1. Yokohama National University, 2. Japan Aerospace Exploration Agency, 3. Kochi Institute for Core Sample Research JAMSTEC, 4. Osaka University, 5. LISA, Université Paris-Est Créteil, 6. Ecole Centrale Paris, 7. Hokkaido University

The Jupiter Trojan asteroids are expected to be a key to understand planet formation and solar system evolution. The Jupiter Trojan asteroids are an asteroid group at the Lagrangian point (L4 and L5) on the Jupiter's orbit, and their spectral types are mainly D and P type, also called "Red" and "Less red", respectively [1,2]. The origin of these asteroids was considered to be trapped by Jupiter according to the classical planet formation theory [3,4]. On the other hand, according to a relatively new theoretical study such as Nice model, the small bodies formed at the Kuiper belt region are disturbed by giant planet migrations, and some of them trapped at the current Jupiter orbit [5]. Thus, constraining planetary formation theories can be possible by investigating whether the Jupiter Trojan asteroids originated from the outer region of the solar system such as the Kuiper belt area or originated from the current Jupiter orbit region (the extension of the main belt asteroids). The stable isotopic ratios of light elements are expected to be an indicator of the origin of the Jupiter Trojan asteroids. Because heavy isotopes such as ^{2}H (D) and ^{15}N tend to incorporate into water and organic matter in low temperatures (<10-100 K) such as in the outer region of the solar system [6,7]. In fact, heavy isotopes are concentrated in materials from the outer region of the solar system such as comets, and materials from main belt asteroids such as chondrites often show relatively light isotopic ratios [8].

The OKEANOS (Outsized Kite-craft for Exploration and AstroNautics in the Outer Solar system) is a candidate for the upcoming strategic middle-class space exploration to rendezvous with and land on a Jupiter Trojan asteroid using a Solar Power Sail (SPS). The mission concept includes sampling and in-situ analysis of the materials of a Jupiter Trojan asteroid [9]. We plan to analyze isotopic and molecular compositions of volatile materials from organic matter, hydrated minerals, and ice, in order to understand origin and evolution of the Jupiter Trojan asteroids, using a multi-turn time-of-flight type high-resolution mass spectrometry (HRMS) system. Our goal is to improve our understanding of (1) planet formation/migration theories, (2) distribution and evolution of volatile substances in protoplanetary disks, (3) origins and evolution of organic matter, and (4) origin and evolution of the Solar System small bodies beyond the snow line.

References: [1] J. P. Emery et al., *Astronomical Journal*, 141, 25, 2011. [2] F. E. DeMeo and B. Carry, *Nature*, 505, 629, 2014. [3] F. Marzari and H. Scholl, *Astronomy & Astrophysics*, 339, 278, 1998. [4] F. Marzari and H. Scholl, *Icarus*, 131, 41, 1998. [5] A. Morbidelli et al., *Nature*, 435, 462, 2005. [6] T. Millar et al., *The Astrophysical Journal*, 340, 906, 1989. [7] R. Terzieva and E. Herbst, *Monthly Notices of the Royal Astronomical Society*, 317, 563, 2000. [8] B. Marty, *Earth. Planet. Sci. Lett.,* 313-314, 56, 2012. [9] T. Okada et al., *Planetary and Space Science*, 161, 99, 2018.

©2019. Japan Geoscience Union. All Right Reserved.

[E] Poster | P (Space and Planetary Sciences)：P-PS Planetary Sciences

Tue. May 28, 2019 3:30 PM - 5:00 PM JST | Tue. May 28, 2019 6:30 AM - 8:00 AM UTC | Poster Hall International Exhibition Hall8, Makuhari Messe_1

[P-PS01] Outer Solar System Exploration Today, and Tomorrow

convener:Jun Kimura(Osaka University), Yasumasa Kasaba(Planetary Plasma and Atmospheric Research Center, Tohoku University), Kunio M. Sayanagi(Hampton University)

The giant planets provide many keys to understanding planetary processes. They play an important role in shaping our solar system, and the physical and chemical processes they harbor also provide a unique opportunity to study the phenomena relevant for studying Earth and other planets, including exoplanetary systems. In this session, we discuss a wide range of topics encompassing the giant planets and their moons, including their origins, interiors, atmospheres, compositions, surface features, and electromagnetic fields. To advocate for current and future outer planets exploration (Cassini, Juno, New Horizons, JUICE, and beyond), we also call for discussions on future missions to explore giant planet systems, including how to develop better international cooperation. Discussion in this latter category will include progress in developing a solar sail mission concept for observing the Jupiter system and its trojan asteroids.

[PPS01-P01] Critical Role of Entry Probes in Giant Planet Exploration

*Sushil K Atreya[1], Olivier Mousis[2] (1.University of Michigan Ann Arbor, 2.Laboratoire d'Astrophysique de Marseille)

[PPS01-P02] OKEANOS – Jupiter Trojan Asteroid Rendezvous and Landing Experiments Using a Solar Power Sail

*Tatsuaki Okada[1,2], Takahiro Iwata[1], Yoko Kebukawa[3], Motoo Ito[4], Jun Aoki[5], Yosuke Kawai[5], Shoichiro Yokota[5], Yoshifumi Saito[1], Kentaro Terada[5], Michisato Toyoda[5], Hikaru Yabuta[6], Hisayoshi Yurimoto[1,7], Shuji Matsuura[8], Kohji Tsumura[9], Daisuke Yonetoku[10], Tatehiro Mihara[11], Ayako Matsuoka[1], Reiko Nomura[12], Hajime Yano[1], Takayuki Hirai[13], Atsushi Kumamoto[9], Ryosuke Nakamura[14], Stephan Ulamec[15], Ralf Jaumann[15], Jean-Pierre Bibring[16], Noel Grand[17], Cyril Szopa[18], Ernesto Palomba[19], Jorn Helbert[15], Alain Herique[20], Matthias Grott[15], Hans-Ulrich Auster[21], Goester Klingelhoefer[22], Fumi Yoshida[13], Makoto Yoshikawa[1], Jun Matsumoto[1], Toshihiro Chujo[1], Masanori Matsushita[1], Takanao Saiki[1], Hideki Kato[1], Osamu Mori[1], Junichiro Kawaguchi[1] (1.Japan Aerospace Exploration Agency, 2.University of Tokyo, 3.Yokohama National University, 4.Japan Agency for Marine-Earth Science and Technology, 5.Osaka University, 6.Hiroshima University, 7.Hokkaido University, 8.Kwansei Gakuin University, 9.Tohoku University, 10.Kanazawa University, 11.RIKEN, 12.National Astronomical Observatory of Japan, 13.Chiba Institute of Technology, 14.National Institute of Advanced Industrial Science and Technology, 15.German Aerospace Center, 16.Institut d'Astrophysique Spatiale, 17.LISA, 18.LATMOS, 19.INAF-IAPS, 20.IPAG, 21.TU Braunschweig, 22.Leibniz Universität Hannover)

[PPS01-P03] Magnetic field model of Jovian magnetosphere

*Naoya Momoki[1], Hiroaki TOH[1] (1.Division of Earth and Planetary Sciences, Graduate School of Science, Kyoto University)

[PPS01-P04] Enhancement of the Jovian thermospheric temperature above the Great Red Spot based on the infrared spectroscopic data obtained with IRTF/iSHELL

*Ayumu Kambara[1], Hajime Kita[2], Takeshi Sakanoi[1], Yasumasa Kasaba[1], Masato Kagitani[1], Haruna Watanabe[1] (1.Planetary Plasma and Atmospheric Research Center, Graduate School of Science, Tohoku University, 2.Institute of Space and Astronautical Science, Japan Aerospace Exploration Agency)

[PPS01-P05] Pulsation-like variation of Jovian infrared polar emission observed by Subaru 8-m: H3+ and methane emissions

*Yasumasa Kasaba[1], Haruna Watanabe[1], Hajime Kita[2], Chihiro Tao[3], Takeshi Sakanoi[1], Masato Kagitani[1], Orton Glenn[1,4], James Sinclair[4] (1.Planetary Plasma and Atmospheric Research Center, 2.ISAS/JAXA,

3.NICT, 4.NASA/JPL)

[PPS01-P06] Structure of Io plasma torus observed with the Tohoku 60-cm telescope

*Masato Kagitani[1], Fuminori Tsuchiya[1], Kazuo Yoshioka[2], Go Murakami[3], Tomoki Kimura[1], Ryoichi Koga[1], Reina Hikida[4], Takeshi Sakanoi[1] (1.Graduate School of Science, Tohoku University, 2.Graduate School of frontier Science, The University of Tokyo, 3.Institute of Space and Astronautical Science, Japan Aerospace Exploration Agency, 4.Department of Earth and Planetary Science, Graduate School of Science, Tokyo University)

[PPS01-P07] Ion Scale Height Variability in Hisaki Io Torus Observations

*Nicholas McCord Schneider[1], Carl Schmidt[2], Masato Kagitani[3], Yasumasa Kasaba[3], Tomoki Kimura[3], Go Murakami[4], Fuminori Tsuchiya[3], Hajime Kita[3], Reina Hikida[5], Ichiro Yoshikawa[5], Kazuo Yoshioka[5] (1.LASP, University of Colorado Boulder, 2.Boston University, 3.Tohoku University, 4.ISAS/JAXA, 5.University of Tokyo)

[PPS01-P08] Size of the Smallest Particles in Saturn's Rings

*Keiji Ohtsuki[1], Hiroshi Kawamura[1], Naoyuki Hirata[1], Hiroshi Daisaka[2], Hiroshi Kimura[3] (1.Graduate School of Science, Kobe University, 2.Graduate School of Commerce and Management, Hitotsubashi University, 3.Planetary Exploration Research Center, Chiba Institute of Technology)

[PPS01-P09] The Radio & Plasma Wave Investigation (RPWI) for JUICE for the investigation of Jupiter and Icy Moons System: Contributions from Japan

*Yasumasa Kasaba[1], Hiroaki Misawa[1], Fuminori Tsuchiya[1], Atsushi Kumamoto[2], Yuto Katoh[2], Tomoki Kimura[2], Hajime Kita[3], J.-E. Wahlund[4] (1.Planetary Plasma and Atmospheric Research Center, Tohoku University, 2.Department of Geophysics, Tohoku University, 3.ISAS/JAXA, 4.IRF Uppsala, Sweden)

[PPS01-P10] Magnetic field experiment at Jupiter icy moons (JUICE J-MAG) and in-flight alignment calibration

*Ayako Matsuoka[1], Michele Karen Dougherty[2], Patrick Brown[2], Futoshi Takahashi[3], Hisayoshi Shimizu[4], Masaki Matsushima[5] (1.Research Division for Space Plasma, Institute of Space and Astronautical Science, Japan Aerospace Exploration Agency, 2.Imperial College London, 3.Kyushu University, 4.University of Tokyo, 5.Tokyo Institute of Technology)

[PPS01-P11] Science targets of the GAnymede Laser Altimeter (GALA) for the JUICE mission

*Jun Kimura[1], Shunichi Kamata[2], Koji Matsumoto[3], Noriyuki Namiki[3], Keigo Enya[4], Masanori Kobayashi[5], Hiroshi Araki[3], Hirotomo Noda[3], Ko Ishibashi[5], Hauke Hussmann[6], Kay Lingenauber[6] (1.Osaka University, 2.Hokkaido University, 3.National Astronomical Observatory Japan, 4.ISAS/JAXA, 5.Chiba Institute of Technology, 6.German Aerospace Center (DLR), Berlin)

[PPS01-P12] Current status of the antenna developments, the data processing, scientific target for JUICE/SWI JAPAN.

*YASUKO KASAI[1], JUICE SWI Japanese Team (1.National Institute of Information and Communications Technology (NICT))

Critical Role of Entry Probes in Giant Planet Exploration

*Sushil K Atreya[1], Olivier Mousis[2]

1. University of Michigan Ann Arbor, 2. Laboratoire d'Astrophysique de Marseille

Flyby and orbiting spacecraft have explored the giant planets since the early 1970’s. In situ measurements in the troposphere are essential, however, for constraining the models of formation, evolution and interior processes of the giant planets. The models employ abundances and isotopic ratios of key elements, in particular C,N, S, O, He, Ne, Ar, Kr, Xe and D/H, derived from the measurement of their (bulk) reservoir species. That was the scientific rationale for the 1995 Galileo Probe at Jupiter and a Saturn Probe in NASA’s New Frontiers list of candidate missions. Considering that the icy giant planets are distinct from the gas giants, they represent the missing pieces of the puzzle of the formation of the outer solar system, besides being the closest analog for nearly half of the confirmed exoplanets. Thus, their comprehensive exploration with an orbiter-probe spacecraft is essential. The principal focus of this talk is the science, feasibility and implementation strategy of in situ measurements with entry probes at the icy giant planets, Uranus and Neptune, guided by thermochemical models and lessons learned from the Galileo Probe and the ongoing Juno Orbiter. [www.umich.edu/~atreya]

Keywords: Icy Giants, Origin and Evolution, Uranus, Neptune, Entry Probes, Exoplanets

©2019. Japan Geoscience Union. All Right Reserved.

OKEANOS –Jupiter Trojan Asteroid Rendezvous and Landing Experiments Using a Solar Power Sail

*Tatsuaki Okada[1,2], Takahiro Iwata[1], Yoko Kebukawa[3], Motoo Ito[4], Jun Aoki[5], Yosuke Kawai[5], Shoichiro Yokota[5], Yoshifumi Saito[1], Kentaro Terada[5], Michisato Toyoda[5], Hikaru Yabuta[6], Hisayoshi Yurimoto[1,7], Shuji Matsuura[8], Kohji Tsumura[9], Daisuke Yonetoku[10], Tatehiro Mihara[11], Ayako Matsuoka[1], Reiko Nomura[12], Hajime Yano[1], Takayuki Hirai[13], Atsushi Kumamoto[9], Ryosuke Nakamura[14], Stephan Ulamec[15], Ralf Jaumann[15], Jean-Pierre Bibring[16], Noel Grand[17], Cyril Szopa[18], Ernesto Palomba[19], Jorn Helbert[15], Alain Herique[20], Matthias Grott[15], Hans-Ulrich Auster[21], Goester Klingelhoefer[22], Fumi Yoshida[13], Makoto Yoshikawa[1], Jun Matsumoto[1], Toshihiro Chujo[1], Masanori Matsushita[1], Takanao Saiki[1], Hideki Kato[1], Osamu Mori[1], Junichiro Kawaguchi[1]

1. Japan Aerospace Exploration Agency, 2. University of Tokyo, 3. Yokohama National University, 4. Japan Agency for Marine-Earth Science and Technology, 5. Osaka University, 6. Hiroshima University, 7. Hokkaido University, 8. Kwansei Gakuin University, 9. Tohoku University, 10. Kanazawa University, 11. RIKEN, 12. National Astronomical Observatory of Japan, 13. Chiba Institute of Technology, 14. National Institute of Advanced Industrial Science and Technology, 15. German Aerospace Center, 16. Institut d’ Astrophysique Spatiale, 17. LISA, 18. LATMOS, 19. INAF-IAPS, 20. IPAG, 21. TU Braunschweig, 22. Leibniz Universität Hannover

The OKEANOS (Oversize Kite-craft for Exploration and AstroNautics in the Outer Solar system) is a mission under study to rendezvous with and land on a Jupiter Trojan asteroid [1]. The target is a Jupiter Trojan but will be the Saturnian system in the future. It is an engineering mission to demonstrate advanced technologies such as the hybrid thrusting with the enhanced ion engine powered by a 40 x 40 m class large area solar cells to explore the outer solar system cost-effectively. With the new technology, the mission will conduct in-depth scientific measurements for understanding the origin and evolution of the solar system and life. The concept is complementary to NASA Lucy mission [2], multi-flybys to six Jupiter Trojans for understanding the variation of Jupiter Trojans.

Jupiter Trojans are D/P-types enriched in volatiles. They might have experienced almost no or only a low degree of alteration. Their origin and evolution, as well as chemical and physical state still remain unknown. Jupiter Trojans should be a missing link of materials that originate from the inner or the outer solar system by gravity scattering due to migration of giant planets [3]. They are key targets to understand the evolution of astromaterials and the radial distribution of elements and isotopes in the early solar system.

The OKEANOS has been downscaled from the previous proposal [4] due to the severe cost cap. The spacecraft of 1400 kg including a 40 kg lander will be launched in 2027 or later, assisted by gravity of Earth and Jupiter. It will arrive at the target asteroid after a 13-year cruise. 30 kg is allocated for science, 12 kg of which is reserved for international collaboration. Bus instruments such as the optical navigation cameras (ONC-T and -W), LIDAR, and radio science are used for scientific purposes. The lander is like Mascot with uprighting capability on the asteroid surface and 12 kg is allocated for science mission.

During the cruise, science experiments will be carried out from the “deep-space platform”. Measurements of IDPs and magnetic fields will continuously monitor their radial distribution in the solar system and sudden events. The gamma-ray polarimeter will be used for precise positioning of gamma-ray bursts using a very long baseline. Visible to near-infrared telescope will map the zodiacal lights and observe the deep sky under a dust-free condition from outside of the asteroid main belt.

©2019. Japan Geoscience Union. All Right Reserved.

After arrival, global mapping is carried out to characterize the asteroid and select the landing site. The asteroid shape, size, rotation state, and geologic features are imaged by ONC. Gravity is measured by radio tracking and LIDAR. Near-infrared spectroscopy characterizes red or less red patterns, the degree of hydration, mineralogy, and abundance of ices, organics, and brines. Thermal infrared multi-bands inform on thermophysical properties, mineralogy and amorphous phases. A radar probes the surface physical state and also contributes to altimetry. *In situ* experiments with the lander will characterize the footprint and surrounding area by imaging and spectroscopy, followed by measurements of mineralogical, elemental, and organic composition as well as physical, thermal, and magnetic properties at the site. The asteroid surface sample is collected to conduct high-resolution mass spectroscopy (HRMS) based on MULTUM system (infi-TOF type mass spectrometer [5]), especially to determine the isotopic ratios of δD and δ^{15}N and the volatile species contained in the sample. Details will be decided during the critical joint study in 2019. Those experiences will be inherited to future missions.

References: [1] Mori O. et al. (2018) Trans. JSASS Aerospace Tech. Japan, 16, 328-333. [2] Levison H.F. et al. (2016) Lunar Planet. Sci. Conf., 47, #2061. [3] Morbidelli A. et al. (2005) *Nature 435*, 462-466. [4] Okada T. et al. (2018) Planet. Space Sci. 161, 99-106. [6] Toyoda M. et al. (2003) J. Mass Spectrom. 38, 1125-1142.

Keywords: Solar Sail, Trojan, Landing

©2019. Japan Geoscience Union. All Right Reserved.

Magnetic field model of Jovian magnetosphere

*Naoya Momoki[1], Hiroaki TOH[1]

1. Division of Earth and Planetary Sciences, Graduate School of Science, Kyoto University

Europa, Ganymede, Callisto are the Jovian icy satellites called Galilean moons, and are possibly with internal oceans each. While ice is almost an insulator electrically, water including ions has high electrical conductivity, and existence of internal oceans can be verified using electromagnetic (EM) induction methods. In this study, we updated the necessary model of the external magnetic field to the icy satellites for the EM induction studies. Namely, parameters of the Euler potential model of the Jovian magnetosphere (Khurana, 1997) were renewed by adding magnetic data from both Galileo and JUNO spacecrafts.

The configuration of the Jovian current sheet was modeled by Khurana [1992] using three parameters, while the Jovian magnetospheric magnetic field modeled by Khurana [1997] was characterized by 14 parameters. We applied a non-linear optimization technique, i.e., the steepest descent method, to the parameters by newly adding magnetic data from Galileo and Juno spacecrafts. We minimized the root mean squared between the model and the data by exploring the parameter space around several initial sets of the parameters.

As a result, time-varying model parameters for each spacecraft orbit were obtained. Their temporal variation may reflect that of both magnetic field and electric current system in the Jovian magnetosphere.The changes of the parameters can be attributed to the interaction between the Jovian magnetosphere and the solar wind. It, therefore, preferable that the temporal variation of the model parameters is incorporated when the updated magnetic field model of the Jovian magnetosphere is applied to the EM induction studies in search for the internal oceans of the icy satellites.

Keywords: Jupiter, Magnetosphere

©2019. Japan Geoscience Union. All Right Reserved.

Enhancement of the Jovian thermospheric temperature above the Great Red Spot based on the infrared spectroscopic data obtained with IRTF/iSHELL

*Ayumu Kambara[1], Hajime Kita[2], Takeshi Sakanoi[1], Yasumasa Kasaba[1], Masato Kagitani[1], Haruna Watanabe[1]

1. Planetary Plasma and Atmospheric Research Center, Graduate School of Science, Tohoku University, 2. Institute of Space and Astronautical Science, Japan Aerospace Exploration Agency

It is known that the thermospheric temperature of all giant planets including Jupiter is several hundred kelvins higher than that expected from solar heating. At mid- to low-latitudes, although the direct atmospheric heating caused by precipitating particles and the energy transportation from high-latitude auroral region have been considered, it is not enough to explain. Another candidate for the heating is energy transportation by atmospheric waves from the lower atmosphere. Recently, O'Donoghue *et al.* [2016] revealed the heating in the thermosphere above the Great red spot from the intensity ratio of two emission lines (3.383um/3.454um) of the vibrational-rotational spectrum of thermospheic H_3^+ taken by IRTF /SpeX (R~2500) in December 2012. They estimated that the temperature above the Great red spot is 1644±161K, and that on surrounding mid- to low-latitude region is 900±42K. They considered that the reason was the energy transport from the lower atmosphere in the Great red spot region, that is, the propagation of atmospheric gravity waves and acousitic waves generated in the Great red spot, the tropospheric anticyclonic storm, to the thermosphere. However, the infrared spectrum observed SpeX might be contaminated by CH_4 line due to its low-resolution capability.
In this study, we carried out the thermosphere temperature observation in the Jovian mid-latitude region near the Great red spot by IRTF/iSHELL on January 11, 2017. This observation was performed with the iSHELL's Lp1-mode (3.265-3.657um), and the data reduction was performed with NASA's data reduction tool Spextool ver. 5.0.1. Similar to the past study by O'Donoghue *et al.* [2016], we adopted the intensity ratio of two emission lines of H_3^+ (3.3839um/3.4548um), and estimated the temperature precisely distinguished from CH_4 line by iSHELL’s higher wavelength resolution (R~75000). As a result, we estimated the thermospheric temperature above the Great red spot to be 910±132K, and that in the surrounding region to be 583±30K, showing about 300K increase on Great red spot. The estimated temperature was lower than that in O’Donoghue *et al.* [2016], there is possibility that the thermosphere temperature varies in time. However, we confirmed the temperature above Great red spot is higher than that in the surrounding region. This suggests the existence of energy transport from the lower to the upper atmosphere in the Great red spot. In the presentation, we report the result of carefully reduction.

Keywords: Jupiter, Great red spot, Thermosphere

©2019. Japan Geoscience Union. All Right Reserved.

Pulsation-like variation of Jovian infrared polar emission observed by Subaru 8-m: H3+ and methane emissions

*Yasumasa Kasaba[1], Haruna Watanabe[1], Hajime Kita[2], Chihiro Tao[3], Takeshi Sakanoi[1], Masato Kagitani[1], Orton Glenn[1,4], James Sinclair[4]

1. Planetary Plasma and Atmospheric Research Center, 2. ISAS/JAXA, 3. NICT, 4. NASA/JPL

In the Jovian high-latitude region, there are emissions with various wavelengths ranges, morphologies, and time variations. They are important tracers of energy injection carried by auroral particles that precipitate from the magnetosphere. The polar IR emissions excited in the Jovian upper atmosphere, which include the H_3^+ aurora and thermal emissions of hydrocarbons, reflect not only the abundance of emission sources but also the thermal structures. Both are affected by auroral precipitation into the source region. It is known that, in the polar region inner than the auroral oval, the flux of auroral precipitation can have time variations over various scales from years to seconds.

The H_3^+ aurora observed in near infrared is emitted in thermosphere / ionosphere from thermally excited H_3^+ ions above the CH_4 homopause. Auroral precipitation ionized H_2 and produce H_3^+ ions through ion chemistries. In previous observational studies, the shortest timescale of H_3^+ auroral intensity change was ~30 min, but detected by ~16-min step imaging. We performed the temporal imaging observation of the Jovian H_3^+ IR aurora with Subaru/IRCS and the H_3^+ narrow-band filter on 31 January 2015 and 25 May 2016. The adaptive optics enabled us to see the target with high spatial resolution (~0.2 arcsec). From the images obtained with time resolution of ~150 s on 25 May 2016, we detected a patch-like auroral feature pulsating with a period of ~10 min in noon sector of northern polar region. On the other hand, we could not find any periodic variations from the data obtained on 31 January 2015, which was obtained as slit-viewer image for the other study, and whose time intervals of ~10–30 min every several images was not optimized to this research. In addition, the location where the patch-like emissions observed with high intensities on 25 May 2016 were not so bright on 31 January 2015. The patch-like auroral feature that was pulsating during our observation period on 25 May 2016 have been sometimes observed in UV, but not always. Previous UV observations reported some pulsating auroral features with the periods of ~2–11 min in the northern polar region. However, the locations of them are not consistent with the patch-like feature in this study. The pulsation period of the X-ray aurora, which has a hot spot coinciding with our patch-like IR aurora, is 40–50 min. This region is estimated to connect magnetically to out of the magnetopause, and auroral precipitation there can be caused by dayside reconnection between the Jovian magnetospheric field and interplanetary field.

On the other hand, the hydrocarbon polar emission observed in mid-infrared is emitted from the whole stratosphere. From their locations and morphologies, it is estimated to be related with auroral particles penetrating under the homopause. However, the mechanisms of this link (composition change and/or heating by particle precipitations) are not well understood. Previous studies found the intensity time variation of polar CH_4 emission over days and months. We tried to detect the time variation of CH_4 emission intensity by continuous imaging observations of the northern polar region over several tens of minutes on 31 March, 24 and 25 May 2018 with Subaru/COMICS. We obtained the images using the 7.8 μm filter, which is sensitive to the CH_4 thermal emissions occurring in the pressure range of 20–0.5 mbar and 1 μbar in the Jovian upper stratosphere, with time resolution of ~1 min. On all observation days, the polar region was not bright in 7.8 μm. In addition, we could not find clear time variations of polar CH_4 emission intensity during our observation periods, 25, 50 and 60 min on 31 March, 24 and 25 May 2018.

©2019. Japan Geoscience Union. All Right Reserved.

This observation result is consistent to the model estimation by *Kuroda et al.* [2014], which suggested the relaxation time of hydrocarbon thermal emissions in the Jovian upper stratosphere, where is a possible source region of polar CH_4 emission, is at least ~10^5 s (~28 h).

Keywords: Jupiter, polar emission, H3+, CH4, short time variations

©2019. Japan Geoscience Union. All Right Reserved.

Structure of Io plasma torus observed with the Tohoku 60-cm telescope

*Masato Kagitani[1], Fuminori Tsuchiya[1], Kazuo Yoshioka[2], Go Murakami[3], Tomoki Kimura[1], Ryoichi Koga[1], Reina Hikida[4], Takeshi Sakanoi[1]

1. Graduate School of Science, Tohoku University, 2. Graduate School of frontier Science, The University of Tokyo, 3. Institute of Space and Astronautical Science, Japan Aerospace Exploration Agency, 4. Department of Earth and Planetary Science, Graduate School of Science, Tokyo University

Volcanic gases (mainly composed of SO_2, SO and S) originated from jovian satellite Io are ionized by interaction with magnetospheric plasma and then form a donut-shaped region called Io plasma torus. Ion pickup is the most significant energy source on the plasma torus though, distribution of pick-up region and its variability is still unclear. Density profiles of ions along the magnetic field line are determined under condition of diffusive equilibrium. Based on the equilibrium, plasma equator is close to the centrifugal equator though, higher ion anisotropy moves the plasma equator toward the magnetic equator. Measuring ion distribution with enough spatial resolution enables us to derive ion anisotropy which is tightly related to the amount of fresh pickup ion. On this study, we focus on variability of latitudinal structure of Io plasma torus as well as its radial structure using ground-based observation over six month period in 2018. The ground-based observation of sulfur ion emission, [SII] 671.6nm and 673.1nm was made at Haleakala observatory in Hawaii during March through August 2018 using the Tohoku 60-cm telescope (T60). A monochromatic imager with coronagraph attached onto the Cassegrain focus of T60 enables to measure distribution of S^+ with spatial resolution of 0.03 jovian radii (R_J). A digital micro-mirror device DMD was employed to block light from Jupiter disk and Galilean moons. Typical integration time of each frame was 20 minutes and total number of reduced image is 480. We also made observation of neutral sodium cloud extending up to several hundred of R_J as a proxy of supply of neutral particles from Io (Yoneda et al., 2015). Based on observation over the six month, [SII] brightness increases from DOY 80 through 140, then gradually decreases though DOY 230 in 2018. The data reduction of iogenic neutral sodium cloud is still undergoing though, neutral sodium cloud seems to increase from DOY 50 through 135, as [SII] brightness increases. The result suggests that increased volcanic activity from DOY 50-135 caused increase of S+ and brightening of [SII] emission. As for variability of shorter duration, we find [SII] brightening event within a short period (< 2 days) at around 28 through 30 July over a small region (< 30 degrees in longitude). [SII] 671.6 and 673.1 nm emissions are sensitive to cold electron (1-10eV) rather than hot electron (>100eV). Thus, increase of cold electron temperature explains the observed [SII] brightening well as the EUV space telescope Hisaki observed brightening of Io plasma torus associated with injection of hot electron. We also find variation of latitudinal structure of Io plasma torus. Longitudinal peak of S^+ emission at the same system III longitude 279 degree are -0.73, -0.80 and -0.79 R_J on 26, 29 July 7 and August, respectively. The shift of S^+ density peak toward magnetic equator implies higher anisotropy 29 on July and 7 August compared with 26 July. One of the possible explanation of the latitudinal shift of S^+ plasma is an increase of flesh pickup ion which makes higher anisotropy. Further study using Colorado Io Plasma Torus Emission Package (CITEP) will be presented on the presentation to take into account for line-of-sight integration effect of the ground-based observation.

Keywords: Io plasma torus

©2019. Japan Geoscience Union. All Right Reserved.

Ion Scale Height Variability in Hisaki Io Torus Observations

*Nicholas McCord Schneider[1], Carl Schmidt[2], Masato Kagitani[3], Yasumasa Kasaba[3], Tomoki Kimura[3], Go Murakami[4], Fuminori Tsuchiya[3], Hajime Kita[3], Reina Hikida[5], Ichiro Yoshikawa[5], Kazuo Yoshioka[5]

1. LASP, University of Colorado Boulder, 2. Boston University, 3. Tohoku University, 4. ISAS/JAXA, 5. University of Tokyo

Ion temperature is a critical variable in Io plasma torus energetics, but is difficult to derive from remote sensing measurements. The relative importance of hot ions vs. hot electrons in powering the torus emissions remains an open question. Torus brightenings, whether caused by episodic changes in the volcanic supply to the torus or periodic System III/IV enhancements, offer the best chance to search for driving variations in hot electrons or ions. Much attention has been paid to hot electron populations, derivable from detailed spectral modeling, but less work has been done on ion temperature. Ground-based studies have successfully derived $T_{\perp}$ from very high resolution spectra, and $T_{||}$ from scale height measurements in images, both over limited datasets. Schneider et al. 1997 found strong longitudinal variations in $T_{||}$ during a week-long dataset, and anti-correlated System III brightness, but more extended followup datasets have not previously been available.

The Hisaki dataset presents the possibility of an unparalleled opportunity to study long-term and short-term variations in ion temperatures. The instrument is not designed to take images of specific emissions, but its large entrance slit accepts the full height and width of the torus. In the ideal case, each spectral emission feature would appear as an image of the torus at its appropriate position in the spectrum, creating an “overlapogram” (as did the Cassini UVIS instrument). In reality, the emissions are blurred due to instrumental resolution and aberrations, and multiple spectral feature overlap. Furthermore, the changing opening angle of the rotating torus adds a spurious apparent scale height variation which must be removed, with special attention to asymmetries introduced by Jupiter's changing tilt. With allowances for all these effects, we will report on our search for ion temperature variations during the first two years of Hisaki observations, and compare our results to a previous independent study by M. Shishido (M.S. thesis, U. Tohoku).

Keywords: Jupiter, Io, plasma torus, magnetosphere , hisaki, ultraviolet

©2019. Japan Geoscience Union. All Right Reserved.

Size of the Smallest Particles in Saturn's Rings

*Keiji Ohtsuki[1], Hiroshi Kawamura[1], Naoyuki Hirata[1], Hiroshi Daisaka[2], Hiroshi Kimura[3]

1. Graduate School of Science, Kobe University, 2. Graduate School of Commerce and Management, Hitotsubashi University, 3. Planetary Exploration Research Center, Chiba Institute of Technology

Spacecraft and ground-based observations have shown that particles in Saturn's main rings have a power-law distribution roughly between centimeter and ten meters, but sub-centimeter particles appear to be lacking. Recent studies based on Cassini observations suggest that the size of the smallest particles is on the order of millimeters. Cohesive force between particles has been proposed to explain the paucity of sub-centimeter particles, but its strength depends on impact velocity. In order to better understand recent Cassini observations about small ring particles, we examine impact velocity between ring particles using N-body simulation including size distribution. We find that most collisions take place at velocities lower than 0.1 cm per second; even in dense rings where particles' velocity dispersion is enhanced by gravitational wakes, they collide at such low velocities because particles tend to move coherently in the wakes. This velocity is too low to detach sub-centimeter particles that are attached to the surface of large ones due to the cohesive force, explaining their paucity in the main rings. On the other hand, more infrequent high-velocity impacts can release millimeter-sized particles strongly attached to the surface of large ones, explaining the observed free millimeter-sized particles with relatively low abundance. We will discuss implications of our results for the observed size of the smallest particles in Saturn's main rings.

Keywords: Saturn, rings, Cassini

©2019. Japan Geoscience Union. All Right Reserved.

The Radio & Plasma Wave Investigation (RPWI) for JUICE for the investigation of Jupiter and Icy Moons System: Contributions from Japan

*Yasumasa Kasaba[1], Hiroaki Misawa[1], Fuminori Tsuchiya[1], Atsushi Kumamoto[2], Yuto Katoh[2], Tomoki Kimura[2], Hajime Kita[3], J.-E. Wahlund[4]

1. Planetary Plasma and Atmospheric Research Center, Tohoku University, 2. Department of Geophysics, Tohoku University, 3. ISAS/JAXA, 4. IRF Uppsala, Sweden

The Radio & Plasma Wave Investigation (RPWI) for the ESA JUICE mission (launch: 2022, Observations: 2030s) provides an elaborate suite of electromagnetic fields and plasma instruments. RPWI focuses on cold plasma studies and will investigate how the transfer of momentum and energy in the Jovian huge magnetosphere and the electrodynamic coupling with the icy Galilean moons. Remote sensing and direction finding of the Jovian radio emissions will be carried out. This capability is also devoted to the ices and the deep interiors of the icy moons. Investigations of the ice shells will be performed by means of a novel passive ground penetrating radar technique, which utilizes Jovian strong radio emissions as the transmitted signal. On the Ganymede orbit, continuous measurements of the electric field with the JUICE Magnetometer (JMAG) measurements will determine the electric coupling between any ocean, the ionosphere, and the magnetosphere, and provide the constraints on the physical characteristics of the subsurface ocean of Ganymede.
For those objectives, RPWI sensors consist of 4 Langmuir probes (LP-PWI) for determination of the vector electric field up to 1.6 MHz and cold plasma properties (including active measurements by LP sweeps and mutual impedance sounding) up to 1.6 MHz, a tri-axial search coil magnetometer (SCM) for determination of the vector magnetic field up to 20 kHz, and a tri-dipole antenna system (RWI) for monitoring of radio emissions (80 kHz - 45 MHz). From Japan, the RWI preamp and its High Frequency receiver with the onboard software will be provided, based on the modifications from the BepiColombo PWI and Arase PWE developments. Since Arase already shows the good performance in the radiation hard environment around Earth, we have enough confidence for the possible functions and performance on the Jovian hard environment. We will also provide Software Wave-Particle Interaction Analyzer (SWPIA) function to RPWI DPU, for the onboard quantitative detection of electromagnetic field - ion interactions, modifying from the Arase SWPIA which is also activating on the space now.
HF reciever will provide the first highly-resolved information of Jovian radio emissions emitted from Jovian multiple regions including lightning activity and icy moons, by the 3-ch receiver system manufactured by Japan and Sweden connected to the 3-elements 1.25-m E-filed dipole antenna system manufactured by Poland and Japan. Highly matured onboard and ground data processing will also be provided by France and Japan. As a byproduct, reflected Jovian emission can also be expected from the boundary of icy crust and conductive liquid subsurface ocean. Such reflection components could be observed as the Lunar surface reflection of terrestrial auroral kilometric radiation (AKR) seen by Kaguya Lunar Radar Sounder. JUICE has the RIME (Radar for Icy Moons Exploration) instrument, an active radar which emits 9 MHz pulse from 16 m tip-to-tip antenna and tries to detect the ocean under ~10 km icy crust. Since the frequency of Jovian radiation is wider (several 100 kHz to several 10s MHz), RPWI will provide complementary information, including the vertical distributions of conductivity and permittivity in the icy crust.
In the srping 2019, we are manufacturing and testing the Flight Models (FM) which will be shipped in June - July 2019 to Europe. The long road are connected to the first Jupiter and outer planet tour of the

©2019. Japan Geoscience Union. All Right Reserved.

hardware from Japan.

Keywords: Jupiter, JUICE, Radio waves

©2019. Japan Geoscience Union. All Right Reserved.

Magnetic field experiment at Jupiter icy moons (JUICE J-MAG) and in-flight alignment calibration

*Ayako Matsuoka[1], Michele Karen Dougherty[2], Patrick Brown[2], Futoshi Takahashi[3], Hisayoshi Shimizu[4], Masaki Matsushima[5]

1. Research Division for Space Plasma, Institute of Space and Astronautical Science, Japan Aerospace Exploration Agency, 2. Imperial College London, 3. Kyushu University, 4. University of Tokyo, 5. Tokyo Institute of Technology

The magnetometer instrument (J-MAG) is one of the core instruments on the JUICE spacecraft and is critical for resolving prime science objectives of the mission. The importance of a magnetometer instrument on JUICE can be described under following themes. Firstly, the magnetic field drives the plasma processes occurring within the Jupiter system. Understanding such observations allows for a better understanding of dynamical plasma processes, of the generation of aurora and of the various current systems which arise within this rapidly rotating magnetosphere. Secondary, the magnetometer science which is unique to JUICE lies in being able to gain an understanding of the interior structure of the icy moons of Jupiter, specifically those of Ganymede, Callisto and Europa. Of particular interest are knowledge of the depth at which the liquid oceans reside beneath their icy surfaces, the strength of any internal magnetic fields such as at Ganymede and the strength of any induced magnetic fields arising within these oceans.

J-MAG science requirements result in a requirement on the spacecraft to determine accurate knowledge of the orientation of the fluxgate sensors (MAGIBS and MAGOB). Due to the long MAG boom it is not possible to meet J-MAG’ s alignment requirement by mechanical stability alone, therefore the spacecraft includes two orthogonal coils mounted around its body. The coils can be driven with a current which produces a measurable magnetic field vector at the fluxgate sensors. This signal can then be used by the fluxgates to track the variation in the sensor alignment. This technical note describes the results of an analysis using an alignment recovery technique that was developed for the Kaguya mission, applied to the specific case of JUICE, considering the relative positions of the fluxgate sensors with respect to the JACS coils.

We derived equations to calculate the directions of the measurement axes in the frame fixed to the spacecraft, namely alignment angles, from the measurement results of reference magnetic fields generated by JACS. The errors of the alignment angle estimation and their dependence on measurement noise as well as inaccuracy of the coil current intensity are examined. Based on the quantitative results, the requirements to the JACS design and operation to satisfy the requests to the alignment accuracy are determined.

Keywords: Jupiter, Jovian moons, magnetometer

©2019. Japan Geoscience Union. All Right Reserved.

Science targets of the GAnymede Laser Altimeter (GALA) for the JUICE mission

*Jun Kimura[1], Shunichi Kamata[2], Koji Matsumoto[3], Noriyuki Namiki[3], Keigo Enya[4], Masanori Kobayashi[5], Hiroshi Araki[3], Hirotomo Noda[3], Ko Ishibashi[5], Hauke Hussmann[6], Kay Lingenauber[6]

1. Osaka University, 2. Hokkaido University, 3. National Astronomical Observatory Japan, 4. ISAS/JAXA, 5. Chiba Institute of Technology, 6. German Aerospace Center (DLR), Berlin

The JUpiter Icy Moons Explorer (JUICE), led by European Space Agency, has started development toward launch in 2022 (arrival at Jupiter in 2029, and Ganymede orbit insertion in 2032), and we are now developing the GALA instrument onboard JUICE spacecraft collaborating with German Aerospace Center (DLR) and other institutions in Europe. GALA will acquire the key information for understanding the evolution of Jovian icy moons and to play an essential role in the JUICE's purpose: exploration of deep habitat.

Jovian icy moon Ganymede, which is the largest moon in the Solar System and the primary target of the JUICE, can be said to be one of the typical solid bodies along with terrestrial planets in terms of its size and the intrinsic magnetic field originated from the metallic core. However, current knowledge provided by previous explorations is extremely limited since it comes from only several fly-bys. The JUICE will unveil the whole picture of Ganymede by the first orbiting in the history around extra-terrestrial moon. Expected new big picture of the origin and evolution of Ganymede will not only be a key to unveil the origin of diversity among the Solar System bodies, but also contribute to an understanding of exoplanets with a wide diversity.

The GALA will measure a distance between the spacecraft and the surface of icy moons and acquire the topography data (globally for Ganymede, and fly-by region for Europa and Callisto). It will be a first-ever laser altimetry for the icy object. Such information makes surface geologies clear and tremendously improves our understanding of the icy tectonics. By comparing their tectonic styles on the rocky planets/moons, GALA data leads to reconsider the Earth's plate tectonics. In addition, the GALA will confirm a presence/absence of the subsurface ocean by measuring tidal and rotational response, and the gravitational information reflecting the interior structure will be greatly improved. Furthermore, strength and waveform of reflected laser pulse have an information about surface reflectance at the laser wavelength and small-scale roughness. Finally we can see degrees of erosion and space weathering without being affected by illumination condition through GALA measurements.

In order to interpret and understand such measurements, accumulated studies for the Earth over the years will be effectively utilized: e.g., the data for surface topography, roughness and albedo will lead to describe the icy tectonics through the knowledge from terrestrial glaciology and experiments on impact and deformation process. The tidal measurements by GALA will also be a window to see its interior based on our knowledge and experiences cultivated through the past geodetic observations, e.g., the SELENE mission for the terrestrial Moon.

Characterization of the icy moons will be achieved not only from the GALA measurements but also synergy of other scientific instruments onboard JUICE spacecraft, for examples, surface images taken by optical camera (JANUS) will confirm the position of GALA laser footprint to complement the GALA "point" data for precise topographic mapping. A radar sounder (RIME) and a radio science experiment (3GM) probe

©2019. Japan Geoscience Union. All Right Reserved.

the interior structure, especially interior of the icy crust to figure out an occurrence of tectonic features. A visible and infrared imaging spectrometer (MAJIS), an ultraviolet imaging spectrograph (UVS) and a sub-millimeter wave instrument (SWI) will acquire a surface and atmosphere compositional data. A magnetometer (J-MAG) monitors moons' inductive response to the Jovian magnetic field and probes the subsurface ocean with the help of a particle environment package (PEP) and a radio and plasma wave investigation (RPWI). The GALA works closely together with these instruments and plays a leading and a supporting role to clarify the whole picture of Ganymede and other icy moons.

Keywords: Jupiter, Icy moons, Laser altimetry

©2019. Japan Geoscience Union. All Right Reserved.

Current status of the antenna developments, the data processing, scientific target for JUICE/SWI JAPAN.

*YASUKO KASAI[1], [Group] JUICE SWI Japanese Team

1. National Institute of Information and Communications Technology (NICT)

The Submillimetre-Wave Instrument (SWI) is one of the 10 scientific payloads on the JUpiter ICy moon Explorer (JUICE). The main scientific objectives of SWI is to investigate the structure, compositions and dynamics of the middle atmosphere of Jupiter and exosphere of its moons, as well as thermophysical properties if the satellite surfaces. SWI observations will provide pioneering direct measurements of atmospheric compositions in Jupiter system. SWI will performed limb and nadir observations in the frequency region 530-600 and 1075-1275 GHz. Japanese contribution is the development of main- and sub- reflectors, actuators for the instruments, feasibility studies, data processing, and scientific contributions. We present Current status of the antenna developments, the data processing, scientific target for JUICE/SWI JAPAN.

Keywords: Jupiter, Jovian moons, submm instrument, JUICE, SWI

©2019. Japan Geoscience Union. All Right Reserved.

[E] Poster | P (Space and Planetary Sciences)：P-PS Planetary Sciences

Tue. May 28, 2019 5:15 PM - 6:30 PM JST | Tue. May 28, 2019 8:15 AM - 9:30 AM UTC | Poster Hall International Exhibition Hall8, Makuhari Messe_1

[P-PS01] Outer Solar System Exploration Today, and Tomorrow

convener:Jun Kimura(Osaka University), Yasumasa Kasaba(Planetary Plasma and Atmospheric Research Center, Tohoku University), Kunio M. Sayanagi(Hampton University)

The giant planets provide many keys to understanding planetary processes. They play an important role in shaping our solar system, and the physical and chemical processes they harbor also provide a unique opportunity to study the phenomena relevant for studying Earth and other planets, including exoplanetary systems. In this session, we discuss a wide range of topics encompassing the giant planets and their moons, including their origins, interiors, atmospheres, compositions, surface features, and electromagnetic fields. To advocate for current and future outer planets exploration (Cassini, Juno, New Horizons, JUICE, and beyond), we also call for discussions on future missions to explore giant planet systems, including how to develop better international cooperation. Discussion in this latter category will include progress in developing a solar sail mission concept for observing the Jupiter system and its trojan asteroids.

[PPS01-P01] Critical Role of Entry Probes in Giant Planet Exploration

*Sushil K Atreya[1], Olivier Mousis[2] (1.University of Michigan Ann Arbor, 2.Laboratoire d'Astrophysique de Marseille)

[PPS01-P02] OKEANOS – Jupiter Trojan Asteroid Rendezvous and Landing Experiments Using a Solar Power Sail

*Tatsuaki Okada[1,2], Takahiro Iwata[1], Yoko Kebukawa[3], Motoo Ito[4], Jun Aoki[5], Yosuke Kawai[5], Shoichiro Yokota[5], Yoshifumi Saito[1], Kentaro Terada[5], Michisato Toyoda[5], Hikaru Yabuta[6], Hisayoshi Yurimoto[1,7], Shuji Matsuura[8], Kohji Tsumura[9], Daisuke Yonetoku[10], Tatehiro Mihara[11], Ayako Matsuoka[1], Reiko Nomura[12], Hajime Yano[1], Takayuki Hirai[13], Atsushi Kumamoto[9], Ryosuke Nakamura[14], Stephan Ulamec[15], Ralf Jaumann[15], Jean-Pierre Bibring[16], Noel Grand[17], Cyril Szopa[18], Ernesto Palomba[19], Jorn Helbert[15], Alain Herique[20], Matthias Grott[15], Hans-Ulrich Auster[21], Goester Klingelhoefer[22], Fumi Yoshida[13], Makoto Yoshikawa[1], Jun Matsumoto[1], Toshihiro Chujo[1], Masanori Matsushita[1], Takanao Saiki[1], Hideki Kato[1], Osamu Mori[1], Junichiro Kawaguchi[1] (1.Japan Aerospace Exploration Agency, 2.University of Tokyo, 3.Yokohama National University, 4.Japan Agency for Marine-Earth Science and Technology, 5.Osaka University, 6.Hiroshima University, 7.Hokkaido University, 8.Kwansei Gakuin University, 9.Tohoku University, 10.Kanazawa University, 11.RIKEN, 12.National Astronomical Observatory of Japan, 13.Chiba Institute of Technology, 14.National Institute of Advanced Industrial Science and Technology, 15.German Aerospace Center, 16.Institut d'Astrophysique Spatiale, 17.LISA, 18.LATMOS, 19.INAF-IAPS, 20.IPAG, 21.TU Braunschweig, 22.Leibniz Universität Hannover)

[PPS01-P03] Magnetic field model of Jovian magnetosphere

*Naoya Momoki[1], Hiroaki TOH[1] (1.Division of Earth and Planetary Sciences, Graduate School of Science, Kyoto University)

[PPS01-P04] Enhancement of the Jovian thermospheric temperature above the Great Red Spot based on the infrared spectroscopic data obtained with IRTF/iSHELL

*Ayumu Kambara[1], Hajime Kita[2], Takeshi Sakanoi[1], Yasumasa Kasaba[1], Masato Kagitani[1], Haruna Watanabe[1] (1.Planetary Plasma and Atmospheric Research Center, Graduate School of Science, Tohoku University, 2.Institute of Space and Astronautical Science, Japan Aerospace Exploration Agency)

[PPS01-P05] Pulsation-like variation of Jovian infrared polar emission observed by Subaru 8-m: H3+ and methane emissions

*Yasumasa Kasaba[1], Haruna Watanabe[1], Hajime Kita[2], Chihiro Tao[3], Takeshi Sakanoi[1], Masato Kagitani[1], Orton Glenn[1,4], James Sinclair[4] (1.Planetary Plasma and Atmospheric Research Center, 2.ISAS/JAXA,

3.NICT, 4.NASA/JPL)

[PPS01-P06] Structure of Io plasma torus observed with the Tohoku 60-cm telescope

*Masato Kagitani[1], Fuminori Tsuchiya[1], Kazuo Yoshioka[2], Go Murakami[3], Tomoki Kimura[1], Ryoichi Koga[1], Reina Hikida[4], Takeshi Sakanoi[1] (1.Graduate School of Science, Tohoku University, 2.Graduate School of frontier Science, The University of Tokyo, 3.Institute of Space and Astronautical Science, Japan Aerospace Exploration Agency, 4.Department of Earth and Planetary Science, Graduate School of Science, Tokyo University)

[PPS01-P07] Ion Scale Height Variability in Hisaki Io Torus Observations

*Nicholas McCord Schneider[1], Carl Schmidt[2], Masato Kagitani[3], Yasumasa Kasaba[3], Tomoki Kimura[3], Go Murakami[4], Fuminori Tsuchiya[3], Hajime Kita[3], Reina Hikida[5], Ichiro Yoshikawa[5], Kazuo Yoshioka[5] (1.LASP, University of Colorado Boulder, 2.Boston University, 3.Tohoku University, 4.ISAS/JAXA, 5.University of Tokyo)

[PPS01-P08] Size of the Smallest Particles in Saturn's Rings

*Keiji Ohtsuki[1], Hiroshi Kawamura[1], Naoyuki Hirata[1], Hiroshi Daisaka[2], Hiroshi Kimura[3] (1.Graduate School of Science, Kobe University, 2.Graduate School of Commerce and Management, Hitotsubashi University, 3.Planetary Exploration Research Center, Chiba Institute of Technology)

[PPS01-P09] The Radio & Plasma Wave Investigation (RPWI) for JUICE for the investigation of Jupiter and Icy Moons System: Contributions from Japan

*Yasumasa Kasaba[1], Hiroaki Misawa[1], Fuminori Tsuchiya[1], Atsushi Kumamoto[2], Yuto Katoh[2], Tomoki Kimura[2], Hajime Kita[3], J.-E. Wahlund[4] (1.Planetary Plasma and Atmospheric Research Center, Tohoku University, 2.Department of Geophysics, Tohoku University, 3.ISAS/JAXA, 4.IRF Uppsala, Sweden)

[PPS01-P10] Magnetic field experiment at Jupiter icy moons (JUICE J-MAG) and in-flight alignment calibration

*Ayako Matsuoka[1], Michele Karen Dougherty[2], Patrick Brown[2], Futoshi Takahashi[3], Hisayoshi Shimizu[4], Masaki Matsushima[5] (1.Research Division for Space Plasma, Institute of Space and Astronautical Science, Japan Aerospace Exploration Agency, 2.Imperial College London, 3.Kyushu University, 4.University of Tokyo, 5.Tokyo Institute of Technology)

[PPS01-P11] Science targets of the GAnymede Laser Altimeter (GALA) for the JUICE mission

*Jun Kimura[1], Shunichi Kamata[2], Koji Matsumoto[3], Noriyuki Namiki[3], Keigo Enya[4], Masanori Kobayashi[5], Hiroshi Araki[3], Hirotomo Noda[3], Ko Ishibashi[5], Hauke Hussmann[6], Kay Lingenauber[6] (1.Osaka University, 2.Hokkaido University, 3.National Astronomical Observatory Japan, 4.ISAS/JAXA, 5.Chiba Institute of Technology, 6.German Aerospace Center (DLR), Berlin)

[PPS01-P12] Current status of the antenna developments, the data processing, scientific target for JUICE/SWI JAPAN.

*YASUKO KASAI[1], JUICE SWI Japanese Team (1.National Institute of Information and Communications Technology (NICT))

Critical Role of Entry Probes in Giant Planet Exploration

*Sushil K Atreya[1], Olivier Mousis[2]

1. University of Michigan Ann Arbor, 2. Laboratoire d'Astrophysique de Marseille

Flyby and orbiting spacecraft have explored the giant planets since the early 1970’s. In situ measurements in the troposphere are essential, however, for constraining the models of formation, evolution and interior processes of the giant planets. The models employ abundances and isotopic ratios of key elements, in particular C,N, S, O, He, Ne, Ar, Kr, Xe and D/H, derived from the measurement of their (bulk) reservoir species. That was the scientific rationale for the 1995 Galileo Probe at Jupiter and a Saturn Probe in NASA’s New Frontiers list of candidate missions. Considering that the icy giant planets are distinct from the gas giants, they represent the missing pieces of the puzzle of the formation of the outer solar system, besides being the closest analog for nearly half of the confirmed exoplanets. Thus, their comprehensive exploration with an orbiter-probe spacecraft is essential. The principal focus of this talk is the science, feasibility and implementation strategy of in situ measurements with entry probes at the icy giant planets, Uranus and Neptune, guided by thermochemical models and lessons learned from the Galileo Probe and the ongoing Juno Orbiter. [www.umich.edu/~atreya]

Keywords: Icy Giants, Origin and Evolution, Uranus, Neptune, Entry Probes, Exoplanets

©2019. Japan Geoscience Union. All Right Reserved.

OKEANOS –Jupiter Trojan Asteroid Rendezvous and Landing Experiments Using a Solar Power Sail

*Tatsuaki Okada[1,2], Takahiro Iwata[1], Yoko Kebukawa[3], Motoo Ito[4], Jun Aoki[5], Yosuke Kawai[5], Shoichiro Yokota[5], Yoshifumi Saito[1], Kentaro Terada[5], Michisato Toyoda[5], Hikaru Yabuta[6], Hisayoshi Yurimoto[1,7], Shuji Matsuura[8], Kohji Tsumura[9], Daisuke Yonetoku[10], Tatehiro Mihara[11], Ayako Matsuoka[1], Reiko Nomura[12], Hajime Yano[1], Takayuki Hirai[13], Atsushi Kumamoto[9], Ryosuke Nakamura[14], Stephan Ulamec[15], Ralf Jaumann[15], Jean-Pierre Bibring[16], Noel Grand[17], Cyril Szopa[18], Ernesto Palomba[19], Jorn Helbert[15], Alain Herique[20], Matthias Grott[15], Hans-Ulrich Auster[21], Goester Klingelhoefer[22], Fumi Yoshida[13], Makoto Yoshikawa[1], Jun Matsumoto[1], Toshihiro Chujo[1], Masanori Matsushita[1], Takanao Saiki[1], Hideki Kato[1], Osamu Mori[1], Junichiro Kawaguchi[1]

1. Japan Aerospace Exploration Agency, 2. University of Tokyo, 3. Yokohama National University, 4. Japan Agency for Marine-Earth Science and Technology, 5. Osaka University, 6. Hiroshima University, 7. Hokkaido University, 8. Kwansei Gakuin University, 9. Tohoku University, 10. Kanazawa University, 11. RIKEN, 12. National Astronomical Observatory of Japan, 13. Chiba Institute of Technology, 14. National Institute of Advanced Industrial Science and Technology, 15. German Aerospace Center, 16. Institut d’ Astrophysique Spatiale, 17. LISA, 18. LATMOS, 19. INAF-IAPS, 20. IPAG, 21. TU Braunschweig, 22. Leibniz Universität Hannover

The OKEANOS (Oversize Kite-craft for Exploration and AstroNautics in the Outer Solar system) is a mission under study to rendezvous with and land on a Jupiter Trojan asteroid [1]. The target is a Jupiter Trojan but will be the Saturnian system in the future. It is an engineering mission to demonstrate advanced technologies such as the hybrid thrusting with the enhanced ion engine powered by a 40 x 40 m class large area solar cells to explore the outer solar system cost-effectively. With the new technology, the mission will conduct in-depth scientific measurements for understanding the origin and evolution of the solar system and life. The concept is complementary to NASA Lucy mission [2], multi-flybys to six Jupiter Trojans for understanding the variation of Jupiter Trojans.

Jupiter Trojans are D/P-types enriched in volatiles. They might have experienced almost no or only a low degree of alteration. Their origin and evolution, as well as chemical and physical state still remain unknown. Jupiter Trojans should be a missing link of materials that originate from the inner or the outer solar system by gravity scattering due to migration of giant planets [3]. They are key targets to understand the evolution of astromaterials and the radial distribution of elements and isotopes in the early solar system.

The OKEANOS has been downscaled from the previous proposal [4] due to the severe cost cap. The spacecraft of 1400 kg including a 40 kg lander will be launched in 2027 or later, assisted by gravity of Earth and Jupiter. It will arrive at the target asteroid after a 13-year cruise. 30 kg is allocated for science, 12 kg of which is reserved for international collaboration. Bus instruments such as the optical navigation cameras (ONC-T and -W), LIDAR, and radio science are used for scientific purposes. The lander is like Mascot with uprighting capability on the asteroid surface and 12 kg is allocated for science mission.

During the cruise, science experiments will be carried out from the “deep-space platform”. Measurements of IDPs and magnetic fields will continuously monitor their radial distribution in the solar system and sudden events. The gamma-ray polarimeter will be used for precise positioning of gamma-ray bursts using a very long baseline. Visible to near-infrared telescope will map the zodiacal lights and observe the deep sky under a dust-free condition from outside of the asteroid main belt.

©2019. Japan Geoscience Union. All Right Reserved.

After arrival, global mapping is carried out to characterize the asteroid and select the landing site. The asteroid shape, size, rotation state, and geologic features are imaged by ONC. Gravity is measured by radio tracking and LIDAR. Near-infrared spectroscopy characterizes red or less red patterns, the degree of hydration, mineralogy, and abundance of ices, organics, and brines. Thermal infrared multi-bands inform on thermophysical properties, mineralogy and amorphous phases. A radar probes the surface physical state and also contributes to altimetry. *In situ* experiments with the lander will characterize the footprint and surrounding area by imaging and spectroscopy, followed by measurements of mineralogical, elemental, and organic composition as well as physical, thermal, and magnetic properties at the site. The asteroid surface sample is collected to conduct high-resolution mass spectroscopy (HRMS) based on MULTUM system (infi-TOF type mass spectrometer [5]), especially to determine the isotopic ratios of δD and δ^{15}N and the volatile species contained in the sample. Details will be decided during the critical joint study in 2019. Those experiences will be inherited to future missions.

References: [1] Mori O. et al. (2018) Trans. JSASS Aerospace Tech. Japan, 16, 328-333. [2] Levison H.F. et al. (2016) Lunar Planet. Sci. Conf., 47, #2061. [3] Morbidelli A. et al. (2005) *Nature 435*, 462-466. [4] Okada T. et al. (2018) Planet. Space Sci. 161, 99-106. [6] Toyoda M. et al. (2003) J. Mass Spectrom. 38, 1125-1142.

Keywords: Solar Sail, Trojan, Landing

©2019. Japan Geoscience Union. All Right Reserved.

Magnetic field model of Jovian magnetosphere

*Naoya Momoki[1], Hiroaki TOH[1]

1. Division of Earth and Planetary Sciences, Graduate School of Science, Kyoto University

Europa, Ganymede, Callisto are the Jovian icy satellites called Galilean moons, and are possibly with internal oceans each. While ice is almost an insulator electrically, water including ions has high electrical conductivity, and existence of internal oceans can be verified using electromagnetic (EM) induction methods. In this study, we updated the necessary model of the external magnetic field to the icy satellites for the EM induction studies. Namely, parameters of the Euler potential model of the Jovian magnetosphere (Khurana, 1997) were renewed by adding magnetic data from both Galileo and JUNO spacecrafts.

The configuration of the Jovian current sheet was modeled by Khurana [1992] using three parameters, while the Jovian magnetospheric magnetic field modeled by Khurana [1997] was characterized by 14 parameters. We applied a non-linear optimization technique, i.e., the steepest descent method, to the parameters by newly adding magnetic data from Galileo and Juno spacecrafts. We minimized the root mean squared between the model and the data by exploring the parameter space around several initial sets of the parameters.

As a result, time-varying model parameters for each spacecraft orbit were obtained. Their temporal variation may reflect that of both magnetic field and electric current system in the Jovian magnetosphere.The changes of the parameters can be attributed to the interaction between the Jovian magnetosphere and the solar wind. It, therefore, preferable that the temporal variation of the model parameters is incorporated when the updated magnetic field model of the Jovian magnetosphere is applied to the EM induction studies in search for the internal oceans of the icy satellites.

Keywords: Jupiter, Magnetosphere

©2019. Japan Geoscience Union. All Right Reserved.

Enhancement of the Jovian thermospheric temperature above the Great Red Spot based on the infrared spectroscopic data obtained with IRTF/iSHELL

*Ayumu Kambara[1], Hajime Kita[2], Takeshi Sakanoi[1], Yasumasa Kasaba[1], Masato Kagitani[1], Haruna Watanabe[1]

1. Planetary Plasma and Atmospheric Research Center, Graduate School of Science, Tohoku University, 2. Institute of Space and Astronautical Science, Japan Aerospace Exploration Agency

It is known that the thermospheric temperature of all giant planets including Jupiter is several hundred kelvins higher than that expected from solar heating. At mid- to low-latitudes, although the direct atmospheric heating caused by precipitating particles and the energy transportation from high-latitude auroral region have been considered, it is not enough to explain. Another candidate for the heating is energy transportation by atmospheric waves from the lower atmosphere. Recently, O'Donoghue *et al.* [2016] revealed the heating in the thermosphere above the Great red spot from the intensity ratio of two emission lines (3.383um/3.454um) of the vibrational-rotational spectrum of thermospheic H_3^+ taken by IRTF /SpeX (R~2500) in December 2012. They estimated that the temperature above the Great red spot is 1644±161K, and that on surrounding mid- to low-latitude region is 900±42K. They considered that the reason was the energy transport from the lower atmosphere in the Great red spot region, that is, the propagation of atmospheric gravity waves and acousitic waves generated in the Great red spot, the tropospheric anticyclonic storm, to the thermosphere. However, the infrared spectrum observed SpeX might be contaminated by CH_4 line due to its low-resolution capability.
In this study, we carried out the thermosphere temperature observation in the Jovian mid-latitude region near the Great red spot by IRTF/iSHELL on January 11, 2017. This observation was performed with the iSHELL's Lp1-mode (3.265-3.657um), and the data reduction was performed with NASA's data reduction tool Spextool ver. 5.0.1. Similar to the past study by O'Donoghue *et al.* [2016], we adopted the intensity ratio of two emission lines of H_3^+ (3.3839um/3.4548um), and estimated the temperature precisely distinguished from CH_4 line by iSHELL’s higher wavelength resolution (R~75000). As a result, we estimated the thermospheric temperature above the Great red spot to be 910±132K, and that in the surrounding region to be 583±30K, showing about 300K increase on Great red spot. The estimated temperature was lower than that in O’Donoghue *et al.* [2016], there is possibility that the thermosphere temperature varies in time. However, we confirmed the temperature above Great red spot is higher than that in the surrounding region. This suggests the existence of energy transport from the lower to the upper atmosphere in the Great red spot. In the presentation, we report the result of carefully reduction.

Keywords: Jupiter, Great red spot, Thermosphere

©2019. Japan Geoscience Union. All Right Reserved.

Pulsation-like variation of Jovian infrared polar emission observed by Subaru 8-m: H3+ and methane emissions

*Yasumasa Kasaba[1], Haruna Watanabe[1], Hajime Kita[2], Chihiro Tao[3], Takeshi Sakanoi[1], Masato Kagitani[1], Orton Glenn[1,4], James Sinclair[4]

1. Planetary Plasma and Atmospheric Research Center, 2. ISAS/JAXA, 3. NICT, 4. NASA/JPL

In the Jovian high-latitude region, there are emissions with various wavelengths ranges, morphologies, and time variations. They are important tracers of energy injection carried by auroral particles that precipitate from the magnetosphere. The polar IR emissions excited in the Jovian upper atmosphere, which include the H_3^+ aurora and thermal emissions of hydrocarbons, reflect not only the abundance of emission sources but also the thermal structures. Both are affected by auroral precipitation into the source region. It is known that, in the polar region inner than the auroral oval, the flux of auroral precipitation can have time variations over various scales from years to seconds.

The H_3^+ aurora observed in near infrared is emitted in thermosphere / ionosphere from thermally excited H_3^+ ions above the CH_4 homopause. Auroral precipitation ionized H_2 and produce H_3^+ ions through ion chemistries. In previous observational studies, the shortest timescale of H_3^+ auroral intensity change was ~30 min, but detected by ~16-min step imaging. We performed the temporal imaging observation of the Jovian H_3^+ IR aurora with Subaru/IRCS and the H_3^+ narrow-band filter on 31 January 2015 and 25 May 2016. The adaptive optics enabled us to see the target with high spatial resolution (~0.2 arcsec). From the images obtained with time resolution of ~150 s on 25 May 2016, we detected a patch-like auroral feature pulsating with a period of ~10 min in noon sector of northern polar region. On the other hand, we could not find any periodic variations from the data obtained on 31 January 2015, which was obtained as slit-viewer image for the other study, and whose time intervals of ~10–30 min every several images was not optimized to this research. In addition, the location where the patch-like emissions observed with high intensities on 25 May 2016 were not so bright on 31 January 2015. The patch-like auroral feature that was pulsating during our observation period on 25 May 2016 have been sometimes observed in UV, but not always. Previous UV observations reported some pulsating auroral features with the periods of ~2–11 min in the northern polar region. However, the locations of them are not consistent with the patch-like feature in this study. The pulsation period of the X-ray aurora, which has a hot spot coinciding with our patch-like IR aurora, is 40–50 min. This region is estimated to connect magnetically to out of the magnetopause, and auroral precipitation there can be caused by dayside reconnection between the Jovian magnetospheric field and interplanetary field.

On the other hand, the hydrocarbon polar emission observed in mid-infrared is emitted from the whole stratosphere. From their locations and morphologies, it is estimated to be related with auroral particles penetrating under the homopause. However, the mechanisms of this link (composition change and/or heating by particle precipitations) are not well understood. Previous studies found the intensity time variation of polar CH_4 emission over days and months. We tried to detect the time variation of CH_4 emission intensity by continuous imaging observations of the northern polar region over several tens of minutes on 31 March, 24 and 25 May 2018 with Subaru/COMICS. We obtained the images using the 7.8 μm filter, which is sensitive to the CH_4 thermal emissions occurring in the pressure range of 20–0.5 mbar and 1 μbar in the Jovian upper stratosphere, with time resolution of ~1 min. On all observation days, the polar region was not bright in 7.8 μm. In addition, we could not find clear time variations of polar CH_4 emission intensity during our observation periods, 25, 50 and 60 min on 31 March, 24 and 25 May 2018.

©2019. Japan Geoscience Union. All Right Reserved.

This observation result is consistent to the model estimation by *Kuroda et al.* [2014], which suggested the relaxation time of hydrocarbon thermal emissions in the Jovian upper stratosphere, where is a possible source region of polar CH_4 emission, is at least ~10^5 s (~28 h).

Keywords: Jupiter, polar emission, H3+, CH4, short time variations

©2019. Japan Geoscience Union. All Right Reserved.

Structure of Io plasma torus observed with the Tohoku 60-cm telescope

*Masato Kagitani[1], Fuminori Tsuchiya[1], Kazuo Yoshioka[2], Go Murakami[3], Tomoki Kimura[1], Ryoichi Koga[1], Reina Hikida[4], Takeshi Sakanoi[1]

1. Graduate School of Science, Tohoku University, 2. Graduate School of frontier Science, The University of Tokyo, 3. Institute of Space and Astronautical Science, Japan Aerospace Exploration Agency, 4. Department of Earth and Planetary Science, Graduate School of Science, Tokyo University

Volcanic gases (mainly composed of SO_2, SO and S) originated from jovian satellite Io are ionized by interaction with magnetospheric plasma and then form a donut-shaped region called Io plasma torus. Ion pickup is the most significant energy source on the plasma torus though, distribution of pick-up region and its variability is still unclear. Density profiles of ions along the magnetic field line are determined under condition of diffusive equilibrium. Based on the equilibrium, plasma equator is close to the centrifugal equator though, higher ion anisotropy moves the plasma equator toward the magnetic equator. Measuring ion distribution with enough spatial resolution enables us to derive ion anisotropy which is tightly related to the amount of fresh pickup ion. On this study, we focus on variability of latitudinal structure of Io plasma torus as well as its radial structure using ground-based observation over six month period in 2018. The ground-based observation of sulfur ion emission, [SII] 671.6nm and 673.1nm was made at Haleakala observatory in Hawaii during March through August 2018 using the Tohoku 60-cm telescope (T60). A monochromatic imager with coronagraph attached onto the Cassegrain focus of T60 enables to measure distribution of S^+ with spatial resolution of 0.03 jovian radii (R_J). A digital micro-mirror device DMD was employed to block light from Jupiter disk and Galilean moons. Typical integration time of each frame was 20 minutes and total number of reduced image is 480. We also made observation of neutral sodium cloud extending up to several hundred of R_J as a proxy of supply of neutral particles from Io (Yoneda et al., 2015). Based on observation over the six month, [SII] brightness increases from DOY 80 through 140, then gradually decreases though DOY 230 in 2018. The data reduction of iogenic neutral sodium cloud is still undergoing though, neutral sodium cloud seems to increase from DOY 50 through 135, as [SII] brightness increases. The result suggests that increased volcanic activity from DOY 50-135 caused increase of S+ and brightening of [SII] emission. As for variability of shorter duration, we find [SII] brightening event within a short period (< 2 days) at around 28 through 30 July over a small region (< 30 degrees in longitude). [SII] 671.6 and 673.1 nm emissions are sensitive to cold electron (1-10eV) rather than hot electron (>100eV). Thus, increase of cold electron temperature explains the observed [SII] brightening well as the EUV space telescope Hisaki observed brightening of Io plasma torus associated with injection of hot electron. We also find variation of latitudinal structure of Io plasma torus. Longitudinal peak of S^+ emission at the same system III longitude 279 degree are -0.73, -0.80 and -0.79 R_J on 26, 29 July 7 and August, respectively. The shift of S^+ density peak toward magnetic equator implies higher anisotropy 29 on July and 7 August compared with 26 July. One of the possible explanation of the latitudinal shift of S^+ plasma is an increase of flesh pickup ion which makes higher anisotropy. Further study using Colorado Io Plasma Torus Emission Package (CITEP) will be presented on the presentation to take into account for line-of-sight integration effect of the ground-based observation.

Keywords: Io plasma torus

©2019. Japan Geoscience Union. All Right Reserved.

Ion Scale Height Variability in Hisaki Io Torus Observations

*Nicholas McCord Schneider[1], Carl Schmidt[2], Masato Kagitani[3], Yasumasa Kasaba[3], Tomoki Kimura[3], Go Murakami[4], Fuminori Tsuchiya[3], Hajime Kita[3], Reina Hikida[5], Ichiro Yoshikawa[5], Kazuo Yoshioka[5]

1. LASP, University of Colorado Boulder, 2. Boston University, 3. Tohoku University, 4. ISAS/JAXA, 5. University of Tokyo

Ion temperature is a critical variable in Io plasma torus energetics, but is difficult to derive from remote sensing measurements. The relative importance of hot ions vs. hot electrons in powering the torus emissions remains an open question. Torus brightenings, whether caused by episodic changes in the volcanic supply to the torus or periodic System III/IV enhancements, offer the best chance to search for driving variations in hot electrons or ions. Much attention has been paid to hot electron populations, derivable from detailed spectral modeling, but less work has been done on ion temperature. Ground-based studies have successfully derived $T_{\perp}$ from very high resolution spectra, and $T_{||}$ from scale height measurements in images, both over limited datasets. Schneider et al. 1997 found strong longitudinal variations in $T_{||}$ during a week-long dataset, and anti-correlated System III brightness, but more extended followup datasets have not previously been available.

The Hisaki dataset presents the possibility of an unparalleled opportunity to study long-term and short-term variations in ion temperatures. The instrument is not designed to take images of specific emissions, but its large entrance slit accepts the full height and width of the torus. In the ideal case, each spectral emission feature would appear as an image of the torus at its appropriate position in the spectrum, creating an “overlapogram” (as did the Cassini UVIS instrument). In reality, the emissions are blurred due to instrumental resolution and aberrations, and multiple spectral feature overlap. Furthermore, the changing opening angle of the rotating torus adds a spurious apparent scale height variation which must be removed, with special attention to asymmetries introduced by Jupiter's changing tilt. With allowances for all these effects, we will report on our search for ion temperature variations during the first two years of Hisaki observations, and compare our results to a previous independent study by M. Shishido (M.S. thesis, U. Tohoku).

Keywords: Jupiter, Io, plasma torus, magnetosphere , hisaki, ultraviolet

©2019. Japan Geoscience Union. All Right Reserved.

Size of the Smallest Particles in Saturn's Rings

*Keiji Ohtsuki[1], Hiroshi Kawamura[1], Naoyuki Hirata[1], Hiroshi Daisaka[2], Hiroshi Kimura[3]

1. Graduate School of Science, Kobe University, 2. Graduate School of Commerce and Management, Hitotsubashi University, 3. Planetary Exploration Research Center, Chiba Institute of Technology

Spacecraft and ground-based observations have shown that particles in Saturn's main rings have a power-law distribution roughly between centimeter and ten meters, but sub-centimeter particles appear to be lacking. Recent studies based on Cassini observations suggest that the size of the smallest particles is on the order of millimeters. Cohesive force between particles has been proposed to explain the paucity of sub-centimeter particles, but its strength depends on impact velocity. In order to better understand recent Cassini observations about small ring particles, we examine impact velocity between ring particles using N-body simulation including size distribution. We find that most collisions take place at velocities lower than 0.1 cm per second; even in dense rings where particles' velocity dispersion is enhanced by gravitational wakes, they collide at such low velocities because particles tend to move coherently in the wakes. This velocity is too low to detach sub-centimeter particles that are attached to the surface of large ones due to the cohesive force, explaining their paucity in the main rings. On the other hand, more infrequent high-velocity impacts can release millimeter-sized particles strongly attached to the surface of large ones, explaining the observed free millimeter-sized particles with relatively low abundance. We will discuss implications of our results for the observed size of the smallest particles in Saturn's main rings.

Keywords: Saturn, rings, Cassini

©2019. Japan Geoscience Union. All Right Reserved.

The Radio & Plasma Wave Investigation (RPWI) for JUICE for the investigation of Jupiter and Icy Moons System: Contributions from Japan

*Yasumasa Kasaba[1], Hiroaki Misawa[1], Fuminori Tsuchiya[1], Atsushi Kumamoto[2], Yuto Katoh[2], Tomoki Kimura[2], Hajime Kita[3], J.-E. Wahlund[4]

1. Planetary Plasma and Atmospheric Research Center, Tohoku University, 2. Department of Geophysics, Tohoku University, 3. ISAS/JAXA, 4. IRF Uppsala, Sweden

The Radio & Plasma Wave Investigation (RPWI) for the ESA JUICE mission (launch: 2022, Observations: 2030s) provides an elaborate suite of electromagnetic fields and plasma instruments. RPWI focuses on cold plasma studies and will investigate how the transfer of momentum and energy in the Jovian huge magnetosphere and the electrodynamic coupling with the icy Galilean moons. Remote sensing and direction finding of the Jovian radio emissions will be carried out. This capability is also devoted to the ices and the deep interiors of the icy moons. Investigations of the ice shells will be performed by means of a novel passive ground penetrating radar technique, which utilizes Jovian strong radio emissions as the transmitted signal. On the Ganymede orbit, continuous measurements of the electric field with the JUICE Magnetometer (JMAG) measurements will determine the electric coupling between any ocean, the ionosphere, and the magnetosphere, and provide the constraints on the physical characteristics of the subsurface ocean of Ganymede.
For those objectives, RPWI sensors consist of 4 Langmuir probes (LP-PWI) for determination of the vector electric field up to 1.6 MHz and cold plasma properties (including active measurements by LP sweeps and mutual impedance sounding) up to 1.6 MHz, a tri-axial search coil magnetometer (SCM) for determination of the vector magnetic field up to 20 kHz, and a tri-dipole antenna system (RWI) for monitoring of radio emissions (80 kHz - 45 MHz). From Japan, the RWI preamp and its High Frequency receiver with the onboard software will be provided, based on the modifications from the BepiColombo PWI and Arase PWE developments. Since Arase already shows the good performance in the radiation hard environment around Earth, we have enough confidence for the possible functions and performance on the Jovian hard environment. We will also provide Software Wave-Particle Interaction Analyzer (SWPIA) function to RPWI DPU, for the onboard quantitative detection of electromagnetic field - ion interactions, modifying from the Arase SWPIA which is also activating on the space now.
HF reciever will provide the first highly-resolved information of Jovian radio emissions emitted from Jovian multiple regions including lightning activity and icy moons, by the 3-ch receiver system manufactured by Japan and Sweden connected to the 3-elements 1.25-m E-filed dipole antenna system manufactured by Poland and Japan. Highly matured onboard and ground data processing will also be provided by France and Japan. As a byproduct, reflected Jovian emission can also be expected from the boundary of icy crust and conductive liquid subsurface ocean. Such reflection components could be observed as the Lunar surface reflection of terrestrial auroral kilometric radiation (AKR) seen by Kaguya Lunar Radar Sounder. JUICE has the RIME (Radar for Icy Moons Exploration) instrument, an active radar which emits 9 MHz pulse from 16 m tip-to-tip antenna and tries to detect the ocean under ~10 km icy crust. Since the frequency of Jovian radiation is wider (several 100 kHz to several 10s MHz), RPWI will provide complementary information, including the vertical distributions of conductivity and permittivity in the icy crust.
In the srping 2019, we are manufacturing and testing the Flight Models (FM) which will be shipped in June - July 2019 to Europe. The long road are connected to the first Jupiter and outer planet tour of the

©2019. Japan Geoscience Union. All Right Reserved.

hardware from Japan.

Keywords: Jupiter, JUICE, Radio waves

©2019. Japan Geoscience Union. All Right Reserved.

Magnetic field experiment at Jupiter icy moons (JUICE J-MAG) and in-flight alignment calibration

*Ayako Matsuoka[1], Michele Karen Dougherty[2], Patrick Brown[2], Futoshi Takahashi[3], Hisayoshi Shimizu[4], Masaki Matsushima[5]

1. Research Division for Space Plasma, Institute of Space and Astronautical Science, Japan Aerospace Exploration Agency, 2. Imperial College London, 3. Kyushu University, 4. University of Tokyo, 5. Tokyo Institute of Technology

The magnetometer instrument (J-MAG) is one of the core instruments on the JUICE spacecraft and is critical for resolving prime science objectives of the mission. The importance of a magnetometer instrument on JUICE can be described under following themes. Firstly, the magnetic field drives the plasma processes occurring within the Jupiter system. Understanding such observations allows for a better understanding of dynamical plasma processes, of the generation of aurora and of the various current systems which arise within this rapidly rotating magnetosphere. Secondary, the magnetometer science which is unique to JUICE lies in being able to gain an understanding of the interior structure of the icy moons of Jupiter, specifically those of Ganymede, Callisto and Europa. Of particular interest are knowledge of the depth at which the liquid oceans reside beneath their icy surfaces, the strength of any internal magnetic fields such as at Ganymede and the strength of any induced magnetic fields arising within these oceans.

J-MAG science requirements result in a requirement on the spacecraft to determine accurate knowledge of the orientation of the fluxgate sensors (MAGIBS and MAGOB). Due to the long MAG boom it is not possible to meet J-MAG’ s alignment requirement by mechanical stability alone, therefore the spacecraft includes two orthogonal coils mounted around its body. The coils can be driven with a current which produces a measurable magnetic field vector at the fluxgate sensors. This signal can then be used by the fluxgates to track the variation in the sensor alignment. This technical note describes the results of an analysis using an alignment recovery technique that was developed for the Kaguya mission, applied to the specific case of JUICE, considering the relative positions of the fluxgate sensors with respect to the JACS coils.

We derived equations to calculate the directions of the measurement axes in the frame fixed to the spacecraft, namely alignment angles, from the measurement results of reference magnetic fields generated by JACS. The errors of the alignment angle estimation and their dependence on measurement noise as well as inaccuracy of the coil current intensity are examined. Based on the quantitative results, the requirements to the JACS design and operation to satisfy the requests to the alignment accuracy are determined.

Keywords: Jupiter, Jovian moons, magnetometer

©2019. Japan Geoscience Union. All Right Reserved.

Science targets of the GAnymede Laser Altimeter (GALA) for the JUICE mission

*Jun Kimura[1], Shunichi Kamata[2], Koji Matsumoto[3], Noriyuki Namiki[3], Keigo Enya[4], Masanori Kobayashi[5], Hiroshi Araki[3], Hirotomo Noda[3], Ko Ishibashi[5], Hauke Hussmann[6], Kay Lingenauber[6]

1. Osaka University, 2. Hokkaido University, 3. National Astronomical Observatory Japan, 4. ISAS/JAXA, 5. Chiba Institute of Technology, 6. German Aerospace Center (DLR), Berlin

The JUpiter Icy Moons Explorer (JUICE), led by European Space Agency, has started development toward launch in 2022 (arrival at Jupiter in 2029, and Ganymede orbit insertion in 2032), and we are now developing the GALA instrument onboard JUICE spacecraft collaborating with German Aerospace Center (DLR) and other institutions in Europe. GALA will acquire the key information for understanding the evolution of Jovian icy moons and to play an essential role in the JUICE's purpose: exploration of deep habitat.

Jovian icy moon Ganymede, which is the largest moon in the Solar System and the primary target of the JUICE, can be said to be one of the typical solid bodies along with terrestrial planets in terms of its size and the intrinsic magnetic field originated from the metallic core. However, current knowledge provided by previous explorations is extremely limited since it comes from only several fly-bys. The JUICE will unveil the whole picture of Ganymede by the first orbiting in the history around extra-terrestrial moon. Expected new big picture of the origin and evolution of Ganymede will not only be a key to unveil the origin of diversity among the Solar System bodies, but also contribute to an understanding of exoplanets with a wide diversity.

The GALA will measure a distance between the spacecraft and the surface of icy moons and acquire the topography data (globally for Ganymede, and fly-by region for Europa and Callisto). It will be a first-ever laser altimetry for the icy object. Such information makes surface geologies clear and tremendously improves our understanding of the icy tectonics. By comparing their tectonic styles on the rocky planets/moons, GALA data leads to reconsider the Earth's plate tectonics. In addition, the GALA will confirm a presence/absence of the subsurface ocean by measuring tidal and rotational response, and the gravitational information reflecting the interior structure will be greatly improved. Furthermore, strength and waveform of reflected laser pulse have an information about surface reflectance at the laser wavelength and small-scale roughness. Finally we can see degrees of erosion and space weathering without being affected by illumination condition through GALA measurements.

In order to interpret and understand such measurements, accumulated studies for the Earth over the years will be effectively utilized: e.g., the data for surface topography, roughness and albedo will lead to describe the icy tectonics through the knowledge from terrestrial glaciology and experiments on impact and deformation process. The tidal measurements by GALA will also be a window to see its interior based on our knowledge and experiences cultivated through the past geodetic observations, e.g., the SELENE mission for the terrestrial Moon.

Characterization of the icy moons will be achieved not only from the GALA measurements but also synergy of other scientific instruments onboard JUICE spacecraft, for examples, surface images taken by optical camera (JANUS) will confirm the position of GALA laser footprint to complement the GALA "point" data for precise topographic mapping. A radar sounder (RIME) and a radio science experiment (3GM) probe

©2019. Japan Geoscience Union. All Right Reserved.

the interior structure, especially interior of the icy crust to figure out an occurrence of tectonic features. A visible and infrared imaging spectrometer (MAJIS), an ultraviolet imaging spectrograph (UVS) and a sub-millimeter wave instrument (SWI) will acquire a surface and atmosphere compositional data. A magnetometer (J-MAG) monitors moons' inductive response to the Jovian magnetic field and probes the subsurface ocean with the help of a particle environment package (PEP) and a radio and plasma wave investigation (RPWI). The GALA works closely together with these instruments and plays a leading and a supporting role to clarify the whole picture of Ganymede and other icy moons.

Keywords: Jupiter, Icy moons, Laser altimetry

©2019. Japan Geoscience Union. All Right Reserved.

Current status of the antenna developments, the data processing, scientific target for JUICE/SWI JAPAN.

*YASUKO KASAI[1], [Group] JUICE SWI Japanese Team

1. National Institute of Information and Communications Technology (NICT)

The Submillimetre-Wave Instrument (SWI) is one of the 10 scientific payloads on the JUpiter ICy moon Explorer (JUICE). The main scientific objectives of SWI is to investigate the structure, compositions and dynamics of the middle atmosphere of Jupiter and exosphere of its moons, as well as thermophysical properties if the satellite surfaces. SWI observations will provide pioneering direct measurements of atmospheric compositions in Jupiter system. SWI will performed limb and nadir observations in the frequency region 530-600 and 1075-1275 GHz. Japanese contribution is the development of main- and sub- reflectors, actuators for the instruments, feasibility studies, data processing, and scientific contributions. We present Current status of the antenna developments, the data processing, scientific target for JUICE/SWI JAPAN.

Keywords: Jupiter, Jovian moons, submm instrument, JUICE, SWI

©2019. Japan Geoscience Union. All Right Reserved.

[E] Oral | P (Space and Planetary Sciences)：P-PS Planetary Sciences

Tue. May 28, 2019 10:45 AM - 12:15 PM JST | Tue. May 28, 2019 1:45 AM - 3:15 AM UTC | A01 TOKYO BAY MAKUHARI HALL

[P-PS03] Solar System Small Bodies: A New Frontier Arising Hayabusa 2, OSIRIS-REx and Other Projects

convener:Masateru Ishiguro(Department of Physics and Astronomy, Seoul National University), Taishi Nakamoto(Tokyo Institute of Technology), Masanao Abe(Institute of Space and Astronautical Science, Japan Aerospace Exploration Agency), Olivier S Barnouin(Johns Hopkins University Applied Physics Laboratory), Chairperson:Masateru Ishiguro(Seoul National University)

In June 2018, the Hayabusa 2 spacecraft arrived at the target asteroid Ryugu after three and half years journey. In addition, another spacecraft, OSIRIS-REx will soon arrive at its destination Bennu. With these arrivals, the solar system research is about to enter a new era. We have organized this small bodies session since 2012 and had a broad range of discussions from viewpoints of laboratory experiments, observations, space explorations, theoretical modeling, and sample analyses. In particular, this time, we aim to hold this session to bring the latest research on solar system small bodies, focusing on the initial results of Hayabusa 2 and OSIRIS-REx. Presentations in the related fields other than these two asteroidal missions are also welcomed.

10:45 AM - 11:00 AM JST | 1:45 AM - 2:00 AM UTC

[PPS03-01] The shape and origin of the rubble-pile asteroid Ryugu

★Invited Papers

*Sei-ichiro WATANABE[1,5], Masatoshi Hirabayashi[2], Naru Hirata[3], Naoyuki Hirata[4], Rina Noguchi[5], Yuri Shimaki[5], Hitoshi Ikeda[6], Eri Tatsumi[7], Makoto Yoshikawa[5], Shota Kikuchi[5], Hikaru Yabuta[8], Tomoki Nakamura[9], Shogo Tachibana[7,5], Yoshiaki Ishihara[10], Tomokatsu Morota[1], Kohei Kitazato[3], Naoya Sakatani[5], Koji Matsumoto[11,12], Koji Wada[13], Hiroki Senshu[13], Chikatoshi Honda[3], Tatsuhiro Michikami[14], Hiroshi Takeuchi[5], Toru Kouyama[15], Rie Honda[16], Robert Gaskell[17], Eric Palmer[17], Olivier S. Barnouin[18], Patrick Michel[19], Paul Abell[20], Yukio Yamamoto[5], Satoshi Tanaka[5], Kei Shirai[5], Moe Matsuoka[5], Seiji Sugita[5,7], Tatsuaki Okada[5], Noriyuki Namiki[11], Masahiko Arakawa[4], Masateru Ishiguro[21], Kazunori Ogawa[4], Fuyuto Terui[5], Takanao Saiki[5], Satoru Nakazawa[5], Yuichi Tsuda[5], Hayabusa2 Science Team (1.Division of Earth and Planetary Sciences, Graduate School of Science, Nagoya University, 2.Auburn University, 3.University of Aizu, 4.Kobe University, 5.ISAS, JAXA, 6.Research and Development Directorate, JAXA, 7.University of Tokyo, 8.Hiroshima University, 9.Tohoku University, 10.National Institute for Environmental Studies, 11.National Astronomical Observatory of Japan, 12.SOKENDAI, 13.Chiba Institute of Technology, 14.Kindai University, 15.National Institute of Advanced Industrial Science and Technology, 16.Kochi University, 17.Planetary Science Institute, 18.John Hopkins University, 19.Universite Cote d'Azur, Observatorie de la Cote d'Azur, 20.NASA, Johnson Space Center, 21.Seoul National University)

11:00 AM - 11:15 AM JST | 2:00 AM - 2:15 AM UTC

[PPS03-02] Results of Hayabusa2 Near Infrared Spectroscopy at Asteroid Ryugu

*Takahiro Iwata[1], Kohei Kitazato[2], Masanao Abe[1], Makiko Ohtake[1], Yusuke Nakauchi[1], Moe Matsuoka[1], KOHJI TSUMURA[3], Shuji Matsuura[4], Lucie Riu[1], NIRS3 Team (1.Institute of Space and Astronautical Science, Japan Aerospace Exploration Agency, 2.The University of Aizu, 3.Tohoku University, 4.Kwansei Gakuin University)

11:15 AM - 11:30 AM JST | 2:15 AM - 2:30 AM UTC

[PPS03-03] Impact experiment on asteroid Ryugu by Small-Carry on impactor of Hayabusa-2 and observation of the impact ejecta by a Deployable CAMera-3

★Invited Papers

*Masahiko Arakawa[1], Takanao Saiki[2], Toshihiko Kadono[3], Yasuhiko Takagi[4], Koji Wada[5], Yu-ichi Iijima[2], Hiroshi Imamura[2], Chisato Okamoto[1], Yuri Shimaki[2], Kei Shirai[2], Satoru Nakazawa[2], Masahiko Hayakawa[2], Naru Hirata[6], Hajime Yano[2], Hirotaka Sawada[2], Kazunori Ogawa[1], Ko Ishibashi[5], Hiroshi

Kimura[5], Masanori Kobayashi[5], Naoya Sakatani[2], Hajime Hayakawa[2], Rie Honda[7], Seiji Sugita[8], Tomokatsu Morota[9], Shingo Kameda[10], ERI TATSUMI[8], Chikatoshi Honda[6], yokota yasuhiro[2], Toru Kouyama[11], Manabu Yamada[5], Hidehiko Suzuki[12], Kazuo Yoshioka[13], Yuichiro Cho[8], Moe Matsuoka[2] (1.Graduate School of Science, Kobe University, 2.Institute of Space and Astronautical Science, Japan Aerospace Exploration Agency, 3.University of Occupational and Environmental Health, 4.Aichi Toho University, 5.Planetary Exploration Research Center, Chiba Institute of Technology, 6.Dep. of Computer Science and Engineering, Univ. of Aizu, 7.Department of Science and Technology, System of Natual Science, Kochi University, 8.Department of Earth and Planetary Science, Graduate School of Science Sciece, The University of Tokyo, 9.Graduate School of Environmental Studies, Nagoya University, 10.School of Science, Rikkyo University, 11.National Institute of Advanced Industrial Science and Technology, 12.Department of physics, Meiji university, 13.Graduate School of frontier Science, The University of Tokyo)

11:30 AM - 11:45 AM JST | 2:30 AM - 2:45 AM UTC

[PPS03-04] Impact cratering experiments on glass beads with bead size frequency distribution: Implications for cratering process on asteroid Ryugu

*Minami Yasui[1], Masahiko Arakawa[1], Sunao Hasegawa[2], Yuya Yamamoto[1], Ryo Sugimura[1] (1.Graduate School of Science, Kobe University, 2.ISAS, JAXA)

11:45 AM - 12:00 PM JST | 2:45 AM - 3:00 AM UTC

[PPS03-05] Enhancement of impact heating in strength-supported media

*Kosuke Kurosawa[1], Hidenori Genda[2], Shigeru Wakita[2], Thomas M Davison[3], Ryuki Hyodo[2], Tomoki Nakamura[4] (1.Planetary Exploration Research Center, Chiba Institute of Technology, 2.Earth-Life Science Institute, Tokyo Institute of Technology, 3.Department of Earth Science & Engineering, Imperial College London, 4.Department of Earth Science, Tohoku University)

12:00 PM - 12:15 PM JST | 3:00 AM - 3:15 AM UTC

[PPS03-06] Global Thermal Inertia and Surface Roughness of Asteroid 162173 Ryugu by TIR on Hayabusa2

*Yuri Shimaki[1], Hiroki Senshu[2], Naoya Sakatani[1], Tatsuaki Okada[1,3], Tetsuya Fukuhara[4], Satoshi Tanaka[1], Makoto Taguchi[4], Takehiko Arai[5], Hirohide Demura[6], Yoshiko Ogawa[6], Kentaro Suko[6], Tomohiko Sekiguchi[7], Toru Kouyama[8], Jun Takita[9], Tsuneo Matsunaga[10], Takeshi Imamura[3], Takehiko Wada[1], Sunao Hasegawa[1] (1.Institute of Space and Astronautical Science, Japan Aerospace Exploration Agency, 2.Chiba Institute of Technology, 3.University of Tokyo, 4.Rikkyo University, 5.Ashikaga University, 6.University of Aizu, 7.Hokkaido University of Education, 8.National Institute of Advanced Industrial Science and Technology, 9.Hokkaido Kitami Hokuto High School, 10.National Institute for Environmental Studies)

The shape and origin of the rubble-pile asteroid Ryugu

*Sei-ichiro WATANABE[1,5], Masatoshi Hirabayashi[2], Naru Hirata[3], Naoyuki Hirata[4], Rina Noguchi[5], Yuri Shimaki[5], Hitoshi Ikeda[6], Eri Tatsumi[7], Makoto Yoshikawa[5], Shota Kikuchi[5], Hikaru Yabuta[8], Tomoki Nakamura[9], Shogo Tachibana[7,5], Yoshiaki Ishihara[10], Tomokatsu Morota[1], Kohei Kitazato[3], Naoya Sakatani[5], Koji Matsumoto[11,12], Koji Wada[13], Hiroki Senshu[13], Chikatoshi Honda[3], Tatsuhiro Michikami[14], Hiroshi Takeuchi[5], Toru Kouyama[15], Rie Honda[16], Robert Gaskell[17], Eric Palmer[17], Olivier S. Barnouin[18], Patrick Michel[19], Paul Abell[20], Yukio Yamamoto[5], Satoshi Tanaka[5], Kei Shirai[5], Moe Matsuoka[5], Seiji Sugita[5,7], Tatsuaki Okada[5], Noriyuki Namiki[11], Masahiko Arakawa[4], Masateru Ishiguro[21], Kazunori Ogawa[4], Fuyuto Terui[5], Takanao Saiki[5], Satoru Nakazawa[5], Yuichi Tsuda[5], Hayabusa2 Science Team

1. Division of Earth and Planetary Sciences, Graduate School of Science, Nagoya University, 2. Auburn University, 3. University of Aizu, 4. Kobe University, 5. ISAS, JAXA, 6. Research and Development Directorate, JAXA, 7. University of Tokyo, 8. Hiroshima University, 9. Tohoku University, 10. National Institute for Environmental Studies, 11. National Astronomical Observatory of Japan, 12. SOKENDAI, 13. Chiba Institute of Technology, 14. Kindai University, 15. National Institute of Advanced Industrial Science and Technology, 16. Kochi University, 17. Planetary Science Institute, 18. John Hopkins University, 19. Universite Cote d'Azur, Observatorie de la Cote d'Azur, 20. NASA, Johnson Space Center, 21. Seoul National University

In June 2018 Hayabusa2 arrived at near-Earth asteroid (NEA) Ryugu and has been successfully conducting remote-sensing observations from ~20-km or less altitudes and deploying rovers and a lander. Based on images taken by ONC-T, we constructed global shape models of Ryugu [1, 2]. In order to obtain a reliable shape model in a short period, we used two independent methods; the stereophotoclinometry (SPC) technique [3] and the Structure-from-Motion (SfM) technique [4]. Except for boulders and high latitudes, the two models are in good agreement with each other.

The total volume of Ryugu derived from an SPC-based shape model is 0.377±0.005 km^3. Gravity measurement revealed that the asteroid's mass is (4.50±0.06) $\times 10^{11}$ kg. The bulk density is thus obtained as 1.19±0.03 g cm^{-3}. The density is significantly smaller than bulk densities (1.6-2.4 g cm^{-3}) measured for Ch- and Cgh-type having the 0.7-μm absorption [5]. However, it remains within the 0.8–1.5 g cm^{-3} range measured for BCG-types (B-, C-, Cb-, and Cg-type), which might be related to unheated icy asteroids [5]. The low bulk density of Ryugu is consistent with the spectral type (Cb-type) measured by ONC-T and NIRS3 [2, 6].

NIRS3 observations indicate that hydrated minerals are widely spread on the surface of Ryugu [6]. The presence of water ice, however, is unlikely for NEA Ryugu because the radiative equilibrium temperature (~250 K) is higher than the ice sublimation temperature (~230 K) at its central pressure of ~8 Pa and the thermal diffusion time of Ryugu is estimated to be much shorter than the typical dynamical lifetime of NEAs [1]. Note that the parent body of Ryugu located in the Main Belt might have water ice and low density of Ryugu could be ascribed to loss of volatile components without subsequent compaction. If we adopt the grain densities of CM carbonaceous chondrites (CCs), the derived total porosity is 57-63%. Adopting those of Orgueil CI CC, we predict the total porosity to be 50-52%. The estimated total porosity is even higher than that of rubble-pile asteroid Itokawa (44±4%) [8, 9], indicating that Ryugu is also a rubble pile.

Hayabusa2 reveals that Ryugu is a top-shape asteroid; a prominent elevated ridge around the equator. Although dozens of top-shaped asteroid have been found by ground-based radar, Ryugu is the first top-shape asteroid to be directly observed up close by a spacecraft. Bennu is the second one.

Derived surface slopes to the equipotential surface assuming the present shape and uniform interior

©2019. Japan Geoscience Union. All Right Reserved.

demonstrate least variation with latitude if, at some epoch, Ryugu had a spin period of 3.5 hours (about half of the current value) [1]. This suggests that the top shape was formed by centrifugally induced structural failure during a rapid rotation era. The deformation occurred either in the initial re-accumulation stage [10] or in the later quasi-statically spin-up stage (due to the YORP thermal effect) [11]. In the later stage, a deformation process might be induced either on the surface or in the interior, depending on the internal structure. The high porosity nature of Ryugu as well as no significant offset between the centers of figure and gravity suggest that the internal tensile strength of the asteroid is uniform and low.
NIR absorption feature of Ryugu obtained by NIRS3 is similar to those of heated/hocked CI/CM chondrites [6]. However, these meteorites are relatively rare whereas BCG types are abundant, so that another meteoritic counterpart of BCG types are expected. High porosity nature of Ryugu suggests that meteorites originated from BCG-type asteroids would be very fragile and should be destroyed at the atmospheric entry. This is consistent with the scanty of BCG-originated meteorites and a hypothesis that pyroxene-rich interplanetary dust particles (IDPs) are originate from BCG-types based on the mid-IR spectroscopy [5]. Thus, comparative studies of Ryugu and Bennu, not only in material science but also in physical properties and internal structure, are the key to understand the delivery system of water and organic materials from the snow line to Earth.

References: [1] S. Watanabe+ (2019) *Science,* under review, [2] S. Sugita+ (2019) *Science,* under review, [3] R.W. Gaskell+ (2008) *Meteoritics & Planet Sci.,* 43, 1049. [4] R. Szeliski (2010) *Computer Vision: Algorithms and Applications* (Science & Business Media, Springer, New York), [5] P. Vernazza+ (2015) *Astrophys. J.,* 806, 204, [6] K. Kitazato+ (2019) *Science*, under review, [7] R.J. Macke+ (2011) *Meteoritics & Planet Sci.*, 46, 1842, [8] A. Fujiwara+ (2006) *Science* 312, 1330, [9] A. Tsuchiyama+ (2011), *Science*, 333, 1125, [10] P. Michel+ (2001) *Science*, 294, 1696, [11] K. J. Walsh (2018) *Ann. Rev. Astron. Astrophys.* 56, 593.

Keywords: Planetary exploration, C-type asteroids, Rubble-pile objects, Hayabusa2

©2019. Japan Geoscience Union. All Right Reserved.

Results of Hayabusa2 Near Infrared Spectroscopy at Asteroid Ryugu

*Takahiro Iwata[1], Kohei Kitazato[2], Masanao Abe[1], Makiko Ohtake[1], Yusuke Nakauchi[1], Moe Matsuoka[1], KOHJI TSUMURA[3], Shuji Matsuura[4], Lucie Riu[1], NIRS3 Team

1. Institute of Space and Astronautical Science, Japan Aerospace Exploration Agency, 2. The University of Aizu, 3. Tohoku University, 4. Kwansei Gakuin University

The Near Infrared Spectrometer (NIRS3) is installed on the Hayabusa2 spacecraft to observe the target C-type asteroid 162173 Ryugu at near infrared wavelengths of 1.8 to 3.2 μm. It aims to obtain reflectance spectra in order to detect absorption bands of hydrated and hydroxide minerals in the 3 μm-band spectral region. Spectra obtained during the cruising and proximity-operation phases have revealed that the performance of NIRS3, using the newly developed linear-image sensor with indium arsenide (InAs) photodiodes, are good enough as expected from the ground performance tests.
Prior to the touch down of Hayabusa2 on the surface of Ryugu, NIRS3 has completed global observations from the Home Position, where the altitude is about 20 km above the surface. NIRS3 also performed low-altitude observations in several opportunities, such as the separation operation of the small rovers and lander, during which the lowest altitude was less than 30 m. Analyzing the spectra, NIRS3 contributed to estimate the temperature of the asteroid surface. After removing the thermal emission, we successfully detected a weak and narrow absorption feature centered at 2.72 μm, which suggests the existence of hydroxyl (OH)-bearing minerals formed by aqueous alteration. This feature is, however, almost uniform over the whole surface in terms of band depth and position. Additionally, it is remarkable that the albedo of Ryugu is extremely low. These results imply the following hypotheses; 1) dehydration caused by heating or space weathering, or 2) masking effects by dark materials on the surface. We will argue about the inspection of the evolution scenario of Ryugu inferred from the above results.

Keywords: Hayabusa2, Ryugu, NIRS3, hydrated mineral

©2019. Japan Geoscience Union. All Right Reserved.

Impact experiment on asteroid Ryugu by Small-Carry on impactor of Hayabusa-2 and observation of the impact ejecta by a Deployable CAMera-3

*Masahiko Arakawa[1], Takanao Saiki[2], Toshihiko Kadono[3], Yasuhiko Takagi[4], Koji Wada[5], Yu-ichi Iijima[2], Hiroshi Imamura[2], Chisato Okamoto[1], Yuri Shimaki[2], Kei Shirai[2], Satoru Nakazawa[2], Masahiko Hayakawa[2], Naru Hirata[6], Hajime Yano[2], Hirotaka Sawada[2], Kazunori Ogawa[1], Ko Ishibashi[5], Hiroshi Kimura[5], Masanori Kobayashi[5], Naoya Sakatani[2], Hajime Hayakawa[2], Rie Honda[7], Seiji Sugita[8], Tomokatsu Morota[9], Shingo Kameda[10], ERI TATSUMI[8], Chikatoshi Honda[6], yokota yasuhiro[2], Toru Kouyama[11], Manabu Yamada[5], Hidehiko Suzuki[12], Kazuo Yoshioka[13], Yuichiro Cho[8], Moe Matsuoka[2]

1. Graduate School of Science, Kobe University, 2. Institute of Space and Astronautical Science, Japan Aerospace Exploration Agency, 3. University of Occupational and Environmental Health, 4. Aichi Toho University, 5. Planetary Exploration Research Center, Chiba Institute of Technology, 6. Dep. of Computer Science and Engineering, Univ. of Aizu, 7. Department of Science and Technology, System of Natual Science, Kochi University, 8. Department of Earth and Planetary Science, Graduate School of Science Sciece, The University of Tokyo, 9. Graduate School of Environmental Studies, Nagoya University, 10. School of Science, Rikkyo University, 11. National Institute of Advanced Industrial Science and Technology, 12. Department of physics, Meiji university, 13. Graduate School of frontier Science, The University of Tokyo

A small carry-on impactor (SCI) equipped on Hayabusa2 is scheduled to be propelled toward to the surface of asteroid Ryugu this spring. Cratering process on Ryugu made by the impactor will simultaneously observed by a deployable camera 3 (DCAM3) detached from Hayabusa2. The mission objective of the impactor is to excavate the asteroid to expose a subsurface material as ejecta deposits around the crater. Thus, not only it enables us to give a good opportunity for obtaining a fresh or subsurface material by a sampler system, remote sensing instruments such as ONC, TIR, NIRS3 onboard Hayabusa2 will also have a good chance to observe the exposed subsurface material. Furthermore, this impact experiment on Ryugu is also a rare opportunity to verify the crater scaling law in the microgravity environment on the real asteroid materials, and is expected to enable us to improve the conventional scaling law, especially for the crater size and the ejecta velocity distribution.

After arrival at Ryugu, the surface morphology observation through remote sensing has turned out that a plenty of boulders cover throughout the surface, and many of the boulders are larger than 10 m. These boulders are distributed almost uniformly and the size frequency distribution of the boulders is a power law distribution with the power law index around -1, indicating relatively large boulders are dominant on the surface. Therefore, taking into account that the precision of an actual impact point toward an aiming point expands several 10 m, the impactor possibly collides with a large boulder, otherwise with small boulders having the power law size distribution, wherever the impactor would aim at on the surface of Ryugu. If the impactor collides with a large boulder, a crater should be formed in the strength regime, and if the impactor collides into a finer-boulder area, a crater will be formed in the gravity regime. The DCAM3 was designed for the observation of not only the impact cratering in the strength regime but also that in the gravity regime.

We believe that we will success to observe impact ejecta induced by the impactor when the SCI and DCAM3 operations are conducted as scheduled. We are planning to present a first report of the DCAM3

©2019. Japan Geoscience Union. All Right Reserved.

observation in this talk, and discuss how to search the impact point on the Ryugu surface using the DCAM3 images, beforehand the onboard imaging instruments. Moreover, the morphology of the ejecta curtain imaged by DCAM3 will bring us a lot of information about the crater formation process. We report the surface condition around the impact point, such as a large block or a small-boulders area, and an excavated area corresponding to the crater size. The DCAM3 will also observe individual dusts in the ejecta curtain to obtain information of the ejecta velocity distribution, so that we may have a chance to introduce these images. However, please note that this presentation strongly depends on the success of the SCI/DCAM3 operation.

Keywords: Asteroid Ryugu, Impact Experiment, Small carry-on impactor, Deployable camera3, Rubble pile body

©2019. Japan Geoscience Union. All Right Reserved.

Impact cratering experiments on glass beads with bead size frequency distribution: Implications for cratering process on asteroid Ryugu

*Minami Yasui[1], Masahiko Arakawa[1], Sunao Hasegawa[2], Yuya Yamamoto[1], Ryo Sugimura[1]

1. Graduate School of Science, Kobe University, 2. ISAS, JAXA

Some impact craters with a diameter of a few hundred meters are found on asteroid Ryugu while there are few small craters of < several meters on the asteroid. Many boulders are found on Ryugu and they have the size frequency distribution similar to that of impact fragments obtained by the impact experiments of rocky materials [1]. When an impactor collided with a larger boulder compared with the impactor size, the boulder could be disrupted but the crater might not form. Some researchers conducted impact experiments on granular targets with a particle size larger than the projectile size and they found that the crater radius became smaller as the size ratio of the target particle to the projectile was larger [e.g., 2]. In this study, we conducted impact cratering experiments on granular targets having the size frequency distribution similar to that of boulders on Ryugu to examine the relationship between the particle size frequency distribution and the crater size.

We conducted cratering experiments by using a one-stage light gas gun at Kobe University and a two-stage light gas gun at ISAS. We used glass beads having the diameters of 0.1, 1, 3, and 10 mm as a target and prepared four types of target; two targets consist of one size of glass bead (0.1 or 3 mm glass beads) and the others consist of mixing three (1-10 mm) or four (0.1-10 mm) different-sized glass beads with the same mass ratio. We used only four glass bead mixing target at ISAS. At Kobe University, the stainless-steel spheres with a diameter of 2 and 3 mm were used as a projectile and the impact velocity was changed from 53 to 181 m/s. At ISAS, the aluminum projectile with a diameter of 1 mm was used and the impact velocity was changed from 1.2 to 4.4 km/s. The collisional phenomena were recorded by high speed camera to observe the rebound of the projectile and the ejection of glass beads.

We observed the ejection of glass beads from the target surface. In the case of 0.1-mm bead target, the beads were ejected radially and the corn-shaped ejecta curtain was observed. In the case of 3-mm bead target, some intact beads were ejected at lower speed. In the case of four bead mixing target, some 0.1-mm beads were ejected like a smoke passing through other beads. Furthermore, the projectile rebounded from the target surface in most cases of 3-mm bead target and two mixing bead targets. When the projectile collided with a 10-mm bead, the amount of the ejected beads decreased drastically.

We applied our results to the crater scaling law showing as $\pi_R = a \cdot \pi_2^{-b}$, where π_R is the non-dimensional parameter related to the crater radius, π_2 is the non-dimensional parameter related to the gravity, the projectile size, and the impact velocity, and a and b are constants. As a result, the π_R of the 0.1-mm bead target was largest. The π_R of the 3-mm bead target and two mixing bead targets matched each other and a little smaller than that of the 0.1-mm bead target when the projectile did not collide with a 10 mm glass bead. Furthermore, the π_R of mixing bead targets was much smaller when the projectile collided with a 10-mm bead.

Finally, we revised the crater scaling law of mixing bead targets by using the scaling law of the 0.1-mm bead target (a=0.58 and b=0.21). In this study, we assumed that the projectile collided with a 3-mm or 10-mm bead and the momentum of the projectile was transferred to the impacted bead, then the bead penetrated into the target slowly and the cavity was formed. On this assumption, we constructed the revised crater scaling law by using the coefficient of the restitution of projectile, e, and the momentum conservation law. As a result, we could obtain e=0.5-1 to match our experimental results with the revised crater scaling law.

[1] Satakani et al. (2018), 2nd Aqua Planetology Symposium, Kobe University. [2] Tatsumi & Sugita (2018),

©2019. Japan Geoscience Union. All Right Reserved.

Icarus 300, 227-248.

Keywords: cratering mechanism, asteroids, boulders, size frequency distribution, crater scaling law

©2019. Japan Geoscience Union. All Right Reserved.

Enhancement of impact heating in strength-supported media

*Kosuke Kurosawa[1], Hidenori Genda[2], Shigeru Wakita[2], Thomas M Davison[3], Ryuki Hyodo[2], Tomoki Nakamura[4]

1. Planetary Exploration Research Center, Chiba Institute of Technology, 2. Earth-Life Science Institute, Tokyo Institute of Technology, 3. Department of Earth Science & Engineering, Imperial College London, 4. Department of Earth Science, Tohoku University

Hypervelocity mutual collisions between small bodies, which include the asteroid Ryugu,occur throughout the history of the solar system. A strong compression and thermal pulse caused by an impact can produce various unique features, such as a change in spectral properties, mosaicism, planer deformation features, high-pressure minerals, atomic diffusion, volatile loss, shock veins, impact melt, and so on. We can obtain these features in samples returned from Ryugu, collected by the Hayabusa2 spacecraft. When we have a reliable model connecting the degree of shock metamorphism with the impactor/target conditions, we can reveal the impact history of Ryugu more correctly.

Frequently, the table from Stöffler et al. (1991, 2018) is used to deduce the shock stage of meteorites using observed shock features, which are subsequently used to infer impact velocities on target bodies. Recently, Kurosawa and Genda (2018) reported that the degree of heating in low-velocity impacts (<10 km/s) is expected to be much higher than previously expected. This is caused by the irreversible heating during plastic deformation against material strength. Low-velocity impacts do not produce large-scale impact melting, but trigger a comminution of both impactor and target materials. Although the materials experiencing compression do not have a tensile strength, they still have a compressive one. Thus, the required impact velocities for producing the unique features produced mainly by the rise in temperature is greatly lowered as shown by Kurosawa and Genda (2018). Another work also confirmed the importance of plastic deformation during impacts to a target embedding hydrous minerals (Wakita and Genda 2019). The experienced temperature at a given shock stage defined by Stöffler’ s table would be revised to somewhat higher temperatures, which would mean that impact histories derived from shock features using the previous table would need to be revised. For example, the target bodies are likely to experience many fewer high-speed energetic impacts than previously expected.

We are planning to revise the Stöffler’ s table by using the state-of-the-art numerical shock physics code, iSALE, which includes both recent equation-of-state (EOS) models and various constitutive models. The Hayabusa2 spacecraft is planning to return to Earth with Ryugu samples in 2020. The revised table would largely help to reproduce the impact history of Ryugu.

In the presentation, we will introduce the work done by Kurosawa and Genda (2018) using the iSALE-2D model and will present some preliminary results from the three-dimensional (3D) model. We newly investigated the effects of impact obliquity using iSALE-3D. As a preliminary result, the enhancement of the impact heating in strength-supported media at oblique impacts becomes larger than the case at vertical impacts to the tangent plane. Although it is widely accepted that the degree of heating correlates well with the vertical component of the impact velocity, our preliminary results show that oblique impacts (45-degrees) produce nearly the same amount of heated volume as vertical impacts do. We are also going to discuss the strategy for reproducting Ryugu’ s impact history.

©2019. Japan Geoscience Union. All Right Reserved.

Acknowledgement: We appreciate the developers of iSALE, including G. Collins, K. Wünnemann, B. Ivanov, J. Melosh, and D. Elbeshausen.

Keywords: Hypervelocity impacts, Impact heating, Shock physics code, Ryugu’s impact history

©2019. Japan Geoscience Union. All Right Reserved.

Global Thermal Inertia and Surface Roughness of Asteroid 162173 Ryugu by TIR on Hayabusa2

*Yuri Shimaki[1], Hiroki Senshu[2], Naoya Sakatani[1], Tatsuaki Okada[1,3], Tetsuya Fukuhara[4], Satoshi Tanaka[1], Makoto Taguchi[4], Takehiko Arai[5], Hirohide Demura[6], Yoshiko Ogawa[6], Kentaro Suko[6], Tomohiko Sekiguchi[7], Toru Kouyama[8], Jun Takita[9], Tsuneo Matsunaga[10], Takeshi Imamura[3], Takehiko Wada[1], Sunao Hasegawa[1]

1. Institute of Space and Astronautical Science, Japan Aerospace Exploration Agency, 2. Chiba Institute of Technology, 3. University of Tokyo, 4. Rikkyo University, 5. Ashikaga University, 6. University of Aizu, 7. Hokkaido University of Education, 8. National Institute of Advanced Industrial Science and Technology, 9. Hokkaido Kitami Hokuto High School, 10. National Institute for Environmental Studies

Thermal infrared imager TIR onboard the Hayabusa2 spacecraft acquired thermal images of the asteroid 162173 Ryugu for one asteroid rotation during Mid-altitude operation on August 1, 2018, with around 5 m/pixel resolution. The thermal images were converted to brightness temperature maps on a shape model based on the ground tests, then temperature profiles of the surface of Ryugu were obtained. For comparison, thermal calculations by a thermophysical model without roughness using the shape model (TPM1) and by one with roughness using fractal rough surfaces (TPM2) were carried out.

Thermal images by TIR reveled that the surface of Ryugu showed ubiquitously high temperature above 300 K, and its temperature profile showed flat pattern at noon. Thermal calculations by TPM1 did not reproduce observed temperature profiles. By comparing maximum temperatures by TIR with those by TPM1, thermal inertia of Ryugu was estimated to be around 160 in MKS unit and reached maximum at the equatorial ridge. By contrast, thermal calculations by TPM2 successfully created flat temperature profile at noon for various thermal inertia and surface roughness. The temperature profiles were fitted by 4-order function to characterize its pattern. A multi linear regression analysis was carried out to estimate thermal inertia and surface roughness from the fitting coefficients. From the regression equations and fitting coefficients by observed temperature profiles, thermal inertia and surface roughness of Ryugu were estimated. Since the estimation is strongly affected by surface tilt angle of a polygon on a shape model, we carried out tilt angle corrections. Finally, thermal inertia of Ryugu by TPM2 was estimated to be around 330 in MKS unit and showed little variation in latitude, and with moderate homogeneous surface roughness. Thermal inertia of Ryugu determined in this study by two TPMs are consistent with that determined by ground observations. Our results suggest that thermal inertia of Ryugu is consistent with that of boulders, indicating porous nature of the boulders widely distributed on Ryugu.

Keywords: Hayabusa2, Thermal Infrared Imager, Asteroid Ryugu

©2019. Japan Geoscience Union. All Right Reserved.

[E] Oral | P (Space and Planetary Sciences)：P-PS Planetary Sciences

Tue. May 28, 2019 1:45 PM - 3:15 PM JST | Tue. May 28, 2019 4:45 AM - 6:15 AM UTC | A01 TOKYO BAY MAKUHARI HALL

[P-PS03] Solar System Small Bodies: A New Frontier Arising Hayabusa 2, OSIRIS-REx and Other Projects

convener:Masateru Ishiguro(Department of Physics and Astronomy, Seoul National University), Taishi Nakamoto(Tokyo Institute of Technology), Masanao Abe(Institute of Space and Astronautical Science, Japan Aerospace Exploration Agency), Olivier S Barnouin(Johns Hopkins University Applied Physics Laboratory), Chairperson:Olivier Barnouin(Johns Hopkins University Applied Physics Laboratory)

In June 2018, the Hayabusa 2 spacecraft arrived at the target asteroid Ryugu after three and half years journey. In addition, another spacecraft, OSIRIS-REx will soon arrive at its destination Bennu. With these arrivals, the solar system research is about to enter a new era. We have organized this small bodies session since 2012 and had a broad range of discussions from viewpoints of laboratory experiments, observations, space explorations, theoretical modeling, and sample analyses. In particular, this time, we aim to hold this session to bring the latest research on solar system small bodies, focusing on the initial results of Hayabusa 2 and OSIRIS-REx. Presentations in the related fields other than these two asteroidal missions are also welcomed.

1:45 PM - 2:00 PM JST | 4:45 AM - 5:00 AM UTC

[PPS03-07] Asteroid Ryugu's parent body and its properties inferred from Haybusa2 multi-band imaging observations

★Invited Papers

*Seiji Sugita[1,6], Rie Honda[2], Tomokatsu Morota[3], Shingo Kameda[4], ERI TATSUMI[1], Chikatoshi Honda[7], yokota yasuhiro[2,5], Toru Kouyama[8], Naoya Sakatani[5], Manabu Yamada[6], Hidehiko Suzuki[10], Kazuo Yoshioka[1], Yuichiro Cho[1], Moe Matsuoka[5], Kazunori Ogawa[9], Deborah Domingue[11], Hideaki Miyamoto[1], Olivier Barnouin[12], Patrick Michel[13], Carolyn Ernst[12], Sei-ichiro WATANABE[3], Yuichi Tsuda[5] (1.University of Tokyo, 2.Kochi University, 3.Nagoya University, 4.Rikkyo University, 5.JAXA/ISAS, 6.Chiba Institute of Technology, PERC, 7.University of Aizu, 8.National Institute of Advanced Industrial Science and Technology, 9.Kobe University, 10.Meiji University, 11.Planetary Science Institute, 12.Johns Hopkins University/Applied Physics Laboratory, 13.Observatoire de la Coˆte d'Azur)

2:00 PM - 2:15 PM JST | 5:00 AM - 5:15 AM UTC

[PPS03-08] REDDENING PROCESS OF THE RYUGU SURFACE BASED ON THE CRATER SIZE-FREQUENCY DISTRIBUTION

*Tomokatsu Morota[1], Yuichiro Cho[2], Masanori Kanamaru[3], Rie Honda[4], Shingo Kameda[5], ERI TATSUMI[2], yokota yasuhiro[6], Toru Kouyama[7], Hidehiko Suzuki[8], Manabu Yamada[9], Naoya Sakatani[6], Chikatoshi Honda[10], Masahiko Hayakawa[6], Kazuo Yoshioka[2], Moe Matsuoka[6], Tatsuhiro Michikami[11], Hideaki Miyamoto[2], Hiroshi Kikuchi[2], Ryodo Hemmi[2], Masatoshi Hirabayashi[12], Naoyuki Hirata[13], Naru Hirata[10], Carolyn Ernst[14], Olivier Barnouin[14], Hirotake Sawada[6], Seiji Sugita[2] (1.Nagoya University, 2.The University of Tokyo, 3.Osaka University, 4.Kochi University, 5.Rikky University, 6.JAXA, 7.AIST, 8.Meiji University, 9.Chiba Institute of Technology, 10.The University of Aizu, 11.Kindai University, 12.Auburn University, 13.Kobe University, 14.Johns Hopkins University/Applied Physics Laboratory)

2:15 PM - 2:30 PM JST | 5:15 AM - 5:30 AM UTC

[PPS03-09] Preliminary report on global distribution visible spectra of asteroid Ryugu based on clustering

*Rie Honda[1], Yasuhiro Yokota[1,2], Eri Tatsumi[3], Antonella Barucci[12], Davide Perna[13], Moe Matsuoka[2], Deborah Domingue[14], Tomokatsu Morota[4], Shingo Kameda[5], Toru Kouyama[15], Hidehiko Suzuki[6], Manabu Yamada[10], Naoya Sakatani[2], Chikatoshi Honda[7], Lucille LeCorre[14], Masahiko Hayakawa[2], Kazuo Yoshioka[3], Yuichiro Cho[3], Yukio Yamamoto[2], Naru Hirata[7], Naoyuki Hirata[8], Tomoki Nakamura[9], Takahiro Hiroi[11], Hirotaka Sawada[2], Yuki Fujii[1], Seiji Sugita[3], Ryo Hayashi[1] (1.Kochi University, 2.ISAS/JAXA, 3.University of Tokyo, 4.Nagoya University, 5.Rikkyo University, 6.Meiji University, 7.Aizu University,

8.Kobe University, 9.Tohoku University, 10.Chiba Institute of Technology, 11.Brown University, 12.Paris Observatory, 13.INAF, 14.Planetary Science Institute, 15.National Institute of Advanced Industrial Science and Technology)

2:30 PM - 2:45 PM JST | 5:30 AM - 5:45 AM UTC

[PPS03-10] Visible spectra of small bright spots on asteroid 162173 Ryugu

*Chiho Sugimoto[1], Eri Tatsumi[1], Yuichiro Cho[1], Kazuo Yoshioka[1], Hirotaka Sawada[2], Yasuhiro Yokota[2], Naoya Sakatani[2], Masahiko Hayakawa[2], Moe Matsuoka[2], Rie Honda[3], Tomokatsu Morota[4], Shingo Kameda[5], Manabu Yamada[6], Toru Kouyama[7], Hidehiko Suzuki[8], Chikatoshi Honda[9], Kazunori Ogawa[10], Deborah Domingue[11], Patrick Michel[12], Seiji Sugita[1] (1.University of Tokyo, 2.JAXA/ISAS, 3.Kochi University, 4.Nagoya University, 5.Rikkyo University, 6.Chiba Institute of Technology, 7.AIST, 8.Meiji University, 9.University of Aizu, 10.Kobe University, 11.Planetary Science Institute, 12.Nice Observatory)

2:45 PM - 3:00 PM JST | 5:45 AM - 6:00 AM UTC

[PPS03-11] Geomorphological characteristics of asteroid Ryugu: implications to its evolutional history

*Hideaki Miyamoto[1], Ryodo Hemmi[1], Hiroshi Kikuchi[1], Goro Komatsu[2], Chikatoshi Honda[3], Tatsuhiro Michikami[4], Tomokatsu Morota[5], Yuichiro Cho[1], Olivier S Barnouin[6], Sho Sasaki[7], Naru Hirata[3], Naoyuki Hirata[8], Rie Honda[10], Shingo Kameda[11], ERI TATSUMI[1], Yasuhiro Yokota[12], Toru Kouyama[13], Hidehiko Suzuki[14], Manabu Yamada[15], Naoya Sakatani[12], Masahiko Hayakawa[12], Kazuo Yoshioka[1], Moe Matsuoka[12], Masatoshi Hirabayashi[9], Hirotaka Sawada[12], Seiji Sugita[1] (1.University of Tokyo, 2.D'Annunzio University, 3.Aizu University, 4.Kinki University, 5.Nagoya University, 6.Johns Hopkins University, 7.Osaka University, 8.Kobe University, 9.Auburn University, 10.Kouchi University, 11.Rikkyo University, 12.ISAS/JAXA, 13.AIST, 14.Meiji University, 15.Chiba Inst Tech)

3:00 PM - 3:15 PM JST | 6:00 AM - 6:15 AM UTC

[PPS03-12] Global distribution of sub-meter boulders measured with texture analysis of Ryugu images

*Naoya Tanabe[1], Yuichiro Cho[1], ERI TATSUMI[1], Tomokatsu Morota[4], Chikatoshi Honda[9], Tatsuhiro Michikami[11], Patrick Michel[12], Carolyn Ernst[13], Olivier S Barnouin[13], Kazuo Yoshioka[1], Sawada Hirotaka[2], yokota yasuhiro[2,3], Naoya Sakatani[2], Masahiko Hayakawa[2], Moe Matsuoka[2], Rie Honda[3], Shingo Kameda[5], Manabu Yamada[6], Toru Kouyama[7], Hidehiko Suzuki[8], Kazunori Ogawa[10], Seiji Sugita[1] (1.University of Tokyo, 2.JAXA/ISAS, 3.Kochi University, 4.Nagoya University, 5.Rikkyo University, 6.Chiba Inst. Tech., PERC, 7.AIST, 8.Meiji University, 9.University of Aizu, 10.Kobe University, 11.Kindai University, 12.Observatoire de la Côte d'Azur, 13.Johns Hopkins University APL)

Asteroid Ryugu's parent body and its properties inferred from Haybusa2 multi-band imaging observations

*Seiji Sugita[1,6], Rie Honda[2], Tomokatsu Morota[3], Shingo Kameda[4], ERI TATSUMI[1], Chikatoshi Honda[7], yokota yasuhiro[2,5], Toru Kouyama[8], Naoya Sakatani[5], Manabu Yamada[6], Hidehiko Suzuki[10], Kazuo Yoshioka[1], Yuichiro Cho[1], Moe Matsuoka[5], Kazunori Ogawa[9], Deborah Domingue[11], Hideaki Miyamoto[1], Olivier Barnouin[12], Patrick Michel[13], Carolyn Ernst[12], Sei-ichiro WATANABE[3], Yuichi Tsuda[5]

1. University of Tokyo, 2. Kochi University, 3. Nagoya University, 4. Rikkyo University, 5. JAXA/ISAS, 6. Chiba Institute of Technology, PERC, 7. University of Aizu, 8. National Institute of Advanced Industrial Science and Technology, 9. Kobe University, 10. Meiji University, 11. Planetary Science Institute, 12. Johns Hopkins University/Applied Physics Laboratory, 13. Observatoire de la Coˆte d’Azur

JAXA’s Hayabusa2 has conducted global observations of Ryugu and revealed many important properties of Ryugu, such as Cb-type average spectrum, the lack of a strong 0.7-um absorption, very low 0.55-um geometric albedo (4.5+/-0.2) %, and very young (< a few Myr) crater retention age for small craters (>10m).

The Cb-type spectrum of Ryugu is consistent with Eulalia and Polana families in the inner main belt, which are dynamically most probable source families. This agreement between the prediction from dynamic calculations and spectral observations suggests that one of the two asteroids is likely Ryugu’s parent body. These families are among the most widely dispersed C-complex families in the inner main belt, allowing to deliver family members at very high flux rate to the resonance zones (nue6 and 3:1) at both inner and outer boundaries of the inner main belt, which are the dominant source of near-Earth objects (NEOs).

Furthermore, high abundance of boulders are found on Ryugu. Evidence for mass wasting indicates mechanically unconsolidated surfaces, allowing surface boulders to move easily. The morphologies of impact craters on Ryugu are consistent with gravity-regime formation, in which impact events produce large ejecta masses. These suggest that large mass of boulders and pebbles can be ejected from Ryugu to space over time.

Consequently, a large mass of Ryugu-like macroscopic objects would enter Earth’s atmosphere, suggesting the presence of counterparts in our meteorite collection. Among such candidates is moderately dehydrated carbonaceous chondrites, which have both very low albedo and flat spectra. They are also found with high abundance in Antarctica, which may represent the long-term average flux of infalling meteorites on Earth. Another is interplanetary dust particles (IDPs), which also have low albedos and account for large influx of extraterrestrial materials to Earth. Although a decisive conclusion may not be obtained before the analysis of Ryugu samples returned to Earth, currently available observational evidence, such as high boulder abundance on Ryugu, favors that its composition may be similar to moderately dehydrated carbonaceous chondrites. This would further suggest that Ryugu’s relatively low abundance of hydrated minerals may be due to partial dehydration on Ryugu’s parent body.

Keywords: Hayabusa2, Ryugu, The evolution of the solar system

©2019. Japan Geoscience Union. All Right Reserved.

REDDENING PROCESS OF THE RYUGU SURFACE BASED ON THE CRATER SIZE-FREQUENCY DISTRIBUTION

*Tomokatsu Morota[1], Yuichiro Cho[2], Masanori Kanamaru[3], Rie Honda[4], Shingo Kameda[5], ERI TATSUMI[2], yokota yasuhiro[6], Toru Kouyama[7], Hidehiko Suzuki[8], Manabu Yamada[9], Naoya Sakatani[6], Chikatoshi Honda[10], Masahiko Hayakawa[6], Kazuo Yoshioka[2], Moe Matsuoka[6], Tatsuhiro Michikami[11], Hideaki Miyamoto[2], Hiroshi Kikuchi[2], Ryodo Hemmi[2], Masatoshi Hirabayashi[12], Naoyuki Hirata[13], Naru Hirata[10], Carolyn Ernst[14], Olivier Barnouin[14], Hirotake Sawada[6], Seiji Sugita[2]

1. Nagoya University, 2. The University of Tokyo, 3. Osaka University, 4. Kochi University, 5. Rikky University, 6. JAXA, 7. AIST, 8. Meiji University, 9. Chiba Institute of Technology, 10. The University of Aizu, 11. Kindai University, 12. Auburn University, 13. Kobe University, 14. Johns Hopkins University/Applied Physics Laboratory

The Hayabusa2 has acquired the high-resolution images and spectra of the Ryugu surface. Although the Ryugu surface has almost homogeneous reflectance and color at the macro scale, the regional variation in the spectral slope is observed by the telescopic optical navigation camera (ONC-T). The redder materials of the Ryugu surface seem to cover bluer materials. Some small craters excavate the red materials on the surface and penetrate the underlying blue materials, suggesting that the craters are younger than the reddening of the surface (space weathering or deposition of red materials). In this study, we performed the crater size-frequency measurements on the Ryugu surface using the ONC image data to constrain the surface age of the Ryugu and the age of reddening event or the timescale of reddening process of the Ryugu surface.

To identify the craters excavating the red materials we used the b-x slope images calculated from multi-band images obtained in the Mid-altitude operation. We identified 15 craters excavating the red materials. These craters have diameters from 10 to 50 m, suggesting that the thickness of the red material layer is less than 1 m.

The cratering chronology models of asteroids have been numerically calculated from the collision rate with other asteroids and scaling laws for crater formation. In this study, we used the intrinsic collision probabilities Pi for the main belt and the NEAs, the population models of the main belt asteroids and NEAs, the mean impact velocities for the main belt (5.3 km/s) and the NEAs (18 km/s), and the new Pi–scaling law developed by Tatsumi and Sugita to develop the cratering chronology model of Ryugu. Because little is known about the bulk strength of materials on Ryugu, we examined two cases (i) the strengthless target (Y = 0 MPa) and (ii) the strength for dry soil (Y = 0.18 MPa).

The density of large craters (D>100 m) on Ryugu is lower than the empirical saturation level and its slope is steeper than that of the saturated distribution, suggesting that craters larger than 100 m are not saturated and the size distribution reflects the crater production function. However, craters smaller than 100 m are significantly under-saturated, suggesting that some crater erasure processes such as seismic shaking and armoring effect are active on the Ryugu surface. Based on cratering chronology model for the main belt, the surface age of Ryugu is estimated to be 5–200 Ma from the size–frequency distribution of craters larger than 100 m.

The observed frequency of craters penetrating the underlying blue materials is ~1/50 of that of craters found on the whole Ryugu. The model age of the reddening is estimated to be 0.1–4 Ma based on the main-belt chronology model and 4–160 Ma based on the NEA chronology model. The NEA model age is roughly close to the median dynamical lifetime of NEAs (~10 Ma), suggesting that the reddening of the Ryugu surface may have some connect with the orbital transition from the main belt to near Earth orbit.

©2019. Japan Geoscience Union. All Right Reserved.

Keywords: Hayabusa2, Ryugu, crater

©2019. Japan Geoscience Union. All Right Reserved.

Preliminary report on global distribution visible spectra of asteroid Ryugu based on clustering

*Rie Honda[1], Yasuhiro Yokota[1,2], Eri Tatsumi[3], Antonella Barucci[12], Davide Perna[13], Moe Matsuoka[2], Deborah Domingue[14], Tomokatsu Morota[4], Shingo Kameda[5], Toru Kouyama[15], Hidehiko Suzuki[6], Manabu Yamada[10], Naoya Sakatani[2], Chikatoshi Honda[7], Lucille LeCorre[14], Masahiko Hayakawa[2], Kazuo Yoshioka[3], Yuichiro Cho[3], Yukio Yamamoto[2], Naru Hirata[7], Naoyuki Hirata[8], Tomoki Nakamura[9], Takahiro Hiroi[11], Hirotaka Sawada[2], Yuki Fujii[1], Seiji Sugita[3], Ryo Hayashi[1]

1. Kochi University, 2. ISAS/JAXA, 3. University of Tokyo, 4. Nagoya University, 5. Rikkyo University, 6. Meiji University, 7. Aizu University, 8. Kobe University, 9. Tohoku University, 10. Chiba Institute of Technology, 11. Brown University, 12. Paris Observatory, 13. INAF, 14. Planetary Science Institute, 15. National Institute of Advanced Industrial Science and Technology

Preliminary result of global distribution of visible spectra of asteroid Ryugu derived from multi-band images obtained by ONC-T onboard Hayabuasa 2 is presented.
The ONC-T is a telescopic charge-coupled-device (CCD) camera with a 6.27˚ ×6.27˚ field of view (FOV) , having a 1024 pixels x 1024 pixels sensor and seven narrow band filters ranging from 395nm and 950nm and one wide-band filter. Images obtained by ONC-T are spatially aligned and converted into seven-band visible spectra (reflectance factor).

The spectra are clustered, and the obtained cluster id are shown on the global map. As the method of clustering, k-means++, x-means, gaussian mixture model via EM are tested for synthetized data and x-means is selected since this method is stable to obtain a suitable number of components.

The obtained spectra are divided into seven to nine groups depending the slope of the spectra. Flat spectrum group is distributed around the equatorial ridge, the redder and darker groups are in the southern hemisphere and the relatively bright and bluer spectra are observed at the polar region, in particular at Otohime Saxum. The distribution of these spectra groups appears to indicate the surface history such as space weathering and erosion and the supply from different sources.

Keywords: asteroid, Ryugu, visible, Hayabusa2, spectra, clustering

©2019. Japan Geoscience Union. All Right Reserved.

Visible spectra of small bright spots on asteroid 162173 Ryugu

*Chiho Sugimoto[1], Eri Tatsumi[1], Yuichiro Cho[1], Kazuo Yoshioka[1], Hirotaka Sawada[2], Yasuhiro Yokota[2], Naoya Sakatani[2], Masahiko Hayakawa[2], Moe Matsuoka[2], Rie Honda[3], Tomokatsu Morota[4], Shingo Kameda[5], Manabu Yamada[6], Toru Kouyama[7], Hidehiko Suzuki[8], Chikatoshi Honda[9], Kazunori Ogawa[10], Deborah Domingue[11], Patrick Michel[12], Seiji Sugita[1]

1. University of Tokyo, 2. JAXA/ISAS, 3. Kochi University, 4. Nagoya University, 5. Rikkyo University, 6. Chiba Institute of Technology, 7. AIST, 8. Meiji University, 9. University of Aizu, 10. Kobe University, 11. Planetary Science Institute, 12. Nice Observatory

The Optical Navigation Camera (ONC) onboard the Hayabusa2 spacecraft has obversed asteroid 162173 Ryugu at various scales and found that Ryugu has a uniform spectrum in km-scale and that boulders exhibit a range of albedo (0.89 −1.3 times of the surface average) and spectra [1]. Higher resolution images taken during descent operations revealed the presence of bright spots, which are typically much brighter than the brightest large boulders. Brightness variation may reflect differences in composition, thermal alteration, or space weathering maturity. Such materials would follow spectral trends seen on other materials on Ryugu. In fact, brightest boulders are the end-members in reflectance/slope statistics and Principal Component Analysis (PCA) of boulders on Ryugu. If bright spots are fragments of the parent body at the origin of Ryugu, they may correspond to the fresher components of the boulder population constituting Ryugu, contributing to the spectral variety observed on the asteroid. In contrast, it is also possible that Ryugu contains materials of exogenous origin. In that case, the spectra of bright spots should not follow the spectral trends observed for other materials on Ryugu and should rather be consistent with the spectra of asteroids found in the inner main belt. In either case, bright spots will help us place important constraints on to the formation and evolution of Ryugu.

In this study, we analyzed the brightest spots whose reflectance is ≧ 1.7 times the reflectance global average. The dimensions of these sports are very small: ≦ 3 m. The spectra of these brightest spots were extracted from I/F images taken at altitudes of Hayabusa2 between 100 and 500 m (i.e., low-altitude descent observations) and 3 −4 km (hovering operation after MASCOT deployment) and were compared with meteorite spectra. As for low altitude images, we conducted a photometric correction because the rotation of Ryugu results in a several degrees phase angle gap between different filters. The spectra of meteorites include 250 carbonaceous chondrite spectra and 106 ordinary chondrite spectra from RELAB of Brown University and they are linearly interpolated to match the bands of ONC-T [2]. We searched for meteorite spectrum that gives minimum residual sum of squares (RSS) of spectra among the 356 samples.

Analysis results indicate that 5 out of 10 bright spots have spectra consistent with carbonaceous chondrites (CC), such as CM2 and CV3, and that the other half are consistent with ordinary chondrite (OC) such as LL6. Some of CC-like bright spot spectra are very similar to that of type3 (bright and molted) boulders found in [1], which was one of the end-members in reflectance/slope statistics and PCA of boulders. This suggests that these bright spots can be new members of this boulder group.

Because Ryugu most likely comes from the inner main bet, OC-like bright spots are consistent with exogenous origin. Preliminary results indicate that two types of spectra are present. One has a spectral peak at v-band (centered at 0.55 micron) and the other has a peak at w-band (0.86 micron). If this spectral variation is large enough to require the delivery of meteoritic materials from asteroids, it would reflect the variety in composition among many projectiles that collided with Ryugu after its formation. In

©2019. Japan Geoscience Union. All Right Reserved.

contrast, if the shift in spectral peak is consistent with spectral modification mechanisms within a large OC-like projectile, such as thermal metamorphism, these bright spots could be remnants of one projectile only. In either case, however, because the average impact velocity in the main belt is very high ~5km/s [3], the fact that we may observe remnants of projectiles impacting at such speeds on the surface of Ryugu has strong implications in our understanding of the impact process and in our interpretation of the compositional heterogeneity of small bodies and meteorites.

[1] Sugita, S. et al., (2019) submitted to *Science*
[2] Tatsumi et al., (2019) *Icarus*
[3] Bottke et al., (1994) *Icarus*

©2019. Japan Geoscience Union. All Right Reserved.

Geomorphological characteristics of asteroid Ryugu: implications to its evolutional history

*Hideaki Miyamoto[1], Ryodo Hemmi[1], Hiroshi Kikuchi[1], Goro Komatsu[2], Chikatoshi Honda[3], Tatsuhiro Michikami[4], Tomokatsu Morota[5], Yuichiro Cho[1], Olivier S Barnouin[6], Sho Sasaki[7], Naru Hirata[3], Naoyuki Hirata[8], Rie Honda[10], Shingo Kameda[11], ERI TATSUMI[1], Yasuhiro Yokota[12], Toru Kouyama[13], Hidehiko Suzuki[14], Manabu Yamada[15], Naoya Sakatani[12], Masahiko Hayakawa[12], Kazuo Yoshioka[1], Moe Matsuoka[12], Masatoshi Hirabayashi[9], Hirotaka Sawada[12], Seiji Sugita[1]

1. University of Tokyo, 2. D'Annunzio University, 3. Aizu University, 4. Kinki University, 5. Nagoya University, 6. Johns Hopkins University, 7. Osaka University, 8. Kobe University, 9. Auburn University, 10. Kouchi University, 11. Rikkyo University, 12. ISAS/JAXA, 13. AIST, 14. Meiji University, 15. Chiba Inst Tech

Observations by Hayabusa 2 spacecraft indicate that Ryugu is a highly porous C-type asteroid. Ryugu’s surface is covered by numerous boulders. These are consistent with the idea that Ryugu is a rubble-pile asteroid. Interestingly, Itokawa, the only other similarly-sized rubble-pile asteroid closely observed by spacecraft, is different from Ryugu in many aspects. For example, while the shape of Ryugu is a top-shape, that of Itokawa is somehow elongated cigar-like. Though Ryugu is generally homogeneous in terms of roughness, Itokawa has two distinctive areas such as smooth and rough terrains. Ryugu has an almost continuous equatorial ridge, though Itokawa does not have such a large-scale topographic feature.

These differences may come from the difference in evolutional processes; a top-shape of rubble pile asteroid is believed to result of rotationally induced deformation or from re-accumulation. Another possibility is that the differences may come from variations in mechanical properties of asteroid forming materials. We are investigating geological characteristics of Ryugu, which may hold clues for these aspects. In this talk, we report initial results of geological investigations mostly using visible images obtained by the Optical Navigation Camera (ONC) onboard the Hayabusa2 spacecraft, and discuss about their implications to evolutional history of Ryugu..

Keywords: asteroid, Hayabusa 2, Ryugu

©2019. Japan Geoscience Union. All Right Reserved.

Global distribution of sub-meter boulders measured with texture analysis of Ryugu images

*Naoya Tanabe[1], Yuichiro Cho[1], ERI TATSUMI[1], Tomokatsu Morota[4], Chikatoshi Honda[9], Tatsuhiro Michikami[11], Patrick Michel[12], Carolyn Ernst[13], Olivier S Barnouin[13], Kazuo Yoshioka[1], Sawada Hirotaka[2], yokota yasuhiro[2,3], Naoya Sakatani[2], Masahiko Hayakawa[2], Moe Matsuoka[2], Rie Honda[3], Shingo Kameda[5], Manabu Yamada[6], Toru Kouyama[7], Hidehiko Suzuki[8], Kazunori Ogawa[10], Seiji Sugita[1]

1. University of Tokyo, 2. JAXA/ISAS, 3. Kochi University, 4. Nagoya University, 5. Rikkyo University, 6. Chiba Inst. Tech., PERC, 7. AIST, 8. Meiji University, 9. University of Aizu, 10. Kobe University, 11. Kindai University, 12. Observatoire de la Côte d'Azur, 13. Johns Hopkins University APL

The spacecraft Hayabusa2 arrived at a C-type asteroid Ryugu on June 27, 2018 and is currently conducting both global and high-resolution observations. These observations have revealed that Ryugu has a very high abundance of boulders; the number density of boulders >20m in diameter is about twice that on Itokawa. However, the sizes of boulders detected in global and regional observations are limited to several to ten meters because the image resolution is 0.5 –2 m in these observations.

In this study, in order to push the limits of boulder detetion, we developed a method that automatically evaluates the abundance of small boulders (sub-pixel to a few pixels in diameter) and applied it to both Ryugu and Itokawa.

The analysis results show that Ryugu has a relatively uniform distribution of boulders over its globe. More specifically, both the power-law index and the coefficient for the boulder cumulative size frequency distribution are very uniform over the entire surface. The power-law index average is -2.53 and the standard deviation due to regional scatter is 0.03 over the globe for boulders > 75 cm. This power-law index is consistent with the result (-2.65 ±0.05) of visual counting for boulders > 5 m [Michikami et al. 2019]. In contrast, Itokawa has a very heterogeneous boulder distribution. The power-law index average is -3.6, and the standard deviation due to regional scatter is 0.83 over the globe. This large regional variation of boulder size distribution on Itokawa strongly suggests the presence of size sorting on its surface, which may be induced by granular convection [Miyamoto et al. 2007].

More detailed analysis has revealed a large variation in boulder number density in both longitudinal and latitudinal directions. In the longitudinal direction, dichotomic contrast in boulder abundance is seen. The boulder density of the eastern hemisphere is ~1.4 times higher than that of the western hemisphere. A similar dichotomic pattern is seen in crater number density [Cho et al. 2019 LPSC] and v-band albedo distribution [Sugita et al. 2019]. Furthermore, the boulder number density is the lowest in troughs surrounding the western hemisphere. The troughs are bluer in the visible wavelengths, similar to the equatorial ridge and polar regions, where newer surfaces are expected to be exposed because of their high geopotential. These lines of evidence suggest that the western hemisphere may be separated from the eastern hemisphere by high mobility zones.

Global observations have revealed that Ryugu exhibits a small but significant latitudinal size sorting in boulders; a larger number of boulders is found at higher latitudes [Sugita et al. 2019]. Our new analysis found a more detailed trend in latitudinal direction. The top of the equatorial ridge exhibits a higher boulder number density, and both southern and northern slopes of the ridge have lower boulder density.

©2019. Japan Geoscience Union. All Right Reserved.

This trend is opposite from the general trend from the equator to the poles and is more pronounced in the eastern hemisphere. We found a significant correlation (R ~ -0.73) between the boulder abundance and the topographic slope with respect to the geopotential. This suggests that the observed boulder distribution is controlled by the current geopotential and not by the paleo-geopotential during a possible past high-spin-rate era.

Keywords: Ryugu, Hayabusa2, boulder

©2019. Japan Geoscience Union. All Right Reserved.

[E] Oral | P (Space and Planetary Sciences)：P-PS Planetary Sciences

Tue. May 28, 2019 3:30 PM - 5:00 PM JST | Tue. May 28, 2019 6:30 AM - 8:00 AM UTC | A01 TOKYO BAY MAKUHARI HALL

[P-PS03] Solar System Small Bodies: A New Frontier Arising Hayabusa 2, OSIRIS-REx and Other Projects

convener:Masateru Ishiguro(Department of Physics and Astronomy, Seoul National University), Taishi Nakamoto(Tokyo Institute of Technology), Masanao Abe(Institute of Space and Astronautical Science, Japan Aerospace Exploration Agency), Olivier S Barnouin(Johns Hopkins University Applied Physics Laboratory), Chairperson:Masanao Abe(Institute of Space and Astronautical Science, JAXA)

In June 2018, the Hayabusa 2 spacecraft arrived at the target asteroid Ryugu after three and half years journey. In addition, another spacecraft, OSIRIS-REx will soon arrive at its destination Bennu. With these arrivals, the solar system research is about to enter a new era. We have organized this small bodies session since 2012 and had a broad range of discussions from viewpoints of laboratory experiments, observations, space explorations, theoretical modeling, and sample analyses. In particular, this time, we aim to hold this session to bring the latest research on solar system small bodies, focusing on the initial results of Hayabusa 2 and OSIRIS-REx. Presentations in the related fields other than these two asteroidal missions are also welcomed.

3:30 PM - 3:45 PM JST | 6:30 AM - 6:45 AM UTC

[PPS03-13] Brightness and morphology variations on surface boulders of 162173 Ryugu: Space Weathering, Breccia, and Thermal Cracks

*Sho Sasaki[1], Seiji Sugita[2], Eri Tatsumi[2], Hideaki Miyamoto[3], Chikatoshi Honda[4], Tomokatsu Morota[5], Masatoshi Hirabayashi[6], Shiho Kanda[1], Naru Hirata[4], Takahiro Hiroi[7], Tomoki Nakamura[8], Takaaki Noguchi[9], Rie Honda[10], Tatsuhiro Michikami[11], Sei-ichiro Watanabe[5], Noriyuki Namiki[12], Patrick Michel[13], Shingo Kameda[14], Toru Kouyama[15], Hidehiko Suzuki[16], Manabu Yamada[17], Hiroshi Kikuchi[3], Yuichiro Cho[2], Kazuo Yoshioka[18], Masahiko Hayakawa[19], Moe Matsuoka[19], Rina Noguchi[19], Naoya Sakatani[19], Hirotaka Sawada[19], yokota yasuhiro[19,10], Makoto Yoshikawa[19] (1.Department of Earth and Space Science, School of Science, Osaka University, 2.Department of Earth and Planetary Science, School of Science, University of Tokyo, 3.Department of Systems Innovation, School of Engineering, University of Tokyo, 4.University of Aizu, 5.Graduate School of Environmental Studies, Nagoya University, 6.Auburn University, 7.Brown University, 8.Department of Earth and Planetary Materials Sciences, Faculty of Science, Tohoku University, 9.Department of Arts and Science, Kyushu University, 10.Department of Science and Technology, System of Natural Science, Kochi University, 11.Faculty of Engineering, Kinki University, 12.RISE Project, National Astronomical Observatory of Japan, 13.Observatoire de la Cote d'Azur, 14.School of Science, Rikkyo University, 15.National Institute of Advanced Industrial Science and Technology, 16.Department of physics, Meiji university, 17.Planetary Exploration Research Center, Chiba Institute of Technology, 18.School of frontier Science, University of Tokyo, 19.Institute of Space and Astronautical Science, Japan Aerospace Exploration Agency)

3:45 PM - 4:00 PM JST | 6:45 AM - 7:00 AM UTC

[PPS03-14] Topography of large craters and equatorial bulge of 162173 Ryugu

*Noriyuki Namiki[1,2], Takahide Mizuno[3], Hiroki Senshu[4], Hirotomo Noda[1,2], Koji Matsumoto[1,2], Naru Hirata[5], Ryuhei Yamada[5], Yoshiaki Ishihara[6], HItoshi Ikeda[3], Hiroshi Araki[1,2], Keiko Yamamoto[1,2], Shinsuke Abe[7], Fumi Yoshida[4], Arika Higuchi[1], Sho Sasaki[10], Shoko Oshigami[1], Seiitsu Tsuruta[1], Kazuyoshi Asari[1], Seiichi Tazawa[1], Makoto Shizugami[1], Hideaki Miyamoto[8], Hirohide Demura[5], Jun Kimura[10], Toshimichi Otsubo[9] (1.National Astronomical Observatory of Japan, 2.SOKENDAI (The Graduate University for Advanced Studies), 3.Japan Aerospace Exploration Agency, Institute of Space and Astronautical Science, 4.Chiba Institute of Technology, 5.The University of Aizu, 6.National Institute of Advanced Industrial Science and Technology, 7.Nihon University,8Osaka University, 8.The University of Tokyo, 9.Hitotsubashi University, 10.Osaka University)

4:00 PM - 4:15 PM JST | 7:00 AM - 7:15 AM UTC

[PPS03-15] Observation of 1064 nm normal albedo around equator of the Ryugu using the Hayabusa2 LIDAR

*Ryuhei Yamada[1], Keiko Yamamoto[2], Hiroshi Araki[2], Hirotomo Noda[2], Hiroki Senshu[3], Noriyuki Namiki[2], Koji Matsumoto[2], Fumi Yoshida[3], Shinsuke Abe[4], Naru Hirata[1] (1.The University of Aizu, Department of Computer Science and Engineering, 2.National Astronomical Observatory of Japan, 3.Chiba Institute of Technology, 4.Nihon University)

4:15 PM - 4:30 PM JST | 7:15 AM - 7:30 AM UTC

[PPS03-16] Improved Trajectory of Hayabusa2 by Combining LIDAR Data and a Shape Model

*Koji Matsumoto[1], Hirotomo Noda[1], Yoshiaki Ishihara[2], Hiroki Senshu[3], Keiko Yamamoto[1], Naru Hirata[4], Naoyuki Hirata[5], Noriyuki Namiki[1], Toshimichi Otsubo[6], Sei-ichiro WATANABE[7], Takahide Mizuno[8], Yukio Yamamoto[8], Hitoshi Ikeda[8], Naoko Ogawa[8], Shota Kikuchi[8], Takanao Saiki[8], Yuichi Tsuda[8] (1.RISE Project, National Astronomical Observatory of Japan, 2.National Institute for Environmental Studie, 3.Chiba Institute of Technology, 4.The University of Aizu, 5.Kobe University, 6.Hitotsubashi University, 7.Nagoya University, 8.JAXA)

4:30 PM - 4:45 PM JST | 7:30 AM - 7:45 AM UTC

[PPS03-17] Present status of preparation for the Ryugu sample curation returned by the Hayabusa2

*Toru Yada[1], Masanao Abe[1], Aiko Nakato[1], Kasumi Yogata[1], Kanako Sakamoto[1], Masahiro Nishimura[1], Tatsuaki Okada[1], Yuki Nakano[2], Miwa Yoshitake[1], Kazuya Kumagai[3], Ayako Iwamae[3], Shizuho Furuya[1], Shogo Tachibana[4,1], Hisayoshi Yurimoto[1,2] (1.Japan Aerospace Exploration Agency, 2.Hokkaido University, 3.Marine Works Japan Ltd., 4.University of Tokyo)

4:45 PM - 5:00 PM JST | 7:45 AM - 8:00 AM UTC

[PPS03-18] Analysis of the grain from the asteroid Ryugu proposed by the Phase 2 curation “Team KOCHI”

*Motoo Ito[1], Naotaka Tomioka[1], Masayuki Uesugi[2], Kentaro Uesugi[2], Ohigashi Takuji[3], Akira Yamaguchi[4], Naoya Imae[4], Yuzuru Karouji[5], Naoki Shirai[6], Toru Yada[5], Masanao Abe[5] (1.Kochi Institute for Core Sample Research, JAMSTEC, 2.JASRI, 3.UVSOR Synchrotron Facility, Institute for Molecular Science, 4.National Institute Polar Research, 5.JAXA, 6.Tokyo Metropolitan University)

Brightness and morphology variations on surface boulders of 162173 Ryugu: Space Weathering, Breccia, and Thermal Cracks

*Sho Sasaki[1], Seiji Sugita[2], Eri Tatsumi[2], Hideaki Miyamoto[3], Chikatoshi Honda[4], Tomokatsu Morota[5], Masatoshi Hirabayashi[6], Shiho Kanda[1], Naru Hirata[4], Takahiro Hiroi[7], Tomoki Nakamura[8], Takaaki Noguchi[9], Rie Honda[10], Tatsuhiro Michikami[11], Sei-ichiro Watanabe[5], Noriyuki Namiki[12], Patrick Michel[13], Shingo Kameda[14], Toru Kouyama[15], Hidehiko Suzuki[16], Manabu Yamada[17], Hiroshi Kikuchi[3], Yuichiro Cho[2], Kazuo Yoshioka[18], Masahiko Hayakawa[19], Moe Matsuoka[19], Rina Noguchi[19], Naoya Sakatani[19], Hirotaka Sawada[19], yokota yasuhiro[19,10], Makoto Yoshikawa[19]

1. Department of Earth and Space Science, School of Science, Osaka University, 2. Department of Earth and Planetary Science, School of Science, University of Tokyo, 3. Department of Systems Innovation, School of Engineering, University of Tokyo, 4. University of Aizu, 5. Graduate School of Environmental Studies, Nagoya University, 6. Auburn University, 7. Brown University, 8. Department of Earth and Planetary Materials Sciences, Faculty of Science, Tohoku University, 9. Department of Arts and Science, Kyushu University, 10. Department of Science and Technology, System of Natural Science, Kochi University, 11. Faculty of Engineering, Kinki University, 12. RISE Project, National Astronomical Observatory of Japan, 13. Observatoire de la Cote d'Azur, 14. School of Science, Rikkyo University, 15. National Institute of Advanced Industrial Science and Technology, 16. Department of physics, Meiji university, 17. Planetary Exploration Research Center, Chiba Institute of Technology, 18. School of frontier Science, University of Tokyo, 19. Institute of Space and Astronautical Science, Japan Aerospace Exploration Agency

Hayabusa2 is the second sample return mission from an asteroid after Hayabusa which visited an S-type asteroid Itokawa. The target asteroid of Hayabusa2 is (162173)Ryugu (1999 JU3),which is a C-type asteroid. Since June 2018, Hayabusa2 observed Ryugu including several low altitude operations, where three surface rovers (MINERVA IIA, IIB, MASCOT) have been deployed successfully.

ONC(Optical Navigation Camera) on board Hayabusa2 captured tantalizing features of 162173 Ryugu, which is a top-shaped dark body with overall visible albedo is 4.6% and photometry standard reflectance is lower than 2%. Color Vis-NIR spectra are flat with little variation (close to B-Cb type, darker). Ryugu would be composed of dark CM meteorite.

Brightness Variation: There are brightness (and associated color u/v bands) variations on the surface. Ryugu’s surface is covered with numerous boulders/rocks whose number density is about twice as large as that of Itokawa. Bright, large boulders are on polar regions and smaller ones with similar brightness are scattered globally. Otohime Saxum is the largest boulder (~180m) on Ryugu; it has bright (and blue) smooth surface and darker surface. Around Otomime Saxum, there observed smooth bright boulders and dark rugged boulders.

The equatorial ridge (Ryujin Dorsum) and some of undulated crater rim zones are brighter. In high-resolution images, Ryugu‘s surface is covered with darker regolith materials (with various size particles >cm) that would cover and bury boulders. Ridge/crater brightness can be ascribed to movement of fine darker materials to potentially lower region, or to abundant brighter fragments. Bright crater rims could be explained by the former process, whereas Ryujin brightness could be also explained by the latter process.

©2019. Japan Geoscience Union. All Right Reserved.

The distinct characteristics of brighter and darker boulders are scale-invariant on Ryugu’ s surface. show brighter boulders with smooth and layered surface and darker boulders with rough (rugged/crumbling) surface. High resolution images obtained by MINERVA-II and MASCOT confirmed the characteristics of bright and dark rocks; MASCOT suggested the existence of bright rugged rocks. We do not observe pond-like deposits of relatively similar size grains as we saw on Eros and Itokawa.

Space Weathering: The brightness/color difference may not be due to compositional variation but to the differences of space weathering maturity. Usually bright boulders are a few 10 % brighter than dark boulders and regolith. Sometimes it is 50% and more brighter. We found the evidence that the interior of a dark small rock is 4 times brighter in v-band (550nm). It should be noted that (bi-directional) reflectance of the bright interior is about 8% (~4 x 2%) and still in the range of CM.

The darker boulders with rough (rugged/crumbling) surface, which would have experienced longer exposure and thus more erosion and weathering. Probably the darkening timescale is so short that usual brightness difference is smaller than a few 10 %.

Breccia A lot of rocks on Ryugu show brecciated structure with brightness variation. The breccia formation would take place by impacts on Ryugu’ s parent body, where the layered structure of boulders would be also formed.

Meridional Cracks: High resolution images show that more than 10 boulders/rocks have a crack in the meridional direction (north –south) on Ryugu. The size range of cracked rocks is a few 10cm to 10m. Boulders with a crack in the meridional direction suggest that thermal stress would play a role in the boulder disruption. Thermal fatigue is an advocated process where difference of thermal properties among minerals should cause disintegration of rocks and it is effective in a smaller scale. Actually thermal timescale of diurnal temperature change is as small as or smaller than 10cm.

In the terrestrial desert area, however, meridional fractures are frequently observed on rocks. Since Ryugu has a large orbital eccentricity 0.19, annual temperature change might bring about thermal stress in longer length scales.

Figure: Rocks with a crack in the meridional direction.

Keywords: Near Earth asteroids, Hayabusa 2, Space weathering, Thermal fatigue, Carbonaceous meteorites

©2019. Japan Geoscience Union. All Right Reserved.

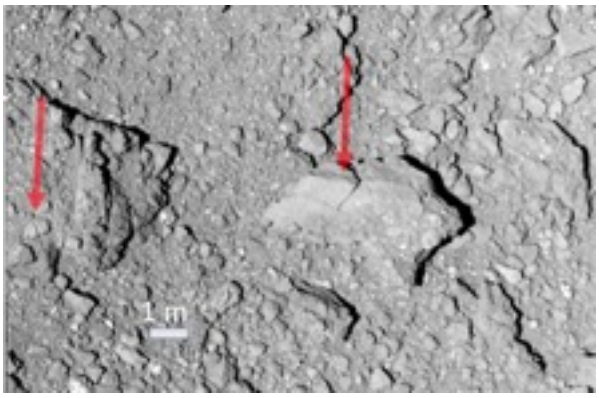

©2019. Japan Geoscience Union. All Right Reserved.

Topography of large craters and equatorial bulge of 162173 Ryugu

*Noriyuki Namiki[1,2], Takahide Mizuno[3], Hiroki Senshu[4], Hirotomo Noda[1,2], Koji Matsumoto[1,2], Naru Hirata[5], Ryuhei Yamada[5], Yoshiaki Ishihara[6], HItoshi Ikeda[3], Hiroshi Araki[1,2], Keiko Yamamoto[1,2], Shinsuke Abe[7], Fumi Yoshida[4], Arika Higuchi[1], Sho Sasaki[10], Shoko Oshigami[1], Seiitsu Tsuruta[1], Kazuyoshi Asari[1], Seiichi Tazawa[1], Makoto Shizugami[1], Hideaki Miyamoto[8], Hirohide Demura[5], Jun Kimura[10], Toshimichi Otsubo[9]

1. National Astronomical Observatory of Japan, 2. SOKENDAI (The Graduate University for Advanced Studies), 3. Japan Aerospace Exploration Agency, Institute of Space and Astronautical Science, 4. Chiba Institute of Technology, 5. The University of Aizu, 6. National Institute of Advanced Industrial Science and Technology, 7. Nihon University,8Osaka University, 8. The University of Tokyo, 9. Hitotsubashi University, 10. Osaka University

In LIDAR topography data, 3 circular depressions are recognized near the equatorial bulge. All of these circular depressions are identified as craters and have been given names approved by IAU, namely Urashima, Kolobok, and Brabo craters. After careful calibration for different passes, consistent and precise cross sections of the craters are derived.

For Urashima crater, topography data of 4 passes are merged. Because these passes are taken in different days of operation, altitude of the spacecraft and sampling rate vary widely from 6 to 21 km and from 1/32 Hz to 1 Hz, respectively. Nonetheless, the cross sections show a good match. Similarly, three passes are merged for Kolobok and Brabo craters, and the match among different passes is very good for these craters, too, except for topography over large boulders.

Depth-to-diameter ratios (d/D) of Urashima, Kolobok, and Brabo craters are 0.2, 0.14, and 0.155, respectively, and are consistent with previous in situ observations of asteroid topography, while there seems marked difference from craters on Itokawa and Bennu. Both Itokawa and Bennu are comparable in size and surface gravity to Ryugu, and these 3 asteroids are regarded as rubble pile bodies. On the contrary, the d/D of Itokawa craters, 0.08 +- 0.03, is significantly shallower than that of Ryugu and other asteroids. The d/D of Bennu is apparently shallower, too. In addition, craters on Ryugu have topographically distinctive raised rim while those on Itokawa do not.

The low d/D of Itokawa is regarded as a result of either an influence of curvature of small body, a lack of raised rim, or fine grains infilling the craters, but has been unsolved. On the other hand, craters of Mathilde have characteristics much alike to those on Ryugu; the d/D ranging from 0.12 to 0.25, prominent raised rim, and a lack of ejecta blanket. While Mathilde is 50 times larger than Ryugu, the bulk density of Mathilde is only 1.34 +- 0.2 g cm^{-3}. Such low density is likely suggesting that Mathilde is as porous as 50 %.

The shapes of the four craters are neither bowl-shaped like 951 Gaspra and Eros nor flat like Itokawa. It is notable that slopes of inner wall of Ryugu craters are linear rather than paraboloidal, and that Kolobok and Brabo craters are flat-bottomed. 3D topography model of Urashima crater shows a central cavity on Urashima crater indicating an agreement with impact cratering experiments into porous targets, while the d/D of Ryugu crates is lower than experimental results which is between 0.2 and 0.5. It is interesting that slopes of the 3 craters are almost identical. Such nearly identical conical shape indicates that either the crater shape is well relaxed, or in the contrary, is holding initial shape.

©2019. Japan Geoscience Union. All Right Reserved.

The slopes of inner walls are measured with respect to local gravity estimated by taking GM of 30.0 m^3 s^{-2} and assuming a constant density inside of Ryugu. The mode of the slopes of inner wall of Urahisma, Kolobok, and Breabo craters are between 16 and 20 degrees, 7 and 15 degrees, 16 and 18 degrees, respectively. The mode of slopes is shallower than the repose angle of regolith which is between 30 and 35 degrees. The shallow slopes and flat bottom may indicate that morphology of Ryugu craters is sufficiently relaxed. However, preservation of entire conical shape as well as central cavity of Urashima crater instead suggest that modification of crater topography on Ryugu is limited volumetrically and is less effective than Itokawa.

Keywords: Hayabusa2, Crater, Ea\quatorial bulge, topography, Ryugu

©2019. Japan Geoscience Union. All Right Reserved.

Observation of 1064 nm normal albedo around equator of the Ryugu using the Hayabusa2 LIDAR

*Ryuhei Yamada[1], Keiko Yamamoto[2], Hiroshi Araki[2], Hirotomo Noda[2], Hiroki Senshu[3], Noriyuki Namiki[2], Koji Matsumoto[2], Fumi Yoshida[3], Shinsuke Abe[4], Naru Hirata[1]

1. The University of Aizu, Department of Computer Science and Engineering, 2. National Astronomical Observatory of Japan, 3. Chiba Institute of Technology, 4. Nihon University

In June 2018, the Japanese asteroid explore Hayabusa2 has arrived to C-type asteroid 162173 Ryugu after three and half years journey. The Hayabusa2 has the laser altimeter (light detection and ranging: LIDAR) for navigation of the spacecraft and scientific uses. The main purpose of the LIDAR is to measure the distance between the spacecraft and the asteroid using time delay between the transmission and reception of the laser. In addition, the Hayabusa2 LIDAR has the function of measuring the intensities of a transmitted laser pulse and received laser pulse reflected from the asteroid surface. In this study, we have derived the normal albedo of the Ryugu at the laser wavelength of 1064 nm using the intensity data. The observation of normal albedo using the LIDAR has never been performed on C-type asteroid. Our observation will provide first knowledge of normal albedo variation at 1064 nm on C-type asteroid.

Usually, the Hayabusa2 spacecraft stands at home position (altitude of 20 km) and the intensity and ranging data are obtained with 1/32 Hz. As special operation, the spacecraft moves to latitudinal and longitudinal direction or descend to low altitude. Then, the LIDAR data are sampled at 1Hz. For analysis of normal albedo, we have selected the data obtained in altitude lower than 7 km. The size of the footprint become smaller with descent of the spacecraft, and mapping resolution is higher. Then, less size of footprint is effective to reduce effect of the surface terrain on the LIDAR return pulse. We have applied the data obtained at July 20, August 1, 6, 7, September 11, 20, 21, October 2, 3, 4, 15, 24, 31 and November 1, 2018 for normal albedo analysis. In these days, the spacecraft has been operated at low altitude, for example, rehearsal of touchdown for sample sampling has been performed in October 15 and 24. From the selected data, we have derived the normal albedo around equator of the Ryugu in range of about 10 degrees in latitude. The total data number is 37,5151.

For calculation of normal albedo, we applied some reflectance models; they are the Lambert, the Lommel-Seeliger and the Oren-Nayar models. The intensity of the reflected pulse calculated by the Oren-Nayar model depends on the applied value of roughness () in degree. We have applied 9 Oren-Nayar model changing the roughness from 10 to 90 degrees with interval of 10 degrees. On a footprint, 11 types of normal albedo have calculated for 11 reflectance models, respectively.

Firstly, we have found that the derived values of the 1064 nm normal albedo are different for each model. The lowest albedo is derived for the Lommel-Seeliger model, and the highest albedo is derived for the Oren-Nayar model with roughness of 90 degrees. Secondary, it has been found that values of normal albedo depend on the incident angle of the laser pulse for some reflectance models. Especially, the normal albedo using the Lambert model are evidently higher with increase in incident angle at many areas

©2019. Japan Geoscience Union. All Right Reserved.

around the equator. This is impossible phenomena for real material as rocks, and this means the Lambert model is inappropriate to represent reflectance of a lot of areas on the Ryugu. Therefore, we have investigated relation between the normal albedo and incident angle in each grid with resolution of 5 5 degrees. In the investigation, slope of normal albedo for incident angle were derived for 11 reflectance models in each grid, and the model which have the smallest slope would be appropriate in the area. From the results, we found that the Lommel-Seeliger model is dominant around equator of the Ryugu. When we apply the Lommel-Seeliger model, the average of normal albedo in the equator area is 0.042, and the deviation is 9.0 %. It corresponds to typical albedo of C-type asteroid (0.03-0.06) observed by ground telescope. In this presentation, we will also discuss regionality of the normal albedo on Ryugu and relation with surface terrain.

Keywords: C-type asteroid , Ryugu, Hayabusa2, LIDAR, Normal albedo

©2019. Japan Geoscience Union. All Right Reserved.

Improved Trajectory of Hayabusa2 by Combining LIDAR Data and a Shape Model

*Koji Matsumoto[1], Hirotomo Noda[1], Yoshiaki Ishihara[2], Hiroki Senshu[3], Keiko Yamamoto[1], Naru Hirata[4], Naoyuki Hirata[5], Noriyuki Namiki[1], Toshimichi Otsubo[6], Sei-ichiro WATANABE[7], Takahide Mizuno[8], Yukio Yamamoto[8], Hitoshi Ikeda[8], Naoko Ogawa[8], Shota Kikuchi[8], Takanao Saiki[8], Yuichi Tsuda[8]

1. RISE Project, National Astronomical Observatory of Japan, 2. National Institute for Environmental Studie, 3. Chiba Institute of Technology, 4. The University of Aizu, 5. Kobe University, 6. Hitotsubashi University, 7. Nagoya University, 8. JAXA

Hayabusa2 spacecraft successfully arrived at the target C-type asteroid 162173 Ryugu on 27 June, 2018, with its “home position” being about 20 km above the sub-Earth point. Soon after arrival, Hayabusa2’s remote sensing instruments started near-global observations. Because map products from these instruments depend on the spacecraft position with respect to the asteroid, it is necessary to provide precise spacecraft trajectory in a timely manner. The basic idea is to find a trajectory correction which makes “LIDAR-derived topography” fit to the reference shape model. The LIDAR-derived topography is, in other words, a sequence of LIDAR footprint positions expressed in asteroid-centered body-fixed rotating frame. The footprints can be computed by using the following information; spacecraft position with respect to the asteroid, spacecraft attitude, LIDAR range, rotational information of the asteroid (orientation and spin period). If all the information above was perfect, the collective footprints would delineate the shape of the asteroid. In reality, however, there are various errors affecting the footprint positions, among which the largest is generally the trajectory error, making the resultant LIDAR footprints deviate from the shape model. We call the deviation as residual. A shape model constructed by stereo photoclinometry (SPC) method is used as reference. We obtain trajectory correction by minimizing the residuals with polynomial functions. We made use of Markov chain Monte Carlo (MCMC) algorithm to explore better parameters. We compared the LIDAR-corrected trajectory with camera positions that are determined through SPC shape modeling. The two estimates agree with each other within about 40 m on 10 July 2018, and 20 m on 20 July 2018. LIDAR-derived topography with such an improved trajectory can be used for analysis of boulder height, crater shape, surface roughness, etc.

Keywords: Hayabusa2, spacecraft trajectory, LIDAR

©2019. Japan Geoscience Union. All Right Reserved.

Present status of preparation for the Ryugu sample curation returned by the Hayabusa2

*Toru Yada[1], Masanao Abe[1], Aiko Nakato[1], Kasumi Yogata[1], Kanako Sakamoto[1], Masahiro Nishimura[1], Tatsuaki Okada[1], Yuki Nakano[2], Miwa Yoshitake[1], Kazuya Kumagai[3], Ayako Iwamae[3], Shizuho Furuya[1], Shogo Tachibana[4,1], Hisayoshi Yurimoto[1,2]

1. Japan Aerospace Exploration Agency, 2. Hokkaido University, 3. Marine Works Japan Ltd., 4. University of Tokyo

Hayabusa2 spacecraft had launched in Dec. 2014 and reached the C-type asteroid Ryugu in June 2018 [1]. It has been observing the asteroid with a series of remote-sensing instruments and plans to perform the first touchdown for sampling at the beginning of this year [1, 2]. It will depart from the asteroid at the end of 2019, and return its re-entry capsule encapsulating Ryugu's surface samples back to the Earth at the end of 2020 [1, 2].

In parallel with the spacecraft operation, JAXA has been preparing for the curation of the samples returned from the asteroid. A new class-1000 clean room for Hayabusa2-returned Ryugu samples was established in Sept. 2017. Installation of newly developed sample-handling clean chamber system (CCs) was accomplished by last Oct. The entire sample-handling system consists of five chambers (CC3-1, CC3-2, CC3-3, CC4-1 and CC4-2).

Because C-type asteroids are likely to be parent bodies of hydrated carbonaceous chondrites [3], volatile components such as water and organic matter are one of essential science target for sample analysis [4]. To return volatile-containing samples without contamination of terrestrial volatiles, a new metal sealing system was developed for the Hayabusa2 sample container [5, 6]. Although the sealing system using double Viton O-rings for the Hayabusa container could not prevent terrestrial air contamination [7], the metal sealing system can keep the air contamination less than 1 Pa for 100 hour in the air [5, 6].

After the recovery of re-entry capsule at the landing point, it will first be transferred to the quick look facility (QLC) nearby there. Following the securing processes to the capsule, the sample container will be extracted, cleaned up and connected to a gas sampling system in a clean booth to extract gaseous volatiles inside the container. After the gaseous volatile recovery from the container, the container will then be delivered to the JAXA's curation facility with being kept in a nitrogen atmosphere during the travel from the QLC to Japan. Then the parts of the container which should not be introduced into the CCs will be removed in the cleanroom. Finally, the sample container will be set to the container opening system and installed into CC3-1.

The container will be opened at the CC3-1 in vacuum condition to take out the sample catcher that encapsulates Ryugu grains. The extracted sample catcher will be transferred to CC3-2. The sample catcher has three chambers for keeping samples collected at different surface locations separately [5, 6], and a lid of the chamber for samples obtained at the first sampling location will be taken apart to pick up a small fraction of grains. The picked-up samples will be kept in CC3-2 for future generations under a vacuum condition. The catcher will be transferred from the CC3-2 to CC3-3 under a vacuum condition, and then CC3-3 will be purged with purified nitrogen. The catcher will be transported to CC4-1 and CC4-2 to take out grains from three chambers of the container. As the initial description called 'phase-1' curation work under purified nitrogen environment in CCs, the grains will be weighed, observed with a stereomicroscope, and examined with visible to near-infrared spectrometers in CC3-3

©2019. Japan Geoscience Union. All Right Reserved.

and CC4-2.

Functional checks of the sample handling system and rehearsals of receiving and handling samples will be initiated in April 2019. The sample handling system will be reconditioned in early 2020 based on feedbacks from the preparation activities to be ready for the sample return in late 2020.

References: [1] Watanabe S. et al. (2018). AGU 2018 fall meet., present. #P21A-02. [2] Watanabe S. et al. (2017) Space Sci. Rev. 208, 3–16. [3] Vilas et al. (2008) Astron. J. 135, 1101–1105. [4] Tachibana S. et al. (2014) Geochem. J., 48, 571-587. [5] Sawada T. et al. (2017) Space Sci. Rev. 208, 81-106. [6] Okazaki R. et al. (2017) Space Sci. Rev. 208, 107-124. [7] Okazaki R. et al. (2011) LPS XLII, abstract #1653.

Keywords: Hayabusa2, C-type asteroid, Ryugu, sample curation, carbonaceous chondrite, Near Earth asteroid

©2019. Japan Geoscience Union. All Right Reserved.

Analysis of the grain from the asteroid Ryugu proposed by the Phase 2 curation “Team KOCHI”

*Motoo Ito[1], Naotaka Tomioka[1], Masayuki Uesugi[2], Kentaro Uesugi[2], Ohigashi Takuji[3], Akira Yamaguchi[4], Naoya Imae[4], Yuzuru Karouji[5], Naoki Shirai[6], Toru Yada[5], Masanao Abe[5]

1. Kochi Institute for Core Sample Research, JAMSTEC, 2. JASRI, 3. UVSOR Synchrotron Facility, Institute for Molecular Science, 4. National Institute Polar Research, 5. JAXA, 6. Tokyo Metropolitan University

Returned samples from asteroids and comets have provided unique characteristics to investigate their origin and nature of the Solar System [1-3]. For example, analytical studies of the S-type asteroid Itokawa by the Hayabusa mission provided new insights for the asteroid-meteorite connections, space weathering processes, small asteroidal body formation in the Solar System [e.g., 1, 3, 4]. JAXA Hayabusa2 and NASA Osiris-REx are both on-going sample return missions from the primitive asteroids, Ryugu (C-type) and Bennu (B-type), respectively [5, 6]. Both missions have complementary scientific goals that are to understand the Solar System evolution in the point of view of organics, water, and associated minerals (i.e., hydrous minerals).

Phase 2 curation teams will be acting under the scientific direction and strong ethic of the Astromaterial Science Research Group (ASRG) of JAXA and was authorized 2 institutes by the steering committee of the ASRG in 2017: (1) Kochi Institute for Core Sample Research (KOCHI), JAMSTEC in collaboration with JASRI/SPring-8, UVSOR Synchrotron Facility/National Institutes of Natural Sciences, Institute for Molecular Science, National Institute of Polar Research (NIPR) and Tokyo Metropolitan University, and (2) the Institute for Planetary Materials, Okayama University at Misasa. The JAXA Curation requested us to make an in-depth analysis of a few grains by the state-of-the-art instruments/techniques and nationwide collaborative research activities. We will conduct on analyses in parallel with the initial analysis team led by the Hayabusa2 project.

Recent reports by the Near-IR Spectrometer (NIRS3) on Hayabusa2 spacecraft presented that the asteroid Ryugu may consist of either CM chondritic materials [8] or shocked/heated carbonaceous chondrites [9]. Matsuoka et al. [9] pointed out that the low albedo of the asteroid Ryugu could be explained by a combination of C-rich material, grains size, porosity and space weathering effects on the asteroid surface materials. This implies that the avoiding terrestrial contaminations (i.e., atmospheric water/air, organics) during sample curation, transportation and analysis are important to obtain original chemical characteristics of Hayabusa2 returned samples.

We have developed novel and universal sample holders (KOCHI grid and KOCHI clamp) for a linkage analysis utilizing micro-analytical instruments of FIB, TEM, STXM and NanoSIMS minimizing terrestrial contaminations and sample lost or broken. We also made an additional sample holder (Okazaki cell) for STXM analysis (Ohigashi T. et al. in preparation), and a sample transport vessel (FFTC: facility to facility transfer container; Uesugi K. et al. in preparation) under vacuum or inert gas in parallel.

We have carried out the development of coordinated synchrotron based-CT (SPring-8) –XRD (SPring-8) –FIB (JAMSTEC KOCHI) –STXM (UVSOR Synchrotron Facility) –NanoSIMS (JAMSTEC KOCHI) –TEM (JAMSTEC KOCHI) analysis to obtain complex structure inside of the sample, light element/isotope images to obtain their spatial distributions, speciation of elements: type of bonding, chemical species, redox state and ultra-fine textural observation: mineralogy and crystallography in fine-grained mineral and

©2019. Japan Geoscience Union. All Right Reserved.

organic assemblages in few tens to hundreds of micrometer-scale Hayabusa2 samples. We, therefore, have chosen Antarctic micrometeorites provided by NIPR as analogues of Hayabusa2 sample because of their size (50 to 800 μm, as an example of small particle) and chemical characteristics.

We will report the current status, ethic and motivation of "Team KOCHI" of Phase2 Curation. In addition, we will present newly developed universal sample holders for FIB, TEM, NanoSIMS, STXM, and a sample transport vessel under vacuum or inert gas among nationwide/international universities and institutes.

References: [1] Nakamura T. et al. (2011) Science 333, 1113–1116. [2] Brownlee D.E. et al. (2006) Science 314, 1711–1716. [3] Yurimoto H. et al. (2011) Science 333, 1116–1119. [4] Noguchi T. et al. (2011) Science 333, 1121–1125. [5] Tachibana S. et al. (2014) Geochem. J. 48, 571–587. [6] Lauretta D.S. et al. (2014) Meteorit. Planet. Sci. 50, 834–849. [7] Uesugi M. et al. (2019) Meteorit. Planet. Sci. 1, 1–29. [8] Hiroi T. et al. (2019) 50th LPSC (LPI Contrib. No. 2132), abstract#1129. [9] Matsuoka et al. (2019) 50th LPSC (LPI Contrib. No. 2132), abstract#1534.

Keywords: Hayabusa2 returned sample, Linkage analysis utilizing micro-analytical instruments

©2019. Japan Geoscience Union. All Right Reserved.

[J] Oral | P (Space and Planetary Sciences)：P-PS Planetary Sciences

Tue. May 28, 2019 9:00 AM - 10:30 AM JST | Tue. May 28, 2019 12:00 AM - 1:30 AM UTC | A01 TOKYO BAY MAKUHARI HALL

[P-PS06] Planetary Sciences

convener:Kenji Kurosaki(Department of Physics, Nagoya University), Yusuke Nakauchi(Japan Aerospace Exploration Agency), Chairperson:Ryo Suetsugu(University of Occupational and Environmental Health, Japan), Keisuke Sugiura(Nagoya University)

We call for general interest papers for Planetary Scienses. Planetary Sciences consist of a variety of studies on the past, present, and future of our solar system and exoplanetary systems, Discussions based on various backgrounds are encouraged.

9:00 AM - 9:15 AM JST | 12:00 AM - 12:15 AM UTC

[PPS06-25] Tensile Strength of Porous Dust Aggregates Measured with Dust N-body Simulations

*Misako Tatsuuma[1,2], Akimasa Kataoka[2], Hidekazu Tanaka[3] (1.The University of Tokyo, 2.National Astronomical Observatory of Japan, 3.Tohoku University)

9:15 AM - 9:30 AM JST | 12:15 AM - 12:30 AM UTC

[PPS06-26] **Filling factor dependence of the thermal conductivity understood from the graph structure of dust aggregates**

*Sota ARAKAWA[1], Masaki TAKEMOTO[1], Taishi NAKAMOTO[1] (1.Tokyo Institute of Technology)

9:30 AM - 9:45 AM JST | 12:30 AM - 12:45 AM UTC

[PPS06-27] Collisional disruption of planetesimals: dependence of material strength

*Ryo Suetsugu[1], Hidekazu Tanaka[2], Hiroshi Kobayashi[3], Hidenori Genda[4] (1.University of Occupational and Environmental Health, 2.Tohoku University, 3.Nagoya University, 4.Tokyo Institute of Technology)

9:45 AM - 10:00 AM JST | 12:45 AM - 1:00 AM UTC

[PPS06-28] Size and cooling rate of chondrules formed thorough collision between planetesimals containing volatile materials

*Sin-iti Sirono[1] (1.Department of Earth and Planetary Sciences, Nagoya University)

10:00 AM - 10:15 AM JST | 1:00 AM - 1:15 AM UTC

[PPS06-29] From Dust to Planet via collisional growth

*Hiroshi Kobayashi[1], Hidekazu Tanaka[2] (1.Department of Physics, Nagoya University, 2.Tohoku University)

10:15 AM - 10:30 AM JST | 1:15 AM - 1:30 AM UTC

[PPS06-30] Impact Conditions for the Formation of the Extremely Elongated Shape of 1I/'Oumuamua

*Keisuke Sugiura[1], Hiroshi Kobayashi[1], Shu-ichiro Inutsuka[1] (1.NAGOYA UNIVERSITY Graduate School of Science)

Tensile Strength of Porous Dust Aggregates Measured with Dust N-body Simulations

*Misako Tatsuuma[1,2], Akimasa Kataoka[2], Hidekazu Tanaka[3]

1. The University of Tokyo, 2. National Astronomical Observatory of Japan, 3. Tohoku University

The formation process of μm-sized dust grains into km-sized planetesimals in planet formation has several theories such as direct coalescence growth and concentration due to instability and has not yet been unraveled. It is difficult to verify the formation process because we cannot directly observe planetesimals forming in protoplanetary disks. Therefore, we focus on comets which are the most primitive bodies in our solar system and are thought to be leftover planetesimals. Comets are capable of detailed observation by spacecraft. In this work, we focused on the tensile strength of 67P/Churyumov-Gerasimenko, which is one of the comets in our solar system and was observed by the Rosetta mission.

In order to investigate whether or not the formation process of planetesimals can be restricted by their tensile strength, we conducted N-body simulations considering the interaction model of dust particles (Wada et al. 2007, ApJ, 661, 320) and investigated the tensile strength of porous dust aggregates. The initial dust aggregates were isotropically and statically compressed to simulate their formation process (Kataoka et al. 2013, A&A, 554, A4). As a result of our numerical simulations, we found that tensile stress gradually increases as tensile displacement increases, and then the tensile stress takes the maximum value. In other words, the tensile strength was obtained. We also confirmed that cutting of contacts between particles in the dust aggregates begins to occur near the maximum tensile stress. We obtained the relation that the tensile strength of dust aggregates is proportional to the 1.8 power of the initial volume filling factor, inversely proportional to the constituent particle radius, and proportional to the surface energy of the constituent material. Moreover, we succeeded in reproducing numerical simulation results by using a semi-analytical model that the tensile strength is determined by cutting of contacts between particles. It was also revealed that the constituent particle radius of comet 67P has to be about 3.3–220 μm to reproduce its tensile strength using our model. In the conventional planet formation theory, the constituent particle radius is assumed to be 0.1 μm same as the interstellar dust radius and is different from the value obtained from our model. It is necessary to reconsider theories such as the time evolution of the constituent particle radius.

Keywords: Protoplanetary disks, Planetesimals, Comets, Tensile Strength

©2019. Japan Geoscience Union. All Right Reserved.

Filling factor dependence of the thermal conductivity understood from the graph structure of dust aggregates

*Sota ARAKAWA[1], Masaki TAKEMOTO[1], Taishi NAKAMOTO[1]

1. Tokyo Institute of Technology

Previous studies (Arakawa *et al*. 2017; 2019) revealed that the thermal conductivity through the solid network of dust aggregates is proportional to the square of the filling factor. However, the reason why the thermal conductivity is given by the power-law function of the filling factor was still unclear. In order to understand the physical reason of this power-law dependence, we need to investigate the geometric structure of highly porous dust aggregates.
In this study, we study the graph structure of fractal aggregates called BCCA aggregates (e.g., Meakin 1991). The fractal dimension of BCCA aggregates is approximately 1.9 (e.g., Okuzumi *et al.* 2009) and the graph structure of BCCA aggregates is classified as a tree. Then the gyration radius r_g and the filling factor ϕ is connected by the following equation, $r_g \simeq \phi^{-1/(3-1.9)}$, and the number of the heat conduction path per unit area, σ, is given by $\sigma \simeq \phi^{2/(3-1.9)}$ for BCCA aggregates. In addition, we calculated the graph-theoretical distances of monomer grains within a BCCA aggregate. We found that the root mean square of the graph-theoretical distance d is given by $d \simeq r_g^{1.2}$. Therefore, the thermal conductivity of BCCA aggregates is proportional to $\sigma r_g / d \simeq \phi^2$.

Keywords: thermal conductivity, dust aggregate, powder and granular material

©2019. Japan Geoscience Union. All Right Reserved.

Collisional disruption of planetesimals: dependence of material strength

*Ryo Suetsugu[1], Hidekazu Tanaka[2], Hiroshi Kobayashi[3], Hidenori Genda[4]

1. University of Occupational and Environmental Health, 2. Tohoku University, 3. Nagoya University, 4. Tokyo Institute of Technology

Collisions are one of the most important processes in planet formation because planetary bodies in the Solar System are thought to have experienced a lot of collisions during the accretion process. Thus, collisional processes have been examined extensively. Roughly speaking, collisional outcomes can be classified into disruptive collisions and erosive collisions by the specific impact energy Q_R. In particular, the specific impact energy required to disperse the largest body such that it has exactly half its total mass after the collision is called the critical specific impact energy Q_{RD}^*. In the case of $Q_R > Q_{RD}^*$, collisions between planetesimals are regarded as disruptive collisions, while they are non-disruptive collisions for $Q_R << Q_{RD}^*$, whose mass ejection is small. The values of Q_{RD}^* have been investigated by laboratory experiments and numerical simulations. When the target is small enough to neglect the effect of the target's gravity, the critical specific impact energy is mainly estimated by laboratory experiments. As target size increases, collision outcomes gradually become dominated by the gravity of the target. However, direct experimental measurements of a large scale collision are difficult to carry out in the laboratory. Thus, the values of Q_{RD}^* for large targets are estimated via shock-physics code calculations, which compute the propagation of the shock wave caused by a high velocity collision: Lagrangian hydrocode such as Smoothed Particle Hydrodynamics (SPH) methods, or a hybrid code of Eulerian hydrocode and N-body. These numerical simulations showed the dependence of the value of Q_{RD}^* on various impact conditions such as target size, impact velocity, material properties, impact angle, and numerical resolution. Recently, we performed impact simulation using the grid-based code (iSALE) in the gravity regime, because almost all high velocity collisions have been examined by the SPH method. We showed that collision outcomes of the iSALE simulation agree well with those of the SPH simulation.
As mentioned above, material properties of the target affect collisional outcomes. However, the dependence of Q_{RD}^* on material properties was not studied in detail. In this study, we perform impact simulations in the gravity regime by using shock-physics code, iSALE. We will discuss the dependence of Q_{RD}^* on material properties and impact conditions for a wide range of specific impact energy, and compare our results with previous studies.

Keywords: Planetary formation, Impact processes

©2019. Japan Geoscience Union. All Right Reserved.

Size and cooling rate of chondrules formed thorough collision between planetesimals containing volatile materials

*Sin-iti Sirono[1]

1. Department of Earth and Planetary Sciences, Nagoya University

Chondrite meteorite contains "chondrules", which are silicate spheres with sizes of 0.1-2 mm. Volume fraction of chondrules exceeds 80% in some chondrites. Its shape and high fraction indicate that chondrules were formed through common heating event in the solar nebula. Cooling rate of chondule has been estimated as 10-1000 K/h from laboratory experiments. The size and cooling rate are the most important quantities which characterize chondrules. Although many models have been proposed, the parameter range suitable for chondrule formation is limited in most models.

Collision of planetesimals has been studied as a chondrule forming mechanism. It requires high velocity collision > km/s which is difficult to attain in the solar nebula. However, the formation of Jupiter can excite the motion of planetesimals. Nagasawa et al. (2019) showed that the impact velocity between planetesimals can exceed 10 km/s due to the exitation. Moreover, the age of chondrules ranges between 1 and 3 Myr after CAI. This is consistent to the timing of Jupiter fomation and duration of excited motion of planetesimals.

In order to form chondrules of 0.1-2mm size, high gas dynamic pressure is necessary. The gas in the solar nebula is too rare to breakup silicate melt down to the size range. If a colliding plantesimal contains volatile materials, they evapolate quickly and expand because of the collisional heating. The velocity difference between silicate melt and gas can lead to breakup of silicate melt. The size of melt droplet is determined by Weber number, which is a ratio between gas dynamic pressure and surface tension. I conducted 1-D numerical simulation of expansion of gas-melt mixture. The simluation parameters are the thickness of the mixture L, mass fraction of volatile materials f, and initial temperature $T_{0.}$ I adopted physical parameters of H_2O, and ideal gas is assumed for simplicity.

Figure shows typical evolution of temperatrure. The temperature of the mixture decreases by the expansion of the gas. In this case, the cooling rate is ~1000 K/h. I conducted simluations with various parameter sets. The range of droplet size is 0.3-2mm. Cooling rate is 100-10000 K/h. These ranges are consistent to those of chondrules.

It is possible that the volatile material is not water but organics. If this is the case, the gas is reducing and Fe becomes Fe metal, not FeO. Then the variation of oxidation condition of Fe can explain by the variation of volatile materials. Moreover, if the inside of a planetesimal is melted due to heating by ^{26}Al, Fe migrates to the center of a planetesimal and avoid collision. Then the variation of Fe content (seen as H, L, LL chondrites) can be explained by the internal melting of a planetesimal.

Keywords: chondrule, volatile material, planetesimal, size, cooling rate

©2019. Japan Geoscience Union. All Right Reserved.

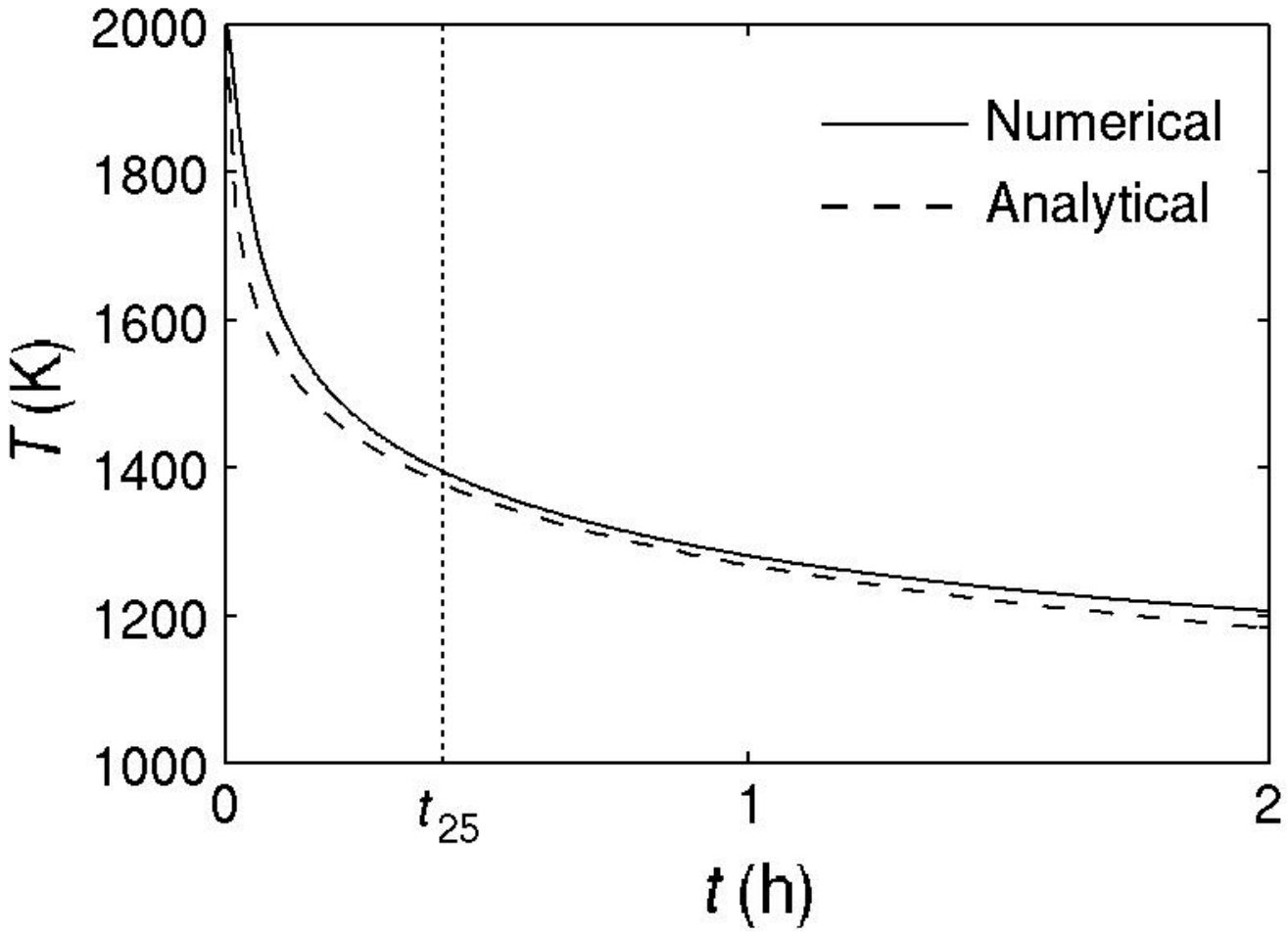

©2019. Japan Geoscience Union. All Right Reserved.

From Dust to Planet via collisional growth

*Hiroshi Kobayashi[1], Hidekazu Tanaka[2]

1. Department of Physics, Nagoya University, 2. Tohoku University

We investigate collisional evolution from dust to planets in protoplanetary disks. For the collisional growth of dust, the bulk density evolution of dust aggregates is important. On the other hand, the random velocity evolution is needed to be considered for planetesimal growth. We take into account both effects consistently and then carry out the simulation for collisional growth from dust to planets. We show planets are possible to be formed via collisional growth of dust.

Keywords: planet formation, protoplanetary disk

©2019. Japan Geoscience Union. All Right Reserved.

Impact Conditions for the Formation of the Extremely Elongated Shape of 1I/’Oumuamua

*Keisuke Sugiura[1], Hiroshi Kobayashi[1], Shu-ichiro Inutsuka[1]

1. NAGOYA UNIVERSITY Graduate School of Science

1I/’Oumuamua is considered to be the first interstellar object observed by the Pan-STARRS telescope on October 2017. The eccentricity of 1I/’Oumuamua is about 1.2, which corresponds to the relative velocity with respect to the sun at infinity of 26 km/s. This relative velocity at infinity is comparable to the relative velocity of solar neighborhoods, and thus we consider that 1I/’Oumuamua came from a nearby planetary system. The absolute magnitude of this object is about 22 magnitude, which corresponds to the size of about 100 m with the albedo of 0.04. This object shows large light curve amplitude of at most 2.5 magnitude, and the shape of 1I/’Oumuamua is estimated to be the extremely elongated one with the ratio of the intermediate to major axis lengths less than 0.3.

To examine whether asteroidal impacts can form the extremely elongated shape of 1I/’Oumuamua or not, we conduct numerical simulations of collisions between asteroids. We use a Smoothed Particle Hydrodynamics code for elastic dynamics with the self gravity, a fracture model for rocky material, and a friction model for completely damaged rocks. We assume that impacting bodies do not have tensile strength of monolith bodies but have frictional forces of granular material. The diameter of target bodies is fixed to 100 m. We conduct impact simulations with various ratios of the masses of two impacting bodies, friction angles, impact angles, and impact velocities, and then we investigate the impact conditions required for the formation of the extremely elongated objects with the ratio of the intermediate to major axis lengths less than 0.3.

As a result of the impact simulations, we find that the formation of the extremely elongated bodies requires the mass ratio larger than 0.5, the friction angle larger than 40 degrees, the impact angle less than 30 degrees, and the impact velocity less than 40 cm/s. The most difficult condition to be realized among these conditions is the impact velocity; the required impact velocity is much smaller than the average impact velocity in the main belt ~ 5 km/s.

The impact velocities less than 40 cm/s require dynamically cold environments in protoplanetary disks. However, turbulent scattering due to gas or gravitational scattering due to larger bodies increase the relative velocities. We estimate required turbulent strength and the size of larger bodies and find that the Shakura-Sunyaev alpha parameter less than $10^{-4}$and the size of larger bodies less than 7 km realize the relative velocities between 100-m sized bodies less than 40 cm/s. This turbulent strength is realized at the places where magnetorotational instability is not active. The size of bodies less than 7 km is realized only in extremely young protoplanetary disks. Therefore,1I/’Oumuamua might have been formed in such an extremely primordial protoplanetary disk, then might have been ejected from the planetary system due to, for example, a stellar encounter, and then visited our solar system.

Keywords: 1I/’Oumuamua, extremely elongated shape, asteroidal impact, numerical simulation, SPH method

©2019. Japan Geoscience Union. All Right Reserved.

[J] Poster | P (Space and Planetary Sciences)：P-PS Planetary Sciences

Tue. May 28, 2019 3:30 PM - 5:00 PM JST | Tue. May 28, 2019 6:30 AM - 8:00 AM UTC | Poster Hall International Exhibition Hall8, Makuhari Messe_2

[P-PS06] Planetary Sciences

convener:Kenji Kurosaki(Department of Physics, Nagoya University), Yusuke Nakauchi(Japan Aerospace Exploration Agency)

We call for general interest papers for Planetary Scienses. Planetary Sciences consist of a variety of studies on the past, present, and future of our solar system and exoplanetary systems, Discussions based on various backgrounds are encouraged.

[PPS06-P01] The Study of Using SLR and GPS Observation Data to Estimate Geocenter Motion.

*Yih Jack Cheng[1], Fang-shii Ning[1] (1.National Chengchi University)

[PPS06-P02] Evolution of Pluto's surface albedo due to sublimation and condensation of ice

*Hisashi Matsui[1], Jun Kimura[1] (1.Osaka University)

[PPS06-P03] ***Origin of the moon*, Reason why Moon is always facing to Earth, Origin of Moon Sea, reasons why there is no Ocean behind Moon**

*Akira Taneko[1] (1.SEED SCIENCE Lab.)

[PPS06-P04] ***Proposed the Good model*** to verify**Origins of Solar System (Planet, Asteroid belt, Earth, Moon)**
*with "Multi Impact Hypothesis ",***from 16' results of one time Evolution *by Abduction.***
cf. Simulation is an example by Abduction from 1.

*Akira Taneko[1] (1.SEED SCIENCE Lab.)

[PPS06-P05] Quantitative evaluation of the cumulus convection schemes for the implementation into the Paleo Martian Global Climate Model

*Katsushige Toriumi[1], Arihiro Kamada[1], Takeshi Kuroda[1,2], Naoki Terada[1], Yasumasa Kasaba[3], Isao Murata[1], Hiromu Nakagawa[1] (1.Tohoku university, Geophysics, Planetary Atmospheric Physics, 2.NICT, 3.Tohoku university, Geophysics, Planetary Plasma and Atmosperic Research Center)

[PPS06-P06] Forced libration of Ganymede including the visco-elastic tidal deformation

*shinichiro kojima[1], Jun Kimura[1], Shunichi Kamata[2] (1.Department of Earth and Space Science, Graduate School of Science, Osaka University, 2.Creative Research Institution, Hokkaido University)

[PPS06-P07] Experimental study on collision destruction simulating the primitive meteorite parent body

*Horikawa Kazuhiro[1], Masahiko Arakawa[1], Minami Yasui[1], Ryo Sugimura[1] (1.Kobe University Faculty of Science)

[PPS06-P08] Evolution of atmospheric composition in the early Martian atmosphere

*Ryosuke Yagi[1], Naoki Terada[1] (1.Planetary Atmospheric Physics Group, Tohoku University, Japan)

[PPS06-P09] Observation of catastrophic destruction of two different targets using X Ray photography

*Takumi Nagano[1], Masahiko Arakawa[1], Minami Yasui[1], masato nakamura[1], Fumiya Nagatomo[1] (1.Faculty of Science Kobe University)

[PPS06-P10] Charge transport between granular particles in an ejecta curtain produced by hypervelocity impacts

*Kosuke Kurosawa[1], Takanori Iwasawa[2], Satoshi Okuzumi[2], Sunao Hasegawa[3], Takayuki Muranushi[4] (1.Planetary Exploration Research Center, Chiba Institute of Technology, 2.Department of Earth and Planetary Sciences, Tokyo Institute of Technology, 3.ISAS, JAXA, 4.AICS, RIKEN)

[PPS06-P11] Nonlinear outcome of gravitational instability in irradiated protoplanetary disks

*Shigenobu Hirose[1], Jiming Shi[2] (1.Japan Agency for Marine-Earth Science and Technology, 2.Spotify USA Inc)

[PPS06-P12] Rheology of clay paste and application to the investigation of formation process of surface topography on the Mars

*Chihiro Uemura[1], Takahiro Iwata[1,2], Akio Nakahara[3], Yosuke Matsuo[3], Tomohiro Usui[2], Rina Noguchi[2] (1.SOKENDAI, 2.ISAS/JAXA, 3.Nihon Univ.)

[PPS06-P13] An Explanation for Physical Mechanism of the Streaming Instability

*Hiroaki Kaneko[1] (1.Tokyo Institude of Technology)

[PPS06-P14] Spatial motion of the Earth-Moon system and Earth pole oscillatory process

*Alexandra Sergeevna Filippova[1], Vadim Vladimirovich Perepelkin[1], Wai Yan Soe[1] (1.Moscow Aviation Institute)

[PPS06-P15] Chondrule formation model by lightning in high dust density regions

*Chihiro Ikeda[1], Taishi Nakamoto[1] (1.Tokyo Institute of Technology)

[PPS06-P16] The transition to superrotation in stratospheric atmospheres

*Motoki Sumi[1] (1.Tokyo Institute of Technology)

[PPS06-P17] **ExPRES: a Tool to Simulate Exoplanetary and Planetary Radio Emissions**

*Corentin LOUIS[1,2,3], Sebastien L. Hess[4], Baptiste Cecconi[2,3], Philippe Zarka[2,3], Laurent Lamy[2,3], Stéphane Aicardi[5], Alan Loh[2] (1.IRAP, Toulouse, 2.LESIA - Observatoire de Paris, 3.USN, Observatoire de Paris, 4.ONERA-The French Aerospace Lab, FR-31055 Toulouse, France, 5.DIO, Observatoire de Paris, PSL Research University, CNRS, Paris, France)

[PPS06-P18] Crustal structures of major mercurian basins

*Qingyun Deng[1], Fei Li[1], Jianguo Yan[1], Zhiyong Xiao[2] (1.State Key Laboratory of Information Engineering in Surveying, Mapping and Remote Sensing, Wuhan University, 2.Planetary Science Institute, China University of Geoscience)

[PPS06-P19] Application of LiDAR Technique for the 3D Digital Documentation of Cultural Heritage Sites

*Sachchidanand [1], Mayank Sharma[1], Rahul Dev Garg[1] (1.Indian Institute of Technology Roorkee)

[PPS06-P20] Tidal Interaction in the Earth-Moon System Treated as a Double Planet

*Aleksandr Aphanasievich Zlenko[1], Irina Michailovna Ryabikova[2] (1.Department of high mathematics, Moscow automobile and road construction state technical university, 2.Department of descriptive geometry, Moscow automobile and road construction state technical university)

[PPS06-P21] **The consequences of Saturn's "ring rain"**

*James O Donoghue[1,2], Luke Moore[3], Jack Connerney[4,1], Henrik Melin[5], Tom Stallard[5], Sean Hsu[6], Steve Miller[7], Kevin Baines[8] (1.NASA Goddard Space Flight Center, USA, 2.Institute of Space and Astronautical Science, Japan Aerospace Exploration Agency (ISAS; JAXA), Japan, 3.Boston University, USA, 4.Space Research Corporation, Maryland, USA, 5.University of Leicester, UK, 6.Laboratory for Atmospheric and

Space Physics, University of Colorado–Boulder, CO, USA, 7.University College London, UK, 8.NASA Jet Propulsion Laboratory, California, USA)

[PPS06-P22] **Calculation of kinetic rate constants using high-level *ab initio* quantum chemical methods for planetary sciences and astrochemistry**

*Shiblee Ratan Barua[1,2], Paul Romani[1] (1.NASA Goddard Space Flight Center, Greenbelt MD USA, 2.Universities Space Research Association (USRA), Columbia MD USA)

[PPS06-P23] How many conditions must be satisfied to produce a habitable planet?

*Shigenori Maruyama[1], Soichi Omori[2] (1.Earth-Life Science Institute, Tokyo Institute of Technology, 2.The Faculty of Liberal Arts, The Open University of Japan)

[PPS06-P24] Quantitative Evaluations for Meteorite Impact Tsunami

*Naotaka YAMAMOTO CHIKASADA[1], Tetsuharu Fuse[2], Toshitaka Baba[3] (1.NIED, 2.NICT, 3.Tokushima University)

The Study of Using SLR and GPS Observation Data to Estimate Geocenter Motion.

*Yih Jack Cheng[1], Fang-shii Ning[1]

1. National Chengchi University

Geocenter motion describes the difference of Center of Figure (CF) respect to Center of Mass of the Earth system (CM) due to the mass re-distribution and deformation of the Earth system. This is a factor that cannot be ignored in the maintenance of the high-precision terrestrial reference frame. As precision requirements and application demands in space geodesy increase, research on estimation of the geocenter motion become increasingly important as the key point to realize a reference frame with its origin fixed to the center of mass of the Earth system. In this study, GPS (Global Positioning System) observation data from IGS (International GNSS Service) and SLR (Satellite Laser Ranging) tracking data in the period of 2007 to 2016 are applied to estimate the coordinates of IGS sites on Earth’ s surface by using the GAMIT/GLOBK and Bernese software. Then, the Helmert transformation model is used to acquire seven parameters between the ITRF (International Terrestrial Reference Frame) reference frame and the CM reference frame. There are three parameters of them are related to the shift in three axes, which are the results of the geocenter motion. Afterwards, the geocenter motion time series are applied with the linear fitting method in order to obtain the amplitudes and phases along three axes of geocenter motion. The annual amplitude of X-, Y-, and Z- components between the years 2007and 2016 are 2.6± 0.2 mm, 4.1±0.2 mm, and 5.6±0.3mm respectively. The annual phase of X-, Y-, and Z- components are 72˚, 330˚, and 145˚ respectively. The accuracy of this study is significant improvement comparing to just using GPS or SLR technique only.

Keywords: Geocenter motion, Global Positioning System, Satellite Laser Ranging

©2019. Japan Geoscience Union. All Right Reserved.

Evolution of Pluto's surface albedo due to sublimation and condensation of ice

*Hisashi Matsui[1], Jun Kimura[1]

1. Osaka University

Observation of the spacecraft New Horizons approached Pluto in 2015 revealed that H_2O, N_2, CH_4, CO ice coexists on the surface of Pluto and that the surface has a strong contrast of bright and dark due to a difference in the amount of ice. However, it is not cleared an origin of the bright and dark color distribution on the surface.
In previous researches about a temporal changing of albedo on the Jovian and Saturnian moons, it has been shown that sublimation of ice due to an insolation affects albedo changing on their surfaces. In addition, condensation of sublimated ice in the atmosphere also should affect Pluto’s surface albedo. Through these processes, ice behavior like sublimation and condensation possibly affects a change of albedo on Pluto’s surface. However, it has been not considered quantitatively so far.
In this study, we evaluate relationship between behavior such as sublimation and condensation of various ices and change of albedo with a numerical simulation, and investigate the origin of the albedo variation on Pluto.
In our model, we assume that bright ice and dark non-ice material exist uniformly mixed and the surface albedo can be modeled by the volume ratio. Subsequently, calculate the surface temperature with a change of insolation on each latitude and thermal inertia and then estimate the sublimation amount of ices from the difference between the vapor pressure at the temperature and the atmospheric pressure. Sublimated ices exist as the atmospheric gas, and these gas should be segregated and deposited on the surface if the surface temperature falls below the segregation temperature. We calculate albedo at the next time step from the volume ratio of ice and non-ice material contained in depth considered to be mixed by micrometeorite bombardment. Finally we examine temporal change of the Pluto’s surface albedo by repeating these cycle.
As a result, using the difference of insolation amount for each latitude caused by the large inclination of the obliquity, we found that a possibility to explain the overall trend of the albedo on current Pluto without special events like a giant impact.

Keywords: Pluto, Albedo

©2019. Japan Geoscience Union. All Right Reserved.

Origin of the moon, Reason why Moon is always facing to Earth, Origin of Moon Sea, reasons why there is no Ocean behind Moon

*Akira Taneko[1]

1. SEED SCIENCE Lab.

In Solar system, Way to verify Mystery of planet origin (evolution creative inference Abduction with Evolution),It is to be able to describe all Multiple results of evolution uniformly using physically meaningful hypothesis,It can be said that it is a verification using evolution that occurs only once.
Initial condition is also unknown, and from Present state where Reproduction experiment can not be done, there is a way that is Only way to infer **Missing Link** to Origin.
Origin of Moon **(2014 U 06 - P 24)**, described Theory of necessity of Moon formation in Model of Multi-Impact Hypothesis. In addition, Origin of Jupiter Large Red Spot, Origin of Asteroid Belt, Origin of Earth Differentiation Meteorite, Origin of Earth Deep Ocean Bottom, Origin of Plate Tectonics, Origin of Driving Force, Origin of Pluto, Origin of Diamond Pipe, Core Eccentricity Also Mentioned Origin.
Origin where Moon is always facing Earth, origin of Moon sea, reason why there is no ocean behind Moon, Earth mantle ejected as shown in Lower right figure has a higher inner density, Moon is biased Center of Moon sea was formed by collision with Meteorite crust which heavy basaltic rocks were heavily on Front side, and Same crustal material does not change even if Meteorite falls on Back side around Common center of gravity of Earth and Moon Rotate Heavy side always to Center (Earth) when Earth rotates each other from its birth, and it is further accelerated and rotating due to Collision.

Y. Toda and Y. Abe Hypothesis that a special mechanism is unnecessary and can be explained as Difference of **random collision number N** between Front side and Back side and **as a result** Tidal lock of Moon will occur after establishment of Crust deformation symmetry [2] . However, since it does not mention the cause of the N number difference, ***it is only a Result Theory.***

Moon Origin Hypothesis up to Present *was a Simulation Deformation in which Differentiated Mars was formed at an arbitrary angle and velocity by Accidental Collision and Moon of only Mantle was formed in the orbital position three times Earth Radius Re.*

In "Multi- Impact Hypothesis", CERRA which was flattened toward the near point side of Jupiter by the perturbation by the gravity of Jupiter formed on the outer side of the Mars sized Differentiated Protoplanet formed at the position of Asteroid Belt by Baudet's Law, And it breaks at Jupiter's gravitational equally dividing point and it revolves around a elliptical orbital with **Train Mantle Fragments** like **a comet of a shoe maker Levi collides** with Earth at the intersection of Earth orbit Time and angle at this time Mooon that is eccentric with **Pacific Ocean** in **the first collision** is formed at current **Moon orbit energy 60 ·Re.**Fragments that collided with Jupiter become **Large Rd Spots** and the mantle of the debris becomes the asteroid belt Origin became an isostasy and became **Origin of Deep Ocean Floor of depth 5 km**, and the multiple collisions became the origin of extinct species species **High Latitude Collision of Tethys Sea formation** is caused by **Earth's gradient** and **Sudden Change in Driving direction** And **Triggered the plate movement**. It can be explained by -Antarctica moving **Center of Shaft** became unchanged **Pacific Rim arc islands and back-arc basins** also **Aisosutashi.**
I can verify **the missing link** by using **the inevitable result of evolution** that I can explain about *the present condition of about 17 items* in **a single Hypothetical model** as **a result of only one Evolution.**

©2019. Japan Geoscience Union. All Right Reserved.

A better **Hypothesis** is presented It seems to be **the best as a provisional model.**

I entered S-CG61, U-08, S-SS12, **P-PS 06**, P-PS 07. Please discuss with oral and poster venue.
[2]The Giant Impact and the Formation of the Moon P46.Des.1-3, 1998 MONTEREY,LIFORNIA

Keywords: Origin of the moon, Verification by Abduction using evolution results, Origin the moon is always facing the earth, origin of the moon sea, reasons why there is no ocean behind the moon

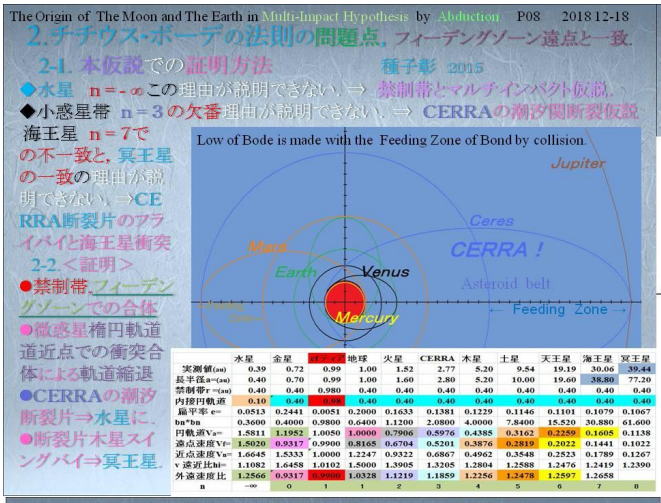

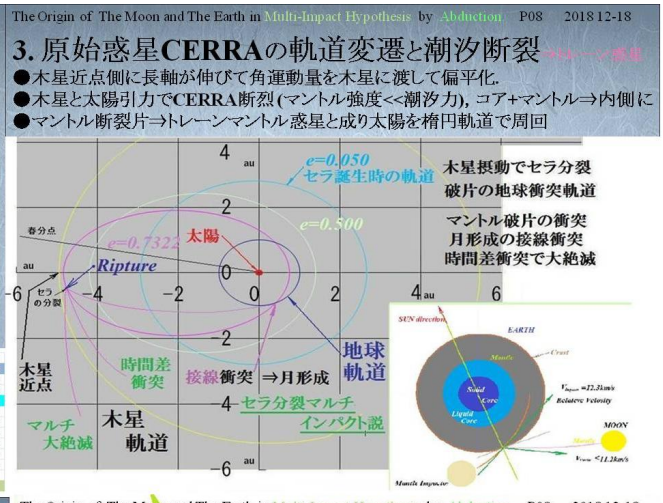

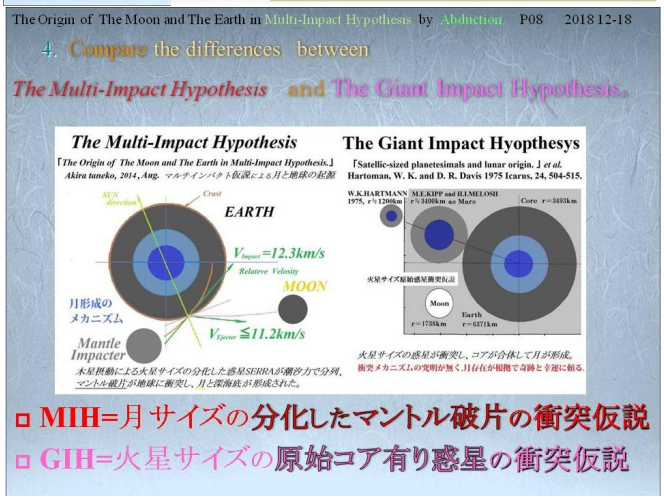

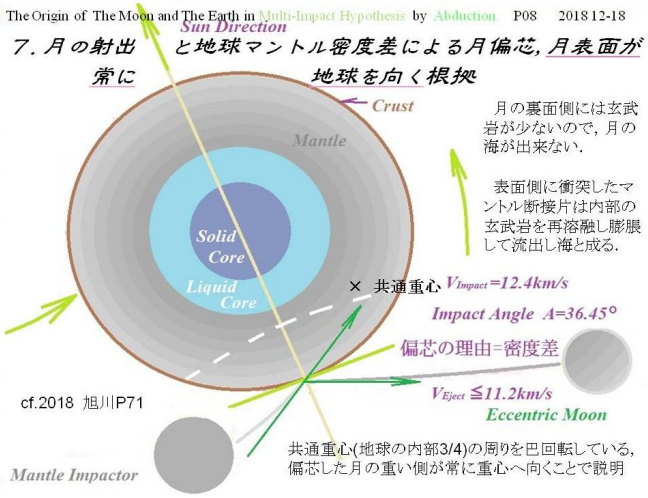

©2019. Japan Geoscience Union. All Right Reserved.

Proposed the Good model to verifyOrigins of Solar System (Planet, Asteroid belt, Earth, Moon) *with "Multi Impact Hypothesis ",*from 16' results of one time Evolution *by Abduction.*

cf. Simulation is an example by Abduction from 1.

*Akira Taneko[1]

1. SEED SCIENCE Lab.

We have been exploring **Origins of Solar System** ***by Induction and Deductive methods*** until now, but since we **can not go back in time to the past**, **Search for Truth** has not **proceeded late.The theory has verified the law by explaining multiple results only for the results of detailed experiments.**
Since **Evolution of Origin Hypothesis** that **Initial State is unknown** and **Impossible to reproduce Experiment is reality**, ***One-Time Evolution happened***, so ***unified*** explanation of **Planet of Solar system**, ***such as Present state,*** and **all of Features** of **Earth and Moon in particular** You can verify by **Method** called **Abduction.**
Origin Hypothesis of Moon **"Giant Impact Hypothesis"** up to now is **a Simulation** that creates **Moon of Mantle alone**, and ***it could not explain*** **one feature of any other Moon. In abduction it is only an illustration of N=1.**
However, the **"multi impact hypothesis"** includes not only **Origin of the moon whose component is Mantle** but also **Moon's Orbital Energy** (60·Re), **Eccentricity of Moon** (always **Moon's Surface** faces the earth), **Origin of Moon Sea** , ***I could explain why*** there is no **Ocean** on **the reverse side.**
Furthermore, although it is Origin Hypothesis of Moon, other features of the solar system, Origins of Asteroid Belt and **Origin of Differentiated Earth Meteorite**, **Origin of Ocean of Earth** (60%>, 5 km depth), **Origin of Plate Boundary, Origin of Plate Tectonics**, **Origin of Driving Force**, **Origin of Pacific Rim Orphan Ocean Island and Back Arc Concave Marine Basin, Origins of Mutual Plate Overlap, Origins of Axis Inclination, Origin of Diamond Mine,** Origin of Van Allen belt eccentricity, Origin of Titian Sea, Origin of tilt, Risk of Sudden Change of Plate Movement Direction, Origin of species extinction, Origin of Jupiter large red spot, Origin of Mercury core rich, Origin of Pluto, Origin of Alps and Tibetan highland, Unified description to **Origin of Continental Drift** It can be said that it was able to be verified as Abduction by being able to do. In particular, Formation of Deep Seabed average of 5 km by Isostasy and **Air Hockey state of the plate by Asthenosphere is Driving force of Earth plate due to eccentricity of the inertial efficiency,** become **Train Asteroid** of the **CERRA Mantle** ***due to CERRA rupture,*** Collision at **the intersection of Moon is Injection of Moon and Earth's Mantle Defect**, it is Origin of several Seas and Origin of extinct species. Cracks in Earth's Mantle are Origin of Plate Boundary, and **the Pacific Rimback Arc Naval Basin is also Origin of Plate Overlap. The high latitude collision is the origin of the earth's axis tilt,** and **Verification of Driving Force** is ***also made that Antarctica fits into the earth's axis and becomes immovable.***
I proposed **a theoretical model to verify Origins of Solar System (Planet, Asteroid belt, Earth, Moon) by Abduction** ***from multiple (16) results of*** **One Time Evolution.** It is particularly noteworthy to show **Collision Speed and Aangle to Earth** ***(12.4 km / s, 36.4 degrees)*** and **Moon orbit energy** ***(60 ·Re).*** At the same time I could show **Feeding Zone and Bowden 's law.** It is **a theory model** and **victory of Abduction.**
I entered S-CG61, U-08, S-SS12, P-PS 06, **P-PS 07.** Please discuss with oral and poster venue.

©2019. Japan Geoscience Union. All Right Reserved.

Keywords: Multi Impact Hypothesis, Verify with Abduction, Origin of the Solar System (Planet, Asteroid Belt, Earth, Moon), Multiple (16) results of one time evolution, Method of verifying Origin

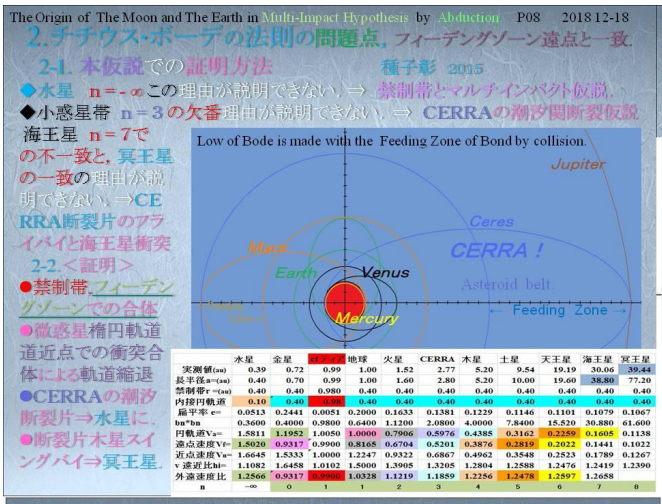

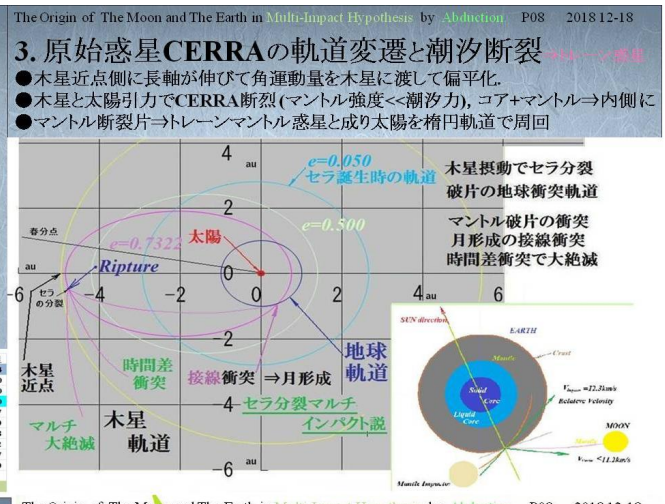

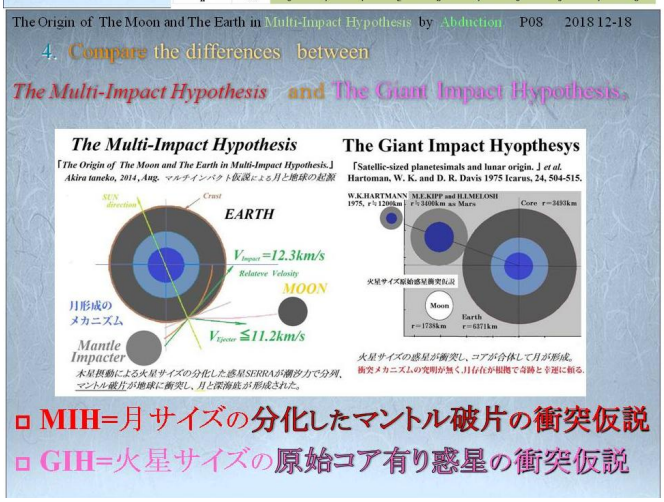

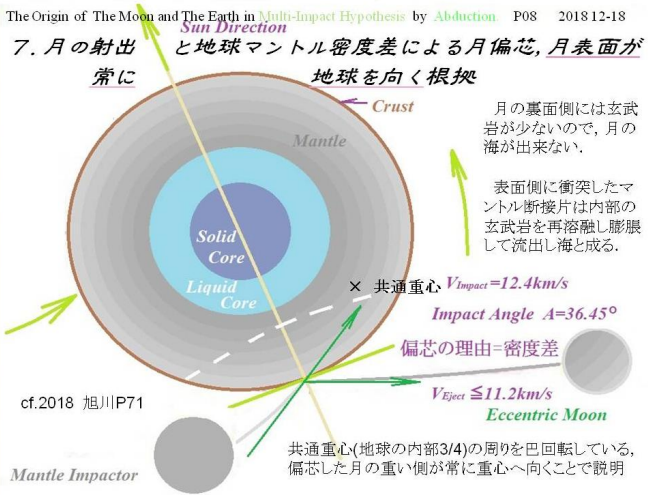

©2019. Japan Geoscience Union. All Right Reserved.

Quantitative evaluation of the cumulus convection schemes for the implementation into the Paleo Martian Global Climate Model

*Katsushige Toriumi[1], Arihiro Kamada[1], Takeshi Kuroda[1,2], Naoki Terada[1], Yasumasa Kasaba[3], Isao Murata[1], Hiromu Nakagawa[1]

1. Tohoku university, Geophysics, Planetary Atmospheric Physics, 2. NICT, 3. Tohoku university, Geophysics, Planetary Plasma and Atmosperic Research Center

Current Mars has a lot of fluvial traces, which are supposed to be made during the late Noachian and early Hesperian boundary (3.85-3.6 Ga). If these traces are created by the fluvial activity, the climate of early Mars should be ‘warm and wet’ enough for the long-term existence of liquid water on its surface. However, solar luminosity at that time would be weaker by 20-30 % of today’s value, which would preclude early Mars from such ‘warm and wet’ climate (‘Faint young Sun paradox’). Previous studies using 3-dimensional Mars Global Climate Models (MGCMs) have revealed that pure CO_2atmosphere, even assuming 2~7 bars, was hard to reproduce the surface temperature above 273 K [e.g. *Kasting*, 1991; *Forget et al*. 2013].

We newly developed a 3-dimensional Paleo MGCM (PMGCM) with ancient ocean on its surface below a sea level of -2.54 km, including the absorptions of CO_2/ H_2O gases, CO_2/ H_2O ice clouds, thermodynamics of land / ocean, and hydrological processes [*Kamada et al*., submitting to Icarus]. This model reproduced a clement surface environment enough for liquid water on surface and could create most of fluvial channels by hydrological processes. However, the fluvial channels reproduced in our model were partly not consistent with observations on current Mars (e.g. *Sabaea Terra*). There are several explanations for the inconsistencies, such as 1) in Noachian and early Hesperian boundary the Tharsis rise had not finished or completed, which would enable wind system to transport water vapor towards the leeward regions such as Sabaea Terra, and/or 2) some of fluvial channels would have formed by glaciation.

Another possible reason is that our modelhad excluded the cumulus convection scheme, considering only the large-scale condensation process for the precipitation. This process could be crucial for resolving atmospheric instability and affect the distribution and the amount of precipitations on early Mars. Therefore, as the next step, we are newly introducing a cumulus convection scheme. One candidate is the Relaxed Arakawa-Schubert scheme [*Moorthi and Suarez*, 1991] which is often introduced to terrestrial GCMs. However, it is not clear whether this scheme could be adapted to early Mars, because it is a simplified scheme taking the empirical processes of the Earth into account for the calculations of the cloud mass flux, which may not be simply adopted to the CO_2/ H_2O atmosphere of early Mars. On the other hand, the Kain-Fritsch scheme [*Kain and Fritsch,* 1993], which is appropriate for middle resolution GCMs to reproduce the cumulus lifetime including creation, developing, declining, and deletion phases by one cumulusin a grid,is considered to be more suitable for PMGCM. It directly calculates the vertical structure of the cumulus without using the empirical assumption of the Earth.Though it is inferior to the Relaxed Arakawa-Schubert scheme in terms of ensemble, it is meaningful to introduce this scheme with high accuracy if we aim for high resolution in the future.Ultimately, we intend to calculate PMGCM with high resolution (both vertical and horizontal), verify the validity of the PMGCM introducing the cumulus convection model, and consider the influence on the running water topography.

In order to do the trade-off between those two schemes, we evaluated the differences of heat balance and

©2019. Japan Geoscience Union. All Right Reserved.

precipitation created by both schemes. First, we did the test under the present terrestrial condition (1bar, N_2/ O_2atmosphere, present solar flux at 1 AU). We supposed that both schemes would show the similar results in radiation balance and precipitation on the present terrestrial models. However, in the actual calculation results, the cloud structure had wider range of clouds in the low altitude with the Kain-Fritch scheme. That is because the characteristics of detrainment for each scheme are different. As the next step, we are changing parameters such as surface pressures (wet CO_2atmosphere of 0.5-2.0 bars), atmospheric compositions, solar flux, and terrain for early Mars as our PMGCM conditions. And we analyze the cloud structure generated by Kain-Fritsch scheme and qualitatively and quantitatively compare the change of water vapor transport with the case without cumulus convection scheme. In this paper, we plan to provide a first summary of those results.

Keywords: Mars, GCM, Valley Networks

©2019. Japan Geoscience Union. All Right Reserved.

Forced libration of Ganymede including the visco-elastic tidal deformation

*shinichiro kojima[1], Jun Kimura[1], Shunichi Kamata[2]

1. Department of Earth and Space Science, Graduate School of Science, Osaka University, 2. Creative Research Institution, Hokkaido University

From spacecraft observations and interior thermal modeling, Ganymede has been expected to possess a global ocean beneath its ice shell. To confirm an existence of the ocean, the JUICE (JUpiter ICy moons Explorer) mission has been prepared by ESA (The European Space Agency) and the spacecraft will be launched in 2022. After arriving at Jupiter system, the JUICE spacecraft is going to make several flybys Europa and Callisto and finally will orbits around Ganymede. During orbiting around Ganymede, the spacecraft will obtain several kinds of scientific data, for instance, surface topography from GALA (GAnymede Laser Altimeter) and surface images from JANUS (camera system). These data will provide important information about the tidal responses of Ganymede.

The tidal responses, e.g., tidal deformation and rotational variation, are caused by the gravitational force of other bodies such as a mother planet. The rotational variation includes libration, obliquity variation, nutation, and precession. In this study, we focus on the libration which is a spin rate variation caused by a torque acted on the aspherical degree-2 order-0 shape of the satellite. The libration changes the centrifugal force of a satellite and affects the tidal deformation. Inversely, tidal deformation affects the aspherical shape of the satellite.

Although Van Hoolst et al. (2013) has modeled the interaction of the tidal deformation and the libration, their tidal deformation models were simplified. In order to estimate an actual libration, we model 5-layered Ganymede interior and use the visco-elastic tidal deformation model constructed by Kamata et al. (2016). Our interior model consists of five layers, which have a homogeneous density and rigidity in each layer. The viscosities of the ocean, the high-pressure ice mantle, the rock mantle and the metallic core are homogeneous in each layer, and the viscosity of the ice shell is not homogeneous and depends on a radial temperature variation.
As a typical case, we use interior parameters which are the ice shell thickness of 155 km, the ice shell density of 940 kg/m^3 , the ocean thickness of 1 km, and the ocean density of 1050 kg/m^3 . Then we also use the three sets of a shell rigidity and a shell viscosity (1) 0.1 GPa and 10^{12} Pas, (2) 0.1 GPa and 10^{17} Pas, and (3) 10 GPa and 10^{17} Pas, respectively. The results for the libration amplitude are 34.1 m, 34.1 m, and 37.5 m respectively. As a conclusion, our calculation of the visco-elastic libration infer that the reference viscosity of ice (temperature-dependent viscosity of ice at a melting point) doesn’ t affect the amplitude of the shell libration. The ice rigidity affects the amplitude of the shell libration of order of a few meters.

Keywords: Ganymede, tidal deformation, libration

©2019. Japan Geoscience Union. All Right Reserved.

Experimental study on collision destruction simulating the primitive meteorite parent body

*Horikawa Kazuhiro[1], Masahiko Arakawa[1], Minami Yasui[1], Ryo Sugimura[1]

1. Kobe University Faculty of Science

We studied the impact strength of weak brittle materials changing the strength continuously from 40kPa to 800kPa, and found that the impact strength could be well scaled by using the non-dimensional impact strength.

Asteroids are believed to be constructed from various materials based on the long-term study related to meteorites. The components of S-type and C-type asteroids could be composed of chondrules and matrix; the chondrules are sub-mm size glass spherules and the matrix could be micron-size fine grained materials such as phyllosilicates and lithic fragments etc. Moreover, these components could have a wide range of porosity inside because they might be residual pore during the compaction process of planetesimals or relics of water ice or volatiles escaping from these bodies. Impact strength is one of the most important physical properties of asteroids because it could control the evolution of the size-frequency distribution of asteroids at the asteroid belt. The impact strength strongly depends on the asteroid size and it is dominated by the material strength at the size smaller than 100m, so that the impact strength should be determined by the laboratory experiments. Therefore, a lot of research have been conducted for rock, ice, and porous materials to investigate the material dependence, however the impact experiments using the target with the strength continuously changed have been hardly conducted so far. Then, we prepared the targets simulating asteroids composed of chondrules, matrix and pore and changed the internal structure of the target such as matrix ratio and porosity; the tensile strength was changed more than one order of magnitude, then we studied the relationship between the internal structure and the impact strength.

Impact experiments were conducted by using two-stage light gas gun at Kobe University, and we used a polycarbonate projectile with the size of 4.7mm and a nylon projectile with the size of 2mm and they were lunched at the velocity from 0.9km/s to 5.7km/s. The impact was conducted at a head-on collision. A spherical target with the size of 60mm were prepared by using quartz sands with the size of 100 μm and porous gypsum, and they are mixed with various mass ratio of quarts to gypsum from 2:1 to 8:1. The tensile strength of these materials (Y_t) was measured by using Brazilian test and it was found that the tensile strength changed from 40kPa to 800kPa with the increase of the gypsum mass ratio. The impact disruption was observed by a high-speed camera at 10^5fps.

The impact strength (Q*) was determined by using a largest fragment mass for each shot, and Q* was found to change from 400J/kg to 1900J/kg with the increase of the gypsum mass ratio. This means that the Q* is directly proportional to the tensile strength. However, the ejection velocity at an antipodal point (v_a), which was measured by using high-speed images, showed the almost similar results, irrespective of the tensile strength. A non-dimensional impact strength (P_I) is defined as the ratio of the target tensile strength to the antipodal pressure such as P_I=Y_t/P_a, where P_a is calculated by ρ C_b v_a/2. This P_I was proposed to scale the target with the different tensile strength. Then, the relationship between the largest fragment mass and P_I was examined to discuss the P_I scaling law for the catastrophic disruption. We found that P_I is able to scale the largest fragment data very well, and this might mean that P_I could be applicable to asteroid components composed of weak brittle materials.

©2019. Japan Geoscience Union. All Right Reserved.

Keywords: collisional disruption, strength, impact strength

©2019. Japan Geoscience Union. All Right Reserved.

Evolution of atmospheric composition in the early Martian atmosphere

*Ryosuke Yagi[1], Naoki Terada[1]

1. Planetary Atmospheric Physics Group, Tohoku University, Japan

The purpose of this study is to investigate the evolution of atmospheric composition in the early Martian atmosphere. Not only hydrogen and oxygen but also carbon escape to space is considered in this study. The early Martian atmosphere was influenced by a stronger Sun’ EUV radiation than today. The escape parameter, defined as the ratio of the gravitational potential to kinetic energy at a given altitude, could be small enough to allow massive escapes of these species under such a strong radiation. For example, the escape parameter of atomic carbon in the Martian atmosphere was estimated 0.8 times smaller than that of atomic oxygen and both densities at the exobase level were comparable at 4.1 Gyr ago (Tian et al., 2009). Hence, we consider that in early Mars, thermal escape of atomic carbon could be stronger than atomic oxygen, and oxygen dissociated from CO2 was left behind in the atmosphere. Assuming that the escape rates of atomic carbon and atomic oxygen were in the same proportion, we get results that carbon disappeared in 5 Myrs from 1 bar of CO2 atmosphere and only 0.4 bar of oxygen atmosphere remained around 4.2 Gyr ago. On the other hand, it was suggested that the Martian atmosphere about 3.5 Gyr ago could have several mbar or more of oxygen partial pressure(Noda et al., 2018). In the present study, we have developed a 1-D photochemical model of the early Martian atmosphere to investigate the evolution of the atmospheric composition, in particular from 4.2 to 3.5 Gyr ago. This model includes not only the effect of escapes of hydrogen, oxygen and carbon but also that of deposition to surface and degassing. In this presentation, we will show the influence of the atomic carbon escape to the evolution of oxygen partial pressure left behind in the early Martian atmosphere.

©2019. Japan Geoscience Union. All Right Reserved.

Observation of catastrophic destruction of two different targets using X Ray photography

*Takumi Nagano[1], Masahiko Arakawa[1], Minami Yasui[1], masato nakamura[1], Fumiya Nagatomo[1]

1. Faculty of Science Kobe University

We studied the dependence of physical properties of planetesimals on the impact strength in the gravity regime, then we made laboratory impact experiments by using a Flash X-ray for porous gypsum and dry clay simulating planetesimals in order to obtain the relationship between impact fragment masses and ejection velocities.

The impact strength of planetesimals is one of the most important physical properties to clarify the planetary accretion process and the formation process of proto-planets and asteroids. Thus, the impact strength in the strength regime applicable to planetary bodies smaller than 100 m has been mainly studied in laboratory experiments. However, the impact strength in the gravity regime applicable to planetary bodies larger than planetesimals has been studied only by numerical simulations, and their results are not consistent with each other. Furthermore, recent numerical results conducted by Jutzi (2016) showed us that the material properties such as friction, cohesion and porosity affected the impact strength in the gravity regime drastically. Then, we made laboratory impact experiments to elucidate the material dependence on the impact strength in the gravity regime.

In order to determine the impact strength in the gravity regime by the laboratory experiments, we should obtain the relationships between the impact fragment masses and the ejection velocities, and especially, the fragments ejected from the interior of the disrupted target must be observed to construct the velocity –mass relationship for all the fragments. Then, we introduced 3 sets of flash X-ray generators and imaging plates to take transmitted X-ray images of a target with 3 mm steel balls arranged in it. These steel balls were used as makers of the motion of impact fragments, and the time sequence of these balls were observed by using X-rays to analyze the local velocities of the target’ s interior.

Impact experiments were conducted by using a polycarbonate projectile with the size of 7mm at the velocity of 2 –5 km/s, and the projectile was impacted on a spherical target with the size of 6 cm in a head-on collision. We used porous gypsum targets with the porosity of 50% and the tensile strength from 1 to 2 MPa and dry clay targets with the porosity of 48 % and the tensile strength different from the porous gypsum. All the targets were catastrophically disrupted into the largest fragment mass less than 0.2. As a result, we determined an upper limit of ejection velocities having a half mass of the target for each experiment, and we defined this upper velocity as a median velocity of V*. So, we studied how V* depended on the energy density, tensile strength and porosity, then we found that V* increased with the energy density for both targets. Moreover, we found that it strongly depended on the target porosity when it was compared with the previous result for the frozen clay with the similar tensile strength but without porosity, the V* for porous gypsum reduced to be 1/3 for the frozen clay. The V* for the dry clay was almost similar to that for the porous gypsum, thus this might mean that the tensile strength does not affect the V* even for the porous target.

Keywords: Destruction

©2019. Japan Geoscience Union. All Right Reserved.

Charge transport between granular particles in an ejecta curtain produced by hypervelocity impacts

*Kosuke Kurosawa[1], Takanori Iwasawa[2], Satoshi Okuzumi[2], Sunao Hasegawa[3], Takayuki Muranushi[4]

1. Planetary Exploration Research Center, Chiba Institute of Technology, 2. Department of Earth and Planetary Sciences, Tokyo Institute of Technology, 3. ISAS, JAXA, 4. AICS, RIKEN

We studied the charge transport between granular particles in an ejecta curtain produced by hypervelocity impacts to access the energy partitioning from the initial kinetic energy to the electrostatic one having the ejecta curtain. We conducted both hypervelocity impact experiments and numerical calculations. The impact experiments were done at ISAS/JAXA hypervelocity impact facility. A vertical gun was used to use granular materials as a target. High-speed video cameras for the visible and infrared were used to observed an impact-generated ejecta curtain. Any light sources were not used in this experiment. We constructed a numerical model by combining the iSALE shock physics code and the REBOUND N-body integrator. The processes of impact ejection under the conditions similar to the laboratory experiments were solved by the iSALE. The time at the ejection, ejection velocity, and the launch position of each particle was extracted as a txt file. Then, the txt file was imported in the REBOUND as a input file. At this time, we added random velocities to simulate the velocity dispersion. Although the dispersion would be inevitably added to each ejected particles in nature, it cannot be modeled in the hydrocode. The absolute magnitude of the random velocity was treated as a free parameter. Subsequent particle motions under the Earth’ s gravity field and the resistance force by the surrounding air were calculated. The decceleration due to inelastic collisions and charge transport between particles were included into the calculations. The restitution coefficient was also treated as a free parameter. The degree of charge separation was given by an empirical law proposed by the previous experiment. The results are summarized as follows; (1) We did not observe a large-scale discharge in an ejecta curtain under the experimental condition, (2) we observed a number of bright points along with an produced-ejection flow, (3) we observed a mesh pattern in the ejecta curtain as well as a previous study, (4) we reproduced the mesh pattern in the REBOUND when we chose the degree of the random velocity to be 5-15% of the ejection velocities at the restitution coefficient of 0.8, (5) mutual collisions between granular particles cease at the early stage of the growth of the ejecta curtain, (6) the end time of the mutual collisions depends on the atmospheric pressure, and (7) the empirical law pertaining to the charge separation yields an unphysically-high electrostatic energy. In the presentation, we will present the current status of our research development and discuss the future plans.

Acknowledgements:We thank the developers of iSALE, including G. Collins, K. Wün- nemann, B. Ivanov, J. Melosh, and D. Elbeshausen. We also appreciate the developers of REBOUND, including Hanno Rein, ShangfeiLiu, David S. Spiegel, Akihiko Fujii, and Dan Tamayo.

Keywords: Hypervelocity impacts, Ejecta curtain, Charge transport

©2019. Japan Geoscience Union. All Right Reserved.

Nonlinear outcome of gravitational instability in irradiated protoplanetary disks

*Shigenobu Hirose[1], Jiming Shi[2]

1. Japan Agency for Marine-Earth Science and Technology, 2. Spotify USA Inc

Using local three dimensional radiation hydrodynamics simulations, the nonlinear outcome of gravitational instability in an irradiated protoplanetary disc is investigated in a parameter space of the surface density Σ and the radius r. Starting from laminar flow, axisymmetric self-gravitating density waves grow first. Their self-gravitating degree becomes larger when Σ is larger or the cooling time is shorter at larger radii. The density waves eventually collapse owing to non-axisymmetric instability, which results in either fragmentation or gravito-turbulence after a transient phase. The boundaries between the two are found at $r \sim 75$ AU as well as at the Σ that corresponds to the initial Toomre's parameter of ~ 0.2. The former boundary corresponds to the radius where the cooling time becomes short, approximating unity in terms of the inverse of the orbital frequency. Even when gravito-turbulence is established around the boundary radius, such a short cooling time inevitably makes the fluctuation of Σ large enough to trigger fragmentation. On the other hand, when Σ is beyond the latter boundary (i.e. the initial Toomre's parameter is less than $\sim$0.2), the initial laminar flow is so unstable against self-gravity that it evolves into fragmentation regardless of the radius or, equivalently, the cooling time. Runaway collapse follows fragmentation when the mass concentration at the centre of a bound object is high enough that the temperature exceeds the H_2 dissociation temperature.

Keywords: Protoplanetary disks, Gravitational instability, Hydrodynamics simulations

©2019. Japan Geoscience Union. All Right Reserved.

Rheology of clay paste and application to the investigation of formation process of surface topography on the Mars

*Chihiro Uemura[1], Takahiro Iwata[1,2], Akio Nakahara[3], Yosuke Matsuo[3], Tomohiro Usui[2], Rina Noguchi[2]

1. SOKENDAI, 2. ISAS/JAXA, 3. Nihon Univ.

Mars is known to have many terrains formed by water, which is one of important candidates for future exploration places. For example, RSL (Reccuring Slope Lineae) is repeating disappearance and occurrence by seasonal variation, so it suggests that RSL was formed by water. However, there is a hypothesis that RSL is formed by sands, and formation process of RSL is still unclear.
Considering that flowing water is mixed with grain of sands and clay powders, and becomes pastes (colloidal suspension). It is valuable to understand properties of pastes. Since pastes have many unique properties, they are attracting widespread interest in various fields. Pastes are classified as attractive or repulsive according to a force among particles. Rheology of repulsive colloidal suspension has been studied so far. On the other hand, rheology of attractive colloidal suspension is still unknown. To understand the surface topography on Mars, it is important to study the rheology of clay paste, one of typical attractive colloidal suspension, because clay minerals are widely found on the surface of Mars. As the formation of some landforms, such as RSL, are considered to be dependent on temperature, we focused on the temperature dependence of their rheology, such as an yield stress and a viscosity, of attractive colloidal suspension.
We used paste of magnesium carbonate hydroxide because their properties are similar to clay minerals; their inter-particle force is attractive and makes a card house structure. We used rheometer (Anton Paar, Physica, MCR-301) for measuring. We measured rheology of paste at four different temperatures and five different solid volume fractions. We found that the yield stress of paste of magnesium carbonate hydroxide is an increasing function of a temperature. The yield stress of usual elastoplastic media is known to decrease as the temperature increases. However, our experimental study revealed that the yield stress of attractive colloidal suspension is an increasing function of the temperature, the result of which is an inverse behavior to that of usual elastoplastic media. The temperature dependence of the yield stress of attractive colloidal suspension is much more drastic when it is compared to the theoretical prediction for the repulsive colloidal suspension with the linear dependence to its absolute temperature.
As for the viscosity of attractive colloidal suspension, its behavior is similar to that of Newtonian viscous fluid with its viscosity a decreasing function of the temperature. We consider that this is because the viscosity of solvent, i. e., water, decreases as the temperature of an colloidal suspension increases.
These facts suggest that temperature dependence of rheology was caused by what kind of force is working among particles. As a mechanism of these results, we suggest that changing charge on the surface of particles or changing viscosity of water. In order to reveal why interaction is changed with increasing temperature, we need further verification.
In the future work, we will make use of these results for understanding the process of forming subsurface terrains on Mars.

Keywords: Mars, RSL, rheology, yield stress, clay paste

©2019. Japan Geoscience Union. All Right Reserved.

An Explanation for Physical Mechanism of the Streaming Instability

*Hiroaki Kaneko[1]

1. Tokyo Institude of Technology

Planets are thought to be formed from planetesimals, which are 1-100 km in size, and planetesimals are formed by accumulating small dust particles. Dust particles of a size of 10 cm-1 m drift sunward at 1 au per a century. Dust particles must grow within a timescale faster than this sunward drift timescale limit, otherwise they cannot form planetesimals. Enhancement of the particle density leads to the self-gravitational instability if the density reaches the Roche density, and the dense dust particles form planetesimals. In this case, the dramatic radial drift of dust particles can be avoided. Youdin & Goodman (2005; YG05) discovered that dust and gas streams mutually interacting via drag force generate local linear instability and a particle clumping occurs. This instability is called the streaming instability (SI). A lot of linear and non-linear numerical simulations conducted and it has been confirmed that SI emerges under certain conditions. But the physical mechanism of SI is not clear yet, because the order of the dispersion relation is as high as 6 and the mechanism seems to be difficult to understand. Applying the terminal velocity approximation (YG05) to particle continuity equation and gas incompressibility, Jacquet, Balbus, & Latter (2011; JBL11) attempted to give a physical explanation about the SI mechanism. Their explanation was as follows:

1. The gas pressure maximum traps dust particles.

2. Dust particles drag the gas toward the gas pressure maximum.

3. The gas pressure maximum is strengthened. Though the gas pressure gradient tends to force out the gas from the maximum, the dust particle drag force on the gas and the Coriolis force make roles to keep the geostrophic balance.

JBL11 suggested the explanation of the mechanism in which all the motion takes place only in the midplane, however, YG05 emphasized that the vertical advection flows toward the density maximum and it dominates the flow in the midplane.

In this study, first, we conduct an analysis on the dispersion relation that employs the terminal velocity approximation (YG05) and calculate phase differences among the perturbed particle density, the perturbed gas pressure, and the perturbed particle velocities for an unstable mode. Then, we give an explanation about the mechanism of SI including the vertical motion unlike the explanation by JBL11.

Our explanation on the SI mechanism is as follows:

1. At the particle density maximum, the gas receives more angular momentum, while at the particle density minimum, the gas receives less. So, the gas radial velocity perturbation and the gas pressure fluctuation along the radial direction are generated.

©2019. Japan Geoscience Union. All Right Reserved.

2. Toward the gas pressure minimum, the gas flows in vertically with dragging dust particles. On the contrary, both gas and dust particles flow out vertically from the gas pressure maximum.

3. The phase velocity of the dust particle density maximum is negative so the particle density maximum moves radially inward. The density maximum encounters the dust particle input due to the vertical converging flow and the density maximum is enhanced.

This explanation is consistent with solutions of the linear stability analysis. In addition, the explanation seems physically reasonable and easy to understand.

Keywords: Streaming Instability, protoplanetary disk, protoplanetesimal formation, hydrodynamics, linear stability analysis

©2019. Japan Geoscience Union. All Right Reserved.

Spatial motion of the Earth-Moon system and Earth pole oscillatory process

*Alexandra Sergeevna Filippova[1], Vadim Vladimirovich Perepelkin[1], Wai Yan Soe[1]

1. Moscow Aviation Institute

The variation of the Chandler and annual components of the polar motion are of a significant interest in the Earth pole oscillatory process research. Generally these variations are quasiperiodic. But some regular oscillations can be isolated from it that correspond with the basic periods of the lunar motion. Here we discuss the theoretical assumptions of the observed effect as well as the experimental rules that illustrate the relationship between the Earth pole oscillations and the lunar motion.
The complex process of the Earth pole oscillations includes components with frequency and amplitude that differ significantly from each other. Processing the pole motion observations over the last 100 years result in statistically convincing definition of the main characteristics in its oscillatory process. Basic components in the Earth pole motion are Chandler wobble, annual oscillation and also polar motion's trend. Observed Earth pole oscillations have a wobbling character. The trajectory of the pole on the Earth surface is a winding and unwinding spiral with a period of about six years.
Actual problem that was stated by P. Melchior (Melchior, 1972) about the instability in the basic components parameters of the Earth pole is still not sufficiently explored. This problem is connected with the exploring the celestial-mechanics' and geophysical causes of such behavior in the Chandler and annual components, and also with the construction of the refined models of the forecasting the Earth orientation parameters for long time intervals.
In this work along with the common methods of the separating the pole oscillation process into the Chandler and annual components we suggest an approach to the resulted Earth pole trajectory research. For the purpose of analyzing the nonstationary resulted pole motion a perturbed trajectory is isolated. For the unperturbed trajectory a “mean” one is chosen –the Earth pole trajectory where the Chandler and annual oscillation parameters have mean values.
The differential equations for the amplitude a and phase ψ of the Earth pole modulation motion can be derived from the dynamical Euler–Liouville equations of Earth motion around its center of mass (Markov, Perepelkin et al, Astronomy Reports, 2018 and Markov, Perepelkin at al, Doklady Physics, 2017).
It is shown that the significant impact into the variations of the basic pole oscillation components is given by the long-term perturbations from the lunar orbit. The analysis of these perturbations is held using the wavelet and Fourier transformations. On the long time interval it shows matching phases of the perturbed polar motion and the lunar orbit motion using the available series of observations C04 and C01 from the International Earth Rotation and Reference Systems Service. This feature can be used to refine the model of the forecasting the Earth pole oscillations. And taking into account these structural features of the oscillations the refined numerical-analytical model of the Earth pole motion is presented.
Thus the graphical correspondence between the Earth pole oscillations and the motion of the lunar orbit is presented. It is shown that the refined model gives a more accurate description of the Earth pole motion by comparing the model computation results with the observations made by the International Earth Rotation and Reference Systems Service.

Keywords: Earth pole oscillations, Numerical-analytical model, Chandler Wobble, Lunar orbit perturbations

©2019. Japan Geoscience Union. All Right Reserved.

Chondrule formation model by lightning in high dust density regions

*Chihiro Ikeda[1], Taishi Nakamoto[1]

1. Tokyo Institute of Technology

Chondrules are spherical objects of 0.1 - 1 mm in radius and are the main component of chondrite meteorites (Scott 2007). It is known that chondrules were formed early in the solar system. So, chondrules may have important information about early solar system nebula. It is believed that chondrules melt with dust particles heated within several minutes and have cooled and solidified at a rate of 1-1000 K/hour in the early solar nebula (Desch et al. 2012). Also, since chondrules contain volatile substances, it is considered that they are formed in a high dust density region (Alexander et al. 2008). Although the formation mechanism of chondrules have not been elucidated, formation theories include the shock wave model, astronomical collision model, X-wind model, and lightning model. In this study, we examine the chondrule formation by lightning from the viewpoint of thermal evolution of chondrules.

Thermal evolution of chondrules has been studied by Horanyi et al. (1995). In that study, assuming the occurrence of lightning in the solar nebula, they calculated the time evolution of the gas and dust in the lightning. As a result, the cooling rate of the chondrule became faster than the cooling inferred from observations of crystals in chondrules. On the other hand, according to studies on the occurrence of lightning, the mass ratio of dust to gas needs to be 100:1 or more for lightning generation (Muranushi 2010). However, Horanyi et al. (1995) considered the situation where only one dust particle is present inside the lightning.

In this study, we consider the occurrence of lightning in the high dust density region and calculate the thermal evolution of chondrules numerically. Especially, we investigate if the cooling rate condition for the chondrule formation is satisfied under the high dust density situation. As a result, it was found that there are circumstances suitable for chondrule formation. It is suggested that chondrule formation by lightning is possible in the solar nebula.

Keywords: chondrule, lightning

©2019. Japan Geoscience Union. All Right Reserved.

The transition to superrotation in stratospheric atmospheres

*Motoki Sumi[1]

1. Tokyo Institute of Technology

Titan is the only satellite with the developed atmosphere and the stable liquid on the ground surface in the solar system. The history of the observation begins with the suggestion of the existence of the atmosphere in 1908. In the 1970's, the temperature structure and atmospheric composition of the Titan atmosphere have been clarified thanks to the progress of observation technology. Also, in the Cassini-Huygens mission, it visited the Saturnian system, made Huygens probes into the Titan atmosphere, and made high-precision observations. Ground-based submillimeter wave observation by the ALMA telescope is currently being carried out, and it is possible to observe at high resolution.
Observations clearly show the existence of superrotation, which is a high-speed zonal wind oriented to overtake the rotation on a global scale as a characteristic of the Titan atmosphere. The wind speed reaches 100 m/s eastward at about 10 degrees south latitude where Huygens entered, but it is difficult to investigate its mechanism from the viewpoint of insufficient observation data and complexity of atmospheric structure. Also, the theory which unified the generation mechanism of superrotation is not established, and various theories are advocated. Representative examples are the Gierasch mechanism proposed by Gierasch or the mechanism by thermal tidal waves proposed by Fels and Lindzen.
In this research, I conducted numerical experiments to generate superrotation by changing only the planetary radius using the Earth model. We used the numerical simulation model DCPAM5 of the planetary atmospheric general circulation developed by GFD Dennou Club. Primitive equations were used as the basic equation system of the model assuming a dry atmosphere. We used the model of Williamson et al.(1998) which added the pressure dependency of stratosphere to the Newtonian cooling process in Held and Suarez (1994). The calculation time was 1080 days where sufficient stationarity was confirmed, and we analyzed the time average of the physical quantities in last 360 days.
First, I output the temperature field, the mass transport distribution, zonal-mean zonal wind speed field, compare the structure of the atmosphere in the meridional space, and investigate the location and the condition. where superrotation is occurring. In the Earth model, eastward jet streams occurred in the mid latitudes of the troposphere and the stratosphere, but on the equator the westward winds are blowing. If the planetary radius is small, in the troposphere even in the equator the eastward wind is accelerated and superrotation has occurred. In the stratosphere, equator superrotation occurred in the lower stratosphere, but in the upper stratosphere the jet occurred only in the middle and high latitudes, and the high-speed eastward wind did not appear in the equator.
Next, in order to investigate the mechanism of keeping the angular momentum in the upper layer of the equator, the dispersion of the band-like disturbance of the temperature, the band-shaped disturbance spectrum of the east-west wind speed field were output, and the structure of the wave existing in the atmosphere was summarized. In the troposphere in the Earth model, many waves with a wave number of 4 or more existed in the mid latitudes, and angular momentum in the east direction was accumulated in mid latitude. However, as the radius of the planet is decreased, the waves with large zonal wavenumbers decrease, and global waves with the wave number of around one dominate. The behavior is similar in the stratosphere, in the Earth model, waves with large wavenumbers are present, although the waves are weaker in the troposhere as the planetary radius is reduced, only waves with small wavenumbers remain. In the stratosphere the equator super rotation and the mid-high latitude jet occur in different altitude, and the mechanism for maintaining superrotation seems somewhat different from the mechanism in the troposphere.

©2019. Japan Geoscience Union. All Right Reserved.

©2019. Japan Geoscience Union. All Right Reserved.

ExPRES: a Tool to Simulate Exoplanetary and Planetary Radio Emissions

*Corentin LOUIS[1,2,3], Sebastien L. Hess[4], Baptiste Cecconi[2,3], Philippe Zarka[2,3], Laurent Lamy[2,3], Stéphane Aicardi[5], Alan Loh[2]

1. IRAP, Toulouse, 2. LESIA - Observatoire de Paris, 3. USN, Observatoire de Paris, 4. ONERA-The French Aerospace Lab, FR-31055 Toulouse, France, 5. DIO, Observatoire de Paris, PSL Research University, CNRS, Paris, France

All magnetized planets are known to produce intense non−thermal radio emissions through a mechanism known as Cyclotron Maser Instability (CMI), requiring the presence of accelerated electrons generally arising from magnetospheric current systems. In return, radio emissions are a good probe of these current systems and acceleration processes. The CMI generates highly anisotropic emissions and leads to important visibility effects, which have to be taken into account when interpreting the data. Several studies showed that modeling the radio source anisotropic beaming pattern can reveal a wealth of physical information about the planetary or exoplanetary magnetospheres that produce these emissions. We present a numerical tool, called ExPRES (Exoplanetary and Planetary Radio Emission Simulator), which is able to reproduce the occurrence in time−frequency plane of CMI−generated radio emissions from planetary magnetospheres, exoplanets or star−planet interacting systems. Special attention is given to the computation of the radio emission beaming at and near its source. We explain what physical information about the system can be drawn from such radio observations, and how it is obtained. These information may include the location and dynamics of the radio sources, the type of current system leading to electron acceleration and their energy and, for exoplanetary systems, the magnetic field strength, the orbital period of the emitting body and the rotation period, tilt and offset of the planetary magnetic field. Most of these parameters can be remotely measured only via radio observations. The ExPRES code provides the proper framework of analysis and interpretation for past (Cassini, Voyager, Galileo. . .), current (*Juno*, ground-based radiotelescopes) and future (BepiColombo, Juice) observations of planetary radio emissions, as well as for future detection of radio emissions from exoplanetary systems (or magnetic white dwarf−planet or white dwarf−brown dwarf systems). Our methodology can be easily adapted to simulate specific observations, once effective detection is achieved.

Keywords: Planetsandsatellites:Aurorae, Radiocontinuum:Planetarysystems, Radioemissions simulation

©2019. Japan Geoscience Union. All Right Reserved.

Crustal structures of major mercurian basins

*Qingyun Deng[1], Fei Li[1], Jianguo Yan[1], Zhiyong Xiao[2]

1. State Key Laboratory of Information Engineering in Surveying, Mapping and Remote Sensing, Wuhan University, 2. Planetary Science Institute, China University of Geoscience

Mercury is the innermost planet in the solar system. Its surface resembles to the Moon, which is characterized with large number of impact basins, indicating an intensive bombardment history. From the data acquired by previous Mercury missions, the spatial distribution, relative age, and morphology of impact basins on Mercury is studied. Gravity data from NASA MESSENGER mission revealed the crustal structures of mercurian basins, providing information about the crust properties of the early Mercury when those basins formed. In this work, the crustal thickness ratio for each basin is calculated from global crustal thickness model obtained by inverting gravity data. The relation between crustal thickness ratio, basin relaxation state, and relative age is investigated and some implication for the early evolution of Mercury is discussed.

Keywords: crustal structures, impact basin, gravity anomaly

©2019. Japan Geoscience Union. All Right Reserved.

Crustal thickness

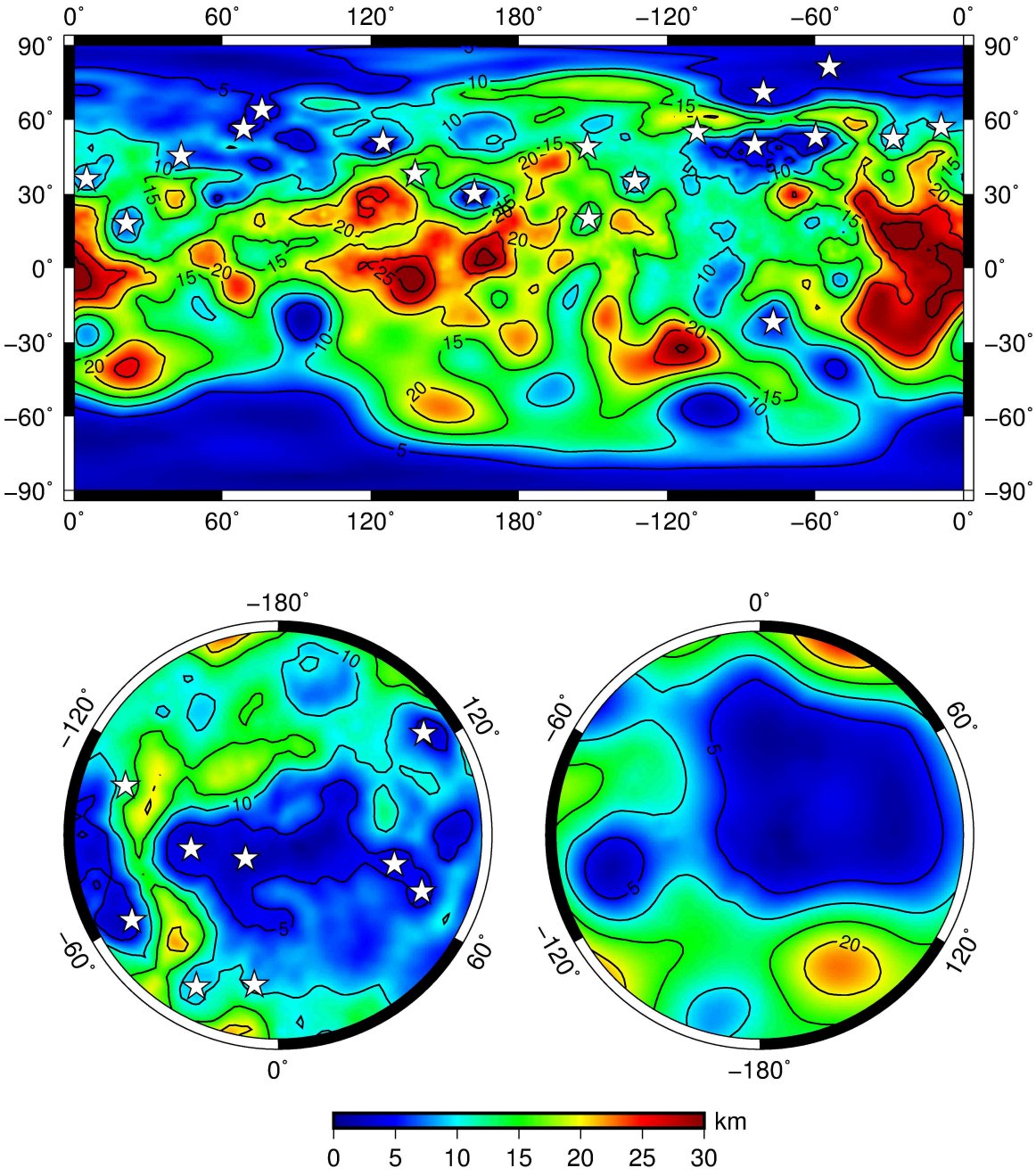

©2019. Japan Geoscience Union. All Right Reserved.

Application of LiDAR Technique for the 3D Digital Documentation of Cultural Heritage Sites

*Sachchidanand -[1], Mayank Sharma[1], Rahul Dev Garg[1]

1. Indian Institute of Technology Roorkee

Now a day’ s remote sensing and geospatial techniques are gaining popularity as they offer correct and precise information of any object situated at a distant place. Advanced remote sensing techniques like terrestrial laser scanning (TLS), mobile laser scanner(MLS), close range photogrammetry(CRP), smart total station(STS) and GNSS are the useful techniques for creating a 3D (three-dimensional) documentation of complex engineering structures or cultural heritage sites. The integration of these techniques with other methods like topographic survey or physical measurement method also offer the potential to the user to perform a complete 3D documentation of any structure.

This paper presents a methodological framework for the 3D digital documentation of cultural heritage sites from laser scanned datasets. The framework includes acquisition of point cloud datasets through laser scanners and their conversion to 3D models. 3D models are useful for planning and surface detail measurements. Detailed planimetric and elevation information or plans could be easily extracted from developed 3D models. These planimetric informations and elevation plans are useful for the conservation and preservation of structure, and can help in restoration of these structures in case of any damage due to natural disasters or other seismic activities.

Keywords: TERRESTRIAL LASER SCANNER, 3D DIGITAL DOCUMENTATION, ELEVATION PLAN, POINT CLOUD, SOLID 3D MODEL

©2019. Japan Geoscience Union. All Right Reserved.

Tidal Interaction in the Earth-Moon System Treated as a Double Planet

*Aleksandr Aphanasievich Zlenko[1], Irina Michailovna Ryabikova[2]

1. Department of high mathematics, Moscow automobile and road construction state technical university, 2. Department of descriptive geometry, Moscow automobile and road construction state technical university

Our approach to the phenomenon of tides differs from the traditional one, in which an empirically tidal potential with Love numbers is introduced. We consider the motion of two viscoelastic bodies, the Earth and the Moon treated as a double planet, in the gravitational field of a massive point, the Sun.The deformations of the bodies are described by the classical theory of small deformations. The influence of viscous forces is described by the dissipative functional of the Kelvin-Voigt model. The quasi-static equation of the elasticity theory is solved for obtaining the displacements of body points. The method of averaging and separation of motion is used for solving of this equation. The displacements of each point of the deformable body consist of displacements caused by centrifugal forces, the forces due to body elasticity and dissipative forces due to body viscosity. Substituting these displacements in the potential formulae and integrating over the each body, we get the potential of the system and the moments of forces acting on the bodies.. Knowing the displacements, we determine the shape of deformable bodies, their moments of inertia and the lagging angle. The results of this approach are compared with the results of the traditional theory.

Keywords: Earth-Moon system, viscoelastic bodies, moments of forces

©2019. Japan Geoscience Union. All Right Reserved.

The consequences of Saturn’s “ring rain”

*James O Donoghue[1,2], Luke Moore[3], Jack Connerney[4,1], Henrik Melin[5], Tom Stallard[5], Sean Hsu[6], Steve Miller[7], Kevin Baines[8]

1. NASA Goddard Space Flight Center, USA, 2. Institute of Space and Astronautical Science, Japan Aerospace Exploration Agency (ISAS; JAXA), Japan, 3. Boston University, USA, 4. Space Research Corporation, Maryland, USA, 5. University of Leicester, UK, 6. Laboratory for Atmospheric and Space Physics, University of Colorado–Boulder, CO, USA, 7. University College London, UK, 8. NASA Jet Propulsion Laboratory, California, USA

Saturn’s upper-atmospheric H3+ emissions have been previously studied using ground-based observations, and found to exhibit peaks in emissions at specific latitudes. The cause of these peaks is due to an influx of charged water products originating from Saturn’s rings known as 'ring rain'. Subsequent modeling using the Saturn Thermosphere Ionosphere Model (STIM) has indicated that these peaks in H3+ emissions are likely driven by an increase in H3+ density, rather than temperature, as a local reduction in electron density (due to charge exchange with water) lengthens the lifetime of H3+. However, a direct observation of the H3+ density is required to estimate the flow rate of material into Saturn with models. Calculation of ring rain’s flow rate into Saturn is a highly important input for determining the age, lifetime and evolution of Saturn’s rings.

Here we present the first ever derivation of H3+ density, temperature and radiance in the non-auroral regions of Saturn, using data taken from the 10-meter Keck telescope in 2011. H3+ density is enhanced near 45 degrees north planetocentric latitude and strongly reduced near 39 degrees south. When compared to STIM modeling results, these densities indicate a small ~50kg/sec water influx in the north and an enormous ~1500 kg/sec influx in the south. The charged grains are pulled in along the magnetic field by gravity, but the southward-inclination of the magnetic field (in the vicinity of the ring plane) means that the grains are preferentially drawn southwards into the planet. Assuming that our (Saturn northern Springtime) measurement represents all seasons, and that the rings are able to disperse over time, the ring rain mechanism alone will drain Saturn’s rings to the planet within 300 million years. If we also add the recent Cassini-spacecraft measured ring-material detected falling into Saturn’s equator (and assume it is constant), then the rings have less than 100 million years to live.

Recent measurements by Cassini again have estimated a ring age of ~50 million years, so it seems that Saturn’s rings are short-lived phenomena, perhaps lasting just 150 million years in total. A long time on human timescales, but compared to the 4.5 billion year age of Saturn, the rings are essentially temporary; i.e. if Saturn were 30 years old, the ring system would exist for just 1 year of its life! These recent findings indicate that ring systems in general are practically doomed to be removed as soon as they are formed. Indeed, the ring rain mechanism itself ought to be universal at any planet with both a ring system and a strong magnetic field. We might ask, did Jupiter, Uranus and Neptune, which have thin rings today, once have magnificent rings in the past that have eroded away?

Keywords: Saturn, Rings, Ionosphere, Magnetosphere, Atmosphere, Ring rain

©2019. Japan Geoscience Union. All Right Reserved.

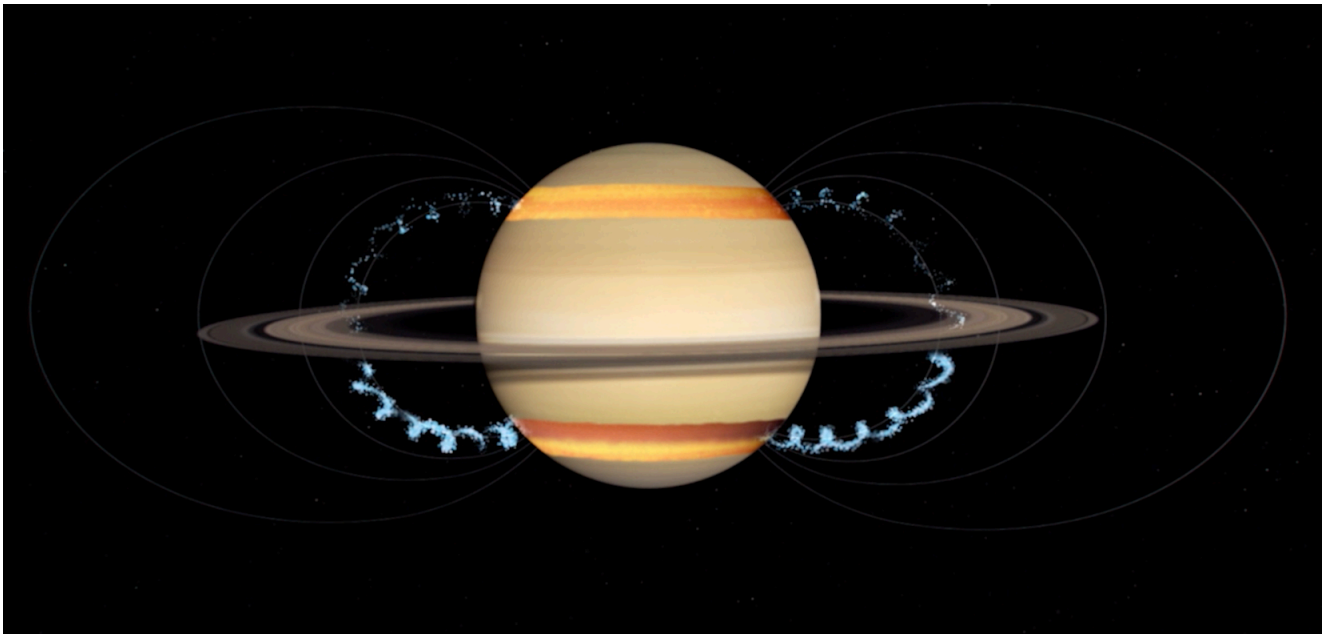

©2019. Japan Geoscience Union. All Right Reserved.

Calculation of kinetic rate constants using high-level *ab initio* quantum chemical methods for planetary sciences and astrochemistry

*Shiblee Ratan Barua[1,2], Paul Romani[1]

1. NASA Goddard Space Flight Center, Greenbelt MD USA, 2. Universities Space Research Association (USRA), Columbia MD USA

Existing photochemical models for the atmospheres of planetary bodies suffer from large errors when predicting the mole fraction profiles of various compounds. Global sensitivity analyses show that a major source of these model errors can be attributed to inaccurate rate coefficients for “key” radical–radical and radical–neutral reactions in low-temperature conditions. Accurate rate coefficients for key reactions thus improve the accuracy of photochemical models. Unfortunately, accurate experimental rate constants for such low-*T* reactions are difficult, if not impossible, to measure, and the lab data are affected by uncertainties in determining the absolute concentrations of radical species. Currently, the most common theoretical approach involves uncertainty extrapolation technique in which uncertainties in room-temperature rate constants are extrapolated to low-temperature conditions, resulting in large errors in the theoretical low-*T* rate constant data. To solve this existing problem, we are employing the two-transition-state (2TS) model developed by Klippenstein and coworkers to calculate high-level *ab initio* rate-constants for key low-*T* (*i.e.* 10–200K) reactions relevant to planetary atmospheres like that of Titan. In particular, we are investigating key reactions that have not yet been studied in the lab, and for which accurate rate coefficients are still unknown. Our calculated *ab initio* rate coefficients will be made available to the astrochemistry community via well-established free online kinetic databases (*e.g.* KIDA). These rate coefficients will be used by scientists in photochemical models to make accurate predictions of mole fraction profiles for planetary atmospheres and improve our understanding of the diverse chemistry of these bodies.

Keywords: Titan atmosphere, Low-temperature reaction kinetics, Ab initio quantum chemistry, Photochemical model, Plantery science, Astrochemistry

©2019. Japan Geoscience Union. All Right Reserved.

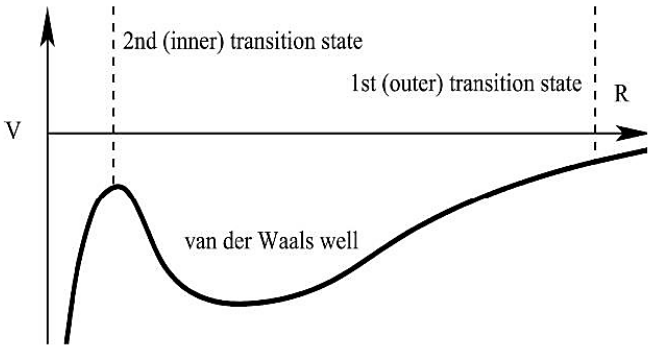

Figure 1. Schematic one-dimensional picture of the potential energy as a function of the reaction coordinate for a neutral–neutral reaction leading to bimolecular products. In its approach, the 2TS model incorporates both the 1st (outer) transition state for barrierless association reaction and the 2nd (inner) transition state for reaction path with a barrier. **Source:** Georgievskii and Klippenstein, 2007.

Table 1: Selected key reactions currently being investigated that are responsible for uncertainties in the mole fractions of major nitrogen species (left-most column) in low-T Titan conditions. Each reaction shown here has an absolute Rank Correlation Coefficient (RCC) value, a quantitative indicator of the sensitivity of model mole fractions on rate constants, greater than the chosen threshold of 0.2 at 100 km or above (right-most column). **Source:** Loison *et al.*, 2015.

Affected N Species	Key Reactions	|RCC| > 0.2
NH_3	$N(^4S) + NH_2 \rightarrow N_2 + H + H$	(100, 900) km
HNC	$N(^4S) + {}^3CH_2 \rightarrow HNC + H$	100 km
CH_2NH	$N(^2D) + CH_4 \rightarrow NH + CH_3$	900 km
CH_3C_3N	$^1CH_2 + CH_4 \rightarrow CH_3 + CH_3$	900 km
CH_3C_3N	$C_2N + H \rightarrow HCN + C$	900 km
C_2H_3CN	$CHCN + H \rightarrow C_2N + H_2$	900 km

©2019. Japan Geoscience Union. All Right Reserved.

How many conditions must be satisfied to produce a habitable planet?

*Shigenori Maruyama[1], Soichi Omori[2]

1. Earth-Life Science Institute, Tokyo Institute of Technology, 2. The Faculty of Liberal Arts, The Open University of Japan

<Purpose>

Concept of habitable zone (HZ below) is regarded as the presence of stability field of liquid water on the surface of planet. HZ is regarded as the most important condition to produce a habitable planet. However, we think the presence of liquid water is not enough to be habitable. We list up other necessary conditions (6+5=11) to produce a habitable planet in the Universe.

<Method>

The best studied habitable planet is the Earth. Therefore, based on the research results of the Earth, we consider necessary conditions. Key points are chemical composition of primordial atmosphere and biosphere.

<Result>

Based on the research of the Earth, I propose there are at least 6 conditions to be a habitable planet in case of the solar system. (1) a planet must be given totally 400 bars CO_2, 300 bars water, and 50-60 bars N_2 as minimum values. In addition, such an amount is given gradually with time (ABEL model) not to become Venus-state, (2) the presence of extremely small amount of ocean water (3km ±1km thickness), (3) the presence of huge landmass (continent above sea level) to finally provide habitable trinity condition to drive the material circulation to give nutrients through water-rock interaction to feed primordial life. (4) Initiation of plate tectonics to keep dynamic equilibria not to become Venus state. (5) selective transportation of CO_2 into mantle, while H_2O remains on the surface, and N_2 remains all in atmosphere, (6) the presence of biosphere, if not, fixation of atmospheric CO_2 is restricted only to inorganic carbonates that would be insufficient to prevent evolving into Venus-state.

<Discussion>

These six conditions are deduced from the history of the Earth. However, if we enlarge the concept to exoplanets based on the research of the solar system, the following five conditions are added; (7) the distance from the central star, (8) the abundance of atmosphere, (9) mass and composition of central star, (10) size and composition of planet, and (11) circular orbital path.

Keywords: habitable planet, conditions to produce a habitable planet

©2019. Japan Geoscience Union. All Right Reserved.

Quantitative Evaluations for Meteorite Impact Tsunami

*Naotaka YAMAMOTO CHIKASADA[1], Tetsuharu Fuse[2], Toshitaka Baba[3]

1. NIED, 2. NICT, 3. Tokushima University

Tsunami induced by earthquakes, submarine landslides, volcanic eruption in submarine and coastal area and meteorological phenomena is one of the most devastating natural disasters. A meteorite impact into the oceans spawn large tsunami depending on the size and velocity of the meteorite and the sea depth at the location of the impact as well. However, we do not have a numerical model to reproduce both of meteorite impacts and tsunami propagations. We have started to develop a new numerical model to simulate tsunamis generated by the meteorite impact combining iSALE (Wünnemann et al., 2006) for simulating impact phenomena and JAGURS (Baba et al., 2017) for simulating tsunami. The iSALE is a multi-material and multi-rheology shock physics code for simulating impact phenomena. JAGURS is a parallelized tsunami simulation code to solve two-dimensional non-linear long-wave equation with Boussinesq terms for representing observed tsunami waveforms, tsunami height and inundation. We set sea-floor deformation, sea-surface disturbance and velocity of gravity wave which is the output from iSALE to the input of JAGURS. We then calculate tsunami height along the coastlines in any place using ASTER GDEM version 2 (Fujisada et al., 2012) and GEBCO_2014 Grid. ASTER GDEM has one arcsecond (about 30 m) spatial resolution and covers land between 56S and 60N latitude as a topographic data. GEBCO’s gridded bathymetric data has thirty arcseconds (about 1 km) spatial resolution for the worldwide.
We first investigate the tsunami generation using iSALE code for creating tsunami source model depending on the meteor size, the velocity of impact, the size of cavity, the width and depth of crater and tsunami propagation speed. We also investigate probabilistic hazard of meteorite impact tsunami using simplified cavity curves with developed JAGURS built-in. Finally, we construct a new numerical model of meteorite impact tsunami combining iSALE and JAGURS. Additionally, we consider the way of automatic detection of meteorite impact using the recode of the highly sensitive seismograph network in real-time.
We gratefully acknowledge the developers of iSALE, including Gareth Collins, Kai Wünnemann, Boris Ivanov, H. Jay Melosh and Dirk Elbeshausen. Data analysis and visualizations of iSALE were carried out on PC cluster and the computers at Center for Computational Astrophysics, National Astronomical Observatory of Japan. This work was partially supported by JSPS KAKENHI Grant Number JP18K04674.

Keywords: Meteorite, Impact, Tsunami

©2019. Japan Geoscience Union. All Right Reserved.

[J] Poster | P (Space and Planetary Sciences)：P-PS Planetary Sciences

Tue. May 28, 2019 5:15 PM - 6:30 PM JST | Tue. May 28, 2019 8:15 AM - 9:30 AM UTC | Poster Hall International Exhibition Hall8, Makuhari Messe_2

[P-PS06] Planetary Sciences

convener:Kenji Kurosaki(Department of Physics, Nagoya University), Yusuke Nakauchi(Japan Aerospace Exploration Agency)

We call for general interest papers for Planetary Scienses. Planetary Sciences consist of a variety of studies on the past, present, and future of our solar system and exoplanetary systems, Discussions based on various backgrounds are encouraged.

[PPS06-P01] The Study of Using SLR and GPS Observation Data to Estimate Geocenter Motion.

*Yih Jack Cheng[1], Fang-shii Ning[1] (1.National Chengchi University)

[PPS06-P02] Evolution of Pluto's surface albedo due to sublimation and condensation of ice

*Hisashi Matsui[1], Jun Kimura[1] (1.Osaka University)

[PPS06-P03] ***Origin of the moon*, Reason why Moon is always facing to Earth, Origin of Moon Sea, reasons why there is no Ocean behind Moon**

*Akira Taneko[1] (1.SEED SCIENCE Lab.)

[PPS06-P04] ***Proposed the Good model*** to verify**Origins of Solar System (Planet, Asteroid belt, Earth, Moon)**
*with "Multi Impact Hypothesis ",***from 16' results of one time Evolution *by Abduction.***
cf. Simulation is an example by Abduction from 1.

*Akira Taneko[1] (1.SEED SCIENCE Lab.)

[PPS06-P05] Quantitative evaluation of the cumulus convection schemes for the implementation into the Paleo Martian Global Climate Model

*Katsushige Toriumi[1], Arihiro Kamada[1], Takeshi Kuroda[1,2], Naoki Terada[1], Yasumasa Kasaba[3], Isao Murata[1], Hiromu Nakagawa[1] (1.Tohoku university, Geophysics, Planetary Atmospheric Physics, 2.NICT, 3.Tohoku university, Geophysics, Planetary Plasma and Atmosperic Research Center)

[PPS06-P06] Forced libration of Ganymede including the visco-elastic tidal deformation

*shinichiro kojima[1], Jun Kimura[1], Shunichi Kamata[2] (1.Department of Earth and Space Science, Graduate School of Science, Osaka University, 2.Creative Research Institution, Hokkaido University)

[PPS06-P07] Experimental study on collision destruction simulating the primitive meteorite parent body

*Horikawa Kazuhiro[1], Masahiko Arakawa[1], Minami Yasui[1], Ryo Sugimura[1] (1.Kobe University Faculty of Science)

[PPS06-P08] Evolution of atmospheric composition in the early Martian atmosphere

*Ryosuke Yagi[1], Naoki Terada[1] (1.Planetary Atmospheric Physics Group, Tohoku University, Japan)

[PPS06-P09] Observation of catastrophic destruction of two different targets using X Ray photography

*Takumi Nagano[1], Masahiko Arakawa[1], Minami Yasui[1], masato nakamura[1], Fumiya Nagatomo[1] (1.Faculty of Science Kobe University)

[PPS06-P10] Charge transport between granular particles in an ejecta curtain produced by hypervelocity impacts

*Kosuke Kurosawa[1], Takanori Iwasawa[2], Satoshi Okuzumi[2], Sunao Hasegawa[3], Takayuki Muranushi[4] (1.Planetary Exploration Research Center, Chiba Institute of Technology, 2.Department of Earth and Planetary Sciences, Tokyo Institute of Technology, 3.ISAS, JAXA, 4.AICS, RIKEN)

[PPS06-P11] Nonlinear outcome of gravitational instability in irradiated protoplanetary disks

*Shigenobu Hirose[1], Jiming Shi[2] (1.Japan Agency for Marine-Earth Science and Technology, 2.Spotify USA Inc)

[PPS06-P12] Rheology of clay paste and application to the investigation of formation process of surface topography on the Mars

*Chihiro Uemura[1], Takahiro Iwata[1,2], Akio Nakahara[3], Yosuke Matsuo[3], Tomohiro Usui[2], Rina Noguchi[2] (1.SOKENDAI, 2.ISAS/JAXA, 3.Nihon Univ.)

[PPS06-P13] An Explanation for Physical Mechanism of the Streaming Instability

*Hiroaki Kaneko[1] (1.Tokyo Institude of Technology)

[PPS06-P14] Spatial motion of the Earth-Moon system and Earth pole oscillatory process

*Alexandra Sergeevna Filippova[1], Vadim Vladimirovich Perepelkin[1], Wai Yan Soe[1] (1.Moscow Aviation Institute)

[PPS06-P15] Chondrule formation model by lightning in high dust density regions

*Chihiro Ikeda[1], Taishi Nakamoto[1] (1.Tokyo Institute of Technology)

[PPS06-P16] The transition to superrotation in stratospheric atmospheres

*Motoki Sumi[1] (1.Tokyo Institute of Technology)

[PPS06-P17] **ExPRES: a Tool to Simulate Exoplanetary and Planetary Radio Emissions**

*Corentin LOUIS[1,2,3], Sebastien L. Hess[4], Baptiste Cecconi[2,3], Philippe Zarka[2,3], Laurent Lamy[2,3], Stéphane Aicardi[5], Alan Loh[2] (1.IRAP, Toulouse, 2.LESIA - Observatoire de Paris, 3.USN, Observatoire de Paris, 4.ONERA-The French Aerospace Lab, FR-31055 Toulouse, France, 5.DIO, Observatoire de Paris, PSL Research University, CNRS, Paris, France)

[PPS06-P18] Crustal structures of major mercurian basins

*Qingyun Deng[1], Fei Li[1], Jianguo Yan[1], Zhiyong Xiao[2] (1.State Key Laboratory of Information Engineering in Surveying, Mapping and Remote Sensing, Wuhan University, 2.Planetary Science Institute, China University of Geoscience)

[PPS06-P19] Application of LiDAR Technique for the 3D Digital Documentation of Cultural Heritage Sites

*Sachchidanand [1], Mayank Sharma[1], Rahul Dev Garg[1] (1.Indian Institute of Technology Roorkee)

[PPS06-P20] Tidal Interaction in the Earth-Moon System Treated as a Double Planet

*Aleksandr Aphanasievich Zlenko[1], Irina Michailovna Ryabikova[2] (1.Department of high mathematics, Moscow automobile and road construction state technical university, 2.Department of descriptive geometry, Moscow automobile and road construction state technical university)

[PPS06-P21] **The consequences of Saturn's "ring rain"**

*James O Donoghue[1,2], Luke Moore[3], Jack Connerney[4,1], Henrik Melin[5], Tom Stallard[5], Sean Hsu[6], Steve Miller[7], Kevin Baines[8] (1.NASA Goddard Space Flight Center, USA, 2.Institute of Space and Astronautical Science, Japan Aerospace Exploration Agency (ISAS; JAXA), Japan, 3.Boston University, USA, 4.Space Research Corporation, Maryland, USA, 5.University of Leicester, UK, 6.Laboratory for Atmospheric and

Space Physics, University of Colorado–Boulder, CO, USA, 7.University College London, UK, 8.NASA Jet Propulsion Laboratory, California, USA)

[PPS06-P22] **Calculation of kinetic rate constants using high-level *ab initio* quantum chemical methods for planetary sciences and astrochemistry**

*Shiblee Ratan Barua[1,2], Paul Romani[1] (1.NASA Goddard Space Flight Center, Greenbelt MD USA, 2.Universities Space Research Association (USRA), Columbia MD USA)

[PPS06-P23] How many conditions must be satisfied to produce a habitable planet?

*Shigenori Maruyama[1], Soichi Omori[2] (1.Earth-Life Science Institute, Tokyo Institute of Technology, 2.The Faculty of Liberal Arts, The Open University of Japan)

[PPS06-P24] Quantitative Evaluations for Meteorite Impact Tsunami

*Naotaka YAMAMOTO CHIKASADA[1], Tetsuharu Fuse[2], Toshitaka Baba[3] (1.NIED, 2.NICT, 3.Tokushima University)

The Study of Using SLR and GPS Observation Data to Estimate Geocenter Motion.

*Yih Jack Cheng[1], Fang-shii Ning[1]

1. National Chengchi University

Geocenter motion describes the difference of Center of Figure (CF) respect to Center of Mass of the Earth system (CM) due to the mass re-distribution and deformation of the Earth system. This is a factor that cannot be ignored in the maintenance of the high-precision terrestrial reference frame. As precision requirements and application demands in space geodesy increase, research on estimation of the geocenter motion become increasingly important as the key point to realize a reference frame with its origin fixed to the center of mass of the Earth system. In this study, GPS (Global Positioning System) observation data from IGS (International GNSS Service) and SLR (Satellite Laser Ranging) tracking data in the period of 2007 to 2016 are applied to estimate the coordinates of IGS sites on Earth’ s surface by using the GAMIT/GLOBK and Bernese software. Then, the Helmert transformation model is used to acquire seven parameters between the ITRF (International Terrestrial Reference Frame) reference frame and the CM reference frame. There are three parameters of them are related to the shift in three axes, which are the results of the geocenter motion. Afterwards, the geocenter motion time series are applied with the linear fitting method in order to obtain the amplitudes and phases along three axes of geocenter motion. The annual amplitude of X-, Y-, and Z- components between the years 2007and 2016 are 2.6± 0.2 mm, 4.1±0.2 mm, and 5.6±0.3mm respectively. The annual phase of X-, Y-, and Z- components are 72˚, 330˚, and 145˚ respectively. The accuracy of this study is significant improvement comparing to just using GPS or SLR technique only.

Keywords: Geocenter motion, Global Positioning System, Satellite Laser Ranging

©2019. Japan Geoscience Union. All Right Reserved.

Evolution of Pluto's surface albedo due to sublimation and condensation of ice

*Hisashi Matsui[1], Jun Kimura[1]

1. Osaka University

Observation of the spacecraft New Horizons approached Pluto in 2015 revealed that H_2O, N_2, CH_4, CO ice coexists on the surface of Pluto and that the surface has a strong contrast of bright and dark due to a difference in the amount of ice. However, it is not cleared an origin of the bright and dark color distribution on the surface.
In previous researches about a temporal changing of albedo on the Jovian and Saturnian moons, it has been shown that sublimation of ice due to an insolation affects albedo changing on their surfaces. In addition, condensation of sublimated ice in the atmosphere also should affect Pluto’s surface albedo. Through these processes, ice behavior like sublimation and condensation possibly affects a change of albedo on Pluto’s surface. However, it has been not considered quantitatively so far.
In this study, we evaluate relationship between behavior such as sublimation and condensation of various ices and change of albedo with a numerical simulation, and investigate the origin of the albedo variation on Pluto.
In our model, we assume that bright ice and dark non-ice material exist uniformly mixed and the surface albedo can be modeled by the volume ratio. Subsequently, calculate the surface temperature with a change of insolation on each latitude and thermal inertia and then estimate the sublimation amount of ices from the difference between the vapor pressure at the temperature and the atmospheric pressure. Sublimated ices exist as the atmospheric gas, and these gas should be segregated and deposited on the surface if the surface temperature falls below the segregation temperature. We calculate albedo at the next time step from the volume ratio of ice and non-ice material contained in depth considered to be mixed by micrometeorite bombardment. Finally we examine temporal change of the Pluto’s surface albedo by repeating these cycle.
As a result, using the difference of insolation amount for each latitude caused by the large inclination of the obliquity, we found that a possibility to explain the overall trend of the albedo on current Pluto without special events like a giant impact.

Keywords: Pluto, Albedo

©2019. Japan Geoscience Union. All Right Reserved.

Origin of the moon, Reason why Moon is always facing to Earth, Origin of Moon Sea, reasons why there is no Ocean behind Moon

*Akira Taneko[1]

1. SEED SCIENCE Lab.

In Solar system, Way to verify Mystery of planet origin (evolution creative inference Abduction with Evolution),It is to be able to describe all Multiple results of evolution uniformly using physically meaningful hypothesis,It can be said that it is a verification using evolution that occurs only once.
Initial condition is also unknown, and from Present state where Reproduction experiment can not be done, there is a way that is Only way to infer **Missing Link** to Origin.
Origin of Moon **(2014 U 06 - P 24)**, described Theory of necessity of Moon formation in Model of Multi-Impact Hypothesis. In addition, Origin of Jupiter Large Red Spot, Origin of Asteroid Belt, Origin of Earth Differentiation Meteorite, Origin of Earth Deep Ocean Bottom, Origin of Plate Tectonics, Origin of Driving Force, Origin of Pluto, Origin of Diamond Pipe, Core Eccentricity Also Mentioned Origin.
Origin where Moon is always facing Earth, origin of Moon sea, reason why there is no ocean behind Moon, Earth mantle ejected as shown in Lower right figure has a higher inner density, Moon is biased Center of Moon sea was formed by collision with Meteorite crust which heavy basaltic rocks were heavily on Front side, and Same crustal material does not change even if Meteorite falls on Back side around Common center of gravity of Earth and Moon Rotate Heavy side always to Center (Earth) when Earth rotates each other from its birth, and it is further accelerated and rotating due to Collision.

Y. Toda and Y. Abe Hypothesis that a special mechanism is unnecessary and can be explained as Difference of **random collision number N** between Front side and Back side and **as a result** Tidal lock of Moon will occur after establishment of Crust deformation symmetry [2] . However, since it does not mention the cause of the N number difference, ***it is only a Result Theory.***

Moon Origin Hypothesis up to Present *was a Simulation Deformation in which Differentiated Mars was formed at an arbitrary angle and velocity by Accidental Collision and Moon of only Mantle was formed in the orbital position three times Earth Radius Re.*

In "Multi- Impact Hypothesis", CERRA which was flattened toward the near point side of Jupiter by the perturbation by the gravity of Jupiter formed on the outer side of the Mars sized Differentiated Protoplanet formed at the position of Asteroid Belt by Baudet's Law, And it breaks at Jupiter's gravitational equally dividing point and it revolves around a elliptical orbital with **Train Mantle Fragments** like **a comet of a shoe maker Levi collides** with Earth at the intersection of Earth orbit Time and angle at this time Mooon that is eccentric with **Pacific Ocean** in **the first collision** is formed at current **Moon orbit energy 60 ·Re.**Fragments that collided with Jupiter become **Large Rd Spots** and the mantle of the debris becomes the asteroid belt Origin became an isostasy and became **Origin of Deep Ocean Floor of depth 5 km**, and the multiple collisions became the origin of extinct species species **High Latitude Collision of Tethys Sea formation** is caused by **Earth's gradient** and **Sudden Change in Driving direction** And **Triggered the plate movement**. It can be explained by -Antarctica moving **Center of Shaft** became unchanged **Pacific Rim arc islands and back-arc basins** also **Aisosutashi.**
I can verify **the missing link** by using **the inevitable result of evolution** that I can explain about *the present condition of about 17 items* in **a single Hypothetical model** as **a result of only one Evolution.**

©2019. Japan Geoscience Union. All Right Reserved.

A better **Hypothesis** is presented It seems to be **the best as a provisional model.**

I entered S-CG61, U-08, S-SS12, **P-PS 06**, P-PS 07. Please discuss with oral and poster venue.
[2]The Giant Impact and the Formation of the Moon P46.Des.1-3, 1998 MONTEREY,LIFORNIA

Keywords: Origin of the moon, Verification by Abduction using evolution results, Origin the moon is always facing the earth, origin of the moon sea, reasons why there is no ocean behind the moon

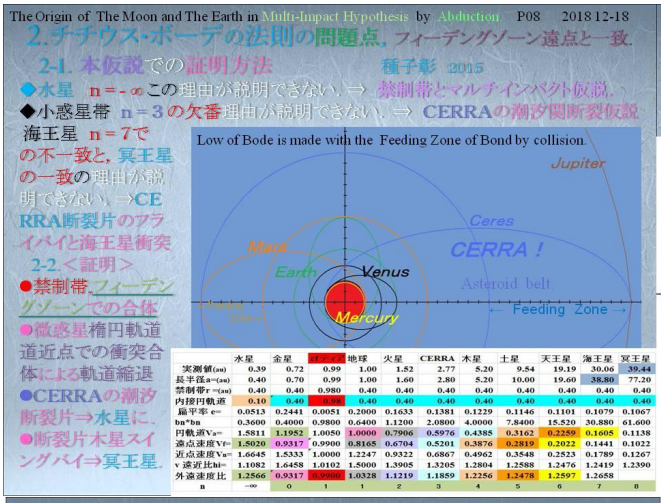

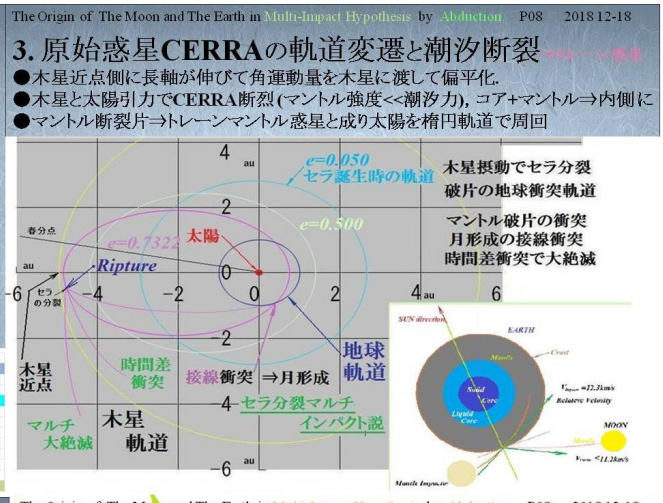

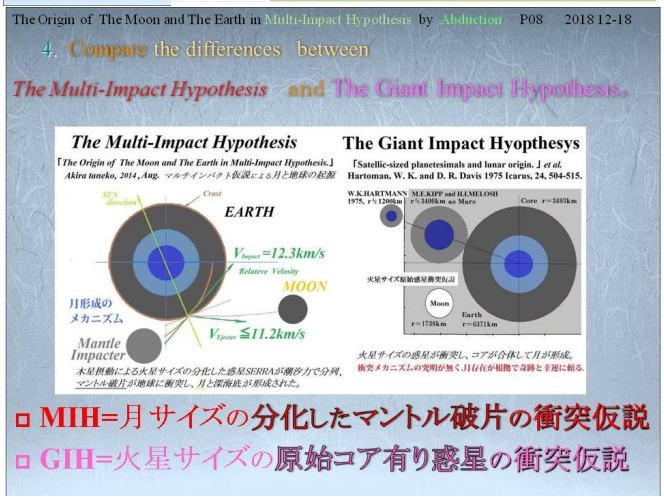

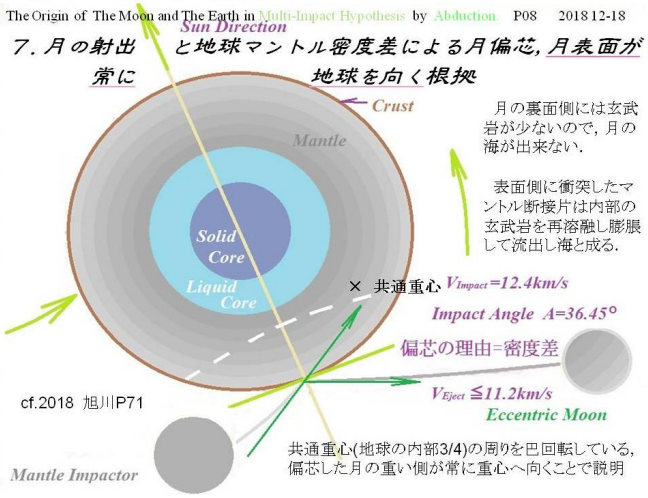

©2019. Japan Geoscience Union. All Right Reserved.

Proposed the Good model to verifyOrigins of Solar System (Planet, Asteroid belt, Earth, Moon) *with "Multi Impact Hypothesis ",*from 16' results of one time Evolution *by Abduction.*

cf. Simulation is an example by Abduction from 1.

*Akira Taneko[1]

1. SEED SCIENCE Lab.

We have been exploring **Origins of Solar System** ***by Induction and Deductive methods*** until now, but since we **can not go back in time to the past**, **Search for Truth** has not **proceeded late.The theory has verified the law by explaining multiple results only for the results of detailed experiments.**
Since **Evolution of Origin Hypothesis** that **Initial State is unknown** and **Impossible to reproduce Experiment is reality**, ***One-Time Evolution happened***, so ***unified*** explanation of **Planet of Solar system**, ***such as Present state,*** and **all of Features** of **Earth and Moon in particular** You can verify by **Method** called **Abduction.**
Origin Hypothesis of Moon **"Giant Impact Hypothesis"** up to now is **a Simulation** that creates **Moon of Mantle alone**, and ***it could not explain*** **one feature of any other Moon. In abduction it is only an illustration of N=1.**
However, the **"multi impact hypothesis"** includes not only **Origin of the moon whose component is Mantle** but also **Moon's Orbital Energy** (60·Re), **Eccentricity of Moon** (always **Moon's Surface** faces the earth), **Origin of Moon Sea** , ***I could explain why*** there is no **Ocean** on **the reverse side.**
Furthermore, although it is Origin Hypothesis of Moon, other features of the solar system, Origins of Asteroid Belt and **Origin of Differentiated Earth Meteorite**, **Origin of Ocean of Earth** (60%>, 5 km depth), **Origin of Plate Boundary, Origin of Plate Tectonics**, **Origin of Driving Force**, **Origin of Pacific Rim Orphan Ocean Island and Back Arc Concave Marine Basin, Origins of Mutual Plate Overlap, Origins of Axis Inclination, Origin of Diamond Mine,** Origin of Van Allen belt eccentricity, Origin of Titian Sea, Origin of tilt, Risk of Sudden Change of Plate Movement Direction, Origin of species extinction, Origin of Jupiter large red spot, Origin of Mercury core rich, Origin of Pluto, Origin of Alps and Tibetan highland, Unified description to **Origin of Continental Drift** It can be said that it was able to be verified as Abduction by being able to do. In particular, Formation of Deep Seabed average of 5 km by Isostasy and **Air Hockey state of the plate by Asthenosphere is Driving force of Earth plate due to eccentricity of the inertial efficiency,** become **Train Asteroid** of the **CERRA Mantle** ***due to CERRA rupture,*** Collision at **the intersection of Moon is Injection of Moon and Earth's Mantle Defect**, it is Origin of several Seas and Origin of extinct species. Cracks in Earth's Mantle are Origin of Plate Boundary, and **the Pacific Rimback Arc Naval Basin is also Origin of Plate Overlap. The high latitude collision is the origin of the earth's axis tilt,** and **Verification of Driving Force** is ***also made that Antarctica fits into the earth's axis and becomes immovable.***
I proposed **a theoretical model to verify Origins of Solar System (Planet, Asteroid belt, Earth, Moon) by Abduction** ***from multiple (16) results of*** **One Time Evolution.** It is particularly noteworthy to show **Collision Speed and Aangle to Earth** ***(12.4 km / s, 36.4 degrees)*** and **Moon orbit energy** ***(60 ·Re).*** At the same time I could show **Feeding Zone and Bowden 's law.** It is **a theory model** and **victory of Abduction.**
I entered S-CG61, U-08, S-SS12, P-PS 06, **P-PS 07.** Please discuss with oral and poster venue.

©2019. Japan Geoscience Union. All Right Reserved.

Keywords: Multi Impact Hypothesis, Verify with Abduction, Origin of the Solar System (Planet, Asteroid Belt, Earth, Moon), Multiple (16) results of one time evolution, Method of verifying Origin

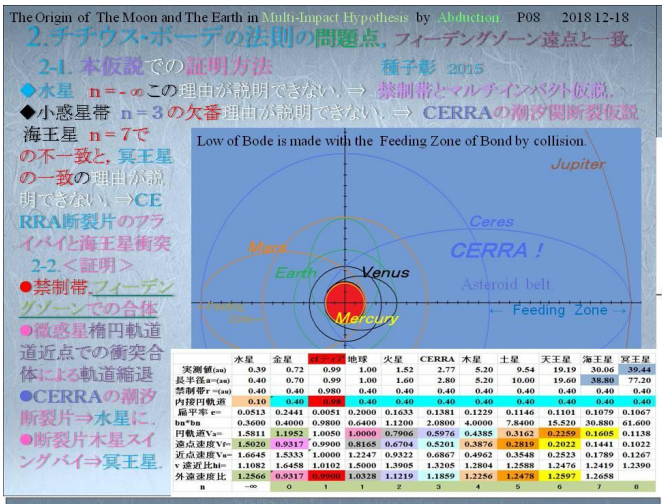

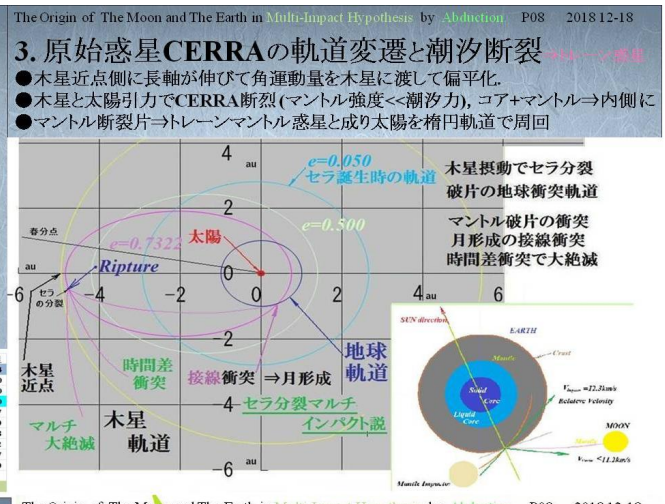

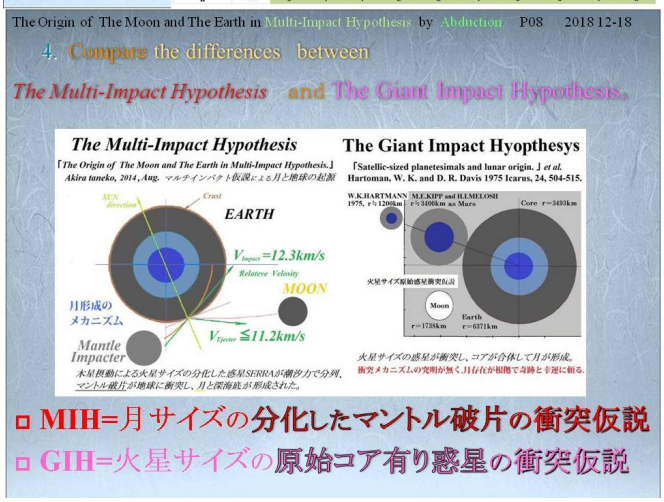

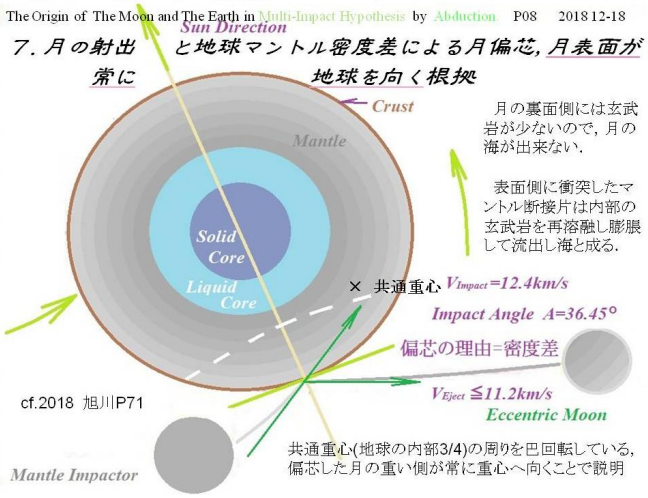

©2019. Japan Geoscience Union. All Right Reserved.

Quantitative evaluation of the cumulus convection schemes for the implementation into the Paleo Martian Global Climate Model

*Katsushige Toriumi[1], Arihiro Kamada[1], Takeshi Kuroda[1,2], Naoki Terada[1], Yasumasa Kasaba[3], Isao Murata[1], Hiromu Nakagawa[1]

1. Tohoku university, Geophysics, Planetary Atmospheric Physics, 2. NICT, 3. Tohoku university, Geophysics, Planetary Plasma and Atmosperic Research Center

Current Mars has a lot of fluvial traces, which are supposed to be made during the late Noachian and early Hesperian boundary (3.85-3.6 Ga). If these traces are created by the fluvial activity, the climate of early Mars should be ‘warm and wet’ enough for the long-term existence of liquid water on its surface. However, solar luminosity at that time would be weaker by 20-30 % of today’s value, which would preclude early Mars from such ‘warm and wet’ climate (‘Faint young Sun paradox’). Previous studies using 3-dimensional Mars Global Climate Models (MGCMs) have revealed that pure CO_2atmosphere, even assuming 2~7 bars, was hard to reproduce the surface temperature above 273 K [e.g. *Kasting*, 1991; *Forget et al*. 2013].

We newly developed a 3-dimensional Paleo MGCM (PMGCM) with ancient ocean on its surface below a sea level of -2.54 km, including the absorptions of CO_2/ H_2O gases, CO_2/ H_2O ice clouds, thermodynamics of land / ocean, and hydrological processes [*Kamada et al*., submitting to Icarus]. This model reproduced a clement surface environment enough for liquid water on surface and could create most of fluvial channels by hydrological processes. However, the fluvial channels reproduced in our model were partly not consistent with observations on current Mars (e.g. *Sabaea Terra*). There are several explanations for the inconsistencies, such as 1) in Noachian and early Hesperian boundary the Tharsis rise had not finished or completed, which would enable wind system to transport water vapor towards the leeward regions such as Sabaea Terra, and/or 2) some of fluvial channels would have formed by glaciation.

Another possible reason is that our modelhad excluded the cumulus convection scheme, considering only the large-scale condensation process for the precipitation. This process could be crucial for resolving atmospheric instability and affect the distribution and the amount of precipitations on early Mars. Therefore, as the next step, we are newly introducing a cumulus convection scheme. One candidate is the Relaxed Arakawa-Schubert scheme [*Moorthi and Suarez*, 1991] which is often introduced to terrestrial GCMs. However, it is not clear whether this scheme could be adapted to early Mars, because it is a simplified scheme taking the empirical processes of the Earth into account for the calculations of the cloud mass flux, which may not be simply adopted to the CO_2/ H_2O atmosphere of early Mars. On the other hand, the Kain-Fritsch scheme [*Kain and Fritsch,* 1993], which is appropriate for middle resolution GCMs to reproduce the cumulus lifetime including creation, developing, declining, and deletion phases by one cumulusin a grid,is considered to be more suitable for PMGCM. It directly calculates the vertical structure of the cumulus without using the empirical assumption of the Earth.Though it is inferior to the Relaxed Arakawa-Schubert scheme in terms of ensemble, it is meaningful to introduce this scheme with high accuracy if we aim for high resolution in the future.Ultimately, we intend to calculate PMGCM with high resolution (both vertical and horizontal), verify the validity of the PMGCM introducing the cumulus convection model, and consider the influence on the running water topography.

In order to do the trade-off between those two schemes, we evaluated the differences of heat balance and

©2019. Japan Geoscience Union. All Right Reserved.

precipitation created by both schemes. First, we did the test under the present terrestrial condition (1bar, N_2/ O_2atmosphere, present solar flux at 1 AU). We supposed that both schemes would show the similar results in radiation balance and precipitation on the present terrestrial models. However, in the actual calculation results, the cloud structure had wider range of clouds in the low altitude with the Kain-Fritch scheme. That is because the characteristics of detrainment for each scheme are different. As the next step, we are changing parameters such as surface pressures (wet CO_2atmosphere of 0.5-2.0 bars), atmospheric compositions, solar flux, and terrain for early Mars as our PMGCM conditions. And we analyze the cloud structure generated by Kain-Fritsch scheme and qualitatively and quantitatively compare the change of water vapor transport with the case without cumulus convection scheme. In this paper, we plan to provide a first summary of those results.

Keywords: Mars, GCM, Valley Networks

©2019. Japan Geoscience Union. All Right Reserved.

Forced libration of Ganymede including the visco-elastic tidal deformation

*shinichiro kojima[1], Jun Kimura[1], Shunichi Kamata[2]

1. Department of Earth and Space Science, Graduate School of Science, Osaka University, 2. Creative Research Institution, Hokkaido University

From spacecraft observations and interior thermal modeling, Ganymede has been expected to possess a global ocean beneath its ice shell. To confirm an existence of the ocean, the JUICE (JUpiter ICy moons Explorer) mission has been prepared by ESA (The European Space Agency) and the spacecraft will be launched in 2022. After arriving at Jupiter system, the JUICE spacecraft is going to make several flybys Europa and Callisto and finally will orbits around Ganymede. During orbiting around Ganymede, the spacecraft will obtain several kinds of scientific data, for instance, surface topography from GALA (GAnymede Laser Altimeter) and surface images from JANUS (camera system). These data will provide important information about the tidal responses of Ganymede.

The tidal responses, e.g., tidal deformation and rotational variation, are caused by the gravitational force of other bodies such as a mother planet. The rotational variation includes libration, obliquity variation, nutation, and precession. In this study, we focus on the libration which is a spin rate variation caused by a torque acted on the aspherical degree-2 order-0 shape of the satellite. The libration changes the centrifugal force of a satellite and affects the tidal deformation. Inversely, tidal deformation affects the aspherical shape of the satellite.

Although Van Hoolst et al. (2013) has modeled the interaction of the tidal deformation and the libration, their tidal deformation models were simplified. In order to estimate an actual libration, we model 5-layered Ganymede interior and use the visco-elastic tidal deformation model constructed by Kamata et al. (2016). Our interior model consists of five layers, which have a homogeneous density and rigidity in each layer. The viscosities of the ocean, the high-pressure ice mantle, the rock mantle and the metallic core are homogeneous in each layer, and the viscosity of the ice shell is not homogeneous and depends on a radial temperature variation.
As a typical case, we use interior parameters which are the ice shell thickness of 155 km, the ice shell density of 940 kg/m^3 , the ocean thickness of 1 km, and the ocean density of 1050 kg/m^3 . Then we also use the three sets of a shell rigidity and a shell viscosity (1) 0.1 GPa and 10^{12} Pas, (2) 0.1 GPa and 10^{17} Pas, and (3) 10 GPa and 10^{17} Pas, respectively. The results for the libration amplitude are 34.1 m, 34.1 m, and 37.5 m respectively. As a conclusion, our calculation of the visco-elastic libration infer that the reference viscosity of ice (temperature-dependent viscosity of ice at a melting point) doesn’ t affect the amplitude of the shell libration. The ice rigidity affects the amplitude of the shell libration of order of a few meters.

Keywords: Ganymede, tidal deformation, libration

©2019. Japan Geoscience Union. All Right Reserved.

Experimental study on collision destruction simulating the primitive meteorite parent body

*Horikawa Kazuhiro[1], Masahiko Arakawa[1], Minami Yasui[1], Ryo Sugimura[1]

1. Kobe University Faculty of Science

We studied the impact strength of weak brittle materials changing the strength continuously from 40kPa to 800kPa, and found that the impact strength could be well scaled by using the non-dimensional impact strength.

Asteroids are believed to be constructed from various materials based on the long-term study related to meteorites. The components of S-type and C-type asteroids could be composed of chondrules and matrix; the chondrules are sub-mm size glass spherules and the matrix could be micron-size fine grained materials such as phyllosilicates and lithic fragments etc. Moreover, these components could have a wide range of porosity inside because they might be residual pore during the compaction process of planetesimals or relics of water ice or volatiles escaping from these bodies. Impact strength is one of the most important physical properties of asteroids because it could control the evolution of the size-frequency distribution of asteroids at the asteroid belt. The impact strength strongly depends on the asteroid size and it is dominated by the material strength at the size smaller than 100m, so that the impact strength should be determined by the laboratory experiments. Therefore, a lot of research have been conducted for rock, ice, and porous materials to investigate the material dependence, however the impact experiments using the target with the strength continuously changed have been hardly conducted so far. Then, we prepared the targets simulating asteroids composed of chondrules, matrix and pore and changed the internal structure of the target such as matrix ratio and porosity; the tensile strength was changed more than one order of magnitude, then we studied the relationship between the internal structure and the impact strength.

Impact experiments were conducted by using two-stage light gas gun at Kobe University, and we used a polycarbonate projectile with the size of 4.7mm and a nylon projectile with the size of 2mm and they were lunched at the velocity from 0.9km/s to 5.7km/s. The impact was conducted at a head-on collision. A spherical target with the size of 60mm were prepared by using quartz sands with the size of 100 μm and porous gypsum, and they are mixed with various mass ratio of quarts to gypsum from 2:1 to 8:1. The tensile strength of these materials (Y_t) was measured by using Brazilian test and it was found that the tensile strength changed from 40kPa to 800kPa with the increase of the gypsum mass ratio. The impact disruption was observed by a high-speed camera at 10^5fps.

The impact strength (Q*) was determined by using a largest fragment mass for each shot, and Q* was found to change from 400J/kg to 1900J/kg with the increase of the gypsum mass ratio. This means that the Q* is directly proportional to the tensile strength. However, the ejection velocity at an antipodal point (v_a), which was measured by using high-speed images, showed the almost similar results, irrespective of the tensile strength. A non-dimensional impact strength (P_I) is defined as the ratio of the target tensile strength to the antipodal pressure such as P_I=Y_t/P_a, where P_a is calculated by ρ C_b v_a/2. This P_I was proposed to scale the target with the different tensile strength. Then, the relationship between the largest fragment mass and P_I was examined to discuss the P_I scaling law for the catastrophic disruption. We found that P_I is able to scale the largest fragment data very well, and this might mean that P_I could be applicable to asteroid components composed of weak brittle materials.

©2019. Japan Geoscience Union. All Right Reserved.

Keywords: collisional disruption, strength, impact strength

©2019. Japan Geoscience Union. All Right Reserved.

Evolution of atmospheric composition in the early Martian atmosphere

*Ryosuke Yagi[1], Naoki Terada[1]

1. Planetary Atmospheric Physics Group, Tohoku University, Japan

The purpose of this study is to investigate the evolution of atmospheric composition in the early Martian atmosphere. Not only hydrogen and oxygen but also carbon escape to space is considered in this study. The early Martian atmosphere was influenced by a stronger Sun’ EUV radiation than today. The escape parameter, defined as the ratio of the gravitational potential to kinetic energy at a given altitude, could be small enough to allow massive escapes of these species under such a strong radiation. For example, the escape parameter of atomic carbon in the Martian atmosphere was estimated 0.8 times smaller than that of atomic oxygen and both densities at the exobase level were comparable at 4.1 Gyr ago (Tian et al., 2009). Hence, we consider that in early Mars, thermal escape of atomic carbon could be stronger than atomic oxygen, and oxygen dissociated from CO2 was left behind in the atmosphere. Assuming that the escape rates of atomic carbon and atomic oxygen were in the same proportion, we get results that carbon disappeared in 5 Myrs from 1 bar of CO2 atmosphere and only 0.4 bar of oxygen atmosphere remained around 4.2 Gyr ago. On the other hand, it was suggested that the Martian atmosphere about 3.5 Gyr ago could have several mbar or more of oxygen partial pressure(Noda et al., 2018). In the present study, we have developed a 1-D photochemical model of the early Martian atmosphere to investigate the evolution of the atmospheric composition, in particular from 4.2 to 3.5 Gyr ago. This model includes not only the effect of escapes of hydrogen, oxygen and carbon but also that of deposition to surface and degassing. In this presentation, we will show the influence of the atomic carbon escape to the evolution of oxygen partial pressure left behind in the early Martian atmosphere.

©2019. Japan Geoscience Union. All Right Reserved.

Observation of catastrophic destruction of two different targets using X Ray photography

*Takumi Nagano[1], Masahiko Arakawa[1], Minami Yasui[1], masato nakamura[1], Fumiya Nagatomo[1]

1. Faculty of Science Kobe University

We studied the dependence of physical properties of planetesimals on the impact strength in the gravity regime, then we made laboratory impact experiments by using a Flash X-ray for porous gypsum and dry clay simulating planetesimals in order to obtain the relationship between impact fragment masses and ejection velocities.

The impact strength of planetesimals is one of the most important physical properties to clarify the planetary accretion process and the formation process of proto-planets and asteroids. Thus, the impact strength in the strength regime applicable to planetary bodies smaller than 100 m has been mainly studied in laboratory experiments. However, the impact strength in the gravity regime applicable to planetary bodies larger than planetesimals has been studied only by numerical simulations, and their results are not consistent with each other. Furthermore, recent numerical results conducted by Jutzi (2016) showed us that the material properties such as friction, cohesion and porosity affected the impact strength in the gravity regime drastically. Then, we made laboratory impact experiments to elucidate the material dependence on the impact strength in the gravity regime.

In order to determine the impact strength in the gravity regime by the laboratory experiments, we should obtain the relationships between the impact fragment masses and the ejection velocities, and especially, the fragments ejected from the interior of the disrupted target must be observed to construct the velocity –mass relationship for all the fragments. Then, we introduced 3 sets of flash X-ray generators and imaging plates to take transmitted X-ray images of a target with 3 mm steel balls arranged in it. These steel balls were used as makers of the motion of impact fragments, and the time sequence of these balls were observed by using X-rays to analyze the local velocities of the target’ s interior.

Impact experiments were conducted by using a polycarbonate projectile with the size of 7mm at the velocity of 2 –5 km/s, and the projectile was impacted on a spherical target with the size of 6 cm in a head-on collision. We used porous gypsum targets with the porosity of 50% and the tensile strength from 1 to 2 MPa and dry clay targets with the porosity of 48 % and the tensile strength different from the porous gypsum. All the targets were catastrophically disrupted into the largest fragment mass less than 0.2. As a result, we determined an upper limit of ejection velocities having a half mass of the target for each experiment, and we defined this upper velocity as a median velocity of V*. So, we studied how V* depended on the energy density, tensile strength and porosity, then we found that V* increased with the energy density for both targets. Moreover, we found that it strongly depended on the target porosity when it was compared with the previous result for the frozen clay with the similar tensile strength but without porosity, the V* for porous gypsum reduced to be 1/3 for the frozen clay. The V* for the dry clay was almost similar to that for the porous gypsum, thus this might mean that the tensile strength does not affect the V* even for the porous target.

Keywords: Destruction

©2019. Japan Geoscience Union. All Right Reserved.

Charge transport between granular particles in an ejecta curtain produced by hypervelocity impacts

*Kosuke Kurosawa[1], Takanori Iwasawa[2], Satoshi Okuzumi[2], Sunao Hasegawa[3], Takayuki Muranushi[4]

1. Planetary Exploration Research Center, Chiba Institute of Technology, 2. Department of Earth and Planetary Sciences, Tokyo Institute of Technology, 3. ISAS, JAXA, 4. AICS, RIKEN

We studied the charge transport between granular particles in an ejecta curtain produced by hypervelocity impacts to access the energy partitioning from the initial kinetic energy to the electrostatic one having the ejecta curtain. We conducted both hypervelocity impact experiments and numerical calculations. The impact experiments were done at ISAS/JAXA hypervelocity impact facility. A vertical gun was used to use granular materials as a target. High-speed video cameras for the visible and infrared were used to observed an impact-generated ejecta curtain. Any light sources were not used in this experiment. We constructed a numerical model by combining the iSALE shock physics code and the REBOUND N-body integrator. The processes of impact ejection under the conditions similar to the laboratory experiments were solved by the iSALE. The time at the ejection, ejection velocity, and the launch position of each particle was extracted as a txt file. Then, the txt file was imported in the REBOUND as a input file. At this time, we added random velocities to simulate the velocity dispersion. Although the dispersion would be inevitably added to each ejected particles in nature, it cannot be modeled in the hydrocode. The absolute magnitude of the random velocity was treated as a free parameter. Subsequent particle motions under the Earth’ s gravity field and the resistance force by the surrounding air were calculated. The decceleration due to inelastic collisions and charge transport between particles were included into the calculations. The restitution coefficient was also treated as a free parameter. The degree of charge separation was given by an empirical law proposed by the previous experiment. The results are summarized as follows; (1) We did not observe a large-scale discharge in an ejecta curtain under the experimental condition, (2) we observed a number of bright points along with an produced-ejection flow, (3) we observed a mesh pattern in the ejecta curtain as well as a previous study, (4) we reproduced the mesh pattern in the REBOUND when we chose the degree of the random velocity to be 5-15% of the ejection velocities at the restitution coefficient of 0.8, (5) mutual collisions between granular particles cease at the early stage of the growth of the ejecta curtain, (6) the end time of the mutual collisions depends on the atmospheric pressure, and (7) the empirical law pertaining to the charge separation yields an unphysically-high electrostatic energy. In the presentation, we will present the current status of our research development and discuss the future plans.

Acknowledgements:We thank the developers of iSALE, including G. Collins, K. Wün- nemann, B. Ivanov, J. Melosh, and D. Elbeshausen. We also appreciate the developers of REBOUND, including Hanno Rein, ShangfeiLiu, David S. Spiegel, Akihiko Fujii, and Dan Tamayo.

Keywords: Hypervelocity impacts, Ejecta curtain, Charge transport

©2019. Japan Geoscience Union. All Right Reserved.

Nonlinear outcome of gravitational instability in irradiated protoplanetary disks

*Shigenobu Hirose[1], Jiming Shi[2]

1. Japan Agency for Marine-Earth Science and Technology, 2. Spotify USA Inc

Using local three dimensional radiation hydrodynamics simulations, the nonlinear outcome of gravitational instability in an irradiated protoplanetary disc is investigated in a parameter space of the surface density Σ and the radius r. Starting from laminar flow, axisymmetric self-gravitating density waves grow first. Their self-gravitating degree becomes larger when Σ is larger or the cooling time is shorter at larger radii. The density waves eventually collapse owing to non-axisymmetric instability, which results in either fragmentation or gravito-turbulence after a transient phase. The boundaries between the two are found at $r \sim 75$ AU as well as at the Σ that corresponds to the initial Toomre's parameter of ~ 0.2. The former boundary corresponds to the radius where the cooling time becomes short, approximating unity in terms of the inverse of the orbital frequency. Even when gravito-turbulence is established around the boundary radius, such a short cooling time inevitably makes the fluctuation of Σ large enough to trigger fragmentation. On the other hand, when Σ is beyond the latter boundary (i.e. the initial Toomre's parameter is less than $\sim$0.2), the initial laminar flow is so unstable against self-gravity that it evolves into fragmentation regardless of the radius or, equivalently, the cooling time. Runaway collapse follows fragmentation when the mass concentration at the centre of a bound object is high enough that the temperature exceeds the H_2 dissociation temperature.

Keywords: Protoplanetary disks, Gravitational instability, Hydrodynamics simulations

©2019. Japan Geoscience Union. All Right Reserved.

Rheology of clay paste and application to the investigation of formation process of surface topography on the Mars

*Chihiro Uemura[1], Takahiro Iwata[1,2], Akio Nakahara[3], Yosuke Matsuo[3], Tomohiro Usui[2], Rina Noguchi[2]

1. SOKENDAI, 2. ISAS/JAXA, 3. Nihon Univ.

Mars is known to have many terrains formed by water, which is one of important candidates for future exploration places. For example, RSL (Reccuring Slope Lineae) is repeating disappearance and occurrence by seasonal variation, so it suggests that RSL was formed by water. However, there is a hypothesis that RSL is formed by sands, and formation process of RSL is still unclear.
Considering that flowing water is mixed with grain of sands and clay powders, and becomes pastes (colloidal suspension). It is valuable to understand properties of pastes. Since pastes have many unique properties, they are attracting widespread interest in various fields. Pastes are classified as attractive or repulsive according to a force among particles. Rheology of repulsive colloidal suspension has been studied so far. On the other hand, rheology of attractive colloidal suspension is still unknown. To understand the surface topography on Mars, it is important to study the rheology of clay paste, one of typical attractive colloidal suspension, because clay minerals are widely found on the surface of Mars. As the formation of some landforms, such as RSL, are considered to be dependent on temperature, we focused on the temperature dependence of their rheology, such as an yield stress and a viscosity, of attractive colloidal suspension.
We used paste of magnesium carbonate hydroxide because their properties are similar to clay minerals; their inter-particle force is attractive and makes a card house structure. We used rheometer (Anton Paar, Physica, MCR-301) for measuring. We measured rheology of paste at four different temperatures and five different solid volume fractions. We found that the yield stress of paste of magnesium carbonate hydroxide is an increasing function of a temperature. The yield stress of usual elastoplastic media is known to decrease as the temperature increases. However, our experimental study revealed that the yield stress of attractive colloidal suspension is an increasing function of the temperature, the result of which is an inverse behavior to that of usual elastoplastic media. The temperature dependence of the yield stress of attractive colloidal suspension is much more drastic when it is compared to the theoretical prediction for the repulsive colloidal suspension with the linear dependence to its absolute temperature.
As for the viscosity of attractive colloidal suspension, its behavior is similar to that of Newtonian viscous fluid with its viscosity a decreasing function of the temperature. We consider that this is because the viscosity of solvent, i. e., water, decreases as the temperature of an colloidal suspension increases.
These facts suggest that temperature dependence of rheology was caused by what kind of force is working among particles. As a mechanism of these results, we suggest that changing charge on the surface of particles or changing viscosity of water. In order to reveal why interaction is changed with increasing temperature, we need further verification.
In the future work, we will make use of these results for understanding the process of forming subsurface terrains on Mars.

Keywords: Mars, RSL, rheology, yield stress, clay paste

©2019. Japan Geoscience Union. All Right Reserved.

An Explanation for Physical Mechanism of the Streaming Instability

*Hiroaki Kaneko[1]

1. Tokyo Institude of Technology

Planets are thought to be formed from planetesimals, which are 1-100 km in size, and planetesimals are formed by accumulating small dust particles. Dust particles of a size of 10 cm-1 m drift sunward at 1 au per a century. Dust particles must grow within a timescale faster than this sunward drift timescale limit, otherwise they cannot form planetesimals. Enhancement of the particle density leads to the self-gravitational instability if the density reaches the Roche density, and the dense dust particles form planetesimals. In this case, the dramatic radial drift of dust particles can be avoided. Youdin & Goodman (2005; YG05) discovered that dust and gas streams mutually interacting via drag force generate local linear instability and a particle clumping occurs. This instability is called the streaming instability (SI). A lot of linear and non-linear numerical simulations conducted and it has been confirmed that SI emerges under certain conditions. But the physical mechanism of SI is not clear yet, because the order of the dispersion relation is as high as 6 and the mechanism seems to be difficult to understand. Applying the terminal velocity approximation (YG05) to particle continuity equation and gas incompressibility, Jacquet, Balbus, & Latter (2011; JBL11) attempted to give a physical explanation about the SI mechanism. Their explanation was as follows:

1. The gas pressure maximum traps dust particles.

2. Dust particles drag the gas toward the gas pressure maximum.

3. The gas pressure maximum is strengthened. Though the gas pressure gradient tends to force out the gas from the maximum, the dust particle drag force on the gas and the Coriolis force make roles to keep the geostrophic balance.

JBL11 suggested the explanation of the mechanism in which all the motion takes place only in the midplane, however, YG05 emphasized that the vertical advection flows toward the density maximum and it dominates the flow in the midplane.

In this study, first, we conduct an analysis on the dispersion relation that employs the terminal velocity approximation (YG05) and calculate phase differences among the perturbed particle density, the perturbed gas pressure, and the perturbed particle velocities for an unstable mode. Then, we give an explanation about the mechanism of SI including the vertical motion unlike the explanation by JBL11.

Our explanation on the SI mechanism is as follows:

1. At the particle density maximum, the gas receives more angular momentum, while at the particle density minimum, the gas receives less. So, the gas radial velocity perturbation and the gas pressure fluctuation along the radial direction are generated.

©2019. Japan Geoscience Union. All Right Reserved.

2. Toward the gas pressure minimum, the gas flows in vertically with dragging dust particles. On the contrary, both gas and dust particles flow out vertically from the gas pressure maximum.

3. The phase velocity of the dust particle density maximum is negative so the particle density maximum moves radially inward. The density maximum encounters the dust particle input due to the vertical converging flow and the density maximum is enhanced.

This explanation is consistent with solutions of the linear stability analysis. In addition, the explanation seems physically reasonable and easy to understand.

Keywords: Streaming Instability, protoplanetary disk, protoplanetesimal formation, hydrodynamics, linear stability analysis

©2019. Japan Geoscience Union. All Right Reserved.

Spatial motion of the Earth-Moon system and Earth pole oscillatory process

*Alexandra Sergeevna Filippova[1], Vadim Vladimirovich Perepelkin[1], Wai Yan Soe[1]

1. Moscow Aviation Institute

The variation of the Chandler and annual components of the polar motion are of a significant interest in the Earth pole oscillatory process research. Generally these variations are quasiperiodic. But some regular oscillations can be isolated from it that correspond with the basic periods of the lunar motion. Here we discuss the theoretical assumptions of the observed effect as well as the experimental rules that illustrate the relationship between the Earth pole oscillations and the lunar motion.
The complex process of the Earth pole oscillations includes components with frequency and amplitude that differ significantly from each other. Processing the pole motion observations over the last 100 years result in statistically convincing definition of the main characteristics in its oscillatory process. Basic components in the Earth pole motion are Chandler wobble, annual oscillation and also polar motion's trend. Observed Earth pole oscillations have a wobbling character. The trajectory of the pole on the Earth surface is a winding and unwinding spiral with a period of about six years.
Actual problem that was stated by P. Melchior (Melchior, 1972) about the instability in the basic components parameters of the Earth pole is still not sufficiently explored. This problem is connected with the exploring the celestial-mechanics' and geophysical causes of such behavior in the Chandler and annual components, and also with the construction of the refined models of the forecasting the Earth orientation parameters for long time intervals.
In this work along with the common methods of the separating the pole oscillation process into the Chandler and annual components we suggest an approach to the resulted Earth pole trajectory research. For the purpose of analyzing the nonstationary resulted pole motion a perturbed trajectory is isolated. For the unperturbed trajectory a “mean” one is chosen –the Earth pole trajectory where the Chandler and annual oscillation parameters have mean values.
The differential equations for the amplitude a and phase ψ of the Earth pole modulation motion can be derived from the dynamical Euler–Liouville equations of Earth motion around its center of mass (Markov, Perepelkin et al, Astronomy Reports, 2018 and Markov, Perepelkin at al, Doklady Physics, 2017).
It is shown that the significant impact into the variations of the basic pole oscillation components is given by the long-term perturbations from the lunar orbit. The analysis of these perturbations is held using the wavelet and Fourier transformations. On the long time interval it shows matching phases of the perturbed polar motion and the lunar orbit motion using the available series of observations C04 and C01 from the International Earth Rotation and Reference Systems Service. This feature can be used to refine the model of the forecasting the Earth pole oscillations. And taking into account these structural features of the oscillations the refined numerical-analytical model of the Earth pole motion is presented.
Thus the graphical correspondence between the Earth pole oscillations and the motion of the lunar orbit is presented. It is shown that the refined model gives a more accurate description of the Earth pole motion by comparing the model computation results with the observations made by the International Earth Rotation and Reference Systems Service.

Keywords: Earth pole oscillations, Numerical-analytical model, Chandler Wobble, Lunar orbit perturbations

©2019. Japan Geoscience Union. All Right Reserved.

Chondrule formation model by lightning in high dust density regions

*Chihiro Ikeda[1], Taishi Nakamoto[1]

1. Tokyo Institute of Technology

Chondrules are spherical objects of 0.1 - 1 mm in radius and are the main component of chondrite meteorites (Scott 2007). It is known that chondrules were formed early in the solar system. So, chondrules may have important information about early solar system nebula. It is believed that chondrules melt with dust particles heated within several minutes and have cooled and solidified at a rate of 1-1000 K/hour in the early solar nebula (Desch et al. 2012). Also, since chondrules contain volatile substances, it is considered that they are formed in a high dust density region (Alexander et al. 2008). Although the formation mechanism of chondrules have not been elucidated, formation theories include the shock wave model, astronomical collision model, X-wind model, and lightning model. In this study, we examine the chondrule formation by lightning from the viewpoint of thermal evolution of chondrules.

Thermal evolution of chondrules has been studied by Horanyi et al. (1995). In that study, assuming the occurrence of lightning in the solar nebula, they calculated the time evolution of the gas and dust in the lightning. As a result, the cooling rate of the chondrule became faster than the cooling inferred from observations of crystals in chondrules. On the other hand, according to studies on the occurrence of lightning, the mass ratio of dust to gas needs to be 100:1 or more for lightning generation (Muranushi 2010). However, Horanyi et al. (1995) considered the situation where only one dust particle is present inside the lightning.

In this study, we consider the occurrence of lightning in the high dust density region and calculate the thermal evolution of chondrules numerically. Especially, we investigate if the cooling rate condition for the chondrule formation is satisfied under the high dust density situation. As a result, it was found that there are circumstances suitable for chondrule formation. It is suggested that chondrule formation by lightning is possible in the solar nebula.

Keywords: chondrule, lightning

©2019. Japan Geoscience Union. All Right Reserved.

The transition to superrotation in stratospheric atmospheres

*Motoki Sumi[1]

1. Tokyo Institute of Technology

Titan is the only satellite with the developed atmosphere and the stable liquid on the ground surface in the solar system. The history of the observation begins with the suggestion of the existence of the atmosphere in 1908. In the 1970's, the temperature structure and atmospheric composition of the Titan atmosphere have been clarified thanks to the progress of observation technology. Also, in the Cassini-Huygens mission, it visited the Saturnian system, made Huygens probes into the Titan atmosphere, and made high-precision observations. Ground-based submillimeter wave observation by the ALMA telescope is currently being carried out, and it is possible to observe at high resolution.
Observations clearly show the existence of superrotation, which is a high-speed zonal wind oriented to overtake the rotation on a global scale as a characteristic of the Titan atmosphere. The wind speed reaches 100 m/s eastward at about 10 degrees south latitude where Huygens entered, but it is difficult to investigate its mechanism from the viewpoint of insufficient observation data and complexity of atmospheric structure. Also, the theory which unified the generation mechanism of superrotation is not established, and various theories are advocated. Representative examples are the Gierasch mechanism proposed by Gierasch or the mechanism by thermal tidal waves proposed by Fels and Lindzen.
In this research, I conducted numerical experiments to generate superrotation by changing only the planetary radius using the Earth model. We used the numerical simulation model DCPAM5 of the planetary atmospheric general circulation developed by GFD Dennou Club. Primitive equations were used as the basic equation system of the model assuming a dry atmosphere. We used the model of Williamson et al.(1998) which added the pressure dependency of stratosphere to the Newtonian cooling process in Held and Suarez (1994). The calculation time was 1080 days where sufficient stationarity was confirmed, and we analyzed the time average of the physical quantities in last 360 days.
First, I output the temperature field, the mass transport distribution, zonal-mean zonal wind speed field, compare the structure of the atmosphere in the meridional space, and investigate the location and the condition. where superrotation is occurring. In the Earth model, eastward jet streams occurred in the mid latitudes of the troposphere and the stratosphere, but on the equator the westward winds are blowing. If the planetary radius is small, in the troposphere even in the equator the eastward wind is accelerated and superrotation has occurred. In the stratosphere, equator superrotation occurred in the lower stratosphere, but in the upper stratosphere the jet occurred only in the middle and high latitudes, and the high-speed eastward wind did not appear in the equator.
Next, in order to investigate the mechanism of keeping the angular momentum in the upper layer of the equator, the dispersion of the band-like disturbance of the temperature, the band-shaped disturbance spectrum of the east-west wind speed field were output, and the structure of the wave existing in the atmosphere was summarized. In the troposphere in the Earth model, many waves with a wave number of 4 or more existed in the mid latitudes, and angular momentum in the east direction was accumulated in mid latitude. However, as the radius of the planet is decreased, the waves with large zonal wavenumbers decrease, and global waves with the wave number of around one dominate. The behavior is similar in the stratosphere, in the Earth model, waves with large wavenumbers are present, although the waves are weaker in the troposhere as the planetary radius is reduced, only waves with small wavenumbers remain. In the stratosphere the equator super rotation and the mid-high latitude jet occur in different altitude, and the mechanism for maintaining superrotation seems somewhat different from the mechanism in the troposphere.

©2019. Japan Geoscience Union. All Right Reserved.

©2019. Japan Geoscience Union. All Right Reserved.

ExPRES: a Tool to Simulate Exoplanetary and Planetary Radio Emissions

*Corentin LOUIS[1,2,3], Sebastien L. Hess[4], Baptiste Cecconi[2,3], Philippe Zarka[2,3], Laurent Lamy[2,3], Stéphane Aicardi[5], Alan Loh[2]

1. IRAP, Toulouse, 2. LESIA - Observatoire de Paris, 3. USN, Observatoire de Paris, 4. ONERA-The French Aerospace Lab, FR-31055 Toulouse, France, 5. DIO, Observatoire de Paris, PSL Research University, CNRS, Paris, France

All magnetized planets are known to produce intense non−thermal radio emissions through a mechanism known as Cyclotron Maser Instability (CMI), requiring the presence of accelerated electrons generally arising from magnetospheric current systems. In return, radio emissions are a good probe of these current systems and acceleration processes. The CMI generates highly anisotropic emissions and leads to important visibility effects, which have to be taken into account when interpreting the data. Several studies showed that modeling the radio source anisotropic beaming pattern can reveal a wealth of physical information about the planetary or exoplanetary magnetospheres that produce these emissions. We present a numerical tool, called ExPRES (Exoplanetary and Planetary Radio Emission Simulator), which is able to reproduce the occurrence in time−frequency plane of CMI−generated radio emissions from planetary magnetospheres, exoplanets or star−planet interacting systems. Special attention is given to the computation of the radio emission beaming at and near its source. We explain what physical information about the system can be drawn from such radio observations, and how it is obtained. These information may include the location and dynamics of the radio sources, the type of current system leading to electron acceleration and their energy and, for exoplanetary systems, the magnetic field strength, the orbital period of the emitting body and the rotation period, tilt and offset of the planetary magnetic field. Most of these parameters can be remotely measured only via radio observations. The ExPRES code provides the proper framework of analysis and interpretation for past (Cassini, Voyager, Galileo. . .), current (*Juno*, ground-based radiotelescopes) and future (BepiColombo, Juice) observations of planetary radio emissions, as well as for future detection of radio emissions from exoplanetary systems (or magnetic white dwarf−planet or white dwarf−brown dwarf systems). Our methodology can be easily adapted to simulate specific observations, once effective detection is achieved.

Keywords: Planetsandsatellites:Aurorae, Radiocontinuum:Planetarysystems, Radioemissions simulation

©2019. Japan Geoscience Union. All Right Reserved.

Crustal structures of major mercurian basins

*Qingyun Deng[1], Fei Li[1], Jianguo Yan[1], Zhiyong Xiao[2]

1. State Key Laboratory of Information Engineering in Surveying, Mapping and Remote Sensing, Wuhan University, 2. Planetary Science Institute, China University of Geoscience

Mercury is the innermost planet in the solar system. Its surface resembles to the Moon, which is characterized with large number of impact basins, indicating an intensive bombardment history. From the data acquired by previous Mercury missions, the spatial distribution, relative age, and morphology of impact basins on Mercury is studied. Gravity data from NASA MESSENGER mission revealed the crustal structures of mercurian basins, providing information about the crust properties of the early Mercury when those basins formed. In this work, the crustal thickness ratio for each basin is calculated from global crustal thickness model obtained by inverting gravity data. The relation between crustal thickness ratio, basin relaxation state, and relative age is investigated and some implication for the early evolution of Mercury is discussed.

Keywords: crustal structures, impact basin, gravity anomaly

©2019. Japan Geoscience Union. All Right Reserved.

Crustal thickness

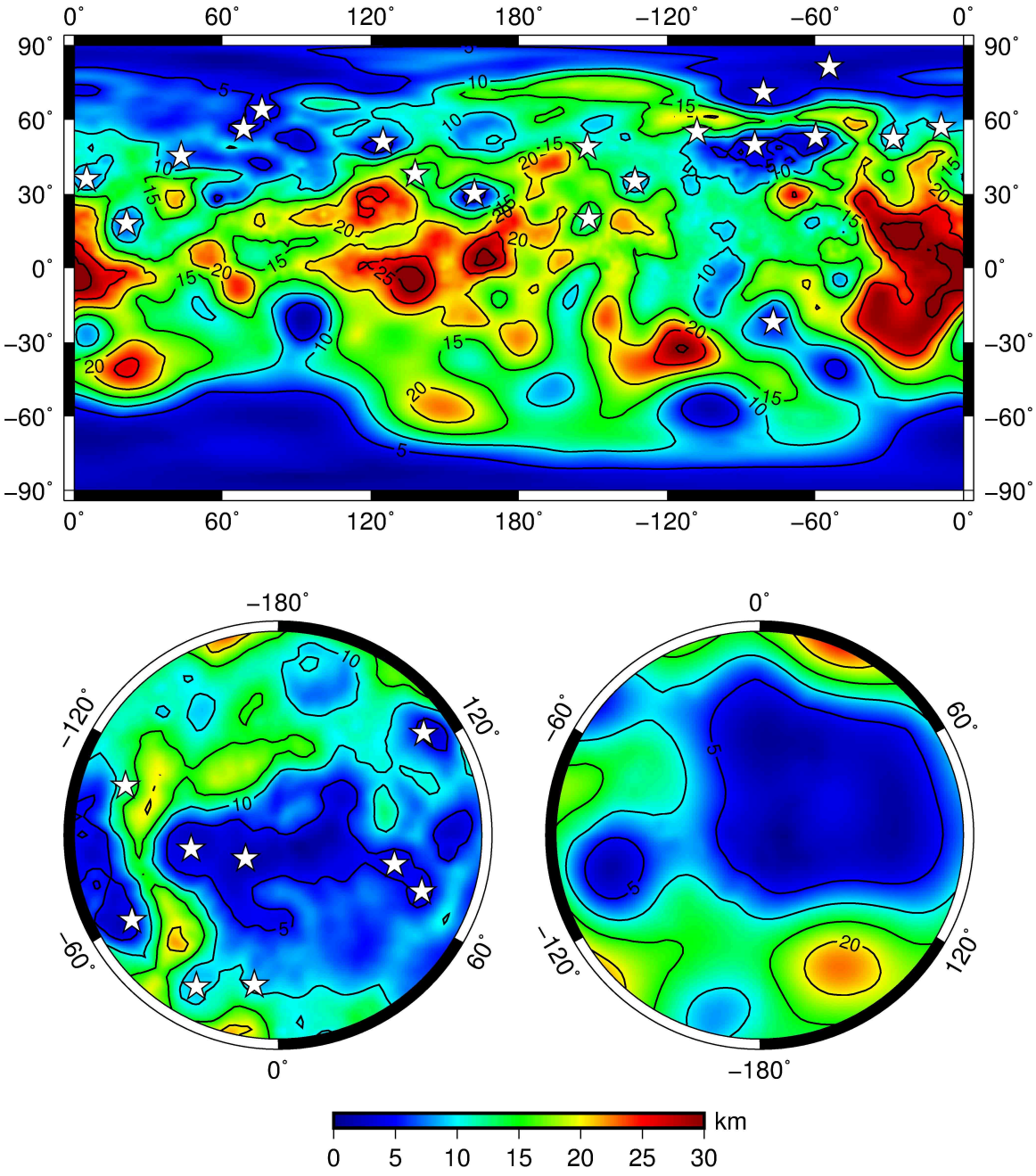

©2019. Japan Geoscience Union. All Right Reserved.

Application of LiDAR Technique for the 3D Digital Documentation of Cultural Heritage Sites

*Sachchidanand -[1], Mayank Sharma[1], Rahul Dev Garg[1]

1. Indian Institute of Technology Roorkee

Now a day’ s remote sensing and geospatial techniques are gaining popularity as they offer correct and precise information of any object situated at a distant place. Advanced remote sensing techniques like terrestrial laser scanning (TLS), mobile laser scanner(MLS), close range photogrammetry(CRP), smart total station(STS) and GNSS are the useful techniques for creating a 3D (three-dimensional) documentation of complex engineering structures or cultural heritage sites. The integration of these techniques with other methods like topographic survey or physical measurement method also offer the potential to the user to perform a complete 3D documentation of any structure.

This paper presents a methodological framework for the 3D digital documentation of cultural heritage sites from laser scanned datasets. The framework includes acquisition of point cloud datasets through laser scanners and their conversion to 3D models. 3D models are useful for planning and surface detail measurements. Detailed planimetric and elevation information or plans could be easily extracted from developed 3D models. These planimetric informations and elevation plans are useful for the conservation and preservation of structure, and can help in restoration of these structures in case of any damage due to natural disasters or other seismic activities.

Keywords: TERRESTRIAL LASER SCANNER, 3D DIGITAL DOCUMENTATION, ELEVATION PLAN, POINT CLOUD, SOLID 3D MODEL

©2019. Japan Geoscience Union. All Right Reserved.

Tidal Interaction in the Earth-Moon System Treated as a Double Planet

*Aleksandr Aphanasievich Zlenko[1], Irina Michailovna Ryabikova[2]

1. Department of high mathematics, Moscow automobile and road construction state technical university, 2. Department of descriptive geometry, Moscow automobile and road construction state technical university

Our approach to the phenomenon of tides differs from the traditional one, in which an empirically tidal potential with Love numbers is introduced. We consider the motion of two viscoelastic bodies, the Earth and the Moon treated as a double planet, in the gravitational field of a massive point, the Sun.The deformations of the bodies are described by the classical theory of small deformations. The influence of viscous forces is described by the dissipative functional of the Kelvin-Voigt model. The quasi-static equation of the elasticity theory is solved for obtaining the displacements of body points. The method of averaging and separation of motion is used for solving of this equation. The displacements of each point of the deformable body consist of displacements caused by centrifugal forces, the forces due to body elasticity and dissipative forces due to body viscosity. Substituting these displacements in the potential formulae and integrating over the each body, we get the potential of the system and the moments of forces acting on the bodies.. Knowing the displacements, we determine the shape of deformable bodies, their moments of inertia and the lagging angle. The results of this approach are compared with the results of the traditional theory.

Keywords: Earth-Moon system, viscoelastic bodies, moments of forces

©2019. Japan Geoscience Union. All Right Reserved.

The consequences of Saturn’s “ring rain”

*James O Donoghue[1,2], Luke Moore[3], Jack Connerney[4,1], Henrik Melin[5], Tom Stallard[5], Sean Hsu[6], Steve Miller[7], Kevin Baines[8]

1. NASA Goddard Space Flight Center, USA, 2. Institute of Space and Astronautical Science, Japan Aerospace Exploration Agency (ISAS; JAXA), Japan, 3. Boston University, USA, 4. Space Research Corporation, Maryland, USA, 5. University of Leicester, UK, 6. Laboratory for Atmospheric and Space Physics, University of Colorado–Boulder, CO, USA, 7. University College London, UK, 8. NASA Jet Propulsion Laboratory, California, USA

Saturn’s upper-atmospheric H3+ emissions have been previously studied using ground-based observations, and found to exhibit peaks in emissions at specific latitudes. The cause of these peaks is due to an influx of charged water products originating from Saturn’s rings known as 'ring rain'. Subsequent modeling using the Saturn Thermosphere Ionosphere Model (STIM) has indicated that these peaks in H3+ emissions are likely driven by an increase in H3+ density, rather than temperature, as a local reduction in electron density (due to charge exchange with water) lengthens the lifetime of H3+. However, a direct observation of the H3+ density is required to estimate the flow rate of material into Saturn with models. Calculation of ring rain’s flow rate into Saturn is a highly important input for determining the age, lifetime and evolution of Saturn’s rings.

Here we present the first ever derivation of H3+ density, temperature and radiance in the non-auroral regions of Saturn, using data taken from the 10-meter Keck telescope in 2011. H3+ density is enhanced near 45 degrees north planetocentric latitude and strongly reduced near 39 degrees south. When compared to STIM modeling results, these densities indicate a small ~50kg/sec water influx in the north and an enormous ~1500 kg/sec influx in the south. The charged grains are pulled in along the magnetic field by gravity, but the southward-inclination of the magnetic field (in the vicinity of the ring plane) means that the grains are preferentially drawn southwards into the planet. Assuming that our (Saturn northern Springtime) measurement represents all seasons, and that the rings are able to disperse over time, the ring rain mechanism alone will drain Saturn’s rings to the planet within 300 million years. If we also add the recent Cassini-spacecraft measured ring-material detected falling into Saturn’s equator (and assume it is constant), then the rings have less than 100 million years to live.

Recent measurements by Cassini again have estimated a ring age of ~50 million years, so it seems that Saturn’s rings are short-lived phenomena, perhaps lasting just 150 million years in total. A long time on human timescales, but compared to the 4.5 billion year age of Saturn, the rings are essentially temporary; i.e. if Saturn were 30 years old, the ring system would exist for just 1 year of its life! These recent findings indicate that ring systems in general are practically doomed to be removed as soon as they are formed. Indeed, the ring rain mechanism itself ought to be universal at any planet with both a ring system and a strong magnetic field. We might ask, did Jupiter, Uranus and Neptune, which have thin rings today, once have magnificent rings in the past that have eroded away?

Keywords: Saturn, Rings, Ionosphere, Magnetosphere, Atmosphere, Ring rain

©2019. Japan Geoscience Union. All Right Reserved.

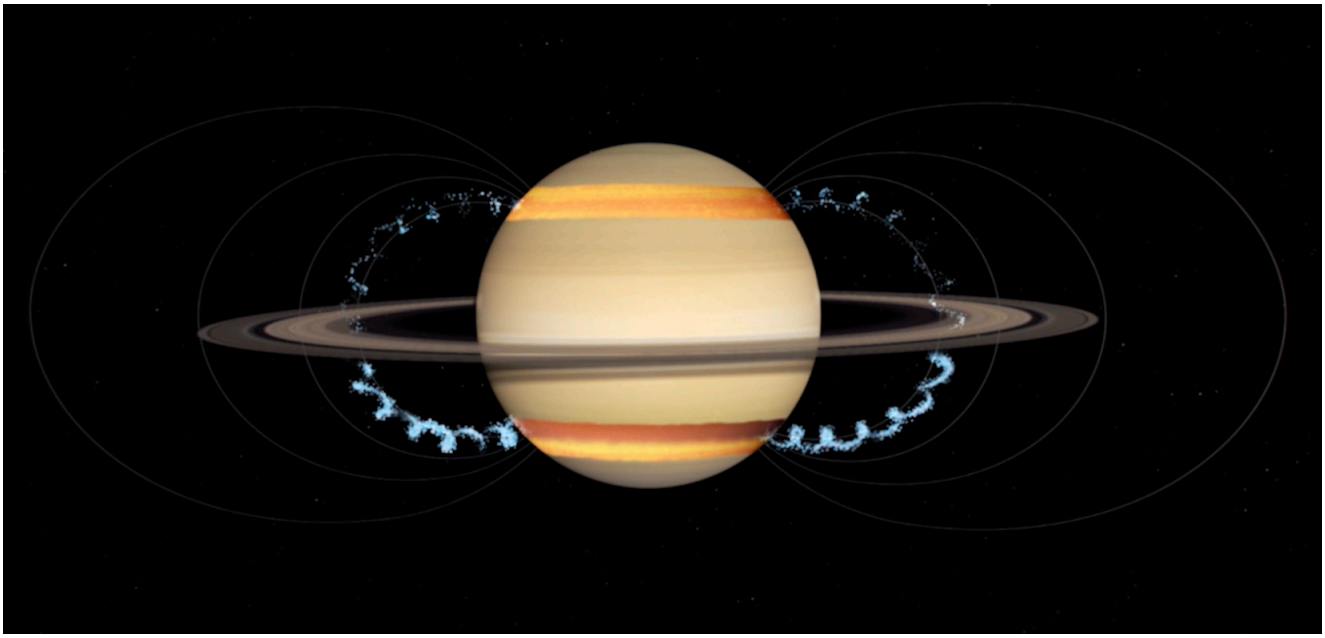

©2019. Japan Geoscience Union. All Right Reserved.

Calculation of kinetic rate constants using high-level *ab initio* quantum chemical methods for planetary sciences and astrochemistry

*Shiblee Ratan Barua[1,2], Paul Romani[1]

1. NASA Goddard Space Flight Center, Greenbelt MD USA, 2. Universities Space Research Association (USRA), Columbia MD USA

Existing photochemical models for the atmospheres of planetary bodies suffer from large errors when predicting the mole fraction profiles of various compounds. Global sensitivity analyses show that a major source of these model errors can be attributed to inaccurate rate coefficients for “key” radical–radical and radical–neutral reactions in low-temperature conditions. Accurate rate coefficients for key reactions thus improve the accuracy of photochemical models. Unfortunately, accurate experimental rate constants for such low-*T* reactions are difficult, if not impossible, to measure, and the lab data are affected by uncertainties in determining the absolute concentrations of radical species. Currently, the most common theoretical approach involves uncertainty extrapolation technique in which uncertainties in room-temperature rate constants are extrapolated to low-temperature conditions, resulting in large errors in the theoretical low-*T* rate constant data. To solve this existing problem, we are employing the two-transition-state (2TS) model developed by Klippenstein and coworkers to calculate high-level *ab initio* rate-constants for key low-*T* (*i.e.* 10–200K) reactions relevant to planetary atmospheres like that of Titan. In particular, we are investigating key reactions that have not yet been studied in the lab, and for which accurate rate coefficients are still unknown. Our calculated *ab initio* rate coefficients will be made available to the astrochemistry community via well-established free online kinetic databases (*e.g.* KIDA). These rate coefficients will be used by scientists in photochemical models to make accurate predictions of mole fraction profiles for planetary atmospheres and improve our understanding of the diverse chemistry of these bodies.

Keywords: Titan atmosphere, Low-temperature reaction kinetics, Ab initio quantum chemistry, Photochemical model, Plantery science, Astrochemistry

©2019. Japan Geoscience Union. All Right Reserved.

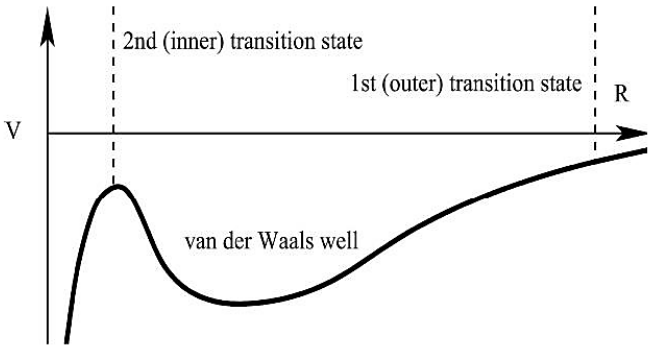

Figure 1. Schematic one-dimensional picture of the potential energy as a function of the reaction coordinate for a neutral–neutral reaction leading to bimolecular products. In its approach, the 2TS model incorporates both the 1st (outer) transition state for barrierless association reaction and the 2nd (inner) transition state for reaction path with a barrier. **Source:** Georgievskii and Klippenstein, 2007.

Table 1: Selected key reactions currently being investigated that are responsible for uncertainties in the mole fractions of major nitrogen species (left-most column) in low-T Titan conditions. Each reaction shown here has an absolute Rank Correlation Coefficient (RCC) value, a quantitative indicator of the sensitivity of model mole fractions on rate constants, greater than the chosen threshold of 0.2 at 100 km or above (right-most column). **Source:** Loison *et al.*, 2015.

Affected N Species	Key Reactions	|RCC| > 0.2
NH_3	$N(^4S) + NH_2 \rightarrow N_2 + H + H$	(100, 900) km
HNC	$N(^4S) + {}^3CH_2 \rightarrow HNC + H$	100 km
CH_2NH	$N(^2D) + CH_4 \rightarrow NH + CH_3$	900 km
CH_3C_3N	$^1CH_2 + CH_4 \rightarrow CH_3 + CH_3$	900 km
CH_3C_3N	$C_2N + H \rightarrow HCN + C$	900 km
C_2H_3CN	$CHCN + H \rightarrow C_2N + H_2$	900 km

©2019. Japan Geoscience Union. All Right Reserved.

How many conditions must be satisfied to produce a habitable planet?

*Shigenori Maruyama[1], Soichi Omori[2]

1. Earth-Life Science Institute, Tokyo Institute of Technology, 2. The Faculty of Liberal Arts, The Open University of Japan

<Purpose>

Concept of habitable zone (HZ below) is regarded as the presence of stability field of liquid water on the surface of planet. HZ is regarded as the most important condition to produce a habitable planet. However, we think the presence of liquid water is not enough to be habitable. We list up other necessary conditions (6+5=11) to produce a habitable planet in the Universe.

<Method>

The best studied habitable planet is the Earth. Therefore, based on the research results of the Earth, we consider necessary conditions. Key points are chemical composition of primordial atmosphere and biosphere.

<Result>

Based on the research of the Earth, I propose there are at least 6 conditions to be a habitable planet in case of the solar system. (1) a planet must be given totally 400 bars CO_2, 300 bars water, and 50-60 bars N_2 as minimum values. In addition, such an amount is given gradually with time (ABEL model) not to become Venus-state, (2) the presence of extremely small amount of ocean water (3km ±1km thickness), (3) the presence of huge landmass (continent above sea level) to finally provide habitable trinity condition to drive the material circulation to give nutrients through water-rock interaction to feed primordial life. (4) Initiation of plate tectonics to keep dynamic equilibria not to become Venus state. (5) selective transportation of CO_2 into mantle, while H_2O remains on the surface, and N_2 remains all in atmosphere, (6) the presence of biosphere, if not, fixation of atmospheric CO_2 is restricted only to inorganic carbonates that would be insufficient to prevent evolving into Venus-state.

<Discussion>

These six conditions are deduced from the history of the Earth. However, if we enlarge the concept to exoplanets based on the research of the solar system, the following five conditions are added; (7) the distance from the central star, (8) the abundance of atmosphere, (9) mass and composition of central star, (10) size and composition of planet, and (11) circular orbital path.

Keywords: habitable planet, conditions to produce a habitable planet

©2019. Japan Geoscience Union. All Right Reserved.

Quantitative Evaluations for Meteorite Impact Tsunami

*Naotaka YAMAMOTO CHIKASADA[1], Tetsuharu Fuse[2], Toshitaka Baba[3]

1. NIED, 2. NICT, 3. Tokushima University

Tsunami induced by earthquakes, submarine landslides, volcanic eruption in submarine and coastal area and meteorological phenomena is one of the most devastating natural disasters. A meteorite impact into the oceans spawn large tsunami depending on the size and velocity of the meteorite and the sea depth at the location of the impact as well. However, we do not have a numerical model to reproduce both of meteorite impacts and tsunami propagations. We have started to develop a new numerical model to simulate tsunamis generated by the meteorite impact combining iSALE (Wünnemann et al., 2006) for simulating impact phenomena and JAGURS (Baba et al., 2017) for simulating tsunami. The iSALE is a multi-material and multi-rheology shock physics code for simulating impact phenomena. JAGURS is a parallelized tsunami simulation code to solve two-dimensional non-linear long-wave equation with Boussinesq terms for representing observed tsunami waveforms, tsunami height and inundation. We set sea-floor deformation, sea-surface disturbance and velocity of gravity wave which is the output from iSALE to the input of JAGURS. We then calculate tsunami height along the coastlines in any place using ASTER GDEM version 2 (Fujisada et al., 2012) and GEBCO_2014 Grid. ASTER GDEM has one arcsecond (about 30 m) spatial resolution and covers land between 56S and 60N latitude as a topographic data. GEBCO’s gridded bathymetric data has thirty arcseconds (about 1 km) spatial resolution for the worldwide.
We first investigate the tsunami generation using iSALE code for creating tsunami source model depending on the meteor size, the velocity of impact, the size of cavity, the width and depth of crater and tsunami propagation speed. We also investigate probabilistic hazard of meteorite impact tsunami using simplified cavity curves with developed JAGURS built-in. Finally, we construct a new numerical model of meteorite impact tsunami combining iSALE and JAGURS. Additionally, we consider the way of automatic detection of meteorite impact using the recode of the highly sensitive seismograph network in real-time.
We gratefully acknowledge the developers of iSALE, including Gareth Collins, Kai Wünnemann, Boris Ivanov, H. Jay Melosh and Dirk Elbeshausen. Data analysis and visualizations of iSALE were carried out on PC cluster and the computers at Center for Computational Astrophysics, National Astronomical Observatory of Japan. This work was partially supported by JSPS KAKENHI Grant Number JP18K04674.

Keywords: Meteorite, Impact, Tsunami

©2019. Japan Geoscience Union. All Right Reserved.

[E] Oral | P (Space and Planetary Sciences)：P-EM Solar-Terrestrial Sciences, Space Electromagnetism & Space Environment

Tue. May 28, 2019 9:00 AM - 10:30 AM JST | Tue. May 28, 2019 12:00 AM - 1:30 AM UTC | A04 TOKYO BAY MAKUHARI HALL

[P-EM12] Space Weather and Space Climate

convener:Ryuho Kataoka(National Institute of Polar Research), Antti A Pulkkinen(NASA Goddard Space Flight Center), Kanya Kusano(Institute for Space-Earth Environmental Research, Nagoya University), Kaori Sakaguchi(National Institute of Information and Communications Technology), Chairperson:Ryuho Kataoka(National Institute of Polar Research)

We share the latest scientific papers to understand how the solar-terrestrial environment changes in various time scales, and to discuss how we will react via international and interdisciplinary collaborations. More specifically, welcomed papers include space climate studies to reconstruct long-term variations from radio isotopes; cutting-edge observational and modeling studies of the ionosphere, geospace, heliosphere and the sun; simulation and statistical studies to predict the future space weather and space climate; applied science such as operational space weather forecast and mitigation of the social impact due to extreme space hazards.

9:00 AM - 9:15 AM JST | 12:00 AM - 12:15 AM UTC

[PEM12-25] Variation of carbon-14 in tree rings around the onset of the Spoerer Minimum

★Invited Papers

*Hiroko Miyahara[1], Fuyuki Tokanai[2], Toru Moriya[2], Motonari Ohyama[3], Masataka Hakozaki[4], Mirei Takeyama[2], Hirohisa Sakurai[2] (1.Musashino Art University, 2.Yamagata University, 3.Tohoku University, 4.Nagoya University)

9:15 AM - 9:30 AM JST | 12:15 AM - 12:30 AM UTC

[PEM12-26] Current Status of WASAVIES: Warning System for Aviation Exposure to Solar Energetic Particles

★Invited Papers

*Tatsuhiko Sato[1], Ryuho Kataoka[2,3], Daikou Shiota[4,5], Yuki Kubo[4], Mamoru Ishii[4], Hiroshi Yasuda[6], Shoko Miyake[7], InChun Park[5], Yoshizumi Miyoshi[5] (1.Japan Atomic Energy Agency, 2.National Institute of Polar Research, 3.SOKENDAI, 4.National Institute of Information and Communications Technology, 5.Nagoya University, 6.Hiroshima University, 7.National Institute of Technology, Ibaraki College)

9:30 AM - 9:45 AM JST | 12:30 AM - 12:45 AM UTC

[PEM12-27] Statistical analysis of solar energetic particle events

*Kosuke Kihara[1], Yuwei Huang[2], Nobuhiko Nishimura[3], Seiji Yashiro[4], Nariaki Nitta[5], Kiyoshi Ichimoto[2], Ayumi Asai[2] (1.Department of Astronomy, Kyoto University, 2.Astronomical Observatory, Kyoto University, 3.Institute for Space Earth Environmental Research, Nagoya University, 4.The Catholic University of America, 5.Lockheed Martin Advanced Technology Center)

9:45 AM - 10:00 AM JST | 12:45 AM - 1:00 AM UTC

[PEM12-28] Long-term variation of galactic cosmic ray intensity observed with the Nagoya multidirectional muon detector

*Kazuoki Munakata[1], Rafael Mendonca[2], Chihiro Kato[1], Munetoshi Tokumaru[3] (1.Department of Physics, Faculty of Science, Shinshu University, 2.INPE, Brazil, 3.ISEE, Nagoya University)

10:00 AM - 10:15 AM JST | 1:00 AM - 1:15 AM UTC

[PEM12-29] Solar modulation of galactic cosmic rays during grand minima: A hybrid simulation

*Shoko Miyake[1], Tomoaki Matsumoto[2,3], Ryuho Kataoka[4,5], Tatsuhiko Sato[6], Daikou Shiota[7], Hiroko Miyahara[8], Shinsuke Imada[9], Haruka Ueno[10] (1.NIT, Ibaraki College, 2.Hosei Univ., 3.Princeton Univ., 4.NIPR, 5.SOKENDAI, 6.JAEA, 7.NICT, 8.Musashino Art Univ., 9.Nagoya Univ., 10.JAXA)

10:15 AM - 10:30 AM JST | 1:15 AM - 1:30 AM UTC

[PEM12-30] Overview of radio propagation project

*Kornyanat Hozumi[1], Hiroyuki Nakata[2], Susumu Saito[3], Takumi Kondo[1], Ryo Nakao[2], Takashi Maruyama[1], Takuya Tsugawa[1], Mamoru Ishii[1] (1.National Institute of Information and Communications Technology, 2.Graduate School of Engineering, Chiba University, Chiba, Japan, 3.National Institute of Maritime, Port and Aviation Technology, Electronic Navigation Research Institute (ENRI), Tokyo, Japan)

Variation of carbon-14 in tree rings around the onset of the Spoerer Minimum

*Hiroko Miyahara[1], Fuyuki Tokanai[2], Toru Moriya[2], Motonari Ohyama[3], Masataka Hakozaki[4], Mirei Takeyama[2], Hirohisa Sakurai[2]

1. Musashino Art University, 2. Yamagata University, 3. Tohoku University, 4. Nagoya University

Solar activity in the past has been reconstructed using carbon-14 in tree rings and beryllium-10 in ice cores, and it has been indicated that the Sun has long-term activity cycles such as Gleissberg cycle (~88 yrs) and the de Vries cycle (~200 yrs). Long-term variations of solar activity sometimes bring the grand minima such as the Dalton Minimum (1800-1820 CE) and the Maunder Minimum (1645-1715 CE). The detailed mechanism of such grand minima, however, remain unsolved. Reconstruction of solar cycles around the onset of the grand minima may shed light on the process of the occurrence of grand minima. We therefore have been conducting high-precision measurement of carbon-14 in tree rings with annual resolution using the Accelerator Mass Spectrometer at the Yamagata University. In this paper, we present our recent results on the measurement of carbon-14 around the onset of the Spoerer Minimum.

Keywords: solar cycle , grand solar minima, cosmogenic nuclide

©2019. Japan Geoscience Union. All Right Reserved.

Current Status of WASAVIES: Warning System for Aviation Exposure to Solar Energetic Particles

*Tatsuhiko Sato[1], Ryuho Kataoka[2,3], Daikou Shiota[4,5], Yuki Kubo[4], Mamoru Ishii[4], Hiroshi Yasuda[6], Shoko Miyake[7], InChun Park[5], Yoshizumi Miyoshi[5]

1. Japan Atomic Energy Agency, 2. National Institute of Polar Research, 3. SOKENDAI, 4. National Institute of Information and Communications Technology, 5. Nagoya University, 6. Hiroshima University, 7. National Institute of Technology, Ibaraki College

A physics-based warning system of aviation exposure to solar energetic particles, WASAVIES, is improved to be capable of real-time and automatic analysis. In the improved system, the count rates of several neutron monitors (NM) at the ground level, as well as the proton fluxes measured by the GOES satellite are continuously downloaded at intervals of 5 min and used for checking the occurrence of ground level enhancement (GLE). When a GLE event is detected, the system automatically determines the model parameters for characterizing the profiles of each GLE event, and nowcasts and forecasts the radiation dose rates all over the world up to 24 h after the flare onset. A web-interface of WASAVIES (see picture below) was also developed, which broadcasts radiation dose rates due to cosmic-ray exposure for all over the world as well as on 9 selected flight routes at intervals of 5 min and 1 day during GLE and the other periods, respectively. It is planned to be in operation from March 2019 through the public server of NICT.

Keywords: solar energetic particle, radiation exposure, space weather

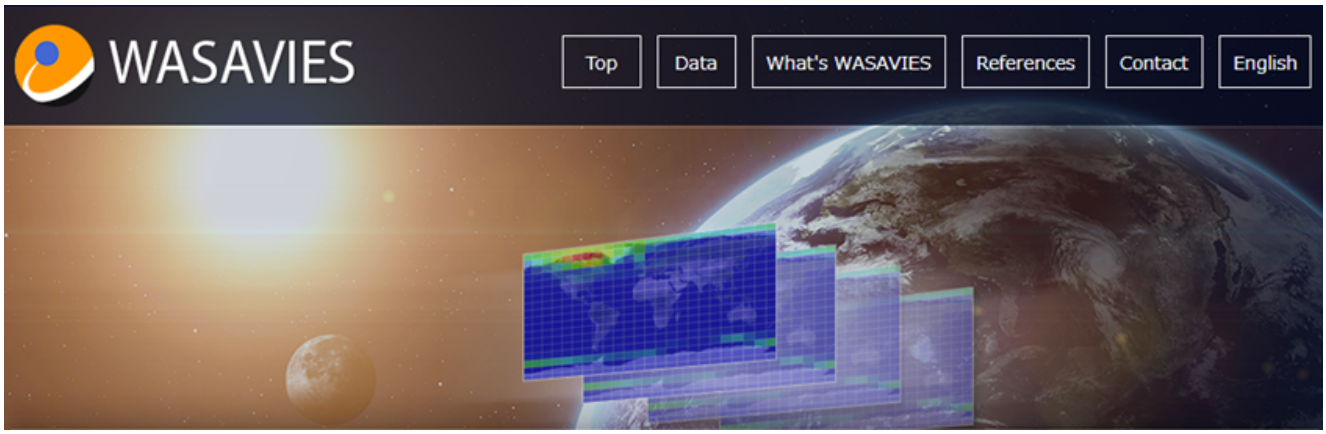

©2019. Japan Geoscience Union. All Right Reserved.

Statistical analysis of solar energetic particle events

*Kosuke Kihara[1], Yuwei Huang[2], Nobuhiko Nishimura[3], Seiji Yashiro[4], Nariaki Nitta[5], Kiyoshi Ichimoto[2], Ayumi Asai[2]

1. Department of Astronomy, Kyoto University, 2. Astronomical Observatory, Kyoto University, 3. Institute for Space Earth Environmental Research, Nagoya University, 4. The Catholic University of America, 5. Lockheed Martin Advanced Technology Center

Solar energetic particles (SEPs), which originate in powerful eruptions in the solar corona, give rise to critical radiation hazards for astronauts and airline passengers, causing damages to satellites, which result in serious societal impacts. The SEP phenomenon encompasses many cross-disciplinary fields, so collaborative research is indispensable. As a part of the Japanese space weather project PSTEP (Project for Solar-Terrestrial Environment Prediction), a Coordinated Data Analysis Workshop (CDAW) was held at Kyoto University in August 2018. As a first step toward building the capabilities to predict SEP events, we need to better understand what solar eruptions lead to SEP events of varying magnitudes. One approach, as adopted by this CDAW, is to start from energetic coronal mass ejections (CMEs) regardless of SEP occurrences, rather than from the actual SEP events. We first identified 197 CMEs between 2006 and 2017 that were faster than 900 km/s and wider than 60 degrees, as determined using data from SOHO/LASCO.

Our first objective is to characterize the basic properties of SEP events, such as the occurrence, proton flux intensity, and their time variations. We examined proton peak intensity, duration, and onset time with respect to the extrapolated CME onset time, using GOES >10-MeV proton data. STEREO LET and HET data were also analyzed to study the longitudinal distribution of the SEPs. We investigated the correlations of these SEP properties with the source longitude and speed of the CMEs, and soft X-ray intensity of the associated solar flares. We found that the SEP onset time is correlated with the source longitude of the CMEs. There were correlations between other parameters that we found in our statistical analysis, which will also be discussed. Finally, we will present examples of peculiar SEP events that were found as outliers in some scatter plots.

Keywords: Solar Energetic Particles, Coronal Mass Ejections, Space Weather

©2019. Japan Geoscience Union. All Right Reserved.

Long-term variation of galactic cosmic ray intensity observed with the Nagoya multidirectional muon detector

*Kazuoki Munakata[1], Rafael Mendonca[2], Chihiro Kato[1], Munetoshi Tokumaru[3]

1. Department of Physics, Faculty of Science, Shinshu University, 2. INPE, Brazil, 3. ISEE, Nagoya University

We have recently developed a correction method of the atmospheric temperature effect on muon count rate by using the GMDN (Global Muon Detector Network) data (R. R. S. Mendonca et al., Astrophys. J., 830:88, 2016). This is a significant step, because it makes possible for the first time to analyze the long-term variation of ~50 GeV cosmic ray density (i.e. isotropic intensity) which has been nalyed only for cosmic ray below ~10 GeV using the neutron monitor data nearly free from the temperature effect. In this paper, we report the 11-year and 22-year variations of cosmic ray density observed with Nagoya muon detector in 1970-2016 and discuss the energy dependence of variations by comparing the observation with neutron monitors.

Keywords: long-term variation of galactic cosmic ray intensity, energy spectrum of galactic cosmic rays, solar modulation

©2019. Japan Geoscience Union. All Right Reserved.

Solar modulation of galactic cosmic rays during grand minima: A hybrid simulation

*Shoko Miyake[1], Tomoaki Matsumoto[2,3], Ryuho Kataoka[4,5], Tatsuhiko Sato[6], Daikou Shiota[7], Hiroko Miyahara[8], Shinsuke Imada[9], Haruka Ueno[10]

1. NIT, Ibaraki College, 2. Hosei Univ., 3. Princeton Univ., 4. NIPR, 5. SOKENDAI, 6. JAEA, 7. NICT, 8. Musashino Art Univ., 9. Nagoya Univ., 10. JAXA

In the current and next weak solar cycles, we expect higher flux of galactic cosmic rays than that in the previous solar cycles because of the decreasing trend of the solar activity. It is important to quantitatively evaluate the high flux of galactic cosmic rays because it leads to the increase in the radiation exposure of aircrews and the increasing rates of single event upset events at spacecraft. However, reliable prediction of the increasing galactic cosmic rays in upcoming weak solar cycles is a challenges topic in the field of space weather forecast. We introduce a new project called Grand Minimum 7 (Gm7) for developing a hybrid simulation of galactic cosmic rays in such a weak solar condition, solving the stochastic differential equations of energetic particles in the MHD solar wind resolved by adaptive mesh refinement technique. We also discuss the possible situation of galactic cosmic rays and the radiation dose during the grand minima such as Maunder Minimum.

Keywords: galactic cosmic ray, solar wind

©2019. Japan Geoscience Union. All Right Reserved.

Overview of radio propagation project

*Kornyanat Hozumi[1], Hiroyuki Nakata[2], Susumu Saito[3], Takumi Kondo[1], Ryo Nakao[2], Takashi Maruyama[1], Takuya Tsugawa[1], Mamoru Ishii[1]

1. National Institute of Information and Communications Technology, 2. Graduate School of Engineering, Chiba University, Chiba, Japan, 3. National Institute of Maritime, Port and Aviation Technology, Electronic Navigation Research Institute (ENRI), Tokyo, Japan

Dated back to early 2016, the radio propagation subgroup was started in the A01 group (Space Weather Forecast System) of the PSTEP (Project for Solar-Terrestrial Environment Prediction). This subgroup has been working on clarifying of space weather (ionosphere is particular) effect on the radio propagation. Day-to-day variation of the bottom side of ionosphere has great influence on availability and integrity of radio waves in high frequency (HF, 3-30 MHz) band. HF is used as a backbone of communication systems for aviation during en-route phase and for amateur radio during disaster relief operation. We, therefore, focused on the HF band. The radio propagation simulator named HF-START (HF Simulator Targeting for All-users' Regional Telecommunications) has been developed. Availability and integrity of HF band are expected to be provided through HF-START interface after receiving users' input/ request. The HF-START project activity and its future operation plan will be overviewed in this talk.

Keywords: HF-START, Radio Propagation Simulator, Space Weather, Ionosphere

©2019. Japan Geoscience Union. All Right Reserved.

[E] Oral | P (Space and Planetary Sciences)：P-EM Solar-Terrestrial Sciences, Space Electromagnetism & Space Environment

Tue. May 28, 2019 10:45 AM - 12:15 PM JST | Tue. May 28, 2019 1:45 AM - 3:15 AM UTC | A04 TOKYO BAY MAKUHARI HALL

[P-EM12] Space Weather and Space Climate

convener:Ryuho Kataoka(National Institute of Polar Research), Antti A Pulkkinen(NASA Goddard Space Flight Center), Kanya Kusano(Institute for Space-Earth Environmental Research, Nagoya University), Kaori Sakaguchi(National Institute of Information and Communications Technology), Chairperson:Kaori Sakaguchi

We share the latest scientific papers to understand how the solar-terrestrial environment changes in various time scales, and to discuss how we will react via international and interdisciplinary collaborations. More specifically, welcomed papers include space climate studies to reconstruct long-term variations from radio isotopes; cutting-edge observational and modeling studies of the ionosphere, geospace, heliosphere and the sun; simulation and statistical studies to predict the future space weather and space climate; applied science such as operational space weather forecast and mitigation of the social impact due to extreme space hazards.

10:45 AM - 11:00 AM JST | 1:45 AM - 2:00 AM UTC

[PEM12-31] Dynamic Spectral Characteristics of Equatorial Plasma Bubbles

★Invited Papers

*Tatsuhiro Yokoyama[1], Charles L Rino[2], Charles S Carrano[2] (1.Kyoto University, 2.Boston College)

11:00 AM - 11:15 AM JST | 2:00 AM - 2:15 AM UTC

[PEM12-32] Recent advances in space weather monitoring using the Super Dual Auroral Radar Network

★Invited Papers

*Evan G Thomas[1], Simon G Shepherd[1] (1.Dartmouth College)

11:15 AM - 11:30 AM JST | 2:15 AM - 2:30 AM UTC

[PEM12-33] **A Study of Solar Flare Effects on Radio Wave Propagation using SuperDARN & riometer**

*Shibaji Chakraborty[1], Joseph Baker[1], John Michael Ruohoniemi[1], Nozomu Nishitani[2] (1.Virginia Tech, 2.Institute for Space-Earth Environmental Research, Nagoya University)

11:30 AM - 11:45 AM JST | 2:30 AM - 2:45 AM UTC

[PEM12-34] Exploring the use of cell phone GNSS receivers for global monitoring of the ionosphere

*Dawn Kellogg Merriman[1], Omar A Nava[1], Jennifer L Meehan[2], Hsien-Liang R Tseng[1] (1.AFIT, 2.NOAA)

11:45 AM - 12:00 PM JST | 2:45 AM - 3:00 AM UTC

[PEM12-35] Large enhancements of global GPS total electron content during a magnetic storm on 7-8 November 2004

*Sori Takuya[1], Yuichi Otsuka[1], Atsuki Shinbori[1], Takuya Tsugawa[2], Michi Nishioka[2] (1.Institute for Space-Earth Environmental Research, Nagoya University, 2.National Institute of Information and Communications Technology)

12:00 PM - 12:15 PM JST | 3:00 AM - 3:15 AM UTC

[PEM12-36] Large scale traveling ionospheric disturbances origin and propagation

*Iurii Cherniak[1,2], Irina Zakharenkova[2,5], Paul Prikryl[3,4], William Schreiner[1] (1.COSMIC Program Office, University Corporation for Atmospheric Research, 2.University of Warmia and Mazury in Olsztyn, 3.Physics Department, University of New Brunswick, 4.Geomagnetic Laboratory, Natural Resources Canada, 5.West Department of IZMIRAN)

Dynamic Spectral Characteristics of Equatorial Plasma Bubbles

*Tatsuhiro Yokoyama[1], Charles L Rino[2], Charles S Carrano[2]

1. Kyoto University, 2. Boston College

Equatorial plasma bubble (EPB) is a well-known phenomenon in the equatorial ionospheric F region. As it causes severe scintillation in the amplitude and phase of radio signals, it is important to understand and forecast the occurrence of EPB from a space weather point of view. In order to simulate the instability in the equatorial ionosphere, a 3D high-resolution bubble (HIRB) model with a grid spacing of as small as 200 m has been developed. It provides a unique opportunity to characterize intermediate-scale EPB structure, which was not well resolved until very recently. Estimation of altitude-dependent power law spectral density function parameters provides an altitude versus time history of the intermediate-scale structure development. Local structure onset is associated with successive bifurcation of rising EPBs. Developed structure characterized by a two-component power law spectral density function ultimately subtends several hundred kilometers in altitude. The EPB simulation data fully support the reported EPB diagnostics from previous in situ measurements. In the near future, HIRB model may be able to directly resolve Fresnel scale of GPS frequency band (300-400m), so that the effects of EPBs on radio wave propagation could be evaluated without any assumption.

Keywords: plasma bubble, scintillation, ionosphere

©2019. Japan Geoscience Union. All Right Reserved.

Recent advances in space weather monitoring using the Super Dual Auroral Radar Network

*Evan G Thomas[1], Simon G Shepherd[1]

1. Dartmouth College

Over the last decade, the Super Dual Auroral Radar Network (SuperDARN) has undergone a dramatic expansion in the Northern Hemisphere with the addition of more than a dozen radars offering improved coverage at midlatitudes (50º–60º magnetic latitude) and in the polar cap (80º–90º magnetic latitude). This has led to the development of new empirical models which better describe both the regional and global morphology of ionospheric convection under a range of solar wind and geomagnetic activity conditions. In addition, real-time measurements of ionospheric plasma motion are once again being collected from more than 15 SuperDARN radar sites to produce nowcasts of the global convection pattern. In this presentation we discuss the operational challenges and space weather applications of these real-time SuperDARN products.

©2019. Japan Geoscience Union. All Right Reserved.

A Study of Solar Flare Effects on Radio Wave Propagation using SuperDARN & riometer

*Shibaji Chakraborty[1], Joseph Baker[1], John Michael Ruohoniemi[1], Nozomu Nishitani[2]

1. Virginia Tech, 2. Institute for Space-Earth Environmental Research, Nagoya University

A prolonged study is underway to improve the understanding of the lower ionospheric (D & lower E layer) response to solar flare and its effects on HF propagation. Over-the-Horizon communication is strongly dependent on the state of the ionosphere, which is fragile to solar X-ray flares. The Super Dual Auroral Radar Network (SuperDARN) is an active HF radio receiver, primarily used to probe ionosphere and upper atmosphere. SuperDARN has one common mode of operation which simulates a ground-to-ground communications link, commonly known as ground scatter. Riometers on the other side are passive HF radio receiver, provides information about HF absorption in the ionosphere by measuring variations in cosmic radio noise. Both instruments' observations get altered due to the well-known effects of Short-Wave Fadeout or SWF. During an SWF the number of SuperDARN ground-scatter echoes drops suddenly (≈1 min) and sharply followed by an apparent increase in Doppler velocity (also known as "Doppler Flash"), often to near zero, reflecting disruption. In addition to that, riometer observe an enhancement in cosmic noise absorption. Since decades, enhanced D and E region electron density are known to be the significant driver of HF radio wave absorption, and we have steadily developed a better understanding of the sources and driving processes of HF absorption. However, the picture is less clear when we talk about the influence of collision frequency in radio wave absorption and Doppler frequency anomaly during SWF. This study aims to propose a relatively newer semi-empirical model to provide insights into the physical significance of collision frequency in HF absorption effect which can be seen in the riometer data. In addition to that, the study also aims to provide physical insights to Doppler frequency anomaly seen in SuperDARN data. Furthermore, this study will help us to advance our understanding of the role of collision frequency in HF absorption and Doppler frequency anomaly, their sources and driving parameters.

Keywords: Solar Flare, Shortwave-Fadeout, HF Absorption

©2019. Japan Geoscience Union. All Right Reserved.

Exploring the use of cell phone GNSS receivers for global monitoring of the ionosphere

*Dawn Kellogg Merriman[1], Omar A Nava[1], Jennifer L Meehan[2], Hsien-Liang R Tseng[1]

1. AFIT, 2. NOAA

Accurate characterization of the ionosphere in response to space weather events has important implications for the effective use of high-frequency (HF) communications in civilian and military operations, including, but not limited to, emergency services, amateur radio, aviation, and over-the-horizon radar. This study investigates the use of cell phone Global Navigation Satellite System (GNSS) technology to monitor and study highly variable phenomena in the ionosphere, such as the aurora at high-latitudes or scintillation at the equator. Field campaigns to high and mid-latitudes will be summarized here, emphasizing the sensitivity of cell phone GNSS receivers to pick up on space weather events such as traveling ionospheric disturbances. Preliminary analysis on the potential to combine data from various cell phone manufacturers (e.g. Hauwei, Samsung, Google, LG and Moto) to enhance data quality will also be presented. Based on this research the potential to collect data from millions of cell phones GNSS technology may allow for real-time monitoring and measuring of the ionosphere to occur on an unprecedented global scale.

Keywords: GNSS, cell phone, space weather

©2019. Japan Geoscience Union. All Right Reserved.

Large enhancements of global GPS total electron content during a magnetic storm on 7-8 November 2004

*Sori Takuya[1], Yuichi Otsuka[1], Atsuki Shinbori[1], Takuya Tsugawa[2], Michi Nishioka[2]

1. Institute for Space-Earth Environmental Research, Nagoya University, 2. National Institute of Information and Communications Technology

Storm enhanced density (SED) with a latitudinally narrow structure is one of the storm-time ionospheric disturbances in the mid- and low-latitude regions. Foster and Rideout [2007] reported that the SED plume occurs in magnetically-conjugate regions in both northern and southern hemispheres. In this study, we analyzed geomagnetic storm events from 2000 to 2012 and found that a TEC enhancement over Japan on 8 November 2004 is the largest. Maruyama [2006] reported that the TEC enhancement appeared during this event, and pointed out that the mid-latitude TEC enhancement observed after the sunset is related to SED. However, since most of the previous studies focus on TEC variation in a specific region, the detail features of global TEC variation associated with the development and decay of the geomagnetic storm have not yet been clarified. The purpose of this study is to understand the generation mechanism of the TEC enhancement in the mid- and low-latitude ionosphere during the geomagnetic storm using global GPS-TEC data with high temporal and spatial resolutions provided by NICT. The GPS-TEC data have spatial and temporal resolutions of 0.5˚×0.5˚ in longitude and latitude and 5 minutes, respectively. Here, we first calculated a difference value (dTEC) between storm-time TEC and average TEC of 10 geomagnetically quiet days. In this calculation, we referred to a list of geomagnetically quiet and disturbed days provided by World Data Center for Kyoto University. Next, we created a two-dimensional map of rTEC (dTEC normalized by the average TEC of 10 geomagnetically quiet days), and analyzed the temporal and spatial variations of rTEC for a geomagnetic storm which occurred on 8 November 2004 with the minimum SYM-H value of -400 nT at 6:00 UT. As a result, the rTEC enhancement in Japan was maintained even after the onset of the recovery phase, and the maximum value reached ~17 (~90 TECU). The enhanced rTEC region in Japan propagates westward with a velocity of 317 m/s. In order to investigate the specific signature of rTEC in Japan in detail, we created the latitude-time plot of TEC at a longitude 142˚E. In this plot, two high TEC regions appear near 5:00 UT and 11:00 UT, and propagate from high to low latitudes. Furthermore, the ion drift meter data obtained from the DMSP satellite traveling over Japan show the westward flow with a velocity of 250 m/s, which is almost consistent with that of the enhanced rTEC velocity. In the two-dimensional global map of rTEC, the TEC enhancements over Japan and Australia occurred simultaneously with a magnetic conjugacy. The rTEC enhancements were larger in the northern hemisphere than that in the southern hemisphere. The rTEC enhancements started near 5:00 UT at magnetic latitude of 50˚ in both the hemispheres, and propagated from high to low latitudes. In order to investigate the global signature of rTEC over Japan and America, we created the magnetic latitude-time plot of rTEC. As a result, we found that the rTEC in Japan and America showed a large enhancement at 5:00 UT with the maximum values of more than 6. In the rTEC map at 5:00 UT, the enhanced rTEC region existed between America and Japan. This rTEC enhancement is thought as a cause of SED. SED is thought to be caused by the westward plasma transportation in the mid- and low-latitude ionosphere due to the storm-time enhanced SAPS [Tsurutani et al., 2004]. Assuming that the propagation velocity is 317 m/s, it takes 9.5 hours to move from America to Japan. However, the time difference of the onsets of the rTEC enhancement between America and Japan is 6 hours. Therefore, the rTEC enhancement cannot be explained by the above mechanism of the westward transportation. These results suggest that the enhanced TEC region associated with the TEC peak over Japan existed between America and Japan. Therefore, mechanism different from the SED generation can cause large TEC enhancement

©2019. Japan Geoscience Union. All Right Reserved.

during nighttime and have a wide extent of longitude (100˚~).

Keywords: Ionosphere, Geomagnetic storm, Total electron content, Magnetic conjugacy

©2019. Japan Geoscience Union. All Right Reserved.

Large scale traveling ionospheric disturbances origin and propagation

*Iurii Cherniak[1,2], Irina Zakharenkova[2,5], Paul Prikryl[3,4], William Schreiner[1]

1. COSMIC Program Office, University Corporation for Atmospheric Research, 2. University of Warmia and Mazury in Olsztyn, 3. Physics Department, University of New Brunswick, 4. Geomagnetic Laboratory, Natural Resources Canada, 5. West Department of IZMIRAN

We investigate an origin, occurrence, and propagation of large-scale traveling ionospheric disturbances (LSTIDs) with an analysis of the total electron content (TEC) perturbation component deduced from the ground-based GPS and GLONASS observations. The high spatio-temporal resolution mapping approach provides a very detailed specification of the ionospheric small- to large-scale disturbances associated with two major sources of the LSTIDs generation: the solar terminator passage during the quiet time and auroral activity caused by auroral particle precipitation and field-aligned currents (FACs) intensification during geomagnetic disturbances. For the first time, the joint analysis of the ionospheric plasma irregularities, FACs, and LSTIDs reveals that a zone with the intense FACs and ionospheric irregularities occurred at the same region that represent the most probable source of LSTIDs excitation. The COSMIC RO electron density profiles confirm the E layer plasma density enhancement within LSTIDs excitation area. Such density enhancement leads to an increase of ionospheric conductivity, intensification of currents in the ionosphere, and release of energy by Joule heating into the lower thermosphere.
This approach was demonstrated for the case of the 19-21 December 2015 geomagnetic storm, when LSTIDs propagated over the European region were detected. During the main phase of the storm, the LSTIDs propagated equatorward from European high latitudes to middle latitudes (35-40N) with the horizontal velocities of ~700-800 m/s. The LSTIDs as deduced from the TEC-disturbed component had a much larger magnitude and propagate much longer distances during the daytime (sunlit part) than in the night. We found that an equatorward expansion of the strong ionospheric irregularities zone and an increase of the FACs magnitude led to a simultaneous intensification of the LSTIDs occurrence at high latitudes. The GPS ROTI (rate of TEC index) technique, a sensitive one for detection of the rapid ionospheric gradients and irregularities, could not recognize any signatures of the TIDs structures.

The research is supported by the NSF CAS AGS-1033112, the NASA LWS grant NNX15AB83G, by the National Science Centre, Poland, through grants 2017/25/B/ST10/00479 and 2017/27/B/ST10/02190, and by RFBR Grant 19-05-00570A.

Keywords: LSTIDs, GNSS, ionosphere, geomagnetic storm, FACs, plasma irregularities

©2019. Japan Geoscience Union. All Right Reserved.

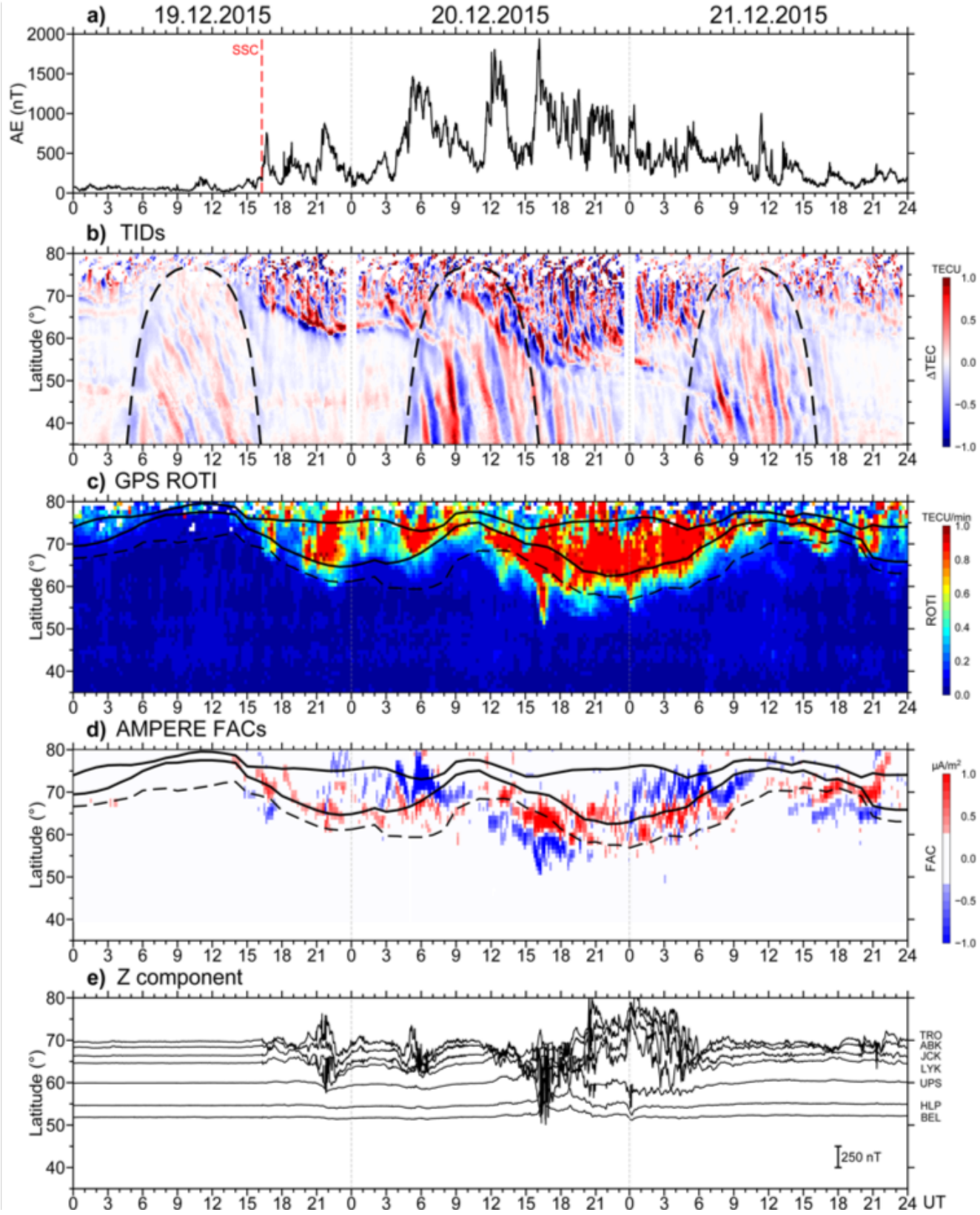

©2019. Japan Geoscience Union. All Right Reserved.

[E] Poster | P (Space and Planetary Sciences)：P-EM Solar-Terrestrial Sciences, Space Electromagnetism & Space Environment

Tue. May 28, 2019 3:30 PM - 5:00 PM JST | Tue. May 28, 2019 6:30 AM - 8:00 AM UTC | Poster Hall International Exhibition Hall8, Makuhari Messe_3

[P-EM12] Space Weather and Space Climate

convener:Ryuho Kataoka(National Institute of Polar Research), Antti A Pulkkinen(NASA Goddard Space Flight Center), Kanya Kusano(Institute for Space-Earth Environmental Research, Nagoya University), Kaori Sakaguchi(National Institute of Information and Communications Technology)

We share the latest scientific papers to understand how the solar-terrestrial environment changes in various time scales, and to discuss how we will react via international and interdisciplinary collaborations. More specifically, welcomed papers include space climate studies to reconstruct long-term variations from radio isotopes; cutting-edge observational and modeling studies of the ionosphere, geospace, heliosphere and the sun; simulation and statistical studies to predict the future space weather and space climate; applied science such as operational space weather forecast and mitigation of the social impact due to extreme space hazards.

[PEM12-P01] Reconnection signatures in solar magnetograms during the solar storms of 4-10 September 2017

*Robert Dean Loper[1,2] (1.Air Force Institute of Technology, Department of Engineering Physics, 2.National Center for Atmospheric Research, High Altitude Observatory)

[PEM12-P02] Statistical Relation between Solar Flares and Coronal Mass Ejections with Respect to Sigmoidal Structures in Active Regions

*Yusuke Kawabata[1,2], Yusuke Iida[3], Takafumi Doi, Sachiko Akiyama[4], Seiji Yashiro[4], Toshifumi Shimizu[2] (1.Earth and Planetary Science, The University of Tokyo, 2.Institute of Space and Astronautical Science, JAXA, 3.Kwansei Gakuin University, 4.The Catholic University of America)

[PEM12-P03] Multi-wavelength Observations of Pre-flare Quasi-periodic Pulsation in the C2.2 Flare on 2012 October 15

*Yung-Chi Yang[1], Ya-Hui Yang[1], Baolin Tan[2], Chengming Tan[2], Y.H. Yan[2] (1.Graduate Institute of Space Science National Central University, 2.Key Laboratory of Solar Activities, National Astronomical Observatories)

[PEM12-P04] Investigation of pre-flare type III solar radio bursts and their potential solar origins

*Shao-Fu Hsieh[1], Ya-Hui Yang[1], Baolin Tan[2], Chengming Tan[2], Y.H. Yan[2] (1.Graduate Institute of Space Science National Central University, 2.Key Laboratory of Solar Activities, National Astronomical Observatories, Chinese Academy of Sciences)

[PEM12-P05] Statistical and observational research of solar flare for constructing total emission spectra prediction model

*Shohei Nishimoto[1], kyoko Watanabe[1], Shinsuke Imada[2], Tomoko Kawate[3], Kyoung-Sun Lee[4] (1.National Defense Academy, 2.Institute for Space-Earth Environmental Research, Nagoya University, 3.Institute Of Space And Astronautical Science, Japan Aerospace Exploration Agency, 4.National Astronomical Observatory of Japan)

[PEM12-P06] Modeling of solar active regions using local linear force-free fields to estimate magnetic twist

*Kento Nakatani[1], Kanya Kusano[1], Sung-Hong Park[1], Leka KD[2] (1.Institute for space-Earth Environmental Research, Nagoya University, 2.North West Reserch Associates)

[PEM12-P07] Magnetohydrodynamic Simulation of an Erupting Magnetic Flux Rope on February 13 2009: Journey to Coronal Mass Ejection

*Satoshi Inoue[1], Antonia Savcheva[2] (1.Institute for Space-Earth Environmental Research, Nagoya University, 2.Harvard-Smithsonian Center for Astrophysics)

[PEM12-P08] Investigation of flow structures in the solar interior through the surface magnetic elements' tracking

*Yusuke Iida[1] (1.Kwansei Gakuin University)

[PEM12-P09] High-precision measurement of carbon-14 in tree rings around the onset of the Maunder Minimum

*Hiroko Miyahara[1], Fuyuki Tokanai[2], Toru Moriya[2], Hideyuki Hotta[3] (1.Musashino Art University, 2.Yamagata University, 3.Chiba University)

[PEM12-P10] Examination of ^{10}Be in travertine sediment as a possible tool to reconstruct past solar activity

*Hongyang Xu[1,2], Hiroko Miyahara[2], Kazuho Horiuchi[3], Hiroyuki Matsuzaki[4], Hailong Sun[5], Weijun Luo[5], Xiangmin Zheng[1], Yusuke Suganuma[6,7], Shijie Wang[5], Limin Zhou[1] (1.East China Normal University, 2.Musashino Art University, 3.Hirosaki University, 4.University of Tokyo, 5.Chinese Academy of Sciences, 6.National Institute of Polar Research, 7.The Graduate University for Advanced Studies (SOKENDAI))

[PEM12-P11] Examination of ^{10}Be in travertine sediment as a possible tool to reconstruct past solar activity II

*Hongyang Xu[1,2], Hiroko Miyahara[2], Kazuho Horiuchi[3], Hiroyuki Matsuzaki[4], Hailong Sun[5], Weijun Luo[5], Xiangmin Zheng[1], Yusuke Suganuma[6,7], Shijie Wang[5], Limin Zhou[1] (1.East China Normal University, 2.Musashino Art University, 3.Hirosaki University, 4.University of Tokyo, 5.Chinese Academy of Sciences, 6.National Institute of Polar Research, 7.The Graduate University for Advanced Studies (SOKENDAI))

[PEM12-P12] 1 year of CR observation at Syowa Station in the Antarctic.

*Chihiro Kato[1], Kazuoki Munakata[1], Akira Kadokura[2], Ryuho Kataoka[2], Paul Evenson[3] (1.Shinshu University, 2.National Institute of Polar Research, 3.University of Delaware)

[PEM12-P13] Space weather forecast archives at NICT: handwritten solar activity charts

*Kaori Sakaguchi[1], Daikou Shiota[1], Kaori Fukunaga[1], Katsuhide Marubashi[1], Hiromitsu Ishibashi[1], Yuki Kubo[1], Mamoru Ishii[1] (1.National Institute of Information and Communications Technology)

[PEM12-P14] IMF dependence on solar wind parameters

*Tohru Araki, Yuki Harada[1] (1.Kyoto University)

[PEM12-P15] **Dipole Tilt Effect of Geomagnetic Activity from Low- to High-latitudes**

*Nowada Motoharu[1] (1.Shandong University at Weihai)

[PEM12-P16] A New Prediction Model for Solar Wind-Triggered Magnetospheric Disturbances Based on Potential Learning (Neural Network)

*Ryozo Kitajima[1], Motoharu Nowada[2], Ryotaro Kamimura[3] (1.Seikei University, 2.Shandong University at Weihai, 3.Tokai University)

[PEM12-P17] Real-time magnetosphere simulator for space weather using REProduce Plasma Universe code

*Yasubumi Kubota[1], Aoi Nakamizo[1], Kaori Sakaguchi[1], Mitsue Den[1], Yuki Kubo[1], Tsutomu Nagatsuma[1], Takashi Tanaka[1,2] (1.National Institute of Information and Communications Technology, 2.Kyushu University)

[PEM12-P18] **Simulation of GIC flowing through the power transmission network (187 kV-500 kV) in Japan**

*Nishida Yuichiro[1,6], Yusuke Ebihara[1], Satoko Nakamura[1], Shinichi Watari[2], Kumiko Hashimoto[3], Kentaro Kitamura[4], Takashi Kikuchi[5] (1.Kyoto University Reserch Institute for Sustainable Humanosphere, 2.National Institute of Information and Communications Technology, 3.Kibi International University, 4.National Insutitute of Technology, Tokuyama College, 5.Nagoya University, 6.Kyoto University Department of Electrical Engineering)

[PEM12-P19] Climatological features of the upper atmosphere reproduced by a revised version of a whole atmosphere-ionosphere coupled model GAIA

*Hidekatsu Jin[1], Yasunobu Miyoshi[2], Chihiro Tao[1], Hiroyuki Shinagawa[1], Hitoshi Fujiwara[3] (1.National Institude of Information and Communications Technology, 2.Kyushu University, 3.Seikei University)

[PEM12-P20] Investigation of the thermospheric mass density variations below 200 km

*Hitoshi Fujiwara[1], Yasunobu Miyoshi[2], Masayoshi Utashima[1], Huixin Liu[2] (1.Faculty of Science and Technology, Seikei University, 2.Department of Earth and Planetary Sciences, Faculty of Sciences, Kyushu University)

[PEM12-P21] Low-latitude HF Doppler observations of magnetospheric electric fields during space weather disturbances

*Kumiko K. Hashimoto[1], Takashi Kikuchi[2], Ichiro Tomizawa[3], Keisuke Hosokawa[3], Jaroslav Chum[4] (1.Kibi International University, 2.Nagoya University, 3.University of Electro-Commnunications, 4.Institute of Atmospheric Physics, Prague)

[PEM12-P22] Stratospheric ionization during magnetic storms

*Ryuho Kataoka[1] (1.National Institute of Polar Research)

[PEM12-P23] Calculating propagation time of HF radio wave using ray-tracing method and simple comparison with the observation.

*Ryo Nakao[1], Hiroyuki Nakata[1], Hiroyo Ohya[1], Toshiaki Takano[1], Kornyanat Hozumi[2], Takuya Tsugawa[2], Susumu Saito[3], Mamoru Ishii[2] (1.Graduate School of Engineering, Chiba University, 2.National Institute of imformation and Communications Technology, 3.Electronic Navigation Research Institute)

[PEM12-P24] Why do some probabilistic forecasts lack reliability?

*Yuki Kubo[1] (1.National Institute of Information and Communications Technology)

[PEM12-P25] An estimation method of GEO spacecraft surface charging for a real-time spacecraft risk assessment

*Masao Nakamura[1], Ryota Kawachi[1], Go Takahashi[1], Tsutomu Nagatsuma[2], Mamoru Ishii[2] (1.Osaka Prefecture University, 2.NICT)

[PEM12-P26] A network of HF Doppler sounding systems in Japan

*Keisuke Hosokawa[1], Hiroyuki Nakata[2], Kumiko K. Hashimoto[3], Ichiro Tomizawa[1], Jun Sakai[1], Takashi Kikuchi[4] (1.University of Electro-Communications, 2.Chiba University, 3.Kibi International University, 4.ISEE, Nagoya University)

Reconnection signatures in solar magnetograms during the solar storms of 4-10 September 2017

*Robert Dean Loper[1,2]

1. Air Force Institute of Technology, Department of Engineering Physics, 2. National Center for Atmospheric Research, High Altitude Observatory

Solar flare forecasting is limited to active region classification and historical correlation, due largely to our lack of understanding of magnetic reconnection as a driving mechanism for solar flares and coronal mass ejections. Photospheric observations indicate magnetic field changes during solar flares, brought about during magnetic reconnection and related to magnetic field helicity on the solar surface. While the neutral point of the reconnection event associated with a flare usually occurs in the solar corona, some signs of the magnetic field changes should manifest as low as the photosphere. This study utilizes data from SDO HMI and Space-Weather HMI Active Regions Patches (SHARPS) to analyze full vector field component data in the photospheric magnetic field during several magnetic reconnection events during the space weather events of 4-10 September 2017.

Keywords: solar atmosphere, sunspots, magnetogram, solar flares

©2019. Japan Geoscience Union. All Right Reserved.

Statistical Relation between Solar Flares and Coronal Mass Ejections with Respect to Sigmoidal Structures in Active Regions

*Yusuke Kawabata[1,2], Yusuke Iida[3], Takafumi Doi, Sachiko Akiyama[4], Seiji Yashiro[4], Toshifumi Shimizu[2]

1. Earth and Planetary Science, The University of Tokyo, 2. Institute of Space and Astronautical Science, JAXA, 3. Kwansei Gakuin University, 4. The Catholic University of America

We will report statistical dependences among features of coronal mass ejections (CMEs), solar flares, and sigmoidal structures in soft-X-ray images (Kawabata et al. 2018). We applied analysis methods to all the features in the same way in order to investigate the reproducibility of the correlations among them, which may be found from previous statistical studies. Samples of 211 M-class and X-class flares, observed between 2006 and 2015 by the Hinode/X-ray telescope, Solar and Heliospheric Observatory/Large Angle and Spectrometric Coronagraph, and Geostationary Operational Environmental Satellite, were examined statistically. Five kinds of analysis were performed: Occurrence rate analysis, linear-correlation analysis, association analysis, the Kolmogorov–Smirnov test, and the Anderson–Darling test. These give three main results. First, the sigmoidal structure and long-duration events (LDEs) have a stronger dependence on CME occurrence than large X-ray-class events in on-disk events. Second, for the limb events, a significant dependence exists between LDEs and CME occurrence, and between X-ray-class events and CME occurrence. Third, 32.4% of on-disk flare events have sigmoidal structure and are not accompanied by CMEs. However, the occurrence probability of CMEs without sigmoidal structure is very small, 8.8%, in on-disk events. While the first and second results are consistent with previous studies, we provide for the first time a difference between the on-disk and limb events. The third result, that non-sigmoidal regions produce fewer eruptive events, is also different from previous results. We suggest that sigmoidal structures in soft X-ray images will be a helpful feature for CME prediction in on-disk flare events.

Keywords: Sun, Solar flares, Coronal mass ejections, Sigmoid

©2019. Japan Geoscience Union. All Right Reserved.

Multi-wavelength Observations of Pre-flare Quasi-periodic Pulsation in the C2.2 Flare on 2012 October 15

*Yung-Chi Yang[1], Ya-Hui Yang[1], Baolin Tan[2], Chengming Tan[2], Y.H. Yan[2]

1. Graduate Institute of Space Science National Central University, 2. Key Laboratory of Solar Activities, National Astronomical Observatories

Quasi-periodic pulsation (QPP) is thought to be the nature of solar flares, which can be observed during and before flares in various wavelengths, such as the radio, microwave, SXR, and EUV. In this study, we analyze a pre-flare QPP event on 2012 October 15 and its association with the following C2.2 flare based on the radio data in the ranges of 2.81-2.85 GHz and 2.91-2.95 GHz from Solar Broadband Radio Spectrometer (SBRS), EUV images from AIA multi-wavelength observations, and wavelet analysis. Our result show that the main period of the radio QPP is ~800 s which is similar to the period of ~13.5 min obtained in SXR by Tan et al. (2016). Moreover, we analyze several localized areas in the flare-eruptive AR 11593 to search for the possible regions responsible for the occurrence of pre-flare QPP. We find that the footpoints of brightening loops in 211 Åshow the quasi-periodic behavior of ~850 s. It is thus suggested that the pre-flare QPP with a period of 13-15 min can be manifested in both of the thermal (SXR, EUV) and nonthermal (radio) radiation processes. The relationship between the pre-flare QPP and the subsequent C2.2 flare will also be discussed.

Keywords: sun, solar flares, solar oscillation

©2019. Japan Geoscience Union. All Right Reserved.

Investigation of pre-flare type III solar radio bursts and their potential solar origins

*Shao-Fu Hsieh[1], Ya-Hui Yang[1], Baolin Tan[2], Chengming Tan[2], Y.H. Yan[2]

1. Graduate Institute of Space Science National Central University, 2. Key Laboratory of Solar Activities, National Astronomical Observatories, Chinese Academy of Sciences

Type III solar radio bursts are characterized as the fast-drifting radio emissions in a dynamic spectrogram, which is believed to be produced by the propagating electron beams and often accompanied with the solar flares or magnetic reconnection. Studying the type III radio bursts in high-frequency range before flares would be important for understanding the trigger of energy release although it is rarely reported previously. Here we present two pre-flare type III burst events found in the range of 2.6-3.8 GHz at Solar Broadband Radio Spectrometer (SBRS). By comparing with the SDO/AIA multi-wavelength observations in flare active regions, the pre-flare type III radio bursts have good temporal correlations with the increases of EUV emissions. Furthermore, we find that one event is related to the EUV brightening with 1-min delay, implying the existence of plasma heating before energy release. The other event has a simultaneous EUV jet with a speed of ~700 km/s indicating the occurrence of magnetic reconnection. We suppose both pre-flare events are associated with small-scale energy release via magnetic reconnection.

Keywords: sun, solar flares, solar radio bursts

©2019. Japan Geoscience Union. All Right Reserved.

Statistical and observational research of solar flare for constructing total emission spectra prediction model

*Shohei Nishimoto[1], kyoko Watanabe[1], Shinsuke Imada[2], Tomoko Kawate[3], Kyoung-Sun Lee[4]

1. National Defense Academy, 2. Institute for Space-Earth Environmental Research, Nagoya University, 3. Institute Of Space And Astronautical Science, Japan Aerospace Exploration Agency, 4. National Astronomical Observatory of Japan

Impulsive energy release phenomena such as solar flares, sometimes affect to the solar-terrestrial environment. Usually, we use soft X-ray flux (GOES class) as the index of flare scale. However, the magnitude of effect to the solar-terrestrial environment is not proportional to this scale. Therefore, it is considered that the GOES class is not optimal parameter for predicting the Sudden Ionospheric Disturbance (SID). To identify the relationship between solar flare phenomena and influence to the solar-terrestrial environment, we need to understand the full spectra of solar flares in detail.
There is the solar flare irradiance model named the Flare Irradiance Spectral Model (FISM) (Chamberlin et al., 2006, 2007, 2008). FISM is the most used model, and can estimate solar flare spectra with high wavelength and temporal resolution. However, this model can not express the time evolution of emitted plasma during the solar flare, and has low accuracy on short wavelength that might strongly affect to the total flare spectra. Therefore, individual SID phenomenon can not be reproduced.
In this work, in order to solve the problems of FISM, we performed statistical analysis on observational data during the solar flares. From This study, we tried to find the parameters that control the solar flare emission spectra. We selected solar flare events larger than M-class from the Hinode flare catalogue (Watanabe et al., 2012). First, we focused on the EUV emission observed by the SDO/EVE. We examined the intensities and time evolutions of five EUV lines (Fe XX, Fe XVIII, Fe XVI, Fe VIII, and He II) for 54 flare events. As a result, we found positive correlation between the “GOES class” and the “EUV peak flux” for all Fe lines. Moreover, we found that hotter lines peaked earlier than cooler lines. On the other hand, He II line data have poor correlation with GOES X-ray data. Furthermore, we considered that the geometrical features of solar flares effect to those time evolutions. We measured flare ribbon length for 33 flare events observed by SDO/AIA, and found positive correlation between the “flare duration” and the “ribbon length”. From the statistical research of these observational data, we found that the time evolution of EUV emission can be explained by the X-ray emission.
Then, we tried to identify parameters that determine the solar flare spectra by comparing the flare emissions derived from physical based numerical model of solar flare with the actual observational data. Consequently, we used numerical simulation same as Imada et al.(2015). This numerical model can reproduce the movement and ionization of the plasma in the flare loop.
In this presentation, we will show some results of numerical simulation, and discuss the parameters for total solar flare emission spectra by comparing of simulation results, observational data and FISM.

Keywords: Space Weather, Solar Flare

©2019. Japan Geoscience Union. All Right Reserved.

Modeling of solar active regions using local linear force-free fields to estimate magnetic twist

*Kento Nakatani[1], Kanya Kusano[1], Sung-Hong Park[1], Leka KD[2]

1. Institute for space-Earth Environmental Research, Nagoya University, 2. North West Reserch Associates

The prediction of solar flares is an important issue for space weather forecasting. Although solar flares are believed to be caused by the magnetohydrodynamic (MHD) instability in solar active regions, the method for accurately evaluating the stability of solar magnetic field is not yet established. Recently, Ishiguro & Kusano (2017) proposed that a new instability called the Double Arc Instability (DAI) plays a role of initial driver of solar flares and the critical parameter for this instability can be used to evaluate the stability of active regions. The parameter can be derived by the integration of the magnetic twist as the function of magnetic flux. One way for it is given by the nonlinear force-free field (NLFFF) extrapolation using the photospheric vector magnetic field data. However, the NLFFF extrapolation demands heavy computation and it sometimes cannot well work as a model of solar coronal magnetic field because the force-free condition is limited on the photosphere. Therefore, in order to improve the efficiency and applicability of the flare prediction using , it may be required to develop a method to approximately but much quickly capture the overall features of magnetic field in solar active regions, especially in the flare triggering region. From this point of view, we try to develop a method to extract the characteristic feature of magnetic field in solar active regions using the linear force-free field (LFFF) model. For this objective, we compare the several methods to accurately capture the structure of using LFFF. In this study, we report the result of the analysis for the solar active region NOAA 11429.

Keywords: Space weather, solar , twist, force-free, photosphere, active region

©2019. Japan Geoscience Union. All Right Reserved.

Magnetohydrodynamic Simulation of an Erupting Magnetic Flux Rope on February 13 2009: Journey to Coronal Mass Ejection

*Satoshi Inoue[1], Antonia Savcheva[2]

1. Institute for Space-Earth Environmental Research, Nagoya University, 2. Harvard-Smithsonian Center for Astrophysics

We performed a magnetohydrodynamic (MHD) simulation of a solar eruption launched from solar active region 11012 on February 13, 2009. We in particular concentrated on the evolution of the magnetic flux rope (MFR) leading a coronal mass ejection. We first extrapolated the pre-eruptive magnetic flux ropes using a flux insertion method, in which the MFRs can be extrapolated from the normal component of the magnetic field (Bz) observed by SOHO/MDI and Extreme-Ultra Violet (EUV) images observed by the STEREO satellite. The extrapolated magnetic field reproduced the sigmoidal magnetic structure observed in EUV image well. Next we performed the MHD simulation using the extrapolated magnetic field.

The resulting simulation showed the dramatic eruption of the magnetic flux rope under which the current sheet and the post-flare loops are formed. This is well explained by the standard CSHKP flare model. The evolution of the MFR did not show simple dynamics, rather it showed very complicated dynamics through a magnetic reconnection. We found, during the eruption, that the coherent MFR is created through the reconnection of multiple pre-existing MFRs. Magnetic reconnection plays a role in producing the coherent, erupting MFR and supplying further twist into it. Furthermore we found that the footpoints of the erupting MFR moves along or away from the polarity inversion line, as seen in two-ribbon flares. The locations of both the footpoints of the MFR correspond to those of dimming regions observed in EUV images. Since the location and shape of the post-flare loops obtained from the simulation is reproduced in the observations, we can confirm the reliability of our simulation.

Keywords: Solar Flare, Solar Eruption, Magnetohydrodynamics

©2019. Japan Geoscience Union. All Right Reserved.

Investigation of flow structures in the solar interior through the surface magnetic elements' tracking

*Yusuke Iida[1]

1. Kwansei Gakuin University

We investigate the correlation of meridional flow and rotation velocity in the solar interior by tracking huge number of the surface magnetic elements.

As reported in JpGU2017 meeting, we found that the meridional flow velocity from the magnetic elements' tracking depends positively on their flux and size. We discussed that it may come from that the larger magnetic elements are rooted in the deeper solar interior. We further investigate this issue by correlating the meridional flow velocity and rotation velocity.

We use line-of-sight magnetograms obtained by SDO/HMI in July 2016. Time cadence is 45 seconds, in which the travel distance of magnetic element is smaller than 1 pixel. The magnetograms are transposed from the Earth-view coordinate to the Stonyhurst coordinate. We use the data within 75 degree from the disk center. Magnetic field strength is converted with an assumption that magnetic field is vertical to the surface and interpolated with a cubic spline interpolation.

We detected approximately 8,000 elements in each magnetogram and 4.5x108 displacements in our data set. The meridional flow and rotation velocity on magnetic flux are investigated. The rotation velocity shows negative dependence on the flux at the latitude within 45 degree while it shows weekly positive dependence at the latitude higher than 45 degree. This result is consistent with the depth dependence of rotation velocity obtained by previous helioseismology researches.

Keywords: Sun, Bigdata, Turbulence

©2019. Japan Geoscience Union. All Right Reserved.

High-precision measurement of carbon-14 in tree rings around the onset of the Maunder Minimum

*Hiroko Miyahara[1], Fuyuki Tokanai[2], Toru Moriya[2], Hideyuki Hotta[3]

1. Musashino Art University, 2. Yamagata University, 3. Chiba University

It is well known that the Sun indicates long-term variations at time scales of a few hundred years to a few millennia. It sometimes brings the grand minima, at which period the sunspots disappear for more than several decades. The detailed process of such long-lasting disappearance of sunspots, however, remains unclear. We therefore have been trying to reconstruct solar cycles around the onset of grand minima based on high-precision measurement of carbon-14 in tree rings. In this paper, we report on our preliminary result on the measurement of carbon-14 around the onset of the Maunder Minimum.

Keywords: solar cycle, grand minima, cosmogenic nuclide

©2019. Japan Geoscience Union. All Right Reserved.

Examination of ^{10}Be in travertine sediment as a possible tool to reconstruct past solar activity

*Hongyang Xu[1,2], Hiroko Miyahara[2], Kazuho Horiuchi[3], Hiroyuki Matsuzaki[4], Hailong Sun[5], Weijun Luo[5], Xiangmin Zheng[1], Yusuke Suganuma[6,7], Shijie Wang[5], Limin Zhou[1]

1. East China Normal University, 2. Musashino Art University, 3. Hirosaki University, 4. University of Tokyo, 5. Chinese Academy of Sciences, 6. National Institute of Polar Research, 7. The Graduate University for Advanced Studies (SOKENDAI)

In this study, we explore the possibility of using travertine sediment for reconstructing the past solar activity. We obtained an annual ^{10}Be record from travertine deposit from the modern period and compared with the neutron monitor data. We discuss a possible methodology to calibrate the climatological impact on ^{10}Be deposition and to obtain the signal of past solar and cosmic-ray variations.

Keywords: Beryllium-10, cosmogenic nuclide, solar activity, endogenic travertine

©2019. Japan Geoscience Union. All Right Reserved.

Examination of ^{10}Be in travertine sediment as a possible tool to reconstruct past solar activity II

*Hongyang Xu[1,2], Hiroko Miyahara[2], Kazuho Horiuchi[3], Hiroyuki Matsuzaki[4], Hailong Sun[5], Weijun Luo[5], Xiangmin Zheng[1], Yusuke Suganuma[6,7], Shijie Wang[5], Limin Zhou[1]

1. East China Normal University, 2. Musashino Art University, 3. Hirosaki University, 4. University of Tokyo, 5. Chinese Academy of Sciences, 6. National Institute of Polar Research, 7. The Graduate University for Advanced Studies (SOKENDAI)

We have been examining the potential of ^{10}Be in travertine sediment as a tool to reconstruct past solar and cosmic-ray variations. In this paper, we compare the ^{10}Be profile in the travertine layers from the rainy and dry seasons, and discuss the nature of ^{10}Be deposition at the two seasons.

Keywords: Beryllium-10, cosmogenic nuclide, solar activity, endogenic travertine

©2019. Japan Geoscience Union. All Right Reserved.

1 year of CR observation at Syowa Station in the Antarctic.

*Chihiro Kato[1], Kazuoki Munakata[1], Akira Kadokura[2], Ryuho Kataoka[2], Paul Evenson[3]

1. Shinshu University, 2. National Institute of Polar Research, 3. University of Delaware

CR observation has been carried out for 1 year at Syowa Station in the Antarctic. There was no serious unavailability of data during the whole year. It is now concluded that this station can contribute to a space weather study as one of the CR monitoring station of Global Muon Detector Network (GMDN). We report observed data and its stability as GMDN.

Keywords: Cosmic Rays, Space Weather

©2019. Japan Geoscience Union. All Right Reserved.

Space weather forecast archives at NICT: handwritten solar activity charts

*Kaori Sakaguchi[1], Daikou Shiota[1], Kaori Fukunaga[1], Katsuhide Marubashi[1], Hiromitsu Ishibashi[1], Yuki Kubo[1], Mamoru Ishii[1]

1. National Institute of Information and Communications Technology

About 40 years ago from 1978 to 1999, at Hiraiso Branch, Radio Research Laboratory; present Space Environment Laboratory of National Institute for Information and Communication Technology (NICT) in Japan, space environment data had been recorded in "solar activity chart" by hand for the operation of the radio wave warning service. The charts were created based on URSIgram codes, which were developed to facilitate the rapid exchange of information by telex in periods when internet was not available. Based on the exchanged codes, sunspots transitions and solar flare occurrences on the solar surface, these effects on shortwave propagation, geomagnetic disturbance, and cosmic ray flux over Japan were written in the solar activity charts together with comments and sketch by recorders. One chart was created for each Bertel’ s solar rotation number between No. 1974 and No. 2254, corresponding to sunspot cycles 21 and 22. We realized that the data exchange is almost only once a day from each observation point and charts was accumulation of the available data in real-time at that time.It might be quite difficult to decide future forecast from such a limited real-time data set. Currently, we are digitizing the solar activities charts and the data shown there. In this poster, we present examples of solar activity charts and possible real-time data set and time delay, as well as the verifying result of the solar flare / geomagnetism storm forecast at the time.

Keywords: Space Weather Archive, URSIgram

©2019. Japan Geoscience Union. All Right Reserved.

IMF dependence on solar wind parameters

*Tohru Araki, Yuki Harada[1]

1. Kyoto University

We studied IMF dependence upon solar wind parameters using OMNI hourly values.

Figure below is a plot of the total force (B), horizontal component (Bxy) in the ecliptic plane and vertical component (Bz) of IMF versus the solar wind density (Nsw). The IMF is averaged over 0.2/cc bin of Nsw. Data number in each bin is also plotted. The data period here is 1979-1981 (maximum SSN phase).

The figure shows (1) that B, Bxy and Bz slowly decrease with decreasing Nsw and (2) that when Nsw approaches further to zero. B and Bxy begin to increase and converges to the same finite value (about 10 nT here) while Bz converges to zero. The property (2) suggests that IMF converges to a typical spiral pattern when solar wind density converges to zero.

Two other data periods, 1999-2001 (SSN maximum) and 2007-2009 (SSN minimum) are examined. IMF observed by MAVEN orbiting Mars is also studied for the period, 2014-2018. The results of the analysis are roughly consistent with the description above. We also checked IMF dependence on solar wind velocity

Keywords: IMF, solar wind density, solar wind melocity

©2019. Japan Geoscience Union. All Right Reserved.

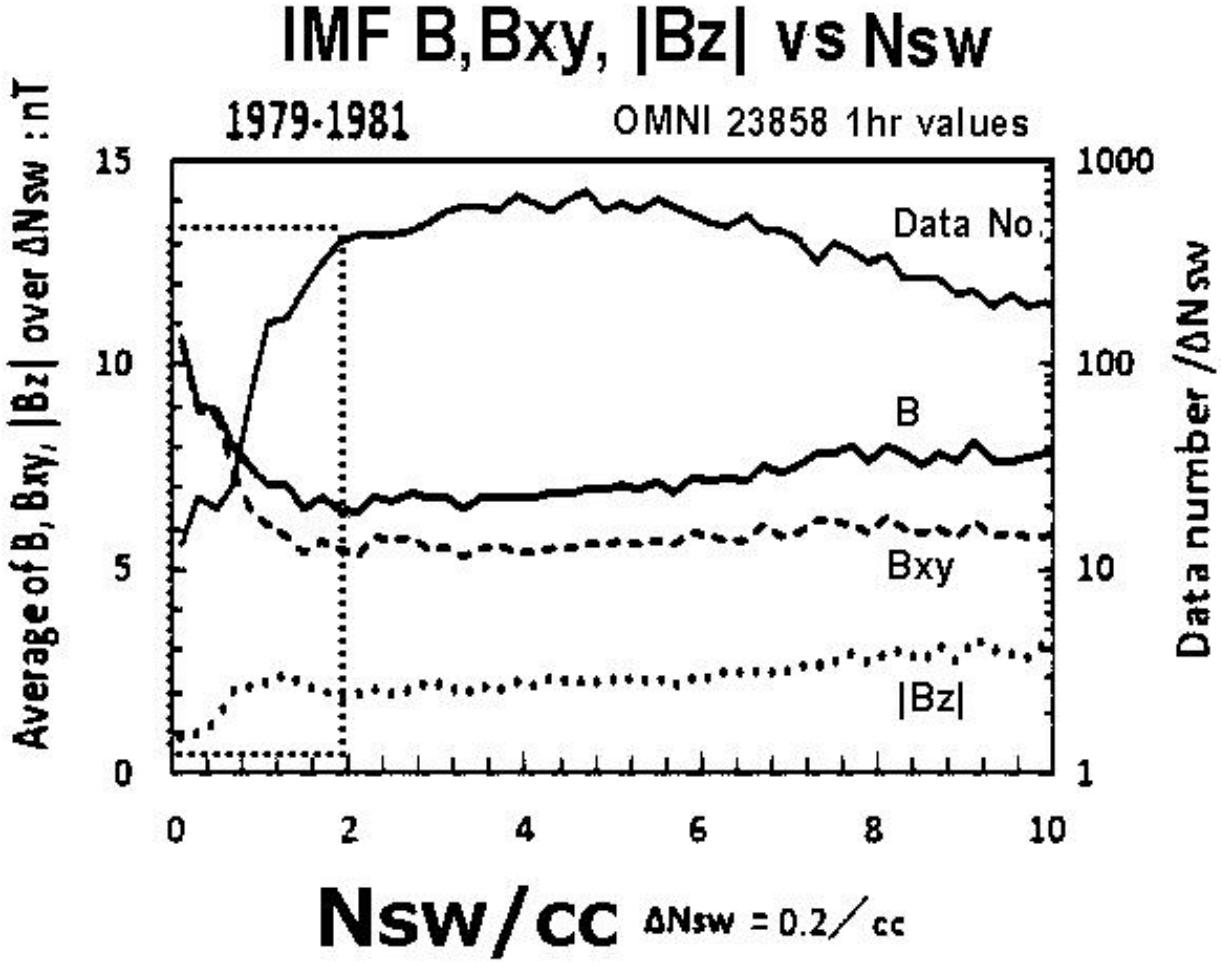

©2019. Japan Geoscience Union. All Right Reserved.

Dipole Tilt Effect of Geomagnetic Activity from Low- to High-latitudes

*Nowada Motoharu[1]

1. Shandong University at Weihai

Geomagnetic activity is dominantly impacted by the orientation of the Interplanetary Magnetic Field (IMF). However, when trying to address why the variations of geomagnetic activity are “semi-annual”, and are greater at equinoxes than at solstices, only IMF control of geomagnetic activity is not enough. This is because these variations are strongly dependent on the Earth’s dipole tilt; the dipole tilt is smaller at the equinoxes than at the solstices. Primitive studies assumed that magnetic reconnection occurs only at the subsolar point of dayside magnetopause. In their studies, the dipole tilt effect was not considered, but only the magnetic field direction between the IMF and the magnetosphere at the subsolar point was discussed in their studies. After them, geomagnetic variations where both dipole tilt effect and IMF direction are taken into account have been investigated. Based on a large database of IMF and AL/AU, we examined the relationship between the IMF clock angle and AL/AU at various dipole tilts. For both positive and negative dipole tilts, geomagnetic activity decrease as the clock angle moves away from 180˚. The AL/AU indices also tend to become smaller for larger dipole tilts. This dipole tilt dependence enhances the semi-annual variation of high-latitude geomagnetic activity.
It also remains unclear how degree energy input rate from solar wind to ring current (dD_{st}^{*}/dt) depends on dipole tilt under various interplanetary magnetic field (IMF) orientation and whether or not ring current development also follows this dipole tilt dependence. We tried to statistically investigate the dependence of dipole tilt and IMF clock angles on low- and middle-latitude geomagnetic activity (D_{st}^{*}), which is a proxy of ring current development, and solar wind energy input rate to ring current (dD_{st}^{*}/dt) over one solar cycle (1978 - 1988). D_{st}^{*} was calculated with the solar wind dynamic pressure and original D_{st} index, and the dipole tilt angle was defined as function of the day of year and universal time. The (dD_{st}^{*}/dt) values were obtained based on the solar wind electric field under the southward IMF conditions. Under positive and negative dipole tilts, the (dD_{st}^{*}/dt) values under low dipole tilt are negatively larger than those in case of high dipole tilt. Further peaks at 180˚ of the IMF clock angle are seen in most of the dipole tilt cases. However, the D_{st}^{*} index shows neither a peak at 180˚ of the IMF clock angle nor particular dipole tilt dependence in case of negative dipole tilt angles. This result suggests that low- and middle latitude geomagnetic activity (ring current development) does not necessarily show dipole tilt dependence and a one-to-one correlation with solar wind energy input rate to ring current (dD_{st}^{*}/dt).

Keywords: Geomagnetic activity (Dst*), Solar wind energy input rate to ring current (dDst*/dt), Semiannual variation , Dipole tilt effect, Interplanetary magnetic field and clock angel, Magnetic reconnection

©2019. Japan Geoscience Union. All Right Reserved.

A New Prediction Model for Solar Wind-Triggered Magnetospheric Disturbances Based on Potential Learning (Neural Network)

*Ryozo Kitajima[1], Motoharu Nowada[2], Ryotaro Kamimura[3]

1. Seikei University, 2. Shandong University at Weihai, 3. Tokai University

Nowadays, it becomes so important in saving our economic activity, and preventing the disasters caused by terrestrial electromagnetic effects to predict a scale and the duration of the geomagnetic disturbances based on in-situ solar wind observations. Recently, one of the notable techniques for the predictions of the magnetospheric disturbances is Neural Network (NN). However, most of these studies are focused on the reproduction of the behaviors of the index values, which represent the geomagnetic disturbances (e.g, D_{st} and AE), by inputting the solar wind parameters measured by the satellites. In our study, we apply a novel neural network model of ‘Potential Learning (PL)’.
Basically, Neural Networks (NNs) are models which imitate the information processing in the nervous system of brain. The nerve is made of cells as referred to as “neurons”, which specializes the information processing. NNs consist of “artificial” neurons, and can process information by learning. Therefore, using NNs, we can obtain some characteristics of the data inputted. The PL is a new kind of the NNs. A feature of the PL is to make a network that can understand the input variables based on learning by “input potentialities”, which are indices as calculated with the variances derived from the input variables. If using this PL, we can specify what input variable(s) is (are) potentially important and influential for a phenomenon.
In this study, introducing the PL technique, we try to specify which solar wind parameter plays an essential role in causing the geomagnetic disturbances. Although the conventional PL, where we used, had automatically selected the variables of interest, we develop a “improved” PL in this study so that the variables can manually be selected. We benchmark this new algorithm using the 4 polar magnetic storm cases occurred under the southward Interplanetary Magnetic Field (IMF)-B_z conditions, and advisedly set the maximum potentiality for the IMF-B_z, so that the IMF-B_z component is the most possible solar wind parameter to cause the geomagnetic disturbances. We note “second” solar wind parameter(s) to possibly cause the magnetospheric disturbances, following the IMF-B_z component. After testing our new technique to actual storm events, we might distinguish the magnetospheric disturbances into two different types, that is, the geomagnetic disturbances driven by “IMF-dominant” and “combination of IMF with solar wind plasma (dynamic pressure)”. The advantages to adopt this new algorithm to space weather, and more detailed results will be discussed in this presentation.

Keywords: Predictions of Geomagnetic Activity, Neural Network Considered Potential Learning, Development of Space Weather

©2019. Japan Geoscience Union. All Right Reserved.

Real-time magnetosphere simulator for space weather using REProduce Plasma Universe code

*Yasubumi Kubota[1], Aoi Nakamizo[1], Kaori Sakaguchi[1], Mitsue Den[1], Yuki Kubo[1], Tsutomu Nagatsuma[1], Takashi Tanaka[1,2]

1. National Institute of Information and Communications Technology, 2. Kyushu University

Surface charging of artificial satellite is one of risks caused by dynamical variations of space environment. It occurs when a satellite exposes high energy electrons around 10 keV created by plasma injection accompanied with substorm. Therefore we want to predict timing and electron energy of plasma injection using magnetosphere-ionosphere coupling global MHD simulation. Now we are developing a real-time numerical simulator for space weather forecast using magnetosphere-ionosphere coupling global MHD simulation called REPPU (REProduce Plasma Universe) code. The feature of the simulation code is highly robust to extreme solar wind parameters because the unstructured grid system has no singular point and is able to calculate in the uniform accuracy over the whole region. We use the real-time solar wind data formatted in the GSM coordinate system observed by DSCOVR spacecraft. Magnetic-dipole axis is fixed to z-direction in our simulation. Therefore daily variation of magnetic-dipole axis is not reproduced. Instead, we convert the input direction of the solar wind velocity and magnetic field into that which tilts including daily variation of magnetic dipole axis in x-z plane. In the method the solar wind structure is not exact. However we can relatively reproduce the magnetosphere response including daily variation of the magnetic-dipole axis against solar wind. The resolution is 7682 grids in the horizontal direction and 240 grids in the radial direction.
In this presentation, we compare the simulation results with the CPCP, AE index, and plasma variations observed by geostationary orbit satellites. Density and temperature of plasma injection derived from MHD simulation tends to estimate larger and smaller values than observation respectively because the MHD simulation does not include kinetic heating effects. We have to interpret MHD simulation results for prediction of electron density and temperature. We will discuss how to interpret electron density and temperature between observation and MHD simulation.

Keywords: global MHD simulation, surface charging

©2019. Japan Geoscience Union. All Right Reserved.

Simulation of GIC flowing through the power transmission network (187 kV-500 kV) in Japan

*Nishida Yuichiro[1,6], Yusuke Ebihara[1], Satoko Nakamura[1], Shinichi Watari[2], Kumiko Hashimoto[3], Kentaro Kitamura[4], Takashi Kikuchi[5]

1. Kyoto University Reserch Institute for Sustainable Humanosphere, 2. National Institute of Information and Communications Technology, 3. Kibi International University, 4. National Insutitute of Technology, Tokuyama College, 5. Nagoya University, 6. Kyoto University Department of Electrical Engineering

The energy released from the sun can enhance electric currents in Earth’ s magnetosphere, which induces an electric field on the ground surface. This electric field, called a geomagnetically induced electric field (GIE), gives rise to geomagnetically induced current (GIC) flowing in a transmission line. Japan is situated at geomagnetically low latitudes, but the potential risk is probably non-zero because a large-amplitude of GIC, as high as 129 A, was recorded in the Japanese power grid during the Halloween storm in October 2003. To evaluate the potential risk of the Japanese power grid properly, we modeled the Japanese power grid with high voltage class over 187 kV on the basis of publicly available data. The model consists of 602 nodes and 763 paths. The uniform GIE imposed on Japan was estimated on the basis of the geoelectric field observed in April 2018 at Kakioka Magnetic Observatory. We applied the uniform GIE on the model. The calculated GIC is roughly in agreement with that measured at 4 substations in Japan. For the westmost substation, a disagreement was found when we considered only the highest class of the power grid (500 kV), which may imply that the lower voltage class of the grid (<500 kV) may have some contribution to the GIC in Japan. We discuss the general tendency of the GIC flowing in the Japanese power grid, and prediction capability of the currently available model.

©2019. Japan Geoscience Union. All Right Reserved.

Simulation of GIC flowing through the power transmission network (187 kV-500 kV) in Japan

Yuichiro Nishida
Yusuke Ebihara
Satoko Nakamura
Shin-Ichi Watari
Kumiko Hashimoto
Kentaro Kitamura
Takashi Kikuchi

Abstract

The energy released from the sun can enhance electric currents in Earth's magnetosphere, which induces an electric field on the ground surface. This electric field, called a geomagnetically induced electric field (GIE), gives rise to geomagnetically induced current (GIC) flowing in a transmission line. Japan is situated at geomagnetically low latitudes, but the potential risk is probably non-zero because a large-amplitude of GIC, as high as 129 A, was recorded in the Japanese power grid during the Halloween storm in October 2003. To evaluate the potential risk of the Japanese power grid properly, we modeled the Japanese power grid with high voltage class over 187 kV on the basis of publicly available data. The model consists of 602 nodes and 763 paths. The uniform GIE imposed on Japan was estimated on the basis of the geoelectric field observed in April 2018 at Kakioka Magnetic Observatory. We applied the uniform GIE on the model. The calculated GIC is roughly in agreement with that measured at 4 substations in Japan. For the westmost substation, a disagreement was found when we considered only the highest class of the power grid (500 kV), which may imply that the lower voltage class of the grid (<500 kV) may have some contribution to the GIC in Japan. We discuss the general tendency of the GIC flowing in the Japanese power grid, and prediction capability of the currently available model.

©2019. Japan Geoscience Union. All Right Reserved.

Climatological features of the upper atmosphere reproduced by a revised version of a whole atmosphere-ionosphere coupled model GAIA

*Hidekatsu Jin[1], Yasunobu Miyoshi[2], Chihiro Tao[1], Hiroyuki Shinagawa[1], Hitoshi Fujiwara[3]

1. National Institude of Information and Communications Technology, 2. Kyushu University, 3. Seikei University

Temporal and spatial variations in the ionospheric electron density and thermospheric mass density could have significant impacts on radio communications between ground and space, and particle and atmospheric drag environments around satellites. Origins of such upper atmospheric variations are not only in the solar atmosphere through the emissions of solar radiation, high-speed plasma gas and high-energy particles, but also in the Earth’ s lower atmosphere, where meteorological phenomena could give rise to atmospheric waves propagating upward. In order to nowcast and forecast the upper atmospheric variations and disturbances, a whole atmospheric model, GAIA, has been developed, which combines a whole atmospheric GCM, an ionospheric model and an electrodynamics model in a self-consistent manner.

So far, for the purpose of its validation, we have compared climatological features of thermosphere and ionosphere reproduced by GAIA with those from ionospheric observation and observation-based empirical models. The comparison indicates that the model and observations are generally in good agreements, but in some condition such as at solar maximum there are significant disagreements in the ionospheric electron density distribution. In order to improve the accuracy of the model, we have made several updates such as ion chemical processes, energetics, parameterization, and so on. We also have introduced magnetospheric effects into the model, such as electrodynamics coupling with magnetosphere and particle precipitation. In this presentation, we discuss how the upper atmospheric model can improve its accuracy and how they can be validated.

Keywords: space weather, whole atmosphere, ionosphere, simulation, thermosphere, assimilation

©2019. Japan Geoscience Union. All Right Reserved.

Investigation of the thermospheric mass density variations below 200 km

*Hitoshi Fujiwara[1], Yasunobu Miyoshi[2], Masayoshi Utashima[1], Huixin Liu[2]

1. Faculty of Science and Technology, Seikei University, 2. Department of Earth and Planetary Sciences, Faculty of Sciences, Kyushu University

Since both the effects from the lower atmosphere and in-situ forcing are significant in the thermospheric region between 100 and 200 km altitude, the thermosphere in the region shows complex variations depending on various conditions. In addition, observations of the thermosphere (neutral atmosphere) between 100 and 200 km are very few compared to the upper thermosphere (above 300 km) and the ionosphere. These make it difficult to improve reliability of empirical and numerical models. Observations from Low Earth Orbit (LOE) satellites would be essential for building up available data sets in the thermospheric region between 100 and 200 km altitude. We will introduce our research project to investigate the thermospheric mass density variations in the 100-200 km altitude region with the LOE satellite, e.g., Tsubame (SLATS), data and a whole atmosphere GCM.

Keywords: thermosphere, mass density, Low Earth Orbit (LOE) satellite, GCM

©2019. Japan Geoscience Union. All Right Reserved.

Low-latitude HF Doppler observations of magnetospheric electric fields during space weather disturbances

*Kumiko K. Hashimoto[1], Takashi Kikuchi[2], Ichiro Tomizawa[3], Keisuke Hosokawa[3], Jaroslav Chum[4]

1. Kibi International University, 2. Nagoya University, 3. University of Electro-Commnunications, 4. Institute of Atmospheric Physics, Prague

Ionospheric electric fields penetrated from the magnetosphere to the low latitude ionosphere have been observed as geomagnetic disturbances caused by ionospheric currents, such as the equatorial electrojet (EEJ) at the dayside equator. The ionospheric currents are too weak to be a detector of the electric field at low latitudes on the dayside and even at the equator on the nightside. The HF Doppler (HFD) sounder is another powerful tool for observations of the electric filed at low latitudes on both the day- and night-sides. We have shown that the electric fields of the geomagnetic sudden commencements (SC) are composed of the preliminary impulse followed by the main impulse, of which directions are opposite to each other and both electric fields are opposite on the day- to night-sides (Kikuchi et al. 2016 JGR). We have also shown that the substorm electric fields are composed of the growth phase followed by expansion phase overshielding electric fields, of which directions are opposite to each other (Hashimoto et al., 2017). In this paper, we show that the HFD sounder is capable of detecting stormtime electric fields and that the electric fields are found to decay rather rapidly over one hour during the main phase with the time scale of a few hours. Combining with the equatorial magnetometer data, we would be able to estimate the decaying rate of the HFD electric fields, which helps obtain the stormtime electric fields quantitatively from the HFD data. We discuss advantages of widely separated HFD sounder operations and cooperations with SuperDARN as well as with magnetometer networks.

Keywords: HF Doppler observation, ionosphere electric field, magnetospheric electric field, geomagnetic storm, equatorial electrojet

©2019. Japan Geoscience Union. All Right Reserved.

Stratospheric ionization during magnetic storms

*Ryuho Kataoka[1]

1. National Institute of Polar Research

Transient mesospheric ionization was detected at an altitude of 65-70 km during the auroral breakup that occurred from 2220 to 2226 UT on June 30, 2017. During this event, the footprint of the Arase satellite was located within the field of view of the all-sky imagers at Syowa Station in the Antarctic. Auroral observations at Syowa Station revealed the dominant precipitation of relatively soft electrons during the auroral breakup. A corresponding spike in cosmic noise absorption was also observed at Syowa Station, while the Arase satellite observed a flux enhancement of >100 keV electrons and a broadband noise without detecting chorus waves or electromagnetic ion cyclotron waves. A general-purpose Monte Carlo particle transport simulation code was used to quantitatively evaluate the ionization in the middle atmosphere. Results of this study indicate that the precipitation of energetic electrons of >100 keV, rather than X-rays from the auroral electrons, played a dominant role in the transient and deep (65-70 km) mesospheric ionization during the observed auroral breakup. Based on the above results of Kataoka et al. (2019), we further discuss a possible role of X-rays to ionize the stratosphere during magnetic storms.

Reference:
Kataoka et al. (2019), Earth, Planets and Space, 71, 9, https://doi.org/10.1186/s40623-019-0989-7

©2019. Japan Geoscience Union. All Right Reserved.

Calculating propagation time of HF radio wave using ray-tracing method and simple comparison with the observation.

*Ryo Nakao[1], Hiroyuki Nakata[1], Hiroyo Ohya[1], Toshiaki Takano[1], Kornyanat Hozumi[2], Takuya Tsugawa[2], Susumu Saito[3], Mamoru Ishii[2]

1. Graduate School of Engineering, Chiba University, 2. National Institute of imformation and Communications Technology, 3. Electronic Navigation Research Institute

To provide the information of nowcast of radio propagation, we have started a project, HF-START (HF simulator Targeting for All user's Regional Telecommunications). In this project, a simulator that is able to predict propagation of HF radio waves is constructed by ray-tracing calculation.
Using this simulator, we have examined whether HF radio wave travels between any two points. In this calculation, the electron density, which is necessary to calculate reflection index is determined by International Reference Ionosphere (IRI).In this project, HF receivers have been installed at Chiba University (Chiba, 35.62N, 140.10E), Sarobetu (Hokkaido, 45.16N, 141.74E), Numata (Gunma, 36.62N, 139.02E), Yamagawa (Kagoshima, 31.20N, 130.61), Ogimi (Okinawa, 26.68, 128.15E) for observing HF radio wave transmitted from radioNIKKEI (Nagara, Chiba, 35.46N, 140.20E) to confirm the results of the ray-tracing calculation. In the ray-tracing calculation, therefore, we set the same locations of the transmitter and receivers as the observatories of HF-START. As a result of simple comparison between the ray-tracing results and the observation, it is found that there was a difference of the propagation time between the ray-tracing results and the observations. It is possible that the radio wave propagation between radioNIKKEI and Ciba University is not ground wave but sky wave that is reflected by ionosphere. As for further calculation, we plan to use the electron density distributions determined by GAIA and GNSS tomography in the ray-tracing calculation.

©2019. Japan Geoscience Union. All Right Reserved.

Why do some probabilistic forecasts lack reliability?

*Yuki Kubo[1]

1. National Institute of Information and Communications Technology

One of the important attributes to be satisfied for the probabilistic forecast system is reliability. However, some probabilistic forecast systems lack reliability. Why do some probabilistic forecasts lack reliability? We investigate a condition for a probabilistic binary forecast to be reliable in this work. We mathematically prove that a necessary, but not sufficient, condition for achieving a reliable probabilistic forecast is maximizing the Peirce skill score (PSS) at the threshold probability of the climatological base rate. The condition is confirmed by using artificially synthesized forecast-outcome pair data and previously published probabilistic solar flare forecast models. The condition gives a partial answer as to why some probabilistic forecast systems lack reliability, because the system, which does not satisfy the proved condition, can never be reliable. The result implies that those who want to develop a reliable probabilistic forecast system must adjust or train the system so as to maximize PSS near the threshold probability of the climatological base rate.

Keywords: Probabilistic forecast, Reliability

©2019. Japan Geoscience Union. All Right Reserved.

An estimation method of GEO spacecraft surface charging for a real-time spacecraft risk assessment

*Masao Nakamura[1], Ryota Kawachi[1], Go Takahashi[1], Tsutomu Nagatsuma[2], Mamoru Ishii[2]

1. Osaka Prefecture University, 2. NICT

Spacecraft anomalies are often induced by electrostatic discharges due to surface charging. Some spacecraft charging simulation software is developed by space agencies and research institutes and used for spacecraft designs and charging analysis. However these simulations cannot be used for a real-time estimation because they need hours or days to calculate the surface potential for a given plasma environment. Therefore we develop a quick estimation method of GEO spacecraft surface charging for the Space Environment Customized Risk Estimation for Spacecraft (SECURES) of the space weather forecast Project for Solar-Terrestrial Environment Prediction (PSTEP). We estimate the surface potentials by interpolation using lookup tables of the pre-simulated surface potentials for combinations of plasma temperatures and densities. We study fitting functions used in the interpolation and how to make the lookup tables for the good estimation. Then we can real-time estimate the surface potentials of the target GEO spacecraft when the on-orbit plasma environment is predicted or observed. The spacecraft risk assessment can be accomplished by additional information about the experimental discharging differential potential of the surface materials.

Keywords: Spacecraft surface charging, Space weather, Spacecraft risk assessment

©2019. Japan Geoscience Union. All Right Reserved.

A network of HF Doppler sounding systems in Japan

*Keisuke Hosokawa[1], Hiroyuki Nakata[2], Kumiko K. Hashimoto[3], Ichiro Tomizawa[1], Jun Sakai[1], Takashi Kikuchi[4]

1. University of Electro-Communications, 2. Chiba University, 3. Kibi International University, 4. ISEE, Nagoya University

Since 2003, a network observation of HF Doppler sounding has been conducted in Japan for remote-sensing the atmospheric, ionospheric and magnetospheric processes. Currently, 1 transmitting station (Tx) and 7 receiving stations (Rx) are operative by a collaborative effort of four difference universities. The main transmitting station is located at Chofu, Tokyo, Japan in the Campus of University of Electro-Communications (JG2XA). JG2XA transmits continuous waves at 5006 kHz and 8006 kHz with a transmitting power of 200 W. By receiving this JG2XA signal at 7 Rx stations (Sugadaira, Oarai, Kure, Kashima, Iitate, Fujisawa and Sugito) we derive the Doppler shift imposed during the propagation and reflection in the ionosphere. In particular, the Doppler shift data can be used to detect vertical motion of the ionospheric F region with a temporal resolution of 10 s. At some stations, we also have observed signals from Radio Nikkei 1 (JOZ at 3925 kHz, JOZ2 at 6055 kHz, and JOZ3 at 9595 kHz) transmitted from Nagara, Chiba, Japan, which allows us to observe the vertical motion of the ionosphere at several altitude levels. The data obtained from this experiment since 2003 are all available at http://gwave.cei.uec.ac.jp/~hfd. Not only quick-look plots but also several types of digital data (raw wave form and Doppler shift data) can be retrieved from this database. The experiment covers various ionospheric phenomena in the Magnetosphere-Ionospheric (M-I) coupling system, such as sporadic E-layer (Es), medium-scale traveling ionospheric disturbances (MSTIDs), large-scale traveling ionospheric disturbances (LSTIDs), global-scale electric field variation, geomagnetic pulsations, and sudden commencement (SC). The data can also be used for the studies of vertical coupling between the lower atmosphere and ionosphere, for example, observations of ionospheric variation after large earthquakes, volcanic eruptions and typhoons. To facilitate analyses of the phenomena listed above, it is desired to observe a wider area in latitude and longitude. For this purpose we plan to extend the network covering the entire ionosphere over Japan in the near future. In the presentation, we will give a brief introduction to the experiments and online database, and then discuss the future direction of the studies of atmosphere, ionosphere and magnetosphere using the HF Doppler sounding in a framework of international collaborations.

Keywords: HF Doppler experiment, Ionosphere

©2019. Japan Geoscience Union. All Right Reserved.

[E] Poster | P (Space and Planetary Sciences)：P-EM Solar-Terrestrial Sciences, Space Electromagnetism & Space Environment

Tue. May 28, 2019 5:15 PM - 6:30 PM JST | Tue. May 28, 2019 8:15 AM - 9:30 AM UTC | Poster Hall International Exhibition Hall8, Makuhari Messe_3

[P-EM12] Space Weather and Space Climate

convener:Ryuho Kataoka(National Institute of Polar Research), Antti A Pulkkinen(NASA Goddard Space Flight Center), Kanya Kusano(Institute for Space-Earth Environmental Research, Nagoya University), Kaori Sakaguchi(National Institute of Information and Communications Technology)

We share the latest scientific papers to understand how the solar-terrestrial environment changes in various time scales, and to discuss how we will react via international and interdisciplinary collaborations. More specifically, welcomed papers include space climate studies to reconstruct long-term variations from radio isotopes; cutting-edge observational and modeling studies of the ionosphere, geospace, heliosphere and the sun; simulation and statistical studies to predict the future space weather and space climate; applied science such as operational space weather forecast and mitigation of the social impact due to extreme space hazards.

[PEM12-P01] Reconnection signatures in solar magnetograms during the solar storms of 4-10 September 2017

*Robert Dean Loper[1,2] (1.Air Force Institute of Technology, Department of Engineering Physics, 2.National Center for Atmospheric Research, High Altitude Observatory)

[PEM12-P02] Statistical Relation between Solar Flares and Coronal Mass Ejections with Respect to Sigmoidal Structures in Active Regions

*Yusuke Kawabata[1,2], Yusuke Iida[3], Takafumi Doi, Sachiko Akiyama[4], Seiji Yashiro[4], Toshifumi Shimizu[2] (1.Earth and Planetary Science, The University of Tokyo, 2.Institute of Space and Astronautical Science, JAXA, 3.Kwansei Gakuin University, 4.The Catholic University of America)

[PEM12-P03] Multi-wavelength Observations of Pre-flare Quasi-periodic Pulsation in the C2.2 Flare on 2012 October 15

*Yung-Chi Yang[1], Ya-Hui Yang[1], Baolin Tan[2], Chengming Tan[2], Y.H. Yan[2] (1.Graduate Institute of Space Science National Central University, 2.Key Laboratory of Solar Activities, National Astronomical Observatories)

[PEM12-P04] Investigation of pre-flare type III solar radio bursts and their potential solar origins

*Shao-Fu Hsieh[1], Ya-Hui Yang[1], Baolin Tan[2], Chengming Tan[2], Y.H. Yan[2] (1.Graduate Institute of Space Science National Central University, 2.Key Laboratory of Solar Activities, National Astronomical Observatories, Chinese Academy of Sciences)

[PEM12-P05] Statistical and observational research of solar flare for constructing total emission spectra prediction model

*Shohei Nishimoto[1], kyoko Watanabe[1], Shinsuke Imada[2], Tomoko Kawate[3], Kyoung-Sun Lee[4] (1.National Defense Academy, 2.Institute for Space-Earth Environmental Research, Nagoya University, 3.Institute Of Space And Astronautical Science, Japan Aerospace Exploration Agency, 4.National Astronomical Observatory of Japan)

[PEM12-P06] Modeling of solar active regions using local linear force-free fields to estimate magnetic twist

*Kento Nakatani[1], Kanya Kusano[1], Sung-Hong Park[1], Leka KD[2] (1.Institute for space-Earth Environmental Research, Nagoya University, 2.North West Reserch Associates)

[PEM12-P07] Magnetohydrodynamic Simulation of an Erupting Magnetic Flux Rope on February 13 2009: Journey to Coronal Mass Ejection

*Satoshi Inoue[1], Antonia Savcheva[2] (1.Institute for Space-Earth Environmental Research, Nagoya University, 2.Harvard-Smithsonian Center for Astrophysics)

[PEM12-P08] Investigation of flow structures in the solar interior through the surface magnetic elements' tracking

*Yusuke Iida[1] (1.Kwansei Gakuin University)

[PEM12-P09] High-precision measurement of carbon-14 in tree rings around the onset of the Maunder Minimum

*Hiroko Miyahara[1], Fuyuki Tokanai[2], Toru Moriya[2], Hideyuki Hotta[3] (1.Musashino Art University, 2.Yamagata University, 3.Chiba University)

[PEM12-P10] Examination of ^{10}Be in travertine sediment as a possible tool to reconstruct past solar activity

*Hongyang Xu[1,2], Hiroko Miyahara[2], Kazuho Horiuchi[3], Hiroyuki Matsuzaki[4], Hailong Sun[5], Weijun Luo[5], Xiangmin Zheng[1], Yusuke Suganuma[6,7], Shijie Wang[5], Limin Zhou[1] (1.East China Normal University, 2.Musashino Art University, 3.Hirosaki University, 4.University of Tokyo, 5.Chinese Academy of Sciences, 6.National Institute of Polar Research, 7.The Graduate University for Advanced Studies (SOKENDAI))

[PEM12-P11] Examination of ^{10}Be in travertine sediment as a possible tool to reconstruct past solar activity II

*Hongyang Xu[1,2], Hiroko Miyahara[2], Kazuho Horiuchi[3], Hiroyuki Matsuzaki[4], Hailong Sun[5], Weijun Luo[5], Xiangmin Zheng[1], Yusuke Suganuma[6,7], Shijie Wang[5], Limin Zhou[1] (1.East China Normal University, 2.Musashino Art University, 3.Hirosaki University, 4.University of Tokyo, 5.Chinese Academy of Sciences, 6.National Institute of Polar Research, 7.The Graduate University for Advanced Studies (SOKENDAI))

[PEM12-P12] 1 year of CR observation at Syowa Station in the Antarctic.

*Chihiro Kato[1], Kazuoki Munakata[1], Akira Kadokura[2], Ryuho Kataoka[2], Paul Evenson[3] (1.Shinshu University, 2.National Institute of Polar Research, 3.University of Delaware)

[PEM12-P13] Space weather forecast archives at NICT: handwritten solar activity charts

*Kaori Sakaguchi[1], Daikou Shiota[1], Kaori Fukunaga[1], Katsuhide Marubashi[1], Hiromitsu Ishibashi[1], Yuki Kubo[1], Mamoru Ishii[1] (1.National Institute of Information and Communications Technology)

[PEM12-P14] IMF dependence on solar wind parameters

*Tohru Araki, Yuki Harada[1] (1.Kyoto University)

[PEM12-P15] **Dipole Tilt Effect of Geomagnetic Activity from Low- to High-latitudes**

*Nowada Motoharu[1] (1.Shandong University at Weihai)

[PEM12-P16] A New Prediction Model for Solar Wind-Triggered Magnetospheric Disturbances Based on Potential Learning (Neural Network)

*Ryozo Kitajima[1], Motoharu Nowada[2], Ryotaro Kamimura[3] (1.Seikei University, 2.Shandong University at Weihai, 3.Tokai University)

[PEM12-P17] Real-time magnetosphere simulator for space weather using REProduce Plasma Universe code

*Yasubumi Kubota[1], Aoi Nakamizo[1], Kaori Sakaguchi[1], Mitsue Den[1], Yuki Kubo[1], Tsutomu Nagatsuma[1], Takashi Tanaka[1,2] (1.National Institute of Information and Communications Technology, 2.Kyushu University)

[PEM12-P18] **Simulation of GIC flowing through the power transmission network (187 kV-500 kV) in Japan**

*Nishida Yuichiro[1,6], Yusuke Ebihara[1], Satoko Nakamura[1], Shinichi Watari[2], Kumiko Hashimoto[3], Kentaro Kitamura[4], Takashi Kikuchi[5] (1.Kyoto University Reserch Institute for Sustainable Humanosphere, 2.National Institute of Information and Communications Technology, 3.Kibi International University, 4.National Insutitute of Technology, Tokuyama College, 5.Nagoya University, 6.Kyoto University Department of Electrical Engineering)

[PEM12-P19] Climatological features of the upper atmosphere reproduced by a revised version of a whole atmosphere-ionosphere coupled model GAIA

*Hidekatsu Jin[1], Yasunobu Miyoshi[2], Chihiro Tao[1], Hiroyuki Shinagawa[1], Hitoshi Fujiwara[3] (1.National Institude of Information and Communications Technology, 2.Kyushu University, 3.Seikei University)

[PEM12-P20] Investigation of the thermospheric mass density variations below 200 km

*Hitoshi Fujiwara[1], Yasunobu Miyoshi[2], Masayoshi Utashima[1], Huixin Liu[2] (1.Faculty of Science and Technology, Seikei University, 2.Department of Earth and Planetary Sciences, Faculty of Sciences, Kyushu University)

[PEM12-P21] Low-latitude HF Doppler observations of magnetospheric electric fields during space weather disturbances

*Kumiko K. Hashimoto[1], Takashi Kikuchi[2], Ichiro Tomizawa[3], Keisuke Hosokawa[3], Jaroslav Chum[4] (1.Kibi International University, 2.Nagoya University, 3.University of Electro-Commnunications, 4.Institute of Atmospheric Physics, Prague)

[PEM12-P22] Stratospheric ionization during magnetic storms

*Ryuho Kataoka[1] (1.National Institute of Polar Research)

[PEM12-P23] Calculating propagation time of HF radio wave using ray-tracing method and simple comparison with the observation.

*Ryo Nakao[1], Hiroyuki Nakata[1], Hiroyo Ohya[1], Toshiaki Takano[1], Kornyanat Hozumi[2], Takuya Tsugawa[2], Susumu Saito[3], Mamoru Ishii[2] (1.Graduate School of Engineering, Chiba University, 2.National Institute of imformation and Communications Technology, 3.Electronic Navigation Research Institute)

[PEM12-P24] Why do some probabilistic forecasts lack reliability?

*Yuki Kubo[1] (1.National Institute of Information and Communications Technology)

[PEM12-P25] An estimation method of GEO spacecraft surface charging for a real-time spacecraft risk assessment

*Masao Nakamura[1], Ryota Kawachi[1], Go Takahashi[1], Tsutomu Nagatsuma[2], Mamoru Ishii[2] (1.Osaka Prefecture University, 2.NICT)

[PEM12-P26] A network of HF Doppler sounding systems in Japan

*Keisuke Hosokawa[1], Hiroyuki Nakata[2], Kumiko K. Hashimoto[3], Ichiro Tomizawa[1], Jun Sakai[1], Takashi Kikuchi[4] (1.University of Electro-Communications, 2.Chiba University, 3.Kibi International University, 4.ISEE, Nagoya University)

Reconnection signatures in solar magnetograms during the solar storms of 4-10 September 2017

*Robert Dean Loper[1,2]

1. Air Force Institute of Technology, Department of Engineering Physics, 2. National Center for Atmospheric Research, High Altitude Observatory

Solar flare forecasting is limited to active region classification and historical correlation, due largely to our lack of understanding of magnetic reconnection as a driving mechanism for solar flares and coronal mass ejections. Photospheric observations indicate magnetic field changes during solar flares, brought about during magnetic reconnection and related to magnetic field helicity on the solar surface. While the neutral point of the reconnection event associated with a flare usually occurs in the solar corona, some signs of the magnetic field changes should manifest as low as the photosphere. This study utilizes data from SDO HMI and Space-Weather HMI Active Regions Patches (SHARPS) to analyze full vector field component data in the photospheric magnetic field during several magnetic reconnection events during the space weather events of 4-10 September 2017.

Keywords: solar atmosphere, sunspots, magnetogram, solar flares

©2019. Japan Geoscience Union. All Right Reserved.

Statistical Relation between Solar Flares and Coronal Mass Ejections with Respect to Sigmoidal Structures in Active Regions

*Yusuke Kawabata[1,2], Yusuke Iida[3], Takafumi Doi, Sachiko Akiyama[4], Seiji Yashiro[4], Toshifumi Shimizu[2]

1. Earth and Planetary Science, The University of Tokyo, 2. Institute of Space and Astronautical Science, JAXA, 3. Kwansei Gakuin University, 4. The Catholic University of America

We will report statistical dependences among features of coronal mass ejections (CMEs), solar flares, and sigmoidal structures in soft-X-ray images (Kawabata et al. 2018). We applied analysis methods to all the features in the same way in order to investigate the reproducibility of the correlations among them, which may be found from previous statistical studies. Samples of 211 M-class and X-class flares, observed between 2006 and 2015 by the Hinode/X-ray telescope, Solar and Heliospheric Observatory/Large Angle and Spectrometric Coronagraph, and Geostationary Operational Environmental Satellite, were examined statistically. Five kinds of analysis were performed: Occurrence rate analysis, linear-correlation analysis, association analysis, the Kolmogorov–Smirnov test, and the Anderson–Darling test. These give three main results. First, the sigmoidal structure and long-duration events (LDEs) have a stronger dependence on CME occurrence than large X-ray-class events in on-disk events. Second, for the limb events, a significant dependence exists between LDEs and CME occurrence, and between X-ray-class events and CME occurrence. Third, 32.4% of on-disk flare events have sigmoidal structure and are not accompanied by CMEs. However, the occurrence probability of CMEs without sigmoidal structure is very small, 8.8%, in on-disk events. While the first and second results are consistent with previous studies, we provide for the first time a difference between the on-disk and limb events. The third result, that non-sigmoidal regions produce fewer eruptive events, is also different from previous results. We suggest that sigmoidal structures in soft X-ray images will be a helpful feature for CME prediction in on-disk flare events.

Keywords: Sun, Solar flares, Coronal mass ejections, Sigmoid

©2019. Japan Geoscience Union. All Right Reserved.

Multi-wavelength Observations of Pre-flare Quasi-periodic Pulsation in the C2.2 Flare on 2012 October 15

*Yung-Chi Yang[1], Ya-Hui Yang[1], Baolin Tan[2], Chengming Tan[2], Y.H. Yan[2]

1. Graduate Institute of Space Science National Central University, 2. Key Laboratory of Solar Activities, National Astronomical Observatories

Quasi-periodic pulsation (QPP) is thought to be the nature of solar flares, which can be observed during and before flares in various wavelengths, such as the radio, microwave, SXR, and EUV. In this study, we analyze a pre-flare QPP event on 2012 October 15 and its association with the following C2.2 flare based on the radio data in the ranges of 2.81-2.85 GHz and 2.91-2.95 GHz from Solar Broadband Radio Spectrometer (SBRS), EUV images from AIA multi-wavelength observations, and wavelet analysis. Our result show that the main period of the radio QPP is ~800 s which is similar to the period of ~13.5 min obtained in SXR by Tan et al. (2016). Moreover, we analyze several localized areas in the flare-eruptive AR 11593 to search for the possible regions responsible for the occurrence of pre-flare QPP. We find that the footpoints of brightening loops in 211 Åshow the quasi-periodic behavior of ~850 s. It is thus suggested that the pre-flare QPP with a period of 13-15 min can be manifested in both of the thermal (SXR, EUV) and nonthermal (radio) radiation processes. The relationship between the pre-flare QPP and the subsequent C2.2 flare will also be discussed.

Keywords: sun, solar flares, solar oscillation

©2019. Japan Geoscience Union. All Right Reserved.

Investigation of pre-flare type III solar radio bursts and their potential solar origins

*Shao-Fu Hsieh[1], Ya-Hui Yang[1], Baolin Tan[2], Chengming Tan[2], Y.H. Yan[2]

1. Graduate Institute of Space Science National Central University, 2. Key Laboratory of Solar Activities, National Astronomical Observatories, Chinese Academy of Sciences

Type III solar radio bursts are characterized as the fast-drifting radio emissions in a dynamic spectrogram, which is believed to be produced by the propagating electron beams and often accompanied with the solar flares or magnetic reconnection. Studying the type III radio bursts in high-frequency range before flares would be important for understanding the trigger of energy release although it is rarely reported previously. Here we present two pre-flare type III burst events found in the range of 2.6-3.8 GHz at Solar Broadband Radio Spectrometer (SBRS). By comparing with the SDO/AIA multi-wavelength observations in flare active regions, the pre-flare type III radio bursts have good temporal correlations with the increases of EUV emissions. Furthermore, we find that one event is related to the EUV brightening with 1-min delay, implying the existence of plasma heating before energy release. The other event has a simultaneous EUV jet with a speed of ~700 km/s indicating the occurrence of magnetic reconnection. We suppose both pre-flare events are associated with small-scale energy release via magnetic reconnection.

Keywords: sun, solar flares, solar radio bursts

©2019. Japan Geoscience Union. All Right Reserved.

Statistical and observational research of solar flare for constructing total emission spectra prediction model

*Shohei Nishimoto[1], kyoko Watanabe[1], Shinsuke Imada[2], Tomoko Kawate[3], Kyoung-Sun Lee[4]

1. National Defense Academy, 2. Institute for Space-Earth Environmental Research, Nagoya University, 3. Institute Of Space And Astronautical Science, Japan Aerospace Exploration Agency, 4. National Astronomical Observatory of Japan

Impulsive energy release phenomena such as solar flares, sometimes affect to the solar-terrestrial environment. Usually, we use soft X-ray flux (GOES class) as the index of flare scale. However, the magnitude of effect to the solar-terrestrial environment is not proportional to this scale. Therefore, it is considered that the GOES class is not optimal parameter for predicting the Sudden Ionospheric Disturbance (SID). To identify the relationship between solar flare phenomena and influence to the solar-terrestrial environment, we need to understand the full spectra of solar flares in detail.
There is the solar flare irradiance model named the Flare Irradiance Spectral Model (FISM) (Chamberlin et al., 2006, 2007, 2008). FISM is the most used model, and can estimate solar flare spectra with high wavelength and temporal resolution. However, this model can not express the time evolution of emitted plasma during the solar flare, and has low accuracy on short wavelength that might strongly affect to the total flare spectra. Therefore, individual SID phenomenon can not be reproduced.
In this work, in order to solve the problems of FISM, we performed statistical analysis on observational data during the solar flares. From This study, we tried to find the parameters that control the solar flare emission spectra. We selected solar flare events larger than M-class from the Hinode flare catalogue (Watanabe et al., 2012). First, we focused on the EUV emission observed by the SDO/EVE. We examined the intensities and time evolutions of five EUV lines (Fe XX, Fe XVIII, Fe XVI, Fe VIII, and He II) for 54 flare events. As a result, we found positive correlation between the “GOES class” and the “EUV peak flux” for all Fe lines. Moreover, we found that hotter lines peaked earlier than cooler lines. On the other hand, He II line data have poor correlation with GOES X-ray data. Furthermore, we considered that the geometrical features of solar flares effect to those time evolutions. We measured flare ribbon length for 33 flare events observed by SDO/AIA, and found positive correlation between the “flare duration” and the “ribbon length”. From the statistical research of these observational data, we found that the time evolution of EUV emission can be explained by the X-ray emission.
Then, we tried to identify parameters that determine the solar flare spectra by comparing the flare emissions derived from physical based numerical model of solar flare with the actual observational data. Consequently, we used numerical simulation same as Imada et al.(2015). This numerical model can reproduce the movement and ionization of the plasma in the flare loop.
In this presentation, we will show some results of numerical simulation, and discuss the parameters for total solar flare emission spectra by comparing of simulation results, observational data and FISM.

Keywords: Space Weather, Solar Flare

©2019. Japan Geoscience Union. All Right Reserved.

Modeling of solar active regions using local linear force-free fields to estimate magnetic twist

*Kento Nakatani[1], Kanya Kusano[1], Sung-Hong Park[1], Leka KD[2]

1. Institute for space-Earth Environmental Research, Nagoya University, 2. North West Reserch Associates

The prediction of solar flares is an important issue for space weather forecasting. Although solar flares are believed to be caused by the magnetohydrodynamic (MHD) instability in solar active regions, the method for accurately evaluating the stability of solar magnetic field is not yet established. Recently, Ishiguro & Kusano (2017) proposed that a new instability called the Double Arc Instability (DAI) plays a role of initial driver of solar flares and the critical parameter for this instability can be used to evaluate the stability of active regions. The parameter can be derived by the integration of the magnetic twist as the function of magnetic flux. One way for it is given by the nonlinear force-free field (NLFFF) extrapolation using the photospheric vector magnetic field data. However, the NLFFF extrapolation demands heavy computation and it sometimes cannot well work as a model of solar coronal magnetic field because the force-free condition is limited on the photosphere. Therefore, in order to improve the efficiency and applicability of the flare prediction using , it may be required to develop a method to approximately but much quickly capture the overall features of magnetic field in solar active regions, especially in the flare triggering region. From this point of view, we try to develop a method to extract the characteristic feature of magnetic field in solar active regions using the linear force-free field (LFFF) model. For this objective, we compare the several methods to accurately capture the structure of using LFFF. In this study, we report the result of the analysis for the solar active region NOAA 11429.

Keywords: Space weather, solar , twist, force-free, photosphere, active region

©2019. Japan Geoscience Union. All Right Reserved.

Magnetohydrodynamic Simulation of an Erupting Magnetic Flux Rope on February 13 2009: Journey to Coronal Mass Ejection

*Satoshi Inoue[1], Antonia Savcheva[2]

1. Institute for Space-Earth Environmental Research, Nagoya University, 2. Harvard-Smithsonian Center for Astrophysics

We performed a magnetohydrodynamic (MHD) simulation of a solar eruption launched from solar active region 11012 on February 13, 2009. We in particular concentrated on the evolution of the magnetic flux rope (MFR) leading a coronal mass ejection. We first extrapolated the pre-eruptive magnetic flux ropes using a flux insertion method, in which the MFRs can be extrapolated from the normal component of the magnetic field (Bz) observed by SOHO/MDI and Extreme-Ultra Violet (EUV) images observed by the STEREO satellite. The extrapolated magnetic field reproduced the sigmoidal magnetic structure observed in EUV image well. Next we performed the MHD simulation using the extrapolated magnetic field.

The resulting simulation showed the dramatic eruption of the magnetic flux rope under which the current sheet and the post-flare loops are formed. This is well explained by the standard CSHKP flare model. The evolution of the MFR did not show simple dynamics, rather it showed very complicated dynamics through a magnetic reconnection. We found, during the eruption, that the coherent MFR is created through the reconnection of multiple pre-existing MFRs. Magnetic reconnection plays a role in producing the coherent, erupting MFR and supplying further twist into it. Furthermore we found that the footpoints of the erupting MFR moves along or away from the polarity inversion line, as seen in two-ribbon flares. The locations of both the footpoints of the MFR correspond to those of dimming regions observed in EUV images. Since the location and shape of the post-flare loops obtained from the simulation is reproduced in the observations, we can confirm the reliability of our simulation.

Keywords: Solar Flare, Solar Eruption, Magnetohydrodynamics

©2019. Japan Geoscience Union. All Right Reserved.

Investigation of flow structures in the solar interior through the surface magnetic elements' tracking

*Yusuke Iida[1]

1. Kwansei Gakuin University

We investigate the correlation of meridional flow and rotation velocity in the solar interior by tracking huge number of the surface magnetic elements.

As reported in JpGU2017 meeting, we found that the meridional flow velocity from the magnetic elements' tracking depends positively on their flux and size. We discussed that it may come from that the larger magnetic elements are rooted in the deeper solar interior. We further investigate this issue by correlating the meridional flow velocity and rotation velocity.

We use line-of-sight magnetograms obtained by SDO/HMI in July 2016. Time cadence is 45 seconds, in which the travel distance of magnetic element is smaller than 1 pixel. The magnetograms are transposed from the Earth-view coordinate to the Stonyhurst coordinate. We use the data within 75 degree from the disk center. Magnetic field strength is converted with an assumption that magnetic field is vertical to the surface and interpolated with a cubic spline interpolation.

We detected approximately 8,000 elements in each magnetogram and 4.5x108 displacements in our data set. The meridional flow and rotation velocity on magnetic flux are investigated. The rotation velocity shows negative dependence on the flux at the latitude within 45 degree while it shows weekly positive dependence at the latitude higher than 45 degree. This result is consistent with the depth dependence of rotation velocity obtained by previous helioseismology researches.

Keywords: Sun, Bigdata, Turbulence

©2019. Japan Geoscience Union. All Right Reserved.

High-precision measurement of carbon-14 in tree rings around the onset of the Maunder Minimum

*Hiroko Miyahara[1], Fuyuki Tokanai[2], Toru Moriya[2], Hideyuki Hotta[3]

1. Musashino Art University, 2. Yamagata University, 3. Chiba University

It is well known that the Sun indicates long-term variations at time scales of a few hundred years to a few millennia. It sometimes brings the grand minima, at which period the sunspots disappear for more than several decades. The detailed process of such long-lasting disappearance of sunspots, however, remains unclear. We therefore have been trying to reconstruct solar cycles around the onset of grand minima based on high-precision measurement of carbon-14 in tree rings. In this paper, we report on our preliminary result on the measurement of carbon-14 around the onset of the Maunder Minimum.

Keywords: solar cycle, grand minima, cosmogenic nuclide

©2019. Japan Geoscience Union. All Right Reserved.

Examination of ^{10}Be in travertine sediment as a possible tool to reconstruct past solar activity

*Hongyang Xu[1,2], Hiroko Miyahara[2], Kazuho Horiuchi[3], Hiroyuki Matsuzaki[4], Hailong Sun[5], Weijun Luo[5], Xiangmin Zheng[1], Yusuke Suganuma[6,7], Shijie Wang[5], Limin Zhou[1]

1. East China Normal University, 2. Musashino Art University, 3. Hirosaki University, 4. University of Tokyo, 5. Chinese Academy of Sciences, 6. National Institute of Polar Research, 7. The Graduate University for Advanced Studies (SOKENDAI)

In this study, we explore the possibility of using travertine sediment for reconstructing the past solar activity. We obtained an annual ^{10}Be record from travertine deposit from the modern period and compared with the neutron monitor data. We discuss a possible methodology to calibrate the climatological impact on ^{10}Be deposition and to obtain the signal of past solar and cosmic-ray variations.

Keywords: Beryllium-10, cosmogenic nuclide, solar activity, endogenic travertine

©2019. Japan Geoscience Union. All Right Reserved.

Examination of ^{10}Be in travertine sediment as a possible tool to reconstruct past solar activity II

*Hongyang Xu[1,2], Hiroko Miyahara[2], Kazuho Horiuchi[3], Hiroyuki Matsuzaki[4], Hailong Sun[5], Weijun Luo[5], Xiangmin Zheng[1], Yusuke Suganuma[6,7], Shijie Wang[5], Limin Zhou[1]

1. East China Normal University, 2. Musashino Art University, 3. Hirosaki University, 4. University of Tokyo, 5. Chinese Academy of Sciences, 6. National Institute of Polar Research, 7. The Graduate University for Advanced Studies (SOKENDAI)

We have been examining the potential of ^{10}Be in travertine sediment as a tool to reconstruct past solar and cosmic-ray variations. In this paper, we compare the ^{10}Be profile in the travertine layers from the rainy and dry seasons, and discuss the nature of ^{10}Be deposition at the two seasons.

Keywords: Beryllium-10, cosmogenic nuclide, solar activity, endogenic travertine

©2019. Japan Geoscience Union. All Right Reserved.

1 year of CR observation at Syowa Station in the Antarctic.

*Chihiro Kato[1], Kazuoki Munakata[1], Akira Kadokura[2], Ryuho Kataoka[2], Paul Evenson[3]

1. Shinshu University, 2. National Institute of Polar Research, 3. University of Delaware

CR observation has been carried out for 1 year at Syowa Station in the Antarctic. There was no serious unavailability of data during the whole year. It is now concluded that this station can contribute to a space weather study as one of the CR monitoring station of Global Muon Detector Network (GMDN). We report observed data and its stability as GMDN.

Keywords: Cosmic Rays, Space Weather

©2019. Japan Geoscience Union. All Right Reserved.

Space weather forecast archives at NICT: handwritten solar activity charts

*Kaori Sakaguchi[1], Daikou Shiota[1], Kaori Fukunaga[1], Katsuhide Marubashi[1], Hiromitsu Ishibashi[1], Yuki Kubo[1], Mamoru Ishii[1]

1. National Institute of Information and Communications Technology

About 40 years ago from 1978 to 1999, at Hiraiso Branch, Radio Research Laboratory; present Space Environment Laboratory of National Institute for Information and Communication Technology (NICT) in Japan, space environment data had been recorded in "solar activity chart" by hand for the operation of the radio wave warning service. The charts were created based on URSIgram codes, which were developed to facilitate the rapid exchange of information by telex in periods when internet was not available. Based on the exchanged codes, sunspots transitions and solar flare occurrences on the solar surface, these effects on shortwave propagation, geomagnetic disturbance, and cosmic ray flux over Japan were written in the solar activity charts together with comments and sketch by recorders. One chart was created for each Bertel’ s solar rotation number between No. 1974 and No. 2254, corresponding to sunspot cycles 21 and 22. We realized that the data exchange is almost only once a day from each observation point and charts was accumulation of the available data in real-time at that time.It might be quite difficult to decide future forecast from such a limited real-time data set. Currently, we are digitizing the solar activities charts and the data shown there. In this poster, we present examples of solar activity charts and possible real-time data set and time delay, as well as the verifying result of the solar flare / geomagnetism storm forecast at the time.

Keywords: Space Weather Archive, URSIgram

©2019. Japan Geoscience Union. All Right Reserved.

IMF dependence on solar wind parameters

*Tohru Araki, Yuki Harada[1]

1. Kyoto University

We studied IMF dependence upon solar wind parameters using OMNI hourly values.

Figure below is a plot of the total force (B), horizontal component (Bxy) in the ecliptic plane and vertical component (Bz) of IMF versus the solar wind density (Nsw). The IMF is averaged over 0.2/cc bin of Nsw. Data number in each bin is also plotted. The data period here is 1979-1981 (maximum SSN phase).

The figure shows (1) that B, Bxy and Bz slowly decrease with decreasing Nsw and (2) that when Nsw approaches further to zero. B and Bxy begin to increase and converges to the same finite value (about 10 nT here) while Bz converges to zero. The property (2) suggests that IMF converges to a typical spiral pattern when solar wind density converges to zero.

Two other data periods, 1999-2001 (SSN maximum) and 2007-2009 (SSN minimum) are examined. IMF observed by MAVEN orbiting Mars is also studied for the period, 2014-2018. The results of the analysis are roughly consistent with the description above. We also checked IMF dependence on solar wind velocity

Keywords: IMF, solar wind density, solar wind melocity

©2019. Japan Geoscience Union. All Right Reserved.

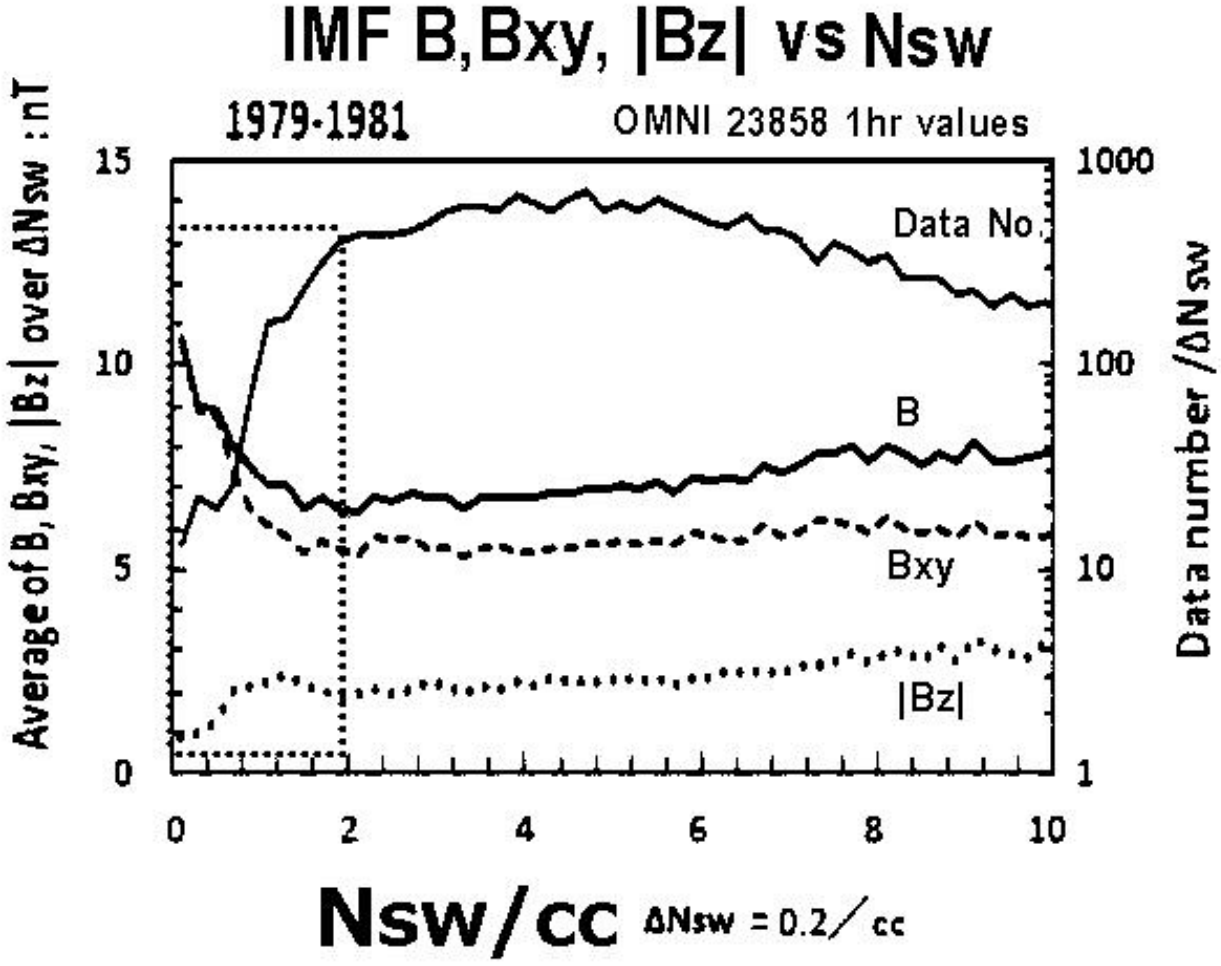

©2019. Japan Geoscience Union. All Right Reserved.

Dipole Tilt Effect of Geomagnetic Activity from Low- to High-latitudes

*Nowada Motoharu[1]

1. Shandong University at Weihai

Geomagnetic activity is dominantly impacted by the orientation of the Interplanetary Magnetic Field (IMF). However, when trying to address why the variations of geomagnetic activity are “semi-annual”, and are greater at equinoxes than at solstices, only IMF control of geomagnetic activity is not enough. This is because these variations are strongly dependent on the Earth’s dipole tilt; the dipole tilt is smaller at the equinoxes than at the solstices. Primitive studies assumed that magnetic reconnection occurs only at the subsolar point of dayside magnetopause. In their studies, the dipole tilt effect was not considered, but only the magnetic field direction between the IMF and the magnetosphere at the subsolar point was discussed in their studies. After them, geomagnetic variations where both dipole tilt effect and IMF direction are taken into account have been investigated. Based on a large database of IMF and AL/AU, we examined the relationship between the IMF clock angle and AL/AU at various dipole tilts. For both positive and negative dipole tilts, geomagnetic activity decrease as the clock angle moves away from 180˚. The AL/AU indices also tend to become smaller for larger dipole tilts. This dipole tilt dependence enhances the semi-annual variation of high-latitude geomagnetic activity.
It also remains unclear how degree energy input rate from solar wind to ring current (dD_{st}^{*}/dt) depends on dipole tilt under various interplanetary magnetic field (IMF) orientation and whether or not ring current development also follows this dipole tilt dependence. We tried to statistically investigate the dependence of dipole tilt and IMF clock angles on low- and middle-latitude geomagnetic activity (D_{st}^{*}), which is a proxy of ring current development, and solar wind energy input rate to ring current (dD_{st}^{*}/dt) over one solar cycle (1978 - 1988). D_{st}^{*} was calculated with the solar wind dynamic pressure and original D_{st} index, and the dipole tilt angle was defined as function of the day of year and universal time. The (dD_{st}^{*}/dt) values were obtained based on the solar wind electric field under the southward IMF conditions. Under positive and negative dipole tilts, the (dD_{st}^{*}/dt) values under low dipole tilt are negatively larger than those in case of high dipole tilt. Further peaks at 180˚ of the IMF clock angle are seen in most of the dipole tilt cases. However, the D_{st}^{*} index shows neither a peak at 180˚ of the IMF clock angle nor particular dipole tilt dependence in case of negative dipole tilt angles. This result suggests that low- and middle latitude geomagnetic activity (ring current development) does not necessarily show dipole tilt dependence and a one-to-one correlation with solar wind energy input rate to ring current (dD_{st}^{*}/dt).

Keywords: Geomagnetic activity (Dst*), Solar wind energy input rate to ring current (dDst*/dt), Semiannual variation , Dipole tilt effect, Interplanetary magnetic field and clock angel, Magnetic reconnection

©2019. Japan Geoscience Union. All Right Reserved.

A New Prediction Model for Solar Wind-Triggered Magnetospheric Disturbances Based on Potential Learning (Neural Network)

*Ryozo Kitajima[1], Motoharu Nowada[2], Ryotaro Kamimura[3]

1. Seikei University, 2. Shandong University at Weihai, 3. Tokai University

Nowadays, it becomes so important in saving our economic activity, and preventing the disasters caused by terrestrial electromagnetic effects to predict a scale and the duration of the geomagnetic disturbances based on in-situ solar wind observations. Recently, one of the notable techniques for the predictions of the magnetospheric disturbances is Neural Network (NN). However, most of these studies are focused on the reproduction of the behaviors of the index values, which represent the geomagnetic disturbances (e.g, D_{st} and AE), by inputting the solar wind parameters measured by the satellites. In our study, we apply a novel neural network model of ‘Potential Learning (PL)’.
Basically, Neural Networks (NNs) are models which imitate the information processing in the nervous system of brain. The nerve is made of cells as referred to as “neurons”, which specializes the information processing. NNs consist of “artificial” neurons, and can process information by learning. Therefore, using NNs, we can obtain some characteristics of the data inputted. The PL is a new kind of the NNs. A feature of the PL is to make a network that can understand the input variables based on learning by “input potentialities”, which are indices as calculated with the variances derived from the input variables. If using this PL, we can specify what input variable(s) is (are) potentially important and influential for a phenomenon.
In this study, introducing the PL technique, we try to specify which solar wind parameter plays an essential role in causing the geomagnetic disturbances. Although the conventional PL, where we used, had automatically selected the variables of interest, we develop a “improved” PL in this study so that the variables can manually be selected. We benchmark this new algorithm using the 4 polar magnetic storm cases occurred under the southward Interplanetary Magnetic Field (IMF)-B_z conditions, and advisedly set the maximum potentiality for the IMF-B_z, so that the IMF-B_z component is the most possible solar wind parameter to cause the geomagnetic disturbances. We note “second” solar wind parameter(s) to possibly cause the magnetospheric disturbances, following the IMF-B_z component. After testing our new technique to actual storm events, we might distinguish the magnetospheric disturbances into two different types, that is, the geomagnetic disturbances driven by “IMF-dominant” and “combination of IMF with solar wind plasma (dynamic pressure)”. The advantages to adopt this new algorithm to space weather, and more detailed results will be discussed in this presentation.

Keywords: Predictions of Geomagnetic Activity, Neural Network Considered Potential Learning, Development of Space Weather

©2019. Japan Geoscience Union. All Right Reserved.

Real-time magnetosphere simulator for space weather using REProduce Plasma Universe code

*Yasubumi Kubota[1], Aoi Nakamizo[1], Kaori Sakaguchi[1], Mitsue Den[1], Yuki Kubo[1], Tsutomu Nagatsuma[1], Takashi Tanaka[1,2]

1. National Institute of Information and Communications Technology, 2. Kyushu University

Surface charging of artificial satellite is one of risks caused by dynamical variations of space environment. It occurs when a satellite exposes high energy electrons around 10 keV created by plasma injection accompanied with substorm. Therefore we want to predict timing and electron energy of plasma injection using magnetosphere-ionosphere coupling global MHD simulation. Now we are developing a real-time numerical simulator for space weather forecast using magnetosphere-ionosphere coupling global MHD simulation called REPPU (REProduce Plasma Universe) code. The feature of the simulation code is highly robust to extreme solar wind parameters because the unstructured grid system has no singular point and is able to calculate in the uniform accuracy over the whole region. We use the real-time solar wind data formatted in the GSM coordinate system observed by DSCOVR spacecraft. Magnetic-dipole axis is fixed to z-direction in our simulation. Therefore daily variation of magnetic-dipole axis is not reproduced. Instead, we convert the input direction of the solar wind velocity and magnetic field into that which tilts including daily variation of magnetic dipole axis in x-z plane. In the method the solar wind structure is not exact. However we can relatively reproduce the magnetosphere response including daily variation of the magnetic-dipole axis against solar wind. The resolution is 7682 grids in the horizontal direction and 240 grids in the radial direction.
In this presentation, we compare the simulation results with the CPCP, AE index, and plasma variations observed by geostationary orbit satellites. Density and temperature of plasma injection derived from MHD simulation tends to estimate larger and smaller values than observation respectively because the MHD simulation does not include kinetic heating effects. We have to interpret MHD simulation results for prediction of electron density and temperature. We will discuss how to interpret electron density and temperature between observation and MHD simulation.

Keywords: global MHD simulation, surface charging

©2019. Japan Geoscience Union. All Right Reserved.

Simulation of GIC flowing through the power transmission network (187 kV-500 kV) in Japan

*Nishida Yuichiro[1,6], Yusuke Ebihara[1], Satoko Nakamura[1], Shinichi Watari[2], Kumiko Hashimoto[3], Kentaro Kitamura[4], Takashi Kikuchi[5]

1. Kyoto University Reserch Institute for Sustainable Humanosphere, 2. National Institute of Information and Communications Technology, 3. Kibi International University, 4. National Insutitute of Technology, Tokuyama College, 5. Nagoya University, 6. Kyoto University Department of Electrical Engineering

The energy released from the sun can enhance electric currents in Earth’ s magnetosphere, which induces an electric field on the ground surface. This electric field, called a geomagnetically induced electric field (GIE), gives rise to geomagnetically induced current (GIC) flowing in a transmission line. Japan is situated at geomagnetically low latitudes, but the potential risk is probably non-zero because a large-amplitude of GIC, as high as 129 A, was recorded in the Japanese power grid during the Halloween storm in October 2003. To evaluate the potential risk of the Japanese power grid properly, we modeled the Japanese power grid with high voltage class over 187 kV on the basis of publicly available data. The model consists of 602 nodes and 763 paths. The uniform GIE imposed on Japan was estimated on the basis of the geoelectric field observed in April 2018 at Kakioka Magnetic Observatory. We applied the uniform GIE on the model. The calculated GIC is roughly in agreement with that measured at 4 substations in Japan. For the westmost substation, a disagreement was found when we considered only the highest class of the power grid (500 kV), which may imply that the lower voltage class of the grid (<500 kV) may have some contribution to the GIC in Japan. We discuss the general tendency of the GIC flowing in the Japanese power grid, and prediction capability of the currently available model.

©2019. Japan Geoscience Union. All Right Reserved.

Simulation of GIC flowing through the power transmission network (187 kV-500 kV) in Japan

Yuichiro Nishida
Yusuke Ebihara
Satoko Nakamura
Shin-Ichi Watari
Kumiko Hashimoto
Kentaro Kitamura
Takashi Kikuchi

Abstract

The energy released from the sun can enhance electric currents in Earth's magnetosphere, which induces an electric field on the ground surface. This electric field, called a geomagnetically induced electric field (GIE), gives rise to geomagnetically induced current (GIC) flowing in a transmission line. Japan is situated at geomagnetically low latitudes, but the potential risk is probably non-zero because a large-amplitude of GIC, as high as 129 A, was recorded in the Japanese power grid during the Halloween storm in October 2003. To evaluate the potential risk of the Japanese power grid properly, we modeled the Japanese power grid with high voltage class over 187 kV on the basis of publicly available data. The model consists of 602 nodes and 763 paths. The uniform GIE imposed on Japan was estimated on the basis of the geoelectric field observed in April 2018 at Kakioka Magnetic Observatory. We applied the uniform GIE on the model. The calculated GIC is roughly in agreement with that measured at 4 substations in Japan. For the westmost substation, a disagreement was found when we considered only the highest class of the power grid (500 kV), which may imply that the lower voltage class of the grid (<500 kV) may have some contribution to the GIC in Japan. We discuss the general tendency of the GIC flowing in the Japanese power grid, and prediction capability of the currently available model.

©2019. Japan Geoscience Union. All Right Reserved.

Climatological features of the upper atmosphere reproduced by a revised version of a whole atmosphere-ionosphere coupled model GAIA

*Hidekatsu Jin[1], Yasunobu Miyoshi[2], Chihiro Tao[1], Hiroyuki Shinagawa[1], Hitoshi Fujiwara[3]

1. National Institude of Information and Communications Technology, 2. Kyushu University, 3. Seikei University

Temporal and spatial variations in the ionospheric electron density and thermospheric mass density could have significant impacts on radio communications between ground and space, and particle and atmospheric drag environments around satellites. Origins of such upper atmospheric variations are not only in the solar atmosphere through the emissions of solar radiation, high-speed plasma gas and high-energy particles, but also in the Earth’ s lower atmosphere, where meteorological phenomena could give rise to atmospheric waves propagating upward. In order to nowcast and forecast the upper atmospheric variations and disturbances, a whole atmospheric model, GAIA, has been developed, which combines a whole atmospheric GCM, an ionospheric model and an electrodynamics model in a self-consistent manner.

So far, for the purpose of its validation, we have compared climatological features of thermosphere and ionosphere reproduced by GAIA with those from ionospheric observation and observation-based empirical models. The comparison indicates that the model and observations are generally in good agreements, but in some condition such as at solar maximum there are significant disagreements in the ionospheric electron density distribution. In order to improve the accuracy of the model, we have made several updates such as ion chemical processes, energetics, parameterization, and so on. We also have introduced magnetospheric effects into the model, such as electrodynamics coupling with magnetosphere and particle precipitation. In this presentation, we discuss how the upper atmospheric model can improve its accuracy and how they can be validated.

Keywords: space weather, whole atmosphere, ionosphere, simulation, thermosphere, assimilation

©2019. Japan Geoscience Union. All Right Reserved.

Investigation of the thermospheric mass density variations below 200 km

*Hitoshi Fujiwara[1], Yasunobu Miyoshi[2], Masayoshi Utashima[1], Huixin Liu[2]

1. Faculty of Science and Technology, Seikei University, 2. Department of Earth and Planetary Sciences, Faculty of Sciences, Kyushu University

Since both the effects from the lower atmosphere and in-situ forcing are significant in the thermospheric region between 100 and 200 km altitude, the thermosphere in the region shows complex variations depending on various conditions. In addition, observations of the thermosphere (neutral atmosphere) between 100 and 200 km are very few compared to the upper thermosphere (above 300 km) and the ionosphere. These make it difficult to improve reliability of empirical and numerical models. Observations from Low Earth Orbit (LOE) satellites would be essential for building up available data sets in the thermospheric region between 100 and 200 km altitude. We will introduce our research project to investigate the thermospheric mass density variations in the 100-200 km altitude region with the LOE satellite, e.g., Tsubame (SLATS), data and a whole atmosphere GCM.

Keywords: thermosphere, mass density, Low Earth Orbit (LOE) satellite, GCM

©2019. Japan Geoscience Union. All Right Reserved.

Low-latitude HF Doppler observations of magnetospheric electric fields during space weather disturbances

*Kumiko K. Hashimoto[1], Takashi Kikuchi[2], Ichiro Tomizawa[3], Keisuke Hosokawa[3], Jaroslav Chum[4]

1. Kibi International University, 2. Nagoya University, 3. University of Electro-Commnunications, 4. Institute of Atmospheric Physics, Prague

Ionospheric electric fields penetrated from the magnetosphere to the low latitude ionosphere have been observed as geomagnetic disturbances caused by ionospheric currents, such as the equatorial electrojet (EEJ) at the dayside equator. The ionospheric currents are too weak to be a detector of the electric field at low latitudes on the dayside and even at the equator on the nightside. The HF Doppler (HFD) sounder is another powerful tool for observations of the electric filed at low latitudes on both the day- and night-sides. We have shown that the electric fields of the geomagnetic sudden commencements (SC) are composed of the preliminary impulse followed by the main impulse, of which directions are opposite to each other and both electric fields are opposite on the day- to night-sides (Kikuchi et al. 2016 JGR). We have also shown that the substorm electric fields are composed of the growth phase followed by expansion phase overshielding electric fields, of which directions are opposite to each other (Hashimoto et al., 2017). In this paper, we show that the HFD sounder is capable of detecting stormtime electric fields and that the electric fields are found to decay rather rapidly over one hour during the main phase with the time scale of a few hours. Combining with the equatorial magnetometer data, we would be able to estimate the decaying rate of the HFD electric fields, which helps obtain the stormtime electric fields quantitatively from the HFD data. We discuss advantages of widely separated HFD sounder operations and cooperations with SuperDARN as well as with magnetometer networks.

Keywords: HF Doppler observation, ionosphere electric field, magnetospheric electric field, geomagnetic storm, equatorial electrojet

©2019. Japan Geoscience Union. All Right Reserved.

Stratospheric ionization during magnetic storms

*Ryuho Kataoka[1]

1. National Institute of Polar Research

Transient mesospheric ionization was detected at an altitude of 65-70 km during the auroral breakup that occurred from 2220 to 2226 UT on June 30, 2017. During this event, the footprint of the Arase satellite was located within the field of view of the all-sky imagers at Syowa Station in the Antarctic. Auroral observations at Syowa Station revealed the dominant precipitation of relatively soft electrons during the auroral breakup. A corresponding spike in cosmic noise absorption was also observed at Syowa Station, while the Arase satellite observed a flux enhancement of >100 keV electrons and a broadband noise without detecting chorus waves or electromagnetic ion cyclotron waves. A general-purpose Monte Carlo particle transport simulation code was used to quantitatively evaluate the ionization in the middle atmosphere. Results of this study indicate that the precipitation of energetic electrons of >100 keV, rather than X-rays from the auroral electrons, played a dominant role in the transient and deep (65-70 km) mesospheric ionization during the observed auroral breakup. Based on the above results of Kataoka et al. (2019), we further discuss a possible role of X-rays to ionize the stratosphere during magnetic storms.

Reference:
Kataoka et al. (2019), Earth, Planets and Space, 71, 9, https://doi.org/10.1186/s40623-019-0989-7

©2019. Japan Geoscience Union. All Right Reserved.

Calculating propagation time of HF radio wave using ray-tracing method and simple comparison with the observation.

*Ryo Nakao[1], Hiroyuki Nakata[1], Hiroyo Ohya[1], Toshiaki Takano[1], Kornyanat Hozumi[2], Takuya Tsugawa[2], Susumu Saito[3], Mamoru Ishii[2]

1. Graduate School of Engineering, Chiba University, 2. National Institute of imformation and Communications Technology, 3. Electronic Navigation Research Institute

To provide the information of nowcast of radio propagation, we have started a project, HF-START (HF simulator Targeting for All user's Regional Telecommunications). In this project, a simulator that is able to predict propagation of HF radio waves is constructed by ray-tracing calculation.
Using this simulator, we have examined whether HF radio wave travels between any two points. In this calculation, the electron density, which is necessary to calculate reflection index is determined by International Reference Ionosphere (IRI).In this project, HF receivers have been installed at Chiba University (Chiba, 35.62N, 140.10E), Sarobetu (Hokkaido, 45.16N, 141.74E), Numata (Gunma, 36.62N, 139.02E), Yamagawa (Kagoshima, 31.20N, 130.61), Ogimi (Okinawa, 26.68, 128.15E) for observing HF radio wave transmitted from radioNIKKEI (Nagara, Chiba, 35.46N, 140.20E) to confirm the results of the ray-tracing calculation. In the ray-tracing calculation, therefore, we set the same locations of the transmitter and receivers as the observatories of HF-START. As a result of simple comparison between the ray-tracing results and the observation, it is found that there was a difference of the propagation time between the ray-tracing results and the observations. It is possible that the radio wave propagation between radioNIKKEI and Ciba University is not ground wave but sky wave that is reflected by ionosphere. As for further calculation, we plan to use the electron density distributions determined by GAIA and GNSS tomography in the ray-tracing calculation.

©2019. Japan Geoscience Union. All Right Reserved.

Why do some probabilistic forecasts lack reliability?

*Yuki Kubo[1]

1. National Institute of Information and Communications Technology

One of the important attributes to be satisfied for the probabilistic forecast system is reliability. However, some probabilistic forecast systems lack reliability. Why do some probabilistic forecasts lack reliability? We investigate a condition for a probabilistic binary forecast to be reliable in this work. We mathematically prove that a necessary, but not sufficient, condition for achieving a reliable probabilistic forecast is maximizing the Peirce skill score (PSS) at the threshold probability of the climatological base rate. The condition is confirmed by using artificially synthesized forecast-outcome pair data and previously published probabilistic solar flare forecast models. The condition gives a partial answer as to why some probabilistic forecast systems lack reliability, because the system, which does not satisfy the proved condition, can never be reliable. The result implies that those who want to develop a reliable probabilistic forecast system must adjust or train the system so as to maximize PSS near the threshold probability of the climatological base rate.

Keywords: Probabilistic forecast, Reliability

©2019. Japan Geoscience Union. All Right Reserved.

An estimation method of GEO spacecraft surface charging for a real-time spacecraft risk assessment

*Masao Nakamura[1], Ryota Kawachi[1], Go Takahashi[1], Tsutomu Nagatsuma[2], Mamoru Ishii[2]

1. Osaka Prefecture University, 2. NICT

Spacecraft anomalies are often induced by electrostatic discharges due to surface charging. Some spacecraft charging simulation software is developed by space agencies and research institutes and used for spacecraft designs and charging analysis. However these simulations cannot be used for a real-time estimation because they need hours or days to calculate the surface potential for a given plasma environment. Therefore we develop a quick estimation method of GEO spacecraft surface charging for the Space Environment Customized Risk Estimation for Spacecraft (SECURES) of the space weather forecast Project for Solar-Terrestrial Environment Prediction (PSTEP). We estimate the surface potentials by interpolation using lookup tables of the pre-simulated surface potentials for combinations of plasma temperatures and densities. We study fitting functions used in the interpolation and how to make the lookup tables for the good estimation. Then we can real-time estimate the surface potentials of the target GEO spacecraft when the on-orbit plasma environment is predicted or observed. The spacecraft risk assessment can be accomplished by additional information about the experimental discharging differential potential of the surface materials.

Keywords: Spacecraft surface charging, Space weather, Spacecraft risk assessment

©2019. Japan Geoscience Union. All Right Reserved.

A network of HF Doppler sounding systems in Japan

*Keisuke Hosokawa[1], Hiroyuki Nakata[2], Kumiko K. Hashimoto[3], Ichiro Tomizawa[1], Jun Sakai[1], Takashi Kikuchi[4]

1. University of Electro-Communications, 2. Chiba University, 3. Kibi International University, 4. ISEE, Nagoya University

Since 2003, a network observation of HF Doppler sounding has been conducted in Japan for remote-sensing the atmospheric, ionospheric and magnetospheric processes. Currently, 1 transmitting station (Tx) and 7 receiving stations (Rx) are operative by a collaborative effort of four difference universities. The main transmitting station is located at Chofu, Tokyo, Japan in the Campus of University of Electro-Communications (JG2XA). JG2XA transmits continuous waves at 5006 kHz and 8006 kHz with a transmitting power of 200 W. By receiving this JG2XA signal at 7 Rx stations (Sugadaira, Oarai, Kure, Kashima, Iitate, Fujisawa and Sugito) we derive the Doppler shift imposed during the propagation and reflection in the ionosphere. In particular, the Doppler shift data can be used to detect vertical motion of the ionospheric F region with a temporal resolution of 10 s. At some stations, we also have observed signals from Radio Nikkei 1 (JOZ at 3925 kHz, JOZ2 at 6055 kHz, and JOZ3 at 9595 kHz) transmitted from Nagara, Chiba, Japan, which allows us to observe the vertical motion of the ionosphere at several altitude levels. The data obtained from this experiment since 2003 are all available at http://gwave.cei.uec.ac.jp/~hfd. Not only quick-look plots but also several types of digital data (raw wave form and Doppler shift data) can be retrieved from this database. The experiment covers various ionospheric phenomena in the Magnetosphere-Ionospheric (M-I) coupling system, such as sporadic E-layer (Es), medium-scale traveling ionospheric disturbances (MSTIDs), large-scale traveling ionospheric disturbances (LSTIDs), global-scale electric field variation, geomagnetic pulsations, and sudden commencement (SC). The data can also be used for the studies of vertical coupling between the lower atmosphere and ionosphere, for example, observations of ionospheric variation after large earthquakes, volcanic eruptions and typhoons. To facilitate analyses of the phenomena listed above, it is desired to observe a wider area in latitude and longitude. For this purpose we plan to extend the network covering the entire ionosphere over Japan in the near future. In the presentation, we will give a brief introduction to the experiments and online database, and then discuss the future direction of the studies of atmosphere, ionosphere and magnetosphere using the HF Doppler sounding in a framework of international collaborations.

Keywords: HF Doppler experiment, Ionosphere

©2019. Japan Geoscience Union. All Right Reserved.

[E] Oral | P (Space and Planetary Sciences)：P-EM Solar-Terrestrial Sciences, Space Electromagnetism & Space Environment

Tue. May 28, 2019 1:45 PM - 3:15 PM JST | Tue. May 28, 2019 4:45 AM - 6:15 AM UTC | A04 TOKYO BAY MAKUHARI HALL

[P-EM13] Inner magnetosphere: Recent understanding and new insights

convener:Yusuke Ebihara(Research Institute for Sustainable Humanosphere, Kyoto University), Danny Summers(Memorial University of Newfoundland), Yoshizumi Miyoshi(Institute for Space-Earth Environmental Research, Nagoya University), Shinji Saito(Graduate School of Science, Nagoya University), Chairperson:Danny Summers, Yoshizumi Miyoshi(ISEE, Nagoya University)

The inner magnetosphere is characterized by the dominance of intrinsic dipolar Earth's magnetic field. The dipolar magnetic field traps charged particles, resulting in the formation of unique particle environment known as the plasmasphere, the ring current, and the radiation belt. The inner magnetosphere is always changing because of incoming energy from the outer magnetosphere and the ionosphere in the forms of particles and electromagnetic fields. In the inner magnetosphere, the particle energy is transferred to the field energy, and vice versa. The mutual coupling between particles and fields also makes the inner magnetosphere unique. The outgoing energy to these regions is also known to be significant, such as precipitation into the upper atmosphere and sub-auroral disturbances. A number of satellites (e.g., DMSP, NOAA, Geotail, Cluster, THEMIS, Van Allen Probes, MMS, and Arase), ground-based instruments (e.g., SuperDARN and EISCAT radars, magnetometers, and cameras), and numerical simulations (e.g., global particle simulation, PIC simulation, and hybrid simulation) have successfully surveyed the inner magnetosphere, which deepen our knowledge significantly. USAF DSX, UCLA Elfin and NASA CeRES will be launched soon, being expected to provide important information. We solicit papers describing recent results on the inner magnetosphere and/or its coupling with the other regions, including the ionosphere and the outer magnetosphere.

1:45 PM - 2:05 PM JST | 4:45 AM - 5:05 AM UTC

[PEM13-01] Developing an improved understanding of Earth’s outer radiation belt electrons with combined observations from Van Allen Probes, MMS, and Arase

★Invited Papers

*Drew L Turner[1], Ian Cohen[2], Alexander Boyd[1,3], Joseph Fennell[1], Geoff Reeves[3], Yoshizumi Miyoshi[4] (1.Aerospace Corporation El Segundo, 2.Johns Hopkins University Applied Physics Lab, 3.Los Alamos National Laboratory, 4.Nagoya University)

2:05 PM - 2:25 PM JST | 5:05 AM - 5:25 AM UTC

[PEM13-02] Recent results from Van Allen Probes and future prospects from the CeREs Cubesat

★Invited Papers

*Shrikanth G Kanekal[1], Daniel N Baker[2], Ashley Greeley[1], Lauren Blum[1], Quintin Schiller[1], David G Sibeck[1], Hong Zhao[2], Xinlin Li[2], Allison Jaynes[3] (1.NASA Goddard Space Flight Center, 2.LASP, University of Colorado, Boulder, 3.Univeristy of Iowa)

2:25 PM - 2:40 PM JST | 5:25 AM - 5:40 AM UTC

[PEM13-03] Optimal Use of Time Lags Between MMS Spacecraft : Application to the Estimation of Wave-Vectors

*Gerard Marcel CHANTEUR[1,2,3], Drew L. Turner, Olivier Le Contel[1,2,3], Alessandro Retino[1,2,3], Laurent Mirioni[1,2,3] (1.CNRS, 2.SORBONNE UNIVERSITE, 3.ECOLE POLYTECHNIQUE)

2:40 PM - 2:55 PM JST | 5:40 AM - 5:55 AM UTC

[PEM13-04] Conjugate observation of EMIC waves by Arase and RBSP with associated POES and AARDDVARK detected electron precipitation

*Aaron T. Hendry[1], Ondrej Santolik[1,2], Yoshizumi Miyoshi[3], Yoshiya Kasahara[4], Yasumasa Kasaba[5], Ayako Matsuoka[6], Craig J Rodger[7], Mark Clilverd[8], Masafumi Shoji[3], Shoya Matsuda[6], Craig Kletzing[9], Iku Shinohara[6] (1.Dept. of Space Physics, Inst. of Atmospheric Physics, Czech Acad. of Science, 2.Fac. of Mathematics and Physics, Charles Univ., 3.Inst. for Space Earth Environmental Research, Nagoya Univ.,

4.Graduate School of Natural Science and Technology, Kanazawa Univ., 5.Planetary Plasma and Atmospheric Research Center, Tohoku Univ., 6.Inst. of Space and Astronautical Science, Japan Aerospace Exploration Agency, 7.Dept. of Physics, Univ. of Otago, 8.British Antarctic Survey (NERC), 9.Dept. of Physics and Astronomy, Univ. of Iowa)

2:55 PM - 3:10 PM JST | 5:55 AM - 6:10 AM UTC

[PEM13-05] Over-darkening pulsating aurora: simultaneous observations with Arase and an all-sky camera in Scandinavia

*Keisuke Hosokawa[1], Yoshizumi Miyoshi[2], Shin-ichiro Oyama[2], Yasunobu Ogawa[3], Satoshi Kurita[2], Yoshiya Kasahara[4], Mitsunori Ozaki[4], Yasumasa Kasaba[5], Satoshi Yagitani[4], Shoya Matsuda[6], Fuminori Tsuchiya[5], Atsushi Kumamoto[5], Iku Shinohara[6], Ryoichi Fujii[7] (1.Department of Communication Engineering and Informatics, University of Electro-Communications, 2.ISEE, Nagoya University, 3.National Institute of Polar Research, 4.Kanazawa University, 5.Tohoku University, 6.ISAS/JAXA, 7.Research Organization of Information and Systems)

3:10 PM - 3:15 PM JST | 6:10 AM - 6:15 AM UTC

Discussion

Developing an improved understanding of Earth's outer radiation belt electrons with combined observations from Van Allen Probes, MMS, and Arase

*Drew L Turner[1], Ian Cohen[2], Alexander Boyd[1,3], Joseph Fennell[1], Geoff Reeves[3], Yoshizumi Miyoshi[4]

1. Aerospace Corporation El Segundo, 2. Johns Hopkins University Applied Physics Lab, 3. Los Alamos National Laboratory, 4. Nagoya University

In this presentation, we focus on two aspects of Earth's outer radiation belt electrons: acceleration due to interactions with whistler-mode chorus waves and losses due to magnetopause incursions and outward radial transport. Using a combination of energetic electron intensities and wave data from NASA's Van Allen Probes and MMS missions plus JAXA's Arase (ERG) mission, we evaluate evidence of local acceleration and losses to outward radial transport based on phase space density and multipoint wave analysis. A telltale sign of local acceleration due to interactions between 100s of keV electrons and chorus waves within the heart of the outer radiation belt is a growing peak in electron phase space density for those energies and pitch angles affected by the acceleration. Sometimes that peak in phase space density might occur beyond the apogee of the Van Allen Probes orbit, but MMS and Arase data can be used to disambiguate dominant acceleration processes for such cases. Losses to the magnetopause and from outward radial transport also result in distinct features in the time history of radial distributions of electron phase space density. Again, with their apogees extending to higher L-shells (including into the magnetosheath for MMS), MMS and Arase can supplement the Van Allen Probes dataset by directly observing evidence of these processes beyond Van Allen Probes apogee. In this presentation, we showcase several examples of these processes using multipoint data from these missions.

Keywords: Radiation belts, Relativistic electrons, Wave-particle interactions

©2019. Japan Geoscience Union. All Right Reserved.

Recent results from Van Allen Probes and future prospects from the CeREs Cubesat

*Shrikanth G Kanekal[1], Daniel N Baker[2], Ashley Greeley[1], Lauren Blum[1], Quintin Schiller[1], David G Sibeck[1], Hong Zhao[2], Xinlin Li[2], Allison Jaynes[3]

1. NASA Goddard Space Flight Center, 2. LASP, University of Colorado, Boulder, 3. Univeristy of Iowa

The Van Allen Probes mission, since its launch in August 2012 has advanced our understanding of fundamental questions regarding the acceleration and loss of outer Van Allen belt electron populations. Electron dynamics in the outer radiation belt are driven by a number of physical processes, which affect low energy cold plasma to relativistic and ultra-relativistic particle populations. I will present recent results from Van Allen Probes mission focusing on the energetic electron dynamics. I will also discuss the significant role of CubeSats that may lead to a paradigm shift in the way space-based observations are carried out, e.g., by enabling multipoint observations. I am currently leading a CubeSat mission, CeREs, the Compact Radiation belt Explorer, CeREs that was launched December 2018 and is currently in the commissioning phase. CeREs will provide high quality measurements of radiation belt electrons, especially microbursts.

Keywords: Radiation belts, CubeSat, energetic electrons

©2019. Japan Geoscience Union. All Right Reserved.

Optimal Use of Time Lags Between MMS Spacecraft : Application to the Estimation of Wave-Vectors

*Gerard Marcel CHANTEUR[1,2,3], Drew L. Turner, Olivier Le Contel[1,2,3], Alessandro Retino[1,2,3], Laurent Mirioni[1,2,3]

1. CNRS, 2. SORBONNE UNIVERSITE, 3. ECOLE POLYTECHNIQUE

Turner et al. (2017) made use of cross-correlations of SCM quasi monochromatic data between pairs of MMS spacecraft to estimate phase lags and to derive wave vectors of whistler mode chorus elements in the inner magnetosphere. A new approach has been developped to revisite this study. For a cluster of four spacecraft there are six pairs of spacecraft, each one giving raise to a scalar equation relating the vector position **R** from the first to the second spacecraft, the wave vector **K** and the phase lag $\Delta\phi$: **R.K**=$\Delta\phi$. A positive weight is attributed to each equation (w_j, j=1 to 6). A statistical ensemble of 6-uplets is built and we look for the 6-uplet giving the lowest condition number of matrix **M**. This procedure warrants the best accuracy of the pseudo-inverse of **M** and hence the best estimate of the wave vector **K**. Adding random perturbations to M and $\Delta\phi$ the procedure allows to estimate the uncertainties on **K.**

Turner, D. L. et al. JGR Space Physics, https://doi.org/10.1002/2017JA024474

Keywords: multi-spacecraft missions, MMS, field analysis, wave vectors, phase shifts

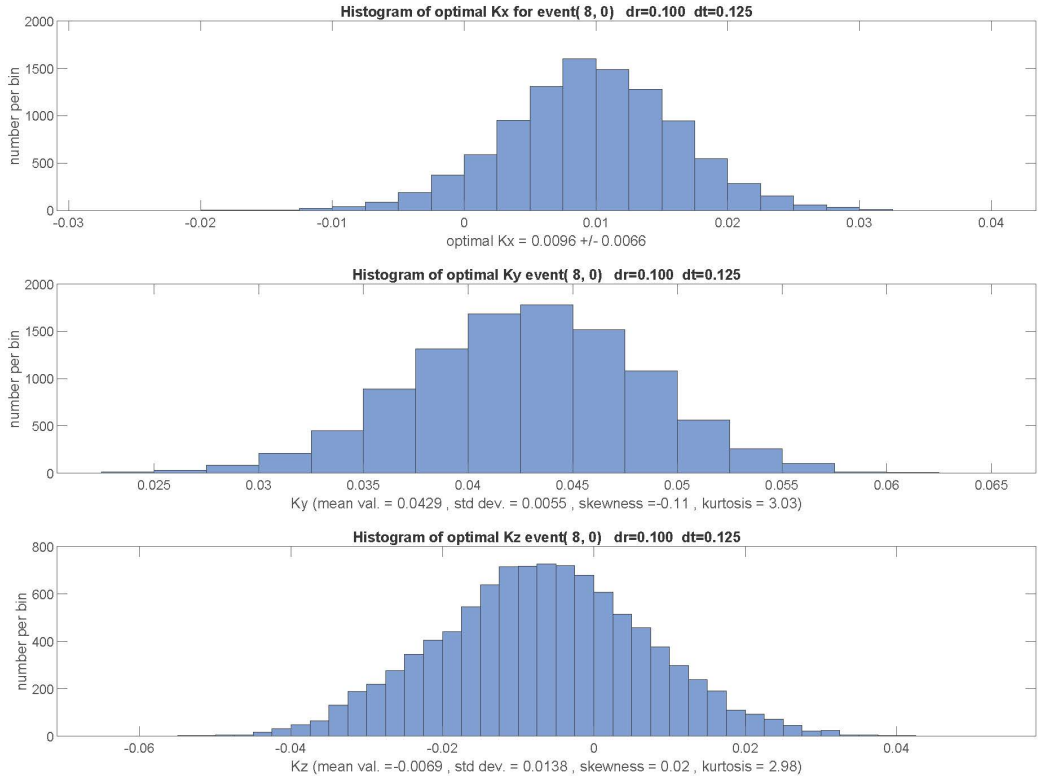

©2019. Japan Geoscience Union. All Right Reserved.

Conjugate observation of EMIC waves by Arase and RBSP with associated POES and AARDDVARK detected electron precipitation

*Aaron T. Hendry[1], Ondrej Santolik[1,2], Yoshizumi Miyoshi[3], Yoshiya Kasahara[4], Yasumasa Kasaba[5], Ayako Matsuoka[6], Craig J Rodger[7], Mark Clilverd[8], Masafumi Shoji[3], Shoya Matsuda[6], Craig Kletzing[9], Iku Shinohara[6]

1. Dept. of Space Physics, Inst. of Atmospheric Physics, Czech Acad. of Science, 2. Fac. of Mathematics and Physics, Charles Univ., 3. Inst. for Space Earth Environmental Research, Nagoya Univ., 4. Graduate School of Natural Science and Technology, Kanazawa Univ., 5. Planetary Plasma and Atmospheric Research Center, Tohoku Univ., 6. Inst. of Space and Astronautical Science, Japan Aerospace Exploration Agency, 7. Dept. of Physics, Univ. of Otago, 8. British Antarctic Survey (NERC), 9. Dept. of Physics and Astronomy, Univ. of Iowa

We present a remarkable case study of strong EMIC wave emissions observed simultaneously by instruments on board the ARASE and RBSP-B satellites, as well as by ground-based observatories, during a period of significant geomagnetic activity. These waves coincided with strong substorm activity (AE>1000 nT) during a southward IMF Bz shift, corresponding to the initial phase of an intense geomagnetic storm (peak Dst < -170 nT). At the time of this observation, the ARASE and RBSP-B satellites were co-located in L and MLT, showing simultaneous observation of the same wave emission, but were significantly separated in magnetic latitude. This separation allows us to examine the evolution of the wave parameters as the wave propagates down the field-line to the Earth.

During this period of wave activity, we also see evidence of energetic electron precipitation into the ionosphere. At the time of the RBSP and ARASE observations, the POES METOP-02 satellite passed through the footprint of the source region and observed bursts of energetic ion and electron precipitation into the ionosphere, matching known signatures of EMIC-driven particle precipitation. This precipitation was then in turn observed from the ground as AARDDVARK-detected sub-ionospheric VLF perturbations. Through analysis of these ground-based observations, we are able to estimate the extent of the EMIC source region.

Keywords: Arase, Van Allen Probes, EMIC, Wave-particle interactions, AARDDVARK

©2019. Japan Geoscience Union. All Right Reserved.

Over-darkening pulsating aurora: simultaneous observations with Arase and an all-sky camera in Scandinavia

*Keisuke Hosokawa[1], Yoshizumi Miyoshi[2], Shin-ichiro Oyama[2], Yasunobu Ogawa[3], Satoshi Kurita[2], Yoshiya Kasahara[4], Mitsunori Ozaki[4], Yasumasa Kasaba[5], Satoshi Yagitani[4], Shoya Matsuda[6], Fuminori Tsuchiya[5], Atsushi Kumamoto[5], Iku Shinohara[6], Ryoichi Fujii[7]

1. Department of Communication Engineering and Informatics, University of Electro-Communications, 2. ISEE, Nagoya University, 3. National Institute of Polar Research, 4. Kanazawa University, 5. Tohoku University, 6. ISAS/JAXA, 7. Research Organization of Information and Systems

Pulsating aurora (PsA) is one of the major classes of aurora often seen in the lower latitude part of the auroral region in the morning side. PsAs are characterized by quasi-periodic variations in the optical intensity whose period typically ranges from a few to a few tens of second. Coordinated ground/satellite observations in the last decade demonstrated that the main optical pulsation well correlates with the intensity modulation of whistler mode chorus waves in the magnetosphere. Recent analyses of high time resolution ground-based optical observations have reported that the brightness of PsA decreases below the diffuse background immediately after the ON phase of the main pulsation. To date, however, the generation mechanism of such “over-darkening PsA” is still unclarified. In this paper, we investigate the characteristics of the over-darkening PsA by using simultaneous observations of PsA with an EMCCD all-sky camera in Sodankylä, Finland (67°N, 26°E, 64°MLAT) and the Arase satellite. The EMCCD all-sky camera captures auroral emission with a temporal resolution of 100 Hz. We make use of data from the PWE/OFA instrument to analyse the temporal variation of chorus wave as a source of PsA. During one of the conjunction events in Scandinavia on March 29, 2017, almost all the PsA pulses showed clear over-darkening characteristics. By analysing the 2D all-sky images at the times of over-darkening we identified that over-darkening areas appeared in the trailing edge of PsA patches and moved in tandem with the poleward propagating patches. It was also found that similar over-darkening characteristics were not seen in the chorus data from PWE/OFA onboard Arase located at the magnetospheric counterpart of PsA. These results indicate that the over-darkening PsA is not caused by a temporal variation of chorus at a fixed point, but is produced by a propagation of over-darkening area with PsA patches. That is, the over-darkening PsA is a spatial structure rather than a temporal variation. In the presentation, we discuss several possible scenarios that can explain the over-darkening along the edge of PsA patches.

Acknowledgement: The operation of the EMCCD camera at Sodankyläas been supported by Sodankylä Geophysical Observatory (SGO).

Keywords: Pulsating Aurora, Chorus Waves

©2019. Japan Geoscience Union. All Right Reserved.

[E] Oral | P (Space and Planetary Sciences)：P-EM Solar-Terrestrial Sciences, Space Electromagnetism & Space Environment

Tue. May 28, 2019 3:30 PM - 5:00 PM JST | Tue. May 28, 2019 6:30 AM - 8:00 AM UTC | A04 TOKYO BAY MAKUHARI HALL

[P-EM13] Inner magnetosphere: Recent understanding and new insights

convener:Yusuke Ebihara(Research Institute for Sustainable Humanosphere, Kyoto University), Danny Summers(Memorial University of Newfoundland), Yoshizumi Miyoshi(Institute for Space-Earth Environmental Research, Nagoya University), Shinji Saito(Graduate School of Science, Nagoya University), Chairperson:Yoshizumi Miyoshi(ISEE, Nagoya University), Danny Summers

The inner magnetosphere is characterized by the dominance of intrinsic dipolar Earth's magnetic field. The dipolar magnetic field traps charged particles, resulting in the formation of unique particle environment known as the plasmasphere, the ring current, and the radiation belt. The inner magnetosphere is always changing because of incoming energy from the outer magnetosphere and the ionosphere in the forms of particles and electromagnetic fields. In the inner magnetosphere, the particle energy is transferred to the field energy, and vice versa. The mutual coupling between particles and fields also makes the inner magnetosphere unique. The outgoing energy to these regions is also known to be significant, such as precipitation into the upper atmosphere and sub-auroral disturbances. A number of satellites (e.g., DMSP, NOAA, Geotail, Cluster, THEMIS, Van Allen Probes, MMS, and Arase), ground-based instruments (e.g., SuperDARN and EISCAT radars, magnetometers, and cameras), and numerical simulations (e.g., global particle simulation, PIC simulation, and hybrid simulation) have successfully surveyed the inner magnetosphere, which deepen our knowledge significantly. USAF DSX, UCLA Elfin and NASA CeRES will be launched soon, being expected to provide important information. We solicit papers describing recent results on the inner magnetosphere and/or its coupling with the other regions, including the ionosphere and the outer magnetosphere.

3:30 PM - 3:50 PM JST | 6:30 AM - 6:50 AM UTC

[PEM13-06] Deformation of electron pitch angle distributions caused by chorus waves observed by the Arase satellite

★Invited Papers

*Satoshi Kurita[1], Yoshizumi Miyoshi[1], Satoshi Kasahara[2], Shoichiro Yokota[3], Yoshiya Kasahara[4], Shoya Matsuda[5], Ayako Matsuoka[5], Iku Shinohara[5] (1.Institute for Space-Earth Environmental Research, Nagoya University, 2.The University of Tokyo, 3.Graduate School of Science, Osaka University, 4.Information Media Center, Kanazawa University, 5.ISAS/JAXA)

3:50 PM - 4:10 PM JST | 6:50 AM - 7:10 AM UTC

[PEM13-07] Electron scattering by isolated chorus elements observed near the magnetospheric equator

★Invited Papers

*Satoshi Kasahara[1], Yoshizumi Miyoshi[2], Shoichiro Yokota[3], Yoshiya Kasahara[4], Shoya Matsuda[5], Ayako Matsuoka[5], Kunihiro Keika[1], Tomoaki Hori[2], Iku Shinohara[5] (1.The university of Tokyo, 2.Nagoya University, 3.Osaka University, 4.Kanazawa University, 5.Institute of Space and Astronautical Science)

4:10 PM - 4:25 PM JST | 7:10 AM - 7:25 AM UTC

[PEM13-08] Continuous precipitation of low-energy electrons associated with pulsating aurora obtained by the Reimei satellite

*Takeshi Sakanoi[1], Fukizawa Mizuki[1], Yoshizumi Miyoshi[2], Yusuke Ebihara[3], Kazushi Asamura[4], Masafumi Hirahara[2] (1.Planetary Plasma and Atmospheric Research Center, Graduate School of Science, Tohoku University, 2.ISEE, Nagoya University, 3.RISH, Kyoto University, 4.ISAS/JAXA)

4:25 PM - 4:40 PM JST | 7:25 AM - 7:40 AM UTC

[PEM13-09] Origin of energetic electron precipitation with fast fluctuation: Data-driven simulations using the ERG plasma wave observations

*Shinji Saito[1], Yoshizumi Miyoshi[2], Shoya Matsuda[3], Satoshi Kurita[2], Yoshiya Kasahara[4], Atsushi Kumamoto[5], Fuminori Tsuchiya[5], Ayako Matsuoka[3] (1.Graduate School of Science, Nagoya University, 2.ISEE, Nagoya University , 3.ISAS/JAXA, 4.Kanazawa University, 5.Tohoku University)

4:40 PM - 4:55 PM JST | 7:40 AM - 7:55 AM UTC

[PEM13-10] Conjugated quasi-periodic ELF/VLF emissions between the Arase satellite and both Van Allen Probes

*Claudia Martinez Calderon[1,2], Frantisek Nemec[3], Kazuo Shiokawa[2], Yuto Katoh[1], Yoshiya Kasahara[4], Shoya Matsuda[2], Fuminori Tsuchiya[1], Atsushi Kumamoto[1], Mariko Teramoto[2], Ayako Matsuoka[5], Yoshizumi Miyoshi[2], Ondrej Santolik[6,3], George Hospodarksy[7] (1.Dept. Geophys., Grad. Sch. Sci., Tohoku University, 2.Instute for Space-Earth Environmental Research, Nagoya University, 3.Faculty of Mathematics and Physics, Charles University, Prague, Czech Republic, 4.Kanazawa University, 5.Japan Aerospace Exploration Agency, 6.Institute of Atmospheric Physics, Prague, Czech Republic, 7.Department of Physics and Astronomy, University of Iowa, USA)

4:55 PM - 5:00 PM JST | 7:55 AM - 8:00 AM UTC

Discussion

Deformation of electron pitch angle distributions caused by chorus waves observed by the Arase satellite

*Satoshi Kurita[1], Yoshizumi Miyoshi[1], Satoshi Kasahara[2], Shoichiro Yokota[3], Yoshiya Kasahara[4], Shoya Matsuda[5], Ayako Matsuoka[5], Iku Shinohara[5]

1. Institute for Space-Earth Environmental Research, Nagoya University, 2. The University of Tokyo, 3. Graduate School of Science, Osaka University, 4. Information Media Center, Kanazawa University, 5. ISAS/JAXA

We report on deformation of electron pitch angle distributions associated with chorus waves observed by the Arase satellite. The deformation is characterized by flux increase of 17-30 keV electrons in a narrow and oblique pitch angle range and by flux decrease in 7-17 keV electron flux in the smaller pitch angle range than the flux increase. Comparison of change in electron pitch angle distributions with resonant ellipses of the upper band chorus shows that the deformation appears where effective wave-particle interaction is expected in the velocity space, and the flux increase takes place along the resonant ellipse of the upper frequency of the wave. This strongly suggests that the deformation is a consequence of wave-particle interactions between electrons and upper band chorus. The Arase observation demonstrates that the deformation occurs within 30 s, which is faster than expected from the quasi-linear diffusion theory.

Keywords: ERG/Arase satellite, Chorus waves, Acceleration

©2019. Japan Geoscience Union. All Right Reserved.

Electron scattering by isolated chorus elements observed near the magnetospheric equator

*Satoshi Kasahara[1], Yoshizumi Miyoshi[2], Shoichiro Yokota[3], Yoshiya Kasahara[4], Shoya Matsuda[5], Ayako Matsuoka[5], Kunihiro Keika[1], Tomoaki Hori[2], Iku Shinohara[5]

1. The university of Tokyo, 2. Nagoya University, 3. Osaka University, 4. Kanazawa University, 5. Institute of Space and Astronautical Science

Theories have predicted significant pitch angle scattering of electron by chorus waves via cyclotron resonance, resulting in electron precipitation into the atmosphere and consequent auroral illumination. Recent observations of chorus waves at the equator, in conjunction with ground observations, have indicated that even a single chorus element can cause sufficient electron scattering causing auroral flashing. Here we report more direct, in-situ evidence that electrons are indeed scattered into the loss cone up to strong diffusion, by an isolated chorus element. We discuss the scattering rate based on the observed parameters.

Keywords: electron scattering, chorus waves

©2019. Japan Geoscience Union. All Right Reserved.

Continuous precipitation of low-energy electrons associated with pulsating aurora obtained by the Reimei satellite

*Takeshi Sakanoi[1], Fukizawa Mizuki[1], Yoshizumi Miyoshi[2], Yusuke Ebihara[3], Kazushi Asamura[4], Masafumi Hirahara[2]

1. Planetary Plasma and Atmospheric Research Center, Graduate School of Science, Tohoku University, 2. ISEE, Nagoya University, 3. RISH, Kyoto University, 4. ISAS/JAXA

We report the results of event and statistical analyses on continuous precipitation of low-energy electrons associated with pulsating aurora using the data taken by the Reimei satellite. From recent data obtained with a magnetospheric satellite like Arase, it is widely supported that chorus waves interact with plasma sheet electrons that produce diffuse aurora mainly in the post-midnight to morning sectors. In addition, temporal (a few Hz) variation of lower band chorus waves cause modulation of pitch-angle scattering of keV-range electrons that generate pulsating aurora in the ionosphere. On the other hand, such temporal variation is not commonly seen in upper band chorus and electrostatic electron cyclotron harmonic (ECH) waves that expected to interact with lower-energy electrons. However, the characteristics of such low-energy electrons and their relationship to pulsating aurora are not understood.
Reimei is a polar-orbiting sun-synchronous satellite at an altitude of 650 km and obtained simultaneous image and particle data with high-time and spatial resolutions. Thanks to its orbit, Reimei covers wide L-value ranges and measures velocity-dispersed electrons travelling from magnetospheric source region to ionosphere. Miyoshi et al. [2015] showed an event that Reimei observed continuous precipitation of low-energy electrons (mainly in the energy range of hundreds eV) in addition to high energy (more than a few keV) temporal electrons that caused pulsating auroral emission. Here, we investigated the characteristics and generation mechanism of continuous low-energy electron precipitation using all of the electron data (5150 paths) taken by Reimei/ESA from November 2005 to August 2008, and compared the data with simulation results. Event selection criteria are 1) existence of continuous precipitation of low-energy electrons below a few keV range, and 2) high-energy (more than a few keV) electrons that distinguished from the continuous low-energy electrons. We also examined simultaneous auroral image data obtained with Reimei/MAC. Using the criteria, we found 155 events of continuous low-energy electron band. From statistical analysis, the continuous low-energy electron evens occurred in 11 % of total observation paths in the nightside sector, while temporal precipitation of high-energy electrons that produced pulsating aurora appeared in 36 % of total observation paths in the nightside sector. From event analysis for several cases, we found in most cases that energy of continuous low-energy electrons increased from ~200 eV to a few keV as the latitude decreased. However, the electron energy decreased near the lower boundary of plasma sheet. In some cases, multiple electron band structures were seen in the low-latitude region. To understand the characteristics and mechanisms of continuous precipitation of low-energy electrons, we carried out simulations of electron pitch angle scattering with chorus waves and ECH waves, respectively. For the simulation of ECH wave resonance, we calculated wavenumber at ECH wave frequency (e.g., 1.6 fce(cyclotron frequency)) based on the Bernstein mode dispersion relation, and estimated electron energy by the cyclotron resonance equation assuming the electron density with GCPM model and magnetic field with IGRF model. From the comparison between the Reimei data with simulation results, we suggest that latitudinal dependence of low-energy electrons can probably be explained with the chorus wave resonance. The decrease of electron energy near the low-latitude boundary is likely to be caused with decrease of plasma density outside of the plamsapause. On the other hand, we showed the possibility for some cases that low-energy electron precipitations were generated by ECH waves.

©2019. Japan Geoscience Union. All Right Reserved.

Keywords: pulsating aurora, inner magnetosphere, Reimei

©2019. Japan Geoscience Union. All Right Reserved.

Origin of energetic electron precipitation with fast fluctuation: Data-driven simulations using the ERG plasma wave observations

*Shinji Saito[1], Yoshizumi Miyoshi[2], Shoya Matsuda[3], Satoshi Kurita[2], Yoshiya Kasahara[4], Atsushi Kumamoto[5], Fuminori Tsuchiya[5], Ayako Matsuoka[3]

1. Graduate School of Science, Nagoya University, 2. ISEE, Nagoya University , 3. ISAS/JAXA, 4. Kanazawa University, 5. Tohoku University

Bursty precipitation of keV electrons can be a source of pulsating aurora which has quasi-periodic on-off switching of luminosity. On the other hand, relativistic electrons also precipitate into the atmosphere with intermittent and bursty nature, which are observed as relativistic electron microbursts. A common cause of the electron bursty precipitation for the pulsating aurora and for the microbursts is expected to be whistler chorus waves propagating along a field line.
In this study, we demonstrate electron precipitation caused by realistic whistler chorus waves using our newly developed test-particle model, GEMSIS-RBW-II simulation code. Wave form data obtained from ERG satellite are applied to the simulation model as a boundary condition at the magnetic equator. The simulation shows that the whistler chorus waves propagating to high magnetic latitudes along the field line can precipitate electrons with energy from keV to MeV. We found that amplitude modulation of a whistler chorus burst observed by ERG causes over ten Hz modulation of keV electron precipitation. At relativistic energies fluctuation with higher frequencies and bursty/intermittent nature appear in time history of precipitation flux. It suggests that whistler chorus bursts can cause electron precipitation associated with pulsating aurora and relativistic electron microbursts.

Keywords: Pulsating Aurora, Relativistic electron microbursts, Whistler chorus bursts, Data-driven test-particle simulation, ERG

©2019. Japan Geoscience Union. All Right Reserved.

Conjugated quasi-periodic ELF/VLF emissions between the Arase satellite and both Van Allen Probes

*Claudia Martinez Calderon[1,2], Frantisek Nemec[3], Kazuo Shiokawa[2], Yuto Katoh[1], Yoshiya Kasahara[4], Shoya Matsuda[2], Fuminori Tsuchiya[1], Atsushi Kumamoto[1], Mariko Teramoto[2], Ayako Matsuoka[5], Yoshizumi Miyoshi[2], Ondrej Santolik[6,3], George Hospodarksy[7]

1. Dept. Geophys., Grad. Sch. Sci., Tohoku University, 2. Instute for Space-Earth Environmental Research, Nagoya University, 3. Faculty of Mathematics and Physics, Charles University, Prague, Czech Republic, 4. Kanazawa University, 5. Japan Aerospace Exploration Agency, 6. Institute of Atmospheric Physics, Prague, Czech Republic, 7. Department of Physics and Astronomy, University of Iowa, USA

Extremely Low (ELF) and Very Low Frequency (VLF) emissions are naturally occurring magnetospheric plasma waves in the frequencies of 3 Hz to 30 kHz. They play a fundamental role in radiation belt dynamics, accelerating or scattering electrons through wave-particle interactions. We report the first quasi-periodic (QP) emission simultaneously observed by the Arase (ERG) satellite and both Van Allen Probes (RBSP). This is one of few known conjugated satellite events where the waves show very similar spectral and temporal features. The event was observed on November 29, 2018 from approximately 11 to 13:30 UT by both RBSP, while ERG observed it from 12 to 14 UT. Using wave analysis, propagation parameters, and intensities simultaneously measured at several locations we will discuss the approximate location of the source region. We will also discuss the eventual timing differences between QP periodicity at different locations. Some slight variation in the spectral shapes is observed. We will discuss possible relationships with the variations of plasma number density, magnetic field, and energetic electron distribution.

Keywords: conjugated event, VLF, QP, Arase, RBSP, plasma waves

©2019. Japan Geoscience Union. All Right Reserved.

[E] Poster | P (Space and Planetary Sciences)：P-CG Complex & General

Tue. May 28, 2019 10:45 AM - 12:15 PM JST | Tue. May 28, 2019 1:45 AM - 3:15 AM UTC | Poster Hall International Exhibition Hall8, Makuhari Messe_1

[P-CG22] Shock responses of planetary materials elucidated from meteorites and dynamic compression experiments

convener:Toshimori Sekine(Center for High Pressure Science and Technology Advanced Research), Takuo Okuchi(Institute for Planetary Materials, Okayama University)

Impact phenomena had played essential roles in the process of planetary evolution. Recent analytical and experimental developments reveal a new prospective on the effects of shock-compression process for planetary materials. For deeper understanding of such shock effects, it is necessary to evaluate the detailed shock conditions from the observations of naturally-shocked planetary materials, and to compare them with the results on the planetary materials experienced a wide range of known shock conditions. Several metastable phases, that have not been known before, have recently been identified in shocked meteorites. They suggest that the shock state is often not in equilibrium and that it is more complicated process than ever thought. Experimental techniques including laser-driven shock compression and x-ray free electron laser diagnostics have been progressed to successfully simulate a wide range of shock conditions. The recent results indicate that shocked grains are fractured and rotated at relatively low pressures, and that they are subsequently transformed into denser phases or melts, or their mixtures at pressures of a few 100s GPa. Understanding of such shock dynamics requires another prospect, which is qualitatively different from the static high pressure and high temperature consensus. Therefore, it is timely to have an international symposium on dynamics of planetary materials.

[PCG22-P01] discussion

*Takuo Okuchi[1], Toshimori Sekine[2] (1.Institute for Planetary Materials, Okayama University, 2.Center for High Pressure Science and Technology Advanced Research)

[PCG22-P02] Shock-compressed behavior of quartz by XFEL

*Tomoko Sato[1], Yoshinori Tange[2], Yusuke Seto[3], Toshimori Sekine[4,5], Norimasa Ozaki[4], Toyohito Nishikawa[4], Kohei Miyanishi[4], Kensuke Matsuoka[4], Ryosuke Kodama[4], Tadashi Togashi[2], Yuichi Inubushi[2], Toshinori Yabuuchi[6], Makina Yabashi[6] (1.Hiroshima University, 2.Japan Synchrotron Radiation Research Institute, 3.Kobe University, 4.Osaka University, 5.Center for High Pressure Science &Technology Advanced Research, 6.RIKEN)

[PCG22-P04] Laser-shock experiments of dense polymorphs of Mg_2SiO_4: technical developments using synthetic single crystals

*Narangoo Purevjav[1], Takuo Okuchi[1], Norimasa Ozaki[2], Takayoshi Sano[3], Yuhei Umeda[2], Shintaro Morioka[2], Nobuki Kamimura[2] (1.Institute for Planetary Materials, Okayama University, 2.Graduate School of Engineering, Osaka University, 3.Institute of Laser Engineering, Osaka University)

[PCG22-P05] Richtmyer-Meshkov instability in inhomogeneous density materials and its application to planetary science

*Takayoshi Sano[1] (1.Institute of Laser Engineering, Osaka University)

[PCG22-P06] Impact-induced dehydration reactions of Fe- and Al-hydrates as potential storage, carrier and source of water

*Tsubasa Tobase[1], Toshimori Sekine[1], Ginga Kitahara[2], Makoto Tokuda[2], Akira Yoshiasa[2], Makoto Takafuji[2], Tsutomu Mashimo[2], Nobuaki Kawai[2] (1.HPSTAR, 2.Graduate School of Science and Technology, Kumamoto University)

[PCG22-P07] Crystallization of amorphous $MgSiO_3$ by shock compression

*Akane Arasuna[1], Masayuki Okuno[1], Nobuaki Kawai[2] (1.Kanazawa University, 2.Kumamoto University)

[PCG22-P08] First-principle study of the structural and electronic properties of N-doped $MgAl_2O_4$ spinel

*Chi Pui Tang[1], Pak Kin Leong[1], Toshimori Sekine[2,3] (1.State Key Laboratory of Lunar and Planetary Sciences, Macau University of Science and Technology, 2.Center for High Pressure Science and Technology Advanced Research (HPSTAR) Shanghai Laboratory of HPSTAR, Shanghai, P.R. China, 3.Graduate School of Engineering, Osaka University)

[PCG22-P09] Transparency of shock-compressed single crystal diamond

*Kento Katagiri[1], Norimasa Ozaki[1,2], Kohei Miyanishi[2], Yuhei Umeda[1], Shintaro Morioka[1], Takayoshi Sano[2], Ryosuke Kodama[1,2] (1.Osaka University, 2.Institute of Laser Engineering, Osaka Unversity)

[PCG22-P10] Pb-Pb dating of the NWA 7203 angrite and relationship to its shock metamorphism

*Hideyuki Hayashi[1], Takashi Mikouchi[1], Yuji Sano[1], Martin Bizzarro[2] (1.The university of Tokyo, 2.University of Copenhagen)

[PCG22-P11] Shock recovery of high-pressure phase of SiO_2 using high-power laser

*Tadashi Kondo[1], Hiromoto Kengo[1], Tatsuhiro Sakaiya[1], Hidenori Terasaki[1], Keisuke Shigemori[2], Youichiro Hironaka[2] (1.Department of Earth and Space Science, Graduate School of Science Osaka University, 2.Institute of Laser Engineering, Osaka University)

[PCG22-P12] Hugoniot measurement of calcite under meteorite collision condition

*Fukui Keiya[1], Norimasa Ozaki[1,2], Yuhei Umeda[1], Kohei Miyanishi[3], Kento Katagiri[1], Shintaro Morioka[1], Takayoshi Sano[3], Ryosuke Kodama[1,2,3] (1.Graduate School of Engineering,Osaka univ., 2.PPC, Osaka Univ., 3.ILE, Osaka Univ.)

[PCG22-P13] Direct observation of the transformation toughening of tetragonal stabilized zirconia under shock deformation condition by ns time-resolved XRD.

*Sota Takagi[1,2], Kouhei Ichiyanagi[2,3], Nobuaki Kawai[4], Ryo Fukaya[2], Shunsuke Nozawa[2], Atsushi Kyono[1], Nobumasa Funamori[2], Shin-ichi Adachi[2] (1.University of Tsukuba, 2.KEK PF, 3.Jichi Medical University, 4.Kumamoto University)

discussion

*Takuo Okuchi[1], Toshimori Sekine[2]

1. Institute for Planetary Materials, Okayama University, 2. Center for High Pressure Science and Technology Advanced Research

We discuss natural and experimendal evidences on impact phenomena, which had played essential roles in the process of early planetary evolution. Recent analytical and experimenotal developments reveal a new prospective on the effects of shock-compression process of planetary materials. For deeper understanding of such shock effects, it is necessary to evaluate the detailed shock conditions from the observations of naturally-shocked planetary materials, as well as to compare them with the results of shock-compression experiments of these materials obtained at laboratory conditions.

Keywords: discussion

©2019. Japan Geoscience Union. All Right Reserved.

Shock-compressed behavior of quartz by XFEL

*Tomoko Sato[1], Yoshinori Tange[2], Yusuke Seto[3], Toshimori Sekine[4,5], Norimasa Ozaki[4], Toyohito Nishikawa[4], Kohei Miyanishi[4], Kensuke Matsuoka[4], Ryosuke Kodama[4], Tadashi Togashi[2], Yuichi Inubushi[2], Toshinori Yabuuchi[6], Makina Yabashi[6]

1. Hiroshima University, 2. Japan Synchrotron Radiation Research Institute, 3. Kobe University, 4. Osaka University, 5. Center for High Pressure Science &Technology Advanced Research, 6. RIKEN

We have conducted x-ray diffraction measurement (XRD) with femtosecond x-ray pulses generated by the x-ray free electron laser (XFEL) to observe lattice dynamics and phase transformation of single-crystal quartz under high strain-rate shock compression (~10^9 s^{-1}) and high pressure. Single-crystal quartz samples were shock-compressed by high-power short- and long-pulse lasers. In the short-pulse experiments, the lattice was reduced to 15% and 1.5% in the direction parallel and perpendicular to the compression axis, respectively. The sample was uniaxially compressed over its known Hugoniot elastic limit. In the long-pulse experiments, three different states were observed. Polycrystalline stishovite appeared at first, and elastically compressed state and a topotaxially transformed new phase were observed successively.

Keywords: Shock compression, in-situ X-ray diffraction, quartz

©2019. Japan Geoscience Union. All Right Reserved.

Laser-shock experiments of dense polymorphs of Mg_2SiO_4: technical developments using synthetic single crystals

*Narangoo Purevjav[1], Takuo Okuchi[1], Norimasa Ozaki[2], Takayoshi Sano[3], Yuhei Umeda[2], Shintaro Morioka[2], Nobuki Kamimura[2]

1. Institute for Planetary Materials, Okayama University, 2. Graduate School of Engineering, Osaka University, 3. Institute of Laser Engineering, Osaka University

Mg_2SiO_4 polymorphs (α-phase as forsterite, β-phase as wadsleyite, and γ-phase as ringwoodite) are the major constituents of our Earth's mantle and also for Earth-like planets. Thus studying these polymorphs at extreme pressure and temperature conditions will lead to understanding their changes of chemical and physical properties at extremely high pressure and temperature conditions, such as those occurring during the giant impacts phenomena of such planets at their final stage of accretion. Shock compression of forsterite has been studied up to ~ 1000 GPa by using polycrystalline and single crystal samples [1-3]. The studies have reported contradicting results for the shock compression of forsterite. Sekine et al (2016) reported that there are several phase transformations in the liquid state of Mg_2SiO_4 at > 270 GPa, while other two studies were reported no phase transformation [1, 3]. Thus it is interesting to see how the Hugonoit relations of Mg_2SiO_4 polymorphs will come up at different pressure and temperature conditions. However, Hugoniot relations of wadsleyite and ringwoodite have not been studied well. Especially, there is any data on the densest polymorph ringwoodite. Shock compression of wadsleyite was carried out up to 200 GPa by using polycrystalline samples [4]. In addition, there are no studies by using single crystal samples for both wadsleyite and ringwoodite. To newly conduct such studies, the denser polymorph of Mg_2SiO_4 are needed to be synthesized and grown at their relevant conditions of deep mantle corresponding to the 15 –21 GPa and 1000 –1500 ˚C in the laboratory. Most importantly, the synthesized minerals must be chemically, physically and optically homogenous and should have suitable sizes for the laser-shock experiments. Here, by utilizing the results of our previous efforts for growing such quality of single crystals, we made possible to obtain Hugoniot relation of wadsleyite and ringwoodite by laser-shock compression. Their crystals were synthesized and grown by using a scaled-up Kawai-type cell by together with applying our pre-established a slow-cooling method at their relevant conditions [5]. Recovered crystals were up to 1 mm in sizes and confirmed to be chemically homogenous and free from twinning, cracks, and inclusions. The crystals were then doubly polished separately down to 100 mm in thickness and with an area of > 500 mm. They were assembled to form targets which are optimized for the laser-shock experiments. laser-shock experiments at GEKKO XII were conducted at Institute of Laser Engineering, Osaka University. The crystals are optical to give very clean VISAR (Velocity Interferometer System for Any Reflector) images. The details of our technical developments will be discussed on the poster.

[1] Root, T., Townsend, J. L., Davies, E., Lemke, R. W., Bliss, D. E., Fratanduono, D. E., et al. (2018). *Geophys. Res. Lett.*, **45**:3865. [2] Sekine, T., Ozaki, N., Miyanishi, K., Asaumi, Y., Kimura, T., Albertazzi, B. et al. (2016). *Sci. Adv.*, **2**:e1600157. [3] Bolis, R. M., Morard, G., Vinci, T., Ravasio, A., Bambrink, E. et al. (2016). *Geophys. Res. Lett.*, **43**:9475. [4] Mosenfelder, J. L., Asimow, P. D. and Ahrens, T. J. (2007). *J. Geophys. Res.*, **112**:B06208. [5] Okuchi, T., Purevjav, N., Tomioka, N., Lin, J. F., Kuribayashi, T. et al. (2015). *Am. Mineral.*, **100**:1483.

Keywords: laser-shock compression, Mg2SiO4 polymorphs

©2019. Japan Geoscience Union. All Right Reserved.

©2019. Japan Geoscience Union. All Right Reserved.

Richtmyer-Meshkov instability in inhomogeneous density materials and its application to planetary science

*Takayoshi Sano[1]

1. Institute of Laser Engineering, Osaka University

Richtmyer-Meshkov instability (RMI) is a hydrodynamic interfacial instability, which occurs by the interaction between a shock wave and corrugated density jump. Because of the corrugation of the interface, the surface profiles of the transmitted and reflected shocks are also rippled. The RMI is driven by the vorticity left by these rippled shocks at the interface and in the fluid. In this study, we consider shock propagation in inhomogeneous density materials (e.g., uniform density materials with small round voids) and the turbulent growth of the interface. For these cases, the vorticity distribution and turbulent motion are much more complicated than the standard RMI cases. Then the spatial fluctuation of pressure or temperature could be significantly large after the shock passage. Using two-dimensional hydrodynamic simulations, we will examine the dependence of the pressure fluctuation on the density inhomogeneity. As the application of this numerical study, we will discuss about the shock propagation in meteorites with large density fluctuation.

Keywords: shock waves, Richtmyer-Meshkov instability

©2019. Japan Geoscience Union. All Right Reserved.

Impact-induced dehydration reactions of Fe- and Al-hydrates as potential storage, carrier and source of water

*Tsubasa Tobase[1], Toshimori Sekine[1], Ginga Kitahara[2], Makoto Tokuda[2], Akira Yoshiasa[2], Makoto Takafuji[2], Tsutomu Mashimo[2], Nobuaki Kawai[2]

1. HPSTAR, 2. Graduate School of Science and Technology, Kumamoto University

Hydrous minerals have been known to play an important role to preserve and carry water because a mechanism is required for water to reach the inner planets such as Earth far beyond the snow line that defines the boundary between water ice and vapor. In order to understand the detailes, we need to know the stability at high temperature and high pressure and impact resistance for possible hydrous minerals. Fe- and Al-hydrates (FeOOH and AlOOH) have been reported to be stable under static high temperature and static high pressure. In addition, they are observed in some meteorites and the surface on Mars. Although there are some data available on clay minerals and serpentine, those Fe- and Al-hydrates are considered to be present in the Earth’ s deep lower mantle according to the recent studies.

We have investigated the impact resistibility through shock recovery techniques. Our peak shock pressures are 24 GPa and 31 GPa for the recovered Fe- and Al-hydrates, respectively, where they displayed significant dehydration. We set various range of sample porosity and peak shock pressure to investing the dehydration reaction. These impact conditions correspond to impact velocities of 2.6 km/s and 4.9 km/s if we assume face to face impacts between carbonaceous chondrite such as Murchison. These are within a range of velocity for possible meteoritic collisions, and we need to know the relationship between impact condition and degree of dehydration. Using TG/DTA analyses of samples we estimated the relationship. The phase changes by impact dehydration are investigated by XRD, XAFS and Raman spectroscopy. We also try to understand dynamical void formation process by dehydration that can occur during adiabatic quenching through observation of void distribution in the recovered samples.

In our previous research for shock recovery experiments of hydrous minerals, we observed heterogenous temperature rise in dehydration process. We tried to confirm whether heterogeneous temperature rise occurs even in Fe- and Al-hydrates by comparison with the results between previously reported hydrous minerals. We will be able to select most possible candidate by comparing the thermal stability and impact resistibility among them.

Keywords: Shock recovered experiments, hydrous mineral, dynamic water loss, Powder x-ray diffraction

©2019. Japan Geoscience Union. All Right Reserved.

Crystallization of amorphous $MgSiO_3$ by shock compression

*Akane Arasuna[1], Masayuki Okuno[1], Nobuaki Kawai[2]

1. Kanazawa University, 2. Kumamoto University

Structural change of synthesized amorphous $MgSiO_3$ by shock compression up to 22.2 GPa has been investigated using XRD and IR analyses. The obtained result provides information for elucidating of the collision behavior of $MgSiO_3$ contained in cosmic dust.

Amorphous $MgSiO_3$ sample was prepared by an aqueous solution of TEOS, Magnesium Nitrate Hexahydrate, and ethanol with ammonia as a catalyst. As-prepared sample was heated at 700 C˚ to dehydrate excess water. TG curve of this sample indicated that the sample contained about 8.8 wt% of water molecules and hydroxyl groups.

A powdered heated (original) sample was put in an aluminum tubes and pressed at 20 kN for 10 minutes to obtain samples for shock compression experiment. These samples were compressed at 13.6, 17.2, and 22.2 GPa using a single-stage propellant gun at Kumamoto University.

XRD pattern of the pressed sample showed no crystalline peak as same as the original sample. However, the XRD pattern of thesample compressed at 13.6 GPa showed the weak crystalline peaks at around 2θ = 28, 31, 35-36˚. These peaks became intense with increasing shock pressure. Crystalline peaks observed in the XRD pattern for the sample of 22.2 GPa were attributed to those of enstatite. However, some peaks was due to the formation of Mg_2SiO_4. IR spectra for the compressed samples showed the similar trend as the result of XRD analysis. But IR analysis indicated that the sample contains water molecules even after the shock compression at 22.2 GPa. Water molecules probably present in the remaining amorphous part. Crystallization of sample by shock compression has not been reported in shock experiments for other crystalline and non-crystalline silicates. The crystallization of our samples at low pressure may be due to the simple chain structure of enstatite. Also, high shock temperature which generated by friction due to the porosity of the sample may promote this crystallization.

Keywords: MgSiO3, amorphous , shock compression, enstatite

©2019. Japan Geoscience Union. All Right Reserved.

First-principle study of the structural and electronic properties of N-doped $MgAl_2O_4$ spinel

*Chi Pui Tang[1], Pak Kin Leong[1], Toshimori Sekine[2,3]

1. State Key Laboratory of Lunar and Planetary Sciences, Macau University of Science and Technology, 2. Center for High Pressure Science and Technology Advanced Research (HPSTAR) Shanghai Laboratory of HPSTAR, Shanghai, P.R. China, 3. Graduate School of Engineering, Osaka University

On basis of the first principle calculation, we report a possible nitrogen doped structure of $MgAl_2O_4$ spinel. The structural and electronic properties (include the band structure, density of states and phonon) of spinel ($MgAl_2O_4$) and N-doped spinel ($MgAl_2O_{3.5}N_{0.5}$) compounds are performed using density functional theory (DFT). The density and space group of two crystal cells are 3.47 g/cm^3 (Fd3m) for $MgAl_2O_4$ and 3.38 g/cm^3 (R3m) for $MgAl_2O_{3.5}N_{0.5}$, respectively. The calculated direct band gaps at the Γ-point are about 5.13 eV for $MgAl_2O_4$ and 4.24 eV for $MgAl_2O_{3.5}N_{0.5}$, respectively. The projected density of states (PDOS) shows that the tops of the valence bands are built up from ~93% of *p*(O) states and ~60% of *p*(N) + ~32% of *p*(O) states (for $MgAl_2O_4$ and $MgAl_2O_{3.5}N_{0.5}$, respectively). In the phonon analysis, the lowest frequency of $MgAl_2O_{3.5}N_{0.5}$ is redshifted to 36.6 cm^{-1} ($MgAl_2O_4$ is 39.8 cm^{-1}) caused by the N-doped. We also calculate their cohesive energy in the pressure range of 0-150 GPa. We found that the cohesive energy of $MgAl_2O_{3.5}N_{0.5}$ is lower than $MgAl_2O_4$ at the pressure higher than ~115 GPa, it implies that $MgAl_2O_{3.5}N_{0.5}$ is more stable than $MgAl_2O_4$ at high pressure. Finally, we suggest that nitrogen atom would replace the oxygen of spinel in the depths of the earth. The results imply the deep mantle may storage a considerable amount of nitrogen.

Keywords: First principle calculation, Density functional theory, Spinel

©2019. Japan Geoscience Union. All Right Reserved.

Transparency of shock-compressed single crystal diamond

*Kento Katagiri[1], Norimasa Ozaki[1,2], Kohei Miyanishi[2], Yuhei Umeda[1], Shintaro Morioka[1], Takayoshi Sano[2], Ryosuke Kodama[1,2]

1. Osaka University, 2. Institute of Laser Engineering, Osaka Unversity

Carbon is one of the most prominent elements in nature and it is abundant in the Earth and many other planets. Diamond, a metastable phase of carbon, is naturally synthesized in deep inside of the Earth where substances are isotropically pressured. Diamond is known for its many unique properties such as high hardness, low compressibility, small thermal expansion coefficient, and transparency. Since it is important to understand how substances behave under high pressure, properties of compressed diamond have been measured in a wide range of pressures up to 5 TPa. However, the transparency of diamond under pressure has not been fully elucidated. Here, we report the measurment of the pressure dependency of the absorption coefficient of laser shock compressed single crystalline diamond. A high-intensity laser was utilized to shock compress the diamond sample along its <100> direction, and velocity interferometer systems for any reflector (VISARs) were used to determine the absorption coefficient and pressure. It was found that single crystalline diamond remains largely transparent to the probe laser for VISAR (λ =532 nm) up to 140 GPa. The pressure dependence of the refractive index will also be discussed.

This experiment was conducted under the joint research of the Institute of Laser Engineering, Osaka University. This work was supported in part by JSPS KAKENHI grant No. 16H02246 and No. 16H01119. The part of work was also supported by Genesis Research Institute, Inc. (Konpon-ken, TOYOTA).

Keywords: Shock-compression, High intensity laser, Diamond, Transparency, Refractive index

©2019. Japan Geoscience Union. All Right Reserved.

Pb-Pb dating of the NWA 7203 angrite and relationship to its shock metamorphism

*Hideyuki Hayashi[1], Takashi Mikouchi[1], Yuji Sano[1], Martin Bizzarro[2]

1. The university of Tokyo, 2. University of Copenhagen

Introduction: Angrite is one of the oldest basaltic achondrites in the early solar system which is depleted in volatile elements and enriched in refractory elements (e.g., Keil, 2012). Almost all angrites show either a quenched or slowly-cooled texture. The crystallization ages of quenched angrites are older (ca. 4564 Ma) than those of slowly-cooled samples (ca. 4558 Ma). One of the most striking mineralogical characteristics about angrites is the lack of shock metamorphism. Thus, quenched angrites can be good time anchors to connect absolute and relative ages, because the age differences between two systems can be ignored due to fast cooling and furthermore there is no chronological reset by shock metamorphism. However, NWA 1670 and NWA 7203 are known to show evidence for shock (Mikouchi et al., 2003; Hayashi et al., 2018), and especially we found that NWA 7203 exhibited remarkable shock metamorphic textures. The Pb-Pb dating of angrites has been done only for angrites without shock textures, indicating the obtained ages are crystallization ages. Pb-Pb age is relatively easy to be reset by shock heating. Therefore, Pb-Pb age of NWA 1670 or especially NWA 7203 may be reset by shock heating. However, there is no study which measured Pb-Pb dating of NWA 1670 or NWA 7203. In this study, we measured Pb isotopic ratios of silico-apatite in NWA 7203 by Nano-SIMS, and discussed the Pb-Pb age of NWA 7203.

Sample: We used NWA 7203 for this study. NWA 7203 is an angrite meteorite showing a quenched texture. NWA 7203 consists of a dendritic texture of olivine and anorthite, and pyroxene fills gaps of the dendrites. Grain size exhibits large variations from fine grains (~1 μm) to coarse grains (>100 μm). This is not a typical characteristic of quenched angrites. NWA 7203 is composed mainly of olivine, pyroxene and anorthite, and the accessory minerals are troilite, ulvospinel and silico-apatite.

Methods: Observation was carried out on thin sections by optical microscope and BSE images of FE-EPMA. Mineral phases were identified by micro-Raman spectroscopic analysis. Pb-Pb dating of NWA 7203 was carried out by measuring Pb isotope ratios of silico-apatites using Nano-SIMS at AORI, Univ. of Tokyo. Measurement conditions were 300 pA for primary ions and $^{16}O^-$ for ion sources. Pre-sputtering was performed for 8 minutes in the range of 10 x 10 μm. In the SIMS measurement, raster diameter of 3 x 3 μm and analysis time of 60 seconds were applied for two magnetic fields, respectively, and repeated for 30 cycles. For the standard, NIST SRM 610 was used.

Result and discussion: Pb isotopic ratios of silico-apatite in the NWA 7203 angrite were obtained. We obtained a weighted approximate straight line for each plot and found the Pb-Pb age to be 4551 ±17 Ma. These plots are relatively variable. This is probably because Pb isotopic ratios were disturbed by shock metamorphism. In fact, the Pb-Pb age of silico-apatite grains that are at least 200 μm away from the shock veins was found to be 4560 ±16 Ma. It is considered that the Pb isotopic ratios of these silico-apatite grains are relatively undisturbed as they are linearly aligned. This age coincides with the crystallization age of other quenched angrites within the error range. Takenouchi et al. (2019) measured the Ar-Ar ages of NWA 7203 and found that it has two plateau ages of 3800 ±440 Ma and 2300 ±140 Ma, and concluded that the shock metamorphism of NWA 7203 occurred at 2300 ±140 Ma. From this result, it is considered that the Pb-Pb age of NWA 7203 is not completely reset, but slightly disturbed.

©2019. Japan Geoscience Union. All Right Reserved.

Keywords: NWA 7203, Angrite, Pb-Pb dating, Shock metamorphism, Parent body

©2019. Japan Geoscience Union. All Right Reserved.

Shock recovery of high-pressure phase of SiO_2 using high-power laser

*Tadashi Kondo[1], Hiromoto Kengo[1], Tatsuhiro Sakaiya[1], Hidenori Terasaki[1], Keisuke Shigemori[2], Youichiro Hironaka[2]

1. Department of Earth and Space Science, Graduate School of Science Osaka University, 2. Institute of Laser Engineering, Osaka University

High-pressure phases in meteorites provide us the important information of shock history in natural materials. Experimental approach to reproduce such high-pressure phase have been studied intensively mainly by light-gas gun so far, though shock condition with impact velocity beyond 10km/s is difficult. Recent technical progress of high-intensity laser as a tool of shock experiment realize the recovery of samples with shock condition above 10km/s(Nagaki et al.,2016). However, the limited shock duration time of about 10 nsec has been too short to drive structural conversion to high-pressure form in single crystal sample. In this study, we explored recovery condition of high-pressure phase of SiO_2 using finely ground samples of quartz, cristobalite and fused silica as starting materials. Laser shock experiments were performed using GXII hyper laser at Institute of Laser Engineering, Osaka University. The whole sample retaining relative locations in the recovered box made of aluminum was quenched without significant scattering in each run. The sectioned sample at shocked center were examined by optical microscope, micro-focused X-ray diffraction and SEM-EDS. We will report the characteristic feature of top portion of sample, which shows layered structure with different metamorphism, and distribution of grass and stishovite phase found in the samples shocked above 100GPa, which have still a residual stress to 10GPa in the ambient condition. We will discuss the dependence of the initial state of crystal to recover the high-pressure phase in shocked samples in nsec.

Keywords: shocked quartz, high-intensity laser, recovery experiments

©2019. Japan Geoscience Union. All Right Reserved.

Hugoniot measurement of calcite under meteorite collision condition

*Fukui Keiya[1], Norimasa Ozaki[1,2], Yuhei Umeda[1], Kohei Miyanishi[3], Kento Katagiri[1], Shintaro Morioka[1], Takayoshi Sano[3], Ryosuke Kodama[1,2,3]

1. Graduate School of Engineering,Osaka univ., 2. PPC, Osaka Univ., 3. ILE, Osaka Univ.

Volatile substances inside planetary materialsare generated and released as gas under the extreme condition caused by collision phenomenon that is thought to contribute greatly to the formation of the planetary atmosphere [1]. Particularly the degassing reaction of carbonate, may generate CO or CO_2as greenhouse gas and affect the temperature of the planetary surface. A typical planetary mineral as carbonate of calcite ($CaCO_3$) is expected degassing above 3300 K at pressure of 150 GPa along the Hugoniot[2].
In the previous study, the experimental investigations for the shock-degassing reaction were carried out only below the impact pressure of 100 GPa. Also, we have not understood when the degassing reaction of calcite occur on a compressed state or a released state [3]
In natural, typical meteorite impacts exceed 10 km/s in impact velocity, and can generate at the pressure above 150 GPa. The purpose of this research is to understand the impact compression characteristics of calcite under the meteorite collision condition.

This experiment was conducted in Shock Drive Laser (Gekko XII) atInstitute for Laser Engineering, Osaka University. The target consists of polypropylene as an ablator aluminum as a piston, quartz as a standard material, and calcite as a sample from laser side. The impact pressures and temperatures were estimated by the measured shock wave velocity using Velocity interferometer system for any reflector (VISAR) and self-emission intensity using radiance thermometer (SOP).
As a result of this experiments, we obtained the Hugoniot date at the puressure from 200 GPa to 1 Tpa at the temperature above 5000 K. The detailed results will be shown as this presentation.
Acknowledgements

This experiment was conducted on the joint research of the Institute of Laser Engineering, Osaka University. This work was supported in part by JSPS KAKENHI grant No. 16H02246 and No. 16H01119. The part of work was also supported by Genesis Research Institute, Inc. (Konpon-ken, TOYOTA).

REFERENCES

[1] T. Matsui and Y.Abe: Nature, 319, 303 - 319 (1986).

[2] B.Ivanov and A. Deutsch: Physics of the Earth and Planetary Interiors, 129, 131-143 (2002).

[3] K.Kawaragi et al.: Earth and Planetary Science Letters, 282, 56 - 64 (2009).

Keywords: Laser-Shock-compression, hugoniot, calcite, degassing

©2019. Japan Geoscience Union. All Right Reserved.

Direct observation of the transformation toughening of tetragonal stabilized zirconia under shock deformation condition by ns time-resolved XRD.

*Sota Takagi[1,2], Kouhei Ichiyanagi[2,3], Nobuaki Kawai[4], Ryo Fukaya[2], Shunsuke Nozawa[2], Atsushi Kyono[1], Nobumasa Funamori[2], Shin-ichi Adachi[2]

1. University of Tsukuba, 2. KEK PF, 3. Jichi Medical University, 4. Kumamoto University

The enhancement of strength and toughness was found in oxide-doped tetragonal stabilized zirconia, with the suggestion that the absorption of energy during the martensitic transformation contribute to the increment [Gravie et al., 1975; Gupta et al., 1977]. Using transmission electron microscopy (TEM), in recovery sample, it was observed that the stress-induced transformation from stabilized tetragonal phase to monoclinic phase can be occurred around the crack tip [Porter et al., 1977], and the transformation-toughening model were devised [McMeeking et al., 1982; Hannink et al., 2000]. In high-pressure experiments, the phase transformation behavior of tetragonal stabilized zirconia has not been clarified in both static and shock compression because a lack of in-situ observation [Ohtaka et al., 1988; Grady et al., 1992]. We tried to observe the behavior of tetragonal stabilized zirconia under shock compression condition using time-resolved XRD method.We performed the experiments at NW14A beamline at PF-AR (Photon Factory Advanced Ring), High Energy Accelerator Research Organization (KEK), Japan. Nd:glass laser with the wavelength of 1064 nm, pulse energy of 16 J, pulse width of 12 ns was used for shock-driving source. The laser beam was focused by optical lens to the size of 500 μm × 500 μm on the sample surface. For TR-XRD experiments, the synchrotron X-ray pulse of PF-AR was used as a probe source. The energy, the pulse width, and the size on the sample were 15.68 keV, about 100 ps, and 450 μm (H) ×250 μm (W), respectively. The irradiation timing between laser pulse and X-ray pulse on the sample surface were controlled by delay generator at ns time scale. The targets consisted of an 25 um PET film ablator with Al coated on the surface and 50 um polycrystalline 3 mol% yttria doped tetragonal stabilized zirconia.
The XRD change were observed up to 35 ns after shock compression started. Before shock, the (101), (002), (110), (102), (112), (200) diffraction of tetragonal phase were observed. 6.5 ns after shock, the diffraction from compression region appeared with maximum compression of 6%. No phase transition occurred at compression states. At release states (~11.4 ns), on the other hand, the (-111), (111), (022), (-221) diffraction peaks of monoclinic phase were appeared. We will discuss the detail of the experimental results and the transformation toughening mechanism.

Keywords: Synchrotron X-ray, Time-resolved XRD, Laser-induced shock wave, Tetragonal stabilized zirconia

©2019. Japan Geoscience Union. All Right Reserved.

[E] Poster | P (Space and Planetary Sciences)：P-CG Complex & General

Tue. May 28, 2019 5:15 PM - 6:30 PM JST | Tue. May 28, 2019 8:15 AM - 9:30 AM UTC | Poster Hall International Exhibition Hall8, Makuhari Messe_4

[P-CG22] Shock responses of planetary materials elucidated from meteorites and dynamic compression experiments

convener:Toshimori Sekine(Center for High Pressure Science and Technology Advanced Research), Takuo Okuchi(Institute for Planetary Materials, Okayama University)

Impact phenomena had played essential roles in the process of planetary evolution. Recent analytical and experimental developments reveal a new prospective on the effects of shock-compression process for planetary materials. For deeper understanding of such shock effects, it is necessary to evaluate the detailed shock conditions from the observations of naturally-shocked planetary materials, and to compare them with the results on the planetary materials experienced a wide range of known shock conditions. Several metastable phases, that have not been known before, have recently been identified in shocked meteorites. They suggest that the shock state is often not in equilibrium and that it is more complicated process than ever thought. Experimental techniques including laser-driven shock compression and x-ray free electron laser diagnostics have been progressed to successfully simulate a wide range of shock conditions. The recent results indicate that shocked grains are fractured and rotated at relatively low pressures, and that they are subsequently transformed into denser phases or melts, or their mixtures at pressures of a few 100s GPa. Understanding of such shock dynamics requires another prospect, which is qualitatively different from the static high pressure and high temperature consensus. Therefore, it is timely to have an international symposium on dynamics of planetary materials.

[PCG22-P01] discussion

*Takuo Okuchi[1], Toshimori Sekine[2] (1.Institute for Planetary Materials, Okayama University, 2.Center for High Pressure Science and Technology Advanced Research)

[PCG22-P02] Shock-compressed behavior of quartz by XFEL

*Tomoko Sato[1], Yoshinori Tange[2], Yusuke Seto[3], Toshimori Sekine[4,5], Norimasa Ozaki[4], Toyohito Nishikawa[4], Kohei Miyanishi[4], Kensuke Matsuoka[4], Ryosuke Kodama[4], Tadashi Togashi[2], Yuichi Inubushi[2], Toshinori Yabuuchi[6], Makina Yabashi[6] (1.Hiroshima University, 2.Japan Synchrotron Radiation Research Institute, 3.Kobe University, 4.Osaka University, 5.Center for High Pressure Science &Technology Advanced Research, 6.RIKEN)

[PCG22-P04] Laser-shock experiments of dense polymorphs of Mg_2SiO_4: technical developments using synthetic single crystals

*Narangoo Purevjav[1], Takuo Okuchi[1], Norimasa Ozaki[2], Takayoshi Sano[3], Yuhei Umeda[2], Shintaro Morioka[2], Nobuki Kamimura[2] (1.Institute for Planetary Materials, Okayama University, 2.Graduate School of Engineering, Osaka University, 3.Institute of Laser Engineering, Osaka University)

[PCG22-P05] Richtmyer-Meshkov instability in inhomogeneous density materials and its application to planetary science

*Takayoshi Sano[1] (1.Institute of Laser Engineering, Osaka University)

[PCG22-P06] Impact-induced dehydration reactions of Fe- and Al-hydrates as potential storage, carrier and source of water

*Tsubasa Tobase[1], Toshimori Sekine[1], Ginga Kitahara[2], Makoto Tokuda[2], Akira Yoshiasa[2], Makoto Takafuji[2], Tsutomu Mashimo[2], Nobuaki Kawai[2] (1.HPSTAR, 2.Graduate School of Science and Technology, Kumamoto University)

[PCG22-P07] Crystallization of amorphous $MgSiO_3$ by shock compression

*Akane Arasuna[1], Masayuki Okuno[1], Nobuaki Kawai[2] (1.Kanazawa University, 2.Kumamoto University)

[PCG22-P08] First-principle study of the structural and electronic properties of N-doped $MgAl_2O_4$ spinel

*Chi Pui Tang[1], Pak Kin Leong[1], Toshimori Sekine[2,3] (1.State Key Laboratory of Lunar and Planetary Sciences, Macau University of Science and Technology, 2.Center for High Pressure Science and Technology Advanced Research (HPSTAR) Shanghai Laboratory of HPSTAR, Shanghai, P.R. China, 3.Graduate School of Engineering, Osaka University)

[PCG22-P09] Transparency of shock-compressed single crystal diamond

*Kento Katagiri[1], Norimasa Ozaki[1,2], Kohei Miyanishi[2], Yuhei Umeda[1], Shintaro Morioka[1], Takayoshi Sano[2], Ryosuke Kodama[1,2] (1.Osaka University, 2.Institute of Laser Engineering, Osaka Unversity)

[PCG22-P10] Pb-Pb dating of the NWA 7203 angrite and relationship to its shock metamorphism

*Hideyuki Hayashi[1], Takashi Mikouchi[1], Yuji Sano[1], Martin Bizzarro[2] (1.The university of Tokyo, 2.University of Copenhagen)

[PCG22-P11] Shock recovery of high-pressure phase of SiO_2 using high-power laser

*Tadashi Kondo[1], Hiromoto Kengo[1], Tatsuhiro Sakaiya[1], Hidenori Terasaki[1], Keisuke Shigemori[2], Youichiro Hironaka[2] (1.Department of Earth and Space Science, Graduate School of Science Osaka University, 2.Institute of Laser Engineering, Osaka University)

[PCG22-P12] Hugoniot measurement of calcite under meteorite collision condition

*Fukui Keiya[1], Norimasa Ozaki[1,2], Yuhei Umeda[1], Kohei Miyanishi[3], Kento Katagiri[1], Shintaro Morioka[1], Takayoshi Sano[3], Ryosuke Kodama[1,2,3] (1.Graduate School of Engineering,Osaka univ., 2.PPC, Osaka Univ., 3.ILE, Osaka Univ.)

[PCG22-P13] Direct observation of the transformation toughening of tetragonal stabilized zirconia under shock deformation condition by ns time-resolved XRD.

*Sota Takagi[1,2], Kouhei Ichiyanagi[2,3], Nobuaki Kawai[4], Ryo Fukaya[2], Shunsuke Nozawa[2], Atsushi Kyono[1], Nobumasa Funamori[2], Shin-ichi Adachi[2] (1.University of Tsukuba, 2.KEK PF, 3.Jichi Medical University, 4.Kumamoto University)

discussion

*Takuo Okuchi[1], Toshimori Sekine[2]

1. Institute for Planetary Materials, Okayama University, 2. Center for High Pressure Science and Technology Advanced Research

We discuss natural and experimendal evidences on impact phenomena, which had played essential roles in the process of early planetary evolution. Recent analytical and experimenotal developments reveal a new prospective on the effects of shock-compression process of planetary materials. For deeper understanding of such shock effects, it is necessary to evaluate the detailed shock conditions from the observations of naturally-shocked planetary materials, as well as to compare them with the results of shock-compression experiments of these materials obtained at laboratory conditions.

Keywords: discussion

©2019. Japan Geoscience Union. All Right Reserved.

Shock-compressed behavior of quartz by XFEL

*Tomoko Sato[1], Yoshinori Tange[2], Yusuke Seto[3], Toshimori Sekine[4,5], Norimasa Ozaki[4], Toyohito Nishikawa[4], Kohei Miyanishi[4], Kensuke Matsuoka[4], Ryosuke Kodama[4], Tadashi Togashi[2], Yuichi Inubushi[2], Toshinori Yabuuchi[6], Makina Yabashi[6]

1. Hiroshima University, 2. Japan Synchrotron Radiation Research Institute, 3. Kobe University, 4. Osaka University, 5. Center for High Pressure Science &Technology Advanced Research, 6. RIKEN

We have conducted x-ray diffraction measurement (XRD) with femtosecond x-ray pulses generated by the x-ray free electron laser (XFEL) to observe lattice dynamics and phase transformation of single-crystal quartz under high strain-rate shock compression (~10^9 s^{-1}) and high pressure. Single-crystal quartz samples were shock-compressed by high-power short- and long-pulse lasers. In the short-pulse experiments, the lattice was reduced to 15% and 1.5% in the direction parallel and perpendicular to the compression axis, respectively. The sample was uniaxially compressed over its known Hugoniot elastic limit. In the long-pulse experiments, three different states were observed. Polycrystalline stishovite appeared at first, and elastically compressed state and a topotaxially transformed new phase were observed successively.

Keywords: Shock compression, in-situ X-ray diffraction, quartz

©2019. Japan Geoscience Union. All Right Reserved.

Laser-shock experiments of dense polymorphs of Mg_2SiO_4: technical developments using synthetic single crystals

*Narangoo Purevjav[1], Takuo Okuchi[1], Norimasa Ozaki[2], Takayoshi Sano[3], Yuhei Umeda[2], Shintaro Morioka[2], Nobuki Kamimura[2]

1. Institute for Planetary Materials, Okayama University, 2. Graduate School of Engineering, Osaka University, 3. Institute of Laser Engineering, Osaka University

Mg_2SiO_4 polymorphs (α-phase as forsterite, β-phase as wadsleyite, and γ-phase as ringwoodite) are the major constituents of our Earth's mantle and also for Earth-like planets. Thus studying these polymorphs at extreme pressure and temperature conditions will lead to understanding their changes of chemical and physical properties at extremely high pressure and temperature conditions, such as those occurring during the giant impacts phenomena of such planets at their final stage of accretion. Shock compression of forsterite has been studied up to ~ 1000 GPa by using polycrystalline and single crystal samples [1-3]. The studies have reported contradicting results for the shock compression of forsterite. Sekine et al (2016) reported that there are several phase transformations in the liquid state of Mg_2SiO_4 at > 270 GPa, while other two studies were reported no phase transformation [1, 3]. Thus it is interesting to see how the Hugonoit relations of Mg_2SiO_4 polymorphs will come up at different pressure and temperature conditions. However, Hugoniot relations of wadsleyite and ringwoodite have not been studied well. Especially, there is any data on the densest polymorph ringwoodite. Shock compression of wadsleyite was carried out up to 200 GPa by using polycrystalline samples [4]. In addition, there are no studies by using single crystal samples for both wadsleyite and ringwoodite. To newly conduct such studies, the denser polymorph of Mg_2SiO_4 are needed to be synthesized and grown at their relevant conditions of deep mantle corresponding to the 15 –21 GPa and 1000 –1500 ˚C in the laboratory. Most importantly, the synthesized minerals must be chemically, physically and optically homogenous and should have suitable sizes for the laser-shock experiments. Here, by utilizing the results of our previous efforts for growing such quality of single crystals, we made possible to obtain Hugoniot relation of wadsleyite and ringwoodite by laser-shock compression. Their crystals were synthesized and grown by using a scaled-up Kawai-type cell by together with applying our pre-established a slow-cooling method at their relevant conditions [5]. Recovered crystals were up to 1 mm in sizes and confirmed to be chemically homogenous and free from twinning, cracks, and inclusions. The crystals were then doubly polished separately down to 100 mm in thickness and with an area of > 500 mm. They were assembled to form targets which are optimized for the laser-shock experiments. laser-shock experiments at GEKKO XII were conducted at Institute of Laser Engineering, Osaka University. The crystals are optical to give very clean VISAR (Velocity Interferometer System for Any Reflector) images. The details of our technical developments will be discussed on the poster.

[1] Root, T., Townsend, J. L., Davies, E., Lemke, R. W., Bliss, D. E., Fratanduono, D. E., et al. (2018). *Geophys. Res. Lett.*, **45**:3865. [2] Sekine, T., Ozaki, N., Miyanishi, K., Asaumi, Y., Kimura, T., Albertazzi, B. et al. (2016). *Sci. Adv.*, **2**:e1600157. [3] Bolis, R. M., Morard, G., Vinci, T., Ravasio, A., Bambrink, E. et al. (2016). *Geophys. Res. Lett.*, **43**:9475. [4] Mosenfelder, J. L., Asimow, P. D. and Ahrens, T. J. (2007). *J. Geophys. Res.*, **112**:B06208. [5] Okuchi, T., Purevjav, N., Tomioka, N., Lin, J. F., Kuribayashi, T. et al. (2015). *Am. Mineral.*, **100**:1483.

Keywords: laser-shock compression, Mg2SiO4 polymorphs

©2019. Japan Geoscience Union. All Right Reserved.

©2019. Japan Geoscience Union. All Right Reserved.

Richtmyer-Meshkov instability in inhomogeneous density materials and its application to planetary science

*Takayoshi Sano[1]

1. Institute of Laser Engineering, Osaka University

Richtmyer-Meshkov instability (RMI) is a hydrodynamic interfacial instability, which occurs by the interaction between a shock wave and corrugated density jump. Because of the corrugation of the interface, the surface profiles of the transmitted and reflected shocks are also rippled. The RMI is driven by the vorticity left by these rippled shocks at the interface and in the fluid. In this study, we consider shock propagation in inhomogeneous density materials (e.g., uniform density materials with small round voids) and the turbulent growth of the interface. For these cases, the vorticity distribution and turbulent motion are much more complicated than the standard RMI cases. Then the spatial fluctuation of pressure or temperature could be significantly large after the shock passage. Using two-dimensional hydrodynamic simulations, we will examine the dependence of the pressure fluctuation on the density inhomogeneity. As the application of this numerical study, we will discuss about the shock propagation in meteorites with large density fluctuation.

Keywords: shock waves, Richtmyer-Meshkov instability

©2019. Japan Geoscience Union. All Right Reserved.

Impact-induced dehydration reactions of Fe- and Al-hydrates as potential storage, carrier and source of water

*Tsubasa Tobase[1], Toshimori Sekine[1], Ginga Kitahara[2], Makoto Tokuda[2], Akira Yoshiasa[2], Makoto Takafuji[2], Tsutomu Mashimo[2], Nobuaki Kawai[2]

1. HPSTAR, 2. Graduate School of Science and Technology, Kumamoto University

Hydrous minerals have been known to play an important role to preserve and carry water because a mechanism is required for water to reach the inner planets such as Earth far beyond the snow line that defines the boundary between water ice and vapor. In order to understand the detailes, we need to know the stability at high temperature and high pressure and impact resistance for possible hydrous minerals. Fe- and Al-hydrates (FeOOH and AlOOH) have been reported to be stable under static high temperature and static high pressure. In addition, they are observed in some meteorites and the surface on Mars. Although there are some data available on clay minerals and serpentine, those Fe- and Al-hydrates are considered to be present in the Earth’ s deep lower mantle according to the recent studies.

We have investigated the impact resistibility through shock recovery techniques. Our peak shock pressures are 24 GPa and 31 GPa for the recovered Fe- and Al-hydrates, respectively, where they displayed significant dehydration. We set various range of sample porosity and peak shock pressure to investing the dehydration reaction. These impact conditions correspond to impact velocities of 2.6 km/s and 4.9 km/s if we assume face to face impacts between carbonaceous chondrite such as Murchison. These are within a range of velocity for possible meteoritic collisions, and we need to know the relationship between impact condition and degree of dehydration. Using TG/DTA analyses of samples we estimated the relationship. The phase changes by impact dehydration are investigated by XRD, XAFS and Raman spectroscopy. We also try to understand dynamical void formation process by dehydration that can occur during adiabatic quenching through observation of void distribution in the recovered samples.

In our previous research for shock recovery experiments of hydrous minerals, we observed heterogenous temperature rise in dehydration process. We tried to confirm whether heterogeneous temperature rise occurs even in Fe- and Al-hydrates by comparison with the results between previously reported hydrous minerals. We will be able to select most possible candidate by comparing the thermal stability and impact resistibility among them.

Keywords: Shock recovered experiments, hydrous mineral, dynamic water loss, Powder x-ray diffraction

©2019. Japan Geoscience Union. All Right Reserved.

Crystallization of amorphous $MgSiO_3$ by shock compression

*Akane Arasuna[1], Masayuki Okuno[1], Nobuaki Kawai[2]

1. Kanazawa University, 2. Kumamoto University

Structural change of synthesized amorphous $MgSiO_3$ by shock compression up to 22.2 GPa has been investigated using XRD and IR analyses. The obtained result provides information for elucidating of the collision behavior of $MgSiO_3$ contained in cosmic dust.

Amorphous $MgSiO_3$ sample was prepared by an aqueous solution of TEOS, Magnesium Nitrate Hexahydrate, and ethanol with ammonia as a catalyst. As-prepared sample was heated at 700 C˚ to dehydrate excess water. TG curve of this sample indicated that the sample contained about 8.8 wt% of water molecules and hydroxyl groups.

A powdered heated (original) sample was put in an aluminum tubes and pressed at 20 kN for 10 minutes to obtain samples for shock compression experiment. These samples were compressed at 13.6, 17.2, and 22.2 GPa using a single-stage propellant gun at Kumamoto University.

XRD pattern of the pressed sample showed no crystalline peak as same as the original sample. However, the XRD pattern of thesample compressed at 13.6 GPa showed the weak crystalline peaks at around 2θ = 28, 31, 35-36˚. These peaks became intense with increasing shock pressure. Crystalline peaks observed in the XRD pattern for the sample of 22.2 GPa were attributed to those of enstatite. However, some peaks was due to the formation of Mg_2SiO_4. IR spectra for the compressed samples showed the similar trend as the result of XRD analysis. But IR analysis indicated that the sample contains water molecules even after the shock compression at 22.2 GPa. Water molecules probably present in the remaining amorphous part. Crystallization of sample by shock compression has not been reported in shock experiments for other crystalline and non-crystalline silicates. The crystallization of our samples at low pressure may be due to the simple chain structure of enstatite. Also, high shock temperature which generated by friction due to the porosity of the sample may promote this crystallization.

Keywords: MgSiO3, amorphous , shock compression, enstatite

©2019. Japan Geoscience Union. All Right Reserved.

First-principle study of the structural and electronic properties of N-doped $MgAl_2O_4$ spinel

*Chi Pui Tang[1], Pak Kin Leong[1], Toshimori Sekine[2,3]

1. State Key Laboratory of Lunar and Planetary Sciences, Macau University of Science and Technology, 2. Center for High Pressure Science and Technology Advanced Research (HPSTAR) Shanghai Laboratory of HPSTAR, Shanghai, P.R. China, 3. Graduate School of Engineering, Osaka University

On basis of the first principle calculation, we report a possible nitrogen doped structure of $MgAl_2O_4$ spinel. The structural and electronic properties (include the band structure, density of states and phonon) of spinel ($MgAl_2O_4$) and N-doped spinel ($MgAl_2O_{3.5}N_{0.5}$) compounds are performed using density functional theory (DFT). The density and space group of two crystal cells are 3.47 g/cm^3 (Fd3m) for $MgAl_2O_4$ and 3.38 g/cm^3 (R3m) for $MgAl_2O_{3.5}N_{0.5}$, respectively. The calculated direct band gaps at the Γ-point are about 5.13 eV for $MgAl_2O_4$ and 4.24 eV for $MgAl_2O_{3.5}N_{0.5}$, respectively. The projected density of states (PDOS) shows that the tops of the valence bands are built up from ~93% of *p*(O) states and ~60% of *p*(N) + ~32% of *p*(O) states (for $MgAl_2O_4$ and $MgAl_2O_{3.5}N_{0.5}$, respectively). In the phonon analysis, the lowest frequency of $MgAl_2O_{3.5}N_{0.5}$ is redshifted to 36.6 cm^{-1} ($MgAl_2O_4$ is 39.8 cm^{-1}) caused by the N-doped. We also calculate their cohesive energy in the pressure range of 0-150 GPa. We found that the cohesive energy of $MgAl_2O_{3.5}N_{0.5}$ is lower than $MgAl_2O_4$ at the pressure higher than ~115 GPa, it implies that $MgAl_2O_{3.5}N_{0.5}$ is more stable than $MgAl_2O_4$ at high pressure. Finally, we suggest that nitrogen atom would replace the oxygen of spinel in the depths of the earth. The results imply the deep mantle may storage a considerable amount of nitrogen.

Keywords: First principle calculation, Density functional theory, Spinel

©2019. Japan Geoscience Union. All Right Reserved.

Transparency of shock-compressed single crystal diamond

*Kento Katagiri[1], Norimasa Ozaki[1,2], Kohei Miyanishi[2], Yuhei Umeda[1], Shintaro Morioka[1], Takayoshi Sano[2], Ryosuke Kodama[1,2]

1. Osaka University, 2. Institute of Laser Engineering, Osaka Unversity

Carbon is one of the most prominent elements in nature and it is abundant in the Earth and many other planets. Diamond, a metastable phase of carbon, is naturally synthesized in deep inside of the Earth where substances are isotropically pressured. Diamond is known for its many unique properties such as high hardness, low compressibility, small thermal expansion coefficient, and transparency. Since it is important to understand how substances behave under high pressure, properties of compressed diamond have been measured in a wide range of pressures up to 5 TPa. However, the transparency of diamond under pressure has not been fully elucidated. Here, we report the measurment of the pressure dependency of the absorption coefficient of laser shock compressed single crystalline diamond. A high-intensity laser was utilized to shock compress the diamond sample along its <100> direction, and velocity interferometer systems for any reflector (VISARs) were used to determine the absorption coefficient and pressure. It was found that single crystalline diamond remains largely transparent to the probe laser for VISAR (λ =532 nm) up to 140 GPa. The pressure dependence of the refractive index will also be discussed.

This experiment was conducted under the joint research of the Institute of Laser Engineering, Osaka University. This work was supported in part by JSPS KAKENHI grant No. 16H02246 and No. 16H01119. The part of work was also supported by Genesis Research Institute, Inc. (Konpon-ken, TOYOTA).

Keywords: Shock-compression, High intensity laser, Diamond, Transparency, Refractive index

©2019. Japan Geoscience Union. All Right Reserved.

Pb-Pb dating of the NWA 7203 angrite and relationship to its shock metamorphism

*Hideyuki Hayashi[1], Takashi Mikouchi[1], Yuji Sano[1], Martin Bizzarro[2]

1. The university of Tokyo, 2. University of Copenhagen

Introduction: Angrite is one of the oldest basaltic achondrites in the early solar system which is depleted in volatile elements and enriched in refractory elements (e.g., Keil, 2012). Almost all angrites show either a quenched or slowly-cooled texture. The crystallization ages of quenched angrites are older (ca. 4564 Ma) than those of slowly-cooled samples (ca. 4558 Ma). One of the most striking mineralogical characteristics about angrites is the lack of shock metamorphism. Thus, quenched angrites can be good time anchors to connect absolute and relative ages, because the age differences between two systems can be ignored due to fast cooling and furthermore there is no chronological reset by shock metamorphism. However, NWA 1670 and NWA 7203 are known to show evidence for shock (Mikouchi et al., 2003; Hayashi et al., 2018), and especially we found that NWA 7203 exhibited remarkable shock metamorphic textures. The Pb-Pb dating of angrites has been done only for angrites without shock textures, indicating the obtained ages are crystallization ages. Pb-Pb age is relatively easy to be reset by shock heating. Therefore, Pb-Pb age of NWA 1670 or especially NWA 7203 may be reset by shock heating. However, there is no study which measured Pb-Pb dating of NWA 1670 or NWA 7203. In this study, we measured Pb isotopic ratios of silico-apatite in NWA 7203 by Nano-SIMS, and discussed the Pb-Pb age of NWA 7203.

Sample: We used NWA 7203 for this study. NWA 7203 is an angrite meteorite showing a quenched texture. NWA 7203 consists of a dendritic texture of olivine and anorthite, and pyroxene fills gaps of the dendrites. Grain size exhibits large variations from fine grains (~1 μm) to coarse grains (>100 μm). This is not a typical characteristic of quenched angrites. NWA 7203 is composed mainly of olivine, pyroxene and anorthite, and the accessory minerals are troilite, ulvospinel and silico-apatite.

Methods: Observation was carried out on thin sections by optical microscope and BSE images of FE-EPMA. Mineral phases were identified by micro-Raman spectroscopic analysis. Pb-Pb dating of NWA 7203 was carried out by measuring Pb isotope ratios of silico-apatites using Nano-SIMS at AORI, Univ. of Tokyo. Measurement conditions were 300 pA for primary ions and $^{16}O^-$ for ion sources. Pre-sputtering was performed for 8 minutes in the range of 10 x 10 μm. In the SIMS measurement, raster diameter of 3 x 3 μm and analysis time of 60 seconds were applied for two magnetic fields, respectively, and repeated for 30 cycles. For the standard, NIST SRM 610 was used.

Result and discussion: Pb isotopic ratios of silico-apatite in the NWA 7203 angrite were obtained. We obtained a weighted approximate straight line for each plot and found the Pb-Pb age to be 4551 ±17 Ma. These plots are relatively variable. This is probably because Pb isotopic ratios were disturbed by shock metamorphism. In fact, the Pb-Pb age of silico-apatite grains that are at least 200 μm away from the shock veins was found to be 4560 ±16 Ma. It is considered that the Pb isotopic ratios of these silico-apatite grains are relatively undisturbed as they are linearly aligned. This age coincides with the crystallization age of other quenched angrites within the error range. Takenouchi et al. (2019) measured the Ar-Ar ages of NWA 7203 and found that it has two plateau ages of 3800 ±440 Ma and 2300 ±140 Ma, and concluded that the shock metamorphism of NWA 7203 occurred at 2300 ±140 Ma. From this result, it is considered that the Pb-Pb age of NWA 7203 is not completely reset, but slightly disturbed.

©2019. Japan Geoscience Union. All Right Reserved.

Keywords: NWA 7203, Angrite, Pb-Pb dating, Shock metamorphism, Parent body

©2019. Japan Geoscience Union. All Right Reserved.

Shock recovery of high-pressure phase of SiO_2 using high-power laser

*Tadashi Kondo[1], Hiromoto Kengo[1], Tatsuhiro Sakaiya[1], Hidenori Terasaki[1], Keisuke Shigemori[2], Youichiro Hironaka[2]

1. Department of Earth and Space Science, Graduate School of Science Osaka University, 2. Institute of Laser Engineering, Osaka University

High-pressure phases in meteorites provide us the important information of shock history in natural materials. Experimental approach to reproduce such high-pressure phase have been studied intensively mainly by light-gas gun so far, though shock condition with impact velocity beyond 10km/s is difficult. Recent technical progress of high-intensity laser as a tool of shock experiment realize the recovery of samples with shock condition above 10km/s(Nagaki et al.,2016). However, the limited shock duration time of about 10 nsec has been too short to drive structural conversion to high-pressure form in single crystal sample. In this study, we explored recovery condition of high-pressure phase of SiO_2 using finely ground samples of quartz, cristobalite and fused silica as starting materials. Laser shock experiments were performed using GXII hyper laser at Institute of Laser Engineering, Osaka University. The whole sample retaining relative locations in the recovered box made of aluminum was quenched without significant scattering in each run. The sectioned sample at shocked center were examined by optical microscope, micro-focused X-ray diffraction and SEM-EDS. We will report the characteristic feature of top portion of sample, which shows layered structure with different metamorphism, and distribution of grass and stishovite phase found in the samples shocked above 100GPa, which have still a residual stress to 10GPa in the ambient condition. We will discuss the dependence of the initial state of crystal to recover the high-pressure phase in shocked samples in nsec.

Keywords: shocked quartz, high-intensity laser, recovery experiments

©2019. Japan Geoscience Union. All Right Reserved.

Hugoniot measurement of calcite under meteorite collision condition

*Fukui Keiya[1], Norimasa Ozaki[1,2], Yuhei Umeda[1], Kohei Miyanishi[3], Kento Katagiri[1], Shintaro Morioka[1], Takayoshi Sano[3], Ryosuke Kodama[1,2,3]

1. Graduate School of Engineering,Osaka univ., 2. PPC, Osaka Univ., 3. ILE, Osaka Univ.

Volatile substances inside planetary materialsare generated and released as gas under the extreme condition caused by collision phenomenon that is thought to contribute greatly to the formation of the planetary atmosphere [1]. Particularly the degassing reaction of carbonate, may generate CO or CO_2as greenhouse gas and affect the temperature of the planetary surface. A typical planetary mineral as carbonate of calcite ($CaCO_3$) is expected degassing above 3300 K at pressure of 150 GPa along the Hugoniot[2].
In the previous study, the experimental investigations for the shock-degassing reaction were carried out only below the impact pressure of 100 GPa. Also, we have not understood when the degassing reaction of calcite occur on a compressed state or a released state [3]
In natural, typical meteorite impacts exceed 10 km/s in impact velocity, and can generate at the pressure above 150 GPa. The purpose of this research is to understand the impact compression characteristics of calcite under the meteorite collision condition.

This experiment was conducted in Shock Drive Laser (Gekko XII) atInstitute for Laser Engineering, Osaka University. The target consists of polypropylene as an ablator aluminum as a piston, quartz as a standard material, and calcite as a sample from laser side. The impact pressures and temperatures were estimated by the measured shock wave velocity using Velocity interferometer system for any reflector (VISAR) and self-emission intensity using radiance thermometer (SOP).
As a result of this experiments, we obtained the Hugoniot date at the puressure from 200 GPa to 1 Tpa at the temperature above 5000 K. The detailed results will be shown as this presentation.
Acknowledgements

This experiment was conducted on the joint research of the Institute of Laser Engineering, Osaka University. This work was supported in part by JSPS KAKENHI grant No. 16H02246 and No. 16H01119. The part of work was also supported by Genesis Research Institute, Inc. (Konpon-ken, TOYOTA).

REFERENCES

[1] T. Matsui and Y.Abe: Nature, 319, 303 - 319 (1986).

[2] B.Ivanov and A. Deutsch: Physics of the Earth and Planetary Interiors, 129, 131-143 (2002).

[3] K.Kawaragi et al.: Earth and Planetary Science Letters, 282, 56 - 64 (2009).

Keywords: Laser-Shock-compression, hugoniot, calcite, degassing

©2019. Japan Geoscience Union. All Right Reserved.

Direct observation of the transformation toughening of tetragonal stabilized zirconia under shock deformation condition by ns time-resolved XRD.

*Sota Takagi[1,2], Kouhei Ichiyanagi[2,3], Nobuaki Kawai[4], Ryo Fukaya[2], Shunsuke Nozawa[2], Atsushi Kyono[1], Nobumasa Funamori[2], Shin-ichi Adachi[2]

1. University of Tsukuba, 2. KEK PF, 3. Jichi Medical University, 4. Kumamoto University

The enhancement of strength and toughness was found in oxide-doped tetragonal stabilized zirconia, with the suggestion that the absorption of energy during the martensitic transformation contribute to the increment [Gravie et al., 1975; Gupta et al., 1977]. Using transmission electron microscopy (TEM), in recovery sample, it was observed that the stress-induced transformation from stabilized tetragonal phase to monoclinic phase can be occurred around the crack tip [Porter et al., 1977], and the transformation-toughening model were devised [McMeeking et al., 1982; Hannink et al., 2000]. In high-pressure experiments, the phase transformation behavior of tetragonal stabilized zirconia has not been clarified in both static and shock compression because a lack of in-situ observation [Ohtaka et al., 1988; Grady et al., 1992]. We tried to observe the behavior of tetragonal stabilized zirconia under shock compression condition using time-resolved XRD method.We performed the experiments at NW14A beamline at PF-AR (Photon Factory Advanced Ring), High Energy Accelerator Research Organization (KEK), Japan. Nd:glass laser with the wavelength of 1064 nm, pulse energy of 16 J, pulse width of 12 ns was used for shock-driving source. The laser beam was focused by optical lens to the size of 500 μm × 500 μm on the sample surface. For TR-XRD experiments, the synchrotron X-ray pulse of PF-AR was used as a probe source. The energy, the pulse width, and the size on the sample were 15.68 keV, about 100 ps, and 450 μm (H) ×250 μm (W), respectively. The irradiation timing between laser pulse and X-ray pulse on the sample surface were controlled by delay generator at ns time scale. The targets consisted of an 25 um PET film ablator with Al coated on the surface and 50 um polycrystalline 3 mol% yttria doped tetragonal stabilized zirconia.
The XRD change were observed up to 35 ns after shock compression started. Before shock, the (101), (002), (110), (102), (112), (200) diffraction of tetragonal phase were observed. 6.5 ns after shock, the diffraction from compression region appeared with maximum compression of 6%. No phase transition occurred at compression states. At release states (~11.4 ns), on the other hand, the (-111), (111), (022), (-221) diffraction peaks of monoclinic phase were appeared. We will discuss the detail of the experimental results and the transformation toughening mechanism.

Keywords: Synchrotron X-ray, Time-resolved XRD, Laser-induced shock wave, Tetragonal stabilized zirconia

©2019. Japan Geoscience Union. All Right Reserved.

[E] Oral | P (Space and Planetary Sciences)：P-CG Complex & General

Tue. May 28, 2019 1:45 PM - 3:15 PM JST | Tue. May 28, 2019 4:45 AM - 6:15 AM UTC | A03 TOKYO BAY MAKUHARI HALL

[P-CG22] Shock responses of planetary materials elucidated from meteorites and dynamic compression experiments

convener:Toshimori Sekine(Center for High Pressure Science and Technology Advanced Research), Takuo Okuchi(Institute for Planetary Materials, Okayama University), Chairperson:Toshimori Sekine(HPSTAR & Osaka University), Ai-Cheng Zhang(Nanjing University)

Impact phenomena had played essential roles in the process of planetary evolution. Recent analytical and experimental developments reveal a new prospective on the effects of shock-compression process for planetary materials. For deeper understanding of such shock effects, it is necessary to evaluate the detailed shock conditions from the observations of naturally-shocked planetary materials, and to compare them with the results on the planetary materials experienced a wide range of known shock conditions. Several metastable phases, that have not been known before, have recently been identified in shocked meteorites. They suggest that the shock state is often not in equilibrium and that it is more complicated process than ever thought. Experimental techniques including laser-driven shock compression and x-ray free electron laser diagnostics have been progressed to successfully simulate a wide range of shock conditions. The recent results indicate that shocked grains are fractured and rotated at relatively low pressures, and that they are subsequently transformed into denser phases or melts, or their mixtures at pressures of a few 100s GPa. Understanding of such shock dynamics requires another prospect, which is qualitatively different from the static high pressure and high temperature consensus. Therefore, it is timely to have an international symposium on dynamics of planetary materials.

1:45 PM - 2:00 PM JST | 4:45 AM - 5:00 AM UTC

[PCG22-01] Shock-induced phase transformation in howardite-eucrite-diogenite meteorites

★Invited Papers

*Ai-Cheng Zhang[1,2], De-Liang Chen[1], Run-Lian Pang[1] (1.School of Earth Sciences and Engineering, Nanjing University, China, 2.CAS Center for Excellence in Comparative Planetary, China)

2:00 PM - 2:15 PM JST | 5:00 AM - 5:15 AM UTC

[PCG22-02] Lattice-shear-induced metastable formation of high-pressure silicates in shocked meteorites

★Invited Papers

*Naotaka Tomioka[1], Takuo Okuchi[2], Masaaki Miyahara[3] (1.Kochi Institute for Core Sample Research, Japan Agency for Marine-Earth Science and Technology, 2.Institute for Planetary Materials, Okayama University, 3.Department of Earth and Planetary Systems Science, Hiroshima University)

2:15 PM - 2:30 PM JST | 5:15 AM - 5:30 AM UTC

[PCG22-03] Can high-pressure polymorphs clarify an ordinary chondrite parent-body breakup?

*Masaaki Miyahara[1], Akira Yamaguchi[2], Masato Saitoh[1], Kanta Fukimoto[1], Takeshi Sakai[3], Hiroaki Ohfuji[3], Naotaka Tomioka[4], Yu Kodama[5], Eiji Ohtani[6] (1.Department of Earth and Planetary Systems Science, Graduate School of Science, Hiroshima University, 2.National Institute of Polar Research, 3.Geodynamics Research Center, Ehime University, 4.Kochi Institute for Core Sample Research, Japan Agency for Marine-Earth Science and Technology, 5.Marine Works Japan, 6.Department of Earth Sciences, Graduate School of Science, Tohoku University)

2:30 PM - 2:45 PM JST | 5:30 AM - 5:45 AM UTC

[PCG22-04] Linking occurrence and texture of dense silicate minerals in shocked meteorites with laser-shock experimental results of Mg_2SiO_4 analyzed by XFEL probe

*Takuo Okuchi[1], Narangoo Purevjav[1], Norimasa Ozaki[2], Takeshi Matsuoka[2], Yusuke Seto[3], Yoshinori Tange[4], Toshinori Yabuuchi[5], Naotaka Tomioka[6], Toshimori Sekine[7], Ryosuke Kodama[2] (1.Institute for Planetary Materials, Okayama University, 2.Graduate School of Engineering, Osaka University, 3.Graduate

School of Science, Kobe University, 4.Japan Synchrotron Radiation Research Institute, 5.RIKEN Harima Branch, 6.Kochi Institute for Core Sample Research, Japan Agency for Marine-Earth Science and Technology, 7.Center for High Pressure Science and Technology Advanced Research)

2:45 PM - 3:00 PM JST | 5:45 AM - 6:00 AM UTC

[PCG22-05] **Laser-shock evolution of organic molecules in carbonaceous meteorite**

*Hikaru Yabuta[1], Hikaru Fujioka[2], Tatsuhiro Sakaiya[2], Tadashi Kondo[2], Sohsuke Ohno[3], Kosuke Kurosawa[3], Toshihiko Kadono[4], Keisuke Shigemori[5], Yoichiro Hironaka[5], Takamitsu Yamanaka[6] (1.Hiroshima University, Department of Earth and Planetary Systems Science, 2.Osaka University, Department of Earth and Space Science, 3.Chiba Institute of Technology, Planetary Exploration Research Center (PERC), 4.University of Occupational and Environmental Health, 5.Osaka University, Institute of Laser Engineering, 6.Center for High Pressure Science & Technology Advanced Research, Shanghai, China)

3:00 PM - 3:15 PM JST | 6:00 AM - 6:15 AM UTC

[PCG22-06] Shock barometer using cathodoluminescence and synchrotron angle-dispersive x-ray diffraction analyses of minerals

★Invited Papers

*Masahiro KAYAMA[1] (1.Tohoku University)

Shock-induced phase transformation in howardite-eucrite-diogenite meteorites

*Ai-Cheng Zhang[1,2], De-Liang Chen[1], Run-Lian Pang[1]

1. School of Earth Sciences and Engineering, Nanjing University, China, 2. CAS Center for Excellence in Comparative Planetary, China

Phase transformation is an important type of mineralogical respects to shock metamorphism in planets and asteroids. It has been widely used to constrain the dynamic conditions (pressure-temperature-time, P-T-*t*) of shock events and the mineral constituents in deep planets. In the past decades, shock-induced phase transformation has been extensively studied in shocked ordinary chondrites, martian and lunar meteorites. However, shock-induced phase transformation in howardite-eucrite-diogenite (HED) meteorites was less studied. In the past five years, a few high-pressure minerals (coesite, stishovite, tissintite, vacancy-rich clinopyroxene, super-silicic garnet, grossular, and a new mineral vestaite (TiFe)Ti_3O_9) have been reported in shocked eucrites (Miyahara et al., 2014; Pang et al., 2016, 2018; Fudge et al., 2017). In this study, we report a few new observations about shock-induced phase transformation in HED meteorites and discuss their potential implications for constraining the shock metamorphism of Vesta.

Four eucrite meteorites NWA 8003 (unbrecciated), NWA 2650 (brecciated), NWA 10245 (unbrecciated), and Dhofar 007 (brecciated) and two unbrecciated diogenite meteorites NWA 8321 and NWA 8326 were studied with scanning electron microscopy, Raman spectroscopy, Electron backscatter diffraction, and transmission electron microscopy.

The four eucrite meteorites NWA 8003, NWA 2650, NWA 10245, and Dhofar 007 have a few similar shock-induced features. All of them contain coesite, stishovite, vacancy-rich clinopyroxene, and tissintite. NWA 8003, NWA 2650, and Dhofar 007 also contain super-silicic garnet in shock-induced melt veins; however, no super-silicic garnet was observed in NWA 10245. In NWA 8003, unique Ti-rich melt pockets have been observed and contain ilmenite, vacancy-rich clinopyroxene, vestaite, corundum, and kyanite. In NWA 2650, an oval-shaped region in a super-silicic garnet-dominant shock-induced melt vein contains grossular, kyanite, and silica glass. Some kyanite crystals are present in the interstitial glass between surrounding super-silicic garnet grains. Some of the grossular grains occur as overgrowth on super-silicic garnet. These textures indicate that the grossular + kyanite + silica assemblage has formed through shock-induced melting of anorthite and recrystallization. Reidite was observed as irregular region and lamellae in zircon from NWA 2650. It might have formed through solid-state phase transformation at a pressure >20 GPa.

The two unbrecciated diogenite meteorites have different shock-induced features. NWA 8321 contains shock-induced melt veins which contain some mineral fragments of olivine, and pyroxene. No high-pressure minerals were detected within and adjacent to shock-induced melt veins. However, in NWA 8326, a few high-pressure minerals have been observed. They include stishovite, xieite, reidite, tuite, and tissintite. Stishovite was observed with two different textures. Xieite was observed as brighter lamellae in chromite adjacent to a thin shock-induced melt veins. Reidite mainly occurs as lamellar phase in zircon. The textures indicate that stishovite, xieite, and reidite have formed through solid-state phase transformation. Tissintite was also observed, closely adjacent to a shock-induced melt vein. It has probably formed through crystallization from high-pressure and high-temperature melt.

©2019. Japan Geoscience Union. All Right Reserved.

Our new observations reveal that shock-induced phase transformation in HED meteorites are more common than previous thought. Most of these HED meteorites have experienced a low to moderate degree of shock metamorphism. However, the presence of reidite and xieite indicates that some of the HED meteorites (NWA 2650 and NWA 8326 have experienced severe shock metamorphism. Generally, the diversity of high-pressure minerals in HED meteorites is consistent with the relatively low impact velocities in the main asteroid belt. In addition, compared to severe shock metamorphism in ordinary chondrites, martian and lunar meteorites, the high-pressure minerals in HED meteorites open a new window to study low to moderate shock metamorphism.

This work is financially supported by NSFC (grant 41673068) and NSF of Jiangsu Province of China (BK20170017).

Keywords: High-pressure minerals, Shock metamorphism, HED meteorites, Vesta

©2019. Japan Geoscience Union. All Right Reserved.

Lattice-shear-induced metastable formation of high-pressure silicates in shocked meteorites

*Naotaka Tomioka[1], Takuo Okuchi[2], Masaaki Miyahara[3]

1. Kochi Institute for Core Sample Research, Japan Agency for Marine-Earth Science and Technology, 2. Institute for Planetary Materials, Okayama University, 3. Department of Earth and Planetary Systems Science, Hiroshima University

Heavily shocked meteorites contain various types of high-pressure polymorphs of silicate minerals. These high-pressure minerals are micron to submicron sized and occurred within and in the vicinity of shock-induced melt in stony meteorites. Their occurrence suggests two types of formation mechanisms: (1) solid-state high-pressure transformation of the host-rock minerals into monomineralic polycrystalline aggregates, and (2) crystallization of chondritic or monomineralic melts under high pressure [1]. In some cases of the former process, high-pressure minerals occur as coherent lamellae within grains of the host low-pressure minerals. A typical example is the (Mg,Fe)SiO_3pyroxene-akimotoite intergrowth in the Tenham meteorite [2]. The akimotoite has relatively high Fe content [Fe/(Mg+Fe)=0.21] but does not have its stability field at any P-T conditions [3]. Therefore, the akimotoite would have been formed metastably due to a rapidly-changing P-T history in the shock event. As another example, a new high-pressure polymorph of olivine, which has been defined as “ε-phase” with a spinelloid structure, was recently discovered as nano-scale lamellae in ringwoodite [$(Mg,Fe)_2SiO_4$-spinel] and wadsleyite [$(Mg,Fe)_2SiO_4$ -spinelloid] grains in Tenham and Miami meteorites, respectively [4]. The phase has never been observed in previous phase equilibrium studies. Both pyroxene-akimotoite and ringwoodite/wadsleyite-ε-phase intergrowths have topotaxy with preserving close-packed oxygen layers for their respective structures. The crystallographic relationships between these host and the product phases suggest that these polymorphic phase transformations are promoted by shear mechanism [5]. This process is achieved by shear deformation of oxygen sublattice associating movements of interstitial cations within single unit-cell dimension. Therefore, shear mechanism is considered to be a favorable mechanism under high differential stress, or under relatively low-temperatures, where atomic diffusion is kinetically hindered. Future experimental studies, which include ultrafast in-situ X-ray diffraction under laser shock compression, and high-resolution electron microscopy on recovered specimens of static high-pressure experiments, would contribute to better understanding of detailed structural changes in naturally shocked samples.

References: [1] Tomioka & Miyahara (2017) *Meteorit. Planet. Sci.*,52, 2017–2039. [2]Tomioka & Fujino (1999) *Amer. Mineral.*, 84, 267–271. [3] e.g. Ito & Yamada (1982) in*High-Pres. Res. Geophys.*, 405–419.[4] e.g. Tomioka & Okuchi (2017) *Sci. Rep.*, 7, 17351. [5] Tomioka (2007) *J. Mineral. Petrol. Sci.* ,102, 226–232.

Keywords: shock metamorphism, meteorites, transformation mechanisms, high-pressure minerals

©2019. Japan Geoscience Union. All Right Reserved.

Can high-pressure polymorphs clarify an ordinary chondrite parent-body breakup?

*Masaaki Miyahara[1], Akira Yamaguchi[2], Masato Saitoh[1], Kanta Fukimoto[1], Takeshi Sakai[3], Hiroaki Ohfuji[3], Naotaka Tomioka[4], Yu Kodama[5], Eiji Ohtani[6]

1. Department of Earth and Planetary Systems Science, Graduate School of Science, Hiroshima University, 2. National Institute of Polar Research, 3. Geodynamics Research Center, Ehime University, 4. Kochi Institute for Core Sample Research, Japan Agency for Marine-Earth Science and Technology, 5. Marine Works Japan, 6. Department of Earth Sciences, Graduate School of Science, Tohoku University

An ordinary chondrite is the biggest clan in the meteorites. The ordinary chondrites are the building blocks of an ordinary chondrite parent-body that broke up by an impact in the solar nebula. The breakup process of the ordinary chondrite parent-body is one of the intriguing conundrums. Most ordinary chondrites have evidence for the impact event. Shock-induced melting textures and high-pressure polymorphs are the most distinct clues for the impact event. Chen et al. (1996) suggested that the high-pressure polymorphs occurring in the shock-induced melt can be a clue for clarifying the impact event occurred on the parent-body because we can constrain several parameters for the impact such as shock pressure and impact velocity based on the formation conditions of the high-pressure polymorph assemblage. Accordingly, many previous studies have worked on the high-pressure polymorphs in the ordinary chondrites for several decades. Most previous investigations have focused on the L6 chondrite because the meteorite type is abundantly recovered on the Earth. On the other hand, few previous studies have worked on other petrologic types such as L5 and L4. The inventories of the high-pressure polymorphs in shocked H- and LL-group ordinary chondrites have been barely described. The ordinary chondrite parent-body is expected to have an onion shell-like structure. H-, L-, and LL-group ordinary chondrites originate from their individual parent-bodies. We have to clarify the inventories of the high-pressure polymorphs included in all petrologic types and groups to elucidate the breakup processes of the ordinary chondrite parent-bodies. Accordingly, we initiated the systematic investigations of the high-pressure polymorphs included in the shocked ordinary chondrites. About sixty H-group, eighty L-group, and fifty LL-group ordinary chondrites with the shock-induced melting textures were systematically investigated by SEM and Raman spectrometer. There was the distinct difference in the modes of shock-induced melting between petrologic type 3–4 and type 5–6 in all groups. In the petrologic type 3–4, the melting occurred at the boundaries between the chondrules and surrounding matrices as a melt-pocket. In the petrologic type 5–6, melting occurred as isolated veins or networks. There was also a clear difference in abundance of the high-pressure polymorphs among H-, L-, and LL-groups: the high-pressure polymorphs are abundant in L- and LL-groups, whereas rare in H-group. The species and assemblages of the high-pressure polymorphs depended on the petrologic types. The abundance and assemblages of the high-pressure polymorphs in L- and LL-group were similar to each other, suggesting that both parent-bodies have similar impact histories. The shock-pressure conditions were estimated based on the identified high-pressure polymorph assemblages: from ~13 to ~24 GPa for L/LL6, from ~3 to ~12 GPa for L/LL4 and L/LL5, and less than ~3 GPa for L/LL3. When we adopted the estimations into the onion-shell-structured parent-body, the shock pressure condition on the parent-body surface is much lower than its interior, which is unlikely for a head-on impact. We cannot explain the parent-body breakup phenomenon based only on the estimation using the high-pressure polymorphs. There are clear differences on their petrographic structures between type 3–4 and type 5–6: the former consists of accumulated chondrules and the latter has equilibrated texture. It is also expected that type 3–4 and type 5–6 chondrites have different initial density and porosity. These differences will affect the

©2019. Japan Geoscience Union. All Right Reserved.

response to the shock metamorphism. Unless we take these factors into the estimation, we cannot clarify the parent-body breakup phenomenon by using the high-pressure polymorphs.

Reference: Chen et al. Science 271: 1570–1573 (1996)

Keywords: Shock, Ordinary chondrite, High-pressure polymorph

©2019. Japan Geoscience Union. All Right Reserved.

Linking occurrence and texture of dense silicate minerals in shocked meteorites with laser-shock experimental results of Mg_2SiO_4 analyzed by XFEL probe

*Takuo Okuchi[1], Narangoo Purevjav[1], Norimasa Ozaki[2], Takeshi Matsuoka[2], Yusuke Seto[3], Yoshinori Tange[4], Toshinori Yabuuchi[5], Naotaka Tomioka[6], Toshimori Sekine[7], Ryosuke Kodama[2]

1. Institute for Planetary Materials, Okayama University, 2. Graduate School of Engineering, Osaka University, 3. Graduate School of Science, Kobe University, 4. Japan Synchrotron Radiation Research Institute, 5. RIKEN Harima Branch, 6. Kochi Institute for Core Sample Research, Japan Agency for Marine-Earth Science and Technology, 7. Center for High Pressure Science and Technology Advanced Research

Primitive meteorites often show features of shock metamorphism, including occurrences of dense polymorphs of major mineral phases. By previous transmission electron microscopy studies it was demonstrated that olivine (alpha-Mg_2SiO_4) often had transformed into its denser polymorphs such as ringwoodite (gamma-Mg_2SiO_4), and as a recently-discovered new structure (epsilon-Mg_2SiO_4: Tomioka and Okuchi, Sci. Rep. 2017). The impact events that produced these polymorphs played essential roles in the history of early solar system evolution. Here we tried to reproduce such a dynamic transformation process starting from forsterite olivine single crystals by using very strong laser beam and x-ray free electron laser (XFEL) beam in combination at SACLA, SPring-8, Japan. A transformation process has been successfully observed with sub-nanosecond resolution by x-ray diffraction using femtosecond XFEL pulses. We discovered an ultrafast transformation process completing only within few nanoseconds, which was not expected to occur during shock metamorphism of meteorites. It can be a shear-induced fast lattice slipping proceeding without any atomic diffusion process. We conclude that formation processes and environments of some of dense Mg_2SiO_4 polymorphs in heavily shocked meteorites are needed to be reconsidered to involve this fast process.

Keywords: dense silicate minerals, laser shock experiments, shock metamorphism, Mg2SiO4

©2019. Japan Geoscience Union. All Right Reserved.

Laser-shock evolution of organic molecules in carbonaceous meteorite

*Hikaru Yabuta[1], Hikaru Fujioka[2], Tatsuhiro Sakaiya[2], Tadashi Kondo[2], Sohsuke Ohno[3], Kosuke Kurosawa[3], Toshihiko Kadono[4], Keisuke Shigemori[5], Yoichiro Hironaka[5], Takamitsu Yamanaka[6]

1. Hiroshima University, Department of Earth and Planetary Systems Science, 2. Osaka University, Department of Earth and Space Science, 3. Chiba Institute of Technology, Planetary Exploration Research Center (PERC), 4. University of Occupational and Environmental Health, 5. Osaka University, Institute of Laser Engineering, 6. Center for High Pressure Science & Technology Advanced Research, Shanghai, China

It has been hypothesized that extraterrestrial organic compounds were delivered to the early Earth by meteorites and comets during the Late Heavy Bombardment (LHB). There have been several experiments that simulated the shock synthesis of organic compounds during the LHB. However, in the past studies using gas guns, it is difficult to perform an open system experiment at higher impact velocities than Earth’ s escape velocity (> 17 km/s). In order to understand what compositions of meteoritic organic molecules were produced by the shock energy of LHB and delivered to the Earth, we carried out a high power laser compression experiment (up to 400 GPa) of carbonaceous chondritic meteorite, which contains 2wt% of organic carbon.

Pellets of Murchison carbonaceous meteorite was prepared by diamond anvil cell, respectively. Pellets of the meteorites in 3mm diameter and 1mm thickness were prepared. The titanium foil was located in front of the sample as the ablator for the laser and for preventing the sample from blowing out. The laser-shock experiment was carried using GEKKO XII/HIPER laser system, Institute of Laser Engineering, Osaka University. The laser wavelength, pulse width, and spot diameter were 1053 nm, ~20 ns, and ~0.4 mm, respectively. The shock pressures were 20, 50, and 400 GPa. The collected meteorite samples were extracted with dichloromethane and methanol. The extracts were concentrated and analyzed by a gas chromatography coupled with mass spectrometry (GCMS).

Molecular compositions of polycyclic aromatic hydrocarbons (PAHs) in Murchison meteorite are not changed before and after the shock experiment at 20 GPa, except that the concentration of naphthalene was depleted. At 50 and 400 GPa, the concentrations of pyrene and fluoranthene increased, while those of biphenyl, fluorenone, and anthracene decreased. Molecular compositions of *n*-alkanes (C_{14} –C_{24}) are not largely changed before and after the shock experiment at 20 GPa. However, at 50 GPa, the concentrations of short chain *n*-alkanes (C_{14} - C_{17}) decreased and those of long chain *n*-alkanes (C_{18} - C_{24}) relatively increased. These results indicate that impact processes promote aromatic ring condensation and elongation of carbon chains of *n*-alkanes.

Keywords: High-power laser, Organic compounds in meteorites, Astrobiology

©2019. Japan Geoscience Union. All Right Reserved.

Shock barometer using cathodoluminescence and synchrotron angle-dispersive x-ray diffraction analyses of minerals

*Masahiro KAYAMA[1]

1. Tohoku University

A part of meteorites record collisional history of asteroidal and cometary impacts. Impactites were created in impact craters by the shock event on the Earth. These materials provide vital information on collision and accumulation processes of asteroid and planet and ejection process from the parent body. The shock pressure is one of the most important parameters to interpret these impact history. Various techniques such as optical and electron microscopy and infrared adsorption and Raman spectrometry have been applied for minerals (e.g., feldspar and silica minerals) in meteorites and impactites to estimate the shock pressure that occurs on the Earth, Moon, and Mars. Although there are many works to evaluate the shock pressure using these techniques, quantitative estimation of a wider dynamic range of shock pressure has not been possible for a micrometer-sized grain to date. Here, cathodoluminescence (CL) and synchrotron angle-dispersive x-ray diffraction (SR-XRD) of experimentally shocked feldspars and quartz and these minerals in meteorite and impactite have been investigated to establish a new shock barometer.

Shock experiments were performed for single crystals of synthetic and terrestrial quartz and terrestrial feldspars at the National Institute for Material Science using a one stage propellant gun. Quartz in an impactite from the Chicxulub crater and alkali feldspar and plagioclase in martian meteorites (NWA 2975, Shergotty, Dhofar 019, and Zagami) were selected here. CL spectroscopy of these samples was conducted at Okayama University of Science. SR-XRD was measured for the powder samples at KEK Photon Factory (PF; beam line: PF BL-4B2).

CL spectra of unshocked feldspars (starting material for the shock recovery experiments) consist of blue, yellow, and/or red emission bands in the wavelength range from 300 to 800 nm. The ultraviolet (UV) to blue emission bands at 330 and 380 nm were obtained from CL spectra of only experimentally shocked feldspars at 20 to 40 GPa. The intensities of all UV-blue emissions correlate positively with the shock pressure. Similar UV-blue emission bands were recognized in CL spectra of the shock-induced feldspar glasses in the martian meteorites and impactites.

CL spectra of unshocked synthetic and terrestrial quartz show an extremely weak blue emission band at 400 nm. The blue emission band was also detected in CL spectra of the experimentally shock recovered samples at 5 to 40 GPa and quartz in the impactite, whereas their blue emission intensities are obviously higher than those of the unshocked quartz. The blue emission intensities increase with the pressure due to shock experiments gradually from 5 to 15 GPa and drastically from 20 to 40 GPa. These correlations obtained from CL spectra of experimentally shocked feldspar and quartz would give quantitative values of the shock pressures that the minerals in martian meteorites and impactite have experienced. Therefore, the CL intensity of feldspar has a potential for a shock barometer with high spatial resolution.

SR-XRD analyses of experimentally shocked quartz demonstrated that the diffraction peaks increase in the intensity and become broader with increasing the shock pressure in the range from 5 to 30 GPa. At the shock pressure above 35 GPa, diffraction peak of quartz was no longer undetectable from the pattern, implying its complete amorphization. Moreover, several crystal planes exhibit peak shifts with the pressure in the pressure range from 15 to 30 GPa. Furthermore, the shock experiments enhance micro strain and

©2019. Japan Geoscience Union. All Right Reserved.

reduce crystallite size. This fact indicates that the shock-induced amorphization was initiated by lattice distortion and structural defects induced by shock compression. The SR-XRD response to the shock pressure suggests the possibility of shock barometer using SR-XRD method, at least in the range from 15 to 30 GPa.

Keywords: Shock impact, Feldspar, Quartz, Cathodoluminescence, Synchrotron angle-dispersive x-ray diffraction

©2019. Japan Geoscience Union. All Right Reserved.

[E] Oral | P (Space and Planetary Sciences)：P-CG Complex & General

Tue. May 28, 2019 3:30 PM - 5:00 PM JST | Tue. May 28, 2019 6:30 AM - 8:00 AM UTC | A03 TOKYO BAY MAKUHARI HALL

[P-CG22] Shock responses of planetary materials elucidated from meteorites and dynamic compression experiments

convener:Toshimori Sekine(Center for High Pressure Science and Technology Advanced Research), Takuo Okuchi(Institute for Planetary Materials, Okayama University), Chairperson:Takuo Okuchi(Okayama University), Yongjae Lee(Yonsei University)

Impact phenomena had played essential roles in the process of planetary evolution. Recent analytical and experimental developments reveal a new prospective on the effects of shock-compression process for planetary materials. For deeper understanding of such shock effects, it is necessary to evaluate the detailed shock conditions from the observations of naturally-shocked planetary materials, and to compare them with the results on the planetary materials experienced a wide range of known shock conditions. Several metastable phases, that have not been known before, have recently been identified in shocked meteorites. They suggest that the shock state is often not in equilibrium and that it is more complicated process than ever thought. Experimental techniques including laser-driven shock compression and x-ray free electron laser diagnostics have been progressed to successfully simulate a wide range of shock conditions. The recent results indicate that shocked grains are fractured and rotated at relatively low pressures, and that they are subsequently transformed into denser phases or melts, or their mixtures at pressures of a few 100s GPa. Understanding of such shock dynamics requires another prospect, which is qualitatively different from the static high pressure and high temperature consensus. Therefore, it is timely to have an international symposium on dynamics of planetary materials.

3:30 PM - 3:45 PM JST | 6:30 AM - 6:45 AM UTC

[PCG22-07] Dynamic Compression at Pohang X-ray Free Electron Laser Facility (PAL-XFEL)

★Invited Papers

*Yongjae Lee[1] (1.Yonsei University, Seoul, Korea)

3:45 PM - 4:00 PM JST | 6:45 AM - 7:00 AM UTC

[PCG22-08] Exploration of extreme melt states of silicate usign high-power laser and XFEL

★Invited Papers

*Norimasa Ozaki[1] (1.Osaka University)

4:00 PM - 4:15 PM JST | 7:00 AM - 7:15 AM UTC

[PCG22-09] Hugoniot measurements for silicate: Understanding silicate magma under the planetary impacts

*Yuhei Umeda[1], Norimasa Ozaki[1], Toshimori Sekine[2], Bruno Albertazzi[3], Alessandra Benuzzi-Mounaix[3], Riccardo Bolis[3], Marco Guaruaglini[3], Kento Katagiri[1], Kodama Ryosuke[1], Michel Koeing[3], Kohei Miyanishi[4], Shintaro Morioka[1], Toyohito Nishikawa[1], Syugo Ohi[5], Alessandra Ravasio[3], Yoichi Sakawa[4], Takayoshi Sano[4], Tomoko Sato[6] (1.Graduate School of Engineering, Osaka Univ., 2.Center for High Pressure Science & Technology Advanced Research, 3.Ecole Polytechnique, 4.Institute of Laser Engineering, Osaka University, 5.Shiga Univ., 6.Graduate School of Science, Hiroshima University)

4:15 PM - 4:30 PM JST | 7:15 AM - 7:30 AM UTC

[PCG22-10] **An experimental design to determine iron melting at the Earth's core conditions via in-situ X-ray diffraction technique at high power laser facility**

★Invited Papers

*Hao Liu[1] (1.Laser fusion research center)

4:30 PM - 4:45 PM JST | 7:30 AM - 7:45 AM UTC

[PCG22-11] **Study on transport properties of liquid iron and iron alloy under high temperature and high pressure using the laser shock technique**

*Kohei Miyanishi[1], Norimasa Ozaki[2], Satoshi Ohmura[3], Marion Harmand[4], Andy Krygier[5], Toyohito Nishikawa[2], Yuhei Umeda[2], Shigemori Keisuke[1], Youichi Sakawa[1], Takayoshi Sano[1], Ryosuke Kodama[1,2] (1.Institute for Laser Engineering, Osaka University, 2.Graduate school of engineering, Osaka University, 3.Faculty of Engineering, Hiroshima Institute of Technology, 4.IMPMC, Sorbonne Université, 5.LLNL)

4:45 PM - 5:00 PM JST | 7:45 AM - 8:00 AM UTC

[PCG22-12] **Laser shock compression in LFRC**

*Liang Sun[1] (1.Laser Fusion Research Center, CAEP)

Dynamic Compression at Pohang X-ray Free Electron Laser Facility (PAL-XFEL)

*Yongjae Lee[1]

1. Yonsei University, Seoul, Korea

We have successfully commissioned dynamic compression studies at the Pohang X-ray Free Electron Laser facility (PAL-XFEL) in Korea by utilizing instrumentations at FXS (Femtosecond X-ray Scattering) –XSS (X-ray Scattering and Spectroscopy) beamline. As the first experiment, a polycrystalline iron foil has been illuminated by an 800 nm wavelength uncompressed optical laser with ~6 mJ in 150 ps pulse length, focused onto a 100 mm FWHM spot. The shock-compressed sample has then been probed by ca. 50 fs quasi-monochromatic (bandwidth 0.4%) X-ray pulse at an energy of ~10 keV with 10^{11} photons per pulse, focused to ca. 30 mm diameter using a CRL optics. The sample is positioned normal to the X-ray pulse at a distance of ca. 12 cm from a Rayonix mx225 detector in a way to cover 2q angles up to ca. 65 degrees. Single-shot diffraction measurements were performed with ca. 100 ps. increment up to one nanosecond. We demonstrate that PAL-XFEL can provide a unique opportunity in probing ultrafast lattice dynamics with sufficient spatial and temporal resolution in intermediate pressure regime.

Keywords: dynamic compression, laser shock, iron, X-ray free electron laser

©2019. Japan Geoscience Union. All Right Reserved.

Exploration of extreme melt states of silicate usign high-power laser and XFEL

*Norimasa Ozaki[1]

1. Osaka University

Recent experimental studies on silicate using high-power lasers and XFEL are reviewed.

Keywords: Shock compression, High power laser, Silicate, X-ray free electron laser

©2019. Japan Geoscience Union. All Right Reserved.

Hugoniot measurements for silicate: Understanding silicate magma under the planetary impacts

*Yuhei Umeda[1], Norimasa Ozaki[1], Toshimori Sekine[2], Bruno Albertazzi[3], Alessandra Benuzzi-Mounaix[3], Riccardo Bolis[3], Marco Guaruaglini[3], Kento Katagiri[1], Kodama Ryosuke[1], Michel Koeing[3], Kohei Miyanishi[4], Shintaro Morioka[1], Toyohito Nishikawa[1], Syugo Ohi[5], Alessandra Ravasio[3], Yoichi Sakawa[4], Takayoshi Sano[4], Tomoko Sato[6]

1. Graduate School of Engineering, Osaka Univ., 2. Center for High Pressure Science & Technology Advanced Research, 3. Ecole Polytechnique, 4. Institute of Laser Engineering, Osaka University, 5. Shiga Univ., 6. Graduate School of Science, Hiroshima University

Two magnesium silicates of $MgSiO_3$(Enstatite) and Mg_2SiO_4(Forsterite) are primary mantle constitutions in the Earth and major components in Earth-type exoplanets.The ordinary chondrite, which accounts for about 90 % of all flying meteorites, consists of silicates as main components. The impacts at collision velocities exceeding 10 km/s are known as common events in the universe and such high energy phenomena could have played an important role to form planets or planetesimals and to evolve planetary environments. For example, a large-scale impact such as the giant impact related to the formation of moon was estimated to be at impact velocity of 15-20 km/s [Melosh, 1990].

In this study, Hugoniot equation of state (EOS) of enstatite has been determined at pressures of ~400 to 560 GPa by laser shock experiments. A coupling of both the present study and the previous data by Fratanduono et al. (2018) shows a discontinuity in the shock velocity-particle velocity at ~380-400 GPa. The measured reflectivity of shocked enstatite indicates three different trends relative to that of quartz; less steep slope at 300-345 GPa, parallel at 345-400 GPa, and a rapid increasing above ~400 GPa, suggesting different phases of enstatite melt, a mixture of metal-like liquid of $SiO_2$and crystalline MgO, and fluid-like enstatite melt above ~380 GPa. We also calculated the release state of thin enstatite using quartz on it as a reference. These results on enstatite imply that reactions in silicate magma occur at pressures of 300-400 GPa and that they may affect the current planet formation model in terms of the stratification of interior, the mantle convection, and the formation of magnetic field in Super-Earths.

©2019. Japan Geoscience Union. All Right Reserved.

An experimental design to determine iron melting at the Earth’s core conditions via in-situ X-ray diffraction technique at high power laser facility

*Hao Liu[1]

1. Laser fusion research center

Phase diagram of iron at the Earth’s core conditions is mandatory for determining the states at the core boundaries and the crystal structure of the solid core. Up to date, the iron phase diagram at high pressure has been investigated experimentally by both static compression (diamond-anvil cell) and dynamic compression (shock wave) techniques. However, the discrepancies among different researches on melting line of iron are still irreconciled. Combining in-situ transient X-ray diffraction and laser compression technique, we propose an investigation which could determine the melting line of iron or the high-pressure high-temperature phase from the lattice level. In this research, high power lasers are applied to drive the iron into melting state. X-ray diffraction pattern interpretation and the criteria for judging iron melting are of great importance. Traditionally, the existence of diffraction peak is used as the only criteria to determine if melting occurs. Nevertheless, this is not enough for shock loading with high heating rate, where the pre-melting or superheating phenomenon occurs. Under these conditions, the diffraction peaks could either disappear at temperature below the melting line or remain even above the melting line. This could lead to misinterpretation for melting temperature. However, the two-dimensional shape of diffraction pattern will change. When melting initiates, the shear modulus of the highly stressed material disappears and the diffraction pattern changes into an ideally circled shape. Therefore, with the information of two-dimensional diffraction pattern, we can make the melting criteria, from the lattice level, more sound and clear. This method could provide experimental judgment with higher precision, which might reconcile the discrepancies on melting temperature of iron at the Earth’s core conditions.

Keywords: laser shock, in-situ x-ray diffraction, iron melting, earth core

©2019. Japan Geoscience Union. All Right Reserved.

Study on transport properties of liquid iron and iron alloy under high temperature and high pressure using the laser shock technique

*Kohei Miyanishi[1], Norimasa Ozaki[2], Satoshi Ohmura[3], Marion Harmand[4], Andy Krygier[5], Toyohito Nishikawa[2], Yuhei Umeda[2], Shigemori Keisuke[1], Youichi Sakawa[1], Takayoshi Sano[1], Ryosuke Kodama[1,2]

1. Institute for Laser Engineering, Osaka University, 2. Graduate school of engineering, Osaka University, 3. Faculty of Engineering, Hiroshima Institute of Technology, 4. IMPMC, Sorbonne Université, 5. LLNL

Information on the thermal and electrical transport properties of iron alloys under high-pressure and high-temperature conditions corresponding to the earth’ s outer core is necessary to clarify the convection phenomena of the earth and the cooling history. In particular, the transport properties in the outer core–mantle boundary condition strongly influence the mantle convection, the outer core convection generating the earth's magnetic field, the growth and inner flow of the inner core, and so on. However, there are very few experimental examples concerning high-pressure and high-temperature liquid iron/iron-alloy which correspond to the outer core conditions, and only a few cases have been reported for pure iron [1]. It is required to investigate transport coefficients of liquid iron alloys containing light elements to simulate actual outer core, experimentally. Laser shock compression technique has several advantages to exploring iron-alloys under high-pressure and high-temperature condition. As there is no mechanical restriction on pressure generation, producing the pressure of even TPa is easy, and high heating rate exceeding 10^{15}K / s is possible, and it is a closed system that is not affected by surroundings. Therefore the technique is effective for generation and observation of high-pressure and high-temperature liquid iron-alloys. In this research, we report optical reflectivity, pressure and temperature measurements of laser shock compressed iron and iron-silicon (Fe-Si) alloy at and above the earth's outer core conditions.

Target assemblies containing polypropylene (CH), aluminum, quartz, iron or iron-silicon alloy and magnesium oxide (MgO) window were shock compressed by laser ablation at the GEKKO XII laser facility, the Institute of Laser Engineering, Osaka University. Iron and iron-silicon alloy were formed by electron beam evaporation on the MgO window. Laser beams with a wavelength of 527 nm were focused onto the target. A focal spot was 1 mm in diameter with a flat-top spatial intensity distribution resulting in a planar shock front. Temporal shape of the laser pulse was approximately a flat-top with a full-width at half-maximum of 2.5 ns. The velocity interferometer system for any reflector (VISAR) measure a particle velocity and a reflectivity at the interface between iron or iron-silicon alloy and MgO. The Ppressure was evaluated using measured particle velocity and a known equation of state of MgO[2]. The optical pyrometer measures the temperature at the interface through the MgO window.

The pressures determined from the measurement results were from 200 to 400 GPa, and the temperatures were up to 15000 K. In the pressure range exceeding 200 GPa, in the case of iron, a decrease in reflectivity was observed as the pressure increased, whereas in the case of the iron-silicon alloy, a continuous increase following a discontinuous decrease in the reflectivity was observed. The decrease in reflectivity of iron suggests a decrease in electronic conductivity due to temperature rise with increasing pressure. On the other hand, the continuous rise seems to indicate an increase in the density of free electrons derived from silicon.

©2019. Japan Geoscience Union. All Right Reserved.

[1] K. Ohta, Y. Kuwayama, K. Hirose, K. Shimizu, Y. Ohisi: Nature, 534, 95-98 (02 June 2016).

[2] S. Root, L. Shulenburger, R. W. Lemke et al.: Phys. Rev. Lett, 115, 198501 (2015).

Keywords: iron alloy

©2019. Japan Geoscience Union. All Right Reserved.

Laser shock compression in LFRC

*Liang Sun[1]

1. Laser Fusion Research Center, CAEP

Shock compression is a major technique used for achieving high pressures dynamically. High-powered lasers are increasingly being used for dynamic loading of materials, especially for extreme high pressure. Ramp loading, a series of weak compress waves, is an another advantage for laser-based dynamics, which can be realized easily by the laser pulse shape and can be applied to compress material in much lower temperature under exoplanetary condition. In this talk, we will present our shock loading and X-Ray diagnostics abilities in LFRC and our shock experiment results. Our research progress will also be mentioned, especially in laser shock compression of iron and ramp compression of Al to 420 GPa. Several problems in the mineralogy of Super-Earth planets will also be mentioned in the end of this talk.

Keywords: laser shock compression, ramp compression, High-powered lasers

©2019. Japan Geoscience Union. All Right Reserved.

[J] Oral | P (Space and Planetary Sciences)：P-CG Complex & General

Tue. May 28, 2019 9:00 AM - 10:30 AM JST | Tue. May 28, 2019 12:00 AM - 1:30 AM UTC | A05 TOKYO BAY MAKUHARI HALL

[P-CG25] Planetary Magnetosphere, Ionosphere, and Atmosphere

convener:Kanako Seki(Graduate School of Science, University of Tokyo), Takeshi Imamura(Graduate School of Frontier Sciences, The University of Tokyo), Hiroyuki Maezawa(Department of Physical Science Osaka Prefecture University), Naoki Terada(Graduate School of Science, Tohoku University), Chairperson:Masaki Nishino(名古屋大学宇宙地球環境研究所), Hiroyuki Maezawa(大阪府立大学大学院理学系研究科)

Exploration of Moon, Venus, Mars, Mercury, Jupiter, Saturn, and beyond together with rapid developments of numerical simulations provides us new view of planetary environment. This session collects general contributions of new findings about planetary magnetosphere, ionosphere, and atmosphere. New methodology and technology development studies for future explorations are also welcome. In order to put the common knowledge at different planets into perspective, this session aims to facilitate discussions on comparative planetary environments.

9:00 AM - 9:30 AM JST | 12:00 AM - 12:30 AM UTC

Introduction

9:30 AM - 9:45 AM JST | 12:30 AM - 12:45 AM UTC

[PCG25-01] On the observational constraint on time and spatial variation of Titan's atmospheric trace gases driven with the ALMA solar system big-data

*Takahiro IINO[1,2], Hideo Sagawa[3], Takashi Tsukagoshi[4] (1.The University of Tokyo, 2.Tokyo Univ. of Agr. and Tech., 3.Kyoto Sangyo University, 4.NAOJ)

9:45 AM - 10:00 AM JST | 12:45 AM - 1:00 AM UTC

[PCG25-02] Transport and energization of planetary ions in the magnetospheric flanks of Mercury

*Sae Aizawa[1], Dominique Delcourt[2], Naoki Terada[1] (1.Graduate School of Science,Tohoku University, 2.LPC2E, CNRS)

10:00 AM - 10:15 AM JST | 1:00 AM - 1:15 AM UTC

[PCG25-03] Exploring the real-time prediction of Mercury's magnetosphere

*Manabu Yagi[1], Kanako Seki[2], Yosuke Matsumoto[3], Dominique C. Delcourt[4], Francois Leblanc[4] (1.RIKEN Center for Computational Science, 2.Graduate School of Science, University of Tokyo, 3.Graduate School of Science, Chiba University, 4.The National Center for Scientific Research)

10:15 AM - 10:30 AM JST | 1:15 AM - 1:30 AM UTC

[PCG25-04] Model study on the contribution of various physical processes for generation and dissipation of Mercury's exosphere

*Yudai Suzuki[1], Kazuo Yoshioka[1] (1.University of Tokyo)

On the observational constraint on time and spatial variation of Titan's atmospheric trace gases driven with the ALMA solar system big-data

*Takahiro IINO[1,2], Hideo Sagawa[3], Takashi Tsukagoshi[4]

1. The University of Tokyo, 2. Tokyo Univ. of Agr. and Tech., 3. Kyoto Sangyo University, 4. NAOJ

Titan's atmosphere is characterized by the presence of the number of trace gases such as hydrocarbons and nitriles produced with complex photochemical processes. Cassini spacecraft, which completed its works in 2017, has played an important role to illustrate the dynamic variation of the trace gases. For example, on the high-latitudinal region of the southern hemisphere, both hydrogen cyanide (HCN) and benzene (C_6H_6) exhibited ~1000 times enhancement of their atmospheric abundances from 2011 to 2015 (Coustenis et al. 2016). For the understanding of complicated photochemical processes of Titan, long-term observation of the spatial distribution of such trace gases are crucial.

ALMA is a suitable tool for that purpose. We have constructed a large spectroscopic data-set of Titan's trace gases by converting ALMA's archival data obtained for the calibration purpose into the scientific data known as "FITS cube", which contains calibrated spectra in each 2-D image pixels. Extracted number of Titan's FITS data is more than 3000. Many trace gases such as carbon monoxide (CO), HCN, acetonitrile (CH_3CN), cyanoacetylene (HC_3N) and their isotopologues and other complex molecules are detected clearly. For the illustration of the time distribution, spectral intensity distribution maps of all detected species were produced.

From the analysis of the spectral intensity distribution map, from mid 2015, intensities of HC_3N measured on southern hemisphere is stronger than that of northern hemisphere. In turn, northern hemispheric CH_3CN and HCN intensities are still stronger than that of south in 2015 and 2017, respectively. Newly found difference of the time variation between the nitriles possibly reflects their photochemical production/destruction timescale against the seasonal variation of UV influx and atmospheric circulation. Currently, we are attempting to develop the semi-automated atmospheric retrieval code to reproduce the 3-D distribution of trace species to constrain the photochemical processes.

Keywords: Titan, ALMA, Planetary atmosphere

©2019. Japan Geoscience Union. All Right Reserved.

Transport and energization of planetary ions in the magnetospheric flanks of Mercury

*Sae Aizawa[1], Dominique Delcourt[2], Naoki Terada[1]

1. Graduate School of Science,Tohoku University, 2. LPC2E, CNRS

The transport and energization of planetary ions within Kelvin-Helmholtz (KH) vortices developing in the magnetospheric flanks of Mercury are investigated using both numerical methods and data analysis. Due to the presence of heavy ions of planetary origin (e.g., O^+, Na^+, and K^+) and the complicated field structure present during the KH vortex development, the scale of electric field variations can be comparable to that of the ion gyromotion. Therefore, ions may experience non-adiabatic energization as they drift across the magnetopause. In this study, we focus on the effects of the spatial/temporal variations of the electric field along the ion path. We show that the intensification, rather than the change in orientation, is responsible for large non-adiabatic energization of heavy ions of planetary origin. This energization systematically occurs for ions with low initial energies in the direction perpendicular to the magnetic field. The energy gain is of the order of the energy corresponding to the maximum *ExB* drift speed. It is also found that the ion transport across the magnetopause is controlled by the orientation of the magnetosheath electric field. Analyzing data from MESSENGER allow us to compare the observational facts with our numerical results. We find that the counts of Na^+-group detected by FIPS increase with the existence of KH waves, which is consistent with our numerical results. Although some differences in the energy distribution are expected in our numerical results, the data show no significant differences. This will be the subject of further studies using the newly developed BepiColombo instruments.

Keywords: Non-adiabatic energization, Mercury's magnetosphere, FIPS/MESSENGER, Kelvin-Helmholtz instability

©2019. Japan Geoscience Union. All Right Reserved.

Exploring the real-time prediction of Mercury's magnetosphere

*Manabu Yagi[1], Kanako Seki[2], Yosuke Matsumoto[3], Dominique C. Delcourt[4], Francois Leblanc[4]

1. RIKEN Center for Computational Science, 2. Graduate School of Science, University of Tokyo, 3. Graduate School of Science, Chiba University, 4. The National Center for Scientific Research

Observations by MESSENGER found that Mercury's magnetosphere is analogous to the Earth's while there are several differences of the two. Big differences from the Earth's magnetosphere are strong IMF-Bx component and dipole offset which could affect to the global configuration of Mercury's magnetosphere. In this study, first we performed many cases of MHD simulation solving an interaction with solar wind plasma and offset dipole of Mercury. Solar wind densities are given betwenn nominal(35cm^{-3}), high(70cm^{-3}), and extreme(140cm^{-3}), with velocities for 400km/s to 800km/s, which are realistic values in the Mercury's orbit. When solar wind density is nominal and no IMF-Bx, the structure of Mercury’s magnetosphere is not far from ‘miniature’ of Earth’s magnetosphere, while north-south asymmetry is outstanding because of the offset dipole. In the realistic IMF case, global configurations of magnetosphere drastically change and become more complicated structures which include stronger north-south and dawn-dusk asymmetry. IMF-Bx also affects to the intensity ratio of north and south cusp pressure. IMF-By component “twist” the cusp region to longitudinal direction. The heavy ions’ trajectories basically obey the global structure of magnetic field, so that the ions’ precipitation concentrate on the ‘magnetic cusp’ defined from MHD simulations, but the precipitation region is wider and diffusive compared to the MHD cusp. In the presentation, we will discuss more details of heavy ion precipitation pattern. The identification of global structures and ions’ precipitation region especially the cusp is important not only on the understanding of magnetospheric physics itself, but also making a proposal to the observational plan of spacecraft such as Bepi-Colombo.

Keywords: Mercury, magnetosphere, MHD

©2019. Japan Geoscience Union. All Right Reserved.

Model study on the contribution of various physical processes for generation and dissipation of Mercury's exosphere

*Yudai Suzuki[1], Kazuo Yoshioka[1]

1. University of Tokyo

Mercury has tenuous atmosphere (~1e-10 Pa), which escapes into space due to weak gravity and constant exposure to strong solar photo pressure and solar wind.Since exosphere directly connects with ground surface, the amount of generated and dissipated atmosphere drastically variesdepending on the environment.

Exosphere contains several elements such as Na, Mg, H, K, Ca, He. H and He are derived from solar wind, while other species are thought to be supplied owing to desorption from ground surface. For example, thermal desorption, charged particle sputtering (CPS), photon stimulated desorption (PSD) and meteorite impact vaporization (MIV) are suggested as desorption process. The amount of thermal desorption depends on the surface temperature, which is a function of the distance between the Sun and Mercury due to revolution. The amount of CPS changes owing to flares and the intensity of solar wind. Variation of PSD amount is due to fluctuation of solar radiation. MIV is dominated by the amount of dust around Mercury. Therefore, estimating how much each process contributes to generation of atmosphere encourages understanding the environment of inner solar system.

Velocity distribution of emitted particles is different from process to process. Thus, contribution of each process is often presumed by temperature of emitted particles which can be estimated by density profile obtained by the observation of MESSENGER spacecraft. However, the accuracy of estimating the abundance of high-temperature component gas is not enough, and besides it is hard to make an estimate of the dominant process in high latitudes in northern hemisphere and mid-latitudes owing to geometry of the spacecraft’ s orbit.

Thermal desorption dominates the distribution of sodium atoms on ground surface since particles emitted by thermal desorption has small energy and return to the surface only in a short time (~10min). CPS is thought to generate the majority of atmosphere in high latitudes of northern hemisphere and mid latitudes.

In this research, the behavior of neutral sodium particle from generation to escape focused on thermal desorption and CPS is simulated using Monte Carlo method. In addition, the contribution of those processes will be discussed by comparing with the MESSENGER/MASCS/UVVS observation.

Keywords: Mercury, tenuous atmosphere , exosphere, thermal desorption, charged particle sputtering

©2019. Japan Geoscience Union. All Right Reserved.

[J] Oral | P (Space and Planetary Sciences)：P-CG Complex & General

Tue. May 28, 2019 10:45 AM - 12:15 PM JST | Tue. May 28, 2019 1:45 AM - 3:15 AM UTC | A05 TOKYO BAY MAKUHARI HALL

[P-CG25] Planetary Magnetosphere, Ionosphere, and Atmosphere

convener:Kanako Seki(Graduate School of Science, University of Tokyo), Takeshi Imamura(Graduate School of Frontier Sciences, The University of Tokyo), Hiroyuki Maezawa(Department of Physical Science Osaka Prefecture University), Naoki Terada(Graduate School of Science, Tohoku University), Chairperson:Hiromu Nakagawa(Planetary Atmosphere Physics Laboratory, Department of Geophysics, Graduate School of Science, Tohoku University), Kanako Seki(Department of Earth and Planetary Science, Graduate School of Science, University of Tokyo,)

Exploration of Moon, Venus, Mars, Mercury, Jupiter, Saturn, and beyond together with rapid developments of numerical simulations provides us new view of planetary environment. This session collects general contributions of new findings about planetary magnetosphere, ionosphere, and atmosphere. New methodology and technology development studies for future explorations are also welcome. In order to put the common knowledge at different planets into perspective, this session aims to facilitate discussions on comparative planetary environments.

10:45 AM - 11:00 AM JST | 1:45 AM - 2:00 AM UTC

[PCG25-05] Updated status and science goals of the BepiColombo mission

*Go Murakami[1], Hajime Hayakawa[1], Masaki Fujimoto[1], BepiColombo Project Team (1.Institute of Space and Astronautical Science, Japan Aerospace Exploration Agency)

11:00 AM - 11:15 AM JST | 2:00 AM - 2:15 AM UTC

[PCG25-06] A Novel High-Moment Multifluid Model for Mercury: From the Planetary Conducting Core to the Dynamic Magnetosphere

*Chuanfei Dong[1], Liang Wang[1], Ammar Hakim[1], Amitava Bhattacharjee[1], James A Slavin[2], Gina A DiBraccio[3], Kai Germaschewski[4] (1.Princeton University, 2.University of Michigan, Ann Arbor, 3.NASA Goddard Space Flight Center, 4.University of New Hampshire)

11:15 AM - 11:30 AM JST | 2:15 AM - 2:30 AM UTC

[PCG25-07] DSMC simulation of slow hydrodynamic escape from terrestrial planets

Kaori Terada[1], *Naoki Terada[1], Hitoshi Fujiwara[2] (1.Graduate School of Science, Tohoku University, 2.Faculty of Science and Technology, Seikei University)

11:30 AM - 11:45 AM JST | 2:30 AM - 2:45 AM UTC

[PCG25-08] The influence of Martian crustal magnetic fields on atmospheric escape

*Dave A Brain[1,2], Robin Ramstad[1], Yaxue Dong[1], Tristan Weber[1], Shogo Inui[2], Kanako Seki[2], Andrew Poppe[3], Riku Jarvinen[4], Jim McFadden[3], Jasper Halekas[5], Jared Espley[6], David Mitchell[3], Laila Andersson[1], Bruce Jakosky[1] (1.University of Colorado, 2.University of Tokyo, 3.University of California Berkeley, 4.Finnish Meteorological Institute, 5.University of Iowa, 6.NASA Goddard Space Flight Center)

11:45 AM - 12:00 PM JST | 2:45 AM - 3:00 AM UTC

[PCG25-09] Effects of the IMF direction on atmospheric escape under a weak intrinsic magnetic field at Mars

*Shotaro Sakai[1], Kanako Seki[1], Naoki Terada[2], Hiroyuki Shinagawa[3], Ryoya Sakata[1], Takashi Tanaka[3,4], Yusuke Ebihara[5] (1.Graduate School of Science, The University of Tokyo, 2.Graduate School of Science, Tohoku University, 3.National Institute of Information and Communications Technology, 4.International Center for Space Weather Science and Education, Kyushu University, 5.Research Institute for Sustainable Humanosphere, Kyoto University)

12:00 PM - 12:15 PM JST | 3:00 AM - 3:15 AM UTC

[PCG25-10] Simulating solar energetic electron precipitation and drift at Mars

*Rebecca Jolitz[1], Chuanfei Dong[2], Dave A Brain[1], Steve Bougher[3], Christina Lee[4], Rob Lillis[4], Shannon Curry[4], Bruce Jakosky[1] (1.Univ. of Colorado Boulder, 2.Princeton Univ., 3.Univ. of Michigan, 4.Univ. of California Berkeley)

Updated status and science goals of the BepiColombo mission

*Go Murakami[1], Hajime Hayakawa[1], Masaki Fujimoto[1], BepiColombo Project Team

1. Institute of Space and Astronautical Science, Japan Aerospace Exploration Agency

The ESA-JAXA joint mission BepiColombo is now on the track to Mercury. Two spacecraft for BepiColombo, "MIO" (Mercury Magnetospheric Orbiter: MMO) and "Bepi" (Mercury Planetary Orbiter: MPO), were launched by Ariane-5 launch vehicle from Kourou in French Guiana on 20 October 2018. During the cruise to Mercury, in addition to two spacecraft MMO Sunshield and Interface Structure (MOSIF) and Mercury Transfer Module (MTM) are all integrated together. The critical phase just after launch and the near Earth commissioning phase were successfully finished in end of 2018, and the first electrical propulsion started from Decemeber 2018. The next activities are delta commissioning of high voltage instruments in mid 2019, and the first flyby around the Earth in April 2020. Here we report the updated status of BepiColombo mission and the overview of its science goals.

©2019. Japan Geoscience Union. All Right Reserved.

A Novel High-Moment Multifluid Model for Mercury: From the Planetary Conducting Core to the Dynamic Magnetosphere

*Chuanfei Dong[1], Liang Wang[1], Ammar Hakim[1], Amitava Bhattacharjee[1], James A Slavin[2], Gina A DiBraccio[3], Kai Germaschewski[4]

1. Princeton University, 2. University of Michigan, Ann Arbor, 3. NASA Goddard Space Flight Center, 4. University of New Hampshire

We have developed a novel three-dimensional ten-moment multifluid model and applied it to investigate the tightly coupled interior-magnetosphere system of Mercury. This new multifluid model self-consistently solves the continuity, momentum and pressure tensor equations of each species, together with the full Maxwell equations. As a result, non-ideal effects including the Hall effect, inertia, and tensorial pressures are self-consistently embedded without the need for explicitly solving a generalized Ohm's law.

Our simulation results from this new model are in good agreement with observations from MErcury Surface, Space ENvironment, GEochemistry, and Ranging (MESSENGER) spacecraft. The model is able to reproduce the magnetic field vectors, field-aligned currents and cross-tail current sheet asymmetry observed by MESSENGER. We also investigate collisionless magnetic reconnection in Mercury's magnetotail and at dayside magnetopause. In addition, we study the magnetospheric response of Mercury to a hypothetical extreme event with an enhanced solar wind dynamic pressure, which demonstrates the significance of electromagnetic induction effects resulting from the coupled interior. Moreover, two plasmoids (or flux ropes) are formed in Mercury's cross-tail current sheet during this hypothetical extreme event, indicating the extremely dynamic nature of Mercury's magnetotail. Thus, this novel high-moment, multifluid, interior-magnetosphere-coupled model is crucial for understanding Mercury's dynamic magnetosphere and has the potential to enhance the science returns of both the MESSENGER and BepiColombo missions.

Keywords: Mercury's dynamic magnetosphere, ten-moment multifluid model, induction effect, tightly coupled interior-magnetosphere system, collisionless magnetic reconnection, extreme events

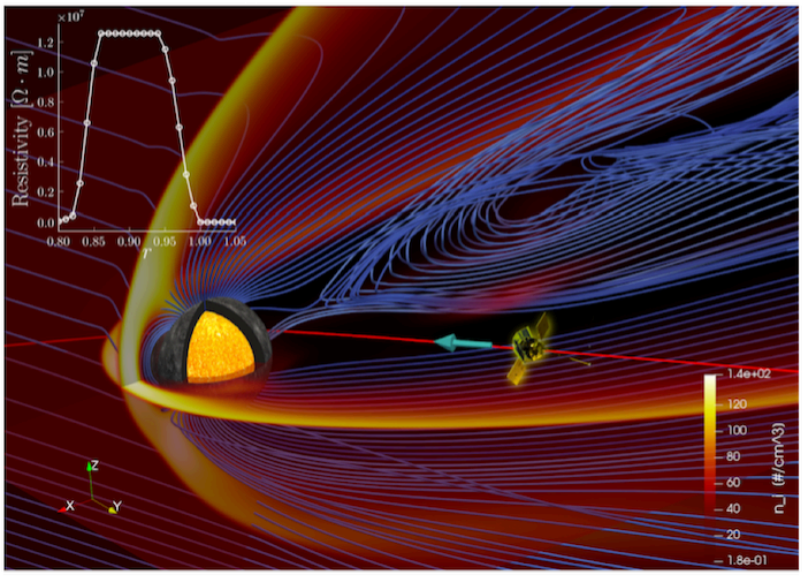

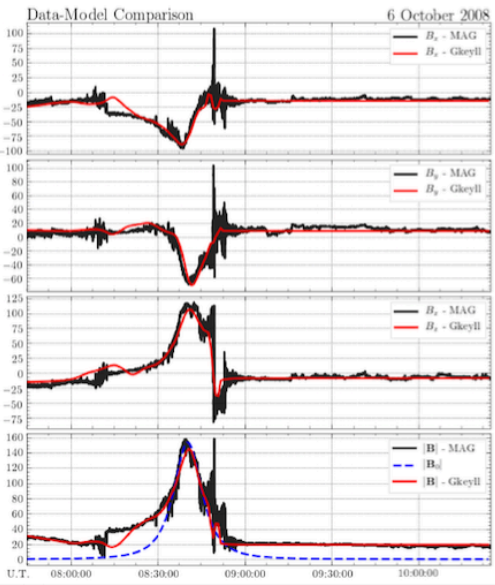

©2019. Japan Geoscience Union. All Right Reserved.

DSMC simulation of slow hydrodynamic escape from terrestrial planets

Kaori Terada[1], *Naoki Terada[1], Hitoshi Fujiwara[2]

1. Graduate School of Science, Tohoku University, 2. Faculty of Science and Technology, Seikei University

Slow hydrodynamic escapes of atmospheric components from terrestrial planets subject to intense EUV radiation are investigated by DSMC simulations to understand the long-term evolution of planetary atmospheric composition.

Sun-like stars in earlier stages of their evolution emit intense EUV radiation. For example, the young sun of 4.5 billion years ago may have emitted 100 times stronger EUV radiation than today. After the formation of planets in a protoplanetary disk, planets get their atmospheres from the remnants of the disk gas and the outgassing due to impacts. The atmospheres were subject to the intense EUV radiation from a young central star, which caused significant heating and massive escape of planetary atmospheres.

The energy-limited escape rate is an upper limit of an atmospheric escape rate. The energy-limited escape is a category of the hydrodynamic escape. After an EUV radiation from a central star became weak, a planetary atmosphere was in hydrostatic equilibrium, and an escape rate became equal to the Jeans escape rate. While hydrodynamic escape and Jeans escape are understood well, there is an incomplete understanding of transition from hydrodynamic to Jeans escapes.

The thermal escape processes such as hydrodynamic escape and Jean escape depend on atmospheric composition. A previous study showed that the exobase temperature of Earth exceeded 10000 K and the atmosphere was well within the hydrodynamic regime when exposed to 20 times stronger EUV levels than present-day Earth. The exobase temperature of a CO2 dominated atmosphere like Mars was not heated as much as Earth’ s exobase because of efficient CO2 IR cooling. Nonetheless a previous simulation study using a fluid model showed that the exobase temperature reached about 2500 K and the Martian atmosphere was not in the hydrostatic equilibrium when exposed to 20 times stronger EUV levels.

In this study, escape rates from Earth-like and Mars-like planets for different EUV radiation intensities are estimated by DSMC simulations. Our full-particle upper thermosphere simulation model can solve the escape rates self-consistently. We show the escape rates of each species including the transition from hydrodynamic through slow hydrodynamic to Jeans escapes to understand the long-term evolution of planetary atmospheric composition.

Keywords: Atmospheric escape, Terrestrial planets, DSMC simulation

©2019. Japan Geoscience Union. All Right Reserved.

The influence of Martian crustal magnetic fields on atmospheric escape

*Dave A Brain[1,2], Robin Ramstad[1], Yaxue Dong[1], Tristan Weber[1], Shogo Inui[2], Kanako Seki[2], Andrew Poppe[3], Riku Jarvinen[4], Jim McFadden[3], Jasper Halekas[5], Jared Espley[6], David Mitchell[3], Laila Andersson[1], Bruce Jakosky[1]

1. University of Colorado, 2. University of Tokyo, 3. University of California Berkeley, 4. Finnish Meteorological Institute, 5. University of Iowa, 6. NASA Goddard Space Flight Center

At present the influence of Martian crustal magnetic fields on atmospheric escape rates is debated. Since Mars lacks a significant global dynamo magnetic field, the presence of strong crustal fields over a significant fraction of the surface could shield portions of the atmosphere from the incident solar wind. The crustal fields could also allow or even enhance atmospheric escape through numerous cusp regions that are magnetically connected to the solar wind. This issue is of interest because the answer has implications for how atmospheric escape has operated on Mars over the history of the planet, including earlier times when Mars was more widely magnetized or even possessed a dynamo field. It is also relevant for assessing whether a global magnetic field is important for atmospheric retention. To this point, both modeling and observational studies appear to disagree on whether crustal fields significantly influence the escape of ions.

We will present the results of a new analysis of ion measurements from the Mars Atmosphere and Volatile EvolutioN (MAVEN) spacecraft mission made over four years. We examine how escape rates vary as Mars rotates and as a function of the solar zenith angle of strong crustal fields, including the dependence on ion energy and species. We also explore whether ion escape rates are larger, in a global sense, above crustal fields compared to non-magnetized regions. Finally, we introduce recent results relevant for evaluating ion escape from individual cusps, including from kinetic models of Martian cusp regions.

Keywords: Mars, Atmospheric escape, Magnetospheres

©2019. Japan Geoscience Union. All Right Reserved.

Effects of the IMF direction on atmospheric escape under a weak intrinsic magnetic field at Mars

*Shotaro Sakai[1], Kanako Seki[1], Naoki Terada[2], Hiroyuki Shinagawa[3], Ryoya Sakata[1], Takashi Tanaka[3,4], Yusuke Ebihara[5]

1. Graduate School of Science, The University of Tokyo, 2. Graduate School of Science, Tohoku University, 3. National Institute of Information and Communications Technology, 4. International Center for Space Weather Science and Education, Kyushu University, 5. Research Institute for Sustainable Humanosphere, Kyoto University

The planetary intrinsic magnetic field is significantly important in considering the atmospheric escape from planets. The strength of intrinsic field particularly affects the interaction between the solar wind and terrestrial-type planets (e.g., Seki et al., 2001), and it would change the escape mechanism. In contrast, Mars would have kept the warm and wet climate around 4 Ga. However, atmosphere and water are lost by certain processes, resulting in that present Mars only leave thin atmosphere. One candidate of the escape mechanism is the ion outflow from the upper atmosphere associated with the magnetic field. It is expected that ancient Mars had a global intrinsic magnetic field because there exists the crustal magnetic field in present Mars, and thus investigating the effect of intrinsic magnetic field on the ion escape leads to understanding the climate change of Mars from past through present.

Sakai et al. (2018) investigated the effect of an intrinsic magnetic field of 100 nT at the Martian equatorial surface on the escape mechanism. It was shown that the existence of the weak field results in an enhancement of the ion escape rate. A parker-spiral interplanetary magnetic field (IMF) was used in order to obtain the escape rate in this earlier study.

In this study, influences of the IMF direction on the ion escape mechanism under the intrinsic magnetic field of 100 nT at the equatorial surface are investigated based on global multispecies single-fluid magnetohydrodynamics simulations (Terada et al., 2009; Sakai et al., 2018). Ion escape processes from Mars under two IMF conditions, namely, a northward and southward cases, are compared to those of the parker-spiral case. For the parker-spiral case, heavy ions escape through the channel associated with the open field lines and another channel associated with a magnetic reconnection between the planetary and solar wind magnetic fields at the flank magnetopause (Sakai et al., 2018). For the north-IMF case, the heavy ions mainly escape through the open or draped field lines formed by double lobe reconnections. The escape rate of heavy ions is about one order of magnitude smaller than for the parker-spiral IMF case and it is even smaller than for the no-dipole case. On the other hand, the heavy ions escape by the mass loading of draped field lines in the ionosphere for the south-IMF case. The escape rate of heavy ions is about one order of magnitude greater than for the parker-spiral case. For the north-IMF case, the interaction of the weak intrinsic magnetic field and IMF forms the firm magnetosphere, resulting in suppressing the ion escape. In contrast, the erosion of IMF into the deep ionosphere yields the increment of the ion escape rate for the south-IMF case.

References:

1. Sakai, S., Seki, K., Terada, N., Shinagawa, H., Tanaka, T., & Ebihara, Y. (2018). Effects of a weak intrinsic magnetic field on atmospheric escape from Mars. *Geophys. Res. Lett.*, *45*, 9336-9343. https://doi.org/10.1029/2018GL079972
2. Seki, K., Elphic, R. C., Hirahara, M., Terasawa, T., & Mukai, T. (2001). On atmospheric loss of oxygen ions from Earth through magnetospheric processes. *Science*, *291*, 1939-1941.

©2019. Japan Geoscience Union. All Right Reserved.

https://doi.org/10.1126/science.1058913
3. Terada, N., Kulikov, Y. N., Lammer, H., Lichtenegger, H. I. M., Tanaka, T., Shinagawa, H., & Zhang, T. (2009). Atmospheric and water loss from early Mars under extreme solar wind and extreme ultraviolet conditions. *Astrobiology*, *9*, 55-70. https://doi.org/10.1089/ast.2008.0250

Keywords: Mars, Atmospheric escape, Intrinsic magnetic field, Interplanetary magnetic field, MHD simulation

©2019. Japan Geoscience Union. All Right Reserved.

Simulating solar energetic electron precipitation and drift at Mars

*Rebecca Jolitz[1], Chuanfei Dong[2], Dave A Brain[1], Steve Bougher[3], Christina Lee[4], Rob Lillis[4], Shannon Curry[4], Bruce Jakosky[1]

1. Univ. of Colorado Boulder, 2. Princeton Univ., 3. Univ. of Michigan, 4. Univ. of California Berkeley

Solar disturbances release energetic charged particles that are expected to directly precipitate into the atmospheres of weakly magnetized planets like Mars. However, draped magnetic fields can influence the motion of energetic electrons. Using a test particle model of 1 keV - 100 keV electrons moving in magnetic fields from a multifluid magnetohydrodynamic simulation, we find that energetic electrons with steep pitch angles are affected by gradient drifts over the dayside of Mars. For an interplanetary magnetic field directed in the away sector, electrons will drift southwards, perpendicular to the direction of the draped magnetic field. Gradient drifts at Mars can facilitate increased precipitation by directing electrons towards the magnetized southern hemisphere and into magnetic field cusps. These findings suggest energetic electrons precipitate non-uniformly and are attenuated at low altitudes above the dayside northern hemisphere of Mars.

Keywords: Mars, solar energetic particles, gradient drift, particle precipitation

©2019. Japan Geoscience Union. All Right Reserved.

[J] Oral | P (Space and Planetary Sciences)：P-CG Complex & General

Tue. May 28, 2019 1:45 PM - 3:15 PM JST | Tue. May 28, 2019 4:45 AM - 6:15 AM UTC | A05 TOKYO BAY MAKUHARI HALL

[P-CG25] Planetary Magnetosphere, Ionosphere, and Atmosphere

convener:Kanako Seki(Graduate School of Science, University of Tokyo), Takeshi Imamura(Graduate School of Frontier Sciences, The University of Tokyo), Hiroyuki Maezawa(Department of Physical Science Osaka Prefecture University), Naoki Terada(Graduate School of Science, Tohoku University), Chairperson:Takeshi Imamura(Graduate School of Frontier Sciences, University of Tokyo), Naoki Terada(School of Science, Tohoku University)

Exploration of Moon, Venus, Mars, Mercury, Jupiter, Saturn, and beyond together with rapid developments of numerical simulations provides us new view of planetary environment. This session collects general contributions of new findings about planetary magnetosphere, ionosphere, and atmosphere. New methodology and technology development studies for future explorations are also welcome. In order to put the common knowledge at different planets into perspective, this session aims to facilitate discussions on comparative planetary environments.

1:45 PM - 2:00 PM JST | 4:45 AM - 5:00 AM UTC

[PCG25-11] Effects of the intrinsic magnetic field on the ion loss from ancient Mars

*Ryoya Sakata[1], Kanako Seki[1], Shotaro Sakai[1], Naoki Terada[2], Hiroyuki Shinagawa[3], Takashi Tanaka[3,4] (1.Department of Earth and Planetary Science, Graduate School of Science, The University of Tokyo, 2.Graduate School of Science, Tohoku University, 3.National Institute of Information and Communications Technology, 4.International Center for Space Weather Science and Education, Kyushu University)

2:00 PM - 2:15 PM JST | 5:00 AM - 5:15 AM UTC

[PCG25-12] Global characterization of wave perturbations in the middle atmosphere on Mars

*Hiromu Nakagawa[1], Naoki Terada[1], Hannes Groller[7], Roger Yelle[7], Montmessin Franck[8], Schneider M Nicholas[4], England Scott[5], Kanako Seki[6], Takeshi Kuroda[3], Hitoshi Fujiwara[2], Takeshi Imamura[6], Kaori Terada[1], Nao Yoshida[1], Justin I Deighan[4], Sonal K Jain[4], Bruce M Jakosky[4] (1.Planetary Atmosphere Physics Laboratory, Department of Geophysics, Graduate School of Science, Tohoku University, 2.Seikei University, 3.National Institute of Information and Communications Technology, 4.Laboratory for Atmospheric and Space Physics, University of Colorado, 5.Aerospace and Ocean Engineering, Virginia Tech, 6.Department of Earth and Planetary Science, University of Tokyo, 7.Lunar and Planetary Laboratory Science, University of Arizona, 8.LATMOS, UVSQ/CNES/IPSL)

2:15 PM - 2:30 PM JST | 5:15 AM - 5:30 AM UTC

[PCG25-13] Seasonal variation of the dayside N_2/CO_2 at 140 km altitude derived from MAVEN/IUVS

*Nao Yoshida[1], Hiromu Nakagawa[1], Naoki Terada[1], Nicholas Schnider[2], Scott Evans[3], Sonal Jain[2], Hitoshi Fujiwara[4], Takeshi Imamura[5], Justin Deighan[2], Ian Stewart[2], Michael Stivens[6], Roger Yelle[7] (1.Dep. Geophysics Graduate School of Science Tohoku University, 2.Laboratory for Atmospheric and Space Physics, Boulder, USA, 3.Computational Physics, Inc., Springfield, Virginia, USA, 4.Faculty of Science and Technology, Seikei University, 5.Department of Complexity Science and Engineering, Graduate School of Frontier Sciences, The University of Tokyo, 6.Naval Research Laboratory, Washington, USA, 7.Department of Planetary Sciences, University of Arizona)

2:30 PM - 2:45 PM JST | 5:30 AM - 5:45 AM UTC

[PCG25-14] Automated segmentation of Martian dust storms in MGS/MOC images using a deep learning technique

*Kazunori Ogohara[1], Ryusei Gichu[2] (1.School of Engineering, University of Shiga Prefecture, 2.Graduate School of Engineering, University of Shiga Prefecture)

2:45 PM - 3:00 PM JST | 5:45 AM - 6:00 AM UTC

[PCG25-15] Investigation of variation mechanisms of the Jovian radiation belt using ALMA

*Hajime Kita[1], Hideo Sagawa[2], Takahiro Iino[3], Chihiro Tao[4], Takeshi Kuroda[4], Fuminori Tsuchiya[5], Hiroaki Misawa[5], Yasumasa Kasaba[5], Masaki Fujimoto[1] (1.Institute of Space and Astronautical Science, Japan Aerospace Exploration Agency , 2.Faculty of Science, Kyoto Sangyo University, 3.Nature and Science Museum, Tokyo University of Agriculture and Technology, 4.National Institute of Information and Communications Technology, 5.Tohoku University)

3:00 PM - 3:15 PM JST | 6:00 AM - 6:15 AM UTC

[PCG25-16] Jupiter's radio Riddle arcs observed by LWA and Juno

*Kazumasa Imai[1], Charles A. Higgins[2], Masafumi Imai[3], Tracy Clarke[4] (1.Department of Social Design Engineering, National Institute of Technology, Kochi College, 2.Middle Tennessee State University, 3.University of Iowa, 4.Naval Research Laboratory)

Effects of the intrinsic magnetic field on the ion loss from ancient Mars

*Ryoya Sakata[1], Kanako Seki[1], Shotaro Sakai[1], Naoki Terada[2], Hiroyuki Shinagawa[3], Takashi Tanaka[3,4]

1. Department of Earth and Planetary Science, Graduate School of Science, The University of Tokyo, 2. Graduate School of Science, Tohoku University, 3. National Institute of Information and Communications Technology, 4. International Center for Space Weather Science and Education, Kyushu University

Mars had a thick atmosphere before 4 Ga, but it lost most of them. Ion escape to space could play an important role in the atmosphere loss. The astronomical observations suggest that the solar XUV (X-ray and extreme ultra-violet) flux and the solar mass loss rate were more intense (Ribas et al., 2005; Wood et al., 2002). Previous studies pointed out that the ion loss was several orders of magnitude stronger under such intensified solar conditions (Terada et al., 2009a). On the other hand, the existence of the crustal magnetic field indicates that Mars had an intrinsic magnetic field before 4.1 Ga. The conventional idea is that the intrinsic magnetic field prevents the direct interaction between the solar wind and the atmosphere and thus restrains the ion loss (Lundin et al., 2007). On the contrary, some studies suggested that the existence of an intrinsic magnetic field promotes the ion loss (Sakai et al., 2018). Thus it is important to clarify the effect of the intrinsic magnetic field on the ion loss to understand the atmospheric evolution at Mars.

In this study, we investigated the ion loss processes from Mars under extreme solar conditions and the existence of an intrinsic magnetic field using a 3D multi-species MHD model (Terada et al., 2009b). The solar wind proton density, the solar wind velocity, and the solar XUV flux were assumed to be 1000 /cm^3, 2000 km/s, and 100 times higher than the present-day XUV flux, respectively. The interplanetary magnetic field was assumed to be in Parker spiral and its strength was 60 nT. These parameters are same as those used in Terada et al. (2009a). We conducted four cases of simulations with different intrinsic magnetic field conditions, i.e., dipole fields with the strength of 0 nT, 100 nT, 1000 nT, and 5000 nT on the equatorial surface.

In 0 nT case, there were two major ion loss processes: escape of O^+, O_2^+ and CO_2^+ from the polar region and pickup O^+ carried by the deflected solar wind. In 1000 nT case, O_2^+ and CO_2^+ mainly came from the dayside cusp region through open magnetic field lines. In 5000 nT case, O^+, O_2^+ and CO_2^+ fluxes had almost the same structure and originated from the dayside cusp region. In 0 nT, 100 nT, and 1000 nT cases, the loss rates of O_2^+ and CO_2^+ were higher under the existence of the stronger dipole field, while the O^+ loss rate was nearly the same in these three cases. In 5000 nT case, the loss rates of O_2^+ and CO_2^+ were about three orders of magnitude lower than those of the other weaker dipole cases, while the O^+ loss rate was five times lower. These results suggest that the existence of a weak intrinsic magnetic field facilitates the loss of heavier ions such as O_2^+ and CO_2^+, and there is a threshold strength of the intrinsic magnetic field for this facilitation effect.

References

Lundin, R., et al. (2007). Planetary magnetic fields and solar forcing: Implications for atmospheric evolution. *Space Sci. Rev.*, *129*(1–3), 245–278. doi:10.1007/s11214-007-9176-4

Ribas, I., et al. (2005). Evolution of the Solar Activity over Time and Effects on Planetary Atmospheres. I. High-Energy Irradiances (1-1700 Å). *ApJ*, *622*(1), 680. doi:10.1086/427977

Sakai, S., et al. (2018). Effects of a Weak Intrinsic Magnetic Field on Atmospheric Escape From Mars. *Geophys. Res. Lett.*, *45*(18), 9336–9343. doi:10.1029/2018GL079972

Terada, N., et al. (2009). A three-dimensional, multispecies, comprehensive MHD model of the solar wind

©2019. Japan Geoscience Union. All Right Reserved.

interaction with the planet Venus. *J. Geophys. Res.*, *114*(9), 1–11. doi:10.1029/2008JA013937
Terada, N., et al. (2009). Atmosphere and Water Loss from Early Mars Under Extreme Solar Wind and Extreme Ultraviolet Conditions. *Astrobiology*, *9*(1), 55–70. doi:10.1089/ast.2008.0250
Wood, B. E., et al. (2002). Measured Mass-Loss Rates of Solar-like Stars as a Function of Ageand Activity. *ApJ*, *574*(1), 412–425. doi:10.1086/340797

Keywords: ancient Mars, multi-species MHD simulation, atmospheric escape, intrinsic magnetic field

©2019. Japan Geoscience Union. All Right Reserved.

Global characterization of wave perturbations in the middle atmosphere on Mars

*Hiromu Nakagawa[1], Naoki Terada[1], Hannes Groller[7], Roger Yelle[7], Montmessin Franck[8], Schneider M Nicholas[4], England Scott[5], Kanako Seki[6], Takeshi Kuroda[3], Hitoshi Fujiwara[2], Takeshi Imamura[6], Kaori Terada[1], Nao Yoshida[1], Justin I Deighan[4], Sonal K Jain[4], Bruce M Jakosky[4]

1. Planetary Atmosphere Physics Laboratory, Department of Geophysics, Graduate School of Science, Tohoku University, 2. Seikei University, 3. National Institute of Information and Communications Technology, 4. Laboratory for Atmospheric and Space Physics, University of Colorado, 5. Aerospace and Ocean Engineering, Virginia Tech, 6. Department of Earth and Planetary Science, University of Tokyo, 7. Lunar and Planetary Laboratory Science, University of Arizona, 8. LATMOS, UVSQ/CNES/IPSL

Small-scale atmospheric waves, such as internal gravity waves, are recognized as an important part of the terrestrial climate system. They ubiquitously exist on the Earth's upper atmosphere and affect the dynamics, composition, and thermal structure of the terrestrial middle atmosphere and thermosphere. Global characteristics of gravity waves on Earth have been extensively investigated over decades. On Mars, large fluctuations in density and temperature with short vertical wavelengths were first detected in Viking, Opportunity, Spirit, and Mars Pathfinder entry profiles. Wave amplitudes in the Martian atmosphere are larger than those in the terrestrial atmosphere and the important role of gravity waves of tropospheric origin in the middle atmosphere has been appreciated in early modeling studies. Gravity waves strongly affect the large-scale winds, thermal balance, density in the mesosphere and lower thermosphere. Since October 2014, NASA's Mars Atmosphere and Volatile EvolutioN (MAVEN) mission have been performed comprehensive studies of the Martian atmosphere. In-situ measurements of the upper atmosphere, from 300 km down to 130 km, revealed that wavelike perturbations ubiquitously exist in ions and neutrals in the upper thermosphere. Wavelike perturbations have also been detected by remote sensing with the Imaging Ultraviolet Spectrograph (IUVS) onboard MAVEN at altitudes between 20 and 150 km. These IUVS measurements provide opportunities for investigating possible links between waves in the Martian troposphere and thermosphere.
In order to clarify a global characteristic of waves and its upward propagating processes, we use IUVS stellar occultation measurements to characterize a global distribution of waves in the middle atmosphere between 24 March 2015 and 12 April 2018 for two Martian Years. This study first revealed global characteristics of wave perturbations in the night side temperature profiles derived from MAVEN/IUVS stellar occultations at 20 - 160 km altitudes on Mars. The peak amplitudes of waves on Mars exceed 20 % which is larger than those in Earth's mesosphere/thermosphere (~5-13 %). Perturbations were found to be notably large in summer hemisphere at L_s = 0-180. These waves can be interpreted as resulting from superposed harmonics of internal gravity waves and thermal tides. The superposition of thermal-tides and small-scale perturbations generate extensive instability layer around 70 - 100 km, which potentially causes wave-breaking and turbulences. Vertical wavenumber spectral density in the Martian middle atmosphere shows a power-law dependence with the logarithmic spectral slope of -3. This is similar to the features seen in the Earth's atmosphere. The spectral density in southern hemisphere at L_s = 225-315 tends to follow the semi-empirical spectrum of saturated gravity waves on the high-wavenumber side. The spectral power at high-wavenumbers is lower at 80 - 160 km than that at 20 - 80 km. This suggests that the strong radiative damping by CO_2 15-micron could effectively dissipates shorter waves. Instead, the spectral power at low-wavenumbers suggests the amplitude growth with height of unsaturated waves toward upper thermosphere.

©2019. Japan Geoscience Union. All Right Reserved.

Keywords: Mars, mesosphere, thermosphere, waves, tides

©2019. Japan Geoscience Union. All Right Reserved.

Seasonal variation of the dayside N_2/CO_2 at 140 km altitude derived from MAVEN/IUVS

*Nao Yoshida[1], Hiromu Nakagawa[1], Naoki Terada[1], Nicholas Schnider[2], Scott Evans[3], Sonal Jain[2], Hitoshi Fujiwara[4], Takeshi Imamura[5], Justin Deighan[2], Ian Stewart[2], Michael Stivens[6], Roger Yelle[7]

1. Dep. Geophysics Graduate School of Science Tohoku University, 2. Laboratory for Atmospheric and Space Physics, Boulder, USA, 3. Computational Physics, Inc., Springfield, Virginia, USA, 4. Faculty of Science and Technology, Seikei University, 5. Department of Complexity Science and Engineering, Graduate School of Frontier Sciences, The University of Tokyo, 6. Naval Research Laboratory, Washington, USA, 7. Department of Planetary Sciences, University of Arizona

It is believed that liquid water was abundant on early Mars, despite Mars being too cold today to sustain significant amounts of liquid water. The most likely explanation is that early Mars had a more-effective greenhouse atmosphere and most part of atmosphere and water have lost to space. Mars Atmosphere and Volatile EvolutioN (MAVEN) mission was designed to explore the loss of gas to space at the present. MAVEN spacecraft revealed highly variable nature of upper atmosphere in density, temperature, and atmospheric compounds (e.g. Mahaffy et al., 2015; Elrod et al., 2017; Stone et al., 2018; Slipski et al., 2018). However, the controlling factor of the variations has yet to be fully characterized due to the limited spatial- and temporal- observing geometry by in-situ measurements. In addition to the effects by the external force, such as solar wind and solar EUV on the upper atmosphere, the effect of lower atmospheric phenomena is also required to account for the substantial variations of upper atmosphere. For instance, the homopause (~120 km altitude) influences the upper thermospheric composition, thereby the species escaping to space [Imamura et al., 2016]. The fractionation between the homopause and exobase determines the relative abundance of species to escape to space [Jakosky et al., 2017]. For this purpose, further investigation around atmospheric boundary from the middle atmosphere to lower thermosphere is crucial for understanding regional coupling between lower and upper atmosphere.
We have investigated the seasonal variation of the N_2/CO_2 ratio at 140 km altitude derived from ultraviolet spectroscopy remote-sensing measurements by Imaging Ultraviolet Spectrograph (IUVS) aboard MAVEN. We used the dataset of level 2 version 13 revision 1 data provided by the Planetary Data System, which includes retrieved CO_2 and N_2 number density profiles derived from dayglow emissions. We analyzed N_2 and CO_2 number densities observed from October 2014 to May 2018. Observations cover in the dayside from 7 to 19 hr. The observations covered almost all solar longitudes within the two Martian Years. The retrieved CO_2 density has small uncertainty but the retrieved N_2 density has relatively larger uncertainty in particular above ~170 km due to the dimmer emission intensity. For precise analysis of the N_2/CO_2 ratio, we confine our analysis to the data at 140 km altitude where N_2/CO_2 has uncertainty less than 50%. We found that the N_2/CO_2 ratio at 140 km altitude significantly varies in the range of 0.02 to 0.20, which shows an annual sinusoidal trend. The higher ratio appears during aphelion and the lower ratio appears during perihelion. CO_2 and N_2 number densities also have similar annual variations. It is noted that the CO_2 density varies by a factor of 100, while N_2 density by a factor of 10. This large CO_2 variation affects the N_2/CO_2 ratio at 140 km. The potential sources of the seasonal variation we found are variations (1) of the surface mixing ratio, (2) of the homopause altitude, and (3) of the thermospheric temperature. In this paper, the effect of surface mixing ratio is discussed using Mars Climate Database version 5.3 [Forget et al., 1999; Lewis et al., 1999]. We also address the effects of other sources by considering the seasonal variation of homopause altitude [Slipski et al., 2018] and background temperature [Bougher et al., 2017; Stone et al., 2018].

©2019. Japan Geoscience Union. All Right Reserved.

Keywords: Thermosphere, Mixing ratio, Homopause, MAVEN, escape

©2019. Japan Geoscience Union. All Right Reserved.

Automated segmentation of Martian dust storms in MGS/MOC images using a deep learning technique

*Kazunori Ogohara[1], Ryusei Gichu[2]

1. School of Engineering, University of Shiga Prefecture, 2. Graduate School of Engineering, University of Shiga Prefecture

The shape, texture, and size of dust storms and the climatology of these characteristics are important clues to understanding Martian dust storms. The relations between such characteristics and the phases of the variety of atmospheric waves as well as the frequency of textured/curvilinear dust storms and the spatial and seasonal variations of the cumulative area are also worth investigating (Wang 2007; Wang et al. 2011; Guzewich et al. 2015, 2017). However, it is time-consuming to detect all dust storms visually because of the vast number of images taken by just two instruments, the MGS/MOC and MRO/MARCI. It is also difficult to objectively define which features characterize dust storms. Even approximate categorization of dust events into textured dust storms, untextured yet discrete dust storms, and haze depends on the subjective experience of the human observer. For these reasons, visual detection and categorization of the three types of dust storm textures introduced by Kulowski et al. (2017) would not be exactly reproduced by another human viewing and characterizing the images. Furthermore, we perceive a need to update the criteria for detecting dust events, especially obscured ones such as untextured yet discrete dust storms and haze, via visual detection. Therefore, it would be useful to be able to automatically detect dust events, measure their shape, pattern, and size, and improve the objectivity and reproducibility of dust storm detection.
We have developed a novel algorithm for automated segmentation of Martian dust storms using a encoder-decoder type of Convolutional Neural Network. We can separate dust storm areas from the surface and cloud areas in subsets of the global swath images taken by MGS/MOC without any information from other instruments (e.g. MGS/TES). Assuming that segmentation based on authors' experience is the ground truth, 84% of the true dust storm areas in the Arabia Terra is recognized as dust strom. On the other hand, just 69% of the true dust storm areas in the Hellas Basin is correctly recognized as dust storm.

Keywords: Mars, dust storm, deep learning

©2019. Japan Geoscience Union. All Right Reserved.

Investigation of variation mechanisms of the Jovian radiation belt using ALMA

*Hajime Kita[1], Hideo Sagawa[2], Takahiro Iino[3], Chihiro Tao[4], Takeshi Kuroda[4], Fuminori Tsuchiya[5], Hiroaki Misawa[5], Yasumasa Kasaba[5], Masaki Fujimoto[1]

1. Institute of Space and Astronautical Science, Japan Aerospace Exploration Agency , 2. Faculty of Science, Kyoto Sangyo University, 3. Nature and Science Museum, Tokyo University of Agriculture and Technology, 4. National Institute of Information and Communications Technology, 5. Tohoku University

Jupiter is now considered as an archetype for gas giants widely exist in extrasolar systems. At the outermost layer of this giant planet, there is a 300 km-depth of the nearly isothermal atmospheric layer (stratosphere) above the massive troposphere. Jupiter is also known to be a fast rotator (with a period of 9.9 h) with an enormous magnetic field. High energy particles trapped in the magnetic field form a radiation belt around the planet, much stronger than the terrestrial Van Allen's belt. In the case of the Earth, the primary control factor of the radiation belt is the solar wind, while the solar wind is difficult to impact the Jovian radiation belt because of the intense magnetic field.

It is theoretically expected that the driving mechanism of Jovian radiation belt is due to the interaction between the radiation belt and the upper atmospheric dynamics: neutral wind perturbations and diurnal wind system control the radial diffusion and spatial distribution of the energetic particles, respectively. Therefore, precise measurements of Jovian wind field are essential for not only the dynamics of the stratosphere but also the magnetosphere.

ALMA's unprecedented high spatial-spectral resolution enables us to extract the limb emission of the trace gasses in the Jovian upper stratosphere with a few tens m/s sensitivity. It is well known that HCN and CS have been injected into Jupiter by the Shoemaker-Levy 9 impact and they distribute only in the upper atmosphere (p ~0.4-1mbar). Therefore, the Doppler shift of those molecular emission lines can be used to investigate the dynamics in the upper atmosphere particularly at the limb of the Jovian disk where the line-of-sight direction is equal to the horizontal direction of the atmosphere. Here we present the sensitivity of ALMA observation to measuring Jovian stratospheric winds, and discuss its capability of constraining the magnetosphere-atmosphere coupling. A test analysis is carried out using JVO ALMA archive data.

Keywords: Jupiter, ALMA, stratosphere, radiation belt

©2019. Japan Geoscience Union. All Right Reserved.

Jupiter's radio Riddle arcs observed by LWA and Juno

*Kazumasa Imai[1], Charles A. Higgins[2], Masafumi Imai[3], Tracy Clarke[4]

1. Department of Social Design Engineering, National Institute of Technology, Kochi College, 2. Middle Tennessee State University, 3. University of Iowa, 4. Naval Research Laboratory

The Riddle arcs were found in the dynamic spectrum of Jupiter's decametric radio emissions observed by the Voyager spacecraft [Riddle, 1983]. On a frequency time plot these Riddle arcs have the same slope at the same frequency and System III longitude. (The typical System III longitude is about 260 degrees at 20 MHz.) An isolated Riddle arc can be easily recognized inside of the Io-A arc structures. This emission of Riddle arcs was concluded to be from the instantaneous Io flux tube.

The modulation lane method [Imai et al., 1992,1997,2002] is based on the measurements of the slope of modulation lanes on the dynamic spectrum of Jupiter's decametric radio emissions. We usually measure the slope with a 1 MHz bandwidth and determine the most probable value of the lead angle between activated flux tubes to fit the value of the slope. The lead angle is the longitudinal angle between the instantaneous Io flux tube and the previously energized flux tube (real emitting region). The longitudinal location of the magnetic field line of the radio emitting sources can be calculated by this lead angle.

The Long Wavelength Array (LWA) is a low-frequency radio telescope designed to produce high-sensitivity, high-resolution spectra in the frequency range of 10-88 MHz. The sensitivity of the LWA, combined with the low radio frequency interference environment, allows us to observe wide band modulation lanes of Jupiter's decametric radio emissions [Clarke et al., 2014]. We have analyzed the modulation lane data including the Riddle arcs observed by LWA. We found almost all of the Riddle arcs correspond to a zero degree lead angle. This means that the radio sources related to the Riddle arcs are located along the instantaneous Io flux tube. This result is consistent with Riddle's conclusion.

The Juno spacecraft [Bolton et al., 2017] was inserted into polar orbit around Jupiter on 04 July 2016. Juno's highly eccentric orbits have a period of about 53 days with apojove near 113 Jovian radii and perijove near 1.06 Jovian radii. With the advantage of this unique orbit, Juno's Waves instrument [Kurth et al., 2017] is observing for the first time the polar beaming patterns and geometry of Jupiter's decametric radio emission sources. The dynamic spectra recorded by the Waves instrument show the Riddle arcs very clearly. We are continuing to analyze the Waves data to find the Riddle arcs in each Juno orbit. The Riddle arcs can be used as a reference point to understand the latitudinal beaming patterns of Jupiter's decametric radio emissions and the location of radio sources. We present the preliminary results of this study.

Keywords: Jupiter radio, decametric emissions, Riddle arcs, modulation lanes, radio source parameters

©2019. Japan Geoscience Union. All Right Reserved.

[J] Poster | P (Space and Planetary Sciences)：P-CG Complex & General

Tue. May 28, 2019 3:30 PM - 5:00 PM JST | Tue. May 28, 2019 6:30 AM - 8:00 AM UTC | Poster Hall International Exhibition Hall8, Makuhari Messe_4

[P-CG25] Planetary Magnetosphere, Ionosphere, and Atmosphere

convener:Kanako Seki(Graduate School of Science, University of Tokyo), Takeshi Imamura(Graduate School of Frontier Sciences, The University of Tokyo), Hiroyuki Maezawa(Department of Physical Science Osaka Prefecture University), Naoki Terada(Graduate School of Science, Tohoku University)

Exploration of Moon, Venus, Mars, Mercury, Jupiter, Saturn, and beyond together with rapid developments of numerical simulations provides us new view of planetary environment. This session collects general contributions of new findings about planetary magnetosphere, ionosphere, and atmosphere. New methodology and technology development studies for future explorations are also welcome. In order to put the common knowledge at different planets into perspective, this session aims to facilitate discussions on comparative planetary environments.

[PCG25-P01] Particle-in-cell simulation on the dayside magnetopause in a small-scale magnetosphere

*Hideyuki Usui[1], Satoki oki[1], Yohei Miyake[1], Naoki Terada[2], Kanako Seki[3], Yuto Katoh[2], Manabu Yagi[4] (1.Graduate school of system informatics Kobe University, 2.Graduate school of science, Tohoku University, 3.Graduate school of science, University of Tokyo, 4.Riken R-CCS)

[PCG25-P02] Developments and performance evaluations of 0.48 THz band heterodyne receivers for the future Mars terahertz sensor missions with micro-satellites

*Ayaka Tomihara[1], Satoshi Matsumoto[1], Hiroyuki Maezawa[1], Yasuko Kasai[2], Shigeru Yamada[2], Takeshi Kuroda[2], Takayoshi Yamada[2], Toshiyuki Nishibori[3], Yutaka Hasegawa[3], Yasumasa Kasaba[4], Richard Larsson[5], Shinichi Nakasuka[6] (1.Osaka Prefecture University, Osaka, Japan, 2.National Institute of Information and Communications Technology (NICT), Tokyo, Japan, 3.Japan Aerospace Exploration Agency, 4.Tohoku University, Tohoku, Japan, 5.Max planck Institute Solar System Research, Göttingen Germany, 6.Tokyo University, Tokyo, Japan)

[PCG25-P03] Time response of the self-regulation of H and O escapes from Mars

*Shungo Koyama[1], Naoki Terada[1], Hiromu Nakagawa[1], Takeshi Kuroda[2] (1.Graduate School of Science, Tohoku University, 2.National Institute of Information and Communications Technology)

[PCG25-P04] Study of ion composition in the polar plume from Mars based on MAVEN observations

*Sakakura Kotaro[1], Kanako Seki[1], Shogo Inui[1], Shotaro Sakai[1], David A Brain[2], James P McFadden[3], Jasper S Halekas[4], Gina A Dibraccio[5], Bruce Jakosky[2] (1.Department of Earth and Planetary Science, Graduate School of Science, University of Tokyo, Tokyo, Japan., 2.Laboratory for Atmospheric and Space Physics, University of Colorado Boulder, Boulder, Colorado, USA., 3.Space Sciences Laboratory, University of California, Berkeley, California, USA., 4.Department of Physics and Astronomy, University of Iowa, Iowa City, Iowa, USA., 5.Solar System Exploration Division, NASA Goddard Space Flight Center, Greenbelt, MD, USA.)

[PCG25-P05] Automated detection of Martian dust devils in multiframe images observed by the MER/Spirit rover.

*Kazuki Yajima[1], Kazunori Ogohara[2] (1.Graduate School of Engineering, The University of Shiga Prefecture, 2.School of Engineering, The University of Shiga Prefecture)

[PCG25-P06] Temperature change during the global dust storm period obtained by ground observation of the Martian mesosphere by infrared heterodyne spectroscopy

*Akiho Miyamoto[1], Hiromu Nakagawa[1], Kosuke Takami[1], Takeshi Kuroda[1,3], Isao Murata[2], Naoki Terada[1], Nao Yoshida[1], Katsushige Toriumi[1], Shohei Aoki[4], Yasumasa Kasaba[1] (1.Graduate School of Sciences in

Tohoku University, 2.Graduate School of Environmental Sciences, 3. National Institute of Information and Communications Technology, 4.Royal Belgian Institute for Space Aeronomy(IASB-BIRA))

[PCG25-P07] Observation of Neptune’s storms with Pirka telescope

*Yuuki Sato[1], Yukihiro Takahashi[1], Seiko Takagi[1], Mitsuteru Sato[1], Ono Tatsuharu[1] (1.Graduate School of Science, Hokkaido University)

[PCG25-P08] The study of Jupiter’s zonal wind formation mechanism based on cumulonimbus observation

*Tatsuharu Ono[1], Yukihiro Takahashi[1], Shigeto Watanabe[1], Seiko Takagi[1] (1.Department of Cosmosciences, Graduate School of Science, Hokkaido University)

[PCG25-P09] Development of a radial diffusion model of Jovian inner magnetospheric plasma aimed at comparison with HISAKI satellite observation

*Kazuki Yamaguchi[1], Takeshi Sakanoi[1], Fuminori Tsuchiya[1], Masato Kagitani[1], Ryoichi Koga[1], Tomoki Kimura[2] (1.Planetary Plasma and Atmospheric Research Center, Graduate School of Science, Tohoku University, 2.Frontier Research Institute for Interdisciplinary Sciences, Tohoku University)

[PCG25-P10] Pitch angle scattering due to elastic collisions between magnetospheric 500eV-50keV electrons and neutral H_2O originated from Enceladus: Test particle simulation

*Hiroyasu Tadokoro[1], Yuto Katoh[2] (1.Musashino University, 2.Tohoku University)

[PCG25-P11] Study of Jovian atmosphere dynamics by a multi-band imaging observation

Hayate Ito[1], Sumito Hirota[2], Isshi Tabe[3], *Hidehiko Suzuki[1] (1.Meiji university, 2.Kawasaki municipal science museum, 3.Association of Lunar and Planetary Observers in Japan)

[PCG25-P12] Examination of the relation between Jupiter's inner magnetosphere and magnetic reconfiguration events

*Hiroaki Misawa[1] (1.Planetary Plasma and Atmospheric Research Center, Graduate School of Science, Tohoku University)

[PCG25-P13] Effects of the charged particles of solar wind on planetary atmospheres

*Shinji Karasawa[1] (1.Miyagi National College of Technology Professor emeritus)

Particle-in-cell simulation on the dayside magnetopause in a small-scale magnetosphere

*Hideyuki Usui[1], Satoki oki[1], Yohei Miyake[1], Naoki Terada[2], Kanako Seki[3], Yuto Katoh[2], Manabu Yagi[4]

1. Graduate school of system informatics Kobe University, 2. Graduate school of science, Tohoku University, 3. Graduate school of science, University of Tokyo, 4. Riken R-CCS

By performing three-dimensional full particle-in-cell plasma simulations, we have been studying a small magnetosphere formed by the interaction between a weakly magnetized small body and the solar wind. In this study, we particularly focus on the electron dynamics at the dayside magnetopause in the equatorial plane. In the simulation model, a weakly magnetized small body is set in the center, and the solar wind having the southward IMF is injected from the boundary of the simulation domain. We define D_p as the distance between the dipole center and a position where the solar wind dynamics pressure balances the magnetic pressure at the dayside. We focus on a small-scale magnetosphere with $\lambda_i/D_p=1$ where we define λ_i as the ion inertia length in the solar wind. When we define R_b as the radius of the sphere, we set $R_b/D_p=0.6$ which implies a relatively large proportion of sphere in the magnetosphere. In the simulation results, we found dawn-dusk asymmetry characteristics of the plasma spatial distribution in the equatorial plane. It is also interesting to observe intense electron flux along the dayside magnetopause in the equator. We found that this intense flux is due to the electrons accelerated by the electric field enhanced at the magnetopause. They encounter the inner region where the southward IMF and the northward magnetic dipole field cancel each other, and they start making meandering motions toward the dawn side between the region of different orientations of the magnetic fields. We examined the mechanism of the intense electron flux in terms of electron trajectory as well electron velocity distribution in detail.

Keywords: small body, particle-in-cell simulation, small scale magnetosphere

©2019. Japan Geoscience Union. All Right Reserved.

Developments and performance evaluations of 0.48 THz band heterodyne receivers for the future Mars terahertz sensor missions with micro-satellites

*Ayaka Tomihara[1], Satoshi Matsumoto[1], Hiroyuki Maezawa[1], Yasuko Kasai[2], Shigeru Yamada[2], Takeshi Kuroda[2], Takayoshi Yamada[2], Toshiyuki Nishibori[3], Yutaka Hasegawa[3], Yasumasa Kasaba[4], Richard Larsson[5], Shinichi Nakasuka[6]

1. Osaka Prefecture University, Osaka, Japan, 2. National Institute of Information and Communications Technology (NICT), Tokyo, Japan, 3. Japan Aerospace Exploration Agency, 4. Tohoku University, Tohoku, Japan, 5. Max planck Institute Solar System Research, Göttingen Germany, 6. Tokyo University, Tokyo, Japan

Mars is an important investigation target for understanding atmospheric environments, habitability, and resources of terrestrial planets. On Mars, methane has been detected, and research continues to study its origin and destruction processes by oxidation reaction networks in the atmosphere and on the surface. In order to understand the evolutionary processes of the Martian atmosphere, detailed and systematic observation of spatial and temporal variation of H_2O and oxidants such as HOx, altitude distribution of O_2 is still an important subject. Mars will also give us valuable information on the extent to which biomarkers O_2 and O_3 are formed abiotically in typical earth type planets with mainly CO_2 atmospheres.
Therefore, we are developing the Bread Board Model (BBM) of lightweight, low power consumption 0.48 THz band heterodyne remote sensing detectors for future Mars terahertz sensor missions with micro-satellites. THz/submillimeter-wave band heterodyne spectroscopy with high frequency resolution allows us to derive the altitude distribution of trace molecules of the planetary atmosphere, and this frequency band is less affected by the absorption and scattering by aerosol and dust because of its long wavelength. Also, regardless of the presence or absence of background light sources like the sun day- and night-side atmospheres are observable. In the BBM receiver system, subharmonic mixer (SHM) detectors with Schottky barrier diodes operating at room temperature were adopted and a circularly polarized wave separating device was united for the RF input port (manufactured by Virginia Diodes, USA), which enabled us to integrate two SHM detectors flatly and compactly. The equivalent noise temperature of the SHM mixers was 1400 - 1500 K (DSB) in the 1 - 6 GHz band. The power consumption and weight of the mixer receiver system are 11.2 W (1.66 A) and 0.6 kg. In the local oscillator system, 13 GHz band signals from the dielectric resonator oscillator with the phase locked to 99.9 MHz reference signal from an oven controlled crystal oscillator are multiplied and amplified with the integrated amplifier-multiplier chains (IAMC). For temperature fluctuations of about 3.5 degrees at room temperature, the frequency drift in the 0.48 THz band was about 100 kHz. Based on the performance of this front-end system, atmospheric radiative transfer simulation confirmed that atmospheric minor constituents such as O_3 and H_2O_2 as well as O_2 and H_2O can be sufficiently observed. In this presentation, we will report on these results.

Keywords: Mars, Planetary atmosphere, Heterodyne remote sensing, Terahertz, Mars lander with Micro-satellite

©2019. Japan Geoscience Union. All Right Reserved.

Time response of the self-regulation of H and O escapes from Mars

*Shungo Koyama[1], Naoki Terada[1], Hiromu Nakagawa[1], Takeshi Kuroda[2]

1. Graduate School of Science, Tohoku University, 2. National Institute of Information and Communications Technology

Atmospheric loss from the Martian upper atmosphere plays an essential role in the evolution of the surface environment of Mars. Especially, water loss through the escapes of hydrogen and oxygen is crucial to determine the habitability. It was shown by McElroy. (1972) that Jeans escape flux of H and H2 and nonthermal escape flux of O were regulated to be in the ratio of 2:1 in a converged model, which is called “self-regulation”. However, it was only confirmed in the atmospheric condition of current Mars and time response of the self-regulation is not well understood.

Here we study time-dependent responses of self-regulation system on different atmospheric conditions. We use a 1D time-dependent photochemical model for various atmospheric conditions and parameters, such as atmospheric CO2 pressure, vertical temperature profile and O escape rate.

We find that timescale of the self-regulation is mainly determined by O escape flux and the CO2 pressure. The timescale is inversely proportional to O escape flux, whereas it increases nonlinearly as the CO2 pressure increases. Our calculations also show that when CO2 pressure drops from the current Martian converged condition, H escape flux increases on a timescale of several days and returns to the twice of O escape flux on a timescale of a hundred thousand years. It implies that seasonal drops of the atmospheric pressure due to the CO2 polar ice cap may contribute to the variation of H escape flux. The effect of vertical temperature profile on self-regulation will also be discussed.

Keywords: Mars, Atmospheric evolution, water

©2019. Japan Geoscience Union. All Right Reserved.

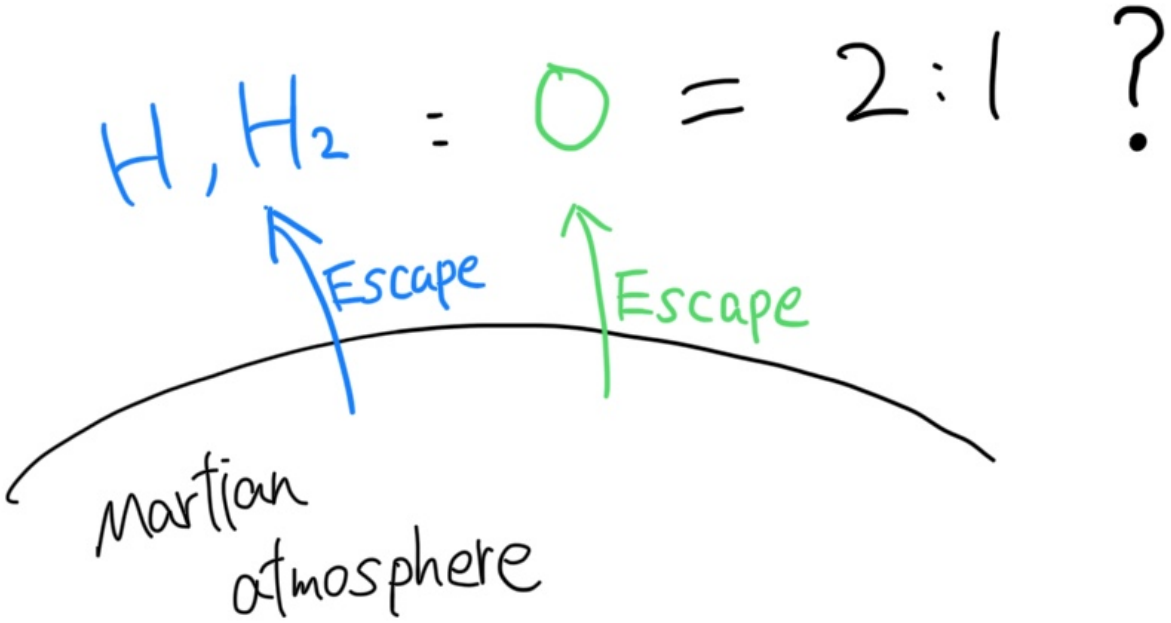

©2019. Japan Geoscience Union. All Right Reserved.

Study of ion composition in the polar plume from Mars based on MAVEN observations

*Sakakura Kotaro[1], Kanako Seki[1], Shogo Inui[1], Shotaro Sakai[1], David A Brain[2], James P McFadden[3], Jasper S Halekas[4], Gina A Dibraccio[5], Bruce Jakosky[2]

1. Department of Earth and Planetary Science, Graduate School of Science, University of Tokyo, Tokyo, Japan., 2. Laboratory for Atmospheric and Space Physics, University of Colorado Boulder, Boulder, Colorado, USA., 3. Space Sciences Laboratory, University of California, Berkeley, California, USA., 4. Department of Physics and Astronomy, University of Iowa, Iowa City, Iowa, USA., 5. Solar System Exploration Division, NASA Goddard Space Flight Center, Greenbelt, MD, USA.

Mars climate was warm and had water on its surface about 4 billion years ago, but there are no liquid water on the surface at present. Escape of the atmosphere to space is considered as the main cause of this climate change. However, the mechanism of the large amount of atmospheric loss is far from understood. Ion escape is one of the important candidates of such mechanism. There are three channels of the ion escape, namely, tailward escape, pickup ion, and polar plume. Polar plume ions are accelerated by solar wind electric field and escape to +E hemisphere of the Mars-Sun-Electric field (MSE) coordinates. It is estimated by Dong et al., (2015) that the escape rate is 23% of the total ion escape. This is not negligible in order to understand ion escape from Mars. However, the composition of the plume is unknown. To fully understand the mechanism of polar plume, it is important to study the composition of the plume.
The purpose of this study is to assess the suggested mechanism of the polar plume based on MAVEN (Mars Atmosphere and Volatile EvolutioN) observations. Spatial distribution of the ion number density ratio can be the evidence that plume is accelerated by electric field because the trajectory of accelerated ions depends on the ion mass. Polar plume contains O^+, O_2^+, and CO_2^+ ions. We focused on molecular ions (O_2^+ and CO_2^+) originating from the ionosphere, since O^+ has corona as its source and its spatial distribution becomes complicated. We analyzed observation data by STATIC (Supra Thermal and Thermal Ion Composition) and MAG (magnetometer) onboard MAVEN. STATIC can measure ion distribution functions with mass discrimination. We selected 12 orbits, in which the plume is observed continuously, from two years of data (from December 2014 to December 2016). To derive CO_2^+ number density, we used fitting method invented by Inui et al., (2018). By fitting a log-normal distribution to O_2^+ count data, we eliminated O_2^+ contamination in the CO_2^+ mass range.
In the event on December 23, 2014, MAVEN moved from the dayside solar wind region to nightside induced magnetosphere in the +E hemisphere of the MSE coordinates. During this event, CO_2^+/O_2^+ number density ratio gradually decreased from ~50 % to ~0.2 %. This tendency is consistent with difference of the trajectories of O_2^+ and CO_2^+, when these ions are accelerated from the same position by the solar wind electric field. We also found high density CO_2^+ plume event in which the CO_2^+ number density is ~1 cm^{-3} and its ratio to O_2^+ is ~500 % at the maximum in the dayside solar wind. We will also report on the statistical tendency of the 12 plume events as well as their dependence on solar wind parameters.

Keywords: Mars, MAVEN, atmospheric escape, carbon dioxide, polar plume

©2019. Japan Geoscience Union. All Right Reserved.

Automated detection of Martian dust devils in multiframe images observed by the MER/Spirit rover.

*Kazuki Yajima[1], Kazunori Ogohara[2]

1. Graduate School of Engineering, The University of Shiga Prefecture, 2. School of Engineering, The University of Shiga Prefecture

Currently, on the surface of Mars the activity range of rovers has spread far more than before, and the Mars environment is gradually becoming clear. Dust devil on Mars is a phenomenon in which dust rolled up from the surface rises in a spiral shape.
Martian dust devils occur everywhere, especially in the middle and low latitudes, and there are various types ranging from small ones like the whirlwind commonly seen on the planet to huge ones much more than tornadoes. In addition, dust that dust devils wind up from the surface of the Martian ground may absorb and block sunlight, sometimes changing the global circulation of the Martian atmosphere. Therefore, in order to understand dynamics of the Mars atmosphere it is necessary to grasp the statistical nature of dust devils.
Previous studies were to count how many dust devils are present in a single image. However, in many cases, the same dust devil is seen in multiple images. Therefore, it was difficult to count the number of dust devil occurences accurately. The number of dust devils that actually occurred has been overestimated unless we detect and count dust devils visually. In this technological study, we propose an algorithm for automatically measuring the population of dust devils correctly by combining template matching and comparison of patch standard deviation.

Keywords: Mars, image processing, dust devil

©2019. Japan Geoscience Union. All Right Reserved.

Temperature change during the global dust storm period obtained by ground observation of the Martian mesosphere by infrared heterodyne spectroscopy

*Akiho Miyamoto[1], Hiromu Nakagawa[1], Kosuke Takami[1], Takeshi Kuroda[1,3], Isao Murata[2], Naoki Terada[1], Nao Yoshida[1], Katsushige Toriumi[1], Shohei Aoki[4], Yasumasa Kasaba[1]

1. Graduate School of Sciences in Tohoku University, 2. Graduate School of Environmental Sciences, 3. National Institute of Information and Communications Technology, 4. Royal Belgian Institute for Space Aeronomy(IASB-BIRA)

In the Martian atmosphere, it is revealed by Mars Express observation that the dust rises to the mesosphere (70-80 [km] in altitude) when dust storm occurs and water vaporis simultaneously transported to the same altitude [Maltagliati et al.,2013 , Heavens et al., 2018]. It leads to Hydrogen atom dissipation due to photodissociation of water vapor at high altitude. It is a new discovery that the phenomenon in the mesosphere can affect the evolution of the Martian environment, and the detailed understanding of the mesosphere is necessary. Therefore, we observed the non-LTE CO_2 emission of 10 μm band by ground observation using Tohoku University heterodyne spectrometer "MILAHI" with wavelength resolution of 10^7(velocity resolution 10 [m/s])to clarify the global mean temperature change during the dust storm period of the Martian mesosphere.
Observations were carried out at the summit of Haleakala, Hawaii from June 2018 (solar longitude Ls = 196, Southern Hemisphere Spring) in the global dust storm to November (Ls = 291 Southern Hemisphere Summer). The spatial resolution is 4 arcsec. (Mars: 19.1 arcsec in June, 10.7 arcsec in November). It is the first time continuous observation by infrared heterodyne spectrometer during the dust storm period at the altitude of 70-80 [km].
The temperature was derived for both kinetic temperature by Doppler width of emission and rotation temperature by line intensity [Sonnabend et al., 2008], and the obtained results were compared.
Kinetic temperature was 150 [K] (68% confidence interval -1sigma122/+1sigma 189 [K]) in June (Ls = 196) and 125 [K] (-1sigma 185/+1sigma 201 [K]) in Sptember(Ls=240), it turned out that the temperature decreased from the global dust storm period to the end.
Compared with the results of the general circulation model [Kuroda et al., 2005,2013,2015] in which dust is not transported at the same altitude, it indicated that 126-129 [K] (Ls = 196) and 132-135 [K] (Ls = 240) which was the opposite tendency to our result. It is thought that the temperature rises at Ls = 240, which is close to the perihelion (Ls = 270), because CO_2 radiation and absorption depend on sunlight. However, the observed higher temperature in Ls = 196 was considered to be caused by the heating by the uplifted dust.
For the rotational temperature, the decrease of line strength of about 1/2 was also detected from the dust storm period to the end. The tendency was similar to the kinetic temperature, and it is clear that absorption around emission was obstructed by dense dust in Ls = 196.
We will compare our results with the stellar occultation observation by MAVEN to validate our result. We will also discuss future prospects such as comparison with observation results at different altitudes in the presentation.

Keywords: Mars, Mesosphere, Temperature, Infrared heterodyne spectrometer

©2019. Japan Geoscience Union. All Right Reserved.

Observation of Neptune’ s storms with Pirka telescope

*Yuuki Sato[1], Yukihiro Takahashi[1], Seiko Takagi[1], Mitsuteru Sato[1], Ono Tatsuharu[1]

1. Graduate School of Science, Hokkaido University

A storm more than 4,000 km in diameter occurrs occasionally in Neptune. In previous study, Voyager 2 observed Neptune on May 24, 1989 and discovered a storm of 13,000 km in diameter called Great Dark Spot(GDS). GDS was located in southern hemisphere like Great Red Spot of Jupiter. But GDS became extinct when Hubble Space Telescope observed it in 1994. It is unknown whether it is a sudden thing or storms such as GDS always occur in Neptune. In addition, a huge storm of 9,000 km was observed on July 2 and June 26, 2017 by Keck observatory. It’ s considered that storms of Neptune occurs at mid latitude in the north and south that an ascending air occurs. However, this huge storm occured near the equator. A rotation axis of Neptune is 29.6 degrees, and the storm possibly occurred near the equator because of seasonal change.
Neptune is observed by large telescopes such as Keck observatory and the Hubble Space Telescope, but it is difficult to always use those telescopes for Neptune observation. Therefore Neptune is not observed for long term on a short time scale. I developed the technique to estimate the drift rate and intensity of storms by observing a whole spectrum of Neptune in this study. When seeing is bad, it’ s possible to observe and aquire the observation data of Neptune for a long term on a short time scale. The purpose is to deepen the understanding of the atmosphere convection structure of Neptune by chasing the detailed change of storms.
In this study, I observed Neptune by using 1.6 m Pirka telescope that Hokkaido University owned. The observation time is from August 7, 2017 to January 17, 2018 and from October 22, 2018 to November 26 2018. The wavelength is 650-1050 nm in 2017, and 890, 855 nm in 2018. In this study, I used methane absorption 890 nm. Storms look brighter at 890 nm because the altitude of storms is higher than that of other areas. In addition, the appearance size of storms from the observation point changes by the rotation of Neptune, so an 890 nm flux changes by the rotation. I took the ratio of an 890 nm flux and an 855 nm flux to correct the effect of the earth atmosphere and calculated the theoretical value of the 890 nm flux by the rotation, compared a relative intensity of the 890nm flux in observation with the theoretical value and estimated the drift rate and intensity of the storms.
I assumed storm's area and calculated the 890 nm reflectance of the storms and estimated the drift rete of storms is 24.9˚/day in 2017, and 47.5˚/day in 2018, 890 nm reflectance is 0.217 in 2018, and 0.105 in 2018. Edward Monlter et al. (2019) study shows that 2017 storm is located at 2˚N and the zonal drift speed is 237.4±0.2 m/s or 47.78±0.04 ˚/day. This drift rate is consistent with the drift rate estimated in my study.

Keywords: Neptune, Ground-based Observations

©2019. Japan Geoscience Union. All Right Reserved.

The study of Jupiter’s zonal wind formation mechanism based on cumulonimbus observation

*Tatsuharu Ono[1], Yukihiro Takahashi[1], Shigeto Watanabe[1], Seiko Takagi[1]

1. Department of Cosmosciences, Graduate School of Science, Hokkaido University

From Galileo spacecraft observation, it is suggested that the zonal jet is created by the small-scale convection and coupling the small-scale eddies made by the vertical convection that involved cumulonimbus [Gierasch et al., 2000]. From the numerical simulation, the intermittency of cumulonimbus is from a few days to one hundred days. However, the observation period of the previous study by spacecraft is from a few days to one month. It is not enough observation period to reveal the relationship between the cumulonimbus and zonal wind. In our study, we observe the cumulonimbus’s time variation by using methane absorption band filters installed 1.6 m Pirka telescope and compare it with the zonal wind velocity variation to reveal this relationship.

In this presentation, we introduce the observational result by ground-based telescope from Jan to June in 2017. And we show the result that compares with the wind velocity time variation. We observed the 727 nm, 756 nm, and 889 nm filters installed at Multi-Spectral Imager (MSI) (pixel scale = 0.39 arcsec/pix) of the 1.6 m Pirka telescope. In our observation, we estimate the existence of cumulonimbus by using the relationship that high cloud top appears as a bright point because the sunlight reflected at cloud top before it is completely absorbed by Jupiter’s atmosphere. We operated the Gaussian High-Pass-Filtering to identify the position of cloud whose cloud top altitude is high like a cumulonimbus. For our observation data, the high cloud top altitude point is extracted in the resolution of one pixel. From the simulation, the intermittency of cumulonimbus would be about 5-100days [Sugiyama et al.,2014]. So, we tried to operate the observation once in a few days. We achieved to operate the observation total 61 times. The interval of observation ranged from successive days to over one week. The average seeing is about 3.0 arcsec. From these observation result,we find the high cloud top altitude point as a possible candidate of cumulonimbus at about latitude -12° and system III longitude 120° on April 20th, 2017. These observation conditions were 2.16 arcsec, equal to about 5000km spatial resolution on Jupiter, and observation covered region was from system III 90° to 180°. Compared with the amateur images that obtained the same day, it is confirmed that the white and bright pattern appeared at that same coordinate position. We observed Jupiter once in every three days from April 20th to the next couple of weeks. However, we couldn’t detect the bright point from data when observed April 23rd, 2017. Compared with the amateur images, we couldn’t confirm the bright and white point around that position. And on April 16th, 2017, from the amateur images, we couldn’t find the bright and white point at the same position. From these results, the lifetime of cumulonimbus at about latitude -12° and system III longitude 120° is about 6 days. We use amateur images to estimate the wind velocity. We compare the wind velocity variation about previous and late date of April 20. From this result, when cumulonimbus is generated, the wind velocity accelerates following the hypothesis. In the other hand, when cumulonimbus is disappeared, the wind velocity decelerates. In the other case, we couldn’t find this relationship. However, the number of data that can compare the wind and cumulonimbus time variation is few. And the accuracy of wind velocity estimated is not enough. So it is not enough to verify the hypothesis suggested by Gierasch and Ingersoll.

Keywords: Jupiter, Cumulonimbus, Convection, Ground-based telescope, thunderstorm

©2019. Japan Geoscience Union. All Right Reserved.

©2019. Japan Geoscience Union. All Right Reserved.

Development of a radial diffusion model of Jovian inner magnetospheric plasma aimed at comparison with HISAKI satellite observation

*Kazuki Yamaguchi[1], Takeshi Sakanoi[1], Fuminori Tsuchiya[1], Masato Kagitani[1], Ryoichi Koga[1], Tomoki Kimura[2]

1. Planetary Plasma and Atmospheric Research Center, Graduate School of Science, Tohoku University, 2. Frontier Research Institute for Interdisciplinary Sciences, Tohoku University

We focus on the development of a diffusion model that estimates interaction and radial transport of various ions and electron in Jovian inner magnetosphere to understand the balance of mass and energy of plasmas and their temporal changes. We also verify the model results with the data obtained by the extreme ultraviolet spectroscope satellite HISAKI.
Jovian first satellite Io has active volcanoes and releases the plasma of the volcanic gas origin to the inner magnetosphere. The plasma is distributed in donut shape along the revolution orbit of Io by co-rotating with Jupiter, and it is called Io plasma torus. 90% of the total mass of Jovian magnetosphere plasma is supplied from Io, and it is transported on the time scale of several tens of days in the radial direction while obtaining energy from the angular momentum of Jovian rotation. Revealing the mass and energy balance of plasma in Jovian inner magnetosphere is an important to understand the macroscopic physical phenomena of the magnetosphere.
The radial distribution model of steady state Jovian magnetospheric plasma was developed based on observation results of Voyager 1, Voyager 2, Cassini spacecrafts. However, there is no report on a model that explains time variation of radial distribution of ions and electrons.

In this study, we are developing a model with the Fokker-Planck equation that can track mass and energy balance of major heavy ions of Io origin (O^+,O^{2+},S^+,S^{2+},S^{3+}) and time evolution of radial transport. We modified the steady state model foe mass and energy transport in Jovian magnetosphere by Delamere *et al.* (2005) to estimate time variations by the Forward Time Central Space (FTCS) method. From Delamere & Bagenal (2003), considering the chemical interaction between ions and electrons by charge exchange, we cited coefficients of electron impact ionization, electron recombination, Coulomb interaction, and radiation due to electron collision excitation. Radiative rate is calculated from the CHIANTI database.The initial temperature and density values of each ion and thermal electron were adopted from HISAKI's observation data in November 2013 when the volcano activity was quiet [Yoshioka *et al.*, 2018]. We assumed that the distribution of neutral atoms (O, S) depends only on the radial direction. For inner boundary conditions, the spatial differentiation of the density was 0 and the ion temperature was 60 eV at 6 R_J. For outer boundary conditions, at 30 R_J, both density and temperature match with values calculated by the function obtained from HISAKI's observation. We compared the model results with the HISAKI's observation data in the region of 6-9 R_J under the steady state conditions. We obtained that the number density of ions with higher valence number tend to be greater than that of observation result. For example, the number density of O^{2+} was 1.2 to 2.0 times greater than observed value. The model estimated the electron temperature to be 6 to 8 eV that was several eV higher than observation value. We considered that the increase in number density of high valence number ions may be due to overestimation of electron impact ionization. We also estimated higher electron temperature than observed value. In addition, we obtained that the temperature with low valence ions was higher than observation value, for example, O^+ temperature was higher than 280 eV at 12 R_J. This discrepancy may be

©2019. Japan Geoscience Union. All Right Reserved.

caused by the heating of pick-up ion gained by high electron temperature. In this presentation, we give detailed comparison between model and observation and quantitative verification.

Keywords: Jupiter, HISAKI

©2019. Japan Geoscience Union. All Right Reserved.

Pitch angle scattering due to elastic collisions between magnetospheric 500eV-50keV electrons and neutral H_2O originated from Enceladus: Test particle simulation

*Hiroyasu Tadokoro[1], Yuto Katoh[2]

1. Musashino University, 2. Tohoku University

Water group neutrals (H_2O, OH, and O) in Saturn’ s inner magnetosphere play the dominant role in loss of energetic electrons and ions because of abundance of the neutrals [e.g., *Paranicas et al.,* 2007; *Sittler et al.,* 2008]. The observations of injected plasmas in the inner magnetosphere suggest that these particles do not survive very long time due to the neutral cloud originated from Enceladus [e.g., Paranicas et al., 2007; 2008]. Thus, the previous studies suggested that the neutral cloud contributes to loss processes of plasma in the inner magnetosphere. However, little has been reported on a quantitative study of the electron loss process due to electron-neutral collisions.

In this study, we focus on the elastic collisional loss process with neutral H_2O originated from Enceladus. Conducting one dimensional test particle simulation, Tadokoro et al., [2014] examined the time variations of equatorial electron pitch angle distribution and electrons within loss cone through 1keV electron pitch angle scattering due to elastic collisions around Enceladus. The result showed that the electrons of 11.4 % are lost in ~380 sec. The time corresponds to the time scale of the co-rotation of the flux tube passing through the region of the dense H_2O in the vicinity of Enceladus. Assuming the uniform azimuth H2O density structure in the Enceladus torus, they estimated the electron loss rate of 33% during one co-rotation.

Next remaining issue is a calculation of energy dependent electron loss rate. We show the loss rates through pitch angle scattering of electrons with 500 eV –50keV and the comparison of the loss rates between the high (in the vicinity of Enceladus) and low (in the Enceladus torus) H_2O density regions. We also show the calculation errors by making several times calculations.

Keywords: Enceladus, Pitch angle scattering, electron-neutral collision, test particle simulation

©2019. Japan Geoscience Union. All Right Reserved.

Study of Jovian atmosphere dynamics by a multi-band imaging observation

Hayate Ito[1], Sumito Hirota[2], Isshi Tabe[3], *Hidehiko Suzuki[1]

1. Meiji university, 2. Kawasaki municipal science museum, 3. Association of Lunar and Planetary Observers in Japan

There are various structures on the surface atmosphere of Jupiter. For example, ‘zones’ or ‘belts’ and vortex structures such as great red spot (GRS) are widely known as quasi-permanent features. Many observations from the ground have revealed dynamical variations both in spatial scale and in visual color for these structures. The changes in apparent color of these structures often occur accompanying dynamical processes such as deformation and change in vorticity. Therefore, it would be a key to understanding Jovian atmosphere dynamics to monitor the change in color of surface structures. The objective of this study is to reveal the mechanism of the variations in Jovian surface structures by a ground-based observation with a multi-band imaging system.
We have developed a multi-band imaging system which can simultaneously obtain both spectral data and spatiotemporal variations of structures. Seven bands in visible range have been selected for the routine observation based on the results from previous spectroscopic works. We have determined the relative sensitivity among these bands which is essential to synthesize a precise natural color image from 7 images. In this talk, we report the initial observation results obtained by the system. The results of the validation for these results by comparing with previous spectroscopic studies using Cassini spacecraft and Hubble space telescope are also shown.

Keywords: Jupiter, Jovian atmosphere, spectroscopy, Multi-band imaging

©2019. Japan Geoscience Union. All Right Reserved.

Examination of the relation between Jupiter's inner magnetosphere and magnetic reconfiguration events

*Hiroaki Misawa[1]

1. Planetary Plasma and Atmospheric Research Center, Graduate School of Science, Tohoku University

It is known that Jupiter's synchrotron radiation (JSR) has information on dynamics of the deep inner magnetosphere. We have made JSR observations in the decimeter radio wavelength more than a decade, and has showed that JSR generally shows short term variations by more than several tens percent with the time scale of days to weeks. A plausible causality of such the short term variations is due to solar UV/EUV variations; i.e., the solar UV/EUV heating for Jupiter's upper atmosphere drives neutral wind perturbations, and the induced dynamo electric field leads to enhancement of radial diffusion of relativistic electrons in the inner magentosphere. and then JSR shows variations. This scenario was initially proposed by Brice and McDonough [1973] and observationally confirmed by Miyoshi et al. [1999], Tsuchiya et al. [2011] and Kita et al., [2013] which is so to speak, an externally driving process. However, this scenario cannot be always applicable to any short term JSR variations, particularly fast variations with the time scale within a few days, and any other processes are required (Kita, 2015; Tsuchiya et al., 2019).
As a process which might explain such a fast variation in Jupiter's magnetosphere, an internally driving process, so-called 'substorm like event', is known (see Louarn et al., 2014). This phenomena is interpreted as a magnetic reconfiguration event occurred in the Jupiter's magnetotail region. Although it is revealed that major magnetic reconfiguration events generally affect the whole magnesphere from 10 to 80-120 Rj (Jupiter's radii), however, it has not been known whether the events affect the inner magnetosphere within 2 Rj.
In order to reveal unknown dynamics of the fast variations in JSR, we have tried to examine relationship between the fast variations and magnetic reconfiguration events. In this study we have used the plasma data explored by the Galileo orbiter in Jupiter's magnetosphere and also Jupiter's particular radio wave component in the hectrometer wave range (see Misawa et al., 2018) for searching magnetic reconfiguration events, and we have compared them with the daily JSR monitoring data at 327MHz observed with the radio telescopes of ISEE, Nagoya University, Japan. In the presentation, we will show results of the examination and discuss a linkage possibility between Jupiter's inner magnetosphere and magnetotail region.

Keywords: Jupiter, radiation belt, fast variation, magnetic reconfiguration

©2019. Japan Geoscience Union. All Right Reserved.

Effects of the charged particles of solar wind on planetary atmospheres

*Shinji Karasawa[1]

1. Miyagi National College of Technology Professor emeritus

The charged particle of H^+ is radiated at an average speed of about 450km/sec from the Sun. It has a rotating component (2km/sec) of the Sun’s rotation. There is no geomagnetic field caused from the inner core of Venus. The charged particles of solar-wind those possess large kinetic momentum. Those collide to the thick atmospheric molecules facing the Sun of Venus. The collisions of the solar wind with angular momentum of anti-clockwise direction causes super-rotation of Venus in the direction of clockwise.
Titan has a super-rotation of 120 m/s at an altitude of 120km. Radius 1.1 million km of the Titan's orbital passes through the stretched portion of the magnetosphere of Saturn at 1.2 million km. Titan's orbital is running through in a part of magnetosphere of Saturn. The rotation period of Titan is about 16 days that is the same as the revolution period of Titan by gravitational lock. So, the surface of Titan receives shower of the charged particle of H^+ in Saturn's magnetosphere at repeating period of 10.7 hours. The movement speed of the magnetosphere in the orbit of the Titan is 200 km/sec**.** The super-rotation of Titan is caused by the difference of moving speed of the H^+ shower on surface of Titan facing Saturn’s side and the backside. Maximum difference of moving speed of the shower is 843 m/sec in counter-clockwise direction. [Website by S. Karasawa,
https://www.youtube.com/watch?v=zPSOD3YAAXw&feature=youtu.be]

Keywords: Solar wind, Magnetoshere, Superrotation, Venus, Saturn, Titan

©2019. Japan Geoscience Union. All Right Reserved.

[J] Poster | P (Space and Planetary Sciences)：P-CG Complex & General

Tue. May 28, 2019 5:15 PM - 6:30 PM JST | Tue. May 28, 2019 8:15 AM - 9:30 AM UTC | Poster Hall International Exhibition Hall8, Makuhari Messe_5

[P-CG25] Planetary Magnetosphere, Ionosphere, and Atmosphere

convener:Kanako Seki(Graduate School of Science, University of Tokyo), Takeshi Imamura(Graduate School of Frontier Sciences, The University of Tokyo), Hiroyuki Maezawa(Department of Physical Science Osaka Prefecture University), Naoki Terada(Graduate School of Science, Tohoku University)

Exploration of Moon, Venus, Mars, Mercury, Jupiter, Saturn, and beyond together with rapid developments of numerical simulations provides us new view of planetary environment. This session collects general contributions of new findings about planetary magnetosphere, ionosphere, and atmosphere. New methodology and technology development studies for future explorations are also welcome. In order to put the common knowledge at different planets into perspective, this session aims to facilitate discussions on comparative planetary environments.

[PCG25-P01] Particle-in-cell simulation on the dayside magnetopause in a small-scale magnetosphere

*Hideyuki Usui[1], Satoki oki[1], Yohei Miyake[1], Naoki Terada[2], Kanako Seki[3], Yuto Katoh[2], Manabu Yagi[4] (1.Graduate school of system informatics Kobe University, 2.Graduate school of science, Tohoku University, 3.Graduate school of science, University of Tokyo, 4.Riken R-CCS)

[PCG25-P02] Developments and performance evaluations of 0.48 THz band heterodyne receivers for the future Mars terahertz sensor missions with micro-satellites

*Ayaka Tomihara[1], Satoshi Matsumoto[1], Hiroyuki Maezawa[1], Yasuko Kasai[2], Shigeru Yamada[2], Takeshi Kuroda[2], Takayoshi Yamada[2], Toshiyuki Nishibori[3], Yutaka Hasegawa[3], Yasumasa Kasaba[4], Richard Larsson[5], Shinichi Nakasuka[6] (1.Osaka Prefecture University, Osaka, Japan, 2.National Institute of Information and Communications Technology (NICT), Tokyo, Japan, 3.Japan Aerospace Exploration Agency, 4.Tohoku University, Tohoku, Japan, 5.Max planck Institute Solar System Research, Göttingen Germany, 6.Tokyo University, Tokyo, Japan)

[PCG25-P03] Time response of the self-regulation of H and O escapes from Mars

*Shungo Koyama[1], Naoki Terada[1], Hiromu Nakagawa[1], Takeshi Kuroda[2] (1.Graduate School of Science, Tohoku University, 2.National Institute of Information and Communications Technology)

[PCG25-P04] Study of ion composition in the polar plume from Mars based on MAVEN observations

*Sakakura Kotaro[1], Kanako Seki[1], Shogo Inui[1], Shotaro Sakai[1], David A Brain[2], James P McFadden[3], Jasper S Halekas[4], Gina A Dibraccio[5], Bruce Jakosky[2] (1.Department of Earth and Planetary Science, Graduate School of Science, University of Tokyo, Tokyo, Japan., 2.Laboratory for Atmospheric and Space Physics, University of Colorado Boulder, Boulder, Colorado, USA., 3.Space Sciences Laboratory, University of California, Berkeley, California, USA., 4.Department of Physics and Astronomy, University of Iowa, Iowa City, Iowa, USA., 5.Solar System Exploration Division, NASA Goddard Space Flight Center, Greenbelt, MD, USA.)

[PCG25-P05] Automated detection of Martian dust devils in multiframe images observed by the MER/Spirit rover.

*Kazuki Yajima[1], Kazunori Ogohara[2] (1.Graduate School of Engineering, The University of Shiga Prefecture, 2.School of Engineering, The University of Shiga Prefecture)

[PCG25-P06] Temperature change during the global dust storm period obtained by ground observation of the Martian mesosphere by infrared heterodyne spectroscopy

*Akiho Miyamoto[1], Hiromu Nakagawa[1], Kosuke Takami[1], Takeshi Kuroda[1,3], Isao Murata[2], Naoki Terada[1], Nao Yoshida[1], Katsushige Toriumi[1], Shohei Aoki[4], Yasumasa Kasaba[1] (1.Graduate School of Sciences in

Tohoku University, 2.Graduate School of Environmental Sciences, 3. National Institute of Information and Communications Technology, 4.Royal Belgian Institute for Space Aeronomy(IASB-BIRA))

[PCG25-P07] Observation of Neptune’s storms with Pirka telescope

*Yuuki Sato[1], Yukihiro Takahashi[1], Seiko Takagi[1], Mitsuteru Sato[1], Ono Tatsuharu[1] (1.Graduate School of Science, Hokkaido University)

[PCG25-P08] The study of Jupiter’s zonal wind formation mechanism based on cumulonimbus observation

*Tatsuharu Ono[1], Yukihiro Takahashi[1], Shigeto Watanabe[1], Seiko Takagi[1] (1.Department of Cosmosciences, Graduate School of Science, Hokkaido University)

[PCG25-P09] Development of a radial diffusion model of Jovian inner magnetospheric plasma aimed at comparison with HISAKI satellite observation

*Kazuki Yamaguchi[1], Takeshi Sakanoi[1], Fuminori Tsuchiya[1], Masato Kagitani[1], Ryoichi Koga[1], Tomoki Kimura[2] (1.Planetary Plasma and Atmospheric Research Center, Graduate School of Science, Tohoku University, 2.Frontier Research Institute for Interdisciplinary Sciences, Tohoku University)

[PCG25-P10] Pitch angle scattering due to elastic collisions between magnetospheric 500eV-50keV electrons and neutral H_2O originated from Enceladus: Test particle simulation

*Hiroyasu Tadokoro[1], Yuto Katoh[2] (1.Musashino University, 2.Tohoku University)

[PCG25-P11] Study of Jovian atmosphere dynamics by a multi-band imaging observation

Hayate Ito[1], Sumito Hirota[2], Isshi Tabe[3], *Hidehiko Suzuki[1] (1.Meiji university, 2.Kawasaki municipal science museum, 3.Association of Lunar and Planetary Observers in Japan)

[PCG25-P12] Examination of the relation between Jupiter's inner magnetosphere and magnetic reconfiguration events

*Hiroaki Misawa[1] (1.Planetary Plasma and Atmospheric Research Center, Graduate School of Science, Tohoku University)

[PCG25-P13] Effects of the charged particles of solar wind on planetary atmospheres

*Shinji Karasawa[1] (1.Miyagi National College of Technology Professor emeritus)

Particle-in-cell simulation on the dayside magnetopause in a small-scale magnetosphere

*Hideyuki Usui[1], Satoki oki[1], Yohei Miyake[1], Naoki Terada[2], Kanako Seki[3], Yuto Katoh[2], Manabu Yagi[4]

1. Graduate school of system informatics Kobe University, 2. Graduate school of science, Tohoku University, 3. Graduate school of science, University of Tokyo, 4. Riken R-CCS

By performing three-dimensional full particle-in-cell plasma simulations, we have been studying a small magnetosphere formed by the interaction between a weakly magnetized small body and the solar wind. In this study, we particularly focus on the electron dynamics at the dayside magnetopause in the equatorial plane. In the simulation model, a weakly magnetized small body is set in the center, and the solar wind having the southward IMF is injected from the boundary of the simulation domain. We define D_p as the distance between the dipole center and a position where the solar wind dynamics pressure balances the magnetic pressure at the dayside. We focus on a small-scale magnetosphere with $\lambda_i/D_p=1$ where we define λ_i as the ion inertia length in the solar wind. When we define R_b as the radius of the sphere, we set $R_b/D_p=0.6$ which implies a relatively large proportion of sphere in the magnetosphere. In the simulation results, we found dawn-dusk asymmetry characteristics of the plasma spatial distribution in the equatorial plane. It is also interesting to observe intense electron flux along the dayside magnetopause in the equator. We found that this intense flux is due to the electrons accelerated by the electric field enhanced at the magnetopause. They encounter the inner region where the southward IMF and the northward magnetic dipole field cancel each other, and they start making meandering motions toward the dawn side between the region of different orientations of the magnetic fields. We examined the mechanism of the intense electron flux in terms of electron trajectory as well electron velocity distribution in detail.

Keywords: small body, particle-in-cell simulation, small scale magnetosphere

©2019. Japan Geoscience Union. All Right Reserved.

Developments and performance evaluations of 0.48 THz band heterodyne receivers for the future Mars terahertz sensor missions with micro-satellites

*Ayaka Tomihara[1], Satoshi Matsumoto[1], Hiroyuki Maezawa[1], Yasuko Kasai[2], Shigeru Yamada[2], Takeshi Kuroda[2], Takayoshi Yamada[2], Toshiyuki Nishibori[3], Yutaka Hasegawa[3], Yasumasa Kasaba[4], Richard Larsson[5], Shinichi Nakasuka[6]

1. Osaka Prefecture University, Osaka, Japan, 2. National Institute of Information and Communications Technology (NICT), Tokyo, Japan, 3. Japan Aerospace Exploration Agency, 4. Tohoku University, Tohoku, Japan, 5. Max planck Institute Solar System Research, Göttingen Germany, 6. Tokyo University, Tokyo, Japan

Mars is an important investigation target for understanding atmospheric environments, habitability, and resources of terrestrial planets. On Mars, methane has been detected, and research continues to study its origin and destruction processes by oxidation reaction networks in the atmosphere and on the surface. In order to understand the evolutionary processes of the Martian atmosphere, detailed and systematic observation of spatial and temporal variation of H_2O and oxidants such as HOx, altitude distribution of O_2 is still an important subject. Mars will also give us valuable information on the extent to which biomarkers O_2 and O_3 are formed abiotically in typical earth type planets with mainly CO_2 atmospheres.
Therefore, we are developing the Bread Board Model (BBM) of lightweight, low power consumption 0.48 THz band heterodyne remote sensing detectors for future Mars terahertz sensor missions with micro-satellites. THz/submillimeter-wave band heterodyne spectroscopy with high frequency resolution allows us to derive the altitude distribution of trace molecules of the planetary atmosphere, and this frequency band is less affected by the absorption and scattering by aerosol and dust because of its long wavelength. Also, regardless of the presence or absence of background light sources like the sun day- and night-side atmospheres are observable. In the BBM receiver system, subharmonic mixer (SHM) detectors with Schottky barrier diodes operating at room temperature were adopted and a circularly polarized wave separating device was united for the RF input port (manufactured by Virginia Diodes, USA), which enabled us to integrate two SHM detectors flatly and compactly. The equivalent noise temperature of the SHM mixers was 1400 - 1500 K (DSB) in the 1 - 6 GHz band. The power consumption and weight of the mixer receiver system are 11.2 W (1.66 A) and 0.6 kg. In the local oscillator system, 13 GHz band signals from the dielectric resonator oscillator with the phase locked to 99.9 MHz reference signal from an oven controlled crystal oscillator are multiplied and amplified with the integrated amplifier-multiplier chains (IAMC). For temperature fluctuations of about 3.5 degrees at room temperature, the frequency drift in the 0.48 THz band was about 100 kHz. Based on the performance of this front-end system, atmospheric radiative transfer simulation confirmed that atmospheric minor constituents such as O_3 and H_2O_2 as well as O_2 and H_2O can be sufficiently observed. In this presentation, we will report on these results.

Keywords: Mars, Planetary atmosphere, Heterodyne remote sensing, Terahertz, Mars lander with Micro-satellite

©2019. Japan Geoscience Union. All Right Reserved.

Time response of the self-regulation of H and O escapes from Mars

*Shungo Koyama[1], Naoki Terada[1], Hiromu Nakagawa[1], Takeshi Kuroda[2]

1. Graduate School of Science, Tohoku University, 2. National Institute of Information and Communications Technology

Atmospheric loss from the Martian upper atmosphere plays an essential role in the evolution of the surface environment of Mars. Especially, water loss through the escapes of hydrogen and oxygen is crucial to determine the habitability. It was shown by McElroy. (1972) that Jeans escape flux of H and H2 and nonthermal escape flux of O were regulated to be in the ratio of 2:1 in a converged model, which is called “self-regulation”. However, it was only confirmed in the atmospheric condition of current Mars and time response of the self-regulation is not well understood.

Here we study time-dependent responses of self-regulation system on different atmospheric conditions. We use a 1D time-dependent photochemical model for various atmospheric conditions and parameters, such as atmospheric CO2 pressure, vertical temperature profile and O escape rate.

We find that timescale of the self-regulation is mainly determined by O escape flux and the CO2 pressure. The timescale is inversely proportional to O escape flux, whereas it increases nonlinearly as the CO2 pressure increases. Our calculations also show that when CO2 pressure drops from the current Martian converged condition, H escape flux increases on a timescale of several days and returns to the twice of O escape flux on a timescale of a hundred thousand years. It implies that seasonal drops of the atmospheric pressure due to the CO2 polar ice cap may contribute to the variation of H escape flux. The effect of vertical temperature profile on self-regulation will also be discussed.

Keywords: Mars, Atmospheric evolution, water

©2019. Japan Geoscience Union. All Right Reserved.

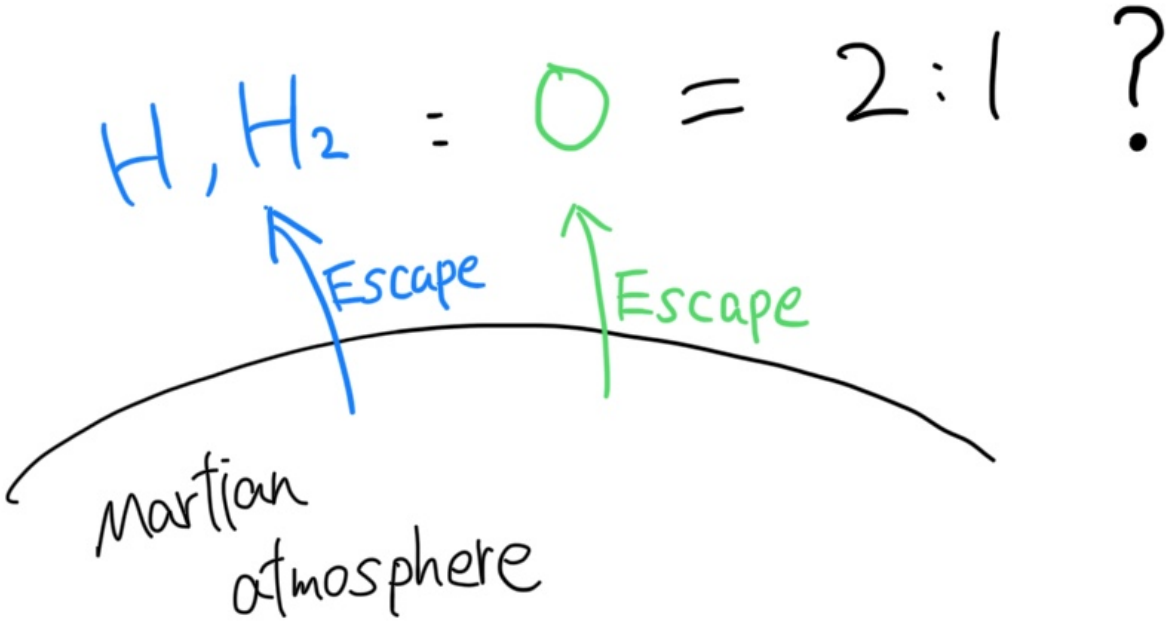

©2019. Japan Geoscience Union. All Right Reserved.

Study of ion composition in the polar plume from Mars based on MAVEN observations

*Sakakura Kotaro[1], Kanako Seki[1], Shogo Inui[1], Shotaro Sakai[1], David A Brain[2], James P McFadden[3], Jasper S Halekas[4], Gina A Dibraccio[5], Bruce Jakosky[2]

1. Department of Earth and Planetary Science, Graduate School of Science, University of Tokyo, Tokyo, Japan., 2. Laboratory for Atmospheric and Space Physics, University of Colorado Boulder, Boulder, Colorado, USA., 3. Space Sciences Laboratory, University of California, Berkeley, California, USA., 4. Department of Physics and Astronomy, University of Iowa, Iowa City, Iowa, USA., 5. Solar System Exploration Division, NASA Goddard Space Flight Center, Greenbelt, MD, USA.

Mars climate was warm and had water on its surface about 4 billion years ago, but there are no liquid water on the surface at present. Escape of the atmosphere to space is considered as the main cause of this climate change. However, the mechanism of the large amount of atmospheric loss is far from understood. Ion escape is one of the important candidates of such mechanism. There are three channels of the ion escape, namely, tailward escape, pickup ion, and polar plume. Polar plume ions are accelerated by solar wind electric field and escape to +E hemisphere of the Mars-Sun-Electric field (MSE) coordinates. It is estimated by Dong et al., (2015) that the escape rate is 23% of the total ion escape. This is not negligible in order to understand ion escape from Mars. However, the composition of the plume is unknown. To fully understand the mechanism of polar plume, it is important to study the composition of the plume.
The purpose of this study is to assess the suggested mechanism of the polar plume based on MAVEN (Mars Atmosphere and Volatile EvolutioN) observations. Spatial distribution of the ion number density ratio can be the evidence that plume is accelerated by electric field because the trajectory of accelerated ions depends on the ion mass. Polar plume contains O^+, O_2^+, and CO_2^+ ions. We focused on molecular ions (O_2^+ and CO_2^+) originating from the ionosphere, since O^+ has corona as its source and its spatial distribution becomes complicated. We analyzed observation data by STATIC (Supra Thermal and Thermal Ion Composition) and MAG (magnetometer) onboard MAVEN. STATIC can measure ion distribution functions with mass discrimination. We selected 12 orbits, in which the plume is observed continuously, from two years of data (from December 2014 to December 2016). To derive CO_2^+ number density, we used fitting method invented by Inui et al., (2018). By fitting a log-normal distribution to O_2^+ count data, we eliminated O_2^+ contamination in the CO_2^+ mass range.
In the event on December 23, 2014, MAVEN moved from the dayside solar wind region to nightside induced magnetosphere in the +E hemisphere of the MSE coordinates. During this event, CO_2^+/O_2^+ number density ratio gradually decreased from ~50 % to ~0.2 %. This tendency is consistent with difference of the trajectories of O_2^+ and CO_2^+, when these ions are accelerated from the same position by the solar wind electric field. We also found high density CO_2^+ plume event in which the CO_2^+ number density is ~1 cm^{-3} and its ratio to O_2^+ is ~500 % at the maximum in the dayside solar wind. We will also report on the statistical tendency of the 12 plume events as well as their dependence on solar wind parameters.

Keywords: Mars, MAVEN, atmospheric escape, carbon dioxide, polar plume

©2019. Japan Geoscience Union. All Right Reserved.

Automated detection of Martian dust devils in multiframe images observed by the MER/Spirit rover.

*Kazuki Yajima[1], Kazunori Ogohara[2]

1. Graduate School of Engineering, The University of Shiga Prefecture, 2. School of Engineering, The University of Shiga Prefecture

Currently, on the surface of Mars the activity range of rovers has spread far more than before, and the Mars environment is gradually becoming clear. Dust devil on Mars is a phenomenon in which dust rolled up from the surface rises in a spiral shape.
Martian dust devils occur everywhere, especially in the middle and low latitudes, and there are various types ranging from small ones like the whirlwind commonly seen on the planet to huge ones much more than tornadoes. In addition, dust that dust devils wind up from the surface of the Martian ground may absorb and block sunlight, sometimes changing the global circulation of the Martian atmosphere. Therefore, in order to understand dynamics of the Mars atmosphere it is necessary to grasp the statistical nature of dust devils.
Previous studies were to count how many dust devils are present in a single image. However, in many cases, the same dust devil is seen in multiple images. Therefore, it was difficult to count the number of dust devil occurences accurately. The number of dust devils that actually occurred has been overestimated unless we detect and count dust devils visually. In this technological study, we propose an algorithm for automatically measuring the population of dust devils correctly by combining template matching and comparison of patch standard deviation.

Keywords: Mars, image processing, dust devil

©2019. Japan Geoscience Union. All Right Reserved.

Temperature change during the global dust storm period obtained by ground observation of the Martian mesosphere by infrared heterodyne spectroscopy

*Akiho Miyamoto[1], Hiromu Nakagawa[1], Kosuke Takami[1], Takeshi Kuroda[1,3], Isao Murata[2], Naoki Terada[1], Nao Yoshida[1], Katsushige Toriumi[1], Shohei Aoki[4], Yasumasa Kasaba[1]

1. Graduate School of Sciences in Tohoku University, 2. Graduate School of Environmental Sciences, 3. National Institute of Information and Communications Technology, 4. Royal Belgian Institute for Space Aeronomy(IASB-BIRA)

In the Martian atmosphere, it is revealed by Mars Express observation that the dust rises to the mesosphere (70-80 [km] in altitude) when dust storm occurs and water vaporis simultaneously transported to the same altitude [Maltagliati et al.,2013 , Heavens et al., 2018]. It leads to Hydrogen atom dissipation due to photodissociation of water vapor at high altitude. It is a new discovery that the phenomenon in the mesosphere can affect the evolution of the Martian environment, and the detailed understanding of the mesosphere is necessary. Therefore, we observed the non-LTE CO_2 emission of 10 μm band by ground observation using Tohoku University heterodyne spectrometer "MILAHI" with wavelength resolution of 10^7(velocity resolution 10 [m/s])to clarify the global mean temperature change during the dust storm period of the Martian mesosphere.
Observations were carried out at the summit of Haleakala, Hawaii from June 2018 (solar longitude Ls = 196, Southern Hemisphere Spring) in the global dust storm to November (Ls = 291 Southern Hemisphere Summer). The spatial resolution is 4 arcsec. (Mars: 19.1 arcsec in June, 10.7 arcsec in November). It is the first time continuous observation by infrared heterodyne spectrometer during the dust storm period at the altitude of 70-80 [km].
The temperature was derived for both kinetic temperature by Doppler width of emission and rotation temperature by line intensity [Sonnabend et al., 2008], and the obtained results were compared.
Kinetic temperature was 150 [K] (68% confidence interval -1sigma122/+1sigma 189 [K]) in June (Ls = 196) and 125 [K] (-1sigma 185/+1sigma 201 [K]) in Sptember(Ls=240), it turned out that the temperature decreased from the global dust storm period to the end.
Compared with the results of the general circulation model [Kuroda et al., 2005,2013,2015] in which dust is not transported at the same altitude, it indicated that 126-129 [K] (Ls = 196) and 132-135 [K] (Ls = 240) which was the opposite tendency to our result. It is thought that the temperature rises at Ls = 240, which is close to the perihelion (Ls = 270), because CO_2 radiation and absorption depend on sunlight. However, the observed higher temperature in Ls = 196 was considered to be caused by the heating by the uplifted dust.
For the rotational temperature, the decrease of line strength of about 1/2 was also detected from the dust storm period to the end. The tendency was similar to the kinetic temperature, and it is clear that absorption around emission was obstructed by dense dust in Ls = 196.
We will compare our results with the stellar occultation observation by MAVEN to validate our result. We will also discuss future prospects such as comparison with observation results at different altitudes in the presentation.

Keywords: Mars, Mesosphere, Temperature, Infrared heterodyne spectrometer

©2019. Japan Geoscience Union. All Right Reserved.

Observation of Neptune’ s storms with Pirka telescope

*Yuuki Sato[1], Yukihiro Takahashi[1], Seiko Takagi[1], Mitsuteru Sato[1], Ono Tatsuharu[1]

1. Graduate School of Science, Hokkaido University

A storm more than 4,000 km in diameter occurrs occasionally in Neptune. In previous study, Voyager 2 observed Neptune on May 24, 1989 and discovered a storm of 13,000 km in diameter called Great Dark Spot(GDS). GDS was located in southern hemisphere like Great Red Spot of Jupiter. But GDS became extinct when Hubble Space Telescope observed it in 1994. It is unknown whether it is a sudden thing or storms such as GDS always occur in Neptune. In addition, a huge storm of 9,000 km was observed on July 2 and June 26, 2017 by Keck observatory. It’ s considered that storms of Neptune occurs at mid latitude in the north and south that an ascending air occurs. However, this huge storm occured near the equator. A rotation axis of Neptune is 29.6 degrees, and the storm possibly occurred near the equator because of seasonal change.
Neptune is observed by large telescopes such as Keck observatory and the Hubble Space Telescope, but it is difficult to always use those telescopes for Neptune observation. Therefore Neptune is not observed for long term on a short time scale. I developed the technique to estimate the drift rate and intensity of storms by observing a whole spectrum of Neptune in this study. When seeing is bad, it’ s possible to observe and aquire the observation data of Neptune for a long term on a short time scale. The purpose is to deepen the understanding of the atmosphere convection structure of Neptune by chasing the detailed change of storms.
In this study, I observed Neptune by using 1.6 m Pirka telescope that Hokkaido University owned. The observation time is from August 7, 2017 to January 17, 2018 and from October 22, 2018 to November 26 2018. The wavelength is 650-1050 nm in 2017, and 890, 855 nm in 2018. In this study, I used methane absorption 890 nm. Storms look brighter at 890 nm because the altitude of storms is higher than that of other areas. In addition, the appearance size of storms from the observation point changes by the rotation of Neptune, so an 890 nm flux changes by the rotation. I took the ratio of an 890 nm flux and an 855 nm flux to correct the effect of the earth atmosphere and calculated the theoretical value of the 890 nm flux by the rotation, compared a relative intensity of the 890nm flux in observation with the theoretical value and estimated the drift rate and intensity of the storms.
I assumed storm's area and calculated the 890 nm reflectance of the storms and estimated the drift rete of storms is 24.9˚/day in 2017, and 47.5˚/day in 2018, 890 nm reflectance is 0.217 in 2018, and 0.105 in 2018. Edward Monlter et al. (2019) study shows that 2017 storm is located at 2˚N and the zonal drift speed is 237.4±0.2 m/s or 47.78±0.04 ˚/day. This drift rate is consistent with the drift rate estimated in my study.

Keywords: Neptune, Ground-based Observations

©2019. Japan Geoscience Union. All Right Reserved.

The study of Jupiter’s zonal wind formation mechanism based on cumulonimbus observation

*Tatsuharu Ono[1], Yukihiro Takahashi[1], Shigeto Watanabe[1], Seiko Takagi[1]

1. Department of Cosmosciences, Graduate School of Science, Hokkaido University

From Galileo spacecraft observation, it is suggested that the zonal jet is created by the small-scale convection and coupling the small-scale eddies made by the vertical convection that involved cumulonimbus [Gierasch et al., 2000]. From the numerical simulation, the intermittency of cumulonimbus is from a few days to one hundred days. However, the observation period of the previous study by spacecraft is from a few days to one month. It is not enough observation period to reveal the relationship between the cumulonimbus and zonal wind. In our study, we observe the cumulonimbus’s time variation by using methane absorption band filters installed 1.6 m Pirka telescope and compare it with the zonal wind velocity variation to reveal this relationship.

In this presentation, we introduce the observational result by ground-based telescope from Jan to June in 2017. And we show the result that compares with the wind velocity time variation. We observed the 727 nm, 756 nm, and 889 nm filters installed at Multi-Spectral Imager (MSI) (pixel scale = 0.39 arcsec/pix) of the 1.6 m Pirka telescope. In our observation, we estimate the existence of cumulonimbus by using the relationship that high cloud top appears as a bright point because the sunlight reflected at cloud top before it is completely absorbed by Jupiter’s atmosphere. We operated the Gaussian High-Pass-Filtering to identify the position of cloud whose cloud top altitude is high like a cumulonimbus. For our observation data, the high cloud top altitude point is extracted in the resolution of one pixel. From the simulation, the intermittency of cumulonimbus would be about 5-100days [Sugiyama et al.,2014]. So, we tried to operate the observation once in a few days. We achieved to operate the observation total 61 times. The interval of observation ranged from successive days to over one week. The average seeing is about 3.0 arcsec. From these observation result,we find the high cloud top altitude point as a possible candidate of cumulonimbus at about latitude -12° and system III longitude 120° on April 20th, 2017. These observation conditions were 2.16 arcsec, equal to about 5000km spatial resolution on Jupiter, and observation covered region was from system III 90° to 180°. Compared with the amateur images that obtained the same day, it is confirmed that the white and bright pattern appeared at that same coordinate position. We observed Jupiter once in every three days from April 20th to the next couple of weeks. However, we couldn’t detect the bright point from data when observed April 23rd, 2017. Compared with the amateur images, we couldn’t confirm the bright and white point around that position. And on April 16th, 2017, from the amateur images, we couldn’t find the bright and white point at the same position. From these results, the lifetime of cumulonimbus at about latitude -12° and system III longitude 120° is about 6 days. We use amateur images to estimate the wind velocity. We compare the wind velocity variation about previous and late date of April 20. From this result, when cumulonimbus is generated, the wind velocity accelerates following the hypothesis. In the other hand, when cumulonimbus is disappeared, the wind velocity decelerates. In the other case, we couldn’t find this relationship. However, the number of data that can compare the wind and cumulonimbus time variation is few. And the accuracy of wind velocity estimated is not enough. So it is not enough to verify the hypothesis suggested by Gierasch and Ingersoll.

Keywords: Jupiter, Cumulonimbus, Convection, Ground-based telescope, thunderstorm

©2019. Japan Geoscience Union. All Right Reserved.

©2019. Japan Geoscience Union. All Right Reserved.

Development of a radial diffusion model of Jovian inner magnetospheric plasma aimed at comparison with HISAKI satellite observation

*Kazuki Yamaguchi[1], Takeshi Sakanoi[1], Fuminori Tsuchiya[1], Masato Kagitani[1], Ryoichi Koga[1], Tomoki Kimura[2]

1. Planetary Plasma and Atmospheric Research Center, Graduate School of Science, Tohoku University, 2. Frontier Research Institute for Interdisciplinary Sciences, Tohoku University

We focus on the development of a diffusion model that estimates interaction and radial transport of various ions and electron in Jovian inner magnetosphere to understand the balance of mass and energy of plasmas and their temporal changes. We also verify the model results with the data obtained by the extreme ultraviolet spectroscope satellite HISAKI.
Jovian first satellite Io has active volcanoes and releases the plasma of the volcanic gas origin to the inner magnetosphere. The plasma is distributed in donut shape along the revolution orbit of Io by co-rotating with Jupiter, and it is called Io plasma torus. 90% of the total mass of Jovian magnetosphere plasma is supplied from Io, and it is transported on the time scale of several tens of days in the radial direction while obtaining energy from the angular momentum of Jovian rotation. Revealing the mass and energy balance of plasma in Jovian inner magnetosphere is an important to understand the macroscopic physical phenomena of the magnetosphere.
The radial distribution model of steady state Jovian magnetospheric plasma was developed based on observation results of Voyager 1, Voyager 2, Cassini spacecrafts. However, there is no report on a model that explains time variation of radial distribution of ions and electrons.

In this study, we are developing a model with the Fokker-Planck equation that can track mass and energy balance of major heavy ions of Io origin (O^+,O^{2+},S^+,S^{2+},S^{3+}) and time evolution of radial transport. We modified the steady state model foe mass and energy transport in Jovian magnetosphere by Delamere *et al.* (2005) to estimate time variations by the Forward Time Central Space (FTCS) method. From Delamere & Bagenal (2003), considering the chemical interaction between ions and electrons by charge exchange, we cited coefficients of electron impact ionization, electron recombination, Coulomb interaction, and radiation due to electron collision excitation. Radiative rate is calculated from the CHIANTI database.The initial temperature and density values of each ion and thermal electron were adopted from HISAKI's observation data in November 2013 when the volcano activity was quiet [Yoshioka *et al.*, 2018]. We assumed that the distribution of neutral atoms (O, S) depends only on the radial direction. For inner boundary conditions, the spatial differentiation of the density was 0 and the ion temperature was 60 eV at 6 R_J. For outer boundary conditions, at 30 R_J, both density and temperature match with values calculated by the function obtained from HISAKI's observation. We compared the model results with the HISAKI's observation data in the region of 6-9 R_J under the steady state conditions. We obtained that the number density of ions with higher valence number tend to be greater than that of observation result. For example, the number density of O^{2+} was 1.2 to 2.0 times greater than observed value. The model estimated the electron temperature to be 6 to 8 eV that was several eV higher than observation value. We considered that the increase in number density of high valence number ions may be due to overestimation of electron impact ionization. We also estimated higher electron temperature than observed value. In addition, we obtained that the temperature with low valence ions was higher than observation value, for example, O^+ temperature was higher than 280 eV at 12 R_J. This discrepancy may be

©2019. Japan Geoscience Union. All Right Reserved.

caused by the heating of pick-up ion gained by high electron temperature. In this presentation, we give detailed comparison between model and observation and quantitative verification.

Keywords: Jupiter, HISAKI

©2019. Japan Geoscience Union. All Right Reserved.

Pitch angle scattering due to elastic collisions between magnetospheric 500eV-50keV electrons and neutral H_2O originated from Enceladus: Test particle simulation

*Hiroyasu Tadokoro[1], Yuto Katoh[2]

1. Musashino University, 2. Tohoku University

Water group neutrals (H_2O, OH, and O) in Saturn’ s inner magnetosphere play the dominant role in loss of energetic electrons and ions because of abundance of the neutrals [e.g., *Paranicas et al.,* 2007; *Sittler et al.,* 2008]. The observations of injected plasmas in the inner magnetosphere suggest that these particles do not survive very long time due to the neutral cloud originated from Enceladus [e.g., Paranicas et al., 2007; 2008]. Thus, the previous studies suggested that the neutral cloud contributes to loss processes of plasma in the inner magnetosphere. However, little has been reported on a quantitative study of the electron loss process due to electron-neutral collisions.

In this study, we focus on the elastic collisional loss process with neutral H_2O originated from Enceladus. Conducting one dimensional test particle simulation, Tadokoro et al., [2014] examined the time variations of equatorial electron pitch angle distribution and electrons within loss cone through 1keV electron pitch angle scattering due to elastic collisions around Enceladus. The result showed that the electrons of 11.4 % are lost in ~380 sec. The time corresponds to the time scale of the co-rotation of the flux tube passing through the region of the dense H_2O in the vicinity of Enceladus. Assuming the uniform azimuth H2O density structure in the Enceladus torus, they estimated the electron loss rate of 33% during one co-rotation.

Next remaining issue is a calculation of energy dependent electron loss rate. We show the loss rates through pitch angle scattering of electrons with 500 eV –50keV and the comparison of the loss rates between the high (in the vicinity of Enceladus) and low (in the Enceladus torus) H_2O density regions. We also show the calculation errors by making several times calculations.

Keywords: Enceladus, Pitch angle scattering, electron-neutral collision, test particle simulation

©2019. Japan Geoscience Union. All Right Reserved.

Study of Jovian atmosphere dynamics by a multi-band imaging observation

Hayate Ito[1], Sumito Hirota[2], Isshi Tabe[3], *Hidehiko Suzuki[1]

1. Meiji university, 2. Kawasaki municipal science museum, 3. Association of Lunar and Planetary Observers in Japan

There are various structures on the surface atmosphere of Jupiter. For example, ‘zones’ or ‘belts’ and vortex structures such as great red spot (GRS) are widely known as quasi-permanent features. Many observations from the ground have revealed dynamical variations both in spatial scale and in visual color for these structures. The changes in apparent color of these structures often occur accompanying dynamical processes such as deformation and change in vorticity. Therefore, it would be a key to understanding Jovian atmosphere dynamics to monitor the change in color of surface structures. The objective of this study is to reveal the mechanism of the variations in Jovian surface structures by a ground-based observation with a multi-band imaging system.
We have developed a multi-band imaging system which can simultaneously obtain both spectral data and spatiotemporal variations of structures. Seven bands in visible range have been selected for the routine observation based on the results from previous spectroscopic works. We have determined the relative sensitivity among these bands which is essential to synthesize a precise natural color image from 7 images. In this talk, we report the initial observation results obtained by the system. The results of the validation for these results by comparing with previous spectroscopic studies using Cassini spacecraft and Hubble space telescope are also shown.

Keywords: Jupiter, Jovian atmosphere, spectroscopy, Multi-band imaging

©2019. Japan Geoscience Union. All Right Reserved.

Examination of the relation between Jupiter's inner magnetosphere and magnetic reconfiguration events

*Hiroaki Misawa[1]

1. Planetary Plasma and Atmospheric Research Center, Graduate School of Science, Tohoku University

It is known that Jupiter's synchrotron radiation (JSR) has information on dynamics of the deep inner magnetosphere. We have made JSR observations in the decimeter radio wavelength more than a decade, and has showed that JSR generally shows short term variations by more than several tens percent with the time scale of days to weeks. A plausible causality of such the short term variations is due to solar UV/EUV variations; i.e., the solar UV/EUV heating for Jupiter's upper atmosphere drives neutral wind perturbations, and the induced dynamo electric field leads to enhancement of radial diffusion of relativistic electrons in the inner magentosphere. and then JSR shows variations. This scenario was initially proposed by Brice and McDonough [1973] and observationally confirmed by Miyoshi et al. [1999], Tsuchiya et al. [2011] and Kita et al., [2013] which is so to speak, an externally driving process. However, this scenario cannot be always applicable to any short term JSR variations, particularly fast variations with the time scale within a few days, and any other processes are required (Kita, 2015; Tsuchiya et al., 2019).
As a process which might explain such a fast variation in Jupiter's magnetosphere, an internally driving process, so-called 'substorm like event', is known (see Louarn et al., 2014). This phenomena is interpreted as a magnetic reconfiguration event occurred in the Jupiter's magnetotail region. Although it is revealed that major magnetic reconfiguration events generally affect the whole magnesphere from 10 to 80-120 Rj (Jupiter's radii), however, it has not been known whether the events affect the inner magnetosphere within 2 Rj.
In order to reveal unknown dynamics of the fast variations in JSR, we have tried to examine relationship between the fast variations and magnetic reconfiguration events. In this study we have used the plasma data explored by the Galileo orbiter in Jupiter's magnetosphere and also Jupiter's particular radio wave component in the hectrometer wave range (see Misawa et al., 2018) for searching magnetic reconfiguration events, and we have compared them with the daily JSR monitoring data at 327MHz observed with the radio telescopes of ISEE, Nagoya University, Japan. In the presentation, we will show results of the examination and discuss a linkage possibility between Jupiter's inner magnetosphere and magnetotail region.

Keywords: Jupiter, radiation belt, fast variation, magnetic reconfiguration

©2019. Japan Geoscience Union. All Right Reserved.

Effects of the charged particles of solar wind on planetary atmospheres

*Shinji Karasawa[1]

1. Miyagi National College of Technology Professor emeritus

The charged particle of H^+ is radiated at an average speed of about 450km/sec from the Sun. It has a rotating component (2km/sec) of the Sun’s rotation. There is no geomagnetic field caused from the inner core of Venus. The charged particles of solar-wind those possess large kinetic momentum. Those collide to the thick atmospheric molecules facing the Sun of Venus. The collisions of the solar wind with angular momentum of anti-clockwise direction causes super-rotation of Venus in the direction of clockwise.
Titan has a super-rotation of 120 m/s at an altitude of 120km. Radius 1.1 million km of the Titan's orbital passes through the stretched portion of the magnetosphere of Saturn at 1.2 million km. Titan's orbital is running through in a part of magnetosphere of Saturn. The rotation period of Titan is about 16 days that is the same as the revolution period of Titan by gravitational lock. So, the surface of Titan receives shower of the charged particle of H^+ in Saturn's magnetosphere at repeating period of 10.7 hours. The movement speed of the magnetosphere in the orbit of the Titan is 200 km/sec**.** The super-rotation of Titan is caused by the difference of moving speed of the H^+ shower on surface of Titan facing Saturn’s side and the backside. Maximum difference of moving speed of the shower is 843 m/sec in counter-clockwise direction. [Website by S. Karasawa,
https://www.youtube.com/watch?v=zPSOD3YAAXw&feature=youtu.be]

Keywords: Solar wind, Magnetoshere, Superrotation, Venus, Saturn, Titan

©2019. Japan Geoscience Union. All Right Reserved.

[E] Poster | A (Atmospheric and Hydrospheric Sciences)：A-AS Atmospheric Sciences, Meteorology & Atmospheric Environment

Tue. May 28, 2019 10:45 AM - 12:15 PM JST | Tue. May 28, 2019 1:45 AM - 3:15 AM UTC | Poster Hall International Exhibition Hall8, Makuhari Messe_2

[A-AS03] Large-scale moisture and organized cloud systems

convener:Hiroaki Miura(The University of Tokyo), Atsushi Hamada(University of Toyama), Satoru Yokoi(Japan Agency for Marine-Earth Science and Technology), Masaki Satoh(Atmosphere and Ocean Research Institute, The University of Tokyo)

Water vapor plays a significant role in regulating the global atmospheric circulation, especially in the troposphere. The overturning circulation is directly driven by the longwave radiative cooling of water vapor and the latent heating/cooling through microphysical processes to balance it. This global circulation is composed of diverse atmospheric phenomena with various spatial and temporal scales. Developments of some significant turbulent motions such as 3D isotropic turbulence in clouds, stratocumulus and cumulus convection, squall lines and tropical cyclones, and the Madden-Julian oscillation, are essentially associated with moisture anomaly in each scale. Moisture is accumulated relatively slowly in larger horizontal scales, but is consumed relatively quickly in smaller ones. This significant scale gaps between the accumulation and consumption may be one of the causes of the long-lasting difficulty in developing the theory of the moist atmosphere. The aim of this session is to share the recent researches about the relationships between moisture and organized cloud systems in wider spatial and temporal scales to enhance collaborations between modeling, observational, and theoretical approaches in tackling this challenging task. Research results relating to the Years of the Maritime Continent (YMC) and Radiative-Convective Equilibrium Model Intercomparison Project (RCEMPI) are welcome.

[AAS03-P01] Numerical investigation on the shape, terminal velocity, and drag coefficient of a small raindrop by the improved immersed boundary method

*Ong Chia Rui[1], Hiroaki Miura[1] (1.The University of Tokyo)

[AAS03-P02] **A diagnostic study of water vapor during an extreme precipitation event in Yili river valleyA diagnostic study of water vapor during an extreme precipitation event in Yili river valley**

*Jing LiU[1], Yushu Zhou[2], Lianmei Yang[1] (1.Institute of Desert Meteorology,CMA, 2.Institute of Atmospheric Physics,CAS)

[AAS03-P03] **The Study on the Characteristics of Weather and Cloud Types in the Summer and Winter Seasons of the South China Sea**

*Jou Ping Hou[1], Bo-Shiou Wei[1], Li-Zhen Su[1] (1.Chung Cheng Institute of Technology)

[AAS03-P04] **Linkages between the South and East Asian Monsoon water vapor transport during boreal summer**

*Yong Liu[1] (1.Institute of Atmospheric Physics, Beijing , China)

[AAS03-P05] Interannual Modulation of the Local Hadley Circulation on Clouds, Radiation and Diagnostic Fields over the Western North Pacific

*Xinyue Wang[1], Hironobu Iwabuchi[1] (1.Tohoku Univ.)

[AAS03-P06] Seasonal and Regional Variation of Diurnal Cycle of Rainfall over Java Island and the Surrounding Area

*Madam Taqiyya Maulana[1], Takeshi Yamazaki[1] (1.Tohoku University)

[AAS03-P07] **Study on atmospheric circulation characteristics of precipitation anomalies in arid region of Central Asia**

*Lianmei Yang[1], Xuefeng Guan[1] (1.Institute of Desert Meteorology, China Meteorological Administration,)

[AAS03-P08] Mechanisms for northward propagation of boreal summer intraseasonal oscillation

*Kanta Nakae[1], Masaki Satoh[1], Daisuke Takasuka[1] (1.Atmosphere and Ocean Research Institute, The University of Tokyo)

[AAS03-P09] Fractality in the perimeter of tropical clouds observed by Himawari-8 or simulated by a high-resolution model

*Takuya Jinno[1] (1.Graduate School of Science, The University of Tokyo)

[AAS03-P10] **Large-scale deformation of tropical cloud band in the ITCZ detected in NICAM simulations**

*Noriyuki Nishi[1], Atsushi Hamada[4], Yohei Yamada[2], Tomoe Nasuno[2], Reona Satoh[5], Masaki Satoh[3] (1.Faculty of Science, Fukuoka Universtiy, 2.JAMSTEC, 3.AORI, University of Tokyo, 4.Graduate School of Science and Engineering for Education, University of Toyama, 5.Graduate School of Science, Fukuoka University)

[AAS03-P11] **Improvement of single-moment bulk microphysics for super-cooled water clouds over the Southern Ocean in NICAM using Joint simulator and double-moment microphysics**

*Woosub Roh[1], Tatsuya Seiki[2], Masaki Satoh[1], Tempei Hashino[3] (1.AORI, the university of Tokyo, 2.JAMSTEC, 3.Kochi university of technology)

[AAS03-P12] High-cloud property responses to SST change: sensitivity study using a global nonhydrostatic model

*Tomoki Ohno[1], Masaki Satoh[2] (1.Japan Agency for Marine-Earth Science and Technology, 2.Atmosphere and Ocean Research Institute, The University of Tokyo)

[AAS03-P13] Effects of different cloud overlapping parameters on simulated total cloud fraction over the globe and East Asian region

*bo hai Wang[1], hua Zhang[2] (1.Institute of Atmospheric Physics, Chinese Academy of Sciences, 2.State Key Laboratory of Severe Weather, Chinese Academy of Meteorological Sciences)

Numerical investigation on the shape, terminal velocity, and drag coefficient of a small raindrop by the improved immersed boundary method

*Ong Chia Rui[1], Hiroaki Miura[1]

1. The University of Tokyo

The cloud microphysical processes play a crucial part in controlling the water cycle, cloud formation, and radiation transfer in the atmosphere. These process are parameterized in a numerical weather prediction model by empirical formulae. In particular, empirical formulae for the prediction of the terminal velocity, drag coefficient, and shape of a free-falling water droplet are used widely in the parameterizations. Despite that the model accuracy is sensitive to the microphysics parameterizations to a considerable extent, these formulae are only verified by experiments which are conducted at room temperature and standard atmospheric pressure or linear theories in an ideal condition. The validity of the parameterizations is therefore questionable under general conditions and the accuracy of the numerical prediction may be affected.
In this work, a new numerical tool, the immersed boundary method, is proposed as an alternative way to investigate the terminal velocity, drag coefficient, and shape of an axisymmetric free-falling raindrop. This improved immersed boundary method for water droplet simulations is applied to verify those commonly used empirical formulae under different conditions. The largest size of the free-falling raindrop in this work is 0.5 mm. To first verify the reliability and robustness of this new method the terminal velocity and drag coefficient obtained from axisymmetric raindrop simulations at standard pressure and temperature fit well with the experimental data. Further simulation results of an axisymmetric free-falling raindrop of diameters of 0.025, 0.01, and 0.5 mm at different altitudes assuming a fixed lapse rate show that the variation of the shape of the raindrop is negligibly small, and there is a significant discrepancy between the numerical results and some of the widely used empirical formulae. The discrepancy is larger at higher altitudes for small raindrops. This is because of the assumption of the fixed drag coefficient in the derivation of those empirical formulae. A new parameterization with better accuracy for terminal velocity aloft of raindrops with diameter smaller than 0.5 mm is proposed. A further sensitivity test of a 0.5 mm free-falling axisymmetric raindrop with different surface tension coefficients are performed and the numerical results suggest that the change in the shape and terminal velocity is negligible with respect to aerosols.

Keywords: Cloud Microphysis, Immersed boundary method, Terminal velocity

©2019. Japan Geoscience Union. All Right Reserved.

A diagnostic study of water vapor during an extreme precipitation event in Yili river valleyA diagnostic study of water vapor during an extreme precipitation event in Yili river valley

*Jing LiU[1], Yushu Zhou[2], Lianmei Yang[1]

1. Institute of Desert Meteorology,CMA, 2. Institute of Atmospheric Physics,CAS

An extreme precipitation events was happened during 31 July to 1 August, 2016 at Yili river valley which multi-stations breakthrough extreme precipitation’ s value. Based on calculation of water vapor transport stream function and the non-divergent (rotational) components, potential function and divergent (irrotational) components, the water vapor transport budget and water vapor transport trajectories for the Yili river valley using the conventional detection,1° x 1° NCEP/NCAR reanalysis, HYSPLIT model based on Lagrangian method, Ground-based GPS observation precipitable water vapor data(GPS-PWV) , the large-scale water vapor transport and convergence characteristics were analyzed during the heavy rainfall period. The results showed that: (1) The Indian, the Pacific and the Atlantic ocean all contributed to the water supply during the heavy rain period, and Indian summer monsoon circulation, the south China sea summer monsoon circulation at low latitudes and Atlantic ocean’ s east airflow at mid-latitude were constituted the water vapor transmission channel, which the Indian Ocean southwest water vapor transport mainly concentrated in the lower troposphere, and middle troposphere water vapor transport was given priority to the west flow of the Atlantic ocean and low trough itself; the valley was in the convergence area of water vapor flux during the heavy rain, and the convergence and uplift of the terrain to the West opening caused vertical motion development provided a favorable dynamic convergence mechanism for the occurrence of local heavy rain.(2) The 3000 m water vapor transmission trajectory included the westward and eastward path at bottom layer and the northward path at middle troposphere as complement of water vapor for the lower troposphere through the vertical motion, the southward path at lower troposphere which water vapor come from the Arabian sea,and the mid-latitude water vapor transport of the westward path was the most powerful ; The 5000 m water vapor transmission trajectory was dominated by the westward path and the low trough itself;(3) During the precipitation period, the water vapor was concentrated in the lower troposphere which transported to the upper level through vertical movement, and the water vapor was positive at the middle and upper layers contrasted with negative at the lower layer. south boundary of water vapor inflow was rapidly increasing at the lower layer while the middle and higher layer water vapor inflow derived from the western boundary during the heavy rainfall period;(4)Yili river valley GPS-PWV jumped caused by the southwest airflow front of low trough before the rainfall happened and steadily maintain the high value influenced by India southwest monsoon during the heavy rainfall period. The large-scale water vapor transport convergence enhancement corresponding local GPS-PWV increased, suggested that the water vapor supply in local heavy rain event was at least associated with the water vapor transport and convergence of hemisphere scale.

Keywords: torrential rain, transfer of water vapor, lagrange trajectory, ground-based GPS

©2019. Japan Geoscience Union. All Right Reserved.

The Study on the Characteristics of Weather and Cloud Types in the Summer and Winter Seasons of the South China Sea

*Jou Ping Hou[1], Bo-Shiou Wei[1], Li-Zhen Su[1]

1. Chung Cheng Institute of Technology

The South China Sea is vast with a tropical maritime climate near the equator and a subtropical climate in the north. Therefore, although it is winter, there are still deep convective and strong precipitation systems in the South China Sea. In summer, thermal convection is strong, sometimes typhoons pass; Dongsha Island and Taiping Island are located in the north and south of the South China Sea. The weather in the region is bound to be significantly affected by various weather systems in the South China Sea. We selected the winter of December 2017 and the summer of June 2018 to study it. The Dongsha Island and Taiping Island areas were subjected to research on the northeast monsoon and tropical convection. The dual island observation and satellite data were combined with numerical models to analyze the mutual interaction between the thermal and dynamic processes in the South China Sea. To enhance the understanding of the weather evolution mechanism in the South China Sea, in order to further clarify the various cloud-phase characteristics of the monsoon circulation and thermal convection in the South China Sea. The results show that the change of northeast monsoon intensity obviously affects the interaction of air-sea in the South China Sea, enhances the intensity of precipitation, and changes the amount and height of the stratus cumulus in the sea. In addition, the northeast monsoon circulation may interact with the surrounding terrain of the South China Sea, thus induces local deep convection. In the summer, the southwest monsoon will be enhanced and thermal convection is very strong. The intensity and life cycle of the typhoon can be maintained when it passes this area.

Keywords: Dongsha Island, Taiping Island, Air-Sea interaction, Deep Convection

©2019. Japan Geoscience Union. All Right Reserved.

Linkages between the South and East Asian Monsoon water vapor transport during boreal summer

*Yong Liu[1]

1. Institute of Atmospheric Physics, Beijing , China

This study provides a water vapor transport (WVT) perspective on the linkages between the South and East Asian summer monsoons (SASM and EASM) and indicates two robustly coupled modes of the vertical integrated WVT (VIWVT) over the two monsoons that accounts for above 90% of the total squared covariance fraction. The first coupled mode (SVD1 mode) depicts a meridional linkage between the meridional dipole VIWVT anomalies over both the SASM and EASM. While the second coupled mode (SVD2 mode) illustrates a zonal connection of an anomalous cyclonic/anticyclone VIWVT over the SASM and a zonal wave-like VIWVT over the EASM. The SVD1 mode is linked through the anomalous subtropical High over the western North Pacific (WNPSH) and primarily associated with the transition phase of El Niñ o/La Niña (ENSO) and simultaneous Indian Ocean Basin mode (IOBM) SST warming/cooling. The meridional connection of the VIWVT in the SVD1 mode experienced a clear intensification since the late-1970s that may be attributed to the strengthened impacts of the ENSO/IOBM on the EASM and SASM after the late-1970s. The SVD2 mode is connected by the Circumglobal teleconnection (CGT) pattern and related to the developing phase of ENSO and summer north Atlantic tripole (NAT) SST anomalies. The zonal VIWVT connection in SVD2 mode is strongly modulated by the SASM-CGT connections and reveals significant weakening since the late-1970s but re-intensifies after the early-1990s. This may be associated with the weakened ENSO-SASM relationship after the late-1970s and interdecadal decreasing of the all Indian summer rainfall since the early-1990s.

Keywords: Water vapor transport, South and East Asian summer monsoon, linkage, interdecadal change

©2019. Japan Geoscience Union. All Right Reserved.

Interannual Modulation of the Local Hadley Circulation on Clouds, Radiation and Diagnostic Fields over the Western North Pacific

*Xinyue Wang[1], Hironobu Iwabuchi[1]

1. Tohoku Univ.

Variation of the local Hadley cell (HC) northern boundary over the western North Pacific, and its interannual imprints on the tropospheric clouds and atmospheric fields are examined with observation and reanalysis data for the winter season from December 1982 to February 2016. The poleward shift of the local HC subsiding edge is marked by anomalous rising motion, large-scale decreased static stability, and corresponding increases of the midlevel cloud amount over the climatological sinking zone around 30N. These responses primarily locate over the continental and coastal areas instead of the open oceans. Concomitant with the increasing cloud fraction, a net negative top-of-atmosphere radiation anomaly is identified, and the main contributor is suggested to be the cumulus congestus, whose top pressures are in a range of 440–680 hPa, and optical thicknesses in a range of 23–60. Interactions between this specific cloud type and the vertical moist instability, and their constrains on the precipitation field is further discussed.

Keywords: Regional Hadley cell, Cloud and radiation, Precipitation pattern

©2019. Japan Geoscience Union. All Right Reserved.

Seasonal and Regional Variation of Diurnal Cycle of Rainfall over Java Island and the Surrounding Area

*Madam Taqiyya Maulana[1], Takeshi Yamazaki[1]

1. Tohoku University

The seasonality and regional variability of diurnal cycle of rainfall (DCR) over Java Island and the surrounding area (coastal region of the Java Sea and the Indian Ocean) are analyzed through satellite observations. This study focus on the area where the studies of the seasonality of DCR over Indonesian Maritime Continent (IMC) are still limited. The DCR is a prominent phenomenon over IMC which is important for aviation industry and related to heavy precipitation events that cause hydro-meteorological disasters.

In this study, **we investigate seasonal and regional variation of DCR (the phase and the amplitude)** through satellite observations. High resolution (spatial and temporal) rainfall estimate is needed to capture feature of DCR over the study area which is difficult to obtain from ground observation. We **mainly employ the high-resolution dataset of Global Satellite Mapping of Precipitation (GSMaP) reanalysis (GSMaP_RNL) and near real time (GSMaP_NRT).** The analysis of DCR seasonal variability is based on investigation throughout boreal winter (December-January-February), boreal spring (March-April-May), boreal summer (June-July-August), and boreal autumn (September-October-November) from 2008-2018 (GSMaP_NRT) and 2009-2014 (GSMaP_RNL).

The results show that hourly data of GSMaP_RNL and GSMaP_NRT with 0.1˚ spatial resolution are able to depict the detailed features of the seasonality and regional variability of DCRover Java Island and surrounding areas. **The comparison between GSMaP_RNL and GSMaP_NRT shows that GSMaP_NRT represents significant time lag of DCR phase over off shore region. GSMaP_NRT shows that the offshore region of the Java Sea is dominated by noon-afternoon rainfall while GSMaP_RNL shows morning rainfall.** However, both of GSMaP_RNL and GSMaP_NRT show similar pattern on phase and amplitude of DCR. Phase of DCR indicates the time when maximum rainfall occurs, while amplitudes indicates the magnitude of DCR. In general, both of GSMaP_RNL and GSMaP_NRT composites, show that the land region with wider landmass area (West Java and western part of East Java) is dominated by evening phase while narrow landmass area (Central Java and eastern part of Java Island) is dominated by late afternoon phase. A large magnitude of the DCR is concentrated inland. The Java Sea has a higher amplitude of DCR compared to the Indian Ocean and the coastal region. The amplitude over the coastal region of the Indian Ocean is higher than over the Indian Ocean and the coastal area of the Java Sea.

Both of rainfall estimates capture inhomogeneous seasonal shifting phase of DCR over this region. The remarkable seasonal shifting phase occurs along the coastal area of the Java Sea. Though, phase shifting over inland of a wide landmass area and the coastal region of the Indian Ocean is not significant. Inhomogeneous seasonal shifting phase of DCR indicated interactions between local circulations, which affected by the topography (e.g. terrain and shape of the coastline), and large circulations (background wind, synoptic conditions, etc.). The analysis of wind profile from reanalysis data confirms the seasonal change of interactions between large and small circulations that caused seasonal shifting phase of DCR.

Keywords: Diurnal cycle of rainfall (DCR), Seasonal variability, Regional variability, Shifting Phase, GSMaP

©2019. Japan Geoscience Union. All Right Reserved.

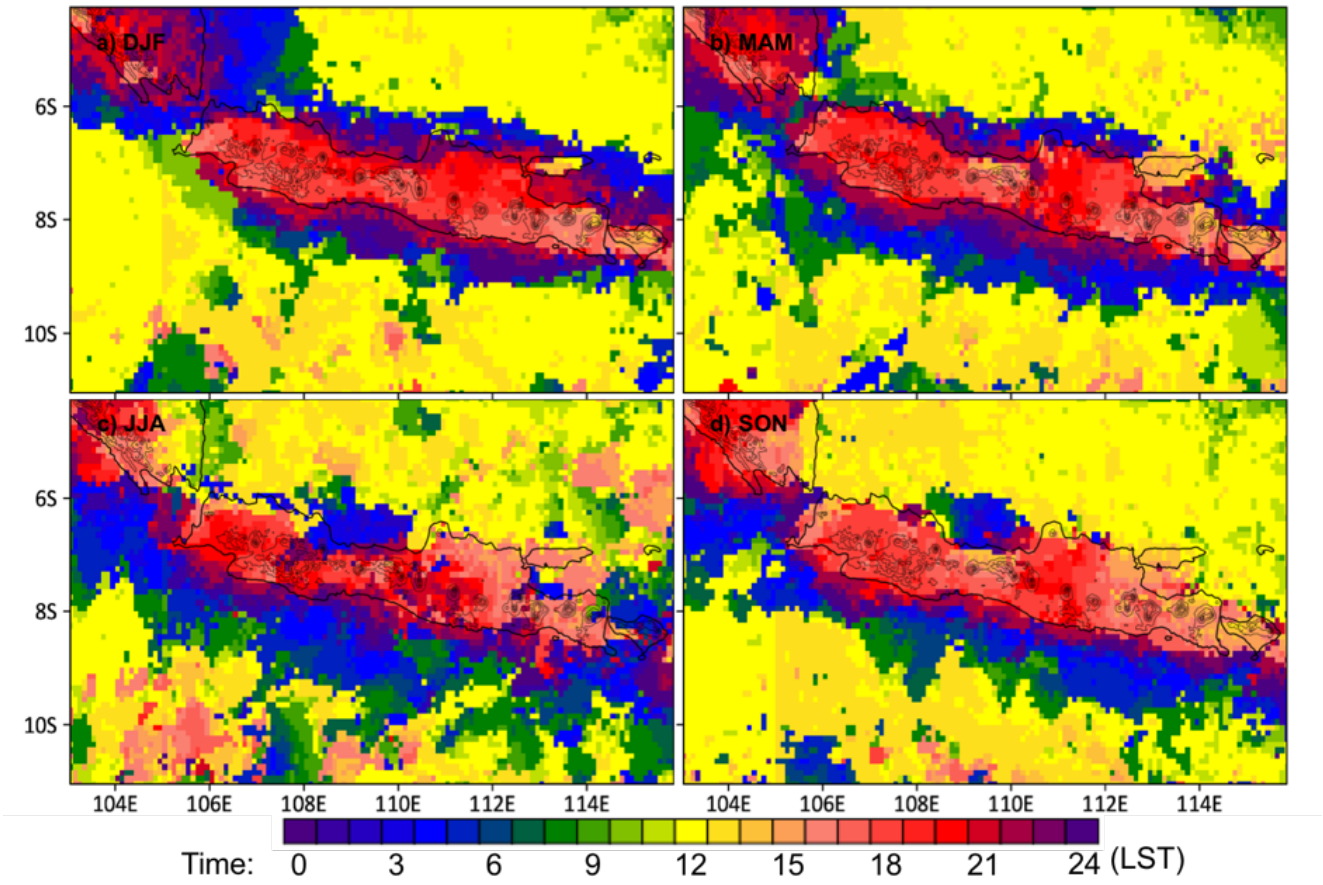

©2019. Japan Geoscience Union. All Right Reserved.

Study on atmospheric circulation characteristics of precipitation anomalies in arid region of Central Asia

*Lianmei Yang[1], Xuefeng Guan[1]

1. Institute of Desert Meteorology, China Meteorological Administration,

As climate transition zone between Mediterranean climate region and East Asian monsoon region, arid region of Central Asia (including five Central Asian countries and Xinjiang province of China) which is influenced by high, middle and low latitude circulations has different synoptic-climatic characteristics from that of Europe and East Asia while its climate characteristics also varies greatly within the region. Central Asia has unique and complicated topography and ecosystem patterns like deserts, oasis, glaciers and basins, forming a highly representative meteorological disaster-breeding environment under the influence of multiple-background, multiple-factor and multiple-scale. This area has abundant solar-heat energy, large evaporation and dramatic temperature changes. Besides, its precipitation is scarce and has extremely uneven distribution with high value in the western and middle parts of Tianshan Mountains. Over the last one hundred years, Central Asia has experienced a warm and wet trend. Central Asia low value system together with the high, middle and low latitude circulation systems linked by West Asia westerly jet stream have contributed to the interdecadal and interannual variations of precipitation in Xinjiang. However, due to the insufficient construction of integrated meteorological observation network, the studies concerning regional featured circulation system, regularity and mechanism of disastrous weathers, high resolution regional numerical model, impacts of land-atmosphere interaction on regional weather and climate change prediction are still inadequate. Correspondingly, to carry out those studies has essential scientific significance and strategic value for the sustainable social and economic development in Silk Road Economic Belt.

Keywords: Arid region of Central Asia, synoptic-climatic characteristics, precipitation anomaly, atmospheric circulation, water vapor

©2019. Japan Geoscience Union. All Right Reserved.

Mechanisms for northward propagation of boreal summer intraseasonal oscillation

*Kanta Nakae[1], Masaki Satoh[1], Daisuke Takasuka[1]

1. Atmosphere and Ocean Research Institute, The University of Tokyo

The 20-90-day Intraseasonal Oscillation (ISO) is one of the dominant modes of tropical variability. In boreal summer northward propagation (NP), which occurs on ISO time scales, originates near the equator and extends to India and western North Pacific Ocean. Understanding the NP of the boreal summer ISO (BSISO) is of vital importance to extended-range weather prediction. Hence, several mechanisms of the NP have been examined. However, they are still incompletely understood. The purpose of this study is to investigate the importance of vertical shear and sea surface temperature (SST) for the NP of the BSISO. In order to obtain a basic structure of the BSISO, we have conducted JJA-perpetual experiments using the Non-hydrostatic Icosahedral Atmospheric Model (NICAM) with a 56-km horizontal mesh.
Although the perpetual experiment has strong Indian monsoon over Arabian sea due to the bias of surface temperature on land, it is found that the NP of the BSISO from Indian Ocean (IO) has two abovementioned mechanisms. One warm SST anomaly north of convection destabilize the lower troposphere, while another tilted vertical shear can generate positive barotropic vorticity to the north of convection. In order to assess the effect of the former mechanism, we made an experiment using fix SST (SSTFIX) obtained from CTL experiment. SSTFIX experiment reproduces the NP of the BSISO from IO, although the amplitude became lower. Therefore, it suggests that the NP of the BSISO from IO doesn’t need warm SST anomaly. To Improve the bias related to basic state like vertical shear, we conducted an experiment using nudging method for surface temperature on land (LNDADJ). In LNDADJ experiment the NP of the BSISO from IO isn’t reproduced due to reduction of column water vapor over Bay of Bengal. Thus, tilted vertical shear can just begin the NP. On the other hand, it is suggested that the NP needs SST and column water vapor to maintain its strength.

Keywords: Boreal summer intraseasonal oscillation, Asian monsoon, Northward propagation

©2019. Japan Geoscience Union. All Right Reserved.

Fractality in the perimeter of tropical clouds observed by Himawari-8 or simulated by a high-resolution model

*Takuya Jinno[1]

1. Graduate School of Science, The University of Tokyo

Cloud clusters show a wide variety of shape and size, and their spatial pattern is often taken up as a typical example of fractal. However, the methods of studying fractal are in an early stage of development. In this study, we conducted fractal analysis on the perimeter of tropical clouds using satellite observation and cloud-resolving simulation of sub-kilometer resolution. We evaluated fractal dimension as a function of spatial scale (transient fractal dimension) and quantified the characteristic spatial scale of the pattern from the scale where self-similarity breaks down. From the observational data from HIMAWARI-8, It is shown that the self-similarity of the cloud perimeter persists only in the spatial scale range from 2 km up to 30 km. The limit of the self-similarity is suggested to be the characteristic scale of the pattern formation of tropical clouds. The cloud-resolving simulation data with NICAM also shows finite-size self-similarity. However, the profile of the transient fractal dimension changed with integration time far more rapidly than HIMAWARI-8 observation, and it lost its self-similarity at the end of the 48-hour simulation. This process is suggested to reflect the increase of stratiform cloud in the upper-troposphere as an adjustment to the transition of spatial resolution.

Keywords: fractal, HIMAWARI-8, cloud-resolving model

©2019. Japan Geoscience Union. All Right Reserved.

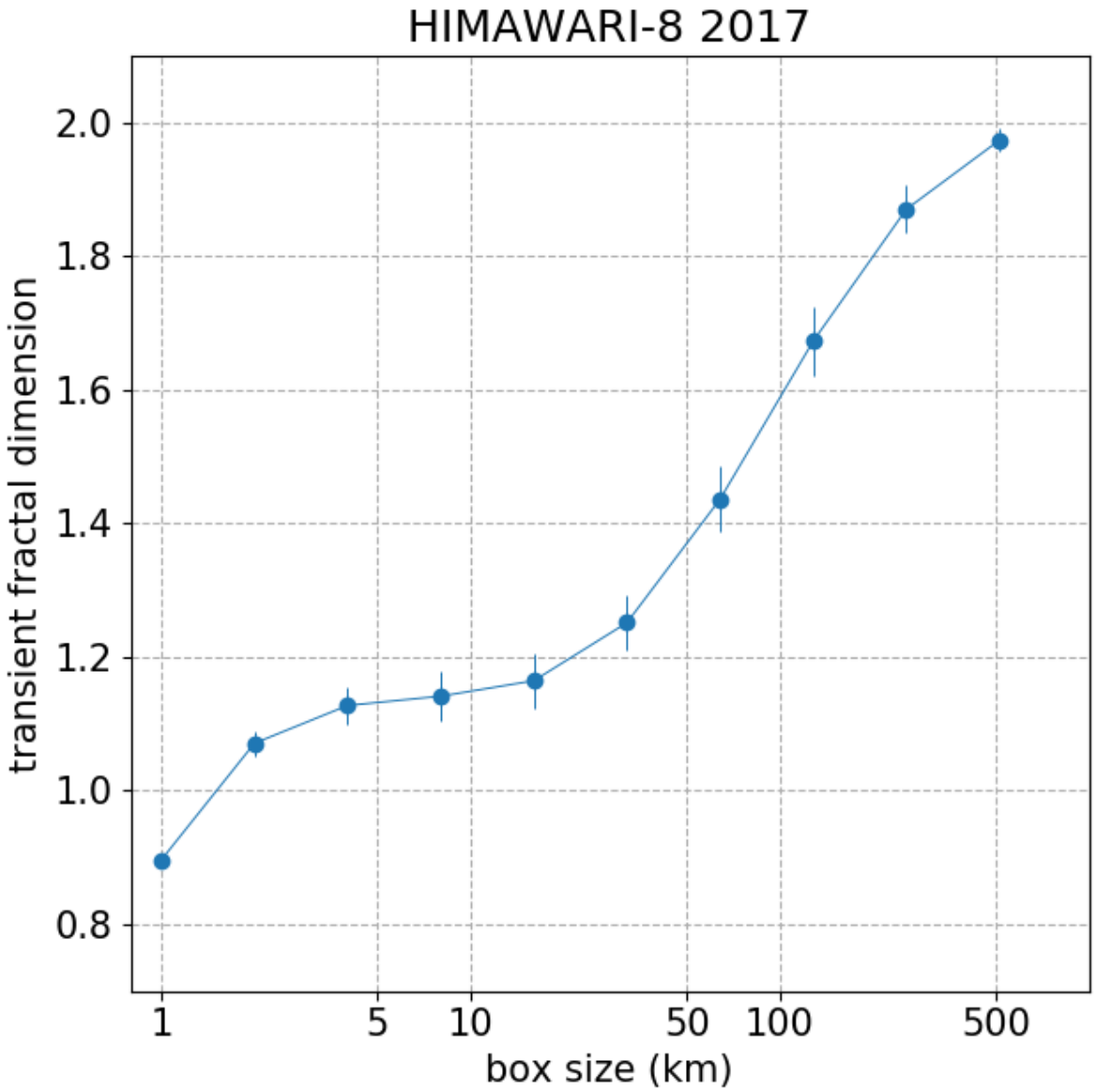

©2019. Japan Geoscience Union. All Right Reserved.

Large-scale deformation of tropical cloud band in the ITCZ detected in NICAM simulations

*Noriyuki Nishi[1], Atsushi Hamada[4], Yohei Yamada[2], Tomoe Nasuno[2], Reona Satoh[5], Masaki Satoh[3]

1. Faculty of Science, Fukuoka Universtiy, 2. JAMSTEC, 3. AORI, University of Tokyo, 4. Graduate School of Science and Engineering for Education, University of Toyama, 5. Graduate School of Science, Fukuoka University

Over the central/eastern tropical Pacific, the Inter Tropical Convergence Zone (ITCZ) is detected in the northern side of the equator. In the ITCZ, we can sometimes observe drastic deformation of the cloud bands elongated zonally with several thousand-kilometer scale. The initial stage of the band, which is composed of deep convective systems, expands meridionally and separates into two or three parallel cirrus bands that keep alive one or two days (Hamada et al., 2013, JMSJ). These separation events cannot be well described in the objective analysis datasets, probably due to lack of the observations over the open ocean; investigation of their mechanism with the analysis data is difficult. In order to study their mechanism, we attempted to use the numerical simulation results of global cloud system resolving model NICAM (Satoh et al. 2014, Progress in Earth and Planetary Science) to find similar events in them. If we can find separation events in the results, we can examine the mechanism with many physical parameters including wind, various kinds of hydrometeors. We have already analyzed several numerical experiment results for different periods, resolution and physical schemes.

We found a similar separation event in an output of the simulation for one year from June 2004 and horizontal resolution 3.5 km. We examined the life cycle of the cirrus bands after separation. One interesting point is on the height of the cirrus clouds in the separated bands. The simulated cirrus clouds in the bands lie in the 13-14 km height level, while the height of the maximum meridional wind that contributes to the meridional movement of the cirrus bands is about 12 km. This difference of the heights means that the cirrus clouds were not just advected by meridional wind but were possibly developed in the course of the separation.

The trigger of zonally simultaneous separation of a long band is another our interest. Inertial instability may be a candidate since vertical exchange of zonal momentum by deep convection would occur in an original band and result in the large meridional shear of the zonal wind in the upper troposphere. We tried to confirm necessary condition for inertial instability by calculating geostrophic vorticity, following the general procedure. However, the position of the bands is too close to the equator (3-7N) to establish geostrophic relationship, and the spatial pattern of the geostrophic vorticity is too noisy to analyze. Therefore, we instead calculate simple absolute vorticity. We found that the absolute vorticity around the separated bands was almost negative. It suggests the possibility of the inertial (or similar kind of) instability.

We are now analyzing another numerical experiment including four kinds of runs using a cloud scheme with different cloud parameter settings. In the real atmosphere, a separation event occurred on 16-17 June 2008 at the just east of the date line. The event can be simulated in all of four runs at 36 hours from the initial time. It suggests that the basic mechanism of the separation is not sensitive to the detail of cloud systems. By analyzing the dynamical fields of these outputs, we are trying to find the key mechanisms to trigger the meridional separation of the cloud bands.

©2019. Japan Geoscience Union. All Right Reserved.

Keywords: tropics, ITCZ, cirrus

©2019. Japan Geoscience Union. All Right Reserved.

Improvement of single-moment bulk microphysics for super-cooled water clouds over the Southern Ocean in NICAM using Joint simulator and double-moment microphysics

*Woosub Roh[1], Tatsuya Seiki[2], Masaki Satoh[1], Tempei Hashino[3]

1. AORI, the university of Tokyo, 2. JAMSTEC, 3. Kochi university of technology

It is important to evaluate and improve the cloud properties in global non-hydrostatic models like a Nonhydrostatic ICosahedral Atmospheric Model (NICAM, Satoh et al. 2014) using observation data. One of the methods is a radiance-based evaluation using satellite data and a satellite simulator (here Joint simulator, Hashino et al. 2013), which avoids making different settings of the microphysics between retrieval algorithms and NICAM.

One of the challenging issues is an evaluation of mixed-phase clouds, which consist of water vapor, ice particles, and supercooled water droplets. It is known one of the main reasons why climate models reveal large errors about the reflection of solar radiation over the Southern Ocean and Arctic.

This study is an evaluation and improvement of mixed-phase clouds over the Southern Ocean in NICAM using a Cloud-Aerosol Lidar and Infrared Pathfinder Satellite Observation (CALIPSO) and a satellite simulator. We evaluated thermodynamics phase of mixed phases clouds over the Southern Ocean in a regional version of NICAM between 45˚S to 65˚S and 170˚E to 170˚W following Yoshida et al. (2010) method. We found underestimation of supercooled water clouds in our single moment scheme. We improved the single moment microphysics scheme using a double moment microphysics and a single column model. We also investigate the impact of microphysics scheme on moisture distributions and the size of cloud systems.

Keywords: microphysics, CALIPSO, Satellite simulator

©2019. Japan Geoscience Union. All Right Reserved.

High-cloud property responses to SST change: sensitivity study using a global nonhydrostatic model

*Tomoki Ohno[1], Masaki Satoh[2]

1. Japan Agency for Marine-Earth Science and Technology, 2. Atmosphere and Ocean Research Institute, The University of Tokyo

Since it has been recognized that the uncertainty of cloud feedback is one of main contributors to the intermodel spread of climate sensitivity, the reduction of the uncertainties associated with cloud response to global warming has been one of central issues for robust projections and predictions of climate variability and change. High clouds have large impacts on the Earth’ s radiative energy budget, and the uncertainty of their response to climate change is known as one of large sources of the climate sensitivity spread although several possible hypotheses to predict the response have been proposed. As the radiation-cloud interaction plays a crucial role in the determination of life time of high clouds, the improvement of the understanding of cloud property responses to global warming helps the reduction of climate-sensitivity variability associated with the high-clouds feedback.

In order to investigate the cloud-property response to climate change, we conducted simulations with RCE configurations using a high-resolution nonhydrostatic global circulation model (the Nonhydrostatic Icosahedral Atmospheric Model; NICAM) with the earth-like sphere for simplifying the problem. Sea surface temperatures (SSTs) are fixed at 300K and 304K and a double-moment bulk scheme are used without cumulus parameterization scheme.

We found that high cloud amount increases with SST increase, as consistent with the previous NICAM studies. It was also determined that the change in particularly optically thin clouds whose optical thicknesses were <3 was dominant, and such thin clouds tended to have large particle sizes. These suggests that the slow evaporative property of ice phase clouds and their representability can play one of key roles in the uncertainty of the high-cloud amount change in global warming.

Keywords: cloud property responses, cloud feedback, climate change

©2019. Japan Geoscience Union. All Right Reserved.

Effects of different cloud overlapping parameters on simulated total cloud fraction over the globe and East Asian region

*bo hai Wang[1], hua Zhang[2]

1. Institute of Atmospheric Physics, Chinese Academy of Sciences, 2. State Key Laboratory of Severe Weather, Chinese Academy of Meteorological Sciences

The cloud overlapping parameter (vertical decorrelation length, L_{cf}) from CloudSat/CALIPSO is implemented in Beijing Climate Center’ s GCM (BCC_AGCM2.0) to reduce the uncertainly in radiation field. Comparing the climate simulation results obtained by using the constant L_{cf} of 2 km with those using the above retrieved L_{cf}, it is found that the total cloud fraction simulation has been obviously improved by using the satellite-based L_{cf}. The error of global mean total cloud fraction between simulations and CERES (Clouds and the Earth's Radiant Energy System) satellite data is decreased by 1.6% in both the winter and summer, of which the positive deviation of total cloud amount at tropical convection area and the negative deviation in subtropical region both are significantly reduced. These improvements are helpful for better simulation of energy budget differences between different regions. In East Asia, using the satellite-based L_{cf} can decrease the error of average total cloud fraction (compared to the CERES) by 1.8% (1.4%) in the winter (summer).Overall, using L_{cf} from CloudSat/CALIPSO satellite data can improve the simulation of total cloud fraction and thus obtain more accurate simulation of radiation field.

Keywords: Cloud overlapping parameter, Vertical decorrelation length, Total cloud fraction

©2019. Japan Geoscience Union. All Right Reserved.

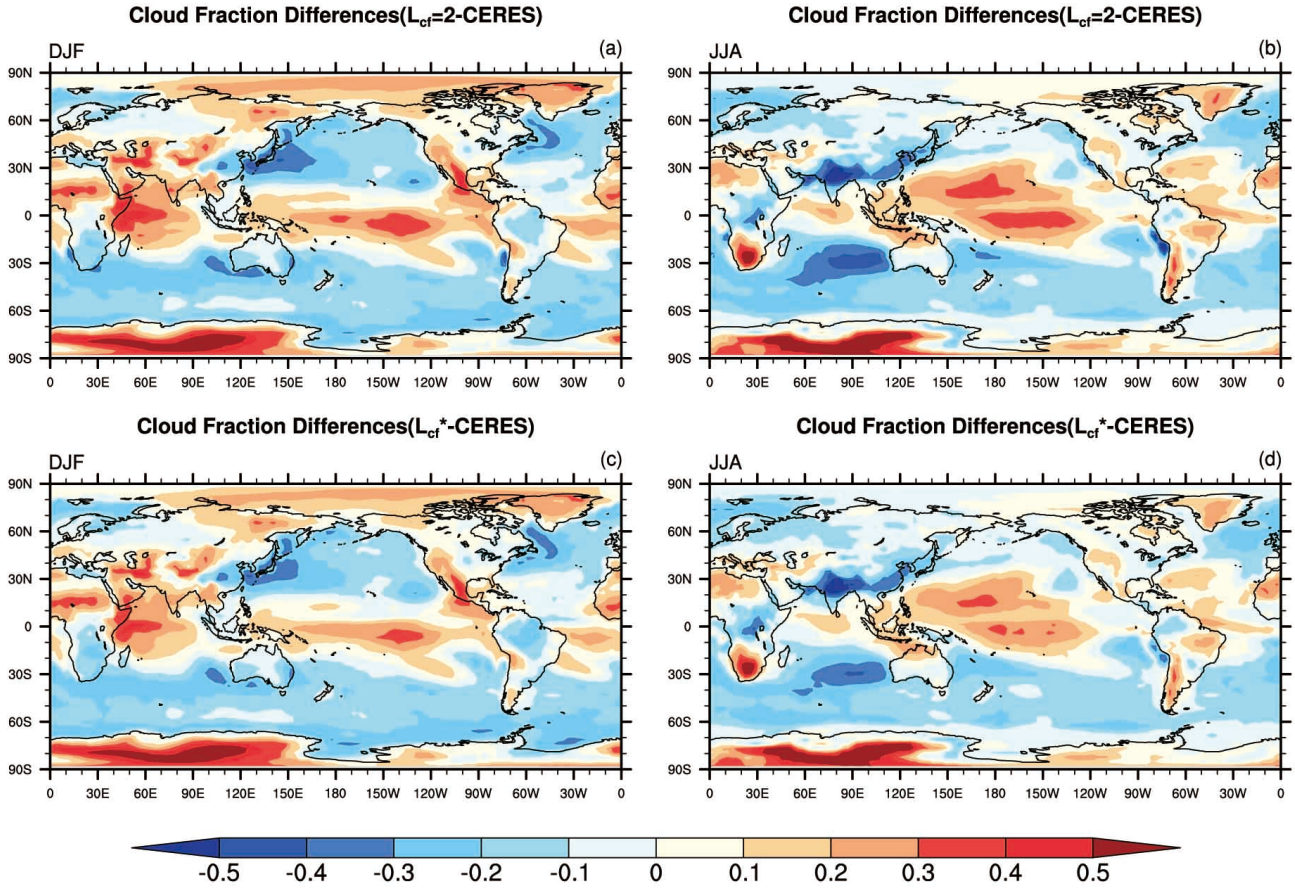

©2019. Japan Geoscience Union. All Right Reserved.

[E] Poster | A (Atmospheric and Hydrospheric Sciences)：A-AS Atmospheric Sciences, Meteorology & Atmospheric Environment

Tue. May 28, 2019 5:15 PM - 6:30 PM JST | Tue. May 28, 2019 8:15 AM - 9:30 AM UTC | Poster Hall International Exhibition Hall8, Makuhari Messe_6

[A-AS03] Large-scale moisture and organized cloud systems

convener:Hiroaki Miura(The University of Tokyo), Atsushi Hamada(University of Toyama), Satoru Yokoi(Japan Agency for Marine-Earth Science and Technology), Masaki Satoh(Atmosphere and Ocean Research Institute, The University of Tokyo)

Water vapor plays a significant role in regulating the global atmospheric circulation, especially in the troposphere. The overturning circulation is directly driven by the longwave radiative cooling of water vapor and the latent heating/cooling through microphysical processes to balance it. This global circulation is composed of diverse atmospheric phenomena with various spatial and temporal scales. Developments of some significant turbulent motions such as 3D isotropic turbulence in clouds, stratocumulus and cumulus convection, squall lines and tropical cyclones, and the Madden-Julian oscillation, are essentially associated with moisture anomaly in each scale. Moisture is accumulated relatively slowly in larger horizontal scales, but is consumed relatively quickly in smaller ones. This significant scale gaps between the accumulation and consumption may be one of the causes of the long-lasting difficulty in developing the theory of the moist atmosphere. The aim of this session is to share the recent researches about the relationships between moisture and organized cloud systems in wider spatial and temporal scales to enhance collaborations between modeling, observational, and theoretical approaches in tackling this challenging task. Research results relating to the Years of the Maritime Continent (YMC) and Radiative-Convective Equilibrium Model Intercomparison Project (RCEMPI) are welcome.

[AAS03-P01] Numerical investigation on the shape, terminal velocity, and drag coefficient of a small raindrop by the improved immersed boundary method

*Ong Chia Rui[1], Hiroaki Miura[1] (1.The University of Tokyo)

[AAS03-P02] **A diagnostic study of water vapor during an extreme precipitation event in Yili river valleyA diagnostic study of water vapor during an extreme precipitation event in Yili river valley**

*Jing LiU[1], Yushu Zhou[2], Lianmei Yang[1] (1.Institute of Desert Meteorology,CMA, 2.Institute of Atmospheric Physics,CAS)

[AAS03-P03] **The Study on the Characteristics of Weather and Cloud Types in the Summer and Winter Seasons of the South China Sea**

*Jou Ping Hou[1], Bo-Shiou Wei[1], Li-Zhen Su[1] (1.Chung Cheng Institute of Technology)

[AAS03-P04] **Linkages between the South and East Asian Monsoon water vapor transport during boreal summer**

*Yong Liu[1] (1.Institute of Atmospheric Physics, Beijing , China)

[AAS03-P05] Interannual Modulation of the Local Hadley Circulation on Clouds, Radiation and Diagnostic Fields over the Western North Pacific

*Xinyue Wang[1], Hironobu Iwabuchi[1] (1.Tohoku Univ.)

[AAS03-P06] Seasonal and Regional Variation of Diurnal Cycle of Rainfall over Java Island and the Surrounding Area

*Madam Taqiyya Maulana[1], Takeshi Yamazaki[1] (1.Tohoku University)

[AAS03-P07] **Study on atmospheric circulation characteristics of precipitation anomalies in arid region of Central Asia**

*Lianmei Yang[1], Xuefeng Guan[1] (1.Institute of Desert Meteorology, China Meteorological Administration,)

[AAS03-P08] Mechanisms for northward propagation of boreal summer intraseasonal oscillation

*Kanta Nakae[1], Masaki Satoh[1], Daisuke Takasuka[1] (1.Atmosphere and Ocean Research Institute, The University of Tokyo)

[AAS03-P09] Fractality in the perimeter of tropical clouds observed by Himawari-8 or simulated by a high-resolution model

*Takuya Jinno[1] (1.Graduate School of Science, The University of Tokyo)

[AAS03-P10] **Large-scale deformation of tropical cloud band in the ITCZ detected in NICAM simulations**

*Noriyuki Nishi[1], Atsushi Hamada[4], Yohei Yamada[2], Tomoe Nasuno[2], Reona Satoh[5], Masaki Satoh[3] (1.Faculty of Science, Fukuoka Universtiy, 2.JAMSTEC, 3.AORI, University of Tokyo, 4.Graduate School of Science and Engineering for Education, University of Toyama, 5.Graduate School of Science, Fukuoka University)

[AAS03-P11] **Improvement of single-moment bulk microphysics for super-cooled water clouds over the Southern Ocean in NICAM using Joint simulator and double-moment microphysics**

*Woosub Roh[1], Tatsuya Seiki[2], Masaki Satoh[1], Tempei Hashino[3] (1.AORI, the university of Tokyo, 2.JAMSTEC, 3.Kochi university of technology)

[AAS03-P12] High-cloud property responses to SST change: sensitivity study using a global nonhydrostatic model

*Tomoki Ohno[1], Masaki Satoh[2] (1.Japan Agency for Marine-Earth Science and Technology, 2.Atmosphere and Ocean Research Institute, The University of Tokyo)

[AAS03-P13] Effects of different cloud overlapping parameters on simulated total cloud fraction over the globe and East Asian region

*bo hai Wang[1], hua Zhang[2] (1.Institute of Atmospheric Physics, Chinese Academy of Sciences, 2.State Key Laboratory of Severe Weather, Chinese Academy of Meteorological Sciences)

Numerical investigation on the shape, terminal velocity, and drag coefficient of a small raindrop by the improved immersed boundary method

*Ong Chia Rui[1], Hiroaki Miura[1]

1. The University of Tokyo

The cloud microphysical processes play a crucial part in controlling the water cycle, cloud formation, and radiation transfer in the atmosphere. These process are parameterized in a numerical weather prediction model by empirical formulae. In particular, empirical formulae for the prediction of the terminal velocity, drag coefficient, and shape of a free-falling water droplet are used widely in the parameterizations. Despite that the model accuracy is sensitive to the microphysics parameterizations to a considerable extent, these formulae are only verified by experiments which are conducted at room temperature and standard atmospheric pressure or linear theories in an ideal condition. The validity of the parameterizations is therefore questionable under general conditions and the accuracy of the numerical prediction may be affected.
In this work, a new numerical tool, the immersed boundary method, is proposed as an alternative way to investigate the terminal velocity, drag coefficient, and shape of an axisymmetric free-falling raindrop. This improved immersed boundary method for water droplet simulations is applied to verify those commonly used empirical formulae under different conditions. The largest size of the free-falling raindrop in this work is 0.5 mm. To first verify the reliability and robustness of this new method the terminal velocity and drag coefficient obtained from axisymmetric raindrop simulations at standard pressure and temperature fit well with the experimental data. Further simulation results of an axisymmetric free-falling raindrop of diameters of 0.025, 0.01, and 0.5 mm at different altitudes assuming a fixed lapse rate show that the variation of the shape of the raindrop is negligibly small, and there is a significant discrepancy between the numerical results and some of the widely used empirical formulae. The discrepancy is larger at higher altitudes for small raindrops. This is because of the assumption of the fixed drag coefficient in the derivation of those empirical formulae. A new parameterization with better accuracy for terminal velocity aloft of raindrops with diameter smaller than 0.5 mm is proposed. A further sensitivity test of a 0.5 mm free-falling axisymmetric raindrop with different surface tension coefficients are performed and the numerical results suggest that the change in the shape and terminal velocity is negligible with respect to aerosols.

Keywords: Cloud Microphysis, Immersed boundary method, Terminal velocity

©2019. Japan Geoscience Union. All Right Reserved.

A diagnostic study of water vapor during an extreme precipitation event in Yili river valleyA diagnostic study of water vapor during an extreme precipitation event in Yili river valley

*Jing LiU[1], Yushu Zhou[2], Lianmei Yang[1]

1. Institute of Desert Meteorology,CMA, 2. Institute of Atmospheric Physics,CAS

An extreme precipitation events was happened during 31 July to 1 August, 2016 at Yili river valley which multi-stations breakthrough extreme precipitation’ s value. Based on calculation of water vapor transport stream function and the non-divergent (rotational) components, potential function and divergent (irrotational) components, the water vapor transport budget and water vapor transport trajectories for the Yili river valley using the conventional detection,1° x 1° NCEP/NCAR reanalysis, HYSPLIT model based on Lagrangian method, Ground-based GPS observation precipitable water vapor data(GPS-PWV) , the large-scale water vapor transport and convergence characteristics were analyzed during the heavy rainfall period. The results showed that: (1) The Indian, the Pacific and the Atlantic ocean all contributed to the water supply during the heavy rain period, and Indian summer monsoon circulation, the south China sea summer monsoon circulation at low latitudes and Atlantic ocean’ s east airflow at mid-latitude were constituted the water vapor transmission channel, which the Indian Ocean southwest water vapor transport mainly concentrated in the lower troposphere, and middle troposphere water vapor transport was given priority to the west flow of the Atlantic ocean and low trough itself; the valley was in the convergence area of water vapor flux during the heavy rain, and the convergence and uplift of the terrain to the West opening caused vertical motion development provided a favorable dynamic convergence mechanism for the occurrence of local heavy rain.(2) The 3000 m water vapor transmission trajectory included the westward and eastward path at bottom layer and the northward path at middle troposphere as complement of water vapor for the lower troposphere through the vertical motion, the southward path at lower troposphere which water vapor come from the Arabian sea,and the mid-latitude water vapor transport of the westward path was the most powerful ; The 5000 m water vapor transmission trajectory was dominated by the westward path and the low trough itself;(3) During the precipitation period, the water vapor was concentrated in the lower troposphere which transported to the upper level through vertical movement, and the water vapor was positive at the middle and upper layers contrasted with negative at the lower layer. south boundary of water vapor inflow was rapidly increasing at the lower layer while the middle and higher layer water vapor inflow derived from the western boundary during the heavy rainfall period;(4)Yili river valley GPS-PWV jumped caused by the southwest airflow front of low trough before the rainfall happened and steadily maintain the high value influenced by India southwest monsoon during the heavy rainfall period. The large-scale water vapor transport convergence enhancement corresponding local GPS-PWV increased, suggested that the water vapor supply in local heavy rain event was at least associated with the water vapor transport and convergence of hemisphere scale.

Keywords: torrential rain, transfer of water vapor, lagrange trajectory, ground-based GPS

©2019. Japan Geoscience Union. All Right Reserved.

The Study on the Characteristics of Weather and Cloud Types in the Summer and Winter Seasons of the South China Sea

*Jou Ping Hou[1], Bo-Shiou Wei[1], Li-Zhen Su[1]

1. Chung Cheng Institute of Technology

The South China Sea is vast with a tropical maritime climate near the equator and a subtropical climate in the north. Therefore, although it is winter, there are still deep convective and strong precipitation systems in the South China Sea. In summer, thermal convection is strong, sometimes typhoons pass; Dongsha Island and Taiping Island are located in the north and south of the South China Sea. The weather in the region is bound to be significantly affected by various weather systems in the South China Sea. We selected the winter of December 2017 and the summer of June 2018 to study it. The Dongsha Island and Taiping Island areas were subjected to research on the northeast monsoon and tropical convection. The dual island observation and satellite data were combined with numerical models to analyze the mutual interaction between the thermal and dynamic processes in the South China Sea. To enhance the understanding of the weather evolution mechanism in the South China Sea, in order to further clarify the various cloud-phase characteristics of the monsoon circulation and thermal convection in the South China Sea. The results show that the change of northeast monsoon intensity obviously affects the interaction of air-sea in the South China Sea, enhances the intensity of precipitation, and changes the amount and height of the stratus cumulus in the sea. In addition, the northeast monsoon circulation may interact with the surrounding terrain of the South China Sea, thus induces local deep convection. In the summer, the southwest monsoon will be enhanced and thermal convection is very strong. The intensity and life cycle of the typhoon can be maintained when it passes this area.

Keywords: Dongsha Island, Taiping Island, Air-Sea interaction, Deep Convection

©2019. Japan Geoscience Union. All Right Reserved.

Linkages between the South and East Asian Monsoon water vapor transport during boreal summer

*Yong Liu[1]

1. Institute of Atmospheric Physics, Beijing , China

This study provides a water vapor transport (WVT) perspective on the linkages between the South and East Asian summer monsoons (SASM and EASM) and indicates two robustly coupled modes of the vertical integrated WVT (VIWVT) over the two monsoons that accounts for above 90% of the total squared covariance fraction. The first coupled mode (SVD1 mode) depicts a meridional linkage between the meridional dipole VIWVT anomalies over both the SASM and EASM. While the second coupled mode (SVD2 mode) illustrates a zonal connection of an anomalous cyclonic/anticyclone VIWVT over the SASM and a zonal wave-like VIWVT over the EASM. The SVD1 mode is linked through the anomalous subtropical High over the western North Pacific (WNPSH) and primarily associated with the transition phase of El Niñ o/La Niña (ENSO) and simultaneous Indian Ocean Basin mode (IOBM) SST warming/cooling. The meridional connection of the VIWVT in the SVD1 mode experienced a clear intensification since the late-1970s that may be attributed to the strengthened impacts of the ENSO/IOBM on the EASM and SASM after the late-1970s. The SVD2 mode is connected by the Circumglobal teleconnection (CGT) pattern and related to the developing phase of ENSO and summer north Atlantic tripole (NAT) SST anomalies. The zonal VIWVT connection in SVD2 mode is strongly modulated by the SASM-CGT connections and reveals significant weakening since the late-1970s but re-intensifies after the early-1990s. This may be associated with the weakened ENSO-SASM relationship after the late-1970s and interdecadal decreasing of the all Indian summer rainfall since the early-1990s.

Keywords: Water vapor transport, South and East Asian summer monsoon, linkage, interdecadal change

©2019. Japan Geoscience Union. All Right Reserved.

Interannual Modulation of the Local Hadley Circulation on Clouds, Radiation and Diagnostic Fields over the Western North Pacific

*Xinyue Wang[1], Hironobu Iwabuchi[1]

1. Tohoku Univ.

Variation of the local Hadley cell (HC) northern boundary over the western North Pacific, and its interannual imprints on the tropospheric clouds and atmospheric fields are examined with observation and reanalysis data for the winter season from December 1982 to February 2016. The poleward shift of the local HC subsiding edge is marked by anomalous rising motion, large-scale decreased static stability, and corresponding increases of the midlevel cloud amount over the climatological sinking zone around 30N. These responses primarily locate over the continental and coastal areas instead of the open oceans. Concomitant with the increasing cloud fraction, a net negative top-of-atmosphere radiation anomaly is identified, and the main contributor is suggested to be the cumulus congestus, whose top pressures are in a range of 440–680 hPa, and optical thicknesses in a range of 23–60. Interactions between this specific cloud type and the vertical moist instability, and their constrains on the precipitation field is further discussed.

Keywords: Regional Hadley cell, Cloud and radiation, Precipitation pattern

©2019. Japan Geoscience Union. All Right Reserved.

Seasonal and Regional Variation of Diurnal Cycle of Rainfall over Java Island and the Surrounding Area

*Madam Taqiyya Maulana[1], Takeshi Yamazaki[1]

1. Tohoku University

The seasonality and regional variability of diurnal cycle of rainfall (DCR) over Java Island and the surrounding area (coastal region of the Java Sea and the Indian Ocean) are analyzed through satellite observations. This study focus on the area where the studies of the seasonality of DCR over Indonesian Maritime Continent (IMC) are still limited. The DCR is a prominent phenomenon over IMC which is important for aviation industry and related to heavy precipitation events that cause hydro-meteorological disasters.

In this study, **we investigate seasonal and regional variation of DCR (the phase and the amplitude)** through satellite observations. High resolution (spatial and temporal) rainfall estimate is needed to capture feature of DCR over the study area which is difficult to obtain from ground observation. We **mainly employ the high-resolution dataset of Global Satellite Mapping of Precipitation (GSMaP) reanalysis (GSMaP_RNL) and near real time (GSMaP_NRT).** The analysis of DCR seasonal variability is based on investigation throughout boreal winter (December-January-February), boreal spring (March-April-May), boreal summer (June-July-August), and boreal autumn (September-October-November) from 2008-2018 (GSMaP_NRT) and 2009-2014 (GSMaP_RNL).

The results show that hourly data of GSMaP_RNL and GSMaP_NRT with 0.1˚ spatial resolution are able to depict the detailed features of the seasonality and regional variability of DCRover Java Island and surrounding areas. **The comparison between GSMaP_RNL and GSMaP_NRT shows that GSMaP_NRT represents significant time lag of DCR phase over off shore region. GSMaP_NRT shows that the offshore region of the Java Sea is dominated by noon-afternoon rainfall while GSMaP_RNL shows morning rainfall.** However, both of GSMaP_RNL and GSMaP_NRT show similar pattern on phase and amplitude of DCR. Phase of DCR indicates the time when maximum rainfall occurs, while amplitudes indicates the magnitude of DCR. In general, both of GSMaP_RNL and GSMaP_NRT composites, show that the land region with wider landmass area (West Java and western part of East Java) is dominated by evening phase while narrow landmass area (Central Java and eastern part of Java Island) is dominated by late afternoon phase. A large magnitude of the DCR is concentrated inland. The Java Sea has a higher amplitude of DCR compared to the Indian Ocean and the coastal region. The amplitude over the coastal region of the Indian Ocean is higher than over the Indian Ocean and the coastal area of the Java Sea.

Both of rainfall estimates capture inhomogeneous seasonal shifting phase of DCR over this region. The remarkable seasonal shifting phase occurs along the coastal area of the Java Sea. Though, phase shifting over inland of a wide landmass area and the coastal region of the Indian Ocean is not significant. Inhomogeneous seasonal shifting phase of DCR indicated interactions between local circulations, which affected by the topography (e.g. terrain and shape of the coastline), and large circulations (background wind, synoptic conditions, etc.). The analysis of wind profile from reanalysis data confirms the seasonal change of interactions between large and small circulations that caused seasonal shifting phase of DCR.

Keywords: Diurnal cycle of rainfall (DCR), Seasonal variability, Regional variability, Shifting Phase, GSMaP

©2019. Japan Geoscience Union. All Right Reserved.

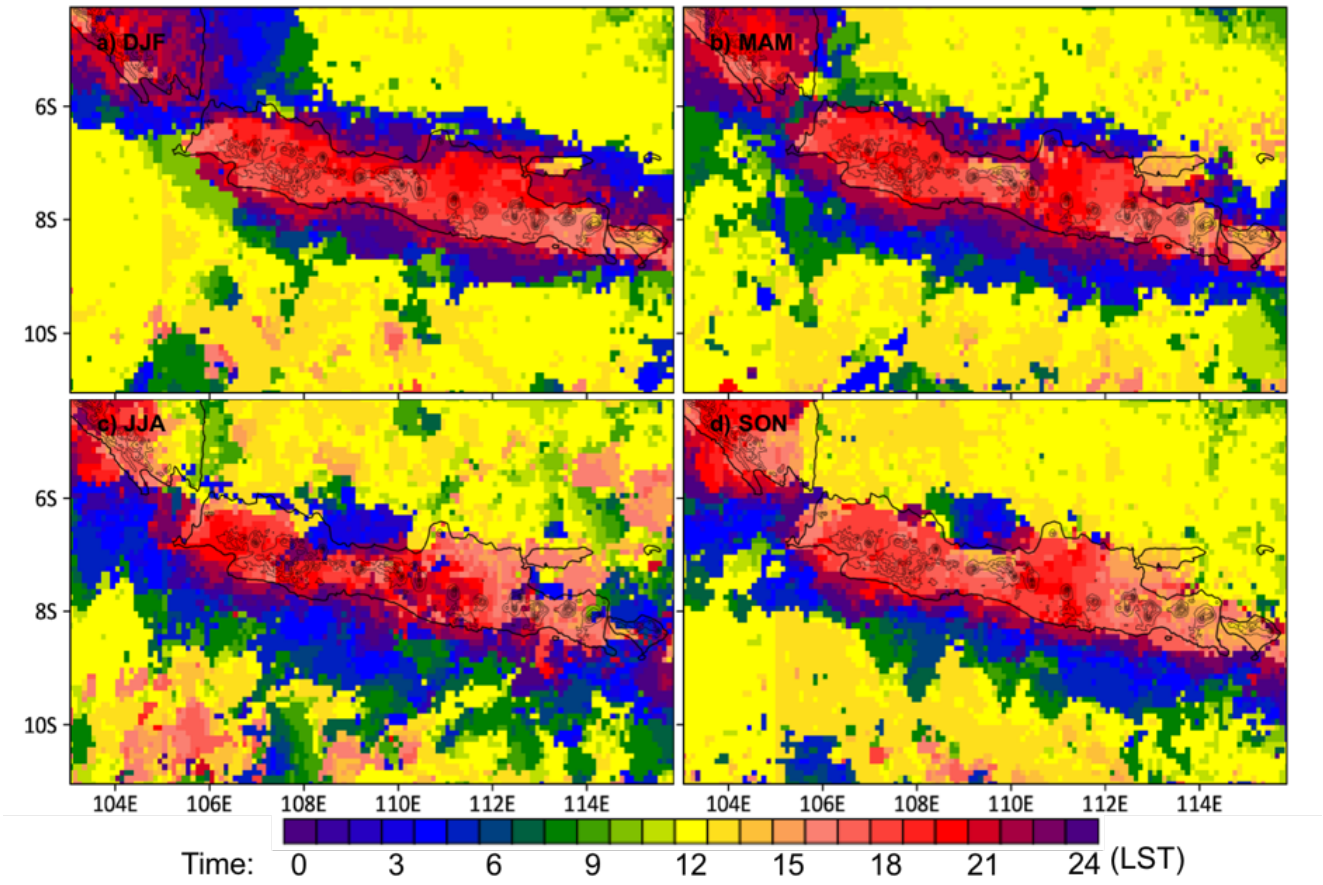

©2019. Japan Geoscience Union. All Right Reserved.

Study on atmospheric circulation characteristics of precipitation anomalies in arid region of Central Asia

*Lianmei Yang[1], Xuefeng Guan[1]

1. Institute of Desert Meteorology, China Meteorological Administration,

As climate transition zone between Mediterranean climate region and East Asian monsoon region, arid region of Central Asia (including five Central Asian countries and Xinjiang province of China) which is influenced by high, middle and low latitude circulations has different synoptic-climatic characteristics from that of Europe and East Asia while its climate characteristics also varies greatly within the region. Central Asia has unique and complicated topography and ecosystem patterns like deserts, oasis, glaciers and basins, forming a highly representative meteorological disaster-breeding environment under the influence of multiple-background, multiple-factor and multiple-scale. This area has abundant solar-heat energy, large evaporation and dramatic temperature changes. Besides, its precipitation is scarce and has extremely uneven distribution with high value in the western and middle parts of Tianshan Mountains. Over the last one hundred years, Central Asia has experienced a warm and wet trend. Central Asia low value system together with the high, middle and low latitude circulation systems linked by West Asia westerly jet stream have contributed to the interdecadal and interannual variations of precipitation in Xinjiang. However, due to the insufficient construction of integrated meteorological observation network, the studies concerning regional featured circulation system, regularity and mechanism of disastrous weathers, high resolution regional numerical model, impacts of land-atmosphere interaction on regional weather and climate change prediction are still inadequate. Correspondingly, to carry out those studies has essential scientific significance and strategic value for the sustainable social and economic development in Silk Road Economic Belt.

Keywords: Arid region of Central Asia, synoptic-climatic characteristics, precipitation anomaly, atmospheric circulation, water vapor

©2019. Japan Geoscience Union. All Right Reserved.

Mechanisms for northward propagation of boreal summer intraseasonal oscillation

*Kanta Nakae[1], Masaki Satoh[1], Daisuke Takasuka[1]

1. Atmosphere and Ocean Research Institute, The University of Tokyo

The 20-90-day Intraseasonal Oscillation (ISO) is one of the dominant modes of tropical variability. In boreal summer northward propagation (NP), which occurs on ISO time scales, originates near the equator and extends to India and western North Pacific Ocean. Understanding the NP of the boreal summer ISO (BSISO) is of vital importance to extended-range weather prediction. Hence, several mechanisms of the NP have been examined. However, they are still incompletely understood. The purpose of this study is to investigate the importance of vertical shear and sea surface temperature (SST) for the NP of the BSISO. In order to obtain a basic structure of the BSISO, we have conducted JJA-perpetual experiments using the Non-hydrostatic Icosahedral Atmospheric Model (NICAM) with a 56-km horizontal mesh.
Although the perpetual experiment has strong Indian monsoon over Arabian sea due to the bias of surface temperature on land, it is found that the NP of the BSISO from Indian Ocean (IO) has two abovementioned mechanisms. One warm SST anomaly north of convection destabilize the lower troposphere, while another tilted vertical shear can generate positive barotropic vorticity to the north of convection. In order to assess the effect of the former mechanism, we made an experiment using fix SST (SSTFIX) obtained from CTL experiment. SSTFIX experiment reproduces the NP of the BSISO from IO, although the amplitude became lower. Therefore, it suggests that the NP of the BSISO from IO doesn’t need warm SST anomaly. To Improve the bias related to basic state like vertical shear, we conducted an experiment using nudging method for surface temperature on land (LNDADJ). In LNDADJ experiment the NP of the BSISO from IO isn’t reproduced due to reduction of column water vapor over Bay of Bengal. Thus, tilted vertical shear can just begin the NP. On the other hand, it is suggested that the NP needs SST and column water vapor to maintain its strength.

Keywords: Boreal summer intraseasonal oscillation, Asian monsoon, Northward propagation

©2019. Japan Geoscience Union. All Right Reserved.

Fractality in the perimeter of tropical clouds observed by Himawari-8 or simulated by a high-resolution model

*Takuya Jinno[1]

1. Graduate School of Science, The University of Tokyo

Cloud clusters show a wide variety of shape and size, and their spatial pattern is often taken up as a typical example of fractal. However, the methods of studying fractal are in an early stage of development. In this study, we conducted fractal analysis on the perimeter of tropical clouds using satellite observation and cloud-resolving simulation of sub-kilometer resolution. We evaluated fractal dimension as a function of spatial scale (transient fractal dimension) and quantified the characteristic spatial scale of the pattern from the scale where self-similarity breaks down. From the observational data from HIMAWARI-8, It is shown that the self-similarity of the cloud perimeter persists only in the spatial scale range from 2 km up to 30 km. The limit of the self-similarity is suggested to be the characteristic scale of the pattern formation of tropical clouds. The cloud-resolving simulation data with NICAM also shows finite-size self-similarity. However, the profile of the transient fractal dimension changed with integration time far more rapidly than HIMAWARI-8 observation, and it lost its self-similarity at the end of the 48-hour simulation. This process is suggested to reflect the increase of stratiform cloud in the upper-troposphere as an adjustment to the transition of spatial resolution.

Keywords: fractal, HIMAWARI-8, cloud-resolving model

©2019. Japan Geoscience Union. All Right Reserved.

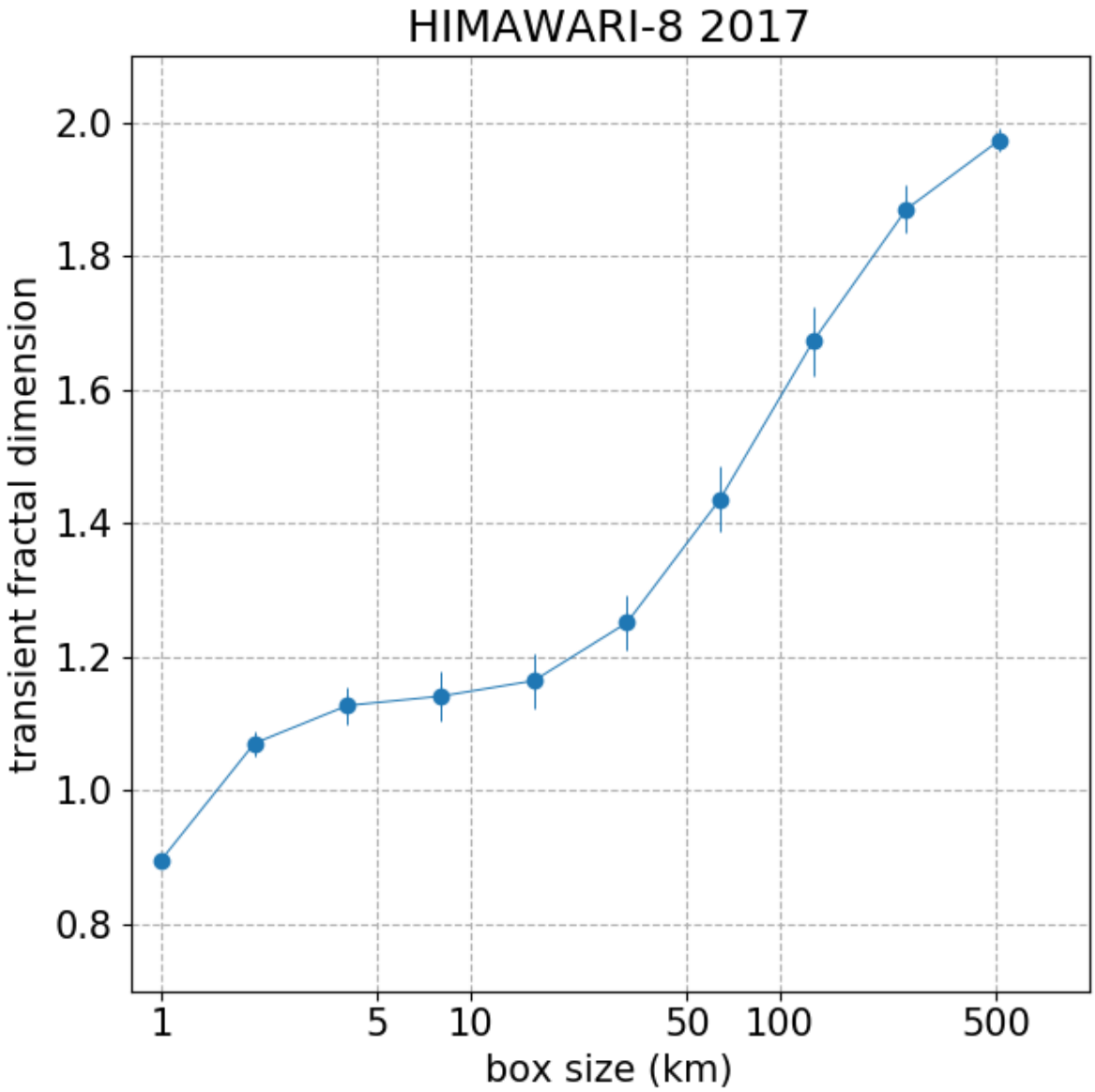

©2019. Japan Geoscience Union. All Right Reserved.

Large-scale deformation of tropical cloud band in the ITCZ detected in NICAM simulations

*Noriyuki Nishi[1], Atsushi Hamada[4], Yohei Yamada[2], Tomoe Nasuno[2], Reona Satoh[5], Masaki Satoh[3]

1. Faculty of Science, Fukuoka Universtiy, 2. JAMSTEC, 3. AORI, University of Tokyo, 4. Graduate School of Science and Engineering for Education, University of Toyama, 5. Graduate School of Science, Fukuoka University

Over the central/eastern tropical Pacific, the Inter Tropical Convergence Zone (ITCZ) is detected in the northern side of the equator. In the ITCZ, we can sometimes observe drastic deformation of the cloud bands elongated zonally with several thousand-kilometer scale. The initial stage of the band, which is composed of deep convective systems, expands meridionally and separates into two or three parallel cirrus bands that keep alive one or two days (Hamada et al., 2013, JMSJ). These separation events cannot be well described in the objective analysis datasets, probably due to lack of the observations over the open ocean; investigation of their mechanism with the analysis data is difficult. In order to study their mechanism, we attempted to use the numerical simulation results of global cloud system resolving model NICAM (Satoh et al. 2014, Progress in Earth and Planetary Science) to find similar events in them. If we can find separation events in the results, we can examine the mechanism with many physical parameters including wind, various kinds of hydrometeors. We have already analyzed several numerical experiment results for different periods, resolution and physical schemes.

We found a similar separation event in an output of the simulation for one year from June 2004 and horizontal resolution 3.5 km. We examined the life cycle of the cirrus bands after separation. One interesting point is on the height of the cirrus clouds in the separated bands. The simulated cirrus clouds in the bands lie in the 13-14 km height level, while the height of the maximum meridional wind that contributes to the meridional movement of the cirrus bands is about 12 km. This difference of the heights means that the cirrus clouds were not just advected by meridional wind but were possibly developed in the course of the separation.

The trigger of zonally simultaneous separation of a long band is another our interest. Inertial instability may be a candidate since vertical exchange of zonal momentum by deep convection would occur in an original band and result in the large meridional shear of the zonal wind in the upper troposphere. We tried to confirm necessary condition for inertial instability by calculating geostrophic vorticity, following the general procedure. However, the position of the bands is too close to the equator (3-7N) to establish geostrophic relationship, and the spatial pattern of the geostrophic vorticity is too noisy to analyze. Therefore, we instead calculate simple absolute vorticity. We found that the absolute vorticity around the separated bands was almost negative. It suggests the possibility of the inertial (or similar kind of) instability.

We are now analyzing another numerical experiment including four kinds of runs using a cloud scheme with different cloud parameter settings. In the real atmosphere, a separation event occurred on 16-17 June 2008 at the just east of the date line. The event can be simulated in all of four runs at 36 hours from the initial time. It suggests that the basic mechanism of the separation is not sensitive to the detail of cloud systems. By analyzing the dynamical fields of these outputs, we are trying to find the key mechanisms to trigger the meridional separation of the cloud bands.

©2019. Japan Geoscience Union. All Right Reserved.

Keywords: tropics, ITCZ, cirrus

©2019. Japan Geoscience Union. All Right Reserved.

Improvement of single-moment bulk microphysics for super-cooled water clouds over the Southern Ocean in NICAM using Joint simulator and double-moment microphysics

*Woosub Roh[1], Tatsuya Seiki[2], Masaki Satoh[1], Tempei Hashino[3]

1. AORI, the university of Tokyo, 2. JAMSTEC, 3. Kochi university of technology

It is important to evaluate and improve the cloud properties in global non-hydrostatic models like a Nonhydrostatic ICosahedral Atmospheric Model (NICAM, Satoh et al. 2014) using observation data. One of the methods is a radiance-based evaluation using satellite data and a satellite simulator (here Joint simulator, Hashino et al. 2013), which avoids making different settings of the microphysics between retrieval algorithms and NICAM.

One of the challenging issues is an evaluation of mixed-phase clouds, which consist of water vapor, ice particles, and supercooled water droplets. It is known one of the main reasons why climate models reveal large errors about the reflection of solar radiation over the Southern Ocean and Arctic.

This study is an evaluation and improvement of mixed-phase clouds over the Southern Ocean in NICAM using a Cloud-Aerosol Lidar and Infrared Pathfinder Satellite Observation (CALIPSO) and a satellite simulator. We evaluated thermodynamics phase of mixed phases clouds over the Southern Ocean in a regional version of NICAM between 45˚S to 65˚S and 170˚E to 170˚W following Yoshida et al. (2010) method. We found underestimation of supercooled water clouds in our single moment scheme. We improved the single moment microphysics scheme using a double moment microphysics and a single column model. We also investigate the impact of microphysics scheme on moisture distributions and the size of cloud systems.

Keywords: microphysics, CALIPSO, Satellite simulator

©2019. Japan Geoscience Union. All Right Reserved.

High-cloud property responses to SST change: sensitivity study using a global nonhydrostatic model

*Tomoki Ohno[1], Masaki Satoh[2]

1. Japan Agency for Marine-Earth Science and Technology, 2. Atmosphere and Ocean Research Institute, The University of Tokyo

Since it has been recognized that the uncertainty of cloud feedback is one of main contributors to the intermodel spread of climate sensitivity, the reduction of the uncertainties associated with cloud response to global warming has been one of central issues for robust projections and predictions of climate variability and change. High clouds have large impacts on the Earth’ s radiative energy budget, and the uncertainty of their response to climate change is known as one of large sources of the climate sensitivity spread although several possible hypotheses to predict the response have been proposed. As the radiation-cloud interaction plays a crucial role in the determination of life time of high clouds, the improvement of the understanding of cloud property responses to global warming helps the reduction of climate-sensitivity variability associated with the high-clouds feedback.

In order to investigate the cloud-property response to climate change, we conducted simulations with RCE configurations using a high-resolution nonhydrostatic global circulation model (the Nonhydrostatic Icosahedral Atmospheric Model; NICAM) with the earth-like sphere for simplifying the problem. Sea surface temperatures (SSTs) are fixed at 300K and 304K and a double-moment bulk scheme are used without cumulus parameterization scheme.

We found that high cloud amount increases with SST increase, as consistent with the previous NICAM studies. It was also determined that the change in particularly optically thin clouds whose optical thicknesses were <3 was dominant, and such thin clouds tended to have large particle sizes. These suggests that the slow evaporative property of ice phase clouds and their representability can play one of key roles in the uncertainty of the high-cloud amount change in global warming.

Keywords: cloud property responses, cloud feedback, climate change

©2019. Japan Geoscience Union. All Right Reserved.

Effects of different cloud overlapping parameters on simulated total cloud fraction over the globe and East Asian region

*bo hai Wang[1], hua Zhang[2]

1. Institute of Atmospheric Physics, Chinese Academy of Sciences, 2. State Key Laboratory of Severe Weather, Chinese Academy of Meteorological Sciences

The cloud overlapping parameter (vertical decorrelation length, L_{cf}) from CloudSat/CALIPSO is implemented in Beijing Climate Center’ s GCM (BCC_AGCM2.0) to reduce the uncertainly in radiation field. Comparing the climate simulation results obtained by using the constant L_{cf} of 2 km with those using the above retrieved L_{cf}, it is found that the total cloud fraction simulation has been obviously improved by using the satellite-based L_{cf}. The error of global mean total cloud fraction between simulations and CERES (Clouds and the Earth's Radiant Energy System) satellite data is decreased by 1.6% in both the winter and summer, of which the positive deviation of total cloud amount at tropical convection area and the negative deviation in subtropical region both are significantly reduced. These improvements are helpful for better simulation of energy budget differences between different regions. In East Asia, using the satellite-based L_{cf} can decrease the error of average total cloud fraction (compared to the CERES) by 1.8% (1.4%) in the winter (summer).Overall, using L_{cf} from CloudSat/CALIPSO satellite data can improve the simulation of total cloud fraction and thus obtain more accurate simulation of radiation field.

Keywords: Cloud overlapping parameter, Vertical decorrelation length, Total cloud fraction

©2019. Japan Geoscience Union. All Right Reserved.

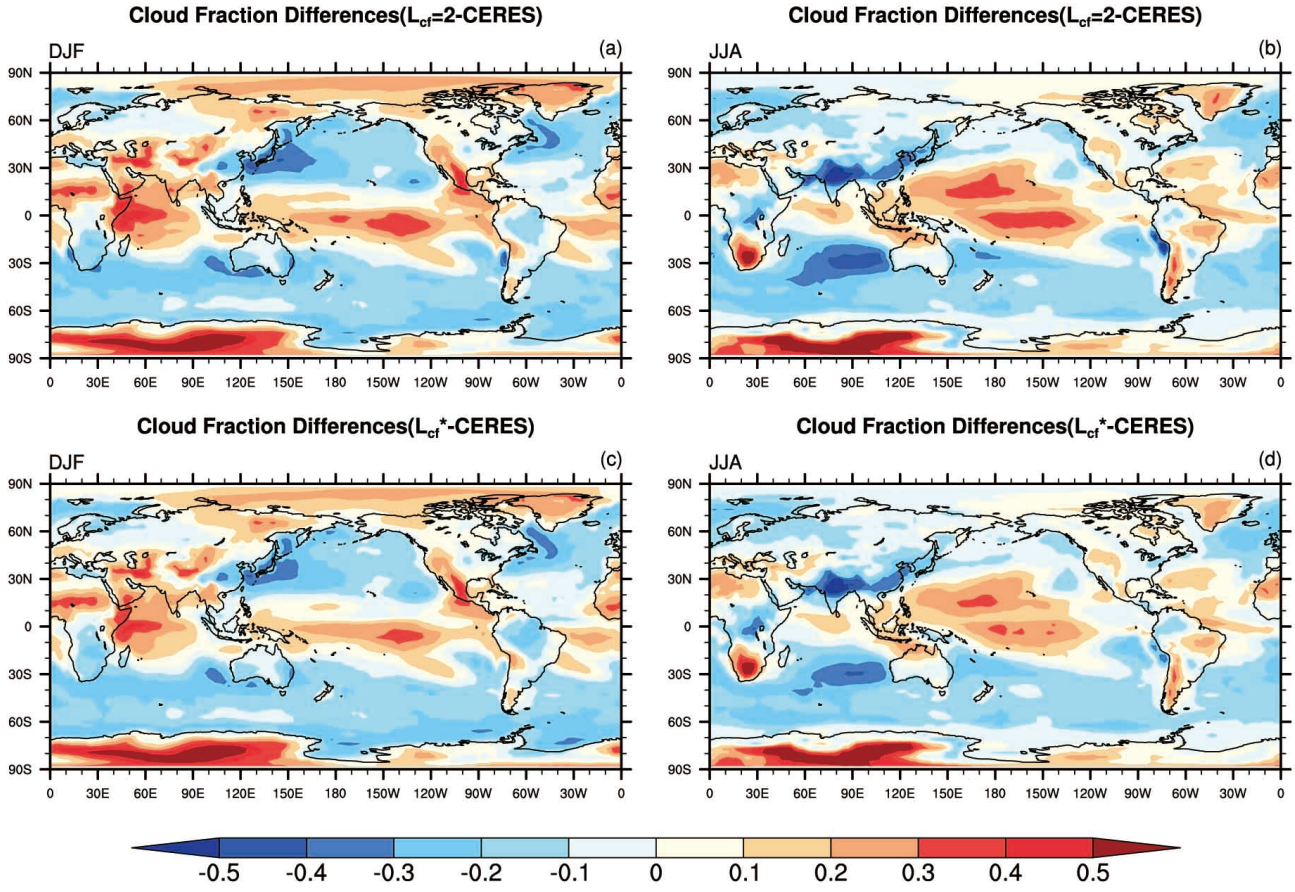

©2019. Japan Geoscience Union. All Right Reserved.

[E] Oral | A (Atmospheric and Hydrospheric Sciences)：A-AS Atmospheric Sciences, Meteorology & Atmospheric Environment

Tue. May 28, 2019 1:45 PM - 3:15 PM JST | Tue. May 28, 2019 4:45 AM - 6:15 AM UTC | 104 1F

[A-AS03] Large-scale moisture and organized cloud systems

convener:Hiroaki Miura(The University of Tokyo), Atsushi Hamada(University of Toyama), Satoru Yokoi(Japan Agency for Marine-Earth Science and Technology), Masaki Satoh(Atmosphere and Ocean Research Institute, The University of Tokyo), Chairperson:Hiroaki Miura

Water vapor plays a significant role in regulating the global atmospheric circulation, especially in the troposphere. The overturning circulation is directly driven by the longwave radiative cooling of water vapor and the latent heating/cooling through microphysical processes to balance it. This global circulation is composed of diverse atmospheric phenomena with various spatial and temporal scales. Developments of some significant turbulent motions such as 3D isotropic turbulence in clouds, stratocumulus and cumulus convection, squall lines and tropical cyclones, and the Madden-Julian oscillation, are essentially associated with moisture anomaly in each scale. Moisture is accumulated relatively slowly in larger horizontal scales, but is consumed relatively quickly in smaller ones. This significant scale gaps between the accumulation and consumption may be one of the causes of the long-lasting difficulty in developing the theory of the moist atmosphere. The aim of this session is to share the recent researches about the relationships between moisture and organized cloud systems in wider spatial and temporal scales to enhance collaborations between modeling, observational, and theoretical approaches in tackling this challenging task. Research results relating to the Years of the Maritime Continent (YMC) and Radiative-Convective Equilibrium Model Intercomparison Project (RCEMPI) are welcome.

1:45 PM - 2:00 PM JST | 4:45 AM - 5:00 AM UTC

[AAS03-01] Boundary-Layer Control on Convective Self-Aggregation

★Invited Papers

*Da YANG[1,2] (1.University of California, Davis, 2.Lawrence Berkeley National Laboratory)

2:00 PM - 2:15 PM JST | 5:00 AM - 5:15 AM UTC

[AAS03-02] Statistical Properties of Cumulus Ensembles in High-Resolution Radiative-Convective Equilibrium Simulations

*Tomoro Yanase[1,2], Tetsuya Takemi[2] (1.Graduate School of Science, Kyoto University, 2.Disaster Prevention Research Institute, Kyoto University)

2:15 PM - 2:30 PM JST | 5:15 AM - 5:30 AM UTC

[AAS03-03] **The role of interactive SST in the cloud-resolving simulations of aggregated convection**

★Invited Papers

*Chien-Ming Wu[1], Yan-Ting Chen[1] (1.National Taiwan University)

2:30 PM - 2:45 PM JST | 5:30 AM - 5:45 AM UTC

[AAS03-04] **Role of coastal convection to moisture buildup during the South China Sea summer monsoon onset**

*Wei-Ting Chen[1], Wei-Ming Tsai[1,2], Chien-Ming Wu[1], Peng-Jen Chen[1] (1.National Taiwan University, 2.University of Miami)

2:45 PM - 3:00 PM JST | 5:45 AM - 6:00 AM UTC

[AAS03-05] Resolution dependencies of tropical convection in a global cloud/cloud-system resolving model

★Invited Papers

*Tomoki Miyakawa[1], Hiroaki Miura[2] (1.Atmosphere and Ocean Research Institute, The University of Tokyo, 2.Graduate School of Science, The University of Tokyo)

3:00 PM - 3:15 PM JST | 6:00 AM - 6:15 AM UTC

[AAS03-06] Effects of the local convection over the western Maritime Continent on the large-scale: numerical study during the YMC Sumatra campaigns

*Tomoe Nasuno[1] (1.Japan Agency for Marine-Earth Science and Technology)

Boundary-Layer Control on Convective Self-Aggregation

*Da YANG[1,2]

1. University of California, Davis, 2. Lawrence Berkeley National Laboratory

The atmosphere can self-organize into overturning circulations over an ocean surface with uniform temperature in cloud-resolving models. The upwelling branch is associated with humid air and deep convection; the downwelling branch is associated with dry air and clear sky. This phenomenon is referred to as convective self-aggregation, and understanding this phenomenon can advance our understanding of the Madden-Julian Oscillation (MJO). In this talk, I will introduce a boundary-layer centric framework for self-aggregation. This framework helps explain what leads to self-aggregation, and what sets the spatial scale of self-aggregation.

Reference:
1. Yang, D., 2018: JAS, https://doi.org/10.1175/JAS-D-17-0150.1
2. Yang, D., 2018: JAMES, https://doi.org/10.1029/2017MS001261

Keywords: Convection, Boundary layer, Self-aggregation

©2019. Japan Geoscience Union. All Right Reserved.

Statistical Properties of Cumulus Ensembles in High-Resolution Radiative-Convective Equilibrium Simulations

*Tomoro Yanase[1,2], Tetsuya Takemi[2]

1. Graduate School of Science, Kyoto University, 2. Disaster Prevention Research Institute, Kyoto University

This study investigates the statistical properties of cumulus ensembles in radiative-convective equilibrium states. Numerical experiments were conducted with the use of the non-hydrostatic Weather Research and Forecasting (WRF) model version 3.8.1 at horizontal grid spacing varied from 1600 m to 200 m in an area of $(200\ km)^2$, with an interactive radiative flux calculation scheme. The experiment with the horizontal grid spacing of 200 m successfully reproduced the diurnal variability of the trimodal characteristics of cumulus convection. With the decrease in the horizontal resolution, intermittent deep convection accompanied by the strong updraft and rainfall becomes dominant. The middle-to-upper troposphere appears to become stabler and drier with the decrease in the horizontal resolution. We further analyzed the cloud structures by using a three-dimensional cloud detection method. It is suggested that the vertical structure of in-cloud properties and the vertical development of cumulus ensembles are strongly affected by horizontal scales of microstructure which are constrained by horizontal resolution. Furthermore, it is suggested that the statistical properties of cumulus ensemble such as horizontal distances and size distribution are related to the horizontal heterogeneity of water vapor.

Keywords: Cumulus Convection, Radiative-Convective Equilibrium, WRF

©2019. Japan Geoscience Union. All Right Reserved.

The role of interactive SST in the cloud-resolving simulations of aggregated convection

*Chien-Ming Wu[1], Yan-Ting Chen[1]

1. National Taiwan University

This study investigates the role of interactive SST in the early development of aggregated convection using a vector vorticity equation cloud-resolving model (VVM) coupled to a slab ocean. The simulations are initialized by a mock Walker circulation driven by initial SST gradient in the elongated x-axis, with an average of 300K and sinusoidal variation of amplitude ranging from 1.5K to 3K. According to large-scale perturbation strength, which is caused by SST variation, the results can be divided into two groups. Under weak perturbation, convection-SST feedback efficiently eliminates SST gradient and moisture anomaly. The large-scale environment is homogenized within two days. Even though SST in the group with stronger perturbation undergoes a similar process, significant moist static energy (MSE) advection in the boundary produces enough moisture difference to introduce virtual temperature effect and aggregation is triggered. Once dry zone starts to expand, radiative and convective effects regenerate SST gradient, which intensifies circulation and accelerates the process. We further show that the evolution of aggregation or not is captured by the trend of MSE-EIS variance. The results highlight the boundary layer processes on the formation of aggregated convection in the tropics.

Keywords: boundary layer processes, large-scale moisture, aggregated convection

©2019. Japan Geoscience Union. All Right Reserved.

Role of coastal convection to moisture buildup during the South China Sea summer monsoon onset

*Wei-Ting Chen[1], Wei-Ming Tsai[1,2], Chien-Ming Wu[1], Peng-Jen Chen[1]

1. National Taiwan University, 2. University of Miami

In this study, the climatological characteristics of object-based precipitation systems (OPS) and moisture development are analyzed over the South China Sea (SCS) during the sharp transition of summer monsoon onset. The satellite observed OPS statistics showed that during the pre-onset period, small (<100 km) to medium size (100-300 km) OPS are active over surrounding land, while convection over the ocean is mostly suppressed. During post-onset, large OPS develop over the coastal ocean and contribute to over 60% of the total precipitation. The results suggest that when the convection is strong over the surrounding islands, a local circulation with anomalous subsidence over the ocean can develop and suppress convection. The number of observed large OPS significantly increases along with the sharp moisture buildup during the SCS onset period. The moisture budgets suggested that local contribution from convection vertical mixing is the major moisture source during monsoon onset pentad, while large-scale moisture advection tends to be weak. The relationship between moisture buildup and convection organization is then examined using a set of idealized cloud-resolving model (CRM) experiments, with a land-ocean configuration approximating the SCS basin. The CRM appropriated represents the observed development of coastal convection. With a non-shear environment, the strong basin-scale circulation is formed, which suppresses the ocean moisture development. When large-scale vertical wind shear is imposed to represent the changes of large-scale circulation during the onset pentad, organized convection systems are increased over the coastal ocean and propagate toward the open ocean, accompanied by fast ocean moistening. We identified through the CRM simulations that the moistening time-scale by the transition of coastal convection organization is within 5-10 days.

Keywords: Convective Organization, Coastal convection, Moisture, TRMM, CloudSat, Cloud-Resolving Model

©2019. Japan Geoscience Union. All Right Reserved.

Resolution dependencies of tropical convection in a global cloud/cloud-system resolving model

*Tomoki Miyakawa[1], Hiroaki Miura[2]

1. Atmosphere and Ocean Research Institute, The University of Tokyo, 2. Graduate School of Science, The University of Tokyo

The properties of tropical convection are evaluated using one-month long simulation datasets produced by the non-hydrostatic icosahedral atmospheric model (NICAM) using 3.5-, 7-, and 14-km horizontal meshes with identical cloud-microphysics configurations. The simulations are targeted on the 2nd Madden-Julian oscillation (MJO) event observed in the CINDY2011/DYNAMO field campaign. An increase of high cloud fraction at 200 hPa level and a reduction of surface precipitation occur as the horizontal resolution increases, corresponding to the reduction of precipitation efficiency due to the shorter residence time inside stronger updrafts that occur at the higher resolution. The increase of high cloud fraction is followed by the warming of the troposphere, which results in an increase in the column water vapor and an elevation of the freezing level. The total water condensation is decreased at higher resolutions, which is likely due to a balance with the decreased outgoing longwave radiation (OLR). The reproduced MJOs, which accounted for a large portion of the tropical convections, were similar in the 3.5-km and 14-km simulations in terms of eastward propagation speeds and structures, including the characteristic westward tilt of the moisture anomaly with height. However, the amplitude of the anomalous MJO circulation was considerably smaller in the 3.5-km simulation. The robust resolution dependence and the interpretations presented in this study underline the necessity for a resolution-aware cloud-microphysics optimization method that will have value in the coming era of global cloud-resolving simulations.

Keywords: resolution dependency , global cloud-resolving model, tropical convection

©2019. Japan Geoscience Union. All Right Reserved.

Effects of the local convection over the western Maritime Continent on the large-scale: numerical study during the YMC Sumatra campaigns

*Tomoe Nasuno[1]

1. Japan Agency for Marine-Earth Science and Technology

The effects of the high-frequency variability on the large-scale, including the intraseasonal oscillation (ISO), over the western Maritime Continent (MC), was quantified using the global nonhydrostatic simulation datasets that marginally resolve mesoscale convective systems. Moisture transport during the Years of the Maritime Continent (YMC) winter field campaigns in 2015 and in 2017 were analyzed, focusing on the land-ocean contrast and their relationship with the ISO events.

The period-mean profiles indicate moistening by low-frequency upward motion in the deep troposphere and drying (moistening) in the lower (middle and upper) troposphere by high-frequency variability. The advection over ocean was greater in 2017 than in 2015, with the opposite occurring over land with smaller interannual differences. These can be related to the longer preconditioning period (rapid transition from the preconditioning to the active, and decaying phases) for the 2015 (2017) case, as well as the relatively suppressed (enhanced) upward motion over ocean under the strong El Niño (moderate La Niña) conditions during 2015 (2017).

The dependence of the land-ocean contrast on the ISO life cycle was more significant in 2015 than in 2017. In the 2015 simulation, moistening over land preceded the major convective period of the ISO, whereas that over ocean preceded the ISO convection not longer than 1 week, consistent with the arguments by previous studies based on precipitation observations. In this case, a nearly in-phase relationship between the moisture advection by high-frequency variability and by low-frequency variability was found over land. In the 2017 case, the land-ocean contrast was weak in low-frequency advection. The relationship between moisture advection by high-frequency variability and by low-frequency variability was indistinct over land, whereas clear relationship was seen over ocean: the high-frequency variability induced lower to middle tropospheric moistening (enhanced upward transport of moisture) during the preconditioning (active) phases of the ISO convection, in common with the 2015 case. These results highlight clear land-ocean contrasts in sensitivity of local convection to background states and its link with the ISO life cycle.

Keywords: Years of the Maritime Conrtinent (YMC), scale interaction, intraseasonal oscillation (ISO), moisture advection, global cloud-system-resolving simulations

©2019. Japan Geoscience Union. All Right Reserved.

[E] Oral | A (Atmospheric and Hydrospheric Sciences)：A-AS Atmospheric Sciences, Meteorology & Atmospheric Environment

Tue. May 28, 2019 3:30 PM - 5:00 PM JST | Tue. May 28, 2019 6:30 AM - 8:00 AM UTC | 104 1F

[A-AS03] Large-scale moisture and organized cloud systems

convener:Hiroaki Miura(The University of Tokyo), Atsushi Hamada(University of Toyama), Satoru Yokoi(Japan Agency for Marine-Earth Science and Technology), Masaki Satoh(Atmosphere and Ocean Research Institute, The University of Tokyo), Chairperson:Satoru Yokoi

Water vapor plays a significant role in regulating the global atmospheric circulation, especially in the troposphere. The overturning circulation is directly driven by the longwave radiative cooling of water vapor and the latent heating/cooling through microphysical processes to balance it. This global circulation is composed of diverse atmospheric phenomena with various spatial and temporal scales. Developments of some significant turbulent motions such as 3D isotropic turbulence in clouds, stratocumulus and cumulus convection, squall lines and tropical cyclones, and the Madden-Julian oscillation, are essentially associated with moisture anomaly in each scale. Moisture is accumulated relatively slowly in larger horizontal scales, but is consumed relatively quickly in smaller ones. This significant scale gaps between the accumulation and consumption may be one of the causes of the long-lasting difficulty in developing the theory of the moist atmosphere. The aim of this session is to share the recent researches about the relationships between moisture and organized cloud systems in wider spatial and temporal scales to enhance collaborations between modeling, observational, and theoretical approaches in tackling this challenging task. Research results relating to the Years of the Maritime Continent (YMC) and Radiative-Convective Equilibrium Model Intercomparison Project (RCEMPI) are welcome.

3:30 PM - 3:45 PM JST | 6:30 AM - 6:45 AM UTC

[AAS03-07] A Mechanism for the Maintenance of Sharp Tropical Margins

★Invited Papers

*Hirohiko Masunaga[1], Brian Earle Mapes[2] (1.Nagoya University, 2.University of Miami)

3:45 PM - 4:00 PM JST | 6:45 AM - 7:00 AM UTC

[AAS03-08] Observational Evidence of Mixed Rossby-Gravity Waves as a Driving Force for the MJO Convective Initiation and Propagation

*Daisuke Takasuka[1,2], Masaki Satoh[1], Satoru Yokoi[2] (1.Atmosphere and Ocean Research Institute, The University of Tokyo, 2.Japan Agency for Marine-Earth Science and Technology)

4:00 PM - 4:15 PM JST | 7:00 AM - 7:15 AM UTC

[AAS03-09] A characteristic of the MJO as a part of enhanced large-scale zonal circulation

*Tamaki Suematsu[1], Hiroaki Miura[2] (1.Atmosphere and Ocean Reaserch Institute, The University of Tokyo, 2.School of Science, The University of Tokyo)

4:15 PM - 4:30 PM JST | 7:15 AM - 7:30 AM UTC

[AAS03-10] **The role of the moisture on the occurrences and distribution of the Amazonian mesoscale convective systems**

*Amanda Rehbein[1,2], Masaki Satoh[2], Tercio Ambrizzi[1] (1.Univ. of Sao Paulo, 2.Univ. of Tokyo)

4:30 PM - 4:45 PM JST | 7:30 AM - 7:45 AM UTC

[AAS03-11] Interdecadal Change of the Impact of Eurasian Snow on Spring Precipitation Over Southern China

*Dingrui Cao[1] (1.Zhejiang University)

4:45 PM - 5:00 PM JST | 7:45 AM - 8:00 AM UTC

[AAS03-12] Atmospheric Rivers and related atmospheric circulations associated with Japanese disastrous precipitation in warm season

Naho Suetou[1], *Akiyo Yatagai[1], Yukari Takayabu[2] (1.Graduate School of Science and Technology/Hirosaki University, 2.Atmosphere and Ocean Research Institute/The University of Tokyo)

A Mechanism for the Maintenance of Sharp Tropical Margins

*Hirohiko Masunaga[1], Brian Earle Mapes[2]

1. Nagoya University, 2. University of Miami

The deep tropics characterized by moist air and deep convection are separated from the dry, quiescent subtropics often by a sharp horizontal gradient of moisture only loosely tied to SST or other geographical constraints. Mapes et al. (GRL, 2018) showed that this margin of the moist tropics is a true PDF minimum (a regime separatrix), along a column water vapor (CWV) contour around 48 mm in instantaneous data. Quasi-meridional statistical composites of observations across the poleward-most excursion of this sinuous contour retain the sharpness of the margin while increasing signal to noise ratio. Observations primarily from a suite of the A-Train satellites show the meridional structure of thermodynamic state and budget terms across the margin of the moist tropics. Composites are computed around the PDF-minimum CWV value of 48 mm as well as a range of other thresholds from 35 mm to 60 mm for comparison. Major findings are summarized as follows. (1) CWV increases equatorward from the subtropics for all CWV thresholds but eventually converges to 48 mm deep into the tropical side. Precipitation abruptly intensifies on the tropical side of the margin but declines equatorward to 85 W/m2 regardless of the CWV thresholds. (2) The diabatic forcing to the atmosphere (radiative heating plus surface heat fluxes) changes its sign across the CWV=48 mm border, being positive on the tropical side and negative on the subtropics. This contrast is owing to the meridional gradient of radiative heating, principally the longwave effect of high clouds. (3) Vertical mode decomposition reveals a transition from bottom-heavy to top-heavy subsidence on the subtropical side of the margin. These observed features are interpreted in terms of a simple theory from the moisture and heat budget perspectives. The model explains the abrupt moistening at the margin as a singularity where the vertical displacement of air costs little energy within a column.

Keywords: Tropical dynamics, Satellite data analysis, Conceptual theory

©2019. Japan Geoscience Union. All Right Reserved.

Observational Evidence of Mixed Rossby-Gravity Waves as a Driving Force for the MJO Convective Initiation and Propagation

*Daisuke Takasuka[1,2], Masaki Satoh[1], Satoru Yokoi[2]

1. Atmosphere and Ocean Research Institute, The University of Tokyo, 2. Japan Agency for Marine-Earth Science and Technology

The Madden-Julian Oscillation (MJO) is known to be the most dominant intraseasonal variability in the tropics, which features large-scale convective envelopes emergening and propagating eastward slowly (~5 m s^{-1}) over the warm pool region. Since its discovery, there have been dedicated efforts to clarify mechanisms about MJO initiation and propagation in terms of large-scale low-frequency dynamics and thermodynamics and a multi-scale interaction with synoptic disturbances. As for the latter standpoint, although some recent observational and idealized numerical studies suggested that mixed Rossby-gravity waves (MRGs) can play a significant role in MJO mechanics, more detailed evidence is necessary because the realistic relationship between MJO and MRGs has had little recognition.

In this study, we examine the contributions of MRGs to the MJO convective initation and propagation in the Indian Ocean during the YMC-Sumatra 2017 field campaign (YMC: Years of the Maritime Continent). The intensive observation captured mid-tropospheric wind variations associated with MRGs, and those signals propagated westward over the Indian Ocean in the MJO suppressed phase. The transition to the MJO active phase follows tight MRG-convection coupling, which is enhanced when the wavelength becomes shorter due to weak mid-level convergence in the western Indian Ocean. Basin-scale anomalous mid-tropospheric moistening caused by MRG shallow circulations is also recognized. These processes lead to the lower-tropospheric MRG wave packet formation and successive triggering of MJO convection, with the eastward MRG group velocity corresponding to MJO propagation. This study suggests that it is worth reconsidering the MJO with a focus on MRG activities at least in the Indian Ocean.

Keywords: Madden-Julian Oscillation, equatorial waves, multi-scale interaction, the Years of the Maritime Continent

©2019. Japan Geoscience Union. All Right Reserved.

A characteristic of the MJO as a part of enhanced large-scale zonal circulation

*Tamaki Suematsu[1], Hiroaki Miura[2]

1. Atmosphere and Ocean Reaserch Institute, The University of Tokyo, 2. School of Science, The University of Tokyo

The Madden-Julian Oscillation (MJO) is known as the dominant mode of intraseasonal variability in the tropics, characterized a region of enhanced convective activities that propagate from the Indian Ocean (IO) to the Western Pacific(WP). However, our understanding of its fundamental role in the atmosphere, and explanation for why it exists is still limited. Taking this into consideration, this study examined how the MJO propagation speed and the intensity of their events were modulated by the background environment and sought for an intrinsic relationship of the MJO with the background atmospheric states. To build on our recent finding of MJO enhancement with background zonal sea surface temperature (SST) gradient, we examined how MJO propagation speed was influenced by the background SST. We constructed a tracking method of MJO convection and calculated the propagation speed of each event. We investigated how the characteristics of the MJO and the background SST states that they occur in varied depending on their propagation speed. The analysis revealed that the slower events were associated with a condition of low-frequency SST (> 60 days) distribution with a positive zonal gradient from the IO to WP. In contrast, high-frequency SST (20 –60 days) distributions associated with the MJO events were much the same between the fast and the slow groups with little zonal SST gradient across IO to WP. Furthermore, the extension of the analysis to rest of the events revealed that the relationship between zonal SST gradient and propagation speed was not a tendency restricted to the fastest and the slowest groups, but is an overall relationship that is displayed by all of the events. Taking note that the presence of zonal SST gradient in the low-frequency range has the potential to enhance large-scale zonal circulation, the component of the zonal wind associated with the background circulation was also analyzed. The analysis showed that there is a tendency for MJO to propagate slower when the background large-scale zonal circulation was stronger, implying that slower MJOs are embedded in enhanced large-scale zonal circulation.

Keywords: Madden-Julian Oscillation , Air-Sea Interaction, Large-Scale Circulation

©2019. Japan Geoscience Union. All Right Reserved.

The role of the moisture on the occurrences and distribution of the Amazonian mesoscale convective systems

*Amanda Rehbein[1,2], Masaki Satoh[2], Tercio Ambrizzi[1]

1. Univ. of Sao Paulo, 2. Univ. of Tokyo

The mesoscale convective systems (MCSs) are large and long-lived organized cloud systems, which have impacts on climate and weather. Studies on MCSs over the Amazon basin have been driven in recent years. They showed that MCSs occur spreadly during the Amazon’ s wet season (November to March) when the Intertropical Convergence Zone is toward northern South America. The MCSs occurrence during wet season months has variations very little known. For instance, during January and March, the MCSs occurrence is greater than in February, being March the month with most occurrences. A similar pattern occurs with the monthly precipitation. During the dry season (May to September), the number of MCSs decreases to a minimum in August, the same as precipitation. However, these MCSs are larger than those occurred in the wet season. Why these differences in the MCSs behavior and occurrence happens is an open question and very important for understanding and improving the MCSs simulations over the Amazon basin. Also, we know very few about the MCSs’ mechanism of genesis and maintenance over that region, mainly due to the lack of data on the Amazon capable of representing the convection time scale. Recently (Jan. 17th, 2019), the European Centre for Medium-Range Weather Forecasts (ECMWF) turn available the highest spatial and temporal reanalysis data (ERA5; hourly temporal and 0.5º spatial resolutions) for global range and long-term data (since 1979 to the present). Therefore, our objective is to use this dataset to investigate the moisture’ s role to the MCSs occurrences on the diurnal, seasonal and interannual scales. To achieve it, we will present temporal and spatial statistical analysis in the hourly, monthly, and annual scales, including vertical moisture profiles. The target period is 2000 to 2013 because of this is the same period of the available MCSs climatology by Rehbein et al. (2017). This investigation is complimentary for a major study where the Amazonian MCSs present and future climates are being investigated.

Keywords: Mesoscale convective systems, Moisture, Amazon basin

©2019. Japan Geoscience Union. All Right Reserved.

Interdecadal Change of the Impact of Eurasian Snow on Spring Precipitation Over Southern China

*Dingrui Cao[1]

1. Zhejiang University

In this study, the relationship between interdecadal and interannual changes of snow cover over Eurasia and precipitation over southern China are investigated. The results show that, the spring precipitation over southern China has experienced a change of positive to negative trend since the end of 1980s. The interannual change of spring precipitation over southern China has a significant positive correlation with the Eurasian snow cover (SCE) anomalies in northwest Lake Baikal. Baroclinic Atmosphere Model (LBM) was utilized in numerical simulation experiment. The results show that The SCE anomalies near northwest Lake Baikal can affect the spring precipitation over southern China by regulating the atmospheric circulation in East Asia and the Northwest Pacific. Further study indicates that the SCE anomalies near Lake Baikal have different contributions to the change of spring precipitation in south China around the end of 1980s. The whole dataset is divided into two periods, 1972-1987 (P1) and 1988-2009 (P2). During P1, the SCE anomalies around Lake Baikal contribute to the formation of regional mono-sign of spring precipitation over southern China. During P2, the SCE anomalies around Lake Baikal are conducive to the formation of north-south dipole modes of spring precipitation. Meanwhile, the SCE anomalies also have experienced an interdecadal change and contributes to precipitation mode over China. During P1, The SCE anomalies near Lake Baikal and its southeast side contribute to the formation of mono-sign of spring precipitation over southern China. During P2, the SCE anomalies near Lake Baikal and its northeast side are favorable for the south China spring precipitation to present the north-south dipole modes of spring precipitation.

Keywords: spring precipitation, snow cover, interdecadal changes

©2019. Japan Geoscience Union. All Right Reserved.

Atmospheric Rivers and related atmospheric circulations associated with Japanese disastrous precipitation in warm season

Naho Suetou[1], *Akiyo Yatagai[1], Yukari Takayabu[2]

1. Graduate School of Science and Technology/Hirosaki University, 2. Atmosphere and Ocean Research Institute/The University of Tokyo

Atmospheric Rivers (ARs) refer to the flow of moisture like an elongated river that reach the mid-troposphere, and water vapor evaporated in the tropics is transported rapidly by subtropical jet streams and extends to mid-latitudes. ARs play an important role in the meridional moisture (i.e. energy) transport in the mid-latitudes; besides bringing down heavy rain on the west coast of North America and the western coast of Europe. Recently, it was found that ARs could emerge around Japan, and the AR occurrence in Hiroshima in August 2014 was reported as one of the factors of heavy rain. However, there are few studies about a relation between heavy precipitation and ARs occurred in Japan. However, previous studies counted the AR occurrence among the heavy precipitation events in entire Japan (longitude 123˚-146˚ and latitude 24˚-46˚). The result during the warm season (April-October) was approximately 70%, which was a high value. It was considered that it included the location of heavy rain did not coincide with the occurrence spot of ARs, because the AR occurrence rate was calculated over a wide range. Therefore, this study analyzed it by dividing Japan into sub-regions, calculating the rate of ARs for heavy rain days that cause disasters in each region, and clarifying the atmospheric circulation field of the day when ARs occurred on heavy rain days.

The target period was 35 years from 1980 to 2014, and a year was divided into two seasons, the warm season (April-October) and the cold season (November-March). This study extracted heavy rain days and detected ARs in the warm season after defined conditions for extracting heavy rain days that cause disasters and conditions for detecting ARs that pass through around Japan. Then, Japan was divided into 13 regions, and it was sorted out the extraction of heavy rain days and AR detection in each region. At this time, AR detection in each area was the detection area up to 100 km in four directions of the area targeted, considering the remote influence of ARs. Only the AR occurrence rate of the warm season was targeted to be analyzed.

The AR occurrence rate in each area was lower than the value calculated in entire Japan. The area with the highest AR occurrence rate was 64.6 % in North Kyushu Region, and the areas with many heavy rain days but a low AR occurrence rate were in Shikoku-Kii Peninsula Region (44.1 %) and South Kyushu Region (45.8%).
This study compared Shikoku-Kii Peninsula Region and North Kyushu Region, and investigated the circulation field. First, the monthly value of AR occurrence rate was the highest in September (61.9 %) in Shikoku-Kii Peninsula Region and in June (83.3 %) in North Kyushu Region. Although the month that took the highest value was different, what common for these two regions were that it was relatively low in July and August and high in rainy seasons.

Regarding the circulation field, the moisture flux in both regions converged on the target areas; however, it diverged over water in the east in Shikoku-Kii Peninsula Region and over water in the south in North Kyushu Region. Both moisture flow comes along the western periphery of the Pacific high where moisture diverges. It is found that there is a trough near the Korean Peninsula in Shikoku-Kii Peninsula Region.

©2019. Japan Geoscience Union. All Right Reserved.

Next, looking into the vertical cross section of the relative humidity and the wind field, the area with high specific humidity anomaly in both regions extended to the mid-troposphere. Also, looking into the specific humidity anomaly and the wind anomaly at the 2 pressure altitudes (500 hPa and 700 hPa) of the mid-troposphere, the areas with high in the specific humidity anomaly existed roughly at the same position as the moisture flux convergence, and the wind anomaly was similar to the flow of the moisture flux in the both regions. The flow of this wind and the moisture flux flown from the southwest to the northeast passing through the sea near Taiwan in Shikoku-Kii Peninsula Region, and from the west-southwest to the east-northeast passing through the mainland of China in North Kyushu Region.

Lastly, from the vertical cross section of the Omega (vertical p-velocity) anomaly, it was seen a strong ascending flow area that was narrow in the east and west and long in the north and south in Shikoku-Kii Peninsula Region, and that was wide in the east and west and narrow in the north and south.

Keywords: AR, APHRO_JP, moisture transport

©2019. Japan Geoscience Union. All Right Reserved.

[J] Oral | A (Atmospheric and Hydrospheric Sciences)：A-OS Ocean Sciences & Ocean Environment

Tue. May 28, 2019 10:45 AM - 12:15 PM JST | Tue. May 28, 2019 1:45 AM - 3:15 AM UTC | 106 1F

[A-OS17] Kuroshio Large Meander

convener:Toru Miyama(Japan Agency for Marine-Earth Science and Technology, Application Laboratory), Norihisa Usui(Meteorological Research Institute), Takashi Setou(National Research Institute of Fisheries Science, Fisheries Research and Education Agency), Chairperson:Toru Miyama, Takashi Setou, Norihisa Usui

The Kuroshio has taken large meander path since the end of August 2017. Although it is unknown whether it is continuing at the time of the JpGU meeting, this notable event of the coastal area south of Japan after 12 years later from the last one has already attracted societal interests. In this session, behaviors, dynamics, influences, comparisons with past cases, etc. are discussed. Presentations from various perspectives of ocean physics, biology, chemistry, and meteorology are welcome.

10:45 AM - 11:00 AM JST | 1:45 AM - 2:00 AM UTC

[AOS17-01] The progress of the Kuroshio large meander in and after 2017

★Invited Papers

*Toshiyuki Sakurai[1], Mikitoshi Hirabara[1], Yoshikazu Fukuda[1], Mika Kimura[1], Kotaro Mine[1], Masaomi Takahashi[1], Kensaku Kobayashi[1], Yuka Okunaka[1], Hiromu Kobayashi[1] (1.Japan Meteorological Agency)

11:00 AM - 11:15 AM JST | 2:00 AM - 2:15 AM UTC

[AOS17-02] Influences of the Kuroshio path variation south of Honshu on summer surface air temperature in Kanto district, Japan

*Shusaku Sugimoto[1] (1.Graduate School of Science, Tohoku University)

11:15 AM - 11:30 AM JST | 2:15 AM - 2:30 AM UTC

[AOS17-03] Bio-chemilcal difference between the large meander and the non case of the Kuroshio current

*Takashi Setou[1], Tuneo Ono[2], Kiyotaka Hidaka[1], Yugo Shimizu[1], Atsushi Nishimoto[1], Sayaka Sogawa[1], Akira Kusaka[1], Daisuke Ambe[1], Daiki Itoh[1], Takashiko Kameda[1], Yutaka Hiroe[3] (1.National Research Institute of Fisheries Science, Fisheries Research and Education Agency , 2.National Research Institute of Far Seas Fisheires,Fisheries Research and Education Agency , 3.National Research Institute of Far Seas Fisheires,Seikai National Fisheries Research Institute)

11:30 AM - 11:45 AM JST | 2:30 AM - 2:45 AM UTC

[AOS17-04] The late arrival of 2017-18 Japanese eel recruitment and its links to ocean circulation

*Yu-Lin Eda Chang[1], Yasumasa Miyazawa[1], Michael Miller[2], Katsumi Tsukamoto[2] (1.Application Laboratory, Japan Agency for Marine-Earth Science and Technology, 2.Department of Aquatic Bioscience, The University of Tokyo)

11:45 AM - 12:00 PM JST | 2:45 AM - 3:00 AM UTC

[AOS17-05] A probabilistic forecast of the Kuroshio current path variability using an 80-member ensemble simulation.

*Kunihiro Aoki[1], Yasumasa Miyazawa[1], Tsutomu Hihara[1] (1.JAMSTEC)

12:00 PM - 12:15 PM JST | 3:00 AM - 3:15 AM UTC

[AOS17-06] Long-term forecast of the Kuroshio large meander in 2017

*Norihisa Usui[1], Nariaki Hirose[1], Kei Sakamoto[1], Yosuke Fujii[1], Nadao Kohno[1] (1.Meteorological Research Institute)

The progress of the Kuroshio large meander in and after 2017

*Toshiyuki Sakurai[1], Mikitoshi Hirabara[1], Yoshikazu Fukuda[1], Mika Kimura[1], Kotaro Mine[1], Masaomi Takahashi[1], Kensaku Kobayashi[1], Yuka Okunaka[1], Hiromu Kobayashi[1]

1. Japan Meteorological Agency

Office of Marine Prediction (OMP) at Japan Meteorological Agency (JMA) has been routinely operating an ocean data assimilation and prediction system for the western North Pacific (MOVE/MRI.COM-WNP) since March 2008. This system aims to represent ocean characteristics such as the Kuroshio/Oyashio current and meso-scale eddies. Using MOVE/MRI.COM-WNP, OMP provides ocean state information of major currents around Japan (Kuroshio/Oyashio/Tsushima-Warm-Current) and water temperatures in the western North Pacific mainly through the JMA website.
In August 2017, the Kuroshio developed a large meander (LM) for the first time in 12 years. A small meander that developed southeast of Japan’ s Kyushu Island in late March 2017 and propagated eastward to waters off the country’ s Tokai region in August is considered to have induced the Kuroshio LM. In August, MOVE/MRI.COM-WNP successfully forecasted the generation of the Kuroshio LM and JMA published a press release about the probabilityof the Kuroshio LM.
This presentation shows the progress of the Kuroshio LM in and after 2017 as contrasted with the past cases.

Keywords: The Kuroshio, Kuroshio large meander, Forecast, Ocean Data Assimilation

©2019. Japan Geoscience Union. All Right Reserved.

Influences of the Kuroshio path variation south of Honshu on summer surface air temperature in Kanto district, Japan

*Shusaku Sugimoto[1]

1. Graduate School of Science, Tohoku University

In the Kuroshio and its extension (KE), the warm surface waters compared to the surrounding waters enhance upward heat release in winter, indicating that the ocean affects the atmosphere. On the other hand, in summer, atmospheric response to the Kuroshio/KE remains unclear because of a small difference between sea surface temperature (SST) and surface air temperature (SAT) over the Kuroshio/KE and of its-associated weak SST gradient. Here we investigated summertime (June-August) SST variations south of Japan, using high spatial resolution satellite-derived measurements of 2003–2018. The result showed that the variation is dominant in the region off Kanto-Tokai district, which was related to the Kuroshio path state; the SST increases off Kanto-Tokai district when the Kuroshio takes the meander path, which would reflect the following two points. In the meander period, (1) the Kuroshio shifted southward around Cape Shionomisaki, moves to the north around the Izu Islands, and then reaches very close to south coast of Kanto district, and (2) westward warm flow, which is a flow on the north edge of the anticlockwise eddy north of the Kuroshio, runs very close to the south coast of Tokai district. To reveal the extent to which the warm surface waters off Kanto-Tokai district influence the atmospheric fields, we conducted regional atmospheric model experiments using the high-resolution Japan Meteorological Agency nonhydrostatic model (JMA-NHM) with 5 km horizontal grid spacing. The experiment showed that, over the warm surface waters, evaporation increased considerably, and the northward water vapor transport by low-level wind caused an increase of moisture in Kanto district. The warm-water-induced moisture increase enhances downward longwave radiation at the surface in Kanto district, leading to the SAT increase. Actually, the SST off Kanto-Tokai district is significantly correlated with the SAT in Kanto district, from the Automated Meteorological Data Acquisition System (AMeDAS) of the Japan Meteorological Agency. Our results indicate that, in summer, the Kuroshio path state (meander or straight path) affect the overlying atmosphere and climate on Japan.

Keywords: Kuroshio meander path, SST off Kanto-Tokai district, SAT in Kanto district, Regional atmospheric model experiment

©2019. Japan Geoscience Union. All Right Reserved.

Bio-chemilcal difference between the large meander and the non case of the Kuroshio current

*Takashi Setou[1], Tuneo Ono[2], Kiyotaka Hidaka[1], Yugo Shimizu[1], Atsushi Nishimoto[1], Sayaka Sogawa[1], Akira Kusaka[1], Daisuke Ambe[1], Daiki Itoh[1], Takashiko Kameda[1], Yutaka Hiroe[3]

1. National Research Institute of Fisheries Science, Fisheries Research and Education Agency , 2. National Research Institute of Far Seas Fisheires,Fisheries Research and Education Agency , 3. National Research Institute of Far Seas Fisheires,Seikai National Fisheries Research Institute

Since 2001, FRA has set up a regular monitoring line, called O-line north and south along 138E off Omaezaki south of Japan and has been conducting the monitoring four or five times a year until now. O-line, the monitoring line was named after Omaezaki City, which is near the starting point of the line. The line has been mainly conducted by the National Research Institute of Fisheries Science and has been carried out for the measure of water temperature, salinity, nutrient, some phytoplankton and zooplankton. In this presentation, the bio-chemical difference on the line between the large meandering case and the non case of the Kuroshio current has been focused on.

Keywords: Kuroshio

©2019. Japan Geoscience Union. All Right Reserved.

The late arrival of 2017-18 Japanese eel recruitment and its links to ocean circulation

*Yu-Lin Eda Chang[1], Yasumasa Miyazawa[1], Michael Miller[2], Katsumi Tsukamoto[2]

1. Application Laboratory, Japan Agency for Marine-Earth Science and Technology, 2. Department of Aquatic Bioscience, The University of Tokyo

In the year 2018, the Japanese eel (*Anguilla japonica*) recruitment almost vanished in Japan in the early recruitment season, and the eel catch peaked up in late recruitment period when the recruitment was usually small. Coincidently, the Kuroshio meander occurring south of Japan was revisiting since the previous event ends in 2005. The role of ocean circulation in 2018 unusual Japanese eel larvae recruitment was investigated using a three-dimensional particle tracking model, in which swimming behaviors of virtue larvae (v-larvae) was included in addition to passively drift by ocean currents. Similar results appeared in the simulation, showing none v-larvae arrival to the south of Japan in early recruitment period and increased substantially in the late recruitment period. The late arrival could be explained by the change of ocean circulation. The southward shifting and weak North Equatorial Current near spawning area, less Subtropical Countercurrent eddies, and weak Kuroshio during the early migration and recruitment period prevented v-larvae transport. In the late recruitment period, the Kuroshio was strengthened and strong near the East China Sea and south of Japan that transported v-larvae downstream efficiently. The maximum eel catch reduction in Tokai region where Kuroshio bifurcated offshore could be related to large meander. The Kuroshio large meander could potentially influence the local eel recruitment, but its actual role remained to be explored.

Keywords: Japanese eel, North Equatorial Current, Kuroshio large meander

©2019. Japan Geoscience Union. All Right Reserved.

A probabilistic forecast of the Kuroshio current path variability using an 80-member ensemble simulation.

*Kunihiro Aoki[1], Yasumasa Miyazawa[1], Tsutomu Hihara[1]

1. JAMSTEC

This study aims to describe the probabilistic behavior of the Kuroshio current path variability using an 80-member ensemble simulation in a high-resolution numerical regional ocean model, JCOPE. This simulation provides the outputs for 4 months starting from the initial conditions optimized by the data assimilation (LETKF) for one months. All the members are found to predict the non-large meander path at first 2 months, but some members predict the large meander path after that. We propose a method of quantifying the occurrence/non-occurrence of the branch, the probabilities of each path, and a set of the mean and spread for each path by a machine learning method.

Keywords: Ensemble forecast, Data assimilation, Clustering

©2019. Japan Geoscience Union. All Right Reserved.

Long-term forecast of the Kuroshio large meander in 2017

*Norihisa Usui[1], Nariaki Hirose[1], Kei Sakamoto[1], Yosuke Fujii[1], Nadao Kohno[1]

1. Meteorological Research Institute

The Kuroshio large meander (KLM) occurred in the end of August 2017 for the first time in 12 years, and has maintained for more than a year. Changes in the oceanic condition south of Japan associated with the KLM have a large impact on various fields such as fisheries, marine transportation, and local weather. The KLM has, therefore, been received much attention. In this presentation, we discuss prospects of the KLM in 2017 on the basis of a long-term forecast experiment using an eddy-resolving ocean model. First, the actual Kuroshio state in the end of August 2018 is reproduced by applying data assimilation. We then conduct ensemble simulations with 40 members, in which atmospheric forcing data are replaced by those on the same day from 1975 to 2014 and the model is integrated for more than three years starting from 28 August 2018. In most cases, the KLM maintains for more than one and a half years (i.e. February 2020). After that, differences in the Kuroshio state among the ensemble members become large. As pointed out be former studies, these behaviors of the Kuroshio path are largely explained by the Sverdrup transport estimated from the wind stress field used in the experiment. In the presentation, we will evaluate the ensemble simulations results using the actual Kuroshio state in May 2019, and will show more detailed results.

Keywords: Kuroshio large meander, Kuroshio transport, long-term forecast

©2019. Japan Geoscience Union. All Right Reserved.

[J] Poster | A (Atmospheric and Hydrospheric Sciences)：A-OS Ocean Sciences & Ocean Environment

Tue. May 28, 2019 3:30 PM - 5:00 PM JST | Tue. May 28, 2019 6:30 AM - 8:00 AM UTC | Poster Hall International Exhibition Hall8, Makuhari Messe_5

[A-OS17] Kuroshio Large Meander

convener:Toru Miyama(Japan Agency for Marine-Earth Science and Technology, Application Laboratory), Norihisa Usui(Meteorological Research Institute), Takashi Setou(National Research Institute of Fisheries Science, Fisheries Research and Education Agency)

The Kuroshio has taken large meander path since the end of August 2017. Although it is unknown whether it is continuing at the time of the JpGU meeting, this notable event of the coastal area south of Japan after 12 years later from the last one has already attracted societal interests. In this session, behaviors, dynamics, influences, comparisons with past cases, etc. are discussed. Presentations from various perspectives of ocean physics, biology, chemistry, and meteorology are welcome.

[AOS17-P01] Temporal and spacial changes in relative vorticity along the Kuroshio axis

*Yuya Hirano[1], Kazuyuki Uehara[1] (1.The Graduate School of Geo-environmental Science, Tokai University)

[AOS17-P02] The Kuroshio large meander in 2017 and its coastal impact reproduced by a 2-km resolution assimilation model

*Nariaki Hirose[1], Norihisa Usui[1], Kei Sakamoto[1], Goro Yamanaka[1], Nadao Kohno[1] (1.Meteorological Research Institute, Japan Meteorological Agency)

[AOS17-P03] Reintesification of the Kuroshio Large Meander in Summer 2018

*Toru Miyama[1], Yasumasa Miyazawa[1] (1.Japan Agency for Marine-Earth Science and Technology, Application Laboratory)

Temporal and spacial changes in relative vorticity along the Kuroshio axis

*Yuya Hirano[1], Kazuyuki Uehara[1]

1. The Graduate School of Geo-environmental Science, Tokai University

The transition process of the Kuroshio path has been investigated by many previous studies. According to these studies, the transition from a non-large-meander path to a large-meander path is considerd to be caused by a eastward propagation of a "Kuroshio small meander" which occurs southeast of Kyushu (e.g. Solomon, 1978; Sekine, 1895; Kawabe, 2003). Not all small-meanders, however, form large-meander-paths. In many cases, magnitudes of small-meanders usually become smaller before reaching at Shionomisaki. In this study, we therefore calculate temporal and spacial changes along the Kuroshio axis in relative vorticities using maps of the absolute sea surface dynamic topography (MADT) providing from AVISO describe transition processes the Kuroshio meandering in detail. Here, we use MADT with weekly mean temporal resolution and 0.25 ×0.25 grid spatial resolution from January 4, 1993 to June 4, 2018. In addition, we also focus on the intensity of the Kuroshio recirculation gyre located stably at south of Shikoku.

Keywords: The Kuroshio, path transition

©2019. Japan Geoscience Union. All Right Reserved.

The Kuroshio large meander in 2017 and its coastal impact reproduced by a 2-km resolution assimilation model

*Nariaki Hirose[1], Norihisa Usui[1], Kei Sakamoto[1], Goro Yamanaka[1], Nadao Kohno[1]

1. Meteorological Research Institute, Japan Meteorological Agency

The Kuroshio large meander (KLM) occurred in the end of August 2017 for the first time in 12 years. In order to reproduce this event and investigate its impact on coastal regions, we conducted assimilation and forecast experiments using a 2-km resolution assimilation model, which has been developed at the Meteorological Research Institute of Japan Meteorological Agency (MRI/JMA) for the purpose of operational use in JMA. The assimilation model succeeded in reproducing formation process of the KLM in 2017 as well as associated variations in sea level and water temperature in coastal regions. It is reported that sudden strong current so-called Kyusho occurred in the southeast coast of Shikoku in September 2017. The assimilation results show that this Kyucho event is caused as a result of propagation of a disturbance with cyclonic circulation along the Kuroshio. Besides, in the end of October, warm Kuroshio water was intruded into coastal regions in Shizuoka, Aichi and Mie prefectures in the central part of Japan. This warm water separates from a northward current in the eastern flank of the large meander. In the presentation, forecast results will also be shown to discuss more detailed process.

©2019. Japan Geoscience Union. All Right Reserved.

Reintesification of the Kuroshio Large Meander in Summer 2018

*Toru Miyama[1], Yasumasa Miyazawa[1]

1. Japan Agency for Marine-Earth Science and Technology, Application Laboratory

More than one year have passed since the Kuroshio large meander started in the end of August. It is already longer than the last event in 2004/2005 and the evert before the last in 1989/1990. If the strength of the cyclonic eddy that makes the large meander was defined with the minimum sea level height in 135-140ºE 30-35ºN of FRA-JCOPE 2 reanalysis (Miyazawa et al. 2009) (a smaller value means a stronger eddy), the cyclonic eddy was strengthened after the large meander started, and was weakened from spring in 2018. However, the eddy has been intensified since summer in 2018. The reintensification of the eddy was also found in the temperature field of the reanalysis. The same tendency can be confirmed by the observed absolute dynamic sea surface height (E.U. Copernicus Marine Service Information). Sekine (1985) reported that the spin-up of the cold eddy occurred from late spring to summer in the 1975-1980 Kuroshio large meander event. Therefore, the reintensification of the cold eddy in summer 2018 could play some role in that the current large meander event is becoming long one. In this talk, the situation and dynamics of the reintensification will be discussed.

Keywords: Kuroshio large meander, ocean reanalysis, eddy

©2019. Japan Geoscience Union. All Right Reserved.

[J] Poster | A (Atmospheric and Hydrospheric Sciences)：A-OS Ocean Sciences & Ocean Environment

Tue. May 28, 2019 5:15 PM - 6:30 PM JST | Tue. May 28, 2019 8:15 AM - 9:30 AM UTC | Poster Hall International Exhibition Hall8, Makuhari Messe_7

[A-OS17] Kuroshio Large Meander

convener:Toru Miyama(Japan Agency for Marine-Earth Science and Technology, Application Laboratory), Norihisa Usui(Meteorological Research Institute), Takashi Setou(National Research Institute of Fisheries Science, Fisheries Research and Education Agency)

The Kuroshio has taken large meander path since the end of August 2017. Although it is unknown whether it is continuing at the time of the JpGU meeting, this notable event of the coastal area south of Japan after 12 years later from the last one has already attracted societal interests. In this session, behaviors, dynamics, influences, comparisons with past cases, etc. are discussed. Presentations from various perspectives of ocean physics, biology, chemistry, and meteorology are welcome.

[AOS17-P01] Temporal and spacial changes in relative vorticity along the Kuroshio axis

*Yuya Hirano[1], Kazuyuki Uehara[1] (1.The Graduate School of Geo-environmental Science, Tokai University)

[AOS17-P02] The Kuroshio large meander in 2017 and its coastal impact reproduced by a 2-km resolution assimilation model

*Nariaki Hirose[1], Norihisa Usui[1], Kei Sakamoto[1], Goro Yamanaka[1], Nadao Kohno[1] (1.Meteorological Research Institute, Japan Meteorological Agency)

[AOS17-P03] Reintesification of the Kuroshio Large Meander in Summer 2018

*Toru Miyama[1], Yasumasa Miyazawa[1] (1.Japan Agency for Marine-Earth Science and Technology, Application Laboratory)

Temporal and spacial changes in relative vorticity along the Kuroshio axis

*Yuya Hirano[1], Kazuyuki Uehara[1]

1. The Graduate School of Geo-environmental Science, Tokai University

The transition process of the Kuroshio path has been investigated by many previous studies. According to these studies, the transition from a non-large-meander path to a large-meander path is considerd to be caused by a eastward propagation of a "Kuroshio small meander" which occurs southeast of Kyushu (e.g. Solomon, 1978; Sekine, 1895; Kawabe, 2003). Not all small-meanders, however, form large-meander-paths. In many cases, magnitudes of small-meanders usually become smaller before reaching at Shionomisaki. In this study, we therefore calculate temporal and spacial changes along the Kuroshio axis in relative vorticities using maps of the absolute sea surface dynamic topography (MADT) providing from AVISO describe transition processes the Kuroshio meandering in detail. Here, we use MADT with weekly mean temporal resolution and 0.25 ×0.25 grid spatial resolution from January 4, 1993 to June 4, 2018. In addition, we also focus on the intensity of the Kuroshio recirculation gyre located stably at south of Shikoku.

Keywords: The Kuroshio, path transition

©2019. Japan Geoscience Union. All Right Reserved.

The Kuroshio large meander in 2017 and its coastal impact reproduced by a 2-km resolution assimilation model

*Nariaki Hirose[1], Norihisa Usui[1], Kei Sakamoto[1], Goro Yamanaka[1], Nadao Kohno[1]

1. Meteorological Research Institute, Japan Meteorological Agency

The Kuroshio large meander (KLM) occurred in the end of August 2017 for the first time in 12 years. In order to reproduce this event and investigate its impact on coastal regions, we conducted assimilation and forecast experiments using a 2-km resolution assimilation model, which has been developed at the Meteorological Research Institute of Japan Meteorological Agency (MRI/JMA) for the purpose of operational use in JMA. The assimilation model succeeded in reproducing formation process of the KLM in 2017 as well as associated variations in sea level and water temperature in coastal regions. It is reported that sudden strong current so-called Kyusho occurred in the southeast coast of Shikoku in September 2017. The assimilation results show that this Kyucho event is caused as a result of propagation of a disturbance with cyclonic circulation along the Kuroshio. Besides, in the end of October, warm Kuroshio water was intruded into coastal regions in Shizuoka, Aichi and Mie prefectures in the central part of Japan. This warm water separates from a northward current in the eastern flank of the large meander. In the presentation, forecast results will also be shown to discuss more detailed process.

©2019. Japan Geoscience Union. All Right Reserved.

Reintesification of the Kuroshio Large Meander in Summer 2018

*Toru Miyama[1], Yasumasa Miyazawa[1]

1. Japan Agency for Marine-Earth Science and Technology, Application Laboratory

More than one year have passed since the Kuroshio large meander started in the end of August. It is already longer than the last event in 2004/2005 and the evert before the last in 1989/1990. If the strength of the cyclonic eddy that makes the large meander was defined with the minimum sea level height in 135-140ºE 30-35ºN of FRA-JCOPE 2 reanalysis (Miyazawa et al. 2009) (a smaller value means a stronger eddy), the cyclonic eddy was strengthened after the large meander started, and was weakened from spring in 2018. However, the eddy has been intensified since summer in 2018. The reintensification of the eddy was also found in the temperature field of the reanalysis. The same tendency can be confirmed by the observed absolute dynamic sea surface height (E.U. Copernicus Marine Service Information). Sekine (1985) reported that the spin-up of the cold eddy occurred from late spring to summer in the 1975-1980 Kuroshio large meander event. Therefore, the reintensification of the cold eddy in summer 2018 could play some role in that the current large meander event is becoming long one. In this talk, the situation and dynamics of the reintensification will be discussed.

Keywords: Kuroshio large meander, ocean reanalysis, eddy

©2019. Japan Geoscience Union. All Right Reserved.

[J] Oral | A (Atmospheric and Hydrospheric Sciences)：A-OS Ocean Sciences & Ocean Environment

Tue. May 28, 2019 1:45 PM - 3:15 PM JST | Tue. May 28, 2019 4:45 AM - 6:15 AM UTC | 106 1F

[A-OS18] Physical Oceanography (General)

convener:Yoshimi Kawai(Research and Development Center for Global Change, Japan Agency for Marine-Earth Science and Technology), Tomoki Tozuka(Department of Earth and Planetary Science, Graduate School of Science, The University of Tokyo), Kitade Yujiro(Tokyo University of Marine Science and Technology), Chairperson:Yoshimi Kawai(Japan Agency for Marine-Earth Science and Technology), Tomoki Tozuka(The University of Tokyo)

This session invites presentations on a wide variety of topics related to physical oceanography.

1:45 PM - 1:50 PM JST | 4:45 AM - 4:50 AM UTC

Introduction

1:50 PM - 2:05 PM JST | 4:50 AM - 5:05 AM UTC

[AOS18-01] **Real-Time Subsurface Moorings as a Promising Component of Global Ocean Monitoring System**

*Jianing Wang[1], Fan Wang[1] (1.Institute of Oceanology, Chinese Academy of Sciences)

2:05 PM - 2:20 PM JST | 5:05 AM - 5:20 AM UTC

[AOS18-02] Seasonal Variation of the Mixed Layer Depth at 60°S and its governing dynamics

*Matheus Ferreira Azevedo[1], Yujiro Kitade[1], Shigeru Aoki[2] (1.Tokyo University of Marine Science and Technology, 2.Institute of Low Temperature Science, Hokkaido University)

2:20 PM - 2:40 PM JST | 5:20 AM - 5:40 AM UTC

[AOS18-03] **21st-Century Flood Hazards along the U.S. Atlantic Coast: Impacts of Sea Level Rise and Tropical Cyclone Climatology Change**

★Invited Papers

*Reza Marsooli[1], Ning Lin[2], Kerry Emanuel[3] (1.Stevens Institute of Technology, 2.Princeton University, 3.Massachusetts Institute of Technology)

2:40 PM - 3:00 PM JST | 5:40 AM - 6:00 AM UTC

[AOS18-04] **The Effect of Ocean Waves on an Explosive Cyclone Development: Investigation with a Coupled Model**

★Invited Papers

*Yuki Kita[1], Takuji Waseda[1] (1.University of Tokyo)

3:00 PM - 3:15 PM JST | 6:00 AM - 6:15 AM UTC

Discussion

Real-Time Subsurface Moorings as a Promising Component of Global Ocean Monitoring System

*Jianing Wang[1], Fan Wang[1]

1. Institute of Oceanology, Chinese Academy of Sciences

Subsurface moorings have advantage in providing long term and full-depth ocean monitoring parameters. Traditional moorings normally release data once a year, which put constraints on the mooring data usage in the weather and short-term climate forecasts. Recently, the Institute of Oceanology, Chinese Academy of Sciences (IOCAS) has overcome difficulties in the long-term transmission of real-time data from subsurface moorings. Data from sensors up to 3000 m depth can be transmitted to the surface floating body through wireless acoustic communications and then to the shore through satellite. In 2016, the IOCAS had realized real-time transmission of three dimensional velocities over the upper 1000 m from one mooring for more than 280 days. In 2017, real-time transmission module was equipped on the majority of the moorings, and the depth range of data has been extended from 1000 to 3000 m; this real-time observing network has successfully been conducted for 300 days until now. The aim of this abstract is to make recommendation for Real-Time Subsurface Moorings (RTSMs) as a promising component of global ocean observing systems.

The present prediction skill of ENSO at short lead time still leaves much to be desired. Beyond surface ocean data delivered by moored buoys and satellites in real time, the RTSMs can provide the time-depth variations of temperature and velocity at the subsurface and intermediate layers (e.g., the Equatorial Undercurrent variability), which also play a crucial role in the evolution of ENSO. Assimilation of these data will further improve the ENSO prediction skill. Deep-sea data acquiring in real time are also useful to many marine applications, including shipping, fishing, ocean emergent search and rescue, and pollution monitoring. RTSMs will provide data without the need of the use of a ship. This reduces the cost of ship and the risk of data loss due to mooring damage, making the fixed observation system in a more cost-effective manner.

Keywords: Real-Time Subsurface Mooring, Global Ocean Observing Systems

©2019. Japan Geoscience Union. All Right Reserved.

Seasonal Variation of the Mixed Layer Depth at 60°S and its governing dynamics

*Matheus Ferreira Azevedo[1], Yujiro Kitade[1], Shigeru Aoki[2]

1. Tokyo University of Marine Science and Technology, 2. Institute of Low Temperature Science, Hokkaido University

In this research, data from a yearlong M-TRITON type mooring system deployed in 2012 is used to study the seasonal variability of the dynamics governing the Southern Ocean and its influence on the mixed layer depth by measuring temperature, salinity and current velocity data. GHRSST Satellite data and reanalysis ERA-interim wind data were used to complement the mooring, identifying spatial variation in wind and sea surface temperature (SST). This is relevant in the context of coupling readily available surface information (via satellite) and punctual information from ship CTD casts with corresponding subsurface phenomena.

A major factor of mixing was identified as the work on upper-ocean inertial motions (period T =13.8186 hours) associated with variable wind forcing, corroborating with the work of Alford (2001, 2003), Watanabe & Hibiya (2002) and Furuichi et al. (2008). Strong wind peaks, were observed to break stability, parametrized as the Buoyancy frequency N^2, which varied from an order of 10^{-4} s^{-2} to 0 or negative values in the original mixed layer depth (MLD) at the period, while enhancing stability at deeper layers in the same proportion it decreases at the layer above. As a consequence, the MLD increases by around 25m during these events. Wind forcing was found to influence stability and MLD not only through the work of storm induced near-inertial motion but also through meso-scale meridional transport, modulating the frontal structure of the Antarctic Convergence. During winter, the system response to wind weakened as surface cooling induced large scale convection. In particular a cold front reached the mooring at May 28th, starting the convection process. MLD responded by deepening to as far as 150m, and upward salinity flux could be observed.

Strong shear could be observed, usually bellow the mixed layer and generally agreeing with other reports of momentum penetration beyond the scalar mixed layer (e.g. Johnston & Rudnick, 2009). Shear comparison could not be made throughout the year, however, as the mixed layer goes bellow the ADCP detection range during winter. The strong stratification at the base of the mixed layer was seen to generate a complex internal wave field, where shear instability dissipates through high frequency internal waves of period between 2 and 4 hours. These waves seem to become trapped at the stratified layer and evolve to inertial period oscillations, increasing in amplitude until they break, generating high frequency waves once again. This process was observed to repeat at every mixed layer deepening event, either in summer or winter. The relation between internal waves, mixing and MLD at the Southern Ocean is a step to understand nutrient availability and the formation of important water masses of global influence.

Keywords: Southern Ocean, Internal waves, Mixing

©2019. Japan Geoscience Union. All Right Reserved.

21st-Century Flood Hazards along the U.S. Atlantic Coast: Impacts of Sea Level Rise and Tropical Cyclone Climatology Change

*Reza Marsooli[1], Ning Lin[2], Kerry Emanuel[3]

1. Stevens Institute of Technology, 2. Princeton University, 3. Massachusetts Institute of Technology

Flooding due to tropical cyclones (TC) is among the most destructive coastal hazards along the U.S. Atlantic Coast. TC-induced coastal flooding will worsen under sea level rise (SLR) and climate change. To effectively adapt to these evolving hazards, it is essential to understand potential changes in future flood return levels. The present study investigates the impact of 21st-century sea level and TC climatology on flood return levels along the U.S. East and Gulf Coasts. We use extreme value theory and combine probabilistic estimates of sea level rise and TC storm tides to determine flood return levels for the historical period of 1980-2005 and the future period of 2070-2100 (under the emission scenario RCP8.5). A basin-scale hydrodynamic model is implemented to simulate storm tides for large numbers of synthetic TCs that are generated by a statistical-deterministic TC model under climate conditions observed during the historical period and projected by six climate models for the future period. We present and discuss flood return level projections and the contribution of sea level rise and TC climatology change to the projected changes in the return levels.

Keywords: Storm Surge, Tropical Cyclone, Sea Level Rise, Climate Change, U.S. Atlantic Coast

©2019. Japan Geoscience Union. All Right Reserved.

The Effect of Ocean Waves on an Explosive Cyclone Development: Investigation with a Coupled Model

*Yuki Kita[1], Takuji Waseda[1]

1. University of Tokyo

Violent ocean waves are generated by the explosive cyclone. Since ocean waves affect the development of tropical cyclones, the impacts of ocean waves on the development of explosive cyclones are expected. Ocean waves have several impacts on the atmospheric surface layer: surface friction, sea spray, and momentum flux. We implemented sensitivity experiments to clarify how much ocean waves affect the development of an explosive cyclone with an atmosphere-ocean-wave coupled model, especially focusing on surface friction affected by ocean waves. The test case is the explosive cyclone emerged in early January 2018 over the Northwestern Atlantic. The atmospheric model is Weather Research and Forecasting Model (WRF), the ocean model is Coastal and Regional Ocean COmmunity model (CROCO), and the ocean wave model is WAVEWATCH III (WW3). We compared the numerical simulation results between the WRF-CROCO model and the WRF-CROCO-WW3 model. In the WRF-CROCO-WW3 coupled model considering ocean wave impacts just on surface friction, it is found that the deepening of the explosive cyclone was intensified by about 2hPa in the central sea level pressure, and the center track slightly shifted. In the fully coupled model, the surface roughness reduced and the wind speed was intensified by and large. Compared with observation data above the ocean, the fully coupled model had more accurate wind speed and sea level pressure than the atmosphere-ocean coupled model. It is also revealed that the boundary surface layer scheme in the atmospheric model is critical for accurate reproduction of surface atmospheric process and ocean waves. To reproduce accurate wind speed and wave height, the YSU (Yonsei University) scheme had a better performance than the MYNN (Mellor-Yamada-Nakanishi-Niino) 3rd scheme. As the next step, it is necessary that a coupled model takes into account the turbulent momentum flux produced by ocean waves to reproduce complete accurate air-sea interactions.

Keywords: Explosive cyclone, Ocean surface waves, Air-sea interaction, Coupled model

©2019. Japan Geoscience Union. All Right Reserved.

[J] Poster | A (Atmospheric and Hydrospheric Sciences)：A-OS Ocean Sciences & Ocean Environment

Tue. May 28, 2019 5:15 PM - 6:30 PM JST | Tue. May 28, 2019 8:15 AM - 9:30 AM UTC | Poster Hall International Exhibition Hall8, Makuhari Messe_8

[A-OS18] Physical Oceanography (General)

convener:Yoshimi Kawai(Research and Development Center for Global Change, Japan Agency for Marine-Earth Science and Technology), Tomoki Tozuka(Department of Earth and Planetary Science, Graduate School of Science, The University of Tokyo), Kitade Yujiro(Tokyo University of Marine Science and Technology)

This session invites presentations on a wide variety of topics related to physical oceanography.

[AOS18-P01] Mathematical modeling for initial profile of tsunami by instantaneous- or slow-faulting

*Chi-Min Liu[1] (1.Chienkuo Technology University)

[AOS18-P02] Geoid height and sea surface changes due to the 2004 Sumatra-Andaman earthquake and the 2012 Indian-Ocean earthquake from satellite gravimetry and satellite altimetry

★Invited Papers

*Yusaku Tanaka[1] (1.Earthquake Research Institute)

[AOS18-P03] An irregularly shaped warm eddy observed by Chinese underwater gliders

*Huabin MAO[1] (1.South China Sea Institute of Oceanology)

[AOS18-P04] sea surface cooling in the northern South China Sea observed using Chinese underwater glider

*Chunhua Qiu[1] (1.Sun Yat-sen University)

[AOS18-P05] Airborne SAR observation of dependence of ocean surface backscattering on wind direction

*Akitsugu Nadai[1] (1.NICT National Institute of Information and Communications Technology)

Mathematical modeling for initial profile of tsunami by instantaneous- or slow-faulting

*Chi-Min Liu[1]

1. Chienkuo Technology University

Tsunami is one of the most catastrophic disasters in the world. Most of them are generated by the faultings. As the faulting speed is of several thousand meters per second, many tsunamis are generated instantaneously and therefore their initial profiles are assumed to be identical to the profiles of the uplifted sea bottom. This assumption is often adopted in numerical simulation for the sake of simplification. However, in some faulting cases, the speed is comparatively slow which results in the profile discrepancy between sea bottom and surface. To this end, present study aims to mathematically analyze the initial wave profiles generated by either the instantaneous or slow faulting. Results show that the initial profiles greatly differ from the variation of sea bottom for the slow-faulting scenarios.

Keywords: tsunami, slow-faulting, initial profile

©2019. Japan Geoscience Union. All Right Reserved.

Geoid height and sea surface changes due to the 2004 Sumatra-Andaman earthquake and the 2012 Indian-Ocean earthquake from satellite gravimetry and satellite altimetry

*Yusaku Tanaka[1]

1. Earthquake Research Institute

A research article about irreversible local geoid height changes on ocean area by the 2004 and 2012 Sumatra huge earthquakes is in press as of 18th February, 2019 (Tanaka et al., accepted by TAO in 2018). I hope to introduce the results in the session of ocean sciences. The abstract of the article is below.

We first report the results from analyzing the GRACE satellite data for the co-seismic and long-term post-seismic changes in the Earth’ s gravity field and geoid height induced by the 2004 Sumatra-Andaman earthquake (Mw9.2) and the 2012 Indian-Ocean earthquake (Mw8.6). The results suggest that the two earthquakes have changed the gravity field and geoid height irreversibly (as opposed to cyclically). We next use satellite ocean altimetry measurements to search for the geoid height change induced by the Sumatra-Andaman earthquake, employing an effective method of extracting coherent space-temporal signals, namely the empirical orthogonal functions (EOF) analysis. Our results demonstrate that the sea level variation in the studied (tropical) area during the studied (10-year) period is dominated by the strong steric changes related to ENSO, to the point that the earthquake-induced signals, even using EOF for the largest earthquakes, are obscured and thus undetectable by ocean altimetry. However, this also means that steric and non-steric changes can be observed separately from artificial satellites.

[Figure] (a) Coseismic geoid height changes induced by the 2004 Sumatra-Andaman earthquake (its rectangular faults are depicted). (b) The sum of short- and long-term post-seismic geoid height changes from the earthquake occurrences till May 2016. (c) The sum of (a) + (b), i.e. co- and post-seismic geoid height changes. (d, e, f) The same as (a, b, c) but for the 2012 Sumatra/Indian-Ocean earthquake. (g) The total geoid height changes by the two earthquakes. The fault mechanisms of the two earthquakes are shown at the epicenters. (h) The time series of geoid height changes at the red circles marked in (a)-(g). The overall mean and average seasonal changes have been removed. The black dots with error bars (assumed uniform in time and have been scaled with post-fit residuals) show monthly gravity data and the red curve is the least-squares fit. The two vertical green lines indicates the occurrences of the two earthquakes.

Keywords: Geoid height change, Sea level variation, Satellite gravimetry (GRACE), Satellite altimetry (Jason), earthquake

©2019. Japan Geoscience Union. All Right Reserved.

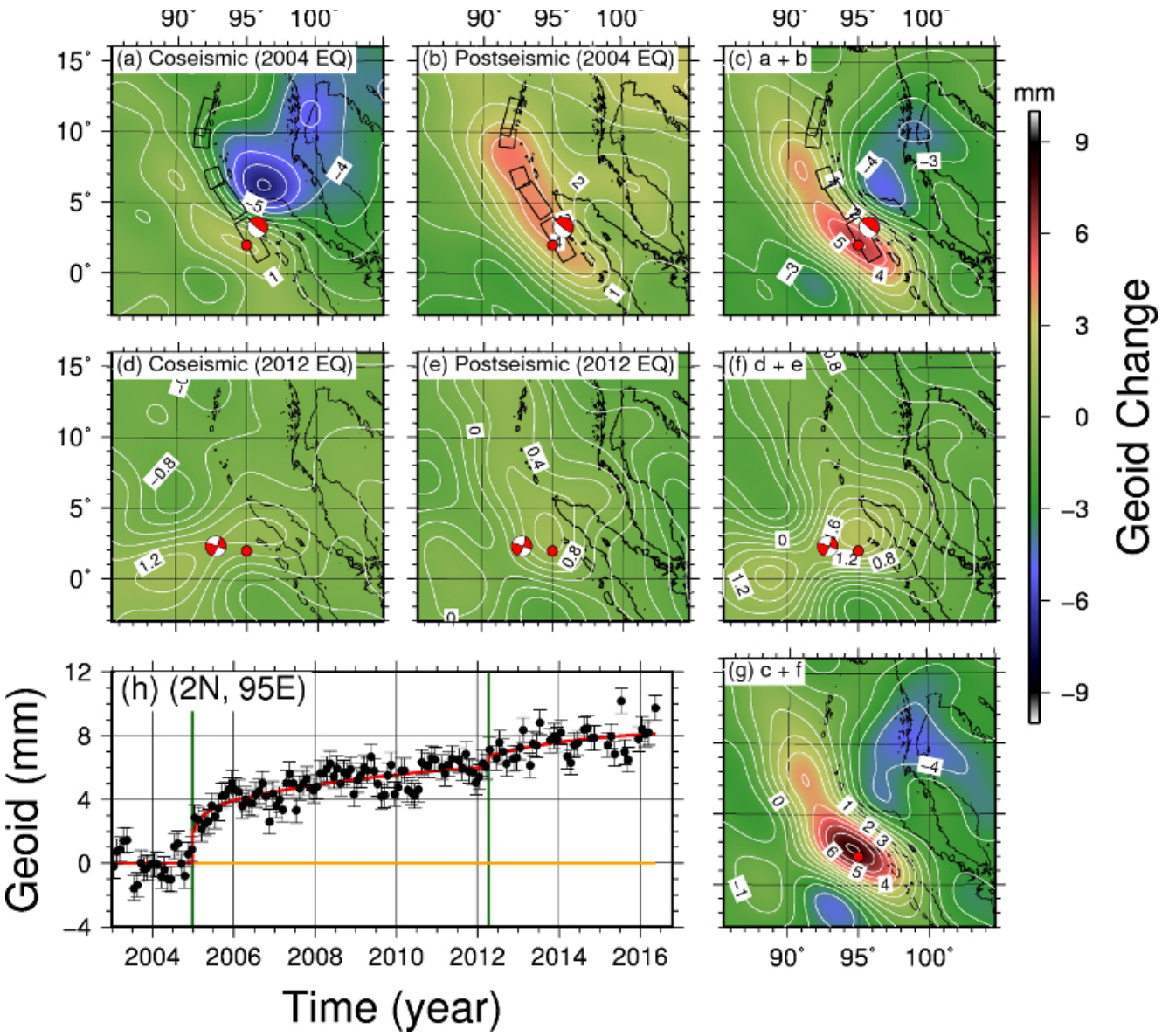

©2019. Japan Geoscience Union. All Right Reserved.

An irregularly shaped warm eddy observed by Chinese underwater gliders

*Huabin MAO[1]

1. South China Sea Institute of Oceanology

Mesoscale eddies are important for transporting oceanic energy and matter. We investigated the three-dimensional structure
of an irregularly shaped warm eddy using three Chinese underwater gliders and satellite data during May 2015 in the northern
South China Sea. The warm eddy lasted for 2 months, remained quasi-steady, and had a mean radius of ~ 70 km from May
10 to May 31. The heat contents observed along the two glider tracks differed markedly, by 2 ×109 J/m2, which reflected an
imbalance in the geostrophic and tangential velocity distributions of the eddy. The geostrophic/tangential velocity decreased/
increased with depth within the warm eddy. The maximum tangential velocities calculated using the datasets from the two
gliders were 0.8 and 0.25 m/s, respectively, confirming that the shape of the warm eddy was horizontally asymmetrical.
Large errors can arise when the heat, energy, and matter transport for an irregularly shaped eddy are estimated using a regular
circular model. We suggest that more intersecting glider tracks should be used to retrieve the three-dimensional eddy structure,
and that those tracks should be better designed. The irregular shape of the warm eddy was likely induced by oceanic
currents such as the wind-induced Ekman current. Further study is needed to elucidate the eddy–current interactions and
the mechanisms thereof.

Keywords: Irregular shape, Warm eddy, Chinese underwater glider

©2019. Japan Geoscience Union. All Right Reserved.

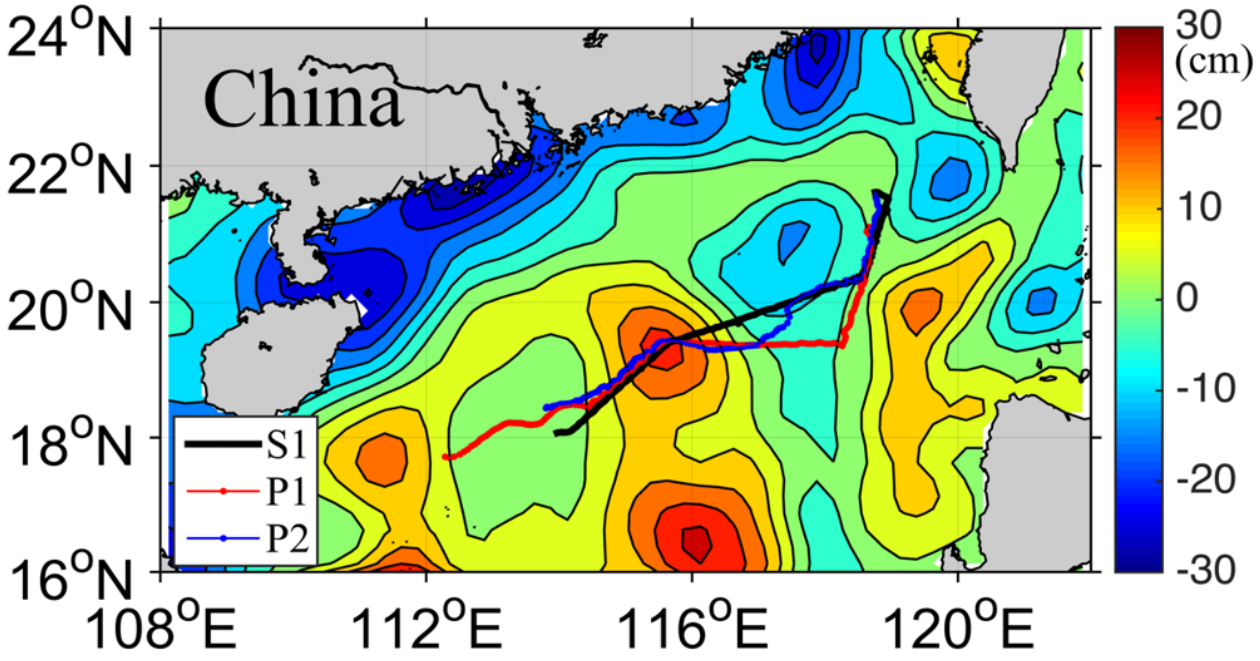

©2019. Japan Geoscience Union. All Right Reserved.

sea surface cooling in the northern South China Sea observed using Chinese underwater glider

*Chunhua Qiu[1]

1. Sun Yat-sen University

Based on 26 days of Chinese Sea-wing underwater glider and satellite microwave data, we documented cooling of the upper mixed layer in response to changes in the wind in 9.19-10.15, 2014. The sea-wing underwater glider measured 177 profiles of temperature, salinity, and pressure. we estimated temperature tendencies using a mixed layer model. The entrainment rate and latent heat flux were the two major components that regulated cooling of the mixed layer, and that the Ekman advection and sensible heat flux were small.

Keywords: mixed layer, glider, south china sea

©2019. Japan Geoscience Union. All Right Reserved.

Airborne SAR observation of dependence of ocean surface backscattering on wind direction

*Akitsugu Nadai[1]

1. NICT National Institute of Information and Communications Technology

Synthetic aperture radar (SAR) has attracted attention as an oceanwinds measurement technique in coastal areas where high spatial resolution is required.

Oceanwinds measurement by SAR requires the normalized radar cross section (NRCS) model of ocean surface backscattering. However, the NRCS models currently developed is statistically analyzed by combination of NRCS measured by spaceborne SAR and meteorological data. In this study, by carrying out airborne SAR observations with multiple illumination directions in a short time, direct measurement of wind direction dependence of the NRCS at a certain wind speed was tried.

Using a model function of NRCS with the same format as the NRCS models, the coefficients of oceanwinds dependence of NRCS are determined by the airborne SAR. The results determined by airborne SAR are compared with NRCS models and results of the airborne scatterometer.

Regarding the wind speed dependence, the results of the airborne SAR showed good agreement with that of the airborne scatterometer. On the other hand, two NRCS models give a fairly large NRCS. In addition, the change of wind speed dependence with incidence angle determined by the airborne SAR and the airborne scatterometer show different tendency with those of NRCS models.

Regarding the wind direction dependence, the results by airborne SAR shows significantly large wind direction dependence compared with the NRCS model at the incidence angle of 32 degrees. On the other hand, the wind direction dependence by the airborne SAR almost agrees with that of the airborne scatterometer at the incidence angle of 32 degrees.

Comparing the measured NRCS by the airborne SAR with that by the airborne scatterometer, the possibility of influence of the observation configuration on measurement accuracy of the wind direction dependence is suggested.

In addition, the influence of size of spatial averaging may be important on the accuracy of oceanwinds measurement using SAR. Though the high spatial resolution oceanwinds measurement is expected for SAR, ocean surface phenomena like swells and ship wakes may influence the oceanwinds measurement by SAR. Moreover, SAR data cannot be free from speckle noise. The influence of spatial averaging size has to be grasped.

Keywords: Oceanwinds, Synthetic aperture radar, Ocean surface backscattering, Normalized radar cross section

©2019. Japan Geoscience Union. All Right Reserved.

[J] Oral | A (Atmospheric and Hydrospheric Sciences)：A-OS Ocean Sciences & Ocean Environment

Tue. May 28, 2019 9:00 AM - 10:30 AM JST | Tue. May 28, 2019 12:00 AM - 1:30 AM UTC | 106 1F

[A-OS20] Global ocean observing systems, obtained results and system optimization: toward OceanObs19

convener:Shigeki Hosoda(Japan Marine-Earth Science and Technology), Shuhei Masuda(Japan Agency for Marine-Earth Science and Technology), Yosuke Fujii(Meteorological Research Institute, Japan Meteorological Agency), Fujiki Tetsuichi(Japan Agency for Marine-Earth Science and Technology), Chairperson:Shigeki Hosoda(Japan Agency for Marine-Earth Science and Technology)

Almost twenty years have been passed since the beginning of Argo programme to construct global ocean observing system. The Argo observing system have been covering the global ocean with more than 3000 Argo floats with collaboration of many countries. The Argo is well known as one of the best practices of ocean observing systems, as lots of scientific results and social/industrial benefits have been gained based on indispensable huge amount of oceanic data which has never obtained before. Recently, the Argo observing system is rapidly expanded to monitor deeper ocean (Deep Argo; >4000m depth) and bio-geochemical parameters (Biogeochemical Argo) in addition to upper layer temperature and salinity (Core Argo; <2000m depth).
On the other hand, sustainability of the Argo is not guaranteed and its observing array is still developing as international infrastructure. For example, Argo float distribution recently tends to be inhomogeneous since a part of float deployment and operation is still conducted by voluntary works. Therefore, improving the observing systems to be more effective and sustainable is a mandatory task in the oceanographic community. In this background, various efforts are forwarded to evaluate impacts of ocean observations by the support of GODAE OceanView which is endorsing the Argo programme. In coming OceanObs19, development, expansion and enhancement of the sustainability of the Argo observing systems will be discussed based on scientific results and application researches.
In this session, current status, recent issues, future works on large-scale ocean observing systems are discussed in related to Argo and other research infrastructures such as GO-SHIP, OceanSITES etc., focusing on the global ocean observing system in coming next decade.

9:00 AM - 9:15 AM JST | 12:00 AM - 12:15 AM UTC

[AOS20-01] Global Ocean Observing System: The Past, the Present and the Future

★Invited Papers

*Toshio Suga[1,2] (1.Graduate School of Science, Tohoku University, 2.JAMSTEC)

9:15 AM - 9:30 AM JST | 12:15 AM - 12:30 AM UTC

[AOS20-02] Observed long-term change and variability in the global upper-ocean stratification

*Ryohei Yamaguchi[1], Toshio Suga[1,2] (1.Graduate School of Science, Tohoku University, 2.Japan Agency for Marine-Earth Science and Technology)

9:30 AM - 9:45 AM JST | 12:30 AM - 12:45 AM UTC

[AOS20-03] Estimation of changes in salinity and dissolved oxygen based on observational networks

★Invited Papers

*Shinya Kouketsu[1] (1.JAMSTEC Japan Agency for Marine-Earth Science and Technology)

9:45 AM - 10:00 AM JST | 12:45 AM - 1:00 AM UTC

[AOS20-04] Remotely forced decadal physical and biogeochemical variability of North Pacific Subtropical Mode Water over the last 40 years

*Daisuke Sasano[1], Eitarou Oka[2], Yudai Yamada[2], Enyo Kazutaka[1], Toshiya Nakano[1], Masao Ishii[3] (1.Japan Meteorological Agency, 2.Atmosphere and Ocean Research Institute, The University of Tokyo, 3.Meteorological Research Institute)

10:00 AM - 10:15 AM JST | 1:00 AM - 1:15 AM UTC

[AOS20-05] Asessing the impact of the global ocean observing system using ocean data assimilation systems

*Yosuke Fujii[1] (1.Meteorological Research Institute, Japan Meteorological Agency)

10:15 AM - 10:30 AM JST | 1:15 AM - 1:30 AM UTC

[AOS20-06] **Global ocean state estimation with new float observations**

*Shuhei Masuda[1], Satoshi Osafune[1], Tadashi Hemmi[1] (1.Japan Agency for Marine-Earth Science and Technology)

Global Ocean Observing System: The Past, the Present and the Future

*Toshio Suga[1,2]

1. Graduate School of Science, Tohoku University, 2. JAMSTEC

A global ocean observing system with the first letters capitalized is the name of the international program led by the Intergovernmental Oceanography Committee (IOC) of the UNESCO: the Global Ocean Observing System (GOOS). GOOS is responsible for coordinating global ocean observations for three critical themes: climate, operational services, and marine ecosystem health. GOOS was launched in 1991 by the IOC in response to calls from the Second World Climate Congress held in 1990. The ocean research community has been intrinsically involved in the subsequent development of GOOS. The two international conferences, OceanObs '99 and OceanObs' 09, were milestones both for GOOS as the international program and for the global ocean observation system as the system consisting of various observing networks. Focusing on the outcomes and significance of these two conferences, the history of GOOS will be briefly described. At the moment, preparation of OceanObs'19 to be held this coming September is going on. The objective of the conference is to "bring people from all over the planet together to communicate the decadal progress of ocean observing networks and to chart innovative solutions to society’ s growing needs for ocean information in the coming decade." The relevant and background information of OceanObs'19 will be presented and the role of the research community will be discussed.

Keywords: Global Ocean Observing System, Essential Climate Variables, Essential Ocean Variables, observing network, Framework for Ocean Observing

©2019. Japan Geoscience Union. All Right Reserved.

Observed long-term change and variability in the global upper-ocean stratification

*Ryohei Yamaguchi[1], Toshio Suga[1,2]

1. Graduate School of Science, Tohoku University, 2. Japan Agency for Marine-Earth Science and Technology

With the progress of global warming, enhanced upper-ocean thermal stratification from the 1970s has been reported by IPCC AR5. Many studies on future climate projection using CMIP climate models also point out that upper-ocean stratification will strengthen in this century. The strengthened stratification will reduce vertical nutrient supply from the subsurface by futher stabilizing the upper-ocean water column, and then the primary production of the whole ocean is concerned to decrease.

However, large uncertainties in the observational estimate of the long-term change in the upper-ocean stratification still remain. Strengthening trend of the upper-ocean thermal stratification due to the surface intensification of the warming signals has been detected from estimation using globally-averaged sea surface and subsurface temperature time series. On the other hand, some observational studies focusing on some specific regions or using relatively short time series demonstrate that the upper-ocean stratifications are weakening in recent decades, rather than strengthening associated with global warming.

We investigated globally the long-term change and variability in the upper-ocean stratification defined here as the difference between the surface and subsurface density. To resolve spatial patterns of the trends and superposed decadal variability, we used temperature and salinity observations with as spatial and temporal coverage as wide as possible from World Ocean Database 2013. As a result, strengthening trends of the upper-ocean stratification associated with global warming were detected over the global ocean, except for the Arctic Ocean. In the global average, the increase in density stratification corresponds to a 6.6–11.8% of the mean stratification from the 1960s. In addition to the well-documented cause, that is the surface intensified warming, the subsurface temperature changes and haline stratification changes also have significant impacts on the long-term changes in the upper-ocean stratification. The decadal/interannual variabilities in the upper-ocean stratification associated with each particular climate mode are also detected in some ocean regions: The density stratification is correlated with the Niño 3.4 index in the tropical Pacific, negatively lagged correlated with the North Atlantic Oscillation (NAO) index in the North Atlantic, and shows correspondences with SST variations associated with the Pacific Decadal Oscillation (PDO) in the North Pacific.

©2019. Japan Geoscience Union. All Right Reserved.

Estimation of changes in salinity and dissolved oxygen based on observational networks

*Shinya Kouketsu[1]

1. JAMSTEC Japan Agency for Marine-Earth Science and Technology

Changes in temperature and salinity can be captured by Argo float networks more clearly than before the 2000s. For example, the global changes in ocean heat content can be comparable to the ones in sea surface height and net radiative flux into the earth system. Furthermore, various studies have been focusing on the changes in water masses, especially around surface layers. However, quantitative evaluation of regional changes has not been sufficiently clarified. For example, the salinity changes in the deeper layers cannot be easily captured by a float observation due to measurement uncertainty, and the changes in dissolved materials (ex. dissolved oxygen) remained not to be observed sufficiently. In this study, with the combination of autonomous observations and high accurate ship-based observations, we try to examine the possibility to capture and evaluate more accurately long-term changes with observation network.

As the first step, I will present the results based on the monthly salinity (temperature) distributions on the isopycnal surfaces obtained from Argo float observations. Based on the dataset, the long-term mean circulation with the spatial distribution of diffusivity coefficients was estimated, and the budgets for salinity (and temperature) changes in the recent decade were calculated. Especially, in the deeper layer (below 400m), the diapycnal diffusion effects were relatively large to the salinity (and temperature) increases. The salinity (and temperature) increases on the isopycnal surfaces might be consistent with the temperature increased on iso-depths. As the large-scale patterns of the changes revealed by the datasets were similar to the ones detected by twice occupations of the highest accurate observations, the salinity (and temperature) changes in this study were not so much influenced by biases in autonomous measurements (especially of salinity), and the present observation systems might be able to detect such small changes potentially.

The dissolved oxygen budgets were also estimated in the North Pacific with a long-term climatological distribution of the oxygen. The residuals of the budgets seemed to be consistent with the oxygen utilization estimation in previous studies. However, in some regions, temporal changes in oxygen, which included in temporal changes due to the changes in circulations and biological activities, were in the same order of magnitude of the residuals. Thus, spatial and temporal dense (and relatively high accurate) observation network will be needed to clarify the roles of mean biological activities on oxygen circulations as well as the temporal variabilities.

In the presentation, I will show some results of comparisons with assimilation or numerical models, and the other results (regional changes) appearing in the dataset.

Keywords: ocean observations, long-term ocean variability

©2019. Japan Geoscience Union. All Right Reserved.

Remotely forced decadal physical and biogeochemical variability of North Pacific Subtropical Mode Water over the last 40 years

*Daisuke Sasano[1], Eitarou Oka[2], Yudai Yamada[2], Enyo Kazutaka[1], Toshiya Nakano[1], Masao Ishii[3]

1. Japan Meteorological Agency, 2. Atmosphere and Ocean Research Institute, The University of Tokyo, 3. Meteorological Research Institute

Half-century-long observations at the 137ºE hydrographic section across the western North Pacific have been analyzed to demonstrate remotely forced decadal physical and biogeochemical variability of Subtropical Mode Water (STMW) over the last 40 years. During unstable periods of the Kuroshio Extension (KE) that lagged the warm phase of the Pacific Decadal Oscillation by 3–4 years, high regional eddy activity reduced the formation rate and salinity of STMW in its main formation region south of the KE. At the 137ºE section south of Japan, decreasing advection of oxygen-rich STMW from the east resulted in decreases of dissolved oxygen and pH and increases of nutrients and dissolved inorganic carbon, accelerating acidification. Such changes reversed and acidification slowed down during stable-KE periods, especially in the current period since 2010 exhibiting a hiatus of acidification. These results indicate a new mechanism by which climate variability affects physical and biogeochemical structure in the ocean interior.

Keywords: North Pacific Subtropical Mode Water, Kuroshio Extension, Decadal variability, physical and biogeochemical linkage

©2019. Japan Geoscience Union. All Right Reserved.

Asessing the impact of the global ocean observing system using ocean data assimilation systems

*Yosuke Fujii[1]

1. Meteorological Research Institute, Japan Meteorological Agency

Ocean and climate prediction systems are one of the important applications of the data observed by the global ocean observing system. In a prediction system, the oceanic field is estimated as accurately as possible through an ocean data assimilation system first, and then forecast integration of a numerical model is started using the estimated field as the oceanic initial condition. Data assimilation systems require ocean observation data for estimating the oceanic field, and the accuracy of the predictions, thus, severely depends on how much oceanic information effective for the predictions are included in the assimilated observation data, as well as the quality of the numerical model and the data assimilation scheme. Therefore, developing observing systems is an important factor of improving the prediction skills. Meanwhile, building up and maintenance of an observing system are conducted by public money or funds by stakeholders, and in order to sustain and to extend the observing system, we need to show that the system brings social benefits that is equivalent to or more than the investigation. Since observation data are exploited in the society mostly through the prediction systems, assessing impact of observation data on the accuracy of analysis and predictions in ocean data assimilation and prediction systems is an effective way to show the value of the observing system in the society.
GODAE OceanView (Its follow-on program “Oceanpredict” will take over the activity from May 2019) has established the Observing System Evaluation Task Team (OS-Eval TT) since the program was started, promotes data-impact assessments and information sharing for that, and builds up international collaboration for the relevant activities. These activities are also supported by CLIVAR Global Synthesis and Observation panel (GSOP). Operational centers, such as JMA and ECMWF, and research institutes, such as JAMSTEC and Scripps Institution of Oceanography, conducted observing system evaluation studies for various observations such as Argo, TAO-TRITON, and satellite altimetry under these supports. Those results are exploited in the evaluation of the TAO-TRIRON array for its reconstruction for example, but they have a limitation due to its system dependency and the importance of multi-system evaluation with common metrics is indicated. Achievements and resent challenges of observing system evaluation studies are summarized in a community white paper for OceanObs’19. This presentation will introduce some achievements of observing system evaluation studies and show a future perspective on this field.

Keywords: Observing System Evaluation, Ocean Data Assimilation, GODAE OceanView, Ocean Prediction, OceanObs'19

©2019. Japan Geoscience Union. All Right Reserved.

Global ocean state estimation with new float observations

*Shuhei Masuda[1], Satoshi Osafune[1], Tadashi Hemmi[1]

1. Japan Agency for Marine-Earth Science and Technology

Argo floats are successfully contributing to global ocean state estimation. As the important roles of deep ocean to global changes has been recognized, sustainable deep ocean monitoring networks that use autonomous profiling floats have been widely proposed by the ocean observation community. An increasing number of deep-float deployment initiatives around the world. Deployed floats promise to provide unprecedented deep ocean information. Here we applied deep float data deployed by JAMSTEC to a deep ocean state estimation by using a four-dimensional variational approach. The results demonstrate that the available float data enables some corrections of the modeled ocean state locally for each float although the impact of the data on a basin-scale deep ocean state estimation was still limited in this study due to sparseness of used float data. This implies strategic deployments of deep float in the world’s ocean can immediately contribute to improvement of a current global deep ocean state estimation.

Keywords: Ocean Observation, Global, data assimilation

©2019. Japan Geoscience Union. All Right Reserved.

[J] Poster | A (Atmospheric and Hydrospheric Sciences)：A-OS Ocean Sciences & Ocean Environment

Tue. May 28, 2019 3:30 PM - 5:00 PM JST | Tue. May 28, 2019 6:30 AM - 8:00 AM UTC | Poster Hall International Exhibition Hall8, Makuhari Messe_6

[A-OS20] Global ocean observing systems, obtained results and system optimization: toward OceanObs19

convener:Shigeki Hosoda(Japan Marine-Earth Science and Technology), Shuhei Masuda(Japan Agency for Marine-Earth Science and Technology), Yosuke Fujii(Meteorological Research Institute, Japan Meteorological Agency), Fujiki Tetsuichi(Japan Agency for Marine-Earth Science and Technology)

Almost twenty years have been passed since the beginning of Argo programme to construct global ocean observing system. The Argo observing system have been covering the global ocean with more than 3000 Argo floats with collaboration of many countries. The Argo is well known as one of the best practices of ocean observing systems, as lots of scientific results and social/industrial benefits have been gained based on indispensable huge amount of oceanic data which has never obtained before. Recently, the Argo observing system is rapidly expanded to monitor deeper ocean (Deep Argo; >4000m depth) and bio-geochemical parameters (Biogeochemical Argo) in addition to upper layer temperature and salinity (Core Argo; <2000m depth).
On the other hand, sustainability of the Argo is not guaranteed and its observing array is still developing as international infrastructure. For example, Argo float distribution recently tends to be inhomogeneous since a part of float deployment and operation is still conducted by voluntary works. Therefore, improving the observing systems to be more effective and sustainable is a mandatory task in the oceanographic community. In this background, various efforts are forwarded to evaluate impacts of ocean observations by the support of GODAE OceanView which is endorsing the Argo programme. In coming OceanObs19, development, expansion and enhancement of the sustainability of the Argo observing systems will be discussed based on scientific results and application researches.
In this session, current status, recent issues, future works on large-scale ocean observing systems are discussed in related to Argo and other research infrastructures such as GO-SHIP, OceanSITES etc., focusing on the global ocean observing system in coming next decade.

[AOS20-P01] Fresh bias with pressure dependency at the measurements of SBE 41CP for deep float

*Taiyo Kobayashi[1] (1.Japan Agency for Marine-Earth Science and Technology)

[AOS20-P02] Long-term thermohaline variations in the North Pacific subtropical gyre observed by repeat hydrography along the 165°E meridian

*Yuma Kawakami[1,2], Yoshiteru Kitamura[1], Toshiya Nakano[1,2] (1.Japan Meteorological Agency, 2.Meteorological Research Institute)

[AOS20-P03] First detection of chlorofluorocarbons into bottom layer in the Melanesian Basin of the North Pacific

*Toshiya NAKANO[1], Kazutaka ENYO[1], Daisuke SASANO[1], Shogo URAKAWA[2], Hiroyuki TSUJINO[2], Hideyuki NAKANO[2], Masao ISHII[2] (1.Japan Meteorological Agency, 2.Meteorological Research Institute)

[AOS20-P04] **Global grid mapping of temperature and salinity based on Argo float data**

*Shigeki Hosoda[1] (1.Japan Marine-Earth Science and Technology)

[AOS20-P05] **Evolutions of water mass anomalies in the upper North Pacific based on Argo data, in STMW, ESTMW, and CMW.**

*Tong Wang[1], Toshio Suga[1,2], Shinya Kouketsu[2] (1.Graduate School of Science, Tohoku University, 2.Research and Development Center for Global Change, JAMSTEC)

[AOS20-P06] Impacts of temperature measurements from sea turtles on seasonal prediction around the Arafura Sea

*Takeshi Doi[1], Andrea Storto[2], Takuya Fukuoka[3], Hiroyuki Suganuma[4], Katsufumi Sato[3] (1.JAMSTEC, 2.CMRE, 3.The University of Tokyo, 4.ELNA)

[AOS20-P07] Physical and biogeochemical processes from winter to spring in the south of the Kuroshio Extension

*Chiho Sukigara[1], Ryuichiro Inoue[2], Takeyoshi Nagai[1], Andrea J Fassbender[3], Yuichiro Takeshita[3], Stuart P Bishop[4], Eitarou Oka[5] (1.Tokyo University of Marine Science and Technology, 2.Japan Agency for Marine-Earth Science and Technology, 3.Monterey Bay Aquarium Research Institute, 4.North Carolina State University, 5.The University of Tokyo)

Fresh bias with pressure dependency at the measurements of SBE 41CP for deep float

*Taiyo Kobayashi[1]

1. Japan Agency for Marine-Earth Science and Technology

Fresh bias was found at the measurements by deep float model of SBE 41CP CTD sensor on Deep NINJA floats. Its details were clarified and possible causes were discussed.

Keywords: Deep Argo, salinity measurements

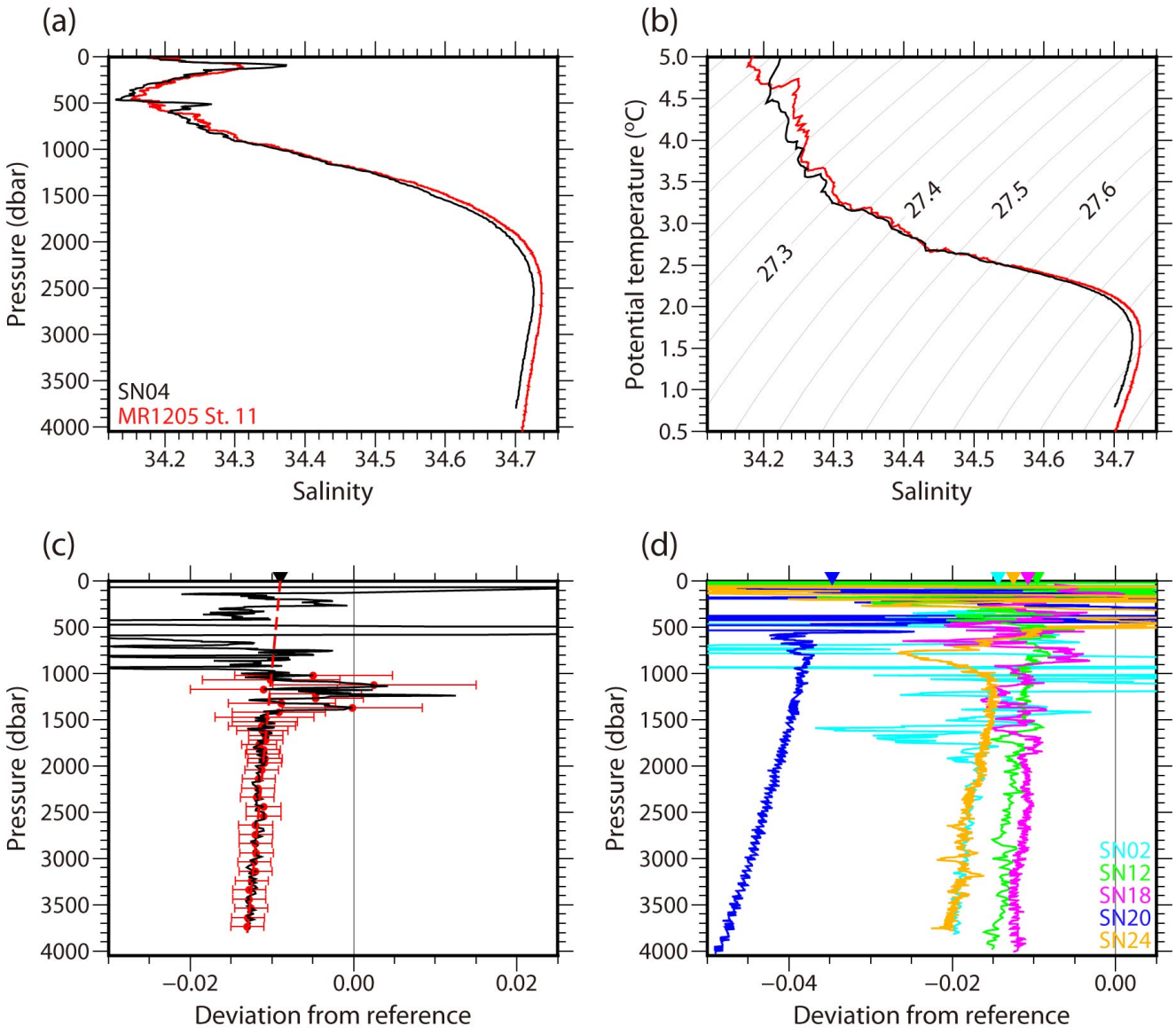

©2019. Japan Geoscience Union. All Right Reserved.

Long-term thermohaline variations in the North Pacific subtropical gyre observed by repeat hydrography along the 165°E meridian

*Yuma Kawakami[1,2], Yoshiteru Kitamura[1], Toshiya Nakano[1,2]

1. Japan Meteorological Agency, 2. Meteorological Research Institute

Recently, long-term thermohaline changes in the surface and subsurface of the world ocean, such as the global warming and the intensification of salinity contrast between basins or regions, are continuously reported. Since changes of temperature and salinity greatly influence not only the density-driven geostrophic ocean circulation but also the marine ecosystem, sea levels and climates, monitoring of the ocean variations and understandings of those mechanisms are important.

Numerous scientific knowledges about thermohaline variations in the subsurface and intermediate layers of the North Pacific subtropical gyre including significant freshening in the thermocline/halocline and fluctuation in a decadal timescale were given by previous researches. However, many of them described in the western part of the subtropical gyre, and studies in its central part have been more limited partially due to the lack of data even though large scale atmospheric forcing generates great long-term thermohaline variations in there. Since thermohaline anomalies in the central North Pacific are mostly transported to the west by the Rossby waves or subsurface water masses flowing along the anticyclonic geostrophic circulation, examinations in the central subtropical gyre may be helpful for better understandings of thermohaline variations in the whole North Pacific.

In this study, we analyzed the repeat hydrography along the 165°E meridian maintained by Japan Meteorological Agency since 1996 to examine long-term thermohaline variations in the North Pacific subtropical gyre. As a result, in the subsurface of the southern part of the subtropical gyre corresponding to North Pacific Tropical Water (NPTW) characterized as the salinity maximum, a significant incresing salinity trend was detected. In this region, potential temperature and salinity also performed an inter-annual variation. On the other hand, in the greater part of the main thermocline/halocline, a significant decreasing trend was observed. In addition, potential temperature and salinity clearly fluctuated in a decadal timescale.

Causes of these variations were further investigated. Then we confirmed that variations in the subsruface around NPTW were originated in the surface mixed layer in the western part of its formation region to the east of the 165°E meridian by temporal changes of freshwater flux and eddy diffusion, and anomalies were transported by the westward geostrophic flow, as demonstrated by previous studies. We also found that thermohaline anomalies in the intermediate layers around the main thermocline/halocline derived from variations of winter mixed layer properties in the central North Pacific. A long-term variation of mixed layer temperature caused by changes of winter atmospheric forcing induced meridional migrations of isopycnal outcrops and thermohaline anomalies on there. Such anomalies were widely distributed to the subtropical gyre by mode waters such as North Pacific Subtropical Mode Water (STMW) in a few years.

Keywords: Repeat hydrography, Long-term changes, Decadal variability

©2019. Japan Geoscience Union. All Right Reserved.

First detection of chlorofluorocarbons into bottom layer in the Melanesian Basin of the North Pacific

*Toshiya NAKANO[1], Kazutaka ENYO[1], Daisuke SASANO[1], Shogo URAKAWA[2], Hiroyuki TSUJINO[2], Hideyuki NAKANO[2], Masao ISHII[2]

1. Japan Meteorological Agency, 2. Meteorological Research Institute

Chlorofluorocarbons (CFCs) are a group of artificial chemical compounds that have no natural sources. The CFC concentrations in the ocean interior have been used to quantify the transit time distribution and transport time-scale since the water masses was ventilated from the formation region, and to estimate rates of formation for many water masses. In addition, the distribution of CFCs in the bottom layer indicates the pathway of the advection/diffusion of bottom waters. From 6 August to 27 September 2018, the Japan Meteorological Agency (JMA) conducted a Global Ocean Ship-based Hydrographic Investigation Program (GO-SHIP) revisit cruise at P13 section along the 165˚E meridian on board the R/V Ryofu Maru. In this cruise, JMA collected data of dissolved CFC-11, -12 and -113, and detected the concentration of CFC-11 greater than its detection limit (0.006±0.0011 pmol/kg) in bottom layer between 17˚N and 3˚S in the Melanesian Basin. This result demonstrates that the Lower Circumpolar Deep Water, i.e., a lower part of ventilated Southern Ocean water, formed after 1960s has already reached to the Melanesian Basin of the North Pacific through the Samoan Passage and across the Equator. From the high-quality historical WOCE and GO-SHIP cruise data in the South Pacific, we estimated that the advection speed of CFC-11 equivalent to current speed of bottom layer is about 1 cm/sec (315 km/year). This estimate is consistent with the results of the CMIP6/OMIP numerical modeling by the Meteorological Research Institute. Our results contribute to the understanding of the thermohaline circulation in the Pacific Ocean and the validation and upgrading of the Earth System Model for the future projection of the global warming.

Keywords: JMA 165˚E section, Melanesian Basin, chlorofluorocarbons, bottom water

©2019. Japan Geoscience Union. All Right Reserved.

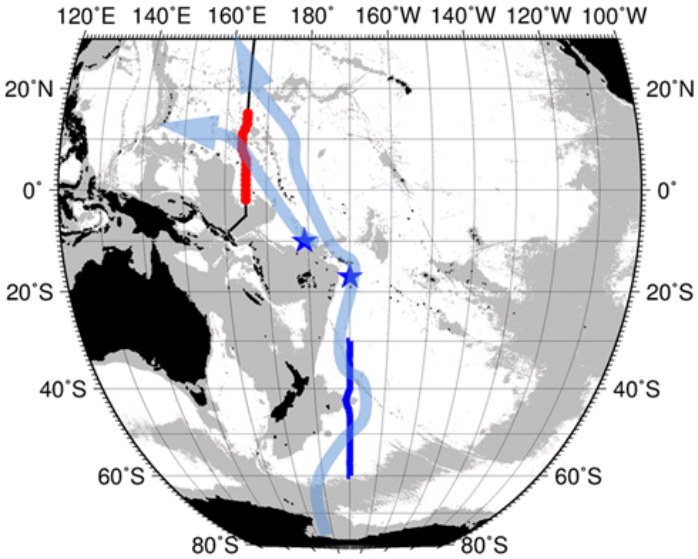

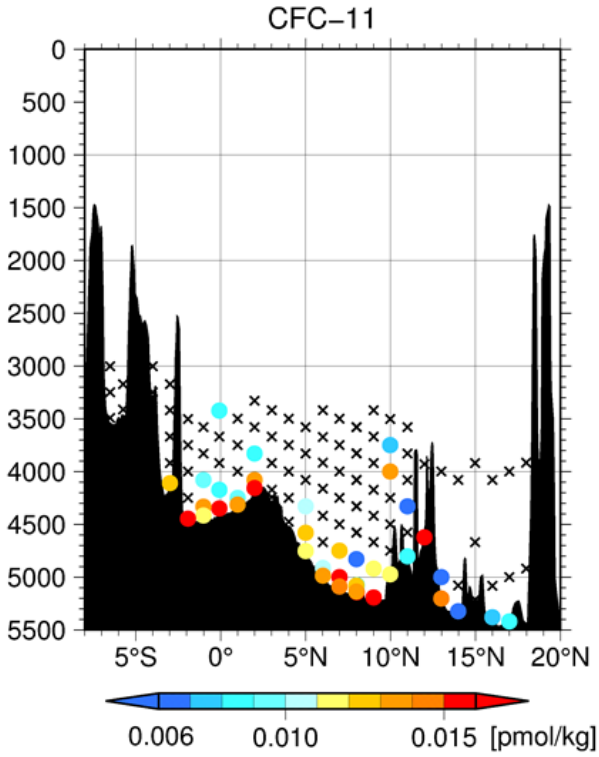

©2019. Japan Geoscience Union. All Right Reserved.

Global grid mapping of temperature and salinity based on Argo float data

*Shigeki Hosoda[1]

1. Japan Marine-Earth Science and Technology

About twenty years have been passed since when Argo programme started in 1999, over 3500 active Argo floats are working to measure temperature and salinity in the upper ocean, accumulating over 2 million profiles. As the situation enables us to construct gridded temperature and salinity data set in the global ocean to be easier, variable kinds of 3-dimensional gridded data set based on purely Argo and Argo plus other observational data are produced from many institutes to investigate global changes in climate and ocean environment.

JAMSTEC produces quasi-real time gridded objective mappings of Argo, MOAA GPV for temperature and salinity fields, and MILA GPV for mixed layer depth every month or 10 days. Those data set are widely used not only to directly analyze the data set but also to validate the state estimate based on data assimilation. The data and its error from MOAA GPV are effectively informed to evaluate representation of temperature and salinity fields, which makes it possible to improve the data assimilation to be more elaborated for accurate analyses of changes in climate and ocean environment. While MILA GPV is produced with characteristics of Argo profiling float which has finer vertical resolution with horizontally homogeneous distribution. That enables us to capture detailed distribution of surface layer mixed layer depth, rapidly progressing physical and biogeochemical researches related to mixed layer variability.

In the future, the objective mapping will be more accurate and useful if the Core Argo array is sustained to obtain long-term statistical characteristics of the upper ocean temperature and salinity. Further, it is expected that improved mapping of physical and biogeochemical parameters will be developed when huge amount of measurement of temperature and salinity in deeper ocean than 2000 m and biogeochemical parameters, with the Deep and BGC Argo arrays.

Keywords: Argo, global ocean, gridded data

©2019. Japan Geoscience Union. All Right Reserved.

Evolutions of water mass anomalies in the upper North Pacific based on Argo data, in STMW, ESTMW, and CMW.

*Tong Wang[1], Toshio Suga[1,2], Shinya Kouketsu[2]

1. Graduate School of Science, Tohoku University, 2. Research and Development Center for Global Change, JAMSTEC

Under the background of climate changes, long-term trends and interannual to decadal variations of water masses have been discovered in recent studies. However, how they evolved in space and time is still not fully investigated, partly due to the insufficiency of observation. With spatially and temporally unbiased data available through Argo floats recently, this study describes three-dimensional evolutions of water mass anomalies during 2004-2015, focusing on three typical water masses in the upper North Pacific: North Pacific Subtropical Mode Water (STMW), Eastern Subtropical Mode Water (ESTMW), and North Pacific Central Mode Water (CMW).

In order to preserve the water mass characteristics as much as possible, the analysis in this study is mainly on neutral density surfaces, along which the advection and mixing of water masses dominantly occur. Because of the compensation between temperature and salinity on isopycnal surfaces, this study mainly investigates salinity as a proxy of spiciness. The main results are listed as follows:

In STMW:
The temporal variations of spiciness are dominated by interannual or longer variations. There is a long-term freshening trend at 0.005/year generally as well as strong decadal variations. The former is related to global warming; the latter are caused by the decadal variations of Kuroshio Extension path stability. These anomalies show rapid southwestward propagations in STMW, and the directions can be explained by geostrophic currents, but the propagation speed are 2-3 times higher than geostrophic currents, which indicates other processes involved. The origins of anomalies are most likely to be the STMW formation region. Another possible origin is found in the subtropics of the central North Pacific through statistical analysis, which needs further verification and explanation. Strikingly, the Eulerian temporal changes of spiciness are preserved well during the large distance propagation, implying the existence and persistence of large-scale spiciness fronts.

In ESTMW:
The temporal variability of ESTMW is higher than STMW and CMW, and interannual or longer variations are dominant. The long-term trend in northeastern ESTMW shows freshening, while the southwestern ESTMW is in salinification. There is an obvious 5-6-year oscillation cycle. The anomalies shift between positive and negative rapidly at the ESTMW formation region, spread to the whole ESTMW along its subduction path in each period, and propagate southwestward to the central subtropics and the western tropics by geostrophic flow.

In CMW:
Both spiciness and its total variations are smaller than the other two water masses, but the seasonal variations are higher, being comparable with interannual or longer variations in the northern CMW. With regard to trends, the northern CMW is in salinification, with the anomalies propagating eastward on both monthly scale and annual mean. However, the majority of CMW shows freshening almost uniformly, with weak but recognizable southward propagations.

©2019. Japan Geoscience Union. All Right Reserved.

In conclusion, this study provides a comprehensive description of the evolutions of water mass anomalies in the upper North Pacific for the first time. The regional variations that have been found by limited observations are confirmed and complemented with three-dimensional presentations. The evolutions occurred in earlier years and documented by previous studies are updated by the present analysis. Furthermore, the new phenomena that should be investigated in future are also raised.

Keywords: Argo float data, Subtropical Mode Water, Eastern Subtropical Mode Water, Central Mode Water, Spiciness anomaly

©2019. Japan Geoscience Union. All Right Reserved.

Impacts of temperature measurements from sea turtles on seasonal prediction around the Arafura Sea

*Takeshi Doi[1], Andrea Storto[2], Takuya Fukuoka[3], Hiroyuki Suganuma[4], Katsufumi Sato[3]

1. JAMSTEC, 2. CMRE, 3. The University of Tokyo, 4. ELNA

In this work, we add the assimilation of temperature measurements from sea turtles, which covered from surface to maximum depth of about 120m around the Arafura Sea during June-August 2017, into an operational seasonal prediction system. The impact of these new observations is explored by conducting so-called Ocean Observing System Experiments. We find that the prediction of sea surface temperature is significantly improved at 3-4 months lead-time. The results show that the addition of temperature measurements from sea turtles into the existing Global Ocean Observing System (including satellite, mooring buoys, ships, and profiling floats) may open a new door to improve regional seasonal prediction through better representation of the initial state of the upper ocean.

Keywords: Seasonal prediction, Biologging, Arafura Sea

©2019. Japan Geoscience Union. All Right Reserved.

Physical and biogeochemical processes from winter to spring in the south of the Kuroshio Extension

*Chiho Sukigara[1], Ryuichiro Inoue[2], Takeyoshi Nagai[1], Andrea J Fassbender[3], Yuichiro Takeshita[3], Stuart P Bishop[4], Eitarou Oka[5]

1. Tokyo University of Marine Science and Technology, 2. Japan Agency for Marine-Earth Science and Technology, 3. Monterey Bay Aquarium Research Institute, 4. North Carolina State University, 5. The University of Tokyo

In a subtropical region south of the Kuroshio Extension (KE) in the Western North Pacific, large ocean heat loss in the surface layer during winter makes a deep mixed layer. Then, a part of CO_2 dissolved from air to surface ocean is transformed to particulate organic matters via photosynthesis using nutrients which are supplied from deeper layer. Eventually particulate organic matters are transported to deeper layer. In this oligotrophic region, winter mixing is a critical process to supply nutrients to the euphotic zone, which supports high chlorophyll concentrations in early spring are clearly seen by satellite observations. Therefore, it is important to understand effects of nutrient transports by physical processes on biogeochemical material transport and cycle in this period. However, there are few physical and biogeochemical data during winter in this region because of the difficult circumstances in observation.

In this study, we deployed two biogeochemical Argo (BGC-Argo) floats in 33°15’ N, 142°30’ E on January 28th, 2018 during the Shinsei-maru KS-18-1 cruise and recovered them in 35°31’ N, 143°11’ E and 35°43’ N, 143°29’ E on April 20th, 2018 during the Shinsei-maru KS-18-4 cruise. During these two cruises, CTD observations and water samplings were conducted to validate sensors (temperature, salinity, oxygen, chlorophyll, nitrate, and backscatter) attached to floats. BGC-Argos observed 82 profiles from 2000 m depth to the surface every day.

Those floats were kept staying around the deployment position for a month, then moved to southwestward in the middle of March, and were to northward near KE until the recovery. In the first half of the observation period, intermittent mixed layer deepening and subsequent restratification were repeated in the top 300 m depth. High chlorophyll concentrations and backscatter values were observed in the surface layer when upper layers were stratified. After March 17th, oxygen concentration increased, nitrate concentration decreased, and chlorophyll concentration and back scatter value were stable in the subsurface (100 to 300 m). After that, oxygen concentration, chlorophyll concentrations and back scatter values increased (nitrate decreased) coincided with stratification in the surface layer until April 2nd. In the subsurface layer, chlorophyll concentration and back scatter value decreased suddenly, which might mean that biogenic particulate organic matters transported by the deep mixing were quickly decomposed in the layer. Furthermore, a water with low oxygen and high nitrate intruded in the layer 50 to 100 m around March 30th. The origin of this water would be relative deeper layer because of low chlorophyll concentration and back scatter values.

The BGC-Argo observation in the south of KE for three months revealed that physical processes with various time scales in the surface layer from winter to spring affect the primary productivity of phytoplankton and the material distribution.

Keywords: BGC-Argo, Spring restratification, biological response, material transport

©2019. Japan Geoscience Union. All Right Reserved.

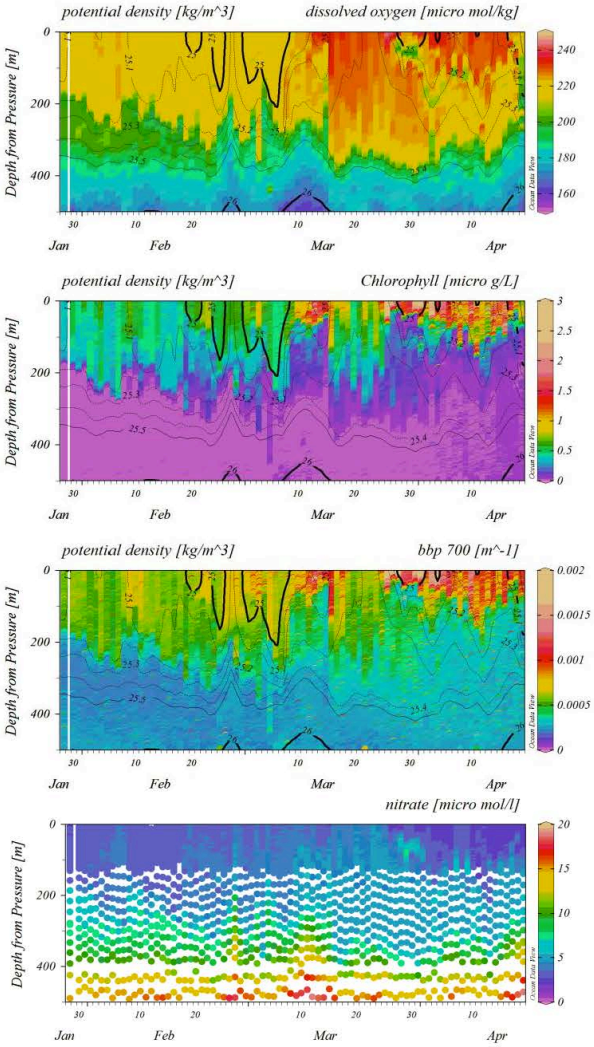

©2019. Japan Geoscience Union. All Right Reserved.

[J] Poster | A (Atmospheric and Hydrospheric Sciences)：A-OS Ocean Sciences & Ocean Environment

Tue. May 28, 2019 5:15 PM - 6:30 PM JST | Tue. May 28, 2019 8:15 AM - 9:30 AM UTC | Poster Hall International Exhibition Hall8, Makuhari Messe_9

[A-OS20] Global ocean observing systems, obtained results and system optimization: toward OceanObs19

convener:Shigeki Hosoda(Japan Marine-Earth Science and Technology), Shuhei Masuda(Japan Agency for Marine-Earth Science and Technology), Yosuke Fujii(Meteorological Research Institute, Japan Meteorological Agency), Fujiki Tetsuichi(Japan Agency for Marine-Earth Science and Technology)

Almost twenty years have been passed since the beginning of Argo programme to construct global ocean observing system. The Argo observing system have been covering the global ocean with more than 3000 Argo floats with collaboration of many countries. The Argo is well known as one of the best practices of ocean observing systems, as lots of scientific results and social/industrial benefits have been gained based on indispensable huge amount of oceanic data which has never obtained before. Recently, the Argo observing system is rapidly expanded to monitor deeper ocean (Deep Argo; >4000m depth) and bio-geochemical parameters (Biogeochemical Argo) in addition to upper layer temperature and salinity (Core Argo; <2000m depth).
On the other hand, sustainability of the Argo is not guaranteed and its observing array is still developing as international infrastructure. For example, Argo float distribution recently tends to be inhomogeneous since a part of float deployment and operation is still conducted by voluntary works. Therefore, improving the observing systems to be more effective and sustainable is a mandatory task in the oceanographic community. In this background, various efforts are forwarded to evaluate impacts of ocean observations by the support of GODAE OceanView which is endorsing the Argo programme. In coming OceanObs19, development, expansion and enhancement of the sustainability of the Argo observing systems will be discussed based on scientific results and application researches.
In this session, current status, recent issues, future works on large-scale ocean observing systems are discussed in related to Argo and other research infrastructures such as GO-SHIP, OceanSITES etc., focusing on the global ocean observing system in coming next decade.

[AOS20-P01] Fresh bias with pressure dependency at the measurements of SBE 41CP for deep float

*Taiyo Kobayashi[1] (1.Japan Agency for Marine-Earth Science and Technology)

[AOS20-P02] Long-term thermohaline variations in the North Pacific subtropical gyre observed by repeat hydrography along the 165°E meridian

*Yuma Kawakami[1,2], Yoshiteru Kitamura[1], Toshiya Nakano[1,2] (1.Japan Meteorological Agency, 2.Meteorological Research Institute)

[AOS20-P03] First detection of chlorofluorocarbons into bottom layer in the Melanesian Basin of the North Pacific

*Toshiya NAKANO[1], Kazutaka ENYO[1], Daisuke SASANO[1], Shogo URAKAWA[2], Hiroyuki TSUJINO[2], Hideyuki NAKANO[2], Masao ISHII[2] (1.Japan Meteorological Agency, 2.Meteorological Research Institute)

[AOS20-P04] **Global grid mapping of temperature and salinity based on Argo float data**

*Shigeki Hosoda[1] (1.Japan Marine-Earth Science and Technology)

[AOS20-P05] **Evolutions of water mass anomalies in the upper North Pacific based on Argo data, in STMW, ESTMW, and CMW.**

*Tong Wang[1], Toshio Suga[1,2], Shinya Kouketsu[2] (1.Graduate School of Science, Tohoku University, 2.Research and Development Center for Global Change, JAMSTEC)

[AOS20-P06] Impacts of temperature measurements from sea turtles on seasonal prediction around the Arafura Sea

*Takeshi Doi[1], Andrea Storto[2], Takuya Fukuoka[3], Hiroyuki Suganuma[4], Katsufumi Sato[3] (1.JAMSTEC, 2.CMRE, 3.The University of Tokyo, 4.ELNA)

[AOS20-P07] Physical and biogeochemical processes from winter to spring in the south of the Kuroshio Extension

*Chiho Sukigara[1], Ryuichiro Inoue[2], Takeyoshi Nagai[1], Andrea J Fassbender[3], Yuichiro Takeshita[3], Stuart P Bishop[4], Eitarou Oka[5] (1.Tokyo University of Marine Science and Technology, 2.Japan Agency for Marine-Earth Science and Technology, 3.Monterey Bay Aquarium Research Institute, 4.North Carolina State University, 5.The University of Tokyo)

Fresh bias with pressure dependency at the measurements of SBE 41CP for deep float

*Taiyo Kobayashi[1]

1. Japan Agency for Marine-Earth Science and Technology

Fresh bias was found at the measurements by deep float model of SBE 41CP CTD sensor on Deep NINJA floats. Its details were clarified and possible causes were discussed.

Keywords: Deep Argo, salinity measurements

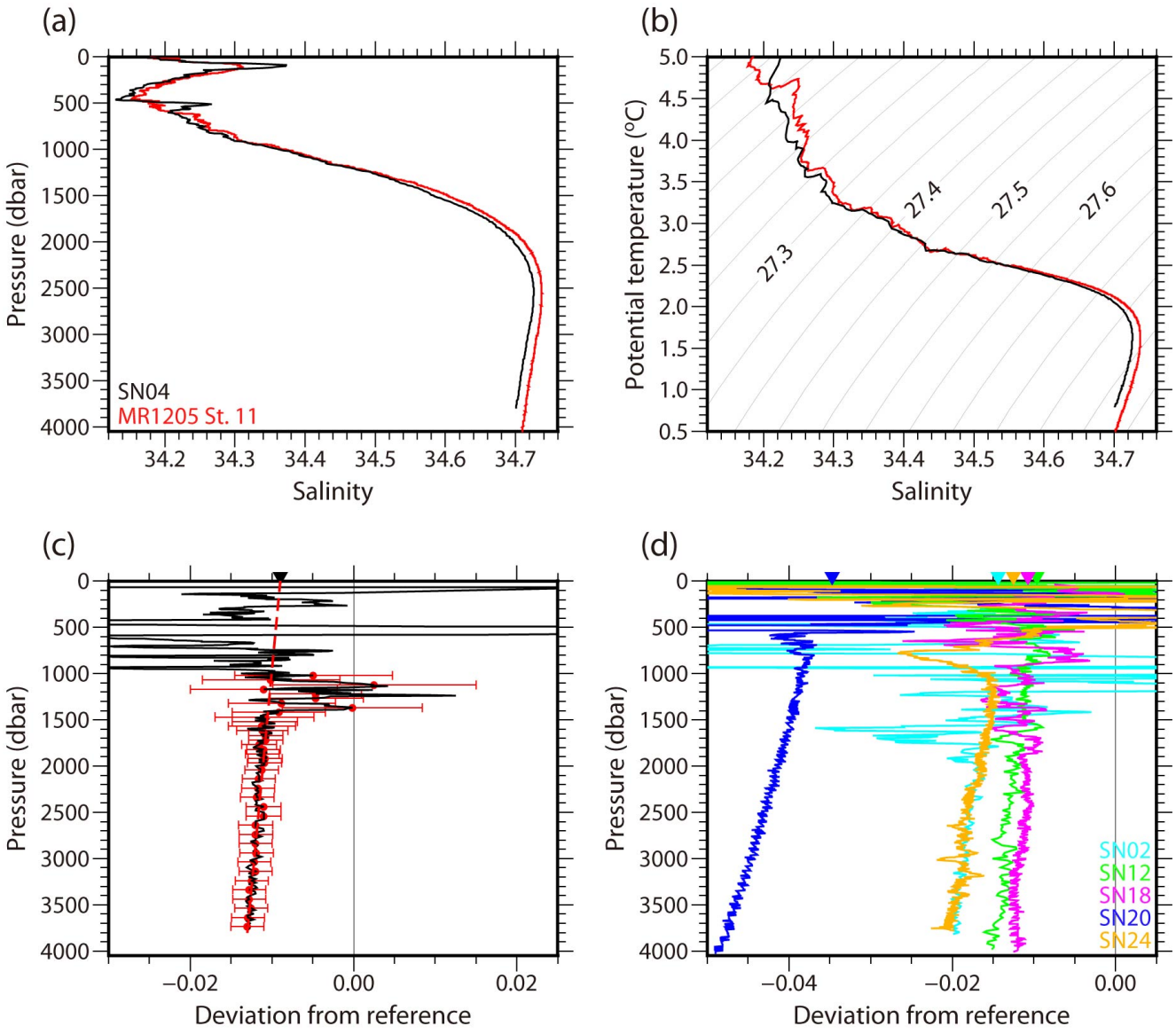

©2019. Japan Geoscience Union. All Right Reserved.

Long-term thermohaline variations in the North Pacific subtropical gyre observed by repeat hydrography along the 165°E meridian

*Yuma Kawakami[1,2], Yoshiteru Kitamura[1], Toshiya Nakano[1,2]

1. Japan Meteorological Agency, 2. Meteorological Research Institute

Recently, long-term thermohaline changes in the surface and subsurface of the world ocean, such as the global warming and the intensification of salinity contrast between basins or regions, are continuously reported. Since changes of temperature and salinity greatly influence not only the density-driven geostrophic ocean circulation but also the marine ecosystem, sea levels and climates, monitoring of the ocean variations and understandings of those mechanisms are important.

Numerous scientific knowledges about thermohaline variations in the subsurface and intermediate layers of the North Pacific subtropical gyre including significant freshening in the thermocline/halocline and fluctuation in a decadal timescale were given by previous researches. However, many of them described in the western part of the subtropical gyre, and studies in its central part have been more limited partially due to the lack of data even though large scale atmospheric forcing generates great long-term thermohaline variations in there. Since thermohaline anomalies in the central North Pacific are mostly transported to the west by the Rossby waves or subsurface water masses flowing along the anticyclonic geostrophic circulation, examinations in the central subtropical gyre may be helpful for better understandings of thermohaline variations in the whole North Pacific.

In this study, we analyzed the repeat hydrography along the 165°E meridian maintained by Japan Meteorological Agency since 1996 to examine long-term thermohaline variations in the North Pacific subtropical gyre. As a result, in the subsurface of the southern part of the subtropical gyre corresponding to North Pacific Tropical Water (NPTW) characterized as the salinity maximum, a significant incresing salinity trend was detected. In this region, potential temperature and salinity also performed an inter-annual variation. On the other hand, in the greater part of the main thermocline/halocline, a significant decreasing trend was observed. In addition, potential temperature and salinity clearly fluctuated in a decadal timescale.

Causes of these variations were further investigated. Then we confirmed that variations in the subsruface around NPTW were originated in the surface mixed layer in the western part of its formation region to the east of the 165°E meridian by temporal changes of freshwater flux and eddy diffusion, and anomalies were transported by the westward geostrophic flow, as demonstrated by previous studies. We also found that thermohaline anomalies in the intermediate layers around the main thermocline/halocline derived from variations of winter mixed layer properties in the central North Pacific. A long-term variation of mixed layer temperature caused by changes of winter atmospheric forcing induced meridional migrations of isopycnal outcrops and thermohaline anomalies on there. Such anomalies were widely distributed to the subtropical gyre by mode waters such as North Pacific Subtropical Mode Water (STMW) in a few years.

Keywords: Repeat hydrography, Long-term changes, Decadal variability

©2019. Japan Geoscience Union. All Right Reserved.

First detection of chlorofluorocarbons into bottom layer in the Melanesian Basin of the North Pacific

*Toshiya NAKANO[1], Kazutaka ENYO[1], Daisuke SASANO[1], Shogo URAKAWA[2], Hiroyuki TSUJINO[2], Hideyuki NAKANO[2], Masao ISHII[2]

1. Japan Meteorological Agency, 2. Meteorological Research Institute

Chlorofluorocarbons (CFCs) are a group of artificial chemical compounds that have no natural sources. The CFC concentrations in the ocean interior have been used to quantify the transit time distribution and transport time-scale since the water masses was ventilated from the formation region, and to estimate rates of formation for many water masses. In addition, the distribution of CFCs in the bottom layer indicates the pathway of the advection/diffusion of bottom waters. From 6 August to 27 September 2018, the Japan Meteorological Agency (JMA) conducted a Global Ocean Ship-based Hydrographic Investigation Program (GO-SHIP) revisit cruise at P13 section along the 165˚E meridian on board the R/V Ryofu Maru. In this cruise, JMA collected data of dissolved CFC-11, -12 and -113, and detected the concentration of CFC-11 greater than its detection limit (0.006±0.0011 pmol/kg) in bottom layer between 17˚N and 3˚S in the Melanesian Basin. This result demonstrates that the Lower Circumpolar Deep Water, i.e., a lower part of ventilated Southern Ocean water, formed after 1960s has already reached to the Melanesian Basin of the North Pacific through the Samoan Passage and across the Equator. From the high-quality historical WOCE and GO-SHIP cruise data in the South Pacific, we estimated that the advection speed of CFC-11 equivalent to current speed of bottom layer is about 1 cm/sec (315 km/year). This estimate is consistent with the results of the CMIP6/OMIP numerical modeling by the Meteorological Research Institute. Our results contribute to the understanding of the thermohaline circulation in the Pacific Ocean and the validation and upgrading of the Earth System Model for the future projection of the global warming.

Keywords: JMA 165˚E section, Melanesian Basin, chlorofluorocarbons, bottom water

©2019. Japan Geoscience Union. All Right Reserved.

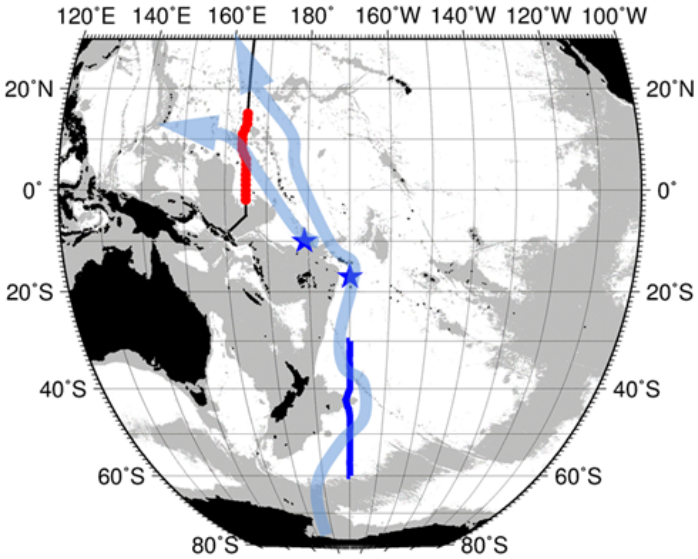

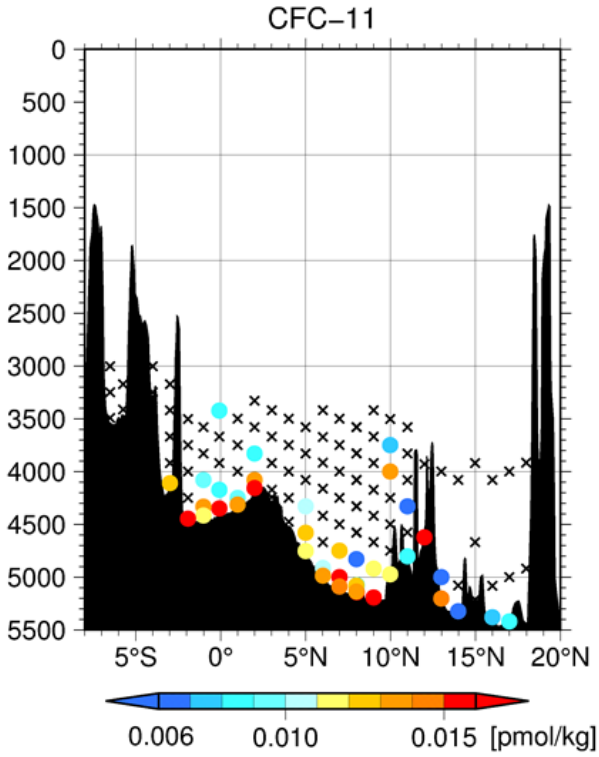

©2019. Japan Geoscience Union. All Right Reserved.

Global grid mapping of temperature and salinity based on Argo float data

*Shigeki Hosoda[1]

1. Japan Marine-Earth Science and Technology

About twenty years have been passed since when Argo programme started in 1999, over 3500 active Argo floats are working to measure temperature and salinity in the upper ocean, accumulating over 2 million profiles. As the situation enables us to construct gridded temperature and salinity data set in the global ocean to be easier, variable kinds of 3-dimensional gridded data set based on purely Argo and Argo plus other observational data are produced from many institutes to investigate global changes in climate and ocean environment.

JAMSTEC produces quasi-real time gridded objective mappings of Argo, MOAA GPV for temperature and salinity fields, and MILA GPV for mixed layer depth every month or 10 days. Those data set are widely used not only to directly analyze the data set but also to validate the state estimate based on data assimilation. The data and its error from MOAA GPV are effectively informed to evaluate representation of temperature and salinity fields, which makes it possible to improve the data assimilation to be more elaborated for accurate analyses of changes in climate and ocean environment. While MILA GPV is produced with characteristics of Argo profiling float which has finer vertical resolution with horizontally homogeneous distribution. That enables us to capture detailed distribution of surface layer mixed layer depth, rapidly progressing physical and biogeochemical researches related to mixed layer variability.

In the future, the objective mapping will be more accurate and useful if the Core Argo array is sustained to obtain long-term statistical characteristics of the upper ocean temperature and salinity. Further, it is expected that improved mapping of physical and biogeochemical parameters will be developed when huge amount of measurement of temperature and salinity in deeper ocean than 2000 m and biogeochemical parameters, with the Deep and BGC Argo arrays.

Keywords: Argo, global ocean, gridded data

©2019. Japan Geoscience Union. All Right Reserved.

Evolutions of water mass anomalies in the upper North Pacific based on Argo data, in STMW, ESTMW, and CMW.

*Tong Wang[1], Toshio Suga[1,2], Shinya Kouketsu[2]

1. Graduate School of Science, Tohoku University, 2. Research and Development Center for Global Change, JAMSTEC

Under the background of climate changes, long-term trends and interannual to decadal variations of water masses have been discovered in recent studies. However, how they evolved in space and time is still not fully investigated, partly due to the insufficiency of observation. With spatially and temporally unbiased data available through Argo floats recently, this study describes three-dimensional evolutions of water mass anomalies during 2004-2015, focusing on three typical water masses in the upper North Pacific: North Pacific Subtropical Mode Water (STMW), Eastern Subtropical Mode Water (ESTMW), and North Pacific Central Mode Water (CMW).

In order to preserve the water mass characteristics as much as possible, the analysis in this study is mainly on neutral density surfaces, along which the advection and mixing of water masses dominantly occur. Because of the compensation between temperature and salinity on isopycnal surfaces, this study mainly investigates salinity as a proxy of spiciness. The main results are listed as follows:

In STMW:
The temporal variations of spiciness are dominated by interannual or longer variations. There is a long-term freshening trend at 0.005/year generally as well as strong decadal variations. The former is related to global warming; the latter are caused by the decadal variations of Kuroshio Extension path stability. These anomalies show rapid southwestward propagations in STMW, and the directions can be explained by geostrophic currents, but the propagation speed are 2-3 times higher than geostrophic currents, which indicates other processes involved. The origins of anomalies are most likely to be the STMW formation region. Another possible origin is found in the subtropics of the central North Pacific through statistical analysis, which needs further verification and explanation. Strikingly, the Eulerian temporal changes of spiciness are preserved well during the large distance propagation, implying the existence and persistence of large-scale spiciness fronts.

In ESTMW:
The temporal variability of ESTMW is higher than STMW and CMW, and interannual or longer variations are dominant. The long-term trend in northeastern ESTMW shows freshening, while the southwestern ESTMW is in salinification. There is an obvious 5-6-year oscillation cycle. The anomalies shift between positive and negative rapidly at the ESTMW formation region, spread to the whole ESTMW along its subduction path in each period, and propagate southwestward to the central subtropics and the western tropics by geostrophic flow.

In CMW:
Both spiciness and its total variations are smaller than the other two water masses, but the seasonal variations are higher, being comparable with interannual or longer variations in the northern CMW. With regard to trends, the northern CMW is in salinification, with the anomalies propagating eastward on both monthly scale and annual mean. However, the majority of CMW shows freshening almost uniformly, with weak but recognizable southward propagations.

©2019. Japan Geoscience Union. All Right Reserved.

In conclusion, this study provides a comprehensive description of the evolutions of water mass anomalies in the upper North Pacific for the first time. The regional variations that have been found by limited observations are confirmed and complemented with three-dimensional presentations. The evolutions occurred in earlier years and documented by previous studies are updated by the present analysis. Furthermore, the new phenomena that should be investigated in future are also raised.

Keywords: Argo float data, Subtropical Mode Water, Eastern Subtropical Mode Water, Central Mode Water, Spiciness anomaly

©2019. Japan Geoscience Union. All Right Reserved.

Impacts of temperature measurements from sea turtles on seasonal prediction around the Arafura Sea

*Takeshi Doi[1], Andrea Storto[2], Takuya Fukuoka[3], Hiroyuki Suganuma[4], Katsufumi Sato[3]

1. JAMSTEC, 2. CMRE, 3. The University of Tokyo, 4. ELNA

In this work, we add the assimilation of temperature measurements from sea turtles, which covered from surface to maximum depth of about 120m around the Arafura Sea during June-August 2017, into an operational seasonal prediction system. The impact of these new observations is explored by conducting so-called Ocean Observing System Experiments. We find that the prediction of sea surface temperature is significantly improved at 3-4 months lead-time. The results show that the addition of temperature measurements from sea turtles into the existing Global Ocean Observing System (including satellite, mooring buoys, ships, and profiling floats) may open a new door to improve regional seasonal prediction through better representation of the initial state of the upper ocean.

Keywords: Seasonal prediction, Biologging, Arafura Sea

©2019. Japan Geoscience Union. All Right Reserved.

Physical and biogeochemical processes from winter to spring in the south of the Kuroshio Extension

*Chiho Sukigara[1], Ryuichiro Inoue[2], Takeyoshi Nagai[1], Andrea J Fassbender[3], Yuichiro Takeshita[3], Stuart P Bishop[4], Eitarou Oka[5]

1. Tokyo University of Marine Science and Technology, 2. Japan Agency for Marine-Earth Science and Technology, 3. Monterey Bay Aquarium Research Institute, 4. North Carolina State University, 5. The University of Tokyo

In a subtropical region south of the Kuroshio Extension (KE) in the Western North Pacific, large ocean heat loss in the surface layer during winter makes a deep mixed layer. Then, a part of CO_2 dissolved from air to surface ocean is transformed to particulate organic matters via photosynthesis using nutrients which are supplied from deeper layer. Eventually particulate organic matters are transported to deeper layer. In this oligotrophic region, winter mixing is a critical process to supply nutrients to the euphotic zone, which supports high chlorophyll concentrations in early spring are clearly seen by satellite observations. Therefore, it is important to understand effects of nutrient transports by physical processes on biogeochemical material transport and cycle in this period. However, there are few physical and biogeochemical data during winter in this region because of the difficult circumstances in observation.

In this study, we deployed two biogeochemical Argo (BGC-Argo) floats in 33°15’ N, 142°30’ E on January 28th, 2018 during the Shinsei-maru KS-18-1 cruise and recovered them in 35°31’ N, 143°11’ E and 35°43’ N, 143°29’ E on April 20th, 2018 during the Shinsei-maru KS-18-4 cruise. During these two cruises, CTD observations and water samplings were conducted to validate sensors (temperature, salinity, oxygen, chlorophyll, nitrate, and backscatter) attached to floats. BGC-Argos observed 82 profiles from 2000 m depth to the surface every day.

Those floats were kept staying around the deployment position for a month, then moved to southwestward in the middle of March, and were to northward near KE until the recovery. In the first half of the observation period, intermittent mixed layer deepening and subsequent restratification were repeated in the top 300 m depth. High chlorophyll concentrations and backscatter values were observed in the surface layer when upper layers were stratified. After March 17th, oxygen concentration increased, nitrate concentration decreased, and chlorophyll concentration and back scatter value were stable in the subsurface (100 to 300 m). After that, oxygen concentration, chlorophyll concentrations and back scatter values increased (nitrate decreased) coincided with stratification in the surface layer until April 2nd. In the subsurface layer, chlorophyll concentration and back scatter value decreased suddenly, which might mean that biogenic particulate organic matters transported by the deep mixing were quickly decomposed in the layer. Furthermore, a water with low oxygen and high nitrate intruded in the layer 50 to 100 m around March 30th. The origin of this water would be relative deeper layer because of low chlorophyll concentration and back scatter values.

The BGC-Argo observation in the south of KE for three months revealed that physical processes with various time scales in the surface layer from winter to spring affect the primary productivity of phytoplankton and the material distribution.

Keywords: BGC-Argo, Spring restratification, biological response, material transport

©2019. Japan Geoscience Union. All Right Reserved.

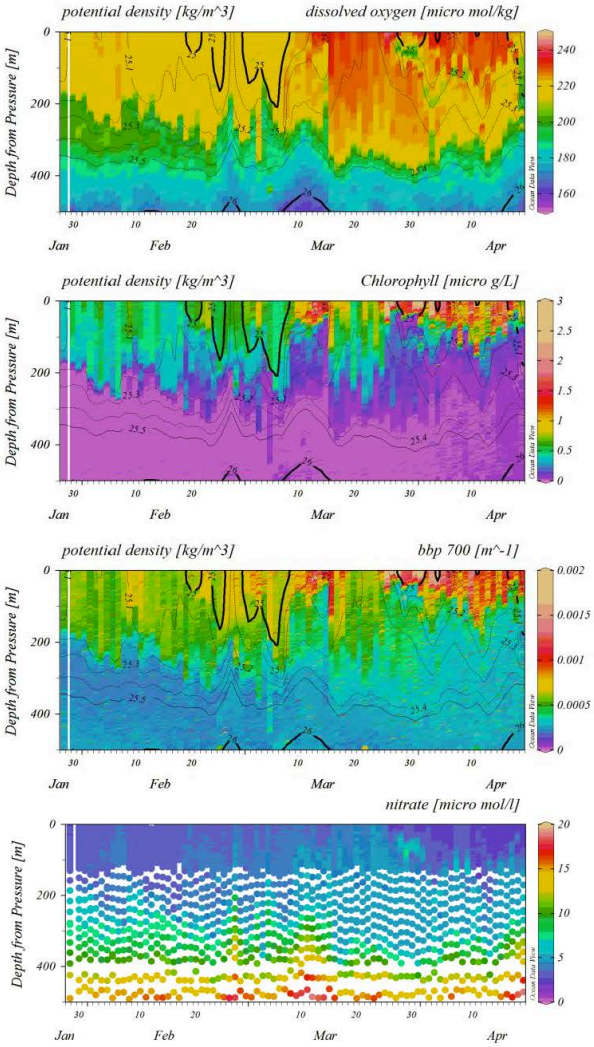

©2019. Japan Geoscience Union. All Right Reserved.

[E] Oral | A (Atmospheric and Hydrospheric Sciences)：A-HW Hydrology & Water Environment

Tue. May 28, 2019 1:45 PM - 3:15 PM JST | Tue. May 28, 2019 4:45 AM - 6:15 AM UTC | 103 1F

[A-HW23] Hydrology & Water Environment

convener:Isao Machida(Geological Survey of Japan), Dai Yamazaki(Institute of Industrial Sciences, The University of Tokyo), Takeshi Hayashi(Faculty of Education and Human Studies, Akita University), Keisuke Fukushi(Institute of Nature & Environmental Technology, Kanazawa University), Chairperson:Isao Machida(Geological Survey of Japan, AIST)

We focus on various issues of water cycle and environment and aim to answer questions of hydrological and earth system sciences including 1) surface, subsurface and evapotranspiration processes of water cycle; 2) natural and anthropogenic hydrothermal systems, 3) environments issues and studies on a watershed or global scale, 4) water-related issues with ecological, environmental, and geochemical aspects, and 5) other issues in hydrological sciences. This session welcomes presentations regarding various kinds of approaches and techniques such as field survey, remote sensing, isotope tracers, numerical simulation, and theoretical analysis.

1:45 PM - 2:00 PM JST | 4:45 AM - 5:00 AM UTC

[AHW23-01] Method for measuring the pore air pressure in the mountainous slope for rainfall-runoff processes research

★Invited Papers

*Sho Iwagami[1], Shoji Noguchi[1], Takanori Shimizu[1], Tayoko Kubota[1], Shin'ichi Iida[1], Makoto Araki[1] (1.Forestry and Forest Products Research Institute, Forest Research and Management Organization, National Research and Development Agency)

2:00 PM - 2:15 PM JST | 5:00 AM - 5:15 AM UTC

[AHW23-02] **A method to quantify the influence of total water storage change on climate elasticity of streamflow**

*Yin Tang[1] (1.Institute of Geographic Sciences and Natural Resources Research, Chinese Academy of Science)

2:15 PM - 2:30 PM JST | 5:15 AM - 5:30 AM UTC

[AHW23-03] **Trade-off analysis of discharge-desiltation-turbidity and sediment simulation of a combined reservoir–river system under multi-phase and multi-layer conjunctive releasing operation**

*Chien-Lin Huang[1], Nien-Sheng Hsu[1], Gene Jiing-Yun You[1] (1.National Taiwan University, Taiwan)

2:30 PM - 2:45 PM JST | 5:30 AM - 5:45 AM UTC

[AHW23-04] Gradient change of soil moisture effect on next-day precipitation identified via a Random Forest-Granger causality model

*Lu Li[1], Wei ShangGuan[1], Shu Peng Zhang[1], Jin Jing Pan[1], Nan Wei[1], Yong Jiu Dai[1] (1.Guangdong Province Key Laboratory for Climate Change and Natural Disaster Studies, School of Atmospheric Sciences, Sun Yat-sen University)

2:45 PM - 3:00 PM JST | 5:45 AM - 6:00 AM UTC

[AHW23-05] **Using data-driven methods to explore the predictability of surface soil moisture with FLUXNET site data**

*jinjing Pan[1] (1.Guangdong Province Key Laboratory for Climate Change and Natural Disaster Studies, School of Atmospheric Sciences, Sun Yat-sen University.)

3:00 PM - 3:15 PM JST | 6:00 AM - 6:15 AM UTC

[AHW23-23] Global Analyis of the Hydrological Sensitivity to Climate Variability

*Marisol Dominguez[1], Hugo Alberto Gutierrez-Jurado[1] (1.University of Texas at El Paso)

Method for measuring the pore air pressure in the mountainous slope for rainfall-runoff processes research

*Sho Iwagami[1], Shoji Noguchi[1], Takanori Shimizu[1], Tayoko Kubota[1], Shin'ichi Iida[1], Makoto Araki[1]

1. Forestry and Forest Products Research Institute, Forest Research and Management Organization, National Research and Development Agency

Many researches have been conducted to clarify the mechanism of rainfall-runoff process in a forested catchment in humid warm-temperate regions. Some results obtained from hydrograph separation using isotopic tracer showed that stream discharge is mainly composed of pre-event old water rather than new water (rainwater). Since the 1980’s, the important issue in rainfall-runoff process studies has been solving how pre-event old water stored in the slope discharge in rapid response during rainstorm event. After 1990’s the role of bedrock groundwater contribution to rainfall-runoff process became to be illustrated. Iwagami et al. (2010) described the contribution of bedrock groundwater during rainfall events in a headwater catchment, however there were some large scale events which were not enough to be explain by the bedrock groundwater contribution. Further possible ideas to explain the rapid outflow of pre-event old water might be effect of pressure wave (Torres et al., 1998) and effect of entrapped air (Marui et al., 1993; Delfs et al., 2013).
Role of pore air effects (e.g., entrapped air and, pressure wave) on rainfall-runoff process are pointed out by previous studies however field evidence of pore air behavior or pore air pressure in the slope scale are still lacking. Also method for pore air pressure observation is not established and not discussed fully. In present study, in order to investigate the behavior of pore air under mountainous slopes, measurements of pore air pressure were conducted at two small headwater catchment in Hitachi Ohta Experimental Watershed and Tsukuba Experimental Watershed, Ibaraki Prefecture, Japan. We measured pore air pressure by detecting the inner pressure of borehole and piezometer. Focusing on the pressure difference between pore air and atmosphere (hereafter we call this as “pressure gap”), it is expected that during a dry period (not during rainfall and ground surface is unsaturated), shallow pore air pressure in the slope is almost at equilibrium state with the atmospheric pressure and the pressure gap might be zero. On the other hand, when the pressure gap was raised remarkably during the rainfall event, pore air is supposed to be entrapped and compressed by infiltrating rainwater (wetting front) and groundwater table (or underlying low permeability layer). During the observation from July 2018 to January 2019, pressure gap rising event have observed in both sites. Also negative pressure gap was observed after the pressure gap rising event. Further observation studies are needed for understanding the effect of entrapped air to rainfall-runoff process which could potentially contribute to the prediction of flash flood or corresponding slope instability.

Keywords: Rainfall-runoff processes, pore air, entrapped air, pressure gap

©2019. Japan Geoscience Union. All Right Reserved.

A method to quantify the influence of total water storage change on climate elasticity of streamflow

*Yin Tang[1]

1. Institute of Geographic Sciences and Natural Resources Research, Chinese Academy of Science

Numerous studies documented the climate elasticity of streamflow (i.e., precipitation elasticity and potential evapotranspiration elasticity) without considering the total water storage change (dS) based on long-term Budyko framework. However, the values of dS have been found to be a significant component of water balance at short time scales (e.g., annual) and some specific watersheds (e.g., arid regions). The purpose of this paper is to develop a new approach based on the extended Budyko framework to quantify the climate elasticity of streamflow with the influence of dS . The available water under the extended Budyko framework is the effective precipitation (Pe), i.e. the difference between precipitation and dS. The climate elasticity of streamflow with the influence of dS are derived from one recent proposed Budyko-type equation based on proportionality relationship under the extended Budyko framework. The performance of this new approach at annual scale as an example is evaluated for 273 MOPEX watersheds in the United States. Results show that climate elasticity of streamflow with the influence of dS are generally larger than that without considering the influence of dS for study watersheds. Results also indicates that the modeled proportional changes in annual streamflow are significantly biased by using the methods without considering the influence of dS, especially for peak values. This study highlights the needs to consider the influence of dS on climate elasticity of streamflow and provides a framework to quantify the climate elasticity of streamflow with the influence of dS.

Keywords: climate elasticity, total water storage change, MOPEX

©2019. Japan Geoscience Union. All Right Reserved.

Trade-off analysis of discharge-desiltation-turbidity and sediment simulation of a combined reservoir–river system under multi-phase and multi-layer conjunctive releasing operation

*Chien-Lin Huang[1], Nien-Sheng Hsu[1], Gene Jiing-Yun You[1]

1. National Taiwan University, Taiwan

Multi-objective reservoir operation considering the trade-off of discharge-desiltation-turbidity during typhoons and sediment concentration simulation modeling are the vital components for sustainable reservoir management. The purpose of this study is to analyze the multi-layer release trade-offs between reservoir desiltation and intake turbidity of downstream purification plants and thus propose a superior conjunctive operation strategy. To this end, this study proposed a methodology to develop (1) a series of multi-phase and multi-layer sediment-flood conjunctive release modes and (2) a specialized sediment concentration numerical model for a combined reservoir–river system. The conjunctive release modes involve (1) an optimization model where the decision variables are multi-phase reduction/scaling ratios and the timings to generate a superior total release hydrograph for flood control (Phase I: phase prior to flood arrival, Phase II/III: phase prior to/subsequent to peak flow) and (2) a combination method with physical limitations regarding separation of the singular hydrograph into multi-layer release hydrographs for sediment control. This study employed the featured signals obtained from statistical quartiles/sediment duration curve in mesh segmentation, and an iterative optimization model with a sediment unit response matrix and corresponding geophysical-based acceleration factors, for efficient parameter calibration. This study applied the developed methodology to the Shihmen Reservoir watershed in Taiwan. The trade-off analytical results using Typhoons Sinlaku and Jangmi as case examples revealed that owing to gravity current and re-suspension effects, Phase I+II can de-silt safely without violating the intake's turbidity limitation before reservoir discharge reaches 2238 m^3/s; however, Phase III can only de-silt after the release at spillway reaches 827 m^3/s, and before reservoir discharge reaches 1924 m^3/s, with corresponding maximum desiltation ratio being 0.221 and 0.323, respectively.

Keywords: Multi-phase sediment-flood management, Sediment concentration modeling, Sediment duration curve, Hydrological statistic, Multi-objective trade-off analysis, Multi-layer conjunctive releasing

©2019. Japan Geoscience Union. All Right Reserved.

Gradient change of soil moisture effect on next-day precipitation identified via a Random Forest-Granger causality model

*Lu Li[1], Wei ShangGuan[1], Shu Peng Zhang[1], Jin Jing Pan[1], Nan Wei[1], Yong Jiu Dai[1]

1. Guangdong Province Key Laboratory for Climate Change and Natural Disaster Studies, School of Atmospheric Sciences, Sun Yat-sen University

Surface soil moisture influences precipitation through its impact on water and energy cycles. Understanding of soil moisture-precipitation (SM-P) coupling on synoptic scale is important for improving short-term weather forecasting. However, the sign and pattern of SM-P feedback are still controversial, mainly caused by the difficulty to establish causal relationship. In this paper, we use empirical models to separate local land-atmosphere coupling effect from low frequency variation and persistence effects, and use Granger causality to identify the casual relationship between surface soil moisture and subsequent precipitation over China. Five experiments are designed to investigate the impact of the discrepancy of datasets and empirical models on SM-P feedback. Differences of SM-P feedback using different SM-P datasets are minor compared to those of empirical models. We improved the SM-P feedback model by using random forest to eliminate low frequency variation and persistence effects instead of generalized linear model. Moreover, we present a novel SM-P feedback framework by considering spatial impact of data, raising a new feature selection method and a new SM-P coupling index. The corresponding pattern of SM-P feedback shows that (1) positive SM-P feedback appears almost all over China. (2) The effect of surface soil moisture on next-day precipitation probability decreases from arid to humid regions over China. (3) The effect of low frequency variation and persistence on precipitation is larger than the effect of soil moisture, but we must emphasize that soil moisture also plays an important role in arid and semi-arid regions. Our finding statically supports the hypothesis that strong SM-P feedback locates in transition zones and SM-P coupling is higher during wet periods for dry regions.

Keywords: Soil moisture-precipitation feedback, random forest, granger causality

©2019. Japan Geoscience Union. All Right Reserved.

Using data-driven methods to explore the predictability of surface soil moisture with FLUXNET site data

*jinjing Pan[1]

1. Guangdong Province Key Laboratory for Climate Change and Natural Disaster Studies, School of Atmospheric Sciences, Sun Yat-sen University.

Soil moisture (SM) is a key variable of land surface-atmosphere interactions. Data-driven methods have been widely used to predict SM, but the predictability of SM has not been well evaluated. This study investigated what variables and methods can be used to better predict SM for leading times of 7 days or longer with a global coverage of FLUXNET site data for the first time. Three machine-learning models, i.e., Bayesian linear regression, random forest and gradient boosting regression tree, are used for the prediction. Variables including atmospheric forcing, surface soil temperature, time variables (year, day of year (DOY) and hour), the Fourier transformation of time variables and lagged SM (7-14 day lagged) were sequentially added into models. A framework with five experiments is designed for factorial exploration of SM predictability. A stepwise method was used to build the best models for each site. The performance of regression models became better when adding more explaining variables in most cases. The results showed that from 47 % to 95% of variation of the best models can be explained. The important explaining variables are lagged surface SM, followed by DOY, year, soil temperature and atmospheric forcing. The predictability of SM depends highly on SM memory characteristics and the persistence of seasonality. The effect of SM memory characteristics on SM prediction as an initial condition question has been widely discussed in this paper. Our results also provide an insight that mechanisms of seasonality effects on SM should be also paid more attention to.

Keywords: A framework with five contrasting experiments is designed to investigate the factors affecting the predictability of soil moisture, The best models can explain between 47% and 95% of variation with different explaining variable combinations at different sites, The most important explaining variable is lagged surface soil moisture, followed by time variables, soil temperature and atmospheric forcing, The predictability of soil moisture depends highly on soil moisture memory characteristics and the persistence of seasonality

©2019. Japan Geoscience Union. All Right Reserved.

Global Analyis of the Hydrological Sensitivity to Climate Variability

*Marisol Dominguez[1], Hugo Alberto Gutierrez-Jurado[1]

1. University of Texas at El Paso

Projected climate changes in the 21st century is expected to have a profound impact in the functioning of Earth's water cycle. Therefore, identifying the components contributing to the sensitivity and resilience of water resources constitutes a research priority of global relevance. Here we present a practical approach to globally assess the hydrologic sensitivity of regions to climate variability. The aim is to identify the regions most vulnerable to changes in their hydrologic functioning as they experience external climatic shifts. For this purpose we present a new metric, the Hydrologic Sensitivity Index (HSI). HSI is calculated for any given location within 50 degrees North and South of the equator using annual values of Potential and Actual Evapotranspiration (PET and AET) obtained from the Moderate Resolution Imaging Spectrometer (MODIS), and Precipitation (P) from the Tropical Rainfall Measuring Mission (TRMM) for all continents for the last 16 years (2001-2016). The HSI defines the hydrologic behavior under a given climatic condition by calculating the change in the Evaporative Index (DAET/P) against the change in the Dryness Index (DPET/P) between consecutive years. For HSI values >=1, regions are classified as Sensitive and for values of <1, Resilient. We calculated the mean, frequency and intensity of the HSI and analyzed the distribution of sensitive areas (HSI >=1) against changes in latitude, elevation, slope and aspect conditions using a 90m elevation dataset from the Shuttle Radar Topography Mission (STRM), as well as according to land cover properties defined by different biome types. Our analysis show the most hydrologically sensitive regions to climate variability occur in Temperate Grasslands along the Great Plains in North American and the Great Dividing Range in Australia, in parts of eastern Asia, in European Temperate Forests, parts of Tropical and Subtropical pampas east of the Amazonian forest and Tropical and Subtropical African Savannas. We also observe a combined latitudinal-elevation control on the HSI that is particularly noticeable along equatorial regions of the globe.

Keywords: Budyko Curve, Climate Variability , Hydrologic Sensitivity, Evapotranspiration, Global Analysis, Elevation and Aspect

©2019. Japan Geoscience Union. All Right Reserved.

[E] Oral | A (Atmospheric and Hydrospheric Sciences)：A-HW Hydrology & Water Environment

Tue. May 28, 2019 3:30 PM - 5:00 PM JST | Tue. May 28, 2019 6:30 AM - 8:00 AM UTC | 103 1F

[A-HW23] Hydrology & Water Environment

convener:Isao Machida(Geological Survey of Japan), Dai Yamazaki(Institute of Industrial Sciences, The University of Tokyo), Takeshi Hayashi(Faculty of Education and Human Studies, Akita University), Keisuke Fukushi(Institute of Nature & Environmental Technology, Kanazawa University), Chairperson:Megumi Watanabe

We focus on various issues of water cycle and environment and aim to answer questions of hydrological and earth system sciences including 1) surface, subsurface and evapotranspiration processes of water cycle; 2) natural and anthropogenic hydrothermal systems, 3) environments issues and studies on a watershed or global scale, 4) water-related issues with ecological, environmental, and geochemical aspects, and 5) other issues in hydrological sciences. This session welcomes presentations regarding various kinds of approaches and techniques such as field survey, remote sensing, isotope tracers, numerical simulation, and theoretical analysis.

3:30 PM - 3:45 PM JST | 6:30 AM - 6:45 AM UTC

[AHW23-06] A review on the global soil property maps for Earth system model

Yongjiu Dai[1], *Wei Shangguan[1], Dagang Wang[2], Nan Wei[1], Qinchuan Xin[2], Hua Yuan[1], Shupeng Zhang[1], Shaofeng Liu[1], Fapeng Yan[3], Xingji Lu[1] (1. Guangdong Province Key Laboratory for Climate Change and Natural Disaster Studies, School of Atmospheric Sciences, Sun Yat-sen University, 2.School of Geography and Planning, Sun Yat-sen University, 3.College of Global Change and Earth System Science, Beijing Normal University)

3:45 PM - 4:00 PM JST | 6:45 AM - 7:00 AM UTC

[AHW23-07] Estimating near surface soil moisture at a high spatial resolution using an in-situ data based model

*Indishe Prabath Senanayake[1], In-Young Yeo[1,2], Natthachet Tangdamrongsub[3,4], Garry R Willgoose[1], Gregory R Hancock[5], Tony Wells[1], Bin Fang[6], Venkataraman Lakshmi[6], Jeffrey P Walker[7] (1.School of Engineering, Faculty of Engineering and Built Environment, The University of Newcastle, Callaghan, NSW 2308, Australia., 2.Department of Geographical Sciences, University of Maryland, College Park, MD 20742, USA., 3.Earth System Science Interdisciplinary Center, University of Maryland, College Park, Maryland, USA., 4.Hydrological Sciences Laboratory, NASA Goddard Space Flight Center, Greenbelt, Maryland, USA., 5.School of Environmental and Life Sciences, Faculty of Science, The University of Newcastle, Callaghan, NSW 2308, Australia., 6.School of Earth Ocean and Environment, University of South Carolina, Columbia, SC 29223, United States., 7.Department of Civil Engineering, Monash University, Clayton, Victoria 3800, Australia.)

4:00 PM - 4:15 PM JST | 7:00 AM - 7:15 AM UTC

[AHW23-08] Representation of dams in global flood inundation simulations by coupling the global hydrological model H08 and the global hydrodynamic model CaMa-Flood

*Julien Eric Boulange[1], Naota Hanasaki[1] (1.National Institute for Environmental Studies)

4:15 PM - 4:30 PM JST | 7:15 AM - 7:30 AM UTC

[AHW23-09] An investigation into a potential long subglacial river beneath the Greenland ice sheet using SICOPOLIS simulations.

*Christopher Chambers[1], Ralf Greve[1], Bas Altena[2], Pierre-Marie Lefeuvre[2] (1.Hokkaido University, 2.University of Oslo)

4:30 PM - 4:45 PM JST | 7:30 AM - 7:45 AM UTC

[AHW23-10] Changes in Annual Rainfall patterns in the Democratic Republic of Congo: Congo river basin

*Chetan Sharma[1], Chandra Shekhar Prasad Ojha[1] (1.Indian Institute of Technology Roorkee)

4:45 PM - 5:00 PM JST | 7:45 AM - 8:00 AM UTC

[AHW23-11] Seasonality in the extreme precipitation events linked to temperature over Japan

*Sridhara Nayak[1], Tetsuya Takemi[1] (1.Disaster Prevention Research Institute, Kyoto University)

A review on the global soil property maps for Earth system model

Yongjiu Dai[1], *Wei Shangguan[1], Dagang Wang[2], Nan Wei[1], Qinchuan Xin[2], Hua Yuan[1], Shupeng Zhang[1], Shaofeng Liu[1], Fapeng Yan[3], Xingji Lu[1]

1. Guangdong Province Key Laboratory for Climate Change and Natural Disaster Studies, School of Atmospheric Sciences, Sun Yat-sen University, 2. School of Geography and Planning, Sun Yat-sen University, 3. College of Global Change and Earth System Science, Beijing Normal University

Soil is an important regulator of Earth system processes, but remains one of the least well-described data layers in Earth System Models (ESMs). We reviewed global soil property maps from the perspective of ESMs, including soil physical and, chemical and biological properties. These soil datasets provide model inputs, initial variables and benchmark datasets. For modeling use, the dataset should be geographically continuous, scalable and with uncertainty estimates. The popular soil datasets used in ESMs are often based on limited soil profiles and coarse resolution soil type maps. Updated and comprehensive soil information needs to be incorporated in ESMs. New generation soil datasets derived by digital soil mapping with abundant, harmonized and quality controlled soil observations and environmental covariates are preferred to those by the taxotransfer rule-based method for ESMs. Because there is no universal pedotransfer function, an ensemble of them may be more suitable to provide derived soil properties to ESMs. Aggregation and upscaling of soil data are needed for model use but can be avoid by taking a subgrid method in ESMs at the cost of increases in model complexity. Uncertainty of soil data needs to be incorporated in ESMs.

Keywords: Earth system model, soil hydrology, soil data, pedotransfer function

©2019. Japan Geoscience Union. All Right Reserved.

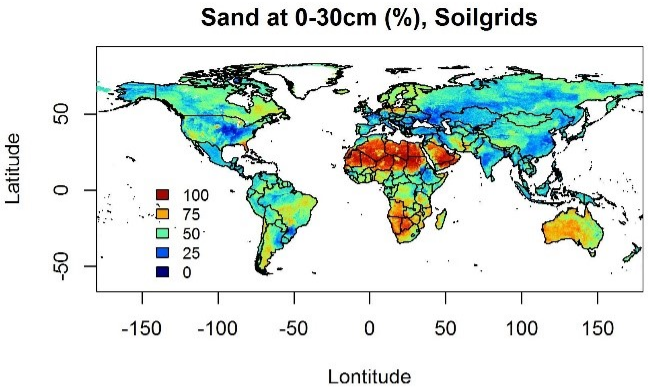

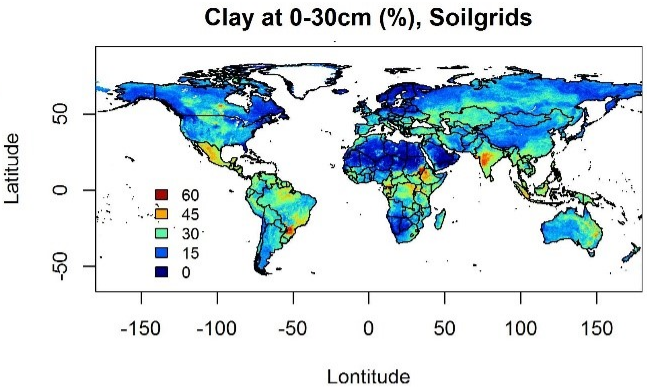

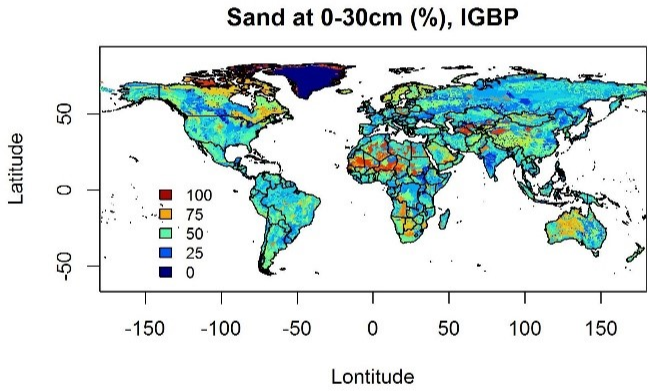

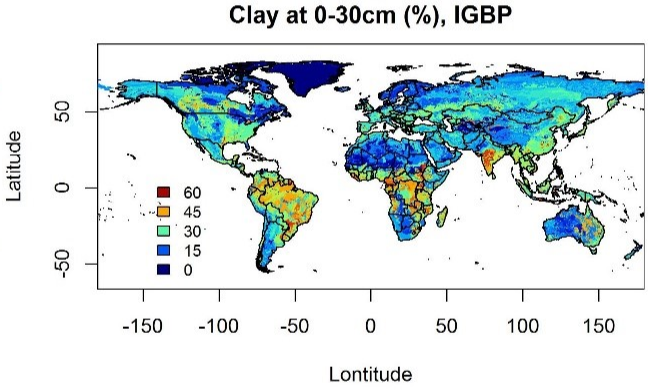

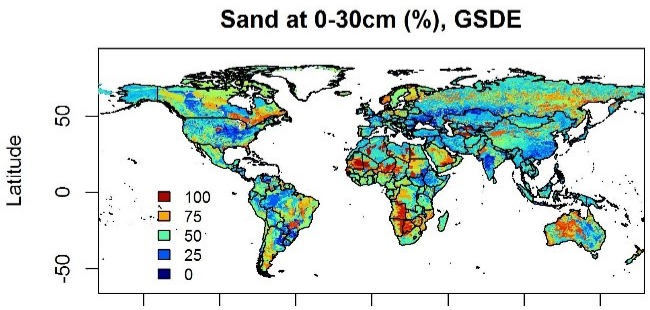

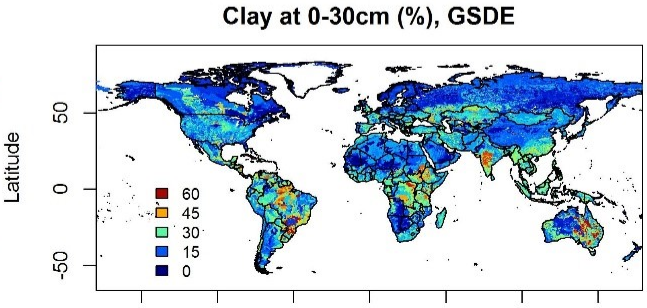

©2019. Japan Geoscience Union. All Right Reserved.

Estimating near surface soil moisture at a high spatial resolution using an in-situ data based model

*Indishe Prabath Senanayake[1], In-Young Yeo[1,2], Natthachet Tangdamrongsub[3,4], Garry R Willgoose[1], Gregory R Hancock[5], Tony Wells[1], Bin Fang[6], Venkataraman Lakshmi[6], Jeffrey P Walker[7]

1. School of Engineering, Faculty of Engineering and Built Environment, The University of Newcastle, Callaghan, NSW 2308, Australia., 2. Department of Geographical Sciences, University of Maryland, College Park, MD 20742, USA., 3. Earth System Science Interdisciplinary Center, University of Maryland, College Park, Maryland, USA., 4. Hydrological Sciences Laboratory, NASA Goddard Space Flight Center, Greenbelt, Maryland, USA., 5. School of Environmental and Life Sciences, Faculty of Science, The University of Newcastle, Callaghan, NSW 2308, Australia., 6. School of Earth Ocean and Environment, University of South Carolina, Columbia, SC 29223, United States., 7. Department of Civil Engineering, Monash University, Clayton, Victoria 3800, Australia.

Soil moisture is a key variable in the hydrologic cycle. Therefore, soil moisture information is important for hydrologic and climatic modelling, and for agricultural applications. However, the available point-scale in-situ observations and coarse resolution (10s of km) satellite soil moisture retrievals are unable to capture the spatial variability of soil moisture at high spatial resolutions as required by many of the local and regional scale applications. The lack of high resolution soil moisture data has resulted uncertainties in the model outcomes in these applications. Downscaling coarse spatial resolution L-band microwave satellite soil moisture products using high spatial resolution optical/thermal satellite data appears to be a feasible option to estimate near surface (~top 5 cm) soil moisture at a high spatial resolution. In this study a model was developed to estimate soil moisture at 1 km spatial resolution by downscaling coarse resolution satellite soil moisture products. This downscaling model was built by using in-situ observations from a long term monitoring network (2004-2015) over two sub-catchments, Krui and Merriwa River, located in the Upper Hunter Region of south-eastern Australia. The model was based on the soil thermal inertia relationship between the diurnal temperature difference (ΔT) and daily mean soil moisture (μSM). A regression tree (RT) was built between ΔT and μSM and classified based on the season, vegetation density and soil clay content. Moderate Resolution Imaging Spectroradiometer (MODIS) land surface temperature (LST) and Normalized Difference Vegetation Index (NDVI) values at 1 km spatial resolution were input to the model to estimate soil moisture at 1 km resolution. Subsequently, SMAP-Enhanced 9 km (L3SMP-E) and SMOS 25 km grid (SMOS CATDS L3 SM 3-DAY) soil moisture products over the study area were downscaled and then compared against in-situ observations. Further, the downscaling algorithm was applied to aggregated soil moisture observations from National Airborne Field Experiment 2005 (NAFE’05) over a 40 x 40 km land area over Krui and Merriwa River catchments. The downscaled products were validated using 1 km airborne data. The SMAP L3SMP-E and SMOS CATDS L3 SM 3-DAY products show unbiased root mean square errors (ubRMSEs) of 0.068 and 0.051 cm^3/cm^3 (R^2 values of 0.40 and 0.61), respectively, against in-situ observations. The downscaled airborne soil moisture data shows an RMSE of 0.07 cm^3/cm^3 (with R value of 0.4). The model performed well in dry conditions compared to wet conditions. This method shows a good potential in developing a long time series of high spatial resolution soil moisture information over arid and semi-arid regions using SMOS and SMAP soil moisture products.

Keywords: Downscaling, remote sensing, SMAP, SMOS, soil moisture, thermal inertia

©2019. Japan Geoscience Union. All Right Reserved.

Representation of dams in global flood inundation simulations by coupling the global hydrological model H08 and the global hydrodynamic model CaMa-Flood

*Julien Eric Boulange[1], Naota Hanasaki[1]

1. National Institute for Environmental Studies

Dams and reservoirs regulate the flow of rivers, storing and releasing water to maximize its availability for human and environmental needs[1]. While regulating water flow is beneficial regarding human water security, it was reported to have rather dire consequences for the environment such as aquatic biota[2,3]. Nevertheless, currently about half of the major global river systems are affected by dams[4].
Global hydrodynamic models have greatly improved in terms of accuracy and computational efficiency in reproducing flood inundation extent[5]. However, to this day, still few such models successfully simulated flood inundation considering the influence of dams.
In this research, the global hydrological model H08[6,7] is coupled to the global hydrodynamic model CaMa-Flood[8] for representing dams in global flood inundation simulation. The input meteorological dataset used in this study were provided by the ISIMIP2b project[9] and consisted of 4 GCMs and 4 scenarios.

The coupled model simulates river discharge and inundation globally at a daily interval, at a spatial resolution of 0.5˚ ×0.5˚. Discharge predicted with the original CaMa-Flood model were compared to those obtained with the coupled model. The seasonal discharge in rivers heavily affected by reservoir operation were very different between the two simulations. Generally, annual minimum (maximum) 7-day discharge was significantly higher (lower) for the simulation explicitly representing dams. In addition, timings of the discharge peaks were also different between the 2 simulations. We deeply investigated the results in several selected river basins.

References:

1 Ehsani, N., Vörösmarty, C. J., Fekete, B. M. & Stakhiv, E. Z. *J. Hydrol.* (2017).
2 Pringle, C., Freeman, M. & Freeman, B. *Regional Effects of Hydrologic Alterations on Riverine Macrobiota in the New World: Tropical–Temperate Comparisons*. Vol. 50 (2000).
3 Kingsford, R. T. *Austral Ecology* (2000).
4 Dynesius, M. & Nilsson, C. *Science* (1994).
5 Teng, J. *et al. Environmental Modelling & Software* (2017).
6 Hanasaki, N. *et al. Hydrol. Earth Syst. Sci.* (2008).
7 Hanasaki, N. *et al. Hydrol. Earth Syst. Sci.* (2008).
8 Yamazaki, D., Kanae, S., Kim, H. & Oki, T. *Water Resour. Res.* (2011).
9 Frieler, K. *et al. Geosci. Model Dev. Discuss.* (2016).

Keywords: Global hydrology, Flood, H08 model, CaMa-Flood model

©2019. Japan Geoscience Union. All Right Reserved.

An investigation into a potential long subglacial river beneath the Greenland ice sheet using SICOPOLIS simulations.

*Christopher Chambers[1], Ralf Greve[1], Bas Altena[2], Pierre-Marie Lefeuvre[2]

1. Hokkaido University, 2. University of Oslo

The Greenland ice sheet appears to be hiding large geographical features at its base that have the potential to affect ice sheet simulations to an unknown degree. One feature is a broken valley extending from Petermann Fjord far into the center of Greenland revealed by the widely used BedMachine basal topographic dataset. The valley appears to be blocked by topographic rises at many points along its route, however it will be demonstrated that these blockages are entirely artificial consequences of data interpolation and that all available data indicate that the valley is not blocked. To test whether opening up this valley could affect ice sheet sliding, SImulation COde for POLythermal Ice Sheets (SICOPOLIS) simulations are used. The simulations show that opening up this valley creates an uninterrupted potential subglacial water pathway from central Greenland to Petermann Fjord (Figure 1) suggesting that water could flow along its length. The reason this is possible is because the valley tracks down a gentle ice thickness gradient as it roughly follows the ice divide. The redistribution of water towards Petermann Glacier focuses increased sliding there. There is also a small reduction of sliding in central west Greenland. Other effects of this valley on the ice-sheet hydrology and dynamics will be presented. If confirmed with further radar bed observations, this would be a great world river the runs under ice for its entire length, a distance that could be up to 1600 km.

Keywords: ice, glacier, river, Greenland, climate

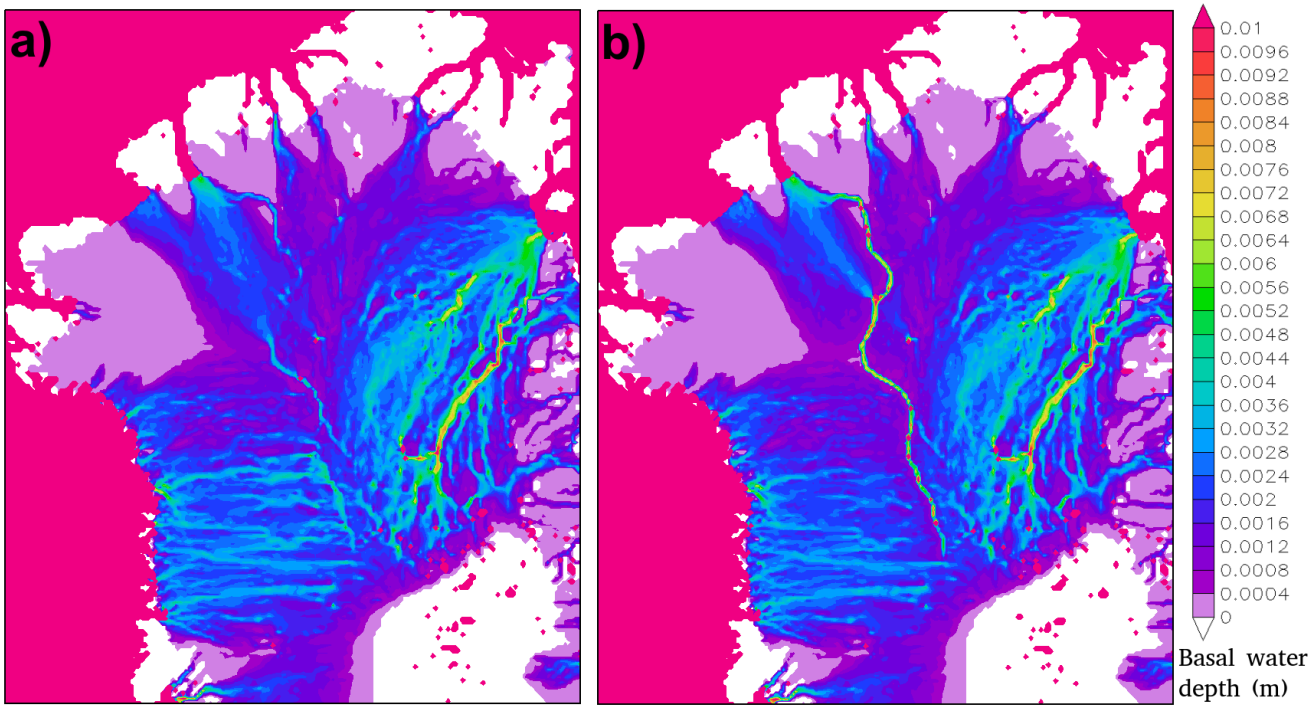

Figure 1: Basal water depth (m) for a) standard bed and b) valley inserted.

©2019. Japan Geoscience Union. All Right Reserved.

Changes in Annual Rainfall patterns in the Democratic Republic of Congo: Congo river basin

*Chetan Sharma[1], Chandra Shekhar Prasad Ojha[1]

1. Indian Institute of Technology Roorkee

This study focuses on the change detection in annual rainfall in the Democratic Republic of Congo (DRC) in the Congo river basin. High resolution gridded rainfall provided by Climate Research Unit (CRU) is used in this study. Trends in the annual rainfall patterns are calculated and the significance of the trends are found out using non-parametric Mann-Kendal test at 10% significance level. It is found that high negative trends are prevailing in Northern and Southern parts and high positive trends are in the Eastern and Western parts of the Congo river basin. Almost all of these locations show a significant trend. Central wetlands don’ t show a significant change in annual rainfall pattern. Change detection studies are carried out to detect year of change when annual rainfall starts showing deviation from its natural state. Mann-Whitney-Pettit method is used to detect year of change at 5% significance level in this study. Change is detected for almost all of the locations where the trend of annual rainfall is significant. Much earlier change is detected in the Eastern regions of the basin, i.e., the change year 1941-1960, while most of the Northern, Southern and Westerns shows change detection year from 1981-1995.
It is evident from this study that rainfall patterns in the Congo river basin are changing and the changes are non-uniform. There is no change detected in the central regions, while Northern and Southern areas show a significant decrease in rainfall and Eastern and Western regions are showing an increase in total annual rainfall. Change detection year also have non-uniform spatial patterns and Eastern regions are found to be affected much earlier by climate change.

Keywords: Change Detection, Congo river basin, Rainfall

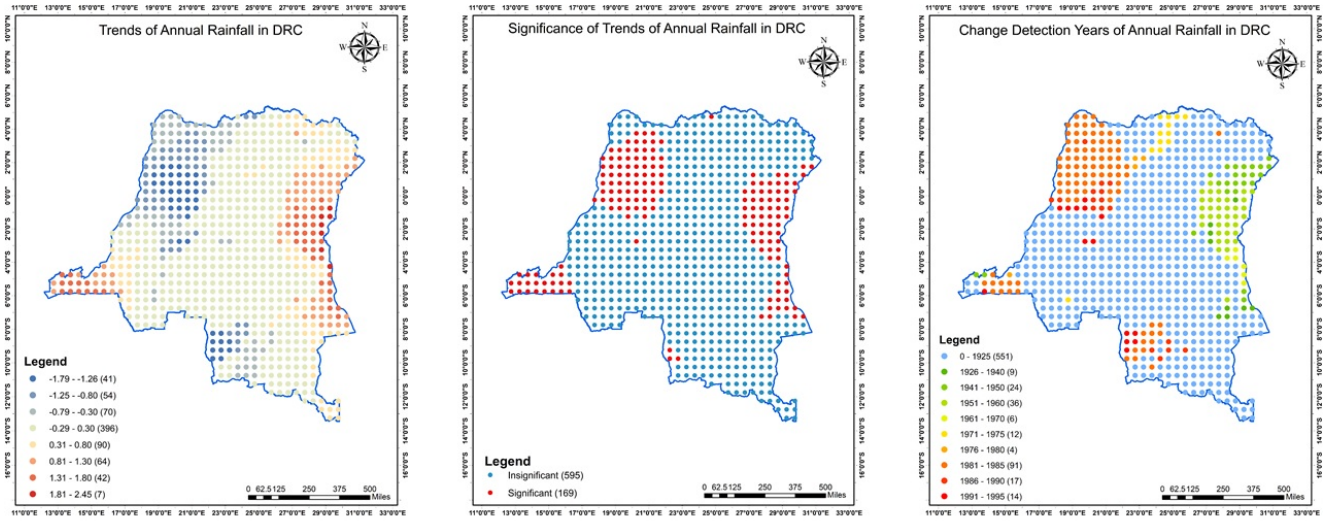

(a) (b) (c)

Fig-1. Annual Rainfall Patterns and Changes in Democratic Republic of Congo (DRC): Congo River basin (a) Trends (b) Significance of rends (c) Change Detection Year

©2019. Japan Geoscience Union. All Right Reserved.

Seasonality in the extreme precipitation events linked to temperature over Japan

*Sridhara Nayak[1], Tetsuya Takemi[1]

1. Disaster Prevention Research Institute, Kyoto University

The frequency of extreme precipitation events is expected to increase in future warmer climate according to the Clausius-Clapeyron (CC) equation which states that atmosphere can hold more moisture in warmer air temperature (about 7 percent per increase of 1ºC). In this study, the extreme precipitation intensities linked to temperature are investigated for different seasons over seven sub-regions of Japan by analyzing the d4PDF dataset at 20 km in present (1951-2010) and future climate (2051-2110). To do this we stratified the precipitation intensities of wet days (defined as excess of 1 mm per day) in different temperature bins at 1º intervals and computed the 99-percentile of the precipitation intensities from each temperature bin. We find that the extreme precipitation intensities linked to temperature is strongly influenced by the seasons and regions of Japan. The extreme precipitation intensities increase with temperature up to 21º over northern Japan, while the extreme precipitation intensities over Okinawa increase up to 24º. Intensities of extreme precipitation events over northern parts of Japan including Hokkaido and Tohoku regions are increased by about 10 mm per day in future warming climate, while over western regions of Japan it is increased by about 20 mm per day. Seasonal analysis indicates a super CC relationship in winter season and a sub CC relationship in summer. Overall results suggest that Japanese regions may experience more extreme precipitations in future warming climate.

Keywords: Extreme Precipitation Events, d4PDF, Clausius-Clapeyron Equation

©2019. Japan Geoscience Union. All Right Reserved.

[J] Oral | A (Atmospheric and Hydrospheric Sciences)：A-CC Cryospheric Sciences & Cold District Environment

Tue. May 28, 2019 9:00 AM - 10:30 AM JST | Tue. May 28, 2019 12:00 AM - 1:30 AM UTC | 201B 2F

[A-CC26] Ice cores and paleoenvironmental modeling

convener:Ryu Uemura(University of the Ryukyus), Kenji Kawamura(National Institute of Polar Research, Research Organization of Information and Systems), Ayako Abe-Ouchi(Atmosphere and Ocean Research Institute, The University of Tokyo), Nozomu Takeuchi(Chiba University), Chairperson:Ryu Uemura(University of the Ryukyus), Ikumi Oyabu(National Institute of Polar Research)

Analyses of ice cores from polar and mountain regions have contributed to the reconstruction and understanding of the past environmental changes on timescales from years to several hundred thousand years. In this session, we welcome paleoenvironmental studies using ice cores and paleoclimatic modeling. Studies on reconstruction methods, recording processes and new paleoenvironmental proxies, technical aspects of paleo-modeling are also welcomed. Studies with marine sediment cores, terrestrial sediment cores and tree-rings on similar timescales are also important and welcomed, in order to discuss past environmental changes from multidisciplinary viewpoints.

9:00 AM - 9:15 AM JST | 12:00 AM - 12:15 AM UTC

[ACC26-01] Aerosols and climate change in the Arctic in the historical experiments using the MRI Earth System Model

★Invited Papers

*Naga Oshima[1], Taichu Y Tanaka[1], Tsuyoshi Koshiro[1], Makoto Deushi[1], Takuro Aizawa[1], Masahiro Hosaka[1], Hideaki Kawai[1], Seiji Yukimoto[1], Iizuka Yoshinori[2], Kumiko Goto-Azuma[3], Teruo Aoki[4] (1.Meteorological Research Institute, 2.Institute of Low Temperature Science, Hokkaido University, 3.National Institute of Polar Research, 4.Okayama University)

9:15 AM - 9:30 AM JST | 12:15 AM - 12:30 AM UTC

[ACC26-02] Particles in ice layers of SIGMA-A ice core, northwestern Greenland

*Kaoru Kawakami[1,2], Yoshinori Iizuka[2], Sumito Matoba[2], Teruo Aoki[3], Shin Sugiyama[2], Takuto Ando[4] (1.Graduate School of Environmental Science, Hokkaido University, 2.Institute of Low Temperature Science, Hokkaido University, 3.Graduate School of Natural Science and Technology, Okayama University, 4.Arctic Research Center, Hokkaido University)

9:30 AM - 9:45 AM JST | 12:30 AM - 12:45 AM UTC

[ACC26-03] Snow modification due to climate change in southeastern high-accumulation area of Greenland over the last 60 years evaluated by physical properties of firn core.

*Takuto Ando[1], Iizuka Yoshinori[2,3], Mai Shibata[2,3], Sumito Matoba[2,3], Shin Sugiyama[2,3], Satoru Adachi[4], Satoru Yamaguchi[4], Koji Fujita[5], Akira Hori[6], Teruo Aoki[7], Shuji Fujita[8] (1.Arctic Research Center, Hokkaido University, 2.Institute of Low Temperature Science, Hokkaido University, 3.Graduate School of Environmental Science, Hokkaido University, 4.National Research Institute for Earth Science and Disaster Resilience, 5.Graduate School of Environmental Studies, Nagoya University, 6.Department of Civil and Environmental Engineering, Kitami Institute of Technology, 7.Graduate School of Natural Science and Technology, Okayama University, 8. National Institute of Polar Research)

9:45 AM - 10:00 AM JST | 12:45 AM - 1:00 AM UTC

[ACC26-04] Temporal variations of concentrations, size distributions, and seasonal variations of anthropogenic and natural black carbon in Greenland

*Kumiko Goto-Azuma[1,2], Yoshimi Ogawa-Tsukagawa[1], Yutaka Kondo[1], Remi Dallmayr[1,10], Motohiro Hirabayashi[1], Jun Ogata[1], Kyotaro Kitamura[1], Kenji Kawamura[1,2], Hideaki Motoyama[1,2], Sumito Matoba[3], Teruo Aoki[4], Nobuhiro Moteki[5], Sho Ohata[5], Tatsuhiro Mori[6], Makoto Koike[5], Yuki Komuro[7], Akane Tsushima[8,9], Naoko Nagatsuka[1], Wataru Shigeyama[1,2], Koji Fujita[9] (1.National Institute of Polar Research, 2.SOKENDAI, 3.Hokkaido University, 4.Okayama University, 5.University of Tokyo, 6.University

of Science, 7.Yamagata University, 8.Research Institute for Humanity and Nature, 9.Nagoya University, 10.AWI)

10:00 AM - 10:15 AM JST | 1:00 AM - 1:15 AM UTC

[ACC26-05] Mineral composition of dust layers in a shallow ice core drilled in Pamir Alay Mountains of Central Asia

*Shunsuke Takeuchi[1], Nozomu Takeuchi[1], Koji Fujita[2], Kenji Kawamura[3], Akane Tsushima[2], Vladimir Aizen[4] (1.Chiba University, 2.Nagoya University, 3.National Institute of Polar Research, 4.Idaho University)

10:15 AM - 10:30 AM JST | 1:15 AM - 1:30 AM UTC

[ACC26-06] Estimation of snow surface patterns from the coast to the inland, Dome-Fuji Station, of Antarctica, using camera images

*Konosuke Sugiura[1], Kengo Watanabe[1], Naohiko Hirasawa[2], Kenji Kawamura[2], Fumio Nakazawa[2], Hiroshi Ohno[3], Shuji Fujita[2], Ikumi Oyabu[2], Takashi Yamanouchi[2], Hideaki Motoyama[2] (1.University of Toyama, 2.National Institute of Polar Research, 3.Kitami Institute of Technology)

Aerosols and climate change in the Arctic in the historical experiments using the MRI Earth System Model

*Naga Oshima[1], Taichu Y Tanaka[1], Tsuyoshi Koshiro[1], Makoto Deushi[1], Takuro Aizawa[1], Masahiro Hosaka[1], Hideaki Kawai[1], Seiji Yukimoto[1], Iizuka Yoshinori[2], Kumiko Goto-Azuma[3], Teruo Aoki[4]

1. Meteorological Research Institute, 2. Institute of Low Temperature Science, Hokkaido University, 3. National Institute of Polar Research, 4. Okayama University

Atmospheric aerosols modify the global radiation budget directly through scattering and absorption of solar radiation and indirectly through modification of the microphysical properties of clouds. However, there remain large uncertainties in estimates of aerosol effects on the climate system because of the insufficient prediction of aerosols in the Arctic by previous climate models.
Meteorological Research Institute (MRI) has developed a new version of MRI Earth System Model (MRI-ESM2) for participating in the Coupled Model Intercomparison Project Phase 6 (CMIP6). MRI-ESM2 is an updated version of MRI-ESM1 and consists of four major component models; an atmospheric general circulation model with land processes (a horizontal resolution of approximately 120 km), an ocean-sea-ice general circulation model, an aerosol model (approximately 180 km), and an atmospheric chemistry model (approximately 280 km). The number of vertical levels of MRI-ESM2 is 80 (model top at 0.01 hPa). As MRI-ESM2 shows the improvement of prediction of aerosol variations in the recent Arctic, we estimate effects of aerosols on climate change in the Arctic from the pre-industrial to present conditions.
We conducted the CMIP6 historical experiment (1850-2014) by MRI-ESM2 and compared the model results with the ice core data in Greenland. In the comparisons, we used three types of model calculation results; the MRI-ESM2 calculation with the CMIP6 emission inventory, the MRI-ESM2 calculation with the CMIP5 emission inventory, and the previous MRI-ESM1 calculation with the CMIP5 emission inventory. The comparison with the Greenland SouthEastern Dome (SE-Dome) ice core data shows that the MRI-ESM2 calculations successfully reproduce the temporal variation of deposition flux of sulfate, although the previous MRI-ESM1 calculation largely underestimates the sulfate. The historical experiments by MRI-ESM2 show that sulfate at SE-Dome was mostly originating from anthropogenic sources in winter, but natural sources also played an important role in summer. The comparison with the ice core data at the D4 site shows that the MRI-ESM2 calculation with the CMIP6 emission could not reproduce the enhancement of black carbon concentrations in the early 20th century, but the MRI-ESM2 calculation with the CMIP5 emission could. This result suggests that there still remain large uncertainties in the emission inventory of black carbon. The CMIP6 historical experiments by MRI-ESM2 suggest that the aerosols play an important role for temperature changes in the Arctic. The predictions of the surface air temperature changes by MRI-ESM2 are improved from the previous model both in global and the Arctic. These results indicate the importance of analyses of ice cores for improvement of predictions of climate models and the usefulness of climate models for interpretation of ice core data.

Keywords: Aerosol, Climate model, Ice core, Climate change, Environmental change, Arctic

©2019. Japan Geoscience Union. All Right Reserved.

Particles in ice layers of SIGMA-A ice core, northwestern Greenland

*Kaoru Kawakami[1,2], Yoshinori Iizuka[2], Sumito Matoba[2], Teruo Aoki[3], Shin Sugiyama[2], Takuto Ando[4]

1. Graduate School of Environmental Science, Hokkaido University, 2. Institute of Low Temperature Science, Hokkaido University, 3. Graduate School of Natural Science and Technology, Okayama University, 4. Arctic Research Center, Hokkaido University

Arctic atmospheric warming accelerates surface melting on the Greenland ice sheet. In the accumulation areas of the Greenland ice sheet, ice layers are formed by snowmelt and refreezing processes during summer. In the snowmelt water, chemical substances originated from atmospheric soluble aerosols exist as dissolved anion and cation species. After refreezing process, the ions are preserved in the state of acid or salt in the refrozen ice layer. However, the behavior of inclusions in refreezing ice layers is still unclear. In this study, we observed salt inclusions in ice layers of a Greenlandic ice core to understand how and where inclusions were formed along the snowmelt and refreezing process.
During spring 2017, a 60m ice core (hereinafter referred to as SIGMA-A core) was drilled on the northwestern Greenland (78º 03′06″N, 67º 37′42″W, 1490 m a.s.l), which covers the past 100 years. The SIGMA-A core has 243 ice layers (longer than 1mm in thickness), whose mean thickness is 13.8mm.Both the number and the thickness of ice layers have increased in recent 30 years. In a -20℃ cold room of Institute of Low Temperature Science, Hokkaido University, ice layers formed in 2006 and 2014 were selected from the SIGMA-A ice core. The two ice layers were cut to three sections of 40*6.56*25 mm(the 2014 sample), 40*5.45*75 mm(the bottom part of 2006 sample), 40*6*80 mm(the top part of 2006 sample) in the -20℃ cold room. Then, the size and location of inclusions in the sections were observed by a measuring microscope (OLYMPUS, STM-UM) in the cold room. The chemical composition of inclusions were identified by Raman spectroscopy in a cold chamber at -30℃ with the same method described in Ohno et al.[1].
The location of inclusions tends to be the bottom part of the both ice layers. The mean particle size is 17.6μm, which is larger than that in other dry ice cores. For example, the mean size of particles in Greenland NEEM core is about 1-4μm[2], and that in Dome Fuji core is 1-3 μm[1]. Also, inclusions are identified as $Na_2SO_4 \cdot 10H_2O$ and $CaSO_4 \cdot 2H_2O$ by the Raman measurements. The snowmelt and refreezing processes may produce huge salt inclusions at the last stage of refreezing due to ion redistribution.

References

[1] Ohno, H., et al. (2006), Characteristics of salt inclusions in polar ice from Dome Fuji, East Antarctica, *Geophysical Research Letters*, **33**, 8, L08501.

[2] Oyabu, I., et al. (2015), Chemical compositions of solid particles present in the Greenland NEEM ice core over the last 110,000 years, *J. Geophys. Res. Atmos.*, **120**, 9789–9813.

Keywords: ice core, Greenland, SIGMA-A

©2019. Japan Geoscience Union. All Right Reserved.

Snow modification due to climate change in southeastern high-accumulation area of Greenland over the last 60 years evaluated by physical properties of firn core.

*Takuto Ando[1], Iizuka Yoshinori[2,3], Mai Shibata[2,3], Sumito Matoba[2,3], Shin Sugiyama[2,3], Satoru Adachi[4], Satoru Yamaguchi[4], Koji Fujita[5], Akira Hori[6], Teruo Aoki[7], Shuji Fujita[8]

1. Arctic Research Center, Hokkaido University, 2. Institute of Low Temperature Science, Hokkaido University, 3. Graduate School of Environmental Science, Hokkaido University, 4. National Research Institute for Earth Science and Disaster Resilience, 5. Graduate School of Environmental Studies, Nagoya University, 6. Department of Civil and Environmental Engineering, Kitami Institute of Technology, 7. Graduate School of Natural Science and Technology, Okayama University, 8. National Institute of Polar Research

Information of ice sheet albedo in the past is necessary for improving climatic models and future prediction. Snow grain size is indispensable property for evaluating surface albedo of ice sheets. The large parts of firn/ice core samples, however, have already lost information of initial snow grain size after densification. It is important to develop indicators to evaluate history of snow grain modification from firn/ice core samples. There is a correlation between specific surface area (SSA) and near-infrared reflectance (NIR). Continuous SSA values of core samples can be obtained by near-infrared reflectance analysis. We collected the firn core from SE-Dome, the southeastern Greenland in 2015. The SE-Dome firn core records the seasonal variations over the last 60 years due to their higher accumulation rate (~1m/year). In the present study, we focused on relationship between density and NIR and reconstructed the relationship between climate change and snow grain modification over the last 60 years.
Density and NIR data from the SE-Dome ice core are negatively correlated in the long-term trend. These negative correlations show SSA values basically decrease with snow densification. On the other hand, there is positive correlation between density and NIR data in the short-time trend. Both density and NIR of summer samples particularly tend to be lower value than those of samples deposited during other seasons in same year. Timing and number of the low-SSA and low-density layers are related to those of the periods in which air temperature reaching over -5 ℃ continued. This relationship shows the formation of low-SSA and low-density layers enhanced even though air temperature was less than 0℃. The low-SSA and low-density layers are caused by density reduction due to snow sublimation on the surface of ice sheet.

Keywords: Greenland, physical property, near-infrared reflectance , firn, snow grain, albedo

©2019. Japan Geoscience Union. All Right Reserved.

Temporal variations of concentrations, size distributions, and seasonal variations of anthropogenic and natural black carbon in Greenland

*Kumiko Goto-Azuma[1,2], Yoshimi Ogawa-Tsukagawa[1], Yutaka Kondo[1], Remi Dallmayr[1,10], Motohiro Hirabayashi[1], Jun Ogata[1], Kyotaro Kitamura[1], Kenji Kawamura[1,2], Hideaki Motoyama[1,2], Sumito Matoba[3], Teruo Aoki[4], Nobuhiro Moteki[5], Sho Ohata[5], Tatsuhiro Mori[6], Makoto Koike[5], Yuki Komuro[7], Akane Tsushima[8,9], Naoko Nagatsuka[1], Wataru Shigeyama[1,2], Koji Fujita[9]

1. National Institute of Polar Research, 2. SOKENDAI, 3. Hokkaido University, 4. Okayama University, 5. University of Tokyo, 6. University of Science, 7. Yamagata University, 8. Research Institute for Humanity and Nature, 9. Nagoya University, 10. AWI

An ice core retrieved at the SIGMA-D site, Northwest Greenland, in 2014 was analyzed down to the depth of 113 m. Between 6 and 113 m depths, we used a Continuous Flow Analysis (CFA) system developed at the National Institute of Polar Research. The CFA system enabled us to obtain high resolution data of black carbon (BC), stable isotopes of water, microparticles and six elements (Na, K, Mg, Ca, Fe, and Al). The top 6 m of the core was cut at a ca 5 cm interval, melted and analyzed. For BC analysis, we used a recently developed Wide-range SP2 (Single Particle Soot Photometer). We dated the core by annual layer counting using mainly Na and water stable isotopes, with occasional use of other impurities. We divided a year into 12 months and calculated monthly averaged BC concentrations and size distributions.
Here we report the variability of monthly resolved BC concentrations and size distributions over the past 350 years. BC number and mass concentrations started to increase in the 1870s, reached its maximum in the 1920s - 1930s, and decreased again since then. The increases are likely due to anthropogenic input. The increases are most significant in fall and winter months. We find anthropogenic changes in seasonality of BC concentration: annual concentration peak shifted from summer to winter. We also find anthropogenic changes in size distribution of BC: the mode diameter of mass concentration and average mass of BC particles became larger. This suggests that anthropogenic BC particles are larger than natural ones in the snow deposited in Greenland. Apart from anthropogenic BC, BC concentration occasionally showed large spikes in summer. They are likely originated from biomass burnings. We will compare the results from the SIGMA-D core with those from other ice cores drilled in Greenland and discuss spatial variations of BC.

Keywords: Black carbon, Greenland, Ice core

©2019. Japan Geoscience Union. All Right Reserved.

Mineral composition of dust layers in a shallow ice core drilled in Pamir Alay Mountains of Central Asia

*Shunsuke Takeuchi[1], Nozomu Takeuchi[1], Koji Fujita[2], Kenji Kawamura[3], Akane Tsushima[2], Vladimir Aizen[4]

1. Chiba University, 2. Nagoya University, 3. National Institute of Polar Research, 4. Idaho University

Dust (mineral particles) contained in the ice core has been used as a proxy of past atmospheric circulation or arid climate condition. Most of dust studies have just analyzed dust flux and size distribution, but little study focused the meteorological type and composition of dust. Since the type and composition of dust varies depending on its origin and transport process, they are potential to reveal detailed source of dust and atmospheric circulation fluctuation. In this study, we analyzed mineral composition of dust layers of a shallow ice core drilled in the Pamir Alay Mountains of Central Asia of Kyrgyz Republic in August 2016, using an optical microscope and a scanning electron microscope.
The depth profiles of dust differed between small size ($1<d\leqq15$ μm) and large size ($d>15$ μm). The dust layers consisting mainly of small size dust contained abundant yellow colored minerals, while those with large size dust contained more abundant red colored minerals. Furthermore, the dust layers of large size dust contained calcite originating from limestone, which is an unique geology of Pamir region, indicating they are originate from near the glacier. Results revealed that the mereological type and composition differed significantly among the dust layers of the ice core. In particular, they are possibly originated from two different sources, including a short distance consisting of calcite and red mineral, and a long-distance without them.

Keywords: Glacier, Ice core, Dust, Colored mineral, Mineral composition, Pamir

©2019. Japan Geoscience Union. All Right Reserved.

Estimation of snow surface patterns from the coast to the inland, Dome-Fuji Station, of Antarctica, using camera images

*Konosuke Sugiura[1], Kengo Watanabe[1], Naohiko Hirasawa[2], Kenji Kawamura[2], Fumio Nakazawa[2], Hiroshi Ohno[3], Shuji Fujita[2], Ikumi Oyabu[2], Takashi Yamanouchi[2], Hideaki Motoyama[2]

1. University of Toyama, 2. National Institute of Polar Research, 3. Kitami Institute of Technology

Snow surface patterns in Antarctica are of practical concern and are important from the standpoint of developing an optimum route in Antarctica. In this study, we estimate snow surface patterns from the coast to the inland of Antarctica using camera images during JARE-59. The interval camera was used to capture the image of snow surface. Snow surface was photographed from November 13, 2017 to December 9, 2017. The number of images from the southern latitude of 69 degrees to 77 degrees was about 14,000 sheets. One sheet was divided into eight zones to distinguish a small-scale snow surface pattern. The pattern of snow surface was classified in three kinds such as 1) deposition, 2) equilibrium, and 3) erosion. We judged the snow surface patterns by sight. When Snow dune/Snow barchan was observed, it was classified as a deposition pattern. When Sastrugi/Glazed surface was observed, it was classified as an erosion pattern. In addition, when snow ripples were observed, it was classified as an equilibrium pattern.
The result of our analysis shows that the frequency of the deposition pattern decreases as latitude rises to 73 degrees south (Katabatic wind region) and then it increases slightly. In contrast, the frequency of the erosion pattern increases as latitude rises to 73 degrees south above which it decreases slightly. On the other hand, there have been no outstanding changes in the equilibrium pattern. The analyzed results of latitude dependence agree with the previous research qualitatively. However, the dominant surface pattern in the inland plateau region was still the erosion pattern. Since we analyzed the data of the outward trip, it is necessary to analyze the data of the return trip from the inland to the coast and to investigate a time scale of the surface pattern changes.

Keywords: snow dune, snow barchan, sastrugi, glazed surface, snow ripple

©2019. Japan Geoscience Union. All Right Reserved.

[J] Oral | A (Atmospheric and Hydrospheric Sciences)：A-CC Cryospheric Sciences & Cold District Environment

Tue. May 28, 2019 10:45 AM - 12:15 PM JST | Tue. May 28, 2019 1:45 AM - 3:15 AM UTC | 201B 2F

[A-CC26] Ice cores and paleoenvironmental modeling

convener:Ryu Uemura(University of the Ryukyus), Kenji Kawamura(National Institute of Polar Research, Research Organization of Information and Systems), Ayako Abe-Ouchi(Atmosphere and Ocean Research Institute, The University of Tokyo), Nozomu Takeuchi(Chiba University), Chairperson:Nozomu Takeuchi(千葉大学), Kenji Kawamura(国立極地研究所)

Analyses of ice cores from polar and mountain regions have contributed to the reconstruction and understanding of the past environmental changes on timescales from years to several hundred thousand years. In this session, we welcome paleoenvironmental studies using ice cores and paleoclimatic modeling. Studies on reconstruction methods, recording processes and new paleoenvironmental proxies, technical aspects of paleo-modeling are also welcomed. Studies with marine sediment cores, terrestrial sediment cores and tree-rings on similar timescales are also important and welcomed, in order to discuss past environmental changes from multidisciplinary viewpoints.

10:45 AM - 11:00 AM JST | 1:45 AM - 2:00 AM UTC

[ACC26-07] Isolation of living fungi from Antarctic ice cores

★Invited Papers

*Masaharu Tsuji[1] (1.National Institute of Polar Research)

11:00 AM - 11:15 AM JST | 2:00 AM - 2:15 AM UTC

[ACC26-08] Study of ancient fungi resting in the polar ice cores and its future prospects

*Fumio Nakazawa[1,2], Masaharu Tsuji[1], Satoshi Imura[1,2] (1.National Institute of Polar Research, 2.SOKENDAI (The Graduate University of Advanced Studies))

11:15 AM - 11:30 AM JST | 2:15 AM - 2:30 AM UTC

[ACC26-09] Flux, provenance and modification of terrestrial dust and sea salt in the Dome C and Dome Fuji ice cores from Last Glacial Maximum to early Holocene by ice-sublimation and single-particle measurement of soluble and insoluble particles

*Ikumi Oyabu[1,2], Iizuka Yoshinori[3], Kenji Kawamura[1,4,5], Eric Wolff[6], Mirko Severi[7], Margareta Hansson[8] (1.National Institute of Polar Research, Research Organization of Information and Systems, 2.Japan Society for the Promotion of Science, 3.Institute of Low Temperature Science, Hokkaido University, 4.SOKENDAI (The Graduate University of Advanced Studies), 5.Japan Agency for Marine Science and Technology (JAMSTEC), 6.Department of Earth Sciences, University of Cambridge, 7.Department of Chemistry “Ugo Schiff”, University of Florence, 8.Department of Physical Geography, Stockholm University)

11:30 AM - 11:45 AM JST | 2:30 AM - 2:45 AM UTC

[ACC26-10] Spatial variation of surface mass balance over the last few millennia in the Dome Fuji area from the analyses of shallow ice cores

*Kenji Kawamura[1], Ikumi Oyabu[1], Fumio Nakazawa[1,2], Shuji Fujita[1,2], Kyohei Yamada[1], Naoyuki Kurita[4], Shun Tsutaki[5], Hiroshi Ohno[6], Konosuke Sugiura[7], Kumiko Goto-Azuma[1,2], Hideaki Motoyama[1,2], Ayako Abe-Ouchi[5,3] (1.National Institute of Polar Research, Research Organization of Information and Systems, 2.SOKENDAI (The Graduate University of Advanced Studies), 3.JAMSTEC, 4.Nagoya University, 5.University of Tokyo, 6.Kitami Institute of Technology, 7.University of Toyama)

11:45 AM - 12:00 PM JST | 2:45 AM - 3:00 AM UTC

[ACC26-11] Sensitivity of global nonhydrostatic atmospheric model to changes in orbital forcing for the early Holocene

*Minoru Chikira[1], Ayako Abe-Ouchi[1], Masaki Satoh[1] (1.Atmosphere and Ocean Research Institute, The University of Tokyo)

12:00 PM - 12:15 PM JST | 3:00 AM - 3:15 AM UTC

[ACC26-12] **Roles of sea ice–surface wind feedback in maintaining contrasting modes of glacial Atlantic meridional overturning circulation and climate**

*Sam Sherriff-Tadano[1], Ayako Abe-Ouchi[1] (1.Atmosphere and Ocean Research Institute, the University of Tokyo)

Isolation of living fungi from Antarctic ice cores

*Masaharu Tsuji[1]

1. National Institute of Polar Research

15 million years ago, the temperature of Antarctica was about 11 ℃ higher than the current temperature [(1)]. Many of fungi reported from Antarctica have also been reported from a variety of extreme, perennial cold environments including the Arctic, Siberia, the Alps, Alaska, Patagonia. Since these fungi have only been reported from the environment like the polar desert, fungi currently inhabited in Antarctica are thought to have come after 15 million years ago. However, the origins of the fungi inhabiting Antarctica are unknown.

In this presentation, to elucidate the origin and evolution of Antarctic fungi, I would like to introduce the isolation of Antarctic fungi from Antarctic ice cores.

Keywords: Ice core, Ancient fungi, Antarctica

©2019. Japan Geoscience Union. All Right Reserved.

Study of ancient fungi resting in the polar ice cores and its future prospects

*Fumio Nakazawa[1,2], Masaharu Tsuji[1], Satoshi Imura[1,2]

1. National Institute of Polar Research, 2. SOKENDAI (The Graduate University of Advanced Studies)

This study attempted to culture ancient fungi preserved in the polar ice cores dated from ~1000 to ~9000 years ago. The samples of several hundred grams of ice collected at depths of 97, 470 and 670 m from Mizuho station (70°42'S, 44°20'E; 2230 m a.s.l.) and at depths of 116, 141 and 169 m from Dome Fuji station (77°19'S, 39°42'E; 3810 m a.s.l.) in Antarctica (Fujii, 1985; Dome-F Deep Coring Group, 1998). The ages of these samples were estimated to be ~1000, ~5500 and ~9000 years for the Mizuho ice core (Nakawo et al., 1989) and ~3000, ~4000 and ~5000 years for the Dome Fuji deep ice core (Dome Fuji Ice Core Project Members, 2017) respectively. In addition, an ice core sample from Åsgardfonna in the northeastern part of Svalbard (79°27'N, 16°43'E; 1140 m a.s.l.) (Uchida et al., 1993) was used for the cultivation. The information on the sample depth and age were unclear. In this study, we successfully cultivated fungi from all the samples. The nucleotide sequences were obtained by DNA analyses of the strains. Many of these sequences showed low homology to those registered in the NCBI DNA database, therefore it was believed that ancient fungi were actually obtained. This suggested that the culture of ancient fungi and its DNA analysis enable to be done over time by using deep ice cores such as the Dome Fuji ice core. This allows to study the physiological ecology of ancient fungi and to use decomposition and fermentation characteristics of ancient fungi for industrial purposes. Also, DNA analyses of the ancient fungi may enable to examine the diversity of fungi with climate and environmental changes and to study the evolutionary history on fungi. In our presentation, we will introduce the results obtained and discuss the prospects and developments of the study using the ancient fungi preserved in the polar ice cores in the future.

References

1. Dome-F Deep Coring Group, Deep ice-core drilling at Dome Fuji and glaciological studies in East Dronning Maud
Land, Antarctica. Annals of Glaciology, 27, 333-337, 1998.
2. Dome Fuji Ice Core Project Members, State dependence of climatic instability over the past 720,000 years from
Antarctic ice cores and climate modeling. Science Advances, 3(2), e1600446, 2017, doi:10.1126/sciadv.1600446.
3. Fujii, Y., Drilling an ice core to a depth of 700 m at Mizuho Station, Kyokuchi, 41, 29–34, 1985. (in Japanese)
Nakawo, M, H. Ohmae, F. Nishio and T. Kameda, Dating the Mizuho 700-m core from core ice fabric data. Proceedings of the NIPR Symposium on Polar. Meteorology and Glaciology, 2, 105–110, 1989.
4. Uchida, T., K. Kamiyama, Y. Fujii., A. Takahashi, T. Suzuki, Y. Yoshimura, M. Igarashi and O. Watanabe, Ice core
analyses and borehole temperature measurements at the drilling site on Asgardfonna, Svalbard, in 1993. Memoirs of National Institute of Polar Research. Special issue, 51, 377–386, 1996.

Keywords: snow and ice, microorganism, ancient DNA, population genetics, evolution, biotechnology

©2019. Japan Geoscience Union. All Right Reserved.

©2019. Japan Geoscience Union. All Right Reserved.

Flux, provenance and modification of terrestrial dust and sea salt in the Dome C and Dome Fuji ice cores from Last Glacial Maximum to early Holocene by ice-sublimation and single-particle measurement of soluble and insoluble particles

*Ikumi Oyabu[1,2], Iizuka Yoshinori[3], Kenji Kawamura[1,4,5], Eric Wolff[6], Mirko Severi[7], Margareta Hansson[8]

1. National Institute of Polar Research, Research Organization of Information and Systems, 2. Japan Society for the Promotion of Science, 3. Institute of Low Temperature Science, Hokkaido University, 4. SOKENDAI (The Graduate University of Advanced Studies), 5. Japan Agency for Marine Science and Technology (JAMSTEC), 6. Department of Earth Sciences, University of Cambridge, 7. Department of Chemistry “Ugo Schiff”, University of Florence, 8. Department of Physical Geography, Stockholm University

We analyzed chemical compositions of dust and sea-salt particles in the EPICA Dome C (EDC) ice core between 26 and 7kyr BP by using an ice sublimation technique, and compared the results with existing data of the Dome Fuji (DF) ice core. Combining the results of non-sea-salt Na and sea-salt Na fractions in total Na from the sublimation measurement and Na^+concentrations from ion measurement, we estimated that sea-salt flux in the two cores are roughly the same, while dust flux in the EDC core is significantly lower than that in the DF core throughout the studied period. Al/Si ratio of dust particles in the EDC core increased since around 16 kyr BP, suggesting that the average mixing ratios of minerals, presumably from different source locations, are different before and after 16 kyr BP. The composition of calcic dust also changed around 16 kyr BP; the fraction of calcium sulfate (calcic dust sulfatized during transport through lower troposphere) decreased and that of calcium nitrate (calcic dust reacted with nitric acid during transport through the middle to upper troposphere) increased. Previous studies on the mineralogy of EDC dust have suggested that dominant dust source area was Patagonia before 16 kyr BP and that multiple dust sources may have contributed thereafter (Siggaard-Andersen et al., 2007; Marino et al., 2008; Vallelonga et al., 2010).On the other hand, atmospheric model simulations have suggested that Patagonian dust is transported via lower troposphere, while Australian dust is transported via middle to upper troposphere (Li et al., 2008; Krinner et al., 2010). Thus, our data collectively confirm the dominance of Patagonian dust during the LGM and support the hypothesis of increased Australian dust contribution during the Termination and Holocene. The Dome Fuji Al/Si ratios were lower than those in the EDC core, and the fraction of calcium sulfate in the DF core are higher than those in the EDC core after around 16 kyr BP. The results suggest that Patagonian dust continued to be the dominant contributor to the Dome Fuji region after 16 kyr BP.

References

Siggaard-Andersen et al. (2007), *Earth Planet. Sci. Lett.*, *258*(1-2), 32-43.
Marino, F., (2008), *Geochem. Geophys. Geosyst.*, *9*(10), Q10018.
Vallelonga, P., et al. (2010), *Quat. Sci. Rev.*, *29*(1-2), 247-255.
Li, F. (2008), *J. Geophys. Res. Oceans*, *113*(D10), 573-515.
Krinner, G. (2010), *Quat. Sci. Rev.*, *29*, 274-284.

Keywords: Ice core, Antarctica, aerosol, dust, sea salt

©2019. Japan Geoscience Union. All Right Reserved.

Spatial variation of surface mass balance over the last few millennia in the Dome Fuji area from the analyses of shallow ice cores

*Kenji Kawamura[1], Ikumi Oyabu[1], Fumio Nakazawa[1,2], Shuji Fujita[1,2], Kyohei Yamada[1], Naoyuki Kurita[4], Shun Tsutaki[5], Hiroshi Ohno[6], Konosuke Sugiura[7], Kumiko Goto-Azuma[1,2], Hideaki Motoyama[1,2], Ayako Abe-Ouchi[5,3]

1. National Institute of Polar Research, Research Organization of Information and Systems, 2. SOKENDAI (The Graduate University of Advanced Studies), 3. JAMSTEC, 4. Nagoya University, 5. University of Tokyo, 6. Kitami Institute of Technology, 7. University of Toyama

One of the main targets in the current Japanese Antarctic program is to identify the drilling site for the oldest ice around Dome Fuji. The site selection activities (during JARE 59 and 60 summer seasons) include national and international ice-penetrating radar surveys, four shallow ice corings, and firn air sampling at one site. In this presentation, we report the shallow drillings and their analytical results for DEP (dielectric profiling) for deducing spatial differences of accumulation rate among the shallow drill sites.

During the JARE 59 surveys (2017-2018), the first core was drilled at 55 km south of Dome Fuji (New Dome Fuji; NDF) to the depth of 151.9 m, second one was drilled at 40 km southeast of Dome Fuji (DFSE) to 41 m, and third one was drilled at 30 km northwest of Dome Fuji (DFNW) to 41 m. The DEP of these cores were analyzed in summer 2018 at the NIPR cold laboratory, and major volcanic signals were identified back to 13thcentury for all three cores. During the JARE 60 surveys (2018-2019), we set up one base camp 5 km north of NDF (~50 km south of Dome Fuji) (NDFN) and drilled a shallow core to 142 m. The DEP analyses will be conducted for detecting volcanic signals along the core.

We also found a visible 20-mm-thick volcanic ash layer at 118.9 m in the NDF core, and a 10-mm-thick layer at 122.18 m in the NDFN core. Visible ash layers from probably the same origin have also been found in the Dome C (< 1-mm-thick layer at 132.6 m) and Vostok (~30-mm-thick layer at 103.04 m) ice cores. These ash layers were dated at 3500–3600 years before present (Basile et al., 2001; Kohno et al., 2004). On the other hand, volcanic ash layer was not found in the first Dome Fuji deep ice core (Narcisi et al., 2005) but in the second Dome Fuji deep ice core at 133.6 m.

The DEP and in-situ density data are used to date the horizons by comparing the DEP peaks to published volcanic data sets from several ice cores including the WAIS Divide core (Sigl et al., 2014), and to deduce surface mass balance between the volcanic signals for the three cores from JARE 59.

We identified 6 volcanic signals to 40-m depth and 12 signals to ~150-m depth (from the DF and NDF cores). We also use the data from the previously drilled cores (e.g. one from 6-km south of DF drilled in JARE 52, and one from 195-km south of DF in JARE 54) to discuss spatial patterns of accumulation rate from the corings. In the near future, the data will be combined with shallow ice-radar data from the JARE

©2019. Japan Geoscience Union. All Right Reserved.

60 international surveys to expand the spatial estimate of accumulation rate over the Dome Fuji area.

Keywords: Ice core, Volcanic ash, Antarctica, Dome Fuji

©2019. Japan Geoscience Union. All Right Reserved.

Sensitivity of global nonhydrostatic atmospheric model to changes in orbital forcing for the early Holocene

*Minoru Chikira[1], Ayako Abe-Ouchi[1], Masaki Satoh[1]

1. Atmosphere and Ocean Research Institute, The University of Tokyo

Various types of geological records have extensively shown consistent patterns of warmer and moister areas over Asia and Africa during the early to mid-Holocene. Previous sensitivity simulations of many global climate models to the changes in the earth’s orbital parameters during this period have equally shown the enhancement of the Asian and African monsoons, providing a successful interpretation on the qualitative patterns of these records. This study aims to shed a new light on the climate of this period by running sensitivity simulations by a global nonhydrostatic atmospheric model which began to be available for climate studies in recent years. The model used in this study is Nonhydrostatic ICosahedoral Atmospheric Model (NICAM) developed by a Japanese meteorological community: a framework of a cloud resolving model which resolves cumulus convection when used with a proper resolution and does not adopt any cumulus parameterizations. Because of the limit of computational resources, we use NICAM with a horizontal resolution of 56km. Despite not resolving cumulus convection, previous studies confirmed that it behaved similarly to the one with much higher resolution and provided practically reasonable mean-states and variability. The simulations were run with a slab ocean model and orbital parameters of 9000 years B.P. (9kBP). The Integrations were continued for 5 years. The seasonal mean precipitation in the control run is largely overestimated, however, it shows very good spatial distributions in terms of the locations of the ITCZs and peak precipitation. In particular, because of the high resolution enough to represent the steep terrain of the Tibetan Plateau, the model successfully reproduces a narrow rain band along its southern edge. The boreal summer precipitation of the 9kBP simulation shows a well-known northward shift of the African ITCZ, consistent with previous studies. Over Asia, the narrow precipitation band at the south of the Tibetan Plateau is significantly enhanced. The precipitation also increases over the Indian ocean. In between, there is a band-like structure of the suppressed precipitation over the India and Indochinese Peninsula. Although the resolution is not sufficient to resolve cumulus convection, the global nonhydrostatic atmospheric model appears to have a potential to represent small structures of the earth’s topography and evaluate its effect on precipitation which had not been discussed in previous studies. It is expected to be useful in discussing regional scale patterns of the geological records.

Keywords: Paleoclimate, Climate model, Holocene

©2019. Japan Geoscience Union. All Right Reserved.

Roles of sea ice–surface wind feedback in maintaining contrasting modes of glacial Atlantic meridional overturning circulation and climate

*Sam Sherriff-Tadano[1], Ayako Abe-Ouchi[1]

1. Atmosphere and Ocean Research Institute, the University of Tokyo

During the glacial period, climate varied on millennial-time scale between two contrasting modes. These climate changes are often associated with drastic reorganizations of North Atlantic sea ice and Atlantic meridional overturning circulation (AMOC). However, processes affecting the periodicity of AMOC and climate variability remain unclear. Here, through performing simulations with a comprehensive climate model, we show that sea ice and associated changes in surface winds play a key role in maintaining the contrasting modes of AMOC and climate. Experiments highlights the importance of the suppression of atmosphere-ocean heat exchange by sea ice in inducing a weakening of surface winds. The surface wind anomaly then causes a reduction of salt transport and weakens AMOC, which triggers further expansion of sea ice. Our results show that sea ice–surface wind interactions over the North Atlantic plays an important role in inducing the long periodicity of the climate variability.

Keywords: millennial time-scale climate variability, sea ice-surface wind interaction, AMOC

©2019. Japan Geoscience Union. All Right Reserved.

[J] Oral | A (Atmospheric and Hydrospheric Sciences)：A-CC Cryospheric Sciences & Cold District Environment

Tue. May 28, 2019 1:45 PM - 3:15 PM JST | Tue. May 28, 2019 4:45 AM - 6:15 AM UTC | 201B 2F

[A-CC26] Ice cores and paleoenvironmental modeling

convener:Ryu Uemura(University of the Ryukyus), Kenji Kawamura(National Institute of Polar Research, Research Organization of Information and Systems), Ayako Abe-Ouchi(Atmosphere and Ocean Research Institute, The University of Tokyo), Nozomu Takeuchi(Chiba University), Chairperson:Ayako Abe-Ouchi(東京大学大気海洋研究所), Sam Sherriff-Tadano(University of Tokyo)

Analyses of ice cores from polar and mountain regions have contributed to the reconstruction and understanding of the past environmental changes on timescales from years to several hundred thousand years. In this session, we welcome paleoenvironmental studies using ice cores and paleoclimatic modeling. Studies on reconstruction methods, recording processes and new paleoenvironmental proxies, technical aspects of paleo-modeling are also welcomed. Studies with marine sediment cores, terrestrial sediment cores and tree-rings on similar timescales are also important and welcomed, in order to discuss past environmental changes from multidisciplinary viewpoints.

1:45 PM - 2:00 PM JST | 4:45 AM - 5:00 AM UTC

[ACC26-13] Simulated Dansgaard-Oeschger like oscillations and abrupt climate changes

*Ayako Abe-Ouchi[1,2,3], Wing-Le Chan[1], Sam Sherriff-Tadano[1], Takashi Obase[1], Masakazu Yoshimori[1], Akira Oka[1], Kenji Kawamura[3], Rumi Ohgaito[2] (1.Atmosphere and Ocean Research Institute, The University of Tokyo, 2.JAMSTEC, 3.National Institute of Polar Research)

2:00 PM - 2:15 PM JST | 5:00 AM - 5:15 AM UTC

[ACC26-14] Reproduction of the increasing amplitude and period in the glacial cycles using a model incorporating diatomaceous activity.

*Tasuku Akagi[1], Takahiro Hasegawa[2] (1.Department of Earth and Planetary Sciences, Faculty of Science, Kyushu University, 2.Graduate School of Science, Kyushu University)

2:15 PM - 2:30 PM JST | 5:15 AM - 5:30 AM UTC

[ACC26-15] Development of an Ice Sheet Model coupled General Circulation Model and application of Energy Balance Model on the estimation of Ice Sheet mass balance

*Ryouta O'ishi[1], Ayako Abe-Ouchi[2,1], Fuyuki SAITO[2], Takashi Obase[1] (1.Atmosphere and Ocean Research Institute, the Universitoy of Tokyo, 2.JAMSTEC)

2:30 PM - 2:45 PM JST | 5:30 AM - 5:45 AM UTC

[ACC26-16] An ice-flow modeling study for evaluation of sites for and oldest ice core around Dome Fuji, Antarctica

★Invited Papers

*Takashi Obase[1], Ayako Abe-Ouchi[1,2], Fuyuki SAITO[2], Shun Tsutaki[1], Shuji Fujita[3], Kenny Matsuoka[4], Kenji Kawamura[3,5,2], Ralf Greve[6] (1.Atmosphere and Ocean Research Institute, the University of Tokyo, 2.Japan Agency for Marine-Earth Science and Technology, 3.National Institute of Polar Research, Research Organization of Information and Systems, 4.Norwegian Polar Institute, 5.SOKENDAI (The Graduate University of Advanced Studies), 6.Institute of Low Temperature Science, Hokkaido University)

2:45 PM - 3:00 PM JST | 5:45 AM - 6:00 AM UTC

[ACC26-17] International studies of ice sheet and bedrock at Dome Fuji, East Antarctica

*Shuji Fujita[1,2], Kenji Kawamura[1,2,10], Prasad Gogineni[3], Ayako Abe-Ouchi[4], David Braaten[5], Jean-Charles Gallet[6], Elisabeth Isaksson[6], Brice van Liefferinge[6], Kenny Matsuoka[6], Charles O'Neill[3], John Paden[5], Fernando Rodriguez-Morales[5], Ryan A. Taylor[3], Shun Tsutaki[4], Jie-Bang Yan[3], Kumiko Goto-Azuma[1,2], Ralf Greve[7], Stephen Hudson[6], Jack Kohler[6], Shriniwas Kolpuke[3], Linfeng Li[3], Geir Moholdt[6], Hideaki Motoyama[1,2], Fumio Nakazawa[1], Takashi Obase[4], Hiroshi Ohno[8], Ikumi Oyabu[9,1], Fuyuki Saito[10],

Konosuke Sugiura[11] (1.National Institute of Polar Research, Research Organization of Information and Systems(ROIS), 2.Department of Polar Science, The Graduate University for Advanced Studies (SOKENDAI), Japan, 3.The University of Alabama, USA, 4.Atmosphere and Ocean Research Institute, The University of Tokyo, Japan, 5.CReSIS, University of Kansas, USA, 6.Norwegian Polar Institute, Norway, 7.Institute of Low Temperature Science, Hokkaido University, Japan, 8.Kitami Institute of Technology, Japan, 9.JSPS, Japan, 10.Japan Agency for Marine-Earth Science and Technology (JAMSTEC), Japan, 11.University of Toyama, Japan)

3:00 PM - 3:15 PM JST | 6:00 AM - 6:15 AM UTC

[ACC26-18] Possible cause for rapid deformation of ice from glacial periods, investigated from laboratory-based deformation experiments and microstructural observations

*Tomotaka Saruya[1], Morimasa Takata[1], Tomoyuki Homma[1], Nobuhiko Azuma[1], Kumiko Goto-Azuma[2,3] (1.Nagaoka University of Technology, 2.National Institute of Polar Research, 3.SOKENDAI (The Graduate University for Advaced Research))

Simulated Dansgaard-Oeschger like oscillations and abrupt climate changes

*Ayako Abe-Ouchi[1,2,3], Wing-Le Chan[1], Sam Sherriff-Tadano[1], Takashi Obase[1], Masakazu Yoshimori[1], Akira Oka[1], Kenji Kawamura[3], Rumi Ohgaito[2]

1. Atmosphere and Ocean Research Institute, The University of Tokyo, 2. JAMSTEC, 3. National Institute of Polar Research

During the last termination of ice age cycle (deglaciation), Heinrich event 1 as well as B/A, Antarctic Cold Reversal (ACR) and Younger Dryas occurred as millennial scale climate changes. On the other hand, millennial scale climate changes such as D-O cycles recorded in ice core and deep sea cores in both hemisphere seem to occur more frequently during the mid-glacial state than during the early or late glacial state. Here we ran several sensitivity experiments and deglaciation simulations using a coupled atmosphere and ocean GCM (MIROC4m AOGCM) developed in Japan and analyzed the stability of AMOC and climate. Many model experiments were run for longer than10000 years under many different conditions of constant Greenhouse Gas levels, obliquity with/without glacial ice sheet and with and without freshwater flux into North Atlantic region. The results show large self-sustained oscillation of AMOC and high latitude temperature change similar to D-O cycles, which are consistent with ice core data and deep-sea data in both low and high latitude. Furthurmore, the results imply that both Northern Atlantic ocean-atmosphere-sea ice coupled system and Southern Ocean are important to maintain the oscillation with periodicity longer than 2000 years, for which we propose “Bipolar thermohaline oscillation” as its mechanism. We show that the D-O like oscillation occur with Glacial ice sheets under limited range of CO2, obliquity, and freshwater forcing. Implication on the mechanism and the conditions of the millennial scale climate changes for the past time period is discussed.

Keywords: Climate, Ice age cycle, Atlantic Meridional Overturning Circulation

©2019. Japan Geoscience Union. All Right Reserved.

Reproduction of the increasing amplitude and period in the glacial cycles using a model incorporating diatomaceous activity.

*Tasuku Akagi[1], Takahiro Hasegawa[2]

1. Department of Earth and Planetary Sciences, Faculty of Science, Kyushu University, 2. Graduate School of Science, Kyushu University

The mode changes in the glacial cycle, smaller amplitudes with 20 kyr periods before 2.7 BP; medium amplitudes with 40 kyr periods between 2.70 and 1 Ma BP; greater amplitudes with around 100 kyr periods after 1 Ma BP, remain unanswered.

Carbon cycling is closely coupled with silicon cycling in the Earth surface. Oceanic silica is supplied from weathering of terrestrial matter, which depends on the atmospheric pCO_2. The atmospheric pCO_2, in turn, is influenced by the diatomaceous biological pump. Silicon can be a crucial driver of the Earth surface environment. Oceanic silica is removed by the burial of amorphous silica produced by diatoms. We have reported that the non-linear dissolution behavior of diatom frustules, where greater diatomaceous production tends to suppress dissolution of dissolved silica forming greater-sized frustule-aggregates.

Here we have developed a numerical model expressing the carbon and silicon cycling in the Earth surface, with diatomaceous biological pump and the non-linear dissolution behavior of diatom frustules being introduced.

The results of the model runs show interesting outcomes: when the amount of circulating carbon is reduced with time, both the amplitude and period of atmospheric pCO_2increase with time. When the insolation changes by Milankovitch forcing were loaded on the model temperature, the mode changes are successfully reproduced.

We propose that the glacial cycles may be understood by the coupling of ice-sheet dynamics and change in the oceanic Si inventory.

Keywords: the glacial cycles, amplitude and period, silicon cycling, diatom activity

©2019. Japan Geoscience Union. All Right Reserved.

Development of an Ice Sheet Model coupled General Circulation Model and application of Energy Balance Model on the estimation of Ice Sheet mass balance

*Ryouta O'ishi[1], Ayako Abe-Ouchi[2,1], Fuyuki SAITO[2], Takashi Obase[1]

1. Atmosphere and Ocean Research Institute, the Universitoy of Tokyo, 2. JAMSTEC

A sea level rise is an important topic in a future climate projection. In the past warm period known as the Last Interglacial (LIG), paleoevidences indicate sea level rise of several meters. Paleoclimate modeling community applies past GCM results on ice sheet models and tries to reproduce past sea level rises.
We designed a coupling procedure between an ice sheet model and a general circulation model and are planning to introduce a surface mass balance of ice sheet not only by a typicall empirical method called PDD (Positive Degree Days) but also surface mass balance on the ice sheet as an upper boundary condition. The PDD only refers the surface atmosphere temperature and snowfall. In the present study, we use a process-based land surface model MATSIRO to estimate surface mas balance forced not only by temperature and snowfall but also by other surface variables including shortwave and longwave radiation. We compare the characteristics of resultant ice melt amount from PDD and MATSIRO to evaluate the inclusion of process-based heat and water balance instead of empirical equation.
We apply this procedure on the estimation of Grennland mass balance in the LIG.

Keywords: ice sheet, mass balance, grneral circulation model

©2019. Japan Geoscience Union. All Right Reserved.

An ice-flow modeling study for evaluation of sites for and oldest ice core around Dome Fuji, Antarctica

*Takashi Obase[1], Ayako Abe-Ouchi[1,2], Fuyuki SAITO[2], Shun Tsutaki[1], Shuji Fujita[3], Kenny Matsuoka[4], Kenji Kawamura[3,5,2], Ralf Greve[6]

1. Atmosphere and Ocean Research Institute, the University of Tokyo, 2. Japan Agency for Marine-Earth Science and Technology, 3. National Institute of Polar Research, Research Organization of Information and Systems, 4. Norwegian Polar Institute, 5. SOKENDAI (The Graduate University of Advanced Studies), 6. Institute of Low Temperature Science, Hokkaido University

The recovery of a new Antarctic ice core to cover one million years will advance our understandings of the Quaternary climate. Previous ice flow modeling studies indicate that such old ice may exist in inland areas of the Antarctic continent, where horizontal ice flow is slow, the ice is thick, accumulation rate is low, basal temperature is well below the pressure melting point (Pattyn 2010; Fischer et al. 2013). We have been analyzing the field data taken by 59th Japanese Antarctic Research Expedition (JARE 59, 2017-2018) and conducting ice flow modelings as the essential parts of the site selection activities. In the present study, we show results of ice flow modeling to estimate the temperature and age of ice, and age resolution of the ice near the bed at a dome of the ice sheet. We use an one-dimensional ice flow-thermodynamic model, in which the vertical velocity of the ice is parameterized with empirical functions applied to the area near ice sheet domes. At first, the calculated age and temperature profiles of the ice are compared with depth-age profile of the Dome Fuji ice core and borehole temperature at Dome Fuji to assess the model performance for our purposes. Next, we investigate the influence of parameters (ice thickness, accumulation rate, geothermal heat flux, profile of vertical velocity of the ice) on the age of ice especially in the lowest few hundred meters. The results indicate that a fine resolution of oldest ice (~age of 1.0 Ma before present) is expected from a thick ice and a low accumulation, but the thick ice increases the chance of basal melting. The one-dimensional model is applied to the vicinity of Dome Fuji along the transect of JARE 59 surveys, using estimated ice thickness and simplified pattern of surface mass balance and geothermal heat flux. The calculated distribution of the age of ice are compared with internal layers of the ice (isochrone) derived from ground radar surveys. The calculated age of ice roughly follows observed internal layers of ice, and a smaller accumulation near NDF compared to Dome Fuji increases the agreement between calculated age of ice and internal layers of ice.

Keywords: Antarctic ice sheet, ice core, modeling, Dome Fuji

©2019. Japan Geoscience Union. All Right Reserved.

International studies of ice sheet and bedrock at Dome Fuji, East Antarctica

*Shuji Fujita[1,2], Kenji Kawamura[1,2,10], Prasad Gogineni[3], Ayako Abe-Ouchi[4], David Braaten[5], Jean-Charles Gallet[6], Elisabeth Isaksson[6], Brice van Liefferinge[6], Kenny Matsuoka[6], Charles O'Neill[3], John Paden[5], Fernando Rodriguez-Morales[5], Ryan A. Taylor[3], Shun Tsutaki[4], Jie-Bang Yan[3], Kumiko Goto-Azuma[1,2], Ralf Greve[7], Stephen Hudson[6], Jack Kohler[6], Shriniwas Kolpuke[3], Linfeng Li[3], Geir Moholdt[6], Hideaki Motoyama[1,2], Fumio Nakazawa[1], Takashi Obase[4], Hiroshi Ohno[8], Ikumi Oyabu[9,1], Fuyuki Saito[10], Konosuke Sugiura[11]

1. National Institute of Polar Research, Research Organization of Information and Systems(ROIS), 2. Department of Polar Science, The Graduate University for Advanced Studies (SOKENDAI), Japan, 3. The University of Alabama, USA, 4. Atmosphere and Ocean Research Institute, The University of Tokyo, Japan, 5. CReSIS, University of Kansas, USA, 6. Norwegian Polar Institute, Norway, 7. Institute of Low Temperature Science, Hokkaido University, Japan, 8. Kitami Institute of Technology, Japan, 9. JSPS, Japan, 10. Japan Agency for Marine-Earth Science and Technology (JAMSTEC), Japan, 11. University of Toyama, Japan

Climatic histories from about 800 kyr BP up to present have been studied using very deep ice cores drilled at dome summits in East Antarctica at Dome Fuji and Dome C. Knowledge gained from ice cores studies are crucial to understand the past and present climate and to predict the impacts of future climate changes. International Partnership for Ice Core Sciences (IPICS) identified that ice cores covering ages of the mid-Pleistocene Transition are necessary step to better understand climate dynamics. Multiple ice cores older than 1 M yrs BP are necessary. Dome Fuji area in East Antarctica is one of the candidate areas where we may be able to find very old ice core near the bottom of the ice sheet. Japanese Antarctic Research Expedition (JARE) has conducted deep ice coring at Dome Fuji twice in the past decade. They recovered ice cores covering ages up to about 720 kyr BP. At the same time, they have accumulated radar sounding data in this area. Alfred Wegener Institute (AWI), Germany, made an extensive airborne radar survey in 2016/2017 season covering Dom Fuji with a basic survey line spacing of 10 km. In the following season of 2017/2018, JARE also made ground-based radar surveys over a distance of 2950 km with a line spacing of 5 km or less. Based on results of these surveys, we conducted a more detailed radar surveys at Dome Fuji in 2018/2019 season as a collaborative research between University of Alabama, the University of Kansas, National Institute of Polar Research under Research Organization of Information and Systems (Japan), and Norwegian Polar Institute. Norwegian Polar Institute joined also collaborating on these efforts with the European framework of Beyond EPICA - Oldest Ice (BE-OI). We used two state-of-the-art radars: A wideband radar ice sounder developed by CReSIS, University of Kansas and ultra-wideband radar developed by University of Alabama. In addition, we used a classical pulse-modulated VHF radar of JARE with high gain antennas. Using a traverse team of JARE and its snow vehicles, we investigated along 2,700 km in an area of about 1,000 km^2. Final spacing between survey lines varied between 0.5 km and 0.25 km. The surveys were completed by the end of December, 2018. We will present preliminary results from these surveys. Preliminary quick-look results indicate that we collected an excellent radar data set with very good layering information including the bottom 10% of the ice. The data will be examined to identify candidate locations to drill very old ice.

Keywords: Antarctica, ice core, ice sheet, radar, paleoclimate, climate change

©2019. Japan Geoscience Union. All Right Reserved.

Possible cause for rapid deformation of ice from glacial periods, investigated from laboratory-based deformation experiments and microstructural observations

*Tomotaka Saruya[1], Morimasa Takata[1], Tomoyuki Homma[1], Nobuhiko Azuma[1], Kumiko Goto-Azuma[2,3]

1. Nagaoka University of Technology, 2. National Institute of Polar Research, 3. SOKENDAI (The Graduate University for Advaced Research)

Deformation mechanism of coarse-grained polycrystalline ice is well investigated by various experiments. However, the deformation of ice-sheet ice is complicated by various factors such as local distributions of impurities and mechanical anisotropies. Detailed analyses of ice cores have revealed that ice from glacial periods (ice-age ice) that has highly-concentrated impurities and small grains deforms rapidly compared with ice from Holocene. Although the causes of the rapid deformation in ice-age ice have been discussed in various studies, the detailed mechanism remains unclear.
The deformation rate in ice sheets is extremely slow; therefore, ice-sheet ice deforms under low dislocation density state. To replicate such deformation mechanism in laboratory experiments, we prepared fine-grained ice which has much grain boundaries. Since grain boundaries can act as sinks of dislocations, a low dislocation density state is kept during deformation like ice sheets.
To investigate the cause of rapid deformation of ice-age ice, we conducted deformation experiments and microstructural observations using artificial ice, with focusing on the influences of microparticles and grain size (grain boundaries). We made pure ice, and silica-dispersed ice with particle diameters of 0.3 μm and mass concentrations of 0.1 and 0.01 %. For the investigation of grain-size-sensitivity of deformation, various-sized ice (mean grain size with 30 μm –2 mm) was prepared.
Our experimental results revealed different trends for softening and hardening effect due to microparticles dispersion, grain-size-sensitivity, and microstructural evolutions during deformation in fine- and coarse-grained ice. Silica-dispersed ice with coarse grains indicated a hardening trend compared with pure ice, while little direct effect on the deformation in fine-grained ice. Grain-size-sensitivity was appeared only in fine-grained ice: the strain rates become larger at finer grains.
In this presentation, we discuss the possible cause for the rapid deformation of ice-age ice based on systematic deformation experiments and microstructural observations.

Keywords: ice-sheet flow, microstructure, microparticles

©2019. Japan Geoscience Union. All Right Reserved.

[J] Poster | A (Atmospheric and Hydrospheric Sciences)：A-CC Cryospheric Sciences & Cold District Environment

Tue. May 28, 2019 3:30 PM - 5:00 PM JST | Tue. May 28, 2019 6:30 AM - 8:00 AM UTC | Poster Hall International Exhibition Hall8, Makuhari Messe_7

[A-CC26] Ice cores and paleoenvironmental modeling

convener:Ryu Uemura(University of the Ryukyus), Kenji Kawamura(National Institute of Polar Research, Research Organization of Information and Systems), Ayako Abe-Ouchi(Atmosphere and Ocean Research Institute, The University of Tokyo), Nozomu Takeuchi(Chiba University)

Analyses of ice cores from polar and mountain regions have contributed to the reconstruction and understanding of the past environmental changes on timescales from years to several hundred thousand years. In this session, we welcome paleoenvironmental studies using ice cores and paleoclimatic modeling. Studies on reconstruction methods, recording processes and new paleoenvironmental proxies, technical aspects of paleo-modeling are also welcomed. Studies with marine sediment cores, terrestrial sediment cores and tree-rings on similar timescales are also important and welcomed, in order to discuss past environmental changes from multidisciplinary viewpoints.

[ACC26-P01] Pollen analysis of ice cores drilled in the Pamir-Arai Mountains, central Asia

*Haruka Ogaya[1], Nozomu Takeuchi[1], Koji Fujita[2], Kenji Kawamura[3], Akane Tsushima[4], Vladimir Aizen[5], Azamat Osmonov[6] (1.Chiba University, 2.Nagoya University, 3.National Institute of Polar Research, 4.Research Institute for Humanity and Nature, 5.University of Idaho, 6.Central Asian Institute of Applied Geo-Science)

[ACC26-P02] Variations in mineralogy of dust in the Greenland SIGMA-D ice core over the past 100 years using SEM

*Naoko Nagatsuka[1], Kumiko Goto-Azuma[1,2], Akane Tsushima, Hideaki Motoyama[1,2], Sumito Matoba[3], Koji Fujita[4], Tetsuhide Yamasaki[5], Yukihiko Onuma[6], Masahiro Minowa[7], Teruo Aoki[8], Motohiro Hirabayashi[1] (1.National Institute of Polar Research, 2.SOKENDAI, 3.Institute of Low Temperature Science, Hokkaido University, 4.Graduate School of Environmental Studies, Nagoya University, 5.Avangnaq Arctic Project Corp., 6.Institute of Industrial Science, University of Tokyo, 7.Universidad Austral de Chile, 8.Graduate School of Natural Science and Technology, Okayama University)

[ACC26-P03] Size and shape of solid particles in a Greenland ice core

*Wataru Shigeyama[1,2], Kumiko Goto-Azuma[2,1], Kaori Fukuda[2], Fumio Nakazawa[2,1], Morimasa Takata[3], Tomoyuki Homma[3], Nobuhiko Azuma[3], Dorthe Dahl-Jensen[4] (1.The Graduate University for Advanced Studies (SOKENDAI), School of Multidisciplinary Sciences, Department of Polar Science, 2.National Institute of Polar Research, 3.Nagaoka University of Technology, 4.University of Copenhagen)

[ACC26-P04] Methane concentration measurements of the Dome Fuji ice core using Continuous Flow Analysis system

Ikumi Oyabu[1], Miho Arai[1,4,5], *Kenji Kawamura[1,2,3], Kyotaro Kitamura[1], Jun Ogata[1], Kumiko Goto-Azuma[1,2] (1.National Institute of Polar Research, Research Organization of Information and Systems, 2.SOKENDAI (The Graduate University of Advanced Studies), 3.JAMSTEC, 4.Yamagata University, 5.Weathernews Inc.)

[ACC26-P05] A basal topographic map in the Dome Fuji region constructed from the ground-based radar survey in the JARE 59

*Shun Tsutaki[1], Takashi Obase[1], Shuji Fujita[2,3], Ayako Abe-Ouchi[1,4], Kenji Kawamura[2,3,4], Kenichi Matsuoka[5], Hiroshi Ohno[6], Ikumi Oyabu[2,7], Fumio Nakazawa[2], Konosuke Sugiura[8] (1.The University of Tokyo, 2.National Institute of Polar Research, 3.The Graduate University for Advanced Studies, 4.Japan Agency for Marine-Earth Science and Technology, 5.Norwegian Polar Institute, 6.Kitami Institute of Technology, 7.Japan Society for the Promotion of Science, 8.University of Toyama)

[ACC26-P06] Performance of RCIP scheme on 1-d age computation of ice sheet.

*Fuyuki SAITO[1], Takashi Obase[2], Ayako Abe-Ouchi[2,1] (1.Japan Agency for Marine-Earth Science and Technology, 2.Atmosphere and Ocean Research Institute, University of Tokyo)

[ACC26-P07] Climate changes of the last deglaciation simulated by MIROC AOGCM

*Takashi Obase[1], Ayako Abe-Ouchi[1,2], Sam Sherriff-Tadano[1] (1.Atmosphere and Ocean Research Institute, the University of Tokyo, 2.Japan Agency for Marine-Earth Science and Technology)

[ACC26-P08] A Last Glacial Maximum experiment using MIROC-ES2L earth system model in comparison with ice core and the other paleo-proxy data

*Rumi Ohgaito[1], Tomohiro Hajima[1], Akitomo Yamamoto[1], Hiroaki Tatebe[1], Michio Kawamiya[1], Ayako Abe-Ouchi[2,1] (1.Japan Agency for Marine-Earth Science and Technology, 2.AORI, Univ. Tokyo)

[ACC26-P09] On the possible bifurcation mechanisms and associated dynamical properties of Dansgaard-Oeschger oscillations

*Takahito Mitsui[1], Ayako Abe-Ouchi[1], Wing-Le Chan[1], Sam Sherriff-Tadano[1] (1.The University of Tokyo)

[ACC26-P10] The role of climate-vegetation feedback in climate changes driven by orbital parameter changes: the Arctic land surfaces and seasonality

*Kanon Kino[1], Ayako Abe-Ouchi[1,2], Ryouta O'ishi[1], Fuyuki SAITO[2], Masakazu Yoshimori[1] (1.Atmosphere and Ocean Research Institute, the University of Tokyo, 2.Japan Agency for Marine-Earth Science and Technology)

Pollen analysis of ice cores drilled in the Pamir-Arai Mountains, central Asia

*Haruka Ogaya[1], Nozomu Takeuchi[1], Koji Fujita[2], Kenji Kawamura[3], Akane Tsushima[4], Vladimir Aizen[5], Azamat Osmonov[6]

1. Chiba University, 2. Nagoya University, 3. National Institute of Polar Research, 4. Research Institute for Humanity and Nature, 5. University of Idaho, 6. Central Asian Institute of Applied Geo-Science

Ice cores drilled from mountain glaciers usually contains abundant pollen grains supplied from vegetation around the glaciers. Pollen grains have been used in ice core studies as markers of annual layer boundary since they are supplied on the glacier in a certain season of a year. Furthermore, they have been used as a proxy of vegetation in the surrounding area since their composition reflects relative abundance of each species in the source area. An ice core from the surface to the bottom was drilled on a glacier in Pamir Arai Mountains in central Asia in 2016. In this study, pollen grains in a part of the ice core and snow pit were analyzed. Annual layers of the ice core, which were determined based on a seasonality of stable isotope, were compared with the variations of pollen grains concentration, and the seasonality of pollen supplies was examined.
Ice cores were recovered at two sites (sites 1 and 2 at 5300 m and 5208 m, respectively) on the glacier. Oxygen stable isotope in the 7 m deep ice cores at both sites showed significant fluctuations. We assumed that they are periodic seasonal signals and determined the annual layers. As a result, the ice cores of Sites 1 and 2 includes layers for 8 years and 9 years, respectively. Microscopic analysis revealed that 6 types of pollen grains, which were identified as Cupressaceae, Artemisia, Chenopodiaceae, Pinaceae, Betulaceae, and Ephedra, were contained in the ice cores. Mean concentration of the pollen grains was highest for Cupressaceae at both sites (2.20, 2.62 grains/ml (74, 67%)), was second highest for Artemisia (0.65, 1.06 grains/ml (22, 27%)). The depth profile of the pollen grain concentrations showed several spikes in the ice cores. The depth of peaks differed between species. The peaks of Artemisia and Chenopodiaceae appeared at the same depth while the peaks of Cupressaceae appeared just below the depth of their peaks. The peak depths of Artemisia and Chenopodiaceae roughly agreed with the depth of the maximum value of the isotope ratio, indicating that these pollens were supplied in the summer or autumn. On the other hand, Cupressaceae found in the layer below is likely to be supplied in spring or summer. There are exceptional annual layers, in which the peaks of all species were not present, and the flux of pollen grains did not agree between two sites. These inconsistencies were likely due to the influence of the melting of the glacier surface. Results shows that the ice cores contain sufficient pollen grains for analysis and pollen profiles can be used to annual layer counting.

Keywords: Mountain glaciers, Ice core, Pollen, Pamir Arai Mountains, Central Asia

©2019. Japan Geoscience Union. All Right Reserved.

Variations in mineralogy of dust in the Greenland SIGMA-D ice core over the past 100 years using SEM

*Naoko Nagatsuka[1], Kumiko Goto-Azuma[1,2], Akane Tsushima, Hideaki Motoyama[1,2], Sumito Matoba[3], Koji Fujita[4], Tetsuhide Yamasaki[5], Yukihiko Onuma[6], Masahiro Minowa[7], Teruo Aoki[8], Motohiro Hirabayashi[1]

1. National Institute of Polar Research, 2. SOKENDAI, 3. Institute of Low Temperature Science, Hokkaido University, 4. Graduate School of Environmental Studies, Nagoya University, 5. Avangnaq Arctic Project Corp., 6. Institute of Industrial Science, University of Tokyo, 7. Universidad Austral de Chile, 8. Graduate School of Natural Science and Technology, Okayama University

Snow and ice on glaciers and the ice sheet in the Arctic contain windblown mineral dust derived from local sediments as well as distant deserts. Dust deposited on the ice sheet in the past can be obtained by ice core drilling, and the variations in its sources and transportation processes can be reconstructed by particle analysis of ice cores. In this study, we analyzed morphology and surface chemistry of mineral dust particles in an ice core drilled in Northwest Greenland with Scanning Electron Microscope (SEM, QUANTA FEG 450) and Energy Dispersive X-ray Spectrometer (EDS).
The ice core was drilled at the SIGMA-D site (N77°64’, W59°12’ [1]) of 2100 m a.s.l. in 2014. The length is 222.72 m and the estimated age at 113 m depth is 350 years before present . The ice samples were collected every five years in plastic bottles and freeze dried on a polycarbonate filter to concentrate micro-particles. Then, the filter was coated with platinum (Pt) for SEM analysis. Here we report the temporal variations in size distributions and compositions of the minerals during the past 100 years (A.D 1920-2013).
The SEM observation revealed that the mean size of mineral dust in the SIGMA-D ice core ranged from 1-3 μm, which is similar to that of the other Greenland ice core dust that seems to be derived from distant areas. This suggests that the SIGMA-D ice core contained mainly long–range transported wind-blown mineral dust.
The EDS analysis revealed the ice core contained mainly silicate minerals, especially clay minerals that showed compositional variation among the samples. For example, the mineralogical composition varied in every 10-15 years and showed a negative correlation between minerals formed by chemical and physical weathering (kaolinite vs illite/micas and chlorite). This indicates that minerals in the ice core were derived from multiple geological sources and the source areas might have varied temporally. Furthermore, quartz and feldspar, which had larger particles than clay minerals and thus were generally used as a short-distant transport, were higher in 1920-1945 and 1990-2013 compared with the other periods. Based on the past temperature record in Greenland, the warming occurred from 1910 to 1945 and after 1990. This may suggest that the minerals were derived not only from distant areas but also from local sources, such as moraine around the ice sheet margin in warmer periods. This is likely due to exposure of ground surface without snow cover.

Keywords: mineral dust, ice core, Greenland , SEM

©2019. Japan Geoscience Union. All Right Reserved.

Size and shape of solid particles in a Greenland ice core

*Wataru Shigeyama[1,2], Kumiko Goto-Azuma[2,1], Kaori Fukuda[2], Fumio Nakazawa[2,1], Morimasa Takata[3], Tomoyuki Homma[3], Nobuhiko Azuma[3], Dorthe Dahl-Jensen[4]

1. The Graduate University for Advanced Studies (SOKENDAI), School of Multidisciplinary Sciences, Department of Polar Science, 2. National Institute of Polar Research, 3. Nagaoka University of Technology, 4. University of Copenhagen

Concentrations and size distributions of insoluble solid particles in ice cores provide us with information on the changes in provenance, aridity, atmospheric circulation, etc. Most of the previous studies have focused on concentrations and size distributions. However, several studies (e.g., Barnes et al., 2002; Lambert et al., 2008; Simonsen et al., 2018) reported that particles formed aggregates and had various shapes. For a better environmental reconstruction, we need to study shapes and aggregation processes of the particles together with concentrations and size distributions.

Using a cryogenic scanning electron microscope (cryo-SEM), we carried out in-situ observations of solid particles in ice core samples without melting them. From the observations on selected ice samples (124 m depth in the present interglacial period, 1548 m depth in the last glacial period and 2406 m in the last interglacial period) retrieved by North Greenland Eemian Ice Drilling (NEEM), we found that many particles formed aggregates, and that individual particles (particles forming the aggregates) had elongated shapes (aspect ratio: 0.4-0.8). We also found that the sizes of the aggregate and individual particles showed log-normal distribution. The aggregates were larger in the interglacial periods than those in the glacial period (median diameter: 4.5 μm in the present interglacial period, 5.9 μm in the last interglacial period, and 2.2 μm in the last glacial period). These results need to be taken into account to interpret the size distribution data obtained by analyses on melted ice cores.

References

Barnes, P.R.F. et al., 2002, Ann. Glaciol. 35. pp 559-566

Lambert, F. et al., 2008, Nature. 452. pp 616-619

Simonsen, M.F. et al., 2018, Clim. Past. 14. pp 601-608

Keywords: solid particles, size distribution, particle shape, aggregate, cryo-SEM, NEEM ice core

©2019. Japan Geoscience Union. All Right Reserved.

Methane concentration measurements of the Dome Fuji ice core using Continuous Flow Analysis system

Ikumi Oyabu[1], Miho Arai[1,4,5], *Kenji Kawamura[1,2,3], Kyotaro Kitamura[1], Jun Ogata[1], Kumiko Goto-Azuma[1,2]

1. National Institute of Polar Research, Research Organization of Information and Systems, 2. SOKENDAI (The Graduate University of Advanced Studies), 3. JAMSTEC, 4. Yamagata University, 5. Weathernews Inc.

At the National Institute of Polar Research (NIPR), Continuous Flow Analyses (CFA) system has been developed. In addition to the measurements of melt water (e.g. water isotopes, micro-particles and major ions), the enclosed air is extracted from the water stream and measured for methane (CH_4) concentration by a customized Cavity Ring-Down Spectrometer (CRDS) (Picarro G2301). The CFA system provides data at much higher resolution than classic discrete measurements, which can improve our knowledge and understanding of past climatic variations.

The CH_4 concentration measured by CFA is affected by several factors, impacting precision, accuracy and resolution. The factors include dissolution of CH_4 in meltwater and its imperfect extraction, sample mixing and smoothing in sample lines, and contamination by room air intrusion into the system at the interface between ice samples. The magnitudes of these effects have been investigated, and the data are corrected accordingly. Here, we report the results of various tests for assessing the performance of our CFA for CH_4 measurement. Furthermore, the results of the measurement campaigns of the Dome Fuji ice core, covering the 8.2-kyr cooling event and a part of the last deglaciation, will also be presented.

Keywords: Continuous Flow Analysis, Ice core, CH4, Dome Fuji

©2019. Japan Geoscience Union. All Right Reserved.

A basal topographic map in the Dome Fuji region constructed from the ground-based radar survey in the JARE 59

*Shun Tsutaki[1], Takashi Obase[1], Shuji Fujita[2,3], Ayako Abe-Ouchi[1,4], Kenji Kawamura[2,3,4], Kenichi Matsuoka[5], Hiroshi Ohno[6], Ikumi Oyabu[2,7], Fumio Nakazawa[2], Konosuke Sugiura[8]

1. The University of Tokyo, 2. National Institute of Polar Research, 3. The Graduate University for Advanced Studies, 4. Japan Agency for Marine-Earth Science and Technology, 5. Norwegian Polar Institute, 6. Kitami Institute of Technology, 7. Japan Society for the Promotion of Science, 8. University of Toyama

Drilling a deep ice core extending 1.5 million years (Ma) back in time is crucial to better understand the transition in the periodicity of the glacial cycles changed from 40 kilo year (ka) to the current 100 ka during the mid-Pleistocene transition (0.9–1.2 Ma). However, continuous ice core records more than 1 Ma have not been retrieved in the Antarctic ice sheet. Sufficient knowledge of the basal topography is crucial to modify numerical experiments that may provide a continuous record of past mechanisms of climate change. A ground-based radar survey was conducted over an area of 20000 km^2 with a line spacing of 5 km in the Dome Fuji area in the 59th Japanese Antarctic Research Expedition (JARE 59, 2017–2018 Antarctic summer). In this study, we analyze the JARE 59 radar data to construct an improved map of basal topography in the Dome Fuji region to progress the identification of a suitable drilling site at the region.

Keywords: Antarctic ice sheet, Basal topography, Radar

©2019. Japan Geoscience Union. All Right Reserved.

Performance of RCIP scheme on 1-d age computation of ice sheet.

*Fuyuki SAITO[1], Takashi Obase[2], Ayako Abe-Ouchi[2,1]

1. Japan Agency for Marine-Earth Science and Technology, 2. Atmosphere and Ocean Research Institute, University of Tokyo

Generally the evolution of ice-sheet thickness, temperature and age in an ice-sheet model are formulated using the transport or advection equation. There are many variation of the formulation, which differ in numerical aspects such as stability, accuracy, numerical diffusivity, conservation and/or computational costs.
Rational Constrained Interpolation Profile scheme (RCIP, Xiao et al. 1996) is a variation of semi-Lagrangian scheme, which has properties in suppressing numerical oscillation and diffusion near large gradients.
In this study, RCIP scheme is implemented on 1d age computation of ice sheet, which is a typical numerical study of ice-core related topics. Comparison with the results of RCIP scheme and those of classical upwind scheme shows that the former keeps fine information (i.e., surface mass balance) recorded at the deposit.

Keywords: Ice core dating simulation

©2019. Japan Geoscience Union. All Right Reserved.

Climate changes of the last deglaciation simulated by MIROC AOGCM

*Takashi Obase[1], Ayako Abe-Ouchi[1,2], Sam Sherriff-Tadano[1]

1. Atmosphere and Ocean Research Institute, the University of Tokyo, 2. Japan Agency for Marine-Earth Science and Technology

During the last deglaciation, a major global warming was punctuated by abrupt climate changes related to Atlantic Meridional Overturning Circulation (AMOC). However, abrupt climate change associated with a rapid increase in the AMOC during Bølling-Allerød (BA) transition was reproduced only by applying a reduction in glacial meltwater, which is not inferred from reconstructions. Here we show that an abrupt increase in the AMOC during the BA transition can occur without reduction in glacial meltwater, from a transient simulation of the last deglaciation using an atmosphere-ocean general circulation model. The abrupt increase in the AMOC accompanied with drastic retreat of sea ice in the North Atlantic, abrupt warming in Greenland, cooling of the Southern Hemisphere, that are consistent with proxies and previous modeling studies. Model-data comparison at specific sites will be presented to evaluate simulated climate changes of the last deglaciation.

©2019. Japan Geoscience Union. All Right Reserved.

A Last Glacial Maximum experiment using MIROC-ES2L earth system model in comparison with ice core and the other paleo-proxy data

*Rumi Ohgaito[1], Tomohiro Hajima[1], Akitomo Yamamoto[1], Hiroaki Tatebe[1], Michio Kawamiya[1], Ayako Abe-Ouchi[2,1]

1. Japan Agency for Marine-Earth Science and Technology, 2. AORI, Univ. Tokyo

We are performing numerical experiments targeting distinctive time period of the past, Last Glacial Maximum (LGM, 21,000 years before present), using MIROC-ES2L. MIROC-ES2L is a newly developed earth system model (ESM) (Hajima et al. in prep.) including atmosphere, ocean, land, and ocean and land biogeochemical cycles in order to contribute Coupled Model Intercomparison Project phase 6 and Intergovernmental Panel on Climate Change 6th assessment report.
Testing climate models using paleoclimate experiments is an irreplaceable opportunity on evaluation of models to simulate climate change significantly different from the present day. In this presentation, we describe how we simulate the LGM experiment, compare with paleo-proxy data and discuss which component contributed for the realization of the LGM climate.
Following protocol of Paleoclimate Modelling Intercomparison Project phase 4 (Kageyama et al. 2017), we are performing a LGM experiment. Because the LGM condition is significantly different from the present day, long spin-up is essential. Hence, before the model development is finalized, we started spin-up using the physical core (Atmosphere-Ocean coupled general circulation model) of MIROC-ES2L. Firstly, an experiment is branched from pre-industrial control (PI) experiment and the greenhouse gas levels are reduced to the LGM values. After integration for 2640 model years, land-sea mask and ice sheets, altitude, river path, orbit of the earth, salinity of ocean, and an erodibility map (concerning dust) of the LGM conditions are applied step by step and the total spin-up reached 6760 model years. Since MIROC-ES2L is ready during this procedure, the initial conditions at the 6760th model year of the spin-up experiment are used to initiate LGM experiment using MIROC-ES2L. In this conversion procedure, the initial conditions for land and ocean biogeochemical cycles were prepared respectively using offline modules to obtain quasi-stabilized states. Global mean temperature drawdown of the last 60 year climatology after 540 years integration with the ESM is -4.4 degree Celsius. Borehole thermometry suggested the cooling over the Eastern Antarctica at LGM was -7 to -10 degree Celsius (Stenni et al. 2010, Uemura et al. 2012). The modelled temperature anomaly is about -6.0 degree Celsius, which suggests weaker cooling compared to the ice core data. For the central Greenland, borehole thermometry suggested -21 to -25 degree Celsius (Cuffey et al. 1995, Johnsen et al. 1995, Dahl-Jensen et al. 1998), whereas the LGM experiment resulted -11.1 degree Celsius. This large discrepancy would be attributed to realization of ocean thermohaline state in the model experiment. The modelled peak value of the Atlantic Meridional Overturning Circulation (AMOC) is 21.0 Sverdrup for LGM and 15.3 Sverdrup for PI. On the other hand, AMOC is thought to be weaker than the present day from paleo proxy data (Lynch-Stieglitz et al. 2007, Hesse et al. 2011). We continue the experiment and analyze which component contributes global cooling and the cooling over the polar regions.

Keywords: Last Glacial Maximum, CMIP6, earth system model

©2019. Japan Geoscience Union. All Right Reserved.

On the possible bifurcation mechanisms and associated dynamical properties of Dansgaard-Oeschger oscillations

*Takahito Mitsui[1], Ayako Abe-Ouchi[1], Wing-Le Chan[1], Sam Sherriff-Tadano[1]

1. The University of Tokyo

Dansgaard-Oeschger (DO) oscillations are millennial-scale abrupt climate changes in the last glacial period (Dansgaard et al. 1993; Johnsen et al. 1992). In particular, they are frequent in the mid-glacial and less frequent at the beginning of the glacial and in the Last Glacial Maximum (McManus et al. 1999; Kawamura et al. 2017). Since its discovery, DO oscillations have been intensively studied, but its detailed mechanisms are still a subject of debate. Our recent modeling study (Abe-Ouchi et al. in prep) with MIROC4m Atmosphere-Ocean general circulation model (Hasumi and Emori 2004) suggests that DO oscillations are spontaneous oscillations which arise from global-scale interactions between the atmosphere and ocean (see also studies in [12] and Brown and Galbraith, 2016). Our simulated oscillations are likely to appear in a certain region of background climate conditions directly related to factors such as ice sheets, orbital elements, and greenhouse gases (Abe-Ouchi et al. in prep; Sam Sherriff-Tadano et al. 2017). This result is consistent with the observations that DO oscillations were most frequent in the mid-glacial.

The bifurcation theory is a field of mathematics which studies qualitative changes of dynamical systems depending on the changes in parameters. In general, we can consider numerous types of dynamical systems, but their bifurcation phenomena are classified into only several types (Strogatz, Nonlinear Dynamics And Chaos, 2000). Identifying bifurcation mechanisms may help us to understand the emergence mechanism of the oscillation and its associated properties like the period or the amplitude. For example, when oscillations emerge/vanish via a Homoclinic bifurcation, the period of oscillations diverges to infinity as the parameter approaches the bifurcation point. On the other hand, when oscillations emerge via a Hopf bifurcation, such divergence of the period does not occur. On the basis of such scaling properties of the period, previous studies [7, 9] suggested onset mechanisms for the oscillations.

In this study, we survey bifurcation mechanisms reported in previous models of DO oscillations [1-12]. We also performed a bifurcation analysis of an extended version of the Winton (1993) 3-box halocline oscillator [2], which has a parameter dependence similar to that of MIROC AOCGM. It is found that, in many models, DO-like oscillations emerge via a Hopf-type bifurcation [1,2,4,5,6,7,10,11] and/or via a Homoclinic-type bifurcation [1,2,3,5,6,7,8,9,11]. The Welander (1982) model [1] and the extended Winton model may generate oscillations via both a Hopf-type bifurcation and a Homoclinic-type bifurcation depending on their parameters, but these bifurcations become identical at a parameter limit. This implies that the oscillation period may increase rapidly even near the Hopf bifurcation points (though it does not diverge). Therefore, identifying onset mechanisms of oscillations on the basis of scaling properties of the period may have a subtle problem. The extended Winton's model has a phase space structure like Homoclinic orbit even near the Hopf bifurcation point, and this phase space structure induces a long oscillation period. In MIROC AOGCM, the onset of oscillation may be related to either a Hopf-type bifurcation or a Homoclinic-type bifurcation, or to both of them. The determination of the bifurcation type in MIROC AOGCM is still difficult because of limited computational time and inherent natural variability. Nevertheless, we observe that noisy 'limit cycles' near bifurcation points show characteristics similar to Homoclinic orbit and have relatively long periods.

©2019. Japan Geoscience Union. All Right Reserved.

[1] Welander, Dyn. Atmos. Oceans (1982)
[2] Winton, Ice in the Climate System. NATO ASI Series (1993)
[3] Cessi, Journal of Physical Oceanography (1996)
[4] Sakai and Peltier, J. Climate (1999)
[5] Timmermann, Schulz, Gildor, and Tzipermann J. Climate (2003)
[6] Abshagen and Timmermann, Journal of Physical Oceanography (2004)
[7] Colin de Verdière, Ben Jelloul, and Sévellec, J. Climate (2006)
[8] Colin de Verdière, Journal of Physical Oceanography (2007)
[9] Sévellec, Huck, and Colin de Verdière, J. Mar. Res (2010)
[10] Roberts and Saha, Clim. Dyn. (2017)
[11] Leifeld, Euro. Jnl. of Applied Mathematics (2018)
[12] W. R. Peltier and G. Vettoretti, GRL (2014)

Keywords: Dansgaard-Oeschger cycles, bifurcation, oscillation

©2019. Japan Geoscience Union. All Right Reserved.

The role of climate-vegetation feedback in climate changes driven by orbital parameter changes: the Arctic land surfaces and seasonality

*Kanon Kino[1], Ayako Abe-Ouchi[1,2], Ryouta O'ishi[1], Fuyuki SAITO[2], Masakazu Yoshimori[1]

1. Atmosphere and Ocean Research Institute, the University of Tokyo, 2. Japan Agency for Marine-Earth Science and Technology

Periodic summer insolation change accompanying Earth’s orbital parameter changes is widely known as a main driver of the glacial cycles. Realistic orbital parameters are prescribed with climate models and ice-sheet models to reproduce and explain the characteristic of the glacial cycles in past several hundred thousand years(e.g. Abe-Ouchi et al., 2007; 2013). On the other way, radiative feedback analyses at the top of the atmosphere enable to understand the Earth’s climate response to the orbital forcing (Mantsis et al., 2011; Erb et al., 2013). In this study, we investigate the surface climate responses to the orbital forcing, by using MIROC-GCM and a surface climate feedback analyses method. We focus on the relationship between summer insolation and summer temperature on the land in the northern high latitude, since the former is a major index and the later is important for the ice-sheets melt.

We use a coupled atmosphere-vegetation GCM with slab ocean of MIROC-GCM (O’ishi and Abe-Ouchi, 2011) and performed numerous experiments by systematically changing the combinations of orbital parameters (maximum, minimum and present values of each parameter). A seasonal surface feedback analysis method (Lu and Cai, 2009) is also applied.

Results show that summer temperature change over the Arctic land due to obliquity change can be larger than that due to precession-eccentricity change, when the summer insolation maxima are the same. The results also show that the different efficiency is mainly caused by vegetation feedback with a meridional shift of a tundra-boreal forest boundary. In the northern high latitude, insolation change due to the summer solstice at the perihelion has a typical pattern of seasonality (increased in the mid-summer decreased in the spring and autumn) with no annual-mean component. This seasonality is unfavorable for snow melt in the spring (hence delay the melt) and surface albedo feedback, which accompany cooling in the spring and prevent boreal forests from growing. On the other hand, insolation change due to large obliquity has the other pattern of seasonality (increased the insolation in half a year) with increased annual mean insolation. This seasonality is favorable for the snow melt (hence promote the melt) and surface albedo feedback, which accompany warming throughout the year and assist the growing. These differences cause that obliquity changes promote vegetation-snow-albedo feedback stronger than precession-eccentricity changes.

Keywords: GCM, orbital parameter, feedback

©2019. Japan Geoscience Union. All Right Reserved.

[J] Poster | A (Atmospheric and Hydrospheric Sciences)：A-CC Cryospheric Sciences & Cold District Environment

Tue. May 28, 2019 5:15 PM - 6:30 PM JST | Tue. May 28, 2019 8:15 AM - 9:30 AM UTC | Poster Hall International Exhibition Hall8, Makuhari Messe_10

[A-CC26] Ice cores and paleoenvironmental modeling

convener:Ryu Uemura(University of the Ryukyus), Kenji Kawamura(National Institute of Polar Research, Research Organization of Information and Systems), Ayako Abe-Ouchi(Atmosphere and Ocean Research Institute, The University of Tokyo), Nozomu Takeuchi(Chiba University)

Analyses of ice cores from polar and mountain regions have contributed to the reconstruction and understanding of the past environmental changes on timescales from years to several hundred thousand years. In this session, we welcome paleoenvironmental studies using ice cores and paleoclimatic modeling. Studies on reconstruction methods, recording processes and new paleoenvironmental proxies, technical aspects of paleo-modeling are also welcomed. Studies with marine sediment cores, terrestrial sediment cores and tree-rings on similar timescales are also important and welcomed, in order to discuss past environmental changes from multidisciplinary viewpoints.

[ACC26-P01] Pollen analysis of ice cores drilled in the Pamir-Arai Mountains, central Asia

*Haruka Ogaya[1], Nozomu Takeuchi[1], Koji Fujita[2], Kenji Kawamura[3], Akane Tsushima[4], Vladimir Aizen[5], Azamat Osmonov[6] (1.Chiba University, 2.Nagoya University, 3.National Institute of Polar Research, 4.Research Institute for Humanity and Nature, 5.University of Idaho, 6.Central Asian Institute of Applied Geo-Science)

[ACC26-P02] Variations in mineralogy of dust in the Greenland SIGMA-D ice core over the past 100 years using SEM

*Naoko Nagatsuka[1], Kumiko Goto-Azuma[1,2], Akane Tsushima, Hideaki Motoyama[1,2], Sumito Matoba[3], Koji Fujita[4], Tetsuhide Yamasaki[5], Yukihiko Onuma[6], Masahiro Minowa[7], Teruo Aoki[8], Motohiro Hirabayashi[1] (1.National Institute of Polar Research, 2.SOKENDAI, 3.Institute of Low Temperature Science, Hokkaido University, 4.Graduate School of Environmental Studies, Nagoya University, 5.Avangnaq Arctic Project Corp., 6.Institute of Industrial Science, University of Tokyo, 7.Universidad Austral de Chile, 8.Graduate School of Natural Science and Technology, Okayama University)

[ACC26-P03] Size and shape of solid particles in a Greenland ice core

*Wataru Shigeyama[1,2], Kumiko Goto-Azuma[2,1], Kaori Fukuda[2], Fumio Nakazawa[2,1], Morimasa Takata[3], Tomoyuki Homma[3], Nobuhiko Azuma[3], Dorthe Dahl-Jensen[4] (1.The Graduate University for Advanced Studies (SOKENDAI), School of Multidisciplinary Sciences, Department of Polar Science, 2.National Institute of Polar Research, 3.Nagaoka University of Technology, 4.University of Copenhagen)

[ACC26-P04] Methane concentration measurements of the Dome Fuji ice core using Continuous Flow Analysis system

Ikumi Oyabu[1], Miho Arai[1,4,5], *Kenji Kawamura[1,2,3], Kyotaro Kitamura[1], Jun Ogata[1], Kumiko Goto-Azuma[1,2] (1.National Institute of Polar Research, Research Organization of Information and Systems, 2.SOKENDAI (The Graduate University of Advanced Studies), 3.JAMSTEC, 4.Yamagata University, 5.Weathernews Inc.)

[ACC26-P05] A basal topographic map in the Dome Fuji region constructed from the ground-based radar survey in the JARE 59

*Shun Tsutaki[1], Takashi Obase[1], Shuji Fujita[2,3], Ayako Abe-Ouchi[1,4], Kenji Kawamura[2,3,4], Kenichi Matsuoka[5], Hiroshi Ohno[6], Ikumi Oyabu[2,7], Fumio Nakazawa[2], Konosuke Sugiura[8] (1.The University of Tokyo, 2.National Institute of Polar Research, 3.The Graduate University for Advanced Studies, 4.Japan Agency for Marine-Earth Science and Technology, 5.Norwegian Polar Institute, 6.Kitami Institute of Technology, 7.Japan Society for the Promotion of Science, 8.University of Toyama)

[ACC26-P06] Performance of RCIP scheme on 1-d age computation of ice sheet.

*Fuyuki SAITO[1], Takashi Obase[2], Ayako Abe-Ouchi[2,1] (1.Japan Agency for Marine-Earth Science and Technology, 2.Atmosphere and Ocean Research Institute, University of Tokyo)

[ACC26-P07] Climate changes of the last deglaciation simulated by MIROC AOGCM

*Takashi Obase[1], Ayako Abe-Ouchi[1,2], Sam Sherriff-Tadano[1] (1.Atmosphere and Ocean Research Institute, the University of Tokyo, 2.Japan Agency for Marine-Earth Science and Technology)

[ACC26-P08] A Last Glacial Maximum experiment using MIROC-ES2L earth system model in comparison with ice core and the other paleo-proxy data

*Rumi Ohgaito[1], Tomohiro Hajima[1], Akitomo Yamamoto[1], Hiroaki Tatebe[1], Michio Kawamiya[1], Ayako Abe-Ouchi[2,1] (1.Japan Agency for Marine-Earth Science and Technology, 2.AORI, Univ. Tokyo)

[ACC26-P09] On the possible bifurcation mechanisms and associated dynamical properties of Dansgaard-Oeschger oscillations

*Takahito Mitsui[1], Ayako Abe-Ouchi[1], Wing-Le Chan[1], Sam Sherriff-Tadano[1] (1.The University of Tokyo)

[ACC26-P10] The role of climate-vegetation feedback in climate changes driven by orbital parameter changes: the Arctic land surfaces and seasonality

*Kanon Kino[1], Ayako Abe-Ouchi[1,2], Ryouta O'ishi[1], Fuyuki SAITO[2], Masakazu Yoshimori[1] (1.Atmosphere and Ocean Research Institute, the University of Tokyo, 2.Japan Agency for Marine-Earth Science and Technology)

Pollen analysis of ice cores drilled in the Pamir-Arai Mountains, central Asia

*Haruka Ogaya[1], Nozomu Takeuchi[1], Koji Fujita[2], Kenji Kawamura[3], Akane Tsushima[4], Vladimir Aizen[5], Azamat Osmonov[6]

1. Chiba University, 2. Nagoya University, 3. National Institute of Polar Research, 4. Research Institute for Humanity and Nature, 5. University of Idaho, 6. Central Asian Institute of Applied Geo-Science

Ice cores drilled from mountain glaciers usually contains abundant pollen grains supplied from vegetation around the glaciers. Pollen grains have been used in ice core studies as markers of annual layer boundary since they are supplied on the glacier in a certain season of a year. Furthermore, they have been used as a proxy of vegetation in the surrounding area since their composition reflects relative abundance of each species in the source area. An ice core from the surface to the bottom was drilled on a glacier in Pamir Arai Mountains in central Asia in 2016. In this study, pollen grains in a part of the ice core and snow pit were analyzed. Annual layers of the ice core, which were determined based on a seasonality of stable isotope, were compared with the variations of pollen grains concentration, and the seasonality of pollen supplies was examined.
Ice cores were recovered at two sites (sites 1 and 2 at 5300 m and 5208 m, respectively) on the glacier. Oxygen stable isotope in the 7 m deep ice cores at both sites showed significant fluctuations. We assumed that they are periodic seasonal signals and determined the annual layers. As a result, the ice cores of Sites 1 and 2 includes layers for 8 years and 9 years, respectively. Microscopic analysis revealed that 6 types of pollen grains, which were identified as Cupressaceae, Artemisia, Chenopodiaceae, Pinaceae, Betulaceae, and Ephedra, were contained in the ice cores. Mean concentration of the pollen grains was highest for Cupressaceae at both sites (2.20, 2.62 grains/ml (74, 67%)), was second highest for Artemisia (0.65, 1.06 grains/ml (22, 27%)). The depth profile of the pollen grain concentrations showed several spikes in the ice cores. The depth of peaks differed between species. The peaks of Artemisia and Chenopodiaceae appeared at the same depth while the peaks of Cupressaceae appeared just below the depth of their peaks. The peak depths of Artemisia and Chenopodiaceae roughly agreed with the depth of the maximum value of the isotope ratio, indicating that these pollens were supplied in the summer or autumn. On the other hand, Cupressaceae found in the layer below is likely to be supplied in spring or summer. There are exceptional annual layers, in which the peaks of all species were not present, and the flux of pollen grains did not agree between two sites. These inconsistencies were likely due to the influence of the melting of the glacier surface. Results shows that the ice cores contain sufficient pollen grains for analysis and pollen profiles can be used to annual layer counting.

Keywords: Mountain glaciers, Ice core, Pollen, Pamir Arai Mountains, Central Asia

©2019. Japan Geoscience Union. All Right Reserved.

Variations in mineralogy of dust in the Greenland SIGMA-D ice core over the past 100 years using SEM

*Naoko Nagatsuka[1], Kumiko Goto-Azuma[1,2], Akane Tsushima, Hideaki Motoyama[1,2], Sumito Matoba[3], Koji Fujita[4], Tetsuhide Yamasaki[5], Yukihiko Onuma[6], Masahiro Minowa[7], Teruo Aoki[8], Motohiro Hirabayashi[1]

1. National Institute of Polar Research, 2. SOKENDAI, 3. Institute of Low Temperature Science, Hokkaido University, 4. Graduate School of Environmental Studies, Nagoya University, 5. Avangnaq Arctic Project Corp., 6. Institute of Industrial Science, University of Tokyo, 7. Universidad Austral de Chile, 8. Graduate School of Natural Science and Technology, Okayama University

Snow and ice on glaciers and the ice sheet in the Arctic contain windblown mineral dust derived from local sediments as well as distant deserts. Dust deposited on the ice sheet in the past can be obtained by ice core drilling, and the variations in its sources and transportation processes can be reconstructed by particle analysis of ice cores. In this study, we analyzed morphology and surface chemistry of mineral dust particles in an ice core drilled in Northwest Greenland with Scanning Electron Microscope (SEM, QUANTA FEG 450) and Energy Dispersive X-ray Spectrometer (EDS).
The ice core was drilled at the SIGMA-D site (N77°64’, W59°12’ [1]) of 2100 m a.s.l. in 2014. The length is 222.72 m and the estimated age at 113 m depth is 350 years before present . The ice samples were collected every five years in plastic bottles and freeze dried on a polycarbonate filter to concentrate micro-particles. Then, the filter was coated with platinum (Pt) for SEM analysis. Here we report the temporal variations in size distributions and compositions of the minerals during the past 100 years (A.D 1920-2013).
The SEM observation revealed that the mean size of mineral dust in the SIGMA-D ice core ranged from 1-3 μm, which is similar to that of the other Greenland ice core dust that seems to be derived from distant areas. This suggests that the SIGMA-D ice core contained mainly long–range transported wind-blown mineral dust.
The EDS analysis revealed the ice core contained mainly silicate minerals, especially clay minerals that showed compositional variation among the samples. For example, the mineralogical composition varied in every 10-15 years and showed a negative correlation between minerals formed by chemical and physical weathering (kaolinite vs illite/micas and chlorite). This indicates that minerals in the ice core were derived from multiple geological sources and the source areas might have varied temporally. Furthermore, quartz and feldspar, which had larger particles than clay minerals and thus were generally used as a short-distant transport, were higher in 1920-1945 and 1990-2013 compared with the other periods. Based on the past temperature record in Greenland, the warming occurred from 1910 to 1945 and after 1990. This may suggest that the minerals were derived not only from distant areas but also from local sources, such as moraine around the ice sheet margin in warmer periods. This is likely due to exposure of ground surface without snow cover.

Keywords: mineral dust, ice core, Greenland , SEM

©2019. Japan Geoscience Union. All Right Reserved.

Size and shape of solid particles in a Greenland ice core

*Wataru Shigeyama[1,2], Kumiko Goto-Azuma[2,1], Kaori Fukuda[2], Fumio Nakazawa[2,1], Morimasa Takata[3], Tomoyuki Homma[3], Nobuhiko Azuma[3], Dorthe Dahl-Jensen[4]

1. The Graduate University for Advanced Studies (SOKENDAI), School of Multidisciplinary Sciences, Department of Polar Science, 2. National Institute of Polar Research, 3. Nagaoka University of Technology, 4. University of Copenhagen

Concentrations and size distributions of insoluble solid particles in ice cores provide us with information on the changes in provenance, aridity, atmospheric circulation, etc. Most of the previous studies have focused on concentrations and size distributions. However, several studies (e.g., Barnes et al., 2002; Lambert et al., 2008; Simonsen et al., 2018) reported that particles formed aggregates and had various shapes. For a better environmental reconstruction, we need to study shapes and aggregation processes of the particles together with concentrations and size distributions.

Using a cryogenic scanning electron microscope (cryo-SEM), we carried out in-situ observations of solid particles in ice core samples without melting them. From the observations on selected ice samples (124 m depth in the present interglacial period, 1548 m depth in the last glacial period and 2406 m in the last interglacial period) retrieved by North Greenland Eemian Ice Drilling (NEEM), we found that many particles formed aggregates, and that individual particles (particles forming the aggregates) had elongated shapes (aspect ratio: 0.4-0.8). We also found that the sizes of the aggregate and individual particles showed log-normal distribution. The aggregates were larger in the interglacial periods than those in the glacial period (median diameter: 4.5 μm in the present interglacial period, 5.9 μm in the last interglacial period, and 2.2 μm in the last glacial period). These results need to be taken into account to interpret the size distribution data obtained by analyses on melted ice cores.

References

Barnes, P.R.F. et al., 2002, Ann. Glaciol. 35. pp 559-566

Lambert, F. et al., 2008, Nature. 452. pp 616-619

Simonsen, M.F. et al., 2018, Clim. Past. 14. pp 601-608

Keywords: solid particles, size distribution, particle shape, aggregate, cryo-SEM, NEEM ice core

©2019. Japan Geoscience Union. All Right Reserved.

Methane concentration measurements of the Dome Fuji ice core using Continuous Flow Analysis system

Ikumi Oyabu[1], Miho Arai[1,4,5], *Kenji Kawamura[1,2,3], Kyotaro Kitamura[1], Jun Ogata[1], Kumiko Goto-Azuma[1,2]

1. National Institute of Polar Research, Research Organization of Information and Systems, 2. SOKENDAI (The Graduate University of Advanced Studies), 3. JAMSTEC, 4. Yamagata University, 5. Weathernews Inc.

At the National Institute of Polar Research (NIPR), Continuous Flow Analyses (CFA) system has been developed. In addition to the measurements of melt water (e.g. water isotopes, micro-particles and major ions), the enclosed air is extracted from the water stream and measured for methane (CH_4) concentration by a customized Cavity Ring-Down Spectrometer (CRDS) (Picarro G2301). The CFA system provides data at much higher resolution than classic discrete measurements, which can improve our knowledge and understanding of past climatic variations.

The CH_4 concentration measured by CFA is affected by several factors, impacting precision, accuracy and resolution. The factors include dissolution of CH_4 in meltwater and its imperfect extraction, sample mixing and smoothing in sample lines, and contamination by room air intrusion into the system at the interface between ice samples. The magnitudes of these effects have been investigated, and the data are corrected accordingly. Here, we report the results of various tests for assessing the performance of our CFA for CH_4 measurement. Furthermore, the results of the measurement campaigns of the Dome Fuji ice core, covering the 8.2-kyr cooling event and a part of the last deglaciation, will also be presented.

Keywords: Continuous Flow Analysis, Ice core, CH4, Dome Fuji

©2019. Japan Geoscience Union. All Right Reserved.

A basal topographic map in the Dome Fuji region constructed from the ground-based radar survey in the JARE 59

*Shun Tsutaki[1], Takashi Obase[1], Shuji Fujita[2,3], Ayako Abe-Ouchi[1,4], Kenji Kawamura[2,3,4], Kenichi Matsuoka[5], Hiroshi Ohno[6], Ikumi Oyabu[2,7], Fumio Nakazawa[2], Konosuke Sugiura[8]

1. The University of Tokyo, 2. National Institute of Polar Research, 3. The Graduate University for Advanced Studies, 4. Japan Agency for Marine-Earth Science and Technology, 5. Norwegian Polar Institute, 6. Kitami Institute of Technology, 7. Japan Society for the Promotion of Science, 8. University of Toyama

Drilling a deep ice core extending 1.5 million years (Ma) back in time is crucial to better understand the transition in the periodicity of the glacial cycles changed from 40 kilo year (ka) to the current 100 ka during the mid-Pleistocene transition (0.9–1.2 Ma). However, continuous ice core records more than 1 Ma have not been retrieved in the Antarctic ice sheet. Sufficient knowledge of the basal topography is crucial to modify numerical experiments that may provide a continuous record of past mechanisms of climate change. A ground-based radar survey was conducted over an area of 20000 km^2 with a line spacing of 5 km in the Dome Fuji area in the 59th Japanese Antarctic Research Expedition (JARE 59, 2017–2018 Antarctic summer). In this study, we analyze the JARE 59 radar data to construct an improved map of basal topography in the Dome Fuji region to progress the identification of a suitable drilling site at the region.

Keywords: Antarctic ice sheet, Basal topography, Radar

©2019. Japan Geoscience Union. All Right Reserved.

Performance of RCIP scheme on 1-d age computation of ice sheet.

*Fuyuki SAITO[1], Takashi Obase[2], Ayako Abe-Ouchi[2,1]

1. Japan Agency for Marine-Earth Science and Technology, 2. Atmosphere and Ocean Research Institute, University of Tokyo

Generally the evolution of ice-sheet thickness, temperature and age in an ice-sheet model are formulated using the transport or advection equation. There are many variation of the formulation, which differ in numerical aspects such as stability, accuracy, numerical diffusivity, conservation and/or computational costs.
Rational Constrained Interpolation Profile scheme (RCIP, Xiao et al. 1996) is a variation of semi-Lagrangian scheme, which has properties in suppressing numerical oscillation and diffusion near large gradients.
In this study, RCIP scheme is implemented on 1d age computation of ice sheet, which is a typical numerical study of ice-core related topics. Comparison with the results of RCIP scheme and those of classical upwind scheme shows that the former keeps fine information (i.e., surface mass balance) recorded at the deposit.

Keywords: Ice core dating simulation

©2019. Japan Geoscience Union. All Right Reserved.

Climate changes of the last deglaciation simulated by MIROC AOGCM

*Takashi Obase[1], Ayako Abe-Ouchi[1,2], Sam Sherriff-Tadano[1]

1. Atmosphere and Ocean Research Institute, the University of Tokyo, 2. Japan Agency for Marine-Earth Science and Technology

During the last deglaciation, a major global warming was punctuated by abrupt climate changes related to Atlantic Meridional Overturning Circulation (AMOC). However, abrupt climate change associated with a rapid increase in the AMOC during Bølling-Allerød (BA) transition was reproduced only by applying a reduction in glacial meltwater, which is not inferred from reconstructions. Here we show that an abrupt increase in the AMOC during the BA transition can occur without reduction in glacial meltwater, from a transient simulation of the last deglaciation using an atmosphere-ocean general circulation model. The abrupt increase in the AMOC accompanied with drastic retreat of sea ice in the North Atlantic, abrupt warming in Greenland, cooling of the Southern Hemisphere, that are consistent with proxies and previous modeling studies. Model-data comparison at specific sites will be presented to evaluate simulated climate changes of the last deglaciation.

©2019. Japan Geoscience Union. All Right Reserved.

A Last Glacial Maximum experiment using MIROC-ES2L earth system model in comparison with ice core and the other paleo-proxy data

*Rumi Ohgaito[1], Tomohiro Hajima[1], Akitomo Yamamoto[1], Hiroaki Tatebe[1], Michio Kawamiya[1], Ayako Abe-Ouchi[2,1]

1. Japan Agency for Marine-Earth Science and Technology, 2. AORI, Univ. Tokyo

We are performing numerical experiments targeting distinctive time period of the past, Last Glacial Maximum (LGM, 21,000 years before present), using MIROC-ES2L. MIROC-ES2L is a newly developed earth system model (ESM) (Hajima et al. in prep.) including atmosphere, ocean, land, and ocean and land biogeochemical cycles in order to contribute Coupled Model Intercomparison Project phase 6 and Intergovernmental Panel on Climate Change 6th assessment report.
Testing climate models using paleoclimate experiments is an irreplaceable opportunity on evaluation of models to simulate climate change significantly different from the present day. In this presentation, we describe how we simulate the LGM experiment, compare with paleo-proxy data and discuss which component contributed for the realization of the LGM climate.
Following protocol of Paleoclimate Modelling Intercomparison Project phase 4 (Kageyama et al. 2017), we are performing a LGM experiment. Because the LGM condition is significantly different from the present day, long spin-up is essential. Hence, before the model development is finalized, we started spin-up using the physical core (Atmosphere-Ocean coupled general circulation model) of MIROC-ES2L. Firstly, an experiment is branched from pre-industrial control (PI) experiment and the greenhouse gas levels are reduced to the LGM values. After integration for 2640 model years, land-sea mask and ice sheets, altitude, river path, orbit of the earth, salinity of ocean, and an erodibility map (concerning dust) of the LGM conditions are applied step by step and the total spin-up reached 6760 model years. Since MIROC-ES2L is ready during this procedure, the initial conditions at the 6760th model year of the spin-up experiment are used to initiate LGM experiment using MIROC-ES2L. In this conversion procedure, the initial conditions for land and ocean biogeochemical cycles were prepared respectively using offline modules to obtain quasi-stabilized states. Global mean temperature drawdown of the last 60 year climatology after 540 years integration with the ESM is -4.4 degree Celsius. Borehole thermometry suggested the cooling over the Eastern Antarctica at LGM was -7 to -10 degree Celsius (Stenni et al. 2010, Uemura et al. 2012). The modelled temperature anomaly is about -6.0 degree Celsius, which suggests weaker cooling compared to the ice core data. For the central Greenland, borehole thermometry suggested -21 to -25 degree Celsius (Cuffey et al. 1995, Johnsen et al. 1995, Dahl-Jensen et al. 1998), whereas the LGM experiment resulted -11.1 degree Celsius. This large discrepancy would be attributed to realization of ocean thermohaline state in the model experiment. The modelled peak value of the Atlantic Meridional Overturning Circulation (AMOC) is 21.0 Sverdrup for LGM and 15.3 Sverdrup for PI. On the other hand, AMOC is thought to be weaker than the present day from paleo proxy data (Lynch-Stieglitz et al. 2007, Hesse et al. 2011). We continue the experiment and analyze which component contributes global cooling and the cooling over the polar regions.

Keywords: Last Glacial Maximum, CMIP6, earth system model

©2019. Japan Geoscience Union. All Right Reserved.

On the possible bifurcation mechanisms and associated dynamical properties of Dansgaard-Oeschger oscillations

*Takahito Mitsui[1], Ayako Abe-Ouchi[1], Wing-Le Chan[1], Sam Sherriff-Tadano[1]

1. The University of Tokyo

Dansgaard-Oeschger (DO) oscillations are millennial-scale abrupt climate changes in the last glacial period (Dansgaard et al. 1993; Johnsen et al. 1992). In particular, they are frequent in the mid-glacial and less frequent at the beginning of the glacial and in the Last Glacial Maximum (McManus et al. 1999; Kawamura et al. 2017). Since its discovery, DO oscillations have been intensively studied, but its detailed mechanisms are still a subject of debate. Our recent modeling study (Abe-Ouchi et al. in prep) with MIROC4m Atmosphere-Ocean general circulation model (Hasumi and Emori 2004) suggests that DO oscillations are spontaneous oscillations which arise from global-scale interactions between the atmosphere and ocean (see also studies in [12] and Brown and Galbraith, 2016). Our simulated oscillations are likely to appear in a certain region of background climate conditions directly related to factors such as ice sheets, orbital elements, and greenhouse gases (Abe-Ouchi et al. in prep; Sam Sherriff-Tadano et al. 2017). This result is consistent with the observations that DO oscillations were most frequent in the mid-glacial.

The bifurcation theory is a field of mathematics which studies qualitative changes of dynamical systems depending on the changes in parameters. In general, we can consider numerous types of dynamical systems, but their bifurcation phenomena are classified into only several types (Strogatz, Nonlinear Dynamics And Chaos, 2000). Identifying bifurcation mechanisms may help us to understand the emergence mechanism of the oscillation and its associated properties like the period or the amplitude. For example, when oscillations emerge/vanish via a Homoclinic bifurcation, the period of oscillations diverges to infinity as the parameter approaches the bifurcation point. On the other hand, when oscillations emerge via a Hopf bifurcation, such divergence of the period does not occur. On the basis of such scaling properties of the period, previous studies [7, 9] suggested onset mechanisms for the oscillations.

In this study, we survey bifurcation mechanisms reported in previous models of DO oscillations [1-12]. We also performed a bifurcation analysis of an extended version of the Winton (1993) 3-box halocline oscillator [2], which has a parameter dependence similar to that of MIROC AOCGM. It is found that, in many models, DO-like oscillations emerge via a Hopf-type bifurcation [1,2,4,5,6,7,10,11] and/or via a Homoclinic-type bifurcation [1,2,3,5,6,7,8,9,11]. The Welander (1982) model [1] and the extended Winton model may generate oscillations via both a Hopf-type bifurcation and a Homoclinic-type bifurcation depending on their parameters, but these bifurcations become identical at a parameter limit. This implies that the oscillation period may increase rapidly even near the Hopf bifurcation points (though it does not diverge). Therefore, identifying onset mechanisms of oscillations on the basis of scaling properties of the period may have a subtle problem. The extended Winton's model has a phase space structure like Homoclinic orbit even near the Hopf bifurcation point, and this phase space structure induces a long oscillation period. In MIROC AOGCM, the onset of oscillation may be related to either a Hopf-type bifurcation or a Homoclinic-type bifurcation, or to both of them. The determination of the bifurcation type in MIROC AOGCM is still difficult because of limited computational time and inherent natural variability. Nevertheless, we observe that noisy 'limit cycles' near bifurcation points show characteristics similar to Homoclinic orbit and have relatively long periods.

©2019. Japan Geoscience Union. All Right Reserved.

[1] Welander, Dyn. Atmos. Oceans (1982)
[2] Winton, Ice in the Climate System. NATO ASI Series (1993)
[3] Cessi, Journal of Physical Oceanography (1996)
[4] Sakai and Peltier, J. Climate (1999)
[5] Timmermann, Schulz, Gildor, and Tzipermann J. Climate (2003)
[6] Abshagen and Timmermann, Journal of Physical Oceanography (2004)
[7] Colin de Verdière, Ben Jelloul, and Sévellec, J. Climate (2006)
[8] Colin de Verdière, Journal of Physical Oceanography (2007)
[9] Sévellec, Huck, and Colin de Verdière, J. Mar. Res (2010)
[10] Roberts and Saha, Clim. Dyn. (2017)
[11] Leifeld, Euro. Jnl. of Applied Mathematics (2018)
[12] W. R. Peltier and G. Vettoretti, GRL (2014)

Keywords: Dansgaard-Oeschger cycles, bifurcation, oscillation

©2019. Japan Geoscience Union. All Right Reserved.

The role of climate-vegetation feedback in climate changes driven by orbital parameter changes: the Arctic land surfaces and seasonality

*Kanon Kino[1], Ayako Abe-Ouchi[1,2], Ryouta O'ishi[1], Fuyuki SAITO[2], Masakazu Yoshimori[1]

1. Atmosphere and Ocean Research Institute, the University of Tokyo, 2. Japan Agency for Marine-Earth Science and Technology

Periodic summer insolation change accompanying Earth’s orbital parameter changes is widely known as a main driver of the glacial cycles. Realistic orbital parameters are prescribed with climate models and ice-sheet models to reproduce and explain the characteristic of the glacial cycles in past several hundred thousand years(e.g. Abe-Ouchi et al., 2007; 2013). On the other way, radiative feedback analyses at the top of the atmosphere enable to understand the Earth’s climate response to the orbital forcing (Mantsis et al., 2011; Erb et al., 2013). In this study, we investigate the surface climate responses to the orbital forcing, by using MIROC-GCM and a surface climate feedback analyses method. We focus on the relationship between summer insolation and summer temperature on the land in the northern high latitude, since the former is a major index and the later is important for the ice-sheets melt.

We use a coupled atmosphere-vegetation GCM with slab ocean of MIROC-GCM (O’ishi and Abe-Ouchi, 2011) and performed numerous experiments by systematically changing the combinations of orbital parameters (maximum, minimum and present values of each parameter). A seasonal surface feedback analysis method (Lu and Cai, 2009) is also applied.

Results show that summer temperature change over the Arctic land due to obliquity change can be larger than that due to precession-eccentricity change, when the summer insolation maxima are the same. The results also show that the different efficiency is mainly caused by vegetation feedback with a meridional shift of a tundra-boreal forest boundary. In the northern high latitude, insolation change due to the summer solstice at the perihelion has a typical pattern of seasonality (increased in the mid-summer decreased in the spring and autumn) with no annual-mean component. This seasonality is unfavorable for snow melt in the spring (hence delay the melt) and surface albedo feedback, which accompany cooling in the spring and prevent boreal forests from growing. On the other hand, insolation change due to large obliquity has the other pattern of seasonality (increased the insolation in half a year) with increased annual mean insolation. This seasonality is favorable for the snow melt (hence promote the melt) and surface albedo feedback, which accompany warming throughout the year and assist the growing. These differences cause that obliquity changes promote vegetation-snow-albedo feedback stronger than precession-eccentricity changes.

Keywords: GCM, orbital parameter, feedback

©2019. Japan Geoscience Union. All Right Reserved.

[J] Oral | A (Atmospheric and Hydrospheric Sciences)：A-GE Geological & Soil Environment

Tue. May 28, 2019 1:45 PM - 3:15 PM JST | Tue. May 28, 2019 4:45 AM - 6:15 AM UTC | 202 2F

[A-GE30] Conservation and Restoration of Soil Environment at Terrestrial Surface

convener:Yasushi Mori(Graduate School of Environmental and Life Science, Okayama University), Chairperson:Yasushi Mori(Okayama University)

Soil is the largest store of carbon of all terrestrial media. Soils also have important functions such as water storage and plant support roles. However, at present, these characteristics do not fully function, because of mismanagement of the field or climate-change-induced heavy rainfall would wash away the organic-rich surface soils. In this session, soil environment research, from soil conservation to restoration technique for degraded soils are welcomed.

1:45 PM - 1:50 PM JST | 4:45 AM - 4:50 AM UTC

Introduction

1:50 PM - 2:05 PM JST | 4:50 AM - 5:05 AM UTC

[AGE30-01] Soil Organic Cabon Contents Estimation using Neural Network System

Ikumi Kaida[1], *Yasushi Mori[1], Takayuki Shuku[1] (1.Graduate School of Environmental and Life Science, Okayama University)

2:05 PM - 2:25 PM JST | 5:05 AM - 5:25 AM UTC

[AGE30-02] Methane emission from rice paddies and its response to climate change

★Invited Papers

*Takeshi Tokida[1] (1.Institute for Agro-Environmental Sciences, National Agriculture and Food Research Organization)

2:25 PM - 2:40 PM JST | 5:25 AM - 5:40 AM UTC

[AGE30-03] **Relationship between degradation of rice grain quality due to chalky kernels and available nutrients in soil**

*Shingo Matsumoto[1], Junko Kasuga[1] (1.Shimane University)

2:40 PM - 2:55 PM JST | 5:40 AM - 5:55 AM UTC

[AGE30-04] The effects of trenching and insertion of crop residue on infiltration and soil erosion in a farmland

*Kazutoshi Osawa[1], Yasushi Mori[2], Akira Hoshikawa (1.Utsunomiya University, 2.Graduate school of Environmental and Life Science, Okayama University)

2:55 PM - 3:15 PM JST | 5:55 AM - 6:15 AM UTC

[AGE30-05] Measuring wide-range soil water content using GPS signals

★Invited Papers

*Kosuke Noborio[1], Natsumi Naganuma[1] (1.Meiji University)

Soil Organic Cabon Contents Estimation using Neural Network System

Ikumi Kaida[1], *Yasushi Mori[1], Takayuki Shuku[1]

1. Graduate School of Environmental and Life Science, Okayama University

Dynamics of organic matter in soil greatly affects the material circulation of the outermost layer of the earth and since it has the largest storage capacity in the terrestrial area, its accumulation and disappearance attracts high attention on global warming. Previous studies showed some achievements on the estimation of soil organic matter. However, since natural process is very complicated, the parameters are extracted from the accumulation of individual research, and are not estimated while considering mutual relationships based on a sufficient amount of data. Therefore, it is going to be waste of time or not realistic to tackle the problem for relating huge sets of soil parameters without understanding functional relationship. With the development of computers in recent years, machine learning and neural networks, which are rapidly becoming to be applied to realistic tasks, read huge amounts of data and learn individual relationships while estimating the target value.

Therefore, in this study, we tried to find deeply related soil parameters using 11000 sets of 16 parameters (limited only in Europe) obtained from Harmonized World Soil Database (FAO, IIASA). Recursive Feature Elimination (RFE method) eliminated the weakly related parameters, and then the deeply related parameters are used to estimate organic carbon using neural network. Among the verifications, the neural network showed the best performance when the parameter selection was set to seven. Clay content, dry bulk density, clay CEC, total CEC, base saturation, exchangeable base, and ESP are evaluated as having high relevance. Interestingly, uncommon parameters were also included in the selection. 70% of the models constructed with these seven parameters estimated the amount of soil organic matter very well, 30% resulted in extremely bad results. In addition, although the selected parameter is deeply related to soil organic matter contents, it is not clear whether each parameter works positive or negative for estimation in the non-linear function. Since the derived relation is nonlinear and very complicated, it is difficult to understand the calculation process. But since the model function is obtained without giving a functional system from the human side, it is going to be a powerful tool in extracting necessary parameters from huge data sets which seems to have unknown relationships. In addition, the research will be more effective, and will greatly contribute to elucidation of environmental dynamics involving complex factors.

Keywords: Soil Organic Carbon, Neural Network, Global Warming

©2019. Japan Geoscience Union. All Right Reserved.

Methane emission from rice paddies and its response to climate change

*Takeshi Tokida[1]

1. Institute for Agro-Environmental Sciences, National Agriculture and Food Research Organization

a, b, c, d, e

Keywords: rice paddy, methane, global warming, FACE (Free-Air CO2 Enrichment)

©2019. Japan Geoscience Union. All Right Reserved.

Relationship between degradation of rice grain quality due to chalky kernels and available nutrients in soil

*Shingo Matsumoto[1], Junko Kasuga[1]

1. Shimane University

a,b,c,d,e,

Keywords: high-temperature damage to rice grain ripening, chalky grain, available silicate

©2019. Japan Geoscience Union. All Right Reserved.

The effects of trenching and insertion of crop residue on infiltration and soil erosion in a farmland

*Kazutoshi Osawa[1], Yasushi Mori[2], Akira Hoshikawa

1. Utsunomiya University, 2. Graduate school of Environmental and Life Science, Okayama University

It has been recognized that dynamics of water and the associated materials such as sediment and nutrients are important to conserve ecosystem existing in a watershed. Among others, excess soil and nutrients transports toward the coastal zones and deposition on corals are one of the major environmental problems in Okinawa, Japan, in which agricultural area is the major source of sediment yield. In this study, we focused on effects of trenching and insertion of crop residue on infiltration and soil erosion in a sugarcane field.

In the term of fallow period, water discharge in the trenching plot was 69% smaller than that in the control plot because the rainwater was infiltrated at the trenches on the surface. However, sediment yield in the trenching plot increased 57% over that in the control prot because soil surface was distubed by subsoiler to make trenches.

In the term of cropping period, water discharge in the plot of trenching and insertion of crop residue was 39% smaller than that in the control plot. The effect of increasing infiltration was continued because trenches did not fill with soil due to insertion of crop residue. Sediment yield in the plot of trenching and insertion of crop residue decreased 64% over that in the control prot. Then, from the view of preventing soil erosion, trenching and insertion of crop residue are effective practice during cropping period.

Keywords: Soil erosion, Infiltration, Trenching, insertion of organic matter, Sugarcane, Okinawa

©2019. Japan Geoscience Union. All Right Reserved.

Measuring wide-range soil water content using GPS signals

*Kosuke Noborio[1], Natsumi Naganuma[1]

1. Meiji University

For prediction of the amount of irrigation water during a crop growing period, estimation of groundwater recharge amount, landslide forecast, and others, measurement of a wide range of soil moisture content is indispensable. Since the introduction of TDR moisture meter by Topp et al. in 1980, measurement of soil water content at a certain point has become possible with high precision, and remote automatic data acquisition. However, when measuring a wide range of soil moisture content as conventional measurements using satellites or cosmic rays, there are concerns on resolution and measurement accuracy so that it has not been applied to routine observation. In 2008 Larson and colleagues reported that there is a significant relationship between the ground reflected wave intensity contained in the GPS signal and the soil moisture content around the GPS antenna. Since GPS satellites are operated to be observed at any location on the earth for 24 hours a day, if we could measure soil moisture content using GPS signals, applicability of this method would be immeasurable. In this report, we outline the principle and examples of wide area soil moisture content measurement using GPS signals.

Keywords: soil moisture, GPS satellite, signal noise ratio

©2019. Japan Geoscience Union. All Right Reserved.

©2019. Japan Geoscience Union. All Right Reserved.

[J] Poster | A (Atmospheric and Hydrospheric Sciences)：A-GE Geological & Soil Environment

Tue. May 28, 2019 3:30 PM - 5:00 PM JST | Tue. May 28, 2019 6:30 AM - 8:00 AM UTC | Poster Hall International Exhibition Hall8, Makuhari Messe_8

[A-GE30] Conservation and Restoration of Soil Environment at Terrestrial Surface

convener:Yasushi Mori(Graduate School of Environmental and Life Science, Okayama University)

Soil is the largest store of carbon of all terrestrial media. Soils also have important functions such as water storage and plant support roles. However, at present, these characteristics do not fully function, because of mismanagement of the field or climate-change-induced heavy rainfall would wash away the organic-rich surface soils. In this session, soil environment research, from soil conservation to restoration technique for degraded soils are welcomed.

[AGE30-P01] Analysis of soil erosion on cropland considering future climate change in Okinawa

*Gen Machida[1], Kazutoshi Osawa[1], Hiroyuki Matsui[1] (1.Utsunomiya University)

[AGE30-P02] Linear Macro pore Installation to Reduce Surface Flow

*Masaki Kiyohiro[1], Yasushi Mori[1], Kazutoshi Osawa[2], Akira Hosihkawa[3] (1.Okayama University Graduate school of Environmental and Life Science, 2.Utsunomiya University Faculty of Agriculture, 3.Fund of Coral reef in Sekisei Lagoon)

[AGE30-P03] Conservation of the Rice Terraces of the Philippine Cordilleras Based on the Soil Environmental Factors.

*Tomoyo Kurozumi[1], Yasushi Mori[2], Hiroaki Somura[2], Milagros Ong How[3] (1.Faculty of Environmental Science and Technology, Okayama University, 2.Graduate School of Environmental and Life Science, Okayama University, 3.Universal Harvester Incorporated)

[AGE30-P04] A preliminary study for water and substances simulation modeling in Cordilleras terraced paddy fields, Philippines

*Hiroaki Somura[1], Yasushi Mori[1], Tomoyo Kurozumi[2], Milagros Ong How[3] (1.Graduate School of Environmental and Life Science, Okayama University, 2.Faculty of Environmental Science and Technology, Okayama University, 3.Universal Harvester Incorporated)

Analysis of soil erosion on cropland considering future climate change in Okinawa

*Gen Machida[1], Kazutoshi Osawa[1], Hiroyuki Matsui[1]

1. Utsunomiya University

In Okinawa Prefecture, excessive red soil runoff due to soil erosion (water erosion) is a problem, and development of prediction method of erosion amount in cropland is required. In previous studies, analysis using a process based model "Water Erosion Prediction Project, WEPP" has been tried. However, methods for assessing soil erosion risk considering future climate change, which are necessary for long-term project for measures to reduce soil erosion, have not been studied yet. In this study, we made climate input data considering future climate change in Okinawa Prefecture using weather simulator "MarkSim" and applied it to WEPP.

In the climate input data created from MarkSim, precipitation tended to increase with the rise in temperature due to global warming. However, in the WEPP analysis under bare soil condition and under sugarcane farming condition, no increase in risk of erosion due to climate change could be confirmed. This is because the infiltration amount in the cropland increased with excessive drying of surface soil due to increasing evaporation. From the above, it is suggested that the increase in precipitation due to future climate change may not necessarily lead to an increase in erosion amount.

Keywords: WEPP Model, MarkSim, Global warming, Red soil runoff

©2019. Japan Geoscience Union. All Right Reserved.

Linear Macro pore Installation to Reduce Surface Flow

*Masaki Kiyohiro[1], Yasushi Mori[1], Kazutoshi Osawa[2], Akira Hosihkawa[3]

1. Okayama University Graduate school of Environmental and Life Science, 2. Utsunomiya University Faculty of Agriculture, 3. Fund of Coral reef in Sekisei Lagoon

Linear-Macropore Installation to Reduce Surface Flow at Subtropical Farmland.

Masaki Kiyohiro, Yasushi Mori, Kazutoshi Osawa, and Akira Hoshikawa

Key words: Soil erosion, Macro pore, Surface flow

Fields in Okinawa is suffering from surface flow which causes soil erosion. Soil erosion affects not only farming but also marine resources such as coral reef. The mechanism of the surface flow is as follows. First, rain drops hit the ground, and soil particles are separated from surface. Second, small soil particles filled the soil pores and crust layer is formed. Finally, surface flow increases. Farmland is the main sources of the soil erosion. Therefore, it’ s important to reduce surface flow with soil particles in farmland. Linear-macropore is one of the countermeasures for soil runoff. Linear-macropore is artificial ditch filling with plant residue which keep its structure. It can be installed easily by using agricultural machine. Furthermore, we can obtain plant residue easily in farmland. The objective of this study was to examine whether surface flow can be reduced by installation of linear macro pore by laboratory experiment.

We setup the lysimeter with soil which taken from sugarcane field in Ishigaki island, Okinawa and we examined 4 treatments (i.e., control, mulching, subsoiler (empty linear macro pore) and linear macro pore (subsoiling with filling gap by sugarcane residue). The soil was sieved through a 2 mm screen, and packed with the bulk density of 1.2 gcm^{-3}. Infiltration experiments with artificial rainfall were conducted in the laboratory at 25℃. Simulated rainfall with intensity of 20 mmh^{-1} was applied 4 hours to the surface, and 24 hours later after the first rainfall, the next rainfall was applied. In each experiment, we measured surface flow, soil moisture, and soil runoff.

As a result, crust layer was formed in all sections, and the ditch was collapsed in the subsoiler treatment. There was more surface flow in control section than mulching section, and no surface flow was confirmed in linear-macropore plot. Soil moisture increased the most in linear macropore. This is because linear-macropore can enhance infiltration and decrease surface flow. As we mentioned above, our research suggest that linear macro pore can increase infiltration and it can reduce soil erosion. It can be one of the countermeasures for surface flow and soil runoff.

Keywords: Soil erosion, Macro pore, Surface flow

©2019. Japan Geoscience Union. All Right Reserved.

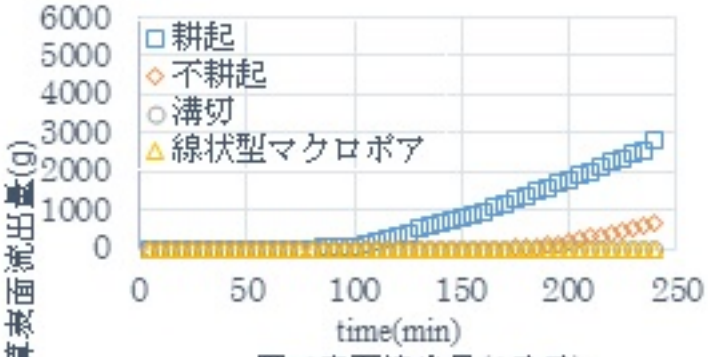

図-1表面流出量(1日目)

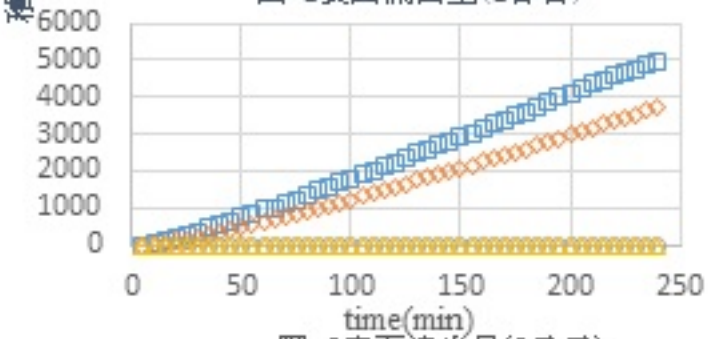

図-2表面流出量(2日目)

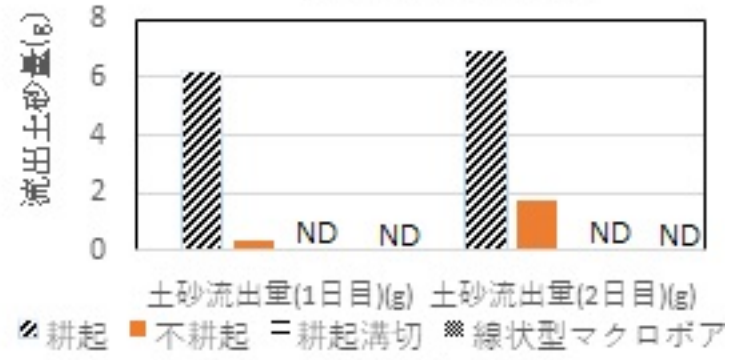

図-3流出土砂量(g)

©2019. Japan Geoscience Union. All Right Reserved.

Conservation of the Rice Terraces of the Philippine Cordilleras Based on the Soil Environmental Factors.

*Tomoyo Kurozumi[1], Yasushi Mori[2], Hiroaki Somura[2], Milagros Ong How[3]

1. Faculty of Environmental Science and Technology, Okayama University, 2. Graduate School of Environmental and Life Science, Okayama University, 3. Universal Harvester Incorporated

Rice terraces of the Philippine Cordilleras in northern Luzon have been damaged seriously. They need proper and efficient agricultural management. In slope failure area including rice terraces, reports said that the infiltration from paddy field surface strongly affected to the short -time ground water level changes. In that situation, the chance of land collapse would be higher when the water infiltration becomes larger. Therefore, in this study, the relationship between soil properties and vertical infiltration was examined. Cone-penetrometer test and infiltration test with ponded paddy was carried out at the site, and soil analysis (C,N and mineral) were at the laboratory. Results showed that both hardpan formation and clogging with organic matter (OM) were considered as factors that control infiltration. At the site, the rice terraces with no-hard pan stored more OM and exchangeable cations had been leached out. Although infiltration control has two patterns, hard pan formation is preferable from the perspective of soil fertility.

Keywords: rice terraces, hardpan, organic matter, Philippines

©2019. Japan Geoscience Union. All Right Reserved.

A preliminary study for water and substances simulation modeling in Cordilleras terraced paddy fields, Philippines

*Hiroaki Somura[1], Yasushi Mori[1], Tomoyo Kurozumi[2], Milagros Ong How[3]

1. Graduate School of Environmental and Life Science, Okayama University, 2. Faculty of Environmental Science and Technology, Okayama University, 3. Universal Harvester Incorporated

In the northern part of Luzon island of the Philippines, the Cordillera terraced paddy fields were registered as a World Heritage site in 1995, and cultivation of paddy rice has been carried out for many years. However, in recent years, maintenance and management of rice paddy fields have become difficult due to lack of personnel and shortage of budget. In addition, some farmers complain about a declining rice yield year by year. In this research, we study methods for stabilizing of crop production, through managing agricultural activities such as irrigation and fertilizer applications, with consideration of environmental conservation. We selected Bangaan village within the Cordillera rice paddy area, and will analyze water and substances dynamics by a simulation model. As results of our preliminary survey, the target area had approximately 11 ha of paddy fields, and the water catchment area flowing into the uppermost paddy field had almost the same area size. Also, using ASTER GDEM, the average slope in the east-west direction was calculated and found to be steep as about 20%. Furthermore, the paddy fields were traced as accurately as possible using the satellite image, and found that more than 130 paddy fields were existed. The largest paddy field in the area was roughly 0.3 ha, with smaller rice paddy fields occupying the majority. As next, we are going to understand the transfer of irrigation water and substances, especially between paddy fields, for modeling analyses.

Keywords: Terraced paddy fields, Irrigation, Agricultural activities, Philippines

©2019. Japan Geoscience Union. All Right Reserved.

[J] Poster | A (Atmospheric and Hydrospheric Sciences)：A-GE Geological & Soil Environment

Tue. May 28, 2019 5:15 PM - 6:30 PM JST | Tue. May 28, 2019 8:15 AM - 9:30 AM UTC | Poster Hall International Exhibition Hall8, Makuhari Messe_11

[A-GE30] Conservation and Restoration of Soil Environment at Terrestrial Surface

convener:Yasushi Mori(Graduate School of Environmental and Life Science, Okayama University)

Soil is the largest store of carbon of all terrestrial media. Soils also have important functions such as water storage and plant support roles. However, at present, these characteristics do not fully function, because of mismanagement of the field or climate-change-induced heavy rainfall would wash away the organic-rich surface soils. In this session, soil environment research, from soil conservation to restoration technique for degraded soils are welcomed.

[AGE30-P01] Analysis of soil erosion on cropland considering future climate change in Okinawa

*Gen Machida[1], Kazutoshi Osawa[1], Hiroyuki Matsui[1] (1.Utsunomiya University)

[AGE30-P02] Linear Macro pore Installation to Reduce Surface Flow

*Masaki Kiyohiro[1], Yasushi Mori[1], Kazutoshi Osawa[2], Akira Hosihkawa[3] (1.Okayama University Graduate school of Environmental and Life Science, 2.Utsunomiya University Faculty of Agriculture, 3.Fund of Coral reef in Sekisei Lagoon)

[AGE30-P03] Conservation of the Rice Terraces of the Philippine Cordilleras Based on the Soil Environmental Factors.

*Tomoyo Kurozumi[1], Yasushi Mori[2], Hiroaki Somura[2], Milagros Ong How[3] (1.Faculty of Environmental Science and Technology, Okayama University, 2.Graduate School of Environmental and Life Science, Okayama University, 3.Universal Harvester Incorporated)

[AGE30-P04] A preliminary study for water and substances simulation modeling in Cordilleras terraced paddy fields, Philippines

*Hiroaki Somura[1], Yasushi Mori[1], Tomoyo Kurozumi[2], Milagros Ong How[3] (1.Graduate School of Environmental and Life Science, Okayama University, 2.Faculty of Environmental Science and Technology, Okayama University, 3.Universal Harvester Incorporated)

Analysis of soil erosion on cropland considering future climate change in Okinawa

*Gen Machida[1], Kazutoshi Osawa[1], Hiroyuki Matsui[1]

1. Utsunomiya University

In Okinawa Prefecture, excessive red soil runoff due to soil erosion (water erosion) is a problem, and development of prediction method of erosion amount in cropland is required. In previous studies, analysis using a process based model "Water Erosion Prediction Project, WEPP" has been tried. However, methods for assessing soil erosion risk considering future climate change, which are necessary for long-term project for measures to reduce soil erosion, have not been studied yet. In this study, we made climate input data considering future climate change in Okinawa Prefecture using weather simulator "MarkSim" and applied it to WEPP.

In the climate input data created from MarkSim, precipitation tended to increase with the rise in temperature due to global warming. However, in the WEPP analysis under bare soil condition and under sugarcane farming condition, no increase in risk of erosion due to climate change could be confirmed. This is because the infiltration amount in the cropland increased with excessive drying of surface soil due to increasing evaporation. From the above, it is suggested that the increase in precipitation due to future climate change may not necessarily lead to an increase in erosion amount.

Keywords: WEPP Model, MarkSim, Global warming, Red soil runoff

©2019. Japan Geoscience Union. All Right Reserved.

Linear Macro pore Installation to Reduce Surface Flow

*Masaki Kiyohiro[1], Yasushi Mori[1], Kazutoshi Osawa[2], Akira Hosihkawa[3]

1. Okayama University Graduate school of Environmental and Life Science, 2. Utsunomiya University Faculty of Agriculture, 3. Fund of Coral reef in Sekisei Lagoon

Linear-Macropore Installation to Reduce Surface Flow at Subtropical Farmland.

Masaki Kiyohiro, Yasushi Mori, Kazutoshi Osawa, and Akira Hoshikawa

Key words: Soil erosion, Macro pore, Surface flow

Fields in Okinawa is suffering from surface flow which causes soil erosion. Soil erosion affects not only farming but also marine resources such as coral reef. The mechanism of the surface flow is as follows. First, rain drops hit the ground, and soil particles are separated from surface. Second, small soil particles filled the soil pores and crust layer is formed. Finally, surface flow increases. Farmland is the main sources of the soil erosion. Therefore, it’ s important to reduce surface flow with soil particles in farmland. Linear-macropore is one of the countermeasures for soil runoff. Linear-macropore is artificial ditch filling with plant residue which keep its structure. It can be installed easily by using agricultural machine. Furthermore, we can obtain plant residue easily in farmland. The objective of this study was to examine whether surface flow can be reduced by installation of linear macro pore by laboratory experiment.

We setup the lysimeter with soil which taken from sugarcane field in Ishigaki island, Okinawa and we examined 4 treatments (i.e., control, mulching, subsoiler (empty linear macro pore) and linear macro pore (subsoiling with filling gap by sugarcane residue). The soil was sieved through a 2 mm screen, and packed with the bulk density of 1.2 gcm^{-3}. Infiltration experiments with artificial rainfall were conducted in the laboratory at 25℃. Simulated rainfall with intensity of 20 mmh^{-1} was applied 4 hours to the surface, and 24 hours later after the first rainfall, the next rainfall was applied. In each experiment, we measured surface flow, soil moisture, and soil runoff.

As a result, crust layer was formed in all sections, and the ditch was collapsed in the subsoiler treatment. There was more surface flow in control section than mulching section, and no surface flow was confirmed in linear-macropore plot. Soil moisture increased the most in linear macropore. This is because linear-macropore can enhance infiltration and decrease surface flow. As we mentioned above, our research suggest that linear macro pore can increase infiltration and it can reduce soil erosion. It can be one of the countermeasures for surface flow and soil runoff.

Keywords: Soil erosion, Macro pore, Surface flow

©2019. Japan Geoscience Union. All Right Reserved.

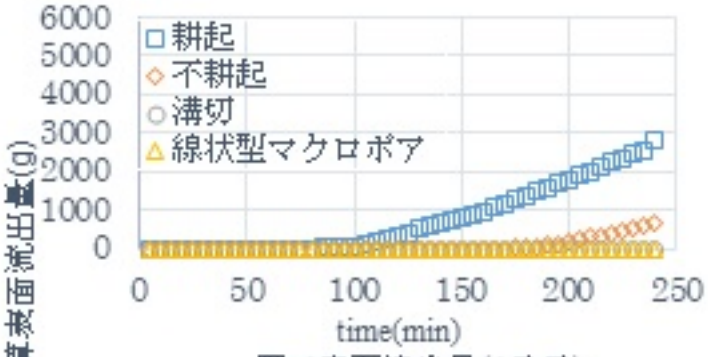

図-1表面流出量(1日目)

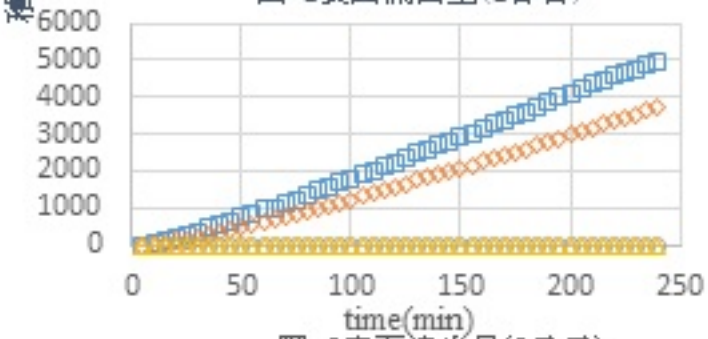

図-2表面流出量(2日目)

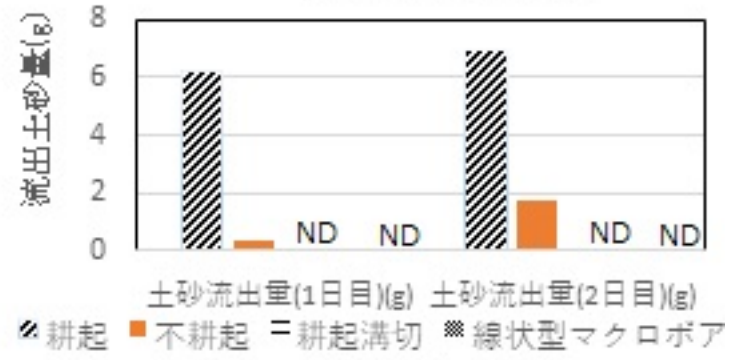

図-3流出土砂量(g)

©2019. Japan Geoscience Union. All Right Reserved.

Conservation of the Rice Terraces of the Philippine Cordilleras Based on the Soil Environmental Factors.

*Tomoyo Kurozumi[1], Yasushi Mori[2], Hiroaki Somura[2], Milagros Ong How[3]

1. Faculty of Environmental Science and Technology, Okayama University, 2. Graduate School of Environmental and Life Science, Okayama University, 3. Universal Harvester Incorporated

Rice terraces of the Philippine Cordilleras in northern Luzon have been damaged seriously. They need proper and efficient agricultural management. In slope failure area including rice terraces, reports said that the infiltration from paddy field surface strongly affected to the short -time ground water level changes. In that situation, the chance of land collapse would be higher when the water infiltration becomes larger. Therefore, in this study, the relationship between soil properties and vertical infiltration was examined. Cone-penetrometer test and infiltration test with ponded paddy was carried out at the site, and soil analysis (C,N and mineral) were at the laboratory. Results showed that both hardpan formation and clogging with organic matter (OM) were considered as factors that control infiltration. At the site, the rice terraces with no-hard pan stored more OM and exchangeable cations had been leached out. Although infiltration control has two patterns, hard pan formation is preferable from the perspective of soil fertility.

Keywords: rice terraces, hardpan, organic matter, Philippines

©2019. Japan Geoscience Union. All Right Reserved.

A preliminary study for water and substances simulation modeling in Cordilleras terraced paddy fields, Philippines

*Hiroaki Somura[1], Yasushi Mori[1], Tomoyo Kurozumi[2], Milagros Ong How[3]

1. Graduate School of Environmental and Life Science, Okayama University, 2. Faculty of Environmental Science and Technology, Okayama University, 3. Universal Harvester Incorporated

In the northern part of Luzon island of the Philippines, the Cordillera terraced paddy fields were registered as a World Heritage site in 1995, and cultivation of paddy rice has been carried out for many years. However, in recent years, maintenance and management of rice paddy fields have become difficult due to lack of personnel and shortage of budget. In addition, some farmers complain about a declining rice yield year by year. In this research, we study methods for stabilizing of crop production, through managing agricultural activities such as irrigation and fertilizer applications, with consideration of environmental conservation. We selected Bangaan village within the Cordillera rice paddy area, and will analyze water and substances dynamics by a simulation model. As results of our preliminary survey, the target area had approximately 11 ha of paddy fields, and the water catchment area flowing into the uppermost paddy field had almost the same area size. Also, using ASTER GDEM, the average slope in the east-west direction was calculated and found to be steep as about 20%. Furthermore, the paddy fields were traced as accurately as possible using the satellite image, and found that more than 130 paddy fields were existed. The largest paddy field in the area was roughly 0.3 ha, with smaller rice paddy fields occupying the majority. As next, we are going to understand the transfer of irrigation water and substances, especially between paddy fields, for modeling analyses.

Keywords: Terraced paddy fields, Irrigation, Agricultural activities, Philippines

©2019. Japan Geoscience Union. All Right Reserved.

[J] Oral | A (Atmospheric and Hydrospheric Sciences)：A-GE Geological & Soil Environment

Tue. May 28, 2019 3:30 PM - 5:00 PM JST | Tue. May 28, 2019 6:30 AM - 8:00 AM UTC | 202 2F

[A-GE31] New Roles of Soil Science for Extraterrestrials

convener:Kosuke Noborio(Meiji University), Masaru Mizoguchi(Graduate school of Agricultural and Life Sciences, The University of Tokyo), Chairperson:Naoto Sato

In recent years water ice and vapor have been discovered in extraterrestrials; however, liquid and ice water behavior in such environments is still not well understood. We will share recent studies how liquid or ice water behavior in porous media in microgravity or vacuum condition.

3:30 PM - 4:00 PM JST | 6:30 AM - 7:00 AM UTC

[AGE31-01] Life search on Mars by Life Detection Microscope (LDM)

★Invited Papers

*Yoshitaka Yoshimura[1] (1.College of Agriculture, Tamagawa University)

4:00 PM - 4:15 PM JST | 7:00 AM - 7:15 AM UTC

[AGE31-02] **Moisture movement in sand during evaporation under reduced pressure**

*Masaru Mizoguchi[1] (1.Graduate school of Agricultural and Life Sciences, The University of Tokyo)

4:15 PM - 4:30 PM JST | 7:15 AM - 7:30 AM UTC

[AGE31-03] Gravity effects on liquid behavior in porous media of uniform glass beads.

*Naoto Sato[1], Natsumi Naganuma[2], Kento Nogawa[2], Yuichi Maruo[2], Kosuke Noborio[1] (1.School of Agriculture, Meiji University, 2.Graduate School of Agriculture, Meiji University)

4:30 PM - 4:45 PM JST | 7:30 AM - 7:45 AM UTC

[AGE31-04] Effects of changes in viscosity under low gravity on infiltration rate

*Kento Nogawa[1], Naoto Sato[2], Yuichi Maruo[1], Natsumi Naganuma[1], Kosuke Noborio[2] (1.Graduate School of Agriculture, Meiji University, 2.School of Agriculture, Meiji University)

4:45 PM - 5:00 PM JST | 7:45 AM - 8:00 AM UTC

[AGE31-05] Differences in infiltration process on the planets under different gravity.

*Yasushi Mori[1] (1.Graduate School of Environmental and Life Science, Okayama University)

Life search on Mars by Life Detection Microscope (LDM)

*Yoshitaka Yoshimura[1]

1. College of Agriculture, Tamagawa University

Recent findings on Mars tend to support the possible presence of living microbes near the surface of Mars. MSL Curiosity has found organic compounds [1], the temporal increase of methane concentration in Martian atmosphere [2] and reduced sulfur compounds such as pyrite in Martian soil [3]. Methane and reduced sulfur compounds can be energy sources to support the growth of chemoautotrophic microbes [4]. The detection of hydrated salts suggested the possible presence of liquid water at Recurring Slope Lineae [5]. Although present Martian environments are hostile to life, terrestrial microorganisms inhabit a wide range of environmental conditions, suggesting some microorganisms may survive near the surface [4]. Though UV radiation is harmful, it would be shielded by thin layers (less than a millimeter) of dust or regolith [6]. A depth of several centimeters from the surface, therefore, could provide sufficient covering for microorganisms to survive.

The Viking mission in 1970’ s did not find evidence for life [7], however, the sensitivity of the GC-MS (mass spectrometer) onboard the Viking mission was found not to be very high, and it was not able to detect 10^6 microbial cells in 1 gram soil [8, 9], indicating that another life detection program is necessary.

The Life Detection Microscope (LDM) that we have proposed [6, 10] has the potential sensitivity much higher than the Viking instrument. Microscopes directly image life forms and identify their shapes, sizes, and other morphological structures and have the potential to detect a single cell in field of view. Therefore, the sensitivity can be as high as desired just by increasing the volume of sample to be scanned in a reasonable duration of experiment. LDM scans about 1 mm^3 and detects less than 10^4 cells in 1 gram soil at a spatial resolution of 1 μm [10]. LDM differentiates among organic compounds surrounded by membranes or with enzyme activity by staining the samples with fluorescent pigments. This technique is especially useful for the detection of living microorganisms.

Our investigation goals are the followings. 1) Identify cell-like structure in which organic compounds are enveloped by membrane, which may represent Martian life. 2) Search for organic compounds in Mars surface samples. The compounds include cells, other biological materials, and abiotic polycyclic aromatic hydrocarbon (PAH). 3) High-resolution characterization of regolith and dust particles. The search for living microorganisms is important not only for scientific interest but for planetary protection. Before future human missions begin, surveys investigating the presence of living microorganisms should be conducted to mitigate the risk of human contact with Martian microorganisms, which may be harmful to human health. The LDM would be also an effective tool for this purpose.

References

[1] Eigenbrode, J. L., et al., *Science*, 360 (2018).

[2] Webster, C. R., et al., *Science*, 360 (2018).

©2019. Japan Geoscience Union. All Right Reserved.

[3] Ming, D., et al., *Science*, 343 (2014).

[4] Yamagishi, A., et al., *Biol. Sci. Space*, 24 (2010).

[5] Ojha, L., et al., *Nature Geosci.*, 8 (2015).

[6] Mancinelli, R. L., et al., *Planetary and Space Sci.*, 48 (2000).

[7] Margulis, L., et al., *J. Mol. Evol.*, 14 (1979).

[8] Glavin, D. P., et al., *Earth and Planetary Sci. Let.*, 185 (2001).

[9] Navarro-Gonzalez, R., et al., *Proc Natl Acad Sci U S A*, 103 (2006).

[10] Yamagishi, A., et al., *Trans. JSASS, Aerospace Tech. Japan*, 16 (2018).

Keywords: fluorescent microscope, extraterrestrial life

©2019. Japan Geoscience Union. All Right Reserved.

Moisture movement in sand during evaporation under reduced pressure

*Masaru Mizoguchi[1]

1. Graduate school of Agricultural and Life Sciences, The University of Tokyo

In order to investigate the mechanism of moisture transfer in the basement of Mars, experiments were conducted to measure the moisture, temperature, and salt distribution in the sand column during the vacuum evaporation process. As a result, it was found that the sample freezes at low salt concentration while it does not freeze at high concentration. In addition, we found that the salt moves to the surface layer with liquid water movement, and that the higher the salt concentration, the higher the evaporation amount. These results may relate to phenomena such as drying accompanied by evaporation under reduced pressure, freezing due to latent heat loss, crust formation due to salt concentration and freezing point depression.

Keywords: under reduced pressure, Moisture movement, evaporation

©2019. Japan Geoscience Union. All Right Reserved.

Gravity effects on liquid behavior in porous media of uniform glass beads.

*Naoto Sato[1], Natsumi Naganuma[2], Kento Nogawa[2], Yuichi Maruo[2], Kosuke Noborio[1]

1. School of Agriculture, Meiji University, 2. Graduate School of Agriculture, Meiji University

In recent years, evidence of the existence of water has been found on the moon and Mars. The water resources on the moon or Mars are expected to be utilized as an in situ resource for future manned exploration. It is necessary to elucidate how the water exists in the porous media and how we can extract it. Under the 1G condition, water flow in porous media is expressed by Richards' equation. According to Richards' equation, water moves by a matric potential gradient and a gravity gradient. It was reported that water movement by a matric potential gradient, however, changed under microgravity. Therefore, water movement under low gravity might be different from estimation by conventional water movement theory. In this study, we observed water movement in porous media made of glass beads under microgravity and evaluated the effects of gravity on liquid behavior in porous media. We conducted infiltration experiments using porous media of 0.4 mm grass beads under microgravity conditions created by parabolic flight. The advances of the gas-liquid interface were captured by a video camera and the infiltration rate was calculated. We also conducted a horizontal infiltration experiment under 1G and compared the infiltration rate under each gravity conditions. The infiltration rate under microgravity was slightly lower than the horizontal infiltration rate under 1G. The decrease of infiltration rate, however, was smaller than the decrease in the previous study using 1.5 mm glass beads.

Keywords: Porous media, Liquid behavior, Gravity

©2019. Japan Geoscience Union. All Right Reserved.

Effects of changes in viscosity under low gravity on infiltration rate

*Kento Nogawa[1], Naoto Sato[2], Yuichi Maruo[1], Natsumi Naganuma[1], Kosuke Noborio[2]

1. Graduate School of Agriculture, Meiji University, 2. School of Agriculture, Meiji University

It is important to clarify water behavior in the porous media to realize cultivation of crops in spacecraft, on Mars or on the Moon. However, Jones et al. (1999) revealed that infiltration rate in porous media under microgravity (μG) is lower than that under 1G. In addition, Maruo (2018) revealed that infiltration rate in the capillary tube under μG is lower than that under 1G. Infiltration in porous media under μG depends on capillary force, so that the decrease infiltration rate in the capillary tube might be a cause of the decrease in infiltration rate in the porous media under μG. It is thought that the decrease of infiltration rate in capillary tube under μG was caused by a decrease in surface tension, an increase in contact angle, and/or an increase in viscosity. Naganuma et al. (2019) reported that the surface tension of water does not vary with gravity. In addition, it was revealed that the contact angle of water droplets under μG does not change compared to under 1G (Naganuma et al., 2018). However, there are few studies that evaluated the gravitational dependence of the viscosity of water. In this research, we evaluated the gravity dependence of the viscosity of water and estimated the influence of viscosity change on infiltration rate. In this experiment, low gravity experiment using parabolic flight was carried out for 2 days using MU-300 (Diamond Air Service Inc., Nagoya, Japan) as an aircraft. The gravity condition was μG (1st day: 3 times, 2nd day: 3 times), 1/6G (1st day: 3 times, 2nd day: 6 times), 1/3G (1st day: 5 times, 2nd: 3 times), and each low gravity duration was 20 to 30 seconds. Changes in gravity were acquired from the accelerometer installed in the aircraft. For the acrylic column with an inner diameter of 64 mm and a height of 41 mm used for the experiment, water repellent treatment was performed on the upper 14 mm of the inner wall of the column, and the water level was adjusted so that the boundary between the processed part and the unprocessed part became the water surface. Degassed water was used as the sample to be filled in the column. For measurement of viscosity, a viscometer (Tuning Fork Vibro Viscometers SV-10, A & D Co., Ltd.) was used. The water temperature was measured by a temperature sensor built in the viscometer. The measurement interval of viscosity and temperature was 2 seconds on the 1st day and 1 second at the 2nd day. I photographed the state of the surface with a video camera (GoPro Hero 4, GoPro Inc.). Experimental results showed a negative correlation between viscosity and gravity in the range of 0G to 1G (Fig. 1). In the range of 1 G to 2 G, the measured values varied due to vibration, and reliable data could not be obtained. Since it is known that the surface tension and the contact angle do not change under μG, it is considered that the decrease infiltration rate in the capillary tube was brought about only by the increase in viscosity. From this, we consider the effect of increase in viscosity under μG on decrease of capillary invasion rate. Maruo (2018) defines the rate of change of infiltration rate in the capillary tube under μG compared to under 1G as a coefficient of delay α and is expressed by equation (1) (Fig. 2). Postulate that values other than viscosity do not change with 1G and μG in equation (1), it is considered that equation (2) holds. Therefore, $1/\alpha^2$ in capillary infiltration experiment by Maruo (2018) is compared with $\eta_{\mu G}/\eta_{1G}$ in this experiment. $1/\alpha^2$ is 2.49 at the capillary diameter of 0.8 mm, 2.78 at 2.37 mm, 3.19 at 5.5 mm, $\eta_{\mu G}/\eta_{1G}$ is at 2.66 on the 1st day and 2.70 on the 2nd day, $1/\alpha^2$ and $\eta_{\mu G}/\eta_{1G}$ are nearly the same value. From this, it is considered that the decrease infiltration rate in the capillary tube under μG was caused by the increase in viscosity.

Keywords: viscosity, low gravity, infiltration rate

©2019. Japan Geoscience Union. All Right Reserved.

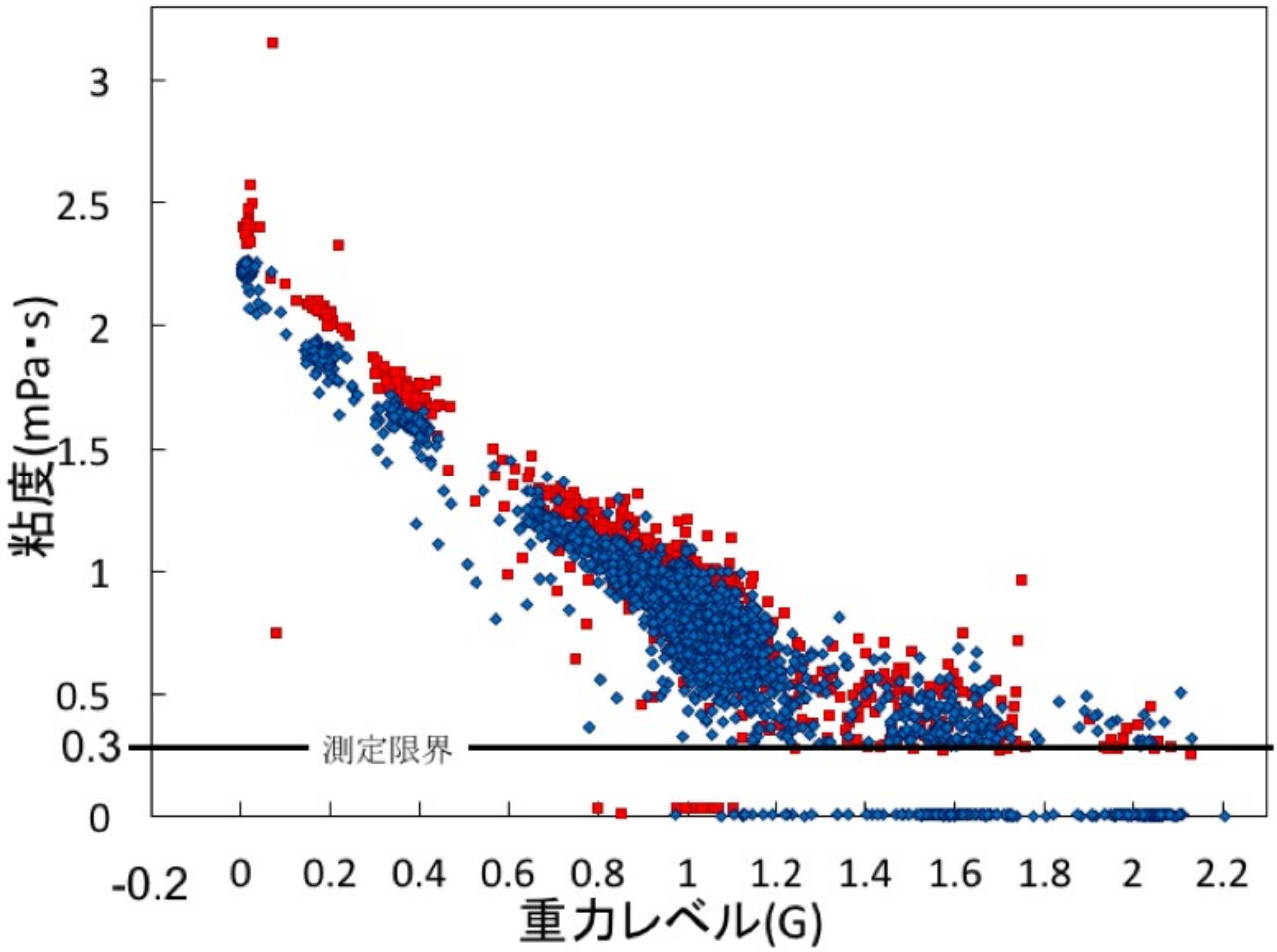

Fig. 1 粘度と重力の関係

$$\alpha = \sqrt{\frac{\sigma_{\mu G}}{\sigma_{1G}} \frac{\cos\theta_{\mu G}}{\cos\theta_{1G}} \frac{\eta_{\mu G}}{\eta_{1G}}}$$

Fig. 2 式 (1)

α ：遅延係数, σ ：表面張力 (N/m),
θ ：接触角(°), η ：粘度(Pa・s)

$$\frac{1}{2} = \frac{\eta_{\mu G}}{}$$

©2019. Japan Geoscience Union. All Right Reserved.

©2019. Japan Geoscience Union. All Right Reserved.

Differences in infiltration process on the planets under different gravity.

*Yasushi Mori[1]

1. Graduate School of Environmental and Life Science, Okayama University

These days, we are trying to conduct the long-term stay in the space station, the various experiments under microgravity by the parabolic flight, and the research to explore the possibility of our stay on the other planets. In addition, we are exploring the existence of water and traces of living things on the other planets and satellites. If such an approach has become realistic, the next approach would be the earth, soil or regolith, where we need to consider how liquid flows and behaves. Here we consider the penetration phenomenon of solution when gravity is different. In the parabolic flight, they report that water in a vessel is sucked into noodles when it becomes zero gravity. When the influence of gravity becomes small, the influence of the capillary force by the porous body becomes relatively large, and the downward movement by the inertial force is restricted. Indeed, preliminary experiments showed that the downward reach of the solution increased as pseudo gravity increased. When we are trying to use regolith as planting on a planet with small gravity, the solution such as water might not move downward as we are estimating.

Keywords: micro-gravity, regolith, infiltration

©2019. Japan Geoscience Union. All Right Reserved.

[J] Poster | A (Atmospheric and Hydrospheric Sciences)：A-GE Geological & Soil Environment

Tue. May 28, 2019 1:45 PM - 3:15 PM JST | Tue. May 28, 2019 4:45 AM - 6:15 AM UTC | Poster Hall International Exhibition Hall8, Makuhari Messe_1

[A-GE31] New Roles of Soil Science for Extraterrestrials

convener:Kosuke Noborio(Meiji University), Masaru Mizoguchi(Graduate school of Agricultural and Life Sciences, The University of Tokyo)

In recent years water ice and vapor have been discovered in extraterrestrials; however, liquid and ice water behavior in such environments is still not well understood. We will share recent studies how liquid or ice water behavior in porous media in microgravity or vacuum condition.

[AGE31-P01] Roles of soil science in ectraterestrial space

*Kosuke Noborio[1] (1.Meiji University)

[AGE31-P02] **Characterization of Soil Organic Matter using Fourier Transform Infrared Spectrometer**

*Iwasaki Masayoshi[1], Yasushi Mori[1] (1.okayama university graduate school environmental and life science)

[AGE31-P03] The slowing down of water movement in capillary tubes under microgravity.

*Yuichi Maruo[1], Naoto Sato[1], Natsumi Naganuma[1], Kento Nogawa[1], Kosuke Noborio[2] (1.Graduate school of Agriculture, Meiji University, 2.Meiji University)

[AGE31-P04] Challenges to measuring of the contact angle and the surface tension of water under reduced gravity

*Natsumi Naganuma[1], Naoto Sato[1], Kento Nogawa[1], Yuichi Maruo[1], Kosuke Noborio[2] (1.Graduate School of Agriculture, Meiji University, 2.School of Agriculture, Meiji University)

Roles of soil science in ectraterestrial space

*Kosuke Noborio[1]

1. Meiji University

Liquid and solid water has recently been deiscovered in the moon, Mars, and other meterorites. Although people talk building bases on the moon and Mars and grow vegetables there, water transport in porous media in such conditions has little attention. Soil physics may play important roles even in extraterestrials as well as on the earth having 1G condition. Overview of water move in spce will be duscussed.

Keywords: extraterrestrial, water, porous media

©2019. Japan Geoscience Union. All Right Reserved.

Characterization of Soil Organic Matter using Fourier Transform Infrared Spectrometer

*Iwasaki Masayoshi[1], Yasushi Mori[1]

1. okayama university graduate school environmental and life science

Combustion method is usually used to measure total carbon (TC). However, the total amount of carbon does not tell the contents such as fresh biomass or old humin. Therefore, detailed organic matter analysis was attempted using Fourier transform infrared spectrometer (FTIR), which could obtain unique spectrum of absorption or emission of soils. First, calibration curve was obtained using a mixture of cellulose and KCl. KCl was newly introduced as a diluent to avoid saturation of the emission peak. Furthermore, in order to extract individual organic matter, heavy liquids were used to select them by specific weight. Then, a total of 12 field soil samples were analyzed to figure out the organic matter differences affected by land management. As a result, the amount of cellulose was successfully measured. In field soils, cellulose was the most abundant organic matter in the surface layer, and the amount was more at the cultivated field than at the no-tillage field. When comparing this result with the result of the total carbon analysis, we estimated that there are much readily decomposable organic matter on the tillage field and much hardly decomposable organic matter on the no-tillage field. This is consistent with the previous reports. However, we should note, in the experiment using heavy liquids for specific gravity fractionation selection, sufficient accuracy was not obtained. So far, quantitative analysis was challenging to examine the organic matter of field soil, but we obtained the possibility that it can be done by specific gravity fractionation. Currently, accurate quantification has not been achieved, but comparison was possible.

Keywords: soil organic matter, specific gravity fractionation, fourier transform infrared spectrometer

©2019. Japan Geoscience Union. All Right Reserved.

The slowing down of water movement in capillary tubes under microgravity.

*Yuichi Maruo[1], Naoto Sato[1], Natsumi Naganuma[1], Kento Nogawa[1], Kosuke Noborio[2]

1. Graduate school of Agriculture, Meiji University, 2. Meiji University

The international deep space gateway is going to be built on the moon orbit from early 2020s. As manned space missions may get farther and longer, the importance of food production in space increases. For food production by growing crops in space, water by the crops plays an important role; however, few workers have conducted research on water movement in porous media under microgravity. It was reported that a water infiltration rate in porous media was slower under microgravity than under 1G. The objective of this study is to reveal what makes water move slower in porous media under microgravity. Capillary rises in capillary tubes, which were simpler pores, were observed under microgravity induced by a free-fall tower. The measured rates of capillary rise were slower than theoretical values calculated by Lucas-Washburn equation for 1G condition. The slower rates could be explained if either surface tension, contact angle, or viscosity are the function of gravity. Previous research reported that larger viscosity was observed under microgravity than under 1G although surface tension and contact angle were not changed by gravity. Slower water flows in capillary tubes under microgravity may be explained by changes in viscosity as a function of gravity.

Keywords: Soil physics , Microgravity, Water movement

©2019. Japan Geoscience Union. All Right Reserved.

Challenges to measuring of the contact angle and the surface tension of water under reduced gravity

*Natsumi Naganuma[1], Naoto Sato[1], Kento Nogawa[1], Yuichi Maruo[1], Kosuke Noborio[2]

1. Graduate School of Agriculture, Meiji University, 2. School of Agriculture, Meiji University

Matric potential gradient is one of the driving forces of water movement in porous media. It has been reported that water movement in porous media under microgravity was slower than that under 1G, and hydraulic characteristic curve changed. Therefore, there is a possibility that the matric potential changes under reduced gravity. Capillary pressure is the main factor of dominating the matric potential value in porous media with a relatively large pore size. In this study we investigated the dependence of capillary force on gravity. Capillary forces are governed by the surface tension and contact angle that the liquid makes with the solid surfaces. We measured the contact angle of droplets on glass plate under microgravity condition to reveal the dependence of the contact angle on gravity. For large droplets, the contact angle under microgravity was larger than that under 1G, but the difference in contact angle between 1G and μG reduced with smaller droplets. We also conducted parabolic experiments to measure the surface tension of water under reduced gravity (μG, 1/6G, 1/3G, 1G). The maximum bubble pressure method which is one of the methods measuring surface tension was used. The bubble pressure greatly changed due to dynamically change of the inboard air pressure during parabolic flight. Evaluation of the surface tension by removing air pressure and hydraulic pressure from bubble pressure will be discussed.

Keywords: capillary pressure, contact angle, surface tension, reduced gravity, maximum bubble method

©2019. Japan Geoscience Union. All Right Reserved.

[J] Poster | A (Atmospheric and Hydrospheric Sciences)：A-GE Geological & Soil Environment

Tue. May 28, 2019 5:15 PM - 6:30 PM JST | Tue. May 28, 2019 8:15 AM - 9:30 AM UTC | Poster Hall International Exhibition Hall8, Makuhari Messe_12

[A-GE31] New Roles of Soil Science for Extraterrestrials

convener:Kosuke Noborio(Meiji University), Masaru Mizoguchi(Graduate school of Agricultural and Life Sciences, The University of Tokyo)

In recent years water ice and vapor have been discovered in extraterrestrials; however, liquid and ice water behavior in such environments is still not well understood. We will share recent studies how liquid or ice water behavior in porous media in microgravity or vacuum condition.

[AGE31-P01] Roles of soil science in ectraterestrial space

*Kosuke Noborio[1] (1.Meiji University)

[AGE31-P02] **Characterization of Soil Organic Matter using Fourier Transform Infrared Spectrometer**

*Iwasaki Masayoshi[1], Yasushi Mori[1] (1.okayama university graduate school environmental and life science)

[AGE31-P03] The slowing down of water movement in capillary tubes under microgravity.

*Yuichi Maruo[1], Naoto Sato[1], Natsumi Naganuma[1], Kento Nogawa[1], Kosuke Noborio[2] (1.Graduate school of Agriculture, Meiji University, 2.Meiji University)

[AGE31-P04] Challenges to measuring of the contact angle and the surface tension of water under reduced gravity

*Natsumi Naganuma[1], Naoto Sato[1], Kento Nogawa[1], Yuichi Maruo[1], Kosuke Noborio[2] (1.Graduate School of Agriculture, Meiji University, 2.School of Agriculture, Meiji University)

Roles of soil science in ectraterestrial space

*Kosuke Noborio[1]

1. Meiji University

Liquid and solid water has recently been deiscovered in the moon, Mars, and other meterorites. Although people talk building bases on the moon and Mars and grow vegetables there, water transport in porous media in such conditions has little attention. Soil physics may play important roles even in extraterestrials as well as on the earth having 1G condition. Overview of water move in spce will be duscussed.

Keywords: extraterrestrial, water, porous media

©2019. Japan Geoscience Union. All Right Reserved.

Characterization of Soil Organic Matter using Fourier Transform Infrared Spectrometer

*Iwasaki Masayoshi[1], Yasushi Mori[1]

1. okayama university graduate school environmental and life science

Combustion method is usually used to measure total carbon (TC). However, the total amount of carbon does not tell the contents such as fresh biomass or old humin. Therefore, detailed organic matter analysis was attempted using Fourier transform infrared spectrometer (FTIR), which could obtain unique spectrum of absorption or emission of soils. First, calibration curve was obtained using a mixture of cellulose and KCl. KCl was newly introduced as a diluent to avoid saturation of the emission peak. Furthermore, in order to extract individual organic matter, heavy liquids were used to select them by specific weight. Then, a total of 12 field soil samples were analyzed to figure out the organic matter differences affected by land management. As a result, the amount of cellulose was successfully measured. In field soils, cellulose was the most abundant organic matter in the surface layer, and the amount was more at the cultivated field than at the no-tillage field. When comparing this result with the result of the total carbon analysis, we estimated that there are much readily decomposable organic matter on the tillage field and much hardly decomposable organic matter on the no-tillage field. This is consistent with the previous reports. However, we should note, in the experiment using heavy liquids for specific gravity fractionation selection, sufficient accuracy was not obtained. So far, quantitative analysis was challenging to examine the organic matter of field soil, but we obtained the possibility that it can be done by specific gravity fractionation. Currently, accurate quantification has not been achieved, but comparison was possible.

Keywords: soil organic matter, specific gravity fractionation, fourier transform infrared spectrometer

©2019. Japan Geoscience Union. All Right Reserved.

The slowing down of water movement in capillary tubes under microgravity.

*Yuichi Maruo[1], Naoto Sato[1], Natsumi Naganuma[1], Kento Nogawa[1], Kosuke Noborio[2]

1. Graduate school of Agriculture, Meiji University, 2. Meiji University

The international deep space gateway is going to be built on the moon orbit from early 2020s. As manned space missions may get farther and longer, the importance of food production in space increases. For food production by growing crops in space, water by the crops plays an important role; however, few workers have conducted research on water movement in porous media under microgravity. It was reported that a water infiltration rate in porous media was slower under microgravity than under 1G. The objective of this study is to reveal what makes water move slower in porous media under microgravity. Capillary rises in capillary tubes, which were simpler pores, were observed under microgravity induced by a free-fall tower. The measured rates of capillary rise were slower than theoretical values calculated by Lucas-Washburn equation for 1G condition. The slower rates could be explained if either surface tension, contact angle, or viscosity are the function of gravity. Previous research reported that larger viscosity was observed under microgravity than under 1G although surface tension and contact angle were not changed by gravity. Slower water flows in capillary tubes under microgravity may be explained by changes in viscosity as a function of gravity.

Keywords: Soil physics , Microgravity, Water movement

©2019. Japan Geoscience Union. All Right Reserved.

Challenges to measuring of the contact angle and the surface tension of water under reduced gravity

*Natsumi Naganuma[1], Naoto Sato[1], Kento Nogawa[1], Yuichi Maruo[1], Kosuke Noborio[2]

1. Graduate School of Agriculture, Meiji University, 2. School of Agriculture, Meiji University

Matric potential gradient is one of the driving forces of water movement in porous media. It has been reported that water movement in porous media under microgravity was slower than that under 1G, and hydraulic characteristic curve changed. Therefore, there is a possibility that the matric potential changes under reduced gravity. Capillary pressure is the main factor of dominating the matric potential value in porous media with a relatively large pore size. In this study we investigated the dependence of capillary force on gravity. Capillary forces are governed by the surface tension and contact angle that the liquid makes with the solid surfaces. We measured the contact angle of droplets on glass plate under microgravity condition to reveal the dependence of the contact angle on gravity. For large droplets, the contact angle under microgravity was larger than that under 1G, but the difference in contact angle between 1G and μG reduced with smaller droplets. We also conducted parabolic experiments to measure the surface tension of water under reduced gravity (μG, 1/6G, 1/3G, 1G). The maximum bubble pressure method which is one of the methods measuring surface tension was used. The bubble pressure greatly changed due to dynamically change of the inboard air pressure during parabolic flight. Evaluation of the surface tension by removing air pressure and hydraulic pressure from bubble pressure will be discussed.

Keywords: capillary pressure, contact angle, surface tension, reduced gravity, maximum bubble method

©2019. Japan Geoscience Union. All Right Reserved.

[E] Poster | A (Atmospheric and Hydrospheric Sciences)：A-CG Complex & General

Tue. May 28, 2019 10:45 AM - 12:15 PM JST | Tue. May 28, 2019 1:45 AM - 3:15 AM UTC | Poster Hall International Exhibition Hall8, Makuhari Messe_3

[A-CG32] Global Carbon Cycle Observation and Analysis

convener:Kazuhito Ichii(Chiba University), Prabir Patra(Research Institute for Global Change, JAMSTEC), Forrest M. Hoffman(Oak Ridge National Laboratory), Makoto Saito(National Institute of Environmental Studies)

The landmark Paris Agreement under the United Nations Framework Convention on Climate Change (UNFCCC) aims at reduction of greenhouse gases (GHGs) emission to keep the global warming below 2 degC. As per the agreement the nationally determined commitments (NDCs) and their progresses should be carefully monitored and verified by international bodies. The emission verification will be based on observation of the time evolution of greenhouse gases and model-based estimations of emissions from time to time.

In recent years, the number of observations and new techniques to monitor GHGs budget have been increasing. The improvements includes observational platforms for monitoring atmospheric GHGs, national or regional emission inventories, top-down models (e.g. atmospheric inverse models), and bottom-up models (e.g. process-based models). However, due to uncertainties in modeling and sparse observation network, high uncertainty exists in GHGs sources/sinks estimations at global and regional scales. These uncertainties lead to large variations in future projection of GHG budgets and climate changes.

The purpose of the session is to discuss state-of-the-art techniques for estimations of GHGs (e.g. CO2, CH4, N2O) budget at global and regional scales. The topic includes natural and anthropogenic processes, various methodologies (e.g. in-situ observation, aircraft monitoring, remote sensing, modeling), and various targets (e.g. atmosphere, terrestrial, and ocean), various spatial and temporal coverage (e.g. regional to global scales and past-present-future). Improved estimates of emissions from land use change, forest fires, and other anthropogenic sources (urban developments and thermal power station etc.) are also of interest. We also welcome discussions for designs and plans for future studies targeting city and country scale emission estimations using sophisticated modeling tools.

[ACG32-P01] Regional budgets of 3 major greenhouse gases using inverse modelling of atmospheric data

*Prabir Patra[1], Naveen Chandra[1], Jagat Bisht[1] (1.Japan Agency for Marine-Earth Science and Technology (JAMSTEC))

[ACG32-P02] Analysis of hot summer in 2018

*Kazutaka Murakami[1], Kazuhito Ichii[1,2], Yukio Yoshida[1], Haruki Oshio[1], Makoto Saito[1] (1.National Institute for Environmental Studies, 2.Chiba University)

[ACG32-P03] Updated Data-Driven GPP and NEE Estimation Using Machine Learning Algorithms with Remote Sensing and Flux Data

*Zhiyan Liu[1], Kazuhito Ichii[1], Yusuke Hayasi[1], Riku Kawase[1], Masahito Ueyama[2], Yuji Kominami[3] (1.Chiba University, 2.Osaka Prefecture University, 3.Forest Research and Management Organization)

[ACG32-P04] Response of a Bornean Rainforest to the Climatic Changes imposed by ENSO during 2009-2016

*Julie Karine Michelon[1], Tomo'omi Kumagai[2,3], Tetsuya Hiyama[3], Hatsuki Fujinami[3], Kazuho Matsumoto[4], Tomonori Kume[5], Takami Saito[6] (1.Graduate School of Environmental Studies, Nagoya University, 2.Graduate School of Agricultural and Life Sciences, The University of Tokyo, 3.Institute for Space-Earth Environmental Research, Nagoya University, 4.Faculty of Agriculture, University of the Ryukyus, 5.Faculty of Agriculture, Kyushu University, 6.Forest Research and Management Organization)

[ACG32-P05] Monitoring and Evaluating CO2 Flux in the Grassland Areas of Mongolia

*Qinxue Wang[1], Tomohiro Okadera[1], Deni Eer[1], Masataka Watanabe[2], Tomohiro Shishime[2], Akihiro Oba[2], Ochirbat Batkhishig[3] (1.National Institute for Environmental Studies, 2.Research and Development Initiative, Chuo University, 3.Institute of Geography and Geoecology, Mongolian Academy of Sciences)

[ACG32-P06] Data-driven monitoring of terrestrial carbon cycle in Mongolia

*ZAYA MART[1], Zhiyan Liu[1], Riku Kawase[1], Kazuhito Ichii[1] (1.Chiba University)

Regional budgets of 3 major greenhouse gases using inverse modelling of atmospheric data

*Prabir Patra[1], Naveen Chandra[1], Jagat Bisht[1]

1. Japan Agency for Marine-Earth Science and Technology (JAMSTEC)

Atmospheric observations of greenhouse gases provide accurate record the changes in their abundance in the Earth's environments, and it has now been well established that the increase in greenhouse gases concentrations is causing the rise in the mean surface air temperature. Using atmospheric chemistry-transport models (ACTM), along with the concentration measurements, we can estimate the sources and sinks of the chemical species. Using MIROC4-ACTM at JAMSTEC, we estimated regional sources and sinks of carbon dioxide (CO2), methane (CH4) and nitrous oxide (N2O) over the period of 1996 to 2016. This will help global stocktake every 5 years, as a independent estimate, when the coutries report their progress on nationally determined contributions (NDCs) under the Paris Agreement and their ammendments, overseen by the UNFCCC.

Keywords: Inverse modelling, Greenhouse gases sources and sinks, Paris Agreement and NDCs

©2019. Japan Geoscience Union. All Right Reserved.

Analysis of hot summer in 2018

*Kazutaka Murakami[1], Kazuhito Ichii[1,2], Yukio Yoshida[1], Haruki Oshio[1], Makoto Saito[1]

1. National Institute for Environmental Studies, 2. Chiba University

Global averaged temperature in 2018 was considerably higher than normal year. Probably it is the fourth highest in the past. Especially, it was memorable that East Asia, Europe, and the southwestern part of the United States were hit by record heat waves in this summer. It is important for the ecological resilience to investigate how much such extreme weather damages the terrestrial ecosystem and how will it change after that. In this study, we analyzed the effect of this extremely high temperature on terrestrial vegetation using satellite remote sensing data. First, we investigated the high temperature area using MODIS land surface temperature (LST) product. Then, focusing on these high LST areas, we analyzed the impact to satellite observed Solar Induced Fluorescence (SIF) that closely related to a photosynthetic activity. As a result, it was found that the LST of 2018 in the East Asia (Japan, Korea and North Korea) was the highest during 2002 - 2018 years. And it also indicated abnormal high LST regions from Germany to northern Europe. Analysis of SIF data showed a positive decline in Europe but did not show a clear trend in Asia. In addition, similar trends were seen from other satellite vegetation indices, and it was found that the terrestrial vegetation shows different responses in both areas affected by the same hot summer.

Keywords: 2018 summer, heat wave, satellite observation, SIF

©2019. Japan Geoscience Union. All Right Reserved.

Updated Data-Driven GPP and NEE Estimation Using Machine Learning Algorithms with Remote Sensing and Flux Data

*Zhiyan Liu[1], Kazuhito Ichii[1], Yusuke Hayasi[1], Riku Kawase[1], Masahito Ueyama[2], Yuji Kominami[3]

1. Chiba University, 2. Osaka Prefecture University, 3. Forest Research and Management Organization

Abstract

Data-driven approach is effective for understanding and up-scaling observation network data of terrestrial carbon fluxes. Recently, the expansion of observation network, the improvement of remote sensing products and more application of machine learning on natural science make it more possible. In this study, we estimated two important parameters of terrestrial ecosystem, terrestrial gross primary productivity (GPP) and net ecosystem exchange (NEE) through re-assessment of previous approaches [Ichii et al. 2017; Kondo et al. 2015]. We tested multiple combinations of input parameters with lagged effect, additional new input parameters and the updated MODIS datasets (Collection C6). Besides, we selected 3 typical machine learning methods (Random Forest, RF; Support Vector Regression, SVR; Artificial Neural Network, ANN) as data-driven method and compare the estimation from 3 different types of machine learning model. The site-level analysis shows that use of the new version data and the time-lagged improved the model performance. Finally, we compared our new estimation of GPP and NEE with several terrestrial models output and other available datasets and we found our new results show better consistency with them. This shows our estimation provides a good benchmark for understanding spatio-temporal variability in terrestrial GPP and NEE.

Acknowledgement

This research was financially supported by the Environment Research and Technology Development Fund (2-1701) of the Environmental Restoration and Conservation Agency of Japan.

Keywords: Terrestrial Carbon Cycle, MODIS Collection6, Data-driven, time-lag effect

©2019. Japan Geoscience Union. All Right Reserved.

Response of a Bornean Rainforest to the Climatic Changes imposed by ENSO during 2009-2016

*Julie Karine Michelon[1], Tomo'omi Kumagai[2,3], Tetsuya Hiyama[3], Hatsuki Fujinami[3], Kazuho Matsumoto[4], Tomonori Kume[5], Takami Saito[6]

1. Graduate School of Environmental Studies, Nagoya University, 2. Graduate School of Agricultural and Life Sciences, The University of Tokyo, 3. Institute for Space-Earth Environmental Research, Nagoya University, 4. Faculty of Agriculture, University of the Ryukyus, 5. Faculty of Agriculture, Kyushu University, 6. Forest Research and Management Organization

Tropical rainforests belong to the most important biomes, as they are one of the largest terrestrial carbon sink and also a consequent source of latent energy. Furthermore, they will be among the first ecosystems to undergo climatic changes in the near future. Understanding how they will response to those changes is essential. El Niño-Southern Oscillation (ENSO) is an opportunity to study ecosystem response under real climatic change conditions.

Transpiration (Tr), net ecosystem exchange (NEE) and heat fluxes were measured with an eddy covariance system in a natural rainforest in Sarawak, Malaysia. Meteorological and soil moisture observations were also conducted. This region does not have phase-locked dry periods, and seasonal variations of both air temperature and solar radiation are small. However, it is directly impacted by ENSO events. During the study period, from November 2009 to December 2016, two events were selected : La Niña 2010-2011 and El Niño 2014-2016. Normal conditions were assumed as a third "neutral" period. Comparisons of measured flux and meteorological drivers between the three periods were carried out, and analysis of environmental controls, as canopy conductance (g_c) were made.

Precipitation and air temperature were significantly different between the three periods. While the water cycle (latent heat flux, Tr, g_c) responded immediately to the changes imposed by La Niña, the enhancement of the ecosystem respiration balanced the gross primary production gain, resulting into a NEE similar to neutral conditions. Conversely, the NEE during El Niño was significantly smaller than during neutral, when the water cycle seemed not impacted. However, further observations of this late rainforest response evolution showed that, during the first part of El Niño, Tr and g_c increased while CO_2 flux reduced. Then, during the second part, the trend reversed : CO_2 flux increased and Tr, as well as g_c, reduced. This may indicate a time lag between the meteorological drivers (precipitation and air temperature) changes imposed by El Niño and the ecosystem response (H_2O and CO_2 fluxes). The response delay may be caused by the rainforest tendency to poorly regulate its water use, being a particular moist environment. As for the response itself, it may be triggered by the depletion of the soil water content.

Those results imply that considering the length of El Niño and the ecosystem response trigger are important to understand and model bornean rainforest fluxes under future climatic scenario.

Keywords: Borneo, Rainforest, ENSO, NEE, Transpiration

©2019. Japan Geoscience Union. All Right Reserved.

Monitoring and Evaluating CO2 Flux in the Grassland Areas of Mongolia

*Qinxue Wang[1], Tomohiro Okadera[1], Deni Eer[1], Masataka Watanabe[2], Tomohiro Shishime[2], Akihiro Oba[2], Ochirbat Batkhishig[3]

1. National Institute for Environmental Studies, 2. Research and Development Initiative, Chuo University, 3. Institute of Geography and Geoecology, Mongolian Academy of Sciences

For verification of data products of the Greenhouse Gas Observing Satellite (GOSAT), in this study, we monitored and evaluated CO2 flux, that is, the absorption and emission of CO2 by ecosystems in the grasslands of Mongolia by the eddy correlation method. Two flux towers were established in 2015 at the Nalaikh site near Ulaanbaatar City and the Hustai site with less influence of cities, respectively. The CO2 analyzers installed on the towers were calibrated every year by using the standard gas imported from Japan. Up to now, about 4-year monitoring data have been accumulated since 2015. The data analysis shows that the CO2 absorption was larger than emissions at both sites, which indicated that the ecosystem at both sites are carbon sinks. The annual mean value of the CO2 absorption at the Nalaikh site was about 2.66 μmol m^{-2} s^{-1} and the emission was about 1.53 μmol m^{-2} s^{-1}, but the absorption at the Hustai site was about 2.11 μmol m^{-2} s^{-1}, and the emission was about 1.37 μmol m^{-2} s^{-1} (Figure 1). Generally, the net CO2 absorption at the Nalaikh site (0.76 μmol m^{-2} s^{-1}) was found to be larger than that at the Hustai site (0.36 μmol m^{-2} s^{-1}).

To compare the GOSAT L4B data with the ground observation at both sites, we extracted the monthly mean value of CO2 absorption/emission from the grid data of GOSAT during 2009-2015 and compared with the observed data. We found that although the seasonal changing pattern and fluctuation range are similar, the CO2 emission derived by GOSAT were larger than absorption, which suggested that the steppe ecosystems at both sites are the carbon sources. However, the ground observations showed that the CO2 absorption at both sites was larger than emission, which suggested that the grassland ecosystems at both sites are carbon sinks (Figure 2). It is essential for us to find the reasons of this difference in the future.

Finally, to evaluate the spatiotemporal distribution of carbon absorption and emission in the whole country, we have developed a carbon budget model considering the influence of grazing density. The primary simulation results showed that the percentage of carbon loss by grazing (CLG) accounted for 19-38% of the net ecosystem production (NEP) in the Nalaikh area around the city of Ulaanbaatar, where the grazing density was 1.5-2.3 sheep/ha during 2012-2016. On the other hand, CLG accounted for only 7-20% of NEP in the Hustai area away from the city, where the grazing density was only 0.4-0.6 sheep/ha (Figure 3). The result implied that the carbon budget was greatly influenced by animal husbandry near cities, where the grazing density is large. The monitoring cameras installed at both sites show that the biomass inside and outside the fence was greatly influenced by the ingestion of livestock.

This study was funded by “the Project to implement MRV and related technological improvements contributing to the Joint Crediting Mechanism (JCM) in Mongolia”, Ministry of the Environment, Japan.

Keywords: Carbon flux, Grassland ecosystem, The Greenhouse Gases Observing Satellite (GOSAT)

©2019. Japan Geoscience Union. All Right Reserved.

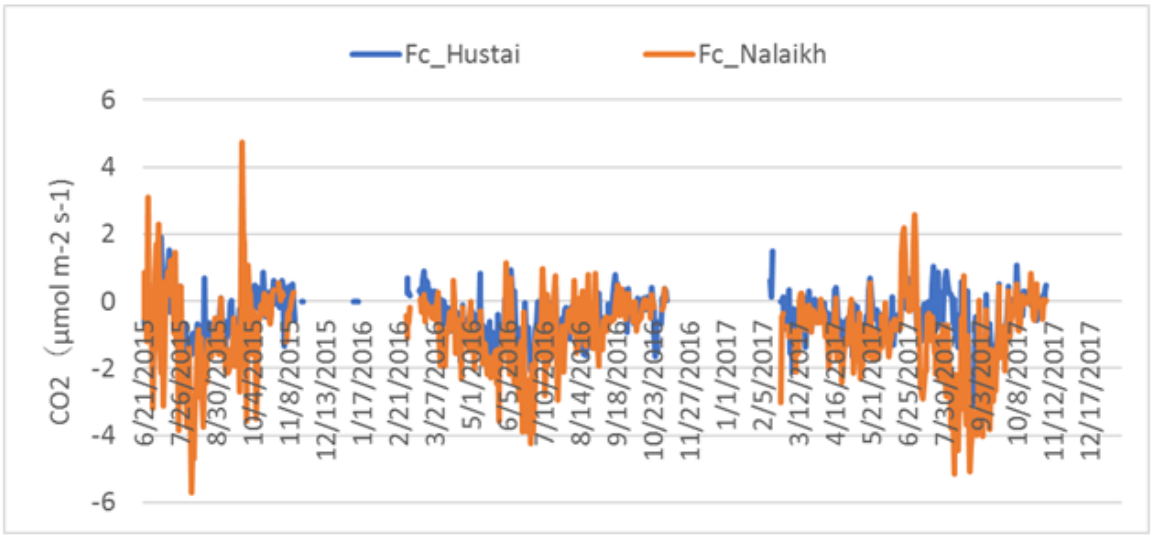

Figure 1 Comparison of CO2 flux observed at Nalaikh Site and Hustai Site

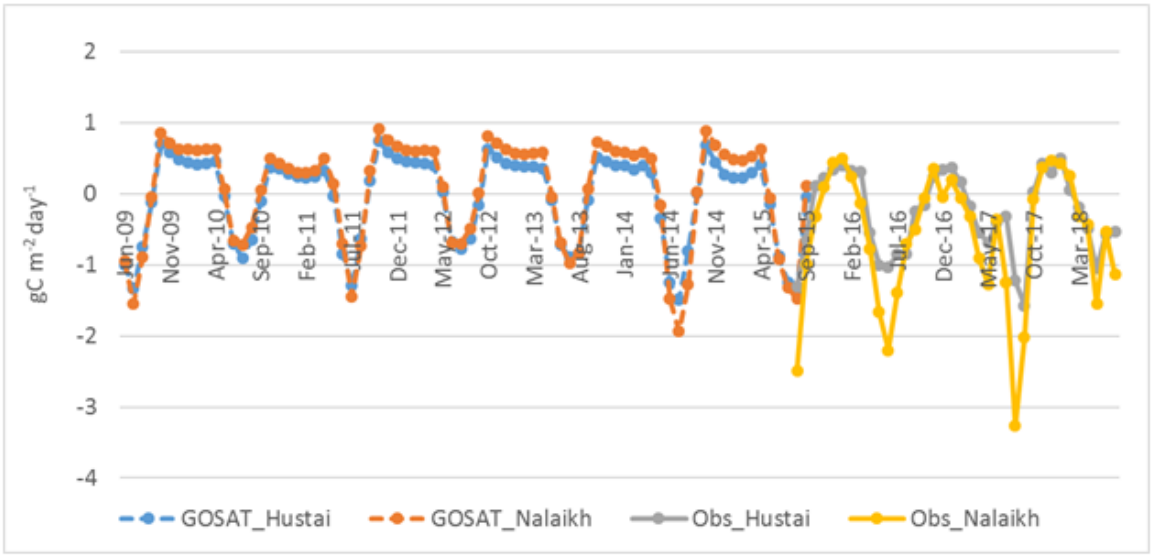

Figure 2 Comparison of GOSAT L4B and observations at Nalaikh Site and Hustai Site

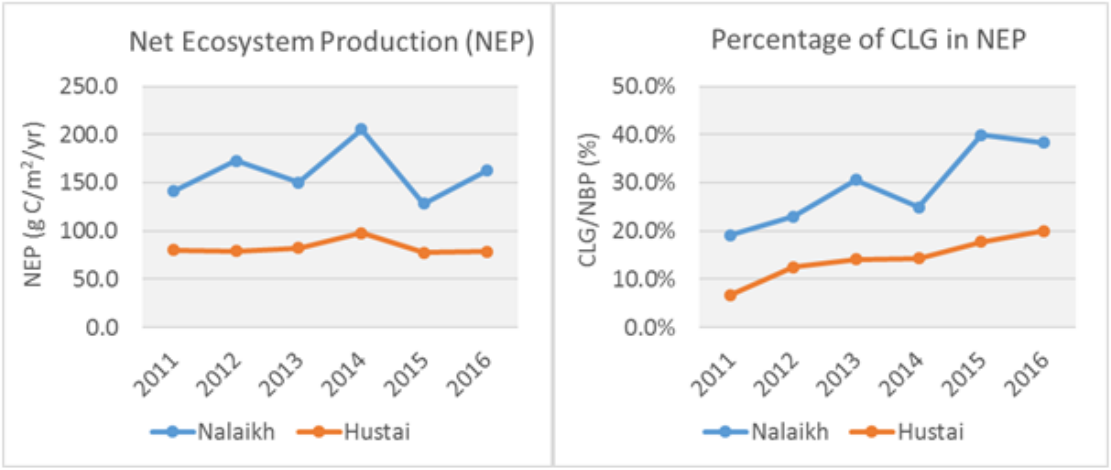

Figure 3 Impact of livestock grazing on NEP at Nalaikh Site and Hustai Site

©2019. Japan Geoscience Union. All Right Reserved.

Data-driven monitoring of terrestrial carbon cycle in Mongolia

*ZAYA MART[1], Zhiyan Liu[1], Riku Kawase[1], Kazuhito Ichii[1]

1. Chiba University

Mongolia has been experiencing both climate changes and anthropogenic environmental changes. Therefore, it is important to monitor environmental changes. In particular, more and more observation-based data sets are available, and synthesis analysis using these multiple observation-based data sets are essential.

We analyzed changes in the terrestrial environmental environment in Mongolia from the 1980s to 2010s. We focused on two different temporal periods, the 1980s to 2010s and 2000 to 2015. As for the first period (1980s to 2010s), we used NOAA AVHRR data sets, observed climate data sets for the analysis. As for the second period (1980s to 2010s), we used multiple remote sensing data sets (e.g. Terra MODIS), empirically upscaled CO2 flux products, and outputs from terrestrial ecosystem models. We will show and discuss the estimated terrestrial environmental changes in Mongolia at the conference.

Keywords: climate change, terrestrial environments, carbon cycle

©2019. Japan Geoscience Union. All Right Reserved.

[E] Poster | A (Atmospheric and Hydrospheric Sciences)：A-CG Complex & General

Tue. May 28, 2019 5:15 PM - 6:30 PM JST | Tue. May 28, 2019 8:15 AM - 9:30 AM UTC | Poster Hall International Exhibition Hall8, Makuhari Messe_13

[A-CG32] Global Carbon Cycle Observation and Analysis

convener:Kazuhito Ichii(Chiba University), Prabir Patra(Research Institute for Global Change, JAMSTEC), Forrest M. Hoffman(Oak Ridge National Laboratory), Makoto Saito(National Institute of Environmental Studies)

The landmark Paris Agreement under the United Nations Framework Convention on Climate Change (UNFCCC) aims at reduction of greenhouse gases (GHGs) emission to keep the global warming below 2 degC. As per the agreement the nationally determined commitments (NDCs) and their progresses should be carefully monitored and verified by international bodies. The emission verification will be based on observation of the time evolution of greenhouse gases and model-based estimations of emissions from time to time.

In recent years, the number of observations and new techniques to monitor GHGs budget have been increasing. The improvements includes observational platforms for monitoring atmospheric GHGs, national or regional emission inventories, top-down models (e.g. atmospheric inverse models), and bottom-up models (e.g. process-based models). However, due to uncertainties in modeling and sparse observation network, high uncertainty exists in GHGs sources/sinks estimations at global and regional scales. These uncertainties lead to large variations in future projection of GHG budgets and climate changes.

The purpose of the session is to discuss state-of-the-art techniques for estimations of GHGs (e.g. CO2, CH4, N2O) budget at global and regional scales. The topic includes natural and anthropogenic processes, various methodologies (e.g. in-situ observation, aircraft monitoring, remote sensing, modeling), and various targets (e.g. atmosphere, terrestrial, and ocean), various spatial and temporal coverage (e.g. regional to global scales and past-present-future). Improved estimates of emissions from land use change, forest fires, and other anthropogenic sources (urban developments and thermal power station etc.) are also of interest. We also welcome discussions for designs and plans for future studies targeting city and country scale emission estimations using sophisticated modeling tools.

[ACG32-P01] Regional budgets of 3 major greenhouse gases using inverse modelling of atmospheric data

*Prabir Patra[1], Naveen Chandra[1], Jagat Bisht[1] (1.Japan Agency for Marine-Earth Science and Technology (JAMSTEC))

[ACG32-P02] Analysis of hot summer in 2018

*Kazutaka Murakami[1], Kazuhito Ichii[1,2], Yukio Yoshida[1], Haruki Oshio[1], Makoto Saito[1] (1.National Institute for Environmental Studies, 2.Chiba University)

[ACG32-P03] Updated Data-Driven GPP and NEE Estimation Using Machine Learning Algorithms with Remote Sensing and Flux Data

*Zhiyan Liu[1], Kazuhito Ichii[1], Yusuke Hayasi[1], Riku Kawase[1], Masahito Ueyama[2], Yuji Kominami[3] (1.Chiba University, 2.Osaka Prefecture University, 3.Forest Research and Management Organization)

[ACG32-P04] Response of a Bornean Rainforest to the Climatic Changes imposed by ENSO during 2009-2016

*Julie Karine Michelon[1], Tomo'omi Kumagai[2,3], Tetsuya Hiyama[3], Hatsuki Fujinami[3], Kazuho Matsumoto[4], Tomonori Kume[5], Takami Saito[6] (1.Graduate School of Environmental Studies, Nagoya University, 2.Graduate School of Agricultural and Life Sciences, The University of Tokyo, 3.Institute for Space-Earth Environmental Research, Nagoya University, 4.Faculty of Agriculture, University of the Ryukyus, 5.Faculty of Agriculture, Kyushu University, 6.Forest Research and Management Organization)

[ACG32-P05] Monitoring and Evaluating CO2 Flux in the Grassland Areas of Mongolia

*Qinxue Wang[1], Tomohiro Okadera[1], Deni Eer[1], Masataka Watanabe[2], Tomohiro Shishime[2], Akihiro Oba[2], Ochirbat Batkhishig[3] (1.National Institute for Environmental Studies, 2.Research and Development Initiative, Chuo University, 3.Institute of Geography and Geoecology, Mongolian Academy of Sciences)

[ACG32-P06] Data-driven monitoring of terrestrial carbon cycle in Mongolia

*ZAYA MART[1], Zhiyan Liu[1], Riku Kawase[1], Kazuhito Ichii[1] (1.Chiba University)

Regional budgets of 3 major greenhouse gases using inverse modelling of atmospheric data

*Prabir Patra[1], Naveen Chandra[1], Jagat Bisht[1]

1. Japan Agency for Marine-Earth Science and Technology (JAMSTEC)

Atmospheric observations of greenhouse gases provide accurate record the changes in their abundance in the Earth's environments, and it has now been well established that the increase in greenhouse gases concentrations is causing the rise in the mean surface air temperature. Using atmospheric chemistry-transport models (ACTM), along with the concentration measurements, we can estimate the sources and sinks of the chemical species. Using MIROC4-ACTM at JAMSTEC, we estimated regional sources and sinks of carbon dioxide (CO2), methane (CH4) and nitrous oxide (N2O) over the period of 1996 to 2016. This will help global stocktake every 5 years, as a independent estimate, when the coutries report their progress on nationally determined contributions (NDCs) under the Paris Agreement and their ammendments, overseen by the UNFCCC.

Keywords: Inverse modelling, Greenhouse gases sources and sinks, Paris Agreement and NDCs

©2019. Japan Geoscience Union. All Right Reserved.

Analysis of hot summer in 2018

*Kazutaka Murakami[1], Kazuhito Ichii[1,2], Yukio Yoshida[1], Haruki Oshio[1], Makoto Saito[1]

1. National Institute for Environmental Studies, 2. Chiba University

Global averaged temperature in 2018 was considerably higher than normal year. Probably it is the fourth highest in the past. Especially, it was memorable that East Asia, Europe, and the southwestern part of the United States were hit by record heat waves in this summer. It is important for the ecological resilience to investigate how much such extreme weather damages the terrestrial ecosystem and how will it change after that. In this study, we analyzed the effect of this extremely high temperature on terrestrial vegetation using satellite remote sensing data. First, we investigated the high temperature area using MODIS land surface temperature (LST) product. Then, focusing on these high LST areas, we analyzed the impact to satellite observed Solar Induced Fluorescence (SIF) that closely related to a photosynthetic activity. As a result, it was found that the LST of 2018 in the East Asia (Japan, Korea and North Korea) was the highest during 2002 - 2018 years. And it also indicated abnormal high LST regions from Germany to northern Europe. Analysis of SIF data showed a positive decline in Europe but did not show a clear trend in Asia. In addition, similar trends were seen from other satellite vegetation indices, and it was found that the terrestrial vegetation shows different responses in both areas affected by the same hot summer.

Keywords: 2018 summer, heat wave, satellite observation, SIF

©2019. Japan Geoscience Union. All Right Reserved.

Updated Data-Driven GPP and NEE Estimation Using Machine Learning Algorithms with Remote Sensing and Flux Data

*Zhiyan Liu[1], Kazuhito Ichii[1], Yusuke Hayasi[1], Riku Kawase[1], Masahito Ueyama[2], Yuji Kominami[3]

1. Chiba University, 2. Osaka Prefecture University, 3. Forest Research and Management Organization

Abstract

Data-driven approach is effective for understanding and up-scaling observation network data of terrestrial carbon fluxes. Recently, the expansion of observation network, the improvement of remote sensing products and more application of machine learning on natural science make it more possible. In this study, we estimated two important parameters of terrestrial ecosystem, terrestrial gross primary productivity (GPP) and net ecosystem exchange (NEE) through re-assessment of previous approaches [Ichii et al. 2017; Kondo et al. 2015]. We tested multiple combinations of input parameters with lagged effect, additional new input parameters and the updated MODIS datasets (Collection C6). Besides, we selected 3 typical machine learning methods (Random Forest, RF; Support Vector Regression, SVR; Artificial Neural Network, ANN) as data-driven method and compare the estimation from 3 different types of machine learning model. The site-level analysis shows that use of the new version data and the time-lagged improved the model performance. Finally, we compared our new estimation of GPP and NEE with several terrestrial models output and other available datasets and we found our new results show better consistency with them. This shows our estimation provides a good benchmark for understanding spatio-temporal variability in terrestrial GPP and NEE.

Acknowledgement

This research was financially supported by the Environment Research and Technology Development Fund (2-1701) of the Environmental Restoration and Conservation Agency of Japan.

Keywords: Terrestrial Carbon Cycle, MODIS Collection6, Data-driven, time-lag effect

©2019. Japan Geoscience Union. All Right Reserved.

Response of a Bornean Rainforest to the Climatic Changes imposed by ENSO during 2009-2016

*Julie Karine Michelon[1], Tomo'omi Kumagai[2,3], Tetsuya Hiyama[3], Hatsuki Fujinami[3], Kazuho Matsumoto[4], Tomonori Kume[5], Takami Saito[6]

1. Graduate School of Environmental Studies, Nagoya University, 2. Graduate School of Agricultural and Life Sciences, The University of Tokyo, 3. Institute for Space-Earth Environmental Research, Nagoya University, 4. Faculty of Agriculture, University of the Ryukyus, 5. Faculty of Agriculture, Kyushu University, 6. Forest Research and Management Organization

Tropical rainforests belong to the most important biomes, as they are one of the largest terrestrial carbon sink and also a consequent source of latent energy. Furthermore, they will be among the first ecosystems to undergo climatic changes in the near future. Understanding how they will response to those changes is essential. El Niño-Southern Oscillation (ENSO) is an opportunity to study ecosystem response under real climatic change conditions.

Transpiration (Tr), net ecosystem exchange (NEE) and heat fluxes were measured with an eddy covariance system in a natural rainforest in Sarawak, Malaysia. Meteorological and soil moisture observations were also conducted. This region does not have phase-locked dry periods, and seasonal variations of both air temperature and solar radiation are small. However, it is directly impacted by ENSO events. During the study period, from November 2009 to December 2016, two events were selected : La Niña 2010-2011 and El Niño 2014-2016. Normal conditions were assumed as a third "neutral" period. Comparisons of measured flux and meteorological drivers between the three periods were carried out, and analysis of environmental controls, as canopy conductance (g_c) were made.

Precipitation and air temperature were significantly different between the three periods. While the water cycle (latent heat flux, Tr, g_c) responded immediately to the changes imposed by La Niña, the enhancement of the ecosystem respiration balanced the gross primary production gain, resulting into a NEE similar to neutral conditions. Conversely, the NEE during El Niño was significantly smaller than during neutral, when the water cycle seemed not impacted. However, further observations of this late rainforest response evolution showed that, during the first part of El Niño, Tr and g_c increased while CO_2 flux reduced. Then, during the second part, the trend reversed : CO_2 flux increased and Tr, as well as g_c, reduced. This may indicate a time lag between the meteorological drivers (precipitation and air temperature) changes imposed by El Niño and the ecosystem response (H_2O and CO_2 fluxes). The response delay may be caused by the rainforest tendency to poorly regulate its water use, being a particular moist environment. As for the response itself, it may be triggered by the depletion of the soil water content.

Those results imply that considering the length of El Niño and the ecosystem response trigger are important to understand and model bornean rainforest fluxes under future climatic scenario.

Keywords: Borneo, Rainforest, ENSO, NEE, Transpiration

©2019. Japan Geoscience Union. All Right Reserved.

Monitoring and Evaluating CO2 Flux in the Grassland Areas of Mongolia

*Qinxue Wang[1], Tomohiro Okadera[1], Deni Eer[1], Masataka Watanabe[2], Tomohiro Shishime[2], Akihiro Oba[2], Ochirbat Batkhishig[3]

1. National Institute for Environmental Studies, 2. Research and Development Initiative, Chuo University, 3. Institute of Geography and Geoecology, Mongolian Academy of Sciences

For verification of data products of the Greenhouse Gas Observing Satellite (GOSAT), in this study, we monitored and evaluated CO2 flux, that is, the absorption and emission of CO2 by ecosystems in the grasslands of Mongolia by the eddy correlation method. Two flux towers were established in 2015 at the Nalaikh site near Ulaanbaatar City and the Hustai site with less influence of cities, respectively. The CO2 analyzers installed on the towers were calibrated every year by using the standard gas imported from Japan. Up to now, about 4-year monitoring data have been accumulated since 2015. The data analysis shows that the CO2 absorption was larger than emissions at both sites, which indicated that the ecosystem at both sites are carbon sinks. The annual mean value of the CO2 absorption at the Nalaikh site was about 2.66 μmol m^{-2} s^{-1} and the emission was about 1.53 μmol m^{-2} s^{-1}, but the absorption at the Hustai site was about 2.11 μmol m^{-2} s^{-1}, and the emission was about 1.37 μmol m^{-2} s^{-1} (Figure 1). Generally, the net CO2 absorption at the Nalaikh site (0.76 μmol m^{-2} s^{-1}) was found to be larger than that at the Hustai site (0.36 μmol m^{-2} s^{-1}).

To compare the GOSAT L4B data with the ground observation at both sites, we extracted the monthly mean value of CO2 absorption/emission from the grid data of GOSAT during 2009-2015 and compared with the observed data. We found that although the seasonal changing pattern and fluctuation range are similar, the CO2 emission derived by GOSAT were larger than absorption, which suggested that the steppe ecosystems at both sites are the carbon sources. However, the ground observations showed that the CO2 absorption at both sites was larger than emission, which suggested that the grassland ecosystems at both sites are carbon sinks (Figure 2). It is essential for us to find the reasons of this difference in the future.

Finally, to evaluate the spatiotemporal distribution of carbon absorption and emission in the whole country, we have developed a carbon budget model considering the influence of grazing density. The primary simulation results showed that the percentage of carbon loss by grazing (CLG) accounted for 19-38% of the net ecosystem production (NEP) in the Nalaikh area around the city of Ulaanbaatar, where the grazing density was 1.5-2.3 sheep/ha during 2012-2016. On the other hand, CLG accounted for only 7-20% of NEP in the Hustai area away from the city, where the grazing density was only 0.4-0.6 sheep/ha (Figure 3). The result implied that the carbon budget was greatly influenced by animal husbandry near cities, where the grazing density is large. The monitoring cameras installed at both sites show that the biomass inside and outside the fence was greatly influenced by the ingestion of livestock.

This study was funded by “the Project to implement MRV and related technological improvements contributing to the Joint Crediting Mechanism (JCM) in Mongolia”, Ministry of the Environment, Japan.

Keywords: Carbon flux, Grassland ecosystem, The Greenhouse Gases Observing Satellite (GOSAT)

©2019. Japan Geoscience Union. All Right Reserved.

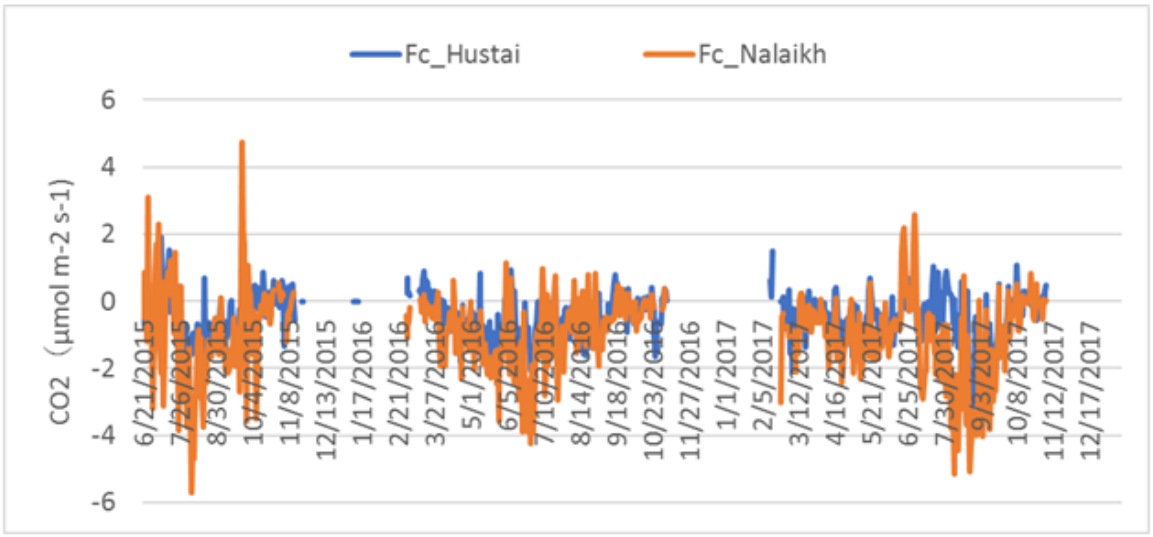

Figure 1 Comparison of CO2 flux observed at Nalaikh Site and Hustai Site

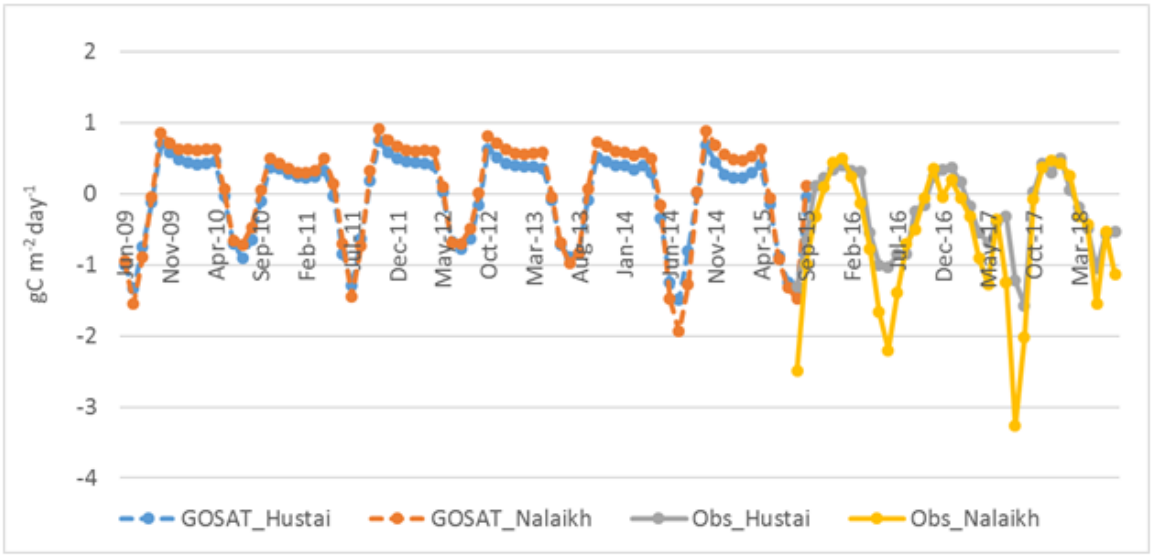

Figure 2 Comparison of GOSAT L4B and observations at Nalaikh Site and Hustai Site

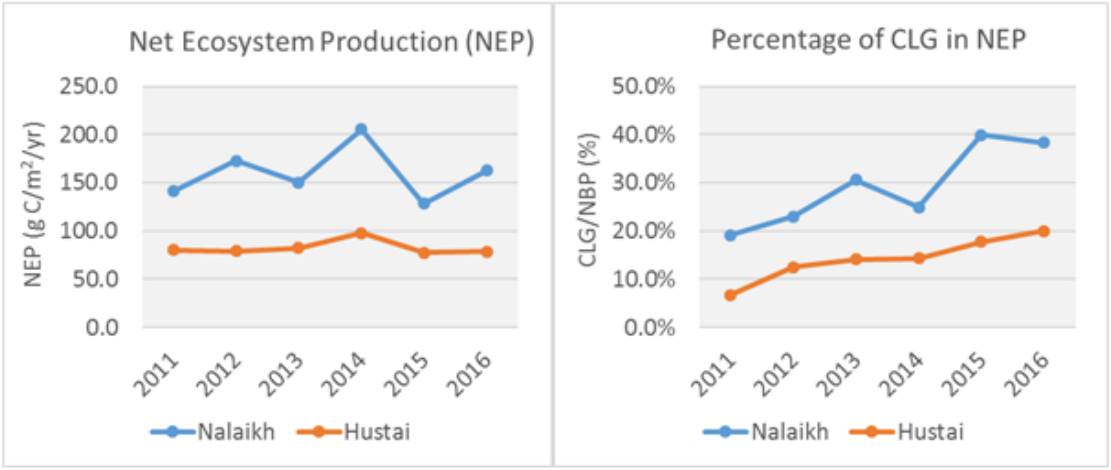

Figure 3 Impact of livestock grazing on NEP at Nalaikh Site and Hustai Site

©2019. Japan Geoscience Union. All Right Reserved.

Data-driven monitoring of terrestrial carbon cycle in Mongolia

*ZAYA MART[1], Zhiyan Liu[1], Riku Kawase[1], Kazuhito Ichii[1]

1. Chiba University

Mongolia has been experiencing both climate changes and anthropogenic environmental changes. Therefore, it is important to monitor environmental changes. In particular, more and more observation-based data sets are available, and synthesis analysis using these multiple observation-based data sets are essential.

We analyzed changes in the terrestrial environmental environment in Mongolia from the 1980s to 2010s. We focused on two different temporal periods, the 1980s to 2010s and 2000 to 2015. As for the first period (1980s to 2010s), we used NOAA AVHRR data sets, observed climate data sets for the analysis. As for the second period (1980s to 2010s), we used multiple remote sensing data sets (e.g. Terra MODIS), empirically upscaled CO2 flux products, and outputs from terrestrial ecosystem models. We will show and discuss the estimated terrestrial environmental changes in Mongolia at the conference.

Keywords: climate change, terrestrial environments, carbon cycle

©2019. Japan Geoscience Union. All Right Reserved.

[E] Oral | A (Atmospheric and Hydrospheric Sciences)：A-CG Complex & General

Tue. May 28, 2019 1:45 PM - 3:15 PM JST | Tue. May 28, 2019 4:45 AM - 6:15 AM UTC | 301A 3F

[A-CG32] Global Carbon Cycle Observation and Analysis

convener:Kazuhito Ichii(Chiba University), Prabir Patra(Research Institute for Global Change, JAMSTEC), Forrest M. Hoffman(Oak Ridge National Laboratory), Makoto Saito(National Institute of Environmental Studies), Chairperson:Kazuhito Ichii

The landmark Paris Agreement under the United Nations Framework Convention on Climate Change (UNFCCC) aims at reduction of greenhouse gases (GHGs) emission to keep the global warming below 2 degC. As per the agreement the nationally determined commitments (NDCs) and their progresses should be carefully monitored and verified by international bodies. The emission verification will be based on observation of the time evolution of greenhouse gases and model-based estimations of emissions from time to time.
In recent years, the number of observations and new techniques to monitor GHGs budget have been increasing. The improvements includes observational platforms for monitoring atmospheric GHGs, national or regional emission inventories, top-down models (e.g. atmospheric inverse models), and bottom-up models (e.g. process-based models). However, due to uncertainties in modeling and sparse observation network, high uncertainty exists in GHGs sources/sinks estimations at global and regional scales. These uncertainties lead to large variations in future projection of GHG budgets and climate changes.
The purpose of the session is to discuss state-of-the-art techniques for estimations of GHGs (e.g. CO2, CH4, N2O) budget at global and regional scales. The topic includes natural and anthropogenic processes, various methodologies (e.g. in-situ observation, aircraft monitoring, remote sensing, modeling), and various targets (e.g. atmosphere, terrestrial, and ocean), various spatial and temporal coverage (e.g. regional to global scales and past-present-future). Improved estimates of emissions from land use change, forest fires, and other anthropogenic sources (urban developments and thermal power station etc.) are also of interest. We also welcome discussions for designs and plans for future studies targeting city and country scale emission estimations using sophisticated modeling tools.

1:45 PM - 2:00 PM JST | 4:45 AM - 5:00 AM UTC

[ACG32-01] A high-resolution fossil fuel CO2 emission gridded dataset for tracer transport simulations and flux inversions: An overview, evaluations, applications and future perspectives

★Invited Papers

*Tomohiro Oda[1,2], Shamil Maksyutov [3], Miguel O. Roman [2,4], Zhousen Wang [4], Thomas Lauvaux[6,5], Sha Feng [5], Rostyslav Bun [7,8], James Wang [2,1], Randy Kawa [1], Lesley Ott[1], Steven Pawson[1] (1.NASA Goddard Space Flight Center, Greenbelt, MD, USA , 2.Universities Space Research Association, Columbia, MD, USA , 3.Center for Global Environmental Research, National Institute for Environmental Studies, Tsukuba, Ibaraki, Japan , 4.Terrestrial Information Systems Laboratory, NASA Goddard Space Flight Center, Greenbelt, MD, USA , 5.Department of Meteorology and Atmospheric Science, Penn. State University, State College, PA, USA , 6.Laboratoire des sciences du climat et de l'environnement, Gif sur Yvette, France, 7.Lviv Polytechnic National University, Lviv, Ukraine , 8.University of Dąbrowa Górnicza, Górnicza, Poland)

2:00 PM - 2:15 PM JST | 5:00 AM - 5:15 AM UTC

[ACG32-02] Towards Decreasing the Uncertainty in Global Carbon Dioxide Emission Inventory

*Richao Cong[1], Makoto Saito[1], Ryuichi Hirata[1], Akihiko Ito[1] (1.Center for Global Environmental Research, National Institute for Environmental Studies)

2:15 PM - 2:30 PM JST | 5:15 AM - 5:30 AM UTC

[ACG32-03] Evaluation of MIROC4-ACTM reanalysis of GHGs concentrations using aircraft

*Jagat Bisht[1], Prabir Patra[1], Naveen Chandra[1], Sergey Gromov[2], Taku Umezawa[3], Andreas Zahn[4], cARL A. M. Brenninkmeijer[5] (1.Japan Agency for Marine-Earth Science and Technology (JAMSTEC), Yokohama, Japan, 2.Max Planck Institute for Chemistry, Mainz, Germany, 3.National Institute for Environmental Studies, Tsukuba, Japan, 4.Karlsruhe Institute of Technology (KIT), Institute for Meteorology and Climate

Research, Karlsruhe, Germany, 5.Max Planck Institute for Chemistry, Air Chemistry Division, Mainz, Germany)

2:30 PM - 2:45 PM JST | 5:30 AM - 5:45 AM UTC

[ACG32-04] **Carbon flux estimation using NICAM-TM 4D-Var and GOSAT data towards GOSAT-2 Level 4 product**

*Tazu Saeki[1], Yosuke Niwa[1], Makoto Saito[1] (1.National Institute for Environmental Studies)

2:45 PM - 3:00 PM JST | 5:45 AM - 6:00 AM UTC

[ACG32-05] **Attribution of the ambiguity in methane's growth rate shifts during 1988-2016.**

*Naveen Chandra[1], Prabir Patra[1] (1.Japan Agency for Marine Earth Science and Technology)

3:00 PM - 3:15 PM JST | 6:00 AM - 6:15 AM UTC

[ACG32-06] **Ocean uptake and land use change emissions suppressed atmospheric CO_2 growth in the 2015/16 El Niño**

*Masayuki Kondo[1], Peter Landschützer[2], Yousuke Iida[3], Richard Houghton[4], Stephen Sitch[5] (1. Center for Environmental Remote Sensing, Chiba University, 2.Max Planck Institute for Meteorology, 3.Global Environment and Marine Department, Japan Meteorological Agency, 4.Woods Hole Research Center, 5.University of Exeter)

A high-resolution fossil fuel CO2 emission gridded dataset for tracer transport simulations and flux inversions: An overview, evaluations, applications and future perspectives

*Tomohiro Oda[1,2], Shamil Maksyutov [3], Miguel O. Roman [2,4], Zhousen Wang [4], Thomas Lauvaux[6,5], Sha Feng [5], Rostyslav Bun [7,8], James Wang [2,1], Randy Kawa [1], Lesley Ott[1], Steven Pawson[1]

1. NASA Goddard Space Flight Center, Greenbelt, MD, USA , 2. Universities Space Research Association, Columbia, MD, USA , 3. Center for Global Environmental Research, National Institute for Environmental Studies, Tsukuba, Ibaraki, Japan , 4. Terrestrial Information Systems Laboratory, NASA Goddard Space Flight Center, Greenbelt, MD, USA , 5. Department of Meteorology and Atmospheric Science, Penn. State University, State College, PA, USA , 6. Laboratoire des sciences du climat et de l'environnement, Gif sur Yvette, France, 7. Lviv Polytechnic National University, Lviv, Ukraine , 8. University of Dąbrowa Górnicza, Górnicza, Poland

Carbon dioxide (CO_2) emissions from fossil fuel combustion (Fossil fuel CO_2, FFCO2) is the largest input to the global carbon cycle over the decadal time scales. FFCO2 needs to be accurately quantified and monitored in order to deduce the carbon uptakes by natural sinks from atmospheric measurements as well as support the emission reduction and management. The Open-source Data Inventory for Anthropogenic CO_2 (ODIAC) is a global, high-spatial resolution (1x1km) gridded FFCO2 emission data product. We first pioneered the combined use of the point source information and satellite-observed nighttime lights data for emission downscaling in order to achieve global 1×1 km spatial resolution emission fields. The use of nightlight data allows us to observe dynamic changes in emissions spatial distributions in a timely manner and incorporate these into the emission field. Since its establishment in 2009, ODIAC has been extensively used in global and regional flux inversions especially with CO_2 data collected by carbon observing satellites, such as the Japanese Greenhouse gas Observing SATellite (GOSAT) and NASA’s Orbiting Carbon Observatory 2 (OCO-2). ODIAC has been also successfully applied to studies for localized emissions point sources such as power plants and cities. In order to further improve the accuracy of the emission downscaling, we have examined NASA’s new Visible Infrared Imaging Spectrometer Suite (VIIRS) Nighttime Environmental Product. An accurate global emission disaggregation is one of the key elements of future Monitoring and Verification Support (MVS) scientific systems that consist of the carbon modeling and data assimilation. Our advanced satellite-based emission downscaling model holds the promise of playing a critical role in such future systems.

Keywords: CO2, fossil fuel CO2 emissions, Carbon cycle, Remote sensing, GOSAT, OCO-2

©2019. Japan Geoscience Union. All Right Reserved.

Towards Decreasing the Uncertainty in Global Carbon Dioxide Emission Inventory

*Richao Cong[1], Makoto Saito[1], Ryuichi Hirata[1], Akihiko Ito[1]

1. Center for Global Environmental Research, National Institute for Environmental Studies

Global carbon dioxide (CO_2) emission inventory are considered as containing large uncertainty. To decrease the uncertainty, we corrected the emissions reported by some famous orgainzations to make a new global CO_2 emission map by top-down approach and to analyze the temporary variation of emissions at global, regional, and national scale. For that purpose, 133 nations across 10 databases which included the values from 2000 to 2010 were picked up for analysis. Then, the emissions are corrected by averaging of the values in the range of 25% to 75% quartile. To visualize the temporary variation for the emissions, we linked the emissions for 133 nations with global boundary map of nations by Geographic Information System (GIS). As our summarization, the total CO_2 emissions for 133 nations in 2010 are about 31,595 Tg CO_2 yr^{-1} which are inside the values reported by IEA (30,434 Tg only from fuel combustion) and CDIAC (33,469 Tg from fuel combustion, cement manufacture, and gas flaring), occupying about 94% of the emissions reported by EDGAR (33,588 Tg). In addition, we also combined the emissions with population, GDP, and area of each nation reported by world bank to summarize the emissions per capita and analyze the trends of them from 2000 to 2010.

©2019. Japan Geoscience Union. All Right Reserved.

Evaluation of MIROC4-ACTM reanalysis of GHGs concentrations using aircraft

*Jagat Bisht[1], Prabir Patra[1], Naveen Chandra[1], Sergey Gromov[2], Taku Umezawa[3], Andreas Zahn[4], cARL A. M. Brenninkmeijer[5]

1. Japan Agency for Marine-Earth Science and Technology (JAMSTEC), Yokohama, Japan, 2. Max Planck Institute for Chemistry, Mainz, Germany, 3. National Institute for Environmental Studies, Tsukuba, Japan, 4. Karlsruhe Institute of Technology (KIT), Institute for Meteorology and Climate Research, Karlsruhe, Germany, 5. Max Planck Institute for Chemistry, Air Chemistry Division, Mainz, Germany

Using the “Atmospheric Chemistry Transport Model” being part of the “Model for Interdisciplinary Research On Climate Earth System Model, version 4” (MIROC4-ACTM), simulations of several important greenhouse gases, such as CH_4, CO_2, SF_6, and N_2O, have been conducted using optimized emissions by inverse modelling of surface measurements for the period 1996-2016 (referred to as “reanalysis data”). Aircraft observations, conducted on board passenger aircraft (projects: CARIBIC and CONTRAIL) over diverse latitude and longitude regions offer independent constraints for evaluating the quality of reanalysis data. MIROC4-ACTM captures the variations in CO_2 and SF_6 observed by CARIBIC and CONTRAIL very well, with a correlation coefficient of above 0.96 and a slope of 0.92 at all atmospheric conditions. However, for CH_4 and N_2O the agreement was worse, with correlation coefficients (slopes) between CONTRAIL observations and model simulations of 0.80(0.49)-0.87(0.66) and 0.74(0.55)-0.77(0.75), respectively, at 0-140°E and poleward of 40°N. Further south, that is between 30° S-40°N latitude (for the Tokyo-Australia flights), the correlation coefficients (slopes) was 0.76(0.83)-0.88(0.89) and 0.92(0.87)-0.98(1.05), respectively. Similarly, the agreement with the CARIBIC observations was moderate for CH_4 and N_2O, with correlation coefficients (slopes) of 0.81(0.55) and 0.88(0.65), respectively.

Keywords: MIROC4-ACTM, CONTRAIL, CARIBIC

©2019. Japan Geoscience Union. All Right Reserved.

Carbon flux estimation using NICAM-TM 4D-Var and GOSAT data towards GOSAT-2 Level 4 product

*Tazu Saeki[1], Yosuke Niwa[1], Makoto Saito[1]

1. National Institute for Environmental Studies

Greenhouse gases (GHG) observations from satellites have contributed to expanding spatial coverage of observational networks for GHGs over the globe. Greenhouse gases Observing SATellite (GOSAT) has been monitoring the column-averaged dry-air mole fractions of atmospheric carbon dioxide (XCO_2) and methane (XCH_4) from space since its launch in January 2009. Its successor GOSAT-2 was successfully launched on 29 October 2018, and the observational data are being processed at GOSAT-2 ground systems. The GOSAT-2 mission aims to continue and enhance spaceborne measurement of GHGs started by GOSAT, and to monitor the impacts of climate change and human activities on the carbon cycle. Both satellites are jointly developed and operated by Ministry of the Environment, Japan Aerospace Exploration Agency (JAXA), and National Institute for Environmental Studies (NIES). NIES is responsible for producing and distributing higher level data products, such as Level 2 products (XCO_2 and XCH_4 etc.) and Level 4 products (surface fluxes of CO_2 and CH_4 and three-dimensional global distributions of CO_2 and CH_4 concentrations) (http://www.gosat-2.nies.go.jp).

We are currently developing an inversion system for operational use to produce GOSAT-2 L4 products. The Non-hydrostatic ICosahedral Atmospheric Model (NICAM)-based Transport Model (NICAM-TM; Niwa et al., 2011) is used for simulating atmospheric CO_2 and CH_4 concentrations, and an inversion system based on the four-dimensional variational (4D-Var) method with NICAM-TM (NICAM-TM 4D-Var; Niwa et al., 2017a,b) is adopted to estimate global surface CO_2 and CH_4 fluxes. In this presentation, we will present test results of CO_2 flux estimation with NICAM-TM 4D-Var using GOSAT data (not GOSAT-2 data), ground-based data, prior fluxes, and their error covariances. NICAM-TM is operated with a horizontal resolution of glevel-5 (an average grid resolution of 223 km) and 40 vertical layers, and its meteorological fields are nudged with JRA-55 data to simulate real atmospheric transport. NICAM-TM 4D-Var is run with stored meteorological data, which successfully reduces computational cost. CO_2 surface fluxes have been estimated at every 223 km grid resolution and at monthly time resolution. Preliminary test results with single-year GOSAT data showed that flux differences between the prior fluxes and estimated fluxes from the GOSAT data inversion appear over a broad area of land regions, even over Siberia and South America where ground sites are sparse, while the ocean regions showed relatively fewer flux changes after the inversion. Our ongoing work includes inversions with multi-year data, the inclusion of other data, and tuning model parameters. The details will be presented at the meeting.

Acknowledgments. The model simulations are performed with the NIES supercomputer system and the Research Computation Facility for GOSAT-2 (RCF2). This research is partly supported by the Environment Research and Technology Development Fund (2-1701) of the Environmental Restoration and Conservation Agency of Japan.

References

Niwa et al. (2011), Journal of the Meteorological Society of Japan. Ser. II, 89(3), 255–268.
Niwa et al. (2017a), Geoscientific Model Development, 10(3), 1157–1174.
Niwa et al. (2017b), Geoscientific Model Development, 10(6), 2201–2219.

©2019. Japan Geoscience Union. All Right Reserved.

Keywords: Carbon budget, Flux estimations of greenhouse gases, Atmospheric inverse model, Top-down approach, Satellite remote sensing

©2019. Japan Geoscience Union. All Right Reserved.

Attribution of the ambiguity in methane’s growth rate shifts during 1988-2016.

*Naveen Chandra[1], Prabir Patra[1]

1. Japan Agency for Marine Earth Science and Technology

Atmospheric (CH_4) is an important greenhouse gas for mitigating climate change in the decadal scale due to its shorter atmospheric lifetime and about 30 times higher warming potential than carbon dioxide. The remarkable shift in CH_4 growth rate (decrease since early 1990s, quasi-stationary state during 1999-2005 and resume increase after 2006) has observed in past three decades (1990s-2010s). However, the attribution of these fluctuations remained highly conflicting. We have used a global inverse modeling system for constraining CH_4 emissions from 53 land regions for the period 1988–2016 using measurements from 19 sites and forward simulation by MIROC4-ACTM. The ACTM realistically represent inter-hemispheric transport and stratospheric age of air, and methyl chloroform concentration decay (proxy for loss OH concentration level) which are key elements for modelling CH4 in atmosphere. A set of 2 inversions is performed for different combinations of a priori emissions due to the wetlands and rice cultivation. We have shown that slowing down of emissions from oil and gas industry in the 1980s and Mt. Pinatubo volcanic eruption in 1991 led to a stabilization in emissions and thus the quasi-stationary state of CH4 concentration. The CH_4 growth after 2006 is attributed to increases in emissions mainly from coal industry and ruminant farming. The climatic variation due to ENSO caused significant interannual variation in the CH_4 growth rate. The role of CH_4 loss by hydroxyl (OH) reaction in CH4 growth rate variability is proposed to be not significant from inter-site differences.

©2019. Japan Geoscience Union. All Right Reserved.

Ocean uptake and land use change emissions suppressed atmospheric CO_2 growth in the 2015/16 El Niño

*Masayuki Kondo[1], Peter Landschützer[2], Yousuke Iida[3], Richard Houghton[4], Stephen Sitch[5]

1. Center for Environmental Remote Sensing, Chiba University, 2. Max Planck Institute for Meteorology, 3. Global Environment and Marine Department, Japan Meteorological Agency, 4. Woods Hole Research Center, 5. University of Exeter

Large variability in El Niño-Southern Oscillation (ENSO) induces anomalous CO_2 fluxes both in biosphere and hydrosphere. In the negative phase of ENSO (i.e., El Niño), dryer climate over lower latitudes decreases productivity of land vegetation and increases vulnerability to biomass burning. At the same time, suppressed upwelling of carbon-rich water near the Pacific South America reduces outgassing of oceanic CO_2 to atmosphere. In years of a strong El Niño, anomalous land and ocean CO_2 fluxes account for a large part of interannual variability of the total net CO_2 flux of the Earth surface. Thus, anomalously large atmospheric CO_2 growth rates co-occur with periods of El Niño events.

Biomass burning is believed to be the dominant component of variability in atmospheric CO_2 growth rate during El Niño. The 1997/98 El Niño induced the most significant anomalous CO_2 release on record, largely due to forest and peat fires in Southeast Asia. Likewise, a massive fire haze over Southeast Asia was found during the recent 2015/16 El Niño. Despite the seemingly large impact of biomass burning in the two events, the 2015/16 El Niño accompanied substantially less atmospheric CO_2 growth compared with that in the 1997/98 El Niño. It turns out that CO_2 emission from biomass burning in 2015 was substantially less than that in 1997 because precipitation before the peak of fire emission (Sept-Oct) shortened the drought length of 2015.

However, it is still arguable that the insignificant biomass burning is the dominate cause behind no obvious signs of large CO_2 release in the 2015/16 El Niño. In the recent decades, both biospheric and hydrospheric CO_2 fluxes has shown trends towards a net sink of CO_2, which suggest a possibility of that increasing CO_2 uptake has suppressed the atmospheric CO_2 growth in the 2015/16 El Niño. To evaluate this possibility, a synthesis of land-ocean CO_2 flux over the period of the two El Niño events is necessary. Here, we explore mechanisms behind differences in the atmospheric CO_2 growth in the 1997/98 and 2015/16 El Niño. The aim of this study is to fully characterize the causes for insignificant atmospheric CO_2 growth in 2015/16 through analyzing types (anomaly/trend) of relative contributions of land-ocean fluxes to atmospheric CO_2 growth between the two El Niño events. Through the analysis, we discuss about components that would likely continue to mitigate atmospheric CO_2 growth in future El Niño.

Keywords: Carbon Cycle, El Nino, Attribution analysis

©2019. Japan Geoscience Union. All Right Reserved.

[E] Oral | A (Atmospheric and Hydrospheric Sciences)：A-CG Complex & General

Tue. May 28, 2019 3:30 PM - 5:00 PM JST | Tue. May 28, 2019 6:30 AM - 8:00 AM UTC | 301A 3F

[A-CG32] Global Carbon Cycle Observation and Analysis

convener:Kazuhito Ichii(Chiba University), Prabir Patra(Research Institute for Global Change, JAMSTEC), Forrest M. Hoffman(Oak Ridge National Laboratory), Makoto Saito(National Institute of Environmental Studies), Chairperson:Prabir Patra

The landmark Paris Agreement under the United Nations Framework Convention on Climate Change (UNFCCC) aims at reduction of greenhouse gases (GHGs) emission to keep the global warming below 2 degC. As per the agreement the nationally determined commitments (NDCs) and their progresses should be carefully monitored and verified by international bodies. The emission verification will be based on observation of the time evolution of greenhouse gases and model-based estimations of emissions from time to time.

In recent years, the number of observations and new techniques to monitor GHGs budget have been increasing. The improvements includes observational platforms for monitoring atmospheric GHGs, national or regional emission inventories, top-down models (e.g. atmospheric inverse models), and bottom-up models (e.g. process-based models). However, due to uncertainties in modeling and sparse observation network, high uncertainty exists in GHGs sources/sinks estimations at global and regional scales. These uncertainties lead to large variations in future projection of GHG budgets and climate changes.

The purpose of the session is to discuss state-of-the-art techniques for estimations of GHGs (e.g. CO2, CH4, N2O) budget at global and regional scales. The topic includes natural and anthropogenic processes, various methodologies (e.g. in-situ observation, aircraft monitoring, remote sensing, modeling), and various targets (e.g. atmosphere, terrestrial, and ocean), various spatial and temporal coverage (e.g. regional to global scales and past-present-future). Improved estimates of emissions from land use change, forest fires, and other anthropogenic sources (urban developments and thermal power station etc.) are also of interest. We also welcome discussions for designs and plans for future studies targeting city and country scale emission estimations using sophisticated modeling tools.

3:30 PM - 3:45 PM JST | 6:30 AM - 6:45 AM UTC

[ACG32-07] Observing vegetation seasonal dynamics in Japan with Himawari-8 hypertemporal data

*Tomoaki Miura[1,2], Shin Nagai[2], Kazuhito Ichii[3], Hiroki Yoshioka[4] (1.University of Hawaii at Manoa, 2.Japan Agency for Marine-Earth Science and Technology, 3.Center for Environmental Remote Sensing, Chiba University, 4.Aichi Prefectural University)

3:45 PM - 4:00 PM JST | 6:45 AM - 7:00 AM UTC

[ACG32-08] Carbon and Water Fluxes at High spatial Resolutions through Down-Scaling

*Jiquan Chen[1], Pietro Sciusco[1], Ranjeet John[1], Zutao Ouyang[1] (1.Michigan State University)

4:00 PM - 4:15 PM JST | 7:00 AM - 7:15 AM UTC

[ACG32-09] **Connecting Satellite Based Spectral Modelling Approach and Forest Inventory to Model Biomass and Carbon Stocks in Natural and Planted Forest over part of Semi-arid zone, India**

*SWATI UNIYAL[1], Siti Raju Rao (1.Andhra University)

4:15 PM - 4:30 PM JST | 7:15 AM - 7:30 AM UTC

[ACG32-10] **Allocation of forest net primary production varies by forest age and air temperature**

*Xiang Song[1], Xiaodong Zeng[1], Dongxiao Tian[2] (1.IAP, CAS, 2.Beijing Meteorological Information Center)

4:30 PM - 4:45 PM JST | 7:30 AM - 7:45 AM UTC

[ACG32-11] Analyzing Model Biases in Terrestrial Carbon Cycle Submodels in Earth System Models and Offline Models

*Kazuhito Ichii[1], Kazutaka Murakami[2], Hiroaki Takayama[3], Tomohiro Hajima[3], Kaoru Tachiiri[3] (1.Chiba University, 2.National Institute for Environmental Studies, 3.Japan Agency for Marine-Earth Science and Technology)

4:45 PM - 5:00 PM JST | 7:45 AM - 8:00 AM UTC

[ACG32-12] Assessing terrestrial biogeochemical feedbacks in a strategically geoengineered climate

*Forrest M. Hoffman[1,2], Cheng-En Yang[2,1], Joshua S. Fu[2,1], Simone Tilmes[3], Lili Xia[4], Douglas G. MacMartin[5], Jadwiga H. Richter[3], Michael Mills[3], Ben Kravitz[6] (1.Oak Ridge National Laboratory, 2.University of Tennessee, 3.National Center for Atmospheric Research, 4.Rutgers University, 5.Cornell University, 6.Pacific Northwest National Laboratory)

Observing vegetation seasonal dynamics in Japan with Himawari-8 hypertemporal data

*Tomoaki Miura[1,2], Shin Nagai[2], Kazuhito Ichii[3], Hiroki Yoshioka[4]

1. University of Hawaii at Manoa, 2. Japan Agency for Marine-Earth Science and Technology, 3. Center for Environmental Remote Sensing, Chiba University, 4. Aichi Prefectural University

Spectral vegetation index (VI) time series data derived from moderate resolution, polar-orbiting satellite sensors, have been used to monitor and characterize the Earth’ s vegetative cover and its dynamics in regional to global scales. Unities of these VI time series data are, however, constrained by frequent cloud covers. That is, the derived VI products from these sensor data are at a weekly or bi-weekly temporal resolution due to the availability of cloud-free observations, resulting in relatively high uncertainties in their seasonal dynamics characterization. A new generation of geostationary satellite sensors equipped with spectral bands suitable for VIs, such as Himawari-8/9, have been launched during the last decade. As they are on geostationary orbit, they can image an Earth’ s hemisphere at 10-15 min intervals, potentially serving as another significant data source for the studies of vegetation dynamics.

In this study, we assessed the utilities of Himawari-8 “hypertemporal” NDVI data for characterizing seasonal dynamics of vegetation and land cover conditions. We compared Himawari NDVI temporal signatures to those derived from a new generation polar-orbiting satellite sensor, Visible Infrared Imaging Radiometer Suite (VIIRS), at select sites in Japan. Our analysis showed that cloud-free observations were available for ~24 days during the 45-day green-up period with Himawari, but ~12 days with VIIRS. In other words, the number of days with cloud-free observations could double with Himawari data compared to VIIRS data. These results indicate the potential of Himawari data for providing higher temporal resolution NDVI time series data and, thus, improved monitoring and characterization of vegetation dynamics in Japan compared to the current polar-orbiting satellite data. One potential drawback would be the fixed view zenith and azimuth angles which might become problematic when one is interested in analyzing vegetation dynamics across space. Validation of Himawari-observed NDVI temporal profiles with ground observational NDVI and carbon flux data will be one required step.

Keywords: Himawari, geostationary satellite, vegetation phenology, land surface phenology, NDVI

©2019. Japan Geoscience Union. All Right Reserved.

Carbon and Water Fluxes at High spatial Resolutions through Down-Scaling

*Jiquan Chen[1], Pietro Sciusco[1], Ranjeet John[1], Zutao Ouyang[1]

1. Michigan State University

We propose an innovative top-down modeling approach to estimate high resolution (30 m) net primary production (NPP), evapotranspiration (ET) and *albedo* from MODIS products by integrating accurately classified land cover from Landsat/Sentinel and MODIS. Assuming that a measure of ecosystem ET in a landscape is a linear sum of ET of cover type (i), MODIS ET of a pixel can be expressed as:

$ET = sum(a_i * ET_i) + e$ [1]

where a_i is the compositional portion of cover type i within a MODIS pixel (where $sum(\alpha_i) = 1$) that can be calculated from classified land cover for the year; ET_i is the ET value of cover type i and can be estimated through multi-linear regression analysis with a zero intercept; and e is the residuals from the empirical model [1] and will be further examined for the potential influences of biophysical and socioeconomic driving forces. MODIS products of NPP, ET, and *albedo* of a landscape are estimated for their monthly and annual values by assuming that land cover during an individual year remains unchanged. This downscaling approach, currently tested for the Kalamazoo watershed in the southwestern Michigan, is only valid at a scale where similar climate, soil, and landforms exist (i.e. value of the same cover type in isolated patches are the same). To assure the validity of this approach, a multilinear regression analysis is performed with external factors such as soil type, climatic zone, and/or disturbance regime. Estimated ecosystem functions is then scaled up based on the 30 m resolution land cover of Landsat imagery for their high resolution spatiotemporal changes.

Keywords: carbon flux, down scaling, MODIS and Landsat

©2019. Japan Geoscience Union. All Right Reserved.

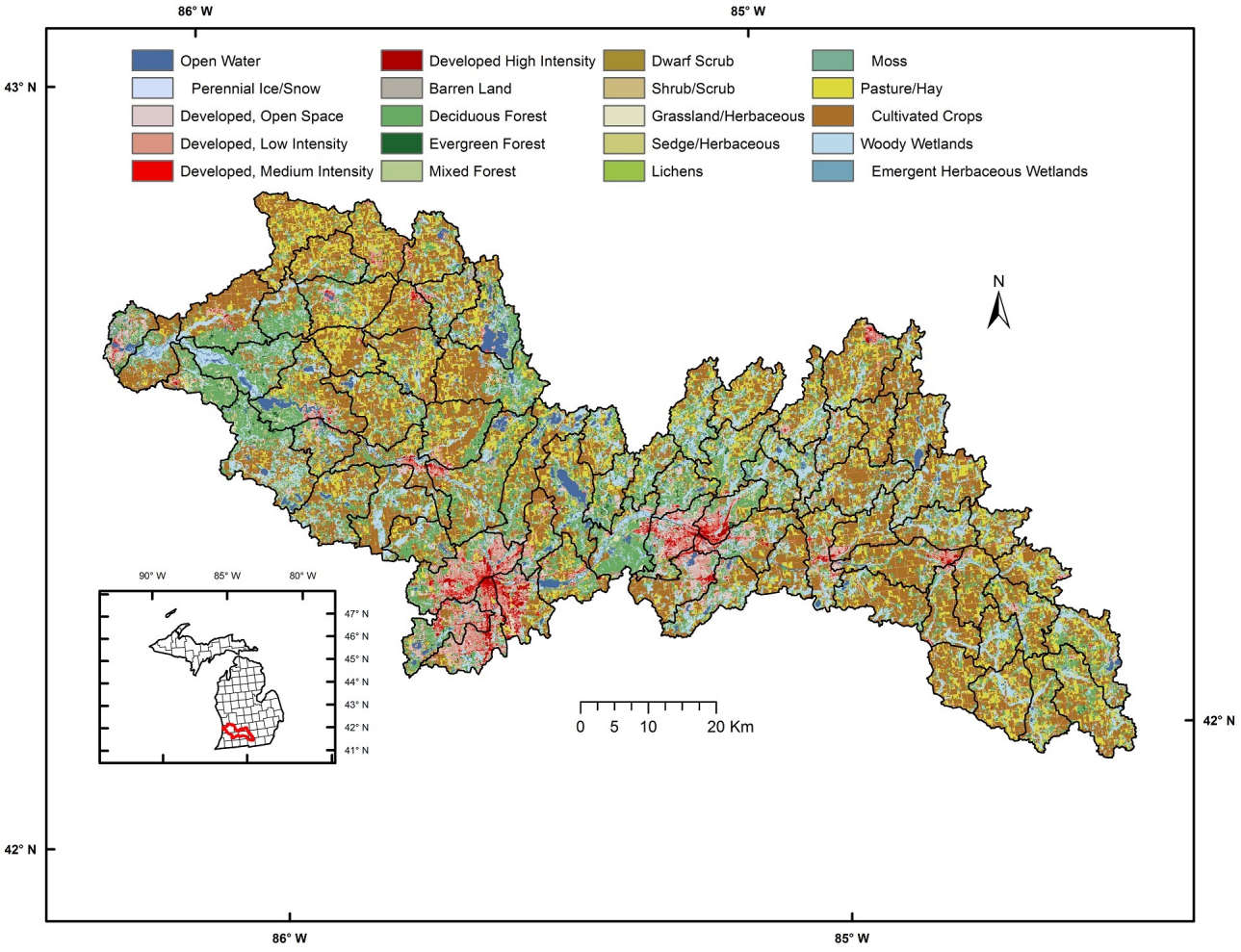

©2019. Japan Geoscience Union. All Right Reserved.

Connecting Satellite Based Spectral Modelling Approach and Forest Inventory to Model Biomass and Carbon Stocks in Natural and Planted Forest over part of Semi-arid zone, India

*SWATI UNIYAL[1], Siti Raju Rao

1. Andhra University

Forests have been recognized as having important mitigation potential because of their critical role in the global carbon cycle and significant potential to capture and hold carbon. Biomass is an important parameter to assess the atmospheric carbon that is harvested by trees.

This study describes an effort to estimate regional level Above Ground Biomass (AGB) and carbon from plot to point from multi-season MODIS data for a part of semi-arid zone i.e. Madhya Pradesh state by establishing a correlation with field observed data. Using clustered sampling approach a total number of 1200 plots were laid on ground for natural forests and planted forests/tress. Stand biomass for each plot was computed from ground inventory using diameter, height, generalized species and interspecies allometric equations.

Spectral modelling was done with red, infra-red and NDVI of different seasons with observed AGB using statistical functions like linear, logarithmic, power and exponential. Various linear and multiple regression models were tested among all seasons and bands, and the best fit model from those was used for predicting biomass and carbon at regional level.

Red band and NDVI spectral reflectance combined with logarithmic function in multiple regression was found to be the best model (r^2=0.5784) for model Y= a +b1* ln (NDVI) + b2 *1/x*(Red) +b3 *sqrt (NDVI) for predicting biomass and Carbon. Predicted biomass value is in the range of 0-134.836t/ha, while total biomass of the area is 5950Tg. Similarly Predicted Carbon content is in the range of 0-64.04tC/ha and total carbon content in the range of 2690TgC.

Results were validated using 50 random points. The observed ABG of these 50 points validated with predicted AGB, a correlation R^2= 0.6003 was obtained indicating biomass and carbon obtained through spectral modelling has given good estimation at regional level.

Comparing biomass and carbon value for natural forest and plantation study explicitly noted that planted forest/trees sequester more carbon because results from a combination of site factors and adaptation of good silvicultural practices, while for natural forest wide variation in stand structure, tree growth, different stages of forest growth cycle, and varying tree density resulted in lower carbon content.

Keywords: Biomass, Spectral Modelling, Carbon Cycle, MODIS

©2019. Japan Geoscience Union. All Right Reserved.

Allocation of forest net primary production varies by forest age and air temperature

*Xiang Song[1], Xiaodong Zeng[1], Dongxiao Tian[2]

1. IAP, CAS, 2. Beijing Meteorological Information Center

Carbon partition among plant parts has a vital influence not only on the growth of individual plants but also on decomposition, carbon and nitrogen sequestration, and plant-atmosphere water exchange. Although many studies have tried to reveal plant growth mechanisms using observational living biomass or the biomass ratio among different organs, knowledge and understanding about carbon partition is still scarce and exists much uncertainty. In this work, a dataset from the Chinese Ecosystem Research Network (CERN) was used to explore the dependences of net primary production (NPP) partition among foliage, stem and branch, and root on forest age, and mean annual temperature (MAT). The results found that (1) younger plants usually allocated a higher proportion of the NPP to stems, branches, and roots; (2) MAT was negatively correlated with the proportions of the NPP allocated to foliage (F_{leaf}; %) and roots (F_{root}; %), while proportions of the NPP allocated to stems and branches (F_{stbr}; %) were positively dependent on MAT; (3) forest age had a larger direct influence on F_{leaf} and F_{root}, while MAT was relatively important for F_{stbr}. This work not only is important for understanding the contribution of climatic factor and forest age on forest NPP partition, but also provides valuable ideas for developing ecological models.

Keywords: net primary production partition, forest age, climate, China’s forest

©2019. Japan Geoscience Union. All Right Reserved.

Analyzing Model Biases in Terrestrial Carbon Cycle Submodels in Earth System Models and Offline Models

*Kazuhito Ichii[1], Kazutaka Murakami[2], Hiroaki Takayama[3], Tomohiro Hajima[3], Kaoru Tachiiri[3]

1. Chiba University, 2. National Institute for Environmental Studies, 3. Japan Agency for Marine-Earth Science and Technology

Improvement of terrestrial models in earth system models (ESMs) is important to reduce uncertainties in future projections of global carbon cycle and climate. Toward an improvement of ESMs, we need to evaluate current performance of terrestrial components in current ESMs and analyze their causes of biases. Therefore, using available observation based products (e.g. satellite-based products), offline ecosystem model outputs, and CMIP-5 ESM outputs, we attempted to characterize causes of biases of modeled terrestrial carbon flux and pools. We found that key climate variables, such as precipitation, is one of the causes of biases in ESM-based carbon fluxes. For example, positive precipitation biases in Africa and Oceania results in positive biases of gross primary productivity (GPP), biomass, and net biome productivity (NBP). Negative precipitation bias in tropical South America leads to negative GPP, biomass and NBP biases. Therefore, improvement of spatial patterns are one of the important next step toward ESM, in particular toward realistic simulations of sub-continental scale terrestrial variations.

Keywords: Terrestrial Carbon Cycle, Remote Sensing, Model, Data-driven estimation

©2019. Japan Geoscience Union. All Right Reserved.

Assessing terrestrial biogeochemical feedbacks in a strategically geoengineered climate

*Forrest M. Hoffman[1,2], Cheng-En Yang[2,1], Joshua S. Fu[2,1], Simone Tilmes[3], Lili Xia[4], Douglas G. MacMartin[5], Jadwiga H. Richter[3], Michael Mills[3], Ben Kravitz[6]

1. Oak Ridge National Laboratory, 2. University of Tennessee, 3. National Center for Atmospheric Research, 4. Rutgers University, 5. Cornell University, 6. Pacific Northwest National Laboratory

Stratospheric geoengineering by injecting sulfur dioxide into the lower stratosphere has been suggested as a possible means of reducing anthropogenic warming. While the impacts of stratospheric aerosol geoengineering on climate change have been investigated in the past few decades, only a few studies have considered the terrestrial biogeochemical feedbacks resulting from such treatment. These feedbacks can alter the atmospheric carbon dioxide concentration by storing or releasing additional carbon in terrestrial and marine ecosystems, thus, changing the climate trajectory and aerosol injection strategy for geoengineering. In this study, we analyzed model output from the recent Stratospheric Aerosol Geoengineering Large Ensemble project to assess the changes in terrestrial biogeochemical feedbacks on climate, particularly the carbon sink strength (CSS), in response to stratospheric aerosol geoengineering. Our results showed that the terrestrial CSS increased globally by 5.2 Pg C during 2070–2089 compared to that during the first twenty years of geoengineering starting from 2020, *i.e.*, an additional 11 ppm CO_2 -equivalent amount of carbon in the atmosphere would be stored on land. Among seven latitude bands, the midlatitudes in the Northern Hemisphere (35˚N–60˚N) had the largest CSS increase (+8.0 Pg C) whereas the Tropics (23.5˚S–23.5˚N) released carbon back to the atmosphere (–2.9 Pg C). Hypotheses regarding the causes of the variations in the differences in regional responses will be presented.

Keywords: geoengineering, biogeochemistry-Earth system interactions, carbon sink strength

©2019. Japan Geoscience Union. All Right Reserved.

[J] Oral | A (Atmospheric and Hydrospheric Sciences)：A-CG Complex & General

Tue. May 28, 2019 9:00 AM - 10:30 AM JST | Tue. May 28, 2019 12:00 AM - 1:30 AM UTC | 104 1F

[A-CG38] Multi-scale ocean-atmosphere interaction in the tropical Indo-Pacific region

convener:Ayako Seiki(Japan Agency for Marine-Earth Science and Technology), Tomoki Tozuka(Department of Earth and Planetary Science, Graduate School of Science, The University of Tokyo), Motoki Nagura(Japan Agency for Marine-Earth Science and Technology), Youichi Kamae(Faculty of Life and Environmental Sciences, University of Tsukuba), Chairperson:Ayako Seiki(Japan Agency for Marine-Earth Science and Technology), Motoki Nagura(Japan Agency for Marine-Earth Science and Technology)

Multi-scale ocean-atmosphere interaction in the tropics exerts a significant imprint on the global climate via atmospheric teleconnection. Since the 1980s, anchored by in-situ and satellite observations, improvements in modeling and theoretical understanding, various aspects of dominant modes of interannual (e.g., ENSO and IOD), intraseasonal (e.g., MJO) variabilities and their impacts on tropical (e.g., monsoons) and extra-tropical (e.g., North America) climate variations have received wide attention. Recent satellite-based salinity measurements indicate for an active role of salinity in the tropical ocean-atmosphere interaction. While recent studies suggest a possible link between interdecadal Pacific oscillation and global warming hiatus in 2000s, changes (if any) in the tropical ocean-atmosphere interaction are yet to be understood. Due to interactions between different time scales, between different ocean basins, and with the extratropics, the tropical ocean and atmosphere play a key role in shaping climate, its variability and change. To better understand and examine these challenging issues from various perspectives, this session offers a forum to discuss recent progress in observational, modeling and theoretical studies of multi-scale tropical ocean-atmosphere interaction.

9:00 AM - 9:15 AM JST | 12:00 AM - 12:15 AM UTC

[ACG38-01] Various aspects of climate system variability associated with ENSO

★Invited Papers

*Shuhei Maeda[1] (1.Climate Prediction Division, Japan Meteorological Agency)

9:15 AM - 9:30 AM JST | 12:15 AM - 12:30 AM UTC

[ACG38-02] Influence and mechanism of the tropical Pacific variability on the Arctic and its seasonality

*Tsubasa Takigawa[1], Yu Kosaka[1], Bunmei Taguchi[1], Lea Svendsen[2] (1.Research Center for Advanced Science and Technology, University of Tokyo, 2.Bjerknes Centre for Climate Research, University of Bergen)

9:30 AM - 9:45 AM JST | 12:30 AM - 12:45 AM UTC

[ACG38-03] Subsurface nonlinear dynamical heating and ENSO asymmetry in CMIP5: Implications for anthropogenic tropical-warming uncertainties

★Invited Papers

*Michiya Hayashi[1], Fei-Fei Jin[1] (1.Department of Atmospheric Sciences, University of Hawaii at Manoa)

9:45 AM - 10:00 AM JST | 12:45 AM - 1:00 AM UTC

[ACG38-04] **Uncertainty in the projections of ENSO amplitude change under global warming: Role of the response of atmospheric circulation to SST anomalies**

*Jun Ying[1] (1.Second institute of Oceanography, Ministry of Natural Resources)

10:00 AM - 10:15 AM JST | 1:00 AM - 1:15 AM UTC

[ACG38-05] Impact of atmospheric variability on Indian Ocean Dipole mode

*Yuya Baba[1] (1.JAMSTEC Japan Agency for Marine-Earth Science and Technology)

10:15 AM - 10:30 AM JST | 1:15 AM - 1:30 AM UTC

[ACG38-06] Do salinity anomalies matter for the evolution of the IOD? –Experimental assessments using a regional ocean model-

*Shoichiro Kido[1], Tomoki Tozuka[1], Weiqing Han[2] (1.Graduate School of Science, The University of Tokyo, 2.Department of Atmospheric and Oceanic Sciences, University of Colorado Boulder)

Various aspects of climate system variability associated with ENSO

*Shuhei Maeda[1]

1. Climate Prediction Division, Japan Meteorological Agency

The El Niño-Southern Oscillation (ENSO) is the most dominant interannual climate variability in the Earth’ s climate system, and its pattern is characterized as zonal east-west see-saw of oceanic and atmospheric conditions in the tropical Pacific, and their associated teleconnections in the atmosphere to the extra-tropics. In addition, various aspects of climate system variability associated with ENSO are observed. For example, (1)vertical distribution of sea sub-surface temperature, (2)global average temperature, (3)energy budget at the top of atmosphere, (4)available potential energy in the atmosphere, (5)atmospheric meridional circulation such as Hadley and Ferrel circulations, (6) sub-tropical jet streams, (7)wave activities in the extra-tropics, and (8) polar vortex. In the presentation, I will review these aspects of climate system variability associated with ENSO, and discuss related mechanisms.

Keywords: ENSO, meridional circulation, polar vortex

©2019. Japan Geoscience Union. All Right Reserved.

Influence and mechanism of the tropical Pacific variability on the Arctic and its seasonality

*Tsubasa Takigawa[1], Yu Kosaka[1], Bunmei Taguchi[1], Lea Svendsen[2]

1. Research Center for Advanced Science and Technology, University of Tokyo, 2. Bjerknes Centre for Climate Research, University of Bergen

Arctic temperature has increased about twice as fast as global mean surface temperature in recent decades. While anthropogenic influence on this Arctic warming is evident, potential contributions from internal climate variability remains to be examined. Svendsen et al. (2018) showed that Pacific decadal variability played a key role in the early twentieth century Arctic warming through a coupled model pacemaker experiments with historical forcing. It is still unclear, however, how much influence the Pacific internal variability induces on the Arctic and how this remote influence is conveyed.
This study investigates the relationship between Arctic climate and tropical Pacific variability (TPV) by using a pre-industrial control experiment with GFDL CM2.1, with the primary aim to quantify the effect of TPV in different timescales. The result shows that the surface temperature response at high latitudes is amplified at multi-decadal timescales compared to sub-decadal one. The Arctic temperature anomalies peak near surface and diminishes with height. Moreover, Arctic temperature and sea ice responses feature strong seasonality with peak in late winter, despite weak seasonality of the tropical SST anomalies associated with decadal TPV. These features bear similarity to radiatively induced Arctic warming, and suggest importance of local feedbacks in Arctic climate variability driven remotely by the TPV.

Keywords: ENSO, Inter-decadal Pacific Oscillation, Teleconnection

©2019. Japan Geoscience Union. All Right Reserved.

Subsurface nonlinear dynamical heating and ENSO asymmetry in CMIP5: Implications for anthropogenic tropical-warming uncertainties

*Michiya Hayashi[1], Fei-Fei Jin[1]

1. Department of Atmospheric Sciences, University of Hawaii at Manoa

El Niño-Southern Oscillation (ENSO) is a dominant interannual tropical variability, playing a key role in worldwide climate. Most climate models participating in CMIP5 (Coupled Model Intercomparison Project phase 5) can produce ENSO amplitude close to observations, but the asymmetry between its warm and cold phases is still poorly simulated in general. Here, using 25 CMIP5 historical simulations and multiple ocean reanalysis datasets, it is shown that the model-to-model diversity of ENSO asymmetry is mostly explained by the representation of nonlinear dynamical heating (NDH) in the subsurface ocean along the equatorial Pacific thermocline. The skewness of sea-surface temperature (SST) anomalies in the Niño-3 region linearly increases with respect to the variability of the subsurface NDH among the CMIP5 models (correlation of 0.8). The NDH variability in most CMIP5 models is under-simulated due to weak Equatorial Undercurrent variability.

Using a small subset of the models having the NDH variability greater than the CMIP5 average, the influence of ENSO amplitude change in CMIP5 anthropogenic warming scenarios is further assessed. The future change in ENSO amplitude still shows a large spread even within this subset. Nevertheless, the long-term change in climatological NDH mean follows the ENSO amplitude change, which is absent in the rest of the CMIP5 models having weak NDH variability. Hence, increasing the rectification effect of the subsurface NDH that deepens the mean-state thermocline to warm the SST can enhance the so-called "El Niño-like" global-warming pattern that exhibits the faster eastern-Pacific surface warming. In contrast, suppressing the subsurface rectification effect can cause a more "La Niña-like" warming pattern. These results suggest that properly simulating ENSO asymmetry and subsurface NDH in climate models is critical on projecting future climate.

Keywords: El Niño-Southern Oscillation, anthropogenic global warming, CMIP5 climate model

©2019. Japan Geoscience Union. All Right Reserved.

Uncertainty in the projections of ENSO amplitude change under global warming: Role of the response of atmospheric circulation to SST anomalies

*Jun Ying[1]

1. Second institute of Oceanography, Ministry of Natural Resources

The study investigates the mechanism of the large inter-model uncertainty in the change of ENSO’s amplitude under global warming, based on 31 CMIP5 models. We find that the uncertainty in ENSO’s amplitude is significantly correlated to that of the change in the response of atmospheric circulation to SST anomalies (SSTAs) in the eastern equatorial Pacific Niño3 region. This effect of the atmospheric response to SSTAs mainly influences the uncertainty in ENSO’s amplitude during El Niño (EN) phases, but not during La Niña (LN) phases, showing pronounced nonlinearity. The effect of the relative SST warming and the present-day response of atmospheric circulation to SSTAs are the two major contributors to the inter-model spread of the change in the atmospheric response to SSTAs, of which the latter is more important. On the one hand, models with a stronger (weaker) mean-state SST warming in the eastern equatorial Pacific, relative to the tropical-mean warming, favor a larger (smaller) increase in the change in the response of atmospheric circulation to SSTAs in the eastern equatorial Pacific during EN. On the other hand, models with a weaker (stronger) present-day response of atmospheric circulation to SSTAs during EN tend to exhibit a larger (smaller) increase in the change under global warming. The result implies that an improved simulation of the present-day response of atmospheric circulation to SSTAs will be effective in lowering the uncertainty in ENSO’s amplitude change under global warming.

Keywords: ENSO amplitude , Global warming, Uncertainty, relative SST warming

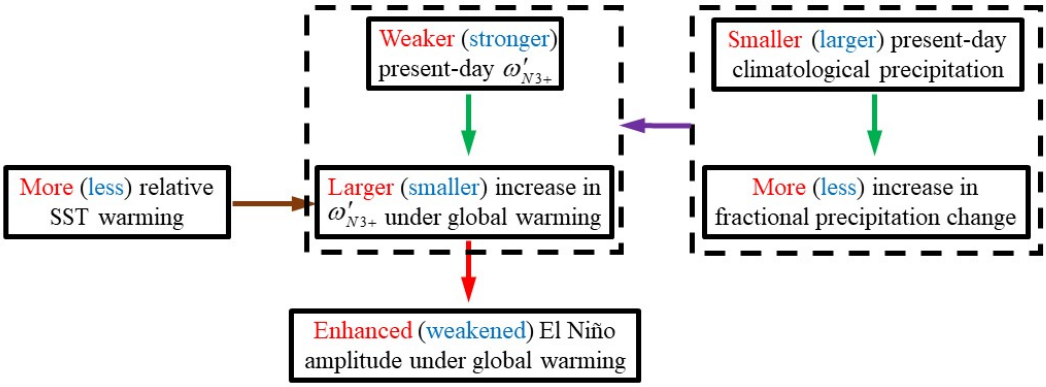

©2019. Japan Geoscience Union. All Right Reserved.

Impact of atmospheric variability on Indian Ocean Dipole mode

*Yuya Baba[1]

1. JAMSTEC Japan Agency for Marine-Earth Science and Technology

Some preceding studies investigated tropical atmospheric internal variability such as Madden-Julian oscillation on the formation of Indian Ocean Dipole mode (IOD), but still number of the studies remains few, and their relationship remains unknown. In this study, we focused on the impact of atmospheric variability especially intraseasonal variability. To reveal the impact, we conducted sensitivity experiments for the IOD during 1980-2009, using an ocean general circulation model and difference atmospheric forcing data, such as (1) climatological forcing, (2) same as (1) but with yearly anomalies, (3) same as (1) but with seasonal anomalies, (4) same as (1) but with monthly anomalies, (5) 90-day low-pass filtered forcing. The simulated Dipole mode index (DMI) indicates that the sensitivity case of (1) could not reproduced realistic DMI at all, (2) and (3) reproduced decreased DMI amplitudes, and (4) and (5) reproduced similar DMI which was simulated with daily forcing data. In this presentation, possible mechanisms that caused different features of simulated IODs will be explained, focusing on the relationship between the variabilities of ocean and atmosphere.

Keywords: Indian Ocean Dipole mode, atmospheric internal variability

©2019. Japan Geoscience Union. All Right Reserved.

Do salinity anomalies matter for the evolution of the IOD? –Experimental assessments using a regional ocean model-

*Shoichiro Kido[1], Tomoki Tozuka[1], Weiqing Han[2]

1. Graduate School of Science, The University of Tokyo, 2. Department of Atmospheric and Oceanic Sciences, University of Colorado Boulder

The Indian Ocean Dipole (IOD), which is a dominant climate mode in the tropical Indian Ocean, is accompanied by significant surface and subsurface salinity anomalies. These salinity anomalies alter density field and stratification in the upper ocean, and thereby have potentials to affect the evolution of the IOD itself. Though many previous studies have attempted to estimate the impacts of the IOD-related salinity anomalies, no comprehensive assessments have been conducted. To this end, a series of sensitivity experiments using a regional ocean model is conducted with a novel experimental strategy. Results from these sensitivity experiments show that interannual salinity anomalies associated with the positive IOD tend to suppress the cooling in the eastern equatorial Indian Ocean by about 1.0˚C. Through an on-line heat budget analysis of each experiment, it is shown that weakening of the upwelling in the eastern Indian Ocean, which originates from the upward shift of the Equatorial Undercurrent, is the primary cause of the suppressed cooling there. These changes are induced by enhanced stratification in the eastern equatorial Indian Ocean associated with negative (positive) salinity anomalies near the surface (pycnocline). Momentum budget analysis and additional sensitivity experiments using a linear continuously stratified ocean model further support these ideas. Therefore, salinity plays an active role in the evolution of the IOD, rather than being passively influenced by atmospheric anomalies.

Keywords: Indian Ocean Dipole, Salinity anomaly, Regional ocean model

©2019. Japan Geoscience Union. All Right Reserved.

[J] Oral | A (Atmospheric and Hydrospheric Sciences)：A-CG Complex & General

Tue. May 28, 2019 10:45 AM - 12:15 PM JST | Tue. May 28, 2019 1:45 AM - 3:15 AM UTC | 104 1F

[A-CG38] Multi-scale ocean-atmosphere interaction in the tropical Indo-Pacific region

convener:Ayako Seiki(Japan Agency for Marine-Earth Science and Technology), Tomoki Tozuka(Department of Earth and Planetary Science, Graduate School of Science, The University of Tokyo), Motoki Nagura(Japan Agency for Marine-Earth Science and Technology), Youichi Kamae(Faculty of Life and Environmental Sciences, University of Tsukuba), Chairperson:Tomoki Tozuka(The University of Tokyo), Youichi Kamae(University of Tsukuba)

Multi-scale ocean-atmosphere interaction in the tropics exerts a significant imprint on the global climate via atmospheric teleconnection. Since the 1980s, anchored by in-situ and satellite observations, improvements in modeling and theoretical understanding, various aspects of dominant modes of interannual (e.g., ENSO and IOD), intraseasonal (e.g., MJO) variabilities and their impacts on tropical (e.g., monsoons) and extra-tropical (e.g., North America) climate variations have received wide attention. Recent satellite-based salinity measurements indicate for an active role of salinity in the tropical ocean-atmosphere interaction. While recent studies suggest a possible link between interdecadal Pacific oscillation and global warming hiatus in 2000s, changes (if any) in the tropical ocean-atmosphere interaction are yet to be understood. Due to interactions between different time scales, between different ocean basins, and with the extratropics, the tropical ocean and atmosphere play a key role in shaping climate, its variability and change. To better understand and examine these challenging issues from various perspectives, this session offers a forum to discuss recent progress in observational, modeling and theoretical studies of multi-scale tropical ocean-atmosphere interaction.

10:45 AM - 11:00 AM JST | 1:45 AM - 2:00 AM UTC

[ACG38-07] Mechanisms of future changes in equatorial upwelling: CMIP5 inter-model analysis

★Invited Papers

*Shoshiro Minobe[1,2], Mio Terada[2], Curtis Deutsch[3] (1.Earth and Planetary Sciences, Faculty of Science, Hokkaido University, 2.Graduate School of Science, Hokkaido University, 3.School of Oceanography, University of Washington)

11:00 AM - 11:15 AM JST | 2:00 AM - 2:15 AM UTC

[ACG38-08] The Indo-Pacific cross-basin interaction of the decadal climate variability under the progress of the global warming

*Yuma Miyaji[1], Youichi Tanimoto[2] (1.Hokkaido University, Graduate School of Environmental Science, 2.Hokkaido University, Faculty of Environmental Earth Science)

11:15 AM - 11:30 AM JST | 2:15 AM - 2:30 AM UTC

[ACG38-09] Air-sea flux observation by unmanned autonomous sea surface vehicle in the Tropics - Application of the Wave Glider -

★Invited Papers

*Iwao Ueki[1] (1.JAMSTEC Japan Agency for Marine-Earth Science and Technology)

11:30 AM - 11:45 AM JST | 2:30 AM - 2:45 AM UTC

[ACG38-10] Radar-derived Fresh water flux and its possible impact to the oceanic stratification observed during the Years of the Maritime Continent (YMC)

*Masaki Katsumata[1], Biao Geng[1], Satoru Yokoi[1], Shuichi Mori[1], Iwao Ueki[1] (1.Japan Agency for Marine-Earth Science and Technology)

11:45 AM - 12:00 PM JST | 2:45 AM - 3:00 AM UTC

[ACG38-11] Driving Mechanism of Inter-Annual Precipitation Variability during Monsoon Season over the Northern Part of Sumatra Island, Indonesia

*Yahya Darmawan[1,2,3], Huang-Hsiung Hsu[2] (1.Taiwan International Graduation Program, Academia Sinica, 2.Research Center for Environmental Changes, Academia Sinica, 3.Indonesian Agency for Meteorology, Climatology and Geophysics (BMKG))

12:00 PM - 12:15 PM JST | 3:00 AM - 3:15 AM UTC

[ACG38-12] The impact of diurnal precipitation over the maritime continent on synoptic disturbances and its relation to the MJO

*Ayako Seiki[1], Satoru Yokoi[1], Masaki Katsumata[1], Kunio Yoneyama[1] (1.Japan Agency for Marine-Earth Science and Technology)

Mechanisms of future changes in equatorial upwelling: CMIP5 inter-model analysis

*Shoshiro Minobe[1,2], Mio Terada[2], Curtis Deutsch[3]

1. Earth and Planetary Sciences, Faculty of Science, Hokkaido University, 2. Graduate School of Science, Hokkaido University, 3. School of Oceanography, University of Washington

The future change in equatorial upwelling is investigated for the Pacific and Atlantic Oceans using data from 24 Coupled *Model* Intercomparison Project Phase 5 (CMIP5) models for the Representative Concentration Pathway 8.5 scenario until 2100. Three-dimensional velocity components of CMIP5 multi-models are used for the first time in an upwelling study, and allow to divide upwelling velocities into diapycnal and isopycnal velocities. This analysis, combined with inter-model regression, revealed that both the multi-model ensemble (MME) mean and the inter-model variability in the upwelling change in the eastern equatorial Pacific, where strong upwelling change occurs, are explained by two mechanisms. One is that the diapycnal upwelling decreases near the surface, which is associated with a weakened Ekman divergence. The other is that the isopycnal upwelling decreases at depths of 75–200 m around the core of the equatorial undercurrent (EUC) due to EUC flattening. Both the weakened Ekman divergence and the EUC flattening are induced by the locally weakened trade wind over the eastern Pacific basin. In the equatorial Atlantic, both the change in MME mean and the inter-model variability of upwellings are significantly related to the weakened trade wind and enhanced stratification, although these drivers are not independent. The results for the Pacific Ocean imply that future reduction in upwelling may impact the sea surface temperature and marine ecosystem by different mechanisms. The rapid warming of sea surface temperature in the eastern Pacific basin may be related to the near-surface diapycnal upwelling reduction, while the decrease in net community production, which is often measured by marine export production at a depth of 100 m, may be related to the isopycnal upwelling reduction.

Keywords: global warming , variability and mean across multiple models , ocean dynamics

©2019. Japan Geoscience Union. All Right Reserved.

The Indo-Pacific cross-basin interaction of the decadal climate variability under the progress of the global warming

*Yuma Miyaji[1], Youichi Tanimoto[2]

1. Hokkaido University, Graduate School of Environmental Science, 2. Hokkaido University, Faculty of Environmental Earth Science

We investigate a relationship of the decadal sea surface temperature (SST) variability between over the Indian Ocean and over the tropical Pacific based on the observed data sets and the multi-model climate simulations. In the present study, by subtracting the multi-model ensemble mean rather than the observed linear trend, we attempt to retain the decadal signals without the effect of the radiative forcing, in the observed long-term records of the ocean and atmosphere.
While several observational studies indicated that the simultaneous correlation coefficient of the long-term SST variability over the two basins changed from positive before 1985 into negative after 1985, our analysis always shows the positive correlation regardless of the selected decades, indicating that the internal dynamics of the Indo-Pacific ocean-atmosphere system for this cross-basin interaction. While the decadal variations of the surface winds over the Indian Ocean are influenced by the SST variability over the tropical Pacific, the SST formation processes by those surface winds are different among the regions north and south of 10˚S, respectively. The effect of the climatological meridional gradient in the thermocline depth on the different formation processes is discussed.

Keywords: Air-sea interaction, cross-basin interaction, Decadal variability

©2019. Japan Geoscience Union. All Right Reserved.

Air-sea flux observation by unmanned autonomous sea surface vehicle in the Tropics - Application of the Wave Glider -

*Iwao Ueki[1]

1. JAMSTEC Japan Agency for Marine-Earth Science and Technology

Air-sea fluxes of heat and momentum are fundamental variables for the ocean and atmosphere interaction, which influence weather and climate. The air-sea flux measurements; actually measurements of air temperature, humidity, sea surface temperature, winds, and radiations, are mainly conducted by research vessels, mooring buoys, and satellites. Based on these measurements, many types of global air-sea flux products are produced. However, these products still remain large biases and uncertainties in the global fields. Reducing inaccuracies in air-sea fluxes is important for improving long-term weather and climate predictions. For that purpose, we should consider about intensification of *in situ* measurements, which contribute to improve bulk algorithms, to understand mechanisms of flux variability, and to validate the products as proposed in Community White Papers of air-sea fluxes with a focus on heat and momentum in OceanObs’19. Due to the relatively high cost of research vessel and mooring buoy operations, number of in situ measurements is limited. The sparsity of the *in situ* measurement in present situation is one of obstacles to improve satellite algorithm development and product validation. Because of recent progress of unmanned autonomous ocean surface vehicles (UAVs) development, we can use these vehicles as a platform for air-sea flux observation. In this study, several field tests and evaluations of the acquired data through comparison with mooring buoys have been conducted especially in the tropical region. The present status of these activities will be introduced in the presentation.

Keywords: Air-sea flux, unmanned autonomous vehicle, Wave Glider

©2019. Japan Geoscience Union. All Right Reserved.

Radar-derived Fresh water flux and its possible impact to the oceanic stratification observed during the Years of the Maritime Continent (YMC)

*Masaki Katsumata[1], Biao Geng[1], Satoru Yokoi[1], Shuichi Mori[1], Iwao Ueki[1]

1. Japan Agency for Marine-Earth Science and Technology

To investigate the air-land-sea interaction in the Maritime Continent (the world's largest archipelago bridging tropical Indian Ocean and tropical western Pacific), a series of the field campaign “YMC-Sumatra” was conducted as part of the project "Years of the Maritime Continent (YMC)". In “YMC-Sumatra 2017”, we deploy the research vessel "Mirai" at one station near the west coast of Sumatra Island to obtain time series.

The continuous dataset from C-band polarimetric radar is converted to the rainrate (i.e. fresh water flux) by utilizing the data from disdrometers and raingauges. The estimated fresh water flux is compared to the oceanic near-surface stratifications measured by the unmanned surface vehicle “wave glider”. The observed salinity at 0.2m and 6m depths differ under a precipitating event with weak wind (< 5 m/s). The event was followed by the strong wind (>10 m/s) precipitation. After the event, low salinity layer was captured down to 30~40 m depth for more than half days.

Keywords: fresh water flux, oceanic near-surface stratification, YMC (Years of the Maritime Continent)

©2019. Japan Geoscience Union. All Right Reserved.

Driving Mechanism of Inter-Annual Precipitation Variability during Monsoon Season over the Northern Part of Sumatra Island, Indonesia

*Yahya Darmawan[1,2,3], Huang-Hsiung Hsu[2]

1. Taiwan International Graduation Program, Academia Sinica, 2. Research Center for Environmental Changes, Academia Sinica, 3. Indonesian Agency for Meteorology, Climatology and Geophysics (BMKG)

The precipitation variability of the Northern part of Sumatra Island in Indonesia has been driven by the complex tropical climate systems along with the local factors. The aim of this study is to investigate the driving mechanism of precipitation variability during the JJA-periods (June, July, and August) over the northern part of Sumatra. Moist Static Energy (MSE) budget analysis was used to model the source of energy which supports the precipitation anomalies. Composite analysis and statistical methods were used for confirming the result of MSE budget. By using 36 years of ERA-interim data, precipitation anomalies of JJA periods were classified into two categories, namely: wet years and dry years. Positive precipitation anomalies are found during the wet years which are supported by the upward motion of vertical velocity. During the wet years, the weaker easterly wind of Indian Summer Monsoon (ISM) associated with the westerly winds of a negative El Niño–Southern Oscillation (ENSO), a positive Indian Ocean Dipole (IOD), and a strong Western North Pacific Subtropical High (WNPSH). As a consequence, these anomalous circulations trigger a moisture flux convergence and positive precipitation anomaly. In the dry years, the downward of vertical velocity leads to negative precipitation anomaly. Generally, a stronger easterly wind of ISM was found during the dry years which is associated with a positive ENSO, a negative IOD, and a weak WNPSH. Even though the precipitation anomalies occur due to the collaboration of those winds, a new finding shows that WNSPH has a stronger impact to the precipitation anomalies than ENSO and IOD in the Northern part of Sumatra Island. In addition to those circulations, higher topography of the Barisan Mountains supports the ascending motion to moisten the lower troposphere and induces a positive precipitation anomaly in this maritime continent.

Keywords: Precipitation, MSE, ENSO, IOD, ISM, Sumatra Island

©2019. Japan Geoscience Union. All Right Reserved.

The impact of diurnal precipitation over the maritime continent on synoptic disturbances and its relation to the MJO

*Ayako Seiki[1], Satoru Yokoi[1], Masaki Katsumata[1], Kunio Yoneyama[1]

1. Japan Agency for Marine-Earth Science and Technology

Diurnal cycle has been known to contribute to a significant amount of precipitation over the maritime continent. In this study, the impact of diurnal precipitation over Sumatra Island, the Indonesian maritime continent, on synoptic disturbances over the surrounding ocean, especially the eastern Indian Ocean, is examined using the Global Satellite Mapping of Precipitation (GSMaP) data. High precipitation area observed over Sumatra in afternoon migrates offshore during night-time and reaches 500 km off the coast in average. Synoptic disturbances represented by eddy kinetic energy are enhanced south of the equator off Sumatra when the diurnal precipitation is strong, then they migrate poleward with cyclonic structures over the eastern Indian Ocean. These results suggest that the diurnal precipitation over Sumatra can excite synoptic disturbances over the eastern Indian Ocean.

Keywords: diurnal precipitation, the maritime continent, synoptic disturbances

©2019. Japan Geoscience Union. All Right Reserved.

[J] Poster | A (Atmospheric and Hydrospheric Sciences)：A-CG Complex & General

Tue. May 28, 2019 3:30 PM - 5:00 PM JST | Tue. May 28, 2019 6:30 AM - 8:00 AM UTC | Poster Hall International Exhibition Hall8, Makuhari Messe_9

[A-CG38] Multi-scale ocean-atmosphere interaction in the tropical Indo-Pacific region

convener:Ayako Seiki(Japan Agency for Marine-Earth Science and Technology), Tomoki Tozuka(Department of Earth and Planetary Science, Graduate School of Science, The University of Tokyo), Motoki Nagura(Japan Agency for Marine-Earth Science and Technology), Youichi Kamae(Faculty of Life and Environmental Sciences, University of Tsukuba)

Multi-scale ocean-atmosphere interaction in the tropics exerts a significant imprint on the global climate via atmospheric teleconnection. Since the 1980s, anchored by in-situ and satellite observations, improvements in modeling and theoretical understanding, various aspects of dominant modes of interannual (e.g., ENSO and IOD), intraseasonal (e.g., MJO) variabilities and their impacts on tropical (e.g., monsoons) and extra-tropical (e.g., North America) climate variations have received wide attention. Recent satellite-based salinity measurements indicate for an active role of salinity in the tropical ocean-atmosphere interaction. While recent studies suggest a possible link between interdecadal Pacific oscillation and global warming hiatus in 2000s, changes (if any) in the tropical ocean-atmosphere interaction are yet to be understood. Due to interactions between different time scales, between different ocean basins, and with the extratropics, the tropical ocean and atmosphere play a key role in shaping climate, its variability and change. To better understand and examine these challenging issues from various perspectives, this session offers a forum to discuss recent progress in observational, modeling and theoretical studies of multi-scale tropical ocean-atmosphere interaction.

[ACG38-P01] Impacts of seasonal transitions of ENSO on frequency of atmospheric rivers over East Asia

*Youichi Kamae[1], Moeka Naoi[2], Hiroaki Ueda[1] (1.Faculty of Life and Environmental Sciences, University of Tsukuba, 2.Graduate School of Life and Environmental Sciences, University of Tsukuba)

[ACG38-P02] Impact of tropical Pacific sea surface temperature on the regional heavy rainfall events in Japan

*Yukiko Imada[1], Hiroaki Kawase[1], Masahiro Watanabe[2], Izuru Takayabu[1] (1.Meteorological Research Institute, Japan Meteorological Agency, 2.Atmosphere and Ocean Research Institute, the University of Tokyo)

[ACG38-P03] The North Pacific pacemaker effect on historical ENSO and its mechanisms

*Yu Kosaka[1], Dillon J. Amaya[2], Wenyu Zhou[2], Yu Zhang[2], Shang-Ping Xie[2], Arthur J. Miller[2] (1.Research Center for Advanced Science and Technology, University of Tokyo, 2.Scripps Institution of Oceanography, University of California San Diego)

[ACG38-P04] **Detection of the dry intrusions from the mid-latitudes to the Equator and their association with MJO**

*Saki Yanagisawa[1], Akiyo Yatagai[1] (1.Hirosaki Univercity)

[ACG38-P05] **Relationship between oceanic and atmospheric variations in the Philippine Sea and modulation of El Nino events**

*Takuya Hasegawa[1], Akira Nagano[2], Iwao Ueki[2], Kentaro Ando[2] (1.Tohoku University, 2.JAMSTEC)

[ACG38-P06] Contribution of oceanic wave propagation from the tropical Pacific to asymmetry of the Ningaloo Nino/Nina

*Hidehiro Kusunoki[1], Shoichiro Kido[1], Tomoki Tozuka[1] (1.Department of Earth and Planetary Science, Graduate School of Science, The University of Tokyo)

[ACG38-P07] The life-cycle of annual waves in the Indian Ocean as identified by a seamless diagnosis for the energy flux

*Zimeng Li[1], Hidenori Aiki[2] (1.Graduate school of environmental studies, Nagoya university, 2.Institute for space-earth environmental research, Nagoya university)

Impacts of seasonal transitions of ENSO on frequency of atmospheric rivers over East Asia

*Youichi Kamae[1], Moeka Naoi[2], Hiroaki Ueda[1]

1. Faculty of Life and Environmental Sciences, University of Tsukuba, 2. Graduate School of Life and Environmental Sciences, University of Tsukuba

Narrow corridors of moisture transport bands over the middle latitudes called atmospheric rivers (ARs) are important phenomena for hydrological cycle and natural disasters. Landfalling ARs associated with extratropical cyclones bring huge amount of rainfall over western coasts of North America and Europe. Previous studies pointed out that large-scale anomalies in atmospheric circulation associated with El Niño-Southern Oscillation (ENSO) are important factors for interannual variability in frequency of wintertime ARs over western North America. Recently, Kamae et al. (2017) revealed that ARs were also frequently observed over East Asia, especially during boreal summer. They also pointed out that preceding winter's El Niño results in anomalously-enhanced AR activity over summertime East Asia with a half-year lag. After the wintertime El Niño development, delayed warming over the Indian Ocean produces an anomalous anticyclone over the western North Pacific and associated increase in summertime AR frequency over East Asia. However, possible impacts of ENSO transition from preceding winter to concurrent summer on summertime AR activity over East Asia are still unclear. Here we extend our understanding on seasonal ENSO-AR relationship by compositing individual ENSO transition cases from winter to summer including rapid transitions from El Niño to La Niña. The rapid transition results in an anomalous AR activity over East Asia associated with the anomalous anticyclone over the western North Pacific. The anomalous anticyclone shifts northward compared to those found in years with sustained El Niño or decayed El Niño. We also found that the impacts of ENSO transition on ARs can be understood as a result of summertime teleconnection from the tropics favored by anomalous convective heating over the tropics associated with anomalous Walker circulation over the equatorial Pacific.

Keywords: ENSO, Atmospheric river, North Pacific High, Indian Ocean capacitor effect

©2019. Japan Geoscience Union. All Right Reserved.

Impact of tropical Pacific sea surface temperature on the regional heavy rainfall events in Japan

*Yukiko Imada[1], Hiroaki Kawase[1], Masahiro Watanabe[2], Izuru Takayabu[1]

1. Meteorological Research Institute, Japan Meteorological Agency, 2. Atmosphere and Ocean Research Institute, the University of Tokyo

To detect the impact of global-scale climate on regional extreme events is challenging especially for disastrous regional heavy rainfall events which are often strongly affected by local topography. Observed records are too short to obtain significant concurrent signals. General circulation models (GCMs) can represent background large-scale circulations causing regional heavy rainfall but cannot resolve the topography. On the other hand, high-resolution regional climate model can resolve orographic rainfall but cannot provide the information of key processes in larger-scale circulation. Here, we prepared a large-ensemble pair of GCM and nonhydrostatic regional model simulations covering 6800-year samples. It enables us to access local rainfall event directly and investigate cause-to-effect pathway to explain the impact of global scale climate. As an example, we cite 2-type heavy rainfall events around precipitous terrains in Japan: western Kyushu type and eastern Kyushu type. The western Kyushu type related to moisture transport is attributed to the development of the Pacific subtropical High which is often forced by an El Nino event during previous winter. On the other hand, the eastern Kyushu type is attributed to TC approach which correlates to the central Pacific El Ninos. Through this new flamework with large-ensemble pairs of global and regional simulations, we can verify various influence pathways of large-scale climate to specific regional extreme events.

Keywords: Heavy rainfall, Atomospheric general circulation model, Regional climate model

©2019. Japan Geoscience Union. All Right Reserved.

The North Pacific pacemaker effect on historical ENSO and its mechanisms

*Yu Kosaka[1], Dillon J. Amaya[2], Wenyu Zhou[2], Yu Zhang[2], Shang-Ping Xie[2], Arthur J. Miller[2]

1. Research Center for Advanced Science and Technology, University of Tokyo, 2. Scripps Institution of Oceanography, University of California San Diego

Recent studies have indicated that North Pacific sea surface temperature (SST) variability can significantly modulate the evolution of the El Niño-Southern Oscillation (ENSO), but there has been little effort to put these extratropical-tropical interactions into the context of historical ENSO events. To quantify the role of the North Pacific in pacing the timing and magnitude of observed ENSO events, we use a fully-coupled climate model to produce the first ensemble of North Pacific Ocean-Global Atmosphere (nPOGA) SST pacemaker simulations. In nPOGA, SST anomalies in the North Pacific (>15˚N) are restored back to observations, but are free to evolve throughout the rest of the globe. We find that North Pacific SST variability has significantly influenced the observed trajectory of historical ENSO, accounting for approximately 15% of the total variance in boreal fall and winter. The interaction between the North and tropical Pacific is the result of two physical pathways: 1. A Wind-Evaporation-SST propagating mechanism in boreal spring, and 2. A convective response associated with the Seasonal Footprinting Mechanism in boreal fall. The latter accounts for 25% of the observed zonal wind variability around the equatorial dateline. On an event-by-event basis, nPOGA most closely reproduces the 2014-2015 and the 2015-2016 El Niño events. In particular, we show that the 2015 Pacific Meridional Mode event increased wind forcing along the equator by 20%, potentially contributing to the extreme nature of the 2015-2016 El Niño. Our results illustrate the significant role of extratropical noise in pacing the initiation and magnitude of ENSO events and may improve the predictability of ENSO on seasonal timescales.

Keywords: Pacific Meridional Mode, ENSO, Pacemaker experiment

©2019. Japan Geoscience Union. All Right Reserved.

Detection of the dry intrusions from the mid-latitudes to the Equator and their association with MJO

*Saki Yanagisawa[1], Akiyo Yatagai[1]

1. Hirosaki Univercity

Dry intrusion is a large-scale intrusion phenomenon of extremely dry air into tropics and it influences on the cumulus convection. However, their large-scale features and statistics have not been revealed yet. The purposes of this study are detecting the dry intrusions using a long-term reanalysis data (the ERA-Interim, 0.75˚ grid) and clarifying relationship between the appearance of the dry intrusions and the Madden-Julian Oscillation (MJO) activity.
First, we drew daily map of precipitable water (PW) from the ERA-interim for the year from 1998 to 2016 (total 10593 days), and we counted the appearance at every 20˚ longitudes according to the following conditions; 1) the dry intrusion arrives at 10˚S-10˚N and is maintained for 2-10 days, 2) It forms a crescent shape with an area that PW of less than 40 mm, 3) It includes areas with a PW of less than 30 mm and 4) The entire dry intrusion fits into an area of roughly 2000 km^2.
Among the 10593 days, we detected 1118 cases in all so the dry intrusions appear about 40 times a year in average, and appearance in the Northern Hemisphere are less (388 cases), and more in the Southern Hemisphere (730 cases). About 90% of the dry intrusions were detected in an area from the Indian Ocean to the western tropical Pacific in both hemispheres. The appearance of the dry intrusions has seasonal dependence; a lot of the dry intrusions are in winter and few are in summer in both hemispheres. Sometimes the dry intrusions by above definitions were appeared in association with the strong tropical cyclones, and they reach 8% of the total number of appearances of the dry intrusions.
We composited 700 hPa and 850 hPa zonal wind when the dry intrusions were appeared around the Indian Ocean, the Maritime Continent and the western tropical Pacific, respectively. As a result, a strong westerly wind blew around an area where dry intrusions were appeared in the Indian Ocean and the western tropical Pacific. In the Maritime Continent, a strong westerly wind blew on the west side of the Maritime Continent. Such wind fields occurred also at the MJO activity and it is called the Westerly wind burst (WWB). The WWB blew over the western tropical Pacific when the dry intrusions occurred in the Maritime Continent and the western tropical Pacific. Therefore, it may be had an association between a convection activity by the MJO and dry air intrusion. Over an entire period, 25.2% of all the dry intrusions detected in the western tropical Pacific occurred when the MJO was active in there and 14.8% occurred in the same area but the MJO was not active. The remaining 60.0% occurred when the MJO was active or non-active in other areas. This percentage has become lower in cases of the dry intrusions occurred in the Indian Ocean and the Maritime Continent.

©2019. Japan Geoscience Union. All Right Reserved.

Relationship between oceanic and atmospheric variations in the Philippine Sea and modulation of El Nino events

*Takuya Hasegawa[1], Akira Nagano[2], Iwao Ueki[2], Kentaro Ando[2]

1. Tohoku University, 2. JAMSTEC

Western Pacific Oscillator model (WPO model), which is the one of the ENSO theory models, shows strong anti-cyclonic anomalies over the wetern tropical Pacific (around Philippine Sea) after a mature phase of El Nino. To check this point, time series of sea level pressure (SLP) anomalies averaged over the Philippine Sea for boreal-winter (i.e., January to March) is made. The result shows that eastern-Pacific (EP)-El Nino events (1982.83, 1986/87, 1991/92, 1997/98) show strong positive SLP anomalies in line with the WPO model. On the other hand, central-Pacific (CP)-El Nino events (1994/95, 2002/03, 2004/05, 2006/07, 2009/10) show weak SLP anomalies. Next, composite maps for SLP and sea surface winds during boreal-winter in the year of occurrence of EP-El Nino and CP-El Nino are made, respectively. It is shown that positive SLP anomalies and related anti-cyclonic sea surface wind pattern appear over the Philippine Sea for EP-El Nino. In the south part of the Philippine Sea, easterly anomaly winds appear and it can lead poleward Ekman transport that decreases warm water volume in the western equatorial Pacific. This situation is consistent with that expected from the WPO model, that is, the equatorial cold Kelvin waves can be generated, and then will terminate the on-going El Nino event to start the next La Nina event. Analysis on the sea surface height anomalies also shows negative sea surface height anomalies in the western equatorial Pacific at that time. In contrast to the EP-El Nino, CP-El Nino does not show such patterns of SLP, sea surface wind, and sea surface height anomalies. Therefore, it can be said that WPO model does not well act after mature phase of CP-El Nino, while the model does well after mature phase of EP-El Nino.

Acknowledgment: This work was partly supported by the Japan Society for the Promotion of Science (JSPS), Grant-in-Aid for Scientific Research (17K05660).

Keywords: El Nino, Philippine Sea, western Pacific Oscillator model

©2019. Japan Geoscience Union. All Right Reserved.

Contribution of oceanic wave propagation from the tropical Pacific to asymmetry of the Ningaloo Nino/Nina

*Hidehiro Kusunoki[1], Shoichiro Kido[1], Tomoki Tozuka[1]

1. Department of Earth and Planetary Science, Graduate School of Science, The University of Tokyo

Ningaloo Nino (Nina) is a climate mode associated with anomalously warm (cool) sea surface temperature (SST) off the Western Australian coast. Considering its large impacts on the local marine ecosystem and precipitation, better understanding of its mechanism and predictability is desirable. Existing studies suggest that both local air-sea interaction and remote forcing contribute to generation and amplification of the Ningaloo Nino/Nina. The latter forcing includes the atmospheric teleconnection and oceanic wave propagation through the Indonesian archipelago, mainly associated with the El Nino/Southern Oscillation (ENSO). One of the important characteristics of Ningaloo Nino/Nina is its asymmetry; the Ningaloo Nino is stronger than the Ningaloo Nina. This suggests the presence of some asymmetry in these processes. However, no studies to date focused on this topic.

Using a regional ocean modeling system (ROMS), the contribution of oceanic wave propagation to the amplitude and asymmetry of SST anomalies associated with the Ningaloo Nino/Nina is investigated. For these purposes, a sensitivity experiment in which oceanic lateral boundary conditions are replaced by the monthly climatology is conducted. The results suggest that downwelling (upwelling) Kelvin waves from the western tropical Pacific associated with La Nina (El Nino) that often co-occur with Ningaloo Nino (Nina) are stronger (weaker) and contribute to the asymmetry.

Keywords: Ningaloo Nino, Regional ocean modeling system, El Nino/Southern Oscillation, coastal Kelvin wave

©2019. Japan Geoscience Union. All Right Reserved.

The life-cycle of annual waves in the Indian Ocean as identified by a seamless diagnosis for the energy flux

*Zimeng Li[1], Hidenori Aiki[2]

1. Graduate school of environmental studies, Nagoya university, 2. Institute for space-earth environmental research, Nagoya university

The role of synoptic-scale waves in tropical-extratropical interactions has been little investigated in terms of the transfers of wave energy, owing to the lack of an appropriate diagnosis scheme in previous studies. A recent theoretical study has derived a seamless scheme that is able to identify the direction of group velocity for both gravity and planetary waves at all latitudes. This new scheme has been used in the present study to provide a first-ever energetic view for the life-cycle of annual waves in the Indian Ocean in a set of shallow-water model experiments with climatological wind forcing. The new scheme is able to show, in particular for the second baroclinic mode, eastward energy fluxes associated with equatorial Kelvin waves (KWs) whose signal are found to span the full zonal extent of the tropical Indian Ocean. For the first and third baroclinic modes, eastward signals at the equator are found to appear in the western and eastern parts of the basin, respectively. Concerning the low-pass filtered time evolution the energy flux, eastward signals associated with equatorial KWs are found to culminate when zonal currents change direction (four times per year) according to monsoon winds. Waves in the tropical and subtropical regions are connected each other at the zonal boundaries of the Indian Ocean that has been viewed, for the first time in the history of geophysical fluid dynamics, in terms of the circulation of wave energy. Near the eastern boundary of the Indian Ocean, the incoming signals of equatorial KW bifurcate polewards along the coasts of Bay of Bengal and Australia and then transmit midlatitude Rossby waves, forming a basin-scale cyclonic energy circulation in each hemisphere. Near the western boundary of the Indian Ocean, the seasonal variations of both the Somali jet and the east African coastal current are found to yield equatorward energy fluxes along the African coast, forming a localized cyclonic energy circulation in each hemisphere. These results for the analysis of climatological annual waves provide a basis for the analysis of waves with interannual variations in a future study to better understand, for example, tropical-extratropical interactions during the Indian Ocean Dipole mode.

Keywords: tropical-extratropical interactions, seasonal variations analysis, wave energy circulation

©2019. Japan Geoscience Union. All Right Reserved.

[J] Poster | A (Atmospheric and Hydrospheric Sciences)：A-CG Complex & General

Tue. May 28, 2019 5:15 PM - 6:30 PM JST | Tue. May 28, 2019 8:15 AM - 9:30 AM UTC | Poster Hall International Exhibition Hall8, Makuhari Messe_14

[A-CG38] Multi-scale ocean-atmosphere interaction in the tropical Indo-Pacific region

convener:Ayako Seiki(Japan Agency for Marine-Earth Science and Technology), Tomoki Tozuka(Department of Earth and Planetary Science, Graduate School of Science, The University of Tokyo), Motoki Nagura(Japan Agency for Marine-Earth Science and Technology), Youichi Kamae(Faculty of Life and Environmental Sciences, University of Tsukuba)

Multi-scale ocean-atmosphere interaction in the tropics exerts a significant imprint on the global climate via atmospheric teleconnection. Since the 1980s, anchored by in-situ and satellite observations, improvements in modeling and theoretical understanding, various aspects of dominant modes of interannual (e.g., ENSO and IOD), intraseasonal (e.g., MJO) variabilities and their impacts on tropical (e.g., monsoons) and extra-tropical (e.g., North America) climate variations have received wide attention. Recent satellite-based salinity measurements indicate for an active role of salinity in the tropical ocean-atmosphere interaction. While recent studies suggest a possible link between interdecadal Pacific oscillation and global warming hiatus in 2000s, changes (if any) in the tropical ocean-atmosphere interaction are yet to be understood. Due to interactions between different time scales, between different ocean basins, and with the extratropics, the tropical ocean and atmosphere play a key role in shaping climate, its variability and change. To better understand and examine these challenging issues from various perspectives, this session offers a forum to discuss recent progress in observational, modeling and theoretical studies of multi-scale tropical ocean-atmosphere interaction.

[ACG38-P01] Impacts of seasonal transitions of ENSO on frequency of atmospheric rivers over East Asia

*Youichi Kamae[1], Moeka Naoi[2], Hiroaki Ueda[1] (1.Faculty of Life and Environmental Sciences, University of Tsukuba, 2.Graduate School of Life and Environmental Sciences, University of Tsukuba)

[ACG38-P02] Impact of tropical Pacific sea surface temperature on the regional heavy rainfall events in Japan

*Yukiko Imada[1], Hiroaki Kawase[1], Masahiro Watanabe[2], Izuru Takayabu[1] (1.Meteorological Research Institute, Japan Meteorological Agency, 2.Atmosphere and Ocean Research Institute, the University of Tokyo)

[ACG38-P03] The North Pacific pacemaker effect on historical ENSO and its mechanisms

*Yu Kosaka[1], Dillon J. Amaya[2], Wenyu Zhou[2], Yu Zhang[2], Shang-Ping Xie[2], Arthur J. Miller[2] (1.Research Center for Advanced Science and Technology, University of Tokyo, 2.Scripps Institution of Oceanography, University of California San Diego)

[ACG38-P04] **Detection of the dry intrusions from the mid-latitudes to the Equator and their association with MJO**

*Saki Yanagisawa[1], Akiyo Yatagai[1] (1.Hirosaki Univercity)

[ACG38-P05] **Relationship between oceanic and atmospheric variations in the Philippine Sea and modulation of El Nino events**

*Takuya Hasegawa[1], Akira Nagano[2], Iwao Ueki[2], Kentaro Ando[2] (1.Tohoku University, 2.JAMSTEC)

[ACG38-P06] Contribution of oceanic wave propagation from the tropical Pacific to asymmetry of the Ningaloo Nino/Nina

*Hidehiro Kusunoki[1], Shoichiro Kido[1], Tomoki Tozuka[1] (1.Department of Earth and Planetary Science, Graduate School of Science, The University of Tokyo)

[ACG38-P07] The life-cycle of annual waves in the Indian Ocean as identified by a seamless diagnosis for the energy flux

*Zimeng Li[1], Hidenori Aiki[2] (1.Graduate school of environmental studies, Nagoya university, 2.Institute for space-earth environmental research, Nagoya university)

Impacts of seasonal transitions of ENSO on frequency of atmospheric rivers over East Asia

*Youichi Kamae[1], Moeka Naoi[2], Hiroaki Ueda[1]

1. Faculty of Life and Environmental Sciences, University of Tsukuba, 2. Graduate School of Life and Environmental Sciences, University of Tsukuba

Narrow corridors of moisture transport bands over the middle latitudes called atmospheric rivers (ARs) are important phenomena for hydrological cycle and natural disasters. Landfalling ARs associated with extratropical cyclones bring huge amount of rainfall over western coasts of North America and Europe. Previous studies pointed out that large-scale anomalies in atmospheric circulation associated with El Niño-Southern Oscillation (ENSO) are important factors for interannual variability in frequency of wintertime ARs over western North America. Recently, Kamae et al. (2017) revealed that ARs were also frequently observed over East Asia, especially during boreal summer. They also pointed out that preceding winter's El Niño results in anomalously-enhanced AR activity over summertime East Asia with a half-year lag. After the wintertime El Niño development, delayed warming over the Indian Ocean produces an anomalous anticyclone over the western North Pacific and associated increase in summertime AR frequency over East Asia. However, possible impacts of ENSO transition from preceding winter to concurrent summer on summertime AR activity over East Asia are still unclear. Here we extend our understanding on seasonal ENSO-AR relationship by compositing individual ENSO transition cases from winter to summer including rapid transitions from El Niño to La Niña. The rapid transition results in an anomalous AR activity over East Asia associated with the anomalous anticyclone over the western North Pacific. The anomalous anticyclone shifts northward compared to those found in years with sustained El Niño or decayed El Niño. We also found that the impacts of ENSO transition on ARs can be understood as a result of summertime teleconnection from the tropics favored by anomalous convective heating over the tropics associated with anomalous Walker circulation over the equatorial Pacific.

Keywords: ENSO, Atmospheric river, North Pacific High, Indian Ocean capacitor effect

©2019. Japan Geoscience Union. All Right Reserved.

Impact of tropical Pacific sea surface temperature on the regional heavy rainfall events in Japan

*Yukiko Imada[1], Hiroaki Kawase[1], Masahiro Watanabe[2], Izuru Takayabu[1]

1. Meteorological Research Institute, Japan Meteorological Agency, 2. Atmosphere and Ocean Research Institute, the University of Tokyo

To detect the impact of global-scale climate on regional extreme events is challenging especially for disastrous regional heavy rainfall events which are often strongly affected by local topography. Observed records are too short to obtain significant concurrent signals. General circulation models (GCMs) can represent background large-scale circulations causing regional heavy rainfall but cannot resolve the topography. On the other hand, high-resolution regional climate model can resolve orographic rainfall but cannot provide the information of key processes in larger-scale circulation. Here, we prepared a large-ensemble pair of GCM and nonhydrostatic regional model simulations covering 6800-year samples. It enables us to access local rainfall event directly and investigate cause-to-effect pathway to explain the impact of global scale climate. As an example, we cite 2-type heavy rainfall events around precipitous terrains in Japan: western Kyushu type and eastern Kyushu type. The western Kyushu type related to moisture transport is attributed to the development of the Pacific subtropical High which is often forced by an El Nino event during previous winter. On the other hand, the eastern Kyushu type is attributed to TC approach which correlates to the central Pacific El Ninos. Through this new flamework with large-ensemble pairs of global and regional simulations, we can verify various influence pathways of large-scale climate to specific regional extreme events.

Keywords: Heavy rainfall, Atomospheric general circulation model, Regional climate model

©2019. Japan Geoscience Union. All Right Reserved.

The North Pacific pacemaker effect on historical ENSO and its mechanisms

*Yu Kosaka[1], Dillon J. Amaya[2], Wenyu Zhou[2], Yu Zhang[2], Shang-Ping Xie[2], Arthur J. Miller[2]

1. Research Center for Advanced Science and Technology, University of Tokyo, 2. Scripps Institution of Oceanography, University of California San Diego

Recent studies have indicated that North Pacific sea surface temperature (SST) variability can significantly modulate the evolution of the El Niño-Southern Oscillation (ENSO), but there has been little effort to put these extratropical-tropical interactions into the context of historical ENSO events. To quantify the role of the North Pacific in pacing the timing and magnitude of observed ENSO events, we use a fully-coupled climate model to produce the first ensemble of North Pacific Ocean-Global Atmosphere (nPOGA) SST pacemaker simulations. In nPOGA, SST anomalies in the North Pacific (>15˚N) are restored back to observations, but are free to evolve throughout the rest of the globe. We find that North Pacific SST variability has significantly influenced the observed trajectory of historical ENSO, accounting for approximately 15% of the total variance in boreal fall and winter. The interaction between the North and tropical Pacific is the result of two physical pathways: 1. A Wind-Evaporation-SST propagating mechanism in boreal spring, and 2. A convective response associated with the Seasonal Footprinting Mechanism in boreal fall. The latter accounts for 25% of the observed zonal wind variability around the equatorial dateline. On an event-by-event basis, nPOGA most closely reproduces the 2014-2015 and the 2015-2016 El Niño events. In particular, we show that the 2015 Pacific Meridional Mode event increased wind forcing along the equator by 20%, potentially contributing to the extreme nature of the 2015-2016 El Niño. Our results illustrate the significant role of extratropical noise in pacing the initiation and magnitude of ENSO events and may improve the predictability of ENSO on seasonal timescales.

Keywords: Pacific Meridional Mode, ENSO, Pacemaker experiment

©2019. Japan Geoscience Union. All Right Reserved.

Detection of the dry intrusions from the mid-latitudes to the Equator and their association with MJO

*Saki Yanagisawa[1], Akiyo Yatagai[1]

1. Hirosaki Univercity

Dry intrusion is a large-scale intrusion phenomenon of extremely dry air into tropics and it influences on the cumulus convection. However, their large-scale features and statistics have not been revealed yet. The purposes of this study are detecting the dry intrusions using a long-term reanalysis data (the ERA-Interim, 0.75˚ grid) and clarifying relationship between the appearance of the dry intrusions and the Madden-Julian Oscillation (MJO) activity.
First, we drew daily map of precipitable water (PW) from the ERA-interim for the year from 1998 to 2016 (total 10593 days), and we counted the appearance at every 20˚ longitudes according to the following conditions; 1) the dry intrusion arrives at 10˚S-10˚N and is maintained for 2-10 days, 2) It forms a crescent shape with an area that PW of less than 40 mm, 3) It includes areas with a PW of less than 30 mm and 4) The entire dry intrusion fits into an area of roughly 2000 km^2.
Among the 10593 days, we detected 1118 cases in all so the dry intrusions appear about 40 times a year in average, and appearance in the Northern Hemisphere are less (388 cases), and more in the Southern Hemisphere (730 cases). About 90% of the dry intrusions were detected in an area from the Indian Ocean to the western tropical Pacific in both hemispheres. The appearance of the dry intrusions has seasonal dependence; a lot of the dry intrusions are in winter and few are in summer in both hemispheres. Sometimes the dry intrusions by above definitions were appeared in association with the strong tropical cyclones, and they reach 8% of the total number of appearances of the dry intrusions.
We composited 700 hPa and 850 hPa zonal wind when the dry intrusions were appeared around the Indian Ocean, the Maritime Continent and the western tropical Pacific, respectively. As a result, a strong westerly wind blew around an area where dry intrusions were appeared in the Indian Ocean and the western tropical Pacific. In the Maritime Continent, a strong westerly wind blew on the west side of the Maritime Continent. Such wind fields occurred also at the MJO activity and it is called the Westerly wind burst (WWB). The WWB blew over the western tropical Pacific when the dry intrusions occurred in the Maritime Continent and the western tropical Pacific. Therefore, it may be had an association between a convection activity by the MJO and dry air intrusion. Over an entire period, 25.2% of all the dry intrusions detected in the western tropical Pacific occurred when the MJO was active in there and 14.8% occurred in the same area but the MJO was not active. The remaining 60.0% occurred when the MJO was active or non-active in other areas. This percentage has become lower in cases of the dry intrusions occurred in the Indian Ocean and the Maritime Continent.

©2019. Japan Geoscience Union. All Right Reserved.

Relationship between oceanic and atmospheric variations in the Philippine Sea and modulation of El Nino events

*Takuya Hasegawa[1], Akira Nagano[2], Iwao Ueki[2], Kentaro Ando[2]

1. Tohoku University, 2. JAMSTEC

Western Pacific Oscillator model (WPO model), which is the one of the ENSO theory models, shows strong anti-cyclonic anomalies over the wetern tropical Pacific (around Philippine Sea) after a mature phase of El Nino. To check this point, time series of sea level pressure (SLP) anomalies averaged over the Philippine Sea for boreal-winter (i.e., January to March) is made. The result shows that eastern-Pacific (EP)-El Nino events (1982.83, 1986/87, 1991/92, 1997/98) show strong positive SLP anomalies in line with the WPO model. On the other hand, central-Pacific (CP)-El Nino events (1994/95, 2002/03, 2004/05, 2006/07, 2009/10) show weak SLP anomalies. Next, composite maps for SLP and sea surface winds during boreal-winter in the year of occurrence of EP-El Nino and CP-El Nino are made, respectively. It is shown that positive SLP anomalies and related anti-cyclonic sea surface wind pattern appear over the Philippine Sea for EP-El Nino. In the south part of the Philippine Sea, easterly anomaly winds appear and it can lead poleward Ekman transport that decreases warm water volume in the western equatorial Pacific. This situation is consistent with that expected from the WPO model, that is, the equatorial cold Kelvin waves can be generated, and then will terminate the on-going El Nino event to start the next La Nina event. Analysis on the sea surface height anomalies also shows negative sea surface height anomalies in the western equatorial Pacific at that time. In contrast to the EP-El Nino, CP-El Nino does not show such patterns of SLP, sea surface wind, and sea surface height anomalies. Therefore, it can be said that WPO model does not well act after mature phase of CP-El Nino, while the model does well after mature phase of EP-El Nino.

Acknowledgment: This work was partly supported by the Japan Society for the Promotion of Science (JSPS), Grant-in-Aid for Scientific Research (17K05660).

Keywords: El Nino, Philippine Sea, western Pacific Oscillator model

©2019. Japan Geoscience Union. All Right Reserved.

Contribution of oceanic wave propagation from the tropical Pacific to asymmetry of the Ningaloo Nino/Nina

*Hidehiro Kusunoki[1], Shoichiro Kido[1], Tomoki Tozuka[1]

1. Department of Earth and Planetary Science, Graduate School of Science, The University of Tokyo

Ningaloo Nino (Nina) is a climate mode associated with anomalously warm (cool) sea surface temperature (SST) off the Western Australian coast. Considering its large impacts on the local marine ecosystem and precipitation, better understanding of its mechanism and predictability is desirable. Existing studies suggest that both local air-sea interaction and remote forcing contribute to generation and amplification of the Ningaloo Nino/Nina. The latter forcing includes the atmospheric teleconnection and oceanic wave propagation through the Indonesian archipelago, mainly associated with the El Nino/Southern Oscillation (ENSO). One of the important characteristics of Ningaloo Nino/Nina is its asymmetry; the Ningaloo Nino is stronger than the Ningaloo Nina. This suggests the presence of some asymmetry in these processes. However, no studies to date focused on this topic.

Using a regional ocean modeling system (ROMS), the contribution of oceanic wave propagation to the amplitude and asymmetry of SST anomalies associated with the Ningaloo Nino/Nina is investigated. For these purposes, a sensitivity experiment in which oceanic lateral boundary conditions are replaced by the monthly climatology is conducted. The results suggest that downwelling (upwelling) Kelvin waves from the western tropical Pacific associated with La Nina (El Nino) that often co-occur with Ningaloo Nino (Nina) are stronger (weaker) and contribute to the asymmetry.

Keywords: Ningaloo Nino, Regional ocean modeling system, El Nino/Southern Oscillation, coastal Kelvin wave

©2019. Japan Geoscience Union. All Right Reserved.

The life-cycle of annual waves in the Indian Ocean as identified by a seamless diagnosis for the energy flux

*Zimeng Li[1], Hidenori Aiki[2]

1. Graduate school of environmental studies, Nagoya university, 2. Institute for space-earth environmental research, Nagoya university

The role of synoptic-scale waves in tropical-extratropical interactions has been little investigated in terms of the transfers of wave energy, owing to the lack of an appropriate diagnosis scheme in previous studies. A recent theoretical study has derived a seamless scheme that is able to identify the direction of group velocity for both gravity and planetary waves at all latitudes. This new scheme has been used in the present study to provide a first-ever energetic view for the life-cycle of annual waves in the Indian Ocean in a set of shallow-water model experiments with climatological wind forcing. The new scheme is able to show, in particular for the second baroclinic mode, eastward energy fluxes associated with equatorial Kelvin waves (KWs) whose signal are found to span the full zonal extent of the tropical Indian Ocean. For the first and third baroclinic modes, eastward signals at the equator are found to appear in the western and eastern parts of the basin, respectively. Concerning the low-pass filtered time evolution the energy flux, eastward signals associated with equatorial KWs are found to culminate when zonal currents change direction (four times per year) according to monsoon winds. Waves in the tropical and subtropical regions are connected each other at the zonal boundaries of the Indian Ocean that has been viewed, for the first time in the history of geophysical fluid dynamics, in terms of the circulation of wave energy. Near the eastern boundary of the Indian Ocean, the incoming signals of equatorial KW bifurcate polewards along the coasts of Bay of Bengal and Australia and then transmit midlatitude Rossby waves, forming a basin-scale cyclonic energy circulation in each hemisphere. Near the western boundary of the Indian Ocean, the seasonal variations of both the Somali jet and the east African coastal current are found to yield equatorward energy fluxes along the African coast, forming a localized cyclonic energy circulation in each hemisphere. These results for the analysis of climatological annual waves provide a basis for the analysis of waves with interannual variations in a future study to better understand, for example, tropical-extratropical interactions during the Indian Ocean Dipole mode.

Keywords: tropical-extratropical interactions, seasonal variations analysis, wave energy circulation

©2019. Japan Geoscience Union. All Right Reserved.

[J] Oral | A (Atmospheric and Hydrospheric Sciences)：A-CG Complex & General

Tue. May 28, 2019 9:00 AM - 10:30 AM JST | Tue. May 28, 2019 12:00 AM - 1:30 AM UTC | 301A 3F

[A-CG39] Biogeochemical cycles in Land Ecosystem

convener:Tomomichi Kato(Research Faculty of Agriculture, Hokkaido University), Kazuhito Ichii(Chiba University), Takeshi Ise(FSERC, Kyoto University), Munemasa Teramoto(National Institute for Environmental Studies), Chairperson:Tomomichi Kato(Hokkaido University)

Terrestrial ecosystem influences global climate through cycles of water, carbon, and nitrogen between land surface and atmosphere. For better understanding of those behaviors, a great effort has been paid for developing varieties of approaches and techniques such as biometric survey, eddy and chamber methods, near and satellite remote sensing, biosphere modeling and so on.
 In particular, the JapanFlux, founded in 2006 as a researchers network of CO2, H2O and other trace gas flux measurement, has promoted the multi-disciplinal studies not only for flux measurement community, but also for remote sensing and biosphere modeling communities. Moreover, the Research-Group-on-Integrated-Land-Processes, which was founded in 2006, also has contributed to build networks between Japanese researchers to better understanding of physical and biological processes on interactions between terrestrial surface and atmosphere.
 This session unites those multi-disciplinal activities, and promotes the oral and poster presentations on the role of terrestrial ecosystem in material circulations of water, carbon, nitrogen, energy and other substances by any approaches and technics. This session takes over the former session in last year: A-CG40.

9:00 AM - 9:15 AM JST | 12:00 AM - 12:15 AM UTC

[ACG39-01] Laboratory examination of combined effects of temperature rising and increased water fluctuation on CO_2 release from volcanic ash soils

*Hirohiko Nagano[1], Mariko Atarashi-Andoh[1], Jun Koarashi[1] (1.Japan Atomic Energy Agency)

9:15 AM - 9:30 AM JST | 12:15 AM - 12:30 AM UTC

[ACG39-02] Field observation of GHGs emission from pome palm oil mill effluent (POME) treatment ponds in an oil palm plantation in tropical peatland.

*Yoshiyuki Takahashi[1], Takashi Onodera[2], Ryuichi Hirata[1], Kazuya Nishina[2], Joseph Wenceslaus Waili[3], Kevin Kemudang Musin[3], Edward Baran Aeries[3], Frankie Kiew[3], Guan Xhuan Wong[3], Zufaqar Sa'adi[3], Lulie Melling[3] (1.Center for Global Environmental Research, National Institute for Environmental Studies, 2.Center for Regional Environmental Research, National Institute for Environmental Studies, 3.Sarawak Tropical Peat Research Institute)

9:30 AM - 9:45 AM JST | 12:30 AM - 12:45 AM UTC

[ACG39-03] Soil CO_2 efflux dynamics with land-use changes in Southeast Asia

*HAJIME TOMIMATSU[1], NAISHEN LIANG[1], MUNEMASA TERAMOTO[1], JIYE ZENG[1], ZHAO XIN[1] (1.National Institute for Environmental Studies)

9:45 AM - 10:00 AM JST | 12:45 AM - 1:00 AM UTC

[ACG39-04] Individual-based analyses of the carry-over effects from recent climatic conditions on the interannual variability of LAI of an evergreen conifer stand

*Akihiro Sumida[1], Tsutomu Watanabe[1], Tomiyasu Miyaura[2] (1.Institute of Low Temperature Science, Hokkaido University, 2.Faculty of Science and Technology, Ryukoku University)

10:00 AM - 10:15 AM JST | 1:00 AM - 1:15 AM UTC

[ACG39-05] Carbon dioxide balance of an oil palm plantation on tropical peat

*Takashi Hirano[1], Frankie Kiew[2], Ryuichi Hirata[3], Guan Xhuan Wong[2], Edward Baran Aries[2], Kevin Kemudang[2], Joseph Wenceslaus[2], Lo Kim San[2], Lulie Melling[2] (1.Research Faculty of Agriculture, Hokkaido University, 2.Sarawak Tropical Peat Research Institute, 3.CGER, National Institute for Environmental Studies)

10:15 AM - 10:30 AM JST | 1:15 AM - 1:30 AM UTC

[ACG39-06] The effect of heat wave in the summer of 2018 on carbon and water fluxes in an open black spruce forest in an interior Alaska

*Hideki Kobayashi[1], Robert Busey[2], Yongwon Kim[2], Sigrid Dengel[3], Stephen Chan[3] (1.Japan Agency for Marine-Earch Science and Technology, 2.International Arctic Research Center, University of Alaska, Fairbanks, 3.Lawrence Berkeley National Laboratory)

Laboratory examination of combined effects of temperature rising and increased water fluctuation on CO_2 release from volcanic ash soils

*Hirohiko Nagano[1], Mariko Atarashi-Andoh[1], Jun Koarashi[1]

1. Japan Atomic Energy Agency

Global warming will alter the precipitation pattern, resulting in the increase in seasonal fluctuation of soil water conditions. Both environmental factors of soil temperature and water fundamentally affect soil CO_2 release, a major carbon flux in terrestrial ecosystems. However, our understandings of soil CO_2 release under the increased temperature and fluctuated water conditions are still insufficient to infer the feedback of terrestrial carbon cycling in future worlds. In the present study, we are conducting laboratory incubation experiments for examining the combined effects of temperature rising and soil water fluctuation on CO_2 release from volcanic ash soils. Volcanic ash soil is the major soil type in Japan and is expected to have great ability to stabilize carbon as soil organic matter. We incubated volcanic ash soils under four combinatorial conditions of two temperatures (20 and 30 ˚C) and two water conditions (a continuously constant water and a fluctuated water conditions). The rate of CO_2 release was periodically measured during the incubation. Then, the ratio of CO_2 release at 20 ˚C to that at 30 ˚C, namely Q_{10}, was expressed as the temperature sensitivity of soil CO_2 release. The fluctuated water condition was maintained with multiple dry-wet cycles to achieve an average water content of 40% of water holding capacity which was equivalent to that under the continuously constant water condition. For the incubation at 20 ˚C, soil CO_2 release under the fluctuated water condition was up to 50% greater than that under the constant water condition. The excess of soil CO_2 release under the fluctuated water condition was, however, reduced to less than 10% for the incubation at 30 ˚C. Thus, Q_{10} under the fluctuated water condition (1.3 to 1.5) was equivalent to or lower than that under the continuously constant water condition (around 1.5). These preliminary results offer the needs of modifying basal CO_2 release extent and Q_{10} value for inferring the soil CO_2 release under increased temperature and fluctuated water conditions. The experiments are still ongoing and results and further insights will be presented at the meeting.

Keywords: greenhouse gas, soil carbon dynamics, global warming

©2019. Japan Geoscience Union. All Right Reserved.

Field observation of GHGs emission from pome palm oil mill effluent (POME) treatment ponds in an oil palm plantation in tropical peatland.

*Yoshiyuki Takahashi[1], Takashi Onodera[2], Ryuichi Hirata[1], Kazuya Nishina[2], Joseph Wenceslaus Waili[3], Kevin Kemudang Musin[3], Edward Baran Aeries[3], Frankie Kiew[3], Guan Xhuan Wong[3], Zufaqar Sa'adi[3], Lulie Melling[3]

1. Center for Global Environmental Research, National Institute for Environmental Studies, 2. Center for Regional Environmental Research, National Institute for Environmental Studies, 3. Sarawak Tropical Peat Research Institute

1. Introduction

Intense land-use change in tropical Asia has a significant influence on greenhouse gases (GHGs) budget in the region. Conversion of tropical peat swamp forest to both acacia and oil palm plantation is a typical land-use change in the region. To evaluate impact of the conversion on GHGs budget, we have to quantify many related processes, for example, enhanced decomposition of peat soil, N_2O emission from fertilization, biogas emission from palm oil mill effluent (POME) treatment ponds, etc. Oil mill facility is built adjacent to oil palm field because fresh oil palm fruit needs to be processed immediately after harvest. Oil palm plantation forms a stationary material cycle system as an integration of palm oil field and mill facility. POME treatment ponds is typical waste water treatment system in an oil palm plantation. Biogas contains high concentration of methane, because methane fermentation is an essential process in waste water purification in the ponds. Measured values of GHGs emission from POME treatment ponds is limited. We conducted field observation of GHGs emission from a POME treatment ponds in an oil palm plantation in tropical peatland as a joint research of National Institute for Environmental Studies and Sarawak Tropical Peat Research Institute.

2. Methods

We conducted field measurement of GHGs emissions from POME treatment ponds in an oil palm plantation on tropical peatland near Sibu Town, Sarawak, Malaysia. The life of the sampling equipment was assumed considerably short in POME treatment ponds due to the exposure to high concentration of corrosive hydrogen sulfide and pollution by oily scum. To quantify GHGs emission from the ponds, we had developed floating chamber system specialized to the POME ponds. The low cost and program controlled system made it possible to perform multi-point simultaneous sampling automatically in a short period of time. We collected biogas from the ponds into balloons of gas-barrier film using the chambers. We measured total amount of biogas in the balloons with modified water replacement method firstly, consequently measured concentration of gases (CH_4, CO_2, O_2, H_2, and H_2S) with portable gas monitor (BIOGAS 5000, Gastech, U.K.). We calculated gas fluxes from covered area, sampling duration, gas volume and gas concentrations. The gas fluxes measurements were conducted in eight ponds in upstream side of whole ten ponds during dry season (June 2018).

3. Results and discussions

Biogas from POME treatment ponds were mainly CO_2 and CH_4. Markedly large biogas flux was found in fourth pond from upper stream. About 65% of the biogas from the fourth pond was CH_4. This might be due to neutral pH and moderate temperature were suitable for methane fermentation in the pond. In the three upper-stream ponds, the pond water was acidic in which CO_2 dominated about 60% of biogas. Biogas flux was small in the ponds in lower-stream of the forth pond.

4. Summary

©2019. Japan Geoscience Union. All Right Reserved.

In the POME treatment ponds, decomposition process of organic matter in POME would be different in each stage because of differences in the various environmental factors such as pH, temperature, organic matter content, etc. It was successful in the integration of data in severe environmental condition in the POME treatment ponds despite various technical challenge. Oil palm plantation is a continuous and stationary material flow system as a whole including plant field, mill facility and POME treatment ponds. To fully understand the impact of land-use change on GHGs budget, it is very important to quantify the relationship between GHGs budget and material cycle in the whole plantation system. Besides field measurements, we also do interviews on material flow in the plantation with the cooperation of business entity of the plantation.
We will introduce the result of wet season (January 2019) during this presentation.

Keywords: Climate change, Land-use change, Tropical Asia, Tropical peat, Greenhouse gases

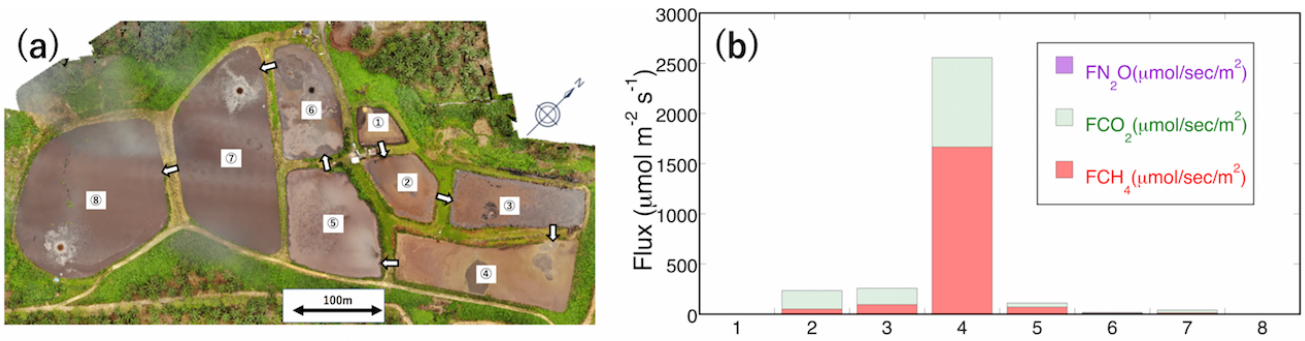

Figure. (a) Location of ponds and (b)GHGs flux from the ponds.

©2019. Japan Geoscience Union. All Right Reserved.

Soil CO_2 efflux dynamics with land-use changes in Southeast Asia

*HAJIME TOMIMATSU[1], NAISHEN LIANG[1], MUNEMASA TERAMOTO[1], JIYE ZENG[1], ZHAO XIN[1]

1. National Institute for Environmental Studies

Land use changes greatly affect carbon cycle of forest ecosystem. Since the 1970s, about 35% of tropical primary forests were lost due to disorderly commercial logging, plantation development such as oil palm and rubber in Southeast Asia. These rapid land use changes cause serious environmental problems such as soil erosion, decrease in soil fertility, and decrease in productivity. As a result, there will be a major change in the regional biochemical cycles.

Soil is an important source of information on the global carbon budget and it is a carbon sink, and soil respiration (R_s) is one of the most important elements of the carbon cycle in terrestrial ecosystems. Land use changes influence the dynamics of R_s. However, most studies on the effects of land use change on R_s focused on the boreal, temperate and subtropical ecosystems. In Southeast Asia, we have addressed the response of R_s to the land use changes, but mostly it is a short period with little spatial or temporal repetition, especially there are few long-term observations in lowland rainforests with no seasonal changes in temperature.

To examine the long-term response of R_s to land use change in Southeast Asia, we selected 4 research sites of different land use type, primary forest (PF), secondary forest (SF), oil palm plantation (OP), and rubber plantation (RP). In 2010, we installed total 30 soil collars (diameter 32 cm) in each site. The 30 collars were distributed in two rows, each with 15 collars and at 5 m intervals. R_s was measured every two weeks using a portable automatic opening and closing chamber system developed by the National Institute for Environmental Studies.

R_s showed synchronicity seasonal change among all sites, suggesting that it is controlled by both soil temperature and moisture. The apparent temperature sensitivity of R_s (Q_{10}) decreased from 4.86 in NF to 2.09 in SF, 2.14 in OP, 3.79 in GP. In addition, the annual average soil respiration rate decreased about 38% in SF, about 33% in OP and about 40% in GP compared with NF. Our results indicate that logging and/or conversions of primary forests to plantations lead severe soil degradation.

Keywords: Land use change, Plantation, Soil respiration

©2019. Japan Geoscience Union. All Right Reserved.

Individual-based analyses of the carry-over effects from recent climatic conditions on the interannual variability of LAI of an evergreen conifer stand

*Akihiro Sumida[1], Tsutomu Watanabe[1], Tomiyasu Miyaura[2]

1. Institute of Low Temperature Science, Hokkaido University, 2. Faculty of Science and Technology, Ryukoku University

The leaf area index (LAI) of a forest stand has been known to remain within a specific range after a peak at relatively young stand ages. For evergreen stands, however, little has been known about interannual variability of LAI and its effects on biomass increase. In this paper we introduce a series of studies ([1], [2]) in which interannual variability of the LAI and the growth rates of stem biomass were investigated with biological and climatic factors affecting them in an evergreen hinoki cypress (*Chamaecyparis obtusa*) stand between 21 and 40 years of stand age. In this long-term investigation, the stem diameter at the crown base (D_{CB}) was recorded for all living trees each year. This allowed us to estimate the leaf area of a tree (tree LA) using an allometric equation, which is known to be little affected by the difference in stand ages. Given the tapered shape of a tree stem within the crown, a rapid rise of the crown base height can lead to a decrease in D_{CB}, or a decrease in the tree LA. The other measurements also allowed us to estimate the stem dry mass for each tree in each year, and then the stand LAI and the stand stem biomass. The prediction intervals of LAI and stand stem biomass were evaluated for each year by propagating errors of those individual-based estimates. Monthly meteorological data were obtained using the climatic measurements recorded at the nearest weather station (AMeDAS).

The LAI varied between 7.1–8.8, with a relatively long fluctuation cycles over the observation period. This LAI range was maintained such that the gradual increase in the LA of the largest trees counterbalanced the gradual loss in LA of the smallest trees. The decrease in LA of the smallest trees resulted in their gradual death. Just before their death year, their tree LA had decreased to ~1% of the LAI of that year. Hence their death did not affect the LAI. These smallest trees were able to survive for many years even as their LA was decreasing, which would be important for LAI to be maintained without a sudden decrease. The total basal area decreased twice during the 20 years, whereas the stand stem biomass never decreased despite the death of trees. This was because the portion of the stem within the crown maintained a certain level of radial growth even in the trees with almost no stem radial growth at breast height.

There was a weak but significant positive relationship (r=0.40) between the LAI and the current-year mean summer temperature (July and August). This indicates that LAI tended to increase in the year with warm summer during which new leaves are produced. Further, we found that the moving average of the summer temperatures of 6 years (the current year and the previous 5 years) indicated a much stronger relationship (r=0.93) with the current-year LAI. According to a previous study in the same forest, the mean turnover time of the canopy leaves was estimated to be 4.3–6.3 years, suggesting that the summer temperature of the past years when the leaves in the current-year canopy accumulated was strongly influential in the LAI of the current year.

As canopy photosynthesis would generally be proportional to LAI, we had expected that the annual stem biomass increase rate (dB_{STEM}) would be greater in a year with a high LAI. However, the relationship

©2019. Japan Geoscience Union. All Right Reserved.

between them was not significant (r=0.09). Instead, dB_{STEM} had a positive significant relationship with the sum of precipitation of early summer (May-July) of the current year. Preceding studies of tree physiology have pointed out that a considerable portion of non-structural carbohydrates (NSC) from photosynthesis are used for purposes other than growth (e.g., maintenance of physiological homeostasis), and that the priority of the NSC to be allotted to growth would be lower than any other uses. This partly explains why dB_{STEM} was not correlated with LAI.

[1] Sumida et al. (2013) Tree Physiology 33, 106–118; [2] Sumida et al. (2018) Scientific Reports 8, 13950.

Keywords: evergreen conifer forest, leaf area index, carry-over effects from recent climatic conditions, biomass growth, competition among individuals, interannual variability

©2019. Japan Geoscience Union. All Right Reserved.

Carbon dioxide balance of an oil palm plantation on tropical peat

*Takashi Hirano[1], Frankie Kiew[2], Ryuichi Hirata[3], Guan Xhuan Wong[2], Edward Baran Aries[2], Kevin Kemudang[2], Joseph Wenceslaus[2], Lo Kim San[2], Lulie Melling[2]

1. Research Faculty of Agriculture, Hokkaido University, 2. Sarawak Tropical Peat Research Institute, 3. CGER, National Institute for Environmental Studies

Oil palm plantations have been expanding rapidly over recent decades especially in Indonesia and Malaysia, the two largest oil palm producers in the world. The greatest concern associated with such expansion is its environmental impact. Carbon rich tropical peat swamp forest is also not excluded from such expansion, because it is accessible for developers. Carbon dioxide (CO_2) release through accelerated oxidative peat decomposition is one of the main environmental concerns in the land conversion from peat swamp forest into oil palm plantations, which were drained and compacted to increase yield. Changes in aboveground biomass also might significantly alter the CO_2 exchange dynamics of the ecosystems. Despite the possible significant changes in the CO_2 balance through the land conversion, there is still no study on the ecosystem-scale CO_2 balance of oil palm plantations established on tropical peat. Thus, we have monitored CO_2 flux above an oil palm plantation established on tropical peatland in Sarawak, Malaysia by the eddy covariance technique since 2011. We quantify the annual CO_2 balance of the oil palm plantation and compare it with that of a secondary peat swamp forest in the same region.

Keywords: CO2 flux, Eddy covariance technique, Tropical peat swamp forest, Deforestation, Drainage

©2019. Japan Geoscience Union. All Right Reserved.

The effect of heat wave in the summer of 2018 on carbon and water fluxes in an open black spruce forest in an interior Alaska

*Hideki Kobayashi[1], Robert Busey[2], Yongwon Kim[2], Sigrid Dengel[3], Stephen Chan[3]

1. Japan Agency for Marine-Earch Science and Technology, 2. International Arctic Research Center, University of Alaska, Fairbanks, 3. Lawrence Berkeley National Laboratory

Temperatures have been increasing at higher rate in the northern high latitudes than any other regions of the globe, especially over the land areas, and are projected to continue to do so during this century. In interior Alaska, where the majority of landscape is covered with evergreen needleleaf forest, an exceptionally hot dry summer heat wave was observed in July 2018. In this study, we investigated the eddy covariance carbon and water fluxes under the hot dry period in July 2018. The study was performed in an open black spruce forest site located in the Poker Flat Research Range in interior Alaska. Three eddy covariance systems (two enclosed path and one open path eddy covariance systems) were utilized in the study period. We found the significant down regulation of net ecosystem exchanges (NEE) during a high temperature period during DOY 201-206, 2018. We will introduce the results from the carbon and water fluxes with meteorological and spectral measurements in order to understand how the environmental conditions regulated the carbon and water fluxes and how these fluxes are related with the continuous spectral measurements.

Keywords: eddy Covariance, heat wave, boreal forest

©2019. Japan Geoscience Union. All Right Reserved.

[J] Oral | A (Atmospheric and Hydrospheric Sciences)：A-CG Complex & General

Tue. May 28, 2019 10:45 AM - 12:15 PM JST | Tue. May 28, 2019 1:45 AM - 3:15 AM UTC | 301A 3F

[A-CG39] Biogeochemical cycles in Land Ecosystem

convener:Tomomichi Kato(Research Faculty of Agriculture, Hokkaido University), Kazuhito Ichii(Chiba University), Takeshi Ise(FSERC, Kyoto University), Munemasa Teramoto(National Institute for Environmental Studies), Chairperson:Tomomichi Kato(Hokkaido University)

Terrestrial ecosystem influences global climate through cycles of water, carbon, and nitrogen between land surface and atmosphere. For better understanding of those behaviors, a great effort has been paid for developing varieties of approaches and techniques such as biometric survey, eddy and chamber methods, near and satellite remote sensing, biosphere modeling and so on.
 In particular, the JapanFlux, founded in 2006 as a researchers network of CO2, H2O and other trace gas flux measurement, has promoted the multi-disciplinal studies not only for flux measurement community, but also for remote sensing and biosphere modeling communities. Moreover, the Research-Group-on-Integrated-Land-Processes, which was founded in 2006, also has contributed to build networks between Japanese researchers to better understanding of physical and biological processes on interactions between terrestrial surface and atmosphere.
 This session unites those multi-disciplinal activities, and promotes the oral and poster presentations on the role of terrestrial ecosystem in material circulations of water, carbon, nitrogen, energy and other substances by any approaches and technics. This session takes over the former session in last year: A-CG40.

10:45 AM - 11:00 AM JST | 1:45 AM - 2:00 AM UTC

[ACG39-07] Evaluation of feasibility of continental vegetation monitoring using Himawari-8.

*Kodai Hayashi[1], Kazuhito Ichii[1], Hiroki Yoshioka[2], Kazutaka Murakami[3], Reiko Ide[3], Kenlo Nasahara[4], Tomoko Akitsu[4], Tomoaki Miura[5] (1.Chiba Univ., 2.Aichi Prefectural Univ., 3.NIES, 4.Tsukuba Univ., 5.Univ. Hawaii)

11:00 AM - 11:15 AM JST | 2:00 AM - 2:15 AM UTC

[ACG39-08] Estimation of global carbon dioxide emissions by fires

*Tomohiro Shiraishi[1], Ryuichi Hirata[1] (1.National Institute for Environmental Studies)

11:15 AM - 11:30 AM JST | 2:15 AM - 2:30 AM UTC

[ACG39-09] Interactions between topography, permafrost, and vegetation in Siberian larch forest: a simulation study

*Hisashi Sato[1] (1.Institute of Arctic Climate and Environment Research, Japan Agency for Marine-Earth Science and Technology (JAMSTEC))

11:30 AM - 11:45 AM JST | 2:30 AM - 2:45 AM UTC

[ACG39-10] Data assimilation experiments with MODIS LAI observation and the dynamic global vegetation model SEIB-DGVM in Japan

*Hazuki Arakida[1], Shunji Kotsuki[1], Shigenori Otsuka[1], Takemasa Miyoshi[1] (1.RIKEN Center for Computational Science)

11:45 AM - 12:15 PM JST | 2:45 AM - 3:15 AM UTC

[ACG39-11] Studying ecosystem dynamics with deep neural networks

★Invited Papers

*Takeshi Ise[1], Masanori Onishi[2] (1.FSERC, Kyoto University, 2.Grad. School of Agriculture, Kyoto University)

Evaluation of feasibility of continental vegetation monitoring using Himawari-8.

*Kodai Hayashi[1], Kazuhito Ichii[1], Hiroki Yoshioka[2], Kazutaka Murakami[3], Reiko Ide[3], Kenlo Nasahara[4], Tomoko Akitsu[4], Tomoaki Miura[5]

1. Chiba Univ., 2. Aichi Prefectural Univ., 3. NIES, 4. Tsukuba Univ., 5. Univ. Hawaii

A new generation geostationary meteorological satellite, Himawari-8, began operation in July 2015. Due to newly attached multiple bands in the visible and near infrared wavelength ranges and improved observation frequency of onboard sensor, AHI (Advanced Himawari Imager), application to terrestrial monitoring is expected.
Himawari-8/AHI data are provided as the radiance or the reflectance at the top of atmosphere (TOA) level. In order to monitor terrestrial vegetation, conversion to surface reflectance (TOC: Top of canopy reflectance) is necessary. However, the methods to estimate and verify TOC reflectance of Himawari-8/AHI data has not yet been established. Furthermore, the TOC reflectance data of Himawari-8/AHI requires careful interpretation due to observational geometric conditions unique to geostationary orbit.
In order to understand the feature of the TOC reflectance and the normalized index by Himawari-8/AHI data and to evaluate the usefulness for terrestrial vegetation monitoring, first, we estimated the TOC reflectance from Himawari-8/AHI data with 6SV. The estimated TOC reflectance from Himawari-8/AHI was further evaluated using independent observations such as Terra, Aqua MODIS data and ground observations (HemiSpherical Spectro-Radiometer (HSSR) at Phenological Eyes Network (PEN) sites).
We compared the Himawari-8 TOA/TOC reflectances with the MODIS TOA/TOC reflectances from Terra and Aqua. In particular, in the shorter wavelengths such as blue and green, the R^2 was greatly improved by atmospheric correction. Furthermore, if we selected data only with similar illumination and geometric condition of AHI and MODIS, both TOC reflectances were very close to each other in all wavelength bands. Then, we checked the monthly variation in the TOC reflectances of AHI, MODIS, and HSSR. We found that the three TOC reflectances are similar in the first half of the year (spring and summer). However, after summer, the TOC reflectances of AHI were higher than those of MODIS and HSSR. It can be explained by the dominant backward scattering component in AHI in Japan. In particular, the difference in intensity between the backward scattering and the forward scattering increases toward winter seasons. Meanwhile normalized index such as NDVI could effectively reduce the anisotropic effect on the TOC reflectance and it can capture vegetation phenology similar to MODIS. As a result of cross-validation, Himawri-8 TOC reflectance estimated in this study was generally consistent with other data. However it is necessary to consider the observation conditions of the Himawari-8 TOC reflectance. In the next step, we will demonstrate how the high temporal resolution of Himawari-8 improve our understandings of terrestrial vegetation dynamics.

Keywords: Himawari-8, atmospheric correction, PEN, MODIS, vegetation monitoring, 6SV

©2019. Japan Geoscience Union. All Right Reserved.

Estimation of global carbon dioxide emissions by fires

*Tomohiro Shiraishi[1], Ryuichi Hirata[1]

1. National Institute for Environmental Studies

Global warming accelerates snow melting and drying which cause forest fires. The forest fire gives positive feedback in global warming because large greenhouse gases are emitted into the atmosphere by the forest fire. The purpose of this study is to estimate carbon emissions caused by forest fire with high spatial and temporal resolution, which are 500 m and daily base.
In this study, we used several satellite observation data to estimate global carbon dioxide emissions by fires from 2001 to 2018. We used MODIS MOD14A 1 product for fire detection, MODIS MCD12Q1 product as land cover classification map, and above ground biomass map created by (Avitabile et al., 2016) in Wageningen university. Carbon dioxide emissions were estimated from burned area, biomass densities, burning efficiencies and emission factors for each land cover categories. The estimated carbon dioxide emissions through 18 years were 6159.77 [Tg/year] on yearly average and 607.26 [Tg/year] on standard deviation. These results underestimated to approximately 11% for GFED4.1s and FINN1.0, 8%, 36% for GFAS 1.0 and G-G (Shi et al., 2015), respectively.

Keywords: Carbon dioxide emissions

©2019. Japan Geoscience Union. All Right Reserved.

Interactions between topography, permafrost, and vegetation in Siberian larch forest: a simulation study

*Hisashi Sato[1]

1. Institute of Arctic Climate and Environment Research, Japan Agency for Marine-Earth Science and Technology (JAMSTEC)

In eastern Siberia, larches (Larix spp.) often exist in pure stands, constructing the world's largest coniferous forest, of which changes can significantly affect the earth's albedo and the global carbon balance. Siberian larch area locates on the environmental edge of existence of forest ecosystem, and hence small difference in environmental condition alters existence of larch trees.

Indeed, there is a quantitative pattern that topographic properties controls the abundance of larch forest via both drought and flooding stresses in this region; larch abundance appears to be controlled by drought stress in mountainous regions, while controlled by flooding stresses in plain areas (Sato& Kobayashi 2018). Besides, this region is underlaid by permafrost, vegetation productivity is constraint by depth of active layer; plant productivity becomes lower for shallower active layer by reducing liquid-state-water holding capacity (Beers et al. 2007). At the same time, active layer depth is a function of soil wetness, because wetland soil has larger ice content in active layer, which facilitates downward heat conduction to the permafrost, resulting in shallow thaw for the active layers (Woo & Xia 1996).

To reconstruct such complicated interactions between topography, permafrost, and vegetation in Siberian larch forest, the TOPMODEL, which is a physically based streamflow and water-table-depth computation scheme was implemented to a dynamic vegetation model SEIB-DGVM (Sato et al. 2016), which works with a thermohydrology model. In this presentation, I will talk how this integrated model reasonably works, and how it can be employed for future projection of environmental conditions of the Siberian larch region.

Citations

Beer, C., et al. (2007). "Effects of soil freezing and thawing on vegetation carbon density in Siberia: A modeling analysis with the Lund-Potsdam-Jena Dynamic Global Vegetation Model (LPJ-DGVM)." Global Biogeochemical Cycles 21(1).

Carey, S. K. and M.-k. Woo (1998). A Case Study of Active Layer Thaw and Its Controlling Factors. 7th International Permafrost Conference. Yellowknife, NWT: 127-132.

Sato, H., et al. (2016). "Endurance of larch forest ecosystems in eastern Siberia under warming trends." Ecol Evol 6(16): 5690-5704.

Sato, H. and H. Kobayashi (2018). "Topography Controls the Abundance of Siberian Larch Forest." Journal of Geophysical Research-Biogeosciences 123(1): 106-116.

Woo, M. K. and Z. J. Xia (1996). "Effects of hydrology on the thermal conditions of the active layer." Nordic Hydrology 27(1-2): 129-142.

Keywords: Permafrost, Dynamic Global Vegetation Models, Larch, TOPMODEL

©2019. Japan Geoscience Union. All Right Reserved.

©2019. Japan Geoscience Union. All Right Reserved.

Data assimilation experiments with MODIS LAI observation and the dynamic global vegetation model SEIB-DGVM in Japan

*Hazuki Arakida[1], Shunji Kotsuki[1], Shigenori Otsuka[1], Takemasa Miyoshi[1]

1. RIKEN Center for Computational Science

In the previous study, Arakida et al. (2017) developed a data assimilation system with the SEIB-DGVM (Spatially Explicit Individual-Based Dynamic Global Vegetation Model), and assimilated satellite-observed Leaf Area Index (LAI) successfully over Siberia. In this study, we extend the experiment to a Japanese forest at the Takayama flux site and investigate the performance of the data assimilation system. We estimate the vegetation functions and structures, and model parameters related to the phenology of the deciduous broad-leaved tree and the undergrowth. For the climate forcing data, we used the global reanalysis dataset known as the ERA5. The original data assimilation system developed for Siberia turned out not to be suitable for the Japanese forest because of different LAI variabilities between Siberia and Japan. Namely, LAI stays at the saturated level for an extended period in Japan, while in Siberia, the LAI starts to drop soon after it reaches to the maximum value. Therefore, a model parameter which controls the saturated LAI level was considered for additional parameter estimation. In addition, the undergrowth was changed from deciduous to evergreen. The results show that the DA system performs generally well in Japan with the additional parameter estimation and the modification to the undergrowth.

Arakida, H., T. Miyoshi, T. Ise, S.-I. Shima, and S. Kotsuki (2017), Non-Gaussian data assimilation of satellite-based leaf area index observations with an individual-based dynamic global vegetation model, Nonlinear Proc. Geoph., 24, 553-567, doi:10.5194/npg-24-553-2017.

Keywords: data assimilation, vegetation model, satellite data

©2019. Japan Geoscience Union. All Right Reserved.

Studying ecosystem dynamics with deep neural networks

*Takeshi Ise[1], Masanori Onishi[2]

1. FSERC, Kyoto University, 2. Grad. School of Agriculture, Kyoto University

Obtaining ecological data by field observation has been labor intensive. In this study, we present several approaches to obtain ecological bid data, using information technology. First, introduction to data-driven science and big-data science will be presented. As an example of these new approaches, deep learning with neural networks has various applications in ecological studies. In fact, digital images from satellite, UAV, or even smartphone can be the big data. We show how these big data are used to identify specific features of organisms and vegetation. Moreover, deep neural networks can be applied to analyze time-series data and project the future conditions.

Keywords: deep learning, neural networks, remote sensing

©2019. Japan Geoscience Union. All Right Reserved.

[J] Poster | A (Atmospheric and Hydrospheric Sciences)：A-CG Complex & General

Tue. May 28, 2019 1:45 PM - 3:15 PM JST | Tue. May 28, 2019 4:45 AM - 6:15 AM UTC | Poster Hall International Exhibition Hall8, Makuhari Messe_2

[A-CG39] Biogeochemical cycles in Land Ecosystem

convener:Tomomichi Kato(Research Faculty of Agriculture, Hokkaido University), Kazuhito Ichii(Chiba University), Takeshi Ise(FSERC, Kyoto University), Munemasa Teramoto(National Institute for Environmental Studies)

Terrestrial ecosystem influences global climate through cycles of water, carbon, and nitrogen between land surface and atmosphere. For better understanding of those behaviors, a great effort has been paid for developing varieties of approaches and techniques such as biometric survey, eddy and chamber methods, near and satellite remote sensing, biosphere modeling and so on.
 In particular, the JapanFlux, founded in 2006 as a researchers network of CO2, H2O and other trace gas flux measurement, has promoted the multi-disciplinal studies not only for flux measurement community, but also for remote sensing and biosphere modeling communities. Moreover, the Research-Group-on-Integrated-Land-Processes, which was founded in 2006, also has contributed to build networks between Japanese researchers to better understanding of physical and biological processes on interactions between terrestrial surface and atmosphere.
 This session unites those multi-disciplinal activities, and promotes the oral and poster presentations on the role of terrestrial ecosystem in material circulations of water, carbon, nitrogen, energy and other substances by any approaches and technics. This session takes over the former session in last year: A-CG40.

[ACG39-P01] Long-term warming effect on heterotrophic respiration in a beech forest on Mount Naeba

*Munemasa Teramoto[1], Naishen Liang[1], Masaaki Naramoto[2], Jiye Zeng[1], Zhao Xin[1], Hajime Tomimastu[1] (1.Center for Global Environmental Research, National Institute for Environmental Studies, 2.Faculty of Agriculture, Shizuoka University)

[ACG39-P02] Simple approach to predict flowering and full blooming dates by bi-directional Self Organizing Maps

*Shin Nagai[1], Hiroshi Morimoto[2], Taku M Saitoh[3] (1.Research and Development Center for Global Change, Japan Agency for Marine-Earth Science and Technology, 2.Nagoya University, 3.River Basin Research Center, Gifu University)

[ACG39-P03] Effects of undergrowth mowing on understory carbon balance in a deciduous broadleaf forest of an urban park in central Japan

Guochao Wang[2], *Tomotsugu Yazaki[1], Toshio Kume[1], Takamitsu Kai[3] (1.School of Agriculture, Meiji University, 2.Graduate School of Agriculture, Meiji University, 3.Kurokawa Field Science Center, Meiji University)

[ACG39-P04] Solar-induced chlorophyll fluorescence for detecting ecosystem photosynthetic activity by high-resolution spectrum measurement in a paddy field in Japan

*KANOKRAT BUAREAL[1], Tomomichi Kato[2], Keisuke Ono[3] (1.Graduate School of Global Food Resources, Hokkaido University, Sapporo, Japan, 2.Research Faculty of Agriculture, Hokkaido University, Sapporo, Japan, 3.National Institute for Agro-Environmental Sciences, Tsukuba, Ibaraki, Japan)

[ACG39-P05] Environmental controls on anomalous variation in solar-induced fluorescence during the last 10 years

*Tomomichi Kato[1], Kazuki Mizuno[2] (1.Research Faculty of Agriculture, Hokkaido University, 2.Graduate School of Agriculture, Hokkaido University)

[ACG39-P06] Estimation of terrestrial carbon cycle in Asia using a machine learning and satellite data

*Riku Kawase[1], Kazuhito Ichii[2], Yusuke hayashi[1], Zhiyan Liu[1], Masahito Ueyama[3], Yuji Kominami[4] (1.Chiba University, 2.Center for Environmental Remote Sensing, Chiba University, 3.Osaka Prefecture University, 4.Forest Research and Management Organization)

[ACG39-P07] Estimation of global solar-induced chlorophyll fluorescence (SIF) by terrestrial ecosystem model VISIT and comparison with SIF observed by GOSAT

*Tatsuya Miyauchi[1], Makoto Saito[1], Hibiki M Noda[1], Yukio Yoshida[1], Haruki Oshio[1], Akihiko Ito[1] (1.National Institute for Environmental Studies)

[ACG39-P08] Automatic vegetation identification in the satellite image using a convolutional neural network

*Watanabe Shuntaro[1], Kazuaki Sumi[2], Takeshi Ise[1,3] (1.Field Science Education and Research Center, Kyoto University, 2.Graduate School of Agriculture, Kyoto University, 3.PRESTO, Japan Science and Technology Agency)

Long-term warming effect on heterotrophic respiration in a beech forest on Mount Naeba

*Munemasa Teramoto[1], Naishen Liang[1], Masaaki Naramoto[2], Jiye Zeng[1], Zhao Xin[1], Hajime Tomimastu[1]

1. Center for Global Environmental Research, National Institute for Environmental Studies, 2. Faculty of Agriculture, Shizuoka University

Soil respiration is the second largest carbon flux in terrestrial ecosystems and the global soil respiration is estimated to be 98 GtC yr^{-1}. Soil respiration consists of root respiration and heterotrophic respiration (R_h), and R_h contributes more than half of the soil respiration. It is commonly observed that R_h exponentially increases with temperature. Therefore, a small increase of temperature can result in a remarkable enhancement of R_h, indicating that it is an important positive feedback factor to accelerate global warming under a warmer environment. However, the long-term warming effect on R_h is not well understood especially in the humid Asian monsoon region.

To examine the long-term response of R_h to global warming in Asian monsoon forests, we set a multi-channel automated chamber measurement system in a beech forest on Mount Naeba in July 2007. We prepared 10 trenched chambers (90 cm ×90 cm ×50 cm) to continuously measure R_h. Half of those trenched chambers were artificially warmed by infrared heaters 1.6 m above the soil surface (+2.5ºC), and the influence of soil warming on R_h was examined by comparing control plots and warming plots. Measurements were conducted mainly during growing season from June to October.

Even though there was a large inter-annual variation, enhancement of R_h by soil warming was confirmed in all 8 years measurements. Soil temperature was the primary factor for the seasonal variation of R_h. The influence of soil moisture on seasonal variation of R_h was relatively small.

Keywords: soil organic carbon, global warming, heterotrophic respiration, chamber, Asian monsoon

©2019. Japan Geoscience Union. All Right Reserved.

Simple approach to predict flowering and full blooming dates by bi-directional Self Organizing Maps

*Shin Nagai[1], Hiroshi Morimoto[2], Taku M Saitoh[3]

1. Research and Development Center for Global Change, Japan Agency for Marine-Earth Science and Technology, 2. Nagoya University, 3. River Basin Research Center, Gifu University

Accurate prediction of blooming phenology is important to evaluate spatio-temporal variability of ecosystem functions and services, and biodiversity under climate change. The process-based phenology models have been developed but they require suitable parameters to account for endodormancy and ecodormancy processes for each species. Our eco-physiological interpretation and observations of these processes are not still enough for various species. Here, we proposed a simple blooming phenology model by the bi-directional Self Organizing Maps (SOM). SOM, which is one of the data mining approaches, is a tool for categorizing patterns in n-dimensional observation data by forming a 2 dimensional lattice (https://clarkdatalabs.github.io/soms/SOM_NBA). The flowering and full blooming dates from 1953 to 2018 in 42 sites, Japan were predicted by the bi-directional SOM. We inputted daily mean air temperature during ecodormancy period (mainly from February to just before the flowering date) into input vectors and observed flowering or full blooming dates into a target vector. The mean absolute errors between predicted and observed flowering and full blooming dates were 2.78 to 4.33 days and 2.77 to 4.76 days, respectively. Compared with the process-based phenology model approach, our proposed approach have a little higher error. However, our approach has a merit that flowering and full blooming dates can be predicted with the very low cost of calculation without accounting for the endodormancy and ecodormancy processes. In this presentation, we show the latest result and discuss usability, uncertainty, and outlook of our proposed method.

Keywords: phenology, Self Organizing Maps, climate change

©2019. Japan Geoscience Union. All Right Reserved.

Effects of undergrowth mowing on understory carbon balance in a deciduous broadleaf forest of an urban park in central Japan

Guochao Wang[2], *Tomotsugu Yazaki[1], Toshio Kume[1], Takamitsu Kai[3]

1. School of Agriculture, Meiji University, 2. Graduate School of Agriculture, Meiji University, 3. Kurokawa Field Science Center, Meiji University

This study evaluated effects of undergrowth mowing on the carbon balance of understory of a deciduous broadleaf forest in urban park near Tokyo Metropolitan, central Japan.

Keywords: understory vegetation management, carbon balance, biomass, soil respiration, soil carbon

©2019. Japan Geoscience Union. All Right Reserved.

Solar-induced chlorophyll fluorescence for detecting ecosystem photosynthetic activity by high-resolution spectrum measurement in a paddy field in Japan

*KANOKRAT BUAREAL[1], Tomomichi Kato[2], Keisuke Ono[3]

1. Graduate School of Global Food Resources, Hokkaido University, Sapporo, Japan, 2. Research Faculty of Agriculture, Hokkaido University, Sapporo, Japan, 3. National Institute for Agro-Environmental Sciences, Tsukuba, Ibaraki, Japan

The terrestrial ecosystem is the main sink of carbon storage through plant photosynthesis which can be expressed as gross primary productivity (GPP). Accurate tracking of photosynthesis in the ecosystem level is essential because it is involved in global carbon cycling and the carbon balance between land and atmosphere. Recently, Solar-Induced Chlorophyll fluorescence (SIF) has been used for tracking changes in plant photosynthesis at the global scale by satellite. However, the coarser spatial-temporal scale by satellite needs to be validated by performing a ground-based SIF assessment to better understand the dynamics of CO2 uptake by plants. The high-resolution spectrum for SIF detection was measured at the Mase eddy flux site (36.05˚N, 140.03˚E, 11 m ASL.) in Tsukuba, Japan. The study area is a rice paddy field (*Oryza sativa* L.; cultivar Koshihikari), which is a main Asia crop type. Transplanting seedlings and harvesting crop were processed in early-May and mid-September, respectively. The spectrum was measured from April to December in 2018 using five spectroradiometers; FLAME, HR4000 x 2, QE Pro x 2 (Ocean Optics, Dunedin, FL, USA) with 0.11-1.08 nm of the full-width at half maximum (FWHM). For recording the irradiance with 5 minutes interval time, the spectroradiometers were connected via fiber switches (FSM1x8, Piezosystem Jena GmbH, Jena, Germany, and MOL-1x8-600-H, LEONI Fiber Optics GmbH, Föritztal, Germany) to three optical fiber cables: the first one was set looking downward at a viewing zenith angle of 45˚ as bare fiber (field of view (FOV) of 25˚, cable length of 15m), the second one was vertically set looking downward with cosine corrector (FOV of 180˚, cable length of 15m), and the third one was vertically set looking upward to the sky with cosine corrector (FOV of 180˚, cable length of 6m). The SIF was calculated by multispectral methods derived from the Fraunhofer Line Depth (FLD) principle 2FLD, 3FLD, iFLD and Spectral Fitting Method (SFM). In this study, the preliminary results of SIF detection are shown together with other conventional vegetation indices such as the normalized difference vegetation index (NDVI) and Enhanced Vegetation Index (EVI) for evaluating their relationship and finally verifying the SIF to be a promising proxy of photosynthesis tracking in the paddy field ecosystem.

Keywords: Ground-based SIF measurement, Fraunhofer Line Depth, Gross primary productivity, Photosynthesis, Spectroradiometers

©2019. Japan Geoscience Union. All Right Reserved.

Environmental controls on anomalous variation in solar-induced fluorescence during the last 10 years

*Tomomichi Kato[1], Kazuki Mizuno[2]

1. Research Faculty of Agriculture, Hokkaido University, 2. Graduate School of Agriculture, Hokkaido University

Solar-Induced Chlorophyll Fluorescence (SIF) has been used to estimate the ecosystem photosynthesis (GPP) recently by Satellite remote sensing and by ground observations. The advantage of use of SIF is to be able to detect the photosynthetic activity on multiple scales. To examine the potential relationship in the anomalies between SIF and environmental factors including the VI, we investigated them from the currently available satellite monthly data from GOME-2 on 0.5o (Joiner et al., 2009) and other observation-based datasets including the inversion biosphere carbon uptake estimated by CarbonTracker, the ground surface CO2 concentration by GOSAT, the CRU climatology from UEA, and multiple climatic teleconnection indices (NiNO3, PDO, NAO etc.) for 10 years from 2007 to 2016.

The SIF and biosphere land carbon uptake by Carbon Tracker 2016 has a strong negative correlationship in Australia and Middle of North America, especially in summer (JJA) in grass, shrub and rangeland. High correlation between SIF and CO2 concentration showed seasonal change. This suggests that the photosynthesis in drier and less productive ecosystems showed directly positive reactions to leaf biomass change increase probably due to simple canopy structure.

Summer SIF anomaly showed relatively high correlation coefficients to the anomalies in temperature, diurnal temperature range, potential evapotranspiration, cloudiness and precipitation depending on region. SIF anomaly also responses strongly to NiNO3 and other teleconnections in Africa, Australia, East and Central Asia, and North America. Land Cover specific analysis shows that cloudiness has negative relationship to the sensitivity of anomalies in SIF to that in cloudiness and precipitation slopes except for desert. Precipitation does not show clear relationship. Temperature shows positive response to sensitivity to cloudiness and precipitation, and negative one to that to temperature.

Keywords: Remote sensing, Carbon dynamics

©2019. Japan Geoscience Union. All Right Reserved.

Estimation of terrestrial carbon cycle in Asia using a machine learning and satellite data

*Riku Kawase[1], Kazuhito Ichii[2], Yusuke hayashi[1], Zhiyan Liu[1], Masahito Ueyama[3], Yuji Kominami[4]

1. Chiba University, 2. Center for Environmental Remote Sensing, Chiba University, 3. Osaka Prefecture University, 4. Forest Research and Management Organization

Gross Primary Productivity (GPP) and Ecosystem Respiration (RE) play an important role in the terrestrial carbon cycle. For large-scale estimation, empirical upscaling by machine learning using observation data is becoming one methodology because of expansion of ground observation network, improvement of satellite data, and development of machine learning [Yang et al. 2007; Jung et al. 2011; Kondo et al., 2015]. In Asia, spatio-temporal variations in terrestrial carbon fluxes were estimated using support vector regression by integrating ground observation network including JapanFlux [Ichii et al., 2017].
MODIS sensor data onboard Terra and Aqua satellite are one of the most widely used data for upscaling. The MODIS dataset used in many of the previous studies was an older version, Collection 5 (C5). C5 data was not able to adequately account for the secular change of sensor sensitivity, and it was improved by the new version, Collection 6 (C6) [Wang et al., 2012]. C5 data were mainly used in the large-scale estimation by machine learning so far. Therefore, we need to upgrade the dataset from C5 to C6.
In this study, we upgraded the MODIS data (from C5 to C6) from the existing study [Ichii et al. 2017]. We upgraded only MODIS data for site-level training and testing and large-scale model application. The satellite data used as input variables include the surface temperature, leaf area index, the vegetation index and the water index. GPP and NEE (Net Ecosystem Exchange) were estimated as output variables.
In the site-level model training and testing, there was no overall big difference in the result of the model (GPP, NEE) between C5 and C6. Spatial variations in GPP and NEE averaged over 2000-2015 were similar except for Southeast Asia. We also found differences in long-term trends in GPP and NPP over Asia. GPP and NEE using C6 shows more increase trends from 2000-2015. We need to evaluate which GPP and NEE changes are more realistic by comparing with other independent datasets.

Acknowledgement

This research was financially supported by the Environment Research and Technology Development Fund (2-1701) of the Environmental Restoration and Conservation Agency of Japan.

REFERENCES:

Ichii et al. (2017) JGR-Biogeosciences, 122, 767–795.

Jung et al. (2011) JGR-Biogeosciences, 116, G00J07.

Kondo et al. (2015) JGR-Biogeosciences, 120, 1226–1245.

Yang et al. (2007) Remote Sens. Environ., 110, 109-122.

©2019. Japan Geoscience Union. All Right Reserved.

Wang et al. (2012) Remote Sens. Environ., 119, 55–61.

Keywords: carbon cycle, terrestrial ecosystem, machine learning

©2019. Japan Geoscience Union. All Right Reserved.

Estimation of global solar-induced chlorophyll fluorescence (SIF) by terrestrial ecosystem model VISIT and comparison with SIF observed by GOSAT

*Tatsuya Miyauchi[1], Makoto Saito[1], Hibiki M Noda[1], Yukio Yoshida[1], Haruki Oshio[1], Akihiko Ito[1]

1. National Institute for Environmental Studies

Many studies for GPP model estimation improved by using solar-induced chlorophyll fluorescence (SIF) were reported after SIF was available from GOSAT's spectrum data. GOSAT-2 was launched in 2018 and SIF product is planted to provide. In this study we implemented the biochemical process for calculating SIF to terrestrial ecosystem model VISIT. Moreover, we estimated SIF for observation direction of GOSAT using a radiation transfer model for atmosphere-canopy. In our presentation, we will report details of model implementation and the method for converting the SIF calculated VISIT to the SIF of satellite-observed direction. We will show the comparison of SIF by VISIT and GOSAT.

Keywords: Solar-induced chlorophyll fluorescence, Terrestrial ecosystem model, GOSAT, GPP, Carbon cycle

©2019. Japan Geoscience Union. All Right Reserved.

Automatic vegetation identification in the satellite image using a convolutional neural network

*Watanabe Shuntaro[1], Kazuaki Sumi[2], Takeshi Ise[1,3]

1. Field Science Education and Research Center, Kyoto University, 2. Graduate School of Agriculture, Kyoto University, 3. PRESTO, Japan Science and Technology Agency

Image based object identification and classification would be a promising tool to implement the mapping the biodiversity with high spatio-temporal resolution. Since convolutional neural network (CNN) technique achieve highly accurate object detection and classification, it has become a new solution in the field of remote sensing. However, detection or classification of vegetation in the satellite images are still challenging task because vegetation in the satellite images often represents ambiguous and amorphous shape.

Recently, Ise et al., (2018) developed a method (chopped picture method) to conveniently classify the ambiguous and amorphous objects. This method dissects the images into numerous small squares and efficiently produces the training images. In this study, we investigated the potential for adapting the chopped picture method to classify the 3 vegetation types (Bamboo, Deciduous forest and Confer forest) in Google Earth images.
We obtained Google Earth images from three regions in Japan. By applying the deep convolutional neural network, the model successfully learned the features of each vegetation in Google Earth images, and the best trained model correctly classify the vegetation types. Our results also show that identification accuracy strongly depends on the image resolution and number of classification class. Our results suggest that CNN and the chopped picture method can potentially become a powerful tool for high accuracy automated detection and mapping of vegetation.

Keywords: Convolutional neural network, Remote sensing, Vegetation mapping, Google Earth imagery

©2019. Japan Geoscience Union. All Right Reserved.

[J] Poster | A (Atmospheric and Hydrospheric Sciences)：A-CG Complex & General

Tue. May 28, 2019 5:15 PM - 6:30 PM JST | Tue. May 28, 2019 8:15 AM - 9:30 AM UTC | Poster Hall International Exhibition Hall8, Makuhari Messe_15

[A-CG39] Biogeochemical cycles in Land Ecosystem

convener:Tomomichi Kato(Research Faculty of Agriculture, Hokkaido University), Kazuhito Ichii(Chiba University), Takeshi Ise(FSERC, Kyoto University), Munemasa Teramoto(National Institute for Environmental Studies)

Terrestrial ecosystem influences global climate through cycles of water, carbon, and nitrogen between land surface and atmosphere. For better understanding of those behaviors, a great effort has been paid for developing varieties of approaches and techniques such as biometric survey, eddy and chamber methods, near and satellite remote sensing, biosphere modeling and so on.
 In particular, the JapanFlux, founded in 2006 as a researchers network of CO2, H2O and other trace gas flux measurement, has promoted the multi-disciplinal studies not only for flux measurement community, but also for remote sensing and biosphere modeling communities. Moreover, the Research-Group-on-Integrated-Land-Processes, which was founded in 2006, also has contributed to build networks between Japanese researchers to better understanding of physical and biological processes on interactions between terrestrial surface and atmosphere.
 This session unites those multi-disciplinal activities, and promotes the oral and poster presentations on the role of terrestrial ecosystem in material circulations of water, carbon, nitrogen, energy and other substances by any approaches and technics. This session takes over the former session in last year: A-CG40.

[ACG39-P01] Long-term warming effect on heterotrophic respiration in a beech forest on Mount Naeba

*Munemasa Teramoto[1], Naishen Liang[1], Masaaki Naramoto[2], Jiye Zeng[1], Zhao Xin[1], Hajime Tomimastu[1] (1.Center for Global Environmental Research, National Institute for Environmental Studies, 2.Faculty of Agriculture, Shizuoka University)

[ACG39-P02] Simple approach to predict flowering and full blooming dates by bi-directional Self Organizing Maps

*Shin Nagai[1], Hiroshi Morimoto[2], Taku M Saitoh[3] (1.Research and Development Center for Global Change, Japan Agency for Marine-Earth Science and Technology, 2.Nagoya University, 3.River Basin Research Center, Gifu University)

[ACG39-P03] Effects of undergrowth mowing on understory carbon balance in a deciduous broadleaf forest of an urban park in central Japan

Guochao Wang[2], *Tomotsugu Yazaki[1], Toshio Kume[1], Takamitsu Kai[3] (1.School of Agriculture, Meiji University, 2.Graduate School of Agriculture, Meiji University, 3.Kurokawa Field Science Center, Meiji University)

[ACG39-P04] Solar-induced chlorophyll fluorescence for detecting ecosystem photosynthetic activity by high-resolution spectrum measurement in a paddy field in Japan

*KANOKRAT BUAREAL[1], Tomomichi Kato[2], Keisuke Ono[3] (1.Graduate School of Global Food Resources, Hokkaido University, Sapporo, Japan, 2.Research Faculty of Agriculture, Hokkaido University, Sapporo, Japan, 3.National Institute for Agro-Environmental Sciences, Tsukuba, Ibaraki, Japan)

[ACG39-P05] Environmental controls on anomalous variation in solar-induced fluorescence during the last 10 years

*Tomomichi Kato[1], Kazuki Mizuno[2] (1.Research Faculty of Agriculture, Hokkaido University, 2.Graduate School of Agriculture, Hokkaido University)

[ACG39-P06] Estimation of terrestrial carbon cycle in Asia using a machine learning and satellite data

*Riku Kawase[1], Kazuhito Ichii[2], Yusuke hayashi[1], Zhiyan Liu[1], Masahito Ueyama[3], Yuji Kominami[4] (1.Chiba University, 2.Center for Environmental Remote Sensing, Chiba University, 3.Osaka Prefecture University, 4.Forest Research and Management Organization)

[ACG39-P07] Estimation of global solar-induced chlorophyll fluorescence (SIF) by terrestrial ecosystem model VISIT and comparison with SIF observed by GOSAT

*Tatsuya Miyauchi[1], Makoto Saito[1], Hibiki M Noda[1], Yukio Yoshida[1], Haruki Oshio[1], Akihiko Ito[1] (1.National Institute for Environmental Studies)

[ACG39-P08] Automatic vegetation identification in the satellite image using a convolutional neural network

*Watanabe Shuntaro[1], Kazuaki Sumi[2], Takeshi Ise[1,3] (1.Field Science Education and Research Center, Kyoto University, 2.Graduate School of Agriculture, Kyoto University, 3.PRESTO, Japan Science and Technology Agency)

Long-term warming effect on heterotrophic respiration in a beech forest on Mount Naeba

*Munemasa Teramoto[1], Naishen Liang[1], Masaaki Naramoto[2], Jiye Zeng[1], Zhao Xin[1], Hajime Tomimastu[1]

1. Center for Global Environmental Research, National Institute for Environmental Studies, 2. Faculty of Agriculture, Shizuoka University

Soil respiration is the second largest carbon flux in terrestrial ecosystems and the global soil respiration is estimated to be 98 GtC yr^{-1}. Soil respiration consists of root respiration and heterotrophic respiration (R_h), and R_h contributes more than half of the soil respiration. It is commonly observed that R_h exponentially increases with temperature. Therefore, a small increase of temperature can result in a remarkable enhancement of R_h, indicating that it is an important positive feedback factor to accelerate global warming under a warmer environment. However, the long-term warming effect on R_h is not well understood especially in the humid Asian monsoon region.

To examine the long-term response of R_h to global warming in Asian monsoon forests, we set a multi-channel automated chamber measurement system in a beech forest on Mount Naeba in July 2007. We prepared 10 trenched chambers (90 cm ×90 cm ×50 cm) to continuously measure R_h. Half of those trenched chambers were artificially warmed by infrared heaters 1.6 m above the soil surface (+2.5ºC), and the influence of soil warming on R_h was examined by comparing control plots and warming plots. Measurements were conducted mainly during growing season from June to October.

Even though there was a large inter-annual variation, enhancement of R_h by soil warming was confirmed in all 8 years measurements. Soil temperature was the primary factor for the seasonal variation of R_h. The influence of soil moisture on seasonal variation of R_h was relatively small.

Keywords: soil organic carbon, global warming, heterotrophic respiration, chamber, Asian monsoon

©2019. Japan Geoscience Union. All Right Reserved.

Simple approach to predict flowering and full blooming dates by bi-directional Self Organizing Maps

*Shin Nagai[1], Hiroshi Morimoto[2], Taku M Saitoh[3]

1. Research and Development Center for Global Change, Japan Agency for Marine-Earth Science and Technology, 2. Nagoya University, 3. River Basin Research Center, Gifu University

Accurate prediction of blooming phenology is important to evaluate spatio-temporal variability of ecosystem functions and services, and biodiversity under climate change. The process-based phenology models have been developed but they require suitable parameters to account for endodormancy and ecodormancy processes for each species. Our eco-physiological interpretation and observations of these processes are not still enough for various species. Here, we proposed a simple blooming phenology model by the bi-directional Self Organizing Maps (SOM). SOM, which is one of the data mining approaches, is a tool for categorizing patterns in n-dimensional observation data by forming a 2 dimensional lattice (https://clarkdatalabs.github.io/soms/SOM_NBA). The flowering and full blooming dates from 1953 to 2018 in 42 sites, Japan were predicted by the bi-directional SOM. We inputted daily mean air temperature during ecodormancy period (mainly from February to just before the flowering date) into input vectors and observed flowering or full blooming dates into a target vector. The mean absolute errors between predicted and observed flowering and full blooming dates were 2.78 to 4.33 days and 2.77 to 4.76 days, respectively. Compared with the process-based phenology model approach, our proposed approach have a little higher error. However, our approach has a merit that flowering and full blooming dates can be predicted with the very low cost of calculation without accounting for the endodormancy and ecodormancy processes. In this presentation, we show the latest result and discuss usability, uncertainty, and outlook of our proposed method.

Keywords: phenology, Self Organizing Maps, climate change

©2019. Japan Geoscience Union. All Right Reserved.

Effects of undergrowth mowing on understory carbon balance in a deciduous broadleaf forest of an urban park in central Japan

Guochao Wang[2], *Tomotsugu Yazaki[1], Toshio Kume[1], Takamitsu Kai[3]

1. School of Agriculture, Meiji University, 2. Graduate School of Agriculture, Meiji University, 3. Kurokawa Field Science Center, Meiji University

This study evaluated effects of undergrowth mowing on the carbon balance of understory of a deciduous broadleaf forest in urban park near Tokyo Metropolitan, central Japan.

Keywords: understory vegetation management, carbon balance, biomass, soil respiration, soil carbon

©2019. Japan Geoscience Union. All Right Reserved.

Solar-induced chlorophyll fluorescence for detecting ecosystem photosynthetic activity by high-resolution spectrum measurement in a paddy field in Japan

*KANOKRAT BUAREAL[1], Tomomichi Kato[2], Keisuke Ono[3]

1. Graduate School of Global Food Resources, Hokkaido University, Sapporo, Japan, 2. Research Faculty of Agriculture, Hokkaido University, Sapporo, Japan, 3. National Institute for Agro-Environmental Sciences, Tsukuba, Ibaraki, Japan

The terrestrial ecosystem is the main sink of carbon storage through plant photosynthesis which can be expressed as gross primary productivity (GPP). Accurate tracking of photosynthesis in the ecosystem level is essential because it is involved in global carbon cycling and the carbon balance between land and atmosphere. Recently, Solar-Induced Chlorophyll fluorescence (SIF) has been used for tracking changes in plant photosynthesis at the global scale by satellite. However, the coarser spatial-temporal scale by satellite needs to be validated by performing a ground-based SIF assessment to better understand the dynamics of CO2 uptake by plants. The high-resolution spectrum for SIF detection was measured at the Mase eddy flux site (36.05˚N, 140.03˚E, 11 m ASL.) in Tsukuba, Japan. The study area is a rice paddy field (*Oryza sativa* L.; cultivar Koshihikari), which is a main Asia crop type. Transplanting seedlings and harvesting crop were processed in early-May and mid-September, respectively. The spectrum was measured from April to December in 2018 using five spectroradiometers; FLAME, HR4000 x 2, QE Pro x 2 (Ocean Optics, Dunedin, FL, USA) with 0.11-1.08 nm of the full-width at half maximum (FWHM). For recording the irradiance with 5 minutes interval time, the spectroradiometers were connected via fiber switches (FSM1x8, Piezosystem Jena GmbH, Jena, Germany, and MOL-1x8-600-H, LEONI Fiber Optics GmbH, Föritztal, Germany) to three optical fiber cables: the first one was set looking downward at a viewing zenith angle of 45˚ as bare fiber (field of view (FOV) of 25˚, cable length of 15m), the second one was vertically set looking downward with cosine corrector (FOV of 180˚, cable length of 15m), and the third one was vertically set looking upward to the sky with cosine corrector (FOV of 180˚, cable length of 6m). The SIF was calculated by multispectral methods derived from the Fraunhofer Line Depth (FLD) principle 2FLD, 3FLD, iFLD and Spectral Fitting Method (SFM). In this study, the preliminary results of SIF detection are shown together with other conventional vegetation indices such as the normalized difference vegetation index (NDVI) and Enhanced Vegetation Index (EVI) for evaluating their relationship and finally verifying the SIF to be a promising proxy of photosynthesis tracking in the paddy field ecosystem.

Keywords: Ground-based SIF measurement, Fraunhofer Line Depth, Gross primary productivity, Photosynthesis, Spectroradiometers

©2019. Japan Geoscience Union. All Right Reserved.

Environmental controls on anomalous variation in solar-induced fluorescence during the last 10 years

*Tomomichi Kato[1], Kazuki Mizuno[2]

1. Research Faculty of Agriculture, Hokkaido University, 2. Graduate School of Agriculture, Hokkaido University

Solar-Induced Chlorophyll Fluorescence (SIF) has been used to estimate the ecosystem photosynthesis (GPP) recently by Satellite remote sensing and by ground observations. The advantage of use of SIF is to be able to detect the photosynthetic activity on multiple scales. To examine the potential relationship in the anomalies between SIF and environmental factors including the VI, we investigated them from the currently available satellite monthly data from GOME-2 on 0.5o (Joiner et al., 2009) and other observation-based datasets including the inversion biosphere carbon uptake estimated by CarbonTracker, the ground surface CO2 concentration by GOSAT, the CRU climatology from UEA, and multiple climatic teleconnection indices (NiNO3, PDO, NAO etc.) for 10 years from 2007 to 2016.

The SIF and biosphere land carbon uptake by Carbon Tracker 2016 has a strong negative correlationship in Australia and Middle of North America, especially in summer (JJA) in grass, shrub and rangeland. High correlation between SIF and CO2 concentration showed seasonal change. This suggests that the photosynthesis in drier and less productive ecosystems showed directly positive reactions to leaf biomass change increase probably due to simple canopy structure.

Summer SIF anomaly showed relatively high correlation coefficients to the anomalies in temperature, diurnal temperature range, potential evapotranspiration, cloudiness and precipitation depending on region. SIF anomaly also responses strongly to NiNO3 and other teleconnections in Africa, Australia, East and Central Asia, and North America. Land Cover specific analysis shows that cloudiness has negative relationship to the sensitivity of anomalies in SIF to that in cloudiness and precipitation slopes except for desert. Precipitation does not show clear relationship. Temperature shows positive response to sensitivity to cloudiness and precipitation, and negative one to that to temperature.

Keywords: Remote sensing, Carbon dynamics

©2019. Japan Geoscience Union. All Right Reserved.

Estimation of terrestrial carbon cycle in Asia using a machine learning and satellite data

*Riku Kawase[1], Kazuhito Ichii[2], Yusuke hayashi[1], Zhiyan Liu[1], Masahito Ueyama[3], Yuji Kominami[4]

1. Chiba University, 2. Center for Environmental Remote Sensing, Chiba University, 3. Osaka Prefecture University, 4. Forest Research and Management Organization

Gross Primary Productivity (GPP) and Ecosystem Respiration (RE) play an important role in the terrestrial carbon cycle. For large-scale estimation, empirical upscaling by machine learning using observation data is becoming one methodology because of expansion of ground observation network, improvement of satellite data, and development of machine learning [Yang et al. 2007; Jung et al. 2011; Kondo et al., 2015]. In Asia, spatio-temporal variations in terrestrial carbon fluxes were estimated using support vector regression by integrating ground observation network including JapanFlux [Ichii et al., 2017].
MODIS sensor data onboard Terra and Aqua satellite are one of the most widely used data for upscaling. The MODIS dataset used in many of the previous studies was an older version, Collection 5 (C5). C5 data was not able to adequately account for the secular change of sensor sensitivity, and it was improved by the new version, Collection 6 (C6) [Wang et al., 2012]. C5 data were mainly used in the large-scale estimation by machine learning so far. Therefore, we need to upgrade the dataset from C5 to C6.
In this study, we upgraded the MODIS data (from C5 to C6) from the existing study [Ichii et al. 2017]. We upgraded only MODIS data for site-level training and testing and large-scale model application. The satellite data used as input variables include the surface temperature, leaf area index, the vegetation index and the water index. GPP and NEE (Net Ecosystem Exchange) were estimated as output variables.
In the site-level model training and testing, there was no overall big difference in the result of the model (GPP, NEE) between C5 and C6. Spatial variations in GPP and NEE averaged over 2000-2015 were similar except for Southeast Asia. We also found differences in long-term trends in GPP and NPP over Asia. GPP and NEE using C6 shows more increase trends from 2000-2015. We need to evaluate which GPP and NEE changes are more realistic by comparing with other independent datasets.

Acknowledgement

This research was financially supported by the Environment Research and Technology Development Fund (2-1701) of the Environmental Restoration and Conservation Agency of Japan.

REFERENCES:

Ichii et al. (2017) JGR-Biogeosciences, 122, 767–795.

Jung et al. (2011) JGR-Biogeosciences, 116, G00J07.

Kondo et al. (2015) JGR-Biogeosciences, 120, 1226–1245.

Yang et al. (2007) Remote Sens. Environ., 110, 109-122.

©2019. Japan Geoscience Union. All Right Reserved.

Wang et al. (2012) Remote Sens. Environ., 119, 55–61.

Keywords: carbon cycle, terrestrial ecosystem, machine learning

©2019. Japan Geoscience Union. All Right Reserved.

Estimation of global solar-induced chlorophyll fluorescence (SIF) by terrestrial ecosystem model VISIT and comparison with SIF observed by GOSAT

*Tatsuya Miyauchi[1], Makoto Saito[1], Hibiki M Noda[1], Yukio Yoshida[1], Haruki Oshio[1], Akihiko Ito[1]

1. National Institute for Environmental Studies

Many studies for GPP model estimation improved by using solar-induced chlorophyll fluorescence (SIF) were reported after SIF was available from GOSAT's spectrum data. GOSAT-2 was launched in 2018 and SIF product is planted to provide. In this study we implemented the biochemical process for calculating SIF to terrestrial ecosystem model VISIT. Moreover, we estimated SIF for observation direction of GOSAT using a radiation transfer model for atmosphere-canopy. In our presentation, we will report details of model implementation and the method for converting the SIF calculated VISIT to the SIF of satellite-observed direction. We will show the comparison of SIF by VISIT and GOSAT.

Keywords: Solar-induced chlorophyll fluorescence, Terrestrial ecosystem model, GOSAT, GPP, Carbon cycle

©2019. Japan Geoscience Union. All Right Reserved.

Automatic vegetation identification in the satellite image using a convolutional neural network

*Watanabe Shuntaro[1], Kazuaki Sumi[2], Takeshi Ise[1,3]

1. Field Science Education and Research Center, Kyoto University, 2. Graduate School of Agriculture, Kyoto University, 3. PRESTO, Japan Science and Technology Agency

Image based object identification and classification would be a promising tool to implement the mapping the biodiversity with high spatio-temporal resolution. Since convolutional neural network (CNN) technique achieve highly accurate object detection and classification, it has become a new solution in the field of remote sensing. However, detection or classification of vegetation in the satellite images are still challenging task because vegetation in the satellite images often represents ambiguous and amorphous shape.

Recently, Ise et al., (2018) developed a method (chopped picture method) to conveniently classify the ambiguous and amorphous objects. This method dissects the images into numerous small squares and efficiently produces the training images. In this study, we investigated the potential for adapting the chopped picture method to classify the 3 vegetation types (Bamboo, Deciduous forest and Confer forest) in Google Earth images.
We obtained Google Earth images from three regions in Japan. By applying the deep convolutional neural network, the model successfully learned the features of each vegetation in Google Earth images, and the best trained model correctly classify the vegetation types. Our results also show that identification accuracy strongly depends on the image resolution and number of classification class. Our results suggest that CNN and the chopped picture method can potentially become a powerful tool for high accuracy automated detection and mapping of vegetation.

Keywords: Convolutional neural network, Remote sensing, Vegetation mapping, Google Earth imagery

©2019. Japan Geoscience Union. All Right Reserved.

[J] Oral | A (Atmospheric and Hydrospheric Sciences)：A-CG Complex & General

Tue. May 28, 2019 9:00 AM - 10:30 AM JST | Tue. May 28, 2019 12:00 AM - 1:30 AM UTC | 102 1F

[A-CG40] Coastal Ecosystems - 1. Water Cycle and Land-Ocean Interactions

convener:Masahiko Fujii(Faculty of Environmental Earth Science), Makoto Yamada(Faculty of Economics, Ryukoku University), Jun Shoji(The University of Tokyo), Ryo Sugimoto(Faculty of Marine Biosciences, Fukui Prefectural University), Chairperson:Masahiko Fujii, Makoto Yamada

Substances from land which are brought by river and/or submarine groundwater discharge are important for the process of biological production in coastal areas. This session focuses on land-ocean interactions through water cycle. The aim of this session is to create interdisciplinary discussions on the research of connectivity of ecosystems, water cycles in terrestrial and coastal areas, fishery resources and biodiversity. Comprehensive discussion on the mechanisms that promote productivity and biodiversity in coastal ecosystems will be made from the viewpoint of land-ocean interactions. Presentations on water-material cycle in terrestrial and coastal areas, fishery resources, biodiversity and connectivity of the ecosystems are encouraged.
A companion session proposed as "Coastal Ecosystems - 2. Coral reefs, seagrass meadows, and mangroves" focuses on benthic communities in shallow-water ecosystems such as coral reefs, seagrass meadows and mangroves and is dedicated to promote researches on comprehensive assessment and monitoring of ecosystem functions and development of effective means for conservation and restoration. Main focuses of these two sessions are different. However, there are much of information that covers both sessions. Scientists who work on the related field will be able to obtain information and share them with other scientists if they attend to both of these sessions.

9:00 AM - 9:05 AM JST | 12:00 AM - 12:05 AM UTC

Introduction

9:05 AM - 9:20 AM JST | 12:05 AM - 12:20 AM UTC

[ACG40-01] Submarine groundwater discharge from Mt. Fuji in Suruga Bay(VI)

*Yasuhide Muranaka[1], Takafumi Kamitani[1], Noriaki Fushimi[1], Tomoya Oka[1], Masahiko Ono[2], Atsunao Marui[2] (1.Shizuoka Institute of Environment and Hygiene, 2.National Institute of Advanced Industrial Science and Technology)

9:20 AM - 9:35 AM JST | 12:20 AM - 12:35 AM UTC

[ACG40-02] Relationship between the distribution of freshwater groundwater under the seabed at Obama Bay and the surrounding terrain of the land

*Makoto Yamada[1], Ryo Sugimoto[2], Toshimi Nakajima[3] (1.Faculty of Economics, Ryukoku University, 2.Fuculty of Marine Biosciences, Fukui Prefectural University, 3.Fukui Prefectural University)

9:35 AM - 9:50 AM JST | 12:35 AM - 12:50 AM UTC

[ACG40-03] Influence of recirculated submarine groundwater discharge on phytoplankton dynamics in Moune Bay, Kesennuma

*Toshimi Nakajima[1], Takahiro Kusunoki[1], Yoshitake Takao[1], Ryo Sugimoto[1] (1.Fukui Prefectural University)

9:50 AM - 10:05 AM JST | 12:50 AM - 1:05 AM UTC

[ACG40-04] Estimation of contribution rate of Submarine Groundwater Discharge to *Ulva pertusa* using nitrogen stable isotope ratio analysis

*Tatsuhiro Ishida[1], Masaru Takeuchi[1], Toshimi Nakajima[1], Ryo Sugimoto[1], Shiho Kobayashi[2], Keisuke Koba[3], Keitaro Fukushima[3], Osamu Tominaga[1] (1.Fukui Prefectural University, 2.Kyoto University, 3.Center for Ecological Research,Kyoto Univrsity)

10:05 AM - 10:20 AM JST | 1:05 AM - 1:20 AM UTC

[ACG40-05] Evaluation of the environmental condition of Submarine Groundwater Discharge (SGD) using carbon and oxygen stable isotope ratio of the sessile bivalve *Crassostrea nippona*

shell

*Osamu Tominaga[1], Takeuchi Masaru[1], Ryo Sugimoto[1], Ishida Tatsuhiro[1], Takeru Hirai[1], Toshimi Nakajima[1], Jun Shoji[2], Hisami Honda[4], Makoto Taniguchi[3] (1.Fukui Prefectural University, 2.Tokyo Univ. AORI, 3.RIHN, 4.Fukui Pref Gov)

10:20 AM - 10:30 AM JST | 1:20 AM - 1:30 AM UTC

Discussion

Submarine groundwater discharge from Mt. Fuji in Suruga Bay(VI)

*Yasuhide Muranaka[1], Takafumi Kamitani[1], Noriaki Fushimi[1], Tomoya Oka[1], Masahiko Ono[2], Atsunao Marui[2]

1. Shizuoka Institute of Environment and Hygiene, 2. National Institute of Advanced Industrial Science and Technology

Around the foot of Mt. Fuji, the main flow passages of groundwater are thought to be in the Younger Fuji volcano, which consists of the pervious basaltic lavas in new volcanic stage. Most of rainfall and melted snow have been considered to be percolating into underground, turning to groundwater, flowing down in the layers of the Younger Fuji volcano and partly discharging from seabed in Suruga Bay. Especially, the Fujikawa-kako fault zone, which stretches south to north in the southwestern side of Mt. Fuji, has a potentially effect on the local groundwater flow system into Suruga Bay. Therefore, precipitation at Mt. Fuji have been considered to be discharging partly from seabed in Suruga Bayand making a impact on the biological production at the coastal sea area.

For the purpose of contribution to make sense of the rich coastal ecosystem in Suruga Bay, we conducted a survey for submarine groundwater discharge (SGD) in Oku-Suruga Bay: from the mouth of the Fuji River, at which the fault is found, to Tagonoura, where the lavas of the Younger Fuji volcano are distributed from 100 to 200 m below sea level. We detected SGD in the top of the cliff in the west of Tagonoura usinga remotelyoperatedvehicle(ROV), sampled seawater containing a high percentage of sea bottom spring water and conducted water quality analyses. In this presentation, we introduce our works noted above.

Keywords: submarine groundwater discharge (SGD), Mt. Fuji, remotely operated vehicle (ROV), water sampling method

©2019. Japan Geoscience Union. All Right Reserved.

Relationship between the distribution of freshwater groundwater under the seabed at Obama Bay and the surrounding terrain of the land

*Makoto Yamada[1], Ryo Sugimoto[2], Toshimi Nakajima[3]

1. Faculty of Economics, Ryukoku University, 2. Fuculty of Marine Biosciences, Fukui Prefectural University, 3. Fukui Prefectural University

In Obama bay at north side of Obama City, Fukui Prefecture, research on submarine groundwater discharge (SGD) has been actively carried out so far, and it is clear that the SGD are discharging in Obama Bay. However, there are still many unclear points about the situation of SGD, that is, the distribution of freshwater groundwater under the seabed. Therefore, in this research, in order to clarify the distribution of freshwater groundwater under the seabed, we conducted the survey of resistivity distribution under the seabed by using a towing electric exploration system (SuperSting: Advanced Geosciences, Inc.). We discussed about relationship between the distribution of freshwater groundwater under the seabed and the surrounding terrain of the land from the results and the surrounding land topography.

The range indicated by the resistivity value under the seabed was approximately 0.1 to 6.2 Ohm-m. The place where the relatively high resistivity value of 1 Ohm-m or more was seen was mainly the place close to the land of the alluvial fan. At the north survey area, Observation towards the offshore direction revealed that the high resistivity area extended towards the offshore area. However, further offshore there was no place of high resistivity. These facts suggest that there is a possibility that freshwater groundwater is present in the high resistivity area extending about 500 m from the shoreline to the offshore.

At the estuary of the Kita-river in the south survey area, a high resistivity area was found at a distance of 1 km from the shoreline, suggesting the possibility that freshwater groundwater is present there. According to the bathymetric chart of Obama bay, the slope of the seabed at the offshore of Kita-river is gentle from estuary towards the ocean, which is considered to be covered with sediments derived from Kita-river. The place where high resistivity was observed corresponds to that part. In other words, it is considered that freshwater groundwater is present in the fan-shaped sediment. The above suggests that the groundwater flowing through the basement of the fan in land area may flow through the alluvial fan sediment under the seabed and supply freshwater groundwater under the seabed.
As a result, it was suggested that the distribution of freshwater groundwater under the seabed in Obama Bay was influenced by the spread of the alluvial sediment at the seabed and related to the shape of the alluvial fan in land area.

Keywords: Submarine Groundwater Discharge, Alluvial fan, Obama Bay

©2019. Japan Geoscience Union. All Right Reserved.

Influence of recirculated submarine groundwater discharge on phytoplankton dynamics in Moune Bay, Kesennuma

*Toshimi Nakajima[1], Takahiro Kusunoki[1], Yoshitake Takao[1], Ryo Sugimoto[1]

1. Fukui Prefectural University

Riverine inputs are often considered as the main terrestrial source of dissolved inorganic nitrogen (DIN), phosphorus (DIP), and silicon (DSi) in coastal seas. However, the fluxes of nutrients through submarine groundwater discharge (SGD) often exceed riverine inputs in different local and regional scale settings. Although the combined effects of riverine and SGD-derived nutrient inputs are crucial for sustaining marine productivity, a difference of nutrient composition in each source may result in a different response of phytoplankton dynamics in coastal seas. In this study, we evaluated the influence of each nutrient source on phytoplankton dynamics in the head of Kesennuma Bay in June, September and November 2018. Using the short-lived radium and radon isotopes, we quantified the contribution rates of four nutrient sources (river water, fresh SGD, recirculated SGD and offshore waters) on surface waters. Simultaneously, we evaluated productivity, biomass, apparent growth rates and species composition of phytoplankton. In brief results, DIP-enriched recirculated SGD affect significant impacts on phytoplankton dynamics. In the presentation, we will discuss more detailed results.

Keywords: Recirculated submarine groundwater discharge, Phytoplankton, Radium isotopes

©2019. Japan Geoscience Union. All Right Reserved.

Estimation of contribution rate of Submarine Groundwater Discharge to *Ulva pertusa* using nitrogen stable isotope ratio analysis

*Tatsuhiro Ishida[1], Masaru Takeuchi[1], Toshimi Nakajima[1], Ryo Sugimoto[1], Shiho Kobayashi[2], Keisuke Koba[3], Keitaro Fukushima[3], Osamu Tominaga[1]

1. Fukui Prefectural University, 2. Kyoto University, 3. Center for Ecological Research,Kyoto Univrsity

In recent years, the influence of Submarine groundwater discharge (SGD) has attracted attention as a source of nutrient that supports biological production in the coastal area. However, the information about the direct influence of SGD on biological production is poor. In this study, in order to examine how much the groundwater contributes to primary production, we collected the primary producer *Ulva pertusa* in Yuza, Yamagata Prefecture, where the groundwater is abundant. On August 27, 2018, we collected sea water, ground water and ambient water around *Ulva* at five sites in the Yuza Coast and simultaneously measured salinity, water temperature, ^{222}Rn concentration which is the indicator of undergroundwater. We also analyzed the nutrient concentration, of sampled water and of *Ulva*. Finally, we estimated the contribution of groundwater to Ulva using two source Bayesian Mixing model. The value of nitrate nitrogen derived from SGD was low. In the high SGD sites (^{222}Rn concentration 427 ~ 22000 Bq/m^3) and the low SGD sites (^{222}Rn concentration 38.1 to 210.6 Bq/m^3), the of *Ulva* was 2.1 to 3.6 and 5.4 to 6.9, respectively. It was suggested that nutrient derived from SGD contributed to the production of *Ulva* in Yuza.

Keywords: Submarine Groundwater Discharge, Biological production, δ 15N

©2019. Japan Geoscience Union. All Right Reserved.

Evaluation of the environmental condition of Submarine Groundwater Discharge (SGD) using carbon and oxygen stable isotope ratio of the sessile bivalve *Crassostrea nippona* shell

*Osamu Tominaga[1], Takeuchi Masaru[1], Ryo Sugimoto[1], Ishida Tatsuhiro[1], Takeru Hirai[1], Toshimi Nakajima[1], Jun Shoji[2], Hisami Honda[4], Makoto Taniguchi[3]

1. Fukui Prefectural University, 2. Tokyo Univ. AORI, 3. RIHN, 4. Fukui Pref Gov

Submarine Groundwater Discharge (SGD) results in various biogeochemical changes in the coastal environments, such as coastal primary production, eutrophication, and benthic production. The SGD condition of 6 sites along volcanic mountain coast in northern Japan was evaluated by using carbon and oxygen stable isotope ratio ($\delta^{13}C$ and $\delta^{18}O$) in the shell of sessile bivalves *Crassostrea nippona*. In order to estimate the proportion of fresh water flow rate in SGD (FR) from the respective $\delta^{13}C$ and $\delta^{18}O$ of *C. nippona* shell, we used the three end member (sea water, riverine water and fresh underground water) bayesian stable isotope mixing model. The significant positive correlation was found between $\delta^{13}C$ and $\delta^{18}O$ of the shell and those of ambient water, respectively. FRs estimated from three source model were 3.1 -8.6% at low ^{222}Rn sites and 21.9-28.5% at high ^{222}Rn sites. At the site (Nishihama) of river mouth, the $\delta^{13}C$ and $\delta^{18}O$ of the shell collected were low (estimated FR 10.6-25.0%) and ^{222}Rn concentration was also low. The contribution of DIC in SGD and riverine water for shell formation was estimated to be 19.8 % and 7.8%, respectively. In the present study, we demonstrated the effectiveness of $\delta^{13}C$ and $\delta^{18}O$ of *C. nippona* shell as the tool for estimating FR.

Keywords: Submarine Groundwater Discharge, carbon stable isotope, oxygen stable isotope, rock oyster shell, bayesian stable isotope mixing model

©2019. Japan Geoscience Union. All Right Reserved.

[J] Oral | A (Atmospheric and Hydrospheric Sciences)：A-CG Complex & General

Tue. May 28, 2019 10:45 AM - 12:15 PM JST | Tue. May 28, 2019 1:45 AM - 3:15 AM UTC | 102 1F

[A-CG40] Coastal Ecosystems - 1. Water Cycle and Land-Ocean Interactions

convener:Masahiko Fujii(Faculty of Environmental Earth Science), Makoto Yamada(Faculty of Economics, Ryukoku University), Jun Shoji(The University of Tokyo), Ryo Sugimoto(Faculty of Marine Biosciences, Fukui Prefectural University), Chairperson:Masahiko Fujii, Makoto Yamada

Substances from land which are brought by river and/or submarine groundwater discharge are important for the process of biological production in coastal areas. This session focuses on land-ocean interactions through water cycle. The aim of this session is to create interdisciplinary discussions on the research of connectivity of ecosystems, water cycles in terrestrial and coastal areas, fishery resources and biodiversity. Comprehensive discussion on the mechanisms that promote productivity and biodiversity in coastal ecosystems will be made from the viewpoint of land-ocean interactions. Presentations on water-material cycle in terrestrial and coastal areas, fishery resources, biodiversity and connectivity of the ecosystems are encouraged.
A companion session proposed as "Coastal Ecosystems - 2. Coral reefs, seagrass meadows, and mangroves" focuses on benthic communities in shallow-water ecosystems such as coral reefs, seagrass meadows and mangroves and is dedicated to promote researches on comprehensive assessment and monitoring of ecosystem functions and development of effective means for conservation and restoration. Main focuses of these two sessions are different. However, there are much of information that covers both sessions. Scientists who work on the related field will be able to obtain information and share them with other scientists if they attend to both of these sessions.

10:45 AM - 11:00 AM JST | 1:45 AM - 2:00 AM UTC

[ACG40-06] Influence of climate change on river and submarine groundwater discharge for three decades and the change of nutrient fluxes from the land to the coastal area

*Saki KATAZAKAI[1], Jing ZHANG[2], Kota NOJIMA[3] (1.Graduate School of Science and Engineer, University of Toyama, 2.Graduate School of Science and Engineering for Science, University of Toyama, 3.University of Toyama)

11:00 AM - 11:15 AM JST | 2:00 AM - 2:15 AM UTC

[ACG40-07] The assessment of human impacts on the distribution patterns of mangroves: a comparative study between the Rewa and Ba delta, Fiji

*Masahiko Fujii[1], Jone Ravuci Sassen[2] (1.Faculty of Environmental Earth Science, 2.Graduate School of Environmental Science)

11:15 AM - 11:30 AM JST | 2:15 AM - 2:30 AM UTC

[ACG40-08] Landscape factors affect persistence and accumulation of organic carbon in sediment of secondary mangrove forests: A preliminary study

*Toshihiro Miyajima[1], Rempei Suwa[2], Keith Limuel C. Bejasa[3], Rene N. Rollon[3], Maria Lourdes San Diego-McGlone[3], Caroline M.B. Jaraula[3], Fernando P. Siringan[3], Kenji Ono[4], Yasmin H. Primavera Tirol[5], Yosuke Miyairi[1], Yusuke Yokoyama[1] (1.Atmosphere and Ocean Research Institute, The University of Tokyo, 2.Japan International Research Center for Agricultural Sciences, 3.Marine Science Institute, University of the Philippines, 4.Forestry and Forest Products Research Institute, 5.Aklan State University)

11:30 AM - 11:45 AM JST | 2:30 AM - 2:45 AM UTC

[ACG40-09] Multiple benefits of blue carbon ecosystems in promoting blue economy and reinforcing resilience in coastal communities

*Atsushi Watanabe[1] (1.The ocean policy research institute, The Sasakawa peace foundation)

11:45 AM - 12:05 PM JST | 2:45 AM - 3:05 AM UTC

[ACG40-10] Significant storage of organic carbon in mineral matrix in both land and ocean and the role of Fe

★Invited Papers

*Rota Wagai[1] (1.NARO, Institute for Agro-Environmental Sciences)

12:05 PM - 12:15 PM JST | 3:05 AM - 3:15 AM UTC

Discussion

Influence of climate change on river and submarine groundwater discharge for three decades and the change of nutrient fluxes from the land to the coastal area

*Saki KATAZAKAI[1], Jing ZHANG[2], Kota NOJIMA[3]

1. Graduate School of Science and Engineer, University of Toyama, 2. Graduate School of Science and Engineering for Science, University of Toyama, 3. University of Toyama

In Toyama prefecture, 10 billion tons of river and submarine groundwater discharge annually flows in to Toyama Bay containing nutrients (Hatta et al., 2005) . Urasawa et al. (2016) shows that 20-40% of nitrate originated on land contributes to the coastal ecosystems. So it is important to evaluate the state of nutrient transport of from the land to the coastal area. However, global warming has caused an increase in rainfall and a decrease in snowfall in Hokuriku area and it is possible that the states of water and material fluxes has changed over the past years. The aim of this study is to clarify the change of nutrient fluxes via river and submarine groundwater discharge into the coastal area, analyzing hydrogen and oxygen stable isotopes as well as chemical composition.
Results of my analysis, should be, data in my study show that the stable isotopes decreased due to increasing rainfall and decreasing snowfall for three decades. Nitrate and phosphate fluxes are shown to have dramatically decreased as forest and paddy field decreased and the water treatment facilities increased over the years.
These results suggest that nutrient fluxes from the land to coastal zone in this region may continue to decrease due to ongoing climate change and the impact of human activities.

Keywords: climate change, nutrients, river , submarine groundwater discharge

©2019. Japan Geoscience Union. All Right Reserved.

The assessment of human impacts on the distribution patterns of mangroves: a comparative study between the Rewa and Ba delta, Fiji

*Masahiko Fujii[1], Jone Ravuci Sassen[2]

1. Faculty of Environmental Earth Science, 2. Graduate School of Environmental Science

Mangrove ecosystems are among the most productive ecosystems on this planet. They are sources of livelihood to many people, the first walls of protection from storm waves, and nursery grounds for some marine organisms. Unfortunately, mangroves in Fiji are observed to have decreased over the years due to human (induced) activities. Moreover, apart from human impacts, there are several other natural impacts like tropical cyclones that may influence the distribution patterns of mangroves. The aims of this study are: (1) to elucidate changes of the distribution patterns of mangroves and the causes, and based on the results, and (2) to provide practical suggestions for sustainable use of mangroves and saving the ecosystems in Fiji.

To estimate changes in the area of mangroves, satellite imagery data from Landsat 7 and 8 were acquired and analyzed by using Geographic Information System (GIS) to produce land use classification maps for the Rewa delta (in 2002, 2005, 2016 and 2017) and Ba delta (in 2004, 2007, 2010 and 2017) in Fiji. A total of five land cover classes, i.e. mangrove, non-mangrove, urban, barren land, and water were used to classify the land cover. To elucidate causes of the changes in the area of mangroves, social survey was conducted in three villages of Kiuva, Muana I ra and Kinoya in the Rewa delta and three villages of Natutu, Nawaqarua and Votua of the Ba delta, respectively.

The trend in distribution patterns of mangroves was different between the study sites. In the Rewa delta, the area of mangroves has increased from 2002 to 2016 and decreased by 5 km² from 2016 to 2017. In Ba delta, on the other hand, the area decreased from 2004 to 2007, increased from 2007 to 2010, and again decreased from 2010 to 2017. The difference is considered to be caused by the difference in the dependency of people on mangrove ecosystems in the two sites, i.e. higher dependency on mangrove ecosystems for livelihood in the Ba delta with less access to urban centers than in the Rewa delta. Impacts of tropical cyclones and subsequent floods to mangrove ecosystems were also examined as possible climate change stressors, but the impacts were not found clearly in this study.

This study suggests that anthropogenic factors have continuously been major causes of mangrove degradation in Fiji. Mangrove protection in Fiji can be improved firstly by raising people’s awareness on the importance of mangroves to their lives. Secondly, amendment of current legislation might administer the protection of mangrove ecosystems by broadening its scope to monitor the domestic use as well as the commercial use of mangroves. Furthermore, mangrove areas are also required to be designated as “protected areas”, which can be an effective way to guard mangrove ecosystems from human impacts.

©2019. Japan Geoscience Union. All Right Reserved.

Landscape factors affect persistence and accumulation of organic carbon in sediment of secondary mangrove forests: A preliminary study

*Toshihiro Miyajima[1], Rempei Suwa[2], Keith Limuel C. Bejasa[3], Rene N. Rollon[3], Maria Lourdes San Diego-McGlone[3], Caroline M.B. Jaraula[3], Fernando P. Siringan[3], Kenji Ono[4], Yasmin H. Primavera Tirol[5], Yosuke Miyairi[1], Yusuke Yokoyama[1]

1. Atmosphere and Ocean Research Institute, The University of Tokyo, 2. Japan International Research Center for Agricultural Sciences, 3. Marine Science Institute, University of the Philippines, 4. Forestry and Forest Products Research Institute, 5. Aklan State University

Mangroves are swamp forest ecosystem that predominates in low-energy brackish environment of subtropical and tropical coastal systems. Mangroves have a remarkable capacity to capture CO_2 by primary production and sequester organic carbon (OC) in the sediment, thereby contributing to climate change mitigation. Typical carbon sequestration rate and OC stock in top 1 m of mangrove sediment have been estimated to be 1030 kg C ha^{-1} $year^{-1}$ and 723 Mg C ha^{-1}, respectively (median values of available data; Alongi 2018). Mangroves have been vastly degraded by human activities and reclaimed and/or converted to aquacultures and agricultural fields for past a few centuries. Current global loss rate of mangroves has been estimated to be up to 2% per year, which corresponds to an emission of 0.27 to 0.59 Pg CO_2 $year^{-1}$ at the maximum, if OC in top 1 m of sediment is assumed to be entirely reoxidized after reclamation and conversion (Alongi 2018, Atwood et al. 2017). However, the degree to which and the rate at which sediment OC is returned to the atmosphere as CO_2 after degradation of mangroves are still uncertain, and presumably depend on land use pattern and hydrodynamic conditions after conversion. Some part of sediment OC may be reoxidized shortly after conversion, while other parts may remain unoxidized in the soil for long term or be flushed out to the ocean by tidal exchange. To estimate the rate of OC loss after degradation and conversion of mangroves and evaluate how the sediment OC stock may be recovered by reforestation, we are now conducting a multidisciplinary research project in coastal areas of Panay Island, Philippines, where various types of habitats typical to once degraded and converted mangroves are found, such as naturally recovered secondary mangroves, artificially reforested mangroves, artificial mangroves planted on originally seagrass-dominated habitats, and tidal marshes and shrubs growing on abandoned aquaculture plots. Here, we introduce first preliminary results on OC characteristics in sediment cores collected from a naturally-recovered secondary mangrove in an estuarine delta (Ibajay) and a replanted mangrove in a well-protected embayment (Batan Bay). Estimated OC stocks in top 1 m of sediment ranged from 40 Mg C ha^{-1} in lower estuary of Ibajay to 420 Mg C ha^{-1} in Batan Bay, which are significantly lower than the world-median OC stock for natural mangroves mentioned above. Radiocarbon dating showed that the cores from the lower estuarine secondary mangrove were predominated by modern carbon down to a depth of 1 m, which suggests that old OC originally stored in the primary mangrove had been reoxidized and/or washed out to the sea soon after the conversion. In contrast, sediment OC in the upper estuarine secondary mangrove showed a radiocarbon age of 400 –1200 yBP throughout the cores, suggesting that old OC stored in original mangroves persisted at least partially through conversion and subsequent regrowth of the forest. The OC loading, i.e. the amount of OC per unit surface area of sediment grains, seemed to be constrained by the hydrodynamic stability of sediment. This implies that detrital particles derived from mangrove litter was stored at the higher concentrations in sediment of the more protected environment. The curvilinear correlation of stable carbon ($\delta^{13}C$) and nitrogen ($\delta^{15}N$) isotope ratios to the OC loading suggests that

©2019. Japan Geoscience Union. All Right Reserved.

mangrove-derived detritus typically exhibits the $\delta^{13}C$ of −28‰ vs. VPDB and the $\delta^{15}N$ of +0.5‰ vs. atmospheric N_2. The other endmember of sediment OC, putatively marine seston, is represented by the $\delta^{13}C$ of around −25‰ and the $\delta^{15}N$ of +3‰ and tended to decrease with increasing sediment depth. Our results overall showed that both the persistence of old sediment OC and the accumulation of newly supplied detrital OC in secondary mangroves are strongly constrained by the hydrodynamic setting of habitat.

Keywords: carbon sequestration function, mangroves, reforestation

©2019. Japan Geoscience Union. All Right Reserved.

Multiple benefits of blue carbon ecosystems in promoting blue economy and reinforcing resilience in coastal communities

*Atsushi Watanabe[1]

1. The ocean policy research institute, The Sasakawa peace foundation

Blue carbon ecosystems (hereafter BCEs) such as seagrass beds and mangrove forests have recently been paid international attention due to their capability in effectively absorbing and storing carbon dioxide and thus mitigating climate change impacts when they are managed properly. BCEs could also be beneficial to the coastal communities in terms of preventing or minimizing climate change impacts, offering better environmental settings for aquaculture and fisheries, and in turn reinforcing their resilience. For instance ecosystem-based disaster risk reduction (Eco-DRR), sustainable food production through fisheries and aquacultures, and sustainable tourism could enhance adaptation capacity of the coastal community to climate change. The properly managed coastal ecosystems are thus the basis for the secure, safe, and circular coastal society, which is one of the main targets of the sustainable blue economy.
In this presentation, the definition and characteristics of BCEs such as mangrove forests, seagrass beds, coral reefs, and their interlinkages will be introduced first. Then some good examples and lessons learned from coastal communities in Japan as well as Palau will be introduced. Restoration of seagrass beds and coral reefs has involved multi-stakeholders and strengthened socioecological systems in Japanese coastal communities with some innovative ideas or continuing efforts of locals. In Palau, beautiful, unique marine ecosystems have attracted tourists from overseas and environmental fees paid by these tourists have contributed to the conservation and monitoring of these ecosystems in return. Through cataloguing and networking of these good examples from world coastal areas with similar natural or socioeconomic backgrounds, sustainable use of BCEs could be mainstreamed for promoting the blue economy and combating loss of these important ecosystems globally.

Keywords: Blue economy, Blue carbon, Seagrass beds, Coral reefs

©2019. Japan Geoscience Union. All Right Reserved.

Significant storage of organic carbon in mineral matrix in both land and ocean and the role of Fe

*Rota Wagai[1]

1. NARO, Institute for Agro-Environmental Sciences

Land-ocean linkage is one of the least understood aspects in biogeochemistry and carbon (C) cycle, which presumably results from insufficient collaboration between land and ocean scientists as well as the inherent complexity of land-to-ocean processes. At a global scale, the largest C reservoir on land is soil (1500-2400 Pg C) in which major portions of C is stored as organic C (OC) in association with soil mineral particles. In ocean, sediment holds similar amounts of OC. Thus, OC stability and reactivity in soils and sediments have been a great concern as their strong impacts on global C cycle and climate change.

In this talk, I focus on the interaction of organic C with minerals (e.g., aluminosilicate clays, hydrous iron oxides) and discuss the similarity and difference in their interaction between soil and sediment based on my own studies and the literature. I also discuss mechanistic reasons why OC is stabilized in mineral matrix in both systems. An emphasis is given to iron-C interaction due to their high reactivity and ecological importance in both terrestrial and aquatic systems. For instance, OC cycle is linked to N and P cycling as many organic compounds contain N and P. Iron can control P cycle due to strong sorption of phosphate to Fe oxides.

I plan to end my talk by emphasizing that basic understanding of soil formation and biogeochemistry would greatly help when tackling C and nutrient-related questions in river and coastal water.

Keywords: iron, organic matter, soil and sediment, soil carbon, carbon cycle

©2019. Japan Geoscience Union. All Right Reserved.

[J] Poster | A (Atmospheric and Hydrospheric Sciences)：A-CG Complex & General

Tue. May 28, 2019 3:30 PM - 5:00 PM JST | Tue. May 28, 2019 6:30 AM - 8:00 AM UTC | Poster Hall International Exhibition Hall8, Makuhari Messe_10

[A-CG40] Coastal Ecosystems - 1. Water Cycle and Land-Ocean Interactions

convener:Masahiko Fujii(Faculty of Environmental Earth Science), Makoto Yamada(Faculty of Economics, Ryukoku University), Jun Shoji(The University of Tokyo), Ryo Sugimoto(Faculty of Marine Biosciences, Fukui Prefectural University)

Substances from land which are brought by river and/or submarine groundwater discharge are important for the process of biological production in coastal areas. This session focuses on land-ocean interactions through water cycle. The aim of this session is to create interdisciplinary discussions on the research of connectivity of ecosystems, water cycles in terrestrial and coastal areas, fishery resources and biodiversity. Comprehensive discussion on the mechanisms that promote productivity and biodiversity in coastal ecosystems will be made from the viewpoint of land-ocean interactions. Presentations on water-material cycle in terrestrial and coastal areas, fishery resources, biodiversity and connectivity of the ecosystems are encouraged.
A companion session proposed as "Coastal Ecosystems - 2. Coral reefs, seagrass meadows, and mangroves" focuses on benthic communities in shallow-water ecosystems such as coral reefs, seagrass meadows and mangroves and is dedicated to promote researches on comprehensive assessment and monitoring of ecosystem functions and development of effective means for conservation and restoration. Main focuses of these two sessions are different. However, there are much of information that covers both sessions. Scientists who work on the related field will be able to obtain information and share them with other scientists if they attend to both of these sessions.

[ACG40-P01] Submarine groundwater discharge and dissolved material fluxes quantified by radium isotopes in sandy beach, central Wakasa Bay

*Toshimi Nakajima[1], Ryo Sugimoto[1], Yuta Sumino[1], Makoto Taniguchi[2], Osamu Tominaga[1] (1.Fukui Prefectural University, 2.Research Institute for Humanity and Nature)

[ACG40-P02] Influence of difference in river shape on heat supply to coastal area by hot spring drainage river

*Makoto Yamada[1], Taketoshi Mishima[2], Shinji Ohsawa[2] (1.Faculty of Economics, Ryukoku University, 2.Institute for Geothermal Sciences, Graduate School of Sciences, Kyoto University)

[ACG40-P03] Construction of an artificial outlet channel affects organic carbon accumulation in a coastal lagoon

*Kenta Watanabe[1], Tomohiro Kuwae[1] (1.Port and Airport Research Institute)

[ACG40-P04] Evaluation of the influence of swans, *Cygnus cygnus* on the distribution of seagrass, *Zostera japonica*

*Yoshiyuki TANAKA[1], Fumiyuki SATO[1] (1.Hachinohe Institute of Technology, Department of Life and Environmental Science)

[ACG40-P05] Assessment and future projection of variational characteristics of ocean warming and acidification proxies in Oshoro Bay, Japan

*Masahiko Fujii[1], Takuto Yamaka[2], Shintaro Takao[3] (1.Faculty of Environmental Earth Science, 2.Graduate School of Environmental Science, 3.National Institute of Polar Research)

Submarine groundwater discharge and dissolved material fluxes quantified by radium isotopes in sandy beach, central Wakasa Bay

*Toshimi Nakajima[1], Ryo Sugimoto[1], Yuta Sumino[1], Makoto Taniguchi[2], Osamu Tominaga[1]

1. Fukui Prefectural University, 2. Research Institute for Humanity and Nature

Submarine groundwater discharge (SGD) is recognized as an important pathway for dissolved materials such as nutrients, carbon, alkalinity and trace metals from the land to the coastal sea. In the last decades, ^{222}Rn and Ra isotopes have been used as a proxy of groundwater discharge. In this study, we measured both SGD tracers (^{222}Rn, ^{223}Ra, ^{224}Ra, and ^{226}Ra) and nutrients, dissolved inorganic carbon (DIC), and total alkalinity (TAlk) of surface seawater and subterranean estuary in sandy beach of central Wakasa Bay to quantify the rate of groundwater discharge and associated material fluxes in May, July, and September 2018. Regardless of the sampling periods, ^{222}Rn, Ra isotopes, nutrients, DIC, and total alkalinity in subterranean estuary showed higher concentrations than in seawater. Activities of ^{222}Rn, ^{223}Ra, and ^{224}Ra in seawater decreased constantly from the tideline to offshore with little variation in salinity. This implies that recirculated saline groundwater seeps around the shoreline. Estimated SGD rates in May, July, and September by using the activities of ^{223}Ra and ^{224}Ra were 0.1 m^3 m^{-1} d^{-1}, 4.5 m^3 m^{-1} d^{-1}, 0.3 m^3 m^{-1} d^{-1} and 1.3 m^3 m^{-1} d^{-1}, 20.3 m^3 m^{-1} d^{-1}, 2.3 m^3 m^{-1} d^{-1}, respectively. High SGD rates in July would be due to heavy rain before the sampling date. If we assume that groundwater discharge occurs along the tideline of the beach (length: 887 m), mean SGD rates were 809.1 m^3 d^{-1} in May, 11192.4 m^3 d^{-1} in July, and 1186.2 m^3 d^{-1} in September. Fluxes of nutrients (DIN, DIP, and DSi), DIC, and TAlk, derived SGD were calculated by multiplying mean SGD rates by its mean concentration in subterranean estuary. Although the nutrients fluxes from SGD were < 1% of those from the Kita River, DIC flux of SGD in May, July, and September corresponds to 6.5%, 94.7%, and 7.7% of the Kita River, respectively. These results mean that DIC transport through groundwater may be significant for carbonate system of Wakasa Bay.

Keywords: Submarine groundwater discharge, Ra isotopes, dissolved materials, Coastal seas

©2019. Japan Geoscience Union. All Right Reserved.

Influence of difference in river shape on heat supply to coastal area by hot spring drainage river

*Makoto Yamada[1], Taketoshi Mishima[2], Shinji Ohsawa[2]

1. Faculty of Economics, Ryukoku University, 2. Institute for Geothermal Sciences, Graduate School of Sciences, Kyoto University

In Beppu City, Oita Prefecture, it is clear that hot spring drainage flows into the river and affects the river ecosystem. On the mouth of the river where hot spring drainage flow into, there are many tropical fish due to the influence of the heat of hot spring drainage. However, even in rivers where hot spring drainage flow into, there are rivers where many of the native fish inhabits, and the influence of heat on the estuary is various. The river in Beppu city is flowing down a volcanic fan, and the length of the river is relatively short, but the shape differs for each river. Depending on the river, river stream is lined entirely with concrete, and the condition of the river is very different. In Beppu, hot spring drainage flows into mainly by the middle part of the river, so it is expected that the degree of heat supplied to the estuary will be different due to the difference in river conditions while reaching the estuary area. Therefore, in this study, in order to clarify the reason for the difference in the amount of heat supply to the coastal area, we compared the two rivers where the hot spring drainage remarkably flows into.
On both rivers, hot spring drainage flows into the river at the area of about 200 m in elevation, flows down about 3 km and reaches the mouth of the estuary. However, the river water temperature at the estuary is lower by 5 deg. C or more in the Haruki-river throughout the year. Compared to the Haruki River where some of the natural river remains, nearly all of the Hirata River is covered with concrete. In the presentation, in addition to these differences, topographical differences such as inclination and linearity, differences in flow rate etc. are compared and the reason why the difference in thermal influence of hot spring drainage at the mouth of the estuary occurs is considered.

Keywords: hot spring drainage, hot spring heat, river water temperature

©2019. Japan Geoscience Union. All Right Reserved.

Construction of an artificial outlet channel affects organic carbon accumulation in a coastal lagoon

*Kenta Watanabe[1], Tomohiro Kuwae[1]

1. Port and Airport Research Institute

Organic carbon (C_{org}) storage is one of the important functions of vegetated coastal ecosystems for mitigating the adverse effects of climate change. The artificial alteration of landforms by coastal constructions would impact on habitats, hydrological conditions, and sediment loads. However, how the coastal constructions change C_{org} accumulation in vegetated coastal ecosystems is poorly understood. In this study, the sediment profiles of geological and biogeochemical characteristics were measured in Komuke Lagoon, Hokkaido. Stable isotope ratios and ^{210}Pb profiles were used to investigate the origin of C_{org} and sediment age. We showed that C_{org} accumulation rates and the origin of accumulated C_{org} significantly changed after the construction of an artificial outlet channel. C_{org} accumulation was enhanced, the contribution of terrestrial-derived C_{org} decreased, and that of microalgae- and seagrass-derived C_{org} increased after the coastal construction at the site. These findings indicate that the construction of an artificial outlet channel alters the frequency of seawater exchange and affects habitat types and C_{org} accumulation.

Keywords: organic carbon storage, seagrass meadows, saltmarshes, coastal construction, age-depth modelling

©2019. Japan Geoscience Union. All Right Reserved.

Evaluation of the influence of swans, *Cygnus cygnus* on the distribution of seagrass, *Zostera japonica*

*Yoshiyuki TANAKA[1], Fumiyuki SATO[1]

1. Hachinohe Institute of Technology, Department of Life and Environmental Science

Distribution and biomass of seagrass are changed by various environmental factors. Grazing pressure by animals is one of the factors. It is pointed out that Zostera japonica growing on the shallow coast of Kominato in Aimori prefecture is affected by Grazing pressures of swans that come every winter. In this study, we investigated seasonal change of Z. japonica in the shallow area and seasonal change of biomass, and analyzed feces of swans, and evaluated the influence of swans on the distribution of Z. japonica. In July, October, November, December 2018, line transect survey was conducted to measure the presence or absence of seagrasses at 57 fixed points, and at some sites seagrass shoots within 20 cm * 20 cm frame were collected, shoot number and biomass was recorded. We also carried out aerial photographs using a drone. In February and March 2018, the feces of the swan was collected, the content of the feces was visually analyzed, and carbon and nitrogen stable isotope ratio analysis was also conducted. As a result of presence or absence survey, the distribution point decreased in November compared with October, and almost disappeared in December. A sharp decline was confirmed even in the Drone images. The shoot number of seagrass slightly decreased from July to October, while the weight of the underground part did not change much, whereas the weight of the aboveground part slightly increased. The shoots number of Z. japnonica in October to November, the weight of the aboveground and the belowground decreased sharply. Plant pieces and seaweed pieces were confirmed as fecal contents in February and rice hulls were confirmed in March and in the isotopic ratio analysis, changes in food quality were confirmed between February and March. It is inferred that the influence of predation by swans and other migratory birds was great for wide range and sudden reduction of distribution and biomass. Because biomass of the Z. japonica becomes extremely small in December, it is reasonable to think that the swans during overwintering depends on bait other than the Z. japonica. It was suggested that in December and March before and after paddy fields were covered with snow, it depended on the heading of paddy fields.

Keywords: seagrass, swan, Cygnus cygnus

©2019. Japan Geoscience Union. All Right Reserved.

Assessment and future projection of variational characteristics of ocean warming and acidification proxies in Oshoro Bay, Japan

*Masahiko Fujii[1], Takuto Yamaka[2], Shintaro Takao[3]

1. Faculty of Environmental Earth Science, 2. Graduate School of Environmental Science, 3. National Institute of Polar Research

As ocean acidification proceeds, it is concerned difficult for calcium carbonate and magnesium carbonate to be produced in the ocean, and calcifying organisms such as corals and shellfish having these skeletons and shells may be adversely affected. Moreover, the diurnal, seasonal and interannual fluctuation are all considered more prominent in coasts than in the open ocean, because of relatively larger amount of sea grass beds and more direct and significant terrestrial impacts. On the other hand, in the subarctic coastal region, it is difficult to maintain observation due to stormy weather in winter, which yields paucity of observational data. In this study, long-term continuous monitoring of physical and biogeochemical parameters was conducted in Oshoro Bay, Otaru City, Hokkaido. Our results show that the timing of increase and decrease of pH and dissolved oxygen almost coincided with each other, and the diurnal variation of pH was larger in spring and summer than in fall and winter. The diurnal variation of pH was 0.1 or more on average from May to August. The variation was 0.15 on average and 0.26 at the maximum, respectively, in August. That was 0.03 on average and 0.07 at the maximum, respectively, in November. Thus, the seasonal difference in the diurnal variation was clear, suggesting significant effects of the photosynthesis in the daytime and the respiration in the nighttime by primary producers. The results suggest relatively predominant biological effects with larger biomass and higher solar radiation in summer compared to those in winter. Results of the temporal variability of the ocean warming and acidification proxies obtained by applying the Regional Ocean Model System (ROMS) to the site will be introduced in the presentation.

Keywords: Ocean acidification, Ocean warming , subarctic, coast, pH, calcium saturation state

©2019. Japan Geoscience Union. All Right Reserved.

[J] Poster | A (Atmospheric and Hydrospheric Sciences)：A-CG Complex & General

Tue. May 28, 2019 5:15 PM - 6:30 PM JST | Tue. May 28, 2019 8:15 AM - 9:30 AM UTC | Poster Hall International Exhibition Hall8, Makuhari Messe_16

[A-CG40] Coastal Ecosystems - 1. Water Cycle and Land-Ocean Interactions

convener:Masahiko Fujii(Faculty of Environmental Earth Science), Makoto Yamada(Faculty of Economics, Ryukoku University), Jun Shoji(The University of Tokyo), Ryo Sugimoto(Faculty of Marine Biosciences, Fukui Prefectural University)

Substances from land which are brought by river and/or submarine groundwater discharge are important for the process of biological production in coastal areas. This session focuses on land-ocean interactions through water cycle. The aim of this session is to create interdisciplinary discussions on the research of connectivity of ecosystems, water cycles in terrestrial and coastal areas, fishery resources and biodiversity. Comprehensive discussion on the mechanisms that promote productivity and biodiversity in coastal ecosystems will be made from the viewpoint of land-ocean interactions. Presentations on water-material cycle in terrestrial and coastal areas, fishery resources, biodiversity and connectivity of the ecosystems are encouraged.
A companion session proposed as "Coastal Ecosystems - 2. Coral reefs, seagrass meadows, and mangroves" focuses on benthic communities in shallow-water ecosystems such as coral reefs, seagrass meadows and mangroves and is dedicated to promote researches on comprehensive assessment and monitoring of ecosystem functions and development of effective means for conservation and restoration. Main focuses of these two sessions are different. However, there are much of information that covers both sessions. Scientists who work on the related field will be able to obtain information and share them with other scientists if they attend to both of these sessions.

[ACG40-P01] Submarine groundwater discharge and dissolved material fluxes quantified by radium isotopes in sandy beach, central Wakasa Bay

*Toshimi Nakajima[1], Ryo Sugimoto[1], Yuta Sumino[1], Makoto Taniguchi[2], Osamu Tominaga[1] (1.Fukui Prefectural University, 2.Research Institute for Humanity and Nature)

[ACG40-P02] Influence of difference in river shape on heat supply to coastal area by hot spring drainage river

*Makoto Yamada[1], Taketoshi Mishima[2], Shinji Ohsawa[2] (1.Faculty of Economics, Ryukoku University, 2.Institute for Geothermal Sciences, Graduate School of Sciences, Kyoto University)

[ACG40-P03] Construction of an artificial outlet channel affects organic carbon accumulation in a coastal lagoon

*Kenta Watanabe[1], Tomohiro Kuwae[1] (1.Port and Airport Research Institute)

[ACG40-P04] Evaluation of the influence of swans, *Cygnus cygnus* on the distribution of seagrass, *Zostera japonica*

*Yoshiyuki TANAKA[1], Fumiyuki SATO[1] (1.Hachinohe Institute of Technology, Department of Life and Environmental Science)

[ACG40-P05] Assessment and future projection of variational characteristics of ocean warming and acidification proxies in Oshoro Bay, Japan

*Masahiko Fujii[1], Takuto Yamaka[2], Shintaro Takao[3] (1.Faculty of Environmental Earth Science, 2.Graduate School of Environmental Science, 3.National Institute of Polar Research)

Submarine groundwater discharge and dissolved material fluxes quantified by radium isotopes in sandy beach, central Wakasa Bay

*Toshimi Nakajima[1], Ryo Sugimoto[1], Yuta Sumino[1], Makoto Taniguchi[2], Osamu Tominaga[1]

1. Fukui Prefectural University, 2. Research Institute for Humanity and Nature

Submarine groundwater discharge (SGD) is recognized as an important pathway for dissolved materials such as nutrients, carbon, alkalinity and trace metals from the land to the coastal sea. In the last decades, ^{222}Rn and Ra isotopes have been used as a proxy of groundwater discharge. In this study, we measured both SGD tracers (^{222}Rn, ^{223}Ra, ^{224}Ra, and ^{226}Ra) and nutrients, dissolved inorganic carbon (DIC), and total alkalinity (TAlk) of surface seawater and subterranean estuary in sandy beach of central Wakasa Bay to quantify the rate of groundwater discharge and associated material fluxes in May, July, and September 2018. Regardless of the sampling periods, ^{222}Rn, Ra isotopes, nutrients, DIC, and total alkalinity in subterranean estuary showed higher concentrations than in seawater. Activities of ^{222}Rn, ^{223}Ra, and ^{224}Ra in seawater decreased constantly from the tideline to offshore with little variation in salinity. This implies that recirculated saline groundwater seeps around the shoreline. Estimated SGD rates in May, July, and September by using the activities of ^{223}Ra and ^{224}Ra were 0.1 m^3 m^{-1} d^{-1}, 4.5 m^3 m^{-1} d^{-1}, 0.3 m^3 m^{-1} d^{-1} and 1.3 m^3 m^{-1} d^{-1}, 20.3 m^3 m^{-1} d^{-1}, 2.3 m^3 m^{-1} d^{-1}, respectively. High SGD rates in July would be due to heavy rain before the sampling date. If we assume that groundwater discharge occurs along the tideline of the beach (length: 887 m), mean SGD rates were 809.1 m^3 d^{-1} in May, 11192.4 m^3 d^{-1} in July, and 1186.2 m^3 d^{-1} in September. Fluxes of nutrients (DIN, DIP, and DSi), DIC, and TAlk, derived SGD were calculated by multiplying mean SGD rates by its mean concentration in subterranean estuary. Although the nutrients fluxes from SGD were < 1% of those from the Kita River, DIC flux of SGD in May, July, and September corresponds to 6.5%, 94.7%, and 7.7% of the Kita River, respectively. These results mean that DIC transport through groundwater may be significant for carbonate system of Wakasa Bay.

Keywords: Submarine groundwater discharge, Ra isotopes, dissolved materials, Coastal seas

©2019. Japan Geoscience Union. All Right Reserved.

Influence of difference in river shape on heat supply to coastal area by hot spring drainage river

*Makoto Yamada[1], Taketoshi Mishima[2], Shinji Ohsawa[2]

1. Faculty of Economics, Ryukoku University, 2. Institute for Geothermal Sciences, Graduate School of Sciences, Kyoto University

In Beppu City, Oita Prefecture, it is clear that hot spring drainage flows into the river and affects the river ecosystem. On the mouth of the river where hot spring drainage flow into, there are many tropical fish due to the influence of the heat of hot spring drainage. However, even in rivers where hot spring drainage flow into, there are rivers where many of the native fish inhabits, and the influence of heat on the estuary is various. The river in Beppu city is flowing down a volcanic fan, and the length of the river is relatively short, but the shape differs for each river. Depending on the river, river stream is lined entirely with concrete, and the condition of the river is very different. In Beppu, hot spring drainage flows into mainly by the middle part of the river, so it is expected that the degree of heat supplied to the estuary will be different due to the difference in river conditions while reaching the estuary area. Therefore, in this study, in order to clarify the reason for the difference in the amount of heat supply to the coastal area, we compared the two rivers where the hot spring drainage remarkably flows into.
On both rivers, hot spring drainage flows into the river at the area of about 200 m in elevation, flows down about 3 km and reaches the mouth of the estuary. However, the river water temperature at the estuary is lower by 5 deg. C or more in the Haruki-river throughout the year. Compared to the Haruki River where some of the natural river remains, nearly all of the Hirata River is covered with concrete. In the presentation, in addition to these differences, topographical differences such as inclination and linearity, differences in flow rate etc. are compared and the reason why the difference in thermal influence of hot spring drainage at the mouth of the estuary occurs is considered.

Keywords: hot spring drainage, hot spring heat, river water temperature

©2019. Japan Geoscience Union. All Right Reserved.

Construction of an artificial outlet channel affects organic carbon accumulation in a coastal lagoon

*Kenta Watanabe[1], Tomohiro Kuwae[1]

1. Port and Airport Research Institute

Organic carbon (C_{org}) storage is one of the important functions of vegetated coastal ecosystems for mitigating the adverse effects of climate change. The artificial alteration of landforms by coastal constructions would impact on habitats, hydrological conditions, and sediment loads. However, how the coastal constructions change C_{org} accumulation in vegetated coastal ecosystems is poorly understood. In this study, the sediment profiles of geological and biogeochemical characteristics were measured in Komuke Lagoon, Hokkaido. Stable isotope ratios and ^{210}Pb profiles were used to investigate the origin of C_{org} and sediment age. We showed that C_{org} accumulation rates and the origin of accumulated C_{org} significantly changed after the construction of an artificial outlet channel. C_{org} accumulation was enhanced, the contribution of terrestrial-derived C_{org} decreased, and that of microalgae- and seagrass-derived C_{org} increased after the coastal construction at the site. These findings indicate that the construction of an artificial outlet channel alters the frequency of seawater exchange and affects habitat types and C_{org} accumulation.

Keywords: organic carbon storage, seagrass meadows, saltmarshes, coastal construction, age-depth modelling

©2019. Japan Geoscience Union. All Right Reserved.

Evaluation of the influence of swans, *Cygnus cygnus* on the distribution of seagrass, *Zostera japonica*

*Yoshiyuki TANAKA[1], Fumiyuki SATO[1]

1. Hachinohe Institute of Technology, Department of Life and Environmental Science

Distribution and biomass of seagrass are changed by various environmental factors. Grazing pressure by animals is one of the factors. It is pointed out that Zostera japonica growing on the shallow coast of Kominato in Aimori prefecture is affected by Grazing pressures of swans that come every winter. In this study, we investigated seasonal change of Z. japonica in the shallow area and seasonal change of biomass, and analyzed feces of swans, and evaluated the influence of swans on the distribution of Z. japonica. In July, October, November, December 2018, line transect survey was conducted to measure the presence or absence of seagrasses at 57 fixed points, and at some sites seagrass shoots within 20 cm * 20 cm frame were collected, shoot number and biomass was recorded. We also carried out aerial photographs using a drone. In February and March 2018, the feces of the swan was collected, the content of the feces was visually analyzed, and carbon and nitrogen stable isotope ratio analysis was also conducted. As a result of presence or absence survey, the distribution point decreased in November compared with October, and almost disappeared in December. A sharp decline was confirmed even in the Drone images. The shoot number of seagrass slightly decreased from July to October, while the weight of the underground part did not change much, whereas the weight of the aboveground part slightly increased. The shoots number of Z. japnonica in October to November, the weight of the aboveground and the belowground decreased sharply. Plant pieces and seaweed pieces were confirmed as fecal contents in February and rice hulls were confirmed in March and in the isotopic ratio analysis, changes in food quality were confirmed between February and March. It is inferred that the influence of predation by swans and other migratory birds was great for wide range and sudden reduction of distribution and biomass. Because biomass of the Z. japonica becomes extremely small in December, it is reasonable to think that the swans during overwintering depends on bait other than the Z. japonica. It was suggested that in December and March before and after paddy fields were covered with snow, it depended on the heading of paddy fields.

Keywords: seagrass, swan, Cygnus cygnus

©2019. Japan Geoscience Union. All Right Reserved.

Assessment and future projection of variational characteristics of ocean warming and acidification proxies in Oshoro Bay, Japan

*Masahiko Fujii[1], Takuto Yamaka[2], Shintaro Takao[3]

1. Faculty of Environmental Earth Science, 2. Graduate School of Environmental Science, 3. National Institute of Polar Research

As ocean acidification proceeds, it is concerned difficult for calcium carbonate and magnesium carbonate to be produced in the ocean, and calcifying organisms such as corals and shellfish having these skeletons and shells may be adversely affected. Moreover, the diurnal, seasonal and interannual fluctuation are all considered more prominent in coasts than in the open ocean, because of relatively larger amount of sea grass beds and more direct and significant terrestrial impacts. On the other hand, in the subarctic coastal region, it is difficult to maintain observation due to stormy weather in winter, which yields paucity of observational data. In this study, long-term continuous monitoring of physical and biogeochemical parameters was conducted in Oshoro Bay, Otaru City, Hokkaido. Our results show that the timing of increase and decrease of pH and dissolved oxygen almost coincided with each other, and the diurnal variation of pH was larger in spring and summer than in fall and winter. The diurnal variation of pH was 0.1 or more on average from May to August. The variation was 0.15 on average and 0.26 at the maximum, respectively, in August. That was 0.03 on average and 0.07 at the maximum, respectively, in November. Thus, the seasonal difference in the diurnal variation was clear, suggesting significant effects of the photosynthesis in the daytime and the respiration in the nighttime by primary producers. The results suggest relatively predominant biological effects with larger biomass and higher solar radiation in summer compared to those in winter. Results of the temporal variability of the ocean warming and acidification proxies obtained by applying the Regional Ocean Model System (ROMS) to the site will be introduced in the presentation.

Keywords: Ocean acidification, Ocean warming , subarctic, coast, pH, calcium saturation state

©2019. Japan Geoscience Union. All Right Reserved.

[J] Poster | A (Atmospheric and Hydrospheric Sciences)：A-CG Complex & General

Tue. May 28, 2019 1:45 PM - 3:15 PM JST | Tue. May 28, 2019 4:45 AM - 6:15 AM UTC | Poster Hall International Exhibition Hall8, Makuhari Messe_3

[A-CG41] Promotion of Application and Utilization of Aircrafts for Earth sciences

convener:Nobuhiro Takahashi(Institute for Space-Earth Environmental Research, Nagoya University), Makoto Koike(Department of Earth and Planetary Science, Graduate School of Science, The University of Tokyo), Toshinobu Machida(National Institute for Environmental Studies), Taro Shinoda(Institute for Space-Earth Environmental Research, Nagoya University)

The problem of global environmental change such as global warming is a problem throughout the Earth and planetary sciences. To confront this problem, progresses of the observations that are dedicated for the monitoring Earth and for the process studies as well as the progresses of numerical prediction models. Aircraft observation has the great advantages of immediate and direct (in-situ) observations which cannot be achieved by Earth observing satellites or ground-based observations. Recently, the importance of aircraft observation is increasing in "in-situ measurements" such as concentration of greenhouse gases, aerosol and cloud particle size distribution, and chemical composition, and "remote sensing" such as three dimensional typhoon observation and observation on forests and vegetation. In addition, the application of aircraft observation to geodesy, study on earthquakes and volcanos are also progressing. However, steady and extensive aircraft observations to fulfill the requirements in Japan are not realized at the present time. Meanwhile, it is also a fact that the aircraft observations which have been carried out has cited the world leading results. In order to realize the effective research by using aircraft, it is necessary to have a close collaborations among researchers to promote aircraft observations, and it is also necessary to carry out as the master plan of national academic council of Japan. In this session, we will discuss the future aircraft observation through the latest research results with aircraft observations.

[ACG41-P01] In situ measurements of aerosol and cloud microphysical properties and cloud seeding experiments over the UAE

*Narihiro Orikasa[1], Masataka Murakami[2,1], Takuya Tajiri[1], Yuji Zaizen[1], Taro Shinoda[2] (1.Meteorological Research Institute, 2.Nagoya Univ., ISEE)

[ACG41-P02] Analysis and Forecast Using Dropsonde Data from the Inner-Core Region of Tropical Cyclone Lan (2017) Obtained during the First Aircraft Missions of T-PARCII

*Kosuke Ito[1], Hiroyuki Yamada[1], Munehiko Yamaguchi[2], Tetsuo Nakazawa[2], Norio Nagahama[3], Kensaku Shimizu[3], Tadayasu Ohigashi[4], Taro Shinoda[5], Kazuhisa Tsuboki[5] (1.University of the Ryukyus, 2.Meteorological Research Institute, 3.Meisei Electric Co. LTD., 4.National Research Institute for Earth Science and Disaster Resilience, 5.Nagoya University)

[ACG41-P03] On the Spatial Distribution of Freezing height of Typhoon Trami

*Nobuhiro Takahashi[1], Yuki Kaneko[2], Kazuhisa Tsuboki[1] (1.Institute for Space-Earth Environmental Research, Nagoya University, 2.Japan Aerospace Exploration Agency)

[ACG41-P04] Revision of Research Plan on “Promotion of Climate and Earth System Science Research by Aircraft Observation”

*Nobuhiro Takahashi[1], Makoto Koike[2] (1.Institute for Space-Earth Environmental Research, Nagoya University, 2.School of Science, The University of Tokyo)

In situ measurements of aerosol and cloud microphysical properties and cloud seeding experiments over the UAE

*Narihiro Orikasa[1], Masataka Murakami[2,1], Takuya Tajiri[1], Yuji Zaizen[1], Taro Shinoda[2]

1. Meteorological Research Institute, 2. Nagoya Univ., ISEE

Our field campaign of aircraft observations had successfully been conducted over the UAE regions, as well as ferries between UAE and Japan, in the summer of 2017. This campaign has mainly two objectives. First, in situ measurements contribute to investigation on microphysical processes in seeded and unseeded clouds as well as elucidation of the mechanism responsible for precipitation augmentation. Secondly, the field observation data is useful to validate numerical simulations of cloud and precipitation and to improve the accuracy and reliability of numerical models.

We had deployed two aircraft whose base was Al Ain International Airport, as well as one ground-based observation site next to the aircraft hangar. One aircraft for in situ measurements was B200T operated by Diamond Air Service Inc., and the other for cloud seeding was C-90 operated by UAE National Center of Meteorology (NCM). We performed 14 research flights (~30 hours in total) from Sep. 5 to Sep. 24. Thirteen of the B200T flights were coordinated with the C-90 flights. As shown in Fig. 1, the B200T installed meteorological instruments, hot-wire water content probes, cloud microphysical probes for in situ measurements, aerosol size distribution instruments, sampling mesh device for electron microscopic analysis, cloud condensation nuclei (CCN) counter, and ice nucleating particle (INP) counter. The C-90 dispersed two types of seeding materials through burn-in-place flare racks: $CaCl_2$ hygroscopic (HYG) and silver iodide (AgI) flares.

As one of the flight patterns, seeding plumes generated from the C-90 were sampled and measured with the instrumented B200T which followed the C-90. We collected excellent data for background (BG) aerosols and seeding plume particles generated by HYG flares, AgI flares, or simultaneously generated by the both types of flares.

In order to investigate cloud seeding effects, the B200T measured the evolution of aerosols and cloud particles from cloud base to upper levels before and after the C-90's flare seeding. Based on the same strategy and method as in previous studies on Japanese field campaigns, the flight data quality check and data analysis have been processed, and results of initial cloud droplet size distributions in terms of the seeding signatures are shown from several cases. In general, it was difficult to find clear seeding signatures in any cases.

Except for the seeding experiments, several flights provided us in situ measurements of natural clouds. We sometimes encountered relatively developed clouds whose top temperature was warmer than -10 C, and most of such clouds had ice crystals and graupels. Those basic data will be useful to fully understand the mechanism of ice formation over the UAE regions and to verify the numerical simulations of cloud and precipitation.

In order to conduct an effective and efficient cloud seeding experiment, it is essential to know the physico-chemical properties of BG aerosols in the atmosphere and to observe their spatial and temporal distributions before the experiment. The vertical profiles of aerosol number concentrations (corrected for STP conditions) showed rather constant below cloud base height. The IN and CCN abilities of BG aerosols

©2019. Japan Geoscience Union. All Right Reserved.

are also essential information to accurately simulate cloud formation and precipitation development. The analysis of number concentrations of INP and CCN is shown from a few cases. The INP concentrations were typically ranged on the order of 1 to 10 L^{-1} and there were no significant height dependency. The CCN concentrations were typically several hundreds cm^{-3}_stp and generally depended on the space and time.

Keywords: Aerosol-Cloud Interactions, Cloud Condensation Nuclei/Ice Nucleating Particles, Cloud Seeding, Hygroscopic Particles

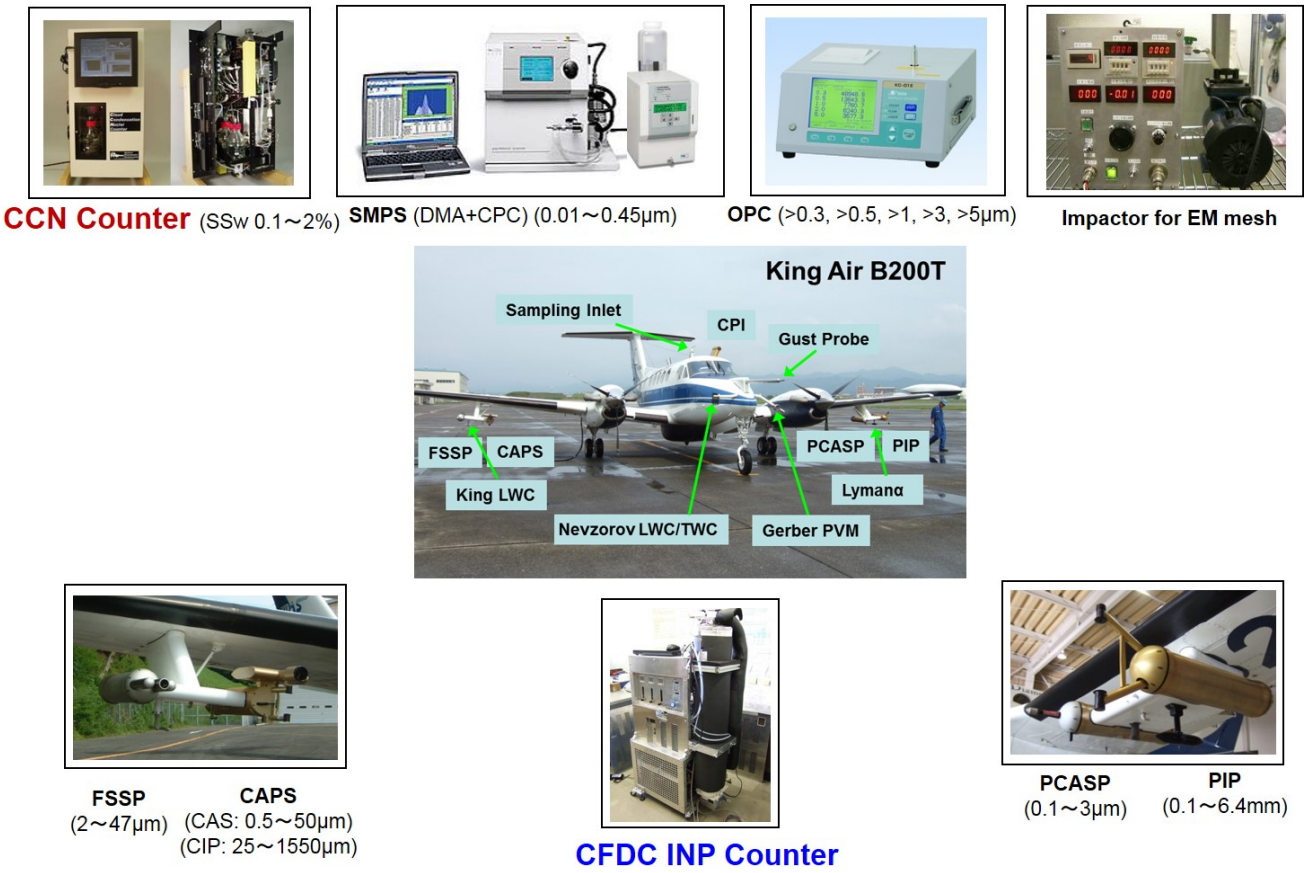

Fig. 1 Aircraft instrumentation.

©2019. Japan Geoscience Union. All Right Reserved.

Analysis and Forecast Using Dropsonde Data from the Inner-Core Region of Tropical Cyclone Lan (2017) Obtained during the First Aircraft Missions of T-PARCII

*Kosuke Ito[1], Hiroyuki Yamada[1], Munehiko Yamaguchi[2], Tetsuo Nakazawa[2], Norio Nagahama[3], Kensaku Shimizu[3], Tadayasu Ohigashi[4], Taro Shinoda[5], Kazuhisa Tsuboki[5]

1. University of the Ryukyus, 2. Meteorological Research Institute, 3. Meisei Electric Co. LTD., 4. National Research Institute for Earth Science and Disaster Resilience, 5. Nagoya University

The inner core of Tropical Cyclone Lan was observed on 21–22 October 2017 by GPS dropsondes during the first aircraft missions of the Tropical Cyclones-Pacific Asian Research Campaign for the Improvement of Intensity Estimations/Forecasts (T-PARCII). To evaluate the impact of dropsondes on forecast skill, 12 36-h forecasts were conducted using a Japan Meteorological Agency non-hydrostatic model (JMA-NHM) with a JMANHM-based mesoscale four-dimensional data assimilation (DA) system. Track forecast skill improved over all forecast times with the assimilation of the dropsonde data. The improvement rate was 8–16% for 27–36-h forecasts. Minimum sea level pressure (Pmin) forecasts were generally degenerated (improved) for relatively short-term (long-term) forecasts by adding the dropsonde data, and maximum wind speed (Vmax) forecasts were degenerated. Some of the changes in the track and Vmax forecasts were statistically significant at the 95% confidence level. It is notable that the dropsonde-derived estimate of Pmin was closer to the realtime analysis by the Regional Specialized Meteorological Center (RSMC) Tokyo than the RSMC Tokyo best track analysis. The degeneration in intensity forecast skill due to uncertainties in the best track data is discussed.

Keywords: tropical cyclone, data assimilation

©2019. Japan Geoscience Union. All Right Reserved.

On the Spatial Distribution of Freezing height of Typhoon Trami

*Nobuhiro Takahashi[1], Yuki Kaneko[2], Kazuhisa Tsuboki[1]

1. Institute for Space-Earth Environmental Research, Nagoya University, 2. Japan Aerospace Exploration Agency

Drop sonde observation from aircraft was conducted for typhoon Trami that occurred in September 2018. The drop sonde observation provides the vertical profile of the temperature and humidity in and around the eye of typhoon. Meanwhile, the global precipitation measuring (GPM) core satellite, which equips dual frequency precipitation radar (DPR), passed over Trami for several times, two of which captured the eye structure. In particular, the over flight case on September 27 by DPR is several hours after the drop sonde observation.

Since DPR can observe the vertical structure of the precipitation system, it is possible to estimate the freezing height in the stratiform precipitation region from the melting layer appearing as the so-called bright band, and an attempt was made to separate snowfall and rainfall by using dual frequency observation which gives information on altitude of transition from rain to snowfall in convective precipitation. In this report, freezing height pattern of typhoon Trami is estimated by combining information from drop sonde and DPR observation, especially around the eye of the typhoon. According to DPR's bright band information, the freezing height increases from 4500 m to 5400 m along the spiral band. Especially on the south side, it rose suddenly about 500 m around the inner core. In the vicinity of the inner core, which is a convective precipitation system, the region of large dual frequency ratio rises to about 6 km. On the other hand, from the observation of the drop sonde, the 0 ℃ altitude rose to about 6500 m in the eye.

Keywords: Typhoon, Spaceborne radar, Freezing height

©2019. Japan Geoscience Union. All Right Reserved.

Revision of Research Plan on “Promotion of Climate and Earth System Science Research by Aircraft Observation”

*Nobuhiro Takahashi[1], Makoto Koike[2]

1. Institute for Space-Earth Environmental Research, Nagoya University, 2. School of Science, The University of Tokyo

The Meteorological Society of Japan proposes on promotion of climate and Earth system science research by introducing a dedicated astronomical observation aircraft for Master Plan 2014 and 2017 of the Science Council of Japan with researchers in a wide field of the Earth and Planetary Sciences. In the Master Plan 2014 and 2017, this proposal was not selected as a priority plan. For Master Plan 2020, we strengthening cooperation with academic societies and researchers in the field of earth planetary science to consolidate the scientific purpose and also stated the cooperation with aeronautical engineering for future evolution of observation system. This research plan, which was originally prepared for the Master Plan 2017, revised to include the updated research field and issued as “Promotion of Climate and Earth System Science Research by Aircraft Observation.” In this presentation, overview of the research plan is introduced in terms of scientific purposes in the various field, proposed aircraft, cost and organization.

Keywords: Aircraft observation

©2019. Japan Geoscience Union. All Right Reserved.

[J] Poster | A (Atmospheric and Hydrospheric Sciences)：A-CG Complex & General

Tue. May 28, 2019 5:15 PM - 6:30 PM JST | Tue. May 28, 2019 8:15 AM - 9:30 AM UTC | Poster Hall International Exhibition Hall8, Makuhari Messe_17

[A-CG41] Promotion of Application and Utilization of Aircrafts for Earth sciences

convener:Nobuhiro Takahashi(Institute for Space-Earth Environmental Research, Nagoya University), Makoto Koike(Department of Earth and Planetary Science, Graduate School of Science, The University of Tokyo), Toshinobu Machida(National Institute for Environmental Studies), Taro Shinoda(Institute for Space-Earth Environmental Research, Nagoya University)

The problem of global environmental change such as global warming is a problem throughout the Earth and planetary sciences. To confront this problem, progresses of the observations that are dedicated for the monitoring Earth and for the process studies as well as the progresses of numerical prediction models. Aircraft observation has the great advantages of immediate and direct (in-situ) observations which cannot be achieved by Earth observing satellites or ground-based observations. Recently, the importance of aircraft observation is increasing in "in-situ measurements" such as concentration of greenhouse gases, aerosol and cloud particle size distribution, and chemical composition, and "remote sensing" such as three dimensional typhoon observation and observation on forests and vegetation. In addition, the application of aircraft observation to geodesy, study on earthquakes and volcanos are also progressing. However, steady and extensive aircraft observations to fulfill the requirements in Japan are not realized at the present time. Meanwhile, it is also a fact that the aircraft observations which have been carried out has cited the world leading results. In order to realize the effective research by using aircraft, it is necessary to have a close collaborations among researchers to promote aircraft observations, and it is also necessary to carry out as the master plan of national academic council of Japan. In this session, we will discuss the future aircraft observation through the latest research results with aircraft observations.

[ACG41-P01] In situ measurements of aerosol and cloud microphysical properties and cloud seeding experiments over the UAE

*Narihiro Orikasa[1], Masataka Murakami[2,1], Takuya Tajiri[1], Yuji Zaizen[1], Taro Shinoda[2] (1.Meteorological Research Institute, 2.Nagoya Univ., ISEE)

[ACG41-P02] Analysis and Forecast Using Dropsonde Data from the Inner-Core Region of Tropical Cyclone Lan (2017) Obtained during the First Aircraft Missions of T-PARCII

*Kosuke Ito[1], Hiroyuki Yamada[1], Munehiko Yamaguchi[2], Tetsuo Nakazawa[2], Norio Nagahama[3], Kensaku Shimizu[3], Tadayasu Ohigashi[4], Taro Shinoda[5], Kazuhisa Tsuboki[5] (1.University of the Ryukyus, 2.Meteorological Research Institute, 3.Meisei Electric Co. LTD., 4.National Research Institute for Earth Science and Disaster Resilience, 5.Nagoya University)

[ACG41-P03] On the Spatial Distribution of Freezing height of Typhoon Trami

*Nobuhiro Takahashi[1], Yuki Kaneko[2], Kazuhisa Tsuboki[1] (1.Institute for Space-Earth Environmental Research, Nagoya University, 2.Japan Aerospace Exploration Agency)

[ACG41-P04] Revision of Research Plan on “Promotion of Climate and Earth System Science Research by Aircraft Observation”

*Nobuhiro Takahashi[1], Makoto Koike[2] (1.Institute for Space-Earth Environmental Research, Nagoya University, 2.School of Science, The University of Tokyo)

In situ measurements of aerosol and cloud microphysical properties and cloud seeding experiments over the UAE

*Narihiro Orikasa[1], Masataka Murakami[2,1], Takuya Tajiri[1], Yuji Zaizen[1], Taro Shinoda[2]

1. Meteorological Research Institute, 2. Nagoya Univ., ISEE

Our field campaign of aircraft observations had successfully been conducted over the UAE regions, as well as ferries between UAE and Japan, in the summer of 2017. This campaign has mainly two objectives. First, in situ measurements contribute to investigation on microphysical processes in seeded and unseeded clouds as well as elucidation of the mechanism responsible for precipitation augmentation. Secondly, the field observation data is useful to validate numerical simulations of cloud and precipitation and to improve the accuracy and reliability of numerical models.

We had deployed two aircraft whose base was Al Ain International Airport, as well as one ground-based observation site next to the aircraft hangar. One aircraft for in situ measurements was B200T operated by Diamond Air Service Inc., and the other for cloud seeding was C-90 operated by UAE National Center of Meteorology (NCM). We performed 14 research flights (~30 hours in total) from Sep. 5 to Sep. 24. Thirteen of the B200T flights were coordinated with the C-90 flights. As shown in Fig. 1, the B200T installed meteorological instruments, hot-wire water content probes, cloud microphysical probes for in situ measurements, aerosol size distribution instruments, sampling mesh device for electron microscopic analysis, cloud condensation nuclei (CCN) counter, and ice nucleating particle (INP) counter. The C-90 dispersed two types of seeding materials through burn-in-place flare racks: $CaCl_2$ hygroscopic (HYG) and silver iodide (AgI) flares.

As one of the flight patterns, seeding plumes generated from the C-90 were sampled and measured with the instrumented B200T which followed the C-90. We collected excellent data for background (BG) aerosols and seeding plume particles generated by HYG flares, AgI flares, or simultaneously generated by the both types of flares.

In order to investigate cloud seeding effects, the B200T measured the evolution of aerosols and cloud particles from cloud base to upper levels before and after the C-90's flare seeding. Based on the same strategy and method as in previous studies on Japanese field campaigns, the flight data quality check and data analysis have been processed, and results of initial cloud droplet size distributions in terms of the seeding signatures are shown from several cases. In general, it was difficult to find clear seeding signatures in any cases.

Except for the seeding experiments, several flights provided us in situ measurements of natural clouds. We sometimes encountered relatively developed clouds whose top temperature was warmer than -10 C, and most of such clouds had ice crystals and graupels. Those basic data will be useful to fully understand the mechanism of ice formation over the UAE regions and to verify the numerical simulations of cloud and precipitation.

In order to conduct an effective and efficient cloud seeding experiment, it is essential to know the physico-chemical properties of BG aerosols in the atmosphere and to observe their spatial and temporal distributions before the experiment. The vertical profiles of aerosol number concentrations (corrected for STP conditions) showed rather constant below cloud base height. The IN and CCN abilities of BG aerosols

©2019. Japan Geoscience Union. All Right Reserved.

are also essential information to accurately simulate cloud formation and precipitation development. The analysis of number concentrations of INP and CCN is shown from a few cases. The INP concentrations were typically ranged on the order of 1 to 10 L^{-1} and there were no significant height dependency. The CCN concentrations were typically several hundreds cm^{-3}_stp and generally depended on the space and time.

Keywords: Aerosol-Cloud Interactions, Cloud Condensation Nuclei/Ice Nucleating Particles, Cloud Seeding, Hygroscopic Particles

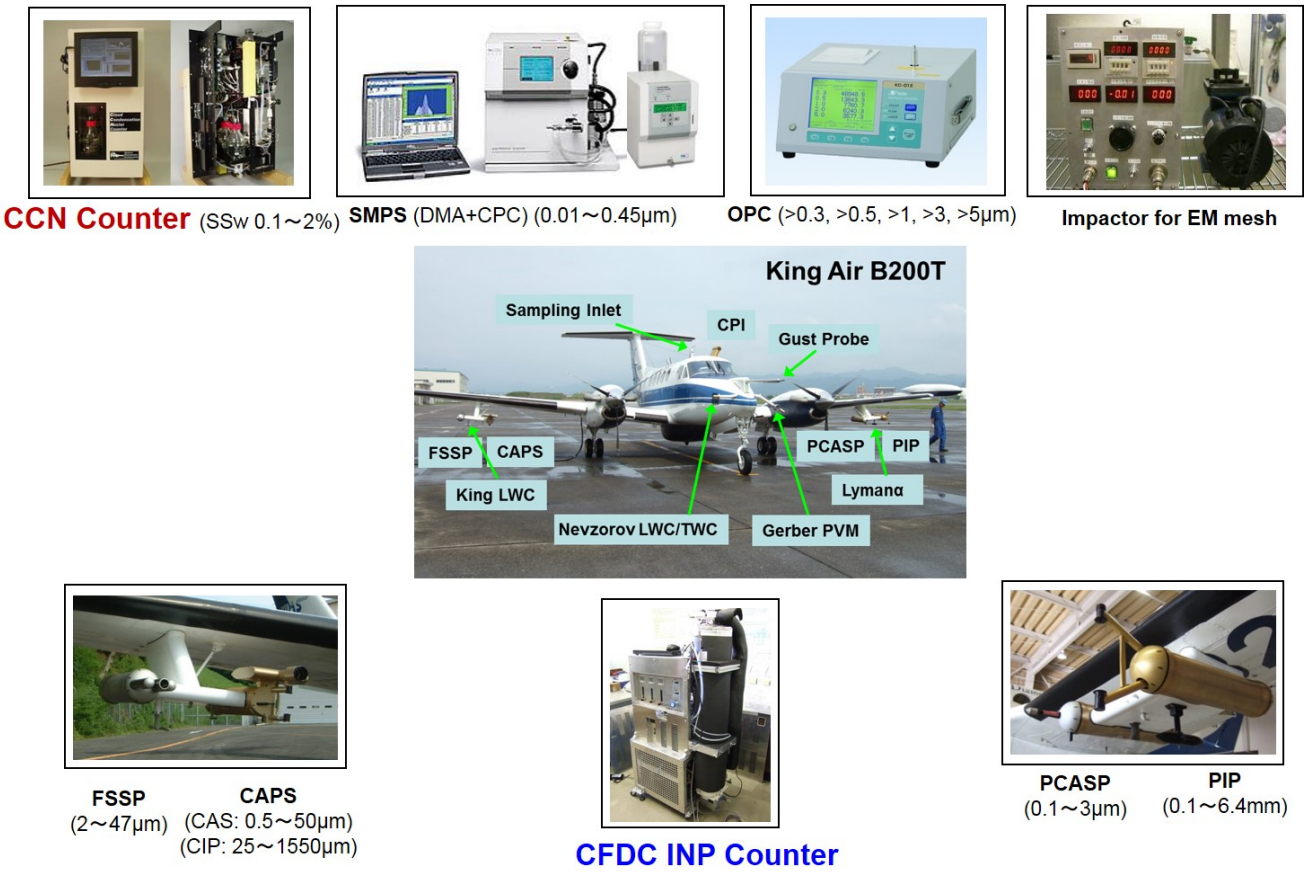

Fig. 1 Aircraft instrumentation.

©2019. Japan Geoscience Union. All Right Reserved.

Analysis and Forecast Using Dropsonde Data from the Inner-Core Region of Tropical Cyclone Lan (2017) Obtained during the First Aircraft Missions of T-PARCII

*Kosuke Ito[1], Hiroyuki Yamada[1], Munehiko Yamaguchi[2], Tetsuo Nakazawa[2], Norio Nagahama[3], Kensaku Shimizu[3], Tadayasu Ohigashi[4], Taro Shinoda[5], Kazuhisa Tsuboki[5]

1. University of the Ryukyus, 2. Meteorological Research Institute, 3. Meisei Electric Co. LTD., 4. National Research Institute for Earth Science and Disaster Resilience, 5. Nagoya University

The inner core of Tropical Cyclone Lan was observed on 21–22 October 2017 by GPS dropsondes during the first aircraft missions of the Tropical Cyclones-Pacific Asian Research Campaign for the Improvement of Intensity Estimations/Forecasts (T-PARCII). To evaluate the impact of dropsondes on forecast skill, 12 36-h forecasts were conducted using a Japan Meteorological Agency non-hydrostatic model (JMA-NHM) with a JMANHM-based mesoscale four-dimensional data assimilation (DA) system. Track forecast skill improved over all forecast times with the assimilation of the dropsonde data. The improvement rate was 8–16% for 27–36-h forecasts. Minimum sea level pressure (Pmin) forecasts were generally degenerated (improved) for relatively short-term (long-term) forecasts by adding the dropsonde data, and maximum wind speed (Vmax) forecasts were degenerated. Some of the changes in the track and Vmax forecasts were statistically significant at the 95% confidence level. It is notable that the dropsonde-derived estimate of Pmin was closer to the realtime analysis by the Regional Specialized Meteorological Center (RSMC) Tokyo than the RSMC Tokyo best track analysis. The degeneration in intensity forecast skill due to uncertainties in the best track data is discussed.

Keywords: tropical cyclone, data assimilation

©2019. Japan Geoscience Union. All Right Reserved.

On the Spatial Distribution of Freezing height of Typhoon Trami

*Nobuhiro Takahashi[1], Yuki Kaneko[2], Kazuhisa Tsuboki[1]

1. Institute for Space-Earth Environmental Research, Nagoya University, 2. Japan Aerospace Exploration Agency

Drop sonde observation from aircraft was conducted for typhoon Trami that occurred in September 2018. The drop sonde observation provides the vertical profile of the temperature and humidity in and around the eye of typhoon. Meanwhile, the global precipitation measuring (GPM) core satellite, which equips dual frequency precipitation radar (DPR), passed over Trami for several times, two of which captured the eye structure. In particular, the over flight case on September 27 by DPR is several hours after the drop sonde observation.

Since DPR can observe the vertical structure of the precipitation system, it is possible to estimate the freezing height in the stratiform precipitation region from the melting layer appearing as the so-called bright band, and an attempt was made to separate snowfall and rainfall by using dual frequency observation which gives information on altitude of transition from rain to snowfall in convective precipitation. In this report, freezing height pattern of typhoon Trami is estimated by combining information from drop sonde and DPR observation, especially around the eye of the typhoon. According to DPR's bright band information, the freezing height increases from 4500 m to 5400 m along the spiral band. Especially on the south side, it rose suddenly about 500 m around the inner core. In the vicinity of the inner core, which is a convective precipitation system, the region of large dual frequency ratio rises to about 6 km. On the other hand, from the observation of the drop sonde, the 0 ℃ altitude rose to about 6500 m in the eye.

Keywords: Typhoon, Spaceborne radar, Freezing height

©2019. Japan Geoscience Union. All Right Reserved.

Revision of Research Plan on “Promotion of Climate and Earth System Science Research by Aircraft Observation”

*Nobuhiro Takahashi[1], Makoto Koike[2]

1. Institute for Space-Earth Environmental Research, Nagoya University, 2. School of Science, The University of Tokyo

The Meteorological Society of Japan proposes on promotion of climate and Earth system science research by introducing a dedicated astronomical observation aircraft for Master Plan 2014 and 2017 of the Science Council of Japan with researchers in a wide field of the Earth and Planetary Sciences. In the Master Plan 2014 and 2017, this proposal was not selected as a priority plan. For Master Plan 2020, we strengthening cooperation with academic societies and researchers in the field of earth planetary science to consolidate the scientific purpose and also stated the cooperation with aeronautical engineering for future evolution of observation system. This research plan, which was originally prepared for the Master Plan 2017, revised to include the updated research field and issued as “Promotion of Climate and Earth System Science Research by Aircraft Observation.” In this presentation, overview of the research plan is introduced in terms of scientific purposes in the various field, proposed aircraft, cost and organization.

Keywords: Aircraft observation

©2019. Japan Geoscience Union. All Right Reserved.

[J] Oral | A (Atmospheric and Hydrospheric Sciences)：A-CG Complex & General

Tue. May 28, 2019 3:30 PM - 5:00 PM JST | Tue. May 28, 2019 6:30 AM - 8:00 AM UTC | 201B 2F

[A-CG41] Promotion of Application and Utilization of Aircrafts for Earth sciences

convener:Nobuhiro Takahashi(Institute for Space-Earth Environmental Research, Nagoya University), Makoto Koike(Department of Earth and Planetary Science, Graduate School of Science, The University of Tokyo), Toshinobu Machida(National Institute for Environmental Studies), Taro Shinoda(Institute for Space-Earth Environmental Research, Nagoya University), Chairperson:Nobuhiro Takahashi(Institute for Space-Earth Environmental Research, Nagoya University)

The problem of global environmental change such as global warming is a problem throughout the Earth and planetary sciences. To confront this problem, progresses of the observations that are dedicated for the monitoring Earth and for the process studies as well as the progresses of numerical prediction models. Aircraft observation has the great advantages of immediate and direct (in-situ) observations which cannot be achieved by Earth observing satellites or ground-based observations. Recently, the importance of aircraft observation is increasing in "in-situ measurements" such as concentration of greenhouse gases, aerosol and cloud particle size distribution, and chemical composition, and "remote sensing" such as three dimensional typhoon observation and observation on forests and vegetation. In addition, the application of aircraft observation to geodesy, study on earthquakes and volcanos are also progressing. However, steady and extensive aircraft observations to fulfill the requirements in Japan are not realized at the present time. Meanwhile, it is also a fact that the aircraft observations which have been carried out has cited the world leading results. In order to realize the effective research by using aircraft, it is necessary to have a close collaborations among researchers to promote aircraft observations, and it is also necessary to carry out as the master plan of national academic council of Japan. In this session, we will discuss the future aircraft observation through the latest research results with aircraft observations.

3:30 PM - 3:45 PM JST | 6:30 AM - 6:45 AM UTC

[ACG41-01] In situ observation of typhoon central pressure using dropsondes

*Kazuhisa Tsuboki[1], Hiroyuki Yamada[2], Yukihiro Takahashi[3], Taro Shinoda[1], Tadayasu Ohigashi[4], Munehiko Yamaguchi[5], Hisayuki Kubota[3], Tetsuo Nakazawa[5], Norio Nagahama[6], Kensaku Shimizu[6], Masaya Kato[1], Sachie Kanada[1], Mayumi Yoshioka[1], Nobuhiro Takahashi[1] (1. Institute for Space-Earth Environmental Research, Nagoya University, 2.University of the Ryukyus, 3.Hokkaido University, 4.National Research Institute for Earth Science and Disaster Resilience, 5.Meteorological Research Institute, Japan Meteorological Agency, 6.Meisei Electric Co. Ltd.)

3:45 PM - 4:00 PM JST | 6:45 AM - 7:00 AM UTC

[ACG41-02] New observation strategies for typhoon intensity over the western North Pacific

*Hiroyuki Yamada[1], Kazuhisa Tsuboki[2], Taro Shinoda[2], Hisayuki Kubota[3], Yukihiro Takahashi[3], Norio Nagahama[4], Kensaku Shimizu[4], Tadayasu Ohigashi[5], Kosuke Ito[1], Munehiko Yamaguchi[6], Tetsuo Nakazawa[6] (1.University of the Ryukyus, 2.Nagoya University, 3.Hokkaido University, 4.Meisei Electric, 5.National Research Institute for Earth Science and Disaster Resilience, 6.Meteorological Research Institute, Japan Meteorological Agency)

4:00 PM - 4:15 PM JST | 7:00 AM - 7:15 AM UTC

[ACG41-03] Observing System Experiment for Typhoon Trami (2018) using T-PARCII dropsondes and JMA Global Forecasting System

*Munehiko Yamaguchi[1], Toshiyuki Ishibashi[1], Tetsuo Nakazawa[1], Kosuke Ito[2], Hiroyuki Yamada[2], Tadayasu Ohigashi[3], Norio Nagahama[4], Kensaku Shimizu[4], Hisayuki Kubota[5], Yukihiro Takahashi[5], Masaya Kato[6], Sachie Kanada[6], Mayumi Yoshioka[6], Taro Shinoda[6], Nobuhiro Takahashi[6], Kazuhisa Tsuboki[6] (1.Meteorological Research Institute, Japan Meteorological Agency, 2.Faculty of Science, University of the Ryukyus, 3.National Research Institute for Earth Science and Disaster Resilience, 4.Meisei Electric, 5.Graduate School of Science, Hokkaido University, 6.Institute for Space-Earth Environmental Research, Nagoya University)

4:15 PM - 4:30 PM JST | 7:15 AM - 7:30 AM UTC

[ACG41-04] Fundamental characteristics of black carbon and iron oxide aerosols in the troposphere revealed from the aircraft measurements

*Nobuhiro Moteki[1], Makoto Koike[1], Sho Ohata[2], Yutaka Kondo[3], Nobuyuki Takegawa[5], Kouji Adachi[4], Naga Oshima[4], Hitoshi Matsui[2], Kazuyuki Kita[6], Tatsuhiro Mori[7], Atsushi Yoshida[1] (1.The Univerisity of Tokyo, 2.Nagoya University, 3.National Institute for Polar Research, 4.Meteorological Research Institute, 5.Tokyo Metropolitan University, 6.Ibaraki University, 7.Tokyo University of Science)

4:30 PM - 4:45 PM JST | 7:30 AM - 7:45 AM UTC

[ACG41-05] Aerosol measurements around the ridge of East Antarctica using a Rogallo wing UAV

*Ryohei Haraguchi[1], Masahiko Hayashi[1], Keiichiro Hara[1], Naohiko Hirasawa[2], Koki Nakata[3], Kei-ichi Ozuka[4,1] (1.Fukuoka University, 2.National Institute of Polar Research, 3.kkt Inovate Co., Ltd, 4.Nippon Tungsten Co., Ltd)

4:45 PM - 5:00 PM JST | 7:45 AM - 8:00 AM UTC

[ACG41-06] Wind Mesurements Based on In-situ Data -Direct Vector Calculation and Hodograph Analyses-

*Masahiko Hayashi[1], Tomoyuki Onohara[1], Ryohei Haraguchi[1,3], Kei-ichi Ozuka[2,4], Kazuo Okabe[3] (1.Faculty of Science, Fukuoka University, 2.Nippon Tungsten Co.,Ltd, 3.SkyRemote Co.,Ltd, 4.FIT-EH, Fukuoka University)

In situ observation of typhoon central pressure using dropsondes

*Kazuhisa Tsuboki[1], Hiroyuki Yamada[2], Yukihiro Takahashi[3], Taro Shinoda[1], Tadayasu Ohigashi[4], Munehiko Yamaguchi[5], Hisayuki Kubota[3], Tetsuo Nakazawa[5], Norio Nagahama[6], Kensaku Shimizu[6], Masaya Kato[1], Sachie Kanada[1], Mayumi Yoshioka[1], Nobuhiro Takahashi[1]

1. Institute for Space-Earth Environmental Research, Nagoya University, 2. University of the Ryukyus, 3. Hokkaido University, 4. National Research Institute for Earth Science and Disaster Resilience, 5. Meteorological Research Institute, Japan Meteorological Agency, 6. Meisei Electric Co. Ltd.

After the US aircraft reconnaissance in the western North Pacific was terminated in 1987, typhoon intensity is estimated by the Dvorak technique using satellite cloud pattern. Consequently, uncertainty of intensity estimation became large for very intense typhoons. Accurate intensity estimations are essential for prevention and mitigation of typhoon disaster. They are also important information for a study of long-term change of typhoon with the climate change. To improve this problem, the T-PARCII (Tropical cyclone-Pacific Asian Research Campaign for Improvement of Intensity estimations/forecasts) project performs an in situ observation of typhoons. In this project, Nagoya University and Meisei Electric Co., Ltd developed a new dropsonde and a four-channel dropsonde receiver. Using these systems on a jet aircraft, the T-PARCII project performed aircraft observations of very intense typhoons in 2017 and 2018. Typhoon Lan (2017) was the most intense typhoon in 2017 and was categorized as a supertyphoon by JTWC. It moved northeastward in the east of the Okinawa main island at 23 N on 21 October and at 28 N on October 22, 2017. In these two days, we made dropsonde observations inside of the eye and in the surrounding area of the eyewall. The T-PARCII team also made aircraft observations of Typhoon Trami (2018) during the period from 25 to 28 September 2018 in collaboration with the SATREPS ULAT group as well as Taiwan DOTSTAR. The observed dropsonde data were transmitted to GTS (Global Telecommunication System) in real time and were used for typhoon forecasts in 2018.

Because the height of dropsonde is derived from GPS, error of height data becomes large just before the dropsonde reaches to the sea surface. As a result, the sea level pressure is uncertain. Typhoon intensity is represented by the central sea level pressure. Accurate estimation of sea level pressure is necessary for a typhoon intensity information. We, therefore, developed two schemes to estimate the sea level pressure from dropsonde data. Temperature, humidity and pressure are measured by sensors of dropsonde. We assume that the accuracy of these data is sufficiently high and height is also accurate above ~500 m in height. In the scheme I, the sea level pressure is calculated by a pressure correction method from 50~100 observed points in 900~750 hPa. The final result is the average of these calculated sea level pressure values. In the scheme II, heights of observed pressure levels below 800 hPa are calculated by the hydrostatic equation using virtual temperature. The sea level pressure is corrected from the lowest grid point.

These schemes were examined by special observations around Minami-Daitojima comparing dropsonde observations with balloon sonde observations launched from Minami-Daitojima Island as well as the JMA surface observation. The maximum difference of sea level pressure is less than 3 hPa. The central sea level pressures of typhoons Lan and Trami were calculated by the schemes I and II. The results by these two schemes agreed well each other. We consider that the sea level pressures were estimated with a sufficient accuracy. They were compared with the JMA best track data. The difference of central pressure of typhoon Trami was about 5 hPa on September 25 when the typhoon was most intense. It was about 10 hPa on September 28 when the typhoon was weakened in the south of the Okinawa main island.

©2019. Japan Geoscience Union. All Right Reserved.

Keywords: typhoon, dropsonde, central pressure

©2019. Japan Geoscience Union. All Right Reserved.

New observation strategies for typhoon intensity over the western North Pacific

*Hiroyuki Yamada[1], Kazuhisa Tsuboki[2], Taro Shinoda[2], Hisayuki Kubota[3], Yukihiro Takahashi[3], Norio Nagahama[4], Kensaku Shimizu[4], Tadayasu Ohigashi[5], Kosuke Ito[1], Munehiko Yamaguchi[6], Tetsuo Nakazawa[6]

1. University of the Ryukyus, 2. Nagoya University, 3. Hokkaido University, 4. Meisei Electric, 5. National Research Institute for Earth Science and Disaster Resilience, 6. Meteorological Research Institute, Japan Meteorological Agency

Recent activities on typhoon intensity observation/estimation using aircraft reconnaissance and ground-based Doppler radars in the western North Pacific are introduced. Since aircraft reconnaissance by the US military was ceased in 1987, new techniques of intensity estimation using microwave radiometer and a geostationary satellite are used in this basin without enough verification. The major obstacle of aircraft reconnaissance is the difficulty of having a specially-designed propeller aircraft that withstands strong turbulence. Since wind speed in a typhoon is stronger in the lower troposphere, it takes a great deal of labor and expense to measure the center position and the central pressure of a typhoon through low-altitude flight with slow speed. On the other hand, since the winds become weaker in the upper troposphere, it is possible to fly into the typhoon center if the risks of heavy icing and severe turbulence in a convective burst can be avoided by using an airborne weather radar. During T-PARCII (Tropical Cyclone-Pacific Asian Research Campaign for Improvement of Intensity Estimations / Forecasts), we succeeded in observing the central pressure of two intense typhoons, Lan (2017) and Trami (2018), by using a commercial jet aircraft (Gulfstream-II) with a newly-developed GPS dropsonde system. These flight missions were made in the upper troposphere (43,000ft, approximately 13.7 km) and were marked by very weak turbulence during eyewall penetration. These flights demonstrated a possibility of typhoon intensity observation using a civil aircraft. In the Pacific coast of Japan and Philippines, Doppler radars became available in this decade. The combination of aircraft reconnaissance off the coast with the ground-based velocity track display (GBVTD) analysis near the coast will provide accurate information on typhoon intensity.

Acknowledgements: This work was supported by JSPS KAKENHI Grant Numbers JP16H06311, JP16H04053, JP18H03805, and the Science and Technology Research Partnership for Sustainable Development (SATREPS) Understanding Lightning and Thunderstorm (ULAT) project.

Keywords: aircraft reconnaissance, tropical cyclone, western North Pacific

©2019. Japan Geoscience Union. All Right Reserved.

Observing System Experiment for Typhoon Trami (2018) using T-PARCII dropsondes and JMA Global Forecasting System

*Munehiko Yamaguchi[1], Toshiyuki Ishibashi[1], Tetsuo Nakazawa[1], Kosuke Ito[2], Hiroyuki Yamada[2], Tadayasu Ohigashi[3], Norio Nagahama[4], Kensaku Shimizu[4], Hisayuki Kubota[5], Yukihiro Takahashi[5], Masaya Kato[6], Sachie Kanada[6], Mayumi Yoshioka[6], Taro Shinoda[6], Nobuhiro Takahashi[6], Kazuhisa Tsuboki[6]

1. Meteorological Research Institute, Japan Meteorological Agency, 2. Faculty of Science, University of the Ryukyus, 3. National Research Institute for Earth Science and Disaster Resilience, 4. Meisei Electric, 5. Graduate School of Science, Hokkaido University, 6. Institute for Space-Earth Environmental Research, Nagoya University

Airborne typhoon observations were conducted for Typhoon Trami (2018) under Tropical cyclones-Pacific Asian Research Campaign for Improvement of Intensity estimations/forecasts (T-PARCII). Using the dropsonde data (zonal and meridional winds, temperature, and relative humidity) and the Japan Meteorological Agency Global Spectral Model (JMA/GSM, TL959L100) and 4 Dimensional Variational data assimilation (4DVAR, TL319L100), we performed Observing System Experiment (OSE) to see the impact of the newly available observational date on the track/intensity predictions by the JMA/GSM.

Three sets of numerical experiments, CNTL, EXP1 and EXP2, were performed. All the T-PARCII dropsonde and typhoon bogus data were used in the data assimilation in CNTL while T-PARCII dropsonde (typhoon bogus) data only were assimilated in the 4DVAR in EXP1 (EXP2). The period of the experiments is from 2018.09.25 00UTC to 2018.09.28 18UTC with a 6-hour data assimilation and forecasting cycle.

The error of the track predictions of EXP1 and EXP2 is smaller than that of CNTL. For example, the 3-day track prediction error of CNTL, EXP1 and EXP2 is 232, 201 and 218 km, respectively. A possible reason of the degradation of the track predictions by CNTL is that some dropsonde data were assimilated at the almost same locations as typhoon bogus data, which might deteriorate the initial structure of the typhoon.

In the operational configuration of the 4DVAR, all dropsonde data were assimilated irrespective of the existence of the typhoon bogus data. The results of a series of these numerical experiments may lead to improvement in the operational setting of dropsonde assimilation.

Keywords: Airborne observation, Typhoon, Weather Prediction

©2019. Japan Geoscience Union. All Right Reserved.

Fundamental characteristics of black carbon and iron oxide aerosols in the troposphere revealed from the aircraft measurements

*Nobuhiro Moteki[1], Makoto Koike[1], Sho Ohata[2], Yutaka Kondo[3], Nobuyuki Takegawa[5], Kouji Adachi[4], Naga Oshima[4], Hitoshi Matsui[2], Kazuyuki Kita[6], Tatsuhiro Mori[7], Atsushi Yoshida[1]

1. The Univerisity of Tokyo, 2. Nagoya University, 3. National Institute for Polar Research, 4. Meteorological Research Institute, 5. Tokyo Metropolitan University, 6. Ibaraki University, 7. Tokyo University of Science

In this presentation, we will talk about the basic behaviors, microphysical and associated optical properties, and transport-and-removal processes of the tropospheric black carbon and iron oxide aerosol which have been elucidated mostly from aircraft measurements. We will clarify the scientific significance and contribution of these findings in the context of the related international research activities on atmospheric aerosols and climate change. In addition, we will suggest some related open problems which need to be investigated through in-situ aircraft measurements in future research.

Keywords: aerosol, aircraft measurement, black carbon, iron oxide, atmospheric chemical composition

©2019. Japan Geoscience Union. All Right Reserved.

Aerosol measurements around the ridge of East Antarctica using a Rogallo wing UAV

*Ryohei Haraguchi[1], Masahiko Hayashi[1], Keiichiro Hara[1], Naohiko Hirasawa[2], Koki Nakata[3], Kei-ichi Ozuka[4,1]

1. Fukuoka University, 2. National Institute of Polar Research, 3. kkt Inovate Co., Ltd, 4. Nippon Tungsten Co., Ltd

Meteorological observations using a UAV in the Antarctica have been carried out at S17 Air Base (69° 02’ S, 40° 06’ E, 606m a.s.l.), near Syowa Base by the 48th, 54th, and 56th Japanese Antarctic Research Expedition, (JARE). The JARE 58th planned to perform meteorological observations including snow, water vapor and aerosols budgets at S17 during December 22nd, 2016 and February 4th, 2017. One of main mission of the observation focused on aerosol processes using automated UAVs with a Rogallo wing, called Kite Planes. Two types of Kite Planes were used for different type observations. One is engine powered Kite Plane for horizontal observations with a condensation particle counter, an optical particle counter, and an aerosol sampler for SEM/EDX analyses. Another is a glider KitePlane supported by electric motor with an optical particle counter for vertical distribution observations. 22 flights were successfully carried out during the campaign of JARE 58th and obtained following results.

1. Uniformity in CN and Mie particle concentrations is very high during January in 2017.
2. Low CN concentrations were sometimes observed near surface.
3. High CN event with low Mie particle concentration from free troposphere was observed on January 23rd, suggesting caused by new particle formation.
4. High CN event with high Mie particle concentration from ocean area was observed on January 27th, 2017, suggesting hygroscopic growth of aerosols from marin boundary layer.

Keywords: Aerosol, UAV, Antarctica, new particle formation

©2019. Japan Geoscience Union. All Right Reserved.

Wind Mesurements Based on In-situ Data -Direct Vector Calculation and Hodograph Analyses-

*Masahiko Hayashi[1], Tomoyuki Onohara[1], Ryohei Haraguchi[1,3], Kei-ichi Ozuka[2,4], Kazuo Okabe[3]

1. Faculty of Science, Fukuoka University, 2. Nippon Tungsten Co.,Ltd, 3. SkyRemote Co.,Ltd, 4. FIT-EH, Fukuoka University

Un-manned Aerial Vehicles have been developing rapidly and performance as observation platform are increasing. Our group have used Rogallo wing UAV, called KitePlane for aerosol measurement about 20 years ago. In-situ wind measurements have tested, becuase of importance for meteorological analyses and technical requirements for safety flight operations. There are two typical methods for atmospheric wind measurements based on in-situ data by in-flight airplane. One is direct calculation method by difference between gound speed and true air speed. The other is that drift of center of hodograph circle for ground speed coinsident with wind vector during flight.
Time and spatial resolutions for the direct calculations are around 1 second and 10 m respectively, and require high accuracy for true wind vectors. On the other hand, those for the hodograph methods are around 1 minuite and several hundreds meters, respectively, however the method only require position and time for calculations.
It will be presented based on actual flight by KitePlane that accuracies of wind speeds and directions are around 0.1m/sec and several degrees for both methods with recently developed small and precision sensors.

Keywords: wind mesurements, UAV, meteorology

©2019. Japan Geoscience Union. All Right Reserved.

[J] Poster | A (Atmospheric and Hydrospheric Sciences)：A-CG Complex & General

Tue. May 28, 2019 10:45 AM - 12:15 PM JST | Tue. May 28, 2019 1:45 AM - 3:15 AM UTC | Poster Hall International Exhibition Hall8, Makuhari Messe_4

[A-CG44] Coastal Ecosystems 2 Coral reefs, seagrass and macroalgal beds, and mangrove

convener:Yu Umezawa(Tokyo University of Agriculture and Technology), Toshihiro Miyajima(Marine Biogeochemistry Group, Division of Ocean-Earth System Science, Atmosphere and Ocean Research Institute, The University of Tokyo), Atsushi Watanabe(The ocean policy research institute, The Sasakawa peace foundation), Tomihiko Higuchi(Atmosphere and Ocean Research Institute, The University of Tokyo)

Coastal marine ecosystems are complex open system interacting with surrounding watersheds, outer ocean, and the atmosphere, providing a wealth of various ecosystem services to human life. Simultaneously, they are also influenced strongly and often negatively by human activities. This session, together with a companion session dedicated for the water cycle and land-ocean interactions, aims to provide a platform for interdisciplinary discussion covering various aspects of frontiers in coastal ecosystem sciences. This session particularly focuses shallow-water benthic communities ranging from temperate to tropical regions, such as coral reefs, seagrass and macroalgal beds, and mangroves. All these communities are characterized by intrinsically high primary production, active material cycling, and biodiversity hot spots. However, increasing human demand for coastal marine resources and industrial development concentrating on coastal regions incur the risk of rapid degradation and diminishment. Comprehensive assessment and monitoring of ecosystem functions and development of effective means for conservation and restoration are urgently needed for such communities. This session is dedicated to organizing and promoting such research and management activities by sharing state-of-the-art science and technology among ecologists, geologists, geochemists, biogeographers, etc. Field-based and modeling studies concerning the following topics are especially welcome: material cycling and ecosystem functions; community connectivity; environmental changes such as global warming, ocean acidification, and sea-level rise; ecosystem services such as carbon sequestration, nutrient regulation, and fisheries production; broad-scale comparison; long-term ecological researches.

[ACG44-P01] Characteristics of organic carbon in coastal carbonate sediment accompanied by seagrass meadows

*Toshihiro Miyajima[1] (1.Marine Biogeochemistry Group, Division of Ocean-Earth System Science, Atmosphere and Ocean Research Institute, The University of Tokyo)

[ACG44-P02] Perceptions of Coastal Communities on Blue Carbon Ecosystems Services at the Municipalities of Eastern Samar and Western Visayas, Philippines

*Jay Mar Dioquito Quevedo[1], Yuta Uchiyama[1], Kaoru Kakinuma[1], Ryo Kohsaka[1] (1.Tohoku University)

[ACG44-P03] Numerical simulation of typhoon events in Sekisei Lagoon, Okinawa, Japan using a coupled ocean-wave model

*Lawrence Patrick Cases Bernardo[1], Takashi Nakamura[1], Kazuo Nadoka[1] (1.Department of Transdisciplinary Science and Engineering, Tokyo Institute of Technology)

[ACG44-P04] Study of macrobenthic community structure at mesophotic depths in the South Ryukyus based on ROV and AUV seafloor imaging

*Marc Humblet[1], Toshihiro Maki[2], Yasuo Furushima[3], Yukiyasu Noguchi[2], Hiroumi Horimoto[2], Hiroya Yatagai[2], Takashi Sakamaki[2], Shohei Ito[4], Sadao Suzuki[5] (1.Department of Earth and Planetary Sciences, Nagoya University, 2.Institute of Industrial Science, The University of Tokyo, 3.JAMSTEC, 4.FullDepth Co., Ltd., 5.ORE)

[ACG44-P05] Enhancement of antioxidant activity of scleractinian coral *Galaxea Fascicularis* by feeding treatment.

*Hiroyuki Fujimura[1], Sayaka Higa[1], Toshihiro Miyajima[2], Tomihiko Higuchi[2], Sylvain Agostini[3], Ikuko Yuyama[3], Takashi Nakamura[4] (1.University of the Ryukyus, 2.The University of Tokyo, 3.Tsukuba University, 4.Tokyo Institute of Technology)

[ACG44-P06] Effects of environmental stresses on coral bleaching

*Tomihiko Higuchi[1] (1.Atmosphere and Ocean Research Institute, The University of Tokyo)

Characteristics of organic carbon in coastal carbonate sediment accompanied by seagrass meadows

*Toshihiro Miyajima[1]

1. Marine Biogeochemistry Group, Division of Ocean-Earth System Science, Atmosphere and Ocean Research Institute, The University of Tokyo

Seagrass meadows are submerged, highly productive ecosystem that occurs in sandy shallow coastal environments from tropical to boreal regions. Colonization of seagrasses in coastal habitats renders originally oligotrophic, organic-poor sandy sediment into a hot spot of organic carbon (OC) sequestration and storage. This function depends on a combination of several characteristics specific to seagrasses, such as very high and efficient photosynthetic ability, production of perennial belowground biomass, and physical attenuation effects of leaf blades and roots that enhance accumulation and stability of sediment. Recent estimates indicate that around 70% of global seagrass meadows are present in tropical and subtropical coastal habitats (Siikamäki et al. 2012), which are often covered with biogenic carbonate sediment especially in archipelagic regions. In fact, carbonate accumulated in global seagrass meadow sediments has been estimated to be up to five times greater than the amount of OC on the carbon basis (Mazarrasa et al. 2015). However, geochemical roles of carbonate sediment in OC sequestration in seagrass meadow sediments is not well understood.
This study focuses on the OC stock and its relationship to mineralogical properties of sediment such as carbonate content, specific surface area (SSA), and mesopore distribution in carbonate sediments accompanied by seagrass meadows in Japan and the Philippines. Here, typical carbonate sediment is defined as sediment with inorganic carbon (IC) content greater than 8 mmol IC g^{-1}(ca. 10%-IC w/w). Obtained results were compared with corresponding properties of temperate, non-carbonate (<0.5 mmol IC g^{-1}) seagrass meadow sediments. The ranges of OC concentration and stock, as well as the degree of accumulation of OC in seagrass meadows relative to adjacent non-vegetated sediment, were similar between carbonate and non-carbonate seagrass habitats. The OC concentration strongly correlated with SSA and total mesopore volume for both carbonate and non-carbonate sediments. However, average OC loading per unit surface area and unit mesopore volume was six-times and three-times greater for carbonate sediments than non-carbonate sediments, respectively. Carbon isotope abundance suggested that the fraction of seagrass-derived OC to total OC was often much greater for carbonate sediments than non-carbonate sediments. Nonetheless, OC tightly associated with carbonate minerals seemed to be derived mainly from non-seagrass sources. These findings as well as the differences between carbonate and non-carbonate sediments may be partially explained by characteristics specific to carbonate sediments, such as presence of basic OC inherited from organisms that originally produced the carbonate, different affinity to soluble organic matter, different mesopore shape and size distribution, and gradual dissolution during early diagenesis. However, what constrains the capacity of carbonate sediments to sequester OC is still unclear. Our results suggest that, although mineralogical control on sediment OC is significant in carbonate sediment, the classical sorptive preservation mechanism originally put forward for explaining the constant OC/SSA ratio in continental shelf sediments is not sufficient to explain the OC sequestration capacity of carbonate sediments supporting seagrass meadows.

Keywords: seagrass beds, calcium carbonate, carbon storage

©2019. Japan Geoscience Union. All Right Reserved.

Perceptions of Coastal Communities on Blue Carbon Ecosystems Services at the Municipalities of Eastern Samar and Western Visayas, Philippines

*Jay Mar Dioquito Quevedo[1], Yuta Uchiyama[1], Kaoru Kakinuma[1], Ryo Kohsaka[1]

1. Tohoku University

The blue carbon ecosystems (mangroves and seagrass) in the Philippines provide a wide range of benefits to the coastal communities; from provisional, regulating and cultural services ranging from supply of food and a natural fish nursery, carbon storage, protection against storm surges and as a tourism site. Existing studies in the Philippines have shown how local people in coastal areas affects the utilization and managing of the blue carbon ecosystems. However, little have recorded and evaluated the perception of people on the importance of these coastal ecosystems at the municipality level in relationship with rate of utilization to the different services these ecosystems provide. It is very important to understand the level of awareness and usage of mangrove, seagrass and associated resources because it can help in contextual formulation and implementation of management plan of coastal ecosystems in the municipality. In this study, household surveys, key informant interviews (KII), and focus group discussions (FGD) using semi-structured questionnaires will be utilized at coastal areas in select municipalities of Eastern Samar and Western Visayas. This study aims to determine the local knowledge of the coastal communities on blue carbon ecosystems, evaluate how they directly or indirectly use the services and identify potential local threats and destructive activities. It will also highlight the perception and evaluation of the existing efforts of the local government and their effectivity on the management of blue carbon ecosystems from local perspectives which has been largely overlooked.

Keywords: Blue Carbon Ecosystems, Coastal Management, Ecosystem Services, Coastal Communities, Awareness, Utilization

©2019. Japan Geoscience Union. All Right Reserved.

Numerical simulation of typhoon events in Sekisei Lagoon, Okinawa, Japan using a coupled ocean-wave model

*Lawrence Patrick Cases Bernardo[1], Takashi Nakamura[1], Kazuo Nadoka[1]

1. Department of Transdisciplinary Science and Engineering, Tokyo Institute of Technology

Sekisei Lagoon is the site of Japan's largest coral reef area and is an important target site for conservation. However, it is affected to varying degrees by typhoons which approach yearly during the summer and autumn seasons. To closely investigate typhoon-driven hydrodynamics in Sekisei Lagoon, a modeling setup was developed using a nested Regional Ocean Modeling System (ROMS) configuration with an outer coarse scale regional model at 1.5 km grid resolution, and an inner model focused on the Sekisei Lagoon domain with a grid resolution of 300 meters. The inner model was configured using the Coupled Ocean-Atmophere-Wave-Sediment Transport (COAWST) modeling framework in order to couple the ROMS ocean model with the Simulating Waves Nearshore (SWAN) wave model. Initial conditions and ocean boundary forcing for the regional model were derived from the global 1/12° Hybrid Coordinate Modeling System analysis data (HYCOM GLBv0.08), and tidal forcing was added using data from the 1/30° OSU Topex/Poseidon Global Inverse tidal solution (TPXO9). Meteorological forcing was derived from Japan Meteorological Agency-Grid Point Value (JMA-GPV) mesoscale model results, and SWAN boundary forcing for the inner model was derived using outputs from the 5-km JMA Coastal Wave Model (CWM) for locations around the Yaeyama Islands where Sekisei Lagoon is located.

The modeling setup was run for specific typhoon events as well as for relatively calmer periods, and model performance was evaluated by comparing simulation results with in-situ observations from sensor deployments around Sekisei Lagoon conducted during the summer months of 2014, 2015, and 2016, as well as from a long term continuous monitoring setup in the Shiraho Reef area in Ishigaki Island. Modeled significant wave heights and peak wave periods at wave sensor locations for relatively calm periods had comparable ranges, but exact temporal trends could not yet be reproduced well. During modeled typhoon passages, trends in significant wave height, such as the timing of increase as the typhoon approached and the maximum wave height reached, were well-reproduced for a wave sensor located at the southeastern part of Sekisei Lagoon. However, the comparison was relatively poor for wave sensors deployed at the northwestern part of the lagoon and offshore of Shiraho Reef on the eastern side of Ishigaki Island, particularly in terms of the timing of wave height increase. In terms of simulating water temperature, running the inner ROMS model without SWAN resulted in Wilmott skill index (Wilmott 1981) scores ranging from 0.72 to 0.95 and root mean-square errors ranging from 0.46 to 1.52 deg C when compared with field observations conducted around Sekisei Lagoon from May to November in 2016. Modeling runs for the coupled ROMS-SWAN model were of shorter duration, but the simulated water temperatures showed some notable differences with the ROMS only case for some locations, suggesting that the influence of wave-driven flows on water temperature trends may need closer investigation.

Adjustments to the modeling setup are ongoing, especially in terms of more properly resolving bathymetric features, as some parts of the domain are characterized by complex barrier and fringing reef structures. Parameter tuning is also being conducted in relation to the physical processes considered in the SWAN wave model, such as the influence of bottom friction and depth-induced wave breaking. With further improvement, this modeling setup may serve as a potentially useful tool to gain further insight into the ways typhoons affect the hydrodynamic conditions in Sekisei Lagoon, as well as estimate potential damage levels, given that typhoon tracks and intensities vary. Even for the non-typhoon case, the setup

©2019. Japan Geoscience Union. All Right Reserved.

may also be useful to help clarify the influence of waves on the overall circulation in the area.

Keywords: hydrodynamics, typhoon, ocean model, wave model, coral reef, sensors

©2019. Japan Geoscience Union. All Right Reserved.

Study of macrobenthic community structure at mesophotic depths in the South Ryukyus based on ROV and AUV seafloor imaging

*Marc Humblet[1], Toshihiro Maki[2], Yasuo Furushima[3], Yukiyasu Noguchi[2], Hiroumi Horimoto[2], Hiroya Yatagai[2], Takashi Sakamaki[2], Shohei Ito[4], Sadao Suzuki[5]

1. Department of Earth and Planetary Sciences, Nagoya University, 2. Institute of Industrial Science, The University of Tokyo, 3. JAMSTEC, 4. FullDepth Co., Ltd., 5. ORE

Mesophotic coral reef habitats (30-150 m) are still largely unexplored despite their importance in biology (e.g., marine biodiversity studies, genetic connectivity between shallow and deep communities, ecological shift from photosynthetic to heterotrophic communities along a depth/light gradient) and in geology (e.g., study of sea-level changes and reef growth history during Quaternary sea-level lowstands). Here we report on new seafloor observations conducted by remotely operated vehicles (ROVs) and an autonomous underwater vehicle (AUV) at depths of 30-65 m around the Sekisei lagoon, Yaeyama Islands, South Ryukyus, Japan. In this study, new seafloor imaging was carried out at six sites along the northern (N1-N2) and southern (S1-S4) margins of the Sekisei Lagoon by two ROVs (BlueRov 2, Blue Robotics Inc., and FullDepth DiveUnit 300, FullDepth Co., Ltd.) and one AUV (HATTORI 2). HATTORI 2 is designed to acquire high-resolution video images of the seafloor at a constant elevation along a pre-programmed path, which enables the creation of a 3D topographic map of the seafloor based on structure-from-motion photogrammetry. In addition, HATTORI 2 was equipped with depth, temperature, salinity and light sensors. We combine these new observations with data obtained during previous ROV and AUV surveys to investigate the community structure of benthic organisms, particularly scleractinian corals, at mesophotic depths, and examine its relationship with water depth, seafloor topography, substrate type, and other major environmental parameters (i.e., light penetration, water temperature and salinity). Previous surveys revealed a clear bathymetric zonation at site S1 with a shift from a “coralgal” community (dominated by scleractinian corals and coralline algae) to a “mixed” community (including scleractinian corals, algae, octocorallians, sponges, and foraminifers) at a depth of ~60 m, and showed also that scleractinian corals become rare below 70 m. A preliminary analysis of images acquired during our latest survey indicates that coral cover in the upper mesophotic zone (30-40 m) varies greatly from one site to another: up to 100% in the area of sites N1 and N2 (*Leptoseris* and *Acropora* colonies locally abundant), 35% or less in the area of S1, close to 0% at sites S2 and S3, and 30-60 % at site S4. Our new data confirm that substrate type and seafloor topography are likely important factors controlling the distribution of corals at upper mesophotic depths (higher coral cover on hard rocky substrate and topographic highs), but they alone cannot explain the full range of our observations.

Keywords: Coral reefs, Mesophotic habitat, Coral communities, ROV, AUV

©2019. Japan Geoscience Union. All Right Reserved.

Enhancement of antioxidant activity of scleractinian coral *Galaxea Fascicularis* by feeding treatment.

*Hiroyuki Fujimura[1], Sayaka Higa[1], Toshihiro Miyajima[2], Tomihiko Higuchi[2], Sylvain Agostini[3], Ikuko Yuyama[3], Takashi Nakamura[4]

1. University of the Ryukyus, 2. The University of Tokyo, 3. Tsukuba University, 4. Tokyo Institute of Technology

In recent years, mass coral bleaching has been recognized around the world. Coral bleaching is a phenomenon that coral loses symbiotic algae “zooxanthellae” due to strong solar radiation and high water temperature, and white coral skeleton can be seen through the transparent its soft tissue. Coral bleaching is caused by a damage of photosynthetic system of zooxanthella by strong light and the damaged part is not repaired by the continuation of the high water temperature, leading to a generation of harmful reactive oxygen species by combining surplus electrons and surrounding oxygen.
Since a translocation of fixed carbon from zooxanthellae to coral decreases during bleaching event, corals are forced to consume the stored lipids in the tissues. Prolonged bleaching event eventually causes the death of coral. Corals that store enough energy by predation have more resistance against bleaching (Ferrier-Pages et al. 2010). An addition of a trace amount of inorganic metals to corals has shown an increase in antioxidant enzyme activity (Sasaki 2013). Feeding activity is not only energy supply for coral but also supply of trace metal elements that can be used for the active center of antioxidant enzyme as a cofactor. It is possible that heterotrophic feeding may improve a tolerance of coral bleaching. Therefore, the aim of this study is to investigate experimentally whether antioxidant capacity can be enhanced by heterotrophic nutrition.
Coral polyps of *Galaxea fascicularis* were incubated with and without a feeding condition for 20 days. Zooplankton was given to coral at the dawn when coral actively extends its tentacles and takes predatory behavior (AM 5: 00 - 8: 00). After 20 days, the water temperature was raised up to 31ºC within 3 days. Finally, all the coral polyps were sacrificed and separated into host tissues and zooxanthella. Superoxide dismutase (SOD) enzyme activity of the antioxidant and concentration of the metal element contained in the protein were measured, respectively.
As a result of feeding experiment, the SOD enzyme activity increased under feeding conditions of 27 ℃ and maintained the activity level after exposure to high water temperature, indicating the enhancement of the antioxidant activity of *G. fascicularis* by feeding process.

Keywords: scleractinian coral, heterotrophic nutrition, antioxidant capacity

©2019. Japan Geoscience Union. All Right Reserved.

Effects of environmental stresses on coral bleaching

*Tomihiko Higuchi[1]

1. Atmosphere and Ocean Research Institute, The University of Tokyo

Coral reefs are threatened by multiple environmental stresses at both the global and the local scales. Declining water quality in coastal reefs has been reported such as due to red soil runoff, agricultural fertilizers, and anti-fouling chemicals. Coral bleaching has been frequently reported and actively studied recently. The synergistic effects of multiple stressors have also been studied, with several studies reporting accelerated bleaching under conditions of high seawater temperature and low water quality. For example, enrichment of nitrate can accelerate coral bleaching under high light or high temperature conditions compared with single stress conditions. If the concentration of nitrate increases damage to coral reefs in coastal areas could significantly increase under high temperature or high light stress. Moreover, environmental bacteria, *Sulfitobacter* sp., which can be found in the seawater of coral reef, enhanced bleaching process under high temperature. These nitrate and bacteria did not affect corals severely under ambient temperature (not high temperature). To mitigate environmental stresses on coral reefs, it is important to evaluate risks due not only to global warming, but also to local stresses.

Keywords: global warming, coral bleaching, multiple stresses

©2019. Japan Geoscience Union. All Right Reserved.

[J] Poster | A (Atmospheric and Hydrospheric Sciences)：A-CG Complex & General

Tue. May 28, 2019 5:15 PM - 6:30 PM JST | Tue. May 28, 2019 8:15 AM - 9:30 AM UTC | Poster Hall International Exhibition Hall8, Makuhari Messe_18

[A-CG44] Coastal Ecosystems 2 Coral reefs, seagrass and macroalgal beds, and mangrove

convener:Yu Umezawa(Tokyo University of Agriculture and Technology), Toshihiro Miyajima(Marine Biogeochemistry Group, Division of Ocean-Earth System Science, Atmosphere and Ocean Research Institute, The University of Tokyo), Atsushi Watanabe(The ocean policy research institute, The Sasakawa peace foundation), Tomihiko Higuchi(Atmosphere and Ocean Research Institute, The University of Tokyo)

Coastal marine ecosystems are complex open system interacting with surrounding watersheds, outer ocean, and the atmosphere, providing a wealth of various ecosystem services to human life. Simultaneously, they are also influenced strongly and often negatively by human activities. This session, together with a companion session dedicated for the water cycle and land-ocean interactions, aims to provide a platform for interdisciplinary discussion covering various aspects of frontiers in coastal ecosystem sciences. This session particularly focuses shallow-water benthic communities ranging from temperate to tropical regions, such as coral reefs, seagrass and macroalgal beds, and mangroves. All these communities are characterized by intrinsically high primary production, active material cycling, and biodiversity hot spots. However, increasing human demand for coastal marine resources and industrial development concentrating on coastal regions incur the risk of rapid degradation and diminishment. Comprehensive assessment and monitoring of ecosystem functions and development of effective means for conservation and restoration are urgently needed for such communities. This session is dedicated to organizing and promoting such research and management activities by sharing state-of-the-art science and technology among ecologists, geologists, geochemists, biogeographers, etc. Field-based and modeling studies concerning the following topics are especially welcome: material cycling and ecosystem functions; community connectivity; environmental changes such as global warming, ocean acidification, and sea-level rise; ecosystem services such as carbon sequestration, nutrient regulation, and fisheries production; broad-scale comparison; long-term ecological researches.

[ACG44-P01] Characteristics of organic carbon in coastal carbonate sediment accompanied by seagrass meadows

*Toshihiro Miyajima[1] (1.Marine Biogeochemistry Group, Division of Ocean-Earth System Science, Atmosphere and Ocean Research Institute, The University of Tokyo)

[ACG44-P02] Perceptions of Coastal Communities on Blue Carbon Ecosystems Services at the Municipalities of Eastern Samar and Western Visayas, Philippines

*Jay Mar Dioquito Quevedo[1], Yuta Uchiyama[1], Kaoru Kakinuma[1], Ryo Kohsaka[1] (1.Tohoku University)

[ACG44-P03] Numerical simulation of typhoon events in Sekisei Lagoon, Okinawa, Japan using a coupled ocean-wave model

*Lawrence Patrick Cases Bernardo[1], Takashi Nakamura[1], Kazuo Nadoka[1] (1.Department of Transdisciplinary Science and Engineering, Tokyo Institute of Technology)

[ACG44-P04] Study of macrobenthic community structure at mesophotic depths in the South Ryukyus based on ROV and AUV seafloor imaging

*Marc Humblet[1], Toshihiro Maki[2], Yasuo Furushima[3], Yukiyasu Noguchi[2], Hiroumi Horimoto[2], Hiroya Yatagai[2], Takashi Sakamaki[2], Shohei Ito[4], Sadao Suzuki[5] (1.Department of Earth and Planetary Sciences, Nagoya University, 2.Institute of Industrial Science, The University of Tokyo, 3.JAMSTEC, 4.FullDepth Co., Ltd., 5.ORE)

[ACG44-P05] Enhancement of antioxidant activity of scleractinian coral *Galaxea Fascicularis* by feeding treatment.

*Hiroyuki Fujimura[1], Sayaka Higa[1], Toshihiro Miyajima[2], Tomihiko Higuchi[2], Sylvain Agostini[3], Ikuko Yuyama[3], Takashi Nakamura[4] (1.University of the Ryukyus, 2.The University of Tokyo, 3.Tsukuba University, 4.Tokyo Institute of Technology)

[ACG44-P06] Effects of environmental stresses on coral bleaching

*Tomihiko Higuchi[1] (1.Atmosphere and Ocean Research Institute, The University of Tokyo)

Characteristics of organic carbon in coastal carbonate sediment accompanied by seagrass meadows

*Toshihiro Miyajima[1]

1. Marine Biogeochemistry Group, Division of Ocean-Earth System Science, Atmosphere and Ocean Research Institute, The University of Tokyo

Seagrass meadows are submerged, highly productive ecosystem that occurs in sandy shallow coastal environments from tropical to boreal regions. Colonization of seagrasses in coastal habitats renders originally oligotrophic, organic-poor sandy sediment into a hot spot of organic carbon (OC) sequestration and storage. This function depends on a combination of several characteristics specific to seagrasses, such as very high and efficient photosynthetic ability, production of perennial belowground biomass, and physical attenuation effects of leaf blades and roots that enhance accumulation and stability of sediment. Recent estimates indicate that around 70% of global seagrass meadows are present in tropical and subtropical coastal habitats (Siikamäki et al. 2012), which are often covered with biogenic carbonate sediment especially in archipelagic regions. In fact, carbonate accumulated in global seagrass meadow sediments has been estimated to be up to five times greater than the amount of OC on the carbon basis (Mazarrasa et al. 2015). However, geochemical roles of carbonate sediment in OC sequestration in seagrass meadow sediments is not well understood.
This study focuses on the OC stock and its relationship to mineralogical properties of sediment such as carbonate content, specific surface area (SSA), and mesopore distribution in carbonate sediments accompanied by seagrass meadows in Japan and the Philippines. Here, typical carbonate sediment is defined as sediment with inorganic carbon (IC) content greater than 8 mmol IC g^{-1}(ca. 10%-IC w/w). Obtained results were compared with corresponding properties of temperate, non-carbonate (<0.5 mmol IC g^{-1}) seagrass meadow sediments. The ranges of OC concentration and stock, as well as the degree of accumulation of OC in seagrass meadows relative to adjacent non-vegetated sediment, were similar between carbonate and non-carbonate seagrass habitats. The OC concentration strongly correlated with SSA and total mesopore volume for both carbonate and non-carbonate sediments. However, average OC loading per unit surface area and unit mesopore volume was six-times and three-times greater for carbonate sediments than non-carbonate sediments, respectively. Carbon isotope abundance suggested that the fraction of seagrass-derived OC to total OC was often much greater for carbonate sediments than non-carbonate sediments. Nonetheless, OC tightly associated with carbonate minerals seemed to be derived mainly from non-seagrass sources. These findings as well as the differences between carbonate and non-carbonate sediments may be partially explained by characteristics specific to carbonate sediments, such as presence of basic OC inherited from organisms that originally produced the carbonate, different affinity to soluble organic matter, different mesopore shape and size distribution, and gradual dissolution during early diagenesis. However, what constrains the capacity of carbonate sediments to sequester OC is still unclear. Our results suggest that, although mineralogical control on sediment OC is significant in carbonate sediment, the classical sorptive preservation mechanism originally put forward for explaining the constant OC/SSA ratio in continental shelf sediments is not sufficient to explain the OC sequestration capacity of carbonate sediments supporting seagrass meadows.

Keywords: seagrass beds, calcium carbonate, carbon storage

©2019. Japan Geoscience Union. All Right Reserved.

Perceptions of Coastal Communities on Blue Carbon Ecosystems Services at the Municipalities of Eastern Samar and Western Visayas, Philippines

*Jay Mar Dioquito Quevedo[1], Yuta Uchiyama[1], Kaoru Kakinuma[1], Ryo Kohsaka[1]

1. Tohoku University

The blue carbon ecosystems (mangroves and seagrass) in the Philippines provide a wide range of benefits to the coastal communities; from provisional, regulating and cultural services ranging from supply of food and a natural fish nursery, carbon storage, protection against storm surges and as a tourism site. Existing studies in the Philippines have shown how local people in coastal areas affects the utilization and managing of the blue carbon ecosystems. However, little have recorded and evaluated the perception of people on the importance of these coastal ecosystems at the municipality level in relationship with rate of utilization to the different services these ecosystems provide. It is very important to understand the level of awareness and usage of mangrove, seagrass and associated resources because it can help in contextual formulation and implementation of management plan of coastal ecosystems in the municipality. In this study, household surveys, key informant interviews (KII), and focus group discussions (FGD) using semi-structured questionnaires will be utilized at coastal areas in select municipalities of Eastern Samar and Western Visayas. This study aims to determine the local knowledge of the coastal communities on blue carbon ecosystems, evaluate how they directly or indirectly use the services and identify potential local threats and destructive activities. It will also highlight the perception and evaluation of the existing efforts of the local government and their effectivity on the management of blue carbon ecosystems from local perspectives which has been largely overlooked.

Keywords: Blue Carbon Ecosystems, Coastal Management, Ecosystem Services, Coastal Communities, Awareness, Utilization

©2019. Japan Geoscience Union. All Right Reserved.

Numerical simulation of typhoon events in Sekisei Lagoon, Okinawa, Japan using a coupled ocean-wave model

*Lawrence Patrick Cases Bernardo[1], Takashi Nakamura[1], Kazuo Nadoka[1]

1. Department of Transdisciplinary Science and Engineering, Tokyo Institute of Technology

Sekisei Lagoon is the site of Japan's largest coral reef area and is an important target site for conservation. However, it is affected to varying degrees by typhoons which approach yearly during the summer and autumn seasons. To closely investigate typhoon-driven hydrodynamics in Sekisei Lagoon, a modeling setup was developed using a nested Regional Ocean Modeling System (ROMS) configuration with an outer coarse scale regional model at 1.5 km grid resolution, and an inner model focused on the Sekisei Lagoon domain with a grid resolution of 300 meters. The inner model was configured using the Coupled Ocean-Atmophere-Wave-Sediment Transport (COAWST) modeling framework in order to couple the ROMS ocean model with the Simulating Waves Nearshore (SWAN) wave model. Initial conditions and ocean boundary forcing for the regional model were derived from the global 1/12° Hybrid Coordinate Modeling System analysis data (HYCOM GLBv0.08), and tidal forcing was added using data from the 1/30° OSU Topex/Poseidon Global Inverse tidal solution (TPXO9). Meteorological forcing was derived from Japan Meteorological Agency-Grid Point Value (JMA-GPV) mesoscale model results, and SWAN boundary forcing for the inner model was derived using outputs from the 5-km JMA Coastal Wave Model (CWM) for locations around the Yaeyama Islands where Sekisei Lagoon is located.

The modeling setup was run for specific typhoon events as well as for relatively calmer periods, and model performance was evaluated by comparing simulation results with in-situ observations from sensor deployments around Sekisei Lagoon conducted during the summer months of 2014, 2015, and 2016, as well as from a long term continuous monitoring setup in the Shiraho Reef area in Ishigaki Island. Modeled significant wave heights and peak wave periods at wave sensor locations for relatively calm periods had comparable ranges, but exact temporal trends could not yet be reproduced well. During modeled typhoon passages, trends in significant wave height, such as the timing of increase as the typhoon approached and the maximum wave height reached, were well-reproduced for a wave sensor located at the southeastern part of Sekisei Lagoon. However, the comparison was relatively poor for wave sensors deployed at the northwestern part of the lagoon and offshore of Shiraho Reef on the eastern side of Ishigaki Island, particularly in terms of the timing of wave height increase. In terms of simulating water temperature, running the inner ROMS model without SWAN resulted in Wilmott skill index (Wilmott 1981) scores ranging from 0.72 to 0.95 and root mean-square errors ranging from 0.46 to 1.52 deg C when compared with field observations conducted around Sekisei Lagoon from May to November in 2016. Modeling runs for the coupled ROMS-SWAN model were of shorter duration, but the simulated water temperatures showed some notable differences with the ROMS only case for some locations, suggesting that the influence of wave-driven flows on water temperature trends may need closer investigation.

Adjustments to the modeling setup are ongoing, especially in terms of more properly resolving bathymetric features, as some parts of the domain are characterized by complex barrier and fringing reef structures. Parameter tuning is also being conducted in relation to the physical processes considered in the SWAN wave model, such as the influence of bottom friction and depth-induced wave breaking. With further improvement, this modeling setup may serve as a potentially useful tool to gain further insight into the ways typhoons affect the hydrodynamic conditions in Sekisei Lagoon, as well as estimate potential damage levels, given that typhoon tracks and intensities vary. Even for the non-typhoon case, the setup

©2019. Japan Geoscience Union. All Right Reserved.

may also be useful to help clarify the influence of waves on the overall circulation in the area.

Keywords: hydrodynamics, typhoon, ocean model, wave model, coral reef, sensors

©2019. Japan Geoscience Union. All Right Reserved.

Study of macrobenthic community structure at mesophotic depths in the South Ryukyus based on ROV and AUV seafloor imaging

*Marc Humblet[1], Toshihiro Maki[2], Yasuo Furushima[3], Yukiyasu Noguchi[2], Hiroumi Horimoto[2], Hiroya Yatagai[2], Takashi Sakamaki[2], Shohei Ito[4], Sadao Suzuki[5]

1. Department of Earth and Planetary Sciences, Nagoya University, 2. Institute of Industrial Science, The University of Tokyo, 3. JAMSTEC, 4. FullDepth Co., Ltd., 5. ORE

Mesophotic coral reef habitats (30-150 m) are still largely unexplored despite their importance in biology (e.g., marine biodiversity studies, genetic connectivity between shallow and deep communities, ecological shift from photosynthetic to heterotrophic communities along a depth/light gradient) and in geology (e.g., study of sea-level changes and reef growth history during Quaternary sea-level lowstands). Here we report on new seafloor observations conducted by remotely operated vehicles (ROVs) and an autonomous underwater vehicle (AUV) at depths of 30-65 m around the Sekisei lagoon, Yaeyama Islands, South Ryukyus, Japan. In this study, new seafloor imaging was carried out at six sites along the northern (N1-N2) and southern (S1-S4) margins of the Sekisei Lagoon by two ROVs (BlueRov 2, Blue Robotics Inc., and FullDepth DiveUnit 300, FullDepth Co., Ltd.) and one AUV (HATTORI 2). HATTORI 2 is designed to acquire high-resolution video images of the seafloor at a constant elevation along a pre-programmed path, which enables the creation of a 3D topographic map of the seafloor based on structure-from-motion photogrammetry. In addition, HATTORI 2 was equipped with depth, temperature, salinity and light sensors. We combine these new observations with data obtained during previous ROV and AUV surveys to investigate the community structure of benthic organisms, particularly scleractinian corals, at mesophotic depths, and examine its relationship with water depth, seafloor topography, substrate type, and other major environmental parameters (i.e., light penetration, water temperature and salinity). Previous surveys revealed a clear bathymetric zonation at site S1 with a shift from a “coralgal” community (dominated by scleractinian corals and coralline algae) to a “mixed” community (including scleractinian corals, algae, octocorallians, sponges, and foraminifers) at a depth of ~60 m, and showed also that scleractinian corals become rare below 70 m. A preliminary analysis of images acquired during our latest survey indicates that coral cover in the upper mesophotic zone (30-40 m) varies greatly from one site to another: up to 100% in the area of sites N1 and N2 (*Leptoseris* and *Acropora* colonies locally abundant), 35% or less in the area of S1, close to 0% at sites S2 and S3, and 30-60 % at site S4. Our new data confirm that substrate type and seafloor topography are likely important factors controlling the distribution of corals at upper mesophotic depths (higher coral cover on hard rocky substrate and topographic highs), but they alone cannot explain the full range of our observations.

Keywords: Coral reefs, Mesophotic habitat, Coral communities, ROV, AUV

©2019. Japan Geoscience Union. All Right Reserved.

Enhancement of antioxidant activity of scleractinian coral *Galaxea Fascicularis* by feeding treatment.

*Hiroyuki Fujimura[1], Sayaka Higa[1], Toshihiro Miyajima[2], Tomihiko Higuchi[2], Sylvain Agostini[3], Ikuko Yuyama[3], Takashi Nakamura[4]

1. University of the Ryukyus, 2. The University of Tokyo, 3. Tsukuba University, 4. Tokyo Institute of Technology

In recent years, mass coral bleaching has been recognized around the world. Coral bleaching is a phenomenon that coral loses symbiotic algae “zooxanthellae” due to strong solar radiation and high water temperature, and white coral skeleton can be seen through the transparent its soft tissue. Coral bleaching is caused by a damage of photosynthetic system of zooxanthella by strong light and the damaged part is not repaired by the continuation of the high water temperature, leading to a generation of harmful reactive oxygen species by combining surplus electrons and surrounding oxygen.
Since a translocation of fixed carbon from zooxanthellae to coral decreases during bleaching event, corals are forced to consume the stored lipids in the tissues. Prolonged bleaching event eventually causes the death of coral. Corals that store enough energy by predation have more resistance against bleaching (Ferrier-Pages et al. 2010). An addition of a trace amount of inorganic metals to corals has shown an increase in antioxidant enzyme activity (Sasaki 2013). Feeding activity is not only energy supply for coral but also supply of trace metal elements that can be used for the active center of antioxidant enzyme as a cofactor. It is possible that heterotrophic feeding may improve a tolerance of coral bleaching. Therefore, the aim of this study is to investigate experimentally whether antioxidant capacity can be enhanced by heterotrophic nutrition.
Coral polyps of *Galaxea fascicularis* were incubated with and without a feeding condition for 20 days. Zooplankton was given to coral at the dawn when coral actively extends its tentacles and takes predatory behavior (AM 5: 00 - 8: 00). After 20 days, the water temperature was raised up to 31ºC within 3 days. Finally, all the coral polyps were sacrificed and separated into host tissues and zooxanthella. Superoxide dismutase (SOD) enzyme activity of the antioxidant and concentration of the metal element contained in the protein were measured, respectively.
As a result of feeding experiment, the SOD enzyme activity increased under feeding conditions of 27 ℃ and maintained the activity level after exposure to high water temperature, indicating the enhancement of the antioxidant activity of *G. fascicularis* by feeding process.

Keywords: scleractinian coral, heterotrophic nutrition, antioxidant capacity

©2019. Japan Geoscience Union. All Right Reserved.

Effects of environmental stresses on coral bleaching

*Tomihiko Higuchi[1]

1. Atmosphere and Ocean Research Institute, The University of Tokyo

Coral reefs are threatened by multiple environmental stresses at both the global and the local scales. Declining water quality in coastal reefs has been reported such as due to red soil runoff, agricultural fertilizers, and anti-fouling chemicals. Coral bleaching has been frequently reported and actively studied recently. The synergistic effects of multiple stressors have also been studied, with several studies reporting accelerated bleaching under conditions of high seawater temperature and low water quality. For example, enrichment of nitrate can accelerate coral bleaching under high light or high temperature conditions compared with single stress conditions. If the concentration of nitrate increases damage to coral reefs in coastal areas could significantly increase under high temperature or high light stress. Moreover, environmental bacteria, *Sulfitobacter* sp., which can be found in the seawater of coral reef, enhanced bleaching process under high temperature. These nitrate and bacteria did not affect corals severely under ambient temperature (not high temperature). To mitigate environmental stresses on coral reefs, it is important to evaluate risks due not only to global warming, but also to local stresses.

Keywords: global warming, coral bleaching, multiple stresses

©2019. Japan Geoscience Union. All Right Reserved.

[J] Oral | A (Atmospheric and Hydrospheric Sciences)：A-CG Complex & General

Tue. May 28, 2019 1:45 PM - 3:15 PM JST | Tue. May 28, 2019 4:45 AM - 6:15 AM UTC | 102 1F

[A-CG44] Coastal Ecosystems 2 Coral reefs, seagrass and macroalgal beds, and mangrove

convener:Yu Umezawa(Tokyo University of Agriculture and Technology), Toshihiro Miyajima(Marine Biogeochemistry Group, Division of Ocean-Earth System Science, Atmosphere and Ocean Research Institute, The University of Tokyo), Atsushi Watanabe(The ocean policy research institute, The Sasakawa peace foundation), Tomihiko Higuchi(Atmosphere and Ocean Research Institute, The University of Tokyo), Chairperson:Yu Umezawa(Tokyo University of Agriculture and Technology), Toshihiro Miyajima(The University of Tokyo), Tomihiko Higuchi(Atmosphere and Ocean Research Institute, The University of Tokyo), Atsushi Watanabe(Tokyo Institute of Technology)

Coastal marine ecosystems are complex open system interacting with surrounding watersheds, outer ocean, and the atmosphere, providing a wealth of various ecosystem services to human life. Simultaneously, they are also influenced strongly and often negatively by human activities. This session, together with a companion session dedicated for the water cycle and land-ocean interactions, aims to provide a platform for interdisciplinary discussion covering various aspects of frontiers in coastal ecosystem sciences. This session particularly focuses shallow-water benthic communities ranging from temperate to tropical regions, such as coral reefs, seagrass and macroalgal beds, and mangroves. All these communities are characterized by intrinsically high primary production, active material cycling, and biodiversity hot spots. However, increasing human demand for coastal marine resources and industrial development concentrating on coastal regions incur the risk of rapid degradation and diminishment. Comprehensive assessment and monitoring of ecosystem functions and development of effective means for conservation and restoration are urgently needed for such communities. This session is dedicated to organizing and promoting such research and management activities by sharing state-of-the-art science and technology among ecologists, geologists, geochemists, biogeographers, etc. Field-based and modeling studies concerning the following topics are especially welcome: material cycling and ecosystem functions; community connectivity; environmental changes such as global warming, ocean acidification, and sea-level rise; ecosystem services such as carbon sequestration, nutrient regulation, and fisheries production; broad-scale comparison; long-term ecological researches.

1:45 PM - 1:50 PM JST | 4:45 AM - 4:50 AM UTC

Introduction

1:50 PM - 2:10 PM JST | 4:50 AM - 5:10 AM UTC

[ACG44-01] Evaluation of mangrove ecosystems as a dissolved iron supplying system to tropical coastal waters

★Invited Papers

*Yasuhiro Nakanishi[1], Ko Hinokidani[1] (1.Tokyo University of Agriculture)

2:10 PM - 2:25 PM JST | 5:10 AM - 5:25 AM UTC

[ACG44-02] Dissolved organic carbon and optical properties in tropical and subtropical mangrove environments

*Raghab Ray[1], Toshihiro Miyajima[1], Charissa M Ferrera[2], Chia-Jung Lu[1], M.L San Diego-McGlone[2], Hiroshi Ogawa[1], Kazuo Nadaoka[3] (1.Atmosphere and Ocean Research Institute, The University of Tokyo, 2.Marine Science Institute, University of the Philippines, Diliman, 3.School of Environment and Society, Tokyo Institute of Technology)

2:25 PM - 2:45 PM JST | 5:25 AM - 5:45 AM UTC

[ACG44-03] Modeling coral polyp-scale bleaching phenomenon and upscaling to reef-scale

★Invited Papers

*Takashi Nakamura[1], Tomihiko Higuchi[2], Toshihiro Miyajima[2], Lawrence Patrick Cases Bernardo[1], Kazuo Nadaoka[1], Atsushi Watanabe[1,3], Hiroyuki Fujimura[4] (1.School of Environment and Society, Tokyo Institute of Technology, 2.AORI, The University of Tokyo, 3.The ocean policy research institute, The Sasakawa peace foundation, 4.University of the Ryukyus)

2:45 PM - 3:00 PM JST | 5:45 AM - 6:00 AM UTC

[ACG44-04] Reversal of surface ocean acidification and recovery potential of calcification: ecology of proton concentration control

*Kazuhiko Ichikawa[1] (1.(post) Graduate School of Environmental Earth Science, Hokkaido University)

3:00 PM - 3:15 PM JST | 6:00 AM - 6:15 AM UTC

[ACG44-05] Revisit of massive *Porites* coral growth under the outbreak of crown-of-thorns starfish and thermal stress in Sekisei Lagoon, Japan

*Kohki Sowa[1] (1.Japan Agency for Marine-Earth Science and Technology)

Evaluation of mangrove ecosystems as a dissolved iron supplying system to tropical coastal waters

*Yasuhiro Nakanishi[1], Ko Hinokidani[1]

1. Tokyo University of Agriculture

Iron, one of the essential micro elements for plants, is normally contained in the insoluble forms in sea water, content of the dissolved forms greatly affects propagations of marine phytoplankton which are origins of the marine food chain and absorb CO_2 in sea water.

As one of the studies on natural systems for dissolved forms of iron from land to sea, we focused on mangrove ecosystems located at boundary between the land and sea in the tropical regions. To clarify the dissolved iron supplying systems, we have conducted studies on polyphenols content in leaves of some mangrove species and elution of dissolved iron generated in reactions between the polyphenols and mangrove floor soils. Additionally, we surveyed dissolved iron elution from the floor soils mixed with fecal materials of benthos, such as *Neosarmatium smith* and *Telebralia palustris* which feed on mangrove leaves.

Keywords: Mangrove, Ecosystem, Dissolved iron, Benthos, Polyphenole

©2019. Japan Geoscience Union. All Right Reserved.

Dissolved organic carbon and optical properties in tropical and subtropical mangrove environments

*Raghab Ray[1], Toshihiro Miyajima[1], Charissa M Ferrera[2], Chia-Jung Lu[1], M.L San Diego-McGlone[2], Hiroshi Ogawa[1], Kazuo Nadaoka[3]

1. Atmosphere and Ocean Research Institute, The University of Tokyo, 2. Marine Science Institute, University of the Philippines, Diliman, 3. School of Environment and Society, Tokyo Institute of Technology

Among different wetland habitats, mangroves are key source of dissolved organic matter (DOM) for the estuarine and coastal waters. However, the quantity and quality of DOM from both natural and rehabilitated mangroves sustained under contrasting hydro-climatological settings of tropical and subtropical regions have not been examined comprehensively. The present study was carried out in areas of such regions in the tropics (Panay and Palawan, Philippines) and sub-tropics (Ishigaki and Iriomote, Japan). Surface water sampling was performed along the salinity gradient of mangrove dominated rivers and estuaries in 2018, aiming to investigate the distribution, mixing and fate of dissolved organic carbon (DOC), δ^{13}C-DOC and optical properties such as chromophoric dissolved organic matter (as CDOM). Preliminary results showed that mean DOC concentration was ~2-fold higher in Ishigaki and Iriomote than Panay and Palawan mangroves (225±111 μM and 103±52 μM, respectively) due to dilution effect by increased rain water flux from the typhoon event during sampling in Panay and Palawan. Strong correlation between DOC and CDOM absorption coefficient at 412 nm was only evident for the Ishigaki and Iriomote mangroves, indicative of dominance of predominantly allochthonous DOM. In the Philippines, there were no significant variations of DOM properties observed between natural (Palawan) and rehabilitated (Panay) mangroves but their mixing pattern along the salinity transect differed significantly. Property-salinity relationship revealed regions of non-linear mixing of DOC for both sites demonstrating dynamic source-sink reaction processes within the river estuaries. During the course of transport to the sea, DOC was added to the waters in Palawan in contrast to the recruited mangroves of Panay reflecting higher mangrove material input for the former site. Other optical descriptors (like spectra slope between 275 nm and 295 nm, and slope ratio in the ranges of 275-295 nm and 350-400 nm) confirmed the shift in DOM origin from terrigenous to marine sources along the salinity transects of the river estuaries. The linear decreasing trend of specific UV absorption at 254 nm ($SUVA_{254}$) further indicated the loss of DOM aromaticity downstream to the sea. Further attempt will be made to better characterize the DOM molecular compositions and fluorescence properties from the same tropical and sub-tropical mangrove sites.

Keywords: Dissolved organic matter, CDOM, Mangrove, Philippines

©2019. Japan Geoscience Union. All Right Reserved.

Modeling coral polyp-scale bleaching phenomenon and upscaling to reef-scale

*Takashi Nakamura[1], Tomihiko Higuchi[2], Toshihiro Miyajima[2], Lawrence Patrick Cases Bernardo[1], Kazuo Nadaoka[1], Atsushi Watanabe[1,3], Hiroyuki Fujimura[4]

1. School of Environment and Society, Tokyo Institute of Technology, 2. AORI, The University of Tokyo, 3. The ocean policy research institute, The Sasakawa peace foundation, 4. University of the Ryukyus

To elucidate the mechanism responsible for coral bleaching and to project the status of coral communities in the near future, a coral bleaching model was developed based on a reef-scale three-dimensional hydrodynamic–biogeochemical model coupled with a polyp-scale coral bleaching model.

The polyp-scale bleaching model was developed by incorporating the dynamics of photoinhibition, reactive oxygen species (ROS), and zooxanthella abundance based on a previously developed coral polyp model by Nakamura et al. (2013). The polyp-scale model assumes that ROS are produced by zooxanthellae and that corals expel zooxanthellae when the concentration of ROS in their tissues exceeds tolerable levels. When temperature increases, corals release more zooxanthellae because the ROS production rate per zooxanthella cell increases with increasing temperature. This mechanism accounts for coral bleaching at high temperatures. The model assumes that ROS are produced from excess electrons transferred from photosystem II (PSII) that are not used in the downstream photosynthetic process. Photoinhibition, which is a key factor in the transfer of electrons from PSII, was included in the model, and the temperature dependence of Rubisco activity was introduced as a blocking factor in the downstream photosynthetic process. The ROS dynamics include detoxification of ROS by antioxidant substances, and the zooxanthella population dynamics include reproduction, mortality, and the rate of zooxanthellae release, which depends on the ROS damage of the coral cell. Results of simulated incubation experiments under different temperature conditions by the bleaching model reproduced the temperature dependence of the coral bleaching phenomenon. Moreover, recovery process after bleaching was also reproduced, and the ability of the model to describe the recovery process is a unique feature. The model also reproduced the phenomenon that coral bleaching is effectively reduced by light shading. A comparison between photoinhibition and its absence revealed that photoinhibition effectively reduced electron transport from PSII and consequently reduced the production of excess electrons that form ROS. Photoinhibition therefore protects the photosystem and tissues from oxidative damage by ROS. A temperature-dependent repair delay from photoinhibition also reduces ROS production and thereby prevents coral bleaching. The delay may be strategically controlled by zooxanthellae.

The polyp-scale bleaching model was coupled with reef-scale hydrodynamic-biogeochemical model based on the model framework by Nakamura et al. (2018). The model was applied to both the Shiraho coral reef based on Nakamura et al. (2018), and Sekisei Lagoon based on Bernardo et al. (2017). The results of the model simulation confirmed that the model accurately reproduced the spatiotemporal variations of bottom water temperatures on the reef. In particular, the temperatures during the daytime were significantly higher on the reef crest and in shallow nearshore areas than in the offshore seawater. The model confirmed that the spatial pattern of zooxanthella density coincided with the spatial pattern of water temperature on the reef. The model can use the internal condition of the corals to output the parameters that characterize coral population dynamics, such as coral growth rates and mortality rates. The coupled model therefore has the potential to simulate long-term spatiotemporal changes in coral

©2019. Japan Geoscience Union. All Right Reserved.

coverage. Although the model still needs some improvement, incorporation of additional modules and improvement of the model will make it a useful tool for evaluating how corals respond to multiple environmental stresses on the reef-scale.

Keywords: coral bleaching, numerical simulation, zooxanthellae, ROS

©2019. Japan Geoscience Union. All Right Reserved.

Reversal of surface ocean acidification and recovery potential of calcification: ecology of proton concentration control

*Kazuhiko Ichikawa[1]

1. (post) Graduate School of Environmental Earth Science, Hokkaido University

Surface ocean ecology is open system under anthropogenic effect on atmosphere. Coral reefs and individual coral polyps are interacting with surrounding watersheds. They are influenced strongly and often negatively by human activities. All the coordinates pointed out by atmospheric PCO2 and surface ocean pH were irregularly scattered at PCO2 > 290ppm under anthropogenic effect on surface ocean. The calcifying organism habitats of surface ocean are controlled by the proton dynamics and chemical physics of comprehensive global-environment. The surface oceans of calcifying organism habitats showed the proper base of ~8.0 < pH < ~8.3 at ~200ppm < P_{CO2} < ~290ppm under no anthropogenic effect on P_{CO2}. The calcifying organism habitats of surface ocean are controlled by the proton dynamics and chemical physics of comprehensive global-environment.Surface ocean ecology is open system under anthropogenic effect on atmosphere. Coral reefs and individual coral polyps are interacting with surrounding watersheds. They are influenced strongly and often negatively by human activities. All the coordinates pointed out by atmospheric PCO2 and surface ocean pH were irregularly scattered at PCO2 > 290ppm under anthropogenic effect on surface ocean. The calcifying organism habitats of surface ocean are controlled by the proton dynamics and chemical physics of comprehensive global-environment. The surface oceans of calcifying organism habitats showed the proper base of ~8.0 < pH < ~8.3 at ~200ppm < P_{CO2} < ~290ppm under no anthropogenic effect on P_{CO2}. The calcifying organism habitats of surface ocean are controlled by the proton dynamics and chemical physics of comprehensive global-environment.

©2019. Japan Geoscience Union. All Right Reserved.

Revisit of massive *Porites* coral growth under the outbreak of crown-of-thorns starfish and thermal stress in Sekisei Lagoon, Japan

*Kohki Sowa[1]

1. Japan Agency for Marine-Earth Science and Technology

Recently, shallow water coral reefs have come under high pressure because of the changes in climate due to global warming and water quality due to pollution. Coral reefs, which are distributed from the tropical to the temperate areas, consist of calcareous biotas such as scleractinian corals. As the coral skeletal growth is one of the candidate proxies for representing the whole coral reef health, it can provide vital information for developing effective conservation strategies for coral reefs. However, there are only a few studies on the long-term and *in-situ* verification of the relationships among coral skeletal growth, and changes in coral ecology and climate information.

Sekisei area is located between the Yaeyama Islands and the largest coral reef lagoon in Japan (approximately 400 km^2). Continual monitoring of coral and crown-of-thorns starfish (COTS) started in 1983, and the results revealed the negative effects of the outbreak of COTS and the thermal stress-induced severe damage to coral reef ecology. Massive *Porites* coral is one of the key species in the framework of coral reefs in North-West Pacific. The coral continuously precipitates carbonate skeleton over its previous frame, which provides us an opportunity to hindcast the skeletal growth for the long term. Therefore, massive *Porites* coral skeleton in Sekisei Lagoon offers an opportunity to verify whether their skeletal growth is an indicator of coral reef health.

This study shows the revisit of long-term massive *Porites* coral growth (extension rate) estimated from the coral cores in Sekisei Lagoon from 1965 to 2000 reported by Omata *et al.* (2002). Eighty-two coral cores were collected from 12 areas, including reef fronts and patch reefs in Sekisei Lagoon. This study then selected seventy-four coral cores. The average growth anomaly decreased from the 1980s to 1990, which corresponded to decreasing coral coverage. The results imply that the growth of *Porites* coral would be an indicator of the changes in coral coverage by biodisturbance in this area. On the contrary, there were several reductions in extension anomaly, but it did not entirely correspond to the coral bleaching events in 1983 and 1998. These results imply that the growth of *Porites* coral does not represent the coral bleaching events in this area.

References

Omata *et al.* (2002) Skeletal growth history of modern corals in Sekisei Lagoon as a bio-indicator. *JAMSTEC-R* 45, 17-30.

Keywords: Coral, Skeleton , Hindcast, COTS, Thermal stress, Sekisei lagoon

©2019. Japan Geoscience Union. All Right Reserved.

[J] Oral | A (Atmospheric and Hydrospheric Sciences)：A-CG Complex & General

Tue. May 28, 2019 3:30 PM - 5:00 PM JST | Tue. May 28, 2019 6:30 AM - 8:00 AM UTC | 102 1F

[A-CG44] Coastal Ecosystems 2 Coral reefs, seagrass and macroalgal beds, and mangrove

convener:Yu Umezawa(Tokyo University of Agriculture and Technology), Toshihiro Miyajima(Marine Biogeochemistry Group, Division of Ocean-Earth System Science, Atmosphere and Ocean Research Institute, The University of Tokyo), Atsushi Watanabe(The ocean policy research institute, The Sasakawa peace foundation), Tomihiko Higuchi(Atmosphere and Ocean Research Institute, The University of Tokyo), Chairperson:Yu Umezawa(Tokyo University of Agriculture and Technology), Toshihiro Miyajima(The University of Tokyo), Atsushi Watanabe(Tokyo Institute of Technology), Tomihiko Higuchi(Atmosphere and Ocean Research Institute, The University of Tokyo)

Coastal marine ecosystems are complex open system interacting with surrounding watersheds, outer ocean, and the atmosphere, providing a wealth of various ecosystem services to human life. Simultaneously, they are also influenced strongly and often negatively by human activities. This session, together with a companion session dedicated for the water cycle and land-ocean interactions, aims to provide a platform for interdisciplinary discussion covering various aspects of frontiers in coastal ecosystem sciences. This session particularly focuses shallow-water benthic communities ranging from temperate to tropical regions, such as coral reefs, seagrass and macroalgal beds, and mangroves. All these communities are characterized by intrinsically high primary production, active material cycling, and biodiversity hot spots. However, increasing human demand for coastal marine resources and industrial development concentrating on coastal regions incur the risk of rapid degradation and diminishment. Comprehensive assessment and monitoring of ecosystem functions and development of effective means for conservation and restoration are urgently needed for such communities. This session is dedicated to organizing and promoting such research and management activities by sharing state-of-the-art science and technology among ecologists, geologists, geochemists, biogeographers, etc. Field-based and modeling studies concerning the following topics are especially welcome: material cycling and ecosystem functions; community connectivity; environmental changes such as global warming, ocean acidification, and sea-level rise; ecosystem services such as carbon sequestration, nutrient regulation, and fisheries production; broad-scale comparison; long-term ecological researches.

3:30 PM - 3:45 PM JST | 6:30 AM - 6:45 AM UTC

[ACG44-06] Reconstructing sedimentation process of lagoon sediment in the Eastern Kume Island, Ryukyus

*Wataru Sano[1], Shoko Hirabayashi[2], Yusuke Yokoyama[3], Yosuke Miyairi[3], Kazuhiko Fujita[4], Hironobu Kan[2], Lauren T. Toth[5], Richard B. Aronson[6] (1.Graduate School of Integrated Sciences for Global Society, Kyushu University, 2.Graduate School of Social and Cultural Studies, Kyushu University, 3.Atmosphere and Ocean Research Institute, University of Tokyo, 4.Department of Physics and Earth Sciences, University of the Ryukyus, 5.United States Geological Survey, 6.Florida Institute of Technology)

3:45 PM - 4:00 PM JST | 6:45 AM - 7:00 AM UTC

[ACG44-07] Addressing challenges in long-term coral reef monitoring: Statistical tools to address the effect of new methods

*Iwao Fujii[1,2], Jennifer Selgrath[3,2], Amanda Vincent[2] (1.The Ocean Policy Research Institute of the Sasakawa Peace Foundation, 2.Project Seahorse, Institute of the Oceans and Fisheries, The University of British Columbia, 3.Hopkins Marine Station, Stanford University)

4:00 PM - 4:20 PM JST | 7:00 AM - 7:20 AM UTC

[ACG44-08] Ocean currents and herbivory drive macroalgae-to-coral community shift under climate warming

★Invited Papers

*Naoki H. Kumagai[1], Jorge García Molinos[2], Hiroya Yamano[1], Shintaro Takao[1], Masahiko Fujii[2], Yasuhiro Yamanaka[2] (1.National Institute for Environmental Studies, 2.Hokkaido University)

4:20 PM - 4:35 PM JST | 7:20 AM - 7:35 AM UTC

[ACG44-09] Estimation of temperature of seaweed bed vegetation boundary in the Western Seto Inland Sea using satellite SST

*Naoki Yoshie[1], Anri Kabe[1], Hiromori Shimabukuro[2], Goro Yoshida[2] (1.Center for Marine Environmental Studies, Ehime University, 2.Japan Fisheries Research and Education Agency)

4:35 PM - 4:55 PM JST | 7:35 AM - 7:55 AM UTC

[ACG44-10] Fate of macroalgal organic matter and its effects on in and outside of algal bed

★Invited Papers

*Shigeki Wada[1], Yuko Omori[1], Takeo Hama[1,2] (1.University of Tsukuba, 2.Dokkyo University)

4:55 PM - 5:00 PM JST | 7:55 AM - 8:00 AM UTC

Discussion

Reconstructing sedimentation process of lagoon sediment in the Eastern Kume Island, Ryukyus

*Wataru Sano[1], Shoko Hirabayashi[2], Yusuke Yokoyama[3], Yosuke Miyairi[3], Kazuhiko Fujita[4], Hironobu Kan[2], Lauren T. Toth[5], Richard B. Aronson[6]

1. Graduate School of Integrated Sciences for Global Society, Kyushu University, 2. Graduate School of Social and Cultural Studies, Kyushu University, 3. Atmosphere and Ocean Research Institute, University of Tokyo, 4. Department of Physics and Earth Sciences, University of the Ryukyus, 5. United States Geological Survey, 6. Florida Institute of Technology

This study aims to reveal the sedimentation process of the barrier reef lagoon in the Eastern Kume Island. We drilled at two sites (the south of Ooha island and the east of Eef beach)in Kume Island and obtained 4 cores. The penetration depth of cores were from 2.4 to 4.2 m. Unlithified sediments in coral reef lagoons in Kume Island were mainly composed of bioclast such as branching coral pebbles, foraminifera, shell, algae and lime mud.
We measured radiocarbon dating of 28 samples (18 coral pebbles and 10 foraminifera) in the cores and estimated their sedimentation rates. The results showed that the sedimentation rate was slow at the south of Ooha Island, but rapid at Eef beach. The timing of rapid sediment accumulation at Ooha Island coincided with the timing of relative sea-level rise around 6.7 ka and reached its highest level at Tonaki Island (Kan et al.,1997) locating next to Kume Island. The sediment accumulation at Eef Beach was from 4.1 to 3.2 ka and it lagged behind Ooha Island. It may be because the coastal plain was developed with three beach ridges behind Eef Beach (Kawana,1990) and the coring sites were located at the front of the coastal plain formation.
This study was supported by JSPS and the U.S. National Science Foundation.

Keywords: Coral reef, Sea-level change, Geomorphological development, Holocene, Ryukyu Islands

©2019. Japan Geoscience Union. All Right Reserved.

Addressing challenges in long-term coral reef monitoring: Statistical tools to address the effect of new methods

*Iwao Fujii[1,2], Jennifer Selgrath[3,2], Amanda Vincent[2]

1. The Ocean Policy Research Institute of the Sasakawa Peace Foundation, 2. Project Seahorse, Institute of the Oceans and Fisheries, The University of British Columbia, 3. Hopkins Marine Station, Stanford University

Tracking how coral responds to marine protected areas (MPA) is critical for the effective coral reef management. Ideally, one method would be employed consistently throughout monitoring, but such longitudinal sampling can pose problems of methodology. Some possible reasons include a possibility of a current method found inappropriate in the course of monitoring or development of new preferred approaches over time. What happens when procedures are suboptimal and must be changed? Our project evaluated how data from two reef survey methods, line intercept transect (LIT) and photoquadrat (PQ), estimated coral cover. We then explored a way of combining data from different sources as one time-series dataset.

Data used in this study were collected in a three-year period of 18-year monitoring, where both LIT and PQ were executed. Monitoring surveys were conducted between 1998 and 2016 in dry and wet seasons (March ~ April, and September ~ October, respectively) at eight MPAs. LIT was used in the first half of monitoring (1998 ~ 2010) and PQ in the later half (2008 ~ 2016). Both methods were used between 2008 and 2010 as a transition period. In LIT, two 20 m transects were set up as fixed transects in each MPA; however, this method was replaced with PQ due to difficulties in maintaining the transects as fixed. In PQ, ten 23 m transects were placed haphazardly at each MPA. The surveys were conducted at the depth shallower than 5 m. LIT data were also sampled from areas between 5 and 10 m, but data from the deep areas were not included in this study.

In a comparison of data from the transition period, LIT showed higher mean percent coral cover than PQ (LIT mean: 40.5 %, PQ mean: 31.1 %). However, a difference between the two methods became insignificant after increasing sample sizes of LIT data by resampling (LIT mean after resampling: 39.0 %). In resampling, two 20 m LIT transects were subsetted by 1 m and thus, 40 samples were generated. In an analysis of coral cover change over time, PQ showed significant results (5.8 % decrease / year) whereas LIT exhibited insignificant results (1.8 % increase / year). This difference can be attributed to characteristics of PQ, where larger sample sizes were collected from wider areas. Although temporal patterns of LIT did not significantly change even after resampling, a comparability between the two methods can increase by adding deep LIT data, given there is no depth effect. These results confirmed that a difference in sample sizes and areas need to be carefully considered when data form different sources are analyzed. In addition, they indicated that resampling can be effective to improve comparability of different datasets. The results from this study can help improve the quality of monitoring data and thus, contributed to more powerful coral reef conservation.

Keywords: Coral reef, Marine protected area, Long-term monitoring , Marine Conservation

©2019. Japan Geoscience Union. All Right Reserved.

Ocean currents and herbivory drive macroalgae-to-coral community shift under climate warming

*Naoki H. Kumagai[1], Jorge García Molinos[2], Hiroya Yamano[1], Shintaro Takao[1], Masahiko Fujii[2], Yasuhiro Yamanaka[2]

1. National Institute for Environmental Studies, 2. Hokkaido University

Range shifts in foundation species induced by global warming are likely to have ecosystem-wide implications for biodiversity, ecological functioning, biogeochemical cycling and resources used by humans. Corals and macroalgae are habitat-forming species in coastal ecosystems that co-occur and compete for space, and thus global degradation of coral reefs and macroalgal beds can have ecosystem-wide implications. However, recent studies in warm temperate zones have documented community shifts from macroalgae to corals, signaling a potential mechanism for coral conservation under climate warming at the expense of macroalgae under climate warming. Although such community shifts are expanding geographically, our understanding of the driving processes is still limited. Here, we reconstruct long-term climate-driven range shifts in 30 species of macroalgae (8 kelp and 22 fucoid species), 12 species of corals and three species of herbivorous fishes (records of overgrazing) from over 60 years records (mainly 1950–2015) stretching across 3,000 km of the Japanese archipelago from tropical to subarctic zones.

The direction and rate of the observed range shifts calculated for each species and coast during the study period showed considerable variation in both distribution centroids and range edges. Expansions were scarcer than contractions in macroalgae, whereas fishes and corals experienced expansions much more frequently than contractions. Expansions were fastest in fishes, followed by corals, fucoids and kelps, whereas macroalgae contracted their range faster than corals and fishes. Based on a revised coastal version of climate velocity trajectories and a Bayesian inference, we found that prediction models combining the effects of climate and ocean currents consistently explained observed community shifts significantly better than those relying on climate alone. Corals and herbivorous fishes performed better at exploiting opportunities offered by this interaction.

The contrasting range dynamics for these taxa suggest that ocean warming is promoting macroalgal-to-coral shifts both directly by increased competition from the expansion of tropical corals into the contracting temperate macroalgae, and indirectly via deforestation by the expansion of tropical herbivorous fish. Beyond individual species' effects, our results provide novel evidence on the important role that the interaction between climate warming and external forces conditioning the dispersal of organisms, such as ocean currents, can have in shaping community-level responses, with concomitant changes to ecosystem structure and functioning. Further, we found that community shifts from macroalgae to corals might accelerate with future climate warming, highlighting the complexity of managing these evolving communities under future climate change. Nevertheless, and although expansion rates are faster than contraction rates overall, we found that not only macroalgae but even corals might be unable to keep pace with climate change. This may suggest that the apparent expansion in overall range might be a transient effect potentially masking risk of metapopulation collapse with decreasing connectivity among local populations and future range collapses. Thus, future conservation of these communities might require of a more proactive management towards climate adaptation including abundance control of herbivorous fishes, artificial assistance for thermal adaptation through selection of thermal-tolerant lineages, or relocation and translocation into cooler areas.

©2019. Japan Geoscience Union. All Right Reserved.

(Kumagai, N. H., J. García Molinos, H. Yamano, S. Takao, M. Fujii, and Y. Yamanaka 2018. Proceedings of the National Academy of Sciences of the United States of America 115: 8990–8995; doi: 10.1073/pnas.1716826115)

Keywords: climate velocity, coastal tropicalization, community phase shifts, range shifts

©2019. Japan Geoscience Union. All Right Reserved.

Estimation of temperature of seaweed bed vegetation boundary in the Western Seto Inland Sea using satellite SST

*Naoki Yoshie[1], Anri Kabe[1], Hiromori Shimabukuro[2], Goro Yoshida[2]

1. Center for Marine Environmental Studies, Ehime University, 2. Japan Fisheries Research and Education Agency

Seaweed bed is algal community in the coastal region, and important for the coastal fishing. It provides various ecosystem services to human society. However, it has been changing seriously, especially in the species and composition and habitat. Therefore, vegetation and distribution of seaweed in the near future is regarded as uneasiness by fisher men. Although several studies had reported the changes associated with the warming of sea surface temperature due to the climate change, they have some problems, such as low spatial-temporal resolution for the coastal region. Moreover, the boundary temperatures of the seaweed vegetation are not clear. In this study, I investigated the boundary temperature of seaweed vegetation in the Bungo Channel by using a satellite sea surface temperature data set (NOAA/AVHRR Pathfinder version5.3 level 3 collated global 4km sea surface temperature) which had enough resolution for the coastal region. The Bungo Channel has large gradient of sea surface temperature and various seaweed vegetation. First, I analyzed the accuracy of the satellite temperature in this region by comparing with ship board observation. The result shows that the accuracy of the satellite temperature in winter is enough high (RMSE<0.74℃), while the accuracy in summer is relative low (RMSE<1.25℃) compared with those in winter. Secondly, I analyzed the time series of the temperatures of three boundaries of seaweed vegetation both winter and summer. One is the restrictive temperature of the southern limit of temperate kelps habitat. Second is the restrictive temperature of the southern limit of the other temperate seaweeds habitat. Third is the restrictive temperature of the southern limit of the transition region between temperate and subtropical seaweeds (i.e., the northern limit of subtropical seaweeds). I found that the restrictive temperatures in winter were 14.5℃, 15.0℃, 16.0℃, and also the restrictive temperatures in summer were 26.0℃, 26.5℃, 27.0℃, respectively. The restrictive temperature of the southern limit of temperate kelps moved northward from 1989 when the winter temperature have been over 14.5℃. It was also affected by warm summer temperature changing in the 2000s. The restrictive temperature of the southern limit of the other temperate seaweed habitat was considered to be strongly affected by the warm winter temperature over 15.0℃ after the 1990s. Invasion of the subtropical seaweed seemed to be related with the disappearance of the temperate seaweed which lived in there after the 1990s.

Keywords: Seaweed bed, climate change, vegetation boundary, remote sensing

©2019. Japan Geoscience Union. All Right Reserved.

Fate of macroalgal organic matter and its effects on in and outside of algal bed

*Shigeki Wada[1], Yuko Omori[1], Takeo Hama[1,2]

1. University of Tsukuba, 2. Dokkyo University

Macroalgal bed is known as one of the most productive biome on the earth’ s surface. Their habitat is limited to shallow coastal region, but the coastal environments are linked with the open oceans. A part of organic matter derived from macroalgae would be exported, and it contributes to ecosystem outside of algal bed. Dislodgement of algal body from their base provide drifting algae which would be partly utilized by organisms in offshore. Another fate of organic matter which is exported would be dissolved organic matter (DOM). DOM is exuded to body surface of macroalgae, and transported with mixing of water mass. Based on quantitative estimates of these fate of macroalgal products, we have tried to evaluate the ecological roles of macroalgae in large special scale.

Dislodgement of macroalgae

Dislodgement of macroalgal body would often happen due to wave action. In order to quantitatively estimate the amount of dislodgement, we labeled the body of *Ecklonia cava* which is dominant species in kelp forest around Shimoda, Izu Peninsula, Shizuoka, Japan. A part of labels was disappeared due to dislodgement, and it accounted for about 20-30% of fixed carbon by *E. cava*. In addition, we collected benthic organisms in offshore region with/without drifting algae, showing settlement of drifting algae increases species diversity of fauna on the seafloor.

Macroalgal DOM

Release rate of DOM is estimated by covering bag on blades of *E. cava*, and approximately 40% of fixed carbon is released as DOM. Horizontal distribution of DOM across algal bed to offshore showed a gradient of macroalgal DOM, being consistent with the fact that *E. cava* releases large amount of DOM in coastal region. We additionally examined the microbial and photochemical decomposition processes of the macroalgal DOM. Macroalgal DOM has a resistance for bacterial mineralization, while it was degraded by exposure to sunlight. Therefore, macroalgal DOM would be exported with mixing of water mass, and it is partly decomposed in surface layer. On the other hand, the fraction transported to deeper layer has resistance for bacterial decomposition, and contributes to carbon sequestration.

Keywords: Macroalgae, Dislodgement, Dissolved Organic Matter, Decomposition

©2019. Japan Geoscience Union. All Right Reserved.

[J] Oral | A (Atmospheric and Hydrospheric Sciences)：A-CG Complex & General

Tue. May 28, 2019 9:00 AM - 10:30 AM JST | Tue. May 28, 2019 12:00 AM - 1:30 AM UTC | 103 1F

[A-CG45] Visible Remote Sensing of Hydrospheric Science and Its Application

convener:Joji Ishizaka(Institute for Space-Earth Environmental Research, Nagoya University), Mitsuhiro Toratani(School of Engineering, Tokai University), Yuji Sakuno(Graduate School of Engineering, Hiroshima University), Toru Hirawake(Faculty of Fisheries Sciences, Hokkaido University), Chairperson:Yuji Sakuno(広島大学大学院工学研究科)

Variety of visible remote sensing data for hydrospheric science is now available. For example, it is known that 20 years of long time series of 1 km resolution ocean color data from OCTS-SeaWiFS-MODIS is available. At the end of 2017, 250 m resolution SGLI (Shikisai) was launched by JAXA, and with 300 m resolution European OLSI it became possible to use high resolution and high frequency data. Furthermore, geostationary satellite data from Korean GOCI is also useful. Not only the satellite variety, diversity of products is also increasing from just phytoplankton pigment, chlorophyll-a, to primary production, phytoplankton community structure and even non-phytoplankton materials and optical properties. Those ocean color satellite data should be useful for various fields of hydrospheric science, combining with higher resolution LANDSAT as well as high frequency Himawari data. In this section, we will discuss the variety of new observations and applications of visible remote sensing in hydrospheric science.

9:00 AM - 9:15 AM JST | 12:00 AM - 12:15 AM UTC

[ACG45-01] Further information in the coastal areas from 250-m resolution multiple bands of GCOM-C “SHIKISAI”

★Invited Papers

*Hiroshi Murakami[1], Manabu Shimizu[2], Goh Onizuka[3] (1.Earth Observation Research Center, Japan Aerospace Exploration Agency, 2.Japan Fisheries Research and Education Agency, 3.National Research Institute of Fisheries and Environment of Inland Sea, Japan Fisheries Research and Education Agency)

9:15 AM - 9:30 AM JST | 12:15 AM - 12:30 AM UTC

[ACG45-02] Features of GCOM-C/SGLI standard atmospheric correction scheme and its processing results

*Mitsuhiro Toratani[1], Kazunori Ogata[2], Hajime Fukushima[3] (1.School of Engineering, Tokai University, 2.Japan Aerospace Exploration Agency/Earth Observation Research Center, 3.Tokai University)

9:30 AM - 9:45 AM JST | 12:30 AM - 12:45 AM UTC

[ACG45-03] Verification of GCOM-C/SGLI-derived chlorophyll *a* data in the western North Pacific during May 2018 aboard the R/V *Shinsei Maru*

*Koji Suzuki[1], Stanford B. Hooker[2], Tomonori Isada[1], Kazunori Ogata[3], Mitsuhiro Toratani[4], Hiroshi Murakami[3] (1.Hokkaido University, 2.NASA, 3.JAXA, 4.Tokai University)

9:45 AM - 10:00 AM JST | 12:45 AM - 1:00 AM UTC

[ACG45-04] Toward a global retrieval of in-water optical properties using Deep Neural Network

*Salem Ibrahim Salem[1], Hiroto Higa[2], Kazuo Oki[1], Taikan Oki[1] (1.The University of Tokyo, 2.Yokohama National University)

10:00 AM - 10:15 AM JST | 1:00 AM - 1:15 AM UTC

[ACG45-05] Development of atmosphere and in-water combining algorithm using GCOM-C/SGLI in Tokyo Bay

*Taiga Nakayama[1], HIROTO HIGA[1], Kazuki Ogata[2] (1.Yokohama National University, 2.Japan Aerospace eXploration Agency)

10:15 AM - 10:30 AM JST | 1:15 AM - 1:30 AM UTC

[ACG45-06] Analysis of the uncertainty of backscattering coefficient by radiative transfer simulation in coastal areas and lakes

*Hidehito Taki[1], Hiroto Higa[1], Yoshiyuki Nakamura[1], Takayuki Suzuki[1] (1.Graduate School of Urban Innovation, Yokohama National University)

Further information in the coastal areas from 250-m resolution multiple bands of GCOM-C “SHIKISAI”

*Hiroshi Murakami[1], Manabu Shimizu[2], Goh Onizuka[3]

1. Earth Observation Research Center, Japan Aerospace Exploration Agency, 2. Japan Fisheries Research and Education Agency, 3. National Research Institute of Fisheries and Environment of Inland Sea, Japan Fisheries Research and Education Agency

Generally, since the optical characteristics of a coastal area is more complicated than an open ocean, it is necessary to take into consideration the regionality of the in-water optical properties (absorption and scattering, and their spectral characteristics) in order to estimate biological variables like a chlorophyll-a concentration from satellite observations. On the other hand, the optical properties may be useful as new environment information if they can be derived correctly.

The Second-generation Global Imager (SGLI) boarded on Global Change Observation Mission - Climate (GCOM-C) has launched in Dec. 2017. Since SGLI has 19 observation channels with 250-m spatial resolution in the visible - infrared wavelengths, applications near the coastal areas are expected to be improved. The SGLI channels (380, 412, 443, 490, 530, 565, 672, and 867 nm) include a near-ultraviolet band (380 nm) and a pair of an absorption and a baseline in comparatively longer wavelengths (530 nm and 565 nm) which can improve estimate of high chlorophyll-a concentration since the absorption is not saturated with the high concentration in the wavelengths.

GCOM-C captured patches where water-leaving reflectance (r_w) of 565-nm, which is derived by the atmospheric radiative transfer code, Pstar-4 (Ota et al., 2010), were especially higher compared with r_w at 530 nm in the central part of the Seto Inland Sea on August 1, 5, and 13 2018. High a_ph/(a_ph+a_dg) ratio areas were captured (Fig. 1) through the in-water optical property model (Lyon and Hoge, 2006; Murakami, 2018) using average spectra of a_ph or a_dg in NOMAD dataset (Werdell, and Bailey, 2005). Generally, difference between absorption coefficients of phytoplankton at 530 nm and 565 nm (a_ph(530nm) - a_ph(565nm)) is larger than difference between absorption coefficient of CDOM + detritus at 530 nm and 565 nm (a_dg(530nm) - a_dg(565nm)). It may correspond to the redtide which has been reported around the area by Fisheries Agency (Fisheries Agency, 2018).

We will continue to make more precise water-leaving spectra to be used for useful information of coastal environment through improvement of correction aerosol absorption and so on.

Reference

Ota, Y., A. Higurashi, T. Nakajima, and T. Yokota, 2010: Matrix formulations of radiative transfer including the polarization effect in a coupled atmosphere-ocean system, *J. Quantitative Spectroscopy and Radiative Transfer*, **111**, 878-894.

Werdell, P. J., and S.W. Bailey, 2005: An improved bio-optical data set for ocean color algorithm development and satellite data product validation, *Remote Sens. Environment,* 98, 122-140.

Lyon, P., and F. Hoge, 2006: The Linear Matrix Inversion Algorithm, Chap. 7 of IOCCG Report Number 5, Remote Sensing of Inherent Optical Properties: Fundamentals, Tests of Algorithms, and Applications, Ed. by Z. Lee.

Murakami, H., “Ocean color”, Chapter 10 of Meteorological Research Notes, Vol. 238, *Geostationary Meteorological Satellites, Himawari-8 and 9 and their applications*, M, Ed. by K. Okamoto, K. Bessho, N.

©2019. Japan Geoscience Union. All Right Reserved.

Yoshizaki, and H. Murata, Japan Meteorological Society 2018.
Fisheries Management Office, Fisheries Agency, "Red tide in the Seto Inland Sea”, August 2018

Keywords: GCOM-C, SHIKISAI, SGLI , ocean color, remote sensing

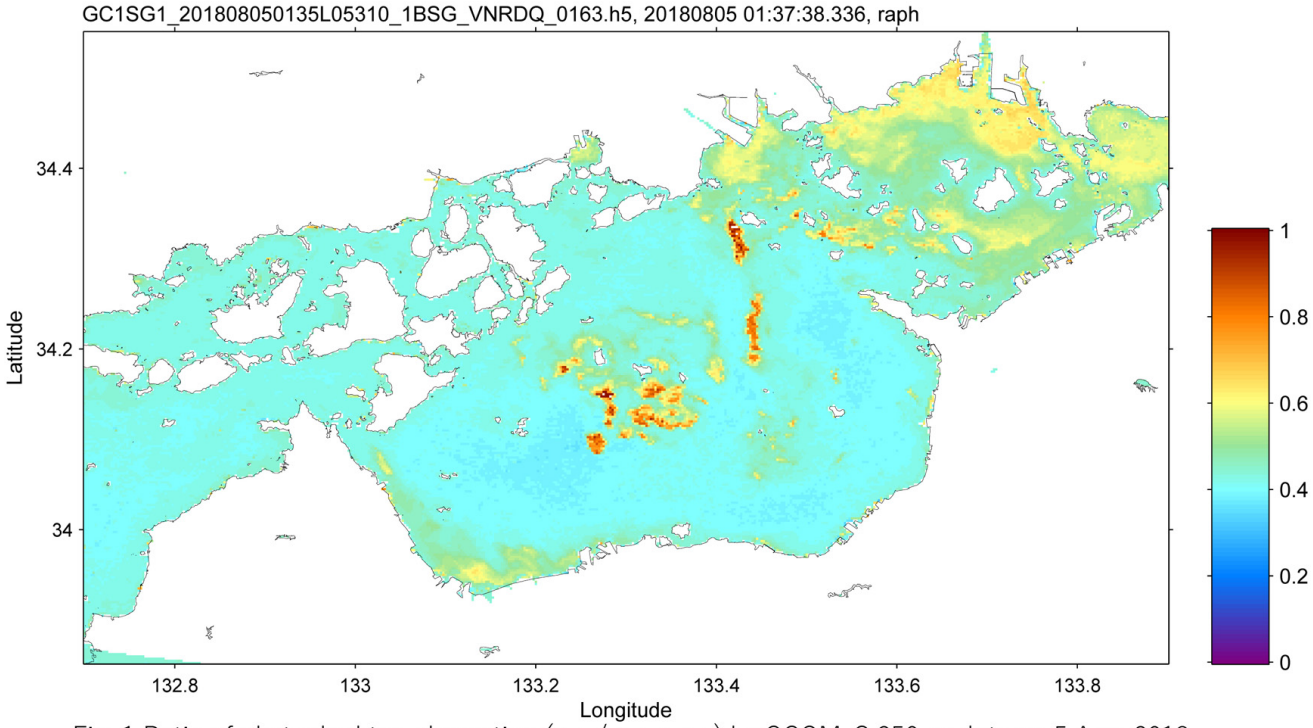

Fig. 1 Ratio of phytoplankton absorption (a_{ph} / a_{ph} + a_{dg}) by GCOM-C 250-m data on 5 Aug. 2018

©2019. Japan Geoscience Union. All Right Reserved.

Features of GCOM-C/SGLI standard atmospheric correction scheme and its processing results

*Mitsuhiro Toratani[1], Kazunori Ogata[2], Hajime Fukushima[3]

1. School of Engineering, Tokai University, 2. Japan Aerospace Exploration Agency/Earth Observation Research Center, 3. Tokai University

On December 23, 2017, the Second-generation Global Imager (SGLI) aboard the Global Climate Observation Mission-C (GCOM-C) satellite "Shikisai" was launched. SGLI has 11 observation bands in the visible and near-infrared region (380-870 nm), designed to detect slight change in water color (spectral water reflectance) with 250m spatial resolution. In order to retrieve accurate water reflectance, the correction of atmospheric absorption and scattering effects (atmospheric correction) is of vital importance. One feature of the JAXA standard atmospheric correction for SGLI is to combined use of the conventional atmospheric correction method for open ocean with the method that utilize the short wavelength infrared bands for coastal high suspended matter concentration waters. We demonstrate the processing results in comparison with MODIS results, and discuss the remaining issues.

Keywords: ocean color remote sensing, atmospheric correction

©2019. Japan Geoscience Union. All Right Reserved.

Verification of GCOM-C/SGLI-derived chlorophyll *a* data in the western North Pacific during May 2018 aboard the R/V *Shinsei Maru*

*Koji Suzuki[1], Stanford B. Hooker[2], Tomonori Isada[1], Kazunori Ogata[3], Mitsuhiro Toratani[4], Hiroshi Murakami[3]

1. Hokkaido University, 2. NASA, 3. JAXA, 4. Tokai University

The Second-generation Global Imager (SGLI) aboard the JAXA GCOM-C satellite was successfully launched on 23 December 2017. We conducted the first GCOM-C field campaign for the western North Pacific during 20–30 May 2018 aboard the R/V *Shinsei Maru*. During this expedition, in situ apparent optical property (AOP) measurements were made using a Compact-Optical Profiling System (C-OPS, Biospherical Instruments Inc.) in order to match up with SGLI data. Also, phytoplankton pigment samples were concomitantly collected from surface waters. A significant linear correlation (R^2 = 0.99, n = 6) was found between ultra-high performance liquid chromatography (UHPLC)-determined chlorophyll (Chl) *a* levels and those derived from C-OPS with the in-water algorithm OC3M6. However, the C-OPS values were underestimated by 32% as compared with the UHPLC data. This could be partly due to the higher pigment extraction efficiency of *N*,*N*-dimethylformamide (DMF) than other organic solvents such as methanol and acetone which are generally used in the world. During the field campaign, SGLI data were successfully matched up with in situ data at a station off Iwate Prefecture, Japan on 21 May. The SGLI-, C-OPS-, UHPLC- and Turner fluorometry-determined surface Chl *a* values were 0.546, 0.709, 0.847 and 1.21 mg m^{-3}, respectively. Other results obtained from the GCOM-C field campaign will also be shown in our presentation.

Keywords: GCOM-C/SGLI, ocean color, satellite remote sensing

©2019. Japan Geoscience Union. All Right Reserved.

Toward a global retrieval of in-water optical properties using Deep Neural Network

*Salem Ibrahim Salem[1], Hiroto Higa[2], Kazuo Oki[1], Taikan Oki[1]

1. The University of Tokyo, 2. Yokohama National University

Reflected sunlight from water bodies, which records by ocean color sensors, contains information of optical properties of water bodies (e.g., chlorophyll-a concentrations, absorption and backscattering coefficients). During the last few decades, researches have been proposed many approaches for monitoring water bodies by retrieving their optical properties. These approaches include bands ratio, semi-analytical algorithms, and spectrum matching. However, there is no accurate continuous monitoring on a global scale, particularly over inland lakes and coastal regions. This is mainly due to the nonlinear complexity of water environment. In additions, there are a few studies that used the synthetic simulated reflectance to train artificial neural network (ANN) models to be applied on a global scale. However, the recent revaluation of these ANN models over the Japanese and European lakes revealed their limitation to provide accurate monitoring of these water bodies. These results could be attributed to two main reasons; (1) inappropriate ANN architecture with one hidden layer which could not be suitable to represent the complex situation of water bodies. (2) the limitation of the synthetic simulated reflectance that used to train these models. The deep neural network (DNN) with multiple hidden layers could provide a promising approach to overcome these complexities. Up to 2006, there is no way to accurately train a DNN due to a Vanishing gradient problem. the recent advances of DNN enable researchers to efficiently use the DNN models with low cost. During the current research, the performance of a DNN model with three-, five- and seven-hidden layers under different architecture conditions will be presented. These conditions include different activation functions (i.e., sigmoid, Relu and TanH), different optimization technique (i.e, Adam optimizer and stochastic gradient descent) and with/without applying dropout technique. The DNN model was designed to receive water leaving reflectance of several ocean color satellites (e.g., Global Change Observation Mission –Climate (GCOM-C)). Nine water quality parameters are generating from the DNN model. Two independent simulated datasets comprising 100,000 water leaving reflectance spectra each were generated for training and testing the DNN models. The two simulated datasets cover wide ranges of Chla (0.01–250 $mg \cdot m^{-3}$), NAP (0.01–250 $g \cdot m^{-3}$), and CDOM (0.001–10 m^{-1}) concentrations, representing the open ocean, coastal areas, and inland lakes. The proposed technique was also validated using in-situ datasets (e.g., NOMAD dataset, and many Japanese lakes and coastal bodies) that represent various trophic statuses. The results reveal the ability of proposed technique to provide accurate retrieval of in-water optical properties as will be discussed.

Keywords: deep neural network, water quality, optical properties, Lakes

©2019. Japan Geoscience Union. All Right Reserved.

Toward a global retrieval of in-water optical properties using Deep Neural Network

Salem Ibrahim Salem[1], Hiroto Higa[2], Kazuo Oki[1], Taikan Oki[1]
[1] Institute of Industrial Science, The University of Tokyo, Japan.
[2] Faculty of Urban Innovation, Yokohama National University, Japan.

Corresponding e-mail: salem@rainbow.iis.u-tokyo.ac.jp and eng.salemsalem@gmail.com

Reflected sunlight from water bodies, which records by ocean color sensors, contains information of optical properties of water bodies (e.g., chlorophyll-a concentrations, absorption and backscattering coefficients). During the last few decades, researches have been proposed many approaches for monitoring water bodies by retrieving their optical properties. These approaches include bands ratio, semi-analytical algorithms, and spectrum matching. However, there is no accurate continuous monitoring on a global scale, particularly over inland lakes and coastal regions. This is mainly due to the nonlinear complexity of water environment. In additions, there are a few studies that used the synthetic simulated reflectance to train artificial neural network (ANN) models to be applied on a global scale. However, the recent revaluation of these ANN models over the Japanese and European lakes revealed their limitation to provide accurate monitoring of these water bodies. These results could be attributed to two main reasons; (1) inappropriate ANN architecture with one hidden layer which could not be suitable to represent the complex situation of water bodies. (2) the limitation of the synthetic simulated reflectance that used to train these models. The deep neural network (DNN) with multiple hidden layers could provide a promising approach to overcome these complexities. Up to 2006, there is no way to accurately train a DNN due to a Vanishing gradient problem. the recent advances of DNN enable researchers to efficiently use the DNN models with low cost. During the current research, the performance of a DNN model with three-, five- and seven-hidden layers under different architecture conditions will be presented. These conditions include different activation functions (i.e., sigmoid, Relu and TanH), different optimization technique (i.e, Adam optimizer and stochastic gradient descent) and with/without applying dropout technique. The DNN model was designed to receive water leaving reflectance of several ocean color satellites (e.g., Global Change Observation Mission – Climate (GCOM-C)). Nine water quality parameters are generating from the DNN model. Two independent simulated datasets comprising 100,000 water leaving reflectance spectra each were generated for training and testing the DNN models. The two simulated datasets cover wide ranges of Chla (0.01–250 $mg \cdot m^{-3}$), NAP (0.01–250 $g \cdot m^{-3}$), and CDOM (0.001–10 m^{-1}) concentrations, representing the open ocean, coastal areas, and inland lakes. The proposed technique was also validated using in-situ datasets (e.g., NOMAD dataset, and many Japanese lakes and coastal bodies) that represent various trophic statuses. The results reveal the ability of proposed technique to provide accurate retrieval of in-water optical properties as will be discussed.

©2019. Japan Geoscience Union. All Right Reserved.

Development of atmosphere and in-water combining algorithm using GCOM-C/SGLI in Tokyo Bay

*Taiga Nakayama[1], HIROTO HIGA[1], Kazuki Ogata[2]

1. Yokohama National University, 2. Japan Aerospace eXploration Agency

GCOM-C / SGLI launched at the end of December 2017, has an excellent spatiotemporal resolution such as one time observation every two or three days at a resolution of 250 m on coastal area, is expected to monitor coastal areas where water environment change is siginificantly large and water area is comparatively small. However, high accuracy of water estimation is exceedingly difficult because coastal light environment in water changes complexly. In the traditional ocean color atmospheric correction algorithm, it is assumed that the water leaving radiance in the near infrared region is 0 and radiance due to air in the visible region is calcuration after estimating the radiance of atmospheric scattering. However, as in the coastal region, in the case of organic matter and inorganic matter increasing significantly, the water leaving radiance in the near infrared region increases and the assumption does not hold. Because of this, an aerosol reflectance is over estimated and an error occurs in the estimation of the water leaving reflectance in the visible region band. To improve this, there is a method of estimating aerosol reflectance while estimating water leaving reflectance in the near infrared region by the iterative method, and if the in-water model is suitable for the water area, highly accurate water leaving reflectance estimation Is possible. SGLI uses this iterative method in a low turbidity water such as the case1 water, and estimates atmospheric reflectance from a short-wavelength infrared channel without using an in-water model in a coastal area or other high turbidity water area, However, its accuracy is not as good as the high turbidity area.

In this study, we tried to develop a combination algorithm of atmospheric correction model, and in-water model which is adequate for coastal areas as a target of Tokyo Bay where organic matter is dominant. This is a modification of the in-water model used at the atmospheric correction stage to the Bio-Optical model created based on the measured SIOPs(Specific inherent optical properties) in Tokyo Bay, an selection aerosol model and estimation of reflectance at each wavelength are conducted by iterative calculation based on three parameters of Chl-a(Chlorophyll-a), CDOM(Color dissolvedorganic matter) and NAP(Non-algal particles). As a result, the suggested model became possible to estimate Chl-a and Rrs with high accuracy compared to normal SGLI atmospheric correction.

Keywords: atmospheric correction, SGLI, TokyoBay

©2019. Japan Geoscience Union. All Right Reserved.

Analysis of the uncertainty of backscattering coefficient by radiative transfer simulation in coastal areas and lakes

*Hidehito Taki[1], Hiroto Higa[1], Yoshiyuki Nakamura[1], Takayuki Suzuki[1]

1. Graduate School of Urban Innovation, Yokohama National University

In coastal areas and lakes, the ocean color change is greatly complicated because of various substances which are derived from terrestrial and internal production coexist in the water. Therefore, in radiative transfer simulation in the water, the inherent optical properties per substance concentration, which is the basic parameter change greatly in spatiotemporal, resulting in errors in calculation accuracy. In particular, it has been pointed out that the uncertainty of the backscattering coefficient is one of the major error factors in radiative transfer simulation. (Lain et al., (2017)). In this study, we have conducted field observations to measure water quality, apparent optical properties and inherent optical properties which are basic parameters in radiative transfer simulation in coastal areas and lakes having different optical characteristics such as Tokyo Bay, Kasumigaura Lake, Thailand Bay, and Seto Inland Sea respectively. Furthermore, we tried to conduct radiative transfer simulation by using Hydrolight 4.1 (Mobley et al., (2000)) based on in-situ specific light absorption coefficient and specific backscattering coefficient in each water areas. As a result, it was found that the simulated remote sensing reflectance: R_{rs} (/str) is remarkably variable due to the fluctuation of backscattering probability expressing the particle scattering form in the water.
It was suggested that this result is because of not considering properly the variations of scattering form related to particle characteristics.

Keywords: Ocean color remote sensing, Coastal areas and lakes, Radiative transfer simulation, Inherent optical properties, Backscattering probability

©2019. Japan Geoscience Union. All Right Reserved.

[J] Oral | A (Atmospheric and Hydrospheric Sciences)：A-CG Complex & General

Tue. May 28, 2019 10:45 AM - 12:15 PM JST | Tue. May 28, 2019 1:45 AM - 3:15 AM UTC | 103 1F

[A-CG45] Visible Remote Sensing of Hydrospheric Science and Its Application

convener:Joji Ishizaka(Institute for Space-Earth Environmental Research, Nagoya University), Mitsuhiro Toratani(School of Engineering, Tokai University), Yuji Sakuno(Graduate School of Engineering, Hiroshima University), Toru Hirawake(Faculty of Fisheries Sciences, Hokkaido University), Chairperson:Joji Ishizaka(名古屋大学宇宙地球環境研究所)

Variety of visible remote sensing data for hydrospheric science is now available. For example, it is known that 20 years of long time series of 1 km resolution ocean color data from OCTS-SeaWiFS-MODIS is available. At the end of 2017, 250 m resolution SGLI (Shikisai) was launched by JAXA, and with 300 m resolution European OLSI it became possible to use high resolution and high frequency data. Furthermore, geostationary satellite data from Korean GOCI is also useful. Not only the satellite variety, diversity of products is also increasing from just phytoplankton pigment, chlorophyll-a, to primary production, phytoplankton community structure and even non-phytoplankton materials and optical properties. Those ocean color satellite data should be useful for various fields of hydrospheric science, combining with higher resolution LANDSAT as well as high frequency Himawari data. In this section, we will discuss the variety of new observations and applications of visible remote sensing in hydrospheric science.

10:45 AM - 11:00 AM JST | 1:45 AM - 2:00 AM UTC

[ACG45-07] Development of a blue tide estimation method based on the optical properties of sulfur colloid particles by geostationary ocean color satellite

*HIROTO HIGA[1], WATARU NAKAMURA[1] (1.Yokohama National University)

11:00 AM - 11:15 AM JST | 2:00 AM - 2:15 AM UTC

[ACG45-08] Characteristics of water quality and red tide distribution in the Seto Inland Sea immediately after heavy rain in the western Japan by GCOM-C SGLI data

*Yuji Sakuno[1], Hiroto Higa[2], Hiroshi Kobayashi[3], Mitsuhiro Toratani[4] (1.Hiroshima University, 2.Yokohama National University, 3.Yamanashi University, 4.Tokai University)

11:15 AM - 11:30 AM JST | 2:15 AM - 2:30 AM UTC

[ACG45-09] Application of Satellite Remote Sensing to Monitor Eutrophication Status of Inland Lakes

*Wei Yang[1], Bunkei Matsushita[2] (1.Chiba University, 2.University of Tsukuba)

11:30 AM - 11:45 AM JST | 2:30 AM - 2:45 AM UTC

[ACG45-10] **Exploring the Potentials of Google Earth Engine for Global Assessment of Coastal Eutrophication Based on Chlorophyll-*a* concentration**

*Eligio de Raus Maure[1], Genki Terauchi[1], Joji Ishizaka[2] (1.Northwest Pacific Region Environmental Cooperation Center, 2.Institute for Space-Earth Environmental Research, Nagoya University)

11:45 AM - 12:00 PM JST | 2:45 AM - 3:00 AM UTC

[ACG45-11] Seasonal and interannual variability of seagrass distribution detected by Landsat TM, ETM+ and OLI images in western Nanao Bay

*Genki Terauchi[1] (1.Northwest Pacific Region Environmental Cooperation Center)

12:00 PM - 12:15 PM JST | 3:00 AM - 3:15 AM UTC

Discussion

Development of a blue tide estimation method based on the optical properties of sulfur colloid particles by geostationary ocean color satellite

*HIROTO HIGA[1], WATARU NAKAMURA[1]

1. Yokohama National University

Blue tides occurs every year from the summer to the fall in Tokyo Bay or Mikawa Bay, Japan. The blue tides occurs by upwelling sulfur colloid particles, which is generated by reacting oxygen with hydrogen sulfide in the hypoxic water at the bottom. The sulfur colloid particles scatter the light strongly at the surface and the ocean color changes to blue-white, therefore, it is called blue tide. When the magnitude of the blue tide is huge, mass mortality of shell and fish occurs and sometimes it is connected to damage of fisheries. Hence, the blue tides are recognized as an important water environment problem. Because the blue tide is short time scale phenomenon, it is difficult to monitor the spatial behavior adequately. Hence, the blue tide monitoring is expected by using geostationary ocean color satellite which spatio-temporal resolution is superior.
In the previous study, simple method of sulfur estimation method based on simple band of Rrs(Remote sensing reflectance) at 660 nm have been suggested(Higa et al., (2017)). However, it is impossible to separate the backscattering of sulfur and other detritus, respectively. In this study, we developed a bio-optical model, which is specialized in blue tide, based on the measured IOPs(Inherent optical properties) of Sulfur colloid particles. Furthermore, a sulfur estimation method was developed to separate the backscattering of sulfur and other detritus based on the QAA(Quasi-Analytical Algorithm).

Keywords: Blue tide, Geostationary Ocean Color Satellite

©2019. Japan Geoscience Union. All Right Reserved.

Characteristics of water quality and red tide distribution in the Seto Inland Sea immediately after heavy rain in the western Japan by GCOM-C SGLI data

*Yuji Sakuno[1], Hiroto Higa[2], Hiroshi Kobayashi[3], Mitsuhiro Toratani[4]

1. Hiroshima University, 2. Yokohama National University, 3. Yamanashi University, 4. Tokai University

The heavy rain in western Japan disaster occurred in early July 2018. After this heavy rain, a large amount of sediment discharge from the river and damage of red tide occurred in the Seto Inland Sea. Meanwhile, Chla (Chlorophyll-a), TSM (Total Suspended Matter), CDOM (Color Dissolved Organic Matter), SST (Sea Surface Temperature), Rrs (Remote Sensing Reflectance) of GCOM-C SGLI launched at the end of December 2017 Standard product data with 250 m spatial resolution will be provided once every 2-3 days from JAXA (The Japan Aerospace Exploration Agency). In this research, the results of accuracy verification of these product data (Level 2) officially released in December 2018 will be reported. Secondly, a method for estimating the distribution of harmful red tides (mainly *Chattonella* and *Karenia*) occurred in the Seto Inland Sea from Rrs products will be examined. The study period is mainly from June to August 2018. As a result, the SGLI product satisfies the target accuracy even in this water area, and the characteristics of the water quality and red tide distributions in the Seto Inland Sea about one month after the heavy rainfall became clear.

Keywords: red tide, heavy rain, satellite

©2019. Japan Geoscience Union. All Right Reserved.

Application of Satellite Remote Sensing to Monitor Eutrophication Status of Inland Lakes

*Wei Yang[1], Bunkei Matsushita[2]

1. Chiba University, 2. University of Tsukuba

Eutrophication of inland lakes is becoming a severe environmental issue all over the world. Routine monitoring of eutrophication status of inland lakes is essential for guaranteeing sustainable development of freshwater resources. The coupled spatial and temporal heterogeneity of water bodies often result in inadequate monitoring and characterization of water quality by using conventional sampling methods. On contrast, satellite remote sensing is quite flexible for monitoring the eutrophication status of inland lakes in terms of being able to cover large spatial areas at very frequent intervals. However, remote sensing of inland lakes has been far less successful than that of open oceans, due mainly to the complex interactions among optically active substances in the lake waters, as well as the difficulties in atmospheric correction. In this presentation, we will introduce our state-of-the-art remote sensing algorithms for estimating Chlorophyll-a concentrations (Chl-*a*) and Secchi disk depth (SDD), which have been widely used to evaluate the eutrophication status of lakes. These algorithms have been extensively validated using extensive in situ collected data sets, yielding satisfactory performances in overcoming the difficulties in remote sensing of turbid inland lakes. Application studies on satellite-based operational monitoring of Chl-*a* and SDD in several lakes of Japan will also be presented. Assessment results demonstrated that the proposed algorithms have the potential of being applied to operationally monitor water quality of inland lakes.

Keywords: inland lake, satellite remote sensing, water quality

©2019. Japan Geoscience Union. All Right Reserved.

Exploring the Potentials of Google Earth Engine for Global Assessment of Coastal Eutrophication Based on Chlorophyll-*a* concentration

*Eligio de Raus Maure[1], Genki Terauchi[1], Joji Ishizaka[2]

1. Northwest Pacific Region Environmental Cooperation Center, 2. Institute for Space-Earth Environmental Research, Nagoya University

Eutrophication is either emerging or growing environmental issue in many parts of the global marine systems in the ocean. This deterioration in water quality in the coastal regions may at times result in the appearance of harmful algal blooms or hypoxic conditions that affects large spatial and temporal scales with serious damages to the environment and economy, and the marine ecosystem itself. To assess the coastal eutrophication the Special Monitoring and Coastal Environment Assessment Regional Activity Centre (of the Action Plan for the Protection, Management and Development of the Marine and Coastal Environment of the Northwest Pacific Region of the United Nations Environmental Programme) developed a screening procedure to detect symptoms of eutrophication based on satellite observations of chlorophyll-a concentration. The methodology was originally developed for the Toyama Bay, Japan and later applied to the whole Northwest Pacific region. In this presentation, we introduced the method and its applicability to the global ocean. Furthermore, we also introduce the potentials of the Google Earth Engine (GEE)—a cloud-based tool with planetary-scale analysis capability—for future coastal eutrophication assessment based on recent higher resolution ocean colour sensors such as SGLI on GCOM-C with 250 m or Sentinel-3 with 300 m spatial resolutions. Once the GEE is proven useful, it will be an important tool in providing rapid assessment of the status of marine systems in many regions where the information on the status and extent of coastal eutrophication is very limited.

Keywords: coastal eutrophication, assessment, satellite, chlorophyll-a concentration, google earth engine

©2019. Japan Geoscience Union. All Right Reserved.

Seasonal and interannual variability of seagrass distribution detected by Landsat TM, ETM+ and OLI images in western Nanao Bay

*Genki Terauchi[1]

1. Northwest Pacific Region Environmental Cooperation Center

Western Nanao Bay is known for being a home to massive seagrass beds. A massive die-off of seagrass was reported in 2012 in this area, possibly due to high water temperature in summer. Archive images of Landsat Thematic Mapper (TM), Enhanced Thematic Mapper Plus (ETM+) and Operational Land Imager (OLI) were obtained from USGS to detect seasonal and interannual variability of seagrass distribution. Ground truthing survey with an underwater video camera were carried out from a small boat to study sea floor substrates on June 1, 2 and 16 in 2016. Still photos were also taken from a Stand Up Paddleboard on June 1, 2016 to study seagrass species in a very shallow (< 1m) water area. Information of sea floor substrates obtained from the field survey was then used to classify sea floor types. Six classes of training data were then prepared for classifying the Landsat OLI image observed on June 1, 2016 namely: (1) dense seagrass, (2) dense seagrass with *Sargassum*, (3) *Sargassum*, (4) sandy bottom, (5) mud and (6) exposed sand. Supervised classification of the bottom substrates was carried out by the maximum likelihood method using bands of Red, Green and Blue or ratios of Green/Blue, Green/Red, Blue/Red and Green/Coastal bands corrected with the Depth Invariant Index (DII) method. Accuracy assessment showed better results in the DII corrected band ratios: overall accuracy of 0.73 and tau coefficient of 0.66.

To study seasonal and interannual variability for seagrass, past Landsat archive images were analyzed to detect seagrass distribution. Since past field data of seagrass distribution were not sufficient, the K means unsupervised classification technique with the six classes was applied for mapping the seagrass distribution from past Landsat archive images. The classification result of the Landsat OLI image on June 1, 2015 was used as a reference to determine seagrass distributions as it had a good compliance with the ground truth data. Since two out of the six classes obtained from the unsupervised classification corresponded to a distribution pattern of (1) the dense seagrass and (2) the dense seagrass with *Sargassum* classes from the June 1, 2015, these two classes were merged into one class to represent seagrass distribution in Western Nanao Bay. A comparison of seasonal patterns of seagrass distribution estimated by the unsupervised classification of the Landsat archive data from November 22, 1991 to June 1, 1992 and from November 21, 2014 to June 1, 2015 showed consistent similar seasonal pattern; indicating seagrass recovery between late fall to early summer, which corresponds to seagrass seed germination periods. The Landsat archive data during the seagrass seed germination periods were also obtained to study interannual variability of seagrass distribution. The obtained results showed that there are fewer seagrass years (1994, 1996 and 1999) and more seagrass years (2000, 2004, 2007 and 2008) during the seagrass seed germination periods, indicating the survival rate of seagrass varied depending on the year.

Keywords: seagrass, landsat, remote sensing, mapping, Nanao Bay

©2019. Japan Geoscience Union. All Right Reserved.

[J] Poster | A (Atmospheric and Hydrospheric Sciences)：A-CG Complex & General

Tue. May 28, 2019 3:30 PM - 5:00 PM JST | Tue. May 28, 2019 6:30 AM - 8:00 AM UTC | Poster Hall International Exhibition Hall8, Makuhari Messe_11

[A-CG45] Visible Remote Sensing of Hydrospheric Science and Its Application

convener:Joji Ishizaka(Institute for Space-Earth Environmental Research, Nagoya University), Mitsuhiro Toratani(School of Engineering, Tokai University), Yuji Sakuno(Graduate School of Engineering, Hiroshima University), Toru Hirawake(Faculty of Fisheries Sciences, Hokkaido University)

Variety of visible remote sensing data for hydrospheric science is now available. For example, it is known that 20 years of long time series of 1 km resolution ocean color data from OCTS-SeaWiFS-MODIS is available. At the end of 2017, 250 m resolution SGLI (Shikisai) was launched by JAXA, and with 300 m resolution European OLSI it became possible to use high resolution and high frequency data. Furthermore, geostationary satellite data from Korean GOCI is also useful. Not only the satellite variety, diversity of products is also increasing from just phytoplankton pigment, chlorophyll-a, to primary production, phytoplankton community structure and even non-phytoplankton materials and optical properties. Those ocean color satellite data should be useful for various fields of hydrospheric science, combining with higher resolution LANDSAT as well as high frequency Himawari data. In this section, we will discuss the variety of new observations and applications of visible remote sensing in hydrospheric science.

[ACG45-P01] About GCOM-C/SGLI Ocean Standard Products

*Kazunori Ogata[1] (1.Japan Aerospace Exploration Agency)

[ACG45-P02] Verification of GCOM-C/SGLI product in coastal area

*Joji Ishizaka[1] (1.Institute for Space-Earth Environmental Research, Nagoya University)

[ACG45-P03] Hyperspectral Radiometry towards Classification of Marine Phytoplankton Groups

*Takafumi Hirata[1], Robert J.W. Brewin[2], Girgio Dall'Olmo[2], Mariana Altenburg Soppa[3], Astrid Bracher[3] (1.Faculty of Environmental Earth Science, Hokkaido University, 2.Plymouth Marine Laboratory, 3.Alfred-Wegener Institute for Polar and Marine Research)

[ACG45-P04] Improvement of absorption-based primary production model for SGLI/GCOM-C

*Toru Hirawake[1], Takuhei Shiozaki[2], Hisatomo Waga[1], Koji Suzuki[1] (1.Hokkaido University, 2.JAMSTEC)

[ACG45-P05] Attempt to distinguish river water influencing concentration of chlorophyll *a* off Miho Peninsula

*Akihiko Tanaka[1], Kyoko Takashima[2], Gen Fukuda[2], Takaaki Katsumata[1], Hiroyuki Tan[1], Masato Niki[2], Daisuke Takahashi[2] (1.Liberal Arts Education Center, Shimizu Campus, Tokai University, 2.School of Marine Science and Technology, Tokai University)

[ACG45-P06] Estimation of chlorophyll-a from RGB digital camera data collected in Ise-Mikawa Bay

*Akiko N. Mizuno[1], Joji Ishizaka[1] (1.Institute for Space-Earth Environmental Research, Nagoya University)

[ACG45-P07] Seasonal variability of MODIS chlorophyll-a and total suspended matter in the spring-neap tidal cycle in the Ariake Bay, Japan

*Mengmeng Yang[1], Joji Ishizaka[2], Joaquim I. Goes[3], Hongzhen Tian[4], Elígio R. Maúre[5], Masataka Hayashi[6] (1.Graduate School of Environmental Studies, Nagoya University, Furo-cho, Chikusa-ku, Nagoya, Aichi, Japan., 2.Institute for Space-Earth Environmental Research (ISEE) Nagoya University Furo-cho, Chikusa-ku, Nagoya, Aichi, Japan., 3.Lamont-Doherty Earth Observatory, Marine Biology and Paleo Environment, Columbia University, 61 Route 9W - PO Box 1000, Palisades, NY 10964-8000, US., 4.School of Management and Economy, Tianjin Polytechnic University, Tianjin 300387, China., 5.Dept. of Research and Study,

Northwest Pacific Region Environmental Cooperation Center, Toyama, Japan., 6.Science and Technology co., Ltd., 3-9-2, Koubai-cho, Showa, Nagoya, Aichi 466-0031, Japan.)

[ACG45-P08] Discrimination of green *Noctiluca scintillans* in the upper Gulf of Thailand using remote sensing techniques

*Jutarak Luang-on[1], Joji Ishizaka[2], Anukul Buranapratheprat[3], Jitraporn Phaksopa[4] (1.Graduate School of Environmental Studies, Nagoya University, 2.Institute for Space-Earth Environmental Research, Nagoya University, Japan, 3.Department of Aquatic Science, Faculty of Science, Burapha University, Thailand, 4.Department of Marine Science, Faculty of Fisheries, Kasetsart University, Thailand)

[ACG45-P09] Monthly variability of Chlorophyll-a distribution in the Gulf of Thailand

*Dudsadee Leenawarat[1], Anukul Buranapratheprat[2], Joji Ishizaka[3] (1.Graduate School of Environmental Studies, Nagoya University, Japan, 2.Department of Aquatic Science, Faculty of Science, Burapha University, Thailand, 3.Institute for Space-Earth Environmental Research, Nagoya University, Japan)

[ACG45-P10] AERONET-Ocean Color time series in Ariake Bay.

*yifei wu[1], Joji Ishizaka[2], Mengmeng Yang[1], Naoki Fujii[3], Masahiro Hori[4] (1. Graduate School of Environmental Studies, Nagoya University, 2. Institute for Space-Earth Environmental Research, Nagoya University, 3. Graduate School of Agriculture, Saga University, 4.EORC, JAXA)

About GCOM-C/SGLI Ocean Standard Products

*Kazunori Ogata[1]

1. Japan Aerospace Exploration Agency

The Global Change Observation Mission - Climate "SHIKISAI" (GCOM-C) was launched on Dec. 23, 2017 by JAXA. The Second Generation Global Imager (SGLI) onboard GCOM-C is optical sensor which has 19 channels from near ultraviolet to thermal infrared wavelengths (380 nm to 12um).
SGLI Ocean standard products consist of 7 parameters and 2 processing levels. The parameters are composed of Normalized water Leaving Radiance (NWLR) at 380, 412, 443, 490, 530, 565 and 673.5 [W/m^2/sr/um], Aerosol optical Thickness (TAUA) at 673.5 and 868.5 [-], Photosynthetically Available Radiation (PAR) [Ein/m^2/day], Chlorophyll-*a* concentration (CHLA) [mg/m^3], Total Suspended Matter concentration (TSM) [g/m^3], Absorption coefficient of Colored dissolved Organic Matter (CDOM) at 412 [m^-1] and Sea Surface Temperature (SST) [degree C]. The processing levels consists of Level-2 and Level-3 from distinctions of time- and spatial resolutions.
After about one year of launch, all ocean standard products had achieved the thresholds of release accuracies, therefore, those products were started to provide on Dec. 20, 2018 from the JAXA G-Portal (https://gportal.jaxa.jp/gpr/).

Keywords: GCOM-C, SGLI, Ocean color, SST, Remote sensing

©2019. Japan Geoscience Union. All Right Reserved.

Verification of GCOM-C/SGLI product in coastal area

*Joji Ishizaka[1]

1. Institute for Space-Earth Environmental Research, Nagoya University

GCOM-C/SGLI was launched on Decmber 2017, and the data distribution was started from December 2018. We obtained verification data of remote sensing reflectance, chlorophyll-a and others in the East China Sea, Ise Bay, Ariake Bay, etc. We will present the results of the verification of the products in the coastal area.

Keywords: validation of ocean color data, coastal area, chlorophyll-a, remote sensing reflectance, suspended matter, colored dissolved organic matter

©2019. Japan Geoscience Union. All Right Reserved.

Hyperspectral Radiometry towards Classification of Marine Phytoplankton Groups

*Takafumi Hirata[1], Robert J.W. Brewin[2], Girgio Dall'Olmo[2], Mariana Altenburg Soppa[3], Astrid Bracher[3]

1. Faculty of Environmental Earth Science, Hokkaido University, 2. Plymouth Marine Laboratory, 3. Alfred-Wegener Institute for Polar and Marine Research

Marine phytoplankton plays an essential role in marine ecosystems as a primary producer. Generally, a trophic transfer food chain via large-sized phytoplankton can be found in the oceans at higher latitudes and/or in coastal waters. On the other hand, a trophic transfer via middle- and/or small-sized phytoplankton can be found in the oceans at lower latitudes. As a first approximation, a cell size of phytoplankton is associated with taxonomic groups (e.g. diatoms are often large in size whereas cyanobacteria are usually small). In addition, phytoplankton in a taxonomic group often possesses a characteristic photosynthetic and/or photoprotective pigment(s) (e.g. diatoms contain fucoxanthin while cyanobacteria zeaxanthin). As a result, a taxonomic group are linked as a first approximation to a specific size class and a pigment(s), so that the groups may be inferred from the size and pigments. Both of the cell size distribution and the pigments affects optical, or spectral signature of phytoplankton. Hence, once the spectral signature of phytoplankton is obtained, their taxonomic detection/classification may be possible. In the present technology, a radiometric observation, either in situ or from space, enables the detection of the signature. Currently, it is an open question what, and how many, spectral bands are required for the accurate detection/classification of the phytoplankton, especially when phytoplankton taxonomic composition is complex and when other optically-active components interplay in the radiometric measurements. In this presentation, a preliminary result towards answering the question is presented using in situ hyperspectral radiometric measurements obtained in the Atlantic Ocean. Our result shows that radiometric measurements at many spectral bands are correlated with each other. While the correlation strength differs among spectral bands in question, radiometric measurements at these bands are correlated to the concentration of chlorophyll-a, a pigment commonly found in phytoplankton groups. The correlation with chlorophyll-a was even found at spectral bands where chlorophyll-a little absorbs the light. This may be due to another correlation between the chlorophyll-a concentration and other phytoplankton pigments, the latter of which absorb the light at the spectral band where chlorophyll-a does not. The pigment co-variation implies that a correlation between the radiometric measurements and any pigment concentration does not guarantee the optical detection of the pigment signature, and a more careful analysis is required when the radiometric measurements are analyzed.

Keywords: hyperspectral, remote sensing, phytoplankton

©2019. Japan Geoscience Union. All Right Reserved.

Improvement of absorption-based primary production model for SGLI/GCOM-C

*Toru Hirawake[1], Takuhei Shiozaki[2], Hisatomo Waga[1], Koji Suzuki[1]

1. Hokkaido University, 2. JAMSTEC

Net primary production (NPP) of phytoplankton is important to understand the global carbon cycle and marine ecosystem. While the majority of satellite NPP models use chlorophyll *a*(chl-*a*) concentration as a proxy of phytoplankton biomass, several NPP models use absorption coefficient of phytoplankton. An NPP models for Japanese new ocean color sensor, Second-generation GLobal Imager (SGLI), was developed based on the phytoplankton absorption to reduce estimation errors of chl-*a*due to pigment packaging and turbid water. However, sufficient validation in the open ocean has not been carried out. In this study, we obtained NPP data in the Pacific Ocean and compared with satellite-derived NPP applying the SGLI NPP model to MODIS data. The model overestimated the lower values of NPP less than 1000 mg m^2d^{-1}. Newly developed model considering response to daily averaged photosynthetically available radiation (PAR) showed better performance than previous one. However, bias and errors were still detected for a part of data. We will also discuss possibility of temperature dependency on this NPP model.

Keywords: ocean color remote sensing, primary production, phytoplankton

©2019. Japan Geoscience Union. All Right Reserved.

Attempt to distinguish river water influencing concentration of chlorophyll *a* off Miho Peninsula

*Akihiko Tanaka[1], Kyoko Takashima[2], Gen Fukuda[2], Takaaki Katsumata[1], Hiroyuki Tan[1], Masato Niki[2], Daisuke Takahashi[2]

1. Liberal Arts Education Center, Shimizu Campus, Tokai University, 2. School of Marine Science and Technology, Tokai University

In Suruga Bay, ocean color remote sensing shows that relatively higher chlorophyll a concentration in the western area than in the eastern part. One reason is that many large rivers flowing into Suruga Bay exist more in the west than the eastern side of Suruga Bay. The Miho Peninsula is located at the western part of Suruga Bay, that there are mouths of the Fuji River and the Okitsu River in the north, and the mouth of the Abe River in the south. High chlorophyll a concentration is also observed off Miho Peninsula. From the chlorophyll a concentration image by ocean color remote sensing, which river that influence high concentration of chlorophyll a off Miho Peninsula can be empirically discriminated, whereas it is sometimes difficult to distinguish with chlorophyll a concentration image. In Suruga Bay, the Ferry Fuji (Suruga Bay Ferry) cruises 4 times a day to Shimizu Port and Toi Port. It has been suggested that the current in the normal direction of the course can be estimated from the AIS (Automatic Identification System) information of the Ferry FUJI. Since the route of the Suruga Bay ferry is approximately in the east-west direction, it is possible to obtain the flow in the north-south direction. In this study, we attempt to distinguish river water affecting chlorophyll a concentration off Miho Peninsula by adding information of current estimated from AIS information to Chlorophyll a concentration image in the Suruga Bay.

Keywords: Ocean color remote sensing, Suruga Bay, AIS

©2019. Japan Geoscience Union. All Right Reserved.

Estimation of chlorophyll-a from RGB digital camera data collected in Ise-Mikawa Bay

*Akiko N. Mizuno[1], Joji Ishizaka[1]

1. Institute for Space-Earth Environmental Research, Nagoya University

Development for survey methods for phototrophs and/or environmental condition using RGB digital camera data has been increasingly studied for two decades. In examples for the ocean are studies of estimation of water quality using smart phone’ s camera (Goddijin et al. 2009, Leeuw and Boss 2018), detection of sea grass from aerial photo images and estimation of chlorophyll-a (Goddijn and White 2006). The portability and convenience of the digital camera are the reasons of interest for the RGB data. It is possible to be used as supplementary observation of satellite sensing because digital camera can use regardless of the cloud. Also, citizen participation surveys may be possible because anyone can take photographs using his or her digital camera.

Thus, we attempted to develop estimation method for chlorophyll-a from RGB digital camera data for Ise-Mikawa Bay, Japan. For Ise-Mikawa Bay, method of estimation of chlorophyll a concentration form SeaWiFS and MODIS data was developed by Hayashi et al (2015), but estimation method with digital camera data was not developed yet.

We used chlorophyll-a concentration, RGB data from photo images of surface water, sky and a photographer’ s 18% reflectance gray card during monthly survey cruises in Ise-Mikawa Bay. Spectral remote sensing reflectance data from RAMSES/TriOS was also obtained. We calculated RGB from spectral remote sensing reflectance data and compared RGB from digital camera. Digital camera RGB data was correlated with RGB from spectral data and in-situ chlorophyll-a concentration. In the future, we will reduce effect of reflection of sunlight from estimation of chlorophyll-a concentration using photographs of sky and gray card.

L.M. Goddijn; M White, Using a digital camera for water quality measurements in Galway Bay, Estuarine, Coastal and Shelf Science (2006), 66, 429-436.

L.M. Goddijn; D. Dailloux; M. White; D. Bowers, Fundamentals of in situ digital camera methodology for water quality monitoring of coast and ocean., Sensors (2009), 9, 5825-5843.

T. Leeuw; E. Boss, The HydroColor App: Above Water Measurements of Remote Sensing Reflectance and Turbidity Using a Smartphone Camera, Sensors (2018), 18, 256-271.

M. Hayashi; J. Ishizaka; M. Toratani; T. Nakamura; Y. Nakashima; S. Yamada; Evaluation and Improvement of MODIS and SeaWIFS-derived Chlorophyll a Concentration in Ise-Mikawa Bay, Journal of The Remote Sensing Society of Japan (2015), 35, 245-259.

Keywords: Coastal region, Estimation of Chl.a concentration, RGB values, digital camera image, sea surface reflection

©2019. Japan Geoscience Union. All Right Reserved.

©2019. Japan Geoscience Union. All Right Reserved.

Seasonal variability of MODIS chlorophyll-a and total suspended matter in the spring-neap tidal cycle in the Ariake Bay, Japan

*Mengmeng Yang[1], Joji Ishizaka[2], Joaquim I. Goes[3], Hongzhen Tian[4], Elígio R. Maúre[5], Masataka Hayashi[6]

1. Graduate School of Environmental Studies, Nagoya University, Furo-cho, Chikusa-ku, Nagoya, Aichi, Japan., 2. Institute for Space-Earth Environmental Research (ISEE) Nagoya University Furo-cho, Chikusa-ku, Nagoya, Aichi, Japan., 3. Lamont-Doherty Earth Observatory, Marine Biology and Paleo Environment, Columbia University, 61 Route 9W - PO Box 1000, Palisades, NY 10964-8000, US., 4. School of Management and Economy, Tianjin Polytechnic University, Tianjin 300387, China., 5. Dept. of Research and Study, Northwest Pacific Region Environmental Cooperation Center, Toyama, Japan., 6. Science and Technology co., Ltd., 3-9-2, Koubai-cho, Showa, Nagoya, Aichi 466-0031, Japan.

Red tide occurs more frequently in the Ariake Bay since 1990s, and it has greatly damaged the local fisheries, especially the nori farms. Increase of water transparency and reduction of tidal currents were also reported recently, and they may be related to the increase of the frequency of red tides. It is also reported that another cause of the red tide is the river discharge. Satellite remote sensing is suggested to be used to monitor the red tide. In this study, the newly developed MODIS-derived chlorophyll-a (Chl-a) and total suspended matter (TSM) was used to investigate the relationship between Chl-a and TSM and the seasonal variations of influences of spring-neap tides and river discharge. We observed that 1) high Chl-a (>5 mg m^{-3}) and high TSM (>5 g m^{-3}) were generally distributed in the areas off Saga, Kumamoto and Yatsushiro, and Isahaya Bay where the main river systems discharge the fresh water; 2) the magnitude of Chl-a was highest in summer, and decreased gradually from autumn to spring, which corresponded to the amount of river discharge which concentrates in summer and early autumn (June-September); 3) in the spring-neap tidal cycle, TSM was much higher in neap to spring (NS) and spring (S) tide than in spring to neap (SN) and neap (N) tide, which was consistent with the tidal suspension. On the other hand, Chl-a was often increased after high river discharge peak and the variation of Chl-a was small when the river discharge peak was small, indicating that the variation of Chl-a was mainly influenced by the river discharge. The variation of TSM in the spring-neap tidal cycle was mainly regulated by the tidal suspension, whereas the variation of Chl-a was more controlled by the river discharge than the tidal resuspension.

Keywords: MODIS, chlorophyll-a, total suspended matter, seasonal variability, spring-neap tides, river discharge

©2019. Japan Geoscience Union. All Right Reserved.

Discrimination of green *Noctiluca scintillans* in the upper Gulf of Thailand using remote sensing techniques

*Jutarak Luang-on[1], Joji Ishizaka[2], Anukul Buranapratheprat[3], Jitraporn Phaksopa[4]

1. Graduate School of Environmental Studies, Nagoya University, 2. Institute for Space-Earth Environmental Research, Nagoya University, Japan, 3. Department of Aquatic Science, Faculty of Science, Burapha University, Thailand, 4. Department of Marine Science, Faculty of Fisheries, Kasetsart University, Thailand

Green *Noctiluca scintillans*, the peculiar single cellular heterotrophic organism containing green algae called *Pedinomonas noctilucae*, frequently causes harmful algal bloom (HAB) in the upper Gulf of Thailand (uGoT). The high density of green *Noctiluca* discolors the water to deep milky green, and it has the potential to generate low dissolved oxygen (hypoxia) in the water column resulting in massive fish mortality. The co-occurrence of green Noctiluca and other phytoplankton species (e.g., *Ceratium furca* and diatoms) was often reported. Heretofore, the behavior of red tides has not been clarified. In this study, we, therefore, focus on investigating the dominant spectral characteristics of each HAB species and developing an algorithm to discriminate green *Noctiluca* from the other harmful species. The ship observations (2017 –2018) were conducted to obtain the apparent and inherent optical properties as well as the pigment information of green *Noctiluca* blooms. Fortunately, the super green *Noctiluca* blooms (>1,500,000 cell L^{-1}) occurred near the west coast of the uGoT in July 2017. The remote sensing reflectance spectra measured by using the RAMSES hyperspectral radiometer (320 nm –950 nm) revealed the crucial features of green *Noctiluca* in near-infrared wavelengths. The different characteristics of green *Noctiluca* and other HAB species were also found in visible wavelengths. The investigated features were used in the discrimination method to detect the green *Noctiluca* bloom using satellite observation in the near future.

Keywords: green Noctiluca, the upper Gulf of Thailand, remote sensing

©2019. Japan Geoscience Union. All Right Reserved.

©2019. Japan Geoscience Union. All Right Reserved.

Monthly variability of Chlorophyll-a distribution in the Gulf of Thailand

*Dudsadee Leenawarat[1], Anukul Buranapratheprat[2], Joji Ishizaka[3]

1. Graduate School of Environmental Studies, Nagoya University, Japan, 2. Department of Aquatic Science, Faculty of Science, Burapha University, Thailand, 3. Institute for Space-Earth Environmental Research, Nagoya University, Japan

The Gulf of Thailand (GoT) is semi-enclosed sea located in the western part of the South China Sea. This area is important to fisheries production in this region. The satellite data can reveal the primary production through chlorophyll-a (Chl-a) which is basic for the food chain. The objectives of this study are to investigate the variation and spatial distribution patterns of Chl-a in the GoT by using long-term satellite data from SeaWiFS (1997-2010), MERIS (2002-2012), MODIS AQUA (2002-2018), and VIIRS (2012-2018) level 3 compared with oceanographic conditions from previous study and circulation model name Princeton Ocean Model (POM). Tide and climatological data of wind, salinity, temperature and river discharge are forcing in the model. The results from averaged monthly Chl-a concentration in the central GoT illustrate low Chl-a concentration occurred in transition periods (April-May, and October) by lowest in May when the water column was stratified. High Chl-a concentration occurred during the northeast monsoon (November to February) with the highest in December when the water column was well mixed, and a small peak was found during June to August. Hight Chl-a was found along the coast, especially near the northern coast in the southwest monsoon (June to October). During the northeast monsoon Chl-a near cape CaMau spread offshore, due to strong surface currents flew into GoT from the southern part of cape CaMau to the middle of GoT mouth.

Keywords: Gulf of Thailand, Chlorophyll-a, Variability

©2019. Japan Geoscience Union. All Right Reserved.

AERONET-Ocean Color time series in Ariake Bay.

*yifei wu[1], Joji Ishizaka[2], Mengmeng Yang[1], Naoki Fujii[3], Masahiro Hori[4]

1. Graduate School of Environmental Studies, Nagoya University, 2. Institute for Space-Earth Environmental Research, Nagoya University, 3. Graduate School of Agriculture, Saga University, 4. EORC, JAXA

The AERONET (**AE**rosol **RO**botic **NET**work) project is a federation of ground-based remote sensing aerosol networks established by **NASA** and **PHOTONS** and is greatly expanded by networks from national agencies, institutes, universities, individual scientists. AERONET –Ocean Color (AERONET-OC) provides the additional capability of measuring the radiance emerging from the sea. In April 2018, a new station of AERONET-OC has been set by JAXA for GCOM-C validation in Ariake Bay located in Kyusyu, Japan where the seaweed (Nori) culture very famous. Aerosol Optical Depth (AOD) and remote sensing reflectance (Rrs) is considered as the most important products of AERONET-OC since the estimation of chlorophyll-a concentration by ocean color satellite is usually not so accurate in coastal areas because of the inaccurate satellite remote sensing reflectance (Rrs) influenced by aerosol. This study is to make a brief description of the time series of the AERONET-OC data from April 2018 to April 2019. Local Chl-a and TSM estimated by using radiances measured by the AERONET-OC is going to use to explain the phytoplankton bloom connect with factors such as precipitation and river discharge in Ariake Bay.

Keywords: chlorophyll-a, remote sensing reflectance, AERONET-OC

©2019. Japan Geoscience Union. All Right Reserved.

[J] Poster | A (Atmospheric and Hydrospheric Sciences)：A-CG Complex & General

Tue. May 28, 2019 5:15 PM - 6:30 PM JST | Tue. May 28, 2019 8:15 AM - 9:30 AM UTC | Poster Hall International Exhibition Hall8, Makuhari Messe_19

[A-CG45] Visible Remote Sensing of Hydrospheric Science and Its Application

convener:Joji Ishizaka(Institute for Space-Earth Environmental Research, Nagoya University), Mitsuhiro Toratani(School of Engineering, Tokai University), Yuji Sakuno(Graduate School of Engineering, Hiroshima University), Toru Hirawake(Faculty of Fisheries Sciences, Hokkaido University)

Variety of visible remote sensing data for hydrospheric science is now available. For example, it is known that 20 years of long time series of 1 km resolution ocean color data from OCTS-SeaWiFS-MODIS is available. At the end of 2017, 250 m resolution SGLI (Shikisai) was launched by JAXA, and with 300 m resolution European OLSI it became possible to use high resolution and high frequency data. Furthermore, geostationary satellite data from Korean GOCI is also useful. Not only the satellite variety, diversity of products is also increasing from just phytoplankton pigment, chlorophyll-a, to primary production, phytoplankton community structure and even non-phytoplankton materials and optical properties. Those ocean color satellite data should be useful for various fields of hydrospheric science, combining with higher resolution LANDSAT as well as high frequency Himawari data. In this section, we will discuss the variety of new observations and applications of visible remote sensing in hydrospheric science.

[ACG45-P01] About GCOM-C/SGLI Ocean Standard Products

*Kazunori Ogata[1] (1.Japan Aerospace Exploration Agency)

[ACG45-P02] Verification of GCOM-C/SGLI product in coastal area

*Joji Ishizaka[1] (1.Institute for Space-Earth Environmental Research, Nagoya University)

[ACG45-P03] Hyperspectral Radiometry towards Classification of Marine Phytoplankton Groups

*Takafumi Hirata[1], Robert J.W. Brewin[2], Girgio Dall'Olmo[2], Mariana Altenburg Soppa[3], Astrid Bracher[3] (1.Faculty of Environmental Earth Science, Hokkaido University, 2.Plymouth Marine Laboratory, 3.Alfred-Wegener Institute for Polar and Marine Research)

[ACG45-P04] Improvement of absorption-based primary production model for SGLI/GCOM-C

*Toru Hirawake[1], Takuhei Shiozaki[2], Hisatomo Waga[1], Koji Suzuki[1] (1.Hokkaido University, 2.JAMSTEC)

[ACG45-P05] Attempt to distinguish river water influencing concentration of chlorophyll *a* off Miho Peninsula

*Akihiko Tanaka[1], Kyoko Takashima[2], Gen Fukuda[2], Takaaki Katsumata[1], Hiroyuki Tan[1], Masato Niki[2], Daisuke Takahashi[2] (1.Liberal Arts Education Center, Shimizu Campus, Tokai University, 2.School of Marine Science and Technology, Tokai University)

[ACG45-P06] Estimation of chlorophyll-a from RGB digital camera data collected in Ise-Mikawa Bay

*Akiko N. Mizuno[1], Joji Ishizaka[1] (1.Institute for Space-Earth Environmental Research, Nagoya University)

[ACG45-P07] Seasonal variability of MODIS chlorophyll-a and total suspended matter in the spring-neap tidal cycle in the Ariake Bay, Japan

*Mengmeng Yang[1], Joji Ishizaka[2], Joaquim I. Goes[3], Hongzhen Tian[4], Elígio R. Maúre[5], Masataka Hayashi[6] (1.Graduate School of Environmental Studies, Nagoya University, Furo-cho, Chikusa-ku, Nagoya, Aichi, Japan., 2.Institute for Space-Earth Environmental Research (ISEE) Nagoya University Furo-cho, Chikusa-ku, Nagoya, Aichi, Japan., 3.Lamont-Doherty Earth Observatory, Marine Biology and Paleo Environment, Columbia University, 61 Route 9W - PO Box 1000, Palisades, NY 10964-8000, US., 4.School of Management and Economy, Tianjin Polytechnic University, Tianjin 300387, China., 5.Dept. of Research and Study,

Northwest Pacific Region Environmental Cooperation Center, Toyama, Japan., 6.Science and Technology co., Ltd., 3-9-2, Koubai-cho, Showa, Nagoya, Aichi 466-0031, Japan.)

[ACG45-P08] Discrimination of green *Noctiluca scintillans* in the upper Gulf of Thailand using remote sensing techniques

*Jutarak Luang-on[1], Joji Ishizaka[2], Anukul Buranapratheprat[3], Jitraporn Phaksopa[4] (1.Graduate School of Environmental Studies, Nagoya University, 2.Institute for Space-Earth Environmental Research, Nagoya University, Japan, 3.Department of Aquatic Science, Faculty of Science, Burapha University, Thailand, 4.Department of Marine Science, Faculty of Fisheries, Kasetsart University, Thailand)

[ACG45-P09] Monthly variability of Chlorophyll-a distribution in the Gulf of Thailand

*Dudsadee Leenawarat[1], Anukul Buranapratheprat[2], Joji Ishizaka[3] (1.Graduate School of Environmental Studies, Nagoya University, Japan, 2.Department of Aquatic Science, Faculty of Science, Burapha University, Thailand, 3.Institute for Space-Earth Environmental Research, Nagoya University, Japan)

[ACG45-P10] AERONET-Ocean Color time series in Ariake Bay.

*yifei wu[1], Joji Ishizaka[2], Mengmeng Yang[1], Naoki Fujii[3], Masahiro Hori[4] (1. Graduate School of Environmental Studies, Nagoya University, 2. Institute for Space-Earth Environmental Research, Nagoya University, 3. Graduate School of Agriculture, Saga University, 4.EORC, JAXA)

About GCOM-C/SGLI Ocean Standard Products

*Kazunori Ogata[1]

1. Japan Aerospace Exploration Agency

The Global Change Observation Mission - Climate "SHIKISAI" (GCOM-C) was launched on Dec. 23, 2017 by JAXA. The Second Generation Global Imager (SGLI) onboard GCOM-C is optical sensor which has 19 channels from near ultraviolet to thermal infrared wavelengths (380 nm to 12um).
SGLI Ocean standard products consist of 7 parameters and 2 processing levels. The parameters are composed of Normalized water Leaving Radiance (NWLR) at 380, 412, 443, 490, 530, 565 and 673.5 [W/m^2/sr/um], Aerosol optical Thickness (TAUA) at 673.5 and 868.5 [-], Photosynthetically Available Radiation (PAR) [Ein/m^2/day], Chlorophyll-*a* concentration (CHLA) [mg/m^3], Total Suspended Matter concentration (TSM) [g/m^3], Absorption coefficient of Colored dissolved Organic Matter (CDOM) at 412 [m^-1] and Sea Surface Temperature (SST) [degree C]. The processing levels consists of Level-2 and Level-3 from distinctions of time- and spatial resolutions.
After about one year of launch, all ocean standard products had achieved the thresholds of release accuracies, therefore, those products were started to provide on Dec. 20, 2018 from the JAXA G-Portal (https://gportal.jaxa.jp/gpr/).

Keywords: GCOM-C, SGLI, Ocean color, SST, Remote sensing

©2019. Japan Geoscience Union. All Right Reserved.

Verification of GCOM-C/SGLI product in coastal area

*Joji Ishizaka[1]

1. Institute for Space-Earth Environmental Research, Nagoya University

GCOM-C/SGLI was launched on Decmber 2017, and the data distribution was started from December 2018. We obtained verification data of remote sensing reflectance, chlorophyll-a and others in the East China Sea, Ise Bay, Ariake Bay, etc. We will present the results of the verification of the products in the coastal area.

Keywords: validation of ocean color data, coastal area, chlorophyll-a, remote sensing reflectance, suspended matter, colored dissolved organic matter

©2019. Japan Geoscience Union. All Right Reserved.

Hyperspectral Radiometry towards Classification of Marine Phytoplankton Groups

*Takafumi Hirata[1], Robert J.W. Brewin[2], Girgio Dall'Olmo[2], Mariana Altenburg Soppa[3], Astrid Bracher[3]

1. Faculty of Environmental Earth Science, Hokkaido University, 2. Plymouth Marine Laboratory, 3. Alfred-Wegener Institute for Polar and Marine Research

Marine phytoplankton plays an essential role in marine ecosystems as a primary producer. Generally, a trophic transfer food chain via large-sized phytoplankton can be found in the oceans at higher latitudes and/or in coastal waters. On the other hand, a trophic transfer via middle- and/or small-sized phytoplankton can be found in the oceans at lower latitudes. As a first approximation, a cell size of phytoplankton is associated with taxonomic groups (e.g. diatoms are often large in size whereas cyanobacteria are usually small). In addition, phytoplankton in a taxonomic group often possesses a characteristic photosynthetic and/or photoprotective pigment(s) (e.g. diatoms contain fucoxanthin while cyanobacteria zeaxanthin). As a result, a taxonomic group are linked as a first approximation to a specific size class and a pigment(s), so that the groups may be inferred from the size and pigments. Both of the cell size distribution and the pigments affects optical, or spectral signature of phytoplankton. Hence, once the spectral signature of phytoplankton is obtained, their taxonomic detection/classification may be possible. In the present technology, a radiometric observation, either in situ or from space, enables the detection of the signature. Currently, it is an open question what, and how many, spectral bands are required for the accurate detection/classification of the phytoplankton, especially when phytoplankton taxonomic composition is complex and when other optically-active components interplay in the radiometric measurements. In this presentation, a preliminary result towards answering the question is presented using in situ hyperspectral radiometric measurements obtained in the Atlantic Ocean. Our result shows that radiometric measurements at many spectral bands are correlated with each other. While the correlation strength differs among spectral bands in question, radiometric measurements at these bands are correlated to the concentration of chlorophyll-a, a pigment commonly found in phytoplankton groups. The correlation with chlorophyll-a was even found at spectral bands where chlorophyll-a little absorbs the light. This may be due to another correlation between the chlorophyll-a concentration and other phytoplankton pigments, the latter of which absorb the light at the spectral band where chlorophyll-a does not. The pigment co-variation implies that a correlation between the radiometric measurements and any pigment concentration does not guarantee the optical detection of the pigment signature, and a more careful analysis is required when the radiometric measurements are analyzed.

Keywords: hyperspectral, remote sensing, phytoplankton

©2019. Japan Geoscience Union. All Right Reserved.

Improvement of absorption-based primary production model for SGLI/GCOM-C

*Toru Hirawake[1], Takuhei Shiozaki[2], Hisatomo Waga[1], Koji Suzuki[1]

1. Hokkaido University, 2. JAMSTEC

Net primary production (NPP) of phytoplankton is important to understand the global carbon cycle and marine ecosystem. While the majority of satellite NPP models use chlorophyll *a*(chl-*a*) concentration as a proxy of phytoplankton biomass, several NPP models use absorption coefficient of phytoplankton. An NPP models for Japanese new ocean color sensor, Second-generation GLobal Imager (SGLI), was developed based on the phytoplankton absorption to reduce estimation errors of chl-*a*due to pigment packaging and turbid water. However, sufficient validation in the open ocean has not been carried out. In this study, we obtained NPP data in the Pacific Ocean and compared with satellite-derived NPP applying the SGLI NPP model to MODIS data. The model overestimated the lower values of NPP less than 1000 mg m^2d^{-1}. Newly developed model considering response to daily averaged photosynthetically available radiation (PAR) showed better performance than previous one. However, bias and errors were still detected for a part of data. We will also discuss possibility of temperature dependency on this NPP model.

Keywords: ocean color remote sensing, primary production, phytoplankton

©2019. Japan Geoscience Union. All Right Reserved.

Attempt to distinguish river water influencing concentration of chlorophyll *a* off Miho Peninsula

*Akihiko Tanaka[1], Kyoko Takashima[2], Gen Fukuda[2], Takaaki Katsumata[1], Hiroyuki Tan[1], Masato Niki[2], Daisuke Takahashi[2]

1. Liberal Arts Education Center, Shimizu Campus, Tokai University, 2. School of Marine Science and Technology, Tokai University

In Suruga Bay, ocean color remote sensing shows that relatively higher chlorophyll a concentration in the western area than in the eastern part. One reason is that many large rivers flowing into Suruga Bay exist more in the west than the eastern side of Suruga Bay. The Miho Peninsula is located at the western part of Suruga Bay, that there are mouths of the Fuji River and the Okitsu River in the north, and the mouth of the Abe River in the south. High chlorophyll a concentration is also observed off Miho Peninsula. From the chlorophyll a concentration image by ocean color remote sensing, which river that influence high concentration of chlorophyll a off Miho Peninsula can be empirically discriminated, whereas it is sometimes difficult to distinguish with chlorophyll a concentration image. In Suruga Bay, the Ferry Fuji (Suruga Bay Ferry) cruises 4 times a day to Shimizu Port and Toi Port. It has been suggested that the current in the normal direction of the course can be estimated from the AIS (Automatic Identification System) information of the Ferry FUJI. Since the route of the Suruga Bay ferry is approximately in the east-west direction, it is possible to obtain the flow in the north-south direction. In this study, we attempt to distinguish river water affecting chlorophyll a concentration off Miho Peninsula by adding information of current estimated from AIS information to Chlorophyll a concentration image in the Suruga Bay.

Keywords: Ocean color remote sensing, Suruga Bay, AIS

©2019. Japan Geoscience Union. All Right Reserved.

Estimation of chlorophyll-a from RGB digital camera data collected in Ise-Mikawa Bay

*Akiko N. Mizuno[1], Joji Ishizaka[1]

1. Institute for Space-Earth Environmental Research, Nagoya University

Development for survey methods for phototrophs and/or environmental condition using RGB digital camera data has been increasingly studied for two decades. In examples for the ocean are studies of estimation of water quality using smart phone’ s camera (Goddijin et al. 2009, Leeuw and Boss 2018), detection of sea grass from aerial photo images and estimation of chlorophyll-a (Goddijn and White 2006). The portability and convenience of the digital camera are the reasons of interest for the RGB data. It is possible to be used as supplementary observation of satellite sensing because digital camera can use regardless of the cloud. Also, citizen participation surveys may be possible because anyone can take photographs using his or her digital camera.

Thus, we attempted to develop estimation method for chlorophyll-a from RGB digital camera data for Ise-Mikawa Bay, Japan. For Ise-Mikawa Bay, method of estimation of chlorophyll a concentration form SeaWiFS and MODIS data was developed by Hayashi et al (2015), but estimation method with digital camera data was not developed yet.

We used chlorophyll-a concentration, RGB data from photo images of surface water, sky and a photographer’ s 18% reflectance gray card during monthly survey cruises in Ise-Mikawa Bay. Spectral remote sensing reflectance data from RAMSES/TriOS was also obtained. We calculated RGB from spectral remote sensing reflectance data and compared RGB from digital camera. Digital camera RGB data was correlated with RGB from spectral data and in-situ chlorophyll-a concentration. In the future, we will reduce effect of reflection of sunlight from estimation of chlorophyll-a concentration using photographs of sky and gray card.

L.M. Goddijn; M White, Using a digital camera for water quality measurements in Galway Bay, Estuarine, Coastal and Shelf Science (2006), 66, 429-436.

L.M. Goddijn; D. Dailloux; M. White; D. Bowers, Fundamentals of in situ digital camera methodology for water quality monitoring of coast and ocean., Sensors (2009), 9, 5825-5843.

T. Leeuw; E. Boss, The HydroColor App: Above Water Measurements of Remote Sensing Reflectance and Turbidity Using a Smartphone Camera, Sensors (2018), 18, 256-271.

M. Hayashi; J. Ishizaka; M. Toratani; T. Nakamura; Y. Nakashima; S. Yamada; Evaluation and Improvement of MODIS and SeaWIFS-derived Chlorophyll a Concentration in Ise-Mikawa Bay, Journal of The Remote Sensing Society of Japan (2015), 35, 245-259.

Keywords: Coastal region, Estimation of Chl.a concentration, RGB values, digital camera image, sea surface reflection

©2019. Japan Geoscience Union. All Right Reserved.

©2019. Japan Geoscience Union. All Right Reserved.

Seasonal variability of MODIS chlorophyll-a and total suspended matter in the spring-neap tidal cycle in the Ariake Bay, Japan

*Mengmeng Yang[1], Joji Ishizaka[2], Joaquim I. Goes[3], Hongzhen Tian[4], Elígio R. Maúre[5], Masataka Hayashi[6]

1. Graduate School of Environmental Studies, Nagoya University, Furo-cho, Chikusa-ku, Nagoya, Aichi, Japan., 2. Institute for Space-Earth Environmental Research (ISEE) Nagoya University Furo-cho, Chikusa-ku, Nagoya, Aichi, Japan., 3. Lamont-Doherty Earth Observatory, Marine Biology and Paleo Environment, Columbia University, 61 Route 9W - PO Box 1000, Palisades, NY 10964-8000, US., 4. School of Management and Economy, Tianjin Polytechnic University, Tianjin 300387, China., 5. Dept. of Research and Study, Northwest Pacific Region Environmental Cooperation Center, Toyama, Japan., 6. Science and Technology co., Ltd., 3-9-2, Koubai-cho, Showa, Nagoya, Aichi 466-0031, Japan.

Red tide occurs more frequently in the Ariake Bay since 1990s, and it has greatly damaged the local fisheries, especially the nori farms. Increase of water transparency and reduction of tidal currents were also reported recently, and they may be related to the increase of the frequency of red tides. It is also reported that another cause of the red tide is the river discharge. Satellite remote sensing is suggested to be used to monitor the red tide. In this study, the newly developed MODIS-derived chlorophyll-a (Chl-a) and total suspended matter (TSM) was used to investigate the relationship between Chl-a and TSM and the seasonal variations of influences of spring-neap tides and river discharge. We observed that 1) high Chl-a (>5 mg m^{-3}) and high TSM (>5 g m^{-3}) were generally distributed in the areas off Saga, Kumamoto and Yatsushiro, and Isahaya Bay where the main river systems discharge the fresh water; 2) the magnitude of Chl-a was highest in summer, and decreased gradually from autumn to spring, which corresponded to the amount of river discharge which concentrates in summer and early autumn (June-September); 3) in the spring-neap tidal cycle, TSM was much higher in neap to spring (NS) and spring (S) tide than in spring to neap (SN) and neap (N) tide, which was consistent with the tidal suspension. On the other hand, Chl-a was often increased after high river discharge peak and the variation of Chl-a was small when the river discharge peak was small, indicating that the variation of Chl-a was mainly influenced by the river discharge. The variation of TSM in the spring-neap tidal cycle was mainly regulated by the tidal suspension, whereas the variation of Chl-a was more controlled by the river discharge than the tidal resuspension.

Keywords: MODIS, chlorophyll-a, total suspended matter, seasonal variability, spring-neap tides, river discharge

©2019. Japan Geoscience Union. All Right Reserved.

Discrimination of green *Noctiluca scintillans* in the upper Gulf of Thailand using remote sensing techniques

*Jutarak Luang-on[1], Joji Ishizaka[2], Anukul Buranapratheprat[3], Jitraporn Phaksopa[4]

1. Graduate School of Environmental Studies, Nagoya University, 2. Institute for Space-Earth Environmental Research, Nagoya University, Japan, 3. Department of Aquatic Science, Faculty of Science, Burapha University, Thailand, 4. Department of Marine Science, Faculty of Fisheries, Kasetsart University, Thailand

Green *Noctiluca scintillans*, the peculiar single cellular heterotrophic organism containing green algae called *Pedinomonas noctilucae*, frequently causes harmful algal bloom (HAB) in the upper Gulf of Thailand (uGoT). The high density of green *Noctiluca* discolors the water to deep milky green, and it has the potential to generate low dissolved oxygen (hypoxia) in the water column resulting in massive fish mortality. The co-occurrence of green Noctiluca and other phytoplankton species (e.g., *Ceratium furca* and diatoms) was often reported. Heretofore, the behavior of red tides has not been clarified. In this study, we, therefore, focus on investigating the dominant spectral characteristics of each HAB species and developing an algorithm to discriminate green *Noctiluca* from the other harmful species. The ship observations (2017 –2018) were conducted to obtain the apparent and inherent optical properties as well as the pigment information of green *Noctiluca* blooms. Fortunately, the super green *Noctiluca* blooms (>1,500,000 cell L^{-1}) occurred near the west coast of the uGoT in July 2017. The remote sensing reflectance spectra measured by using the RAMSES hyperspectral radiometer (320 nm –950 nm) revealed the crucial features of green *Noctiluca* in near-infrared wavelengths. The different characteristics of green *Noctiluca* and other HAB species were also found in visible wavelengths. The investigated features were used in the discrimination method to detect the green *Noctiluca* bloom using satellite observation in the near future.

Keywords: green Noctiluca, the upper Gulf of Thailand, remote sensing

©2019. Japan Geoscience Union. All Right Reserved.

©2019. Japan Geoscience Union. All Right Reserved.

Monthly variability of Chlorophyll-a distribution in the Gulf of Thailand

*Dudsadee Leenawarat[1], Anukul Buranapratheprat[2], Joji Ishizaka[3]

1. Graduate School of Environmental Studies, Nagoya University, Japan, 2. Department of Aquatic Science, Faculty of Science, Burapha University, Thailand, 3. Institute for Space-Earth Environmental Research, Nagoya University, Japan

The Gulf of Thailand (GoT) is semi-enclosed sea located in the western part of the South China Sea. This area is important to fisheries production in this region. The satellite data can reveal the primary production through chlorophyll-a (Chl-a) which is basic for the food chain. The objectives of this study are to investigate the variation and spatial distribution patterns of Chl-a in the GoT by using long-term satellite data from SeaWiFS (1997-2010), MERIS (2002-2012), MODIS AQUA (2002-2018), and VIIRS (2012-2018) level 3 compared with oceanographic conditions from previous study and circulation model name Princeton Ocean Model (POM). Tide and climatological data of wind, salinity, temperature and river discharge are forcing in the model. The results from averaged monthly Chl-a concentration in the central GoT illustrate low Chl-a concentration occurred in transition periods (April-May, and October) by lowest in May when the water column was stratified. High Chl-a concentration occurred during the northeast monsoon (November to February) with the highest in December when the water column was well mixed, and a small peak was found during June to August. Hight Chl-a was found along the coast, especially near the northern coast in the southwest monsoon (June to October). During the northeast monsoon Chl-a near cape CaMau spread offshore, due to strong surface currents flew into GoT from the southern part of cape CaMau to the middle of GoT mouth.

Keywords: Gulf of Thailand, Chlorophyll-a, Variability

©2019. Japan Geoscience Union. All Right Reserved.

AERONET-Ocean Color time series in Ariake Bay.

*yifei wu[1], Joji Ishizaka[2], Mengmeng Yang[1], Naoki Fujii[3], Masahiro Hori[4]

1. Graduate School of Environmental Studies, Nagoya University, 2. Institute for Space-Earth Environmental Research, Nagoya University, 3. Graduate School of Agriculture, Saga University, 4. EORC, JAXA

The AERONET (**AE**rosol **RO**botic **NET**work) project is a federation of ground-based remote sensing aerosol networks established by **NASA** and **PHOTONS** and is greatly expanded by networks from national agencies, institutes, universities, individual scientists. AERONET –Ocean Color (AERONET-OC) provides the additional capability of measuring the radiance emerging from the sea. In April 2018, a new station of AERONET-OC has been set by JAXA for GCOM-C validation in Ariake Bay located in Kyusyu, Japan where the seaweed (Nori) culture very famous. Aerosol Optical Depth (AOD) and remote sensing reflectance (Rrs) is considered as the most important products of AERONET-OC since the estimation of chlorophyll-a concentration by ocean color satellite is usually not so accurate in coastal areas because of the inaccurate satellite remote sensing reflectance (Rrs) influenced by aerosol. This study is to make a brief description of the time series of the AERONET-OC data from April 2018 to April 2019. Local Chl-a and TSM estimated by using radiances measured by the AERONET-OC is going to use to explain the phytoplankton bloom connect with factors such as precipitation and river discharge in Ariake Bay.

Keywords: chlorophyll-a, remote sensing reflectance, AERONET-OC

©2019. Japan Geoscience Union. All Right Reserved.

[E] Oral | H (Human Geosciences)：H-DS Disaster geosciences

Tue. May 28, 2019 9:00 AM - 10:30 AM JST | Tue. May 28, 2019 12:00 AM - 1:30 AM UTC | 304 3F

[H-DS09] Landslides and related phenomena

convener:Masahiro Chigira(Disaster Prevention Research Institute, Kyoto University), Gonghui Wang(Disaster Prevention Research Institute, Kyoto University), Fumitoshi Imaizumi(Faculty of Agriculture, Shizuoka University), Chairperson:Fumitoshi Imaizumi

Mass movements, such as landslides, rockfalls, and debris flows, have been occurring extensively in a large number of countries, causing heavy damage. In order to understand them and mitigate induced disasters, we invite contributions that report and discuss on mass movements and related phenomena, focusing on improved understanding of their characteristics; new insights into landslide mechanisms; the development of new approaches to monitoring; novel approaches to behavior forecasting and prediction; studies of successful landslide management; and the development of methods for hazard and risk evaluation. In particular, papers about recent landslide hazards, induced by 2017 northern Kyushu rainstorm, 2018 Osaka earthquake, 2018 western Japan rainstorm, and 2018 Hokkaido earthquake are welcome.

9:00 AM - 9:15 AM JST | 12:00 AM - 12:15 AM UTC

[HDS09-01] Mechanical behavior modulated by shear surface morphology of simulated shear zone

*Yao Jiang[1], Gonghui Wang[2], Toshitaka Kamai[2] (1.Institute of Mountain Hazards and Environment, Chinese Academy of Sciences, China, 2.Research Center on Landslide, Disaster Prevention Research Institute, Kyoto University, Japan)

9:15 AM - 9:30 AM JST | 12:15 AM - 12:30 AM UTC

[HDS09-02] On the Pre-failure Shear Behavior of Clayey Soil

*Chengrui Chang[1], Gonghui Wang[1] (1.Disaster Prevention Research Institute, Kyoto University)

9:30 AM - 9:45 AM JST | 12:30 AM - 12:45 AM UTC

[HDS09-03] GeoGuard: low-cost GNSS sensors for the continuous monitoring of landslides and structures

*Andrea Gatti[1], Giulio Tagliaferro[1], Eugenio Realini[1], Stefano Caldera[1] (1.Geomatics Research & Development srl)

9:45 AM - 10:00 AM JST | 12:45 AM - 1:00 AM UTC

[HDS09-04] Landslide Susceptibility Analysis in the Chenyulan River Watershed, Taiwan

*Po-Tsun Yeh[1], Kuang-Tsung Chang[1] (1.National Chung Hsing University, Taiwan)

10:00 AM - 10:15 AM JST | 1:00 AM - 1:15 AM UTC

[HDS09-05] Investigating the Relationship Between Tree Height and Landslide Occurrence in the Ikawa Catchment, Central Japan

*Jamie Rhys Evans[1], Fumitoshi Imaizumi [1] (1.Faculty of Agriculture, Shizuoka University)

10:15 AM - 10:30 AM JST | 1:15 AM - 1:30 AM UTC

[HDS09-06] Landslides induced by the knickpoint migration in the southern and the eastern margins of the Tibetan Plateau.

*Masahiro Chigira[1], Ching-Ying Tsou[2], Siyuan Zhao[4], Xiong Wu[3] (1.Disaster Prevention Research Institute, Kyoto University, 2.Hirosaki University, 3.Souithwest Jiaotong University, 4.Graduate School of Science, Kyoto University)

Mechanical behavior modulated by shear surface morphology of simulated shear zone

*Yao Jiang[1], Gonghui Wang[2], Toshitaka Kamai[2]

1. Institute of Mountain Hazards and Environment, Chinese Academy of Sciences, China, 2. Research Center on Landslide, Disaster Prevention Research Institute, Kyoto University, Japan

Mechanical behaviors of geologic granular materials in shear provide fundamental insights into the mobility mechanisms related to the dynamics of landslides and tectonic faults. Some previous experimental studies have shown that the mineralogy of constituent materials plays a first-order control on the transitions of mechanical behaviors, including sliding stability or instability. Moreover, other laboratory investigations have demonstrated the importance of shear rate as a primary control on the strength properties, leading to rate-strengthening or rate-weakening. Despite these efforts, however, neither the knowledge of general relationships between material properties and failure modes nor the underlying processes are well understood. Here we report on a series of ring-shear friction experiments designed to investigate the shear surface morphology on the mechanical behaviors along pre-existing granular shear zones. Two kinds of commercial granular materials were used in our experiments, say, halite and silica. Results directly show that only inclusion a low proportion of granular halite can produce the transition from stable sliding to stick-slip instability. The visual observations of shear surfaces further indicate that the variations with halite content form different morphologies. By analyzing the shear displacement and acoustic emission data, the microslip precursors were identified to stick-slip instability. It is expected that the mechanical behavior transition may constrain the evolution of asperity mechanism in nucleating rupture instability along heterogeneous shear surfaces owing to breakage of grain interfaces.

Keywords: granular materials, mechanical behavior, shear surface, acoustic emission, ring shear apparatus

©2019. Japan Geoscience Union. All Right Reserved.

On the Pre-failure Shear Behavior of Clayey Soil

*Chengrui Chang[1], Gonghui Wang[1]

1. Disaster Prevention Research Institute, Kyoto University

Introduction

Landslides are significant natural hazard that cause substantial economic loss and extensive loss of life. Triggering in landslides occurs as a result of highly dynamic processes and the hydrological state has a profound influence on the stability of the slopes. For rainfall-induced landslides, the increase of pore water pressure as a result of rainfall infiltration progressively reduces the normal effective stress of the slope materials acting on a potential shear surface and the shear resistance decreases as the inter-particle friction is reduced by the buoyancy force. Saito (1965) first proposed a linear trend when the inverse velocity before failure is plotted against time which has made a significant contribution to the understanding and monitoring of landslides (Voight, 1988, 1989; Fukozono, 1990). Many studies focusing on the deformation and pore water pressure noted that the rate of strain was initially small but showed a very rapid increase towards failure (Anderson & Sitar, 1995; Zhu & Anderson, 1998; Dai et al, 1999; Ng & Petley,

Methods

The aim of this study is to investigate experimentally the nature of the interactions between the pore pressure variation and the development of the displacement in the pre-failure stage. All the soil samples were taken from the Nishiwaki landslide, which was induced by the heavy rainfall accompanying the No. 21 Typhoon on Oct. 22rd, 2017 in Wakayama Prefecture. Subsequently, two different series of tests were undertaken under the combined condition of predefined normal stress and shear stress simulating consolidated nature slope in the ring shear apparatus. One series of test is the pore-pressure-controlled test, which uses a serially connected air tank and water tank to increase the pore water pressure (PWP) in the shear box of ring shear apparatus. This series of tests aims at simulating the effect of decreasing the effective stress state whilst holding constant shear stress to reproduce a slope undergoing heavy rainfall. The pore water pressure was increased deliberately and then hold or decrease the pore water pressure as a short-term movement was detected. Such a procedure has been repeated until the shear resistance dropped, which indicates the shear failure. The shear-stress-controlled series is aiming to investigate the shear displacement pattern with a gently cumulative increase in shear stress under undrained condition, which involves an increase of the shear stress in a flattened gradient after consolidation. Both series of tests are conducted in three kinds of consolidated conditions to examine the correlation between velocity and acceleration.

Results and discussions

In pore-pressure-controlled tests, the displacement shows a creep-like pattern before failure. During the whole test, several periods of constant velocity had been identified. We also found that shear swelling occurred in the drained shear test, therefore, we inferred that the possible infiltration of water into the shear zone may enable the continuous increase of pore water pressure so that the shear resistance will be lowered to initiate the accelerating movement. We also found that “stick-slip” behavior (short-term movements) occurred in the shear tests. We inferred that the increment of the PWP initiates the shear displacement rather than the amount of the PWP.

The results indicate that the increment of PWP can initiate larger and more rapid shear displacement when the level of the PWP is higher. A series of creep-like movements leads to final failure. The role of increasing pore water pressure in the initiation of the tertiary acceleration will be key for us to understand the creep behavior, and further tests and detailed examination on this issue will be continued.

©2019. Japan Geoscience Union. All Right Reserved.

©2019. Japan Geoscience Union. All Right Reserved.

GeoGuard: low-cost GNSS sensors for the continuous monitoring of landslides and structures

*Andrea Gatti[1], Giulio Tagliaferro[1], Eugenio Realini[1], Stefano Caldera[1]

1. Geomatics Research & Development srl

The United Nation Office for Disaster Risk Reduction warned that economic losses from landslides, floods, earthquakes, and drought will continue to escalate unless businesses take action to reduce their exposure to disaster risks. Structures can suffer structural deterioration due to aging, misuse or lack of proper maintenance. In addition, they are subject to exposure to natural hazards such as landslides, floods, and earthquakes. Traditional visual inspection techniques are both time consuming and expensive. They are also qualitative and can only assess outward appearance. Structures and natural hazard control and management are becoming one of the key issues in the approach to sustainable development of modern countries. In this framework, structural health monitoring is representing one of the most valuable approaches for the decision-making process. Global Navigation Satellite System (GNSS) technology can provide position information with accuracy to a few millimeters in near real-time. However, the widespread adoption of GNSS monitoring is hindered by the high cost of dual-/multi-frequency geodetic GNSS receivers.

In 2015, through a partnership with the Italian company Softeco, GReD started GeoGuard, an innovative end-to-end service for the continuous monitoring of landslides and structures by means of single-frequency GNSS low-cost receivers and antennas. GeoGuard provides accurate positioning with centimeter-level accuracy in near real-time, or millimeter-level accuracy for daily/sub-daily solutions. The GNSS network observations are processed by means of both Bernese software, and an ad-hoc evolution of goGPS, a free and open source positioning software package developed by the GReD team. A software platform was developed for the management of a GNSS positioning service, and for the visualization and delivery of results. Currently, GeoGuard uses GPS L1 observations for its operational activities; however, promising results are being obtained with the addition of Galileo E1 observations, especially for sites with limited sky visibility, and to improve the accuracy of sub-daily (e.g. hourly) solutions. Currently, the GeoGuard service is operational on two landslides, a highway bridge, a dam, and two penstocks.

Keywords: Monitoring, GNSS, GPS, Landslide, Structures, low-cost

©2019. Japan Geoscience Union. All Right Reserved.

Landslide Susceptibility Analysis in the Chenyulan River Watershed, Taiwan

*Po-Tsun Yeh[1], Kuang-Tsung Chang[1]

1. National Chung Hsing University, Taiwan

Many rainfall-triggered landslides occurred in the Chenyulan river watershed of central Taiwan during typhoon Morakot. In order to prevent rainfall-triggered landslide disasters, it is important to understand the relation of the disasters and the factors of rainfall, geology, and topography. In this study, the landslide susceptibility model of the Chenyulan river watershed was built and evaluated under the multiple logistic regression analysis based on slope units. These units were delineated by topography and 249 units out of them were chosen because orientation data of weak planes were included. The detection of the binary dependent variables (landslide and non-landslide samples) were based on the geomorphic change using satellite imageries before and after typhoon Morakot. Then the independent variables include geological, topographic and rainfall factors. Especially, we considered the orientation of weak planes and the spatial and temporal variability of rainfall. The result showed that the p-value of Hosmer-Lemeshow test and the Area Under the Curve of ROC are over 0.1 and 0.75, respectively. As the result, the chosen factors in the model could predict landslides in the Chenyulan river watershed effectively. It could be reference for follow-up research.

Keywords: Landslide susceptibility, Spatial and temporal variability of rainfall, Multiple logistic regression, Orientation of weak plane, Slope unit

©2019. Japan Geoscience Union. All Right Reserved.

Investigating the Relationship Between Tree Height and Landslide Occurrence in the Ikawa Catchment, Central Japan

*Jamie Rhys Evans[1], Fumitoshi Imaizumi [1]

1. Faculty of Agriculture, Shizuoka University

The occurrence of landslides in forested terrain can have large impacts on the future productivity of soil and the quality of water that drains from a catchment, as well as damaging a valuable asset in the forest itself. The relationship between tree height and landslide occurrence in the Ikawa catchment, Northern Shizuoka prefecture, is investigated to gain a better insight into the distribution of landslides. Root depth profile, measured for trees of various height via trenches, is used in conjunction with tree height when assessing the distribution of landslides. Root tensile strength for unit areas of soil is calculated from individual root diameters to better understand the effect of the root network on slope stability. Landslide ratios in the Ikawa catchment show that landslides occur more frequently in shorter forests, with occurrence decreasing as tree height increases. This is likely due to stabilizing features of trees being accentuated as they grow, which is supported by both total root area and total root tensile strength data showing a significant increase between that of the 6.5m Kumashide, 8m Momi, and 12m Kumashide. The random distribution of results when comparing landslide depth to tree height suggests that while tree height, and hence total root tensile strength, has an impact upon whether a landslide is to occur or not, the depth of the landslides that do occur are independent of the height of trees. This suggests that slope stability increases alongside tree height and that landslide depth is not controlled by tree height so is therefore controlled by other factors. While there is no relationship between tree height and landslide depth, both Kumashide trees surveyed show decreases in total root tensile strength around the average depth of landslides in the Ikawa catchment of 0.46m.

Keywords: Landslide depth, Tree height, Root tensile strength, LiDAR

©2019. Japan Geoscience Union. All Right Reserved.

Landslides induced by the knickpoint migration in the southern and the eastern margins of the Tibetan Plateau.

*Masahiro Chigira[1], Ching-Ying Tsou[2], Siyuan Zhao[4], Xiong Wu[3]

1. Disaster Prevention Research Institute, Kyoto University, 2. Hirosaki University, 3. Souithwest Jiaotong University, 4. Graduate School of Science, Kyoto University

Because of the collision of Indian plate to Eurasian continent, Himalaya, which is the southern margin of the Tibetan Plateau, is uplifting very rapidly and also the eastern margin of the Tibetan Plateau is uplifting. Those mountains are the sites of uplift and also the sites of rapid erosion and mass movements. We made field survey, using PRISM image with a resolution of 5 m and 5-m ALOS AW3D in both areas. We studied gravitational slope deformation and landslide, which are the response of mountain slopes to river incision, along the Kaligandaki River in Nepal Himalaya and the Minjiang River in Sichuan and found that gigantic landslides have occurred due to the slope instability made by the upstream migration of knickpoints and undercutting of the nearby slopes.

Along the Kaligandaki River, there are two outstanding knickpoints at Kalopani and Talbagar, respectively. The knickpoint at Kalopani is located at the largest landslide dam, which is called Kalopani landslide or Lete landslide. This landslide is inferred to be preceded by buckling deformation of calc gneiss. It is located near the lower margin of the glaciated area, and the slope could have been eroded by a glacier at the foot of the slope. Downstream of the Lete landslide are aligned 4 gigantic landslides, of which the most upstream one is the Talbagar landslide. It occurred on the left bank just downstream of an outstanding knickpoint of the Kali Gandaki River. This knickpoint propagated from downstream forming a slope break 200-400 m high from the riverbed. Talbagar landslide is a rock compound slide and the other three gigantic landslides were of two mica gneiss and occurred on slopes that had been toppled above the slope break.

There are two significant knickpoints along the Minjian River upstream of the Longmenshan fault. The effects of the knickpoint propagation and inner gorge formation on slope stability are dependent on the geometrical relationships between the river and geological structures. When the geological trend is normal or highly oblique to the river axis, landslides generally do not occur, but gigantic catastrophic landslides have occurred on one side of the Minjiang valley, which can be attributed to a wedge structure consisting of bedding planes and joints with intersections dipping valleyward and tight folds with hinges plunging valleyward. Diexi landslide, the largest landslide along the Minjian River was a wedge failure induced by this knickpoint migration.

Keywords: Landslide, Tibetan Plateau, Himalaya, Minjan, Knickpoint

©2019. Japan Geoscience Union. All Right Reserved.

[E] Oral | H (Human Geosciences)：H-DS Disaster geosciences

Tue. May 28, 2019 10:45 AM - 12:15 PM JST | Tue. May 28, 2019 1:45 AM - 3:15 AM UTC | 304 3F

[H-DS09] Landslides and related phenomena

convener:Masahiro Chigira(Disaster Prevention Research Institute, Kyoto University), Gonghui Wang(Disaster Prevention Research Institute, Kyoto University), Fumitoshi Imaizumi(Faculty of Agriculture, Shizuoka University), Chairperson:Wang Gonghui, Issei Doi

Mass movements, such as landslides, rockfalls, and debris flows, have been occurring extensively in a large number of countries, causing heavy damage. In order to understand them and mitigate induced disasters, we invite contributions that report and discuss on mass movements and related phenomena, focusing on improved understanding of their characteristics; new insights into landslide mechanisms; the development of new approaches to monitoring; novel approaches to behavior forecasting and prediction; studies of successful landslide management; and the development of methods for hazard and risk evaluation. In particular, papers about recent landslide hazards, induced by 2017 northern Kyushu rainstorm, 2018 Osaka earthquake, 2018 western Japan rainstorm, and 2018 Hokkaido earthquake are welcome.

10:45 AM - 11:15 AM JST | 1:45 AM - 2:15 AM UTC

[HDS09-07] Landslides caused by the 2018 Hokkaido Eastern Iburi Earthquake

★Invited Papers

*Shin-ichiro Hayashi[1], Nobutomo Osanai[1], Takashi Yamada[1], Shin'ya Katsura[1], Takahisa Furuichi[1], Seiji Yanai[2], Yasuharo Murakami[3], Tomoyoshi Miyazaki[4], Yuichiro Tanioka[1], Shigetaka Takiguchi[5], Mayumi Miyazaki[6] (1.Hokkaido University, 2.Ishikawa Prefectural University, 3.Civil Engineering Research Institute for Cold Region, PWRI, 4.Shin Engineering Consultant, Co., Ltd., 5.Ministry of Land, Infrastructure, Transport and Tourism, 6.Pasco Corporation)

11:15 AM - 11:45 AM JST | 2:15 AM - 2:45 AM UTC

[HDS09-08] On the coseismic landslides occurring on tephra slopes during the 2018 Hokkaido Eastern Iburi Earthquake

★Invited Papers

*Gonghui Wang[1], Gen Furuya[2] (1.Disaster Prevention Research Institute, Kyoto University, 2.Toyama Prefectural University)

11:45 AM - 12:00 PM JST | 2:45 AM - 3:00 AM UTC

[HDS09-09] Seismological and geotechnical surveys on the landslides induced by the 2018 Hokkaido Eastern Iburi earthquake

*Issei Doi[1], Hikaru Osawa[2], Sumio Matsuura[1] (1.Disaster Prevention Research Institute, Kyoto University, 2.Mountain Science Center, University of Tsukuba)

12:00 PM - 12:15 PM JST | 3:00 AM - 3:15 AM UTC

Discussion

Landslides caused by the 2018 Hokkaido Eastern Iburi Earthquake

*Shin-ichiro Hayashi[1], Nobutomo Osanai[1], Takashi Yamada[1], Shin'ya Katsura[1], Takahisa Furuichi[1], Seiji Yanai[2], Yasuharo Murakami[3], Tomoyoshi Miyazaki[4], Yuichiro Tanioka[1], Shigetaka Takiguchi[5], Mayumi Miyazaki[6]

1. Hokkaido University, 2. Ishikawa Prefectural University, 3. Civil Engineering Research Institute for Cold Region, PWRI, 4. Shin Engineering Consultant, Co., Ltd., 5. Ministry of Land, Infrastructure, Transport and Tourism, 6. Pasco Corporation

The 2018 Hokkaido Eastern Iburi Earthquake struck the eastern Iburi region (epicenter: 42.691˚N, 142.007˚E, depth: 37.0km) of Hokkaido, Japan, at 3:07.59 JST, September 6, 2018 (18:07.59, September 5, 2018 UTC). Many shallow landslides and several large-scale deep-seated landslides, generating a landslide dam in the Hidaka-horonai River, were triggered by this magnitude 6.6 M_w (6.7 M_j) earthquake. The sedimentary rock in the affected area was covered by thick pyroclastic fall deposits derived from the Tarumae Volcano etc.. Landslides were densely distributed over hilly regions (elevation: 200–400 m) within an area of approximately 400 km^2 in Atsuma, causing 36 deaths, Abira and Mukawa, and representing the largest total area of earthquake-related landslides in Japan since the Meiji Era (1868–1912). The shallow landslides were characterized as follows: 1) pyroclastic fall deposits on sedimentary rock (basement complex) were moved by the strong seismic shock, 2) slip surface types included weathered tephra, weathered bedrock, and buried humus layers, 3) many occurred at relatively gentle slopes (< 30˚), 4) shallow landslides moving along valley type topography tended to travel longer than those moving along planar slope topography, and 5) concentrated shallow landslides occurred in tributary catchments of the Atsuma and Abira Rivers. Large-scale deep-seated landslides were characterized as follows: 1) rare occurrence and 2) slip surface within sedimentary rock.

Keywords: 2018 Hokkaido Eastern Iburi Earthquake, pyroclastic fall deposits, shallow landslide, landslide dam

©2019. Japan Geoscience Union. All Right Reserved.

On the coseismic landslides occurring on tephra slopes during the 2018 Hokkaido Eastern Iburi Earthquake

*Gonghui Wang[1], Gen Furuya[2]

1. Disaster Prevention Research Institute, Kyoto University, 2. Toyama Prefectural University

Numerous landslides were triggered by 2018 Hokkaido Eastern Iburi Earthquake on the tephra slopes, resulting in 36 casualties. Although one large landslide was initiated with its sliding surface being in the bedrock of sandstone and siltstone, most of them occurred on the tephra slope. To understand the initiation and movement mechanisms of these landslides occurring on tephra slopes, we performed field investigation (including geophysical survey, penetration test and field director shear box tests), and also conducted dynamic shear tests on the tephra samples taken from the sliding surface. The results will be presented in this report.

Keywords: Coseismic landslide, 2018 Hokkaido Eastern Iburi Earthquake, Tephra slope, Initiation mechanism, Movement mechanism

©2019. Japan Geoscience Union. All Right Reserved.

Seismological and geotechnical surveys on the landslides induced by the 2018 Hokkaido Eastern Iburi earthquake

*Issei Doi[1], Hikaru Osawa[2], Sumio Matsuura[1]

1. Disaster Prevention Research Institute, Kyoto University, 2. Mountain Science Center, University of Tsukuba

Atsuma Town, central part of Hokkaido, Japan, suffered from numerous landslides induced by the 2018 Hokkaido Eastern Iburi earthquake (Mw 6.7). We had a seismological and geotechnical surveys on some of the landslides. We selected a shallow landslide within tephra layers and a huge landslide of rockslide. Aftershock observation was conducted to grasp the vibration characteristics of the large landslide. Frequency components of ~2 Hz were dominant for S- and coda parts, with long durations of monochroic vibrations. Surface wave surveys, in both active and passive ways, were deployed to understand the vertical profile of the shallow landslide area. Very low (~ 50 m/s) Vs layers with the thickness ~ 1 m, which were consistent to the landslide depth, were detected along the survey line beside the landslide area, while such layers did not exist inside the landslide.

Acknowlegement: Hirokazu Fukui, a graduate student in Kyoto University, helped us for conducting the surveys.

©2019. Japan Geoscience Union. All Right Reserved.

[E] Oral | H (Human Geosciences)：H-DS Disaster geosciences

Tue. May 28, 2019 1:45 PM - 3:15 PM JST | Tue. May 28, 2019 4:45 AM - 6:15 AM UTC | 304 3F

[H-DS09] Landslides and related phenomena

convener:Masahiro Chigira(Disaster Prevention Research Institute, Kyoto University), Gonghui Wang(Disaster Prevention Research Institute, Kyoto University), Fumitoshi Imaizumi(Faculty of Agriculture, Shizuoka University), Chairperson:Fumitoshi Imaizumi, Chigira Masahiro

Mass movements, such as landslides, rockfalls, and debris flows, have been occurring extensively in a large number of countries, causing heavy damage. In order to understand them and mitigate induced disasters, we invite contributions that report and discuss on mass movements and related phenomena, focusing on improved understanding of their characteristics; new insights into landslide mechanisms; the development of new approaches to monitoring; novel approaches to behavior forecasting and prediction; studies of successful landslide management; and the development of methods for hazard and risk evaluation. In particular, papers about recent landslide hazards, induced by 2017 northern Kyushu rainstorm, 2018 Osaka earthquake, 2018 western Japan rainstorm, and 2018 Hokkaido earthquake are welcome.

1:45 PM - 2:15 PM JST | 4:45 AM - 5:15 AM UTC

[HDS09-10] Initiation conditions of debris flows in Ohsawa landslide, Mt. Fuji

★Invited Papers

*Fumitoshi Imaizumi[1], Kazuki Yamamoto[1], Atsushi Ikeda[4], Okihiro Ohsaka[1], Hiroyuki Sugimoto[2], Satoru Suzuki[2], Shinichi Sato[2], Yoshiaki Kashiwabara[3], Naoki Nishimura[3] (1.Faculty of Agriculture, Shizuoka University, 2.Fuji Sabo Office, Ministry of Land, Infrastructure and Transport, 3.Asia Air Survey Co., Ltd., 4.Faculty of Life and Environmental Sciences, Tsukuba University)

2:15 PM - 2:30 PM JST | 5:15 AM - 5:30 AM UTC

[HDS09-11] The role of thrust faults with incohesive clayey fault materials to generate deep-seated gravitational slope deformations and catastrophic landslides in the Shimanto accretionary complex

*Noriyuki Arai[1], Masahiro Chigira[1] (1.Disaster Prevention Research Institute,Kyoto University)

2:30 PM - 2:45 PM JST | 5:30 AM - 5:45 AM UTC

[HDS09-12] Control effect of huge faults on the structure of surrounding regional rock mass in the whole mountain: implications for the distribution pattern of coseismic landslides

*Chao HUANG[1,2], Yusheng LI[1], Chunhao WU[3], Shujian YI[1,3], Kai LIU[1,4], Gonghui WANG[2] (1.State Key Laboratory of Geohazard Prevention and Geoenvironment Protection, Chengdu University of Technology, China, 2.Disaster Prevention Research Institute, Kyoto University, Japan, 3.Institute of Mountain Hazards and Environment, Chinese Academy of Sciences, China, 4.China Railway Eryuan Engineering Group CO. LTD, China)

2:45 PM - 3:15 PM JST | 5:45 AM - 6:15 AM UTC

Discussion

Initiation conditions of debris flows in Ohsawa landslide, Mt. Fuji

*Fumitoshi Imaizumi[1], Kazuki Yamamoto[1], Atsushi Ikeda[4], Okihiro Ohsaka[1], Hiroyuki Sugimoto[2], Satoru Suzuki[2], Shinichi Sato[2], Yoshiaki Kashiwabara[3], Naoki Nishimura[3]

1. Faculty of Agriculture, Shizuoka University, 2. Fuji Sabo Office, Ministry of Land, Infrastructure and Transport, 3. Asia Air Survey Co., Ltd., 4. Faculty of Life and Environmental Sciences, Tsukuba University

Initiation condition of the debris flow is generally explained only using rainfall threshold. However, the rainfall threshold possibly changes in cold seasons because of decreasing in the infiltration rate by freezing of the ground water. Snow cover and volume of unstable sediment in the debris flow torrent are also potential factor affecting the rainfall threshold. We have studied initiation condition of debris flow in Ohsawa landslide, Mt. Fuji, where the ground freezes for a long period due to high elevation. Snow cover period was estimated by the degree-day method. Progress of the freezing and melting of the groundwater toward deeper part of the ground was estimated using freezing degree days and degree days, respectively. In addition, effect of the freezing, snow cover, and volume of storage was studied by analyzing the rainfall and debris flow records over fifty years. Rainfall intensity and total rainfall needed for occurrence of debris flows in freezing periods is lower than that in the non-freezing periods. Rainfall threshold in the non-freezing periods with small volume of storage is lower than that in the non-freezing periods with large volume of storage. Influence of snow cover on the occurrence of debris flow and slash avalanche was not clear.

Keywords: Debris flow, Landslide, Mt. Fuji, Frozen soil

©2019. Japan Geoscience Union. All Right Reserved.

The role of thrust faults with incohesive clayey fault materials to generate deep-seated gravitational slope deformations and catastrophic landslides in the Shimanto accretionary complex

*Noriyuki Arai[1], Masahiro Chigira[1]

1. Disaster Prevention Research Institute,Kyoto University

The purpose of this study is to clarify the geological and geomorphological background of deep-seated catastrophic landslides (DCLs) and related gravitational slope deformations (DGSDs) that occur in mountain areas of accretionary complexes. We performed the detailed geological survey for the area of 25 km^2 in the Shimanto accretionary complex in the middle of the Kii Mountains, Japan. In this area, six DCLs were induced by the heavy rain of Typhoon Talas in 2011. Using the 1-m DTMs made from LiDAR data taken before and after the landslides by the Kinki Regional Development Bureau, Ministry of Land, Infrastructure, Transport and Tourism, and Nara Prefecture, we investigated the distribution of the thrust faults with the incohesive clayey fault materials in the mountain slopes and the inner structures of these thrusts. Mineralogy, permeability and shear strength were measured for the fault gouge.
As a result, we obtained the following results and conclusions.
1. Low-angle thrust faults with incohesive fault rocks thicker than approximately 1 m were newly found to develop at intervals of a few km in the study area.
2. Many of these thrust faults were different from previously reported thrust faults. The thrust faults with incohesive fault rocks include clayey crush materials that form a weak and impermeable layer, which becomes the base of a DGSD and would accommodate a sliding surface of a DCL.
3. The DGSDs and rain-induced DCLs in the study area preferentially occur in the hanging walls of those thrust faults and their areal alignments are controlled by the thrust faults.
4. Thrust faults commonly extend for kilometers as planar features but are sometimes locally folded with their nearby rocks. When a syncline involving thrust faults plunges valleyward, this structure also facilitates DGSDs.

Keywords: deep-seated catastrophic landslide, gravitational slope deformation, incohesive clayey fault material, accretionary complex

©2019. Japan Geoscience Union. All Right Reserved.

Control effect of huge faults on the structure of surrounding regional rock mass in the whole mountain: implications for the distribution pattern of coseismic landslides

*Chao HUANG[1,2], Yusheng LI[1], Chunhao WU[3], Shujian YI[1,3], Kai LIU[1,4], Gonghui WANG[2]

1. State Key Laboratory of Geohazard Prevention and Geoenvironment Protection, Chengdu University of Technology, China, 2. Disaster Prevention Research Institute, Kyoto University, Japan, 3. Institute of Mountain Hazards and Environment, Chinese Academy of Sciences, China, 4. China Railway Eryuan Engineering Group CO. LTD, China

Introduction

Earthquakes and earthquake induced landslides are the most threatening geological disasters in nature. Coseismic landslide, as a surface catastrophic effect induced by earthquakes, has drawn much scientific attention. The fact that seismic faults play a control role in the occurrence of landslide has been generally recognized. Many relating researches focused on the relationship between landslide distribution patterns and the distance to the co-seismic fault, peak ground acceleration (PGA) of the earthquake, and types of faults based on remote sensing interpretation and GIS method. Many statistical methods including fuzzy analytic hierarchy process, principal component analysis, and logistic regression, were used to evaluate landslide susceptibility in an earthquake event considering the main role of faults. However, how the faults affect the distribution patterns of coseismic landslides has not been clearly understood.Therefore, in this study we examined this issue based on a case study on the landslides triggered by the 2008 Wenchuan earthquake, in China.

Method

We selected Qingping part of Longmenshan faults generating the Ms 8.0 earthquake as a target region. First, measurements of rock mass structure were conduceted. In-situ field rock mass structure investigations, 2m*2m measurement network was used, in laboratory, fractures that were visible to the naked eye in the field were sketched and counted using a square frame (0.3 *0.3 m) along profiles oriented across the faults. Then fracture density was calculated to determine the characteristics of fractured system of the crustal rock mass in the fault zone area. Finally, Wenchuan earthquake landslides distribution patterns was combined to deeply discuss the effects of faults on landslides.

Result

The results of spatial variations in fracture density with increasing distance from the Jiangyou-Dujiangyan fault were shown in Fig 1. As can be seen in Fig. 1, fracture density is much higher in the faults zone than other areas and sharply decreases with further increase after it exceeds a certain distance (CD) from the main fault. In Yingxiu-Beichuan fault, this CD is 3030 m in hanging wall and 1170 m in footwall, while in Jiangyou-Dujiangyan fault, this CD is 1350m in the hanging wall. Fracture density also increases when subsidiary faults across. The results showed that occurrences of fractures are strongly concentrated around the faults zone, such as Yingxiu-Beichuan fault and Jiangyou-Dujiangyan fault, presence of secondary faults also has a strong relation with fracture density distribution. Most co-seismic landslides for wenchuan earthquake in the research area distributed on the concentration part of rockmass factures.

Discussion

In this study, we found that there are control effects confined to a certain range of huge faults on the surrounding regional rock mass structure, showing a great impact on rock mass structure in a large scale. A concept named “fracture zone” was defined to express this phenomenon.

The results suggest the existence of remarkable hanging wall effect of rock mass structure, since the width of fracture zone in the hanging wall is greater than that in the foot wall. The fracture zone of Yingxiu-beichuan fault hanging wall is much wider than that of Jiangyou-dujaingyan fault, indicating that

©2019. Japan Geoscience Union. All Right Reserved.

there is a stronger control effect on rockmass structure of Yingxiu-beichuan fault compared with Jiangyou-dujaingyan fault.

Most co-seismic landslides for wenchuan earthquake distributed on the concentration part of rockmass factures, namely fracture zone. Distinct “hanging wall” effect of rockmass structure is consistent with the distribution pattern of coseismic landslides in the research area. Results indicate that the control effect has directly impacts on the distribution pattern of Wenchuan coseismic landslides

Conclusion

1. A control effect confined to a certain range of huge faults on the structure of surrounding regional rock mass in the whole mountain by using fracture density method, this effect was defined as “fracture zone” effect, which has directly impacts on the distribution pattern of Wenchuan earthquake induced landslides.
2. The control effect on surrounding regional rock mass structure were also founded in other huge faults, we argue that this effect is universal, which could be also suitable for other huge faults. The control effect marks long-term dangerous zones, since fragmented rock mass is vulnerable to subjected to failure, which has implications for disaster prevention in mountainous areas where faults are active.

Reference

Keefer, D. K. (1984). Landslides caused by earthquakes. GSA Bulletin 95(4): 406-42

Keywords: Huge fault, Rock mass structure, Coseismic landslide

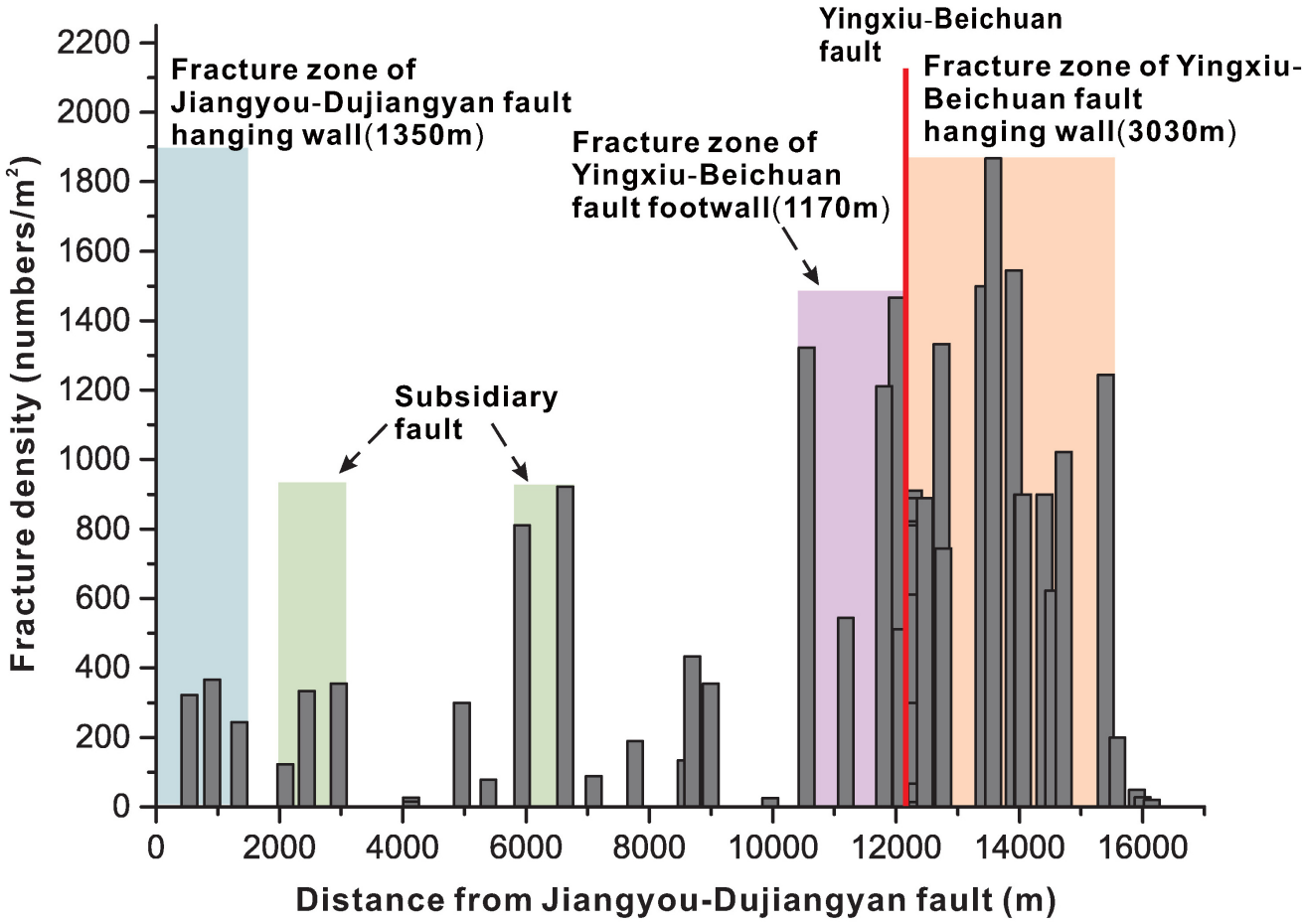

©2019. Japan Geoscience Union. All Right Reserved.

[E] Poster | H (Human Geosciences)：H-DS Disaster geosciences

Tue. May 28, 2019 3:30 PM - 5:00 PM JST | Tue. May 28, 2019 6:30 AM - 8:00 AM UTC | Poster Hall International Exhibition Hall8, Makuhari Messe_12

[H-DS09] Landslides and related phenomena

convener:Masahiro Chigira(Disaster Prevention Research Institute, Kyoto University), Gonghui Wang(Disaster Prevention Research Institute, Kyoto University), Fumitoshi Imaizumi(Faculty of Agriculture, Shizuoka University)

Mass movements, such as landslides, rockfalls, and debris flows, have been occurring extensively in a large number of countries, causing heavy damage. In order to understand them and mitigate induced disasters, we invite contributions that report and discuss on mass movements and related phenomena, focusing on improved understanding of their characteristics; new insights into landslide mechanisms; the development of new approaches to monitoring; novel approaches to behavior forecasting and prediction; studies of successful landslide management; and the development of methods for hazard and risk evaluation. In particular, papers about recent landslide hazards, induced by 2017 northern Kyushu rainstorm, 2018 Osaka earthquake, 2018 western Japan rainstorm, and 2018 Hokkaido earthquake are welcome.

[HDS09-P01] **Fluidized landslides triggered by the liquefaction of subsurface volcanic deposits during the 2018 Iburi–Tobu earthquake, Hokkaido**

*Jun Kameda[1], Hiro Kamiya[2], Hirokazu Masumoto[1], Tomonori Morisaki[1], Toru Hiratsuka[2], Chisaki Inaoi (1.Department of Natural History Sciences, Graduate School of Science, Hokkaido University, 2.Department of Earth and Planetary Sciences, School of Science, Hokkaido University)

[HDS09-P02] A comparison between the acoustic signals and seismic signals generated during a dam-break test

★Invited Papers

*Zheng-yi Feng[1], Hao-yang Huang[1], Chia-Ming Chuang[1] (1.Department of Soil and Water Conservation, National Chung Hsing University, Taichung, Taiwan)

[HDS09-P03] Evaluation of factors of safety and landslide risk for a watershed by Scoops3D

*Zheng-yi Feng[1], Chia-Ming Chuang[1], Hao-yang Huang[1] (1.Department of Soil and Water Conservation, National Chung Hsing University, Taichung, Taiwan)

[HDS09-P04] **Fuzzy Clustering Algorithms for Establishing Landslide Susceptibility Map**

*Pei-hsun Tsai[1], Syuan-yi Wang[1], Jie-shin Cheng[1] (1.Chaoyang University of Technology)

[HDS09-P05] **A Study on Landslides and Debris Flows Susceptibility Mapping Using Unmanned Aerial Vehicles**

*Sheng-Jia Liu[1] (1.qwepoi13@gmail.com)

[HDS09-P06] Largescale landslide induced by AD1586 Tensho-Earthquake in Gifu Prefecture, central Japan

*Takahiro Kurimoto[1], Yoshihiko Kariya[2], Kuniyasu Mokudai[3], Ryuji Yamada[4], Takashi Kimura[4] (1.Undergraduate Senshu University, 2.Department of Geography, Senshu University, 3.Japan Geoservice Incorporated, 4.National Research Institute for Earth Science and Disaster Resilience)

[HDS09-P07] Failure Probability of Lushan Landslide, Taiwan

*Wei-Ting Lin[1], Kuang-Tsung Chang[1] (1.National Chung Hsing University)

[HDS09-P08] Interpretation of landslide surface deformation in Kali Gandaki River watershed, Nepal using ALOS-2/PALSAR-2 InSAR image

*Hiroshi, P. Sato[1] (1.College of Humanities and Sciences, Nihon University)

[HDS09-P09] A depth-integrated model for granular flows on the transition of different bed conditions

*Ling-Yi Hsu[1], Chi-Yao Hung[1] (1.National Chung Hsing University)

[HDS09-P10] A viscous granular flow experiment with new refractive index matching material

*Tsai-Jung Lin[1], Chi-Yao Hung[1] (1.National Chung Hsing University)

[HDS09-P11] Sandbox experiments of submarine landslide caused by water film in low permeability layer

*Shogo Kawakita[1], Daisuke Asahina[2], Keiji Kitajima[3], Mitsukazu Nakanishi[3] (1.Graduate School of Science & Technology, Nihon Univ., 2.National Institute of Advanced Industrial Science and Technology, 3.College of Science & Technology, Nihon Univ.)

[HDS09-P12] **Study on Creep Properties of Sand and Cemented Sand**

*JIN-YI YU[1], KUANG-TSUNG CHANG[1] (1.National Chung Hsing University)

[HDS09-P13] The effects of seepage force and the Poisson's ratio on slope stability

*Hirokazu Fukui[1], Tomomi Terajima[2] (1.Graduate school of Science, Kyoto University, 2.Disaster Prevention Research Institute, Kyoto University)

[HDS09-P14] Study on the factors of seepage erosion

*Szu-Wei Fu[1], Kuang-Tsung Chang[1] (1.National Chung Hsing University)

[HDS09-P15] Deformation of slope models with different orientations of weak planes

*taeyuan tseng[1], Kuang-Tsung Chang[1] (1.National Chung Hsing University)

Fluidized landslides triggered by the liquefaction of subsurface volcanic deposits during the 2018 Iburi–Tobu earthquake, Hokkaido

*Jun Kameda[1], Hiro Kamiya[2], Hirokazu Masumoto[1], Tomonori Morisaki[1], Toru Hiratsuka[2], Chisaki Inaoi

1. Department of Natural History Sciences, Graduate School of Science, Hokkaido University, 2. Department of Earth and Planetary Sciences, School of Science, Hokkaido University

The Iburi–Tobu earthquake of M_w = 6.7 occurred at 3:07 AM (local time) on 6 September 2018, in southern Hokkaido, Japan. The earthquake caused power cuts and destroyed distribution networks across Hokkaido, creating widespread disruption. A total of 41 people were killed during the earthquake, with most of these (36 people) perishing in landslides near the epicenter. The hills in southwestern Hokkaido are widely covered by volcanic deposits, derived from the repeated eruptions of nearby volcanoes such as Tarumai, Eniwa, and Shikotsu (e.g., Nakagawa et al., 2018). On 4 September, Typhoon Jebi caused heavy rainfall in this area, which likely soaked and weakened the volcanic soils. Subsequent earthquake ground motion (with a maximum intensity of 7 on the intensity scale of Japan Meteorology Agency; Japan Meteorology Agency, 2018) may have triggered sudden whole-slope failures. The total number of the present landslides was ~6000 (Yamagishi and Yamazaki, 2018), and most of the recorded landslides are shallow and show features characteristic of fluidized landslides, such as long runouts of debris on a flat depositional area.
To investigate the mechanism generating the landslides triggered by the Iburi–Tobu earthquake, we conducted a field survey at a typical landslide in the Tomisato area of Atsuma, and we found a distinctive occurrence of liquefaction in the field, which could be a precursive condition for the generation of the fluidized landslides triggered by the earthquake. In the scarp of the landslide, an altered halloysite-bearing volcanic layer is observed at a level almost coincident with the sliding surface. The layer is intensely undulating and can be divided into an upper clay-rich layer and a lower pumice-rich layer, suggesting that the altered layer had liquefied as a result of the strong coseismic ground motion. The layer had been soaked by heavy rainfall just one day before the earthquake and could have liquefied by interstitial fluid pressurization, producing a weak and slippery plane, resulting in the catastrophic landslides in this area.

Keywords: fluidized landslide, 2018 Iburi–Tobu earthquake, halloysite

©2019. Japan Geoscience Union. All Right Reserved.

A comparison between the acoustic signals and seismic signals generated during a dam-break test

*Zheng-yi Feng[1], Hao-yang Huang[1], Chia-Ming Chuang[1]

1. Department of Soil and Water Conservation, National Chung Hsing University, Taichung, Taiwan

Natural events, such as landslide, sediment transport, flooding, etc., usually release energy to produce acoustic waves and seismic waves. Acoustic wave is transmitted through air and seismic wave is transmitted through geologic structure. Therefore, the characteristics of acoustic waves and the seismic waves induced by these events should be different. This study focus on the differences in the acoustic signals and seismic signals during a dam-break test performed by the authors. We built a model dam and slope in a creek for the test. We filled the dam with water and caused it to overflow. The overflow water caused the downward erosion of the dam. The flood due to the dam-break eroded the toe of the model slope causing the slope to collapse locally. We set up microphones to collect acoustic signals and installed accelerometers to collect vertical seismic signals generated by the flood and collapse events during the test. During the test we also used unmanned aerial vehicle (UAV) to continuously take photos for the collapsed areas for making the digital surface model (DSM) of the slope to analyze the volumes of the collapsed materials. We used Hilbert-Huang Transform (HHT) to obtain the time-frequency spectra for the acoustic signals and seismic signals. From the spectra, we compared the energy and frequency content of the two kinds of signals and their differences. The results show that the acoustic signal showing earlier indication of overtopping than that of the seismic signal. In addition, the acoustic and seismic signals generated during the flood can correspond to each other. The collapse events of the slope during the flood can be investigated also by examining the time-frequency spectrum of the seismic signal. Usually the signals of the collapse events can be distinguished from the flooding signals.

Keywords: dam break, landslide, slope, acoustic signal, seismic signal, flood

©2019. Japan Geoscience Union. All Right Reserved.

Evaluation of factors of safety and landslide risk for a watershed by Scoops3D

*Zheng-yi Feng[1], Chia-Ming Chuang[1], Hao-yang Huang[1]

1. Department of Soil and Water Conservation, National Chung Hsing University, Taichung, Taiwan

In this study, the Scoops3D code (USGS, 2015) is used to analyze the three-dimensional stability of the slopes in a watershed in Taiwan. To perform Scoops3D it requires the inputs such as digital elevation model (DEM), geological materials, groundwater level, earthquake, etc. The code calculates the minimum factor of safety (F.S.) and the associated potential failure volumes by using three-dimensional limit equilibrium method. We performed a comprehensive analysis of slope stability for the research areas using the Scoops3D code. The ArcMap software was used to present the F.S. that are less than unity as a 2D contoured map. We can observe this contoured map to understand the overall slope stability of the studied watershed. We perform a parametrical study by set three different sizes of sliding volume, “large”, “medium” and “small”, for evaluating the risk of landslide for the three different volume sizes.

Keywords: Landslide, Scoops3D, Factor of safety, Risk

©2019. Japan Geoscience Union. All Right Reserved.

Fuzzy Clustering Algorithms for Establishing Landslide Susceptibility Map

*Pei-hsun Tsai[1], Syuan-yi Wang[1], Jie-shin Cheng[1]

1. Chaoyang University of Technology

In recent years, the rainfall distribution is not uniform because of extreme weather events, the occurrence frequency of heavy rain increases. Coupled with steep terrain and complicated geological condition, so that the slope often occurred landslide when typhoon or heavy rain. Landslide susceptibility map delineates the potential zones for landslide occurrence. To develop the landslide model, we used several independent data layers that are recognized as effective factors in landslide occurrence, including slope, aspect, shear strength of rock or soil, dip and dip direction of stratum, and distance to road. All data layers were converted to raster layers with a 30 m ×30 m cell size. A total of 231336 cells were derived in study area. For assessing landslide susceptibility spatially, this study used fuzzy c-means clustering algorithm to classify the aforementioned data set in the study area into six clusters. Each cluster has similar natural environmental conditions and collapse situation. It is helpful to establish the monitoring management system and it can be applied to an early warning system in the landslide. Results of validation show that this model can accurately predict the occurrence of new landslides.

Keywords: Landslide susceptibility map, Fuzzy c-means , Clustering algorithm

©2019. Japan Geoscience Union. All Right Reserved.

A Study on Landslides and Debris Flows Susceptibility Mapping Using Unmanned Aerial Vehicles

*Sheng-Jia Liu[1]

1. qwepoi13@gmail.com

The geology of Taiwan is generally vulnerable due to the natural adverse conditions such as younger strata, steep topography, active orogeny, frequent seismic activity, weathering and erosion, frequent typhoons, high rainfall, etc. Furthermore, the human factors like immature law and regulations, the weak execution, and improper land use and development also play an important role in reducing the slope stability. These factors to some degree worsen the slope conditions, lead to a more frequent natural disaster and cause the loss of life and property.

In order to effectively evaluate the landslide susceptibility and map the high risk areas, the Soil and Water Conservation Bureau of Taiwan Executive Yuan (SWCB) provides an assessment method for assessing the risk level of landslide susceptibility by selecting the combinations of impact factors that may trigger landslides. However, the accuracy and efficiency of data acquisitions, in a conventional way, for the assessment method are still limited.
With the advantages of UAVs, the digital image with high resolutions for a wider area without terrain restrictions can be obtained efficiently. Its applications have become more widespread, from battlefield detections and communications to forest management and mapping. This study utilizes the latest Dynamic Post-Processing Motion (PPK) positioning system to capture high-resolution image data from a chosen site in the northern part of Taiwan. The terrain information was extracted from aerial images using Pix4Dmapper with aerial triangulation techniques, thus the external direction of each image and the camera's internal direction parameters can be obtained, the point cloud data can be matched automatically, and a digital surface mode can be established. Further, a three-dimensional model with topographic map and landslide susceptibility evaluations can be established and performed by comparing with historical data and monitoring the slope conditions. A modified assessment method is proposed using the three factors (slope, the volume of soil and rock accumulations, and rainfall) to assess the landslide susceptibility of the study area. The evaluations made by the proposed method are in agreement with the SWCB method. The results from this study can be used in slope management and precaution, and rescue and recovery.

Keywords: UAVs, landslides, debris flows, susceptibility evaluation

©2019. Japan Geoscience Union. All Right Reserved.

Largescale landslide induced by AD1586 Tensho-Earthquake in Gifu Prefecture, central Japan

*Takahiro Kurimoto[1], Yoshihiko Kariya[2], Kuniyasu Mokudai[3], Ryuji Yamada[4], Takashi Kimura[4]

1. Undergraduate Senshu University, 2. Department of Geography, Senshu University, 3. Japan Geoservice Incorporated, 4. National Research Institute for Earth Science and Disaster Resilience

On the basis of field investigation and topographic analysis by using GIS, we clarified the geological and geomorphological features of a large-scale landslide (V=2.2×10^7 m^3) called Mizore Landslide (ML) in Gujo City of Gifu Prefecture, central Japan. According to old documents, it is thought to ML was caused by AD1586 Tensho earthquake (generated from the Shokawa fault zone close to the ML and estimated M=7 to 8). However, there are few studies on geomorphological and geological basis. The main results are as follows: a) The ML holds a set of three head scarps and three landslide bodies both showing multiple activities of slope movement; b) The ML shows unique sedimentological and geomorphological characteristics such as a jigsaw crack structure in landslide deposits and hummocks and depressions upon the ground surface of the landslide bodies; c) Both involved buried soils in the landslide deposits and fossil wood logs in the dammed lake deposits enable us to date the landslide events; d) According to those ^{14}C dates of soils and logs, the latest landslide event is thought to occur in the period from cal AD1436 to 1650; e) The latest landslide event would be triggered by AD1586 Tensho earthquake. AD1596 Keicho-Fushimi earthquake occurred around Kyoto is a candidate event for further consideration.

Keywords: AD1586 Tensho-earthquake, Large-scale landslide, Shokawa fault zone, Dammed lake

©2019. Japan Geoscience Union. All Right Reserved.

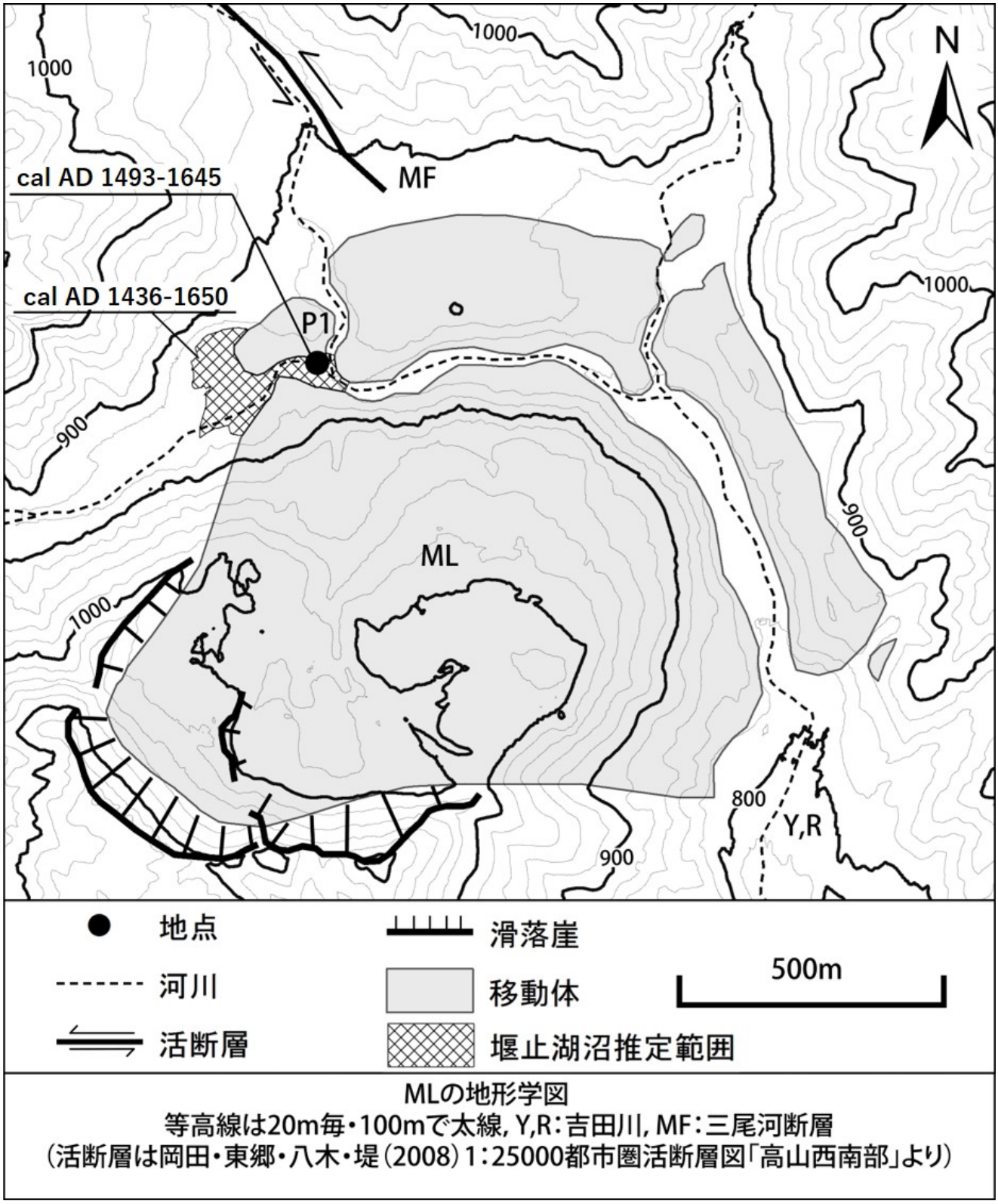

MLの地形学図
等高線は20m毎・100mで太線, Y,R:吉田川, MF:三尾河断層
(活断層は岡田・東郷・八木・堤(2008)1:25000都市圏活断層図「高山西南部」より)

©2019. Japan Geoscience Union. All Right Reserved.

Failure Probability of Lushan Landslide, Taiwan

*Wei-Ting Lin[1], Kuang-Tsung Chang[1]

1. National Chung Hsing University

The Lushan landslide located in the middle of Taiwan, has slid and damaged the road due to typhoons or heavy rainfalls for recent decades. It’ s seriously affecting the safety of life and property of the Lushan Hot Spring Tourist Area and local residents in the lower slope. In order to understand the probability of failure (Pf) of Lushan landslide, we built a numerical model by Plaxis2D, which is validated by the monitoring data of the 2009 typhoon Morakot. However, due to the lack of complete parameter data, uncertainties exist and may affect the simulation result of the collapse. With the back calculated friction angle (∅) and cohesion (c) from Plaxis2D, we used the Monte Carlo Simulation (MCS) to consider the friction angle and the cohesion of sliding body as random variables with uncertainty. The results are statistically analyzed to obtain the Probability Density Function (PDF) of the two parameters. Based on the parameter settings above, with the designed rainfall events at 24hr, 48hr and 72hr rainfall duration and 10, 25, 50, 100 and 200 years of recurrence interval, we calculate the factor of safety (SF) of the Lushan landslide in these 18 simulated rainfall events. Finally, we can obtain the distribution of factor of safety (SF) and probability of failure (Pf) of the Lushan landslide in different rainfall durations and recurrence intervals.

Keywords: probability of failure, Monte Carlo Simulation, uncertainty

©2019. Japan Geoscience Union. All Right Reserved.

Interpretation of landslide surface deformation in Kali Gandaki River watershed, Nepal using ALOS-2/PALSAR-2 InSAR image

*Hiroshi, P. Sato[1]

1. College of Humanities and Sciences, Nihon University

Previous studies have revealed and mapped glacial landform, fluvial terraces, and landslide landform in Thakkohla-Muktinath region, between Kagbeni and Ghasa along Kali Gandaki River, Nepal. And many attentions were paid to detect landslides that brock channels in the region, especially after Gorkha earthquake (25 Apr 2015; Mw7.8). Therefore, I tried to interpret landslide surface deformation on mountain slopes in Kali Gandaki River watershed after the earthquake, using Synthetic Aperture Radar interferometry (InSAR) image. The number of produced InSAR images was six, which is master image/slave image in order from ALOS-2/PALSAR-2 data, 08Oct2015/17Dec2015, 08Oct2015/30Nov2017, 25Feb2016/06Oct2016, 30Nov2017/24Jan2019, 08Mar2018/24Jan2019 and 31May2018/24Jan2019. In these InSAR images clear precursory landslide surface deformation was not interpreted on mountain slopes facing main stream of Kali Gandaki River. However, whose tributary watershed; i.e., Myagdi River watershed gave some landslide surface deformations (e.g., in 83.3983E, 28.4842N) clearly interpreted in the InSAR image of 08Oct2015/17Dec2015, which was relatively better coherence than the rest five images.

Keywords: SAR, earthquake, landslide, interpretation

©2019. Japan Geoscience Union. All Right Reserved.

A depth-integrated model for granular flows on the transition of different bed conditions

*Ling-Yi Hsu[1], Chi-Yao Hung[1]

1. National Chung Hsing University

The different basal boundary conditions profoundly affected the flow behavior of debris flow. However, it is hard to have a general and straightforward model to describe the flow profile switching from different bed conditions. In this study, we purpose a new depth-averaged model to simulate the dense granular flow transition between the rigid and mobile bed. The model is based on mass conservation, momentum conservation, and kinetic energy conservation. We apply the linearized mu(I) rheology to describe granular deformation and assume Coulomb friction along the sidewalls. By incorporating the basal shear rate term into the equations, the theory can balance the extra force from rigid bed friction force. To check the model approach, we conducted an equilibrium and non-equilibrium heap flow experiments using the narrow see-saw channel, which can be tilted to different angles between runs or during flows. To compare the experimental results with the theory, the flow fields are monitored using high-speed video and particle-tracking velocimetry.

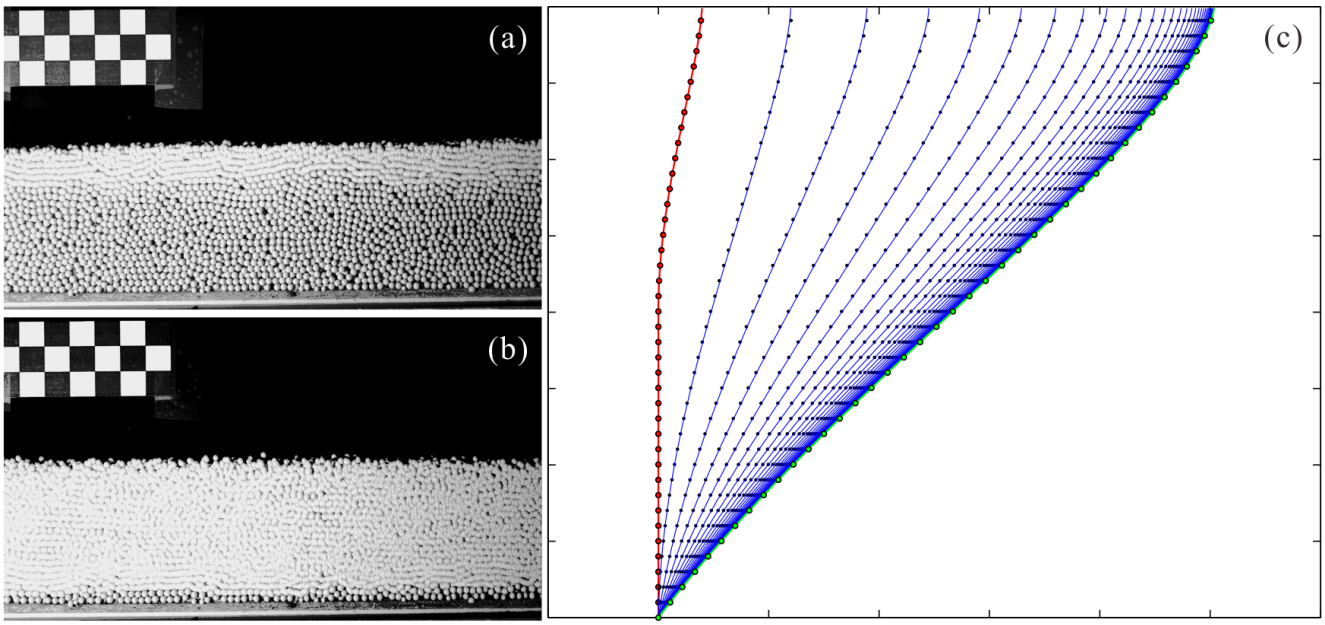

Fig.1 Experimental longexpousre image (a) over deposition bed; (b) over rigid bed; and (c) the transition velocity profile of theory prediction.

©2019. Japan Geoscience Union. All Right Reserved.

A viscous granular flow experiment with new refractive index matching material

*Tsai-Jung Lin[1], Chi-Yao Hung[1]

1. National Chung Hsing University

Entrainment rate at base controls how far the debris flow can travel and how large the debris flow becomes. Flow rheology of Refractive Index Matching (RIM) material are generally limited by the mono-particle properties (such as polymethyl methacrylate/liquid para-cymene etc.). In this study, a new RIM material (polyacrylamide polymer/18% Methanol solution) having a wide range of particle size distribution and viscosity (Fig. 1L) are purposed to visualize and measure the erosion process of mobile bed dam break experiments. Various rheology models may be formed by the different ratio of particle size. To improve the contrast between the particle phase and the liquid phase, a dye is used to make the particles bright under laser illumination. By varying the dye concentration, the entraining/detraining processes are easily distinguished (Fig. 1R). Granular motion is captured through a high-speed camera and Particle Tracking Velocimetry (PTV) method. Finally, an empirical relationship between the rheology and the entraining/ detraining process is developed.

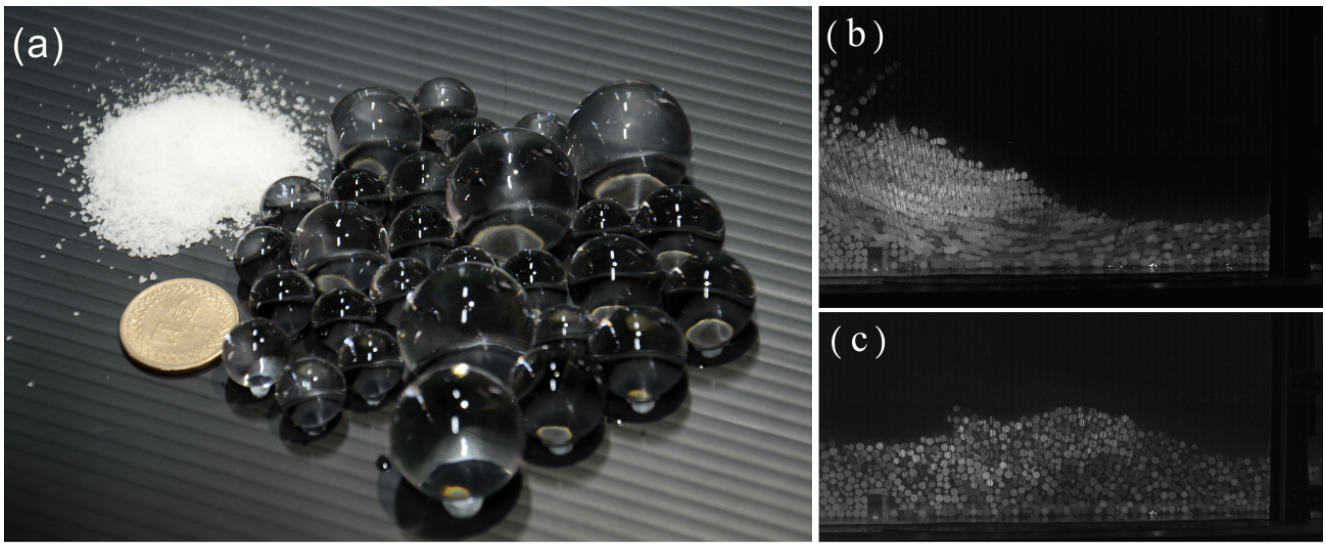

Fig.1 Experimental image (a)wide range of particle size; (b)longexposure image of dam break occurrence; (c)particles with different concentration of dye.

©2019. Japan Geoscience Union. All Right Reserved.

Sandbox experiments of submarine landslide caused by water film in low permeability layer

*Shogo Kawakita[1], Daisuke Asahina[2], Keiji Kitajima[3], Mitsukazu Nakanishi[3]

1. Graduate School of Science & Technology, Nihon Univ., 2. National Institute of Advanced Industrial Science and Technology, 3. College of Science & Technology, Nihon Univ.

Submarine landslides can be serious geohazards since they potentially cause tsunamis and damage seafloor infrastructure. Submarine landslides can be larger in scale than landslides on land. Direct measurements/observations of submarine landslides at deep seafloor still remain a challenging task. Kokusho et al. (2000) proposed a water film effect and its mechanism on lateral flow with less frictional resistance to explain a driving force of large-scale submarine landslides

In this study, we conducted laboratory experiments to understand the relationship between sand liquefaction and lateral flow by water film, and investigate the influence of water film formation on lateral flow of upper layer. In general, it is difficult to observe the formations of liquefaction and lateral flow at the same time. This is because sand particles of sloping layer model start to move when vibration is applied, and inclination disappears before liquefaction. To solve this problem, we devised a mechanism to prevent the flow of the lower layer by providing a weir plate in inside the soil tank. This mechanism enables to distinguish and observe the movement of sand by the liquefaction and the lateral flow by the water film.

The results obtained in this study clearly show three stages: first, the lower layer was liquefied; then pore water was stored below the low permeability layer; and finally, the lateral flow was occurred by the water film effect. The experimental results show that there was no clear correlation between the increase in the angle of sloping layer and the travel distance or the maximum flow velocity. We also discuss the relationship between the layer angle and the location of sand boil. The location where sand soiling occurred moved to the upper side of the slope as the layer angle become larger.

[Reference]

Kokusho, T.: Mechanism for water film generation and lateral flow in liquefied sand layer, Soils and Foundations, Vol.40, No.5, p 99-111, 2000.

Keywords: Submarine Landslides, Pore Water Pressure, Water Film, Lateral Flow

©2019. Japan Geoscience Union. All Right Reserved.

Study on Creep Properties of Sand and Cemented Sand

*JIN-YI YU[1], KUANG-TSUNG CHANG[1]

1. National Chung Hsing University

In this study, we investigated the effects of creep on sand and cemented sand, using triaxial test. Sand represents a non-cohesive material, while cemented sand represents a brittle material. Before the failure of specimens, the deviator stress was fixed and the cyclic mean stress was applied to study the influence of creep on the materials. According to the test results, the axial strain accumulation of sand caused by creep is less, and the peak strength is larger than that of the monotonic loading when the axial loading is resumed. For cemented sand, creep causes microcracks inside the specimens, gradually forming a failure surface. When the axial strain accumulation is large enough, the reapplication of the axial loading shows a reduction of peak strength. We conclude that the influence of creep on non-cohesive material (sand) is limited, whereas creep can reduce the strength of the brittle material (cemented sand) and even cause failure.

Keywords: creep, triaxial test, sand, cemented sand, strength, failure

©2019. Japan Geoscience Union. All Right Reserved.

The effects of seepage force and the Poisson’s ratio on slope stability

*Hirokazu Fukui[1], Tomomi Terajima[2]

1. Graduate school of Science, Kyoto University, 2. Disaster Prevention Research Institute, Kyoto University

To predict accurately the timing of shallow landslide occurrence, we need to consider the direction and magnitude of seepage force and earth pressure. A model sandy slope (L: 9m, W:1m, H:4m) was used to measure the hydraulic gradient and seepage force with the tensiometers under the artificial rainfall of 80mm/h. We incorporated not only the seepage force but also the Poisson’s ratio into conventional slope stability analysis by the limit equilibrium method. As a result, the calculated timing of shallow landslide occurrence was almost agree with the timing of that in the experiment and also more accurate than the timing calculated by the Spenser method which took into account the magnitude and moment equilibrium of the force. These results imply that, based on both monitoring at fields and conducting more experiments by a real-size model slope, we need to verify the effects of seepage force and earth pressure as the important factors causing rainfall-induced slope instability.

Keywords: process-based model, Seepage force, the Poisson's ratio, Shallow landslide, Sandy model slope

©2019. Japan Geoscience Union. All Right Reserved.

Study on the factors of seepage erosion

*Szu-Wei Fu[1], Kuang-Tsung Chang[1]

1. National Chung Hsing University

The causes of many slope disasters are often related to the seepage behaviors of soil. For instance, groundwater seepage may cause internal erosion of the soil. The soil particles are taken away by seepage water to form void or pipe. In addition , the earth pressure leads to the collapse of the overlying soil.

In this study, we designed a set of apparatus that can add confining pressure to the outside of the specimen. In order to simulate the situation of sand in slopes, we investigated the critical seepage velocity of sands caused by seepage erosion failure under different confining pressure, with different particle size distributions, sizes of outflow, etc. Then a failure criterion for seepage erosion is developed based on the drag equation in fluid dynamics and confirm with experimental data.

The results show that the critical seepage velocity at failure is affected by the particle size distributions, sizes of outflow and the confining pressure. The theoretical results are compared well to the experimental data.

Keywords: seepage erosion, Drag equation

©2019. Japan Geoscience Union. All Right Reserved.

Deformation of slope models with different orientations of weak planes

*taeyuan tseng[1], Kuang-Tsung Chang[1]

1. National Chung Hsing University

Weak planes influence failure and deformation of slopes. We conducted experiments to simulate slopes of different orientations of weak planes, including cataclinal and analcinal slopes with 30˚ and 60˚ inclination angles of weak planes. We stacked artificial bricks to make small-sized slope models. The artificial bricks were made of gypsum, sand, cement and water with different weight proportion. In view of the scaling law, the artificial bricks were made less strength than natural rocks. The slope models were weakened under rainfall, resulting in deformation and final collapse. The slope deformation processes were photographed by a camera, and the displacement vector fields were analyzed using the Particle Image Velocimetry (PIV). The deformation and accumulated displacements were compared between slopes of different orientations of weak planes.

Keywords: cataclinal slope, analcinal slopes, rainfall, Particle Image Velocimetry (PIV), weak planes, deformation

©2019. Japan Geoscience Union. All Right Reserved.

[E] Poster | H (Human Geosciences)：H-DS Disaster geosciences

Tue. May 28, 2019 5:15 PM - 6:30 PM JST | Tue. May 28, 2019 8:15 AM - 9:30 AM UTC | Poster Hall International Exhibition Hall8, Makuhari Messe_20

[H-DS09] Landslides and related phenomena

convener:Masahiro Chigira(Disaster Prevention Research Institute, Kyoto University), Gonghui Wang(Disaster Prevention Research Institute, Kyoto University), Fumitoshi Imaizumi(Faculty of Agriculture, Shizuoka University)

Mass movements, such as landslides, rockfalls, and debris flows, have been occurring extensively in a large number of countries, causing heavy damage. In order to understand them and mitigate induced disasters, we invite contributions that report and discuss on mass movements and related phenomena, focusing on improved understanding of their characteristics; new insights into landslide mechanisms; the development of new approaches to monitoring; novel approaches to behavior forecasting and prediction; studies of successful landslide management; and the development of methods for hazard and risk evaluation. In particular, papers about recent landslide hazards, induced by 2017 northern Kyushu rainstorm, 2018 Osaka earthquake, 2018 western Japan rainstorm, and 2018 Hokkaido earthquake are welcome.

[HDS09-P01] **Fluidized landslides triggered by the liquefaction of subsurface volcanic deposits during the 2018 Iburi–Tobu earthquake, Hokkaido**

*Jun Kameda[1], Hiro Kamiya[2], Hirokazu Masumoto[1], Tomonori Morisaki[1], Toru Hiratsuka[2], Chisaki Inaoi (1.Department of Natural History Sciences, Graduate School of Science, Hokkaido University, 2.Department of Earth and Planetary Sciences, School of Science, Hokkaido University)

[HDS09-P02] A comparison between the acoustic signals and seismic signals generated during a dam-break test

★Invited Papers

*Zheng-yi Feng[1], Hao-yang Huang[1], Chia-Ming Chuang[1] (1.Department of Soil and Water Conservation, National Chung Hsing University, Taichung, Taiwan)

[HDS09-P03] Evaluation of factors of safety and landslide risk for a watershed by Scoops3D

*Zheng-yi Feng[1], Chia-Ming Chuang[1], Hao-yang Huang[1] (1.Department of Soil and Water Conservation, National Chung Hsing University, Taichung, Taiwan)

[HDS09-P04] **Fuzzy Clustering Algorithms for Establishing Landslide Susceptibility Map**

*Pei-hsun Tsai[1], Syuan-yi Wang[1], Jie-shin Cheng[1] (1.Chaoyang University of Technology)

[HDS09-P05] **A Study on Landslides and Debris Flows Susceptibility Mapping Using Unmanned Aerial Vehicles**

*Sheng-Jia Liu[1] (1.qwepoi13@gmail.com)

[HDS09-P06] Largescale landslide induced by AD1586 Tensho-Earthquake in Gifu Prefecture, central Japan

*Takahiro Kurimoto[1], Yoshihiko Kariya[2], Kuniyasu Mokudai[3], Ryuji Yamada[4], Takashi Kimura[4] (1.Undergraduate Senshu University, 2.Department of Geography, Senshu University, 3.Japan Geoservice Incorporated, 4.National Research Institute for Earth Science and Disaster Resilience)

[HDS09-P07] Failure Probability of Lushan Landslide, Taiwan

*Wei-Ting Lin[1], Kuang-Tsung Chang[1] (1.National Chung Hsing University)

[HDS09-P08] Interpretation of landslide surface deformation in Kali Gandaki River watershed, Nepal using ALOS-2/PALSAR-2 InSAR image

*Hiroshi, P. Sato[1] (1.College of Humanities and Sciences, Nihon University)

[HDS09-P09] A depth-integrated model for granular flows on the transition of different bed conditions

*Ling-Yi Hsu[1], Chi-Yao Hung[1] (1.National Chung Hsing University)

[HDS09-P10] A viscous granular flow experiment with new refractive index matching material

*Tsai-Jung Lin[1], Chi-Yao Hung[1] (1.National Chung Hsing University)

[HDS09-P11] Sandbox experiments of submarine landslide caused by water film in low permeability layer

*Shogo Kawakita[1], Daisuke Asahina[2], Keiji Kitajima[3], Mitsukazu Nakanishi[3] (1.Graduate School of Science & Technology, Nihon Univ., 2.National Institute of Advanced Industrial Science and Technology, 3.College of Science & Technology, Nihon Univ.)

[HDS09-P12] **Study on Creep Properties of Sand and Cemented Sand**

*JIN-YI YU[1], KUANG-TSUNG CHANG[1] (1.National Chung Hsing University)

[HDS09-P13] The effects of seepage force and the Poisson's ratio on slope stability

*Hirokazu Fukui[1], Tomomi Terajima[2] (1.Graduate school of Science, Kyoto University, 2.Disaster Prevention Research Institute, Kyoto University)

[HDS09-P14] Study on the factors of seepage erosion

*Szu-Wei Fu[1], Kuang-Tsung Chang[1] (1.National Chung Hsing University)

[HDS09-P15] Deformation of slope models with different orientations of weak planes

*taeyuan tseng[1], Kuang-Tsung Chang[1] (1.National Chung Hsing University)

Fluidized landslides triggered by the liquefaction of subsurface volcanic deposits during the 2018 Iburi–Tobu earthquake, Hokkaido

*Jun Kameda[1], Hiro Kamiya[2], Hirokazu Masumoto[1], Tomonori Morisaki[1], Toru Hiratsuka[2], Chisaki Inaoi

1. Department of Natural History Sciences, Graduate School of Science, Hokkaido University, 2. Department of Earth and Planetary Sciences, School of Science, Hokkaido University

The Iburi–Tobu earthquake of M_w = 6.7 occurred at 3:07 AM (local time) on 6 September 2018, in southern Hokkaido, Japan. The earthquake caused power cuts and destroyed distribution networks across Hokkaido, creating widespread disruption. A total of 41 people were killed during the earthquake, with most of these (36 people) perishing in landslides near the epicenter. The hills in southwestern Hokkaido are widely covered by volcanic deposits, derived from the repeated eruptions of nearby volcanoes such as Tarumai, Eniwa, and Shikotsu (e.g., Nakagawa et al., 2018). On 4 September, Typhoon Jebi caused heavy rainfall in this area, which likely soaked and weakened the volcanic soils. Subsequent earthquake ground motion (with a maximum intensity of 7 on the intensity scale of Japan Meteorology Agency; Japan Meteorology Agency, 2018) may have triggered sudden whole-slope failures. The total number of the present landslides was ~6000 (Yamagishi and Yamazaki, 2018), and most of the recorded landslides are shallow and show features characteristic of fluidized landslides, such as long runouts of debris on a flat depositional area.
To investigate the mechanism generating the landslides triggered by the Iburi–Tobu earthquake, we conducted a field survey at a typical landslide in the Tomisato area of Atsuma, and we found a distinctive occurrence of liquefaction in the field, which could be a precursive condition for the generation of the fluidized landslides triggered by the earthquake. In the scarp of the landslide, an altered halloysite-bearing volcanic layer is observed at a level almost coincident with the sliding surface. The layer is intensely undulating and can be divided into an upper clay-rich layer and a lower pumice-rich layer, suggesting that the altered layer had liquefied as a result of the strong coseismic ground motion. The layer had been soaked by heavy rainfall just one day before the earthquake and could have liquefied by interstitial fluid pressurization, producing a weak and slippery plane, resulting in the catastrophic landslides in this area.

Keywords: fluidized landslide, 2018 Iburi–Tobu earthquake, halloysite

©2019. Japan Geoscience Union. All Right Reserved.

A comparison between the acoustic signals and seismic signals generated during a dam-break test

*Zheng-yi Feng[1], Hao-yang Huang[1], Chia-Ming Chuang[1]

1. Department of Soil and Water Conservation, National Chung Hsing University, Taichung, Taiwan

Natural events, such as landslide, sediment transport, flooding, etc., usually release energy to produce acoustic waves and seismic waves. Acoustic wave is transmitted through air and seismic wave is transmitted through geologic structure. Therefore, the characteristics of acoustic waves and the seismic waves induced by these events should be different. This study focus on the differences in the acoustic signals and seismic signals during a dam-break test performed by the authors. We built a model dam and slope in a creek for the test. We filled the dam with water and caused it to overflow. The overflow water caused the downward erosion of the dam. The flood due to the dam-break eroded the toe of the model slope causing the slope to collapse locally. We set up microphones to collect acoustic signals and installed accelerometers to collect vertical seismic signals generated by the flood and collapse events during the test. During the test we also used unmanned aerial vehicle (UAV) to continuously take photos for the collapsed areas for making the digital surface model (DSM) of the slope to analyze the volumes of the collapsed materials. We used Hilbert-Huang Transform (HHT) to obtain the time-frequency spectra for the acoustic signals and seismic signals. From the spectra, we compared the energy and frequency content of the two kinds of signals and their differences. The results show that the acoustic signal showing earlier indication of overtopping than that of the seismic signal. In addition, the acoustic and seismic signals generated during the flood can correspond to each other. The collapse events of the slope during the flood can be investigated also by examining the time-frequency spectrum of the seismic signal. Usually the signals of the collapse events can be distinguished from the flooding signals.

Keywords: dam break, landslide, slope, acoustic signal, seismic signal, flood

©2019. Japan Geoscience Union. All Right Reserved.

Evaluation of factors of safety and landslide risk for a watershed by Scoops3D

*Zheng-yi Feng[1], Chia-Ming Chuang[1], Hao-yang Huang[1]

1. Department of Soil and Water Conservation, National Chung Hsing University, Taichung, Taiwan

In this study, the Scoops3D code (USGS, 2015) is used to analyze the three-dimensional stability of the slopes in a watershed in Taiwan. To perform Scoops3D it requires the inputs such as digital elevation model (DEM), geological materials, groundwater level, earthquake, etc. The code calculates the minimum factor of safety (F.S.) and the associated potential failure volumes by using three-dimensional limit equilibrium method. We performed a comprehensive analysis of slope stability for the research areas using the Scoops3D code. The ArcMap software was used to present the F.S. that are less than unity as a 2D contoured map. We can observe this contoured map to understand the overall slope stability of the studied watershed. We perform a parametrical study by set three different sizes of sliding volume, “large”, “medium” and “small”, for evaluating the risk of landslide for the three different volume sizes.

Keywords: Landslide, Scoops3D, Factor of safety, Risk

©2019. Japan Geoscience Union. All Right Reserved.

Fuzzy Clustering Algorithms for Establishing Landslide Susceptibility Map

*Pei-hsun Tsai[1], Syuan-yi Wang[1], Jie-shin Cheng[1]

1. Chaoyang University of Technology

In recent years, the rainfall distribution is not uniform because of extreme weather events, the occurrence frequency of heavy rain increases. Coupled with steep terrain and complicated geological condition, so that the slope often occurred landslide when typhoon or heavy rain. Landslide susceptibility map delineates the potential zones for landslide occurrence. To develop the landslide model, we used several independent data layers that are recognized as effective factors in landslide occurrence, including slope, aspect, shear strength of rock or soil, dip and dip direction of stratum, and distance to road. All data layers were converted to raster layers with a 30 m ×30 m cell size. A total of 231336 cells were derived in study area. For assessing landslide susceptibility spatially, this study used fuzzy c-means clustering algorithm to classify the aforementioned data set in the study area into six clusters. Each cluster has similar natural environmental conditions and collapse situation. It is helpful to establish the monitoring management system and it can be applied to an early warning system in the landslide. Results of validation show that this model can accurately predict the occurrence of new landslides.

Keywords: Landslide susceptibility map, Fuzzy c-means , Clustering algorithm

©2019. Japan Geoscience Union. All Right Reserved.

A Study on Landslides and Debris Flows Susceptibility Mapping Using Unmanned Aerial Vehicles

*Sheng-Jia Liu[1]

1. qwepoi13@gmail.com

The geology of Taiwan is generally vulnerable due to the natural adverse conditions such as younger strata, steep topography, active orogeny, frequent seismic activity, weathering and erosion, frequent typhoons, high rainfall, etc. Furthermore, the human factors like immature law and regulations, the weak execution, and improper land use and development also play an important role in reducing the slope stability. These factors to some degree worsen the slope conditions, lead to a more frequent natural disaster and cause the loss of life and property.

In order to effectively evaluate the landslide susceptibility and map the high risk areas, the Soil and Water Conservation Bureau of Taiwan Executive Yuan (SWCB) provides an assessment method for assessing the risk level of landslide susceptibility by selecting the combinations of impact factors that may trigger landslides. However, the accuracy and efficiency of data acquisitions, in a conventional way, for the assessment method are still limited.
With the advantages of UAVs, the digital image with high resolutions for a wider area without terrain restrictions can be obtained efficiently. Its applications have become more widespread, from battlefield detections and communications to forest management and mapping. This study utilizes the latest Dynamic Post-Processing Motion (PPK) positioning system to capture high-resolution image data from a chosen site in the northern part of Taiwan. The terrain information was extracted from aerial images using Pix4Dmapper with aerial triangulation techniques, thus the external direction of each image and the camera's internal direction parameters can be obtained, the point cloud data can be matched automatically, and a digital surface mode can be established. Further, a three-dimensional model with topographic map and landslide susceptibility evaluations can be established and performed by comparing with historical data and monitoring the slope conditions. A modified assessment method is proposed using the three factors (slope, the volume of soil and rock accumulations, and rainfall) to assess the landslide susceptibility of the study area. The evaluations made by the proposed method are in agreement with the SWCB method. The results from this study can be used in slope management and precaution, and rescue and recovery.

Keywords: UAVs, landslides, debris flows, susceptibility evaluation

©2019. Japan Geoscience Union. All Right Reserved.

Largescale landslide induced by AD1586 Tensho-Earthquake in Gifu Prefecture, central Japan

*Takahiro Kurimoto[1], Yoshihiko Kariya[2], Kuniyasu Mokudai[3], Ryuji Yamada[4], Takashi Kimura[4]

1. Undergraduate Senshu University, 2. Department of Geography, Senshu University, 3. Japan Geoservice Incorporated, 4. National Research Institute for Earth Science and Disaster Resilience

On the basis of field investigation and topographic analysis by using GIS, we clarified the geological and geomorphological features of a large-scale landslide (V=2.2×10^7 m^3) called Mizore Landslide (ML) in Gujo City of Gifu Prefecture, central Japan. According to old documents, it is thought to ML was caused by AD1586 Tensho earthquake (generated from the Shokawa fault zone close to the ML and estimated M=7 to 8). However, there are few studies on geomorphological and geological basis. The main results are as follows: a) The ML holds a set of three head scarps and three landslide bodies both showing multiple activities of slope movement; b) The ML shows unique sedimentological and geomorphological characteristics such as a jigsaw crack structure in landslide deposits and hummocks and depressions upon the ground surface of the landslide bodies; c) Both involved buried soils in the landslide deposits and fossil wood logs in the dammed lake deposits enable us to date the landslide events; d) According to those ^{14}C dates of soils and logs, the latest landslide event is thought to occur in the period from cal AD1436 to 1650; e) The latest landslide event would be triggered by AD1586 Tensho earthquake. AD1596 Keicho-Fushimi earthquake occurred around Kyoto is a candidate event for further consideration.

Keywords: AD1586 Tensho-earthquake, Large-scale landslide, Shokawa fault zone, Dammed lake

©2019. Japan Geoscience Union. All Right Reserved.

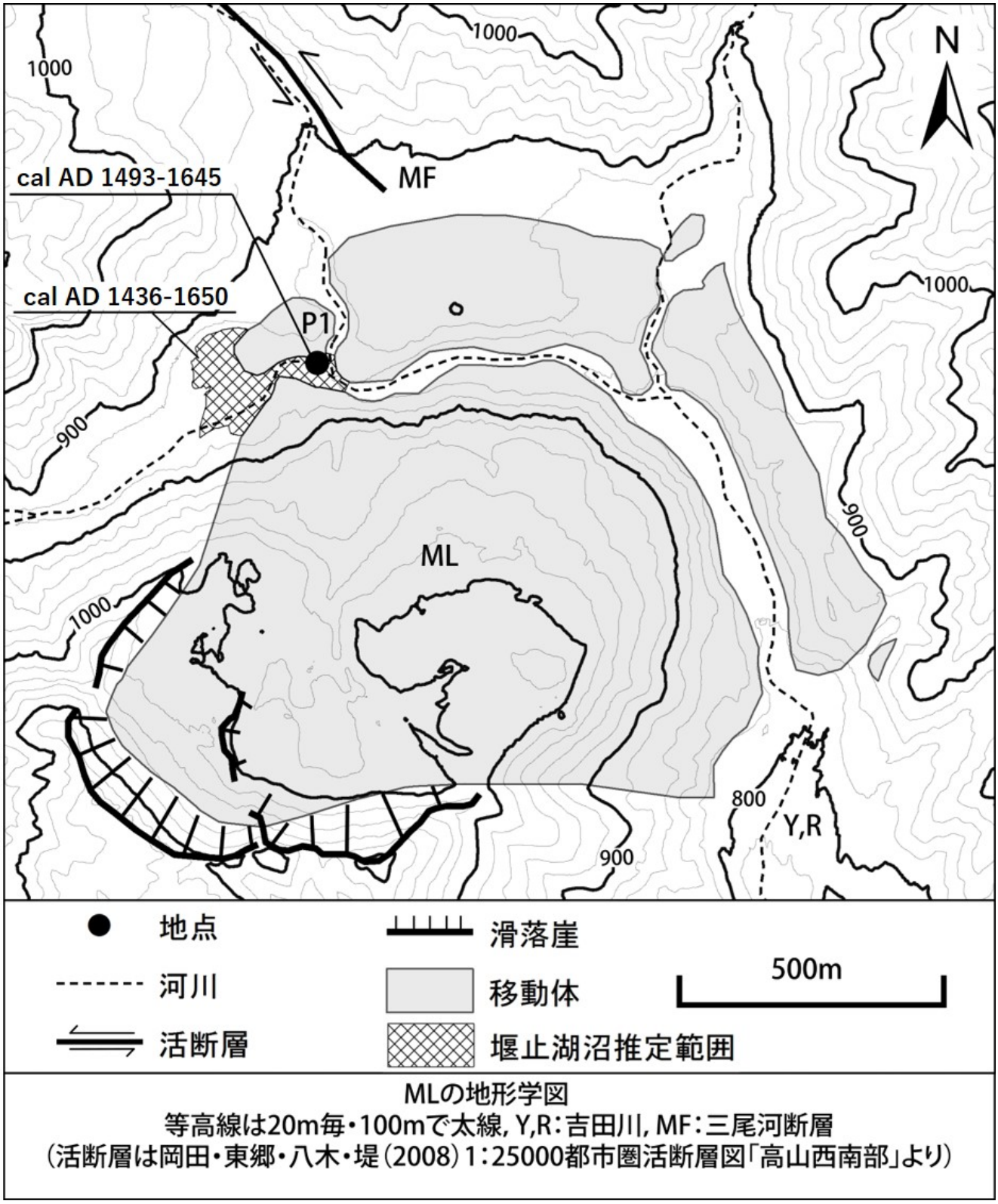

MLの地形学図
等高線は20m毎・100mで太線, Y,R:吉田川, MF:三尾河断層
(活断層は岡田・東郷・八木・堤(2008)1:25000都市圏活断層図「高山西南部」より)

©2019. Japan Geoscience Union. All Right Reserved.

Failure Probability of Lushan Landslide, Taiwan

*Wei-Ting Lin[1], Kuang-Tsung Chang[1]

1. National Chung Hsing University

The Lushan landslide located in the middle of Taiwan, has slid and damaged the road due to typhoons or heavy rainfalls for recent decades. It’ s seriously affecting the safety of life and property of the Lushan Hot Spring Tourist Area and local residents in the lower slope. In order to understand the probability of failure (Pf) of Lushan landslide, we built a numerical model by Plaxis2D, which is validated by the monitoring data of the 2009 typhoon Morakot. However, due to the lack of complete parameter data, uncertainties exist and may affect the simulation result of the collapse. With the back calculated friction angle (∅) and cohesion (c) from Plaxis2D, we used the Monte Carlo Simulation (MCS) to consider the friction angle and the cohesion of sliding body as random variables with uncertainty. The results are statistically analyzed to obtain the Probability Density Function (PDF) of the two parameters. Based on the parameter settings above, with the designed rainfall events at 24hr, 48hr and 72hr rainfall duration and 10, 25, 50, 100 and 200 years of recurrence interval, we calculate the factor of safety (SF) of the Lushan landslide in these 18 simulated rainfall events. Finally, we can obtain the distribution of factor of safety (SF) and probability of failure (Pf) of the Lushan landslide in different rainfall durations and recurrence intervals.

Keywords: probability of failure, Monte Carlo Simulation, uncertainty

©2019. Japan Geoscience Union. All Right Reserved.

Interpretation of landslide surface deformation in Kali Gandaki River watershed, Nepal using ALOS-2/PALSAR-2 InSAR image

*Hiroshi, P. Sato[1]

1. College of Humanities and Sciences, Nihon University

Previous studies have revealed and mapped glacial landform, fluvial terraces, and landslide landform in Thakkohla-Muktinath region, between Kagbeni and Ghasa along Kali Gandaki River, Nepal. And many attentions were paid to detect landslides that brock channels in the region, especially after Gorkha earthquake (25 Apr 2015; Mw7.8). Therefore, I tried to interpret landslide surface deformation on mountain slopes in Kali Gandaki River watershed after the earthquake, using Synthetic Aperture Radar interferometry (InSAR) image. The number of produced InSAR images was six, which is master image/slave image in order from ALOS-2/PALSAR-2 data, 08Oct2015/17Dec2015, 08Oct2015/30Nov2017, 25Feb2016/06Oct2016, 30Nov2017/24Jan2019, 08Mar2018/24Jan2019 and 31May2018/24Jan2019. In these InSAR images clear precursory landslide surface deformation was not interpreted on mountain slopes facing main stream of Kali Gandaki River. However, whose tributary watershed; i.e., Myagdi River watershed gave some landslide surface deformations (e.g., in 83.3983E, 28.4842N) clearly interpreted in the InSAR image of 08Oct2015/17Dec2015, which was relatively better coherence than the rest five images.

Keywords: SAR, earthquake, landslide, interpretation

©2019. Japan Geoscience Union. All Right Reserved.

A depth-integrated model for granular flows on the transition of different bed conditions

*Ling-Yi Hsu[1], Chi-Yao Hung[1]

1. National Chung Hsing University

The different basal boundary conditions profoundly affected the flow behavior of debris flow. However, it is hard to have a general and straightforward model to describe the flow profile switching from different bed conditions. In this study, we purpose a new depth-averaged model to simulate the dense granular flow transition between the rigid and mobile bed. The model is based on mass conservation, momentum conservation, and kinetic energy conservation. We apply the linearized mu(I) rheology to describe granular deformation and assume Coulomb friction along the sidewalls. By incorporating the basal shear rate term into the equations, the theory can balance the extra force from rigid bed friction force. To check the model approach, we conducted an equilibrium and non-equilibrium heap flow experiments using the narrow see-saw channel, which can be tilted to different angles between runs or during flows. To compare the experimental results with the theory, the flow fields are monitored using high-speed video and particle-tracking velocimetry.

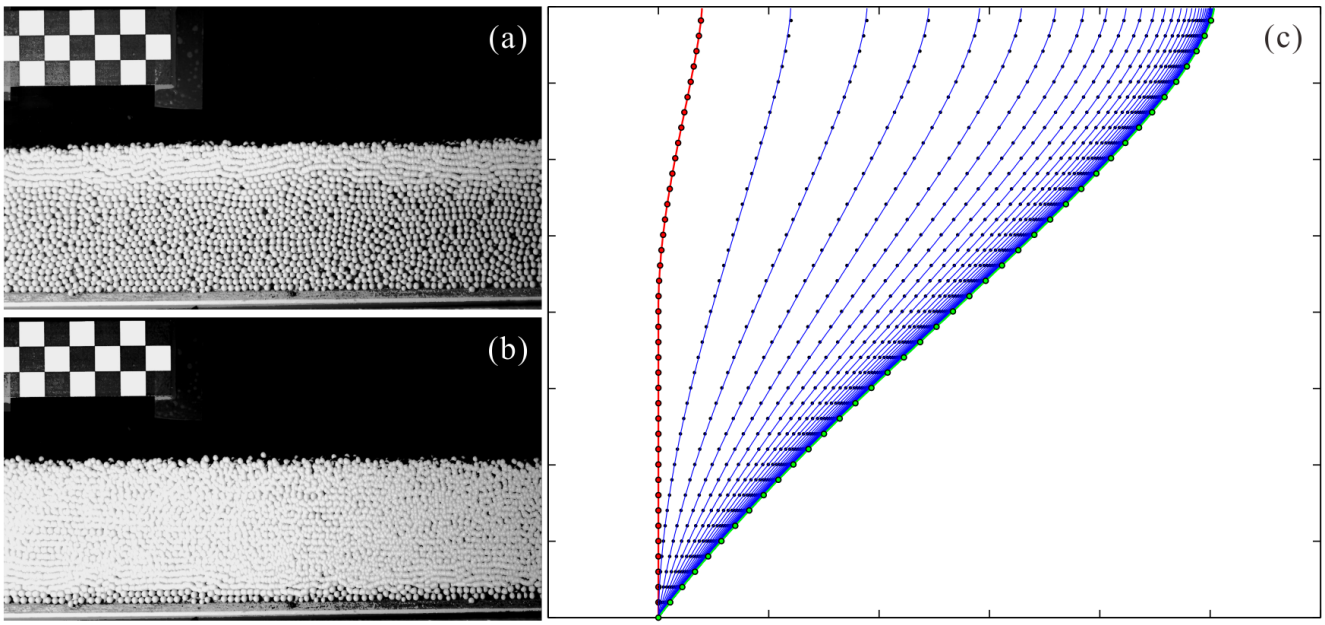

Fig.1 Experimental longexpousre image (a) over deposition bed; (b) over rigid bed; and (c) the transition velocity profile of theory prediction.

©2019. Japan Geoscience Union. All Right Reserved.

A viscous granular flow experiment with new refractive index matching material

*Tsai-Jung Lin[1], Chi-Yao Hung[1]

1. National Chung Hsing University

Entrainment rate at base controls how far the debris flow can travel and how large the debris flow becomes. Flow rheology of Refractive Index Matching (RIM) material are generally limited by the mono-particle properties (such as polymethyl methacrylate/liquid para-cymene etc.). In this study, a new RIM material (polyacrylamide polymer/18% Methanol solution) having a wide range of particle size distribution and viscosity (Fig. 1L) are purposed to visualize and measure the erosion process of mobile bed dam break experiments. Various rheology models may be formed by the different ratio of particle size. To improve the contrast between the particle phase and the liquid phase, a dye is used to make the particles bright under laser illumination. By varying the dye concentration, the entraining/detraining processes are easily distinguished (Fig. 1R). Granular motion is captured through a high-speed camera and Particle Tracking Velocimetry (PTV) method. Finally, an empirical relationship between the rheology and the entraining/ detraining process is developed.

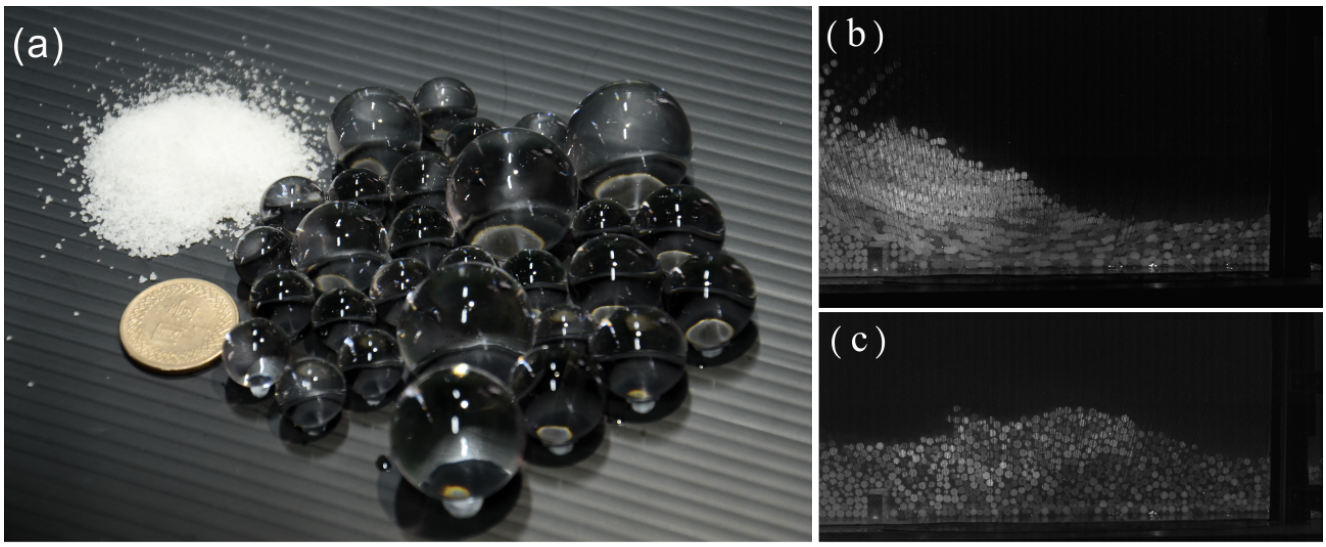

Fig.1 Experimental image (a)wide range of particle size; (b)longexposure image of dam break occurrence; (c)particles with different concentration of dye.

©2019. Japan Geoscience Union. All Right Reserved.

Sandbox experiments of submarine landslide caused by water film in low permeability layer

*Shogo Kawakita[1], Daisuke Asahina[2], Keiji Kitajima[3], Mitsukazu Nakanishi[3]

1. Graduate School of Science & Technology, Nihon Univ., 2. National Institute of Advanced Industrial Science and Technology, 3. College of Science & Technology, Nihon Univ.

Submarine landslides can be serious geohazards since they potentially cause tsunamis and damage seafloor infrastructure. Submarine landslides can be larger in scale than landslides on land. Direct measurements/observations of submarine landslides at deep seafloor still remain a challenging task. Kokusho et al. (2000) proposed a water film effect and its mechanism on lateral flow with less frictional resistance to explain a driving force of large-scale submarine landslides

In this study, we conducted laboratory experiments to understand the relationship between sand liquefaction and lateral flow by water film, and investigate the influence of water film formation on lateral flow of upper layer. In general, it is difficult to observe the formations of liquefaction and lateral flow at the same time. This is because sand particles of sloping layer model start to move when vibration is applied, and inclination disappears before liquefaction. To solve this problem, we devised a mechanism to prevent the flow of the lower layer by providing a weir plate in inside the soil tank. This mechanism enables to distinguish and observe the movement of sand by the liquefaction and the lateral flow by the water film.

The results obtained in this study clearly show three stages: first, the lower layer was liquefied; then pore water was stored below the low permeability layer; and finally, the lateral flow was occurred by the water film effect. The experimental results show that there was no clear correlation between the increase in the angle of sloping layer and the travel distance or the maximum flow velocity. We also discuss the relationship between the layer angle and the location of sand boil. The location where sand soiling occurred moved to the upper side of the slope as the layer angle become larger.

[Reference]

Kokusho, T.: Mechanism for water film generation and lateral flow in liquefied sand layer, Soils and Foundations, Vol.40, No.5, p 99-111, 2000.

Keywords: Submarine Landslides, Pore Water Pressure, Water Film, Lateral Flow

©2019. Japan Geoscience Union. All Right Reserved.

Study on Creep Properties of Sand and Cemented Sand

*JIN-YI YU[1], KUANG-TSUNG CHANG[1]

1. National Chung Hsing University

In this study, we investigated the effects of creep on sand and cemented sand, using triaxial test. Sand represents a non-cohesive material, while cemented sand represents a brittle material. Before the failure of specimens, the deviator stress was fixed and the cyclic mean stress was applied to study the influence of creep on the materials. According to the test results, the axial strain accumulation of sand caused by creep is less, and the peak strength is larger than that of the monotonic loading when the axial loading is resumed. For cemented sand, creep causes microcracks inside the specimens, gradually forming a failure surface. When the axial strain accumulation is large enough, the reapplication of the axial loading shows a reduction of peak strength. We conclude that the influence of creep on non-cohesive material (sand) is limited, whereas creep can reduce the strength of the brittle material (cemented sand) and even cause failure.

Keywords: creep, triaxial test, sand, cemented sand, strength, failure

©2019. Japan Geoscience Union. All Right Reserved.

The effects of seepage force and the Poisson’s ratio on slope stability

*Hirokazu Fukui[1], Tomomi Terajima[2]

1. Graduate school of Science, Kyoto University, 2. Disaster Prevention Research Institute, Kyoto University

To predict accurately the timing of shallow landslide occurrence, we need to consider the direction and magnitude of seepage force and earth pressure. A model sandy slope (L: 9m, W:1m, H:4m) was used to measure the hydraulic gradient and seepage force with the tensiometers under the artificial rainfall of 80mm/h. We incorporated not only the seepage force but also the Poisson’s ratio into conventional slope stability analysis by the limit equilibrium method. As a result, the calculated timing of shallow landslide occurrence was almost agree with the timing of that in the experiment and also more accurate than the timing calculated by the Spenser method which took into account the magnitude and moment equilibrium of the force. These results imply that, based on both monitoring at fields and conducting more experiments by a real-size model slope, we need to verify the effects of seepage force and earth pressure as the important factors causing rainfall-induced slope instability.

Keywords: process-based model, Seepage force, the Poisson's ratio, Shallow landslide, Sandy model slope

©2019. Japan Geoscience Union. All Right Reserved.

Study on the factors of seepage erosion

*Szu-Wei Fu[1], Kuang-Tsung Chang[1]

1. National Chung Hsing University

The causes of many slope disasters are often related to the seepage behaviors of soil. For instance, groundwater seepage may cause internal erosion of the soil. The soil particles are taken away by seepage water to form void or pipe. In addition , the earth pressure leads to the collapse of the overlying soil.

In this study, we designed a set of apparatus that can add confining pressure to the outside of the specimen. In order to simulate the situation of sand in slopes, we investigated the critical seepage velocity of sands caused by seepage erosion failure under different confining pressure, with different particle size distributions, sizes of outflow, etc. Then a failure criterion for seepage erosion is developed based on the drag equation in fluid dynamics and confirm with experimental data.

The results show that the critical seepage velocity at failure is affected by the particle size distributions, sizes of outflow and the confining pressure. The theoretical results are compared well to the experimental data.

Keywords: seepage erosion, Drag equation

©2019. Japan Geoscience Union. All Right Reserved.

Deformation of slope models with different orientations of weak planes

*taeyuan tseng[1], Kuang-Tsung Chang[1]

1. National Chung Hsing University

Weak planes influence failure and deformation of slopes. We conducted experiments to simulate slopes of different orientations of weak planes, including cataclinal and analcinal slopes with 30˚ and 60˚ inclination angles of weak planes. We stacked artificial bricks to make small-sized slope models. The artificial bricks were made of gypsum, sand, cement and water with different weight proportion. In view of the scaling law, the artificial bricks were made less strength than natural rocks. The slope models were weakened under rainfall, resulting in deformation and final collapse. The slope deformation processes were photographed by a camera, and the displacement vector fields were analyzed using the Particle Image Velocimetry (PIV). The deformation and accumulated displacements were compared between slopes of different orientations of weak planes.

Keywords: cataclinal slope, analcinal slopes, rainfall, Particle Image Velocimetry (PIV), weak planes, deformation

©2019. Japan Geoscience Union. All Right Reserved.

[J] Poster | H (Human Geosciences)：H-DS Disaster geosciences

Tue. May 28, 2019 1:45 PM - 3:15 PM JST | Tue. May 28, 2019 4:45 AM - 6:15 AM UTC | Poster Hall International Exhibition Hall8, Makuhari Messe_4

[H-DS13] Tsunami and Tsunami Forecast

convener:Naotaka YAMAMOTO CHIKASADA(National Research Institute for Earth Science and Disaster Resilience), Hiroaki Tsushima(Japan Meteorological Agency), Tatsuya Kubota(National Research Institute for Earth Science and Disaster Resilience)

This session discusses issues related to improving real-time and long-term prediction accuracy of tsunami from earthquakes, landslides, and volcanoes, which include such as a better understanding of tsunami dynamics, new real-time tsunami observing systems deployed in the open ocean and coastal waters, methodologies of more rapid and accurate prediction during tsunami emergencies, more extensive and accurate inundation maps, and long-term tsunami potential forecast.

[HDS13-P01] Possible submarine landslides as sources of the 2018 Sulawesi tsunami

*Kenji Nakata[1], Akio Katsumata[1], Abdul Muhari[2] (1.Meteorological Research Institute, Japan Meteorological Agency, 2.Ministry of Marine Affairs and Fisheries, Indonesia)

[HDS13-P02] Tsunami Data Assimilation of the 2015 Torishima Earthquake

*Yuchen Wang[1], Kenji Satake[1], Osamu Sandanbata[1], Takuto Maeda[2] (1.Earthquake Research Institute, University of Tokyo, 2.Graduate School of Science and Technology, Hirosaki University)

[HDS13-P03] Method for real-time estimation of tsunami sources using a network of dense ocean bottom pressure sensors

*Mayu Inoue[1], Yuichiro Tanioka[1], Yusuke Yamanaka[2] (1.Hokkaido University, 2.The University of Tokyo)

[HDS13-P04] Application of AI Technology for Tsunami Prediction by Oceanographic Radar

*hiromu yokosu[1], Yoshihito - Tanaka[1], Kenji - hayashi[2], Kentarou - Uehara[2] (1.Chubu Electric Power Co., Inc., 2.Japan Weather Association)

[HDS13-P05] Development of the Tsunami Prediction System using fault plane solution of W-phase inversion

*Seolhan You[1], Mikyung Choi[1], Sun-Cheon Park[1], Hye-Won Lee[1], Duk Kee Lee[1] (1.Korea Meteorological Administration)

[HDS13-P06] Can we detect tsunami magnetic signals at on-land observatories prior to tsunami arrivals? : From the perspective of numerical experiments

*Takuto Minami[1], Tungcheng Ho[1], Zhiheng Lin[2], Hiroaki TOH[2] (1.Earthquake Research Institute,The University of Tokyo, 2.Graduate School of Science, Kyoto University)

[HDS13-P07] Probability of Tsunami Inundation Estimated from Tsunami Database and G-R law

*Toru Takeda[1], Toshitaka Baba[1], Tsuneo Ohsumi[2], Hiroyuki Fujiwara[2] (1.Tokushima Univ, 2.NIED)

[HDS13-P08] The Detection of Tsunami Propagation Path by Using Sensitivity Kernel Distribution

*Norihiko Hashimoto[1], Kyosuke Okamoto[2], Seiji Tsuno[3] (1.ITOCHU Techno-Solutions Corporation, 2.National Institute of Advanced Industrial Science and Technology, 3.Railway Technical Research Institute)

[HDS13-P09] Estimation of local seismic waves and rapid magnitudes for ‘slow tsunami earthquakes’ based on moment rate spectrum

*Takahito Nishimiya[1], Akio Katsumata[1] (1.Meteorological Research Institute, Japan Meteorological Agency)

[HDS13-P10] Development of tsunami simulator TNS and release of version 1.0

*Takayuki Miyoshi[1], Wataru Suzuki[1], Naotaka YAMAMOTO CHIKASADA[1], Shin Aoi[1], Sho Akagi[2], Toshihiko Hayakawa[2] (1.National Research Institute for Earth Science and Disaster Resilience, 2.Mitsubishi Space Software Co.,Ltd.)

[HDS13-P11] A Study on Tsunami Inundation Simulation for the Nankai Trough Earthquake for Osaka City

*Kaoru Kawaji[1], Seiji Tsuno[2] (1.ITOCHU Techno-Solutions Corporation, 2.Railway Technical Research Institute)

[HDS13-P12] Database construction of Tsunami inundation simulation for large subduction earthquakes

*Mariko Korenaga[1], Seiji Tsuno[2], Kaoru Kawaji[1] (1.ITOCHU Techno-Solutions Corporation, 2.Railway Technical Research Institute)

[HDS13-P13] Sediment Transport Modeling due to Tsunamis caused by the Nankai great earthquakes

*Takuya Saito[1], Kei Yamashita[2], Toshitaka Baba[1] (1.Tokushima Univ., 2.Tohoku Univ.)

[HDS13-P14] Tsunami model of the 2011 Tohoku Earthquake reproducing the wave gauge record offshore the Fukushima Daiichi NPP

*Toshimichi Kaneto[1], Ayumi Nishi[2], Tadashi Annaka[2] (1.Tokyo Electric Power Company Holdings,Inc, 2.Tokyo Electric Power Services Co,Ltd)

[HDS13-P15] Development of tsunami fragility curves on railway structures based on the 2011 off the Pacific coast of Tohoku earthquake

*Teppei Ono[1], Seiji Tsuno[2], Yuko Sato[2], Marioko Korenaga[1] (1.ITOCHU Techno-Solutions Corporation, 2.Railway Technical Research Institute)

[HDS13-P16] The characteristic of the cause of death in each city in Miyagi prefecture during the Great East Japan Earthquake

*Shuji SETO[1], Fumihiko IMAMURA[1] (1.IRIDeS, Tohoku University)

[HDS13-P17] The reflective south going current, accompanied by the third wave of Tsunammi at Iioka , Asahi City , Chiba Prefecture in 2011.

*Mitsuo Harukawa[1], Noboru Hashimoto[1], Fumio Ooshima[1] (1.The Group of Recording for Tsunami Damage of Asahi City in 2011)

Possible submarine landslides as sources of the 2018 Sulawesi tsunami

*Kenji Nakata[1], Akio Katsumata[1], Abdul Muhari[2]

1. Meteorological Research Institute, Japan Meteorological Agency, 2. Ministry of Marine Affairs and Fisheries, Indonesia

Tsunami struck coastal areas of Palu bay, Slawesi Islands after an earthquake of Mw 7.5. Muhari et al. (2018) hypothesized that the tsunami was generated inside the Palu bay based on the evidence of tide gauge station records, videos, inundation distance, damage characteristics from post-tsunami surveys and so on. Furthermore, Arikawa et al. (2018) pointed out that subsidence of coastal areas may have related to tsunami generation, and that the tsunami heights were not high at the mouth of the Palu bay. While Heidarzadeh et al. (2018) reported that the tide gauge records in Palu bay were successfully simulated by the USGS’ s finite fault model, they also pointed out the possibility of the submarine landslide, following extremely large tsunamis. In this study we assumed that the recorded tsunami was caused by a submarine landslide. We investigated the possible locations and size of the submarine landslide that could express the waveform at the tide gauge station and the possibility of the tsunami generation at the shallow depth by tsunami simulations.
Results of tsunami simulation showed that it was necessary that tsunami wave source was at the shallow depth to simulate the observed period of tsunami wave. Calculated tsunami waveforms that closely matches the observed waveform was obtained at three locations in the bay. By calculating the landslide source for several fluidities, we reached a conclution sediments with low fluidity near coastal line was necessary for the landslide source.

Keywords: 2018 Sulawesi earthquake, submarine landslide, tsunami simulation

©2019. Japan Geoscience Union. All Right Reserved.

Tsunami Data Assimilation of the 2015 Torishima Earthquake

*Yuchen Wang[1], Kenji Satake[1], Osamu Sandanbata[1], Takuto Maeda[2]

1. Earthquake Research Institute, University of Tokyo, 2. Graduate School of Science and Technology, Hirosaki University

The 2015 Torishima earthquake (M5.9) occurred at the Smith caldera, on May 2, 2015. It had a CLVD-type focal mechanism and generated larger tsunami waves compared to its seismic magnitude (Sandanbata et al., 2018). Therefore, it was regarded as a ‘volcanic tsunami earthquake’ –a tsunami earthquake with volcanic origin. The tsunami reached Hachijo Island, Boso Peninsula and Shikoku Island, and were recorded by tide gauges and ocean bottom pressure gauges (Kubota, 2018). Fukao et al. (2018) proposed an opening horizontal sill model to explain its origin. The abnormal mechanism makes it difficult to forecast tsunami from its seismic magnitude.

Tsunami data assimilation forecasts the tsunami by assimilating offshore observed data into a numerical simulation, without the need of calculating the initial sea surface height at the source (Maeda et al., 2015). In the Nankai region, the Dense Oceanfloor Network System for Earthquakes and Tsunamis (DONET) records the water pressure and has real-time data transmission. Synthetic experiments showed that this observational system was able to forecast the waveforms at Shikoku Island by tsunami data assimilation approach (Wang et al., 2018). Here, we performed this method to retroactively forecast the tsunami of the 2015 Torishima earthquake. We assimilated the observations of 16 DONET stations and two ocean bottom gauges off Muroto. The tsunami waveforms at the tide gauges Tosashimizu and Kushimoto were forecasted, and compared with the actual records.

The comparison between forecasted and observed waveforms at two tide gauges suggested that our method could forecast the tsunami amplitudes and arrival time accurately. The tsunami warning could be issued to local residents of Shikoku Island more than one hour before its arrival. Our method is merely based on offshore observations, and could be implemented for future tsunami warning systems.

Keywords: Tsunami Data Assimilation, Tsunami Forecasting, Torishima Earthquake

©2019. Japan Geoscience Union. All Right Reserved.

Method for real-time estimation of tsunami sources using a network of dense ocean bottom pressure sensors

*Mayu Inoue[1], Yuichiro Tanioka[1], Yusuke Yamanaka[2]

1. Hokkaido University, 2. The University of Tokyo

After the 2011 hazardous tsunami, the Seafloor observation network for earthquakes and tsunamis along the Japan Trench (S-net) was installed by National Research Institute for Earth Science and Disaster Resilience in Japan (NIED). Various real-time tsunami-forecast methods using this S-net were developed by several researchers. The objective of this study is to develop a new method for real-time tsunami source estimation using S-net data, a simpler method than the previous methods. This study focuses on tsunami generated by great underthrust earthquakes at the plate interface off the Pacific coast of Hokkaido, Japan. First, we numerically computed tsunamis from fault models of M8.0 to M8.8 classes distributed along the plate interface along the Kurile Trench. Virtual observational waveforms at locations of sensors in S-net during each tsunami were estimated by converting the simulated tsunami waveform into a waveform of water pressure change. We tried to estimate a tsunami source area by classifying the virtual observational waveforms within 500 seconds after the origin time of the earthquake into the following three types. Type1 waveform goes down and stays down within 500 seconds. Type2 waveform includes one complete up-pulse waveform. All of the other waveforms were regarded as Type3. We found that a sensor with the type1 waveform is located in the initial uplifted area, and sensors with the type2 waveform is located not in the area but near the initial uplifted area, and the sensor with the type3 is located far from the initial uplifted area. After the tsunami source area was estimated, the magnitude of the earthquake can be estimated using the scaling relationship between the earthquake fault area and the magnitude of the earthquake. We tested four different scaling relationships suggested by previous studies to find the error of the magnitude estimation. The estimation error was found to be M ±0.08. Finally, this new method was applied to the 1952 Tokachi-oki earthquake and the 1968 Tokachi-oki earthquake source models. The tsunami source area and the magnitude of the earthquake were estimated well for both cases. Therefore, the new method should be useful for the rapid estimation of a tsunami source as a part of the tsunami early warning system.

Keywords: Tsunami forecast, S-net

©2019. Japan Geoscience Union. All Right Reserved.

Application of AI Technology for Tsunami Prediction by Oceanographic Radar

*hiromu yokosu[1], Yoshihito - Tanaka[1], Kenji - hayashi[2], Kentarou - Uehara[2]

1. Chubu Electric Power Co., Inc., 2. Japan Weather Association

At Hamaoka Nuclear Power Station, oceanographic radar (HF radar) is installed to detect the tsunami early.We can observe sea surface velocity distribution up to offshore of about 40 km approximately every minute.When a tsunami occurs, it is expected to capture the situation which the tsunami approaches and to predict the arriving tsunami.

Oceanographic radar observation captures a wide range of flow velocity distribution at once and obtains numerical result.By using the distribution situation of the change of the flow velocity on sea surface by the tsunami, we investigated the tsunami prediction by the image recognition method using AI technology.AlexNet (convolution neural network) was used for the image recognition method.

For the prediction of the tsunami, the tsunami height (first wave) and the arrival time are important, the tsunami height was classified into 1 m interval (tsunami height 10 m or less) or 2 m interval (tsunami height 10 m to 22 m), and the arrival time was classified as one minute interval (1 min to 22 min). The total was classified into 374 categories.Using the image recognition method, we examined the accuracy of the classification based on the observation situation.

In this study, the result of the tsunami simulation exceeding 5000 tsunami caused by the Nankai Trough earthquake which will have the most influence on Hamaoka Nuclear Power Station.Since the number of large-scale tsunami cases is small, we devised such as using data in seconds.Also, since AlexNet can handle color images (RGB), the current flow time change (current time, 1 minute before the current time, 2 minutes before the current time) of three steps in the learning data was applied to R, G, B.As a result, regularity such as time series of flow velocity and position information can be reflected, and the feature of image change (change in flow velocity distribution) became easier to capture.

Although the scale of the tsunami varies, it is important to predict a large-scale tsunami (tsunami height 10 m or more) at Hamaoka Nuclear Power Station, so the result of "Tsunami height 10 m or more" is described here.As for the verification of the AI prediction, the data (verification data) not used for learning data in simulation data was used.The ratio between learning data and verification data was set at about 80% and about 20%.The accuracy rate was about 77%.Regarding time, if one category (arrival time ±1 minute) is permitted, the accuracy rate improves to about 94%.So, it can be said that the error of the tsunami height is smaller than the arrival time with this image recognition method.

Keywords: tsunami prediction, oceanographic radar, AI, AlexNet

©2019. Japan Geoscience Union. All Right Reserved.

Development of the Tsunami Prediction System using fault plane solution of W-phase inversion

*Seolhan You[1], Mikyung Choi[1], Sun-Cheon Park[1], Hye-Won Lee[1], Duk Kee Lee[1]

1. Korea Meteorological Administration

Tsunami is a long-wave caused by earthquakes, submarine volcanoes or coastal landslides. The Korean Peninsula experienced tsunami damage followed by 1983 and 1993 Japan earthquakes. To respond to possible tsunamis in the surrounding seas, the Korea Meteorological Administration has operated tsunami warning system based on tsunami scenario database. Tsunami scenario database was constructed with the results (tsunami height and arrival time) of simulating tsunami assuming virtual earthquakes at each grid point spacing with 0.2˚ interval in surrounding seas of the Korean peninsula(120˚~142˚E, 25˚~45˚N) . Earthquakes were assumed with magnitude 6.0 to 9.0 having intervals of 0.2 on the fault plane which is from known information or which is assumed to generate higher tsunami in the coastal area. Therefore tsunami scenario database has a limitation that does not reflect the characteristics of earthquakes when they actually occur because the fault plane will be different from assumed one.
In this study, we have developed an algorithm for tsunami prediction capable of analyzing fault plane solution using W phase and simulating tsunami using the fault plane information. We tested the performance of the developed algorithm applying into the case of 1993 Japan tsunami. W phase inversion results were as follows: moment magnitude=7.7, depth=25.5km, strike=170.2˚, dip=45.3˚ and rake=77.8˚. As a result of tsunami simulation using the inversion results, the difference between the numerical results (tsunami height and arrival time) and measured data at tide stations was small. Therefore the algorithm for tsunami prediction may be used for tsunami warning as a complement to tsunami scenario database.

Keywords: tsunami, tsunami scenario database, W phase, tsunami prediction system

©2019. Japan Geoscience Union. All Right Reserved.

Can we detect tsunami magnetic signals at on-land observatories prior to tsunami arrivals? : From the perspective of numerical experiments

*Takuto Minami[1], Tungcheng Ho[1], Zhiheng Lin[2], Hiroaki TOH[2]

1. Earthquake Research Institute,The University of Tokyo, 2. Graduate School of Science, Kyoto University

Tsunami flow crossing the geomagnetic field generates electric currents in the ocean and associated secondary magnetic fields due to the electromotive force. This tsunami-generated magnetic (TGM) variations are observable not only at the seafloor (e.g. Toh et al. 2011) but also at on-land magnetic observatories on islands or along coastlines (e.g. Tatehata et al. 2015). Most of the TGM data reported in previous studies are from the seafloor observations since TGM signals are much stronger at the seafloor, which implies that usage of off-shore seafloor magnetic observations is a sensible solution for tsunami early warning. On the other hand, much cheaper on-land magnetic observations may be useful because the vertical component of the TGM field precedes the tsunami arrival by approximately a quarter of the tsunami period in shallow oceans (< ~ 1000 m; Minami et al. 2015). Previous studies have never carefully investigated possibilities of using on-land magnetic data in tsunami early warning, because of the difficulty in evaluating the effect of realistic topography on the TGM variations at on-land observatories.

We conduct three-dimensional simulations of TGM signals to investigate feasibility of using on-land magnetic data for tsunami early warning, with the aid of the finite element simulation code by Minami et al. (2017). This study focuses on three devastating tsunami events in the past, the 1960 Chilean tsunami (Mw 9.5), the 2011 Tohoku tsunami (Mw 9.0), and the 1707 Hoei tsunami (Mw 8.7). For the three tsunamis, we adopt the source models of Ho et al. (2019), Satake et al. (2013), and Furumura et al. (2010), respectively. Although all the three large tsunamis did extensive damage, features of their topographies are distinct from each other. One of the features of coastlines in Tohoku is ria coast, while Nankai area of Japan includes capes and bays. As for Chilean coast for the 1960 event, a straight long coastline is present in the vicinity of Santiago, Chile. We set many virtual magnetic observatories and tide stations along the coastlines and investigate arrival times of tsunamis and TGM signals. In the presentation, we compare the arrival times of tsunamis and TGM signals at each virtual observatory and to discuss feasibility of using on-land TGM signals for tsunami hazard mitigation.

Keywords: tsunami, electromagnetic, simulation

©2019. Japan Geoscience Union. All Right Reserved.

Probability of Tsunami Inundation Estimated from Tsunami Database and G-R law

*Toru Takeda[1], Toshitaka Baba[1], Tsuneo Ohsumi[2], Hiroyuki Fujiwara[2]

1. Tokushima Univ, 2. NIED

Studies on probabilistic hazard assessments considering uncertainties such as the timing and magnitude of earthquake occurrence, diversity of heterogeneous slip, etc. are common in recent years. For tsunami, probabilistic tsunami height assessments along the coast were shown. But probabilistic tsunami inundation assessments are not shown yet because tsunami inundation modeling needs highly resolved topographic data (~10m) and probabilistic approach needs calculations from huge number of earthquake scenarios. Recent development of high-performance computers enables us to make a probabilistic tsunami inundation map if the study area narrowed down. In this study, we attempt to probabilistically assess tsunami inundation in an area of the Nankai subduction zone using a tsunami database and G-R law.

In the creation of the tsunami database, we used the Nankai earthquake slip models shown by Hirata et al. (2017). The propagation and inundation of the tsunami generated by each fault model were carried out by the nonlinear shallow water equations. A nesting algorism was applied to improve the spatial resolution in the study area. Coastal structures such as seawall were defined in the tsunami calculations, but they were disable if the tsunami height is higher than the height of seawall. We defined the relative weights among the earthquake fault models using the G-R law. The weights were used in superimposing of the all inundation maps to estimate probabilities of tsunami inundation.

As a result, it was confirmed that the probability of inundation depends on the topographic features, such as the region where the probability is high in the area end of the V-shaped bay and around the upstream area of the river. We will carry out an analysis that takes into consideration the uncertainty in earthquake occurrence and tsunami height estimations. We also investigate effects of costal structures on the inundation probability.

Keywords: probabilistically assess tsunami inundation, G-R law

©2019. Japan Geoscience Union. All Right Reserved.

The Detection of Tsunami Propagation Path by Using Sensitivity Kernel Distribution

*Norihiko Hashimoto[1], Kyosuke Okamoto[2], Seiji Tsuno[3]

1. ITOCHU Techno-Solutions Corporation, 2. National Institute of Advanced Industrial Science and Technology, 3. Railway Technical Research Institute

Predicting the inundation height and arrival time by tsunami propagation analysis are very important in the tsunami disaster prevention. On the other hand, it is also an important issue to elucidate tsunami propagation path. The tsunami propagation path has been commonly calculated by wave ray method, it has used in combination with the tsunami propagation analysis based on linear long wave theory and, shallow water theory. However, in the wave ray method, it’ s difficult to set an appropriate initial value and boundary conditions consistent with tsunami propagation analysis. So we must pay attention these characteristics in considering the analysis result.
Anyway, applying the sensitivity kernel distribution and adjoint field which used in seismic tomography to the tsunami wave field, we investigated the tsunami propagation path. In this method, it is also possible to detect a propagation path of the specific component extracted from a tsunami waveform by adding a routine for propagating a tsunami waveform in the reverse direction to the general tsunami propagation analysis code.
First, we verified this method whether it is possible to detect tsunami propagation path to the observed point in the ideal space. It was assumed water of constant depth and Gaussian distribution as an initial water level.
In addition, we used this method to detect how the far-field tsunami propagate to the Japan coast. We set the calculation target range that can be covered almost whole Pacific Ocean area whose mesh size is 10 sec, the wave source was the 1960 Chilean tsunami. Analyzing characteristics of tsunami is propagated which comes from Hawaiian island across the north-south, we confirmed the result as same as previous method by wave ray method.
An issue in the future, it’ s necessary to consider a practical method to extract and propagate specific components of the tsunami waveform, and verify the possibility of applying this method for the tsunami propagation analysis based on dispersive wave theory and shallow water theory. It is thought that they will be expanded the range of application.

Keywords: Tsunami propagation path, Tsunami propagation analysis, Wave ray method, Adjoint method, Adjoint field, Sensitivity kernel distribution

©2019. Japan Geoscience Union. All Right Reserved.

Estimation of local seismic waves and rapid magnitudes for ‘slow tsunami earthquakes’ based on moment rate spectrum

*Takahito Nishimiya[1], Akio Katsumata[1]

1. Meteorological Research Institute, Japan Meteorological Agency

The tsunami height estimation at earliest stage in JMA is based on the estimated hypocenter and rapid magnitude (rapid-M) from local seismic wave data. The amplitudes of seismic waves from ‘slow tsunami earthquakes’ are usually smaller than those from normal earthquakes because those earthquakes radiate relatively low seismic energies in the short period range. Therefore it is difficult to estimate rapid-M of ‘slow tsunami earthquakes’ accurately. We would like to evaluate rapid-M of them quantitatively. However local seismic wave data of slow tsunami earthquakes is almost not available.

We estimated moment rate spectra of ‘slow tsunami earthquakes’ using tele-seismic wave data (in JpGU Meeting 2018), and calculated synthetic local seismic waves based on those spectra (in Seismological Society Fall Meeting 2018). We estimated rapid-M from the synthetic wave data here.

JMA magnitude (M_J) and M_{100} (Katsumata et al., 2013) are evaluated as the rapid-M. M_{100} is introduced by JMA to avoid underestimation of magnitude for huge earthquakes because M_J tends to indicate “magnitude saturation” for huge earthquakes. We calculated M_J and M_{100} from the synthetic wave data. REGARD (Kawamoto, 2017) based on GNSS data is also a kind of rapid-M. However we use seismic wave data from which smaller magnitude can be estimated compared with REGARD.

We assumed that a ‘slow tsunami earthquake’ occurs at the plate-boundary off the Pacific coast of Tohoku. It has the same moment rate spectrum as the Java tsunami earthquake (M_w7.8) in 1994. M_J estimated from those synthetic waves was smaller than M_w by more than 1.0. M_{100} is larger than M_J, but M_{100} is smaller than M_w by more than 0.5. We also evaluated magnitudes for an earthquake which has the same moment rate spectrum as the Sumatera tsunami earthquake (M_w7.8) in 2010. The difference from M_w reduced for the earthquake, while both M_J and M_{100} are lower than M_w.
USGS published M_s of significant earthquakes. M_s of the 1994 Java earthquake was lower than M_w by more than 0.5 although M_s of the 2010 Sumatera earthquake was about the same as M_w.

Our results suggest that big difference between M_{100} and M_J is useful for early discriminating ‘slow tsunami earthquakes’ from normal earthquakes. Even if M_{100} is much greater than M_J, M_{100} may be underestimated for slow tsunami earthquakes.

Keywords: tsunami earthquake, spectrum, local seismic wave, magnitude

©2019. Japan Geoscience Union. All Right Reserved.

Development of tsunami simulator TNS and release of version 1.0

*Takayuki Miyoshi[1], Wataru Suzuki[1], Naotaka YAMAMOTO CHIKASADA[1], Shin Aoi[1], Sho Akagi[2], Toshihiko Hayakawa[2]

1. National Research Institute for Earth Science and Disaster Resilience, 2. Mitsubishi Space Software Co.,Ltd.

A tsunami is a natural phenomenon in which disturbance generated in the sea by abrupt submarine deformation, propagates to the surrounding sea area with the gravity as restoring force, and often runs up to the land area. The National Research Institute for Earth Science and Disaster Resilience (NIED) has developed a software that can calculate a tsunami phenomenon including inundation on a computer by numerical simulation using finite-difference method (Miyoshi et al., 2018 JpGU). The software was named Tsunami Simulator (TNS: TsuNami Simulator).

Numerical codes of the TNS was developed to operate on the Central Processing Unit (CPU) and the Graphics Processing Unit (GPU), the main code of the CPU written in Fortran 90 and the GPU written in CUDA C in accordance with CUDA 7.5. The concept of the codes is basically equivalent to TUNAMI-N2 (Imamura et al., 2006), and tsunami propagation and inundation based on two-dimensional nonlinear long wave theory can be implemented using a nesting grid with a space grid ratio of 1: 3 in the Cartesian coordinate system. The initial wave height is calculated by the crustal movement in the semi-infinite medium with respect to a fault plane using the program DC3D (Okada, 1992 BSSA). Horizontal crustal movement (Tanioka and Satake, 1996 GRL) and hydraulic filters by Kajiura (1963, BERI) are also applicable. In the offshore boundary, the transmission boundary (Imamura et al., 2006) and the absorb area (e.g. Clayton et al., 1977 BSSA) are applied, and inundation boundary is used in the land side (Kotani et al., 1998 Coastal Engineering Journal). For distant tsunamis, a spherical coordinate system is introduced and connects to the region in the Cartesian coordinate where inundation simulation is carried out. In the spherical coordinate, Coriolis force and dispersion effect can be considered as the previous study, and loading effect (Inazu and Saito, 2013 EPS) can also be applied.

Real-time tsunami inundation forecast system using numerical database requires a large amount of tsunami scenario. From the TNS development version, we packaged the essential parts for constructing a tsunami scenario bank and released as TNS Version 1.0 (Miyoshi et al., 2019 Technical Note of the NIED). The users are assumed to be researchers, engineers, officers of local governments who is responsible for disaster prevention, and make it possible to calculate on the general Linux environment. The package included an operation guide, executable files precompiled on Linux, and some examples. The solver can conduct sequential computation by single CPU, and can conduct parallel computation using OpenMP, and the general-purpose computing on graphics processing units (GPGPU) in order to achieve reduction of calculation time.

Acknowledgements: This work is partly supported by Council for Science, Technology and Innovation (CSTI), Cross-ministerial Strategic Innovation Promotion Program (SIP), “Enhancement of societal resiliency against natural disasters” (Funding agency: JST).

Keywords: Tsunami, Inundation, Finite-difference method, Nesting grid, GPU

©2019. Japan Geoscience Union. All Right Reserved.

A Study on Tsunami Inundation Simulation for the Nankai Trough Earthquake for Osaka City

*Kaoru Kawaji[1], Seiji Tsuno[2]

1. ITOCHU Techno-Solutions Corporation, 2. Railway Technical Research Institute

In planning disaster prevention measure against the tsunami, it is a very important factor how will the tsunami occur by occurrence of an earthquake and how it will attack. Since the Scenario of the Nankai Trough fault seismic source model was announced from the Cabinet Office as the maximum assumed wave source , various local governments and others are considering various disaster prevention measures and others. In this research, we carried out the tsunami inundation simulation for Osaka City using all 11 case fault models of the Nankai Trough's large earthquake model study meeting (2nd report) announced by the Cabinet Office in August 2012 , and examined the results.

Topographical model in tsunami inundation simulation was using topographic data published by the Cabinet Office, and we modeled with a 1215m grid about range of 1200km ×800km including from the fault to the coast. The calculation time was set to a maximum of 6 hours so that the maximum inundation area and the maximum inundation depth due to the tsunami could be calculated, and the calculation time interval was set to 0.01 second interval so that the calculation was stable.

If the parameters (slip angle, position, epicenter) etc in the fault seismic source model are different, the tsunami characteristics such as the tsunami wave height, the arrival time of the tsunami and the inundation range of tsunami should be different. However, it was different that the location of the large slip region and the epicenter in the fault model of 11 cases, but almost the same tsunami level and arrival time were found in the observation points in Osaka Bay in all cases. It was also found that the maximum wave height appearance time is within 30 minutes from the start of rupture regardless of the case. This trend can be seen similarly in the vicinity of the Kii Channel, off the coast of Osaka Bay, and this trend is thought to be the influence of the topographic of the intricate straits sandwiched between Kii Peninsula and Kochi / Kagawa. We will continue further multilateral investigation in the future and report on the results as well.

Keywords: Tsunami inundation simulation, Nankai Trough Earthquake, Osaka-bay

©2019. Japan Geoscience Union. All Right Reserved.

Database construction of Tsunami inundation simulation for large subduction earthquakes

*Mariko Korenaga[1], Seiji Tsuno[2], Kaoru Kawaji[1]

1. ITOCHU Techno-Solutions Corporation, 2. Railway Technical Research Institute

In the area facing the Nankai Trough, the danger of the tsunami caused by the large subduction earthquake is an urgent task. Because the earthquake occurrence area is too close, it is very important to grasp the possibility of inundation in advance, not after the earthquake occurred.

Therefore, from the viewpoint of tsunami protection against railway structures, databases of tsunami height near the coast and tsunami inundation zones were created, assuming a large number of scenario earthquakes for specific cities on the Pacific coast. Using this result we will investigate the risk of risk assessment due to the maximum inundation area and the delay time of evacuation compared to the coastal prediction results.

Coastal tsunami height tends to increase when large slip regions and super large slip regions exist in front of the coastline in each target area, but the spread of the inundation area is also related to the position in the dip direction of the large slip region. We would like to discuss what kind of information is important for mitigating tsunami damage from the standpoint of railroad disaster prevention while quantitatively examining the various inundated areas obtained.

Keywords: Tsunami simulation, Nankai trough, Reduction of disaster damage

©2019. Japan Geoscience Union. All Right Reserved.

Sediment Transport Modeling due to Tsunamis caused by the Nankai great earthquakes

*Takuya Saito[1], Kei Yamashita[2], Toshitaka Baba[1]

1. Tokushima Univ., 2. Tohoku Univ.

Tsunami that comes to the area in shallow water causes massive erosion and deposition of the coastal area. This causes damage such as collapse of coastal structures, burial of routes and blockage of water intakes at power stations. In the 2011 Tohoku Region Pacific Offshore Earthquake, collapses of coastal levees and burial of routes were caused by scouring. Damage caused by sediment transport will be prolonged, affecting recovery activities after the disaster. On the other hand, for disaster mitigations, it is necessary to accurately investigate the earthquakes and tsunamis back to the past as much as possible in order to estimate the maximum size of the earthquake and tsunami. Tsunami sediments are important information in studies of the historical earthquakes. Therefore, we simulated sediment transport using a numerical model developed by Takahashi et al. (1999, 2000, and 2011) for the great Nankai earthquakes.

The first study area is Tachibana-Bay classified as an important port having the rias coast in Shikoku, the southwestern Japan. In the simulation results, erosions were predicted in the straits between the islands, at the tip of the cape, near the estuary of the river and near the coastal levees. Sediment depositions were predicted in the vicinity. The maximum changes in erosion and sediment were about 10 m, about 6 m, respectively, for the great Nankai earthquakes (Mw 9.1). These were about 6 m and about 2 m, respectively, for the 1707 Hoei earthquake.

The other study area is a pond near the Cape Kamoda where tsunami sediment was found in the sediment layer about 2000 years ago (Okamura et al, 2012). However, all simulations we conducted in this study did not deposit sediment into the pond.

Acknowledgments: We thank Dr. Takahashi for providing us with the sediment transport software. This research is supported by Grant-in-Aid for Scientific Research 15H05718.

Keywords: Nankai Trough Earthquake, Sediment Transport software

©2019. Japan Geoscience Union. All Right Reserved.

Tsunami model of the 2011 Tohoku Earthquake reproducing the wave gauge record offshore the Fukushima Daiichi NPP

*Toshimichi Kaneto[1], Ayumi Nishi[2], Tadashi Annaka[2]

1. Tokyo Electric Power Company Holdings,Inc, 2. Tokyo Electric Power Services Co,Ltd

1. Objectives of research
During the 2011 off the Pacific coast of Tohoku Earthquake, severe core damage accidents occurred in unit one, two and three in Fukushima Daiichi nuclear power plant due to the failure of core cooling after the reactor shutdown. For understanding the process of tsunami caused by the earthquake and for utilizing tsunami evaluation at the nuclear power plants, tsunami source model, L67, of the 2011 Tohoku Earthquake was determined based on the data of the tsunami waves, crustal deformation and run-up height.
Although the model L67 can simulate the first tsunami and the first crest of the secondary tsunami of wave gauge record offshore the Fukushima Daiichi NPP, it cannot reproduce the second crest of the secondary tsunami. Imamura et al. (2016) proposed the revised model of Sugino et al. (2013) which reproduce the second crest of the secondary tsunami. In this research we improve the reproducibility of the wave gauge record based on the following approach.

2. Contents of research
(1) Joint inversion of tsunami wave and 1-second sampling GPS data
For developing the model L67, we took the consideration of the problem that the slip process of the previous tsunami source models such as Cabinet office (2012), Sugino et al. (2013) and Satake et al. (2013), has long duration compared with those of models based on earthquake ground motion data and that of 1-second sampling GPS data by Geospatial Information Authority, Japan. In order to resolve this problem we used the short time window for inversion as 30 sec times 3. Consequently the slip process of the model L67 has shorter duration compared with the above tsunami source models.
In this research we conducted the joint inversion using tsunami wave and 1-second sampling GPS data. It seems that the duration of slip process will become naturally shorter by using the 1-second sampling GPS data.

(2) Inversion using “hypothetical tsunami records”
Non-linear effect is strong in the wave gauge record offshore the Fukushima Daiichi NPP. So we can use only initial portion of the record for the linear inversion. In order to improve the reproducibility of the wave gauge record, “a hypothetical tsunami record” at the depth of 50 m offshore the Fukushima Daiichi NPP was simulated using the initial fault model and the green functions and the adjusted hypothetical tsunami record was added to the inversion as observed record. The calculated tsunami wave became similar to the wave gauge record through a trial and error process.
The same approach was used for improving the K and kappa for the run-up height data.

3. Conclusions
The tsunami source model of the 2011 Tohoku Earthquake reproducing the wave gauge record offshore the Fukushima Daiichi NPP was determined based on the above inversion approach. The duration of slip process became naturally shorter by using the 1-second sampling GPS data. The reproducibility of the wave gauge record was much improved compared with the model L67 by using the “hypothetical tsunami record”. Goodness of fit for tsunami wave and run-up height is same as that for model L67.

©2019. Japan Geoscience Union. All Right Reserved.

References
Imamura et al. (2016) The re-examination of the tsunami affected on the Fukushima Daiichi nuclear power plant by revising the tsunami model for the 2011 Tohoku Pacific Ocean earthquake tsunami, Journal of JSCE (Coastal Engineering), Vol.72, No.2,I-361-I-366

Acknowledgments
We thank GSI (Geospatial Information Authority, japan), NGDS (Nippon GPS Data Service, Japan), Hitz (Hitachi Zosen Co., Japan), GPSS (GPS Solutions Boulder, CO, USA), and VERIPOS for providing “1Hz_2hr_files”.

Keywords: tsunami source model, the 2011 off the Pacific coast of Tohoku Earthquake, Fukushima Daiichi nuclear power plant, 1-second sampling GPS data

©2019. Japan Geoscience Union. All Right Reserved.

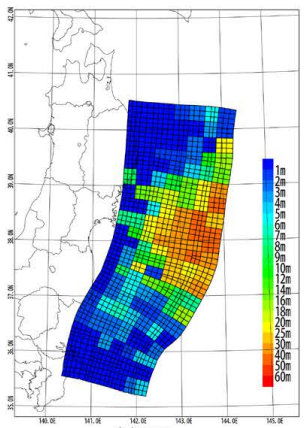
(a)L67

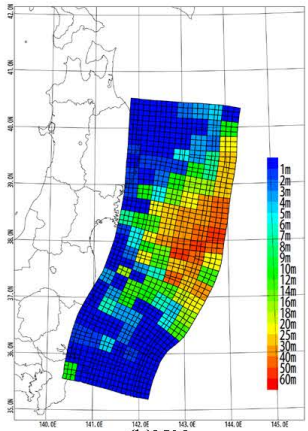
(b)N03

図1　波源の比較

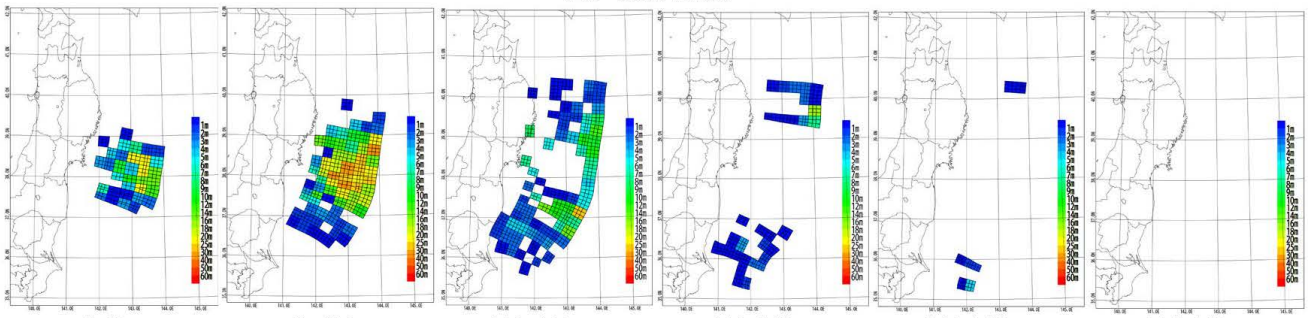

図2　破壊進展図(L67)

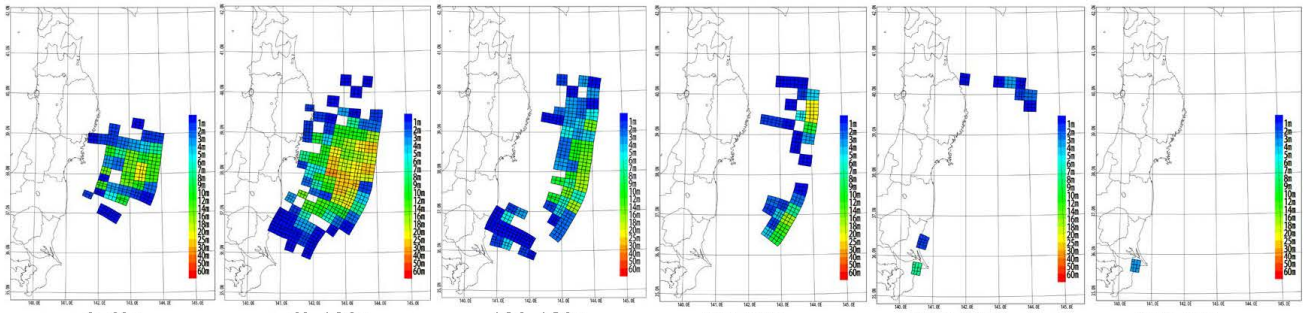

図3　破壊進展図(N03)

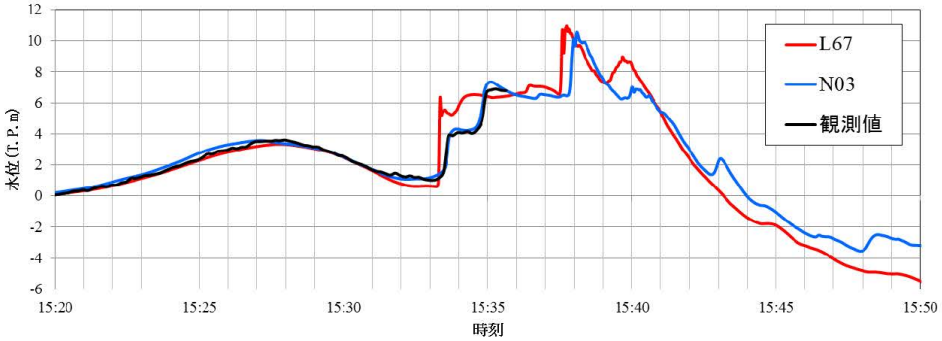

図4　波高計での観測値と計算値の水位時刻歴

表1　適合度表 (K, κ)

	L67		N03	
	K	κ	K	κ
北海道～千葉 (3882 点)	1.00	1.34	1.00	1.34
福島第一 (19 点)	1.00	1.10	0.99	1.11
福島第二 (71 点)	0.99	1.18	1.00	1.13

©2019. Japan Geoscience Union. All Right Reserved.

Development of tsunami fragility curves on railway structures based on the 2011 off the Pacific coast of Tohoku earthquake

*Teppei Ono[1], Seiji Tsuno[2], Yuko Sato[2], Marioko Korenaga[1]

1. ITOCHU Techno-Solutions Corporation, 2. Railway Technical Research Institute

The Great Tsunami associated with the 2011 off the Pacific coast of Tohoku earthquake caused severe damage to railway structures on the coast of the Tohoku region in Japan. It is effective to obtain fragility curve from damaged data in this disaster to predict the risks of railway structures to the tsunami in the future. It is generally represented by a lognormal distribution or a normal distribution. In this study, we obtained fragility curve by integrating spatial damage data for railway structures and spatial inundation data accompanying the 2011 off the Pacific coast of Tohoku earthquake on GIS. The method of obtaining tsunami fragility curves were referred to Koshimura et al. (2009).
In this study, we collected the data of damage and location for railway structures located in the Tohoku region to refer multiple documents. First, the data of inundation depth at intervals of 100 meters of the 2011 off the Pacific coast of Tohoku earthquake published by the Ministry of Land, Infrastructure and Transport was utilized to grasp the inundation depth where the railway structure is located. Second, we used the railway data of MLIT and Geospatial Information Authority to grasp the location of the railway structure. The kinds of structure in railway structures are different from station, bridge, tunnel, railway crossing, roadbed, retaining wall, cage, embankments, cuts and so on. The kinds of material in railway structures are also such as soil, C, RC. The tsunami fragility curves were obtained by using the all data and the case of using only RC to consider the influence of the structural kind.
As a result, it was shown that the gradient of tsunami fragility curve becomes smaller as compared with the tsunami fragility curve for buildings in the 2011 off the Pacific coast of Tohoku earthquake shown at Koshimura and Gokon (2012). The reason is to obtain the tsunami fragility curve from various railway structures. Furthermore, tsunami damage probability for railway structure on Ishinomaki in Miyagi Prefecture and Shimanokoshi in Iwate Prefecture were shown to confirm the reproducibility of the obtained tsunami fragility curve by using the spatial inundation depth calculated by using the Cabinet Office model.

Keywords: Tsunami fragility curve, The 2011 off the Pacific coast of Tohoku earthquake, Railway structures

©2019. Japan Geoscience Union. All Right Reserved.

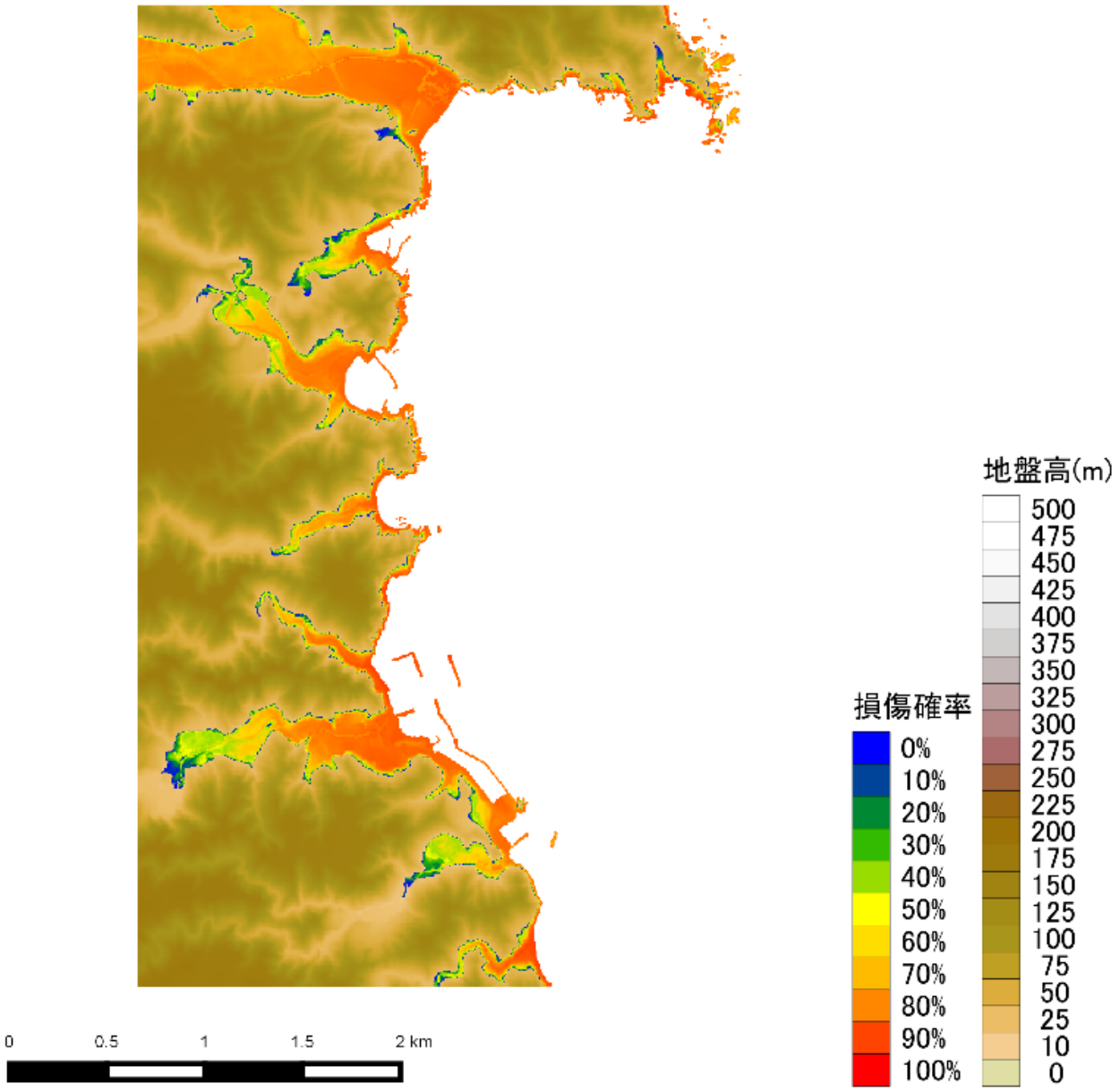

©2019. Japan Geoscience Union. All Right Reserved.

The characteristic of the cause of death in each city in Miyagi prefecture during the Great East Japan Earthquake

*Shuji SETO[1], Fumihiko IMAMURA[1]

1. IRIDeS, Tohoku University

About 20,000 people died in the Great East Japan Earthquake tsunami that occurred in 2011. According to the National Police Agency (2012), 90% of the victims in Iwate, Miyagi and Fukushima prefectures were drowned. Aoki et al. (2012) reported the results of questionnaires to physicians who actually examined in the affected areas. The questionnaire result showed that the National Police Agency's cause of death statistical result was reasonable, and that some physicians could not but describe it as drowning as a realistic problem.

This suggests that victims in a tsunami disaster may diefromcause of death other than drowning. According to Kahoku Shimpo(2011), the survivors witnessed the victims who died of symptoms like hypothermia after exposure to the tsunami. However, the details of the cause of death excluding drowning has not been elucidated yet.

Seto and Imamura(2019) classified the causes of death in Miyagi Prefecture during the 2011 Great East Japan Earthquake tsunami using victim information provided by Miyagi Prefecture Police Headquarters. As a result,the cause of death was classified into the following 12 kinds; Injuries to the head, Injuries to the neck, Injuries to the thorax, traumatic shock, Unspecified multiple injuries, Asphyxiation, Drowning, death due to fire, Hypothermia, Heart disease, Othrers and Unknown. And, they showed the proportion of each cause of death in Miyagi prefecture. The proportion in each city are needed to clarify the casualty in the Great East Japan Earthquake in more detail.

In this study, wecarried outthe analysis using the address data in victim information provided by Miyagi Prefecture Police Headquarters. The data are resident address and bodies found location. Combining each address data and the above 12 kinds of cause of death, we showed characteristics of each cause of death in each city in Miyagi prefecture.

Keywords: The 2011 Tohoku earthquake tsunami, Disaster science

©2019. Japan Geoscience Union. All Right Reserved.

The reflective south going current, accompanied by the third wave of Tsunammi at Iioka , Asahi City , Chiba Prefecture in 2011.

*Mitsuo Harukawa[1], Noboru Hashimoto[1], Fumio Ooshima[1]

1. The Group of Recording for Tsunami Damage of Asahi City in 2011

Shortly after the third wave of tsunami had gone to the north, Iioka was attacked abruptly by the south going current, which caused the disaster. The question is why the south going current occurred. The purpose of this thesis is to explain this issue.
After the disaster, we soon began to visit all the houses along the coast of Asahi City for interviews, and gathered about 650 personal experiences and eyewitness accounts. We found some of them very important. The summary is as follows.
When the third wave of tsunami reached the north coast of Iioka , it was reflected slightly eastward . Then the reflected current went down south along the seawall of west coast of Iioka. After a while, the south going current ran against the succeeding north going current that belonged to the third wave of tsunami. As a result of that collision, the wave height of south going current was increased so much that the wave got over the seawall and destroyed the houses from north to south.
By oblique mono photogrammetry, we calculated the strikes of the wave planes of south going current, and made a wave plane map, which we think proves the eyewitness accounts mentioned above to be right.
A TV program said that *the south going current was the edge wave of the first wave of tsunami*(April 9,2014 FNN), but we don't think it is the case. After the first wave of tsunami had gone, the tidal wave went far off the shore, leaving no seawater along the north coast of Iioka. The large area of the sea floor was visible. It is clear that no edge wave of the first wave stayed there.
Conclusion The south going current was not the edge wave of the first wave of tsunami. It was the reflective current of the third wave of tsunami.
Reference Mitsuo Harukawa(2013) Maps and speeds of Tsunami measured by oblique mono photogrammetry with video image in Asahi City , Chiba Prefecture (JGUMeeting2013HDS26-15)

Keywords: strike of wave plane, photogrammetry, reflective wave , Chiba Prefecture, Asahi City, Iioka

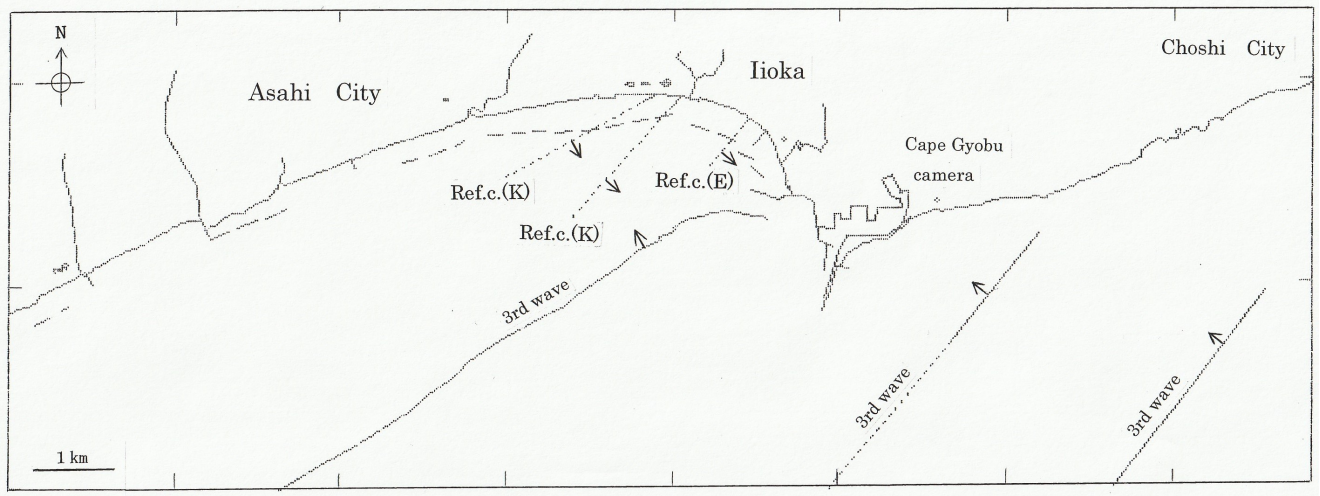

©2019. Japan Geoscience Union. All Right Reserved.

[J] Poster | H (Human Geosciences)：H-DS Disaster geosciences

Tue. May 28, 2019 5:15 PM - 6:30 PM JST | Tue. May 28, 2019 8:15 AM - 9:30 AM UTC | Poster Hall International Exhibition Hall8, Makuhari Messe_21

[H-DS13] Tsunami and Tsunami Forecast

convener:Naotaka YAMAMOTO CHIKASADA(National Research Institute for Earth Science and Disaster Resilience), Hiroaki Tsushima(Japan Meteorological Agency), Tatsuya Kubota(National Research Institute for Earth Science and Disaster Resilience)

This session discusses issues related to improving real-time and long-term prediction accuracy of tsunami from earthquakes, landslides, and volcanoes, which include such as a better understanding of tsunami dynamics, new real-time tsunami observing systems deployed in the open ocean and coastal waters, methodologies of more rapid and accurate prediction during tsunami emergencies, more extensive and accurate inundation maps, and long-term tsunami potential forecast.

[HDS13-P01] Possible submarine landslides as sources of the 2018 Sulawesi tsunami

*Kenji Nakata[1], Akio Katsumata[1], Abdul Muhari[2] (1.Meteorological Research Institute, Japan Meteorological Agency, 2.Ministry of Marine Affairs and Fisheries, Indonesia)

[HDS13-P02] Tsunami Data Assimilation of the 2015 Torishima Earthquake

*Yuchen Wang[1], Kenji Satake[1], Osamu Sandanbata[1], Takuto Maeda[2] (1.Earthquake Research Institute, University of Tokyo, 2.Graduate School of Science and Technology, Hirosaki University)

[HDS13-P03] Method for real-time estimation of tsunami sources using a network of dense ocean bottom pressure sensors

*Mayu Inoue[1], Yuichiro Tanioka[1], Yusuke Yamanaka[2] (1.Hokkaido University, 2.The University of Tokyo)

[HDS13-P04] Application of AI Technology for Tsunami Prediction by Oceanographic Radar

*hiromu yokosu[1], Yoshihito - Tanaka[1], Kenji - hayashi[2], Kentarou - Uehara[2] (1.Chubu Electric Power Co., Inc., 2.Japan Weather Association)

[HDS13-P05] Development of the Tsunami Prediction System using fault plane solution of W-phase inversion

*Seolhan You[1], Mikyung Choi[1], Sun-Cheon Park[1], Hye-Won Lee[1], Duk Kee Lee[1] (1.Korea Meteorological Administration)

[HDS13-P06] Can we detect tsunami magnetic signals at on-land observatories prior to tsunami arrivals? : From the perspective of numerical experiments

*Takuto Minami[1], Tungcheng Ho[1], Zhiheng Lin[2], Hiroaki TOH[2] (1.Earthquake Research Institute,The University of Tokyo, 2.Graduate School of Science, Kyoto University)

[HDS13-P07] Probability of Tsunami Inundation Estimated from Tsunami Database and G-R law

*Toru Takeda[1], Toshitaka Baba[1], Tsuneo Ohsumi[2], Hiroyuki Fujiwara[2] (1.Tokushima Univ, 2.NIED)

[HDS13-P08] The Detection of Tsunami Propagation Path by Using Sensitivity Kernel Distribution

*Norihiko Hashimoto[1], Kyosuke Okamoto[2], Seiji Tsuno[3] (1.ITOCHU Techno-Solutions Corporation, 2.National Institute of Advanced Industrial Science and Technology, 3.Railway Technical Research Institute)

[HDS13-P09] Estimation of local seismic waves and rapid magnitudes for ‘slow tsunami earthquakes’ based on moment rate spectrum

*Takahito Nishimiya[1], Akio Katsumata[1] (1.Meteorological Research Institute, Japan Meteorological Agency)

[HDS13-P10] Development of tsunami simulator TNS and release of version 1.0

*Takayuki Miyoshi[1], Wataru Suzuki[1], Naotaka YAMAMOTO CHIKASADA[1], Shin Aoi[1], Sho Akagi[2], Toshihiko Hayakawa[2] (1.National Research Institute for Earth Science and Disaster Resilience, 2.Mitsubishi Space Software Co.,Ltd.)

[HDS13-P11] A Study on Tsunami Inundation Simulation for the Nankai Trough Earthquake for Osaka City

*Kaoru Kawaji[1], Seiji Tsuno[2] (1.ITOCHU Techno-Solutions Corporation, 2.Railway Technical Research Institute)

[HDS13-P12] Database construction of Tsunami inundation simulation for large subduction earthquakes

*Mariko Korenaga[1], Seiji Tsuno[2], Kaoru Kawaji[1] (1.ITOCHU Techno-Solutions Corporation, 2.Railway Technical Research Institute)

[HDS13-P13] Sediment Transport Modeling due to Tsunamis caused by the Nankai great earthquakes

*Takuya Saito[1], Kei Yamashita[2], Toshitaka Baba[1] (1.Tokushima Univ., 2.Tohoku Univ.)

[HDS13-P14] Tsunami model of the 2011 Tohoku Earthquake reproducing the wave gauge record offshore the Fukushima Daiichi NPP

*Toshimichi Kaneto[1], Ayumi Nishi[2], Tadashi Annaka[2] (1.Tokyo Electric Power Company Holdings,Inc, 2.Tokyo Electric Power Services Co,Ltd)

[HDS13-P15] Development of tsunami fragility curves on railway structures based on the 2011 off the Pacific coast of Tohoku earthquake

*Teppei Ono[1], Seiji Tsuno[2], Yuko Sato[2], Marioko Korenaga[1] (1.ITOCHU Techno-Solutions Corporation, 2.Railway Technical Research Institute)

[HDS13-P16] The characteristic of the cause of death in each city in Miyagi prefecture during the Great East Japan Earthquake

*Shuji SETO[1], Fumihiko IMAMURA[1] (1.IRIDeS, Tohoku University)

[HDS13-P17] The reflective south going current, accompanied by the third wave of Tsunammi at Iioka , Asahi City , Chiba Prefecture in 2011.

*Mitsuo Harukawa[1], Noboru Hashimoto[1], Fumio Ooshima[1] (1.The Group of Recording for Tsunami Damage of Asahi City in 2011)

Possible submarine landslides as sources of the 2018 Sulawesi tsunami

*Kenji Nakata[1], Akio Katsumata[1], Abdul Muhari[2]

1. Meteorological Research Institute, Japan Meteorological Agency, 2. Ministry of Marine Affairs and Fisheries, Indonesia

Tsunami struck coastal areas of Palu bay, Slawesi Islands after an earthquake of Mw 7.5. Muhari et al. (2018) hypothesized that the tsunami was generated inside the Palu bay based on the evidence of tide gauge station records, videos, inundation distance, damage characteristics from post-tsunami surveys and so on. Furthermore, Arikawa et al. (2018) pointed out that subsidence of coastal areas may have related to tsunami generation, and that the tsunami heights were not high at the mouth of the Palu bay. While Heidarzadeh et al. (2018) reported that the tide gauge records in Palu bay were successfully simulated by the USGS’ s finite fault model, they also pointed out the possibility of the submarine landslide, following extremely large tsunamis. In this study we assumed that the recorded tsunami was caused by a submarine landslide. We investigated the possible locations and size of the submarine landslide that could express the waveform at the tide gauge station and the possibility of the tsunami generation at the shallow depth by tsunami simulations.
Results of tsunami simulation showed that it was necessary that tsunami wave source was at the shallow depth to simulate the observed period of tsunami wave. Calculated tsunami waveforms that closely matches the observed waveform was obtained at three locations in the bay. By calculating the landslide source for several fluidities, we reached a conclution sediments with low fluidity near coastal line was necessary for the landslide source.

Keywords: 2018 Sulawesi earthquake, submarine landslide, tsunami simulation

©2019. Japan Geoscience Union. All Right Reserved.

Tsunami Data Assimilation of the 2015 Torishima Earthquake

*Yuchen Wang[1], Kenji Satake[1], Osamu Sandanbata[1], Takuto Maeda[2]

1. Earthquake Research Institute, University of Tokyo, 2. Graduate School of Science and Technology, Hirosaki University

The 2015 Torishima earthquake (M5.9) occurred at the Smith caldera, on May 2, 2015. It had a CLVD-type focal mechanism and generated larger tsunami waves compared to its seismic magnitude (Sandanbata et al., 2018). Therefore, it was regarded as a ‘volcanic tsunami earthquake’ –a tsunami earthquake with volcanic origin. The tsunami reached Hachijo Island, Boso Peninsula and Shikoku Island, and were recorded by tide gauges and ocean bottom pressure gauges (Kubota, 2018). Fukao et al. (2018) proposed an opening horizontal sill model to explain its origin. The abnormal mechanism makes it difficult to forecast tsunami from its seismic magnitude.

Tsunami data assimilation forecasts the tsunami by assimilating offshore observed data into a numerical simulation, without the need of calculating the initial sea surface height at the source (Maeda et al., 2015). In the Nankai region, the Dense Oceanfloor Network System for Earthquakes and Tsunamis (DONET) records the water pressure and has real-time data transmission. Synthetic experiments showed that this observational system was able to forecast the waveforms at Shikoku Island by tsunami data assimilation approach (Wang et al., 2018). Here, we performed this method to retroactively forecast the tsunami of the 2015 Torishima earthquake. We assimilated the observations of 16 DONET stations and two ocean bottom gauges off Muroto. The tsunami waveforms at the tide gauges Tosashimizu and Kushimoto were forecasted, and compared with the actual records.

The comparison between forecasted and observed waveforms at two tide gauges suggested that our method could forecast the tsunami amplitudes and arrival time accurately. The tsunami warning could be issued to local residents of Shikoku Island more than one hour before its arrival. Our method is merely based on offshore observations, and could be implemented for future tsunami warning systems.

Keywords: Tsunami Data Assimilation, Tsunami Forecasting, Torishima Earthquake

©2019. Japan Geoscience Union. All Right Reserved.

Method for real-time estimation of tsunami sources using a network of dense ocean bottom pressure sensors

*Mayu Inoue[1], Yuichiro Tanioka[1], Yusuke Yamanaka[2]

1. Hokkaido University, 2. The University of Tokyo

After the 2011 hazardous tsunami, the Seafloor observation network for earthquakes and tsunamis along the Japan Trench (S-net) was installed by National Research Institute for Earth Science and Disaster Resilience in Japan (NIED). Various real-time tsunami-forecast methods using this S-net were developed by several researchers. The objective of this study is to develop a new method for real-time tsunami source estimation using S-net data, a simpler method than the previous methods. This study focuses on tsunami generated by great underthrust earthquakes at the plate interface off the Pacific coast of Hokkaido, Japan. First, we numerically computed tsunamis from fault models of M8.0 to M8.8 classes distributed along the plate interface along the Kurile Trench. Virtual observational waveforms at locations of sensors in S-net during each tsunami were estimated by converting the simulated tsunami waveform into a waveform of water pressure change. We tried to estimate a tsunami source area by classifying the virtual observational waveforms within 500 seconds after the origin time of the earthquake into the following three types. Type1 waveform goes down and stays down within 500 seconds. Type2 waveform includes one complete up-pulse waveform. All of the other waveforms were regarded as Type3. We found that a sensor with the type1 waveform is located in the initial uplifted area, and sensors with the type2 waveform is located not in the area but near the initial uplifted area, and the sensor with the type3 is located far from the initial uplifted area. After the tsunami source area was estimated, the magnitude of the earthquake can be estimated using the scaling relationship between the earthquake fault area and the magnitude of the earthquake. We tested four different scaling relationships suggested by previous studies to find the error of the magnitude estimation. The estimation error was found to be M ±0.08. Finally, this new method was applied to the 1952 Tokachi-oki earthquake and the 1968 Tokachi-oki earthquake source models. The tsunami source area and the magnitude of the earthquake were estimated well for both cases. Therefore, the new method should be useful for the rapid estimation of a tsunami source as a part of the tsunami early warning system.

Keywords: Tsunami forecast, S-net

©2019. Japan Geoscience Union. All Right Reserved.

Application of AI Technology for Tsunami Prediction by Oceanographic Radar

*hiromu yokosu[1], Yoshihito - Tanaka[1], Kenji - hayashi[2], Kentarou - Uehara[2]

1. Chubu Electric Power Co., Inc., 2. Japan Weather Association

At Hamaoka Nuclear Power Station, oceanographic radar (HF radar) is installed to detect the tsunami early.We can observe sea surface velocity distribution up to offshore of about 40 km approximately every minute.When a tsunami occurs, it is expected to capture the situation which the tsunami approaches and to predict the arriving tsunami.

Oceanographic radar observation captures a wide range of flow velocity distribution at once and obtains numerical result.By using the distribution situation of the change of the flow velocity on sea surface by the tsunami, we investigated the tsunami prediction by the image recognition method using AI technology.AlexNet (convolution neural network) was used for the image recognition method.

For the prediction of the tsunami, the tsunami height (first wave) and the arrival time are important, the tsunami height was classified into 1 m interval (tsunami height 10 m or less) or 2 m interval (tsunami height 10 m to 22 m), and the arrival time was classified as one minute interval (1 min to 22 min). The total was classified into 374 categories.Using the image recognition method, we examined the accuracy of the classification based on the observation situation.

In this study, the result of the tsunami simulation exceeding 5000 tsunami caused by the Nankai Trough earthquake which will have the most influence on Hamaoka Nuclear Power Station.Since the number of large-scale tsunami cases is small, we devised such as using data in seconds.Also, since AlexNet can handle color images (RGB), the current flow time change (current time, 1 minute before the current time, 2 minutes before the current time) of three steps in the learning data was applied to R, G, B.As a result, regularity such as time series of flow velocity and position information can be reflected, and the feature of image change (change in flow velocity distribution) became easier to capture.

Although the scale of the tsunami varies, it is important to predict a large-scale tsunami (tsunami height 10 m or more) at Hamaoka Nuclear Power Station, so the result of "Tsunami height 10 m or more" is described here.As for the verification of the AI prediction, the data (verification data) not used for learning data in simulation data was used.The ratio between learning data and verification data was set at about 80% and about 20%.The accuracy rate was about 77%.Regarding time, if one category (arrival time ±1 minute) is permitted, the accuracy rate improves to about 94%.So, it can be said that the error of the tsunami height is smaller than the arrival time with this image recognition method.

Keywords: tsunami prediction, oceanographic radar, AI, AlexNet

©2019. Japan Geoscience Union. All Right Reserved.

Development of the Tsunami Prediction System using fault plane solution of W-phase inversion

*Seolhan You[1], Mikyung Choi[1], Sun-Cheon Park[1], Hye-Won Lee[1], Duk Kee Lee[1]

1. Korea Meteorological Administration

Tsunami is a long-wave caused by earthquakes, submarine volcanoes or coastal landslides. The Korean Peninsula experienced tsunami damage followed by 1983 and 1993 Japan earthquakes. To respond to possible tsunamis in the surrounding seas, the Korea Meteorological Administration has operated tsunami warning system based on tsunami scenario database. Tsunami scenario database was constructed with the results (tsunami height and arrival time) of simulating tsunami assuming virtual earthquakes at each grid point spacing with 0.2˚ interval in surrounding seas of the Korean peninsula(120˚~142˚E, 25˚~45˚N) . Earthquakes were assumed with magnitude 6.0 to 9.0 having intervals of 0.2 on the fault plane which is from known information or which is assumed to generate higher tsunami in the coastal area. Therefore tsunami scenario database has a limitation that does not reflect the characteristics of earthquakes when they actually occur because the fault plane will be different from assumed one.
In this study, we have developed an algorithm for tsunami prediction capable of analyzing fault plane solution using W phase and simulating tsunami using the fault plane information. We tested the performance of the developed algorithm applying into the case of 1993 Japan tsunami. W phase inversion results were as follows: moment magnitude=7.7, depth=25.5km, strike=170.2˚, dip=45.3˚ and rake=77.8˚. As a result of tsunami simulation using the inversion results, the difference between the numerical results (tsunami height and arrival time) and measured data at tide stations was small. Therefore the algorithm for tsunami prediction may be used for tsunami warning as a complement to tsunami scenario database.

Keywords: tsunami, tsunami scenario database, W phase, tsunami prediction system

©2019. Japan Geoscience Union. All Right Reserved.

Can we detect tsunami magnetic signals at on-land observatories prior to tsunami arrivals? : From the perspective of numerical experiments

*Takuto Minami[1], Tungcheng Ho[1], Zhiheng Lin[2], Hiroaki TOH[2]

1. Earthquake Research Institute,The University of Tokyo, 2. Graduate School of Science, Kyoto University

Tsunami flow crossing the geomagnetic field generates electric currents in the ocean and associated secondary magnetic fields due to the electromotive force. This tsunami-generated magnetic (TGM) variations are observable not only at the seafloor (e.g. Toh et al. 2011) but also at on-land magnetic observatories on islands or along coastlines (e.g. Tatehata et al. 2015). Most of the TGM data reported in previous studies are from the seafloor observations since TGM signals are much stronger at the seafloor, which implies that usage of off-shore seafloor magnetic observations is a sensible solution for tsunami early warning. On the other hand, much cheaper on-land magnetic observations may be useful because the vertical component of the TGM field precedes the tsunami arrival by approximately a quarter of the tsunami period in shallow oceans (< ~ 1000 m; Minami et al. 2015). Previous studies have never carefully investigated possibilities of using on-land magnetic data in tsunami early warning, because of the difficulty in evaluating the effect of realistic topography on the TGM variations at on-land observatories.

We conduct three-dimensional simulations of TGM signals to investigate feasibility of using on-land magnetic data for tsunami early warning, with the aid of the finite element simulation code by Minami et al. (2017). This study focuses on three devastating tsunami events in the past, the 1960 Chilean tsunami (Mw 9.5), the 2011 Tohoku tsunami (Mw 9.0), and the 1707 Hoei tsunami (Mw 8.7). For the three tsunamis, we adopt the source models of Ho et al. (2019), Satake et al. (2013), and Furumura et al. (2010), respectively. Although all the three large tsunamis did extensive damage, features of their topographies are distinct from each other. One of the features of coastlines in Tohoku is ria coast, while Nankai area of Japan includes capes and bays. As for Chilean coast for the 1960 event, a straight long coastline is present in the vicinity of Santiago, Chile. We set many virtual magnetic observatories and tide stations along the coastlines and investigate arrival times of tsunamis and TGM signals. In the presentation, we compare the arrival times of tsunamis and TGM signals at each virtual observatory and to discuss feasibility of using on-land TGM signals for tsunami hazard mitigation.

Keywords: tsunami, electromagnetic, simulation

©2019. Japan Geoscience Union. All Right Reserved.

Probability of Tsunami Inundation Estimated from Tsunami Database and G-R law

*Toru Takeda[1], Toshitaka Baba[1], Tsuneo Ohsumi[2], Hiroyuki Fujiwara[2]

1. Tokushima Univ, 2. NIED

Studies on probabilistic hazard assessments considering uncertainties such as the timing and magnitude of earthquake occurrence, diversity of heterogeneous slip, etc. are common in recent years. For tsunami, probabilistic tsunami height assessments along the coast were shown. But probabilistic tsunami inundation assessments are not shown yet because tsunami inundation modeling needs highly resolved topographic data (~10m) and probabilistic approach needs calculations from huge number of earthquake scenarios. Recent development of high-performance computers enables us to make a probabilistic tsunami inundation map if the study area narrowed down. In this study, we attempt to probabilistically assess tsunami inundation in an area of the Nankai subduction zone using a tsunami database and G-R law.

In the creation of the tsunami database, we used the Nankai earthquake slip models shown by Hirata et al. (2017). The propagation and inundation of the tsunami generated by each fault model were carried out by the nonlinear shallow water equations. A nesting algorism was applied to improve the spatial resolution in the study area. Coastal structures such as seawall were defined in the tsunami calculations, but they were disable if the tsunami height is higher than the height of seawall. We defined the relative weights among the earthquake fault models using the G-R law. The weights were used in superimposing of the all inundation maps to estimate probabilities of tsunami inundation.

As a result, it was confirmed that the probability of inundation depends on the topographic features, such as the region where the probability is high in the area end of the V-shaped bay and around the upstream area of the river. We will carry out an analysis that takes into consideration the uncertainty in earthquake occurrence and tsunami height estimations. We also investigate effects of costal structures on the inundation probability.

Keywords: probabilistically assess tsunami inundation, G-R law

©2019. Japan Geoscience Union. All Right Reserved.

The Detection of Tsunami Propagation Path by Using Sensitivity Kernel Distribution

*Norihiko Hashimoto[1], Kyosuke Okamoto[2], Seiji Tsuno[3]

1. ITOCHU Techno-Solutions Corporation, 2. National Institute of Advanced Industrial Science and Technology, 3. Railway Technical Research Institute

Predicting the inundation height and arrival time by tsunami propagation analysis are very important in the tsunami disaster prevention. On the other hand, it is also an important issue to elucidate tsunami propagation path. The tsunami propagation path has been commonly calculated by wave ray method, it has used in combination with the tsunami propagation analysis based on linear long wave theory and, shallow water theory. However, in the wave ray method, it’ s difficult to set an appropriate initial value and boundary conditions consistent with tsunami propagation analysis. So we must pay attention these characteristics in considering the analysis result.
Anyway, applying the sensitivity kernel distribution and adjoint field which used in seismic tomography to the tsunami wave field, we investigated the tsunami propagation path. In this method, it is also possible to detect a propagation path of the specific component extracted from a tsunami waveform by adding a routine for propagating a tsunami waveform in the reverse direction to the general tsunami propagation analysis code.
First, we verified this method whether it is possible to detect tsunami propagation path to the observed point in the ideal space. It was assumed water of constant depth and Gaussian distribution as an initial water level.
In addition, we used this method to detect how the far-field tsunami propagate to the Japan coast. We set the calculation target range that can be covered almost whole Pacific Ocean area whose mesh size is 10 sec, the wave source was the 1960 Chilean tsunami. Analyzing characteristics of tsunami is propagated which comes from Hawaiian island across the north-south, we confirmed the result as same as previous method by wave ray method.
An issue in the future, it’ s necessary to consider a practical method to extract and propagate specific components of the tsunami waveform, and verify the possibility of applying this method for the tsunami propagation analysis based on dispersive wave theory and shallow water theory. It is thought that they will be expanded the range of application.

Keywords: Tsunami propagation path, Tsunami propagation analysis, Wave ray method, Adjoint method, Adjoint field, Sensitivity kernel distribution

©2019. Japan Geoscience Union. All Right Reserved.

Estimation of local seismic waves and rapid magnitudes for ‘slow tsunami earthquakes’ based on moment rate spectrum

*Takahito Nishimiya[1], Akio Katsumata[1]

1. Meteorological Research Institute, Japan Meteorological Agency

The tsunami height estimation at earliest stage in JMA is based on the estimated hypocenter and rapid magnitude (rapid-M) from local seismic wave data. The amplitudes of seismic waves from ‘slow tsunami earthquakes’ are usually smaller than those from normal earthquakes because those earthquakes radiate relatively low seismic energies in the short period range. Therefore it is difficult to estimate rapid-M of ‘slow tsunami earthquakes’ accurately. We would like to evaluate rapid-M of them quantitatively. However local seismic wave data of slow tsunami earthquakes is almost not available.

We estimated moment rate spectra of ‘slow tsunami earthquakes’ using tele-seismic wave data (in JpGU Meeting 2018), and calculated synthetic local seismic waves based on those spectra (in Seismological Society Fall Meeting 2018). We estimated rapid-M from the synthetic wave data here.

JMA magnitude (M_J) and M_{100} (Katsumata et al., 2013) are evaluated as the rapid-M. M_{100} is introduced by JMA to avoid underestimation of magnitude for huge earthquakes because M_J tends to indicate “magnitude saturation” for huge earthquakes. We calculated M_J and M_{100} from the synthetic wave data. REGARD (Kawamoto, 2017) based on GNSS data is also a kind of rapid-M. However we use seismic wave data from which smaller magnitude can be estimated compared with REGARD.

We assumed that a ‘slow tsunami earthquake’ occurs at the plate-boundary off the Pacific coast of Tohoku. It has the same moment rate spectrum as the Java tsunami earthquake (M_w7.8) in 1994. M_J estimated from those synthetic waves was smaller than M_w by more than 1.0. M_{100} is larger than M_J, but M_{100} is smaller than M_w by more than 0.5. We also evaluated magnitudes for an earthquake which has the same moment rate spectrum as the Sumatera tsunami earthquake (M_w7.8) in 2010. The difference from M_w reduced for the earthquake, while both M_J and M_{100} are lower than M_w.
USGS published M_s of significant earthquakes. M_s of the 1994 Java earthquake was lower than M_w by more than 0.5 although M_s of the 2010 Sumatera earthquake was about the same as M_w.

Our results suggest that big difference between M_{100} and M_J is useful for early discriminating ‘slow tsunami earthquakes’ from normal earthquakes. Even if M_{100} is much greater than M_J, M_{100} may be underestimated for slow tsunami earthquakes.

Keywords: tsunami earthquake, spectrum, local seismic wave, magnitude

©2019. Japan Geoscience Union. All Right Reserved.

Development of tsunami simulator TNS and release of version 1.0

*Takayuki Miyoshi[1], Wataru Suzuki[1], Naotaka YAMAMOTO CHIKASADA[1], Shin Aoi[1], Sho Akagi[2], Toshihiko Hayakawa[2]

1. National Research Institute for Earth Science and Disaster Resilience, 2. Mitsubishi Space Software Co.,Ltd.

A tsunami is a natural phenomenon in which disturbance generated in the sea by abrupt submarine deformation, propagates to the surrounding sea area with the gravity as restoring force, and often runs up to the land area. The National Research Institute for Earth Science and Disaster Resilience (NIED) has developed a software that can calculate a tsunami phenomenon including inundation on a computer by numerical simulation using finite-difference method (Miyoshi et al., 2018 JpGU). The software was named Tsunami Simulator (TNS: TsuNami Simulator).

Numerical codes of the TNS was developed to operate on the Central Processing Unit (CPU) and the Graphics Processing Unit (GPU), the main code of the CPU written in Fortran 90 and the GPU written in CUDA C in accordance with CUDA 7.5. The concept of the codes is basically equivalent to TUNAMI-N2 (Imamura et al., 2006), and tsunami propagation and inundation based on two-dimensional nonlinear long wave theory can be implemented using a nesting grid with a space grid ratio of 1: 3 in the Cartesian coordinate system. The initial wave height is calculated by the crustal movement in the semi-infinite medium with respect to a fault plane using the program DC3D (Okada, 1992 BSSA). Horizontal crustal movement (Tanioka and Satake, 1996 GRL) and hydraulic filters by Kajiura (1963, BERI) are also applicable. In the offshore boundary, the transmission boundary (Imamura et al., 2006) and the absorb area (e.g. Clayton et al., 1977 BSSA) are applied, and inundation boundary is used in the land side (Kotani et al., 1998 Coastal Engineering Journal). For distant tsunamis, a spherical coordinate system is introduced and connects to the region in the Cartesian coordinate where inundation simulation is carried out. In the spherical coordinate, Coriolis force and dispersion effect can be considered as the previous study, and loading effect (Inazu and Saito, 2013 EPS) can also be applied.

Real-time tsunami inundation forecast system using numerical database requires a large amount of tsunami scenario. From the TNS development version, we packaged the essential parts for constructing a tsunami scenario bank and released as TNS Version 1.0 (Miyoshi et al., 2019 Technical Note of the NIED). The users are assumed to be researchers, engineers, officers of local governments who is responsible for disaster prevention, and make it possible to calculate on the general Linux environment. The package included an operation guide, executable files precompiled on Linux, and some examples. The solver can conduct sequential computation by single CPU, and can conduct parallel computation using OpenMP, and the general-purpose computing on graphics processing units (GPGPU) in order to achieve reduction of calculation time.

Acknowledgements: This work is partly supported by Council for Science, Technology and Innovation (CSTI), Cross-ministerial Strategic Innovation Promotion Program (SIP), “Enhancement of societal resiliency against natural disasters” (Funding agency: JST).

Keywords: Tsunami, Inundation, Finite-difference method, Nesting grid, GPU

©2019. Japan Geoscience Union. All Right Reserved.

A Study on Tsunami Inundation Simulation for the Nankai Trough Earthquake for Osaka City

*Kaoru Kawaji[1], Seiji Tsuno[2]

1. ITOCHU Techno-Solutions Corporation, 2. Railway Technical Research Institute

In planning disaster prevention measure against the tsunami, it is a very important factor how will the tsunami occur by occurrence of an earthquake and how it will attack. Since the Scenario of the Nankai Trough fault seismic source model was announced from the Cabinet Office as the maximum assumed wave source , various local governments and others are considering various disaster prevention measures and others. In this research, we carried out the tsunami inundation simulation for Osaka City using all 11 case fault models of the Nankai Trough's large earthquake model study meeting (2nd report) announced by the Cabinet Office in August 2012 , and examined the results.

Topographical model in tsunami inundation simulation was using topographic data published by the Cabinet Office, and we modeled with a 1215m grid about range of 1200km ×800km including from the fault to the coast. The calculation time was set to a maximum of 6 hours so that the maximum inundation area and the maximum inundation depth due to the tsunami could be calculated, and the calculation time interval was set to 0.01 second interval so that the calculation was stable.

If the parameters (slip angle, position, epicenter) etc in the fault seismic source model are different, the tsunami characteristics such as the tsunami wave height, the arrival time of the tsunami and the inundation range of tsunami should be different. However, it was different that the location of the large slip region and the epicenter in the fault model of 11 cases, but almost the same tsunami level and arrival time were found in the observation points in Osaka Bay in all cases. It was also found that the maximum wave height appearance time is within 30 minutes from the start of rupture regardless of the case. This trend can be seen similarly in the vicinity of the Kii Channel, off the coast of Osaka Bay, and this trend is thought to be the influence of the topographic of the intricate straits sandwiched between Kii Peninsula and Kochi / Kagawa. We will continue further multilateral investigation in the future and report on the results as well.

Keywords: Tsunami inundation simulation, Nankai Trough Earthquake, Osaka-bay

©2019. Japan Geoscience Union. All Right Reserved.

Database construction of Tsunami inundation simulation for large subduction earthquakes

*Mariko Korenaga[1], Seiji Tsuno[2], Kaoru Kawaji[1]

1. ITOCHU Techno-Solutions Corporation, 2. Railway Technical Research Institute

In the area facing the Nankai Trough, the danger of the tsunami caused by the large subduction earthquake is an urgent task. Because the earthquake occurrence area is too close, it is very important to grasp the possibility of inundation in advance, not after the earthquake occurred.

Therefore, from the viewpoint of tsunami protection against railway structures, databases of tsunami height near the coast and tsunami inundation zones were created, assuming a large number of scenario earthquakes for specific cities on the Pacific coast. Using this result we will investigate the risk of risk assessment due to the maximum inundation area and the delay time of evacuation compared to the coastal prediction results.

Coastal tsunami height tends to increase when large slip regions and super large slip regions exist in front of the coastline in each target area, but the spread of the inundation area is also related to the position in the dip direction of the large slip region. We would like to discuss what kind of information is important for mitigating tsunami damage from the standpoint of railroad disaster prevention while quantitatively examining the various inundated areas obtained.

Keywords: Tsunami simulation, Nankai trough, Reduction of disaster damage

©2019. Japan Geoscience Union. All Right Reserved.

Sediment Transport Modeling due to Tsunamis caused by the Nankai great earthquakes

*Takuya Saito[1], Kei Yamashita[2], Toshitaka Baba[1]

1. Tokushima Univ., 2. Tohoku Univ.

Tsunami that comes to the area in shallow water causes massive erosion and deposition of the coastal area. This causes damage such as collapse of coastal structures, burial of routes and blockage of water intakes at power stations. In the 2011 Tohoku Region Pacific Offshore Earthquake, collapses of coastal levees and burial of routes were caused by scouring. Damage caused by sediment transport will be prolonged, affecting recovery activities after the disaster. On the other hand, for disaster mitigations, it is necessary to accurately investigate the earthquakes and tsunamis back to the past as much as possible in order to estimate the maximum size of the earthquake and tsunami. Tsunami sediments are important information in studies of the historical earthquakes. Therefore, we simulated sediment transport using a numerical model developed by Takahashi et al. (1999, 2000, and 2011) for the great Nankai earthquakes.

The first study area is Tachibana-Bay classified as an important port having the rias coast in Shikoku, the southwestern Japan. In the simulation results, erosions were predicted in the straits between the islands, at the tip of the cape, near the estuary of the river and near the coastal levees. Sediment depositions were predicted in the vicinity. The maximum changes in erosion and sediment were about 10 m, about 6 m, respectively, for the great Nankai earthquakes (Mw 9.1). These were about 6 m and about 2 m, respectively, for the 1707 Hoei earthquake.

The other study area is a pond near the Cape Kamoda where tsunami sediment was found in the sediment layer about 2000 years ago (Okamura et al, 2012). However, all simulations we conducted in this study did not deposit sediment into the pond.

Acknowledgments: We thank Dr. Takahashi for providing us with the sediment transport software. This research is supported by Grant-in-Aid for Scientific Research 15H05718.

Keywords: Nankai Trough Earthquake, Sediment Transport software

©2019. Japan Geoscience Union. All Right Reserved.

Tsunami model of the 2011 Tohoku Earthquake reproducing the wave gauge record offshore the Fukushima Daiichi NPP

*Toshimichi Kaneto[1], Ayumi Nishi[2], Tadashi Annaka[2]

1. Tokyo Electric Power Company Holdings,Inc, 2. Tokyo Electric Power Services Co,Ltd

1. Objectives of research
During the 2011 off the Pacific coast of Tohoku Earthquake, severe core damage accidents occurred in unit one, two and three in Fukushima Daiichi nuclear power plant due to the failure of core cooling after the reactor shutdown. For understanding the process of tsunami caused by the earthquake and for utilizing tsunami evaluation at the nuclear power plants, tsunami source model, L67, of the 2011 Tohoku Earthquake was determined based on the data of the tsunami waves, crustal deformation and run-up height.
Although the model L67 can simulate the first tsunami and the first crest of the secondary tsunami of wave gauge record offshore the Fukushima Daiichi NPP, it cannot reproduce the second crest of the secondary tsunami. Imamura et al. (2016) proposed the revised model of Sugino et al. (2013) which reproduce the second crest of the secondary tsunami. In this research we improve the reproducibility of the wave gauge record based on the following approach.

2. Contents of research
(1) Joint inversion of tsunami wave and 1-second sampling GPS data
For developing the model L67, we took the consideration of the problem that the slip process of the previous tsunami source models such as Cabinet office (2012), Sugino et al. (2013) and Satake et al. (2013), has long duration compared with those of models based on earthquake ground motion data and that of 1-second sampling GPS data by Geospatial Information Authority, Japan. In order to resolve this problem we used the short time window for inversion as 30 sec times 3. Consequently the slip process of the model L67 has shorter duration compared with the above tsunami source models.
In this research we conducted the joint inversion using tsunami wave and 1-second sampling GPS data. It seems that the duration of slip process will become naturally shorter by using the 1-second sampling GPS data.

(2) Inversion using “hypothetical tsunami records”
Non-linear effect is strong in the wave gauge record offshore the Fukushima Daiichi NPP. So we can use only initial portion of the record for the linear inversion. In order to improve the reproducibility of the wave gauge record, “a hypothetical tsunami record” at the depth of 50 m offshore the Fukushima Daiichi NPP was simulated using the initial fault model and the green functions and the adjusted hypothetical tsunami record was added to the inversion as observed record. The calculated tsunami wave became similar to the wave gauge record through a trial and error process.
The same approach was used for improving the K and kappa for the run-up height data.

3. Conclusions
The tsunami source model of the 2011 Tohoku Earthquake reproducing the wave gauge record offshore the Fukushima Daiichi NPP was determined based on the above inversion approach. The duration of slip process became naturally shorter by using the 1-second sampling GPS data. The reproducibility of the wave gauge record was much improved compared with the model L67 by using the “hypothetical tsunami record”. Goodness of fit for tsunami wave and run-up height is same as that for model L67.

©2019. Japan Geoscience Union. All Right Reserved.

References
Imamura et al. (2016) The re-examination of the tsunami affected on the Fukushima Daiichi nuclear power plant by revising the tsunami model for the 2011 Tohoku Pacific Ocean earthquake tsunami, Journal of JSCE (Coastal Engineering), Vol.72, No.2,I-361-I-366

Acknowledgments
We thank GSI (Geospatial Information Authority, japan), NGDS (Nippon GPS Data Service, Japan), Hitz (Hitachi Zosen Co., Japan), GPSS (GPS Solutions Boulder, CO, USA), and VERIPOS for providing “1Hz_2hr_files”.

Keywords: tsunami source model, the 2011 off the Pacific coast of Tohoku Earthquake, Fukushima Daiichi nuclear power plant, 1-second sampling GPS data

©2019. Japan Geoscience Union. All Right Reserved.

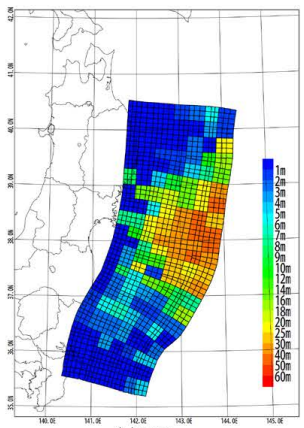
(a)L67

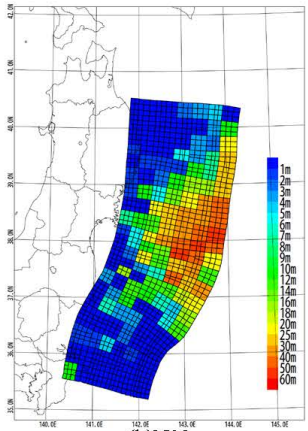
(b)N03

図1　波源の比較

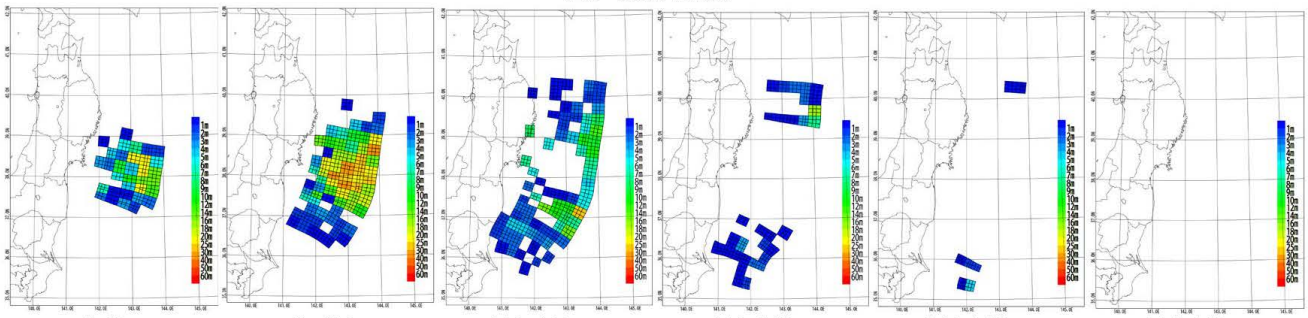

図2　破壊進展図(L67)

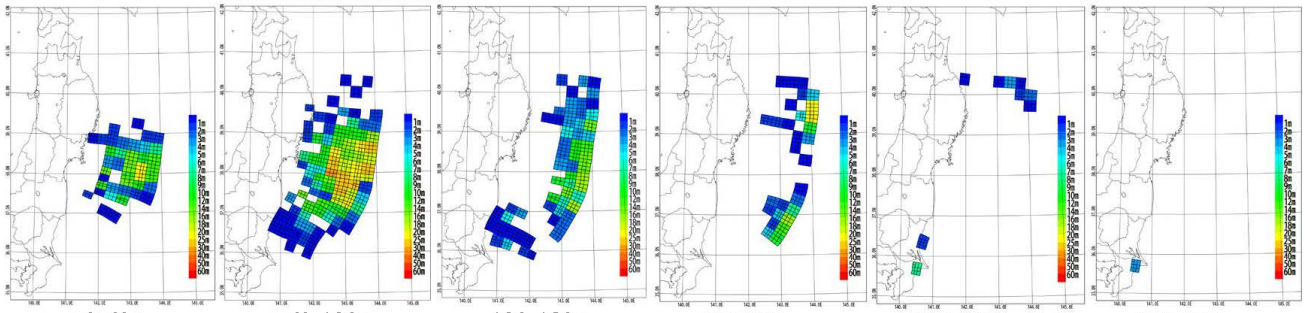

図3　破壊進展図(N03)

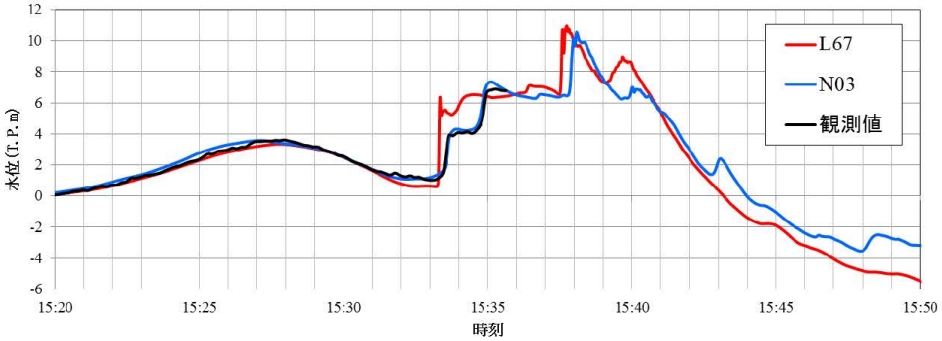

図4　波高計での観測値と計算値の水位時刻歴

表1　適合度表 (K, κ)

	L67		N03	
	K	κ	K	κ
北海道～千葉 (3882 点)	1.00	1.34	1.00	1.34
福島第一 (19 点)	1.00	1.10	0.99	1.11
福島第二 (71 点)	0.99	1.18	1.00	1.13

©2019. Japan Geoscience Union. All Right Reserved.

Development of tsunami fragility curves on railway structures based on the 2011 off the Pacific coast of Tohoku earthquake

*Teppei Ono[1], Seiji Tsuno[2], Yuko Sato[2], Marioko Korenaga[1]

1. ITOCHU Techno-Solutions Corporation, 2. Railway Technical Research Institute

The Great Tsunami associated with the 2011 off the Pacific coast of Tohoku earthquake caused severe damage to railway structures on the coast of the Tohoku region in Japan. It is effective to obtain fragility curve from damaged data in this disaster to predict the risks of railway structures to the tsunami in the future. It is generally represented by a lognormal distribution or a normal distribution. In this study, we obtained fragility curve by integrating spatial damage data for railway structures and spatial inundation data accompanying the 2011 off the Pacific coast of Tohoku earthquake on GIS. The method of obtaining tsunami fragility curves were referred to Koshimura et al. (2009).
In this study, we collected the data of damage and location for railway structures located in the Tohoku region to refer multiple documents. First, the data of inundation depth at intervals of 100 meters of the 2011 off the Pacific coast of Tohoku earthquake published by the Ministry of Land, Infrastructure and Transport was utilized to grasp the inundation depth where the railway structure is located. Second, we used the railway data of MLIT and Geospatial Information Authority to grasp the location of the railway structure. The kinds of structure in railway structures are different from station, bridge, tunnel, railway crossing, roadbed, retaining wall, cage, embankments, cuts and so on. The kinds of material in railway structures are also such as soil, C, RC. The tsunami fragility curves were obtained by using the all data and the case of using only RC to consider the influence of the structural kind.
As a result, it was shown that the gradient of tsunami fragility curve becomes smaller as compared with the tsunami fragility curve for buildings in the 2011 off the Pacific coast of Tohoku earthquake shown at Koshimura and Gokon (2012). The reason is to obtain the tsunami fragility curve from various railway structures. Furthermore, tsunami damage probability for railway structure on Ishinomaki in Miyagi Prefecture and Shimanokoshi in Iwate Prefecture were shown to confirm the reproducibility of the obtained tsunami fragility curve by using the spatial inundation depth calculated by using the Cabinet Office model.

Keywords: Tsunami fragility curve, The 2011 off the Pacific coast of Tohoku earthquake, Railway structures

©2019. Japan Geoscience Union. All Right Reserved.

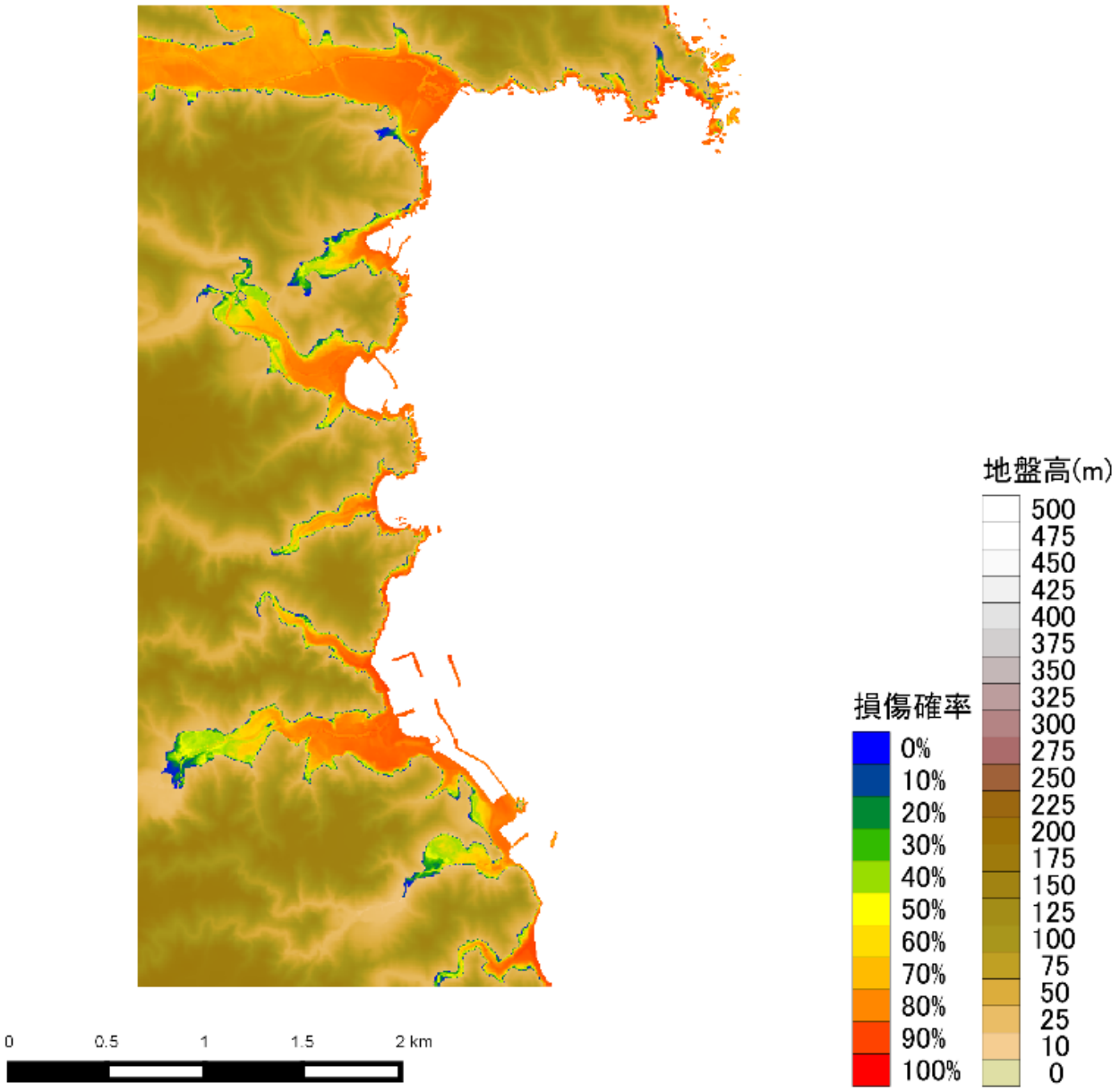

©2019. Japan Geoscience Union. All Right Reserved.

The characteristic of the cause of death in each city in Miyagi prefecture during the Great East Japan Earthquake

*Shuji SETO[1], Fumihiko IMAMURA[1]

1. IRIDeS, Tohoku University

About 20,000 people died in the Great East Japan Earthquake tsunami that occurred in 2011. According to the National Police Agency (2012), 90% of the victims in Iwate, Miyagi and Fukushima prefectures were drowned. Aoki et al. (2012) reported the results of questionnaires to physicians who actually examined in the affected areas. The questionnaire result showed that the National Police Agency's cause of death statistical result was reasonable, and that some physicians could not but describe it as drowning as a realistic problem.

This suggests that victims in a tsunami disaster may diefromcause of death other than drowning. According to Kahoku Shimpo(2011), the survivors witnessed the victims who died of symptoms like hypothermia after exposure to the tsunami. However, the details of the cause of death excluding drowning has not been elucidated yet.

Seto and Imamura(2019) classified the causes of death in Miyagi Prefecture during the 2011 Great East Japan Earthquake tsunami using victim information provided by Miyagi Prefecture Police Headquarters. As a result,the cause of death was classified into the following 12 kinds; Injuries to the head, Injuries to the neck, Injuries to the thorax, traumatic shock, Unspecified multiple injuries, Asphyxiation, Drowning, death due to fire, Hypothermia, Heart disease, Othrers and Unknown. And, they showed the proportion of each cause of death in Miyagi prefecture. The proportion in each city are needed to clarify the casualty in the Great East Japan Earthquake in more detail.

In this study, wecarried outthe analysis using the address data in victim information provided by Miyagi Prefecture Police Headquarters. The data are resident address and bodies found location. Combining each address data and the above 12 kinds of cause of death, we showed characteristics of each cause of death in each city in Miyagi prefecture.

Keywords: The 2011 Tohoku earthquake tsunami, Disaster science

©2019. Japan Geoscience Union. All Right Reserved.

The reflective south going current, accompanied by the third wave of Tsunammi at Iioka , Asahi City , Chiba Prefecture in 2011.

*Mitsuo Harukawa[1], Noboru Hashimoto[1], Fumio Ooshima[1]

1. The Group of Recording for Tsunami Damage of Asahi City in 2011

Shortly after the third wave of tsunami had gone to the north, Iioka was attacked abruptly by the south going current, which caused the disaster. The question is why the south going current occurred. The purpose of this thesis is to explain this issue.
After the disaster, we soon began to visit all the houses along the coast of Asahi City for interviews, and gathered about 650 personal experiences and eyewitness accounts. We found some of them very important. The summary is as follows.
When the third wave of tsunami reached the north coast of Iioka , it was reflected slightly eastward . Then the reflected current went down south along the seawall of west coast of Iioka. After a while, the south going current ran against the succeeding north going current that belonged to the third wave of tsunami. As a result of that collision, the wave height of south going current was increased so much that the wave got over the seawall and destroyed the houses from north to south.
By oblique mono photogrammetry, we calculated the strikes of the wave planes of south going current, and made a wave plane map, which we think proves the eyewitness accounts mentioned above to be right.
A TV program said that *the south going current was the edge wave of the first wave of tsunami*(April 9,2014 FNN), but we don't think it is the case. After the first wave of tsunami had gone, the tidal wave went far off the shore, leaving no seawater along the north coast of Iioka. The large area of the sea floor was visible. It is clear that no edge wave of the first wave stayed there.
Conclusion The south going current was not the edge wave of the first wave of tsunami. It was the reflective current of the third wave of tsunami.
Reference Mitsuo Harukawa(2013) Maps and speeds of Tsunami measured by oblique mono photogrammetry with video image in Asahi City , Chiba Prefecture (JGUMeeting2013HDS26-15)

Keywords: strike of wave plane, photogrammetry, reflective wave , Chiba Prefecture, Asahi City, Iioka

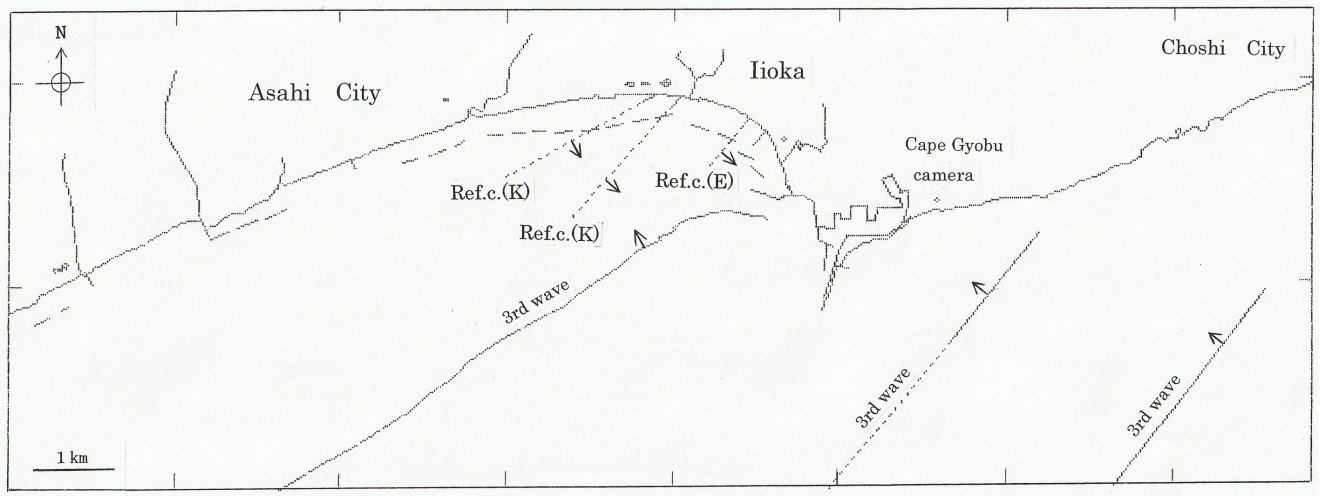

©2019. Japan Geoscience Union. All Right Reserved.

[J] Oral | H (Human Geosciences)：H-DS Disaster geosciences

Tue. May 28, 2019 3:30 PM - 5:00 PM JST | Tue. May 28, 2019 6:30 AM - 8:00 AM UTC | Convention Hall B 2F

[H-DS13] Tsunami and Tsunami Forecast

convener:Naotaka YAMAMOTO CHIKASADA(National Research Institute for Earth Science and Disaster Resilience), Hiroaki Tsushima(Japan Meteorological Agency), Tatsuya Kubota(National Research Institute for Earth Science and Disaster Resilience), Chairperson:Osamu Sandanbata, Tatsuya Kubota

This session discusses issues related to improving real-time and long-term prediction accuracy of tsunami from earthquakes, landslides, and volcanoes, which include such as a better understanding of tsunami dynamics, new real-time tsunami observing systems deployed in the open ocean and coastal waters, methodologies of more rapid and accurate prediction during tsunami emergencies, more extensive and accurate inundation maps, and long-term tsunami potential forecast.

3:30 PM - 3:45 PM JST | 6:30 AM - 6:45 AM UTC

[HDS13-01] Sensibility analysis for the inundation tsunami height due to 2018 Sulawesi earthquake and tsunami

★Invited Papers

*Taro Arikawa[1], Abdul Muhari[3], Shota Takeda[1], Anawat Suppasri[2], Fumihiko Imamura[2] (1.Chuo University, 2.IRIDES, Tohoku University, 3.Ministry of Marine Affairs and Fisheries, Indonesia)

3:45 PM - 4:00 PM JST | 6:45 AM - 7:00 AM UTC

[HDS13-02] Tsunami Source of the 2018 Sulawesi Earthquake Estimated from Tsunami and InSAR Data

*Tungcheng Ho[1], Kenji Satake[1], Shingo Watada[1], Ray Y Chuang[2], Chih-Heng Lu[2] (1.Earthquake Research Institute,The University of Tokyo, 2.Department of Geography, National Taiwan University)

4:00 PM - 4:15 PM JST | 7:00 AM - 7:15 AM UTC

[HDS13-03] **Source Models of the Two September and December 2018 Indonesia Tsunamis Based on Spectral Analyses and Numerical Modeling**

*Mohammad Heidarzadeh[1], Abdul Muhari[2], Tomoya HARADA[3], Takeo Ishibe[4], Antonius Wijanarto[5] (1.Brunel University London, 2.Ministry of Marine Affairs and Fisheries, Jakarta 10110, Indonesia, 3.Earthquake Research Institute, The University of Tokyo, Japan, 4.Association for the Development of Earthquake Prediction, Tokyo, 101-0064, Japan, 5.Badan Informasi Geospasial, Cibinong, Indonesia)

4:15 PM - 4:30 PM JST | 7:15 AM - 7:30 AM UTC

[HDS13-04] Abrupt Large Uplift Caused by Volcanic Tsunami Earthquakes near the Kermadec Islands, New Zealand

*Osamu Sandanbata[1], Shingo Watada[1], Kenji Satake[1] (1.Earthquake Research Institute, the University of Tokyo)

4:30 PM - 4:45 PM JST | 7:30 AM - 7:45 AM UTC

[HDS13-05] **Adaptive tsunami waveform inversion for estimating coseismic vertical displacements and slip distribution**

*Iyan E. Mulia[1], Aditya Riadi Gusman[2], M. Jakir Hossen[3], Kenji Satake[1] (1.Earthquake Research Institute, The University of Tokyo, 2.GNS Science, 3.BRAC University)

4:45 PM - 5:00 PM JST | 7:45 AM - 8:00 AM UTC

[HDS13-06] Real-time tsunami prediction in a coastal zone, using a superposition of Green's function

*Seiji Tsuno[1], Norihiko Hashimoto[2] (1.Railway Technical Research Institute, 2.ITOCHU Techno-Solutions Corporation)

Sensibility analysis for the inundation tsunami height due to 2018 Sulawesi earthquake and tsunami

*Taro Arikawa[1], Abdul Muhari[3], Shota Takeda[1], Anawat Suppasri[2], Fumihiko Imamura[2]

1. Chuo University, 2. IRIDES, Tohoku University, 3. Ministry of Marine Affairs and Fisheries, Indonesia

Today’s Japan has conducted immediate, wide-area tsunami forecasts using the quantitative tsunami forecasting system that databases results of numerous preliminary tsunami simulations. In the future, in order to conduct more accurate tsunami forecasts, it is necessary to verify the accuracy of the tsunami run-up calculation. However, there were few studies about the variation of run-up tsunami force by calculating on-site. In this study, we conducted the on-site tsunami run-up calculation using the two-dimensional simulator and analyzed the variation of run-up tsunami force.

We focused on the earthquake near Palu, Indonesia on September 28, 2018. We set some tsunami sources based on the results of the field study, (by Arikawa *et al.*) and conducted the 300 cases of two-dimensional tsunami run-up simulations by changing the fault parameters. Next, we investigated statistically the variation of the maximum inundation depth and Froude number at the maximum inundation depth. Using the calculation results of all cases we conducted, we made groups every 0.2m from the small inundation depth and made histograms of the maximum inundation depth and Froude number for each group.
As a result, the average of Froude number increased monotonically as the maximum inundation depth increased, and the variance of Froude number tended to increase about 4 times as the maximum inundation depth increased. This corresponds to a value of Froude number of 1.5 to 2.0 times. This indicates that even if the inundation depth is the same, there is a possibility that there is a difference in tsunami force, so it is necessary to investigate the variance of the Tsunami force in the area where the inundation depth is large. In addition, it is also necessary to further study the variance of the flow velocity in numerical calculation.

Keywords: 2018 Sulawesi earthquake and tsunami, Landslide tsuanmi, Inundation simulation

©2019. Japan Geoscience Union. All Right Reserved.

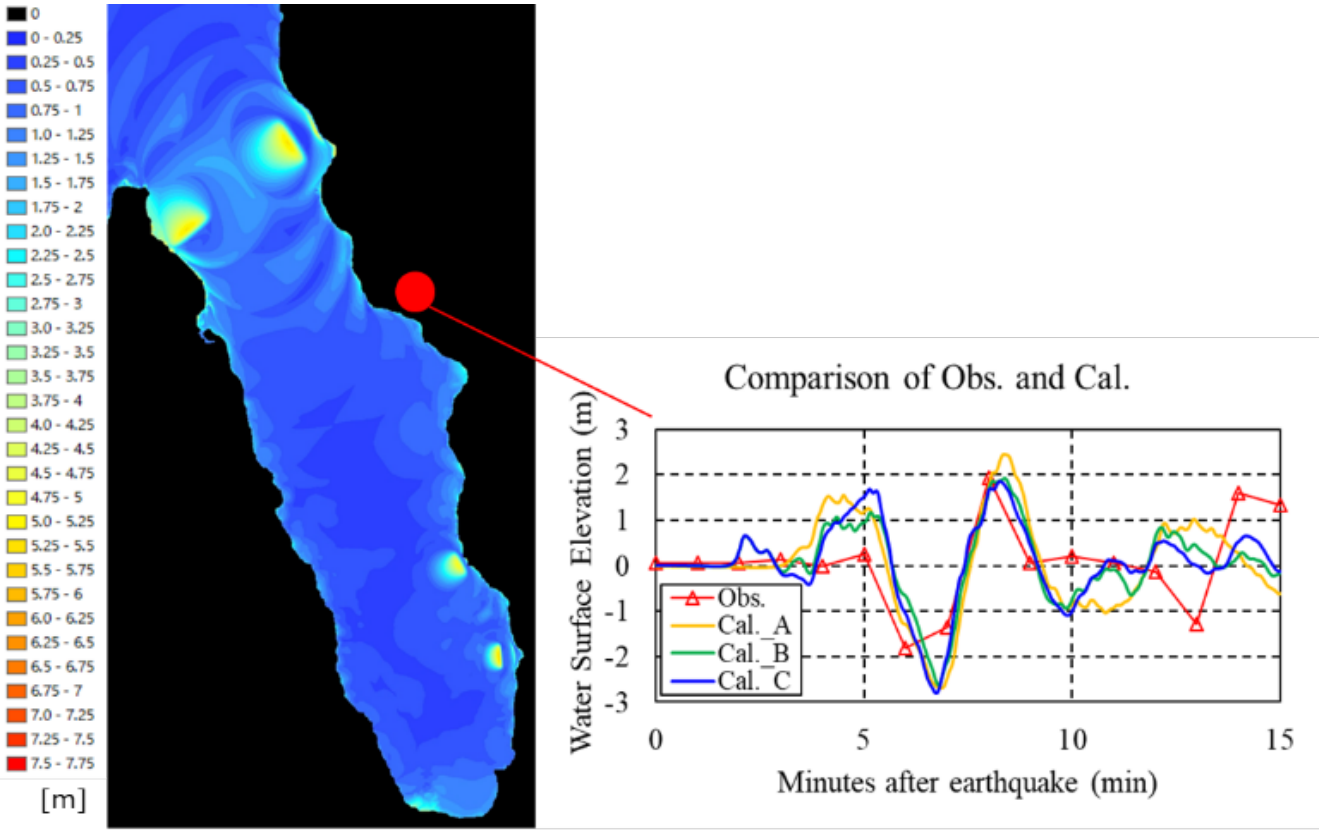

©2019. Japan Geoscience Union. All Right Reserved.

Tsunami Source of the 2018 Sulawesi Earthquake Estimated from Tsunami and InSAR Data

*Tungcheng Ho[1], Kenji Satake[1], Shingo Watada[1], Ray Y Chuang[2], Chih-Heng Lu[2]

1. Earthquake Research Institute,The University of Tokyo, 2. Department of Geography, National Taiwan University

An unexpected destructive tsunami struck Palu Bay after the Mw 7.5 strike-slip faulting earthquake in Sulawesi, Indonesia, on 28 September 2018. This tsunami impacted Palu city with 5 m to 10 m runup. The combined effects of the earthquake and tsunami caused a few thousand casualties. The tsunami waves were observed by two tide gauges in Sulawesi. One tide gauge at Pantoloan port in the bay recorded tsunami waves starting at about 5 minutes after the earthquake with amplitudes of up to 2 m. The other tide gauge at Mamuju port recorded tsunami waves after about 20 minutes with peaks of about 10 cm. To understand the mechanism of this unusual tsunami, we jointly utilized the tsunami records and InSAR data to analyze the source of this earthquake. The InSAR data observed by Sentinel-1 well resolved the offset of horizontal ground movement in the direction of the orbit azimuth along the fault strike. The data show a strike of about 358˚ in the north of the bay and about 352˚ in the south of the bay. The magnitude of the offsets varied from about 1 m in the north to up to 5 m in the south. Our simple modeling result suggests a slip of about 5 m at the north and a slip up to 8 m at the south to reproduce the observed tsunami waveform at Pantoloan. The southern asperity extended about 40 km from the bay with a width of about 16 km. Tsunami travel time analysis showed that the main tsunami arrived at the Mamuju station after about 45 minutes which means the first tsunami wave at this station was triggered by another source.

Keywords: Palu, tsunami, InSAR, Sulawesi Earthquake, source inversion

©2019. Japan Geoscience Union. All Right Reserved.

Source Models of the Two September and December 2018 Indonesia Tsunamis Based on Spectral Analyses and Numerical Modeling

*Mohammad Heidarzadeh[1], Abdul Muhari[2], Tomoya HARADA[3], Takeo Ishibe[4], Antonius Wijanarto[5]

1. Brunel University London, 2. Ministry of Marine Affairs and Fisheries, Jakarta 10110, Indonesia, 3. Earthquake Research Institute, The University of Tokyo, Japan, 4. Association for the Development of Earthquake Prediction, Tokyo, 101-0064, Japan, 5. Badan Informasi Geospasial, Cibinong, Indonesia

Indonesia was struck by two tsunamis in September and December 2018 in Sulawesi and Sunda strait, respectively. The combined fatalities from the two events were ~2500 people which made 2018 as one of the deadliest year for Indonesia in terms of natural disasters. The 2018 twin tsunamis were unique because both events were not generated by typical earthquake-generated seafloor deformation. The Sulawesi tsunami in September 2018 was most likely associated with a large submarine landslide (Heidarzadeh et al., 2018, Pure & Appl. Geophys. 176) and the Sunda event was of volcanic origin. Therefore, there have been intense speculations in the scientific community about the origins and mechanisms of these twin tsunamis without any clear clues about the source mechanisms so far (February 2019). Our methodology here to address the puzzle of the 2018 twin tsunamis is analyzing the observed tide gauges records of both events and then applying numerical simulations. For the Sulawesi tsunami, two tide gauge records were analyzed belonging to Pantoloan (inside the Palu Bay) and Mamuju (outside the Palu Bay). Maximum tsunami trough-to-crest heights of 380 and 24 cm, were measured in Pantoloan and Mamuju, respectively. Spectral analyses of the tide gauge records revealed dominating wave periods of 3.6–4.4 and 10 min at the aforesaid stations, respectively. Spectral results indicate that the tsunami source dimensions should have been most likely in the range of 3.4–4.1 km and 32.5 km, for inside and outside of the Palu Bay, respectively. We were able to reproduce the two observed tide gauge records using numerical simulations. However, the maximum simulated runup was approximately 2 m which was less than the observed runup of 11 m. It is likely that a secondary source, i.e. submarine landslide(s), has contributed to the tectonic source of the tsunami. We identify the southern part of the Palu Bay, around the latitude of -0.82°S, as the most likely location of a potential landslide based on our backward tsunami ray tracing analysis. For the Sunda tsunami, four tide gauges were analyzed revealing wave amplitudes in the range of 44-139 cm. The dominating period of the waves were ~7 min which are shorter than tsunamis generated by earthquakes. We have considered several landslide scenarios and conducted numerical modeling in order to reproduce the observed tsunami waves on the tide gauges and propose a source model for this tsunami.

Keywords: Tsunami, Indonesia, Sulawesi, Krakatoa Volcano

©2019. Japan Geoscience Union. All Right Reserved.

Abrupt Large Uplift Caused by Volcanic Tsunami Earthquakes near the Kermadec Islands, New Zealand

*Osamu Sandanbata[1], Shingo Watada[1], Kenji Satake[1]

1. Earthquake Research Institute, the University of Tokyo

Abnormal non-double-couple (NDC) earthquakes are sometimes observed near volcanic or geothermal areas [e.g. Shuler et al., 2013, JGR], some of which generate large tsunamis despite their moderate seismic magnitudes, M5-6. The Torishima earthquakes are ones of the few examples and were attributed to a large crustal uplift associated with some volcanic activity at a submarine caldera edifice on Izu-Bonin Ridge [Fukao et al., 2018, Sci. Adv.; Sandanbata et al., 2018, PAGEOPH]. This type of earthquakes therefore can be regarded as "volcanic tsunami earthquakes."

Another series of volcanic tsunami earthquake were observed near the Curtis and Cheeseman Islands, parts of the Kermadec Islands, north of New Zealand, on 17 Feb 2009 and 8 Dec 2017 (UTC). Tsunamis were recorded at tide gauges and ocean bottom pressure gauges with a maximum amplitude of ~40 cm. The two earthquakes are remarkably similar in seismic magnitudes (M~6.0), focal mechanisms (dominant NDC components), centroid locations (gap of ~10 km) and observed tsunami waves.

In order to investigate their tsunami sources, we numerically solved two-dimensional Boussinesq-like equations with the simulation code, JAGURS [Baba et al., 2015, PAGEOPH]. We first located their source region in the vicinity of the Curtis and Cheeseman Islands, by assuming Gaussian-shaped sea-surface uplifts at 9 locations. We then conducted the tsunami waveform inversion with Green’s functions computed from cosine-tapered uplift distributed around the islands. The estimated tsunami source has a large sea-surface uplift concentrated just over a bathymetric depression that is a characteristic structure of calderas. This suggests a large uplift on seafloor was caused by the earthquakes associated with a volcanic activity of the submarine caldera.

Large uplift events called “resurgence” have been observed at calderas in nature and experiments, which are often attributed to reactivation of ring faults due to overpressure of a magma reservoir [e.g. Acocella et al., 2001, JVGR]. We modeled crustal deformation of a caldera with an interacted system of a ring-fault structure and a shallow sill-like magma reservoir [Liu et al., 2017, AGU Fall Meeting]. Our modeling suggests that the system can cause a large uplift concentrated just over the caldera. The uplift also reproduced tsunami waves similar to the observations, while the gap between seismic and tsunami magnitudes can be explained qualitatively. We therefore suggest that a ring-fault reactivation due to overpressure in a sill-like magma reservoir as a possible mechanism of the earthquakes and their resultant tsunamis.

Keywords: volcanic earthquake, volcanic tsunami, volcanic tsunami earthquake, caldera, tsunami, submarine volcano

©2019. Japan Geoscience Union. All Right Reserved.

Adaptive tsunami waveform inversion for estimating coseismic vertical displacements and slip distribution

*Iyan E. Mulia[1], Aditya Riadi Gusman[2], M. Jakir Hossen[3], Kenji Satake[1]

1. Earthquake Research Institute, The University of Tokyo, 2. GNS Science, 3. BRAC University

We developed an advanced two-step tsunami source inversion method with adaptive Green's functions by applying an optimization and a reciprocity principle (Mulia et al., 2018 JGR). In the first step, the method reconstructs the sea surface displacement from observed tsunami waveforms based on a superposition of Gaussian-shaped unit sources. Here, we optimize the unit source locations that give the best fit of waveforms to observations. This leads to non-equidistantly distributed unit sources, in which the synthetic waveforms from such sources to the observation points are generated using the reciprocity principle to save computational efforts of Green's functions. In the second step, the reconstructed sea surface displacement is used to estimate the slip on a finite fault plane. We also optimize the fault parameters that produce the closest displacement pattern to the first step result. Therefore, our method provides best fitting of waveforms and optimum fault parameters with automation for the process. The current method improves our previous studies, in terms of the construction of tsunami Green's functions using the reciprocity principle and determination of fault parameters through the optimizations.

We tested the proposed method using tsunami data of the 2004 Kii Peninsula, Japan event generated by an M_w 7.4 intraplate earthquake. Our result revealed a maximum initial displacement of approximately 0.5 m with the uplift region extended northwest to the epicenter. This value is slightly higher than that of most source models by the previous studies (e.g. Baba et al., 2005 EPS, Satake et al., 2005 EPS), but yields more accurate tsunami waveforms, particularly at the later phase of waveform recorded at a Global Positioning System buoy station off Cape Muroto. In terms of fault slip distribution, our model produced a maximum slip of 2.1 m, located at the uplift region of the coseismic displacement. Furthermore, the shallow fault depth resulted from our simulation is consistent with the more reliably relocated aftershock distribution by Bai et al. (2006 EPS).

Keywords: Tsunami, Inversion, Optimization

©2019. Japan Geoscience Union. All Right Reserved.

Real-time tsunami prediction in a coastal zone, using a superposition of Green’ s function

*Seiji Tsuno[1], Norihiko Hashimoto[2]

1. Railway Technical Research Institute, 2. ITOCHU Techno-Solutions Corporation

Recently, S-net (Seafloor observation network for earthquakes and tsunamis along the Japan Trench) and DONET 1 & 2 (Dense Oceanfloor Network system for Earthquakes and Tsunamis) are installed off the Pacific Ocean, Japan by NIED (National Research Institute for Earth Science and Disaster Resilience) and JAMSTEC (Japan Agency for Marine-Earth Science and Technology); therefore, real-time tsunami forecasting methods using directly tsunami data observed in oceanfloor are proposed (e.g. Yamamoto, 2016; Tanioka, 2018). In this study, focusing on the immediacy and the robustness of tsunami forecasting, we investigated real-time tsunami prediction method in a coastal zone, using a superposition of previously calculated Green’ s function.

In this method, we divide the entire source area of tsunami into element sources (for example, 50 km x 50 km), and we, in advance, calculate the Green’ s function to a coastal point for the unit tsunami water level (1 m) in the element source. Assuming that the tsunami water level is the same within the element source when a tsunami occurs, we the Green’ s function to the element source –the coastal point for the maximum value of the tsunami water level observed at one point in the element source. By applying this to all the divided element sources and superimposing these Green’ s functions, we can obtain the tsunami water level in a coastal zone for the entire source area. Comparing the result predicted by this method to a tsunami simulation result simulated from source model proposed by the Cabinet Office, Government of Japan, for the 2011 off the Pacific coast of Tohoku earthquake, we confirmed that two results are in good agreements.

Moreover, to use the amount of tsunami water level in the source area due to heterogeneous fault rupture, we investigated the possibility to replace the time series of tsunami data observed at a point in the element source with the amount of tsunami water level within the element source area. We confirmed that the time series of tsunami data can be used for real-time tsunami prediction using a superposition of Green’ s functions by appropriately estimating the time when the tsunami propagates within the element source.

Keywords: Real-time tsunami prediction, Green’ s function, Superposition, 2011 off the Pacific coast of Tohoku earthquake

©2019. Japan Geoscience Union. All Right Reserved.

[J] Poster | H (Human Geosciences)：H-RE Resource and Engineering Geology

Tue. May 28, 2019 1:45 PM - 3:15 PM JST | Tue. May 28, 2019 4:45 AM - 6:15 AM UTC | Poster Hall International Exhibition Hall8, Makuhari Messe_5

[H-RE17] Application of earth science data towards the renewable energy field

convener:Hideaki Ohtake(National Institute of Advanced Industrial Science and Technology), Fumichika Uno(National Institute of Advanced Industrial Science and Technology), Teruhisa Shimada(Graduate School of Science and Technology, Hirosaki University), Daisuke Nohara(Central Research Institute of Electric Power Industry)

Renewable energy (RE) penetration is increasing dramatically in the world. RE power generations have made their presence felt in an electric power system. However, it is a challenge for RE to be stable power sources due in part to natural variability of RE and the distributed resources. For effective use of RE, a combination between power resources and energy storage technologies (e.g., pumped-storage power generation, storage battery system and electric vehicle) is required to provide power and energy flexibility. Therefore, we need to understand the amount of REs, causes of variation, and the predictability of power output. Then, enormous and diverse observation data sets and modeling technologies from earth science field should be analyzed and applied to power energy field to achieve easy use of earth science databases.
 This proposed session needs your presentation from the whole of RE fields (solar power, wind power, geothermal power, tidal power, wave power and biomass power generations). Our goal of this session is to exchange views with various researchers between RE field and earth science field (e.g., usage-trends of earth science datasets for RE field, the subjects in hand, earth science datasets availability, and cooperation between RE and earth science fields, and so on).

[HRE17-P01] Evaluation of spring, groundwater and stream water quality for use as a cooling heat source at Iwaki volcano

*Seiichiro Ioka[1], Kazuyoshi Asai[2], Kazumi Asai[2] (1.Institute of Regional Innovation, Hirosaki University, 2.Geo Science Laboratory)

[HRE17-P02] Characteristics of the confined groundwater based on the monitoring results in the western part of Osaka area: For thermal utilization of groundwater

*Hiroko Ito[1], Naoko Kitada[1], Tomoo Echigo[1], Teruyuki Fujiwara[1] (1.Geo-Research Institute)

[HRE17-P03] Predictability of Wind Power Ramp Events based on Dynamical and Statistical Ensemble Prediction

*Daisuke Nohara[1], Takeshi Watanabe[1], Masamichi Ohba[1], Shinji Kadokura[1] (1.Central Research Institute of Electric Power Industry)

[HRE17-P04] Offshore wind resource in the vicinity of Cape Erimo

*Teruhisa Shimada[1] (1.Graduate School of Science and Technology, Hirosaki University)

[HRE17-P05] An Efficient Method for Estimating the Surface Solar Irradiance Based on Satellite-Observed Scattered Solar Radiation

*Keiichi Nishizawa[1] (1.Central Research Institute of Electric Power Industry)

[HRE17-P06] Advance detection method of large forecast error on surface solar radiation considering atmospheric circulation patterns

*Fumichika Uno[1,3], Mio Matsueda[2], Takashi oozeki[1], Hideaki Ohtake[1,3], Yoshinori Yamada[3] (1.National Institute of Advanced Industrial Science and Technology, 2.University of Tsukuba, 3.Meteorological Research Institute)

Evaluation of spring, groundwater and stream water quality for use as a cooling heat source at Iwaki volcano

*Seiichiro Ioka[1], Kazuyoshi Asai[2], Kazumi Asai[2]

1. Institute of Regional Innovation, Hirosaki University, 2. Geo Science Laboratory

There is a lack of existing research concerning cooling heat sources that are necessary for geothermal power development at Iwaki volcano. In this study, we evaluate the availability of spring water, groundwater and stream water as a cooling heat source for geothermal power generation. We are mainly concerned with water quality characteristics for geothermal binary power generation, and with scale formation more specifically.

We studied 10 spring water, two groundwater and 18 stream water samples from the Iwaki volcano area. We measured pH, electrical conductivity, water temperature, and flow rate. We conducted analyses for Li^+, Na^+, NH_4^+, K^+, Mg^{2+}, Ca^{2+}, F^-, Cl^-, Br^-, NO_3^-, SO_4^{2-}, Fe, Mn, Sr, Ba, Cu, B, Si, alkalinity, dissolved organic carbon, $\delta^{18}O$ and δD in each sample. The evaluation of scale formation was carried out using PHREEQC Interactive Version 3.4.0.12927.

Scale formation was evaluated at an average temperature of 10 ˚C at the time of water sampling, as well as at a temperature of 15 ˚C assumed to be applicable to a scenario following utilization of the water as a cooling heat source. The saturation index results for calcite and amorphous silica indicated that all spring water, groundwater and stream water were undersaturated at 10 ˚C and 15 ˚C and scale formation was unlikely to occur. However, the saturation index for iron indicated oversaturation at an Fe concentration of 0.005 mg/L or higher, but concentrations of 0.1 mg/L or higher were only detected at two sites. We therefore conclude that these factors are not important provided that those two sites are not used. From the perspective of scale formation, this study indicates that spring water, groundwater and stream water in this area can be effectively utilized as a cooling heat source for geothermal power generation.

Keywords: Iwaki Volcano, water quality, cooling heat source use

©2019. Japan Geoscience Union. All Right Reserved.

Characteristics of the confined groundwater based on the monitoring results in the western part of Osaka area: For thermal utilization of groundwater

*Hiroko Ito[1], Naoko Kitada[1], Tomoo Echigo[1], Teruyuki Fujiwara[1]

1. Geo-Research Institute

Utilization of renewable thermal energies has been promoted for several years in Japan. For the purpose of reduction of CO_2 emissions using renewable energies, thermal utilization of groundwater has been focused in Osaka area, where large amount of groundwater is potentially available for thermal sources. Recently, a demonstration experiment of Aquifer Thermal Energy Storage (ATES) system, which is one of the open-loop systems for large-scaled thermal utilization of groundwater, was performed at the redeveloped site near the Osaka Station. However, since widely ground subsidence was caused by excessive pumping of shallow groundwater in 1960’s, appropriate managements must be performed for effective use of groundwater. On the basis of these backgrounds, we observed groundwater chemistries, levels, and temperatures in order to clarify the initial characteristics and evaluate the possibilities of utilization for ATES system in the western part of Osaka area.

Pliocene to Quaternary sediments reach a maximum thickness of 1,500 m beneath the Osaka plain, and more than 20 marine clay layers deposited in association with cyclic global sea level changes are intercalated with freshwater sand and gravel layers. In this study, we investigated the confined groundwaters in Pleistocene sandy gravel layers so-called Dg1, Dg2 and Dg3. These three confined aquifers are widely distributed in the western part of Osaka Plain within the depth of 100 m from ground surface.

Seasonal variations of the chemical compositions were negligibly small. The analyzed groundwater samples mostly had reductive characteristics, e.g., about 80 % of iron was existed as dissolved ions. In order to long-term utilization of ATES system, it is necessary to maintain reductive groundwater condition to prevent precipitation of iron hydroxides which may cause clogging of well screens. All of sampled waters had Na^+-Cl^- type characteristic as major composition, however, the total concentrations of dissolved ions were higher in the groundwater samples of Dg1 than those of Dg2 and Dg3. Comparing the same aquifer, total concentrations of dissolved ions were lower in the northern part (Umeda-Fukushima area) than in the southern part (Nakanoshima area) of the studied area. Because groundwater chemistries were significantly different in each aquifer, pumped groundwater must be surely recharged into the original aquifer.

Groundwater levels had few variations at each monitoring site for all of the above three aquifers. Therefore, it is suggested that water flow velocities were very slow, stagnant groundwater environment. Artificial sharp declines in the groundwater levels of Dg2 were observed several times in 2017. Such remarkable declines of groundwater levels could not be observed in Dg1 and Dg3, i.e., these three aquifers must be independent at least in the studied area.

Groundwater temperatures were measured 4 times per year for every 1m depth. Both seasonal and locational variations were observed at the shallower than 30 m depth, however, the groundwater temperatures at the depth of more than 30 m showed constant trend around 18 celsius degree in the

©2019. Japan Geoscience Union. All Right Reserved.

western part of Osaka area. On the other hand, they were about 2 celsius degree higher in the northeastern part of Osaka city (near Uemachi Upland) than that of in the western regions.

Finally, this study is based on the results obtained from a “Renewable energy heat utilization technology development” project commissioned by the New Energy and Industrial Technology Development Organization (NEDO), a Japanese national agency.

Keywords: western part of Osaka area, Aquifer Thermal Energy Storage (ATES) system, confined groundwater

©2019. Japan Geoscience Union. All Right Reserved.

Predictability of Wind Power Ramp Events based on Dynamical and Statistical Ensemble Prediction

*Daisuke Nohara[1], Takeshi Watanabe[1], Masamichi Ohba[1], Shinji Kadokura[1]

1. Central Research Institute of Electric Power Industry

Abrupt change in wind power generation, known as ramp events, due to fluctuating wind speeds present challenges to the stability of the electric power supply. In Japan, the ramp events are generally induced by extratropical cyclones along their track. Since prediction for the behavior of the cyclones entails uncertainty caused by nonlinear dynamics, probabilistic prediction is more effective. For this study, we developed a regional ensemble prediction method using the Weather Research and Forecasting model (WRF). To obtain dynamically consistent perturbations with a synoptic weather pattern, both initial and lateral boundary perturbations were determined by differences between the control and an ensemble member of the Japan Meteorological Agency (JMA)'s operational one-week ensemble forecast. This method provides 11 ensemble members with a horizontal resolution of 15 km for 75 hours at 30 minutes interval outputs by downscaling JMA's operational global forecast along with the perturbations. Wind power is projected using power curve which is estimated by relationship between area averaged wind speed and wind power generation. In addition to the dynamical ensemble, we expanded the ensemble member using Monte Carlo method to take account of the impact on uncertainty in the power curve. The expanded ensemble has 100 members. Forecast for the ramp events using the expanded ensemble exhibits high statistical consistency and reliability of ability to capture the ramp events compared with the dynamical ensemble prediction.

Keywords: Wind power, ramp events, prediction

©2019. Japan Geoscience Union. All Right Reserved.

Offshore wind resource in the vicinity of Cape Erimo

*Teruhisa Shimada[1]

1. Graduate School of Science and Technology, Hirosaki University

Wind energy technology is rapidly developing and, above all, offshore wind energy is becoming a center of renewable energy in the world. In northern Japan, to examine the possibility of the offshore wind energy and to promote the development, detailed wind observations, examination for zoning, and plans to build offshore wind turbines are ongoing.

The latest offshore wind maps such as NeoWins (http://app10.infoc.nedo.go.jp/Nedo_Webgis/top.html) shows the largest wind energy resources in the vicinity of Cape Erimo, Hokkaido. Along the Japanese coast, there are only two offshore regions in which annual mean wind speeds exceed 10 m/s within approximately 20 km from the coast. One is the south of Cape Erimo.

However, few studies have paid attention to the strong winds in the vicinity of Cape Erimo and have investigated the mechanism of the strong winds or large wind energy. Although some studies demonstrated the strong winds which locally develops near the Cape Erimo by satellite wind observations (Shimada and Kawamura, 2004, 2007), there are remaining issues for further understanding of wind energy map and of the impact of the locally strong wind on the wind energy statistics. Therefore, this study investigate the locally strong wind developing near the Cape Erimo.

Keywords: offshore wind resource assessment, satellite observation, meteorological simulation

©2019. Japan Geoscience Union. All Right Reserved.

An Efficient Method for Estimating the Surface Solar Irradiance Based on Satellite-Observed Scattered Solar Radiation

*Keiichi Nishizawa[1]

1. Central Research Institute of Electric Power Industry

In order to estimate cloud optical thickness, which substantially affects the surface solar radiation, we intend to analyze the scattered solar radiation observed from satellites. For the inverse analysis of cloud optical thickness, “bidirectional reflectivity” of the earth-atmosphere system at 0.51 mm in wavelength has been calculated by using Rstar6b (a radiative transfer model developed by the University of Tokyo) for various sets of related parameters (i.e., cloud optical thickness, ice cloud fraction, solar zenith angle, satellite zenith angle, azimuth angle difference between sun and satellite, and surface albedo). The results from these calculations have been compiled into a six-dimensional look-up table. By using the table, the cloud optical thickness to reproduce the satellite-observed scattered solar radiation can be estimated very efficiently. When the surface global solar radiation is estimated from the obtained cloud optical thickness, however, uncertain variables, such as the surface albedo and ice cloud fraction, are anticipated causing considerable errors in the estimations.

Keywords: satellite observation, scattered solar radiation, surface solar irradiance

©2019. Japan Geoscience Union. All Right Reserved.

Advance detection method of large forecast error on surface solar radiation considering atmospheric circulation patterns

*Fumichika Uno[1,3], Mio Matsueda[2], Takashi oozeki[1], Hideaki Ohtake[1,3], Yoshinori Yamada[3]

1. National Institute of Advanced Industrial Science and Technology, 2. University of Tsukuba, 3. Meteorological Research Institute

Prediction of surface solar radiation (SSR) using numerical weather prediction (NWP) models usually use at several hours to several days forecast. Large forecast errors (forecast busts) for SSR and therefore photovoltaic power generation may lead to either a shortage of power supply or production of excessive surplus power.

Previous study proposed the detection method of forecast busts using lognormal ensemble spread (standard deviation of ensemble forecast). This study also evaluates lognormal ensemble spread as the four NWP centers (Japan Meteorological Agency: JMA, European Centre for Medium-Range Weather Forecasts: ECMWF, National Centers for Environmental Prediction: NCEP, United Kingdom Met Office: UKMO) and a multi-center grand ensemble (MCGE). However, this study assessed the detectability each atmospheric circulation patterns. The detectability was assessed using ROC diagram. The study period is January 2014 to May 2017 in five winter months (January, February, May, November, December), and forecast lead time is from 24 to 144 hour every 24hours. The forecast busts were defined as the top 5, 10, 15, 20, 25, 30% absolute forecast error. The atmospheric circulation patterns are categorized Winter monsoon (WM), Winter Pacific (WP), High Pressure (HP), Low Pressure (LP), Southerly Flow (SF) using 500hPa height.

As the results, the proposed method in this study indicate higher detectability of forecast bust than the non-categorized detection (previous study) method. For instance, the WP and SF patterns are higher than the non-categorized detection method. Particularly, the hit rate on proposed method was improved more large forecast error event (top 5% forecast busts events), false alarm rate was improved almost all forecast lead time and fix forecast busts cases.

Keywords: Prediction of surface solar radiation, Ensemble forecast, Forecast busts

©2019. Japan Geoscience Union. All Right Reserved.

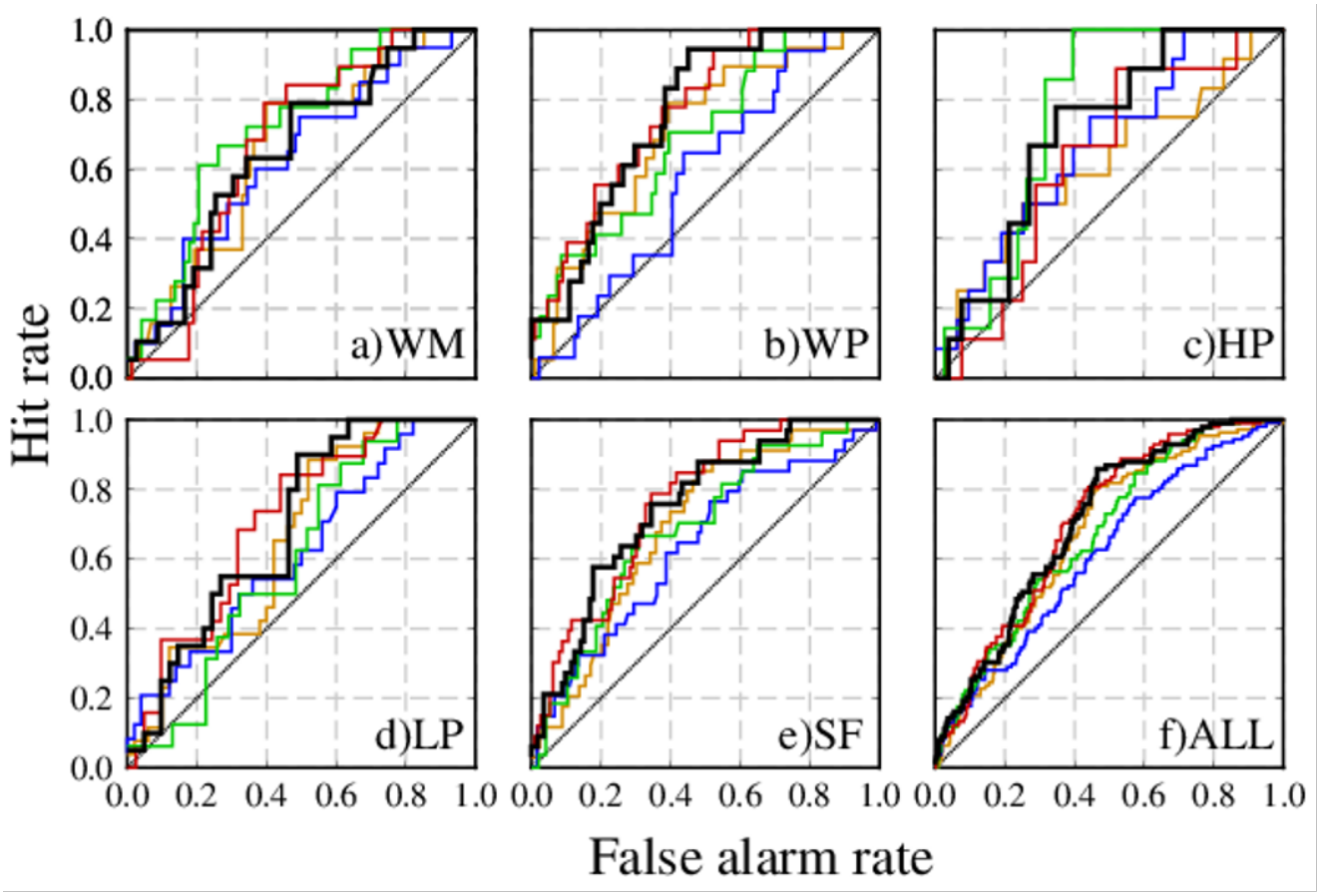

Fig. ROC diagram each circulation patterns (a-e) and non-categorized (f) curve at 24 hours forecast lead time. The forecast busts was defined as the top 20%. The black thick line indicate MCGE, color thin lines indicate JMA (red), ECMWF(Yellow), NCEP (green), UKMO(blue).

©2019. Japan Geoscience Union. All Right Reserved.

[J] Poster | H (Human Geosciences)：H-RE Resource and Engineering Geology

Tue. May 28, 2019 5:15 PM - 6:30 PM JST | Tue. May 28, 2019 8:15 AM - 9:30 AM UTC | Poster Hall International Exhibition Hall8, Makuhari Messe_22

[H-RE17] Application of earth science data towards the renewable energy field

convener:Hideaki Ohtake(National Institute of Advanced Industrial Science and Technology), Fumichika Uno(National Institute of Advanced Industrial Science and Technology), Teruhisa Shimada(Graduate School of Science and Technology, Hirosaki University), Daisuke Nohara(Central Research Institute of Electric Power Industry)

Renewable energy (RE) penetration is increasing dramatically in the world. RE power generations have made their presence felt in an electric power system. However, it is a challenge for RE to be stable power sources due in part to natural variability of RE and the distributed resources. For effective use of RE, a combination between power resources and energy storage technologies (e.g., pumped-storage power generation, storage battery system and electric vehicle) is required to provide power and energy flexibility. Therefore, we need to understand the amount of REs, causes of variation, and the predictability of power output. Then, enormous and diverse observation data sets and modeling technologies from earth science field should be analyzed and applied to power energy field to achieve easy use of earth science databases.
 This proposed session needs your presentation from the whole of RE fields (solar power, wind power, geothermal power, tidal power, wave power and biomass power generations). Our goal of this session is to exchange views with various researchers between RE field and earth science field (e.g., usage-trends of earth science datasets for RE field, the subjects in hand, earth science datasets availability, and cooperation between RE and earth science fields, and so on).

[HRE17-P01] Evaluation of spring, groundwater and stream water quality for use as a cooling heat source at Iwaki volcano

*Seiichiro Ioka[1], Kazuyoshi Asai[2], Kazumi Asai[2] (1.Institute of Regional Innovation, Hirosaki University, 2.Geo Science Laboratory)

[HRE17-P02] Characteristics of the confined groundwater based on the monitoring results in the western part of Osaka area: For thermal utilization of groundwater

*Hiroko Ito[1], Naoko Kitada[1], Tomoo Echigo[1], Teruyuki Fujiwara[1] (1.Geo-Research Institute)

[HRE17-P03] Predictability of Wind Power Ramp Events based on Dynamical and Statistical Ensemble Prediction

*Daisuke Nohara[1], Takeshi Watanabe[1], Masamichi Ohba[1], Shinji Kadokura[1] (1.Central Research Institute of Electric Power Industry)

[HRE17-P04] Offshore wind resource in the vicinity of Cape Erimo

*Teruhisa Shimada[1] (1.Graduate School of Science and Technology, Hirosaki University)

[HRE17-P05] An Efficient Method for Estimating the Surface Solar Irradiance Based on Satellite-Observed Scattered Solar Radiation

*Keiichi Nishizawa[1] (1.Central Research Institute of Electric Power Industry)

[HRE17-P06] Advance detection method of large forecast error on surface solar radiation considering atmospheric circulation patterns

*Fumichika Uno[1,3], Mio Matsueda[2], Takashi oozeki[1], Hideaki Ohtake[1,3], Yoshinori Yamada[3] (1.National Institute of Advanced Industrial Science and Technology, 2.University of Tsukuba, 3.Meteorological Research Institute)

Evaluation of spring, groundwater and stream water quality for use as a cooling heat source at Iwaki volcano

*Seiichiro Ioka[1], Kazuyoshi Asai[2], Kazumi Asai[2]

1. Institute of Regional Innovation, Hirosaki University, 2. Geo Science Laboratory

There is a lack of existing research concerning cooling heat sources that are necessary for geothermal power development at Iwaki volcano. In this study, we evaluate the availability of spring water, groundwater and stream water as a cooling heat source for geothermal power generation. We are mainly concerned with water quality characteristics for geothermal binary power generation, and with scale formation more specifically.

We studied 10 spring water, two groundwater and 18 stream water samples from the Iwaki volcano area. We measured pH, electrical conductivity, water temperature, and flow rate. We conducted analyses for Li^+, Na^+, NH_4^+, K^+, Mg^{2+}, Ca^{2+}, F^-, Cl^-, Br^-, NO_3^-, SO_4^{2-}, Fe, Mn, Sr, Ba, Cu, B, Si, alkalinity, dissolved organic carbon, $\delta^{18}O$ and δD in each sample. The evaluation of scale formation was carried out using PHREEQC Interactive Version 3.4.0.12927.

Scale formation was evaluated at an average temperature of 10 ˚C at the time of water sampling, as well as at a temperature of 15 ˚C assumed to be applicable to a scenario following utilization of the water as a cooling heat source. The saturation index results for calcite and amorphous silica indicated that all spring water, groundwater and stream water were undersaturated at 10 ˚C and 15 ˚C and scale formation was unlikely to occur. However, the saturation index for iron indicated oversaturation at an Fe concentration of 0.005 mg/L or higher, but concentrations of 0.1 mg/L or higher were only detected at two sites. We therefore conclude that these factors are not important provided that those two sites are not used. From the perspective of scale formation, this study indicates that spring water, groundwater and stream water in this area can be effectively utilized as a cooling heat source for geothermal power generation.

Keywords: Iwaki Volcano, water quality, cooling heat source use

©2019. Japan Geoscience Union. All Right Reserved.

Characteristics of the confined groundwater based on the monitoring results in the western part of Osaka area: For thermal utilization of groundwater

*Hiroko Ito[1], Naoko Kitada[1], Tomoo Echigo[1], Teruyuki Fujiwara[1]

1. Geo-Research Institute

Utilization of renewable thermal energies has been promoted for several years in Japan. For the purpose of reduction of CO_2 emissions using renewable energies, thermal utilization of groundwater has been focused in Osaka area, where large amount of groundwater is potentially available for thermal sources. Recently, a demonstration experiment of Aquifer Thermal Energy Storage (ATES) system, which is one of the open-loop systems for large-scaled thermal utilization of groundwater, was performed at the redeveloped site near the Osaka Station. However, since widely ground subsidence was caused by excessive pumping of shallow groundwater in 1960’s, appropriate managements must be performed for effective use of groundwater. On the basis of these backgrounds, we observed groundwater chemistries, levels, and temperatures in order to clarify the initial characteristics and evaluate the possibilities of utilization for ATES system in the western part of Osaka area.

Pliocene to Quaternary sediments reach a maximum thickness of 1,500 m beneath the Osaka plain, and more than 20 marine clay layers deposited in association with cyclic global sea level changes are intercalated with freshwater sand and gravel layers. In this study, we investigated the confined groundwaters in Pleistocene sandy gravel layers so-called Dg1, Dg2 and Dg3. These three confined aquifers are widely distributed in the western part of Osaka Plain within the depth of 100 m from ground surface.

Seasonal variations of the chemical compositions were negligibly small. The analyzed groundwater samples mostly had reductive characteristics, e.g., about 80 % of iron was existed as dissolved ions. In order to long-term utilization of ATES system, it is necessary to maintain reductive groundwater condition to prevent precipitation of iron hydroxides which may cause clogging of well screens. All of sampled waters had Na^+-Cl^- type characteristic as major composition, however, the total concentrations of dissolved ions were higher in the groundwater samples of Dg1 than those of Dg2 and Dg3. Comparing the same aquifer, total concentrations of dissolved ions were lower in the northern part (Umeda-Fukushima area) than in the southern part (Nakanoshima area) of the studied area. Because groundwater chemistries were significantly different in each aquifer, pumped groundwater must be surely recharged into the original aquifer.

Groundwater levels had few variations at each monitoring site for all of the above three aquifers. Therefore, it is suggested that water flow velocities were very slow, stagnant groundwater environment. Artificial sharp declines in the groundwater levels of Dg2 were observed several times in 2017. Such remarkable declines of groundwater levels could not be observed in Dg1 and Dg3, i.e., these three aquifers must be independent at least in the studied area.

Groundwater temperatures were measured 4 times per year for every 1m depth. Both seasonal and locational variations were observed at the shallower than 30 m depth, however, the groundwater temperatures at the depth of more than 30 m showed constant trend around 18 celsius degree in the

©2019. Japan Geoscience Union. All Right Reserved.

western part of Osaka area. On the other hand, they were about 2 celsius degree higher in the northeastern part of Osaka city (near Uemachi Upland) than that of in the western regions.

Finally, this study is based on the results obtained from a “Renewable energy heat utilization technology development” project commissioned by the New Energy and Industrial Technology Development Organization (NEDO), a Japanese national agency.

Keywords: western part of Osaka area, Aquifer Thermal Energy Storage (ATES) system, confined groundwater

©2019. Japan Geoscience Union. All Right Reserved.

Predictability of Wind Power Ramp Events based on Dynamical and Statistical Ensemble Prediction

*Daisuke Nohara[1], Takeshi Watanabe[1], Masamichi Ohba[1], Shinji Kadokura[1]

1. Central Research Institute of Electric Power Industry

Abrupt change in wind power generation, known as ramp events, due to fluctuating wind speeds present challenges to the stability of the electric power supply. In Japan, the ramp events are generally induced by extratropical cyclones along their track. Since prediction for the behavior of the cyclones entails uncertainty caused by nonlinear dynamics, probabilistic prediction is more effective. For this study, we developed a regional ensemble prediction method using the Weather Research and Forecasting model (WRF). To obtain dynamically consistent perturbations with a synoptic weather pattern, both initial and lateral boundary perturbations were determined by differences between the control and an ensemble member of the Japan Meteorological Agency (JMA)'s operational one-week ensemble forecast. This method provides 11 ensemble members with a horizontal resolution of 15 km for 75 hours at 30 minutes interval outputs by downscaling JMA's operational global forecast along with the perturbations. Wind power is projected using power curve which is estimated by relationship between area averaged wind speed and wind power generation. In addition to the dynamical ensemble, we expanded the ensemble member using Monte Carlo method to take account of the impact on uncertainty in the power curve. The expanded ensemble has 100 members. Forecast for the ramp events using the expanded ensemble exhibits high statistical consistency and reliability of ability to capture the ramp events compared with the dynamical ensemble prediction.

Keywords: Wind power, ramp events, prediction

©2019. Japan Geoscience Union. All Right Reserved.

Offshore wind resource in the vicinity of Cape Erimo

*Teruhisa Shimada[1]

1. Graduate School of Science and Technology, Hirosaki University

Wind energy technology is rapidly developing and, above all, offshore wind energy is becoming a center of renewable energy in the world. In northern Japan, to examine the possibility of the offshore wind energy and to promote the development, detailed wind observations, examination for zoning, and plans to build offshore wind turbines are ongoing.

The latest offshore wind maps such as NeoWins (http://app10.infoc.nedo.go.jp/Nedo_Webgis/top.html) shows the largest wind energy resources in the vicinity of Cape Erimo, Hokkaido. Along the Japanese coast, there are only two offshore regions in which annual mean wind speeds exceed 10 m/s within approximately 20 km from the coast. One is the south of Cape Erimo.

However, few studies have paid attention to the strong winds in the vicinity of Cape Erimo and have investigated the mechanism of the strong winds or large wind energy. Although some studies demonstrated the strong winds which locally develops near the Cape Erimo by satellite wind observations (Shimada and Kawamura, 2004, 2007), there are remaining issues for further understanding of wind energy map and of the impact of the locally strong wind on the wind energy statistics. Therefore, this study investigate the locally strong wind developing near the Cape Erimo.

Keywords: offshore wind resource assessment, satellite observation, meteorological simulation

©2019. Japan Geoscience Union. All Right Reserved.

An Efficient Method for Estimating the Surface Solar Irradiance Based on Satellite-Observed Scattered Solar Radiation

*Keiichi Nishizawa[1]

1. Central Research Institute of Electric Power Industry

In order to estimate cloud optical thickness, which substantially affects the surface solar radiation, we intend to analyze the scattered solar radiation observed from satellites. For the inverse analysis of cloud optical thickness, “bidirectional reflectivity” of the earth-atmosphere system at 0.51 mm in wavelength has been calculated by using Rstar6b (a radiative transfer model developed by the University of Tokyo) for various sets of related parameters (i.e., cloud optical thickness, ice cloud fraction, solar zenith angle, satellite zenith angle, azimuth angle difference between sun and satellite, and surface albedo). The results from these calculations have been compiled into a six-dimensional look-up table. By using the table, the cloud optical thickness to reproduce the satellite-observed scattered solar radiation can be estimated very efficiently. When the surface global solar radiation is estimated from the obtained cloud optical thickness, however, uncertain variables, such as the surface albedo and ice cloud fraction, are anticipated causing considerable errors in the estimations.

Keywords: satellite observation, scattered solar radiation, surface solar irradiance

©2019. Japan Geoscience Union. All Right Reserved.

Advance detection method of large forecast error on surface solar radiation considering atmospheric circulation patterns

*Fumichika Uno[1,3], Mio Matsueda[2], Takashi oozeki[1], Hideaki Ohtake[1,3], Yoshinori Yamada[3]

1. National Institute of Advanced Industrial Science and Technology, 2. University of Tsukuba, 3. Meteorological Research Institute

Prediction of surface solar radiation (SSR) using numerical weather prediction (NWP) models usually use at several hours to several days forecast. Large forecast errors (forecast busts) for SSR and therefore photovoltaic power generation may lead to either a shortage of power supply or production of excessive surplus power.

Previous study proposed the detection method of forecast busts using lognormal ensemble spread (standard deviation of ensemble forecast). This study also evaluates lognormal ensemble spread as the four NWP centers (Japan Meteorological Agency: JMA, European Centre for Medium-Range Weather Forecasts: ECMWF, National Centers for Environmental Prediction: NCEP, United Kingdom Met Office: UKMO) and a multi-center grand ensemble (MCGE). However, this study assessed the detectability each atmospheric circulation patterns. The detectability was assessed using ROC diagram. The study period is January 2014 to May 2017 in five winter months (January, February, May, November, December), and forecast lead time is from 24 to 144 hour every 24hours. The forecast busts were defined as the top 5, 10, 15, 20, 25, 30% absolute forecast error. The atmospheric circulation patterns are categorized Winter monsoon (WM), Winter Pacific (WP), High Pressure (HP), Low Pressure (LP), Southerly Flow (SF) using 500hPa height.

As the results, the proposed method in this study indicate higher detectability of forecast bust than the non-categorized detection (previous study) method. For instance, the WP and SF patterns are higher than the non-categorized detection method. Particularly, the hit rate on proposed method was improved more large forecast error event (top 5% forecast busts events), false alarm rate was improved almost all forecast lead time and fix forecast busts cases.

Keywords: Prediction of surface solar radiation, Ensemble forecast, Forecast busts

©2019. Japan Geoscience Union. All Right Reserved.

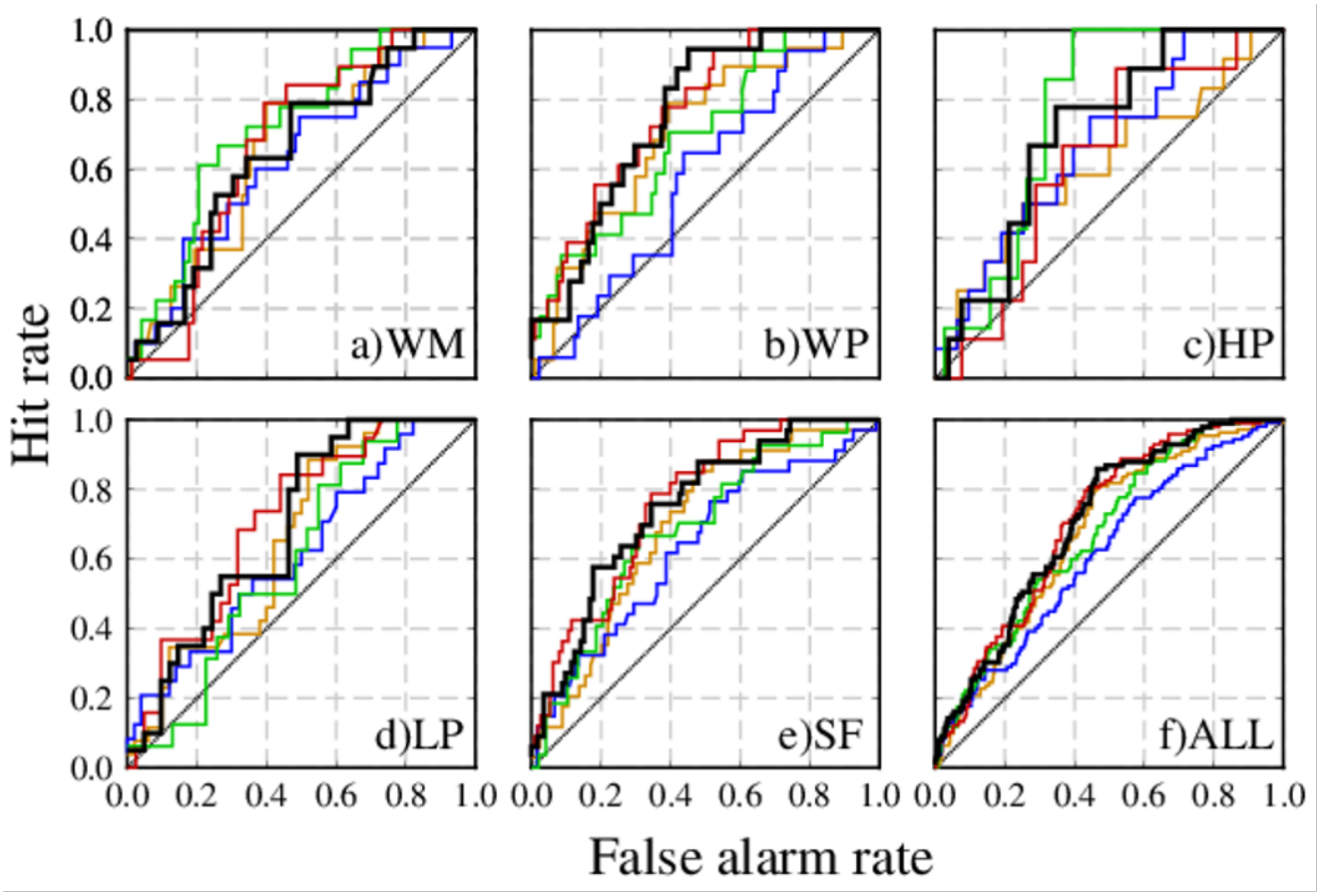

Fig. ROC diagram each circulation patterns (a-e) and non-categorized (f) curve at 24 hours forecast lead time. The forecast busts was defined as the top 20%. The black thick line indicate MCGE, color thin lines indicate JMA (red), ECMWF(Yellow), NCEP (green), UKMO(blue).

©2019. Japan Geoscience Union. All Right Reserved.

[J] Oral | H (Human Geosciences)：H-RE Resource and Engineering Geology

Tue. May 28, 2019 3:30 PM - 5:00 PM JST | Tue. May 28, 2019 6:30 AM - 8:00 AM UTC | 301B 3F

[H-RE17] Application of earth science data towards the renewable energy field

convener:Hideaki Ohtake(National Institute of Advanced Industrial Science and Technology), Fumichika Uno(National Institute of Advanced Industrial Science and Technology), Teruhisa Shimada(Graduate School of Science and Technology, Hirosaki University), Daisuke Nohara(Central Research Institute of Electric Power Industry), Chairperson:Hideaki Ohtake(National Institute of Advanced Industrial Science and Technology (AIST))

Renewable energy (RE) penetration is increasing dramatically in the world. RE power generations have made their presence felt in an electric power system. However, it is a challenge for RE to be stable power sources due in part to natural variability of RE and the distributed resources. For effective use of RE, a combination between power resources and energy storage technologies (e.g., pumped-storage power generation, storage battery system and electric vehicle) is required to provide power and energy flexibility. Therefore, we need to understand the amount of REs, causes of variation, and the predictability of power output. Then, enormous and diverse observation data sets and modeling technologies from earth science field should be analyzed and applied to power energy field to achieve easy use of earth science databases.
 This proposed session needs your presentation from the whole of RE fields (solar power, wind power, geothermal power, tidal power, wave power and biomass power generations). Our goal of this session is to exchange views with various researchers between RE field and earth science field (e.g., usage-trends of earth science datasets for RE field, the subjects in hand, earth science datasets availability, and cooperation between RE and earth science fields, and so on).

3:30 PM - 3:55 PM JST | 6:30 AM - 6:55 AM UTC

[HRE17-01] Application of geological dara to ground source heat pump systems with special reference to thermal conductivity of geological materials

★Invited Papers

*Masakatsu SASADA[1] (1.Geo-Heat Promotion Association of Japan)

3:55 PM - 4:10 PM JST | 6:55 AM - 7:10 AM UTC

[HRE17-02] Use of groundwater in the Nishi-Osaka Area and its activities.

*Naoko Kitada[1], Hiroko Ito[1], Tomoo Echigo[1], Teruyuki Fujiwara[1], Makoto Nishigaki[2] (1.Geo-Research Institute, 2.Okayama University)

4:10 PM - 4:25 PM JST | 7:10 AM - 7:25 AM UTC

[HRE17-03] Improvement of prediction of wind power ramp by using monitoring data

*Shinji Kadokura[1], Daisuke Nohara[1], Masamichi Ohba[1], Atsushi Hashimoto[1], Keisuke Nakao[1], Yasuo Hattori[1], Takeshi Watanabe[1], Hiromaru Hirakuchi[1] (1.Central Research Institute of Electric Power Industry)

4:25 PM - 4:40 PM JST | 7:25 AM - 7:40 AM UTC

[HRE17-04] **A study of the use of meteorological data for energy management**

*Hideaki Ohtake[1], Takashi Oozeki[1], Junichi Imura[2] (1.National Institute of Advanced Industrial Science and Technology, 2.Tokyo institute of technology)

4:40 PM - 5:00 PM JST | 7:40 AM - 8:00 AM UTC

Discussion

Application of geological dara to ground source heat pump systems with special reference to thermal conductivity of geological materials

*Masakatsu SASADA[1]

1. Geo-Heat Promotion Association of Japan

Ground source heat pump systems are getting popular in Japan. Ground source means low temperature energy in geological units shallower than 200 meters below the surface. A geothermal heat pump system is much more efficient than a conventional air source heat pump system. A ground source heat pump system also contributes to mitigating a heat island phenomenon in large urban areas like Tokyo, because it does not emit exhaust heat outside in summer.
Effective thermal conductivity is one of the most important parameters to design ground source heat pump systems. Thermal response tests result in effective thermal conductivity of geological units under the building site. The reference values of thermal conductivity for several geological units are also available to building designers.
The regulation of Energy Conservation Standards came into effect in April 2016. Under the regulation annual primary energy consumption for every type of building is standardized. An owner of building has to submit building certification application with data of annual energy consumption calculated by Web Program of Building Research Institute. When ground source heat pump systems are installed in the building, the thermal conductivity of the building site must be input the Web Program for calculation of annual primary energy consumption.
Thermal response test is the best method to estimate the thermal conductivity of the geological units under the building site. However, it is not always applied to residential houses and small size buildings. The reference data of thermal conductivity are usually applied to them. Since geological units are so diverse in the Japanese Islands that much more measured data of thermal conductivity are required for reference database.

Keywords: Ground source heat pump, Effective thermal conductivity, Thermal response test

©2019. Japan Geoscience Union. All Right Reserved.

Use of groundwater in the Nishi-Osaka Area and its activities.

*Naoko Kitada[1], Hiroko Ito[1], Tomoo Echigo[1], Teruyuki Fujiwara[1], Makoto Nishigaki[2]

1. Geo-Research Institute, 2. Okayama University

On the west side of Osaka plain, several clay layers accompanying repeated sea level change accumulate in layers, and the gravel layer between the clay layers forms a submerged aquifer where abundant underground water resides. On the other hand, due to the severe ground subsidence caused by the massive pumping up of factory water in the 1960s, pumping is currently strictly regulated. However, in recent years, especially in Osaka city, consideration is being made on effective utilization of groundwater, such as the promotion of underground water use project as regenerative thermal energy.

Therefore, we conducted survey of water level, water temperature, and water quality using existing observation holes near Nakanoshima from around Osaka Station for the purpose of acquiring background data on the properties of groundwater at the present time. The aquifer covered in this study is a sand gravel layer (1st aqueduct layer: Dg1) distributed beneath the clay layer (Ma13) of the Holocene, and the gravel layer (the second caught aquifer: Dg 2) distributed under the clay layer (Ma12). Regarding the water quality, we analyzed the composition of the principal components etc. for groundwater sampled 4 times in total in June, September, November 2016 and January 2017. As a result, it was revealed that both Dg 1 and Dg 2 were reductive and showed a Na - Cl type water quality composition, especially Dg 1 had a higher salt concentration.

Keywords: Borehole Database, goundwater, gravel layer

©2019. Japan Geoscience Union. All Right Reserved.

Improvement of prediction of wind power ramp by using monitoring data

*Shinji Kadokura[1], Daisuke Nohara[1], Masamichi Ohba[1], Atsushi Hashimoto[1], Keisuke Nakao[1], Yasuo Hattori[1], Takeshi Watanabe[1], Hiromaru Hirakuchi[1]

1. Central Research Institute of Electric Power Industry

Introduction of power generation by renewable energy such as photovoltaics(PV) and wind power (WT) is worldwidely progressing. Since PV and WT power generation are markedly fluctuated due to the change of the wheather, there is concern about the stability of the electric power system. Therefore, we have been developing a prediction method of wind power generation output to contribute for the stabilization of electric power system. In this method, the numerical forecast value provided by the Japan Meteorological Agency is downscaled using the weather model WRF and CFD model to predict the wind speed at the wind turbine, and the power output is predicted using the power curve. By adding the generated power output for each wind turbine obtained, the total output of the area is obtained. In this study, we have improved the prediction of wind speed and power generation output by using the monitoring data for each wind turbine, by making correction based on multiple regression and by using empirical power curve. Furthermore, we have corrected the accuracy of the area total power output by sequentially correcting the windfarms where data for each windmill is not acquired. In addition, by performing multiple regression on the amplitude of the output change, we have improved the supplementation rate of the wind power generation rapid change henomenon, ramp.

Keywords: Wind power output prediction, wind power ramp, wind power generation, SCADA, Weather forecast

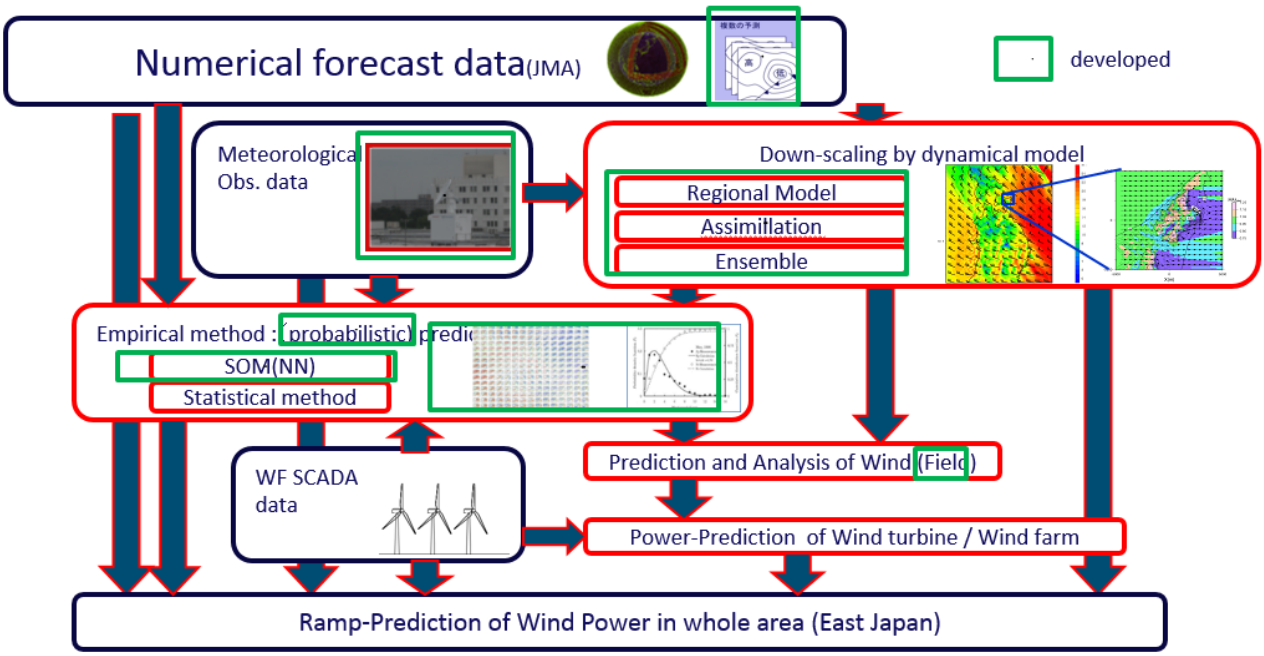

©2019. Japan Geoscience Union. All Right Reserved.

A study of the use of meteorological data for energy management

*Hideaki Ohtake[1], Takashi Oozeki[1], Junichi Imura[2]

1. National Institute of Advanced Industrial Science and Technology, 2. Tokyo institute of technology

Recently, a large amount of photovoltaics (PV) power systems (approximately 45 GW as of June 2018) have been connected to a power grid in Japan. Electric power supply with PV power generation exceed electric power demand in a power grid. For safety control of an energy manage system (EMS) with variable PV power generation, optimal use of other power plants (thermal power plants etc) and battery systems will be required in a future energy network (Fig.1). PV power monitoring and forecasts based on a meteorological data can be useful information for an optimal control of other power systems. In our research group (referred as a HARPS in a JST CREST project), we developed a communication tool between meteorology and EMS research fields. Impacts of meteorological data have been also investigated in an EMS (e.g., optimal control of electrical power systems and battery systems) under large PV installations. Furthermore, real time monitoring of regional PV power estimation have been also tried using a new geostationary satellite, Himawari 8/9. In this presentation, we will introduce research topic of meteorological data in the EMS field.

Keywords: photovoltaic, energy manage system, meteorological data

©2019. Japan Geoscience Union. All Right Reserved.

[E] Oral | H (Human Geosciences)：H-TT Technology & Techniques

Tue. May 28, 2019 9:00 AM - 10:30 AM JST | Tue. May 28, 2019 12:00 AM - 1:30 AM UTC | 302 3F

[H-TT18] Development and application of environmental traceability methods

convener:Ichiro Tayasu(Research Institute for Humanity and Nature), Nobuhito Ohte(Department of Social Informatics, Graduate School of Informatics, Kyoto University), Gabriel J Bowen(University of Utah), Chairperson:Nobuhito Ohte(Kyoto University)

Modern society uses almost all the elements present in the natural world. Although there have long been calls for the sustainable use of the resources that provide these elements and the building of human societies that are in harmony with the environment, the survival of the human race is increasingly at risk as a result of qualitative changes to the environment as a whole. Implementation by the society of methodologies for diagnosing and tracking these various elements of the natural environment and their relationships with humans are now required.
Elements cycle within and among the Earth system spheres, human society and the human body. Information on the concentrations and stable isotopes of elements is powerful tool for tracing this cycling and has been applied in studies of atmosphere-hydrosphere circulation, ecological systems, and the life, health and history of humans. We propose a session to discuss development and applications of environmental traceability methods toward the goal of establishing traceability in natural and human systems.
We encourage the presentation of research integrating isotopic information in various disciplines, such as geochemistry, hydrology, ecology, geology, mineralogy, anthropology, food science, and forensics. Studies applying "Isoscapes", maps of spatial isotopic variation, in addition to traditional database-based approaches, are strongly encouraged.

9:00 AM - 9:15 AM JST | 12:00 AM - 12:15 AM UTC

[HTT18-01] Environmental traceability methodology by multi-isoscapes

*Ichiro Tayasu[1], Lei Fujiyoshi[1], Shiho Yabusaki[1], Ki-Cheol Shin[1], Takanori Nakano[1], Makoto Taniguchi[1] (1.Research Institute for Humanity and Nature)

9:15 AM - 9:45 AM JST | 12:15 AM - 12:45 AM UTC

[HTT18-02] Exploring physical and biological connections using isoscapes

★Invited Papers

*Gabriel J Bowen[1] (1.University of Utah)

9:45 AM - 10:00 AM JST | 12:45 AM - 1:00 AM UTC

[HTT18-03] Spatial and temporal variations in stable isotopes and soluble ions on high mountain snow surface of Mt. Tateyama, Toyama Prefecture, Japan

*Nozomu Takeuchi[1], Ryo Sugiyama[1] (1.Chiba University)

10:00 AM - 10:15 AM JST | 1:00 AM - 1:15 AM UTC

[HTT18-04] Using Sr isotopes to determine the contribution of volcanic ash to Sr and Ca in stream waters in a chert watershed.

*Masami Koshikawa[1], Mirai Watanabe[1], Tomoyoshi Murata[1], Takejiro Takamatsu[1], Shingo Miura[1], Ki-Cheol Shin[2], Takanori Nakano[2] (1.National Institute for Environmental Studies, 2.Research Institute for Humanity and Nature)

10:15 AM - 10:30 AM JST | 1:15 AM - 1:30 AM UTC

[HTT18-05] Influences of soil dust, sea salt and anthropogenic activities on ionic and Sr isotopic compositions of wet deposition in Iran

*Yoriko Yokoo[1], Kosuke Asai[1], Sae Horii[1], Ryo Anma[2], Shiva Mehrabani[3], KiCheol Shin[4] (1.Faculty of Science and Engineering, Doshisha University, 2.Tokushima University, 3.Kurdistan University, 4.RIHN)

Environmental traceability methodology by multi-isoscapes

*Ichiro Tayasu[1], Lei Fujiyoshi[1], Shiho Yabusaki[1], Ki-Cheol Shin[1], Takanori Nakano[1], Makoto Taniguchi[1]

1. Research Institute for Humanity and Nature

Stable isotope ratios of elements, together with the concentrations of elements, can trace a matter flow, the environmental condition of sites, ecosystem structure and food products. Spatio-temporal variation of multiple isotope ratios can be used for studying the earth systems from local to global point of view. By using the traceability function of the multiple isotope ratios, we can conduct research that contributes to solving global environmental problems covering various regions and time scales. Spatio-temporal variation of multiple isotope ratios can be used for studying earth systems, ranging from local to global scales. The information may serve as a key decision- making factor for local people to consider water, food and environmental security, all of which are fundamental for the sustainability of human society.

We are conducting a research for establishing a methodology for how to use the concept of environmental traceability. A combination of quantitative and qualitative tools, including “Multi-Isoscapes” (use of multiple elements and multiple isotope ratios, together with GIS-based mapping technique), social surveys, and workshops, are deployed to investigate the role of environmental traceability in confronting environmental issues. We hypothesize that the role and perception of traceability methods in transdisciplinary processes will differ among stakeholders and that the co-production of “Multi-Isoscapes” can act as an effective “bridging tool” for understanding and explaining variation in local environments. The ultimate objective of this research is to demonstrate the effectiveness of multi-isotopic information in solving global environmental issues. Research is taking place at sites in Ono City, Fukui; Otsuchi Town, Iwate; Saijo City, Ehime; Oshino Village, Yamanashi; the Chikusa river watershed, Hyogo; Lake Biwa and Yasu river watershed in Shiga; and Silang-Santa Rosa sub-watershed in the Philippines.

Keywords: Stable isotopes, Milti-isoscapes, Environmental traceability

©2019. Japan Geoscience Union. All Right Reserved.

Exploring physical and biological connections using isoscapes

*Gabriel J Bowen[1]

1. University of Utah

Environmental chemistry data provide a wealth of information on Earth system processes, but perhaps one of the most general and widely useful applications of such data is in to identify within- and between-system connectivity. Chemical signatures have been used to establish hydrological connectivity, identify the provenance of geological materials, artefacts and forensic evidence, and trace the migration of humans and other animals. Particularly useful are spatial and temporal patterns of environmental isotope variation, which are often predictable based on large-scale databases and/or fundamental physio-chemical theory. I will review case studies demonstrating how the resulting quantitative data products, called isoscapes, have led to new advances and applications in fields as diverse as forensic science, water resources research, and aquatic ecology. I will also discuss how community data and computational infrastructure, including the Waterisotopes Database (wiDB; http://waterisotopes.org) and Isoscape Modeling, Analysis and Prediction tool (http://isomap.org) are facilitating and promoting the use of geochemical data in connectivity research and related outreach and education.

Keywords: stable isotopes, traceability, connectivity, water resources, forensics, hydrology

©2019. Japan Geoscience Union. All Right Reserved.

Spatial and temporal variations in stable isotopes and soluble ions on high mountain snow surface of Mt. Tateyama, Toyama Prefecture, Japan

*Nozomu Takeuchi[1], Ryo Sugiyama[1]

1. Chiba University

A great amount of snow accumulates during winter in mountain regions in Japan due to strong westerly of the Asian monsoon. Snow can preserve various aerosols in the atmosphere, such as sea spay, anthropogenic pollutants, mineral dust, and volcanic substances. Thus, studies of snow chemistry provide a means to understand spatial and seasonal variabilities of aerosols. Furthermore, soluble chemists in snow affect alpine vegetations and also affect microbes growing on snow surface during snow melting season. In this study, we investigated spatial variations in water stable isotopes and major soluble ions on snow surface of high alpine area of Mt. Tateyama (2300 - 2700 m a.s.l.) from spring to summer to understand sources and transportation of aerosols affecting the surface snow chemistry. The soluble ion concentrations in the surface snow are generally higher in April, when the surface snow did not melt yet, than those in May to August, when the snow melted significantly. We found high anomaly in Cl and stable isotope in the area along a small valley, called Raicho-zawa throughout the seasons. They are likely to originate from an active volcanic fumarole, called Jigokudani, located in this area. Results shows that the chemical conditions of the snow surface in this mountain area are mostly influenced by sea spay and anthropogenic pollutants supplied by westerly before melting season, and are also partially influenced by the volcanic fumarole of the mountain throughout the melting seasons.

Keywords: snow, stable isotope, soluble ion

©2019. Japan Geoscience Union. All Right Reserved.

Using Sr isotopes to determine the contribution of volcanic ash to Sr and Ca in stream waters in a chert watershed.

*Masami Koshikawa[1], Mirai Watanabe[1], Tomoyoshi Murata[1], Takejiro Takamatsu[1], Shingo Miura[1], Ki-Cheol Shin[2], Takanori Nakano[2]

1. National Institute for Environmental Studies, 2. Research Institute for Humanity and Nature

The sources of Ca in forest ecosystems in Japan have been considered to be sea salt, weathering product of bedrock, and weak-acid soluble minerals in Kosa (Asian dust). However, we believe that volcanic ash in soil also plays an important contributor of Ca in areas with volcanic ash soil (e.g., Andosols), especially in the regions where the Ca supply from bedrock is anticipated to be low. We reported the significant contribution of volcanic ash in soil to Ca in stream waters and plants in a granite watershed of Tsukuba area, using stable isotope of Sr, a good proxy of Ca (Koshikawa et al. 2016). To evaluate the contribution of volcanic substances to soil-vegetation-stream systems, we conducted a similar study at the forest on Mount Amamaki where volcanic ash in soil would be more abundant than Tsukuba area and chert with high resistance to chemical weathering are widely distributed. In this presentation, we report the concentrations of Sr and Ca and the isotope ratio of Sr in the 42 stream waters, and those of precipitation, bedrock and volcanic ash which are considered to be the end component, and estimate the contribution of volcanic ash to Sr and Ca in stream waters.

Keywords: Volcanic ash, Sr isotopes, Stream water, Ca sources, Chert

©2019. Japan Geoscience Union. All Right Reserved.

Influences of soil dust, sea salt and anthropogenic activities on ionic and Sr isotopic compositions of wet deposition in Iran

*Yoriko Yokoo[1], Kosuke Asai[1], Sae Horii[1], Ryo Anma[2], Shiva Mehrabani[3], KiCheol Shin[4]

1. Faculty of Science and Engineering, Doshisha University, 2. Tokushima University, 3. Kurdistan University, 4. RIHN

We collected monthly wet deposition in four western cities (Hamedan, Ilam, Shiraz and Ahvaz) from January 2014 to May 2017 and in three eastern cities (Mashhad, Birjand and Zahedan) from January 2016 to May 2017 and in Rezvanshahr from May 2016 to May 2017 in Iran, and determined their pH values, electrical conductivity (EC), major ionic concentration (Na^+, Mg^{2+}, K^+, Ca^{2+}, Cl^-, NO_3^-, SO_4^{2-} and HCO_3^-) and Sr isotope ratios ($^{87}Sr/^{86}Sr$) in order to elucidate the influences of soil dust, sea salt and anthropogenic activities on wet deposition chemistry. In no-rainfall months, we rinsed the sampler with ultrapure water and collected it to understand the influence of aerosols. The climate in Iran is semiarid, and the dry and wet seasons are from June to September and from October to May, respectively.
The wet deposition and rinsed water samples in western and eastern Iran were neutral to slightly alkaline ranging from 6.26 to 9.04 and from 6.71 to 11.08 in pH, respectively. Those in Rezvanshahr were neutral to acidic ranging from 3.88 to 7.48 in pH. The ionic compositions of most precipitation samples were enriched in $Ca^{2+}$and HCO_3^-. Although the pH of natural rain in equilibrium state with atmospheric CO_2 is typically 5.6, precipitation in western Iran is not acidic because of neutralization by aeolian minerals such as calcite originating from arid areas. The $^{87}Sr/^{86}Sr$ of samples fell in a narrow range of 0.708±0.001. These values were most likely due to the dissolution of calcite. Small, but detectable seasonal variation was found in the $^{87}Sr/^{86}Sr$ ratio that suggests different provenances of calcite/gypsum controlled by changing wind direction.
The ionic compositions of several samples were abundant in NO_3^- and SO_4^{2-} in Hamedan, Ilam, Shiraz and Mashhad. These samples were collected during dry season and wet season immediately after the dry season. These results suggest that the samples dissolved NO_3^- and SO_4^{2-} derived from anthropogenic activities and/or soil dust such as sulfate minerals concentrated in atmosphere during the dry season. The ionic compositions of samples in Ahvaz, Rezvanshahr, Birjand and Zahedan were relatively enriched in Na^+ and Cl^-. Ahvaz and Rezvanshahr are closer to the Persian Gulf and the Caspian Sea, respectively. These indicate that the wet deposition samples in Ahvaz and Rezvanshahr are subject to salt from sea and salt lake.

Keywords: wet deposition, ionic composition, Sr isotope ratio, West Asia

©2019. Japan Geoscience Union. All Right Reserved.

[E] Oral | H (Human Geosciences)：H-TT Technology & Techniques

Tue. May 28, 2019 10:45 AM - 12:15 PM JST | Tue. May 28, 2019 1:45 AM - 3:15 AM UTC | 302 3F

[H-TT18] Development and application of environmental traceability methods

convener:Ichiro Tayasu(Research Institute for Humanity and Nature), Nobuhito Ohte(Department of Social Informatics, Graduate School of Informatics, Kyoto University), Gabriel J Bowen(University of Utah), Chairperson:Gabriel Bowen(The University of Utah)

Modern society uses almost all the elements present in the natural world. Although there have long been calls for the sustainable use of the resources that provide these elements and the building of human societies that are in harmony with the environment, the survival of the human race is increasingly at risk as a result of qualitative changes to the environment as a whole. Implementation by the society of methodologies for diagnosing and tracking these various elements of the natural environment and their relationships with humans are now required.
Elements cycle within and among the Earth system spheres, human society and the human body. Information on the concentrations and stable isotopes of elements is powerful tool for tracing this cycling and has been applied in studies of atmosphere-hydrosphere circulation, ecological systems, and the life, health and history of humans. We propose a session to discuss development and applications of environmental traceability methods toward the goal of establishing traceability in natural and human systems.
We encourage the presentation of research integrating isotopic information in various disciplines, such as geochemistry, hydrology, ecology, geology, mineralogy, anthropology, food science, and forensics. Studies applying "Isoscapes", maps of spatial isotopic variation, in addition to traditional database-based approaches, are strongly encouraged.

10:45 AM - 11:00 AM JST | 1:45 AM - 2:00 AM UTC

[HTT18-06] Long-term increasing trend of line-conditioned excess in groundwater

*Masanori Katsuyama[1] (1.Graduate School of Agriculture, Kyoto University)

11:00 AM - 11:15 AM JST | 2:00 AM - 2:15 AM UTC

[HTT18-07] Geochemistry of river water in the Okayama and Tottori Prefectures, Japan

*Katsuyuki Yamashita[1], Takahiro Kamei[1], Yuga Kishimoto[1], Masahiko Mori[1], Aya Ooi[2], Ayaka Onishi[2], Yoko Kurihara[2], Hitoshi CHIBA[1], Takanori Nakano[3], Ki-Cheol Shin[4] (1.Graduate School of Natural Science and Technology, Okayama University, 2.Faculty of Science, Okayama University, 3.Ono City, 4.Research Institute for Humanity and Nature)

11:15 AM - 11:30 AM JST | 2:15 AM - 2:30 AM UTC

[HTT18-08] Study on groundwater flow system at Oshino Village in Yamanashi Prefecture – Report 5. Estimation of the residence time in spring water and groundwater at Oshino Village.

*Shiho Yabusaki[1], Makoto Taniguchi[1], Ichiro Tayasu[1], Tomoya Akimichi[1], Noboru Ohomori[2], Ken Gotou[2], Souichirou Watanabe[2], Hitoshi Watanabe[2] (1.Research Institute for Humanity and Nature, 2.Oshino Village)

11:30 AM - 11:45 AM JST | 2:30 AM - 2:45 AM UTC

[HTT18-09] The hydrogen and oxygen isotopic compositions of water in the Chikusa River

*Ken'ichi Ohkushi[1], Shiho Yabusaki[2], Ichiro Tayasu[2], Lei Fujiyoshi[2], Takanori Nakano[2], Ki-Cheol Shin[2], Tadashi Yokoyama[3], Hiromune Mitsuhashi[4], Masayuki Itoh[1], Kazuki Yasugi[1] (1.Kobe University, 2.The Research Institute for Humanity and Nature, 3.Ako School for Students with Special Ne, 4.University of Hyogo)

11:45 AM - 12:00 PM JST | 2:45 AM - 3:00 AM UTC

[HTT18-10] Dynamics of sulfate and nitrate inferred from stable isotope techniques in Chikusa river watershed, Hyogo Prefecture

*Lei Fujiyoshi[1], Ichiro Tayasu[1], Shiho Yabusaki[1], Takashi F Haraguchi[1], Chikage Yoshimizu[1], Ken'ichi Ohkushi[2], Fumiko Furukawa[2], Masayuki Itoh[2], Yudai Yamamoto[3], Tadashi Yokoyama[4], Hiromune

Mitsuhashi[5] (1.The Research Institute for Humanity and Nature, 2.Kobe University, 3.Nagoya University, 4.Hyogo prefectural Ako School for Students with Special Needs, 5.University of Hyogo)

12:00 PM - 12:15 PM JST | 3:00 AM - 3:15 AM UTC

[HTT18-11] Chemistry and sulfur and oxygen isotope ratios of sulfate ion of water soluble component of suspended particulate matter at Okayama city.

*Hitoshi CHIBA[1], Tsubasa Yamamoto[1] (1.Graduate School of Natural Science and Technology, Okayama University)

Long-term increasing trend of line-conditioned excess in groundwater

*Masanori Katsuyama[1]

1. Graduate School of Agriculture, Kyoto University

The isotope composition in water is commonly used for the analysis of hydrological processes. According to the recently proposed two water world hypothesis, precipitation will separated into two water pools such as the stored portion in soil pore which is much evaporated and used by vegetation, and the rapidly infiltrated portion which is less affected by evaporation and recharge the stored ground- and stream water. The line-conditioned excess (or lc-excess) is an appropriate indicator to find these separation. This method defines the offset between a meteoric water line and each water samples, with a negative value indicate the effect of evaporation. The long-term observation of isotope composition is ongoing at the Kiryu Experimental Watershed (KEW). The isotope composition in the rain water does not have a clear increasing or decreasing trends for the observation period. The long-term trend of the lc-excess was also not found in soil water and shallow groundwater. On the other hand, the increasing trend of the lc-excess was found in deeper groundwater. This fact means that the effects of evaporation on the infiltrating water are decreasing. The d18O in the groundwater was slightly decreasing. If the global warming directly effects on the isotope composition in the groundwater, the d18O may increase. Thus, the decreasing d18O and the increasing lc-excess may be the results of the change of local hydrological processes. Recently, it is reported that the extreme rainfall events are increasing in Japan, including in KEW. Therefore, the trend of lc-excess in groundwater suggest that change of rainfall patterns cause the increase of rapid infiltration and recharge of groundwater body. Moreover, the long-term trend of groundwater isotope composition was observed at five locations, Hokkaido, Toyama, Yamanashi, Tottori, and Miyazaki prefectures in Japan and one location in California, USA using commercially available bottled waters. Within these locations, similar trend as KEW was found at Tottori and California. Although the depth and size of groundwater body and their residence time may effect on the patterns and trends of isotope composition, the results shown here suggest that the importance of the long-term monitoring of the groundwater. The effects of extreme rainfall events and vulnerability of each region should be evaluated based on the intensive observations at highly installed watersheds, as well as the utilization of easily available samples such as bottled waters.

Keywords: Groundwater, Stable isotope in water, local meteoric water line, line-conditioned excess, two water world hypothesis, extreme events

©2019. Japan Geoscience Union. All Right Reserved.

Geochemistry of river water in the Okayama and Tottori Prefectures, Japan

*Katsuyuki Yamashita[1], Takahiro Kamei[1], Yuga Kishimoto[1], Masahiko Mori[1], Aya Ooi[2], Ayaka Onishi[2], Yoko Kurihara[2], Hitoshi CHIBA[1], Takanori Nakano[3], Ki-Cheol Shin[4]

1. Graduate School of Natural Science and Technology, Okayama University, 2. Faculty of Science, Okayama University, 3. Ono City, 4. Research Institute for Humanity and Nature

In order to evaluate the effect of water-soil (rock) interaction, as well as human impact on the geochemical nature of river water, we have collected 695 river water samples from 454 locations in the Okayama and Tottori Prefectures, Japan. The area is ideal for such study because (1) the geology of the area is well studied, (2) there is a sharp contrast in the amount of precipitation between the southern Okayama and northern Okayama to Tottori, and (3) the population density is highly variable. We have measured the major dissolved components, trace element concentrations, and O-H isotope ratios for all of the samples, along with Sr and S isotope ratios of the selected samples. Using these data, the high-resolution geochemical maps of the two prefectures were constructed.
Both the oxygen and hydrogen isotope ratios display a clear altitude effect. The d-excess, on the other hand, is high in the northern Okayama and Tottori Prefectures (>20), and gradually decreases towards the southern Okayama (5~15). This pattern can be explained by considering the O-H isotopic signatures of the precipitation (e.g Mao 2017), as well as the difference in the amount of precipitation in the two areas. The concentration of some elements seems to correlate well with the type of rocks exposed in the area. For example, Ca and Sr concentrations are high in the areas where limestones are exposed, whereas Cr and Ni concentrations are generally high in the areas dominated by ultra-mafic rocks. In the Mt. Daisen area of the western Tottori Prefecture where dacitic volcanic rocks are common, the concentration of Si, V, Rb, Cs is high. These observations suggest that the concentration of some elements in the river water is strongly controlled by the geochemistry of rocks exposed in the area. The concentration of some dissolved constituents such as SO_4 and NO_3, on the other hand, seem to correlate well with the population density. This may imply that human activity (industrial and agricultural) is responsible for the elevation of SO_4 and NO_3 concentrations in the river water.

Keywords: River water, Okayama Prefecture, Tottori Prefecture

©2019. Japan Geoscience Union. All Right Reserved.

Study on groundwater flow system at Oshino Village in Yamanashi Prefecture –Report 5. Estimation of the residence time in spring water and groundwater at Oshino Village.

*Shiho Yabusaki[1], Makoto Taniguchi[1], Ichiro Tayasu[1], Tomoya Akimichi[1], Noboru Ohomori[2], Ken Gotou[2], Souichirou Watanabe[2], Hitoshi Watanabe[2]

1. Research Institute for Humanity and Nature, 2. Oshino Village

Oshino Village is located in southern part of Yamanashi Prefecture, Japan. The elevation is 936 m a.s.l. and the area of village is about 8 km from east to west and about 4 km from north to south. The Oshino Hakkai springs that is registered as World Cultural Heritage Site are located in Oshino Village. It is suggested that the Oshino Hakkai springs are recharged at Mt. Fuji as a result of field observation. The objective in this study to clarify the detailed groundwater flow and residence time of spring water and groundwater in Oshino Village. In this presentation, the authors will report about average residence time of groundwater and spring water.

The water samples for estimating the residence time by using the CFCs and SF_6 have been collected at 2 spring water sites, 1 shallow groundwater site and 11 deep groundwater sites. For ^3H analysis, water samples have been collected at 4 spring water sites and 4 deep groundwater sites. In this study, “shallow groundwater” is defined as several meters to some dozen meters depth, and “deep groundwater” is defined as about 100 m to 400 m depth.

As a result of analysis, the average residence time of spring water is about 10 to 26 years, shallow groundwater is about 30 to 40 years and deep groundwater is about 40 to 60 years. In addition, it is estimated that the average residence time of spring water which show the specific water quality (Na-SO_4 type, $\delta^{18}O$ and δD is relatively low) is more than 70 years. We will consider the relation between average residence time and water quality/ stable isotopes in future.

The continuous observation of water temperature and EC at 2 sites of Oshino Hakkai has been implemented since August, 2018. We will continue the field observation of Oshino village at 2019, and estimate the groundwater flow system and residence time more clearly.

Keywords: Oshino Village, groundwater, water quality, stable isotopes, groundwater flow, residence time

©2019. Japan Geoscience Union. All Right Reserved.

The hydrogen and oxygen isotopic compositions of water in the Chikusa River

*Ken'ichi Ohkushi[1], Shiho Yabusaki[2], Ichiro Tayasu[2], Lei Fujiyoshi[2], Takanori Nakano[2], Ki-Cheol Shin[2], Tadashi Yokoyama[3], Hiromune Mitsuhashi[4], Masayuki Itoh[1], Kazuki Yasugi[1]

1. Kobe University, 2. The Research Institute for Humanity and Nature, 3. Ako School for Students with Special Ne, 4. University of Hyogo

Chikusa River is the class B river facing the Seto Inland Sea in southwest Japan. Because of heavy rain, this river sometimes flows over and its basin is damaged, so Hyogo prefecture has carried out river reforming works to improve the capacity of flow until May, 2016. But the works changed the environment of this river, the impact on the quality of river water and the river ecosystem is concerned and we need the basic data of this river to measure this impact scientifically. In this study, we analyzed concentrations of dissolved ion and trace elements, stable isotopic ratio of water (δ 2H, δ 18O). In addition, we plotted the result of analysis on a basin map with a geographical information system so that the result could be seen easily and we aimed to offer the basic data which was easy to use. Furthermore, we estimated the formation factor of dissolved ion, trace elements and stable isotopic ratio of the river water through a comparison between the result of analysis and the land use, geological features and topography of the basin.

In Chikusa River, Chikusa River Conservation Committee has been holding “The simultaneous survey of water temperature all around Chikusa River” in every August since 2002. In this survey, the committee and many local residents measure water temperature at 94 sites, from headwaters to river-mouth and some tributaries. From 2015, Research Institute for Humanity and Nature, Kobe University and University of Hyogo has joined in this survey and started collecting water samples. In the survey of 2018 (held in August 5, 13:00~16:00), we received the water samples from local residents and we filtered them at once, with cellulose acetate filters whose diameters of holds are 0.2 μm. After filtering, we subdivided the samples into some polyethylene bottles and a glass vial and stored them at 20℃ or -30℃. We analyzed stable isotopic compositions of water. Stable isotopic composition of water was lower in the upstream and higher from the middle reaches to the downstream. From the upstream toward the middle reaches, the ratio became lower as the altitude became higher because of the precipitation affected by the altitude effects. On the other hand, the ratio was higher from the middle reaches to the downstream in spite of the altitude. These areas’ river became shallower and wider in the river reforming works, so the effects of sunlight on the river became big and the evaporation from the surface of river became more active.

©2019. Japan Geoscience Union. All Right Reserved.

Dynamics of sulfate and nitrate inferred from stable isotope techniques in Chikusa river watershed, Hyogo Prefecture

*Lei Fujiyoshi[1], Ichiro Tayasu[1], Shiho Yabusaki[1], Takashi F Haraguchi[1], Chikage Yoshimizu[1], Ken'ichi Ohkushi[2], Fumiko Furukawa[2], Masayuki Itoh[2], Yudai Yamamoto[3], Tadashi Yokoyama[4], Hiromune Mitsuhashi[5]

1. The Research Institute for Humanity and Nature, 2. Kobe University, 3. Nagoya University, 4. Hyogo prefectural Ako School for Students with Special Needs, 5. University of Hyogo

The Chikusa river watershed is located in the southwestern part of Hyogo prefecture. Recent river improvement in the watershed has posed concerns about changes in water quality and river ecosystem. This study aims to clarify the dynamics of dissolved ions especially sulfate and nitrate using stable isotope techniques, and to contribute to the evaluation of water environment in the watershed.

Water samples were collected from headwaters to the river mouth in August (2015, 2016, and 2017) and in February (2018), and measured ion concentrations, sulfur (δ^{34}S) and oxygen (δ^{18}O) stable isotope ratios of sulfate, and nitrogen (δ^{15}N) and oxygen (δ^{18}O) stable isotope ratios of nitrate.

Sulfate concentration was lower upstream and higher downstream in all periods, and the nearest point to the river mouth showed topically high concentration (1156 mgl^{-1}). The δ^{34}S and δ^{18}O values of sulfate suggested that the sulfate was mainly derived from soil sulfate, and the sulfate near the river mouth was derived from the seawater. In contrast, nitrate concentration was higher upstream and lower downstream in August, however the trend reversed in February. The δ^{15}N and δ^{18}O values of nitrate imply that the contribution of primary production and/or denitrification in water caused the reversed trend of nitrate concentration. The spatial distribution of δ^{15}N of nitrate showed a significant correlation with the proportion of fertilized land use (paddy field, farmland, and golf course) in all periods, suggesting an influence of fertilization.

Keywords: sulfate, nitrate, sulfur stable isotope, nitrogen isotope, oxygen stable isotope, Chikusa River watershed in Hyogo

©2019. Japan Geoscience Union. All Right Reserved.

Chemistry and sulfur and oxygen isotope ratios of sulfate ion of water soluble component of suspended particulate matter at Okayama city.

*Hitoshi CHIBA[1], Tsubasa Yamamoto[1]

1. Graduate School of Natural Science and Technology, Okayama University

Suspended particulate matters (SPM and PM2.5) have been collected at Okayama University, Okayama city in order to elucidate their chemical nature, origin and relationship with sulfate ion in precipitation. SPM and PM2.5 were sampled once a month and duration of the sampling is 96 hours. Water soluble components of SPM and PM2.5 were extracted ultrasonically. Their chemical compositions were analyzed by ion chromatography and sulfur and oxygen isotope ratios were analyzed by EA-IRMS and TC/EA-IRMS, respectively.

Soluble components of PM and PM2.5 are overwhelmingly composed NH_4^+ and SO_4^{2-}, thus seems to be mainly $(NH_4)_2SO_4$. There is no significant compositional difference in SPM and PM2.5.

Sulfur isotopic ratio of sulfate in water soluble components in SPM and PM2.5 at Okayama city is high in winter and low in other seasons, similar to nss-sulfate in precipitation. However, their sulfur isotope ratios in autumn and winter are 1 to 2‰ higher than those of nss-sulfate in precipitation. High sulfur isotope ratios in winter seem to be affected by sulfur compounds originated from coal combustion in China. However, they are clearly lower than those of sulfate in total suspended particulate matter in Beijing (Han et al., 2016) and indicate that, even in winter, contribution of sulfur originated from coal-combustion in China seems to be small at Okayama city and local source may mainly contribute to sulfate of suspended particulate matter. Furthermore, sulfur isotope ratios of nss-sulfate in PM2.5 at Niigata city (Inomata et al., 2016) agree generally with our data at Okayama city.

Oxygen isotope ratios of soluble components in SPM and PM2.5 seem to be high in winter. Oxygen isotope ratios of nss-sulfate of precipitation is also high in spring. However, the cause of this phenomena is not clear now.

Present data suggests that the direct contribution of trans-border transport of SPM and PM2.5 from China is limited at Okayama city and/or that sulfur and oxygen isotope signatures of sulfate in water soluble components of SPM and PM2.5 are greatly altered during transport from China to Okayama.

Keywords: Water soluble components of suspended particulate matter, Okayama, Sulfur isotope ratio of sulfate, Oxygen isotope ratio of sulfate

©2019. Japan Geoscience Union. All Right Reserved.

[E] Oral | H (Human Geosciences)：H-TT Technology & Techniques

Tue. May 28, 2019 1:45 PM - 3:15 PM JST | Tue. May 28, 2019 4:45 AM - 6:15 AM UTC | 302 3F

[H-TT18] Development and application of environmental traceability methods

convener:Ichiro Tayasu(Research Institute for Humanity and Nature), Nobuhito Ohte(Department of Social Informatics, Graduate School of Informatics, Kyoto University), Gabriel J Bowen(University of Utah), Chairperson:Ichiro Tayasu(Research Institute for Humanity and Nature)

Modern society uses almost all the elements present in the natural world. Although there have long been calls for the sustainable use of the resources that provide these elements and the building of human societies that are in harmony with the environment, the survival of the human race is increasingly at risk as a result of qualitative changes to the environment as a whole. Implementation by the society of methodologies for diagnosing and tracking these various elements of the natural environment and their relationships with humans are now required.
Elements cycle within and among the Earth system spheres, human society and the human body. Information on the concentrations and stable isotopes of elements is powerful tool for tracing this cycling and has been applied in studies of atmosphere-hydrosphere circulation, ecological systems, and the life, health and history of humans. We propose a session to discuss development and applications of environmental traceability methods toward the goal of establishing traceability in natural and human systems.
We encourage the presentation of research integrating isotopic information in various disciplines, such as geochemistry, hydrology, ecology, geology, mineralogy, anthropology, food science, and forensics. Studies applying "Isoscapes", maps of spatial isotopic variation, in addition to traditional database-based approaches, are strongly encouraged.

1:45 PM - 2:00 PM JST | 4:45 AM - 5:00 AM UTC

[HTT18-12] **Do mountain-climbing mammals protect plants from global warming by their vertical seed dispersal?**

*Shoji NAOE[1], Ichiro Tayasu[2] (1.Forestry and Forest Products Research Institute, Forest Research and Management Organization, 2.Research Institute for Humanity and Nature)

2:00 PM - 2:15 PM JST | 5:00 AM - 5:15 AM UTC

[HTT18-13] Spatial distribution of nitrogen stable isotope ratio in deer feces in an agro-environment, Osaka

*Takashi F Haraguchi[1], Ryosuke Koda[2], Ichiro Tayasu[1] (1.Research Institute for Humanity and Nature, 2.RIEAF, Osaka)

2:15 PM - 2:30 PM JST | 5:15 AM - 5:30 AM UTC

[HTT18-14] Nutrient supply from forest to river in eastern Toyama: carbon and nitrogen isotopic composition of Epilithic Organic Matter

*JING ZHANG[1], Ryosuke Masuda[1], SAKI KATAZAKAI[1], Tamihisa Ohta[1], OSAMU INAMURA[2], Fumiko Nakagawa[3] (1.University of Toyama, 2.Uozu Aquarium, 3.Nagoya University)

2:30 PM - 2:45 PM JST | 5:30 AM - 5:45 AM UTC

[HTT18-15] Investigation on the possibility of the identification of air pollutant sources using stable isotope ratios of lead and strontium

*Shinji Sakurai[1], Takao Nakagiri[1], Kosuke Tanaka[1], Haruhiko Horino[1], Ki-Cheol Shin[2], Ichiro Tayasu[2], Shiho Yabusaki[2] (1.Osaka Prefecture University, 2.Research Institute for Humanity and Nature)

2:45 PM - 3:00 PM JST | 5:45 AM - 6:00 AM UTC

[HTT18-16] **Magnesium and zinc stable isotopes in stream ecology**

*Kai Nils Nitzsche[1], Yoshikazu Kato[1], Ki-Cheol Shin[1], Hiromitsu Kamauchi[1], Ichiro Tayasu[1] (1.Research Institute for Humanity and Nature)

3:00 PM - 3:15 PM JST | 6:00 AM - 6:15 AM UTC

[HTT18-17] A mechanitic metabolic model of nitrogen stable isotope dynamics in trophic processes

*Reiichiro Ishii[1], Maki Noguchi Aita[2], Eitaro Wada (1.Research Institute for Humanity and Nature, 2.Japan Agency for Marine-Earth Science and Technology)

Do mountain-climbing mammals protect plants from global warming by their vertical seed dispersal?

*Shoji NAOE[1], Ichiro Tayasu[2]

1. Forestry and Forest Products Research Institute, Forest Research and Management Organization, 2. Research Institute for Humanity and Nature

Today, global warming is progressing rapidly, and attention is focused on how trees that make up the forest respond. The easiest and most powerful means for trees to escape from global warming is to move to colder areas, that is, higher altitude or latitude, by seed dispersal. Considering that the temperature drop with increasing altitude is one hundred to a thousand times larger than that of the equivalent latitudinal distance, vertical seed dispersal seems a key process for plant escape from warming temperatures. However, no study has evaluated vertical seed dispersal itself due to technical difficulty or high cost. By using negative correlation between altitudes and oxygen isotope ratio of seeds, we evaluated the vertical seed dispersal of summer-fruiting wild cherry and autumn-fruiting wild kiwi by mammals in central Japan. The results were contrasting: while seeds of cherry were dispersed toward mountain tops (by bear; mean +307.2, marten; +193.0 m), seeds of kiwifruit were dispersed toward the foot of mountains (by bear; -393.1, monkey; -98.5, raccoon dog; +4.5, marten; -226.9 m). These were probably because mammals followed plant phenology in temperate zone which proceeds from the foot to the top of mountains in spring to summer and from the top to the foot in autumn to winter. Downhill seed dispersal will likely lead to a serious population decrease of plants under global warming, because their performance is strongly reduced by novel competitive plants in the lower altitude environment. Considering that many of trees depend on animals and fruit in autumn to winter, forest composition in temperate zone might dramatically change under global warming due to biased vertical seed dispersal by animal.

Keywords: seed dispersal, global warming, temperate forest, mammal, cherry, kiwi

©2019. Japan Geoscience Union. All Right Reserved.

Spatial distribution of nitrogen stable isotope ratio in deer feces in an agro-environment, Osaka

*Takashi F Haraguchi[1], Ryosuke Koda[2], Ichiro Tayasu[1]

1. Research Institute for Humanity and Nature, 2. RIEAF, Osaka

A rapid increase in the number of sika deer (*Cervus nippon*) in the last decades aroused needs for quantitatively estimating crop herbivory by them, in order to evaluate how much damage they cause to agriculture. Analysis of ingredients in deer feces using observation under microscopes or molecular techniques is useful to reveal whether they consumed crops. Nevertheless, these techniques in common tend to underestimate crop herbivory, because crops are usually digested more easily than wild plants and less likely to remain in the feces. Measurement of fecal nitrogen stable isotope ratio (fecal δ^{15}N) can be a complement to the molecular technique, considering that application of fertilizer leads to distinctively higher δ^{15}N values of crops than the adjacent wild plants. In our previous study using captive deer individuals, we estimated the fecal δ^{15}N values are 2.0 to 3.5‰ lower than those of deer diets. Based on the test using captive individuals, the uncertainties of the fecal δ^{15}N values associated with the variations in isotopic fractionation were far less than the difference of δ^{15}N values between fertilized crops and wild plants. In this study, for a field validation of the fecal δ^{15}N measurements as an indicator of crop consumption, we examined the spatial distribution of the fecal δ^{15}N, assuming the crop consumption should occur in the individuals of sika deer inhabiting close to cropland.

Deer feces were collected in 80 forested sites in the northern part of Osaka prefecture in the 2014 to 2015 winter period. The fecal samples, which were dried at 60℃, ground, and homogenized for each of the fecal mass, were used for δ^{15}N measurements. Based on GPS telemetry of sika deer in the region (Ishizuka et al., 2007), we assumed that short-time moving range of sika deer is around 500 m in radius and the accessibility of crops for the deer is reflected by surrounding land use within the distance from sampling points. Land use surrounding sampling points were categorized into four components; forest, crop field, herbal vegetation, residential area and area of each component were calculated. Land use data are obtained from MoE National Surveys on the Natural Environment and area (m^2) of the surrounding sampling points. We conducted Spatial AutoRegressive model (SAR) and PCNM-RDA analyses to analyze the effects of surrounding areas of these landscape components on the fecal δ^{15}N values and concentrations of nitrogen in the feces.

The surrounding area of crop field was selected as a single variable to explain the fecal δ^{15}N values, and the positive correlation between the fecal δ^{15}N values and crop field area indicated the availability of crop to deer was a factor of the increase in the fecal δ^{15}N values. Based on the result, this study supported our hypothesis that fecal δ^{15}N values are an effective indicator of crop consumption by sika deer. In our presentation, we will further discuss about the relationships among concentration of nitrogen in the feces, which is known as an indicator of nutritional status of the defecated individual, estimated deer population density, and land use to elucidate factors inducing crop consuming behavior of sika deer.

Keywords: wildlife control, spatial analysis, biologging

©2019. Japan Geoscience Union. All Right Reserved.

Nutrient supply from forest to river in eastern Toyama: carbon and nitrogen isotopic composition of Epilithic Organic Matter

*JING ZHANG[1], Ryosuke Masuda[1], SAKI KATAZAKAI[1], Tamihisa Ohta[1], OSAMU INAMURA[2], Fumiko Nakagawa[3]

1. University of Toyama, 2. Uozu Aquarium, 3. Nagoya University

River water has higher concentrations of dissolved components than precipitation because dissolved components are added when precipitation passes through forest areas interacting with rocks and vegetation. To clarify the supply of nutrients from the forest area to the river, in this study we focused on catchment areas and conducted research at river upstream areas in eastern Toyama prefecture where there is with very little human influence. River waters and Epilithic Organic Matter (EOM) were collected from 2016 to 2018. We measured the concentration of major chemical components, stable isotope composition of oxygen and hydrogen (d18O, dD) in water samples, and stable carbon and nitrogen isotopic ratios of EOM. Analysis results are discussed together with topographical data and the vegetation map obtained by GIS. The results are as follows.

1) Judging from d18O values and dD values, river waters were formed by a mixture of precipitation in summer and in winter in an altitude range of 300 ~ 2000 m.

2) There was a correlation between d13C values of EOM and both Calcium and bicarbonate concentration. This suggests that Ca in river water is supplied by carbonate (CaCO3) weathering of rock and soil in the catchment area. Ca, Na, K and Mg concentrations showed a significant positive correlation with the coniferous proportion, it suggests that these chemicals are added into river water when passing through the forest area. Compared to rain water, chemical components were higher in rivers, about 200 times for Ca, 6 times for Na, 8 times for K and 10 times for Mg respectively.

3) A negative correlation exists between riverine nitrate concentration and evergreen percentage of vegetation in the catchment, and more than 90% of nitrate in river water is derived from the forest using oxygen isotopic ratio Δ17O of nitrate. It means the amount of nitrate in precipitation is trapped in the forest and then the forest originated nitrogen discharges into the rivers.

4) Δ15N in EOM, which possibility “records" the nitrogen supply information for several days to weeks when using nitrate from river water, is bounded at the altitude of 1500 m and reflects the vegetation within the catchment areas. In addition, the δ15N value showed a positive correlation with the evergreen percentage in the Catchment area, suggesting that vegetation affects nitrate outflow to rivers.

Keywords: Epilithic Organic Matter, carbon and nitrogen isotopic composition, nutrient supply, forest area, eastern Toyama

©2019. Japan Geoscience Union. All Right Reserved.

Investigation on the possibility of the identification of air pollutant sources using stable isotope ratios of lead and strontium

*Shinji Sakurai[1], Takao Nakagiri[1], Kosuke Tanaka[1], Haruhiko Horino[1], Ki-Cheol Shin[2], Ichiro Tayasu[2], Shiho Yabusaki[2]

1. Osaka Prefecture University, 2. Research Institute for Humanity and Nature

In Japan, transboundary air pollution coming from neighboring countries is concerned as one of the serious threads on the health. However, it is not easy to assess the actual impact because of difficulty to identifying the detailed transport path and the source of pollutants. Although it is expected that stable isotope ratios (hereafter, isotope ratios) of lead (Pb) and strontium (Sr) can be used as environment tracers to identify the pollutant source, even the basic information on their characteristics such as chronological and/or seasonal variations at resolution of rainfall event as well as the relationship between the ratios and other water quality parameters is still not enough to consider the possibility.
In our study, rainwater was collected in a polyethylene bottle, on the top of which a polypropylene funnel was set, separately in every rainfall event from June 2016 to August 2018 at the campus of Osaka Prefecture University in Sakai, Osaka, Japan. The isotope ratios of Pb and Sr ($^{207}Pb/^{206}Pb$, $^{208}Pb/^{206}Pb$, and $^{87}Sr/^{86}Sr$) in the rainwater samples were measured using a multi-collector inductively coupled plasma mass spectrometer. Concentrations of heavy metals (Fe, Mn, Cd, Cu, Ni, and Pb), inorganic ions, pH, EC, TOC, COD, T-N, and T-P were measured as water quality parameters. Rainfall amount was measured with a rain gauge set near the rainwater sampling point. Other meteorological data needed to investigate and estimate the pollutant sources, such as air temperature, wind direction, and duration of drought, were obtained from the Japan Meteorological Agency.
There was no obvious trend either chronologically or seasonally for $^{207}Pb/^{206}Pb$ or $^{87}Sr/^{86}Sr$. The values of the $^{207}Pb/^{206}Pb$ ratio declined slightly during the observation period, but the $^{87}Sr/^{86}Sr$ ratio did not show this chronological variation.
There was no obvious correspondence between most of water quality parameters and each isotope ratio. The $^{207}Pb/^{206}Pb$ varied widely during events in which Cr and Fe concentrations were low, but was close to 0.871 as the concentrations of these metals were getting higher. There is similar tendency in $^{87}Sr/^{86}Sr$ for Fe and Cr. It was suggested that these metals might be derived from the same source.
For correspondence with meteorological factors, the monthly rainfall amount weighted average of $^{207}Pb/^{206}Pb$ fluctuated when the wind from the west or the west-southwest was dominant, while it took almost a unique value for the south-southwest. It was suggested that Pb was originated from various sources with the west wind.
Plots of the obtained data on the $^{207}Pb/^{206}Pb$ vs. $^{208}Pb/^{206}Pb$ were distributed upside and parallel to the lead isotope growth curve. When comparing our plots with the previous global studies, we found that ours were distributed in a manner similar to those from China and Russia. It was indicated that it is difficult to identify pollutant sources from these countries, which are thought to cause transboundary pollution in Japan.
Further research, including the collection of data on isotope ratios as environmental tracers, is necessary to identify pollutant sources using isotope ratio of Pb and/or Sr.

Keywords: stable isotope ratio, air pollution, heavy metal, lead, strontium, rainwater

©2019. Japan Geoscience Union. All Right Reserved.

Magnesium and zinc stable isotopes in stream ecology

*Kai Nils Nitzsche[1], Yoshikazu Kato[1], Ki-Cheol Shin[1], Hiromitsu Kamauchi[1], Ichiro Tayasu[1]

1. Research Institute for Humanity and Nature

Magnesium (Mg) and zinc (Zn) play important roles in biological production in stream ecosystems. Aquatic organisms take up metals from the diet and the water; however, relative contributions are largely unknown, which is assumed to depend on feeding habits. We determined Mg and Zn stable isotope ratios (δ^{26}Mg, δ^{66}Zn) of aquatic macroinvertebrates and of small goby, and their potential Mg and Zn sources (periphyton, plant litter, stream water) from upper and lower reaches of two temperate streams in the Lake Biwa catchment. Our goal was to understand Mg and Zn sources to aquatic organisms, and to explore δ^{26}Mg and δ^{66}Zn variations across feeding habits. δ^{26}Mg and δ^{66}Zn did not correlate with each other indicating that Mg and Zn sources differ across functional feeding groups and/or different degrees of isotopic fractionation during Mg and Zn uptake. Grazers, shredders and predators showed offsets to higher δ^{26}Mg values compared to metal sources indicating isotope fractionation during Mg accumulation, while stream water was the main Mg source to filter-feeders. In contrast, δ^{66}Zn of grazers and filter-feeders indicated Zn was often a mixture between periphyton and stream water, while δ^{66}Zn of shredders and predators gave evidence for Zn isotopic fractionation. Our results demonstrate the usefulness of applying non-traditional isotopes to understand metal sources to aquatic organisms, which could be used to trace the ultimate origin of metals from the catchment.

Keywords: Aquatic animals, Stream food web, Magnesium, Zinc, Non-traditional isotopes

©2019. Japan Geoscience Union. All Right Reserved.

A mechanitic metabolic model of nitrogen stable isotope dynamics in trophic processes

*Reiichiro Ishii[1], Maki Noguchi Aita[2], Eitaro Wada

1. Research Institute for Humanity and Nature, 2. Japan Agency for Marine-Earth Science and Technology

Stable isotope analysis of nitrogen and carbon have been a powerful tool used for identifying trophic structure of ecosystems. Our previous studies suggested that the ratios of trophic fractionation of carbon and nitrogen isotopes ($Dd^{15}N/Dd^{13}C$) throughout food chain are similar in various ecosystems (Aita et al. 2011, Wada et al. 2013), although the general mechanisms determining isotopic incorporation rates and discrimination factors are not understood mechanistically yet. On the other hand, recent studies revealed the 15N enrichment factor for trophic processes varies among amino acids from which new method of estimation of the trophic level of animal samples (e.g., Chikaraishi et al. 2009).
Based on these observations, we developed a simple dynamic model of the isotopic fractionation in nitrogen metabolic processes that are common to animals composing most grazing food chains. Particularly, we focused on and incorporated the transamination and deamination processes of two classes of amino acid, essential and non-essential, respectively into the model. With this model we investigated how d15N signatures of the two amino acid classes and whole-body change. Preliminary result suggests that the instant isotopic composition of animals are sensitive to the change of their diet composition and growth rate, but on the other hand, the isotopic composition converges as the integrating period becomes long. Based on this model we will discuss possible negative feedback processes in isotopic enrichment for nitrogen to explain the commonly observed trophic-step 15N-enrichment factor through many food chains.

Keywords: metabolic model, nitrogen stable isotope, ecological conditions

©2019. Japan Geoscience Union. All Right Reserved.

[E] Poster | H (Human Geosciences)：H-TT Technology & Techniques

Tue. May 28, 2019 3:30 PM - 5:00 PM JST | Tue. May 28, 2019 6:30 AM - 8:00 AM UTC | Poster Hall International Exhibition Hall8, Makuhari Messe_13

[H-TT18] Development and application of environmental traceability methods

convener:Ichiro Tayasu(Research Institute for Humanity and Nature), Nobuhito Ohte(Department of Social Informatics, Graduate School of Informatics, Kyoto University), Gabriel J Bowen(University of Utah)

Modern society uses almost all the elements present in the natural world. Although there have long been calls for the sustainable use of the resources that provide these elements and the building of human societies that are in harmony with the environment, the survival of the human race is increasingly at risk as a result of qualitative changes to the environment as a whole. Implementation by the society of methodologies for diagnosing and tracking these various elements of the natural environment and their relationships with humans are now required.
Elements cycle within and among the Earth system spheres, human society and the human body. Information on the concentrations and stable isotopes of elements is powerful tool for tracing this cycling and has been applied in studies of atmosphere-hydrosphere circulation, ecological systems, and the life, health and history of humans. We propose a session to discuss development and applications of environmental traceability methods toward the goal of establishing traceability in natural and human systems.
We encourage the presentation of research integrating isotopic information in various disciplines, such as geochemistry, hydrology, ecology, geology, mineralogy, anthropology, food science, and forensics. Studies applying "Isoscapes", maps of spatial isotopic variation, in addition to traditional database-based approaches, are strongly encouraged.

[HTT18-P01] Isotopic study on seasonal nitrogen dynamics at Lake Biwa

*Takaaki Ishibashi[1], Ken'ichi Osaka[1], Keisuke Koba[2], Takashi Nakamura[3], Kei Nishida[3] (1.Department of ecosystem study, University of Shiga Prefecture, 2.Center for Ecological Research, Kyoto University, 3.International Research Center for River Basin Environment, University of YAMANASHI)

[HTT18-P02] Relationship between residence time, water quality, and stable isotopes of spring water and groundwater in coastal area of Fukushima prefecture

*Shiho Yabusaki[1], Kazuyoshi Asai[2] (1. Research Institute for Humanity and Nature・Faculty of Symbiotic Systems Science, Fukushima University, 2.Geo Science Laboratory)

[HTT18-P03] Applicability evaluation of CIA due to river and lake

*yusuke hataya[1], SEIKI KAWAGOE[1], Shiho Yabusaki[2], KEN Suzuki[1] (1.fukushima university, 2.Research Institute for Humanity and Nature)

[HTT18-P04] Chemical property analysis of short time scale to determine snowfall source

*Suzuki hiromichi[1], SEIKI KAWAGOE[1], SHO ADACHI[1], Shiho Yabusaki[2] (1.Fukushima University, 2.Research Institute for Humanity and Nature)

[HTT18-P05] Analyzing the origin of surface water in the Saijo Plain, Japan, based on the antimony concentration in the water

*Minoru TOKUMASU[1,2], Ki-Cheol SHIN[3], Yoshihiro YAMADA[4] (1.The United Graduate School of Agricultural Sciences, Ehime University, 2.Saijo City, 3.The Research Institute for Humanity and Nature (RIHN) , 4.Kagawa University, Faculty of Agriculture)

[HTT18-P06] Basic kinetic study on stable isotope ratios of nitrogen compounds: a case study for groundwater in the Kathmandu Valley, Nepal

*Ken Yokozawa[1,2], Kei Nishida[1,3], Takashi Nakamura[1,3], Ken'ichi Osaka[4] (1.University of Yamanashi, 2.Special Graduate Program on River Basin Environmental Science,, 3.ICRE, 4.Department of ecosystem study Univercity of Shiga prefecture)

[HTT18-P07] Usefulness of strontium isotope composition for determining the geographical origin of wasabi and potato

*Takafumi Kamitani[1], Ki-Cheol Shin[2], Sachiko Nakamura[1], Rika Koda[1], Tomoya Oka[1], Noriaki Fushimi[1], Yasuhide Muranaka[1] (1.Shizuoka Institute of Environment and Hygiene, 2.Research Institute for Humanity and Nature)

[HTT18-P08] Reconstruction of sea surface temperature and salinity for the Medieval Climatic Anomaly using a long-lived fossil coral collected at Ishigaki Island, southwestern Japan

*Osamu Abe[1], Maki Morimoto[2], Ryuji Asami[3], Takeshi Nakatsuka[1,4] (1.Graduate School of Environmental Studies, Nagoya University, 2.School of Education, Gifu University, 3.Graduate School of Science, Tohoku University, 4.Research Institute for Humanity and Nature)

[HTT18-P09] Development of the analytical method for sulfur isotope in SO_2 gas

*Masaaki Takahashi[1], Hiroyuki Sase[1], Tsuyoshi Ohizumi[1] (1.Asia Center for Air Pollution Research)

[HTT18-P10] Zinc isotope analysis on human tooth enamel samples to reconstruct diet of the Jomon period.

*Soichiro Kusaka[1], Ki-Cheol Shin[2] (1.Tokai Univ., 2.Research Institute for Humanity and Nature)

[HTT18-P11] Zinc stable isotope analysis of environmental reference materials

*Ki-Cheol Shin[1] (1.Research Institute for Humanity and Nature)

Isotopic study on seasonal nitrogen dynamics at Lake Biwa

*Takaaki Ishibashi[1], Ken'ichi Osaka[1], Keisuke Koba[2], Takashi Nakamura[3], Kei Nishida[3]

1. Department of ecosystem study, University of Shiga Prefecture, 2. Center for Ecological Research, Kyoto University, 3. International Research Center for River Basin Environment, University of YAMANASHI

To clarify nitrogen dynamics in Lake Biwa, we measured the concentrations of nitrogen compounds and their nitrogen stable isotopic ratios in 14 depths in north basin of Lake Biwa. In the lake, particulate nitrogen (PN), such as phytoplankton, is generally decomposed to dissolved nitrogen (DN); in order of dissolved organic nitrogen (DON), ammonia nitrogen (NH_4^+) and nitrate nitrogen (NO_3^-). These dissolved nitrogen compounds are taken up by phytoplankton again, and the nitrogen circulation in the lake is established. To predict the water quality in future, it is necessary to understand the nitrogen cycle in the lake, as well as nutrient load to the lake.

In this study, we collected lake water sample at 14 depths in north basin of Lake Biwa (water depth is 90 m) in 1-2 months interval. The lake waster sample was analyzed for the concentration of PN, PC, DN, NO_3^-, NO_2^- and NH_4^+, $d^{15}N$ of PN, DN and NO_3^-.

NO_3^- concentration was lower in the surface layer (0-20m), and higher in the deep layer (20-90m) during the stratification period, whereas NO_3^- concentration was constant in all layers during the circulation period. PN concentration also increased in the surface layer from April to June, decreased sharply in July. These indicate that phytoplankton which grew on the surface layer from April to June used NO_3^-, thereafter, NO_3^- was depleted after June, then, phytoplankton decreased after July respectively. On the other hand, NO_3^- concentration is considered to be increased by decomposition of the precipitated PN from surface layer. It is considered that the NO_3^- concentration became constant in all layers because of mixing of deep layer and the surface layer.

The weighted average $d^{15}N_{DN}$, $d^{15}N_{NO3}$ in the unit water columns decreased about 3‰ in the circulation period, in the circulation period, then, increased during the stratification period. The decrease of $d^{15}N_{DN}$, $d^{15}N_{NO3}$ at the water column during circulation period can not be explained by mixing of deep layer and the surface layer. We will discuss the mechanisms of $d^{15}N_{DN}$, $d^{15}N_{NO3}$ decrease during circulation period in the presentation.

Keywords: nitrogen dynamics, nitrogen isotope, seasonality

©2019. Japan Geoscience Union. All Right Reserved.

Relationship between residence time, water quality, and stable isotopes of spring water and groundwater in coastal area of Fukushima prefecture

*Shiho Yabusaki[1], Kazuyoshi Asai[2]

1. Research Institute for Humanity and Nature・Faculty of Symbiotic Systems Science, Fukushima University, 2. Geo Science Laboratory

After the Great East Japan Earthquake occurred, the investigation near the coast area in northern part of Fukushima prefecture has been carried out to clarify the groundwater flow and residence time in this area. The measuring of EC, pH, water temperature, ORP and sampling of groundwater, spring water and river water have been carried out several times at Shinchi town, Soma city, Minamisoma city, Namie town, Okuma town, Iitate village and Date city since September in 2012. The inorganic ions, stable isotopes of oxygen and hydrogen, trace elements were analyzed for all samples by using the IC (ICS-3000), CRDS (Picarro L2130-i) and ICP-MS (Agilent 7500cx). For estimating the residence time, tritium concentration, CFCs and SF_6 measurements were made in several samples.

The water quality of river water and shallow groundwater indicates mainly Ca-HCO_3 type. In the part of the flooded area by a tsunami, the water quality of shallow groundwater and spring water is Na-Cl type. The Ca-SO_4 type and mixed type were also confirmed in some sites. In the case of deep groundwater, the water quality shows the Na-HCO_3 type and Ca-HCO_3 type. The concentration of Fe, Mn and Al were relatively high in some parts of deep groundwater. It is considered that the origin of these trace elements is soil.

The stable isotopes of oxygen and hydrogen ($\delta^{18}O$ and δD) in river water of Niida river, Mano river and Kamimano river indicate altitude effect. Because the stable isotopes in deep groundwater is relatively low, it is anticipated the recharge are of deep groundwater is about 300 m higher than that of shallow groundwater. It is expected that the recharge area of deep groundwater is around the Abukuma Mountains.

The average residence time of deep groundwater and spring water which indicate the Na-HCO_3 type is about 60 to 70 years. On the other hand, the average residence time of shallow groundwater which indicate the Ca-HCO_3 type is less than 10 years.

The information of groundwater flow is useful for considering the groundwater use with revival of the coastal area. We will continue the investigation of coastal area and make clear the groundwater flow system.

Keywords: Minamisoma city, Fukushima prefecture, CFCs・SF6, residence time, water quality, stable isotopes, groundwater flow

©2019. Japan Geoscience Union. All Right Reserved.

Applicability evaluation of CIA due to river and lake

*yusuke hataya[1], SEIKI KAWAGOE[1], Shiho Yabusaki[2], KEN Suzuki[1]

1. fukushima university, 2. Research Institute for Humanity and Nature

Water resources management must be further attention because extreme weather condition generate to predict climate change. However, a water area have the various regional characteristics. Therefore a universal way may not also be able to indicate the effect management. If categorized basin tool is developing to obtain characteristic, it is possible to choose suitable management technique in water areas. We tried to develop database to manage basin as chemical and geographical information. In this research, Water factors (Chemical condition, land use condition, soil condition and geological condition) between basins (rivers and reservoirs) were compared to develop data base. Especially, we applied to Chemical Index of Alteration (CIA) as chemical condition factor. As results, It was possible to obtain the basin area scale to apply CIA.

Keywords: CIA, water resource, Numerical geographic information

©2019. Japan Geoscience Union. All Right Reserved.

Chemical property analysis of short time scale to determine snowfall source

*Suzuki hiromichi[1], SEIKI KAWAGOE[1], SHO ADACHI[1], Shiho Yabusaki[2]

1. Fukushima University, 2. Research Institute for Humanity and Nature

Occurrence of the strange weather phenomenon is predicted from the current state depending on climate change. To ask this influence, we have to advance the match which raises the future predictability. And, we have to mark a phenomenon of the current state detail. This study targets to obtain chemically snow environment. The aim of this study was to analyse and predict the stable water isotopic composition of the snow cover at specific basin (Agano river). In addition, the dependence of short time step isotopic composition of the entire snow cover was analysed. Snow in 3 catchments was sampled at the end of the accumulation period from December 2016 to April 2018. The observed variability of short time step isotopic composition of the snow cover was analysed chemical verification. Especially, basin The Inawashiro-Lake north side of the northern upstream region indicated the low chemical feature (Suzuki et al 2018). I'm working on the investigation analysis to grasp the chemical special quality of the snow event of the short time scale at present based on this result (2016-2018). It was that a chemical analysis makes the sample which sampled and acquired it by each day the time of a snowfall at Fukushima, Hibara and Yonezawa located in an upstream region in a basin, and we tried to follow up a snowfall origin of the short time scale.

As results, a strong pressure pattern of southern high and northern low could admit January 22nd-the 25th, the result obtained from the result of analysis also reacted to the weather situation sensitively. And influence of a characteristic snowfall origin was admitted at 3 spots. The difference in the spatial time lags was done clearly.

Keywords: d-excess value, isotope, short time scale

©2019. Japan Geoscience Union. All Right Reserved.

Analyzing the origin of surface water in the Saijo Plain, Japan, based on the antimony concentration in the water

*Minoru TOKUMASU[1,2], Ki-Cheol SHIN[3], Yoshihiro YAMADA[4]

1. The United Graduate School of Agricultural Sciences, Ehime University, 2. Saijo City, 3. The Research Institute for Humanity and Nature (RIHN) , 4. Kagawa University, Faculty of Agriculture

1. Introduction

The flow of river water in many medium and small rivers is managed for water use and flood control. However, it is almost impossible to understand how the water taken from the rivers circulates throughout a basin. The source of water in the Saijo Plain in Ehime Prefecture is from the Kamo River surface water flow, shallow groundwater (unconfined ground water), and deep groundwater (confined ground water). Therefore, it is necessary to quantitatively clarify the source of water for sustainable water use. In this study, we tried to quantify the origin of river water in the plain based on the concentration of some chemical elements. In particular, antimony (Sb) was used as the main trace element because of large differences in its concentration between the water sources.

2. Materials and Methods

On November 25 and 26, 2017, during the non-irrigation period and on the 27th and 28th of July, 2018, during the irrigation period, surface water was collected at a total of 43 sites on small and medium rivers and waterways in the Saijo Plain. Multi-element analysis was carried out on the collected water using ICP-MS 7500 cx.

3. Results and Discussion

There was a large difference in the concentration of Sb among the sites. The highest concentration was found in the water from the Ichino River (Stn. 2) at 113 (2017) and 158 μg/L (2018). There was once an antimony mine in the Ichino River basin, so high concentrations of the element in the river water can be regarded as reflecting the influence of the geology. In the main stream of the Kamo River before joining the Ichinose River (Stn. 1), the Sb concentration was as low as 0.2 μg/L, and after the junction of the two rivers (Stn. 3), the concentration increased to 4.3 (2017) and 7.2 μg/L (2018). The concentration was 4.2 (2017) and 7.2 μg/L (2018) at Stn. 4 of the Kamo River, 11.6 (2017) and 11.7 μg/L (2018) in the unconfined ground water (average of Stns. 13, 14, 15), and 0.4 (2017) and 0.5 μg/L (2018) in the confined ground water (average of Stns. 28, 29, 40, 41, 43). The concentration of Si was 2.7 (2017) and 3.2 mg/L (2018) at Stn. 4 of the Kamo River, 3.4 (2017) and 2.9 mg/L (2018) in the unconfined ground water (average of Stns. 13, 14, 15), and 4.1 (2017) and 3.9 mg/L (2018) in the confined ground water (average of Stns. 28, 29, 40, 41, 43).
The ratio of water origin at each survey site was estimated using the above three sources as end members. In the upstream area, the irrigation water taken from the Kamo River occupied most of the surface water. In the middlestream area, the ratio of water taken from the rivers was smaller, and the contribution of

©2019. Japan Geoscience Union. All Right Reserved.

unconfined ground water exceeded 80%. In the downstream area, the confined ground water contribution exceeded 40% at many sites. In the Saijo Plain, the water origins are different in the upstream, middlestream, and downstream areas, where the contribution of irrigation water is small overall, and the contribution of the confined ground water is large.

©2019. Japan Geoscience Union. All Right Reserved.

Basic kinetic study on stable isotope ratios of nitrogen compounds: a case study for groundwater in the Kathmandu Valley, Nepal

*Ken Yokozawa[1,2], Kei Nishida[1,3], Takashi Nakamura[1,3], Ken'ichi Osaka[4]

1. University of Yamanashi, 2. Special Graduate Program on River Basin Environmental Science,, 3. ICRE, 4. Department of ecosystem study Univercity of Shiga prefecture

Groundwater is a valuable source of water in developing countries where water demand is increasing with population increase. At the same time, nitrogen contamination by industrial wastewater, domestic wastewater and agricultural activities has been reported. In underground environments, it is not unusual to identify sources of contamination since the forms and the concentrations of nitrogen compounds vary at different water flow or microbial metabolism. Stable isotopic analysis is one of the effective methods to detail the variations. However, the isotope value is also greatly affected by environmental conditions, and the theoretical enforcement for describing the variation of the isotope value is needed. In this study, we aimed to quantitatively understand and identify the factors of mixing and isotopic fractionation that determine the stable isotope ratio with a case study on groundwater contamination in the Kathmandu Valley, Nepal.

The data used for the analysis was obtained from the groundwater survey of the Kathmandu Valley conducted from September 2014 to August 2018. Based on the stable isotope ratios of nitrogen and oxygen of nitrate, the contamination patterns were roughly categorized. The mixing line and the denitrification line were prepared based on the dynamic fractionation for the stable isotope ratios of nitrate nitrogen, and the spatial distribution of denitrification-related samples was examined on the map. In addition, assuming that the reactants exist sufficiently and homogeneously in the system, an equilibrium fractionation model was formulated by combining nitrification and denitrification for oxygen stable isotope ratios of nitrate and water. The range of the model parameters were determined by using the measured data from the filed survey, the influence of each process on the stable oxygen isotope ratio of nitrate was quantified.

The result showed that the nitrate in shallow groundwater partially originated from the atmospheric source through infiltration of rainwater. A characteristic of denitrification was observed, which was initiated and proceeded over the valley. Additionally, the correspondent isotopic fractionation differed at the location and the season, particularly controlled by ammonia oxidation, nitrite reduction and oxygen exchange between nitrite and water.

Keywords: groundwater , nitrogen and oxygen stable isotope ratios, nitrification, denitrification, mixing, fractionation

©2019. Japan Geoscience Union. All Right Reserved.

Usefulness of strontium isotope composition for determining the geographical origin of wasabi and potato

*Takafumi Kamitani[1], Ki-Cheol Shin[2], Sachiko Nakamura[1], Rika Koda[1], Tomoya Oka[1], Noriaki Fushimi[1], Yasuhide Muranaka[1]

1. Shizuoka Institute of Environment and Hygiene, 2. Research Institute for Humanity and Nature

Originally, the use of strontium isotope ratios ($^{87}Sr/^{86}Sr$) was restricted to geology and petrology, but they have been used as a particularly effective tracer of geographical food origin, as plants reflect the strontium isotope composition of the regionally based rock, soil, and water. This study aims to evaluate the usefulness of $^{87}Sr/^{86}Sr$ for determining the geographical origin of wasabi (Japanese horseradish) and potato, which are specialty crops in Shizuoka Prefecture, Japan.

Wasabi is cultivated in springs and streams located at the top of rivers, where dissolved element and isotopic compositions in water would reflect the geological characteristics without the effects of atmospheric deposition and human activity. We collected wasabi and water samples from 40 locations of major production areas in Japan: Shizuoka, Iwate, Nagano, Tokyo, and Shimane. These samples were subjected to trace elements and $^{87}Sr/^{86}Sr$ analyses. The $^{87}Sr/^{86}Sr$ values differed, based on the geological characteristics of their site locations, and the value of wasabi was well accorded with that of water in the same location. The wasabi samples collected from Izu Peninsula and Mt. Fuji regions in Shizuoka, where young volcanic rocks such as Quaternary basalts are distributed, had low $^{87}Sr/^{86}Sr$ (below 0.7040), whereas those from Nagano and Tokyo, where older rocks such as Mesozoic granites and accretionary complex are distributed, showed higher ratios (over 0.7095). We conclude that $^{87}Sr/^{86}Sr$ value of wasabi allowed us to distinguish the production area clearly.

On the other hand, the $^{87}Sr/^{86}Sr$ values of crops cultivated in the field are considered to be partly affected by precipitation and fertilizer. Therefore we conducted field survey and planter test for potato in Shizuoka. Field survey was conducted at Mishima, in eastern part of Shizuoka prefecture, and at Mikatahara, in western part of it, and $^{87}Sr/^{86}Sr$ of potato and soil exchangeable fraction were compared. As a result, there was a correlation between potato and soil in $^{87}Sr/^{86}Sr$, although the effects of precipitation and fertilizer were observed. The planter test suggests that the influence of fertilizer on $^{87}Sr/^{86}Sr$ varies depending on the amount of exchangeable Sr contained in the original soil.

Keywords: geographical origin, strontium isotope ratio, wasabi, potato, Shizuoka

©2019. Japan Geoscience Union. All Right Reserved.

Reconstruction of sea surface temperature and salinity for the Medieval Climatic Anomaly using a long-lived fossil coral collected at Ishigaki Island, southwestern Japan

*Osamu Abe[1], Maki Morimoto[2], Ryuji Asami[3], Takeshi Nakatsuka[1,4]

1. Graduate School of Environmental Studies, Nagoya University, 2. School of Education, Gifu University, 3. Graduate School of Science, Tohoku University, 4. Research Institute for Humanity and Nature

The period between 950 and 1250CE is called as the Medieval Climate Anomaly (MCA; Masson-Delmotte et al., 2013), at the time when the warmer climate seemed dominant globally (Bradley et al., 2003). Recent investigations based on the proxy record such as tree-ring widths, speleothems, ice cores, and historical documents indicated that a significant climate change occurred during the latter half of the 10th century. Mann et al. (2009) found that an increase of the average air temperature in the northern hemisphere at the late 10c. coincided with an increase of sea surface temperature at northern subpolar oceans. Yan et al. (2011) indicated that atmospheric environments in the equatorial Pacific shifted from the La Nina like condition to the El Nino like condition around 1000CE. In East Asia, Zhang et al. (2008) and Ge et al. (2013) described that the activity of East Asian Summer Monsoon (EASM) had been enhanced during the late 10c., then the climate in China shifted to warmer and wetter. Whereas Lie et al. (2014) showed that the EASM had been weakened during the 11th century. In addition, the climate in southern China was reported as relatively dry (Chen et al., 2015).

These studies demonstrated that a large climatic shift occurred around 1000CE, however, most of them have relied on records collected on land. There is little long-term high-resolution marine record during the MCA.

We reconstructed sea surface temperature (SST) and salinity with a temporal resolution of one month for 300 years using a long-lived fossil coral collected at Ishigaki Island, southwestern Japan. Based on the U/Th dating in the youngest part of the coral skeletons as well as the band counting, this coral sample had lived between 845 and 1130CE, largely covered the MCA period. Skeletal Sr/Ca and oxygen isotopic composition were analyzed for about 4,000 samples.

The empirical equations between Sr/Ca and water temperature; between oxygen isotopic composition of coral skeleton and seawater, and water temperature, were established using the present coral records, observed water temperature and oxygen isotopic composition of seawater. With these equations and the relationship between seawater salinity and oxygen isotopic composition, proposed by Abe et al. (2009), SST and seawater salinity from 845 to 1130CE were reconstructed from the fossil coral Sr/Ca and oxygen isotopic composition.

Through the entire period, average summer and winter SSTs were 2 and 1 deg. C higher than the present, respectively. In addition, SST increased significantly after 1040CE; 0.9 for the annual average, 0.7 for summer and 1.1 for winter. Salinity also increased after 990CE; 0.8 all for the annual average, summer and winter. Salinity was significantly higher through the entire period than the present, however, its absolute value seems unconfirmed yet.

©2019. Japan Geoscience Union. All Right Reserved.

Increasing SST and salinity found in this study during ca. 1000 and 1130CE were consistent with the weakening of EASM during the 11th and 12th centuries shown by Liu et al. (2014). They argued the weakening occurred as a consequence of weakening of the solar activity and the decrease of SST at the western Pacific warm pool. In this study region, the decrease of precipitation during the Baiu period induced the increase of salinity as well as local SST increase due to the decrease of the cloud cover. Our results were also consistent with the warming of China in the late 10c. (Ge et al., 2013), and a drier condition in southern China (Chen et al., 2015).

The periodicity of SST and salinity based on the spectral analysis will be discussed in the presentation.

Keywords: Coral annual bands, Medieval Climate Anomaly

©2019. Japan Geoscience Union. All Right Reserved.

Development of the analytical method for sulfur isotope in SO_2 gas

*Masaaki Takahashi[1], Hiroyuki Sase[1], Tsuyoshi Ohizumi[1]

1. Asia Center for Air Pollution Research

1. Introduction

Sulfur is a major source of acid deposition. Usually sulfur is emitted as SO_2 and it is oxidized to SO_4^{2-} in atmosphere. S isotopic analysis of water and particulate samples were conducted in many studies. But gaseous SO_2 was rarely used for isotopic study. Isotopic ratio of SO_2 is strongly influenced by emission source near the sampling point. Because most of SO_2 emitted far from sampling point is oxidized to SO_4^{2-} during transportation. It is possible to distinguish domestic emission from transboundary emission. Moreover, dry deposition processes of SO_2 and particulate SO_4^{2-} and their interactions with tree canopy could be discussed more precisely. Isotopic analysis of SO_2 is considered as a powerful method to investigate the behavior of S in the atmosphere and ecosystems. We studied about the analytical method for S isotope in SO_2.

2. Method

(1) Equipment

SO_2 concentration in Japan is very low (e.g. annual 0.02ppb at Sado). We need to collect air sample at least $1m^3$ that is the amount we can obtain 1.2mg of $BaSO_4$ precipitation enough for isotopic analysis. High volume air sampler is generally used to collect around $1m^3$ of air sample. It uses filter, so we examined filter collection of SO_2 by K_2CO_3 filter generally used to collect SO_2 in filter-pack method.

(2) Filters

We used quarts filter for particulate SO_4^{2-} and K_2CO_3 filter for gaseous SO_2 next to it. K_2CO_3 filter is made on the basis of EANET manual. But to get enough flow rate for high volume air sampler, the size of K_2CO_3 filter is larger (20×26 cm, same size with quarts filter) than the manual and already dried before sampling.

(3) Flow rate/leak test

Under flow rate 100~400 L/min in this system, we confirmed weather sampling can be carried out stably. And we checked leak using two K_2CO_3 filters.

(4) Sample treatment

©2019. Japan Geoscience Union. All Right Reserved.

On the basis of EANET manual, the sample was extracted with 0.05% H_2O_2aq and filtered. Then 2N HCl was added and concentrated to remove CO_3^{2-}. Next 1%(w/w)$BaCl_2$ was added. We filtered forming $BaSO_4$ precipitation. We examined the method to get $BaSO_4$ precipitation and to remove the components from K_2CO_3 filter.

3. Results

(1) Sampling and sample treatment

Sampling could be conducted under flow rate 100~400 L/min. Sampling efficiency was about 80%..

Several conditions to get $BaSO_4$ precipitation ware examined, it could be gotten by the method as below.

Filter was cut and ultrasonic extracted with 0.05% H_2O_2aq 30 minutes and filtered. 2.5 ml of 2N HCl was added and concentrated to around 10 ml. Then 1 ml of heated 1 %(w/w) $BaCl_2$ was added under pH 4~6. Next evaporated all solvent and added 10 ml of water. $BaSO_4$ precipitation was observed. After put for one night, the precipitation was separated by centrifuge 3,600 rpm for 10 minutes and we removed the solvent. The precipitation was washed twice by 10 ml of water and filtered. At last the filter was ashed for four hours in muffle furnace in 800 ℃ .

(2) Actual analysis

We used two K_2CO_3 filters and collected 2160.2 m^3 of air sample under flow rate 300 L/min. 3.80 mg of particular SO_4^{2-} and 0.89 mg (first) and 0.14 mg (second) of SO_4^{2-} from SO_2 were obtained. $\delta^{34}S$ of particular SO_4^{2-} was 8.64 ‰and that of SO_2 from the first filter was -1.54 ‰. The amount of precipitation from second filter was not enough for isotopic analysis. This difference was caused by effect of sea salt mainly. But nss- $\delta^{34}S$ of particular SO_4^{2-} was 4.78 ‰. It was still higher than SO_2. It suggested that nss- SO_4^{2-} contains both transboundary SO_4^{2-} and domestic SO_4^{2-}. According to the relevant literature, domestic SO_2 may have negative isotopic values because of imported oil from Middle East. Considering that this sampling was carried out in January, possible effect of transboundary SO_2 with higher isotopic values should also be taken into account for source identification of the collected SO_2.
We would like to discuss at the conference with the latest data.

Keywords: sulfur isotope, SO2 gas

©2019. Japan Geoscience Union. All Right Reserved.

Zinc isotope analysis on human tooth enamel samples to reconstruct diet of the Jomon period.

*Soichiro Kusaka[1], Ki-Cheol Shin[2]

1. Tokai Univ., 2. Research Institute for Humanity and Nature

This study investigates zinc isotope ratios in tooth enamels of human skeletal remains of the Jomon period in Japan. Carbon and nitrogen isotope analysis on bone collagen were traditionary used to reconstruct diet and trophic levels on prehistoric people. The progress of isotope measurements using MC-ICP-MS enables us to analyze isotope ratios of zinc and other metals. Some researches report that the zinc isotope ratios of animals reflect dietary sources and vary according to trophic levels. This study newly develops zinc isotope analysis on human tooth enamels. The zinc isotope analysis has great potential to reconstruct dietary information from inorganic materials of archaeological bones or fossils.

The material used in this study is SRM1400 (bone ash), six samples of human tooth enamels from the Yoshigo and Inariyama shell mounds of Aichi prefecture, and faunal remains (six deer enamels, three boar enamels, six marine fish bones, and six modern plant leaves). Zinc was purified from these samples using anion exchange resin. Zinc isotope ratios were measured by MC-ICP-MS with the zinc standard solution of AA-ETH. The mass bias was corrected with Cu standard solution added to all standards and samples. The zinc isotope ratios of SRM1400 showed similar value with the value previously reported. The difference of zinc isotope ratios between washed and unwashed samples with acetic acids were very small, suggesting no significant diagenetic alteration. The deer and marine fish samples showed the value expected from their dietary ecology. The zinc isotope ratios of Jomon skeletal remains was higher than those of plants, but lower than deer and marine fish. This result indicates that sources of zinc for humans were terrestrial and marine meat as well as terrestrial plants.

Keywords: Zinc Isotope, Jomon period, Human skeletal remains

©2019. Japan Geoscience Union. All Right Reserved.

Zinc stable isotope analysis of environmental reference materials

*Ki-Cheol Shin[1]

1. Research Institute for Humanity and Nature

Zinc has atomic number 30 and atomic mass 65.39. It is a trace element of terrestrial rocks and widely distributed throughout the lithosphere and biosphere. It is chalcophile features and has rich coordination chemistry, participates in a large number of important biological compounds and reactions. The zinc plays an important role as an essential trace metal in all living systems from bacteria to humans. Zn has five stable isotopes ^{64}Zn, ^{66}Zn, ^{67}Zn, ^{68}Zn, and ^{70}Zn. Their isotopic fractionation could provide valuable information about environmental processes, especially in biological processes.

With the advent of multi-collector ICP-MS, it is possible to measure the precise value of ^{66}Zn/^{64}Zn in Zn solution. To promote the environmental stable isotope traceability, RIHN is desired to determine the isotope ratios of zinc for environmental reference materials with high precision and accuracy, rapidness, and convenience.

Here, I report a simple and efficient method for zinc isotope analysis. The various environmental samples over 20 types were used for the study. All samples have purified with an anion exchange resin to separated Zn and Fe at a time. Zinc isotope ratios were measured by MC-ICP-MS (NEPTUNE plus) with AA-ETH, which is a new zinc isotopic standard solution reported by Archer et al. (2017). The mass bias correction conducted with Cu standard solution (NIST SRM 976).

Keywords: stable isotope , Zinc, environmental reference materials

©2019. Japan Geoscience Union. All Right Reserved.

[E] Poster | H (Human Geosciences)：H-TT Technology & Techniques

Tue. May 28, 2019 5:15 PM - 6:30 PM JST | Tue. May 28, 2019 8:15 AM - 9:30 AM UTC | Poster Hall International Exhibition Hall8, Makuhari Messe_23

[H-TT18] Development and application of environmental traceability methods

convener:Ichiro Tayasu(Research Institute for Humanity and Nature), Nobuhito Ohte(Department of Social Informatics, Graduate School of Informatics, Kyoto University), Gabriel J Bowen(University of Utah)

Modern society uses almost all the elements present in the natural world. Although there have long been calls for the sustainable use of the resources that provide these elements and the building of human societies that are in harmony with the environment, the survival of the human race is increasingly at risk as a result of qualitative changes to the environment as a whole. Implementation by the society of methodologies for diagnosing and tracking these various elements of the natural environment and their relationships with humans are now required.
Elements cycle within and among the Earth system spheres, human society and the human body. Information on the concentrations and stable isotopes of elements is powerful tool for tracing this cycling and has been applied in studies of atmosphere-hydrosphere circulation, ecological systems, and the life, health and history of humans. We propose a session to discuss development and applications of environmental traceability methods toward the goal of establishing traceability in natural and human systems.
We encourage the presentation of research integrating isotopic information in various disciplines, such as geochemistry, hydrology, ecology, geology, mineralogy, anthropology, food science, and forensics. Studies applying "Isoscapes", maps of spatial isotopic variation, in addition to traditional database-based approaches, are strongly encouraged.

[HTT18-P01] Isotopic study on seasonal nitrogen dynamics at Lake Biwa

*Takaaki Ishibashi[1], Ken'ichi Osaka[1], Keisuke Koba[2], Takashi Nakamura[3], Kei Nishida[3] (1.Department of ecosystem study, University of Shiga Prefecture, 2.Center for Ecological Research, Kyoto University, 3.International Research Center for River Basin Environment, University of YAMANASHI)

[HTT18-P02] Relationship between residence time, water quality, and stable isotopes of spring water and groundwater in coastal area of Fukushima prefecture

*Shiho Yabusaki[1], Kazuyoshi Asai[2] (1. Research Institute for Humanity and Nature・Faculty of Symbiotic Systems Science, Fukushima University, 2.Geo Science Laboratory)

[HTT18-P03] Applicability evaluation of CIA due to river and lake

*yusuke hataya[1], SEIKI KAWAGOE[1], Shiho Yabusaki[2], KEN Suzuki[1] (1.fukushima university, 2.Research Institute for Humanity and Nature)

[HTT18-P04] Chemical property analysis of short time scale to determine snowfall source

*Suzuki hiromichi[1], SEIKI KAWAGOE[1], SHO ADACHI[1], Shiho Yabusaki[2] (1.Fukushima University, 2.Research Institute for Humanity and Nature)

[HTT18-P05] Analyzing the origin of surface water in the Saijo Plain, Japan, based on the antimony concentration in the water

*Minoru TOKUMASU[1,2], Ki-Cheol SHIN[3], Yoshihiro YAMADA[4] (1.The United Graduate School of Agricultural Sciences, Ehime University, 2.Saijo City, 3.The Research Institute for Humanity and Nature (RIHN) , 4.Kagawa University, Faculty of Agriculture)

[HTT18-P06] Basic kinetic study on stable isotope ratios of nitrogen compounds: a case study for groundwater in the Kathmandu Valley, Nepal

*Ken Yokozawa[1,2], Kei Nishida[1,3], Takashi Nakamura[1,3], Ken'ichi Osaka[4] (1.University of Yamanashi, 2.Special Graduate Program on River Basin Environmental Science,, 3.ICRE, 4.Department of ecosystem study Univercity of Shiga prefecture)

[HTT18-P07] Usefulness of strontium isotope composition for determining the geographical origin of wasabi and potato

*Takafumi Kamitani[1], Ki-Cheol Shin[2], Sachiko Nakamura[1], Rika Koda[1], Tomoya Oka[1], Noriaki Fushimi[1], Yasuhide Muranaka[1] (1.Shizuoka Institute of Environment and Hygiene, 2.Research Institute for Humanity and Nature)

[HTT18-P08] Reconstruction of sea surface temperature and salinity for the Medieval Climatic Anomaly using a long-lived fossil coral collected at Ishigaki Island, southwestern Japan

*Osamu Abe[1], Maki Morimoto[2], Ryuji Asami[3], Takeshi Nakatsuka[1,4] (1.Graduate School of Environmental Studies, Nagoya University, 2.School of Education, Gifu University, 3.Graduate School of Science, Tohoku University, 4.Research Institute for Humanity and Nature)

[HTT18-P09] Development of the analytical method for sulfur isotope in SO_2 gas

*Masaaki Takahashi[1], Hiroyuki Sase[1], Tsuyoshi Ohizumi[1] (1.Asia Center for Air Pollution Research)

[HTT18-P10] Zinc isotope analysis on human tooth enamel samples to reconstruct diet of the Jomon period.

*Soichiro Kusaka[1], Ki-Cheol Shin[2] (1.Tokai Univ., 2.Research Institute for Humanity and Nature)

[HTT18-P11] Zinc stable isotope analysis of environmental reference materials

*Ki-Cheol Shin[1] (1.Research Institute for Humanity and Nature)

Isotopic study on seasonal nitrogen dynamics at Lake Biwa

*Takaaki Ishibashi[1], Ken'ichi Osaka[1], Keisuke Koba[2], Takashi Nakamura[3], Kei Nishida[3]

1. Department of ecosystem study, University of Shiga Prefecture, 2. Center for Ecological Research, Kyoto University, 3. International Research Center for River Basin Environment, University of YAMANASHI

To clarify nitrogen dynamics in Lake Biwa, we measured the concentrations of nitrogen compounds and their nitrogen stable isotopic ratios in 14 depths in north basin of Lake Biwa. In the lake, particulate nitrogen (PN), such as phytoplankton, is generally decomposed to dissolved nitrogen (DN); in order of dissolved organic nitrogen (DON), ammonia nitrogen (NH_4^+) and nitrate nitrogen (NO_3^-). These dissolved nitrogen compounds are taken up by phytoplankton again, and the nitrogen circulation in the lake is established. To predict the water quality in future, it is necessary to understand the nitrogen cycle in the lake, as well as nutrient load to the lake.

In this study, we collected lake water sample at 14 depths in north basin of Lake Biwa (water depth is 90 m) in 1-2 months interval. The lake waster sample was analyzed for the concentration of PN, PC, DN, NO_3^-, NO_2^- and NH_4^+, $d^{15}N$ of PN, DN and NO_3^-.

NO_3^- concentration was lower in the surface layer (0-20m), and higher in the deep layer (20-90m) during the stratification period, whereas NO_3^- concentration was constant in all layers during the circulation period. PN concentration also increased in the surface layer from April to June, decreased sharply in July. These indicate that phytoplankton which grew on the surface layer from April to June used NO_3^-, thereafter, NO_3^- was depleted after June, then, phytoplankton decreased after July respectively. On the other hand, NO_3^- concentration is considered to be increased by decomposition of the precipitated PN from surface layer. It is considered that the NO_3^- concentration became constant in all layers because of mixing of deep layer and the surface layer.

The weighted average $d^{15}N_{DN}$, $d^{15}N_{NO3}$ in the unit water columns decreased about 3‰ in the circulation period, in the circulation period, then, increased during the stratification period. The decrease of $d^{15}N_{DN}$, $d^{15}N_{NO3}$ at the water column during circulation period can not be explained by mixing of deep layer and the surface layer. We will discuss the mechanisms of $d^{15}N_{DN}$, $d^{15}N_{NO3}$ decrease during circulation period in the presentation.

Keywords: nitrogen dynamics, nitrogen isotope, seasonality

©2019. Japan Geoscience Union. All Right Reserved.

Relationship between residence time, water quality, and stable isotopes of spring water and groundwater in coastal area of Fukushima prefecture

*Shiho Yabusaki[1], Kazuyoshi Asai[2]

1. Research Institute for Humanity and Nature・Faculty of Symbiotic Systems Science, Fukushima University, 2. Geo Science Laboratory

After the Great East Japan Earthquake occurred, the investigation near the coast area in northern part of Fukushima prefecture has been carried out to clarify the groundwater flow and residence time in this area. The measuring of EC, pH, water temperature, ORP and sampling of groundwater, spring water and river water have been carried out several times at Shinchi town, Soma city, Minamisoma city, Namie town, Okuma town, Iitate village and Date city since September in 2012. The inorganic ions, stable isotopes of oxygen and hydrogen, trace elements were analyzed for all samples by using the IC (ICS-3000), CRDS (Picarro L2130-i) and ICP-MS (Agilent 7500cx). For estimating the residence time, tritium concentration, CFCs and SF_6 measurements were made in several samples.

The water quality of river water and shallow groundwater indicates mainly Ca-HCO_3 type. In the part of the flooded area by a tsunami, the water quality of shallow groundwater and spring water is Na-Cl type. The Ca-SO_4 type and mixed type were also confirmed in some sites. In the case of deep groundwater, the water quality shows the Na-HCO_3 type and Ca-HCO_3 type. The concentration of Fe, Mn and Al were relatively high in some parts of deep groundwater. It is considered that the origin of these trace elements is soil.

The stable isotopes of oxygen and hydrogen ($\delta^{18}O$ and δD) in river water of Niida river, Mano river and Kamimano river indicate altitude effect. Because the stable isotopes in deep groundwater is relatively low, it is anticipated the recharge are of deep groundwater is about 300 m higher than that of shallow groundwater. It is expected that the recharge area of deep groundwater is around the Abukuma Mountains.

The average residence time of deep groundwater and spring water which indicate the Na-HCO_3 type is about 60 to 70 years. On the other hand, the average residence time of shallow groundwater which indicate the Ca-HCO_3 type is less than 10 years.

The information of groundwater flow is useful for considering the groundwater use with revival of the coastal area. We will continue the investigation of coastal area and make clear the groundwater flow system.

Keywords: Minamisoma city, Fukushima prefecture, CFCs・SF6, residence time, water quality, stable isotopes, groundwater flow

©2019. Japan Geoscience Union. All Right Reserved.

Applicability evaluation of CIA due to river and lake

*yusuke hataya[1], SEIKI KAWAGOE[1], Shiho Yabusaki[2], KEN Suzuki[1]

1. fukushima university, 2. Research Institute for Humanity and Nature

Water resources management must be further attention because extreme weather condition generate to predict climate change. However, a water area have the various regional characteristics. Therefore a universal way may not also be able to indicate the effect management. If categorized basin tool is developing to obtain characteristic, it is possible to choose suitable management technique in water areas. We tried to develop database to manage basin as chemical and geographical information. In this research, Water factors (Chemical condition, land use condition, soil condition and geological condition) between basins (rivers and reservoirs) were compared to develop data base. Especially, we applied to Chemical Index of Alteration (CIA) as chemical condition factor. As results, It was possible to obtain the basin area scale to apply CIA.

Keywords: CIA, water resource, Numerical geographic information

©2019. Japan Geoscience Union. All Right Reserved.

Chemical property analysis of short time scale to determine snowfall source

*Suzuki hiromichi[1], SEIKI KAWAGOE[1], SHO ADACHI[1], Shiho Yabusaki[2]

1. Fukushima University, 2. Research Institute for Humanity and Nature

Occurrence of the strange weather phenomenon is predicted from the current state depending on climate change. To ask this influence, we have to advance the match which raises the future predictability. And, we have to mark a phenomenon of the current state detail. This study targets to obtain chemically snow environment. The aim of this study was to analyse and predict the stable water isotopic composition of the snow cover at specific basin (Agano river). In addition, the dependence of short time step isotopic composition of the entire snow cover was analysed. Snow in 3 catchments was sampled at the end of the accumulation period from December 2016 to April 2018. The observed variability of short time step isotopic composition of the snow cover was analysed chemical verification. Especially, basin The Inawashiro-Lake north side of the northern upstream region indicated the low chemical feature (Suzuki et al 2018). I'm working on the investigation analysis to grasp the chemical special quality of the snow event of the short time scale at present based on this result (2016-2018). It was that a chemical analysis makes the sample which sampled and acquired it by each day the time of a snowfall at Fukushima, Hibara and Yonezawa located in an upstream region in a basin, and we tried to follow up a snowfall origin of the short time scale.

As results, a strong pressure pattern of southern high and northern low could admit January 22nd-the 25th, the result obtained from the result of analysis also reacted to the weather situation sensitively. And influence of a characteristic snowfall origin was admitted at 3 spots. The difference in the spatial time lags was done clearly.

Keywords: d-excess value, isotope, short time scale

©2019. Japan Geoscience Union. All Right Reserved.

Analyzing the origin of surface water in the Saijo Plain, Japan, based on the antimony concentration in the water

*Minoru TOKUMASU[1,2], Ki-Cheol SHIN[3], Yoshihiro YAMADA[4]

1. The United Graduate School of Agricultural Sciences, Ehime University, 2. Saijo City, 3. The Research Institute for Humanity and Nature (RIHN) , 4. Kagawa University, Faculty of Agriculture

1. Introduction

The flow of river water in many medium and small rivers is managed for water use and flood control. However, it is almost impossible to understand how the water taken from the rivers circulates throughout a basin. The source of water in the Saijo Plain in Ehime Prefecture is from the Kamo River surface water flow, shallow groundwater (unconfined ground water), and deep groundwater (confined ground water). Therefore, it is necessary to quantitatively clarify the source of water for sustainable water use. In this study, we tried to quantify the origin of river water in the plain based on the concentration of some chemical elements. In particular, antimony (Sb) was used as the main trace element because of large differences in its concentration between the water sources.

2. Materials and Methods

On November 25 and 26, 2017, during the non-irrigation period and on the 27th and 28th of July, 2018, during the irrigation period, surface water was collected at a total of 43 sites on small and medium rivers and waterways in the Saijo Plain. Multi-element analysis was carried out on the collected water using ICP-MS 7500 cx.

3. Results and Discussion

There was a large difference in the concentration of Sb among the sites. The highest concentration was found in the water from the Ichino River (Stn. 2) at 113 (2017) and 158 μg/L (2018). There was once an antimony mine in the Ichino River basin, so high concentrations of the element in the river water can be regarded as reflecting the influence of the geology. In the main stream of the Kamo River before joining the Ichinose River (Stn. 1), the Sb concentration was as low as 0.2 μg/L, and after the junction of the two rivers (Stn. 3), the concentration increased to 4.3 (2017) and 7.2 μg/L (2018). The concentration was 4.2 (2017) and 7.2 μg/L (2018) at Stn. 4 of the Kamo River, 11.6 (2017) and 11.7 μg/L (2018) in the unconfined ground water (average of Stns. 13, 14, 15), and 0.4 (2017) and 0.5 μg/L (2018) in the confined ground water (average of Stns. 28, 29, 40, 41, 43). The concentration of Si was 2.7 (2017) and 3.2 mg/L (2018) at Stn. 4 of the Kamo River, 3.4 (2017) and 2.9 mg/L (2018) in the unconfined ground water (average of Stns. 13, 14, 15), and 4.1 (2017) and 3.9 mg/L (2018) in the confined ground water (average of Stns. 28, 29, 40, 41, 43).
The ratio of water origin at each survey site was estimated using the above three sources as end members. In the upstream area, the irrigation water taken from the Kamo River occupied most of the surface water. In the middlestream area, the ratio of water taken from the rivers was smaller, and the contribution of

©2019. Japan Geoscience Union. All Right Reserved.

unconfined ground water exceeded 80%. In the downstream area, the confined ground water contribution exceeded 40% at many sites. In the Saijo Plain, the water origins are different in the upstream, middlestream, and downstream areas, where the contribution of irrigation water is small overall, and the contribution of the confined ground water is large.

©2019. Japan Geoscience Union. All Right Reserved.

Basic kinetic study on stable isotope ratios of nitrogen compounds: a case study for groundwater in the Kathmandu Valley, Nepal

*Ken Yokozawa[1,2], Kei Nishida[1,3], Takashi Nakamura[1,3], Ken'ichi Osaka[4]

1. University of Yamanashi, 2. Special Graduate Program on River Basin Environmental Science,, 3. ICRE, 4. Department of ecosystem study Univercity of Shiga prefecture

Groundwater is a valuable source of water in developing countries where water demand is increasing with population increase. At the same time, nitrogen contamination by industrial wastewater, domestic wastewater and agricultural activities has been reported. In underground environments, it is not unusual to identify sources of contamination since the forms and the concentrations of nitrogen compounds vary at different water flow or microbial metabolism. Stable isotopic analysis is one of the effective methods to detail the variations. However, the isotope value is also greatly affected by environmental conditions, and the theoretical enforcement for describing the variation of the isotope value is needed. In this study, we aimed to quantitatively understand and identify the factors of mixing and isotopic fractionation that determine the stable isotope ratio with a case study on groundwater contamination in the Kathmandu Valley, Nepal.

The data used for the analysis was obtained from the groundwater survey of the Kathmandu Valley conducted from September 2014 to August 2018. Based on the stable isotope ratios of nitrogen and oxygen of nitrate, the contamination patterns were roughly categorized. The mixing line and the denitrification line were prepared based on the dynamic fractionation for the stable isotope ratios of nitrate nitrogen, and the spatial distribution of denitrification-related samples was examined on the map. In addition, assuming that the reactants exist sufficiently and homogeneously in the system, an equilibrium fractionation model was formulated by combining nitrification and denitrification for oxygen stable isotope ratios of nitrate and water. The range of the model parameters were determined by using the measured data from the filed survey, the influence of each process on the stable oxygen isotope ratio of nitrate was quantified.

The result showed that the nitrate in shallow groundwater partially originated from the atmospheric source through infiltration of rainwater. A characteristic of denitrification was observed, which was initiated and proceeded over the valley. Additionally, the correspondent isotopic fractionation differed at the location and the season, particularly controlled by ammonia oxidation, nitrite reduction and oxygen exchange between nitrite and water.

Keywords: groundwater , nitrogen and oxygen stable isotope ratios, nitrification, denitrification, mixing, fractionation

©2019. Japan Geoscience Union. All Right Reserved.

Usefulness of strontium isotope composition for determining the geographical origin of wasabi and potato

*Takafumi Kamitani[1], Ki-Cheol Shin[2], Sachiko Nakamura[1], Rika Koda[1], Tomoya Oka[1], Noriaki Fushimi[1], Yasuhide Muranaka[1]

1. Shizuoka Institute of Environment and Hygiene, 2. Research Institute for Humanity and Nature

Originally, the use of strontium isotope ratios ($^{87}Sr/^{86}Sr$) was restricted to geology and petrology, but they have been used as a particularly effective tracer of geographical food origin, as plants reflect the strontium isotope composition of the regionally based rock, soil, and water. This study aims to evaluate the usefulness of $^{87}Sr/^{86}Sr$ for determining the geographical origin of wasabi (Japanese horseradish) and potato, which are specialty crops in Shizuoka Prefecture, Japan.

Wasabi is cultivated in springs and streams located at the top of rivers, where dissolved element and isotopic compositions in water would reflect the geological characteristics without the effects of atmospheric deposition and human activity. We collected wasabi and water samples from 40 locations of major production areas in Japan: Shizuoka, Iwate, Nagano, Tokyo, and Shimane. These samples were subjected to trace elements and $^{87}Sr/^{86}Sr$ analyses. The $^{87}Sr/^{86}Sr$ values differed, based on the geological characteristics of their site locations, and the value of wasabi was well accorded with that of water in the same location. The wasabi samples collected from Izu Peninsula and Mt. Fuji regions in Shizuoka, where young volcanic rocks such as Quaternary basalts are distributed, had low $^{87}Sr/^{86}Sr$ (below 0.7040), whereas those from Nagano and Tokyo, where older rocks such as Mesozoic granites and accretionary complex are distributed, showed higher ratios (over 0.7095). We conclude that $^{87}Sr/^{86}Sr$ value of wasabi allowed us to distinguish the production area clearly.

On the other hand, the $^{87}Sr/^{86}Sr$ values of crops cultivated in the field are considered to be partly affected by precipitation and fertilizer. Therefore we conducted field survey and planter test for potato in Shizuoka. Field survey was conducted at Mishima, in eastern part of Shizuoka prefecture, and at Mikatahara, in western part of it, and $^{87}Sr/^{86}Sr$ of potato and soil exchangeable fraction were compared. As a result, there was a correlation between potato and soil in $^{87}Sr/^{86}Sr$, although the effects of precipitation and fertilizer were observed. The planter test suggests that the influence of fertilizer on $^{87}Sr/^{86}Sr$ varies depending on the amount of exchangeable Sr contained in the original soil.

Keywords: geographical origin, strontium isotope ratio, wasabi, potato, Shizuoka

©2019. Japan Geoscience Union. All Right Reserved.

Reconstruction of sea surface temperature and salinity for the Medieval Climatic Anomaly using a long-lived fossil coral collected at Ishigaki Island, southwestern Japan

*Osamu Abe[1], Maki Morimoto[2], Ryuji Asami[3], Takeshi Nakatsuka[1,4]

1. Graduate School of Environmental Studies, Nagoya University, 2. School of Education, Gifu University, 3. Graduate School of Science, Tohoku University, 4. Research Institute for Humanity and Nature

The period between 950 and 1250CE is called as the Medieval Climate Anomaly (MCA; Masson-Delmotte et al., 2013), at the time when the warmer climate seemed dominant globally (Bradley et al., 2003). Recent investigations based on the proxy record such as tree-ring widths, speleothems, ice cores, and historical documents indicated that a significant climate change occurred during the latter half of the 10th century. Mann et al. (2009) found that an increase of the average air temperature in the northern hemisphere at the late 10c. coincided with an increase of sea surface temperature at northern subpolar oceans. Yan et al. (2011) indicated that atmospheric environments in the equatorial Pacific shifted from the La Nina like condition to the El Nino like condition around 1000CE. In East Asia, Zhang et al. (2008) and Ge et al. (2013) described that the activity of East Asian Summer Monsoon (EASM) had been enhanced during the late 10c., then the climate in China shifted to warmer and wetter. Whereas Lie et al. (2014) showed that the EASM had been weakened during the 11th century. In addition, the climate in southern China was reported as relatively dry (Chen et al., 2015).

These studies demonstrated that a large climatic shift occurred around 1000CE, however, most of them have relied on records collected on land. There is little long-term high-resolution marine record during the MCA.

We reconstructed sea surface temperature (SST) and salinity with a temporal resolution of one month for 300 years using a long-lived fossil coral collected at Ishigaki Island, southwestern Japan. Based on the U/Th dating in the youngest part of the coral skeletons as well as the band counting, this coral sample had lived between 845 and 1130CE, largely covered the MCA period. Skeletal Sr/Ca and oxygen isotopic composition were analyzed for about 4,000 samples.

The empirical equations between Sr/Ca and water temperature; between oxygen isotopic composition of coral skeleton and seawater, and water temperature, were established using the present coral records, observed water temperature and oxygen isotopic composition of seawater. With these equations and the relationship between seawater salinity and oxygen isotopic composition, proposed by Abe et al. (2009), SST and seawater salinity from 845 to 1130CE were reconstructed from the fossil coral Sr/Ca and oxygen isotopic composition.

Through the entire period, average summer and winter SSTs were 2 and 1 deg. C higher than the present, respectively. In addition, SST increased significantly after 1040CE; 0.9 for the annual average, 0.7 for summer and 1.1 for winter. Salinity also increased after 990CE; 0.8 all for the annual average, summer and winter. Salinity was significantly higher through the entire period than the present, however, its absolute value seems unconfirmed yet.

©2019. Japan Geoscience Union. All Right Reserved.

Increasing SST and salinity found in this study during ca. 1000 and 1130CE were consistent with the weakening of EASM during the 11th and 12th centuries shown by Liu et al. (2014). They argued the weakening occurred as a consequence of weakening of the solar activity and the decrease of SST at the western Pacific warm pool. In this study region, the decrease of precipitation during the Baiu period induced the increase of salinity as well as local SST increase due to the decrease of the cloud cover. Our results were also consistent with the warming of China in the late 10c. (Ge et al., 2013), and a drier condition in southern China (Chen et al., 2015).

The periodicity of SST and salinity based on the spectral analysis will be discussed in the presentation.

Keywords: Coral annual bands, Medieval Climate Anomaly

©2019. Japan Geoscience Union. All Right Reserved.

Development of the analytical method for sulfur isotope in SO_2 gas

*Masaaki Takahashi[1], Hiroyuki Sase[1], Tsuyoshi Ohizumi[1]

1. Asia Center for Air Pollution Research

1. Introduction

Sulfur is a major source of acid deposition. Usually sulfur is emitted as SO_2 and it is oxidized to SO_4^{2-} in atmosphere. S isotopic analysis of water and particulate samples were conducted in many studies. But gaseous SO_2 was rarely used for isotopic study. Isotopic ratio of SO_2 is strongly influenced by emission source near the sampling point. Because most of SO_2 emitted far from sampling point is oxidized to SO_4^{2-} during transportation. It is possible to distinguish domestic emission from transboundary emission. Moreover, dry deposition processes of SO_2 and particulate SO_4^{2-} and their interactions with tree canopy could be discussed more precisely. Isotopic analysis of SO_2 is considered as a powerful method to investigate the behavior of S in the atmosphere and ecosystems. We studied about the analytical method for S isotope in SO_2.

2. Method

(1) Equipment

SO_2 concentration in Japan is very low (e.g. annual 0.02ppb at Sado). We need to collect air sample at least $1m^3$ that is the amount we can obtain 1.2mg of $BaSO_4$ precipitation enough for isotopic analysis. High volume air sampler is generally used to collect around $1m^3$ of air sample. It uses filter, so we examined filter collection of SO_2 by K_2CO_3 filter generally used to collect SO_2 in filter-pack method.

(2) Filters

We used quarts filter for particulate SO_4^{2-} and K_2CO_3 filter for gaseous SO_2 next to it. K_2CO_3 filter is made on the basis of EANET manual. But to get enough flow rate for high volume air sampler, the size of K_2CO_3 filter is larger (20×26 cm, same size with quarts filter) than the manual and already dried before sampling.

(3) Flow rate/leak test

Under flow rate 100~400 L/min in this system, we confirmed weather sampling can be carried out stably. And we checked leak using two K_2CO_3 filters.

(4) Sample treatment

©2019. Japan Geoscience Union. All Right Reserved.

On the basis of EANET manual, the sample was extracted with 0.05% H_2O_2aq and filtered. Then 2N HCl was added and concentrated to remove CO_3^{2-}. Next 1%(w/w)$BaCl_2$ was added. We filtered forming $BaSO_4$ precipitation. We examined the method to get $BaSO_4$ precipitation and to remove the components from K_2CO_3 filter.

3. Results

(1) Sampling and sample treatment

Sampling could be conducted under flow rate 100~400 L/min. Sampling efficiency was about 80%..

Several conditions to get $BaSO_4$ precipitation ware examined, it could be gotten by the method as below.

Filter was cut and ultrasonic extracted with 0.05% H_2O_2aq 30 minutes and filtered. 2.5 ml of 2N HCl was added and concentrated to around 10 ml. Then 1 ml of heated 1 %(w/w) $BaCl_2$ was added under pH 4~6. Next evaporated all solvent and added 10 ml of water. $BaSO_4$ precipitation was observed. After put for one night, the precipitation was separated by centrifuge 3,600 rpm for 10 minutes and we removed the solvent. The precipitation was washed twice by 10 ml of water and filtered. At last the filter was ashed for four hours in muffle furnace in 800 ℃ .

(2) Actual analysis

We used two K_2CO_3 filters and collected 2160.2 m^3 of air sample under flow rate 300 L/min. 3.80 mg of particular SO_4^{2-} and 0.89 mg (first) and 0.14 mg (second) of SO_4^{2-} from SO_2 were obtained. $\delta^{34}S$ of particular SO_4^{2-} was 8.64 ‰and that of SO_2 from the first filter was -1.54 ‰. The amount of precipitation from second filter was not enough for isotopic analysis. This difference was caused by effect of sea salt mainly. But nss- $\delta^{34}S$ of particular SO_4^{2-} was 4.78 ‰. It was still higher than SO_2. It suggested that nss- SO_4^{2-} contains both transboundary SO_4^{2-} and domestic SO_4^{2-}. According to the relevant literature, domestic SO_2 may have negative isotopic values because of imported oil from Middle East. Considering that this sampling was carried out in January, possible effect of transboundary SO_2 with higher isotopic values should also be taken into account for source identification of the collected SO_2.
We would like to discuss at the conference with the latest data.

Keywords: sulfur isotope, SO2 gas

©2019. Japan Geoscience Union. All Right Reserved.

Zinc isotope analysis on human tooth enamel samples to reconstruct diet of the Jomon period.

*Soichiro Kusaka[1], Ki-Cheol Shin[2]

1. Tokai Univ., 2. Research Institute for Humanity and Nature

This study investigates zinc isotope ratios in tooth enamels of human skeletal remains of the Jomon period in Japan. Carbon and nitrogen isotope analysis on bone collagen were traditionary used to reconstruct diet and trophic levels on prehistoric people. The progress of isotope measurements using MC-ICP-MS enables us to analyze isotope ratios of zinc and other metals. Some researches report that the zinc isotope ratios of animals reflect dietary sources and vary according to trophic levels. This study newly develops zinc isotope analysis on human tooth enamels. The zinc isotope analysis has great potential to reconstruct dietary information from inorganic materials of archaeological bones or fossils.

The material used in this study is SRM1400 (bone ash), six samples of human tooth enamels from the Yoshigo and Inariyama shell mounds of Aichi prefecture, and faunal remains (six deer enamels, three boar enamels, six marine fish bones, and six modern plant leaves). Zinc was purified from these samples using anion exchange resin. Zinc isotope ratios were measured by MC-ICP-MS with the zinc standard solution of AA-ETH. The mass bias was corrected with Cu standard solution added to all standards and samples. The zinc isotope ratios of SRM1400 showed similar value with the value previously reported. The difference of zinc isotope ratios between washed and unwashed samples with acetic acids were very small, suggesting no significant diagenetic alteration. The deer and marine fish samples showed the value expected from their dietary ecology. The zinc isotope ratios of Jomon skeletal remains was higher than those of plants, but lower than deer and marine fish. This result indicates that sources of zinc for humans were terrestrial and marine meat as well as terrestrial plants.

Keywords: Zinc Isotope, Jomon period, Human skeletal remains

©2019. Japan Geoscience Union. All Right Reserved.

Zinc stable isotope analysis of environmental reference materials

*Ki-Cheol Shin[1]

1. Research Institute for Humanity and Nature

Zinc has atomic number 30 and atomic mass 65.39. It is a trace element of terrestrial rocks and widely distributed throughout the lithosphere and biosphere. It is chalcophile features and has rich coordination chemistry, participates in a large number of important biological compounds and reactions. The zinc plays an important role as an essential trace metal in all living systems from bacteria to humans. Zn has five stable isotopes ^{64}Zn, ^{66}Zn, ^{67}Zn, ^{68}Zn, and ^{70}Zn. Their isotopic fractionation could provide valuable information about environmental processes, especially in biological processes.

With the advent of multi-collector ICP-MS, it is possible to measure the precise value of ^{66}Zn/^{64}Zn in Zn solution. To promote the environmental stable isotope traceability, RIHN is desired to determine the isotope ratios of zinc for environmental reference materials with high precision and accuracy, rapidness, and convenience.

Here, I report a simple and efficient method for zinc isotope analysis. The various environmental samples over 20 types were used for the study. All samples have purified with an anion exchange resin to separated Zn and Fe at a time. Zinc isotope ratios were measured by MC-ICP-MS (NEPTUNE plus) with AA-ETH, which is a new zinc isotopic standard solution reported by Archer et al. (2017). The mass bias correction conducted with Cu standard solution (NIST SRM 976).

Keywords: stable isotope , Zinc, environmental reference materials

©2019. Japan Geoscience Union. All Right Reserved.

[J] Oral | H (Human Geosciences)：H-TT Technology & Techniques

Tue. May 28, 2019 9:00 AM - 10:30 AM JST | Tue. May 28, 2019 12:00 AM - 1:30 AM UTC | 301B 3F

[H-TT22] New Developments in Shallow Geophysics

convener:Kyosuke Onishi(Public Works Research Institute), Kunio Aoike(Oyo corporation), Keisuke Inoue(National Agriculture and Food Research Organization), Tishiyuki Yokota(National Institute of Advanced Industrial Science and Technology), Chairperson:Toshiyuki Yokota, Keisuke Inoue

The session of shallow geophysics calls many research contributions on geophysical exploration techniques for the near surface. Our target depth is strictly restricted in the depth zone from 5 cm to 30 m (or from 2 in to 100 ft) below the surface of the ground. It may be the closest unknown territory for human society and advanced societies cannot have controlled yet to avoid disasters caused by dynamics in the shallow near surface. Peoples require techniques to manage levee, landslide and earth constructions also knowledge to control groundwater, liquefaction and soil pollution. The near surface has many geotechnical, environmental and hydrogeologic problems.
Major survey techniques are surface wave method, electric exploration, ground-penetrating radar and land streamer, but any methods will be discussed if your target is located in the specified depths. This session welcomes to discuss laboratory tests and rock physics for unconsolidated porous media in the vadose zone. Also, we will welcome not only cutting-edge technologies but also classic theory, if the knowledge is useful for human living.

9:00 AM - 9:15 AM JST | 12:00 AM - 12:15 AM UTC

[HTT22-01] High-frequency seismic reflection measurements for imaging internal structure of a sabo dam damaged by a huge debris flow

*Tomio INAZAKI[1], Hiroshi Kisanuki[2], Takanori Ogahara[1], Takeshi Shimizu[1], Naoki Fujimura[1] (1.Public Works Research Institute, Tsukuba Central Institute, 2.PWRI (Present address: OYO Corporation))

9:15 AM - 9:30 AM JST | 12:15 AM - 12:30 AM UTC

[HTT22-02] Development and applications of 3D ambient noise tomography

*Chisato Konishi[1], Koichi Hayashi[1] (1.OYO Corporation)

9:30 AM - 9:45 AM JST | 12:30 AM - 12:45 AM UTC

[HTT22-03] An Attempt to Estimate the Level of Non-confind Groundwater by Earthing Resistance (I) - Outline of Theory -

*Kunihiro Ryoki[1] (1.Polytechnic University)

9:45 AM - 10:00 AM JST | 12:45 AM - 1:00 AM UTC

[HTT22-04] Experimental and Theoretical Studies for Seafloor Survey by Ground Penetrating Radar

*Jun Sonoda[1], Tomoyuki Kimoto[2] (1.National Institute of Technology, Sendai College, 2.National Institute of Technology, Oita College)

10:00 AM - 10:15 AM JST | 1:00 AM - 1:15 AM UTC

[HTT22-05] Evaluation of the 3-D Distribution of Fractures in a Rock Mass using Directional Borehole Radar Data from a Horizontal Borehole

*Kazuhiko Masumoto[1], Tomoaki Matsushita[2], Suguru Shirasagi[1], Takashi Ueki[3], Shinsuke Karasawa[3], Daiki Makino[3], Kazushige Wada[4] (1.Kajima Technical Research Institute, 2.Kajima Corporation, 3.Matsunaga Geo-Survey Co., Ltd., 4.Mitsui Mineral Development Engineering Co., Ltd.)

10:15 AM - 10:30 AM JST | 1:15 AM - 1:30 AM UTC

[HTT22-06] Automatic Detection of Deteriorated Concrete Bridge Deck using 2 GHz Horn Antennae

*Kunio Aoike[1], Shogo Tanaka[2], Naoto Takase[1], Akio Matsuyama[1], Masaya Yamauchi[1], Yoshinori Uno[1] (1.OYO Corporation, 2.Professor Emeritus of Yamaguchi Univ.)

High-frequency seismic reflection measurements for imaging internal structure of a sabo dam damaged by a huge debris flow

*Tomio INAZAKI[1], Hiroshi Kisanuki[2], Takanori Ogahara[1], Takeshi Shimizu[1], Naoki Fujimura[1]

1. Public Works Research Institute, Tsukuba Central Institute, 2. PWRI (Present address: OYO Corporation)

We conducted high-frequency, high-resolution seismic reflection measurements on the rear face of a sabo dam which had been damaged by a huge debris flow attack in July 9, 2014. The debris flow swept away the top 5 m part of the dam and segmented the dam body into several blocks associated with horizontal cracks. Estimated surface dislocation was at most 20 cm.
iezoelectric type high-frequency accelerometers were pasted on the surface at 10 cm intervals, and manual hit using a rock hammer was employed for generating high-frequency signals. High-performance data acquisition systems were also employed to obtain high-resolution and high sampling seismic data. Minimum sampling rate was set to 2 microseconds. We set 5 horizontal lines and 1 vertical line on the rear surface during December 2014 to April 2016. Relative height was about 5 m between the first and the last horizontal line. Assuming the RMS velocity to the constant value to 2,500 m/s, which was the typical S-wave velocity of concrete, we processed the dataset to reconstruct migrated depth sections. Clear flat reflection events appeared at 10 m and 7 to 5 meters. The former or deeper reflection event was correlated to the frontal face of the dam. The latter events were possible to be correlated to a horizontal joint which had dislocated the dam body caused by the debris flow attack. A gently dipping reflector, which started from the point just the survey line intersected a vertical fracture, was recognized in the lowest depth section.
In conclusion, field measurements demonstrated that high-frequency and high-resolution seismic reflection surveying was helpful to image the internal fracture distributions in a damaged concrete dam body.

Keywords: Sabo dam, debris flow, seismic reflection survey, high-frequency accelerometer

©2019. Japan Geoscience Union. All Right Reserved.

Development and applications of 3D ambient noise tomography

*Chisato Konishi[1], Koichi Hayashi[1]

1. OYO Corporation

In a microtremor array measurement, receivers are usually placed on a center and the circumference of a circle or a center and the vertexes of a triangle to observe ambient noise from omni-directions for 1D S-wave velocity delineation. We developed 2D/3D ambient noise tomography as an extension of the normal microtremor array method, and we have conducted several field experiments. Cable-less seismographs including GPS clock, AD converter, battery, and SD card memory are used for the survey, and that makes a receiver array deployment flexible. Additionally, the estimated phase velocity is not affected by a specific direction of the ambient noise because several tens of receivers are deployed in X and Y directions on the ground surface. Furthermore, high quality data can be obtained due to a stacking of the multiple receiver pairs even if the observation time is limited.
CMP-SPAC analysis that is a modification of the CMPCC analysis in the 2D surface wave method is used in the 3D ambient noise tomography. SPAC coefficients are calculated for all possible pairs of the receiver arrays, and these are stacked and sorted by receiver separations at each CMP bin to make CMP-SPAC gathers. The frequency versus phase velocity image is obtained by comparing the CMP-SPAC gather with Bessel function. Dispersion curve is obtained from the frequency versus phase velocity image at all CMPs. By the same procedure to the 2D surface wave method, 1D S-wave velocity structure can be estimated by an inversion based on the non-linear least square method. And then 3D S-wave velocity is created by interpolating the 1D velocity structure at all CMPs. The computation time for this analysis is comparable to the 2D surface wave method, so we can easily obtain the 3D S-wave velocity.
Several field experiments have been conducted and the results almost agree with the existing geological information and other geophysical survey results. We found that the accuracy of the estimated S-wave velocity structure is lower around the edge of the survey area, and the estimated phase velocity around the edge might be affected by the direction of the ambient noise due to the limited receiver pairs. Nevertheless, we can eliminate this issue by extending the survey area, which is a usual countermeasure in most of geophysical surveys. Another finding is that even if the ambient noise does not include high frequency or short-wave length, we can investigate the shallow subsurface by adding a manmade vibration around the receiver array easily.

Keywords: Microtremor, S-wave velocity, 3D exploration

©2019. Japan Geoscience Union. All Right Reserved.

An Attempt to Estimate the Level of Non-confind Groundwater by Earthing Resistance (I) - Outline of Theory -

*Kunihiro Ryoki[1]

1. Polytechnic University

1. Introduction

In the Musashino district of the Kanto plain, some loam layers for several meters with good permeability cover the Musashino gravel layer. The groundwater under no pressure here uses the Musashino gravel layer as the main aquifer. However, the seasonal recharge may raise the water level to the upper loam layer. The impermeable layer, which has a clay-rich lens shape, is often present in the loam layer (Kakuda, 2017). As the perchied water level rises to near the surface of the earth, flood damage is brought about occasionally (for example, Tokyo Metropolitan Geological Survey Association, 2000). Therefore, observation of such groundwater level fluctuation at many points is required to prepare for flood damage. Ohshima *et al*. (2015) examined the stability of these earthing resistances, in order to use the housing foundation as the earthing electrode to ensure safety for the electrical equipment, using a small model foundation of about 2 m ×2 m or the building foundation of a real scale housing. According to this, it was shown that there is a seasonal fluctuation in earthing resistance of about 200% in the small model or about 20% to 30% in the real scale. It is thought that this fluctuation is caused by the characteristic accompanying the temperature change. On the other hand, the observations of groundwater level at the wells around Inokashira pond, from the beginning of December 1988 until March 2001, showed that the peak-to-peak annual change of 2 m to 3 m (Kokubu, 2005). These variation in the groundwater level makes to change the earthing resistivity, and it becomes a factor of changing the earthing resistance of the electrode (Ryoki, 2019). In this memoir, the conseption is introduced, and then, it has been proposed that a method for estimating the level, based on the contribution of the variation of the groundwater level to the earthing resistance.

2. Theory

Consider the point current I flowing from the origin O to the ground of the semi-infinite medium with the resistivity ρ, the potential V_r, that is created on the surface of the distance r, is $V_r=\rho I/2\pi r$. When the hemispherical metal electrode of the radius a, which instead of the point current source, is grounded, the potential in the metal becomes equal to the potential $V_a=\rho I/2\pi a$ on the surface. Therefore, R, as the resistance of the origin O (*eq*. the resistance value of the hemispherical metal electrode) viewed from infinity, is expressed as follows; $R=V_a/I=\rho/2\pi a$. This is the earthing resistance of the hemispherical metal electrode.

Next, let us consider the ground potential when the earth is regarded as a horizontal two-layers structure. According to the mirror image method (Figure 1) shown by Hagiwara (1951), the potential $V_{0(r,\,z=0)}$ on the ground surface, z=0, at the distance r made by the point current source is as follows; $V_{0(r,\,z=0)}=\rho_1 I(1/r+2\Sigma^{\infty}_{k=1}(Q^k/(r^2+(2kd)^2)^{1/2}))/2\pi$. Where Q is the reflection coefficient with respect to the current density; $Q=(\rho_2-\rho_1)/(\rho_2+\rho_1)$. ρ_1 and ρ_2 are the resistivities of the first layer and the second layer, respectively. d is the layer thickness of the first layer. Now, consider R_a, the earthing resistance of the earth electrode on the two-layer structure, as in the case of Wenner's method which is a vertical electrical prospecting, letting $r=a$; $R_a=V_a/I=\rho_1(1/a+2\Sigma^{\infty}_{k=1}(Q^k/(a^2+(2kd)^2)^{1/2}))/2\pi$. This is able to call the equivalent earthing resistance. Consider the ratio of R_a to the earthing resistance R_1 which is in the semi-infinite medium consisting only of the first layer of resistivity ρ_1; $R_a/R_1=1+2\Sigma^{\infty}_{k=1}(Q^k/(1+4k^2(d/a)^2)^{1/2})$. This is able to call the apparent resistivity with respect to the equivalent earthing resistance.

©2019. Japan Geoscience Union. All Right Reserved.

Fig. 2 shows the relationship between d/a and R_a/R_1, here, d: thickness of the first layer, a: radius of the hemispherical conductive electrode. Shown in Fig. 2, it is able to understand that the equivalent earthing resistance takes a change when the groundwater level varies. Therefore, it is able to expect that variations in groundwater level is sensed by monitoring fluctuation of earthing resistance.

3. Future plans

In order to verify the method introduced here, the observation well will be drilled, and the fluctuation of the groundwater level *etc.* will be measured there. Then, the earthing resistance of the earth electrode for safety of electrical equipment will be continuously measured. The planned observations are (1) the groundwater level, (2) also the temperature, (3) also the electrical conductivity, (4) the apparent resistivity of the earth, and (5) the earthing resistance. Preliminary measurement results will be shown at the JpGU meeting.

Keywords: electrical equipment, Musashino district, loam layers, perchied water, flood damage, equivalent earthing resistance

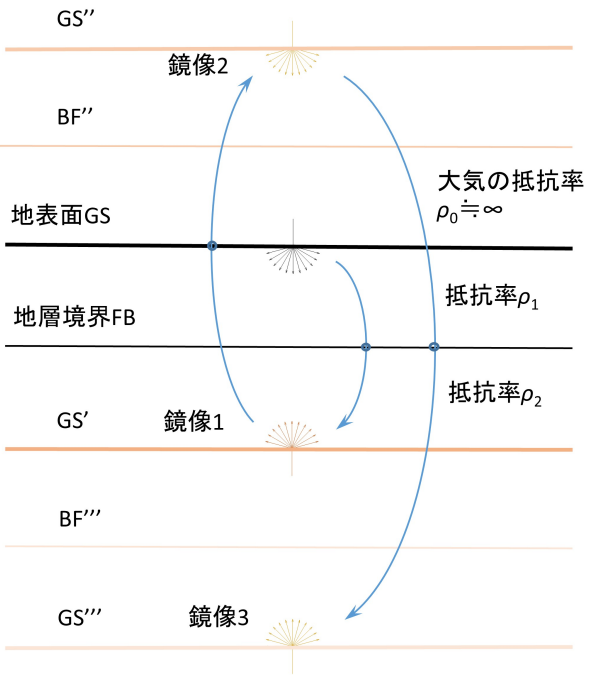

図1　鏡像法の概念図 (領木, 2019).
Fig. 1. Conceptual diagram of the mirror imaging method (Ryoki, 2019).

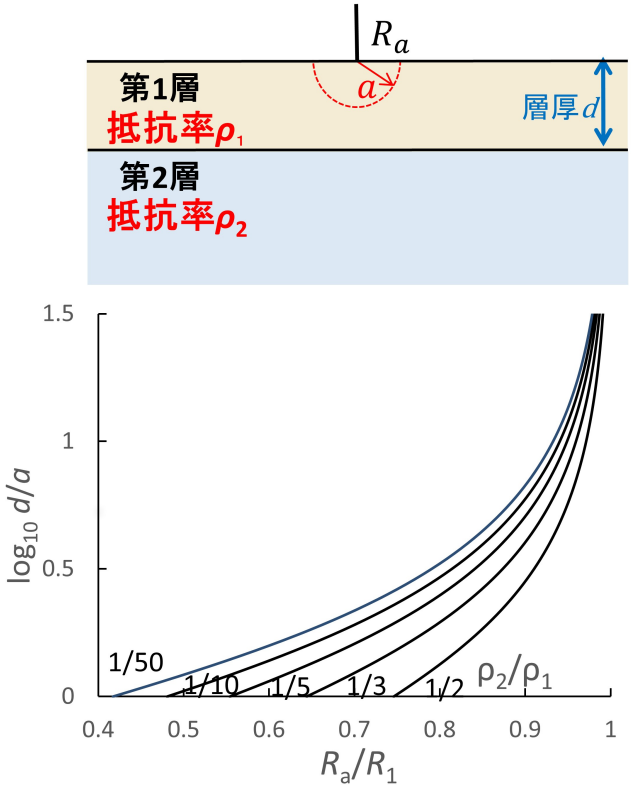

図2　等価接地抵抗と第1層の層厚との関係　それぞれ，半無限媒質での接地抵抗と半球導体電極の半径で基準化してある (領木, 2019).
Fig. 2. Relationship between the equivalent earthing resistance and the 1st layer thickness. Parameters are nor-malized by the earthing resistance in the semi infinite medium and the radius of the hemi-spherical conductor electrode, respectively (Ryoki, 2019).

©2019. Japan Geoscience Union. All Right Reserved.

Experimental and Theoretical Studies for Seafloor Survey by Ground Penetrating Radar

*Jun Sonoda[1], Tomoyuki Kimoto[2]

1. National Institute of Technology, Sendai College, 2. National Institute of Technology, Oita College

The electromagnetic wave (EM) do not propagate in the seawater because of high conductivity. In recent, the ultrasonic wave is widely used in the sea, such as the fish-finder, the side-scan sonar, and so on. We have used the ground penetrating radar (GPR) by several hundred MHz to search missing persons and rubbers in the sea after the tsunami caused by the Great East Japan earthquake. In this study, we have studied the under seawater prospecting using 350/400 MHz GPR in Hiroura Bay, Natori city, in Isohama fisher port, and off the coast of Sakamoto, Yamamoto town, Miyagi prefecture. At first, frequency characteristics of complex permittivity of several seawater samples by the time domain reflectometry (TDR), and conductivity in the depth of seawater by the conductivity temperature depth profiler (CTD) have been shown. Also, it is shown that the reflected wave from several objects at the about 10 meters depth has been observed using the 350 MHz GPR. Finally, the EM wave propagation in the seawater has been analyzed using the FDTD method with the graphics processing unit (GPU).

Keywords: ground penetrating radar, seafloor survey, FDTD

©2019. Japan Geoscience Union. All Right Reserved.

Evaluation of the 3-D Distribution of Fractures in a Rock Mass using Directional Borehole Radar Data from a Horizontal Borehole

*Kazuhiko Masumoto[1], Tomoaki Matsushita[2], Suguru Shirasagi[1], Takashi Ueki[3], Shinsuke Karasawa[3], Daiki Makino[3], Kazushige Wada[4]

1. Kajima Technical Research Institute, 2. Kajima Corporation, 3. Matsunaga Geo-Survey Co., Ltd., 4. Mitsui Mineral Development Engineering Co., Ltd.

Evaluation of the distribution of fractures in a rock mass ahead of a tunnel face is required for safe and reasonable tunnel excavation. To evaluate not only the position of fractures, but also their inclination before tunnel excavation, a directional borehole radar may be a suitable technique. A directional borehole radar can determine the inclination of fractures with a single pilot boring because it can estimate the arrival direction of the waves reflected by fractures, which are measured by a dipole array antenna with multiple elements. This study first examined the application of a directional borehole radar to investigate within a horizontal pilot boring. Next, field test using the directional borehole radar was conducted in a horizontal borehole drilled in the sidewall of a tunnel in order to confirm the applicability of the directional borehole radar for evaluating the three-dimensional distributions of fractures.

To apply the borehole radar for horizontal pilot boring in a tunnel, a casing is needed to prevent collapse of the borehole. Because the steel casing pipe which is typically used for pilot borings cannot be used for radar measurements, the applicability of a glass fiber reinforced plastic (GFRP) tube was verified as the borehole casing in this study. As the results of the experimental study, it could be concluded that GFRP tubes with steel joint couplers can be used as a borehole casing for measurements with radar.

Next, a directional borehole radar was applied to the survey of fractures in granite in a horizontal borehole drilled in the sidewall of a tunnel in order to confirm its applicability for evaluating the three-dimensional distribution of fractures. The results indicated that the strike and dip of each reflector estimated by the directional borehole radar measurements approximately corresponded to the fractures observed with a borehole scanner. Therefore, it was concluded that a survey with a directional borehole radar in a horizontal borehole could evaluate the three-dimensional distribution of fractures surrounding the borehole.

Keywords: borehole radar, horizontal borehole, distribution of fractures

©2019. Japan Geoscience Union. All Right Reserved.

Automatic Detection of Deteriorated Concrete Bridge Deck using 2 GHz Horn Antennae

*Kunio Aoike[1], Shogo Tanaka[2], Naoto Takase[1], Akio Matsuyama[1], Masaya Yamauchi[1], Yoshinori Uno[1]

1. OYO Corporation, 2. Professor Emeritus of Yamaguchi Univ.

In 10 years, about 40% road bridges in Japan will become over 50 years old after the construction. Although many inspections have been conducted to the aged road bridges, the upper part of the bridge deck is impossible to inspect visually because of the asphalt concrete layer covering the bridge decks. It is becoming an important problem that slab deterioration is often generated in the upper part of the aged concrete bridge deck. Thus, it is becoming urgently necessary for the deterioration of the aged concrete bridge deck to be detected and repaired to elongate the life of the bridge. Ground penetrating radar (GPR) mounted on a vehicle is one of the effective non-destructive methods, which enables us to inspect the deterioration under no traffic control. A high pulse resolution is required to the GPR to detect anomalies beneath the asphalt concrete layer of the thickness of about 8cm. Adding to it, both a high scan rate in data acquisition and a safe mounting way of the GPR on vehicle are required to achieve the accurate and high-resolution inspection with a high speed traveling of the inspection cars. We adopted the horn antenna, produced by GSSI, whose central frequency is 2 GHz. The antenna can detect reflection waves from the boundary between the asphalt layer and the concrete bridge deck, and also can distinguish them from the surface reflection wave of the asphalt surface. SIR-30 type radar system having 8 channels enables us to realize 989 scans per second with 512 samples, thus it can realize the inspection under the vehicle speed up to 80km/h. We also mount the GPR antennae to the height of 45cm (i.e., lift off) from the road surface. This mounting is important for safe traveling of the inspection vehicle. 8 antennae are mounted on a boat trailer towed by vehicle and aligned in the transverse line to the moving direction. It allows us to scan about 1.7m width at one time. For the inspection of the deterioration of the concrete bridge deck, we developed an automatic processing system. This method predicts a received signal by using two empirical reflection waveforms. We acquired in advance surface reflection waveform and asphalt bottom reflection waveform from an experiment using a real size physical model. We determined the arrival time and the amplitude for each empirical waveform by matching the linear combination of the two empirical waveforms and the actual received signal. To visualize the anomaly distribution of the concrete bridge deck and to inspect the deterioration, we made three types of 2 dimensional maps on thickness of asphalt layer, relative reflectivity at the asphalt bottom, and the fitness between the received and the predicted waveforms. As the results, we could successfully detect the anomalies and delineate their extents. Fig. 1 shows an example of the processing results on a concrete bridge deck model which simulated slab deterioration. We have a plan to continue to modify and update the proposed method by applying the method to real road bridges as a future work.

Keywords: Ground Panetrating Radar, horn antenna, bridge deck

©2019. Japan Geoscience Union. All Right Reserved.

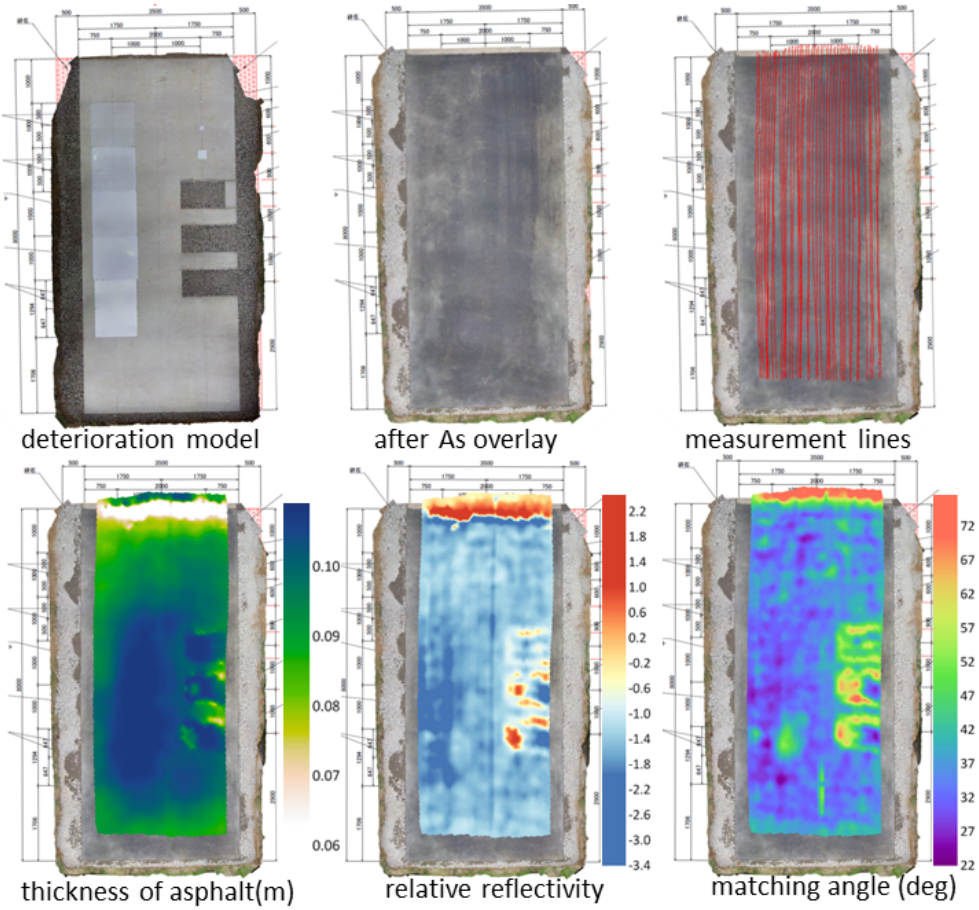

Fig. 1 Simulated deterioration model of concrete bridge deck and the results of automatic processing

©2019. Japan Geoscience Union. All Right Reserved.

[J] Poster | H (Human Geosciences)：H-TT Technology & Techniques

Tue. May 28, 2019 3:30 PM - 5:00 PM JST | Tue. May 28, 2019 6:30 AM - 8:00 AM UTC | Poster Hall International Exhibition Hall8, Makuhari Messe_14

[H-TT22] New Developments in Shallow Geophysics

convener:Kyosuke Onishi(Public Works Research Institute), Kunio Aoike(Oyo corporation), Keisuke Inoue(National Agriculture and Food Research Organization), Tishiyuki Yokota(National Institute of Advanced Industrial Science and Technology)

The session of shallow geophysics calls many research contributions on geophysical exploration techniques for the near surface. Our target depth is strictly restricted in the depth zone from 5 cm to 30 m (or from 2 in to 100 ft) below the surface of the ground. It may be the closest unknown territory for human society and advanced societies cannot have controlled yet to avoid disasters caused by dynamics in the shallow near surface. Peoples require techniques to manage levee, landslide and earth constructions also knowledge to control groundwater, liquefaction and soil pollution. The near surface has many geotechnical, environmental and hydrogeologic problems.
Major survey techniques are surface wave method, electric exploration, ground-penetrating radar and land streamer, but any methods will be discussed if your target is located in the specified depths. This session welcomes to discuss laboratory tests and rock physics for unconsolidated porous media in the vadose zone. Also, we will welcome not only cutting-edge technologies but also classic theory, if the knowledge is useful for human living.

[HTT22-P01] The shallow structure imaging of integrated geophysical surveying of GPR and ERT at Oyunuma in the Goshougake geothermal area, northeast of Japan

*Inoue Yusuke[1], Tomoki Tsutsui[1], Shinya Sakanaka[1] (1.Graduate School of International Resource Sciences in Akita University)

[HTT22-P02] The P and S wave velocity and geological conditions of shallow surrounding tunnel ground by velocity logging on tunnel side wall

*Kenji OKAZAKI[1], Toshiyuki KURAHASHI[1], Hiroumi NIWA[2] (1.Civil Engineering Research Institute for cold region, Public Works Research Institute, 2.FUJITA corporation)

[HTT22-P03] Rock physical interpretation of the relationship between S-wave velocity and fluid saturation in rocks

*Toru Takahashi[1] (1.Fukada Geological Institute)

[HTT22-P04] Estimation of Rayleigh wave group velocities in Zushi City using seismic interferometry in the short period range

*jun ueno[1], Yoshiya - Oda[1] (1.Tokyo Metropolitan University)

[HTT22-P05] Acquiring distributions of phase velocity for wave frequency to use DAS for surface wave method

*Kyosuke Onishi[1], Kobayashi Takayuki[1], Takanori Ogahara[1], Tomio INAZAKI[1] (1.Public Works Research Institute)

[HTT22-P06] Imaging of deteriorated floor slabs using a test model by ground-penetrating radar

*Kyosuke Onishi[1] (1.Public Works Research Institute)

The shallow structure imaging of integrated geophysical surveying of GPR and ERT at Oyunuma in the Goshougake geothermal area, northeast of Japan

*Inoue Yusuke[1], Tomoki Tsutsui[1], Shinya Sakanaka[1]

1. Graduate School of International Resource Sciences in Akita University

The Goshougake geothermal area is surrounded in active volcanoes of Akita Yakeyama volcanoes and Hachimantai volcanoes. In this area, we can observe active geothermal phenomena, such as hot springs, high temperature water marshes including Oyunuma, and mud volcanoes. In this field, a part of sidewalk was broken by mud volcanic eruption, and has closed to walk since autumn 2016. The event inspires our motivation to research the shallow structure at the field by geophysical method.
The previous studies with geophysical methods were applied to the area including the Goshougake geothermal area. The gravitational survey, magnetic survey, electrical survey, and seismic survey in the north Hachimantai area were carried out by Yora and Ito (1974). Airborne electromagnetic survey, MT survey, and electrical survey were carried out by Uchida and Mitsuhata (1995). The research target of these studies focused on the wide area and the studies imaging shallow structure have never reported at Oyunuma in the in the Goshougake geothermal area. Our research purpose is revealing the shallow structures at Oyunuma in the Goshougake geothermal area by the integrated geophysical surveying of GPR (Ground Penetrating Radar) and ERT (Electrical Resistivity Tomography).
In GPR survey, a line of 172 m long was arranged on the southeast of Oyunuma. We used 4 different antennas of 100 MHz, 270 MHz, 400 MHz, and 900 MHz with the GPR equipment SIR-3000 made by GSSI (Geophysical Survey System, Inc.) and adopted the profile measurement with keeping interval of transmitter and receiver antennas. In ERT, a line of 188 m long was arranged along the GPR survey line. We used the equipment SYSCAL Pro made by IRIS Instruments and adopted the array system of the dipole-dipole method. The number of electrode is 48 and the intervals of the electrodes were 4 m.
A series of the GPR analysis, that is, time-zero correction, background removal, bandpass filter (BPF), autocorrelation, predictive deconvolution, velocity analysis, and depth conversion were applied to the obtained data. Clear reflections appeared at two way time of 75-100 ns in the time sections derived by BPF in the records of 4 kinds of antennas. Especially, clear reflections appeared in the reflection record of 270 MHz antenna. We picked up 4 blocks (sections) with remarkably clear reflections in the GPR survey line and carried out detailed analyses on each classified block.
The reflection records obtained in GPR survey are presented in the time sections. In order to convert them in the depth sections, it is necessary to know the exact EM (electromagnetic) wave velocity. We developed an original computer program for the EM velocity analysis which can be applicable for GPR profiling using Visual Studio 2015 C#. Based on calculation using the program, we can draw the contour chart of velocity spectrum which evaluates the most appropriate mean velocity by the semblance values. The semblance value is the ratio of the energy of stacked waves included in a time window to the total input energy of the waves in the same window (Honda, 2014). The exact mean EM velocity in ground medium is estimated to be 0.093-0.147 m/ns for each block. When multiple reflectors appear in reflection records, appropriate velocities are obtained by the predictive deconvolution processing. The original program also calculates the autocorrelation function which is the parameter used in the predictive deconvolution processing. Using the EM velocity by the velocity analysis, we can convert GPR data to the depth sections and the clear reflections revealed in the depth of 4-5 m from the surface of the sidewalk.
The 2D resistivity inversion by the finite difference method is used in the analysis of ERT. The part of the

©2019. Japan Geoscience Union. All Right Reserved.

continuity of an extreme low resistivity zone to the ground surface matches the location of the outcrop of the vents of sulfur gas. Consequently, the zone of the extreme low resistivity is suggested to be a layer of the pass of thermal water.
Comparing the results of GPR and ERT in the depth sections, the clear reflections in the blocks (from block1 to block 4) in GPR sections are located at the area steeply changing from the low resistivity to the high resistivity in ERT section. We can conclude that the some features of the shallow structure in Goshougake geothermal area obtained by the geophysical methods provide the key to elucidate the mechanism and the prediction of the eruption of mud volcanoes.

Keywords: GPR, Velocity spectrum, Resistivity

©2019. Japan Geoscience Union. All Right Reserved.

The P and S wave velocity and geological conditions of shallow surrounding tunnel ground by velocity logging on tunnel side wall

*Kenji OKAZAKI[1], Toshiyuki KURAHASHI[1], Hiroumi NIWA[2]

1. Civil Engineering Research Institute for cold region, Public Works Research Institute, 2. FUJITA corporation

In the tunnel maintenance, the information for the condition of tunnel ground may be necessary to grasp its loosening or deterioration of the surrounding tunnel ground. One way method to estimate these condition is velocity logging. The velocity logging is a method of measuring P and S wave velocity in a borehole, and the condition of the tunnel ground can be estimated based on the velocity distribution. Normally, the S-wave velocity is measured by applying a top load to a thick plate placed horizontally on the ground surface and tapping it. However, in order to measure the S-wave velocity in a horizontal ground in a tunnel, it is necessary to vibrate the concrete surface of the side wall, and it is necessary to fix the thick plate used for its vibration to the side wall surface is there. Touyama et al. 2018 show the results of striking with a thick plate fixed to the ground by a spike of 30 cm in length, and clear and equivalent waveforms are measured compared with the case where it is not fixed by spikes, and the amplitude of the S-wave has been amplified to about 2 times.

In this study, a core drill (Niwa et al. 2017) at the two points A and B on the side wall part covers 5.0 meters at point A, 3.8 meters at point B was excavated and the these core were collected in the tunnel that constructed by the sheet pile construction method. In addition, velocity logging by the downhole method was performed in each hole, and the correspondence between the properties of the excavation core and the P and S wave velocity was compared. The P-wave velocity was measured by directly hitting the concrete surface of the side wall around the boring hole with a steel hammer. The S-wave velocity was measured by driving four anchors on the concrete surface of the side wall, fixing the thick plate so as to be in close contact with a screw type anchor bar, and hitting a thick plate with a hammer from both directions.

As a result of drilling by the core drill, at the point A, the andesite was confirmed on the back side of the liner concrete of 0.87 m. An andesitic rocks were collected as rod-shaped cores that emit metal sounds somewhat by hammer consultation. At point B, we also confirmed the andesitic rocks at the back of the liner concrete of 0.75 m in the same way. The andesite was collected as a short columnar core up to about 40 cm which emits a voiced sound at hammering consultation. As a result of velocity logging, the P-wave velocity at point A was 2170 m/s and the S-wave velocity was 1050 m/s. In addition, it was confirmed that inverted waveforms could be measured symmetrically with S-waves hit from both directions. The P-wave velocity at point B was 980 m/s and the S-wave velocity was 550 m/s, confirming a tendency lower than point A. It is thought that this is due to the fact that the same andesite is distributed at both sites, but the site B is in a situation with more degradation and cracks than at point A. It was confirmed that the inverted waveform of S-wave at point B was also measured symmetrically. In this survey, we measured the S-wave velocity for the ground in the horizontal direction of the tunnel with the vertical surface of the side wall concrete on tunnel, and we were able to obtain good waveform. By the simple method like this survey, we could grasp the velocity distribution of the shallow part of the tunnel and obtained information to evaluate the condition of the surrounding tunnel ground.

Keywords: tunnel, velocity logging, geological survey, core drill

©2019. Japan Geoscience Union. All Right Reserved.

©2019. Japan Geoscience Union. All Right Reserved.

Rock physical interpretation of the relationship between S-wave velocity and fluid saturation in rocks

*Toru Takahashi[1]

1. Fukada Geological Institute

There have been many studies on the relationship between seismic velocity and fluid (water) saturation in rocks. As for the S-wave velocity, it is reported that it increases and decreases with the increase of the saturation degree, and it shows a more complicated aspect than the P wave velocity. In recent years, the application of seismic exploration and monitoring methods using surface waves has rapidly expanded and the importance of S-wave velocity of rocks which governs surface wave propagation is further increasing. In this study, to understand and model the relationship between S-wave velocity and fluid saturation, the data on the relationship between seismic velocity, especially S-wave velocity, and fluid saturation obtained in the laboratory tests are analyzed. It is also examined whether the observation data as described above can be explained or not by the proposed model. As a result, it is confirmed that the relationship between the S-wave velocity and fluid saturation is changed according to the type and age of the rock, and that the relationship can be represented by the rock physical model.

Keywords: S-wave velocity, fluid saturation, rock physics model

©2019. Japan Geoscience Union. All Right Reserved.

Estimation of Rayleigh wave group velocities in Zushi City using seismic interferometry in the short period range

*jun ueno[1], Yoshiya - Oda[1]

1. Tokyo Metropolitan University

To estimate Rayleigh wave group velocities in the short period range from microtremor data, we have applied seismic interferometry method to microtremor data observed in Zushi City, Kanagawa, Japan. The group velocities for the 82 station pairs from 58 observation points have been calculated by using the multiple filter analysis. As the result, we found that there is a good correlation with the results of microtremor array method carried out at the same area.

Keywords: seismic interferometry, group velocity, short period range

©2019. Japan Geoscience Union. All Right Reserved.

Acquiring distributions of phase velocity for wave frequency to use DAS for surface wave method

*Kyosuke Onishi[1], Kobayashi Takayuki[1], Takanori Ogahara[1], Tomio INAZAKI[1]

1. Public Works Research Institute

Recently, the distributed acoustic sensing (DAS) technology has been developed and the development speed is accelerated. Test surveys using test wells of petroleum production are frequency reported. In shallow geophysics, DAS will be useful technology for a low-cost sensor to monitor for long ranges. The main method of geophysical exploration using elastic wave for river banks and shallow soil structures is surface wave method. When we want to use DAS technology to survey shallow soil structure, it is important to acquire and analyze surface waves. We acquired events of surface wave on DAS records using optical fiber set in shallow ground in our research institute (PWRI, Tsukuba). DAS records show lower s/n than the records from standard geophones, but we can find propagation of surface wave on the DAS records. We analyzed phase velocities on different frequencies using CMP-CC method and acquired fine images of dispersion property. The minimum wave length we specified is about 6.5 m to acquire phase velocity. However, we cannot analyze phase velocity in some CMP points and we search reasons to improve analysis methods. When phase velocity curves will be stably acquired, surface wave method is applied by DAS technology and development of DAS for shallow geophysics will be accelerated.

Keywords: optical fiber, surface wave method

©2019. Japan Geoscience Union. All Right Reserved.

Imaging of deteriorated floor slabs using a test model by ground-penetrating radar

*Kyosuke Onishi[1]

1. Public Works Research Institute

The concrete floor slab of bridge sometimes has special deterioration, which is faster than standard deteriorations. Previous detecting methods without visual examination will be developed for sudden problems. Ground-penetrating radar (GPR) is frequently and widely used for survey underground cavities and it becomes one of effective tools to detect deterioration areas of floor slabs. However, GPR is difficult to detect deterioration of a concrete slab in many situations. One of the reasons is that the target depth is shallow. The deterioration of concrete slab occurs from the top surface. The depth of the top surface from the surface of road is decided from the thickness of pavement. The value of pavement thickness is frequently ranged from 5 cm to 10 cm. The thickness values is travel time including direct waves in air and on ground, which becomes difficult to separate important event signals. We made a model of floor slab and measured several GPR equipment. We show some results of GPR records. The model has a special design to remove an asphalt pavement layer and to easily change conditions of a concrete slab. We find GPR can detect anomalous areas in the upper zone with deterioration of a concrete slab, when dielectric characteristic shows enough different from around areas. However, it is difficult to detect abnormal conditions, such as thickness, particle size, moisture from characteristic signals detected on GPR records. We conclude that tests of slab model and numerical simulations should be used to understand characteristic signals of many conditions and to use them to interpret actual data acquired from bridges.

Keywords: ground-penetrating radar, floor slab

©2019. Japan Geoscience Union. All Right Reserved.

[J] Poster | H (Human Geosciences)：H-TT Technology & Techniques

Tue. May 28, 2019 5:15 PM - 6:30 PM JST | Tue. May 28, 2019 8:15 AM - 9:30 AM UTC | Poster Hall International Exhibition Hall8, Makuhari Messe_24

[H-TT22] New Developments in Shallow Geophysics

convener:Kyosuke Onishi(Public Works Research Institute), Kunio Aoike(Oyo corporation), Keisuke Inoue(National Agriculture and Food Research Organization), Tishiyuki Yokota(National Institute of Advanced Industrial Science and Technology)

The session of shallow geophysics calls many research contributions on geophysical exploration techniques for the near surface. Our target depth is strictly restricted in the depth zone from 5 cm to 30 m (or from 2 in to 100 ft) below the surface of the ground. It may be the closest unknown territory for human society and advanced societies cannot have controlled yet to avoid disasters caused by dynamics in the shallow near surface. Peoples require techniques to manage levee, landslide and earth constructions also knowledge to control groundwater, liquefaction and soil pollution. The near surface has many geotechnical, environmental and hydrogeologic problems.
Major survey techniques are surface wave method, electric exploration, ground-penetrating radar and land streamer, but any methods will be discussed if your target is located in the specified depths. This session welcomes to discuss laboratory tests and rock physics for unconsolidated porous media in the vadose zone. Also, we will welcome not only cutting-edge technologies but also classic theory, if the knowledge is useful for human living.

[HTT22-P01] The shallow structure imaging of integrated geophysical surveying of GPR and ERT at Oyunuma in the Goshougake geothermal area, northeast of Japan

*Inoue Yusuke[1], Tomoki Tsutsui[1], Shinya Sakanaka[1] (1.Graduate School of International Resource Sciences in Akita University)

[HTT22-P02] The P and S wave velocity and geological conditions of shallow surrounding tunnel ground by velocity logging on tunnel side wall

*Kenji OKAZAKI[1], Toshiyuki KURAHASHI[1], Hiroumi NIWA[2] (1.Civil Engineering Research Institute for cold region, Public Works Research Institute, 2.FUJITA corporation)

[HTT22-P03] Rock physical interpretation of the relationship between S-wave velocity and fluid saturation in rocks

*Toru Takahashi[1] (1.Fukada Geological Institute)

[HTT22-P04] Estimation of Rayleigh wave group velocities in Zushi City using seismic interferometry in the short period range

*jun ueno[1], Yoshiya - Oda[1] (1.Tokyo Metropolitan University)

[HTT22-P05] Acquiring distributions of phase velocity for wave frequency to use DAS for surface wave method

*Kyosuke Onishi[1], Kobayashi Takayuki[1], Takanori Ogahara[1], Tomio INAZAKI[1] (1.Public Works Research Institute)

[HTT22-P06] Imaging of deteriorated floor slabs using a test model by ground-penetrating radar

*Kyosuke Onishi[1] (1.Public Works Research Institute)

The shallow structure imaging of integrated geophysical surveying of GPR and ERT at Oyunuma in the Goshougake geothermal area, northeast of Japan

*Inoue Yusuke[1], Tomoki Tsutsui[1], Shinya Sakanaka[1]

1. Graduate School of International Resource Sciences in Akita University

The Goshougake geothermal area is surrounded in active volcanoes of Akita Yakeyama volcanoes and Hachimantai volcanoes. In this area, we can observe active geothermal phenomena, such as hot springs, high temperature water marshes including Oyunuma, and mud volcanoes. In this field, a part of sidewalk was broken by mud volcanic eruption, and has closed to walk since autumn 2016. The event inspires our motivation to research the shallow structure at the field by geophysical method.
The previous studies with geophysical methods were applied to the area including the Goshougake geothermal area. The gravitational survey, magnetic survey, electrical survey, and seismic survey in the north Hachimantai area were carried out by Yora and Ito (1974). Airborne electromagnetic survey, MT survey, and electrical survey were carried out by Uchida and Mitsuhata (1995). The research target of these studies focused on the wide area and the studies imaging shallow structure have never reported at Oyunuma in the in the Goshougake geothermal area. Our research purpose is revealing the shallow structures at Oyunuma in the Goshougake geothermal area by the integrated geophysical surveying of GPR (Ground Penetrating Radar) and ERT (Electrical Resistivity Tomography).
In GPR survey, a line of 172 m long was arranged on the southeast of Oyunuma. We used 4 different antennas of 100 MHz, 270 MHz, 400 MHz, and 900 MHz with the GPR equipment SIR-3000 made by GSSI (Geophysical Survey System, Inc.) and adopted the profile measurement with keeping interval of transmitter and receiver antennas. In ERT, a line of 188 m long was arranged along the GPR survey line. We used the equipment SYSCAL Pro made by IRIS Instruments and adopted the array system of the dipole-dipole method. The number of electrode is 48 and the intervals of the electrodes were 4 m.
A series of the GPR analysis, that is, time-zero correction, background removal, bandpass filter (BPF), autocorrelation, predictive deconvolution, velocity analysis, and depth conversion were applied to the obtained data. Clear reflections appeared at two way time of 75-100 ns in the time sections derived by BPF in the records of 4 kinds of antennas. Especially, clear reflections appeared in the reflection record of 270 MHz antenna. We picked up 4 blocks (sections) with remarkably clear reflections in the GPR survey line and carried out detailed analyses on each classified block.
The reflection records obtained in GPR survey are presented in the time sections. In order to convert them in the depth sections, it is necessary to know the exact EM (electromagnetic) wave velocity. We developed an original computer program for the EM velocity analysis which can be applicable for GPR profiling using Visual Studio 2015 C#. Based on calculation using the program, we can draw the contour chart of velocity spectrum which evaluates the most appropriate mean velocity by the semblance values. The semblance value is the ratio of the energy of stacked waves included in a time window to the total input energy of the waves in the same window (Honda, 2014). The exact mean EM velocity in ground medium is estimated to be 0.093-0.147 m/ns for each block. When multiple reflectors appear in reflection records, appropriate velocities are obtained by the predictive deconvolution processing. The original program also calculates the autocorrelation function which is the parameter used in the predictive deconvolution processing. Using the EM velocity by the velocity analysis, we can convert GPR data to the depth sections and the clear reflections revealed in the depth of 4-5 m from the surface of the sidewalk.
The 2D resistivity inversion by the finite difference method is used in the analysis of ERT. The part of the

©2019. Japan Geoscience Union. All Right Reserved.

continuity of an extreme low resistivity zone to the ground surface matches the location of the outcrop of the vents of sulfur gas. Consequently, the zone of the extreme low resistivity is suggested to be a layer of the pass of thermal water.
Comparing the results of GPR and ERT in the depth sections, the clear reflections in the blocks (from block1 to block 4) in GPR sections are located at the area steeply changing from the low resistivity to the high resistivity in ERT section. We can conclude that the some features of the shallow structure in Goshougake geothermal area obtained by the geophysical methods provide the key to elucidate the mechanism and the prediction of the eruption of mud volcanoes.

Keywords: GPR, Velocity spectrum, Resistivity

©2019. Japan Geoscience Union. All Right Reserved.

The P and S wave velocity and geological conditions of shallow surrounding tunnel ground by velocity logging on tunnel side wall

*Kenji OKAZAKI[1], Toshiyuki KURAHASHI[1], Hiroumi NIWA[2]

1. Civil Engineering Research Institute for cold region, Public Works Research Institute, 2. FUJITA corporation

In the tunnel maintenance, the information for the condition of tunnel ground may be necessary to grasp its loosening or deterioration of the surrounding tunnel ground. One way method to estimate these condition is velocity logging. The velocity logging is a method of measuring P and S wave velocity in a borehole, and the condition of the tunnel ground can be estimated based on the velocity distribution. Normally, the S-wave velocity is measured by applying a top load to a thick plate placed horizontally on the ground surface and tapping it. However, in order to measure the S-wave velocity in a horizontal ground in a tunnel, it is necessary to vibrate the concrete surface of the side wall, and it is necessary to fix the thick plate used for its vibration to the side wall surface is there. Touyama et al. 2018 show the results of striking with a thick plate fixed to the ground by a spike of 30 cm in length, and clear and equivalent waveforms are measured compared with the case where it is not fixed by spikes, and the amplitude of the S-wave has been amplified to about 2 times.

In this study, a core drill (Niwa et al. 2017) at the two points A and B on the side wall part covers 5.0 meters at point A, 3.8 meters at point B was excavated and the these core were collected in the tunnel that constructed by the sheet pile construction method. In addition, velocity logging by the downhole method was performed in each hole, and the correspondence between the properties of the excavation core and the P and S wave velocity was compared. The P-wave velocity was measured by directly hitting the concrete surface of the side wall around the boring hole with a steel hammer. The S-wave velocity was measured by driving four anchors on the concrete surface of the side wall, fixing the thick plate so as to be in close contact with a screw type anchor bar, and hitting a thick plate with a hammer from both directions.

As a result of drilling by the core drill, at the point A, the andesite was confirmed on the back side of the liner concrete of 0.87 m. An andesitic rocks were collected as rod-shaped cores that emit metal sounds somewhat by hammer consultation. At point B, we also confirmed the andesitic rocks at the back of the liner concrete of 0.75 m in the same way. The andesite was collected as a short columnar core up to about 40 cm which emits a voiced sound at hammering consultation. As a result of velocity logging, the P-wave velocity at point A was 2170 m/s and the S-wave velocity was 1050 m/s. In addition, it was confirmed that inverted waveforms could be measured symmetrically with S-waves hit from both directions. The P-wave velocity at point B was 980 m/s and the S-wave velocity was 550 m/s, confirming a tendency lower than point A. It is thought that this is due to the fact that the same andesite is distributed at both sites, but the site B is in a situation with more degradation and cracks than at point A. It was confirmed that the inverted waveform of S-wave at point B was also measured symmetrically. In this survey, we measured the S-wave velocity for the ground in the horizontal direction of the tunnel with the vertical surface of the side wall concrete on tunnel, and we were able to obtain good waveform. By the simple method like this survey, we could grasp the velocity distribution of the shallow part of the tunnel and obtained information to evaluate the condition of the surrounding tunnel ground.

Keywords: tunnel, velocity logging, geological survey, core drill

©2019. Japan Geoscience Union. All Right Reserved.

©2019. Japan Geoscience Union. All Right Reserved.

Rock physical interpretation of the relationship between S-wave velocity and fluid saturation in rocks

*Toru Takahashi[1]

1. Fukada Geological Institute

There have been many studies on the relationship between seismic velocity and fluid (water) saturation in rocks. As for the S-wave velocity, it is reported that it increases and decreases with the increase of the saturation degree, and it shows a more complicated aspect than the P wave velocity. In recent years, the application of seismic exploration and monitoring methods using surface waves has rapidly expanded and the importance of S-wave velocity of rocks which governs surface wave propagation is further increasing. In this study, to understand and model the relationship between S-wave velocity and fluid saturation, the data on the relationship between seismic velocity, especially S-wave velocity, and fluid saturation obtained in the laboratory tests are analyzed. It is also examined whether the observation data as described above can be explained or not by the proposed model. As a result, it is confirmed that the relationship between the S-wave velocity and fluid saturation is changed according to the type and age of the rock, and that the relationship can be represented by the rock physical model.

Keywords: S-wave velocity, fluid saturation, rock physics model

©2019. Japan Geoscience Union. All Right Reserved.

Estimation of Rayleigh wave group velocities in Zushi City using seismic interferometry in the short period range

*jun ueno[1], Yoshiya - Oda[1]

1. Tokyo Metropolitan University

To estimate Rayleigh wave group velocities in the short period range from microtremor data, we have applied seismic interferometry method to microtremor data observed in Zushi City, Kanagawa, Japan. The group velocities for the 82 station pairs from 58 observation points have been calculated by using the multiple filter analysis. As the result, we found that there is a good correlation with the results of microtremor array method carried out at the same area.

Keywords: seismic interferometry, group velocity, short period range

©2019. Japan Geoscience Union. All Right Reserved.

Acquiring distributions of phase velocity for wave frequency to use DAS for surface wave method

*Kyosuke Onishi[1], Kobayashi Takayuki[1], Takanori Ogahara[1], Tomio INAZAKI[1]

1. Public Works Research Institute

Recently, the distributed acoustic sensing (DAS) technology has been developed and the development speed is accelerated. Test surveys using test wells of petroleum production are frequency reported. In shallow geophysics, DAS will be useful technology for a low-cost sensor to monitor for long ranges. The main method of geophysical exploration using elastic wave for river banks and shallow soil structures is surface wave method. When we want to use DAS technology to survey shallow soil structure, it is important to acquire and analyze surface waves. We acquired events of surface wave on DAS records using optical fiber set in shallow ground in our research institute (PWRI, Tsukuba). DAS records show lower s/n than the records from standard geophones, but we can find propagation of surface wave on the DAS records. We analyzed phase velocities on different frequencies using CMP-CC method and acquired fine images of dispersion property. The minimum wave length we specified is about 6.5 m to acquire phase velocity. However, we cannot analyze phase velocity in some CMP points and we search reasons to improve analysis methods. When phase velocity curves will be stably acquired, surface wave method is applied by DAS technology and development of DAS for shallow geophysics will be accelerated.

Keywords: optical fiber, surface wave method

©2019. Japan Geoscience Union. All Right Reserved.

Imaging of deteriorated floor slabs using a test model by ground-penetrating radar

*Kyosuke Onishi[1]

1. Public Works Research Institute

The concrete floor slab of bridge sometimes has special deterioration, which is faster than standard deteriorations. Previous detecting methods without visual examination will be developed for sudden problems. Ground-penetrating radar (GPR) is frequently and widely used for survey underground cavities and it becomes one of effective tools to detect deterioration areas of floor slabs. However, GPR is difficult to detect deterioration of a concrete slab in many situations. One of the reasons is that the target depth is shallow. The deterioration of concrete slab occurs from the top surface. The depth of the top surface from the surface of road is decided from the thickness of pavement. The value of pavement thickness is frequently ranged from 5 cm to 10 cm. The thickness values is travel time including direct waves in air and on ground, which becomes difficult to separate important event signals. We made a model of floor slab and measured several GPR equipment. We show some results of GPR records. The model has a special design to remove an asphalt pavement layer and to easily change conditions of a concrete slab. We find GPR can detect anomalous areas in the upper zone with deterioration of a concrete slab, when dielectric characteristic shows enough different from around areas. However, it is difficult to detect abnormal conditions, such as thickness, particle size, moisture from characteristic signals detected on GPR records. We conclude that tests of slab model and numerical simulations should be used to understand characteristic signals of many conditions and to use them to interpret actual data acquired from bridges.

Keywords: ground-penetrating radar, floor slab

©2019. Japan Geoscience Union. All Right Reserved.

[E] Poster | H (Human Geosciences)：H-CG Complex & General

Tue. May 28, 2019 1:45 PM - 3:15 PM JST | Tue. May 28, 2019 4:45 AM - 6:15 AM UTC | Poster Hall International Exhibition Hall8, Makuhari Messe_6

[H-CG28] Implementing Integrated Research for Sustainable Future

convener:Yukio Himiyama(Emeritus Professor, Hokkaido University of Education), Akihiko Kondoh(Center for Environmental Remote Sensing, Chiba University), Takeshi Sakurai(Graduate School of Agricultural and Life Sciences, The University of Tokyo), Kenichi Abe(Research Institute for Humanity and Nature)

The world global environmental studies are being re-organized in the framework of Future Earth, which is considered to be an important driver to achieve the Sustainable Development Goals (SDGs) set by UN in 2015. Geoscience, which has traditionally been concerned about the dynamic nature and phenomena of the Earth, including lithosphere, hydrosphere, atmosphere and biosphere, is now increasingly committed to human sphere and human dimensions of global change, assuming unique roles in Future Earth and the SDGs. The session is intended to discuss the crucial issues related with them, particularly in reference to such SDGs as good health and well-being, quality education, clean water and sanitation, sustainable cities and communities, climate action, life below water and life on land. Those interested in Future Earth, SDGs, and ESD (Education for Sustainable Development) particularly those who have already started or are about to start related projects, or are interested in Future Earth Knowledge-Action Networks (KANs), such as Ocean, Food-Water-Energy Nexus, Health, Disasters, Cities, Natural Assets, will find this Session an ideal place to present his/her research results, to exchange information and ideas, and to seek new collaborative relations with other research groups and even with partners in the society.

[HCG28-P01] Ground Motion Instrumentation Network and Earthquake Early Warning System for Uttarakhand

*Pankaj Kumar[1,2], Ashok - Kumar[1,2], Ajay - Gairola[1,2] (1.Indian Institute of Technology Roorkee, India, 2.Earthquake Early Warning Laboratory, Centre of Excellence in Disaster Mitigation & Management, IIT Roorkee)

[HCG28-P02] Linking Socioeconomic and Geographical Model to Analyze Land Use Changes in the Jakarta - Bandung Mega Urban Regions

*Didit Okta Pribadi[1,2] (1.Center for Regional Systems Analysis, Planning and Development (CrestPent) - IPB University, 2.Research Center for Plant Conservation and Botanic Gardens - Indonesian Institute of Sciences)

[HCG28-P03] Development of an Integrated Model for Evaluation of Pasture Carrying Capacity and its Vulnerability based on Water Resources in Arid and Semi-arid Regions-----A Case Study in Mongolia

★Invited Papers

*Qinxue Wang[1], Tomohiro Okadera[1], Tadanobu Nakayama[1], Deni Eer[1], Ochirbat Batkhishig[2], Dorjgotov Battogtokh[2], Uudus Bayasaikhan[3] (1.National Institute for Environmental Studies, 2.Institute of Geography and Geoecology, Mongolian Academy of Sciences, 3.School of Arts and Sciences, National University of Mongolia)

[HCG28-P04] Influence of land use histories on vegetation and ecosystem services of restored wetlands in Tumen River basin, China

*CAO GUANGLAN[1], Kazuaki Tsuchiya[1], Weihong Zhu[2], OKURO TOSHIYA[1] (1.The University of Tokyo, 2.Yanbian University)

[HCG28-P05] The spatial flow of freshwater ecosystem services: A case study of Tumen River watershed

*JIAN ZHANG[1], Shizuka hashimoto[1], Kazuaki Tsuchiya[1], Weihong Zhu[2], OKURO TOSHIYA[1] (1.The University of Tokyo, 2.Yanbian University)

Ground Motion Instrumentation Network and Earthquake Early Warning System for Uttarakhand

*Pankaj Kumar[1,2], Ashok - Kumar[1,2], Ajay - Gairola[1,2]

1. Indian Institute of Technology Roorkee, India, 2. Earthquake Early Warning Laboratory, Centre of Excellence in Disaster Mitigation & Management, IIT Roorkee

An Earthquake Early Warning System (EEWS) has been developed by Indian institute of Technology Roorkee (IIT Roorkee) for Uttarakhand, a Himalayan province of India. The region behind to set up first EEWS in India for Uttarakhand is that the main central thrust (MCT) and main boundary thrust (MBT) passes through it and central seismic gap exists in its region and seismologist envisaged a big earthquake will hit this region in near future. Under this project, 155 accelerometers have been installed in 53,483 km^2 area in the Himalayan part of Uttarakhand. These accelerometers are installed on the ground floor of government owned offices of Bharat Sanchar Nigam Limited (BSNL) mobile towers and State Wide Area Network (SWAN) available in the province. The average station to station distance is kept between 10 to 20 km which ensure the triggering of more than 6 accelerometers if an earthquake of magnitude greater than 6 triggers in the region. The data is streamed at the central server located in Earthquake Early Warning Laboratory at Centre of Excellence in Disaster Mitigation & Management in IIT Roorkee through private network of BSNL and SWAN on 24 ×7 basis. The location of installed accelerometers and their streaming at the Earthquake Early Warning Laboratory is shown in figure 1. Whole system is automatic and the early warning parameter is peak displacement (Pd). When an earthquake of magnitude greater than 6 will strike in the instrumented region an earthquake warning will be issued to public through the sirens. The early warning sirens are installed in the public offices, government buildings, schools, colleges of the two major cities, Dehradun and Haldwani, and all 13 district emergency operation center of the province. After hearing, earthquake alarm, people can take necessary precautionary measures. This paper presents the details of instrumentation and working of the EEWS.

Fig 1. Installed accelerometers are shown in Uttarakhand’ s map. MCT and MBT passes through the Himalayan province. Streaming of the data from accelerometer to central server at EEW laboratory is shown in the snapshot.

Keywords: Instrumentation, Accelerometers, Seismic gap, EEWS, Sirens

©2019. Japan Geoscience Union. All Right Reserved.

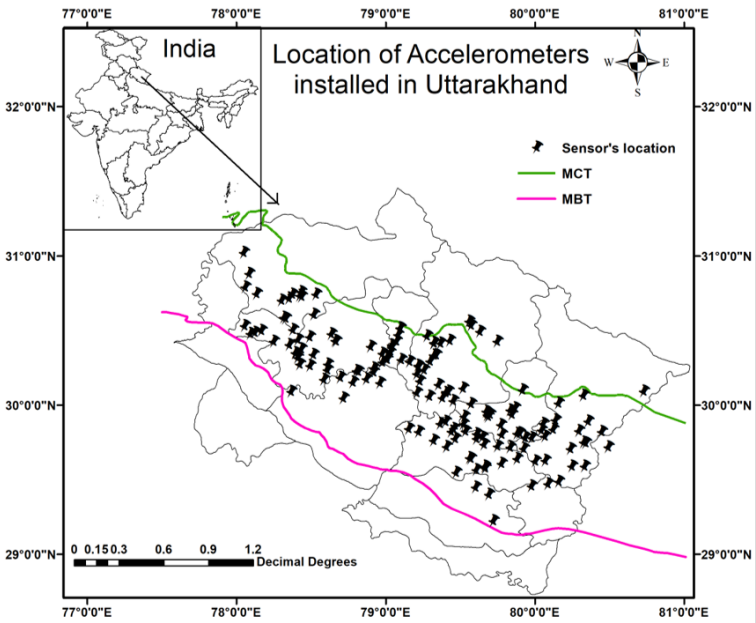

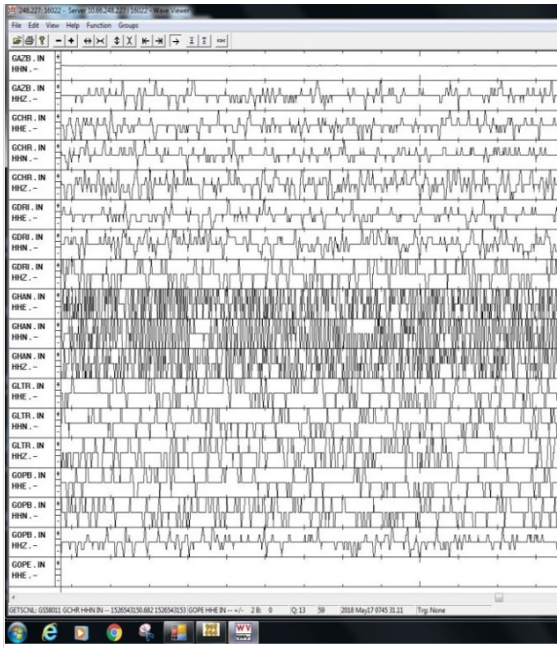

©2019. Japan Geoscience Union. All Right Reserved.

Linking Socioeconomic and Geographical Model to Analyze Land Use Changes in the Jakarta - Bandung Mega Urban Regions

*Didit Okta Pribadi[1,2]

1. Center for Regional Systems Analysis, Planning and Development (CrestPent) - IPB University, 2. Research Center for Plant Conservation and Botanic Gardens - Indonesian Institute of Sciences

Continuing rapid urbanization has led to escalating socio-economic and physical interaction between two adjacent megacities in Indonesia namely Jakarta and Bandung megacity. Physically, enhancing the connection over time has formed urban corridors that stimulate rapid land use changes as well as the expansion of urban-rural land use mixture in the vast area between the two big cities. As land use composition is essential to achieve urban sustainability, modelling land use changes is required as a tool for decision makers to assess the sustainability of different urban form. Nowadays, land use changes model has been rapidly developed owing to increasing computation capacity which is capable of incorporating previous trend of land use changes (e.g. Markov Chain), spatial correlation (e.g. Cellular Automata), and related driving factors (e.g. Logistic Regression or Neural Network) within the model. However, this model is too focused on geographical aspect, while lacking to consider socio-economic factors which spatially might have distinctive properties such as spatial heterogeneity, spatial network, and spatial multiplier effect. This paper aims to combine socioeconomic and geographical factors to analyze complex and dynamic land use systems as found in Jakarta-Bandung Megacity corridors. Land Change Modeler (LCM) from Idrisi Tersset software as a combination of Neural Network and CA-Markov model would be enhanced by incorporating socioeconomic aspects analyzed by GWR (Geographical Weighted Regression) for detecting spatial heterogeneity, gravity model for analyzing spatial network, and spatial autocorrelation model (SAM) for defining spatial multiplier effect. This model would be compared to the results of LCM as a single approach. A new model is suggested as an enhanced approach to understand multiple factors that influence land use changes in Jakarta-Bandung megacity corridors, thus more comprehensive policies can be formulated.

Keywords: Urbanization, Socioeconomic model, Geographical Model, Land Use Changes, Jakarta-Bandung Mega Urban Regions

©2019. Japan Geoscience Union. All Right Reserved.

Development of an Integrated Model for Evaluation of Pasture Carrying Capacity and its Vulnerability based on Water Resources in Arid and Semi-arid Regions------A Case Study in Mongolia

*Qinxue Wang[1], Tomohiro Okadera[1], Tadanobu Nakayama[1], Deni Eer[1], Ochirbat Batkhishig[2], Dorjgotov Battogtokh[2], Uudus Bayasaikhan[3]

1. National Institute for Environmental Studies, 2. Institute of Geography and Geoecology, Mongolian Academy of Sciences, 3. School of Arts and Sciences, National University of Mongolia

Arid and semi-arid regions cover 41% of the global land area and near 2 billion people (34.7%) live there, where fragile environment is getting more vulnerable due to climate change and human activities. Pasture carrying capacity and its vulnerability can be recognized as the integrated indicators for SDGs in arid and semi-arid regions. Our previous study revealed that climate change in past few decades caused the obvious degradation of permafrost, the water deficit of land-surface, and then the decrease of pasture productivity and carrying capacity. However, beside climate change, land use/cover changes caused by human activities such as urbanization, cultivation and mining industry may also have a large influence on pasture carrying capacity. In such regions, it is essential for us to develop some indicators to be used for sustainable management of pasture ecosystems.

In this study, we have developed an integrated model based on water resources to evaluate the pasture Carrying Capacity (CC), Grazing Pressure (GP) and Vulnerability Index (VI) under the influences of both climate change and land use/cover changes, such as urbanization, cultivation and mining & so on (Figure 1). The input data include the pasture net primary production, land use, gradient of slope and grazing density, etc. In order to evaluate the impact of land use/cover changes, we applied the model to four target areas: urban area (Ulaanbaatar City) and steppe area (Altanbulag Soum) in semi-arid regions of northern Mongolia and mining area (Khanbogd Soum) and desert (Manlai Soum) in arid regions of southern Mongolia, and the estimated result was shown in Figure 2, which indicates:

Carrying Capacity (CC): steppe area > urban area > desert area > mining area
Grazing Pressure (GP): urban area > steppe area > mining area > desert area
Vulnerability Index (VI): urban area > mining area > desert area > steppe area

We also applied the model to the Soum level in Mongolia and found that the areas with high vulnerability expanded rapidly, especially in central Mongolia in last decades. We are now trying to use the model to do sensitivity analysis to parameters, such as water accessibility, harvest index and so on, to be able to evaluate the efficiency of adaptation strategies, such as well construction for enhancing groundwater usage, forage plantation for enhancing harvest index and so on.

Keywords: Pasture Carrying Capacity, Environmental Vulnerability, Arid and Semi-arid Regions, Water Resources

©2019. Japan Geoscience Union. All Right Reserved.

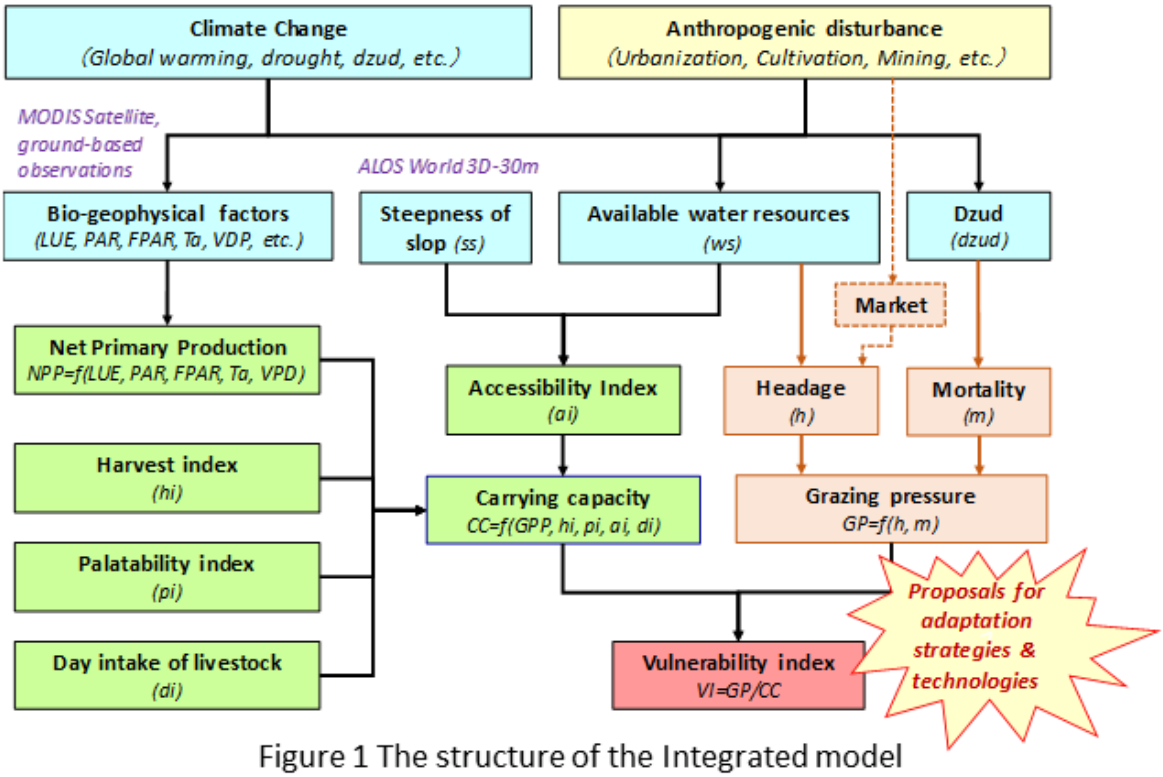

Figure 1 The structure of the Integrated model

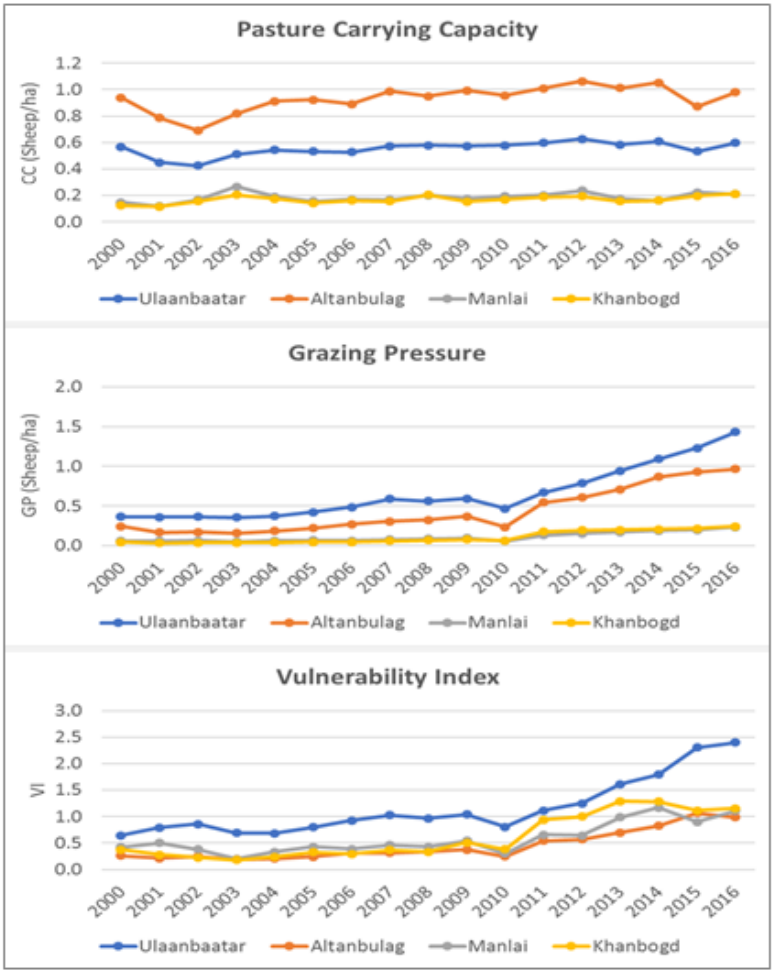

Figure 2 Evaluated pasture CC and VI in four target areas

©2019. Japan Geoscience Union. All Right Reserved.

Influence of land use histories on vegetation and ecosystem services of restored wetlands in Tumen River basin, China

*CAO GUANGLAN[1], Kazuaki Tsuchiya[1], Weihong Zhu[2], OKURO TOSHIYA[1]

1. The University of Tokyo, 2. Yanbian University

Wetlands are among the world’ s most productive and valuable ecosystems. They are important habitats for a variety of flora and fauna, and are vital ecosystems that provide diverse services. They not only are essential for ecological functions such as maintaining biodiversity, controlling floods, and removing pollutants, but also serve necessary economic functions in rice and fish production, transport, and hydropower energy. Despite this, they have suffered a loss of 54%–57% of their area worldwide, which continues under pressures from agriculture, urban expansion, industrialization, and resource extraction. Conservation and restoration of wetland ecosystems is important issues for conservation biodiversity and sustainable use of ecosystem services. In this study, we focus on the lower of Tumen River, Northeast China where the wetlands decreased dramatically because of reclamation. Our objective was to determine the influence of land use and management histories on vegetation structure and ecosystem services and future analyse their associations with environmental factors. The results of this study are of great significance to the impact of management measures on wetland ecosystems, as well as the analysis and evaluation of vegetation restoration.

Keywords: land use histories, vegetation dynamics, wetland restoration, ecosystem services

©2019. Japan Geoscience Union. All Right Reserved.

The spatial flow of freshwater ecosystem services: A case study of Tumen River watershed

*JIAN ZHANG[1], Shizuka hashimoto[1], Kazuaki Tsuchiya[1], Weihong Zhu[2], OKURO TOSHIYA[1]

1. The University of Tokyo, 2. Yanbian University

Freshwater is widely regarded as the most essential natural resource underpinning the well-being of human society, and while scientists translate it into ecosystem services' valuable processes, the supply of clean freshwater has the highest value among various provisioning services. However, due to the land-use intensification and projected warming climate, an increasing likelihood of persistent drought condition, and inadequate conservation, freshwater scarcity issues continue to gain urgency in science and policies. The fusion of the concept of ecosystem services with natural resources management nowadays represents a new conservation paradigm, but still faces notable limitations. Some scientists, noticing the occurrence of spatial mismatch between the supply and demand of ecosystem services, put forward the concept of ecosystem services flow to deal with the problem. Ecosystem services flow research brings out a spatio-temporal connection between the supply and demand, and an deepened understanding about when ,where, and how those benefits were enjoyed. Many papers also suggested that studies at landscape scale may offer a better understanding of ecosystem processes, ecosystem functions, ecosystem services and link them from one to another, as landscape patterns have long been discussed as tools for explaining numerous ecological consequences. In 2017, the annual meeting of IALE in USA as well emphasized the pressing need of integrating landscape patterns to ecosystem services. Thus the study attempt to conduct an analysis of freshwater ecosystem services flow in an intact watershed with the combination of landscape ecology theories. The conceptual framework and progress of this study will be introduced.

Keywords: freshwater ecosystem services, services flow, andscape pattern, watershed

©2019. Japan Geoscience Union. All Right Reserved.

[E] Poster | H (Human Geosciences)：H-CG Complex & General

Tue. May 28, 2019 5:15 PM - 6:30 PM JST | Tue. May 28, 2019 8:15 AM - 9:30 AM UTC | Poster Hall International Exhibition Hall8, Makuhari Messe_25

[H-CG28] Implementing Integrated Research for Sustainable Future

convener:Yukio Himiyama(Emeritus Professor, Hokkaido University of Education), Akihiko Kondoh(Center for Environmental Remote Sensing, Chiba University), Takeshi Sakurai(Graduate School of Agricultural and Life Sciences, The University of Tokyo), Kenichi Abe(Research Institute for Humanity and Nature)

The world global environmental studies are being re-organized in the framework of Future Earth, which is considered to be an important driver to achieve the Sustainable Development Goals (SDGs) set by UN in 2015. Geoscience, which has traditionally been concerned about the dynamic nature and phenomena of the Earth, including lithosphere, hydrosphere, atmosphere and biosphere, is now increasingly committed to human sphere and human dimensions of global change, assuming unique roles in Future Earth and the SDGs. The session is intended to discuss the crucial issues related with them, particularly in reference to such SDGs as good health and well-being, quality education, clean water and sanitation, sustainable cities and communities, climate action, life below water and life on land. Those interested in Future Earth, SDGs, and ESD (Education for Sustainable Development) particularly those who have already started or are about to start related projects, or are interested in Future Earth Knowledge-Action Networks (KANs), such as Ocean, Food-Water-Energy Nexus, Health, Disasters, Cities, Natural Assets, will find this Session an ideal place to present his/her research results, to exchange information and ideas, and to seek new collaborative relations with other research groups and even with partners in the society.

[HCG28-P01] Ground Motion Instrumentation Network and Earthquake Early Warning System for Uttarakhand

*Pankaj Kumar[1,2], Ashok - Kumar[1,2], Ajay - Gairola[1,2] (1.Indian Institute of Technology Roorkee, India, 2.Earthquake Early Warning Laboratory, Centre of Excellence in Disaster Mitigation & Management, IIT Roorkee)

[HCG28-P02] Linking Socioeconomic and Geographical Model to Analyze Land Use Changes in the Jakarta - Bandung Mega Urban Regions

*Didit Okta Pribadi[1,2] (1.Center for Regional Systems Analysis, Planning and Development (CrestPent) - IPB University, 2.Research Center for Plant Conservation and Botanic Gardens - Indonesian Institute of Sciences)

[HCG28-P03] Development of an Integrated Model for Evaluation of Pasture Carrying Capacity and its Vulnerability based on Water Resources in Arid and Semi-arid Regions-----A Case Study in Mongolia

★Invited Papers

*Qinxue Wang[1], Tomohiro Okadera[1], Tadanobu Nakayama[1], Deni Eer[1], Ochirbat Batkhishig[2], Dorjgotov Battogtokh[2], Uudus Bayasaikhan[3] (1.National Institute for Environmental Studies, 2.Institute of Geography and Geoecology, Mongolian Academy of Sciences, 3.School of Arts and Sciences, National University of Mongolia)

[HCG28-P04] Influence of land use histories on vegetation and ecosystem services of restored wetlands in Tumen River basin, China

*CAO GUANGLAN[1], Kazuaki Tsuchiya[1], Weihong Zhu[2], OKURO TOSHIYA[1] (1.The University of Tokyo, 2.Yanbian University)

[HCG28-P05] The spatial flow of freshwater ecosystem services: A case study of Tumen River watershed

*JIAN ZHANG[1], Shizuka hashimoto[1], Kazuaki Tsuchiya[1], Weihong Zhu[2], OKURO TOSHIYA[1] (1.The University of Tokyo, 2.Yanbian University)

Ground Motion Instrumentation Network and Earthquake Early Warning System for Uttarakhand

*Pankaj Kumar[1,2], Ashok - Kumar[1,2], Ajay - Gairola[1,2]

1. Indian Institute of Technology Roorkee, India, 2. Earthquake Early Warning Laboratory, Centre of Excellence in Disaster Mitigation & Management, IIT Roorkee

An Earthquake Early Warning System (EEWS) has been developed by Indian institute of Technology Roorkee (IIT Roorkee) for Uttarakhand, a Himalayan province of India. The region behind to set up first EEWS in India for Uttarakhand is that the main central thrust (MCT) and main boundary thrust (MBT) passes through it and central seismic gap exists in its region and seismologist envisaged a big earthquake will hit this region in near future. Under this project, 155 accelerometers have been installed in 53,483 km^2 area in the Himalayan part of Uttarakhand. These accelerometers are installed on the ground floor of government owned offices of Bharat Sanchar Nigam Limited (BSNL) mobile towers and State Wide Area Network (SWAN) available in the province. The average station to station distance is kept between 10 to 20 km which ensure the triggering of more than 6 accelerometers if an earthquake of magnitude greater than 6 triggers in the region. The data is streamed at the central server located in Earthquake Early Warning Laboratory at Centre of Excellence in Disaster Mitigation & Management in IIT Roorkee through private network of BSNL and SWAN on 24 ×7 basis. The location of installed accelerometers and their streaming at the Earthquake Early Warning Laboratory is shown in figure 1. Whole system is automatic and the early warning parameter is peak displacement (Pd). When an earthquake of magnitude greater than 6 will strike in the instrumented region an earthquake warning will be issued to public through the sirens. The early warning sirens are installed in the public offices, government buildings, schools, colleges of the two major cities, Dehradun and Haldwani, and all 13 district emergency operation center of the province. After hearing, earthquake alarm, people can take necessary precautionary measures. This paper presents the details of instrumentation and working of the EEWS.

Fig 1. Installed accelerometers are shown in Uttarakhand’ s map. MCT and MBT passes through the Himalayan province. Streaming of the data from accelerometer to central server at EEW laboratory is shown in the snapshot.

Keywords: Instrumentation, Accelerometers, Seismic gap, EEWS, Sirens

©2019. Japan Geoscience Union. All Right Reserved.

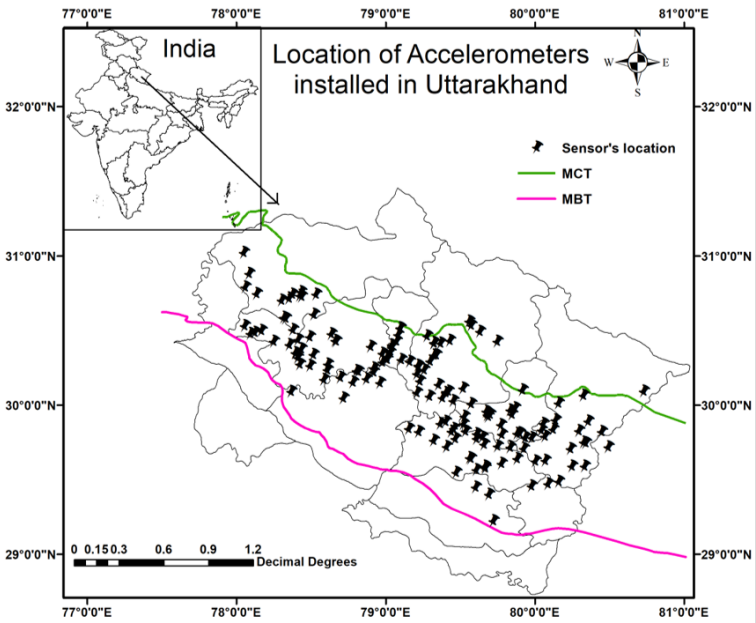

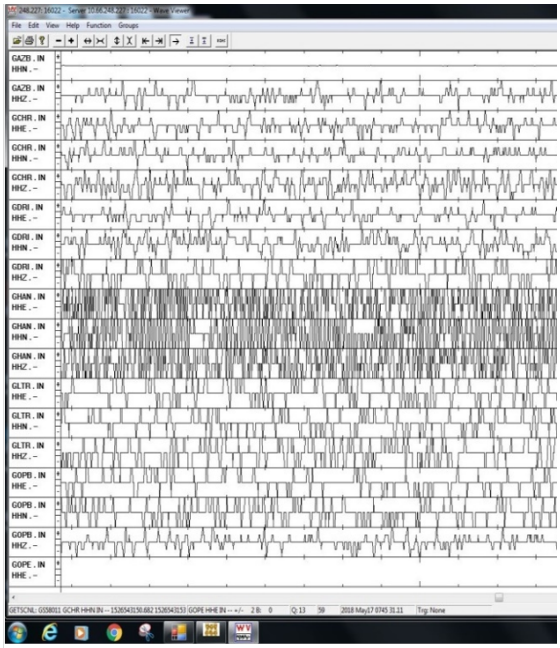

©2019. Japan Geoscience Union. All Right Reserved.

Linking Socioeconomic and Geographical Model to Analyze Land Use Changes in the Jakarta - Bandung Mega Urban Regions

*Didit Okta Pribadi[1,2]

1. Center for Regional Systems Analysis, Planning and Development (CrestPent) - IPB University, 2. Research Center for Plant Conservation and Botanic Gardens - Indonesian Institute of Sciences

Continuing rapid urbanization has led to escalating socio-economic and physical interaction between two adjacent megacities in Indonesia namely Jakarta and Bandung megacity. Physically, enhancing the connection over time has formed urban corridors that stimulate rapid land use changes as well as the expansion of urban-rural land use mixture in the vast area between the two big cities. As land use composition is essential to achieve urban sustainability, modelling land use changes is required as a tool for decision makers to assess the sustainability of different urban form. Nowadays, land use changes model has been rapidly developed owing to increasing computation capacity which is capable of incorporating previous trend of land use changes (e.g. Markov Chain), spatial correlation (e.g. Cellular Automata), and related driving factors (e.g. Logistic Regression or Neural Network) within the model. However, this model is too focused on geographical aspect, while lacking to consider socio-economic factors which spatially might have distinctive properties such as spatial heterogeneity, spatial network, and spatial multiplier effect. This paper aims to combine socioeconomic and geographical factors to analyze complex and dynamic land use systems as found in Jakarta-Bandung Megacity corridors. Land Change Modeler (LCM) from Idrisi Tersset software as a combination of Neural Network and CA-Markov model would be enhanced by incorporating socioeconomic aspects analyzed by GWR (Geographical Weighted Regression) for detecting spatial heterogeneity, gravity model for analyzing spatial network, and spatial autocorrelation model (SAM) for defining spatial multiplier effect. This model would be compared to the results of LCM as a single approach. A new model is suggested as an enhanced approach to understand multiple factors that influence land use changes in Jakarta-Bandung megacity corridors, thus more comprehensive policies can be formulated.

Keywords: Urbanization, Socioeconomic model, Geographical Model, Land Use Changes, Jakarta-Bandung Mega Urban Regions

©2019. Japan Geoscience Union. All Right Reserved.

Development of an Integrated Model for Evaluation of Pasture Carrying Capacity and its Vulnerability based on Water Resources in Arid and Semi-arid Regions------A Case Study in Mongolia

*Qinxue Wang[1], Tomohiro Okadera[1], Tadanobu Nakayama[1], Deni Eer[1], Ochirbat Batkhishig[2], Dorjgotov Battogtokh[2], Uudus Bayasaikhan[3]

1. National Institute for Environmental Studies, 2. Institute of Geography and Geoecology, Mongolian Academy of Sciences, 3. School of Arts and Sciences, National University of Mongolia

Arid and semi-arid regions cover 41% of the global land area and near 2 billion people (34.7%) live there, where fragile environment is getting more vulnerable due to climate change and human activities. Pasture carrying capacity and its vulnerability can be recognized as the integrated indicators for SDGs in arid and semi-arid regions. Our previous study revealed that climate change in past few decades caused the obvious degradation of permafrost, the water deficit of land-surface, and then the decrease of pasture productivity and carrying capacity. However, beside climate change, land use/cover changes caused by human activities such as urbanization, cultivation and mining industry may also have a large influence on pasture carrying capacity. In such regions, it is essential for us to develop some indicators to be used for sustainable management of pasture ecosystems.

In this study, we have developed an integrated model based on water resources to evaluate the pasture Carrying Capacity (CC), Grazing Pressure (GP) and Vulnerability Index (VI) under the influences of both climate change and land use/cover changes, such as urbanization, cultivation and mining & so on (Figure 1). The input data include the pasture net primary production, land use, gradient of slope and grazing density, etc. In order to evaluate the impact of land use/cover changes, we applied the model to four target areas: urban area (Ulaanbaatar City) and steppe area (Altanbulag Soum) in semi-arid regions of northern Mongolia and mining area (Khanbogd Soum) and desert (Manlai Soum) in arid regions of southern Mongolia, and the estimated result was shown in Figure 2, which indicates:

Carrying Capacity (CC): steppe area > urban area > desert area > mining area
Grazing Pressure (GP): urban area > steppe area > mining area > desert area
Vulnerability Index (VI): urban area > mining area > desert area > steppe area

We also applied the model to the Soum level in Mongolia and found that the areas with high vulnerability expanded rapidly, especially in central Mongolia in last decades. We are now trying to use the model to do sensitivity analysis to parameters, such as water accessibility, harvest index and so on, to be able to evaluate the efficiency of adaptation strategies, such as well construction for enhancing groundwater usage, forage plantation for enhancing harvest index and so on.

Keywords: Pasture Carrying Capacity, Environmental Vulnerability, Arid and Semi-arid Regions, Water Resources

©2019. Japan Geoscience Union. All Right Reserved.

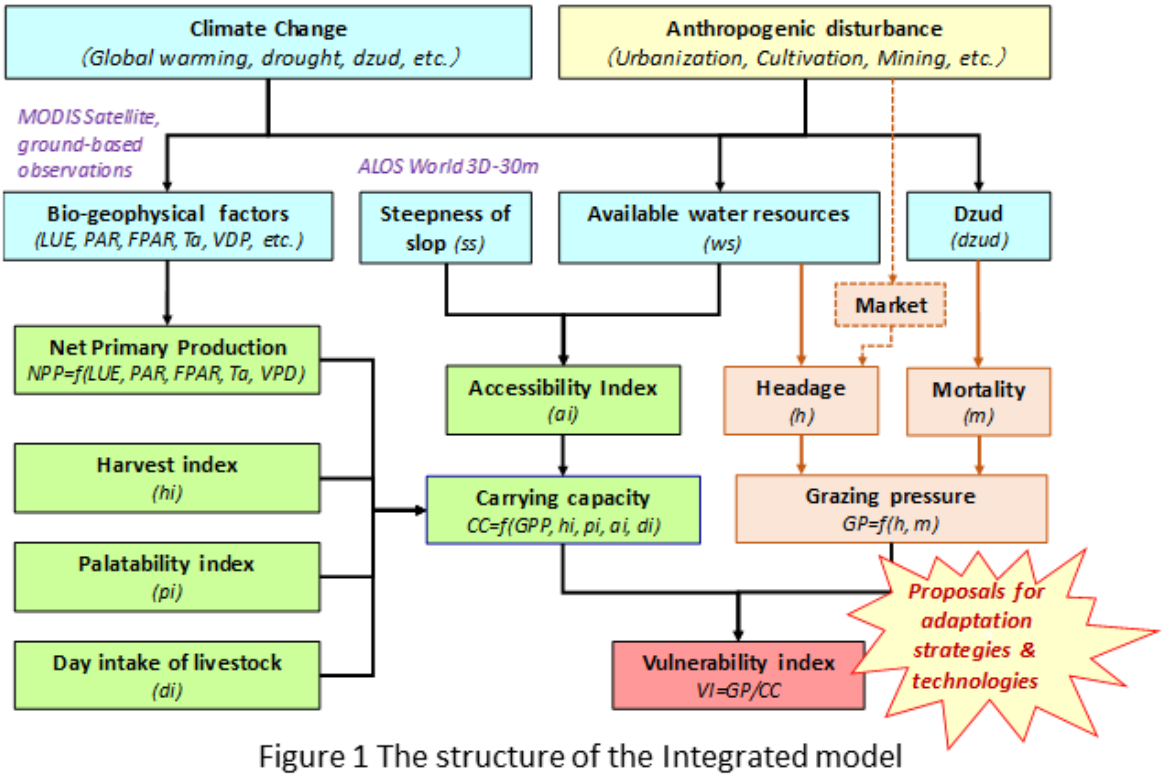

Figure 1 The structure of the Integrated model

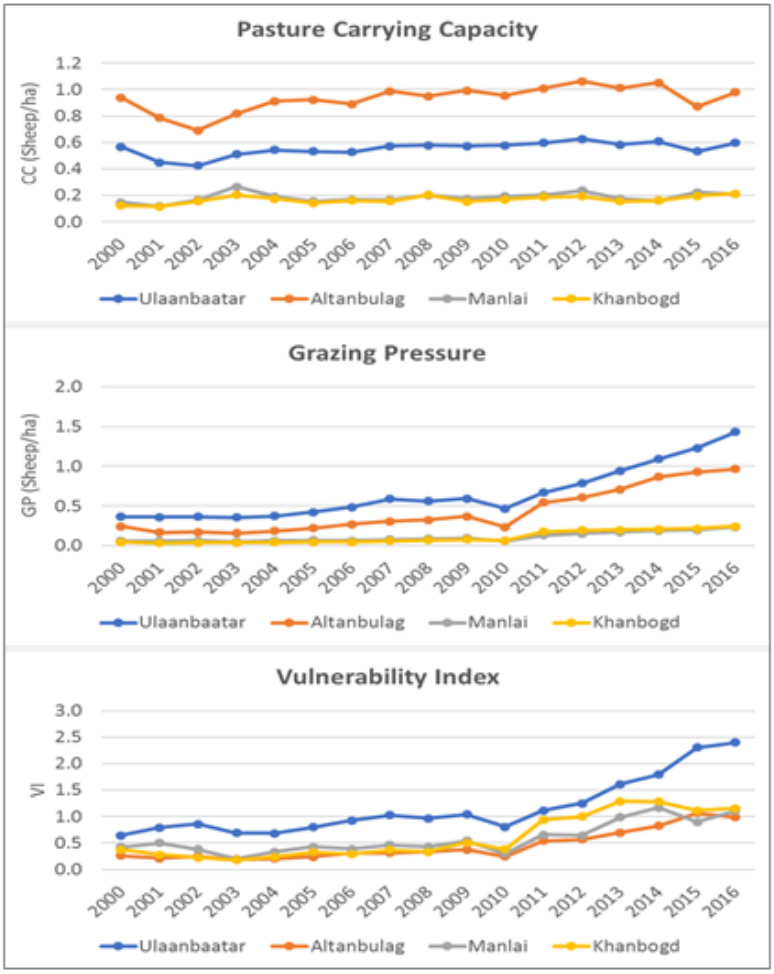

Figure 2 Evaluated pasture CC and VI in four target areas

©2019. Japan Geoscience Union. All Right Reserved.

Influence of land use histories on vegetation and ecosystem services of restored wetlands in Tumen River basin, China

*CAO GUANGLAN[1], Kazuaki Tsuchiya[1], Weihong Zhu[2], OKURO TOSHIYA[1]

1. The University of Tokyo, 2. Yanbian University

Wetlands are among the world’ s most productive and valuable ecosystems. They are important habitats for a variety of flora and fauna, and are vital ecosystems that provide diverse services. They not only are essential for ecological functions such as maintaining biodiversity, controlling floods, and removing pollutants, but also serve necessary economic functions in rice and fish production, transport, and hydropower energy. Despite this, they have suffered a loss of 54%–57% of their area worldwide, which continues under pressures from agriculture, urban expansion, industrialization, and resource extraction. Conservation and restoration of wetland ecosystems is important issues for conservation biodiversity and sustainable use of ecosystem services. In this study, we focus on the lower of Tumen River, Northeast China where the wetlands decreased dramatically because of reclamation. Our objective was to determine the influence of land use and management histories on vegetation structure and ecosystem services and future analyse their associations with environmental factors. The results of this study are of great significance to the impact of management measures on wetland ecosystems, as well as the analysis and evaluation of vegetation restoration.

Keywords: land use histories, vegetation dynamics, wetland restoration, ecosystem services

©2019. Japan Geoscience Union. All Right Reserved.

The spatial flow of freshwater ecosystem services: A case study of Tumen River watershed

*JIAN ZHANG[1], Shizuka hashimoto[1], Kazuaki Tsuchiya[1], Weihong Zhu[2], OKURO TOSHIYA[1]

1. The University of Tokyo, 2. Yanbian University

Freshwater is widely regarded as the most essential natural resource underpinning the well-being of human society, and while scientists translate it into ecosystem services' valuable processes, the supply of clean freshwater has the highest value among various provisioning services. However, due to the land-use intensification and projected warming climate, an increasing likelihood of persistent drought condition, and inadequate conservation, freshwater scarcity issues continue to gain urgency in science and policies. The fusion of the concept of ecosystem services with natural resources management nowadays represents a new conservation paradigm, but still faces notable limitations. Some scientists, noticing the occurrence of spatial mismatch between the supply and demand of ecosystem services, put forward the concept of ecosystem services flow to deal with the problem. Ecosystem services flow research brings out a spatio-temporal connection between the supply and demand, and an deepened understanding about when ,where, and how those benefits were enjoyed. Many papers also suggested that studies at landscape scale may offer a better understanding of ecosystem processes, ecosystem functions, ecosystem services and link them from one to another, as landscape patterns have long been discussed as tools for explaining numerous ecological consequences. In 2017, the annual meeting of IALE in USA as well emphasized the pressing need of integrating landscape patterns to ecosystem services. Thus the study attempt to conduct an analysis of freshwater ecosystem services flow in an intact watershed with the combination of landscape ecology theories. The conceptual framework and progress of this study will be introduced.

Keywords: freshwater ecosystem services, services flow, andscape pattern, watershed

©2019. Japan Geoscience Union. All Right Reserved.

[E] Oral | H (Human Geosciences)：H-CG Complex & General

Tue. May 28, 2019 3:30 PM - 5:00 PM JST | Tue. May 28, 2019 6:30 AM - 8:00 AM UTC | 302 3F

[H-CG28] Implementing Integrated Research for Sustainable Future

convener:Yukio Himiyama(Emeritus Professor, Hokkaido University of Education), Akihiko Kondoh(Center for Environmental Remote Sensing, Chiba University), Takeshi Sakurai(Graduate School of Agricultural and Life Sciences, The University of Tokyo), Kenichi Abe(Research Institute for Humanity and Nature), Chairperson:Ernan Rustiadi(Bogor Agricultural University), Qinxue Wang(National Institute for environmental Studies), takeshi sakurai

The world global environmental studies are being re-organized in the framework of Future Earth, which is considered to be an important driver to achieve the Sustainable Development Goals (SDGs) set by UN in 2015. Geoscience, which has traditionally been concerned about the dynamic nature and phenomena of the Earth, including lithosphere, hydrosphere, atmosphere and biosphere, is now increasingly committed to human sphere and human dimensions of global change, assuming unique roles in Future Earth and the SDGs. The session is intended to discuss the crucial issues related with them, particularly in reference to such SDGs as good health and well-being, quality education, clean water and sanitation, sustainable cities and communities, climate action, life below water and life on land. Those interested in Future Earth, SDGs, and ESD (Education for Sustainable Development) particularly those who have already started or are about to start related projects, or are interested in Future Earth Knowledge-Action Networks (KANs), such as Ocean, Food-Water-Energy Nexus, Health, Disasters, Cities, Natural Assets, will find this Session an ideal place to present his/her research results, to exchange information and ideas, and to seek new collaborative relations with other research groups and even with partners in the society.

3:30 PM - 3:45 PM JST | 6:30 AM - 6:45 AM UTC

[HCG28-01] Implementing Integrated Research for Sustainable Future - a human geoscience perspective

*Yukio Himiyama[1] (1.Emeritus Professor, Hokkaido University of Education)

3:45 PM - 4:00 PM JST | 6:45 AM - 7:00 AM UTC

[HCG28-02] Application of environmental carrying capacity analysis and land cover change scenarios in collaborative spatial planning process: The Jakarta Megacity Case

★Invited Papers

*ERNAN RUSTIADI[1], Andrea Emma Pravitasari[2], Diar Shiddiq[1], Laode Syamsul Iman[1], Setyardi Pratika Mulya[2], Mia Ermyanila[1], Nur Etika Karyati[1] (1.Center for Regional System Analysis, Planning and Development, Bogor Agricultural University , 2.Department of Soil Science and Land Resource, Faculty of Agriculture, Bogor Agricultural University)

4:00 PM - 4:15 PM JST | 7:00 AM - 7:15 AM UTC

[HCG28-03] Does the Market Economy Save the Local Natural Resources While Improving Human Welfare? The Case of 101 Natural Forests in the Middle Hills of Nepal

*Takeshi Sakurai[1], Towa Tachibana[2], Santosh Rayamajhi [3] (1.The University of Tokyo, 2.Chiba University , 3.Tribhuvan University)

4:15 PM - 4:30 PM JST | 7:15 AM - 7:30 AM UTC

[HCG28-04] Academic-public-private partnerships for sustainable herding under increasing frequency of climate hazards

*Masato Shinoda[1] (1.Graduate School of Environmental Studies Nagoya University)

4:30 PM - 4:45 PM JST | 7:30 AM - 7:45 AM UTC

[HCG28-05] Land use after death and funeral of citizen mainly based on public cemeteries in modern Beijing city

*Haruhiro Doi[1], Yanwei Chai[2], Peiwei Xu[3] (1.Faculty of Education, Oita University, 2.Peking University, 3.Beijing Normal University)

4:45 PM - 5:00 PM JST | 7:45 AM - 8:00 AM UTC

[HCG28-06] Restoration and sustainable land management of degraded landscapes in Asia and Africa

★Invited Papers

*OKURO TOSHIYA[1] (1.Graduate School of Agricultural and Life Sciences, The University of Tokyo)

Implementing Integrated Research for Sustainable Future - a human geoscience perspective

*Yukio Himiyama[1]

1. Emeritus Professor, Hokkaido University of Education

Global environmental programmes are re-organized under the framework of Future Earth, which is intend to play a leading role in guiding or coordinating world research communities for sustainability. Human geoscience, which has been built on geoscience which studies dynamic nature and phenomena of the Earth including its resources, geo-hazards and environmental changes, is uniquely committed to human sphere, where human, the environment, environmental problems and disasters are, and to the world sustainability. It hence has strong human/social scientific, as well as physical scientific, viewpoint, and assumes important roles in Future Earth, SDGs (Sustainable Development Goals), and other programmes for global sustainability or disaster risk reduction. This session is intended to discuss crucial issues related with them, and to seek right ways to implement needed integrated research for sustainable future in human geoscience perspective.

Keywords: Future Earth, SDGs, sustainability, human geoscience, disaster, environmental problem

©2019. Japan Geoscience Union. All Right Reserved.

Application of environmental carrying capacity analysis and land cover change scenarios in collaborative spatial planning process: The Jakarta Megacity Case

*ERNAN RUSTIADI[1], Andrea Emma Pravitasari[2], Diar Shiddiq[1], Laode Syamsul Iman[1], Setyardi Pratika Mulya[2], Mia Ermyanila[1], Nur Etika Karyati[1]

1. Center for Regional System Analysis, Planning and Development, Bogor Agricultural University , 2. Department of Soil Science and Land Resource, Faculty of Agriculture, Bogor Agricultural University

In the National Spatial Plan, the Jabodetabekpunjur area (Jakarta Megacity) is designated as a national strategic area. Due to the increasing environmental problems, the Indonesian government carried out a revision process of spatial plan based on an environmental carrying capacity assessment. This research is intended to explain how the study of land-based carrying capacity assessment was applied to the spatial planning process. First, this research is carried out by developing scenarios for land cover changes. Projections of land use change are carried out by extrapolating 20-year time series data on land cover change backward to forecast 20 years of future land use. The study of environmental carrying capacity against current and future conditions is based on the concept of land capability, land suitability, and multi-criteria analysis. The results of the study of carrying capacity were then used to revise existing spatial plans. The decision-making process on revising spatial plan was carried out by a collaborative process involving relevant stakeholders in serial workshop processes by considering the results of the carrying capacity study.

Keywords: urban sprawl, land capability, land use cover changes, regional planning

©2019. Japan Geoscience Union. All Right Reserved.

Does the Market Economy Save the Local Natural Resources While Improving Human Welfare? The Case of 101 Natural Forests in the Middle Hills of Nepal

*Takeshi Sakurai[1], Towa Tachibana[2], Santosh Rayamajhi [3]

1. The University of Tokyo, 2. Chiba University , 3. Tribhuvan University

To pursue a sustainable human development, while expanding human frontiers into space, we need to conserve the natural environment of our mother planet. In low-income countries, deterioration of local natural resources such as forests for firewood, inshore fishery for home and local consumption has been the most urgent environment issue. Various measures have been taken to stem excessive harvesting of local natural resources in the course of the population increase: e.g., community management. Little attention has been paid, however, to the seemingly most powerful lifesaver for the overuse of local natural resources: the market economy. Out-migration from the marginally productive rural areas along with the investments in urban areas would attain both the conservation of natural resources and improvements in human welfare. With 101 randomly-sampled natural forests in the Middle Hills of Nepal, we compare the impacts of community management and those of out-migration on forest conditions. Forest condition was evaluated by forest inventory conducted in 1997-1999 and 2014-2016.

©2019. Japan Geoscience Union. All Right Reserved.

Academic-public-private partnerships for sustainable herding under increasing frequency of climate hazards

*Masato Shinoda[1]

1. Graduate School of Environmental Studies Nagoya University

Socio-ecological damage from climate-related disasters has increased worldwide, including a slow-onset cold-season disaster that is unique to Mongolia, known as *dzud*. *Dzuds* are defined, bio-geophysically, as anomalous climatic and/or land-surface (i.e. snow) conditions that lead to reduced accessibility and/or availability of pastures, and ultimately to significant livestock mortality during winter–spring. Our studies showed that recent *dzuds* were caused by a half-to-half combination of multi-climate hazards and man-made vulnerability, including inadequate pasture management, poverty, and insufficient winter preparedness. With this background, for the first time, our academia produced a new *dzud* risk map to predict risky areas at the national level for the 2015/2016 winter. Subsequently, the early warning system developed together with the risk map has been implemented and successfully applied for sustainable herding under the framework of partnerships among universities/research institutes, Mongolian government, international aid organizations, and herders. This action was supported by the Grant-in-Aid for Scientific Research from the Japan Society for the Promotion of Science ‘Integrating Dryland Disaster Science’ and nominated as a top case study of early warning early action at the Asian Ministerial Conference on Disaster Risk Reduction in July 2018.

Keywords: Transdisciplinary approach, Disaster risk map, Climate disaster, Livestock mortality, Mongolia

©2019. Japan Geoscience Union. All Right Reserved.

Land use after death and funeral of citizen mainly based on public cemeteries in modern Beijing city

*Haruhiro Doi[1], Yanwei Chai[2], Peiwei Xu[3]

1. Faculty of Education, Oita University, 2. Peking University, 3. Beijing Normal University

After death, a person builds a graveyard by occupying a certain land, such as by relatives left behind. Therefore, in urban areas of China where economic growth and population growth continue, the demand for the land used for the deceased is large, so controlling the cemetery area as part of the management of land resources is an important policy task.
In modern Beijing City, large-scale public cemeteries have been developed throughout the city over the last few decades in order to cope with the increasing demand for land use after death. These public cemeteries are mainly located in rural areas that are relatively adjacent to built-up areas and suitable fountains on Feng shui in suburban areas (Doi and Chai, 2017).
The present report intends to examine the history of maintenance of these public cemeteries and its relations with neighboring rural communities and to consider the relationship between the funeral of the ethnic minorities other than the Han tribe in modern Beijing.

Keywords: Urban policy, suburban rural areas, ethnic group

©2019. Japan Geoscience Union. All Right Reserved.

Restoration and sustainable land management of degraded landscapes in Asia and Africa

*OKURO TOSHIYA[1]

1. Graduate School of Agricultural and Life Sciences, The University of Tokyo

Land degradation causes reduction or loss of the biological or economic productivity and complexity, resulting from land uses or from processes arising from human activities and habitation patterns. As land degradation is also defined as “the processes of landscape changes caused by miss-match between natural land conditions and land use by human”, it is necessary to reconstruct new land use systems based on new human-environment relations which can realize sustainable use of ecosystem services. This paper introduces case studies on the sustainable land management (SLM) approaches, focusing on human-environment relations, or social-ecological systems in rangelands of Asia and Africa. Firstly, I show a modelling of trade-offs in ecosystem services and assessment of effectiveness of countermeasures on land restoration. Secondly, I show a concept and methodology of grassland management systems in consideration of biodiversity-ecosystem functioning relationships. Finally I propose future perspectives, possible research topics which should be further developed, and implication to SDGs.

Keywords: social-ecological system, threshold, biodiversity, ecosystem functioning, sustainable land management, non-equilibrium

©2019. Japan Geoscience Union. All Right Reserved.

[J] Poster | S (Solid Earth Sciences)：S-GD Geodesy

Tue. May 28, 2019 10:45 AM - 12:15 PM JST | Tue. May 28, 2019 1:45 AM - 3:15 AM UTC | Poster Hall International Exhibition Hall8, Makuhari Messe_5

[S-GD01] Gravity and Geoid

convener:Tokuro Kodama(Geospatial Information Authority of Japan), Daisuke Oka(Geological Survey of Hokkaido, Environmental and Geological Research Department, Local Independent Administrative Agency, Hokkaido Research Organization)

Recent precise gravity measurements lead to advances in many kinds of applications, e.g., geophysical exploration of internal structure of the Earth and Moon, studies of earthquake, volcano, subsidence, landslide and tsunami, monitoring ice mass balance, and so on.
In this session, we call wide range of papers related to topics of gravity and geoid, including theory of gravity field, absolute/relative gravity measurements, data analysis of satellite gravity missions, and development of gravity sensors.

[SGD01-P01] An Improved GRACE time-varying gravity field model and its application in China and Antarctica

*Yunlong Wu[1], Yi Zhang[1], Zhengbo Zou[1], Minzhang Hu[1] (1.Institute of Seismology, China Earthquake Administration)

[SGD01-P02] Numerical modeling of crustal deformation and gravity change caused by glacier melting in Southeast Alaska

*Kazuhiro Naganawa[1], Takahito Kazama[1] (1.Graduate School of Science, Kyoto University)

[SGD01-P03] Gravity gradient variations considered to have occured 3 months before the Tohoku-Oki earthquake

*Naoki Hasumi[1], Kosuke Heki[1] (1.Hokkaido University Graduate School of Science)

[SGD01-P04] Density structure inferred from gravity and airborne gravity gradiometry data in the northwestern part of Kuju volcano, Oita prefecture

*Jun Nishijima[1], Yasuhiro Fujimitsu[1] (1.Department of Earth Resources Engineering, Graduate School of Engineering, Kyushu University)

[SGD01-P05] On the effect of higher-order terms in the gravity sensor of the superconducting gravimeter

*Yuichi Imanishi[1], Kazunari Nawa[2], Yoshiaki Tamura[3], Hiroshi Ikeda[4] (1.Earthquake Research Institute, The University of Tokyo, 2.AIST, 3.NAOJ, 4.University of Tsukuba)

[SGD01-P06] **Gravity Effect of Local Snow Accumulation obtained from Superconducting Gravimeter and UAV survey at Syowa Station**

*Akihisa Hattori[1], Yuichi Aoyama[1,2], Koichiro Doi[1,2], Hajime Oishi[3], Jun Nishijima[4], Hiroshi Ikeda[5] (1.SOKENDAI (The Graduate University of Advanced Studies), 2.National Institute of Polar Research, 3.NEC Networks & System Integration Corporation, 4.Kyushu University, 5.University of Tsukuba)

An Improved GRACE time-varying gravity field model and its application in China and Antarctica

*Yunlong Wu[1], Yi Zhang[1], Zhengbo Zou[1], Minzhang Hu[1]

1. Institute of Seismology, China Earthquake Administration

A cross correlation analysis is carried out on the time-varying gravity field models derived from GRACE observations and provided by CSR, GFZ, JPL and ITSG. This is used to propose an improved weight determination method for producing a combined time-varying gravity field model. Taking the Antarctic region as a test area, the reliability and accuracy of the combined model is verified by comparing the changes of Antarctic ice sheet mass inferred from it and the other gravity field solutions considered. The results show that the minimum difference in mass changes (expressed as equivalent water height) between the combined model and the ITSG inversion is concentrated between -0.2 cm to 0.4 cm. To further verify the new method, China’ s Three Gorges region, the North China Plain region, and the Tianshan region are assessed. The results indicate that the new combined time-varying gravity field model is consistent with those models published by CSR, GFZ and JPL, and conforms best to ITSG. The combined time-varying gravity field model proposed in this paper provides a reference for the application of such models and the optimization of time-varying gravity field for future gravity satellite missions.

Keywords: GRACE, Time-varying gravity field, Combined model, Forward modeling, Equivalent water height

©2019. Japan Geoscience Union. All Right Reserved.

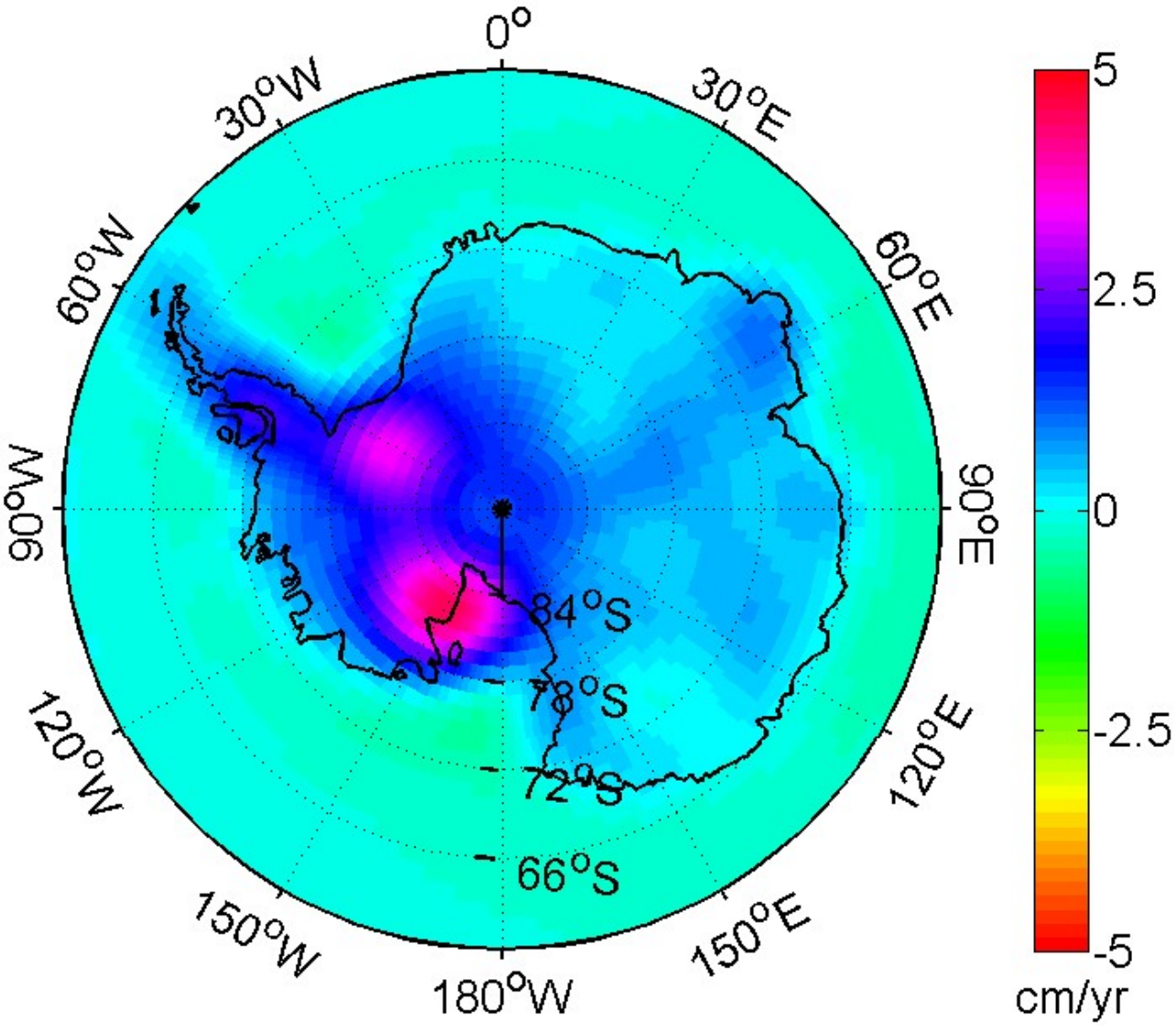

©2019. Japan Geoscience Union. All Right Reserved.

Numerical modeling of crustal deformation and gravity change caused by glacier melting in Southeast Alaska

*Kazuhiro Naganawa[1], Takahito Kazama[1]

1. Graduate School of Science, Kyoto University

Glacier melting caused by global warming is of great interest as a factor of sea level rise. Spatiotemporal variations in glacier melting have been monitored by geodetic observations such as altimetry, gravimetry and GNSS. However, since these observations contain various responses of solid earth, many devices are necessary in order to estimate glacier melting from observation data. As one of the devices, it is considered to construct numerical model of solid earth deformations caused by glacier melting. Because glacier melting involve variation of mass distribution in earth’ s surface and deformation of solid earth (GIA : Glacial Isostatic Adjustment), glacier melting cause various spatiotemporal deformations such as sea level change, crustal deformation, and gravity change. Therefore, in order to quantify the present spatiotemporal variations in glacier melting directly, it is necessary to improve numerical model regularly.

In Southeast Alaska that is the main area of this study, about 16 km^3/yr of glaciers melt at present (Larsen et al., 2007) and those melting speed may be accelerated these days (Arendt et al., 2002). GNSS stations has been installed in this area since the 2000s, and they observed large ground uplift of up to 3 cm/yr associated with GIA (Larsen et al., 2004). The spatial variation of the uplift was already modeled by Larsen et al. (2005) and Sato et al. (2012) numerically. On the other hand, absolute gravity values have been measured in this area sinse 2006, and absolute gravity changes of -4~-7 microGal/yr were detected (Sun et al., 2010). However, any previous studies have not considered the observed gravity changes in their numerical model, so the gravity variations are not reproduced quantitatively as of now.

Therefore, we numerically model spatiotemporal variations in crustal deformation and gravity change derived from GIA in Southeast Alaska as follows. Both of crustal deformation and gravity change are mainly composed of two effects: the elastic deformation due to the present glacier melting, and the viscoelastic deformation due to the past glacier melting. Gravity change is additionally caused by the time variation in the attraction effect due to the present glacier melting. We here estimate these effects expected at six absolute gravity points in Southeast Alaska, by numerically computing the spatiotemporal integral of the present-day ice melting model (Larsen et al., 2007) and the ice melting history model (e.g., ICE-6G; Peltier et al., 2015). We compare the estimated results with the data observed in Southeast Alaska until 2015, to discuss the present glacier melting in this area.

Keywords: glacier melting, glacial isostatic adjustment, Alaska, gravity change, crustal uplift

©2019. Japan Geoscience Union. All Right Reserved.

Gravity gradient variations considered to have occured 3 months before the Tohoku-Oki earthquake

*Naoki Hasumi[1], Kosuke Heki[1]

1. Hokkaido University Graduate School of Science

Since the launch in 2002, the Gravity Recovery And Climate Experiment (GRACE) satellite system has been measuring global gravity field of the Earth. It has produced various scientific results by measuring redistribution of land water storage and snow/ice as time-variable gravity. Fault dislocations associated with earthquakes also redistribute mass and cause subtle changes of gravity. GRACE has also enabled observations of coseismic and postseismic gravity changes of recent megathrust earthquakes, contributing to seismology (Tanaka & Heki, 2017). Preseismic gravity changes have not been considered a target of researches with GRACE. Recently, Panet et al. (2018) reported possible detection of significant change of gravity gradients around Japan a few months before the Mw9.0 2011 Tohoku-Oki earthquake. Their approach differs from conventional studies in several ways. First, they analyzed gravity gradients, which has better spatial resolution than gravity. Second, they searched for signals over wide range of temporal and spatial scales. Third, they concentrated on components with wavelengths of 800-1600 km. We tried to reproduce the results of Panet et al. (2018) by analyzing GRACE level-2 data (Stokes' coefficients) and examining gravity gradient changes a few months before the 2011 Tohoku-Oki earthquake. We could obtain preseismic gravity gradient changes fairly similar to Panet et al. (2018), although we still see certain differences due to unknown reasons. We will also report if we see similar gravity gradient changes before the other two M9 class earthquakes, 2004 Sumatra-Andaman and 2010 Maule earthquakes.

References

Panet, I., S. Bonvalot , C. Narteau , D. Remy, and J.-M. Lemoine (2018), Migrating pattern of deformation prior to the Tohoku-Oki earthquake revealed by GRACE data, *Nature Geosci., 11,* 367-373, Doi:10.1038/s41561-018-0099-3

Tanaka, Y.-S. and K. Heki (2017), GRACE seismology: Review and perspective of satellite gravimetry for earthquake sciences, Zisin2, 69, 69-85, doi:10.4294/zisin.69.69.

Keywords: GRACE, gravity gradient

©2019. Japan Geoscience Union. All Right Reserved.

Density structure inferred from gravity and airborne gravity gradiometry data in the northwestern part of Kuju volcano, Oita prefecture

*Jun Nishijima[1], Yasuhiro Fujimitsu[1]

1. Department of Earth Resources Engineering, Graduate School of Engineering, Kyushu University

There are many geothermal fields, hot springs and the geothermal power plants (Otake, Hatchobaru and Takigami) in the northwestern part of Kuju volcano, Oita prefecture. This area is included in the Hohi geothermal area. Many geothermal explorations have been conducted in this area since 1960. The gravity data which is measured by many institute, company and university was recorded in some gravity database. Moreover, an airborne gravity gradiometry (AGG) survey was conducted by the Japan Oil, Gas and Metals National Corporation (JOGMEC) in 2012 and 2017. The underground density structure is estimated by the gravity and AGG data inversion analysis using VOXI Earth modeling on Geosoft Oasis montaj. This result is integrated with the other geological, geophysical and geochemical data on the GIS software. Finally, the conceptual hydrothermal model is estimated by the integrated interpretation using GIS software.The high-density (2400 –2550 kg/m^3) areas were estimated below the middle and late Pleistocene volcanoes in the shouthern part of the study area at a depth of 0 to 2000 m below sea level. These high-density areas correspond to the distributions of the older Hohi volcanic rocks. Moreover, the depression structure was detected in the western side of Mt. Waita. Some hot springs (Yamakawa, Asozuru, Nuruyu and Tsuetate) are located on the edge of this structure.

Keywords: Gravity anomaly, Gravity gradient, Kuju volcano

©2019. Japan Geoscience Union. All Right Reserved.

On the effect of higher-order terms in the gravity sensor of the superconducting gravimeter

*Yuichi Imanishi[1], Kazunari Nawa[2], Yoshiaki Tamura[3], Hiroshi Ikeda[4]

1. Earthquake Research Institute, The University of Tokyo, 2. AIST, 3. NAOJ, 4. University of Tsukuba

The superconducting gravimeter CT #036 operated at the VERA Ishigakijima station, Okinawa, Japan, indicates several kinds of behaviors characteristic to this site. Imanishi et al. (2018), by developing a theoretical model for the static and dynamic properties of the gravity sensor, showed that the effect of the movements of a nearby VLBI antenna on the gravimeter is explained quantitatively by the coupling between the horizontal and vertical components in the gravity sensor. However, it remained unresolved whether the apparent gravity increase associated with enhanced ground noise, as typically seen when typhoons approach the Ishigakijima island, is explained by the same model, because the magnitude of the higher-order terms representing vertical nonlinearity were unknown. Here we will report our result on the measurements of the higher-order terms obtained by injecting artificial signals to CT #036, and discuss its impact on the dynamic properties of the gravity sensor.

Keywords: superconducting gravimeter, Ishigakijima, nonlinearity

©2019. Japan Geoscience Union. All Right Reserved.

Gravity Effect of Local Snow Accumulation obtained from Superconducting Gravimeter and UAV survey at Syowa Station

*Akihisa Hattori[1], Yuichi Aoyama[1,2], Koichiro Doi[1,2], Hajime Oishi[3], Jun Nishijima[4], Hiroshi Ikeda[5]

1. SOKENDAI (The Graduate University of Advanced Studies), 2. National Institute of Polar Research, 3. NEC Networks & System Integration Corporation, 4. Kyushu University, 5. University of Tsukuba

Continuous gravity observation has been conducted with a superconducting gravimeter (SG) at the Japanese Antarctic station, Syowa Station (69°0.2646' S, 39°34.9074' E) since 1993. The first SG, TT70#016, was replaced by the second SG, CT#043, in 2003, then CT#043 was replaced by the third OSG#058 in 2010, and OSG#058 is in operation. It is considered that the gravity observations with SGs, which have a high sensitivity, are detecting the gravitational signal of local snow accumulation in Syowa Station. It is necessary to correct the accumulated snow effect for monitoring the geophysically important but weak signals, such as one associated with Glacial Isostatic Adjustment (GIA).

The distribution of snow depth in Syowa Station was estimated from digital surface models (DSMs) made from unmanned aerial vehicle (UAV) photographic survey by applying structure from motion (SfM) processing methods to the aerial photographs. In the 59th Japanese Antarctic Research Expedition (JARE-59) activity (2017-2019), we conducted aerial photogrammetry by the fixed-wing drone "senseFly eBee Plus," which has dual-frequency GNSS receiver, over Syowa Station in January (austral summer season). Besides, we have conducted aerial photogrammetry by the rotary wing drone "DJI Inspire 2" and "DJI Phantom" in the same area, about every one month from May to November (austral winter season). The DSM and the orthomosaic photo were generated from each set of the geotagged photos using the SfM software "Pix4D."

For improving the accuracy of DSM, we used the geodetic triangulation survey points operated by GSI (Geospatial Information Authority of Japan) as GCP (ground control points) in SfM analysis. We also calibrated the height of DSM by using the ground area uncovered by snow characterized by Brown color as fixed height sites. Thereby, we obtained the time-series of snow depth distributions by calculating height differences among DSMs.

We calculated the attractive changes on OSG#058 estimated from the obtained snow depth distribution. Consequently, it was revealed that the local snow accumulation changes in the Syowa Station caused a seasonal gravity variation of at least 0.1-0.3 μGal (1 μGal = 10^{-8} m/s^2).

In this presentation, we show the details of observed changes in snow distribution, and discuss the comparison between the estimated gravity effect of local snow accumulation and the gravity change observed by OSG#058.

Keywords: Superconducting gravimeter, Unmanned aerial vehicle (UAV), Structure from Motion (SfM)

©2019. Japan Geoscience Union. All Right Reserved.

[J] Poster | S (Solid Earth Sciences)：S-GD Geodesy

Tue. May 28, 2019 5:15 PM - 6:30 PM JST | Tue. May 28, 2019 8:15 AM - 9:30 AM UTC | Poster Hall International Exhibition Hall8, Makuhari Messe_26

[S-GD01] Gravity and Geoid

convener:Tokuro Kodama(Geospatial Information Authority of Japan), Daisuke Oka(Geological Survey of Hokkaido, Environmental and Geological Research Department, Local Independent Administrative Agency, Hokkaido Research Organization)

Recent precise gravity measurements lead to advances in many kinds of applications, e.g., geophysical exploration of internal structure of the Earth and Moon, studies of earthquake, volcano, subsidence, landslide and tsunami, monitoring ice mass balance, and so on.
In this session, we call wide range of papers related to topics of gravity and geoid, including theory of gravity field, absolute/relative gravity measurements, data analysis of satellite gravity missions, and development of gravity sensors.

[SGD01-P01] An Improved GRACE time-varying gravity field model and its application in China and Antarctica

*Yunlong Wu[1], Yi Zhang[1], Zhengbo Zou[1], Minzhang Hu[1] (1.Institute of Seismology, China Earthquake Administration)

[SGD01-P02] Numerical modeling of crustal deformation and gravity change caused by glacier melting in Southeast Alaska

*Kazuhiro Naganawa[1], Takahito Kazama[1] (1.Graduate School of Science, Kyoto University)

[SGD01-P03] Gravity gradient variations considered to have occured 3 months before the Tohoku-Oki earthquake

*Naoki Hasumi[1], Kosuke Heki[1] (1.Hokkaido University Graduate School of Science)

[SGD01-P04] Density structure inferred from gravity and airborne gravity gradiometry data in the northwestern part of Kuju volcano, Oita prefecture

*Jun Nishijima[1], Yasuhiro Fujimitsu[1] (1.Department of Earth Resources Engineering, Graduate School of Engineering, Kyushu University)

[SGD01-P05] On the effect of higher-order terms in the gravity sensor of the superconducting gravimeter

*Yuichi Imanishi[1], Kazunari Nawa[2], Yoshiaki Tamura[3], Hiroshi Ikeda[4] (1.Earthquake Research Institute, The University of Tokyo, 2.AIST, 3.NAOJ, 4.University of Tsukuba)

[SGD01-P06] **Gravity Effect of Local Snow Accumulation obtained from Superconducting Gravimeter and UAV survey at Syowa Station**

*Akihisa Hattori[1], Yuichi Aoyama[1,2], Koichiro Doi[1,2], Hajime Oishi[3], Jun Nishijima[4], Hiroshi Ikeda[5] (1.SOKENDAI (The Graduate University of Advanced Studies), 2.National Institute of Polar Research, 3.NEC Networks & System Integration Corporation, 4.Kyushu University, 5.University of Tsukuba)

An Improved GRACE time-varying gravity field model and its application in China and Antarctica

*Yunlong Wu[1], Yi Zhang[1], Zhengbo Zou[1], Minzhang Hu[1]

1. Institute of Seismology, China Earthquake Administration

A cross correlation analysis is carried out on the time-varying gravity field models derived from GRACE observations and provided by CSR, GFZ, JPL and ITSG. This is used to propose an improved weight determination method for producing a combined time-varying gravity field model. Taking the Antarctic region as a test area, the reliability and accuracy of the combined model is verified by comparing the changes of Antarctic ice sheet mass inferred from it and the other gravity field solutions considered. The results show that the minimum difference in mass changes (expressed as equivalent water height) between the combined model and the ITSG inversion is concentrated between -0.2 cm to 0.4 cm. To further verify the new method, China’ s Three Gorges region, the North China Plain region, and the Tianshan region are assessed. The results indicate that the new combined time-varying gravity field model is consistent with those models published by CSR, GFZ and JPL, and conforms best to ITSG. The combined time-varying gravity field model proposed in this paper provides a reference for the application of such models and the optimization of time-varying gravity field for future gravity satellite missions.

Keywords: GRACE, Time-varying gravity field, Combined model, Forward modeling, Equivalent water height

©2019. Japan Geoscience Union. All Right Reserved.

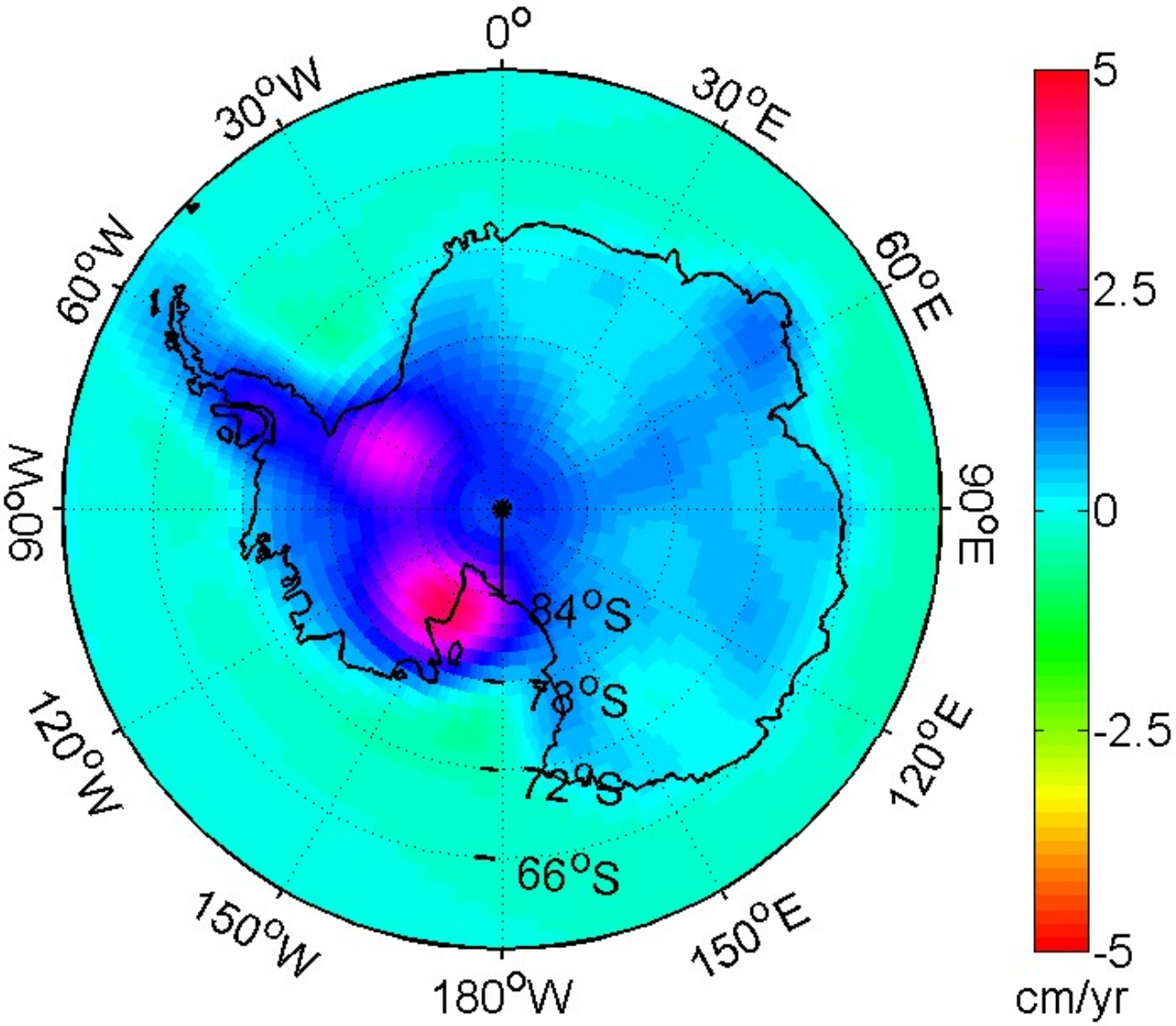

©2019. Japan Geoscience Union. All Right Reserved.

Numerical modeling of crustal deformation and gravity change caused by glacier melting in Southeast Alaska

*Kazuhiro Naganawa[1], Takahito Kazama[1]

1. Graduate School of Science, Kyoto University

Glacier melting caused by global warming is of great interest as a factor of sea level rise. Spatiotemporal variations in glacier melting have been monitored by geodetic observations such as altimetry, gravimetry and GNSS. However, since these observations contain various responses of solid earth, many devices are necessary in order to estimate glacier melting from observation data. As one of the devices, it is considered to construct numerical model of solid earth deformations caused by glacier melting. Because glacier melting involve variation of mass distribution in earth’ s surface and deformation of solid earth (GIA : Glacial Isostatic Adjustment), glacier melting cause various spatiotemporal deformations such as sea level change, crustal deformation, and gravity change. Therefore, in order to quantify the present spatiotemporal variations in glacier melting directly, it is necessary to improve numerical model regularly.

In Southeast Alaska that is the main area of this study, about 16 km^3/yr of glaciers melt at present (Larsen et al., 2007) and those melting speed may be accelerated these days (Arendt et al., 2002). GNSS stations has been installed in this area since the 2000s, and they observed large ground uplift of up to 3 cm/yr associated with GIA (Larsen et al., 2004). The spatial variation of the uplift was already modeled by Larsen et al. (2005) and Sato et al. (2012) numerically. On the other hand, absolute gravity values have been measured in this area sinse 2006, and absolute gravity changes of -4~-7 microGal/yr were detected (Sun et al., 2010). However, any previous studies have not considered the observed gravity changes in their numerical model, so the gravity variations are not reproduced quantitatively as of now.

Therefore, we numerically model spatiotemporal variations in crustal deformation and gravity change derived from GIA in Southeast Alaska as follows. Both of crustal deformation and gravity change are mainly composed of two effects: the elastic deformation due to the present glacier melting, and the viscoelastic deformation due to the past glacier melting. Gravity change is additionally caused by the time variation in the attraction effect due to the present glacier melting. We here estimate these effects expected at six absolute gravity points in Southeast Alaska, by numerically computing the spatiotemporal integral of the present-day ice melting model (Larsen et al., 2007) and the ice melting history model (e.g., ICE-6G; Peltier et al., 2015). We compare the estimated results with the data observed in Southeast Alaska until 2015, to discuss the present glacier melting in this area.

Keywords: glacier melting, glacial isostatic adjustment, Alaska, gravity change, crustal uplift

©2019. Japan Geoscience Union. All Right Reserved.

Gravity gradient variations considered to have occured 3 months before the Tohoku-Oki earthquake

*Naoki Hasumi[1], Kosuke Heki[1]

1. Hokkaido University Graduate School of Science

Since the launch in 2002, the Gravity Recovery And Climate Experiment (GRACE) satellite system has been measuring global gravity field of the Earth. It has produced various scientific results by measuring redistribution of land water storage and snow/ice as time-variable gravity. Fault dislocations associated with earthquakes also redistribute mass and cause subtle changes of gravity. GRACE has also enabled observations of coseismic and postseismic gravity changes of recent megathrust earthquakes, contributing to seismology (Tanaka & Heki, 2017). Preseismic gravity changes have not been considered a target of researches with GRACE. Recently, Panet et al. (2018) reported possible detection of significant change of gravity gradients around Japan a few months before the Mw9.0 2011 Tohoku-Oki earthquake. Their approach differs from conventional studies in several ways. First, they analyzed gravity gradients, which has better spatial resolution than gravity. Second, they searched for signals over wide range of temporal and spatial scales. Third, they concentrated on components with wavelengths of 800-1600 km. We tried to reproduce the results of Panet et al. (2018) by analyzing GRACE level-2 data (Stokes' coefficients) and examining gravity gradient changes a few months before the 2011 Tohoku-Oki earthquake. We could obtain preseismic gravity gradient changes fairly similar to Panet et al. (2018), although we still see certain differences due to unknown reasons. We will also report if we see similar gravity gradient changes before the other two M9 class earthquakes, 2004 Sumatra-Andaman and 2010 Maule earthquakes.

References

Panet, I., S. Bonvalot , C. Narteau , D. Remy, and J.-M. Lemoine (2018), Migrating pattern of deformation prior to the Tohoku-Oki earthquake revealed by GRACE data, *Nature Geosci., 11,* 367-373, Doi:10.1038/s41561-018-0099-3

Tanaka, Y.-S. and K. Heki (2017), GRACE seismology: Review and perspective of satellite gravimetry for earthquake sciences, Zisin2, 69, 69-85, doi:10.4294/zisin.69.69.

Keywords: GRACE, gravity gradient

©2019. Japan Geoscience Union. All Right Reserved.

Density structure inferred from gravity and airborne gravity gradiometry data in the northwestern part of Kuju volcano, Oita prefecture

*Jun Nishijima[1], Yasuhiro Fujimitsu[1]

1. Department of Earth Resources Engineering, Graduate School of Engineering, Kyushu University

There are many geothermal fields, hot springs and the geothermal power plants (Otake, Hatchobaru and Takigami) in the northwestern part of Kuju volcano, Oita prefecture. This area is included in the Hohi geothermal area. Many geothermal explorations have been conducted in this area since 1960. The gravity data which is measured by many institute, company and university was recorded in some gravity database. Moreover, an airborne gravity gradiometry (AGG) survey was conducted by the Japan Oil, Gas and Metals National Corporation (JOGMEC) in 2012 and 2017. The underground density structure is estimated by the gravity and AGG data inversion analysis using VOXI Earth modeling on Geosoft Oasis montaj. This result is integrated with the other geological, geophysical and geochemical data on the GIS software. Finally, the conceptual hydrothermal model is estimated by the integrated interpretation using GIS software.The high-density (2400 –2550 kg/m^3) areas were estimated below the middle and late Pleistocene volcanoes in the shouthern part of the study area at a depth of 0 to 2000 m below sea level. These high-density areas correspond to the distributions of the older Hohi volcanic rocks. Moreover, the depression structure was detected in the western side of Mt. Waita. Some hot springs (Yamakawa, Asozuru, Nuruyu and Tsuetate) are located on the edge of this structure.

Keywords: Gravity anomaly, Gravity gradient, Kuju volcano

©2019. Japan Geoscience Union. All Right Reserved.

On the effect of higher-order terms in the gravity sensor of the superconducting gravimeter

*Yuichi Imanishi[1], Kazunari Nawa[2], Yoshiaki Tamura[3], Hiroshi Ikeda[4]

1. Earthquake Research Institute, The University of Tokyo, 2. AIST, 3. NAOJ, 4. University of Tsukuba

The superconducting gravimeter CT #036 operated at the VERA Ishigakijima station, Okinawa, Japan, indicates several kinds of behaviors characteristic to this site. Imanishi et al. (2018), by developing a theoretical model for the static and dynamic properties of the gravity sensor, showed that the effect of the movements of a nearby VLBI antenna on the gravimeter is explained quantitatively by the coupling between the horizontal and vertical components in the gravity sensor. However, it remained unresolved whether the apparent gravity increase associated with enhanced ground noise, as typically seen when typhoons approach the Ishigakijima island, is explained by the same model, because the magnitude of the higher-order terms representing vertical nonlinearity were unknown. Here we will report our result on the measurements of the higher-order terms obtained by injecting artificial signals to CT #036, and discuss its impact on the dynamic properties of the gravity sensor.

Keywords: superconducting gravimeter, Ishigakijima, nonlinearity

©2019. Japan Geoscience Union. All Right Reserved.

Gravity Effect of Local Snow Accumulation obtained from Superconducting Gravimeter and UAV survey at Syowa Station

*Akihisa Hattori[1], Yuichi Aoyama[1,2], Koichiro Doi[1,2], Hajime Oishi[3], Jun Nishijima[4], Hiroshi Ikeda[5]

1. SOKENDAI (The Graduate University of Advanced Studies), 2. National Institute of Polar Research, 3. NEC Networks & System Integration Corporation, 4. Kyushu University, 5. University of Tsukuba

Continuous gravity observation has been conducted with a superconducting gravimeter (SG) at the Japanese Antarctic station, Syowa Station (69°0.2646' S, 39°34.9074' E) since 1993. The first SG, TT70#016, was replaced by the second SG, CT#043, in 2003, then CT#043 was replaced by the third OSG#058 in 2010, and OSG#058 is in operation. It is considered that the gravity observations with SGs, which have a high sensitivity, are detecting the gravitational signal of local snow accumulation in Syowa Station. It is necessary to correct the accumulated snow effect for monitoring the geophysically important but weak signals, such as one associated with Glacial Isostatic Adjustment (GIA).

The distribution of snow depth in Syowa Station was estimated from digital surface models (DSMs) made from unmanned aerial vehicle (UAV) photographic survey by applying structure from motion (SfM) processing methods to the aerial photographs. In the 59th Japanese Antarctic Research Expedition (JARE-59) activity (2017-2019), we conducted aerial photogrammetry by the fixed-wing drone "senseFly eBee Plus," which has dual-frequency GNSS receiver, over Syowa Station in January (austral summer season). Besides, we have conducted aerial photogrammetry by the rotary wing drone "DJI Inspire 2" and "DJI Phantom" in the same area, about every one month from May to November (austral winter season). The DSM and the orthomosaic photo were generated from each set of the geotagged photos using the SfM software "Pix4D."

For improving the accuracy of DSM, we used the geodetic triangulation survey points operated by GSI (Geospatial Information Authority of Japan) as GCP (ground control points) in SfM analysis. We also calibrated the height of DSM by using the ground area uncovered by snow characterized by Brown color as fixed height sites. Thereby, we obtained the time-series of snow depth distributions by calculating height differences among DSMs.

We calculated the attractive changes on OSG#058 estimated from the obtained snow depth distribution. Consequently, it was revealed that the local snow accumulation changes in the Syowa Station caused a seasonal gravity variation of at least 0.1-0.3 μGal (1 μGal = 10^{-8} m/s^2).

In this presentation, we show the details of observed changes in snow distribution, and discuss the comparison between the estimated gravity effect of local snow accumulation and the gravity change observed by OSG#058.

Keywords: Superconducting gravimeter, Unmanned aerial vehicle (UAV), Structure from Motion (SfM)

©2019. Japan Geoscience Union. All Right Reserved.

[J] Oral | S (Solid Earth Sciences)：S-GD Geodesy

Tue. May 28, 2019 1:45 PM - 3:15 PM JST | Tue. May 28, 2019 4:45 AM - 6:15 AM UTC | 303 3F

[S-GD01] Gravity and Geoid

convener:Tokuro Kodama(Geospatial Information Authority of Japan), Daisuke Oka(Geological Survey of Hokkaido, Environmental and Geological Research Department, Local Independent Administrative Agency, Hokkaido Research Organization), Chairperson:Toshiyuki Tanaka, Takahito Kazama

Recent precise gravity measurements lead to advances in many kinds of applications, e.g., geophysical exploration of internal structure of the Earth and Moon, studies of earthquake, volcano, subsidence, landslide and tsunami, monitoring ice mass balance, and so on.
In this session, we call wide range of papers related to topics of gravity and geoid, including theory of gravity field, absolute/relative gravity measurements, data analysis of satellite gravity missions, and development of gravity sensors.

1:45 PM - 2:00 PM JST | 4:45 AM - 5:00 AM UTC

[SGD01-01] Seasonal variation of gravity values at the Ishioka Geodetic Observing Station

*Akira Tomiyama[1], Tokuro Kodama[1], Shuichi Oomori[1], Yoshifumi Hiraoka[1], Toshihiro Yahagi[1] (1.GSI of Japan)

2:00 PM - 2:15 PM JST | 5:00 AM - 5:15 AM UTC

[SGD01-02] Installation of the First Gravity Station in the Mount Fuji Research Institute, and the Phase-Free gravity measurement

*Ryo Honda[1], Yuichi Imanishi[2], Kazunari Nawa[3], Toshiyuki Tanaka[4], Tokuro Kodama[5], Akira Tomiyama[5] (1.MFRI, Yamanashi Prefectural Government, 2.ERI, University of Tokyo, 3.GSJ, AIST, 4.TRIES, ADEP, 5.GSI)

2:15 PM - 2:30 PM JST | 5:15 AM - 5:30 AM UTC

[SGD01-03] Absolute gravity and GNSS measurements on bedrock outcrops in Dronning Maud Land, East Antarctica

*Takahito Kazama[1], Yuichi Aoyama[2], Yoichi Fukuda[1], Koichiro Doi[2] (1.Graduate School of Science, Kyoto University, 2.National Institute of Polar Research)

2:30 PM - 2:45 PM JST | 5:30 AM - 5:45 AM UTC

[SGD01-04] **Capability of ICA Method for separating GIA and Ice Mass Signals in Antarctica**

*SHI TIANYAN[1], Yoichi Fukuda[1] (1.Graduate School of Science, Kyoto University)

2:45 PM - 3:00 PM JST | 5:45 AM - 6:00 AM UTC

[SGD01-05] Preliminary result of continuous observation with an iGrav superconducting gravimeter at the Teshikaga observatory, eastern Hokkaido, Japan

*Kazunari Nawa[1], Hiroaki Takahashi[2], Mako Ohzono[2], Kazumi Okada[2], Teruhiro Yamaguchi[2], Daisuke Oka[3], Noritoshi Okazaki[3], Ryo Honda[4], Hiroshi Ikeda[5] (1.National Institute of Advanced Industrial Science and Technology, 2.Hokkaido University, 3.Geological Survey of Hokkaido, 4.Mount Fuji Research Institute, 5.University of Tsukuba)

3:00 PM - 3:15 PM JST | 6:00 AM - 6:15 AM UTC

[SGD01-06] On the anomalous temporal gravity change between VERA and F-net stations at Ishigakijima, Japan

*Kazunari Nawa[1], Yuichi Imanishi[2], Yoshiaki Tamura[3], Hiroshi Ikeda[4], Takeshi Kimura[5] (1.National Institute of Advanced Industrial Science and Technology, 2.Earthquake Research Institute, The University of Tokyo, 3.National Astronomical Observatory of Japan, 4.University of Tsukuba, 5.National Research Institute for Earth Science and Disaster Resilience)

Seasonal variation of gravity values at the Ishioka Geodetic Observing Station

*Akira Tomiyama[1], Tokuro Kodama[1], Shuichi Oomori[1], Yoshifumi Hiraoka[1], Toshihiro Yahagi[1]

1. GSI of Japan

Conventionally consistency between absolute gravimeters has been confirmed through the International Comparison of Absolute Gravimeters (ICAG) which is offered by the Comité International des Poids et Mesures (CIPM) with supports of the International Association of Geodesy (IAG). In order to extent the consistency to inside Japan, the Domestic Comparison of Absolute Gravimeters (DCAG) has been conducted by the Geospatial Information Authority of Japan (GSI) since 2002. Thanks to the opening of a new facility of GSI, named the Ishioka Geodetic Observing Station, the DCAG has been held there with inviting several domestic organizations which own absolute gravimeters. In order to evaluate validity of obtained data, it is necessary to collect data inside the Ishioka station and to examine influences of external factors. Therefore, we carried out periodic measurements using one of our FG5 absolute gravimeters for about one week every month throughout one year at the fundamental gravity point, “Ishioka FGS”, which is installed inside the Ishioka station. In this presentation, we will report the seasonal variation of gravity values obtained from our verification work.

Keywords: Absolute gravimeter, Seasonal variation

©2019. Japan Geoscience Union. All Right Reserved.

Installation of the First Gravity Station in the Mount Fuji Research Institute, and the Phase-Free gravity measurement

*Ryo Honda[1], Yuichi Imanishi[2], Kazunari Nawa[3], Toshiyuki Tanaka[4], Tokuro Kodama[5], Akira Tomiyama[5]

1. MFRI, Yamanashi Prefectural Government, 2. ERI, University of Tokyo, 3. GSJ, AIST, 4. TRIES, ADEP, 5. GSI

Mount Fuji is an active volcano, the difficult situation is that we can’ t tell where the vent will open. Moreover, the eruption is thought to occur rapidly after the precursors such as grand deformations or increase of the seismic activities, because of its low viscosity magma. As a part of the volcano monitoring system, we are now constructing the gravity monitoring network. We are planning to install multiple continuous gravity monitoring stations. We installed the First Gravity Station in Mount Fuji Research Institute (MFRI) last year, where the absolute gravity value is measured by GSI. We are going to start the continuous observation in this station. Although low frequency events or tremors are observed sporadically, Mount Fuji is quiet at this point of time. So, the purpose of our observation at the beginning is to comprehend the precipitation and ground water effect, including snow melting effect in the spring time.

There is another interesting point for the gravity observation in Mount Fuji. The gravity difference between MFRI and the fifth station of the Yoshida trail is about 320 mGal, and the travel time between two points is about 30 minutes. It means that this is a good observation line for the verification of the gravimeters. Now we suggest the "phase-free" gravity measurement (https://phasefree.org/). The idea of "phase-free" is to eliminate the social phases (time, state) of normal times and disasters, so that goods or services normally used can be appropriately used at the time of disaster. If we continuously use the gravity observation line for the verification by various gravimeters in the normal time, that will be the important data for the volcano monitoring when the Mount Fuji is starting to prepare the eruption.

Keywords: Gravity, Mount Fuji, Volcano Monitoring, Verification of Gravimeter, Phase-Free

©2019. Japan Geoscience Union. All Right Reserved.

Absolute gravity and GNSS measurements on bedrock outcrops in Dronning Maud Land, East Antarctica

*Takahito Kazama[1], Yuichi Aoyama[2], Yoichi Fukuda[1], Koichiro Doi[2]

1. Graduate School of Science, Kyoto University, 2. National Institute of Polar Research

The Antarctic ice sheet plays a significant role in the long-term global climate change, so the spatiotemporal variations in the Antarctic ice sheet should be precisely monitored to forecast future climate changes. The ice sheet variations can be detected as loading deformations of the solid Earth, which are composed of the elastic deformation due to the present-day ice melting and the viscoelastic deformation due to the past ice melting. These effects can be separated by measuring both of the crustal deformation and land gravity variation, but enough gravity data has not been collected in the Antarctic region as of now. In order to understand more about the ice sheet variations in terms of solid-earth geophysics, land gravity data should be repeatedly measured at more sites in the Antarctic region.
We therefore collected new absolute gravity data using the FG5-210 absolute gravimeter at two stations located on bedrock outcrops in Dronning Maud Land, East Antarctica in November-December 2018. We first stayed at the Norwegian station, Troll (72.01S, 2.53E) from November 13 to 26, and installed the gravimeter on the benchmark (Troll AA) of the gravity hut. We needed to take more time to vacuum the dropping chamber of the gravimeter during the installation, because vacuuming pumps did not work normally, mainly associated with the cold weather in Troll Station. We started to measure absolute gravity values on November 18, and obtained the average gravity value of 982,360,741.41 +/- 1.16 +/- 1.82 microGal from the 178 sets of the gravity data collected for 5 days. We also stayed at the Indian station, Maitri (70.77S, 11.73E) from November 26 to December 4, and started to measure gravity values on the benchmark (Maitri AB) of the gravity hut on November 28. We obtained the 112 sets of the gravity data for 4 days, and determined the average gravity value of 982,576,883.10 +/- 1.23 +/- 1.83 microGal.
Our absolute gravity values collected in November-December 2018 was found to be smaller than those obtained in January-February 2012 (Dr. Jaakko Mäkinen, personal communication) by -4.4 and -4.2 microGal at Troll and Maitri stations, respectively. The gravity decrease may be caused by ground subsidence and/or ice mass decrease around the stations. The cause of the gravity decrease will be investigated in detail by analyzing the GNSS data which was collected simultaneously with the absolute gravity data at two stations.

Keywords: Antarctic ice sheet, absolute gravity, relative gravity, GNSS, Troll Station, Maitri Station

©2019. Japan Geoscience Union. All Right Reserved.

Capability of ICA Method for separating GIA and Ice Mass Signals in Antarctica

*SHI TIANYAN[1], Yoichi Fukuda[1]

1. Graduate School of Science, Kyoto University

The Gravity Recovery and Climate Experiment (GRACE) mission provided global gravity change data with a spatial resolution of a few hundred kilometers and a temporal resolution of 30 days. The GRACE data revealed the total mass changes in Antarctica and contributed to Antarctic Ice Sheet (AIS) mass balance researches. However, there are large uncertainties in Glacial Isostatic Adjustment (GIA) effects, which should be removed from the GRACE data, for estimating the AIS mass balance. While many studies have been conducted for estimating or removing the GIA effects thus far, we try to use a statistical analysis method called Independent Component Analysis (ICA) and investigated its capability of separating GIA and AIS mass signals.

We primarily employed GRACE RL05 mascon data provided by NASA Jet Propulsion Laboratory (JPL) of all the GRACE available period from January 2002 to June 2017 with the spatial coverage of all Antarctica. And we used three ICA methods, namely, spatial ICA (sICA), temporal ICA (tICA), and spatio-temporal ICA (stICA), for testing the characteristics and/or the capabilities of the methods.

The results showed that the GIA like signal can be recovered successfully with sICA which separated GIA signals and AIS mass change signals into two statistical independent components. On the other hand, tICA decomposed the GIA signal into two independent components. This suggested that tICA could not solve the signals mixing problem completely. Nevertheless, tICA detected an extra anomaly snow-fall signal around 2010. This shows that tICA may have the potential to separate long-term trend signals with different time scales. The results of stICA suggested that its characteristics could be seen as a combination of the above two methods. Thus, an appropriate combination of the methods should be examined.

We also tested other datasets and revealed the different datasets and/or pre-processing of the datasets largely affected the obtained results. It is impossible to assess the validity of the results only using the GRACE data. Therefore, additional information should be necessary to validate and interpret the results.

Keywords: GRACE, GIA, ICA

©2019. Japan Geoscience Union. All Right Reserved.

Preliminary result of continuous observation with an iGrav superconducting gravimeter at the Teshikaga observatory, eastern Hokkaido, Japan

*Kazunari Nawa[1], Hiroaki Takahashi[2], Mako Ohzono[2], Kazumi Okada[2], Teruhiro Yamaguchi[2], Daisuke Oka[3], Noritoshi Okazaki[3], Ryo Honda[4], Hiroshi Ikeda[5]

1. National Institute of Advanced Industrial Science and Technology, 2. Hokkaido University, 3. Geological Survey of Hokkaido, 4. Mount Fuji Research Institute, 5. University of Tsukuba

In November, 2018, continuous observation with the iGrav type superconducting gravimeter (# 017) was started at the Teshikaga Observatory of the Hokkaido University in order to carry out high spatiotemporal resolution gravity monitoring in the caldera / volcanic area in eastern Hokkaido. The gravity meter used in CCS project of Tomakomai site was temporarily relocated to the Minami-shinkawa Observatory in September of the same year and then moved to the Teshikaga Observatory from Minami-shinkawa at the timing before entering the snowy season . We report what kind of record is obtained by the superconducting gravimeter at each observatory in wide frequency band from the seismic to the geodetic band. The observation data will be registered in the Crustal Deformation Database of Hokkaido University for the purpose of archive, distribution and comparative analysis with other principle data.

©2019. Japan Geoscience Union. All Right Reserved.

On the anomalous temporal gravity change between VERA and F-net stations at Ishigakijima, Japan

*Kazunari Nawa[1], Yuichi Imanishi[2], Yoshiaki Tamura[3], Hiroshi Ikeda[4], Takeshi Kimura[5]

1. National Institute of Advanced Industrial Science and Technology, 2. Earthquake Research Institute, The University of Tokyo, 3. National Astronomical Observatory of Japan, 4. University of Tsukuba, 5. National Research Institute for Earth Science and Disaster Resilience

Continuous gravity and hydrological observations at Ishigakijima revealed that the gravity difference between the F-net station (gPhone) and the VERA station (superconducting gravimeter) is closely related with the change in the soil water content near the F-net station. It was also noted, however, that the gravity difference did not indicate significant changes on some occasions of heavy rainfall. In addition, our precipitation response model did not predict the observed gravity change well for a particular period expanding a few tens of days. Here we reexamine our data of precipitation, soil moisture, and underground water level as well as gravity, to refine our model of the hydrological effects on gravity at Ishigakijima.

©2019. Japan Geoscience Union. All Right Reserved.

[J] Oral | S (Solid Earth Sciences)：S-GD Geodesy

Tue. May 28, 2019 3:30 PM - 5:00 PM JST | Tue. May 28, 2019 6:30 AM - 8:00 AM UTC | 303 3F

[S-GD01] Gravity and Geoid

convener:Tokuro Kodama(Geospatial Information Authority of Japan), Daisuke Oka(Geological Survey of Hokkaido, Environmental and Geological Research Department, Local Independent Administrative Agency, Hokkaido Research Organization), Chairperson:Kazunari Nawa, Ryo Honda(山梨県富士山科学研究所)

Recent precise gravity measurements lead to advances in many kinds of applications, e.g., geophysical exploration of internal structure of the Earth and Moon, studies of earthquake, volcano, subsidence, landslide and tsunami, monitoring ice mass balance, and so on.
In this session, we call wide range of papers related to topics of gravity and geoid, including theory of gravity field, absolute/relative gravity measurements, data analysis of satellite gravity missions, and development of gravity sensors.

3:30 PM - 3:45 PM JST | 6:30 AM - 6:45 AM UTC

[SGD01-07] **Absolute gravity signals at the Sakurajima volcano since 2009 through 2018**

*Shuhei Okubo[1], Keigo Yamamoto[2], Masato Iguchi[2], Yoshiyuki Tanaka[3], Yuichi Imanishi[1], Ryuichi Nishiyama[1], Miwako Ando[1], Atsushi Watanabe[1] (1.Earthquake Research Institute, The University of Tokyo, 2.Disaster Prevention Research Institute, Kyoto University, 3.Graduate School of Science, The University of Tokyo)

3:45 PM - 4:00 PM JST | 6:45 AM - 7:00 AM UTC

[SGD01-08] Detection of Earthquake-induced Prompt Gravity Signals in Multi-channel Data

*Masaya Kimura[1], Nobuki Kame[1], Shingo Watada[1], Makiko Ohtani[2], Akito Araya[1], Yuichi Imanishi[1], Masaki Ando[3], Takashi Kunugi[4] (1.Earthquake Research Institute,The University of Tokyo, 2.National Institute of Advanced Industrial Science and Technology, 3.Department of Physics, The University of Tokyo, 4.National Research Institute for Earth Science and Disaster Resilience)

4:00 PM - 4:15 PM JST | 7:00 AM - 7:15 AM UTC

[SGD01-09] Evaluation of atmospheric attraction effect using local-scale objective analysis (LANAL)

*Toshiyuki Tanaka[1] (1.Tono Research Institute of Earthquake Science, Association for the Development of Earthquake Prediction)

4:15 PM - 4:30 PM JST | 7:15 AM - 7:30 AM UTC

[SGD01-10] Airborne gravity survey for establishment of a new precise gravimetric geoid model

*Tokuro Kodama[1], Akira Tomiyama[1], Shuichi Oomori[1], Erika Wada[1], Toshihiro Yahagi[1], Yoshifumi Hiraoka[1], Hiroshi Kawawa[1] (1.GSI of Japan)

4:30 PM - 4:45 PM JST | 7:30 AM - 7:45 AM UTC

[SGD01-11] Gravimetric geoid modeling using airborne gravity data : a case study in Colorado, U.S.A.

*Koji Matsuo[1], Rene Forsberg[2] (1.GSI of Japan, 2.Denmark Technical University)

4:45 PM - 5:00 PM JST | 7:45 AM - 8:00 AM UTC

Discussion

Absolute gravity signals at the Sakurajima volcano since 2009 through 2018

*Shuhei Okubo[1], Keigo Yamamoto[2], Masato Iguchi[2], Yoshiyuki Tanaka[3], Yuichi Imanishi[1], Ryuichi Nishiyama[1], Miwako Ando[1], Atsushi Watanabe[1]

1. Earthquake Research Institute, The University of Tokyo, 2. Disaster Prevention Research Institute, Kyoto University, 3. Graduate School of Science, The University of Tokyo

In this paper, we present gravity signals based on continuous absolute gravity measurements since 2009 through 2018. During this period, several hundreds to a thousand eruptions/explosions were observed every year during 2009 through 2015 (phase 1). Significant seismicity and crustal deformations were observed on Aug. 15, 2015 (phase 2), followed by unusual quiescence since August 2015 (phase 3). Gravity signal after eliminating groundwater disturbance showed remarkable features according to the phase of volcanic activity as described below. During the phase 1 characterized by frequent vulcanian eruptions from the Showa crater, gravity fluctuated about a mean with rather small amplitude of 10 microgals, suggesting dynamic equilibrium is achieved at the magma chamber; magma supply from deeper interior is balanced with mass loss through eruptions. The phase 2 is interpreted as a dyke intrusion event, which causes elastic deformation and short-term gravity change almost simultaneously. In the current phase 3 (2016-2018), gravity shows monotonous increase of 10 microgal/yr, suggesting deflation of magma.

Keywords: Absolute Gravity, Sakurajima

©2019. Japan Geoscience Union. All Right Reserved.

Detection of Earthquake-induced Prompt Gravity Signals in Multi-channel Data

*Masaya Kimura[1], Nobuki Kame[1], Shingo Watada[1], Makiko Ohtani[2], Akito Araya[1], Yuichi Imanishi[1], Masaki Ando[3], Takashi Kunugi[4]

1. Earthquake Research Institute,The University of Tokyo, 2. National Institute of Advanced Industrial Science and Technology, 3. Department of Physics, The University of Tokyo, 4. National Research Institute for Earth Science and Disaster Resilience

Seismic waves radiating from an earthquake rupture induce density perturbations of the medium, which in turn generate widespread transient gravity perturbations before the arrival of P-waves. Recently, signal detections of such prompt gravity perturbations from the 2011 Tohoku-Oki earthquake were reported. However, the data used for the detections were only a small subset of the available data, and the statistical significance of the signals were not sufficient nor discussed. In this study, we optimized multi-channel data recorded by several instruments and searched for the signals from the 2011 event. Though the single-trace records did not show any signal, the stacked trace of the broadband seismometer array data in Japan showed a signal clearly standing above the noise level, and this detection was confirmed with a sufficient statistical significance. This result provides the first constraint on the amplitude of prompt gravity signals by observation and will work as a reference for future detections.

Keywords: earthquake-induced gravity perturbation, transient deformation, time variable gravity, 2011 Tohoku-Oki earthquake

©2019. Japan Geoscience Union. All Right Reserved.

Evaluation of atmospheric attraction effect using local-scale objective analysis (LANAL)

*Toshiyuki Tanaka[1]

1. Tono Research Institute of Earthquake Science, Association for the Development of Earthquake Prediction

Tono Research Institute of Earthquake Science (TRIES) has been conducting continuous gravity observations both above the ground and below the ground of Mizunami Underground Research Institute in order to monitor the underground mass fluctuation including groundwater (Tanaka and Honda, 2018, doi: 10.1002 / 2017EA000311). The mass fluctuation between these two gravimeters can be evaluated from the difference between the two gravimeter values. Also, the sum of the two gravimeter values reflects the gravitational effects both from above the ground gravimeter position and from the below the underground gravimeter position. In order to extract the gravity fluctuation related to earthquake phenomena, that is, the gravitational effect only from below the subsurface gravimeter position, it is necessary to correct the atmospheric attraction effects above the ground gravimeter. Here, for the sake of simplicity, it is assumed that the atmospheric loading deformation effects and the existence of high altitude near the observation point are negligible. TRIES has been used the meso-scale objective analysis (MANAL) to calculate the atmospheric attraction effect in the range of 10 ˚×10 ˚×100 hPa–surf (approximately, 900 km in latitudinal direction ×1100 km in longitudinal direction ×16 km in altitudinal direction) centered on a gravity observation point before now. This attraction effect accounts for approximately 60% of the time-variating amplitude of the global summation. Local-scale objective analysis (LANAL) began publishing since 2018. The lattice spacing was 5 km, the same as MANAL, but LANAL increased the number of isobaric surfaces by 1 (975 hPa surface) from MANAL. This increase improved the spatial resolution of the altitude close to the observation point. Moreover, the time resolution improved as time interval changed from three hours of MANAL to one hour. Therefore, the updating from MANAL to LANAL to calculate the atmospheric attraction effect have to been evaluated quantitatively. Like other objective analysis data, LANAL is also offered in GRIB 2 format. We accessed LANAL using the GrADS software (http://cola.gmu.edu/grads/), but as it was seen in MANAL, it was not possible to display correctly with the control file generated by the g2clt or alt_g2ctl commands. In the PDEF line of the control file, you need to change the jref variable set to 1 to the value of the jsize variable. Also, from the necessity both of atmospheric density calculation on the topographic surface and comparison between isobaric surfaces and a topographic altitude, we use the enclosed terrain data (4-byte real binary). This feature is also the same specification as MANAL, and the GrADS draws the North-South direction reversed figure. In order to correct this problem, the data stored with the northwest end as the starting point was restored as the start point at the southwest end (byte swapping is necessary depending on the processing system). After that, the atmospheric attraction effect was calculated according to the procedure developed for MANAL. At the time of this writing, it was an evaluation for only one month in March 2018. The standard deviation of the difference of simultaneous numerical values between MANAL and LANAL was 0.66 microGal, and the maximum difference of instantaneous values was 2.4 microGal. It turned out that there was a significant difference. In the future, we would like to evaluate the difference from using MANAL by applying to gravity observation data.

Keywords: gravity, local-scale objective analysis, atmosphere

©2019. Japan Geoscience Union. All Right Reserved.

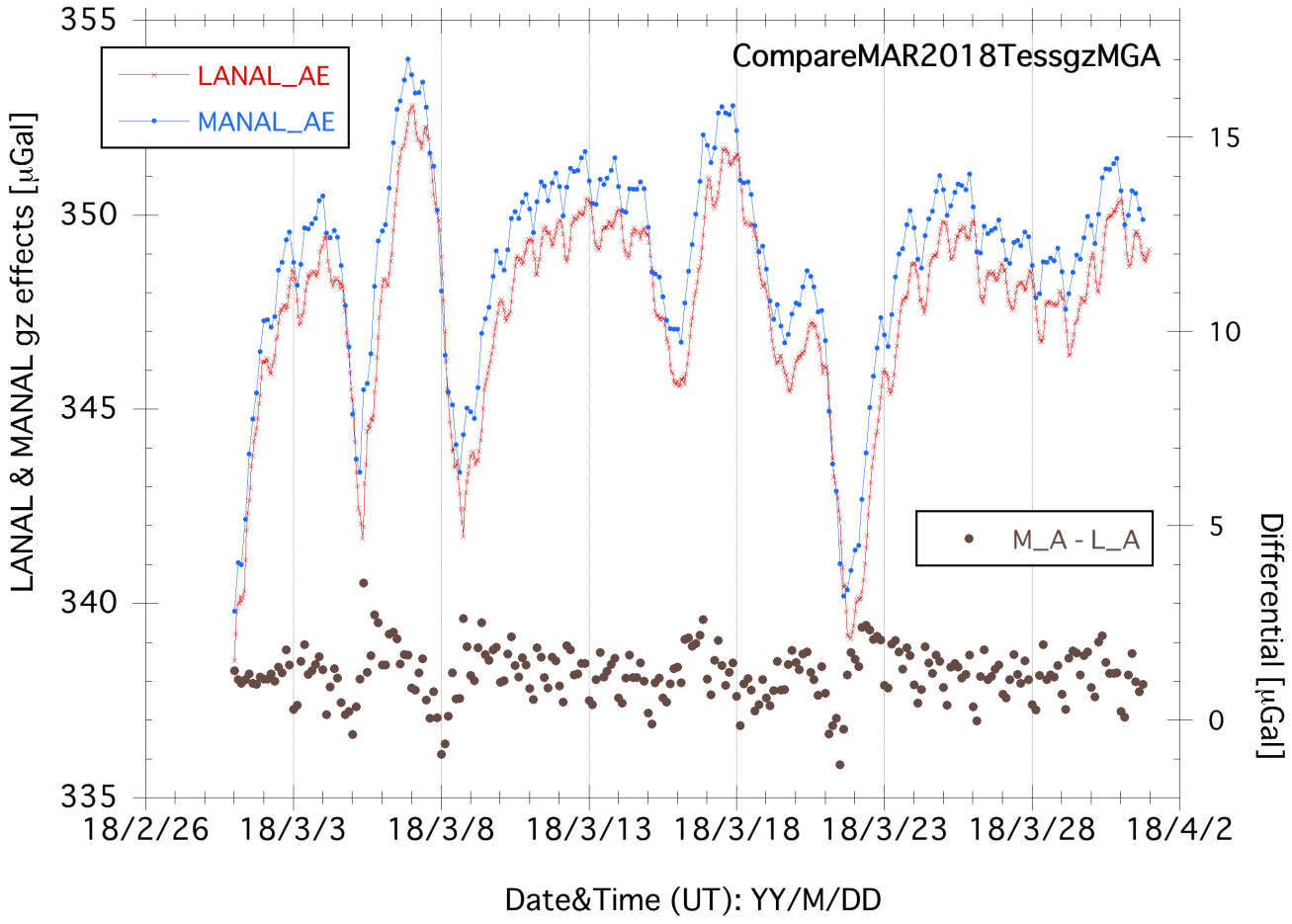

©2019. Japan Geoscience Union. All Right Reserved.

Airborne gravity survey for establishment of a new precise gravimetric geoid model

*Tokuro Kodama[1], Akira Tomiyama[1], Shuichi Oomori[1], Erika Wada[1], Toshihiro Yahagi[1], Yoshifumi Hiraoka[1], Hiroshi Kawawa[1]

1. GSI of Japan

The vertical datum of Japan has been maintained by the Geospatial Information Authority of Japan (GSI) since more than 130 years ago. Basically it has been realized by conducting periodical leveling surveys in order to determine orthometric height of benchmarks, which are installed at approximately 2 km intervals along main national highways, based on the mean sea level of the Tokyo Bay. However, since this method takes much time and costs a lot, it is quite difficult to reflect vertical land movements quickly caused by such as plate motions and big earthquakes.

In order to tackle this situation, the GSI established a geoid model, called GSIGEO2011+2000, in April 2013 and also implemented a new manual for utilizing the model for public surveys in order to obtain orthometric height from GNSS data. It in fact played a certain role in improving the efficiency of surveying. Geoid models released by the GSI so far are all hybrid, which are constructed of a gravimetric geoid model and geoid heights directly measured by GNSS/leveling surveys, in order to compensate the lack of precision of the gravimetric geoid model. However, since the GNSS/leveling data are based on results of the leveling surveys, they are unavailable once crustal deformation occurs until the leveling surveys are conducted again. In order to improve the precision of the gravimetric geoid model, it is necessary to prepare high quality gravity data all over Japan. But current gravity data contain some problems such as blank areas in both mountainous areas and coastal waters , age of data and inaccuracy of location information decided by topographic map.

In order to solve these problems and make it possible to measure precise orthometric height more quickly, the GSI has been carrying out a new airborne gravity survey project since FY2018. First, we will collect high quality nationwide gravity data using aircraft, then calculate a new precise gravimetric geoid model combined the airborne gravity data with other ones such as terrestrial, marine and satellite gravity data. We are planning to introduce a new height system based on this new geoid model and ellipsoidal heights obtained from GEONET by 2014. Since the geoid model is basically very stable against the crustal deformation, it is expected to update the orthometric height immediately by GNSS data even if crustal deformation occurs.

In this presentation, we will review our future vision of the new height system and report the progress of GSI’ s airborne gravity survey project.

Keywords: Airborne gravity survey, Gravimetric geoid model, Height system

©2019. Japan Geoscience Union. All Right Reserved.

Gravimetric geoid modeling using airborne gravity data : a case study in Colorado, U.S.A.

*Koji Matsuo[1], Rene Forsberg[2]

1. GSI of Japan, 2. Denmark Technical University

We present the conputational results of gravimetric geoid over Colorado using airborne gravity data. The gravity data and degital elevation model were provided by IAG JWG2.2.2 with the colaboration of National Geodetic Survey. Here we show the gravimetric geoid based on the two Stokes-Helmert approaches, i.e. the classical approach (Moritz, 1980) and UNB approach (Vanicek et al., 2013).

Keywords: Geodesy, Gravity and Geoid, Airborne gravimetry

©2019. Japan Geoscience Union. All Right Reserved.

[J] Oral | S (Solid Earth Sciences)：S-GD Geodesy

Tue. May 28, 2019 9:00 AM - 10:30 AM JST | Tue. May 28, 2019 12:00 AM - 1:30 AM UTC | 105 1F

[S-GD02] Engineering Application of Space Geodesy

convener:Seiichi Shimada(Graduate School of Frontier Sciences, University of Tokyo Nippo Co. Ltd.), Shuichi Rokugawa(The University of Tokyo), Basara Miyahara(GSI of Japan), Toshiaki Tsujii(Department of Aerospace Engineering, Osaka Prefecture University), Chairperson:Masaatsu Aichi, Kazuki Sakai

In the space geodetic community in Japan, geoscience and other scientific researches, such as seismology, volcanology and meteorology, are predominant. However, engineering application researches are also actively conducted in academic societies abroad. Recent advances in GNSS and InSAR measurement techniques are progressing towards widely engineering usage of space geodetic measurements even in domestic Japan. In addition, the Geospatial Information Authority of Japan (GSI) is about to shift from conventional leveling survey to space geodetic surveying such as GNSS levelling, and the space geodetic method could spread rapidly even in many engineering fields using conventional leveling survey. In this session, we introduce advanced engineering research using space geodetic measurements such as ground measurement / self-driving in particular to young earth scientists. We will also welcome a wide range of general presentations on measurements/research in engineering fields using space geodetic technology.

9:00 AM - 9:15 AM JST | 12:00 AM - 12:15 AM UTC

[SGD02-01] Future vision of the society for utilizing highly precise three dimensional positioning data by applying crustal deformation and precise gravimetric geoid model

*Toshihiro Yahagi[1], Kensuke Kokado[1], Kenji Yoshida[1], Takashi Toyofuku[1], Masao Iwata[1], Basara Miyahara[1] (1.GSI of Japan)

9:15 AM - 9:30 AM JST | 12:15 AM - 12:30 AM UTC

[SGD02-02] Preliminary study on the application of satelite-based monitoring for land surface displacement to inverse analyses of groundater flow/land subsidence modeling

*Masaatsu Aichi[1] (1.Graduate School of Frontier Sciences, The University of Tokyo)

9:30 AM - 9:45 AM JST | 12:30 AM - 12:45 AM UTC

[SGD02-03] Monitoring of ground deformation all over Japan by InSAR and utilizing 2.5-D analysis

*Kazuki Sakai[1], Kyonosuke Hayahsi[1], Masaki Kuwahara[1], Tatsuya Yamashita[1], Masaki Honda[1], Hiroshi Munekane[1] (1.GSI of Japan)

9:45 AM - 10:00 AM JST | 12:45 AM - 1:00 AM UTC

[SGD02-04] Resource Exploration using Interferometric Synthetic Aperture Radar Measurement Technology

*Shuichi Rokugawa[1], Takako Nakamura[1] (1.The University of Tokyo)

10:00 AM - 10:15 AM JST | 1:00 AM - 1:15 AM UTC

[SGD02-05] The application example of GNSS for natural gas development together with PDCA Management Method

★Invited Papers

*Yoshiyuki Muramoto[1], Susumu Hayatsu[1], Michiharu Hiyama[1], Daisuke Murai[1], Shoji Kunisue[1] (1.KANTO NATURAL GAS DEVELOPMENT CO., LTD)

10:15 AM - 10:30 AM JST | 1:15 AM - 1:30 AM UTC

[SGD02-06] New threats and countermeasures in the aviation field where the use of GNSS satellite navigation expands

★Invited Papers

*Takeshi Fujiwara[1], Toshiaki Tsujii[2] (1.Japan Aerospace Exploration Agency, 2.Osaka Prefecture University)

Future vision of the society for utilizing highly precise three dimensional positioning data by applying crustal deformation and precise gravimetric geoid model

*Toshihiro Yahagi[1], Kensuke Kokado[1], Kenji Yoshida[1], Takashi Toyofuku[1], Masao Iwata[1], Basara Miyahara[1]

1. GSI of Japan

Global Navigation Satellite System (GNSS) are conventionally used for determining reference positions in Japan by static survey activities following a uniform standard based on the survey low. In recent years, thanks to improvement of satellite positioning techniques, the utilization of GNSS positioning has been expanded to various real-time positioning services such as autonomous driving system, intelligent construction, smart agriculture and drone delivery. This trend would accelerate in the future due to new services like Centimeter Level Augmentation Service (CLAS) offered by Quasi-Zenith Satellite System (QZSS) or Precise Point Positioning (PPP) provided by private companies. Basically those kind of real-time positioning data give us ‘current’ location though most geospatial information, represented by maps, are built based on the certain ‘past’ epoch. The difference between them becomes larger year by year because of active crustal deformation in Japan. The more precise the real-time position are decided, the more careful we should treat this difference.

Therefore GSI has been developing a new system for correcting this difference in order to fully utilize the real-time positioning data by keeping consistency between existed geospatial information. The prototype of the system was offered to public from January to March in 2019 to collect feedbacks from stakeholders. We plan to launch this system officially until 2020.

It is also important to obtain precise elevation for three dimensional positioning. Historically the height system in Japan has been maintained by conducting nationwide split leveling surveys for more than 130 years. However, since it needs a lot of time and cost, it is necessary to prepare a precise geoid model for determining an orthometric height directly from an ellipsoidal height obtained by GNSS data. Hence GSI launched a new airborne gravity survey project in 2018 to collect high quality gravity data all over Japan, which is necessary to construct a new precise gravimetric geoid model within several centimeters precision. It is expected to introduce a new height system based on the new geoid model and GNSS data up to 2014. It will enable users to determine reasonable elevation data by GNSS without leveling surveys.

Through these efforts, GSI will contribute to realize the future society which fully utilize precise three dimensional position data for various geospatial information services. In this presentation, we will review the current actions of GSI and share a future vision derived from them.

Keywords: Crustal deformation model , Gravimetric geoid model, Airborne gravity survey

©2019. Japan Geoscience Union. All Right Reserved.

Preliminary study on the application of satelite-based monitoring for land surface displacement to inverse analyses of groundater flow/land subsidence modeling

*Masaatsu Aichi[1]

1. Graduate School of Frontier Sciences, The University of Tokyo

Incerasing land subsidence monitoring data with InSAR and GNSS techniques are expected to improve a calibration process of groundwater flow/land subsidence model. However, the observed data possibly includes the displacement caused not only by known groundwater abstraction but also natural displacements such as seismic/post-seismic crustal motion. Then, it is not straight forward to use the observed data for inverse analysis. It is important to separate known and unknown components from monitoring data with a simultaneous
calibration of land subsidence model.
This study presents a new method based on the prior assumption that the crustal deformation is smooth in space relative to land subsidence cone caused by groundwater abstraction. It consists of the iteration of the following three steps. In the first step, the map of difference between the observed data and the calculated result of the land subsidence model with assumed parameters. In the next step, the spatial roughness of difference map is evaluated from the rotational energy. In the final step, the model parameters are modified to minimize the spatial roughness of unknown components.
This method was tested by a synthetic data composed of land subsidence from the assumed groundwater abstraction, the assumed sudden and long-term displacement like earthquake and post seismic motion. The proposed method successfully separated the land subsidence caused by groundwater abstraction and other components, and exactly found the model parameters. The results suggest that the porposed method has the possibility to enhance the application of satellite-based land subsidence monitoring data to the calibration of land subsidence models.

Keywords: groundwater, land subsidence modeling, inverse analysis, satellite-based monitoring

©2019. Japan Geoscience Union. All Right Reserved.

Monitoring of ground deformation all over Japan by InSAR and utilizing 2.5-D analysis

*Kazuki Sakai[1], Kyonosuke Hayahsi[1], Masaki Kuwahara[1], Tatsuya Yamashita[1], Masaki Honda[1], Hiroshi Munekane[1]

1. GSI of Japan

GSI (Geospatial Information Authority of Japan) has been conducting SAR interferometry (InSAR) analysis with ALOS-2 data to monitor ground deformation all over JAPAN. In addition, we have conducted InSAR urgent analyses once natural disasters such as volcanic crisis or large earthquakes occur. We provide InSAR-derived deformation data to the Earthquake Research Committee, the Coordinating Committee for Prediction of Volcanic Eruptions and others. Furthermore, we publish those data on GSI website for general users.

InSAR analysis with a pair of observation data can reveal only line-of-sight (LOS) deformation. However, quasi-up-down and quasi-east-west component deformation may be calculated by combining LOS deformations observed from both east and west direction. This analysis method is called 2.5-D analysis (Fujiwara et al., 2000). “Quasi” means that the directions of obtained deformation by 2.5-D analysis are slightly different from up-down and east-west.

LOS deformation from InSAR analysis is usually represented in rainbow color, and is difficult to understand intuitively. Furthermore, deformation direction can’t be identified from such InSAR image. On the other hand, 2.5-D analysis image is easier to understand and deformation direction can be identified. GSI has been considering a way to make InSAR image more understandable to general public, and 2.5-D analysis is one of the candidates. The 2018 Hokkaido Eastern Iburi Earthquake is an example of utilizing 2.5-D analysis. The quasi-up-down component deformation was utilized in setting a recovery survey area.

In this presentation, we will introduce ground deformations detected by InSAR analysis and some examples of 2.5-D analysis derived from earthquakes and volcanic activities.

*Acknowledgment

ALOS-2 data were provided based on the joint research agreement with JAXA (Japan Aerospace Exploration Agency). The ownership of ALOS-2 data belongs to JAXA.

Keywords: InSAR, 2.5-D analysis, Ground deformation, ALOS-2

©2019. Japan Geoscience Union. All Right Reserved.

Resource Exploration using Interferometric Synthetic Aperture Radar Measurement Technology

*Shuichi Rokugawa[1], Takako Nakamura[1]

1. The University of Tokyo

InSAR using synthetic aperture radar (SAR) is a technology that enables the detection of the earth surface deformation without any observation points on the ground. The L-band SAR mounted on ALOS / PALSAR-2 is effective even in the vegetated areas because of relatively long wavelength of the sensor. InSAR has the potential to be used in the various technical applications. This technique has been primarily used to analyze fluctuations due to natural disasters and large-scale deformations such as crustal movement caused by earthquakes and volcanic eruptions. However, the extraction of the small deformation is also possible by continuously monitoring the ground deformation. Compared with the leveling and global navigation satellite system, InSAR provides the advantage of wide range observation capability. However, accumulating a certain amount of data is required for this kind of analysis. In this study, the second largest oil filed in Kuwait and East Kanto gas field in the Chiba prefecture, were analyzed as case study fields. InSAR data from 2004 to 2010 are applied to derive the surface deformation. The results of the detailed analysis confirmed remarkable ground deformation mainly at four locations in Kuwait. It was confirmed that each of these four points coincided with the positions of the Burgan, Minagishu, Umm Gudair and the Wafra oil fields, respectively. Therefore, it was discovered that InSAR can accurately grasp the ground deformation near the oil production wells. Moreover, these results reveal that there was a linear correlation between the influence range of the oil and the production amount of the oil field. A high correlation was also observed between the subsidence amount of the oil field and the actual production amount. Therefore, it is established that the InSAR analysis results can be applicable in production management, as well. Similarly, in Chiba prefecture, the InSAR time series analysis was conducted to grasp the spatial distribution of the ground change in time series. It also demonstrate the possibility of the tools for monitoring and management of the actual oil/gas fields.

Keywords: InSAR, ALOS/PALSAR-2, oil/gas fields

©2019. Japan Geoscience Union. All Right Reserved.

The application example of GNSS for natural gas development together with PDCA Management Method

*Yoshiyuki Muramoto[1], Susumu Hayatsu[1], Michiharu Hiyama[1], Daisuke Murai[1], Shoji Kunisue[1]

1. KANTO NATURAL GAS DEVELOPMENT CO., LTD

[Background]
We have been developing the Southern Kanto gas field for many years. This field which contains natural gas dissolved in water is located primarily under Chiba prefecture, and it extends across a wide area of the Kanto region, including Ibaraki, Saitama and Kanagawa prefectures as well as Tokyo Metropolis. This field's recoverable reserves are estimated 368.5 billion cubic meters, making it the largest field of gas dissolved in water in Japan. The gas is dissolved in formation water which is called brine, so it is produced together with brine. Commercial production of natural gas has been conducted in Chiba prefecture since 1931 and has contributed to the growth in the region. Formerly, it was mainly used for industrial gas, but now most common usage is for city gas. On the other hand, land subsidence has been confirmed in Kujukuri area, east of Chiba prefecture. Brine production is considered as one of possible causes of it. Companies producing natural gas in this area including our company have made a land subsidence prevention agreement with the Chiba prefectural government to prevent and control land subsidence. Also, from the technical point of view, we conduct joint study on environmental issues with other gas production companies as a member of "Environmental Technology Research Association for Natural Gas Dissolved in Water".

[Observation of land subsidence]
The Chiba prefectural government has conducted leveling every year. We also have conducted it, but it takes a lot of time to get the survey result because we have to revise the observation data based on the leveling result conducted by local government. On the other hand, GNSS observation which is one of the surface level observation techniques has been prevailed recently. The advantage of GNSS is that continuous observation is possible at the place where it is installed. In Japan, the Geographical Survey Institute has established GEONET (GNSS Earth Observation Network System) throughout the country. We installed GNSS stations in our operating area and analyze these data together with GEONET's since 2013 to get circumstance of land subsidence quickly.

[Application example of GNSS for natural gas production]
We installed GNSS station to monitor the land subsidence in a certain area where natural gas is newly developed. The reason for that is because we need to adjust the brine production rate based on land subsidence. We use GNSS data in "PDCA Management for Land Subsidence Control", one method for controlling land subsidence systematically. This method consists of four elements. "P", Plan, means making of production plan based on the simulation result. "D", Do, means production of natural gas based on the production plan. "C", Check, means observation and evaluation of land subsidence by GNSS and leveling. "A", Act, means update of simulation model. By repeating this method every year, we will improve the way of subsidence management.
In the presentation, we will introduce the application example of GNSS for natural gas development together with PDCA Management Method.

Keywords: GNSS, Natural gas dissolved in water, Southern Kanto gas field

©2019. Japan Geoscience Union. All Right Reserved.

©2019. Japan Geoscience Union. All Right Reserved.

New threats and countermeasures in the aviation field where the use of GNSS satellite navigation expands

*Takeshi Fujiwara[1], Toshiaki Tsujii[2]

1. Japan Aerospace Exploration Agency, 2. Osaka Prefecture University

To contribute to the realization of the next-generation air transportation system, JAXA is promoting the research and development project named DREAMS (Distributed and Revolutionary Efficient Air-safety Management System). Research and development of high precision and reliable navigation system is one of the most important targets of this project. In this paper, the impact of the plasma bubble, a kind of ionospheric anomalies, on the availability of GBAS precision approach is investigated based on the collected data under the actual plasma bubbles and the mathematical models of the plasma bubbles are introduced to be used in the Monte-Carlo simulations to estimate the availability.

Keywords: aviation, GNSS, satellite navigation

©2019. Japan Geoscience Union. All Right Reserved.

[J] Poster | S (Solid Earth Sciences)：S-GD Geodesy

Tue. May 28, 2019 3:30 PM - 5:00 PM JST | Tue. May 28, 2019 6:30 AM - 8:00 AM UTC | Poster Hall International Exhibition Hall8, Makuhari Messe_15

[S-GD02] Engineering Application of Space Geodesy

convener:Seiichi Shimada(Graduate School of Frontier Sciences, University of Tokyo Nippo Co. Ltd.), Shuichi Rokugawa(The University of Tokyo), Basara Miyahara(GSI of Japan), Toshiaki Tsujii(Department of Aerospace Engineering, Osaka Prefecture University)

In the space geodetic community in Japan, geoscience and other scientific researches, such as seismology, volcanology and meteorology, are predominant. However, engineering application researches are also actively conducted in academic societies abroad. Recent advances in GNSS and InSAR measurement techniques are progressing towards widely engineering usage of space geodetic measurements even in domestic Japan. In addition, the Geospatial Information Authority of Japan (GSI) is about to shift from conventional leveling survey to space geodetic surveying such as GNSS levelling, and the space geodetic method could spread rapidly even in many engineering fields using conventional leveling survey. In this session, we introduce advanced engineering research using space geodetic measurements such as ground measurement / self-driving in particular to young earth scientists. We will also welcome a wide range of general presentations on measurements/research in engineering fields using space geodetic technology.

[SGD02-P01] Dynamic map for engineering use of GNSS positioning

*Mikio Satomura[1], Seiichi Shimada[1,2], Hirokazu Ito[1], UKEI KAZUYUKI[1], Mikio Sueno[1,3], Shigeru Nakao[4] (1.Nippo Company, Limited, 2.Graduate School of Frontier Sciences, University of Tokyo, 3.Calsystem Company, Limited, 4.Graduate School of Scienece and Engineering, Kagoshima Univeresity)

[SGD02-P02] Utilization of Interferometric Synthetic Aperture Radar Time Series Analysis Technology for Disaster Prevention

*Takako Nakamura[1], Shuichi Rokugawa[1] (1.The University of Tokyo)

[SGD02-P03] The annual and secular movements of vertical component in GEONET sites caused by groundwater usages

*Seiichi Shimada[1], Masaatsu Aichi[1] (1.Graduate School of Frontier Sciences, University of Tokyo)

Dynamic map for engineering use of GNSS positioning

*Mikio Satomura[1], Seiichi Shimada[1,2], Hirokazu Ito[1], UKEI KAZUYUKI[1], Mikio Sueno[1,3], Shigeru Nakao[4]

1. Nippo Company, Limited, 2. Graduate School of Frontier Sciences, University of Tokyo, 3. Calsystem Company, Limited, 4. Graduate School of Scienece and Engineering, Kagoshima Univeresity

1. Introduction

We have obtained the RINEX data of the electronic reference points of the Geospatial Information Authority of Japan every day from 2008, and automatically process it using GAMIT/GLOBK software and accumulate the coordinate data of day value and week value (Shimada et al., 2014; 2015). We used ITRF 2005 from April 2008 to October 2011, ITRF 2008 from October 2011 to May 2017, and ITRF 2014 from May 2017 onwards so that the reference coordinate system of that analysis conforms to the latest coordinate system as much as possible. In the processing, observation data of 30 IGS points around Japan is used as reference points for constraining to the ITRF coordinate system, and it is solved together with electronic reference point data in Japan. In addition, we processed using Bernese Ver. 5.2 under the same conditions, and checked whether or not there is no difference in the results depending on processing software.

2. Application to dynamic map (4 dimensional map) management for engineering use

By using the above data, as the Japanese Information System of Land Deformation (JISLaD), changes in the position of the electronic reference point and the baseline length have already been disclosed. We also plan to announce the results of monitoring the fluctuation of area distortion etc.
Furthermore, we plan to calculate the fluctuation speed of an arbitrary point from the fluctuation at the GEONET point. Specifically, we are considering application to dynamic map management which is a 4-dimensional map.

As one of the items of the Cross-ministerial Strategic Innovation Promotion Program (SIP), an automatic driving system is mentioned in both the first and second phases. Automatic traveling system is a system to combine various technologies, but high-precision digital map is an important item among them. For self-location estimation for automatic driving, it is important to recognize self-position using satellite positioning information etc. However, if there is no map corresponding to it, it is meaningless only by self-position recognition.

Needless to say, the crustal deformation in Japan is intense. Therefore, once you have made a precise digital map you cannot use the map forever.

The idea of crustal deformation in Japan's map is based on semi-dynamic system. In other words, the idea is to decide the initial stage and to take the correspondence with the map by returning the latest position coordinates measured at the present time to the value of the coordinates of the original period, based on the observation of the crustal deformation.

Although this system is suitable for use such as the registration of land, it is not suitable for the automatic traveling system which corresponds the position and the map of the car every moment in the Japanese

©2019. Japan Geoscience Union. All Right Reserved.

islands where the crustal deformation is intense. Therefore, we consider the dynamic map which makes the coordinates of the map itself new every day considering the change accompanying the crustal deformation, considering application of JISLaD data to dynamic map management. In the Tohoku region, the postseismic movements exceed 10 cm per year continues still after the 2011 Tohoku Earthquake. We believe that an accuracy of about 10 cm is necessary as a basic map used for automatic driving, which means that even if crustal deformation due to a new earthquake does not occur, update the map at least once a year is necessary in the Tohoku region.

This way of thinking is not limited to cars with both roads and autonomous driving, it is important for all engineering applications where acquisition of precise coordinates is considered to be effective, especially for aircraft using electronic navigation and airport. It is a very important thing for checking the positional relationship etc.

Keywords: dynamic map, 4 dimensional coordinate management, precise GNSS positioning

©2019. Japan Geoscience Union. All Right Reserved.

Utilization of Interferometric Synthetic Aperture Radar Time Series Analysis Technology for Disaster Prevention

*Takako Nakamura[1], Shuichi Rokugawa[1]

1. The University of Tokyo

In this research, we investigate the possibility of extraction and monitoring of the ground changes before and after disasters such as landslides using interference synthetic aperture radar (InSAR) time series analysis. An analysis was conducted using the satellite image data obtained before and after the occurrence of the disaster from the location with a past disaster occurrence. The obtained results may be effective in predicting to some extent the occurrence timing of the sediment-related disasters in hazardous areas caused due to frequent earthquakes, volcanic eruptions, and local heavy rains in recent years. Several regions affected due to these sediment-related disasters were considered and a ground deformation analysis was performed on a model area using the InSAR analysis technology.
The Miyazaki prefecture Mimikawa upper basin, southwestern part of the Hiroshima prefecture, Kyushu Northwest and a few other regions were considered for analysis. These are the areas with landslide risks and past occurrences of sediment-related disasters. The image data of a HH polarized wave with an incident angle of 34.3˚ acquired during the satellite operation period was retrieved from the archive data of ALOS/PALSAR and used for the analysis.
Interference SAR time series analysis enables the detection of minute fluctuations using smoothing restraint inversion method for integrally analyzing the interference images of multiple orbits. We also performed a 2.5 dimensional analysis using two orbits of descending and ascending nodes. During the analysis, strong displacements were observed not only in the collapse track, but also at other points in the upper stream of the Mimi River. Those points that demonstrated a high possibility of collapse were then extracted. Such a phenomenon was also observed in some instances of other analyses. From the 2.5 dimensional analysis of the area around the affected area in the southwestern part of Hiroshima Prefecture, actual sediment-related disasters were extracted, almost pinpoint, from the variation diagram of the eastern component. In the area, the faults in the northeast and the southwest directions were dominant and the continuous slope of the mountain extended in the same directions. The characteristic topography of these areas possibly affected the direction of the ground surface fluctuation. In the northwestern part of Kyushu, several points with earlier occurrences of landslides were detected in addition to the actual landslide site by employing the median filter plus histogram extraction processing and Laplacian filter processing together. As a result, it was determined that various measures were necessary for the interference SAR time series analysis to extract the fine ground fluctuation immediately before the disaster, as these fluctuations are unlike the relatively large fluctuations that occur during the disaster.
To actually implement monitoring using the InSAR analysis, it is important to sufficiently consider the geology of the target area and its topographical features and accumulate and maintain the base information on the target area in times of peace. In case of emergencies, the latest observation data can be obtained immediately by retrieving from the archives to perform the required analysis.

Keywords: Interferometric Synthetic Aperture Radar Time Series Analysis, disaster prevention, ground deformation analysis

©2019. Japan Geoscience Union. All Right Reserved.

The annual and secular movements of vertical component in GEONET sites caused by groundwater usages

*Seiichi Shimada[1], Masaatsu Aichi[1]

1. Graduate School of Frontier Sciences, University of Tokyo

Annual and secular movements are observed in vertical components of many GEONET sites caused by the groundwater usage. Observation of vertical movements associated with groundwater drawing is an indispensable observation element for establishing groundwater circulation model, as well as observations of groundwater level and meteorological factors. The Geospatial Information Authority of Japan plans to switch the monitoring method of vertical movements from conventional leveling survey to the space geodetic techniques such as GNSS measurements, and in the near future vertical movement monitoring by GNSS observations is likely to become an observation tool indispensable for groundwater usage and management through groundwater circulation model. In order to observe ground subsidence, one of the largest obstacles in the groundwater usage, installation of antenna pillar for GNSS observations will become indispensable near the water well that pumps a large amount of groundwater, in the near future.

In this presentation, we show examples of annual and long-term secular variations associated with groundwater usage, which we find by the analyses of GEONET sites in the Kanto region and Niigata prefecture. In the analysis, we determine at first the daily coordinates of the GEONET sites with 23 fiducial sites of IGS network in East Asia and the surrounding area. We apply the ITRF 2014 coordinates and the VMF1 mapping function as well as 10° cutoff elevation angle. We estimate every hourly zenith delay and every four-hourly atmospheric gradient simultaneously with the site coordinates and ambiguities. Then we apply the 30-day window Kalman filter to eliminate the short cycle fluctuation and clarify the annual/semi-annual and secular vertical movements from long-term observation data.

In the GEONET sites in the Kanto region, vertical movements due to agricultural usage of ground water are detected in the central to northern part of the Kanto plain, centering on Saitama prefecture. For example, at the Tsukuba1 site (92110 site) in the campus of the Geospatial Information Authority of Japan, annual variations that subside in summer are observed caused by the groundwater usage of the rise field around the site, that are harmonious with VLBI and groundwater level observations (Tobita et al., 2004; Munekane et al., 2010; Shimada et al., 2017).

In the Kujukuri area, a large amount of subsiding is observed caused by the groundwater mining for refining natural gas. At the Oami-Shirasato site (93027 point) and the Chosei site (93033 site) in this area, in addition to the annual variation subsiding in the winter, the long-term ground subsidence are detected harmonizing with the level survey and the InSAR observations (Harada, 2018; Shimada et al., 2018).

In Niigata prefecture including the Niigata plain, groundwater usage for snow melting is widespread, and vertical subsidence is observed caused by the groundwater usage. For example, at the Niigata Sakae site (970810 site) in Sanjo city, as well as the annual variation that settling in winter, progress of inelastic secular subsidence is seen especially in the years when the amount of snow fall is large and the amount of ground subsidence also large (Shimada, 2018).

©2019. Japan Geoscience Union. All Right Reserved.

Keywords: GNSS measurements, GEONET, Groundwater usage, Annual movements, Secular movements

©2019. Japan Geoscience Union. All Right Reserved.

[J] Poster | S (Solid Earth Sciences)：S-GD Geodesy

Tue. May 28, 2019 5:15 PM - 6:30 PM JST | Tue. May 28, 2019 8:15 AM - 9:30 AM UTC | Poster Hall International Exhibition Hall8, Makuhari Messe_27

[S-GD02] Engineering Application of Space Geodesy

convener:Seiichi Shimada(Graduate School of Frontier Sciences, University of Tokyo Nippo Co. Ltd.), Shuichi Rokugawa(The University of Tokyo), Basara Miyahara(GSI of Japan), Toshiaki Tsujii(Department of Aerospace Engineering, Osaka Prefecture University)

In the space geodetic community in Japan, geoscience and other scientific researches, such as seismology, volcanology and meteorology, are predominant. However, engineering application researches are also actively conducted in academic societies abroad. Recent advances in GNSS and InSAR measurement techniques are progressing towards widely engineering usage of space geodetic measurements even in domestic Japan. In addition, the Geospatial Information Authority of Japan (GSI) is about to shift from conventional leveling survey to space geodetic surveying such as GNSS levelling, and the space geodetic method could spread rapidly even in many engineering fields using conventional leveling survey. In this session, we introduce advanced engineering research using space geodetic measurements such as ground measurement / self-driving in particular to young earth scientists. We will also welcome a wide range of general presentations on measurements/research in engineering fields using space geodetic technology.

[SGD02-P01] Dynamic map for engineering use of GNSS positioning

*Mikio Satomura[1], Seiichi Shimada[1,2], Hirokazu Ito[1], UKEI KAZUYUKI[1], Mikio Sueno[1,3], Shigeru Nakao[4] (1.Nippo Company, Limited, 2.Graduate School of Frontier Sciences, University of Tokyo, 3.Calsystem Company, Limited, 4.Graduate School of Scienece and Engineering, Kagoshima Univeresity)

[SGD02-P02] Utilization of Interferometric Synthetic Aperture Radar Time Series Analysis Technology for Disaster Prevention

*Takako Nakamura[1], Shuichi Rokugawa[1] (1.The University of Tokyo)

[SGD02-P03] The annual and secular movements of vertical component in GEONET sites caused by groundwater usages

*Seiichi Shimada[1], Masaatsu Aichi[1] (1.Graduate School of Frontier Sciences, University of Tokyo)

Dynamic map for engineering use of GNSS positioning

*Mikio Satomura[1], Seiichi Shimada[1,2], Hirokazu Ito[1], UKEI KAZUYUKI[1], Mikio Sueno[1,3], Shigeru Nakao[4]

1. Nippo Company, Limited, 2. Graduate School of Frontier Sciences, University of Tokyo, 3. Calsystem Company, Limited, 4. Graduate School of Scienece and Engineering, Kagoshima Univeresity

1. Introduction

We have obtained the RINEX data of the electronic reference points of the Geospatial Information Authority of Japan every day from 2008, and automatically process it using GAMIT/GLOBK software and accumulate the coordinate data of day value and week value (Shimada et al., 2014; 2015). We used ITRF 2005 from April 2008 to October 2011, ITRF 2008 from October 2011 to May 2017, and ITRF 2014 from May 2017 onwards so that the reference coordinate system of that analysis conforms to the latest coordinate system as much as possible. In the processing, observation data of 30 IGS points around Japan is used as reference points for constraining to the ITRF coordinate system, and it is solved together with electronic reference point data in Japan. In addition, we processed using Bernese Ver. 5.2 under the same conditions, and checked whether or not there is no difference in the results depending on processing software.

2. Application to dynamic map (4 dimensional map) management for engineering use

By using the above data, as the Japanese Information System of Land Deformation (JISLaD), changes in the position of the electronic reference point and the baseline length have already been disclosed. We also plan to announce the results of monitoring the fluctuation of area distortion etc.
Furthermore, we plan to calculate the fluctuation speed of an arbitrary point from the fluctuation at the GEONET point. Specifically, we are considering application to dynamic map management which is a 4-dimensional map.

As one of the items of the Cross-ministerial Strategic Innovation Promotion Program (SIP), an automatic driving system is mentioned in both the first and second phases. Automatic traveling system is a system to combine various technologies, but high-precision digital map is an important item among them. For self-location estimation for automatic driving, it is important to recognize self-position using satellite positioning information etc. However, if there is no map corresponding to it, it is meaningless only by self-position recognition.

Needless to say, the crustal deformation in Japan is intense. Therefore, once you have made a precise digital map you cannot use the map forever.

The idea of crustal deformation in Japan's map is based on semi-dynamic system. In other words, the idea is to decide the initial stage and to take the correspondence with the map by returning the latest position coordinates measured at the present time to the value of the coordinates of the original period, based on the observation of the crustal deformation.

Although this system is suitable for use such as the registration of land, it is not suitable for the automatic traveling system which corresponds the position and the map of the car every moment in the Japanese

©2019. Japan Geoscience Union. All Right Reserved.

islands where the crustal deformation is intense. Therefore, we consider the dynamic map which makes the coordinates of the map itself new every day considering the change accompanying the crustal deformation, considering application of JISLaD data to dynamic map management. In the Tohoku region, the postseismic movements exceed 10 cm per year continues still after the 2011 Tohoku Earthquake. We believe that an accuracy of about 10 cm is necessary as a basic map used for automatic driving, which means that even if crustal deformation due to a new earthquake does not occur, update the map at least once a year is necessary in the Tohoku region.

This way of thinking is not limited to cars with both roads and autonomous driving, it is important for all engineering applications where acquisition of precise coordinates is considered to be effective, especially for aircraft using electronic navigation and airport. It is a very important thing for checking the positional relationship etc.

Keywords: dynamic map, 4 dimensional coordinate management, precise GNSS positioning

©2019. Japan Geoscience Union. All Right Reserved.

Utilization of Interferometric Synthetic Aperture Radar Time Series Analysis Technology for Disaster Prevention

*Takako Nakamura[1], Shuichi Rokugawa[1]

1. The University of Tokyo

In this research, we investigate the possibility of extraction and monitoring of the ground changes before and after disasters such as landslides using interference synthetic aperture radar (InSAR) time series analysis. An analysis was conducted using the satellite image data obtained before and after the occurrence of the disaster from the location with a past disaster occurrence. The obtained results may be effective in predicting to some extent the occurrence timing of the sediment-related disasters in hazardous areas caused due to frequent earthquakes, volcanic eruptions, and local heavy rains in recent years. Several regions affected due to these sediment-related disasters were considered and a ground deformation analysis was performed on a model area using the InSAR analysis technology.
The Miyazaki prefecture Mimikawa upper basin, southwestern part of the Hiroshima prefecture, Kyushu Northwest and a few other regions were considered for analysis. These are the areas with landslide risks and past occurrences of sediment-related disasters. The image data of a HH polarized wave with an incident angle of 34.3˚ acquired during the satellite operation period was retrieved from the archive data of ALOS/PALSAR and used for the analysis.
Interference SAR time series analysis enables the detection of minute fluctuations using smoothing restraint inversion method for integrally analyzing the interference images of multiple orbits. We also performed a 2.5 dimensional analysis using two orbits of descending and ascending nodes. During the analysis, strong displacements were observed not only in the collapse track, but also at other points in the upper stream of the Mimi River. Those points that demonstrated a high possibility of collapse were then extracted. Such a phenomenon was also observed in some instances of other analyses. From the 2.5 dimensional analysis of the area around the affected area in the southwestern part of Hiroshima Prefecture, actual sediment-related disasters were extracted, almost pinpoint, from the variation diagram of the eastern component. In the area, the faults in the northeast and the southwest directions were dominant and the continuous slope of the mountain extended in the same directions. The characteristic topography of these areas possibly affected the direction of the ground surface fluctuation. In the northwestern part of Kyushu, several points with earlier occurrences of landslides were detected in addition to the actual landslide site by employing the median filter plus histogram extraction processing and Laplacian filter processing together. As a result, it was determined that various measures were necessary for the interference SAR time series analysis to extract the fine ground fluctuation immediately before the disaster, as these fluctuations are unlike the relatively large fluctuations that occur during the disaster.
To actually implement monitoring using the InSAR analysis, it is important to sufficiently consider the geology of the target area and its topographical features and accumulate and maintain the base information on the target area in times of peace. In case of emergencies, the latest observation data can be obtained immediately by retrieving from the archives to perform the required analysis.

Keywords: Interferometric Synthetic Aperture Radar Time Series Analysis, disaster prevention, ground deformation analysis

©2019. Japan Geoscience Union. All Right Reserved.

The annual and secular movements of vertical component in GEONET sites caused by groundwater usages

*Seiichi Shimada[1], Masaatsu Aichi[1]

1. Graduate School of Frontier Sciences, University of Tokyo

Annual and secular movements are observed in vertical components of many GEONET sites caused by the groundwater usage. Observation of vertical movements associated with groundwater drawing is an indispensable observation element for establishing groundwater circulation model, as well as observations of groundwater level and meteorological factors. The Geospatial Information Authority of Japan plans to switch the monitoring method of vertical movements from conventional leveling survey to the space geodetic techniques such as GNSS measurements, and in the near future vertical movement monitoring by GNSS observations is likely to become an observation tool indispensable for groundwater usage and management through groundwater circulation model. In order to observe ground subsidence, one of the largest obstacles in the groundwater usage, installation of antenna pillar for GNSS observations will become indispensable near the water well that pumps a large amount of groundwater, in the near future.

In this presentation, we show examples of annual and long-term secular variations associated with groundwater usage, which we find by the analyses of GEONET sites in the Kanto region and Niigata prefecture. In the analysis, we determine at first the daily coordinates of the GEONET sites with 23 fiducial sites of IGS network in East Asia and the surrounding area. We apply the ITRF 2014 coordinates and the VMF1 mapping function as well as 10° cutoff elevation angle. We estimate every hourly zenith delay and every four-hourly atmospheric gradient simultaneously with the site coordinates and ambiguities. Then we apply the 30-day window Kalman filter to eliminate the short cycle fluctuation and clarify the annual/semi-annual and secular vertical movements from long-term observation data.

In the GEONET sites in the Kanto region, vertical movements due to agricultural usage of ground water are detected in the central to northern part of the Kanto plain, centering on Saitama prefecture. For example, at the Tsukuba1 site (92110 site) in the campus of the Geospatial Information Authority of Japan, annual variations that subside in summer are observed caused by the groundwater usage of the rise field around the site, that are harmonious with VLBI and groundwater level observations (Tobita et al., 2004; Munekane et al., 2010; Shimada et al., 2017).

In the Kujukuri area, a large amount of subsiding is observed caused by the groundwater mining for refining natural gas. At the Oami-Shirasato site (93027 point) and the Chosei site (93033 site) in this area, in addition to the annual variation subsiding in the winter, the long-term ground subsidence are detected harmonizing with the level survey and the InSAR observations (Harada, 2018; Shimada et al., 2018).

In Niigata prefecture including the Niigata plain, groundwater usage for snow melting is widespread, and vertical subsidence is observed caused by the groundwater usage. For example, at the Niigata Sakae site (970810 site) in Sanjo city, as well as the annual variation that settling in winter, progress of inelastic secular subsidence is seen especially in the years when the amount of snow fall is large and the amount of ground subsidence also large (Shimada, 2018).

©2019. Japan Geoscience Union. All Right Reserved.

Keywords: GNSS measurements, GEONET, Groundwater usage, Annual movements, Secular movements

©2019. Japan Geoscience Union. All Right Reserved.

[E] Oral | S (Solid Earth Sciences)：S-SS Seismology

Tue. May 28, 2019 1:45 PM - 3:15 PM JST | Tue. May 28, 2019 4:45 AM - 6:15 AM UTC | Convention Hall B 2F

[S-SS06] Nankai Trough Seismogenic Zone Experiment: Logging and sampling the seismogenic megathrust

convener:Kyuichi Kanagawa(Graduate School of Science, Chiba University), Demian M Saffer(Pennsylvania State University), Masataka Kinoshita(Earthquake Research Institute, University of Tokyo), Chairperson:Kyuichi Kanagawa(Graduate School of Science, Chiba University), Demian Saffer(Department of Geosciences, Pennsylvania State University), Masataka Kinoshita(Earthquake Research Institute, the University of Tokyo)

The Nankai Trough Seismogenic Zone Experiment (NanTroSEIZE) is a multidisciplinary investigation of fault mechanics and seismogenesis along the megathrust at the Nankai Trough subduction zone, and includes reflection and refraction seismic imaging, direct sampling by drilling, in situ measurements, and long-term monitoring in conjunction with laboratory and numerical modeling studies. During the past 12 IODP expeditions off Kii Peninsula since 2007, 15 sites have been drilled by D/V "Chikyu" down to depths from 100s of meters to more than 3000 meters below seafloor, where the inner and outer wedge of the Nankai margin has been logged and sampled extensively, and three state-of-the-art real-time downhole observatories are now in operation. The final NanTroSEIZE expedition aiming to log and sample the seismogenic megathrust at ~5200 meters below seafloor is now ongoing from October, 2018 to March, 2019.
In this session, we expect presentations not only on scientific outcomes from the past NanTroSEIZE expeditions, but also on the exciting preliminary results of the final NanTroSEIZE expedition. We welcome presentations on, but are not limited to, seismic imaging, borehole logging and monitoring, chemical analyses of pore water and mud gas, lithology, structures, physical properties and laboratory experiments of cuttings and core samples, and theoretical and numerical modeling.

1:45 PM - 2:00 PM JST | 4:45 AM - 5:00 AM UTC

[SSS06-01] Geoscientific information about plate boundary along the Nankai Trough provided by the GNSS-A

★Invited Papers

*Yusuke Yokota[1], Tadashi Ishikawa[2] (1.Institute of Industrial Science, The University of Tokyo, 2.Hydrographic and Oceanographic department, Japan Coast Guard)

2:00 PM - 2:15 PM JST | 5:00 AM - 5:15 AM UTC

[SSS06-02] Deep Drilling at the Nankai Trough: IODP NanTroSEIZE Expedition 358 Summary and First Results

★Invited Papers

*Harold Tobin[1], Takehiro Hirose[7], Matt Ikari[5], Kyuichi Kanagawa[10], Gaku Kimura[3], Masataka Kinoshita[8], Hiroko Kitajima[6], Demian M Saffer[4], Asuka Yamaguchi[9], Lena Maeda[2], Nobu Eguchi[2], Sean Toczko[2] (1.Department of Earth and Space Sciences, University of Washington, 2.JAMSTEC-CDEX, 3.Tokyo Un. of Marine Science-Technology, 4.Penn State University, 5.MARUM Un. of Bremen, 6.Texas A&M University, 7.JAMSTEC-KCC, 8.Un. of Tokyo Earthquake Research Institute, 9.Un. of Tokyo AORI, 10.Chiba University)

2:15 PM - 2:30 PM JST | 5:15 AM - 5:30 AM UTC

[SSS06-03] Coexistence of soft and hard sediments at deep Nankai accretionary prism, NanTro SEIZE Project, IODP Exp.358

*Arito Sakaguchi[1,2], Michael Strasser[3], Mari Hamahashi[4,5], Takehiro Hirose[2], Hiroko Kitajima[6], Expedition 358 Scientists IODP (1.Yamaguchi Univ., 2.JAMSTEC, 3.University of Innsbruck, 4.University of Tokyo, 5.Nanyang Technological University, 6.Texas A&M University)

2:30 PM - 2:45 PM JST | 5:30 AM - 5:45 AM UTC

[SSS06-04] Active and passive seismic experiment during the IODP Exp. 358 deep riser drilling in the Nankai Trough, Japan

*Toshinori Kimura[1], Takashi Tonegawa[1], Kazuya Shiraishi[1], Eiichiro Araki[1], Yasuyuki Nakamura[1], Yuka Kaiho[1], Gou Fujie[1], Seiichi Miura[1], Shuichi Kodaira[1], Noriaki Sakurai[1], Yoshinori Sanada[1], Yukari Kido[1], Masataka Kinoshita[2], Narumi Takahashi[3,1], Yuya Machida[1], Shuhei Nishida[1] (1.Japan Agency for Marine-Earth Science and Technology, 2.Earthquake Research Institute, The University of Tokyo, 3.National Research Institute for Earth Science and Disaster Resilience)

2:45 PM - 3:00 PM JST | 5:45 AM - 6:00 AM UTC

[SSS06-05] Microfabric analysis of damaged zone of principal shear zone in the frontal megathrust in the Nankai Trough

*Gaku Kimura[1], Asuka Yamaguchi[2], Yohei Hamada[3], Suguru Yabe[4] (1.Tokyo University of Marine Science and Technology, 2.Atomosphere and Ocean Research Institute, The University of Tokyo, 3.Kochi Institute for Core Sample Research, Japan Agency for Marine-Earth Science and Technology, 4.Japan Agency for Marine-Earth Science and Technology)

3:00 PM - 3:15 PM JST | 6:00 AM - 6:15 AM UTC

[SSS06-06] Seismic Imaging of Mud Diapirs in Northern Kumano Basin, Nankai Trough

*Gregory F Moore[1], Miho Asada[2], Shuichi Kodaira[2], Achim Kopf[3] (1.University of Hawaii at Manoa, 2.JAMSTEC, 3.MARUM)

Geoscientific information about plate boundary along the Nankai Trough provided by the GNSS-A

*Yusuke Yokota[1], Tadashi Ishikawa[2]

1. Institute of Industrial Science, The University of Tokyo, 2. Hydrographic and Oceanographic department, Japan Coast Guard

In the last decade, many geophysical implications were provided by the GNSS-A seafloor geodetic network. Along the Japan Trench, coseismic and postseismic deformations following the 2011 Tohoku-oki earthquake were detected [Sato et al., 2011, Science; Watanabe et al., 2014, GRL; Tomita et al., 2017, Sci. Adv.]. Coseismic monitoring result was applied for many seismological research [e.g., Ozawa et al., 2012, JGR] and geological research and monitoring plan. Postseismic viscoelastic behavior and afterslip event [Sun et al., 2016, Nature; Iinuma et al., 2016, Nature Comm.] could not be identified without our monitoring results.

After 2015, more important geoscientific suggestions were obtained from monitoring in the Nankai Trough. Yokota et al. [2016, Nature] showed undersea interseismic coupling condition. This observation result has been broadly applied to various geophysical studies while being modified [e.g., Nishimura et al., 2018, Gesphere; Noda et al., 2018, JGR] and constrains earthquake prediction research including numerical simulation and submarine drilling research.

In addition, recently, we improved the GNSS-A technology and upgraded observation frequency and precision [Yokota et al., 2017, Rep. Hydro. Ocean. Res; Yokota et al., 2018, MGR]. With the present observation ability, yearly time change of the amount of undersea crustal deformation was newly unclosed. This new version data suggests that there were longer-term sequences of slow slip events (SSEs) around strong coupling regions [Yokota and Ishikawa, this JpGU meeting].

These results provide several suggestions about property and condition on the plate boundary. The simple and biggest question is what is the reason for separating strong coupling and SSE conditions. Since the difference between the generation patterns of SSE and other slow earthquakes is also considered to be due to physical properties, some dominant factor can be assumed. Differences and similarities between deep and shallow SSEs are also important. What physical properties control the behaviors of deep and shallow SSEs?

For answering these questions, additional experiments and observations from many different viewpoints will be necessary. At the same time, continuous GNSS-A monitoring and upgrading its density and accuracy are required for understanding shallow coupling conditions and SSEs.

Keywords: GNSS-A, Nankai Trough, SSE, plate boundary, coupling condition

©2019. Japan Geoscience Union. All Right Reserved.

Deep Drilling at the Nankai Trough: IODP NanTroSEIZE Expedition 358 Summary and First Results

*Harold Tobin[1], Takehiro Hirose[7], Matt Ikari[5], Kyuichi Kanagawa[10], Gaku Kimura[3], Masataka Kinoshita[8], Hiroko Kitajima[6], Demian M Saffer[4], Asuka Yamaguchi[9], Lena Maeda[2], Nobu Eguchi[2], Sean Toczko[2]

1. Department of Earth and Space Sciences, University of Washington, 2. JAMSTEC-CDEX, 3. Tokyo Un. of Marine Science-Technology, 4. Penn State University, 5. MARUM Un. of Bremen, 6. Texas A&M University, 7. JAMSTEC-KCC, 8. Un. of Tokyo Earthquake Research Institute, 9. Un. of Tokyo AORI, 10. Chiba University

IODP Expedition 358 was carried out beginning October 10, 2018 and scheduled to continue until March 31, 2019. The primary objective was to sample and make geophysical measurements in and around the megasplay fault/plate boundary fault at Site C0002, by extending the riser borehole (Hole C0002P) established during previous Integrated Ocean Drilling Program NanTroSEIZE expeditions. After Expedition 348 in 2014, Hole C0002P was left suspended, with steel casing in pace holding the borehole open to 2922 meters below the sea floor (mbsf). The primary seismic reflector target interpreted as the main plate boundary fault zone was estimated to lie at a little more than 5000 mbsf, necessitating a plan to re-enter that hole and then add about 2000 meters of new depth drilling to reach and cross it.

Drilling commenced with a sidetracking operation to establish Hole C0002Q, which was advanced to 3263 mbsf, but operational difficulties precluded going any deeper. Two more attempts were made to advance the riser hole over many weeks, but ultimately did not result in further progress toward the objective. At the time of this writing, coring operations are ongoing at the site at a depth of about 2900 mbsf, in deformed and steeply-dipping mid-Miocene age inner accretionary wedge rocks. There are plans to end riser operations at Site C0002 at the end of February 2019 despite not reaching the primary target, and instead commence drilling at a new site to target the frontal thrust portion of the plate boundary near previous IODP Site C0006. First results from the expedition will be reviewed in this presentation, and a preliminary assessment of the scientific outcomes will be made.

Keywords: Nankai Trough, IODP , megathrust

©2019. Japan Geoscience Union. All Right Reserved.

Coexistence of soft and hard sediments at deep Nankai accretionary prism, NanTro SEIZE Project, IODP Exp.358

*Arito Sakaguchi[1,2], Michael Strasser[3], Mari Hamahashi[4,5], Takehiro Hirose[2], Hiroko Kitajima[6], Expedition 358 Scientists IODP

1. Yamaguchi Univ., 2. JAMSTEC, 3. University of Innsbruck, 4. University of Tokyo, 5. Nanyang Technological University, 6. Texas A&M University

It was believed that sediment strengthened irreversibly with depth, and same lithology has same strength in same depth. It was found that quite soft portions were developed within hard sedimentary rock at deep Nankai accretionary prism, southwest Japan, during the NanTro Seize Project, IODP Expedition 348 and 358.

The site C0002 is located at the Tonankai Earthquake (1944 M=8.0) area and penetrates 3262 m below sea floor (mbsf) through the Kumano basin and Nankai accretionary prism. The porosity decreases, and hardness increases with depth gradually. Deeper than approximately 2000 mbsf, the Silty claystone of dark gray lithified hard rock with low porosity less than 20% is occurred for main lithology. Interleaved between this hard rock, the Fine silty claystone with high porosity upper than 30% was observed deeper than 2360 mbsf (Tobin et al., 2015). This soft sediment is similar with the Silty claystone in grain size and mineral assemblages, but strength is totally difference. Such soft stuffs are commonly generated during drilling. In this site, various types of drill tools of bit and reamers were operated due to unstable hole condition. However, no relationship was found between drilling tool and occurrence of the Fine silty claystone. Optical microscope and micro X-CT observations revealed that some sedimentary laminations and burrows of benthos were preserved within the Fine silty claystone. These show that the fine silty claystone is natural sediment, but not drilling induced artifact.

The reason for coexistence of soft and hard sediments in same depth can be explained by conceptual idea as below. In initial state of diagenesis, some crystals will grow larger having smaller surface energy than the other. This surface energy difference in same solution causes that smaller crystal dissolution and larger crystal grow further. Resulting of this process, well crystalline and less crystalline parts probably have marked contrast in strength. This implies that present of heterogeneous strength distribution around the initiation depth of diagenesis.

Keywords: Nankai trough, IODP Exp.358, CHIKYU, Diagenesis

©2019. Japan Geoscience Union. All Right Reserved.

Active and passive seismic experiment during the IODP Exp. 358 deep riser drilling in the Nankai Trough, Japan

*Toshinori Kimura[1], Takashi Tonegawa[1], Kazuya Shiraishi[1], Eiichiro Araki[1], Yasuyuki Nakamura[1], Yuka Kaiho[1], Gou Fujie[1], Seiichi Miura[1], Shuichi Kodaira[1], Noriaki Sakurai[1], Yoshinori Sanada[1], Yukari Kido[1], Masataka Kinoshita[2], Narumi Takahashi[3,1], Yuya Machida[1], Shuhei Nishida[1]

1. Japan Agency for Marine-Earth Science and Technology, 2. Earthquake Research Institute, The University of Tokyo, 3. National Research Institute for Earth Science and Disaster Resilience

Stress and strain should be crucial parameter to understand preparation/generation cycle of mega-thrust earthquakes which repeatedly occur along subduction zone. Recent studies suggest that seismic approach (c.f. seismic anisotropy analysis and seismic velocity monitoring) could be alternative tool to monitor stress/strain field in the seismogenic zone. The IODP Exp. 358, which includes deep riser drilling by D/V Chikyu around the IODP C0002 hole in the Nankai Trough region, is a great opportunity to observe the seismic dataset, which would be used to discuss the relationship between seismic parameters and stress field before, after and while the deep borehole drilling.

We performed a series of seismic experiments including passive and active surveys. The experiments include: 1) Seismic velocity monitoring near the C0002 hole by seismic interferometry using drilling/vessel noise. 2) Seismic anisotropy survey around the C0002 hole by air-gun circular shooting. 3) Microearthquakes and tremors monitoring to identify stress condition around the borehole. In this region, real-time borehole seismic observatory and seafloor seismic observatory, named LTBMS (Long-Term Borehole Monitoring System) and DONET (Dense Oceanfloor Network system for Earthqukae and Tsunamis), have been already installed and operated. These observatories can be used as seismic receivers for this experiment. 10 OBSs (Ocean Bottom Seismicmeter) were additionally deployed near the C0002 hole for dense seismic observation within 10 km from the C0002 hole. 6 OBSs were deployed by R/V Yokosuka during the YK18-14 cruise. Another 4 OBSs were deployed by Chikyu’s ROV (Remotely Operated Vehicle) with distances of 90 m to 300 m from the C0002 hole. These OBSs will be recovered from May to Oct. 2019. As active seismic survey, R/V Kaimei fired circular shooting line around the C0002 hole during the KM18-10 cruise. The air-gun signals were clearly observed by LTBMS seismometer and seafloor DONET seismometers. The observed data show clear seismic events which should be caused by seismic anisotropy. Since 2013 to 2016, we have performed the same survey around the C0002 hole by R/V Kairei in every year. Therefore, time-lapse discussion on seismic anisotropy should be possible by using the newly and existing dataset.

Phase analysis and beam-forming processing would be possible by using the OBS array dataset to discuss distributions of microearthquake and tremors. OBS array data can be also used for seismic interferometry analysis to discuss velocity structure monitoring during the drilling. In this presentation, we will show initial data observed by OBS if the data were available after the recovery. Also, we will show initial results of active seismic survey observed by LTBMS and DONET seismometers including time-lapse discussion on seismic anisotropy.

Keywords: Nankai Trough, Seismic experiment, Deep drilling, Monitoring

©2019. Japan Geoscience Union. All Right Reserved.

Microfabric analysis of damaged zone of principal shear zone in the frontal megathrust in the Nankai Trough

*Gaku Kimura[1], Asuka Yamaguchi[2], Yohei Hamada[3], Suguru Yabe[4]

1. Tokyo University of Marine Science and Technology, 2. Atomosphere and Ocean Research Institute, The University of Tokyo, 3. Kochi Institute for Core Sample Research, Japan Agency for Marine-Earth Science and Technology, 4. Japan Agency for Marine-Earth Science and Technology

The outer wedge of the Nankai forearc is located to the south of the splay fault, which is the traditional southern margin of the seismogenic rupture zone. The evidence for seismo-tsunamigenic slip was, however, recognized on the basis of a thermal anomaly along ~2 mm thick fault gouge indicative of frictional heating at the frontal thrust. This fact suggested a rupture propagation to the Nankai Trough in the past. Recently, slow slips along the megathrust beneath the outer wedge were observed and an intimate relationship between the coseismo-tsunamigenic large and fast slip and interseismic slow slips is a matter of great concern.

The underlying micro-mechanical processes responsible for the fast or slow slips are, however, poorly known.

We revisited the recovered core sample of the frontal thrust and added further micro-textural observations for damaged zone to already reported principal shear zone. The detailed mineralogical, chemical and micro fabric analysis for a principal shear zone presents the nearly complete transformation from smectite to illite, which is consistent with frictional heating. The observed micro-texture of the gouge and its surroundings of damaged zone is characteristic of experimentally-produced brittle textures for slow slip. This suggests an overprint of slow slip on the previous seismo-tsunamigenic fast slip. This micro-tectonic based interpretation is consistent with the recent observation of inter-sesimic slow slip beneath the outer wedge and around the frontal megathrust. We suggest that the illite-smectite lithology of gouge and surrounding is conditionally stable, allowing it to transition from co-seismic rapid slip to inter-seismic slow slip at different times.

Keywords: Nankai trough, frontal thrust, principal shear zone, slow slip, fault fabric, tsunamigenic fault

©2019. Japan Geoscience Union. All Right Reserved.

Seismic Imaging of Mud Diapirs in Northern Kumano Basin, Nankai Trough

*Gregory F Moore[1], Miho Asada[2], Shuichi Kodaira[2], Achim Kopf[3]

1. University of Hawaii at Manoa, 2. JAMSTEC, 3. MARUM

Mud volcanoes (MV), the surface expression of deeper-seated diapirs are now well known in Kumano Basin. Fifteen years ago, Morita et al. (2004) published a seismic line across the basin showing mud diapirs sourcing the MVs, but the extent of these diapirs has remained underappreciated. We present JAMSTEC 2D seismic lines across and along the basin axis showing that significant deformation of the shallow sedimentary section in the northern part of the basin is caused by mud diapirs. The diapirs feed at least 11 MVs in the northern part of the basin, all of which have been surveyed with multibeam bathymetry, high-resolution sonar and sampling. The diapirs range in diameter from 4-6 km and have seismic expression to at least 2-3 km below the seafloor. Older sedimentary layers are tilted upward adjacent to the diapirs and have internal onlap features that indicate several stages of uplift. Bottom simulating reflections (BSRs) that cross-cut the sediment and diapirs are locally disrupted under the MVs, indicating upward migration of fluids through the methane hydrate layers to the surface. Morita et al. (2004) report that mudstone fragments carried to the surface by the MVs range in age from 18.2-13.6 Ma (late Early Miocene –early Middle Miocene), indicating that the mud diapirs, which probably originate within the underlying accretionary prism, passed through the older layers of the forearc basin.

Reference: Morita, S., Ashi, J., Aoike, K., and Kuramoto, S. (2004), Evolution of Kumano basin and sources of clastic ejecta and pore fluid in Kumano mud volcanoes, Eastern Nanaki Trough, In: Proceedings of the International Symposium on Methane Hydrates and Fluid Flow in Upper Accretionary Prisms, Engineering Geology Laboratory, Department of Civil & Earth Resources Engineering, Kyoto University, Kyoto, pp. 92–99.

Keywords: Nankai Trough, Mud diapir, Accretionary prism

©2019. Japan Geoscience Union. All Right Reserved.

[E] Poster | S (Solid Earth Sciences)：S-SS Seismology

Tue. May 28, 2019 3:30 PM - 5:00 PM JST | Tue. May 28, 2019 6:30 AM - 8:00 AM UTC | Poster Hall International Exhibition Hall8, Makuhari Messe_16

[S-SS06] Nankai Trough Seismogenic Zone Experiment: Logging and sampling the seismogenic megathrust

convener:Kyuichi Kanagawa(Graduate School of Science, Chiba University), Demian M Saffer(Pennsylvania State University), Masataka Kinoshita(Earthquake Research Institute, University of Tokyo)

The Nankai Trough Seismogenic Zone Experiment (NanTroSEIZE) is a multidisciplinary investigation of fault mechanics and seismogenesis along the megathrust at the Nankai Trough subduction zone, and includes reflection and refraction seismic imaging, direct sampling by drilling, in situ measurements, and long-term monitoring in conjunction with laboratory and numerical modeling studies. During the past 12 IODP expeditions off Kii Peninsula since 2007, 15 sites have been drilled by D/V "Chikyu" down to depths from 100s of meters to more than 3000 meters below seafloor, where the inner and outer wedge of the Nankai margin has been logged and sampled extensively, and three state-of-the-art real-time downhole observatories are now in operation. The final NanTroSEIZE expedition aiming to log and sample the seismogenic megathrust at ~5200 meters below seafloor is now ongoing from October, 2018 to March, 2019.
In this session, we expect presentations not only on scientific outcomes from the past NanTroSEIZE expeditions, but also on the exciting preliminary results of the final NanTroSEIZE expedition. We welcome presentations on, but are not limited to, seismic imaging, borehole logging and monitoring, chemical analyses of pore water and mud gas, lithology, structures, physical properties and laboratory experiments of cuttings and core samples, and theoretical and numerical modeling.

[SSS06-P01] Crustal structure in the Nankai Trough seismogenic zone based on renewed depth images and seismic attribute analysis

*Kazuya Shiraishi[1], Yasuhiro Yamada[1], Masataka Kinoshita[2], Gaku Kimura[3] (1.Japan Agency for Marine-Earth Science and Technology, 2.Earthquake Research Institute, The University of Tokyo, 3.Tokyo University of Marine Science and Technology)

[SSS06-P02] Along-strike variations in protothrust zone characteristics at the Nankai Trough subduction margin

*Hannah Tilley[1], Gregory F Moore[1], Mikiya Yamashita[2], Shuichi Kodaira[2] (1.University of Hawaii at Manoa, 2.JAMSTEC)

[SSS06-P03] Temporal change in seismic velocity in the Nankai subduction zone from cross-correlation analysis of ambient noise

*Tatsunori Ikeda[1], Takeshi Tsuji[1] (1.Kyushu University)

[SSS06-P04] Strength profile of the Nankai accretionary prism evaluated from drilling parameters

★Invited Papers

*Yohei Hamada[1], Manami Kitamura[2], Takehiro Hirose[1], Yasuhiro Yamada[1], Yoshinori Sanada[1], Takamitsu Sugihara[1], Saneatsu Saito[1], KYAW MOE[1] (1.Japan Agency for Marine-Earth Science and Technology, 2.National Institute of Advanced Industrial Science andTechnology)

[SSS06-P05] Paleotemperature anomalies deduced from thermal-maturity parameters within the décollement, off Cape of Muroto, Japan

*Nana Kamiya[1,2], Takehiro Hirose[2], Yuzuru Yamamoto[2], Yohei Hamada[2], Stephen A Bowden[3], Man-Yin Tsang[4], Kiho Yang[5], Satoshi Tonai[6], Weiren Lin[1,2] (1.Graduate School of Engineering, Kyoto University, 2.JAMSTEC, 3.University of Aberdeen, 4.University of Toronto, 5.Yonsei University, 6.Kochi University)

[SSS06-P06] Modelling thermal maturity of an accretionary wedge

Utsav Mannu[2], *Masataka Kinoshita[1], Taras Gerya[3] (1.Earthquake Research Institute, University of Tokyo, 2.Department of Earth and Climate Science, IISER Pune, 3.Institute of Geophysics, ETH Zürich)

Crustal structure in the Nankai Trough seismogenic zone based on renewed depth images and seismic attribute analysis

*Kazuya Shiraishi[1], Yasuhiro Yamada[1], Masataka Kinoshita[2], Gaku Kimura[3]

1. Japan Agency for Marine-Earth Science and Technology, 2. Earthquake Research Institute, The University of Tokyo, 3. Tokyo University of Marine Science and Technology

To better understand geological structure in the Nankai Trough seismogenic zone, we investigate deformations in the accretionary prism based on renewed depth images and seismic attribute analyses. We reprocessed subareas of the Kumano-nada 3D MCS data acquired in 2006: 25 km x 12 km area including IODP C0002 site in Phase 1 (2015-2016) and 20 km x 12 km area including IODP C0006 site in Phase 2 (2017-2018). We also reprocessed 2D MCS data along a 50-km line crossing C0002 site in NW-SE direction, which was selected from a 2D survey ODKM03 in 2003 with a longer streamer cable (6 km) than streamer cables of the 3D survey (4.5 km). Quality improvement of reflection signals was achieved by applying recent broadband processing and advanced process to attenuate noise and multiple reflections. Depth domain reflection images were obtained after applying new pre-stack depth migration methods. Then, we calculated several seismic attributes from the 3D reflection image volumes, such as coherence and structure dips which are useful to interpret structural features.
As a result of our investigation, deformed structure within the inner accreted sediments and its relation with the megathrust fault are clearer than before. Anticlines are identified just below the Kumano forearc basin and fragmented reflections can be seen below the anticlines. Characteristic patterns of folds can be recognized on the horizontal section of the coherence cube, which are corresponding to the anticlines on the vertical sections. These reflection features imply development of fold structures due to thrust faults with branched minor faults. In the reprocessed 2D section, curved reflectors with stepwise displacement are imaged in the region of 4 - 6 km depth. These reflectors may represent multiple thrust faults with back-thrusts, and the thrust faults are consistent with the structural features in the 3D images. The detachments of the thrust faults seem to converge to wavy points on the megathrust fault surface. Furthermore, details of deformation and fracture in the outer accretionary prism are imaged clearer than the previous images. Lithological boundaries with displacement along imbricated thrusts can be traced beyond the fault, and conjugate faults due to horizontal compression which cut the in-sequence thrusts are recognized on the horizontal section from superimposed view of the coherence and dip angles. Reflectors within underthrusted sediments beneath the imbricated thrust layer are clearly imaged. Some of the reflectors can be identified as parts of detachment of the thrust faults. The topographic relief of the oceanic crust should be considered when the deformed structures in the overburden sediments and distribution of décollement are revisited.

Acknowledgements:
This research is supported by JSPS KAKENHI (JP15H05717).

Keywords: Nankai Trough seismogenic zone, crustal structure, reflection seismic, seismic attribute

©2019. Japan Geoscience Union. All Right Reserved.

Along-strike variations in protothrust zone characteristics at the Nankai Trough subduction margin

*Hannah Tilley[1], Gregory F Moore[1], Mikiya Yamashita[2], Shuichi Kodaira[2]

1. University of Hawaii at Manoa, 2. JAMSTEC

Protothrust zones (PTZs) are assumed to control the development of new frontal thrusts at subduction zones. PTZs are areas of incipient thrust faulting between the deformation front and the frontal thrust. However, limited resolution of previous seismic studies has hindered the study of their role in subduction accretion. New high-resolution seismic reflection surveys enabled detailed analysis of the PTZ along the Nankai Trough, SE Japan. Seventeen multichannel seismic reflection lines were collected perpendicular to the trench axis between Cape Ashizuri and Cape Muroto using a 1200m long, 192 channel hydrophone cable and a 380 in^3 (5.24L) cluster airgun array. These lines were processed using pre-stack depth migration. PTZs only existed where a turbidite sequence was present beneath the trench wedge. The PTZs consisted of closely spaced, sub-parallel protothrusts that decreased in spacing and increased in length landward. Where the turbidites were truncated by basement topography, there was a transitional PTZ heterogeneous protothrusts and small displacement thrust faults. We hypothesize that elevated pore pressures due to the low permeability hemipelagic sediment inhibit the formation of PTZs and favor small displacement thrusts in a narrow trench wedge. Conversely, turbidite layers within the hemipelagic sediment allow drainage and reduce the pore pressure. This increases the effective stress and shear strength on faults, resulting in strain localizing protothrusts. This implies that the changes in pore pressure imposed by differences in the sediment permeability control the style of deformation in the trench wedge and consequently, the geometry of the accretionary wedge.

Keywords: Nankai Trough, Protothrust Zone, Subduction zone

©2019. Japan Geoscience Union. All Right Reserved.

Temporal change in seismic velocity in the Nankai subduction zone from cross-correlation analysis of ambient noise

*Tatsunori Ikeda[1], Takeshi Tsuji[1]

1. Kyushu University

To investigate the temporal variation of stress or strain in the Nankai subduction zone, we estimated the temporal variation of seismic velocity by using cross-correlations of ambient noise in the frequency range 0.7–2.0 Hz, which was dominated by ACR waves, recorded by the DONET offshore seismic network from 1 October 2014 to 30 November 2017. The 1 April 2016 Off-Mie earthquake (M_W 5.9) and its aftershocks occurred beneath the seismic network.

Our results document a clear decrease in seismic velocity at the time of the earthquake. These coseismic velocity drops were correlated with peak ground velocities at each station, suggesting that dynamic stress changes due to strong ground motions are a primary factor in coseismic velocity variations. Differences in the sensitivity of seismic velocity changes to peak ground velocity may reflect subsurface conditions at each station, such as geological structures and effective pressure conditions. We also observed a long-term increase in seismic velocities, independent of the 2016 earthquake, that may reflect tectonic strain accumulation around the Nankai subduction zone. After removing the long-term trend, we found that the coseismic velocity drops had not completely recovered by the end of the observation period, possibly indicating nonlinear effects of the 2016 earthquake. Our results suggest that ambient noise cross-correlation might be used to monitor the stress state in the Nankai accretionary prism in offshore environments, which would contribute to a better understanding of earthquake processes.

Keywords: Nankai Trough, 2016 Off-Mie earthquake, monitoring, ambient noise, seismic interferometry

©2019. Japan Geoscience Union. All Right Reserved.

Strength profile of the Nankai accretionary prism evaluated from drilling parameters

*Yohei Hamada[1], Manami Kitamura[2], Takehiro Hirose[1], Yasuhiro Yamada[1], Yoshinori Sanada[1], Takamitsu Sugihara[1], Saneatsu Saito[1], KYAW MOE[1]

1. Japan Agency for Marine-Earth Science and Technology, 2. National Institute of Advanced Industrial Science andTechnology

In-situ rock strength with depth under the ground/seafloor is a critical parameter for various studies in geology and seismology. The measurements on rock/core samples, however, hardly have been done with success due to lack of drilled cores and sufficient knowledge about the in situ conditions. We proposed a new indicator of the strength, equivalent strength (EST) developing previous mechanical parameter (Mechanical specific energy: Teal, 1964) from the oil industry, which is converted only from drilling performance parameters such as drillstring rotational torque, bit depth and drillstring rotational per minute. The data processing was applied to the data taken from International Ocean Discovery Program (IODP) expeditions in the Nankai Trough (sites C0002 and C0023). The depth profiles of the EST at Site C0002 are drawn from 0 to 3000 meter-below-seafloor (mbsf), across the forearc basin and the accretionary prism, and the values of the calculated EST are consistent with compressive strength measured on core samples under estimated in situ stress conditions in laboratory. The high (~20 MPa) EST in the forearc basin sediments corresponds to the high $CaCO_3$ content indicating the carbonate is cementing the shallow formation. The EST did not show a significant increase at the forearc basin–accretionary prism boundary, however clearly increased within the prism, ca. below 1500 mbsf. This result may indicate that even the shallow accretionary prism has been strengthened by horizontal compression derived from plate subduction. At the site C0023, where the toe of the accretionary prism area off Cape Muroto, the EST trend increases with depth and suddenly changes between 600–650 mbsf, 840–870 mbsf, and 1120 ~ mbsf, corresponding to tuff0rich zone, top of the subducting sediments and the basement igneous rocks, respectively. This EST trend shows good agreement with P-wave velocity curve measured on core samples. The EST decreases from ~20 MPa to 5 MPa below the frontal decollement with sharp negative peak. This low-EST zone probably indicate the existence of excess fluid pressure.

Keywords: The Nankai Trough, Equivalent strength, Nankai Trough SeismogenicZone Experiment, T-Limit of the Deep Biosphere off Muroto

©2019. Japan Geoscience Union. All Right Reserved.

Paleotemperature anomalies deduced from thermal-maturity parameters within the décollement, off Cape of Muroto, Japan

*Nana Kamiya[1,2], Takehiro Hirose[2], Yuzuru Yamamoto[2], Yohei Hamada[2], Stephen A Bowden[3], Man-Yin Tsang[4], Kiho Yang[5], Satoshi Tonai[6], Weiren Lin[1,2]

1. Graduate School of Engineering, Kyoto University, 2. JAMSTEC, 3. University of Aberdeen, 4. University of Toronto, 5. Yonsei University, 6. Kochi University

Heat flow is characteristically high at the toe of the Nankai accretionary prism, off cape Muroto, and this is considered to be a consequence of the subduction of a hot and active ridge (e.g. Yamano et al., 2003). Despite present-day heat flow being known, how heat has changed over time in this area remains uncertain and is poorly constrained. To address this question, we have investigated palaeotemperatures using thermal maturity parameters measured on cores collected during IODP Expedition 370. Paleotemperature data were evaluated within the context of present-day heat flow and expected changes in temperature with respect to depth; e.g., numerical constraint whether present-day temperatures are too hot or cold to explain thermal maturity measurements, and whether there are anomalies with respect to depth. This is particularly important for Expedition 370 (T-limits) which selected the Muroto-site (Site C0023) because of its high heat flow and the chance this offers to investigate the habitability of the deep biosphere with respect to the temperature. Site C0023 is located 120 km from Cape Muroto, and is in the protothrust-zone of the Nankai accretionary prism. The hole encountered the décollement at 758-795 mbsf, and present-day temperatures were measured down to ~350 mbsf. Vitrinite reflectance was used to estimate maximum paleotemperatures and to look for thermal anomalies. The vitrinite reflectance increases with depth from 0.2 to 0.6 % from 200 to 700 mbsf, typical of conventional burial metamorphism, but changes little from 700 to 1000 mbsf (values stay about 0.6 %). There is a notable high value at 1090 mbsf (about 1%). There are anomalously high values of both vitrinite reflectance and sterane and hopane biomarker data at about 800 mbsf. For heating durations of 400, 4000, 40000 and 400000 years, and assuming thermal maturation using the EasyVit model of Burnham and Sweeny (1990), temperatures of 40~140 ℃ can explain data between 200 to 750 mbsf. To match measurements of vitrinite reflectance at 750 mbsf, a maximum paleotemperature of 140 ℃ is required. At 1090 mbsf, temperatures as high as ~200 ℃ could be needed. The difference between the paleo- and present-day temperatures is the notably the greatest at the décollement, strongly suggesting an elevated heat flow at some time. A heating duration of 400 years, an elevated a heat flow of 130 ±90 mW/m^2 and a temperature > 150 ℃ can explain the observations on the vitrinite reflectance. Considering the scales of space and time of thermal advection, a high-temperature fluid along the décollement zone is our currently preferred explanation.

Keywords: Muroto, Décollement, Paleotemperature anomalies

©2019. Japan Geoscience Union. All Right Reserved.

Modelling thermal maturity of an accretionary wedge

Utsav Mannu[2], *Masataka Kinoshita[1], Taras Gerya[3]

1. Earthquake Research Institute, University of Tokyo, 2. Department of Earth and Climate Science, IISER Pune, 3. Institute of Geophysics, ETH Zürich

In accretionary margins, the estimation of peak heating through the thermal maturity of organic material reveals differentiated deformational pathways in the adjoining sections of the wedge. As the thermal maturity of the deformed structures is a function of both the geothermal gradient and the duration of time it has been exposed to different gradients, the distribution of vitrinite reflectance (the measure of thermal maturity) in the wedge does not necessarily reveal the temporal deformational pathway of the individual pockets. As a result, the different portions of the accretionary wedge exhibit different correlations between the thermal maturity and a unique deformational pathway. These different correlations can be explored through the means of geodynamic modelling which can then be used in the field to ascertain a more holistic picture of deformation in an accretionary wedge. Therefore, in this study, we use a 2D plate subduction thermomechanical model, to simulate formation of accretionary wedge and the track the evolution of the vitrinite reflectance in the accretionary wedge.

Keywords: thermal maturity, accretionary wedge, numerical simulation

©2019. Japan Geoscience Union. All Right Reserved.

[E] Poster | S (Solid Earth Sciences)：S-SS Seismology

Tue. May 28, 2019 5:15 PM - 6:30 PM JST | Tue. May 28, 2019 8:15 AM - 9:30 AM UTC | Poster Hall International Exhibition Hall8, Makuhari Messe_28

[S-SS06] Nankai Trough Seismogenic Zone Experiment: Logging and sampling the seismogenic megathrust

convener:Kyuichi Kanagawa(Graduate School of Science, Chiba University), Demian M Saffer(Pennsylvania State University), Masataka Kinoshita(Earthquake Research Institute, University of Tokyo)

The Nankai Trough Seismogenic Zone Experiment (NanTroSEIZE) is a multidisciplinary investigation of fault mechanics and seismogenesis along the megathrust at the Nankai Trough subduction zone, and includes reflection and refraction seismic imaging, direct sampling by drilling, in situ measurements, and long-term monitoring in conjunction with laboratory and numerical modeling studies. During the past 12 IODP expeditions off Kii Peninsula since 2007, 15 sites have been drilled by D/V "Chikyu" down to depths from 100s of meters to more than 3000 meters below seafloor, where the inner and outer wedge of the Nankai margin has been logged and sampled extensively, and three state-of-the-art real-time downhole observatories are now in operation. The final NanTroSEIZE expedition aiming to log and sample the seismogenic megathrust at ~5200 meters below seafloor is now ongoing from October, 2018 to March, 2019.
In this session, we expect presentations not only on scientific outcomes from the past NanTroSEIZE expeditions, but also on the exciting preliminary results of the final NanTroSEIZE expedition. We welcome presentations on, but are not limited to, seismic imaging, borehole logging and monitoring, chemical analyses of pore water and mud gas, lithology, structures, physical properties and laboratory experiments of cuttings and core samples, and theoretical and numerical modeling.

[SSS06-P01] Crustal structure in the Nankai Trough seismogenic zone based on renewed depth images and seismic attribute analysis

*Kazuya Shiraishi[1], Yasuhiro Yamada[1], Masataka Kinoshita[2], Gaku Kimura[3] (1.Japan Agency for Marine-Earth Science and Technology, 2.Earthquake Research Institute, The University of Tokyo, 3.Tokyo University of Marine Science and Technology)

[SSS06-P02] Along-strike variations in protothrust zone characteristics at the Nankai Trough subduction margin

*Hannah Tilley[1], Gregory F Moore[1], Mikiya Yamashita[2], Shuichi Kodaira[2] (1.University of Hawaii at Manoa, 2.JAMSTEC)

[SSS06-P03] Temporal change in seismic velocity in the Nankai subduction zone from cross-correlation analysis of ambient noise

*Tatsunori Ikeda[1], Takeshi Tsuji[1] (1.Kyushu University)

[SSS06-P04] Strength profile of the Nankai accretionary prism evaluated from drilling parameters

★Invited Papers

*Yohei Hamada[1], Manami Kitamura[2], Takehiro Hirose[1], Yasuhiro Yamada[1], Yoshinori Sanada[1], Takamitsu Sugihara[1], Saneatsu Saito[1], KYAW MOE[1] (1.Japan Agency for Marine-Earth Science and Technology, 2.National Institute of Advanced Industrial Science andTechnology)

[SSS06-P05] Paleotemperature anomalies deduced from thermal-maturity parameters within the décollement, off Cape of Muroto, Japan

*Nana Kamiya[1,2], Takehiro Hirose[2], Yuzuru Yamamoto[2], Yohei Hamada[2], Stephen A Bowden[3], Man-Yin Tsang[4], Kiho Yang[5], Satoshi Tonai[6], Weiren Lin[1,2] (1.Graduate School of Engineering, Kyoto University, 2.JAMSTEC, 3.University of Aberdeen, 4.University of Toronto, 5.Yonsei University, 6.Kochi University)

[SSS06-P06] Modelling thermal maturity of an accretionary wedge

Utsav Mannu[2], *Masataka Kinoshita[1], Taras Gerya[3] (1.Earthquake Research Institute, University of Tokyo, 2.Department of Earth and Climate Science, IISER Pune, 3.Institute of Geophysics, ETH Zürich)

Crustal structure in the Nankai Trough seismogenic zone based on renewed depth images and seismic attribute analysis

*Kazuya Shiraishi[1], Yasuhiro Yamada[1], Masataka Kinoshita[2], Gaku Kimura[3]

1. Japan Agency for Marine-Earth Science and Technology, 2. Earthquake Research Institute, The University of Tokyo, 3. Tokyo University of Marine Science and Technology

To better understand geological structure in the Nankai Trough seismogenic zone, we investigate deformations in the accretionary prism based on renewed depth images and seismic attribute analyses. We reprocessed subareas of the Kumano-nada 3D MCS data acquired in 2006: 25 km x 12 km area including IODP C0002 site in Phase 1 (2015-2016) and 20 km x 12 km area including IODP C0006 site in Phase 2 (2017-2018). We also reprocessed 2D MCS data along a 50-km line crossing C0002 site in NW-SE direction, which was selected from a 2D survey ODKM03 in 2003 with a longer streamer cable (6 km) than streamer cables of the 3D survey (4.5 km). Quality improvement of reflection signals was achieved by applying recent broadband processing and advanced process to attenuate noise and multiple reflections. Depth domain reflection images were obtained after applying new pre-stack depth migration methods. Then, we calculated several seismic attributes from the 3D reflection image volumes, such as coherence and structure dips which are useful to interpret structural features.
As a result of our investigation, deformed structure within the inner accreted sediments and its relation with the megathrust fault are clearer than before. Anticlines are identified just below the Kumano forearc basin and fragmented reflections can be seen below the anticlines. Characteristic patterns of folds can be recognized on the horizontal section of the coherence cube, which are corresponding to the anticlines on the vertical sections. These reflection features imply development of fold structures due to thrust faults with branched minor faults. In the reprocessed 2D section, curved reflectors with stepwise displacement are imaged in the region of 4 - 6 km depth. These reflectors may represent multiple thrust faults with back-thrusts, and the thrust faults are consistent with the structural features in the 3D images. The detachments of the thrust faults seem to converge to wavy points on the megathrust fault surface. Furthermore, details of deformation and fracture in the outer accretionary prism are imaged clearer than the previous images. Lithological boundaries with displacement along imbricated thrusts can be traced beyond the fault, and conjugate faults due to horizontal compression which cut the in-sequence thrusts are recognized on the horizontal section from superimposed view of the coherence and dip angles. Reflectors within underthrusted sediments beneath the imbricated thrust layer are clearly imaged. Some of the reflectors can be identified as parts of detachment of the thrust faults. The topographic relief of the oceanic crust should be considered when the deformed structures in the overburden sediments and distribution of décollement are revisited.

Acknowledgements:
This research is supported by JSPS KAKENHI (JP15H05717).

Keywords: Nankai Trough seismogenic zone, crustal structure, reflection seismic, seismic attribute

©2019. Japan Geoscience Union. All Right Reserved.

Along-strike variations in protothrust zone characteristics at the Nankai Trough subduction margin

*Hannah Tilley[1], Gregory F Moore[1], Mikiya Yamashita[2], Shuichi Kodaira[2]

1. University of Hawaii at Manoa, 2. JAMSTEC

Protothrust zones (PTZs) are assumed to control the development of new frontal thrusts at subduction zones. PTZs are areas of incipient thrust faulting between the deformation front and the frontal thrust. However, limited resolution of previous seismic studies has hindered the study of their role in subduction accretion. New high-resolution seismic reflection surveys enabled detailed analysis of the PTZ along the Nankai Trough, SE Japan. Seventeen multichannel seismic reflection lines were collected perpendicular to the trench axis between Cape Ashizuri and Cape Muroto using a 1200m long, 192 channel hydrophone cable and a 380 in^3 (5.24L) cluster airgun array. These lines were processed using pre-stack depth migration. PTZs only existed where a turbidite sequence was present beneath the trench wedge. The PTZs consisted of closely spaced, sub-parallel protothrusts that decreased in spacing and increased in length landward. Where the turbidites were truncated by basement topography, there was a transitional PTZ heterogeneous protothrusts and small displacement thrust faults. We hypothesize that elevated pore pressures due to the low permeability hemipelagic sediment inhibit the formation of PTZs and favor small displacement thrusts in a narrow trench wedge. Conversely, turbidite layers within the hemipelagic sediment allow drainage and reduce the pore pressure. This increases the effective stress and shear strength on faults, resulting in strain localizing protothrusts. This implies that the changes in pore pressure imposed by differences in the sediment permeability control the style of deformation in the trench wedge and consequently, the geometry of the accretionary wedge.

Keywords: Nankai Trough, Protothrust Zone, Subduction zone

©2019. Japan Geoscience Union. All Right Reserved.

Temporal change in seismic velocity in the Nankai subduction zone from cross-correlation analysis of ambient noise

*Tatsunori Ikeda[1], Takeshi Tsuji[1]

1. Kyushu University

To investigate the temporal variation of stress or strain in the Nankai subduction zone, we estimated the temporal variation of seismic velocity by using cross-correlations of ambient noise in the frequency range 0.7–2.0 Hz, which was dominated by ACR waves, recorded by the DONET offshore seismic network from 1 October 2014 to 30 November 2017. The 1 April 2016 Off-Mie earthquake (M_W 5.9) and its aftershocks occurred beneath the seismic network.

Our results document a clear decrease in seismic velocity at the time of the earthquake. These coseismic velocity drops were correlated with peak ground velocities at each station, suggesting that dynamic stress changes due to strong ground motions are a primary factor in coseismic velocity variations. Differences in the sensitivity of seismic velocity changes to peak ground velocity may reflect subsurface conditions at each station, such as geological structures and effective pressure conditions. We also observed a long-term increase in seismic velocities, independent of the 2016 earthquake, that may reflect tectonic strain accumulation around the Nankai subduction zone. After removing the long-term trend, we found that the coseismic velocity drops had not completely recovered by the end of the observation period, possibly indicating nonlinear effects of the 2016 earthquake. Our results suggest that ambient noise cross-correlation might be used to monitor the stress state in the Nankai accretionary prism in offshore environments, which would contribute to a better understanding of earthquake processes.

Keywords: Nankai Trough, 2016 Off-Mie earthquake, monitoring, ambient noise, seismic interferometry

©2019. Japan Geoscience Union. All Right Reserved.

Strength profile of the Nankai accretionary prism evaluated from drilling parameters

*Yohei Hamada[1], Manami Kitamura[2], Takehiro Hirose[1], Yasuhiro Yamada[1], Yoshinori Sanada[1], Takamitsu Sugihara[1], Saneatsu Saito[1], KYAW MOE[1]

1. Japan Agency for Marine-Earth Science and Technology, 2. National Institute of Advanced Industrial Science andTechnology

In-situ rock strength with depth under the ground/seafloor is a critical parameter for various studies in geology and seismology. The measurements on rock/core samples, however, hardly have been done with success due to lack of drilled cores and sufficient knowledge about the in situ conditions. We proposed a new indicator of the strength, equivalent strength (EST) developing previous mechanical parameter (Mechanical specific energy: Teal, 1964) from the oil industry, which is converted only from drilling performance parameters such as drillstring rotational torque, bit depth and drillstring rotational per minute. The data processing was applied to the data taken from International Ocean Discovery Program (IODP) expeditions in the Nankai Trough (sites C0002 and C0023). The depth profiles of the EST at Site C0002 are drawn from 0 to 3000 meter-below-seafloor (mbsf), across the forearc basin and the accretionary prism, and the values of the calculated EST are consistent with compressive strength measured on core samples under estimated in situ stress conditions in laboratory. The high (~20 MPa) EST in the forearc basin sediments corresponds to the high $CaCO_3$ content indicating the carbonate is cementing the shallow formation. The EST did not show a significant increase at the forearc basin–accretionary prism boundary, however clearly increased within the prism, ca. below 1500 mbsf. This result may indicate that even the shallow accretionary prism has been strengthened by horizontal compression derived from plate subduction. At the site C0023, where the toe of the accretionary prism area off Cape Muroto, the EST trend increases with depth and suddenly changes between 600–650 mbsf, 840–870 mbsf, and 1120 ~ mbsf, corresponding to tuff0rich zone, top of the subducting sediments and the basement igneous rocks, respectively. This EST trend shows good agreement with P-wave velocity curve measured on core samples. The EST decreases from ~20 MPa to 5 MPa below the frontal decollement with sharp negative peak. This low-EST zone probably indicate the existence of excess fluid pressure.

Keywords: The Nankai Trough, Equivalent strength, Nankai Trough SeismogenicZone Experiment, T-Limit of the Deep Biosphere off Muroto

©2019. Japan Geoscience Union. All Right Reserved.

Paleotemperature anomalies deduced from thermal-maturity parameters within the décollement, off Cape of Muroto, Japan

*Nana Kamiya[1,2], Takehiro Hirose[2], Yuzuru Yamamoto[2], Yohei Hamada[2], Stephen A Bowden[3], Man-Yin Tsang[4], Kiho Yang[5], Satoshi Tonai[6], Weiren Lin[1,2]

1. Graduate School of Engineering, Kyoto University, 2. JAMSTEC, 3. University of Aberdeen, 4. University of Toronto, 5. Yonsei University, 6. Kochi University

Heat flow is characteristically high at the toe of the Nankai accretionary prism, off cape Muroto, and this is considered to be a consequence of the subduction of a hot and active ridge (e.g. Yamano et al., 2003). Despite present-day heat flow being known, how heat has changed over time in this area remains uncertain and is poorly constrained. To address this question, we have investigated palaeotemperatures using thermal maturity parameters measured on cores collected during IODP Expedition 370. Paleotemperature data were evaluated within the context of present-day heat flow and expected changes in temperature with respect to depth; e.g., numerical constraint whether present-day temperatures are too hot or cold to explain thermal maturity measurements, and whether there are anomalies with respect to depth. This is particularly important for Expedition 370 (T-limits) which selected the Muroto-site (Site C0023) because of its high heat flow and the chance this offers to investigate the habitability of the deep biosphere with respect to the temperature. Site C0023 is located 120 km from Cape Muroto, and is in the protothrust-zone of the Nankai accretionary prism. The hole encountered the décollement at 758-795 mbsf, and present-day temperatures were measured down to ~350 mbsf. Vitrinite reflectance was used to estimate maximum paleotemperatures and to look for thermal anomalies. The vitrinite reflectance increases with depth from 0.2 to 0.6 % from 200 to 700 mbsf, typical of conventional burial metamorphism, but changes little from 700 to 1000 mbsf (values stay about 0.6 %). There is a notable high value at 1090 mbsf (about 1%). There are anomalously high values of both vitrinite reflectance and sterane and hopane biomarker data at about 800 mbsf. For heating durations of 400, 4000, 40000 and 400000 years, and assuming thermal maturation using the EasyVit model of Burnham and Sweeny (1990), temperatures of 40~140 ℃ can explain data between 200 to 750 mbsf. To match measurements of vitrinite reflectance at 750 mbsf, a maximum paleotemperature of 140 ℃ is required. At 1090 mbsf, temperatures as high as ~200 ℃ could be needed. The difference between the paleo- and present-day temperatures is the notably the greatest at the décollement, strongly suggesting an elevated heat flow at some time. A heating duration of 400 years, an elevated a heat flow of 130 ±90 mW/m^2 and a temperature > 150 ℃ can explain the observations on the vitrinite reflectance. Considering the scales of space and time of thermal advection, a high-temperature fluid along the décollement zone is our currently preferred explanation.

Keywords: Muroto, Décollement, Paleotemperature anomalies

©2019. Japan Geoscience Union. All Right Reserved.

Modelling thermal maturity of an accretionary wedge

Utsav Mannu[2], *Masataka Kinoshita[1], Taras Gerya[3]

1. Earthquake Research Institute, University of Tokyo, 2. Department of Earth and Climate Science, IISER Pune, 3. Institute of Geophysics, ETH Zürich

In accretionary margins, the estimation of peak heating through the thermal maturity of organic material reveals differentiated deformational pathways in the adjoining sections of the wedge. As the thermal maturity of the deformed structures is a function of both the geothermal gradient and the duration of time it has been exposed to different gradients, the distribution of vitrinite reflectance (the measure of thermal maturity) in the wedge does not necessarily reveal the temporal deformational pathway of the individual pockets. As a result, the different portions of the accretionary wedge exhibit different correlations between the thermal maturity and a unique deformational pathway. These different correlations can be explored through the means of geodynamic modelling which can then be used in the field to ascertain a more holistic picture of deformation in an accretionary wedge. Therefore, in this study, we use a 2D plate subduction thermomechanical model, to simulate formation of accretionary wedge and the track the evolution of the vitrinite reflectance in the accretionary wedge.

Keywords: thermal maturity, accretionary wedge, numerical simulation

©2019. Japan Geoscience Union. All Right Reserved.

[J] Poster | S (Solid Earth Sciences)：S-SS Seismology

Tue. May 28, 2019 10:45 AM - 12:15 PM JST | Tue. May 28, 2019 1:45 AM - 3:15 AM UTC | Poster Hall International Exhibition Hall8, Makuhari Messe_6

[S-SS10] Seismicity

convener:Kei Katsumata(Institute of Seismology and Volcanology, Hokkaido University)

This session aims to improve our understanding on seismicity. Any contribution on behavior of earthquakes as a cluster, such as regional seismicity and aftershocks, are welcomed. We also welcome contribution on temporal and spatial interactions that control seismicity, and tectonic processes, and geological and thermal structures that regulate seismicity.

[SSS10-P01] Spatial-temporal and seismogram characteristics of foreshock and aftershock activities for tsunami earthquakes

*Yifeng Liu[1], Yoshihiro Ito[2], Kazuaki Ohta[2], Satoshi Katakami[1] (1.Division of Earth and Planetary Sciences, Graduate School of Science, Kyoto University, 2.Disaster Prevention Research Institude, Kyoto University)

[SSS10-P02] Successively occurring large earthquakes in the world – comparison of real cases with expectations by the space-time ETAS

*Tetsuo Hashimoto[1], Takashi YOKOTA[2] (1.Seismology and Tsunami Research Department, Meteorological Reaserch Institute, 2.Aichi Institue Technology)

[SSS10-P03] Seismicity beneath stable oceanic plate

*Yasushi Ishihara[1] (1.R&D Center for Earthquake and Tsunami, JAMSTEC)

[SSS10-P04] Relation between long-term slow slip events and correlation between tidal triggering effect and deep low-frequency earthquakes in Bungo Channel: Part 2

*Fuyuki Hirose[1], Akio Kobayashi[1], Kenji Maeda[2] (1.Seismology and Tsunami Research Department, Meteorological Research Institute, 2.Seismology and Volcanology Department, Japan Meteorological Agency)

[SSS10-P05] Arrival-time and hypocenter determination using S-net

*Tomomi Okada[1], Ryota Takagi[1], Takashi NAKAYAMA[1], Syuichi Suzuki[1], Ryosuke Azuma[1], Genti Toyokuni[1], Keisuke Yoshida[1], Naoki Uchida[1], Ryota Hino[1] (1.Research Center for Prediction of Earthquakes and Volcanic Eruptions, Graduate School of Science, Tohoku University)

[SSS10-P06] Focal mechanisms of the double seismic zone in the Pacific plate, off Boso: Temporal change after the 2011 Tohoku EQ

*Guanyu Chen[1], Toshinori Sato[2], Tomoharu Sato[1], Asami Terada, Masanao Shinohara[3], Kimihiro Mochizuki[3], Tomoaki Yamada[3], Kenji Uehira[4], Takashi Shimbo[5], Shuichi Kodaira[5], Yuya Machida[5], Ryota Hino[6], Ryosuke Azuma[6], Yoshio Murai[7], Yoshihiro Ito[8], Hiroshi Yakiwara[9], Kenji Hirata[4], Akinori Hashima[3], Andrew M. Freed[10] (1.Faculty of Science, Chiba University, 2.Graduate School of Science, Chiba University, 3.Earthquake Research Institute, University of Tokyo, 4.National Research Institute for Earth Science and Disaster Resilience, 5.Japan Agency for Marine-Earth Science and Technology, 6.Graduate School of Science, Tohoku University, 7.Institute of Seismology and Volcanology, Faculty of Science, Hokkaido University, 8.Disaster Prevention Research Institute, Kyoto University, 9.Nansei-toko Observatory for Earthquakes and Volcanoes, Kagoshima University, 10.Purdue University)

[SSS10-P07] Ocean bottom seismographic observation and similar earthquake detection in the northern part of the Nansei Islands

*Yukihiro Nakatani[1], Hiroshi Yakiwara[1], Shuichiro Hirano[1], Reiji Kobayashi[2], Hiroki Miyamachi[2], Shigeru Nakao[2], Kazunari Uchida[3], Takeshi Matsushima[3], Hiroshi Shimizu[3], Kazuo Nakahigashi[4], Yusuke Yamashita[5], Hideji Abe[6], Tomoaki Yamada[6], Masanao Shinohara[6] (1.Nansei-Toko Observatory for Earthquakes and Volcanoes, Kagoshima University, 2.Graduate School of Science and Engineering,

Kagoshima University, 3.Institute of Seismology and Volcanology, Faculty of Science, Kyushu University, 4.Tokyo University of Marine Science and Technology, 5.Disaster Prevention Research Institute, Kyoto University, 6.Earthquake Research Institute, the University of Tokyo)

[SSS10-P08] Seismicity and crustal structure in the Okinawa Trough

*Azusa Nishizawa[1], Takeshi Kimura[1], Kentaro Kaneda[2] (1.National Research Institute for Earth Science and Disaster Resilience, 2.Japan Coast Guard)

[SSS10-P09] Time series analyses of the seismic activities in southwestern Japanese Island to southeastern Korean Peninsula excited by the deep fluid heat flow

*Takayuki Kawabe[1] (1.Faculty of Education, Arts and Sciences, Yamagata University)

[SSS10-P10] Integrated monitoring of seismicity in and around the Suruga Bay using Ocean Bottom Seismometers and inland stations.

*Yannis Panayotopoulos[1], Hisatoshi Baba[2], Takahito Nishimiya[3], Taiyo Sotani[4], Nakao Nagisa[4] (1.Association for the Development of Earthquake Prediction, 2.Department of Marine and Earth Science, Tokai University, 3.Meteorological Research Institute, Japan Meteorological Agency, 4.Tokai University)

[SSS10-P11] Linear distribution of the intraslab earthquakes in Tokai

*Sadaomi Suzuki[1] (1.Tono Research Institute of Earthquake Science, Association for the Development of Earthquake Prediction)

[SSS10-P12] The stress change of Chubu region before and after the 2011 Tohoku-oki Earthquake(Mw9.0)

*Yuki Susukida[1], Kei Katsumata[1] (1.Institute of Seismology and Volcanology, Hokkaido University)

[SSS10-P13] Repeating earthquake activity off Miyagi Prefecture triggered by the 2011 Tohoku-oki earthquake

*Kenshiro Tsumura[1] (1.Association for Developement of Earthquake Prediction)

[SSS10-P14] Seismic Moments of Inland Small Earthquakes in Japan: Spectral Analyses Using the Hi-net

*Tomotake Ueno[1], Tatsuhiko Saito[1] (1.National Research Institute for Earth Science and Disaster Resilience)

[SSS10-P15] Spatiotemporal variations of stress field in the 2016 Kumamoto earthquake (M 7.3) area

*Dapeng Zhao[1], Zhiteng Yu[2], Jiabiao Li[2], Zhouchuan Huang[3] (1.Department of Geophysics, Tohoku University, 2.State Oceanic Administration, 3.School of Earth Sciences and Engineering, Nanjing University)

[SSS10-P16] Seismicity and crustal deformation following the 2016 Kumamoto earthquakes

*Kazuyoshi Nanjo[1], Jun Izutsu[2], Yoshiaki Orihara[3], Masashi Kamogawa[4], Toshiyasu Nagao[3] (1.University of Shizuoka, 2.Chubu University, 3.Tokai University, 4.Tokyo Gakugei University)

[SSS10-P17] The unique characters of intensity distribution of the 2018 Sep. 6 Mw6.6 Earthquake of Iburi region in Hokkaido, Japan

*Ritsuko S. Matsu'ura[1], Hiroto Tanaka[2], Mitsuko Furumura[1], Tsutomu Takahama[2] (1.Earthquake Research Center, Association for the Development of Earthquake Prediction, 2.Kozo Keikaku Engineering Inc.)

[SSS10-P18] **Determination of Hypocenter Location in Sumani and Sianok Fault Segments, West Sumatra region Using Oct-Tree Importance Sampling Method**

*Ade Surya Putra[1], Nanang Tyasbudi Puspito[2], Andri Dian Nugraha[2], Pepen Supendi[3,1] (1.Geophysical Engineering, Faculty of Mining and Petroleoum Engineering, Institute of Technology Bandung, 2.Global Geophysics Research Group, Faculty of Mining and Petroleoum Engineering, Institute of Technology Bandung, 3.Agency of Meteorology, Climatology and Geohysics (BMKG), Indonesia, Bandung, Indonesia)

[SSS10-P19] **1D Seismic Velocity Modelling and Hypocenter Relocation around Central and East Java Region: Preliminary Result**

*Faiz Muttaqy[1], Andri Dian Nugraha[2], Nanang Tyasbudi Puspito[2] (1.Geophysical Engineering Study Program, Faculty of Mining and Petroleum Engineering, Institut Teknologi Bandung, 2.Global Geophysics Research Group, Faculty of Mining and Petroleum Engineering, Institut Teknologi Bandung)

[SSS10-P20] ***Seismicity and Tectonics of the Bingöl Area: Eastern Anatolia***

*Dogan Kalafat[1] (1.Bogazici University Kandilli Observatory and Earthquake Research Institute Cengelkoy, Istanbul Turkey)

[SSS10-P21] Seismicity along the North Anatolian Fault beneath the Marmara Sea, deduced from long-term ocean bottom seismographic observations

*Yojiro Yamamoto[1], Narumi Takahashi[2,1], Dogan Kalafat[3], Ali Pinar[3], Remzi Polat[3], Zeynep Coskun[3], Haluk Ozener[3], Yoshiyuki Kaneda[4] (1.Japan Agency for Marine-Earth Science and Technology (JAMSTEC), 2.NIED, 3.KOERI, Bogaziti University, 4.Kagawa University)

[SSS10-P22] **Microseismic Monitoring of the Sultandagi Fault Zone: Western Turkey**

*Dogan Kalafat[1], Yavuz Gunes[1], Mehmet Kara[1], Kivanc Kekovali[1] (1.Bogazici University Kandilli Observatory and Earthquake Research Institute Cengelkoy, Istanbul Turkey)

[SSS10-P23] Analysis of radiated seismic energy distributing in aftershock sequences at the Guerrero, Mexico subduction zone.

*Raymundo Omar Plata Martinez[1], Xyoli Pérez Campos[2], Krishna Shri Singh[2] (1.Kyoto University, 2.Geophysics Institute, UNAM)

Spatial-temporal and seismogram characteristics of foreshock and aftershock activities for tsunami earthquakes

*Yifeng Liu[1], Yoshihiro Ito[2], Kazuaki Ohta[2], Satoshi Katakami[1]

1. Division of Earth and Planetary Sciences, Graduate School of Science, Kyoto University, 2. Disaster Prevention Research Institude, Kyoto University

A tsunami earthquake is an abnormal earthquake type causing a large tsunami compared to the magnitude measured by short-period seismic waves. There is a high risk to induce a massive tsunami damage for the reason that people who live in the coastal area do not feel quakes a lot, and it is difficult to keep themselves safe after the unusual earthquake happened. Additionally, as for the tsunami earthquakes, their observation cases are much fewer than ordinary earthquakes, so the mechanism of its occurrence is still an open question. To address spatio-temporal features and the mechanism of tsunami earthquakes, we focus on three typical examples of tsunami earthquake and their foreshock & aftershock sequences, which are (Nicaragua (1992/09/02, Mw 7.7), Jawa island (2006/07/17, Mw 7.7) and Mentawai (2010/10/25, Mw 7.8)). We also investigated whether a small earthquake showing the same characteristics as the tsunami earthquake is contained in the foreshock and aftershock activity.

First, we use seismic catalogs and waveform recording provided by ISC/USGS and IRIS respectively to extract the foreshock and aftershock activity, then evaluate the spatio-temporal features. We have found that four foreshock sequences (1992/08/10 06:09:20 Mb 5.2, 1992/08/10 06:34:14 Mb4.7, 1992/08/11 05:23:51 Mb 5.1, 1992/08/13 08:41:17 Mb 4.7) near the epicenter of mainshock area were observed before the occurrence of the Nicaragua mainshock. We have also analyzed the regional and spatio-temporal characteristics of three tsunami earthquake regions by dividing the area of 5*5 around the epicenter into twenty-five segments with the size of 1*1. As a result, in each of the three regions, we have found out that there is a seismic quiescence period in the vicinity of the mainshock area in each tsunami earthquake. Meanwhile, regarding aftershocks of the Nicaragua earthquake, seismic quiescence area is still detected in the same segment as the foreshock.

Migration phenomenon is observed in the foreshock activity near the focal region of the mainshock, especially before the mainshock of the Nicaragua earthquake. Meanwhile, the waveforms of aftershocks occurring in the same area as the events included in the migration have been compared with those of the mainshock. Next, we have calculated the ratio of maximum absolute amplitude of surface wave to that of body wave, in order to address features on waveforms of tsunami earthquake. As a result, the ratio of the mainshock, such as the tsunami earthquake shows extremely high value, whereas for the foreshocks and aftershocks, it does not show the same characteristic as the tsunami earthquake does. This suggests that small earthquakes occurring within the tsunami seismogenic region show the same phenomenon as ordinary earthquakes, but only the mainshock has the characteristics of the tsunami earthquake.

Keywords: tsunami earthquake, seismic activity, waveform analysis

©2019. Japan Geoscience Union. All Right Reserved.

Successively occurring large earthquakes in the world –comparison of real cases with expectations by the space-time ETAS

*Tetsuo Hashimoto[1], Takashi YOKOTA[2]

1. Seismology and Tsunami Research Department, Meteorological Reaserch Institute, 2. Aichi Institue Technology

In the government for evaluating criteria on abnormal phenomena along the Nankai Trough for disaster prevention measures, they made the criteria for events to announce the Nankai Trough Earthquake Information. In order to implement specific ways of disaster prevention, they discussed about specific criteria for what kind of phenomenon corresponds to the abnormal event. In this time, we presented the real cases of the successive occurrence of large earthquakes in the world on the newly revised ISC-GEM version 5.1 data (1904-2014) for contributing to the above discussion. And we estimated the large earthquakes occurrence by using the space-time ETAS (Ogata and Zhuang, 2006).The 103 earthquakes of Mw 8.0 over were extracted about the earthquakes in the world for about the last 100 years. There were 9, 10 and 13 earthquakes which were accompanied with the earthquake of Mw 7.8 over occurred within the epicentral distances 500 km within 3 days, 7 days and 30 days, respectively.We estimated occurrences earthquakes from summations of expectations by the space-temporal ETAS which was applied with the parameters around Japan of Ogata and Zhaung (2006) and b=0.92 estimated with the JMA earthquake catalog. And then there were 5.3, 6.5 and 8.0 earthquakes of Mw 8 over which accompanied to the earthquake of Mw 7.8 over within the epicentral distances 500km within 3days, 7days and 30 days, respectively.The expected frequency of occurrence and the decreasing trend accompanying the elapsed time since the preceding earthquake were generally consistent with the above actual case.Acknowledgment: We used ISCGEMver 5.1 from ISC. In addition, we received great cooperation from the Earthquake Prediction and Information Division, Seismology and Volcanology Department, Japan Meteorological Agency.

Keywords: Nankai trough earthquake, Large earthquake, occurring in succession, ETAS

©2019. Japan Geoscience Union. All Right Reserved.

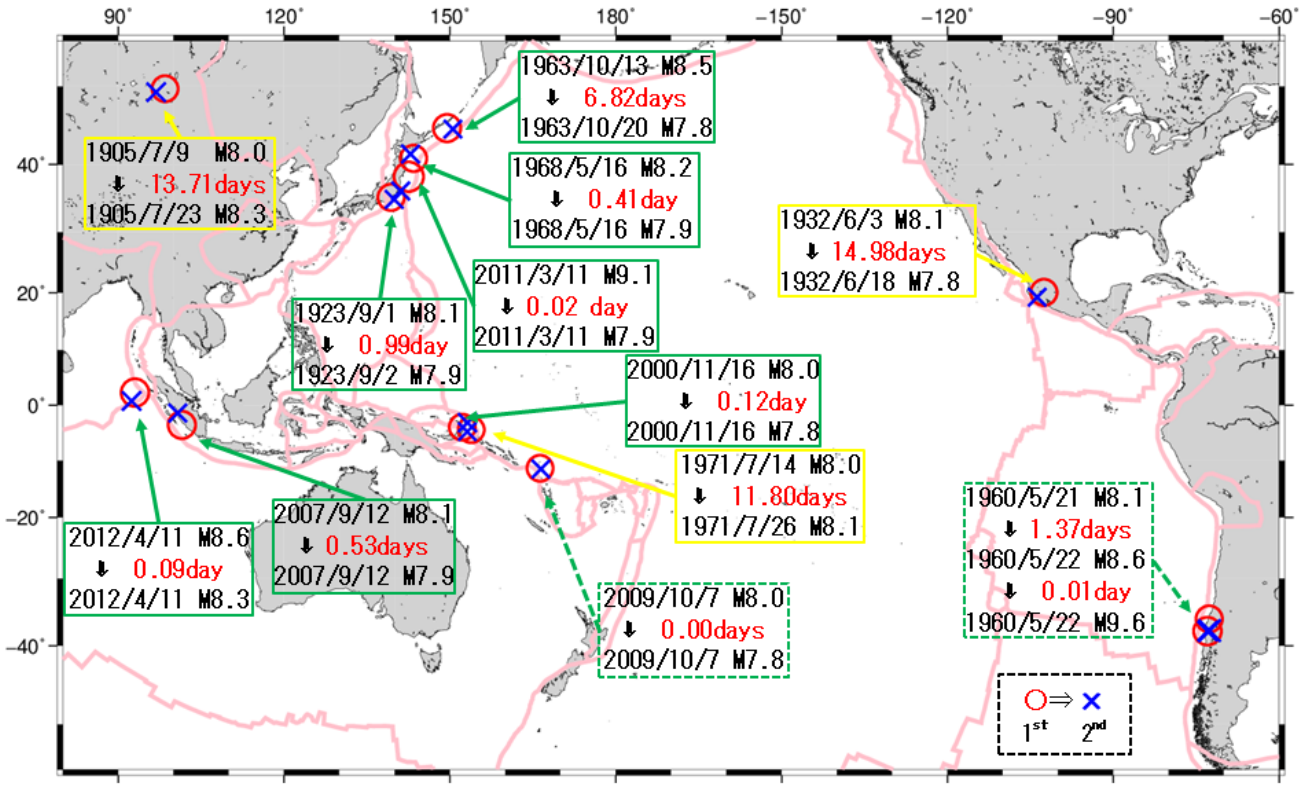

Epicentral distribution of pairs of the over Mw8 as 1st event(upper) and over Mw7.8 as 2nd event(lower) within 500km of the 1st. Time differences of two events are shown as red (yellow frames are over 7days). Pairs of less 50km of distance are shown as dashed frame. Plate boundaries data from Bird(2003). Map is drawn with GMT.

©2019. Japan Geoscience Union. All Right Reserved.

Seismicity beneath stable oceanic plate

*Yasushi Ishihara[1]

1. R&D Center for Earthquake and Tsunami, JAMSTEC

Stable oceanic plate has low seismic activity generally. Real tectonic deformation is also stable? To survey this topics, high quality and long-term observation. Pacific21 broadband seismic network deploys stations in Micronesia area. At present five islands station are under operation. Two of all have already telemetered to our data center via internet connection and transfer to other organization and institute.
In this year new telemeter station (station code: CHUK) is completed successfully. Chuuk (Truk) island locates on old oceanic plate about 900-1,000km southeast of Mariana trench and Guam. CHUK station locates inside deep tunnel made in more than 70 years ago, WWII era. The site condition is fine in basalt mountain, under stable temperature and on rigid floor. We deployed STS-2 broadband sensor in sensor room, high-resolution data logger and stable power supply system. CHUK station will contribute monitor and location of earthquake around Mariana trench and outer rise area.
Though CHUK station locates in small oceanic island and records strong ocean microseism, background noise level is lower level than standard model. CHUK station is excellent site to monitor including small local earthquake. CHUK station operates for about four years. We review continuous data and pick up local regional seismic events. Not only outer rise region but also Chuuk island area and hidden tectonic zone has active seismicity. By trial analysis, depth of these seismic events is beneath 20km. It implies stress concentration in oceanic plate and its deformation.

Keywords: oceanic plate, seismicity

©2019. Japan Geoscience Union. All Right Reserved.

Relation between long-term slow slip events and correlation between tidal triggering effect and deep low-frequency earthquakes in Bungo Channel: Part 2

*Fuyuki Hirose[1], Akio Kobayashi[1], Kenji Maeda[2]

1. Seismology and Tsunami Research Department, Meteorological Research Institute, 2. Seismology and Volcanology Department, Japan Meteorological Agency

Long-term slow slip events (LSSEs) have occurred with the interval of 5-6 years beneath the Bungo Channel [e.g., Kobayashi, 2017, EPS]. Deep low-frequency tremors and earthquakes (LFEs) have synchronized with the LSSEs and have activated [Hirose et al., 2010, Science]. It is pointed out that tremors have high tidal correlation [Ide, 2010, Nature; Ide & Tanaka, 2014, GRL]. There is no study that investigated long-term changes of the tidal correlation of LFEs.
On the other hand, the correlation between regular seismicity and tide also have been investigated energetically, and then there is a report that the tidal correlation became higher before the large earthquake around the focal region and became lower after the mainshock [e.g., Tanaka et al., 2012, GRL]. In addition, it is also pointed out that a leading period of high tidal correlation corresponded with the magnitude of a following earthquake.
Accordingly, we investigated temporal changes of tidal correlation of LFEs before and after LSSEs beneath the Bungo Channel on the analogy of tidal correlation of background seismicity before and after large earthquakes.
We extracted LFEs from the earthquake catalog unified by Japan Meteorological Agency (JMA) that occurred beneath the Bungo Channel from 2000 to March 21, 2018. Accuracy of locations of LFEs is lower than that of regular earthquakes. Note that hypocenter determination method for LFE by JMA changed since March 22, 2018, and then detection level also changed at the border. Taking int consideration that the change is not suitable in order to investigate long-term changes of tidal correlation of LFEs, we selected LFEs data.
It is necessary to set fault parameters in order to estimate the theoretical below-ground tidal response. Because our study area was narrow area with 15 km square, we set one fault plane (strike angle 237˚, dip angle 16˚, and rake angle 103˚) taking into consideration the plate configuration [Hirose et al., 2008, JGR] and MT solutions of deep very LFEs [Ide & Yabe, 2014, GRL]. In addition, we set hypocenters of LFEs to the common location (longitude 132.254˚, latitude 33.142˚, and depth 32 km). We used only occurrence times of LFEs determined by the JMA.
We summed temporal variations of the solid and oceanic tide loading effects for six independent components of the strain tensor, as estimated at the hypocenter of each event. Then we converted them to temporal variations of volumetric strain (ΔV) at the hypocenter, and shear stress ($\Delta\tau$), normal stress ($\Delta\sigma$), and the Coulomb failure function (ΔCFF) on the assumed fault plane. In the ΔCFF calculation, we assumed values of 0.1, 0.4, and 0.7 for the apparent friction coefficient μ'. In the case of ΔV and $\Delta\sigma$, we defined expansion/dilatation as positive and contraction/compression as negative; consequently, positive $\Delta\sigma$ values promote fault slip. We also defined $\Delta\tau$ and ΔCFF as positive when they promote fault slip. Using the time series of tidal stress (strain) levels, we assigned phase angles of −180˚ and 180˚ to the minimum tidal stress (strain) levels before and after an event, respectively, and 0˚ to the maximum tidal stress (strain) that occurred between these two minima. The phase angle at the earthquake occurrence time was estimated by linear interpolation in the time interval between −180º and 0˚ or between 0˚ and 180˚. The possible occurrence of LFEs at certain tidal phase angles was evaluated using the *p* value, as

©2019. Japan Geoscience Union. All Right Reserved.

calculated by Schuster [1897].
We found that LFEs tended to occur near a tidal phase angle of 0° for $\Delta\tau$ (when the tidal force promoted fault slip). This result indicates extremely low μ' and high pore pressure, being consistent with the existence of fluid inferred from the seismic velocity structure [Hirose et al., 2008]. LSSEs occurred three times (in 2003-2004, 2009-2011, and 2014) during the study period. Temporal changes of *p* value showed to tend to become lower before the LSSEs and become higher after ones (Tidal correlation tended to become higher before the LSSEs and become lower after ones). This result is similar to temporal changes of *p* value for background seismicity before and after large earthquakes. Accordingly, temporal tidal correlation of LFEs indicates to be affected by stress perturbation associated with LSSEs. Note that *p* value at March in 2018 falls to a level just before past LSSEs.

Keywords: Earth tide, Schuster's p value, Low frequency event, Long-term slow slip event, Bungo Channel

©2019. Japan Geoscience Union. All Right Reserved.

Arrival-time and hypocenter determination using S-net

*Tomomi Okada[1], Ryota Takagi[1], Takashi NAKAYAMA[1], Syuichi Suzuki[1], Ryosuke Azuma[1], Genti Toyokuni[1], Keisuke Yoshida[1], Naoki Uchida[1], Ryota Hino[1]

1. Research Center for Prediction of Earthquakes and Volcanic Eruptions, Graduate School of Science, Tohoku University

Hypocenter distribution is basic information for understanding seismogenesis.
For east off Honshu from Hokkaido, Tohoku, Kanto, S-net has been deployed by NIED. S-net is expected to improve accuracy of hypocenter location. In this study, we show a preliminary result of hypocenter determination using S-net and onshore stations.
We used hypomh (Hirata and Matsu’ura (1984)) with seismic velocity structure of Hasegawa et al. (1978). In our case, we used waveform converted to vertical, north-south, east-west components by Takagi et al. (this meeting).
For the earthquake near coast line, we can determine reliable hypocenter location, which is correspond to the location determined by F-net CMT or AQUA catalog. However, large travel time residuals over 3 seconds earlier are estimated for distant stations including the stations east of trench. This would mainly be due to the high velocity Pacific plate (e.g., Toyokuni et al., this meeting). To improve the velocity structure and use station correction are necessary for further study.

Acknowledgements: We used S-net, Hi-net and stations by universities (Hokkaido, Hirosaki, Tokyo and others), Aomori and Tokyo Pref., ADEP (Association for the development of earthquake prediction) and JMA. Profs. Matsuzawa, Zhao, Umino and Hasegawa and Mr. Hirahara give us valuable suggestions.

Keywords: S-net

©2019. Japan Geoscience Union. All Right Reserved.

Focal mechanisms of the double seismic zone in the Pacific plate, off Boso: Temporal change after the 2011 Tohoku EQ

*Guanyu Chen[1], Toshinori Sato[2], Tomoharu Sato[1], Asami Terada, Masanao Shinohara[3], Kimihiro Mochizuki[3], Tomoaki Yamada[3], Kenji Uehira[4], Takashi Shimbo[5], Shuichi Kodaira[5], Yuya Machida[5], Ryota Hino[6], Ryosuke Azuma[6], Yoshio Murai[7], Yoshihiro Ito[8], Hiroshi Yakiwara[9], Kenji Hirata[4], Akinori Hashima[3], Andrew M. Freed[10]

1. Faculty of Science, Chiba University, 2. Graduate School of Science, Chiba University, 3. Earthquake Research Institute, University of Tokyo, 4. National Research Institute for Earth Science and Disaster Resilience, 5. Japan Agency for Marine-Earth Science and Technology, 6. Graduate School of Science, Tohoku University, 7. Institute of Seismology and Volcanology, Faculty of Science, Hokkaido University, 8. Disaster Prevention Research Institute, Kyoto University, 9. Nansei-toko Observatory for Earthquakes and Volcanoes, Kagoshima University, 10. Purdue University

1. Introduction

The Pacific plate and the Philippine Sea plate subduct off the Boso Peninsula, and the Pacific plate has a double seismic zone at this place (e.g. Terada et. al., JpGU, 2016). Sato et. al. (JpGU, 2018) revealed that most focal mechanisms for the lower surface events have down-dip extension before the 2011 Tohoku EQ, and down-dip compression during 3 months after the EQ using land and ocean bottom seismic observations. This presentation shows 1 year temporal change of focal mechanisms for the double seismic zone’ s events after the 2011 Tohoku EQ.

2. Data and analysis

The used data are waveform data from Hi-net by NIED, and the aftershock survey of the 2011 Tohoku EQ using ocean bottom seismometers (2011/3/15-2012/3/31). We select events in the double seismic zone, and pick polarities of the P wave first motions. We calculate emergent azimuth and dip of each event-receiver pair using a 3D structure determined by Terada et al. (JpGU, 2016), and search optimal focal mechanisms using a grid search method.

3. Results

During 1 year after the 2011 Tohoku EQ, most focal mechanisms have down-dip compression for the upper surface events. For the lower surface events, on the other hand, most focal mechanisms have down-dip compression by July, 2011, and many mechanisms have down-dip extension after September, 2011. This may indicate that a compressional stress change occurred at the depth of the Pacific plate just after the 2011 Tohoku EQ, because the EQ moved the Pacific plate downward at the shallower part, and compressed the deeper part of the plate. After that, the compressional stress may had relaxed about a half a year.

Acknowledgements

We thank captains and crew of aftershock observation cruises of the 2011 Tohoku Earthquake. We used waveform data from Hi-net by NIED.

Keywords: Double seismic zone, temporal change of focal mechanism, the Pacific plate, off the Boso Peninsula, the 2011 Tohoku Earthquake

©2019. Japan Geoscience Union. All Right Reserved.

©2019. Japan Geoscience Union. All Right Reserved.

Ocean bottom seismographic observation and similar earthquake detection in the northern part of the Nansei Islands

*Yukihiro Nakatani[1], Hiroshi Yakiwara[1], Shuichiro Hirano[1], Reiji Kobayashi[2], Hiroki Miyamachi[2], Shigeru Nakao[2], Kazunari Uchida[3], Takeshi Matsushima[3], Hiroshi Shimizu[3], Kazuo Nakahigashi[4], Yusuke Yamashita[5], Hideji Abe[6], Tomoaki Yamada[6], Masanao Shinohara[6]

1. Nansei-Toko Observatory for Earthquakes and Volcanoes, Kagoshima University, 2. Graduate School of Science and Engineering, Kagoshima University, 3. Institute of Seismology and Volcanology, Faculty of Science, Kyushu University, 4. Tokyo University of Marine Science and Technology, 5. Disaster Prevention Research Institute, Kyoto University, 6. Earthquake Research Institute, the University of Tokyo

The Ryukyu Trench subduction zone is seismically active region. In the northern part of the Nansei Islands, both seismic and aseismic events have occurred along the subducting plate interface. Spatial distribution of small local earthquakes in this region seems to show some seismic clusters and gaps. Short-term slow slip events and shallow low-frequency tremors have been also observed by recent onshore seismic and geodetic data. However, patterns of their slip behavior and spatiotemporal relationship between regular and slow earthquakes are less well understood because seismic stations are located only at the islands that are linearly arranged; at least 100 km away from the Ryukyu Trench.
We have therefore conducted repeating long-term ocean bottom seismographic observation off the northern part of the Nansei Islands since 2014. First, we deployed three pop-up type ocean bottom seismometers (OBSs) in April 2014. Then, three more OBSs were added to the network in July 2015, and after that deployment and retrieval of OBSs at the same position have been repeatedly carried out every about one year. The station interval is about 40–60 km.
In this study, we focus on regular local earthquakes, particularly seismic clusters beneath the central part of the observation network. In order to obtain key properties of the clusters and to detect missing earthquakes, we apply a matched-filter technique to OBS continuous waveform data. As template event waveforms, we select events determined by Nansei-Toko Observatory for Earthquakes and Volcanoes, Kagoshima University. The hypocenters of the template events are relocated by merging manual pick data of P phases and S phases recorded on the OBSs with those on the onshore stations. As a preliminary result, we achieve detection of missing earthquakes using example template events and a threshold rule based on the median absolute deviation of the mean correlation coefficient. In this presentation, we further discuss the characteristics of waveform similarity of the OBS data.

Acknowledgements: This work is supported by Earthquake and Volcano Hazards Observation and Research Program, the MEXT of Japan and by ERI JURP.

Keywords: OBS observation, the Ryukyu Trench, similar earthquakes

©2019. Japan Geoscience Union. All Right Reserved.

Seismicity and crustal structure in the Okinawa Trough

*Azusa Nishizawa[1], Takeshi Kimura[1], Kentaro Kaneda[2]

1. National Research Institute for Earth Science and Disaster Resilience, 2. Japan Coast Guard

The Okinawa Trough is an active backarc basin of the Nansei-Shoto (Ryukyu) island arc–trench system, where the crustal thinning caused by backarc rifting is currently in progress in the entire trough. The characteristics of the seismic activity around the Ryukyu Trench and the Okinawa Trough are not enough investigated due to several reasons; 1) the number of large earthquakes related to the plate subduction along the Ryukyu Trench is not many compared with those in the Nankai Trough and the Japan Trench, 2) the coupling of the plate boundary is considered to be weak, and 3) the sparse distribution of the seismic stations on the Nansei-Shoto island arc makes difficult to obtain enough seismic data in the Ryukyu subduction zone and the Okinawa Trough.

The distribution of the shallow earthquakes in the Okinawa Trough by obtained Japan Metrological Agency during 1923–2018 is spatially inhomogeneous and shows several clusters. The seismic activity in the trough should be related to the seismic crustal structures. Recently, the Japan Coast Guard has reported the detailed seismic structure in the Okinawa Trough. We compared the active seismic areas with the seismic crustal models. The *M*7.1 Satsuma-hanto Seiho-oki Earthquake occurred on Nov. 14, 2015, in the western margin of the northern trough, the transition area between the East China Sea shelf and the Okinawa Trough, where the crust is thinner than the center of the trough with the deepest water. The source mechanisms of the main shock and intense aftershock activity compiled in the NIED (National Research Institute for Earth Science and Disaster Resilience) F-net moment tensor catalog have NW–SE extension axis, indicating that the area is undergoing tectonic rifting.

The largest shallow earthquakes with depths < 30 km observed in the trough is the 1938 Miyako-jima–Hokusei-oki Earthquake (*M*7.2) near the north of Miyako-jima Island and a tsunami with a height of 1.5 m hit Miyako-jima Island. The location of the hypocenter is estimated at the structurally discontinuous area where the northern extension of the Yaeyama Rift, the deepest elongated depression in the Okinawa Trough, meets Miyako Seamount, a fragment of the continental crust of the East China Sea shelf. Active seismicity including three events with $M > 6$ on Apr. 20, 2007 was observed in the Miyako Rift to the north of Miyako Seamount. Multichannel seismic profiles show many normal faults and deformation in sedimentary layers beneath the Miyako Rift. However, the accuracy of hypocenter locations in this region is poor, and the CMT locations are different over 20 km at the maximum between the NIED F-net and Global CMT.

The P-wave velocity models beneath the Okinawa Trough generally show an extended arc crust of the Ryukyu Islands which consists of upper, middle, and lower crusts. Although the crustal thickness becomes thinner from the north to the south, the crust is thicker than those of typical oceanic crusts or backarc basin crusts such as the Shikoku Basin. Therefore, the seismogenic layer in the Okinawa Trough is thicker than in mid-oceanic ridges, indicating that larger earthquakes could occur in the trough.

Keywords: Okinawa Trough, seismic activity, marine seismics

©2019. Japan Geoscience Union. All Right Reserved.

Time series analyses of the seismic activities in southwestern Japanese Island to southeastern Korean Peninsula excited by the deep fluid heat flow

*Takayuki Kawabe[1]

1. Faculty of Education, Arts and Sciences, Yamagata University

More than eight series of large damaging earthquakes occurred since November 2015 in southwestern Japanese Islands. They are as follows;
1) 2015/11/15 earthquakes of Northwestern margin of Okinawa Trough N31.33050˚, E128.71733˚, Depth: 9.4km, M5.9.
Foreshock: M5.1 (11/14), largest aftershock: M5.5 (2016/05/07).
2) 2016/04/16 2016 Kumamoto Earthquakes N32.75450˚ E130.76300˚, Depth: 12.45km, M7.3.
Foreshock: M6.5 (04/14), M6.4 (04/15), largesrt aftershock: (04/16) M5.9.
3) 2016/09/12 earthquake of Southeastern Korean Peninsula N35.79817˚ E129.27167˚, Depth: 36.0km, M5.8.
Foreshock: M5.2 (40 minutes before), Largest aftershock: M5.2 (2017/11/15).

4) 2016/10/21 earthquake of Central Tottori in 2016 N35.38050˚ E133.85617˚, Depth: 10.61km, M6.6.
Foreshocks: low frequency earthquakes, aftershocks: containing low frequency earthquakes.
5) 2017/11/15 earthquake of Southeastern Korean Peninsula N36.19584˚ E129.39417˚, Depth: 11.0km, M5.6.
6) 2018/02/11 earthquake of Southeastern Korean Peninsula N36.09883˚ E129.45700˚, Depth: 4.0km, M4.6.
7) 2018/04/09 earthquake of Western Shimane Prefecture in 2018 N35.18467˚ E132.58667˚, Depth: 12.13km, M6.1.
8) 2018/06/18 Northern Osaka Earthquake in 2018 N34.84433˚ E135.62167˚, Depth: 12.98km, M6.1.

Positions of the formar four eathquakes and the later four earthquakes shift from the west to the east. The number and scale of the earthquakes of Northwestern margin of Ryukyu Trough is reduced just several days berore the 2016 Kumamoto Earthquakes, and the number and scale of them is just restored after the 2016 Kumamoto Earthquakes. This seems to have a strong relationship between the earthquakes of Northwestern margin of Okinawa Trough and the 2016 Kumamoto Earthquakes. This suggests that such two strongly related earthquakes may be drived by the migration of thermal enargy because the earthquake activities are restored.
Seismic activity contined more than two years in the case of the earthquakes of Southeastern Korean Peninsula and large eathquakes often recured there. Their hypocenters show remarkable distribution. That is to say, they distribute not along any plane but along three dimensionally bent lines. on the lines, earthquakes occurred from the bellow to the upper in the lower to the upper crust. This means that the earthquakes of southeastern Korean Peninsula occurred not in an elastomechanical system but other system as thermal energy. Next earthquakes, just after the earthquakes of southeastern Korean Peninsula, occuring in the central Tottori in 2016 contains large number of low frequency earthquakes through the foreshocks to the aftershocks. The main shock of the ceentral Tottori in 2016 is actually drived by the thermal liquid enargy.
According to such evidences of the liquid flow causing the earthquakes, the large earthquakes occuring in

©2019. Japan Geoscience Union. All Right Reserved.

the upper crust of Southwest Japan would be driven by the eastward transmigrating thermal energy in the upper mantle (Tsunoda et al., 2013).

Reference:
Tsunoda, F., Choi, D.R. and Kawabe, T., 2013. Thermal energy transmigration and fluctuation. NCGT Journal, v.1, p.65-80.

Keywords: time series analyses of seismic activities, deep fluid heat flow, southwestern Japanese Island

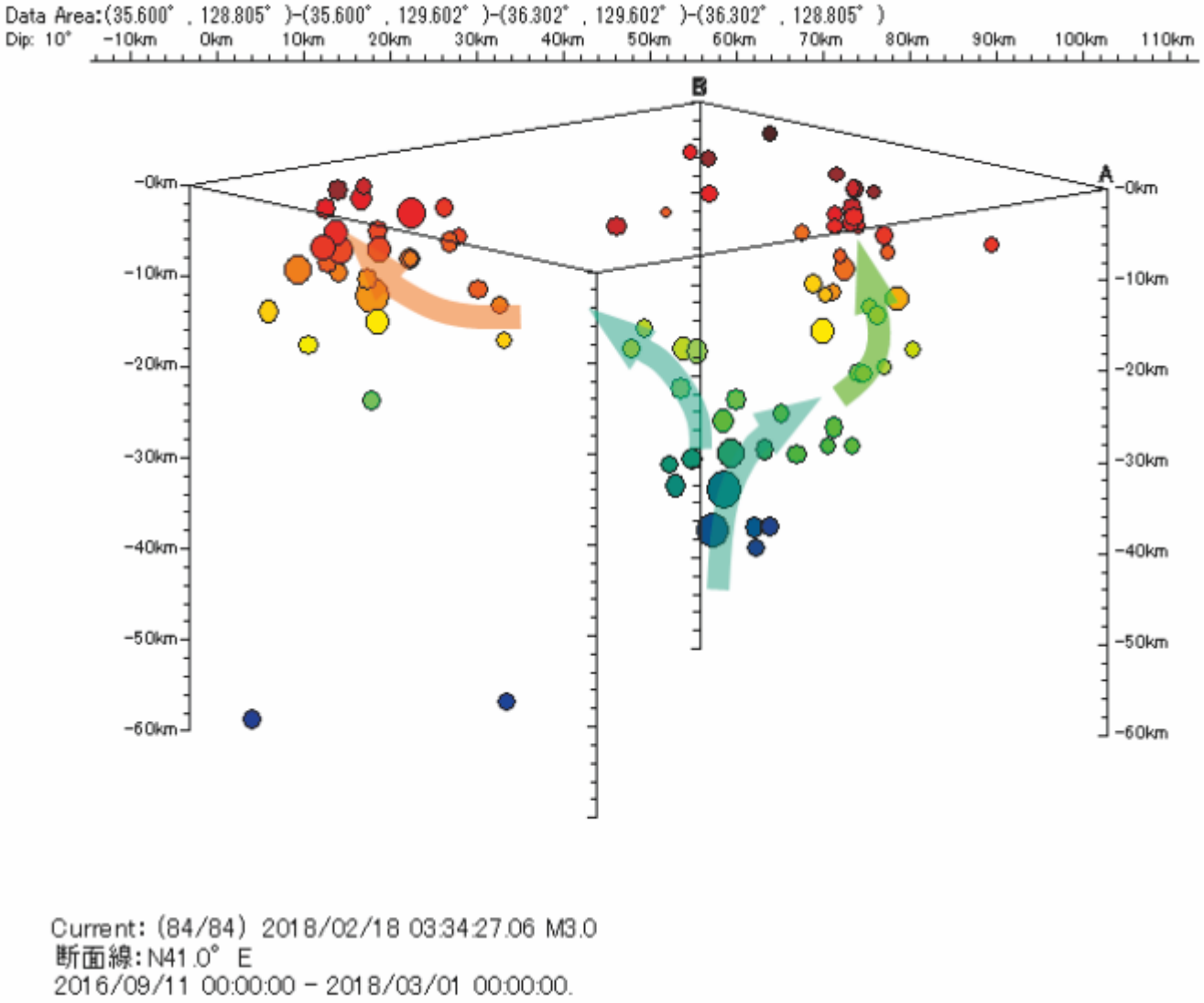

©2019. Japan Geoscience Union. All Right Reserved.

Integrated monitoring of seismicity in and around the Suruga Bay using Ocean Bottom Seismometers and inland stations.

*Yannis Panayotopoulos[1], Hisatoshi Baba[2], Takahito Nishimiya[3], Taiyo Sotani[4], Nakao Nagisa[4]

1. Association for the Development of Earthquake Prediction, 2. Department of Marine and Earth Science, Tokai University, 3. Meteorological Research Institute, Japan Meteorological Agency, 4. Tokai University

The Suruga bay is located in the western flank of the Izu Peninsula in central Japan. It marks the easternmost boundary of the Nankai trough, of the Philippine Sea plate subduction zone. The Fujikawa fault zone located at the northern tip of the Suruga Bay is considered to be the landward extension of the megathrust boundary between the Philippine Sea plate and the Eurasia plate (e.g.: Yamazaki, 1992). This megathrust boundary produced the M8.4 Ansei-Tokai Earthquake (e.g.: Ishibashi, 1981), and is assumed to be the source region of the next Tokai Earthquake. We closely monitored the seismicity in the vicinity of the Suruga Trough axial region from May, 2018 to September, 2018, using 6 pop-up type Ocean Bottom Seismometers (OBS). In recent years, several moderate size earthquakes have occurred in the Suruga Trough axial region (M6.5 in 2009 and M6.2 in 2011), that resulted in a prominent excitation of seismicity in the area. Using the inland routine observation network alone, those earthquakes are estimated to have occurred on the subduction zone of the Philippine Sea Plate. However, there is a considerable amount of hypocenter depth location error due to the lack of stations in the sea areas.

In this study, we will report the results of the OBSs observations, which enabled us to make more accurate estimations of the frequency and hypocenter depth distribution of the earthquakes occurring in the Suruga Trough axial region.

Keywords: Suruga bay, Earthquake cluster, Seismicity

©2019. Japan Geoscience Union. All Right Reserved.

Linear distribution of the intraslab earthquakes in Tokai

*Sadaomi Suzuki[1]

1. Tono Research Institute of Earthquake Science, Association for the Development of Earthquake Prediction

Figure 1 show an epicenter map of the earthquakes shallower than 60 km in the Tokai area occurring from June 2002 to April 2018. The intraslab earthquakes were shown by yellow, green, or blue small circles, because they occurred in the depth from 30 −50 km. They distribute not homogeneously but linearly as shown in the epicenter map. Elongated ellipses by broken lines show linear distributions (LDs) of the intraslab earthquakes. LD-A and LD-d arranged NW-SE are main distribution in the Tokai area. On the east of them there are small LD-e and LD-f. In contrast LD-B which is arranged NNE from near the port of Nagoya makes an angle of 70° with LD-A. There is small LD-c on the west of LD-B. LD-B and LD-c may be suggested by Miyoshi and Obara (2010a). We studied focal mechanism solutions of 12 earthquakes (Group A) belonging to LD-A and 146 earthquakes (Group B) belonging to LD-B, respectively, using JMA data. We obtained the average values of the azimuths of P- and T-axis for each group as the following. The average values for Group A are 171° and 350° in P-axes and 91° and 256° in T-axes, respectively (see Figure 1). The average values for Group B are 172° and 358° in P-axes and 82° and 254° in T-axes, respectively (see Figure 1). There are no large differences in their corresponding values between Group A and B. This result suggests that there is no large difference in the average stress generating earthquakes between Group A and B. We, therefore, have to consider other reasons for causing those linear distributions.

Figure 2 is a seismological cross section that crosses the Tokai area from NNW to SSE referred from Suzuki et al., 2018. Schematic interpretation of seismic structures including S wave tomography (Nakajima and Hasegawa, 2016) and two earthquake groups consisiting of LFEs and intraslab earthquakes are represented. The most of intraslab earthquakes distributes in the low velocity area of *S* wave in the uppermost oceanic mantle. The relatively low velocities of *S* wave in the subducting oceanic crust and its surrounding areas are interpreted as being indicative of fluids released by progressive metamorphic dehydration reactions in the oceanic crust (e.g., Abers et al., 2013) under increasing temperature and pressure conditions. We suppose that the intraslab earthquakes occur because these fluids penetrate into the uppermost oceanic mantle. Therefore the pore fluids may penetrate from the oceanic crust into not homogeneously but linearly in plane. It is presumed that old fracture zones that had been formed before the Philippine Sea plate subducted below the Tokai area existed at the uppermost oceanic mantle.

Abers GA, Nakajima J, van Keken PE, Kita S, Hacker BR (2013) Thermal–petrological controls on the location of earthquakes within subducting plates. Earth Planet Sci Lett 369–370:178–187

Hirose F, Nakajima J, Hasegawa A (2008) Three-dimensional seismic velocity structure and configuration of the Philippine Sea slab in southwestern Japan estimated by double-difference tomography, J. Geophys. Res., 113:B09315. doi:10.1029/2007JB005274.

Miyoshi,T. and K. Obara (2010a), Seismogenic stress field of the double seismic zone within the Philippine Sea plate beneath Ise Bay to the Kii Peninsula, Abstract of the 2010 meeting of Japan Geoscience Union, S-SS013 P14 (in Japanese).

Miyoshi,T. and K. Obara (2010b), Double seismic zone within the ridge-shaped slab beneath southwest Japan, Earth Planets Space, 62, 949-954.

Nakajima, J., and A. Hasegawa (2016), Tremor activity inhibited by well-drained conditions above a megathrust, Nature communications 7, Article number: 13863 (2016), doi:10.1038/ncomms13863, 2016.

Suzuki, S., Okubo, M., Imanishi, K., Takeda, N. (2018) , Detection method for pairs of *P* and *S* waves of

©2019. Japan Geoscience Union. All Right Reserved.

deep low-frequency earthquakes using a 3-D array in the Tokai area of the Nankai subduction and its application to hypocenter determination, Geochemistry, Geophysics, Geosytems, 19,.https://doi.org/10.1029/2018GC007479.

Keywords: intraslab earthquakes , linear distribution of earthquakes , oceanic mantle

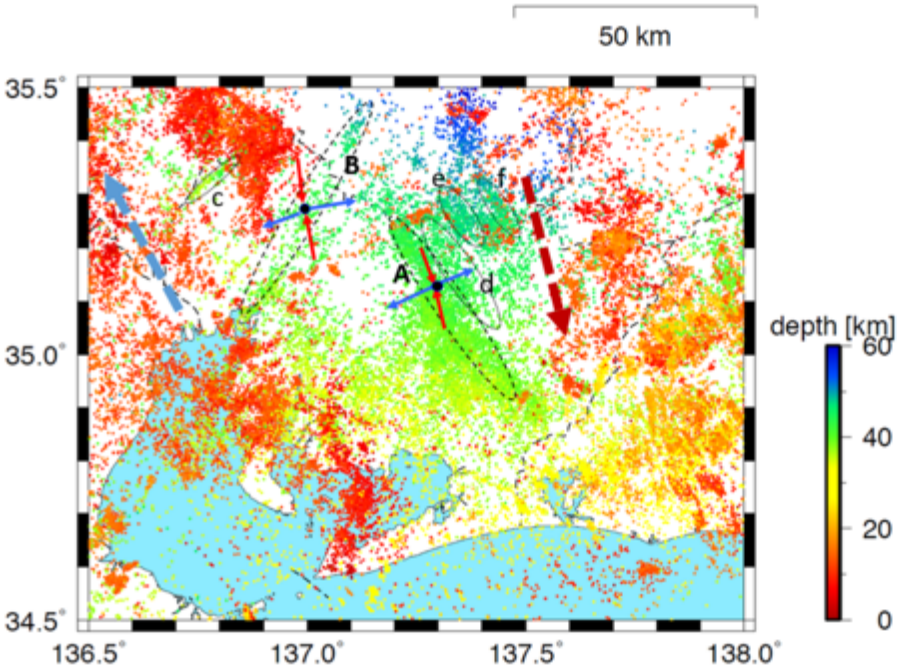

Figure 1. Epicenter map (presented by Osamu Murakami) of the earthquakes shallower than 60 km in the Tokai area occurring from June 2002 to April 2018 (JMA data). Elongated ellipses by broken lines show linear distributions of the intraslab earthquakes. Red and blue allows indicate P-axes and T-axes, respectively. A brown and blue broken lines show the ridge and valley of the slab shape (Hirose et al., 2008), respectively

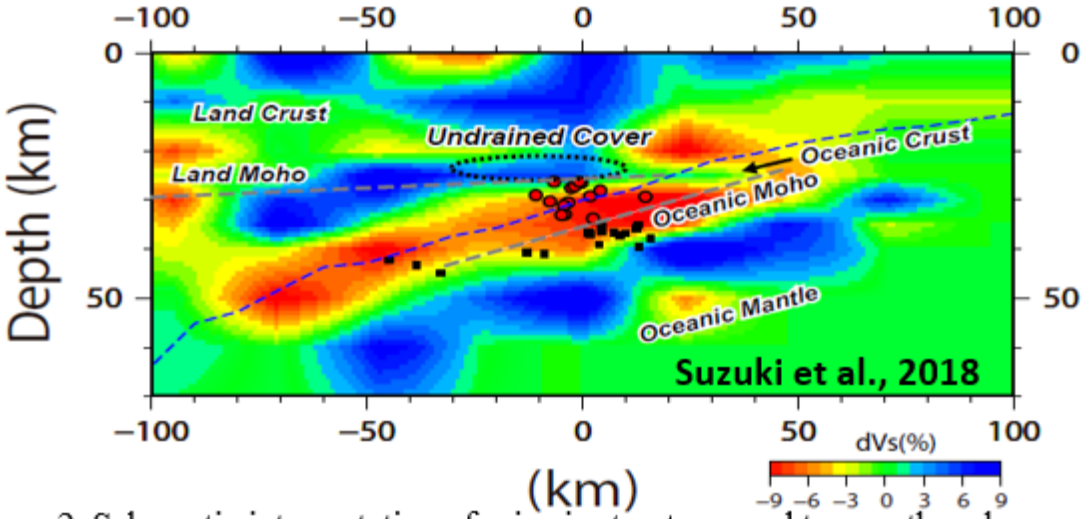

Figure 2. Schematic interpretation of seismic structures and two earthquake groups consisiting of LFEs (red circles) and intraslab earthquakes (black squares) referred from Suzuki et al., 2018.

©2019. Japan Geoscience Union. All Right Reserved.

The stress change of Chubu region before and after the 2011 Tohoku-oki Earthquake(Mw9.0)

*Yuki Susukida[1], Kei Katsumata[1]

1. Institute of Seismology and Volcanology, Hokkaido University

Great subduction-zone earthquakes occur frequently off coast of the Pacific Ocean in Japan. And the Chubu region (central part of Honshu, Japan) has risk not only subduction-zone earthquake but also inland earthquake. In 1891, Nobi earthquake (M8.0) occurred at Neodani fault system in Chubu region, which is the largest inland earthquake in Japan. (Milne 1893) Furthermore, after Tohoku-oki earthquake, seismicity of northern part of Neodani fault system was activated. (Toda et al, 2011) In this study, I examined effect of Tohoku-oki earthquake on seismicity around the Neodani fault system by inferring of stress change before and after Tohoku-oki earthquake.

At first, I demonstrated the stress field inversion method (Hardebeck & Michael, 2006) by synthetic data to check the performance of this inversion method. As a result, I found that the inversion method will analyze real data well.

Next, I conduct stress field inversion for the joint observation data by eight Universities in Japan and NIED (National Research Institute for Earth Science and Disaster Resilience in Japan) in the Chubu region between 2009 and 2013. As a result, I found the stress field in Neodani fault system didn’ t change significantly before and after Tohoku-oki earthquake.

Keywords: Tohoku-oki Earthquake, Inland Earthquake, Neodani fault system, stress field inversion

©2019. Japan Geoscience Union. All Right Reserved.

Repeating earthquake activity off Miyagi Prefecture triggered by the 2011 Tohoku-oki earthquake

*Kenshiro Tsumura[1]

1. Association for Developement of Earthquake Prediction

A remarkable repeating earthquke activity off Miyagi Prefecture tiggered by the 2011 Tohoku-oki earthquake was analized in detail. The epicenters of repeating earthquakes ditributed in a very small area with a diameter of about 1km , centered at 38°38′N and 141°54′E, and with depth 46-49km. The recurrence intervals were about 20 days in the initial period then gradually changed longer, about 100 days in 2018. Magnitude of earthquake was about 4.0 in the initial period then gradually changed smaller, about 3.5 in 2018. For this activity, based on its repeating regularity, mid-term prediction was tried and obtaied good result for a certain period.

Keywords: repeating earthquakes, 2011 Tohoku-oki earthquake, mid-term erathquake prediction

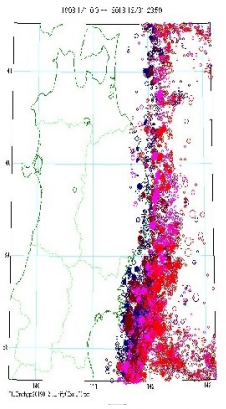

図１. 震央分布図

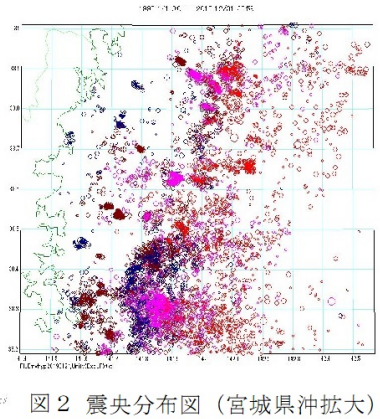

図２ 震央分布図（宮城県沖拡大）

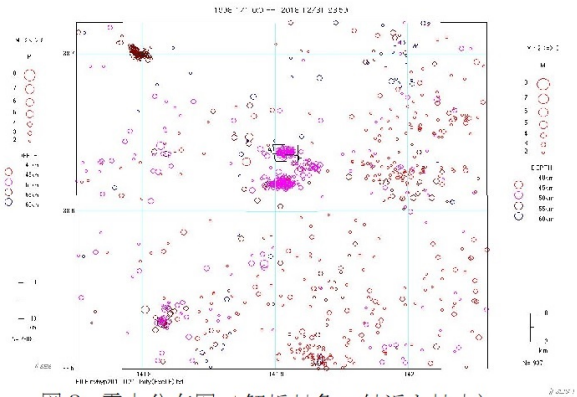

図３. 震央分布図（解析対象の付近を拡大）

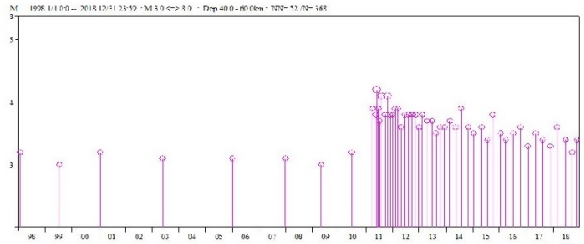

図５. 対象とする繰り返し地震活動のＭＴ図

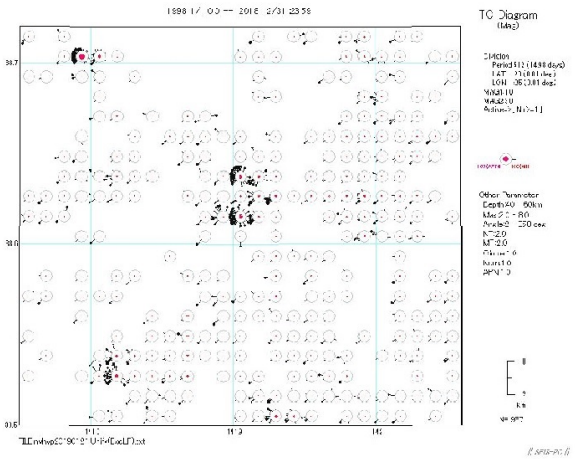

図４ 図3に対応する時間円表示図（TC-M図）

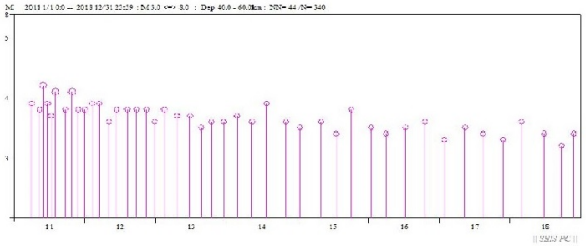

図６. 対象とする繰り返し地震活動のＭＴ図（2011年以降を拡大）

©2019. Japan Geoscience Union. All Right Reserved.

Seismic Moments of Inland Small Earthquakes in Japan: Spectral Analyses Using the Hi-net

*Tomotake Ueno[1], Tatsuhiko Saito[1]

1. National Research Institute for Earth Science and Disaster Resilience

Seismic moments and moment magnitudes are one of the most important quantities in characterizing earthquakes. NIED reports moment magnitudes for moderate and large earthquakes (M_W > ~3.5) using the F-net or the KiK-net/K-NET. However, the moment magnitudes of small earthquakes (M_W < 3.5) aren't well determined because of sparse station distributions of the F-net and low sensitivity sensors of the KiK-net/K-NET. These earthquakes' magnitudes are determined using maximum amplitudes of the seismograms of the Hi-net, a dense seismic observations with high-sensitivity sensors. Such high sensitivity seismometers are also used to estimate seismic moments (e.g., Uchide and Imanishi, 2018). This study estimated seismic moments and moment magnitudes for inland earthquakes in Japan using the Hi-net.

We calculated seismic moment for inland earthquakes shallower than 20 km deep with magnitudes from 3 to 4 occurred in 2013 to 2017. Firstly, we calculated a source spectrum from waveform data during 1s before to 9s after the S-wave arrival time. Then, correcting path, site, and the instrumental response, we estimated source spectra. Comparing the observed source spectra with a theoretical one supposing the ω^2 model, we obtained the seismic moment.

The Hi-net detected 455 inland earthquakes with the magnitude from 3 to 4 in 2017. We successfully estimated the seismic moments more than 90 % of those earthquakes. We could estimate the moment magnitudes more than 90 % except 2016. Because the aftershocks of the Kumamoto earthquakes contaminated Hi-net records, we calculated the seismic moments only for 70 % of the 1730 earthquakes in 2016. We compared the moment magnitudes determined by the Hi-net with those by a moment tensor inversion of the F-net. The moment magnitude of Hi-net was smaller than those of the F-net by 0.13±0.11. On the other hand, the magnitude using the maximum amplitude of the Hi-net was larger than the F-net by 0.06±0.21.

Keywords: seismic moment, Hi-net, small earthquakes

©2019. Japan Geoscience Union. All Right Reserved.

Spatiotemporal variations of stress field in the 2016 Kumamoto earthquake (M 7.3) area

*Dapeng Zhao[1], Zhiteng Yu[2], Jiabiao Li[2], Zhouchuan Huang[3]

1. Department of Geophysics, Tohoku University, 2. State Oceanic Administration, 3. School of Earth Sciences and Engineering, Nanjing University

Focal mechanism solutions of 349 local crustal earthquakes and stress tensors in central-north Kyushu are determined using a large number of P-wave polarity data and a 3-D velocity model. The obtained tensional ($\sigma 3$) axis trends NNW-SSE or N-S horizontally, and the compressive ($\sigma 1$) axis trends WSW-ENE or E-W. The direction of the $\sigma 3$ axis is consistent with the spreading direction at the Okinawa Trough. The stress field in the 2016 Kumamoto earthquake area is attributed to rollback of the Philippine Sea plate and northward extension of the Okinawa Trough. The orientation of the $\sigma 3$ axis is quite stable, whereas the $\sigma 1$ and $\sigma 2$ axes are distributed in a wide range. With the 3-D velocity model, the principal stress axes can be better determined by inverting a large number of FMSs. Spatial and temporal variations of the stress field are well revealed in the Kumamoto source area. The $\sigma 3$ axis significantly rotated counterclockwise after the M 6.5 foreshock, and rotated clockwise after the M 7.3 mainshock on the Futagawa fault segment. The stress rotation suggests a small magnitude of deviatoric stress in the source area, which indicates a small friction coefficient on the seismogenic faults. In addition, a generally small value of friction (~0.4) on the faults is obtained by the stress inversions, indicating that the faults in the Kumamoto earthquake area are weak. The fault weakening may be caused by the arc magma and fluids ascending from the mantle wedge associated with the dehydration reactions of the subducting Philippine Sea slab.

Keywords: Kumamoto earthquake, crustal stress, focal mechanism

©2019. Japan Geoscience Union. All Right Reserved.

Seismicity and crustal deformation following the 2016 Kumamoto earthquakes

*Kazuyoshi Nanjo[1], Jun Izutsu[2], Yoshiaki Orihara[3], Masashi Kamogawa[4], Toshiyasu Nagao[3]

1. University of Shizuoka, 2. Chubu University, 3. Tokai University, 4. Tokyo Gakugei University

The 2016 Kumamoto earthquakes include a magnitude *M*7.3 mainshock that struck April 16, 2016, as well as *M*6-class foreshocks (*M*6.5 and *M*6.4) and many *M*5-class aftershocks. This seismicity that fulfils sections along the Futagawa and Hinagu faults, is still being active. Seismicity and crustal deformation in the Kumamoto region were investigated to get implications of future seismic-activity trends.

We referred our previous work (Nanjo et al., 2016) that examined the spatial and temporal trend in *b* value of the Gutenberg-Richter's law, based on seismicity prior to the Kumamoto earthquakes. For the spatial distribution of *b* values, which shows data for a post-period (January 2017-January 2019), excluding the active aftershock period, we found a zone with low *b* values (130.6-130.8˚E, 32.5-32.6˚N), which lays further to the southwest of the *M*6.5 and *M*6.4 foreshocks along the Hinagu fault. A comparison with the spatial distribution of *b* values calculated for the seismicity from January 2000 to immediately before the Kumamoto earthquakes (Nanjo et al., 2016) reveals a zone where the *b* value decreased. This zone coincides with the low-*b*-value locations seen for seismicity after 2017. We compared the spatial distribution of earthquakes with *M*>5 in the Kumamoto sequence and the *b*-value distribution based on seismicity after 2017. Earthquakes with *M*> 5 have not occurred in the low-*b*-value zone.

While referring previous studies of crustal deformation associated with the Kumamoto earthquakes by GEONET (e.g., Hiyama et al., 2016), we investigated baseline changes of control stations near the Futagawa and Hinagu faults (the period from January 2013 until the end of 2018, with the "Misumi" (Shimane pref.) taken as a fixed station). A step-like change associated with the mainshock occurrence, followed by gradual changes associated with postseismic formation, is seen for all the baselines investigated. The same is true for the control station "Izumi" (130.79˚E, 32.58˚N), located in the low-*b* -value zone identified for seismicity after 2017, although the postseismic deformation is coming to an end. Therefore, active seismicity is expected to continue in the future.

Our method pinpointed the zone of low *b* values along the Hinagu fault, and this is the only one where the *b* value has decreased, compared to before the Kumamoto earthquakes. Nanjo et al. (2016) compared the *b*-value map with the sequence of foreshocks, mainshock, and aftershocks with *M*5 or greater, and showed that areas of low *b* values contained a high percentage (84%) of the sequence. If the *b* value is regarded, for the Kumamoto region, as an indicator for estimating the occurrence location of a relatively large earthquake in the future, the current low-*b*-value zone shows the high likelihood of "seismic gap", a segment considered to suffer a future *M*>5 earthquake.

Keywords: 2016 Kumamoto earthquakes, b value, crustal deformation

©2019. Japan Geoscience Union. All Right Reserved.

The unique characters of intensity distribution of the 2018 Sep. 6 Mw6.6 Earthquake of Iburi region in Hokkaido, Japan

*Ritsuko S. Matsu'ura[1], Hiroto Tanaka[2], Mitsuko Furumura[1], Tsutomu Takahama[2]

1. Earthquake Research Center, Association for the Development of Earthquake Prediction, 2. Kozo Keikaku Engineering Inc.

On Sep. 6, 2018, the Mw6.6 (M_{JMA}6.7) earthquake of 35km depth (JMA depth 37km) occurred in the eastern part of Iburi region, Hokkaido, Japan. Waves from this event are characterized by the very high level in high frequency part. Although it is just an Mw6.6 earthquake, and the shortest distance to the land is larger than its depth, Japanese Instrumental Seismic Intensity (JISI) 7 was recorded at Shikanuma station, 43km away from the source. The comparison of observed waves with the various prediction equations of PGV or PGA for Japan, such as Si and Midorikawa(1999) shows that the observation was remarkably larger than most equations in distances less than 50km [e.g. Nishimura and Miyakoshi (2018)].

We applied the new prediction equation of JISI, which was classified by the physical source types, and in which the surface ground effect was removed by the term dependent on AVS30 of each station [Matsu'ura et al. (2018)], to this event. The equation for the PAC-intra type fits well to stations in distances less than 100km, while the equation for the PAC-inter type fits well to further stations in Iwate or southeastern part of Hokkaido (Fig.). It apparently shows the high stress-drop source feature like an event of intra slab, but the abnormal intensity effect due to the PAC is weaker than that of the PAC-intra type, and similar to that of the PAC-inter type. These features are well explained when this Mw6.6 event occurred within the rather cold shallow mantle overriding on the slab on the western foot of Hidaka Mountains. The high frequency waves were transferred very efficiently from the source to the PAC slab like those from interplate events, which suggests that the source lies in fairly homogeous area than the ordinary Japanese crust.

This study was done as a part of the Supporting Project for the Headquarters for Earthquake Research Promotion (HERP) sponsored by the Ministry of Education, Culture, Sports, Science and Technology (MEXT), Japan.

References

Matsu'ura, R. S. et al. (2018). A new multidimensional prediction equation of instrumental seismic intensity of Japan reflecting source type characteristics, submitted to BSSA.

Nishimura, T., and K. Miyakoshi (2018). Comparison of Hokkaido-Iburi-Tobu earthquake with existed prediction equations of ground motions, Fall meeting of Seismological Society of Japan, S25-P19.

Si, H. and S. Midorikawa (1999). New attenuation relationships for peak ground acceleration and velocity considering effects of fault type and site condition, J. Struct. Constr. Eng. AIJ, 523, 63-70.

Keywords: Prediction Equation of Japanese Instrumental Intensity, 2018 Sep. 6 Mw6.6 Earthquake of Iburi region, earthquake in the uppermost mantle

©2019. Japan Geoscience Union. All Right Reserved.

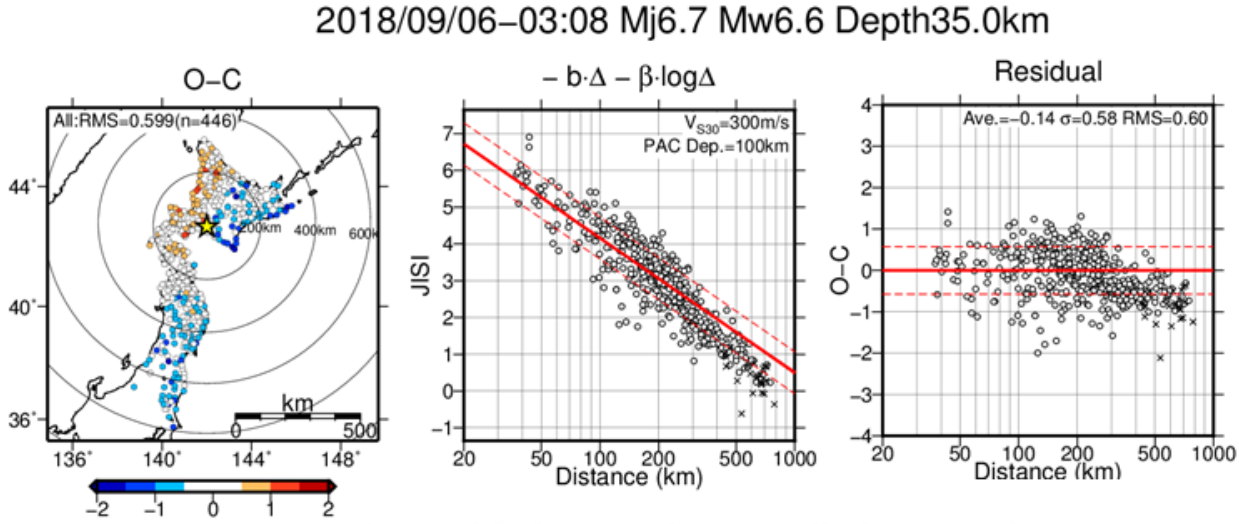

comparison with the PAC intra prediction equation

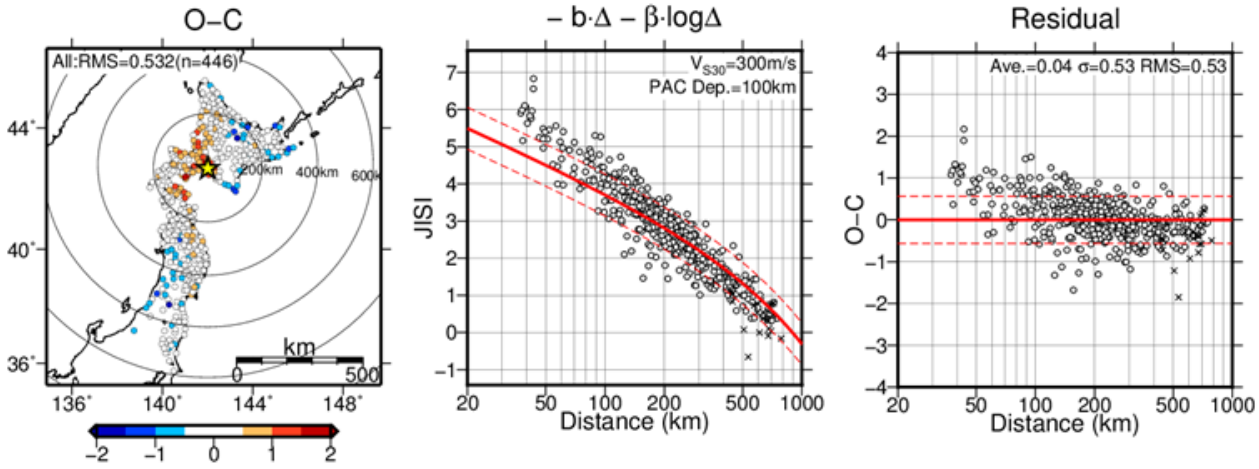

comparison with the PAC inter prediction equation

©2019. Japan Geoscience Union. All Right Reserved.

Determination of Hypocenter Location in Sumani and Sianok Fault Segments, West Sumatra region Using Oct-Tree Importance Sampling Method

*Ade Surya Putra[1], Nanang Tyasbudi Puspito[2], Andri Dian Nugraha[2], Pepen Supendi[3,1]

1. Geophysical Engineering, Faculty of Mining and Petroleoum Engineering, Institute of Technology Bandung, 2. Global Geophysics Research Group, Faculty of Mining and Petroleoum Engineering, Institute of Technology Bandung, 3. Agency of Meteorology, Climatology and Geohysics (BMKG), Indonesia, Bandung, Indonesia

Sumani and Sianok segments are two of the many fault segments in Sumatra Fault Zone (SFZ) that have a considerable history of seismicity and cause significant impacts. An important effort to overcome this problem is the need to analyze tectonic structures in detail through one of them by elaborating an accurate hypocenter location. In this study, we conducted hypocenter determination by using a non-linear approach with the oct-tree importance sampling method through NonLinLoc software by using local velocity components for earthquakes in Sumani and Sianok Segments in the range of 2009-2017. The results of hypocenter determination in this study indicate an improvement in picking arrival time of P and S wave. The increment is denoted by the results of residual picking P and S wave arrival times using oct-tree sampling method that dominant at frequency of 0.1 seconds and there is a correlation between hypocenter location cluster in this study with a location of major earthquakes that have occurred in Sumani and Sianok Segments.

Keywords: Hypocenter, Oct-tree importance sampling, Fault segment, Sumatra Fault Zone

©2019. Japan Geoscience Union. All Right Reserved.

1D Seismic Velocity Modelling and Hypocenter Relocation around Central and East Java Region: Preliminary Result

*Faiz Muttaqy[1], Andri Dian Nugraha[2], Nanang Tyasbudi Puspito[2]

1. Geophysical Engineering Study Program, Faculty of Mining and Petroleum Engineering, Institut Teknologi Bandung,
2. Global Geophysics Research Group, Faculty of Mining and Petroleum Engineering, Institut Teknologi Bandung

Central and East Java are part of Sunda Arc which has relatively high seismicity and complex geological system as a result of Indo-Australian plate that subducted under the Eurasian plate. The early stage of seismic tomography study in order to obtain a reliable geometry about the velocity structure beneath the study area is to define the precise earthquake location and 1D seismic velocity model. In this study, we manually picked P- and S-wave arrival time recorded by BMKG network for the time period from January 2009 to September 2017. We determined the hypocenter location around Central and East Java region by using an NLLoc program. We also conducted a velocity inversion using the VELEST program to obtain an updated 1D velocity model in the study area. Afterward, the hypocenters were relocated using the double-difference algorithm and the updated 1D velocity model to improve the accuracy of the hypocenter locations. Our results indicate that the seismicity around Central and East Java is generally distributed in the southern part of the island, such as in the south of Kebumen, Yogyakarta, Pacitan, Malang, and Banyuwangi that associated with the subduction activity. Moreover, the shallow seismicity is probably controlled by the presence of active inland faults, such as Opak Fault and Kendeng Thrust. As further studies, we will determine the focal mechanism of selected events related to the active inland fault in this region and conduct 3D seismic tomography imaging beneath Central and East Java region.

Keywords: Central Java, East Java, Hypocenter Relocation, 1D Velocity Model

©2019. Japan Geoscience Union. All Right Reserved.

Seismicity and Tectonics of the Bingöl Area: Eastern Anatolia

*Dogan Kalafat[1]

1. Bogazici University Kandilli Observatory and Earthquake Research Institute Cengelkoy, Istanbul Turkey

In this study, Bingöl Earthquakes which have occurred in recent years have been evaluated from seismological point of view. The Eastern Anatolia Region is the most seismologically deformed area of the Anatolian plate and is under compression due to the relative movement of the Arabian and Eurasian plates in general. The Anatolian plate bounded by the North Anatolian Fault Zone (NAFZ) and Eastern Anatolian Fault Zones (EAFZ) moves relatively westward. Bingöl Earthquakes are located within the Eastern Anatolian Fault Zone and this fault zone occurs due to the movement of the parts. Bingöl and the surrounding area is the most active regions in Turkey in terms of seismicity. The most important earthquakes in Bingöl during the instrumental period were the 1971 and 2003 earthquakes. Bingöl Fault starts from the south of Bingöl and extends along the Göynuk stream valley. This fault length is about 75 km. which is northern part of the Eastern Anatolian Fault Zone and joins the North Anatolian Fault Zone after passing through the villages of Serpmekaya and Sakaören. During the 1971 Bingöl Earthquake, about 38 km surface rupture occured which it started from Ormanardi to the southeast of Bingöl and extends to the N45ºE degree in the southwestern direction of Goynuk. The observed faults showed a strike-slip and a left lateral movement and the fault plane solutions supported the field observations.
The other important earthquake occurred on May 1, 2003. In this earthquake, 176 citizens were killed and 521 citizens were injured in various places. In particular, public buildings were severely damaged. The episantr area is between the Balikcay village plateau, Hanocayiri-Kurtulus and Sudugunu Plateau. Stepped fractures with NW-SE trending N20-30ºW trending were observed in Hanocayiri, which is one of the closest settlements of earthquake. As a result of earthquake, a great deal of collapses and mud currents were formed due to the effect of groundwater pressure. The fault traces in the region continued on the slopes of the NW-SE trending Kade mountains. Liquefaction, sitting, collapse and faulting samples were seen together in Hanocayiri hamlet. The earthquake caused severe damage, destruction and death in the buildings located on the alluvial terrace of Göynuk Creek in Bingöl province. During the earthquake, the Celtiksuyu Boarding School of Bingöl province was completely destroyed and 84 students died under the rubble. In addition, many public buildings were damaged. The macroseismic epicenter of the earthquake is approximately 12 km. distance between the district of Elcagini-Elmacayiri and Sudugunu plateaus. The area is mountainous and there are no frequent settlements. The nearest settlements are Balikcay, Hanocayiri Village, Elmacayiri village and Kurtulus village. It was observed that the epicenter of Bingöl Earthquake was highly compatible with the NW-SE trending faults. The fault of N-NW, which passes between Kurtulus-Elmacayiri-Hanocayiri and towards the Balikcay-Cimenli villages, was defined as the fault which was broken by the 2003 Bingöl Earthquake. In this study, 12 earthquakes fault plane solutions have given (magnitude Mw> 5.0) between 1971-2015 time period in Bingöl. The fault plane solution of 6 earthquakes was conducted within the scope of the study. The stress analysis shows that the dominant stress axes in the region are dominated by NW-SE directional compression and strike-slip faulting which are characterized by NE-SW extension axes.
The recent earthquakes showed that the ongoing deformation in the region continued with the strike-slip fault systems as the dominant. Structural heavy damages caused by earthquakes were mostly due to poor soil conditions, improper production, low quality and missing materials.

Keywords: Bingöl, East Anatolia, Göynük Stream, Fault Plane, Strike-Slip faulting

©2019. Japan Geoscience Union. All Right Reserved.

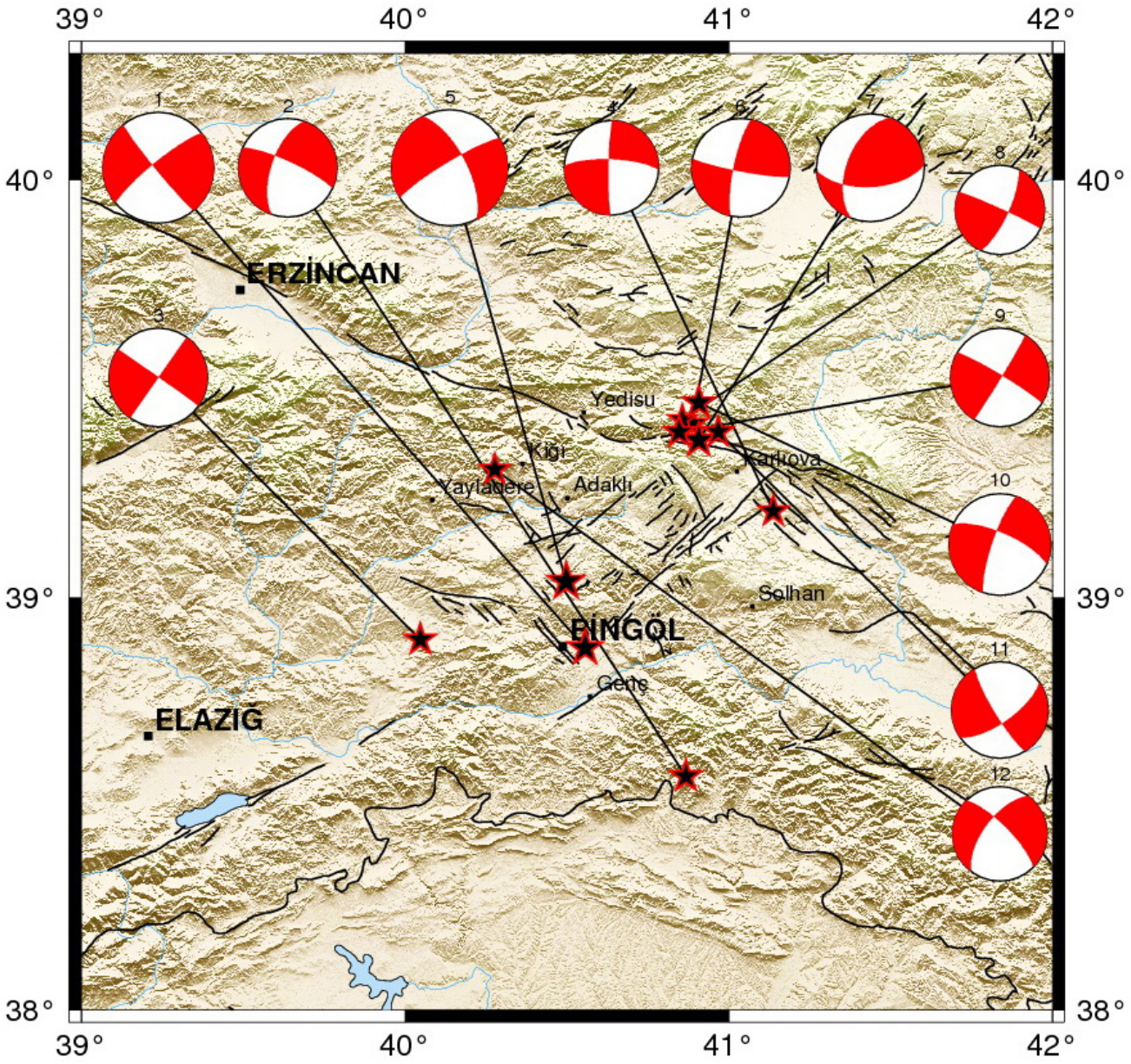

©2019. Japan Geoscience Union. All Right Reserved.

Seismicity along the North Anatolian Fault beneath the Marmara Sea, deduced from long-term ocean bottom seismographic observations

*Yojiro Yamamoto[1], Narumi Takahashi[2,1], Dogan Kalafat[3], Ali Pinar[3], Remzi Polat[3], Zeynep Coskun[3], Haluk Ozener[3], Yoshiyuki Kaneda[4]

1. Japan Agency for Marine-Earth Science and Technology (JAMSTEC), 2. NIED, 3. KOERI, Bogaziti University, 4. Kagawa University

The North Anatolian Fault (NAF) beneath the Marmara Sea is recognized as a seismic gap for M >7 earthquake during more than 100 years. Earthquake hazard and disaster mitigation studies in Marmara region are sensitive to detailed information on fault geometry and its coupling status beneath the Marmara Sea. Although hypocenter distribution could help us to estimate them, it is difficult to obtain precise hypocenter location from only onshore permanent seismic stations. Thus, we have started a series of long-term ocean bottom seismographic (OBS) observations beneath the western and central Marmara Sea since 2014. We have installed 10~15 OBSs along the Main Marmara Fault(MMF) for each observation phases, and observation length is about 10 or 11 months. Based on the first phase observation, conducted from 2014 to 2015, Yamamoto et al. (2017) identified a segment boundary of the MMF beneath the central basin of the Marmara Sea (28.05˚E). Besides, they proposed that the zones of no seismicity within the upper crust appear to indicate locked sections of the MMF.
In this study, we analyze the second (from 2015 to 2016) and third phases (from 2016 to 2017) observation data. The OBS distribution of second phase is same as first phase,whereas that of third phase is about 20 km shifted to eastward relative to first and second phases. The tentative result shows that the feature of hypocenter distribution, including the location of no seismicity zones obtained by Yamamoto et al. (2017), is not changed for all phases, suggesting that the coupling status along the fault is almost same during at least three years. In the west of 28.05˚E, seismicity located not only the upper but also lower crust. On the other hand, the lower limit of the seismogenic zone in the east of 28.05˚E is about 15 km, shallower than the Conrad discontinuity. The largest no seismicity zone extended over the upper crust is located between 28.45˚E and 28.65˚E, where strong coupling is suggested from seafloor geodetic observation (Sakic et al., 2016).
According to the spatial relationship between the epicenter of microearthquakes and fault trace on the sea floor (Armijo et al., 2005) suggests that the MMF around 28.75˚E is near vertical to slightly northward dipping. Since previous study indicates that the east of 28.05˚E MMF is southward dipping (Yamamoto et al., 2017), there might be another segment boundary west of 28.75˚E. We also find an active seismic cluster around 40.8˚N, 28.7˚E, 14 km depth. There is a possibility that this cluster relates to the southern branch of NAF.

Keywords: The North Anatolian Fault, Marmara Sea, Seismicity

©2019. Japan Geoscience Union. All Right Reserved.

Microseismic Monitoring of the Sultandagi Fault Zone: Western Turkey

*Dogan Kalafat[1], Yavuz Gunes[1], Mehmet Kara[1], Kivanc Kekovali[1]

1. Bogazici University Kandilli Observatory and Earthquake Research Institute Cengelkoy, Istanbul Turkey

Western Turkey is one of the seismically active region in Turkey. The high seismic activity is a result of the complex tectonic deformation of the Anatolian plate which has been dominated by the N–S extensional tectonic regime in the western edge. In western Turkey, relatively 3 major earthquakes (Mw≧6.0) were identified on the Sultandagi Fault Zone (Afyon-Aksehir Graben) between years of 2000–2002. In this study, mentioned local earthquake activity, have been investigated to understand their nature and relation of the regional seismic activity and tectonic deformation on the Sultandagi Fault Zone (SFZ) in western Turkey. Due to these activities along the SFZ it is decided to monitor microseismic activity (M<2.5) by establishing low-magnitude threshold seismic network. For this purpose, 3 new broadband (BB) seismic stations were temporarily established to control the northern part of the Sultandagi Fault Zone, and the micro-seismicity of the fault zone was started to be observed in July 2017. Thus, the earthquake activity in the region started to be monitored sensitively. So we started to get 2 times more earthquakes than permanent stations in the region. The one of the biggest primary outcome by this study that there is a significant microseismic activity (M<2.5) at the SFZ which was not seen from prior studies and long-term seismicity catalogues from permanent network (M>2.5). At first, we started to analyze the distribution of micro-earthquakes in the region. During the data analysis, it was predicted that some intensive micro-earthquake activity in the project area could be caused by quary-blasting and some locations were visited during the field study. Relocation of common earthquakes recorded by KOERI and the study was carried out, and the earthquake epicenters were displaced approximately as ±0.8–6 km. There were also some positive changes in the depth distribution of earthquakes. Consequently, thanks to the stations established within the scope of the study, horizontal (distance) and vertical error (depth) margins of the events in the region have been reduced. As a result of the evaluation of the data obtained, it was observed that the Sultandagi Fault Zone has especially intense seismic activity in the middle and northwest part. In addition, a significant seismic activity was observed in NW-SE direction at the north of Isparta city .
This research is funded by Bogazici University Research Fund within the scope of Project Number 12280. We thank to Bogazici University Research Fund Commission and members.

Keywords: Sultandagi Fault Zone, Western Turkey, extensional tectonic regime, micro-seismicity

©2019. Japan Geoscience Union. All Right Reserved.

Analysis of radiated seismic energy distributing in aftershock sequences at the Guerrero, Mexico subduction zone.

*Raymundo Omar Plata Martinez[1], Xyoli Pérez Campos[2], Krishna Shri Singh[2]

1. Kyoto University, 2. Geophysics Institute, UNAM

Radiated seismic energy is valuable parameter in seismic source studies, as it can be a good criterion to evaluate earthquakes size but also very useful to analyze the dynamics of the rupture process. Significant large thrust earthquakes have occurred over the last decades at the Mexican, subduction zone, however just a few researches have been done to understand the distribution of seismic energy release in the area. For this purpose, we calculated source spectra to estimate radiated seismic energy of three large earthquakes and their aftershocks (*M* larger than 4.0) in the Guerrero segment of the Mexican subductions zone; the 2012 Ometepec-Pinotepa Nacional (*Mw* 7.5), the 2014 Papanoa (*Mw* 7.2) and the 2018 Pinotepa Nacional (*Mw* 7.2) earthquakes. We found a mean value of the log of radiated seismic energy scaled with the seismic moment (Mo/Es) of -5.05 ±0.25, as well as, regional estimations tend to be higher than the teleseismic estimations by a factor of 1.3 to 6.3. A small dependence of scaled seismic energy with distance from the trench was seen, however distribution of seimsic energy seems to be spatially heterogeneous along the trench. We found four different regions with characteristic behaviors in energy release. One of the regions reveals recurrent low energies with possible slow rupturing close to the trench. Opposingly, high energy seismicity was present, adjacent to the Guerrero gap, which has not had a large earthquake in over 115 years. This suggests that radiated seismic energy can be highly influenced by complexities at the plate interphase, variations on the shear strength and/or coupling at the interface where seismic slip interacts over previous rupture patches.

Keywords: Radiated energy, aftershocks, subduction

©2019. Japan Geoscience Union. All Right Reserved.

[J] Poster | S (Solid Earth Sciences)：S-SS Seismology

Tue. May 28, 2019 5:15 PM - 6:30 PM JST | Tue. May 28, 2019 8:15 AM - 9:30 AM UTC | Poster Hall International Exhibition Hall8, Makuhari Messe_29

[S-SS10] Seismicity

convener:Kei Katsumata(Institute of Seismology and Volcanology, Hokkaido University)

This session aims to improve our understanding on seismicity. Any contribution on behavior of earthquakes as a cluster, such as regional seismicity and aftershocks, are welcomed. We also welcome contribution on temporal and spatial interactions that control seismicity, and tectonic processes, and geological and thermal structures that regulate seismicity.

[SSS10-P01] Spatial-temporal and seismogram characteristics of foreshock and aftershock activities for tsunami earthquakes

*Yifeng Liu[1], Yoshihiro Ito[2], Kazuaki Ohta[2], Satoshi Katakami[1] (1.Division of Earth and Planetary Sciences, Graduate School of Science, Kyoto University, 2.Disaster Prevention Research Institude, Kyoto University)

[SSS10-P02] Successively occurring large earthquakes in the world – comparison of real cases with expectations by the space-time ETAS

*Tetsuo Hashimoto[1], Takashi YOKOTA[2] (1.Seismology and Tsunami Research Department, Meteorological Reaserch Institute, 2.Aichi Institue Technology)

[SSS10-P03] Seismicity beneath stable oceanic plate

*Yasushi Ishihara[1] (1.R&D Center for Earthquake and Tsunami, JAMSTEC)

[SSS10-P04] Relation between long-term slow slip events and correlation between tidal triggering effect and deep low-frequency earthquakes in Bungo Channel: Part 2

*Fuyuki Hirose[1], Akio Kobayashi[1], Kenji Maeda[2] (1.Seismology and Tsunami Research Department, Meteorological Research Institute, 2.Seismology and Volcanology Department, Japan Meteorological Agency)

[SSS10-P05] Arrival-time and hypocenter determination using S-net

*Tomomi Okada[1], Ryota Takagi[1], Takashi NAKAYAMA[1], Syuichi Suzuki[1], Ryosuke Azuma[1], Genti Toyokuni[1], Keisuke Yoshida[1], Naoki Uchida[1], Ryota Hino[1] (1.Research Center for Prediction of Earthquakes and Volcanic Eruptions, Graduate School of Science, Tohoku University)

[SSS10-P06] Focal mechanisms of the double seismic zone in the Pacific plate, off Boso: Temporal change after the 2011 Tohoku EQ

*Guanyu Chen[1], Toshinori Sato[2], Tomoharu Sato[1], Asami Terada, Masanao Shinohara[3], Kimihiro Mochizuki[3], Tomoaki Yamada[3], Kenji Uehira[4], Takashi Shimbo[5], Shuichi Kodaira[5], Yuya Machida[5], Ryota Hino[6], Ryosuke Azuma[6], Yoshio Murai[7], Yoshihiro Ito[8], Hiroshi Yakiwara[9], Kenji Hirata[4], Akinori Hashima[3], Andrew M. Freed[10] (1.Faculty of Science, Chiba University, 2.Graduate School of Science, Chiba University, 3.Earthquake Research Institute, University of Tokyo, 4.National Research Institute for Earth Science and Disaster Resilience, 5.Japan Agency for Marine-Earth Science and Technology, 6.Graduate School of Science, Tohoku University, 7.Institute of Seismology and Volcanology, Faculty of Science, Hokkaido University, 8.Disaster Prevention Research Institute, Kyoto University, 9.Nansei-toko Observatory for Earthquakes and Volcanoes, Kagoshima University, 10.Purdue University)

[SSS10-P07] Ocean bottom seismographic observation and similar earthquake detection in the northern part of the Nansei Islands

*Yukihiro Nakatani[1], Hiroshi Yakiwara[1], Shuichiro Hirano[1], Reiji Kobayashi[2], Hiroki Miyamachi[2], Shigeru Nakao[2], Kazunari Uchida[3], Takeshi Matsushima[3], Hiroshi Shimizu[3], Kazuo Nakahigashi[4], Yusuke Yamashita[5], Hideji Abe[6], Tomoaki Yamada[6], Masanao Shinohara[6] (1.Nansei-Toko Observatory for Earthquakes and Volcanoes, Kagoshima University, 2.Graduate School of Science and Engineering,

Kagoshima University, 3.Institute of Seismology and Volcanology, Faculty of Science, Kyushu University, 4.Tokyo University of Marine Science and Technology, 5.Disaster Prevention Research Institute, Kyoto University, 6.Earthquake Research Institute, the University of Tokyo)

[SSS10-P08] Seismicity and crustal structure in the Okinawa Trough

*Azusa Nishizawa[1], Takeshi Kimura[1], Kentaro Kaneda[2] (1.National Research Institute for Earth Science and Disaster Resilience, 2.Japan Coast Guard)

[SSS10-P09] Time series analyses of the seismic activities in southwestern Japanese Island to southeastern Korean Peninsula excited by the deep fluid heat flow

*Takayuki Kawabe[1] (1.Faculty of Education, Arts and Sciences, Yamagata University)

[SSS10-P10] Integrated monitoring of seismicity in and around the Suruga Bay using Ocean Bottom Seismometers and inland stations.

*Yannis Panayotopoulos[1], Hisatoshi Baba[2], Takahito Nishimiya[3], Taiyo Sotani[4], Nakao Nagisa[4] (1.Association for the Development of Earthquake Prediction, 2.Department of Marine and Earth Science, Tokai University, 3.Meteorological Research Institute, Japan Meteorological Agency, 4.Tokai University)

[SSS10-P11] Linear distribution of the intraslab earthquakes in Tokai

*Sadaomi Suzuki[1] (1.Tono Research Institute of Earthquake Science, Association for the Development of Earthquake Prediction)

[SSS10-P12] The stress change of Chubu region before and after the 2011 Tohoku-oki Earthquake(Mw9.0)

*Yuki Susukida[1], Kei Katsumata[1] (1.Institute of Seismology and Volcanology, Hokkaido University)

[SSS10-P13] Repeating earthquake activity off Miyagi Prefecture triggered by the 2011 Tohoku-oki earthquake

*Kenshiro Tsumura[1] (1.Association for Developement of Earthquake Prediction)

[SSS10-P14] Seismic Moments of Inland Small Earthquakes in Japan: Spectral Analyses Using the Hi-net

*Tomotake Ueno[1], Tatsuhiko Saito[1] (1.National Research Institute for Earth Science and Disaster Resilience)

[SSS10-P15] Spatiotemporal variations of stress field in the 2016 Kumamoto earthquake (M 7.3) area

*Dapeng Zhao[1], Zhiteng Yu[2], Jiabiao Li[2], Zhouchuan Huang[3] (1.Department of Geophysics, Tohoku University, 2.State Oceanic Administration, 3.School of Earth Sciences and Engineering, Nanjing University)

[SSS10-P16] Seismicity and crustal deformation following the 2016 Kumamoto earthquakes

*Kazuyoshi Nanjo[1], Jun Izutsu[2], Yoshiaki Orihara[3], Masashi Kamogawa[4], Toshiyasu Nagao[3] (1.University of Shizuoka, 2.Chubu University, 3.Tokai University, 4.Tokyo Gakugei University)

[SSS10-P17] The unique characters of intensity distribution of the 2018 Sep. 6 Mw6.6 Earthquake of Iburi region in Hokkaido, Japan

*Ritsuko S. Matsu'ura[1], Hiroto Tanaka[2], Mitsuko Furumura[1], Tsutomu Takahama[2] (1.Earthquake Research Center, Association for the Development of Earthquake Prediction, 2.Kozo Keikaku Engineering Inc.)

[SSS10-P18] **Determination of Hypocenter Location in Sumani and Sianok Fault Segments, West Sumatra region Using Oct-Tree Importance Sampling Method**

*Ade Surya Putra[1], Nanang Tyasbudi Puspito[2], Andri Dian Nugraha[2], Pepen Supendi[3,1] (1.Geophysical Engineering, Faculty of Mining and Petroleoum Engineering, Institute of Technology Bandung, 2.Global Geophysics Research Group, Faculty of Mining and Petroleoum Engineering, Institute of Technology Bandung, 3.Agency of Meteorology, Climatology and Geohysics (BMKG), Indonesia, Bandung, Indonesia)

[SSS10-P19] **1D Seismic Velocity Modelling and Hypocenter Relocation around Central and East Java Region: Preliminary Result**

*Faiz Muttaqy[1], Andri Dian Nugraha[2], Nanang Tyasbudi Puspito[2] (1.Geophysical Engineering Study Program, Faculty of Mining and Petroleum Engineering, Institut Teknologi Bandung, 2.Global Geophysics Research Group, Faculty of Mining and Petroleum Engineering, Institut Teknologi Bandung)

[SSS10-P20] ***Seismicity and Tectonics of the Bingöl Area: Eastern Anatolia***

*Dogan Kalafat[1] (1.Bogazici University Kandilli Observatory and Earthquake Research Institute Cengelkoy, Istanbul Turkey)

[SSS10-P21] Seismicity along the North Anatolian Fault beneath the Marmara Sea, deduced from long-term ocean bottom seismographic observations

*Yojiro Yamamoto[1], Narumi Takahashi[2,1], Dogan Kalafat[3], Ali Pinar[3], Remzi Polat[3], Zeynep Coskun[3], Haluk Ozener[3], Yoshiyuki Kaneda[4] (1.Japan Agency for Marine-Earth Science and Technology (JAMSTEC), 2.NIED, 3.KOERI, Bogaziti University, 4.Kagawa University)

[SSS10-P22] **Microseismic Monitoring of the Sultandagi Fault Zone: Western Turkey**

*Dogan Kalafat[1], Yavuz Gunes[1], Mehmet Kara[1], Kivanc Kekovali[1] (1.Bogazici University Kandilli Observatory and Earthquake Research Institute Cengelkoy, Istanbul Turkey)

[SSS10-P23] Analysis of radiated seismic energy distributing in aftershock sequences at the Guerrero, Mexico subduction zone.

*Raymundo Omar Plata Martinez[1], Xyoli Pérez Campos[2], Krishna Shri Singh[2] (1.Kyoto University, 2.Geophysics Institute, UNAM)

Spatial-temporal and seismogram characteristics of foreshock and aftershock activities for tsunami earthquakes

*Yifeng Liu[1], Yoshihiro Ito[2], Kazuaki Ohta[2], Satoshi Katakami[1]

1. Division of Earth and Planetary Sciences, Graduate School of Science, Kyoto University, 2. Disaster Prevention Research Institude, Kyoto University

A tsunami earthquake is an abnormal earthquake type causing a large tsunami compared to the magnitude measured by short-period seismic waves. There is a high risk to induce a massive tsunami damage for the reason that people who live in the coastal area do not feel quakes a lot, and it is difficult to keep themselves safe after the unusual earthquake happened. Additionally, as for the tsunami earthquakes, their observation cases are much fewer than ordinary earthquakes, so the mechanism of its occurrence is still an open question. To address spatio-temporal features and the mechanism of tsunami earthquakes, we focus on three typical examples of tsunami earthquake and their foreshock & aftershock sequences, which are (Nicaragua (1992/09/02, Mw 7.7), Jawa island (2006/07/17, Mw 7.7) and Mentawai (2010/10/25, Mw 7.8)). We also investigated whether a small earthquake showing the same characteristics as the tsunami earthquake is contained in the foreshock and aftershock activity.

First, we use seismic catalogs and waveform recording provided by ISC/USGS and IRIS respectively to extract the foreshock and aftershock activity, then evaluate the spatio-temporal features. We have found that four foreshock sequences (1992/08/10 06:09:20 Mb 5.2, 1992/08/10 06:34:14 Mb4.7, 1992/08/11 05:23:51 Mb 5.1, 1992/08/13 08:41:17 Mb 4.7) near the epicenter of mainshock area were observed before the occurrence of the Nicaragua mainshock. We have also analyzed the regional and spatio-temporal characteristics of three tsunami earthquake regions by dividing the area of 5*5 around the epicenter into twenty-five segments with the size of 1*1. As a result, in each of the three regions, we have found out that there is a seismic quiescence period in the vicinity of the mainshock area in each tsunami earthquake. Meanwhile, regarding aftershocks of the Nicaragua earthquake, seismic quiescence area is still detected in the same segment as the foreshock.

Migration phenomenon is observed in the foreshock activity near the focal region of the mainshock, especially before the mainshock of the Nicaragua earthquake. Meanwhile, the waveforms of aftershocks occurring in the same area as the events included in the migration have been compared with those of the mainshock. Next, we have calculated the ratio of maximum absolute amplitude of surface wave to that of body wave, in order to address features on waveforms of tsunami earthquake. As a result, the ratio of the mainshock, such as the tsunami earthquake shows extremely high value, whereas for the foreshocks and aftershocks, it does not show the same characteristic as the tsunami earthquake does. This suggests that small earthquakes occurring within the tsunami seismogenic region show the same phenomenon as ordinary earthquakes, but only the mainshock has the characteristics of the tsunami earthquake.

Keywords: tsunami earthquake, seismic activity, waveform analysis

©2019. Japan Geoscience Union. All Right Reserved.

Successively occurring large earthquakes in the world –comparison of real cases with expectations by the space-time ETAS

*Tetsuo Hashimoto[1], Takashi YOKOTA[2]

1. Seismology and Tsunami Research Department, Meteorological Reaserch Institute, 2. Aichi Institue Technology

In the government for evaluating criteria on abnormal phenomena along the Nankai Trough for disaster prevention measures, they made the criteria for events to announce the Nankai Trough Earthquake Information. In order to implement specific ways of disaster prevention, they discussed about specific criteria for what kind of phenomenon corresponds to the abnormal event. In this time, we presented the real cases of the successive occurrence of large earthquakes in the world on the newly revised ISC-GEM version 5.1 data (1904-2014) for contributing to the above discussion. And we estimated the large earthquakes occurrence by using the space-time ETAS (Ogata and Zhuang, 2006).The 103 earthquakes of Mw 8.0 over were extracted about the earthquakes in the world for about the last 100 years. There were 9, 10 and 13 earthquakes which were accompanied with the earthquake of Mw 7.8 over occurred within the epicentral distances 500 km within 3 days, 7 days and 30 days, respectively.We estimated occurrences earthquakes from summations of expectations by the space-temporal ETAS which was applied with the parameters around Japan of Ogata and Zhaung (2006) and b=0.92 estimated with the JMA earthquake catalog. And then there were 5.3, 6.5 and 8.0 earthquakes of Mw 8 over which accompanied to the earthquake of Mw 7.8 over within the epicentral distances 500km within 3days, 7days and 30 days, respectively.The expected frequency of occurrence and the decreasing trend accompanying the elapsed time since the preceding earthquake were generally consistent with the above actual case.Acknowledgment: We used ISCGEMver 5.1 from ISC. In addition, we received great cooperation from the Earthquake Prediction and Information Division, Seismology and Volcanology Department, Japan Meteorological Agency.

Keywords: Nankai trough earthquake, Large earthquake, occurring in succession, ETAS

©2019. Japan Geoscience Union. All Right Reserved.

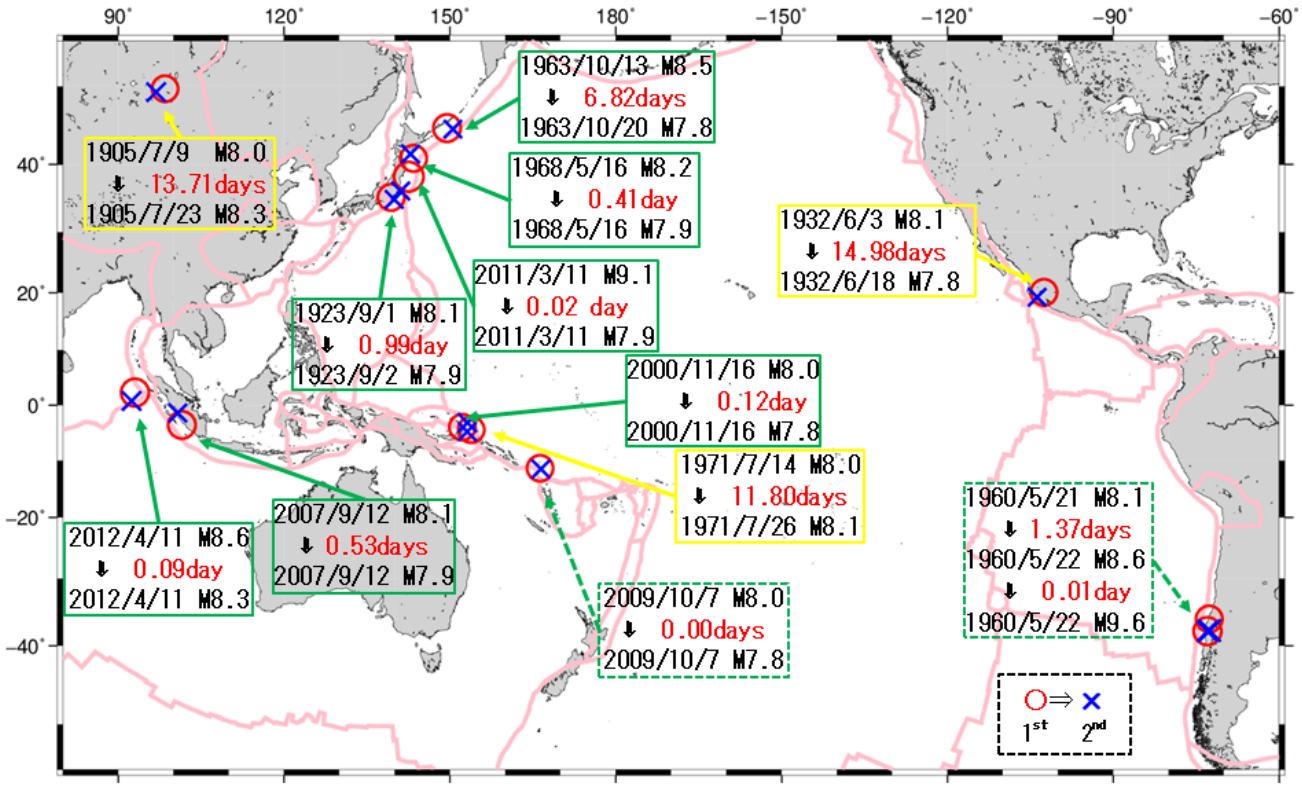

Epicentral distribution of pairs of the over Mw8 as 1st event(upper) and over Mw7.8 as 2nd event(lower) within 500km of the 1st. Time differences of two events are shown as red (yellow frames are over 7days). Pairs of less 50km of distance are shown as dashed frame. Plate boundaries data from Bird(2003). Map is drawn with GMT.

©2019. Japan Geoscience Union. All Right Reserved.

Seismicity beneath stable oceanic plate

*Yasushi Ishihara[1]

1. R&D Center for Earthquake and Tsunami, JAMSTEC

Stable oceanic plate has low seismic activity generally. Real tectonic deformation is also stable? To survey this topics, high quality and long-term observation. Pacific21 broadband seismic network deploys stations in Micronesia area. At present five islands station are under operation. Two of all have already telemetered to our data center via internet connection and transfer to other organization and institute.
In this year new telemeter station (station code: CHUK) is completed successfully. Chuuk (Truk) island locates on old oceanic plate about 900-1,000km southeast of Mariana trench and Guam. CHUK station locates inside deep tunnel made in more than 70 years ago, WWII era. The site condition is fine in basalt mountain, under stable temperature and on rigid floor. We deployed STS-2 broadband sensor in sensor room, high-resolution data logger and stable power supply system. CHUK station will contribute monitor and location of earthquake around Mariana trench and outer rise area.
Though CHUK station locates in small oceanic island and records strong ocean microseism, background noise level is lower level than standard model. CHUK station is excellent site to monitor including small local earthquake. CHUK station operates for about four years. We review continuous data and pick up local regional seismic events. Not only outer rise region but also Chuuk island area and hidden tectonic zone has active seismicity. By trial analysis, depth of these seismic events is beneath 20km. It implies stress concentration in oceanic plate and its deformation.

Keywords: oceanic plate, seismicity

©2019. Japan Geoscience Union. All Right Reserved.

Relation between long-term slow slip events and correlation between tidal triggering effect and deep low-frequency earthquakes in Bungo Channel: Part 2

*Fuyuki Hirose[1], Akio Kobayashi[1], Kenji Maeda[2]

1. Seismology and Tsunami Research Department, Meteorological Research Institute, 2. Seismology and Volcanology Department, Japan Meteorological Agency

Long-term slow slip events (LSSEs) have occurred with the interval of 5-6 years beneath the Bungo Channel [e.g., Kobayashi, 2017, EPS]. Deep low-frequency tremors and earthquakes (LFEs) have synchronized with the LSSEs and have activated [Hirose et al., 2010, Science]. It is pointed out that tremors have high tidal correlation [Ide, 2010, Nature; Ide & Tanaka, 2014, GRL]. There is no study that investigated long-term changes of the tidal correlation of LFEs.
On the other hand, the correlation between regular seismicity and tide also have been investigated energetically, and then there is a report that the tidal correlation became higher before the large earthquake around the focal region and became lower after the mainshock [e.g., Tanaka et al., 2012, GRL]. In addition, it is also pointed out that a leading period of high tidal correlation corresponded with the magnitude of a following earthquake.
Accordingly, we investigated temporal changes of tidal correlation of LFEs before and after LSSEs beneath the Bungo Channel on the analogy of tidal correlation of background seismicity before and after large earthquakes.
We extracted LFEs from the earthquake catalog unified by Japan Meteorological Agency (JMA) that occurred beneath the Bungo Channel from 2000 to March 21, 2018. Accuracy of locations of LFEs is lower than that of regular earthquakes. Note that hypocenter determination method for LFE by JMA changed since March 22, 2018, and then detection level also changed at the border. Taking int consideration that the change is not suitable in order to investigate long-term changes of tidal correlation of LFEs, we selected LFEs data.
It is necessary to set fault parameters in order to estimate the theoretical below-ground tidal response. Because our study area was narrow area with 15 km square, we set one fault plane (strike angle 237˚, dip angle 16˚, and rake angle 103˚) taking into consideration the plate configuration [Hirose et al., 2008, JGR] and MT solutions of deep very LFEs [Ide & Yabe, 2014, GRL]. In addition, we set hypocenters of LFEs to the common location (longitude 132.254˚, latitude 33.142˚, and depth 32 km). We used only occurrence times of LFEs determined by the JMA.
We summed temporal variations of the solid and oceanic tide loading effects for six independent components of the strain tensor, as estimated at the hypocenter of each event. Then we converted them to temporal variations of volumetric strain (ΔV) at the hypocenter, and shear stress ($\Delta\tau$), normal stress ($\Delta\sigma$), and the Coulomb failure function (ΔCFF) on the assumed fault plane. In the ΔCFF calculation, we assumed values of 0.1, 0.4, and 0.7 for the apparent friction coefficient μ'. In the case of ΔV and $\Delta\sigma$, we defined expansion/dilatation as positive and contraction/compression as negative; consequently, positive $\Delta\sigma$ values promote fault slip. We also defined $\Delta\tau$ and ΔCFF as positive when they promote fault slip. Using the time series of tidal stress (strain) levels, we assigned phase angles of −180˚ and 180˚ to the minimum tidal stress (strain) levels before and after an event, respectively, and 0˚ to the maximum tidal stress (strain) that occurred between these two minima. The phase angle at the earthquake occurrence time was estimated by linear interpolation in the time interval between −180º and 0˚ or between 0˚ and 180˚. The possible occurrence of LFEs at certain tidal phase angles was evaluated using the *p* value, as

©2019. Japan Geoscience Union. All Right Reserved.

calculated by Schuster [1897].
We found that LFEs tended to occur near a tidal phase angle of 0° for $\Delta\tau$ (when the tidal force promoted fault slip). This result indicates extremely low μ' and high pore pressure, being consistent with the existence of fluid inferred from the seismic velocity structure [Hirose et al., 2008]. LSSEs occurred three times (in 2003-2004, 2009-2011, and 2014) during the study period. Temporal changes of *p* value showed to tend to become lower before the LSSEs and become higher after ones (Tidal correlation tended to become higher before the LSSEs and become lower after ones). This result is similar to temporal changes of *p* value for background seismicity before and after large earthquakes. Accordingly, temporal tidal correlation of LFEs indicates to be affected by stress perturbation associated with LSSEs. Note that *p* value at March in 2018 falls to a level just before past LSSEs.

Keywords: Earth tide, Schuster's p value, Low frequency event, Long-term slow slip event, Bungo Channel

©2019. Japan Geoscience Union. All Right Reserved.

Arrival-time and hypocenter determination using S-net

*Tomomi Okada[1], Ryota Takagi[1], Takashi NAKAYAMA[1], Syuichi Suzuki[1], Ryosuke Azuma[1], Genti Toyokuni[1], Keisuke Yoshida[1], Naoki Uchida[1], Ryota Hino[1]

1. Research Center for Prediction of Earthquakes and Volcanic Eruptions, Graduate School of Science, Tohoku University

Hypocenter distribution is basic information for understanding seismogenesis.
For east off Honshu from Hokkaido, Tohoku, Kanto, S-net has been deployed by NIED. S-net is expected to improve accuracy of hypocenter location. In this study, we show a preliminary result of hypocenter determination using S-net and onshore stations.
We used hypomh (Hirata and Matsu’ura (1984)) with seismic velocity structure of Hasegawa et al. (1978). In our case, we used waveform converted to vertical, north-south, east-west components by Takagi et al. (this meeting).
For the earthquake near coast line, we can determine reliable hypocenter location, which is correspond to the location determined by F-net CMT or AQUA catalog. However, large travel time residuals over 3 seconds earlier are estimated for distant stations including the stations east of trench. This would mainly be due to the high velocity Pacific plate (e.g., Toyokuni et al., this meeting). To improve the velocity structure and use station correction are necessary for further study.

Acknowledgements: We used S-net, Hi-net and stations by universities (Hokkaido, Hirosaki, Tokyo and others), Aomori and Tokyo Pref., ADEP (Association for the development of earthquake prediction) and JMA. Profs. Matsuzawa, Zhao, Umino and Hasegawa and Mr. Hirahara give us valuable suggestions.

Keywords: S-net

©2019. Japan Geoscience Union. All Right Reserved.

Focal mechanisms of the double seismic zone in the Pacific plate, off Boso: Temporal change after the 2011 Tohoku EQ

*Guanyu Chen[1], Toshinori Sato[2], Tomoharu Sato[1], Asami Terada, Masanao Shinohara[3], Kimihiro Mochizuki[3], Tomoaki Yamada[3], Kenji Uehira[4], Takashi Shimbo[5], Shuichi Kodaira[5], Yuya Machida[5], Ryota Hino[6], Ryosuke Azuma[6], Yoshio Murai[7], Yoshihiro Ito[8], Hiroshi Yakiwara[9], Kenji Hirata[4], Akinori Hashima[3], Andrew M. Freed[10]

1. Faculty of Science, Chiba University, 2. Graduate School of Science, Chiba University, 3. Earthquake Research Institute, University of Tokyo, 4. National Research Institute for Earth Science and Disaster Resilience, 5. Japan Agency for Marine-Earth Science and Technology, 6. Graduate School of Science, Tohoku University, 7. Institute of Seismology and Volcanology, Faculty of Science, Hokkaido University, 8. Disaster Prevention Research Institute, Kyoto University, 9. Nansei-toko Observatory for Earthquakes and Volcanoes, Kagoshima University, 10. Purdue University

1. Introduction

The Pacific plate and the Philippine Sea plate subduct off the Boso Peninsula, and the Pacific plate has a double seismic zone at this place (e.g. Terada et. al., JpGU, 2016). Sato et. al. (JpGU, 2018) revealed that most focal mechanisms for the lower surface events have down-dip extension before the 2011 Tohoku EQ, and down-dip compression during 3 months after the EQ using land and ocean bottom seismic observations. This presentation shows 1 year temporal change of focal mechanisms for the double seismic zone’ s events after the 2011 Tohoku EQ.

2. Data and analysis

The used data are waveform data from Hi-net by NIED, and the aftershock survey of the 2011 Tohoku EQ using ocean bottom seismometers (2011/3/15-2012/3/31). We select events in the double seismic zone, and pick polarities of the P wave first motions. We calculate emergent azimuth and dip of each event-receiver pair using a 3D structure determined by Terada et al. (JpGU, 2016), and search optimal focal mechanisms using a grid search method.

3. Results

During 1 year after the 2011 Tohoku EQ, most focal mechanisms have down-dip compression for the upper surface events. For the lower surface events, on the other hand, most focal mechanisms have down-dip compression by July, 2011, and many mechanisms have down-dip extension after September, 2011. This may indicate that a compressional stress change occurred at the depth of the Pacific plate just after the 2011 Tohoku EQ, because the EQ moved the Pacific plate downward at the shallower part, and compressed the deeper part of the plate. After that, the compressional stress may had relaxed about a half a year.

Acknowledgements

We thank captains and crew of aftershock observation cruises of the 2011 Tohoku Earthquake. We used waveform data from Hi-net by NIED.

Keywords: Double seismic zone, temporal change of focal mechanism, the Pacific plate, off the Boso Peninsula, the 2011 Tohoku Earthquake

©2019. Japan Geoscience Union. All Right Reserved.

©2019. Japan Geoscience Union. All Right Reserved.

Ocean bottom seismographic observation and similar earthquake detection in the northern part of the Nansei Islands

*Yukihiro Nakatani[1], Hiroshi Yakiwara[1], Shuichiro Hirano[1], Reiji Kobayashi[2], Hiroki Miyamachi[2], Shigeru Nakao[2], Kazunari Uchida[3], Takeshi Matsushima[3], Hiroshi Shimizu[3], Kazuo Nakahigashi[4], Yusuke Yamashita[5], Hideji Abe[6], Tomoaki Yamada[6], Masanao Shinohara[6]

1. Nansei-Toko Observatory for Earthquakes and Volcanoes, Kagoshima University, 2. Graduate School of Science and Engineering, Kagoshima University, 3. Institute of Seismology and Volcanology, Faculty of Science, Kyushu University, 4. Tokyo University of Marine Science and Technology, 5. Disaster Prevention Research Institute, Kyoto University, 6. Earthquake Research Institute, the University of Tokyo

The Ryukyu Trench subduction zone is seismically active region. In the northern part of the Nansei Islands, both seismic and aseismic events have occurred along the subducting plate interface. Spatial distribution of small local earthquakes in this region seems to show some seismic clusters and gaps. Short-term slow slip events and shallow low-frequency tremors have been also observed by recent onshore seismic and geodetic data. However, patterns of their slip behavior and spatiotemporal relationship between regular and slow earthquakes are less well understood because seismic stations are located only at the islands that are linearly arranged; at least 100 km away from the Ryukyu Trench.
We have therefore conducted repeating long-term ocean bottom seismographic observation off the northern part of the Nansei Islands since 2014. First, we deployed three pop-up type ocean bottom seismometers (OBSs) in April 2014. Then, three more OBSs were added to the network in July 2015, and after that deployment and retrieval of OBSs at the same position have been repeatedly carried out every about one year. The station interval is about 40–60 km.
In this study, we focus on regular local earthquakes, particularly seismic clusters beneath the central part of the observation network. In order to obtain key properties of the clusters and to detect missing earthquakes, we apply a matched-filter technique to OBS continuous waveform data. As template event waveforms, we select events determined by Nansei-Toko Observatory for Earthquakes and Volcanoes, Kagoshima University. The hypocenters of the template events are relocated by merging manual pick data of P phases and S phases recorded on the OBSs with those on the onshore stations. As a preliminary result, we achieve detection of missing earthquakes using example template events and a threshold rule based on the median absolute deviation of the mean correlation coefficient. In this presentation, we further discuss the characteristics of waveform similarity of the OBS data.

Acknowledgements: This work is supported by Earthquake and Volcano Hazards Observation and Research Program, the MEXT of Japan and by ERI JURP.

Keywords: OBS observation, the Ryukyu Trench, similar earthquakes

©2019. Japan Geoscience Union. All Right Reserved.

Seismicity and crustal structure in the Okinawa Trough

*Azusa Nishizawa[1], Takeshi Kimura[1], Kentaro Kaneda[2]

1. National Research Institute for Earth Science and Disaster Resilience, 2. Japan Coast Guard

The Okinawa Trough is an active backarc basin of the Nansei-Shoto (Ryukyu) island arc–trench system, where the crustal thinning caused by backarc rifting is currently in progress in the entire trough. The characteristics of the seismic activity around the Ryukyu Trench and the Okinawa Trough are not enough investigated due to several reasons; 1) the number of large earthquakes related to the plate subduction along the Ryukyu Trench is not many compared with those in the Nankai Trough and the Japan Trench, 2) the coupling of the plate boundary is considered to be weak, and 3) the sparse distribution of the seismic stations on the Nansei-Shoto island arc makes difficult to obtain enough seismic data in the Ryukyu subduction zone and the Okinawa Trough.

The distribution of the shallow earthquakes in the Okinawa Trough by obtained Japan Metrological Agency during 1923–2018 is spatially inhomogeneous and shows several clusters. The seismic activity in the trough should be related to the seismic crustal structures. Recently, the Japan Coast Guard has reported the detailed seismic structure in the Okinawa Trough. We compared the active seismic areas with the seismic crustal models. The *M*7.1 Satsuma-hanto Seiho-oki Earthquake occurred on Nov. 14, 2015, in the western margin of the northern trough, the transition area between the East China Sea shelf and the Okinawa Trough, where the crust is thinner than the center of the trough with the deepest water. The source mechanisms of the main shock and intense aftershock activity compiled in the NIED (National Research Institute for Earth Science and Disaster Resilience) F-net moment tensor catalog have NW–SE extension axis, indicating that the area is undergoing tectonic rifting.

The largest shallow earthquakes with depths < 30 km observed in the trough is the 1938 Miyako-jima–Hokusei-oki Earthquake (*M*7.2) near the north of Miyako-jima Island and a tsunami with a height of 1.5 m hit Miyako-jima Island. The location of the hypocenter is estimated at the structurally discontinuous area where the northern extension of the Yaeyama Rift, the deepest elongated depression in the Okinawa Trough, meets Miyako Seamount, a fragment of the continental crust of the East China Sea shelf. Active seismicity including three events with $M > 6$ on Apr. 20, 2007 was observed in the Miyako Rift to the north of Miyako Seamount. Multichannel seismic profiles show many normal faults and deformation in sedimentary layers beneath the Miyako Rift. However, the accuracy of hypocenter locations in this region is poor, and the CMT locations are different over 20 km at the maximum between the NIED F-net and Global CMT.

The P-wave velocity models beneath the Okinawa Trough generally show an extended arc crust of the Ryukyu Islands which consists of upper, middle, and lower crusts. Although the crustal thickness becomes thinner from the north to the south, the crust is thicker than those of typical oceanic crusts or backarc basin crusts such as the Shikoku Basin. Therefore, the seismogenic layer in the Okinawa Trough is thicker than in mid-oceanic ridges, indicating that larger earthquakes could occur in the trough.

Keywords: Okinawa Trough, seismic activity, marine seismics

©2019. Japan Geoscience Union. All Right Reserved.

Time series analyses of the seismic activities in southwestern Japanese Island to southeastern Korean Peninsula excited by the deep fluid heat flow

*Takayuki Kawabe[1]

1. Faculty of Education, Arts and Sciences, Yamagata University

More than eight series of large damaging earthquakes occurred since November 2015 in southwestern Japanese Islands. They are as follows;
1) 2015/11/15 earthquakes of Northwestern margin of Okinawa Trough N31.33050˚, E128.71733˚, Depth: 9.4km, M5.9.
Foreshock: M5.1 (11/14), largest aftershock: M5.5 (2016/05/07).
2) 2016/04/16 2016 Kumamoto Earthquakes N32.75450˚ E130.76300˚, Depth: 12.45km, M7.3.
Foreshock: M6.5 (04/14), M6.4 (04/15), largesrt aftershock: (04/16) M5.9.
3) 2016/09/12 earthquake of Southeastern Korean Peninsula N35.79817˚ E129.27167˚, Depth: 36.0km, M5.8.
Foreshock: M5.2 (40 minutes before), Largest aftershock: M5.2 (2017/11/15).

4) 2016/10/21 earthquake of Central Tottori in 2016 N35.38050˚ E133.85617˚, Depth: 10.61km, M6.6.
Foreshocks: low frequency earthquakes, aftershocks: containing low frequency earthquakes.
5) 2017/11/15 earthquake of Southeastern Korean Peninsula N36.19584˚ E129.39417˚, Depth: 11.0km, M5.6.
6) 2018/02/11 earthquake of Southeastern Korean Peninsula N36.09883˚ E129.45700˚, Depth: 4.0km, M4.6.
7) 2018/04/09 earthquake of Western Shimane Prefecture in 2018 N35.18467˚ E132.58667˚, Depth: 12.13km, M6.1.
8) 2018/06/18 Northern Osaka Earthquake in 2018 N34.84433˚ E135.62167˚, Depth: 12.98km, M6.1.

Positions of the formar four eathquakes and the later four earthquakes shift from the west to the east. The number and scale of the earthquakes of Northwestern margin of Ryukyu Trough is reduced just several days berore the 2016 Kumamoto Earthquakes, and the number and scale of them is just restored after the 2016 Kumamoto Earthquakes. This seems to have a strong relationship between the earthquakes of Northwestern margin of Okinawa Trough and the 2016 Kumamoto Earthquakes. This suggests that such two strongly related earthquakes may be drived by the migration of thermal enargy because the earthquake activities are restored.
Seismic activity contined more than two years in the case of the earthquakes of Southeastern Korean Peninsula and large eathquakes often recured there. Their hypocenters show remarkable distribution. That is to say, they distribute not along any plane but along three dimensionally bent lines. on the lines, earthquakes occurred from the bellow to the upper in the lower to the upper crust. This means that the earthquakes of southeastern Korean Peninsula occurred not in an elastomechanical system but other system as thermal energy. Next earthquakes, just after the earthquakes of southeastern Korean Peninsula, occuring in the central Tottori in 2016 contains large number of low frequency earthquakes through the foreshocks to the aftershocks. The main shock of the ceentral Tottori in 2016 is actually drived by the thermal liquid enargy.
According to such evidences of the liquid flow causing the earthquakes, the large earthquakes occuring in

©2019. Japan Geoscience Union. All Right Reserved.

the upper crust of Southwest Japan would be driven by the eastward transmigrating thermal energy in the upper mantle (Tsunoda et al., 2013).

Reference:
Tsunoda, F., Choi, D.R. and Kawabe, T., 2013. Thermal energy transmigration and fluctuation. NCGT Journal, v.1, p.65-80.

Keywords: time series analyses of seismic activities, deep fluid heat flow, southwestern Japanese Island

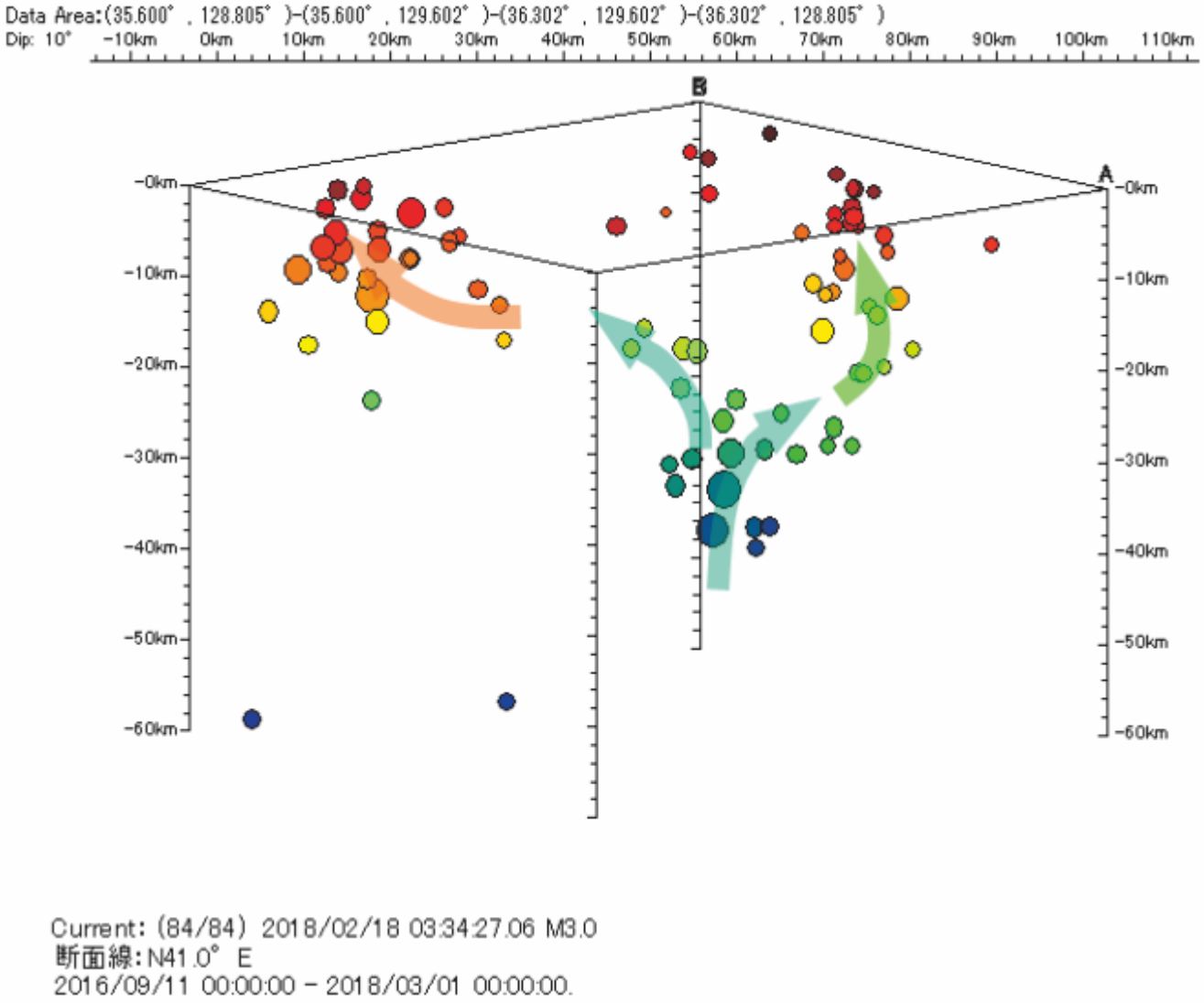

©2019. Japan Geoscience Union. All Right Reserved.

Integrated monitoring of seismicity in and around the Suruga Bay using Ocean Bottom Seismometers and inland stations.

*Yannis Panayotopoulos[1], Hisatoshi Baba[2], Takahito Nishimiya[3], Taiyo Sotani[4], Nakao Nagisa[4]

1. Association for the Development of Earthquake Prediction, 2. Department of Marine and Earth Science, Tokai University, 3. Meteorological Research Institute, Japan Meteorological Agency, 4. Tokai University

The Suruga bay is located in the western flank of the Izu Peninsula in central Japan. It marks the easternmost boundary of the Nankai trough, of the Philippine Sea plate subduction zone. The Fujikawa fault zone located at the northern tip of the Suruga Bay is considered to be the landward extension of the megathrust boundary between the Philippine Sea plate and the Eurasia plate (e.g.: Yamazaki, 1992). This megathrust boundary produced the M8.4 Ansei-Tokai Earthquake (e.g.: Ishibashi, 1981), and is assumed to be the source region of the next Tokai Earthquake. We closely monitored the seismicity in the vicinity of the Suruga Trough axial region from May, 2018 to September, 2018, using 6 pop-up type Ocean Bottom Seismometers (OBS). In recent years, several moderate size earthquakes have occurred in the Suruga Trough axial region (M6.5 in 2009 and M6.2 in 2011), that resulted in a prominent excitation of seismicity in the area. Using the inland routine observation network alone, those earthquakes are estimated to have occurred on the subduction zone of the Philippine Sea Plate. However, there is a considerable amount of hypocenter depth location error due to the lack of stations in the sea areas.

In this study, we will report the results of the OBSs observations, which enabled us to make more accurate estimations of the frequency and hypocenter depth distribution of the earthquakes occurring in the Suruga Trough axial region.

Keywords: Suruga bay, Earthquake cluster, Seismicity

©2019. Japan Geoscience Union. All Right Reserved.

Linear distribution of the intraslab earthquakes in Tokai

*Sadaomi Suzuki[1]

1. Tono Research Institute of Earthquake Science, Association for the Development of Earthquake Prediction

Figure 1 show an epicenter map of the earthquakes shallower than 60 km in the Tokai area occurring from June 2002 to April 2018. The intraslab earthquakes were shown by yellow, green, or blue small circles, because they occurred in the depth from 30 −50 km. They distribute not homogeneously but linearly as shown in the epicenter map. Elongated ellipses by broken lines show linear distributions (LDs) of the intraslab earthquakes. LD-A and LD-d arranged NW-SE are main distribution in the Tokai area. On the east of them there are small LD-e and LD-f. In contrast LD-B which is arranged NNE from near the port of Nagoya makes an angle of 70° with LD-A. There is small LD-c on the west of LD-B. LD-B and LD-c may be suggested by Miyoshi and Obara (2010a). We studied focal mechanism solutions of 12 earthquakes (Group A) belonging to LD-A and 146 earthquakes (Group B) belonging to LD-B, respectively, using JMA data. We obtained the average values of the azimuths of P- and T-axis for each group as the following. The average values for Group A are 171° and 350° in P-axes and 91° and 256° in T-axes, respectively (see Figure 1). The average values for Group B are 172° and 358° in P-axes and 82° and 254° in T-axes, respectively (see Figure 1). There are no large differences in their corresponding values between Group A and B. This result suggests that there is no large difference in the average stress generating earthquakes between Group A and B. We, therefore, have to consider other reasons for causing those linear distributions.

Figure 2 is a seismological cross section that crosses the Tokai area from NNW to SSE referred from Suzuki et al., 2018. Schematic interpretation of seismic structures including S wave tomography (Nakajima and Hasegawa, 2016) and two earthquake groups consisiting of LFEs and intraslab earthquakes are represented. The most of intraslab earthquakes distributes in the low velocity area of *S* wave in the uppermost oceanic mantle. The relatively low velocities of *S* wave in the subducting oceanic crust and its surrounding areas are interpreted as being indicative of fluids released by progressive metamorphic dehydration reactions in the oceanic crust (e.g., Abers et al., 2013) under increasing temperature and pressure conditions. We suppose that the intraslab earthquakes occur because these fluids penetrate into the uppermost oceanic mantle. Therefore the pore fluids may penetrate from the oceanic crust into not homogeneously but linearly in plane. It is presumed that old fracture zones that had been formed before the Philippine Sea plate subducted below the Tokai area existed at the uppermost oceanic mantle.

Abers GA, Nakajima J, van Keken PE, Kita S, Hacker BR (2013) Thermal–petrological controls on the location of earthquakes within subducting plates. Earth Planet Sci Lett 369–370:178–187

Hirose F, Nakajima J, Hasegawa A (2008) Three-dimensional seismic velocity structure and configuration of the Philippine Sea slab in southwestern Japan estimated by double-difference tomography, J. Geophys. Res., 113:B09315. doi:10.1029/2007JB005274.

Miyoshi,T. and K. Obara (2010a), Seismogenic stress field of the double seismic zone within the Philippine Sea plate beneath Ise Bay to the Kii Peninsula, Abstract of the 2010 meeting of Japan Geoscience Union, S-SS013 P14 (in Japanese).

Miyoshi,T. and K. Obara (2010b), Double seismic zone within the ridge-shaped slab beneath southwest Japan, Earth Planets Space, 62, 949-954.

Nakajima, J., and A. Hasegawa (2016), Tremor activity inhibited by well-drained conditions above a megathrust, Nature communications 7, Article number: 13863 (2016), doi:10.1038/ncomms13863, 2016.

Suzuki, S., Okubo, M., Imanishi, K., Takeda, N. (2018) , Detection method for pairs of *P* and *S* waves of

©2019. Japan Geoscience Union. All Right Reserved.

deep low-frequency earthquakes using a 3-D array in the Tokai area of the Nankai subduction and its application to hypocenter determination, Geochemistry, Geophysics, Geosytems, 19,.https://doi.org/10.1029/2018GC007479.

Keywords: intraslab earthquakes , linear distribution of earthquakes , oceanic mantle

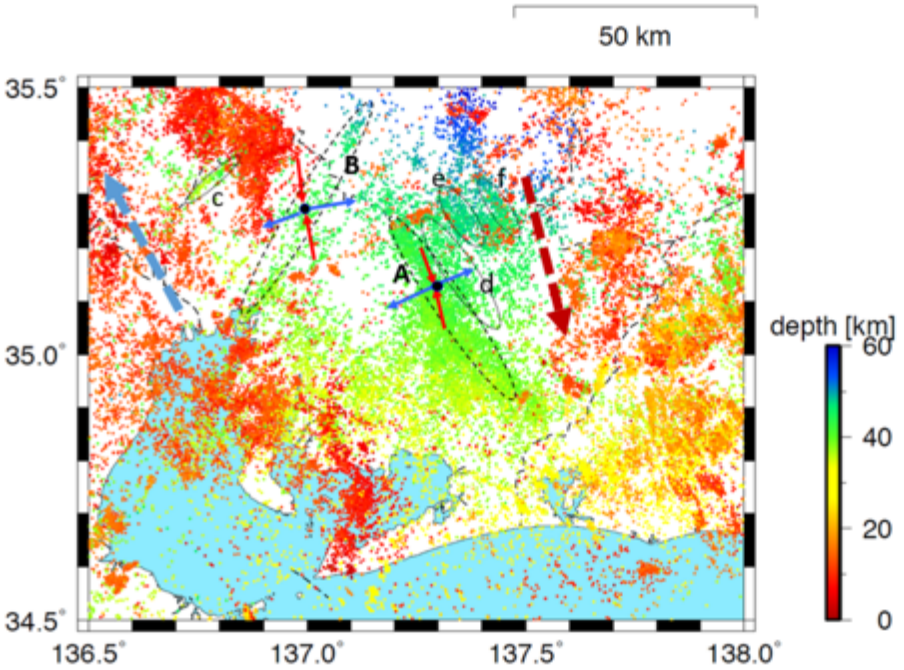

Figure 1. Epicenter map (presented by Osamu Murakami) of the earthquakes shallower than 60 km in the Tokai area occurring from June 2002 to April 2018 (JMA data). Elongated ellipses by broken lines show linear distributions of the intraslab earthquakes. Red and blue allows indicate P-axes and T-axes, respectively. A brown and blue broken lines show the ridge and valley of the slab shape (Hirose et al., 2008), respectively

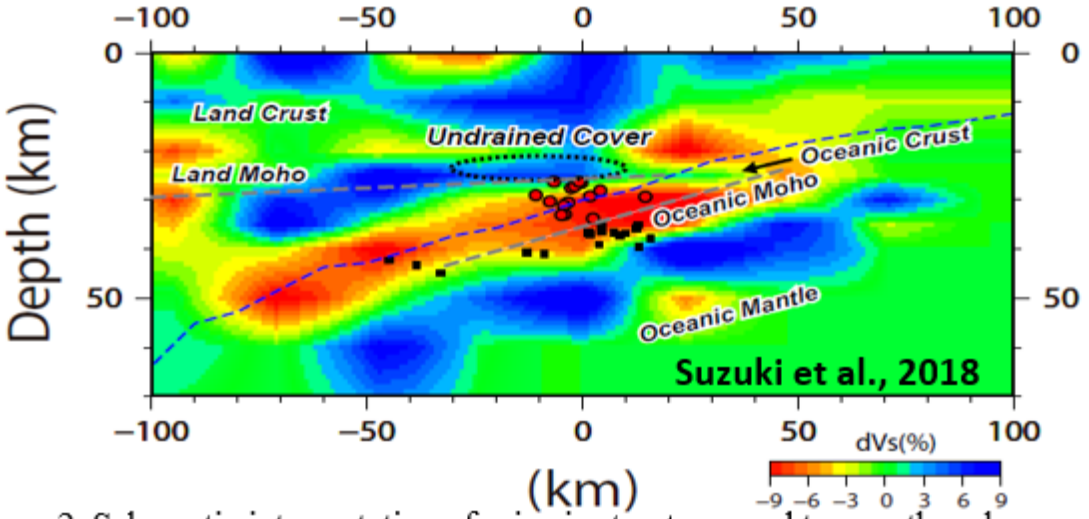

Figure 2. Schematic interpretation of seismic structures and two earthquake groups consisiting of LFEs (red circles) and intraslab earthquakes (black squares) referred from Suzuki et al., 2018.

©2019. Japan Geoscience Union. All Right Reserved.

The stress change of Chubu region before and after the 2011 Tohoku-oki Earthquake(Mw9.0)

*Yuki Susukida[1], Kei Katsumata[1]

1. Institute of Seismology and Volcanology, Hokkaido University

Great subduction-zone earthquakes occur frequently off coast of the Pacific Ocean in Japan. And the Chubu region (central part of Honshu, Japan) has risk not only subduction-zone earthquake but also inland earthquake. In 1891, Nobi earthquake (M8.0) occurred at Neodani fault system in Chubu region, which is the largest inland earthquake in Japan. (Milne 1893) Furthermore, after Tohoku-oki earthquake, seismicity of northern part of Neodani fault system was activated. (Toda et al, 2011) In this study, I examined effect of Tohoku-oki earthquake on seismicity around the Neodani fault system by inferring of stress change before and after Tohoku-oki earthquake.

At first, I demonstrated the stress field inversion method (Hardebeck & Michael, 2006) by synthetic data to check the performance of this inversion method. As a result, I found that the inversion method will analyze real data well.

Next, I conduct stress field inversion for the joint observation data by eight Universities in Japan and NIED (National Research Institute for Earth Science and Disaster Resilience in Japan) in the Chubu region between 2009 and 2013. As a result, I found the stress field in Neodani fault system didn’ t change significantly before and after Tohoku-oki earthquake.

Keywords: Tohoku-oki Earthquake, Inland Earthquake, Neodani fault system, stress field inversion

©2019. Japan Geoscience Union. All Right Reserved.

Repeating earthquake activity off Miyagi Prefecture triggered by the 2011 Tohoku-oki earthquake

*Kenshiro Tsumura[1]

1. Association for Developement of Earthquake Prediction

A remarkable repeating earthquke activity off Miyagi Prefecture tiggered by the 2011 Tohoku-oki earthquake was analized in detail. The epicenters of repeating earthquakes ditributed in a very small area with a diameter of about 1km , centered at 38°38′N and 141°54′E, and with depth 46-49km. The recurrence intervals were about 20 days in the initial period then gradually changed longer, about 100 days in 2018. Magnitude of earthquake was about 4.0 in the initial period then gradually changed smaller, about 3.5 in 2018. For this activity, based on its repeating regularity, mid-term prediction was tried and obtaied good result for a certain period.

Keywords: repeating earthquakes, 2011 Tohoku-oki earthquake, mid-term erathquake prediction

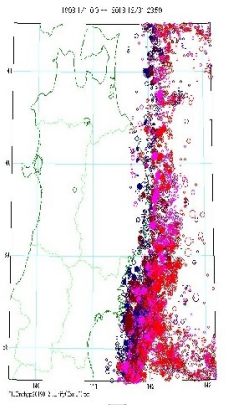

図１. 震央分布図

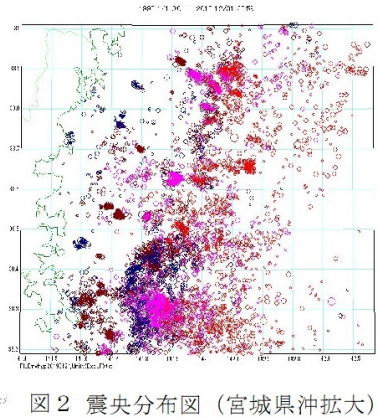

図２ 震央分布図（宮城県沖拡大）

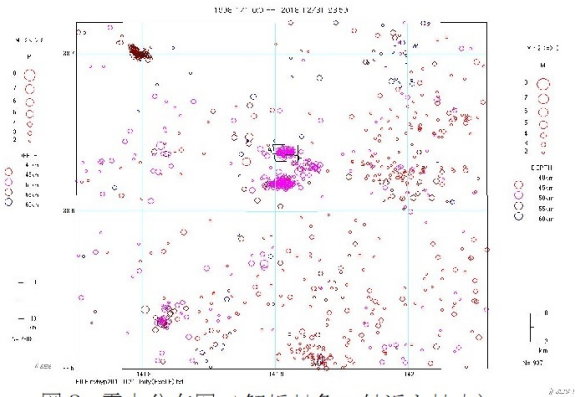

図３. 震央分布図（解析対象の付近を拡大）

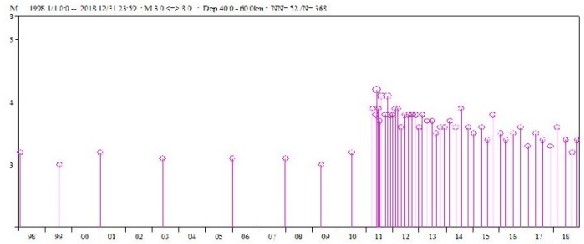

図５. 対象とする繰り返し地震活動のＭＴ図

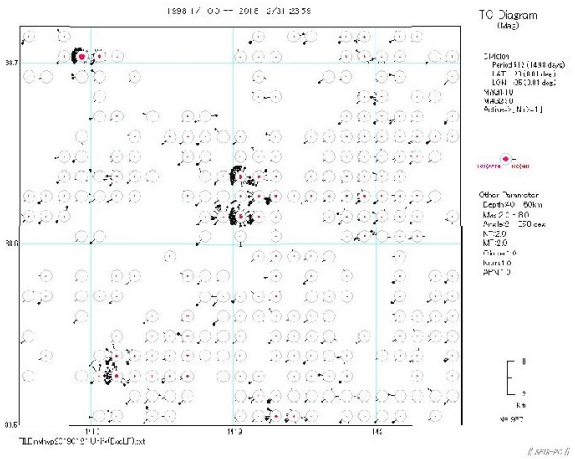

図４ 図3に対応する時間円表示図（TC-M図）

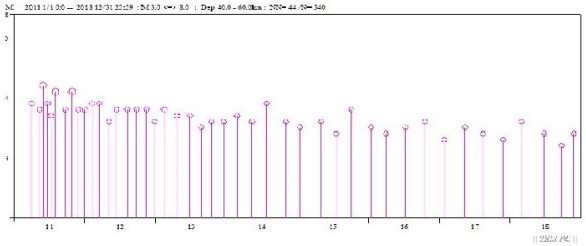

図６. 対象とする繰り返し地震活動のＭＴ図（2011年以降を拡大）

©2019. Japan Geoscience Union. All Right Reserved.

Seismic Moments of Inland Small Earthquakes in Japan: Spectral Analyses Using the Hi-net

*Tomotake Ueno[1], Tatsuhiko Saito[1]

1. National Research Institute for Earth Science and Disaster Resilience

Seismic moments and moment magnitudes are one of the most important quantities in characterizing earthquakes. NIED reports moment magnitudes for moderate and large earthquakes (M_W > ~3.5) using the F-net or the KiK-net/K-NET. However, the moment magnitudes of small earthquakes (M_W < 3.5) aren't well determined because of sparse station distributions of the F-net and low sensitivity sensors of the KiK-net/K-NET. These earthquakes' magnitudes are determined using maximum amplitudes of the seismograms of the Hi-net, a dense seismic observations with high-sensitivity sensors. Such high sensitivity seismometers are also used to estimate seismic moments (e.g., Uchide and Imanishi, 2018). This study estimated seismic moments and moment magnitudes for inland earthquakes in Japan using the Hi-net.

We calculated seismic moment for inland earthquakes shallower than 20 km deep with magnitudes from 3 to 4 occurred in 2013 to 2017. Firstly, we calculated a source spectrum from waveform data during 1s before to 9s after the S-wave arrival time. Then, correcting path, site, and the instrumental response, we estimated source spectra. Comparing the observed source spectra with a theoretical one supposing the ω^2 model, we obtained the seismic moment.

The Hi-net detected 455 inland earthquakes with the magnitude from 3 to 4 in 2017. We successfully estimated the seismic moments more than 90 % of those earthquakes. We could estimate the moment magnitudes more than 90 % except 2016. Because the aftershocks of the Kumamoto earthquakes contaminated Hi-net records, we calculated the seismic moments only for 70 % of the 1730 earthquakes in 2016. We compared the moment magnitudes determined by the Hi-net with those by a moment tensor inversion of the F-net. The moment magnitude of Hi-net was smaller than those of the F-net by 0.13±0.11. On the other hand, the magnitude using the maximum amplitude of the Hi-net was larger than the F-net by 0.06±0.21.

Keywords: seismic moment, Hi-net, small earthquakes

©2019. Japan Geoscience Union. All Right Reserved.

Spatiotemporal variations of stress field in the 2016 Kumamoto earthquake (M 7.3) area

*Dapeng Zhao[1], Zhiteng Yu[2], Jiabiao Li[2], Zhouchuan Huang[3]

1. Department of Geophysics, Tohoku University, 2. State Oceanic Administration, 3. School of Earth Sciences and Engineering, Nanjing University

Focal mechanism solutions of 349 local crustal earthquakes and stress tensors in central-north Kyushu are determined using a large number of P-wave polarity data and a 3-D velocity model. The obtained tensional ($\sigma 3$) axis trends NNW-SSE or N-S horizontally, and the compressive ($\sigma 1$) axis trends WSW-ENE or E-W. The direction of the $\sigma 3$ axis is consistent with the spreading direction at the Okinawa Trough. The stress field in the 2016 Kumamoto earthquake area is attributed to rollback of the Philippine Sea plate and northward extension of the Okinawa Trough. The orientation of the $\sigma 3$ axis is quite stable, whereas the $\sigma 1$ and $\sigma 2$ axes are distributed in a wide range. With the 3-D velocity model, the principal stress axes can be better determined by inverting a large number of FMSs. Spatial and temporal variations of the stress field are well revealed in the Kumamoto source area. The $\sigma 3$ axis significantly rotated counterclockwise after the M 6.5 foreshock, and rotated clockwise after the M 7.3 mainshock on the Futagawa fault segment. The stress rotation suggests a small magnitude of deviatoric stress in the source area, which indicates a small friction coefficient on the seismogenic faults. In addition, a generally small value of friction (~0.4) on the faults is obtained by the stress inversions, indicating that the faults in the Kumamoto earthquake area are weak. The fault weakening may be caused by the arc magma and fluids ascending from the mantle wedge associated with the dehydration reactions of the subducting Philippine Sea slab.

Keywords: Kumamoto earthquake, crustal stress, focal mechanism

©2019. Japan Geoscience Union. All Right Reserved.

Seismicity and crustal deformation following the 2016 Kumamoto earthquakes

*Kazuyoshi Nanjo[1], Jun Izutsu[2], Yoshiaki Orihara[3], Masashi Kamogawa[4], Toshiyasu Nagao[3]

1. University of Shizuoka, 2. Chubu University, 3. Tokai University, 4. Tokyo Gakugei University

The 2016 Kumamoto earthquakes include a magnitude *M*7.3 mainshock that struck April 16, 2016, as well as *M*6-class foreshocks (*M*6.5 and *M*6.4) and many *M*5-class aftershocks. This seismicity that fulfils sections along the Futagawa and Hinagu faults, is still being active. Seismicity and crustal deformation in the Kumamoto region were investigated to get implications of future seismic-activity trends.

We referred our previous work (Nanjo et al., 2016) that examined the spatial and temporal trend in *b* value of the Gutenberg-Richter's law, based on seismicity prior to the Kumamoto earthquakes. For the spatial distribution of *b* values, which shows data for a post-period (January 2017-January 2019), excluding the active aftershock period, we found a zone with low *b* values (130.6-130.8˚E, 32.5-32.6˚N), which lays further to the southwest of the *M*6.5 and *M*6.4 foreshocks along the Hinagu fault. A comparison with the spatial distribution of *b* values calculated for the seismicity from January 2000 to immediately before the Kumamoto earthquakes (Nanjo et al., 2016) reveals a zone where the *b* value decreased. This zone coincides with the low-*b*-value locations seen for seismicity after 2017. We compared the spatial distribution of earthquakes with *M*>5 in the Kumamoto sequence and the *b*-value distribution based on seismicity after 2017. Earthquakes with *M*> 5 have not occurred in the low-*b*-value zone.

While referring previous studies of crustal deformation associated with the Kumamoto earthquakes by GEONET (e.g., Hiyama et al., 2016), we investigated baseline changes of control stations near the Futagawa and Hinagu faults (the period from January 2013 until the end of 2018, with the "Misumi" (Shimane pref.) taken as a fixed station). A step-like change associated with the mainshock occurrence, followed by gradual changes associated with postseismic formation, is seen for all the baselines investigated. The same is true for the control station "Izumi" (130.79˚E, 32.58˚N), located in the low-*b* -value zone identified for seismicity after 2017, although the postseismic deformation is coming to an end. Therefore, active seismicity is expected to continue in the future.

Our method pinpointed the zone of low *b* values along the Hinagu fault, and this is the only one where the *b* value has decreased, compared to before the Kumamoto earthquakes. Nanjo et al. (2016) compared the *b*-value map with the sequence of foreshocks, mainshock, and aftershocks with *M*5 or greater, and showed that areas of low *b* values contained a high percentage (84%) of the sequence. If the *b* value is regarded, for the Kumamoto region, as an indicator for estimating the occurrence location of a relatively large earthquake in the future, the current low-*b*-value zone shows the high likelihood of "seismic gap", a segment considered to suffer a future *M*>5 earthquake.

Keywords: 2016 Kumamoto earthquakes, b value, crustal deformation

©2019. Japan Geoscience Union. All Right Reserved.

The unique characters of intensity distribution of the 2018 Sep. 6 Mw6.6 Earthquake of Iburi region in Hokkaido, Japan

*Ritsuko S. Matsu'ura[1], Hiroto Tanaka[2], Mitsuko Furumura[1], Tsutomu Takahama[2]

1. Earthquake Research Center, Association for the Development of Earthquake Prediction, 2. Kozo Keikaku Engineering Inc.

On Sep. 6, 2018, the Mw6.6 (M_{JMA}6.7) earthquake of 35km depth (JMA depth 37km) occurred in the eastern part of Iburi region, Hokkaido, Japan. Waves from this event are characterized by the very high level in high frequency part. Although it is just an Mw6.6 earthquake, and the shortest distance to the land is larger than its depth, Japanese Instrumental Seismic Intensity (JISI) 7 was recorded at Shikanuma station, 43km away from the source. The comparison of observed waves with the various prediction equations of PGV or PGA for Japan, such as Si and Midorikawa(1999) shows that the observation was remarkably larger than most equations in distances less than 50km [e.g. Nishimura and Miyakoshi (2018)].

We applied the new prediction equation of JISI, which was classified by the physical source types, and in which the surface ground effect was removed by the term dependent on AVS30 of each station [Matsu'ura et al. (2018)], to this event. The equation for the PAC-intra type fits well to stations in distances less than 100km, while the equation for the PAC-inter type fits well to further stations in Iwate or southeastern part of Hokkaido (Fig.). It apparently shows the high stress-drop source feature like an event of intra slab, but the abnormal intensity effect due to the PAC is weaker than that of the PAC-intra type, and similar to that of the PAC-inter type. These features are well explained when this Mw6.6 event occurred within the rather cold shallow mantle overriding on the slab on the western foot of Hidaka Mountains. The high frequency waves were transferred very efficiently from the source to the PAC slab like those from interplate events, which suggests that the source lies in fairly homogeous area than the ordinary Japanese crust.

This study was done as a part of the Supporting Project for the Headquarters for Earthquake Research Promotion (HERP) sponsored by the Ministry of Education, Culture, Sports, Science and Technology (MEXT), Japan.

References

Matsu'ura, R. S. et al. (2018). A new multidimensional prediction equation of instrumental seismic intensity of Japan reflecting source type characteristics, submitted to BSSA.

Nishimura, T., and K. Miyakoshi (2018). Comparison of Hokkaido-Iburi-Tobu earthquake with existed prediction equations of ground motions, Fall meeting of Seismological Society of Japan, S25-P19.

Si, H. and S. Midorikawa (1999). New attenuation relationships for peak ground acceleration and velocity considering effects of fault type and site condition, J. Struct. Constr. Eng. AIJ, 523, 63-70.

Keywords: Prediction Equation of Japanese Instrumental Intensity, 2018 Sep. 6 Mw6.6 Earthquake of Iburi region, earthquake in the uppermost mantle

©2019. Japan Geoscience Union. All Right Reserved.

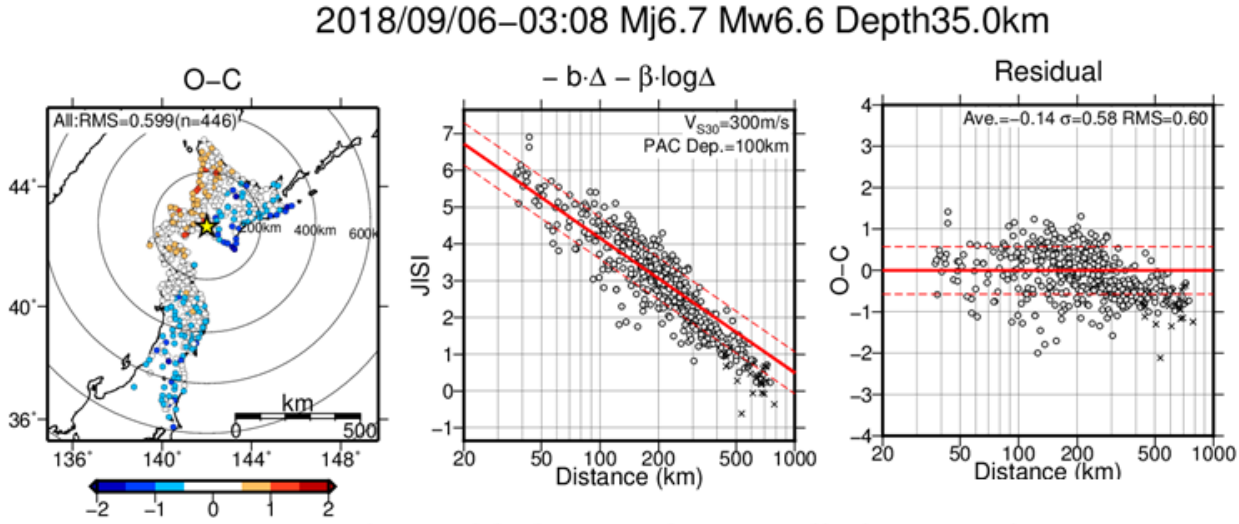

comparison with the PAC intra prediction equation

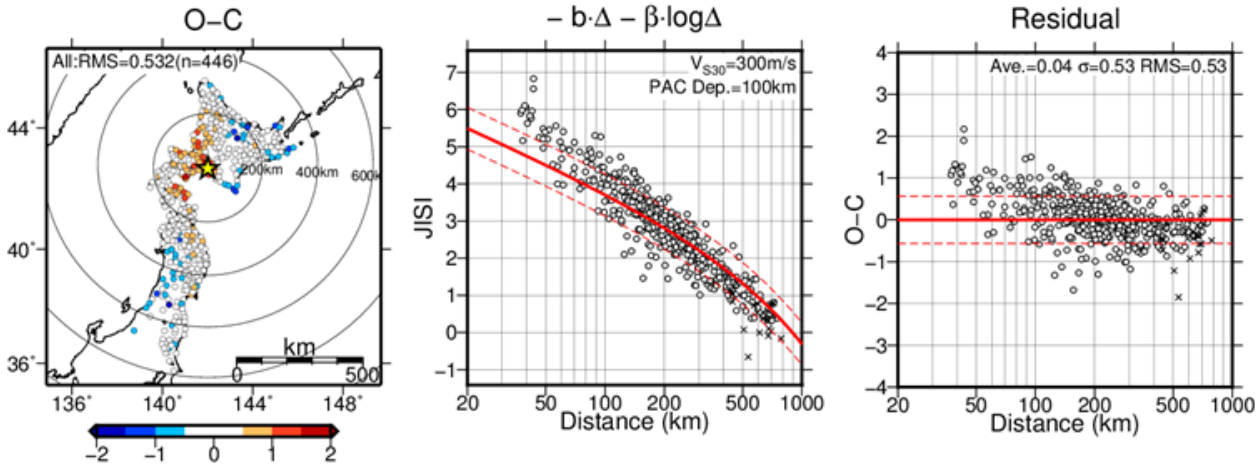

comparison with the PAC inter prediction equation

©2019. Japan Geoscience Union. All Right Reserved.

Determination of Hypocenter Location in Sumani and Sianok Fault Segments, West Sumatra region Using Oct-Tree Importance Sampling Method

*Ade Surya Putra[1], Nanang Tyasbudi Puspito[2], Andri Dian Nugraha[2], Pepen Supendi[3,1]

1. Geophysical Engineering, Faculty of Mining and Petroleoum Engineering, Institute of Technology Bandung, 2. Global Geophysics Research Group, Faculty of Mining and Petroleoum Engineering, Institute of Technology Bandung, 3. Agency of Meteorology, Climatology and Geohysics (BMKG), Indonesia, Bandung, Indonesia

Sumani and Sianok segments are two of the many fault segments in Sumatra Fault Zone (SFZ) that have a considerable history of seismicity and cause significant impacts. An important effort to overcome this problem is the need to analyze tectonic structures in detail through one of them by elaborating an accurate hypocenter location. In this study, we conducted hypocenter determination by using a non-linear approach with the oct-tree importance sampling method through NonLinLoc software by using local velocity components for earthquakes in Sumani and Sianok Segments in the range of 2009-2017. The results of hypocenter determination in this study indicate an improvement in picking arrival time of P and S wave. The increment is denoted by the results of residual picking P and S wave arrival times using oct-tree sampling method that dominant at frequency of 0.1 seconds and there is a correlation between hypocenter location cluster in this study with a location of major earthquakes that have occurred in Sumani and Sianok Segments.

Keywords: Hypocenter, Oct-tree importance sampling, Fault segment, Sumatra Fault Zone

©2019. Japan Geoscience Union. All Right Reserved.

1D Seismic Velocity Modelling and Hypocenter Relocation around Central and East Java Region: Preliminary Result

*Faiz Muttaqy[1], Andri Dian Nugraha[2], Nanang Tyasbudi Puspito[2]

1. Geophysical Engineering Study Program, Faculty of Mining and Petroleum Engineering, Institut Teknologi Bandung,
2. Global Geophysics Research Group, Faculty of Mining and Petroleum Engineering, Institut Teknologi Bandung

Central and East Java are part of Sunda Arc which has relatively high seismicity and complex geological system as a result of Indo-Australian plate that subducted under the Eurasian plate. The early stage of seismic tomography study in order to obtain a reliable geometry about the velocity structure beneath the study area is to define the precise earthquake location and 1D seismic velocity model. In this study, we manually picked P- and S-wave arrival time recorded by BMKG network for the time period from January 2009 to September 2017. We determined the hypocenter location around Central and East Java region by using an NLLoc program. We also conducted a velocity inversion using the VELEST program to obtain an updated 1D velocity model in the study area. Afterward, the hypocenters were relocated using the double-difference algorithm and the updated 1D velocity model to improve the accuracy of the hypocenter locations. Our results indicate that the seismicity around Central and East Java is generally distributed in the southern part of the island, such as in the south of Kebumen, Yogyakarta, Pacitan, Malang, and Banyuwangi that associated with the subduction activity. Moreover, the shallow seismicity is probably controlled by the presence of active inland faults, such as Opak Fault and Kendeng Thrust. As further studies, we will determine the focal mechanism of selected events related to the active inland fault in this region and conduct 3D seismic tomography imaging beneath Central and East Java region.

Keywords: Central Java, East Java, Hypocenter Relocation, 1D Velocity Model

©2019. Japan Geoscience Union. All Right Reserved.

Seismicity and Tectonics of the Bingöl Area: Eastern Anatolia

*Dogan Kalafat[1]

1. Bogazici University Kandilli Observatory and Earthquake Research Institute Cengelkoy, Istanbul Turkey

In this study, Bingöl Earthquakes which have occurred in recent years have been evaluated from seismological point of view. The Eastern Anatolia Region is the most seismologically deformed area of the Anatolian plate and is under compression due to the relative movement of the Arabian and Eurasian plates in general. The Anatolian plate bounded by the North Anatolian Fault Zone (NAFZ) and Eastern Anatolian Fault Zones (EAFZ) moves relatively westward. Bingöl Earthquakes are located within the Eastern Anatolian Fault Zone and this fault zone occurs due to the movement of the parts. Bingöl and the surrounding area is the most active regions in Turkey in terms of seismicity. The most important earthquakes in Bingöl during the instrumental period were the 1971 and 2003 earthquakes. Bingöl Fault starts from the south of Bingöl and extends along the Göynuk stream valley. This fault length is about 75 km. which is northern part of the Eastern Anatolian Fault Zone and joins the North Anatolian Fault Zone after passing through the villages of Serpmekaya and Sakaören. During the 1971 Bingöl Earthquake, about 38 km surface rupture occured which it started from Ormanardi to the southeast of Bingöl and extends to the N45ºE degree in the southwestern direction of Goynuk. The observed faults showed a strike-slip and a left lateral movement and the fault plane solutions supported the field observations.
The other important earthquake occurred on May 1, 2003. In this earthquake, 176 citizens were killed and 521 citizens were injured in various places. In particular, public buildings were severely damaged. The episantr area is between the Balikcay village plateau, Hanocayiri-Kurtulus and Sudugunu Plateau. Stepped fractures with NW-SE trending N20-30ºW trending were observed in Hanocayiri, which is one of the closest settlements of earthquake. As a result of earthquake, a great deal of collapses and mud currents were formed due to the effect of groundwater pressure. The fault traces in the region continued on the slopes of the NW-SE trending Kade mountains. Liquefaction, sitting, collapse and faulting samples were seen together in Hanocayiri hamlet. The earthquake caused severe damage, destruction and death in the buildings located on the alluvial terrace of Göynuk Creek in Bingöl province. During the earthquake, the Celtiksuyu Boarding School of Bingöl province was completely destroyed and 84 students died under the rubble. In addition, many public buildings were damaged. The macroseismic epicenter of the earthquake is approximately 12 km. distance between the district of Elcagini-Elmacayiri and Sudugunu plateaus. The area is mountainous and there are no frequent settlements. The nearest settlements are Balikcay, Hanocayiri Village, Elmacayiri village and Kurtulus village. It was observed that the epicenter of Bingöl Earthquake was highly compatible with the NW-SE trending faults. The fault of N-NW, which passes between Kurtulus-Elmacayiri-Hanocayiri and towards the Balikcay-Cimenli villages, was defined as the fault which was broken by the 2003 Bingöl Earthquake. In this study, 12 earthquakes fault plane solutions have given (magnitude Mw> 5.0) between 1971-2015 time period in Bingöl. The fault plane solution of 6 earthquakes was conducted within the scope of the study. The stress analysis shows that the dominant stress axes in the region are dominated by NW-SE directional compression and strike-slip faulting which are characterized by NE-SW extension axes.
The recent earthquakes showed that the ongoing deformation in the region continued with the strike-slip fault systems as the dominant. Structural heavy damages caused by earthquakes were mostly due to poor soil conditions, improper production, low quality and missing materials.

Keywords: Bingöl, East Anatolia, Göynük Stream, Fault Plane, Strike-Slip faulting

©2019. Japan Geoscience Union. All Right Reserved.

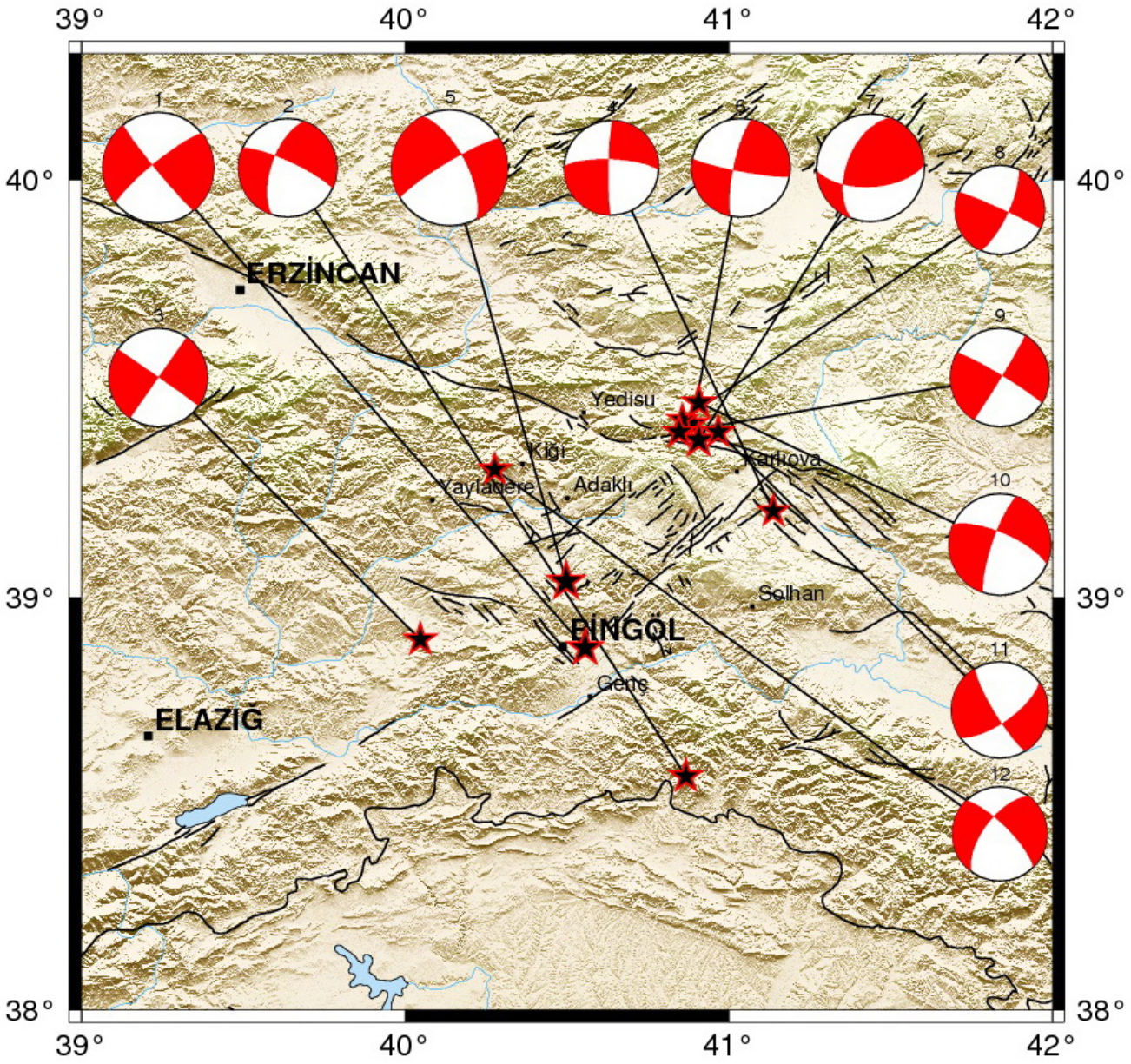

©2019. Japan Geoscience Union. All Right Reserved.

Seismicity along the North Anatolian Fault beneath the Marmara Sea, deduced from long-term ocean bottom seismographic observations

*Yojiro Yamamoto[1], Narumi Takahashi[2,1], Dogan Kalafat[3], Ali Pinar[3], Remzi Polat[3], Zeynep Coskun[3], Haluk Ozener[3], Yoshiyuki Kaneda[4]

1. Japan Agency for Marine-Earth Science and Technology (JAMSTEC), 2. NIED, 3. KOERI, Bogaziti University, 4. Kagawa University

The North Anatolian Fault (NAF) beneath the Marmara Sea is recognized as a seismic gap for M >7 earthquake during more than 100 years. Earthquake hazard and disaster mitigation studies in Marmara region are sensitive to detailed information on fault geometry and its coupling status beneath the Marmara Sea. Although hypocenter distribution could help us to estimate them, it is difficult to obtain precise hypocenter location from only onshore permanent seismic stations. Thus, we have started a series of long-term ocean bottom seismographic (OBS) observations beneath the western and central Marmara Sea since 2014. We have installed 10~15 OBSs along the Main Marmara Fault(MMF) for each observation phases, and observation length is about 10 or 11 months. Based on the first phase observation, conducted from 2014 to 2015, Yamamoto et al. (2017) identified a segment boundary of the MMF beneath the central basin of the Marmara Sea (28.05˚E). Besides, they proposed that the zones of no seismicity within the upper crust appear to indicate locked sections of the MMF.
In this study, we analyze the second (from 2015 to 2016) and third phases (from 2016 to 2017) observation data. The OBS distribution of second phase is same as first phase,whereas that of third phase is about 20 km shifted to eastward relative to first and second phases. The tentative result shows that the feature of hypocenter distribution, including the location of no seismicity zones obtained by Yamamoto et al. (2017), is not changed for all phases, suggesting that the coupling status along the fault is almost same during at least three years. In the west of 28.05˚E, seismicity located not only the upper but also lower crust. On the other hand, the lower limit of the seismogenic zone in the east of 28.05˚E is about 15 km, shallower than the Conrad discontinuity. The largest no seismicity zone extended over the upper crust is located between 28.45˚E and 28.65˚E, where strong coupling is suggested from seafloor geodetic observation (Sakic et al., 2016).
According to the spatial relationship between the epicenter of microearthquakes and fault trace on the sea floor (Armijo et al., 2005) suggests that the MMF around 28.75˚E is near vertical to slightly northward dipping. Since previous study indicates that the east of 28.05˚E MMF is southward dipping (Yamamoto et al., 2017), there might be another segment boundary west of 28.75˚E. We also find an active seismic cluster around 40.8˚N, 28.7˚E, 14 km depth. There is a possibility that this cluster relates to the southern branch of NAF.

Keywords: The North Anatolian Fault, Marmara Sea, Seismicity

©2019. Japan Geoscience Union. All Right Reserved.

Microseismic Monitoring of the Sultandagi Fault Zone: Western Turkey

*Dogan Kalafat[1], Yavuz Gunes[1], Mehmet Kara[1], Kivanc Kekovali[1]

1. Bogazici University Kandilli Observatory and Earthquake Research Institute Cengelkoy, Istanbul Turkey

Western Turkey is one of the seismically active region in Turkey. The high seismic activity is a result of the complex tectonic deformation of the Anatolian plate which has been dominated by the N–S extensional tectonic regime in the western edge. In western Turkey, relatively 3 major earthquakes (Mw≧6.0) were identified on the Sultandagi Fault Zone (Afyon-Aksehir Graben) between years of 2000–2002. In this study, mentioned local earthquake activity, have been investigated to understand their nature and relation of the regional seismic activity and tectonic deformation on the Sultandagi Fault Zone (SFZ) in western Turkey. Due to these activities along the SFZ it is decided to monitor microseismic activity (M<2.5) by establishing low-magnitude threshold seismic network. For this purpose, 3 new broadband (BB) seismic stations were temporarily established to control the northern part of the Sultandagi Fault Zone, and the micro-seismicity of the fault zone was started to be observed in July 2017. Thus, the earthquake activity in the region started to be monitored sensitively. So we started to get 2 times more earthquakes than permanent stations in the region. The one of the biggest primary outcome by this study that there is a significant microseismic activity (M<2.5) at the SFZ which was not seen from prior studies and long-term seismicity catalogues from permanent network (M>2.5). At first, we started to analyze the distribution of micro-earthquakes in the region. During the data analysis, it was predicted that some intensive micro-earthquake activity in the project area could be caused by quary-blasting and some locations were visited during the field study. Relocation of common earthquakes recorded by KOERI and the study was carried out, and the earthquake epicenters were displaced approximately as ±0.8–6 km. There were also some positive changes in the depth distribution of earthquakes. Consequently, thanks to the stations established within the scope of the study, horizontal (distance) and vertical error (depth) margins of the events in the region have been reduced. As a result of the evaluation of the data obtained, it was observed that the Sultandagi Fault Zone has especially intense seismic activity in the middle and northwest part. In addition, a significant seismic activity was observed in NW-SE direction at the north of Isparta city .
This research is funded by Bogazici University Research Fund within the scope of Project Number 12280. We thank to Bogazici University Research Fund Commission and members.

Keywords: Sultandagi Fault Zone, Western Turkey, extensional tectonic regime, micro-seismicity

©2019. Japan Geoscience Union. All Right Reserved.

Analysis of radiated seismic energy distributing in aftershock sequences at the Guerrero, Mexico subduction zone.

*Raymundo Omar Plata Martinez[1], Xyoli Pérez Campos[2], Krishna Shri Singh[2]

1. Kyoto University, 2. Geophysics Institute, UNAM

Radiated seismic energy is valuable parameter in seismic source studies, as it can be a good criterion to evaluate earthquakes size but also very useful to analyze the dynamics of the rupture process. Significant large thrust earthquakes have occurred over the last decades at the Mexican, subduction zone, however just a few researches have been done to understand the distribution of seismic energy release in the area. For this purpose, we calculated source spectra to estimate radiated seismic energy of three large earthquakes and their aftershocks (*M* larger than 4.0) in the Guerrero segment of the Mexican subductions zone; the 2012 Ometepec-Pinotepa Nacional (*Mw* 7.5), the 2014 Papanoa (*Mw* 7.2) and the 2018 Pinotepa Nacional (*Mw* 7.2) earthquakes. We found a mean value of the log of radiated seismic energy scaled with the seismic moment (Mo/Es) of -5.05 ±0.25, as well as, regional estimations tend to be higher than the teleseismic estimations by a factor of 1.3 to 6.3. A small dependence of scaled seismic energy with distance from the trench was seen, however distribution of seimsic energy seems to be spatially heterogeneous along the trench. We found four different regions with characteristic behaviors in energy release. One of the regions reveals recurrent low energies with possible slow rupturing close to the trench. Opposingly, high energy seismicity was present, adjacent to the Guerrero gap, which has not had a large earthquake in over 115 years. This suggests that radiated seismic energy can be highly influenced by complexities at the plate interphase, variations on the shear strength and/or coupling at the interface where seismic slip interacts over previous rupture patches.

Keywords: Radiated energy, aftershocks, subduction

©2019. Japan Geoscience Union. All Right Reserved.

[J] Oral | S (Solid Earth Sciences)：S-SS Seismology

Tue. May 28, 2019 1:45 PM - 3:15 PM JST | Tue. May 28, 2019 4:45 AM - 6:15 AM UTC | A10 TOKYO BAY MAKUHARI HALL

[S-SS10] Seismicity

convener:Kei Katsumata(Institute of Seismology and Volcanology, Hokkaido University), Chairperson:Aitaro Kato(Earthquake Research Institute, University of Tokyo), Shinji Toda(東北大学)

This session aims to improve our understanding on seismicity. Any contribution on behavior of earthquakes as a cluster, such as regional seismicity and aftershocks, are welcomed. We also welcome contribution on temporal and spatial interactions that control seismicity, and tectonic processes, and geological and thermal structures that regulate seismicity.

1:45 PM - 2:00 PM JST | 4:45 AM - 5:00 AM UTC

[SSS10-01] Seasonal variations in crustal seismicity in San-in district, southwest Japan

*Taku Ueda[1], Aitaro Kato[1] (1.Earthquake Research Institute, the University of Tokyo)

2:00 PM - 2:15 PM JST | 5:00 AM - 5:15 AM UTC

[SSS10-02] **Source fault model of the 2018 M_W 5.6 northern Osaka earthquake, Japan, inferred from the aftershock sequence**

*Aitaro Kato[1], Taku Ueda[1] (1.Earthquake Research Institute, the University of Tokyo)

2:15 PM - 2:30 PM JST | 5:15 AM - 5:30 AM UTC

[SSS10-03] The 2018 Hokkaido Eastern Iburi earthquake (M_{JMA} = 6.7) was triggered by a strike-slip faulting in a stepover segment: Insights from the aftershock distribution and the focal mechanism solution of the mainshock

*Kei Katsumata[1], Mako Ohzono[1], Hiroshi Aoyama[1], Ryo Tanaka[1], Masamitsu Takada[1], Masayoshi Ichiyanagi[1], Teruhiro Yamaguchi[1], Kazumi Okada[1], Hiroaki Takahashi[1], Shin'ichi Sakai[2], Satoshi Matsumoto[3], Tomomi Okada[4], Toru Matsuzawa[4], Shuichiro Hirano[5], Toshiko Terakawa[6], Shinichiro Horikawa[6], Masahiro Kosuga[7], Hiroshi Katao[8], Yoshihisa Iio[8], Airi Nagaoka[8], Noriko Tsumura[9], Tomotake Ueno[10], the Group for the Aftershock Observations of the 2018 Hokkaido Eastern Iburi Earthquake (1.Institute of Seismology and Volcanology, Faculty of Science, Hokkaido University, 2.Earthquake Research Institute, University of Tokyo, 3.Institute of Seismology and Volcanology, Faculty of Science, Kyushu University, 4.Research Center for Prediction of Earthquakes and Volcanic Eruptions, Graduate School of Science, Tohoku University, 5.Nansei-Toko Observatory for Earthquakes and Volcanoes, Graduate School of Science and Engineering, Kagoshima University, 6.Earthquake and Volcano Research Center, Graduate School of Environmental Studies, Nagoya University, 7.Graduate School of Science and Technology, Hirosaki University, 8.Research Center for Earthquake Prediction, Disaster Prevention Research Institute, Kyoto University, 9.Graduate School of Science, Chiba University, 10.National Research Institute for Earth Science and Disaster Prevention)

2:30 PM - 2:45 PM JST | 5:30 AM - 5:45 AM UTC

[SSS10-04] Layered structure of the upper mantle and the crust revealed in the time series analyses of the aftershocks of the 2018 Hokkaido Eastern Iburi Earthquake

*Takayuki Kawabe[1] (1.Faculty of Education, Arts and Sciences, Yamagata University)

2:45 PM - 3:00 PM JST | 5:45 AM - 6:00 AM UTC

[SSS10-05] Aftershock sequence of the 1847 Zenkoji earthquake: Temporal decay presented in four historical materials and best fit values of paramaters for Omori-Utsu law

*Kentaro Hattori[1], Ichiro Nakanishi[1] (1.Kyoto Univ.)

3:00 PM - 3:15 PM JST | 6:00 AM - 6:15 AM UTC

[SSS10-06] The aseismic islands, Amakusa-Kamishima and Shimoshima, Kumamoto Prefecture, southwest Japan: What persistently shuts off regional seismicity

*Shinji Toda[1] (1.International Research Institute of Disaster Science, Tohoku University)

Seasonal variations in crustal seismicity in San-in district, southwest Japan

*Taku Ueda[1], Aitaro Kato[1]

1. Earthquake Research Institute, the University of Tokyo

A growing body of evidence suggests that seismicity is seasonally modulated in a variety of tectonic environments (e.g., Gao et al., 2000; Heki, 2003; Bettinelli et al., 2008; Ben-Zion & Allam, 2013; Amos et al., 2014; Johnson et al., 2017). Identifying cyclic variations in seismicity leads to an improvement of our understanding about the physics of earthquake triggering.

San-in district, southwest Japan, is an active seismicity zone characterized as high shear strain rate by geodetic measurement (Nishimura and Takada, 2017). Moreover, Ogata (1983) has pointed out a possibility of seasonal variations in seismicity rate in the Inner Zone of southwest Japan. We here focus on seasonal variations in crustal seismicity in San-in district.

We used the JMA catalog (constructed by Japan Meteorological Agency) from 1975 through 2017 (magnitude M >= 3.0 and depth <= 20 km). We applied space-time Epidemic Type Aftershock Sequence (ETAS) model (e.g., Ogata, 1998; Zhuang et al., 2004) to the catalog and used a probability-based declustering procedure based on the work of Zhuang et al. (2002) to evaluate the significance of the seasonal variations, adopting uncertainties derived from the declustering scheme.

We demonstrated that semiannual variations in background seismicity rate, which increases in spring and autumn, are statistically significant from 1980 through 2017. The distribution of large historic and modern earthquakes (from 1850 through 2017, magnitude M >= 6.2, constructed by Chronological Scientific Tables) shows a similar pattern to recent background seismicity, suggesting that seismicity in San-in district has shown seasonal variations for over 150 years. There is some correlation between the monthly averaged background rate shifted backward 2 months and monthly averaged rain amount in the studied region. These results infer that seasonal variations in seismicity in San-in district can be explained by increasing pore pressure within fault zones, caused by infiltration of rainfall in autumn and decreasing surface mass due to snow melting in spring. Some correlation between seismicity and precipitation suggests that modulation of precipitation may be a key ingredient to produce time-dependence of background seismicity.

Keywords: Seismicity, Seasonal variations, Stochastic declustering, San-in shear zone

©2019. Japan Geoscience Union. All Right Reserved.

Source fault model of the 2018 M_w 5.6 northern Osaka earthquake, Japan, inferred from the aftershock sequence

*Aitaro Kato[1], Taku Ueda[1]

1. Earthquake Research Institute, the University of Tokyo

We reconstructed the spatiotemporal evolution of seismicity associated with the 2018 M_w 5.6 northern Osaka earthquake, Japan, to discuss the source fault model of the mainshock rupture, the possible link between this rupture and known active faults, and subsequent crustal deformation. We first relocated the hypocenters listed in the earthquake catalog determined by the Japan Meteorological Agency using a double-difference relocation algorithm. We then searched for the earthquake waveforms that closely resembled those of the relocated hypocenters by applying a matched filtering technique to the continuous waveform data. The relocated hypocenters revealed two distinct planar alignments with different fault geometries. A combination of the relocated hypocenters and focal mechanisms suggests that the mainshock rupture initiated on a NNW–SSE-striking thrust fault, dipping ~45° to the east, with the rupture propagating to an adjacent sub-vertical ENE–WSW-striking strike-slip fault ~0.3 s after the initial mainshock rupture, resulting in the simultaneous propagation of dynamic rupture along the two faults. The strike-slip fault is oblique to the strike of the Arima-Takatsuki Fault, indicating that blind strike-slip faulting occurred. While the east-dipping thrust fault is located deeper than the modeled extent of the Uemachi Fault, a simple extrapolation of the near-surface geometry of the Uemachi fault partially overlaps the mainshock rupture area. Although it is unclear as to whether a blind thrust fault or a deep portion of the Uemachi Fault ruptured during this mainshock–aftershock sequence, a mainshock rupture would have transferred a static stress change of >0.1 MPa to a portion of the east-dipping thrust fault system. Intensive aftershocks have persisted along the northern and southern edges of the source area, including moderate-magnitude events, whereas the seismicity in the central part of the source area has shown a rapid decay over time. Delayed triggered aftershocks were clearly identified along the northern extension of the rupture area. Because the background seismicity is predominant in this northern area, we interpret that aseismic deformation, such as cataclastic flow lubricated by crustal fluids, triggered this off-fault seismicity.

Keywords: the 2018 Mw 5.6 northern Osaka earthquake, afershocks, Source fault model

©2019. Japan Geoscience Union. All Right Reserved.

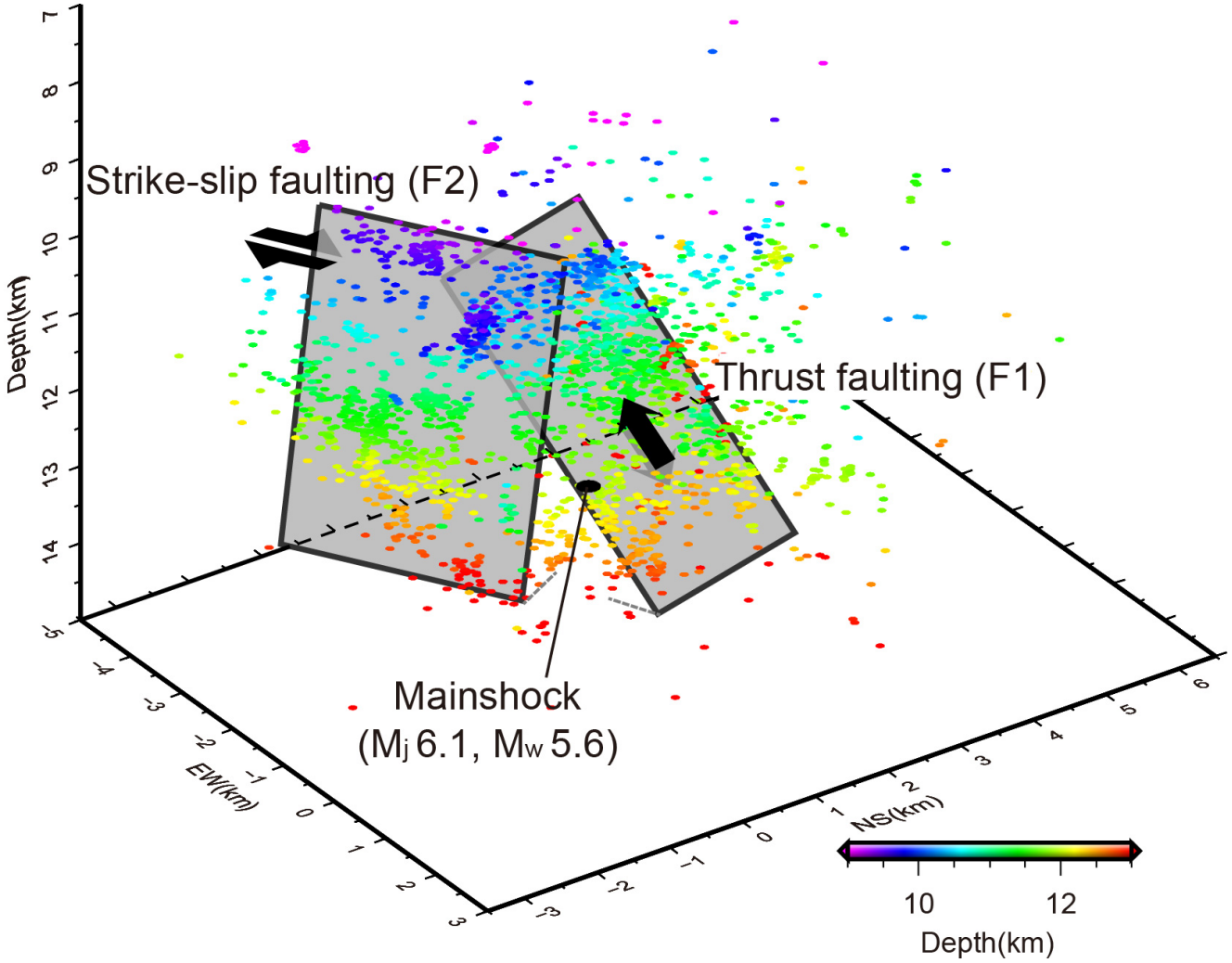

©2019. Japan Geoscience Union. All Right Reserved.

The 2018 Hokkaido Eastern Iburi earthquake (M_{JMA} = 6.7) was triggered by a strike-slip faulting in a stepover segment: Insights from the aftershock distribution and the focal mechanism solution of the mainshock

*Kei Katsumata[1], Mako Ohzono[1], Hiroshi Aoyama[1], Ryo Tanaka[1], Masamitsu Takada[1], Masayoshi Ichiyanagi[1], Teruhiro Yamaguchi[1], Kazumi Okada[1], Hiroaki Takahashi[1], Shin'ichi Sakai[2], Satoshi Matsumoto[3], Tomomi Okada[4], Toru Matsuzawa[4], Shuichiro Hirano[5], Toshiko Terakawa[6], Shinichiro Horikawa[6], Masahiro Kosuga[7], Hiroshi Katao[8], Yoshihisa Iio[8], Airi Nagaoka[8], Noriko Tsumura[9], Tomotake Ueno[10], the Group for the Aftershock Observations of the 2018 Hokkaido Eastern Iburi Earthquake

1. Institute of Seismology and Volcanology, Faculty of Science, Hokkaido University, 2. Earthquake Research Institute, University of Tokyo, 3. Institute of Seismology and Volcanology, Faculty of Science, Kyushu University, 4. Research Center for Prediction of Earthquakes and Volcanic Eruptions, Graduate School of Science, Tohoku University, 5. Nansei-Toko Observatory for Earthquakes and Volcanoes, Graduate School of Science and Engineering, Kagoshima University, 6. Earthquake and Volcano Research Center, Graduate School of Environmental Studies, Nagoya University, 7. Graduate School of Science and Technology, Hirosaki University, 8. Research Center for Earthquake Prediction, Disaster Prevention Research Institute, Kyoto University, 9. Graduate School of Science, Chiba University, 10. National Research Institute for Earth Science and Disaster Prevention

The Hokkaido Eastern Iburi earthquake (M_{JMA} = 6.7) occurred on 6 September 2018 in the Hokkaido-corner region where the Kurile and the northeastern Japan island arcs meet. We relocated aftershocks of this intraplate event immediately after the mainshock by using data from a permanent local seismic network and found that the aftershocks concentrated in depths from 20 to 40 km, which is extraordinarily deep when comparing with other shallow intraplate earthquakes in the inland area of Honshu and Kyushu, Japan. Moreover, we found that the aftershock area consists of three segments. The first one is located in the northern part of the aftershock area, the second one is located in the southern part, and the third one is located in a stepover segment between the first one and the second one. The hypocenter of the mainshock, which is a rupture initiation point, is located in the stepover segment. The centroid moment tensor solution for the mainshock indicates a reverse faulting, whereas the focal mechanism solution determined by using a first motion polarity of *P* wave indicates a strike-slip faulting. To explain this mismatch qualitatively, we present a model that the rupture started as a small strike-slip faulting in the stepover segment of the aftershock area and it is followed by the large rupture of two reverse faulting in the northern and the southern segments.

Keywords: the Hokkaido Eastern Iburi earthquake, aftershock distribution, focal mechanism solution

©2019. Japan Geoscience Union. All Right Reserved.

Layered structure of the upper mantle and the crust revealed in the time series analyses of the aftershocks of the 2018 Hokkaido Eastern Iburi Earthquake

*Takayuki Kawabe[1]

1. Faculty of Education, Arts and Sciences, Yamagata University

The 2018 Hokkaido Eastern Iburi Earthquake, occurred at September 6, 2018 03:07:57 am. Many aftershocks occurred along a plane which is striking north-northeastward and is dipping to the east at an inclination of 70 ˚. The depth of the upper limit at which aftershocks occurred has been becoming shallow over time.
According to time series analyses of the aftershocks, four depth zones are recognized. They are as follows;
Depth zone of 45 to 30 km deep: Many aftershocks occurred in the zone just after the main shock.
Depth zone of 30 to 20 km deep: Less aftershocks occur. However the magnitude of many of them are larger.
Depth zone of 20 to 10 km deep: Many small aftershocks were active. They distribute not uniformly but on multiple radial lines, and they occurred line by line.
Depth zone of 10 to 5 km deep: less aftershocks occur. However the dip of the plane on which aftershocks occurred is gentle as 45 ˚
These recognized zones seems to show the difference in physical properties of the underground geology. According to the slow development of aftershock and distribution form of epicenters suggest strongly the involvement of the deep hot water flow along the fault plane.

Keywords: Layered structure of the Crust, the 2018 Hokkaido Eastern Iburi Earthquake, time series analyses of the aftershocks

©2019. Japan Geoscience Union. All Right Reserved.

Aftershock sequence of the 1847 Zenkoji earthquake: Temporal decay presented in four historical materials and best fit values of paramaters for Omori-Utsu law

*Kentaro Hattori[1], Ichiro Nakanishi[1]

1. Kyoto Univ.

Seismic intensities estimated from damage caused by earthquakes have been most commonly used to locate earthquake epicentral area since Irish seismologist Mallet used degree of damage by the great Napoli earthquake of 1857 to locate earthquake source area. However, the scales of seismic intensity are different among countries. The seismic intensities are somewhat subjective and are affected by ground conditions.

Matsui and Oike (1997) proposed the use of the numbers of felt aftershocks right after large historical earthquakes to locate source area. A problem in their approach is that it is usually difficult to count the number of aftershocks in epicentral area or places close to the area.

We attempt to fit Omori-Utsu law (Utsu, 1961) to aftershock sequences of a historical large earthquake to overcome the above mentioned problem of the location of epicentral area. The value from counting aftershocks is integer, and seems to be more robust than the estimation of ground motion from the description in historical materials. The temporal decay of the number of aftershocks n(t) is described by the empirical Omori-Utsu law as $n(t) = K (t+c)^{-p}$, where t is the lapse time after the mainshock, p is an exponent showing the decay rate, c is a time scale, and K is a parameter showing aftershock activity.

We use aftershock sequence data of the 1847 Zenkoji earthquake presented in four historical materials owned in Matsushiro, Suwa, Fujinomiya, Gifu, in order of the distance from the epicentral area. We assume c=0.1 and p is common in four data, and obtain the best fitting p and four K. The result is shown in Fig.1. In the figure, it is clear that Omori-Utsu law does not fit the time range right after the earthquake occurrence for Matsushiro, Gifu, Suwa data, but fits Fujinomiya data. Another clear feature in Fig.1 is that the parameter K for Gifu data is 300. This value is much larger than those for Suwa (K=80) and Fujinomiya (K=6), both places are located closer to epicental area than Gifu. Fig.1 may suggest that the data preserved in Gifu were not written in Gifu, but in a place much closer to epicentral area.

Keywords: the 1847 Zenkoji earthquake, aftershock sequence, Omori-Utsu law

©2019. Japan Geoscience Union. All Right Reserved.

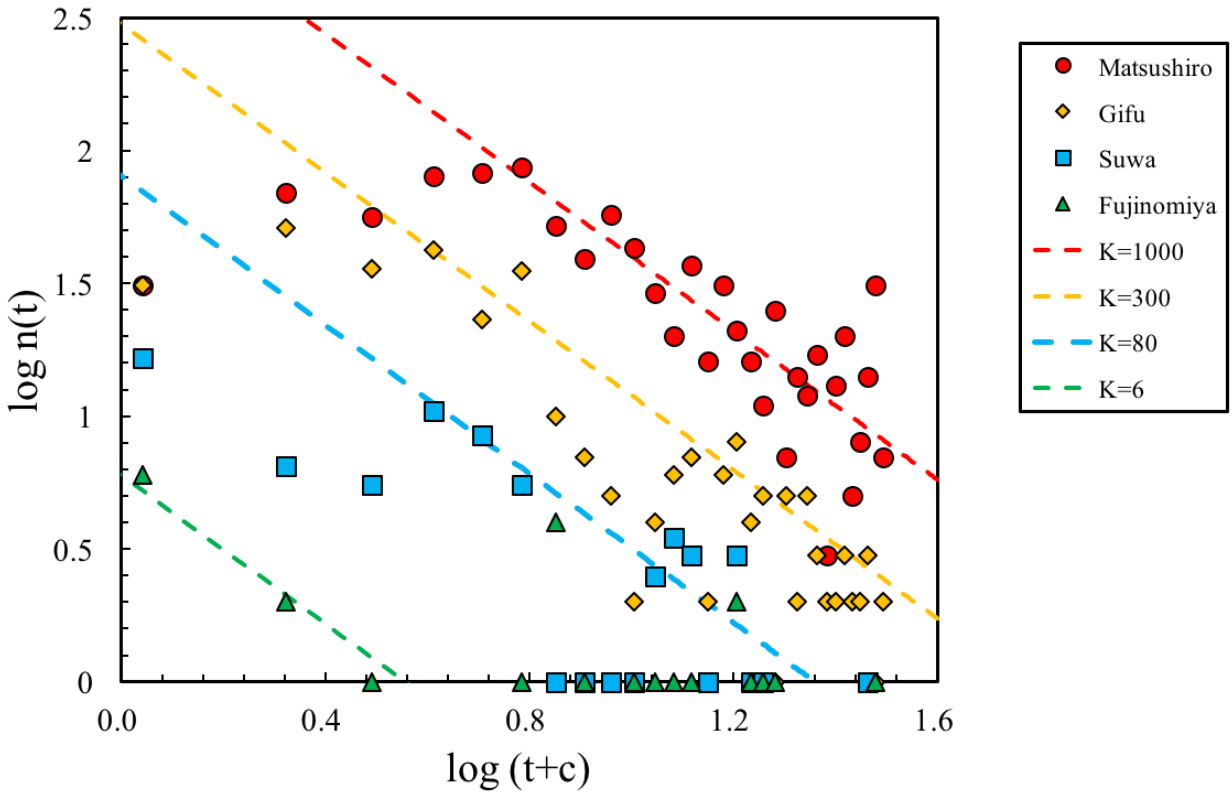

Fig. 1 Temporal decay of the aftershocks of the 1847 Zenkoji earthquake with lines (p=1.4) from Omori-Utsu law (Utsu, 1961)

©2019. Japan Geoscience Union. All Right Reserved.

The aseismic islands, Amakusa-Kamishima and Shimoshima, Kumamoto Prefecture, southwest Japan: What persistently shuts off regional seismicity

*Shinji Toda[1]

1. International Research Institute of Disaster Science, Tohoku University

Is there any inland region in Japan totally aseismic? This is a simple question against the frequently releasing comment by seismologists to the general public “none of the region in Japan can be avoided from strong ground motion.” To strictly check if this is true, we simply examined the Japan Meteorological Agency (JMA) earthquake catalog of 1923-January 2019, and then found one of the significantly aseismic regions in Kumamoto Prefecture, Amakusa-Kamishima and Shimoshima islands that extend about an area of 2,000 km^2 (hereinafter AAR). Neither historical destructive earthquake is documented in the AAR (Usami et al, 2013). Instead the AAR is surrounded by tectonically and seismically active zones of the Beppu-Shimabara graben to the north, Amakusa-nada graben to the west, the Futagawa-Hinagu fault system that caused the 2016 Kumamoto earthquake to the east, and highly seismic zone to the south. The AAR is characterized by high-Bouguer gravity anomaly possibly related to the underlying metamorphic rocks, while the most of the area exposes upper Cretaceous to Paleogene sedimentary rocks folded along NNE-trending axes (Takai and Sato, 1982). Numerous WNW-trending strike-slip faults, transverse these anticlines and synclines, are thought to have developed in the Miocene period but not been active during the late Quaternary period. Although the coastal geomorphologic features suggest uplifted marine terraces to the north and rias-type subsidence to the south formed during the late Quaternary, we infer long-term very gradual crustal uplift has been lasting since late Miocene due to the lack of sediments. Since the recent GNSS observation indicates a very low rate of strain in the AAR (GSI, 2018), we believe the AAR behaves as a rigid block enclosed by active tectonic zones mentioned above, those condition brings long-term stress shadow to bear such a persistent aseismic region.

Keywords: aseismicity, inland earthquake, seismicity

©2019. Japan Geoscience Union. All Right Reserved.

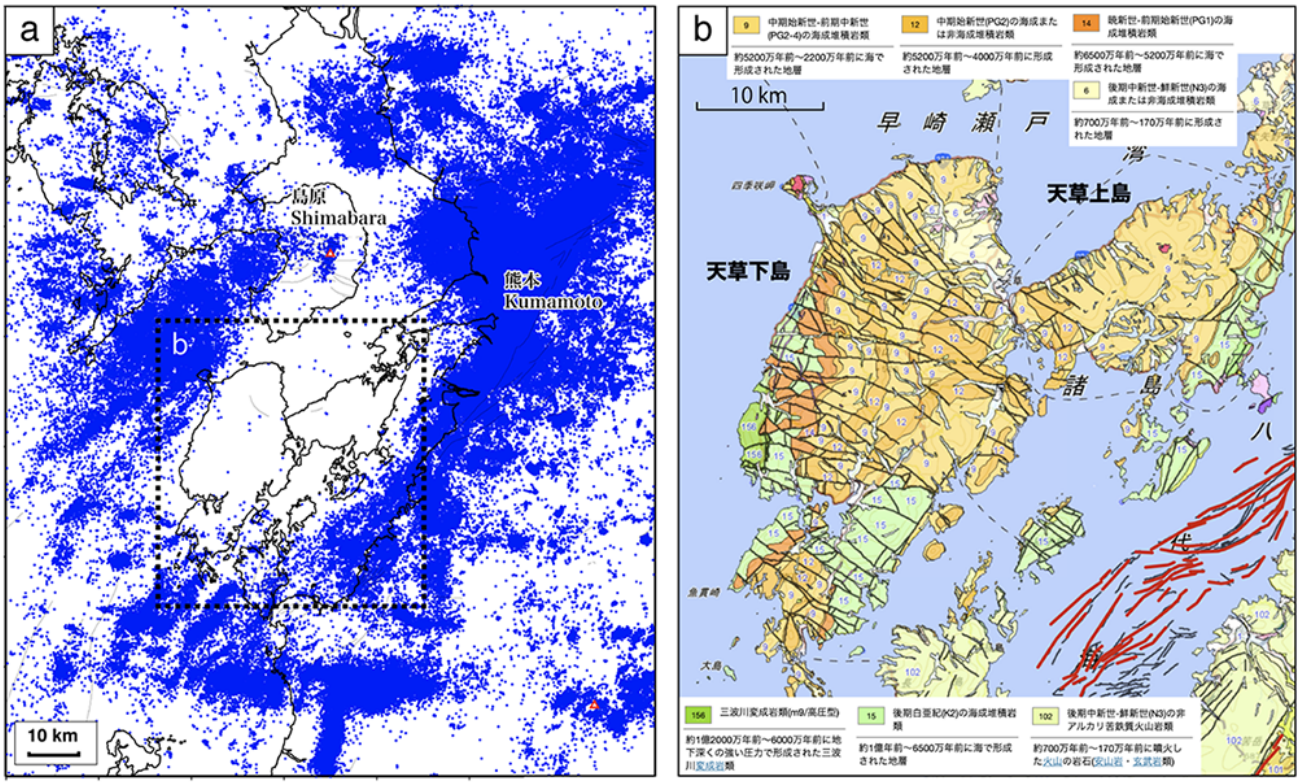

©2019. Japan Geoscience Union. All Right Reserved.

[J] Oral | S (Solid Earth Sciences)：S-SS Seismology

Tue. May 28, 2019 3:30 PM - 5:00 PM JST | Tue. May 28, 2019 6:30 AM - 8:00 AM UTC | A10 TOKYO BAY MAKUHARI HALL

[S-SS10] Seismicity

convener:Kei Katsumata(Institute of Seismology and Volcanology, Hokkaido University), Chairperson:Akio Katsumata(気象研究所地震津波研究部第一研究室), Yasushi Harada(東海大学)

This session aims to improve our understanding on seismicity. Any contribution on behavior of earthquakes as a cluster, such as regional seismicity and aftershocks, are welcomed. We also welcome contribution on temporal and spatial interactions that control seismicity, and tectonic processes, and geological and thermal structures that regulate seismicity.

3:30 PM - 3:45 PM JST | 6:30 AM - 6:45 AM UTC

[SSS10-07] Seismicity in the matle wedge around Ogasawara Islands and Lesser Antilles

*Akio Katsumata[1], Kenji Nakata[1], Akio Kobayashi[1], Fuyuki Hirose[1], Takahito Nishimiya[1] (1.Meteorological Research Institute, Japan Meteorological Agency)

3:45 PM - 4:00 PM JST | 6:45 AM - 7:00 AM UTC

[SSS10-08] Improvement of the accuracy of the unified Japan Earthquake Catalog using ocean bottom seismographs

*Hiroshi UENO[1], Mitsuharu Ueda[1], Hiromi Misu[1], Hirofumi Yokoyama[1], Yuriko Iwasaki[1], Iwakiri Kazuhiro[1] (1.Seismology and Volcanology Department, Japan Meteorological Agency)

4:00 PM - 4:15 PM JST | 7:00 AM - 7:15 AM UTC

[SSS10-09] Spatial distribution of seismic activity and stress field in the source region after the 2011 Tohoku-Oki earthquake

Tomoya Nishimori[1], *Ryota Hino[1], Masanao Shinohara[2] (1.Graduate School of Science, Tohoku University, 2.Earthquake Research Institute, The University of Tokyo)

4:15 PM - 4:30 PM JST | 7:15 AM - 7:30 AM UTC

[SSS10-10] Assessment for a large earthquake occurrence on the northern side of the focal region of the 2011 off-Tohoku mega-thrust earthquake

*Kazuyoshi Nanjo[1], Kazuki Miyaoka[2], Akio Yoshida[3] (1.University of Shizuoka, 2.Japan Meteorological Agency, 3.Shizuoka University)

4:30 PM - 4:45 PM JST | 7:30 AM - 7:45 AM UTC

[SSS10-11] Spatial and temporal distributions of *b*-values related to long-term slow-slip and low-frequency earthquakes in the Bungo Channel and Hyuga-nada regions, Japan

*Keita Chiba[1] (1.Institute of Seismology and Volcanology, Faculty of Science, Kyushu University)

4:45 PM - 5:00 PM JST | 7:45 AM - 8:00 AM UTC

[SSS10-12] 4D b-Value Mapping for Japan

*Yasushi Harada[1], Yuichi Akamine[1], Masayoshi Anzai[1] (1.School of Marine Science and Technology, Tokai University)

Seismicity in the matle wedge around Ogasawara Islands and Lesser Antilles

*Akio Katsumata[1], Kenji Nakata[1], Akio Kobayashi[1], Fuyuki Hirose[1], Takahito Nishimiya[1]

1. Meteorological Research Institute, Japan Meteorological Agency

Nakata et al. (2018) deployed ocean bottom seismometers around Ogasawara Islands from July to October in 2015, and observed seismicity of the area. Double seismic zone and seismicity in the mantle wedge (green circles in the figure) were identified. Some hypocenters were distributed in the 20-50 km depth range inside the mantle wedge. These earthquakes are located beneath the Ogasawara Trough without forming any clusters. Ogasawara Trough is a forearc basin between the the current volcanic arc and the Ogasawara ridge.
Seismic activity is usually low in the mantle wedge in areas without complex plate interactions. However, seismicities in the mantle wedge have been reported for other regions. Uchida et al. (2010) found supraslab seismicity off Sanriku coast. Davey and Ristau (2011) reported seismicity observed in the mantle wedge beneath northeast New Zealand. Laigle et al. (2013) reported seismicity in the mantle wedge along the Lesser Antilles subduction zone. The seismicity in the mantle wedge beneath Lesser Antilles is distributed over trench-normal distance more than 50 km, which is wider than that seen in the figure.
Supraslab earthquakes offshore Sanriku (Uchida et al. 2010) are distributed mainly near the toe of the mantle wedge, and form clusters. Earthquakes in the mantle wedge beneath northeast New Zealand form clusters near the boundary of subducting slab. The seismicity around Ogasawara Islands looks like that of Lesser Antilles rather than those offshore Sanriku and beneath northeast New Zealand.
The tectonic features of the forearc basins in the Lesser Antilles and Ogasawara Island regions are similar. Ogasawara ridge was formed with volcanic activities in 41-48 Ma related to beginning of the Pacific plate subduction in this area (Ishizuka et al. 2006). The backarc and forearc basins of the Lesser Antilles were formed as a single structure, and the Lesser Antilles were formed by volcanic activities with dividing the single basin into the two (Aitken et al. 2011). The volcanic activity started at about 40 Ma (Briden et al. 1979) due to the rollback of the Atlantic oceanic slab subduction (Aitken et al. 2011). Both forearc basins around Ogasawara Islands and Lesser Antilles are related to beginning of oceanic slab subduction. The seismic activity in mantle wedge may be related to dehydration of minerals which were formed at the time of subduction onset.

Keywords: Ogasawara Islands, the Lesser Antilles, seismicity in the mantle wedge, onset of oceanic slab subduction

©2019. Japan Geoscience Union. All Right Reserved.

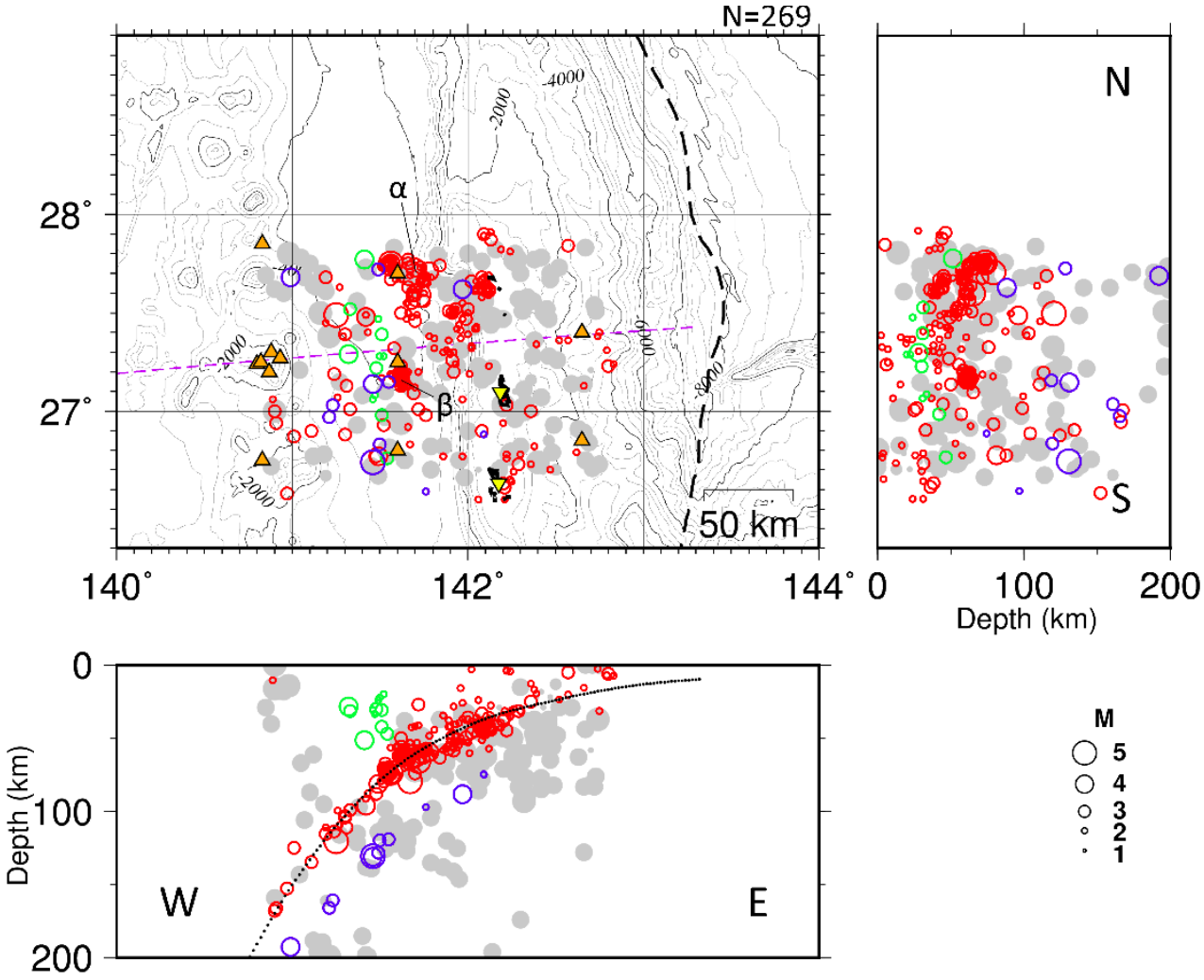

©2019. Japan Geoscience Union. All Right Reserved.

Improvement of the accuracy of the unified Japan Earthquake Catalog using ocean bottom seismographs

*Hiroshi UENO[1], Mitsuharu Ueda[1], Hiromi Misu[1], Hirofumi Yokoyama[1], Yuriko Iwasaki[1], Iwakiri Kazuhiro[1]

1. Seismology and Volcanology Department, Japan Meteorological Agency

The Unified Earthquake catalog for Japan has already been made available to the public by the Japan Meteorological Agency (JMA). In this catalog, hypocenters are determined using high-density seismic data collected by Japanese institutes and universities.

Recently, many ocean bottom seismographs(OBS) were installed around Japan Trench and Nankai trough.

In order to utilize many OBS data, we will optimize the hypocenter determination method of JMA from the following viewpoints.
1. Applications of the correction travel times of OBS for sedimentary beneath OBS.
2. Applications of velocity structures for OBS stations estimated from some velocity structure investigations.
3. Applications of the correction values of OBS for calculating magnitude with velocity amplitudes.

Keywords: Unified Japan Earthquake Catalog, Ocean bottom seismograph, hypocenter determination

©2019. Japan Geoscience Union. All Right Reserved.

Spatial distribution of seismic activity and stress field in the source region after the 2011 Tohoku-Oki earthquake

Tomoya Nishimori[1], *Ryota Hino[1], Masanao Shinohara[2]

1. Graduate School of Science, Tohoku University, 2. Earthquake Research Institute, The University of Tokyo

The 2011 Tohoku-Oki earthquake changed the stress field around its source region. Significant coseismic rotation of the principal stress axes was observed and it was suggested that almost all the accumulated shear stress was released on the ruptured plate boundary (e.g. Hasegawa et al. 2011). Therefore, it is important to study the spatial variation of the stress state after the Tohoku-Oki earthquake in detail to understand not only the coseismic stress change but also the stress state before the occurrence of the earthquake. Since previous studies used the focal mechanism solutions to estimate stress field inversion are based on the data of the onshore seismic networks, it has been difficult to discuss detailed features of the spatial variation of the stress state, especially of the depth variation, because accuracies of focal depths (centroid depths) of offshore earthquakes are not sufficient. In this study, we relocated the hypocenters by using arrival time data of ocean bottom seismic stations deployed in the central part of the Japan trench where the coseismic slip was large to improve three-dimensional distribution of the focal mechanism solutions of the earthquakes in the area occurred before and after the Tohoku-Oki earthquake. As a result of stress field estimation based on the improved focal mechanism catalogue, it was shown that the stress field after the Tohoku-Oki earthquake shows clear difference between the overring and the subducting plates in the west side of the coseismic slip region. This sharp change in the stress field across the plate boundary suggests that the shear stress along the plate interface is extremely small. The area corresponds to the region with extensive afterslip estimated from the postseismic deformation data. A remarkable intraplate seismicity extending upward from the plate interface by ~ 25 km was identified after the Tohoku-Oki earthquake at the western rim of the large coseismic slip area. By applying a moment tensor inversion to these earthquakes, we investigated the depth variation of the stress field in the upper plate above the large coseismic slip zone. As a result, the minimum principal stress axis was found to orient almost in the direction of the coseismic slip just above the plate boundary, whereas its direction changed to the along-strike direction in the shallow depth range. The change can be interpreted by the decrease of the tensional stress associated with the coseismic slip with the increasing distance from the rupture plane.

Keywords: 2011 Tohoku-Oki Earthquake, Stress tensor inversion, postseismic processes

©2019. Japan Geoscience Union. All Right Reserved.

Assessment for a large earthquake occurrence on the northern side of the focal region of the 2011 off-Tohoku mega-thrust earthquake

*Kazuyoshi Nanjo[1], Kazuki Miyaoka[2], Akio Yoshida[3]

1. University of Shizuoka, 2. Japan Meteorological Agency, 3. Shizuoka University

Eight years have passed since the occurrence of the 2011 off-Tohoku mega-thrust earthquake (off-Tohoku earthquake). Seismic activity in the central part of the focal region has settled down. However, magnitude (*M*) 5 to 6 earthquakes occur occasionally along the coast and inland areas of Tohoku and Kanto. Therefore, it can be said that seismic activity in a wide area is still in a higher level than that before the off-Tohoku earthquake.

Soon after the off-Tohoku earthquake, it was worried that a large earthquake might occur in the northern or southern adjacent regions, for it is not rare that a mega-thrust earthquake was succeeded by an occurrence of another large shock within several years. Last year, Matsu’ura (2018) warned impendence of a large earthquake occurrence in east-off Hokkaido, based on analysis of seismicity changes as well as historical records about great earthquake occurrence in the concerned area. Here, we report results of a detailed investigation about changes in the seismicity and the *b* value in the sea area on the northern side of the focal region of the east-off Tohoku earthquake.

Based on a *b* value analysis using data in three years after the off-Tohoku earthquake, Tormann et al. (2015) inferred that stress level in the focal region had already returned to the state before the earthquake, and presented an idea that a large earthquake may not repeat at an interval of a characteristic period, but rather occur at random. On the other hand, Nanjo and Yoshida (2017) showed, by re-analyzing data of a longer time period, that such a feature of the notable lowering of the *b* value as was observed before the off-Tohoku earthquake in the large-slip area was not seen. However, it was found that the *b* value in the northern adjacent area, far-east off Aomori Prefecture, is notably low. The area covers the focal region of the 1994 far-off Sanriku earthquake partly and extends further north. Further, it was seen that seismicity there has been decreasing in recent years.

Based on seismicity in the study region covering from off Aomori Prefecture to east-off Hokkaido, we found, in this study, spatiotemporal variability in *b* value. In particular, the 2003 *M*8.0 Tokachi earthquake did not show a transition of *b* value to normal levels but further lowered *b* value and expanded zones of low *b* values. The result obtained here is consistent with that by our previous work (Nanjo and Yoshida, 2017). From these observations, we think that a large earthquake may occur in the northern adjacent area of the focal region of the off-Tohoku earthquake in the near future.

Seismicity along the coast of Tohoku on the down-dip side of the coupling region is still high. A seismic quiescence as well as lowering of the *b* value is often observed before occurrence of an *M*5~6-class earthquake in the area around their foci. Although effectiveness of the observation of seismic quiescence and lowering of the *b* value in the prediction of a large-earthquake occurrence is still a problem under debate, we would like to propose here that extent of the low-*b* value area and the *b* value at the center of the area may be useful indices in evaluating results of the *b* value analysis. This is an analogy of a typhoon where their magnitude and intensity are evaluated by an extent of the storm area and air pressure at the central point. We expect further that imminence of a large earthquake occurrence may be assessed by noting tendency of the lowering of the *b* value.

Keywords: 2011 off-Tohoku mega-thrust earthquake, b value , seismicity

©2019. Japan Geoscience Union. All Right Reserved.

Spatial and temporal distributions of *b*-values related to long-term slow-slip and low-frequency earthquakes in the Bungo Channel and Hyuga-nada regions, Japan

*Keita Chiba[1]

1. Institute of Seismology and Volcanology, Faculty of Science, Kyushu University

Long-term slow-slip events (SSEs) and low-frequency earthquakes (LFEs) repeatedly occur in the area encompassing the Bungo Channel and Hyuga-nada region in Japan (e.g., Shelly et al., 2006; Ide et al., 2007; Ozawa et al., 2013; Ozawa, 2017). SSEs are slow earthquake events with a duration of months to years, characterized by a type of slip that is considered transitional between the fast rupture of regular earthquakes and stable sliding along a plate interface, and have characteristics sensitive to stress states near the plate interface (e.g., Obara and Kato, 2016). In addition, since LFEs are also thought to occur at the plate interface, it would be useful to infer the stress state in this region. This study focuses on the stress-dependent characteristics of the *b*-value of regular earthquakes, SSEs, and LFEs, as well as the spatio-temporal relationships between *b*-values and these events in this area, using the Japan Unified high-resolution relocated Catalog for Earthquakes (JUICE) (Yano et al., 2017). The *b*-value, which represents the relative proportion of large to small earthquakes (Gutenberg and Richter, 1944), is inversely related to differential stress or effective stress (e.g., Scholz, 1968, 2015; Wyss, 1973; Urbancic, 1992). As a result, the *b*-values are moderate to low (b = 0.6–1.1) in regions with a high incidence of long-term SSEs. This spatial anomaly in *b*-values is attributed to a partial release of the accumulated stress in regions with relatively high differential stress that are characterized by SSEs. In addition, the *b*-values in the Bungo Channel region are relatively higher than those in the Hyuga-nada region. It was also found that the difference of the *b*-values in the vertical direction within the plate for the Bungo Channel region is larger than that for the Hyuga-nada region. These findings support a generation model of LFEs by Nakajima and Hasegawa (2016), in which undrained conditions in the overlying plate are a key factor for generating LFEs. On the other hand, the *b*-values increase and decrease before and during periods of enhanced LFE activity in the Bungo Channel, respectively. The increase and following decrease in *b* -values are thought to reflect episodes of low and high shear strength along the plate interface, which were caused by the presence of abundant fluids supplied from the subducting slab under undrained conditions above the plate interface and the decreased pore pressure related to fluid consumptions by the generation of the LFEs, respectively.

Keywords: b-value, stress states, long-term slow slip, low-frequency earthquake

©2019. Japan Geoscience Union. All Right Reserved.

4D b-Value Mapping for Japan

*Yasushi Harada[1], Yuichi Akamine[1], Masayoshi Anzai[1]

1. School of Marine Science and Technology, Tokai University

b-value is considered as an index for seismicity, and smaller b-value means relatively more earthquakes of large magnetude, larger b-value means relatively less earthquakes of large magnetude. We tied to produce 4D b-value map for Japan to examine the difference of seismicity before and after the M9-class 2011 Tohoku quake. Dr. Kazuki Nanjo kindly provided us his code for calculating b-value and the standard deviation(SD). We created not only 4D b-value maps of Japan but also maps of the SD of b-value. Since large SD may mean a failure of Gutenberg–Richter law. Also from the map of b-value around Japan, we noticed a tendency of smaller b-value at distant area from the coastline. The tendency can be explained by the fact that seismometers cannot detect small distant earthqukes. Therefore we constructed a correction formula for b-values. With this formula, the most of the effect of smaller b-value around the M9-class 2011 Tohoku quake are disappeared. However the current formula is not good enough and it have to be improved in future studies.

Keywords: b-Value Mapping for Japan, 4D analysis, maps of SD of b-value, correction formula

©2019. Japan Geoscience Union. All Right Reserved.

[J] Oral | S (Solid Earth Sciences)：S-SS Seismology

Tue. May 28, 2019 9:00 AM - 10:30 AM JST | Tue. May 28, 2019 12:00 AM - 1:30 AM UTC | A09 TOKYO BAY MAKUHARI HALL

[S-SS11] Seismic wave propagation: Theory and Application

convener:Kiwamu Nishida(Earthquake Research Institute, University of Tokyo), Kazuya Shiraishi(Japan Agency for Marine-Earth Science and Technology), Takao Nibe(JAPEX), Kaoru Sawazaki(National Research Institute for Earth Science and Disaster Resilience), Chairperson:Shunsuke Takemura(防災科研)

Seismic wave propagation provides rich information of earth's heterogeneities and the excitation sources. In order to extract the information, integrated studies are needed among mathematical/numerical studies based on the wave theory, miniature physical experiments using rock specimens, and practical data analyses. Furthermore, it is greatly beneficial to conduct comparative studies of various kinds of waves, such as elastic, acoustic, traveling ionospheric disturbances, and oceanic waves. This session widely invites presentations about the theories and applications related to seismic and other geophysical waves.

9:00 AM - 9:01 AM JST | 12:00 AM - 12:01 AM UTC

Introduction

9:01 AM - 9:23 AM JST | 12:01 AM - 12:23 AM UTC

[SSS11-13] Fluid flows inferred from microseismic events associated with injection test in Okuaizu Geothermal Field

★Invited Papers

*Kyosuke Okamoto[1], Li Yi[2], Hiroshi Asanuma[1], Takashi Okabe[3], Yasuyuki Abe[4], Masatoshi Tsuzuki[5] (1.National Institute of Advanced Industrial Science and Technology, 2.Osaka University, 3.Geothermal Energy Research and Development Co., Ltd., 4.Okuaizu Geothermal Co., Ltd., 5.Japan Oil, Gas and Metals National Corporation)

9:23 AM - 9:45 AM JST | 12:23 AM - 12:45 AM UTC

[SSS11-14] 3D distribution of intrinsic attenuation factors and random velocity fluctuations in southwestern Japan inferred from seismogram envelopes

★Invited Papers

*Masashi Ogiso[1] (1.Meteorological Research Institute, Japan Meteorological Agency)

9:45 AM - 10:00 AM JST | 12:45 AM - 1:00 AM UTC

[SSS11-15] Regional to teleseismic strong ground motions from a 610 km deep 24 May 2013 Sea of Okhotsk earthquake

*Takashi Furumura[1], Brian LN Kennett[2] (1.Earthquake Research Institute The University of Tokyo, 2.Research School of Earth Sciences, The Australian National University)

10:00 AM - 10:15 AM JST | 1:00 AM - 1:15 AM UTC

[SSS11-16] Trial estimation of eclogitization depths within subducting oceanic crust of the Philippine Sea slab inferred from head wave propagating along the oceanic Moho

*Shunsuke Takemura[1], Takashi Tonegawa[2], Junichi Nakajima[3], Katsuhiko Shiomi[1] (1.National Research Institute for Earth Science and Disaster Resilience, 2.Japan Agency for Marine-Earth Science and Technology , 3.Tokyo Institute of Technology)

10:15 AM - 10:30 AM JST | 1:15 AM - 1:30 AM UTC

[SSS11-17] **Transient gravity perturbations due to a buried gravitational source in a homogeneous elastic half space**

*Aditya Nitin Deshmukh[1], Pratik Laxman Borate[1], Abhishek Venkatesh Chitgopkar[1], Nobuki Kame[2], Ranjith Kunnath[1] (1.Mahindra Ecole Centrale, Hyderabad, India , 2.Division of Theoretical Geoscience, Earthquake Research Institute, University of Tokyo, Japan)

Fluid flows inferred from microseismic events associated with injection test in Okuaizu Geothermal Field

*Kyosuke Okamoto[1], Li Yi[2], Hiroshi Asanuma[1], Takashi Okabe[3], Yasuyuki Abe[4], Masatoshi Tsuzuki[5]

1. National Institute of Advanced Industrial Science and Technology, 2. Osaka University, 3. Geothermal Energy Research and Development Co., Ltd., 4. Okuaizu Geothermal Co., Ltd., 5. Japan Oil, Gas and Metals National Corporation

In the Okuaizu geothermal field (Yanaizu, Fukushima Prefecture), a recharge water injection test has been carried out to stabilize the steam production since 2015. In order to avoid cooling of the geothermal reservoir by the water injection and to obtain a larger recharge effect, it is important to grasp and anticipate the flows of the injected water. On the other hand, subsurface structures are generally complicated, especially within the brittle region. Therefore, it is difficult to predict the flows with a simple homogeneous model because the following phenomena are expected in real cases; selective flows passing through a highly permeable region such as a fracture zone as well as creation of a new flow path by shearing. In the shearing, the mechanism of its creation (e.g., reduction of effective stress due to in-flow into fractures, propagation of stress change, stress accumulation due to thermal change) is hard to identify, which is essential information to expect new flow paths.

In the Okuaizu geothermal field, a microseismic monitoring network has been established as part of the JOGMEC project named "Geothermal Reservoir Evaluation and Management Technology" since fiscal year 2015. In this study, we use the seismic record to estimate the subsurface fluid flows associated with the injection test. We investigate factors of the creation of microseismicity associated with the injection test by using elastic wave velocity changes in fractures estimated by seismic scattering analysis as well as pressure and temperature information.

Keywords: Microseismic monitoring, Scattering analysis, Geothermal reservoir

©2019. Japan Geoscience Union. All Right Reserved.

3D distribution of intrinsic attenuation factors and random velocity fluctuations in southwestern Japan inferred from seismogram envelopes

*Masashi Ogiso[1]

1. Meteorological Research Institute, Japan Meteorological Agency

Hi-frequency (> 1 Hz) seismogram envelopes show various envelope shapes due to the influence of seismic scattering as well as intrinsic attenuation of the medium. Intrinsic and scattering attenuation structures inferred from seismogram envelopes are important for precise strong ground motion prediction as well as understanding the Earth structure. Ogiso (2019) have proposed a two-step approach to estimate the 3D distribution of intrinsic attenuation factors and scattering coefficients using envelope fitting method and sensitivity kernels proposed by Takeuchi (2016). In this study, we propose the method to estimate 3D distribution of intrinsic attenuation factors and random velocity fluctuations, which is the improved version of Ogiso (2019).

The same as Ogiso (2019), the proposed method consists of two steps. First, we estimate appropriate attenuation parameters (intrinsic attenuation factor and strength of random velocity fluctuation) for each observed envelope. Second, we map the estimated attenuation parameters in step 1 into 3D space using sensitivity kernels. Radiative transfer theory with non-isotropic scattering coefficients based on the Born approximation is used to model seismogram envelopes. The effect of depth-dependent velocity structure is also considered for modeling envelopes.

The proposed method is applied in southwestern Japan. The estimated structure has three main features: (1) both intrinsic attenuation factors and random velocity fluctuations are stronger in the Kyushu than the other regions, (2) both intrinsic attenuation factors and random velocity fluctuations are smaller in the lower crust than the upper crust, which is clearly found in the Chugoku region, and (3) horizontal heterogeneity in intrinsic attenuation factors at the depth of 10-50 km of the Shikoku region. These features, probably reflecting the tectonic settings of southwestern Japan, seem to be consistent with previous studies.

Acknowledgment

We used seismic waveforms recorded by Hi-net operated by the NIED. This study was financially supported by the JSPS KAKENHI Grand No. JP17H02064 and JP18K13622.

Keywords: seismogram envelope, seismic wave scattering, seismic attenuation structure, southwestern Japan

©2019. Japan Geoscience Union. All Right Reserved.

Regional to teleseismic strong ground motions from a 610 km deep 24 May 2013 Sea of Okhotsk earthquake

*Takashi Furumura[1], Brian LN Kennett[2]

1. Earthquake Research Institute The University of Tokyo, 2. Research School of Earth Sciences, The Australian National University

A very large deep earthquake (Mw8.3, 610 km depth) occurred in the Sea of Okhotsk near Kamchatka on 24 May 2013 producing a large shocks across the Japanese Islands. The maximum shaking intensity reached 3 on the JMA scale at Sarufutsu, Hokkaido and Akita, and the felt area spread to Kagoshima, 3000 km from the hypocenter. According to USGS, the shake was also reported in Northern India, California, and Dubai 6000 km away; also CNN reported that people in Moscow were evacuated from the buildings. Kuge (2015) analyzed teleseismic records and claimed that shaking at large distance is consistent with the radiation pattern of P wave, similar to the 1994 Bolivia Mw8.3 earthquake (Anderson et al., 2015). In this study we aim to understand the cause of large ground motion at regional to teleseismic distances from this very deep event using dense F-net, Hi-net, and IRIS DMC observations, complemented by 3D FDM simulation of seismic wave propagation.

Observed strong ground motion in Japanese Islands

The observed pattern of peak ground velocity (PGV) over Japan demonstrates large motions in Sea of Japan side, opposite to the large shake on the Pacific Ocean side as is usually seen in deep earthquakes. The PGV does not attenuate monotonically with distance, and a second PGV peak was seen at distance of about 2000 km.

At shorter distances (<2000 km) upward travelling waves arrive from the 610 km deep source, waves emitted downwards overlap somewhat and dominate beyond 2000 km. The large PGV is associated with successive arrivals of upgoing and downgoing S waves (near a caustic). S waves incident on the surface at the critical angle generates large sP conversions, which propagate in the crust and uppermost mantle to sustain PGV. Furthermore, a third PGV peak occurs at distances around 3000 km created by the SS wave traveling through deep mantle and reflected twice on the surface. Similar anomalous PGV attenuation is found for other deep earthquakes e.g. near Sakhalin in 2012 (Mw7.7; 600 km).

Strong motion simulation of deep earthquake

FDM simulations using ak135 model demonstrate the ways in which the S wave caustics and sP conversion create the second large PGV peak at regional distances, which moves from 1500 to 3000 km as the source depth increases from 200 to 610 km. The efficiency of sP and SS conversion and reflection is very sensitive to the thickness of the crust; SS is large and sP is weak by reflection from thick continental crust, and thin oceanic crust gives the reverse. The large SS observed over Japanese Island is due to the reflection of S wave at the thicker crust (20-30 km) in the Sea of Okhotsk, and large sP phase at Izu-Ogasawara Islands and the Northwest Pacific, corresponds well with the simulation results.

With a Pacific slab model (Yokota et al., 2017) in the 3D FDM simulation model, we find that S waves traveling through the High-V plate are refracted into the Low-V mantle, making large ground motions on the Sea of Japan side. This anti-waveguide effect differs from the stochastic waveguide effects in the plate at high-frequency (>1-2 Hz) waveguide effect, which is weak for the long-period wave of this distant earthquake with oblique transmission.

Shaking at thousands of kilometers due to long-period ground motion?

©2019. Japan Geoscience Union. All Right Reserved.

The IRIS DMC records show that the PGV has large peak at distance of about 3500 km due to the arrival of the SS wave. Then, PGV attenuate gently until the next large PGV peak around 7000 km with the arrival of the SSS phase. Shaking in the distance range 4000-6000 km from the Sea of Okhotsk earthquake comes from long-period SS and SSS waves. At Obinisk (OBN; 6050 km) near Moscow long-period S and SS produce 0.7 cm/s ground velocity at a period of 3.5 s. With amplification of long-period ground motions in sedimentary basins, the ground motion can grow to the JMA’s long-period intensity scale 1 (> 5 cm/s).

Keywords: Deep earthquake, Strong ground motion

©2019. Japan Geoscience Union. All Right Reserved.

Trial estimation of eclogitization depths within subducting oceanic crust of the Philippine Sea slab inferred from head wave propagating along the oceanic Moho

*Shunsuke Takemura[1], Takashi Tonegawa[2], Junichi Nakajima[3], Katsuhiko Shiomi[1]

1. National Research Institute for Earth Science and Disaster Resilience, 2. Japan Agency for Marine-Earth Science and Technology , 3. Tokyo Institute of Technology

To investigate structural properties within the subducting oceanic crust of the Philippine Sea slab, we analyzed head wave propagating along the oceanic Moho (P_{PHS}). In the case of offshore earthquakes occurred at depths shallower than oceanic Moho, P_{PHS} is first arrival at onshore seismic stations (e.g., Takemura et al., 2016 EPS). During southeast off Mie earthquake, observed Hi-net seismograms illustrated first arrivals with an apparent velocity of 7.2 km/s, which correspond to apparent velocity of P_{PHS}, at epicentral distances of 70-200 km. At distances greater than approximately 200 km, apparent velocity of first arrivals was increased. Such distance change of apparent velocities is related with velocity structure at depths below the continental Moho.

We conducted two-dimensional (2D) finite-difference method (FDM) simulations of seismic wave propagation using the realistic slab model (Hirose et al., 2008 JGR). Thickness of subducting oceanic crust was assumed to be 7 km. Crust and mantle structures were referred from the F-net 1D model (Kubo et al., 2002 Tectonophys.). Although P_{PHS} was clearly found in simulated seismograms, the simulation result with oceanic crust at deeper (> 70 km) depths did not reproduced observed first arrivals at greater (>200 km) distances. By replacing structural properties of the oceanic crust with ones of the oceanic mantle at depths of 40-60 km, simulated first arrivals were changed depending on structural change depth. A structural change depth of 52 km is the optimal model for explaining observed first arrivals. This depth well corresponds to an eclogitization depth of the subducting oceanic crust beneath the Kii Peninsula (Kato et al., 2014 EPS).

We consider that estimated structural change depth within the oceanic crust is linked with transformation to anhydrous eclogitic oceanic crust (Fukao et al., 1983 Nature; Abers et al., 2003 GRL; Hacker et al., 2003 JGR). Our analysis using head wave propagating along the oceanic Moho may provide depth of eclogitization within the oceanic crust.

Acknowledgement
NIED F-net MT catalog and Hi-net velocity seismograms were used. Finite-different method simulations were conducted on the Earth Simulator at the JAMSTEC.

Keywords: Nankai Trough, Philippine Sea Slab, Oceanic crust, Eclogitization, Head wave

©2019. Japan Geoscience Union. All Right Reserved.

Transient gravity perturbations due to a buried gravitational source in a homogeneous elastic half space

*Aditya Nitin Deshmukh[1], Pratik Laxman Borate[1], Abhishek Venkatesh Chitgopkar[1], Nobuki Kame[2], Ranjith Kunnath[1]

1. Mahindra Ecole Centrale, Hyderabad, India , 2. Division of Theoretical Geoscience, Earthquake Research Institute, University of Tokyo, Japan

Earthquake ruptures induce transient deformations which result in changes in the gravity field (Harms, *et. al* (2015)). Prompt elastogravity signals due to the earthquake source arrive before any seismic wave from the source and it has been proposed that these signals could be used for earthquake early warning systems. In this work, we study the model of a buried gravitational load in an isotropic, homogenous elastic half-plane or half-space. The response at the surface is determined for a suddenly applied gravitational line-load in an elastic half-plane. Also, the response at the surface is calculated for a suddenly applied gravitational point-load in an elastic half-space. Due to the gravitational field induced by a suddenly applied line-mass, every point in the half-plane acts as a source by itself. The elastic response due to each point in the half-plane is calculated using the solution of Garvin (1956) for a buried line blast load in an elastic half-plane. The total response at the receiver point on the surface of the half-plane is determined numerically by the convolution of Garvin’ s solution with the gravitational force. Similarly, the elastogravitational response to a suddenly applied point mass in a half-space is determined using the solution of Johnson (1974) to Lamb’ s problem of a source buried in a half-space. We show that in both these models, prompt gravity signals are obtained.Earlier, Kame and Kimura (2018) had considered the elastic response to a suddenly applied point mass in an unbounded medium. They showed that the ground acceleration at any receiver point is exactly cancelled by the gravity perturbation during the entire duration of the prompt period so that a gravimeter at the receiver will not detect any prompt signals. This appears to be a peculiarity of the model of an unbounded medium.

References:

Harms, J., Ampuero, J.-P., Barsuglia, M., Chassande-Mottin, E., Montagner, J.-P., Somala, S. N. and Whiting, B. F. (2015). Transient gravity perturbations induced by earthquake rupture, *Geophys. J. Int.* **201**, 1416-1425.

Garvin, W. W. (1956). Exact transient solution of the buried line source problem, *Proc. R. Soc. Lond. A* **234**, 529-541.

Johnson, L.R. (1974). Green’ s function for the Lamb’ s Problem. *Geophys. J. R. astr. Soc.* **37**, 99-131.

Kame, N. and Kimura, M. (2018). The fundamental nature of a transient elastic response to prompt gravity perturbations, submitted to *Geophy. J. Int.*

Keywords: Geomechanics , Elastogravity, Transient deformation, Computational mechanics

©2019. Japan Geoscience Union. All Right Reserved.

[J] Poster | S (Solid Earth Sciences)：S-SS Seismology

Tue. May 28, 2019 3:30 PM - 5:00 PM JST | Tue. May 28, 2019 6:30 AM - 8:00 AM UTC | Poster Hall International Exhibition Hall8, Makuhari Messe_17

[S-SS11] Seismic wave propagation: Theory and Application

convener:Kiwamu Nishida(Earthquake Research Institute, University of Tokyo), Kazuya Shiraishi(Japan Agency for Marine-Earth Science and Technology), Takao Nibe(JAPEX), Kaoru Sawazaki(National Research Institute for Earth Science and Disaster Resilience)

Seismic wave propagation provides rich information of earth's heterogeneities and the excitation sources. In order to extract the information, integrated studies are needed among mathematical/numerical studies based on the wave theory, miniature physical experiments using rock specimens, and practical data analyses. Furthermore, it is greatly beneficial to conduct comparative studies of various kinds of waves, such as elastic, acoustic, traveling ionospheric disturbances, and oceanic waves. This session widely invites presentations about the theories and applications related to seismic and other geophysical waves.

[SSS11-P01] Estimation of Love wave phase velocity based on array analysis in the northern Tokyo bay area : Numerical experiments using synthetic seismograms

*Kaori Shimazu[1], Kazuo Yoshimoto[1], Shunsuke Takemura[2] (1.Graduate School of Nanobioscience, Yokohama City University, 2.National Research Institute for Earth Science and Disaster Resilience)

[SSS11-P02] Similutanious estimation of amplitude and travel time variation in the transfer function with ACROSS

*Shuhei Tsuji[1], Koshun Yamaoka[1], Takahiro Kunitomo[1], Toshiki Watanabe[1], Ikuta Ryoya[2] (1.Graduate School of Environmental Studies, Nagoya University, 2.Faculty of Science, Shizuoka University)

[SSS11-P03] Temporal variation in travel time of P and S-waves using ACROSS

*rina suzuki[1], Koshun Yamaoka[2] (1.Graduate School of Environmental Studies, Nagoya University, 2.Earthquake and Volcano Research Center,Graduate School of Environmental Studies,Nagoya University)

[SSS11-P04] Inversion analysis of S coda wave envelope based on radiation transfer theory - Estimation of heterogeneous structure of Izu Oshima volcano -

*Takahiro Ueda[1] (1.Department of Geophysics, Graduate School of Science, Tohoku University)

[SSS11-P05] Strong motion characteristics at Nagomi-machi, Eta, during the northern Kumamoto pref. earthquake of Jan. 3rd, 2019

*Tomotaka Iwata[1], Kimiyuki Asano[1], Masayuki Yoshimi[2], Takeshi Sugiyama (1.Disaster Prevention Research Institute, Kyoto University, 2.Geological Survey of Japan, AIST)

[SSS11-P06] **Effects of the heterogeneous crustal structure on the amplitude fluctuation of high-frequency seismic waves**

*Kazuo Yoshimoto[1], Shunsuke Takemura[2] (1.Graduate School of Nanobioscience, Yokohama City University, 2.National Research Institute for Earth Science and Disaster Resilience)

[SSS11-P07] Long-duration long-period ground motion in Hokkaido during off-Tohoku earthquakes (2) Roles of crust and Pacific slab

*Shinako Noguchi[1], Takuto Maeda[2], Takashi Furumura[3] (1.Association for the Development of Earthquake Prediction, 2.Faculty of Science and Technology, Hirosaki University, 3.Earthquake Research Institute, The University of Tokyo)

[SSS11-P08] Measuring the NCF dispersion without the long inter-station distance limitation – a new method based on hybrid peak time matching

*Ying-Nien Chen[1], Yuancheng Gung[2], Ling-Yun Chiao[3] (1.Institute of Seismology, National Chung Cheng University, Taiwan., 2.Department of Geosciences, National Taiwan University, Taipei, Taiwan., 3.Institute of Oceanography, National Taiwan University, Taipei, Taiwan.)

[SSS11-P09] Dynamic Triggering Earthquakes Exploration by Sonification of Seismograms

*Takahiko Uchide[1], Yota Morimoto[2], Masaki Matsubara[3] (1.Research Institute of Earthquake and Volcano Geology, Geological Survey of Japan, National Institute of Advanced Industrial Science and Technology (AIST), 2.Institute of Sonology, Royal Conservatory of the Hague, 3.University of Tsukuba)

[SSS11-P10] The effect of P-wave velocity on the ellipticity of Rayleigh waves in a transversely isotropic medium

*Shun Fukushima[1], Kiyoshi Yomogida[1] (1.Hokkaido University,Graduate school of Science,Department of Natural History Sciences,Seismology Laboratory)

[SSS11-P11] Time series analyses of amplitude of the Earth's background free oscillations

*Ryuichi Kunugi[1], Naoki Suda[1] (1.Hiroshima University)

[SSS11-P12] Regional shear waves from an unusually deep earthquake beneath Ogasawara Islands: 660 km discontinuity and anisotropy

*Keiko Kuge[1] (1.Department of Geophysics, Graduate School of Science, Kyoto University)

[SSS11-P13] On the estimation of G discontinuity in the oceanic upper mantle using ScS reverberations

*Jumpei Maruyama[1], Hitoshi Kawakatsu[1], Nozomu Takeuchi[1] (1.University of Tokyo, Earthquake Research Institute)

[SSS11-P14] Short-period body wave (1-3 Hz) extraction from ambient noise records observed at seafloor and borehole in the Nankai subduction zone

*Takashi Tonegawa[1], Toshinori Kimura[1] (1.Research and Development center for Earthquake and Tsunami, Japan Agency for Marine-Earth Science and Technology)

[SSS11-P15] Characteristics of T-wave envelopes observed by S-net

*Kentaro Emoto[1], Hisashi Nakahara[1] (1.Graduate School of Science, Tohokuk University)

[SSS11-P16] Reverse time reflection imaging of active and passive seismic data with ocean-bottom seismographs

*Kazuya Shiraishi[1], Takao Nibe[2], Yasuhiro Yamada[1] (1.Japan Agency for Marine-Earth Science and Technology, 2.Japan Petroleum Exploration Co. Ltd.)

Estimation of Love wave phase velocity based on array analysis in the northern Tokyo bay area : Numerical experiments using synthetic seismograms

*Kaori Shimazu[1], Kazuo Yoshimoto[1], Shunsuke Takemura[2]

1. Graduate School of Nanobioscience, Yokohama City University, 2. National Research Institute for Earth Science and Disaster Resilience

In the Kanto sedimentary basin, long-period ground motions have been frequently observed during shallow moderate-to-large earthquakes [e.g. Yoshimoto and Takemura (2014)]. Strong long-period ground motions, which are caused by surface waves, complicatedly propagate within the Kanto basin due to 3D structures of low-velocity sediments and bedrock topography [e.g., Furumura and Hayakawa (2007)]. For the precise prediction of long-period ground motions, we should investigate propagation characteristics of surface waves and subsurface structure within the Kanto basin. Array analysis using dense seismic stations in the Kanto basin may be useful to capture propagation characteristics of surface waves and structural properties. In this study, as a basic study for investigating a seismic velocity structure of the Kanto sedimentary basin, we applied a beamforming technique to the seismograms synthesized based on FDM simulations.

We selected shallow moderate earthquakes for our beamforming analysis, e.g. the northern Ibaraki prefecture earthquake on March 19, 2011 (Mw 5.8), the northern Tochigi prefecture earthquake on February 25, 2013 (Mw 5.8), and the northern Nagano prefecture earthquake on November 22, 2014 (Mw 6.3). We synthesized velocity seismograms based on the FDM simulations using a velocity structural model SBVSM [Masuda *et al.*(2014); Takemura *et al.* (2015)]. Virtual seismic stations were distributed at an interval of 750 m in the range of 35.5˚N to 35.9˚N and 139.4˚E to 139.9˚E. Our FDM simulations can evaluate ground motions for periods longer than 4 s. In our array analysis using a three-component beamforming [Riahi *et al.*(2013)], the size of the small local array was adjusted according to the analyzed period of Love waves. The analysis was conducted on the six periods: 5.9, 6.4, 7.3, 8.5, 10.2 and 12.8 s. We analyzed the seismograms for time window of 51.2 s, including the maximum amplitude of energy envelope for horizontal components.

By comparing the estimated phase velocities by our array analysis with theoretical ones from local 1D structure of SBVSM, we confirmed that the phase velocities of Love waves propagating in the large sedimentary basin are successfully obtained. Observed dispersion curves show clear normal dispersions. At the period of 5.9 s, the phase velocity was estimated stably for seismograms of all earthquakes. This period corresponds to the dominant period of long-period ground motions within the Kanto sedimentary basin [e.g. Yoshimoto and Takemura (2014)]. We also found that the phase velocity tends to be estimated stably in large PGV areas of long-period ground motions. These results imply that the propagation of surface waves may characterize the magnitude of long-period ground motions. The other results in detail will be exhibited in our presentation.

Acknowledgement

FDM simulations of seismic wave propagation were conducted on the Earth Simulator of the Japan Agency for Marine-Earth Science and Technology. F-net MT solutions were provided by the National Research Institute for Earth Science and Disaster Resilience.

©2019. Japan Geoscience Union. All Right Reserved.

Keywords: Love wave, Kanto sedimentary basin, array analysis, phase velocity, FDM simulation

©2019. Japan Geoscience Union. All Right Reserved.

Similutanious estimation of amplitude and travel time variation in the transfer function with ACROSS

*Shuhei Tsuji[1], Koshun Yamaoka[1], Takahiro Kunitomo[1], Toshiki Watanabe[1], Ikuta Ryoya[2]

1. Graduate School of Environmental Studies, Nagoya University, 2. Faculty of Science, Shizuoka University

Summary

We developed a method for simultaneous estimation of deviation of the amplitude and the travel time of the transfer functions obtained by an artificial seismic source, ACROSS.

Background

Variation of the amplitude is important information for monitoring the strength of the fault plane (e.g. Nagata et al, 2008). However, studies on the variation of propagation properties were mainly discussing the deviation of the travel time (e.g. Ikuta et al., 2002; Hobiger et al., 2016). The conventional method using the signal envelope is affected by the noise level, which is the shortcoming of the method. Thus, we developed a new method to make a simultaneous estimation of the deviation of both the amplitude and travel time.

Method

The simultaneous estimation method is basically a maximum likelihood estimation using a least square method. We adopt the least square method for deviation functions which are obtained by dividing each transfer function by averaged transfer function on the complex plane in the frequency domain. This is incontrast to the cross-spectrum method which was commonly used for calculation of the deviation of the travel time. In our method, the amplitudes as well as the deviation of travel time is calculated similarly to the cross-spectrum method. We estimated the deviation of the amplitudes and travel times as a nonlinear model fitting problem. We made a model of the deviation function with an assumption that the deviation of the amplitude and travel time is independent of frequency. We searched for the best fitting parameters so that minimizing the sum of the square lengths on the complex plane by grid search. As a result, we could estimate the deviations for smaller SNR data. We also could estimate the errors of the obtained deviations.

Results

We applied the method to High Sensitivity Seismograph Network Japan (Hi-net) stations around an ACROSS seismic source which is deployed at Toki City, the middle part of Honshu Island, Japan. The estimated deviation of the travel time with this method generally coincides with the results with the conventional cross spectrum method. When the data has low SNR, the average of the deviation of the amplitude did not become one due to averaging in the complex domain. This is because the least square fitting is made on the complex plane which does not mathematically guarantee the averaging of amplitude.

Keywords: Deviation of the amplitude, Deviation of the tarvel time, velocity change, Artificial seismic source, ACROSS

©2019. Japan Geoscience Union. All Right Reserved.

Temporal variation in travel time of P and S-waves using ACROSS

*rina suzuki[1], Koshun Yamaoka[2]

1. Graduate School of Environmental Studies, Nagoya University, 2. Earthquake and Volcano Research Center,Graduate School of Environmental Studies,Nagoya University

We analyzed the temporal variation of travel time of P and S wave using observation data for one year by an artificial seismic source ACROSS which can generate controlled vibration repeatedly. In this study, we used a new type of ACROSS called ACR2014 that is installed in Toyohashi City, Aichi Prefecture. This ACROSS source can excite vertical vibration as well as horizontal vibration by rotation of the weight around the horizontal rotation axis to excite P wave efficiently. We used records at three observation stations called NU.MIK, N.THNH, and N.MKBH installed around ACR2014 and calculated transfer functions. From the components of transfer function, we chose the vertical component by vertical excitation and horizontal component by horizontal excitation for calculation of travel time of P and S wave, respectively. We calculated travel time variations from these components of transfer function using cross spectrum method. In this calculation, a window ranging 0.2 to 0.3 seconds was applied to the P and the S wave part, respectively. We compared the travel time variations with the precipitation data of nearby AMeDAS at Toyohashi and Mikkabi. In NU.MIK, short-term change with a step-like delay and following recovery occurred in both P and S waves at rains. The tendency of this recovery was different between the P and S wave. On the other hand, the long-term variation differs between the P and S waves at some observation stations. We interpreted the influence of rainfall on these short-term and long-term travel time variations, using a theoretical effect of the crack density and fluid saturation on the seismic velocity change. The observed difference in the P and S wave change can be explained with the difference in the response of crack density and fluid saturation between P and S waves. The long-term travel time variations in the P and S waves can be interpreted by assuming that the fluid saturation increases in the periods with high precipitation and decrease in the periods with low precipitation. The short-term change with the difference of the recovery between the P and S wave can be interpreted in similar way as the long-term variation.

Keywords: travel time variation, velocity change

©2019. Japan Geoscience Union. All Right Reserved.

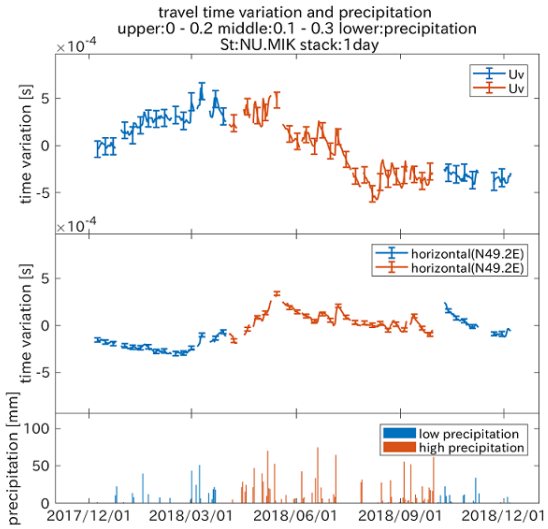

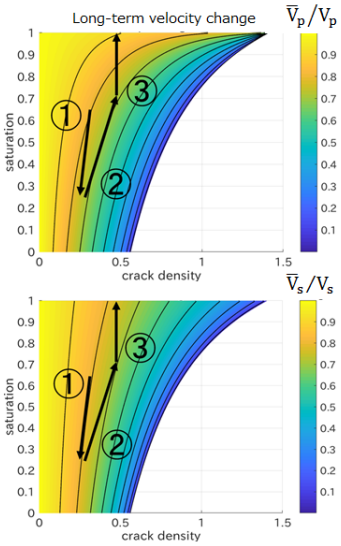

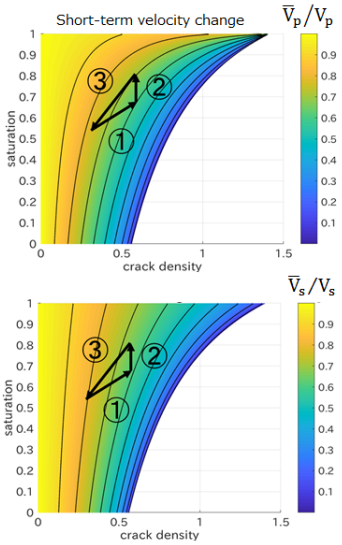

©2019. Japan Geoscience Union. All Right Reserved.

Inversion analysis of S coda wave envelope based on radiation transfer theory - Estimation of heterogeneous structure of Izu Oshima volcano -

*Takahiro Ueda[1]

1. Department of Geophysics, Graduate School of Science, Tohoku University

It is well known that short period seismic waves are strongly influenced by heterogeneous structures in the crust or shallow structures. Analyses using seismic sources near the ground surface such as artificial sources and seismic wave interferometry have reported that strong heterogeneity appears remarkably due to shallow sediments of volcanoes. On the other hand, there are few studies in which volcano-tectonic earthquakes are used, and the characteristics of heterogeneous structure down to deep regions (10 km) of the volcanoes have not been well investigated. In this study, based on the Multiple Lapse Time Window method (Fehler et al. 1992) based on radiative transfer theory, we evaluate heterogeneity of the volcano structures, using an inversion method to obtain the intrinsic attenuation value, scattering attenuation value, the energy radiated from the source, and the site amplification factor, a of the Izu Oshima volcano. We use the seismic waveforms recorded at 4 V-net stations at Izu Oshima. From January 2014 to January 2018, events of M1.5 to M3.5, 150 earthquakes within 10 km deep are analyzed. Bandpass filters of 1-2 Hz, 2-4 Hz, 4-8 Hz, and 8-16 Hz bands are applied, and the envelope waveforms of the direct waves and coda waves of S waves are obtained in each frequency band. The Green’ s function is calculated based on the radiative transfer theory of the S wave multi isotropic scattering. The amplitude is expressed by the product of the site amplification factor, the energy radiated from the source, and Green’ s function. We fit the observation envelope with the theory and determine the internal attenuation and the scattering attenuation as well as site factors and source energy.
The results show that the scattering attenuations are 0.0393, 0.0210, 0.0027, 0.0001 in the 1-2 Hz, 2-4 Hz, 4-8 Hz, and 8-16 Hz bands, respectively, and the intrinsic attenuation was 0.0054, 0.0056, 0.0029, 0.0006. The average values of Japan's crustal structure (Calocoré and Sato, 2010) are almost same with intrinsic attenuation of this study, while the value of the scattering attenuation is larger by about 10 times in the low frequency region around 1.5 Hz. In addition, it is smaller than the results for very shallow part (Yamamoto and Sato., 2010, Hirose et al., 2019) by 1 to 2 orders of magnitude.
Based on the above results, the scattering attenuation parameter is dominant in Izu Oshima compared to the Japanese crust, compared to the internal damping, which is in harmony with the results of the previous study that the scattering damping is large around the active volcano , And it seems that the influence of the minute heterogeneous structure of the shallow part of the crust appeared strongly. In addition, theoretical envelope was well obtained by the envelope inversion method proposed in this research, and it was shown that it is effective as a method to evaluate the radiation energy and the radiation energy of the epicenter.

Keywords: coda wave, volcanic structure

©2019. Japan Geoscience Union. All Right Reserved.

Strong motion characteristics at Nagomi-machi, Eta, during the northern Kumamoto pref. earthquake of Jan. 3rd, 2019

*Tomotaka Iwata[1], Kimiyuki Asano[1], Masayuki Yoshimi[2], Takeshi Sugiyama

1. Disaster Prevention Research Institute, Kyoto University, 2. Geological Survey of Japan, AIST

We estimate ground motion characteristics of Eta, Nagomi-machi, Kumamoto, during the 2019 Jan. 3rd northern Kumamoto earthquake (MJ5.5). The JMA seismic intensity of 6weak was observed at the site. Before this event, we have conducted the microtremor array measurement and obtained that the thin (about 20m) superficial layer with a S-wave velocity of less than 0.2km/s. We also estimated site amplification factor by the spectral inversion method (Somei et al., 2018). The site amplification factor shows the predominant period of about 0.4s for weak motion data. After the mainshock, we have conducted additional microtremor array measurement to give a more in-detail information in the area and single station H/V observations just beside of the seismic intensity meter and outside of the building for checking the effects of station setting of this site. In this moment, there is no significant effect of the station setting because of the similar H/V spectral ratio between the site and the one outside of the building in this period range. We also noticed that the predominant period of observed horizontal motions of the mainshock is about 0.5s, that is a little bit longer than that of the site effect for the weak motions. This would be caused by the non-linear behavior of the superficial layer during the strong shaking. Strong motion data are provided by JMA and Kumamoto prefecture. Microtremor observations and spectral inversion were conducted by the Comprehensive Research Project for the major active faults related to The 2016 Kumamoto Earthquake (2016FY-2018FY), Mext.

Keywords: 2019 Northern Kumamoto prefecture earthquake , Eta, Nagomi-machi

©2019. Japan Geoscience Union. All Right Reserved.

Effects of the heterogeneous crustal structure on the amplitude fluctuation of high-frequency seismic waves

*Kazuo Yoshimoto[1], Shunsuke Takemura[2]

1. Graduate School of Nanobioscience, Yokohama City University, 2. National Research Institute for Earth Science and Disaster Resilience

It is considered in the seismic scattering analyses that crustal heterogeneity may be modeled by combining deterministic heterogeneity and stochastic heterogeneity. A simple technique of this modeling adopts a uniform averaged structure model (background structure model) for deterministic heterogeneity and a uniform random heterogeneity model for stochastic heterogeneity. Although this technique may be adequate for the seismic scattering analysis with a small target area, the simplification might lead erroneous results if the target area of the analysis becomes large. In this study, we investigated the effect of the deterministic crustal heterogeneity on the amplitude fluctuation of high-frequency (0.5-4 Hz) seismic waves on the basis of finite-difference method (FDM) simulations.
We conducted FDM simulations of shallow moderate earthquakes, including a target earthquake occurred on 25 November 2011 at a depth of 14 km beneath the Chugoku region, western Japan. Our simulation model covered a volume of 256×256×80 km^3, which was discretized by a uniform grid spacing of 0.05 km. Technical details are the same as those of Takemura et al. (2017). The background velocity structure was referred from the Japan Integrated Velocity Structure Model (JIVSM; Koketsu et al., 2012). Small-scale random velocity heterogeneity (Takemura et al., 2017) was superposed on the crust of the JIVSM. We adopted a double-couple point source with a focal mechanism reported by the F-net MT catalog. This model setting well reproduced observed high-frequency seismograms at the Hi-net borehole stations (Takemura et al., 2017). Because we employed a finer FDM grid compared to previous simulations (Takemura et al., 2017), our FDM simulation can evaluate seismic wave propagation for higher (~ 8 Hz) frequencies. To investigate fluctuation of seismic amplitudes, we evaluated peak ground velocity (PGV) from filtered synthetic seismograms.
Simulation results of a strike-slip source model showed that the cross-shaped (four-lobed) large PGV distribution in the epicentral area becomes unclear in the surrounding area as the hypocentral distance increases. Theoretical and empirical models of high-frequency seismic amplitudes also predicted a similar characteristic of apparent radiation pattern (Yoshimoto et al., 2015; Takemura et al., 2016). Although this phenomenon, which is mainly caused by the seismic scattering due to random heterogeneity, showed azimuthal symmetry, the symmetry was found to be broken for a certain focal depth condition. Our additional simulations using different properties of background structure model indicated that, at least in our target region, the reflection due to a small velocity contrast of the Conrad discontinuity (about 10% in JIVSM) may cause the large amplitude fluctuation of high-frequency seismic waves in the surrounding area of the epicenter (distance > 40 km).

Keywords: High-frequency seismic ground motion, Amplitude fluctuation, Random crustal heterogeneity, Conrad discontinuity, Seismic ground motion simulation

©2019. Japan Geoscience Union. All Right Reserved.

Long-duration long-period ground motion in Hokkaido during off-Tohoku earthquakes (2) Roles of crust and Pacific slab

*Shinako Noguchi[1], Takuto Maeda[2], Takashi Furumura[3]

1. Association for the Development of Earthquake Prediction, 2. Faculty of Science and Technology, Hirosaki University, 3. Earthquake Research Institute, The University of Tokyo

Anomalously large, long-time-lasting long-period later phases were observed widely in Hokkaido, Japan during moderate to large (M>6.5) earthquakes occurred at off-Tohoku Pacific earthquakes. Such long-period signals spread widely over Hokkaido not only at deep Ishikari basin as reported by Noguchi et al. (2017; JpGU). In this study we discuss new mechanisms to generate this later phase in addition to well recognized deep sediment effect by means of 3D FDM simulations of seismic wave propagation using 3D heterogeneous subsurface structure model.

This long-period later phase caused by off Tohoku earthquakes appeared at most F-net stations in Hokkaido except for a few stations at southwestern Hokkaido. However, these later phases did not appear from inland earthquakes, outer-rise earthquakes and earthquakes occurred near Hokkaido. Dominant period of this later phases lay within the range between 15 s to 25 s, varying among earthquakes. The later phase in transverse component expected to be Love wave showed longer period and appeared earlier than that in radial and vertical components expected to be Rayleigh wave. Both waves showed normal dispersion.

The FDM simulations of seismic wave propagation in 3D heterogeneous crust and mantle structure was conducted using OpenSWPC (Maeda et al., 2017). This simulation model consists of sea water, topography, sediments and subducting plates based on Japan Integrated Velocity Structur Model (JIVSM; Koketsu et al., 2012) and the depth of Moho and Pacific slab is based on Matsubara et al. (2017) and Kita et al. (2010), respectively.

We confirmed two distinct phenomena from the FDM simulations as follows; Firstly, long tail of Rayleigh wave (< 3 km/s) propagating north and southward at western-side of Japan trench following the main packet of surface wave were generated. Then the long wavetrains spreading over Hokkaido were generated by conversion from the Rayleigh wave northward along trench at the edge of deep sediment at off Ishikari. Secondly, Love wave appearing at the junction of Japan trench and Kuril trench extended over Hokkaido in earlier time than the converted Rayleigh wave.

We investigated the phase and group velocities for Rayleigh wave and Love waves from off Tohoku to Hokkaido; we found a lower-wavespeed zone of group and phase velocities for Rayleigh wave at period around 20 s guiding Rayleigh wave along the west side of Japan trench, where was formed by the subsurface low-velocity layer covering over the Pacific slab. Such low-wavespeed zone was not appeared for Love wave. However, strong velocity contrast between the Pacific side and Japan side of trench due to different crustal thickness was confirmed which bended the ray of Love wave toward low-velocity side. Thus, Love waves traveling along low-velocity side released seismic energy toward Hokkaido at the junction of Japan trench and Kuril trench, producing anomalously large and long-time lasting long-period ground motions.

We conclude that the long period later phase observed over Hokkaido during off Tohoku earthquakes

©2019. Japan Geoscience Union. All Right Reserved.

were caused by the deep subsurface structure including crustal thickness and subducting slab in addition to deep sediments at off Ishikari.

Keywords: Long period ground motion, Subduction zone, Wave propagation simulation

©2019. Japan Geoscience Union. All Right Reserved.

Measuring the NCF dispersion without the long inter-station distance limitation –a new method based on hybrid peak time matching

*Ying-Nien Chen[1], Yuancheng Gung[2], Ling-Yun Chiao[3]

1. Institute of Seismology, National Chung Cheng University, Taiwan., 2. Department of Geosciences, National Taiwan University, Taipei, Taiwan., 3. Institute of Oceanography, National Taiwan University, Taipei, Taiwan.

Over the past decade, the probing of Earth structures using seismic ambient noises has been widely used by seismologists and is now a well-developed technique. Based on an implicit high-frequency approximation, the consensus is that the noise cross-correlation function (NCF) of continuous seismic records resembles the Green’ s Function (GF) of the far-field surface wave between sensors. This perspective leads to the application of the long interstation distance criterion in the dispersion measurements, and, accordingly, much of the low-frequency content in the NCF is rejected. Herein we show that, for a far-field source, the NCF used in most surface wave studies should not be considered as representative of the empirical Green’ s Function (EGF); instead, it is simply the interference product between sensors. We present a theoretical derivation of an explicit definition for a “high-frequency approximation” and clarify the relationship between the NCF and the EGF. Furthermore, we propose a new method to measure the NCF dispersion, in which the phase velocity is estimated by matching the peak delay time observed in the time domain NCF to the one predicted by the theoretical complex NCF signals. In this hybrid peak time matching technique, the long interstation distance is no longer a required condition and phase velocities can be determined more precisely at lower frequencies. Therefore, this permits the investigation of deeper structures using noise data.

Keywords: phase velocity measurement, Empirical Green’ s Function, ambient noise

©2019. Japan Geoscience Union. All Right Reserved.

Dynamic Triggering Earthquakes Exploration by Sonification of Seismograms

*Takahiko Uchide[1], Yota Morimoto[2], Masaki Matsubara[3]

1. Research Institute of Earthquake and Volcano Geology, Geological Survey of Japan, National Institute of Advanced Industrial Science and Technology (AIST), 2. Institute of Sonology, Royal Conservatory of the Hague, 3. University of Tsukuba

We have been proposing the sonification of seismograms for exploring dynamic triggering earthquakes (Uchide et al., JpGU, 2016, 2018; Matsubara et al., 2016). The seismic sonification for the 2011 Tohoku-oki earthquake successfully revealed a dynamic triggering event in the Hida area, Central Japan. For the ease of the seismic sonification for seismologists, we are developing the Sonification of Seismograms (SoS) system (Uchide et al., JpGU, 2018), which assigns sound whose amplitude and tone correspond to the maximum absolute value and the number of zero-crossings of seismograms in short time windows.

This study investigates dynamic triggering events by recent major earthquakes using the SoS software. In the case of the 2011 Tohoku-oki earthquake, the dynamic triggering event in the Hida area was M 4.2 (Ohmi et al., 2012) which is relatively large. Identification of smaller dynamic triggering events may be a challenge. Limiting areas of stations for the sonification help us identify where a dynamic triggering event may or may not occur.

In front of our poster, we will provide the opportunity to listen sonified sounds and demonstrate the interactive sonification process using the SoS.

Acknowledgement

We used the Global CMT Catalog and seismic data from Hi-net of NIED, seismic data from JMA, Hokkaido University, Hirosaki University, Tohoku University, the University of Tokyo, Nagoya University, Kyoto University, Kochi University, Kyushu University, Kagoshima University, and AIST. This work was supported by JSPS KAKENHI 17K14386.

Keywords: Seismograms, Sonification, Dynamic Triggering Earthquakes

©2019. Japan Geoscience Union. All Right Reserved.

The effect of P-wave velocity on the ellipticity of Rayleigh waves in a transversely isotropic medium

*Shun Fukushima[1], Kiyoshi Yomogida[1]

1. Hokkaido University,Graduate school of Science,Department of Natural History Sciences,Seismology Laboratory

The study of surface waves is one of effective approaches for the internal structure of the earth. Phase and group velocities data have ever been used, but the ellip- ticity of Rayleigh waves can be also used to infer it (e.g., Tsuboi & Saito, 1983) . The ellipticity of Rayleigh waves is defined as a V(vertical amplitude)/H(horizontal amplitude) ratio, which is more sensitive to shallow structures than the conventional phase or group dispersion data. Fundamentally, it is the same principle as strong ground motions with horizontal and vertical amplitudes of microtremors to evaluate near-surface structures easily. Tsuboi & Saito (1983) and Tanimoto & Tsuboi (2009) derived and calculated partial derivatives of ellipticity in an isotropic medium. In addition to the well-known anisotropy in the asthenosphere such as that included in PREM, the influence of a transversely isotropic medium may be important for shallow structures such as a sedimentary layer. A transversely isotropic medium has five elastic moduli (A, C , L, N .F) but propagations of surface waves can be formulated in a compact manner, similar to the isotropic case.
In this study, we first formulated partial derivatives of ellipticity in a transversely isotropic medium. In the same way as the isotropic medium, we determine the linear relationship using the variational principle and the reciprocal theorem. Then, we set an artificial eigenfunction for the boundary condition of non-zero normal stress at the surface in addition to the natural eigenfunction for the normal condition (i.e., zero stress at the surface). We then derived partial derivatives with the two kinds of eigenfuncitons combined. Several important features of PV-waves and PH-waves are revealed in comparison with those of P-waves in the isotropic case. P-waves have little effects on the ellipticity in an isotropic medium. In the transversely isotropic medium, partial derivatives of PV wave are quite different from those of PH wave with a relatively large amplitude in a shallow part. The reason of the small P-wave effect in the isotropic case comes from the sum of those of PV and PH waves of opposite signs. PH wave in a shallow part has a large positive effect on ellipticity while PV wave has a weak negative one. If there is a strongly laminated sedimentary layer near the surface, for example, the ellipticity does not vary so much, despite of small SV there. It is because the shallow PH velocity is not reduced in such a layer, in contrast with small SV and PV waves, and its partial derivatives is large and of the sign opposite to SV and PV waves. If we performed the inversion for the shallow structure with the data of ellipticity (i.e., only slightly anomalous), under the isotropic model with the dominance of SV wave velocity, the inversion result would lead to slightly small SV velocity near the surface with virtually no changes in P-wave velocity because partial derivatives in the isotropic case are large for SV but small for P wave.

Keywords: Particle motion, Transverse isotropy, Rayleigh wave

©2019. Japan Geoscience Union. All Right Reserved.

Time series analyses of amplitude of the Earth’s background free oscillations

*Ryuichi Kunugi[1], Naoki Suda[1]

1. Hiroshima University

The Earth’s background free oscillations (BFO) are slightly and continuously excited free oscillations of the solid Earth persistent even in seismically quiet periods [Nawa et al. 1998; Suda et al. 1998; Kobayashi and Nishida 1998; Tanimoto et al. 1998]. The observed modes are fundamental modes, suggesting that the excitation sources are atmospheric and oceanic disturbances [e.g. Nishida 2013]. Amplitude of BFO exhibits seasonal variations [Nishida et al. 2000]. Along with such a periodic variation, there may exist transient variations correlated with atmospheric/oceanic phenomena.

The target modes are fundamental modes ${}_0S_{22}$-${}_0S_{43}$ at frequencies between 3 and 5 mHz because they are most clearly observed in the frequency domain. We used vertical records of STS-1 broadband seismometers at 65 quite seismic stations downloaded from IRIS DMC. The data periods are from 2000 to 2017. The analysis method is mainly the same as used in Nishida et al. (2000). Continuous records were divided into 3-days records with a step of 1 day. After applying the Hanning taper, each record was converted into power spectral density (PSD) with the correction of system response. To reject noisy data, we used the data whose mean PSD values at 3-5 mHz are between 10^{-19} and 10^{-18} m^2/s^3. The remained PSDs were then stacked over all the stations to create monthly averaged PSDs. To avoid the influence of temporally changing PSD baseline due to the random background noise, we averaged the PSD values in the mode and the noise frequency bands, and then the averaged noise PSD is subtracted from the averaged signal PSD.

We used two methods of time series analysis for the statistical analysis of long-term variations in amplitude of BFO: one is based on the state-space model and the other is on the regression model. In the state-space analysis we adopted the local level model with seasonal variations, which divide time series into random noise, seasonal variations and a long-term trend. In the regression analysis we adopted the model that consist of random noise, seasonal variations and a long-term trend. We used the R packages dlm and prophet for the state-space and the regression analyses, respectively.

The result obtained in the space-state analysis shows the long-term variation with a time scale of 10 years from 2002 to 2012: the minimum is in 2002 and 2012 and the maximum is in 2008. The long-term trend obtained in the regression analysis shows almost the same characteristics: the minimums in 2000 and 2012 and the maximum in 2008. Thus, we for the first time robustly obtained the nearly 10-year variation in amplitude of BFO from the two different time-series analyses. We can utilize data of infragravity waves at frequencies between 3-30 mHz from WAVEWATCH III. We will show the result of comparison between BFO and infragravity waves in the presentation.

©2019. Japan Geoscience Union. All Right Reserved.

©2019. Japan Geoscience Union. All Right Reserved.

Regional shear waves from an unusually deep earthquake beneath Ogasawara Islands: 660 km discontinuity and anisotropy

*Keiko Kuge[1]

1. Department of Geophysics, Graduate School of Science, Kyoto University

Following a large deep earthquake beneath Ogasawara Islands on 30 May, 2015, an aftershock (mb 4.9) took place at a depth of 678 km (USGS). P and S waves from the aftershock were recorded by F-net broadband stations in Japan at distances of 1 to 18 degrees. The aftershock is small enough to neglect source effect. Here I explore structure effect on the shear wave propagation. SH waves recorded by the transverse directions in western Japan were generally characterized by a single pulse. The peaks of the SH waves tend to arrive earlier than those of the SV waves in the radial directions. The dominance of a single pulse in the SH waves can be explained by the iasp91 model with the 660 km discontinuity shallower than the aftershock. When the 660 km discontinuity is assumed to be deeper than the aftershock, additional signals predicted in radial components can apparently cause different peak time arrivals between SH and SV waves. However, in these cases, the SV peaks arrive earlier than the SH peaks, which cannot fit the observations. It is thus more likely that the observed peak time difference is attributed to anisotropy. Because signals due to crustal reflection are predicted in the radial components ~6 sec after the direct S waves, shear wave splitting parameters were carefully estimated by using initial portions of S waves. The fast directions obtained in western Japan are nearly in the east-west, which looks different from the fast direction observed for a nearby deep earthquake in the Wadati-Benioff zone. We cannot see systematically early arrivals of SH peaks from Fiji earthquakes in a similar back azimuth. The anisotropic regions may be located deep.

©2019. Japan Geoscience Union. All Right Reserved.

On the estimation of G discontinuity in the oceanic upper mantle using ScS reverberations

*Jumpei Maruyama[1], Hitoshi Kawakatsu[1], Nozomu Takeuchi[1]

1. University of Tokyo, Earthquake Research Institute

On the upper mantle shear wave velocity structure in the northwestern Pacific, there is a disagreement between the estimations using ScS reverberations (Bagley et al. 2009) and Rayleigh waves (Isse et al., 2019). This may be ascribed to the difference between the sensitivities of these waves to η_κ, the new fifth parameter of VTI (Kawakatsu, 2016), and reflect a characteristic of anisotropy in the oceanic lithosphere-asthenosphere system (LAS).

The method used by previous work (Revenaugh & Jordan, 1991) employs two-step analysis: 0th order analysis for whole mantle parameters and 1st order analysis for the characteristics of mantle discontinuities. Since this method was introduced to investigate the land area of the western circum-Pacific, there has been no detailed verification if it is compatible for the oceanic area whose upper mantle structure significantly differs from that of the continental area. We applied a simplified analysis method to full wave synthetic waveforms generated for an oceanic model with G, and revealed that the conventional method might fail in estimating the upper mantle structure and the whole mantle quality factor Q because of a strong reflected wave from G.

We will attempt to improve ScS reverberation analysis method and to compare its result for the northwest Pacific area with the existing model.

Keywords: ScS reverberations, G discontinuity, lithosphere-asthenosphere system, northwest Pacific

©2019. Japan Geoscience Union. All Right Reserved.

Short-period body wave (1-3 Hz) extraction from ambient noise records observed at seafloor and borehole in the Nankai subduction zone

*Takashi Tonegawa[1], Toshinori Kimura[1]

1. Research and Development center for Earthquake and Tsunami, Japan Agency for Marine-Earth Science and Technology

In the Nankai subduction zone, a cabled-network, named DONET (Dense Oceanfloor Network system for Earthquakes and Tsunamis), and borehole stations connected to the DONET have been constructed. The station spacing of DONET is 15-20 km, but, corporating it with borehole sensors, some of station pairs have station spacing less than 15 km. We attempted to extract body waves by applying cross correlation analysis to ambient noise records observed at the southern part of those stations, because borehole sensors have constructed near the trough.
As a result, we found eight pairs showing P wave in the cross correlation functions (CCFs) at frequencies of 1–3 Hz, which emerged before T-wave. In the case of station spacing less than 5 km (2 pairs), P wave extraction required only one-day stacking of ambient noise records, but other pairs required 10–30 days. Although the reason for unstable retrieval on the pairs and time periods for stacking is still under debate, the retrieved P-wave was stable over the observation periods.

Keywords: Seismic interferometry, ambient noise, body wave

©2019. Japan Geoscience Union. All Right Reserved.

Characteristics of T-wave envelopes observed by S-net

*Kentaro Emoto[1], Hisashi Nakahara[1]

1. Graduate School of Science, Tohokuk University

S-net enables us to access continuous sea-floor network observation data. Different from observed data in the inland area, the strong signal of the T-wave appears following the P- and S-waves in the seismograms recorded by S-net stations. T-wave is the acoustic wave propagating in the ocean. The low-velocity layer called SOFAR channel efficiently delivers the T-wave to distant stations. Owing to this property, T-wave has been used to monitor nuclear tests and activities of submarine volcanoes [Okal, 2008]. The pulse width and the amplitude of the T-wave can be used as a proxy to distinguish the explosion source and the natural earthquake [Talandier & Okal, 2001]. The rise time of the T-wave and the amplitude ratio of the T-wave and the body wave is related to the focal depth [Yang & Forsyth, 2003; Dziak et al., 2005; Wech et al., 2018]. These features were derived from observations of the T-wave at distant stations. On the other hand, we now become able to investigate the detailed process of the conversion between seismic waves and T wave because we can analyze the T-wave generated by local earthquakes by using the S-net. In this study, we summarize the characteristics of envelopes of T-waves recorded by S-net stations.

We calculate envelopes of T-waves by summing squared three components velocity seismograms band-passed in the frequency range of 8-16 Hz. The duration of the envelope is characterized by $\tau_{1/3}$ or T_{rms} which do not depend on the onset, because the onset of the T-wave is gradual and sometimes buried in the S-wave coda. $\tau_{1/3}$ is the duration during which the amplitude is higher than the one-third of the peak. T_{rms} corresponds to the standard deviation of the envelope. The strength of the T-wave is defined by the TPEF (T-phase energy flux) [Okal et al., 2003].

The propagation velocity is about 1.5 km/s in general, but it is sometimes higher in deeper stations. The onset is not clear and the amplitude gradually increases to the peak. Different from the envelope of the seismic wave which shows the long coda compared to the rise time, the time scales of the increase and the decrease of the T-wave are almost the same. This indicates that the generation process is more dominant than the scattering effect in the propagation process. However, the scattering effect also exists, because the T_{rms} increases with the propagation distance. This result is different from the observation in the relatively flat bathymetry area [Yang & Forsyth, 2003]. $\tau_{1/3}$ in the shallow station is smaller than that in the deeper station, although it shows a large variation. Regarding the energy of the T-wave, TPEF is larger in the deeper stations. This is because the T-wave is reflected by the up-slope of the ocean trench and enough energy can't reach the shallower stations. T-waves generated by the earthquakes near the triple junction mainly propagates along the trench. The TPEF shows a power-law decay with distance. The power law exponent varies from -1 to -6 depending on the source location. Outer rise earthquakes generate strong T-wave compared to inter- and intra-plate earthquakes. This is because the T-waves converted at the down-slope of the trench enter the SOFAR channel with lower incident angles and are efficiently trapped. The conversion point for the case of the intra-plate earthquake whose focal depth is about 100 km is located around the trench. The seismic wave traveling along the slab is converted to the acoustic wave at the trench. This conversion shows strong directivity.

©2019. Japan Geoscience Union. All Right Reserved.

As we mentioned above, T-wave recorded by the S-net stations is strongly affected by the bathymetry and the Earth structure. The modeling of the T-wave by considering both the elastic and the seawater media is necessary to correctly model the T-wave envelopes. By modeling the characteristics observed in this study, we can understand the details of the conversion process between the elastic and acoustic waves.

Acknowledgement

We used seismograms recorded by S-net managed by National Research Institute for Earth Science and Disaster Resilience (NIED).

Keywords: T-wave, Envelope, S-net

©2019. Japan Geoscience Union. All Right Reserved.

Reverse time reflection imaging of active and passive seismic data with ocean-bottom seismographs

*Kazuya Shiraishi[1], Takao Nibe[2], Yasuhiro Yamada[1]

1. Japan Agency for Marine-Earth Science and Technology, 2. Japan Petroleum Exploration Co. Ltd.

Introduction

In most case of crustal seismic surveys or earthquake observations using ocean-bottom seismometers, however, because receiver spacing is generally large in the wide range survey/observation, technical improvements of imaging methods are required to interpolate the lack of subsurface imaging area. On the other hand, high-dense and continuous seismic (earthquake) observation using new and existing optic fiber cables have been advancing. Development of an efficient imaging method is also necessary to utilize the enormous data. Reverse time migration (RTM) in reflection seismic exploration is one of effective seismic imaging techniques for complex subsurface structures with reconstructing full wavefield. In this study, we developed reverse time reflection imaging method which is available in active seismic survey and passive seismic observation, and we conducted a field data application and a numerical feasibility study.

Method

A. basic RTM: source-to-receiver pairs

In case of active survey with artificial seismic sources or a passive observation with accurate source locating, basic imaging principle using primary reflections between the sources and receivers is available. In the basic reverse time reflection imaging, reflected waves are focused on subsurface imaging points by a temporal integration of product between forward-extrapolated wavefields from source and backward-extrapolated wavefields of the recorded seismic data from receiver points.

B. modified RTM: receiver-to-receiver (source-to-source) pairs

We propose a modified reverse time reflection imaging method in passive seismic survey without determining source information. Both forward and backward wavefield extrapolations are performed from all receiver locations with the recorded seismograms, and the surface-reflected multiple reflections are focused on the subsurface imaging points as pseudo-primary reflections. Based on source-receiver reciprocity, this method can be applied to source-to-source pairs to use multiple reflections in airgun-OBS surveys.

Case study

(1) Airgun-OBS survey data in the Nankai Trough

We applied the proposed method to a 2D wide-angle reflection survey data acquired along 170 km survey line (200 m spacing of airgun shots, and 1 - 10 km spacing of OBSs) in the Nankai Trough. In wavefield reconstruction in the imaging process, sources and receivers are exchanged based on source-receiver reciprocity. A final reflection profile can be obtained by stacking two results derived from the primary reflections from OBS to airgun locations with the basic RTM method and from the multiple reflections between different airgun locations with the modified RTM method. Deep structures including the subducting plate and its relationship with old and young accretionary prisms are imaged with long offset reflections. Shallow structures are also clearly shown including sea floor and topographic relief of the base surface of sedimentary basin without lack of imaging area.

(2) Numerical simulation of earthquake observation

We tested reflection imaging with the modified RTM method by using numerical simulation data of both on-land and ocean-bottom earthquake observation. There is a big difference on a boundary condition (i.e. presence of a water layer above receivers) between the ocean-bottom and on-land observation. Multiple

©2019. Japan Geoscience Union. All Right Reserved.

reflections due to the water layer is significant in the ocean-bottom observation. We confirmed that reflection imaging is possible from passive observations both of the on-land and ocean-bottom seismometers with the modified RTM method. The multiple reflections are helpful to illuminate subsurface reflectors more effectively in the ocean-bottom observation in case of spars receiver deployment.

Acknowledgements
This research was supported by JAMSTEC innovation awards Houga research program.

Keywords: reflection imaging, reverse time migration, ocean-bottom seismograph

©2019. Japan Geoscience Union. All Right Reserved.

[J] Poster | S (Solid Earth Sciences)：S-SS Seismology

Tue. May 28, 2019 5:15 PM - 6:30 PM JST | Tue. May 28, 2019 8:15 AM - 9:30 AM UTC | Poster Hall International Exhibition Hall8, Makuhari Messe_30

[S-SS11] Seismic wave propagation: Theory and Application

convener:Kiwamu Nishida(Earthquake Research Institute, University of Tokyo), Kazuya Shiraishi(Japan Agency for Marine-Earth Science and Technology), Takao Nibe(JAPEX), Kaoru Sawazaki(National Research Institute for Earth Science and Disaster Resilience)

Seismic wave propagation provides rich information of earth's heterogeneities and the excitation sources. In order to extract the information, integrated studies are needed among mathematical/numerical studies based on the wave theory, miniature physical experiments using rock specimens, and practical data analyses. Furthermore, it is greatly beneficial to conduct comparative studies of various kinds of waves, such as elastic, acoustic, traveling ionospheric disturbances, and oceanic waves. This session widely invites presentations about the theories and applications related to seismic and other geophysical waves.

[SSS11-P01] Estimation of Love wave phase velocity based on array analysis in the northern Tokyo bay area : Numerical experiments using synthetic seismograms

*Kaori Shimazu[1], Kazuo Yoshimoto[1], Shunsuke Takemura[2] (1.Graduate School of Nanobioscience, Yokohama City University, 2.National Research Institute for Earth Science and Disaster Resilience)

[SSS11-P02] Similutanious estimation of amplitude and travel time variation in the transfer function with ACROSS

*Shuhei Tsuji[1], Koshun Yamaoka[1], Takahiro Kunitomo[1], Toshiki Watanabe[1], Ikuta Ryoya[2] (1.Graduate School of Environmental Studies, Nagoya University, 2.Faculty of Science, Shizuoka University)

[SSS11-P03] Temporal variation in travel time of P and S-waves using ACROSS

*rina suzuki[1], Koshun Yamaoka[2] (1.Graduate School of Environmental Studies, Nagoya University, 2.Earthquake and Volcano Research Center,Graduate School of Environmental Studies,Nagoya University)

[SSS11-P04] Inversion analysis of S coda wave envelope based on radiation transfer theory - Estimation of heterogeneous structure of Izu Oshima volcano -

*Takahiro Ueda[1] (1.Department of Geophysics, Graduate School of Science, Tohoku University)

[SSS11-P05] Strong motion characteristics at Nagomi-machi, Eta, during the northern Kumamoto pref. earthquake of Jan. 3rd, 2019

*Tomotaka Iwata[1], Kimiyuki Asano[1], Masayuki Yoshimi[2], Takeshi Sugiyama (1.Disaster Prevention Research Institute, Kyoto University, 2.Geological Survey of Japan, AIST)

[SSS11-P06] **Effects of the heterogeneous crustal structure on the amplitude fluctuation of high-frequency seismic waves**

*Kazuo Yoshimoto[1], Shunsuke Takemura[2] (1.Graduate School of Nanobioscience, Yokohama City University, 2.National Research Institute for Earth Science and Disaster Resilience)

[SSS11-P07] Long-duration long-period ground motion in Hokkaido during off-Tohoku earthquakes (2) Roles of crust and Pacific slab

*Shinako Noguchi[1], Takuto Maeda[2], Takashi Furumura[3] (1.Association for the Development of Earthquake Prediction, 2.Faculty of Science and Technology, Hirosaki University, 3.Earthquake Research Institute, The University of Tokyo)

[SSS11-P08] Measuring the NCF dispersion without the long inter-station distance limitation – a new method based on hybrid peak time matching

*Ying-Nien Chen[1], Yuancheng Gung[2], Ling-Yun Chiao[3] (1.Institute of Seismology, National Chung Cheng University, Taiwan., 2.Department of Geosciences, National Taiwan University, Taipei, Taiwan., 3.Institute of Oceanography, National Taiwan University, Taipei, Taiwan.)

[SSS11-P09] Dynamic Triggering Earthquakes Exploration by Sonification of Seismograms

*Takahiko Uchide[1], Yota Morimoto[2], Masaki Matsubara[3] (1.Research Institute of Earthquake and Volcano Geology, Geological Survey of Japan, National Institute of Advanced Industrial Science and Technology (AIST), 2.Institute of Sonology, Royal Conservatory of the Hague, 3.University of Tsukuba)

[SSS11-P10] The effect of P-wave velocity on the ellipticity of Rayleigh waves in a transversely isotropic medium

*Shun Fukushima[1], Kiyoshi Yomogida[1] (1.Hokkaido University,Graduate school of Science,Department of Natural History Sciences,Seismology Laboratory)

[SSS11-P11] Time series analyses of amplitude of the Earth's background free oscillations

*Ryuichi Kunugi[1], Naoki Suda[1] (1.Hiroshima University)

[SSS11-P12] Regional shear waves from an unusually deep earthquake beneath Ogasawara Islands: 660 km discontinuity and anisotropy

*Keiko Kuge[1] (1.Department of Geophysics, Graduate School of Science, Kyoto University)

[SSS11-P13] On the estimation of G discontinuity in the oceanic upper mantle using ScS reverberations

*Jumpei Maruyama[1], Hitoshi Kawakatsu[1], Nozomu Takeuchi[1] (1.University of Tokyo, Earthquake Research Institute)

[SSS11-P14] Short-period body wave (1-3 Hz) extraction from ambient noise records observed at seafloor and borehole in the Nankai subduction zone

*Takashi Tonegawa[1], Toshinori Kimura[1] (1.Research and Development center for Earthquake and Tsunami, Japan Agency for Marine-Earth Science and Technology)

[SSS11-P15] Characteristics of T-wave envelopes observed by S-net

*Kentaro Emoto[1], Hisashi Nakahara[1] (1.Graduate School of Science, Tohokuk University)

[SSS11-P16] Reverse time reflection imaging of active and passive seismic data with ocean-bottom seismographs

*Kazuya Shiraishi[1], Takao Nibe[2], Yasuhiro Yamada[1] (1.Japan Agency for Marine-Earth Science and Technology, 2.Japan Petroleum Exploration Co. Ltd.)

Estimation of Love wave phase velocity based on array analysis in the northern Tokyo bay area : Numerical experiments using synthetic seismograms

*Kaori Shimazu[1], Kazuo Yoshimoto[1], Shunsuke Takemura[2]

1. Graduate School of Nanobioscience, Yokohama City University, 2. National Research Institute for Earth Science and Disaster Resilience

In the Kanto sedimentary basin, long-period ground motions have been frequently observed during shallow moderate-to-large earthquakes [e.g. Yoshimoto and Takemura (2014)]. Strong long-period ground motions, which are caused by surface waves, complicatedly propagate within the Kanto basin due to 3D structures of low-velocity sediments and bedrock topography [e.g., Furumura and Hayakawa (2007)]. For the precise prediction of long-period ground motions, we should investigate propagation characteristics of surface waves and subsurface structure within the Kanto basin. Array analysis using dense seismic stations in the Kanto basin may be useful to capture propagation characteristics of surface waves and structural properties. In this study, as a basic study for investigating a seismic velocity structure of the Kanto sedimentary basin, we applied a beamforming technique to the seismograms synthesized based on FDM simulations.

We selected shallow moderate earthquakes for our beamforming analysis, e.g. the northern Ibaraki prefecture earthquake on March 19, 2011 (Mw 5.8), the northern Tochigi prefecture earthquake on February 25, 2013 (Mw 5.8), and the northern Nagano prefecture earthquake on November 22, 2014 (Mw 6.3). We synthesized velocity seismograms based on the FDM simulations using a velocity structural model SBVSM [Masuda *et al.*(2014); Takemura *et al.* (2015)]. Virtual seismic stations were distributed at an interval of 750 m in the range of 35.5˚N to 35.9˚N and 139.4˚E to 139.9˚E. Our FDM simulations can evaluate ground motions for periods longer than 4 s. In our array analysis using a three-component beamforming [Riahi *et al.*(2013)], the size of the small local array was adjusted according to the analyzed period of Love waves. The analysis was conducted on the six periods: 5.9, 6.4, 7.3, 8.5, 10.2 and 12.8 s. We analyzed the seismograms for time window of 51.2 s, including the maximum amplitude of energy envelope for horizontal components.

By comparing the estimated phase velocities by our array analysis with theoretical ones from local 1D structure of SBVSM, we confirmed that the phase velocities of Love waves propagating in the large sedimentary basin are successfully obtained. Observed dispersion curves show clear normal dispersions. At the period of 5.9 s, the phase velocity was estimated stably for seismograms of all earthquakes. This period corresponds to the dominant period of long-period ground motions within the Kanto sedimentary basin [e.g. Yoshimoto and Takemura (2014)]. We also found that the phase velocity tends to be estimated stably in large PGV areas of long-period ground motions. These results imply that the propagation of surface waves may characterize the magnitude of long-period ground motions. The other results in detail will be exhibited in our presentation.

Acknowledgement

FDM simulations of seismic wave propagation were conducted on the Earth Simulator of the Japan Agency for Marine-Earth Science and Technology. F-net MT solutions were provided by the National Research Institute for Earth Science and Disaster Resilience.

©2019. Japan Geoscience Union. All Right Reserved.

Keywords: Love wave, Kanto sedimentary basin, array analysis, phase velocity, FDM simulation

©2019. Japan Geoscience Union. All Right Reserved.

Similutanious estimation of amplitude and travel time variation in the transfer function with ACROSS

*Shuhei Tsuji[1], Koshun Yamaoka[1], Takahiro Kunitomo[1], Toshiki Watanabe[1], Ikuta Ryoya[2]

1. Graduate School of Environmental Studies, Nagoya University, 2. Faculty of Science, Shizuoka University

Summary

We developed a method for simultaneous estimation of deviation of the amplitude and the travel time of the transfer functions obtained by an artificial seismic source, ACROSS.

Background

Variation of the amplitude is important information for monitoring the strength of the fault plane (e.g. Nagata et al, 2008). However, studies on the variation of propagation properties were mainly discussing the deviation of the travel time (e.g. Ikuta et al., 2002; Hobiger et al., 2016). The conventional method using the signal envelope is affected by the noise level, which is the shortcoming of the method. Thus, we developed a new method to make a simultaneous estimation of the deviation of both the amplitude and travel time.

Method

The simultaneous estimation method is basically a maximum likelihood estimation using a least square method. We adopt the least square method for deviation functions which are obtained by dividing each transfer function by averaged transfer function on the complex plane in the frequency domain. This is incontrast to the cross-spectrum method which was commonly used for calculation of the deviation of the travel time. In our method, the amplitudes as well as the deviation of travel time is calculated similarly to the cross-spectrum method. We estimated the deviation of the amplitudes and travel times as a nonlinear model fitting problem. We made a model of the deviation function with an assumption that the deviation of the amplitude and travel time is independent of frequency. We searched for the best fitting parameters so that minimizing the sum of the square lengths on the complex plane by grid search. As a result, we could estimate the deviations for smaller SNR data. We also could estimate the errors of the obtained deviations.

Results

We applied the method to High Sensitivity Seismograph Network Japan (Hi-net) stations around an ACROSS seismic source which is deployed at Toki City, the middle part of Honshu Island, Japan. The estimated deviation of the travel time with this method generally coincides with the results with the conventional cross spectrum method. When the data has low SNR, the average of the deviation of the amplitude did not become one due to averaging in the complex domain. This is because the least square fitting is made on the complex plane which does not mathematically guarantee the averaging of amplitude.

Keywords: Deviation of the amplitude, Deviation of the tarvel time, velocity change, Artificial seismic source, ACROSS

©2019. Japan Geoscience Union. All Right Reserved.

Temporal variation in travel time of P and S-waves using ACROSS

*rina suzuki[1], Koshun Yamaoka[2]

1. Graduate School of Environmental Studies, Nagoya University, 2. Earthquake and Volcano Research Center,Graduate School of Environmental Studies,Nagoya University

We analyzed the temporal variation of travel time of P and S wave using observation data for one year by an artificial seismic source ACROSS which can generate controlled vibration repeatedly. In this study, we used a new type of ACROSS called ACR2014 that is installed in Toyohashi City, Aichi Prefecture. This ACROSS source can excite vertical vibration as well as horizontal vibration by rotation of the weight around the horizontal rotation axis to excite P wave efficiently. We used records at three observation stations called NU.MIK, N.THNH, and N.MKBH installed around ACR2014 and calculated transfer functions. From the components of transfer function, we chose the vertical component by vertical excitation and horizontal component by horizontal excitation for calculation of travel time of P and S wave, respectively. We calculated travel time variations from these components of transfer function using cross spectrum method. In this calculation, a window ranging 0.2 to 0.3 seconds was applied to the P and the S wave part, respectively. We compared the travel time variations with the precipitation data of nearby AMeDAS at Toyohashi and Mikkabi. In NU.MIK, short-term change with a step-like delay and following recovery occurred in both P and S waves at rains. The tendency of this recovery was different between the P and S wave. On the other hand, the long-term variation differs between the P and S waves at some observation stations. We interpreted the influence of rainfall on these short-term and long-term travel time variations, using a theoretical effect of the crack density and fluid saturation on the seismic velocity change. The observed difference in the P and S wave change can be explained with the difference in the response of crack density and fluid saturation between P and S waves. The long-term travel time variations in the P and S waves can be interpreted by assuming that the fluid saturation increases in the periods with high precipitation and decrease in the periods with low precipitation. The short-term change with the difference of the recovery between the P and S wave can be interpreted in similar way as the long-term variation.

Keywords: travel time variation, velocity change

©2019. Japan Geoscience Union. All Right Reserved.

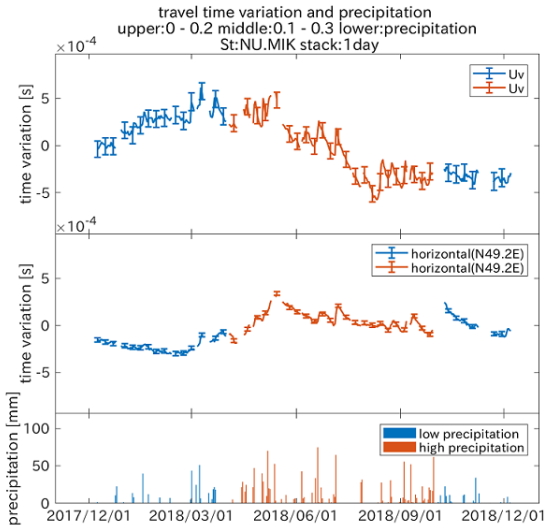

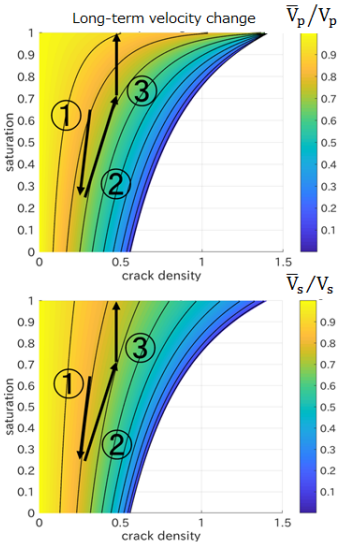

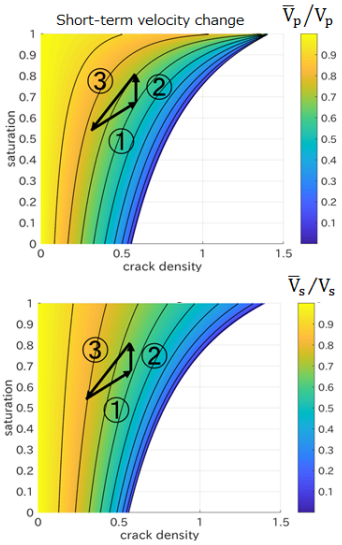

©2019. Japan Geoscience Union. All Right Reserved.

Inversion analysis of S coda wave envelope based on radiation transfer theory - Estimation of heterogeneous structure of Izu Oshima volcano -

*Takahiro Ueda[1]

1. Department of Geophysics, Graduate School of Science, Tohoku University

It is well known that short period seismic waves are strongly influenced by heterogeneous structures in the crust or shallow structures. Analyses using seismic sources near the ground surface such as artificial sources and seismic wave interferometry have reported that strong heterogeneity appears remarkably due to shallow sediments of volcanoes. On the other hand, there are few studies in which volcano-tectonic earthquakes are used, and the characteristics of heterogeneous structure down to deep regions (10 km) of the volcanoes have not been well investigated. In this study, based on the Multiple Lapse Time Window method (Fehler et al. 1992) based on radiative transfer theory, we evaluate heterogeneity of the volcano structures, using an inversion method to obtain the intrinsic attenuation value, scattering attenuation value, the energy radiated from the source, and the site amplification factor, a of the Izu Oshima volcano. We use the seismic waveforms recorded at 4 V-net stations at Izu Oshima. From January 2014 to January 2018, events of M1.5 to M3.5, 150 earthquakes within 10 km deep are analyzed. Bandpass filters of 1-2 Hz, 2-4 Hz, 4-8 Hz, and 8-16 Hz bands are applied, and the envelope waveforms of the direct waves and coda waves of S waves are obtained in each frequency band. The Green’ s function is calculated based on the radiative transfer theory of the S wave multi isotropic scattering. The amplitude is expressed by the product of the site amplification factor, the energy radiated from the source, and Green’ s function. We fit the observation envelope with the theory and determine the internal attenuation and the scattering attenuation as well as site factors and source energy.
The results show that the scattering attenuations are 0.0393, 0.0210, 0.0027, 0.0001 in the 1-2 Hz, 2-4 Hz, 4-8 Hz, and 8-16 Hz bands, respectively, and the intrinsic attenuation was 0.0054, 0.0056, 0.0029, 0.0006. The average values of Japan's crustal structure (Calocoré and Sato, 2010) are almost same with intrinsic attenuation of this study, while the value of the scattering attenuation is larger by about 10 times in the low frequency region around 1.5 Hz. In addition, it is smaller than the results for very shallow part (Yamamoto and Sato., 2010, Hirose et al., 2019) by 1 to 2 orders of magnitude.
Based on the above results, the scattering attenuation parameter is dominant in Izu Oshima compared to the Japanese crust, compared to the internal damping, which is in harmony with the results of the previous study that the scattering damping is large around the active volcano , And it seems that the influence of the minute heterogeneous structure of the shallow part of the crust appeared strongly. In addition, theoretical envelope was well obtained by the envelope inversion method proposed in this research, and it was shown that it is effective as a method to evaluate the radiation energy and the radiation energy of the epicenter.

Keywords: coda wave, volcanic structure

©2019. Japan Geoscience Union. All Right Reserved.

Strong motion characteristics at Nagomi-machi, Eta, during the northern Kumamoto pref. earthquake of Jan. 3rd, 2019

*Tomotaka Iwata[1], Kimiyuki Asano[1], Masayuki Yoshimi[2], Takeshi Sugiyama

1. Disaster Prevention Research Institute, Kyoto University, 2. Geological Survey of Japan, AIST

We estimate ground motion characteristics of Eta, Nagomi-machi, Kumamoto, during the 2019 Jan. 3rd northern Kumamoto earthquake (MJ5.5). The JMA seismic intensity of 6weak was observed at the site. Before this event, we have conducted the microtremor array measurement and obtained that the thin (about 20m) superficial layer with a S-wave velocity of less than 0.2km/s. We also estimated site amplification factor by the spectral inversion method (Somei et al., 2018). The site amplification factor shows the predominant period of about 0.4s for weak motion data. After the mainshock, we have conducted additional microtremor array measurement to give a more in-detail information in the area and single station H/V observations just beside of the seismic intensity meter and outside of the building for checking the effects of station setting of this site. In this moment, there is no significant effect of the station setting because of the similar H/V spectral ratio between the site and the one outside of the building in this period range. We also noticed that the predominant period of observed horizontal motions of the mainshock is about 0.5s, that is a little bit longer than that of the site effect for the weak motions. This would be caused by the non-linear behavior of the superficial layer during the strong shaking. Strong motion data are provided by JMA and Kumamoto prefecture. Microtremor observations and spectral inversion were conducted by the Comprehensive Research Project for the major active faults related to The 2016 Kumamoto Earthquake (2016FY-2018FY), Mext.

Keywords: 2019 Northern Kumamoto prefecture earthquake , Eta, Nagomi-machi

©2019. Japan Geoscience Union. All Right Reserved.

Effects of the heterogeneous crustal structure on the amplitude fluctuation of high-frequency seismic waves

*Kazuo Yoshimoto[1], Shunsuke Takemura[2]

1. Graduate School of Nanobioscience, Yokohama City University, 2. National Research Institute for Earth Science and Disaster Resilience

It is considered in the seismic scattering analyses that crustal heterogeneity may be modeled by combining deterministic heterogeneity and stochastic heterogeneity. A simple technique of this modeling adopts a uniform averaged structure model (background structure model) for deterministic heterogeneity and a uniform random heterogeneity model for stochastic heterogeneity. Although this technique may be adequate for the seismic scattering analysis with a small target area, the simplification might lead erroneous results if the target area of the analysis becomes large. In this study, we investigated the effect of the deterministic crustal heterogeneity on the amplitude fluctuation of high-frequency (0.5-4 Hz) seismic waves on the basis of finite-difference method (FDM) simulations.
We conducted FDM simulations of shallow moderate earthquakes, including a target earthquake occurred on 25 November 2011 at a depth of 14 km beneath the Chugoku region, western Japan. Our simulation model covered a volume of 256×256×80 km^3, which was discretized by a uniform grid spacing of 0.05 km. Technical details are the same as those of Takemura et al. (2017). The background velocity structure was referred from the Japan Integrated Velocity Structure Model (JIVSM; Koketsu et al., 2012). Small-scale random velocity heterogeneity (Takemura et al., 2017) was superposed on the crust of the JIVSM. We adopted a double-couple point source with a focal mechanism reported by the F-net MT catalog. This model setting well reproduced observed high-frequency seismograms at the Hi-net borehole stations (Takemura et al., 2017). Because we employed a finer FDM grid compared to previous simulations (Takemura et al., 2017), our FDM simulation can evaluate seismic wave propagation for higher (~ 8 Hz) frequencies. To investigate fluctuation of seismic amplitudes, we evaluated peak ground velocity (PGV) from filtered synthetic seismograms.
Simulation results of a strike-slip source model showed that the cross-shaped (four-lobed) large PGV distribution in the epicentral area becomes unclear in the surrounding area as the hypocentral distance increases. Theoretical and empirical models of high-frequency seismic amplitudes also predicted a similar characteristic of apparent radiation pattern (Yoshimoto et al., 2015; Takemura et al., 2016). Although this phenomenon, which is mainly caused by the seismic scattering due to random heterogeneity, showed azimuthal symmetry, the symmetry was found to be broken for a certain focal depth condition. Our additional simulations using different properties of background structure model indicated that, at least in our target region, the reflection due to a small velocity contrast of the Conrad discontinuity (about 10% in JIVSM) may cause the large amplitude fluctuation of high-frequency seismic waves in the surrounding area of the epicenter (distance > 40 km).

Keywords: High-frequency seismic ground motion, Amplitude fluctuation, Random crustal heterogeneity, Conrad discontinuity, Seismic ground motion simulation

©2019. Japan Geoscience Union. All Right Reserved.

Long-duration long-period ground motion in Hokkaido during off-Tohoku earthquakes (2) Roles of crust and Pacific slab

*Shinako Noguchi[1], Takuto Maeda[2], Takashi Furumura[3]

1. Association for the Development of Earthquake Prediction, 2. Faculty of Science and Technology, Hirosaki University, 3. Earthquake Research Institute, The University of Tokyo

Anomalously large, long-time-lasting long-period later phases were observed widely in Hokkaido, Japan during moderate to large (M>6.5) earthquakes occurred at off-Tohoku Pacific earthquakes. Such long-period signals spread widely over Hokkaido not only at deep Ishikari basin as reported by Noguchi et al. (2017; JpGU). In this study we discuss new mechanisms to generate this later phase in addition to well recognized deep sediment effect by means of 3D FDM simulations of seismic wave propagation using 3D heterogeneous subsurface structure model.

This long-period later phase caused by off Tohoku earthquakes appeared at most F-net stations in Hokkaido except for a few stations at southwestern Hokkaido. However, these later phases did not appear from inland earthquakes, outer-rise earthquakes and earthquakes occurred near Hokkaido. Dominant period of this later phases lay within the range between 15 s to 25 s, varying among earthquakes. The later phase in transverse component expected to be Love wave showed longer period and appeared earlier than that in radial and vertical components expected to be Rayleigh wave. Both waves showed normal dispersion.

The FDM simulations of seismic wave propagation in 3D heterogeneous crust and mantle structure was conducted using OpenSWPC (Maeda et al., 2017). This simulation model consists of sea water, topography, sediments and subducting plates based on Japan Integrated Velocity Structur Model (JIVSM; Koketsu et al., 2012) and the depth of Moho and Pacific slab is based on Matsubara et al. (2017) and Kita et al. (2010), respectively.

We confirmed two distinct phenomena from the FDM simulations as follows; Firstly, long tail of Rayleigh wave (< 3 km/s) propagating north and southward at western-side of Japan trench following the main packet of surface wave were generated. Then the long wavetrains spreading over Hokkaido were generated by conversion from the Rayleigh wave northward along trench at the edge of deep sediment at off Ishikari. Secondly, Love wave appearing at the junction of Japan trench and Kuril trench extended over Hokkaido in earlier time than the converted Rayleigh wave.

We investigated the phase and group velocities for Rayleigh wave and Love waves from off Tohoku to Hokkaido; we found a lower-wavespeed zone of group and phase velocities for Rayleigh wave at period around 20 s guiding Rayleigh wave along the west side of Japan trench, where was formed by the subsurface low-velocity layer covering over the Pacific slab. Such low-wavespeed zone was not appeared for Love wave. However, strong velocity contrast between the Pacific side and Japan side of trench due to different crustal thickness was confirmed which bended the ray of Love wave toward low-velocity side. Thus, Love waves traveling along low-velocity side released seismic energy toward Hokkaido at the junction of Japan trench and Kuril trench, producing anomalously large and long-time lasting long-period ground motions.

We conclude that the long period later phase observed over Hokkaido during off Tohoku earthquakes

©2019. Japan Geoscience Union. All Right Reserved.

were caused by the deep subsurface structure including crustal thickness and subducting slab in addition to deep sediments at off Ishikari.

Keywords: Long period ground motion, Subduction zone, Wave propagation simulation

©2019. Japan Geoscience Union. All Right Reserved.

Measuring the NCF dispersion without the long inter-station distance limitation –a new method based on hybrid peak time matching

*Ying-Nien Chen[1], Yuancheng Gung[2], Ling-Yun Chiao[3]

1. Institute of Seismology, National Chung Cheng University, Taiwan., 2. Department of Geosciences, National Taiwan University, Taipei, Taiwan., 3. Institute of Oceanography, National Taiwan University, Taipei, Taiwan.

Over the past decade, the probing of Earth structures using seismic ambient noises has been widely used by seismologists and is now a well-developed technique. Based on an implicit high-frequency approximation, the consensus is that the noise cross-correlation function (NCF) of continuous seismic records resembles the Green’ s Function (GF) of the far-field surface wave between sensors. This perspective leads to the application of the long interstation distance criterion in the dispersion measurements, and, accordingly, much of the low-frequency content in the NCF is rejected. Herein we show that, for a far-field source, the NCF used in most surface wave studies should not be considered as representative of the empirical Green’ s Function (EGF); instead, it is simply the interference product between sensors. We present a theoretical derivation of an explicit definition for a “high-frequency approximation” and clarify the relationship between the NCF and the EGF. Furthermore, we propose a new method to measure the NCF dispersion, in which the phase velocity is estimated by matching the peak delay time observed in the time domain NCF to the one predicted by the theoretical complex NCF signals. In this hybrid peak time matching technique, the long interstation distance is no longer a required condition and phase velocities can be determined more precisely at lower frequencies. Therefore, this permits the investigation of deeper structures using noise data.

Keywords: phase velocity measurement, Empirical Green’ s Function, ambient noise

©2019. Japan Geoscience Union. All Right Reserved.

Dynamic Triggering Earthquakes Exploration by Sonification of Seismograms

*Takahiko Uchide[1], Yota Morimoto[2], Masaki Matsubara[3]

1. Research Institute of Earthquake and Volcano Geology, Geological Survey of Japan, National Institute of Advanced Industrial Science and Technology (AIST), 2. Institute of Sonology, Royal Conservatory of the Hague, 3. University of Tsukuba

We have been proposing the sonification of seismograms for exploring dynamic triggering earthquakes (Uchide et al., JpGU, 2016, 2018; Matsubara et al., 2016). The seismic sonification for the 2011 Tohoku-oki earthquake successfully revealed a dynamic triggering event in the Hida area, Central Japan. For the ease of the seismic sonification for seismologists, we are developing the Sonification of Seismograms (SoS) system (Uchide et al., JpGU, 2018), which assigns sound whose amplitude and tone correspond to the maximum absolute value and the number of zero-crossings of seismograms in short time windows.

This study investigates dynamic triggering events by recent major earthquakes using the SoS software. In the case of the 2011 Tohoku-oki earthquake, the dynamic triggering event in the Hida area was M 4.2 (Ohmi et al., 2012) which is relatively large. Identification of smaller dynamic triggering events may be a challenge. Limiting areas of stations for the sonification help us identify where a dynamic triggering event may or may not occur.

In front of our poster, we will provide the opportunity to listen sonified sounds and demonstrate the interactive sonification process using the SoS.

Acknowledgement

We used the Global CMT Catalog and seismic data from Hi-net of NIED, seismic data from JMA, Hokkaido University, Hirosaki University, Tohoku University, the University of Tokyo, Nagoya University, Kyoto University, Kochi University, Kyushu University, Kagoshima University, and AIST. This work was supported by JSPS KAKENHI 17K14386.

Keywords: Seismograms, Sonification, Dynamic Triggering Earthquakes

©2019. Japan Geoscience Union. All Right Reserved.

The effect of P-wave velocity on the ellipticity of Rayleigh waves in a transversely isotropic medium

*Shun Fukushima[1], Kiyoshi Yomogida[1]

1. Hokkaido University,Graduate school of Science,Department of Natural History Sciences,Seismology Laboratory

The study of surface waves is one of effective approaches for the internal structure of the earth. Phase and group velocities data have ever been used, but the ellip- ticity of Rayleigh waves can be also used to infer it (e.g., Tsuboi & Saito, 1983) . The ellipticity of Rayleigh waves is defined as a V(vertical amplitude)/H(horizontal amplitude) ratio, which is more sensitive to shallow structures than the conventional phase or group dispersion data. Fundamentally, it is the same principle as strong ground motions with horizontal and vertical amplitudes of microtremors to evaluate near-surface structures easily. Tsuboi & Saito (1983) and Tanimoto & Tsuboi (2009) derived and calculated partial derivatives of ellipticity in an isotropic medium. In addition to the well-known anisotropy in the asthenosphere such as that included in PREM, the influence of a transversely isotropic medium may be important for shallow structures such as a sedimentary layer. A transversely isotropic medium has five elastic moduli (A, C , L, N .F) but propagations of surface waves can be formulated in a compact manner, similar to the isotropic case.
In this study, we first formulated partial derivatives of ellipticity in a transversely isotropic medium. In the same way as the isotropic medium, we determine the linear relationship using the variational principle and the reciprocal theorem. Then, we set an artificial eigenfunction for the boundary condition of non-zero normal stress at the surface in addition to the natural eigenfunction for the normal condition (i.e., zero stress at the surface). We then derived partial derivatives with the two kinds of eigenfuncitons combined. Several important features of PV-waves and PH-waves are revealed in comparison with those of P-waves in the isotropic case. P-waves have little effects on the ellipticity in an isotropic medium. In the transversely isotropic medium, partial derivatives of PV wave are quite different from those of PH wave with a relatively large amplitude in a shallow part. The reason of the small P-wave effect in the isotropic case comes from the sum of those of PV and PH waves of opposite signs. PH wave in a shallow part has a large positive effect on ellipticity while PV wave has a weak negative one. If there is a strongly laminated sedimentary layer near the surface, for example, the ellipticity does not vary so much, despite of small SV there. It is because the shallow PH velocity is not reduced in such a layer, in contrast with small SV and PV waves, and its partial derivatives is large and of the sign opposite to SV and PV waves. If we performed the inversion for the shallow structure with the data of ellipticity (i.e., only slightly anomalous), under the isotropic model with the dominance of SV wave velocity, the inversion result would lead to slightly small SV velocity near the surface with virtually no changes in P-wave velocity because partial derivatives in the isotropic case are large for SV but small for P wave.

Keywords: Particle motion, Transverse isotropy, Rayleigh wave

©2019. Japan Geoscience Union. All Right Reserved.

Time series analyses of amplitude of the Earth’s background free oscillations

*Ryuichi Kunugi[1], Naoki Suda[1]

1. Hiroshima University

The Earth’s background free oscillations (BFO) are slightly and continuously excited free oscillations of the solid Earth persistent even in seismically quiet periods [Nawa et al. 1998; Suda et al. 1998; Kobayashi and Nishida 1998; Tanimoto et al. 1998]. The observed modes are fundamental modes, suggesting that the excitation sources are atmospheric and oceanic disturbances [e.g. Nishida 2013]. Amplitude of BFO exhibits seasonal variations [Nishida et al. 2000]. Along with such a periodic variation, there may exist transient variations correlated with atmospheric/oceanic phenomena.

The target modes are fundamental modes ${}_0S_{22}$-${}_0S_{43}$ at frequencies between 3 and 5 mHz because they are most clearly observed in the frequency domain. We used vertical records of STS-1 broadband seismometers at 65 quite seismic stations downloaded from IRIS DMC. The data periods are from 2000 to 2017. The analysis method is mainly the same as used in Nishida et al. (2000). Continuous records were divided into 3-days records with a step of 1 day. After applying the Hanning taper, each record was converted into power spectral density (PSD) with the correction of system response. To reject noisy data, we used the data whose mean PSD values at 3-5 mHz are between 10^{-19} and 10^{-18} m^2/s^3. The remained PSDs were then stacked over all the stations to create monthly averaged PSDs. To avoid the influence of temporally changing PSD baseline due to the random background noise, we averaged the PSD values in the mode and the noise frequency bands, and then the averaged noise PSD is subtracted from the averaged signal PSD.

We used two methods of time series analysis for the statistical analysis of long-term variations in amplitude of BFO: one is based on the state-space model and the other is on the regression model. In the state-space analysis we adopted the local level model with seasonal variations, which divide time series into random noise, seasonal variations and a long-term trend. In the regression analysis we adopted the model that consist of random noise, seasonal variations and a long-term trend. We used the R packages dlm and prophet for the state-space and the regression analyses, respectively.

The result obtained in the space-state analysis shows the long-term variation with a time scale of 10 years from 2002 to 2012: the minimum is in 2002 and 2012 and the maximum is in 2008. The long-term trend obtained in the regression analysis shows almost the same characteristics: the minimums in 2000 and 2012 and the maximum in 2008. Thus, we for the first time robustly obtained the nearly 10-year variation in amplitude of BFO from the two different time-series analyses. We can utilize data of infragravity waves at frequencies between 3-30 mHz from WAVEWATCH III. We will show the result of comparison between BFO and infragravity waves in the presentation.

©2019. Japan Geoscience Union. All Right Reserved.

©2019. Japan Geoscience Union. All Right Reserved.

Regional shear waves from an unusually deep earthquake beneath Ogasawara Islands: 660 km discontinuity and anisotropy

*Keiko Kuge[1]

1. Department of Geophysics, Graduate School of Science, Kyoto University

Following a large deep earthquake beneath Ogasawara Islands on 30 May, 2015, an aftershock (mb 4.9) took place at a depth of 678 km (USGS). P and S waves from the aftershock were recorded by F-net broadband stations in Japan at distances of 1 to 18 degrees. The aftershock is small enough to neglect source effect. Here I explore structure effect on the shear wave propagation. SH waves recorded by the transverse directions in western Japan were generally characterized by a single pulse. The peaks of the SH waves tend to arrive earlier than those of the SV waves in the radial directions. The dominance of a single pulse in the SH waves can be explained by the iasp91 model with the 660 km discontinuity shallower than the aftershock. When the 660 km discontinuity is assumed to be deeper than the aftershock, additional signals predicted in radial components can apparently cause different peak time arrivals between SH and SV waves. However, in these cases, the SV peaks arrive earlier than the SH peaks, which cannot fit the observations. It is thus more likely that the observed peak time difference is attributed to anisotropy. Because signals due to crustal reflection are predicted in the radial components ~6 sec after the direct S waves, shear wave splitting parameters were carefully estimated by using initial portions of S waves. The fast directions obtained in western Japan are nearly in the east-west, which looks different from the fast direction observed for a nearby deep earthquake in the Wadati-Benioff zone. We cannot see systematically early arrivals of SH peaks from Fiji earthquakes in a similar back azimuth. The anisotropic regions may be located deep.

©2019. Japan Geoscience Union. All Right Reserved.

On the estimation of G discontinuity in the oceanic upper mantle using ScS reverberations

*Jumpei Maruyama[1], Hitoshi Kawakatsu[1], Nozomu Takeuchi[1]

1. University of Tokyo, Earthquake Research Institute

On the upper mantle shear wave velocity structure in the northwestern Pacific, there is a disagreement between the estimations using ScS reverberations (Bagley et al. 2009) and Rayleigh waves (Isse et al., 2019). This may be ascribed to the difference between the sensitivities of these waves to η_κ, the new fifth parameter of VTI (Kawakatsu, 2016), and reflect a characteristic of anisotropy in the oceanic lithosphere-asthenosphere system (LAS).

The method used by previous work (Revenaugh & Jordan, 1991) employs two-step analysis: 0th order analysis for whole mantle parameters and 1st order analysis for the characteristics of mantle discontinuities. Since this method was introduced to investigate the land area of the western circum-Pacific, there has been no detailed verification if it is compatible for the oceanic area whose upper mantle structure significantly differs from that of the continental area. We applied a simplified analysis method to full wave synthetic waveforms generated for an oceanic model with G, and revealed that the conventional method might fail in estimating the upper mantle structure and the whole mantle quality factor Q because of a strong reflected wave from G.

We will attempt to improve ScS reverberation analysis method and to compare its result for the northwest Pacific area with the existing model.

Keywords: ScS reverberations, G discontinuity, lithosphere-asthenosphere system, northwest Pacific

©2019. Japan Geoscience Union. All Right Reserved.

Short-period body wave (1-3 Hz) extraction from ambient noise records observed at seafloor and borehole in the Nankai subduction zone

*Takashi Tonegawa[1], Toshinori Kimura[1]

1. Research and Development center for Earthquake and Tsunami, Japan Agency for Marine-Earth Science and Technology

In the Nankai subduction zone, a cabled-network, named DONET (Dense Oceanfloor Network system for Earthquakes and Tsunamis), and borehole stations connected to the DONET have been constructed. The station spacing of DONET is 15-20 km, but, corporating it with borehole sensors, some of station pairs have station spacing less than 15 km. We attempted to extract body waves by applying cross correlation analysis to ambient noise records observed at the southern part of those stations, because borehole sensors have constructed near the trough.
As a result, we found eight pairs showing P wave in the cross correlation functions (CCFs) at frequencies of 1–3 Hz, which emerged before T-wave. In the case of station spacing less than 5 km (2 pairs), P wave extraction required only one-day stacking of ambient noise records, but other pairs required 10–30 days. Although the reason for unstable retrieval on the pairs and time periods for stacking is still under debate, the retrieved P-wave was stable over the observation periods.

Keywords: Seismic interferometry, ambient noise, body wave

©2019. Japan Geoscience Union. All Right Reserved.

Characteristics of T-wave envelopes observed by S-net

*Kentaro Emoto[1], Hisashi Nakahara[1]

1. Graduate School of Science, Tohokuk University

S-net enables us to access continuous sea-floor network observation data. Different from observed data in the inland area, the strong signal of the T-wave appears following the P- and S-waves in the seismograms recorded by S-net stations. T-wave is the acoustic wave propagating in the ocean. The low-velocity layer called SOFAR channel efficiently delivers the T-wave to distant stations. Owing to this property, T-wave has been used to monitor nuclear tests and activities of submarine volcanoes [Okal, 2008]. The pulse width and the amplitude of the T-wave can be used as a proxy to distinguish the explosion source and the natural earthquake [Talandier & Okal, 2001]. The rise time of the T-wave and the amplitude ratio of the T-wave and the body wave is related to the focal depth [Yang & Forsyth, 2003; Dziak et al., 2005; Wech et al., 2018]. These features were derived from observations of the T-wave at distant stations. On the other hand, we now become able to investigate the detailed process of the conversion between seismic waves and T wave because we can analyze the T-wave generated by local earthquakes by using the S-net. In this study, we summarize the characteristics of envelopes of T-waves recorded by S-net stations.

We calculate envelopes of T-waves by summing squared three components velocity seismograms band-passed in the frequency range of 8-16 Hz. The duration of the envelope is characterized by $\tau_{1/3}$ or T_{rms} which do not depend on the onset, because the onset of the T-wave is gradual and sometimes buried in the S-wave coda. $\tau_{1/3}$ is the duration during which the amplitude is higher than the one-third of the peak. T_{rms} corresponds to the standard deviation of the envelope. The strength of the T-wave is defined by the TPEF (T-phase energy flux) [Okal et al., 2003].

The propagation velocity is about 1.5 km/s in general, but it is sometimes higher in deeper stations. The onset is not clear and the amplitude gradually increases to the peak. Different from the envelope of the seismic wave which shows the long coda compared to the rise time, the time scales of the increase and the decrease of the T-wave are almost the same. This indicates that the generation process is more dominant than the scattering effect in the propagation process. However, the scattering effect also exists, because the T_{rms} increases with the propagation distance. This result is different from the observation in the relatively flat bathymetry area [Yang & Forsyth, 2003]. $\tau_{1/3}$ in the shallow station is smaller than that in the deeper station, although it shows a large variation. Regarding the energy of the T-wave, TPEF is larger in the deeper stations. This is because the T-wave is reflected by the up-slope of the ocean trench and enough energy can't reach the shallower stations. T-waves generated by the earthquakes near the triple junction mainly propagates along the trench. The TPEF shows a power-law decay with distance. The power law exponent varies from -1 to -6 depending on the source location. Outer rise earthquakes generate strong T-wave compared to inter- and intra-plate earthquakes. This is because the T-waves converted at the down-slope of the trench enter the SOFAR channel with lower incident angles and are efficiently trapped. The conversion point for the case of the intra-plate earthquake whose focal depth is about 100 km is located around the trench. The seismic wave traveling along the slab is converted to the acoustic wave at the trench. This conversion shows strong directivity.

©2019. Japan Geoscience Union. All Right Reserved.

As we mentioned above, T-wave recorded by the S-net stations is strongly affected by the bathymetry and the Earth structure. The modeling of the T-wave by considering both the elastic and the seawater media is necessary to correctly model the T-wave envelopes. By modeling the characteristics observed in this study, we can understand the details of the conversion process between the elastic and acoustic waves.

Acknowledgement

We used seismograms recorded by S-net managed by National Research Institute for Earth Science and Disaster Resilience (NIED).

Keywords: T-wave, Envelope, S-net

©2019. Japan Geoscience Union. All Right Reserved.

Reverse time reflection imaging of active and passive seismic data with ocean-bottom seismographs

*Kazuya Shiraishi[1], Takao Nibe[2], Yasuhiro Yamada[1]

1. Japan Agency for Marine-Earth Science and Technology, 2. Japan Petroleum Exploration Co. Ltd.

Introduction

In most case of crustal seismic surveys or earthquake observations using ocean-bottom seismometers, however, because receiver spacing is generally large in the wide range survey/observation, technical improvements of imaging methods are required to interpolate the lack of subsurface imaging area. On the other hand, high-dense and continuous seismic (earthquake) observation using new and existing optic fiber cables have been advancing. Development of an efficient imaging method is also necessary to utilize the enormous data. Reverse time migration (RTM) in reflection seismic exploration is one of effective seismic imaging techniques for complex subsurface structures with reconstructing full wavefield. In this study, we developed reverse time reflection imaging method which is available in active seismic survey and passive seismic observation, and we conducted a field data application and a numerical feasibility study.

Method

A. basic RTM: source-to-receiver pairs

In case of active survey with artificial seismic sources or a passive observation with accurate source locating, basic imaging principle using primary reflections between the sources and receivers is available. In the basic reverse time reflection imaging, reflected waves are focused on subsurface imaging points by a temporal integration of product between forward-extrapolated wavefields from source and backward-extrapolated wavefields of the recorded seismic data from receiver points.

B. modified RTM: receiver-to-receiver (source-to-source) pairs

We propose a modified reverse time reflection imaging method in passive seismic survey without determining source information. Both forward and backward wavefield extrapolations are performed from all receiver locations with the recorded seismograms, and the surface-reflected multiple reflections are focused on the subsurface imaging points as pseudo-primary reflections. Based on source-receiver reciprocity, this method can be applied to source-to-source pairs to use multiple reflections in airgun-OBS surveys.

Case study

(1) Airgun-OBS survey data in the Nankai Trough

We applied the proposed method to a 2D wide-angle reflection survey data acquired along 170 km survey line (200 m spacing of airgun shots, and 1 - 10 km spacing of OBSs) in the Nankai Trough. In wavefield reconstruction in the imaging process, sources and receivers are exchanged based on source-receiver reciprocity. A final reflection profile can be obtained by stacking two results derived from the primary reflections from OBS to airgun locations with the basic RTM method and from the multiple reflections between different airgun locations with the modified RTM method. Deep structures including the subducting plate and its relationship with old and young accretionary prisms are imaged with long offset reflections. Shallow structures are also clearly shown including sea floor and topographic relief of the base surface of sedimentary basin without lack of imaging area.

(2) Numerical simulation of earthquake observation

We tested reflection imaging with the modified RTM method by using numerical simulation data of both on-land and ocean-bottom earthquake observation. There is a big difference on a boundary condition (i.e. presence of a water layer above receivers) between the ocean-bottom and on-land observation. Multiple

©2019. Japan Geoscience Union. All Right Reserved.

reflections due to the water layer is significant in the ocean-bottom observation. We confirmed that reflection imaging is possible from passive observations both of the on-land and ocean-bottom seismometers with the modified RTM method. The multiple reflections are helpful to illuminate subsurface reflectors more effectively in the ocean-bottom observation in case of spars receiver deployment.

Acknowledgements
This research was supported by JAMSTEC innovation awards Houga research program.

Keywords: reflection imaging, reverse time migration, ocean-bottom seismograph

©2019. Japan Geoscience Union. All Right Reserved.

[J] Oral | S (Solid Earth Sciences)：S-SS Seismology

Tue. May 28, 2019 3:30 PM - 5:00 PM JST | Tue. May 28, 2019 6:30 AM - 8:00 AM UTC | A05 TOKYO BAY MAKUHARI HALL

[S-SS14] Fault Rheology and Earthquake Physics

convener:Keishi Okazaki(Japan Agency for Marine-Earth Science and Technology), Hideki Mukoyoshi(Department of Geoscience Interdisciplinary Graduate School of Science and Engineering, Shimane University), Hiroyuki Noda(Kyoto University, Disaster Prevention Research Institute), Keisuke Yoshida(Tohoku University), Chairperson:Keisuke Yoshida(東北大学大学院理学研究科 地球物理学専攻), Keishi Okazaki(JAMSTEC)

The goal of this session is to integrate theoretical, experimental, observational, and numerical perspectives from various fields such as seismology, geodesy, geology, mineralogy, and so on, to define what is known about earthquake source processes and the physical and chemical elementary processes of faulting. This session welcomes studies that address such issues as pre-, co-, and post-seismic processes, the rheology of seismogenic faults and fault rocks, laboratory experiments on elementary processes, numerical models based on frictional laws, and estimates of the stress field in the seismogenic zones. We also welcome studies on fault-zone drilling projects and in situ stress measurements.

3:30 PM - 3:45 PM JST | 6:30 AM - 6:45 AM UTC

[SSS14-01] **Spatio-temporal Evolution of Micro-Earthquakes illuminated by “0.1 manten” Hyper Dense Seismic Observation: Implication of Fault Growth**

*Aitaro Kato[1], Shin'ichi Sakai[1], Satoshi Matsumoto[2], Yoshihisa Iio[3] (1.Earthquake Research Institute, the University of Tokyo, 2.Kyushu University, 3.Kyoto University)

3:45 PM - 4:00 PM JST | 6:45 AM - 7:00 AM UTC

[SSS14-02] Estimation of fault model of the 2017 Pohang, South Korea earthquake using seismic and geodetic analyses

*Sun-Cheon Park[1], Won-Jin Lee[2], Geunyoung Song[1], Duk Kee Lee[1] (1.Korea Meteorological Administration, 2.National Institute of Environmental Research)

4:00 PM - 4:15 PM JST | 7:00 AM - 7:15 AM UTC

[SSS14-03] Estimation of rupture directivity, fault plane, and stress drop of small earthquakes in inland areas of Japan

*Keisuke Yoshida[1], Tatsuhiko Saito[2], Kentaro Emoto[1], Yumi Urata[2] (1.Tohoku University, 2.NIED)

4:15 PM - 4:30 PM JST | 7:15 AM - 7:30 AM UTC

[SSS14-04] **Possible aseismic phenomena causing the hypocenter migration in the precursory activity and aftershocks of the 2017 M 5.3 Kagoshima Bay earthquake, Kyusyu, SW Japan**

*Yoshiaki Matsumoto[1], Keisuke Yoshida[1], Toru Matsuzawa[1], Akira Hasegawa[1] (1.Research Center for Prediction of Earthquakes and Volcanic Eruptions, Tohoku University)

4:30 PM - 4:45 PM JST | 7:30 AM - 7:45 AM UTC

[SSS14-05] Stress and pore fluid pressure changes in fault zone preceding the earthquake occurrence

*Teruo Yamashita

4:45 PM - 5:00 PM JST | 7:45 AM - 8:00 AM UTC

[SSS14-06] Micromechanical model of fluid-induced seismicity to reproduce observed spatiotemporal changes in source parameters and on-fault fluid diffusion

*Daisuke Sato[1], Keisuke Yoshida[2] (1.Disaster Prevention Research Institute, Kyoto University, 2.Tohoku University)

Spatio-temporal Evolution of Micro-Earthquakes illuminated by “0.1 manten” Hyper Dense Seismic Observation: Implication of Fault Growth

*Aitaro Kato[1], Shin'ichi Sakai[1], Satoshi Matsumoto[2], Yoshihisa Iio[3]

1. Earthquake Research Institute, the University of Tokyo, 2. Kyushu University, 3. Kyoto University

To deepen fundamental understanding of earthquake faulting, it is of crucial importance to image fine scale structure of fault zone. We installed a thousand of seismic stations in the source area, which covers an entire aftershock zone of the 2000 Western-Tottori earthquake (Mw 6.7) from March 2017 to March 2018. The spatial interval of each seismic station ranges from 1 to 2 km. We initially detected ~3000 earthquakes from the continuous waveforms, using automatic arrival time picking technique. Applying a double-difference algorithm to the arrival data-set, we relocated more precise hypocenters in the studied region. The completeness magnitude of the catalog is around -0.7.

From the center to the southeast part, the relocated hypocenters are aligned along sharp fault planes, which are dipping almost vertically. In contrast, at the northwest area, the hypocenter distributions are complex, including several fault planes which are conjugate to the main NW-SE aftershock trend.

We focus on a tiny seismic cluster associated with Mj 1.7 event (main event) in the aftershock zone, which took place on 24th Dec., 2017. Following this event, a total of ~80 micro-earthquakes were detected by automatic-processng and matched filter technique. We visually picked up P-wave arrival times for each micro-earthquake. Using differential travel times derived from waveform cross-correlation technique, we succeeded to relocate them very precicely. The relative hypocenter acuuray appears to be less than 5 m. The relocated micro-earthquakes are sharply aligned along vertically NNW-SSE-striking fault. The length and dip-width of the fault dimension is about 200 m, respectively. This hypoenter alignment is well consisten with a focal mechanism of the main event. Based on the distribution of the earthquakes, the fault zone width is estimated to be ~10 m. The ratio of the fault (process) zone width to the fault length is ~0.01, which fairly matches with that geological observation of fault exposure.

In addition, we identify spatial-temporal evolution of the micro-earthquakes after the main Mj 1.7 event. Interestingly, these migrating events occurred so that they did not overlap events that occurred earlier, like complementary manner. The migration speed is estimated to be < ~0.1 km/day, which is quite lower than that slow slip events observed typically along subduction. This slow migration is similar to fluid migration speeds inferred from seismic observation of induced seismicities following the 2011 Tohoku-Oki earthquake. These results indicate a growth of fault network on a scale of tens of meters.

©2019. Japan Geoscience Union. All Right Reserved.

Estimation of fault model of the 2017 Pohang, South Korea earthquake using seismic and geodetic analyses

*Sun-Cheon Park[1], Won-Jin Lee[2], Geunyoung Song[1], Duk Kee Lee[1]

1. Korea Meteorological Administration, 2. National Institute of Environmental Research

After the 2017 Pohang, South Korea earthquake with magnitude (ML) 5.4, surface deformation was observed using Interferometric Synthetic Aperture Radar (InSAR) technique. This observation of surface deformation can be a constraint to estimate the fault model in addition to aftershock distribution and other seismic information. As the result of InSAR processing using X-band Cosmo-Sky-Med and C-band Sentinel-1 data, we observed the maximum deformation of about 4 cm in Line-Of-Sight (LOS) direction. Considering this observation, we estimated the fault model of the 2017 Pohang earthquake. We determined hypocenters of the earthquake sequence and carried out moment tensor inversion. Then we estimated the dimension and depth of the fault plane using aftershock distribution and displacement on the fault using the seismic moment. Surface deformation was calculated using the formula of Okada (1985) and assuming several models of slip distribution on the fault and was compared with the surface deformation pattern in LOS direction. Larger surface deformation toward the satellite was observed to the northeast from the epicenter and this pattern was well explained by fault models having the slip on the shallow fault plane. During the presentation, we will discuss more about the fault model comparing surface deformation and the aftershock distribution.

Keywords: 2017 Pohang earthquake, surface deformation, aftershock distribution, fault model

©2019. Japan Geoscience Union. All Right Reserved.

Estimation of rupture directivity, fault plane, and stress drop of small earthquakes in inland areas of Japan

*Keisuke Yoshida[1], Tatsuhiko Saito[2], Kentaro Emoto[1], Yumi Urata[2]

1. Tohoku University, 2. NIED

Dominant frequency or duration of seismic waves is considered to reflect the fault size. Some studies used the dominant frequency for the estimation of fault size and stress drop for small earthquakes assuming simple fault models (e.g., Brune, 1970; Sato & Hirasawa, 1973; Madariaga, 1976) without estimating heterogeneous slip distribution on the fault. Some of the simple source models are based on a symmetrical circular fault model (Madariaga & Ruiz, 2016). The assumption of the isotropic rupture evolution on a symmetrical circular fault can lead to a large estimation error of the fault size and thus the stress drops if the real source process is asymmetrical or exhibits a significant directivity effect (e.g., Kaneko & Shearer, 2015). We should carefully check if we can assume a symmetrical source model when we apply it in analyzing seismograms of small earthquakes.

We investigated the rupture directivities of small and moderate-sized earthquakes (M_JMA>2) in the Yamagata-Fukushima border earthquake swarm which was estimated to be triggered by the upward fluid movement after the 2011 Tohoku-Oki earthquake. We utilized the dense nationwide seismic network in Japan to estimate the rupture directivity. Apparent source time functions were calculated at each station for 1,782 earthquakes based on the waveform deconvolution technique with nearby (< 300 m) small earthquakes to remove the propagation- and site-effects. We found clear directional dependences of the peak amplitude and the pulse width in the apparent source time functions, suggesting the earthquake rupture directivity, for 904 of 1,782 events.

Based on the unilateral rupture model, we estimated the direction, duration, and velocity of rupture for each earthquake. Rupture directions of most earthquakes tend to be different from those of the hypocenter migration. This difference between the microscopic and macroscopic propagations of rupture might be explained by the spatial variation of the frictional strength; ruptures of each earthquake are hindered to develop toward shallower part due to higher frictional strength ahead of the pore-pressure front (shallower part) than behind (deeper part). It suggests the importance of the knowledge of frictional strength on fault to understand fracture dynamics of small earthquakes.

Besides, we estimated fault planes of small and moderate-sized earthquakes based on focal mechanism and rupture directivity (Fig.). Most of fault planes are parallel to the macroscopic planar structures, which suggests that they were triggered by fluid intrusions along those common planar structures. By taking the limitation of the resolution of hypocenter relocation, information from the rupture directivity can be unique data to reliably determine the fault planes of small and moderate-sized earthquakes.

By considering the estimated fault planes and areas of small earthquakes, we confirmed the temporal increase in stress drop reported by Yoshida et al. (2017, JGR). The systematic temporal changes in frictional strength, stress drop, background seismicity rate, b-values, the upward hypocenter migration along the planar structures, and the rupture directivity rather opposite to the hypocenter migration can be explained in a consistent manner by the effects of the upward fluid flow along several pre-existing planes after the 2011 M9 Tohoku-Oki earthquake.

©2019. Japan Geoscience Union. All Right Reserved.

Keywords: frictional strength, stress drop, hypocenter migration

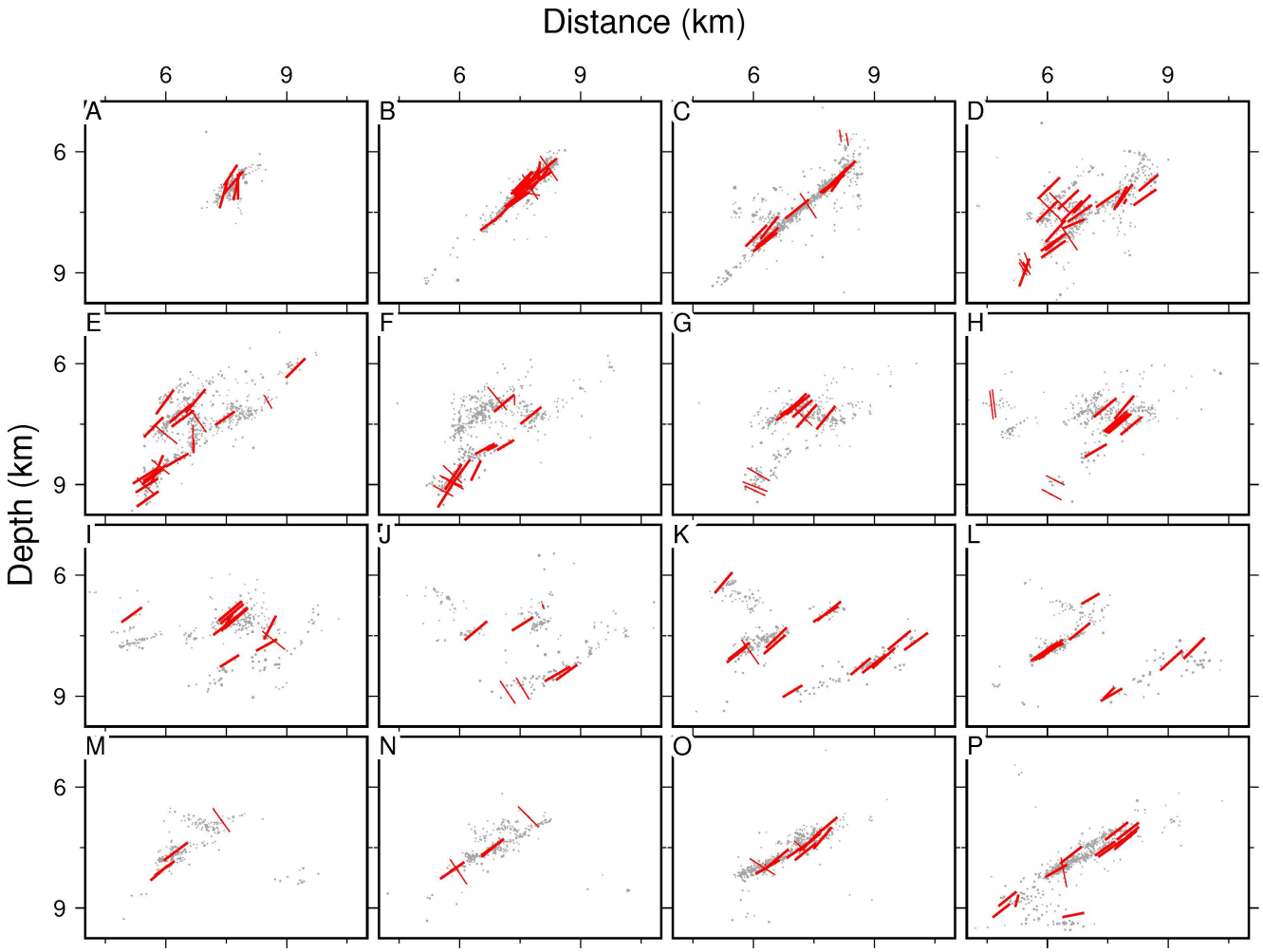

©2019. Japan Geoscience Union. All Right Reserved.

Possible aseismic phenomena causing the hypocenter migration in the precursory activity and aftershocks of the 2017 M 5.3 Kagoshima Bay earthquake, Kyusyu, SW Japan

*Yoshiaki Matsumoto[1], Keisuke Yoshida[1], Toru Matsuzawa[1], Akira Hasegawa[1]

1. Research Center for Prediction of Earthquakes and Volcanic Eruptions, Tohoku University

An earthquake occurs when the shear stress acting on the fault plane reaches the frictional strength. It has been suggested that an increase in pore pressure plays an important role in earthquake occurrence (e.g. Hasegawa, 2017; Hubbert & Rubey, 1959; Nur & Booker, 1972; Sibson, 1992). Migration behavior of earthquake hypocenters is considered to be caused by aseismic processes such as fluid movements or aseismic slip propagations. It is expected that information on aseismic processes in the crust can be obtained by examining the hypocenter migration in detail.

On 11 July 2017, an M 5.3 earthquake occurred at approximately 10 km depth in Kagoshima Bay, Kyusyu, SW Japan. Near the main shock hypocenter, seismicity had been activated since December 2016. In order to investigate the generation mechanism of this seismic sequence, we improved relative locations of hypocenters of the precursory activity and aftershocks by using waveform cross correlations.

First, precise differential arrival times were obtained by calculating cross correlations of a pair of waveforms out of the earthquakes that occurred after January 2010 in the Southern Kagoshima Bay region. We used waveform data observed at 20 stations located around the main shock hypocenter. Calculations of cross correlations of waveforms were performed in the same way as Yoshida & Hasegawa (2018). Then, we applied the double-difference relocation method (Waldhauser and Ellsworth, 2000) to the differential arrival time data thus obtained by cross correlations and those listed in the JMA (Japan Meteorological Agency) unified catalog. We used hypocenters listed in the JMA unified hypocenter catalog as the initial hypocenters in the relocation.

The relocated hypocenters are concentrated forming several thin “planes”. The dominant orientations of the planes agree with the eithers of nodal planes of focal mechanisms of the main shock and aftershocks.

Hypocenters of the precursory activity are neatly concentrated along one of the planes and exhibit distinct migration behavior. Hypocenter distribution of the precursory activity along that plane shows a clear seismic gap located adjacent to the main shock hypocenter. Most of aftershock hypocenters are distributed along the same plane but did not fill this seismic gap. We calculated the corner frequency of the mainshock source spectrum using the spectral ratio method and estimated the mainshock fault size. The estimated fault size is consistent with the size of the seismic gap. It suggests that the seismic gap reflects the main shock rupture area (e.g. Wetzler et al., 2018).

Aftershocks tend to move upward with time along several thin planes. This spatiotemporal feature of earthquake hypocenters is similar to those observed in the earthquake swarms in central Tohoku that were triggered by the 2011 M9 Tohoku-Oki earthquake probably due to the upward movement of fluids (Yoshida & Hasegawa, 2018)

©2019. Japan Geoscience Union. All Right Reserved.

We explain the characteristics of the precursory activity, main shock and aftershocks as follows. (1) Prior to the occurrence of the main shock, crustal fluids penetrated into an existing weak plane from below and reduced the frictional strength, which caused the precursory seismic activity along the plane and the migration of hypocenters. Aseismic slip might also contribute to the hypocenter migration. (2) Then the seismic gap, which had not been ruptured by the precursory activity, was finally ruptured by the main shock. (3) Due to the stress change associated with the main shock, aftershocks were triggered in the region surrounding the main shock hypocenter. Aftershock hypocenters moved upward due to the upward fluid movements after the main shock.

Keywords: seismic activity in Kagoshima Bay, precursory seismic activity, aftershocks, hypocenter migration, seismic gap

©2019. Japan Geoscience Union. All Right Reserved.

Stress and pore fluid pressure changes in fault zone preceding the earthquake occurrence

*Teruo Yamashita

I theoretically study stress and fluid pressure changes in fluid-saturated fault zone that deforms elasto-plastically. Such study will be useful to gain an insight into the process leading to the earthquake occurrence. I employ poro-elasto-plasticity theory (Coussy,2006) and assume a Capped Drucker-Prager model as the yield criterion (Figure 1). The line segment (A) is described by the equation $f= \tau_J + f_m \sigma_{eff} + \kappa = 0$, where f_m and κ are the internal friction coefficient and a function of the hardening variable; $(\tau_J)^2$ and σ_{eff} denote the second deviatoric stress invariant and the effective mean stress. The point I represents the initial state in the elastic region and the yield criterion is satisfied first at point P on A; relatively low effective normal stress is assumed. The stresses τ_J and σ_{eff} move in a direction indicated by the arrow along the line segment A with the increase in the remotely applied stresses. I assume a non-associated flow law; the plastic potential corresponding to the line segment A is given by the equation $g= \tau_J + f_d \sigma_{eff} + \kappa$, where f_d is the dilatancy factor. It is known that the plastic component of volumetric strain is positive on the line segment A, so that the fluid pressure change will be negative there. It is known that f_m is larger for larger values of porosity (Chang et al.,2006). It is also known for low porosity rocks that permeability is higher at locations closer to the fault core, so that it will be allowed to assume that f_m is smaller at locations closer to the fault core. I therefore assume a 1D model such that f_m takes a minimum value just outside the fault core ($|y|=c+0$) and it increases linearly with the distance and attains a constant value (Figure 2). The f_m-increase zone is defined as the fault damage zone. Since the porosity is sufficiently low in the fault core, the value of f_m in the fault core is assumed to be equal to that at $y=\infty$; the boundary at $|y|=c$ is assumed to be impermeable. I also assume the absolute values of the remotely applied principal stresses ($\sigma_1 < \sigma_2 < \sigma_3 < 0$) increase quasi-statically with time. Hence, the yield criterion is first satisfied at $|y|=c+0$; the plastic zone expands with further stress accumulation. The plastic deformation never occurs in the fault core during the calculation. In this model, the time scale is governed by the magnitude of permeability. I assume that the increase rate of the maximum principal stress σ_1 that is remotely applied is 0.2MPa/year. Figure 3 shows examples of fluid pressure change at $|y|=c+0$ for the permeability$10^{-18}m^2$. The curve A is the case of plastic hardening. While both B and C are the cases of perfect plasticity, the damage zone width for C is twice as large as that for B. The figure shows that the fluid pressure decrease is larger for smaller degree of plastic hardening or for larger damage zone width. However, the elastic component of fluid pressure change (elevation) is estimated to be about 10MPa at time t/dt=10,000. Hence, the plastic decrease of fluid pressure is almost negligible. The calculation also shows that the values of $|\sigma_1 - \sigma_3|$ and $|\sigma_1 + \sigma_3|$ in the plastic zone are, respectively, smaller and larger than those in the elastic zone; the difference grows with the expansion of plastic zone. This suggests that the fault damage zone become more stable with the expansion of plastic zone, while the sudden stress and fluid pressure changes formed at $|y|=c$ may damage the impermeable boundary there. However, such stable situation never lasts indefinitely. The yield criterion such as represented by the curve B in Figure 1 seems to be satisfied once stresses exceeds a critical threshold. The plastic component of volumetric strain turns negative on the curve B, so that the damage zone may become unstable. Hence, the stress point is required to move onto the curve B for the occurrence of earthquake. I will show numerical examples of the whole process leading to the earthquake occurrence in the presentation.

Keywords: poro-elasto-plasticity theory, Drucker-Prager model, fault zone

©2019. Japan Geoscience Union. All Right Reserved.

©2019. Japan Geoscience Union. All Right Reserved.

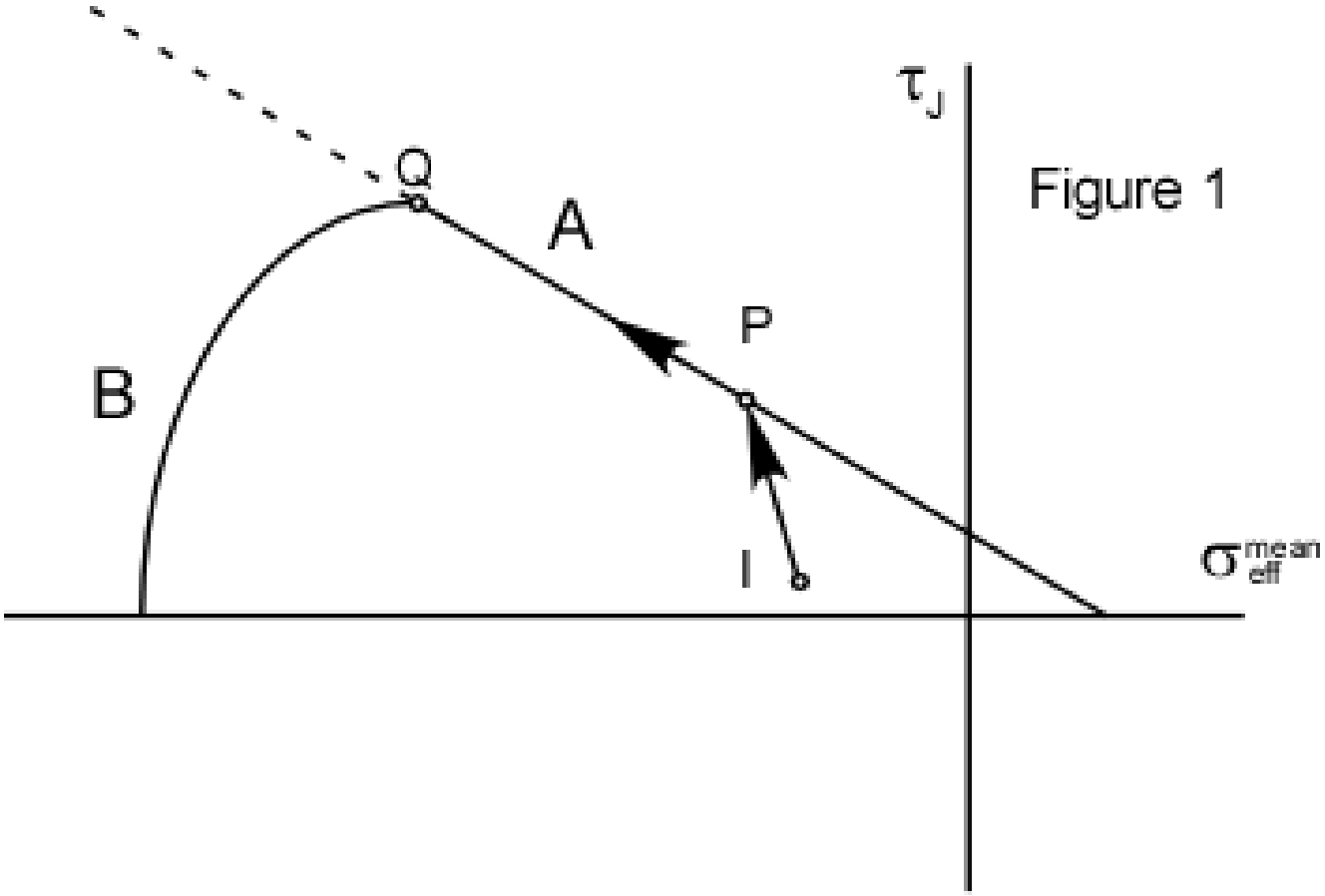

Figure 1

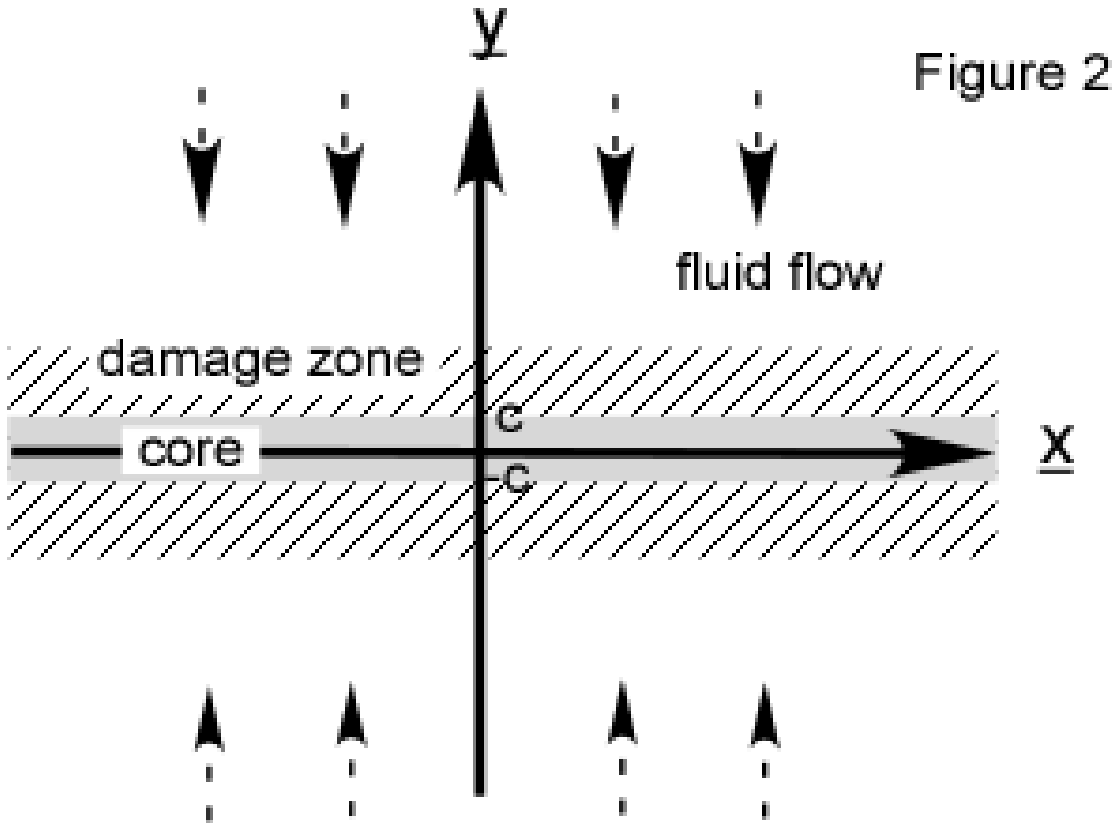

Figure 2

Figure 3

©2019. Japan Geoscience Union. All Right Reserved.

©2019. Japan Geoscience Union. All Right Reserved.

Micromechanical model of fluid-induced seismicity to reproduce observed spatiotemporal changes in source parameters and on-fault fluid diffusion

*Daisuke Sato[1], Keisuke Yoshida[2]

1. Disaster Prevention Research Institute, Kyoto University, 2. Tohoku University

Fluid and seisimicity are considered to be related, as suggested from earthquake swams of natural earthquakes and man-made earhtquakes induced by fluid injection. Some data analysis with relocation techniques of earthquake sources showed that the earthquake activities propagete facially (e.g., Yukutake et al., 2010), and that some source parameters (such as stres drops, strength, b-value, seismicity rate) are functions of elapsed time from fluid injection (Bachmann et al., 2012) or sudden increase of (possibly fluid-induced) seisimicity rate not following mainshocks (Yoshida et al., 2017). In this research, by considering strength heterogeneity of faults expected from experimentally verified physics, we provide the micromechanical model of such seismicity induced by on-fault fluid diffusion, and explain the results of the above data-driven analysis.

Presentation contains following four contents. First, the micromechanical model is proposed. In the model, many patches are distributed randomly on a fault so that the patches are sufficiently small (or distant) to interact with each other; those patches rupture when the effective strength becomes smaller than applied shear stress due to the fluid diffusion. Second, the spatiotemporal changes of the source parameters are obtained as the solutions of the model. Consequently, multiple source parameters are parametrized by injected pressure, diffusion raidus of fluid, normal stress on the fault, and the fluctuation of the exess strength; after the parametrization, those source parameters are shown to follow the common master curve. Third, the observed data is fitted, and the consistency between the theory and the observation is suggested. Fourth, the thoretical prediction for the temporal transience in the moment release rate is checked by the data of Yoshida et al. (2017), and the result strongly supports the theory.

Keywords: earthquake swarms and induced-seismicity, micromechanical model, source paraemters

©2019. Japan Geoscience Union. All Right Reserved.

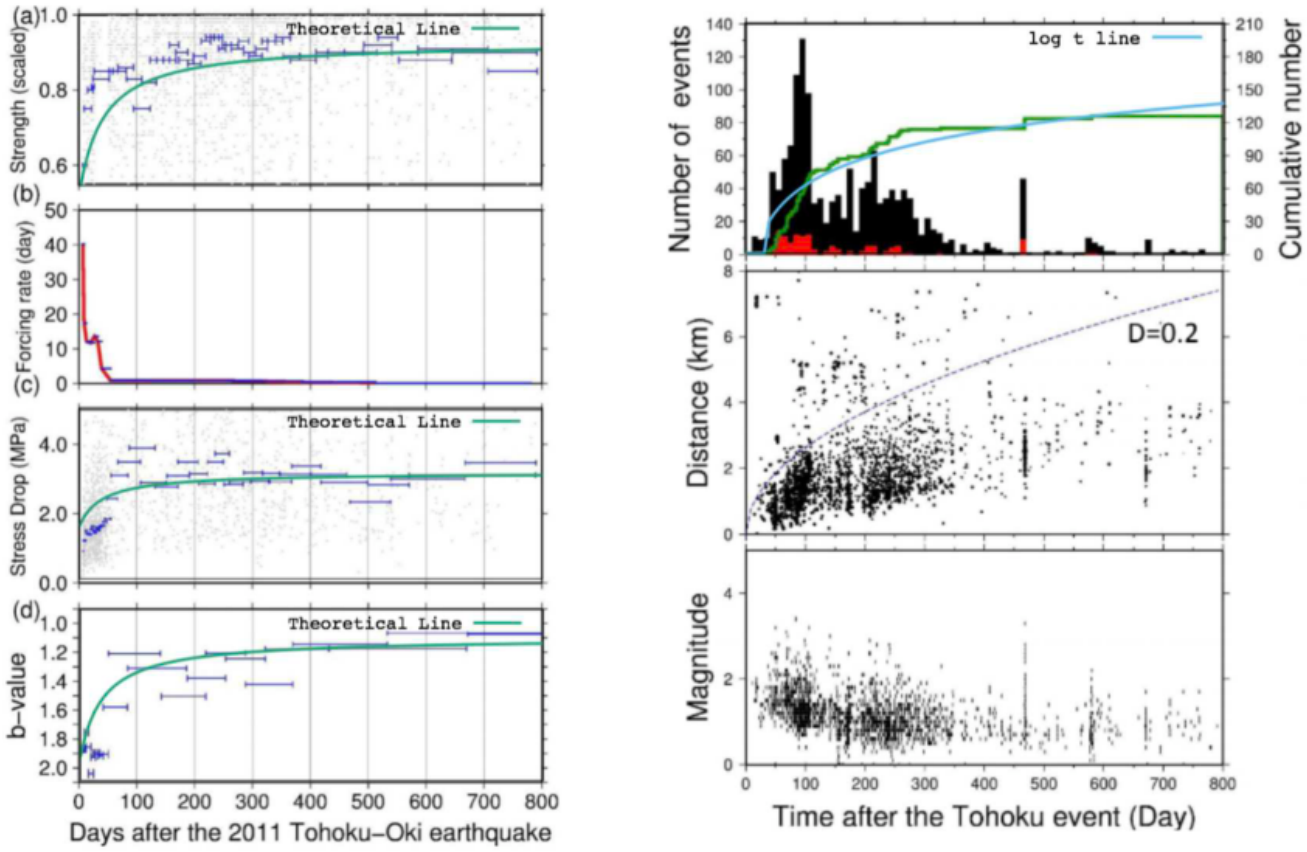

Yoshida et al. (2017)

Fig. 1. A data example of Yoshida et al. (2017) fitted by our theoretical model (written as theoretical or log t line in the figure), after Yoshida et al (2017). (Left) Temporal evolution of the source paramters. (Right) Number of events and the spatial patterns of the seismicity.

©2019. Japan Geoscience Union. All Right Reserved.

[J] Poster | S (Solid Earth Sciences)：S-SS Seismology

Tue. May 28, 2019 1:45 PM - 3:15 PM JST | Tue. May 28, 2019 4:45 AM - 6:15 AM UTC | Poster Hall International Exhibition Hall8, Makuhari Messe_7

[S-SS15] Active faults and paleoseismology

convener:Mamoru Koarai(Earth Science course, College of Science, Ibaraki University), Takashi OGAMI(National Institute of Advanced Industrial Science and Technology), Ryosuke Doke(Hot Springs Research Institute of Kanagawa Prefecture), Hisao Kondo(Geological Survey of Japan, National Institute of Advanced Industrial Science and Technology)

Geologic and historic information on seismic cycles and on the magnitude and source faults of past earthquakes is essential information to understand future large earthquakes. The study of past faulting and seismicity is an important issue for an interdisciplinary community of seismologists, geologists, geomorphologists, archaeologists, and historians.

[SSS15-P01] Paleoseismicity of Atsuma Town , Hokkaido: Evidence from landslide deposits

*Jun Tajika[1], Tetsuya Inui[2] (1.Docon Co.,Ltd., 2.Board of Education, Atsuma Town)

[SSS15-P02] Gravity survey and subsurface structure across the Aomoriwan-Seigan Fault Zone, Northeast Japan(part 2; estimation of the subsurface structure using the density of rock samples)

*Shinsuke Okada[1], Hideki Kosaka[2], Kyoko Kagohara[3], Toshifumi Imaizumi[4], Kohei Abe[5], Susumu Sakashita[5], Atsushi Miwa[5], Kouta Koshika[5], Yusuke Oda[5], Yuki tsukamoto[6], Takahiro Miyauchi[7], Tomoo Echigo[8] (1.International Research Institute of Disaster Science, Tohoku University, 2.Kankyo Chishitsu, Co. Ltd., 3.Faculty of Education, Yamaguchi University, 4.Emeritus professor of Tohoku University, 5.OYO Corporation, 6.Graduate School of Science, Tohoku University, 7.Department of Earth Sciences, Graduate School and Faculty of Science, Chiba University, 8.Geo-Research Institute)

[SSS15-P03] Was the 1611 Keicho earthquake a giant interplate event like the 2011 Tohoku earthquake?

*Tomoya Harada[1], Akihito Nishiyama[1], Kenji Satake[1], Takashi Furumura[1] (1.Earthquake Research Institute, The University of Tokyo)

[SSS15-P04] **Neotectonic characteristics along both flanks of the Ou Backbone Range, Tohoku Region, Japan, from fluvial geomorphic analyses**

*Jhih Hao Liao[1], J Bruce H Shyu[1], Yasufumi Iryu[2], Hiroyuki Tsutsumi[3], Chia-Yu Chen[1] (1.Department of Geosciences, National Taiwan University, Taipei, Taiwan, 2.Graduate School of Science, Tohoku University, Sendai, Japan, 3.Department of Environmental Systems Science, Doshisha University, Kyotanabe, Japan)

[SSS15-P05] Tsunami record of the last 700 years in bottom sediment of lake Kasumi-ga-ura, southeastern part of Ibaragi Prefecture

*Yoshio Inouchi[1] (1.Faculty of Human Sciences, Waseda University)

[SSS15-P06] Detecting concealed fault by microtremor H/V study in Miura Peninsula

*Kazuzi Ogawa[1], Yasuyuki Iwase[1], Takumi Murakoshi[1], Toshihisa Itano[1] (1.National Defense Academy)

[SSS15-P07] Distribution, geometry and slip rates of branch faults around the Kita-Izu fault zone

*Ryuhei Oda[1], Daisuke Ishimura[1], Takehiko Suzuki[1] (1.Tokyo Metropolitan University)

[SSS15-P08] Paleoseismology of the southern part of Kamishiro fault, ISTL active fault zone, central Japan

*Kotaro Mizutani[1], Daisuke Hirouchi[1], Nobuhisa Matsuta[2], Tatsuya Ishiyama[3], Nobuhiko Sugito[4], Kenichi Yasue[5], Yoshihiro Takeshita[1], Natsuko Fujita[6], Hiroshi Sawa[7], Ryosuke Doke[8], Haruo Maruyama[9], Kazutaka Ikeda[10], Kamishiro Fault (1.Shinshu University, 2.Okayama University, 3.ERI, University of Tokyo, 4.Hosei University, 5.Toyama University, 6.JAEA, 7.Tsuruoka Nat.Col.Tech., 8. Hot Springs Research Institute of Kanagawa Pref., 9.Kisoseiho High school, 10.Mochiduki Elementary School)

[SSS15-P09] **Geotectonic history of the Inadani fault zone in southern part of Nagano prefecture, central Japan**

*Shuuhei Tsukui[1], Kenta Kobayashi[1] (1.Department of Geology, Faculty of Science, Niigata University)

[SSS15-P10] Characteristics of the fault zone with only the recent slips in the Atera Fault

Atsushi Nishida[1], *Tomoyuki Ohtani[1], Takuya Niimi[1], Jun'ichi Tsubaki[1], Keiichi Ueta[2] (1.Department of Civil Engineering, Gifu University, 2.CRIEPI)

[SSS15-P11] Identification of active fault location using real-time ground measurements of atmospheric methane concentration by portable Cavity Ring-down Spectroscopy system: Case study at the Atera fault

*Michito Shimo[1], Masakazu Niwa[2], Kenji Amano[2], Tomochika Tokunaga[3], Kenichi Tonokura[3], Toshifumi Matsuoka[1], Sebastien Biraud[4] (1.Fukada Geological Institute, 2.Japan Atomic Energy Agency, 3.Department of Environment Systems, University of Tokyo, 4.Lawrence Berkeley National Laboratory, USA)

[SSS15-P12] Geomorphological evudence of a newly found active fault along the Shirakawa fault in western part Gifu Prefecture

*Yorihide Kohriya[1], Masashi Omata[1], Hiroshi Yokota[1] (1.PASCO CORPORATION)

[SSS15-P13] Active faults around the Niu Mountains, northern part of Fukui Prefecture, Japan

*Masayoshi Tajikara[1], Takashi Nakata[2], Hiroyuki Tsutsumi[3], Hideaki Goto[2] (1.Association for the Development of Earthquake Prediction, 2.Hiroshima University, 3.Doshisha University)

[SSS15-P14] Gifu-Ichinomiya Fault shown from the characteristics of the damage of the Nobi earthquake

*Nobuhisa Matsuta[1,2], Fumiaki KIMATA[2] (1.Okayama University Graduate School of Education, 2.Tono Research Institute of Earthquake Science)

[SSS15-P15] Electrical resistivity structure from the surface to the seismogenic zone below the Gomura fault zone, Kyoto, Southwest Japan

*Satoru Yamaguchi[1], Akira Mimura[1], Kazuki Fukue[1], Shigehiro Katoh[2], Hideki Murakami[3], Makoto Uyeshima[4] (1.Department of Geosciences, Graduate School of Science, Osaka City University, 2.The Museum of Nature and Human Activities, Hyogo, 3.Science and Technology Unit, Research and Education Faculty, Kochi University, 4.Earthquake Research Institute, The University of Tokyo)

[SSS15-P16] Re-analysis and re-interpretation of the very shallow land seismic reflection survey data across the Naruto-South fault, north side of Tokushima Plain.

*Kobayashi Takayuki[1], Dai Nobuoka[2], Tomio Inazaki[1] (1.Public Works Research Institute Japan, 2.OYO Corporation)

[SSS15-P17] Bathymetric mapping and seafloor imaging for finding historical records of Nankai earthquakes at Nomi bay in Susaki city, Kochi Prefecture, Japan

*Wataru Tanikawa[1], Masafumi MURAYAMA[2], Hidekazu Tokuyama[3], Kouki Tanaka[4], Akira Ijiri[1], Tatsuhiko Hoshino[1], Takehiro Hirose[1], Kazuya Kitada[5], Toshiya Fujiwara[5] (1.Japan Agency for Marine-Earth Science and Technology, Kochi Instutute for Core Sample Research, 2.Kochi Univerisity, Faculty of Agriculture and

Marine Science, 3.Kochi Univerisity, Center for Advanced Marine Core Research , 4.Kochi Univerisity, 5.Japan Agency for Marine-Earth Science and Technology)

[SSS15-P18] Tectonic geomorphological and paleoseismological study in the Anoriguchi Canyon: Foraminiferal analysis and ^{14}C dating

*Nobuhiko Sugito[1], Masao Iwai[2], Hitomi Wakaki-Uchimura[2], Hiroki Matsui[2], Yasuhiro Suzuki[3] (1.Faculty of Sustainability Studies, Hosei University, 2.Center for Advanced Marine Core Research, Kochi University, 3.Disaster Mitigation Research Center, Nagoya University)

[SSS15-P19] Subsurface survey around the Matoishi-bokujo 1 Fault in the northwest of the outer rim of the Aso caldera, southwestern Japan

*Takayuki Nakano[1], Hiroshi Une[1], Hiroshi, P. Sato[2], Keitaro Komura[3] (1.GSI of Japan, 2.Nihon Univ., 3.CRIEPI)

[SSS15-P20] Past activity of 'triggered fault' in the northwest of outer rim of Aso caldera estimated from the results of excurvation survey and displacement topography

*Hiroshi Une[1], Takayuki Nakano[1], Hiroshi, P. Sato[2], Hiroshi YAGI[3], Keitaro Komura[4] (1.Geospatial Information Authority of Japan, 2.Nihon University, 3.Yamagata University, 4.Central Research Institute of Electric Power Industry)

[SSS15-P21] Visualization of three-dimensional SAR analysis data by stereo isogram map: Precise detection of surface ruptures of the 2016 Kumamoto earthquake sequence

*Yasuo Awata[1] (1.Institute of Earthquake and Volcano Geology, Geological Survey of Japan, National Institute of Advanced Industrial Science and Technology)

[SSS15-P22] Preliminary active fault mapping of Mongolia by interpretation of ALOS 30 DEM image

*Takashi Nakata[1], Yasuhiro Suzuki[2], Mitsuhisa Watanabe[3] (1.Hiroshima University, 2.Nagoya University, 3.Toyo University)

[SSS15-P23] Ground penetrating radar profiling across the Sanchiao fault in northeast Taiwan

*Mamoru Nakamura[1], How-wei Chen[2] (1.Faculty of Science, University of the Ryukyus, 2.National Central University, Taiwan)

[SSS15-P24] Paleo-earthquake records of the Hengchun offshore structure, southern Taiwan

*Sze-Chieh Liu[1], J Bruce H Shyu[1], Yuan-Lu Tsai[1], Chuan-Chou Shen[1] (1.National Taiwan University)

[SSS15-P25] LC-InSAR analysis of the Sulawesi earthquake in Indonesia

*Jun Sugimoto[1], Masashi Omata[1], Yoshiteru Akiyama[1], Yutaka Horaku[1] (1.PASCO CORPORATION)

[SSS15-P26] **Risk evaluation and disaster education around the coastal areas of Sea of Marmara, Turkey through the fault model construction of the North Anatolian Fault**

*Yoshiyuki Kaneda[1,2,3], Haluk Ozener[4], Nurcan Meral Ozel[4,5], Dogan Kalafat[4], Seckin Ozgur Citak , Narumi Takashi[2,3], Takane Hori[2], Muneo Hori[2,6], Mayumi Sakamoto[10,7], Ali Pinar[4], Asim Oguz Ozel[11], Ahmet Cevdet Yalciner[8], Gulum Tanircan[4], Ahmet Demirtas[9] (1.Kagawa University, 2.JAMSTEC, 3.NIED, 4.Bogazici University, 5.CTBTO, 6.ERI, 7.Nagoya University, 8.Middle East Technical University, 9.AFAD, 10. University of Hyogo, 11.Istanbul University)

[SSS15-P27] Estimation of fault activity by multivariate analysis using chemical composition of fault gouge

*Ryo Tateishi[1], Koji Shimada[2], Tadamasa Ueki[2], Mayuko Shimizu[2], Tetsuya Komatsu[2], Shigeru Sueoka[2], Masakazu Niwa[2], Ken-ichi Yasue[1], Tsuneari Ishimaru[2] (1.University of Toyama, 2.Japan Atomic Energy

Agency)

[SSS15-P28] Bayesian optimization of fault-shape parameters using finite element analysis: parameter sets for strong slip partitioning

*Hidetaka Saomoto[1] (1.National Institute of Advanced Industrial Science and Technology)

Paleoseismicity of Atsuma Town , Hokkaido: Evidence from landslide deposits

*Jun Tajika[1], Tetsuya Inui[2]

1. Docon Co.,Ltd., 2. Board of Education, Atsuma Town

Many landslides occurred by the 2018 Hokkaido Eastern Iburi Earthquake in Atsuma-cho. We reported about discovering of ancient landslide deposit from an archeological site of the Jomon period in Atsuma in 2004 and 2016. It was inferred that this landslide was caused by an earthquake and it probably occurred at activity event of the Ishikari teichi-toen active fault zone. The morphological characteristic of the landslide deposit resembles that of landslide caused by this earthquake. The archeological findings of the past remains excavation in Atsuma-cho area shows that the event of a lot of landslides caused by earth quake is only 2018 Hokkaido Eastern Iburi Earthquake and an earthquake of the Jomon period during last 9,000 years.

Keywords: Paleo seismology, Liquefaction, landslide body

©2019. Japan Geoscience Union. All Right Reserved.

Gravity survey and subsurface structure across the Aomoriwan-Seigan Fault Zone, Northeast Japan(part 2; estimation of the subsurface structure using the density of rock samples)

*Shinsuke Okada[1], Hideki Kosaka[2], Kyoko Kagohara[3], Toshifumi Imaizumi[4], Kohei Abe[5], Susumu Sakashita[5], Atsushi Miwa[5], Kouta Koshika[5], Yusuke Oda[5], Yuki tsukamoto[6], Takahiro Miyauchi[7], Tomoo Echigo[8]

1. International Research Institute of Disaster Science, Tohoku University, 2. Kankyo Chishitsu, Co. Ltd., 3. Faculty of Education, Yamaguchi University, 4. Emeritus professor of Tohoku University, 5. OYO Corporation, 6. Graduate School of Science, Tohoku University, 7. Department of Earth Sciences, Graduate School and Faculty of Science, Chiba University, 8. Geo-Research Institute

The Aomoriwan-Seigan Fault Zone is a fault zone of NNW-SSE trending western dipping reverse faults, which is composed of Aomoriwan West Fault, Nogiwa Fault, and Nyunai Fault. The fault zone is distributed about 31-km long along the eastern foot of the Tsugaru Mountains from Yomogita village of Aomori prefecture to Aomori city (Headquarters of Earthquake Research Promotion, 2004). We carried out a seismic reflection survey and CSAMT (Controlled Source Audio-frequency Magnetic Telluric) survey across the Aomoriwan West Fault (Kagohara et al., 2017; Sakashita et al., 2017) in 2016-2017. The low angle thrust faults of Tsugaru Fault and inclined geological structure until the depth of 1.5 km were revealed in these results. In addition to these surveys, we conducted gravity survey along the seismic survey line, and obtained the Bouguer gravity anomaly (Okada et al., 2018).
In the previous our presentation in the 2018 JpGU (Okada et al., 2018), we use the Talwani method (Talwani et al., 1959) to calculated the Bouguer gravity anomaly, in which the subsurface density structure is determined from the interpretation of the seismic and CSAMT surveys (Kagohara et al., 2017; Sakashita et al., 2017). In a part of the western part of the profile, there were some discrepancies between calculated and observed gravity anomalies. And it was also difficult to estimate the density of each layers. To resolve these problems, we conducted additional field survey and obtained several rock samplings from outcrops around the survey line, which we measured the density of samplings based on the method of Murata et al. eds. (1991). The discrepancies between calculated and observed gravity anomaly were improved by take into the layer densities from samplings.

[References]
Headquarters for Earthquake Research and Promotion, 2014, Survey Results and Evaluation of the Aomoriwan-Seigan Active Fault Zone, 16 p.
Kagohara K., et al., 2017, Seismic reflection profiling survey across the eastern foot of Tsugaru Mountains, SSS12-P08, in JpGU-AGU Joint Meeting 2017, Makuhari Messe International Convention Complex, 2017-05-23.
Okada S., et al., 2018, Gravity survey and subsurface structure across the Aomoriwan-Seigan Fault Zone, Northeast Japan, JpGU Meeting 2018, SSS08-P05, Makuhari Messe International Convention Complex, 2018-05-22.
Murata Y., et al. eds., 1991, Rock Physical Properties of Japan –Density, Magnetism, P-wave Velocity, Porosity, Thermal Conductivity –, Report of ,
Sakashita S., et al., 2017, Application of high density CSAMT exploration for active fault investing by using multi-channel electromagnetic suvey system, SSS12-P18, in JpGU-AGU Joint Meeting 2017, Makuhari Messe International Convention Complex, 2017-05-23.

©2019. Japan Geoscience Union. All Right Reserved.

Talwani M., et al., Rapid gravity computations for 2-dimensional bodies with application to the Mendocino submarine fracture zone, J. Geophys. Res., 64, 49-59, doi:10.1029/JZ064i001p00049.

Keywords: Gravity survey, Bouguer gravity anomaly, Rock density measuring, Aomoriwan-Seigan Fault Zone, Seismic reflection survey, CSAMT survey

©2019. Japan Geoscience Union. All Right Reserved.

Was the 1611 Keicho earthquake a giant interplate event like the 2011 Tohoku earthquake?

*Tomoya Harada[1], Akihito Nishiyama[1], Kenji Satake[1], Takashi Furumura[1]

1. Earthquake Research Institute, The University of Tokyo

After the 2011 Tohoku earthquake (M9.0), the 1611 Keicho earthquake along the Japan trench has been regarded as a giant interplate event. In this study, from the examination of reliability of the historical records about the 1611 event and comparison between the impact on Kanto by the 2011 and 1611 events, we consider that the 1611 earthquake was not a giant interplate event but a tsunami/outer-rise earthquake.
From the historical documents, the Dec. 2nd, 1611 Keicho earthquake generated large tsunami on the Pacific Coasts of Tohoku and Hokkaido while this event caused no seismic damage in Tohoku and Kanto. Since the 1896 tsunami earthqauke (M8.1) and 1933 outer-rise earthquake (M8.1) had similar features, the 1611 event had been regarded as an M~8 tsunami/outer-rise earthquake (Hatori, 1975; Aida, 1977; Watanabe, 1998). After the 2011 Tohoku earthquake, however, some studies claimed that the 1611 earthquake was probably a giant event because the tsunami heights and inundation areas estimated from the historical documents (e.g. Hatori, 1975; Tsuji et al., 2011; Ebina and Imai, 2014) are comparable to (or larger than) those of the 2011 event (e.g. Ebina, 2014; Iwamoto, 2013). Following this claim, tsunami researchers attempted to make fault models to reproduce the 1611 tsunami by the tsunami numerical simulation. Imai et al. (2015) proposed two fault models. One is a giant interplate event (fault size: 400km*200km, Mw8.7), another is a model (Mw8.4) of simultaneous occurrence of a great interplate event (fault size: 400km*150km) and a great outer-rise event (fault size: 400km*50km). Fukuhara and Tanioka (2017) considered that the 1611 event was a giant tsunami earthquake (fault size: 250km*50km, the maximum slip: 80m, Mw9.0).
In this study, however, we considered that the 1611 Keicho earthquake was not a giant interplate event but a M~8 tsunami/outer-rise earthquake from the following reasons: (1) Reliability of the 1611 tsunami heights and inundation areas is not high because they are estimated from the historical records without examination of reliability. There are historians who dispute the 1611 giant earthquake based on the unreliable historical records (e.g. Kan’no, 2014; Sasaki, 2014; Saino, 2017); (2) Strong shaking by the 2011 mainshock caused severe damage in Kanto and aftershocks and induced events caused additional damage and successive shakings in this region for several weeks. Whereas, as for the 1611 earthquake, only two shakings in Edo (present Tokyo) are recorded in the court nobles' diaries and there is no record of the seismic damage in Kanto. From the primary historical documents, Ieyasu Tokugawa went hunting with hawks to the present Saitama Pref. and court nobles went sightseeing to environs of Edo on the next day of the 1611 event. Therefore, the 1611 earthquake was probably an event which didn’t impact on Kanto, i.e. not a giant interplate event like the 2011 earthquake. M~8 interplate event in 1793 offshore present Miyagi Pref. caused minor seismic damage in Edo and its 2-days aftershocks shocked Edo more than 50 times (Usami et al. 2013); (3) Even if the 1611 earthquake was an M~9 tsunami event, ~80m slip on the large fault (250km*50km) should cause many aftershocks and widely induce earthquakes including M7-8 events. As mentioned above, however, there is no record about the successive earthquakes after the 1611 event; (4) No tsunami deposit by the 1611 event is discovered at the ruins in Sendai Plain excepting Taka-ose Ruin in the present Iwanuma City (Saino, 2017), while they are discovered on the Sanriku Coasts (e.g. Takada et al., 2016). In addition, they are not discovered at the Idagawa marsh in the present Fukushima Pref. (Kusumoto, et al. 2018). Therefor, 1611 tsunami probably didn’t inundate deeply in the lowlands on the Pacific Coast in Miyagi and Fukushima Pref. Recently, Goto et al. (2019) reported that the

©2019. Japan Geoscience Union. All Right Reserved.

1611 tsunami deposits were not discovered at the Numano-hama of Sanriku Coast.

Keywords: 1611 Keicho earthquake, a giant interplate earthquake, reliability of historical records, primary historical documents, tsunami heights and inundation areas, tsunami traces

©2019. Japan Geoscience Union. All Right Reserved.

Neotectonic characteristics along both flanks of the Ou Backbone Range, Tohoku Region, Japan, from fluvial geomorphic analyses

*Jhih Hao Liao[1], J Bruce H Shyu[1], Yasufumi Iryu[2], Hiroyuki Tsutsumi[3], Chia-Yu Chen[1]

1. Department of Geosciences, National Taiwan University, Taipei, Taiwan, 2. Graduate School of Science, Tohoku University, Sendai, Japan, 3. Department of Environmental Systems Science, Doshisha University, Kyotanabe, Japan

The islands of Japan are located at the boundaries between the Eurasian, Philippine Sea, and Pacific plates, with frequent earthquakes and numerous active structures. In the Tohoku Region, for example, the Ou Backbone Range is bounded on its both sides by two major active structural systems: the Eastern Marginal Fault Zone of the Yokote Basin in the west and the Western Marginal Fault Zone of the Kitakami Lowland in the east. However, the relative activeness and characteristics of these two systems are still not clear. As fluvial systems are capable of recording variations of topography caused by tectonic, climatic, lithologic, and anthropogenic influences, we hope to further understand these two structural systems using fluvial geomorphology of the Ou Backbone Range area.
In this study, we analyzed river profiles to obtain the geomorphic index χ and the river steepness index (k_{sn}). The results show that the steepness index of river channels along the two flanks of the Ou Backbone Range are different, likely indicating different tectonic activities. However, we also found a number of knickpoints along several river networks. We investigated these knickpoints with satellite imagery and field surveys. Our results show that these knickpoints are mostly produced by local resistant rock layers or check dams, instead of reflecting different states of tectonic activity.
Therefore, we were able to exclude the influence of the knickpoints and to focus only on the results of river steepness index. The results show that rivers along the western flank of the Ou Backbone Range generally have steeper channels than those along the eastern flank. This suggests that the uplift rate of the range’s western flank is higher, and the structures in the west may have higher activity. The results are consistent with the vertical slip rate estimates of the faults; ~1 mm/yr for the western flank and 0.2-0.4 mm/yr for the eastern flank. Moreover, the northern segment of the range’s western flank has the steepest river channels. This result appears to correspond with the surface ruptures of the Senya fault, Ota fault, and other related faults during the 1896 Rikuu earthquake. As a result, we propose that the northern segment of the Eastern Marginal Fault Zone of the Yokote Basin may be the primary structural system in the region, producing the faster uplift of the range and rapid subsidence of the basin, and steeper channels along the western flank of the Ou Backbone Range.

Keywords: Neotectonic activity, river steepness index, fluvial geomorphic index χ, Ou Backbone Range, Japan

©2019. Japan Geoscience Union. All Right Reserved.

Tsunami record of the last 700 years in bottom sediment of lake Kasumi-ga-ura, southeastern part of Ibaragi Prefecture

*Yoshio Inouchi[1]

1. Faculty of Human Sciences, Waseda University

Lake Kasumi-ga-ura connects the Pacific Ocean via Tone River. Sampling site in this lake lies more than 50km far from the river mouth of Tone. Maximum tidal height at March 11, 2011 was +2.5m at the river mouth of Tone and +1.6m at water gate located 18km from the river mouth. Based on these facts, we started studies on tsunamiites in bottom sediment of Lake Kasumi-ga-ura. Cored sediment of 77cm length was taken at the central part of the lake where water depth is 6m on August 21, 2018. CT scan photograph was taken and samples for grain size analysis at each 1cm thickness were taken. Tephra seams of Asama-A in 1873 A.D. and Fuji Hoei in 1707 A.D. were observed at depth 42cm and 50cm respectively. Shells of *Corbicula japonica* were observed at depth from 70 to 73cm. More than 10 event layers were observed having more than 10 micrometers in mean diameter and relatively less transparency in X-ray. Sand size particles are chiefly composed of minerals of quartz, feldspar, pyroxene etc. and fragments of pumices and scorias and sometimes minor plant fragments and shell fragments. Sedimentary ages of event layers estimated based on dry weight of sediment and ages and depths of tephras show good correlation to historical large tsunamis. As mentioned above, Lake Kasumi-ga-ura locates more than 50km far from the river mouth of Tone. Tidal height is supposed to decrease rapidly. But existence of event sediments in Lake Kasumi-ga-ura shows that large tsunamis could reach that lake. Those sediment can be correlated to tsunamis of Showa Sanriku in 1933, Chiba Boso in 1909, Meiji Sanriku in 1896, Chile in 1877 or 1837, Genroku in 1703, Enpou Boso in 1677, keichou in 1605 or Keichou Sanriku in 1611, Tenshou in 1586, Meiou in 1498 or Kyouroku in 1454 and Shouhei in 1361.

Keywords: tsunami, earthquake, lake, sediment, grain size

©2019. Japan Geoscience Union. All Right Reserved.

Detecting concealed fault by microtremor H/V study in Miura Peninsula

*Kazuzi Ogawa[1], Yasuyuki Iwase[1], Takumi Murakoshi[1], Toshihisa Itano[1]

1. National Defense Academy

The Miura Peninsula in the southern part of the Kanto region has many active faults. According to geologic map described by Geological Survey of Japan, there is a concealed fault that has about E-W strike in the center of Shonankokusaimura (Etoh et al., 1998). Therefore, in this study, we adopted a microtremor H/V study to detect this concealed fault. Microtremor is a vibration that is constantly shaking the ground even when there is no earthquake. It occurs from natural phenomena and human activities. It contains information on the ground which is the medium of propagation of tremor though it seems random noise. Currently, method of microtremor H/V spectral ratio is widely used such as site effects assessment (Nakamura et al., 1986), underground structure estimation (Gueguen et al., 2000) and detecting active fault (Shibuya, 2008; Sant et al., 2017).

In this study, we carried out microtremor measurements at 15 points across the fault using the JU410 seismometer. Sampling rate was 100 Hz and 15 minutes measurements were conducted for each observational point. In the analysis, the averaged H/V spectral ratio was calculated from the non-overlapped data sets in which the data window length and number were set to 20 seconds and 45, respectively, and noisy portions were removed. The calculation method of the H/V spectral ratio in this study is as follows. At first, Fourier spectra of N-S, E-W, and U-D wave components are calculated. Secondly, H/V spectral ratio is calculated from dividing the square root of the sum of N-S and E-W components by U-D components. Finally, NS/UD and EW/UD are obtained from dividing the N-S by the U-D components and dividing the E-W by the U-D components, respectively. Final process is performed separately from the second in order to take into account the anisotropy for the N-S and E-W directions.

As a result, change of the peak frequencies of the H/V spectral ratio in the direction perpendicular to the fault strike is confirmed and the peak frequencies of the H/V spectral ratio are about 5 Hz in the northern part and about 3 Hz in the southern part, respectively, and its boundary locates approximately 100 meters south of the concealed faults described in the geological map. This suggests the depth of the boundary between the basement rock and sedimentary layer is decreasing from the north to the south in the center of Shonankokusaimura. Focusing on the direction, EW/UD tends to be larger than NS/UD at the frequency that shows the peak in the H/V spectral ratio. These results may show the possibility of existence of the concealed fault in the center of Shonankokusaimura and imply the occurrence of anisotropy of the H/V spectral ratio near the fault. It is expected that the microtremor measurements and analysis considering anisotropy of wave components can lead to future fault research.

Keywords: Microtremor, H/V spectral ratio, Concealed fault, Anisotropy

©2019. Japan Geoscience Union. All Right Reserved.

Distribution, geometry and slip rates of branch faults around the Kita-Izu fault zone

*Ryuhei Oda[1], Daisuke Ishimura[1], Takehiko Suzuki[1]

1. Tokyo Metropolitan University

In the northeastern part of the Izu Peninsula, there is the Kita-Izu fault zone which extends N-S direction. A branch fault group showing NW-SE strike (Earthquake Research Committee, 2005) is distributed in the east side of the Kita-Izu fault zone. However, slip rates of branch faults have not been estimated. Additionally, the distribution and formation ages of geomorphic surfaces around the Kita-Izu fault zone have not been revealed. Thus, we focus on branch faults (oblique, subparallel to the Tanna fault or Ukihashi central fault) and clarify the distribution, geometry and slip rates of them. Furthermore, we reveal the distribution of geomorphic surfaces around the Kita-Izu fault zone and consider formation ages of them.
In this study, we carried out geomorphic interpretation, field surveys, and measuring the amount of displacements of branch faults using DEM data. In field surveys, we observed fault topographies along active faults and deposits forming geomorphic surfaces around active faults.
From geomorphic interpretation, branch faults are located mainly on the east side of the Tanna fault and the Ukihashi central fault. They are composed of left-lateral slip faults striking N-S and right-lateral slip faults striking NW-SE or E-W. From field surveys, deposits that can estimate formation ages of geomorphic surfaces were not identified. Therefore, we used ages of geology (Oikawa et al., 2011) as lower limits of formation ages of geomorphic surfaces.
Lower limits of slip rates of branch faults were estimated using vertical and horizontal displacements and lower limits of formation ages of geomorphic surfaces. As a result, lower limits of horizontal and vertical slip rates of branch faults were estimated to be 0.10-1.0 mm/yr and 0.01-0.10 mm/yr, respectively. Similarly, we estimated horizontal slip rates of the Tanna and Ukihashi central faults and compared to those of branch faults. Then, we found that horizontal slip rates of Tanna and Ukihashi central faults are one order larger than those of branch faults. Thus, the activity of branch faults is considered to be lower than that of Tanna and Ukihashi central faults. In the north of the Tanna fault, left-lateral slip active faults striking N-S or NW-SE are located. These faults and the Tanna fault form right-stepping en echelon arrays and their slip rates are larger than those of branch faults. Furthermore, there is a possibility that they acted with the Tanna fault in Kita-Izu earthquake in 1930. Thus, some left-lateral slip active faults located in the north of the Tanna fault may constitute the northern end of the Tanna fault.

Keywords: Kita-Izu fault zone, Tanna fault, Ukihashi central fault, branch faults, slip rate

©2019. Japan Geoscience Union. All Right Reserved.

Paleoseismology of the southern part of Kamishiro fault, ISTL active fault zone, central Japan

*Kotaro Mizutani[1], Daisuke Hirouchi[1], Nobuhisa Matsuta[2], Tatsuya Ishiyama[3], Nobuhiko Sugito[4], Ken-ichi Yasue[5], Yoshihiro Takeshita[1], Natsuko Fujita[6], Hiroshi Sawa[7], Ryosuke Doke[8], Haruo Maruyama[9], Kazutaka Ikeda[10], Kamishiro Fault

1. Shinshu University, 2. Okayama University, 3. ERI, University of Tokyo, 4. Hosei University, 5. Toyama University, 6. JAEA, 7. Tsuruoka Nat.Col.Tech., 8. Hot Springs Research Institute of Kanagawa Pref., 9. Kisoseiho High school, 10. Mochiduki Elementary School

Please read the Japanese text.

Keywords: Itoigawa-Shizuoka Tectonic Line, Paleoearthquake, Kamishiro fault, Active fault

©2019. Japan Geoscience Union. All Right Reserved.

Geotectonic history of the Inadani fault zone in southern part of Nagano prefecture, central Japan

*Shuuhei Tsukui[1], Kenta Kobayashi[1]

1. Department of Geology, Faculty of Science, Niigata University

Central Japan is a region where many active faults are distributed, one of Japan's most active fault-dense areas (active fault study, 1991). Many of these active faults are characterized as high angle strike slip fault group with NE-SW strike and NW-SE strike. The Inadani fault zone, which is located in the southern part of Nagano Prefecture, is a unique fault zone characterized as a low-angle reverse fault, while the lateral slippage is dominant in this area.
The Inadani fault zone has been considered as a parallel reverse fault group of the conventional NE trending, but in recent years the evaluation of the activity to the fault group in the southern fault zone was revised, and the Inadani fault zone main part and the southeast part of the Inadani fault zone. The Inadani fault zone main part and the southeastern part were connected by the Shimojo sanroku fault which is the active fault of the NW strike, and it turned out that it is forming complicated fault geometry than conventionally thought. In this way, it is an important task to understand the tectonics of the Central Japan to elucidate how the Inadani fault zone, whose recognition for its motion image has been modified, has developed a unique form It is considered to be.
In order to elucidate the structural development history of the Inadani fault zone, a survey was conducted in the granitic distribution area expected to record longer deformation. Surface survey focused on the form of the fault, sense of movement, properties of the fault rock and so on. Stress analysis using multiple inverse method (Yamaji, 1999) was carried out in indoor work from the data obtained in the survey.In addition, XRD analysis was performed on the obtained fault rock samples to identify clay minerals contained.
From the cutting relationship between faults and the estimation of stress field, the deformation of the area was divided into three deformation stages. Stage: 1 ~ Stage: 2 is deformation with cataclasite with high angle N - S stroke, and Stage: 3 was deformation with fault gouge at low angle to medium angle. In Stage: 1, lateral shear stress solution of EW compression was detected, lateral stress stress solution of NW - SE compression in Stage: 2, and lateral shift to reverse tomographic stress solution of ENE - WSW compression in Stage: 3.
As a result of the XRD analysis, Illite and Smectite were included in all fault gouges, and the quantity ratio was changed depending on the sample.
This area is located in eastern south of southwestern Japan and is subject to clockwise rotation of the massive mass accompanying the enlargement of the Sea of Japan and counterclockwise rotation of the mass due to collision of the Izu arc. In order to discuss the stress direction , It is necessary to correct this influence. The corrected stress field is Stage: 1: E-W compressive stress field, Stage: 2: N-S compressive stress field, Stage: 3: E-W to NE-SW compressive stress field, and the Scaenzuyama fault detected by Katori (2016 MS) This is in good agreement with the stress direction in which the same correction is applied to the stress direction. Therefore, it can be said that the stress detected this time is stress acting widely on the Chubu region. If the cause of the wide area stress is required for the motion of the plate, it is possible that the cataclasite which is the oldest fault rock in this area was formed by driving the westward movement of the Pacific plate after 40 Ma.

Keywords: Inadani fault zone, Fault rock, Active fault, Clay mineral

©2019. Japan Geoscience Union. All Right Reserved.

©2019. Japan Geoscience Union. All Right Reserved.

Characteristics of the fault zone with only the recent slips in the Atera Fault

Atsushi Nishida[1], *Tomoyuki Ohtani[1], Takuya Niimi[1], Jun'ichi Tsubaki[1], Keiichi Ueta[2]

1. Department of Civil Engineering, Gifu University, 2. CRIEPI

The activity assessment of the active faults basically needs younger sediments. To understand the fault activity in the area with no younger sediments, it is desired to develop the new method which assesses the fault activity from the fault rocks in the basement rocks. As the recent slip zone in the active fault exposure is displaced not only in the recent slip event but also the other previous events, the recent slip zone may record many slip experiences. This suggests that the characteristics of the latest slip zone reflect not only the recent slips near surface but also the other older slips in the deeper part. The fault zone with only the recent slips should be studied to understand the phenomenon that occurred in the recent slips near surface. The purpose of this study is to clarify the characteristics of the fault zone with only the recent slips. For this purpose, the Atera Fault zone has studied to understand the above characteristics. The studied exposure of the Atera Fault is located at Tase, Tsukechi, Nakatsuawa in Gifu Prefecture. In this exposure, the fault is mainly a boundary between the Quaternary sedimentary layers and the Cretaceous granite. The fault is divided into two in the upper part of the exposure. The upper and lower faults are located in the granite and at the boundary of the sediments and granite, respectively. The upper fault contacts with the sand and gravel layer in the uppermost part. Toda *et al.* (1994) have clarified that the three seismic events are detected from the exposure and that the upper fault have displaced in recent several seismic events.

The detailed observation of the fault structure, thin section observation, the powder X-ray diffraction (XRD) and the X-ray fluorescence analysis (XRF) were performed using the samples collected along the upper fault. The detailed observation of the fault structure revealed that the upper fault consists of A1 and A2 fault zone and their branch point is consistent with that of the upper and lower faults. The brown fault gouges distributes in the recent slip zone from the branch point of A1 and A2 to 4 m away from the branch point, and the light gray fault gouge far from 4 m. The latest slip occurred in the A1 fault zone based on the radiocarbon dating (Toda et al., 1994), and the cumulative amount of A1 displacement is 2.5 m from the upper plane of the granite. These fault zones involve the fragments of the surrounding weathered granite. The XRD results show that smectite appears within 1 m from the branch point. The XRF results show that Mn-rich zones are within 4 m and 3 m, respectively.
The lower fault zone had been displaced before the upper fault zone was formed, and the brown fault gouge, smectite and Mn-rich zone are included in the lower fault zone. This indicates that some of them in the upper fault zone should be displaced from the lower zone. The distribution of brown fault gouge and Mn-rich zone in the upper zone, however, cannot be explained only the fault displacement. This suggests that the recent Mn concentration would be occurred in the upper fault zone within recent several thousand years.

Keywords: fault zone, recent slips, Atera Fault

©2019. Japan Geoscience Union. All Right Reserved.

Identification of active fault location using real-time ground measurements of atmospheric methane concentration by portable Cavity Ring-down Spectroscopy system: Case study at the Atera fault

*Michito Shimo[1], Masakazu Niwa[2], Kenji Amano[2], Tomochika Tokunaga[3], Kenichi Tonokura[3], Toshifumi Matsuoka[1], Sebastien Biraud[4]

1. Fukada Geological Institute, 2. Japan Atomic Energy Agency, 3. Department of Environment Systems, University of Tokyo, 4. Lawrence Berkeley National Laboratory, USA

Faults and associated fracture zones often provide pathways for the migration of gases, such as methane, hydrogen and helium, formed in the deep subsurface formations. It is expected that information on fault location and fault activity may be obtained by measuring trace gas concentration at the ground surface.

Development of atmospheric trace gas measurement technology using Cavity Ring-Down Spectroscopy (CRDS) enabled us to measure methane gas concentration with an accuracy and precision of a few ppb and a dynamic range of 0 to 5000 ppm.

In order to investigate the applicability of this technology to active fault survey, we conducted field measurements of methane gas concentration using two portable CRDS gas analyzers (Manufacturer: Picarro Inc, models G4301 and G4302) at the Atera fault area in Gifu prefecture. Both instruments have capability of measuring methane concentration with accuracy of 3 ppb and a response time of less than 1 second. Field measurements were carried out at two locations, a fault outcrop at Tase and a fault cliff at Tsukechi town both in the Nakatsugawa city.

For measurement at the fault outcrop, a soil chamber, connected to the G4301 instrument was placed on the ground surface. Concentration of methane released from the fault was measured to be between 20 to 30 ppm. Methane release was confirmed only at the vicinity of the fault gouge and concentration 1m away from the gouge was found to be close to atmospheric background level, 1.85 to 1.88 ppm. Kurosawa et al. (2010, JAEA - Data / Code 2010 - 36) reported that maximum methane concentration was 168 ppm from their measurement using shallow boreholes excavated at the six locations along the outcrop of the Atera fault.

In the vicinity of the fault cliff, two CRDS instruments were mounted in a car and methane gas concentration in the atmosphere along the road was measured continuously with a car speed of several km/h to 30 km/h. Location of the measurements were also recorded using a GPS system. The measurement results showed anomalies of methane concentration at the two locations, approximately 1 km apart from each other, where the road and the extension of the cliff crosses. The peak atmospheric concentration of the anomalies were 1.95 to 2.05 ppm. The nearly 100 ppb difference between the anomaly peaks and the background is significant compared to the measurement accuracy of 3 ppb of the instrument. The anomalies were detected repeatedly at each location when we crossed the fault cliff. Furthermore, the methane concentration obtained by the two instruments were almost identical, confirming that these anomalies were the real responses and not associated with instrument noise.

The anomaly of 100 ppb from background suggests the methane gas emitted from the fault is diluted to about 1/200 to 1/1000 of source gas concentration. Such a small concentration signal was hardly

©2019. Japan Geoscience Union. All Right Reserved.

detected by conventional technology and was successfully detected by using the CRDS technology we employed this time.

In summary, we have confirmed that methane is emitted at the very vicinity of the fault plane at the Atera fault. We also found that the location of the fault can be successfully detected using the CRDS instrument installed on a survey vehicle. From these results, we expect that trace gas measurement using a CRDS technology can be one of the promising approaches to delineate the locations of the active faults creating migration paths of the deep-seated fluids.

This report is part of the achievement in FY2018 by the "Research Committee on Application of High-Accuracy Trace Gas Measurement Technology to Geological Exploration (chairman: Professor Tomochika Tokunaga, the University of Tokyo)" that is operated by the Fukada Geological Institute.

Keywords: Methane, Active fault, Gas Migration, Cavity Ring-Down Spectroscopy, Exploration, Concentration Measurement

©2019. Japan Geoscience Union. All Right Reserved.

Geomorphological evudence of a newly found active fault along the Shirakawa fault in western part Gifu Prefecture

*Yorihide Kohriya[1], Masashi Omata[1], Hiroshi Yokota[1]

1. PASCO CORPORATION

Recently, expression of micro topography was made possible by improvement of LiDER DEM technology.
The surface rupture in the southern part of Mt. Kunimi, Oshu City, Iwate Prefecture that occurred in the 2008 Iwate-Miyagi Nairiku earthquake was expressed using airborne LiDAR-derived 0.5-m-grid DEM (Maruyama et al. 2011).
It is difficult to detect fault traces in the forest zone using photographs, and it is effective to use LiDER DEM.
When 1 m grid DEM was prepared from LiDER data along Shougawa village of Shogawa village, Gifu prefecture, we confirmed new fault topography with possibility of sub fault of Shirakawa fault.
The LiDER data was measured by Jinzu River Sabo Office, Hokuriku Regional Development Bureau, MLIT in 2016.
The photograph taken at the same time as LiDER is difficult to recognize fault topography because it is a forest zone.

At the Kiya point along the Sho river, west side of study area, the trench of the Shirakawa fault was investigated (Sugiyama et al. 1993).
In the trench survey, at least one earthquake event has been certified since 2,500 y.B.P.
However, the last event and activity interval are unclear.
A new fault trace is found on the right bank slope of Nonomata Valley on the east side of Kiya, Shokawa village, Gifu Prefecture, and the length reaches 1.3 km.
The fault topography along the trace is a gentle slope and a reverse-facing fault scarplet which are linearly continuous on the slope of the mountain.
The vertical component is a western uplift similar to the Shirakawa fault, and is about 10 to 20 m from the topography section.
There is a weak left offset ridge across the fault topography.
In addition, a left offset ridge with a slope top of about 200 m is found on the northern side of the fault topography.
From these evidences we assume that this fault has repeated activity.
In the southern part of the fault topography there are reverse-facing fault scarplet and relatively wide gentle slopes, which are suitable for trench survey.
At this point there is no accumulation of coarse-grained sediments by rivers, and there is little loss of formation. Therefore it is possible to identify the last event of the Shirakawa fault.
Reference
Maruyama, T., Toda, S., Yoshimi, M., Ando, R., Takada, Y., Saito, E., Lin, Z., Omata, M., 2011, Characteristics of the northernmost part of the surface rupture associated with the 2008 Iwate-Miyagi Nairiku, Japan, earthquake, Active Fault Research, 34, 1-12.
Nakata, T., Imaizumi, T., 2002,
Sugiyama, Y., Awata, Y., Tsukuda, E., 1993, Trenching Study of the Shirakawa Fault of the Miboro Fault System at Kidani, Gifu Prefecture in 1990, Active Fault Research, 11, 65-70.

©2019. Japan Geoscience Union. All Right Reserved.

Keywords: Shirakawa Fault, fault topography, Digital elevation model

©2019. Japan Geoscience Union. All Right Reserved.

Active faults around the Niu Mountains, northern part of Fukui Prefecture, Japan

*Masayoshi Tajikara[1], Takashi Nakata[2], Hiroyuki Tsutsumi[3], Hideaki Goto[2]

1. Association for the Development of Earthquake Prediction, 2. Hiroshima University, 3. Doshisha University

The Niu Mountains is located between Japan Sea and the Fukui Plain, northern Fukui Prefecture. Many active faults have already been reported around the Niu Mountains (e.g., Research Group for Active Faults, 1991). Along the eastern coastal area of the Niu Mountains, the Yanagase-Sekigahara Fault develops in submarine area, and the Ayukawa Faults develop in the land area, respectively. In the eastern side of the Niu Mountains, the Sarage Fault, the Asahi Fault, the Semiguchi Fault, the Sabae Fault, and the Ozowara Fault are mapped, but tectonic landforms of these active faults have not been described in detail. In this study, we mapped distribution of faults somewhat different from previous studies by interpretation of 1/10000 air photographs and stereoscopic image created from 5-10 m DEM of GSI. In this presentation, we report the precise distribution and characteristics of tectonic landforms of these active faults, and discuss their tectonic implications briefly.

This study was done as a part of the Supporting Project for the Headquarters for Earthquake Research Promotion sponsored by the Ministry of Education, Culture, Sports, Science and Technology, Japan.

Keywords: Niu Mountains, active fault, Sarage fault, Semiguchi fault, Asahi fault

©2019. Japan Geoscience Union. All Right Reserved.

Gifu-Ichinomiya Fault shown from the characteristics of the damage of the Nobi earthquake

*Nobuhisa Matsuta[1,2], Fumiaki KIMATA[2]

1. Okayama University Graduate School of Education, 2. Tono Research Institute of Earthquake Science

The record of the historical earthquake in Japan shows that the ratio of the number of victims to the number of completely destroyed houses increases in the case of the earthquake in which the surface rupture. Using this relationship, we discussed the question "Is there a surface rupture along the Gifu-Ichinomiya fault at the time of the Nobi earthquake?" The record used for the examination is the damaged data in the municipality at the time. As a result, it was found that the ratio of the number of victims to the number of completely destroyed houses is higher along the Gifu - Ichinomiya fault than in the surrounding area. Therefore, Gifu - Ichinomiya fault existed, we believe there was a displacement in the Nobi earthquake.

Keywords: Nobi earthquake, Gifu-Ichinomiya line, surface rupture, completely destroyed house, victim

©2019. Japan Geoscience Union. All Right Reserved.

Electrical resistivity structure from the surface to the seismogenic zone below the Gomura fault zone, Kyoto, Southwest Japan

*Satoru Yamaguchi[1], Akira Mimura[1], Kazuki Fukue[1], Shigehiro Katoh[2], Hideki Murakami[3], Makoto Uyeshima[4]

1. Department of Geosciences, Graduate School of Science, Osaka City University, 2. The Museum of Nature and Human Activities, Hyogo, 3. Science and Technology Unit, Research and Education Faculty, Kochi University, 4. Earthquake Research Institute, The University of Tokyo

The Gomura Fault Zone in the Tango Peninsula, Kyoto, consists of three fault segments, the Go-seihou, Gomura, and Chuzenji Faults. They show different features in fault activity (average slip rates, the latest events etc.). The Go-seihou Fault is a very short in length (~2.8km long) with no clear displacement. Along the Gomura Fault, a clear surface rupture has appeared at the 1927 Kita-Tango earthquake. Cumulative geomorphological displacement is well recognized along the Chuzenji Fault, but no surface rupture appeared at the 1927 Kita-Tango earthquake. Conductivity structure can be one of the crucial elements to clarify subsurface structure of active faults. Furthermore, the Gomura fault zone is especially suitable for studying the relationships between conductivity structure and fault activity because three faults run nearly parallel within about 3km in simple geological setting.
We proposed the conductivity models of the Gomura Fault Zone combining the two conductivity models; one is the shallow model (0 –1.5 km in depth) and the deep model (0 -12 km in depth). The shallow model is determined based on the result obtained using an audio-frequency magnetotelluric (AMT) method which is excellent in shallow part resolution. While, the deep model is determined based on the result using a wide-band magnetotelluric (WBMT) method which is suitable for wide- and deep-range survey.
The final model is characterized and interpreted as follows.
(1) The final model covers from the surface to a depth of 12 km including the epicenter of the 1927 Kita-Tango earthquake and three faults (the Go-seihou, Gomura and Chuzenji Faults).
(2) The final model is characterized by six conductive zones and one resistive zone.
(3) The fault plane of the Gomura Fault starts the hypocenter of the 1927 Kita-Tango earthquake, goes through seismogenic and conductive region, and reaches to the Gomura Fault.
(4) The clear conductive zones were detected below both the Gomura and Chuzenji Faults in the shallow model. The conductive zone below the Gomura Fault is wider and more conductive than that below the Chuzenji Fault. We interpreted these differences reflect the latest faulting event age: that of the Gomura Fault (~90 yrs. ago) is much younger than that of the Chuzenji Fault. The conductive zones are formed by intruding groundwater into a damage zone around the faults.
(5) No conductive zone is recognized below the Go-seihou Fault and the result indicates that the fault is a secondary fault.
(6) The bottom of the resistive zone can be interpreted as that of the Miyazu granite.

Keywords: Gomura fault, Electrical conductivity, active fault, Magnetotellurics

©2019. Japan Geoscience Union. All Right Reserved.

Re-analysis and re-interpretation of the very shallow land seismic reflection survey data across the Naruto-South fault, north side of Tokushima Plain.

*Kobayashi Takayuki[1], Dai Nobuoka[2], Tomio Inazaki[1]

1. Public Works Research Institute Japan, 2. OYO Corporation

We conducted re-analysis and re-interpretation of the very shallow land seismic reflection survey data across the Naruto-South fault, north side of Tokushima Plain. In this study, we show that more detailed active fault structures are obtained by re-analysis and re-interpret old data to give useful information for urban disaster planning. The Naruto-south fault is located in Tokushima Prefecture, the eastern part of Shikoku island, Japan. It is the branch of the Median Tectonic Line (MTL) active fault system. The Naruto south fault is situated 500m to 1000m south of Naruto fault, and cut the Tokushima alluvial plain. The length of the it is expected about 8km (Tokushima Prefecture, 1998). The last faulting event is in 16th century or later. The probability of earthquake indicated the MTL active fault is very low, 0 to 0.4% within 30 years. In the other hand, the expected magnitude of earthquake is very high, 8, and, when the earthquake are occurred, its damage will be tremendous. From this fact, to minimize damages, the clarifying fault structure is required. So, we re-analyze and re-interpret the very shallow S-wave land seismic reflection survey data across the Naruto-South fault acquired in 1998 to obtain more detailed structure of the fault. Measurement length is 100m, receiver spacing is 0.5m and shot source interval is 1.0m. S-wave portable vibrator is utilized for seismic source. Sweep frequency is 40 to 300Hz and sweep length is 7s. As the result of re-analysis, we obtained more detailed active fault structure less than 50m depth. In this study, we can identify the position of the about 70 degrees dip fault, lied from 15m to 50m depth, with more resolution. Also, we achieved to show the continuous structure, not cut off by the active fault, more clearly than conventional. Also, by applying the dating method results, we could estimate the displacement of fault. Maximum displacement is 14.4m, 10.8kyBP to 12.2kyBP, and deformation rate is 1.77mm/yr.

Keywords: Active fault, seismic reflection survey

©2019. Japan Geoscience Union. All Right Reserved.

Bathymetric mapping and seafloor imaging for finding historical records of Nankai earthquakes at Nomi bay in Susaki city, Kochi Prefecture, Japan

*Wataru Tanikawa[1], Masafumi MURAYAMA[2], Hidekazu Tokuyama[3], Kouki Tanaka[4], Akira Ijiri[1], Tatsuhiko Hoshino[1], Takehiro Hirose[1], Kazuya Kitada[5], Toshiya Fujiwara[5]

1. Japan Agency for Marine-Earth Science and Technology, Kochi Instutute for Core Sample Research, 2. Kochi Univerisity, Faculty of Agriculture and Marine Science, 3. Kochi Univerisity, Center for Advanced Marine Core Research , 4. Kochi Univerisity, 5. Japan Agency for Marine-Earth Science and Technology

In a coastal area of Nomi bay (Susaki city, Kochi Prefecture, Japan), a traditional tale about a village named Kuroda-gori (or Nomi sengen, Otani sengen), which was probably submerged during the Hakuho Nankai earthquake of AD 684, has been passed down orally. Local residents reported a well on the seabed at Nomi bay. However, evidence linking Kuroda-gori to these sites and to historical earthquake is lacking. Therefore, we investigated seabed at Nomi bay near Heshima Island and Otani area to find the artifacts that can be related to historical earthquakes.

Our data were obtained from a research boat “Neptune” of Kochi University. The detailed bathymetric maps and the acoustic reflection distribution maps were acquired by a side-scan sonar system. A sub-bottom profiler was also used to obtain a geological structure below the seabed. Underwater omnidirectional camera was used to observe seafloor carefully.

In a bathymetrical map, the small submarine plateaus (200m×300m in area) was found on the north-western part of Heshima Island, delimited by a steep slope. The plateau was located at the depth of around 10 m. Sediment sampling by gravity corers and underwater images from camera showed that the seafloor on the plateau was composed by hard sandy materials and large conglomerate blocks. On the contrary, the seafloors on the outside of the plateau was composed by soft clayey sediments. No artifact or artificial structure were observed from the sub-bottom profiling data. Several strange mosaic images were obtained from the side scan sonar, and then divers identified some of the strange images were artifacts (an octopus pot, a vinyl sheet). We did not discover a well on the seafloor from mosaic images, underwater camera, or sub-bottom images.
The submarine plateau was probably formed by wave-induced erosion, and Shimomura (1980) reported the similar submarine structures and concluded that the plateaus was formed by the subsidence during the Hakuho Nankai earthquake of AD 684. While any well-like structures were not found, gravels (boulder) arranged in a circle were observed. Therefore, the well that local residents suggested might be the gravels. We plan to perform dating analysis (e.g. radiocarbon dating) using subsea floor sediments at the plateau to assess the co-seismic subsidence. We present preliminary results obtained from a scientific cruise at Urano-uchi Bay on March 2019.

Keywords: coseismic subsidence, Kuroda-gori, submarine plateaus, side scan sonnar , sub-bottom profiling

©2019. Japan Geoscience Union. All Right Reserved.

Tectonic geomorphological and paleoseismological study in the Anoriguchi Canyon: Foraminiferal analysis and ^{14}C dating

*Nobuhiko Sugito[1], Masao Iwai[2], Hitomi Wakaki-Uchimura[2], Hiroki Matsui[2], Yasuhiro Suzuki[3]

1. Faculty of Sustainability Studies, Hosei University, 2. Center for Advanced Marine Core Research, Kochi University, 3. Disaster Mitigation Research Center, Nagoya University

It is well known that there exist numerous submarine active faults in the Nankai Trough area. We have to reveal geometry and slip history of these faults, to reveal the origins of the past destructive earthquakes as well as to predict future large earthquakes in more detail. From this point of view, we have conducted a tectonic geomorphological and paleoseismological feasibility study on a submarine active fault of the Nankai Trough area in the Anoriguchi Canyon from FY2016 (Sugito et al., 2018). In this presentation, we report our result of a series of core analysis, including foraminiferal analysis and radiocarbon dating. Based on the data obtained, we infer that the submarine active fault across the Anoriguchi Canyon probably slipped one or more time(s) during this ~10,000 years to produce north-side-up vertical offset of ~10 m. This study illustrates the importance of the tectonic geomorphological and paleoseismological approaches in the studies of historical earthquakes and near-future earthquake potentials.

<Acknowledgements>
The drilled cores have been stored and analyzed under the cooperative research program of Center for Advanced Marine Core Research, Kochi University (16B070, 17A030, 17B030, 18A027, and 18B025). Takuya Matsuzaki and the colleagues (Kochi University) supported our research. Radiocarbon dating was conducted by Institute of Accelerator Analysis Ltd. We thank Hideaki Goto (Hiroshima University) for his constructive suggestion to this abstract. This study was supported by MEXT, under its Earthquake and Volcano Hazards Observation and Research Program, and JSPS KAKENHI Grant Number 15H02959.

<References>
Sugito et al., 2018, The 125th Ann. Meet. Geol. Soc. Japan, R8-P-7.

Keywords: Submarine active fault, Multi-beam echo sounding, Piston coring, Foraminiferal assemblage, Fault-related landform, Nankai Trough

©2019. Japan Geoscience Union. All Right Reserved.

Subsurface survey around the Matoishi-bokujo 1 Fault in the northwest of the outer rim of the Aso caldera, southwestern Japan

*Takayuki Nakano[1], Hiroshi Une[1], Hiroshi, P. Sato[2], Keitaro Komura[3]

1. GSI of Japan, 2. Nihon Univ., 3. CRIEPI

1. Introduction

A lot of linear surface displacement derived by the 2016 Kumamoto Earthquake (Mj 7.3) were detected by InSAR analysis around the northwest of the outer rim of the Aso caldera, central Kyushu Island, southwestern Japan, and it is estimated that they were displaced passively. Many of them appeared along the known active faults. We have investigated the detail topography and geology to elucidate the mechanism around Matoishi-bokujo 1 Fault. In this presentation, we report the results of the subsurface structure survey found by using topographical/geological survey and ground-penetrating radar (GPR) survey.

2. Result & Discussion

The trenching survey at the foot of fault scarp of the Matoishi-bokujo 1 Fault showed that a white color pyroclastic layer presumed as Aso-4 pyroclastic flow deposit (89Ka) was observed around GL-3.5m (EL= ca. 917.4m) in deep case and GL-0.3m (EL= ca. 921.6m) in shallow case (Une et al., 2018). Also, the topographical and geological survey around the fault showed that the Aso-4 pyroclastic flow deposit was observed at the stream bed on the north side of the fault (EL= ca. 917.8m) and at the gully bed on the south side of the fault (EL= ca. 935.0m). Furthermore, on the east side of the site, the outcrop of stratum considered to be representative of the sedimentary structure in this area can be observed, and it was found that blackish soil layer and loam layer sandwiching multiple tephra layers above the Aso-4 pyroclastic flow deposit accumulated ca. 5m in thickness.

GPR profiles performed on the survey line crossing the fault showed clear echoes in GL-2m to -4m on the south side of the fault. It is presumed from the trenching survey and geological survey in the waterway on the south side of the fault so far that these clear echoes correspond to the upper surface of loam layer below the subsurface blackish soil or riverbed gravel layer covering the loam. On the north side of the fault, since GPR echoes are decayed drastically at deeper than GL-1 to -1.5m (EL= ca. 930.5 to 931.0m), it is suggested that there are a layer with a relative dielectric constant greater than that of the upper layer (blackish soil) at GL -1.5m or deeper. In addition, there is a weak echo around GL -4 to -5m (EL= ca. 927 to 928m). It is possible that this weak echo corresponds to the upper surface of the Aso-4 pyroclastic flow deposit from its continuity.

From these result, although the shape of the upper surface of the Aso-4 pyroclastic flow deposit is roughly similar to the present topography surface, it is located at GL-5m deeper on the south side of the fault and around GL-4 to -5m at the north side of the fault. Therefore, its relative height difference is estimated to be about 13 m or more, and this is considered to be the apparent vertical offset of the fault for ca. 90,000 years.

3. Summary and Challenges

As a result of topographical and geological investigation and the subsurface structure survey around the Matoishi-bokujo 1 Fault which was secondarily displaced associated with the Kumamoto Earthquake, we could presume the subsurface structure and the apparent vertical offset of the Aso-4 pyroclastic flow deposit surface. We plan to analyze and interpret the GPR profile in more detail with reference to the result of percussion boring in the future.

©2019. Japan Geoscience Union. All Right Reserved.

Acknowledgements:
The authors would like to express the deepest appreciation to Prof. Yasuhiro Suzuki at Nagoya Univ. for borrowing GPR survey devices. The part of this work was supported by JSPS KAKENHI Grant Number JP17K01234.

References:

Fujiwara et al. (2016): Earth, Planets and Space, 68:160.
Nakano et al. (2018): AGU Fall Meeting 2018.
Une et al. (2018): JSAF Fall Meeting in 2018.

Keywords: Matoishi-bokujo 1 Fault, GPR survey, topographical and geological investigation, trenching survey, the 2016 Kumamoto Earthquake

©2019. Japan Geoscience Union. All Right Reserved.

Past activity of 'triggered fault' in the northwest of outer rim of Aso caldera estimated from the results of excurvation survey and displacement topography

*Hiroshi Une[1], Takayuki Nakano[1], Hiroshi, P. Sato[2], Hiroshi YAGI[3], Keitaro Komura[4]

1. Geospatial Information Authority of Japan, 2. Nihon University, 3. Yamagata University, 4. Central Research Institute of Electric Power Industry

Matoishi Bokujo 1 Fault is one of the "triggered faults" in the northwest of outer rim of Aso caldera associated with the Kumamoto Earthquake in 2016 with clear tectonic geomorphology, significant phase discontinuity appeared in SAR interferometry and surface displacement in the field. We carried out a geomorphological and geological survey including a pit excavation, ground penetrating radar (GPR) survey and simple core samplings in a site on the fault, and discussed the history of past activities. We excavated a pit with 10 m long and 4 m deep at maximum at the bottom of the fault scarp and observed the both walls. A white Aso-4 pyroclastic flow deposit appeared at the bottom of the walls, directly covered by a river bed deposit composed of medium sand and granule and a debris flow deposit composed of rubble on the pit valley side, and the slope sediments of brown sand and mud with rubble on the pit mountain side. They are covered with slope sediments of black sand and mud that accompanies with rubble or that are scarce in rubble. At least two fault ruptures appeared with displacements of these strata and disorientation of gravel. We assume that the upper surface of Aso-4 at the bottom of the walls shows the unconformity of the deposition surface when the pyroclastic flow arrived in 90,000 year BP, for the low relief surface surrounds this area which is the deposition surface of Aso-4 pyroclastic flow, and outcrops of Aso-4 pyroclastic flow deposit are widely observed at a comparatively shallow position, i.e. several meters below the surface of the earth. From the pit survey and the simple core samplings, it is estimated that the upper layer of the white layer gradually lowers its altitude from the south to the north toward the fault scarp, and is raised about 10 m above the fault scarp, consistent with the topography and displacement pattern by SAR interferometry. Considering the results of the ^{14}C dating of the black soil of the slope sediments collected from the wall, a faulting event which brought the movement of slope deposits from the mountain side resulting the coverage of river deposit at the valley side occurred in between about 3,500 and about 3,400 years ago, followed by another faulting event that caused two fault ruptures in between about 3,500 and about 2,000 years ago or younger. It is suggested that the number of events experienced by lower slope sediments is larger than that of upper one (the amount of displacement of upper one is about 2 times). This suggests that the accumulation of displacements like this time formed fault scarp of Matoishi Bokujo I Fault.

ACKNOWLEDGMENT: This work was supported by JSPS KAKENHI Grant Number (JP17K01234) (Research Director: Hiroshi P. Sato). The ownership of Daichi 2 (ALOS-2) data is in the Japan Aerospace Exploration Agency (JAXA). In the field survey and analysis of the materials, we received great cooperation from the students of the Kaneda laboratory of the Graduate School of Science of Chiba University and the Department of Geography of the Nihon University School of Science and Engineering.

Keywords: Kumamoto Earthquake, SAR Interferometry, surface rupture, triggered fault, cumulativeness

©2019. Japan Geoscience Union. All Right Reserved.

Visualization of three-dimensional SAR analysis data by stereo isogram map: Precise detection of surface ruptures of the 2016 Kumamoto earthquake sequence

*Yasuo Awata[1]

1. Institute of Earthquake and Volcano Geology, Geological Survey of Japan, National Institute of Advanced Industrial Science and Technology

Advances in geodetic surveying technology make it possible to grasp the crustal deformation in a wide range from several cms to several meters. In particular, the observation by the spaceborne SAR enables high-resolution detection of crustal deformation using interferometric and three-dimensional analysis. These advances are bringing about a major change to the conventional field investigation method of surface ruptures associated with earthquakes. Here, I tried to visualize the 3D-SAR data of the 2016 Kumamoto earthquake sequence (Kobayashi, 2017) to detect the regional and local surficial deformations with high accuracy.

For visualization of 3D-SAR data to high-resolution and high-dynamic-range images, the stereo contour and relief mapping method is applied. The 3D data is divided into three components, the east-west, north-south, and vertical components, each consists of geographic coordinates and a single value. The isogram map having fine line interval up to the equivalent to the accuracy of data is generated from the data. For east-west and vertical components having the high accuracy, practically fine isogram at a line interval up to 1 cm are drown. Those isogram images are processed into anaglyph capable of stereoscopic viewing with a wide field of view.

In the visual interpretation using an anaglyph image at a line interval of 1 cm, both the main fault zones (Futagawa River, Idenokuchi and Takagi earthquake faults) accompanied by regional crustal deformation and numerous small ruptures scattered in a 50 km square area are observed in a single image. The interpretation results of small ruptures are generally consistent with that of Fijiwara et al. (2016) based on conventional InSAR images that spatial resolution is assumed to be one digit higher. It is easy to detect the ruptures with a displacement of east-west and north-south components of about 5 cm using the image. Furthermore, ruptures up to 2 cm in displacement are recognizable in the Kumamoto urban area where the gradient of regional deformation is small. In the field survey based on the 3D-image interpretation, I found those small ruptures and measured the displacements of guardrails, road curbs, and concrete structures.

Keywords: 3D-SAR, stereo isogram map, 2016 Kumamoto earthquake sequence, surface rupture

©2019. Japan Geoscience Union. All Right Reserved.

Preliminary active fault mapping of Mongolia by interpretation of ALOS 30 DEM image

*Takashi Nakata[1], Yasuhiro Suzuki[2], Mitsuhisa Watanabe[3]

1. Hiroshima University, 2. Nagoya University, 3. Toyo University

Mongolia has experienced huge earthquakes generated from extensive active faults in the 20th Century, namely 1905 Tsetserleg (M7.9), 1905 Bulnai (M8.4), 1931 Fu-Yun (M8.0), 1857 Gobi-Altai (8.1) and 1967 Mogod (M7.1). These earthquakes were generated from pre-existing active faults that have been studied in detail. However most of the other extensive active faults were mapped mainly based by 2D satellite and Google Earth imageries, and they are commonly delineated along distinctive topographic boundaries sometimes without enough evidence for late Pleistocene activities. In order to map active faults throughout Mongolia, we employ stereoscopic interpretation of anaglyph images processed from ALOS 30 DSM images to obtain topographic evidence such as fault scarps across late Pleistocene and Holocene topography and lateral stream offset for late Quaternary activities, and we compiled a preliminary active fault map of Mongolia.

Keywords: Mongolia, active fault, ALOS 30

©2019. Japan Geoscience Union. All Right Reserved.

Ground penetrating radar profiling across the Sanchiao fault in northeast Taiwan

*Mamoru Nakamura[1], How-wei Chen[2]

1. Faculty of Science, University of the Ryukyus, 2. National Central University, Taiwan

Keelung earthquake (M 6.9-7.2) occurred on December 18, 1867, in northeast Taiwan. The seismic intensity distribution and tsunami runup height distribution for this earthquake were estimated from a review of relevant literature. The seismic intensity of the earthquake reached a maximum of VII at downtown Jinshan (northeast Taiwan) according to the scale of the Central Weather Bureau of Taiwan (Cheng et al., 2016 TAO), whilst the tsunami runup height reached 6-15 m along the northeast coast of Taiwan. From the seismic intensity distribution, the source fault of the Keelung earthquake is estimated to have been at the seaward extension of the Sanchiao fault (Cheng et al., 2016 TAO). The Sanchiao fault is a normal fault, approximately 53 km in length, and passes from the south of Taipei through to Jinshan (Shyu et al., 2015 TAO). From morphological surveys, borehole surveys, and seismic reflection surveys, the Sanchiao fault is estimated to pass along the foot of the mountain to the north of downtown Jinshan. However, it is unclear whether the land area of the Sanchiao fault moved in 1867. Therefore, we carried out a Ground Penetrating Radar (GPR) survey to detect the location of the Sanchiao fault.

The GPR survey was carried out on a coastal dune to the north of Jinshan. The coastal sand dune runs in a northwest-southeast direction along the shore, perpendicularly to the Sanchiao fault. The following two types of GPR survey lines were set up: a long range type (100-200 m) running parallel to the coastal dune, and a short range type (20 m) running perpendicularly to the coastal dune. Surveys were carried out from August 15-17, 2017 and from August 13-17, 2018. Three short lines were set up parallel to the dune and two lines perpendicularly to the dune. The pulseEKKO from Sensors & Software Inc. was used for the GPR survey, and the survey frequency of the radar was 50 MHz, 100 MHz, and 250 MHz.

A conspicuous radar reflector was found in the survey line running parallel to the coastal dune. The depth of this reflection changed near the fault trace of the Sanchiao fault, as estimated from boreholes. Furthermore, the depth of the reflection at the northwestern region of the fault was approximately 1 m deeper than that at the southeastern region. This is inconsistent with the vertical displacement of the normal faulting of the Sanchiao fault that dips southeastward, and suggests that the deformation could have been caused by the branching off of the splay fault from the main Sanchiao fault.

Keywords: active fault, 1867 Keelung earthquake, Ground Penetrating Radar

©2019. Japan Geoscience Union. All Right Reserved.

Paleo-earthquake records of the Hengchun offshore structure, southern Taiwan

*Sze-Chieh Liu[1], J Bruce H Shyu[1], Yuan-Lu Tsai[1], Chuan-Chou Shen[1]

1. National Taiwan University

In the southernmost part of Taiwan, the Western Hengchun Tableland is a prominent topographic feature, with several steps of late Pleistocene uplifted marine terraces forming the top of the tableland, and uplifted Holocene coral reefs along the coast. To interpret the formation of this tableland, an inferred Hengchun offshore structure has been proposed as an active structure located offshore to the tableland’ s west. The uplift and the eastward tilting of the tableland are therefore produced by neotectonic activities of this structure. However, the presence of this structure is still debated, and no record of paleo-earthquakes related to this structure has been identified. To solve this, we utilized fossil coral microatolls as paleo-sea-level indicators to identify possible paleo-earthquake records produced by this structure. The highest level of survival (HLS) of corals is limited by the low tide level. Once living corals grow to this level, the upward growth will stop and they will grow outward instead, forming microatoll morphology with a flat top surface. This makes microatolls great tools to record local sea level history. If microatolls were uplifted and killed by co-seismic uplift, the elevation difference between microatolls and the HLS would represent the amount of uplift, and the age of the coral would constrain the age of the earthquake event. In this study, we surveyed six sites along the coast surrounding the Western Hengchun Tableland. Based on our field survey data and U-Th dating results of uplifted corals, we reconstructed a coastal uplift history of the area, and proposed several paleo-earthquake events in the past 2,500 years. These results enabled us to further understand the seismogenic properties and the possible earthquake recurrence intervals of the Hengchun offshore structure.

Keywords: coral microatolls, Hengchun offshore structure, Paleo-earthquake event

©2019. Japan Geoscience Union. All Right Reserved.

©2019. Japan Geoscience Union. All Right Reserved.

LC-InSAR analysis of the Sulawesi earthquake in Indonesia

*Jun Sugimoto[1], Masashi Omata[1], Yoshiteru Akiyama[1], Yutaka Horaku[1]

1. PASCO CORPORATION

On 28 September 2018, a shallow, large earthquake struck in the neck of the Minahasa Peninsula, Indonesia, with its epicenter located in the mountainous area, Central Sulawesi. The magnitude was 7.5.The main active onshore structure in the western part of Central Sulawesi is the left-lateral NNW-SSE trending Palu-Koro strike-slip fault that forms the boundary between the North Sula and Makassar blocks. It was reported that the earthquake caused major soil liquefaction in and around Palu.
In this study, the authors conducted the interferometry analysis using ALOS-2 data and found out the followings:
1) A phase discontinuity lines found in the LC-InSAR diagram can be Palu-Koro fault and other small strike-slip faults around Palu-Koro.
2) In the LC-InSAR diagram, areas with low coherence are distributed in a wider range than the range where damage was caused by liquefaction. This shows the possibility that the ground change has occurred in a wider range than the extent of damage caused by liquefaction.

The authors confirmed that analysis using ALOS-2 data can identify places and scopes of disasters with extensive damages occurred not only in Japan but also in other countries.

Keywords: InSAR, LC-InSAR diagram, 2018 Sulawesi earthquake, Palu-Koro fault

©2019. Japan Geoscience Union. All Right Reserved.

Risk evaluation and disaster education around the coastal areas of Sea of Marmara, Turkey through the fault model construction of the North Anatolian Fault

*Yoshiyuki Kaneda[1,2,3], Haluk Ozener[4], Nurcan Meral Ozel[4,5], Dogan Kalafat[4], Seckin Ozgur Citak , Narumi Takashi[2,3], Takane Hori[2], Muneo Hori[2,6], Mayumi Sakamoto[10,7], Ali Pinar[4], Asim Oguz Ozel[11], Ahmet Cevdet Yalciner[8], Gulum Tanircan[4], Ahmet Demirtas[9]

1. Kagawa University, 2. JAMSTEC, 3. NIED, 4. Bogazici University, 5. CTBTO, 6. ERI, 7. Nagoya University, 8. Middle East Technical University, 9. AFAD, 10. University of Hyogo, 11. Istanbul University

Recent, many destructive earthquakes and tsunamis occurred around the plate boundary in the world, which are, 2004 Sumatra Earthquake/Tsunami, 2011 East Japan Earthquake/Tsunami in Japan, and so on. Along plate boundary in Turkey, the North Anatolian Fault (NAF) distributes and the large earthquakes has occurred there. The one of the events along NAF in Turkey is the 1999 Izmit Earthquake, and severe damages was brought to residents The NAF between the eastern end of Turkey and the Aegean Sea has been ruptured in turn from the both ends, and the part off Istanbul city still remains as unruptured zone. It is considered that future large event brings fatal damages not only Istanbul city but also the entire of Turkish economy.

To prepare future large earthquake there, Japan and Turkey made an agreement to start a multidisciplinary research project, MarDiM SATREPS in 2003. The Project has four research groups with the following goals. Group 1 is Marmara Earthquake Source region observational research group to clarify seismicity, crustal structures and crustal displacement, and to construct a possible fault model. Group 2 focuses on scenario researches of earthquake occurrence along NAF and precise tsunami simulation in the Marmara region. Group 3 aims improvements and constructions of seismic characterizations and damage predictions based on observation researches and precise simulations. Group 4 promotes disaster educations using research result visuals and construct strategies of disaster mitigation.

Group 1 constructed a fault model along NAF with some asperities and with variation on the dip. The segment boundary was also identified through the modeling and it is consistent with the past rupture pattern and fluid distribution. The NAF on the western region of Sea of Marmara has creep and the rate is nearly half of block motion based on direct seafloor observation for crustal displacement. Group 2 calculated cyclic rupture pattern along NAF using heterogeneous fault model and constructed monitoring system “SWIFT” for crustal stress field by mechanisms of many events estimated automatically. We developed tsunami calculation code to image inundation around the coastal area. Group 3 investigated ground structure through regular fine shake observation, and constructed city model of industrial region supporting Turkish economy. We simulated strong motion using ground structure, city model and fault model derived from Group 1 and made a new hazard map. Group 4 considered teaching materials for disaster prevention including Japanese animation technique based on above results of three groups. These materials are utilized for disaster mitigation in Marmara region and disaster education in Turkey.

Keywords: North Anatolian Fault, Sae of Marmara , Risk evaluation, Disaster education

©2019. Japan Geoscience Union. All Right Reserved.

Estimation of fault activity by multivariate analysis using chemical composition of fault gouge

*Ryo Tateishi[1], Koji Shimada[2], Tadamasa Ueki[2], Mayuko Shimizu[2], Tetsuya Komatsu[2], Shigeru Sueoka[2], Masakazu Niwa[2], Ken-ichi Yasue[1], Tsuneari Ishimaru[2]

1. University of Toyama, 2. Japan Atomic Energy Agency

Introduction: Active faults are recognized by displacement / deformation of current topography and the Quaternary strata. However, in the absence of them, it is very difficult to decide whether the fault there is an active fault or not. In this study, we tried multivariate analysis using chemical composition data of fault gouge of active faults and inactive faults in Japan, and tried to determine the presence or absence of fault activity.
Methods: This research was carried out in the following order; collection of papers, extraction of chemical composition data of fault gouge, addition of new chemical analysis data, formatting of input data, variable selection, linear discriminant analysis. First, chemical composition data of fault gouge of active faults and inactive faults in Japan was extracted from existing publications. In this case, the extraction condition clearly describes whether the analysis target is an active fault or an inactive fault and that the basement rock is diverse. In addition, a chemical analysis of the fault gouge sample possessed by the JAEA was carried out, and we created a database that integrates both of them. In this database, in addition to the sample name and analytical value of each sample, 2 categories of active fault and inactive fault were given. Then, we decided elements to be candidates for explanatory variables from this database and arranged them as input data. Since the chemical elements extracted from the literature are not all analyzed for the same element, common elements are chosen so that the number of samples can be taken as much as possible. In order to further extract elements suitable for discrimination between active fault and inactive fault from these elements, variables were selected by two methods of Akaike Information Criterion (AIC: Akaike, 1973) and principal component analysis. Finally, linear discriminant analysis was performed using as an explanatory variable a combination of an element selected by AIC and an element whose factor loading amount was considered to be high in the principal component analysis.
Results: As a result of collection of papers, chemical composition data of fault gouge was extracted from 7 existing papers and 5 reports of the JAEA. We extracted 17 elements as candidates for variables from the database, to which a chemical analysis result of 6 fault gouge samples possessed by the JAEA was added. The number of data was 41 samples for active fault and 16 samples for inactive fault, totaling 57 samples. From these 17 elements, 13 elements were extracted as optimum combination of elements in AIC. In the principal component analysis, synthesis expressions from the first principal component to the 17th principal component were obtained, and elements with high factor loading amounts were calculated for each synthesis formula. From these results, linear discriminant analysis was carried out with a following combination of elements; (a) 13 elements of AIC, combination of elements whose average value of factor load amounts falls in the top 10 of (b) Up to the 3rd principal component of principal component analysis (explain the scattering degree of chemical composition by 65%), (c) Up to the 5th principal component (also 80%), (d) Up to the 8th principal component (also 90%). As a result, a combination of (a), (c) and (d) gives a primary equation that accurately divides the 2 groups of active fault and inactive fault.
Consideration: The elements common to the combination of the above are 6 elements of TiO_2, Al_2O_3, MgO, Na_2O, P_2O_5, Ba. Linear discriminant analysis was carried out again with (e) the combination of these 6 elements, and it resulted in accurate division of the 2 groups. Since these elements are selected by different methods or filters, there is a possibility of elements representing the difference between active faults and inactive faults. Also, as a result of assigning data of 3 specimens of fault gouge of another active

©2019. Japan Geoscience Union. All Right Reserved.

fault to each primary equation, values which are judged to be active faults in all equations were obtained. However, these values were out of the distribution range of the population, and the tendency was more conspicuous as the number of elements was larger. From this, the primary equation consisting of 6 elements of (e) was considered to be the best formula to separate active fault and inactive fault.
This study was carried out under a contract with Ministry of Economy, Trade and Industry of Japan as part of its R&D supporting program for developing geological disposal technology.
Referrence: Akaike, H., Proceedings of the 2nd International Symposium on Information Theory, Petrov, B. N., and Caski, F. (eds.), p. 267-281, 1973.

Keywords: Chemical composition of fault gouge, Multivariate analysis, Active faults and inactive faults

©2019. Japan Geoscience Union. All Right Reserved.

Bayesian optimization of fault-shape parameters using finite element analysis: parameter sets for strong slip partitioning

*Hidetaka Saomoto[1]

1. National Institute of Advanced Industrial Science and Technology

The Bayesian optimization algorithm is now a key technique in various scientific and engineering fields that require the parameter optimization. The technique can reduce the number of simulation trials as compared with the grid-search because the algorithm can act as an artificial intelligence with a statistical decision-making. Because a three-dimensional finite element analysis (FEA) for seismic faulting consumes much CPU time, the use of the Bayesian optimization with the FEA is logical and is expected to accelerate the parameter detection process.

Here, I present the method of combining an open source library Optuna (1) based on a Bayesian optimization algorithm, Tree-Structured Parzen Estimator (TPE) with the seismic faulting FEA based on COMSOL Multiphysics and then demonstrate a Baysian optimization for the fault-shape parameters that activates strong slip partitioning.

The parameter sets obtained from the Bayesian optimization algorithm result in a stronger slip partitioning than that obtained from the grid-search. More specifically, the optimized parameter set was found as a dip angle for the reverse-slip fault of 54.5 degree, a dip angle for the strile-slip fault of 86.3 degree, and the principal stress direction of 56.1 degree clockwise from the strike direction.

The Bayesian optimization detected the parameter set after 50 trials, whereas the grid-search was composed of 784 trials. In summary, the use of the Bayesian optimization algorithm is an effective and efficient way of a parameter optimization for a seismic faulting simulation that requires long CPU time.

References:

(1) Preferred Networks, Inc.: https://optuna.org/

Keywords: Active Fault, Finite Element Method, Bayesian Optimization, Slip Partitioning

©2019. Japan Geoscience Union. All Right Reserved.

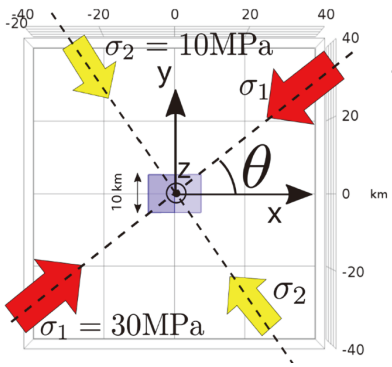

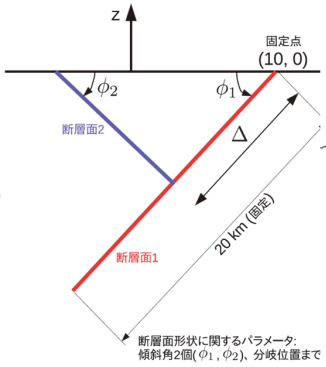

最適化するパラメータ：
主応力方位と断層面形状に関するパラメータ

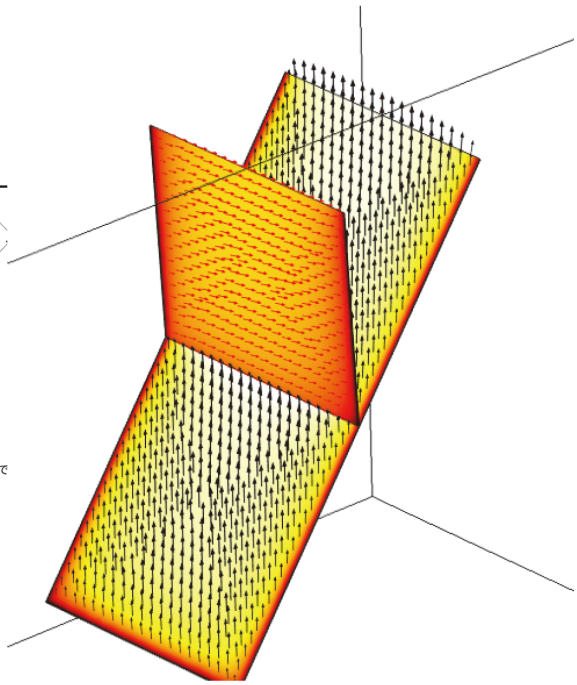

Θ= 33.8°, ϕ1= 54.5°, ϕ2= 86.3°, Δ=10 km のとき、スリップパーティショニングが生じやすいと考える

©2019. Japan Geoscience Union. All Right Reserved.

[J] Poster | S (Solid Earth Sciences)：S-SS Seismology

Tue. May 28, 2019 5:15 PM - 6:30 PM JST | Tue. May 28, 2019 8:15 AM - 9:30 AM UTC | Poster Hall International Exhibition Hall8, Makuhari Messe_31

[S-SS15] Active faults and paleoseismology

convener:Mamoru Koarai(Earth Science course, College of Science, Ibaraki University), Takashi OGAMI(National Institute of Advanced Industrial Science and Technology), Ryosuke Doke(Hot Springs Research Institute of Kanagawa Prefecture), Hisao Kondo(Geological Survey of Japan, National Institute of Advanced Industrial Science and Technology)

Geologic and historic information on seismic cycles and on the magnitude and source faults of past earthquakes is essential information to understand future large earthquakes. The study of past faulting and seismicity is an important issue for an interdisciplinary community of seismologists, geologists, geomorphologists, archaeologists, and historians.

[SSS15-P01] Paleoseismicity of Atsuma Town , Hokkaido: Evidence from landslide deposits

*Jun Tajika[1], Tetsuya Inui[2] (1.Docon Co.,Ltd., 2.Board of Education, Atsuma Town)

[SSS15-P02] Gravity survey and subsurface structure across the Aomoriwan-Seigan Fault Zone, Northeast Japan(part 2; estimation of the subsurface structure using the density of rock samples)

*Shinsuke Okada[1], Hideki Kosaka[2], Kyoko Kagohara[3], Toshifumi Imaizumi[4], Kohei Abe[5], Susumu Sakashita[5], Atsushi Miwa[5], Kouta Koshika[5], Yusuke Oda[5], Yuki tsukamoto[6], Takahiro Miyauchi[7], Tomoo Echigo[8] (1.International Research Institute of Disaster Science, Tohoku University, 2.Kankyo Chishitsu, Co. Ltd., 3.Faculty of Education, Yamaguchi University, 4.Emeritus professor of Tohoku University, 5.OYO Corporation, 6.Graduate School of Science, Tohoku University, 7.Department of Earth Sciences, Graduate School and Faculty of Science, Chiba University, 8.Geo-Research Institute)

[SSS15-P03] Was the 1611 Keicho earthquake a giant interplate event like the 2011 Tohoku earthquake?

*Tomoya Harada[1], Akihito Nishiyama[1], Kenji Satake[1], Takashi Furumura[1] (1.Earthquake Research Institute, The University of Tokyo)

[SSS15-P04] **Neotectonic characteristics along both flanks of the Ou Backbone Range, Tohoku Region, Japan, from fluvial geomorphic analyses**

*Jhih Hao Liao[1], J Bruce H Shyu[1], Yasufumi Iryu[2], Hiroyuki Tsutsumi[3], Chia-Yu Chen[1] (1.Department of Geosciences, National Taiwan University, Taipei, Taiwan, 2.Graduate School of Science, Tohoku University, Sendai, Japan, 3.Department of Environmental Systems Science, Doshisha University, Kyotanabe, Japan)

[SSS15-P05] Tsunami record of the last 700 years in bottom sediment of lake Kasumi-ga-ura, southeastern part of Ibaragi Prefecture

*Yoshio Inouchi[1] (1.Faculty of Human Sciences, Waseda University)

[SSS15-P06] Detecting concealed fault by microtremor H/V study in Miura Peninsula

*Kazuzi Ogawa[1], Yasuyuki Iwase[1], Takumi Murakoshi[1], Toshihisa Itano[1] (1.National Defense Academy)

[SSS15-P07] Distribution, geometry and slip rates of branch faults around the Kita-Izu fault zone

*Ryuhei Oda[1], Daisuke Ishimura[1], Takehiko Suzuki[1] (1.Tokyo Metropolitan University)

[SSS15-P08] Paleoseismology of the southern part of Kamishiro fault, ISTL active fault zone, central Japan

*Kotaro Mizutani[1], Daisuke Hirouchi[1], Nobuhisa Matsuta[2], Tatsuya Ishiyama[3], Nobuhiko Sugito[4], Kenichi Yasue[5], Yoshihiro Takeshita[1], Natsuko Fujita[6], Hiroshi Sawa[7], Ryosuke Doke[8], Haruo Maruyama[9], Kazutaka Ikeda[10], Kamishiro Fault (1.Shinshu University, 2.Okayama University, 3.ERI, University of Tokyo, 4.Hosei University, 5.Toyama University, 6.JAEA, 7.Tsuruoka Nat.Col.Tech., 8. Hot Springs Research Institute of Kanagawa Pref., 9.Kisoseiho High school, 10.Mochiduki Elementary School)

[SSS15-P09] **Geotectonic history of the Inadani fault zone in southern part of Nagano prefecture, central Japan**

*Shuuhei Tsukui[1], Kenta Kobayashi[1] (1.Department of Geology, Faculty of Science, Niigata University)

[SSS15-P10] Characteristics of the fault zone with only the recent slips in the Atera Fault

Atsushi Nishida[1], *Tomoyuki Ohtani[1], Takuya Niimi[1], Jun'ichi Tsubaki[1], Keiichi Ueta[2] (1.Department of Civil Engineering, Gifu University, 2.CRIEPI)

[SSS15-P11] Identification of active fault location using real-time ground measurements of atmospheric methane concentration by portable Cavity Ring-down Spectroscopy system: Case study at the Atera fault

*Michito Shimo[1], Masakazu Niwa[2], Kenji Amano[2], Tomochika Tokunaga[3], Kenichi Tonokura[3], Toshifumi Matsuoka[1], Sebastien Biraud[4] (1.Fukada Geological Institute, 2.Japan Atomic Energy Agency, 3.Department of Environment Systems, University of Tokyo, 4.Lawrence Berkeley National Laboratory, USA)

[SSS15-P12] Geomorphological evudence of a newly found active fault along the Shirakawa fault in western part Gifu Prefecture

*Yorihide Kohriya[1], Masashi Omata[1], Hiroshi Yokota[1] (1.PASCO CORPORATION)

[SSS15-P13] Active faults around the Niu Mountains, northern part of Fukui Prefecture, Japan

*Masayoshi Tajikara[1], Takashi Nakata[2], Hiroyuki Tsutsumi[3], Hideaki Goto[2] (1.Association for the Development of Earthquake Prediction, 2.Hiroshima University, 3.Doshisha University)

[SSS15-P14] Gifu-Ichinomiya Fault shown from the characteristics of the damage of the Nobi earthquake

*Nobuhisa Matsuta[1,2], Fumiaki KIMATA[2] (1.Okayama University Graduate School of Education, 2.Tono Research Institute of Earthquake Science)

[SSS15-P15] Electrical resistivity structure from the surface to the seismogenic zone below the Gomura fault zone, Kyoto, Southwest Japan

*Satoru Yamaguchi[1], Akira Mimura[1], Kazuki Fukue[1], Shigehiro Katoh[2], Hideki Murakami[3], Makoto Uyeshima[4] (1.Department of Geosciences, Graduate School of Science, Osaka City University, 2.The Museum of Nature and Human Activities, Hyogo, 3.Science and Technology Unit, Research and Education Faculty, Kochi University, 4.Earthquake Research Institute, The University of Tokyo)

[SSS15-P16] Re-analysis and re-interpretation of the very shallow land seismic reflection survey data across the Naruto-South fault, north side of Tokushima Plain.

*Kobayashi Takayuki[1], Dai Nobuoka[2], Tomio Inazaki[1] (1.Public Works Research Institute Japan, 2.OYO Corporation)

[SSS15-P17] Bathymetric mapping and seafloor imaging for finding historical records of Nankai earthquakes at Nomi bay in Susaki city, Kochi Prefecture, Japan

*Wataru Tanikawa[1], Masafumi MURAYAMA[2], Hidekazu Tokuyama[3], Kouki Tanaka[4], Akira Ijiri[1], Tatsuhiko Hoshino[1], Takehiro Hirose[1], Kazuya Kitada[5], Toshiya Fujiwara[5] (1.Japan Agency for Marine-Earth Science and Technology, Kochi Instutute for Core Sample Research, 2.Kochi Univerisity, Faculty of Agriculture and

Marine Science, 3.Kochi Univerisity, Center for Advanced Marine Core Research , 4.Kochi Univerisity, 5.Japan Agency for Marine-Earth Science and Technology)

[SSS15-P18] Tectonic geomorphological and paleoseismological study in the Anoriguchi Canyon: Foraminiferal analysis and ^{14}C dating

*Nobuhiko Sugito[1], Masao Iwai[2], Hitomi Wakaki-Uchimura[2], Hiroki Matsui[2], Yasuhiro Suzuki[3] (1.Faculty of Sustainability Studies, Hosei University, 2.Center for Advanced Marine Core Research, Kochi University, 3.Disaster Mitigation Research Center, Nagoya University)

[SSS15-P19] Subsurface survey around the Matoishi-bokujo 1 Fault in the northwest of the outer rim of the Aso caldera, southwestern Japan

*Takayuki Nakano[1], Hiroshi Une[1], Hiroshi, P. Sato[2], Keitaro Komura[3] (1.GSI of Japan, 2.Nihon Univ., 3.CRIEPI)

[SSS15-P20] Past activity of 'triggered fault' in the northwest of outer rim of Aso caldera estimated from the results of excurvation survey and displacement topography

*Hiroshi Une[1], Takayuki Nakano[1], Hiroshi, P. Sato[2], Hiroshi YAGI[3], Keitaro Komura[4] (1.Geospatial Information Authority of Japan, 2.Nihon University, 3.Yamagata University, 4.Central Research Institute of Electric Power Industry)

[SSS15-P21] Visualization of three-dimensional SAR analysis data by stereo isogram map: Precise detection of surface ruptures of the 2016 Kumamoto earthquake sequence

*Yasuo Awata[1] (1.Institute of Earthquake and Volcano Geology, Geological Survey of Japan, National Institute of Advanced Industrial Science and Technology)

[SSS15-P22] Preliminary active fault mapping of Mongolia by interpretation of ALOS 30 DEM image

*Takashi Nakata[1], Yasuhiro Suzuki[2], Mitsuhisa Watanabe[3] (1.Hiroshima University, 2.Nagoya University, 3.Toyo University)

[SSS15-P23] Ground penetrating radar profiling across the Sanchiao fault in northeast Taiwan

*Mamoru Nakamura[1], How-wei Chen[2] (1.Faculty of Science, University of the Ryukyus, 2.National Central University, Taiwan)

[SSS15-P24] Paleo-earthquake records of the Hengchun offshore structure, southern Taiwan

*Sze-Chieh Liu[1], J Bruce H Shyu[1], Yuan-Lu Tsai[1], Chuan-Chou Shen[1] (1.National Taiwan University)

[SSS15-P25] LC-InSAR analysis of the Sulawesi earthquake in Indonesia

*Jun Sugimoto[1], Masashi Omata[1], Yoshiteru Akiyama[1], Yutaka Horaku[1] (1.PASCO CORPORATION)

[SSS15-P26] **Risk evaluation and disaster education around the coastal areas of Sea of Marmara, Turkey through the fault model construction of the North Anatolian Fault**

*Yoshiyuki Kaneda[1,2,3], Haluk Ozener[4], Nurcan Meral Ozel[4,5], Dogan Kalafat[4], Seckin Ozgur Citak , Narumi Takashi[2,3], Takane Hori[2], Muneo Hori[2,6], Mayumi Sakamoto[10,7], Ali Pinar[4], Asim Oguz Ozel[11], Ahmet Cevdet Yalciner[8], Gulum Tanircan[4], Ahmet Demirtas[9] (1.Kagawa University, 2.JAMSTEC, 3.NIED, 4.Bogazici University, 5.CTBTO, 6.ERI, 7.Nagoya University, 8.Middle East Technical University, 9.AFAD, 10. University of Hyogo, 11.Istanbul University)

[SSS15-P27] Estimation of fault activity by multivariate analysis using chemical composition of fault gouge

*Ryo Tateishi[1], Koji Shimada[2], Tadamasa Ueki[2], Mayuko Shimizu[2], Tetsuya Komatsu[2], Shigeru Sueoka[2], Masakazu Niwa[2], Ken-ichi Yasue[1], Tsuneari Ishimaru[2] (1.University of Toyama, 2.Japan Atomic Energy

Agency)

[SSS15-P28] Bayesian optimization of fault-shape parameters using finite element analysis: parameter sets for strong slip partitioning

*Hidetaka Saomoto[1] (1.National Institute of Advanced Industrial Science and Technology)

Paleoseismicity of Atsuma Town , Hokkaido: Evidence from landslide deposits

*Jun Tajika[1], Tetsuya Inui[2]

1. Docon Co.,Ltd., 2. Board of Education, Atsuma Town

Many landslides occurred by the 2018 Hokkaido Eastern Iburi Earthquake in Atsuma-cho. We reported about discovering of ancient landslide deposit from an archeological site of the Jomon period in Atsuma in 2004 and 2016. It was inferred that this landslide was caused by an earthquake and it probably occurred at activity event of the Ishikari teichi-toen active fault zone. The morphological characteristic of the landslide deposit resembles that of landslide caused by this earthquake. The archeological findings of the past remains excavation in Atsuma-cho area shows that the event of a lot of landslides caused by earth quake is only 2018 Hokkaido Eastern Iburi Earthquake and an earthquake of the Jomon period during last 9,000 years.

Keywords: Paleo seismology, Liquefaction, landslide body

©2019. Japan Geoscience Union. All Right Reserved.

Gravity survey and subsurface structure across the Aomoriwan-Seigan Fault Zone, Northeast Japan(part 2; estimation of the subsurface structure using the density of rock samples)

*Shinsuke Okada[1], Hideki Kosaka[2], Kyoko Kagohara[3], Toshifumi Imaizumi[4], Kohei Abe[5], Susumu Sakashita[5], Atsushi Miwa[5], Kouta Koshika[5], Yusuke Oda[5], Yuki tsukamoto[6], Takahiro Miyauchi[7], Tomoo Echigo[8]

1. International Research Institute of Disaster Science, Tohoku University, 2. Kankyo Chishitsu, Co. Ltd., 3. Faculty of Education, Yamaguchi University, 4. Emeritus professor of Tohoku University, 5. OYO Corporation, 6. Graduate School of Science, Tohoku University, 7. Department of Earth Sciences, Graduate School and Faculty of Science, Chiba University, 8. Geo-Research Institute

The Aomoriwan-Seigan Fault Zone is a fault zone of NNW-SSE trending western dipping reverse faults, which is composed of Aomoriwan West Fault, Nogiwa Fault, and Nyunai Fault. The fault zone is distributed about 31-km long along the eastern foot of the Tsugaru Mountains from Yomogita village of Aomori prefecture to Aomori city (Headquarters of Earthquake Research Promotion, 2004). We carried out a seismic reflection survey and CSAMT (Controlled Source Audio-frequency Magnetic Telluric) survey across the Aomoriwan West Fault (Kagohara et al., 2017; Sakashita et al., 2017) in 2016-2017. The low angle thrust faults of Tsugaru Fault and inclined geological structure until the depth of 1.5 km were revealed in these results. In addition to these surveys, we conducted gravity survey along the seismic survey line, and obtained the Bouguer gravity anomaly (Okada et al., 2018).
In the previous our presentation in the 2018 JpGU (Okada et al., 2018), we use the Talwani method (Talwani et al., 1959) to calculated the Bouguer gravity anomaly, in which the subsurface density structure is determined from the interpretation of the seismic and CSAMT surveys (Kagohara et al., 2017; Sakashita et al., 2017). In a part of the western part of the profile, there were some discrepancies between calculated and observed gravity anomalies. And it was also difficult to estimate the density of each layers. To resolve these problems, we conducted additional field survey and obtained several rock samplings from outcrops around the survey line, which we measured the density of samplings based on the method of Murata et al. eds. (1991). The discrepancies between calculated and observed gravity anomaly were improved by take into the layer densities from samplings.

[References]
Headquarters for Earthquake Research and Promotion, 2014, Survey Results and Evaluation of the Aomoriwan-Seigan Active Fault Zone, 16 p.
Kagohara K., et al., 2017, Seismic reflection profiling survey across the eastern foot of Tsugaru Mountains, SSS12-P08, in JpGU-AGU Joint Meeting 2017, Makuhari Messe International Convention Complex, 2017-05-23.
Okada S., et al., 2018, Gravity survey and subsurface structure across the Aomoriwan-Seigan Fault Zone, Northeast Japan, JpGU Meeting 2018, SSS08-P05, Makuhari Messe International Convention Complex, 2018-05-22.
Murata Y., et al. eds., 1991, Rock Physical Properties of Japan –Density, Magnetism, P-wave Velocity, Porosity, Thermal Conductivity –, Report of ,
Sakashita S., et al., 2017, Application of high density CSAMT exploration for active fault investing by using multi-channel electromagnetic suvey system, SSS12-P18, in JpGU-AGU Joint Meeting 2017, Makuhari Messe International Convention Complex, 2017-05-23.

©2019. Japan Geoscience Union. All Right Reserved.

Talwani M., et al., Rapid gravity computations for 2-dimensional bodies with application to the Mendocino submarine fracture zone, J. Geophys. Res., 64, 49-59, doi:10.1029/JZ064i001p00049.

Keywords: Gravity survey, Bouguer gravity anomaly, Rock density measuring, Aomoriwan-Seigan Fault Zone, Seismic reflection survey, CSAMT survey

©2019. Japan Geoscience Union. All Right Reserved.

Was the 1611 Keicho earthquake a giant interplate event like the 2011 Tohoku earthquake?

*Tomoya Harada[1], Akihito Nishiyama[1], Kenji Satake[1], Takashi Furumura[1]

1. Earthquake Research Institute, The University of Tokyo

After the 2011 Tohoku earthquake (M9.0), the 1611 Keicho earthquake along the Japan trench has been regarded as a giant interplate event. In this study, from the examination of reliability of the historical records about the 1611 event and comparison between the impact on Kanto by the 2011 and 1611 events, we consider that the 1611 earthquake was not a giant interplate event but a tsunami/outer-rise earthquake.
From the historical documents, the Dec. 2nd, 1611 Keicho earthquake generated large tsunami on the Pacific Coasts of Tohoku and Hokkaido while this event caused no seismic damage in Tohoku and Kanto. Since the 1896 tsunami earthqauke (M8.1) and 1933 outer-rise earthquake (M8.1) had similar features, the 1611 event had been regarded as an M~8 tsunami/outer-rise earthquake (Hatori, 1975; Aida, 1977; Watanabe, 1998). After the 2011 Tohoku earthquake, however, some studies claimed that the 1611 earthquake was probably a giant event because the tsunami heights and inundation areas estimated from the historical documents (e.g. Hatori, 1975; Tsuji et al., 2011; Ebina and Imai, 2014) are comparable to (or larger than) those of the 2011 event (e.g. Ebina, 2014; Iwamoto, 2013). Following this claim, tsunami researchers attempted to make fault models to reproduce the 1611 tsunami by the tsunami numerical simulation. Imai et al. (2015) proposed two fault models. One is a giant interplate event (fault size: 400km*200km, Mw8.7), another is a model (Mw8.4) of simultaneous occurrence of a great interplate event (fault size: 400km*150km) and a great outer-rise event (fault size: 400km*50km). Fukuhara and Tanioka (2017) considered that the 1611 event was a giant tsunami earthquake (fault size: 250km*50km, the maximum slip: 80m, Mw9.0).
In this study, however, we considered that the 1611 Keicho earthquake was not a giant interplate event but a M~8 tsunami/outer-rise earthquake from the following reasons: (1) Reliability of the 1611 tsunami heights and inundation areas is not high because they are estimated from the historical records without examination of reliability. There are historians who dispute the 1611 giant earthquake based on the unreliable historical records (e.g. Kan’no, 2014; Sasaki, 2014; Saino, 2017); (2) Strong shaking by the 2011 mainshock caused severe damage in Kanto and aftershocks and induced events caused additional damage and successive shakings in this region for several weeks. Whereas, as for the 1611 earthquake, only two shakings in Edo (present Tokyo) are recorded in the court nobles' diaries and there is no record of the seismic damage in Kanto. From the primary historical documents, Ieyasu Tokugawa went hunting with hawks to the present Saitama Pref. and court nobles went sightseeing to environs of Edo on the next day of the 1611 event. Therefore, the 1611 earthquake was probably an event which didn’t impact on Kanto, i.e. not a giant interplate event like the 2011 earthquake. M~8 interplate event in 1793 offshore present Miyagi Pref. caused minor seismic damage in Edo and its 2-days aftershocks shocked Edo more than 50 times (Usami et al. 2013); (3) Even if the 1611 earthquake was an M~9 tsunami event, ~80m slip on the large fault (250km*50km) should cause many aftershocks and widely induce earthquakes including M7-8 events. As mentioned above, however, there is no record about the successive earthquakes after the 1611 event; (4) No tsunami deposit by the 1611 event is discovered at the ruins in Sendai Plain excepting Taka-ose Ruin in the present Iwanuma City (Saino, 2017), while they are discovered on the Sanriku Coasts (e.g. Takada et al., 2016). In addition, they are not discovered at the Idagawa marsh in the present Fukushima Pref. (Kusumoto, et al. 2018). Therefor, 1611 tsunami probably didn’t inundate deeply in the lowlands on the Pacific Coast in Miyagi and Fukushima Pref. Recently, Goto et al. (2019) reported that the

©2019. Japan Geoscience Union. All Right Reserved.

1611 tsunami deposits were not discovered at the Numano-hama of Sanriku Coast.

Keywords: 1611 Keicho earthquake, a giant interplate earthquake, reliability of historical records, primary historical documents, tsunami heights and inundation areas, tsunami traces

©2019. Japan Geoscience Union. All Right Reserved.

Neotectonic characteristics along both flanks of the Ou Backbone Range, Tohoku Region, Japan, from fluvial geomorphic analyses

*Jhih Hao Liao[1], J Bruce H Shyu[1], Yasufumi Iryu[2], Hiroyuki Tsutsumi[3], Chia-Yu Chen[1]

1. Department of Geosciences, National Taiwan University, Taipei, Taiwan, 2. Graduate School of Science, Tohoku University, Sendai, Japan, 3. Department of Environmental Systems Science, Doshisha University, Kyotanabe, Japan

The islands of Japan are located at the boundaries between the Eurasian, Philippine Sea, and Pacific plates, with frequent earthquakes and numerous active structures. In the Tohoku Region, for example, the Ou Backbone Range is bounded on its both sides by two major active structural systems: the Eastern Marginal Fault Zone of the Yokote Basin in the west and the Western Marginal Fault Zone of the Kitakami Lowland in the east. However, the relative activeness and characteristics of these two systems are still not clear. As fluvial systems are capable of recording variations of topography caused by tectonic, climatic, lithologic, and anthropogenic influences, we hope to further understand these two structural systems using fluvial geomorphology of the Ou Backbone Range area.
In this study, we analyzed river profiles to obtain the geomorphic index χ and the river steepness index (k_{sn}). The results show that the steepness index of river channels along the two flanks of the Ou Backbone Range are different, likely indicating different tectonic activities. However, we also found a number of knickpoints along several river networks. We investigated these knickpoints with satellite imagery and field surveys. Our results show that these knickpoints are mostly produced by local resistant rock layers or check dams, instead of reflecting different states of tectonic activity.
Therefore, we were able to exclude the influence of the knickpoints and to focus only on the results of river steepness index. The results show that rivers along the western flank of the Ou Backbone Range generally have steeper channels than those along the eastern flank. This suggests that the uplift rate of the range’s western flank is higher, and the structures in the west may have higher activity. The results are consistent with the vertical slip rate estimates of the faults; ~1 mm/yr for the western flank and 0.2-0.4 mm/yr for the eastern flank. Moreover, the northern segment of the range’s western flank has the steepest river channels. This result appears to correspond with the surface ruptures of the Senya fault, Ota fault, and other related faults during the 1896 Rikuu earthquake. As a result, we propose that the northern segment of the Eastern Marginal Fault Zone of the Yokote Basin may be the primary structural system in the region, producing the faster uplift of the range and rapid subsidence of the basin, and steeper channels along the western flank of the Ou Backbone Range.

Keywords: Neotectonic activity, river steepness index, fluvial geomorphic index χ, Ou Backbone Range, Japan

©2019. Japan Geoscience Union. All Right Reserved.

Tsunami record of the last 700 years in bottom sediment of lake Kasumi-ga-ura, southeastern part of Ibaragi Prefecture

*Yoshio Inouchi[1]

1. Faculty of Human Sciences, Waseda University

Lake Kasumi-ga-ura connects the Pacific Ocean via Tone River. Sampling site in this lake lies more than 50km far from the river mouth of Tone. Maximum tidal height at March 11, 2011 was +2.5m at the river mouth of Tone and +1.6m at water gate located 18km from the river mouth. Based on these facts, we started studies on tsunamiites in bottom sediment of Lake Kasumi-ga-ura. Cored sediment of 77cm length was taken at the central part of the lake where water depth is 6m on August 21, 2018. CT scan photograph was taken and samples for grain size analysis at each 1cm thickness were taken. Tephra seams of Asama-A in 1873 A.D. and Fuji Hoei in 1707 A.D. were observed at depth 42cm and 50cm respectively. Shells of *Corbicula japonica* were observed at depth from 70 to 73cm. More than 10 event layers were observed having more than 10 micrometers in mean diameter and relatively less transparency in X-ray. Sand size particles are chiefly composed of minerals of quartz, feldspar, pyroxene etc. and fragments of pumices and scorias and sometimes minor plant fragments and shell fragments. Sedimentary ages of event layers estimated based on dry weight of sediment and ages and depths of tephras show good correlation to historical large tsunamis. As mentioned above, Lake Kasumi-ga-ura locates more than 50km far from the river mouth of Tone. Tidal height is supposed to decrease rapidly. But existence of event sediments in Lake Kasumi-ga-ura shows that large tsunamis could reach that lake. Those sediment can be correlated to tsunamis of Showa Sanriku in 1933, Chiba Boso in 1909, Meiji Sanriku in 1896, Chile in 1877 or 1837, Genroku in 1703, Enpou Boso in 1677, keichou in 1605 or Keichou Sanriku in 1611, Tenshou in 1586, Meiou in 1498 or Kyouroku in 1454 and Shouhei in 1361.

Keywords: tsunami, earthquake, lake, sediment, grain size

©2019. Japan Geoscience Union. All Right Reserved.

Detecting concealed fault by microtremor H/V study in Miura Peninsula

*Kazuzi Ogawa[1], Yasuyuki Iwase[1], Takumi Murakoshi[1], Toshihisa Itano[1]

1. National Defense Academy

The Miura Peninsula in the southern part of the Kanto region has many active faults. According to geologic map described by Geological Survey of Japan, there is a concealed fault that has about E-W strike in the center of Shonankokusaimura (Etoh et al., 1998). Therefore, in this study, we adopted a microtremor H/V study to detect this concealed fault. Microtremor is a vibration that is constantly shaking the ground even when there is no earthquake. It occurs from natural phenomena and human activities. It contains information on the ground which is the medium of propagation of tremor though it seems random noise. Currently, method of microtremor H/V spectral ratio is widely used such as site effects assessment (Nakamura et al., 1986), underground structure estimation (Gueguen et al., 2000) and detecting active fault (Shibuya, 2008; Sant et al., 2017).

In this study, we carried out microtremor measurements at 15 points across the fault using the JU410 seismometer. Sampling rate was 100 Hz and 15 minutes measurements were conducted for each observational point. In the analysis, the averaged H/V spectral ratio was calculated from the non-overlapped data sets in which the data window length and number were set to 20 seconds and 45, respectively, and noisy portions were removed. The calculation method of the H/V spectral ratio in this study is as follows. At first, Fourier spectra of N-S, E-W, and U-D wave components are calculated. Secondly, H/V spectral ratio is calculated from dividing the square root of the sum of N-S and E-W components by U-D components. Finally, NS/UD and EW/UD are obtained from dividing the N-S by the U-D components and dividing the E-W by the U-D components, respectively. Final process is performed separately from the second in order to take into account the anisotropy for the N-S and E-W directions.

As a result, change of the peak frequencies of the H/V spectral ratio in the direction perpendicular to the fault strike is confirmed and the peak frequencies of the H/V spectral ratio are about 5 Hz in the northern part and about 3 Hz in the southern part, respectively, and its boundary locates approximately 100 meters south of the concealed faults described in the geological map. This suggests the depth of the boundary between the basement rock and sedimentary layer is decreasing from the north to the south in the center of Shonankokusaimura. Focusing on the direction, EW/UD tends to be larger than NS/UD at the frequency that shows the peak in the H/V spectral ratio. These results may show the possibility of existence of the concealed fault in the center of Shonankokusaimura and imply the occurrence of anisotropy of the H/V spectral ratio near the fault. It is expected that the microtremor measurements and analysis considering anisotropy of wave components can lead to future fault research.

Keywords: Microtremor, H/V spectral ratio, Concealed fault, Anisotropy

©2019. Japan Geoscience Union. All Right Reserved.

Distribution, geometry and slip rates of branch faults around the Kita-Izu fault zone

*Ryuhei Oda[1], Daisuke Ishimura[1], Takehiko Suzuki[1]

1. Tokyo Metropolitan University

In the northeastern part of the Izu Peninsula, there is the Kita-Izu fault zone which extends N-S direction. A branch fault group showing NW-SE strike (Earthquake Research Committee, 2005) is distributed in the east side of the Kita-Izu fault zone. However, slip rates of branch faults have not been estimated. Additionally, the distribution and formation ages of geomorphic surfaces around the Kita-Izu fault zone have not been revealed. Thus, we focus on branch faults (oblique, subparallel to the Tanna fault or Ukihashi central fault) and clarify the distribution, geometry and slip rates of them. Furthermore, we reveal the distribution of geomorphic surfaces around the Kita-Izu fault zone and consider formation ages of them.
In this study, we carried out geomorphic interpretation, field surveys, and measuring the amount of displacements of branch faults using DEM data. In field surveys, we observed fault topographies along active faults and deposits forming geomorphic surfaces around active faults.
From geomorphic interpretation, branch faults are located mainly on the east side of the Tanna fault and the Ukihashi central fault. They are composed of left-lateral slip faults striking N-S and right-lateral slip faults striking NW-SE or E-W. From field surveys, deposits that can estimate formation ages of geomorphic surfaces were not identified. Therefore, we used ages of geology (Oikawa et al., 2011) as lower limits of formation ages of geomorphic surfaces.
Lower limits of slip rates of branch faults were estimated using vertical and horizontal displacements and lower limits of formation ages of geomorphic surfaces. As a result, lower limits of horizontal and vertical slip rates of branch faults were estimated to be 0.10-1.0 mm/yr and 0.01-0.10 mm/yr, respectively. Similarly, we estimated horizontal slip rates of the Tanna and Ukihashi central faults and compared to those of branch faults. Then, we found that horizontal slip rates of Tanna and Ukihashi central faults are one order larger than those of branch faults. Thus, the activity of branch faults is considered to be lower than that of Tanna and Ukihashi central faults. In the north of the Tanna fault, left-lateral slip active faults striking N-S or NW-SE are located. These faults and the Tanna fault form right-stepping en echelon arrays and their slip rates are larger than those of branch faults. Furthermore, there is a possibility that they acted with the Tanna fault in Kita-Izu earthquake in 1930. Thus, some left-lateral slip active faults located in the north of the Tanna fault may constitute the northern end of the Tanna fault.

Keywords: Kita-Izu fault zone, Tanna fault, Ukihashi central fault, branch faults, slip rate

©2019. Japan Geoscience Union. All Right Reserved.

Paleoseismology of the southern part of Kamishiro fault, ISTL active fault zone, central Japan

*Kotaro Mizutani[1], Daisuke Hirouchi[1], Nobuhisa Matsuta[2], Tatsuya Ishiyama[3], Nobuhiko Sugito[4], Ken-ichi Yasue[5], Yoshihiro Takeshita[1], Natsuko Fujita[6], Hiroshi Sawa[7], Ryosuke Doke[8], Haruo Maruyama[9], Kazutaka Ikeda[10], Kamishiro Fault

1. Shinshu University, 2. Okayama University, 3. ERI, University of Tokyo, 4. Hosei University, 5. Toyama University, 6. JAEA, 7. Tsuruoka Nat.Col.Tech., 8. Hot Springs Research Institute of Kanagawa Pref., 9. Kisoseiho High school, 10. Mochiduki Elementary School

Please read the Japanese text.

Keywords: Itoigawa-Shizuoka Tectonic Line, Paleoearthquake, Kamishiro fault, Active fault

©2019. Japan Geoscience Union. All Right Reserved.

Geotectonic history of the Inadani fault zone in southern part of Nagano prefecture, central Japan

*Shuuhei Tsukui[1], Kenta Kobayashi[1]

1. Department of Geology, Faculty of Science, Niigata University

Central Japan is a region where many active faults are distributed, one of Japan's most active fault-dense areas (active fault study, 1991). Many of these active faults are characterized as high angle strike slip fault group with NE-SW strike and NW-SE strike. The Inadani fault zone, which is located in the southern part of Nagano Prefecture, is a unique fault zone characterized as a low-angle reverse fault, while the lateral slippage is dominant in this area.
The Inadani fault zone has been considered as a parallel reverse fault group of the conventional NE trending, but in recent years the evaluation of the activity to the fault group in the southern fault zone was revised, and the Inadani fault zone main part and the southeast part of the Inadani fault zone. The Inadani fault zone main part and the southeastern part were connected by the Shimojo sanroku fault which is the active fault of the NW strike, and it turned out that it is forming complicated fault geometry than conventionally thought. In this way, it is an important task to understand the tectonics of the Central Japan to elucidate how the Inadani fault zone, whose recognition for its motion image has been modified, has developed a unique form It is considered to be.
In order to elucidate the structural development history of the Inadani fault zone, a survey was conducted in the granitic distribution area expected to record longer deformation. Surface survey focused on the form of the fault, sense of movement, properties of the fault rock and so on. Stress analysis using multiple inverse method (Yamaji, 1999) was carried out in indoor work from the data obtained in the survey.In addition, XRD analysis was performed on the obtained fault rock samples to identify clay minerals contained.
From the cutting relationship between faults and the estimation of stress field, the deformation of the area was divided into three deformation stages. Stage: 1 ~ Stage: 2 is deformation with cataclasite with high angle N - S stroke, and Stage: 3 was deformation with fault gouge at low angle to medium angle. In Stage: 1, lateral shear stress solution of EW compression was detected, lateral stress stress solution of NW - SE compression in Stage: 2, and lateral shift to reverse tomographic stress solution of ENE - WSW compression in Stage: 3.
As a result of the XRD analysis, Illite and Smectite were included in all fault gouges, and the quantity ratio was changed depending on the sample.
This area is located in eastern south of southwestern Japan and is subject to clockwise rotation of the massive mass accompanying the enlargement of the Sea of Japan and counterclockwise rotation of the mass due to collision of the Izu arc. In order to discuss the stress direction , It is necessary to correct this influence. The corrected stress field is Stage: 1: E-W compressive stress field, Stage: 2: N-S compressive stress field, Stage: 3: E-W to NE-SW compressive stress field, and the Scaenzuyama fault detected by Katori (2016 MS) This is in good agreement with the stress direction in which the same correction is applied to the stress direction. Therefore, it can be said that the stress detected this time is stress acting widely on the Chubu region. If the cause of the wide area stress is required for the motion of the plate, it is possible that the cataclasite which is the oldest fault rock in this area was formed by driving the westward movement of the Pacific plate after 40 Ma.

Keywords: Inadani fault zone, Fault rock, Active fault, Clay mineral

©2019. Japan Geoscience Union. All Right Reserved.

©2019. Japan Geoscience Union. All Right Reserved.

Characteristics of the fault zone with only the recent slips in the Atera Fault

Atsushi Nishida[1], *Tomoyuki Ohtani[1], Takuya Niimi[1], Jun'ichi Tsubaki[1], Keiichi Ueta[2]

1. Department of Civil Engineering, Gifu University, 2. CRIEPI

The activity assessment of the active faults basically needs younger sediments. To understand the fault activity in the area with no younger sediments, it is desired to develop the new method which assesses the fault activity from the fault rocks in the basement rocks. As the recent slip zone in the active fault exposure is displaced not only in the recent slip event but also the other previous events, the recent slip zone may record many slip experiences. This suggests that the characteristics of the latest slip zone reflect not only the recent slips near surface but also the other older slips in the deeper part. The fault zone with only the recent slips should be studied to understand the phenomenon that occurred in the recent slips near surface. The purpose of this study is to clarify the characteristics of the fault zone with only the recent slips. For this purpose, the Atera Fault zone has studied to understand the above characteristics. The studied exposure of the Atera Fault is located at Tase, Tsukechi, Nakatsuawa in Gifu Prefecture. In this exposure, the fault is mainly a boundary between the Quaternary sedimentary layers and the Cretaceous granite. The fault is divided into two in the upper part of the exposure. The upper and lower faults are located in the granite and at the boundary of the sediments and granite, respectively. The upper fault contacts with the sand and gravel layer in the uppermost part. Toda *et al.* (1994) have clarified that the three seismic events are detected from the exposure and that the upper fault have displaced in recent several seismic events.

The detailed observation of the fault structure, thin section observation, the powder X-ray diffraction (XRD) and the X-ray fluorescence analysis (XRF) were performed using the samples collected along the upper fault. The detailed observation of the fault structure revealed that the upper fault consists of A1 and A2 fault zone and their branch point is consistent with that of the upper and lower faults. The brown fault gouges distributes in the recent slip zone from the branch point of A1 and A2 to 4 m away from the branch point, and the light gray fault gouge far from 4 m. The latest slip occurred in the A1 fault zone based on the radiocarbon dating (Toda et al., 1994), and the cumulative amount of A1 displacement is 2.5 m from the upper plane of the granite. These fault zones involve the fragments of the surrounding weathered granite. The XRD results show that smectite appears within 1 m from the branch point. The XRF results show that Mn-rich zones are within 4 m and 3 m, respectively.
The lower fault zone had been displaced before the upper fault zone was formed, and the brown fault gouge, smectite and Mn-rich zone are included in the lower fault zone. This indicates that some of them in the upper fault zone should be displaced from the lower zone. The distribution of brown fault gouge and Mn-rich zone in the upper zone, however, cannot be explained only the fault displacement. This suggests that the recent Mn concentration would be occurred in the upper fault zone within recent several thousand years.

Keywords: fault zone, recent slips, Atera Fault

©2019. Japan Geoscience Union. All Right Reserved.

Identification of active fault location using real-time ground measurements of atmospheric methane concentration by portable Cavity Ring-down Spectroscopy system: Case study at the Atera fault

*Michito Shimo[1], Masakazu Niwa[2], Kenji Amano[2], Tomochika Tokunaga[3], Kenichi Tonokura[3], Toshifumi Matsuoka[1], Sebastien Biraud[4]

1. Fukada Geological Institute, 2. Japan Atomic Energy Agency, 3. Department of Environment Systems, University of Tokyo, 4. Lawrence Berkeley National Laboratory, USA

Faults and associated fracture zones often provide pathways for the migration of gases, such as methane, hydrogen and helium, formed in the deep subsurface formations. It is expected that information on fault location and fault activity may be obtained by measuring trace gas concentration at the ground surface.

Development of atmospheric trace gas measurement technology using Cavity Ring-Down Spectroscopy (CRDS) enabled us to measure methane gas concentration with an accuracy and precision of a few ppb and a dynamic range of 0 to 5000 ppm.

In order to investigate the applicability of this technology to active fault survey, we conducted field measurements of methane gas concentration using two portable CRDS gas analyzers (Manufacturer: Picarro Inc, models G4301 and G4302) at the Atera fault area in Gifu prefecture. Both instruments have capability of measuring methane concentration with accuracy of 3 ppb and a response time of less than 1 second. Field measurements were carried out at two locations, a fault outcrop at Tase and a fault cliff at Tsukechi town both in the Nakatsugawa city.

For measurement at the fault outcrop, a soil chamber, connected to the G4301 instrument was placed on the ground surface. Concentration of methane released from the fault was measured to be between 20 to 30 ppm. Methane release was confirmed only at the vicinity of the fault gouge and concentration 1m away from the gouge was found to be close to atmospheric background level, 1.85 to 1.88 ppm. Kurosawa et al. (2010, JAEA - Data / Code 2010 - 36) reported that maximum methane concentration was 168 ppm from their measurement using shallow boreholes excavated at the six locations along the outcrop of the Atera fault.

In the vicinity of the fault cliff, two CRDS instruments were mounted in a car and methane gas concentration in the atmosphere along the road was measured continuously with a car speed of several km/h to 30 km/h. Location of the measurements were also recorded using a GPS system. The measurement results showed anomalies of methane concentration at the two locations, approximately 1 km apart from each other, where the road and the extension of the cliff crosses. The peak atmospheric concentration of the anomalies were 1.95 to 2.05 ppm. The nearly 100 ppb difference between the anomaly peaks and the background is significant compared to the measurement accuracy of 3 ppb of the instrument. The anomalies were detected repeatedly at each location when we crossed the fault cliff. Furthermore, the methane concentration obtained by the two instruments were almost identical, confirming that these anomalies were the real responses and not associated with instrument noise.

The anomaly of 100 ppb from background suggests the methane gas emitted from the fault is diluted to about 1/200 to 1/1000 of source gas concentration. Such a small concentration signal was hardly

©2019. Japan Geoscience Union. All Right Reserved.

detected by conventional technology and was successfully detected by using the CRDS technology we employed this time.

In summary, we have confirmed that methane is emitted at the very vicinity of the fault plane at the Atera fault. We also found that the location of the fault can be successfully detected using the CRDS instrument installed on a survey vehicle. From these results, we expect that trace gas measurement using a CRDS technology can be one of the promising approaches to delineate the locations of the active faults creating migration paths of the deep-seated fluids.

This report is part of the achievement in FY2018 by the "Research Committee on Application of High-Accuracy Trace Gas Measurement Technology to Geological Exploration (chairman: Professor Tomochika Tokunaga, the University of Tokyo)" that is operated by the Fukada Geological Institute.

Keywords: Methane, Active fault, Gas Migration, Cavity Ring-Down Spectroscopy, Exploration, Concentration Measurement

©2019. Japan Geoscience Union. All Right Reserved.

Geomorphological evudence of a newly found active fault along the Shirakawa fault in western part Gifu Prefecture

*Yorihide Kohriya[1], Masashi Omata[1], Hiroshi Yokota[1]

1. PASCO CORPORATION

Recently, expression of micro topography was made possible by improvement of LiDER DEM technology.
The surface rupture in the southern part of Mt. Kunimi, Oshu City, Iwate Prefecture that occurred in the 2008 Iwate-Miyagi Nairiku earthquake was expressed using airborne LiDAR-derived 0.5-m-grid DEM (Maruyama et al. 2011).
It is difficult to detect fault traces in the forest zone using photographs, and it is effective to use LiDER DEM.
When 1 m grid DEM was prepared from LiDER data along Shougawa village of Shogawa village, Gifu prefecture, we confirmed new fault topography with possibility of sub fault of Shirakawa fault.
The LiDER data was measured by Jinzu River Sabo Office, Hokuriku Regional Development Bureau, MLIT in 2016.
The photograph taken at the same time as LiDER is difficult to recognize fault topography because it is a forest zone.

At the Kiya point along the Sho river, west side of study area, the trench of the Shirakawa fault was investigated (Sugiyama et al. 1993).
In the trench survey, at least one earthquake event has been certified since 2,500 y.B.P.
However, the last event and activity interval are unclear.
A new fault trace is found on the right bank slope of Nonomata Valley on the east side of Kiya, Shokawa village, Gifu Prefecture, and the length reaches 1.3 km.
The fault topography along the trace is a gentle slope and a reverse-facing fault scarplet which are linearly continuous on the slope of the mountain.
The vertical component is a western uplift similar to the Shirakawa fault, and is about 10 to 20 m from the topography section.
There is a weak left offset ridge across the fault topography.
In addition, a left offset ridge with a slope top of about 200 m is found on the northern side of the fault topography.
From these evidences we assume that this fault has repeated activity.
In the southern part of the fault topography there are reverse-facing fault scarplet and relatively wide gentle slopes, which are suitable for trench survey.
At this point there is no accumulation of coarse-grained sediments by rivers, and there is little loss of formation. Therefore it is possible to identify the last event of the Shirakawa fault.
Reference
Maruyama, T., Toda, S., Yoshimi, M., Ando, R., Takada, Y., Saito, E., Lin, Z., Omata, M., 2011, Characteristics of the northernmost part of the surface rupture associated with the 2008 Iwate-Miyagi Nairiku, Japan, earthquake, Active Fault Research, 34, 1-12.
Nakata, T., Imaizumi, T., 2002,
Sugiyama, Y., Awata, Y., Tsukuda, E., 1993, Trenching Study of the Shirakawa Fault of the Miboro Fault System at Kidani, Gifu Prefecture in 1990, Active Fault Research, 11, 65-70.

©2019. Japan Geoscience Union. All Right Reserved.

Keywords: Shirakawa Fault, fault topography, Digital elevation model

©2019. Japan Geoscience Union. All Right Reserved.

Active faults around the Niu Mountains, northern part of Fukui Prefecture, Japan

*Masayoshi Tajikara[1], Takashi Nakata[2], Hiroyuki Tsutsumi[3], Hideaki Goto[2]

1. Association for the Development of Earthquake Prediction, 2. Hiroshima University, 3. Doshisha University

The Niu Mountains is located between Japan Sea and the Fukui Plain, northern Fukui Prefecture. Many active faults have already been reported around the Niu Mountains (e.g., Research Group for Active Faults, 1991). Along the eastern coastal area of the Niu Mountains, the Yanagase-Sekigahara Fault develops in submarine area, and the Ayukawa Faults develop in the land area, respectively. In the eastern side of the Niu Mountains, the Sarage Fault, the Asahi Fault, the Semiguchi Fault, the Sabae Fault, and the Ozowara Fault are mapped, but tectonic landforms of these active faults have not been described in detail. In this study, we mapped distribution of faults somewhat different from previous studies by interpretation of 1/10000 air photographs and stereoscopic image created from 5-10 m DEM of GSI. In this presentation, we report the precise distribution and characteristics of tectonic landforms of these active faults, and discuss their tectonic implications briefly.

This study was done as a part of the Supporting Project for the Headquarters for Earthquake Research Promotion sponsored by the Ministry of Education, Culture, Sports, Science and Technology, Japan.

Keywords: Niu Mountains, active fault, Sarage fault, Semiguchi fault, Asahi fault

©2019. Japan Geoscience Union. All Right Reserved.

Gifu-Ichinomiya Fault shown from the characteristics of the damage of the Nobi earthquake

*Nobuhisa Matsuta[1,2], Fumiaki KIMATA[2]

1. Okayama University Graduate School of Education, 2. Tono Research Institute of Earthquake Science

The record of the historical earthquake in Japan shows that the ratio of the number of victims to the number of completely destroyed houses increases in the case of the earthquake in which the surface rupture. Using this relationship, we discussed the question "Is there a surface rupture along the Gifu-Ichinomiya fault at the time of the Nobi earthquake?" The record used for the examination is the damaged data in the municipality at the time. As a result, it was found that the ratio of the number of victims to the number of completely destroyed houses is higher along the Gifu - Ichinomiya fault than in the surrounding area. Therefore, Gifu - Ichinomiya fault existed, we believe there was a displacement in the Nobi earthquake.

Keywords: Nobi earthquake, Gifu-Ichinomiya line, surface rupture, completely destroyed house, victim

©2019. Japan Geoscience Union. All Right Reserved.

Electrical resistivity structure from the surface to the seismogenic zone below the Gomura fault zone, Kyoto, Southwest Japan

*Satoru Yamaguchi[1], Akira Mimura[1], Kazuki Fukue[1], Shigehiro Katoh[2], Hideki Murakami[3], Makoto Uyeshima[4]

1. Department of Geosciences, Graduate School of Science, Osaka City University, 2. The Museum of Nature and Human Activities, Hyogo, 3. Science and Technology Unit, Research and Education Faculty, Kochi University, 4. Earthquake Research Institute, The University of Tokyo

The Gomura Fault Zone in the Tango Peninsula, Kyoto, consists of three fault segments, the Go-seihou, Gomura, and Chuzenji Faults. They show different features in fault activity (average slip rates, the latest events etc.). The Go-seihou Fault is a very short in length (~2.8km long) with no clear displacement. Along the Gomura Fault, a clear surface rupture has appeared at the 1927 Kita-Tango earthquake. Cumulative geomorphological displacement is well recognized along the Chuzenji Fault, but no surface rupture appeared at the 1927 Kita-Tango earthquake. Conductivity structure can be one of the crucial elements to clarify subsurface structure of active faults. Furthermore, the Gomura fault zone is especially suitable for studying the relationships between conductivity structure and fault activity because three faults run nearly parallel within about 3km in simple geological setting.
We proposed the conductivity models of the Gomura Fault Zone combining the two conductivity models; one is the shallow model (0 –1.5 km in depth) and the deep model (0 -12 km in depth). The shallow model is determined based on the result obtained using an audio-frequency magnetotelluric (AMT) method which is excellent in shallow part resolution. While, the deep model is determined based on the result using a wide-band magnetotelluric (WBMT) method which is suitable for wide- and deep-range survey.
The final model is characterized and interpreted as follows.
(1) The final model covers from the surface to a depth of 12 km including the epicenter of the 1927 Kita-Tango earthquake and three faults (the Go-seihou, Gomura and Chuzenji Faults).
(2) The final model is characterized by six conductive zones and one resistive zone.
(3) The fault plane of the Gomura Fault starts the hypocenter of the 1927 Kita-Tango earthquake, goes through seismogenic and conductive region, and reaches to the Gomura Fault.
(4) The clear conductive zones were detected below both the Gomura and Chuzenji Faults in the shallow model. The conductive zone below the Gomura Fault is wider and more conductive than that below the Chuzenji Fault. We interpreted these differences reflect the latest faulting event age: that of the Gomura Fault (~90 yrs. ago) is much younger than that of the Chuzenji Fault. The conductive zones are formed by intruding groundwater into a damage zone around the faults.
(5) No conductive zone is recognized below the Go-seihou Fault and the result indicates that the fault is a secondary fault.
(6) The bottom of the resistive zone can be interpreted as that of the Miyazu granite.

Keywords: Gomura fault, Electrical conductivity, active fault, Magnetotellurics

©2019. Japan Geoscience Union. All Right Reserved.

Re-analysis and re-interpretation of the very shallow land seismic reflection survey data across the Naruto-South fault, north side of Tokushima Plain.

*Kobayashi Takayuki[1], Dai Nobuoka[2], Tomio Inazaki[1]

1. Public Works Research Institute Japan, 2. OYO Corporation

We conducted re-analysis and re-interpretation of the very shallow land seismic reflection survey data across the Naruto-South fault, north side of Tokushima Plain. In this study, we show that more detailed active fault structures are obtained by re-analysis and re-interpret old data to give useful information for urban disaster planning. The Naruto-south fault is located in Tokushima Prefecture, the eastern part of Shikoku island, Japan. It is the branch of the Median Tectonic Line (MTL) active fault system. The Naruto south fault is situated 500m to 1000m south of Naruto fault, and cut the Tokushima alluvial plain. The length of the it is expected about 8km (Tokushima Prefecture, 1998). The last faulting event is in 16th century or later. The probability of earthquake indicated the MTL active fault is very low, 0 to 0.4% within 30 years. In the other hand, the expected magnitude of earthquake is very high, 8, and, when the earthquake are occurred, its damage will be tremendous. From this fact, to minimize damages, the clarifying fault structure is required. So, we re-analyze and re-interpret the very shallow S-wave land seismic reflection survey data across the Naruto-South fault acquired in 1998 to obtain more detailed structure of the fault. Measurement length is 100m, receiver spacing is 0.5m and shot source interval is 1.0m. S-wave portable vibrator is utilized for seismic source. Sweep frequency is 40 to 300Hz and sweep length is 7s. As the result of re-analysis, we obtained more detailed active fault structure less than 50m depth. In this study, we can identify the position of the about 70 degrees dip fault, lied from 15m to 50m depth, with more resolution. Also, we achieved to show the continuous structure, not cut off by the active fault, more clearly than conventional. Also, by applying the dating method results, we could estimate the displacement of fault. Maximum displacement is 14.4m, 10.8kyBP to 12.2kyBP, and deformation rate is 1.77mm/yr.

Keywords: Active fault, seismic reflection survey

©2019. Japan Geoscience Union. All Right Reserved.

Bathymetric mapping and seafloor imaging for finding historical records of Nankai earthquakes at Nomi bay in Susaki city, Kochi Prefecture, Japan

*Wataru Tanikawa[1], Masafumi MURAYAMA[2], Hidekazu Tokuyama[3], Kouki Tanaka[4], Akira Ijiri[1], Tatsuhiko Hoshino[1], Takehiro Hirose[1], Kazuya Kitada[5], Toshiya Fujiwara[5]

1. Japan Agency for Marine-Earth Science and Technology, Kochi Instutute for Core Sample Research, 2. Kochi Univerisity, Faculty of Agriculture and Marine Science, 3. Kochi Univerisity, Center for Advanced Marine Core Research , 4. Kochi Univerisity, 5. Japan Agency for Marine-Earth Science and Technology

In a coastal area of Nomi bay (Susaki city, Kochi Prefecture, Japan), a traditional tale about a village named Kuroda-gori (or Nomi sengen, Otani sengen), which was probably submerged during the Hakuho Nankai earthquake of AD 684, has been passed down orally. Local residents reported a well on the seabed at Nomi bay. However, evidence linking Kuroda-gori to these sites and to historical earthquake is lacking. Therefore, we investigated seabed at Nomi bay near Heshima Island and Otani area to find the artifacts that can be related to historical earthquakes.

Our data were obtained from a research boat “Neptune” of Kochi University. The detailed bathymetric maps and the acoustic reflection distribution maps were acquired by a side-scan sonar system. A sub-bottom profiler was also used to obtain a geological structure below the seabed. Underwater omnidirectional camera was used to observe seafloor carefully.

In a bathymetrical map, the small submarine plateaus (200m×300m in area) was found on the north-western part of Heshima Island, delimited by a steep slope. The plateau was located at the depth of around 10 m. Sediment sampling by gravity corers and underwater images from camera showed that the seafloor on the plateau was composed by hard sandy materials and large conglomerate blocks. On the contrary, the seafloors on the outside of the plateau was composed by soft clayey sediments. No artifact or artificial structure were observed from the sub-bottom profiling data. Several strange mosaic images were obtained from the side scan sonar, and then divers identified some of the strange images were artifacts (an octopus pot, a vinyl sheet). We did not discover a well on the seafloor from mosaic images, underwater camera, or sub-bottom images.
The submarine plateau was probably formed by wave-induced erosion, and Shimomura (1980) reported the similar submarine structures and concluded that the plateaus was formed by the subsidence during the Hakuho Nankai earthquake of AD 684. While any well-like structures were not found, gravels (boulder) arranged in a circle were observed. Therefore, the well that local residents suggested might be the gravels. We plan to perform dating analysis (e.g. radiocarbon dating) using subsea floor sediments at the plateau to assess the co-seismic subsidence. We present preliminary results obtained from a scientific cruise at Urano-uchi Bay on March 2019.

Keywords: coseismic subsidence, Kuroda-gori, submarine plateaus, side scan sonnar , sub-bottom profiling

©2019. Japan Geoscience Union. All Right Reserved.

Tectonic geomorphological and paleoseismological study in the Anoriguchi Canyon: Foraminiferal analysis and ^{14}C dating

*Nobuhiko Sugito[1], Masao Iwai[2], Hitomi Wakaki-Uchimura[2], Hiroki Matsui[2], Yasuhiro Suzuki[3]

1. Faculty of Sustainability Studies, Hosei University, 2. Center for Advanced Marine Core Research, Kochi University, 3. Disaster Mitigation Research Center, Nagoya University

It is well known that there exist numerous submarine active faults in the Nankai Trough area. We have to reveal geometry and slip history of these faults, to reveal the origins of the past destructive earthquakes as well as to predict future large earthquakes in more detail. From this point of view, we have conducted a tectonic geomorphological and paleoseismological feasibility study on a submarine active fault of the Nankai Trough area in the Anoriguchi Canyon from FY2016 (Sugito et al., 2018). In this presentation, we report our result of a series of core analysis, including foraminiferal analysis and radiocarbon dating. Based on the data obtained, we infer that the submarine active fault across the Anoriguchi Canyon probably slipped one or more time(s) during this ~10,000 years to produce north-side-up vertical offset of ~10 m. This study illustrates the importance of the tectonic geomorphological and paleoseismological approaches in the studies of historical earthquakes and near-future earthquake potentials.

<Acknowledgements>
The drilled cores have been stored and analyzed under the cooperative research program of Center for Advanced Marine Core Research, Kochi University (16B070, 17A030, 17B030, 18A027, and 18B025). Takuya Matsuzaki and the colleagues (Kochi University) supported our research. Radiocarbon dating was conducted by Institute of Accelerator Analysis Ltd. We thank Hideaki Goto (Hiroshima University) for his constructive suggestion to this abstract. This study was supported by MEXT, under its Earthquake and Volcano Hazards Observation and Research Program, and JSPS KAKENHI Grant Number 15H02959.

<References>
Sugito et al., 2018, The 125th Ann. Meet. Geol. Soc. Japan, R8-P-7.

Keywords: Submarine active fault, Multi-beam echo sounding, Piston coring, Foraminiferal assemblage, Fault-related landform, Nankai Trough

©2019. Japan Geoscience Union. All Right Reserved.

Subsurface survey around the Matoishi-bokujo 1 Fault in the northwest of the outer rim of the Aso caldera, southwestern Japan

*Takayuki Nakano[1], Hiroshi Une[1], Hiroshi, P. Sato[2], Keitaro Komura[3]

1. GSI of Japan, 2. Nihon Univ., 3. CRIEPI

1. Introduction

A lot of linear surface displacement derived by the 2016 Kumamoto Earthquake (Mj 7.3) were detected by InSAR analysis around the northwest of the outer rim of the Aso caldera, central Kyushu Island, southwestern Japan, and it is estimated that they were displaced passively. Many of them appeared along the known active faults. We have investigated the detail topography and geology to elucidate the mechanism around Matoishi-bokujo 1 Fault. In this presentation, we report the results of the subsurface structure survey found by using topographical/geological survey and ground-penetrating radar (GPR) survey.

2. Result & Discussion

The trenching survey at the foot of fault scarp of the Matoishi-bokujo 1 Fault showed that a white color pyroclastic layer presumed as Aso-4 pyroclastic flow deposit (89Ka) was observed around GL-3.5m (EL= ca. 917.4m) in deep case and GL-0.3m (EL= ca. 921.6m) in shallow case (Une et al., 2018). Also, the topographical and geological survey around the fault showed that the Aso-4 pyroclastic flow deposit was observed at the stream bed on the north side of the fault (EL= ca. 917.8m) and at the gully bed on the south side of the fault (EL= ca. 935.0m). Furthermore, on the east side of the site, the outcrop of stratum considered to be representative of the sedimentary structure in this area can be observed, and it was found that blackish soil layer and loam layer sandwiching multiple tephra layers above the Aso-4 pyroclastic flow deposit accumulated ca. 5m in thickness.

GPR profiles performed on the survey line crossing the fault showed clear echoes in GL-2m to -4m on the south side of the fault. It is presumed from the trenching survey and geological survey in the waterway on the south side of the fault so far that these clear echoes correspond to the upper surface of loam layer below the subsurface blackish soil or riverbed gravel layer covering the loam. On the north side of the fault, since GPR echoes are decayed drastically at deeper than GL-1 to -1.5m (EL= ca. 930.5 to 931.0m), it is suggested that there are a layer with a relative dielectric constant greater than that of the upper layer (blackish soil) at GL -1.5m or deeper. In addition, there is a weak echo around GL -4 to -5m (EL= ca. 927 to 928m). It is possible that this weak echo corresponds to the upper surface of the Aso-4 pyroclastic flow deposit from its continuity.

From these result, although the shape of the upper surface of the Aso-4 pyroclastic flow deposit is roughly similar to the present topography surface, it is located at GL-5m deeper on the south side of the fault and around GL-4 to -5m at the north side of the fault. Therefore, its relative height difference is estimated to be about 13 m or more, and this is considered to be the apparent vertical offset of the fault for ca. 90,000 years.

3. Summary and Challenges

As a result of topographical and geological investigation and the subsurface structure survey around the Matoishi-bokujo 1 Fault which was secondarily displaced associated with the Kumamoto Earthquake, we could presume the subsurface structure and the apparent vertical offset of the Aso-4 pyroclastic flow deposit surface. We plan to analyze and interpret the GPR profile in more detail with reference to the result of percussion boring in the future.

©2019. Japan Geoscience Union. All Right Reserved.

Acknowledgements:
The authors would like to express the deepest appreciation to Prof. Yasuhiro Suzuki at Nagoya Univ. for borrowing GPR survey devices. The part of this work was supported by JSPS KAKENHI Grant Number JP17K01234.

References:

Fujiwara et al. (2016): Earth, Planets and Space, 68:160.
Nakano et al. (2018): AGU Fall Meeting 2018.
Une et al. (2018): JSAF Fall Meeting in 2018.

Keywords: Matoishi-bokujo 1 Fault, GPR survey, topographical and geological investigation, trenching survey, the 2016 Kumamoto Earthquake

©2019. Japan Geoscience Union. All Right Reserved.

Past activity of 'triggered fault' in the northwest of outer rim of Aso caldera estimated from the results of excurvation survey and displacement topography

*Hiroshi Une[1], Takayuki Nakano[1], Hiroshi, P. Sato[2], Hiroshi YAGI[3], Keitaro Komura[4]

1. Geospatial Information Authority of Japan, 2. Nihon University, 3. Yamagata University, 4. Central Research Institute of Electric Power Industry

Matoishi Bokujo 1 Fault is one of the "triggered faults" in the northwest of outer rim of Aso caldera associated with the Kumamoto Earthquake in 2016 with clear tectonic geomorphology, significant phase discontinuity appeared in SAR interferometry and surface displacement in the field. We carried out a geomorphological and geological survey including a pit excavation, ground penetrating radar (GPR) survey and simple core samplings in a site on the fault, and discussed the history of past activities. We excavated a pit with 10 m long and 4 m deep at maximum at the bottom of the fault scarp and observed the both walls. A white Aso-4 pyroclastic flow deposit appeared at the bottom of the walls, directly covered by a river bed deposit composed of medium sand and granule and a debris flow deposit composed of rubble on the pit valley side, and the slope sediments of brown sand and mud with rubble on the pit mountain side. They are covered with slope sediments of black sand and mud that accompanies with rubble or that are scarce in rubble. At least two fault ruptures appeared with displacements of these strata and disorientation of gravel. We assume that the upper surface of Aso-4 at the bottom of the walls shows the unconformity of the deposition surface when the pyroclastic flow arrived in 90,000 year BP, for the low relief surface surrounds this area which is the deposition surface of Aso-4 pyroclastic flow, and outcrops of Aso-4 pyroclastic flow deposit are widely observed at a comparatively shallow position, i.e. several meters below the surface of the earth. From the pit survey and the simple core samplings, it is estimated that the upper layer of the white layer gradually lowers its altitude from the south to the north toward the fault scarp, and is raised about 10 m above the fault scarp, consistent with the topography and displacement pattern by SAR interferometry. Considering the results of the ^{14}C dating of the black soil of the slope sediments collected from the wall, a faulting event which brought the movement of slope deposits from the mountain side resulting the coverage of river deposit at the valley side occurred in between about 3,500 and about 3,400 years ago, followed by another faulting event that caused two fault ruptures in between about 3,500 and about 2,000 years ago or younger. It is suggested that the number of events experienced by lower slope sediments is larger than that of upper one (the amount of displacement of upper one is about 2 times). This suggests that the accumulation of displacements like this time formed fault scarp of Matoishi Bokujo I Fault.

ACKNOWLEDGMENT: This work was supported by JSPS KAKENHI Grant Number (JP17K01234) (Research Director: Hiroshi P. Sato). The ownership of Daichi 2 (ALOS-2) data is in the Japan Aerospace Exploration Agency (JAXA). In the field survey and analysis of the materials, we received great cooperation from the students of the Kaneda laboratory of the Graduate School of Science of Chiba University and the Department of Geography of the Nihon University School of Science and Engineering.

Keywords: Kumamoto Earthquake, SAR Interferometry, surface rupture, triggered fault, cumulativeness

©2019. Japan Geoscience Union. All Right Reserved.

Visualization of three-dimensional SAR analysis data by stereo isogram map: Precise detection of surface ruptures of the 2016 Kumamoto earthquake sequence

*Yasuo Awata[1]

1. Institute of Earthquake and Volcano Geology, Geological Survey of Japan, National Institute of Advanced Industrial Science and Technology

Advances in geodetic surveying technology make it possible to grasp the crustal deformation in a wide range from several cms to several meters. In particular, the observation by the spaceborne SAR enables high-resolution detection of crustal deformation using interferometric and three-dimensional analysis. These advances are bringing about a major change to the conventional field investigation method of surface ruptures associated with earthquakes. Here, I tried to visualize the 3D-SAR data of the 2016 Kumamoto earthquake sequence (Kobayashi, 2017) to detect the regional and local surficial deformations with high accuracy.

For visualization of 3D-SAR data to high-resolution and high-dynamic-range images, the stereo contour and relief mapping method is applied. The 3D data is divided into three components, the east-west, north-south, and vertical components, each consists of geographic coordinates and a single value. The isogram map having fine line interval up to the equivalent to the accuracy of data is generated from the data. For east-west and vertical components having the high accuracy, practically fine isogram at a line interval up to 1 cm are drown. Those isogram images are processed into anaglyph capable of stereoscopic viewing with a wide field of view.

In the visual interpretation using an anaglyph image at a line interval of 1 cm, both the main fault zones (Futagawa River, Idenokuchi and Takagi earthquake faults) accompanied by regional crustal deformation and numerous small ruptures scattered in a 50 km square area are observed in a single image. The interpretation results of small ruptures are generally consistent with that of Fijiwara et al. (2016) based on conventional InSAR images that spatial resolution is assumed to be one digit higher. It is easy to detect the ruptures with a displacement of east-west and north-south components of about 5 cm using the image. Furthermore, ruptures up to 2 cm in displacement are recognizable in the Kumamoto urban area where the gradient of regional deformation is small. In the field survey based on the 3D-image interpretation, I found those small ruptures and measured the displacements of guardrails, road curbs, and concrete structures.

Keywords: 3D-SAR, stereo isogram map, 2016 Kumamoto earthquake sequence, surface rupture

©2019. Japan Geoscience Union. All Right Reserved.

Preliminary active fault mapping of Mongolia by interpretation of ALOS 30 DEM image

*Takashi Nakata[1], Yasuhiro Suzuki[2], Mitsuhisa Watanabe[3]

1. Hiroshima University, 2. Nagoya University, 3. Toyo University

Mongolia has experienced huge earthquakes generated from extensive active faults in the 20th Century, namely 1905 Tsetserleg (M7.9), 1905 Bulnai (M8.4), 1931 Fu-Yun (M8.0), 1857 Gobi-Altai (8.1) and 1967 Mogod (M7.1). These earthquakes were generated from pre-existing active faults that have been studied in detail. However most of the other extensive active faults were mapped mainly based by 2D satellite and Google Earth imageries, and they are commonly delineated along distinctive topographic boundaries sometimes without enough evidence for late Pleistocene activities. In order to map active faults throughout Mongolia, we employ stereoscopic interpretation of anaglyph images processed from ALOS 30 DSM images to obtain topographic evidence such as fault scarps across late Pleistocene and Holocene topography and lateral stream offset for late Quaternary activities, and we compiled a preliminary active fault map of Mongolia.

Keywords: Mongolia, active fault, ALOS 30

©2019. Japan Geoscience Union. All Right Reserved.

Ground penetrating radar profiling across the Sanchiao fault in northeast Taiwan

*Mamoru Nakamura[1], How-wei Chen[2]

1. Faculty of Science, University of the Ryukyus, 2. National Central University, Taiwan

Keelung earthquake (M 6.9-7.2) occurred on December 18, 1867, in northeast Taiwan. The seismic intensity distribution and tsunami runup height distribution for this earthquake were estimated from a review of relevant literature. The seismic intensity of the earthquake reached a maximum of VII at downtown Jinshan (northeast Taiwan) according to the scale of the Central Weather Bureau of Taiwan (Cheng et al., 2016 TAO), whilst the tsunami runup height reached 6-15 m along the northeast coast of Taiwan. From the seismic intensity distribution, the source fault of the Keelung earthquake is estimated to have been at the seaward extension of the Sanchiao fault (Cheng et al., 2016 TAO). The Sanchiao fault is a normal fault, approximately 53 km in length, and passes from the south of Taipei through to Jinshan (Shyu et al., 2015 TAO). From morphological surveys, borehole surveys, and seismic reflection surveys, the Sanchiao fault is estimated to pass along the foot of the mountain to the north of downtown Jinshan. However, it is unclear whether the land area of the Sanchiao fault moved in 1867. Therefore, we carried out a Ground Penetrating Radar (GPR) survey to detect the location of the Sanchiao fault.

The GPR survey was carried out on a coastal dune to the north of Jinshan. The coastal sand dune runs in a northwest-southeast direction along the shore, perpendicularly to the Sanchiao fault. The following two types of GPR survey lines were set up: a long range type (100-200 m) running parallel to the coastal dune, and a short range type (20 m) running perpendicularly to the coastal dune. Surveys were carried out from August 15-17, 2017 and from August 13-17, 2018. Three short lines were set up parallel to the dune and two lines perpendicularly to the dune. The pulseEKKO from Sensors & Software Inc. was used for the GPR survey, and the survey frequency of the radar was 50 MHz, 100 MHz, and 250 MHz.

A conspicuous radar reflector was found in the survey line running parallel to the coastal dune. The depth of this reflection changed near the fault trace of the Sanchiao fault, as estimated from boreholes. Furthermore, the depth of the reflection at the northwestern region of the fault was approximately 1 m deeper than that at the southeastern region. This is inconsistent with the vertical displacement of the normal faulting of the Sanchiao fault that dips southeastward, and suggests that the deformation could have been caused by the branching off of the splay fault from the main Sanchiao fault.

Keywords: active fault, 1867 Keelung earthquake, Ground Penetrating Radar

©2019. Japan Geoscience Union. All Right Reserved.

Paleo-earthquake records of the Hengchun offshore structure, southern Taiwan

*Sze-Chieh Liu[1], J Bruce H Shyu[1], Yuan-Lu Tsai[1], Chuan-Chou Shen[1]

1. National Taiwan University

In the southernmost part of Taiwan, the Western Hengchun Tableland is a prominent topographic feature, with several steps of late Pleistocene uplifted marine terraces forming the top of the tableland, and uplifted Holocene coral reefs along the coast. To interpret the formation of this tableland, an inferred Hengchun offshore structure has been proposed as an active structure located offshore to the tableland’ s west. The uplift and the eastward tilting of the tableland are therefore produced by neotectonic activities of this structure. However, the presence of this structure is still debated, and no record of paleo-earthquakes related to this structure has been identified. To solve this, we utilized fossil coral microatolls as paleo-sea-level indicators to identify possible paleo-earthquake records produced by this structure. The highest level of survival (HLS) of corals is limited by the low tide level. Once living corals grow to this level, the upward growth will stop and they will grow outward instead, forming microatoll morphology with a flat top surface. This makes microatolls great tools to record local sea level history. If microatolls were uplifted and killed by co-seismic uplift, the elevation difference between microatolls and the HLS would represent the amount of uplift, and the age of the coral would constrain the age of the earthquake event. In this study, we surveyed six sites along the coast surrounding the Western Hengchun Tableland. Based on our field survey data and U-Th dating results of uplifted corals, we reconstructed a coastal uplift history of the area, and proposed several paleo-earthquake events in the past 2,500 years. These results enabled us to further understand the seismogenic properties and the possible earthquake recurrence intervals of the Hengchun offshore structure.

Keywords: coral microatolls, Hengchun offshore structure, Paleo-earthquake event

©2019. Japan Geoscience Union. All Right Reserved.

©2019. Japan Geoscience Union. All Right Reserved.

LC-InSAR analysis of the Sulawesi earthquake in Indonesia

*Jun Sugimoto[1], Masashi Omata[1], Yoshiteru Akiyama[1], Yutaka Horaku[1]

1. PASCO CORPORATION

On 28 September 2018, a shallow, large earthquake struck in the neck of the Minahasa Peninsula, Indonesia, with its epicenter located in the mountainous area, Central Sulawesi. The magnitude was 7.5.The main active onshore structure in the western part of Central Sulawesi is the left-lateral NNW-SSE trending Palu-Koro strike-slip fault that forms the boundary between the North Sula and Makassar blocks. It was reported that the earthquake caused major soil liquefaction in and around Palu.
In this study, the authors conducted the interferometry analysis using ALOS-2 data and found out the followings:
1) A phase discontinuity lines found in the LC-InSAR diagram can be Palu-Koro fault and other small strike-slip faults around Palu-Koro.
2) In the LC-InSAR diagram, areas with low coherence are distributed in a wider range than the range where damage was caused by liquefaction. This shows the possibility that the ground change has occurred in a wider range than the extent of damage caused by liquefaction.

The authors confirmed that analysis using ALOS-2 data can identify places and scopes of disasters with extensive damages occurred not only in Japan but also in other countries.

Keywords: InSAR, LC-InSAR diagram, 2018 Sulawesi earthquake, Palu-Koro fault

©2019. Japan Geoscience Union. All Right Reserved.

Risk evaluation and disaster education around the coastal areas of Sea of Marmara, Turkey through the fault model construction of the North Anatolian Fault

*Yoshiyuki Kaneda[1,2,3], Haluk Ozener[4], Nurcan Meral Ozel[4,5], Dogan Kalafat[4], Seckin Ozgur Citak , Narumi Takashi[2,3], Takane Hori[2], Muneo Hori[2,6], Mayumi Sakamoto[10,7], Ali Pinar[4], Asim Oguz Ozel[11], Ahmet Cevdet Yalciner[8], Gulum Tanircan[4], Ahmet Demirtas[9]

1. Kagawa University, 2. JAMSTEC, 3. NIED, 4. Bogazici University, 5. CTBTO, 6. ERI, 7. Nagoya University, 8. Middle East Technical University, 9. AFAD, 10. University of Hyogo, 11. Istanbul University

Recent, many destructive earthquakes and tsunamis occurred around the plate boundary in the world, which are, 2004 Sumatra Earthquake/Tsunami, 2011 East Japan Earthquake/Tsunami in Japan, and so on. Along plate boundary in Turkey, the North Anatolian Fault (NAF) distributes and the large earthquakes has occurred there. The one of the events along NAF in Turkey is the 1999 Izmit Earthquake, and severe damages was brought to residents The NAF between the eastern end of Turkey and the Aegean Sea has been ruptured in turn from the both ends, and the part off Istanbul city still remains as unruptured zone. It is considered that future large event brings fatal damages not only Istanbul city but also the entire of Turkish economy.

To prepare future large earthquake there, Japan and Turkey made an agreement to start a multidisciplinary research project, MarDiM SATREPS in 2003. The Project has four research groups with the following goals. Group 1 is Marmara Earthquake Source region observational research group to clarify seismicity, crustal structures and crustal displacement, and to construct a possible fault model. Group 2 focuses on scenario researches of earthquake occurrence along NAF and precise tsunami simulation in the Marmara region. Group 3 aims improvements and constructions of seismic characterizations and damage predictions based on observation researches and precise simulations. Group 4 promotes disaster educations using research result visuals and construct strategies of disaster mitigation.

Group 1 constructed a fault model along NAF with some asperities and with variation on the dip. The segment boundary was also identified through the modeling and it is consistent with the past rupture pattern and fluid distribution. The NAF on the western region of Sea of Marmara has creep and the rate is nearly half of block motion based on direct seafloor observation for crustal displacement. Group 2 calculated cyclic rupture pattern along NAF using heterogeneous fault model and constructed monitoring system “SWIFT” for crustal stress field by mechanisms of many events estimated automatically. We developed tsunami calculation code to image inundation around the coastal area. Group 3 investigated ground structure through regular fine shake observation, and constructed city model of industrial region supporting Turkish economy. We simulated strong motion using ground structure, city model and fault model derived from Group 1 and made a new hazard map. Group 4 considered teaching materials for disaster prevention including Japanese animation technique based on above results of three groups. These materials are utilized for disaster mitigation in Marmara region and disaster education in Turkey.

Keywords: North Anatolian Fault, Sae of Marmara , Risk evaluation, Disaster education

©2019. Japan Geoscience Union. All Right Reserved.

Estimation of fault activity by multivariate analysis using chemical composition of fault gouge

*Ryo Tateishi[1], Koji Shimada[2], Tadamasa Ueki[2], Mayuko Shimizu[2], Tetsuya Komatsu[2], Shigeru Sueoka[2], Masakazu Niwa[2], Ken-ichi Yasue[1], Tsuneari Ishimaru[2]

1. University of Toyama, 2. Japan Atomic Energy Agency

Introduction: Active faults are recognized by displacement / deformation of current topography and the Quaternary strata. However, in the absence of them, it is very difficult to decide whether the fault there is an active fault or not. In this study, we tried multivariate analysis using chemical composition data of fault gouge of active faults and inactive faults in Japan, and tried to determine the presence or absence of fault activity.
Methods: This research was carried out in the following order; collection of papers, extraction of chemical composition data of fault gouge, addition of new chemical analysis data, formatting of input data, variable selection, linear discriminant analysis. First, chemical composition data of fault gouge of active faults and inactive faults in Japan was extracted from existing publications. In this case, the extraction condition clearly describes whether the analysis target is an active fault or an inactive fault and that the basement rock is diverse. In addition, a chemical analysis of the fault gouge sample possessed by the JAEA was carried out, and we created a database that integrates both of them. In this database, in addition to the sample name and analytical value of each sample, 2 categories of active fault and inactive fault were given. Then, we decided elements to be candidates for explanatory variables from this database and arranged them as input data. Since the chemical elements extracted from the literature are not all analyzed for the same element, common elements are chosen so that the number of samples can be taken as much as possible. In order to further extract elements suitable for discrimination between active fault and inactive fault from these elements, variables were selected by two methods of Akaike Information Criterion (AIC: Akaike, 1973) and principal component analysis. Finally, linear discriminant analysis was performed using as an explanatory variable a combination of an element selected by AIC and an element whose factor loading amount was considered to be high in the principal component analysis.
Results: As a result of collection of papers, chemical composition data of fault gouge was extracted from 7 existing papers and 5 reports of the JAEA. We extracted 17 elements as candidates for variables from the database, to which a chemical analysis result of 6 fault gouge samples possessed by the JAEA was added. The number of data was 41 samples for active fault and 16 samples for inactive fault, totaling 57 samples. From these 17 elements, 13 elements were extracted as optimum combination of elements in AIC. In the principal component analysis, synthesis expressions from the first principal component to the 17th principal component were obtained, and elements with high factor loading amounts were calculated for each synthesis formula. From these results, linear discriminant analysis was carried out with a following combination of elements; (a) 13 elements of AIC, combination of elements whose average value of factor load amounts falls in the top 10 of (b) Up to the 3rd principal component of principal component analysis (explain the scattering degree of chemical composition by 65%), (c) Up to the 5th principal component (also 80%), (d) Up to the 8th principal component (also 90%). As a result, a combination of (a), (c) and (d) gives a primary equation that accurately divides the 2 groups of active fault and inactive fault.
Consideration: The elements common to the combination of the above are 6 elements of TiO_2, Al_2O_3, MgO, Na_2O, P_2O_5, Ba. Linear discriminant analysis was carried out again with (e) the combination of these 6 elements, and it resulted in accurate division of the 2 groups. Since these elements are selected by different methods or filters, there is a possibility of elements representing the difference between active faults and inactive faults. Also, as a result of assigning data of 3 specimens of fault gouge of another active

©2019. Japan Geoscience Union. All Right Reserved.

fault to each primary equation, values which are judged to be active faults in all equations were obtained. However, these values were out of the distribution range of the population, and the tendency was more conspicuous as the number of elements was larger. From this, the primary equation consisting of 6 elements of (e) was considered to be the best formula to separate active fault and inactive fault.
This study was carried out under a contract with Ministry of Economy, Trade and Industry of Japan as part of its R&D supporting program for developing geological disposal technology.
Referrence: Akaike, H., Proceedings of the 2nd International Symposium on Information Theory, Petrov, B. N., and Caski, F. (eds.), p. 267-281, 1973.

Keywords: Chemical composition of fault gouge, Multivariate analysis, Active faults and inactive faults

©2019. Japan Geoscience Union. All Right Reserved.

Bayesian optimization of fault-shape parameters using finite element analysis: parameter sets for strong slip partitioning

*Hidetaka Saomoto[1]

1. National Institute of Advanced Industrial Science and Technology

The Bayesian optimization algorithm is now a key technique in various scientific and engineering fields that require the parameter optimization. The technique can reduce the number of simulation trials as compared with the grid-search because the algorithm can act as an artificial intelligence with a statistical decision-making. Because a three-dimensional finite element analysis (FEA) for seismic faulting consumes much CPU time, the use of the Bayesian optimization with the FEA is logical and is expected to accelerate the parameter detection process.

Here, I present the method of combining an open source library Optuna (1) based on a Bayesian optimization algorithm, Tree-Structured Parzen Estimator (TPE) with the seismic faulting FEA based on COMSOL Multiphysics and then demonstrate a Baysian optimization for the fault-shape parameters that activates strong slip partitioning.

The parameter sets obtained from the Bayesian optimization algorithm result in a stronger slip partitioning than that obtained from the grid-search. More specifically, the optimized parameter set was found as a dip angle for the reverse-slip fault of 54.5 degree, a dip angle for the strile-slip fault of 86.3 degree, and the principal stress direction of 56.1 degree clockwise from the strike direction.

The Bayesian optimization detected the parameter set after 50 trials, whereas the grid-search was composed of 784 trials. In summary, the use of the Bayesian optimization algorithm is an effective and efficient way of a parameter optimization for a seismic faulting simulation that requires long CPU time.

References:

(1) Preferred Networks, Inc.: https://optuna.org/

Keywords: Active Fault, Finite Element Method, Bayesian Optimization, Slip Partitioning

©2019. Japan Geoscience Union. All Right Reserved.

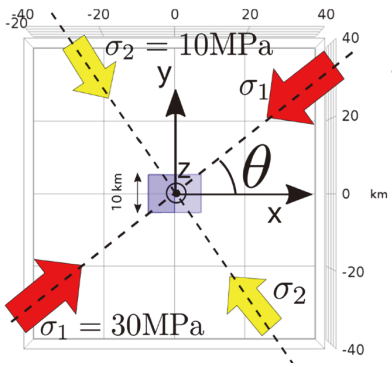

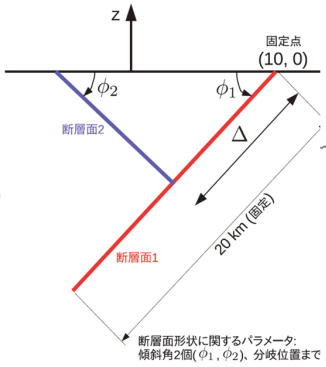

最適化するパラメータ：
主応力方位と断層面形状に関するパラメータ

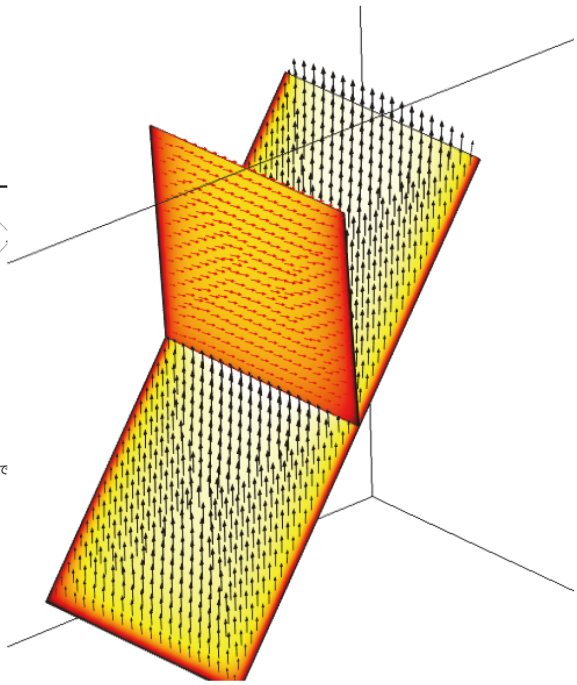

Θ= 33.8°, ϕ1= 54.5°, ϕ2= 86.3°, Δ=10 km のとき、スリップパーティショニングが生じやすいと考える

©2019. Japan Geoscience Union. All Right Reserved.

[J] Oral | S (Solid Earth Sciences)：S-SS Seismology

Tue. May 28, 2019 3:30 PM - 5:00 PM JST | Tue. May 28, 2019 6:30 AM - 8:00 AM UTC | A02 TOKYO BAY MAKUHARI HALL

[S-SS15] Active faults and paleoseismology

convener:Mamoru Koarai(Earth Science course, College of Science, Ibaraki University), Takashi OGAMI(National Institute of Advanced Industrial Science and Technology), Ryosuke Doke(Hot Springs Research Institute of Kanagawa Prefecture), Hisao Kondo(Geological Survey of Japan, National Institute of Advanced Industrial Science and Technology), Chairperson:Mamoru KOARAI(Ibaraki University), Taku Komatsubara(産業技術総合研究所)

Geologic and historic information on seismic cycles and on the magnitude and source faults of past earthquakes is essential information to understand future large earthquakes. The study of past faulting and seismicity is an important issue for an interdisciplinary community of seismologists, geologists, geomorphologists, archaeologists, and historians.

3:30 PM - 4:00 PM JST | 6:30 AM - 7:00 AM UTC

[SSS15-01] Historical documents and oral transmissions on historical tsunamis in the Paciffic coast of Tohoku

★Invited Papers

*ebina yuichi[1] (1.International Research Institute of Disaster Science)

4:00 PM - 4:15 PM JST | 7:00 AM - 7:15 AM UTC

[SSS15-02] Co-seismic crustal movements along reverse faults which subsidence component is larger than uplifting component

*Taku Komatsubara[1] (1.Institute of Geology and Geoinformation, Advanced Industrial Science and Technology)

4:15 PM - 4:30 PM JST | 7:15 AM - 7:30 AM UTC

[SSS15-03] The Iyo-Bungo, southwest Japan, earthquake on September 1st, 1596 as deduced from contemporary historical records

*Katsuhiko Ishibashi[1] (1.Emeritus Professor, Kobe University)

4:30 PM - 4:45 PM JST | 7:30 AM - 7:45 AM UTC

[SSS15-04] Geologically recorded historical and prehistoric tsunamis in the Tonankai region

*Shigehiro Fujino[1], Haruo Kimura[2], Junko Komatsubara[3], Dan Matsumoto[3], Yuichi Namegaya[3], Yuki Sawai[3], Masanobu Shishikura[3] (1.Faculty of Life and Environmental Sciences, University of Tsukuba, 2.Civil Engineering Research Laboratory, Central Research Institute of Electric Power Industry, 3.Geological Survey of Japan, National Institute of Advanced Industrial Science and Technology (AIST))

4:45 PM - 5:00 PM JST | 7:45 AM - 8:00 AM UTC

Discussion

Historical documents and oral transmissions on historical tsunamis in the Paciffic coast of Tohoku

*ebina yuichi[1]

1. International Research Institute of Disaster Science

I analyzed historical tsunamis which attacked the Pacific coast of Tohoku, especially on the AD 1611 Keicho Oshu earthquake and tsunami (commonly called as the Keicho Sanriku earthquake and tsunami), based on historical documents, oral transmissions, and formation process of them.

After the AD 2011 Great East Japan Earthquake, huge historical tsunamis which damaged in the Pacific coast of Tohoku district have received attention. Some people consider the AD 869 Jogan earthquake as the precursor of AD 2011 earthquake and believe huge tsunamis occur once a thousand years. People also recognize the importance of oral transmission and the place name comes from past disasters. Previous studies pointed out the underestimation of the AD 1611 Keicho Oshu earthquake and tsunami but reinvestigated the earthquake and tsunami based on historical documents (Ebina and Imai 2014). Recently, some studies considered the AD 1454 Kyotoku earthquake as a similar event to AD 1611 Keicho oshu earthquake (Namegaya and Yata 2014; Sawai et al., 2015). Furthermore, the tsunami deposit can be correlated with this event have been found in Miyagi and Iwate Prefectures (e.g., Sawai et al., 2012; Takada et al., 2016).

According to “Sunpu Seiji Roku” and “Sunpu Ki", a vassal of the Date family said that another vassal of that encountered the tsunami on the boat during fishing and the boat was driven to the top of the mountain “Senganmatsu”. This event was estimated to occur near the mouth of Abukumagawa River in Iwanuma City. Watanabe (1998) considered this story was not true because Senganmatsu area is too high to be inundated. However, the pictorial map around Iwanuma created in Edo period indicates that Abukumagawa River was located inland from the present position of the river in that time, where a fishing village has been located since the middle ages (Ebina, 2014). Therefore, it is likely that the tsunami actually attacked the area although the story has a little exaggeration.
It is important to restore old geographical features for constraining the sizes of earthquakes and tsunamis. For instance, Fukuhara and Tanioka (2018) estimated that the magnitude of the Keicho earthquake is similar to or large than that of AD 2011 earthquake based on the data of tsunami height inferred from historical documents and oral transmissions in Miyako City, Iwate Prefecture compiled by Ebina and Imai (2014). However, the restored geographical features show that places inundated by the Keicho tsunami were located near the old channel. Therefore, the inundation in Miyako can be interpreted as the result of river run-up.

The knowledge of historical earthquakes and tsunamis along the Pacific coast of Tohoku have not been known by local residents before AD 2011 earthquake and tsunami. According to “Zishigaku Oyobi Chirigaku Kenkyu Zairyo Hokoku”, when the Imperial Science University of Tokyo (present the University of Tokyo) carried out a questionnaire about the existence of "Kaisyo" to municipal corporations all over the country in the 1890s, those in the coastal regions of Iwate answered that there are no historical records and oral transmissions on the historical earthquakes and tsunamis before AD 1856 Ansei Hachinohe-oki earthquake tsunami (Ebina and Satake 2018). This report shows that the coastal residents did not recognize that tsunamis frequently attack the Pacific coast of Tohoku in those days. Shoshin Yamana reevaluated the historical records and oral transmissions still remained in the coastal area. He

©2019. Japan Geoscience Union. All Right Reserved.

carried out the survey after the AD 1896 Meiji Sanriku earthquake tsunami and wrote “Sanriku Engan Daikaisyo Torisirabe Syo”. This book includes that the description of the damage in many areas and Keicho Oshu earthquake tsunami hand-copied from the reference books of "Muto Rokuemon Syozo Komonzyo" and “Miyako Yurai Ki. These materials are obtained by the survey for influential local persons in various places. Yamana also studied the place name may be coming from driftage by past tsunamis through the interview survey to the local residents and compiled those as “Iwate Engan Kochimei Ko”. Among those 40 place names, half of them still exist (Muranaka et al., 2017). However, it is difficult to consider that many of those places were inundated by tsunamis. The possibility that some oral transmissions of those place names newly generated under the confusion by the Meiji Sanriku earthquake and tsunami.
Considering the historical viewpoint on formation processes of historical documents and oral transmissions will be useful for studies on paleo earthquakes and tsunamis.

Keywords: historical tsunamis, historical documents and oral transmissions, Interdisciplinary research, Keicho Oshu earthquake and tsunami

©2019. Japan Geoscience Union. All Right Reserved.

Co-seismic crustal movements along reverse faults which subsidence component is larger than uplifting component

*Taku Komatsubara[1]

1. Institute of Geology and Geoinformation, Advanced Industrial Science and Technology

Introduction

Reverse faulting should cause crustal movement which uplifting component is larger than subsidence component. There are many reverse faults which subsidence component is larger than uplifting one in the Niigata-Kobe and eastern margin of Japan Sea tectonic zones during geological era, Presenter gathered examples of historical co-seismic crustal movement along such faults.

Example 1. Kuwana fault and AD 1586 Tensho Earthquake, Mie Pref., central Japan

Height of the MIS5e shoreline in the uplift area of the Kuwana fault is +63m, it of the upper surface of MIS5e marine deposits in the subsidence area is -92 to -72m.

This fault is one of the source of the 1586 Tensho Earthquake, however a house built on AD 1576 is existing in the subsidence area near the coast at that time. Almost all medieval structural remain surfaces in the subsidence area are less than 1m beneath ground in depth.

Example 2. Hyuuga fault and AD 1662 Kambun Ohmi-Wakasa Earthquake, Fukui Pref., central Japan

Height of the MIS5e shoreline in the uplift area of the Hyuuga fault is +15 to +16m, and it of the upper surface of the MIS5 lacustrine sediments in the subsidence area is -90 to -80 m.

Ahistorical document reported 2.4 m uplift on the north eastern side of Lake Mikata (Suga) and 1.5 m subsidence on the south western side of it occurred during the 1662 Kambun Ohmi-Wakasa Earthquake.

Example 3. Noshiro fault zone and AD1694 Genroku Noshiro Earthquake, Akita Pref., north eastern Japan

Height of the MIS5e shoreline in the uplift area of the Noshiro fault is +30 to 60m, it of the upper surface of the MIS5e marine deposits in the subsidence area is -85m. The 1694 Genroku Noshiro Earthquake induced uplifting of northern bank of the Hachiro-gata lagoon, but no reports describes subsidence in the footwall side of it.

Conclusion

These three historical co-seismic crustal movement along the subsidence prevailing reverse fault did not go with distinct subsidence. This suggests aseismic subsidence in the footwall side of these faults have occurred in the geological era.

Keywords: historical earthquake, co-seismic crustal movement, reverse fault, Niigata-Kobe tectonic zone, eastern margin of Japan Sea tectonic zone

©2019. Japan Geoscience Union. All Right Reserved.

The Iyo-Bungo, southwest Japan, earthquake on September 1st, 1596 as deduced from contemporary historical records

*Katsuhiko Ishibashi[1]

1. Emeritus Professor, Kobe University

In leap July of the 5th year of the Bunroku era (in the old Japanese lunar calendar; September, 1596 in the Gregorian calendar) Bungo province (present-day Oita Prefecture) in Kyushu, southwest Japan, suffered from severe earthquake and tsunami disasters. Concerning the occurrence date of the causative earthquake, currently prevailing idea is that a large earthquake took place on leap July 9 in Iyo province (present-day Ehime Prefecture) in Shikoku, on the eastward opposite shore of Bungo, and another large earthquake occurred on leap July 12 around Bungo. Against this idea I claim that a single event which could be called "the Iyo-Bungo earthquake" occurred around seven p.m. on leap July 9 in the Iyo-Bungo region based on reliable contemporary historical records.

There are more than 70 documents on this (these) earthquake(s) printed in the existing collections of historical earthquake materials, but their values as historical records vary considerably. Since the essential principle of historiographical seismology is to utilize only reliable first-grade documents, I performed historical source criticism to select 16 contemporary materials. I referred to their original or best texts, not using texts printed in the collections.

According to the contemporary records, in Bungo, violent earthquake ground motion collapsed shrines around seven to nine p.m. on leap July 9 and a large tsunami hit Fuchu (Oita) in the twilight (*"Yusuhara-no-miya Nendai Ryakki"*). *"Kodo-ji Daihan'nyakyo Okugaki"* and *"Shibayama Kanbei Ki"* also describe strong earthquake shaking and large tsunami around Fuchu on that day. In Kyoto, roughly 430 km east-northeast of Bungo, earthquake ground motion was felt around seven to nine p.m. on leap July 9 (*"Kotokuni-kyo Ki"*), or around seven p.m. on the same day rather strongly (*"Ozuki-Takasuke-Sukune Ki"*). In Hiroshima Prefecture, at Hatsuka-ichi and Itsukushima strong ground motions were felt at night on leap July 9 without damages (*"Hoida Motokiyo's letter"*), and at Mihara strong earthquake tremors continued from leap July 9 till 12 (*"Buttsu-zenji Juji Ki"*). In Iyo, *"Yakushi-ji Daihan'nyakyo Okugaki"* says a severe earthquake tremor occurred on leap July 9 and the whole Iyo province had trouble, suggesting earthquake disaster in a wide area. In Satsuma and Osumi provinces (present-day Kagoshima Prefecture), *"Kabayama Shoken Jiki"* writes a strong earthquake on leap July 9, and *"Nanko Nikki Zankan"* also writes an earthquake on the same day. *"Chosa Yachi's letter"* written on leap July 29 describes that since leap July 8 earthquake tremors had continued.

As a fundamental methodology of historiographical seismology, these tremors and tsunami in Bungo, Iyo, Kyoto, Hiroshima and Kagoshima on leap July 9 are considered to have been produced by an identical earthquake unless there is any counter-evidence. Leap July 12, the other proposed date of the Bungo earthquake, comes from historical materials written after 1698, which probably mistook the great Kyoto earthquake in the midnight of leap July 12 for the Bungo event. The seismic intensities are evaluated to be stronger 6 in some places in Bungo and Iyo, 4 in Hiroshima, stronger 3 in Kyoto, and about 3 in Kagoshima on the JMA scale. The most simple and reasonable interpretation is that a large earthquake with the source region from around Oita to the midst of Iyo took place around seven p.m. on leap July 9, whose magnitude being around 7.5, and the tsunami on the Bungo coast followed. The rupture of the Kawakami fault in the MTL fault zone during this earthquake suggested by Tsutsumi *et al.* (2000) may have

©2019. Japan Geoscience Union. All Right Reserved.

occurred.

Keywords: 1596, Iyo-Bungo earthquake, historical source criticism, contemporary historical documents, MTL fault zone

©2019. Japan Geoscience Union. All Right Reserved.

Geologically recorded historical and prehistoric tsunamis in the Tonankai region

*Shigehiro Fujino[1], Haruo Kimura[2], Junko Komatsubara[3], Dan Matsumoto[3], Yuichi Namegaya[3], Yuki Sawai[3], Masanobu Shishikura[3]

1. Faculty of Life and Environmental Sciences, University of Tsukuba, 2. Civil Engineering Research Laboratory, Central Research Institute of Electric Power Industry, 3. Geological Survey of Japan, National Institute of Advanced Industrial Science and Technology (AIST)

A coring survey at a coastal lowland in Mie Prefecture exposed 10 sand layers deposited from about 4500 to 500 years ago. The layers are interpreted as tsunami deposits because of the presence of abundant bioclasts of marine organisms such as foraminifers and gastropods, and sedimentary structures common in modern tsunami deposits. At the study site, no substantial seawater inundations and sand depositions have been recorded even for the largest typhoons to ever hit the region. On the other hand, written document tells that the Ansei-Tokai earthquake tsunami (1854 CE) inundated the study site and deposited substantial sand layer. Estimated ages of the youngest three sand layers overlap well with tsunamis in 1498, 1096, and 684 CE. Our results support the hypothesis suggested by archaeological studies that the 684 CE rupture extended farther eastward than the historical record indicates or that another tsunami occurred at some time close to 684 CE. We did not find any sand layers that were definitely correlated with the tsunamis of 1361 and 887 CE, which are thought to have occurred by multi-segment ruptures of the Nankai Trough that includes the segment directly offshore from the study site. If the sand layers found at the study site were deposited by the tsunamis of 1498, 1096, and 684 CE, and if the tsunamis of 1361 and 887 CE did not inundate the study site, the tsunami recurrence interval during the relevant time period was about 400 years. This finding does not support the widely believed hypothesis that earthquakes and tsunamis occur at regular intervals of approximately 100 years in this area. In addition, similar to the historical tsunamis, intervals of geologically recorded prehistoric tsunamis at the study site vary from about 100 to 600 years. The hypothesis of variable recurrence of earthquakes and tsunamis along the Nankai Trough should be tested by future geological and historical studies in unbiased way.

Keywords: tsunami deposit, Nankai Trough, recurrence interval

©2019. Japan Geoscience Union. All Right Reserved.

[E] Oral | S (Solid Earth Sciences)：S-IT Science of the Earth's Interior & Techtonophysics

Tue. May 28, 2019 9:00 AM - 10:30 AM JST | Tue. May 28, 2019 12:00 AM - 1:30 AM UTC | A10 TOKYO BAY MAKUHARI HALL

[S-IT21] Interaction and Coevolution of the Core and Mantle in the Earth and Planets

convener:Kenji Kawai(Department of Earth and Planetary Science, School of Science, University of Tokyo), Tsuyoshi Iizuka(University of Tokyo), Kenji Ohta(Department of Earth and Planetary Sciences, Tokyo Institute of Technology), Taku Tsuchiya(Geodynamics Research Center, Ehime University), Chairperson:Kenji Kawai, Sebastian Ritterbex

Recent observational and experimental investigations have significantly advanced our understanding of the structure and constituent materials of the deep Earth. Yet, even fundamental properties intimately linked with formation and evolution of the planet, such as details of the chemical heterogeneity in the mantle and light elements dissolved in the core, remained unclear. Seismological evidence has suggested a vigorous convection in the lower mantle, whereas geochemistry has suggested the presence of stable regions there that hold ancient chemical signatures. The amounts of radioactive isotopes that act as heat sources and drive dynamic behaviors of the deep Earth are also still largely unknown. We provide an opportunity to exchange the achievements and ideas, and encourage persons who try to elucidate these unsolved issues of the core-mantle evolution using various methods, including high-pressure and high-temperature experiments, high-precision geochemical and paleomagnetic analyses, high-resolution geophysical observations, geo-neutrino observations, and large-scale numerical simulations. Papers stimulating an interdisciplinary collaboration relating to establishment of the Japan-SEDI community are also welcomed.

9:00 AM - 9:15 AM JST | 12:00 AM - 12:15 AM UTC

[SIT21-19] Seismological Explorations of Earth's Outer Core: Normal Mode and Body Wave Analyses

★Invited Papers

*Jessica C E Irving[1], Sanne Cottaar[2], Vedran Lekic[3], Wenbo Wu[4] (1.Princeton University, 2.University of Cambridge, 3.University of Maryland, College Park, 4.California Institute of Technology)

9:15 AM - 9:30 AM JST | 12:15 AM - 12:30 AM UTC

[SIT21-20] Discussion

*Kenji Kawai[1] (1.University of Tokyo)

9:30 AM - 9:45 AM JST | 12:30 AM - 12:45 AM UTC

[SIT21-21] On the 1-D radial convective structure of the Earth’s core inferred from a coupled core-mantle evolution model

*Takashi Nakagawa[1] (1.Department of Earth Sciences, The University of Hong Kong)

9:45 AM - 10:00 AM JST | 12:45 AM - 1:00 AM UTC

[SIT21-22] Structural and transport properties of liquid iron-light-element mixtures under outer core conditions

*Satoshi Ohmura[1], Taku Tsuchiya[2] (1.Hiroshima Inst. of Tech., 2.Ehime Univ.)

10:00 AM - 10:15 AM JST | 1:00 AM - 1:15 AM UTC

[SIT21-23] Development of New Technology for Geoneutrino Directional Measurement

*Hiroko Watanabe[1] (1.Research Center for Neutrino Science, Tohoku University)

10:15 AM - 10:30 AM JST | 1:15 AM - 1:30 AM UTC

[SIT21-24] Investigation of multi light elements in iron-silicate-water system using high pressure and temperature neutron experiments: Implications for the Earth's evolution

★Invited Papers

*Riko Iizuka-Oku[1], Hirotada Gotou[2], Ko Fukuyama[1], Hiroyuki Kagi[1] (1.Geochemical Research Center, Graduate School of Science, The University of Tokyo, 2.The Institute for Solid State Physics, The

University of Tokyo)

Seismological Explorations of Earth's Outer Core: Normal Mode and Body Wave Analyses

*Jessica C E Irving[1], Sanne Cottaar[2], Vedran Lekic[3], Wenbo Wu[4]

1. Princeton University, 2. University of Cambridge, 3. University of Maryland, College Park, 4. California Institute of Technology

Earth's outer core is a source of both the geodynamo and heat for mantle convection. However, we still do not fully understand its chemical composition, and there is debate about whether the uppermost outer core may contain a stratified layer enriched in light elements. We present low frequency normal mode and high frequency body wave investigations of the outer core's properties.

Normal mode oscillations of the whole Earth, excited by large earthquakes, are sensitive to the large-scale variations in velocity and density. We use reported centre frequencies of hundreds of normal mode oscillations to investigate the bulk properties of the outer core. We carry out a Bayesian inversion using a mineralogical Equation-of-State framework to infer the outer core's velocity, density and mineralogical properties, under the assumption that the outer core is well mixed and adiabatic. The model we produce, EPOC, describes the Elastic Parameters of the Outer Core. EPOC predicts seismic velocities at the top of the outer core which are closer to some existing body-wave models than to PREM, resolving a long-standing discrepancy. EPOC also fits normal-mode data better than the Preliminary Reference Earth Model. We also consider the effects of relaxing our assumptions that (i) there is no stratified layer at the top of the outer core, and (ii) that PREM is correct outside the outer core.

To better assess the uppermost outer core, often referred to as the E' layer, we use a novel, iterative technique to measure SmKS differential travel times. SmKS waves are particularly sensitive to the E' layer, and reflect (m-1) times from the underside of the core-mantle boundary. We find that the SmKS differential travel times are better described by models with seismic velocities in the E' layer slower than PREM, such as EPOC or body-wave derived KHOMC (Kaneshima and Helffrich, 2013).

Keywords: Outer Core, Normal Modes, Body waves

©2019. Japan Geoscience Union. All Right Reserved.

Discussion

*Kenji Kawai[1]

1. University of Tokyo

Discussion

©2019. Japan Geoscience Union. All Right Reserved.

On the 1-D radial convective structure of the Earth’s core inferred from a coupled core-mantle evolution model

*Takashi Nakagawa[1]

1. Department of Earth Sciences, The University of Hong Kong

A coupled core-mantle evolution model in the global heat and mass balance of the Earth’s mantle and core is to reveal the 1-D radial convective structure of the Earth’s core over the geologic time-scale. Since tracking the convective structure of the Earth’s core over the geologic time-scale is not still available for numerical geodynamo simulations, the assessment with the global heat and mass balance model of Earth’s core and mantle is quite powerful. Regarding the global heat balance of the Earth’s mantle, the global heat balance approach incorporating with the heat transport by the partial melting is assumed, which is the parameterized mantle convection based on the modified version of Driscoll and Bercovici (2014). The heat flow across the core-mantle boundary computed from this parameterized convection model is used to compute the thermal and chemical structure of the Earth’s core based on the global heat balance of the Earth’s core with the realistic material properties of the Earth’s core provided from Labrosse (2003; 2015) However, on the assessment of convective structure, the effects of compositional convection caused by releasing the light elements associated with inner core growth and/or the metal-silicate partitioning are included (e.g. Takehiro and Sasaki, 2018). As indicated in Takehiro and Sasaki (2018), the effects of compositional convection are essential for understanding the convective structure of the Earth’s core even if the realistic density structure of the Earth’s core is included in the energy flux computations. On the magnetic field generation caused by geodynamo actions, again, the compositional convection plays a significant role under the high thermal conductivity expected from the high-pressure physics. In the presentation, I will indicate the evolution of the convective structure described as the entropy flux of the Earth’s outer core over 4 billion years as a function of the evolution of the heat flows across the core-mantle boundary and oceanic lithosphere.

Keywords: Earth's core, Evolution, Convective structure

©2019. Japan Geoscience Union. All Right Reserved.

Structural and transport properties of liquid iron-light-element mixtures under outer core conditions

*Satoshi Ohmura[1], Taku Tsuchiya[2]

1. Hiroshima Inst. of Tech., 2. Ehime Univ.

It is widely believed that Earth’ s outer core consists of liquid iron (or liquid-nickel alloy) with light element (LE) impurities. For understanding magnetic and thermal behaviors of the Earth, it is required to explore electrical and thermal conductivities of liquid iron and influence of the light elements on these properties.

For this reason, we have investigated influences of light elements on transport properties of liquid iron under high pressure by using ab initio molecular dynamics simulations. We reported the structural and transport properties of liquid Fe-LE binary systems in connection with a microscopic structural properties. This times, in addition to binary systems, we have investigated transport properties of Fe-LE ternary systems. To provide further details of the effects of light-element, we discuss structural and transport properties of liquid Fe alloys in terms of the type and amount of light elements.

Keywords: liquid iron alloy, ab initio molecular dynamics simulation, transport properties, high pressure properties

©2019. Japan Geoscience Union. All Right Reserved.

Development of New Technology for Geoneutrino Directional Measurement

*Hiroko Watanabe[1]

1. Research Center for Neutrino Science, Tohoku University

Neutrino is an elusive particle and it can penetrate even astronomical objects. While neutrino experiments continue to explore the neutrino propertied, e.g. oscillation nature of neutrino flavor transformation, mass-square differences and mixing angles, we have began to utilize neutrino as a tool to look into the Earth. Anti-neutrinos emitted from radioactive isotopes, geo-neutrinos, bring unique and direct information of the Earth's interior and thermal dynamics.

KamLAND, Kamioka Liquid-scintillator Anti-neutrino Detector, has 1 kton ultra pure liquid scintillator. They reported the first experimental study of geo-neutrino in 2005. Later the geo-neutrino signals were used to estimate the Earth's radiogenic heat production and constrain the composition models of the bulk silicate Earth. Following the Fukusima reactor accident in March 2011, the entire Japanese nuclear reactor industry has been subjected to a protected shutdown. This unexpected situation allows us to improve the sensitivity for geo-neutrinos.

The liquid scintillator detectors have the sensitivity for measuring total amount of geo-neutrinos from the Earth's crust and mantle. However, we do not have the technology to track the direction of incoming geo-neutrinos at present due to the high miss-identification in a neutrino's track reconstruction. The direction-sensitive detector can map out the U and Th distribution inside the Earth and this technic is also applicable to resolving crust versus mantle contributions. Recent progress in studying this this new technology confirmed that a signify improvement is possible in neutrino tracking identification with a combination of ^{6}Li-loaded liquid scintillator and imaging detector. We developed prototype detector to measure 3D image of scintillation light and study the methodology for the image reconstruction. We will present recent status of our prototype detector and achievement of dark noise reduction of pixelated detector.

Keywords: geoneutrino, radiogenic power

©2019. Japan Geoscience Union. All Right Reserved.

Investigation of multi light elements in iron-silicate-water system using high pressure and temperature neutron experiments: Implications for the Earth's evolution

*Riko Iizuka-Oku[1], Hirotada Gotou[2], Ko Fukuyama[1], Hiroyuki Kagi[1]

1. Geochemical Research Center, Graduate School of Science, The University of Tokyo, 2. The Institute for Solid State Physics, The University of Tokyo

Introduction:

The Earth’s core is considered to consist of Fe alloy and some light elements (O, S, Si, H, C). Hydrogen (H) is the most abundant element in the universe and one of the promising candidates existing in the Earth’s core. However, its amount dissolved in the core and its process are still unknown because H cannot be detected by X-ray diffraction (XRD) and it easily escapes from iron by the release of pressure. Recently, H content in *fcc*-Fe at high pressure and high temperature (high-PT) has been determined using in-situ neutron diffraction measurements at J-PARC [1], suggesting that H had preferentially dissolved into iron before any other light elements have dissolved in the very early stage of Earth’s evolution. It is important to further study the partitioning of the other light elements between iron hydride (not pure iron) and silicates. To clarify the effects of multi light elements on the core-mantle segregation in the Earth’s formation, we have focused on sulfur (S) and investigated its effect on hydrogenation of iron.

Experimental:

Iron fine powder was pelletized with/without S powder and placed at the center of the graphite sample capsule. Powder mixture of quartz (SiO_2), brucite $Mg(OD)_2$ (or MgO for comparison of the water existence) surrounds the Fe pellet. Sample composition of Fe:$Mg(OD)_2$:SiO_2=2:1:1 of molar ratio with 5wt.% of S simulates an ideal condition of the primitive Earth.

In-situ high-PT neutron experiments were carried out using a six-axis multi-anvil press “Atsuhime” installed at MLF, PLANET (BL11), J-PARC. An originally improved multi-anvil 6-6 type assembly was applied. Three samples were pressurized up to 6–7 GPa and then heated up to 700 ˚C step by step. The reaction processes (dehydration of $Mg(OD)_2$, phase transformations of Fe (*bcc*-*fcc*) and FeS, formation of silicates) were carefully checked in real time. The diffraction patterns of *fcc*-Fe were measured at 550 ˚C and 700 ˚C for long time and analyzed using the Rietveld refinement method to determine structural and atomic parameters of *fcc*-Fe and sub-products. The recovered samples were examined by XRD and SEM-EDS to more precisely identify the products, their compositions, and the elements partition.

Results and Discussion:

The cell volume changes in *fcc*-Fe and sub-phase of FeS-V were investigated for every hour during the long-time measurements at 700 ˚C. For the sample including water, the volume of *fcc*-Fe was significantly increased with time, while the sample without water showed no change regardless of temperatures. The cell volume of FeS-V did not increase, suggesting that the formation of FeS was promoted in the existence of water, but its hydrogenation was negligible. Fe gradually incorporated D in the existence of water and FeD_x formed (x~0.10 at a maximum). From the results of SEM, the inhibition of deuterization might be due to the formation of FeS layer surrounding Fe pellet, whereas such a thick layer was not observed when using the Fe+S pellet. The sample without water did not include FeS layer nor Fe-bearing silicates.

It is suggested that both S and Fe were not mobile and could not react with each other without the existence of water. H and S can be preferentially incorporated into solid Fe at lower-T (~700 ˚C) before melting. The other light elements (C, O, Si) could have dissolved into molten iron hydride and/or FeS in the later process of Earth’s core-mantle differentiation at much higher-PT condition.

©2019. Japan Geoscience Union. All Right Reserved.

Reference:
[1] R. Iizuka-Oku, T. Yagi, H. Gotou, T. Okuchi, T. Hattori, A. Sano-Furukawa, Nature Commun. 8, 14096 (2017).

Keywords: Hydrogen, Sulfur, In situ high pressure and high temperature observation, Core-mantle formation, light elements

©2019. Japan Geoscience Union. All Right Reserved.

[E] Oral | S (Solid Earth Sciences)：S-IT Science of the Earth's Interior & Techtonophysics

Tue. May 28, 2019 10:45 AM - 12:15 PM JST | Tue. May 28, 2019 1:45 AM - 3:15 AM UTC | A10 TOKYO BAY MAKUHARI HALL

[S-IT21] Interaction and Coevolution of the Core and Mantle in the Earth and Planets

convener:Kenji Kawai(Department of Earth and Planetary Science, School of Science, University of Tokyo), Tsuyoshi Iizuka(University of Tokyo), Kenji Ohta(Department of Earth and Planetary Sciences, Tokyo Institute of Technology), Taku Tsuchiya(Geodynamics Research Center, Ehime University), Chairperson:Noriyoshi Tsujino, Kenta Ueki

Recent observational and experimental investigations have significantly advanced our understanding of the structure and constituent materials of the deep Earth. Yet, even fundamental properties intimately linked with formation and evolution of the planet, such as details of the chemical heterogeneity in the mantle and light elements dissolved in the core, remained unclear. Seismological evidence has suggested a vigorous convection in the lower mantle, whereas geochemistry has suggested the presence of stable regions there that hold ancient chemical signatures. The amounts of radioactive isotopes that act as heat sources and drive dynamic behaviors of the deep Earth are also still largely unknown. We provide an opportunity to exchange the achievements and ideas, and encourage persons who try to elucidate these unsolved issues of the core-mantle evolution using various methods, including high-pressure and high-temperature experiments, high-precision geochemical and paleomagnetic analyses, high-resolution geophysical observations, geo-neutrino observations, and large-scale numerical simulations. Papers stimulating an interdisciplinary collaboration relating to establishment of the Japan-SEDI community are also welcomed.

10:45 AM - 11:00 AM JST | 1:45 AM - 2:00 AM UTC

[SIT21-25] Low hydrogen contents in the cores of terrestrial planets

★Invited Papers

*Vincent Clesi[1], Mohamed Ali Bouhifd[2], Nathalie Bolfan-Casanova[2], Geeth Manthilake[2], Federica Schiavi[2], Caroline Raepsaet[3], Hélène Bureau[4], Hicham Khodja[3], Denis Andrault[2] (1.Laboratoire de Geologie de Lyon - Terre, Planètes, Environnement, Université Claude Bernard Lyon 1, CNRS, ENS-Lyon, 69622 Villeurbanne, France., 2.Laboratoire Magmas et Volcans, Université Clermont Auvergne, CNRS UMR 6524, OPGC–IRD, Campus Universitaire des Cézeaux, 6 Avenue Blaise Pascal, 63178 Aubière Cedex, France., 3.Laboratoire d'Etude des Eléments Légers, NIMBE, CEA, CNRS, Université Paris-Saclay, CEA Saclay, 91191 Gif sur Yvette Cedex, France., 4.Institut de Minéralogie et de Physique de la Matière et de Cosmochimie, Sorbonne Universités, UMR CNRS-UPMC 7590, 4 place Jussieu, 75252 Paris, France.)

11:00 AM - 11:15 AM JST | 2:00 AM - 2:15 AM UTC

[SIT21-26] Discussion

*Taku Tsuchiya[1] (1.Geodynamics Research Center, Ehime University)

11:15 AM - 11:30 AM JST | 2:15 AM - 2:30 AM UTC

[SIT21-27] Fe_2S: the most iron-rich Fe-S compound at pressures of the inner core

*Shigehiko Tateno[1,2], Haruka Ozawa[2,3], Kei Hirose[1,4], Toshihiro Suzuki[5] (1.Earth-Life Science Institute, Tokyo Institute of Technology, 2.Institute for Planetary Materials, Okayama University, 3.Nuclear Science and Engineering Center, Japan Atomic Energy Agency, 4.Department of Earth and Planetart Science, The University of Tokyo, 5.Geochemical Research Center, The University of Tokyo)

11:30 AM - 11:45 AM JST | 2:30 AM - 2:45 AM UTC

[SIT21-28] First-principles Investigation of Iron Diffusion Properties with Implications to Inner Core Plasticity

★Invited Papers

*Sebastian Ritterbex[1], Taku Tsuchiya[1] (1.GRC Ehime University)

11:45 AM - 12:00 PM JST | 2:45 AM - 3:00 AM UTC

[SIT21-29] Dependence of the dipole component dominancy on the Rayleigh number and inner core size in geodynamo simulations

*Yuki Nishida[1], Yuto Katoh[1], Hiroaki Matsui[2], Masaki Matsushima[3], Atsushi Kumamoto[1] (1.Department of Geophysics, Graduate School of Science, Tohoku University, 2.Dept. of Earth and Planetary Sciences, University of California, Davis, 3.Department of Earth and Planetary Sciences, School of Science, Tokyo Institute of Technology)

12:00 PM - 12:15 PM JST | 3:00 AM - 3:15 AM UTC

[SIT21-30] Elasticity of Fe-Si Alloy

*Taku Tsuchiya[1], Yu Fukunaga[1] (1.Geodynamics Research Center, Ehime University)

Low hydrogen contents in the cores of terrestrial planets

*Vincent Clesi[1], Mohamed Ali Bouhifd[2], Nathalie Bolfan-Casanova[2], Geeth Manthilake[2], Federica Schiavi[2], Caroline Raepsaet[3], Hélène Bureau[4], Hicham Khodja[3], Denis Andrault[2]

1. Laboratoire de Geologie de Lyon - Terre, Planètes, Environnement, Université Claude Bernard Lyon 1, CNRS, ENS-Lyon, 69622 Villeurbanne, France., 2. Laboratoire Magmas et Volcans, Université Clermont Auvergne, CNRS UMR 6524, OPGC–IRD, Campus Universitaire des Cézeaux, 6 Avenue Blaise Pascal, 63178 Aubière Cedex, France., 3. Laboratoire d’ Etude des Eléments Légers, NIMBE, CEA, CNRS, Université Paris-Saclay, CEA Saclay, 91191 Gif sur Yvette Cedex, France., 4. Institut de Minéralogie et de Physique de la Matière et de Cosmochimie, Sorbonne Universités, UMR CNRS-UPMC 7590, 4 place Jussieu, 75252 Paris, France.

The accretion of planets from primordial materials and their subsequent differentiation to form a core and a mantle are fundamental questions in terrestrial and solar system. Many of the questions about the processes are still open and much debated. For example, could the presenceof water during the metallic phase segregation affect the planet-accretion models? The existing studies on the elemental metal-silicate partitioning under hydrous conditions were extended recently to a range of P, T, f_{O2} and water content (5 - 20 GPa, 2000 - 2500 K, from 1 to 5 log units below the iron-wüstite buffer, and for X_{H2O} varying from 500 ppm to 1.5 wt%) [1]. These experimental results show that except for Fe, there is no effect of water on the partitioning of moderately siderophile elements. It allowed us to build consistent models of planetary accretion from reducing to oxidized conditions. Furthermore, for the range of water concentrations studied, there is no evidence of important hydrogen incorporation into planetary cores, thus making unlikely for hydrogen to be a major light element of the core as previsously assumed [2]. We report H metal-silicate partition coefficients of about 0.2, up to two orders of magnitude lower than reported previously, and indicative of lithophile behavior. Our results imply H content of ~60 ppm in the Earth and Martian cores [3].

[1] Clesi et al. (2016) Geochim. Cosmochim. Acta 192, 97-121.

[2] Okuchi, T. (1997) Science 278, 1781-1784.

[3] Clesi et al. (2018) Science Advances 4: e1701876

Keywords: Hydrogen, Core formation, Primitive Earth, Experimental Petrology

©2019. Japan Geoscience Union. All Right Reserved.

Discussion

*Taku Tsuchiya[1]

1. Geodynamics Research Center, Ehime University

Discussion

©2019. Japan Geoscience Union. All Right Reserved.

Fe_2S: the most iron-rich Fe-S compound at pressures of the inner core

*Shigehiko Tateno[1,2], Haruka Ozawa[2,3], Kei Hirose[1,4], Toshihiro Suzuki[5]

1. Earth-Life Science Institute, Tokyo Institute of Technology, 2. Institute for Planetary Materials, Okayama University, 3. Nuclear Science and Engineering Center, Japan Atomic Energy Agency, 4. Department of Earth and Planetart Science, The University of Tokyo, 5. Geochemical Research Center, The University of Tokyo

Sulfur is considered to be one of the light elements in the Earth’ s core as iron sulfides are universally found in iron meteorites. The phase diagram of the Fe–FeS system at the high-pressure and high-temperature (P-T) conditions of the core has particular importance to understand the composition and state of the Earth’ s core. Because Fe3S is known as the most iron-rich Fe–S compound at > 20 GPa, the iron–sulfur core model has been discussed considering Fe and Fe_3S in the solid core. However, our previous experiment reveals that Fe_3S decomposes into S-bearing hcp-Fe and CsCl (B2)-type phase above ~250 GPa from X-ray diffraction measurements (XRD) (Ozawa et al., 2013 GRL). Furthermore, TEM analysis on the recovered sample exhibits that S-poor phase, likely to be a former hcp-Fe, coexisted with S-rich phase with >33.5 atm% S. Hence, the S-rich end-member compound has not been constrained under pressure more than 250 GPa. In order to re-investigated the phase relations in Fe-FeS system, we studied phase relations in Fe_2S at multi-megabar pressure range.

High P-T conditions were generated in a laser-heated diamond-anvil cell (DAC) using double-beveled diamond anvils with 40 or 60 μm culets. We used the Fe_2S phase as the starting material, which was synthesized beforehand at high pressures in a multianvil apparatus and confirmed by microprobe analysis. SiO_2 glass and MgO were used for thermal insulation and pressure calibration. We loaded such sample assembly as MgO/SiO_2-glass/Fe_2S/SiO_2-glass so that MgO was detached from an iron sample, in order to avoid possible chemical reaction at high temperature. Angle-dispersive XRD measurements were conducted at BL10XU, SPring-8. Heating was performed from both sides of the sample by employing a pair of 100 W Yb fiber lasers.

We performed three separate sets of experiments at pressures between from 120-310 GPa and temperature up to 3000 K. When we heated the Fe_2S sample being mostly amorphous by compression to 300 GPa at 300 K, the 20 new peaks appeared in a few minutes and became spotty with further heating. All peaks are assigned to the orthorhombic structure, which agrees well with Pnma symmetry phase proposed by the theoretical prediction (Bazhanova et al., 2017). This observation indicates that Fe_2S composition crystallizes as a single phase. In the following decompression and re-heating the sample, its stability was confirmed to be 150-310 GPa.

Our previous study (Mori et al., 2017 EPSL) reported that hcp-Fe and B2 phase crystallizes in Fe-6wt% S bulk composition at 270 GPa and 2400 K. Then, the peaks from the B2 phase become weak at further hearting. We re-analyzed the series of XRD datum, and found that such apparent weakening was caused due to the appearance of Fe_2S phase. Indeed, in the XRD patten collected at 3500 K, we confirmed that additional weak peaks from Pnma-Fe_2S were clearly visible and the reflection from the coexisting hcp-Fe phase became intense simultaneously. This indicates that stable phase assemblage in Fe-6wt% S bulk composition changes from hcp-Fe + B2-FeS into hcp-Fe + Pnma-Fe_2S. Hence, Fe_2S is the sulfur-rich end-member compound after the decomposition of Fe_3S at 250 GPa. The slope of eutectic melting curve should have kink at the decomposition of Fe_3S. Also, pressure evolution of the eutectic composition should change as well. Since the extrapolation from lower pressure data <250 GPa is not available, higher P-T experiments are necessary to establish the phase diagram at the pressure of inner core boundary.

©2019. Japan Geoscience Union. All Right Reserved.

©2019. Japan Geoscience Union. All Right Reserved.

First-principles Investigation of Iron Diffusion Properties with Implications to Inner Core Plasticity

*Sebastian Ritterbex[1], Taku Tsuchiya[1]

1. GRC Ehime University

The mechanical properties of Earth’ s inner core are key for understanding the evolution and dynamics of the core. However, little is known about the mechanical properties of iron (alloys) at inner core conditions. Therefore, long-standing questions remain open about the viscous strength of the inner core (Yoshida et al., 1996; Karato, 1999), about the origin of its seismic anisotropy (Deuss, 2014) and about its rotational dynamics (Buffett, 1997). All these issues rely on plastic deformation of the inner core, which is barely constrained.

Under extreme conditions of the Earth’ s deep interior, plasticity is expected to be rate limited by atomic diffusion. Experimental studies of diffusion in iron-nickel alloys at elevated P,T conditions finally rely on extrapolation to inner core conditions (Yunker and Van Orman, 2007; Reaman et al., 2012). Here, we investigate vacancy diffusion in iron at the appropriate inner core conditions. We use a density functional approach to calculate all quantities entering the diffusion coefficient, including the role of pressure and temperature, and quantify the self-diffusion coefficient of hcp iron according to transition state theory (TST).

Vacancy diffusion controls many deformation mechanisms such as dislocation creep, an effective strain producing mechanism in metals. We derived a creep model (based on Weertman, 1955 and Nabarro, 1967) to quantify the rate limiting bounds of climb-controlled dislocation creep in hcp iron to provide the first theoretical estimates of the inner core viscosity. Our results suggest an inner core viscosity that is significantly lower than that of Earth’ s mantle.

Keywords: Inner Core, Self-diffusion, Plasticity

©2019. Japan Geoscience Union. All Right Reserved.

Dependence of the dipole component dominancy on the Rayleigh number and inner core size in geodynamo simulations

*Yuki Nishida[1], Yuto Katoh[1], Hiroaki Matsui[2], Masaki Matsushima[3], Atsushi Kumamoto[1]

1. Department of Geophysics, Graduate School of Science, Tohoku University, 2. Dept. of Earth and Planetary Sciences, University of California, Davis, 3. Department of Earth and Planetary Sciences, School of Science, Tokyo Institute of Technology

Geomagnetic field is generated by a dynamo action in the fluid outer core. Studies of the thermochemical evolutions of the Earth's core suggest that the solid inner core has been growing up for approximately one billion years [e.g., O'Rourke and Stevenson, 2016]. Results of numerical dynamo simulations with various aspect ratios (ratios of inner to outer core radii) indicates that the sustained magnetic field is categorized into dipolar-dominated or non-dipolar-dominated regime [e.g., Hori et al., 2010; Driscoll, 2016]. However, any dominant factors controlling the regime have not been fully understood. In the present study, we perform dynamo simulations with various inner core radii using a geodynamo code Calypso to investigate the characteristics of the generated magnetic field. We fix the Ekman, Prandtl, and magnetic Prandtl numbers to be $E = 10^{-3}$, $Pr = 1$, and $Pm = 5$, respectively, and change the Rayleigh number and the aspect ratio to be $r_i/r_o = 0.15$, 0.25, and 0.35. Then we examine the dominancy of the dipole component in two approaches; one is calculating the dipolarity, f_{dip}, which is the ratio of the amplitude of the axial dipole magnetic field to the total amplitude, and the other is comparing magnetic energy for the dipole component with extrapolated magnetic energy for $l = 1$ using an exponential function for odd degree components from $l = 3$ to $l = 19$. The magnetic energy for the dipole component is compared with that extrapolated from the fitting curve.

In $r_i/r_o = 0.25$ and 0.35 cases, f_{dip} is approximately 0.8 at $Ra/Ra_{crit} \fallingdotseq 2.0$ and gradually decreases to approximately 0.45 with increase of Ra/Ra_{crit} up to around 6.0, where Ra_{crit} is the critical Rayleigh number. By referring to the obtained fitting curve, we find that the magnetic energy for the dipole component is more than 5 times larger than the extrapolated value for $l = 1$ at $Ra/Ra_{crit} \fallingdotseq 2.0$ and decreases with increase of Ra/Ra_{crit} in both aspect ratios. The dependency of the dipole component dominancy on the Rayleigh number is similar in both aspect ratio cases. However, in the $r_i/r_o = 0.15$ case, f_{dip} is approximately 0.4 at $Ra/Ra_{crit} \fallingdotseq 8.0$ and decreases to approximately 0.1 with increase of Ra/Ra_{crit} up to around 15.6. At $Ra/Ra_{crit} = 8.1$ and 9.0, the amplitude of the dipole component is comparable to extrapolated value from the fitting curves. At $Ra/Ra_{crit} > 10.1$, the magnetic energy for $l = 1$ component is smaller than that for the $l = 2$ component. Consequently, the magnetic field obtained in the simulation results is non-dipolar. To summarize above, we categorize the present dynamo simulations as shown in Figure 1. Here we define strong/weak dipolar dynamo by a condition that the magnetic energy is larger/smaller than the kinetic energy. The axial dipolar component becomes small in all three ratio cases for larger Rayleigh numbers. Non-dipolar components become larger for the smaller inner core. In other words, for $r_i/r_o < 0.35$, it is likely that the dipolar magnetic field is dominant for larger inner core.

Keywords: Geodynamo, Inner core size, Rayleigh number, Dipole component dominancy

©2019. Japan Geoscience Union. All Right Reserved.

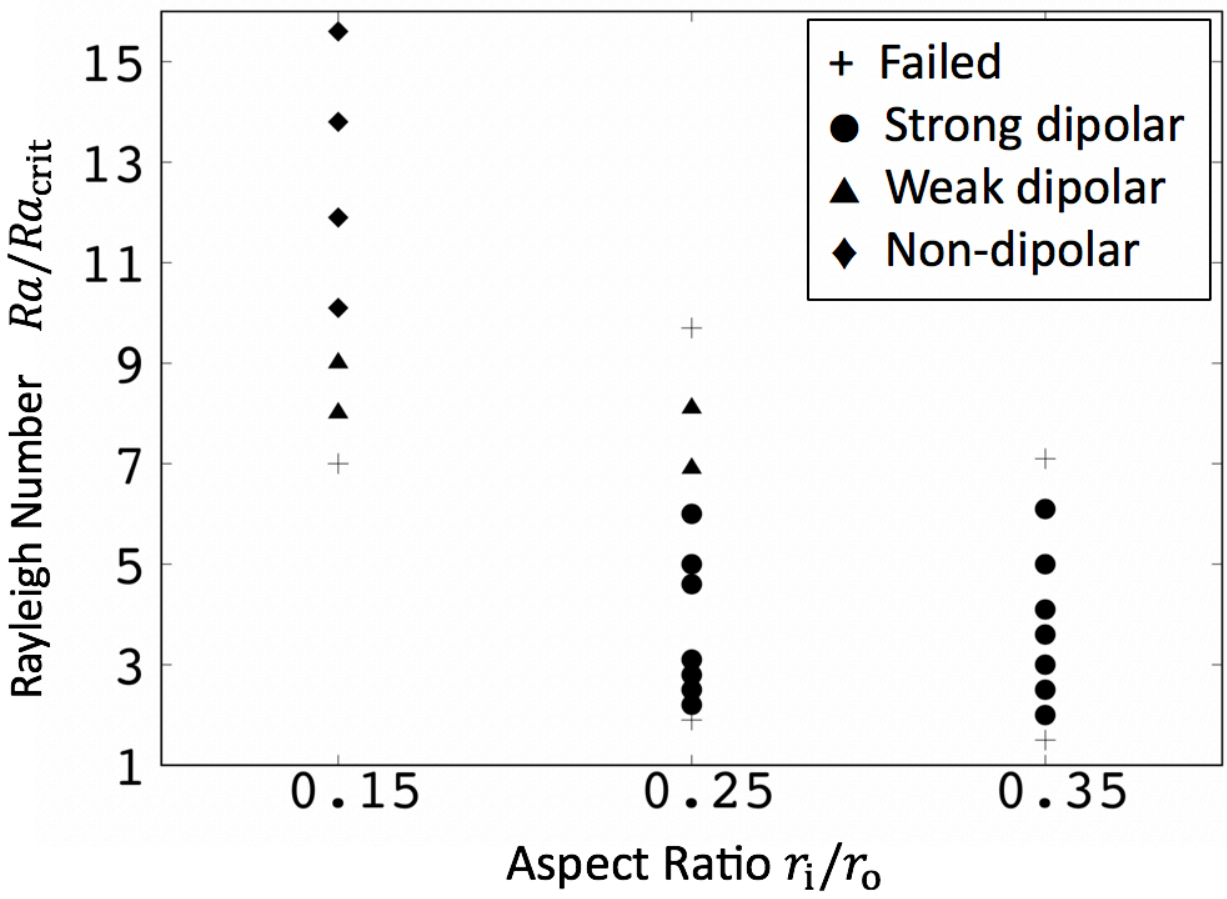

Figure 1 Dynamo regime in various aspect ratios. Cross, circle, triangle, and diamond symbols represent failed, strong dipolar, weak dipolar, and non-dipolar dynamo cases, respectively.

©2019. Japan Geoscience Union. All Right Reserved.

Elasticity of Fe-Si Alloy

*Taku Tsuchiya[1], Yu Fukunaga[1]

1. Geodynamics Research Center, Ehime University

Earth’ s inner core (329~364 GPa and 5000~6000 K) is thought to be composed of solid Fe-Ni alloy with some unknown light elements (e.g., Mao et al., 1998). Thermoelasticity of iron alloys is therefore a key to interpreting seismological information of the inner core: density, seismic wave velocities, and their anisotropy. So far, several studies reported that pure hcp iron has a shear modulus distinctly larger than that of the inner core and a small P-wave anisotropy (e.g., Mao et al., 1998; Vocadlo et al., 2009). This large V_P/V_S ratio of the inner core is one of the remaining inexplicable features of the deep Earth, and it suggests the presence of mechanisms to lower the S-wave velocity in the inner core, such as a low-velocity component (Prescher et al., 2015), pre-melting effect (Martorell et al., 2013), anelasticity, and so on.

In this study, we perform ab initio molecular dynamics simulations on the thermoelasticity of alloy compositions including potential light element candidate of Si. Computations are conducted at the inner core P,T conditions. The obtained velocities, density and aggregate anisotropies are compared against seismological constraints, and we show the first evidential result on the suitable compositions to the inner core constituents, which can reproduce all of V_P, V_S, V_Φ, and ρ of the inner core simultaneously. We also report why Fe-Si alloy can have a large V_P/V_S ratio.

Research supported by KAKENHI .JPN15H05834.

Keywords: Ab initio density functional computation, High-P,T elasticity, Inner core

©2019. Japan Geoscience Union. All Right Reserved.

[E] Poster | S (Solid Earth Sciences)：S-MP Mineralogy & Petrology

Tue. May 28, 2019 10:45 AM - 12:15 PM JST | Tue. May 28, 2019 1:45 AM - 3:15 AM UTC | Poster Hall International Exhibition Hall8, Makuhari Messe_7

[S-MP29] Oceanic and Continental Subduction Processes

convener:REHMAN Ur Hafiz(Department of Earth and Environmental Sciences, Graduate School of Science and Engineering, Kagoshima University), Tatsuki Tsujimori(Tohoku University), Chin-Ho Tsai(Department of Natural Resources and Environmental Studies, National Dong Hwa University), Kazuaki Okamoto(Faculty of Education, Saitama University)

This JpGU-AGU joint session aims at bringing earth scientists from Japan and overseas to present their research related to the processes of oceanic and continent subduction, continent-continent collisions, metamorphism of crustal rocks, formation of the oceanic/continental arcs, and accretion/ tectonic erosion of material along subduction boundaries.

Topics such as role of the fore- and back-arcs in the subduction zones, process of accretion of volcaniclastic and terrigenous sediments along the subduction/collision boundaries, deformation and metamorphism of subducted crust, and exhumation will be the main focus of the session.

In addition to the above mentioned topics, our focus for the10th anniversary of this international session will be towards our understanding and progress on the ultrahigh-pressure/temperature metamorphic terranes in the world.

Exchange of ideas among geoscientists applying different approaches on problems related to the theme of the session are most welcome.

[SMP29-P01] Zircon U-Pb ages of metasedimentary rocks in the Hakogase (Hida Marginal) area, Fukui Prefecture.

*Atsushi MIYASHITA[1], Tatsuki Tsujimori[2], Daniel Pastor-Galán[3], Yi Keewook[4] (1.Seikei University, 2.Tohoku University, 3.Salamanca University, 4.Korea Basic Science Institue)

[SMP29-P02] Late Permian to Early Triassic back-arc type volcanism in the southern Mongolia volcano-plutonic belt of the Central Asian Orogenic Belt: Implication for timing of the final closure of the Palaeo-Asian Ocean

*Takeshi Imayama[1], Yoichiro Koh[2], Kazumasa Aoki[3], Mototaka Saneyoshi[4], Koshi Yagi[5], Shogo Aoki[4], Yoshihiro Sawada[6], Chiaki Ikawa[5], Tomoya Terada[4], Shinobu Ishigaki[4], Shin Toyoda[3], Khishigjav Tsogtbaatar[7], Buuvei Mainbayar[7] (1.Research Institute of Natural Sciences, Okayama University of Science, 2.Graduate School of Environmental Science, Hokkaido University, 3.Faculty of Science, Okayama University of Science, 4.Faculty of Biosphere - Geosphere Science, Okayama University of Science, 5.Hiruzen Institute for Geology and Chronology, 6.Emeritus Professor of Shimane University, 7.Institute of Paleontology and Geology, Mongolian Academy of Sciences)

[SMP29-P03] Mantle dynamics of slab breakoff constrained from the temporal change of the melting depth estimated from the Cumulate Member of the Ordovician Hayachine-Miyamori Ophiolite

*Takafumi Kimura[1], Kazuhito Ozawa[1] (1.Department of Earth and Planetary Science, The University of Tokyo)

[SMP29-P04] **Evidence of HIMU seamount on the Farallon Plate: Application of *in-situ* Sr-Pb isotope analysis to Franciscan lawsonite-bearing metagreywacke**

*Tomomi Hara[1], Tatsuki Tsujimori[1], Jun-Ichi Kimura[2] (1.Tohoku University, 2.Japan Agency for Marine-Earth Science and Technology)

[SMP29-P05] Boron isotope variations of antigorite serpentinites associated with high-pressure metamorphic rocks: A case study in the Itoigawa–Omi area of the Hida-Gaien Belt, Japan

*Chinatsu Yamada[1], Tatsuki Tsujimori[1], King Chang[2], Jun-Ichi Kimura[2] (1.Tohoku University, 2.Japan Aegency for Marine-Earth Science and Technology)

[SMP29-P06] **Study of zircons structures from the Miocene Shibi-san Granodiorite, Kagoshima Prefecture, Japan**

*Nakabayashi Marimo[1], REHMAN Ur Hafiz[1] (1.Kagoshima University)

[SMP29-P07] **Experimental modeling of eclogite and C-O-H fluid interaction in the subduction zones**

*Nadezda Chertkova[1], Shigeru Yamashita[2], Hiroaki Ohfuji[1], Tetsuo Irifune[1], Hirokazu Kadobayashi[1], Yoshitaka Yamamoto[3] (1.Ehime University, Geodynamics Research Center, 2.Okayama University, Institute for Planetary Materials, 3.National Institute of Advanced Industrial Science and Technology)

[SMP29-P08] Microfabrics of omphacite and garnet in eclogite from the Lanterman Range, northern Victoria Land, Antarctica

*Daeyeong Kim[1], Taehwan Kim[2], Jungmin Kim[3] (1.Division of Polar-Earth Sciences, Korea Polar Research Institute, 2.School of Earth and Environmental Sciences, Seoul National University, 3.Earth and Environmental Sciences, Korea University)

[SMP29-P09] Primordial Apatite from Ophiolite in Taiwan

*Nobuaki Niitsuma[1], Reishi Takashima[2], Yuan Hsi Lee[3] (1.Institute of Geosciences,Shizuoka University, 2.Tohoku University Museum, 3.National Chung-Cheng University, Taiwan)

[SMP29-P10] The evolution of the Cretaceous Jinan Basin in South Korea and the age and tectonic setting for the volcanic rocks in it

*Seung Hwan LEE[1], Chang Whan Oh[1] (1.Department of earth and environmental sciences Chonbuk national university)

[SMP29-P11] GEOCHORONOLOGY AND PETROCHEMISTREY OF LATE PALEOZOIC MAGMATIC ROCKS OF THE MANDAKH AREA, SOUTHEAST MONGOLIA

*Undarmaa Batsaikhan[1], Noriyoshi Tsuchiya[1], Masaoki Uno[1], Yukio Isozaki[2], Uyanga Bold[2], Hikaru Sawada[2] (1.Graduate School of Environmental Studies, Tohoku University, 2.Graduate School of Arts and Sciences The University of Tokyo)

[SMP29-P12] Feedbacks Offshore the Cascadia Margin

*Joan S Gomberg[1] (1.USGS Earthquake Science Center)

Zircon U-Pb ages of metasedimentary rocks in the Hakogase (Hida Marginal) area, Fukui Prefecture.

*Atsushi MIYASHITA[1], Tatsuki Tsujimori[2], Daniel Pastor-Galán[3], Yi Keewook[4]

1. Seikei University, 2. Tohoku University, 3. Salamanca University, 4. Korea Basic Science Institue

Combined chronological study using detrital zircon U-Pb dating and phengite K-Ar dating enables to understand the tectonic evolution of the high *P/T* metamorphic belt. The youngest age of detrital zircon U-Pb ages of psamites in the Hida marginal metamorphic rocks (HMMR = Renge belt) approximate its depositional ages (Tsutsumi et al., 2009). The closure temperature of the phengite K-Ar ages are controlled by deformation and recrystallization during exhumation of the metamorphic rocks(Itaya and Tsujimori, 2015). Therefore, the gap between the youngest age of detrital zircons and phengite K-Ar ages are the age difference between subuduction and uplift of metamorphics.
The Hakogase (Nigure-gawa, Kuzuryu, Fukui Prefecture) metamorphic rocks belong to HMMR member as the olistolith in the Cretaceous Tedori Group. It consists mainly pelites with small amount of basites and mables. The main index mineral assemblage of metasediments are garnet + chlorite, and the phenigite K-Ar ages are 287.8 - 283.6 Ma (Kunugiza et al., 2004). Relic Lawsonite was also found in the basaites and psamites (Miyakawa, 1982).
The detrital Zircons U-Pb ages in the two pelites are obtained by the SHRIMP II of KBSI. The youngest U-Pb ages of detrital zircons are 307Ma. The gap of the sedimentation between uplift of the Hakogase metamorphics is estimated 20 Ma. This value means the migration speed of the HMMR metamorphic rocks are 1/10 of plate motion. This rapid migration speed is common for the high *P/T* metamorphic rocks.

Keywords: high P/T metamorphic rocks, Zircon U-Pb ages, Phengite K-Ar ages

©2019. Japan Geoscience Union. All Right Reserved.

Late Permian to Early Triassic back-arc type volcanism in the southern Mongolia volcano-plutonic belt of the Central Asian Orogenic Belt: Implication for timing of the final closure of the Palaeo-Asian Ocean

*Takeshi Imayama[1], Yoichiro Koh[2], Kazumasa Aoki[3], Mototaka Saneyoshi[4], Koshi Yagi[5], Shogo Aoki[4], Yoshihiro Sawada[6], Chiaki Ikawa[5], Tomoya Terada[4], Shinobu Ishigaki[4], Shin Toyoda[3], Khishigjav Tsogtbaatar[7], Buuvei Mainbayar[7]

1. Research Institute of Natural Sciences, Okayama University of Science, 2. Graduate School of Environmental Science, Hokkaido University, 3. Faculty of Science, Okayama University of Science, 4. Faculty of Biosphere - Geosphere Science, Okayama University of Science, 5. Hiruzen Institute for Geology and Chronology, 6. Emeritus Professor of Shimane University, 7. Institute of Paleontology and Geology, Mongolian Academy of Sciences

The timing of final subduction and closure of the Palaeo-Asian Ocean is still controversial in the eastern segments of the Central Asian Orogenic Belt (CAOB). A more detailed understanding is needed with respect to the formation of volcanic rocks and sediments associated with the final closure of the Palaeo-Asian Ocean in southern Mongolia. We investigated alkali series volcanic rocks newly discovered in the southern Mongolia volcano-plutonic belt of the CAOB and classified as basalt, basaltic trachyandesite, andesite, trachyandesite, and trachyte, mainly showing andesitic-dacitic compositions. In Harker diagrams, the TiO_2, FeO, MnO, Al_2O_3, CaO, and MgO contents generally decrease with increasing SiO_2, representing a series of differentiated volcanic rocks. The primitive mantle-normalized trace element spider diagram is characterized by incompatible element-rich patterns and negative Nb anomalies. The tectonic discrimination diagrams show that the volcanic rocks were formed by arc-related volcanism rather than within-plate volcanism. K-Ar dating of feldspars from six volcanic rocks yields ages ranging from 270 to 239 Ma, indicating that andesitic and dacitic magmatism occurred during this period. These geochemical and geochronological data indicate that the differentiated volcanic rocks intruding middle to late Palaeozoic volcanic sediments were formed by back-arc type subduction ca. 270–240 Ma. Based on detrital zircon U-Pb ages, the terrigenous sandstones underlain by the volcanic sediments record a maximum depositional age of Late Triassic (ca. 220–200 Ma) and include a main cluster of Early Devonian ages (ca. 410–390 Ma), possibly derived from the Devonian-Carboniferous arc complex observed surrounding this study area. These results from the volcanic and sedimentary rocks in this study, combined with investigations in previous studies, imply that subduction beneath the eastern segments of the CAOB to consume the Palaeo-Asian Ocean continued until Late Permian to Early Triassic.

Keywords: Palaeo-Asian Ocean, southern Mongolia, Central Asian Orogenic Belt, back-arc type volcanism

©2019. Japan Geoscience Union. All Right Reserved.

Mantle dynamics of slab breakoff constrained from the temporal change of the melting depth estimated from the Cumulate Member of the Ordovician Hayachine-Miyamori Ophiolite

*Takafumi Kimura[1], Kazuhito Ozawa[1]

1. Department of Earth and Planetary Science, The University of Tokyo

Slab breakoff, detachment of oceanic lithosphere highly expected during arc-continent collision, is one of the important mechanisms inducing passive upwelling of the asthenosphere and magma generation in arc environments [1]. In order to better understand the mantle dynamics of slab breakoff, we need to use continuous geological record with high time resolution. In this study, we have extracted a record of temporal change of the magma generation depth from cumulates in an Ordovician arc ophiolite at a time resolution of several tens of million years.
The Hayachine-Miyamori Ophiolite, northern Japan, is one of the Ordovician ophiolite formed in an arc environment [2]. The ultramafic member was built up by three main magmatic stages, which are recorded in three rock units: Tectonite Member, Cumulate Member, and ultramafic dikes, in the order of formation ages. The last two units in the entire evolution of the ophiolite is explained by decompressional melting of sub-slab mantle triggered by slab breakoff [2][3]. The melting depth of an ultramafic magma solidified as dikes in the Cumulate Member is estimated to be ~170km [3]. Our recent field study clarified a large-scale stratification characterized by alternation of wehrlite-dominant and dunite-dominant layers in the Cumulate Member. Each layer has a thickness from several meters to ~1 km and, the total thickness attains ~3km. Moreover, we succeeded in specifying the strike and plunge of the gravity field to be ~N48°E and ~20°NE during the cumulate formation from field information and westward stratigraphic younging [4].
We estimated the temporal change of generation depth of parent magmas of the Cumulate Member by garnet signature in heavy rare earth elements (HREEs) as depth proxy. The information may constrain the mantle dynamics during the slab breakoff. We examined stratigraphic variation of HREE ratio at the core of clinopyroxenes over the thickness of ~2km in the Cumulate Member. The obtained variation of the Dy/Lu increases from ~12.9 to ~16.5 with increasing the stratigraphic height. We estimated the extent of melting in the garnet stability field increasing from ~50 to ~90% of the total melting by applying an open-system fractional melting model to reproduce the Dy/Lu variation.
We also estimated the time scale of formation of the Cumulate Member by using cm –10cm scale heterogeneity recorded in contact zone of intruded magma and the host. The profile of Mg# of olivine in xenoliths of the Tectonite Member occurring at the bottom of the Cumulate Member shows that the cooling time is less than several tens of million years [5]. The dunite of the Cumulate Member contacting the ultramafic dike shows a systematic decrease of Mg# from 90 to 86.8 over the distance of 54 mm towards the contact. We calculated the time scale of subsolidus diffusional exchange between the dunite and dike and obtained several tens of million years at ~1000℃. The host was kept at a high temperature when the dikes intruded because of the absence of chilled margin. We thus estimated time scale of formation of the Cumulate Member to be < several tens of million years.
We propose the following tectonic model in the Ordovician northern Japan on the basis of the above result. The slab breakoff took place at the depth slightly deeper than the boundary of spinel and garnet stability fields (~80 km) and induced counter flow and adiabatic melting of the sub-slab mantle. The melting depth deepened down to ~170 km on the time scale of several tens of million years, which corresponds to the time scale to complete the slab breakoff. The sinking velocity of the slab is more than

©2019. Japan Geoscience Union. All Right Reserved.

a few millimeters per year.

[1]: Davies et al., 1995. [2]: Ozawa et al., 2015. [3],[4]: Kimura et al., 2017, 2018, JpGU abstract. [5]: Ozawa, 1983.

Keywords: slab breakoff, arc ophiolite, cumulate

©2019. Japan Geoscience Union. All Right Reserved.

Evidence of HIMU seamount on the Farallon Plate: Application of *in-situ* Sr-Pb isotope analysis to Franciscan lawsonite-bearing metagreywacke

*Tomomi Hara[1], Tatsuki Tsujimori[1], Jun-Ichi Kimura[2]

1. Tohoku University, 2. Japan Agency for Marine-Earth Science and Technology

Since bulk isotopic composition of oceanic basalt is susceptible to element remobilization during alteration process, there is a risk of causing misread of geochemical signatures from bulk metabasaltic rocks in subduction complex. As Hara et al. (2018) demonstrated, however, *in-situ* Sr-Pb isotope analysis of lawsonite in high-pressure metabasaltic rocks has a great potential for tracing the geochemical signatures reflecting the igneous protolith. In this study, we have applied the method to lawsonite in metasedimentary rocks to explore clastic components of a trench-fill sediment. A jadeite-bearing Franciscan metagreywacke from Pacheco Pass area, east-central Diablo Range, California Coast Ranges was selected for geochemical reconnaissance.

Lawsonites in the Franciscan metagreywacke record a high initial Pb isotope ratios ($^{206}Pb/^{204}Pb$ = 18.74–19.66, $^{207}Pb/^{204}Pb$ = 15.58–15.70 and $^{208}Pb/^{204}Pb$ = 38.41–39.34). This Pb-isotope signature suggests that a protolith of the metagreywacke have contained a debris derived from a HIMU-type basalt. Considering the maximum depositional age of the metagreywacke at ~102 Ma, the underflow of the Farallon Plate beneath continental crust of the North American Plate would have carried a HIMU seamount to a Franciscan trench.

Our study has demonstrated the potential application of 'lawsonitology' as sedimentary provenance analyses for metamorphosed accretionary complex. Moreover, the results would manifest that Pb isotopic signature of ancient oceanic basalt can be detectable from Ca-Al silicate mineral, such as lawsonite, epidote and pumpellyite, in metamorphic rocks.

Keywords: Lawsonite, Sr-Pb isotope, LA-MC-ICPMS, HIMU, Metasediment

©2019. Japan Geoscience Union. All Right Reserved.

Boron isotope variations of antigorite serpentinites associated with high-pressure metamorphic rocks: A case study in the Itoigawa–Omi area of the Hida-Gaien Belt, Japan

*Chinatsu Yamada[1], Tatsuki Tsujimori[1], King Chang[2], Jun-Ichi Kimura[2]

1. Tohoku University, 2. Japan Aegency for Marine-Earth Science and Technology

Boron isotope study of serpentinites in the Franciscan Complex using an ablation volume correction (AVC) LA-MC-ICPMS discriminates two groups (Yamada et al., 2018 JpGU abstr.; Yamada et al. 2019, in press). Serpentinites associated with blueschists are characterized by lighter boron isotope than serpentinites without blueschist-facies rocks. The lighter boron isotope signature (< ~10 ‰) of blueschist-bearing serpentinites results from interaction with forearc slab fluids with low δ^{11}B in deeper depth. In order to evaluate the versatility of B isotopes and composition of high-pressure metamorphosed serpentinites, we investigated antigorite serpentinites associated with three different type of high-pressure metamorphic rocks in the Itoigawa–Omi area.

The investigated serpentinites can be grouped into two types based on the B isotopes. Antigorite serpentinite with blueschist- and eclogite-facies metamorphic rocks in the Yunotani Valley is characterized by moderate boron (12.5–48.4 $\mu g \cdot g^{-1}$) and lower δ^{11}B (+6.6 to +12.3‰ [mostly smaller than +8‰]; n= 10); Brucite-bearing antigorite serpentinite with barroisite-bearing mafic schist in the Kotaki-gawa River is characterized by very high boron (37.5 –302 $\mu g \cdot g^{-1}$) and lower δ^{11}B (+5.8 to +10.7‰ [mostly smaller than +8‰]; n= 10). In contrast, antigorite serpentinite with garnet amphibolite in the Omi-gawa River is characterized by a wide range of boron (9.1–145 $\mu g \cdot g^{-1}$) and relatively high δ^{11}B (+11.5 to + 14.8 ‰; n= 10).

Our preliminary reconnaissance shows significantly lower δ^{11}B (smaller than +8‰) in antigorite serpentinites of the 'Eclogite Unit' proposed by Tsujimori (2002). This trend is consistent with our earlier study in the Franciscan Complex. The antigorite serpentinites in the 'Eclogite Unit' might have been affected by a deep forearc slab fluids.

Keywords: Serpentinite, boron isotope, subduction zone

©2019. Japan Geoscience Union. All Right Reserved.

Study of zircons structures from the Miocene Shibi-san Granodiorite, Kagoshima Prefecture, Japan

*Nakabayashi Marimo[1], REHMAN Ur Hafiz[1]

1. Kagoshima University

The Miocene granodiorite body (zircon fission track age by Miyachi, 1985) of the Mount Shibi, Kagoshima prefecture is a lenticular stock that intrudes the Cretaceous sedimentary rocks of the Shimanto belt. Previous studies subdivided the granodiorite body into the Kusu-bae (core facies) and Hira-bae (marginal facies) types based on the changes in litho-facies and distinct chemical composition of biotite and amphibole (Yamamoto et al., 1988). We conducted field survey in the study area and found no clear contrasts to sub-divide the body, instead it represents a single pluton with local chemical variation along the marginal portions. Based on detailed petrography, the entire body appears as homogeneous stock exhibiting identical mineral assemblage with no clear evidence that can mark the boundary between Kusu-bae and Hira-bae types. Moreover, to understand the processes of magmatic crystallization we investigated more than 600 zircon grains from about 8 samples for external (applying the zircon morphology method of Pupin, 1980) and internal morphology using the Cathodoluminescence imaging. Based on the Pupin’ s method, the deduced temperature range for the zircon crystallization was between 750 and 850℃. In addition, internal structures of zircon (CL images) showed oscillatory zoning with continuous growth domains and abundant apatite inclusions, suggesting the magma was fluid-rich and have been crystallized under relatively higher temperature. We also investigated zircons from the surrounding hornfels (Shimanto belt rocks) that were affected thermally due to the contact metamorphism. Zircons from the hornfels are completely different and rounded with different internal structures. Zircons from the so-called Kusu-bae and Hira-bae types are identical and suggest their crystallization from a single parental magma hence the pluton cannot be sub divisible.

References
Miyachi M. (1985). Fission track ages of some granitic rocks in Outer Zone ofKyushu, Japan. Journal of Mineralogical and Petrological Sciences 80, 406-409.
Pupin J. P. (1980). Zircon and granite petrology. Contribution to Mineralogy and Petrology 73, 207-220.
Yamamoto M., Oniwa N., Toyota K. (1988). Compositional Variation of the Shibi-san Granodioraite Body, Kagoshima Prefecture, Japan. Bulletin of the Kagoshima University Science Faculty 21, 35-49.

Keywords: zircon, granodiorite, crystal shape

©2019. Japan Geoscience Union. All Right Reserved.

Experimental modeling of eclogite and C-O-H fluid interaction in the subduction zones

*Nadezda Chertkova[1], Shigeru Yamashita[2], Hiroaki Ohfuji[1], Tetsuo Irifune[1], Hirokazu Kadobayashi[1], Yoshitaka Yamamoto[3]

1. Ehime University, Geodynamics Research Center, 2. Okayama University, Institute for Planetary Materials, 3. National Institute of Advanced Industrial Science and Technology

The presence of volatile components controls melting relationships in the subducting oceanic plate and the overlying mantle wedge, affecting their physical properties and seismic observables. The major volatile species in the mantle low oxygen fugacity environment are considered to be H_2O and CH_4, as estimated for mantle xenoliths and C-O-H fluid speciation in equilibrium with diamond [1,2]. Experimental studies with the direct monitoring of phase assemblages and melting relationships in the silicate systems with C-O-H components can shed light on the processes, which take place in the subduction zones, and provide important data for interpretation of observed physical parameters.
In this study, we employed *in situ* spectroscopic methods in combination with the diamond anvil cell (DAC) technique for investigation of C-O-H fluid behavior and its influence on phase relationships in the eclogite–5.75H_2O–CH_4 system at temperatures up to 1000 degree C and pressures exceeding 5 GPa. We designed a new cell assembly for Mao-type symmetric diamond anvil cell with large optical access to the sample in order to make it suitable for infrared and Raman measurements directly at high-pressure and high-temperature conditions. Mineral phase assemblages, observed during experiments, are consistent with those described in the dry system of the similar basaltic composition [3]. At the same time, miscibility between aqueous and carbonaceous components in the fluid phase coexisting with silicate minerals was confirmed at temperatures above 800 degree C and pressures above 3.2 GPa.

References

[1] Shirey, S.B., Cartigny, P., Frost, D.J., Keshav, S., Nestola, F., Nimis, P., Pearson, D.G., Sobolev, N.V. and Walter, M.J. (2013) *Rev. Mineral. Geochem.*, **75**, 355-421.
[2] Belonoshko, A. and Saxena, S. (1992) *Geochim. Cosmochim. Acta*, **56**, 3611-3626.
[3] Yasuda, A., Fujii, T. and Kurita, K. (1994) *J. Geophys. Res.: Solid Earth*, **99**, 9401-9414.

©2019. Japan Geoscience Union. All Right Reserved.

Microfabrics of omphacite and garnet in eclogite from the Lanterman Range, northern Victoria Land, Antarctica

*Daeyeong Kim[1], Taehwan Kim[2], Jungmin Kim[3]

1. Division of Polar-Earth Sciences, Korea Polar Research Institute, 2. School of Earth and Environmental Sciences, Seoul National University, 3. Earth and Environmental Sciences, Korea University

Layered structures in metamorphic rocks are sometimes crucial to occur strain localization then affect to seismic properties. We conducted microstructural analyses omphacite and garnet in foliated eclogite from the Lanterman Range, northern Victoria Land, Antarctica, to determine the influence of the layered structure on seismic observations in subduction zone. The analyzed eclogite, composed of layered garnet-rich and omphacite-rich layers, shows the low aspect ratios, similar angular distribution of long axes relative to the foliation, uniform grain size distribution, near-random crystallographic preferred orientations (CPOs), and misorientation angle distributions of garnet and opposite characteristics of omphacite in both layers. The results of fabric analyses are consistent with strain localization into omphacite or omphacite-rich layers rather than garnet or garnet-rich layers. Our results therefore demonstrate the importance of the layered structure in strain localization and in the development of the seismic anisotropies of subducting oceanic crust.

Keywords: Eclogite, EBSD, Layered structure

©2019. Japan Geoscience Union. All Right Reserved.

Primordial Apatite from Ophiolite in Taiwan

*Nobuaki Niitsuma[1], Reishi Takashima[2], Yuan Hsi Lee[3]

1. Institute of Geosciences,Shizuoka University, 2. Tohoku University Museum, 3. National Chung-Cheng University, Taiwan

Apatite is a common accessory mineral in igneous rocks. Because apatite has a wide range of trace element compositions as well as strong resistance to diagenetic alteration, the trace element composition of apatite has been used for tracing petrogenetic processes of plutonic bodies as well as the tephrochronology of Paleozoic tephras and Quaternary volcaniclastic deposits.

We studied trace element compositions of apatites from Ophiolite in Taiwan. The Ophiolite with mafic-ulatramafic rocks (150811-14) expose along the anticlinal axes of the metamorphic belts in Backbone Range of Taiwan, and exotic gabbro block (MA-15B) in chaotic deposits of Lichi Melange, in the southern end of Longitudinal Valley, in East Taiwan.

Lee (2015 JpGU; Chen et al., 2017 Tectonics) reported that zircon ages of Ophiolites in Taiwan are concentrated to 15 Ma, which should relate with termination of spreading in South China Sea and Shikoku & Parece Vela Basin just before Japan Sea Opening, and large scale igneous activities in the Outer Zone of Southwest Japan just after Japan Sea Opening (Niitsuma & Lee, 2018 JpGU).

Fifteen and twelve apatite phenocrysts from samples of MA-15B and 150811-14 were analyzed for major and minor elements using a JEOL 8530F wavelength dispersive Electron Probe Micro Analyzer (Takashima et al., 2017 Quaternary Geochronology) in weight % as follow;
__major elements: P=17.956 +/-0.100, 17.926 +/-0.129
_____Ca=38.362 +/-0.329, 38.128 +/-0.273
_____F=1.082+/-0.151, 0.445+/-0.046
__trace elements: Cl<0.01, 0.04 Mg<0.01, 0.01 Mn<0.04, 0.05
_____Fe<0.03, 0.17 Ce<0.09, 0.05 Y<0.13, 0.04

The contents of trace elements are extremely low and we concluded the apatite might be primordial without any contaminations and petrogenetic effect, and crystallized directly in the magma above rifted mantle along the northwestern margin of West Philippine Basin just before Japan Sea Opening.

Keywords: Apatite, trace element , Ophiolite, Taiwan, Opening of Japan Sea

©2019. Japan Geoscience Union. All Right Reserved.

The evolution of the Cretaceous Jinan Basin in South Korea and the age and tectonic setting for the volcanic rocks in it

*Seung Hwan LEE[1], Chang Whan Oh[1]

1. Department of earth and environmental sciences Chonbuk national university

The Jinan Basin is one of the Cretaceous pull-apart basins in the South Korea. It locates along the Yongdong-Gwangju fault system and consists of non-marine sediments with volcanic and pyroclastic rocks. The sinistral strike slip movement which formed the Cretaceous pull apart basins was occurred by the collision between Siberian and Manchuria blocks at ca. 130~100Ma. LA-MC-ICPMS age dating on the zircons from sedimentary and igneous rocks indicates followings. The sedimentation in the Jinan Basin had started at least from 97.7Ma and continued until 89.47Ma. During the sedimentation, basaltic andesite extruded at 90-92 Ma and later rhyolitc and andesitic magma intruded the Jinan Basin at 90-89 Ma and 85-84 Ma respectively. Later the Jinan Basin uplifted to form Noryeong mountain range due to the compression which was related with dextral strike slip fault movement. This fault movement is expected to be caused by the collision between Indian plate and Eurasian plate at ca. 55~25Ma. AFT(Apatite Fission Track) age from sediments in the Jinan Basin is approximately 68Ma. Due to the formation of Noryeong mountain range, the *Coreoleuciscus splendidus* was differentiated into two species, these two species of *Coreoleuciscus splendidus* have the same ancestors at around 38Ma. These data indicate that the Noryeong mountain range including the Jinan Basin are expected to have uplifted at around 68-38Ma. Rhyolitic volcanic rocks in and around the Jinan Basin are plotted on the VAG (Volcanic Arc Granite) field and basaltic to intermediated volcanic rocks are plotted on the CAB (Calc-Alkaline Basalt) and WPB (WIthin Plate Basalt) fields in the tectonic discrimination diagrams. There was a roll back of subduction zone toward Pacific ocean at ca. 100 Ma. These data suggest that the igneous rocks in the Jinan Basin formed by the mantle upwelling due to extension caused by the roll back of subduction zone. The upwelling asthenospheric mantle supplied heat which caused the felsic magma by the melting of the lithospheric mantle and crust which had been contaminated by crustal material supplied from subducting sediment or ocean before roll back of the subduction zone. The upwelling asthenospheric mantle was also melted to form basaltic magma. The deep faults formed by sinistral strike slip movement around the Jinan Basin at the Cretaceous, gave the path toward surface for the magma at deep depth.

Keywords: Jinan Basin, pull-apart basin, Igneous rock, Cretaceous

©2019. Japan Geoscience Union. All Right Reserved.

(a) ca. 97 ~90 Ma.

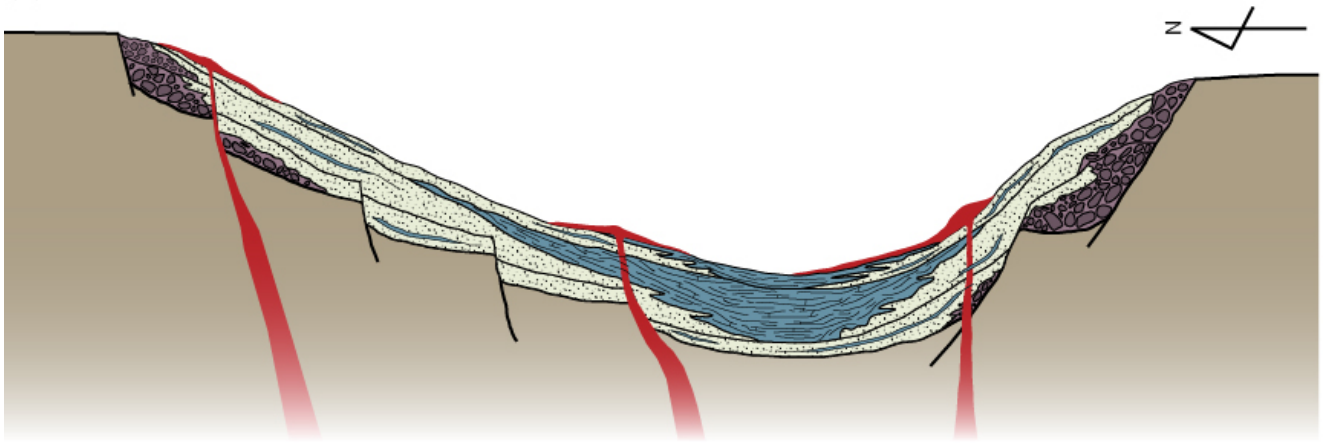

Deposition of lower part sedimentary rocks in the Jinan Basin (97~92 Ma) with extrusion of basaltic andesite (92~90 Ma)

(b) ca. 90 ~89 Ma.

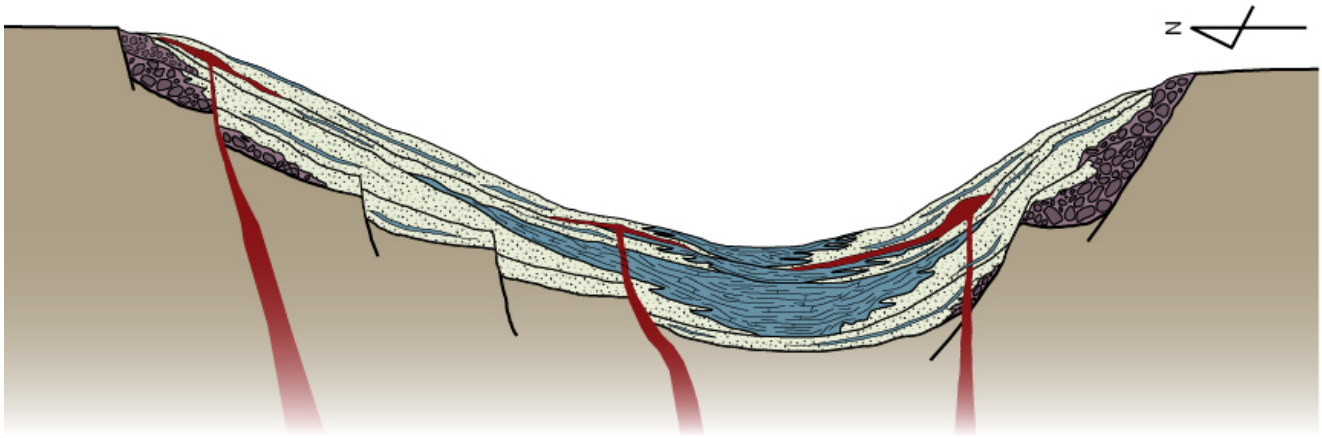

Deposition of upper part sedimentary rocks on the lower part sedimentary rocks and basaltic andesite extrusive volcanic rocks

(c) ca. 89 ~84 Ma.

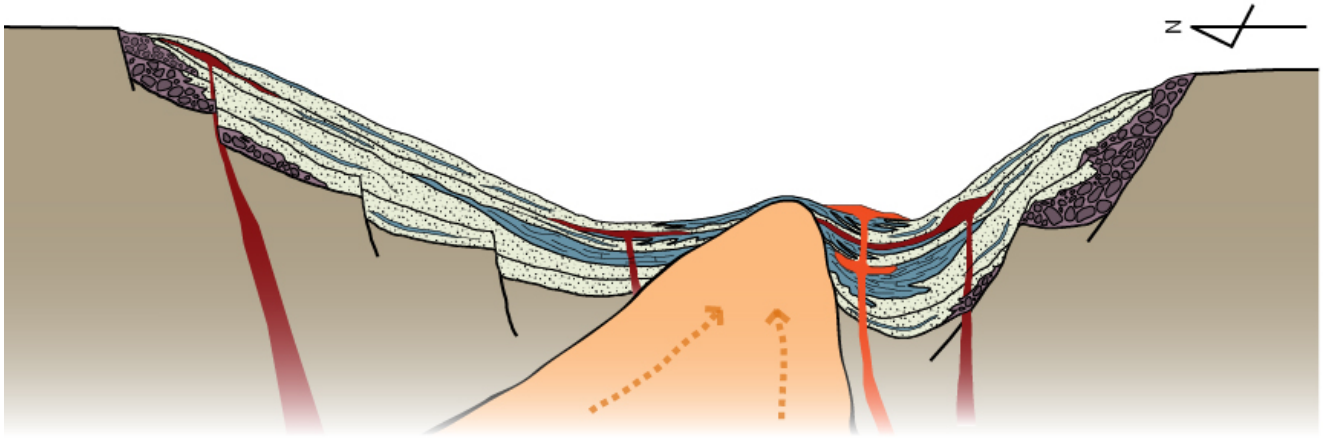

Intrusion and extrusion of rhyolite (ca. 89Ma) with late intrusion of andesitic volcanic rocks (ca. 84Ma)

Intrusive andesitic volcanic rocks
Rhyolite
Basalt and basaltic andesite
Conglomerate
Sandstone
Shale or mudstone

©2019. Japan Geoscience Union. All Right Reserved.

©2019. Japan Geoscience Union. All Right Reserved.

GEOCHORONOLOGY AND PETROCHEMISTREY OF LATE PALEOZOIC MAGMATIC ROCKS OF THE MANDAKH AREA, SOUTHEAST MONGOLIA

*Undarmaa Batsaikhan[1], Noriyoshi Tsuchiya[1], Masaoki Uno[1], Yukio Isozaki[2], Uyanga Bold[2], Hikaru Sawada[2]

1. Graduate School of Environmental Studies, Tohoku University, 2. Graduate School of Arts and Sciences The University of Tokyo

The southeast Mongolia has become a major survey area for unraveling the Paleozoic tectonic evolution because Mongolia occupies the central part of the CAOB which is enormous and composed of a multiplicity of terranes including ancient island and continental arcs, ophiolites, passive continental margins, Precambrian continental blocks and high-T/low-P metamorphic zones and where porphyry Cu deposits occur. The late Paleozoic magmatic rocks are widely distributed in the Mandakh area which is located in the Curvansaikhan and Manlai terrains, in the southeast Mongolia. We will discuss petrochemical features, mineral assemblage and new geochronological constrain of magmatic rocks in the Mandakh area. Furthermore, we compared petrochemical characteristics of the Mandakh area with Tampakan deposit (Philippines), Cerro Colorado deposit (Chili) and negative criteria of Cu deposits (Japan) in order to characterize potential of the porphyry copper deposit in Mandakh area.

The Mandakh area’ s igneous rocks the geochemical features are calc-alkaline, magnetite-series, I type and similar to adakite type. The Devonian intrusive rocks comprised of syenite and syenogranite, while the Carboniferous intrusive rocks consist of granodiorite, monzodiorite, quartz-monzonite and hornblende granite. Devonian magmatic rocks are more alkali in composition. Although Devonian and Carboniferous igneous rocks in the Mandakh area are a little different each other, these igneous rocks are possibility copper deposits as suggested by petrochemical comparisions with bonanza copper deposits in the world.

Keywords: Petrochemistry, Geochoronology, Southeastern Mongolia, Porphyry Copper deposits

©2019. Japan Geoscience Union. All Right Reserved.

Feedbacks Offshore the Cascadia Margin

*Joan S Gomberg[1]

1. USGS Earthquake Science Center

A growing body of evidence from the Cascadia subduction zone in the U.S. Pacific Northwest suggests that there are significant feedbacks among the offshore upper-plate material properties, geologic and geomorphic structures, seismic shaking, sediment redistribution, and mega-thrust slip behaviors. Analyses of seafloor seismic data show that the thick accretionary wedge sediments amplify and prolong shaking by low-frequency seismic waves and attenuate high frequencies (Gomberg, 2018). This strong contrast in shaking feeds back into reshaping the sediments, by controlling where they are likely to be destabilized and redistributed by shaking. Analyses of submarine landslide morphology and numerical modeling of slope strength suggest that different feedbacks, perhaps related to shaking-induced sediment compaction, may actually make sediments stronger (ten Brink et al., 2016; Scholz et al., 2016). Understanding of these contrasting influences in turn feeds into interpretations of turbidites as proxies for paleo-earthquakes, and hazard assessments based on earthquake recurrence models derived from them; for example, regions with greater numbers of turbidites may reflect permanent features of the shaking that are more suitable to trigger failure, but may be interpreted as indicative of a greater rate of earthquakes. Abrupt strike-perpendicular changes in shaking characteristics, apparent along most of the length of the margin, coincide with sharp gradients in topography and structure along the edge of the continental shelf. This same apparent boundary along the shelf-edge also coincides with concentrations of methane bubble plumes, with gas characteristics indicative of origins within the accretionary prism. One explanation is that the shelf is bounded by faults that connect with the megathrust and act as conduits for gas extrusion, some of which may connect with the megathrust directly or indirectly. This suggests another feedback, as structural changes promote or are caused by faulting, which itself permits pore pressure changes that modify the potential for additional faulting. Taken together, the aforementioned correlations and others observed between areas of non-volcanic tremor with gravity lows, crustal faulting patterns, and marginal basins, imply feedbacks between processes along the megathrust and upper plate structure (Wells et al., 2017). To reduce the degree of speculation about some of these feedbacks, several major experiments are planned and underway. These experiments, to be summarized in this presentation, will image the margin structure with sufficient resolution to identify and characterize faults, map changes in material properties, and more, along nearly the entire length of the Cascadia margin.

Gomberg, J. (2018). Cascadia onshore- offshore site response, submarine sediment mobilization, and earthquake recurrence. Journal of Geophysical Research: Solid Earth, 123, 1381–1404. https://doi.org/10.1002/2017JB014985
Johnson, H. P., Miller, U. K., Salmi, M. S., & Solomon, E. A. (2015). Analysis of bubble plume distributions to evaluate methane hydrate decomposition on the continental slope. Geochemistry, Geophysics, Geosystems, 16, 3825–3839. https://doi.org/10.1002/2015GC005955
Scholz, N. A., Riedel, M., Urlaub, M., Spence, G. D., & Hyndman, R. D. (2016). Submarine landslides offshore Vancouver Island along the northern Cascadia margin, British Columbia: Why preconditioning is likely required to trigger slope failure. Geo-Marine Letters, 36(5), 323–337. https://doi.org/10.1007/s00367-016-0452-8
ten Brink, U. S., Andrews, B. D., & Miller, N. C. (2016). Seismicity and sedimentation rate effects on submarine slope stability. Geology, 44(7), 563–566. https://doi.org/10.1130/G37866.1
Wells, R.E., R.J. Blakely, A.G. Wech, P.A. McCrory, and A. Michael (2017). Cascadia subduction tremor

©2019. Japan Geoscience Union. All Right Reserved.

muted by crustal faults, Geology, 45(6), 515-518, doi:10.1130/G38835.1

©2019. Japan Geoscience Union. All Right Reserved.

[E] Poster | S (Solid Earth Sciences)：S-MP Mineralogy & Petrology

Tue. May 28, 2019 5:15 PM - 6:30 PM JST | Tue. May 28, 2019 8:15 AM - 9:30 AM UTC | Poster Hall International Exhibition Hall8, Makuhari Messe_32

[S-MP29] Oceanic and Continental Subduction Processes

convener:REHMAN Ur Hafiz(Department of Earth and Environmental Sciences, Graduate School of Science and Engineering, Kagoshima University), Tatsuki Tsujimori(Tohoku University), Chin-Ho Tsai(Department of Natural Resources and Environmental Studies, National Dong Hwa University), Kazuaki Okamoto(Faculty of Education, Saitama University)

This JpGU-AGU joint session aims at bringing earth scientists from Japan and overseas to present their research related to the processes of oceanic and continent subduction, continent-continent collisions, metamorphism of crustal rocks, formation of the oceanic/continental arcs, and accretion/ tectonic erosion of material along subduction boundaries.

Topics such as role of the fore- and back-arcs in the subduction zones, process of accretion of volcaniclastic and terrigenous sediments along the subduction/collision boundaries, deformation and metamorphism of subducted crust, and exhumation will be the main focus of the session.

In addition to the above mentioned topics, our focus for the10th anniversary of this international session will be towards our understanding and progress on the ultrahigh-pressure/temperature metamorphic terranes in the world.

Exchange of ideas among geoscientists applying different approaches on problems related to the theme of the session are most welcome.

[SMP29-P01] Zircon U-Pb ages of metasedimentary rocks in the Hakogase (Hida Marginal) area, Fukui Prefecture.

*Atsushi MIYASHITA[1], Tatsuki Tsujimori[2], Daniel Pastor-Galán[3], Yi Keewook[4] (1.Seikei University, 2.Tohoku University, 3.Salamanca University, 4.Korea Basic Science Institue)

[SMP29-P02] Late Permian to Early Triassic back-arc type volcanism in the southern Mongolia volcano-plutonic belt of the Central Asian Orogenic Belt: Implication for timing of the final closure of the Palaeo-Asian Ocean

*Takeshi Imayama[1], Yoichiro Koh[2], Kazumasa Aoki[3], Mototaka Saneyoshi[4], Koshi Yagi[5], Shogo Aoki[4], Yoshihiro Sawada[6], Chiaki Ikawa[5], Tomoya Terada[4], Shinobu Ishigaki[4], Shin Toyoda[3], Khishigjav Tsogtbaatar[7], Buuvei Mainbayar[7] (1.Research Institute of Natural Sciences, Okayama University of Science, 2.Graduate School of Environmental Science, Hokkaido University, 3.Faculty of Science, Okayama University of Science, 4.Faculty of Biosphere - Geosphere Science, Okayama University of Science, 5.Hiruzen Institute for Geology and Chronology, 6.Emeritus Professor of Shimane University, 7.Institute of Paleontology and Geology, Mongolian Academy of Sciences)

[SMP29-P03] Mantle dynamics of slab breakoff constrained from the temporal change of the melting depth estimated from the Cumulate Member of the Ordovician Hayachine-Miyamori Ophiolite

*Takafumi Kimura[1], Kazuhito Ozawa[1] (1.Department of Earth and Planetary Science, The University of Tokyo)

[SMP29-P04] **Evidence of HIMU seamount on the Farallon Plate: Application of *in-situ* Sr-Pb isotope analysis to Franciscan lawsonite-bearing metagreywacke**

*Tomomi Hara[1], Tatsuki Tsujimori[1], Jun-Ichi Kimura[2] (1.Tohoku University, 2.Japan Agency for Marine-Earth Science and Technology)

[SMP29-P05] Boron isotope variations of antigorite serpentinites associated with high-pressure metamorphic rocks: A case study in the Itoigawa–Omi area of the Hida-Gaien Belt, Japan

*Chinatsu Yamada[1], Tatsuki Tsujimori[1], King Chang[2], Jun-Ichi Kimura[2] (1.Tohoku University, 2.Japan Aegency for Marine-Earth Science and Technology)

[SMP29-P06] **Study of zircons structures from the Miocene Shibi-san Granodiorite, Kagoshima Prefecture, Japan**

*Nakabayashi Marimo[1], REHMAN Ur Hafiz[1] (1.Kagoshima University)

[SMP29-P07] **Experimental modeling of eclogite and C-O-H fluid interaction in the subduction zones**

*Nadezda Chertkova[1], Shigeru Yamashita[2], Hiroaki Ohfuji[1], Tetsuo Irifune[1], Hirokazu Kadobayashi[1], Yoshitaka Yamamoto[3] (1.Ehime University, Geodynamics Research Center, 2.Okayama University, Institute for Planetary Materials, 3.National Institute of Advanced Industrial Science and Technology)

[SMP29-P08] Microfabrics of omphacite and garnet in eclogite from the Lanterman Range, northern Victoria Land, Antarctica

*Daeyeong Kim[1], Taehwan Kim[2], Jungmin Kim[3] (1.Division of Polar-Earth Sciences, Korea Polar Research Institute, 2.School of Earth and Environmental Sciences, Seoul National University, 3.Earth and Environmental Sciences, Korea University)

[SMP29-P09] Primordial Apatite from Ophiolite in Taiwan

*Nobuaki Niitsuma[1], Reishi Takashima[2], Yuan Hsi Lee[3] (1.Institute of Geosciences,Shizuoka University, 2.Tohoku University Museum, 3.National Chung-Cheng University, Taiwan)

[SMP29-P10] The evolution of the Cretaceous Jinan Basin in South Korea and the age and tectonic setting for the volcanic rocks in it

*Seung Hwan LEE[1], Chang Whan Oh[1] (1.Department of earth and environmental sciences Chonbuk national university)

[SMP29-P11] GEOCHORONOLOGY AND PETROCHEMISTREY OF LATE PALEOZOIC MAGMATIC ROCKS OF THE MANDAKH AREA, SOUTHEAST MONGOLIA

*Undarmaa Batsaikhan[1], Noriyoshi Tsuchiya[1], Masaoki Uno[1], Yukio Isozaki[2], Uyanga Bold[2], Hikaru Sawada[2] (1.Graduate School of Environmental Studies, Tohoku University, 2.Graduate School of Arts and Sciences The University of Tokyo)

[SMP29-P12] Feedbacks Offshore the Cascadia Margin

*Joan S Gomberg[1] (1.USGS Earthquake Science Center)

Zircon U-Pb ages of metasedimentary rocks in the Hakogase (Hida Marginal) area, Fukui Prefecture.

*Atsushi MIYASHITA[1], Tatsuki Tsujimori[2], Daniel Pastor-Galán[3], Yi Keewook[4]

1. Seikei University, 2. Tohoku University, 3. Salamanca University, 4. Korea Basic Science Institue

Combined chronological study using detrital zircon U-Pb dating and phengite K-Ar dating enables to understand the tectonic evolution of the high *P/T* metamorphic belt. The youngest age of detrital zircon U-Pb ages of psamites in the Hida marginal metamorphic rocks (HMMR = Renge belt) approximate its depositional ages (Tsutsumi et al., 2009). The closure temperature of the phengite K-Ar ages are controlled by deformation and recrystallization during exhumation of the metamorphic rocks(Itaya and Tsujimori, 2015). Therefore, the gap between the youngest age of detrital zircons and phengite K-Ar ages are the age difference between subuduction and uplift of metamorphics.
The Hakogase (Nigure-gawa, Kuzuryu, Fukui Prefecture) metamorphic rocks belong to HMMR member as the olistolith in the Cretaceous Tedori Group. It consists mainly pelites with small amount of basites and mables. The main index mineral assemblage of metasediments are garnet + chlorite, and the phenigite K-Ar ages are 287.8 - 283.6 Ma (Kunugiza et al., 2004). Relic Lawsonite was also found in the basaites and psamites (Miyakawa, 1982).
The detrital Zircons U-Pb ages in the two pelites are obtained by the SHRIMP II of KBSI. The youngest U-Pb ages of detrital zircons are 307Ma. The gap of the sedimentation between uplift of the Hakogase metamorphics is estimated 20 Ma. This value means the migration speed of the HMMR metamorphic rocks are 1/10 of plate motion. This rapid migration speed is common for the high *P/T* metamorphic rocks.

Keywords: high P/T metamorphic rocks, Zircon U-Pb ages, Phengite K-Ar ages

©2019. Japan Geoscience Union. All Right Reserved.

Late Permian to Early Triassic back-arc type volcanism in the southern Mongolia volcano-plutonic belt of the Central Asian Orogenic Belt: Implication for timing of the final closure of the Palaeo-Asian Ocean

*Takeshi Imayama[1], Yoichiro Koh[2], Kazumasa Aoki[3], Mototaka Saneyoshi[4], Koshi Yagi[5], Shogo Aoki[4], Yoshihiro Sawada[6], Chiaki Ikawa[5], Tomoya Terada[4], Shinobu Ishigaki[4], Shin Toyoda[3], Khishigjav Tsogtbaatar[7], Buuvei Mainbayar[7]

1. Research Institute of Natural Sciences, Okayama University of Science, 2. Graduate School of Environmental Science, Hokkaido University, 3. Faculty of Science, Okayama University of Science, 4. Faculty of Biosphere - Geosphere Science, Okayama University of Science, 5. Hiruzen Institute for Geology and Chronology, 6. Emeritus Professor of Shimane University, 7. Institute of Paleontology and Geology, Mongolian Academy of Sciences

The timing of final subduction and closure of the Palaeo-Asian Ocean is still controversial in the eastern segments of the Central Asian Orogenic Belt (CAOB). A more detailed understanding is needed with respect to the formation of volcanic rocks and sediments associated with the final closure of the Palaeo-Asian Ocean in southern Mongolia. We investigated alkali series volcanic rocks newly discovered in the southern Mongolia volcano-plutonic belt of the CAOB and classified as basalt, basaltic trachyandesite, andesite, trachyandesite, and trachyte, mainly showing andesitic-dacitic compositions. In Harker diagrams, the TiO_2, FeO, MnO, Al_2O_3, CaO, and MgO contents generally decrease with increasing SiO_2, representing a series of differentiated volcanic rocks. The primitive mantle-normalized trace element spider diagram is characterized by incompatible element-rich patterns and negative Nb anomalies. The tectonic discrimination diagrams show that the volcanic rocks were formed by arc-related volcanism rather than within-plate volcanism. K-Ar dating of feldspars from six volcanic rocks yields ages ranging from 270 to 239 Ma, indicating that andesitic and dacitic magmatism occurred during this period. These geochemical and geochronological data indicate that the differentiated volcanic rocks intruding middle to late Palaeozoic volcanic sediments were formed by back-arc type subduction ca. 270–240 Ma. Based on detrital zircon U-Pb ages, the terrigenous sandstones underlain by the volcanic sediments record a maximum depositional age of Late Triassic (ca. 220–200 Ma) and include a main cluster of Early Devonian ages (ca. 410–390 Ma), possibly derived from the Devonian-Carboniferous arc complex observed surrounding this study area. These results from the volcanic and sedimentary rocks in this study, combined with investigations in previous studies, imply that subduction beneath the eastern segments of the CAOB to consume the Palaeo-Asian Ocean continued until Late Permian to Early Triassic.

Keywords: Palaeo-Asian Ocean, southern Mongolia, Central Asian Orogenic Belt, back-arc type volcanism

©2019. Japan Geoscience Union. All Right Reserved.

Mantle dynamics of slab breakoff constrained from the temporal change of the melting depth estimated from the Cumulate Member of the Ordovician Hayachine-Miyamori Ophiolite

*Takafumi Kimura[1], Kazuhito Ozawa[1]

1. Department of Earth and Planetary Science, The University of Tokyo

Slab breakoff, detachment of oceanic lithosphere highly expected during arc-continent collision, is one of the important mechanisms inducing passive upwelling of the asthenosphere and magma generation in arc environments [1]. In order to better understand the mantle dynamics of slab breakoff, we need to use continuous geological record with high time resolution. In this study, we have extracted a record of temporal change of the magma generation depth from cumulates in an Ordovician arc ophiolite at a time resolution of several tens of million years.
The Hayachine-Miyamori Ophiolite, northern Japan, is one of the Ordovician ophiolite formed in an arc environment [2]. The ultramafic member was built up by three main magmatic stages, which are recorded in three rock units: Tectonite Member, Cumulate Member, and ultramafic dikes, in the order of formation ages. The last two units in the entire evolution of the ophiolite is explained by decompressional melting of sub-slab mantle triggered by slab breakoff [2][3]. The melting depth of an ultramafic magma solidified as dikes in the Cumulate Member is estimated to be ~170km [3]. Our recent field study clarified a large-scale stratification characterized by alternation of wehrlite-dominant and dunite-dominant layers in the Cumulate Member. Each layer has a thickness from several meters to ~1 km and, the total thickness attains ~3km. Moreover, we succeeded in specifying the strike and plunge of the gravity field to be ~N48°E and ~20°NE during the cumulate formation from field information and westward stratigraphic younging [4].
We estimated the temporal change of generation depth of parent magmas of the Cumulate Member by garnet signature in heavy rare earth elements (HREEs) as depth proxy. The information may constrain the mantle dynamics during the slab breakoff. We examined stratigraphic variation of HREE ratio at the core of clinopyroxenes over the thickness of ~2km in the Cumulate Member. The obtained variation of the Dy/Lu increases from ~12.9 to ~16.5 with increasing the stratigraphic height. We estimated the extent of melting in the garnet stability field increasing from ~50 to ~90% of the total melting by applying an open-system fractional melting model to reproduce the Dy/Lu variation.
We also estimated the time scale of formation of the Cumulate Member by using cm –10cm scale heterogeneity recorded in contact zone of intruded magma and the host. The profile of Mg# of olivine in xenoliths of the Tectonite Member occurring at the bottom of the Cumulate Member shows that the cooling time is less than several tens of million years [5]. The dunite of the Cumulate Member contacting the ultramafic dike shows a systematic decrease of Mg# from 90 to 86.8 over the distance of 54 mm towards the contact. We calculated the time scale of subsolidus diffusional exchange between the dunite and dike and obtained several tens of million years at ~1000℃. The host was kept at a high temperature when the dikes intruded because of the absence of chilled margin. We thus estimated time scale of formation of the Cumulate Member to be < several tens of million years.
We propose the following tectonic model in the Ordovician northern Japan on the basis of the above result. The slab breakoff took place at the depth slightly deeper than the boundary of spinel and garnet stability fields (~80 km) and induced counter flow and adiabatic melting of the sub-slab mantle. The melting depth deepened down to ~170 km on the time scale of several tens of million years, which corresponds to the time scale to complete the slab breakoff. The sinking velocity of the slab is more than

©2019. Japan Geoscience Union. All Right Reserved.

a few millimeters per year.

[1]: Davies et al., 1995. [2]: Ozawa et al., 2015. [3],[4]: Kimura et al., 2017, 2018, JpGU abstract. [5]: Ozawa, 1983.

Keywords: slab breakoff, arc ophiolite, cumulate

©2019. Japan Geoscience Union. All Right Reserved.

Evidence of HIMU seamount on the Farallon Plate: Application of *in-situ* Sr-Pb isotope analysis to Franciscan lawsonite-bearing metagreywacke

*Tomomi Hara[1], Tatsuki Tsujimori[1], Jun-Ichi Kimura[2]

1. Tohoku University, 2. Japan Agency for Marine-Earth Science and Technology

Since bulk isotopic composition of oceanic basalt is susceptible to element remobilization during alteration process, there is a risk of causing misread of geochemical signatures from bulk metabasaltic rocks in subduction complex. As Hara et al. (2018) demonstrated, however, *in-situ* Sr-Pb isotope analysis of lawsonite in high-pressure metabasaltic rocks has a great potential for tracing the geochemical signatures reflecting the igneous protolith. In this study, we have applied the method to lawsonite in metasedimentary rocks to explore clastic components of a trench-fill sediment. A jadeite-bearing Franciscan metagreywacke from Pacheco Pass area, east-central Diablo Range, California Coast Ranges was selected for geochemical reconnaissance.

Lawsonites in the Franciscan metagreywacke record a high initial Pb isotope ratios ($^{206}Pb/^{204}Pb$ = 18.74–19.66, $^{207}Pb/^{204}Pb$ = 15.58–15.70 and $^{208}Pb/^{204}Pb$ = 38.41–39.34). This Pb-isotope signature suggests that a protolith of the metagreywacke have contained a debris derived from a HIMU-type basalt. Considering the maximum depositional age of the metagreywacke at ~102 Ma, the underflow of the Farallon Plate beneath continental crust of the North American Plate would have carried a HIMU seamount to a Franciscan trench.

Our study has demonstrated the potential application of 'lawsonitology' as sedimentary provenance analyses for metamorphosed accretionary complex. Moreover, the results would manifest that Pb isotopic signature of ancient oceanic basalt can be detectable from Ca-Al silicate mineral, such as lawsonite, epidote and pumpellyite, in metamorphic rocks.

Keywords: Lawsonite, Sr-Pb isotope, LA-MC-ICPMS, HIMU, Metasediment

©2019. Japan Geoscience Union. All Right Reserved.

Boron isotope variations of antigorite serpentinites associated with high-pressure metamorphic rocks: A case study in the Itoigawa–Omi area of the Hida-Gaien Belt, Japan

*Chinatsu Yamada[1], Tatsuki Tsujimori[1], King Chang[2], Jun-Ichi Kimura[2]

1. Tohoku University, 2. Japan Aegency for Marine-Earth Science and Technology

Boron isotope study of serpentinites in the Franciscan Complex using an ablation volume correction (AVC) LA-MC-ICPMS discriminates two groups (Yamada et al., 2018 JpGU abstr.; Yamada et al. 2019, in press). Serpentinites associated with blueschists are characterized by lighter boron isotope than serpentinites without blueschist-facies rocks. The lighter boron isotope signature (< ~10 ‰) of blueschist-bearing serpentinites results from interaction with forearc slab fluids with low δ^{11}B in deeper depth. In order to evaluate the versatility of B isotopes and composition of high-pressure metamorphosed serpentinites, we investigated antigorite serpentinites associated with three different type of high-pressure metamorphic rocks in the Itoigawa–Omi area.

The investigated serpentinites can be grouped into two types based on the B isotopes. Antigorite serpentinite with blueschist- and eclogite-facies metamorphic rocks in the Yunotani Valley is characterized by moderate boron (12.5–48.4 $\mu g \cdot g^{-1}$) and lower δ^{11}B (+6.6 to +12.3‰ [mostly smaller than +8‰]; n= 10); Brucite-bearing antigorite serpentinite with barroisite-bearing mafic schist in the Kotaki-gawa River is characterized by very high boron (37.5 –302 $\mu g \cdot g^{-1}$) and lower δ^{11}B (+5.8 to +10.7‰ [mostly smaller than +8‰]; n= 10). In contrast, antigorite serpentinite with garnet amphibolite in the Omi-gawa River is characterized by a wide range of boron (9.1–145 $\mu g \cdot g^{-1}$) and relatively high δ^{11}B (+11.5 to + 14.8 ‰; n= 10).

Our preliminary reconnaissance shows significantly lower δ^{11}B (smaller than +8‰) in antigorite serpentinites of the 'Eclogite Unit' proposed by Tsujimori (2002). This trend is consistent with our earlier study in the Franciscan Complex. The antigorite serpentinites in the 'Eclogite Unit' might have been affected by a deep forearc slab fluids.

Keywords: Serpentinite, boron isotope, subduction zone

©2019. Japan Geoscience Union. All Right Reserved.

Study of zircons structures from the Miocene Shibi-san Granodiorite, Kagoshima Prefecture, Japan

*Nakabayashi Marimo[1], REHMAN Ur Hafiz[1]

1. Kagoshima University

The Miocene granodiorite body (zircon fission track age by Miyachi, 1985) of the Mount Shibi, Kagoshima prefecture is a lenticular stock that intrudes the Cretaceous sedimentary rocks of the Shimanto belt. Previous studies subdivided the granodiorite body into the Kusu-bae (core facies) and Hira-bae (marginal facies) types based on the changes in litho-facies and distinct chemical composition of biotite and amphibole (Yamamoto et al., 1988). We conducted field survey in the study area and found no clear contrasts to sub-divide the body, instead it represents a single pluton with local chemical variation along the marginal portions. Based on detailed petrography, the entire body appears as homogeneous stock exhibiting identical mineral assemblage with no clear evidence that can mark the boundary between Kusu-bae and Hira-bae types. Moreover, to understand the processes of magmatic crystallization we investigated more than 600 zircon grains from about 8 samples for external (applying the zircon morphology method of Pupin, 1980) and internal morphology using the Cathodoluminescence imaging. Based on the Pupin’ s method, the deduced temperature range for the zircon crystallization was between 750 and 850℃. In addition, internal structures of zircon (CL images) showed oscillatory zoning with continuous growth domains and abundant apatite inclusions, suggesting the magma was fluid-rich and have been crystallized under relatively higher temperature. We also investigated zircons from the surrounding hornfels (Shimanto belt rocks) that were affected thermally due to the contact metamorphism. Zircons from the hornfels are completely different and rounded with different internal structures. Zircons from the so-called Kusu-bae and Hira-bae types are identical and suggest their crystallization from a single parental magma hence the pluton cannot be sub divisible.

References
Miyachi M. (1985). Fission track ages of some granitic rocks in Outer Zone ofKyushu, Japan. Journal of Mineralogical and Petrological Sciences 80, 406-409.
Pupin J. P. (1980). Zircon and granite petrology. Contribution to Mineralogy and Petrology 73, 207-220.
Yamamoto M., Oniwa N., Toyota K. (1988). Compositional Variation of the Shibi-san Granodioraite Body, Kagoshima Prefecture, Japan. Bulletin of the Kagoshima University Science Faculty 21, 35-49.

Keywords: zircon, granodiorite, crystal shape

©2019. Japan Geoscience Union. All Right Reserved.

Experimental modeling of eclogite and C-O-H fluid interaction in the subduction zones

*Nadezda Chertkova[1], Shigeru Yamashita[2], Hiroaki Ohfuji[1], Tetsuo Irifune[1], Hirokazu Kadobayashi[1], Yoshitaka Yamamoto[3]

1. Ehime University, Geodynamics Research Center, 2. Okayama University, Institute for Planetary Materials, 3. National Institute of Advanced Industrial Science and Technology

The presence of volatile components controls melting relationships in the subducting oceanic plate and the overlying mantle wedge, affecting their physical properties and seismic observables. The major volatile species in the mantle low oxygen fugacity environment are considered to be H_2O and CH_4, as estimated for mantle xenoliths and C-O-H fluid speciation in equilibrium with diamond [1,2]. Experimental studies with the direct monitoring of phase assemblages and melting relationships in the silicate systems with C-O-H components can shed light on the processes, which take place in the subduction zones, and provide important data for interpretation of observed physical parameters.
In this study, we employed *in situ* spectroscopic methods in combination with the diamond anvil cell (DAC) technique for investigation of C-O-H fluid behavior and its influence on phase relationships in the eclogite–5.75H_2O–CH_4 system at temperatures up to 1000 degree C and pressures exceeding 5 GPa. We designed a new cell assembly for Mao-type symmetric diamond anvil cell with large optical access to the sample in order to make it suitable for infrared and Raman measurements directly at high-pressure and high-temperature conditions. Mineral phase assemblages, observed during experiments, are consistent with those described in the dry system of the similar basaltic composition [3]. At the same time, miscibility between aqueous and carbonaceous components in the fluid phase coexisting with silicate minerals was confirmed at temperatures above 800 degree C and pressures above 3.2 GPa.

References

[1] Shirey, S.B., Cartigny, P., Frost, D.J., Keshav, S., Nestola, F., Nimis, P., Pearson, D.G., Sobolev, N.V. and Walter, M.J. (2013) *Rev. Mineral. Geochem.*, **75**, 355-421.
[2] Belonoshko, A. and Saxena, S. (1992) *Geochim. Cosmochim. Acta*, **56**, 3611-3626.
[3] Yasuda, A., Fujii, T. and Kurita, K. (1994) *J. Geophys. Res.: Solid Earth*, **99**, 9401-9414.

©2019. Japan Geoscience Union. All Right Reserved.

Microfabrics of omphacite and garnet in eclogite from the Lanterman Range, northern Victoria Land, Antarctica

*Daeyeong Kim[1], Taehwan Kim[2], Jungmin Kim[3]

1. Division of Polar-Earth Sciences, Korea Polar Research Institute, 2. School of Earth and Environmental Sciences, Seoul National University, 3. Earth and Environmental Sciences, Korea University

Layered structures in metamorphic rocks are sometimes crucial to occur strain localization then affect to seismic properties. We conducted microstructural analyses omphacite and garnet in foliated eclogite from the Lanterman Range, northern Victoria Land, Antarctica, to determine the influence of the layered structure on seismic observations in subduction zone. The analyzed eclogite, composed of layered garnet-rich and omphacite-rich layers, shows the low aspect ratios, similar angular distribution of long axes relative to the foliation, uniform grain size distribution, near-random crystallographic preferred orientations (CPOs), and misorientation angle distributions of garnet and opposite characteristics of omphacite in both layers. The results of fabric analyses are consistent with strain localization into omphacite or omphacite-rich layers rather than garnet or garnet-rich layers. Our results therefore demonstrate the importance of the layered structure in strain localization and in the development of the seismic anisotropies of subducting oceanic crust.

Keywords: Eclogite, EBSD, Layered structure

©2019. Japan Geoscience Union. All Right Reserved.

Primordial Apatite from Ophiolite in Taiwan

*Nobuaki Niitsuma[1], Reishi Takashima[2], Yuan Hsi Lee[3]

1. Institute of Geosciences,Shizuoka University, 2. Tohoku University Museum, 3. National Chung-Cheng University, Taiwan

Apatite is a common accessory mineral in igneous rocks. Because apatite has a wide range of trace element compositions as well as strong resistance to diagenetic alteration, the trace element composition of apatite has been used for tracing petrogenetic processes of plutonic bodies as well as the tephrochronology of Paleozoic tephras and Quaternary volcaniclastic deposits.

We studied trace element compositions of apatites from Ophiolite in Taiwan. The Ophiolite with mafic-ulatramafic rocks (150811-14) expose along the anticlinal axes of the metamorphic belts in Backbone Range of Taiwan, and exotic gabbro block (MA-15B) in chaotic deposits of Lichi Melange, in the southern end of Longitudinal Valley, in East Taiwan.

Lee (2015 JpGU; Chen et al., 2017 Tectonics) reported that zircon ages of Ophiolites in Taiwan are concentrated to 15 Ma, which should relate with termination of spreading in South China Sea and Shikoku & Parece Vela Basin just before Japan Sea Opening, and large scale igneous activities in the Outer Zone of Southwest Japan just after Japan Sea Opening (Niitsuma & Lee, 2018 JpGU).

Fifteen and twelve apatite phenocrysts from samples of MA-15B and 150811-14 were analyzed for major and minor elements using a JEOL 8530F wavelength dispersive Electron Probe Micro Analyzer (Takashima et al., 2017 Quaternary Geochronology) in weight % as follow;
__major elements: P=17.956 +/-0.100, 17.926 +/-0.129
_____Ca=38.362 +/-0.329, 38.128 +/-0.273
_____F=1.082+/-0.151, 0.445+/-0.046
__trace elements: Cl<0.01, 0.04 Mg<0.01, 0.01 Mn<0.04, 0.05
_____Fe<0.03, 0.17 Ce<0.09, 0.05 Y<0.13, 0.04

The contents of trace elements are extremely low and we concluded the apatite might be primordial without any contaminations and petrogenetic effect, and crystallized directly in the magma above rifted mantle along the northwestern margin of West Philippine Basin just before Japan Sea Opening.

Keywords: Apatite, trace element , Ophiolite, Taiwan, Opening of Japan Sea

©2019. Japan Geoscience Union. All Right Reserved.

The evolution of the Cretaceous Jinan Basin in South Korea and the age and tectonic setting for the volcanic rocks in it

*Seung Hwan LEE[1], Chang Whan Oh[1]

1. Department of earth and environmental sciences Chonbuk national university

The Jinan Basin is one of the Cretaceous pull-apart basins in the South Korea. It locates along the Yongdong-Gwangju fault system and consists of non-marine sediments with volcanic and pyroclastic rocks. The sinistral strike slip movement which formed the Cretaceous pull apart basins was occurred by the collision between Siberian and Manchuria blocks at ca. 130~100Ma. LA-MC-ICPMS age dating on the zircons from sedimentary and igneous rocks indicates followings. The sedimentation in the Jinan Basin had started at least from 97.7Ma and continued until 89.47Ma. During the sedimentation, basaltic andesite extruded at 90-92 Ma and later rhyolitc and andesitic magma intruded the Jinan Basin at 90-89 Ma and 85-84 Ma respectively. Later the Jinan Basin uplifted to form Noryeong mountain range due to the compression which was related with dextral strike slip fault movement. This fault movement is expected to be caused by the collision between Indian plate and Eurasian plate at ca. 55~25Ma. AFT(Apatite Fission Track) age from sediments in the Jinan Basin is approximately 68Ma. Due to the formation of Noryeong mountain range, the *Coreoleuciscus splendidus* was differentiated into two species, these two species of *Coreoleuciscus splendidus* have the same ancestors at around 38Ma. These data indicate that the Noryeong mountain range including the Jinan Basin are expected to have uplifted at around 68-38Ma. Rhyolitic volcanic rocks in and around the Jinan Basin are plotted on the VAG (Volcanic Arc Granite) field and basaltic to intermediated volcanic rocks are plotted on the CAB (Calc-Alkaline Basalt) and WPB (WIthin Plate Basalt) fields in the tectonic discrimination diagrams. There was a roll back of subduction zone toward Pacific ocean at ca. 100 Ma. These data suggest that the igneous rocks in the Jinan Basin formed by the mantle upwelling due to extension caused by the roll back of subduction zone. The upwelling asthenospheric mantle supplied heat which caused the felsic magma by the melting of the lithospheric mantle and crust which had been contaminated by crustal material supplied from subducting sediment or ocean before roll back of the subduction zone. The upwelling asthenospheric mantle was also melted to form basaltic magma. The deep faults formed by sinistral strike slip movement around the Jinan Basin at the Cretaceous, gave the path toward surface for the magma at deep depth.

Keywords: Jinan Basin, pull-apart basin, Igneous rock, Cretaceous

©2019. Japan Geoscience Union. All Right Reserved.

(a) ca. 97 ~90 Ma.

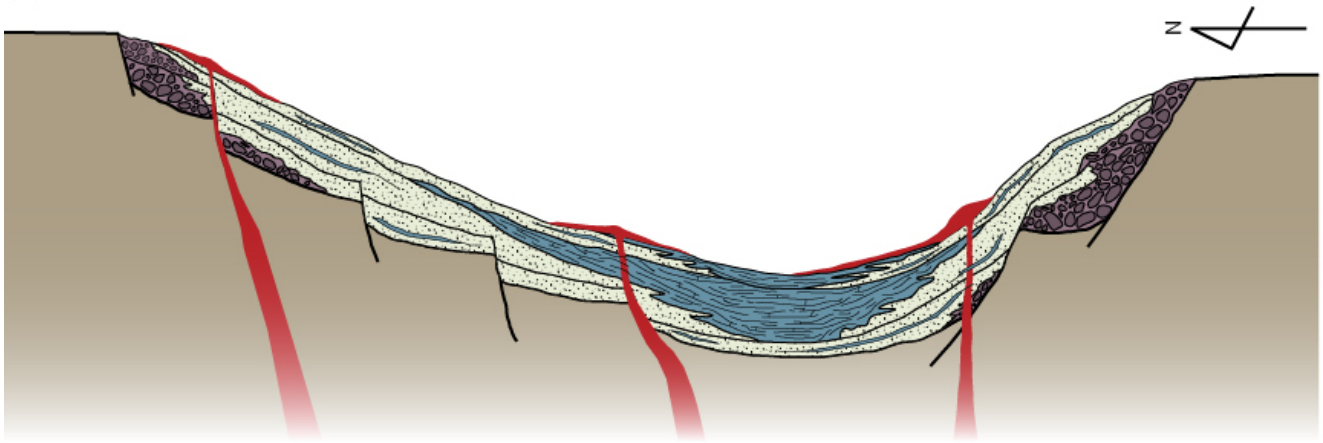

Deposition of lower part sedimentary rocks in the Jinan Basin (97~92 Ma) with extrusion of basaltic andesite (92~90 Ma)

(b) ca. 90 ~89 Ma.

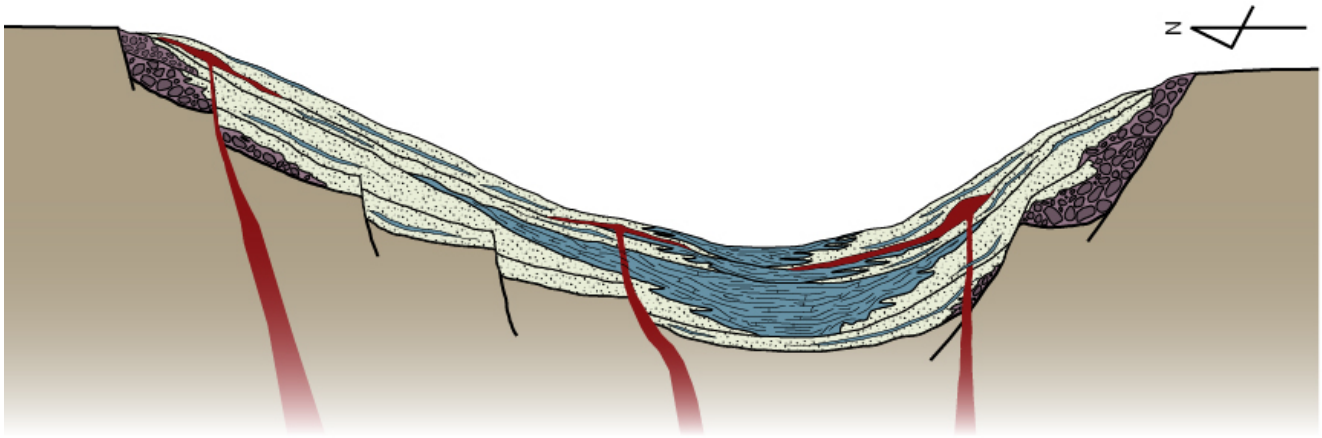

Deposition of upper part sedimentary rocks on the lower part sedimentary rocks and basaltic andesite extrusive volcanic rocks

(c) ca. 89 ~84 Ma.

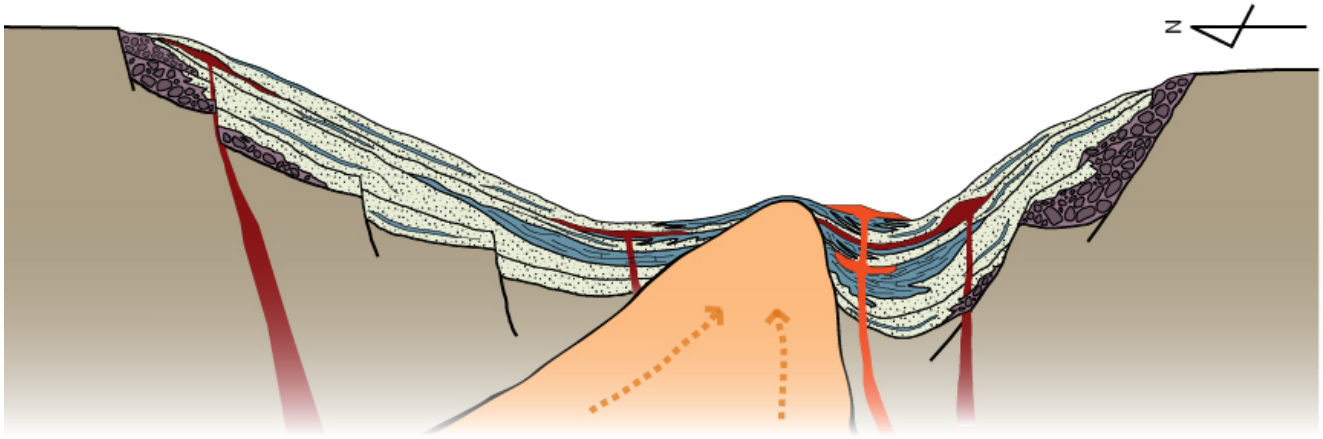

Intrusion and extrusion of rhyolite (ca. 89Ma) with late intrusion of andesitic volcanic rocks (ca. 84Ma)

Intrusive andesitic volcanic rocks
Rhyolite
Basalt and basaltic andesite
Conglomerate
Sandstone
Shale or mudstone

©2019. Japan Geoscience Union. All Right Reserved.

©2019. Japan Geoscience Union. All Right Reserved.

GEOCHORONOLOGY AND PETROCHEMISTREY OF LATE PALEOZOIC MAGMATIC ROCKS OF THE MANDAKH AREA, SOUTHEAST MONGOLIA

*Undarmaa Batsaikhan[1], Noriyoshi Tsuchiya[1], Masaoki Uno[1], Yukio Isozaki[2], Uyanga Bold[2], Hikaru Sawada[2]

1. Graduate School of Environmental Studies, Tohoku University, 2. Graduate School of Arts and Sciences The University of Tokyo

The southeast Mongolia has become a major survey area for unraveling the Paleozoic tectonic evolution because Mongolia occupies the central part of the CAOB which is enormous and composed of a multiplicity of terranes including ancient island and continental arcs, ophiolites, passive continental margins, Precambrian continental blocks and high-T/low-P metamorphic zones and where porphyry Cu deposits occur. The late Paleozoic magmatic rocks are widely distributed in the Mandakh area which is located in the Curvansaikhan and Manlai terrains, in the southeast Mongolia. We will discuss petrochemical features, mineral assemblage and new geochronological constrain of magmatic rocks in the Mandakh area. Furthermore, we compared petrochemical characteristics of the Mandakh area with Tampakan deposit (Philippines), Cerro Colorado deposit (Chili) and negative criteria of Cu deposits (Japan) in order to characterize potential of the porphyry copper deposit in Mandakh area.

The Mandakh area’ s igneous rocks the geochemical features are calc-alkaline, magnetite-series, I type and similar to adakite type. The Devonian intrusive rocks comprised of syenite and syenogranite, while the Carboniferous intrusive rocks consist of granodiorite, monzodiorite, quartz-monzonite and hornblende granite. Devonian magmatic rocks are more alkali in composition. Although Devonian and Carboniferous igneous rocks in the Mandakh area are a little different each other, these igneous rocks are possibility copper deposits as suggested by petrochemical comparisions with bonanza copper deposits in the world.

Keywords: Petrochemistry, Geochoronology, Southeastern Mongolia, Porphyry Copper deposits

©2019. Japan Geoscience Union. All Right Reserved.

Feedbacks Offshore the Cascadia Margin

*Joan S Gomberg[1]

1. USGS Earthquake Science Center

A growing body of evidence from the Cascadia subduction zone in the U.S. Pacific Northwest suggests that there are significant feedbacks among the offshore upper-plate material properties, geologic and geomorphic structures, seismic shaking, sediment redistribution, and mega-thrust slip behaviors. Analyses of seafloor seismic data show that the thick accretionary wedge sediments amplify and prolong shaking by low-frequency seismic waves and attenuate high frequencies (Gomberg, 2018). This strong contrast in shaking feeds back into reshaping the sediments, by controlling where they are likely to be destabilized and redistributed by shaking. Analyses of submarine landslide morphology and numerical modeling of slope strength suggest that different feedbacks, perhaps related to shaking-induced sediment compaction, may actually make sediments stronger (ten Brink et al., 2016; Scholz et al., 2016). Understanding of these contrasting influences in turn feeds into interpretations of turbidites as proxies for paleo-earthquakes, and hazard assessments based on earthquake recurrence models derived from them; for example, regions with greater numbers of turbidites may reflect permanent features of the shaking that are more suitable to trigger failure, but may be interpreted as indicative of a greater rate of earthquakes. Abrupt strike-perpendicular changes in shaking characteristics, apparent along most of the length of the margin, coincide with sharp gradients in topography and structure along the edge of the continental shelf. This same apparent boundary along the shelf-edge also coincides with concentrations of methane bubble plumes, with gas characteristics indicative of origins within the accretionary prism. One explanation is that the shelf is bounded by faults that connect with the megathrust and act as conduits for gas extrusion, some of which may connect with the megathrust directly or indirectly. This suggests another feedback, as structural changes promote or are caused by faulting, which itself permits pore pressure changes that modify the potential for additional faulting. Taken together, the aforementioned correlations and others observed between areas of non-volcanic tremor with gravity lows, crustal faulting patterns, and marginal basins, imply feedbacks between processes along the megathrust and upper plate structure (Wells et al., 2017). To reduce the degree of speculation about some of these feedbacks, several major experiments are planned and underway. These experiments, to be summarized in this presentation, will image the margin structure with sufficient resolution to identify and characterize faults, map changes in material properties, and more, along nearly the entire length of the Cascadia margin.

Gomberg, J. (2018). Cascadia onshore- offshore site response, submarine sediment mobilization, and earthquake recurrence. Journal of Geophysical Research: Solid Earth, 123, 1381–1404. https://doi.org/10.1002/2017JB014985
Johnson, H. P., Miller, U. K., Salmi, M. S., & Solomon, E. A. (2015). Analysis of bubble plume distributions to evaluate methane hydrate decomposition on the continental slope. Geochemistry, Geophysics, Geosystems, 16, 3825–3839. https://doi.org/10.1002/2015GC005955
Scholz, N. A., Riedel, M., Urlaub, M., Spence, G. D., & Hyndman, R. D. (2016). Submarine landslides offshore Vancouver Island along the northern Cascadia margin, British Columbia: Why preconditioning is likely required to trigger slope failure. Geo-Marine Letters, 36(5), 323–337. https://doi.org/10.1007/s00367-016-0452-8
ten Brink, U. S., Andrews, B. D., & Miller, N. C. (2016). Seismicity and sedimentation rate effects on submarine slope stability. Geology, 44(7), 563–566. https://doi.org/10.1130/G37866.1
Wells, R.E., R.J. Blakely, A.G. Wech, P.A. McCrory, and A. Michael (2017). Cascadia subduction tremor

©2019. Japan Geoscience Union. All Right Reserved.

muted by crustal faults, Geology, 45(6), 515-518, doi:10.1130/G38835.1

©2019. Japan Geoscience Union. All Right Reserved.

[E] Oral | S (Solid Earth Sciences)：S-MP Mineralogy & Petrology

Tue. May 28, 2019 1:45 PM - 3:15 PM JST | Tue. May 28, 2019 4:45 AM - 6:15 AM UTC | A08 TOKYO BAY MAKUHARI HALL

[S-MP29] Oceanic and Continental Subduction Processes

convener:REHMAN Ur Hafiz(Department of Earth and Environmental Sciences, Graduate School of Science and Engineering, Kagoshima University), Tatsuki Tsujimori(Tohoku University), Chin-Ho Tsai(Department of Natural Resources and Environmental Studies, National Dong Hwa University), Kazuaki Okamoto(Faculty of Education, Saitama University), Chairperson:Hafiz REHMAN(Kagoshima University), Tatsuki Tsujimori

This JpGU-AGU joint session aims at bringing earth scientists from Japan and overseas to present their research related to the processes of oceanic and continent subduction, continent-continent collisions, metamorphism of crustal rocks, formation of the oceanic/continental arcs, and accretion/ tectonic erosion of material along subduction boundaries.

Topics such as role of the fore- and back-arcs in the subduction zones, process of accretion of volcaniclastic and terrigenous sediments along the subduction/collision boundaries, deformation and metamorphism of subducted crust, and exhumation will be the main focus of the session.

In addition to the above mentioned topics, our focus for the10th anniversary of this international session will be towards our understanding and progress on the ultrahigh-pressure/temperature metamorphic terranes in the world.

Exchange of ideas among geoscientists applying different approaches on problems related to the theme of the session are most welcome.

1:45 PM - 2:00 PM JST | 4:45 AM - 5:00 AM UTC

[SMP29-01] Pb-isotope of Fe-Ni alloy associated with serpentinite: Geochemical constraints on the fluid-mediated hyper-reducing environment in mantle wedge

★Invited Papers

*Mayu Kakefuda[1], Tatsuki Tsujimori[1], Katsuyuki Yamashita[2], Yoshiyuki Iizuka[3] (1.Tohoku University, 2.Graduate School of Natural Science and Technology, Okayama University, 3.Institute of Earth Sciences, Academia Sinica)

2:00 PM - 2:15 PM JST | 5:00 AM - 5:15 AM UTC

[SMP29-02] PETROCHEMISTRY AND AGE DETERMINATION OF THE NEWLY DISCOVERED ECLOGITE IN THE WESTERN MONGOLIA

*Kosuke Naemura[1], Erdenjargal Choindonjamts[4], Takenori Kato[5], Otgonkhuu Javkhlan[3], Katsuyoshi Michibayashi[2] (1.Nagoya University Museum, 2.Nagoya University Graduate school of environmental studies, 3.Chinese Academy of Geological Sciences, 4.Mongolian Academy of Sciences, 5.Nagoya University Space-Earth Environmental Research)

2:15 PM - 2:45 PM JST | 5:15 AM - 5:45 AM UTC

[SMP29-03] Continental subduction, "*Intraslab UHP Metasomatism*", and the formation of metamorphic diamond

★Invited Papers

*Yoshihide Ogasawara[1] (1.Department of Earth Sciences, Waseda University)

2:45 PM - 3:00 PM JST | 5:45 AM - 6:00 AM UTC

[SMP29-04] Ultrahigh-pressure pseudotachylyte in a marble

★Invited Papers

*Tadao Nishiyama[1], Tomoya Fujimoto[1] (1.Department of Earth and Environmental Sciences, School of Science, Graduate School of Science and Technology, Kumamoto University)

3:00 PM - 3:15 PM JST | 6:00 AM - 6:15 AM UTC

[SMP29-05] Dehydration and Deformation process of subducted large Oceanic Pleateau -case study of the Mikabu blueschist-

*Kazuaki Okamoto[1] (1.Faculty of Education, Saitama University)

Pb-isotope of Fe-Ni alloy associated with serpentinite: Geochemical constraints on the fluid-mediated hyper-reducing environment in mantle wedge

*Mayu Kakefuda[1], Tatsuki Tsujimori[1], Katsuyuki Yamashita[2], Yoshiyuki Iizuka[3]

1. Tohoku University, 2. Graduate School of Natural Science and Technology, Okayama University, 3. Institute of Earth Sciences, Academia Sinica

Although the occurrence of Fe-Ni alloy is very limited in the vicinity of modern Earth’s surface due to the highly oxidized state, serpentinization in the forearc mantle wedge can rarely provide extraordinary reducing environments that stabilizes the Fe-Ni alloy.

In order to understand those fluid-mediated hyper-reducing environments in serpentinizing mantle wedge of an active convergent plate margin, we revisited so-called ‘josephinite' —an unusual ‘metallic rock' composed mainly of Fe-Ni alloy (awaruite)— found in the Josephine Ophiolite, by engaging in microtextural and geochemical analyses.

Microtextural analyses using high-resolution FE-SEM and FE-EPMA found the presence of Ni-As mineral within aggregates of Fe-Ni alloy; the Ni-As mineral also occurs as discrete grains in ‘josephinite'-hosting serpentinite, suggesting that Ni-As mineral acted as a precursor seed before the crystallization of Fe-Ni alloy.

Since each leachate obtained by stepwise leaching of a ‘josephinite' pebble confirmed compositional homogeneity, this allows to calculate weighted mean values that give much precise Pb isotope compositions of aliquots of seventeen leaching steps determined by ID-TIMS; the values yielded $^{207}Pb/^{204}Pb$ = 18.3378 ±0.0016, $^{206}Pb/^{204}Pb$ = 15.5693 ±0.0015, and $^{208}Pb/^{204}Pb$ = 38.0879 ± 0.0044. These newly obtained high precision Pb isotope compositions revealed that the ‘josephinite'-forming fluids have a minor GLOSS-like sedimentary component. The presence of Ni arsenide also supports the infiltration of arsenic-bearing external fluids derived from sedimentary rocks.

Considering the geological context of the Josephine Ophiolite, the ‘josephinite’-forming fluids might have been derived from the top layer of subducting sediments. The lack of high-pressure metamorphic rocks such as blueschist in ‘josephinite'-hosted serpentinite implies that the ‘josephinite' formation might have occurred at a relatively shallow level of serpentinizing mantle wedge.
The absence of carbonate minerals further postulates that redox agent of the ‘josephinite' forming hyper-reducing environment was H_2 evolved by the serpentinization rather than CH_4 that is commonly preserved in blueschist and eclogites. This fact would speculate a widespread hyper-reducing environment caused by H_2 fluids in a shallow level of serpentinizing mantle wedge.

Keywords: Fe-Ni alloy, serpentinization, Pb isotope composition, reducing fluid, mantle wedge

©2019. Japan Geoscience Union. All Right Reserved.

PETROCHEMISTRY AND AGE DETERMINATION OF THE NEWLY DISCOVERED ECLOGITE IN THE WESTERN MONGOLIA

*Kosuke Naemura[1], Erdenjargal Choindonjamts[4], Takenori Kato[5], Otgonkhuu Javkhlan[3], Katsuyoshi Michibayashi[2]

1. Nagoya University Museum, 2. Nagoya University Graduate school of environmental studies, 3. Chinese Academy of Geological Sciences, 4. Mongolian Academy of Sciences, 5. Nagoya University Space-Earth Environmental Research

This study report on newly discovered eclogite from the Western Mongolia in the Central Asian Orogenic Belt. Lenticular eclogite bodies with several meters in length are enclosed in quartzite of the Shubun/Urgamal formation in the southernmost part of the Zavkhan block which forms a part of the Neoproterozoic Tuva-Mongolian arc. Trace element patterns of eclogites are like those of OIB. We used relatively fresh eclogite sample and amphibolite sample to reconstruct the pressure-temperature history. Fresh eclogite preserves omphacite (with jadeite 38 mole%) coexisting with garnet ($Alm_{56}Gros_{35}Pyr_{8}$), barroisite, phengite (Si=3.36 apfu, O=11), quartz, epidote, rutile with accessory apatite, calcite, and hematite (assemblage 1). Garnet-core includes paragonite and kyanite coexisting with titanite, quartz, barroisite, which represents prograde stage mineral assemblage (Stage 0). The eclogite assemblages are variably retrogressed into amphibolite assemblage of hornblende, plagioclase, quartz, biotite, Mg-rich garnet-rim ($Alm_{61}Gros_{29}Pyr_{9}$), epidote and titanite (assemblage-2). In amphibolite sample, atoll-shaped garnet is ubiquitously observed. The atoll-shaped garnet consists of the eclogite facies core, Ca-rich mantle ($Alm_{53}Gros_{44}Pyr_{3}$) probably formed during the amphibolite facies stage 2, and a Ca-poor Mg-rich rim (or shell) ($Alm_{64}Gros_{25}Pyr_{10}$). The last Ca-poor garnet rim coexists with plagioclase, hornblende, epidote, quartz, titanite (assemblage-3). The earliest stage of metamorphism might happen in the "lawsonite stability field" if we interpret kyanite formed from paragonite. Subsequent Stage 1 P-T condition was determined at about 2 GPa and 480 ºC by garnet-clinopyroxene-phengite geothermobarometry. The eclogite once experienced decompression to the epidote-amphibolite assembalge equilibrated at ca. 0.8 GPa and 400 ºC during the Stage 2, determined by garnet-hornblende-plagioclase geothermobarometry. After the initial exhumation, the eclogite experienced heating to the high-pressure amphibolite stage 3 formed at ca. 600 ºC and 1.2 GPa. Such multiple P-T paths have been reported from eclogites from collision zones such as Sesia Alps and W.Tianshan. Additionally, we determined U-Pb age of zircon by CHIME method. Zircon typically exhibit oscillatory zoning and are sometimes included at the garnet core. Most zircons are severely altered, with rare fresh core only in large zircon grains (>0.1 mm). We obtained three populations of age at 1170 Ma, 680 Ma and 340 Ma for such zircon fresh cores. If we interpret these ages as igeneous protolith ages, the eclogite-facies metamorphism should have taken place after 340 Ma. Combining the metamorphic history and U-Pb zircon ages, we speculated that the eclogite primarily formed at the ocean island on the Mongol-Okhotsk (MO) ocean. If so, eclogite-facies metamorphism (assemblage 0→1) should have taken place when the MO plate subducted beneath the Siberian craton. Subsequently the eclogite probably separated from the subducting plate and come up to the crustal depth through the subduction channel, and was transformed into epidote-amphibolite assemblage (assemblage 2). Finally, continental collision took place when the N. China craton collide with the Siberian craton to close the MO ocean at 140 Ma, which transformed the rock to high-pressure amphibolite (assemblage 3).

Keywords: Eclogite, Central Asian Orogenic Belt, Mongol-Okhotsk Ocean

©2019. Japan Geoscience Union. All Right Reserved.

Continental subduction, “*Intraslab UHP Metasomatism*”, and the formation of metamorphic diamond

*Yoshihide Ogasawara[1]

1. Department of Earth Sciences, Waseda University

Deep continental subduction is the process carrying supracrustal materials into deep mantle, and UHP metamorphic rocks are the direct evidence for this process as the materials having the information of P-T and the chemical environments during subduction, escaped from the homogenization with mantle rocks. Usually, UHPM silicate rocks have been strongly retrograded during exhumation, and the preservation of UHPM information is limited excepting inclusions in refractory minerals; decoding the chemical processes in subducted materials is difficult. In carbonate and calc-silicate rocks, UHPM information has been well preserved and can be decoded even in the matrix because the chemical reactions in these rocks make distinct changes from the protolith chemistries, not erased during exhumation.

Carbonate-bearing assemblages have large P-T stabilities at HP/UHP and low H_2O activity, and this indicates high possibility of survival of carbonates and transportation of carbon into deep mantle. H_2O-fluid supply is necessary for metamorphic reactions in these rocks because H_2O-fluid lowers temperatures of decarbonations. As a model showing the processes in deeply subducting continental materials, *Intraslab UHP Metasomatism* (metasomatism within subducting continental materials at UHP mantle depths) will be introduced on the basis of our last 20 years research on the Kokchetav UHPM rocks. In this model, key materials are H_2O and CO_2 in the subducting continental slab, and a key process is H_2O-fluid infiltration within the slab. The outline of this model is as follows. 1) In the subducting slab, silicate rocks (gneisses and eclogite) were a H_2O reservoir, and carbonate and calc-silicate rocks were a CO_2 reservoir. 2) During subduction, H_2O-fluid with several components (e.g. C, K, Ti) occurred by dehydrations of silicate rocks. 3) Dehydrations in silicate rocks preceded decarbonation reactions in carbonate and calc-silicate rocks. 4) Infiltration of H_2O-fluid into carbonate and calc-silicate rocks was a trigger for decarbonations. 5) H_2O-fluid infiltration was controlled by the timing of dehydrations in silicate rocks and vaired in mm to cm scales to form or to characterize the mineral assemblages in carbonate and calc-silicate rocks. 6) H_2O-fluid (with C-bearing species) contributed to the formation of diamond in some carbonate calc-silicate rocks. 7) Modal compositions of carbonates in the protoliths controlled the survival of carbonate depending on the intensity of fluid infiltration.

The following subjects from the Kokchetav UHPM rocks support this model. A) Dolomite marble contains abundant diamond formed at two stages; 2nd stage diamond ($\delta^{13}C$: -17 to -27 ‰) from H_2O-fluid. Dol + Di is not the highest-T assemblage and was controlled by fluid composition, XCO_2 as 0.1, which was suitable for diamond formation. B) Dolomitic marble has the highest-T assemblages, Arg-Fo, Arg-Ti-Chum, but diamond was unstable because of low XCO_2 as 0.01. C) Calcite (after Arg) marble with Coe exsolution in Ttn contains diamond only in Di layer, and other parts do not; this indicates short-term stability of diamond in this rock depending on changing XCO_2. The later fluid was low XCO_2 as 0.02; too low for diamond formation. D) Two types of Grt-Cpx rocks occur; diamond-bearing and diamond-free. Their protoliths are a mixture of silicates and carbonates. Minor diamond occurs as two modes in diamond-bearing Grt-Cpx rock; one is fine-grained (several μm) and the other is cubic (max. 200 μm). A cubic diamond has fine core and crystallized slowly from H_2O-fluid on a fine grain as a seed crystal. E) In gneisses, diamond occurrence is diverse; several morphologies with different colors were observed. Two-stage growth was not confirmed. Dissolution of carbon from diamond in gneisses could be possible,

©2019. Japan Geoscience Union. All Right Reserved.

and carbon was carried into dolomite marble by H_2O-fluid to crystallize 2^{nd} stage diamond.

Many of the subjects being still unclear will be mentioned as the targets of future research.

Keywords: intraslab UHP metasomatism, UHP metamorphism, diamond, carbonate, fluid, Kokchetav Massif

©2019. Japan Geoscience Union. All Right Reserved.

Ultrahigh-pressure pseudotachylyte in a marble

*Tadao Nishiyama[1], Tomoya Fujimoto[1]

1. Department of Earth and Environmental Sciences, School of Science, Graduate School of Science and Technology, Kumamoto University

A black vein in a marble from the Higo metamorphic rock in central Kyushu, Japan, represents a signature of dolomite growth from a carbonate melt and also evidence of liquid immiscibility between carbonate and silicate melts. The formation condition is estimated to be 3.5 GPa and 1280 C by the dolomite composition based on the phase diagram in the system CaCO3– MgCO3. This is a peculiar example of pseudotachylyte formed under ultrahigh-pressure condition.

The Higo metamorphic rock is Cretaceous low P/T metamorphic rock, however, some authors have suggested the existence of high to ultrahigh-pressure metamorphism prior to the low P/T metamorphism. In the south of Mt. Kousadake, Tomochi Town, Kumamoto Prefecture, marble occurs as several layers intercalated with pelitic and siliceous gneisses. The thickness of the marble layer is variable from several meters to several tens of meters. In one of the marble layers, near the contact with the surrounding pelitic gneiss, we found a black vein 10 cm thick and 1 m long, of which strike crosscuts that of the boundary between the marble and gneiss. It shows a branching texture, extending perpendicular to the vein strike from the vein towards the country rock (marble). The branching is a signature typical to the pseudotachylyte.
The marble consists of pure calcite, whereas the black vein consists of dolomite domain and silicate domain. The dolomite domain is composed of aggregates of anhedral to subhedral dolomite grains of 10 micrometers in size with oscillatory or complex zoning in terms of Ca, Mg and Fe. The dolomite grains do not show any deformation texture. The dolomite domain occasionally includes fractured quartz clasts, of which fractures are filled with dolomite. The silicate domain occurs as rounded or irregular-shaped aggregates of several hundred micrometres in size. It consists of rounded quartz grains, fibrous aggregates of hydrous alumino-silicate (unknown clay mineral) and minor dolomite grains. The silicate domains occur sporadically in the dolomite domains, and some silicate domains are connected with each other by network veins of silicates of the same material as the silicate domain. Rounded zircon rarely occurs in the silicate domain. In some parts of the vein, thin marble layers several millimeters thick occur, showing a flow folding.
Subhedral shape, oscillatory zoning and non-deformed texture of dolomite in the dolomite domain indicates the origin of dolomite either as precipitates from the fluid or as growth in the melt. If dolomite precipitated from the C-O-H fluid, the assemblage of dolomite + quartz, which occurs both in the dolomite and silicate domains, is stable at relatively low T, high P and high XCO2 region. Outside the stability field, it will react to form diopside. Diopside is common in calc-silicate gneisses in this region, therefore, the assemblage of dolomite + quartz + C-O-H fluid would imply temperature condition lower than that of the regional metamorphic condition. This observation leads to a conclusion that the dolomite grew from the melt, because fault rocks should show temperature condition higher than that of the country rock owing to frictional heating. The silicate domain may represent recrystallized silicate melt, and the coexistence of carbonate and silicate domains implies the liquid immiscibility between carbonate and silicate melts. In such a case, dolomite should represent a minimum melt composition in the system CaCO3 –MgCO3. The minimum melt composition and its temperature depends strongly on pressure (Irvine and Wyllie, 1975 and Buob et al., 2006), therefore, we can estimate the melting temperature and pressure from the dolomite composition. The effect of FeCO3 component is evaluated to be small based

©2019. Japan Geoscience Union. All Right Reserved.

on the experiment of Shatsky et al. (2014). The estimated pressure and temperature conditions are 3.5 GPa and 1280 C. Thus, we interpret that the black vein is a pseudotachylyte formed under ultrahigh-pressure condition, indicating that the Higo metamorphic rock has experienced the ultrahigh-pressure.

References: Buob, A., et al. (2006) Amer. Mineral., 91, 435-440; Irvine, A.J. and Wyllie, P.J. (1975) GCA, 39, 35-53; Shatsky, A. et al. (2014) Amer. Mineral., 99, 773-785.

Keywords: Ultrahigh-pressure metamorphism, pseudotachylyte, Higo metamorphic rock

©2019. Japan Geoscience Union. All Right Reserved.

Dehydration and Deformation process of subducted large Oceanic Pleateau -case study of the Mikabu blueschist-

*Kazuaki Okamoto[1]

1. Faculty of Education, Saitama University

In order to know an origin of mega-earthquake related to subducted large seamount, observation of deformation process recorded in the blueschist (high P/T metamorphic rock) is the best method. Mikabu blueschist is considered as accreted large oceanic plateau and suffered blueschist facies metamorphism at Jurassic time. It extends approximately 1000 km in EW direction from the Kanto Mountain to Kyushu Island. In north-south direction, succession of ocean plateau stratigraphy can be reconstructed although accretion thrusts duplicate them. We have done detailed field observation along the N-S route and collected the rock sample systematically. In the outcrop, the Mikabu blueschist is well foliated with mineral lineation. However, we have identified massive, cataclastic samples in the structural middle in the NS section. Under the microscope, glassy parts suffered brittle and ductile deformation. Origin of the most glass part can be ascribed as igneous product. However, some glass layers along the deformation band in stilpnomelane aggregates might be formed as melt due to shear heating. If this zone is related to earthquake fault zone, it indicates that a huge earthquake has occurred. Metamorphic petrology based on mineral assemblage devides the Mikabu belt as three zones; the North, Mid, and the South zone, respectively. Psseudo-section analysis concludes that the North zone suffered relatively higher T metamorphism compated to the South zone. In the Mid zone, local temperature increase stabilized stilpnomelane after chlorite.

Keywords: subducted large-ocean plateau, blue schist metamorphism, deformation and metamorphic process

©2019. Japan Geoscience Union. All Right Reserved.

[E] Oral | S (Solid Earth Sciences)：S-MP Mineralogy & Petrology

Tue. May 28, 2019 3:30 PM - 5:00 PM JST | Tue. May 28, 2019 6:30 AM - 8:00 AM UTC | A08 TOKYO BAY MAKUHARI HALL

[S-MP29] Oceanic and Continental Subduction Processes

convener:REHMAN Ur Hafiz(Department of Earth and Environmental Sciences, Graduate School of Science and Engineering, Kagoshima University), Tatsuki Tsujimori(Tohoku University), Chin-Ho Tsai(Department of Natural Resources and Environmental Studies, National Dong Hwa University), Kazuaki Okamoto(Faculty of Education, Saitama University), Chairperson:Tsai Chin-HO(National Dong Hwa University), Hafiz REHMAN(Kagoshima University)

This JpGU-AGU joint session aims at bringing earth scientists from Japan and overseas to present their research related to the processes of oceanic and continent subduction, continent-continent collisions, metamorphism of crustal rocks, formation of the oceanic/continental arcs, and accretion/ tectonic erosion of material along subduction boundaries.

Topics such as role of the fore- and back-arcs in the subduction zones, process of accretion of volcaniclastic and terrigenous sediments along the subduction/collision boundaries, deformation and metamorphism of subducted crust, and exhumation will be the main focus of the session.

In addition to the above mentioned topics, our focus for the10th anniversary of this international session will be towards our understanding and progress on the ultrahigh-pressure/temperature metamorphic terranes in the world.

Exchange of ideas among geoscientists applying different approaches on problems related to the theme of the session are most welcome.

3:30 PM - 3:45 PM JST | 6:30 AM - 6:45 AM UTC

[SMP29-06] Unusually high Nb/Ta ratio of fluid-precipitated jadeites from New Idria serpentinite body, California: Implications for extreme fractionation in slab fluids

*Naoko Takahashi[1], Tatsuki Tsujimori[2], Qing Chang[3], Jun-Ichi Kimura[3] (1.Graduate School of Science, Tohoku Univ., 2.CNEAS, Tohoku Univ., 3.Department of Solid Earth Geochemistry, JAMSTEC)

3:45 PM - 4:00 PM JST | 6:45 AM - 7:00 AM UTC

[SMP29-07] The collision process interpreted using the systematic change of metamorphic pattern along theQinling–Dabie–Odesan collisional belt between the North and South Korea-China Cratons

★Invited Papers

*Chang Whan Oh[1,2] (1.Department of Earth and Environmental Sciences, Chonbuk National University, Jeonju, Republic of Korea, 2.Environmental Science System Research Center, Chonbuk National University,Jeonju, Republic of Korea)

4:00 PM - 4:15 PM JST | 7:00 AM - 7:15 AM UTC

[SMP29-08] Contrasting collision processes between northwest and central Himalaya: examination from the "Lesser Himalayan granites” in Pakistan

*Masatsugu Ogasawara[1], Mayuko Fukuyama[2], Rehanul H Siddiqui[3] (1.Institute of Geology and Geoinformation, Geological Survey of Japan, National Institute of Advanced Industrial Science and Technology, 2.Graduate School of Engineering Science, Akita University, 3.Balochistan University of Information Technology, Engineering and Management Sciences)

4:15 PM - 4:30 PM JST | 7:15 AM - 7:30 AM UTC

[SMP29-09] New petrologic indications of subduction metamorphism in the Yuli belt, eastern Taiwan

*Chin-Ho Tsai[1], Chih-Ying Yeh[1], Dominikus Deka Dewangga[1], Yui Kouketsu[2], Masaki Enami[3] (1.Department of Natural Resources & Environmental Studies, National Dong Hwa Univ., 2.Department of Earth & Planetary Sciences, Nagoya Univ., 3.Institute for Space-Earth Environmental Research, Nagoya Univ.)

4:30 PM - 4:45 PM JST | 7:30 AM - 7:45 AM UTC

[SMP29-10] **The importance of Mn-nodules on the sea floor during subduction for the formation of ophiolitic diamond**

*Richard Wirth[1] (1.Helmholtz Centre Potsdam GFZ German Research Centre for Geosciences 3.5 Surface Geochemistry)

4:45 PM - 5:00 PM JST | 7:45 AM - 8:00 AM UTC

[SMP29-11] **Along-strike variability of primitive magmas inferred from olivine-hosted melt inclusions, southernmost Andean Southern Volcanic Zone, Chile**

*Derek Weller[1,2], Charles R Stern[2] (1.Earthquake Research Institute, 2.University of Colorado)

Unusually high Nb/Ta ratio of fluid-precipitated jadeites from New Idria serpentinite body, California: Implications for extreme fractionation in slab fluids

*Naoko Takahashi[1], Tatsuki Tsujimori[2], Qing Chang[3], Jun-Ichi Kimura[3]

1. Graduate School of Science, Tohoku Univ., 2. CNEAS, Tohoku Univ., 3. Department of Solid Earth Geochemistry, JAMSTEC

Fractionation of Nb and Ta, which are conventionally thought as geochemical twins, is a key to understanding the evolution of the silicate Earth. The subchondritic Nb/Ta ratio of the continental crust (12-13; Barth et al., 2000), which is a long-standing problem, has been explained by Nb/Ta fractionation during subduction processes such as slab melting and/or dehydration. However, recent studies have revealed that extreme Nb/Ta fractionation of subduction-zone fluids from minerals in eclogite (up to 87; Xiao et al., 2006; Liang et al., 2009) and metagranite (up to 239; Chen and Zheng, 2015). In order to decipher Nb-Ta (and Zr-Hf) behavior of slab-derived fluids in shallower levels, we investigated a veined jadeitite from the New Idria serpentinite body, which is regarded as direct precipitates from slab-derived fluids at forearc depth. We applied *in-situ* measurements of trace element abundance of jadeites using a LA-ICP-QMS. The New Idria jadeites is characterized by remarkably high Nb concentration but depleted in Ta. Consequently Nb/Ta ratio varies from 10 to 115; Zr/Hf ratio also shows a wide range of 38–164. Nb–Ta and Zr–Hf correlations suggest coupling behaviors of those elemental pairs in fluids during the jadeitite vein formation. A simple Rayleigh fractional crystallization model for jadeite growth using partitioning coefficient D_{Nb} and D_{Ta} between clinopyroxene-aqueous fluid (Stalder et al., 1998) is also unlikely to explain the data. Although the extreme Nb/Ta and Zr/Hf fractionation can occur in seawater (Firdaus et al., 2011), oxygen isotope composition of New Idria jadeites ($\delta^{18}O$ = +8.4 to +9.9‰; Sorensen et al., 2006) eliminates a possibility that jadeitite-forming fluid source was originated from pore fluids derived from seawater. Alternatively, the Nb-Ta behavior might be explained by breakdown of hydrous minerals with high Nb/Ta ratio such as phengitic mica and/or consequences of high degree of fluid-rock interaction in a case of $D_{Nb}/D_{Ta} > \sim 10$ for fluid-rock system. New Idria jadeitite veins would provide an evidence for the presence of highly Nb/Ta fractionated fluids in serpentinized mantle wedge beneath forearc, supporting the idea that Nb and Ta are highly mobile and fractionate during the early stage of oceanic plate subduction before the appearance of rutile.

Keywords: Nb/Ta fractionation, subduction, fluid, water-rock interaction, jadeite

©2019. Japan Geoscience Union. All Right Reserved.

The collision process interpreted using the systematic change of metamorphic pattern along theQinling–Dabie–Odesan collisional belt between the North and South Korea-China Cratons

*Chang Whan Oh[1,2]

1. Department of Earth and Environmental Sciences, Chonbuk National University, Jeonju, Republic of Korea, 2. Environmental Science System Research Center, Chonbuk National University,Jeonju, Republic of Korea

Along the Qinling–Dabie–Odesan collisional belt between the North Korea-China and South Korea-China Cratons, the peak metamorphic conditions reflect systematically changing metamorphic regimes from east to west: ultra-high temperature (UHT) granulite-facies metamorphism in the Odesan area (905–1160˚C, 9-10.6 kbar) at 247-245 Ma; high pressure (HP) eclogite-facies metamorphism in the Hongseong area (819–835˚C, 23-25 kbar) at 250 Ma; ultra-high pressure (UHP) eclogite-facies metamorphism in the Sulu, Dabie and Hong’an areas (620–880˚C, 26–43 kbar) at 220-240 Ma; HP eclogite facies metamorphism in the Tonbai area (530–610˚C, 17–20 kbar) at 216 Ma; epidote–amphibolite and blueschist facies metamorphism in the Wudang area (505–550˚C, 10–13 kbar) at 216 Ma ; and HP granulite-facies metamorphism in the western Qinling area (657–772˚C, 9.7–13.2 kbar) at 214 Ma. Additionally, the Triassic post-collisional igneous rocks regionally intruded at both ends of the collision belt, in the Hongseong–Odesan areas at 230 Ma and in the west Qinling at 210 Ma. These observations indicate that the following collisional processes occurred along the Qinling–Dabie–Odesan collisional belt. The collision between the North Korea-China Craton and South Korea-China Craton first occurred in the eastern margin of the collision belt (the Odesan area) with an angle of approximately 60˚ between their long axes of two Cratons and propagated towards west. The amount of oceanic slab subducted before the collision increased from the Odesan area to the Sulu area due to westwards increase in the width of the ocean between the North Korea-China and South Korea-China Cratons, resulting an increase in the depth of slab break-off. After slab break-off occurred in the Sulu area, the lateral tearing force strengthened, resulting a decrease in the depth of slab break-off from the Sulu area to the western Qinling area as collision propagated westward. At both ends of the collision belt, post collisional igneous activities occurred with metamorphism higher than granulite facies relating to high heat supply from upwelling mantle due to shallow depth of slab break-off.

Keywords: Qinling-Dabie-Odesan collision belt, The depth of slab break-off, Peak metamorphism, Post collisional igneous activity, Collisional process

©2019. Japan Geoscience Union. All Right Reserved.

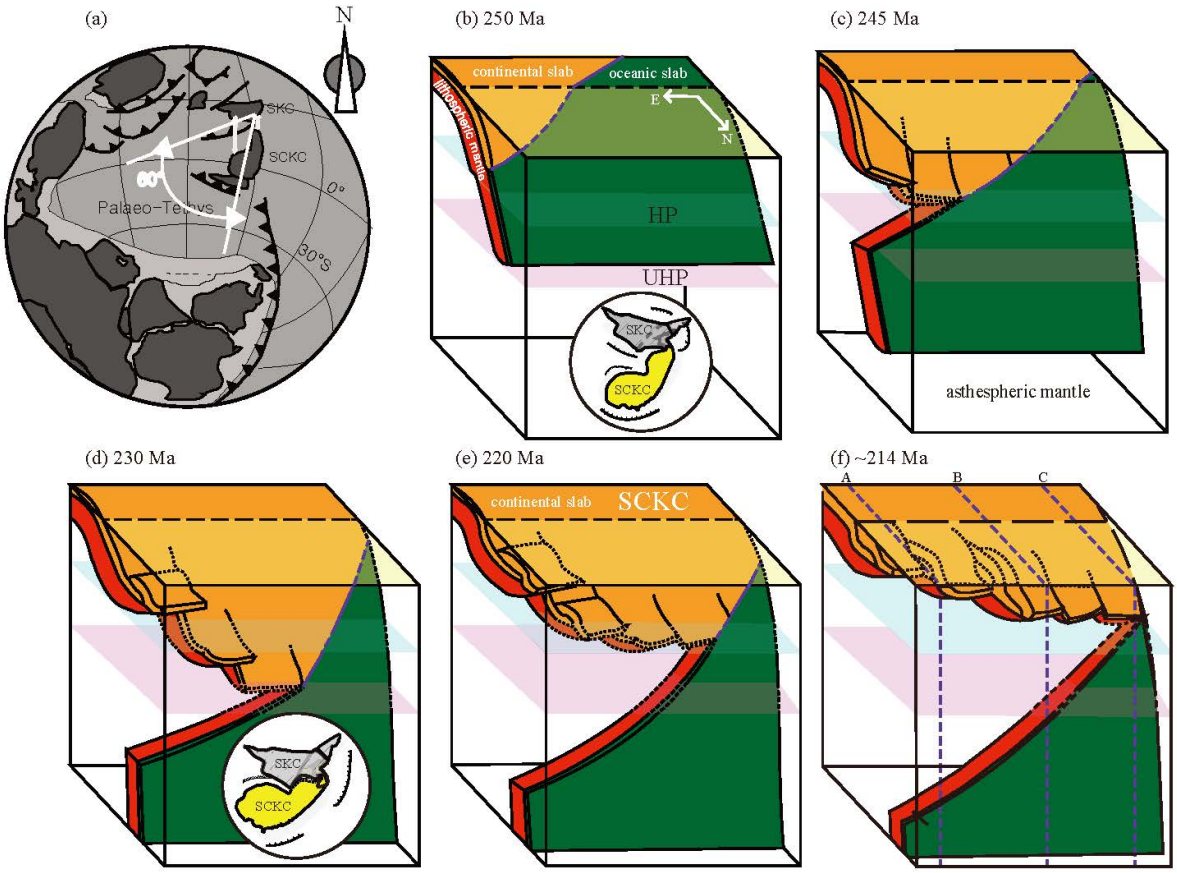

Fig. 16 Oh and Lee,

©2019. Japan Geoscience Union. All Right Reserved.

Contrasting collision processes between northwest and central Himalaya: examination from the "Lesser Himalayan granites" in Pakistan

*Masatsugu Ogasawara[1], Mayuko Fukuyama[2], Rehanul H Siddiqui[3]

1. Institute of Geology and Geoinformation, Geological Survey of Japan, National Institute of Advanced Industrial Science and Technology, 2. Graduate School of Engineering Science, Akita University, 3. Balochistan University of Information Technology, Engineering and Management Sciences

The Himalayan orogenic belt was formed by the Cenozoic collision of Indian and Eurasian plates. In the eastern and central part of the Himalaya, four main tectonostratigraphic zones have been recognized, such as from south to north, Sub-Himalaya, Lesser Himalaya, Greater Himalaya and Tethys Himalaya. However, the northwest Himalaya in Pakistan and northwest India shows some distinct features differ from the main part of the Himalaya, i.e., (1) Presence of the Cretaceous island arc blocks between the Indian and the Eurasian blocks: (2) Boundary between the Lesser Himalaya and Greater Himalaya is not well defined: (3) Presence of UHP eclogites: (4) Extensive exposure of "Lesser Himalayan granites" represented by the Mansehra granite in Pakistan. As granite and granitic gneiss are major components of the Himalayan orogenic belt, we have examined geochemical and isotopic characteristics of the Mansehra granite and compared those with "Lesser Himalaya granites" and granite gneisses of the Greater Himalaya in the central part of the Himalaya. Before the collision of the India to the Eurasian, granites similar to the Mansehra granite were present along the northern margin of the India continent. The collision of India continent with the Tibet of the Eurasia plate formed two separate zones of granites, the "Lesser Himalayan granites" and extensively deformed granite gneiss in the Greater Himalaya. In the collision of India to the Cretaceous island arc blocks in northwest Himalaya did not disturbed distribution of the granite, resulting large exposure of the Mansehra granite. The southern extension of the Karakoram Fault which is a dextral strike-slip fault separating the Tibet and the Karakoram/Pamir block, approximates a boundary between the northwest Himalaya and the eastern and central Himalaya.

Keywords: collision, Himalaya, granite

©2019. Japan Geoscience Union. All Right Reserved.

New petrologic indications of subduction metamorphism in the Yuli belt, eastern Taiwan

*Chin-Ho Tsai[1], Chih-Ying Yeh[1], Dominikus Deka Dewangga[1], Yui Kouketsu[2], Masaki Enami[3]

1. Department of Natural Resources & Environmental Studies, National Dong Hwa Univ., 2. Department of Earth & Planetary Sciences, Nagoya Univ., 3. Institute for Space-Earth Environmental Research, Nagoya Univ.

Previous reports of high-pressure (HP) metamorphism in the Yuli belt are mainly from meta-igneous and meta-volcaniclastic rocks, which are minor constituents within allochthonous metabasite-serpentinite blocks embedded in the dominant metasedimentary schists. By contrast, no HP minerals have yet been found in the metasedimentary rocks, whereas serpentinite is not suitable for pressure constraint. Thus skepticism on whether the Yuli belt is truly a HP metamorphic belt still exists. To solve this problem, we have investigated garnet-bearing pelitic schists using quartz-inclusion Raman spectroscopy barometry and surveyed the metasomatic zones around the Tsunkuanshan serpentinite body. Our Raman spectroscopic analyses on quartz inclusions in garnet from three metapelitic samples yielded residual (entrapment) pressures of 11-15 kbar at temperatures of 420-620˚C (constrained by Raman spectra of carbonaceous material thermometry). These results are essentially consistent with those of HP metabasites, glaucophane schists, and metaplagiogranites in the Yuli belt by recent pseudosection modeling. In the Tsunkuanshan area, meter-scale metasomatic zones crop out at the contact between serpentinite and surrounding pelitic schists. We discovered rare early-stage glaucophane (crossite) in an intermediate amphibole-albite rich rock in the metasomatic zones. This new occurrence indicates that serpentinite bodies might have been incorporated into a (paleo) subduction channel and subsequently recrystallized together with the host metasediments in HP conditions. Both the new pressure-temperature constraints from metasedimentary rocks and the finding of blue amphibole in metasomatic zones around serpentinite bodies indicate that the Yuli belt was subject to ‘warm’ subduction metamorphism.

Keywords: glaucophane, metasomatic zone, serpentinite, garnet, quartz-inclusion Raman barometry

©2019. Japan Geoscience Union. All Right Reserved.

The importance of Mn-nodules on the sea floor during subduction for the formation of ophiolitic diamond

*Richard Wirth[1]

1. Helmholtz Centre Potsdam GFZ German Research Centre for Geosciences 3.5 Surface Geochemistry

Diamonds, native elements and unusual metal alloys from chromitites in ophiolites have been reported already almost 20 years ago (Bai et al., 2000). However, the genesis of these diamonds enclosed in chromite is still challenged. A major question is the origin of all the unusual elements and alloys recorded so far such as W, Co, Ta, CrFe, NiCu, AgAu, CoFeNi and most important Mn-Ni-Co alloys. Meanwhile, diamonds in chromite in ophiolites have been reported from several different locations on the planet (Tibet, Mongolia, Polar Urals, Turkey, Albania), which are separated from each other by long distances (Yang et al., 2014). There is one common feature observed in these diamonds, they usually contain small inclusions (from nanometre up to a few micrometre in size) of a Mn-Ni-Co alloy. The composition of the alloy is varying in diamond from different locations. These diamonds are natural diamonds that is demonstrated by the presence or coexistence of several additional nanoinclusions in diamond such as oxides, silicates and sulphides and selenides. Thinking about the genesis of these ophiolitic diamonds the question arises where all these strange elements and alloys come from? They are not typical Upper Mantle components. However, it is well known that Mn-nodules from the sea floor contain all these rare and unusual elements (Wegorzweski et al., 2015 and ref. therein). Subduction of the sea floor transports the nodules to a depth where melting of the nodules finally occurs. Depending on the Co-concentration melting of a Mn-Ni-Co ally will start at temperatures < 900˚C with increasing Co-concentration at much lower temperature. Under local reducing conditions such Mn-Ni-Co alloy melt pools might exist in the subducted slab. The sea floor also contains plenty of organic material that could potentially supply the carbon necessary for the formation of diamond. Carbon rich fluids might react with the Mn-Ni-Co alloy melt, the melt acting as a catalyst to reduce the C-rich fluid to C. Carbon is dissolved in the alloy melt to a high amount depending on pressure and temperature. A change in PT during uplift then will result in the precipitation of solid carbon from the melt. If that happens in the diamond stability field diamond will precipitate. That process would explain the presence of such kind of Mn-Ni-Co alloy inclusions in diamond. Mn-nodules with their content of a wide variety of elements from the periodic system cannot only explain the unusual occurrence of diamond in chromitite in ophiolites but also the presence of other unusual elements and compounds. The details of the processes involved are not fully understood and they are subject of future investigations.

Bai, W.J., Robinson, P.T., Fang, Q., Hu, X-F., Zhou, M., (2000) Origin of PGE and base metal allloysin podifoem chromitites of he Luobusa ophiolite, southern Tiet. Canadian Mineralogist, 38, 585-598.

Wegorzewski, A.V., Kuhn, T., Dohrmann, R., Wirth, R., Grangeon, S. (2015) Mineralogical characterization of individual growth structures of Mn-nodules with different Ni+Cu content from the central Pacific Ocean. Amer. Min., 100, 2497-2508.

©2019. Japan Geoscience Union. All Right Reserved.

Yang, J., Meng, F., Xu.X, Robinson, P.T., Dilek, Y., Makeyev, A.B., Wirth, R., Wiedenbeck, M., Griffin, W.L., Cliff, J. (2014) Diamonds, native elements and metal alloys from chromitites of the Ray-Iz ophiolite of the Polar Urals. Gondwana Research, http://dx.doi.org/10.1016/j.gr.2014.07.004.

Keywords: Subduction, Mn-nodules, ophiolitic diamond

©2019. Japan Geoscience Union. All Right Reserved.

Along-strike variability of primitive magmas inferred from olivine-hosted melt inclusions, southernmost Andean Southern Volcanic Zone, Chile

*Derek Weller[1,2], Charles R Stern[2]

1. Earthquake Research Institute, 2. University of Colorado

Glass compositions of melt inclusions in olivine phenocrysts found in tephras derived from explosive eruptions of the four volcanoes along the volcanic front of the southernmost Andean Southern Volcanic Zone (SSVZ) are used to constrain primitive magma compositions and melt generation parameters. Primitive magmas from Hudson, Macá, and Melimoyu have similar compositions and are formed by low degrees (8-18 %) of partial melting. Compared to these other three centers, primitive magmas from Mentolat have higher Al_2O_3 and lower MgO, TiO_2 and other incompatible minor elements, and are generated by somewhat higher degrees (12-20%) of partial melting. The differences in the estimated primitive parental magma compositions between Mentolat and the other three volcanic centers are consistent with difference in the more evolved magmas erupted from these centers, Mentolat magmas having higher Al_2O_3 and lower MgO, TiO_2 and other incompatible minor element contents, suggesting that these differences are controlled by melting processes in the mantle source region above the subducted oceanic plate. The observed along-arc changes in parental magma chemistry may be due to the close proximity below Mentolat of the subducted Guamblin Fracture Zone that could efficiently transport hydrous mineral phases, seawater, and sediment into the mantle, driving enhanced volatile fluxed melting beneath this center compared to the others.

Keywords: Andean volcanism, tephra, olivine melt inclusions, primitive magma

©2019. Japan Geoscience Union. All Right Reserved.

[E] Poster | S (Solid Earth Sciences)：S-MP Mineralogy & Petrology

Tue. May 28, 2019 10:45 AM - 12:15 PM JST | Tue. May 28, 2019 1:45 AM - 3:15 AM UTC | Poster Hall International Exhibition Hall8, Makuhari Messe_8

[S-MP30] Crust-Mantle Connections

convener:Yoshihiko Tamura(Research Institute for Marine Geodynamics, Japan Agency for Maine-Earth Science and Technology), Osamu Ishizuka(Geological Survey of Japan, AIST), Chris Conway(Geological Survey of Japan)

A paradigm of the solid Earth geochemical cycles is that the Earth's crust forms by melting of the Earth's upper peridotitic mantle. How divers is the spectrum of primary melts and which factors may contribute to its variations? What is the influence of crustal processing vs. primary magma diversity in creating the diversity of the Earth's crust? The session seeks to explore the crust-mantle connections at divergent and convergent plate boundaries, and oceanic island settings based on volcanology, petrology, geochemistry, geophysics, geochronology, and geodynamics studies.

[SMP30-P01] Secular evolution of proto-Izu-Bonin-Mariana arc volcanism: Constraints from statistical analysis of melt inclusion compositions

*Morihisa Hamada[1], Hikaru Iwamori[1,2], Philipp A. Brandl[3], Takayuki Ushikubo[4], Kenji Shimizu[4], Motoo Ito[4], He Li[5], Ivan P. Savov[6] (1.Department of Solid Earth Geochemistry, Japan Agency for Marine-Earth Science and Technology, 2.Earthquake Research Institute, University of Tokyo, 3.GEOMAR Helmholtz Centre for Ocean Research Kiel, 4.Kochi Institute for Core Sample Research, Japan Agency for Marine-Earth Science and Technology, 5.Institute of Oceanology, Chinese Academy of Sciences, 6.School of Earth and Environment, University of Leeds)

[SMP30-P02] The Jurassic magmatism of protoliths of Mikabu greenstones in SW Japan: zircon U-Pb dating and trace element analysis

*Hikaru Sawada[1], Yukio Isozaki[1], Shogo Aoki[3], Shuhei Sakata[2], Ryo Hasegawa[1], Yasuo Nakamura[1] (1.Department of General Systems Studies, the University of Tokyo, 2.Department of Chemistry, Gakushuin Universtiy, 3.Department of Applied Science, Okayama University of Science)

[SMP30-P03] Origin of variable CaO/Al_2O_3 in olivine-hosted melt inclusions from Kibblewhite Volcano, Kermadec Arc

*Yasuhiro Hirai[1], Yoshihiko Tamura[2], Kaj Hoernle[3], Christian Timm[4], Folkmar Hauff[3], Reinhard Werner[3], Takeshi Hanyu[2], Bogdan Vaglarov[2], Qing Chang[2], Takashi Miyazaki[2], Jun-Ichi Kimura[2] (1.Graduate School of Natural Science and Technology, Kanazawa University, Japan, 2.Japan Agency for Marine-Earth Science and Technology (JAMSTEC), Yokosuka, Kanagawa, Japan, 3.GEOMAR Helmholtz Centre for Ocean Research, Kiel, Germany, 4.GNS Science, Lower Hutt, New Zealand)

[SMP30-P04] Ankaramite from Doyo seamount in the Izu-Ogasawara arc: A precursor of continents?

*Yoshihiko Tamura[1], Tomoki Sato[1], Osamu Ishizuka[1,2], Takashi Miyazaki[1], Yasuhiro Hirai[1,3], Mami Takehara[4], Eri Sakamoto[5] (1.JAMSTEC, 2.AIST, 3.Kanazawa Univ., 4.NIPR, 5.NME)

[SMP30-P05] Different Moho reflections adjacent to Minami-Tori Shima and their petrologic origins

*Yoshihiko Tamura[1], Kentaro Kaneda[2], Gou Fujie[1], Akane Ohira[1], Eiichi TAKAZAWA[3], Georges Ceuleneer[4], Katsuyoshi Michibayashi[5], Tomoki Sato[1], Shuichi Kodaira[1], Seiichi Miura[1] (1.Japan Agency for Maine-Earth Science and Technology, 2.Japan Coast Guard, 3.Niigata University, 4.Universite de Toulouse, 5.Nagoya University)

[SMP30-P06] Melt-rock interaction in plagioclase peridotites from the southern Palawan Ophiolite, Philippines

*FLORENCE ANNETTE CRUSPERO LABIS[1], BETCHAIDA D PAYOT[1], GABRIEL THEOPHILUS V VALERA[1], JULIUS A PASCO[1], JESLEY MEI A DYCOCO[1] (1.UNIVERSITY OF THE PHILIPPINES)

[SMP30-P07] Intra-oceanic arc magma genesis: a case study from Havre volcano, Kermadec arc

*Chris Conway[1], Kenichiro Tani[2] (1.Geological Survey of Japan, 2.National Museum of Nature and Science)

Secular evolution of proto-Izu-Bonin-Mariana arc volcanism: Constraints from statistical analysis of melt inclusion compositions

*Morihisa Hamada[1], Hikaru Iwamori[1,2], Philipp A. Brandl[3], Takayuki Ushikubo[4], Kenji Shimizu[4], Motoo Ito[4], He Li[5], Ivan P. Savov[6]

1. Department of Solid Earth Geochemistry, Japan Agency for Marine-Earth Science and Technology, 2. Earthquake Research Institute, University of Tokyo, 3. GEOMAR Helmholtz Centre for Ocean Research Kiel, 4. Kochi Institute for Core Sample Research, Japan Agency for Marine-Earth Science and Technology, 5. Institute of Oceanology, Chinese Academy of Sciences, 6. School of Earth and Environment, University of Leeds

International Ocean Discovery Program (IODP) Expedition 351 'Izu–Bonin–Mariana (IBM) Arc Origins' drilled Site U1438, situated in the north-western margin of the Philippine Sea, into volcaniclastic sediments of the proto-IBM arc. Brandl *et al.* (2017, *Earth and Planetary Science Letters*) have analysed the major, trace and volatile elements of 304 melt inclusions hosted in fresh silicate minerals to unveil the magmatic evolution of the proto-IBM arc between 30 and 40 Ma, when the arc volcanism matured following subduction initiation at 52 Ma. Brandl *et al.* (2017) concluded that: (1) volcanism of the proto-IBM arc shifted from calc-alkaline affinity to tholeiitic affinity over time; and (2) such compositional shift is linked to both the volcanic productivity and the maturation of an evolving island arc. To better integrate the composition of melt inclusions with the magmatic evolution of the proto-IBM arc, this study extends the dataset of Brandl *et al.* (2017) by: (1) additional analysis of volatiles (H_2O, S, F and Cl) and P_2O_5 for 47 carefully selected melt inclusions by Secondary Ion Mass Spectrometry (SIMS); and (2) statistical analysis on the composition of 237 representative melt inclusions covering the full time range (30–40 Ma) of the dataset. Based on statistical analysis of the melt inclusion compositions and by considering trace element compositions and volatile concentrations, we can confidently distinguish five main clusters of melt inclusion compositions which can be further separated into a total of nine sub-clusters. Among the nine sub-clusters, we identified three major magma types: (1) medium-K enriched magmas which form a tholeiitic trend (30–38 Ma); (2) less-depleted medium-K melts which form a calc-alkaline trend (35–39 Ma); and (3) low-K depleted magmas which form a calc-alkaline trend (35–40 Ma). We demonstrate that: (1) volcanism of calc-alkaline depleted magmas lasted until 35 Ma; (2) the volcanism of calc-alkaline depleted magmas and that of more enriched normal arc magmas (tholeiitic and calc-alkaline affinities) overlap between 35 and 38–39 Ma and; (iii) the volcanism of normal arc magmas became predominant thereafter at the proto-IBM arc. Such identification of three major magma types is distinct from that of Brandl *et al.* (2017), in which less-depleted medium-K calc-alkaline magmas amd depleted low-K calc-alkaline gammas were not distinguished. We infer that depleted source mantle had been replaced by enriched mantle due to mantle convection beneath the proto-IBM arc from >40 Ma to 35 Ma. Statistical analysis is a useful tool to partition a mixture of multivariable dataset, such as datasets of melt inclusion compositions, into several distinct groups and potentially reconstruct their geological evolution.

Keywords: Amami Sankaku Basin, International Ocean Discovery Ptrogram, Izu-Bonin-Mariana arc, Melt inclusion, Statistical analysis, Volatiles

©2019. Japan Geoscience Union. All Right Reserved.

The Jurassic magmatism of protoliths of Mikabu greenstones in SW Japan: zircon U-Pb dating and trace element analysis

*Hikaru Sawada[1], Yukio Isozaki[1], Shogo Aoki[3], Shuhei Sakata[2], Ryo Hasegawa[1], Yasuo Nakamura[1]

1. Department of General Systems Studies, the University of Tokyo, 2. Department of Chemistry, Gakushuin Universtiy, 3. Department of Applied Science, Okayama University of Science

The Mikabu greenstones, incorporated with the Cretaceous high P/T-type Sanbagawa metamorphic belt in SW Japan, are accreted fragments of an oceanic plateau. We identified a Late Jurassic igneous age for the protoliths of the Mikabu greenstones in the eastern Kii Peninsula, by measuring U-Pb age and trace element composition (REE, Y, Sc, Nb, Ta, Hf, U, Th) of zircon grains with an Agilent 8800 single-collector triple quadrupole ICPMS coupled to a NWR-213 laser-ablation system. The U-Pb ages have a weighted average of 154.6 ±1.6 Ma (the Kimmeridgian, Late Jurassic) with an overlap within 2-sigma error. The igneous age is slightly younger than the previously reported radiolarian ages (Middle Jurassic) of deep-sea pelagic chert associated with the Mikabu greenstones. The age difference between them suggests that mafic magmas intruded pelagic deep-sea sediments on the pre-existing oceanic lithosphere. Trace element composition further indicates that the dated zircon grains are more similar to those in oceanic crusts than in granitic continental crusts, and the host mafic magma of the zircon grains was derived from depleted mantle like the mid-oceanic ridge-type source, rather than fertile mantle sources like Hawaii and Iceland. As rocks from the Shatsky Rise in the modern NW Pacific Ocean have similar age and compositional characteristics, this study concluded that the protoliths of the Mikabu greenstones had formed a part of an oceanic plateau, which was generated by the Late Jurassic intra-oceanic plate mafic magmatism in the ancient Pacific Ocean.

Keywords: Mikabu greenstones, zircon, Jurassic, oceanic plateau, U-Pb age, trace element

©2019. Japan Geoscience Union. All Right Reserved.

Origin of variable CaO/Al_2O_3 in olivine-hosted melt inclusions from Kibblewhite Volcano, Kermadec Arc

*Yasuhiro Hirai[1], Yoshihiko Tamura[2], Kaj Hoernle[3], Christian Timm[4], Folkmar Hauff[3], Reinhard Werner[3], Takeshi Hanyu[2], Bogdan Vaglarov[2], Qing Chang[2], Takashi Miyazaki[2], Jun-Ichi Kimura[2]

1. Graduate School of Natural Science and Technology, Kanazawa University, Japan, 2. Japan Agency for Marine-Earth Science and Technology (JAMSTEC), Yokosuka, Kanagawa, Japan, 3. GEOMAR Helmholtz Centre for Ocean Research, Kiel, Germany, 4. GNS Science, Lower Hutt, New Zealand

During R/V SONNE expedition SO-255 mafic basaltic to magnesian andesitic lavas containing melt inclusion hosting forsteritic olivines ($Fo_{90.3–92.4}$) were recovered from Kibblewhite Volcano, southern Kermadec Arc. The re-homogenized melt inclusions have compositions similar to primitive basalt (49.6–52.0 wt.% SiO_2; 12.7–15.9 wt.% MgO). Their CaO/Al_2O_3 values, however, range from 0.9 to 1.6, which cannot be explained by melting of lherzolite. Moreover, CaO/Al_2O_3 values in the melt inclusions correlate negatively with Ni contents of their host olivines suggesting that the high CaO/Al_2O_3 values result from interaction between mafic melts and subarc lithospheric mantle. Prior to the interaction the mafic magma must have had high Ni contents and low CaO/Al_2O_3 values, thus they crystallized high Ni olivines trapping low CaO/Al_2O_3 melt inclusions. During the interaction the olivines crystallized from the mafic magmas and its latent heat assimilated pyroxenes from the surrounding lithospheric mantle. This assimilation of pyroxenes allowed the Ni content of the melt to decrease and CaO/Al_2O_3 to increase while buffering the the Mg-number of the mafic magmas during the ascent. Thus, magmas during and after the interaction could crystallize low Ni olivines bearing high CaO/Al_2O_3 melt inclusions.

Keywords: Subduction zone, Kermadec Arc, Kibblewhite Volcano, SO-255, Olivine-hosted melt inclusion

©2019. Japan Geoscience Union. All Right Reserved.

Ankaramite from Doyo seamount in the Izu-Ogasawara arc: A precursor of continents?

*Yoshihiko Tamura[1], Tomoki Sato[1], Osamu Ishizuka[1,2], Takashi Miyazaki[1], Yasuhiro Hirai[1,3], Mami Takehara[4], Eri Sakamoto[5]

1. JAMSTEC, 2. AIST, 3. Kanazawa Univ., 4. NIPR, 5. NME

Izu-Ogasawara-Mariana (IOM) system of arcs (also known as the Izu-Bonin-Mariana arc system) is a typical oceanic arc produced by subduction of the Pacific Plate beneath the Philippine Sea Plate. Volcanoes along the southern segment of the Izu-Ogasawara arc are underlain by thin crust (10-20 km). According to the hypothesis presented by Tamura *et al.* (2016), rising mantle diapirs stall near the base of the oceanic crust at depths controlled by the thickness of the overlying crust. Where the crust is thin, melting occurs at relatively low pressures in the mantle wedge producing andesitic magmas. Andesites erupted from Nishinoshima that were produced in the recent history of the volcano have been generated by olivine fractionation of primary andesitic magmas (Tamura *et al.*, 2019).

To further examine this hypothesis, we have dived Doyo Seamount by using manned submersible SHINKAI 6500 to sample primitive magmas from the volcano, which is located about 50 km north of Nishinoshima and is underlain by thinner curst (15 km) compared to Nishinoshima. Doyo Seamount is located approximately 900 km south of Tokyo at 27˚41’ N, 140˚48’ E in the Ogasawara Arc. The seamount attained an elevation of ~400 m below sea level (mbsl) and its submarine flanks extend to the depth of 3,200 mbsl. The basal dimeter of the volcano is about 30 km. The deeper parts of this large submarine edifice have yet to be explored. Primitive lavas tend to erupt in the deeper parts of submarine volcanoes at the depth of ~2,000 m. Deeper satellite vents are expected to erupt more primitive magmas compared to the main summit vents because primitive magmas could bypass the shallow magma chambers where crystal fractionation and magma mixing happen.

There is a small satellite cone about 11 km east of the summit of Doyo Seamount at the depth of ~3,000 m. A ridge extends on the flank of the volcano from the summit in the ENE direction to the depth of ~2,400 m. Thus, we tried to sample this satellite cone and the deeper part of the ridge. Interestingly, 13 samples out of all 21 samples, which we have recovered during this dive 6K#1519, are olivine-clinopyroxene basalts containing 20-40 % of very coarse clinopyroxene phenocrysts, which could be called ankaramite (Figure 1). Ankaramites are strongly vesiculated and their blocks have rough and rugged surface, which are different from smooth surface of basaltic pillow lavas. Some of ankaramite magmas might have had explosive eruptions at the depth of 2,000~3,000 m, which have resulted in volcaniclastic cones or brecciated lava flows.

Similar primitive and phenocryst-rich ankaramitic basalts were recovered from the old submarine knolls near Nishinoshima (Tamura et al., 2019). We suggested that lithospheric mantle was thicker before the development of Nishinoshima volcano (Figure 2). Primary basaltic magmas could have been generated at depth beneath the thicker lithospheric lid, and these magmas might have interacted with the lithospheric uppermost mantle during their ascent and have resulted in the unique ankaramite magmas (Figure 1). The temperature of the upper part of the mantle wedge increases with frequent passage of magmas through it, and continuous subduction beneath it will drench the whole mantle wedge, thus, the thickness of the lithosphere will decrease and approach the thickness of the curst in mature arcs. Doyo Seamount could represent the early stage of Nishinoshima volcano, and thus, ankaramite magma is deemed to be a

©2019. Japan Geoscience Union. All Right Reserved.

precursor of andesitic magmas.

References

Tamura et al. (2016). Advent of continents: A new hypothesis. *Scientific Reports* **6,** 33517.
Tamura et al. (2019). Nishinoshima volcano in the Ogasawara Arc: New continent from the ocean? *Island Arc* **28,** e12285.

Keywords: ankaramite, andesite, continent, oceanic arc, lithosphere, mantle wedge

©2019. Japan Geoscience Union. All Right Reserved.

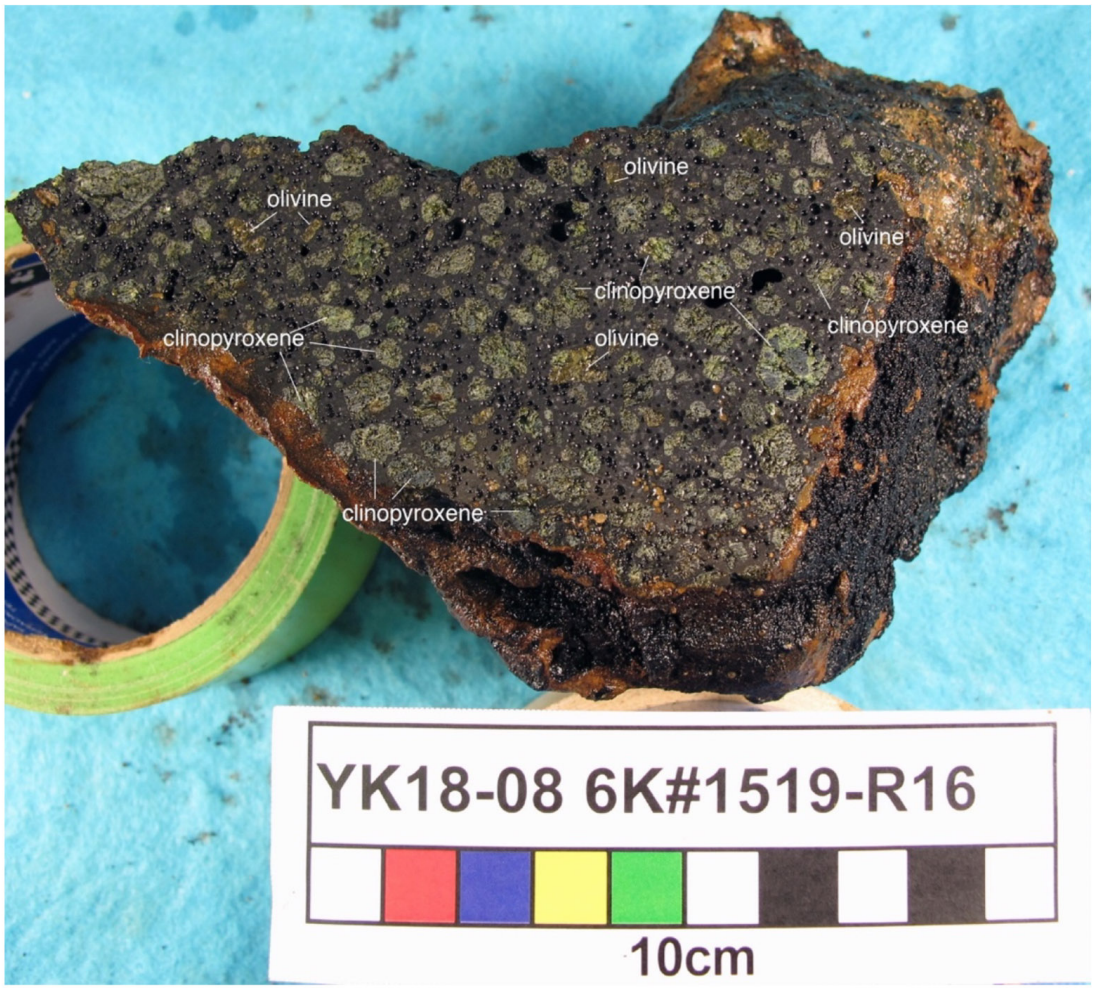

Figure 1. Ankaramite recovered from Doyo Seamount.

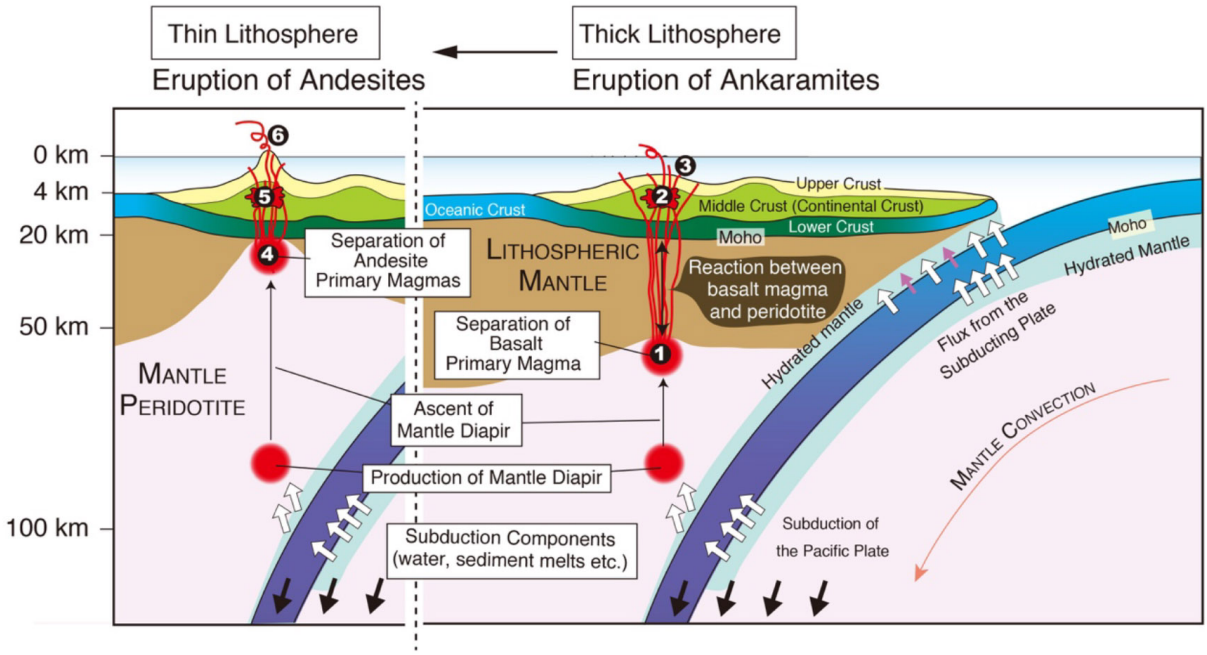

Figure 2. Schematic diagrams showing the genesis of andesite and ankaramite magmas in the Ogasawara arc.

©2019. Japan Geoscience Union. All Right Reserved.

Different Moho reflections adjacent to Minami-Tori Shima and their petrologic origins

*Yoshihiko Tamura[1], Kentaro Kaneda[2], Gou Fujie[1], Akane Ohira[1], Eiichi TAKAZAWA[3], Georges Ceuleneer[4], Katsuyoshi Michibayashi[5], Tomoki Sato[1], Shuichi Kodaira[1], Seiichi Miura[1]

1. Japan Agency for Maine-Earth Science and Technology, 2. Japan Coast Guard, 3. Niigata University, 4. Universite de Toulouse, 5. Nagoya University

It is the common knowledge that Moho is the boundary between the crust and mantle, which was discovered by and named after Croatian seismologist Mohorovičić. We have shown that Moho is not the crust-mantle boundary and presented a new hypothesis about the origin of Moho based on seismological and petrological observations (Tamura et al., EGU2018-11069-2; JpGU2018 SMP36-05; AGCC2018 abstract volume590; Tamura et al., in preparation). Direct drilling and sampling of Moho could be the best scenario to examine the hypothesis. However, IODP drillings of basaltic crust could estimate the petrologic origins of the crust-mantle boundary far below the seafloor, which could be useful to examine the hypothesis of formation of Moho.

Kaneda et al. (2010) conducted seismic surveys across the Marcus-Wake seamount chain near Minami-Tori Shima, which is the Japanese easternmost and one and only island on the Pacific Plate. They found contrasting seafloor in the north and south of the seamount chain, which were referred to the northern and southern basins (Figure 1). Average water depths in the northern and southern basins are about 5900 m and 5700 m, respectively. Magnetic anomalies suggest Jurassic ages of M32 (159 Ma) and M42 (167 Ma) for the northern and southern basins, respectively. The southern basin has the clear Moho reflections, which are characteristically sharp, single, flat, and continuous, and of large amplitude, but in the northern basin, Moho reflections are extremely weak or even absent. Interestingly, the crust of the southern basin has a constant thickness of 7.5-8.0 km, but the crust of the northern basin shows a constant thickness of 6 km, 1.5-2 km thinner than that of the northern basin.The correlation between Moho reflections and crustal thicknesses have been generally observed in other seismic profiles (e.g. Ohira et al., 2017).

The boundary between mantle peridotite and layered gabbro from the lower oceanic crust in the Oman ophiolite consists of a dunitic transition zone (DTZ), mostly made of olivine + scattered Cr-spinel. The thickness of DTZ ranges from a few meters to a few hundred meters. When mantle melts under hydrous conditions, the liquidus field of forsterite expands relative to that of enstatite and enstatite melts incongruently to produce dunites and andesitic melts.

We present here a new hypothesis that (1) accidental influx of seawater at the mid-ocean ridges results in hydrous melting of mantle peridotite just beneath the crust and produces thick dunite at the crust-mantle boundaries, (2) the thick dunite represents reflective Moho, and (3) this additional hydrous melting of shallowest mantle increases the thickness of oceanic crust.

Although the andesitic melts, which are the outgrowth of dunites, would be mixed with dominant basaltic melts extracted from the deeper parts of melting column of MORB, there must be systematic and significant differences between crustal materials with Moho and those without Moho. Comparative drillings of oceanic crust in the northern and southern basins for future IODP expeditions will reveal the differences of basalts and examine the models for Moho.

©2019. Japan Geoscience Union. All Right Reserved.

Keywords: Moho, Minami-Tori Shima, dunite, mantle, crust, basalt

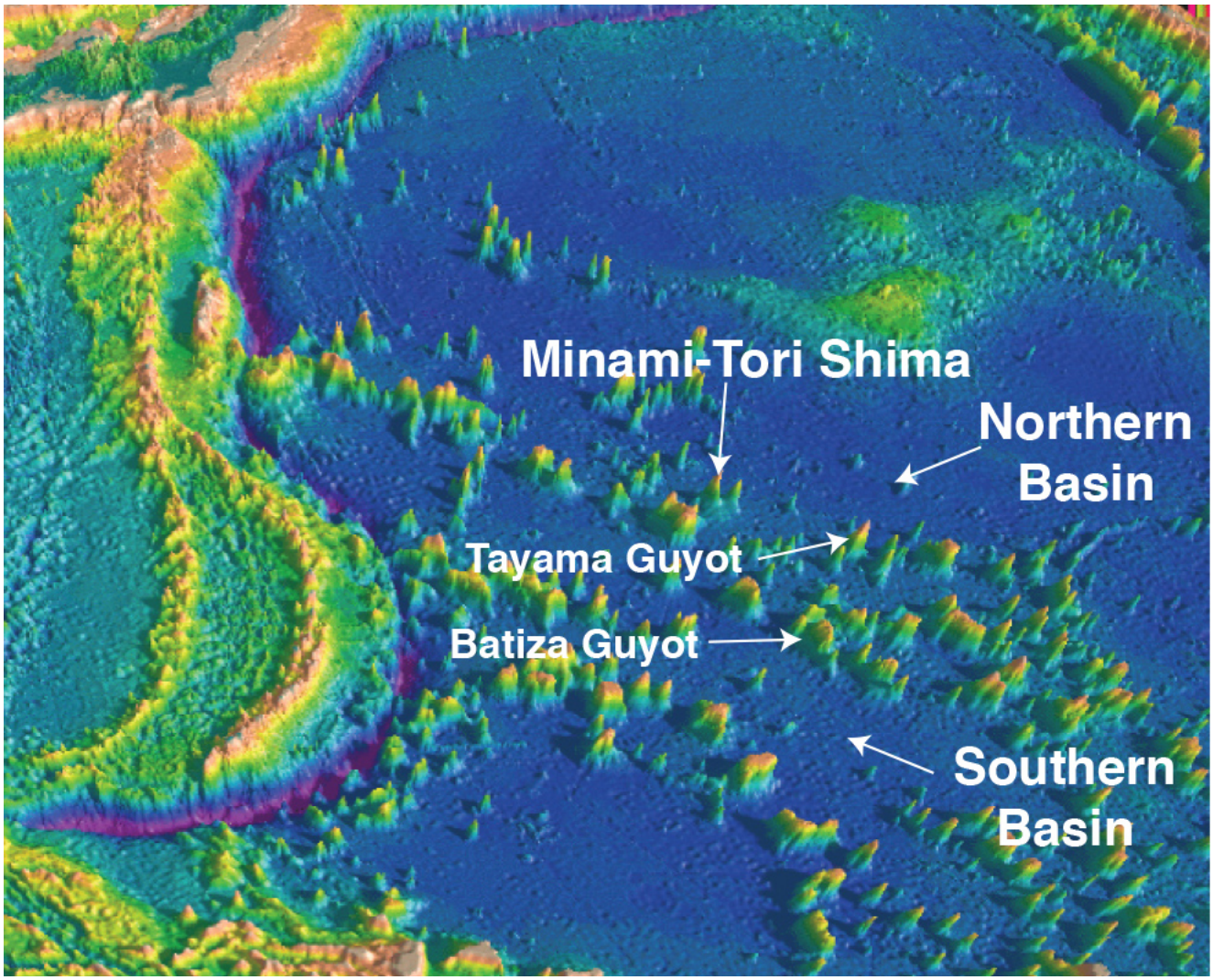

©2019. Japan Geoscience Union. All Right Reserved.

Melt-rock interaction in plagioclase peridotites from the southern Palawan Ophiolite, Philippines

*FLORENCE ANNETTE CRUSPERO LABIS[1], BETCHAIDA D PAYOT[1], GABRIEL THEOPHILUS V VALERA[1], JULIUS A PASCO[1], JESLEY MEI A DYCOCO[1]

1. UNIVERSITY OF THE PHILIPPINES

This work presents new petrographic and geochemical data on the plagioclase peridotites and the spinel harzburgites of the mantle section of the southern Palawan Ophiolite. The plagioclase peridotites show peculiar textures evident of melt-rock interaction as indicated by: (1) interstitial clinopyroxene and subhedral orthopyroxene around plagioclase, and (2) plagioclase blebs within the peridotite matrix. The spinel harzburgites display protogranular to porphyroclastic textures and dominantly composed of olivine, orthopyroxene, and small amounts of clinopyroxene and spinel. These minerals show kink banding and bent lamellae which are indicative of plastic deformation. Major element geochemistry of the spinel harzburgites reveals high Cr# (0.53-0.78) and Mg# (0.40-0.51) in spinel, and high NiO wt.% (0.40-0.43) and Fo contents (89.9-90.5) in olivine reflecting residual origin. Their geochemical composition is comparable to the residual peridotites in arc settings. Consequently, the plagioclase peridotites have lower Mg# (0.23-0.34) and relatively high Cr# (0.60-0.61) in spinel, as well as lower Fo (83.3-85.9) contents in olivine. Spinel and clinopyroxene in the plagioclase peridotites have higher TiO_2 contents compared with those of the spinel harzburgites. Clinopyroxene in plagioclase peridotites are marked by strong depletion in LREE and flat MREE to HREE with significant negative Eu and Sr anomalies. In contrast, the spinel harzburgites have lower REE abundances which suggest higher degrees of partial melting. We propose that the spinel harzburgites of the southern Palawan Ophiolite are residual peridotites formed by high degrees of partial melting above a subduction zone and were subsequently infiltrated by melts leading to the formation of the plagioclase peridotites.

Keywords: Palawan Ophiolite, plagioclase peridotites, melt-rock interaction

©2019. Japan Geoscience Union. All Right Reserved.

Intra-oceanic arc magma genesis: a case study from Havre volcano, Kermadec arc

*Chris Conway[1], Kenichiro Tani[2]

1. Geological Survey of Japan, 2. National Museum of Nature and Science

The Kermadec intra-oceanic arc comprises 33 active arc front volcanoes along its ~1200 km length, which represent key targets for studying the formation of Earth’ s crust. The discovery of numerous submarine caldera volcanoes and dacitic to rhyolitic pumice deposits from this setting has prompted new models for the genesis of intra-oceanic silicic arc magmas. A detailed investigation of the 2012 eruption of rhyolite pumice and lava at Havre volcano has provided a valuable opportunity to test these models. Moreover, the retrieval of older volcanic deposits from the edifice has given critical context for studying magma genesis throughout the lifetime of the volcano. Here we present whole-rock, mineral and glass major and trace element data for volcanic rock samples collected from Havre volcano. The samples, which span a compositional range from basalt to rhyolite, display several key features that support arguments against the derivation of silicic magmas primarily through crustal anatexis: (1) the range of sample compositions fit along coherent crystal fractionation trends; (2) low-MgO aphyric andesites fill the gap within the general bimodality of eruptive products from the Kermadec arc; and (3) there is a scarcity of tonalitic xenoliths. These features favour crystal fractionation over crustal anatexis as the dominant process for generating the compositional diversity seen at Havre volcano.

Keywords: rhyolite, magma genesis, Havre volcano

©2019. Japan Geoscience Union. All Right Reserved.

[E] Poster | S (Solid Earth Sciences)：S-MP Mineralogy & Petrology

Tue. May 28, 2019 5:15 PM - 6:30 PM JST | Tue. May 28, 2019 8:15 AM - 9:30 AM UTC | Poster Hall International Exhibition Hall8, Makuhari Messe_33

[S-MP30] Crust-Mantle Connections

convener:Yoshihiko Tamura(Research Institute for Marine Geodynamics, Japan Agency for Maine-Earth Science and Technology), Osamu Ishizuka(Geological Survey of Japan, AIST), Chris Conway(Geological Survey of Japan)

A paradigm of the solid Earth geochemical cycles is that the Earth's crust forms by melting of the Earth's upper peridotitic mantle. How divers is the spectrum of primary melts and which factors may contribute to its variations? What is the influence of crustal processing vs. primary magma diversity in creating the diversity of the Earth's crust? The session seeks to explore the crust-mantle connections at divergent and convergent plate boundaries, and oceanic island settings based on volcanology, petrology, geochemistry, geophysics, geochronology, and geodynamics studies.

[SMP30-P01] Secular evolution of proto-Izu-Bonin-Mariana arc volcanism: Constraints from statistical analysis of melt inclusion compositions

*Morihisa Hamada[1], Hikaru Iwamori[1,2], Philipp A. Brandl[3], Takayuki Ushikubo[4], Kenji Shimizu[4], Motoo Ito[4], He Li[5], Ivan P. Savov[6] (1.Department of Solid Earth Geochemistry, Japan Agency for Marine-Earth Science and Technology, 2.Earthquake Research Institute, University of Tokyo, 3.GEOMAR Helmholtz Centre for Ocean Research Kiel, 4.Kochi Institute for Core Sample Research, Japan Agency for Marine-Earth Science and Technology, 5.Institute of Oceanology, Chinese Academy of Sciences, 6.School of Earth and Environment, University of Leeds)

[SMP30-P02] The Jurassic magmatism of protoliths of Mikabu greenstones in SW Japan: zircon U-Pb dating and trace element analysis

*Hikaru Sawada[1], Yukio Isozaki[1], Shogo Aoki[3], Shuhei Sakata[2], Ryo Hasegawa[1], Yasuo Nakamura[1] (1.Department of General Systems Studies, the University of Tokyo, 2.Department of Chemistry, Gakushuin Universtiy, 3.Department of Applied Science, Okayama University of Science)

[SMP30-P03] Origin of variable CaO/Al_2O_3 in olivine-hosted melt inclusions from Kibblewhite Volcano, Kermadec Arc

*Yasuhiro Hirai[1], Yoshihiko Tamura[2], Kaj Hoernle[3], Christian Timm[4], Folkmar Hauff[3], Reinhard Werner[3], Takeshi Hanyu[2], Bogdan Vaglarov[2], Qing Chang[2], Takashi Miyazaki[2], Jun-Ichi Kimura[2] (1.Graduate School of Natural Science and Technology, Kanazawa University, Japan, 2.Japan Agency for Marine-Earth Science and Technology (JAMSTEC), Yokosuka, Kanagawa, Japan, 3.GEOMAR Helmholtz Centre for Ocean Research, Kiel, Germany, 4.GNS Science, Lower Hutt, New Zealand)

[SMP30-P04] Ankaramite from Doyo seamount in the Izu-Ogasawara arc: A precursor of continents?

*Yoshihiko Tamura[1], Tomoki Sato[1], Osamu Ishizuka[1,2], Takashi Miyazaki[1], Yasuhiro Hirai[1,3], Mami Takehara[4], Eri Sakamoto[5] (1.JAMSTEC, 2.AIST, 3.Kanazawa Univ., 4.NIPR, 5.NME)

[SMP30-P05] Different Moho reflections adjacent to Minami-Tori Shima and their petrologic origins

*Yoshihiko Tamura[1], Kentaro Kaneda[2], Gou Fujie[1], Akane Ohira[1], Eiichi TAKAZAWA[3], Georges Ceuleneer[4], Katsuyoshi Michibayashi[5], Tomoki Sato[1], Shuichi Kodaira[1], Seiichi Miura[1] (1.Japan Agency for Maine-Earth Science and Technology, 2.Japan Coast Guard, 3.Niigata University, 4.Universite de Toulouse, 5.Nagoya University)

[SMP30-P06] Melt-rock interaction in plagioclase peridotites from the southern Palawan Ophiolite, Philippines

*FLORENCE ANNETTE CRUSPERO LABIS[1], BETCHAIDA D PAYOT[1], GABRIEL THEOPHILUS V VALERA[1], JULIUS A PASCO[1], JESLEY MEI A DYCOCO[1] (1.UNIVERSITY OF THE PHILIPPINES)

[SMP30-P07] Intra-oceanic arc magma genesis: a case study from Havre volcano, Kermadec arc

*Chris Conway[1], Kenichiro Tani[2] (1.Geological Survey of Japan, 2.National Museum of Nature and Science)

Secular evolution of proto-Izu-Bonin-Mariana arc volcanism: Constraints from statistical analysis of melt inclusion compositions

*Morihisa Hamada[1], Hikaru Iwamori[1,2], Philipp A. Brandl[3], Takayuki Ushikubo[4], Kenji Shimizu[4], Motoo Ito[4], He Li[5], Ivan P. Savov[6]

1. Department of Solid Earth Geochemistry, Japan Agency for Marine-Earth Science and Technology, 2. Earthquake Research Institute, University of Tokyo, 3. GEOMAR Helmholtz Centre for Ocean Research Kiel, 4. Kochi Institute for Core Sample Research, Japan Agency for Marine-Earth Science and Technology, 5. Institute of Oceanology, Chinese Academy of Sciences, 6. School of Earth and Environment, University of Leeds

International Ocean Discovery Program (IODP) Expedition 351 'Izu–Bonin–Mariana (IBM) Arc Origins' drilled Site U1438, situated in the north-western margin of the Philippine Sea, into volcaniclastic sediments of the proto-IBM arc. Brandl *et al.* (2017, *Earth and Planetary Science Letters*) have analysed the major, trace and volatile elements of 304 melt inclusions hosted in fresh silicate minerals to unveil the magmatic evolution of the proto-IBM arc between 30 and 40 Ma, when the arc volcanism matured following subduction initiation at 52 Ma. Brandl *et al.* (2017) concluded that: (1) volcanism of the proto-IBM arc shifted from calc-alkaline affinity to tholeiitic affinity over time; and (2) such compositional shift is linked to both the volcanic productivity and the maturation of an evolving island arc. To better integrate the composition of melt inclusions with the magmatic evolution of the proto-IBM arc, this study extends the dataset of Brandl *et al.* (2017) by: (1) additional analysis of volatiles (H_2O, S, F and Cl) and P_2O_5 for 47 carefully selected melt inclusions by Secondary Ion Mass Spectrometry (SIMS); and (2) statistical analysis on the composition of 237 representative melt inclusions covering the full time range (30–40 Ma) of the dataset. Based on statistical analysis of the melt inclusion compositions and by considering trace element compositions and volatile concentrations, we can confidently distinguish five main clusters of melt inclusion compositions which can be further separated into a total of nine sub-clusters. Among the nine sub-clusters, we identified three major magma types: (1) medium-K enriched magmas which form a tholeiitic trend (30–38 Ma); (2) less-depleted medium-K melts which form a calc-alkaline trend (35–39 Ma); and (3) low-K depleted magmas which form a calc-alkaline trend (35–40 Ma). We demonstrate that: (1) volcanism of calc-alkaline depleted magmas lasted until 35 Ma; (2) the volcanism of calc-alkaline depleted magmas and that of more enriched normal arc magmas (tholeiitic and calc-alkaline affinities) overlap between 35 and 38–39 Ma and; (iii) the volcanism of normal arc magmas became predominant thereafter at the proto-IBM arc. Such identification of three major magma types is distinct from that of Brandl *et al.* (2017), in which less-depleted medium-K calc-alkaline magmas amd depleted low-K calc-alkaline gammas were not distinguished. We infer that depleted source mantle had been replaced by enriched mantle due to mantle convection beneath the proto-IBM arc from >40 Ma to 35 Ma. Statistical analysis is a useful tool to partition a mixture of multivariable dataset, such as datasets of melt inclusion compositions, into several distinct groups and potentially reconstruct their geological evolution.

Keywords: Amami Sankaku Basin, International Ocean Discovery Ptrogram, Izu-Bonin-Mariana arc, Melt inclusion, Statistical analysis, Volatiles

©2019. Japan Geoscience Union. All Right Reserved.

The Jurassic magmatism of protoliths of Mikabu greenstones in SW Japan: zircon U-Pb dating and trace element analysis

*Hikaru Sawada[1], Yukio Isozaki[1], Shogo Aoki[3], Shuhei Sakata[2], Ryo Hasegawa[1], Yasuo Nakamura[1]

1. Department of General Systems Studies, the University of Tokyo, 2. Department of Chemistry, Gakushuin Universtiy, 3. Department of Applied Science, Okayama University of Science

The Mikabu greenstones, incorporated with the Cretaceous high P/T-type Sanbagawa metamorphic belt in SW Japan, are accreted fragments of an oceanic plateau. We identified a Late Jurassic igneous age for the protoliths of the Mikabu greenstones in the eastern Kii Peninsula, by measuring U-Pb age and trace element composition (REE, Y, Sc, Nb, Ta, Hf, U, Th) of zircon grains with an Agilent 8800 single-collector triple quadrupole ICPMS coupled to a NWR-213 laser-ablation system. The U-Pb ages have a weighted average of 154.6 ±1.6 Ma (the Kimmeridgian, Late Jurassic) with an overlap within 2-sigma error. The igneous age is slightly younger than the previously reported radiolarian ages (Middle Jurassic) of deep-sea pelagic chert associated with the Mikabu greenstones. The age difference between them suggests that mafic magmas intruded pelagic deep-sea sediments on the pre-existing oceanic lithosphere. Trace element composition further indicates that the dated zircon grains are more similar to those in oceanic crusts than in granitic continental crusts, and the host mafic magma of the zircon grains was derived from depleted mantle like the mid-oceanic ridge-type source, rather than fertile mantle sources like Hawaii and Iceland. As rocks from the Shatsky Rise in the modern NW Pacific Ocean have similar age and compositional characteristics, this study concluded that the protoliths of the Mikabu greenstones had formed a part of an oceanic plateau, which was generated by the Late Jurassic intra-oceanic plate mafic magmatism in the ancient Pacific Ocean.

Keywords: Mikabu greenstones, zircon, Jurassic, oceanic plateau, U-Pb age, trace element

©2019. Japan Geoscience Union. All Right Reserved.

Origin of variable CaO/Al_2O_3 in olivine-hosted melt inclusions from Kibblewhite Volcano, Kermadec Arc

*Yasuhiro Hirai[1], Yoshihiko Tamura[2], Kaj Hoernle[3], Christian Timm[4], Folkmar Hauff[3], Reinhard Werner[3], Takeshi Hanyu[2], Bogdan Vaglarov[2], Qing Chang[2], Takashi Miyazaki[2], Jun-Ichi Kimura[2]

1. Graduate School of Natural Science and Technology, Kanazawa University, Japan, 2. Japan Agency for Marine-Earth Science and Technology (JAMSTEC), Yokosuka, Kanagawa, Japan, 3. GEOMAR Helmholtz Centre for Ocean Research, Kiel, Germany, 4. GNS Science, Lower Hutt, New Zealand

During R/V SONNE expedition SO-255 mafic basaltic to magnesian andesitic lavas containing melt inclusion hosting forsteritic olivines ($Fo_{90.3–92.4}$) were recovered from Kibblewhite Volcano, southern Kermadec Arc. The re-homogenized melt inclusions have compositions similar to primitive basalt (49.6–52.0 wt.% SiO_2; 12.7–15.9 wt.% MgO). Their CaO/Al_2O_3 values, however, range from 0.9 to 1.6, which cannot be explained by melting of lherzolite. Moreover, CaO/Al_2O_3 values in the melt inclusions correlate negatively with Ni contents of their host olivines suggesting that the high CaO/Al_2O_3 values result from interaction between mafic melts and subarc lithospheric mantle. Prior to the interaction the mafic magma must have had high Ni contents and low CaO/Al_2O_3 values, thus they crystallized high Ni olivines trapping low CaO/Al_2O_3 melt inclusions. During the interaction the olivines crystallized from the mafic magmas and its latent heat assimilated pyroxenes from the surrounding lithospheric mantle. This assimilation of pyroxenes allowed the Ni content of the melt to decrease and CaO/Al_2O_3 to increase while buffering the the Mg-number of the mafic magmas during the ascent. Thus, magmas during and after the interaction could crystallize low Ni olivines bearing high CaO/Al_2O_3 melt inclusions.

Keywords: Subduction zone, Kermadec Arc, Kibblewhite Volcano, SO-255, Olivine-hosted melt inclusion

©2019. Japan Geoscience Union. All Right Reserved.

Ankaramite from Doyo seamount in the Izu-Ogasawara arc: A precursor of continents?

*Yoshihiko Tamura[1], Tomoki Sato[1], Osamu Ishizuka[1,2], Takashi Miyazaki[1], Yasuhiro Hirai[1,3], Mami Takehara[4], Eri Sakamoto[5]

1. JAMSTEC, 2. AIST, 3. Kanazawa Univ., 4. NIPR, 5. NME

Izu-Ogasawara-Mariana (IOM) system of arcs (also known as the Izu-Bonin-Mariana arc system) is a typical oceanic arc produced by subduction of the Pacific Plate beneath the Philippine Sea Plate. Volcanoes along the southern segment of the Izu-Ogasawara arc are underlain by thin crust (10-20 km). According to the hypothesis presented by Tamura *et al.* (2016), rising mantle diapirs stall near the base of the oceanic crust at depths controlled by the thickness of the overlying crust. Where the crust is thin, melting occurs at relatively low pressures in the mantle wedge producing andesitic magmas. Andesites erupted from Nishinoshima that were produced in the recent history of the volcano have been generated by olivine fractionation of primary andesitic magmas (Tamura *et al.*, 2019).

To further examine this hypothesis, we have dived Doyo Seamount by using manned submersible SHINKAI 6500 to sample primitive magmas from the volcano, which is located about 50 km north of Nishinoshima and is underlain by thinner curst (15 km) compared to Nishinoshima. Doyo Seamount is located approximately 900 km south of Tokyo at 27˚41’ N, 140˚48’ E in the Ogasawara Arc. The seamount attained an elevation of ~400 m below sea level (mbsl) and its submarine flanks extend to the depth of 3,200 mbsl. The basal dimeter of the volcano is about 30 km. The deeper parts of this large submarine edifice have yet to be explored. Primitive lavas tend to erupt in the deeper parts of submarine volcanoes at the depth of ~2,000 m. Deeper satellite vents are expected to erupt more primitive magmas compared to the main summit vents because primitive magmas could bypass the shallow magma chambers where crystal fractionation and magma mixing happen.

There is a small satellite cone about 11 km east of the summit of Doyo Seamount at the depth of ~3,000 m. A ridge extends on the flank of the volcano from the summit in the ENE direction to the depth of ~2,400 m. Thus, we tried to sample this satellite cone and the deeper part of the ridge. Interestingly, 13 samples out of all 21 samples, which we have recovered during this dive 6K#1519, are olivine-clinopyroxene basalts containing 20-40 % of very coarse clinopyroxene phenocrysts, which could be called ankaramite (Figure 1). Ankaramites are strongly vesiculated and their blocks have rough and rugged surface, which are different from smooth surface of basaltic pillow lavas. Some of ankaramite magmas might have had explosive eruptions at the depth of 2,000~3,000 m, which have resulted in volcaniclastic cones or brecciated lava flows.

Similar primitive and phenocryst-rich ankaramitic basalts were recovered from the old submarine knolls near Nishinoshima (Tamura et al., 2019). We suggested that lithospheric mantle was thicker before the development of Nishinoshima volcano (Figure 2). Primary basaltic magmas could have been generated at depth beneath the thicker lithospheric lid, and these magmas might have interacted with the lithospheric uppermost mantle during their ascent and have resulted in the unique ankaramite magmas (Figure 1). The temperature of the upper part of the mantle wedge increases with frequent passage of magmas through it, and continuous subduction beneath it will drench the whole mantle wedge, thus, the thickness of the lithosphere will decrease and approach the thickness of the curst in mature arcs. Doyo Seamount could represent the early stage of Nishinoshima volcano, and thus, ankaramite magma is deemed to be a

©2019. Japan Geoscience Union. All Right Reserved.

precursor of andesitic magmas.

References

Tamura et al. (2016). Advent of continents: A new hypothesis. *Scientific Reports* **6,** 33517.
Tamura et al. (2019). Nishinoshima volcano in the Ogasawara Arc: New continent from the ocean? *Island Arc* **28,** e12285.

Keywords: ankaramite, andesite, continent, oceanic arc, lithosphere, mantle wedge

©2019. Japan Geoscience Union. All Right Reserved.

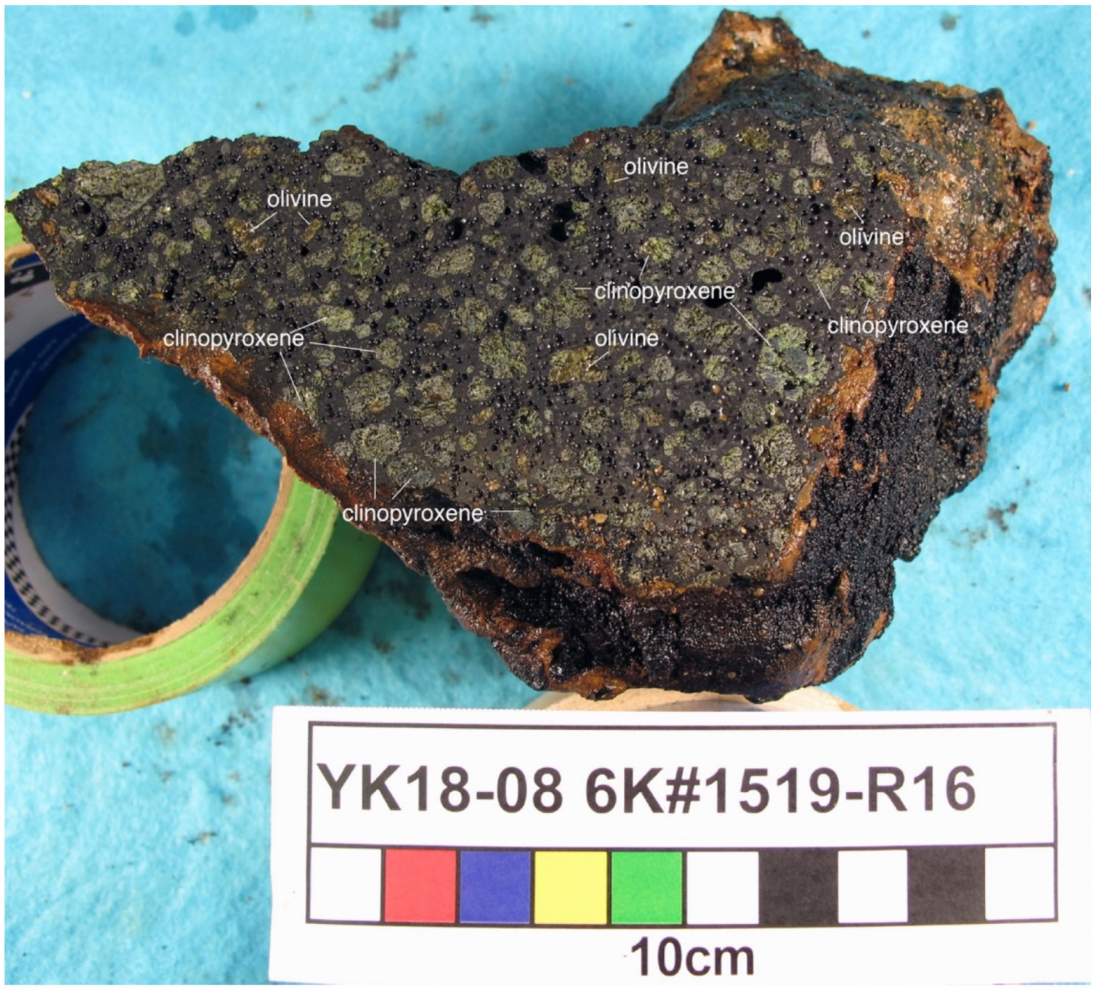

Figure 1. Ankaramite recovered from Doyo Seamount.

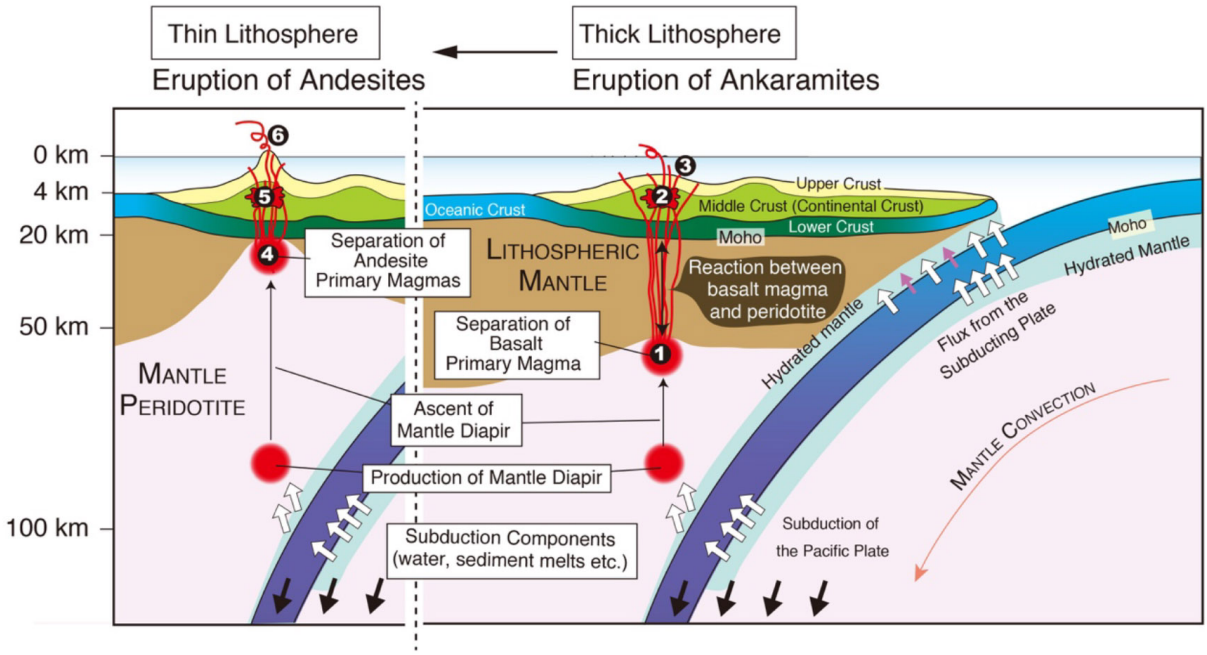

Figure 2. Schematic diagrams showing the genesis of andesite and ankaramite magmas in the Ogasawara arc.

©2019. Japan Geoscience Union. All Right Reserved.

Different Moho reflections adjacent to Minami-Tori Shima and their petrologic origins

*Yoshihiko Tamura[1], Kentaro Kaneda[2], Gou Fujie[1], Akane Ohira[1], Eiichi TAKAZAWA[3], Georges Ceuleneer[4], Katsuyoshi Michibayashi[5], Tomoki Sato[1], Shuichi Kodaira[1], Seiichi Miura[1]

1. Japan Agency for Maine-Earth Science and Technology, 2. Japan Coast Guard, 3. Niigata University, 4. Universite de Toulouse, 5. Nagoya University

It is the common knowledge that Moho is the boundary between the crust and mantle, which was discovered by and named after Croatian seismologist Mohorovičić. We have shown that Moho is not the crust-mantle boundary and presented a new hypothesis about the origin of Moho based on seismological and petrological observations (Tamura et al., EGU2018-11069-2; JpGU2018 SMP36-05; AGCC2018 abstract volume590; Tamura et al., in preparation). Direct drilling and sampling of Moho could be the best scenario to examine the hypothesis. However, IODP drillings of basaltic crust could estimate the petrologic origins of the crust-mantle boundary far below the seafloor, which could be useful to examine the hypothesis of formation of Moho.

Kaneda et al. (2010) conducted seismic surveys across the Marcus-Wake seamount chain near Minami-Tori Shima, which is the Japanese easternmost and one and only island on the Pacific Plate. They found contrasting seafloor in the north and south of the seamount chain, which were referred to the northern and southern basins (Figure 1). Average water depths in the northern and southern basins are about 5900 m and 5700 m, respectively. Magnetic anomalies suggest Jurassic ages of M32 (159 Ma) and M42 (167 Ma) for the northern and southern basins, respectively. The southern basin has the clear Moho reflections, which are characteristically sharp, single, flat, and continuous, and of large amplitude, but in the northern basin, Moho reflections are extremely weak or even absent. Interestingly, the crust of the southern basin has a constant thickness of 7.5-8.0 km, but the crust of the northern basin shows a constant thickness of 6 km, 1.5-2 km thinner than that of the northern basin.The correlation between Moho reflections and crustal thicknesses have been generally observed in other seismic profiles (e.g. Ohira et al., 2017).

The boundary between mantle peridotite and layered gabbro from the lower oceanic crust in the Oman ophiolite consists of a dunitic transition zone (DTZ), mostly made of olivine + scattered Cr-spinel. The thickness of DTZ ranges from a few meters to a few hundred meters. When mantle melts under hydrous conditions, the liquidus field of forsterite expands relative to that of enstatite and enstatite melts incongruently to produce dunites and andesitic melts.

We present here a new hypothesis that (1) accidental influx of seawater at the mid-ocean ridges results in hydrous melting of mantle peridotite just beneath the crust and produces thick dunite at the crust-mantle boundaries, (2) the thick dunite represents reflective Moho, and (3) this additional hydrous melting of shallowest mantle increases the thickness of oceanic crust.

Although the andesitic melts, which are the outgrowth of dunites, would be mixed with dominant basaltic melts extracted from the deeper parts of melting column of MORB, there must be systematic and significant differences between crustal materials with Moho and those without Moho. Comparative drillings of oceanic crust in the northern and southern basins for future IODP expeditions will reveal the differences of basalts and examine the models for Moho.

©2019. Japan Geoscience Union. All Right Reserved.

Keywords: Moho, Minami-Tori Shima, dunite, mantle, crust, basalt

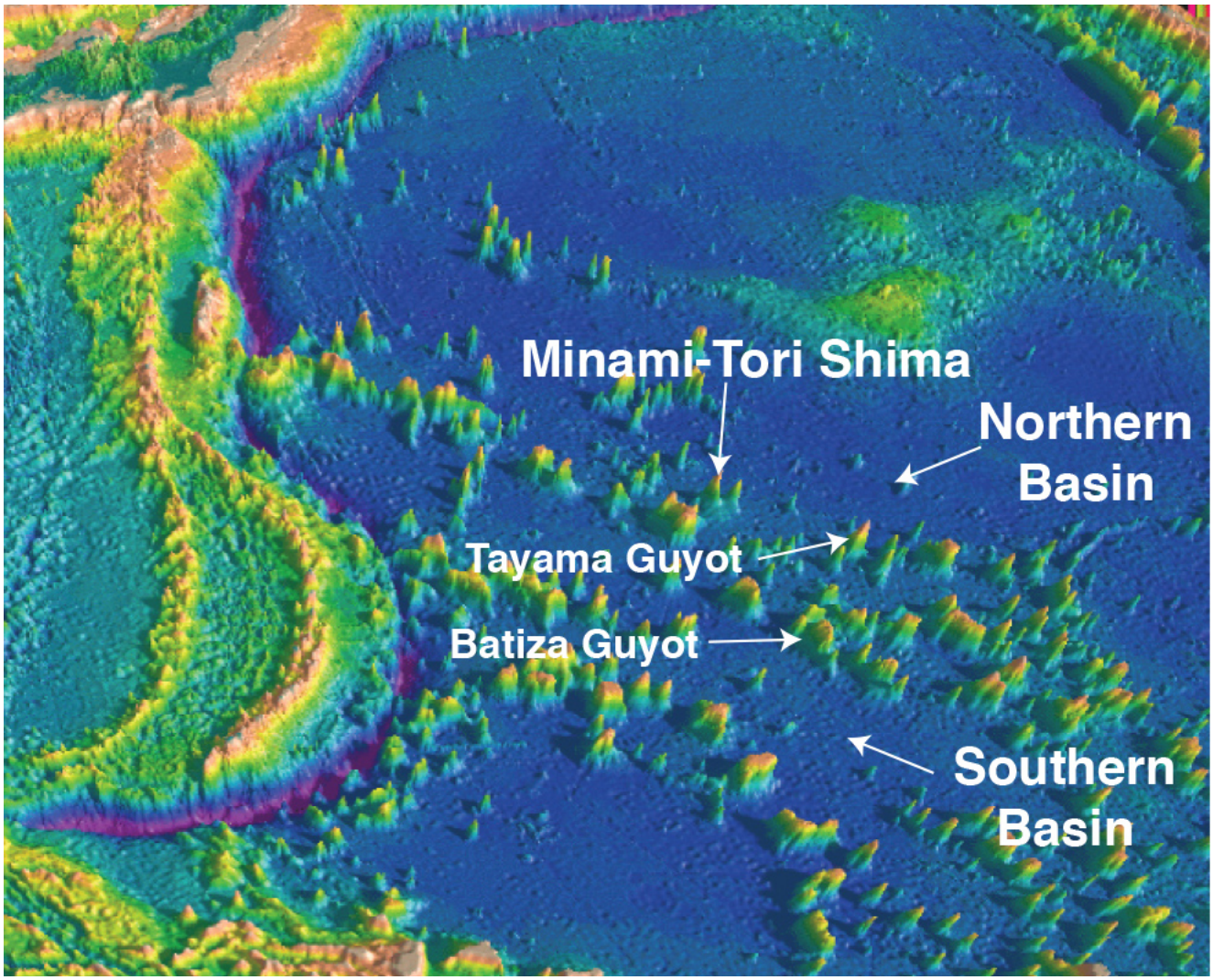

©2019. Japan Geoscience Union. All Right Reserved.

Melt-rock interaction in plagioclase peridotites from the southern Palawan Ophiolite, Philippines

*FLORENCE ANNETTE CRUSPERO LABIS[1], BETCHAIDA D PAYOT[1], GABRIEL THEOPHILUS V VALERA[1], JULIUS A PASCO[1], JESLEY MEI A DYCOCO[1]

1. UNIVERSITY OF THE PHILIPPINES

This work presents new petrographic and geochemical data on the plagioclase peridotites and the spinel harzburgites of the mantle section of the southern Palawan Ophiolite. The plagioclase peridotites show peculiar textures evident of melt-rock interaction as indicated by: (1) interstitial clinopyroxene and subhedral orthopyroxene around plagioclase, and (2) plagioclase blebs within the peridotite matrix. The spinel harzburgites display protogranular to porphyroclastic textures and dominantly composed of olivine, orthopyroxene, and small amounts of clinopyroxene and spinel. These minerals show kink banding and bent lamellae which are indicative of plastic deformation. Major element geochemistry of the spinel harzburgites reveals high Cr# (0.53-0.78) and Mg# (0.40-0.51) in spinel, and high NiO wt.% (0.40-0.43) and Fo contents (89.9-90.5) in olivine reflecting residual origin. Their geochemical composition is comparable to the residual peridotites in arc settings. Consequently, the plagioclase peridotites have lower Mg# (0.23-0.34) and relatively high Cr# (0.60-0.61) in spinel, as well as lower Fo (83.3-85.9) contents in olivine. Spinel and clinopyroxene in the plagioclase peridotites have higher TiO_2 contents compared with those of the spinel harzburgites. Clinopyroxene in plagioclase peridotites are marked by strong depletion in LREE and flat MREE to HREE with significant negative Eu and Sr anomalies. In contrast, the spinel harzburgites have lower REE abundances which suggest higher degrees of partial melting. We propose that the spinel harzburgites of the southern Palawan Ophiolite are residual peridotites formed by high degrees of partial melting above a subduction zone and were subsequently infiltrated by melts leading to the formation of the plagioclase peridotites.

Keywords: Palawan Ophiolite, plagioclase peridotites, melt-rock interaction

©2019. Japan Geoscience Union. All Right Reserved.

Intra-oceanic arc magma genesis: a case study from Havre volcano, Kermadec arc

*Chris Conway[1], Kenichiro Tani[2]

1. Geological Survey of Japan, 2. National Museum of Nature and Science

The Kermadec intra-oceanic arc comprises 33 active arc front volcanoes along its ~1200 km length, which represent key targets for studying the formation of Earth’ s crust. The discovery of numerous submarine caldera volcanoes and dacitic to rhyolitic pumice deposits from this setting has prompted new models for the genesis of intra-oceanic silicic arc magmas. A detailed investigation of the 2012 eruption of rhyolite pumice and lava at Havre volcano has provided a valuable opportunity to test these models. Moreover, the retrieval of older volcanic deposits from the edifice has given critical context for studying magma genesis throughout the lifetime of the volcano. Here we present whole-rock, mineral and glass major and trace element data for volcanic rock samples collected from Havre volcano. The samples, which span a compositional range from basalt to rhyolite, display several key features that support arguments against the derivation of silicic magmas primarily through crustal anatexis: (1) the range of sample compositions fit along coherent crystal fractionation trends; (2) low-MgO aphyric andesites fill the gap within the general bimodality of eruptive products from the Kermadec arc; and (3) there is a scarcity of tonalitic xenoliths. These features favour crystal fractionation over crustal anatexis as the dominant process for generating the compositional diversity seen at Havre volcano.

Keywords: rhyolite, magma genesis, Havre volcano

©2019. Japan Geoscience Union. All Right Reserved.

[E] Oral | S (Solid Earth Sciences)：S-MP Mineralogy & Petrology

Tue. May 28, 2019 1:45 PM - 3:15 PM JST | Tue. May 28, 2019 4:45 AM - 6:15 AM UTC | A07 TOKYO BAY MAKUHARI HALL

[S-MP30] Crust-Mantle Connections

convener:Yoshihiko Tamura(Research Institute for Marine Geodynamics, Japan Agency for Maine-Earth Science and Technology), Osamu Ishizuka(Geological Survey of Japan, AIST), Chris Conway(Geological Survey of Japan), Chairperson:Yoshihiko Tamura(JAMSTEC), Chris Conway, Tomoaki Morishita(Kanazawa University)

A paradigm of the solid Earth geochemical cycles is that the Earth's crust forms by melting of the Earth's upper peridotitic mantle. How divers is the spectrum of primary melts and which factors may contribute to its variations? What is the influence of crustal processing vs. primary magma diversity in creating the diversity of the Earth's crust? The session seeks to explore the crust-mantle connections at divergent and convergent plate boundaries, and oceanic island settings based on volcanology, petrology, geochemistry, geophysics, geochronology, and geodynamics studies.

1:45 PM - 2:00 PM JST | 4:45 AM - 5:00 AM UTC

[SMP30-01] **Noble gas and carbon isotopic compositions of petit-spot lavas from southeast of Marcus Island**

★Invited Papers

*Junji Yamamoto[1], Tetsuma Kawano[2], Naoto Takahata[3], Yuji Sano[3] (1.Hokkaido University Museum, 2.Graduate School of Science, Hokkaido University, 3.Atmosphere and Ocean Research Institute)

2:00 PM - 2:15 PM JST | 5:00 AM - 5:15 AM UTC

[SMP30-02] A series of cummingtonite-bearing rhyolites in Niijima, Izu-Bonin arc, Japan: petrological and geochemical constraints

★Invited Papers

*Yoji Arakawa[1], Daisuke Endo[2], Junya Oshika[3], Taro Shinmura[4], Kei Ikehata[1] (1.Earth Evolution Sciences, Faculty of Life and Environmental Sciences, University of Tsukuba, 2.Shimane Prefectural Sanbe Nature Museum Sahimeru (Shimane) , 3.Earth Resoueces Faculty, China University of Geosciences, 4.Faculty of Economics, Kumanoto-Gakuen University)

2:15 PM - 2:30 PM JST | 5:15 AM - 5:30 AM UTC

[SMP30-03] **Generation of primary andesitic magma in oceanic arcs: Evidence from Kibblewhite Volcano, Kermadec Arc**

★Invited Papers

*Yasuhiro Hirai[1,2], Yoshihiko Tamura[2], Kaj Hoernle[3], Christian Timm[4], Folkmar Hauff[3], Reinhard Werner[3], Bogdan Vaglarov[2], Qing Chang[2], Takashi Miyazaki[2], Jun-Ichi Kimura[2] (1.Graduate School of Natural Science and Technology, Kanazawa University, Japan, 2.Japan Agency for Marine-Earth Science and Technology (JAMSTEC), Yokosuka, Kanagawa, Japan, 3.GEOMAR Helmholtz Centre for Ocean Research, Kiel, Germany, 4.GNS Science, Lower Hutt, New Zealand)

2:30 PM - 2:45 PM JST | 5:30 AM - 5:45 AM UTC

[SMP30-04] Petrogenesis of high-Mg# andesite lavas from Ruapehu volcano, New Zealand

*Chris Conway[1], Katy Chamberlain[2], Yumiko Harigane[1], Daniel Morgan[3] (1.Geological Survey of Japan, 2.Univ. Derby, 3.Univ. Leeds)

2:45 PM - 3:00 PM JST | 5:45 AM - 6:00 AM UTC

[SMP30-05] Hydrous felsic magma generated by unmixing of slab-derived supercritical liquid: evidence from Rishiri Volcano, Kuril Arc

★Invited Papers

*Hajime Taniuchi[1], Takeshi Kuritani[2,3], Tetsuya Yokoyama[4,3], Eizo Nakamura[3], Mitsuhiro Nakagawa[2] (1.Department of Natural History Science, Graduate School of Science, Hokkaido University, 2.Department of Earth and Planetary Science, Faculty of Science, Hokkaido University, 3.Institute for

Planetary Materials, Okayama University, 4.Department of Earth and Planetary Sciences, Tokyo Institute of Technology)

3:00 PM - 3:15 PM JST | 6:00 AM - 6:15 AM UTC

[SMP30-06] Genesis of recent mafic volcanism in the Taupo Volcanic Zone, New Zealand: insights into the birth and death of cataclysmic caldera-forming systems?

*Georg F Zellmer[1], Jun-Ichi Kimura[2], Claudine Stirling[3], Gert Lube[1], Phil A Shane[4] (1.Volcanic Risk Solutions, Massey University, Tennent Drive, Palmerston North 4410, New Zealand, 2.Department of Solid Earth Geochemistry, Japan Agency for Marine-Earth Science and Technology [JAMSTEC], Natsushima-cho 2-15, Yokosuka 237-0061, Japan, 3.Department of Chemistry, University of Otago, Dunedin 9054, New Zealand, 4.School of Environment, University of Auckland, Auckland 1142, New Zealand)

Noble gas and carbon isotopic compositions of petit-spot lavas from southeast of Marcus Island

*Junji Yamamoto[1], Tetsuma Kawano[2], Naoto Takahata[3], Yuji Sano[3]

1. Hokkaido University Museum, 2. Graduate School of Science, Hokkaido University, 3. Atmosphere and Ocean Research Institute

We measured noble gas isotopic compositions of quenched lavas sampled from seamounts, so-called petit-spot volcanoes, on the 160-million-year-old northwestern Pacific Plate. The samples $^{3}He/^{4}He$ and $^{40}Ar/^{36}Ar$ ratios were, respectively, 2.5–8.3 Ra and up to 1735, where Ra stands for atmospheric $^{3}He/^{4}He$, which are analogous to or lower than those of MORB. Considering narrow sampling regions, a secondary effect might be responsible for variation of the data.
During ascent and subsequent cooling of magma in the oceanic lithosphere, chemical components in the magma will be assimilated with those in the lithosphere. Correlation between $CO_2/^{3}He$ ratios and carbon isotopic ratios suggests that carbon was affected by the incorporation of seafloor carbonate. The same would be true of noble gases. The mixing of noble gases among a mantle source, an atmospheric component dissolved in seawater and a radiogenic component can explain the data distribution. There is no $^{3}He/^{4}He$ ratio exceeding MORB-like value. The mantle source of the petit-spot magma was likely to have had a MORB-like $^{3}He/^{4}He$ ratio originally. The eruption of petit-spot magma shows a close relation with the bending of subducting oceanic plates. The MORB-like $^{3}He/^{4}He$ ratio supports the hypothesis that the petit-spot magma is derived from the lithosphere–asthenosphere boundary.

Keywords: noble gases, carbon isotope, petit-spot, lithosphere-asthenosphere boundary, crustal assimilation

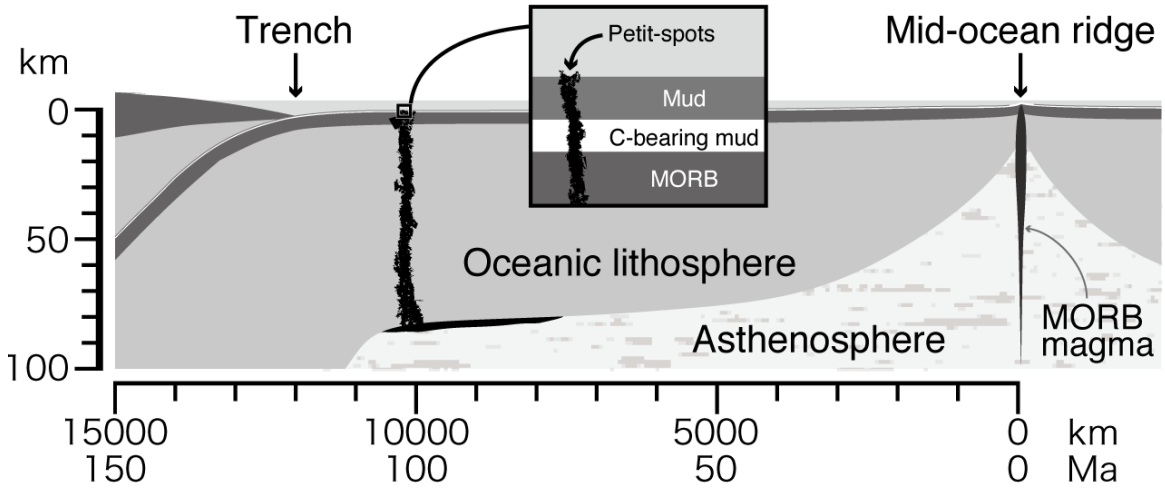

©2019. Japan Geoscience Union. All Right Reserved.

A series of cummingtonite-bearing rhyolites in Niijima, Izu-Bonin arc, Japan: petrological and geochemical constraints

*Yoji Arakawa[1], Daisuke Endo[2], Junya Oshika[3], Taro Shinmura[4], Kei Ikehata[1]

1. Earth Evolution Sciences, Faculty of Life and Environmental Sciences, University of Tsukuba, 2. Shimane Prefectural Sanbe Nature Museum Sahimeru (Shimane) , 3. Earth Resoueces Faculty, China University of Geosciences, 4. Faculty of Economics, Kumanoto-Gakuen University

Niijima volcano in the northern part of the Quaternary Izu–Bonin volcanic arc, Japan, consists predominantly of rhyolitic volcanic units and minor basaltic and andesitic units. Most of the rhyolites are characterized by a phenocryst assemblage of orthopyroxene (Opx), cummingtonite (Cum), biotite (Bt), and hornblende, and a lack of clinopyroxene (Cpx). These rocks can be classified into four types: Opx–Cum, Cum, Cum–Bt, and Bt according to their eruption sequence (e.g., Isshiki, 1987; Endo et al., 2010). Cummingtonite is a common phenocryst phase and is present in most of the rhyolitic units. This sequence of cummingtonite-bearing rhyolites is a unique feature amongst the silicic volcanoes of the northern Izu–Bonin volcanic arc, most of which have an Opx–Cpx phenocryst assemblage (Shukono et al., 2006; Tamura et al., 2009; Haraguchi et al., 2017).

The decreasing anorthite contents (An mol.%) of plagioclase and Mg values (Mg#) of cummingtonite and biotite with time possibly indicate a gradual decrease in the temperature (and pressure) of the magmas. The rhyolites have high whole-rock SiO_2 (73–78 wt.%) and K_2O (1.5–3.3 wt.%) contents, and their trace element contents and patterns differ slightly amongst and within the four types. Highly differentiated rare earth element (REE) patterns characterize most of the rhyolites from Niijima volcano. All rock types from Niijima volcano have limited ranges of isotope values ($^{87}Sr/^{86}Sr$ = 0.70317–0.70339; $^{143}Nd/^{144}Nd$ = 0.51303–0.51308). The phenocryst assemblages and mineral chemistries of the rhyolitic volcanic rocks suggest that these magmas were produced under low temperatures (<800˚C) and low pressures (<3 kbar), and possibly water-saturated conditions, which is consistent with the experimental results for similar dacites and rhyolites from other volcanic arcs (Geschwind and Rutherford, 1992; Nicholls et al., 1992). Major and trace element variations indicate that fractionation of mostly plagioclase and amphibole was the dominant process during evolution of the rhyolitic magma, as supported by the presence of tonalite–granite xenoliths with cumulate textures and chemistries.

The coeval basaltic and andesitic volcanic units and mafic–intermediate inclusions (or enclaves) indicate that these magmas played an important role in the generation and evolution of the dominant rhyolitic magmas. The parental rhyolitic magmas are likely to have been generated by partial melting of lower to middle crust as a result of basaltic underplating, after which the magmas ascended and fractionated into more silicic magmas, producing more than 13 magma units at shallow crustal levels. At deeper crustal levels, basaltic and rhyolitic (or dacitic) parental magmas were mixed to produce andesitic to dacitic magmas, and these magmas ascended and mingled with the shallow rhyolitic magmas before eruption. The complex magmatic system beneath Niijima volcano was developed within a relatively thick crustal sequence on the rear-arc side of the Izu–Bonin volcanic arc.

Keywords: Niijima volcano, Cummingtonite, High-silica rhyolite, Izu-Bonin arc, basaltic-andesitic inclusions

©2019. Japan Geoscience Union. All Right Reserved.

Generation of primary andesitic magma in oceanic arcs: Evidence from Kibblewhite Volcano, Kermadec Arc

*Yasuhiro Hirai[1,2], Yoshihiko Tamura[2], Kaj Hoernle[3], Christian Timm[4], Folkmar Hauff[3], Reinhard Werner[3], Bogdan Vaglarov[2], Qing Chang[2], Takashi Miyazaki[2], Jun-Ichi Kimura[2]

1. Graduate School of Natural Science and Technology, Kanazawa University, Japan, 2. Japan Agency for Marine-Earth Science and Technology (JAMSTEC), Yokosuka, Kanagawa, Japan, 3. GEOMAR Helmholtz Centre for Ocean Research, Kiel, Germany, 4. GNS Science, Lower Hutt, New Zealand

Melting of hydrous subarc mantle at low pressure (<1 GPa) may produce primary andesitic melts, suggesting that primary andesitic lavas can be expected in oceanic arcs where the crust is thin (Tamura et al., 2016). Beneath thick crust, melting of hydrous mantle at higher pressures will occur at higher pressures below the thick crust, generating basaltic primary melts. Recently, Tamura et al. (2018) discovered olivine-bearing andesites derived from primary andesitic melts at the Nishinoshima volcano in the Ogasawara Arc, Japan, where the crustal thickness is 21 km. Here, we will present another example for generation of primary andesitic melts in the southern Kermadec arc.

During R/V SONNE expedition in 2017 (SO-255), phenocryst-poor andesites (57.5–57.6 wt.% SiO_2) were recovered from Kibblewhite volcanic complex, southern Kermadec Arc. These andesites contain skeletal olivine and clinopyroxene microphenocrysts with similar and restricted Mg-numbers (Mg/[Mg+Fe] = 0.84–0.85) and a few euhedral olivine xenocrysts with a magnesian cores (Mg/[Mg+Fe] = ~0.92). The magnesian andesites (5.5–5.6 wt.% MgO; Mg# = 56.8–57.3) have relatively high Ni (~50 ppm) and Cr (~180 ppm) contents. These lavas have depleted high-field strength element and enriched large-ion lithophile element compositions (e.g., Nb/Yb = 0.75–0.80; Ba/Nb = 148–175), similar to the coeval Kibblewhite basalts and typical for other southern Kermadec Arc lavas. Sr-Nd-Hf-Pb isotope compositions for the andesites and basalts of the Kibblewhite Volcano also cannot be distinguished from each other and are consistent with the range of published data for the southern Kermadec Arc (Todd et al., 2011; Timm et al., 2014).

Calculation of equilibrium olivine compositions and olivine fractionation trends (Tamura et al., 2000) indicate that olivine microphenocrysts in the andesites are in equilibrium with host rocks and that the andesites have experienced 10% olivine fractionation from mantle-derived primary melts. Primary melt compositions for the andesites (estimated by addition of 10 wt.% equilibrium olivines) are still andesitic (55.9–56.0 wt.% SiO_2; 9.58–9.68 wt.% MgO) in composition and similar to the estimated primary andesite melt of the Nishinoshima volcano. According to thermo-barometric modelling of Lee et al. (2009) the primary melts for the andesites are segregated from mantle peridotite at temperatures of 1190–1220℃ and pressures of 0.45–0.55 GPa assuming primary H_2O contents to be 1.0–3.0 wt.%. The low primary magma segregation pressures, corresponding to 15–18 km depths, are consistent with thin (9–12 km; Bassett et al., 2016) crust beneath the southern Kermadec Arc.

Keywords: Subduction zone, Kermadec Arc, Kibblewhite Volcano, SO-255

©2019. Japan Geoscience Union. All Right Reserved.

Petrogenesis of high-Mg# andesite lavas from Ruapehu volcano, New Zealand

*Chris Conway[1], Katy Chamberlain[2], Yumiko Harigane[1], Daniel Morgan[3]

1. Geological Survey of Japan, 2. Univ. Derby, 3. Univ. Leeds

The eruption of high-magnesium andesites (HMA) with Mg# values >60 at continental arc volcanoes conflicts with the expectation that mantle-equilibrated primitive magmas produced at subduction zones are basaltic. Studies of the origins of HMA lavas provide details on how primitive magmas transit through arc lithosphere, which has implications for constraints on crust-mantle connections as well as volcanic hazards.

Here we report on the occurrence and origin of a sequence of HMA lavas erupted at ~45 ka from Ruapehu volcano, which is a frequently active andesite-dacite stratovolcano in the Taupo Volcanic Zone (TVZ). The suite of lavas forms linear trends on bivariate whole-rock major and trace element plots that are distinctly elevated for MgO, Ni and Cr compared with all other lavas of Ruapehu and most other calk-alkaline andesites of the TVZ. The relatively primitive whole-rock geochemical characteristics are attributed to the involvement of mafic sources during magma genesis, as revealed by the presence of sharply reverse-zoned pyroxene phenocrysts with rims of $Mg\#_{85-89}$ and olivine xenocrysts with cores of Fo_{88-93} and Cr-spinel inclusions. The contribution of felsic end-members to the genesis of Ruapehu HMA magmas is recorded by the presence of rhyolitic glass within partially fused metasedimentary xenoliths and the low Mg# cores for pyroxenes within crystal clots that also preserve rhyolitic interstitial glass and melt inclusions.

The petrological and geochemical features of the samples indicate that the assembly of HMA magmas involved influxes of mafic magmas from the mantle that entrained olivine xenocrysts into mush zones of bulk (rhyo-) dacitic composition, which had evolved via preceding assimilation, fractionation and mixing processes in the crust. Timescale results from Fe-Mg interdiffusion modelling of orthopyroxene indicate that eruptions occurred within days to weeks of magma mixing events. Ruapehu HMA lavas are valuable samples of high-Mg# magmas collected from the global subduction zone system that were formed by crustal level magma hybridization processes (cf. Streck and Leeman, 2018) rather than directly by mantle melting processes (cf. Mitchell and Grove et al. 2016).

Keywords: andesite, magma mixing, active volcano

©2019. Japan Geoscience Union. All Right Reserved.

Hydrous felsic magma generated by unmixing of slab-derived supercritical liquid: evidence from Rishiri Volcano, Kuril Arc

*Hajime Taniuchi[1], Takeshi Kuritani[2,3], Tetsuya Yokoyama[4,3], Eizo Nakamura[3], Mitsuhiro Nakagawa[2]

1. Department of Natural History Science, Graduate School of Science, Hokkaido University, 2. Department of Earth and Planetary Science, Faculty of Science, Hokkaido University, 3. Institute for Planetary Materials, Okayama University, 4. Department of Earth and Planetary Sciences, Tokyo Institute of Technology

Introduction

Water-rich components released from the subducting slab play important roles in the generation of subduction-zone magmas in the mantle wedge (e.g. Elliott, 2003). With increasing fluid releasing depths, the slab-derived water-rich materials would become supercritical liquid (e.g. Bureau and Keppler, 1999).Experimental studies have suggested that slab-derived supercritical liquid is separated into hydrous silicate melt and aqueous fluid during the ascent in the mantle wedge (e.g. Kawamoto et al., 2012). However, the occurrence of magmas corresponding to this hydrous melt has not been reported so far. In this context, we have carried out a detailed petrological, geochemical, and chronological study on calc-alkaline andesite and dacite at Rishiri Volcano.

Results

Rishiri Volcano is a Quaternary stratovolcano in southern Kuril arc, and is 300 km above the Wadati-Benioff Zone. The volcanic activity started at ~0.2 Ma, which is characterized by coexistence of alkali basalt, tholeiitic andesite to dacite, and calc-alkaline andesite to dacite. The calc-alkaline andesitic products and the following dacitic lavas, investigated in this study, comprise Middle stage of the volcanic activity (Ishizuka, 1999). Our new $^{40}Ar/^{39}Ar$ age data for the dacitic and andesitic lavas are 35.5 ±1.4 ka and 34.6 ±3.0 ka, respectively.

The phenocryst assemblage of the dacitic lavas is Cpx + Opx + Pl, and that of the andesitic lavas is Ol + Cpx + Opx + Pl. All phenocrysts in the dacite have homogeneous compositions or show normal zonation with limited variations. In contrast, those in the andesite occasionally show reverse zonation. Some olivine and plagioclase phenocrysts have core compositions with up to Mg#89 and An#88, respectively. The dacitic lavas are characterized by high Sr/Y and La/Yb ratios (adakitic signature), no Eu anomaly, homogeneous Sr, Nd, and Pb isotopic ratios, and ^{230}Th-excesses. On the other hand, the andesitic lavas are heterogeneous in whole-rock major, trace, and isotopic compositions.

Discussion

The petrological and geochemical features of the andesitic products suggest that they were produced by mixing between felsic magma and primitive mafic magma. On the other hand, the dacitic lavas do not show any evidence of magma mixing. The absence of Eu anomaly negates a primary role of fractional crystallization in the magma genesis. In addition, the adakitic signature cannot be produced by crustal melting, because the underlying crust is too thin (Niu et al., 2016) for garnet to be stable (e.g. Rapp and Watson, 1995). Therefore, it is suggested that the dacitic magma was derived from the upper mantle, most plausibly, from the subducting slab. The slab origin of the magma is consistent with the ^{230}Th-excess

©2019. Japan Geoscience Union. All Right Reserved.

signature and the Pb isotopic compositions, which can be explained by mixing of a sediment component and an altered oceanic crust component of the slab.

One possible origin of the dacitic magma would be direct partial melting of the subducted slab (e.g. Defant and Drummont, 1990). However, extremely high temperatures with >1300ºC (Mibe et al., 2011) is required to melt the slab at ~300 km depth, which is highly unlikely. The andesitic and dacitic lavas erupted almost contemporaneously (~35 ka), with the former preceding the latter. The primitive mafic magma, involved in the generation of the andesitic magma, is considered to have been generated through fluid-fluxed melting of the mantle. These observations suggest that slab-derived aqueous fluid and slab-derived hydrous melt, corresponding to the dacitic magma, were almost simultaneously present in the upper mantle beneath the Rishiri Volcano at ~35 ka. Therefore, it is suggested that the dacitic magma may represent hydrous melt, which was separated from the ascending slab-derived supercritical liquid at the depth corresponding to the critical end point, leaving behind aqueous fluid (e.g. Kawamoto et al., 2012) that induced the generation of the primitive basaltic magma.

Keywords: Supercritical liquid, Unmixing, Subduction zone magmatism

©2019. Japan Geoscience Union. All Right Reserved.

Genesis of recent mafic volcanism in the Taupo Volcanic Zone, New Zealand: insights into the birth and death of cataclysmic caldera-forming systems?

*Georg F Zellmer[1], Jun-Ichi Kimura[2], Claudine Stirling[3], Gert Lube[1], Phil A Shane[4]

1. Volcanic Risk Solutions, Massey University, Tennent Drive, Palmerston North 4410, New Zealand, 2. Department of Solid Earth Geochemistry, Japan Agency for Marine-Earth Science and Technology [JAMSTEC], Natsushima-cho 2-15, Yokosuka 237-0061, Japan, 3. Department of Chemistry, University of Otago, Dunedin 9054, New Zealand, 4. School of Environment, University of Auckland, Auckland 1142, New Zealand

Mafic magmatism of the actively extending Taupo Volcanic Zone (TVZ) of the North Island, New Zealand, is volumetrically minor, but thought to tap the material that provides the heat source for voluminous rhyolite production through partial melting of the crust, which ultimately results in cataclysmic caldera-forming eruptions. We have studied the major and trace element chemistry 14 mafic samples from across the entire TVZ, and the uranium isotopic composition of whole rocks, groundmasses and separates of mafic mineral phases from a selection of 9 samples (with the remaining 5 too sparsely phyric for mineral separation). Some minerals yield significant ^{234}U enrichments despite groundmass and whole rock close to ^{238}U-^{234}U secular equilibrium, pointing to uptake of variably hydrothermally altered antecrystic minerals prior to the eruption of originally sparsely pyric to aphyric mafic magmas. However, incompatible trace element pattern indicate that there are three chemically distinct groups of samples, and that all but one sample may be used to derive primary melt compositions. We employ the latest version of the Arc Basalt Simulator (ABS5) to forward model these compositions, deriving mantle source parameters including mantle fertility, slab liquid flux, mantle volatile content, degree of melting, and P-T conditions of melt segregation. We show that mafic rocks erupted in areas of old, now inactive calderas constitute low-degree, deep melts, while those in areas of active caldera-volcanism are high-degree partial melts segregated from a less depleted source at an intermediate depth. Finally high-Mg basaltic andesites erupted in the southwest and the northeast of the TVZ point to a fertile, shallow mantle source. Our data are consistent with a petrogenetic model where mantle melting is dominated by decompression, rather than fluid fluxing, and progresses from shallow to deeper levels with time. Melt volumes initially increase to a tipping point, at which large scale crustal melting and caldera volcanism become prominent, and then decrease due to progressive depletion of the mantle wedge by melting, resulting in the dearth of heat provided and eventual cessation of rhyolitic cataclysim. For the first time, a direct link becomes apparent between the chemistry of recently erupted mafic magmas and the long-term activity and evolution of caldera volcanism in the TVZ.

Keywords: Arc Basalt Simulator, uranium isotopes, basaltic magmatism, rhyolitic magmatism, subduction zone processes

©2019. Japan Geoscience Union. All Right Reserved.

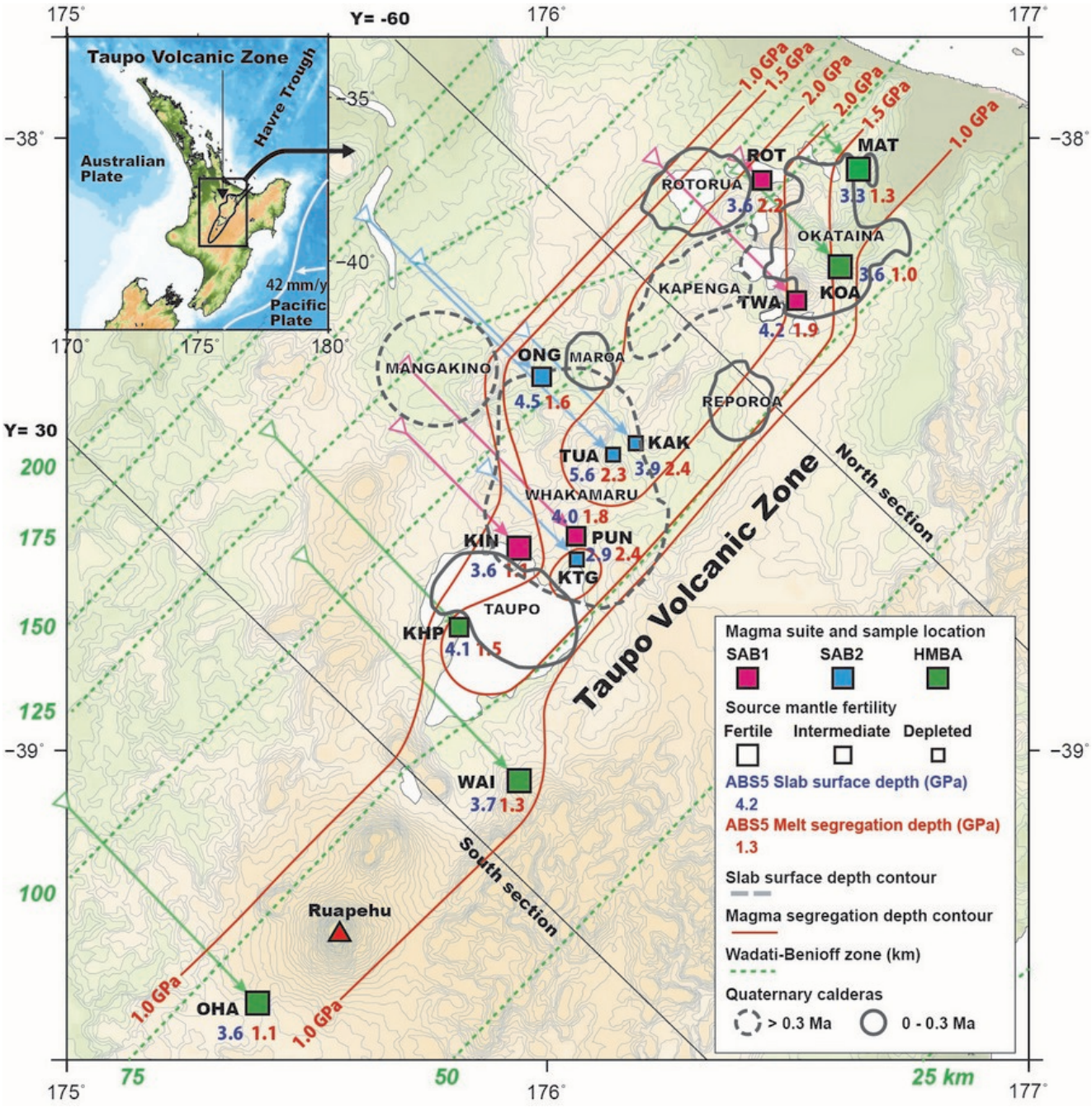

©2019. Japan Geoscience Union. All Right Reserved.

[E] Oral | S (Solid Earth Sciences)：S-MP Mineralogy & Petrology

Tue. May 28, 2019 3:30 PM - 5:00 PM JST | Tue. May 28, 2019 6:30 AM - 8:00 AM UTC | A07 TOKYO BAY MAKUHARI HALL

[S-MP30] Crust-Mantle Connections

convener:Yoshihiko Tamura(Research Institute for Marine Geodynamics, Japan Agency for Maine-Earth Science and Technology), Osamu Ishizuka(Geological Survey of Japan, AIST), Chris Conway(Geological Survey of Japan), Chairperson:Chris Conway, Yoshihiko Tamura(JAMSTEC)

A paradigm of the solid Earth geochemical cycles is that the Earth's crust forms by melting of the Earth's upper peridotitic mantle. How divers is the spectrum of primary melts and which factors may contribute to its variations? What is the influence of crustal processing vs. primary magma diversity in creating the diversity of the Earth's crust? The session seeks to explore the crust-mantle connections at divergent and convergent plate boundaries, and oceanic island settings based on volcanology, petrology, geochemistry, geophysics, geochronology, and geodynamics studies.

3:30 PM - 3:45 PM JST | 6:30 AM - 6:45 AM UTC

[SMP30-07] Introducing an oceanic core complex in the Shikoku Basin: Mado Megamullion

★Invited Papers

*Yasuhiko Ohara[1,2], Kyoko Okino[3], Norikatsu Akizawa[3], Masakazu Fujii[4], Yumiko Harigane[5], Naoto Hirano[6], Ken-ichi Hirauchi[7], Osamu Ishizuka[5], Shiki Machida[8], Katsuyoshi Michibayashi[9], Alessio Sanfilippo[10], Jonathan E. Snow[11], Hiroyuki Yamashita[12] (1.Hydrographic and Oceanographic Department of Japan, 2.Japan Agency for Marine-Earth Science and Technology, 3.Atmosphere and Ocean Research Institute, University of Tokyo, 4.National Institute of Polar Research, 5.Geological Survey of Japan/AIST, 6.Tohoku University, 7.Shizuoka University, 8.Chiba Institute of Technology, 9.Nagoya University, 10.University of Pavia, 11.University of Houston, 12.Kanagawa Prefectural Museum of Natural History)

3:45 PM - 4:00 PM JST | 6:45 AM - 7:00 AM UTC

[SMP30-08] Spatial variation of petrological and geochemical characteristics of mantle peridotites in Mado Megamullion, Shikoku Basin

*Norikatsu Akizawa[1], Shiki Machida[2], Kyoko Okino[1], Yasuhiko Ohara[3] (1.Atmosphere and Ocean Research Institute, The University of Tokyo, 2.Ocean Resources Research Center for Next Generation, Chiba Institute of Technology, 3.Hydrographic and Oceanographic Department of Japan)

4:00 PM - 4:15 PM JST | 7:00 AM - 7:15 AM UTC

[SMP30-09] Magmatism-hydrothermalism interaction along the crust-mantle transition below oceanic spreading centres

★Invited Papers

*Mathieu Rospabe[1,2], Mathieu Benoit[1], Georges Ceuleneer[1] (1.GET, OMP, Univ. of Toulouse, CNRS, IRD, F-31400 Toulouse, France, 2.JAMSTEC, Yokosuka 237-0061, Japan.)

4:15 PM - 4:30 PM JST | 7:15 AM - 7:30 AM UTC

[SMP30-10] Serpentinization and carbonation of dunites in the western part of the Isua Supracrustal Belt, Southwestern Greenland

*Juan Miguel Ramirez Guotana[1], Tomoaki Morishita[1], Akihiro Tamura[1], Ikuya Nishio[1], Kenichiro Tani[2], Yumiko Harigane[3], Kristoffer Szilas[4], D. Graham Pearson[5] (1.Kanazawa University, 2.National Museum of Nature and Science, Japan, 3.Institute of Geology and Geoinformation Geological Survey of Japan/AIST, 4.University of Copenhagen, 5.University of Alberta)

4:30 PM - 4:45 PM JST | 7:30 AM - 7:45 AM UTC

[SMP30-11] Petrogenesis of fertile abyssal peridotites of the Pujada Ophiolite, SE Mindanao, Philippines

*Valerie Shayne Vargas Olfindo[1], Betchaida Duetes Payot[1], Gabriel Theophilus Valera[1], Shoji Arai[2], Tomoyuki Shibata[4], Masako Yoshikawa[3] (1.Rushurgent Working Group, National Institute of Geological

Sciences, University of the Philippines, 2.Department of Earth Sciences, Kanazawa University, Kakuma, Kanazawa, Ishikawa 920-1192, Japan, 3.Institute for Geothermal Sciences, Graduate School of Science, Kyoto University, Beppu 874-0903, Japan, 4.Department of Earth and Planetary Systems Science, Hiroshima University, Hiroshima 739-8526, Japan)

4:45 PM - 5:00 PM JST | 7:45 AM - 8:00 AM UTC

[SMP30-12] Ultramafic rock in the Hida metamorphic belt: an example of arc plutons

Yohei Ogusu[1], *Tomoaki Morishita[1], Akihiro Tamura[1] (1.Kanazawa University)

Introducing an oceanic core complex in the Shikoku Basin: Mado Megamullion

*Yasuhiko Ohara[1,2], Kyoko Okino[3], Norikatsu Akizawa[3], Masakazu Fujii[4], Yumiko Harigane[5], Naoto Hirano[6], Ken-ichi Hirauchi[7], Osamu Ishizuka[5], Shiki Machida[8], Katsuyoshi Michibayashi[9], Alessio Sanfilippo[10], Jonathan E. Snow[11], Hiroyuki Yamashita[12]

1. Hydrographic and Oceanographic Department of Japan, 2. Japan Agency for Marine-Earth Science and Technology, 3. Atmosphere and Ocean Research Institute, University of Tokyo, 4. National Institute of Polar Research, 5. Geological Survey of Japan/AIST, 6. Tohoku University, 7. Shizuoka University, 8. Chiba Institute of Technology, 9. Nagoya University, 10. University of Pavia, 11. University of Houston, 12. Kanagawa Prefectural Museum of Natural History

Oceanic core complexes (OCCs) are domal bathymetric highs with axis-normal corrugations, and with exposure of serpentinized peridotite and gabbroic rocks, interpreted as exhumed footwalls of low-angle detachment faults. OCCs provide a valuable opportunity to directly study the architecture of oceanic lithosphere, together with the tectono-magmatic processes associated with its formation and evolution.

A significant fraction of the ocean floor is created in backarc basins where water plays a major role in generating backarc basin basalts, strikingly contrasting to magmatic process at mid-ocean ridges. The opportunity to explore the recent formation of backarc basin lower crust and upper mantle is, therefore, an important contribution to understanding the ocean basins. The extensive multi-beam bathymetric mapping by Japan’ s continental shelf survey has revealed the presence of potential OCCs in the multiple portions of the Philippine Sea Plate, such as in the Parece Vela Basin, Shikoku Basin, Kita-Daito Basin and West Philippine Basin. Among these, Godzilla Megamullion in the Parece Vela Basin is the largest known OCC on the Earth, and is one of the well-studied OCCs in the world.

In order to advance our understanding of the lithospheric composition of the Philippine Sea Plate, we need to utilize the potential Philippine Sea OCCs as tectonic windows to sample the lower crust and upper mantle materials. However, these potential OCCs have been remained largely unsampled and unstudied except only a few locations. We thus have started a new project focusing on the Shikoku Basin OCCs. Two cruises in the 2018 summer (YK18-07 and KH-18-2) collected peridotites and gabbros from the main Shikoku Basin OCC, here we named “Mado Megamullion”. The scheduled YK19-04S cruise in 2019 April will collect more datasets on this OCC.

In this contribution, we will show the general tectono-magmatic characteristics of Mado Megamullion. The OCC provides the information on the Shikoku Basin lower crust and upper mantle for the first time. Mado Megamullion is an ~20 km square OCC, the areal size is comparable to Kane Magamullion in the Mid-Atlantic Ridge. Thus it should be easier for us to make a comparative study between the two OCCs, providing useful information to understand the difference of the lithospheric characteristics between the two major ocean environments.

©2019. Japan Geoscience Union. All Right Reserved.

Keywords: Mado Megamullion, Shikoku Basin, Oceanic Core Complex

©2019. Japan Geoscience Union. All Right Reserved.

Spatial variation of petrological and geochemical characteristics of mantle peridotites in Mado Megamullion, Shikoku Basin

*Norikatsu Akizawa[1], Shiki Machida[2], Kyoko Okino[1], Yasuhiko Ohara[3]

1. Atmosphere and Ocean Research Institute, The University of Tokyo, 2. Ocean Resources Research Center for Next Generation, Chiba Institute of Technology, 3. Hydrographic and Oceanographic Department of Japan

Oceanic core complex is one of the tectonic windows, where mantle peridotites are exposed directly to the ocean floor. The mantle peridotites can provide petrological and geochemical information of the inaccessible oceanic mantle. However, the mantle peridotites from the oceanic core complex bear a possibility that their petrological and geochemical characteristics were modified during exhumation to the ocean floor via detachment faulting. Thus, formation process of the oceanic core complex must be elucidated in order to better presume the pristine oceanic mantle materials therein. Here, we present petrological and geochemical characteristics of mantle peridotites collected from a newly termed backarc oceanic core complex, “Mado (window in Japanese)” Megamullion in the Shikoku Basin, Philippine Sea. The samples were collected through a series of scientific cruises, YK18-07 by R/V Yokosuka with DSV Shinkai 6500, and KH-18-2 by R/V Hakuho. A total of 16 samples is used here: 13 peridotites and 3 dunites. Vein-like oxide gabbros are included in some peridotite samples from a region close to the ridge axis (proximal region), whereas none of the peridotites showing such lithological characteristics were found from a region far from the ridge axis (distal region). In contrast, the dunite samples were found only from the distal region. Since dunites are commonly interpreted as fossil channels for primitive (silica-depleted) melts beneath mid-ocean ridges, they likely transported parental melts of mid-ocean ridge basalt (MORB) beneath paleo-ridge axis. With regards to the spatial variation of petrological and geochemical characteristics of the mantle peridotites, we delineate a scenario of Mado Megamullion formation, where the exhumed mantle materials were getting modified by evolved magmas with time proceeding, indicating magma stagnation due probably to time-dependent cooling of the ridge spreading system. Therefore, the mantle peridotites in the distal region might show relatively pristine geochemical compositions in comparison with those in the proximal region.

Keywords: Oceanic core complex, Peridotite, Dunite, MORB, Whole-rock chemical composition, Mineral chemical composition

©2019. Japan Geoscience Union. All Right Reserved.

Magmatism-hydrothermalism interaction along the crust-mantle transition below oceanic spreading centres

*Mathieu Rospabe[1,2], Mathieu Benoit[1], Georges Ceuleneer[1]

1. GET, OMP, Univ. of Toulouse, CNRS, IRD, F-31400 Toulouse, France, 2. JAMSTEC, Yokosuka 237-0061, Japan.

Beneath oceanic spreading centres, the transition from the upwelling and partially molten peridotitic mantle and the accreting gabbroic lower crust appears as a major chemical, thermal and rheological interface. In most ophiolites worldwide, it is underlined by a dunitic horizon whatever the paleo-tectonic setting (mid-ocean ridges vs. supra-subduction zone). Since dunite is observed in present-day oceans in different geodynamic environments, in association with mantle harzburgite and with troctolitic-gabbroic veins and sills, it is reasonable to suppose that ophiolitic dunitic transition zone (DTZ) formed prior to the intra-oceanic thrusting leading to obduction.

As a matter of fact, the understanding of the petrological processes occurring in the mantle-crust transition zone beneath oceanic ridges can be studied in the Oman ophiolite. Particularly, the Maqsad area (Sumail massif) evolved in a MORB-like magmatic environment and presently exposes a >300 m thick DTZ above a paleo-mantle diapiric structure. It has been attributed to peridotite reactional melting or to the accumulation of olivine from Mg-rich melts, whether a combined origin is more likely. Following the reactional origin, a partially molten harzburgite reacts with interstitial melts, enhancing the orthopyroxene dissolution and the crystallization of secondary olivine, resulting in a rock essentially made of olivine. Interstitial mineral fractionation during melt migration between olivine grains (or melt-rock reaction) is partly responsible of the extensive petrological and geochemical variability observed at Moho level.

Recent studies evidenced a large interstitial mineral variety in dunites from the DTZ with, in addition to plagioclase and clinopyroxene expected in a MORB magmatic environment, the presence of orthopyroxene and amphibole among others. These minerals are also observed, together with mica, as silicate inclusions in chromite grains scattered in the dunite. This calls for the early involvement of hydrated, Si- and alkali-rich melts in the formation of dunite and chromitite ore bodies at Moho level beneath oceanic ridges. Since the presence of this peculiar mineralogy is ubiquitous within the DTZ and absent in mantle harzburgite, this distribution supports that the hydrated component originated from above, probably seawater in origin. These fluids interacted with surrounding rocks and with the variably evolved MORB issued from the Maqsad diapir, allowing to generate the hybrid melts, i.e. a blend between supercritical hydrothermal fluids rich in silica or trondhjemitic melts issued from hydrous melting of the country rocks.

The chemical variations observed along the Maqsad DTZ define trends with a characteristic vertical scale of few tens of meters. The chemical variation patterns are spatially correlated to the distribution of ridge-related faults or fracture zones (i.e. active at an early, high temperature magmatic stage), not only for fluid-mobile elements but also for immobile elements (e.g. REE, HFSE). These faults seem to have

©2019. Japan Geoscience Union. All Right Reserved.

enhanced (i) melt migration and extraction, from the mantle to the crust, and (ii) deep hydrothermal fluids introduction down to the Moho level. In other words, they are the main vectors for upwelling melt modification by hybridization, with hydrothermal fluids and/or silicic hydrous melts, and crystallization. In this context, the DTZ appears as a reactive interface that developed by the combination of three primary processes: tectonics, magmatism and deep, high temperature hydrothermal circulations. Fluid-melt-rocks reactions occurring at Moho level may have a significant impact on the MORB variability surveyed along present-day mid-ocean ridges and may contribute to part of the signatures observed at hydrothermal vents.

Keywords: Oman ophiolite, dunitic transition zone, melt-rock reactions

©2019. Japan Geoscience Union. All Right Reserved.

Serpentinization and carbonation of dunites in the western part of the Isua Supracrustal Belt, Southwestern Greenland

*Juan Miguel Ramirez Guotana[1], Tomoaki Morishita[1], Akihiro Tamura[1], Ikuya Nishio[1], Kenichiro Tani[2], Yumiko Harigane[3], Kristoffer Szilas[4], D. Graham Pearson[5]

1. Kanazawa University, 2. National Museum of Nature and Science, Japan, 3. Institute of Geology and Geoinformation Geological Survey of Japan/AIST, 4. University of Copenhagen, 5. University of Alberta

The 3.7 Ga Isua supracrustal belt (ISB) hosted in Itsaq Gneiss Complex in southwestern Greenland preserves one of the oldest metamorphosed mafic-ultramafic complex in the world which provides opportunity to study early petrological processes on Earth. Ultramafic bodies are common throughout the Isua supracrustal belt. These ultramafic rocks are interpreted to be possible mantle residues while other studies consider a cumulate origin. In the western limb of the ISB, less altered dunitic bodies enveloped by metasomatized dunites and amphibolites are exposed. The studied dunite lens is also referred as Lens B by previous studies. The northern part of Lens B dunites are highly deformed, highly serpentinized and carbonatized. The central and lower Lens B are less deformed and composed of olivine, serpentine, magnesite, magnetite, stichtite and Ti-rich humites. Ti-chondrodite (Ti-Chn) and Ti-clinohumite (Ti-Chu) are present in the central and southern part of Lens B. Ti-Chn and Ti-Chu occur commonly as irregular patches in olivine. In some portions, intergrowths of Ti-Chn and Ti-Chu are present. The F contents of the the Ti-Chn and Ti-Chu are also very low. Olivine grains are highly forsteritic and are comparable to those derived by deserpentinization process. The major serpentine phase is antigorite which occur as platy grains and minor amounts as inclusion in olivine. Stichtite, a magnesium-chromium hydroxycarbonate mineral, also includes clinohumite minerals. The clinohumite intergrowth in ISB dunites can be associated to the breakdown of Ti-Chn to Ti-Chu (Ti-Chn+Atg+Ol=Ti-Chu+H2O). The clinohumites are also almost F-free which suggests a lower temperature within the antigorite stability field compared to F-bearing clinohumites. Petrographic and geochemical results suggest that the dunites reached P-T conditions within the Ti-Ch and Atg stability field and retrogressed and carbonated (stichtite and magnesite) at lower pressure and temperature where Ti-Chu is stable.

Keywords: Isua Supracrustal Belt, archaean, peridotites

©2019. Japan Geoscience Union. All Right Reserved.

Petrogenesis of fertile abyssal peridotites of the Pujada Ophiolite, SE Mindanao, Philippines

*Valerie Shayne Vargas Olfindo[1], Betchaida Duetes Payot[1], Gabriel Theophilus Valera[1], Shoji Arai[2], Tomoyuki Shibata[4], Masako Yoshikawa[3]

1. Rushurgent Working Group, National Institute of Geological Sciences, University of the Philippines, 2. Department of Earth Sciences, Kanazawa University, Kakuma, Kanazawa, Ishikawa 920-1192, Japan, 3. Institute for Geothermal Sciences, Graduate School of Science, Kyoto University, Beppu 874-0903, Japan, 4. Department of Earth and Planetary Systems Science, Hiroshima University, Hiroshima 739-8526, Japan

Fresh mantle peridotites of the Pujada Ophiolite are extensively exposed in southeast Mindanao, Philippines. Despite its good preservation, its origin and formation is not constrained due to lacking geologic data. In this study, petrographic and geochemical characteristics of the mantle section of the Pujada Ophiolite are investigated to determine its tectonic setting and the magmatic processes operating during its formation.

The mantle section of the Pujada Ophiolite is composed of massive and pyroxene-rich lherzolites and harzburgites and interlayers of variably serpentinized lherzolites, harzburgites and dunites. Mineral chemistry of the spinel peridotites reveal spinel Cr# =0.10-0.50 and olivine Fo =89-91 typical of abyssal peridotites. The mantle peridotites are classified into three based on their field occurrence and spinel Cr#: Group I - massive lherzolites and harzburgites with Cr# =0.10-0.40, Group II - interlayered lherzolites and harzburgites with Cr# =0.10-0.40, and Group III - interlayered harzburgites and dunites with Cr# >0.4. The Group I peridotites are protogranular with minor vermicular spinel. The Group II peridotites are highly serpentinized. Preserved portions show porphyroclastic texture with vermicular to subhedral spinel. The Group III peridotites are also highly serpentinized but porphyroclastic texture in the harzburgites can be observed. Clinopyroxene and orthopyroxene compositions of the peridotites reveal an increasing depletion in Al_2O_3 from Group I to Group II and III with increasing Mg#. Groups I and II show lower Mg# =0.90-0.93 and 0.92-0.93, respectively. The Group III peridotites have the highest Mg# =0.925-0.935. The clinopyroxene Na_2O and TiO_2 of the three groups are within the same range of 0.10-0.40 and 0.10-0.25, respectively. The orthopyroxenes also show the same range of Na_2O and TiO_2 of 0.01-0.10 and 0.01-0.20, respectively. In general, rare earth element composition shows depletion of light rare earth element (LREE) and relatively flat heavy rare earth element (HREE) which further suggest an abyssal origin. Trace element compositions of the peridotites are indicative of low degrees of partial melting within 6%-14%. A few peridotite samples also show LREE enrichment suggesting that metasomatism may have affected these rocks.

Keywords: Pujada Ophiolite, peridotites, mid-oceanic ridge, LREE enrichment

©2019. Japan Geoscience Union. All Right Reserved.

Ultramafic rock in the Hida metamorphic belt: an example of arc plutons

Yohei Ogusu[1], *Tomoaki Morishita[1], Akihiro Tamura[1]

1. Kanazawa University

We report petrology and mineral compositions of ultramafic rocks in the Hida metamorphic belt, which was metamorphosed at around 235-250 Ma (Takahashi et al., 2018, Island Arc). It was pointed out in a graduation thesis of Kanazawa University that a small ultramafic body exists in the Hida metamorphic blet of Ozoe area, Hakusan City (Nagaoka, 1970). A preliminary result revealed that this ultramafic rock of the Hakusan City is mainly composed of large poikilitic amphibole grains enclosing many olivine grains, which are traditionally called as cortlandite (Williams, 1893 Jour. Geol.). These amphibole-rich plutonic rocks are expected in deeper part of island arc (e.g., Davidson et al., 2007 Geology). In fact, cortlandite and/or amphibole-rich plutonic rocks in granitic rocks/felsic metamorphic rocks were reported from all over the world (e.g., Tiepolo et al., 2011 Jour. Petrol.). Although these formation ages are different, it is noticed that they formed at convergent plate boundaries (Tiepolo et al., 2011). Cortlandite is minor but is reported from the Ryoke metamorphic belt, Japan (e.g., Kutsukake, 1978, Memoir. Kyoto Univ. Ser. Geol. Mineral.). Cortlandite and related amphibole-rich rocks would shed light on magmatic processes occurred beneath island arcs.

Ultramafic rocks of the Hakusan city (simply call Hakusan Ultramafic rock hereafter) is mainly composed of large poikilitic amphibole and orthopyroxene enclosing olivine grains. These olivine grains contain chromian spinels. Olivine with spinel existed phases before amphibole and orthopyroxene were crystallized. Orthopyroxene are sometimes included in amphibole and amphibole shows euhedral shape against the next orthopyroxene grain indicating amphibole is an early crystallization phase. The Fo content of olivine is around 84 and XMg of amphibole is around 90. High XMg of mafic minerals indicate that the Hakusan Ultramafic rock was formed from a relatively primitive melt. Poikilitic amphibole is pargasitic in composition. Calculated melt compositions from trace element compositions of the poikilitic amphibole are characterized by high in LILEs with negative anomalies of HFSEs, and are similar to arc magmas. We concluded that the Hokuriku Ultramafic rocks are formed from arc-related magma. It is important to study the origin of cortlandite and related amphibole-rich plutons from other metamorphic belts with different ages to understand the differences in mode and conditions of arc formation.

©2019. Japan Geoscience Union. All Right Reserved.

[E] Oral | S (Solid Earth Sciences)：S-MP Mineralogy & Petrology

Tue. May 28, 2019 10:45 AM - 12:15 PM JST | Tue. May 28, 2019 1:45 AM - 3:15 AM UTC | A08 TOKYO BAY MAKUHARI HALL

[S-MP31] Supercontinents and Crustal Evolution

convener:Madhusoodhan Satish-Kumar(Department of Geology, Faculty of Science, Niigata University), Tomokazu Hokada(National Institute of Polar Research), Krishnan Sajeev(Centre for Earth Sciences, Indian Institute of Science), Yasuhito Osanai(Division of Evolution of Earth Environments, Faculty of Social and Cultural Studies, Kyushu University), Chairperson:M. Satish-Kumar(Niigata University), Tomokazu Hokada(National Institute of Polar Research)

Supercontinent formation and dispersion has been enigmatic in the Earth's history. Eurasia is one such current supercontinent and incredible progress in the understanding of its geological evolution has been achieved in the past decade. Earlier supercontinents in the Earth's history such as Gondwana (0.5 Ga), Rodinia (1.0 Ga), Columbia/Nuna (2.0 Ga), Kenorland (2.5 Ga) and Vaalbara (3.1 Ga), have been the focus of several studies, however limited information on older supercontinents has restricted an understanding of their tectonic evolution. In this session, we invite authors around the world to present new data as well as review existing results on the continental scale crustal processes and tectonic evolution that are associated with supercontinent formation and breakup events in the Earth's history. The well-studied Eurasia and Gondwana supercontinents are of particular focus. Topics of interest include, but not restricted to, extremes in metamorphism, P-T-d-t evolution, magmatism, and the role of fluids. We hope to provide a platform for scientific discussions that will enlighten our understanding of the physical and chemical processes in the continental crust that records episodes of orogenesis that contributed to the formation and evolution of supercontinents.

10:45 AM - 11:00 AM JST | 1:45 AM - 2:00 AM UTC

[SMP31-01] Tectonic development of the East Indian cratonic margin and its status in Columbia Supercontinent

★Invited Papers

*Kaushik Das[1] (1.Hiroshima University)

11:00 AM - 11:15 AM JST | 2:00 AM - 2:15 AM UTC

[SMP31-02] **Continental crust formation and metamorphism during the Neoarchean–Paleoproterozoic: an example from the Nilgiri Block, southern India**

★Invited Papers

*VINOD O SAMUEL[1] (1.Yonsei University)

11:15 AM - 11:30 AM JST | 2:15 AM - 2:30 AM UTC

[SMP31-03] Preliminary paleomagnetic studies on the mafic dykes in Western Dharwar craton, South India.

*Silpa Ammini Sasidharan[1], Madhusoodhan Satish-Kumar[2], Naoto Ishikawa[3], Krishnan Sajeev[4] (1.Graduate School of Science and Technology, Niigata University, 2.Department of Geology, Faculty of Science, Niigata University, 3.Graduate School of Human and Environmental Studies, Kyoto University, Kyoto, Japan, 4.Centre for Earth Sciences, Indian Institute of Science, Bangalore, India)

11:30 AM - 11:45 AM JST | 2:30 AM - 2:45 AM UTC

[SMP31-04] Syn-metamorphic boron-bearing fluid infiltrations deduced from tourmaline in the Main Central Thrust zone, eastern Nepal Himalayas

★Invited Papers

*Tetsuo Kawakami[1], Harutaka Sakai[1], Katsushi Sato[1] (1.Graduate School of Science, Kyoto University)

11:45 AM - 12:00 PM JST | 2:45 AM - 3:00 AM UTC

[SMP31-05] **Geochemical characteristics of mafic and felsic igneous rocks (1.9-1.75 Ga) in the Lesser Himalaya: Regional variation and its implications for tectonic setting**

*Ryuichi Shinjo[1], Tomoki Amuro[1], Kohei Oura[1], Kazuya Oshiro[1], Shiro Tahara[1], Harutaka Sakai[2] (1.Department of Physics and Earth Sciences, University of the Ryukyus, 2.Faculty of Science, Kyoto University)

12:00 PM - 12:15 PM JST | 3:00 AM - 3:15 AM UTC

[SMP31-06] Petrogenesis and tectonic implications of orbicular granodiorite from Yangtze cratonic nucleus

*Yihe Li[1] (1.China University of Geosciences Wuhan)

Tectonic development of the East Indian cratonic margin and its status in Columbia Supercontinent

*Kaushik Das[1]

1. Hiroshima University

The East Indian cratonic margin is an important geological area towards understanding the tectonic development of the Precambrian India co-evolving with its erstwhile continental neighbors, including Antarctica. It, at present spreads out several linearly arranged Mesoproterozoic sedimentary basins (Chhattisgarh Basin and its satelite basins) unconformably lying on the Archean Bastar cratonic basement rocks and also juxtaposed on its east by a Proterozoic orogenic belt (Eastern Ghats Belt, EGB). While the basement rocks reveal the origin and evolution of the Archean craton and later tectonics affecting it, the sedimentary basins preserve the history of basin tectonics and fluctuation of different geological and geochemical proxies indicating the fluctuation of paleoenvironment, and also the tectonics of surrounding areas. The adjacent orogenic belt also has a variegated history of its developement and final cratonization, at least the tectonic history of the southern part was older while major part of the northern part was younger than the formation of those sedimenatry basins.
Our group in recent years have carried out detailed sedimentological, geochemical, and geochronological studies of the early sediment fills of these Mesoproterozoic basins (Chakraborty et al., 2012, Precam. Res., 200-203, 129-148; Das et al., 2015, Geol. Soc. London, Memoirs, 43, 207–221; Saha et al., 2016, Precam. Res., 281, 363-383) In this presentation, the collated data on the paleo-environmental facies analysis, variation in Nd-isotope geochemistry and U-Pb detrital zircon geochronology will be presented for the sediments of Singhora Basin, Khariar Basin and Ampani Basin, and also the geochemical character with tectonic affinity of the ca. 1450 Ma felsic porcellanitic tuff layer in all these basins. This will help to have an integrated understanding of the evolution of deep- to shallow continental crust in the East Indian Craton margin, as well as the connection between its neighbors in the supercontinent, "Columbia".

Keywords: East Indian Craton margin, Mesoproterozoic Chhattisgarh Basin, Felsic volcanism, Columbia Supercontinent

©2019. Japan Geoscience Union. All Right Reserved.

Continental crust formation and metamorphism during the Neoarchean–Paleoproterozoic: an example from the Nilgiri Block, southern India

*VINOD O SAMUEL[1]

1. Yonsei University

Earth is a unique planetary body with an evolved felsic continental crust on its surface. Had this continental crust not evolved, Earth’ s crust would have been basaltic/gabbroic in composition, and covered almost completely by water. It is important to understand how the mafic crust, which formed after the differentiation of Planet Earth transformed to one that is felsic in composition. Presently active processes capable of transforming crust from mafic to felsic composition, on a large scale, are subduction and subsequent arc magmatism. However, whether such processes were active during the Hadean–Archean eon is highly debated. Field evidence from major cratons show that partial melting of the earlier formed mafic crust (e.g., processes like sagduction) formed felsic continental crust. Thus, understanding when subduction-related process started on the planet is important. Here we present evidence from metamorphosed magmatic rocks such as pyroxenite, metagabbro, two-pyroxene granulite, charnockite, hornblende-biotite gneiss and rhyolite from the Nilgiri Block, southern India. U-Pb zircon age data shows that all these rocks formed during the late Neoarchean (core ages between 2600–2500Ma) and that they underwent subsequent metamorphism during the early Paleoproterozoic (rim ages between 2500–2450Ma). If felsic rocks formed from the partial melting of earlier formed mafic rocks, the mafic rocks should be older. Since all these rocks were formed and metamorphosed simultaneously, it is possible that protoliths of these rocks formed through melt differentiation followed by partial melting in the mantle wedge during the subduction-related arc magmatic process. An enrichment in light field strength elements and REE compared to heavy ones, and Nb-Ta depletion are common signatures in rocks formed through the arc magmatic process, where fluids or melts formed from subducted basaltic crust and the overlying sediments enrich the mantle wedge in lighter elements. Further, during metamorphism, these rocks could partially melt and form granitic melts. However there is no field evidence that suggests partial melting during metamorphism in these rocks. Textural relations and vein networks of silicate-oxide-sulfide-phosphate minerals in these rocks suggest that they could have possibly metasomatized in the presence of saline fluids during the early Paleoproterozoic. Such saline fluids could have been released during the waning stages of the magmatic process, probably due to the collapse and mixing of the accretionary wedge to the mantle wedge.

Keywords: Arc Magmatism, Metamorphism, southern India

©2019. Japan Geoscience Union. All Right Reserved.

Preliminary paleomagnetic studies on the mafic dykes in Western Dharwar craton, South India.

*Silpa Ammini Sasidharan[1], Madhusoodhan Satish-Kumar[2], Naoto Ishikawa[3], Krishnan Sajeev[4]

1. Graduate School of Science and Technology, Niigata University, 2. Department of Geology, Faculty of Science, Niigata University, 3. Graduate School of Human and Environmental Studies, Kyoto University, Kyoto, Japan, 4. Centre for Earth Sciences, Indian Institute of Science, Bangalore, India

Mafic dykes of varying dimensions and ages are well exposed all along the Archean Dharwar craton of south India. The mafic dykes in the Eastern Dharwar craton (EDC) have been studied in detail by several researchers previously (French and Heaman, 2010; Kumar et al., 2012, Srivastava et al., 2014). However, limited information is available for the dyke in Western Dharwar craton (WDC) and is considered in the present study. Representative samples were collected from dykes in the WDC and detailed petrography and geochemistry were carried out. The thin section observation revealed two different types of dykes based on the mineral assemblage, texture and the degree of alteration. First category of dykes is dolerites with typical ophitic texture and lath-shaped plagioclase. The other group of dyke samples showed high degree of alteration and remnant ophitic textures with the preservation of very less plagioclase laths as well as original mineralogy. This group termed as meta-dolerites, because of the prominent metamorphism. The dolerites and meta-dolerites are found to exhibit different distribution of major oxides as well as distinct trace and rare-earth element concentrations (Silpa and Satish-Kumar, 2018). The difference in petrography and geochemistry between the dolerites and meta-dolerites can lead to a preliminary inference that these two suits of rocks might not be co-genetic.

Understanding paleo- positions in which the dykes were emplaced is key while correlating the present, spatially distant cratons. Paleomagnetic studies will help to understand the paleo-position of the cratons and mafic dykes are expected to provide excellent records of the earth’s magnetic field as they cool rapidly when emplaced (Belica et al., 2014). For the preliminary paleomagnetic analyses, 86 core specimens were prepared from 33 sites including both dolerite and meta-dolerites and progressive demagnetization experiment has been conducted to assess the stability of natural remanent magnetization (NRM). Pilot specimens were subjected to alternating-field or thermal demagnetization and the NRMs were measured with a spinner magnetometer. Dolerite specimens yielded better magnetic behaviors with stable magnetic components. On the other hand, meta-dolerites show magnetic components probably carried by pyrrhotite and the magnetic behaviors were very unstable. Fig. 1 shows demagnetization behaviors of dolerite sample plotted on orthogonal vector-endpoint diagrams and equal area stereonets.

Studying the dykes in the Dharwar craton is key to understanding the evolution of the mantle during the Precambrian, especially in the Archean to Proterozoic transitional period. Dykes are emplaced after the period of major continental crust formation at around 2.7 Ga and hence the variation in mantle composition through time can be constrained. The dykes can be a result of a plume activity or an indicator of large igneous province and hence the study of which will give valuable information about the mantle source, the degree of melting and the source regions where melting occurred. Dyke swarms and LIPs are the products of major magmatic events in the Earth’s history that probably was the driving force in the breaking up of supercontinents, and they provide clues regarding the cratonic evolution through time. Due to their wide distribution, geochemically coherent dykes can be found in many cratons, thus providing key information on the close proximity of now separated supercontinents.

©2019. Japan Geoscience Union. All Right Reserved.

References

Belica, M.E., Piispa, E.J., Meert, J.G., Pesonen, L. J., Plado, J., Pandit, M.K., Celestino, M. Precambr. Res. 244, 100–122 (2014).

French, J. E., Heaman, L. M. Precambrian Res. 183, 416–441 (2010).

Kumar, A., Nagaraju, E., Besse, J.,. Rao ,Y. J. J. B. Precambrian Res. 220-221, 123–138 (2012).

Silpa, A. S., Satish-Kumar, M. J. Indian Inst. Sci. 98: 4, 365-378 (2018).

Srivastava, R. K.,Samal, A. K., Gautam, G. C. Int. Geol. Rev. 57, 11-12(2014).

Keywords: Mafic dykes, Precambrian, Paleomagetism, Geochemistry

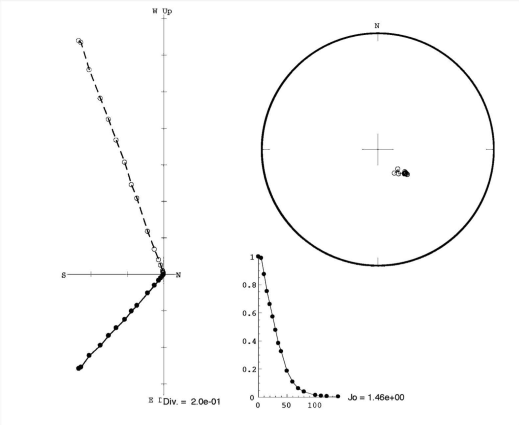

Fig. 1. Orthogonal vector plot, equal area stereonet and alternating-field demagnetization behavior for the dolerite showing typical characteristic remanent magnetization directions.

©2019. Japan Geoscience Union. All Right Reserved.

Syn-metamorphic boron-bearing fluid infiltrations deduced from tourmaline in the Main Central Thrust zone, eastern Nepal Himalayas

*Tetsuo Kawakami[1], Harutaka Sakai[1], Katsushi Sato[1]

1. Graduate School of Science, Kyoto University

Mode of occurrence and chemical composition of tourmaline in pelitic schists from the Main Central Thrust (MCT) zone of the Lesser Himalayan Sequences (LHS) are described in detail to deduce the chemical characteristics of tourmaline formed through boron-bearing fluid infiltration, and to estimate the syn-metamorphic fluid compositions.

Metasomatic tourmaline from the tourmalinized wall rocks of tourmaline-quartz veins and a plagioclase-quartz vein shows significant increase in X_{Ca} [=Ca/(Ca+Na)] at almost constant X_{Mg} [=Mg/(Mg+Fe_{total})]. Plagioclase present in such veins are anorthite-rich, and is not in equilibrium with tourmaline. These chemical characteristics of tourmaline are also confirmed in some of the tourmaline-rich pelitic schists that contain more than 1.0 vol% tourmaline. The tourmaline-rich pelitic schists, therefore, are considered to have formed through boron-bearing fluid infiltration. Ca-metasomatism observed in the pelitic schists adjacent to the metadolostone layers points to Ca-enrichment of the fluid composition when passing through the metadolostone layers. Episodic infiltration of such fluids into pelitic schists resulted in production of abundant tourmaline with increasing X_{Ca} trend at almost constant X_{Mg}. Most of the tourmaline in tourmaline-rich pelitic schists are in equilibrium with plagioclase, suggesting rock-buffered environment during the fluid infiltration. The pelitic schists without tourmaline enrichment mostly show increase in X_{Ca} at broad X_{Mg} values, reflecting its growth during longer range of metamorphism.

The fluid compositions that coexisted with tourmaline were estimated by applying experimentally-determined fluid/tourmaline chemical relationships to the vein, tourmaline-rich pelitic schist and tourmaline-poor pelitic schist samples. Assuming coexisting anion to be Cl, they all gave salinity similar to the sea water (~0.6 mol/l NaCl) and slightly above it (~0.4-0.9 mol/l NaCl+$CaCl_2$). The tourmaline-bearing veins and tourmaline-rich pelitic schists indicative of syn-metamorphic boron-bearing fluid infiltrations are widely distributed in the MCT zone of the LHS.

This observation supports that such fluid infiltrations into the High Himalayan Crystallines (HHC), contemporaneous with the inverted metamorphism of the MCT zone, caused vapor-saturated partial melting of the HHC and formed tourmaline leucogranite melts.

Keywords: metamorphic fluid , boron, tourmaline, inverted metamorphism

©2019. Japan Geoscience Union. All Right Reserved.

Geochemical characteristics of mafic and felsic igneous rocks (1.9-1.75 Ga) in the Lesser Himalaya: Regional variation and its implications for tectonic setting

*Ryuichi Shinjo[1], Tomoki Amuro[1], Kohei Oura[1], Kazuya Oshiro[1], Shiro Tahara[1], Harutaka Sakai[2]

1. Department of Physics and Earth Sciences, University of the Ryukyus, 2. Faculty of Science, Kyoto University

We present geochemical characteristics of mafic and felsic intrusive rocks (1.9-1.75 Ga) in the Lesser Himalaya and discuss about its tectonic setting. Rocks are taken from wide range of the Lesser Himalaya.

Models of tectonic setting for these rocks are controversial, which include subduction-zone setting (Kohn et al., 2010) and continental rift setting (Sakai et al., 2013).

Analyses of immobile trace element compositions suggest that mafic rocks (metagabbro) from the eastern Nepal have within-plate (or OIB) type composition, while the rocks from central and western Nepal have chemical compositions similar to subduction-related (active continental margin) basalt. It is noted that both types occur in the western Nepal. Based on these results, we suggest that plume-related rift system is more likely tectonic setting for these mafic magmatism than arc setting. Arc-like signature in western Nepal rocks may be derived from sub-continental lithospheric mantle.

Similar regional variation in trace element compositions for felsic rocks was observed. Initial 143Nd/144Nd and 176Hf/177Hf of felsic rocks are lower than those of mafic rocks; thus crustal component might involved significantly in generation of felsic magmas.

Keywords: Nepal, Lesser Himalaya, tectonic setting

©2019. Japan Geoscience Union. All Right Reserved.

Petrogenesis and tectonic implications of orbicular granodiorite from Yangtze cratonic nucleus

*Yihe Li[1]

1. China University of Geosciences Wuhan

Orbicular granodiorite outcropped in the Yangtze cratonic nucleus (Huangling Dome), where at least six Precambrian (3.4-0.8 Ga) tectonic events have been recorded. Hence, Huangling Orbicluar Granodiorite (HOG) could help us to investigate both petrogenesis and tectonic implications.

The HOG exposed in the northern margin of Neoproterozoic (~0.8 Ga) Huangling batholith, merely 30 meters long and 5 meters wide. They are composed of obicules (5-12 centimeters in diameter) and matrix. The obicules have different structure as no shell, one-layer shell and multiple-layer shells. In detail, one-layer shell are formed by dark color minerals such as amphibole and biotite; multiple-layer shells are made up of dark layers (dominated by amphibole) and light layers (dominated by plagioclase) at random intervals (0.2-4.3 millimeters). Their inner parts (core) are major plagioclase with minor amphiboles.

Mineral chemistry data are obtained by Electron Probe Micro Analyzer (EPMA) from two profiles crossing obicules. The An (An=100 Ca/(Ca+Na+K)) of plagioclase in matrix, shell and core from one-layer obicule are 26-30, 30-35 and 35-40, indicating the crystallization sequence is from core to shell and then matrix. The An of plagioclase in matrix, shell and core from multiple-layer obicule are more complicate, as 33, 36-46 and 42-45. The data suggest that the obicule crystallized before matrix, without distinct sequence between core and shells.

P-T conditions are calculated by Hb-Pl thermobarometry (Holland and Blundy, 1994; Bhadra and Bhattacharya, 2007). 0.63 GPa and 728℃ are obtained from core of one-layer obicule, while 0.49 GPa and 706℃ are gained from core of multiple-layer obicule. Moreover, P-T condition of multiple-layer shells vary from 0.50-0.80 Gpa and 669-713 ℃, showing pressure decrease towards core with few sharp increasing. The average P-T condition of shells are 0.60 Gpa and 700 ℃, whose pressure is higher than the core. As a result, the multiple-layer obicules may form during decompression. Besides, the sharp increase of An and P-T condition suggest that more basic (Ca-rich) composition may be added into shells during formation.

Chemical distribution patterns of shells and *in-situ* zircon structure have been examined by field emission scanning electron microscopy (FESEM). Energy-dispersive X-ray spectrometers (EDS) mapping shows that no obvious chemical differentiation have been observed in the rhythm shells. Core-mantle-rim structure zircons have been found in the matrix near the shells of obicules. Short columnar zircons with oscillatory bands have been found in amphiboles, while long columnar zircons with wide bands and overgrowth rims/patches have been found in plagioclase.

Zircons with Core-mantle-rim structure present concordant U-Pb ages as 1.95 Ga, 1.85 Ga and 0.88 Ga, with corresponding Epsilon Hf(t) values of -17.2 to -4.6, -10.8 to 0.36 and -23.6 to -21.5. Both short and long columnar zircons present concordant U-Pb ages of 0.88 Ga with Epsilon Hf(t) values of -23.7 to -19.85.

Based on new data and geological background, a model for generation of the HOG has been proposed as:

©2019. Japan Geoscience Union. All Right Reserved.

1) sediments metamorphosed at 1.95 Ga during continent-continent collision (Yin et al., 2013); 2) A-type granitic magma intruded the metasediments at 1.85 Ga (Xiong et al., 2009); 3) dioritic magma intruded the metasediments via the A-type granitic channel at 0.88 Ga; 4) water-rich superheating caused by dehydration of metasediments; 5) rapid crystallzation caused by undercooling while pressure decreasing.

Keywords: Huangling Orbicluar Granodiorite, Cratonic nucleus, Petrogenesis, Tectonic implications

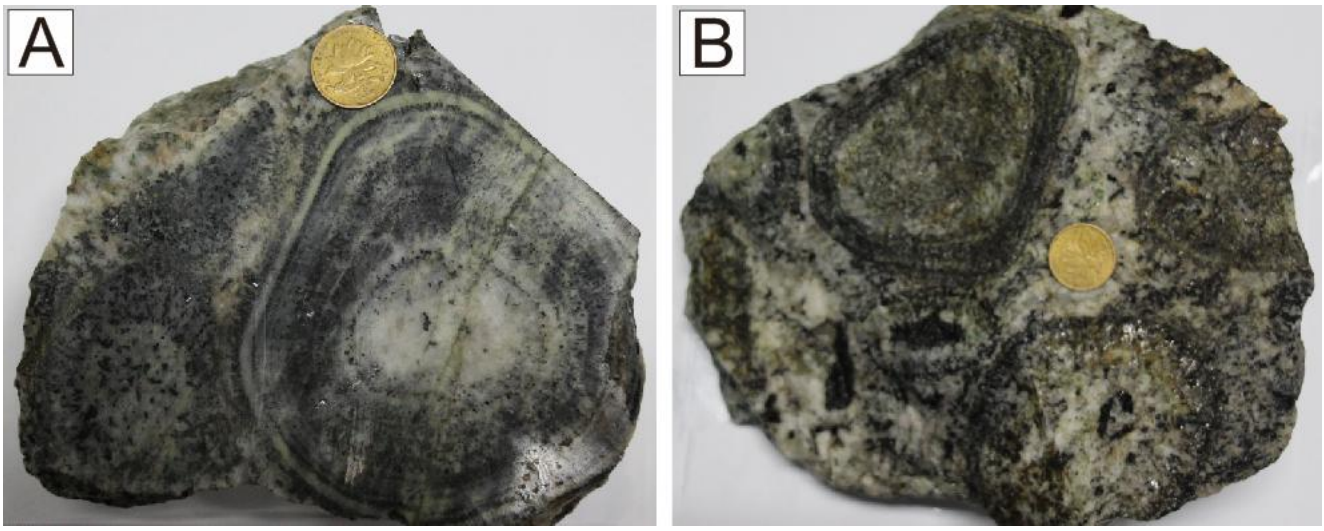

©2019. Japan Geoscience Union. All Right Reserved.

[E] Poster | S (Solid Earth Sciences)：S-MP Mineralogy & Petrology

Tue. May 28, 2019 3:30 PM - 5:00 PM JST | Tue. May 28, 2019 6:30 AM - 8:00 AM UTC | Poster Hall International Exhibition Hall8, Makuhari Messe_18

[S-MP31] Supercontinents and Crustal Evolution

convener:Madhusoodhan Satish-Kumar(Department of Geology, Faculty of Science, Niigata University), Tomokazu Hokada(National Institute of Polar Research), Krishnan Sajeev(Centre for Earth Sciences, Indian Institute of Science), Yasuhito Osanai(Division of Evolution of Earth Environments, Faculty of Social and Cultural Studies, Kyushu University)

Supercontinent formation and dispersion has been enigmatic in the Earth's history. Eurasia is one such current supercontinent and incredible progress in the understanding of its geological evolution has been achieved in the past decade. Earlier supercontinents in the Earth's history such as Gondwana (0.5 Ga), Rodinia (1.0 Ga), Columbia/Nuna (2.0 Ga), Kenorland (2.5 Ga) and Vaalbara (3.1 Ga), have been the focus of several studies, however limited information on older supercontinents has restricted an understanding of their tectonic evolution. In this session, we invite authors around the world to present new data as well as review existing results on the continental scale crustal processes and tectonic evolution that are associated with supercontinent formation and breakup events in the Earth's history. The well-studied Eurasia and Gondwana supercontinents are of particular focus. Topics of interest include, but not restricted to, extremes in metamorphism, P-T-d-t evolution, magmatism, and the role of fluids. We hope to provide a platform for scientific discussions that will enlighten our understanding of the physical and chemical processes in the continental crust that records episodes of orogenesis that contributed to the formation and evolution of supercontinents.

[SMP31-P01] Re-examination of metamorphic and geochronologic events in Rayner Complex and Western Rayner Complex in Antarctica

*Tomokazu Hokada[1,2], Sotaro Baba[3], Atsushi Kamei[4], Ippei Kitano[5], Kenji Horie[1,2], Yoshikuni Hiroi[1,6], Yoichi Motoyoshi[1,2], Mami Takehara[1], Kazuyuki Shiraishi[1] (1.National Institute of Polar Research, 2.The Graduate University for Advanced Studies (SOKENDAI), 3.University of the Ryukyus, 4.Shimane University, 5.Kyushu University, 6.Chiba University)

[SMP31-P02] Composition of constituent minerals in corona-bearing and -free mafic gneisses from the Lützow-Holm Complex at Skallen, East Antarctica

*Yuki Mori[1], Takeshi Ikeda[2] (1.Department of Earth and Planetary Sciences, Graduate School of Sciences, Kyushu University, 2.Department of Earth and Planetary Sciences, Faculty of Sciences, Kyushu University)

[SMP31-P03] “Pseudo-concordance” of U-Pb system in zircon at Harvey Nunatak, Napier Complex, East Antarctica

*Mami Takehara[1] (1.National Institute of Polar Research)

[SMP31-P04] Rapid UHT metamorphism and exhumation of the Lützow-Holm Complex in Antarctica

*Yoshikuni Hiroi[1], Tomokazu Hokada[2], Tatsuro Adachi[3], Yasuhito Osanai[3], Yoichi Motoyoshi[2], Kazuyuki Shiraishi[2] (1.Chiba Univ, 2.National Institute of Polar Research, 3.Kyushu University)

[SMP31-P05] Tectonic History of Hiroo Complex and its implication inpaleo-Kuril Arc evolution

*Sreehari Lakshmanan[1], Tsuyoshi Toyoshima[2], Futoshi Nanayama[3] (1.Graduate School of Science and Technology, Niigata University, Niigata, Japan, 2.Department of Geology, Faculty of Science, Niigata Univ. , 3.Geological Survey of Japan, AIST)

[SMP31-P06] Behaviour of C, O, Sr, Nd and Pb isotopes in high-grade metacarbonate rocks

*Madhusoodhan Satish-Kumar[1], Akari Imura[1], Momoko Shirakawa[2], Gen Shimoda[3], Kosuke T. Goto[3], M A Sanjeewa P K Malaviarachchi[4] (1.Department of Geology, Faculty of Science, Niigata University, 2.Graduate School of Science and Technology, Niigata University, 3.Geological Survey of Japan, 4.University of Peradeniya, Sri Lanka)

Re-examination of metamorphic and geochronologic events in Rayner Complex and Western Rayner Complex in Antarctica

*Tomokazu Hokada[1,2], Sotaro Baba[3], Atsushi Kamei[4], Ippei Kitano[5], Kenji Horie[1,2], Yoshikuni Hiroi[1,6], Yoichi Motoyoshi[1,2], Mami Takehara[1], Kazuyuki Shiraishi[1]

1. National Institute of Polar Research, 2. The Graduate University for Advanced Studies (SOKENDAI), 3. University of the Ryukyus, 4. Shimane University, 5. Kyushu University, 6. Chiba University

Enderby Land in Antarctica comprises of Neoproterozoic-Cambrian (c.650-500 Ma) high-grade metamorphic terranes that constituting Gondwana supercontinent (e.g., Shiraishi et al., 2008). Easternmost part is “Western Rayner Complex” of which granulite-facies and partly UHT metamorphism (Motoyoshi et al., 1994, 1995) and 2400-1000 Ma protolith and 540-520 Ma metamorphic ages were reported (Shiraishi et al., 1997). Neighboring “Rayner Complex” is characterized by >2500-1000 Ma protolith and 980-910 Ma granulite-facies metamorphic ages. Boundary between the Rayner and the Western Rayner Complex has been not clearly defined until when Horie et al. (2016) obtained 934-894 Ma SHIRMP zircon U-Pb ages from Mt. Lira, Condon Hills and Mt. Yuzhnaya regions with minor 590-570 Ma zircons from Mt. Yuzhnaya. Hiroi (unpublished data) also demonstrated contrasting metamorphic P-T evolution among the Mt. Lira, Condon Hills and Mt. Yuzhnaya regions.

JARE-58 (2016-2017) geology team made a short visit and sampling at a small nunatak of west of Mt. Yuzhnaya, a small nunatak of east of Forefinger Point, and Point Widdows in order to assess the relationship between the Rayner and the Western Rayner Complexes. We will report and discuss the update of the characteristic features of the Rayner and the Western Rayner Complexes.

Keywords: Antarctica, Gondwana, Supercontinent, metamorphism, geochronology

©2019. Japan Geoscience Union. All Right Reserved.

Composition of constituent minerals in corona-bearing and -free mafic gneisses from the Lützow-Holm Complex at Skallen, East Antarctica

*Yuki Mori[1], Takeshi Ikeda[2]

1. Department of Earth and Planetary Sciences, Graduate School of Sciences, Kyushu University, 2. Department of Earth and Planetary Sciences, Faculty of Sciences, Kyushu University

Corona is one of the non-equilibrium microstructures and has been employed to infer pressure-temperature path of the metamorphic rocks. The corona around garnet is common in mafic to ultramafic gneisses in the Lützow-Holm Complex (LHC) of East Antarctica (e.g., Hiroi et al., 1991). However, not every garnet in mafic to ultramafic gneisses accompanies the corona. In our ongoing study to reveal the controlling factors of presence and absence of the corona, we compare the composition of garnet and hornblende of the corona-bearing (no. I-223) and -free (no. I-232) mafic gneisses from Skallen.

The metamorphic grade of the complex increases progressively from the upper amphibolite facies to granulite facies toward the southwest, and the LHC is divided into three zones referred to as the amphibolite-facies zone, transitional zone, and granulite-facies zone (Hiroi et al., 1991). Recent studies have revealed that both transitional and granulite-facies zones had undergone high temperatures that exceed 800 ˚C (e.g., Iwamura et al, 2013; Kawakami et al., 2016). Skallen is an exposure located in the granulite-facies zone.

The constituent minerals in the matrix of the studied samples are almost same (garnet, hornblende, plagioclase with minor amounts of clinopyroxene and orthopyroxene), but I-223 further contains biotite. The microstructure and chemical composition of I-223 is as follows. The garnet grain is coarse (15 mm in diameter) and surrounded by a symplectitic corona composed of orthopyroxene and plagioclase. Garnet is clearly divided into two domains of Ca-rich core (Xgrs=0.23) and Ca-poor rim (Xgrs=0.18). X_{Mg} [=Mg/(Mg+Fe)] increases toward rim from 0.22 to 0.27, and that in the outer part of the rim decreases toward the boundary between the garnet and the corona from 0.27 to 0.22. The Ca-poor rim of the garnet includes irregular-shaped nanogranite composed of quartz, biotite, plagioclase, and K-feldspar. Hornblende is brown to brownish-green and polygonal. The X_{Mg} of the hornblende is 0.46-0.50. Matrix plagioclase often shows antiperthite intergrowing An50 plagioclase with Or96 K-feldspar. The coronal plagioclase has higher anorthite content (An80) than that in the matrix (An50). The microstructure and chemical composition of I-232 is as follows. The garnet grain is coarse (10 mm long) and elongated. The garnet and the hornblende define foliation of the rock. The hornblende is brown to pale brown. The composition of garnet gradually changes from core (Alm52Prp31Grs14Sps3) to rim (Alm52Prp28Grs17Sps3). The X_{Mg} in the hornblende varies from 0.60-0.70, and the composition is heterogeneous even in one grain. Most part of plagioclase is An45, and some parts of rim of the plagioclase have higher anorthite content of 70.

The garnet and hornblende in the corona-bearing gneiss have lower X_{Mg} than those in the corona-free gneiss. In addition, calcium content of the garnet and matrix plagioclase in the corona-bearing gneiss is higher than that in the corona-free gneiss. Therefore, we consider that bulk composition is one of the factors controlling the corona formation. The presence of nanogranite in the garnet surrounded by the corona suggests that partial melting and transport of the melt would cause the change of bulk composition in part.

©2019. Japan Geoscience Union. All Right Reserved.

Keywords: corona, garnet, nanogranite, Lützow-Holm Complex, Antarctica

©2019. Japan Geoscience Union. All Right Reserved.

“Pseudo-concordance” of U-Pb system in zircon at Harvey Nunatak, Napier Complex, East Antarctica

*Mami Takehara[1]

1. National Institute of Polar Research

U-Pb zircon dating has played a pivotal role in geochronology due to zircon’s high durability and high closure temperature. In addition, the paired decay scheme of two U isotopes allows us to verify the determined U-Pb zircon age. The Napier Complex in East Antarctica is well known because it preserves both of evidence of ultrahigh-temperature (UHT) metamorphism (e.g., Sheraton et al., 1987; Harley & Hensen 1990) and long Archaean crustal history from 3800 Ma to 2500 Ma (e.g., Harley & Black 1997). Previous researchers also reported the possibilities of the early Archean crust in the Napier Complex (e.g., Compston and Williams, 1982). Some previous researchers pointed out discordant U-Pb data including reverse discordance which was derived from the redistribution of radiogenic Pb isotopes in zircon in the Napier Complex samples (e.g., Kusiak et al., 2013). The some discordant U-Pb data looks concordant but actually reflect the Pb redistribution, namely “pseudo-concordance.” They suggest the redistribution of the radiogenic Pb isotopes in zircons was associated with the UHT metamorphism based on the Pb isotope mapping of the zircons. This report is critical for accurate U-Pb zircon geochronology in the UHT metamorphic region, such as the Napier Complex. Therefore, in this study, the zircons from the rock sample of the Napier Complex were characterized on the basis of the observation and trace-element contents, and the information was utilized for interpretation of the U-Pb data.
Zircons collected from a tonalitic gneiss (170223-2A-09) were first analyzed using sensitive high resolution ion-microprobes (SHRIMP IIe and SHRIMP IIe/AMC) at the National Institute of Polar Research, Japan. The sample was collected at the Harvey Nunatak, which is located close to Mt. Sones. The geochronological data from the Harvey Nunatak had never been reported. The sample was crushed by a high-voltage pulse power fragmentation device (Selfrag Lab) to preserve the external morphology of zircons and prevent contamination (Takehara et al., 2018). After pulverizing, the zircon grains were concentrated using conventional mineral separation techniques, including heavy liquid separation with methylene iodide and magnetic separation.
The zircon grains include fractures and slightly mineral inclusion based on the observation of transmitted light images by an optical microscope. BSE images show that some zircon grains have darker BSE-response domains, which suggests depletion of contents of Zr and Si during hydrothermal alteration of zircon. The zircons show typically high U contents (average is ~2500 ppm), and the U-Pb age from the high U zircons was corrected for the matrix effect derived from the high U contents according to the method by Williams & Hergt (2000) and White & Ireland (2012). It seems that the unaltered zircons show concordant data from about 2450 Ma to 2540 Ma with discordance (Disc.(%) = 1 −(206Pb/238U age)/(207Pb/206Pb age)} ×100 (e.g, Song et al., 1996)) ranges from -5 to +9%. On the other hand, trace element geochemistry of zircons does not support detritus protolith. In this presentation, the information of trace-element contents in zircons was utilized for the interpretation of U-Pb data and “pseudo-concordance.”

©2019. Japan Geoscience Union. All Right Reserved.

Rapid UHT metamorphism and exhumation of the Lützow-Holm Complex in Antarctica

*Yoshikuni Hiroi[1], Tomokazu Hokada[2], Tatsuro Adachi[3], Yasuhito Osanai[3], Yoichi Motoyoshi[2], Kazuyuki Shiraishi[2]

1. Chiba Univ, 2. National Institute of Polar Research, 3. Kyushu University

The Lützow-Holm Complex in Antarctica is a part of Neoproterozoic-Cambrian (c.650-500 Ma) collisional orogen to form Gondwana supercontinent. It is characterized by progressive metamorphism from upper amphibolite facies in the eastern part of the Prince Olav Coast to upper granulite facies in the southern Sôya Coast (e.g., Hiroi et al., 1991). UHT metamorphism is evidenced by such diagnostic mineral assemblages as Opx + Sil + Grt + Rt + Qz and Spr + Qz in Mg-Al-rich pelitic granulites in Rundvågshetta. Intimate intergrowths of Ky + Spr + Grt and Sil + Spr + Grt as well as andalusite-bearing falsite-nanogranite inclusions are included in the same porphyroblastic garnet, which is compositionally zoned, with Mg-rich core, Fe–Mn-rich rim, and core-to-rim oscillation of Ca. Integration of these new data with those previously documented leads to the inference of a rapid change in pressure–temperature conditions during regional UHT metamorphism in this part of the late Neoproterozoic to early Paleozoic ‘large and hot orogen’. Several lines of evidence indicate that partial melting and melt extraction took place even in mafic granulites of fragmented gabbro origin.

Keywords: Antarctica, Gondwana, Supercontinent, UHT metamorphism

©2019. Japan Geoscience Union. All Right Reserved.

Tectonic History of Hiroo Complex and its implication inpaleo-Kuril Arc evolution

*Sreehari Lakshmanan[1], Tsuyoshi Toyoshima[2], Futoshi Nanayama[3]

1. Graduate School of Science and Technology, Niigata University, Niigata, Japan, 2. Department of Geology, Faculty of Science, Niigata Univ. , 3. Geological Survey of Japan, AIST

Melanges records information about deformation history and tectonic events in plate margins and orogens and hence they are important in evolution of accretionary complexes [1]. Mélange facies rocks and brocken formations distributed in Nakanogawa Group of Hidaak Belt in Central Hokkaido is known as Hiroo Complex. We carried out detailed field mapping and structural studies on melange facies rocks distributed around Tachiiwa, Kamitoyoni and Daimaruyama region of Hiroo Complex. Four different deformation processes (D1,D2,D3 and D4) are identified from field to micro-scale observations. D1 event shear zones are wide and considerd as penitrative but D2, D3 and D4 shear zones observed in narrow deformation zones and considerd as less penitrative local events. D1 shearzones are identified as scaly fabric in mudstone and asymmetrically sheared sandstone clast distributed in it. This is similar to 'block in matrix' structure, typical of tectonic melange devoloped in accretionary complexes. D1 foliation trends in N-NNW direction. Tectonic evolution of theses rocks confirmed by pressure solution cleavage, composite planar fabrics (P-Y-R shear), asymmetrical folds and dip-parallel streching lineation. P-Y-R shear relation and other asymmetrical structures in both field and microscale observation shows east-side-up sense of movement. This shear sense suggest that major penetrative deformatoin phase in melange was connected to accretionary complex devolopment in paleo-Kuril-Arc region, where initial subduction was directed in N-S direction and later it rotated clockwise and attained its present position. D2, D3 and D4 events were recognized as dextral strike-slip movement, sinistral-strike-slip to oblique-slip movement and west-side-down movement sense respectively . Mega-micro scale observation of D2 and D3 events show the properties of cataclastic deformation and D4 event is that of fault gouge. Based on this D2, D3 and D4 events are considered as upper crustal or local deformation processes. We consider these are linked to post-melange deformation processes and related to final stages of devolopment of Hidaka Metamorphic Belt (HMB). Recent geochemical studies from Daimaruyama region and geochronological studies from Nakanogawa Group region points that Hiroo Complex was part of initiallly northward subducting Paleo-Kuril Arc region [2]. Through detailed strucural analysis, this study also confirms that Hiroo Complex was devoloped in accretionary complex of paleo- Kuril-Arc by an offscrapping mode of evolution. Later Hiroo Complex became part of Nakanogawa Group through a series of deformation processes asocciated with arc-arc colission between paleo-Kuril Arc and paleo-Japan Arc.
[1]A. Festa et al., 2012. Tectonophysics, 568, 7-24 [2] T.Yamasaki, F. Nanayama, 2018. Lithos. 302, 224-241

Keywords: Hiroo Complex, Paleo Kuri lArc, Mélange tectonics, Accretionary Complex, Nakanogawa Group

©2019. Japan Geoscience Union. All Right Reserved.

Behaviour of C, O, Sr, Nd and Pb isotopes in high-grade metacarbonate rocks

*Madhusoodhan Satish-Kumar[1], Akari Imura[1], Momoko Shirakawa[2], Gen Shimoda[3], Kosuke T. Goto[3], M A Sanjeewa P K Malaviarachchi[4]

1. Department of Geology, Faculty of Science, Niigata University, 2. Graduate School of Science and Technology, Niigata University, 3. Geological Survey of Japan, 4. University of Peradeniya, Sri Lanka

Tectonic environment of metasedimentary sequences deposit in orogenic belts is of importance in understanding the formation and evolution of supercontinents. In particular, chemically deposited carbonate rocks are supposed to hold key information of extinct paleo-oceans, since they are directly precipitated from seawater. In this study, we carried out a comprehensive trace and rare earth element analysis, carbon, oxygen, strontium, neodymium and lead isotope measurements in metacarbonate rocks from the Highland Complex, Sri Lanka. The isotopic systems studied have distinct residence and mixing time in seawater, and are also controlled by the input from surrounding continents. We present here the behaviour of each isotopic system with respect to different processes right from the deposition of carbonate from the seawater through diagenesis and then prograde and retrograde metamorphism. TheProterozoic basement of Sri Lanka is subdivided into four lithotectonic units, namely, the Highland Complex (HC), the Wanni Complex (WC), the Vijayan Complex (VC), and the Kadugannawa Complex (KC), based on Nd isotope model ages. The HC is mainly composed of metasedimentary rocks (granulite facies metaquartzites, metapelitic gneisses and metacarbonate rocks), whereas exposures of the WC and the VC are mainly metaigneous rocks. The metacarbonate rocks in the HC generally occur as layers parallel with other metasedimentary lithological units, and show a NE trend.

We measured oxygen and carbon isotope ratios to understand the effect of diagenetic to metamorphic alterations, which can be recognized in negative isotope shifts. In general, the metacarbonate rocks have positive oxygen isotopic composition comparable with the Proterozoic unmetamorphosed carbonates, suggesting that these rocks were not affected by external fluids during digenesis, dolomitization or metamorphism. However, some of the rock units have been affected by later fluid infiltration as seen in major shifts in oxygen isotopic composition. Negative shifts in both carbon and oxygen isotopes correspond to the metamorphic decarbonation reactions being prominent. Strontium isotope chemostratigraphy was applied for the selected samples with least signatures of alteration. The depositional ages show a younging direction of sedimentation from the Wanni-side to the Vijayan-side. In the case of Nd isotopes, the values correspond to variable mixing of continent derived and oceanic crust derived components during carbonate deposition. This is clearly depicted in the ε Sr vs. ε Nd cross-plots where typical seawater-rock mixing relationship in metacarbonate rocks associated with continents and oceanic crusts can be deduced.Pb isotopic composition of the metacarbonate rocks in Sri Lanka indicated significant differences within the HC; the Vijayan side is more radiogenic than that of Wanni side. This might be due to the difference of initial composition, as well as the relationship to depositional basin and seawater composition. We also observed very low U/Pb ratios, which are considered to have occurred due to the U-loss during metamorphic recrystallization.Thus, the Sr-Nd-Pb isotopic composition in metacarbonate rocks suggests interaction between the oceanic crust and carbonate rocks on the Wanni side whereas on the Vijayan side, carbonate sedimentation was accompanied by interaction with cratonic continental crust.Thus, by applying a multi-element isotope geochemical approach on metacarbonate rocks collected from continental collisional zones, and by comparing the data with basement rocks from various neighbouring Gondwana continents, regional affinities could be established.

©2019. Japan Geoscience Union. All Right Reserved.

Sr, Nd and Pb isotopic compositions provide important information about the depositional settings of sedimentary rocks and provide key information about the surrounding terrains of oceanic and continental affinities during the time of deposition. This can lead to a better understanding of paleo-tectonic settings of crustal fragments that assemble to form supercontinents.

Keywords: metacarbonates, Sr-Nd-Pb isotopes, Sri Lanka

©2019. Japan Geoscience Union. All Right Reserved.

[E] Poster | S (Solid Earth Sciences)：S-MP Mineralogy & Petrology

Tue. May 28, 2019 5:15 PM - 6:30 PM JST | Tue. May 28, 2019 8:15 AM - 9:30 AM UTC | Poster Hall International Exhibition Hall8, Makuhari Messe_34

[S-MP31] Supercontinents and Crustal Evolution

convener:Madhusoodhan Satish-Kumar(Department of Geology, Faculty of Science, Niigata University), Tomokazu Hokada(National Institute of Polar Research), Krishnan Sajeev(Centre for Earth Sciences, Indian Institute of Science), Yasuhito Osanai(Division of Evolution of Earth Environments, Faculty of Social and Cultural Studies, Kyushu University)

Supercontinent formation and dispersion has been enigmatic in the Earth's history. Eurasia is one such current supercontinent and incredible progress in the understanding of its geological evolution has been achieved in the past decade. Earlier supercontinents in the Earth's history such as Gondwana (0.5 Ga), Rodinia (1.0 Ga), Columbia/Nuna (2.0 Ga), Kenorland (2.5 Ga) and Vaalbara (3.1 Ga), have been the focus of several studies, however limited information on older supercontinents has restricted an understanding of their tectonic evolution. In this session, we invite authors around the world to present new data as well as review existing results on the continental scale crustal processes and tectonic evolution that are associated with supercontinent formation and breakup events in the Earth's history. The well-studied Eurasia and Gondwana supercontinents are of particular focus. Topics of interest include, but not restricted to, extremes in metamorphism, P-T-d-t evolution, magmatism, and the role of fluids. We hope to provide a platform for scientific discussions that will enlighten our understanding of the physical and chemical processes in the continental crust that records episodes of orogenesis that contributed to the formation and evolution of supercontinents.

[SMP31-P01] Re-examination of metamorphic and geochronologic events in Rayner Complex and Western Rayner Complex in Antarctica

*Tomokazu Hokada[1,2], Sotaro Baba[3], Atsushi Kamei[4], Ippei Kitano[5], Kenji Horie[1,2], Yoshikuni Hiroi[1,6], Yoichi Motoyoshi[1,2], Mami Takehara[1], Kazuyuki Shiraishi[1] (1.National Institute of Polar Research, 2.The Graduate University for Advanced Studies (SOKENDAI), 3.University of the Ryukyus, 4.Shimane University, 5.Kyushu University, 6.Chiba University)

[SMP31-P02] Composition of constituent minerals in corona-bearing and -free mafic gneisses from the Lützow-Holm Complex at Skallen, East Antarctica

*Yuki Mori[1], Takeshi Ikeda[2] (1.Department of Earth and Planetary Sciences, Graduate School of Sciences, Kyushu University, 2.Department of Earth and Planetary Sciences, Faculty of Sciences, Kyushu University)

[SMP31-P03] “Pseudo-concordance” of U-Pb system in zircon at Harvey Nunatak, Napier Complex, East Antarctica

*Mami Takehara[1] (1.National Institute of Polar Research)

[SMP31-P04] Rapid UHT metamorphism and exhumation of the Lützow-Holm Complex in Antarctica

*Yoshikuni Hiroi[1], Tomokazu Hokada[2], Tatsuro Adachi[3], Yasuhito Osanai[3], Yoichi Motoyoshi[2], Kazuyuki Shiraishi[2] (1.Chiba Univ, 2.National Institute of Polar Research, 3.Kyushu University)

[SMP31-P05] Tectonic History of Hiroo Complex and its implication inpaleo-Kuril Arc evolution

*Sreehari Lakshmanan[1], Tsuyoshi Toyoshima[2], Futoshi Nanayama[3] (1.Graduate School of Science and Technology, Niigata University, Niigata, Japan, 2.Department of Geology, Faculty of Science, Niigata Univ. , 3.Geological Survey of Japan, AIST)

[SMP31-P06] Behaviour of C, O, Sr, Nd and Pb isotopes in high-grade metacarbonate rocks

*Madhusoodhan Satish-Kumar[1], Akari Imura[1], Momoko Shirakawa[2], Gen Shimoda[3], Kosuke T. Goto[3], M A Sanjeewa P K Malaviarachchi[4] (1.Department of Geology, Faculty of Science, Niigata University, 2.Graduate School of Science and Technology, Niigata University, 3.Geological Survey of Japan, 4.University of Peradeniya, Sri Lanka)

Re-examination of metamorphic and geochronologic events in Rayner Complex and Western Rayner Complex in Antarctica

*Tomokazu Hokada[1,2], Sotaro Baba[3], Atsushi Kamei[4], Ippei Kitano[5], Kenji Horie[1,2], Yoshikuni Hiroi[1,6], Yoichi Motoyoshi[1,2], Mami Takehara[1], Kazuyuki Shiraishi[1]

1. National Institute of Polar Research, 2. The Graduate University for Advanced Studies (SOKENDAI), 3. University of the Ryukyus, 4. Shimane University, 5. Kyushu University, 6. Chiba University

Enderby Land in Antarctica comprises of Neoproterozoic-Cambrian (c.650-500 Ma) high-grade metamorphic terranes that constituting Gondwana supercontinent (e.g., Shiraishi et al., 2008). Easternmost part is “Western Rayner Complex” of which granulite-facies and partly UHT metamorphism (Motoyoshi et al., 1994, 1995) and 2400-1000 Ma protolith and 540-520 Ma metamorphic ages were reported (Shiraishi et al., 1997). Neighboring “Rayner Complex” is characterized by >2500-1000 Ma protolith and 980-910 Ma granulite-facies metamorphic ages. Boundary between the Rayner and the Western Rayner Complex has been not clearly defined until when Horie et al. (2016) obtained 934-894 Ma SHIRMP zircon U-Pb ages from Mt. Lira, Condon Hills and Mt. Yuzhnaya regions with minor 590-570 Ma zircons from Mt. Yuzhnaya. Hiroi (unpublished data) also demonstrated contrasting metamorphic P-T evolution among the Mt. Lira, Condon Hills and Mt. Yuzhnaya regions.

JARE-58 (2016-2017) geology team made a short visit and sampling at a small nunatak of west of Mt. Yuzhnaya, a small nunatak of east of Forefinger Point, and Point Widdows in order to assess the relationship between the Rayner and the Western Rayner Complexes. We will report and discuss the update of the characteristic features of the Rayner and the Western Rayner Complexes.

Keywords: Antarctica, Gondwana, Supercontinent, metamorphism, geochronology

©2019. Japan Geoscience Union. All Right Reserved.

Composition of constituent minerals in corona-bearing and -free mafic gneisses from the Lützow-Holm Complex at Skallen, East Antarctica

*Yuki Mori[1], Takeshi Ikeda[2]

1. Department of Earth and Planetary Sciences, Graduate School of Sciences, Kyushu University, 2. Department of Earth and Planetary Sciences, Faculty of Sciences, Kyushu University

Corona is one of the non-equilibrium microstructures and has been employed to infer pressure-temperature path of the metamorphic rocks. The corona around garnet is common in mafic to ultramafic gneisses in the Lützow-Holm Complex (LHC) of East Antarctica (e.g., Hiroi et al., 1991). However, not every garnet in mafic to ultramafic gneisses accompanies the corona. In our ongoing study to reveal the controlling factors of presence and absence of the corona, we compare the composition of garnet and hornblende of the corona-bearing (no. I-223) and -free (no. I-232) mafic gneisses from Skallen.

The metamorphic grade of the complex increases progressively from the upper amphibolite facies to granulite facies toward the southwest, and the LHC is divided into three zones referred to as the amphibolite-facies zone, transitional zone, and granulite-facies zone (Hiroi et al., 1991). Recent studies have revealed that both transitional and granulite-facies zones had undergone high temperatures that exceed 800 ˚C (e.g., Iwamura et al, 2013; Kawakami et al., 2016). Skallen is an exposure located in the granulite-facies zone.

The constituent minerals in the matrix of the studied samples are almost same (garnet, hornblende, plagioclase with minor amounts of clinopyroxene and orthopyroxene), but I-223 further contains biotite. The microstructure and chemical composition of I-223 is as follows. The garnet grain is coarse (15 mm in diameter) and surrounded by a symplectitic corona composed of orthopyroxene and plagioclase. Garnet is clearly divided into two domains of Ca-rich core (Xgrs=0.23) and Ca-poor rim (Xgrs=0.18). X_{Mg} [=Mg/(Mg+Fe)] increases toward rim from 0.22 to 0.27, and that in the outer part of the rim decreases toward the boundary between the garnet and the corona from 0.27 to 0.22. The Ca-poor rim of the garnet includes irregular-shaped nanogranite composed of quartz, biotite, plagioclase, and K-feldspar. Hornblende is brown to brownish-green and polygonal. The X_{Mg} of the hornblende is 0.46-0.50. Matrix plagioclase often shows antiperthite intergrowing An50 plagioclase with Or96 K-feldspar. The coronal plagioclase has higher anorthite content (An80) than that in the matrix (An50). The microstructure and chemical composition of I-232 is as follows. The garnet grain is coarse (10 mm long) and elongated. The garnet and the hornblende define foliation of the rock. The hornblende is brown to pale brown. The composition of garnet gradually changes from core (Alm52Prp31Grs14Sps3) to rim (Alm52Prp28Grs17Sps3). The X_{Mg} in the hornblende varies from 0.60-0.70, and the composition is heterogeneous even in one grain. Most part of plagioclase is An45, and some parts of rim of the plagioclase have higher anorthite content of 70.

The garnet and hornblende in the corona-bearing gneiss have lower X_{Mg} than those in the corona-free gneiss. In addition, calcium content of the garnet and matrix plagioclase in the corona-bearing gneiss is higher than that in the corona-free gneiss. Therefore, we consider that bulk composition is one of the factors controlling the corona formation. The presence of nanogranite in the garnet surrounded by the corona suggests that partial melting and transport of the melt would cause the change of bulk composition in part.

©2019. Japan Geoscience Union. All Right Reserved.

Keywords: corona, garnet, nanogranite, Lützow-Holm Complex, Antarctica

©2019. Japan Geoscience Union. All Right Reserved.

“Pseudo-concordance” of U-Pb system in zircon at Harvey Nunatak, Napier Complex, East Antarctica

*Mami Takehara[1]

1. National Institute of Polar Research

U-Pb zircon dating has played a pivotal role in geochronology due to zircon’s high durability and high closure temperature. In addition, the paired decay scheme of two U isotopes allows us to verify the determined U-Pb zircon age. The Napier Complex in East Antarctica is well known because it preserves both of evidence of ultrahigh-temperature (UHT) metamorphism (e.g., Sheraton et al., 1987; Harley & Hensen 1990) and long Archaean crustal history from 3800 Ma to 2500 Ma (e.g., Harley & Black 1997). Previous researchers also reported the possibilities of the early Archean crust in the Napier Complex (e.g., Compston and Williams, 1982). Some previous researchers pointed out discordant U-Pb data including reverse discordance which was derived from the redistribution of radiogenic Pb isotopes in zircon in the Napier Complex samples (e.g., Kusiak et al., 2013). The some discordant U-Pb data looks concordant but actually reflect the Pb redistribution, namely “pseudo-concordance.” They suggest the redistribution of the radiogenic Pb isotopes in zircons was associated with the UHT metamorphism based on the Pb isotope mapping of the zircons. This report is critical for accurate U-Pb zircon geochronology in the UHT metamorphic region, such as the Napier Complex. Therefore, in this study, the zircons from the rock sample of the Napier Complex were characterized on the basis of the observation and trace-element contents, and the information was utilized for interpretation of the U-Pb data.
Zircons collected from a tonalitic gneiss (170223-2A-09) were first analyzed using sensitive high resolution ion-microprobes (SHRIMP IIe and SHRIMP IIe/AMC) at the National Institute of Polar Research, Japan. The sample was collected at the Harvey Nunatak, which is located close to Mt. Sones. The geochronological data from the Harvey Nunatak had never been reported. The sample was crushed by a high-voltage pulse power fragmentation device (Selfrag Lab) to preserve the external morphology of zircons and prevent contamination (Takehara et al., 2018). After pulverizing, the zircon grains were concentrated using conventional mineral separation techniques, including heavy liquid separation with methylene iodide and magnetic separation.
The zircon grains include fractures and slightly mineral inclusion based on the observation of transmitted light images by an optical microscope. BSE images show that some zircon grains have darker BSE-response domains, which suggests depletion of contents of Zr and Si during hydrothermal alteration of zircon. The zircons show typically high U contents (average is ~2500 ppm), and the U-Pb age from the high U zircons was corrected for the matrix effect derived from the high U contents according to the method by Williams & Hergt (2000) and White & Ireland (2012). It seems that the unaltered zircons show concordant data from about 2450 Ma to 2540 Ma with discordance (Disc.(%) = 1 −(206Pb/238U age)/(207Pb/206Pb age)} ×100 (e.g, Song et al., 1996)) ranges from -5 to +9%. On the other hand, trace element geochemistry of zircons does not support detritus protolith. In this presentation, the information of trace-element contents in zircons was utilized for the interpretation of U-Pb data and “pseudo-concordance.”

©2019. Japan Geoscience Union. All Right Reserved.

Rapid UHT metamorphism and exhumation of the Lützow-Holm Complex in Antarctica

*Yoshikuni Hiroi[1], Tomokazu Hokada[2], Tatsuro Adachi[3], Yasuhito Osanai[3], Yoichi Motoyoshi[2], Kazuyuki Shiraishi[2]

1. Chiba Univ, 2. National Institute of Polar Research, 3. Kyushu University

The Lützow-Holm Complex in Antarctica is a part of Neoproterozoic-Cambrian (c.650-500 Ma) collisional orogen to form Gondwana supercontinent. It is characterized by progressive metamorphism from upper amphibolite facies in the eastern part of the Prince Olav Coast to upper granulite facies in the southern Sôya Coast (e.g., Hiroi et al., 1991). UHT metamorphism is evidenced by such diagnostic mineral assemblages as Opx + Sil + Grt + Rt + Qz and Spr + Qz in Mg-Al-rich pelitic granulites in Rundvågshetta. Intimate intergrowths of Ky + Spr + Grt and Sil + Spr + Grt as well as andalusite-bearing falsite-nanogranite inclusions are included in the same porphyroblastic garnet, which is compositionally zoned, with Mg-rich core, Fe–Mn-rich rim, and core-to-rim oscillation of Ca. Integration of these new data with those previously documented leads to the inference of a rapid change in pressure–temperature conditions during regional UHT metamorphism in this part of the late Neoproterozoic to early Paleozoic ‘large and hot orogen’. Several lines of evidence indicate that partial melting and melt extraction took place even in mafic granulites of fragmented gabbro origin.

Keywords: Antarctica, Gondwana, Supercontinent, UHT metamorphism

©2019. Japan Geoscience Union. All Right Reserved.

Tectonic History of Hiroo Complex and its implication inpaleo-Kuril Arc evolution

*Sreehari Lakshmanan[1], Tsuyoshi Toyoshima[2], Futoshi Nanayama[3]

1. Graduate School of Science and Technology, Niigata University, Niigata, Japan, 2. Department of Geology, Faculty of Science, Niigata Univ. , 3. Geological Survey of Japan, AIST

Melanges records information about deformation history and tectonic events in plate margins and orogens and hence they are important in evolution of accretionary complexes [1]. Mélange facies rocks and brocken formations distributed in Nakanogawa Group of Hidaak Belt in Central Hokkaido is known as Hiroo Complex. We carried out detailed field mapping and structural studies on melange facies rocks distributed around Tachiiwa, Kamitoyoni and Daimaruyama region of Hiroo Complex. Four different deformation processes (D1,D2,D3 and D4) are identified from field to micro-scale observations. D1 event shear zones are wide and considerd as penitrative but D2, D3 and D4 shear zones observed in narrow deformation zones and considerd as less penitrative local events. D1 shearzones are identified as scaly fabric in mudstone and asymmetrically sheared sandstone clast distributed in it. This is similar to 'block in matrix' structure, typical of tectonic melange devoloped in accretionary complexes. D1 foliation trends in N-NNW direction. Tectonic evolution of theses rocks confirmed by pressure solution cleavage, composite planar fabrics (P-Y-R shear), asymmetrical folds and dip-parallel streching lineation. P-Y-R shear relation and other asymmetrical structures in both field and microscale observation shows east-side-up sense of movement. This shear sense suggest that major penetrative deformatoin phase in melange was connected to accretionary complex devolopment in paleo-Kuril-Arc region, where initial subduction was directed in N-S direction and later it rotated clockwise and attained its present position. D2, D3 and D4 events were recognized as dextral strike-slip movement, sinistral-strike-slip to oblique-slip movement and west-side-down movement sense respectively . Mega-micro scale observation of D2 and D3 events show the properties of cataclastic deformation and D4 event is that of fault gouge. Based on this D2, D3 and D4 events are considered as upper crustal or local deformation processes. We consider these are linked to post-melange deformation processes and related to final stages of devolopment of Hidaka Metamorphic Belt (HMB). Recent geochemical studies from Daimaruyama region and geochronological studies from Nakanogawa Group region points that Hiroo Complex was part of initiallly northward subducting Paleo-Kuril Arc region [2]. Through detailed strucural analysis, this study also confirms that Hiroo Complex was devoloped in accretionary complex of paleo- Kuril-Arc by an offscrapping mode of evolution. Later Hiroo Complex became part of Nakanogawa Group through a series of deformation processes asocciated with arc-arc colission between paleo-Kuril Arc and paleo-Japan Arc.
[1]A. Festa et al., 2012. Tectonophysics, 568, 7-24 [2] T.Yamasaki, F. Nanayama, 2018. Lithos. 302, 224-241

Keywords: Hiroo Complex, Paleo Kuri lArc, Mélange tectonics, Accretionary Complex, Nakanogawa Group

©2019. Japan Geoscience Union. All Right Reserved.

Behaviour of C, O, Sr, Nd and Pb isotopes in high-grade metacarbonate rocks

*Madhusoodhan Satish-Kumar[1], Akari Imura[1], Momoko Shirakawa[2], Gen Shimoda[3], Kosuke T. Goto[3], M A Sanjeewa P K Malaviarachchi[4]

1. Department of Geology, Faculty of Science, Niigata University, 2. Graduate School of Science and Technology, Niigata University, 3. Geological Survey of Japan, 4. University of Peradeniya, Sri Lanka

Tectonic environment of metasedimentary sequences deposit in orogenic belts is of importance in understanding the formation and evolution of supercontinents. In particular, chemically deposited carbonate rocks are supposed to hold key information of extinct paleo-oceans, since they are directly precipitated from seawater. In this study, we carried out a comprehensive trace and rare earth element analysis, carbon, oxygen, strontium, neodymium and lead isotope measurements in metacarbonate rocks from the Highland Complex, Sri Lanka. The isotopic systems studied have distinct residence and mixing time in seawater, and are also controlled by the input from surrounding continents. We present here the behaviour of each isotopic system with respect to different processes right from the deposition of carbonate from the seawater through diagenesis and then prograde and retrograde metamorphism. TheProterozoic basement of Sri Lanka is subdivided into four lithotectonic units, namely, the Highland Complex (HC), the Wanni Complex (WC), the Vijayan Complex (VC), and the Kadugannawa Complex (KC), based on Nd isotope model ages. The HC is mainly composed of metasedimentary rocks (granulite facies metaquartzites, metapelitic gneisses and metacarbonate rocks), whereas exposures of the WC and the VC are mainly metaigneous rocks. The metacarbonate rocks in the HC generally occur as layers parallel with other metasedimentary lithological units, and show a NE trend.

We measured oxygen and carbon isotope ratios to understand the effect of diagenetic to metamorphic alterations, which can be recognized in negative isotope shifts. In general, the metacarbonate rocks have positive oxygen isotopic composition comparable with the Proterozoic unmetamorphosed carbonates, suggesting that these rocks were not affected by external fluids during digenesis, dolomitization or metamorphism. However, some of the rock units have been affected by later fluid infiltration as seen in major shifts in oxygen isotopic composition. Negative shifts in both carbon and oxygen isotopes correspond to the metamorphic decarbonation reactions being prominent. Strontium isotope chemostratigraphy was applied for the selected samples with least signatures of alteration. The depositional ages show a younging direction of sedimentation from the Wanni-side to the Vijayan-side. In the case of Nd isotopes, the values correspond to variable mixing of continent derived and oceanic crust derived components during carbonate deposition. This is clearly depicted in the ε Sr vs. ε Nd cross-plots where typical seawater-rock mixing relationship in metacarbonate rocks associated with continents and oceanic crusts can be deduced.Pb isotopic composition of the metacarbonate rocks in Sri Lanka indicated significant differences within the HC; the Vijayan side is more radiogenic than that of Wanni side. This might be due to the difference of initial composition, as well as the relationship to depositional basin and seawater composition. We also observed very low U/Pb ratios, which are considered to have occurred due to the U-loss during metamorphic recrystallization.Thus, the Sr-Nd-Pb isotopic composition in metacarbonate rocks suggests interaction between the oceanic crust and carbonate rocks on the Wanni side whereas on the Vijayan side, carbonate sedimentation was accompanied by interaction with cratonic continental crust.Thus, by applying a multi-element isotope geochemical approach on metacarbonate rocks collected from continental collisional zones, and by comparing the data with basement rocks from various neighbouring Gondwana continents, regional affinities could be established.

©2019. Japan Geoscience Union. All Right Reserved.

Sr, Nd and Pb isotopic compositions provide important information about the depositional settings of sedimentary rocks and provide key information about the surrounding terrains of oceanic and continental affinities during the time of deposition. This can lead to a better understanding of paleo-tectonic settings of crustal fragments that assemble to form supercontinents.

Keywords: metacarbonates, Sr-Nd-Pb isotopes, Sri Lanka

©2019. Japan Geoscience Union. All Right Reserved.

[J] Oral | S (Solid Earth Sciences)：S-VC Volcanology

Tue. May 28, 2019 9:00 AM - 10:30 AM JST | Tue. May 28, 2019 12:00 AM - 1:30 AM UTC | IC 2F

[S-VC38] Active Volcanism

convener:Yuta Maeda(Nagoya University), Takahiro Miwa(National research institute for earth science and disaster prevention), Takeshi Nishimura(Department of Geophysics, Graduate School of Science, Tohoku University), Chairperson:Fukashi Maeno, Yosuke Aoki

This session discusses various aspects of active volcanisms including, but not limited to, recent and historical eruptions, various phenomena associated with the volcanic activities, underground structures of the volcanoes, and developments of new instruments based on geophysical, geochemical, geological, and multidiscipline approaches. We also welcome studies on understanding and predicting the transitions of the eruptive activities from observational, theoretical, and experimental approaches.

9:00 AM - 9:15 AM JST | 12:00 AM - 12:15 AM UTC

[SVC38-06] A sequence of volcanic flank collapse and tsunami event on 22 December 2018 at Anak Krakatau volcano, Indonesia

*Fukashi Maeno[1], Takayuki Kaneko[1] (1.Earthquake Research Institute, University of Tokyo)

9:15 AM - 9:30 AM JST | 12:15 AM - 12:30 AM UTC

[SVC38-07] The 2018 eddifice collapse event of Anak Krakatau, Indonesia: Telseismic waveform analysis and tsunami simulation

*Shingo Watada[1], Iyan E. Mulia[1], Masumi Yamada[2], Dimas Sianipar[3] (1.Earthquake Research Institute, University of Tokyo, 2.Disaster Prevention Research Institute, Kyoto University, 3.TIGP-ESS Academia Sinica, National Central University, Taiwan)

9:30 AM - 9:45 AM JST | 12:30 AM - 12:45 AM UTC

[SVC38-08] The 2018 edifice collapse event of Anak Krakatau, Indonesia: Landslide movement history estimated from seismic waveforms

*Masumi Yamada[1], Shingo Watada[2], Haruhisa Nakamichi[1], Iyan Mulia[2], Karyono Dr.[3] (1.Disaster Prevention Research Institute, Kyoto University, 2.Earthquake Research Institute, University of Tokyo, 3.Center for Earthquake and Tsunami, BMKG)

9:45 AM - 10:00 AM JST | 12:45 AM - 1:00 AM UTC

[SVC38-09] Intense Swarm Activity in the Vicinity of Yake-dake Volcano, Central Japan, Started in November 2018

*Shiro Ohmi[1] (1.Earthquake Hazards Division, Disaster Prevention Research Institute, Kyoto University)

10:00 AM - 10:15 AM JST | 1:00 AM - 1:15 AM UTC

[SVC38-10] Change of the volcanic activity at Kuju volcano.

*Mori Takehiko[1], Muga Yaguchi[1], Yasushi Kawamura[2], Hideyuki Hiramatsu[3], Keiji Ikeda[2], Sugai Akira[2], Michitomo Sugahara[2], Kenichi Takata[2], Kyo Matsumoto[2], Fukuoka Regional Headquarters Japan Meteorological Agency, Oita Meteorological Office Japan Meteorological Agency (1. Meteorological Research Institute, Japan Meteorological Agency, 2.Fukuoka Regional Headquarters, Japan Meteorological Agency, 3.Oita Meteorological Office, Japan Meteorological Agency)

10:15 AM - 10:30 AM JST | 1:15 AM - 1:30 AM UTC

[SVC38-11] Posteruptive Thermoelastic Deflation of Intruded Magma in Usu Volcano, Japan, 1992–2017

*Yosuke Aoki[1], Xiaowen Wang[1] (1.Earthquake Research Institute, University of Tokyo)

A sequence of volcanic flank collapse and tsunami event on 22 December 2018 at Anak Krakatau volcano, Indonesia

*Fukashi Maeno[1], Takayuki Kaneko[1]

1. Earthquake Research Institute, University of Tokyo

Tsunamis were generated at the Sunda Strait, Indonesia, on 22 December 2018 (~21:00 local time), and a disaster (>430 victims) occurred along the coastal area close to Krakatau. As it became clear that the southwest side of Anak Krakatau Island that has continued eruptive activity in recent years had collapsed, the tsunamis are thought to have occurred with the edifice collapse of this volcanic island (PVMBG, 2018). The volume of collapsed material, the process of the collapse event, the tsunami generation and propagation processes, and the relationship between these and the eruption activity are still unclear. Therefore we investigated the sequence of the eruption and tsunami event at Anak Krakatau on 22 Dec 2018 based on satellite images and tsunami numerical simulation. Infrared data of Himawari-8 showed that thermal anomaly has continued since the middle of June 2018 but no specific anomaly signals were detected before the collapse-tsunami event. Then the data showed that the eruptive plume occurred from ~13:50 UTC on 22 December 2018. This time was 40-70 min before tsunami arrival at the coastal areas around Sunda Strait (~14:30-15:00 UTC). The first eruptive plume developed after ~13:50 but soon declined within an hour, then the second eruptive plume developed from ~15:20. It became much higher than the first one and sustained in the next couple of days. Numerical simulation of tsunami and volcanic flank collapse was carried out with the two-layer shallow water model based on non-linear long wave theory that has been developed for the tsunamis generated by gravity flows (pyroclastic flows, debris avalanche, etc.) flowing into the water. It was solved with a finite difference method. Bathymetry data is the same as that used in Maeno and Imamura (2011). The bottom friction coefficient of the gravity current was set to be 0.01 for subaerial condition and 0.06-0.12 for submarine condition. The interfacial drag coefficients between the gravity current and seawater were set to be 0.2. The four cases with different collapsed volumes (0.16, 0.21, 0.26, 0.31 km^3) were examined. The computed tsunami waveforms were compared with tide gauge records (PVMBG, 2018) at representative locations. The most likely initial condition to explain the tide gauge records was the initial collapse volume of 0.21-0.26 km^3. Other parameters don't significantly affect the results. Numerical results also showed that, for all cases, the maximum wave height (>3 m) in the SW coast of Java became higher than other areas. This tendency is consistent with the observational records that the SW coast of Java was more heavily damaged by tsunamis. This is probably because the direction of the collapse was southwestward but the direction of tsunami propagation was gradually changed from SW to S-SE by the effect of bathymetry. We also calculated tsunami travel times and estimated the occurrence time at the source, comparing with tsunami arrival times recorded in the tide gauges. As a result it seems that the tsunamis were caused by 13:54±2 min. We conclude that the collapse occurred almost simultaneously with the small eruption from ~13:50 UTC then followed by the main sustained eruption from ~15:20. In order to determine the timing and mechanism of the collapse event more precisely, it is necessary to further evaluate initial conditions and models as well as to compare with other geological and geophysical data.

Keywords: volcanic flank collapse, tsunami, Anak Krakatau

©2019. Japan Geoscience Union. All Right Reserved.

The 2018 eddifice collapse event of Anak Krakatau, Indonesia: Telseismic waveform analysis and tsunami simulation

*Shingo Watada[1], Iyan E. Mulia[1], Masumi Yamada[2], Dimas Sianipar[3]

1. Earthquake Research Institute, University of Tokyo, 2. Disaster Prevention Research Institute, Kyoto University, 3. TIGP-ESS Academia Sinica, National Central University, Taiwan

On December 22, 2018 at around 14:30 UT, a tsunami hit the coast of Java and Sumatra islands near the Sunda Strait, Indonesia and claimed more than 400 lives. The Anak Krakatau volcano island in the Sunda Strait erupted coeval with the tsunami and the summit elevation decreased from 300 m before the eruption to 100 m after the eruption, suggesting that the tsunami was generated by the subaerial or submarine edifice collapse of Anak Krakatau. SAR images show that the edifice including the summit collapsed toward southwest and disappeared into the sea. Tide gauge records around the strait suggest that the tsunami was generated at around 13:58. There were no report of a strong seismic event in Indonesia before the tsunami event, although broadband seismic networks in and around Indonesia clearly recorded unusual seismic waves (S-waves and Rayleigh waves) dominated by the long-period (50-100 sec) components. S-waves arrived at the Ryukyu islands at 14:11 and Hokkaido at 14:16. Rayleigh waves arrived at Hokkaido at 14:27. All seismic waveforms indicate occurrence of a long-period seismic event at around 13:56 near Anak Krakatau. Teleseismic body waves hint that the source duration is less than 100 sec (about 1min). Three-component broadband seismic records from four stations near the Sunda Strait can be explained by a near horizontal slightly upward force of $5x10^{11}$ N acting toward northeast for the first 20 sec followed by a near horizontal slightly dipping force of the similar magnitude acting toward southwest for about 50 sec. The force direction and angle is consistent with a collapse model predicted by Giachetti et al. (2012, Geol. Soc. London) in which a resurgent volcano Anak Krakatau collapses into the bottom of submarine Krakatau caldera at 250 m deep along a sliding slope with a dip of 8 deg. The estimated total mass of the edifice collapse is $3x10^{11}$ kg based on the empirical formula between the maximum force and the total mass of landslides (Ekström and Stark 2013, Science). Assuming the soil density 2 g/cm^3 the volume is about 0.15 km^3, roughly consistent with the submarine landslide volume 0.2 km^3 estimated from our numerical tsunami simulation for tide gauge records. Based on the routine seismic monitoring no large earthquake enough to cause tsunami was registered. On the other hand, long-period seismic waves from the seismic event at Anak Krakatau coeval with the tsunamis arrived at Jakarta 40 sec after the event. If long-period seismic events were routinely monitored in Indonesia, we could have detect the edifice collapse of the Anak Krakatau volcano and were aware of the possibility of tsunami generation prior to the arrivals of disastrous tsunamis to the coasts.

Keywords: 2018 tsunami in Sunda Strait, 2018 Anak Krakatau volcano eruption edifice collapse, seismic waves and tsunamis from the edifice collapse, submarine landslide

©2019. Japan Geoscience Union. All Right Reserved.

The 2018 edifice collapse event of Anak Krakatau, Indonesia: Landslide movement history estimated from seismic waveforms

*Masumi Yamada[1], Shingo Watada[2], Haruhisa Nakamichi[1], Iyan Mulia[2], Karyono Dr.[3]

1. Disaster Prevention Research Institute, Kyoto University, 2. Earthquake Research Institute, University of Tokyo, 3. Center for Earthquake and Tsunami, BMKG

On December 22, 2018, a huge Tsunami occurred at the Sunda strait in Indonesia, and more than 400 people were killed. There was no large earthquake at that time and the tsunami was associated with the volcanic eruption and edifice collapse in Anak Krakatau island.

The seismic signals due to this event are recorded by the broadband seismic network in Indonesia. There are about 170 broadband stations all over Indonesia, with a spacing 50-100 km. We performed the seismic waveform inversion using long-period component (20-100 s) at the near-field distance (60-200 km), assuming a single force mechanism. We also performed a grid search with 10 km spacing to estimate the location of the source.

Our result shows that the onset of the event was about 14:55:50 (UTC), December 22, 2018. The duration of the source time function is about 1 min with a large amplitude, followed by a smaller signal about a few min. The particle motion of the source time function suggests the event was occurred from northeast to southwest direction with very low dipping angle (about 10 degree). The location of the event was estimated at the Anak Krakatau.

This seismic event was most likely caused by the edifice collapse of the Anak Krakatau. The satellite image shows that the southwest half of the island was subsided after the collapse, and there is a oceanic basin at the depth of 200 m in the southwest of the island, which was the old crater created by the eruption in 1883. These geometries are consistent with the movement history estimated by the seismic waveform inversion.

Based on the scaling relationship between single force amplitude vs mass of the landslide (Ekström and Sterk, 2013), the mass was estimated as 0.2-0.4 * 10^12 kg. This number is consistent with the volume estimated by the tsunami waveform simulation (Maeno and Kaneko 2019; Watada et al., 2019). We think that the edifice collapse was very low-dipping and moved like a landslide, and the mass sliding into the ocean caused the huge tsunami.

The relationship between this landslide and volcanic eruption is still debating, but Center for Volcanology and Geological Disaster Mitigation in Indonesia officially reported the timing of the eruption was 15:03 (UTC). Since the occurrence of the landslide was estimated as 14:55:50, the eruption may be triggered by the landslide, such as the 1980 eruption of Mount St. Helens triggered by the massive landslide.

Keywords: Anak Krakatau, Volcanic eruption, Landslide, Seismic waveform inversion

©2019. Japan Geoscience Union. All Right Reserved.

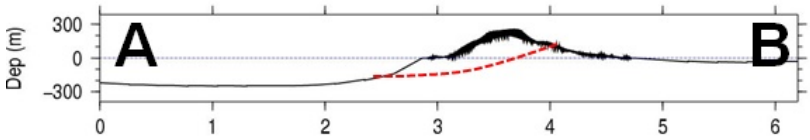

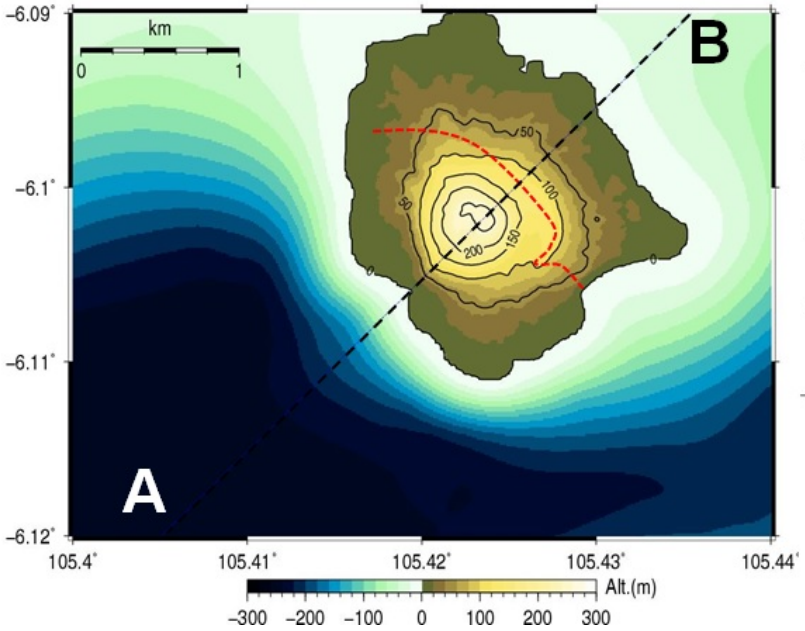

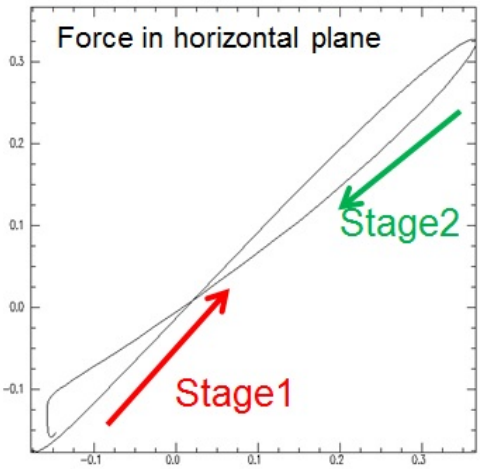

©2019. Japan Geoscience Union. All Right Reserved.

Intense Swarm Activity in the Vicinity of Yake-dake Volcano, Central Japan, Started in November 2018

*Shiro Ohmi[1]

1. Earthquake Hazards Division, Disaster Prevention Research Institute, Kyoto University

An intense seismic swarm activity started in November, 2018 in the vicinity of the Yakedake volcano, Hida mountain range, central Japan. It started on November 22 and lasted for about 10 days (hereafter sited as Series A) . Hypocenters are located at the western flank of the Yakedake volcano in the depth range from 3 km to 4 km below sea level. On December 4, a small swarm activity occurred in the Kamikochi area, where is the eastern flank of Yake-dake volvano, that lasted for two days (Series B). Other small activities took place at the end of January 2019 (Series C) to the western area of the activity of Series A, as well as an activity just beneath the ridge of Hida mountain range where is several kilometers south to the summit of the Yake-dake volcano in the beginning of February 2019 (Series D).

Earthquakes in Series A exhibit ordinary characteristics of tectonic earthquakes with NW-SE compressional stress field and neither significant hypocenter migration nor change in source mechanism were observed during the activity. Earthquakes in Series B, however, some exhibit normal fault type stress field which is not coincide with the regional stress field.

The maximum intensity reported by JMA was less or equal to level 2 for all the events during the activity, however, instrumental seismic intensity observed nearby hypocentral area by DPRI recorded as large as level 4 for some earthquakes. Monitoring data of Yakedake volcano, that include crustal movement by GNSS and tiltmeter, geomagnetic total intensity by proton magnetometer, and ground temperature nearby summit, did not show the anomalous behavior during the swarm activity.

Keywords: Yake-dake volcano, volcano tectonic earthquakes, swarm activity

©2019. Japan Geoscience Union. All Right Reserved.

Change of the volcanic activity at Kuju volcano.

*Mori Takehiko[1], Muga Yaguchi[1], Yasushi Kawamura[2], Hideyuki Hiramatsu[3], Keiji Ikeda[2], Sugai Akira[2], Michitomo Sugahara[2], Kenichi Takata[2], Kyo Matsumoto[2], Fukuoka Regional Headquarters Japan Meteorological Agency, Oita Meteorological Office Japan Meteorological Agency

1. Meteorological Research Institute, Japan Meteorological Agency, 2. Fukuoka Regional Headquarters, Japan Meteorological Agency, 3. Oita Meteorological Office, Japan Meteorological Agency

In Kuju volcano, after an eruption occurs at the east-hillside of Mt. Hossyo (near Mt. Iwo) in October 1995 and January 1996, the eruption has not occurred. The continuous volcanological observation by a research institution and Japan Meteorological Agency started after the eruption in 1995. Although the active seismicity which has the hypocenter in the shallow zone under Mt. Iwo was observed, the activity became calm after 2005. Moreover, after 1995, continued cooling in the shallow zone under Mt. Iwo was obtained by the geomagnetic observation, and the trend for fumarolic activity to decline gradually was seen. In this way, the declining volcanic activity was captured by various observation data.
Changes in volcanic activity of Kuju volcano began to appear around 2012. First, the GNSS observation showed that the length of the base line between the two points crossing Kuju volcano began to grow slightly. Next, the geomagnetic observation began showing the heat-reserve trend in the shallow region of Mt. Iwo from 2014. The gradual increase in fumarolic activity starts around 2015, and the slight increase in seismic activity also started around 2016.
Before the 1995 eruption, continuous volcano observation at Kuju volcano was not done, so the change of various phenomena preceding the eruption was not sufficiently obtained. We have not been able to judge whether the current volcanic activity change is an activity suggesting future eruptive activity. However, we believe that accumulation of observational data will help predict future volcanic activity. Then, by continuous observation of multiple items not only including geophysical observations but a volcano chemistry observation, the character of the volcanic activity in Kuju Volcano is grasped, and change of volcanic activity is monitored.

Keywords: volcanic activity, crustal deformation, geomagnetic variation, Volcanic Gas, phreatic explosion

©2019. Japan Geoscience Union. All Right Reserved.

Posteruptive Thermoelastic Deflation of Intruded Magma in Usu Volcano, Japan, 1992–2017

*Yosuke Aoki[1], Xiaowen Wang[1]

1. Earthquake Research Institute, University of Tokyo

Secular ground subsidence at Usu volcano (Japan) has been reported around the eruption vents following the four eruptions in 1910, 1943, 1977, and 2000. However, the mechanisms accounting for the subsidence have not been well understood. In this study, we systematically investigated the posteruptive deformation at Usu volcano using interferometric synthetic aperture radar based on 111 JERS, ALOS-1, and ALOS-2 images acquired from 1992 to 2017. We also calculated quasi east-west and vertical ground displacements between 2006 and 2017. Our results show three localized deformation regions from west to east of Usu volcano with their locations corresponding to the 2000, 1977, and 1943 eruption vents, respectively. All the deformation sites show patterns of east-west contraction and subsidence. The extent and rate of posteruptive subsidence declined dramatically at the vent of the 2000 eruption site from 2006 to 2017, decreased gradually at the 1977 vent, and show a steady pattern for the 1943 site during 1992-2017. We ascribed the observed posteruptive subsidence to thermoelastic contraction of a sphere intruded at the time of the eruptions to constrain locations, depths, and volumes of heat sources with the assumption of the spherical source shapes. Thermoelastic modeling reveals that the heat sources are embedded at shallow depths not deeper than 400 m below sea level with volumes of about (8.72 ±0.19) $\times 10^6$, (132.18 ±5.21) $\times 10^6$, and (49.51 ±2.02) $\times 10^6$ m^3 for the 2000, 1977, and 1943 eruption sites, respectively. The modeling also highlights the importance of underground water in assessing the thermal diffusion process and the associated posteruptive deformation.

Keywords: Lava dome, Thermal contraction, InSAR

©2019. Japan Geoscience Union. All Right Reserved.

[J] Oral | S (Solid Earth Sciences)：S-VC Volcanology

Tue. May 28, 2019 10:45 AM - 12:15 PM JST | Tue. May 28, 2019 1:45 AM - 3:15 AM UTC | IC 2F

[S-VC38] Active Volcanism

convener:Yuta Maeda(Nagoya University), Takahiro Miwa(National research institute for earth science and disaster prevention), Takeshi Nishimura(Department of Geophysics, Graduate School of Science, Tohoku University), Chairperson:Jun Oikawa, Takeshi Tameguri

This session discusses various aspects of active volcanisms including, but not limited to, recent and historical eruptions, various phenomena associated with the volcanic activities, underground structures of the volcanoes, and developments of new instruments based on geophysical, geochemical, geological, and multidiscipline approaches. We also welcome studies on understanding and predicting the transitions of the eruptive activities from observational, theoretical, and experimental approaches.

10:45 AM - 11:00 AM JST | 1:45 AM - 2:00 AM UTC

[SVC38-12] Volcanic tremors and ash fall volumes associated with the 2018 vulcanian eruptions of Shinmoe-dake

*Jun Oikawa[1], Yasuhisa Tajima[2] (1.Earthquake Research Institute, University of Tokyo, 2.NIPPON KOEI CO.,LTD.)

11:00 AM - 11:15 AM JST | 2:00 AM - 2:15 AM UTC

[SVC38-13] Crustal deformation around the Kirishima Volcano Group detected by GNSS and SAR observation after 2018 eruption.

*Hiroshi Yarai[1], Tomokazu Kobayashi[1], Satoshi Fujiwara[1], Tomokazu Kobayashi[1], Hiroshi Munekane[1], Masaki Honda[1], Kyonosuke Hayahsi[1], Satoshi Kawamoto[1], Atsuko Oowaki[1] (1.GSI of Japan)

11:15 AM - 11:30 AM JST | 2:15 AM - 2:30 AM UTC

[SVC38-14] Harmonic tremor during 2011 eruption at Shinmoedake, Japan

*Minoru Takeo[1] (1.Earthquake Research Institute, University of Tokyo)

11:30 AM - 11:45 AM JST | 2:30 AM - 2:45 AM UTC

[SVC38-15] Forecasting Volcanic Eruption of Sakurajima Volcano Based on Magma Intrusion Rate

*Masato Iguchi[1], Takeshi Tameguri[1], Jun-ichi Hirabayashi, Haruhisa Nakamichi[1] (1.Sakurajima Volcano Research Center, Disaster Prevention Research Institute, Kyoto University)

11:45 AM - 12:00 PM JST | 2:45 AM - 3:00 AM UTC

[SVC38-16] Tilt and strain change before and after the explosion at Minami-dake, Sakurajima, in 2017

*Kohei Hotta[1], Masato Iguchi[2] (1.University of Toyama, 2.Disaster Prevention Research Institute, Kyoto University)

12:00 PM - 12:15 PM JST | 3:00 AM - 3:15 AM UTC

[SVC38-17] Pyroclastic Flow Accompanied with an Eruption on June 16, 2018 at Sakurajima Volcano

*Takeshi Tameguri[1], Masato Iguchi[1], Masayuki Maki[2], Haruhisa Nakamichi[1], Daisuke Miki[1] (1.Sakurajima Volcano Research Center,Disaster Prevention Research Institute, Kyoto University, 2.Research Field in Integrated Studies,Kagoshima University)

Volcanic tremors and ash fall volumes associated with the 2018 vulcanian eruptions of Shinmoe-dake

*Jun Oikawa[1], Yasuhisa Tajima[2]

1. Earthquake Research Institute, University of Tokyo, 2. NIPPON KOEI CO.,LTD.

Kirishima volcanic chain is one of the active volcanoes in southern Kyushu, Japan and is categorized into a composite volcano whose active vents are Shinmoe-dake and Ohachi. The latest eruptive activity of Shinmoe-dake started on August 22, 2008. Subsequently, it erupted on March 30, April 17, May 27, June 27 and 28, and July 5 and 10, 2010. In 2011, the eruption started on January 19 included subplinian and vulcanian explosions. and was followed by sub-Pulinian eruption on 27 January. Eruptive activity gradually ceased since February 2, and moved to Vulcanian activities. It erupted on October in 2017 and on March in 2018. Eruptions continued until June 27. Tajima et. al (JpGU 2019) show volcanic ashfall volumes for each eruption in 2018 and we discuss the relation of ashfall volumes and durations of eruptions that is characterized by the power law: ashfall volume is proportional to durations to the second power.

Keywords: vulcanian eruption, volcanic tremor, ashfall volumes, Shinmoe-dake volcano

©2019. Japan Geoscience Union. All Right Reserved.

Fig. 1

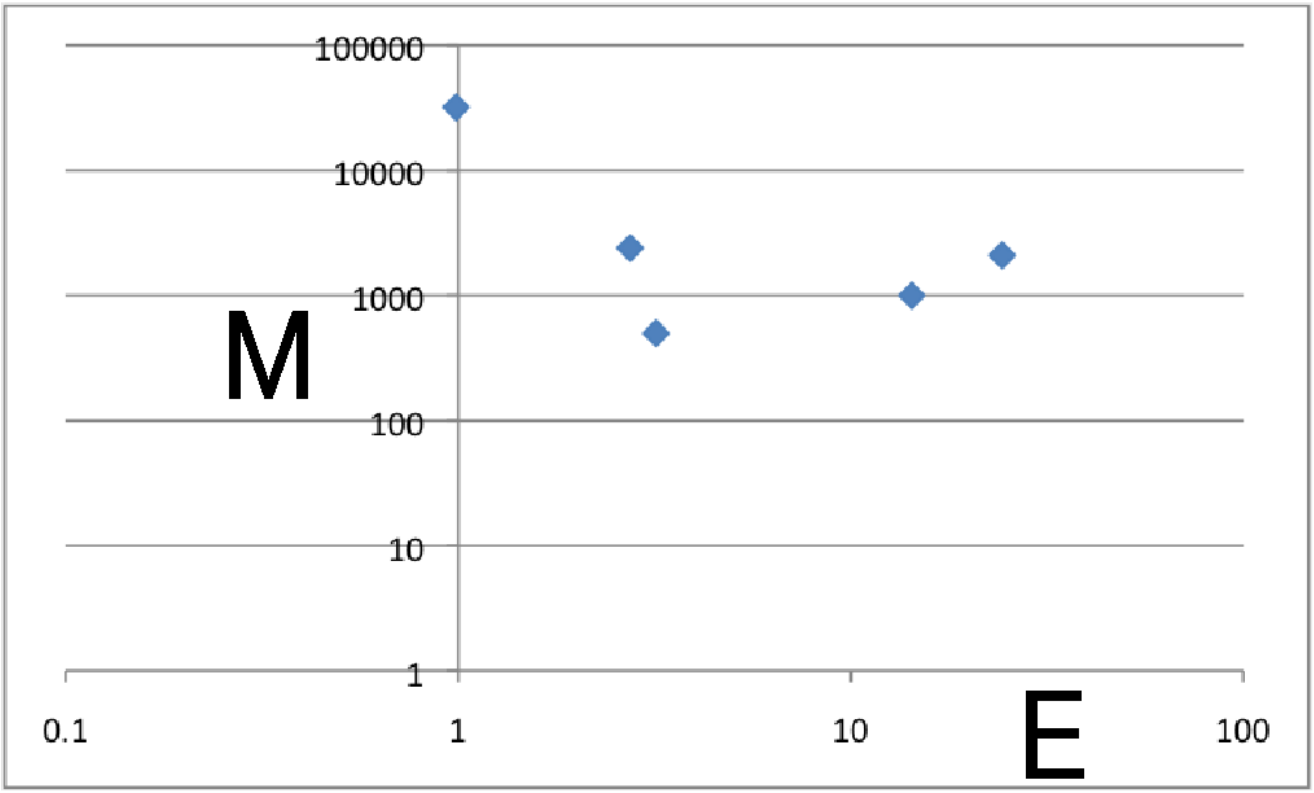

Fig. 2

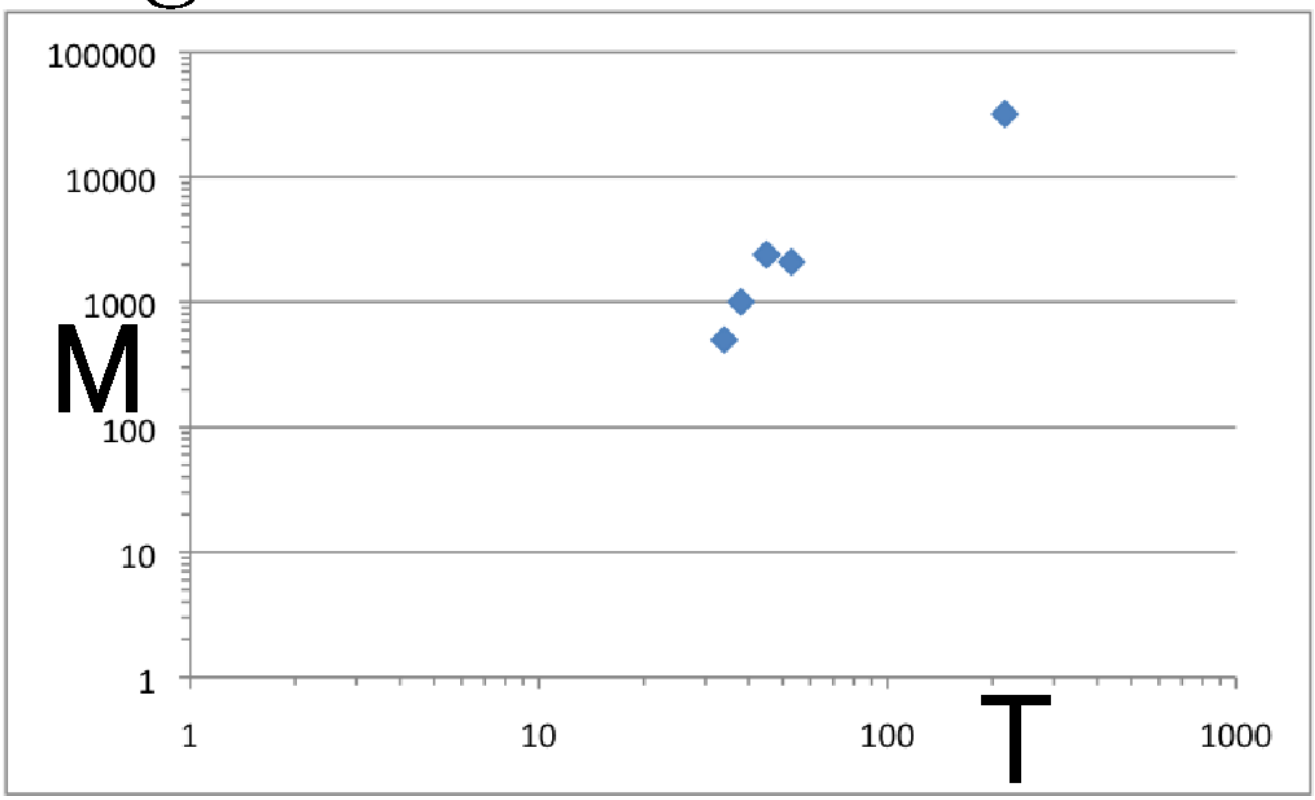

©2019. Japan Geoscience Union. All Right Reserved.

Crustal deformation around the Kirishima Volcano Group detected by GNSS and SAR observation after 2018 eruption.

*Hiroshi Yarai[1], Tomokazu Kobayashi[1], Satoshi Fujiwara[1], Tomokazu Kobayashi[1], Hiroshi Munekane[1], Masaki Honda[1], Kyonosuke Hayahsi[1], Satoshi Kawamoto[1], Atsuko Oowaki[1]

1. GSI of Japan

Since July 2017, GNSS Earth Observation Network (GEONET) maintained by Geospatial Information Authority of Japan (GSI) has observed elongation at the baseline surrounding the Kirishima volcano group. Sharp shortening occurred at the eruption of Shinmoedake volcano in March, 2018, after which elongation was observed again. Similar crustal deformations are also observed during the Shinmoedake eruption in 2011, and at that time expansion and contraction of magma reservoir of about 6 to 7 km northwest of Shinmoedake is presumed (for example, Kobayashi et al., 2012) . In addition, in the Iwo-yama located in the northwest of Kirishima-yama, expansive crustal deformation centered the Iwo-yama was captured by analysis of Daichi 2 (ALOS-2) SAR data. In April 2018, an eruption took place in Iwooyama for the first time in 250 years.

Detailed investigation of crustal deformation of the Kirishima volcano group is important in grasping the situation of volcanic activity. In this research, we investigated the crustal deformation of the Kirishima volcano group including Shinmoe-dake and Iwo-yama after the eruption of Shinmoedake and Iwozan in 2018, using GNSS observation and ALOS-2 (Daichi 2) SAR data analysis.

Keywords: Kisihisma volcano Group, Shinmoe-dake, Iwo-yama, crustal deformation, GNSS, SAR

©2019. Japan Geoscience Union. All Right Reserved.

Harmonic tremor during 2011 eruption at Shinmoedake, Japan

*Minoru Takeo[1]

1. Earthquake Research Institute, University of Tokyo

Volcanic tremor is a continuous seismic signal that is observed near active volcanoes and is often accompanied by evidence of subterranean movement or pressure fluctuation due to a physical or chemical process inside the volcano. However, the source of volcanic tremor is still poorly understood. Most existing tremor’ s models, except for Julian’ s nonlinear channel flow model (Julian, 1994), consider an acoustic resonance in the magma channels, but mechanism to excite this resonance has not been identified until now.

During 2011 eruption at Shinmoedake, Japan, we observed a series of volcanic tremors including harmonic tremor which exhibits a set of narrow, evenly spaced frequency peaks. Natsume *et al.*(2018) perform non-linear time-series analysis on a harmonic tremor recorded near the crater. They found that the stable oscillation of the harmonic tremor is predominantly a limit cycle, implying that the harmonic tremor is generated by self-sustained oscillation. In this paper, I propose a new model of harmonic tremor and reproduce the topological characteristics of observed harmonic tremor using the new model. I formulate a lumped-parameter model of incompressible viscous fluid flow through a partially constrictive path, which seems to be realistic modeling in a shallow part of conduit. I consider inertias and resistances in the upstream and in downstream pipes. The upstream pipe is connected to a large chamber with pressure of Po. Lengths and radiuses of the pipes and the constrictive path could be set flexibly in this model. This model leads to a third-order system of nonlinear ordinary differential equations with functions of area of throat, fluid velocities in upper stream and in downstream. The equations of the model are as follows:
Mass conservations in upstream and in downstream of the constricting path; Conservation of momentum in upstream and in downstream of the constricting path; Equations of motion in upstream pipe and in downstream pipe; Elastic law of the constrictive path;
Typical frequency of the harmonic tremor is 1~2Hz and the wavelength seems to be hundreds meter, so these signals were recorded within a distance of one wavelength, being little affected by wave propagation. Therefore, assuming that these observed signals represent only linear transformations of one parametric function of the nonlinear tremor model, we can compare topological characteristics of observed and simulated signals to evaluate validity of the new model. When the resistance of downstream is larger than that of upstream, a self-sustained oscillation starts in a suitable parameter range. For different driving pressure (Po), numerical solutions exhibit steady flow, simple limit-cycle oscillation, limit-cycle oscillation with double-loops or with quadruple-loops, and a chaotic oscillation. Changing Po in time, I succeed in simulating a harmonic tremor which has same topological characteristics with the observed harmonic tremor in several portions of time series (see Figure 1).

Keywords: volcanic tremor, nonlinear oscillation, chaos

©2019. Japan Geoscience Union. All Right Reserved.

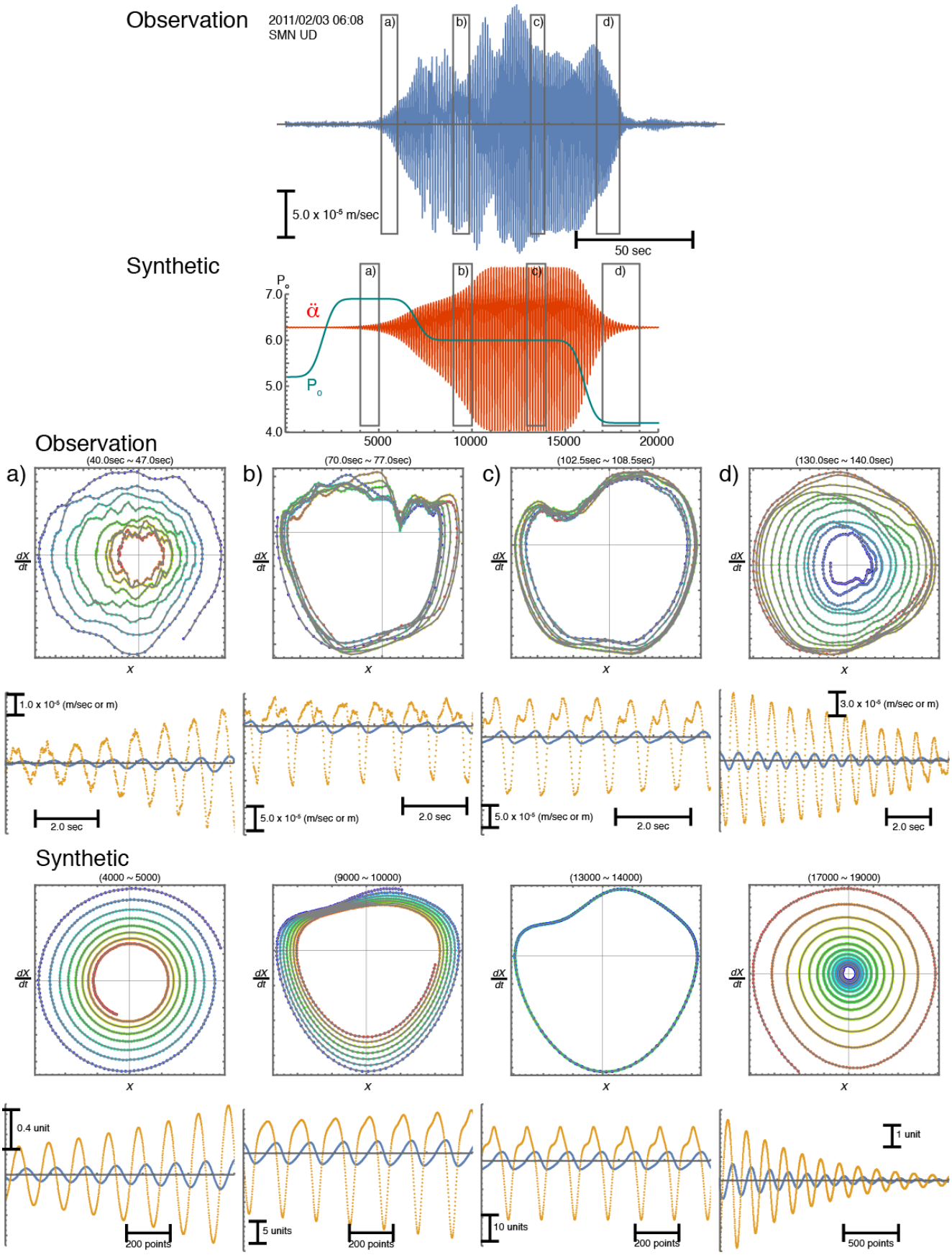

Figure 1

©2019. Japan Geoscience Union. All Right Reserved.

Forecasting Volcanic Eruption of Sakurajima Volcano Based on Magma Intrusion Rate

*Masato Iguchi[1], Takeshi Tameguri[1], Jun-ichi Hirabayashi, Haruhisa Nakamichi[1]

1. Sakurajima Volcano Research Center, Disaster Prevention Research Institute, Kyoto University

In order to find an empirical event branch logic from abnormal phenomena to following volcanic activity for forecasting scale and type of eruption, the magma intrusion rate prior to eruptions of Sakurajima volcano is examined using ground deformation mostly from observation data and partially based on legends, for eruptions after the 20th century: the 1914 eruption starting with plinian eruption followed by effusion of lava, the 1946 eruptions with lava effusion, eruptions at the summit crater of Minamidake during the period from 1955 to 2005, and vulcanian eruptions at Showa crater east of the summit from 2006 to 2017. Prior to the 1914 eruption, it is estimated that the magma intrusion rate attained a level of approximately 10^8 m^3/day and was on the order of 10^6 m^3/day during the effusion of lava in the 1946 eruption. During the eruptive period of Minamidake summit crater, three types of eruption occurred: vulcanian eruption, strombolian/lava fountain and continuous emission of volcanic ash. In cases of intrusion of magma forming a new conduit, the intrusion rate immediately before the 1914 eruption exceeded 10^8 m^3/day, but only 10^6m^3/day in the dyke-forming event of August 15, 2015. Magma intrusion rate into a pre-existing conduit prior to eruptions at Minamidake summit crater are ordered as follows: vulcanian eruption ($1x10^5$ to $8x10^5$ m^3/day) > continuous emission of volcanic ash (approximately $1x10^5$m^3/day) > strombolian/lava fountain ($0.2x10^5$ to $2x10^5$ m^3/day). The magma intrusion rate prior to vulcanian eruptions at Showa crater is smaller (approximately 10^4m^3/day) than for eruptions at Minamidake summit crater. However, the rate reached an order of 10^5m^3/day prior to lava fountain on August 22, 2017. Magma intrusion rates well correspond to the scale and type of eruption. In the case of magma intrusion under detection, the change of volcanic gas and increase in the heat discharge rate are available for the empirical event branch logic.

Keywords: magma intrusion rate, Sakurajima, volcanic earthquake, vulcanian eruption, strombolian eruption, plinian eruption

©2019. Japan Geoscience Union. All Right Reserved.

Tilt and strain change before and after the explosion at Minami-dake, Sakurajima, in 2017

*Kohei Hotta[1], Masato Iguchi[2]

1. University of Toyama, 2. Disaster Prevention Research Institute, Kyoto University

A deformation source associated with each eruption at Sakurajima have been estimated beneath Minami-dake [Ishihara, 1990; Iguchi et al., 2013]. Deformation sources for mid-long-term magma intrusion event were estimated beneath Aira caldera, Kita-dake and Minami-dake; and the deformation source beneath Kita-dake was found to act as a buffer of mid-long eruptive activity at Sakurajima [Hotta et al., 2016].

On November 13, 2017, an explosion with an infrasound occurred at Minami-dake at 22:07. Ground deformation was accompanied and kept for approximately five hours. For the period of 22:07–22:10 (period I), a large strain change at Arimura observation tunnel, which is the nearest tilt/strain station from Minami-dake crater and operated by Ministry of Land Infrastructure, Transport and Tourism, was detected whereas no significant change in tilt/strain was detected at other tilt/strain stations. For the period of 22:10–22:50 (period II), tilt/strain change was detected at all tilt/strain stations associated with violent eruptive activity. At around 23:00, style of eruption shifted from Vulcanian to Strombolian. For the period of 22:50–3:00 of the next day (period III), a pattern of tilt change at Japan Meteoritical Agency (JMA)-A station, which located on western area of Sakurajima, and tilt/strain gradually stopped.

We modeled the detected tilt/strain change using a finite spherical source model [McTigue, 1987]. Because of the poor constraint of the radius of the source, we assumed the radius of the source as 20 m for period I and 200 m for periods II and III. A shallow deflation source was located at a depth of 0.1 km above sea level beneath Minami-dake for period I. A deeper deflation source was located at a depth of 5.9 km below sea level beneath Minami-dake for period II. Then, a deflation source was located at a depth of 5.9 km below sea level beneath Kita-dake for period III. Deformation sources beneath Minami-dake for periods I and II are corresponding to the deformation sources previously found for each eruption at Sakurajima. Meanwhile, the deformation source beneath Kita-dake for period III is corresponding to the deformation source beneath Kita-dake which was found during mid-long eruptive activity. Each eruption at Sakurajima revealed to cause deflation of not only Minami-dake source but also Kita-dake one, which considered to repeat inflation/deflation during mid-long eruptive activity at Sakurajima. Temporal development of deflation accompanied by the eruption on November 13, 2017, will be revealed in our future study.

Keywords: Sakurajima Volcano, Explosion at Minami-dake, Ground deformation, Tilt and strain

©2019. Japan Geoscience Union. All Right Reserved.

Pyroclastic Flow Accompanied with an Eruption on June 16, 2018 at Sakurajima Volcano

*Takeshi Tameguri[1], Masato Iguchi[1], Masayuki Maki[2], Haruhisa Nakamichi[1], Daisuke Miki[1]

1. Sakurajima Volcano Research Center,Disaster Prevention Research Institute, Kyoto University, 2. Research Field in Integrated Studies,Kagoshima University

At Sakurajima volcano, the explosive eruption has repeated at the summit crater since 1955. The eruption resumed for the first time in 58 years in the Showa crater on the eastern flank of the mountain, and the eruption activity was particularly active from 2009. The eruption activity has been transitioning again from the Showa crater to Minamidake summit crater since 2018. Characteristics of the explosive eruption include ejection of volcanic bombs, generation of shock waves, the release of sudden volcanic ash and gases. Besides, although the frequency is small, the explosive eruption of the Minamidake summit crater and Showa crater produces small pyroclastic flows. The pyroclastic flow is one of the most dangerous phenomena of volcanic eruption, with pyroclastic flow of high temperature and volcanic gas flowing down the flank at high speed, prediction of the pyroclastic flow occurrence is important for volcanic disaster prevention.
Seven pyroclastic flows have been confirmed with the eruption at Minamidake summit crater between 1967 and 1985 (Kamo and Ishihara, 1986). Furthermore, 37 pyroclastic flows have been reported to occur in the Showa crater from 2006 to 2014 with the eruption by the Japan Meteorological Agency. Travel distance of the pyroclastic flows from the Minamidake and Showa craters were less than 2 km. Although it is Sakurajima which continues active eruption activity, pyroclastic flow is minor phenomenon and the mechanism of pyroclastic flow generation in Sakurajima has not been elucidated. In the future, when the eruption activity becomes active, it is necessary to consider the occurrence of a large pyroclastic flow, and it is important to understand the occurrence mechanism of the pyroclastic flow. In this study, we will clarify the characteristics of precursory seismic activity and ground deformation data on the pyroclastic flow occurred in the Mimamidake and Showa craters between 2012 and 2018. In addition, we investigate whether it is possible to predict the scale and travel distance of the pyroclastic flow from the data of the precursory earthquakes and ground deformation.
In the explosive eruption at Minamidake summit crater that occurred on June 16, the volcanic ash reached to 4700 m and the pyroclastic flow went down 1.3 km from the crater in the southwest direction. The expansion of the ground deformation was observed about 18 hours before the occurrence of the eruption. The precursory earthquake sporadically occurred about 1 hour before the eruption, but it was not a clear activity compared to the eruption of the Showa crater. The pictures of the pyroclastic flow shows that the ejected material dropped from the plume flowed down the slope about 1 minute after the eruption started to rise. The pyroclastic flow does not occur simultaneously with the eruption, which has the same characteristics as the pyroclastic flow that occurred during the Minamidake activity period (Kamo and Ishihara, 1986). Amount of ejecta by the eruption is estimated to be 280,000 m3 from the ground deformation data. Not all of the ejecta will be pyroclastic flow. It is necessary to estimate the amount of pyroclastic flow out of the ejecta in order to predict the flow down distance. Estimate the amount of ejecta that became a pyroclastic flow from the calculation of fall volcanic ash using weather radar.

Keywords: Sakurajima volcano, pyroclastic flow

©2019. Japan Geoscience Union. All Right Reserved.

[J] Oral | S (Solid Earth Sciences)：S-VC Volcanology

Tue. May 28, 2019 1:45 PM - 3:15 PM JST | Tue. May 28, 2019 4:45 AM - 6:15 AM UTC | IC 2F

[S-VC38] Active Volcanism

convener:Yuta Maeda(Nagoya University), Takahiro Miwa(National research institute for earth science and disaster prevention), Takeshi Nishimura(Department of Geophysics, Graduate School of Science, Tohoku University), Chairperson:Hiroshi Aoyama, Satoshi Miura

This session discusses various aspects of active volcanisms including, but not limited to, recent and historical eruptions, various phenomena associated with the volcanic activities, underground structures of the volcanoes, and developments of new instruments based on geophysical, geochemical, geological, and multidiscipline approaches. We also welcome studies on understanding and predicting the transitions of the eruptive activities from observational, theoretical, and experimental approaches.

1:45 PM - 2:00 PM JST | 4:45 AM - 5:00 AM UTC

[SVC38-18] Ground deformation observed at the crater area of Tokachidake volcano

*Hiroshi Aoyama[1], Takeshi Hashimoto[1], Ryo Tanaka[1], Hiromitsu Oshima[1], Koichiro Saito[2], Tsuyoshi Michishita[2], Satoshi Okuyama[2], Volcanic Observation and Warning Center Sapporo Regional Headquarters[2] (1.Institute of Seismology and Volcanology, Faculty of Science, Hokkaido University, 2.Japan Meteorological Agency)

2:00 PM - 2:15 PM JST | 5:00 AM - 5:15 AM UTC

[SVC38-19] Moment tensor inversion of very-long-period seismicity at Stromboli volcano based on a very-near-field observation

*Shunsuke Sugimura[1,2], Maurizio Ripepe[2], Giorgio Lacanna[2], Denis Legrand[3], Sébastien Valade[4], Takeshi Nishimura[1] (1.Department of Geophysics, Graduate School of Science, Tohoku University, 2.Department of Earth Sciences, University of Florence, Italy, 3.UNAM University, Mexico, 4.GFZ-German Research Centre for Geosciences, Potsdam, Germany)

2:15 PM - 2:30 PM JST | 5:15 AM - 5:30 AM UTC

[SVC38-20] Pressure source estimation of tilt changes associated with small explosions at Stromboli volcano

*Ayumu Ishikawa[1], Takeshi Nishimura[1], Hiroshi Aoyama[2], Ryohei Kawaguchi[3], Eisuke Fujita[4], Takahiro Miwa[4], Taishi Yamada[4], Maurizio Ripepe[5], Riccardo Genco[5] (1.Graduate school of science, Tohoku university, 2.Faculty of science, Hokkaido university, 3.Meteorological Research Institute, 4.National Research Institute for Earth Science and Disaster Resilience, 5.University of Florence)

2:30 PM - 2:45 PM JST | 5:30 AM - 5:45 AM UTC

[SVC38-21] Seismic and acoustic waves excited by volcanic explosion: analyses of energy ratio and source spectra

*Mohammad Hasib[1], Takeshi Nishimura[1], Hisashi Nakahara[1] (1.Department of Geophysics, Graduate School of Science, Tohoku University)

2:45 PM - 3:00 PM JST | 5:45 AM - 6:00 AM UTC

[SVC38-22] Field survey report on Zao Volcano (2012−2018)

*Akio Goto[1], Noriyoshi Tsuchiya[2], Nobuo Hirano[2], Miwa Kuri[3], Tetsuya Matsunaka[4], Kengo Sawayama[2] (1.Center for Northeast Asian Studies, Tohoku University, 2.Graduate School of Environmental Studies, Tohoku University, 3.International Research Institute of Disaster Science, Tohoku University, 4.Institute of Nature and Environmental Technology, Kanazawa University)

3:00 PM - 3:15 PM JST | 6:00 AM - 6:15 AM UTC

[SVC38-23] Inflation Event of Zao Volcano in 2015

*Satoshi Miura[1], Mare Yamamoto[1], Masahiro Ichiki[1], Tomotsugu Demachi[1] (1.Graduate School of Science, Tohoku University)

Ground deformation observed at the crater area of Tokachidake volcano

*Hiroshi Aoyama[1], Takeshi Hashimoto[1], Ryo Tanaka[1], Hiromitsu Oshima[1], Koichiro Saito[2], Tsuyoshi Michishita[2], Satoshi Okuyama[2], Volcanic Observation and Warning Center Sapporo Regional Headquarters[2]

1. Institute of Seismology and Volcanology, Faculty of Science, Hokkaido University, 2. Japan Meteorological Agency

Tokachidake is an active volcano that repeated magmatic eruptions in 1926, 1962 and 1988. Prior to these eruptions, phreatic eruptions had been confirmed from several years ago. Although there has been no magmatic eruption in the last 30 years, long-term expansion centered around the 62-2 crater has been observed since around 2006. One of the GNSS stations near the crater moved more than 50 cm in total till the end of 2017. Coinciding with this expansive crustal deformation, long-term demagnetization under the 62-2 crater has also been observed.

Repetitive GNSS observations around the crater for more than 10 years suggested the fluctuation of deformation area centered around 62-2 crater and Taisho crater. Analysis of the temporal change of the motion vector assuming an isotropic deformation source at these two places revealed that the two inflation sources expanded at a substantially constant rate as a whole while changing the rate complementarily. Since the assumed fluctuation source is extremely shallow and flowing out of hot muddy water at the bottom of the 62-2 crater has occasionally been observed, we consider that this long-term deformation reflects the mechanical response of the shallow hydrothermal system.

Geodetic observation revealed that the long-term expansive deformation turned into stagnation in the period from the end of 2017 to the beginning of 2018. Almost at the same time, the total magnetic force data showed change in its trend of demagnetization. Also, in the Furikozawa fumaroles, an expansion of the geothermal area and an increase in fumarolic activity have been reported since around 2017.

Under such circumstances, number of volcanic earthquakes and tremors temporarily increased from late May 2018. A volcanic tremor on May 29th which activated seismicity was accompanied by a tilt motion showing a stepwise subsidence in the crater direction. Therefore, we visually examined the tiltmeter record from January 2018 which were obtained at the station MTKW (about 650 m west of the crater). Although there were few tilt events until around the end of March, occurrence frequency of such event increased thereafter, and it further increased on May 29th. A total of 117 events were identified by the end of August, 10 events by the end of March, 30 events in April and May and 77 events by August. Tilt events generally show a stepwise subsidence in the crater direction, but careful examination of each event revealed that there are various types of events: tilt change following a small preceding phase, inflation –deflation pattern, gradual change more than a few minutes, and events associated with VLP-like seismic signals, etc. Examining the direction of the tilt motion vector at MTKW about these 117 events, almost 90 % shows subsidence in the crater direction of N120 –135°E. For the event on May 29th, a preliminary analysis using tilt data around the crater showed that the tilt motion can be roughly explained by an isotropic deflation source of 130 m^3 located at 1300 m above sea level slightly south of the 62-2 crater.

Summarizing the shallow activities of Tokachidake volcano, expansion of the geothermal area and increase in fumarolic activity appeared almost at the same time with the latest stagnation of long-term expansive deformation and demagnetization for over 10 years. Volcanic earthquakes and tremors

©2019. Japan Geoscience Union. All Right Reserved.

accompanying stepwise subsidence in the crater direction increased around the same time with the deflation of the crater area. We can roughly consider two hypotheses for the latest deflation: one is a decrease in the amount of hot water supplied from the deep part, and the other is a change in supply / release balance due to an increase in discharge amount from fumaroles. Expansion of the fumarolic area, increase of the fumarolic activity, and increase of the tilt event strongly suggest the possibility of the latter hypothesis, although it is difficult to discuss the amount supplied from the deep part.

Keywords: Volcano, Earthquake, Crustal Deformation, Hydrothermal System, Phreatic Eruption

©2019. Japan Geoscience Union. All Right Reserved.

Moment tensor inversion of very-long-period seismicity at Stromboli volcano based on a very-near-field observation

*Shunsuke Sugimura[1,2], Maurizio Ripepe[2], Giorgio Lacanna[2], Denis Legrand[3], Sébastien Valade[4], Takeshi Nishimura[1]

1. Department of Geophysics, Graduate School of Science, Tohoku University, 2. Department of Earth Sciences, University of Florence, Italy, 3. UNAM University, Mexico, 4. GFZ-German Research Centre for Geosciences, Potsdam, Germany

In recent decades, moment tensor inversion of very-long-period (VLP, 2-100 s) earthquakes associated with explosive/non-explosive activities has been applied to estimate the optimal source location and mechanism. Source mechanism of VLP associated with explosions at Stromboli volcano has been interpreted as the pressure source of opening/closing cracks embedded in the volcanic medium (Chouet et al., 2003). However, the nearest temporal station is 300 m away from the craters so that the source mechanism might have not been constrained well to discuss the detail processes of the magma motion in the conduit. In this study, we analyze broadband seismic data observed in the very-near-field condition, only 100-300 m away from the active craters, to obtain a more precise source mechanism solution.

We use the seismic data recorded at eight broadband seismic stations including temporary and permanent networks. Infrasonic array analyses show that the explosive eruptions mostly occurred at the north-east (NE) crater during the observation period in the end of September 2016. We apply a moment tensor inversion method to VLP (0.05-0.2 Hz) signals associated with the largest explosion occurring at the NE crater. The result shows that the optimal centroid is located at 200 m southwest of, 160 m beneath the NE crater. The source mechanism is greatly dominated by the vertical component of the moment tensor (Mzz), although the polarity inverts with other two diagonal components (Mxx, Myy). The squared error between the observed and synthetic waves (Ohminato et al. 1998) is only 11%.

We note that the squared errors less than 20 % are widely distributed around the optimal location: 300 m ×300 m in horizontal distances and 250 m in the vertical direction. For example, the solution obtained at a depth of 160 m beneath the NE crater shows the error of 18 %, which is within the confidence interval 95 % range of the residual at the optimal location. At this location, the inverted source mechanism is dominated by three diagonal components with a same polarity. This is much different from the best solution.

To examine why such different source mechanisms are obtained for nearby source locations, we calculate a model resolution matrix using the Green’ s functions computed from a point source at the optimal location and investigate how well the moment tensors can be resolved. The minimum singular value in the model resolution matrix is assumed to be 2.1 % of the maximum. We replace this value with zero and consider the pseudoinverse. The model resolution matrix for the pseudoinverse shows that the resolution of the diagonal components of moment tensors is lower than deviatoric ones. This suggests that the amplitudes of diagonal components are not well constrained from the moment tensor inversion even using near-by stations in our temporal observations. These results will be indispensable for discussing the spatial distribution of the volumetric change in the conduit or magma chamber accompanying the explosions.

©2019. Japan Geoscience Union. All Right Reserved.

Keywords: moment tensor inversion, source mechanism, VLP, Stromboli volcano, very-near-field, model resolution matrix

©2019. Japan Geoscience Union. All Right Reserved.

Pressure source estimation of tilt changes associated with small explosions at Stromboli volcano

*Ayumu Ishikawa[1], Takeshi Nishimura[1], Hiroshi Aoyama[2], Ryohei Kawaguchi[3], Eisuke Fujita[4], Takahiro Miwa[4], Taishi Yamada[4], Maurizio Ripepe[5], Riccardo Genco[5]

1. Graduate school of science, Tohoku university, 2. Faculty of science, Hokkaido university, 3. Meteorological Research Institute, 4. National Research Institute for Earth Science and Disaster Resilience, 5. University of Florence

Stromboli volcano is characterized by continuous activities of Strombolian explosions (small explosions) at summit craters. A lot of studies have investigated volcanic processes by multi-parameter observations. However, pressure source determination by geodetic measurements, which is indispensable to understand shallow magma reservoir which is a key for understanding magma dynamics, have not yet been well conducted because of insufficient geodetic observation network. In the present study, we analyze tilt records at 3 temporal and 2 permanent stations located closely to the summit craters to determine the locations and size of pressure source by comparing the observed tilt vectors with the theoretical ones that are calculated by using finite element method.

Temporal stations CPL, PZZ, RFR were equipped with Applied Geomechanics 701-2A, and installed at a distance of <500 m from the active craters. Continuous stations LFS, OHO, LSC, operated by University of Florence, were equipped with Pinnacle 5000T. We analyze continuous tilt records of 5 stations during July 1 to July 15 when small explosion activity was high. We extract uplift and subsidence tilt signals associated with each of small explosion and classify them in 4 stages: (A) Gradual uplift prior to small explosions, (B) Rapid uplift just before small explosions, (C) Rapid subsidence after small explosions, (D) Small uplift after (C). Tilt azimuths and amplitudes are almost same for the stages of (A) –(C), although LFS show about 30 degrees difference. We use the tilt vectors averaged for 680 events in the following analyses. We suppose that the pressure source is represented by an ellipsoidal cavity at (1) beneath the summit craters or (2) VLP source (Chouet et al., 2003; 200 m NW from the summit craters). We searched optimal source model which could explain the observed tilt vectors by changing the size and shape of the ellipsoidal cavity. The results show that simple shape sources such as a sphere cannot explain the observed tilts both for the locations of (1) and (2). A spheroidal source that is modeled from the VLP source mechanism do not explain the observed tilts, either. By changing the size and directions of ellipsoidal cavity, we find that the ellipsoidal cavity with a size of 300×150×600 m at 400 m depth beneath the summit craters can well explain the observed tilts. The pressure applied during the episode (A) is estimated to be about 1 kPa.

The size and position of the estimated ellipsoid is basically consistent with the picture of shallow magma reservoir inferred from an analysis of temporal evolution of flank lava effusion in 2007(Ripepe et al., 2015). The mass and volume of magma supplied for conduit during a small explosion that are estimated from the obtained pressure change, appropriate conduit radius and magma density is comparable to the ejected mass and volume of one small explosion estimated from the observations of surface phenomena.

Keywords: Strombolian eruption, Tilt, FEM

©2019. Japan Geoscience Union. All Right Reserved.

Seismic and acoustic waves excited by volcanic explosion: analyses of energy ratio and source spectra

*Mohammad Hasib[1], Takeshi Nishimura[1], Hisashi Nakahara[1]

1. Department of Geophysics, Graduate School of Science, Tohoku University

Volcanic eruptions generally accompany both seismic and acoustic signals, and these signals are used to understand volcanic fluid motions in the conduit and/or its effusion process from active vents. In the present study, we compare these two kinds of signals observed at three volcanoes in Japan, systematically examining the temporal changes of radiated energy. We further examine the basic spectral characteristics of seismic and acoustic signal radiations during large and small Vulcanian explosions at Sakurajima volcano. We use seismic and acoustic records at seismic-acoustic stations operated by Japan Meteorological Agency (JMA).

We first examine the energy ratio between seismic and acoustic signals of volcanic explosions at Sakurajima, Kirishima, and Kuchinoerabu-jima volcanoes. We calculate the time series of energy ratio of acoustic signals to three-component seismic signals by calculating their envelopes at the frequency band of 1-5 Hz. To obtain averaged characteristics, we stack the energy ratios of seismic and acoustic signals of about 900 explosions at Sakurajima and 8 explosions Shinmoe-dake (Kirishima) volcanoes, respectively. We analyze only one eruption at Kuchinoerabu-jima. The results at Sakurajima and Shinmoedake (Kirishima) show the following characteristics in the temporal changes: the ratio of seismic energies to acoustic energies rapidly decreases at the beginning and reaches the minimum in about 10 s -20 s; then the ratio gradually increases for 20 s - 40 s; the seismic signals continue after the acoustic energy decreases down to the noise level. Although we can analyze one eruption data for Kuchinoerabu-jima volcano (18 December 2018), similar characteristics are recognized. These results suggest that the volcanic fluid motions are strong in the shallow parts in the beginning, and the active zone gradually becomes deep.

Next, we investigate the source spectra of acoustic signals of volcanic explosions. Applying the spectral ratio method that has been often used for seismic signals, we clarify the difference of source spectra between large and small acoustic signals. We stack the spectral ratios of acoustic signals according to their maximum amplitudes, and classify them into Classes IV, III, II, and I from the largest to the smallest. The maximum amplitude of the largest event is about 10 Pa, while the smallest is about 2.5 Pa. Since the wind around the volcano may disturb the wave propagations, we only select the acoustic signals excited by volcanic explosions occurring during a low wind speed (< 3.3 m/s) condition, using the assimilation wind data recorded by ECMWF (European Centre for Medium-Range Weather Forecasts). We observe that the spectral ratios of acoustic signals are similar among different stations both for direct and coda waves. This means that the spectral ratio method is applicable for the acoustic signals of volcanic explosions during low wind speeds. All pair of the observed source spectral ratios of acoustic signals (Class IV/I, III/I, II/I) are characterized by almost flat amplitudes at the frequency range of about 0.2 -10 Hz. The difference between the classes is the amplitude. This characteristic is much different from the seismic signals excited by Vulcanian explosions (Hasib et al., 2018), in which a flat amplitude at low frequency range (about 0.5 - 2 Hz), a gradual decrease with frequency at an intermediate frequency range (about 2–3.5 Hz), and a flat amplitude at high frequency range (about 3.5 –10 Hz). These differences suggest the differences in the generation mechanisms between seismic and acoustic signals, which may reflect the difference of excitation region: the seismic waves are in the volcanic conduit beneath the vent, while the

©2019. Japan Geoscience Union. All Right Reserved.

acoustic waves are at the orifice of the conduit.

Acknowledgements: We used JMA seismic and acoustic signal records.

Keywords: Seismic wave, Acoustic wave, Energy ratio, Source spectra, Volcanic explosion

©2019. Japan Geoscience Union. All Right Reserved.

Field survey report on Zao Volcano (2012–2018)

*Akio Goto[1], Noriyoshi Tsuchiya[2], Nobuo Hirano[2], Miwa Kuri[3], Tetsuya Matsunaka[4], Kengo Sawayama[2]

1. Center for Northeast Asian Studies, Tohoku University, 2. Graduate School of Environmental Studies, Tohoku University, 3. International Research Institute of Disaster Science, Tohoku University, 4. Institute of Nature and Environmental Technology, Kanazawa University

We have been conducting field surveys on Zao volcano since 2012, such as temperature monitoring and water sampling on Maruyama-sawa geothermal area, ruin of Niizeki hotspring and Okama crater lake, based on the expectation that Zao volcano may be activated by 2011 Great East Japan Earthquake. Geophysical observation network by Japan Meteorological Agency, which has started 24-hour monitoring in September 2010, detected volcanic tremor in January 2013 for the first time, and a tremor and preceding tilting occurred in April (JMA, 2013). Since then Zao volcano sustains its higher activity than usual. Volcanic warning, Level 2: Do not approach the crater, were issued in April 2015 due to the increase in volcanic earthquake and in January 2018 due to the occurrence of volcanic tremor with largest-ever amplitude and continuous tilt motion. In harmony with these activities our field surveys also detect some changes in surface activities. Here we review our field survey results since 2012, especially focusing on the 2017-2018 results which has not reported yet.

Temperature of over 20 fumaroles has been measured repeatedly on Maruyama-sawa geothermal area, where small phreatic explosion occurred in 1940 (Toraishi and Tominaga, 1940; Anzai, 1941). The highest temperature exceeded 102 ˚C in 2012, but decreased over 7 ˚C within four months in 2013; fumarole temperature overall fell lower than 95 ˚C by 2014. After the first volcanic warning in 2015, the highest fumarole temperature reached nearly 100 ˚C temporarily, and then overall temperature rise occurred in 2016. In 2018, after volcanic warning was issued for the second time in January, the highest fumarole temperature exceeded 100 ˚C in June and reached 104 ˚C in July, which is the highest record in our survey since 2012.

We have paid attention to ruin of Niizeki hotspring, where high temperature and high concentration hotsprings gushed as a result of activization in the past, but no activity was recognized between 2012 and 2014. In September 2015, five months later from the first volcanic warning, we found that Niizeki hotspring resumed welling up with multiple hotsprings at around 32˚C. But in 2016 surveys, Niizeki hotspring had only a few weak cold-water springs, and no remarkable activity was recognized after the second volcanic warning in 2018.

In contrast with Maruyama-sawa and ruin of Niizeki hotspring, no thermal activity has been recognized on Okama crater lake thus far. The bottom temperature was around 4 ˚C in late May and early June (2014 and 2016), and around 7 ˚C in early September (2014, 2015, 2017 and 2018). We installed thermocouples in 2017 and 2018 on the bottom of Okama crater lake to record the temperature change one hour interval. We found that 3-4 ˚C temperature rise occurred in early October in 2017 and 2018, which is probably not be the results of thermal activity of Zao volcano but seasonal variation, because the degree of temperature change and the time of the year were identical. In 2018 other research group conducted topography survey of Okama crater lake bottom using a multiple-frequency sonar system and detected vertically extending reflection over a small mound on the center of the lake bottom, which may be caused by a chain of rising volcanic gas bubbles or hot water plume (Yamasaki et al., 2018). One of our

©2019. Japan Geoscience Union. All Right Reserved.

thermocouple is set within 10 m from the reflection source. Our thermocouple may catch the temperature change if thermal activity occurs there.

Keywords: Zao volcano, surface activity

©2019. Japan Geoscience Union. All Right Reserved.

Inflation Event of Zao Volcano in 2015

*Satoshi Miura[1], Mare Yamamoto[1], Masahiro Ichiki[1], Tomotsugu Demachi[1]

1. Graduate School of Science, Tohoku University

Volcanic earthquakes and tremors have been occurring beneath Zao volcano located in the northern Honshu, Japan since 2013, following the increase in the number of deep low frequency earthquakes from around 2012. Tohoku University has deployed some new seismological, geodetic, and geomagnetic stations to enhance rather poor observation network prior to the activity. On account of a burst of volcanic earthquakes initiated in April 2015, the Japan Meteorological Agency announced a warning of eruption, however, the number of events gradually decreased for the next two months and the warning was canceled in June 2015. In the same time period, minor expansive deformation was observed by GNSS. Small-scale volcanic earthquakes and tremors are occasionally occurring, and long-period earthquakes have taken place sometimes accompanied by static tilt changes. In this talk, We report the outcome obtained from the five-year observational research to monitor the preparatory process going under the volcano for evaluation of the eruption potential.

Figure 1 demonstrate the horizontal and vertical movement around Zao, respectively, from Jan. to Jun. of 2015. The black arrows show the observed ground movement. The radial pattern of movement around the summit of the volcano is clearly seen and the upheaval indicated by the black bars also centered around the summit. These characteristics of deformation can be modeled by a infinitesimal pressure source underground (so called Mogi model). We tried inversion analyses to find its location and magnitude. It is located about 0.8 km east of the crater lake with depth of about 5.6 km, and the volumetric change equivalent to the pressure change is $3.8 \times 10^6 m^3$. The calculated displacements are shown in the figure by white arrows and bars.

Comparing the hypocenter map, the pressure source is located just above the deep low frequency earthquakes cluster. This suggests that the pressure source might be activated by geothermal heat supplied by magma or fluid. Ogawa et al. (2014) found a conductive zone beneath Zao volcano deeper than about 5km and this may support our result.

Keywords: Volcano, deformation, Pressure source

©2019. Japan Geoscience Union. All Right Reserved.

(a) 水平変動 (2015年1月～6月)

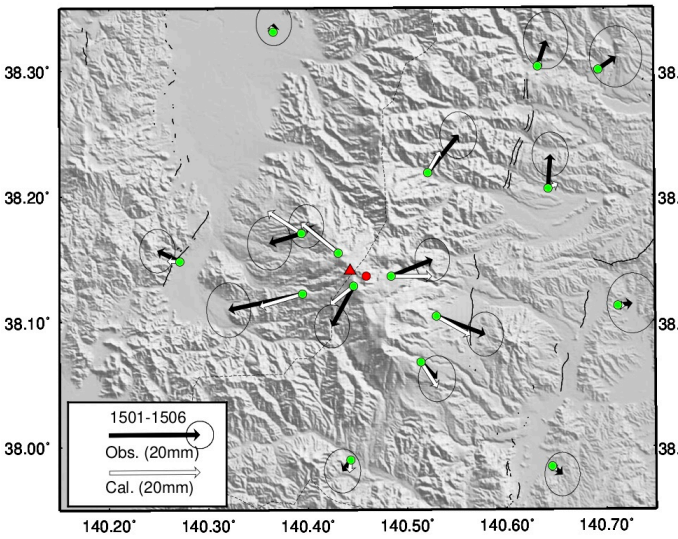

(b) 上下変動

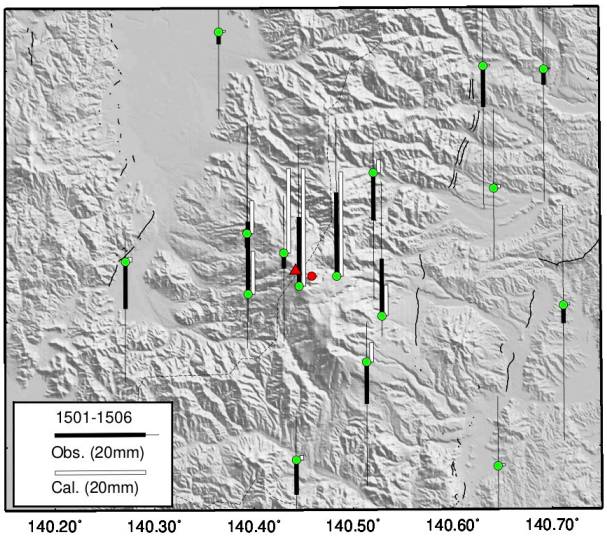

©2019. Japan Geoscience Union. All Right Reserved.

[J] Oral | S (Solid Earth Sciences)：S-VC Volcanology

Tue. May 28, 2019 3:30 PM - 5:00 PM JST | Tue. May 28, 2019 6:30 AM - 8:00 AM UTC | IC 2F

[S-VC38] Active Volcanism

convener:Yuta Maeda(Nagoya University), Takahiro Miwa(National research institute for earth science and disaster prevention), Takeshi Nishimura(Department of Geophysics, Graduate School of Science, Tohoku University), Chairperson:Mare Yamamoto, Yuta Maeda(Nagoya University)

This session discusses various aspects of active volcanisms including, but not limited to, recent and historical eruptions, various phenomena associated with the volcanic activities, underground structures of the volcanoes, and developments of new instruments based on geophysical, geochemical, geological, and multidiscipline approaches. We also welcome studies on understanding and predicting the transitions of the eruptive activities from observational, theoretical, and experimental approaches.

3:30 PM - 3:45 PM JST | 6:30 AM - 6:45 AM UTC

[SVC38-24] A machine-learning-based estimation of large amplitude regions for monitoring volcano seismicity

*Yuta Maeda[1] (1.Nagoya University)

3:45 PM - 4:00 PM JST | 6:45 AM - 7:00 AM UTC

[SVC38-25] Development of a technique for automatic determination of volcanic earthquakes with unclear onsets - Application to Mt. Asama -

*Takao Ohminato[1], Shigeki Horiuchi[2] (1.Earthquake Research Institute, Tokyo University, 2.Home Seismometer Corporation)

4:00 PM - 4:15 PM JST | 7:00 AM - 7:15 AM UTC

[SVC38-26] Amplitude source location method with depth-dependent scattering and attenuation structures for volcano-seismic signals

*Hiroyuki Kumagai[1], John Makario Lonodno[2], Alvaro Esteban Acevedo Rivas[2], Yuta Maeda[1] (1.Graduate School of Environmental Studies, Nagoya University, 2.Colombian Geological Survey)

4:15 PM - 4:30 PM JST | 7:15 AM - 7:30 AM UTC

[SVC38-27] Seismic interferometry at active volcanoes in Japan: Analyses of seismic records of JMA for the period from 2012 to 2018

*Takeshi Nishimura[1], Tomoya Takano[1], Takashi Hirose[1], Hisashi Nakahara[1] (1.Department of Geophysics, Graduate School of Science, Tohoku University)

4:30 PM - 4:45 PM JST | 7:30 AM - 7:45 AM UTC

[SVC38-28] Empirical relation for Q factors of crack resonances and its use to estimate source properties of volcanic LP events

*Kimiko Taguchi[1], Hiroyuki Kumagai[1], Yuta Maeda[1], Roberto Torres[2] (1.Nagoya University Environmental Studies, 2.Colombian Geological Survey)

4:45 PM - 5:00 PM JST | 7:45 AM - 8:00 AM UTC

[SVC38-29] A study on the radiation pattern for resonating fluid-filled crack

*Mare Yamamoto[1] (1.Research Center for Prediction of Earthquakes and Volcanic Eruptions, Graduate School of Science, Tohoku University)

A machine-learning-based estimation of large amplitude regions for monitoring volcano seismicity

*Yuta Maeda[1]

1. Nagoya University

The seismic network of Mt. Ontake has improved after the 2014 eruption, producing one of the most dense observational networks in the world composed of 9 stations within 1 km of the summit, 17 within 4 km, and 29 within 10 km. This network has recorded long-period (LP) events and tremors which had been considered quite rare at Mt. Ontake (Maeda et al., 2018, JPGU). These signals are attributed to movements and volume changes of shallow volcanic fluids according to studies of similar signals at other volcanoes; thus they are important markers to understand the state and behavior of the fluids. However, despite finding several events, the entire activity of them are not known at Mt. Ontake; it is not easy to manually create an event catalog because of abundance of spurious events (i.e., local wind noise) and difficulty of distinguishing them from real volcano-seismic signals. This is partly related to a difficulty of comparing the records at many stations with a sufficient temporal resolution using a small number of figures. A new strategy to extract useful information from the large number of stations is thus needed.

In this study, we developed a method to investigate a spatiotemporal distribution of large amplitude regions to easily monitor the activities of earthquakes and tremors. The amplitudes could be a measure to monitor the seismicity including those without clear initial motions, but could be affected by local structures beneath the stations. To reduce this effect, we used information of whether the amplitudes are significantly larger than the normal level. We determined a threshold to distinguish significantly large and normal amplitudes from every 5-min-long window of each data trace, based on an idea that Gaussian and non-Gaussian portions of the frequency distribution of the amplitudes are normal and significantly large parts, respectively. This idea is implemented by creating a cumulative frequency distribution of absolute amplitudes in the 5-min-long window using only the smallest N data samples; calculating the fitting error between this distribution and an error function; and searching for an optimal N which minimizes the fitting error. The amplitude corresponding to this optimal N was regarded as the threshold. We then computed the ratio of large amplitude samples in every 1-sec-long window of each trace. We used the spatial distribution of this ratio as the input to a machine learning of a neural network model to investigate the large amplitude region for the 1-sec window. In this way, the spatial distribution of the large amplitude region is investigated for every 1-sec window, which could be used to distinguish true volcano-seismic signals from spurious ones.

We applied this method to the continuous records in November and December 2017 at Mt. Ontake. For most earthquakes occurred in the analysis domain, the large amplitude region distributed within a narrow area around the epicenter or spread with time from the epicentral area to a wider region. For distant earthquakes and local noise, the large amplitude region extended over the entire analysis domain with a small probability. These different patterns of the large amplitude regions were useful to distinguish the true volcano-seismic signals from spurious ones, although there were some missing detections of small earthquakes and tremors. Using the large amplitude region, only one figure is needed for each second, enabling a seismicity monitoring easier than detailed evaluations of continuous waveform records. We are now trying the 2nd stage of the machine learning to automatically detect earthquakes and tremors, which uses the spatiotemporal distribution of the large amplitude as the input, giving 93% success as a preliminary result.

©2019. Japan Geoscience Union. All Right Reserved.

Keywords: Volcano seismology, Machine learning, Mt. Ontake

©2019. Japan Geoscience Union. All Right Reserved.

Development of a technique for automatic determination of volcanic earthquakes with unclear onsets - Application to Mt. Asama -

*Takao Ohminato[1], Shigeki Horiuchi[2]

1. Earthquake Research Institute, Tokyo University, 2. Home Seismometer Corporation

Some of volcanic earthquakes have clear P and S-wave onsets, and other has unclear onsets. In the traditional classification of volcanic earthquakes, the former is called A-type, VT, or HF earthquakes, and the latter is called B-type, LP, or LF earthquakes. The source process of the former is thought to be the rock rupture due to the stress changes in the volcanic edifice. For the latter, various source processes involving volcanic fluids such as gas, hot water or magma, have been proposed.

Numerous B-type earthquakes are often detected by the seismic network near the active volcanic vent of a volcano even if the activity level of the volcano is not high. In addition, a sharp increase in the number of B-type earthquakes is often observed when volcanic activity increases. Because shallow B-type earthquakes reflect the state of the magma plumbing system or the shallow hydrothermal system, constant monitoring of their activity is important. However, since B-type earthquakes are numerous and it is difficult to read their onset by human eyes, manual processing is not easy. Therefore, it is necessary to develop a automatic method to detect the event and to determine the hypocenter location. For events with unclear onsets, various methods, such as obtaining travel time differences by using waveform correlation, using particle motion, using spatial distribution of amplitude, etc., have been proposed so far. In particular, methods using waveform amplitude are widely used for hypocenter determination of B-type earthquakes due to their excellent performance.

In this study, we first examine how effective the Horiuchi et al. (2010)'s method for hypocenter determination of volcanic earthquakes with unclear onset. This method has been used in hypocenter determination of non-volcanic earthquakes. The basic idea of this method is, first, to define an evaluation function that imitates the comprehensive judgment of experienced human beings, then, to optimize the parameters of the evaluation function automatically so that the results of automatic readings approach the human readings. Furthermore, the influence of noise is reduced by giving a higher score values to observation stations where the difference between the theoretical and the observed travel times is smaller and by choosing a solution with the sum of the score values of all observation stations is maximum. In order to further improve signal-to-noise ratio, S-waveforms are appropriately rotated before reading S-arrival.

When we applied the method in its original form to Mt. Asama data, the accuracy of the result was poor. Possible reasons would be, in addition to difficulty in onset reading itself, the influence of various factors such as poor human readings which are the basis of parameter optimization, and high noise level of the data. In order to improve the performance of the method, we have tried various remedy such as improving onset reading, utilizing amplitude, reducing noise, etc. and have finally reached the stage where automatic determination is satisfactory. The measures we have taken and their results are as follows.
1) If the conventional automatic reading method is applied as it is, the accuracy of S-reading is not good enough. We examined a method in which an approximate hypocenter location is determined first using the waveform amplitude, then the S-wave arrival is read using the correlation. In order for improving the accuracy of S-reading, we used the correlation of the S-waveform envelope. We then computed the hypocenter location by using both the amplitude and the travel time. But the high accuracy of the

©2019. Japan Geoscience Union. All Right Reserved.

S-reading was not reached. We abandoned this approach.
2) The hypocenters were determined by using both the automatic reading of S-arrival and amplitude, but accuracy was not satisfactory.
3) We performed following four remedy first: "To avoid reading noisy waveforms", "To discriminate between distant earthquakes and local volcanic earthquakes", "Not to use readings with low signal-to-noise ratio", "To remove amplitude data with inconsistent S-arrival". We then carried out hypocenter determination by using waveform amplitude alone. The results obtained by this procedure were most satisfactory.

When we apply above-mentioned improved method to the data for three months from November 2017 to January 2018, we could determine hypocenters of about 1900 events near the summit of Mt. Asama. The number of events that was determined manually during the same period was less than 100 events. Although we need to investigate more about the accuracy of the obtained hypocenter location, we believe that the improved version of this method is fairly promising.

Keywords: volcanic earthquakes, hypocenter determination, amplitude of waveforms, unclear onset

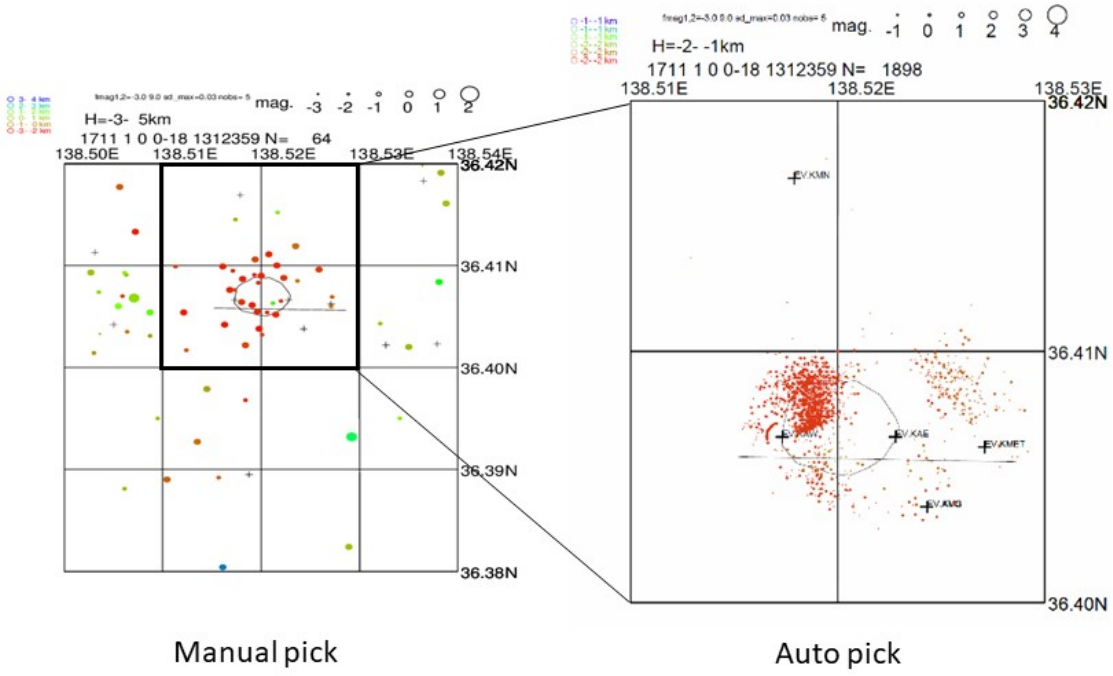

©2019. Japan Geoscience Union. All Right Reserved.

Amplitude source location method with depth-dependent scattering and attenuation structures for volcano-seismic signals

*Hiroyuki Kumagai[1], John Makario Londono[2], Alvaro Esteban Acevedo Rivas[2], Yuta Maeda[1]

1. Graduate School of Environmental Studies, Nagoya University, 2. Colombian Geological Survey

The amplitude source location (ASL) method has been used to locate seismic events and tremor at various volcanoes. It has been indicated that the far-field and isotropic radiation equation for *S* waves used in the ASL method is valid in highly scattering wavefields. A constant *Q* value in the far-field and isotropic radiation equation has been commonly used in previous studies. This implicitly assumes homogenous distributions of scattering characteristics represented by the mean free path (l_0) and intrinsic attenuation (Q_i) beneath volcanoes. Wegler (JGR, 2004) and Kumagai et al. (JGR, 2018) showed that highly heterogeneous structures at volcanoes only exist in a surface thin layer with a thickness of about 1 km, below which less heterogeneous layers comparable to those in the normal crust exist. To evaluate the effects of such layered structures for ASL determinations, we performed synthetic tests using envelope waveforms simulated with the Monte Carlo method of Yoshimoto (JGR, 2000) for a two layer model based on the l_0 and Q_i structures at Nevado del Ruiz volcano (NRV) estimated by Kumagai et al. (2018). Our results indicated that the input source locations were estimated by the ASL method when appropriate values of *Q* values for the two layered model were used in the far-field and isotropic radiation equation. When a constant *Q* value was used, the estimated locations were largely deviated from the input locations especially in the depth direction. We then determined ASLs of volcano-tectonic (VT) earthquakes at NRV, which were compared with their hypocenters determined by the onset arrival times. Our results indicated that the differences between the ASLs and hypocenters of VT earthquakes became smaller when using a two layer *Q* model than those using a constant *Q* model. Our estimated ASLs of long-period (LP) events and tremor at NRV using the two layer *Q* model were more sharply clustered beneath the SW flank compared to those using the constant *Q* model. These locations corresponded to high *P*-wave to *S*-wave velocity ratio regions (Londono and Kumagai, JVGR, 2018), suggesting that the LP events and tremor were generated by fragmentation processes in a shallow magma storage region. These results indicate that use of appropriate *Q* values in the ASL method accommodating a thin surface heterogeneous layer is important to estimate precise source locations.

©2019. Japan Geoscience Union. All Right Reserved.

Seismic interferometry at active volcanoes in Japan: Analyses of seismic records of JMA for the period from 2012 to 2018

*Takeshi Nishimura[1], Tomoya Takano[1], Takashi Hirose[1], Hisashi Nakahara[1]

1. Department of Geophysics, Graduate School of Science, Tohoku University

We analyze the seismic records of JMA stations deployed at active volcanoes in Japan, to examine the basic characteristics of daily variations of seismic velocity changes in the shallow medium. About 20 active volcanoes are systematically analyzed at the frequency range of 0.5-4 Hz. Temporal changes of the seismic velocity changes calculated from comparison of 7 years averaged cross-correlations and 5-days ones show long-period changes with periods of a year and/or a few months. The frequency distributions of seismic velocity changes at each station pairs roughly follow the normal distributions with a standard deviation of about 0.2 to 1 percents. Several phreatic eruptions occurred at Kuchinoerabu-jima, Ontake, Hakone and Aso volcanoes during the observation period, but no significant change is observed in the seismic velocity changes. On the other hand, seismic velocity changes due to the strain changes by volcanic pressure sources, moderate and large earthquakes, and/or dike intrusion are observed at, for example, Sakurajima, Miyakejima, Izu-Ohshima, Azuma and Tarumae volcanoes.

Keywords: Seismic interferometry, active volcanoes, seismic velocity change

©2019. Japan Geoscience Union. All Right Reserved.

Empirical relation for *Q* factors of crack resonances and its use to estimate source properties of volcanic LP events

*Kimiko Taguchi[1], Hiroyuki Kumagai[1], Yuta Maeda[1], Roberto Torres[2]

1. Nagoya University Environmental Studies, 2. Colombian Geological Survey

Long-period (LP) seismic events are thought to arise from the oscillations of a fluid-filled resonator. The resonator geometry and fluid properties of LP sources have been estimated by comparing observed frequencies and *Q* factors to those calculated from a crack model (Chouet, *J. Geophys. Res.*, 1986). Taguchi et al. (*J. Geophys. Res.*, 2018) developed a method based on an analytical formula for the crack resonance frequencies proposed by Maeda and Kumagai (*Geophys. J. Int.*, 2017). This method enables us to estimate all the parameters of crack geometry and fluid properties. But the comparison of *Q* factors was conducted by numerical simulations of the crack model, which took extensive computational time, especially for LP events with large *Q* factors. So we systematically investigated the relation between *Q* factors and the crack model parameters by numerical simulations. It is known that *Q* factors of the crack resonances are proportional to α/a, where α is the *P* wave velocity of the solid and *a* is the sound speed of the fluid in the crack (Kumagai and Chouet, *J. Geophys. Res.*, 2000). We additionally found an empirical relation, indicating that the proportional constant depends on $\log(W/L)$, where *L* and *W* are crack length and width, respectively. To test the applicability of this empirical relation, we used it to analyze LP events at Galeras volcano, Colombia, in January 1993. These LP events have been thought to be generated by resonances of the crack filled with dusty gas. Our estimates of the crack model parameters displayed decreasing trends in both crack volume (*V*) and gas-weight fraction of water vapor (*n*) in the crack. These trends are similar to those shown by Taguchi et al. (2018). We further analyzed LP events at Galeras in May 1993 and December 2006 with the empirical relation for *Q* factors assuming dusty gas as the fluid in the crack. Because of their large *Q* factors, the determinations of crack geometry and fluid properties for these LP events with numerical simulations of the crack model were computationally expensive. The empirical relation for *Q* factors enables us to estimate all the crack model parameters for these LP events easily, and we found similar decreasing trends in both *V* and *n* to those in January 1993. This similarity implies that these variations during the individual periods of LP events were caused by the similar processes at this volcano.

These results demonstrate that the empirical relation obtained in this study is applicable to estimate all the parameters of LP sources, and may contribute to improved monitoring of fluid states under volcanoes and better understanding of LP source processes.

©2019. Japan Geoscience Union. All Right Reserved.

A study on the radiation pattern for resonating fluid-filled crack

*Mare Yamamoto[1]

1. Research Center for Prediction of Earthquakes and Volcanic Eruptions, Graduate School of Science, Tohoku University

Volcanic earthquakes observed around active volcanoes often exhibit harmonic characteristics having multiple spectral peaks, and thus the oscillation of fluid inclusions beneath volcanoes have been considered as one of the most plausible source models of these signals. As examples of such resonator model, the resonance of fluid inclusions whose shapes are sphere, cylinder, and crack have been proposed and successfully applied to the analyses of observed signals to explain the spectral characteristics of volcanic earthquakes. In recent years, it becomes more common that we have dense seismic observation close to the source of volcanic earthquakes, and we often observe varieties of spectral shapes showing different amplitude pattern between spectral peaks and between stations. To utilize the amplitude information of observed spectral peaks, in this study, I model the radiation pattern for a resonating fluid-filled crack, and discuss about the possibility to estimate the orientation and size of the fluid-filled crack.

In this study, the radiation of elastic waves from a resonating thin fluid-filled crack in 3-D infinite medium is considered. First, I compute the oscillation of fluid-filled crack, and compute the wave radiation from the crack by numerically integrating the elastic waves generated by the tensile dislocation on the crack surface. By computing the energy at each direction, the radiation pattern is then obtained as a function of distance from the crack. Because Yamamoto and Kawakatsu (2008) showed that the distribution of the tensile dislocation on the crack surface can be described by small numbers of Chebyshev polynomials as far as we consider the low-frequency oscillation of the crack, for the sake of comparison, I also calculate the wave propagation using this analytical expression. If we consider only far-field compressional wave, the model setting is same as that discussed in Chouet (1986). In contrast, in this study, I use analytical Green’s function including both near- and far-field terms for P and S waves to study the radiation pattern for the resonating fluid-filled crack.

In the case of the crack containing hydrothermal fluids, which have rather large acoustic velocity contrast between inside and outside of the crack, the radiation pattern of each resonant mode becomes almost comparable to that obtained only with far-field compressional term at distance larger than about 50 times of the crack size. On the other hand, the radiation pattern in short distance range is severely distorted due to the contribution of near-field term and the interference of waves emitted from different point of the crack. In addition, there exists the difference between even- and odd-modes of the resonant mode. These results can be explained by considering the following mainly two points: the wavelength of radiated elastic waves is same order of the crack size, and thus the distant range in which the contribution of near-field term dominates is proportional to the wavelength of each resonant mode; the distribution of tensile dislocation have different symmetry for odd/even modes, and thus the effect of the interference of waves emitted from different point of crack surface depends on the direction, as already pointed out by Kumagai et al. (2002). It also becomes clear that there exists the distant dependency of amplitude ratio between resonant modes.

These results indicate the possibility to estimate the orientation and size of fluid-filled crack beneath volcanoes by observing amplitude ratio between stations and between spectral peaks. Because the

©2019. Japan Geoscience Union. All Right Reserved.

spectral amplitude ignoring phase information is less affected by the wave scattering caused by small-scale heterogeneity in shallow volcanic edifice compared to the waveform itself, the methodology has an advantage in practical data analyses. These results also suggest the importance of near-field dense observation to understand the detailed source mechanism and source process of volcanic earthquakes.

Keywords: Volcanic earthquakes, Fluid-filled crack, Source mechanism

©2019. Japan Geoscience Union. All Right Reserved.

[E] Oral | S (Solid Earth Sciences)：S-CG Complex & General

Tue. May 28, 2019 9:00 AM - 10:30 AM JST | Tue. May 28, 2019 12:00 AM - 1:30 AM UTC | A07 TOKYO BAY MAKUHARI HALL

[S-CG49] Hard-Rock Drilling Science: From Continental to Deep Sea Drilling, and Oman Project

convener:Katsuyoshi Michibayashi(Department of Earth and Planetary Sciences, Nagoya University), Eiichi TAKAZAWA(Department of Geology, Faculty of Science, Niigata University), Norikatsu Akizawa(Department of Ocean Floor Geoscience, Atmosphere and Ocean Research Institute, The University of Tokyo), Chairperson:Eiichi Takazawa(Niigata University), Norikatsu Akizawa(AORI The University of Tokyo)

The Oman Drilling Project (OmDP) has completed to drill numerous hard-rock cores within ancient oceanic lithosphere and the underlying subduction zone of the Samail ophiolite in Oman, with support from ICDP, IODP, Japan Society for the Promotion of Science, the Sloan Foundation's Deep Carbon Observatory, US, and European research agencies. Moreover, a number of IODP expeditions have focused on hard-rock drilling over the last several years including Expedition 352 in 2014, which drilled the volcanic sequence associated with subduction initiation in the Bonin fore-arc, Expedition 357, which drilled the Lost City hydrothermal field, Expedition 360, which drilled the lithosphere associated with ultraslow-spreading at the Southwest Indian Ridge in 2016, and Expedition 366, which drilled the serpentinite seamounts in the Mariana fore-arc. In this session, we invite presentations on the scientific results of hard-rock drilling at these and other sites. We also invite related presentations on oceanic lithosphere, island arc formation, and any other significant issue that could be addressed by future hard-rock drilling. This includes marine studies of oceanic lithosphere and on-land geological investigations of ophiolites, accreted arcs, and subduction complexes. The session is intended to be interdisciplinary, including the fields of geophysics, geochemistry, petrology, engineering, and biology.

9:00 AM - 9:15 AM JST | 12:00 AM - 12:15 AM UTC

[SCG49-06] Melt transport and compositional heterogeneity of the mantle: a case study of peridotite, dunite, and wehrlite from Atlantis Massif

*Norikatsu Akizawa[1], Gretchen L. Früh-Green[2], Akihiro Tamura[3], Chiori Tamura[1], Tomoaki Morishita[3] (1.Atmosphere and Ocean Research Institute, The University of Tokyo, 2.Department of Earth Sciences, Eidgenössische Technische Hochschule-Zürich, 3.Institute of Science and Engineering, Kanazawa University)

9:15 AM - 9:30 AM JST | 12:15 AM - 12:30 AM UTC

[SCG49-07] Lower crustal accretion processes revealed from the study of gabbroic cores in Holes GT1A and GT2A, the ICDP Oman Drilling Project

*Sayantani Chatterjee[1], Eiichi TAKAZAWA[1], Katsuyoshi Michibayashi[2], Peter B Kelemen[3], Damon A.H. Teagle[4], Oman Drilling Project Phase I Science Party (1.Department of Geology, Faculty of Sciences, Niigata University, Japan, 2.Department of Earth and Environmental Sciences, Nagoya University, Japan, 3.Lamont Doherty Earth Observatory, Columbia University, USA, 4.Southampton Marine and Maritime Institute, University of Southampton, United Kingdom)

9:30 AM - 9:45 AM JST | 12:30 AM - 12:45 AM UTC

[SCG49-08] Petrology of Oman listvenite : Implications for carbon cycle in the subduction zone

*Toma Takahashi[1], Tomoaki Morishita[2], Hiroki Sato[3], Juan Miguel Guotana[2], Tatsuhiko Kawamoto[4], Peter B Kelemen[5], Jude Ann Coggon[6], Michelle Harris[7], Juerg Michael Matter[6], Katsuyoshi Michibayashi[8], Eiichi TAKAZAWA[9], Damon A H Teagle[6], The Oman Drilling Project Phase 1 science Party (1.Faculty of Geosciences and Civil Engineering, Kanazawa university, 2.Division of Natural Sciences, Graduate School of Natural Science and Technology, Kanazawa university, 3.Faculty of Science, Kyoto university, 4.Department of Geoscience, Faculty of Science, Shizuoka university, 5.Lamont-Doherty Earth Observatory, Columbia university, 6.School of Ocean and Earth Science, National Oceanography Center Southampton, University of Southampton, 7.School of Geography, Earth and Environmental Sciences,

Plymouth University, 8.Department of Earth Planetary Sciences, Graduate School of Environmental Studies, Nagoya university, 9.Institute of Science and Technology, Niigata university)

9:45 AM - 10:00 AM JST | 12:45 AM - 1:00 AM UTC

[SCG49-09] PGE and Os isotope variation in the gabbros and peridotites from the Oman DP drilling cores in the Samail ophiolite, Oman

*Ryoko Senda[1,2], Katsuhiko Suzuki[2], Tomoaki Morishita[3], Eiichi TAKAZAWA[4], Katsuyoshi Michibayashi[5], Peter B Kelemen[6], Damon AH Teagle[7], Jude Ann Coggon[7], Marguerite Godard[8], The Oman DP Science Party (1.Faculty of Social and Cultural Studies, Kyushu University, 2.Research and Development Center for Submarine Resources, JAMSTEC, 3.School of Natural System, Colleage of Science and Technology, Kanazawa University, 4.SDepartment of Geology, Faculty of Science, Niigata University, 5.Department of Earth and Planetary Sciences, Nagoya University, 6.Columbia University, 7.University of Southampton, 8.Géosciences Montpellier)

10:00 AM - 10:15 AM JST | 1:00 AM - 1:15 AM UTC

[SCG49-10] Overview of drilling of crust-mantle boundary at CM1&2 sites of Wadi Tayin massif of Oman ophiolite: the ICDP Oman Drilling Project

*Eiichi TAKAZAWA[1], Damon A H Teagle[2], Katsuyoshi Michibayashi[3], Yoshihiko Tamura[4], Jude Ann Coggon[2], Juerg Matter[2], Peter B Kelemen[5], Oman Drilling Project Phase 2 Science Party (1.Department of Geology, Faculty of Science, Niigata University, 2.University of Southampton, 3.Nagoya University, 4.JAMSTEC, 5.Columbia University)

10:15 AM - 10:30 AM JST | 1:15 AM - 1:30 AM UTC

[SCG49-11] Petrological observation of core samples drilled from a mantle section of the Oman ophiolite: A preliminary report of the Oman Drilling Project Phase 2

*Yuji Ichiyama[1], Oman Drilling Project Phase 2 Scientific Party (1.Chiba University)

Melt transport and compositional heterogeneity of the mantle: a case study of peridotite, dunite, and wehrlite from Atlantis Massif

*Norikatsu Akizawa[1], Gretchen L. Früh-Green[2], Akihiro Tamura[3], Chiori Tamura[1], Tomoaki Morishita[3]

1. Atmosphere and Ocean Research Institute, The University of Tokyo, 2. Department of Earth Sciences, Eidgenö ssische Technische Hochschule-Zürich, 3. Institute of Science and Engineering, Kanazawa University

Harzburgitic, dunitic, and wehrlitic rocks drilled at Atlantis Massif (Mid-Atlantic Ridge, 30˚N), where mantle-derived rocks were exhumed to the sea floor via detachment faulting, were investigated employing *in situ* geochemical analyses. Since dunitic and wehrlitic rocks are commonly interpreted as fossil melt channels, they likely represent transported parental melts of mid-ocean ridge basalt (MORB) beneath the paleo-ridge axis. Although the rocks are severely serpentinized, primary olivines, chromian spinels, orthopyroxenes, and clinopyroxenes were found in several samples. The Cr/(Cr + Al) ratios (Cr#) of the chromian spinel show a bimodal distribution, where one group records higher Cr# (0.35–0.5) and the other group is represented by lower Cr# (0.2–0.3). The extent of mantle melting is strongly correlated to the Cr# of the chromian spinel, thus the mantle-derived lithologies of the Atlantis Massif record at least two end-members with regards to the extent of melting: refractory mantle material with higher Cr#, and enriched mantle material with lower Cr#. To quantitatively evaluate mantle melting and melt transport mechanisms in the suboceanic mantle beneath this section of the Mid-Atlantic Ridge, a one-dimensional, steady-state decompositional mantle melting model was carried out based on rare-earth element concentrations of clinopyroxene. Our modelling results demonstrate that the melting region of the mantle extends unevenly across the ridge axis, with deeper melting occurring on-axis from the garnet-stability field, and shallower melting occurring off-axis from the spinel-stability field. We propose that depleted melts generated at depths in the absence of garnet within the off-axis region were possibly focused to the ridge axis via fracture-induced melt channels and produced wehrlite. It is likely that fracture-induced melt migration was dominantly a response to a decrease of temperature as the mantle was exhumed during detachment faulting.

Keywords: IODP Exp 357, Mid-Atlantic Ridge, Harzburgite, Melt transport, MORB, ultra-depleted melt

©2019. Japan Geoscience Union. All Right Reserved.

Lower crustal accretion processes revealed from the study of gabbroic cores in Holes GT1A and GT2A, the ICDP Oman Drilling Project

*Sayantani Chatterjee[1], Eiichi TAKAZAWA[1], Katsuyoshi Michibayashi[2], Peter B Kelemen[3], Damon A.H. Teagle[4], Oman Drilling Project Phase I Science Party

1. Department of Geology, Faculty of Sciences, Niigata University, Japan, 2. Department of Earth and Environmental Sciences, Nagoya University, Japan, 3. Lamont Doherty Earth Observatory, Columbia University, USA, 4. Southampton Marine and Maritime Institute, University of Southampton, United Kingdom

Transition between middle crustal foliated and to lower crustal layered gabbros of Oman ophiolite was drilled at Hole GT2A and GT1A in Wadi Gideah of Wadi Tayin massif (22˚51.793'E/58˚31.198'N and 22˚53.535'/58˚30.904' respectively) during Phase 1 of Oman drilling project. With total depth of 406.77m long Hole GT2A core samples the middle foliated to layered gabbro. Hole GT1A drilled the lower crustal section in the southern Oman ophiolite and recovered 401.52 m of total cores (99.6% recovery). Petrographic observation of representative samples from GT2A and GT1A, we found two dominant rock types: gabbbro and olivine gabbro, where later dominates the lower part of the drill hole.

The layered structure is mainly controlled by the variable grain size and modal composition of minerals. Gabbros contain plagioclase and clinopyroxene (showing poikilitic texture) as primary minerals associated with few amounts of oxides. Clinopyroxenes are often replaced by brown amphibole along cleavages or at the rim. Olivine gabbros are constituted of plagioclase, clinopyroxene, olivine, some orthopyroxene and oxide minerals. Texturally, olivine grains are present as subhedral to skeletal in nature. Magmatic foliation is often demarcated by laths of plagioclase followed by elongated clinopyroxene. The contact between olivine and plagioclase frequently marked by presence of symplectitic intergrowth between spinel and orthopyroxenewhich suggests, olivine was reacting with late stage liquid and produce simultaneous coprecipitation of magnetite and orthopyroxene. Downhole evolution present from bottom to top for both in gabbro and olivine gabbro samples in terms of Mg#,TiO2, and Cr2O3 in clinopyroxene, olivine and plagioclase, particularly at 270mt and 130mt Mg# increase (influx of primitive melts at several intervals). TiO2 and Cr2O3 correspond with Mg#, and eventually follow fractionation trend. Data from rare earth elements implies that ol-gabbros are crystallized from different parent melts (at least two types) supported by the evidence from evolution with depth profile.

Gabbroic lithologies in GT1A represented by anhedral olivine with tabular to elongate shape. Plagioclase are partly or totally enclosed by large clinopyroxene. Clinopyroxenes are tabular to subequant in habit. Some thin films of orthopyroxene present as corona around olivine. Most of the samples have undergone alteration and obscured the igneous origin. In case of Hole GT2A, gabbros are much less affected by alteration compared to GT1A. Downhole variation in mineral composition (in-situ composition) can be correlated with several cycles of crystallization history. Detailed petrographic, microstructural and geochemical study of all the representative samples will be presented. We have also attempted to determine the oxygen fugacity, where (fO2 vs.T plot) oxide pairs are plotted within FMQ field (fO2 vs. T plot). Temperature estimation ranges from 600-800˚C (shallow level gabbro to deeper gabbro) cover total range of temperature from high to low and also have a clue to determine the thermal evolution by rate of cooling.

Keywords: Oman Drilling Project, Lower crust, Gabbro

©2019. Japan Geoscience Union. All Right Reserved.

©2019. Japan Geoscience Union. All Right Reserved.

Petrology of Oman listvenite : Implications for carbon cycle in the subduction zone

*Toma Takahashi[1], Tomoaki Morishita[2], Hiroki Sato[3], Juan Miguel Guotana[2], Tatsuhiko Kawamoto[4], Peter B Kelemen[5], Jude Ann Coggon[6], Michelle Harris[7], Juerg Michael Matter[6], Katsuyoshi Michibayashi[8], Eiichi TAKAZAWA[9], Damon A H Teagle[6], The Oman Drilling Project Phase 1 science Party

1. Faculty of Geosciences and Civil Engineering, Kanazawa university, 2. Division of Natural Sciences, Graduate School of Natural Science and Technology, Kanazawa university, 3. Faculty of Science, Kyoto university, 4. Department of Geoscience, Faculty of Science, Shizuoka university, 5. Lamont-Doherty Earth Observatory, Columbia university, 6. School of Ocean and Earth Science, National Oceanography Center Southampton, University of Southampton, 7. School of Geography, Earth and Environmental Sciences, Plymouth University, 8. Department of Earth Planetary Sciences, Graduate School of Environmental Studies, Nagoya university, 9. Institute of Science and Technology, Niigata university

Listvenites obtained during the Phase 1 of the Oman Drilling Project can be generally divided into two main groups based on color: red series and green-white series. Although there is a clear color difference, the mineral assemblage is mainly composed of magnesite and quartz. Dolomite occurs as late veins and/or small patches. Opaque minerals are abundant in the red series which occur either as veins or disseminated grains which are commonly enveloped by carbonate minerals and quartz. The opaque minerals are hematite based on Raman spectrometry analysis. In the green-white listvenite series, opaque minerals are very scarce. Greenish portions in both listvenites were observed on a hand sample scale. In the green-white series, dark green and light green portions are present while only light green portions are observed in the red listvenites. These greenish features are interpreted as mainly polymineralic pseudomorphic replacement of orthopyroxene. In the same hole, pyroxene relics in serpentinites exhibit the same shape as with the previously described greenish pseudomorphs. The dark green portions in the green-white listevenites contain fuchsite (Cr-mica) around spinel relics. Silicified relic pyroxenes with fuchsite along relic cleavages are also present in the light green portions. On the other hand, the greenish portions in the red listvenite series are characterized by magnesite with intergranular fuchsite (?). Hematites in the red listvenites have similarities in form with the opaque minerals occurring as discontinuous veinlets in the serpentinite. The combined similarities in the petrographic features suggest that some listvenites were formed from serpentitnites. Quartz veins with Ni-bearing magnesite were observed in the red series and were formed in the last stage.

Keywords: Listvenite, Oman drilling project, Oman ophiolite, elements mobility, Carbonation

©2019. Japan Geoscience Union. All Right Reserved.

PGE and Os isotope variation in the gabbros and peridotites from the Oman DP drilling cores in the Samail ophiolite, Oman

*Ryoko Senda[1,2], Katsuhiko Suzuki[2], Tomoaki Morishita[3], Eiichi TAKAZAWA[4], Katsuyoshi Michibayashi[5], Peter B Kelemen[6], Damon AH Teagle[7], Jude Ann Coggon[7], Marguerite Godard[8], The Oman DP Science Party

1. Faculty of Social and Cultural Studies, Kyushu University, 2. Research and Development Center for Submarine Resources, JAMSTEC, 3. School of Natural System, Colleage of Science and Technology, Kanazawa University, 4. SDepartment of Geology, Faculty of Science, Niigata University, 5. Department of Earth and Planetary Sciences, Nagoya University, 6. Columbia University, 7. University of Southampton, 8. Géosciences Montpellier

It is well known that oceanic crust covers almost 70 % of Earth’ s surface. It is formed at mid-ocean ridge and is subducted into mantle at convergent plate margin. This plate motion is pull many kinds of surface materials in inside the mantle and contributed to a global recycling system. However the details of the oceanic crusts and underlain upper mantle are still poor understanding. The construction of the oceanic crusts is defined by constructions of ophiolites which were the ancient oceanic plates exposed onto land.

To have better understandings of the oceanic crust, underlain upper-most mantle and related other things, the Oman Drilling Project by ICDP was done the drilling from 2016 to 2018 in Samail ophiolite, Oman. The Samail ophiolite in the northern part of Oman is the largest and having better exposed section of the oceanic lithosphere in the world.

We will report the preliminary results of the PGE abundances and Os isotope ratios in the whole-rock gabbros and mantle related peridotites from the drilling cores and compering to the data from the Oman surface data. These data will be help us to better understanding of the relationships between the oceanic crust and underlying upper mantle, mechanisms of making oceanic crust, and planning the future Mohole projects.

Keywords: Oman DP, gabbro, peridotite, Os isotope ratio, PGE abundance

©2019. Japan Geoscience Union. All Right Reserved.

Overview of drilling of crust-mantle boundary at CM1&2 sites of Wadi Tayin massif of Oman ophiolite: the ICDP Oman Drilling Project

*Eiichi TAKAZAWA[1], Damon A H Teagle[2], Katsuyoshi Michibayashi[3], Yoshihiko Tamura[4], Jude Ann Coggon[2], Juerg Matter[2], Peter B Kelemen[5], Oman Drilling Project Phase 2 Science Party

1. Department of Geology, Faculty of Science, Niigata University, 2. University of Southampton, 3. Nagoya University, 4. JAMSTEC, 5. Columbia University

At the boundary between the crustal section and the mantle section of the Oman ophiolite there are several tens to hundreds of meters thick, mainly composed of dunite called the crust-mantle transition zone (MTZ) [1]. Since it often accompanies thin veins or clots of plagioclase and clinopyroxene and several centimeters to meters thick gabbro sills, it leaves traces of magma activity right under the ridge. The origin of dunite in MTZ is still under debate: the accumulation of olivine crystallized from melt [2], or the reaction of harzburgite with pyroxene-undersatulated melt [3], or both [4]. Recently, the presence of water at the time of formation has also been pointed out [5]. To clarify the origin of MTZ, more detailed research by continuous core through MTZ is necessary.

From November 2017 to January 2018 MTZ of Wadi Zeeb (CM1&2 sites) in Wadi Tayin massif was drilled by the International Continental Scientific Drilling ProgramOman Drilling Project [6]. Geological mapping on ground associated with information from the recovered cores the thickness of the MTZ is estimated as about 150 m. The upper and lower boundaries of the MTZ has a strike in the east-west direction, and it is inclined about 30 degrees south. In the summer of 2018, the drilled cores were carefully described by scientists on the deep-sea drilling vessel "CHIKYU". The stratigraphy has been divided into four igneous sequences based on the abundance of different lithologies: Layered Gabbro Sequence, Dunite Sequence, Dunite with Gabbro Sequence, and Mantle Sequence. Dunite Sequence and Dunite with Gabbro Sequence are summarized as Crust - Mantle Transition.

Hole CM1A is inclined 60˚ northward. The upper 160 m of the core is the Layered Gabbro Sequence, mostly composed of olivine gabbro, interlayered with gabbro and a small amount of wehrlite, dunite, anorthosite and troctolite. From 160 to 310 m the Crust-Mantle Transition is divided into an upper 90 m Dunite Sequence and a lower 60 m Dunite with Gabbro Sequence containing small lenses of gabbro, troctolite and wehrlite. The dunites are highly serpentinized, and rodingite and diopsidite commonly replace minor gabbroic rocks in these sequences. The lower 80 m of the hole is the Mantle Sequence, with alternating layers of dunite and increasingly abundant, residual mantle harzburgite.

Hole CM2B is a vertical hole located 400 m north of CM1A, and samples the Crust-Mantle Transition and the Mantle Sequence. As in CM1A, the transition is divided into an upper Dunite Sequence and a lower Dunite with Gabbro Sequence. In contrast to Hole CM1A, a small amount of olivine has escaped complete serpentinization in the lower portions of the CM2B transition zone. In the Mantle Sequence, harzburgite is dominant. Dunite accounts for about 25% of this Sequence, less than in CM1A. The lowermost peridoties in Hole CM2B are strongly altered to talc+carbonate.

[1] Boudier and Nicolas, 1995, J. Petrol., 36, 777-796, [2] Pallister and Hopson, 1981, J. Geophys. Res., 86, 2593-2644, [3] Kelemen et al., 1995, Nature, 375, 747-753, [4] Abily and Ceuleneer, 2013, Geology, 41, 67-70, [5] Rospabé et al., 2017, Geol. Soc. Am., Data Rep. 2017139, [6] Kelemen et al., 2013, Scientific Drilling, 15, 64-71.

©2019. Japan Geoscience Union. All Right Reserved.

Keywords: ophiolite, crust-mantle boundary, Moho Transition Zone, ICDP, Oman Drilling Project

©2019. Japan Geoscience Union. All Right Reserved.

Petrological observation of core samples drilled from a mantle section of the Oman ophiolite: A preliminary report of the Oman Drilling Project Phase 2

*Yuji Ichiyama[1], Oman Drilling Project Phase 2 Scientific Party

1. Chiba University

The Oman ophiolite is the world’s largest ophiolite and will help us to understand the crustal formation, processes in the mantle, and evolution and modification of the oceanic lithosphere through the time. The drillings and investigations of the crust-mantle boundaries and mantle sections were operated in the Oman Drilling Project Phase 2. We report the preliminary results of the petrological observation of the drilling samples from the mantle sections in the Phase 2 Holes BA1B, BA3A, and BA4A.

The Hole BA1B is composed of upper dunite and lower harzburgite associated with mafic dikes. The Hole BA3A is dominated mainly by harzburgite and also contains a minor amount of thin dunitic layers and mafic dikes. The Hole BA4A consists of alternation of dunite and harzburgite with abundant mafic dikes. The mafic dikes observed in each hole are gabbro to olivine gabbro, and sometimes wehrlitic. Brown to pale brown hornblende is usually included in almost all lithology. Phlogopite is also present in association with hornblende. Chromian spinel in an olivine-gabbro sample from the BA4A is characterized by high $Fe^{3+}/(Cr + Al + Fe^{3+})$ ratio (>0.15) and intermediate TiO_2 content (1–2 wt.%), which are comparable with those in island arc basalts. In the contact between the mafic dikes and peridotite, orthopyroxene is formed as a reaction product between the mantle peridotite and mafic melt. The petrological characteristics of the mafic dikes indicate that they crystallized from hydrous, oxidized magmas, which imply that the intrusion event occurred in a convergent margin rather than a typical spreading axis.

Keywords: ICDP, Oman ophiolite, Mantle peridotite, Mafic dike

©2019. Japan Geoscience Union. All Right Reserved.

[E] Oral | S (Solid Earth Sciences)：S-CG Complex & General

Tue. May 28, 2019 10:45 AM - 12:15 PM JST | Tue. May 28, 2019 1:45 AM - 3:15 AM UTC | A07 TOKYO BAY MAKUHARI HALL

[S-CG49] Hard-Rock Drilling Science: From Continental to Deep Sea Drilling, and Oman Project

convener:Katsuyoshi Michibayashi(Department of Earth and Planetary Sciences, Nagoya University), Eiichi TAKAZAWA(Department of Geology, Faculty of Science, Niigata University), Norikatsu Akizawa(Department of Ocean Floor Geoscience, Atmosphere and Ocean Research Institute, The University of Tokyo), Chairperson:Tomoaki Morishita(Kanazawa University), Katsuyoshi Michibayashi

The Oman Drilling Project (OmDP) has completed to drill numerous hard-rock cores within ancient oceanic lithosphere and the underlying subduction zone of the Samail ophiolite in Oman, with support from ICDP, IODP, Japan Society for the Promotion of Science, the Sloan Foundation's Deep Carbon Observatory, US, and European research agencies. Moreover, a number of IODP expeditions have focused on hard-rock drilling over the last several years including Expedition 352 in 2014, which drilled the volcanic sequence associated with subduction initiation in the Bonin fore-arc, Expedition 357, which drilled the Lost City hydrothermal field, Expedition 360, which drilled the lithosphere associated with ultraslow-spreading at the Southwest Indian Ridge in 2016, and Expedition 366, which drilled the serpentinite seamounts in the Mariana fore-arc. In this session, we invite presentations on the scientific results of hard-rock drilling at these and other sites. We also invite related presentations on oceanic lithosphere, island arc formation, and any other significant issue that could be addressed by future hard-rock drilling. This includes marine studies of oceanic lithosphere and on-land geological investigations of ophiolites, accreted arcs, and subduction complexes. The session is intended to be interdisciplinary, including the fields of geophysics, geochemistry, petrology, engineering, and biology.

10:45 AM - 11:00 AM JST | 1:45 AM - 2:00 AM UTC

[SCG49-12] Structural analyses of ultramafic rocks used by X-ray CT core imaging (Oman Drilling Project Phase 2, D/V CHIKYU)

*Katsuyoshi Michibayashi[1], Yuki Kakihata[1], Ikuo Katayama[2], Atsushi Okamoto[3], Keishi Okazaki[4], Peter B Kelemen[5], Eiichi TAKAZAWA[6], Damon A H Teagle[7], Oman Drilling Project Phase 2 Science Party[8] (1.Department of Earth and Planetary Sciences, Graduate School of Environmental Studies, Nagoya University, 2.Hiroshima University, 3.Tohoku University, 4.KCC, JAMSTEC, 5.Columbia University of New York, 6.Niigata University, 7.Southampton University, 8.ICDP)

11:00 AM - 11:15 AM JST | 2:00 AM - 2:15 AM UTC

[SCG49-13] Petrophysical characteristics of serpentinized peridotites of Hole BA1B, BA3A and BA4A

*Kakihata Yuki[1], Katsuyoshi Michibayashi[2], Laura Crispini[3], Bjorn Jamtveit[4], Samuel Barbier[5], Joe Aslin[6], Manuel Menzel[7], Marguerite Godard[8] (1.Graduate School of Science, Shizuoka University, 2.Graduate School of Environmental Studies, Nagoya University, 3.University of Genova, 4.University of Oslo, 5.Claude Bernard University Lyon 1, 6.University of Liverpool, 7.Andalusian Earth Science Institute, 8.Géosciences Montpellier, CNRS, Univ. Montpellier)

11:15 AM - 11:30 AM JST | 2:15 AM - 2:30 AM UTC

[SCG49-14] Physical properties of the Moho TZ: Implications from ICDP Oman Drilling Project Phase I & II on-board measurements

*Natsue Abe[1,12], Keishi Okazaki[1], Ikuo Katayama[2], Kohei Hatakeyama[2], Yuya Akamatsu[2], Benoit Ildefonse[3], Ulven Ivar Ole[4], Gilvert Hong[5], Wenlu Zhu[6], Benoit Cordonnier[4], Katsuyoshi Michibayashi[7], Eiichi TAKAZAWA[8], Michell Harris[10], Damon Teagle[11], Peter Kelemen[9], Marguerite Godard[3], Jurg Matter[11], Jude Coggon[11], Oman Drilling Project Scientific Party (1.Japan Agency for Marine-Earth Science and Technology, 2.Hiroshima University, 3.Universitè de Montpellier, 4.University of Oslo, 5.Seoul National University, 6.University of Maryland, 7.Nagoya University, 8.Niigata University, 9.Columbia University, 10.Polymouth University, 11.University of Southampton, 12.Kanazawa University)

11:30 AM - 11:45 AM JST | 2:30 AM - 2:45 AM UTC

[SCG49-15] **Seismic anisotropy under high pressure conditions of harzburgite collected from Oman Drilling Project Phase II**

*Kohei Hatakeyama[1], Ikuo Katayama[1], Natsue Abe[2], The Oman Drilling Project Phase II Science Party (1.Department of earth and planetary systems science, Hiroshima University , 2.JAMSTEC)

11:45 AM - 12:00 PM JST | 2:45 AM - 3:00 AM UTC

[SCG49-16] Understanding of the mode of seafloor spreading and the architecture of upper oceanic crust by oceanfloor drilling at off-Hawaii MoHole candidate site

*Susumu Umino[1], Tomoaki Morishita[1], Mikiya Yamashita[2], Osamu Ishizuka[3] (1.Department of Earth Sciences, Kanazawa University, 2.Japan Agency for Marine-Earth Science and Technology, 3.Geological Survey of Japan, AIST)

12:00 PM - 12:15 PM JST | 3:00 AM - 3:15 AM UTC

Discussion

Structural analyses of ultramafic rocks used by X-ray CT core imaging (Oman Drilling Project Phase 2, D/V CHIKYU)

*Katsuyoshi Michibayashi[1], Yuki Kakihata[1], Ikuo Katayama[2], Atsushi Okamoto[3], Keishi Okazaki[4], Peter B Kelemen[5], Eiichi TAKAZAWA[6], Damon A H Teagle[7], Oman Drilling Project Phase 2 Science Party[8]

1. Department of Earth and Planetary Sciences, Graduate School of Environmental Studies, Nagoya University, 2. Hiroshima University, 3. Tohoku University, 4. KCC, JAMSTEC, 5. Columbia University of New York, 6. Niigata University, 7. Southampton University, 8. ICDP

X-ray computed tomography (X-ray CT) images were obtained on all cores drilled during Oman Drilling Project (OmanDP) Phase 2 (Holes CM1A, CM2B, BA1B, BA3A and BA4A) as a routine part of the IODP measurement protocol onboard D/V Chikyu. X-ray CT scanning enables the non-destructive observation of the internal structure of the core, providing information about chemical composition and density. The data are useful for assessing sample locations and quality. X-ray CT images can be used for 3D fabric analyses even after core has been cut in half and subsampled for other analyses.

The X-ray CT scanner (Discovery CT 750HD, GE Medical Systems) scans and reconstructs an image of a 1.4 m section in 10 minutes and produces a series of scan images, each 0.625 mm thick. The X-ray source and detector are installed inside of the gantry opposite each other. The excitation voltage and current for X-ray tube are 140kV and 100 mA, respectively.

Core samples are scanned in the gantry with a scanning rate of 20 mm/sec. The distribution of attenuation values mapped to an individual slice comprises the raw data that are used for subsequent image processing. Successive two-dimensional (2D) slices of 512 x 512 pixels yield a representation of attenuation values in three-dimensional (3D) voxels of 512 x 512 by ~1600 in length. Data generated for each core consist of core-axis-normal planes (XY planes) of X-ray attenuation values with dimensions of 512 ×512 pixels in 9 cm ×9 cm cross-section, with a resolution of 0.176 mm/pixel.

X-ray intensity varies as a function of X-ray path length and the linear attenuation coefficient (LAC) of the target material, which is a function of the chemical composition and density of the target material. The basic measure of attenuation, radiodensity, is the CT number given in Hounsfield units (HU). CT numbers of air and water are -1000 and 0, respectively.

CT numbers of OmanDP cores reveal structural features such as the attitude of foliation in primary peridotites, defined by spinel and orthopyroxene crystal shape. Combined with microstructural analyses such as EBSD mapping, we can study petrophysical properties of the uppermost mantle in the mantle section. Moreover, comparing with density profiles measured onboard, we can also estimate the degree of serpentinization in core from Holes BA1B, BA3A and BA4A, ranging from 80 to almost 100%. Profiles of

©2019. Japan Geoscience Union. All Right Reserved.

the degree of serpentinization with depth may provide insight into ongoing serpentinization processes.

Keywords: Oman, XCT, Structural Analyses, Serpentinization

©2019. Japan Geoscience Union. All Right Reserved.

Petrophysical characteristics of serpentinized peridotites of Hole BA1B, BA3A and BA4A

*Kakihata Yuki[1], Katsuyoshi Michibayashi[2], Laura Crispini[3], Bjorn Jamtveit[4], Samuel Barbier[5], Joe Aslin[6], Manuel Menzel[7], Marguerite Godard[8]

1. Graduate School of Science, Shizuoka University, 2. Graduate School of Environmental Studies, Nagoya University, 3. University of Genova, 4. University of Oslo, 5. Claude Bernard University Lyon 1, 6. University of Liverpool, 7. Andalusian Earth Science Institute, 8. Géosciences Montpellier, CNRS, Univ. Montpellier

Structural characteristics within peridotites of Hole BA1B, BA3A and BA4A have been described during the Oman Drilling Project Phase 2 from 5th August to 3rd September, 2018 on D/V Chikyu. The peridotites consisted of intensely serpentinized harzburgite and dunite, which exhibited foliations defined by elongation and alignment of constituent minerals. Crystal plastic fabrics in harzburgite were described prior to those in dunite because orthopyroxene grains are clearer than spinel grains in serpentinized peridotites at macro scale.

Harzburgites in BA1B show variously deformed textures ranging from pophyroclastic to protomylonitic textures in dependent on the depth. In BA3A, harzburgites with protogranular texture were observed in relatively shallow sections (10-90 m), whereas porphyroclastic to strongly foliated textures were dominant in deeper sections. Most of hartzburgites in BA4A show porphyroclastic texture, partly clear foliation and protomylonitic textures by strongly elongated orthopyroxene grains. Dip angles of measured foliations in BA1B are mostly 0-20˚, which are nearly horizontal. Most of dip angles in BA3A are at around 30˚, up to 50˚. In BA4A, dip angles of orthopyroxene grains take various values between 10-50˚. In BA3A and BA4A show similar dip angles, but significantly steeper than those in BA1B. In each hole, dip angles were nearly constant independent on the depth.

Pyroxene and spinel grains in strongly foliated to protomylonitic peridotites are intensely elongated and aligned, exhibiting clear foliation at thin section scale. In protogranular peridotites, pyroxene and spinel grains have rounded shapes and are not elongated and aligned, and foliations are unclear. Elongated pyroxene and olivine grains in protomylonitic peridotites show kink bands and wavy extinction, whereas few rounded pyroxene grains in protogranular peridotites show these features.

Keywords: Oman Drilling Project, Peridotite, Crystal plastic fabric

©2019. Japan Geoscience Union. All Right Reserved.

Physical properties of the Moho TZ: Implications from ICDP Oman Drilling Project Phase I & II on-board measurements

*Natsue Abe[1,12], Keishi Okazaki[1], Ikuo Katayama[2], Kohei Hatakeyama[2], Yuya Akamatsu[2], Benoit Ildefonse[3], Ulven Ivar Ole[4], Gilvert Hong[5], Wenlu Zhu[6], Benoit Cordonnier[4], Katsuyoshi Michibayashi[7], Eiichi TAKAZAWA[8], Michell Harris[10], Damon Teagle[11], Peter Kelemen[9], Marguerite Godard[3], Jurg Matter[11], Jude Coggon[11], Oman Drilling Project Scientific Party

1. Japan Agency for Marine-Earth Science and Technology, 2. Hiroshima University, 3. Universitè de Montpellier, 4. University of Oslo, 5. Seoul National University, 6. University of Maryland, 7. Nagoya University, 8. Niigata University, 9. Columbia University, 10. Polymouth University, 11. University of Southampton, 12. Kanazawa University

We report physical property measurements of core samples from the Samail ophiolite in Oman, drilled by the ICDP Oman Drilling Project. Onboard core logging was conducted on D/V Chikyu for 4 months in total in the summers of 2017 and 2018. We analyzed 4 holes (GT1A, GT2A, GT3A and BT1B) in 2017, and 5 holes (CM1A, CM2B, BA1B, BA3A and BA4A) in 2018. The total core length of those 9 holes is about 3200 m. Cores from Holes GT1A and GT2A in the lower crust section of the ophiolite are mainly composed of gabbros (gabbro and olivine gabbro), with small amounts of ultramafic rocks (wehrlite and dunite), whereas those from Hole GT3A at the boundary between the sheeted dikes and gabbro are mainly composed of basalt and diabase, followed by gabbros (gabbro, olivine gabbro and oxide gabbro). Minor felsic trondhjemite and tonalite dikes intrude the mafic rocks. In contrast, Hole BT1B penetrated from mantle section through the basal thrust and into the metamorphic sole. The CM holes were drilled through the crust-mantle transition, from gabbroic lower crust, through dunite with minor gabbros, and in to residual mantle harzburgite. BA holes were taken from the mantle section and are composed of dunite and harzburgite intruded by minor gabbroic and pyroxenite dikes. Ultramafic rocks at both sites were extensively serpentinized, but the names of igneous protoliths are used here.

Whole-round data, including X-ray CT images, natural gamma radiation (NGR), gamma ray attenuation (GRA) density, magnetic susceptibility (MS), P-wave velocity (Vp) and noncontact electrical resistivity were obtained. Split core color spectroscopy data were also collected. Magnetic susceptibility, electrical resistivity under both nominally dry and brine-saturated conditions, P-wave velocity, bulk/grain density, porosity and thermal conductivity were measured in discrete samples. Nearly 100% core recovery allowed us to take a large data set of petrophysical data on the cores from Oman ophiolite including fault zones and highly altered intervals.

Generally, gabbroic rock types have higher density, P-wave velocity, and electrical resistivity, and lower porosity than ultramafic lithologies. Serpentinized dunite have lower density, P-wave velocity and electrical resistivity, and higher porosity than serpentinized harzburgite, and these physical properties are correlated with magnetic susceptibility, probably due to crystallization of magnetite during alteration. Average X-ray CT values are also correlated with many other physical properties in most lithologies. Those physical property data and the lithological characteristics of the Moho transition zone in the Oman ophiolite revealed apparent difference and similarities with the oceanic data, especially in the seismic profiles from the oceanic plate. In this paper, we would like to compare the data from ocean drilling, Oman Drilling and seismic profiles.

Keywords: ICDP, Oman Drilling Project, ophiolite, Moho TZ, Oceanic crust

©2019. Japan Geoscience Union. All Right Reserved.

©2019. Japan Geoscience Union. All Right Reserved.

Seismic anisotropy under high pressure conditions of harzburgite collected from Oman Drilling Project Phase II

*Kohei Hatakeyama[1], Ikuo Katayama[1], Natsue Abe[2], The Oman Drilling Project Phase II Science Party

1. Department of earth and planetary systems science, Hiroshima University , 2. JAMSTEC

The Oman ophiolite interpreted as ancient oceanic lithosphere has been drilled recently, and core samples of harzburgite were collected from mantle section (Oman Drilling Project). These compressional wave velocity of three orthogonal directions (X, Y and Z axis) was measured under ambient condition onboard D/V Chikyu. Velocity of Z axis was lower than that of orthogonal directions (X and Y axis), showing approximately 4% of anisotropy. Although anisotropy caused by preferred orientation of olivine was observed at oceanic mantle, olivine in harzburgite collected from ophiolite is almost transformed to serpentine, implying that anisotropy of core samples is caused by preferred orientation of pyroxene. In addition, the preferred orientation of cracks also causes anisotropy, which is sensitive to the type of pore fluid (Anderson et al., 1974). However, the dominant factor of anisotropy is unclear because both effects are included in the measurement under the ambient condition. In this study, we measured elastic wave velocity of harzburgite under high confining pressure where most pores are closed, and determine a dominant factor causing seismic anisotropy.
Harzburgite collected from Hole BA1B and BA3A were selected as the experimental samples. Density and porosity of these samples are 2.60 to 2.64 g/cm^{3}and 0.5% to 1.0%, respectively.Intra-vessel deformation and fluid flow apparatus at Hiroshima University were used to conduct the measurements under high confining pressure of up to 200 MPa. Two loading cycles were applied to each specimen to measure velocity successively under both dry and wet conditions. In wet condition, pore pressure was set at 10 MPa using a syringe pump.Both compressional and shear wave velocity ($V_P$andV_S) on two orthogonal directions (Y and Z axis) were measured from the pulse transmission method with the amplitude and the frequency of a trigger wave of 5 V and 2 MHz, respectively.
In the preliminary results at 200 MPa of confining pressure under dry conditions, harzburgite collected from Hole BA3A shows V_P = 5.86 km/s and V_S = 3.03 km/s on the direction of Y axis, and V_P = 5.49 km/s and V_S = 2.95 km/s on the direction of Z axis. Anisotropy under high confining pressure indicates 6.5% and 2.7% for compressional and shear wave velocity, respectively. Therefore, the preferred orientation of minerals is likely to be a dominant factor.

Keywords: Oman Drilling Project, Harzburgite, Anisotropy, Preferred orientation, Pyroxene, Crack

©2019. Japan Geoscience Union. All Right Reserved.

Understanding of the mode of seafloor spreading and the architecture of upper oceanic crust by oceanfloor drilling at off-Hawaii MoHole candidate site

*Susumu Umino[1], Tomoaki Morishita[1], Mikiya Yamashita[2], Osamu Ishizuka[3]

1. Department of Earth Sciences, Kanazawa University, 2. Japan Agency for Marine-Earth Science and Technology, 3. Geological Survey of Japan, AIST

Understanding how seafloor spreading and mantle melting are linked to ocean crust architecture is Challenge 9 of the IODP Science Plan for 2013-2023 and is one of the major goals of the mantle drilling project MoHole to Mantle (M2M). Deep basement drilling is skewed to young and slow-spread crust, with a wide gap of crust age between 20 and 110 Ma, including the world average of 62.5 Ma and spreading rate of 7.6 cm/a. Among the three candidate sites of M2M, only off-Hawaii site can provide the information of oceanic crust of the missing age and spreading rate. We propose a deep drilling off-Hawaii to penetrate through the upper crust and into the gabbros to understand the architecture and governing processes of the upper oceanic crust.

ODP Holes 504B and 1256D have brought invaluable information and fruitful insight into the architecture and formation processes of the upper oceanic crust.

Hole 504B is the deepest drill hole that penetrated 1815 m into 6.9-Ma basement formed at an intermediate rate of 6.6 cm/a at the Costa Rica Rift (Dick et al., 1992). The 504B upper crust, consisting of less dense extrusive rocks underlain by denser sheeted dikes than their source magmas, yields an apparent level of neutral buoyancy that traps accreted magma as dike intrusions. Thus, the 504B crust relaxes stress induced by plate movement and extends by both fault displacement and dike intrusions, which leads to development of rugged summit and axial troughs.

On the contrary, the 15-Ma 1256D crust, formed at the East Pacific Rise, has a distinctly high extrusive to intrusive ratio (814 m / 343 m) compared to that of the 504B crust (780 m / >1056 m). As is expected for the ultrafast spreading rate of 22 cm/a, the extrusive rocks are dominantly of massive and lobate sheet flows, which are as dense as the extruding magma (Umino et al., 2008). This results crust without an apparent level of neutral buoyancy and the persistently over pressurized axial magma chamber (AMC). Only a small increase in magmatic pressure or reduction in horizontal stress leads to dike intrusions followed by eruptions. Conversely, extension of the 1256D upper crust was primarily accomplished by dike intrusions without large faults.

These examples articulate how the density structures of upper crust partition magma into extrusive and intrusive rocks and form characteristic architectures.

Density structures are intimately correlated with magma budget, the amount of magma supplied and consumed to keep the same cross-sectional area of the ridge for a time scale of 100 ky.

The Galapagos Spreading Center (GSC) shows thickening on-axis and thinning total extrusive rocks with AMC depth, indicating axial valleys develop to trap thick on-axis flows with deepening AMC and decreasing magma budget (Blacic et al., 2004). For the GSC spreading rate of 4.5–5.5 cm/a, more than

©2019. Japan Geoscience Union. All Right Reserved.

50 % of flows in the axial valleys are pillows. Consequently, the GSC is underlain by less dense pillows interbedded with fault breccias. The density structure of this crust is essentially the same as the 504B crust.

Likewise, the magmatically robust East Pacific Rise (EPR) shows a negative correlation of total extrusive thickness and AMC depth, while on-axis flow thickness remains constant (Hooft et al., 1996, 1997). Accordingly, the axial troughs do not develop, and the upper crust extends mainly by dikes intrusions. This is facilitated by the presence of dense extrusive rocks comprising more than 80 % sheet flows, considering the spreading rates of 11–14 cm/a, primarily the same as the 1256D crust.

How two types of upper crust architecture change from one type to the other is yet to be understood. If any critical threshold that distinguishes two crust types exists, it would reside in the crust with a spread rate between 7 cm/a and 10 cm/a. The off-Hawaii crust spread at 7–8 cm/a will provide a missing link that connects the two crust architectures and brings us thorough understanding of the seafloor spreading.

Keywords: Oceanfloor Drilling, MoHole, Off-Hawaii site, Upper crust architecture, Density structure, Plate spreading

©2019. Japan Geoscience Union. All Right Reserved.

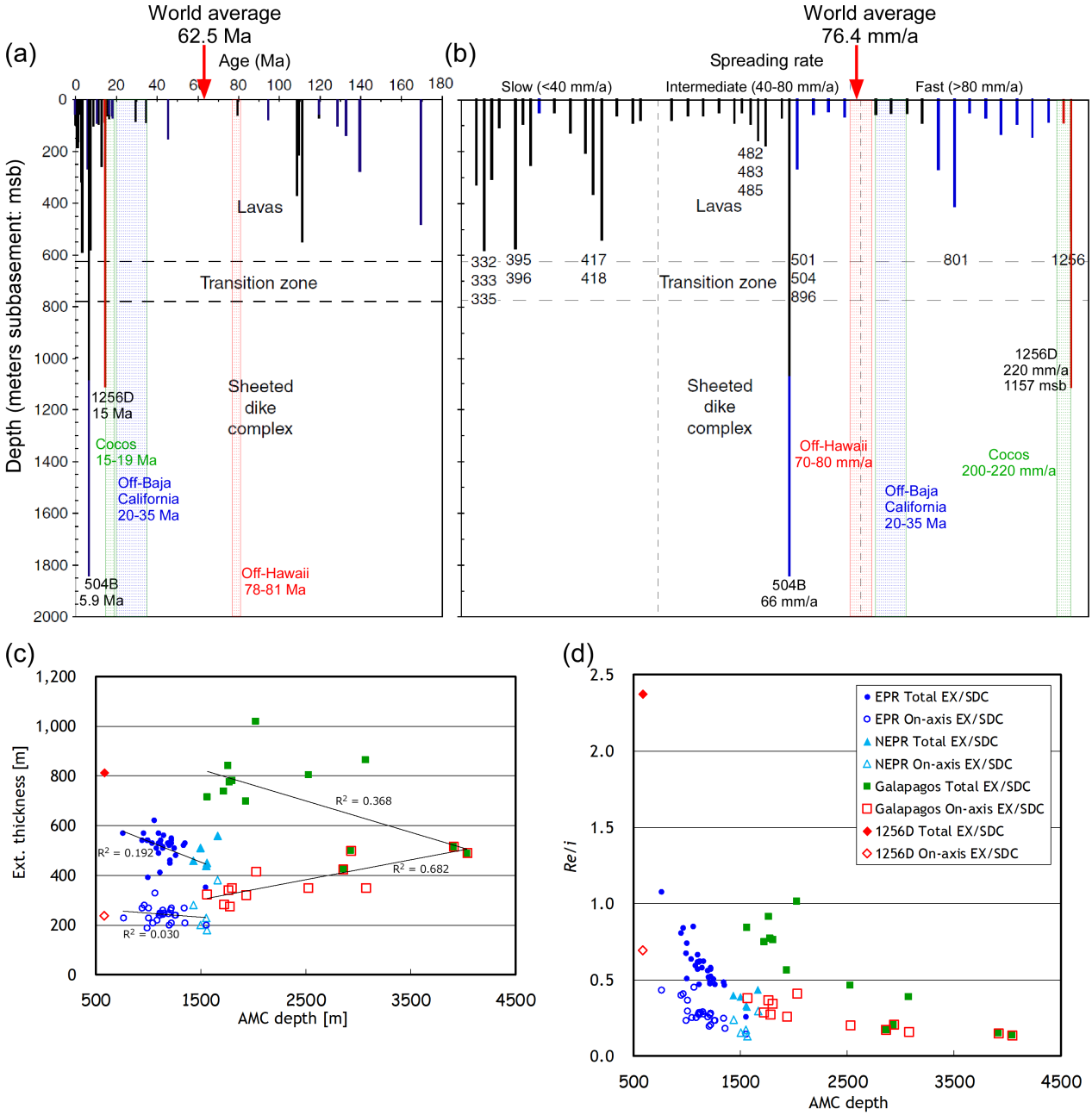

Above: Ocean drill holes deeper than 50 m into the oceanic basement plotted against the basement age (a) and categorized on the basis of spreading rate that formed the basement crust (b). World average age and spreading rate are based on the 3.6 min grid data from EarthByte agegrid 2008 (Muller et al., 2008).
Below: Extrusive thickness (c) and Re/i (ratio of extrusive to intrusive thickness) (d) plotted against the AMC depth for the present GSC and EPR segments and the 15-Ma 1256D crust. Solid and open symbols are data based on total and on-axis extrusive thicknesses.

©2019. Japan Geoscience Union. All Right Reserved.

[E] Poster | S (Solid Earth Sciences)：S-CG Complex & General

Tue. May 28, 2019 3:30 PM - 5:00 PM JST | Tue. May 28, 2019 6:30 AM - 8:00 AM UTC | Poster Hall International Exhibition Hall8, Makuhari Messe_19

[S-CG49] Hard-Rock Drilling Science: From Continental to Deep Sea Drilling, and Oman Project

convener:Katsuyoshi Michibayashi(Department of Earth and Planetary Sciences, Nagoya University), Eiichi TAKAZAWA(Department of Geology, Faculty of Science, Niigata University), Norikatsu Akizawa(Department of Ocean Floor Geoscience, Atmosphere and Ocean Research Institute, The University of Tokyo)

The Oman Drilling Project (OmDP) has completed to drill numerous hard-rock cores within ancient oceanic lithosphere and the underlying subduction zone of the Samail ophiolite in Oman, with support from ICDP, IODP, Japan Society for the Promotion of Science, the Sloan Foundation's Deep Carbon Observatory, US, and European research agencies. Moreover, a number of IODP expeditions have focused on hard-rock drilling over the last several years including Expedition 352 in 2014, which drilled the volcanic sequence associated with subduction initiation in the Bonin fore-arc, Expedition 357, which drilled the Lost City hydrothermal field, Expedition 360, which drilled the lithosphere associated with ultraslow-spreading at the Southwest Indian Ridge in 2016, and Expedition 366, which drilled the serpentinite seamounts in the Mariana fore-arc. In this session, we invite presentations on the scientific results of hard-rock drilling at these and other sites. We also invite related presentations on oceanic lithosphere, island arc formation, and any other significant issue that could be addressed by future hard-rock drilling. This includes marine studies of oceanic lithosphere and on-land geological investigations of ophiolites, accreted arcs, and subduction complexes. The session is intended to be interdisciplinary, including the fields of geophysics, geochemistry, petrology, engineering, and biology.

[SCG49-P01] Permeability profile in the Oman Drilling Project inferred from resistivity measurements

*Ikuo Katayama[1], Keishi Okazaki[2], Natsue Abe[2], Ole Ivar Ulven[3], Gilbert Hong[4], Wenlu Zhu[5], Benoit Cordonnier[3], Kohei Hatakeyama[1], Yuya Akamatsu[1], Katsuyoshi Michibayashi[6], Marguerite Godard[7], Peter Kelemen[8], Science Party The Oman Drilling Project Phase 2 (1.Hiroshima University, 2.JAMSTEC, 3.University of Oslo, 4.Seoul National University, 5.University of Maryland, 6.Nagoya University, 7.Universitè Montpellier, 8.Columbia University)

[SCG49-P02] Relationship between alteration intensity and elastic wave velocity of gabbroic rocks from ICDP Hole CM1A, Oman Drilling Project Phase II

*Kosuke Kimura[1], Ikuo Katayama[1], Kohei Hatakeyama[1], Yuya Akamatsu[1], Natsue Abe[2], Keishi Okazaki[2], The Oman Drilling Project Phase II Science Party (1.Hiroshima University, 2.JAMSTEC)

[SCG49-P03] Physical property of the fossilized crust-mantle transition zone from ICDP Oman Drilling Project Hole CM1A and CM2B measured onboard D/V Chikyu

*Keishi Okazaki[1], Natsue Abe[1], Kohei Hatakeyama[2], Yuya Akamatsu[2], Ikuo Katayama[2], Eiichi TAKAZAWA[3], Damon A H Teagle[4], Peter B Kelemen[5], Jude Coggon[4], The Oman Drilling Project Phase 2 Science Party (1.Japan Agency for Marine-Earth Science and Technology, 2.Hiroshima University, 3.Niigata University, 4.University of Southampton, 5.Columbia University)

[SCG49-P04] Microstructures of lower crust gabbros from the Oman Ophiolite: Analyses of the drilled cores of the Oman Drilling Project

*Koki Iida[1], Takahiro Fudai[1], Susumu Umino[1], Yuki Kusano[2] (1.Kanazawa University, 2.Geological Survey of Japan)

[SCG49-P05] Olivine fabric and mineral compositions in the Maqsad area of the Samail massif, the southern Oman ophiolite

*Kaho Takahashi[1], Eiichi TAKAZAWA[2,3], Katsuyoshi Michibayashi[4], Kakihata Yuki[4], Ryoko Senda[5] (1.Graduate School of Science and Technology, Niigata University, 2.Department of Geology, Faculty of

Science, Niigata University, 3.JAMSTEC, 4.Nagoya University, 5.Kyushu University)

[SCG49-P06] The evolution of melt inclusions in podiform chromitite in Oman

*Yuan YAO[1], Eiichi TAKAZAWA[2,3], Oman Drilling Project Phase 2 Science Party (1.Graduate School of Sciences& Technology, Niigata University, Japan, 2.Department of Geology, Faculty of Science, Niigata University, Japan, 3.Research and Development Center for Ocean Drilling Science, JAMSTEC, Japan)

[SCG49-P07] Melt/fluid - rock reaction inferred from the Wadi Tayin mantle section in the southern Oman ophiolite

*Keisuke ISHII[1], Eiichi TAKAZAWA[2], Akihiro kuriyama[2], Kyouka Someya[2], Yoshihiko Tamura[3] (1.Graduate School of Science and Technology, Niigata University, 2.Department of Geology, Faculty of Science, Niigata University , 3.R&D Center for Ocean Drilling Science, Japan Agency for Marine-Earth Science and Technology)

[SCG49-P08] Numerical simulations for reaction-induced fracture formation of layered gabbro during hydration process

*Kazuki Yoshida[1], Hiroyuki Shimizu[2], Noriyoshi Tsuchiya[1], Atsushi Okamoto[1], Phase 2 Science Party Oman Drilling Project[3] (1.Tohoku university, 2.Geotechnical Analysis Group, Advanced Analysis Department, Civil Engineering Design Division, Kajima Corporation, 3.Oman Drilling Project Phase 2 Science Party)

[SCG49-P09] X-ray CT images of oceanic lithologies obtained on Oman Drilling Project drillcores during ChikyuOman 2017 and 2018

*Katsuyoshi Michibayashi[1], Peter B Kelemen[2], Margurette Godard[3], Eiichi TAKAZAWA[4], Damon A H Teagle[5], The Oman Drilling Project Science Party[6] (1.Department of Earth and Planetary Sciences, Nagoya University, 2.Columbia University, 3.Université Montpellier, 4.Niigata University, 5.Southampton University, 6.ICDP)

[SCG49-P10] Re-examination of the crystallization process of clinopyroxene oikocrysts in layered gabbros at Hess Deep Rift, EPR

*Akane Yasui[1], Takashi Hoshide[1] (1.Graduate School of International Resource Sciences, Akita University)

[SCG49-P11] Structural petrology of peridotites from the Kalaymyo ophiolite

*Kouhei Asano[1,2], Katsuyoshi Michibayashi[1], Jung-Woo Park[3] (1.Graduate School of Environmental Studies, Nagoya University, 2.Shizuoka University, 3.Seoul National University)

[SCG49-P12] Reevaluation of the origin of mafic layers in the Upper Zone of the Horoman Peridotite

*Yumeto KOGURE[1], Eiichi TAKAZAWA[1] (1.Department of Geology, Faculty of Science, Niigata University)

[SCG49-P13] A structural and petrological study of "Shibukawa ultramafic body" in the Sanbagawa belt, western Shizuoka, Japan

*Hikaru Shioya[1,2], Katsuyoshi Michibayashi[1], Ken-ichi Hirauchi[2] (1.Graduate School of Environmental Studies, Nagoya University, 2.Institute of Geosciences, Shizuoka University)

Permeability profile in the Oman Drilling Project inferred from resistivity measurements

*Ikuo Katayama[1], Keishi Okazaki[2], Natsue Abe[2], Ole Ivar Ulven[3], Gilbert Hong[4], Wenlu Zhu[5], Benoit Cordonnier[3], Kohei Hatakeyama[1], Yuya Akamatsu[1], Katsuyoshi Michibayashi[6], Marguerite Godard[7], Peter Kelemen[8], Science Party The Oman Drilling Project Phase 2

1. Hiroshima University, 2. JAMSTEC, 3. University of Oslo, 4. Seoul National University, 5. University of Maryland, 6. Nagoya University, 7. Universitè Montpellier, 8. Columbia University

Permeability is a key property that controls heat and chemical exchange in the oceanic lithosphere as well as microbial activity in the sub-seafloor. Although direct measurements of permeability were not made on board D/V Chikyu during analysis of cores from the Oman Drilling Project, we estimated permeability profiles based on onboard measurements of electrical resistivity. For each core sample, we measure its resistivity at nominally dry conditions to obtain the dry resistivity. We then saturate the sample with NaCl solution (3.5g/L) and repeat the resistivity measurements at brine-saturated conditions to obtain the wet resistivity. Owing to the conductive brine in the pore space, the wet resistivity is systematically lower than dry resistivity. Because the difference between dry and wet resistivity is predominantly controlled by the movement of dissolved ions in the brine that occupied the pore space, we can use the resistivity data to infer the volume fraction of pores that contribute to electrical transport (termed “transport porosity”). We apply the Hashin-Shtrikman upper bound to estimate transport porosity. The estimated transport porosity shows a positive correlation with bulk porosity measured on board (MAD analysis), but is approximately one order of magnitude lower. Using an empirical cubic law between transport porosity and permeability, we produce estimated permeability profiles for the crust-mantle transition zone and the serpentinized mantle sections in the Hole CM1A, BA1B, BA3A and BA4A. The results indicate, (1) the gabbro sequence exhibits a markedly lower permeability than the underlying mantle sequence, (2) serpentinized dunites have higher permeability compared to serpentinized harzburgites, and (3) the general variation of discrete sample permeability is correlated with fault zone and intervals with abundant fractures. These permeability structures are most likely modified by alteration and juxtapositions, and do not represent the in-situ profile of the oceanic lithosphere; but this technique can be applicable to infer on-board permeability in future hard rock drilling.

©2019. Japan Geoscience Union. All Right Reserved.

Relationship between alteration intensity and elastic wave velocity of gabbroic rocks from ICDP Hole CM1A, Oman Drilling Project Phase II

*Kosuke Kimura[1], Ikuo Katayama[1], Kohei Hatakeyama[1], Yuya Akamatsu[1], Natsue Abe[2], Keishi Okazaki[2], The Oman Drilling Project Phase II Science Party

1. Hiroshima University, 2. JAMSTEC

The mafic to ultramafic rocks suffer metamorphism and metasomatism by the seafloor hydrothermal activities. These alterations can influence the elastic wave velocity due to the change of mineral assemblages during the ocean floor metamorphism. However, most previous studies have measured the elastic wave velocity of relatively unaltered samples. In this study, we measured elastic wave velocity of the altered gabbro from the Semail ophiolite collected from the Oman Drilling Project Phase II in order to estimate the effect of ocean floor metamorphism on the elastic wave velocity.

Gabbro samples were collected from CM1A site that is reported to be a layered gabbro sequence. Total seven samples those have different alteration intensity were measured. We use intra-vessel deformation and fluid flow apparatus at Hiroshima University to measure elastic wave velocity under confining pressure up to 200 MPa. Elastic wave velocity was measured by the pulse transmission method, with the amplitude and the frequency of a trigger wave of 5 V and 2 MHz, respectively. After measurements under dry condition, measurements under wet conditions injecting pore water were performed (P_P = 10 MPa). Alteration intensity is recognized by the relative abundances of the secondary minerals.

On the basis of the petrography, alteration group could be divided into four types. First type is almost fresh, olivine altered to serpentine and chlorite partially with less green minerals present. Second type has saussuritized plagioclase dominantly and also some sample shows alteration of clinopyroxene to amphibole. In the third type amphibolitization of clinopyroxene is dominant, and also saussuritization of plagioclase occur. Fourth type is the most altered sample showing alteration halo along the veins. Almost of the minerals are changed to prehnite except a few relict clinopyroxene. This type has higher porosity than other types.

Sample density ranges from 2.77-3.08 g/cm^3, and porosity ranges from 0.02-0.22% except ca. 1% from halo alteration sample. Data from these samples show a trend that elastic wave velocities (V_P and V_S) increase with increasing the confining pressure from 20 to 200 MPa. V_P increases from 5.68-6.80 to 6.16-6.91 km/s, V_S slightly increases from 3.65-3.97 to 3.69-3.99 km/s and V_P/V_S is almost constant ranging between 1.56-1.86 to 1.64-1.88 under dry condition, and on the other hand, V_P increases from 6.08-6.82 to 6.31-6.93 km/s, V_S slightly increases from 3.64-3.98 to 3.69-4.00 km/s and V_P/V_S is almost constant 1.67-1.86 to 1.68-1.87 under fluid-saturated condition, respectively. This result is mostly consistent with the layered gabbro occur in a normal oceanic crust (e.g. White et al., 1992; Shinohara et al., 2008).

At 200 MPa and under dry condition, V_P moderately decreases with increase in alteration intensity. About 0.75 km/s decreases in response to the increase in alteration intensity from 10 to 80 %. Comparing dV_P (difference in calculated and measured values) from the back-calculated original mineral assemblages of gabbro and peridotite reveled that the decrease in dV_P for the former is less than the latter. Moreover, both the curves of V_P and impedance change cross-over each other for gabbro and peridotite after nearly 50% of alteration.

©2019. Japan Geoscience Union. All Right Reserved.

From the above results, we suggest that if both gabbro and peridotite suffer more than 50% alteration, reversal of seismic velocity and impedance occurs, which effectively would affect the determination of geophysical Moho.

Reference: White et al. (1992) J. Geophys. Res. 97, 19,683-19,715. Shinohara et al. (2008) Phys. Earth Plan. Inter., 170, 95-106. Christensen (2004) Inter. Geol. Rev., 46, 795-816.

Keywords: Oman ophiolite, Gabbroic rocks, Elastic Wave Velocity, alteration

©2019. Japan Geoscience Union. All Right Reserved.

Physical property of the fossilized crust-mantle transition zone from ICDP Oman Drilling Project Hole CM1A and CM2B measured onboard D/V Chikyu

*Keishi Okazaki[1], Natsue Abe[1], Kohei Hatakeyama[2], Yuya Akamatsu[2], Ikuo Katayama[2], Eiichi TAKAZAWA[3], Damon A H Teagle[4], Peter B Kelemen[5], Jude Coggon[4], The Oman Drilling Project Phase 2 Science Party

1. Japan Agency for Marine-Earth Science and Technology, 2. Hiroshima University, 3. Niigata University, 4. University of Southampton, 5. Columbia University

To understand physical properties of the oceanic crust and the mantle is fundamentally important to reveal the dynamics of plate tectonics, and the global circulations of H_2O and CO_2 fluids. We report results on physical property measurements of core samples from Oman Drilling Project (OmanDP) Holes CM1A and CM2B, which drilled from the lower igneous crust into the upper mantle in the Samail Ophiolite, Sultanate of Oman.

X-ray CT, bulk/grain density, porosity, magnetic susceptibility, P-wave velocity, electrical resistivity and thermal conductivity were measured onboard D/V Chikyu using whole-round cores and discrete samples for core sections from CM1A and CM2B.

The paleo-Moho in CM1A may not preserve the original structure due to minor faulting, possibly during obduction. The gabbro-dunite transition (paleo-Moho) in Hole CM1A is characterized by a sharp change in physical property data. For example, P-wave velocity decreases from ~6.7 km/s in the layered gabbro sequence to ~4.9 km/s in the MTZ. Low P-wave velocity and density (~2.6 g/cm^3) in serpentinized dunites reflect the fact that olivine in the dunites is almost completely serpentinized. Serpentinization could have occurred during hydrothermal alteration near the spreading ridge axis, during subduction of 100’s of km of oceanic crust and sediment beneath the ophiolite, during obduction onto the Arabian continental margin, and/or during present-day weathering. In contrast to the paleo-Moho, the boundary between the Crust-Mantle Transition (CMT) sequences (i.e., dunites and dunites with gabbro lenses) and the underlying, residual mantle harzburgites is somewhat gradual. P-wave velocity gradually increases from ~4.9 km/s for dunite in the CMT to ~5.5 km/s for harzburgite in the mantle sequence. The thickness of the CMT is 50–70 m in Holes CM1A and CM2B. We also report on correlations between physical properties, especially electrical conductivity and magnetic susceptibility, and the fault intensity and alteration intensity from the core descriptions.

Keywords: ophiolite, mantle, oceanic crust, moho

©2019. Japan Geoscience Union. All Right Reserved.

Microstructures of lower crust gabbros from the Oman Ophiolite: Analyses of the drilled cores of the Oman Drilling Project

*Koki Iida[1], Takahiro Fudai[1], Susumu Umino[1], Yuki Kusano[2]

1. Kanazawa University, 2. Geological Survey of Japan

Oman Drilling Project in 2016 to 2017 recovered 400 m long cores of layered gabbros at Site GT1 in the Wadi Tayin Massif of the Oman Ophiolilte. The purpose of this research is to describe microstructures of the layered gabbro core samples and to discuss the conditions of magmatic and hypersolidus deformation that operated in the lower crust beneath the Oman paleoridge.

Core samples were cut into slabs parallel to foliation and slabs normal to foliation and parallel to lineation, which were made into thin sections for microscopic observations. Structural fabrics and the relationships between crystal shapes and alliginment were described to identify magmatic and hypersolidus deformation structures.

Cored samples are predominantly olivine gabbros consisting of anhedral olivine, anhedral to subhedral clinopyroxene and subhedral to euhedral plagioclase. Grain size ranges from 0.5 mm to a few millimeters irrespective of mineral species.

The structures shown by the gabbros are classified into three regimes by temperature or the amount of melt present: Regime I, magmatic conditions without or minimal plastic deformation; regime Ⅱ, plastic deformation assisted by interstitial melt (Dunn, 2000); regime Ⅲ, near solidus deformation. Regime Ⅱ is identified by ameboid grain boundaries with no intracrystalline deformation and equigranular textures, resulted from decreasing internal strain energy by at high temperatures. The presence of melt is evidenced by the clear euhedral plagioclase rims with resorbed turbid cores as discussed below.

Regime I. Magmatic structures are identified as modal layering due to changes in mineral mode, no preferred orientation or shape-preferred orientation of clinopyroxene and plagioclase, poikilitic texture of olivine enclosing plagioclase laths and ophitic texture of clinopyroxene including plagioclase laths.

Regime II. The hypersolidus deformation structures overprint igneous structures: ameboid olivine with or without strain in the crystal, elongated olivine, and lenticular aggregates of olivine grains with an asymmetric quarter structure. Single clinopyroxene crystals show an asymmetric quarter structure like olivine aggregates. Ophitic clinopyroxenes consist of subgrains with slightly different orientations <10˚. Plagioclase shows deformation twin and undulose extinction. Equigranular fine-grained plagioclase with grain boundaries intersecting at 120˚ are common. Large plagioclases have a resorbed core with a wavy outline and are surrounded by euhedral rim.

Regime III. Subsolidus recrystallization includes buldging and grain boundary migration resulted in ameoboid grain boundaries of clinopyroxene. Undulose extinction and kinked twinning of plagioclase are observed.

It is well known that mid-ocean ridge basalt magma commonly crystallizes in the order of olivine, plagioclase and clinopyroxene, which is also true for the gabbros of the Oman Ophiolite (Adachi and Miyashita, 2003). Nevertheless, only plagioclase shows euhedral to subhedral shapes in the observed

©2019. Japan Geoscience Union. All Right Reserved.

layered gabbro core samples. Deformed olivine aggregates and clinopyroxene with quarter structures are embedded in plagioclase with equilibrium granoblastic textures and large euhedral plagioclases with resorbed turbid cores. Considering these textures combined with the mechanical strength of the three constituent minerals, these gabbros suffered deformation under the presence of melt, which assisted complete recovery of strain through recrystallization of fine-grained plagioclase and overgrowth of euhedral rims around magmatic plagioclase cores. Poikilitic olivine occurs through the hole, whereas ophitic Cpx occurs at 73 m and 220 m in depth. Most deformation structures of regime II are present irrespective to depth. The asymmetric structures of olivine and clinopyroxene were used to determine the relative sense of shear. Both dextral and sinistral sense of shear are observed within the same samples.

Keywords: Oman ophiolite, Oman Drilling Project , Layered gabbro , Foliated gabbro , Microstructures , Lower crust

©2019. Japan Geoscience Union. All Right Reserved.

Olivine fabric and mineral compositions in the Maqsad area of the Samail massif, the southern Oman ophiolite

*Kaho Takahashi[1], Eiichi TAKAZAWA[2,3], Katsuyoshi Michibayashi[4], Kakihata Yuki[4], Ryoko Senda[5]

1. Graduate School of Science and Technology, Niigata University, 2. Department of Geology, Faculty of Science, Niigata University, 3. JAMSTEC, 4. Nagoya University, 5. Kyushu University

In this study, we conducted structural and chemical analysis of oriented samples of 17 harzburgites and 4 dunites collected from the Maqsad area of Samail massif in the southern Oman ophiolite. We investigated the degree of partial melting and the mantle-melt reaction with relation to mantle diapir structure.

The crystallographic preferred orientation (CPO) of olivine grains were measured in highly polished XZ thin sections using a scanning electron microscope equipped with an electron-back scatter diffraction system at Shizuoka University. After plotting the results in the Vp Flinn plot expanded for olivine fabric types [1,2], the fabric type of peridotites in this study are summarized as follows. The distribution of A type is limited in the southeastern part where the diapir structure has been identified [3], whereas D type is dominant in the peripheral part of the diapir. Minor amounts of AG type and E type are also observed in the peripheral part. From these, the olivine in the southeastern part (diapir area) of this study area is likely to have been deformed under high temperature whereas the peripheral part was deformed at slightly lower temperature. The CPOs of olivine in both areas do not show any influence from the presence of H2O except for only one sample with E type CPO. Moreover, strong alignment of [100] to the vertical orientation was observed in the southeastern part (diapir area) of this study area. Since vertical mantle flow has been estimated in this diapir area, our results are consistent with the previous study [3,4].

The Cr# (=Cr/[Cr+Al] atomic ratio) of spinel in the harzburgites and dunites are as high as 0.55-0.58 in the central part of the southeastern part (diapir area) and along the paleo-ridge axis running in the NW - SE direction [3,4]. On the other hand, the Cr# of spinel in the peripheral part is 0.41-0.55 indicating slightly less depleted than in the central part. In addition, the REE abundance of clinopyroxenes in the central part of the diapir area is lower than in the peripheral part being consistent with the distribution of spinel Cr#.

We consider that the upwelling rate in the southeastern part (diapir area) may have been greater than the peripheral part possibly due to higher temperature in the focused vertical mantle flow. This model is consistent with the distribution of the Cr# of spinel: the degree of melting was greater in the diapir area where Cr# of spinel are higher than the peripheral part. The strongly focused pipe-like model for axis location [3,5] is well fitted by our observations in this study.

[1] Karato et al., 2008, Ann. Rev. Earth Planet. Sci., 36, 59-95. [2] Michibayashi, 2015, J. Geography, 124, 397-409. [3] Jousselin et al., 1998, JGR, 103, 18153-18170. [4] Nicolas et al., 2000, Marine Geophys. Res., 21, 147-179. [5] Nicolas and Boudier, 1995, JGR, 100, 6179-6197.

Keywords: Oman ophiolite, crystalographic preferred orientation, olivine, fabric, peridotite, mantle flow

©2019. Japan Geoscience Union. All Right Reserved.

The evolution of melt inclusions in podiform chromitite in Oman

*Yuan YAO[1], Eiichi TAKAZAWA[2,3], Oman Drilling Project Phase 2 Science Party

1. Graduate School of Sciences& Technology, Niigata University, Japan, 2. Department of Geology, Faculty of Science, Niigata University, Japan, 3. Research and Development Center for Ocean Drilling Science, JAMSTEC, Japan

Melt inclusions are tiny inclusions which trapped in the host magmatic minerals. After trapping, the host mineral can be considered as a closed and isolated system (Roedder, 1984). Thus, melt inclusions behave as time capsules, which record the liquid line of descent of magmatic systems (Frezzotti, 2001). Therefore, melt inclusions can provide important information of the primary melts (Kent, 2008).

We studied the melt inclusions in chromite from a chromitite deposit mine in the north of Maqsad and the core sample from the Oman drilling project phase 2. The silicate inclusions range in diameter from 5 μm to 200 μm, contain pargasite, tremolite, aspidolite, high Cr# (=Cr/[Cr+Al] atomic ratio) chromite, diopside, enstatite, forsterite, grossular, albite, titanite, pentlandite, apatite, chlorite, wollastonite and serpentine. We found the high Cr# chromite occurs as lining of the inclusion, moreover the daughter minerals precipitated in the high Cr# chromite lining. Those phenomenon can be explained by the crystallization of chromite on the wall of inclusion. In addition, this is the first report about the necking down of melt inclusion in chromitite. The necking down of inclusions is an originally large, liquid-filled inclusion divided into smaller inclusions. If the necking down happens after the phase change of inclusion, the compositions of smaller inclusions probably are inhomogeneity. Last year, we conducted the high temperature homogenized experiments, the result showed that the homogenized quenching glass are heterogeneous. We consider the inhomogeneity of inclusions perhaps caused by the necking down. Based above all, we suggest the composition of homogenized inclusion can not represent the parental melt.

To summarize, we suggest before analysis and experiment of inclusions in chromite, the origin and the evolution of inclusions should be carefully studied.

Reference

Frezzotti, M. (2001). "Silicate-melt inclusions in magmatic rocks: applications to petrology." Lithos **55** (1-4): 273-299.
Kent, A. J. R. (2008). "Melt Inclusions in Basaltic and Related Volcanic Rocks." Reviews in Mineralogy and Geochemistry **69** (1): 273-331.
Roedder, E. (1984). Fluid inclusions, Walter de Gruyter GmbH & Co KG.

Keywords: melt inclusion, Oman, chromitite

©2019. Japan Geoscience Union. All Right Reserved.

Melt/fluid - rock reaction inferred from the Wadi Tayin mantle section in the southern Oman ophiolite

*Keisuke ISHII[1], Eiichi TAKAZAWA[2], Akihiro kuriyama[2], Kyouka Someya[2], Yoshihiko Tamura[3]

1. Graduate School of Science and Technology, Niigata University, 2. Department of Geology, Faculty of Science, Niigata University , 3. R&D Center for Ocean Drilling Science, Japan Agency for Marine-Earth Science and Technology

We report the petrology and the mineral compositions of peridotites from the Wadi Tayin massif in the southern Oman ophiolite [1-3] to investigate the influence of arc related magmatism during oceanic thrusting of the ophiolite. Harzburgites, dunites and a small number of lherzolite were systematically corrected along wadis to cover the mantle section from the boundary between lower crust and uppermost mantle namely “Moho” to the basal thrust. Spinel Cr# [=Cr/(Cr+Al) atomic ratio] of harzburgite varies from 0.22 to 0.58 similar to the range in abyssal peridotites [4]. Moreover, it gradually increases from the basal part to the Moho indicating the compositional variation expected for the residual mantle column formed at a mid ocean ridge. On the other hand, the spinel Cr# of dunite often exceeds 0.6 in the NW-SE striking shear zone in the middle part of the study area. The chondrite-normalized rare earth element (REE) patterns of clinopyroxenes in peridotites from the shear zone show a linear pattern that monotonously decreases from heavy REE to light REE (LREE). Calculated melt compositions in equilibrium with these clinopyroxenes are equivalent with the V2 (Type2) lava reported in the northern Oman ophiolite [5-6].

The plots in Cr# of spinel versus Ce/Yb ratio of clinopyroxenes show a linear trend with a positive correlation. It indicates that the LREE enrichment of clinopyroxene is associated with an increase in the degree of melting. Clinopyroxenes in the dunite from the shear zone are most significantly enriched in LREE to middle REE and have REE abundances being in equilibrium with the V2 lava. We consider that harzburgites were suffered from a flux melting by infiltration of H2O-rich fluid producing V2 lava. Comparing to the results from the northern massifs the linear trend in the diagram of Cr# of spinel versus Ce/Yb ratio of clinopyroxenes in the southern massif is obviously shifted toward lower in Cr#. It suggests that the infiltration of H2O-rich fluid may have started at early stage of melting in the Wadi Tayin massif relative to the northern massifs.

[1] Kelemen et al., 1995, Nature, 375, 747-753, [2] Godard al., 2000, EPSL, 180, 133-148, [3] HanghØj et al., 2010, J. Petrol., 51, 201-227, [4] Dick and Bullen, 1984, CMP, 86, 54-76, [5] Godard et al., 2003, G-cubed, 4, 8609, [6] Kusano et al., 2016, Chem. Geol., 449, 206-225.

Keywords: Oman ophiolite, Mantle section, Peridotite, Melt/rock reaction

©2019. Japan Geoscience Union. All Right Reserved.

Numerical simulations for reaction-induced fracture formation of layered gabbro during hydration process

*Kazuki Yoshida[1], Hiroyuki Shimizu[2], Noriyoshi Tsuchiya[1], Atsushi Okamoto[1], Phase 2 Science Party Oman Drilling Project[3]

1. Tohoku university, 2. Geotechnical Analysis Group, Advanced Analysis Department, Civil Engineering Design Division, Kajima Corporation, 3. Oman Drilling Project Phase 2 Science Party

Serpentinization of oceanic lithosphere is important for various geological processes, including magmatism and earthquake at subduction zone, and generation of hydrogen and hydrocarbon at seafloor. For understanding the extent of the water infiltration into mantle within the oceanic lithosphere, permeability of the lower crust is an important factor, since gabbro has low permeability at high confining pressure (Katayama et al., 2012). In natural olivine-bearing gabbro, serpentinization of olivine grains produced radial fractures within the plagioclase matrix, which can potentially enhance the permeability (Jamtveit et al., 2008). Based on the numerical simulations using discrete element method (DEM), Jamtveit et al. (2008) shows that fracture network is produced by the volume expansion of olivine grains during hydration. However, their model dos not treat the advective fluid flow explicitly, it is not clear how permeability evolves during such processes. In this study, inspired by the natural textures of olivine gabbro taken from CM1A-7A (Wazi Zeeb, Oman Drilling Project), we conducted the DEM simulation for understanding the feedback of the fluid flow –olivine hydration –fracturing to the layered gabbro, which consists of olivine-rich layer and olivine-poor layer alternately. In particular, we focus on the contrasting fracture patterns between olivine and plagioclase, the evolution and anisotropy of permeability produced by the reaction-induced fracturing within the layered gabbro.

We conducted the two-dimensional DEM model, and the details of the model follows Okamoto and Shimizu (2015) and Shimizu and Okamoto (2016). We consider a simple volume increasing hydration reaction ($A + H_2O \rightarrow B$; 50% volume increase), and the reaction rate is defined as a linear function of fluid pressure. In the model, advective fluid flow occurs through apertures between particles, in response to difference of fluid pressure of individual domains. The rock model is consist of reactive part (it can change from olivine to sperneitne) and non-reactive part (e.g., plagioclase and clnopyronene). The reaction rate constant and aperture width of matrix and fracture are defined based on the non-dimensional numbers based on Shimizu and Okamoto (2016).

Firstly, we conducted the simulations for the model in which a single olivine exists in non-reactive matrix. When fluid is supplied through matrix, hydration of olivine starts, which produces the mesh-like textures inside the olivine grain and radial cracks within the unreactive matrix, which is consistent with those observed in the gabbro sample from CM1A. Second, we conducted a case where several olivine grains exist in matrix. In this case, we found the formation of fracture network that connects among the olivine grains, and positive relationship between the reaction rate and permeability. Finally, we tested the case of the layered structure that consists of olivine-rich layer and olivine-absent layer, and that fluid flows in direction perpendicular to the layers. The results of the simulations reveals that the development of vertical fractures in both olivine-rich and non-reactive layers, whereas the horizontal fractures are only developed in the olivine-rich layers. These features of fracture orientation are consistent with the natural observations and indicate that he reaction-induced fracturing could significantly enhance the fluid infiltration through layered gabbro.

©2019. Japan Geoscience Union. All Right Reserved.

References

Katayama I, Terada T, Okazaki K, Tanikawa W (2012) Nat Geosci 5:731–734.

Jamtveit B., Malthe-Sørenssen A., Kostenko O., 2008. Earth Planet. Sci. Lett., 267, pp. 620-627

Okamoto,A.,Shimizu,H., 2015. Earth and Planetary Science Letters 415, 9–18.

Shimizu, H., Okamoto, A., 2016. Contributions to Mineralogy and Petrology, 171, 73.

Keywords: Oman Drilling Project, layered gabbro, permeability, Discrete Element Method, serpentinization

©2019. Japan Geoscience Union. All Right Reserved.

X-ray CT images of oceanic lithologies obtained on Oman Drilling Project drillcores during ChikyuOman 2017 and 2018

*Katsuyoshi Michibayashi[1], Peter B Kelemen[2], Margurette Godard[3], Eiichi TAKAZAWA[4], Damon A H Teagle[5], The Oman Drilling Project Science Party[6]

1. Department of Earth and Planetary Sciences, Nagoya University, 2. Columbia University, 3. Université Montpellier, 4. Niigata University, 5. Southampton University, 6. ICDP

The Oman Drilling Project (OmanDP) has drilled >3,200 meters of the Oman ophiolite during Phases 1 and 2 in Holes GT1A, GT2A, GT3A, BT1B, CM1A, CM2B, BA1B, BA3A and BA4A. All cores have been described on board D/V Chikyu during the summers of 2017 and 2018. X-ray computed tomography (X-ray CT) images were obtained on all cores as a routine part of the IODP measurement protocol onboard D/V Chikyu.

The X-ray CT scanner (Discovery CT 750HD, GE Medical Systems) scans and reconstructs an image of a 1.4 m section in 10 minutes and produces a series of scan images, each 0.625 mm thick. The X-ray source and detector are installed inside of the gantry opposite each other. The excitation voltage and current for X-ray tube are 140 kV and 100 mA, respectively. Core samples are scanned in the gantry with a scanning rate of 20 mm/sec. The distribution of attenuation values mapped to an individual slice comprises the raw data that are used for subsequent image processing. Successive two-dimensional (2D) slices of 512 x 512 pixels yield a representation of attenuation values in three-dimensional (3D) voxels of 512 x 512 by ~1600 in length. Data generated for each core consist of core-axis-normal planes (XY planes) of X-ray attenuation values with dimensions of 512 ×512 pixels in 9 cm ×9 cm cross-section, with a resolution of 0.176 mm/pixel.

As a consequence, we have >3,200 meters length of X-ray CT images from the dyke/gabbro transition zone to the gabbroic sequence to the mantle sequence to the basal thrust of the ophiolite. All X-ray CT images have been processed to match with individual photo images of the archive halves of the cores. The data are useful for assessing sample locations and quality. X-ray CT images can be used for 3D fabric analyses even after core has been cut in half and subsampled for other analyses.

Keywords: OmanDP, XCT, image

©2019. Japan Geoscience Union. All Right Reserved.

Re-examination of the crystallization process of clinopyroxene oikocrysts in layered gabbros at Hess Deep Rift, EPR

*Akane Yasui[1], Takashi Hoshide[1]

1. Graduate School of International Resource Sciences, Akita University

In the Hess Deep Rift, located about 60km east of the East Pacific Rise, the lower crustal gabbros which have been formed at the fast-spreading ridge are exposed. In the IODP Exp. 345, primitive layered gabbros were collected from the lower crust as mainly three drill cores (U1415 I, J, P; Gillis et al., 2014). From the U1415J, unique gabbroic rocks (troctolites) with poikilitic clinopyroxenes (oikocrysts) including many small plagioclase laths have been found (Maeda and Kaise, 2015, Abstracts of the Geological Society of Japan).

Recently, on the origins of clinopyroxene-oikocryst-bearing gabbroic rocks, the different hypotheses have been proposed by Leuthold et al. (2018) and Maeda and Kaise (2015).
Leuthold et al. (2018) proposed that initial olivine gabbros had been partially molten by the intrusion of a primitive melt and then clinopyroxene oikocrysts had crystallized from clinopyroxene-rich basaltic melts formed by the mixing between the partial melt and the primitive magma.
On the other hands, Maeda and Kaise (2015) proposed that clinopyroxenes have first crystallized from a primitive magma and after molten by the encounter with another primitive magma they have continued to grow further and then, the clinopyroxene rim has simultaneously crystallized with matrix olivine and plagioclase. Several hypotheses other than those above (e.g.,Tegner et al., 1995; Nicolas and Boudier., 2011) have been also proposed for the origin of the clinopyroxene oikocrysts in gabbroic rocks. The question is still open to discussion.
Therefore, I re-examine the process of clinopyroxene-oikocryst formation through the textural observation and chemical analysis of the constituent minerals for 8 samples of clinopyroxene-oikocryst-bearing gabbros from 3R, 5R, 7G, 8R and 15G of the U1415J core collected at the IODP Exp. 345.

The matrix part is troctolite consisting mainly of olivine (about 0.5 mm - 2 mm in size, amoeboidal, Fo85~) and plagioclase (about 1 mm in size, An#77-82). Spherical to ellipsoidal clinopyroxene oikocrysts (5-10 mm in size, Mg#85 to 88) is distributed in the matrix troctolite. In addition, clinopyroxene oikocrysts exhibit the following characteristics:

(1) Clinopyroxene oikocrysts basically do not contain any olivine crystals. Rarely, they contain aggregates of plagioclase and olivine.
(2) Orthopyroxene rims (about 100 μm thick, film-like, Mg#85-87) are observed only in matrix olivines (Fo85~) near the rim of the clinopyroxene oikocryst. The olivine crystals rimmed by orthopyroxene are shrinked.
(3) The decreases in Al and Cr contents towards the plagioclase chadacrysts are observed in clinopyroxene oikocrysts.
(4) In the core of the clinopyroxene oikocrysts, we can find parts with Mg# higher than the values which can be in the Fe/Mg equilibrium with olivine in the matrix troctolite.

The facts of (1) and (2) indicate that the assemblage of olivine and plagioclase had already existed when the clinopyroxene oikocrysts crystallized from the melt. In additions, these facts suggest that the melt which formed clinopyroxene oikocryst was in a reaction relationship with olivine. These interpretations

©2019. Japan Geoscience Union. All Right Reserved.

are consistent with the hypothesis of Leuthold et al. (2018).

Keywords: clinopyroxene oikocrysts, Hess Deep, troctolite, Magma mixing, MORB

©2019. Japan Geoscience Union. All Right Reserved.

Structural petrology of peridotites from the Kalaymyo ophiolite

*Kouhei Asano[1,2], Katsuyoshi Michibayashi[1], Jung-Woo Park[3]

1. Graduate School of Environmental Studies, Nagoya University, 2. Shizuoka University, 3. Seoul National University

The Kalaymyo ophiolite is located at Myanmar. The Kalaymyo ophiolite includes large peridotite massifs, where peridotites are commonly well preserved. In recent years, petrologic and geochemical studies have been carried out on the Kalaymyo peridotites. These results suggest that the Kalaymyo peridotites have been undergone melt-rock interactions. In this study, we used fourteen samples from outcrops and drill cores, and carried out analyses of crystal preferred orientations (CPOs) of olivine and of major elements of olivine and spinel. The samples show coarse-grained equigranular textures. The mineral compositions in spinel Cr# and olivine Mg# plot in the field of OSMA (olivine-spinel mantle array) indicate that these samples represent residual upper mantle rocks after partial melting. Spinel grains with Cr# higher than 0.3 have relatively high TiO_2 contents (0.10-0.20 wt.%). Because Ti is incompatible element, high spinel TiO_2 content suggests that these peridotites have experienced melt-rock interaction. There is a positive correlation between J-index and spinel Cr# in the samples. The correlation also has two trends: high and low positive relationships between J-index and spinel Cr#, respectively. Samples experienced melt-rock interaction belong to the low positive trend. It suggests that melt percolation by melt-rock interaction could have an impact on deformation, in particular on CPO development. We propose that melt-rock interaction was synchronous with deformation. It is noted that peridotites experienced melt-rock interaction are intensely located on a narrow range with respect to the elevation, indicating that the occurrence of melt-rock interaction was localized within the Kalaymyo ophiolite.

Keywords: Kalaymyo ophiolite, peridotite, melt-rock interaction, J-index

©2019. Japan Geoscience Union. All Right Reserved.

Reevaluation of the origin of mafic layers in the Upper Zone of the Horoman Peridotite

*Yumeto KOGURE[1], Eiichi TAKAZAWA[1]

1. Department of Geology, Faculty of Science, Niigata University

Horoman peridotite is situated at the southern tip of the Hidaka mountain range, spreads 8 km east-west, 10 km north-south, and has a layer thickness of 3,000 m. We reevaluated the origin of the mafic layer in the Upper Zone of the Horoman Peridotite. We studied Fumo section in the Upper Zone. This section has total thickness of 263 m and consists of plagioclase lherzolite, harzburgite and mafic layer. In the Fumo section, the mafic layer is only interlayered in the plagioclase lherzolite. In the Al2O3, CaO, and Na2O vs. MgO diagrams of whole rock compositions, the mafic layer is plotted on the extension of the linear composition trend indicated by plagioclase lherzolite and harzburgite. There are two types of mafic layer, one plotted in the vicinity of N-MORB and the other plotted in the vicinity of plagioclase lherzolite. The plagioclase lherzolites which have higher Al2O3, CaO, and Na2O and lower MgO contents than the Depleted MORB Mantle (DMM) [1] contain amphiboles whereas the other plagioclase lherzolite which has lower Al2O3, CaO, and Na2O contents and higher MgO content than the DMM do not contain amphibole. Chondrite-normalized whole rock rare earth element (REE) patterns of plagioclase lherzolites are flat from heavy REE to middle REE and show convex upward pattern with depletion in light REE. The mafic layers also show the similar pattern although the abundances of REE is much lower than N-MORB.

From these results, the mafic layers in the Fumo section do not have the composition of primary melt and is considered to be cumulate [2,3]. Also, in the whole rock FeO, TiO2 vs. MgO diagrams, the compositional trends suddenly bend at the most fertile plagioclase lherzolite and becomes depleted in FeO, TiO2 toward the thin mafic layers. On the extension of this bent trends reach to the composition of Cpx and plagioclase. The mafic layer in the Fumo section suggests the possibility that Cpx and plagioclase were crystallized from a melt penetrated into plagioclase lherzolite in a relatively low pressure where the combination of Cpx and plagioclase was stable.

[1] Workman and Hart, 2005, EPSL, 231, 53-72. [2] Shiotani and Niida, 1997, Memoir. Geol. Soc. Japan, 47, 123–137. [3] Takazawa et al., 1999, J. Petrol., 40, 1827-1851.

Keywords: Horoman Peridotite, mantle, mafic layer, orogenic lherzolite, Hidaka Metamorphic Belt

©2019. Japan Geoscience Union. All Right Reserved.

A structural and petrological study of "Shibukawa ultramafic body" in the Sanbagawa belt, western Shizuoka, Japan

*Hikaru Shioya[1,2], Katsuyoshi Michibayashi[1], Ken-ichi Hirauchi[2]

1. Graduate School of Environmental Studies, Nagoya University, 2. Institute of Geosciences, Shizuoka University

We studied an ultramafic body, which is named "Shibukawa ultramafic body" in this study, in the Sanbagawa belt located to the western Shizuoka, focusing on their primary mineral olivine to reveal its petrogenesis. Shibukawa ultramafic body is composed of dunites and wehlites, although the body was heavily weathered due to serpentinization. Yet, most of samples still contain olivine, spinel and a few amounts of clinopyroxene. The olivine crystal preferred orientations (CPOs) of this body were divided into two types: D type and single maxima type. The CPO intensities were relatively high in the north area, whereas those in the south area were relatively low. Considering the grain size distribution of olivine in the samples, the samples in the south area was weakly deformed as they preserve porphyroclastic olivine grains in the fine-grained matrix. In contrast, grain size reduction due to deformation has been completed in the north area. Olivine CPO patterns and major elements composition of both olivine and spinel indicate that the origin of this ultramafic body could be cumulate such as the Mikabu belt and is different from those of Shikoku mountains in the Sanbagawa belt.

Keywords: Sanbagawa belt, Mikabu belt, Cumulate, Ultramafic, Olivine fabrics, Dunite

©2019. Japan Geoscience Union. All Right Reserved.

[E] Poster | S (Solid Earth Sciences)：S-CG Complex & General

Tue. May 28, 2019 5:15 PM - 6:30 PM JST | Tue. May 28, 2019 8:15 AM - 9:30 AM UTC | Poster Hall International Exhibition Hall8, Makuhari Messe_35

[S-CG49] Hard-Rock Drilling Science: From Continental to Deep Sea Drilling, and Oman Project

convener:Katsuyoshi Michibayashi(Department of Earth and Planetary Sciences, Nagoya University), Eiichi TAKAZAWA(Department of Geology, Faculty of Science, Niigata University), Norikatsu Akizawa(Department of Ocean Floor Geoscience, Atmosphere and Ocean Research Institute, The University of Tokyo)

The Oman Drilling Project (OmDP) has completed to drill numerous hard-rock cores within ancient oceanic lithosphere and the underlying subduction zone of the Samail ophiolite in Oman, with support from ICDP, IODP, Japan Society for the Promotion of Science, the Sloan Foundation's Deep Carbon Observatory, US, and European research agencies. Moreover, a number of IODP expeditions have focused on hard-rock drilling over the last several years including Expedition 352 in 2014, which drilled the volcanic sequence associated with subduction initiation in the Bonin fore-arc, Expedition 357, which drilled the Lost City hydrothermal field, Expedition 360, which drilled the lithosphere associated with ultraslow-spreading at the Southwest Indian Ridge in 2016, and Expedition 366, which drilled the serpentinite seamounts in the Mariana fore-arc. In this session, we invite presentations on the scientific results of hard-rock drilling at these and other sites. We also invite related presentations on oceanic lithosphere, island arc formation, and any other significant issue that could be addressed by future hard-rock drilling. This includes marine studies of oceanic lithosphere and on-land geological investigations of ophiolites, accreted arcs, and subduction complexes. The session is intended to be interdisciplinary, including the fields of geophysics, geochemistry, petrology, engineering, and biology.

[SCG49-P01] Permeability profile in the Oman Drilling Project inferred from resistivity measurements

*Ikuo Katayama[1], Keishi Okazaki[2], Natsue Abe[2], Ole Ivar Ulven[3], Gilbert Hong[4], Wenlu Zhu[5], Benoit Cordonnier[3], Kohei Hatakeyama[1], Yuya Akamatsu[1], Katsuyoshi Michibayashi[6], Marguerite Godard[7], Peter Kelemen[8], Science Party The Oman Drilling Project Phase 2 (1.Hiroshima University, 2.JAMSTEC, 3.University of Oslo, 4.Seoul National University, 5.University of Maryland, 6.Nagoya University, 7.Universitè Montpellier, 8.Columbia University)

[SCG49-P02] Relationship between alteration intensity and elastic wave velocity of gabbroic rocks from ICDP Hole CM1A, Oman Drilling Project Phase II

*Kosuke Kimura[1], Ikuo Katayama[1], Kohei Hatakeyama[1], Yuya Akamatsu[1], Natsue Abe[2], Keishi Okazaki[2], The Oman Drilling Project Phase II Science Party (1.Hiroshima University, 2.JAMSTEC)

[SCG49-P03] Physical property of the fossilized crust-mantle transition zone from ICDP Oman Drilling Project Hole CM1A and CM2B measured onboard D/V Chikyu

*Keishi Okazaki[1], Natsue Abe[1], Kohei Hatakeyama[2], Yuya Akamatsu[2], Ikuo Katayama[2], Eiichi TAKAZAWA[3], Damon A H Teagle[4], Peter B Kelemen[5], Jude Coggon[4], The Oman Drilling Project Phase 2 Science Party (1.Japan Agency for Marine-Earth Science and Technology, 2.Hiroshima University, 3.Niigata University, 4.University of Southampton, 5.Columbia University)

[SCG49-P04] Microstructures of lower crust gabbros from the Oman Ophiolite: Analyses of the drilled cores of the Oman Drilling Project

*Koki Iida[1], Takahiro Fudai[1], Susumu Umino[1], Yuki Kusano[2] (1.Kanazawa University, 2.Geological Survey of Japan)

[SCG49-P05] Olivine fabric and mineral compositions in the Maqsad area of the Samail massif, the southern Oman ophiolite

*Kaho Takahashi[1], Eiichi TAKAZAWA[2,3], Katsuyoshi Michibayashi[4], Kakihata Yuki[4], Ryoko Senda[5] (1.Graduate School of Science and Technology, Niigata University, 2.Department of Geology, Faculty of

Science, Niigata University, 3.JAMSTEC, 4.Nagoya University, 5.Kyushu University)

[SCG49-P06] The evolution of melt inclusions in podiform chromitite in Oman

*Yuan YAO[1], Eiichi TAKAZAWA[2,3], Oman Drilling Project Phase 2 Science Party (1.Graduate School of Sciences& Technology, Niigata University, Japan, 2.Department of Geology, Faculty of Science, Niigata University, Japan, 3.Research and Development Center for Ocean Drilling Science, JAMSTEC, Japan)

[SCG49-P07] Melt/fluid - rock reaction inferred from the Wadi Tayin mantle section in the southern Oman ophiolite

*Keisuke ISHII[1], Eiichi TAKAZAWA[2], Akihiro kuriyama[2], Kyouka Someya[2], Yoshihiko Tamura[3] (1.Graduate School of Science and Technology, Niigata University, 2.Department of Geology, Faculty of Science, Niigata University , 3.R&D Center for Ocean Drilling Science, Japan Agency for Marine-Earth Science and Technology)

[SCG49-P08] Numerical simulations for reaction-induced fracture formation of layered gabbro during hydration process

*Kazuki Yoshida[1], Hiroyuki Shimizu[2], Noriyoshi Tsuchiya[1], Atsushi Okamoto[1], Phase 2 Science Party Oman Drilling Project[3] (1.Tohoku university, 2.Geotechnical Analysis Group, Advanced Analysis Department, Civil Engineering Design Division, Kajima Corporation, 3.Oman Drilling Project Phase 2 Science Party)

[SCG49-P09] X-ray CT images of oceanic lithologies obtained on Oman Drilling Project drillcores during ChikyuOman 2017 and 2018

*Katsuyoshi Michibayashi[1], Peter B Kelemen[2], Margurette Godard[3], Eiichi TAKAZAWA[4], Damon A H Teagle[5], The Oman Drilling Project Science Party[6] (1.Department of Earth and Planetary Sciences, Nagoya University, 2.Columbia University, 3.Université Montpellier, 4.Niigata University, 5.Southampton University, 6.ICDP)

[SCG49-P10] Re-examination of the crystallization process of clinopyroxene oikocrysts in layered gabbros at Hess Deep Rift, EPR

*Akane Yasui[1], Takashi Hoshide[1] (1.Graduate School of International Resource Sciences, Akita University)

[SCG49-P11] Structural petrology of peridotites from the Kalaymyo ophiolite

*Kouhei Asano[1,2], Katsuyoshi Michibayashi[1], Jung-Woo Park[3] (1.Graduate School of Environmental Studies, Nagoya University, 2.Shizuoka University, 3.Seoul National University)

[SCG49-P12] Reevaluation of the origin of mafic layers in the Upper Zone of the Horoman Peridotite

*Yumeto KOGURE[1], Eiichi TAKAZAWA[1] (1.Department of Geology, Faculty of Science, Niigata University)

[SCG49-P13] A structural and petrological study of "Shibukawa ultramafic body" in the Sanbagawa belt, western Shizuoka, Japan

*Hikaru Shioya[1,2], Katsuyoshi Michibayashi[1], Ken-ichi Hirauchi[2] (1.Graduate School of Environmental Studies, Nagoya University, 2.Institute of Geosciences, Shizuoka University)

Permeability profile in the Oman Drilling Project inferred from resistivity measurements

*Ikuo Katayama[1], Keishi Okazaki[2], Natsue Abe[2], Ole Ivar Ulven[3], Gilbert Hong[4], Wenlu Zhu[5], Benoit Cordonnier[3], Kohei Hatakeyama[1], Yuya Akamatsu[1], Katsuyoshi Michibayashi[6], Marguerite Godard[7], Peter Kelemen[8], Science Party The Oman Drilling Project Phase 2

1. Hiroshima University, 2. JAMSTEC, 3. University of Oslo, 4. Seoul National University, 5. University of Maryland, 6. Nagoya University, 7. Universitè Montpellier, 8. Columbia University

Permeability is a key property that controls heat and chemical exchange in the oceanic lithosphere as well as microbial activity in the sub-seafloor. Although direct measurements of permeability were not made on board D/V Chikyu during analysis of cores from the Oman Drilling Project, we estimated permeability profiles based on onboard measurements of electrical resistivity. For each core sample, we measure its resistivity at nominally dry conditions to obtain the dry resistivity. We then saturate the sample with NaCl solution (3.5g/L) and repeat the resistivity measurements at brine-saturated conditions to obtain the wet resistivity. Owing to the conductive brine in the pore space, the wet resistivity is systematically lower than dry resistivity. Because the difference between dry and wet resistivity is predominantly controlled by the movement of dissolved ions in the brine that occupied the pore space, we can use the resistivity data to infer the volume fraction of pores that contribute to electrical transport (termed “transport porosity”). We apply the Hashin-Shtrikman upper bound to estimate transport porosity. The estimated transport porosity shows a positive correlation with bulk porosity measured on board (MAD analysis), but is approximately one order of magnitude lower. Using an empirical cubic law between transport porosity and permeability, we produce estimated permeability profiles for the crust-mantle transition zone and the serpentinized mantle sections in the Hole CM1A, BA1B, BA3A and BA4A. The results indicate, (1) the gabbro sequence exhibits a markedly lower permeability than the underlying mantle sequence, (2) serpentinized dunites have higher permeability compared to serpentinized harzburgites, and (3) the general variation of discrete sample permeability is correlated with fault zone and intervals with abundant fractures. These permeability structures are most likely modified by alteration and juxtapositions, and do not represent the in-situ profile of the oceanic lithosphere; but this technique can be applicable to infer on-board permeability in future hard rock drilling.

©2019. Japan Geoscience Union. All Right Reserved.

Relationship between alteration intensity and elastic wave velocity of gabbroic rocks from ICDP Hole CM1A, Oman Drilling Project Phase II

*Kosuke Kimura[1], Ikuo Katayama[1], Kohei Hatakeyama[1], Yuya Akamatsu[1], Natsue Abe[2], Keishi Okazaki[2], The Oman Drilling Project Phase II Science Party

1. Hiroshima University, 2. JAMSTEC

The mafic to ultramafic rocks suffer metamorphism and metasomatism by the seafloor hydrothermal activities. These alterations can influence the elastic wave velocity due to the change of mineral assemblages during the ocean floor metamorphism. However, most previous studies have measured the elastic wave velocity of relatively unaltered samples. In this study, we measured elastic wave velocity of the altered gabbro from the Semail ophiolite collected from the Oman Drilling Project Phase II in order to estimate the effect of ocean floor metamorphism on the elastic wave velocity.

Gabbro samples were collected from CM1A site that is reported to be a layered gabbro sequence. Total seven samples those have different alteration intensity were measured. We use intra-vessel deformation and fluid flow apparatus at Hiroshima University to measure elastic wave velocity under confining pressure up to 200 MPa. Elastic wave velocity was measured by the pulse transmission method, with the amplitude and the frequency of a trigger wave of 5 V and 2 MHz, respectively. After measurements under dry condition, measurements under wet conditions injecting pore water were performed (P_P = 10 MPa). Alteration intensity is recognized by the relative abundances of the secondary minerals.

On the basis of the petrography, alteration group could be divided into four types. First type is almost fresh, olivine altered to serpentine and chlorite partially with less green minerals present. Second type has saussuritized plagioclase dominantly and also some sample shows alteration of clinopyroxene to amphibole. In the third type amphibolitization of clinopyroxene is dominant, and also saussuritization of plagioclase occur. Fourth type is the most altered sample showing alteration halo along the veins. Almost of the minerals are changed to prehnite except a few relict clinopyroxene. This type has higher porosity than other types.

Sample density ranges from 2.77-3.08 g/cm^3, and porosity ranges from 0.02-0.22% except ca. 1% from halo alteration sample. Data from these samples show a trend that elastic wave velocities (V_P and V_S) increase with increasing the confining pressure from 20 to 200 MPa. V_P increases from 5.68-6.80 to 6.16-6.91 km/s, V_S slightly increases from 3.65-3.97 to 3.69-3.99 km/s and V_P/V_S is almost constant ranging between 1.56-1.86 to 1.64-1.88 under dry condition, and on the other hand, V_P increases from 6.08-6.82 to 6.31-6.93 km/s, V_S slightly increases from 3.64-3.98 to 3.69-4.00 km/s and V_P/V_S is almost constant 1.67-1.86 to 1.68-1.87 under fluid-saturated condition, respectively. This result is mostly consistent with the layered gabbro occur in a normal oceanic crust (e.g. White et al., 1992; Shinohara et al., 2008).

At 200 MPa and under dry condition, V_P moderately decreases with increase in alteration intensity. About 0.75 km/s decreases in response to the increase in alteration intensity from 10 to 80 %. Comparing dV_P (difference in calculated and measured values) from the back-calculated original mineral assemblages of gabbro and peridotite reveled that the decrease in dV_P for the former is less than the latter. Moreover, both the curves of V_P and impedance change cross-over each other for gabbro and peridotite after nearly 50% of alteration.

©2019. Japan Geoscience Union. All Right Reserved.

From the above results, we suggest that if both gabbro and peridotite suffer more than 50% alteration, reversal of seismic velocity and impedance occurs, which effectively would affect the determination of geophysical Moho.

Reference: White et al. (1992) J. Geophys. Res. 97, 19,683-19,715. Shinohara et al. (2008) Phys. Earth Plan. Inter., 170, 95-106. Christensen (2004) Inter. Geol. Rev., 46, 795-816.

Keywords: Oman ophiolite, Gabbroic rocks, Elastic Wave Velocity, alteration

©2019. Japan Geoscience Union. All Right Reserved.

Physical property of the fossilized crust-mantle transition zone from ICDP Oman Drilling Project Hole CM1A and CM2B measured onboard D/V Chikyu

*Keishi Okazaki[1], Natsue Abe[1], Kohei Hatakeyama[2], Yuya Akamatsu[2], Ikuo Katayama[2], Eiichi TAKAZAWA[3], Damon A H Teagle[4], Peter B Kelemen[5], Jude Coggon[4], The Oman Drilling Project Phase 2 Science Party

1. Japan Agency for Marine-Earth Science and Technology, 2. Hiroshima University, 3. Niigata University, 4. University of Southampton, 5. Columbia University

To understand physical properties of the oceanic crust and the mantle is fundamentally important to reveal the dynamics of plate tectonics, and the global circulations of H_2O and CO_2 fluids. We report results on physical property measurements of core samples from Oman Drilling Project (OmanDP) Holes CM1A and CM2B, which drilled from the lower igneous crust into the upper mantle in the Samail Ophiolite, Sultanate of Oman.

X-ray CT, bulk/grain density, porosity, magnetic susceptibility, P-wave velocity, electrical resistivity and thermal conductivity were measured onboard D/V Chikyu using whole-round cores and discrete samples for core sections from CM1A and CM2B.

The paleo-Moho in CM1A may not preserve the original structure due to minor faulting, possibly during obduction. The gabbro-dunite transition (paleo-Moho) in Hole CM1A is characterized by a sharp change in physical property data. For example, P-wave velocity decreases from ~6.7 km/s in the layered gabbro sequence to ~4.9 km/s in the MTZ. Low P-wave velocity and density (~2.6 g/cm^3) in serpentinized dunites reflect the fact that olivine in the dunites is almost completely serpentinized. Serpentinization could have occurred during hydrothermal alteration near the spreading ridge axis, during subduction of 100’s of km of oceanic crust and sediment beneath the ophiolite, during obduction onto the Arabian continental margin, and/or during present-day weathering. In contrast to the paleo-Moho, the boundary between the Crust-Mantle Transition (CMT) sequences (i.e., dunites and dunites with gabbro lenses) and the underlying, residual mantle harzburgites is somewhat gradual. P-wave velocity gradually increases from ~4.9 km/s for dunite in the CMT to ~5.5 km/s for harzburgite in the mantle sequence. The thickness of the CMT is 50–70 m in Holes CM1A and CM2B. We also report on correlations between physical properties, especially electrical conductivity and magnetic susceptibility, and the fault intensity and alteration intensity from the core descriptions.

Keywords: ophiolite, mantle, oceanic crust, moho

©2019. Japan Geoscience Union. All Right Reserved.

Microstructures of lower crust gabbros from the Oman Ophiolite: Analyses of the drilled cores of the Oman Drilling Project

*Koki Iida[1], Takahiro Fudai[1], Susumu Umino[1], Yuki Kusano[2]

1. Kanazawa University, 2. Geological Survey of Japan

Oman Drilling Project in 2016 to 2017 recovered 400 m long cores of layered gabbros at Site GT1 in the Wadi Tayin Massif of the Oman Ophiolilte. The purpose of this research is to describe microstructures of the layered gabbro core samples and to discuss the conditions of magmatic and hypersolidus deformation that operated in the lower crust beneath the Oman paleoridge.

Core samples were cut into slabs parallel to foliation and slabs normal to foliation and parallel to lineation, which were made into thin sections for microscopic observations. Structural fabrics and the relationships between crystal shapes and alliginment were described to identify magmatic and hypersolidus deformation structures.

Cored samples are predominantly olivine gabbros consisting of anhedral olivine, anhedral to subhedral clinopyroxene and subhedral to euhedral plagioclase. Grain size ranges from 0.5 mm to a few millimeters irrespective of mineral species.

The structures shown by the gabbros are classified into three regimes by temperature or the amount of melt present: Regime I, magmatic conditions without or minimal plastic deformation; regime Ⅱ, plastic deformation assisted by interstitial melt (Dunn, 2000); regime Ⅲ, near solidus deformation. Regime Ⅱ is identified by ameboid grain boundaries with no intracrystalline deformation and equigranular textures, resulted from decreasing internal strain energy by at high temperatures. The presence of melt is evidenced by the clear euhedral plagioclase rims with resorbed turbid cores as discussed below.

Regime I. Magmatic structures are identified as modal layering due to changes in mineral mode, no preferred orientation or shape-preferred orientation of clinopyroxene and plagioclase, poikilitic texture of olivine enclosing plagioclase laths and ophitic texture of clinopyroxene including plagioclase laths.

Regime II. The hypersolidus deformation structures overprint igneous structures: ameboid olivine with or without strain in the crystal, elongated olivine, and lenticular aggregates of olivine grains with an asymmetric quarter structure. Single clinopyroxene crystals show an asymmetric quarter structure like olivine aggregates. Ophitic clinopyroxenes consist of subgrains with slightly different orientations <10˚. Plagioclase shows deformation twin and undulose extinction. Equigranular fine-grained plagioclase with grain boundaries intersecting at 120˚ are common. Large plagioclases have a resorbed core with a wavy outline and are surrounded by euhedral rim.

Regime III. Subsolidus recrystallization includes buldging and grain boundary migration resulted in ameoboid grain boundaries of clinopyroxene. Undulose extinction and kinked twinning of plagioclase are observed.

It is well known that mid-ocean ridge basalt magma commonly crystallizes in the order of olivine, plagioclase and clinopyroxene, which is also true for the gabbros of the Oman Ophiolite (Adachi and Miyashita, 2003). Nevertheless, only plagioclase shows euhedral to subhedral shapes in the observed

©2019. Japan Geoscience Union. All Right Reserved.

layered gabbro core samples. Deformed olivine aggregates and clinopyroxene with quarter structures are embedded in plagioclase with equilibrium granoblastic textures and large euhedral plagioclases with resorbed turbid cores. Considering these textures combined with the mechanical strength of the three constituent minerals, these gabbros suffered deformation under the presence of melt, which assisted complete recovery of strain through recrystallization of fine-grained plagioclase and overgrowth of euhedral rims around magmatic plagioclase cores. Poikilitic olivine occurs through the hole, whereas ophitic Cpx occurs at 73 m and 220 m in depth. Most deformation structures of regime II are present irrespective to depth. The asymmetric structures of olivine and clinopyroxene were used to determine the relative sense of shear. Both dextral and sinistral sense of shear are observed within the same samples.

Keywords: Oman ophiolite, Oman Drilling Project , Layered gabbro , Foliated gabbro , Microstructures , Lower crust

©2019. Japan Geoscience Union. All Right Reserved.

Olivine fabric and mineral compositions in the Maqsad area of the Samail massif, the southern Oman ophiolite

*Kaho Takahashi[1], Eiichi TAKAZAWA[2,3], Katsuyoshi Michibayashi[4], Kakihata Yuki[4], Ryoko Senda[5]

1. Graduate School of Science and Technology, Niigata University, 2. Department of Geology, Faculty of Science, Niigata University, 3. JAMSTEC, 4. Nagoya University, 5. Kyushu University

In this study, we conducted structural and chemical analysis of oriented samples of 17 harzburgites and 4 dunites collected from the Maqsad area of Samail massif in the southern Oman ophiolite. We investigated the degree of partial melting and the mantle-melt reaction with relation to mantle diapir structure.

The crystallographic preferred orientation (CPO) of olivine grains were measured in highly polished XZ thin sections using a scanning electron microscope equipped with an electron-back scatter diffraction system at Shizuoka University. After plotting the results in the Vp Flinn plot expanded for olivine fabric types [1,2], the fabric type of peridotites in this study are summarized as follows. The distribution of A type is limited in the southeastern part where the diapir structure has been identified [3], whereas D type is dominant in the peripheral part of the diapir. Minor amounts of AG type and E type are also observed in the peripheral part. From these, the olivine in the southeastern part (diapir area) of this study area is likely to have been deformed under high temperature whereas the peripheral part was deformed at slightly lower temperature. The CPOs of olivine in both areas do not show any influence from the presence of H2O except for only one sample with E type CPO. Moreover, strong alignment of [100] to the vertical orientation was observed in the southeastern part (diapir area) of this study area. Since vertical mantle flow has been estimated in this diapir area, our results are consistent with the previous study [3,4].

The Cr# (=Cr/[Cr+Al] atomic ratio) of spinel in the harzburgites and dunites are as high as 0.55-0.58 in the central part of the southeastern part (diapir area) and along the paleo-ridge axis running in the NW - SE direction [3,4]. On the other hand, the Cr# of spinel in the peripheral part is 0.41-0.55 indicating slightly less depleted than in the central part. In addition, the REE abundance of clinopyroxenes in the central part of the diapir area is lower than in the peripheral part being consistent with the distribution of spinel Cr#.

We consider that the upwelling rate in the southeastern part (diapir area) may have been greater than the peripheral part possibly due to higher temperature in the focused vertical mantle flow. This model is consistent with the distribution of the Cr# of spinel: the degree of melting was greater in the diapir area where Cr# of spinel are higher than the peripheral part. The strongly focused pipe-like model for axis location [3,5] is well fitted by our observations in this study.

[1] Karato et al., 2008, Ann. Rev. Earth Planet. Sci., 36, 59-95. [2] Michibayashi, 2015, J. Geography, 124, 397-409. [3] Jousselin et al., 1998, JGR, 103, 18153-18170. [4] Nicolas et al., 2000, Marine Geophys. Res., 21, 147-179. [5] Nicolas and Boudier, 1995, JGR, 100, 6179-6197.

Keywords: Oman ophiolite, crystalographic preferred orientation, olivine, fabric, peridotite, mantle flow

©2019. Japan Geoscience Union. All Right Reserved.

The evolution of melt inclusions in podiform chromitite in Oman

*Yuan YAO[1], Eiichi TAKAZAWA[2,3], Oman Drilling Project Phase 2 Science Party

1. Graduate School of Sciences& Technology, Niigata University, Japan, 2. Department of Geology, Faculty of Science, Niigata University, Japan, 3. Research and Development Center for Ocean Drilling Science, JAMSTEC, Japan

Melt inclusions are tiny inclusions which trapped in the host magmatic minerals. After trapping, the host mineral can be considered as a closed and isolated system (Roedder, 1984). Thus, melt inclusions behave as time capsules, which record the liquid line of descent of magmatic systems (Frezzotti, 2001). Therefore, melt inclusions can provide important information of the primary melts (Kent, 2008).

We studied the melt inclusions in chromite from a chromitite deposit mine in the north of Maqsad and the core sample from the Oman drilling project phase 2. The silicate inclusions range in diameter from 5 μm to 200 μm, contain pargasite, tremolite, aspidolite, high Cr# (=Cr/[Cr+Al] atomic ratio) chromite, diopside, enstatite, forsterite, grossular, albite, titanite, pentlandite, apatite, chlorite, wollastonite and serpentine. We found the high Cr# chromite occurs as lining of the inclusion, moreover the daughter minerals precipitated in the high Cr# chromite lining. Those phenomenon can be explained by the crystallization of chromite on the wall of inclusion. In addition, this is the first report about the necking down of melt inclusion in chromitite. The necking down of inclusions is an originally large, liquid-filled inclusion divided into smaller inclusions. If the necking down happens after the phase change of inclusion, the compositions of smaller inclusions probably are inhomogeneity. Last year, we conducted the high temperature homogenized experiments, the result showed that the homogenized quenching glass are heterogeneous. We consider the inhomogeneity of inclusions perhaps caused by the necking down. Based above all, we suggest the composition of homogenized inclusion can not represent the parental melt.

To summarize, we suggest before analysis and experiment of inclusions in chromite, the origin and the evolution of inclusions should be carefully studied.

Reference

Frezzotti, M. (2001). "Silicate-melt inclusions in magmatic rocks: applications to petrology." Lithos **55** (1-4): 273-299.
Kent, A. J. R. (2008). "Melt Inclusions in Basaltic and Related Volcanic Rocks." Reviews in Mineralogy and Geochemistry **69** (1): 273-331.
Roedder, E. (1984). Fluid inclusions, Walter de Gruyter GmbH & Co KG.

Keywords: melt inclusion, Oman, chromitite

©2019. Japan Geoscience Union. All Right Reserved.

Melt/fluid - rock reaction inferred from the Wadi Tayin mantle section in the southern Oman ophiolite

*Keisuke ISHII[1], Eiichi TAKAZAWA[2], Akihiro kuriyama[2], Kyouka Someya[2], Yoshihiko Tamura[3]

1. Graduate School of Science and Technology, Niigata University, 2. Department of Geology, Faculty of Science, Niigata University , 3. R&D Center for Ocean Drilling Science, Japan Agency for Marine-Earth Science and Technology

We report the petrology and the mineral compositions of peridotites from the Wadi Tayin massif in the southern Oman ophiolite [1-3] to investigate the influence of arc related magmatism during oceanic thrusting of the ophiolite. Harzburgites, dunites and a small number of lherzolite were systematically corrected along wadis to cover the mantle section from the boundary between lower crust and uppermost mantle namely “Moho” to the basal thrust. Spinel Cr# [=Cr/(Cr+Al) atomic ratio] of harzburgite varies from 0.22 to 0.58 similar to the range in abyssal peridotites [4]. Moreover, it gradually increases from the basal part to the Moho indicating the compositional variation expected for the residual mantle column formed at a mid ocean ridge. On the other hand, the spinel Cr# of dunite often exceeds 0.6 in the NW-SE striking shear zone in the middle part of the study area. The chondrite-normalized rare earth element (REE) patterns of clinopyroxenes in peridotites from the shear zone show a linear pattern that monotonously decreases from heavy REE to light REE (LREE). Calculated melt compositions in equilibrium with these clinopyroxenes are equivalent with the V2 (Type2) lava reported in the northern Oman ophiolite [5-6].

The plots in Cr# of spinel versus Ce/Yb ratio of clinopyroxenes show a linear trend with a positive correlation. It indicates that the LREE enrichment of clinopyroxene is associated with an increase in the degree of melting. Clinopyroxenes in the dunite from the shear zone are most significantly enriched in LREE to middle REE and have REE abundances being in equilibrium with the V2 lava. We consider that harzburgites were suffered from a flux melting by infiltration of H2O-rich fluid producing V2 lava. Comparing to the results from the northern massifs the linear trend in the diagram of Cr# of spinel versus Ce/Yb ratio of clinopyroxenes in the southern massif is obviously shifted toward lower in Cr#. It suggests that the infiltration of H2O-rich fluid may have started at early stage of melting in the Wadi Tayin massif relative to the northern massifs.

[1] Kelemen et al., 1995, Nature, 375, 747-753, [2] Godard al., 2000, EPSL, 180, 133-148, [3] HanghØj et al., 2010, J. Petrol., 51, 201-227, [4] Dick and Bullen, 1984, CMP, 86, 54-76, [5] Godard et al., 2003, G-cubed, 4, 8609, [6] Kusano et al., 2016, Chem. Geol., 449, 206-225.

Keywords: Oman ophiolite, Mantle section, Peridotite, Melt/rock reaction

©2019. Japan Geoscience Union. All Right Reserved.

Numerical simulations for reaction-induced fracture formation of layered gabbro during hydration process

*Kazuki Yoshida[1], Hiroyuki Shimizu[2], Noriyoshi Tsuchiya[1], Atsushi Okamoto[1], Phase 2 Science Party Oman Drilling Project[3]

1. Tohoku university, 2. Geotechnical Analysis Group, Advanced Analysis Department, Civil Engineering Design Division, Kajima Corporation, 3. Oman Drilling Project Phase 2 Science Party

Serpentinization of oceanic lithosphere is important for various geological processes, including magmatism and earthquake at subduction zone, and generation of hydrogen and hydrocarbon at seafloor. For understanding the extent of the water infiltration into mantle within the oceanic lithosphere, permeability of the lower crust is an important factor, since gabbro has low permeability at high confining pressure (Katayama et al., 2012). In natural olivine-bearing gabbro, serpentinization of olivine grains produced radial fractures within the plagioclase matrix, which can potentially enhance the permeability (Jamtveit et al., 2008). Based on the numerical simulations using discrete element method (DEM), Jamtveit et al. (2008) shows that fracture network is produced by the volume expansion of olivine grains during hydration. However, their model dos not treat the advective fluid flow explicitly, it is not clear how permeability evolves during such processes. In this study, inspired by the natural textures of olivine gabbro taken from CM1A-7A (Wazi Zeeb, Oman Drilling Project), we conducted the DEM simulation for understanding the feedback of the fluid flow –olivine hydration –fracturing to the layered gabbro, which consists of olivine-rich layer and olivine-poor layer alternately. In particular, we focus on the contrasting fracture patterns between olivine and plagioclase, the evolution and anisotropy of permeability produced by the reaction-induced fracturing within the layered gabbro.

We conducted the two-dimensional DEM model, and the details of the model follows Okamoto and Shimizu (2015) and Shimizu and Okamoto (2016). We consider a simple volume increasing hydration reaction ($A + H_2O \rightarrow B$; 50% volume increase), and the reaction rate is defined as a linear function of fluid pressure. In the model, advective fluid flow occurs through apertures between particles, in response to difference of fluid pressure of individual domains. The rock model is consist of reactive part (it can change from olivine to sperneitne) and non-reactive part (e.g., plagioclase and clnopyronene). The reaction rate constant and aperture width of matrix and fracture are defined based on the non-dimensional numbers based on Shimizu and Okamoto (2016).

Firstly, we conducted the simulations for the model in which a single olivine exists in non-reactive matrix. When fluid is supplied through matrix, hydration of olivine starts, which produces the mesh-like textures inside the olivine grain and radial cracks within the unreactive matrix, which is consistent with those observed in the gabbro sample from CM1A. Second, we conducted a case where several olivine grains exist in matrix. In this case, we found the formation of fracture network that connects among the olivine grains, and positive relationship between the reaction rate and permeability. Finally, we tested the case of the layered structure that consists of olivine-rich layer and olivine-absent layer, and that fluid flows in direction perpendicular to the layers. The results of the simulations reveals that the development of vertical fractures in both olivine-rich and non-reactive layers, whereas the horizontal fractures are only developed in the olivine-rich layers. These features of fracture orientation are consistent with the natural observations and indicate that he reaction-induced fracturing could significantly enhance the fluid infiltration through layered gabbro.

©2019. Japan Geoscience Union. All Right Reserved.

References

Katayama I, Terada T, Okazaki K, Tanikawa W (2012) Nat Geosci 5:731–734.

Jamtveit B., Malthe-Sørenssen A., Kostenko O., 2008. Earth Planet. Sci. Lett., 267, pp. 620-627

Okamoto,A.,Shimizu,H., 2015. Earth and Planetary Science Letters 415, 9–18.

Shimizu, H., Okamoto, A., 2016. Contributions to Mineralogy and Petrology, 171, 73.

Keywords: Oman Drilling Project, layered gabbro, permeability, Discrete Element Method, serpentinization

©2019. Japan Geoscience Union. All Right Reserved.

X-ray CT images of oceanic lithologies obtained on Oman Drilling Project drillcores during ChikyuOman 2017 and 2018

*Katsuyoshi Michibayashi[1], Peter B Kelemen[2], Margurette Godard[3], Eiichi TAKAZAWA[4], Damon A H Teagle[5], The Oman Drilling Project Science Party[6]

1. Department of Earth and Planetary Sciences, Nagoya University, 2. Columbia University, 3. Université Montpellier, 4. Niigata University, 5. Southampton University, 6. ICDP

The Oman Drilling Project (OmanDP) has drilled >3,200 meters of the Oman ophiolite during Phases 1 and 2 in Holes GT1A, GT2A, GT3A, BT1B, CM1A, CM2B, BA1B, BA3A and BA4A. All cores have been described on board D/V Chikyu during the summers of 2017 and 2018. X-ray computed tomography (X-ray CT) images were obtained on all cores as a routine part of the IODP measurement protocol onboard D/V Chikyu.

The X-ray CT scanner (Discovery CT 750HD, GE Medical Systems) scans and reconstructs an image of a 1.4 m section in 10 minutes and produces a series of scan images, each 0.625 mm thick. The X-ray source and detector are installed inside of the gantry opposite each other. The excitation voltage and current for X-ray tube are 140 kV and 100 mA, respectively. Core samples are scanned in the gantry with a scanning rate of 20 mm/sec. The distribution of attenuation values mapped to an individual slice comprises the raw data that are used for subsequent image processing. Successive two-dimensional (2D) slices of 512 x 512 pixels yield a representation of attenuation values in three-dimensional (3D) voxels of 512 x 512 by ~1600 in length. Data generated for each core consist of core-axis-normal planes (XY planes) of X-ray attenuation values with dimensions of 512 ×512 pixels in 9 cm ×9 cm cross-section, with a resolution of 0.176 mm/pixel.

As a consequence, we have >3,200 meters length of X-ray CT images from the dyke/gabbro transition zone to the gabbroic sequence to the mantle sequence to the basal thrust of the ophiolite. All X-ray CT images have been processed to match with individual photo images of the archive halves of the cores. The data are useful for assessing sample locations and quality. X-ray CT images can be used for 3D fabric analyses even after core has been cut in half and subsampled for other analyses.

Keywords: OmanDP, XCT, image

©2019. Japan Geoscience Union. All Right Reserved.

Re-examination of the crystallization process of clinopyroxene oikocrysts in layered gabbros at Hess Deep Rift, EPR

*Akane Yasui[1], Takashi Hoshide[1]

1. Graduate School of International Resource Sciences, Akita University

In the Hess Deep Rift, located about 60km east of the East Pacific Rise, the lower crustal gabbros which have been formed at the fast-spreading ridge are exposed. In the IODP Exp. 345, primitive layered gabbros were collected from the lower crust as mainly three drill cores (U1415 I, J, P; Gillis et al., 2014). From the U1415J, unique gabbroic rocks (troctolites) with poikilitic clinopyroxenes (oikocrysts) including many small plagioclase laths have been found (Maeda and Kaise, 2015, Abstracts of the Geological Society of Japan).

Recently, on the origins of clinopyroxene-oikocryst-bearing gabbroic rocks, the different hypotheses have been proposed by Leuthold et al. (2018) and Maeda and Kaise (2015).
Leuthold et al. (2018) proposed that initial olivine gabbros had been partially molten by the intrusion of a primitive melt and then clinopyroxene oikocrysts had crystallized from clinopyroxene-rich basaltic melts formed by the mixing between the partial melt and the primitive magma.
On the other hands, Maeda and Kaise (2015) proposed that clinopyroxenes have first crystallized from a primitive magma and after molten by the encounter with another primitive magma they have continued to grow further and then, the clinopyroxene rim has simultaneously crystallized with matrix olivine and plagioclase. Several hypotheses other than those above (e.g.,Tegner et al., 1995; Nicolas and Boudier., 2011) have been also proposed for the origin of the clinopyroxene oikocrysts in gabbroic rocks. The question is still open to discussion.
Therefore, I re-examine the process of clinopyroxene-oikocryst formation through the textural observation and chemical analysis of the constituent minerals for 8 samples of clinopyroxene-oikocryst-bearing gabbros from 3R, 5R, 7G, 8R and 15G of the U1415J core collected at the IODP Exp. 345.

The matrix part is troctolite consisting mainly of olivine (about 0.5 mm - 2 mm in size, amoeboidal, Fo85~) and plagioclase (about 1 mm in size, An#77-82). Spherical to ellipsoidal clinopyroxene oikocrysts (5-10 mm in size, Mg#85 to 88) is distributed in the matrix troctolite. In addition, clinopyroxene oikocrysts exhibit the following characteristics:

(1) Clinopyroxene oikocrysts basically do not contain any olivine crystals. Rarely, they contain aggregates of plagioclase and olivine.
(2) Orthopyroxene rims (about 100 μm thick, film-like, Mg#85-87) are observed only in matrix olivines (Fo85~) near the rim of the clinopyroxene oikocryst. The olivine crystals rimmed by orthopyroxene are shrinked.
(3) The decreases in Al and Cr contents towards the plagioclase chadacrysts are observed in clinopyroxene oikocrysts.
(4) In the core of the clinopyroxene oikocrysts, we can find parts with Mg# higher than the values which can be in the Fe/Mg equilibrium with olivine in the matrix troctolite.

The facts of (1) and (2) indicate that the assemblage of olivine and plagioclase had already existed when the clinopyroxene oikocrysts crystallized from the melt. In additions, these facts suggest that the melt which formed clinopyroxene oikocryst was in a reaction relationship with olivine. These interpretations

©2019. Japan Geoscience Union. All Right Reserved.

are consistent with the hypothesis of Leuthold et al. (2018).

Keywords: clinopyroxene oikocrysts, Hess Deep, troctolite, Magma mixing, MORB

©2019. Japan Geoscience Union. All Right Reserved.

Structural petrology of peridotites from the Kalaymyo ophiolite

*Kouhei Asano[1,2], Katsuyoshi Michibayashi[1], Jung-Woo Park[3]

1. Graduate School of Environmental Studies, Nagoya University, 2. Shizuoka University, 3. Seoul National University

The Kalaymyo ophiolite is located at Myanmar. The Kalaymyo ophiolite includes large peridotite massifs, where peridotites are commonly well preserved. In recent years, petrologic and geochemical studies have been carried out on the Kalaymyo peridotites. These results suggest that the Kalaymyo peridotites have been undergone melt-rock interactions. In this study, we used fourteen samples from outcrops and drill cores, and carried out analyses of crystal preferred orientations (CPOs) of olivine and of major elements of olivine and spinel. The samples show coarse-grained equigranular textures. The mineral compositions in spinel Cr# and olivine Mg# plot in the field of OSMA (olivine-spinel mantle array) indicate that these samples represent residual upper mantle rocks after partial melting. Spinel grains with Cr# higher than 0.3 have relatively high TiO_2 contents (0.10-0.20 wt.%). Because Ti is incompatible element, high spinel TiO_2 content suggests that these peridotites have experienced melt-rock interaction. There is a positive correlation between J-index and spinel Cr# in the samples. The correlation also has two trends: high and low positive relationships between J-index and spinel Cr#, respectively. Samples experienced melt-rock interaction belong to the low positive trend. It suggests that melt percolation by melt-rock interaction could have an impact on deformation, in particular on CPO development. We propose that melt-rock interaction was synchronous with deformation. It is noted that peridotites experienced melt-rock interaction are intensely located on a narrow range with respect to the elevation, indicating that the occurrence of melt-rock interaction was localized within the Kalaymyo ophiolite.

Keywords: Kalaymyo ophiolite, peridotite, melt-rock interaction, J-index

©2019. Japan Geoscience Union. All Right Reserved.

Reevaluation of the origin of mafic layers in the Upper Zone of the Horoman Peridotite

*Yumeto KOGURE[1], Eiichi TAKAZAWA[1]

1. Department of Geology, Faculty of Science, Niigata University

Horoman peridotite is situated at the southern tip of the Hidaka mountain range, spreads 8 km east-west, 10 km north-south, and has a layer thickness of 3,000 m. We reevaluated the origin of the mafic layer in the Upper Zone of the Horoman Peridotite. We studied Fumo section in the Upper Zone. This section has total thickness of 263 m and consists of plagioclase lherzolite, harzburgite and mafic layer. In the Fumo section, the mafic layer is only interlayered in the plagioclase lherzolite. In the Al2O3, CaO, and Na2O vs. MgO diagrams of whole rock compositions, the mafic layer is plotted on the extension of the linear composition trend indicated by plagioclase lherzolite and harzburgite. There are two types of mafic layer, one plotted in the vicinity of N-MORB and the other plotted in the vicinity of plagioclase lherzolite. The plagioclase lherzolites which have higher Al2O3, CaO, and Na2O and lower MgO contents than the Depleted MORB Mantle (DMM) [1] contain amphiboles whereas the other plagioclase lherzolite which has lower Al2O3, CaO, and Na2O contents and higher MgO content than the DMM do not contain amphibole. Chondrite-normalized whole rock rare earth element (REE) patterns of plagioclase lherzolites are flat from heavy REE to middle REE and show convex upward pattern with depletion in light REE. The mafic layers also show the similar pattern although the abundances of REE is much lower than N-MORB.

From these results, the mafic layers in the Fumo section do not have the composition of primary melt and is considered to be cumulate [2,3]. Also, in the whole rock FeO, TiO2 vs. MgO diagrams, the compositional trends suddenly bend at the most fertile plagioclase lherzolite and becomes depleted in FeO, TiO2 toward the thin mafic layers. On the extension of this bent trends reach to the composition of Cpx and plagioclase. The mafic layer in the Fumo section suggests the possibility that Cpx and plagioclase were crystallized from a melt penetrated into plagioclase lherzolite in a relatively low pressure where the combination of Cpx and plagioclase was stable.

[1] Workman and Hart, 2005, EPSL, 231, 53-72. [2] Shiotani and Niida, 1997, Memoir. Geol. Soc. Japan, 47, 123–137. [3] Takazawa et al., 1999, J. Petrol., 40, 1827-1851.

Keywords: Horoman Peridotite, mantle, mafic layer, orogenic lherzolite, Hidaka Metamorphic Belt

©2019. Japan Geoscience Union. All Right Reserved.

A structural and petrological study of "Shibukawa ultramafic body" in the Sanbagawa belt, western Shizuoka, Japan

*Hikaru Shioya[1,2], Katsuyoshi Michibayashi[1], Ken-ichi Hirauchi[2]

1. Graduate School of Environmental Studies, Nagoya University, 2. Institute of Geosciences, Shizuoka University

We studied an ultramafic body, which is named "Shibukawa ultramafic body" in this study, in the Sanbagawa belt located to the western Shizuoka, focusing on their primary mineral olivine to reveal its petrogenesis. Shibukawa ultramafic body is composed of dunites and wehlites, although the body was heavily weathered due to serpentinization. Yet, most of samples still contain olivine, spinel and a few amounts of clinopyroxene. The olivine crystal preferred orientations (CPOs) of this body were divided into two types: D type and single maxima type. The CPO intensities were relatively high in the north area, whereas those in the south area were relatively low. Considering the grain size distribution of olivine in the samples, the samples in the south area was weakly deformed as they preserve porphyroclastic olivine grains in the fine-grained matrix. In contrast, grain size reduction due to deformation has been completed in the north area. Olivine CPO patterns and major elements composition of both olivine and spinel indicate that the origin of this ultramafic body could be cumulate such as the Mikabu belt and is different from those of Shikoku mountains in the Sanbagawa belt.

Keywords: Sanbagawa belt, Mikabu belt, Cumulate, Ultramafic, Olivine fabrics, Dunite

©2019. Japan Geoscience Union. All Right Reserved.

[J] Oral | S (Solid Earth Sciences)：S-CG Complex & General

Tue. May 28, 2019 10:45 AM - 12:15 PM JST | Tue. May 28, 2019 1:45 AM - 3:15 AM UTC | A09 TOKYO BAY MAKUHARI HALL

[S-CG54] Rheology, fracture and friction in Earth and planetary sciences

convener:Miki Tasaka(Shimane University), Osamu Kuwano(Japan Agency for Marine-Earth Science and Technology), Ichiko Shimizu(Division of Earth and Planetary Sciences, Graduate School of Science, Kyoto University), Hidemi Ishibashi(Faculty of Science, Shizuoka University), Chairperson:Osamu Kuwano(Japan Agency for Marine-Earth Science and Technology (JAMSTEC)), Ichiko Shimizu

The aim of this session is to join people from various research area in the earth and planetary sciences and to stimulate discussion beyond the boundaries of each research area. Our goal is to deepen our understanding of dynamics in geosciences by looking over whole areas in the earth and planetary sciences from the viewpoint of PHYSICS OF DEFORMATION, FLOW, AND FRACTURE. We welcome any field (e.g., earthquake, volcano, earth surface, crust, mantle and the core, and other planets and satellites) and any approach (e.g., laboratory experiments, numerical simulations, field observations, and theories).

10:45 AM - 11:00 AM JST | 1:45 AM - 2:00 AM UTC

[SCG54-01] Rheology of granular materials near the jamming transition under oscillatory shear

★Invited Papers

*Michio Otsuki[1], Hisao Hayakawa[2] (1.Graduate School of Engineering Science, Osaka University, 2.Yukawa Institute for Theoretical Physics, Kyoto University)

11:00 AM - 11:15 AM JST | 2:00 AM - 2:15 AM UTC

[SCG54-02] The real-scale numerical sandbox experiments for understanding stress state in accretionary prisms

*Mikito Furuichi[1], Arthur Bauville[1], Daisuke Nishiura[1], Takane Hori[1], Osamu Kuwano[1] (1.Japan Agency for Marine-Earth Science and Technology)

11:15 AM - 11:30 AM JST | 2:15 AM - 2:30 AM UTC

[SCG54-03] Numerical analysis on the fracture of Maxwell fluid by phase field models

*Masaharu Kameda[1], Keita Yamanishi[1], Akinori Yamanaka[1], Mie Ichihara[2] (1.Department of Mechanical Systems Engineering, Tokyo University of Agriculture and Technology, 2.Earthquake Research Institute, The University of Tokyo)

11:30 AM - 11:45 AM JST | 2:30 AM - 2:45 AM UTC

[SCG54-04] Diagenesis- and earthquake-driven transformations of carbonaceous materials and their implication for frictional strength and earthquake rupture dynamics in carbon-bearing plate-subduction faults

*Shunya Kaneki[1], Tetsuro Hirono[1] (1.Graduate School of Science, Osaka University)

11:45 AM - 12:00 PM JST | 2:45 AM - 3:00 AM UTC

[SCG54-05] Viscous behavior of chert during frictional melting

*Ginta Motohashi[1], Kiyokazu Oohashi[2], Kohtaro Ujiie[1] (1.University of Tsukuba, 2.Yamaguchi University)

12:00 PM - 12:15 PM JST | 3:00 AM - 3:15 AM UTC

[SCG54-06] Effect of friction and comminution on the optically-stimulated luminescence of quartz grains

*Kiyokazu Oohashi[1], Koji Akasegawa[2], Yuki Minomo[1], Noriko Hasebe[3], Kazumasa Miura[4] (1.Graduate School of Sciences and Technology for Innovation, Yamaguchi University, 2.Daiwa Exploration & Consulting Co., Ltd., 3.Institute of Nature and Environmental Technology, Kanazawa University, 4.Graduate School of Natural Science & Technology, Kanazawa University)

Rheology of granular materials near the jamming transition under oscillatory shear

*Michio Otsuki[1], Hisao Hayakawa[2]

1. Graduate School of Engineering Science, Osaka University, 2. Yukawa Institute for Theoretical Physics, Kyoto University

Amorphous materials consisting of repulsive and dissipative particles such as granular materials, colloidal suspensions, foams, and emulsions behave like liquids below a critical value of the packing fraction, while they behave like solids above that value. This sudden change is known as a jamming transition [1]. In this talk, we present our recent numerical results on the rheological properties of granular materials near the jamming transition under oscillatory shear. It is confirmed that the shear modulus depends on the amplitude of the initial oscillatory shear before the measurement [2]. Even at densities below the transition point, where isotropic jamming occurs without shear, the initial oscillatory shear can induce the finite shear modulus. This behavior is consistent with a transition known as shear jamming. We also discuss the yielding transition above the jamming point under sufficiently large strain.

[1] M. van Hecke, J. Phys.: Condens. Matter 22, 033101 (2009).
[2] M. Otsuki and H. Hayakawa, arXiv:1810.03846.

Keywords: Rheology, Granular materials, Jamming transition

©2019. Japan Geoscience Union. All Right Reserved.

The real-scale numerical sandbox experiments for understanding stress state in accretionary prisms

*Mikito Furuichi[1], Arthur Bauville[1], Daisuke Nishiura[1], Takane Hori[1], Osamu Kuwano[1]

1. Japan Agency for Marine-Earth Science and Technology

The sandbox experiment is known as a scaled physical analog model of accretionary prisms. Thus, understanding the stress state inside the sand layer is the interesting challenge of the geology. However, measuring stress states in laboratory sandbox experiments is still practically infeasible. Here we performed real-scale numerical sandbox experiments using the Discrete Element Method (DEM) to understand the 3D stress state in the accretionary prism. The critical bottleneck of DEM was the limited number of particles acceptable for practical computation time and it was difficult to simulate a system with a huge number of particles required by such as our target sandbox test with realistic particle size. We had overcome this issue by developing the dynamic load balancing technique for the DEM codes and run the real-scale numerical sandbox simulation using up to 2.4 billion particles [Furuichi et.al. 2017]. We also performed the large-scale stress chain analysis. One of the interesting findings was that the simulation of the horizontal shortening of the granular layer showed undulated margins similar to those observed in accretionary prism, despite the nearly uniform initial conditions. The 3D stress chain analysis that is practically infeasible for the laboratory experiment studies, revealed that arcuate faults emerge from micro-scale perturbations owing to the formation of the stress arch [Furuichi et.al. 2018]. Furthermore, analyses demonstrate that the in-situ stress orientation from borehole data can be a signal of either the regional direction of plate convergence or the local stress orientation associated with such a stress arch. The results may greatly enhance the outcome of long-term monitoring in areas, such as the Nankai Trough. In this contribution, we also investigated the stress state associated with a seamount (indenter) entering the accretionary prisms. The role of indenter was significant as a frictional heterogeneity to control the tomography (taper angle), material transport and stress chain distribution. Especially, amount of sediment covering the indenter was transported inward without deformation. This mechanism potentially constructs the thick low-velocity zone into the plate boundary, the subduction channel. In this presentation, we discuss the detail mechanism of these observed compressional events inside the sand layers.

[Furuichi et.al. 2017] M. Furuichi, D. Nishiura, Comput. Phys. Comm. (2017) DOI:10.1016/j.cpc.2017.05.015

[Furuichi et.al. 2018] M. Furuichi, D. Nishiura, O. Kuwano, A. Bauville, T. Hori, H. Sakaguchi, Scientific Reports (2018), DOI:10.1038/s41598-018-26534-x

Keywords: Accretionary prism, Stress, DEM

©2019. Japan Geoscience Union. All Right Reserved.

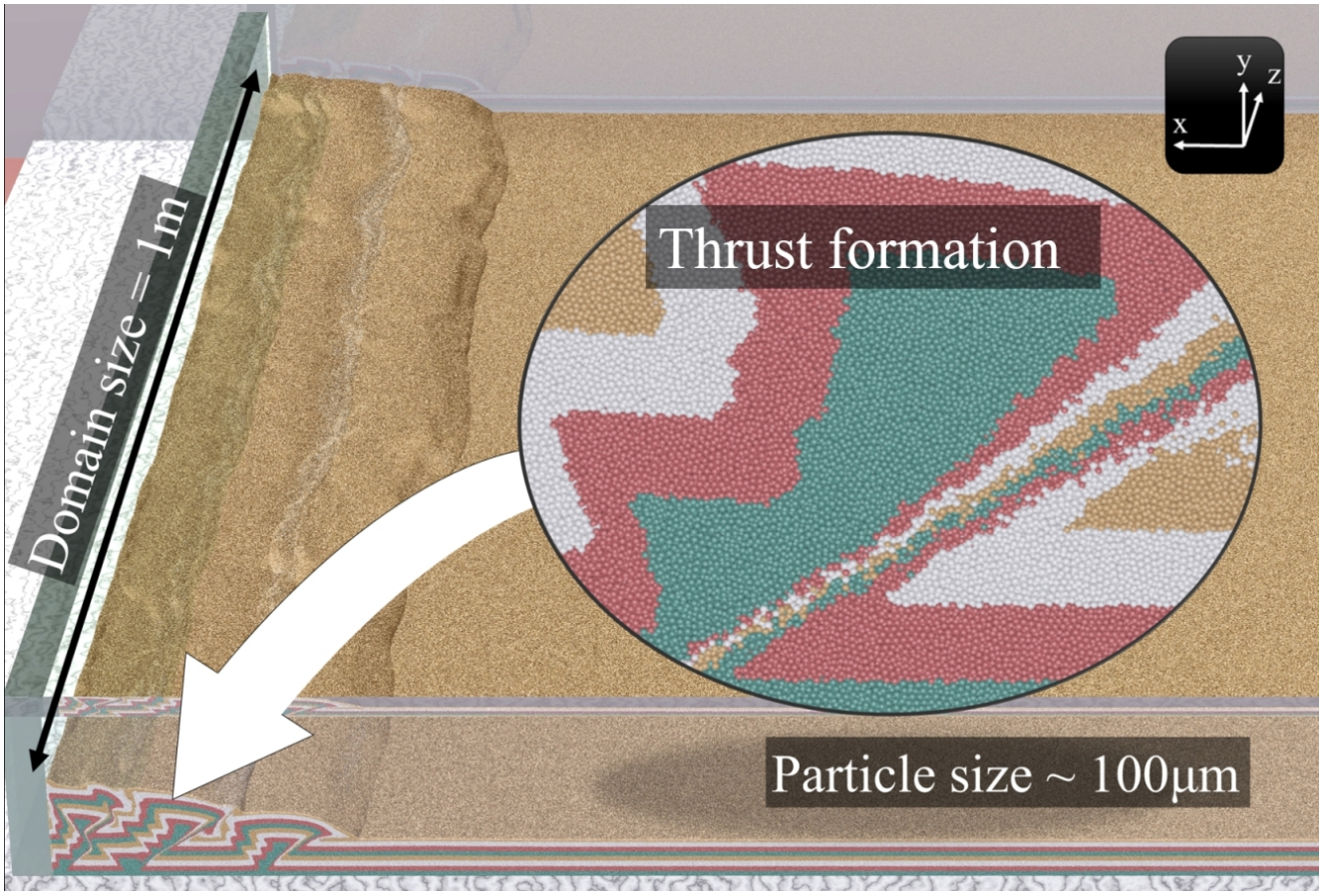

©2019. Japan Geoscience Union. All Right Reserved.

Numerical analysis on the fracture of Maxwell fluid by phase field models

*Masaharu Kameda[1], Keita Yamanishi[1], Akinori Yamanaka[1], Mie Ichihara[2]

1. Department of Mechanical Systems Engineering, Tokyo University of Agriculture and Technology, 2. Earthquake Research Institute, The University of Tokyo

Brittle fragmentation of vesicular magma is a key process in explosive eruption. Recent estimation on the decompression time in real explosive events indicates that the style of fragmentation is to be “brittle-like fragmentation” (Kameda et al. JVGR 2013). The solid-like fracture of the material occurs even if the bulk rheological properties is close to fluid state. We also found the fact that the spatial inhomogeneity of bubble distribution is a major source of crack development that lead to brittle-like fragmentation (Kameda et al. Sci. Rep. 2017).

In order to model our findings by numerical approach, we propose a continuum description of fracture in viscoelastic fluid using the phase field fracture model developed by Kuhn et al. (Comput. Mat. Sci. 2015). The phase-field modes with sharp interfaces consist in incorporating a continuous field variable so-called “order parameter,” by which the magma and the bubbles (or the cracks) are distinguished. The evolution of fracture is obtained implicitly by solving the coupled mathematical models formed by the phase field fracture model and the dynamics of the material. A commercial multiphysics solver (COMSOL) is used as the platform of numerical simulation. The phase field fracture model is solved using PDE solver of COMSOL. The dynamics of the material is calculated using conventional finite element analysis (FEM) prepared in the solver, in which the rheology of unbroken magma is assumed to be a linear Maxwell fluid.

First, we simulated crack propagation in a two-dimensional notched plate in a tensile test at a constant extension rate. We obtained the extension of crack with a sharp tip in pure elastic body (Fig. 1(a)) or viscoelastic body with sufficiently high viscosity (Fig. 1(b)). On the contrary, in the viscoelastic liquid with moderate viscosity the blunted tip occurs after the crack extension starts (Fig. 1(c)). Subsequently, the crack propagates again due to further extension.

Second, we simulated crack initiation and propagation in a porous material, which is a sphere including a large bubble at the center. Additionally, we placed two satellite bubbles nearby the large bubble. The pressure at the outer surface of the material was reduced to generate the non-uniform stress field in the material. As a result, the plane crack was generated between the satellite bubbles. The crack reached outer boundary, then a sharp crack was opened. The computed time scale in the crack propagation was equivalent to the scale observed in the experiment (Kameda et al. Sci. Rep. 2017). This time scale is much smaller than the scale simulated with another phase field fracture model proposed by Karma et al. (Phys. Rev. Lett. 2001).

Keywords: Magma, Fracture, Phase field model

©2019. Japan Geoscience Union. All Right Reserved.

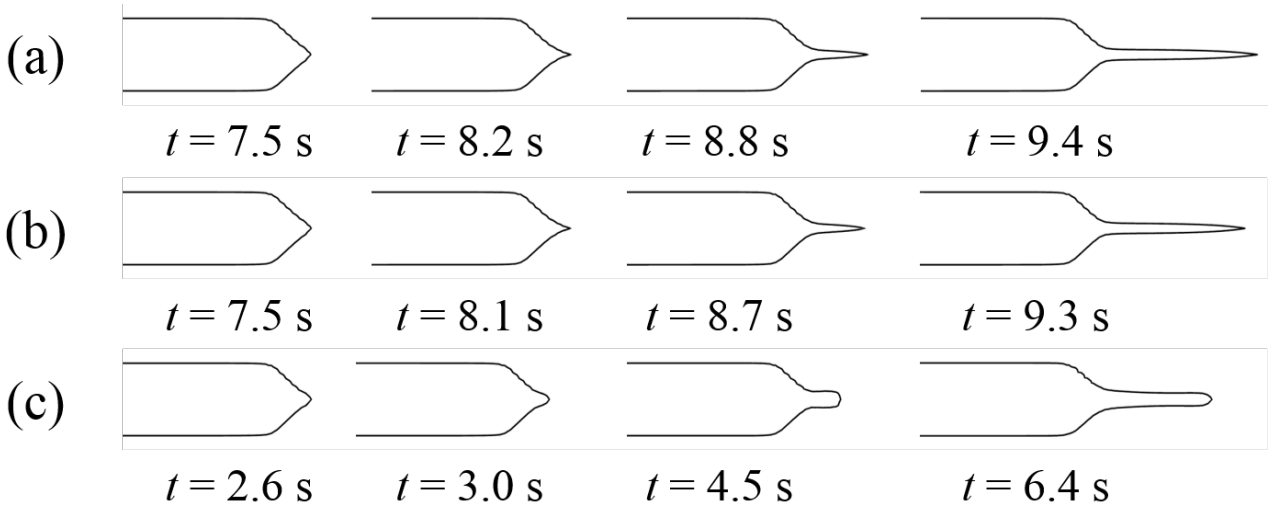

©2019. Japan Geoscience Union. All Right Reserved.

Diagenesis- and earthquake-driven transformations of carbonaceous materials and their implication for frictional strength and earthquake rupture dynamics in carbon-bearing plate-subduction faults

*Shunya Kaneki[1], Tetsuro Hirono[1]

1. Graduate School of Science, Osaka University

Various physicochemical reactions on fault-forming materials, such as illitization of smectite and crystallization of amorphous silica, have been suggested as possible controls on frictional strength of rocks and thus on earthquake dynamics in plate-subduction zones. Carbonaceous material is one of the universal materials that exist in and around both active plate-boundary and inland faults, and previous studies suggest that transformation of carbonaceous material may affect its frictional strength during frictional slip. However, there is currently no systematic study attempting to investigate the relationship of maturity of carbonaceous material to its frictional strength, and thus how diagenesis- and earthquake-driven transformations of carbonaceous material can affect frictional strength and rupture dynamics of carbon-bearing faults, still remains unknown. We conducted high-velocity friction experiments together with elemental analysis, transmission electron microscope observation, X-ray diffraction analysis, and infrared and Raman spectroscopies, on four grades of carbonaceous material in the form of lignite, bituminous coal, anthracite, and graphite. Our experimental results clearly show that an increase in maturity and crystallinity of carbonaceous material results in a decrease in the peak friction coefficient at the initial stage of slip, from 0.5 (lignite) to 0.2 (graphite). We also infer from our results of spectroscopic analyses that low- (lignite and bituminous coal) and intermediate-grade carbonaceous material (anthracite) increases its maturity by high-velocity frictional slip, but friction applied to high-grade carbonaceous material (graphite) induces an opposite trend. Furthermore, by considering systematic decrease and increase in fracture energy and stress ratio with increasing maturity of carbonaceous material, both of which strongly affect rupture propagation process during earthquake, both diagenesis- and earthquake-driven transformations of carbonaceous material can strongly affect the frictional strength of carbon-bearing faults, potentially affecting the depth-dependences of not only frictional strength but also rupture dynamics on plate-subduction faults.

Keywords: Earthquake, Carbonaceous material, Thermal maturation, Friction coefficient, Plate subduction zone, Rupture dynamics

©2019. Japan Geoscience Union. All Right Reserved.

Viscous behavior of chert during frictional melting

*Ginta Motohashi[1], Kiyokazu Oohashi[2], Kohtaro Ujiie[1]

1. University of Tsukuba, 2. Yamaguchi University

Pelagic chert is one of the major lithology in accretionary complexes. Thus, frictional properties of chert at seismic slip rates are important for understanding of earthquake faulting in subduction zones. Here, we conducted high-velocity friction experiments on chert collected from the Jurassic accretionary complex in central Japan at a slip rate of 1.3 m/s and normal stresses of 5–13 MPa under room humidity conditions. The results show that initial slip weakening was followed by slip strengthening and subsequent second slip weakening toward a steady-state shear strength. Slip strengthening resulted from the formation of a silica-rich melt layer (experimentally generated pseudotachylyte) at lower melting temperatures than expected. The chemical composition of the pseudotachylyte matrix suggests the frictional melting of quartz with a small amount of illite, which may contribute to reduce melting temperatures. The second slip weakening occurred despite an increasing shear strain rate because of the thinning of the melt layer, implying that the viscosity of the melt layer decreased with slip. The estimated temperatures before and after the second slip weakening and microstructural and chemical features of experimentally generated pseudotachylytes suggest that the viscosity decrease during the second slip weakening is not due to a change in the chemical composition of melt layer, but rather a temperature increase in the melt layer.

Keywords: frictional melting , chert, high-velocity friction experiments

©2019. Japan Geoscience Union. All Right Reserved.

Effect of friction and comminution on the optically-stimulated luminescence of quartz grains

*Kiyokazu Oohashi[1], Koji Akasegawa[2], Yuki Minomo[1], Noriko Hasebe[3], Kazumasa Miura[4]

1. Graduate School of Sciences and Technology for Innovation, Yamaguchi University, 2. Daiwa Exploration & Consulting Co., Ltd., 3. Institute of Nature and Environmental Technology, Kanazawa University, 4. Graduate School of Natural Science & Technology, Kanazawa University

Optically-stimulated luminescence(OSL) dating is considered to be applicable for fault dating owing to its instability even for short-time heating such as frictional heating. However, fault zone material may experience not only heat but also friction and comminution with coseismic faulting. If the OSL signal becomes small or disappear due to friction and comminution that is also accompanied by stable sliding (fault creep), OSL signal zeroing in natural fault zone can not be simply attributed to earthquake event. Here we report an increment of OSL signal of quartz during a low- to intermediate-velocity frictional sliding. The increments of OSL signal intensities were found from finely ground recovered sample (<75 μm). We also recognized an increment of fast to medium component of OSL with increasing sliding velocity. These results can be explained by (1) trapping of electron on newly-formed mineral surface, (2) rate-dependent emission of electron, such as triboemission, at asperity contact.

[Acknowledgements] This work was supported by grants from the Nuclear Regulation Authority (FY 2015–2018).

Keywords: Optically stimulated luminescence, Friction experiment, BET specific surface area, Triboluminescence

©2019. Japan Geoscience Union. All Right Reserved.

[J] Oral | S (Solid Earth Sciences)：S-CG Complex & General

Tue. May 28, 2019 1:45 PM - 3:15 PM JST | Tue. May 28, 2019 4:45 AM - 6:15 AM UTC | A09 TOKYO BAY MAKUHARI HALL

[S-CG54] Rheology, fracture and friction in Earth and planetary sciences

convener:Miki Tasaka(Shimane University), Osamu Kuwano(Japan Agency for Marine-Earth Science and Technology), Ichiko Shimizu(Division of Earth and Planetary Sciences, Graduate School of Science, Kyoto University), Hidemi Ishibashi(Faculty of Science, Shizuoka University), Chairperson:Miki Tasaka(島根大学), Hidemi Ishibashi(Shizuoka University)

The aim of this session is to join people from various research area in the earth and planetary sciences and to stimulate discussion beyond the boundaries of each research area. Our goal is to deepen our understanding of dynamics in geosciences by looking over whole areas in the earth and planetary sciences from the viewpoint of PHYSICS OF DEFORMATION, FLOW, AND FRACTURE. We welcome any field (e.g., earthquake, volcano, earth surface, crust, mantle and the core, and other planets and satellites) and any approach (e.g., laboratory experiments, numerical simulations, field observations, and theories).

1:45 PM - 2:00 PM JST | 4:45 AM - 5:00 AM UTC

[SCG54-07] Frictional behaviors of smectite clay: constraints for the mobility of slow-moving landslides in the cold season

★Invited Papers

*Tatsuya Shibasaki[1], Sumio Matsuura[2] (1.Japan Conservation Engineers and Co., Ltd, 2.DPRI, Kyoto University)

2:00 PM - 2:15 PM JST | 5:00 AM - 5:15 AM UTC

[SCG54-08] Strength of a deep fault zone along the Median Tectonic Line: Influence of chrolite friction

*Ichiko Shimizu[1], Ayumi S. Okamoto, Andre R. Niemeijer[2], Christopher J. Spiers[2], Shun Arai[3], Toru Takeshita[4] (1.Division of Earth and Planetary Sciences, Graduate School of Science, Kyoto University, 2.Faculty of Geosciences, Utrecht University, 3.Tohoku University, 4.Hokkaido University)

2:15 PM - 2:30 PM JST | 5:15 AM - 5:30 AM UTC

[SCG54-09] Changes in seismic wave velocity during brittle deformation of gabbro and peridotite

*Yuya Akamatsu[1], Ikuo Katayama[1] (1.Hiroshima University)

2:30 PM - 2:45 PM JST | 5:30 AM - 5:45 AM UTC

[SCG54-10] Dislocation textures in shock-compressed MgO and their formation mechanisms

*Kiyoshi Fujino[1], Xun Liu[2], Tsutomu Mashimo[2] (1.Geodynamics Research Center, Ehime University, 2.Institute of Pulsed Power Science, Kumamoto University)

2:45 PM - 3:00 PM JST | 5:45 AM - 6:00 AM UTC

[SCG54-11] Development of rotational diamond anvil cell and large strain deformation experiments of lower-mantle materials

★Invited Papers

*Shintaro Azuma[1,2], Ryuichi Nomura[3,4], Kentaro Uesugi[5], Yu Nishihara[4], Doi Shunta[4], Takeshi Arimoto[4], Tetsuo Irifune[4] (1.Tokyo Tech., 2.Kyushu Univ., 3.Kyoto Univ., 4.Ehime Univ., 5.Japan Synchrotron Radiation Research Institute (JASRI))

3:00 PM - 3:15 PM JST | 6:00 AM - 6:15 AM UTC

[SCG54-12] Rheology of hcp-iron

*Yu Nishihara[1], Doi Shunta[1], Noriyoshi Tsujino[2], Daisuke Yamazaki[2], Yuji Higo[3] (1.Geodynamics Research Center, Ehime University, 2.Institute of Planetary Materials, Okayama University, 3.Japan Synchrotron

Radiation Research Institute)

Frictional behaviors of smectite clay: constraints for the mobility of slow-moving landslides in the cold season

*Tatsuya Shibasaki[1], Sumio Matsuura[2]

1. Japan Conservation Engineers and Co., Ltd, 2. DPRI, Kyoto University

In Japan, reactivated landslides are distributed on gentle clayey slopes in specific geological settings, such as Neogene soft sedimentary rock areas and hydrothermally altered rock areas around active and inactive volcanoes. These strata are typically composed of smectite-bearing high-plasticity soils. Of all the clay minerals, smectite shows an extremely low residual friction angle. Therefore, landslides consisting of these soils can easily become unstable and be reactivated on very gentle slopes. In many cases, such landslides are likely to be reactivated during certain seasons every year, moving slowly with typical velocities ranging from 0.01 to 0.1 mm/min. According to behavioral data of landslides in the Niigata Prefecture, a well-known landslide-prone area in Japan, some landslides begin to move during the early cold season (late autumn or early winter). Some landslides are activated during the winter, and display continuous movement, while others are activated predominantly during the snow-melting period. These various behaviors cannot be explained solely by fluctuations in pore-water pressure (ground water levels), and this therefore raises the question of what the key controlling mechanisms are. Shallow landslides, less than 10 m deep, are sometimes activated in the early cold season. We inferred that the change in ground temperature may play a key role in activating landslides. In order to verify this, we investigated the effect of temperature on residual shear strength of various clayey soils. Reversal box shear experiments and ring shear experiments were performed on undisturbed slip-surface soils and reconstituted soil samples, respectively. The test results revealed that the shear strength of smectite-rich soils decreases with decreasing temperatures under slow shearing rates of lower than 0.1 mm/min. This finding implies that seasonal fluctuation in ground temperature can influence slope instability, especially for shallow, slow-moving landslides. It is also evident that the effect of temperature on residual strength changes with the shearing rate. We infer that the velocity-dependent characteristic is strongly regulated by the fabric of smectite particles along the shearing plane.

References

1) Shibasaki T., Matsuura S., and Okamoto T. (2016): Experimental evidence for shallow, slow-moving landslides activated by a decrease in ground temperature. Geophysical Research Letters, 43, 13, 6975-6984. doi.org/10.1002/2016GL069604
2) Shibasaki T., Matsuura S., and Hasegawa Y. (2017): Temperature-dependent residual shear strength characteristics of smectite-bearing landslide soils. Journal of Geophysical Research: Solid Earth, 122, 2, 1449-1469. doi.org/10.1002/2016JB013241

Keywords: Landslide, Smectite, Residual strength, Temperature dependency

©2019. Japan Geoscience Union. All Right Reserved.

Strength of a deep fault zone along the Median Tectonic Line: Influence of chrolite friction

*Ichiko Shimizu[1], Ayumi S. Okamoto, Andre R. Niemeijer[2], Christopher J. Spiers[2], Shun Arai[3], Toru Takeshita[4]

1. Division of Earth and Planetary Sciences, Graduate School of Science, Kyoto University, 2. Faculty of Geosciences, Utrecht University, 3. Tohoku University, 4. Hokkaido University

To explore the fault strength at the middle crustal levels, we conducted high-pressure hydrothermal experiments using natural fault rocks exposed along the Median Tectonic Line (MTL), focusing on the role of chlorite in fault weakening. Chlorite is a hydrous mineral commonly observed in basic metamorphic rocks and fault zones, and is known to have low friction coefficients around 0.3–0.4 at room temperature water saturated conditions (Behnsen and Faulkner, 2012), and about 0.3 at hydrothermal conditions (Okamoto et al., *in review*).

The experiments were performed on powdered samples of cataclasite and protomylonite, which are originated from tonalite or basic rocks in the Ryoke belt on the northern side of MTL. Cataclasites contain ~30 wt.% mica and clay minerals. Among them, chlorite-rich cataclasite (Chl-cataclasite) contains ~14 wt.% chlorite, and mica-rich cataclasite (Ms-cataclasite) contains ~14 wt.% white mica. Chlorite geothermometer (Bourdelle *et al*., 2013, CMP) yields a bimodal distribution (230–240˚C and 290–340˚C) for the protomylonite sample. The low-temperature chlorite occurs as blobs with the diameter of ~1–2 mm, which contain lamella of white mica. These chlorite grains are considered as pseudomorphs of biotite. The high-temperature chlorite filled fractures and interstice of grains. We therefore interpreted that brittle deformation first occurred at a temperature around 300˚C and subsequent hydrothermal alteration occurred at 230–240˚C. Chl-cataclasite also shows a bimodal temperature distribution (180–220˚C and 240–300˚C), although no clear relationships between temperatures and microstructures were found.

To simulate the deformation conditions at depth, friction experiments were conducted at temperature of 300˚C, normal stress of 300 MPa, and pore fluid pressures of 120 MPa and 240 MPa, using the hydrothermal ring shear apparatus at Utrecht University. Sliding velocities were varied from 0.001 mm/s to 0.1 mm/s. The steady-state friction coefficients obtained for protomylonite were ~0.68, whereas those for Ms- and Chl-cataclasites were ~0.65 and ~0.56 at 120 MPa, and ~0.87 and ~0.66 at 240 MPa, respectively. Velocity stepping tests yielded velocity-weakening or neutral behaviours, although existing laboratory data for pure chlorite gouges mostly show velocity-strengthening behaviours. Our results indicate that fault strengths and sliding behaviours in the middle crusts are not drastically changed by the presence of phyllosilicates even if chlorite contents in fault zones are relatively high (<14 wt.%).

Keywords: friction, fault strength, high-PT experiments

©2019. Japan Geoscience Union. All Right Reserved.

Changes in seismic wave velocity during brittle deformation of gabbro and peridotite

*Yuya Akamatsu[1], Ikuo Katayama[1]

1. Hiroshima University

The Moho is defined as a discontinuity of seismic wave velocity and often interpreted to be the crust-mantle boundary. The oceanic crust is continuously created by magma system at the mid ocean ridge; consequently, the discontinuity of seismic wave velocity and/or sharp seismic reflection at the Moho is expected to be laterally uniform. However, recent seismic observations reported regional variations of the Moho reflectivity (e.g., Mutter and Carton, 2013; Ohira et al., 2018). As seismic wave velocity is greatly influenced by nucleation and growth of microcracks, such seismic anomaly at the Moho can be influenced by microcracks. We found that minor amounts of dilatancy in peridotite relative to mafic rocks based on strain measurements during triaxial deformation tests using these rocks (Akamatsu et al., 2019). This contrasting dilatant behaviors possibly lead to different evolution of seismic wave velocity between crust and mantle, and potentially cause the regional seismic anomaly in the oceanic plate. In this study, we measured elastic wave velocities of gabbro and peridotite during triaxial deformation experiments, and discussed how brittle deformation influences on the seismic velocity and reflectivity.

We used gabbro collected from the Oman ophiolite, and peridotite collected from the Horoman Complex. Triaxial deformation experiments were performed with intra-vessel deformation and fluid flow apparatus at room temperature, a constant strain rate of ~10^{-6} s^{-1}, and a constant confining pressure of 20 MPa. Compressional and shear waves traveling in a direction normal to the loading axis were measured during deformation, where shear waves were polarized normal and parallel to the loading axis. Seismic wave velocities were determined by a pulse transmission method, in which travel times of seismic waves through the sample were measured.

In gabbros, both Vp and Vs markedly decreased (Vp: ~40%, Vs: ~30%) as the samples approache failure. Crack density inverted from the velocities showed anisotropic crack orientation, where microcracks parallel to the loading axis (axial microcracks) were dominantly created. These results correspond to strain data and microstructural observation of recovered samples after deformation (Akamatsu et al., 2019). On the other hand, in peridotites, a small decrease in Vp and Vs (<20%) were observed up to the maximum stress, and inverted crack density showed no significant increase in axial microcracks. This indicates that microcracks developed in peridotites were mainly “mode II” shear microcracks, corresponding to strain data and microstructural observation. These contrasting evolutions of seismic wave velocity and crack density between gabbro and peridotite during brittle deformation can modify the seismic discontinuity and reflectivity at the Moho, and contribute to the variation of the Moho in the oceanic plate.

Keywords: Peridotite, Gabbro, Seismic wave velocity, Brittle deformation, Dilatancy, Microcrack

©2019. Japan Geoscience Union. All Right Reserved.

Dislocation textures in shock-compressed MgO and their formation mechanisms

*Kiyoshi Fujino[1], Xun Liu[2], Tsutomu Mashimo[2]

1. Geodynamics Research Center, Ehime University, 2. Institute of Pulsed Power Science, Kumamoto University

Deformation phenomena under high-pressure in Earth and planetary science occur under the shock compression as well as under the static or quasi-static compression. However, the studies on dislocation textures of materials under the shock compression are very limited, compared to those under the static or quasi-static compression. To fill such gap, the shock compression experiments on MgO were carried out and the dislocation textures of the recovered samples were examined under TEM to consider the formation mechanisms of those dislocation textures.

The shock compression experiments of single-crystal MgO were performed with a powder gun at the Institute of Pulsed Power Science, Kumamoto Univ. The shock compression experiments were done along the <100> and <110> directions. The recovered MgO samples were examined under 200 kV TEM at the Geodynamics Research Center, Ehime University.

In the previous studies, the Burgers vector of MgO is always $(\boldsymbol{a}_1 + \boldsymbol{a}_2)/2$ and the slip planes are mostly {110} and {100}. The present TEM examination showed that the sample under the <100> compression has dislocations of only the {110} slip plane, while under the <110> compression the sample has dislocations of only the {110} slip plane at low pressure but has dislocations of both {110} and {100} slip planes at higher pressure, indicating that the slip plane changes from {110} to {100} with increasing pressure. In addition to these results the dislocation textures which are usually not observed in the static or quasi-static compression, were also observed. In the presentation, the formation mechanisms of the observed dislocation textures are also discussed.

Keywords: shock compression, MgO, TEM observation, slip system of dislocation

©2019. Japan Geoscience Union. All Right Reserved.

Development of rotational diamond anvil cell and large strain deformation experiments of lower-mantle materials

*Shintaro Azuma[1,2], Ryuichi Nomura[3,4], Kentaro Uesugi[5], Yu Nishihara[4], Doi Shunta[4], Takeshi Arimoto[4], Tetsuo Irifune[4]

1. Tokyo Tech., 2. Kyushu Univ., 3. Kyoto Univ., 4. Ehime Univ., 5. Japan Synchrotron Radiation Research Institute (JASRI)

The rheological properties of lower-mantle materials are key to understanding the dynamics and evolution in the Earth’ s interior. However, the pressure range of deformation apparatuses which can achieve large strain is limited to ~30–40 GPa due to a technical reason. We developed the rotational diamond anvil cell (rDAC) which can conduct deformation experiments with large strain under ultra-high pressure conditions, corresponding to those of core-mantle boundary [Nomura et al., 2017]. The rDAC can apply the torsional deformation to sample with constant strain rate by a gearbox and diamond anvils with grooves [Azuma et al., 2018]. However, the stress measurement and high temperature conditions has not been achieved in rDAC. To solve these problems, the vacuum chamber newly designed for rDAC was installed and the stress measurements using X-ray Diffraction (XRD) were applied to deformation experiments in rDAC at SPring-8 (Japan). In this presentation, we will present the preliminary results of stress measurements, high temperature techniques in rDAC, and the results of deformation experiments of lower-mantle materials.

In this study, the mixture of bridgmanite $(Mg,Fe)SiO_3$ and ferropericlase (Mg,Fe)O, which was synthesized from San Carlos olivine, was deformed under torsion geometry using the rDAC. The experimental conditions are ranging 26–130 GPa, 300–673 K. Starting material was grooved by FIB and the groove was deposited by Pt as a strain-marker. Recovered samples were cut by FIB to observe the deformation microstructures in each cross-section. Deformation experiments were conducted at BL47XU, SPring-8 (Japan) and 3D visualization of strain marker within samples was performed every rotation angle of upper anvil of 5–30 degree using X-ray laminography technique [Nomura and Uesugi, 2016]. Stress was measured by collecting X-ray diffraction pattern at twelve different azimuthal angles, Ψ= 0º, ±30º, ±60º, ± 90º, ±120º, ±150º, and 180º. Testing of the new vacuum chamber was also performed at SPring-8. The vacuum chamber has a removable Kapton window for incident and diffracted X-ray, and can keep the vacuum state (<~10 Pa) to prevent the diamond anvils from oxidation during high-temperature deformation experiments. Platinum wires were used as a resistance heater surrounding the sample and Rhenium gasket.

The geometry of strain-marker in cross-section of deformed samples show nearly simple shear (or general shear). Deformed microstructure of recovered samples was observed using FE-SEM and we determined the 2D surface area of ferropericlase and aspect ratio of bridgmanite. The deformation microstructures of the recovered samples showed that ferropericlase highly deformed and formed an interconnected weak layer. On the other hand, the aspect ratio of bridgmanite did not change with the strain, indicating that bridgmanite has high viscosity compared with ferropericlase. These results imply that ferropericlase dominates the deformation in the regions where large shear strain occurs under relatively low-temperature conditions in the lower mantle (e.g., mantle portion in subducted slabs).

Stress in bridgmanite was estimated by using diffraction peaks (110) and (112) at P = 50 GPa and T= 673 K. Shear stress in bridgmanite was relatively constant values, whereas uniaxial stress changed during

©2019. Japan Geoscience Union. All Right Reserved.

deformation experiments. This preliminary experiment was performed under low-temperature and high-pressure conditions, thus the equivalent stress in bridgmanite was about three times higher than that in previous studies [Girard et al., 2016].

In heating experiments using new vacuum chamber, temperature was monitored by Pt/Rh thermocouple placed close to the sample and and we succeeded in increasing temperature up to ~1000 K. However, the resistance heater (Pt) was unstable in vacuum. In the future, high-temperature deformation experiments using rDAC will be conducted in reducing atmosphere produced by inactive gas or internal heating system should be developed for rDAC.

Keywords: Lower mantle, Rotational diamond anvil cell, Deformation

©2019. Japan Geoscience Union. All Right Reserved.

Rheology of hcp-iron

*Yu Nishihara[1], Doi Shunta[1], Noriyoshi Tsujino[2], Daisuke Yamazaki[2], Yuji Higo[3]

1. Geodynamics Research Center, Ehime University, 2. Institute of Planetary Materials, Okayama University, 3. Japan Synchrotron Radiation Research Institute

Seismic observations have revealed presence of axi-symmetric anisotropy with respect to polar direction in the Earth’ s inner core which consists of solid metal, where a P- wave propagating along the polar direction is ~3% faster than that along the equatorial direction. Although many hypotheses have been proposed for origin of seismic anisotropy in the inner core, there is no general consensus for its origin. Lasbleis and Deguen (2015) discussed that dominant mechanism of the inner core dynamics depends on the inner core age and viscosity, and there are several candidate mechanisms which includes anisotropic growth model (Yoshida et al., 1996) and thermal convection model (Jeanloz and Wenk, 1988). Since the inner core is considered to consist of hexagonal close-packed iron(hcp-iron), information of viscosity of hcp-iron is a key for the understanding of the inner core dynamics. In this study, we have studied rheology of hcp-iron based on high-pressure and high-temperature deformation experiments.
Uniaxial deformation experiments were carried out using a D111-type apparatus installed on a beamline NE7A at PF-AR, KEK and a deformation-DIA apparatus installed on a beamline BL04B1 at SPring-8. Using polycrystalline bcc-iron as a starting material, deformation experiments were carried out at pressure of 16.9-22.6 GPa, temperature of 423-873 K, and strain rate of $0.2–5.2\times10^{-5}$ s^{-1}. Stress and strain during deformation were determined based on two-dimensional X-ray diffraction and X-radiography, respectively, using monochromatized synchrotron X-ray with energy of 60 keV.
A preliminary analysis of the observed data suggests that power-law dislocation creep with stress exponent of ~5 is dominant at >700 K whereas power-law breakdown occurs at lower temperatures. Extrapolation of the data based on homologous temperature scaling suggests that viscosity of hcp-iron at the inner core conditions is ~10^{21} Pa s or higher.

Keywords: hcp-iron, inner core, rheology

©2019. Japan Geoscience Union. All Right Reserved.

[J] Poster | S (Solid Earth Sciences)：S-CG Complex & General

Tue. May 28, 2019 3:30 PM - 5:00 PM JST | Tue. May 28, 2019 6:30 AM - 8:00 AM UTC | Poster Hall International Exhibition Hall8, Makuhari Messe_20

[S-CG54] Rheology, fracture and friction in Earth and planetary sciences

convener:Miki Tasaka(Shimane University), Osamu Kuwano(Japan Agency for Marine-Earth Science and Technology), Ichiko Shimizu(Division of Earth and Planetary Sciences, Graduate School of Science, Kyoto University), Hidemi Ishibashi(Faculty of Science, Shizuoka University)

The aim of this session is to join people from various research area in the earth and planetary sciences and to stimulate discussion beyond the boundaries of each research area. Our goal is to deepen our understanding of dynamics in geosciences by looking over whole areas in the earth and planetary sciences from the viewpoint of PHYSICS OF DEFORMATION, FLOW, AND FRACTURE. We welcome any field (e.g., earthquake, volcano, earth surface, crust, mantle and the core, and other planets and satellites) and any approach (e.g., laboratory experiments, numerical simulations, field observations, and theories).

[SCG54-P01] First-principles study on frictional characteristics of gibbsite

*Hanaya Okuda[1], Kenji Kawai[1], Hiroshi Sakuma[2] (1.Department of Earth and Planetary Science, School of Science, University of Tokyo, 2.Research Center for Functional Materials, National Institute for Materials Science)

[SCG54-P02] Feasibility Study of Morphological Characterization to Comminuted Particles by A Particle Characterization Approach (4)

*Daisuke Sasakura[1], Osamu Kuwano[2] (1.MalvernPanalytical Japan ,Div of Spectris Co.Ltd,., 2.JAMSTEC)

[SCG54-P03] Rheological property of basaltic lava at rigid-deformable transition

*Akio Goto[1] (1.Center for Northeast Asian Studies, Tohoku University)

[SCG54-P04] Cataclasitic texture in gabbroic xenoliths of the Fuji 1707 eruption, Japan

*Hidemi Ishibashi[1], Yumiko Harigane[2], ATSUSHI YASUDA[3], Natsumi Hokanishi[3] (1.Faculty of Science, Shizuoka University, 2.Geological Survey of Japan, AIST, 3.Earthquake Research Institute, University of Tokyo)

[SCG54-P05] Heterogeneous deformation and intragranular recrystallization in experimentally deformed fossil-bearing limestone

*Nahyeon Kim[1], Miki Takahashi[2], Jin-Han Ree[1], Haemyeong Jung[3] (1.Korea University, 2.Geological Survey of Japan, AIST, 3.Seoul National University)

[SCG54-P06] Development of the geobarometer using size and mineral species dependence of residual pressure of fluid inclusions

*Yuuki Hagiwara[1], Junji Yamamoto[1] (1.Hokkaido University)

[SCG54-P07] Microstructures and misorientation analysis of quartz in the Sanbagawa metamorphic belt, Shikoku, Japan

*Tadamasa Ueda[1], Ichiko Shimizu[1] (1.Division of Earth and Planetary Sciences, Graduate School of Science, Kyoto University)

[SCG54-P08] Microstructural & petrological analysis of peridotite xenolith in Noyama-dake, Shimane prefecture ~ implication of plastic deformation during Japan sea opening

*Miki Tasaka[1], Shunsuke Inagawa[1] (1.Shimane University)

[SCG54-P09] Thermodynamic approach to grain boundary premelting in a binary eutectic system

*Akihiro Tsunoda[1], Yasuko Takei[1], Hatsuki Yamauchi[1] (1.Earthquake Research Institute, The University of Tokyo)

[SCG54-P10] Size effects on hardness and fracture toughness of olivine

*Sanae Koizumi[1], Tohru S Suzuki[2], Takehiko Hiraga[1] (1.Earthquake Research Institute,The University of Tokyo, 2.National Institute for Materials Science)

[SCG54-P11] Dislocation creep of dry orthoenstatite aggregates under high *P-T* conditions

*Yumiko Tsubokawa[1], Tomohiro Ohuchi[1], Yuji Higo[2], Yoshinori Tange[2], Tetsuo Irifune[1] (1.Ehime University Geodynamics Research Center, 2.Japan Synchrotron Radiation Research Institute)

First-principles study on frictional characteristics of gibbsite

*Hanaya Okuda[1], Kenji Kawai[1], Hiroshi Sakuma[2]

1. Department of Earth and Planetary Science, School of Science, University of Tokyo, 2. Research Center for Functional Materials, National Institute for Materials Science

Sheet-structure minerals, which have layered crystal structures, are known to be observed in natural faults (e.g. Chester et al., 2013). The fault slip behaviors are considered to be controlled by the frictional characteristics of sheet-structure minerals because they have lower and diverse friction coefficients than general minerals (Byerlee, 1978; Moore & Lockner, 2004). Recent studies suggested that the low and diverse frictional characteristics of sheet-structure minerals can be estimated by the variation of the potential energy between layers while being sheared (Sakuma et al., 2018; Okuda et al., submitted).

In this study, we focus on the frictional characteristics of two sheet-structure minerals, brucite (magnesium hydroxides) and gibbsite (aluminum hydroxides). Brucite has the friction coefficient of 0.42 and shows stick-slip behavior, whereas gibbsite has the friction coefficient of 0.75 and shows stable sliding (Moore & Lockner, 2004). These two minerals were composed by MgO_6 and AlO_6 octahedral sheets, respectively (Fig. 1). The difference between them was brucite has no vacant site within the octahedral sheet, whereas gibbsite has 1/3 vacancy with in the sheet (Fig. 2). These two octahedral sheets were the main component of phyllosilicates and their influence of crystal structures on frictional characteristics is important for understanding the frictional characteristics of sheet-structure minerals. We theoretically examined the frictional characteristics of brucite in our previous study (Okuda et al., submitted). Here we calculate atomic-scale frictional characteristics of gibbsite using first-principles calculations based on the density functional theory and compare the results of gibbsite with those of brucite.

Preliminary results showed that gibbsite has lower atomic-scale shear stress than brucite. This is because the hydroxyls of gibbsite can be easily moved due to the vacancy within the octahedral sheet of gibbsite and that makes the potential energy low and increases the structural stability while being sheared. On the other hand, the yield strength of gibbsite is 1~2 GPa estimated by Mohs hardness (Mehrotra et al., 2015; Broz et al., 2006). This yield strength is lower then that of brucite (4.0 GPa (Okuda et al., submitted)) and this low yield strength increases the macroscopic friction coefficient when considering the adhesion theory of friction. We will quantitatively discuss the atomic-scale shear stress and yield strength of gibbsite and investigate what controls the difference of frictional characteristics between brucite and gibbsite.

Keywords: Sheet-structure minerals, Crystal structure, Frictional characteristics, Gibbsite, First-principles calculation

©2019. Japan Geoscience Union. All Right Reserved.

Figure 1

Figure 2

Gibbsite ($Al(OH)_3$)

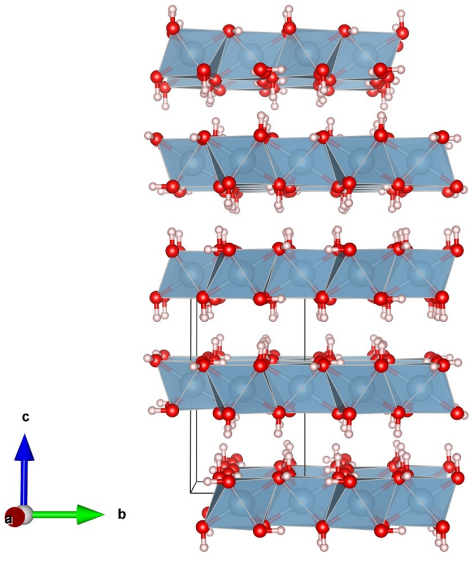

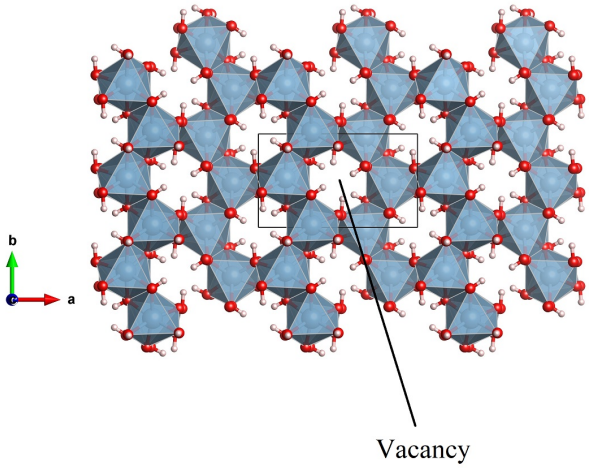

Brucite ($Mg(OH)_2$)

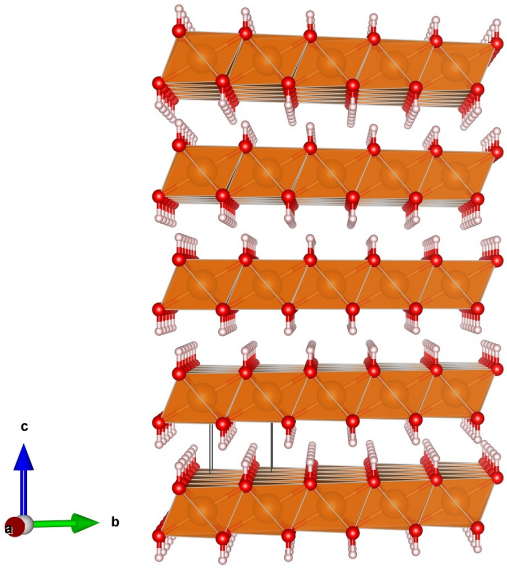

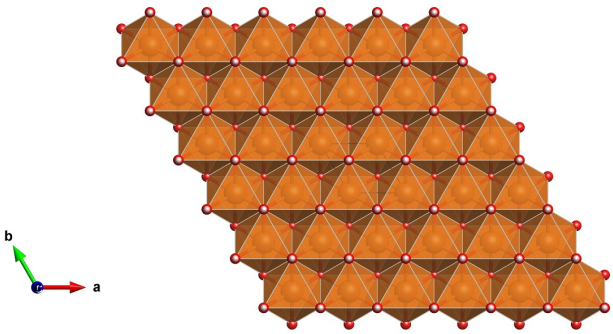

©2019. Japan Geoscience Union. All Right Reserved.

Feasibility Study of Morphological Characterization to Comminuted Particles by A Particle Characterization Approach (4)

*Daisuke Sasakura[1], Osamu Kuwano[2]

1. MalvernPanalytical Japan ,Div of Spectris Co.Ltd,., 2. JAMSTEC

A faults zone contains fine rock powders called gouge that have been ground up by past fault motions. Particle size distribution and particle shape of gouge particles may affect the frictional properties of the fault and reflect the comminution process by the past fault motions. It is well known that particle size distribution (PSD) of fault gouge show power-law distributions. Exponent of this power law is considered to reflect the style and degree of deformation. In this report, we will discuss about the relationship between the PSD and the degree of comminution of model particles by automated particle image analysis and laser diffraction as a particle characterization method.

We did several shear experiments using a rotary shear apparatus with the shear displacement ranges between10mm to 1m. As an automated particle image analysis, Morphologi G3-SE (Malvern Instruments) was used for evaluation of particle size and shape. The observation mode was diascopic mode (Transmittance mode) and a magnification was choose to sufficient to cover 1 to 10,000um. The sample was dispersed with SDU (Sample Dispersion Unit) which attached Morphologi G3-SE. Number of measured particles was over than ten thousand and a parameter filter function on software was used based on shape and pixel number of particle image.

Keywords: Fault gouge, Particle size, Particles Shape, Commutation, Fractal Distributions

©2019. Japan Geoscience Union. All Right Reserved.

Rheological property of basaltic lava at rigid-deformable transition

*Akio Goto[1]

1. Center for Northeast Asian Studies, Tohoku University

The viscosity of Izu Oshima basaltic lava flows, effused from summit crater in 1950-1951 and 1986 eruptions, were estimated from slope angle, thickness and surface velocity with supposed density of the flowing lava (Murauchi, 1950; Minakami, 1951; Shirao, 1986). They seem to be curious in that the viscosity of 1950 lava changed over two orders within 15 ˚C (1.7×10^4 Pa s at 1063 ˚C and 3.3×10^6 Pa s at 1048 ˚C), and 1950 lava at 1048 ˚C had over two orders higher viscosity than 1951 lava at 1038 ˚C (2.3×10^4 Pa s). Minakami (1951) also pointed out that the viscosity from field observation were several tens times higher than the measured viscosity in laboratory by Kani (1934). To solve these paradoxical observation results uniaxial compression viscometry was performed for 1986 LC lava cored cylindrically with 15 mm diameter and 30 mm high (Goto, 2017, JpGU meeting). Contrary to the expectation before the experiment that the viscosity decreases continuously with increasing temperature, the lava became deformable drastically at around 1100 ˚C, which did not seem to be by fluidization but by brittle failure; the middle of the cylindrical core was crushed and their surface skin was pushed out brittly. Below this temperature viscosity changed continuously with temperature, although they were almost at solid state range and much higher than the observed viscosity. These rheological properties were common for other Izu Oshima lavas: 1777 pahoehoe, 1950 aa and two types of 1951 pahoehoe (Goto, 2018, VSJ Fall meeting). A new question arose whether these properties were also common for other basaltic lavas. To confirm it Miyake-jima 1983 lava and Mt. Fuji Kemnarubi 1 (porphyritic) and 2 (aphyric) lavas were newly used for uniaxial compressional viscometry.

Similar deformation was seen for Miyake-jima and Mt. Fuji basaltic lavas, indicating that brittle behavior is common for most, if not all, basaltic lava when the drastic deformation occurs. As was also seen for Izu Oshima lavas the highly deformed sample had enough strength not to separate into pieces after the experiments, indicating melt phase surely existed. Melt composition analysis was impossible for Izu Oshima samples after the uniaxial compression experiments due to dendrite crystallization during cooling (10 ˚C/min); alternatively samples quenched after annealing was used for melt composition analysis to calculate the viscosity using the model by Giordano et al. (2008). The melt phase viscosity scattered within few orders even in each sample, i.e., at the same annealed temperature, due to the variation of the melt composition, and was almost similar with or within few orders higher than the viscosity observed by Murauchi (1950) and Minakami (1951) at the same temperature range. If 1 wt% water was supposed 2 orders viscosity decrease was expected, but high crystallinity (e.g., 50 vol% at 1105 ˚C and 78 vol% at 1095 ˚C in annealed sample) might compensate the viscosity decrease by water or rather heighten the bulk viscosity than observed lava flow viscosity. The mechanism of brittle deformation is not interpreted yet, but high mobility after the brittle deformation may sustain the low bulk viscosity of lava flow, and variation of melt composition at the same temperature may be the source of the above mentioned curious observed viscosity.

Acknowledgements

Mt. Fuji Kenmarubi lavas were provided by Dr. M. Yoshimoto in Mount Fuji Research Institute. This study is supported by grant in aid for cooperative work from Earthquake Research Institute, University of Tokyo.

©2019. Japan Geoscience Union. All Right Reserved.

Keywords: basaltic lava, viscosity, brittle failure

©2019. Japan Geoscience Union. All Right Reserved.

Cataclasitic texture in gabbroic xenoliths of the Fuji 1707 eruption, Japan

*Hidemi Ishibashi[1], Yumiko Harigane[2], ATSUSHI YASUDA[3], Natsumi Hokanishi[3]

1. Faculty of Science, Shizuoka University, 2. Geological Survey of Japan, AIST, 3. Earthquake Research Institute, University of Tokyo

Gabbroic xenoliths are often found in the volcanic products of the 1707 eruption at Fuji volcano, Japan. These xenoliths offer an opportunity to investigate processes occurred in an active magma reservoir. We observed ~300 samples of the gabbroic xenoliths and found several samples which show cataclasitic textures. Cataclasite is typically formed by brittle fracturing associated with a fault. Therefore, the gabbroic xenolths with cataclastic textures may imply interaction between fault and magma plumbing system. In this study, we performed textural observations and chemical analyses of minerals and glasses for the gabbro cataclaseite xenolths to clarify the formation process of the cataclasitic textures.

The gabbro cataclaseite xenolth samples mainly consists of clast and fine-grained matrix, that we also observed a foliated cataclasite at several samples. Mineral assemblage is plagioclase + olivine + pyroxenes + FeTi oxides and interstitial glass is often observed; this is similar to the xenoliths without cataclaseite-like textures. Fine-grained fragmented plagioclase grains sometimes show undulatory extinction whereas less-fragmented coarse plagioclase grains do not show it. Cracks in less-fragmented parts are filled by rhyolitic melt of ~75 wt.% SiO_2. The melt is chemically different from the melt erupted during the 1707 eruption, indicating that the melt is not derived from host magma. In addition, pyroxene reaction rims are found between the melt and olivine, suggesting that the melt was not the product of deformation-induced melting. Plagioclase-hosted melt inclusions in the gabbroic rocks have similar composition with the crack-filling melt. Therefore, the melt was derived from interstitial melt in crystal mush and infiltrated into cracks during formation of cataclastic textures. Compositional relation of FeTi oxide-plagioclase-melt constrains the temperature-water content condition of the crack-filling melt to be ~800 degree C and ~8 wt.%, which is similar to those of melts in the xenoliths without cataclastic textures. Saturation pressure of the water content is calculated to be ~290 MPa, which corresponds to the depth of ~11 km, indicating that the cataclastic textures were formed at the depth.
One of possible causes of the cataclastic textures is the fault at the depth of 5-15 km beneath the SW flank of Fuji volcano. The fault is recognized by Shizuoka-Tobu earthquake occurred at March 15, 2011; the NE edge of the fault is located beneath the vent of the 1707 eruption, implying interaction between the fault and the magma plumbing system of the 1707 eruption. However, the estimated temperature for the gabbro is higher than that at which a tectonic earthquake occurs. Alternatively, deformation of magma reservoir, associated with magma supply and/or compaction of crystal mush, may induce strain localization and local fault movement, resulting in the formation of the cataclastic textures in gabbros.

Keywords: Gabbro, Cataclasitic texture, xenliths, Fuji volcano

©2019. Japan Geoscience Union. All Right Reserved.

Heterogeneous deformation and intragranular recrystallization in experimentally deformed fossil-bearing limestone

*Nahyeon Kim[1], Miki Takahashi[2], Jin-Han Ree[1], Haemyeong Jung[3]

1. Korea University, 2. Geological Survey of Japan, AIST, 3. Seoul National University

Deformation of rocks is heterogeneous particularly when constituent minerals have significant difference in crystallography and/or grain size. Recrystallized grains usually develop from the intragranular region of calcite porphyroclasts in natural shear zones, leading to grain-size reduction and thereby causing rheological change of deforming. However, detailed processes of the intragranular recrystallization and microfabric evolution still remain unclear. To investigate the intragranular recrystallization processes we performed experimental deformation on fossil-bearing limestone using triaxial testing machine. The fossils in the limestone are mainly crinoids and trilobites. The crinoids mostly occur as monocrystalline calcites with larger grain size (700 μm) than that of the matrix (tens μm). In contrast, the trilobites occur as polycrystalline calcites with their grain size (7 μm) much finer than that of matrix. The experiments were performed at temperatures of 500 ~700 ℃, strain rate of 10^{-4}~10^{-5} s^{-1}, confining pressure of 200 MPa and axial strain of up to 30 %. Our strain analyses show that bulk strain is more accommodated in the fine-grained calcites with increase in temperature. In deformed fine-grained calcites of trilobites, fabric strength becomes much weaker with increasing temperature and some grain growth occurs forming equant shape of grains with straight boundaries. These suggest that intergranular process is important in fine-grained calcites of trilobites. In contrast, dynamic recrystallization occurs within the monocrystalline fossil domain of deformed crinoids. The recrystallized grains develop along or near e-twin boundaries and have similar grain size to that of the subgrains (30 μm) formed adjacent to e-twin boundaries. There is a strong correlation of misorientation distribution between the recrystallized grains and e-twin boundaries, suggesting that the intragranular recrystallization in the crinoid fossil is dominated by rotation recrystallization along e-twin boundaries, resulting in misorientation inheritance from the e-twin boundaries. Thus, e-twin boundaries play an important role in intragranular recrystallization processes and grain-size reduction of deforming calcites.

Keywords: Rock deformation, Fossil-bearing limestone, Intragranular recrystallization

©2019. Japan Geoscience Union. All Right Reserved.

Development of the geobarometer using size and mineral species dependence of residual pressure of fluid inclusions

*Yuuki Hagiwara[1], Junji Yamamoto[1]

1. Hokkaido University

Accurate measurements of the residual pressure of the fluid inclusions at given temperature has a potential to guess the depth provenance and *P–T–t* path of the rocks from the equilibrium temperature of the rocks and the equation of state of the fluid (Levresse et al. 2016; Oglialoro et al. 2017). Since this method does not depend on mineral species, it can also be applied to rocks which cannot use conventional geobarometer based on the mineral composition. Furthermore, since fluid density quickly responds to ambient temperature and pressure change, it is possible to trace a phenomenon on a short time scale. Although the existence of mineral species and size dependence of residual pressure (Yamamoto et al. 2008; Campione 2018) has been pointed out, but its geological significance is not well understood. Therefore, in this study, we measured the residual pressure of the fluid inclusions in the various mineral species by Raman spectroscopy, and discussed the possibilities of fluid density variations as the geothermometer, geobarometer, and geospeedmeter.

However, in order to assess re-equilibration processes of the fluid inclusions, it is necessary to obtain physicochemical information of fluid inclusions of various sizes including very small ones since the fluid retentivity depends on the sizes of the fluid inclusions (Bodnar et al., 1989; Doppler et al., 2013; Campione, 2018). Particularly with respect to the residual pressure, the most reliable size range of fluid inclusions for density calculation is close to the submicrometer level since the smaller the fluid inclusions are, the higher the pressure retentivity is (Bodnar et al., 1989; Wanamaker et al., 1990; Campione et al., 2015; Campione, 2018). Although microthermometry is available to determine the residual pressure of H_2O–CO_2 fluid inclusions (Bakker and Diamond, 2000), for fluid inclusion smaller than ~5 μm and/or those in which the CO_2 liquid and vapor homogenize to the vapor phase upon heating, it is difficult to estimate the internal pressure of the fluid accurately (Rosso and Bodnar, 1995; Kobayashi et al., 2012).

Alternatively, in order to measure the residual pressure of the smaller fluid inclusions, several previous studies have described the application of Raman spectroscopy for quantitative analysis of the residual pressure for various fluid composition. Several groups have improved CO_2 barometers (densimeters) and shown the pressure (density) dependence of the wave number difference (Δ) between the two large peaks of the Raman spectrum of CO_2 (e.g. Hagiwara et al. 2018). In case of H_2O–CO_2 mixture, relationship between Δ and pressure (density) can be altered since some H_2O will be dissolved in the CO_2 depending on fluid pressure even at ambient temperature. However, how the H_2O affects the CO_2 peak positions is still unknown. Practically, some studies have shown that other fluids in a gas mixture affect the Raman spectral features of Δ (Seitz et al. 1996; Lamadrid et al. 2018). Therefore, we experimentally confirmed that the Raman based CO_2 barometer can extend to high pressure H_2O–CO_2 system that may be encountered in natural systems, which is common in fluid inclusions in mantle xenoliths (Roedder, 1984; Frezzotti et al., 2012). By using this method, we measured the residual pressure of fluid inclusions in submicron to 10 μm in mantle xenoliths.

Raman spectra were acquired using excitation by a diode pumped solid-state laser (532 nm, Gem 532; Laser Quantum), and using a spectrometer with 75 cm focal length (Acton SP-2750; Princeton Instruments, Inc.) and a CCD camera (1650 ×200 pixels, 16 μm width, iVac; Andor Technology). The

©2019. Japan Geoscience Union. All Right Reserved.

laser power was ~10 mW at the sample. The respective sizes and depths of the fluid inclusions were measured using a 2000× objective (VH-ZST; Keyence Co.) with a digital microscope (VHX-5000; Keyence Co.). The fluid inclusion size was measured automatically by identifying the outline of a fluid inclusion using the brightness contrast.
The results show that the residual pressure of the fluid inclusion systematically changes depending on the diameter of the fluid inclusion, and the smaller the fluid inclusions are, the higher the pressure retentivity is. Furthermore, the absolute value of the residual pressure retained by the mineral species are also different. Based on these data, we discuss the cause of the variation of the residual pressure of the fluid inclusions from the viewpoint of the brittleness, elasticity and plasticity characteristics of the fluid inclusion-host mineral system.

Keywords: Fluid inclusion, Raman spectroscopy, Geobarometer, Mantle xenolith

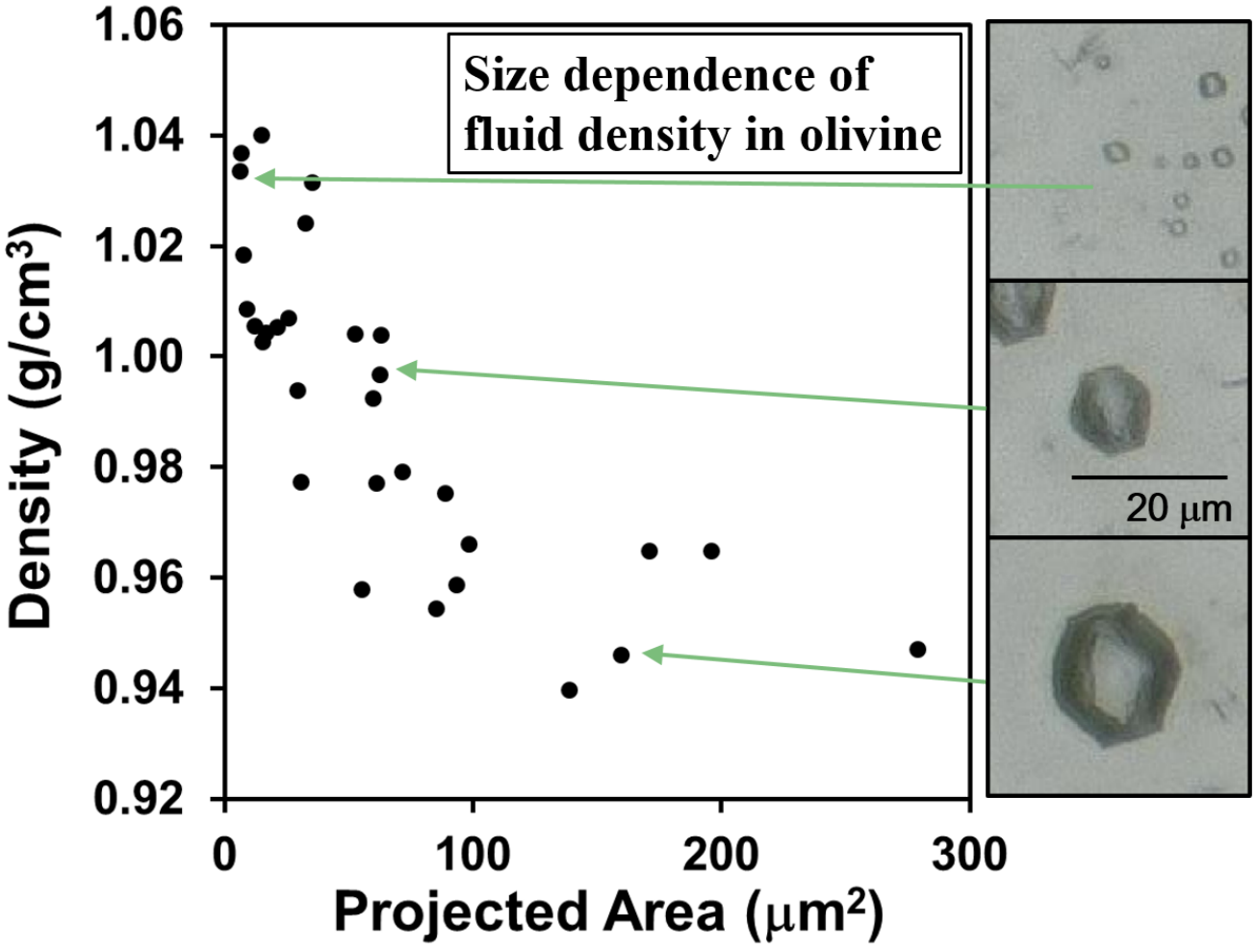

©2019. Japan Geoscience Union. All Right Reserved.

Microstructures and misorientation analysis of quartz in the Sanbagawa metamorphic belt, Shikoku, Japan

*Tadamasa Ueda[1], Ichiko Shimizu[1]

1. Division of Earth and Planetary Sciences, Graduate School of Science, Kyoto University

It was previously revealed that quartz grains in the Sanbagawa metamorphic belt show microstructures of subgrain rotation and strain-driven grain migration irrespective of metamorphic grades along Asemi river route (Ueda and Shimizu, 2018 JpGU). This study scrutinized intracrystalline misorientation of quartz to investigate the subgrain rotation process in the schists, using electron back-scattered diffraction (EBSD) maps obtained by the previous study.

To extract boundaries in single grains from the total data set, the misorientation analysis was conducted by making data sets of grains that are larger than about 9 times the mapping step sizes and are not in contact with each other. The grain detection before this procedure was conducted with 12˚ threshold excluding dauphine-twin boundaries. Such extraction of grains was conducted for a few times for each thin section so that the sum of the data sets covers most (>~80% in area) of indexed quartz grains and no quartz grain is duplicated in the data sets. To eliminate boundaries arising from dauphine-twin-type misindexed grains, the grains smaller than 5 times the mapping step sizes that occur in grain detection without excluding dauphine-twin boundaries were excluded from the data set.

Samples showed the following features irrespective of metamorphic grades. Misorientation angle distributions show two peaks; one is at low angles (<10˚) and the other is at 60˚. Boundaries with 30-40˚ misorientation are nearly absent and those with >65˚ misorientation are absent. The frequency of misorientation gradually decreases from low angle to ~30˚, gradually increases from ~45˚ to 60˚, and rapidly decreases above 60˚. In the crystal coordinate system, misorientation axis distributions of <~12˚ misorientation show weak concentration about c-axis and do not show concentration about the pole to the m planes, even though most samples show c-axis concentration subnormal to the foliation. Compared to the concentration of low-angle misorientation axis about c-axis, misorientation axis distributions of ~15-40˚ generally show concentration off the c-axis direction. Misorientation axis distributions of 45-65˚ show strong concentration at the direction of c-axis. Grains with c-axis nearly normal to the foliation show weaker concentration of misorientation axis of low-angle boundaries about c-axis than grains with c-axis parallel to the foliation and perpendicular to the lineation, but general characteristics of misorientation in crystal coordinate system are similar. In the sample coordinate system, misorientation axis distribution of <~12˚ show weak concentration about the direction parallel to the foliation and perpendicular to the lineation for samples in which flattened planes of quartz grains are subparallel to the foliation. For samples in which flattened planes of quartz are at high angle (>~45˚) to the foliation, misorientation axes of <~12˚ are weakly concentrated about the direction subparallel to the quartz flattening plane and perpendicular to the lineation.

©2019. Japan Geoscience Union. All Right Reserved.

The misorientation angle distributions and misorientation axis distributions indicate that the misorientation of boundaries formed solely by subgrain rotation is less than ~40° and high angle boundaries of ~45-60° are formed by the combination of dauphine twinning and subgrain rotation. The weak concentration of misorientation axes about c-axis for low angle boundaries, which implies prism-a slip, is enigmatic, considering most samples show c-axis concentration nearly perpendicular to the foliation, which is generally interpreted as basal-a slip. However, the coexistence of the misorientation feature and c-axis fabric may be justified, considering that subgrain boundaries are annealed dislocation structures and that most dislocations in crystals suffering steady-state deformation are generally supposed to be forest dislocations. Misorientation axis of subgrain boundaries may indicate rather subsidiary slip systems than main ones.

Keywords: Quartz, Dislocation creep, EBSD, Subgrain rotation, Sanbagawa metamorphic belt, Misorientation analysis

©2019. Japan Geoscience Union. All Right Reserved.

Microstructural & petrological analysis of peridotite xenolith in Noyama-dake, Shimane prefecture ~ implication of plastic deformation during Japan sea opening

*Miki Tasaka[1], Shunsuke Inagawa[1]

1. Shimane University

A number of Cenozoic ultramafic xenoliths are located on the southwest Japan arc. In this study, we conducted microstructural and petrological analyses using peridotite xenoliths in Noyama-dake, Shimane prefecture. These microstructural and petrological results imply that these textures are formed by plastic deformation during Japan Sea opening (=15 Ma) with various stress conditions before Noramadake eruption (~7 Ma).

The microstructure of peridotites is classified into three types, including (1) coarse-grained equigranular texture (~ 1mm), (2) fine-grained texture (~50 um), and (3) large- and fine-grained fractured texture. Based on electron backscattered diffraction (EBSD) analysis, the olivine crystals in (1) coarse-grained equigranular texture and (2) fine-grained texture have a crystallographic preferred orientation (CPO), indicating plastic deformation with various stress condition. Straight cracks are observed in large olivine grains in (3) large- and fine-grained fractured texture. Basaltic melt and fine-grained olivine aggregates with CPO intrude in these cracks. These features indicate that large- and fine-grained fractured texture results from brittle-ductile deformation during volcanic eruption.

Based on electron probe micro analyzer (EPMA), (1) coarse-grained equigranular texture has origin of residual mantle, whereas (2) fine-grained texture and (3) large- and fine-grained fractured textures are originated from cumulus mantle. Two pyroxene geothermometer indicates that the rock has equilibrium temperature T ~ 1200C, resulting from high temperature at the pressure of spinel stability field (P ~ 1 to 2 GPa).

Keywords: peridotite xenolith, Japan sea opening

©2019. Japan Geoscience Union. All Right Reserved.

Thermodynamic approach to grain boundary premelting in a binary eutectic system

*Akihiro Tsunoda[1], Yasuko Takei[1], Hatsuki Yamauchi[1]

1. Earthquake Research Institute, The University of Tokyo

The structure of a weak asthenosphere and a rigid lithosphere constitutes the essential element of plate tectonics. The weakness of asthenosphere has been attributed to the partial melting of rocks. However, in the recent experimental study by using a rock analogue (borneol + diphenylamine binary eutectic system), anelastic relaxation and viscous creep were significantly enhanced from just below the eutectic temperature, where melt does not exist (Yamauchi and Takei, 2016). The mechanisms of anelasticity and viscosity are related to grain boundary sliding and grain boundary diffusion respectively, which implies that thesechanges in the mechanical properties resulted from the changes in grain boundary properties. That means that the “weak asthenosphere” can be explained by “weak grain boundaries” at near solidus temperatures without invoking melt. However, the mechanism causing the change in grain boundary properties is unclear.

In the areas of material science and physics, it is known that the grain boundary is disordered just below the melting temperature or solidus, which is called grain boundary premelting. The results of experiment are expected to be explained by grain boundary premelting. In this study, we investigate the possible occurrence of grain boundary premelting in the upper mantle and its effects on the mechanical properties of rock by using a theoretical model developed in these areas.

In this study, we use a thermodynamic model called phase-field model. We consider a two component bicrystal containing a single grain boundary at x=0. Tang et al. (2006) modeled this system by using three field parameters, composition c(x), crystal orientation θ(x), and crystallinity η(x).(η is sometimes called order parameter or phase-field parameter.) Using the theory of Cahn and Hilliard (1958), they phenomenologically derived the free energy of this nonuniform system as a function of c(x), θ(x), and η(x). By calculating the condition which minimize the free energy, we can predict the equilibrium composition and crystallinity of the grain boundary as functions of temperature. Occurrence of grain boundary premelting can be predicted as an increase in grain boundary disorder (decrease in η at x=0) near the eutectic temperature. We investigate the effects of various model parameters, such as melting temperature, melting enthalpy, and grain boundary misorientation, on the grain boundary crystallinity.

Keywords: premelting, phase-field model

©2019. Japan Geoscience Union. All Right Reserved.

Size effects on hardness and fracture toughness of olivine

*Sanae Koizumi[1], Tohru S Suzuki[2], Takehiko Hiraga[1]

1. Earthquake Research Institute,The University of Tokyo, 2. National Institute for Materials Science

We conducted Vickers indentation tests on Fe-free (Mg_2SiO_4) and Fe-bearing ($Mg_{1.8}Fe_{0.2}SiO_4$) olivine. Their single crystals and highly-dense polycrystalline materials with various average grain sizes (d) from 170 to 890 nm were tested. The largest Vickers microhardness (H_v) of 18 GPa at the lowest load of 0.1 N, which corresponds an indentation depth (h) of 0.6 μm was measured from the polycrystalline material with the finest grain size. The H_v decreases with increasing d and h, both of which are represented by $H_v \propto l^x$ where l corresponds to both sizes with a common x value of ~0.09. The relationship no longer holds at of > 4 μm and of > 1 μm where H_v take constant values of ~9.5 and ~8 GPa for Fe-free and Fe-bearing olivine, respectively. Fracture toughness (K_{IC}) measured from indentation diagonal size and length of cracks radiated outward from the indentation corners is ~0.8 MPa・$m^{1/2}$ for the polycrystalline materials, whose value does not change with the applied load, and olivine chemistry and grain size. The single crystals exhibit lower and orientation dependent toughness from 0.4 to 0.7 MPa・$m^{1/2}$.

Keywords: Olivine, Hardness, Fracture toughness, Indentation size effect, Grain size effect

©2019. Japan Geoscience Union. All Right Reserved.

Dislocation creep of dry orthoenstatite aggregates under high *P-T* conditions

*Yumiko Tsubokawa[1], Tomohiro Ohuchi[1], Yuji Higo[2], Yoshinori Tange[2], Tetsuo Irifune[1]

1. Ehime University Geodynamics Research Center, 2. Japan Synchrotron Radiation Research Institute

Large-scale tectonic processes such as subduction of slabs depend critically on the rheological behaviour of major mantle minerals. Because olivine is the most dominant mineral under the lithospheric conditions, viscosity of dry olivine have been considered to control the strength of the oceanic lithosphere. However, this assumption needs to be reconsidered because olivine is too strong to allow the operation of plate tectonics (Kohlstedt et al., 1995). Ohuchi et al. (2011) showed that orthoenstatite, the second most abundant mineral, could be much weaker than olivine at lithospheric temperatures. Creep strength of polycrystalline orthoenstatite needs to be considered when we discuss the strength of lithosphere because mechanical data on single crystals give the upper/lower limits of the strength of orthoenstatite.

In order to determine the flow-law parameters for dislocation creep of orthoenstatite under the lithospheric conditions, deformation experiments of dry orthoenstatite aggregates were conducted at high temperatures (up to 1473 K) and high pressures (1.8-4.7 GPa) using a deformation DIA (D-DIA) apparatus combined with synchrotron X-ray radiation. Orthoenstatite aggregates, fabricated from powdered natural single crystals, were fired under controlled oxygen fugacity conditions near the FMQ-buffer to remove dissolved water in the samples. Applied differential stress and axial strain were measured using monochromatic X-ray diffraction patterns of orthoenstatite and radiograph images, respectively.

At a constant strain rate ranging from 7.7×10^{-6} to 5.2×10^{-5} s^{-1} , a steady-state creep strength (200-1200 MPa) was achieved at a strain higher than 4% during the uniaxial compression. The water content of samples was mostly less than 50 ppm (H/Si) through a sample deformation. Steady-state creep strength at each experimental conditions followed the power-law dislocation creep with the stress exponent n~3. TEM observations showed development of dislocations with the Burgers vector of either [001] or [0kl] in the recovered samples. The n and the activation energy (Q^* ~170 kJ/mol) , and Burgers vector determined in this study are comparable to those for the [001](010) slip system of dry orthoenstatite (Ohuchi et al., 2011). Viscosity of dry orthoenstatite is ~10 times lower than that of dry olivine (calculated from the flow law by Karato and Jung, 2003) under our experimental conditions (in the case of uniform stress at lithospheric conditions), suggesting that operation of plate tectonics is possible if the strength of a subducting slab is controlled by orthoenstatite.

Keywords: Deformation experiments, Orthoenstatite, Dislocation creep, Lithosphere

©2019. Japan Geoscience Union. All Right Reserved.

[J] Poster | S (Solid Earth Sciences)：S-CG Complex & General

Tue. May 28, 2019 5:15 PM - 6:30 PM JST | Tue. May 28, 2019 8:15 AM - 9:30 AM UTC | Poster Hall International Exhibition Hall8, Makuhari Messe_36

[S-CG54] Rheology, fracture and friction in Earth and planetary sciences

convener:Miki Tasaka(Shimane University), Osamu Kuwano(Japan Agency for Marine-Earth Science and Technology), Ichiko Shimizu(Division of Earth and Planetary Sciences, Graduate School of Science, Kyoto University), Hidemi Ishibashi(Faculty of Science, Shizuoka University)

The aim of this session is to join people from various research area in the earth and planetary sciences and to stimulate discussion beyond the boundaries of each research area. Our goal is to deepen our understanding of dynamics in geosciences by looking over whole areas in the earth and planetary sciences from the viewpoint of PHYSICS OF DEFORMATION, FLOW, AND FRACTURE. We welcome any field (e.g., earthquake, volcano, earth surface, crust, mantle and the core, and other planets and satellites) and any approach (e.g., laboratory experiments, numerical simulations, field observations, and theories).

[SCG54-P01] First-principles study on frictional characteristics of gibbsite

*Hanaya Okuda[1], Kenji Kawai[1], Hiroshi Sakuma[2] (1.Department of Earth and Planetary Science, School of Science, University of Tokyo, 2.Research Center for Functional Materials, National Institute for Materials Science)

[SCG54-P02] Feasibility Study of Morphological Characterization to Comminuted Particles by A Particle Characterization Approach (4)

*Daisuke Sasakura[1], Osamu Kuwano[2] (1.MalvernPanalytical Japan ,Div of Spectris Co.Ltd,., 2.JAMSTEC)

[SCG54-P03] Rheological property of basaltic lava at rigid-deformable transition

*Akio Goto[1] (1.Center for Northeast Asian Studies, Tohoku University)

[SCG54-P04] Cataclasitic texture in gabbroic xenoliths of the Fuji 1707 eruption, Japan

*Hidemi Ishibashi[1], Yumiko Harigane[2], ATSUSHI YASUDA[3], Natsumi Hokanishi[3] (1.Faculty of Science, Shizuoka University, 2.Geological Survey of Japan, AIST, 3.Earthquake Research Institute, University of Tokyo)

[SCG54-P05] Heterogeneous deformation and intragranular recrystallization in experimentally deformed fossil-bearing limestone

*Nahyeon Kim[1], Miki Takahashi[2], Jin-Han Ree[1], Haemyeong Jung[3] (1.Korea University, 2.Geological Survey of Japan, AIST, 3.Seoul National University)

[SCG54-P06] Development of the geobarometer using size and mineral species dependence of residual pressure of fluid inclusions

*Yuuki Hagiwara[1], Junji Yamamoto[1] (1.Hokkaido University)

[SCG54-P07] Microstructures and misorientation analysis of quartz in the Sanbagawa metamorphic belt, Shikoku, Japan

*Tadamasa Ueda[1], Ichiko Shimizu[1] (1.Division of Earth and Planetary Sciences, Graduate School of Science, Kyoto University)

[SCG54-P08] Microstructural & petrological analysis of peridotite xenolith in Noyama-dake, Shimane prefecture ~ implication of plastic deformation during Japan sea opening

*Miki Tasaka[1], Shunsuke Inagawa[1] (1.Shimane University)

[SCG54-P09] Thermodynamic approach to grain boundary premelting in a binary eutectic system

*Akihiro Tsunoda[1], Yasuko Takei[1], Hatsuki Yamauchi[1] (1.Earthquake Research Institute, The University of Tokyo)

[SCG54-P10] Size effects on hardness and fracture toughness of olivine

*Sanae Koizumi[1], Tohru S Suzuki[2], Takehiko Hiraga[1] (1.Earthquake Research Institute,The University of Tokyo, 2.National Institute for Materials Science)

[SCG54-P11] Dislocation creep of dry orthoenstatite aggregates under high *P-T* conditions

*Yumiko Tsubokawa[1], Tomohiro Ohuchi[1], Yuji Higo[2], Yoshinori Tange[2], Tetsuo Irifune[1] (1.Ehime University Geodynamics Research Center, 2.Japan Synchrotron Radiation Research Institute)

First-principles study on frictional characteristics of gibbsite

*Hanaya Okuda[1], Kenji Kawai[1], Hiroshi Sakuma[2]

1. Department of Earth and Planetary Science, School of Science, University of Tokyo, 2. Research Center for Functional Materials, National Institute for Materials Science

Sheet-structure minerals, which have layered crystal structures, are known to be observed in natural faults (e.g. Chester et al., 2013). The fault slip behaviors are considered to be controlled by the frictional characteristics of sheet-structure minerals because they have lower and diverse friction coefficients than general minerals (Byerlee, 1978; Moore & Lockner, 2004). Recent studies suggested that the low and diverse frictional characteristics of sheet-structure minerals can be estimated by the variation of the potential energy between layers while being sheared (Sakuma et al., 2018; Okuda et al., submitted).

In this study, we focus on the frictional characteristics of two sheet-structure minerals, brucite (magnesium hydroxides) and gibbsite (aluminum hydroxides). Brucite has the friction coefficient of 0.42 and shows stick-slip behavior, whereas gibbsite has the friction coefficient of 0.75 and shows stable sliding (Moore & Lockner, 2004). These two minerals were composed by MgO_6 and AlO_6 octahedral sheets, respectively (Fig. 1). The difference between them was brucite has no vacant site within the octahedral sheet, whereas gibbsite has 1/3 vacancy with in the sheet (Fig. 2). These two octahedral sheets were the main component of phyllosilicates and their influence of crystal structures on frictional characteristics is important for understanding the frictional characteristics of sheet-structure minerals. We theoretically examined the frictional characteristics of brucite in our previous study (Okuda et al., submitted). Here we calculate atomic-scale frictional characteristics of gibbsite using first-principles calculations based on the density functional theory and compare the results of gibbsite with those of brucite.

Preliminary results showed that gibbsite has lower atomic-scale shear stress than brucite. This is because the hydroxyls of gibbsite can be easily moved due to the vacancy within the octahedral sheet of gibbsite and that makes the potential energy low and increases the structural stability while being sheared. On the other hand, the yield strength of gibbsite is 1~2 GPa estimated by Mohs hardness (Mehrotra et al., 2015; Broz et al., 2006). This yield strength is lower then that of brucite (4.0 GPa (Okuda et al., submitted)) and this low yield strength increases the macroscopic friction coefficient when considering the adhesion theory of friction. We will quantitatively discuss the atomic-scale shear stress and yield strength of gibbsite and investigate what controls the difference of frictional characteristics between brucite and gibbsite.

Keywords: Sheet-structure minerals, Crystal structure, Frictional characteristics, Gibbsite, First-principles calculation

©2019. Japan Geoscience Union. All Right Reserved.

Figure 1

Figure 2

Gibbsite ($Al(OH)_3$)

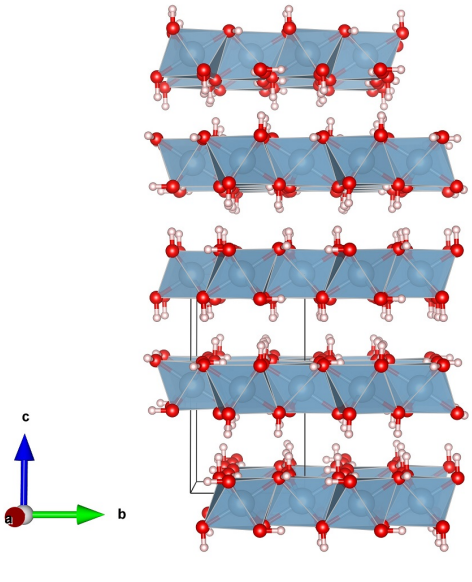

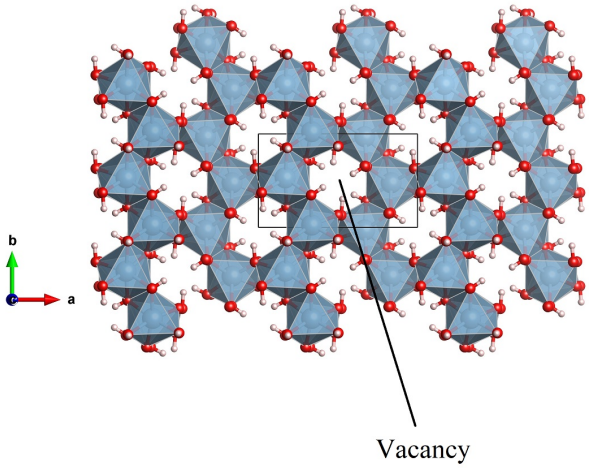

Brucite ($Mg(OH)_2$)

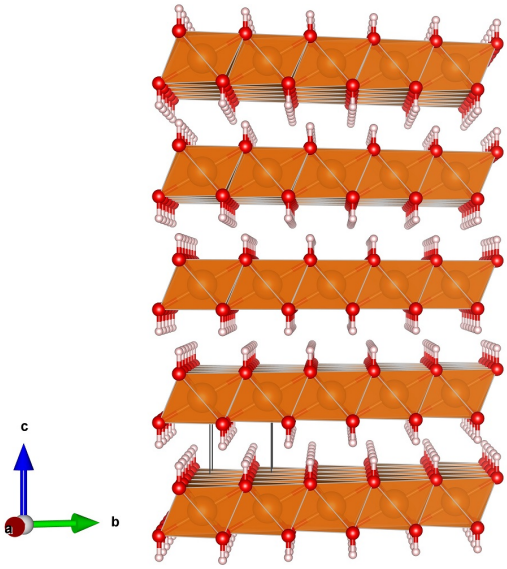

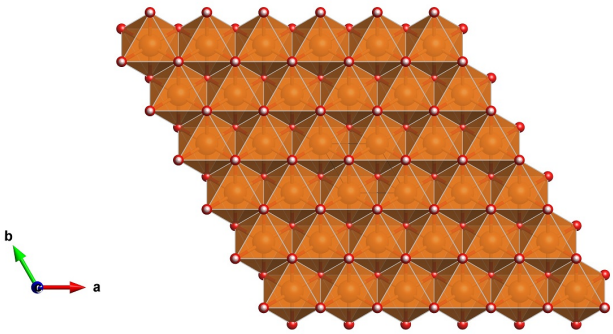

©2019. Japan Geoscience Union. All Right Reserved.

Feasibility Study of Morphological Characterization to Comminuted Particles by A Particle Characterization Approach (4)

*Daisuke Sasakura[1], Osamu Kuwano[2]

1. MalvernPanalytical Japan ,Div of Spectris Co.Ltd,., 2. JAMSTEC

A faults zone contains fine rock powders called gouge that have been ground up by past fault motions. Particle size distribution and particle shape of gouge particles may affect the frictional properties of the fault and reflect the comminution process by the past fault motions. It is well known that particle size distribution (PSD) of fault gouge show power-law distributions. Exponent of this power law is considered to reflect the style and degree of deformation. In this report, we will discuss about the relationship between the PSD and the degree of comminution of model particles by automated particle image analysis and laser diffraction as a particle characterization method.

We did several shear experiments using a rotary shear apparatus with the shear displacement ranges between10mm to 1m. As an automated particle image analysis, Morphologi G3-SE (Malvern Instruments) was used for evaluation of particle size and shape. The observation mode was diascopic mode (Transmittance mode) and a magnification was choose to sufficient to cover 1 to 10,000um. The sample was dispersed with SDU (Sample Dispersion Unit) which attached Morphologi G3-SE. Number of measured particles was over than ten thousand and a parameter filter function on software was used based on shape and pixel number of particle image.

Keywords: Fault gouge, Particle size, Particles Shape, Commutation, Fractal Distributions

©2019. Japan Geoscience Union. All Right Reserved.

Rheological property of basaltic lava at rigid-deformable transition

*Akio Goto[1]

1. Center for Northeast Asian Studies, Tohoku University

The viscosity of Izu Oshima basaltic lava flows, effused from summit crater in 1950-1951 and 1986 eruptions, were estimated from slope angle, thickness and surface velocity with supposed density of the flowing lava (Murauchi, 1950; Minakami, 1951; Shirao, 1986). They seem to be curious in that the viscosity of 1950 lava changed over two orders within 15 ˚C (1.7×10^4 Pa s at 1063 ˚C and 3.3×10^6 Pa s at 1048 ˚C), and 1950 lava at 1048 ˚C had over two orders higher viscosity than 1951 lava at 1038 ˚C (2.3×10^4 Pa s). Minakami (1951) also pointed out that the viscosity from field observation were several tens times higher than the measured viscosity in laboratory by Kani (1934). To solve these paradoxical observation results uniaxial compression viscometry was performed for 1986 LC lava cored cylindrically with 15 mm diameter and 30 mm high (Goto, 2017, JpGU meeting). Contrary to the expectation before the experiment that the viscosity decreases continuously with increasing temperature, the lava became deformable drastically at around 1100 ˚C, which did not seem to be by fluidization but by brittle failure; the middle of the cylindrical core was crushed and their surface skin was pushed out brittly. Below this temperature viscosity changed continuously with temperature, although they were almost at solid state range and much higher than the observed viscosity. These rheological properties were common for other Izu Oshima lavas: 1777 pahoehoe, 1950 aa and two types of 1951 pahoehoe (Goto, 2018, VSJ Fall meeting). A new question arose whether these properties were also common for other basaltic lavas. To confirm it Miyake-jima 1983 lava and Mt. Fuji Kemnarubi 1 (porphyritic) and 2 (aphyric) lavas were newly used for uniaxial compressional viscometry.

Similar deformation was seen for Miyake-jima and Mt. Fuji basaltic lavas, indicating that brittle behavior is common for most, if not all, basaltic lava when the drastic deformation occurs. As was also seen for Izu Oshima lavas the highly deformed sample had enough strength not to separate into pieces after the experiments, indicating melt phase surely existed. Melt composition analysis was impossible for Izu Oshima samples after the uniaxial compression experiments due to dendrite crystallization during cooling (10 ˚C/min); alternatively samples quenched after annealing was used for melt composition analysis to calculate the viscosity using the model by Giordano et al. (2008). The melt phase viscosity scattered within few orders even in each sample, i.e., at the same annealed temperature, due to the variation of the melt composition, and was almost similar with or within few orders higher than the viscosity observed by Murauchi (1950) and Minakami (1951) at the same temperature range. If 1 wt% water was supposed 2 orders viscosity decrease was expected, but high crystallinity (e.g., 50 vol% at 1105 ˚C and 78 vol% at 1095 ˚C in annealed sample) might compensate the viscosity decrease by water or rather heighten the bulk viscosity than observed lava flow viscosity. The mechanism of brittle deformation is not interpreted yet, but high mobility after the brittle deformation may sustain the low bulk viscosity of lava flow, and variation of melt composition at the same temperature may be the source of the above mentioned curious observed viscosity.

Acknowledgements

Mt. Fuji Kenmarubi lavas were provided by Dr. M. Yoshimoto in Mount Fuji Research Institute. This study is supported by grant in aid for cooperative work from Earthquake Research Institute, University of Tokyo.

©2019. Japan Geoscience Union. All Right Reserved.

Keywords: basaltic lava, viscosity, brittle failure

©2019. Japan Geoscience Union. All Right Reserved.

Cataclasitic texture in gabbroic xenoliths of the Fuji 1707 eruption, Japan

*Hidemi Ishibashi[1], Yumiko Harigane[2], ATSUSHI YASUDA[3], Natsumi Hokanishi[3]

1. Faculty of Science, Shizuoka University, 2. Geological Survey of Japan, AIST, 3. Earthquake Research Institute, University of Tokyo

Gabbroic xenoliths are often found in the volcanic products of the 1707 eruption at Fuji volcano, Japan. These xenoliths offer an opportunity to investigate processes occurred in an active magma reservoir. We observed ~300 samples of the gabbroic xenoliths and found several samples which show cataclasitic textures. Cataclasite is typically formed by brittle fracturing associated with a fault. Therefore, the gabbroic xenolths with cataclastic textures may imply interaction between fault and magma plumbing system. In this study, we performed textural observations and chemical analyses of minerals and glasses for the gabbro cataclaseite xenolths to clarify the formation process of the cataclasitic textures.

The gabbro cataclaseite xenolth samples mainly consists of clast and fine-grained matrix, that we also observed a foliated cataclasite at several samples. Mineral assemblage is plagioclase + olivine + pyroxenes + FeTi oxides and interstitial glass is often observed; this is similar to the xenoliths without cataclaseite-like textures. Fine-grained fragmented plagioclase grains sometimes show undulatory extinction whereas less-fragmented coarse plagioclase grains do not show it. Cracks in less-fragmented parts are filled by rhyolitic melt of ~75 wt.% SiO_2. The melt is chemically different from the melt erupted during the 1707 eruption, indicating that the melt is not derived from host magma. In addition, pyroxene reaction rims are found between the melt and olivine, suggesting that the melt was not the product of deformation-induced melting. Plagioclase-hosted melt inclusions in the gabbroic rocks have similar composition with the crack-filling melt. Therefore, the melt was derived from interstitial melt in crystal mush and infiltrated into cracks during formation of cataclastic textures. Compositional relation of FeTi oxide-plagioclase-melt constrains the temperature-water content condition of the crack-filling melt to be ~800 degree C and ~8 wt.%, which is similar to those of melts in the xenoliths without cataclastic textures. Saturation pressure of the water content is calculated to be ~290 MPa, which corresponds to the depth of ~11 km, indicating that the cataclastic textures were formed at the depth.
One of possible causes of the cataclastic textures is the fault at the depth of 5-15 km beneath the SW flank of Fuji volcano. The fault is recognized by Shizuoka-Tobu earthquake occurred at March 15, 2011; the NE edge of the fault is located beneath the vent of the 1707 eruption, implying interaction between the fault and the magma plumbing system of the 1707 eruption. However, the estimated temperature for the gabbro is higher than that at which a tectonic earthquake occurs. Alternatively, deformation of magma reservoir, associated with magma supply and/or compaction of crystal mush, may induce strain localization and local fault movement, resulting in the formation of the cataclastic textures in gabbros.

Keywords: Gabbro, Cataclasitic texture, xenliths, Fuji volcano

©2019. Japan Geoscience Union. All Right Reserved.

Heterogeneous deformation and intragranular recrystallization in experimentally deformed fossil-bearing limestone

*Nahyeon Kim[1], Miki Takahashi[2], Jin-Han Ree[1], Haemyeong Jung[3]

1. Korea University, 2. Geological Survey of Japan, AIST, 3. Seoul National University

Deformation of rocks is heterogeneous particularly when constituent minerals have significant difference in crystallography and/or grain size. Recrystallized grains usually develop from the intragranular region of calcite porphyroclasts in natural shear zones, leading to grain-size reduction and thereby causing rheological change of deforming. However, detailed processes of the intragranular recrystallization and microfabric evolution still remain unclear. To investigate the intragranular recrystallization processes we performed experimental deformation on fossil-bearing limestone using triaxial testing machine. The fossils in the limestone are mainly crinoids and trilobites. The crinoids mostly occur as monocrystalline calcites with larger grain size (700 μm) than that of the matrix (tens μm). In contrast, the trilobites occur as polycrystalline calcites with their grain size (7 μm) much finer than that of matrix. The experiments were performed at temperatures of 500 ~700 ℃, strain rate of 10^{-4}~10^{-5} s^{-1}, confining pressure of 200 MPa and axial strain of up to 30 %. Our strain analyses show that bulk strain is more accommodated in the fine-grained calcites with increase in temperature. In deformed fine-grained calcites of trilobites, fabric strength becomes much weaker with increasing temperature and some grain growth occurs forming equant shape of grains with straight boundaries. These suggest that intergranular process is important in fine-grained calcites of trilobites. In contrast, dynamic recrystallization occurs within the monocrystalline fossil domain of deformed crinoids. The recrystallized grains develop along or near e-twin boundaries and have similar grain size to that of the subgrains (30 μm) formed adjacent to e-twin boundaries. There is a strong correlation of misorientation distribution between the recrystallized grains and e-twin boundaries, suggesting that the intragranular recrystallization in the crinoid fossil is dominated by rotation recrystallization along e-twin boundaries, resulting in misorientation inheritance from the e-twin boundaries. Thus, e-twin boundaries play an important role in intragranular recrystallization processes and grain-size reduction of deforming calcites.

Keywords: Rock deformation, Fossil-bearing limestone, Intragranular recrystallization

©2019. Japan Geoscience Union. All Right Reserved.

Development of the geobarometer using size and mineral species dependence of residual pressure of fluid inclusions

*Yuuki Hagiwara[1], Junji Yamamoto[1]

1. Hokkaido University

Accurate measurements of the residual pressure of the fluid inclusions at given temperature has a potential to guess the depth provenance and *P–T–t* path of the rocks from the equilibrium temperature of the rocks and the equation of state of the fluid (Levresse et al. 2016; Oglialoro et al. 2017). Since this method does not depend on mineral species, it can also be applied to rocks which cannot use conventional geobarometer based on the mineral composition. Furthermore, since fluid density quickly responds to ambient temperature and pressure change, it is possible to trace a phenomenon on a short time scale. Although the existence of mineral species and size dependence of residual pressure (Yamamoto et al. 2008; Campione 2018) has been pointed out, but its geological significance is not well understood. Therefore, in this study, we measured the residual pressure of the fluid inclusions in the various mineral species by Raman spectroscopy, and discussed the possibilities of fluid density variations as the geothermometer, geobarometer, and geospeedmeter.

However, in order to assess re-equilibration processes of the fluid inclusions, it is necessary to obtain physicochemical information of fluid inclusions of various sizes including very small ones since the fluid retentivity depends on the sizes of the fluid inclusions (Bodnar et al., 1989; Doppler et al., 2013; Campione, 2018). Particularly with respect to the residual pressure, the most reliable size range of fluid inclusions for density calculation is close to the submicrometer level since the smaller the fluid inclusions are, the higher the pressure retentivity is (Bodnar et al., 1989; Wanamaker et al., 1990; Campione et al., 2015; Campione, 2018). Although microthermometry is available to determine the residual pressure of H_2O–CO_2 fluid inclusions (Bakker and Diamond, 2000), for fluid inclusion smaller than ~5 μm and/or those in which the CO_2 liquid and vapor homogenize to the vapor phase upon heating, it is difficult to estimate the internal pressure of the fluid accurately (Rosso and Bodnar, 1995; Kobayashi et al., 2012).

Alternatively, in order to measure the residual pressure of the smaller fluid inclusions, several previous studies have described the application of Raman spectroscopy for quantitative analysis of the residual pressure for various fluid composition. Several groups have improved CO_2 barometers (densimeters) and shown the pressure (density) dependence of the wave number difference (Δ) between the two large peaks of the Raman spectrum of CO_2 (e.g. Hagiwara et al. 2018). In case of H_2O–CO_2 mixture, relationship between Δ and pressure (density) can be altered since some H_2O will be dissolved in the CO_2 depending on fluid pressure even at ambient temperature. However, how the H_2O affects the CO_2 peak positions is still unknown. Practically, some studies have shown that other fluids in a gas mixture affect the Raman spectral features of Δ (Seitz et al. 1996; Lamadrid et al. 2018). Therefore, we experimentally confirmed that the Raman based CO_2 barometer can extend to high pressure H_2O–CO_2 system that may be encountered in natural systems, which is common in fluid inclusions in mantle xenoliths (Roedder, 1984; Frezzotti et al., 2012). By using this method, we measured the residual pressure of fluid inclusions in submicron to 10 μm in mantle xenoliths.

Raman spectra were acquired using excitation by a diode pumped solid-state laser (532 nm, Gem 532; Laser Quantum), and using a spectrometer with 75 cm focal length (Acton SP-2750; Princeton Instruments, Inc.) and a CCD camera (1650 ×200 pixels, 16 μm width, iVac; Andor Technology). The

©2019. Japan Geoscience Union. All Right Reserved.

laser power was ~10 mW at the sample. The respective sizes and depths of the fluid inclusions were measured using a 2000× objective (VH-ZST; Keyence Co.) with a digital microscope (VHX-5000; Keyence Co.). The fluid inclusion size was measured automatically by identifying the outline of a fluid inclusion using the brightness contrast.
The results show that the residual pressure of the fluid inclusion systematically changes depending on the diameter of the fluid inclusion, and the smaller the fluid inclusions are, the higher the pressure retentivity is. Furthermore, the absolute value of the residual pressure retained by the mineral species are also different. Based on these data, we discuss the cause of the variation of the residual pressure of the fluid inclusions from the viewpoint of the brittleness, elasticity and plasticity characteristics of the fluid inclusion-host mineral system.

Keywords: Fluid inclusion, Raman spectroscopy, Geobarometer, Mantle xenolith

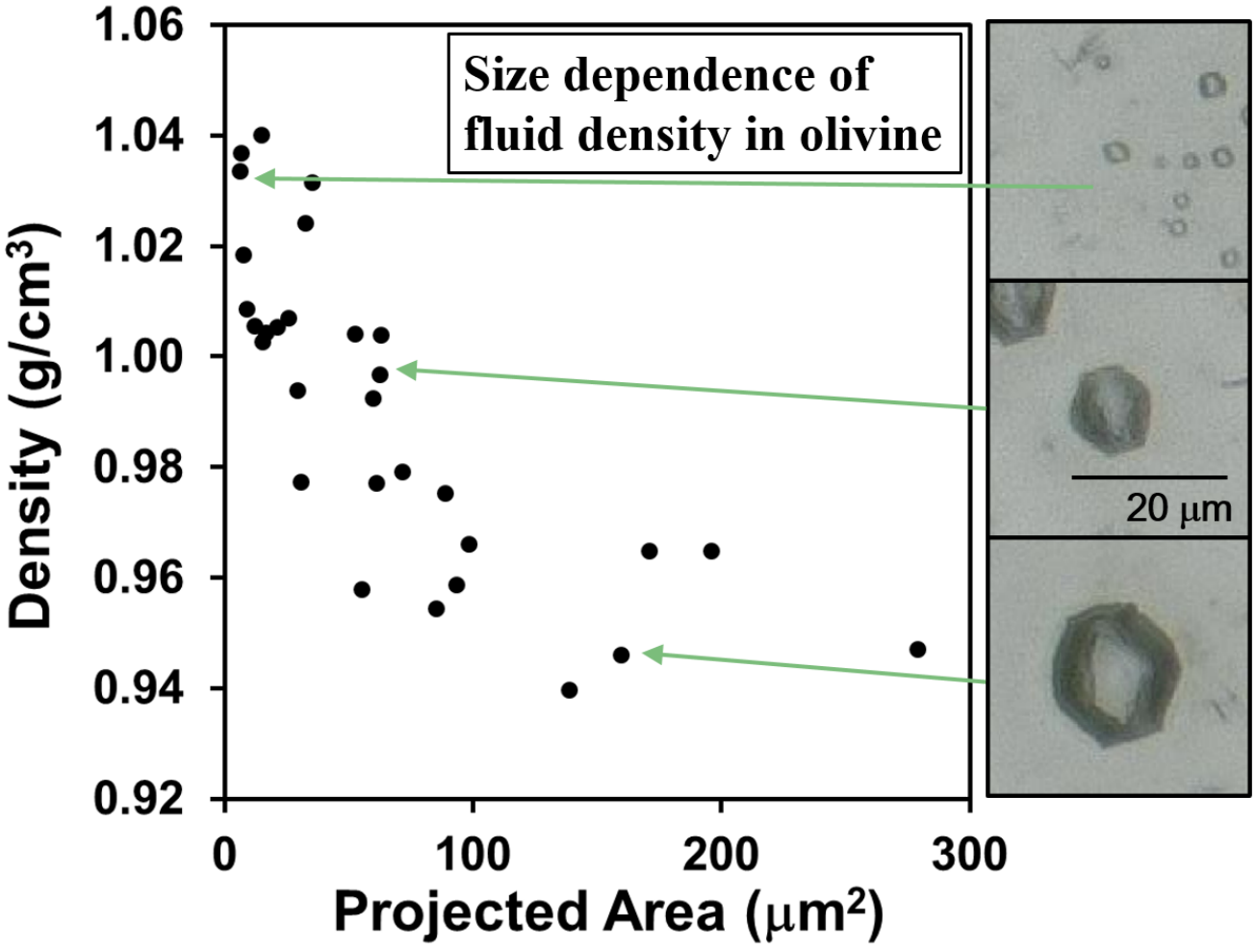

©2019. Japan Geoscience Union. All Right Reserved.

Microstructures and misorientation analysis of quartz in the Sanbagawa metamorphic belt, Shikoku, Japan

*Tadamasa Ueda[1], Ichiko Shimizu[1]

1. Division of Earth and Planetary Sciences, Graduate School of Science, Kyoto University

It was previously revealed that quartz grains in the Sanbagawa metamorphic belt show microstructures of subgrain rotation and strain-driven grain migration irrespective of metamorphic grades along Asemi river route (Ueda and Shimizu, 2018 JpGU). This study scrutinized intracrystalline misorientation of quartz to investigate the subgrain rotation process in the schists, using electron back-scattered diffraction (EBSD) maps obtained by the previous study.

To extract boundaries in single grains from the total data set, the misorientation analysis was conducted by making data sets of grains that are larger than about 9 times the mapping step sizes and are not in contact with each other. The grain detection before this procedure was conducted with 12˚ threshold excluding dauphine-twin boundaries. Such extraction of grains was conducted for a few times for each thin section so that the sum of the data sets covers most (>~80% in area) of indexed quartz grains and no quartz grain is duplicated in the data sets. To eliminate boundaries arising from dauphine-twin-type misindexed grains, the grains smaller than 5 times the mapping step sizes that occur in grain detection without excluding dauphine-twin boundaries were excluded from the data set.

Samples showed the following features irrespective of metamorphic grades. Misorientation angle distributions show two peaks; one is at low angles (<10˚) and the other is at 60˚. Boundaries with 30-40˚ misorientation are nearly absent and those with >65˚ misorientation are absent. The frequency of misorientation gradually decreases from low angle to ~30˚, gradually increases from ~45˚ to 60˚, and rapidly decreases above 60˚. In the crystal coordinate system, misorientation axis distributions of <~12˚ misorientation show weak concentration about c-axis and do not show concentration about the pole to the m planes, even though most samples show c-axis concentration subnormal to the foliation. Compared to the concentration of low-angle misorientation axis about c-axis, misorientation axis distributions of ~15-40˚ generally show concentration off the c-axis direction. Misorientation axis distributions of 45-65˚ show strong concentration at the direction of c-axis. Grains with c-axis nearly normal to the foliation show weaker concentration of misorientation axis of low-angle boundaries about c-axis than grains with c-axis parallel to the foliation and perpendicular to the lineation, but general characteristics of misorientation in crystal coordinate system are similar. In the sample coordinate system, misorientation axis distribution of <~12˚ show weak concentration about the direction parallel to the foliation and perpendicular to the lineation for samples in which flattened planes of quartz grains are subparallel to the foliation. For samples in which flattened planes of quartz are at high angle (>~45˚) to the foliation, misorientation axes of <~12˚ are weakly concentrated about the direction subparallel to the quartz flattening plane and perpendicular to the lineation.

©2019. Japan Geoscience Union. All Right Reserved.

The misorientation angle distributions and misorientation axis distributions indicate that the misorientation of boundaries formed solely by subgrain rotation is less than ~40° and high angle boundaries of ~45-60° are formed by the combination of dauphine twinning and subgrain rotation. The weak concentration of misorientation axes about c-axis for low angle boundaries, which implies prism-a slip, is enigmatic, considering most samples show c-axis concentration nearly perpendicular to the foliation, which is generally interpreted as basal-a slip. However, the coexistence of the misorientation feature and c-axis fabric may be justified, considering that subgrain boundaries are annealed dislocation structures and that most dislocations in crystals suffering steady-state deformation are generally supposed to be forest dislocations. Misorientation axis of subgrain boundaries may indicate rather subsidiary slip systems than main ones.

Keywords: Quartz, Dislocation creep, EBSD, Subgrain rotation, Sanbagawa metamorphic belt, Misorientation analysis

©2019. Japan Geoscience Union. All Right Reserved.

Microstructural & petrological analysis of peridotite xenolith in Noyama-dake, Shimane prefecture ~ implication of plastic deformation during Japan sea opening

*Miki Tasaka[1], Shunsuke Inagawa[1]

1. Shimane University

A number of Cenozoic ultramafic xenoliths are located on the southwest Japan arc. In this study, we conducted microstructural and petrological analyses using peridotite xenoliths in Noyama-dake, Shimane prefecture. These microstructural and petrological results imply that these textures are formed by plastic deformation during Japan Sea opening (=15 Ma) with various stress conditions before Noramadake eruption (~7 Ma).

The microstructure of peridotites is classified into three types, including (1) coarse-grained equigranular texture (~ 1mm), (2) fine-grained texture (~50 um), and (3) large- and fine-grained fractured texture. Based on electron backscattered diffraction (EBSD) analysis, the olivine crystals in (1) coarse-grained equigranular texture and (2) fine-grained texture have a crystallographic preferred orientation (CPO), indicating plastic deformation with various stress condition. Straight cracks are observed in large olivine grains in (3) large- and fine-grained fractured texture. Basaltic melt and fine-grained olivine aggregates with CPO intrude in these cracks. These features indicate that large- and fine-grained fractured texture results from brittle-ductile deformation during volcanic eruption.

Based on electron probe micro analyzer (EPMA), (1) coarse-grained equigranular texture has origin of residual mantle, whereas (2) fine-grained texture and (3) large- and fine-grained fractured textures are originated from cumulus mantle. Two pyroxene geothermometer indicates that the rock has equilibrium temperature T ~ 1200C, resulting from high temperature at the pressure of spinel stability field (P ~ 1 to 2 GPa).

Keywords: peridotite xenolith, Japan sea opening

©2019. Japan Geoscience Union. All Right Reserved.

Thermodynamic approach to grain boundary premelting in a binary eutectic system

*Akihiro Tsunoda[1], Yasuko Takei[1], Hatsuki Yamauchi[1]

1. Earthquake Research Institute, The University of Tokyo

The structure of a weak asthenosphere and a rigid lithosphere constitutes the essential element of plate tectonics. The weakness of asthenosphere has been attributed to the partial melting of rocks. However, in the recent experimental study by using a rock analogue (borneol + diphenylamine binary eutectic system), anelastic relaxation and viscous creep were significantly enhanced from just below the eutectic temperature, where melt does not exist (Yamauchi and Takei, 2016). The mechanisms of anelasticity and viscosity are related to grain boundary sliding and grain boundary diffusion respectively, which implies that thesechanges in the mechanical properties resulted from the changes in grain boundary properties. That means that the “weak asthenosphere” can be explained by “weak grain boundaries” at near solidus temperatures without invoking melt. However, the mechanism causing the change in grain boundary properties is unclear.

In the areas of material science and physics, it is known that the grain boundary is disordered just below the melting temperature or solidus, which is called grain boundary premelting. The results of experiment are expected to be explained by grain boundary premelting. In this study, we investigate the possible occurrence of grain boundary premelting in the upper mantle and its effects on the mechanical properties of rock by using a theoretical model developed in these areas.

In this study, we use a thermodynamic model called phase-field model. We consider a two component bicrystal containing a single grain boundary at x=0. Tang et al. (2006) modeled this system by using three field parameters, composition c(x), crystal orientation θ(x), and crystallinity η(x).(η is sometimes called order parameter or phase-field parameter.) Using the theory of Cahn and Hilliard (1958), they phenomenologically derived the free energy of this nonuniform system as a function of c(x), θ(x), and η(x). By calculating the condition which minimize the free energy, we can predict the equilibrium composition and crystallinity of the grain boundary as functions of temperature. Occurrence of grain boundary premelting can be predicted as an increase in grain boundary disorder (decrease in η at x=0) near the eutectic temperature. We investigate the effects of various model parameters, such as melting temperature, melting enthalpy, and grain boundary misorientation, on the grain boundary crystallinity.

Keywords: premelting, phase-field model

©2019. Japan Geoscience Union. All Right Reserved.

Size effects on hardness and fracture toughness of olivine

*Sanae Koizumi[1], Tohru S Suzuki[2], Takehiko Hiraga[1]

1. Earthquake Research Institute,The University of Tokyo, 2. National Institute for Materials Science

We conducted Vickers indentation tests on Fe-free (Mg_2SiO_4) and Fe-bearing ($Mg_{1.8}Fe_{0.2}SiO_4$) olivine. Their single crystals and highly-dense polycrystalline materials with various average grain sizes (d) from 170 to 890 nm were tested. The largest Vickers microhardness (H_v) of 18 GPa at the lowest load of 0.1 N, which corresponds an indentation depth (h) of 0.6 μm was measured from the polycrystalline material with the finest grain size. The H_v decreases with increasing d and h, both of which are represented by $H_v \propto l^x$ where l corresponds to both sizes with a common x value of ~0.09. The relationship no longer holds at of > 4 μm and of > 1 μm where H_v take constant values of ~9.5 and ~8 GPa for Fe-free and Fe-bearing olivine, respectively. Fracture toughness (K_{IC}) measured from indentation diagonal size and length of cracks radiated outward from the indentation corners is ~0.8 MPa・$m^{1/2}$ for the polycrystalline materials, whose value does not change with the applied load, and olivine chemistry and grain size. The single crystals exhibit lower and orientation dependent toughness from 0.4 to 0.7 MPa・$m^{1/2}$.

Keywords: Olivine, Hardness, Fracture toughness, Indentation size effect, Grain size effect

©2019. Japan Geoscience Union. All Right Reserved.

Dislocation creep of dry orthoenstatite aggregates under high *P-T* conditions

*Yumiko Tsubokawa[1], Tomohiro Ohuchi[1], Yuji Higo[2], Yoshinori Tange[2], Tetsuo Irifune[1]

1. Ehime University Geodynamics Research Center, 2. Japan Synchrotron Radiation Research Institute

Large-scale tectonic processes such as subduction of slabs depend critically on the rheological behaviour of major mantle minerals. Because olivine is the most dominant mineral under the lithospheric conditions, viscosity of dry olivine have been considered to control the strength of the oceanic lithosphere. However, this assumption needs to be reconsidered because olivine is too strong to allow the operation of plate tectonics (Kohlstedt et al., 1995). Ohuchi et al. (2011) showed that orthoenstatite, the second most abundant mineral, could be much weaker than olivine at lithospheric temperatures. Creep strength of polycrystalline orthoenstatite needs to be considered when we discuss the strength of lithosphere because mechanical data on single crystals give the upper/lower limits of the strength of orthoenstatite.

In order to determine the flow-law parameters for dislocation creep of orthoenstatite under the lithospheric conditions, deformation experiments of dry orthoenstatite aggregates were conducted at high temperatures (up to 1473 K) and high pressures (1.8-4.7 GPa) using a deformation DIA (D-DIA) apparatus combined with synchrotron X-ray radiation. Orthoenstatite aggregates, fabricated from powdered natural single crystals, were fired under controlled oxygen fugacity conditions near the FMQ-buffer to remove dissolved water in the samples. Applied differential stress and axial strain were measured using monochromatic X-ray diffraction patterns of orthoenstatite and radiograph images, respectively.

At a constant strain rate ranging from 7.7×10^{-6} to 5.2×10^{-5} s^{-1} , a steady-state creep strength (200-1200 MPa) was achieved at a strain higher than 4% during the uniaxial compression. The water content of samples was mostly less than 50 ppm (H/Si) through a sample deformation. Steady-state creep strength at each experimental conditions followed the power-law dislocation creep with the stress exponent n~3. TEM observations showed development of dislocations with the Burgers vector of either [001] or [0kl] in the recovered samples. The n and the activation energy (Q^* ~170 kJ/mol) , and Burgers vector determined in this study are comparable to those for the [001](010) slip system of dry orthoenstatite (Ohuchi et al., 2011). Viscosity of dry orthoenstatite is ~10 times lower than that of dry olivine (calculated from the flow law by Karato and Jung, 2003) under our experimental conditions (in the case of uniform stress at lithospheric conditions), suggesting that operation of plate tectonics is possible if the strength of a subducting slab is controlled by orthoenstatite.

Keywords: Deformation experiments, Orthoenstatite, Dislocation creep, Lithosphere

©2019. Japan Geoscience Union. All Right Reserved.

[J] Oral | S (Solid Earth Sciences)：S-CG Complex & General

Tue. May 28, 2019 9:00 AM - 10:30 AM JST | Tue. May 28, 2019 12:00 AM - 1:30 AM UTC | Convention Hall A 2F

[S-CG61] Dynamics in mobile belts

convener:Yukitoshi Fukahata(Disaster Prevention Research Institute, Kyoto University), Toru Takeshita(Department of Natural History Sciences, Graduate School of Science, Hokkaido University), Hikaru Iwamori(Geochemical Evolution Research Program, Japan Agency for Marine-Earth Science and Technology), Chairperson:Keisuke Yoshida(東北大学大学院理学研究科 地球物理学専攻), Masaoki Uno(東北大学)

The dynamic behaviours of mobile belts are expressed across a wide range of time scales, from the seismic and volcanic events that impact society during our lifetimes, to orogeny and the formation of large-scale fault systems which can take place over millions of years. Deformation occurs on length scales from microscopic fracture and flow to macroscopic deformation to plate-scale tectonics. To gain a physical understanding of the dynamics of mobile belts, we must determine the relationships between deformation and the driving stresses due to plate motion and other causes, which are connected through the rheological properties of the materials. To understand the full physical system, an integration of geophysics, geomorphology, and geology is necessary, as is the integration of observational, theoretical and experimental approaches. In addition, because rheological properties are greatly affected by fluids in the crust and fluid chemical reactions, petrological and geochemical approaches are also important. After the 2011 great Tohoku-oki earthquake, large-scale changes in seismic activity and regional scale crustal deformation were observed, making present-day Japan a unique natural laboratory for the study of the dynamics of mobile belts. This session welcomes presentations from different disciplines, such as seismology, geodesy, tectonic geomorphology, structural geology, petrology, and hydrology, as well as interdisciplinary studies, that relate to the dynamic behaviours of mobile belts.

9:00 AM - 9:15 AM JST | 12:00 AM - 12:15 AM UTC

[SCG61-13] Deciphering dynamics of thermal events at lithosphere-asthenosphere boundary from peridotite xenoliths of Ichinomegata maar, NE Japan

*Yuto Sato[1], Kazuhito Ozawa[1] (1.Department of Earth and Planetary Science, Graduate School of Science, The University of Tokyo)

9:15 AM - 9:30 AM JST | 12:15 AM - 12:30 AM UTC

[SCG61-14] Experimental investigation of reaction-induced stress and permeability evolution in $MgO–H_2O$ system

*Masaoki Uno[1], Hisamu Kasahara[1], Atsushi Okamoto[1], Noriyoshi Tsuchiya[1] (1.Graduate School of Environmental Studies, Tohoku University)

9:30 AM - 9:45 AM JST | 12:30 AM - 12:45 AM UTC

[SCG61-15] Fluid-Flow, Resistivity and Elastic Wave Velocity Simulation of Digital Rock Fracture and Comparison with Experimental Data

*Kazuki Sawayama[1], Fei Jiang[2], Takuya ISHIBASHI[3], Takeshi Tsuji[4], Yasuhiro Fujimitsu[4] (1.Department of Earth Resources Engineering, Graduate school of engineering, Kyushu University, 2.Department of Mechanical Engineering, Faculty of Engineering, Yamaguchi University, 3.Fukushima Renewable Energy Institute, National Institute of Advanced Industrial Science and Technology, 4.Department of Earth Resources Engineering, Faculty of engineering, Kyushu University)

9:45 AM - 10:00 AM JST | 12:45 AM - 1:00 AM UTC

[SCG61-16] Fluid distribution in the crust – inference from seismic velocity and electrical conductivity

*Tohru Watanabe[1], Kenta Yoshida[2] (1.Gradudate School of Science and Engineering, University of Toyama, 2.Research and Development Center for Ocean Drilling Science, Japan Agency for Marine-earth Science and Technology)

10:00 AM - 10:15 AM JST | 1:00 AM - 1:15 AM UTC

[SCG61-17] The seismological structure about fault zone extending to the lower crust in the northern Kinki district, southwestern Japan

*Shinya Kato[1], Yoshihisa Iio[1], Takuo Shibutani[1], Hiroshi Katao[1], Masayo Sawada[1], Kazuhide Tomisaka[1] (1.Disater Prevention Research Institute, Kyoto University)

10:15 AM - 10:30 AM JST | 1:15 AM - 1:30 AM UTC

[SCG61-18] Inland repeating earthquakes in the vicinity of low frequency earthquakes around Hakodate, Hokkaido

*Keisuke Yoshida[1], Akira Hasegawa[1], Shinako Noguchi[2], Keiji Kasahara[2] (1.Tohoku University, 2. Association for the Development of Earthquake Prediction)

Deciphering dynamics of thermal events at lithosphere-asthenosphere boundary from peridotite xenoliths of Ichinomegata maar, NE Japan

*Yuto Sato[1], Kazuhito Ozawa[1]

1. Department of Earth and Planetary Science, Graduate School of Science, The University of Tokyo

Mantle xenoliths are fragments of mantle materials almost instantaneously transported to the surface by alkali basalt or kimberlite magmas (Nixon, 1987). They are unique in that they record temporal changes of mantle processes in chemical zonings and microstructures of constituent minerals. Thus, such information can potentially constrain time-dependent dynamic processes occurring in the lithosphere-asthenosphere boundary (LAB) zone, where mechanisms of heat and material transfer drastically change (Sleep, 2005, 2006). In this regard, Takahashi (1980) and Koyaguchi (1986) achieved key contributions. They examined chemical zonings of olivine and pyroxenes in spinel peridotite xenoliths from Ichinomegata, a latest Pleistocene andesitic-dacitic maar located in the back-arc side of NE Japan arc (Katsui et al., 1979). They clarified a variety of thermal history that the xenoliths underwent, but processes responsible for the diversity is not resolved yet because the derivation depth was not constrained. We have conducted very careful geothermobarometry of spinel peridotite xenoliths from Ichinomegata maar and successfully reconstructed the thermal, chemical, and rheological structures of the LAB zone beneath NE Japan arc at the time of Ichinomegata maar formation (80-60 ka) (Sato and Ozawa, 2017, 2018, JpGU meeting; Sato and Ozawa, 2016, 2017, AGU fall meeting; see our companion presentation in this meeting). We examined temporal changes of the structures through analyses of chemical zonings of pyroxenes in 9 plagioclase and spinel peridotite xenoliths from Ichinomegata.

In our previous study, the depths and temperatures of 8 of the 9 xenoliths just before the xenolith extraction are estimated to range 28-55 km and 828-1081 ˚C. The mantle beneath Ichinomegata consists of shallow (28-32 km), low temperature, granular (less strained), and amphibole-bearing zone and deep (41-55 km), high temperature, porphyroclastic (strained), and amphibole-free and melt-bearing zone. We identified the shallower zone as lithospheric mantle, the deeper zone as LAB zone, and that their boundary was controlled by wet solidus.

We obtained Ca, Al, Cr, and Ti zonings of large clinopyroxene and orthopyroxene using EPMA at the University of Tokyo and analyzed them with a diffusion model. The zoning patterns of Ca, Al, and Cr of pyroxenes allow us to identify 4 different thermal histories from 4 types of chemical zonings for orthopyroxene (O1-O4) and 3 types for clinopyroxene (C1-C3) as summarized in Table 1. They are (1) continuous cooling at a cooling rate of ~$1x10^{-4}$ ˚C/y over the time scale of ~1-10 million years from ~1000 to ~830 ˚C (constrained from O1 and C1), (2) cooling followed by weak heating at ~900 ˚C over the time scale of ~10-100 thousand years (from O2 and C1), (3) cooling followed by strong heating at ~1050 ˚C over the time scale of ~1-100 thousand years (from O3 and C2), and (4) prolonged cooling and heating at ~1000 ˚C (from O4 and C3). There is a systematic depth variation of thermal histories as summarized in Table 2. It is notable that the shallow lithospheric mantle is characterized by simple cooling or cooling followed by weak heating and the deep LAB zone by cooling followed by strong heating. This systematic depth variation requires a thermal perturbation of asthenospheric mantle beneath the deeper LAB zone, most plausibly asthenospheric upwelling.

The age of the Japan Sea opening is comparable to the time scale of cooling estimated from O1 and C1, and the continuous cooling at the shallow lithospheric mantle is attributable to the cooling of the

©2019. Japan Geoscience Union. All Right Reserved.

back-arc basin lithosphere, The timescale of the heating event in the deep LAB zone is too short to be explained by LAB-fixed heat conduction model. Effective heat transportation mechanisms are necessary, either partial crystallization of melt generated in the asthenosphere that passed through the LAB zone as advocated by Takahashi (1980) or extensive lithosphere thinning.

Keywords: lithosphere-asthenosphere boundary zone, spinel peridotite xenolith, thermal history, chemical zoning

Table 1. Patterns of chemical zonings in orthopyroxene and clinopyroxene.

Zoning type	Patterns of zoning profiles from core to rim		
	Ca	Al	Cr
Orthopyroxene			
O1	simple decrease	simple decrease	
O2	decrease followed by weak increase	decrease followed by weak increase	
		decrease followed by weak increase	simple decrease
O3	decrease followed by intense increase	decrease followed by intense increase	
O4	faint increase	faint decrease	
Clinopyroxene			
C1	simple increase	simple decrease	
C2	simple decrease	simple increase or decrease followed by intense increase	
C3	flat	faint decrease	

Table 2. Depth variations of chemical zoning types of pyroxenes and thermal hisotry.

Sample name	Pressure (GPa)	Depth (km)	Temperature (°C)	Chemical zoning of pyroxenes	
				Types	Decoded thermal history
HK64081206g	0.72 ± .52	28 ± 16	829 ± 23	O1 & C1	Simple cooling.
HK64081206c	0.80 ± .70	30 ± 21	828 ± 30	O1 & C1	Simple cooling.
HK64081206d	(0.82)	(31)	(875)	O2 & C1	Cooling followed by weak heating.
HK66031502	0.85 ± .42	32 ± 13	905 ± 19	O2 & C1	Cooling followed by weak heating.
IC81-5	1.16 ± .29	41 ± 9	1017 ± 15	O4 & C3	Cooling and long heating.
HK64081205a	1.29 ± .24	45 ± 7	1050 ± 12	O3 & C2	Cooling followed by strong heating.
IC81-8	1.46 ± .37	50 ± 11	1052 ± 19	O3 & C2	Cooling followed by strong heating.
HK66031501	1.51 ± .36	52 ± 11	1057 ± 18	O3 & C2	Cooling followed by strong heating.
HK64081205b	1.62 ± .44	55 ± 13	1081 ± 23	O3 & C2	Cooling followed by strong heating.

©2019. Japan Geoscience Union. All Right Reserved.

Experimental investigation of reaction-induced stress and permeability evolution in MgO–H_2O system

*Masaoki Uno[1], Hisamu Kasahara[1], Atsushi Okamoto[1], Noriyoshi Tsuchiya[1]

1. Graduate School of Environmental Studies, Tohoku University

Crustal and mantle hydration reactions at subduction zones accompany large solid volume change as much as several vol.% to several tens of vol.%. Such large solid volume change can generate stress and fractures, accelerate reactions and fluid migrations (e.g., Kelemen and Hirth, 2012), and potentially influence the fluid transport in the crust and mantle (e.g., Jamtveit et al., 2000). Field observations of serpentinization and peridotite carbonation suggest fracture generation and permeability enhancement by such “reaction-induced stress” (e.g., Jamtveit et al., 2008; Plumer et al., 2012). However, the permeability enhancement during hydration reaction have not been reproduced by experiments, and the mechanisms and conditions of permeability enhancement by volume-increasing reactions remain largely unknown.

To understand the controlling mechanisms of fluid flow during hydration reactions, we show one of the first experimental trial to measure the permeability evolution during hydration reactions. We use MgO–H_2O system, where periclase (MgO) react with H_2O to produce brucite ($Mg(OH)_2$). The reaction involves solid volume increase of as much as +119%. Our earlier experiments have revealed that the reaction-induced stress in this system are controlled by the competition of reaction rate and stress-dependent deformation rate, and exceeds 40 MPa in this system which well exceeds the tensile strength of crustal rocks.

In this presentation, we have conducted flow thorough experiments to reveal the permeability evolution during hydration reactions. Experiments were conducted with sintered MgO with 4–14 vol.% porosity, under 100–300˚C with 5–50 MPa confining pressure and 5–15 fluid pressures. Preliminary experiments showed rapid permeability decrease in 2–3 orders, and finally the stainless sleeve broke by the reaction-induced expansion. The rate of permeability decrease is a function of the confining pressure, suggesting that the deformation of the reactant (brucite) has significant control over the permeability evolution during hydration reactions. We will present further experiments with various reaction rate/deformation rate ratios, and discuss the controlling factors of permeability enhancement/reduction during hydration reactions.

[References]

Jamtveit, B., Austrheim., H., Mathe-Sørenssen, A., 2000. *Nature* **408**, 75–78.

Jamtveit, B., Mathe-Sørenssen, A., Kstenko, Olga., 2008. *Earth and Planetary Science Letters* **267**, 620–627.

Kelemen, P.B., Hirth, G., 2012. *Earth and Planetary Science Letters* **345–348**, 81–89.

Plümper O., Røyne, A., Magrasó, A., Jamtveit, B., 2012. *Geology* **40**, 1103–1106.

Keywords: Reaction-induced stress, Reaction-induced fracturing, permeability

©2019. Japan Geoscience Union. All Right Reserved.

Fluid-Flow, Resistivity and Elastic Wave Velocity Simulation of Digital Rock Fracture and Comparison with Experimental Data

*Kazuki Sawayama[1], Fei Jiang[2], Takuya ISHIBASHI[3], Takeshi Tsuji[4], Yasuhiro Fujimitsu[4]

1. Department of Earth Resources Engineering, Graduate school of engineering, Kyushu University, 2. Department of Mechanical Engineering, Faculty of Engineering, Yamaguchi University, 3. Fukushima Renewable Energy Institute, National Institute of Advanced Industrial Science and Technology, 4. Department of Earth Resources Engineering, Faculty of engineering, Kyushu University

Fluid-flow in the fracture plays a key role to evaluate the mechanism of earthquake and fractured reservoirs (e.g., geothermal and shale) since fracture flow constrains the fluid-flow behavior and rock strength under the ground. To predict the fluid-flow and its distribution under the ground, geophysical explorations (seismic and electromagnetic methods) have been broadly applied. However, there is no established rock physical model to estimate the fluid-flow properties (e.g., permeability) in the fracture from resistivity or elastic wave velocity, and thereby fluid-flow behavior in the fracture are difficult to be precisely interpreted by geophysical explorations. For the better interpretation of these exploration data, more detailed investigation about the effect of fluid-flow behavior on resistivity and elastic wave velocity of fractured rocks is required. In this study, in order to discuss this effect, we measured and calculated them by using fractured rock samples which have different apertures.

We conducted laboratory fluid-flow testby using fractured Inada granite (50 mm in a diameter, 80 mm in a length) which have single tensile fracture with different aperture. For the numerical model, we digitalized this real rock fracture (0.1 mm grid resolution) to calculate fluid-flow, resistivity and elastic wave velocity under the same condition with experiment. Three dimensional fracture flow was simulated by using Lattice Boltzmann Method and we applied Finite Element Analysis to calculate resistivity and elastic wave velocity after this fluid-flow simulation.

As a result, permeability decreases with pressure increase under laboratory experiment and calculated permeability also shows the decrease as the aperture increases. This agreement suggests that fracture permeability is constrained by aperture closure due to the pressure effect. From the permeability matching approach, we found that permeability dramatically decreases after the fracture contact area exceeds ~80%. At this threshold value, fluid-flow path, resistivity and elastic wave velocity show inflections. Our results suggest that permeability change caused by aperture closure could be estimated by seismic and electromagnetic explorations.

Keywords: digital rock physics, elastic wave velocity, resistivity, fracture flow, Lattice Boltzmann Method

©2019. Japan Geoscience Union. All Right Reserved.

Fluid distribution in the crust –inference from seismic velocity and electrical conductivity

*Tohru Watanabe[1], Kenta Yoshida[2]

1. Gradudate School of Science and Engineering, University of Toyama, 2. Research and Development Center for Ocean Drilling Science, Japan Agency for Marine-earth Science and Technology

Aqueous fluids must play important roles in crustal dynamics including seismicity. Geophysical mapping of fluids will thus give us insights into crustal dynamics. Electrical conductivity profiles have suggested that fluids exist pervasively in the crust. However, the fluid distribution has not been quantitatively constrained. It must be due to our poor understanding of pores that govern seismic velocity and electrical conductivity under high pressures.

In order to understand pores governing physical properties under pressures, simultaneous measurements of elastic wave velocities and electrical conductivity were conducted on a brine saturated granitic rock (Aji granite) under pressures up to 150 MPa and microstructure of pores was observed by X-ray micro CT and SEM with ion-milling and FIB. X-ray micro CT images show that many grain boundaries are open at atmospheric pressure. Elastic wave velocity increases and electrical conductivity decreases with increasing confining pressure. Most of grain bouundary cracks are closed under high pressures (>100 MPa). The electrical conductivity is, however, still much higher than that of the solid phase. The brine must be interconnected under high pressures. SEM images suggest that wide aperture parts in grain boundaries are open even at high pressures and form conduction paths.

There should be cracks with various sizes in the crust: from grain boundaries to large faults. Though cracks are closed under pressure, there must be a variation in the aperture. Wide aperture parts may form conduction paths even under high pressures. The influence of wide aperture parts on physical properties can be evaluated by tube model. Electrical conductivity is proportional to the fluid volume fraction. A change in conductivity by 4 orders of magnitude requires a change in fluid volume fraction by 4 orders of magnitude. However, seismic velocity for tube model is insenstive to fluid volume fraction. Seismic velocity will thus show relatively small decrease for a large change in fluid fraction. Observed large variation in conductivity and relatively small variation in seismic velocity (e.g., Ogawa et al., 2001; Matsubara et al., 2004) are consistent with tube model. The variation in fluid fraction must reflect that in the amount of wide aperture parts, which is attributed to the variation the amount of cracks.

Keywords: seismic velcoity, resistivity, fluid

©2019. Japan Geoscience Union. All Right Reserved.

The seismological structure about fault zone extending to the lower crust in the northern Kinki district, southwestern Japan

*Shinya Kato[1], Yoshihisa Iio[1], Takuo Shibutani[1], Hiroshi Katao[1], Masayo Sawada[1], Kazuhide Tomisaka[1]

1. Disater Prevention Research Institute, Kyoto University

The “water-weakened lower crust model” has been proposed to explain the mechanism of stress concentration on faults of inland earthquakes (Iio et al. 2002). According to this model, it is necessary that heterogeneous structure caused by the fluid exists locally in the deeper part of fault zones in the lower crust, but it has not been clearly confirmed in previous researches. This is because we do not resolve the heterogeneous structure due to fluid in the deeper part of fault zones in the lower crust. In order to solve this problem, in this study, we tried to image the heterogeneous structure in the lower crust in detail.

We conducted S-wave reflection analysis to detect the horizontal distribution of the heterogeneous structure (reflector), and receiver function analysis to estimate the structure beneath the reflector, in the northern Kinki district, southwestern Japan. As a result of the S-wave reflection analysis, it is found that the reflector exists on the north side of the Arima-Takatsuki fault zone and does not exist on the south side of it. We consider that the distribution of the reflector is related to the Arima-Takatsuki fault zone. From a result of the receiver function analysis, it is found that reflector is a thin layer with low S-wave velocity.

It is concluded that the thin layer with low S-wave velocity exists in the lower crust of the northern Kinki region. As the origin of it, it is possible to consider fluid dehydrated from the Philippine Sea slab subducting beneath the Arima-Takatsuki fault zone. In the vicinity of the Arima-Takatsuki fault zone, it is known that fluid that seems to originate in the mantle springs out (Kazahaya et al. (2014)). In the lower crust, pores between minerals exist independently (Yoshino et al. 2002), and fractures caused by faulting is thought to be necessary for fluid movement (Mibe et al. (2000)). Furthermore, since the spatial distribution of the reflector is related to the Arima-Takatsuki fault zone, we consider that the reflector in the lower crust indicates that fluid exists in fractures caused by faulting. This result supports the water-weakened lower crust model.

Keywords: S-wave reflection analysis, receiver function analysis, lower crust, fault zone, fluid

©2019. Japan Geoscience Union. All Right Reserved.

Inland repeating earthquakes in the vicinity of low frequency earthquakes around Hakodate, Hokkaido

*Keisuke Yoshida[1], Akira Hasegawa[1], Shinako Noguchi[2], Keiji Kasahara[2]

1. Tohoku University, 2. Association for the Development of Earthquake Prediction

Strength reduction due to pore pressure increase plays an important role for the generation of earthquakes. Earthquake swarms in central Tohoku activated after the 2011 Tohoku-Oki earthquake are examples of this; they are estimated to be caused by the upward fluid migration due to the decrease of WNW-ESE compressional stress after the earthquake (Yoshida & Hasegawa, 2018a and b). Inland deep low frequency earthquakes are also considered to be closely related to the fluids (e.g., Hasegawa & Yamamoto, 1994), but their detailed mechanism is poorly understood. In this presentation, we introduce our recent study on earthquakes occurring in Hakodate, Hokkdaido, which are covered by a dense seismic network installed by the Association for the Development of Earthquake Prediction (ADEP) (Noguchi et al., 2017). In this area many low frequency earthquakes are occurring, shallow ones of which occur in the immediate vicinity of ordinary earthquakes. This provides a unique opportunity to investigate the relationship between the diversity of fault motions and the fluid behavior.

We start by relocating hypocenters of ordinary earthquakes and low frequency earthquakes by applying the double-difference location method (Waldhauser & Ellsworth, 2002). We used precise differential arrival time data of P- and S-waves obtained by the waveform cross-correlation following Yoshida & Hasegawa (2018), which largely improved the accuracy of relative hypocenter locations. We relocated hypocenters of 198 earthquakes for the period from 2003 to Oct. 2018, which are listed in the JMA unified catalog or in the ADEP catalog; 22 of them are ordinary earthquakes and 176 are low frequency earthquakes. Relative locations of ordinary earthquakes are very precisely determined due to the similarity of waveform, but those of low frequency earthquakes are almost controlled by the manually picked arrival time data because of the diversity of their waveforms.

Relocated hypocenters show that low frequency earthquakes are distributed in a plate shape dipping eastward with focal depths from 5 to 35 km, which are confirmed by the S-P times obtained at the stations just above their epicenters. Low frequency earthquakes occurring in the shallow part of the crust are located in the immediate vicinity of ordinary earthquakes. We found that the initial parts of P- and S-waves of these low frequency earthquakes have similar waveform characteristics with those of the nearby ordinary earthquakes. Furthermore, ordinary earthquakes occurring near the low frequency earthquakes have very similar waveforms themselves. They turned out to be inland repeating earthquakes based on the hypocenter relocations using precise differential arrival times obtained by the waveform cross-correlation. Other repeating earthquake sequences were also found based on the template matching method (Shelly et al., 2013). Some earthquakes in one of those repeating earthquake sequences occur with a time interval of about ten minutes or so. Similar repeating earthquake occurrences with such a short time interval have been found in an induced seismicity of a recent fluid-injection experiment (Lengline et al., 2014), which suggests that natural repeating earthquakes are also caused by a similar mechanism to the fluid injection induced seismicity; slips are repeatedly caused in the same locations due to successive reduction in frictional strength by the pore pressure increase.

Keywords: low frequency earthquakes, earthquake detection

©2019. Japan Geoscience Union. All Right Reserved.

©2019. Japan Geoscience Union. All Right Reserved.

[J] Oral | S (Solid Earth Sciences)：S-CG Complex & General

Tue. May 28, 2019 10:45 AM - 12:15 PM JST | Tue. May 28, 2019 1:45 AM - 3:15 AM UTC | Convention Hall A 2F

[S-CG61] Dynamics in mobile belts

convener:Yukitoshi Fukahata(Disaster Prevention Research Institute, Kyoto University), Toru Takeshita(Department of Natural History Sciences, Graduate School of Science, Hokkaido University), Hikaru Iwamori(Geochemical Evolution Research Program, Japan Agency for Marine-Earth Science and Technology), Chairperson:Bunichiro Shibazaki, Daisuke Sato

The dynamic behaviours of mobile belts are expressed across a wide range of time scales, from the seismic and volcanic events that impact society during our lifetimes, to orogeny and the formation of large-scale fault systems which can take place over millions of years. Deformation occurs on length scales from microscopic fracture and flow to macroscopic deformation to plate-scale tectonics. To gain a physical understanding of the dynamics of mobile belts, we must determine the relationships between deformation and the driving stresses due to plate motion and other causes, which are connected through the rheological properties of the materials. To understand the full physical system, an integration of geophysics, geomorphology, and geology is necessary, as is the integration of observational, theoretical and experimental approaches. In addition, because rheological properties are greatly affected by fluids in the crust and fluid chemical reactions, petrological and geochemical approaches are also important. After the 2011 great Tohoku-oki earthquake, large-scale changes in seismic activity and regional scale crustal deformation were observed, making present-day Japan a unique natural laboratory for the study of the dynamics of mobile belts. This session welcomes presentations from different disciplines, such as seismology, geodesy, tectonic geomorphology, structural geology, petrology, and hydrology, as well as interdisciplinary studies, that relate to the dynamic behaviours of mobile belts.

10:45 AM - 11:00 AM JST | 1:45 AM - 2:00 AM UTC

[SCG61-19] Modeling strain concentration and mountain building processes in central Japan considering heterogeneous rheological structure

*Bunichiro Shibazaki[1] (1.International Institute of Seismology and Earthquake Engineering, Building Research Institute)

11:00 AM - 11:15 AM JST | 2:00 AM - 2:15 AM UTC

[SCG61-20] Inelastic strain rate and deviatoric stress field of the seismic gap in west part of Kyushu, Japan, estimated from seismic and geodetic data

*Yuhei Yuasa[1], Satoshi Matsumoto[2], Shigeru Nakao[3], Takeshi Matsushima[2], Takahiro Ohkura[4] (1.Department of Earth and Planetary Sciences, Graduate School of Science, Kyushu University, 2.Institute of Seismology and Volcanology, Faculty of Sciences, Kyushu University, 3.Department of Earth and Environmental Sciences, Graduate School of Science and Engineering, Kagoshima University, 4.Aso Volcanological Laboratory, Institute for Geothermal Sciences, Graduate School of Science, Kyoto University)

11:15 AM - 11:30 AM JST | 2:15 AM - 2:30 AM UTC

[SCG61-21] Persistent and time-dependent crustal deformation in northern Fossa Magna and its tectonic implications

*Takeshi Sagiya[1], Koki Kumagai[2], Angela Meneses-Gutierrez[3], Nobuhisa Matsuta[4], Daisuke Hirouchi[5], Kenjiro Matsuhiro[2], Takashi OKUDA[2] (1.Disaster Mitigation Research Center, Nagoya University, 2.Graduate School of Environmental Studies, Nagoya University, 3.Disaster Prevention Research Institute, Kyoto University, 4.Graduate School of Education, Okayama University, 5.Faculty of Education, Shinshu University)

11:30 AM - 11:45 AM JST | 2:30 AM - 2:45 AM UTC

[SCG61-22] Unexpected relationship between ΔCFF and the strain-rate paradox: separation of plastic strain from inelastic strain

*Yukitoshi Fukahata[1], Angela Meneses-Gutierrez[1], Takeshi Sagiya[2] (1.Disaster Prevention Research Institute, Kyoto University, 2.Disaster Mitigation Research Center, Nagoya University)

11:45 AM - 12:00 PM JST | 2:45 AM - 3:00 AM UTC

[SCG61-23] Active period of inland earthquakes based on numerical simulation of megathrust earthquake cycle incorporating viscoelasticity

*Tsukasa MITOGAWA[1], Takuya NISHIMURA[2] (1.Graduate School of Science, Kyoto University, 2.Disaster Prevention Research Institute, Kyoto University)

12:00 PM - 12:15 PM JST | 3:00 AM - 3:15 AM UTC

[SCG61-24] Influence of viscoelastic relaxation on estimated interplate coupling along the Nankai Trough, southwest Japan

*Takuya NISHIMURA[1], Fred F Pollitz[2] (1.Disaster Prevention Research Institute, Kyoto University, 2.U.S. Geological Survey)

Modeling strain concentration and mountain building processes in central Japan considering heterogeneous rheological structure

*Bunichiro Shibazaki[1]

1. International Institute of Seismology and Earthquake Engineering, Building Research Institute

Recent analysis of crustal deformation using GEONET data has revealed the existence of several strain concentration zones in the Niigata–Kobe Tectonic Zone (Sagiya, et al., 2000), in the Ou backbone range (Miura et al., 2004), in Kyushu, and San-in (Nishimura et al., 2018), etc. Many large inland earthquakes have occurred in the strain concentration zones. Elucidating the mechanism of strain concentration leads to understanding generation processes of large inland earthquakes. We develop a model of strain concentration and mountain building in the island-arc crust of central Japan, where several high mountain ranges have been formed by active crustal deformation. We use the finite element code with nonlinear viscoelasticity and plasticity based on Mohr-Coulomb criterion (e.g. Shibazaki et al., 2016). We consider gravitational force as a body force because the plasticity and the flow law depend on absolute stress.

Based on dense geothermal gradient data from Hi-net (Matsumoto et al., 2007) and the Geological Survey of Japan (Tanaka et al., 2004), we develop a thermal structure. We also consider a thick sedimentary layer where the friction coefficient is low based on the J-SHIS deep subsurface structure (NIED). Numerical results show that under the compressional tectonic setting, mountains are reproduced along high geothermal gradient regions. We can reproduce the Hida mountain range, Chikuma mountain, Echigo mountain range, and others, where a geothermal anomaly exists. Our model can also reproduce strain concentration in the Hida region. Furthermore, we can reproduce a strain concentration zone by setting the frictional coefficient to be low in the basement of the Niigata region.

However, the model cannot reproduce the strain concentration zone in the Atotsugawa and Kinki regions where strike slip faulting is dominant; therefore, we consider the boundary condition that yields the stress state of the strike-slip faulting and the effect of water distribution or rheology of partial melting based on seismic velocity anomalies (Nakajima and Hasegawa, 2007). We can reproduce strain concentration along the seismic velocity anomalies. Our results suggest that the Niigata-Kobe strain concentration zone is developed by several factors: thermal anomaly, pre-existing rift structure, and the presence of fluid and partial melting in the crust and the upper mantle.

Keywords: Central Japan, Strain concentration zone, Mountain building, Finite element method, Nonlinear viscoelasticity , Plasticity based on Mohr-Coulomb criterion

©2019. Japan Geoscience Union. All Right Reserved.

Inelastic strain rate and deviatoric stress field of the seismic gap in west part of Kyushu, Japan, estimated from seismic and geodetic data

*Yuhei Yuasa[1], Satoshi Matsumoto[2], Shigeru Nakao[3], Takeshi Matsushima[2], Takahiro Ohkura[4]

1. Department of Earth and Planetary Sciences, Graduate School of Science, Kyushu University, 2. Institute of Seismology and Volcanology, Faculty of Sciences, Kyushu University, 3. Department of Earth and Environmental Sciences, Graduate School of Science and Engineering, Kagoshima University, 4. Aso Volcanological Laboratory, Institute for Geothermal Sciences, Graduate School of Science, Kyoto University

An earthquake is a phenomenon that differential stress loading on the Earth’ s crust is released. Thus, we need to know state of stress in the crust to understand the earthquake generation mechanism. The state in the crust has been investigated in many studies, based on data of the focal mechanisms and seismic moment tensors (e.g., Michael 1984; Horiuchi et al. 1995; Terakawa & Matsu’ ura 2008). However, information on the stress fields in non-active seismic areas is insufficient because accurate stress estimation requires the data from a number of earthquakes. A key factor for acquiring knowledge of the stress field in an aseismic zone is the inelastic strain, which is related to the deviatoric stress based on the flow rule in plasticity theory (Matsumoto 2016). Thus, the strain rate due to inelastic deformation source needs to be separated from the total strain rate measured via geodetic observation. Here, we propose a new method for estimation of the deviatoric stress field through inelastic strain analysis that combines the seismic moment tensor and geodetic data. In this method, the deformation source of inelastic strain in the upper crust is estimated from short wavelength component of the observed total strain rate field, and the inelastic source tensor yields tensor shape of deviatoric stress field based on the flow rule. This method is applied to data for a region in and around the aseismic zone of Amakusa located at west part of Kyushu Island, Japan. It was found that the inelastic deformation in the seismic gap exhibits either normal-fault or strike-slip type. Furthermore, the deviatoric stress field estimated from the inelastic deformation has same trend as the surroundings. In addition, the estimated stress explained slip vectors of event rarely occurring there. These results might provide us with important information regarding the origin of the seismic gap and stress concentration on the surrounding fault.

©2019. Japan Geoscience Union. All Right Reserved.

Persistent and time-dependent crustal deformation in northern Fossa Magna and its tectonic implications

*Takeshi Sagiya[1], Koki Kumagai[2], Angela Meneses-Gutierrez[3], Nobuhisa Matsuta[4], Daisuke Hirouchi[5], Kenjiro Matsuhiro[2], Takashi OKUDA[2]

1. Disaster Mitigation Research Center, Nagoya University, 2. Graduate School of Environmental Studies, Nagoya University, 3. Disaster Prevention Research Institute, Kyoto University, 4. Graduate School of Education, Okayama University, 5. Faculty of Education, Shinshu University

In the northern Fossa Magna of the northern Nagano Prefecture, GNSS observations over last two decades identified a rapid E-W contraction around the northern Itoigawa-Shizuoka Tectonic Line (ISTL) and the Western Nagano Basin Fault (WNBF). After the 2011 Tohoku-oki earthquake, postseismic deformation with a large E-W extension occurred throughout northeast Japan. However, the northern Nagano area has been still under contraction, implying that the local contraction is a persistent deformation feature. Similar persistent deformation was identified in the Niigata area by Meneses-Gutierrez and Sagiya (2016) and around other active faults in central Japan. These observations illustrate that there exists persistent localized deformation in the lower crust beneath active faults, driven by the regional stress field. This localized deformation in the lower crust is the driving force for faults in the upper crust. The persistent local crustal deformation around active faults suggests that the long-term inland deformation and resultant inland seismic activity are steady over a longer time scale than that of an earthquake cycle at subduction zones. On the other hand, after the 2014 Northern Nagano Earthquake (Mw6.3) along the northern ISTL, an acceleration of contraction along the WNBF was identified. This observation implies that the northern ISTL and WNBF are not independent but mechanically interact each other, forming an active deformation system that accommodates regional deformation. Such a complicated behavior of the fault system implies that the long-term activity of each fault in the system is not steady but time-dependent. Such a time-dependence may be a cause of irregular activity of inland faults and such a possibility should be considered for evaluation of seismic hazard.

Keywords: inland earthquake, active fault, inelastic deformation, persistent crustal deformation, fault interaction

©2019. Japan Geoscience Union. All Right Reserved.

Unexpected relationship between ΔCFF and the strain-rate paradox: separation of plastic strain from inelastic strain

*Yukitoshi Fukahata[1], Angela Meneses-Gutierrez[1], Takeshi Sagiya[2]

1. Disaster Prevention Research Institute, Kyoto University, 2. Disaster Mitigation Research Center, Nagoya University

In the field of seismic activity, the phenomena of stress shadow is well known, that is to say, the area with negative ΔCFF after an large earthquake tends to have fewer aftershocks (e.g., Toda et al. 2011, GRL). The concept of ΔCFF is also usful to understand earthquake activity for longer time scales as exemplified by Shikakura et al. (2014, JGR), which shows that large inland earthquakes that happened in western Japan recent 500 years can be very well exlpained by the change history of ΔCFF, which is mainly controled by the repeated occurrences of the Nankai earthquakes and secular increase of east-west compression.

Meneses-Gutierrez and Sagiya (2016, EPSL) have successfully separated the component of inelastic strain from the analysis of pre- and post-seismic GNSS data of the 2011 Tohoku-oki earthquake in the area around the Niigata prefecture. However, when we examine the observed GNSS data in detail, the separated inelastic strain rate is slightly but clearly faster before the Tohoku-oki earthquake. If the inelastic strain is due to viscous flow that depends only on the absolute stress, it is difficult to explain the observed GNSS data, because the stress change due to the 2011 Tohoku-oki earthquake in this area is less than 1 MPa, which is likely to be much smaller than the absolute stress.

Therefore, we consider that the concept of ΔCFF could be applicable not only to seismic activity but also to crustal deformation. In other words, we consider that the change of the inelastic strain rate is caused by plastic strain, which was active before the 2011 Tohoku-oki earthquake but ceased after the earthquake, because the stress level is dropped due to the occurrence of the 2011 Tohoku-oki earthquake, although inelastic strain due to viscous flow occurs essentially in the same manner before and after the 2011 Tohoku-oki earthquake.

If we accept this concept, the strain rate paradox of Japan is viewed differently, that is, the strain rate was exceptionally faster before the 2011 Tohoku-oki earthquake. It might also be possible to issue more effective warnings of large inland earthquakes in western Japan from detailed analyses of crustal deformation data.

Keywords: plastic strain, ΔCFF, inelastic strain, strain-rate paradox

©2019. Japan Geoscience Union. All Right Reserved.

Active period of inland earthquakes based on numerical simulation of megathrust earthquake cycle incorporating viscoelasticity

*Tsukasa MITOGAWA[1], Takuya NISHIMURA[2]

1. Graduate School of Science, Kyoto University, 2. Disaster Prevention Research Institute, Kyoto University

In the subduction zone, megathrust earthquakes may modulate shallow crustal seismicity in the overriding plate. Historical documents demonstrate that large inland earthquakes frequently occurred for 50 years before and 10 years after megathrust earthquakes along the Nankai trough, southwest Japan. Previous studies suggest that inland earthquakes cannot occur until recovering the stress reduced by a megathrust earthquake on the fault. In this study, we modeled megathrust earthquake cycle in a simple oblique subduction zone and calculated temporal evolution of the Coulomb’ s Failure Stress changes (ΔCFS) on inland right-lateral strike-slip faults. And we examined the influence of megathrust earthquake cycle on the activity tune of inland earthquake.

Sources for loading inland faults are assumed to be interseismic locking and coseismic slip on the megathrust fault, stress changes due to inland earthquake and interaction between inland earthquake, and creep on a deeper extension of the inland faults. The stress change due to the megathrust fault was computed with numerical code by Fukahata and Matsu'ura (2006), assuming a medium composed of an elastic layer overlying a Maxwell viscoelastic half-space. We focus on ΔCFS depending on the distance from the megathrust fault, not its along-strike variation. In other words, only two-dimensional stress change at the center of a sufficiently long thrust fault plane (length 2000 km) is calculated. The megathrust fault is represented by a single rectangular fault whose depth, width, strike, dip, and rake are 11 km, 108 km, 270˚, 10˚, and 117˚, respectively. We assigned 6 m of coseismic slip at an interval of 100 years and 6 cm/year of back-slip during the interseismic period on the megathrust fault.The inland faults are located at 150 km (hereafter fault A) and 300 km (hereafter fault B) away from the upper edge of the megathrust fault and their depth, length, width, strike, dip, and rake are 4 km, 30 km, 6 km, 110˚, 90˚, and 180˚, respectively. Coseismic slip of 2 m was assigned when ΔCFS at the center of the inland faults exceeded 4.4 MPa.Becuase the code of Fukahata and Matsu'ura (2006) approximates a rectangular fault by numbers of point sources, a stress change on the fault plane can’ t be calculated. Therefore, we calculated a coseismic stress change on the fault plane assuming a semi-infinite elastic medium (Okada, 1992). In addition, stress loading by creep on a deeper extension of the inland faults was given to each inland fault at a constant rate.

ΔCFS on both inland faults is negative at the megathrust earthquake. When the stress loading rate is 5 kPa/year, the inland earthquake does not occur for 42 years on fault A and 15 years on fault B after the megathrust earthquake. Our interpretation is that viscoelastic effects of megathrust earthquakes makes these quiescence periods shorter and longer for faults A and B, respectively. Also, when the stress loading rate is 0.5 kPa/year, the quiescence period is 83 and 71 years for faults A and B. It is interesting that the quiescence period is not much dependent on the distance from the megathrust fault if the stress loading rate is small, though ΔCFS on both inland faults is highly dependent on the distance at the megathrust earthquake.

Keywords: seismic cycle, coulomb stress change, viscoelasticity

©2019. Japan Geoscience Union. All Right Reserved.

Influence of viscoelastic relaxation on estimated interplate coupling along the Nankai Trough, southwest Japan

*Takuya NISHIMURA[1], Fred F Pollitz[2]

1. Disaster Prevention Research Institute, Kyoto University, 2. U.S. Geological Survey

Viscoelastic relaxation in asthenosphere is an important factor for understanding crustal deformation in the subduction zone. Although interplate coupling on subduction interface has often been estimated from geodetic data using a purely elastic dislocation model, several recent studies (e.g., Li et al., 2015) pointed out that ignoring viscoelasticity in the medium made estimated coupling distribution biased. Pollitz and Evans (2017) developed viscoelastic block models introducing a viscoelastic correction term for earthquake cycles to estimate both interplate coupling and rigid rotation of microplates in western US. Once you subtracted the viscoelastic correction velocities from observed ones, the corrected velocities can be inverted by conventional elastic block models. The viscoelastic correction term consists of two components. One (hereafter, 1st component) is viscoelastic velocities due to interplate locking in the past, which is constant over the interseismic period. The other (hereafter, 2nd component) is total postseismic velocities of past earthquakes repeated with a certain recurrence interval, which is dependent on a time from the last earthquake. Here we examine these viscoelastic correction components for megathrust earthquake cycles along the Nankai trough.

We calculated viscoelastic deformation using VISCO1D (Pollitz, 1997) and assumed a 35 km thick elastic plate overriding a Maxwell viscoelastic half-space with a viscosity of 10^{19} Pa s. Coseismic fault model for the 1944 Tonankai and 1946 Nankai earthquakes estimated by Sagiya and Thatcher (1999) is used for viscoelastic calculation. A recurrence interval of megathrust earthquakes is 117 years and slip deficit accumulated for the interseismic period is completely released by the megathrust earthquakes. Figs. A-C show 1st and 2nd components as well as the sum of them as of 2007. 1st component represent a difference between elastic and viscoelastic responses of locking that has continued since the infinite past. It reaches 2 cm/yr along the Pacific coast and several mm/yr even along the coast of Sea of Japan (Fig. A). 2nd component is generally reverse to 1st component and decays with time from the last earthquake. Amplitude of 2nd component is roughly equal to that of 1st component 30 years after the last earthquake. Therefore, total viscoelastic correction is minimized 30 years after the last earthquakes during the interseismic period. Even after 61 years of the last earthquakes, velocities of 2nd component is still comparable to those of 1st component (Fig. B). Total correction velocities, therefore, exceed 2 mm/yr only near peninsulas along the Pacific Ocean (Fig. C). 2nd component reaches several mm/yr in the last years of the interseismic period for the Nankai subduction zone and cannot be ignored for better viscoelastic correction.

We present a result of applying viscoelastic correction to the block model of Nishimura et al.(2018) which models onshore GNSS and offshore GNSS-Acoustic velocities in southwest Japan.

Keywords: Crustal deformation, Viscoelastic relaxation, Nankai trough, Viscoelastic block model

©2019. Japan Geoscience Union. All Right Reserved.

(a)Velocity for viscoelastic correction of slip-deficit

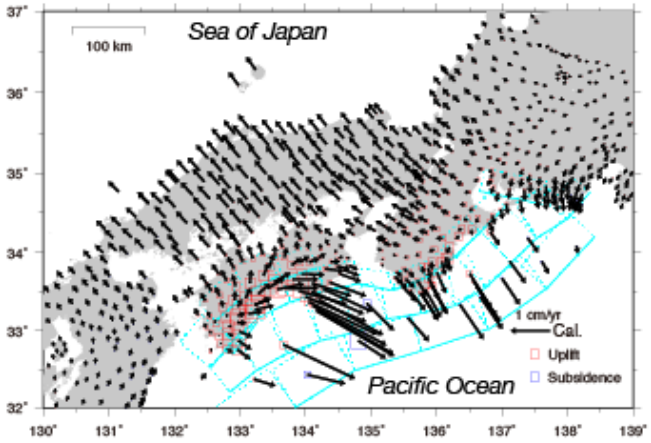

(b) Velocity for viscoelastic correction of past earthquakes

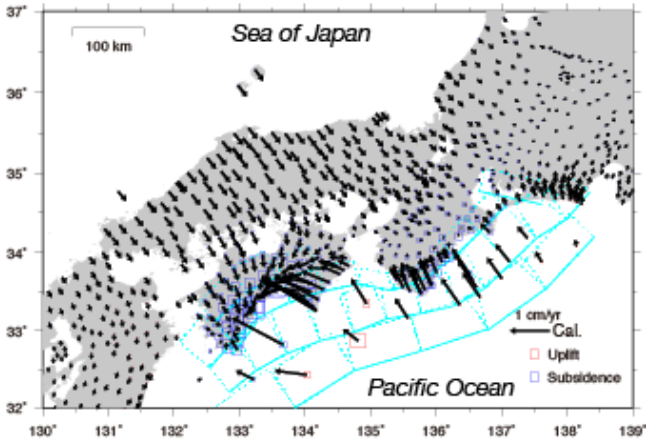

(c) Velocity for total viscoelastic correction

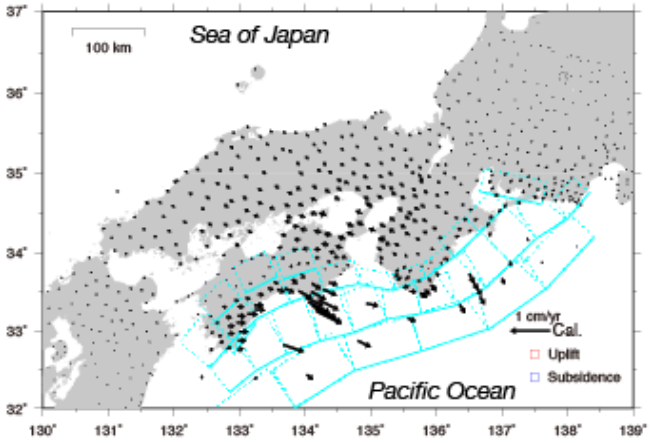

©2019. Japan Geoscience Union. All Right Reserved.

[J] Oral | S (Solid Earth Sciences)：S-CG Complex & General

Tue. May 28, 2019 1:45 PM - 3:15 PM JST | Tue. May 28, 2019 4:45 AM - 6:15 AM UTC | Convention Hall A 2F

[S-CG61] Dynamics in mobile belts

convener:Yukitoshi Fukahata(Disaster Prevention Research Institute, Kyoto University), Toru Takeshita(Department of Natural History Sciences, Graduate School of Science, Hokkaido University), Hikaru Iwamori(Geochemical Evolution Research Program, Japan Agency for Marine-Earth Science and Technology), Chairperson:Naoki Uchida, Takeshi Iinuma

The dynamic behaviours of mobile belts are expressed across a wide range of time scales, from the seismic and volcanic events that impact society during our lifetimes, to orogeny and the formation of large-scale fault systems which can take place over millions of years. Deformation occurs on length scales from microscopic fracture and flow to macroscopic deformation to plate-scale tectonics. To gain a physical understanding of the dynamics of mobile belts, we must determine the relationships between deformation and the driving stresses due to plate motion and other causes, which are connected through the rheological properties of the materials. To understand the full physical system, an integration of geophysics, geomorphology, and geology is necessary, as is the integration of observational, theoretical and experimental approaches. In addition, because rheological properties are greatly affected by fluids in the crust and fluid chemical reactions, petrological and geochemical approaches are also important. After the 2011 great Tohoku-oki earthquake, large-scale changes in seismic activity and regional scale crustal deformation were observed, making present-day Japan a unique natural laboratory for the study of the dynamics of mobile belts. This session welcomes presentations from different disciplines, such as seismology, geodesy, tectonic geomorphology, structural geology, petrology, and hydrology, as well as interdisciplinary studies, that relate to the dynamic behaviours of mobile belts.

1:45 PM - 2:00 PM JST | 4:45 AM - 5:00 AM UTC

[SCG61-25] Revisiting the Forearc Sliver Scenario Along the Southern Kurile Trench to Reconcile Interdisciplinary Observations

*Yuji ITOH[1], Kelin WANG[2], Takuya NISHIMURA[3] (1.Graduate School of Science, Kyoto University, 2.Pacific Geoscience Centre, Geological Survey of Canada, 3.Disaster Prevention Research Institute, Kyoto University)

2:00 PM - 2:15 PM JST | 5:00 AM - 5:15 AM UTC

[SCG61-26] Segmentation of crustal deformation area within the Sanriku coast, northeast Japan, on the basis of spatial distribution of millennial-scale crustal movements

*Yuichi Niwa[1] (1.Faculty of Science and Engineering, Chuo University)

2:15 PM - 2:30 PM JST | 5:15 AM - 5:30 AM UTC

[SCG61-27] Shear wave splitting east off NE Japan based on the S-net data

*Naoki Uchida[1], Junichi Nakajima[2], Ryota Takagi[1], Keisuke Yoshida[1], Takashi NAKAYAMA[1], Ryota Hino[1], Tomomi Okada[1], Youichi Asano[3], Sachiko Tanaka[3] (1.Research Center for Prediction of Earthquakes and Volcanic Eruptions Graduate School of Science, Tohoku University, 2.Department of Earth and Planetary Sciences, Graduate School of Science and Engineering, Tokyo Institute of Technology, Tokyo, 3.National Research Institute for Earth Science and Disaster Resilience)

2:30 PM - 2:45 PM JST | 5:30 AM - 5:45 AM UTC

[SCG61-28] Gravity anomaly due to active faults and crustal rheology in the northeastern Japan arc inferred by fault dislocation model

*Mitsuhiro Hirano[1], Hiroyuki Nagahama[1], Jun Muto[1] (1.tohoku university)

2:45 PM - 3:00 PM JST | 5:45 AM - 6:00 AM UTC

[SCG61-29] On the temporal decay of the localized strain rate in the Tohoku region after the Tohoku-Oki earthquake

*Youichiro Takada[1], Tomomi Inamatsu[2] (1.Faculty of Science, Hokkaido University, 2.Dept. Natural History Sciences, Hokkaido University)

3:00 PM - 3:15 PM JST | 6:00 AM - 6:15 AM UTC

[SCG61-30] Revisiting the Coseismic Slip Distribution of the 2011 Tohoku-oki Earthquake Considering Early Postseismic Deformation, Non-linear Viscoelasticity, and Heterogeneous Structure

*Takeshi Iinuma[1], Ryoichiro Agata[1], Yusaku Ohta[2], Ryota Hino[2], Takane Hori[1] (1.Japan Agency for Marine-Earth Science and Technology (JAMSTEC), 2.Graduate School of Science, Tohoku University)

Revisiting the Forearc Sliver Scenario Along the Southern Kurile Trench to Reconcile Interdisciplinary Observations

*Yuji ITOH[1], Kelin WANG[2], Takuya NISHIMURA[3]

1. Graduate School of Science, Kyoto University, 2. Pacific Geoscience Centre, Geological Survey of Canada, 3. Disaster Prevention Research Institute, Kyoto University

Forearc sliver has been proposed as a mechanism to accommodate margin-parallel component of oblique plate convergence along the southern Kurile trench. The sliver scenario was established based mostly on the presence of the margin-perpendicular Hidaka Mountain Range (HMR), graben at Bussol Strait, en echelon Kurile Islands and high temperature metamorphic and intrusive rocks exposed at HMR. Along the volcanic front, geological faults including Kamishi-Yubetsu tectonic zone with 50 km right-lateral displacement was reported. Seismic velocity tomography and refraction/reflection experiments beneath HMR show the heterogeneous crustal structure relating to collision of the Kurile forearc and Northeast Japan arc, indicating upwelling of upper mantle, sinking of crustal material and delamination of upper mantle beneath HMR, and shortening in the foreland of HMR. Anomalous deep crustal earthquakes beneath HMR such as the 1970 M6.7 Hidaka and 1982 M7.1 Urakawa-oki earthquakes show active margin-parallel compression. However, other observations cast doubt on the forearc sliver being presently active. Although some active faults are reported along the volcanic front, they are not right-lateral faults. Interseismic GNSS velocities do not show localized right-lateral shear deformation along the volcanic front, although they show active margin-normal shortening in the foreland of HMR consistent with active collision. In this study, we propose a new scenario of forearc kinematics and strain partitioning along the southern Kurile trench to reconcile these seemingly discordant observations.

A mountain like HMR pushes sideways because of gravity and acts as a buttress of the forearc sliver to impede its migration. We compared the stress field inferred from CMT solution with that predicted from a buttressed sliver model. The comparison suggests that (1) the forearc sliver is buttressed at HMR and (2) resistance to right-lateral shear along the volcanic front is very large. Therefore, we propose a scenario as follows. The forearc sliver had been increasingly buttressed as HMR rose, so that the rate of strain partitioning diminished with time. Eventually, the forearc migration became too slow to cause recurring large earthquakes and to maintain a mature active fault zone along the volcanic front. As a result, the fault zone healed with time. At present, the forearc and backarc deform together without active faulting and localized shear along the volcanic front.

We also compared Kurile with other oblique subduction zones and found that margin (trench) curvature appears to principal control forearc kinematics. At Cascadia and Nankai where the margin is concave seaward, interseismic GNSS velocities do not show discernable localized shear to define the forearc sliver but strong margin-parallel shortening towards the area of maximum margin curvature. In contrast, in southernmost Chile where the trench is approximately straight, there is little margin-parallel shortening but significant forearc sliver migration. However, at Kamchatka, although the margin is concave off-Kamchatka Peninsula, significant margin-parallel migration of Aleutian Islands is still occurring, which we speculate is due to the extreme obliquity of plate convergence here. Even in this case, significant shortening is observed at the leading edge of the forearc sliver. The concave margin has buttressed the forearc sliver and caused shortening in the area of maximum curvature in the geological time scale as well because the tectonic setting itself, such as the margin curvature and the obliquity of plate convergence, is the controlling factor of the forearc kinematics.

©2019. Japan Geoscience Union. All Right Reserved.

Keywords: Kurile Trench, Forearc Sliver, Oblique Subduction, Hidaka Mountain Range, Strain Partitioning, Volcanic Front

©2019. Japan Geoscience Union. All Right Reserved.

Segmentation of crustal deformation area within the Sanriku coast, northeast Japan, on the basis of spatial distribution of millennial-scale crustal movements

*Yuichi Niwa[1]

1. Faculty of Science and Engineering, Chuo University

Along the Sanriku coast, northeast Japan, discrepancies in crustal movement have been reported between uplift on a timescale of 10^5 years (Koike and Machida, 2001) and subsidence on a timescale of 10^1 –10^2 years (Kato, 1983; Ozawa et al., 2011). Some hypothetical models, which explain these discrepancies, are proposed in relation to megathrust earthquake cycle (e.g., Ikeda et al., 2012; Nishimura, 2014). These models assume that crustal movement style is same within whole part of the Sanriku coast, and show that amount of accumulation of uplift exceeds that of subsidence during one earthquake cycle. However, because of lack of age data of marine terrace except for Hachinohe to Kuji (Miyazaki and Ishimura, 2018) and of putative marine terrace along the southern part of the Sanriku coast (Koike and Machida, 2001), spatial distribution of crustal movement cannot be estimated on the basis of only feature of Pleistocene marine terrace. On the other hand, sedimentary successions in alluvial plains distributed along the Sanriku coast may offer records of millennial-scale crustal movements during the Holocene.

Recent sediment core analyses and radiocarbon dating shows sedimentary succession influenced by sea-level changes during the past 10,000 years. In the Rikuzen-takata plain, Kesennuma Okawa plain, and Onuma, on the southern Sanriku coast, a millennial-scale subsidence is inferred on the basis of height distribution of intertidal sediments which is lower than non-tectonic relative sea-level (Niwa et al., 2014, 2015; Ishimura and Miyauchi, 2017). Depositional environment estimated from a sediment core of the Tsuya plain, between Kesennuma plain and Onuma, also support a millennial-scale subsidence (Niwa et al., 2016). In the Tsugaruishi plain, on the central coast, height distribution of intertidal sediments and aggradation of delta sediments since ca. 7500 cal BP indicates subsidence on a millennial-scale (Niwa et al., 2017). On the other hand, sedimentary feature typical of subsidence area is not identified in sediment cores obtained from Omoto plain, northern Sanriku coast, suggesting no noticeable subsidence on a millennial-scale (Niwa et al., in press).

Inferred millennial-scale crustal movements shows subsidence trend on central to southern Sanriku coast and relatively uplifting trend on northern part of the coast. This spatial distribution of millennial-scale crustal movements is consistent with geodetically estimated subsidence rate on a timescale of 10^1 –10^2 years (Kato, 1983) and the amount of subsidence at 2011 Tohoku-oki earthquake (Ozawa et al., 2011), indicating that the Sanriku coast presents a variety of crustal movement styles. These results suggest that the northern and the central to southern parts of the Sanriku coast should be considered separately when assessing crustal deformation related to subduction.

Ikeda et al. (2012) Jour. Geol. Soc. Japan, 118, 294-312. (in Japanese with English abstract) Ishimura and Miyauchi (2017) Mar. Geol., 386, 126-139. Kato (1983) Tectonophysics, 97, 183-200. Koike and Machida (2001) The University of Tokyo Press, p105. (in Japanese with English abstract) Miyazaki and Ishimura (2018) J. Geogr. (Chigaku-zasshi), 127, 735-757. (in Japanese with English abstract) Nishimura

©2019. Japan Geoscience Union. All Right Reserved.

(2014) J. Disaster Res., 9, 294-302. Niwa et al. (2014) Quat. Res. (Dai-yonki kenkyu), 53, 311-312. (in Japanese with English abstract) Niwa et al. (2015) J. Geogr. (Chigaku-zasshi), 124, 545-560. (in Japanese with English abstract) Niwa et al. (2016) J. Geogr. (Chigaku-zasshi), 125, 395-407. (in Japanese with English abstract) Niwa et al. (2017) Quat. Int., 456, 1-16. Niwa et al. (in press) Quat. Int.. Ozawa et al. (2011) Nature, 475, 373-377.

Keywords: the Sanriku coast, earthquake cycle, millennial-scale, crustal deformation area

©2019. Japan Geoscience Union. All Right Reserved.

Shear wave splitting east off NE Japan based on the S-net data

*Naoki Uchida[1], Junichi Nakajima[2], Ryota Takagi[1], Keisuke Yoshida[1], Takashi NAKAYAMA[1], Ryota Hino[1], Tomomi Okada[1], Youichi Asano[3], Sachiko Tanaka[3]

1. Research Center for Prediction of Earthquakes and Volcanic Eruptions Graduate School of Science, Tohoku University, 2. Department of Earth and Planetary Sciences, Graduate School of Science and Engineering, Tokyo Institute of Technology, Tokyo, 3. National Research Institute for Earth Science and Disaster Resilience

We estimated the anisotropy of seismic wave speed by using shear wave splitting data in the offshore area of NE Japan. The analysis was made possible by the deployment of the Seafloor Observation Network for Earthquakes and Tsunamis along the Japan Trench (S-net) by National Research Institute for Earth Science and Disaster Resilience (NIED). We used the waveforms of 421 interplate earthquakes from August 2016 to October 2018 which are selected based on the focal mechanisms of Full Range Seismograph Network of Japan (F-net) operated by NIED and located under the S-net stations (within 35 degree from the vertical). We determined the fast polarization directions and delay times between fast- and slow-shear waves by the cross-correlation method.

The results show that the shear wave splitting tends to have trench parallel fast polarization direction for the region east off Chiba to Hokkaido which is the same with the observations in the land area of the forearc. Since we used earthquakes on the plate boundary, the anisotropy must be located in mantle wedge or forearc crust. The interpretation of the polarization includes the flow-normal fast direction of B-type olivine fabric in the forearc mantle-wedge and cracks aligned in the trench parallel direction due to the present forearc stress-field or fossil structures developed during the formation of the forearc.

Acknowledgements: We used S-net data which is deployed and maintained by NIED.

Keywords: Shear wave splitting, S-net, forearc

©2019. Japan Geoscience Union. All Right Reserved.

Gravity anomaly due to active faults and crustal rheology in the northeastern Japan arc inferred by fault dislocation model

*Mitsuhiro Hirano[1], Hiroyuki Nagahama[1], Jun Muto[1]

1. tohoku university

Short-wavelength Bouguer gravity anomaly reflects crustal structures including effective elastic thickness distribution in the northeastern (NE) Japan arc [1-3]. Moreover, earthquake epicenters and active faults tend to be located in the region of the negative gravity anomaly or high gradient in the anomaly in the NE Japan arc [1-3]. Following the relationship between gravity anomaly and active fault distributions, Yamazaki and Nagahama [4] derive an equation of static gravity change by volumetric strain due to fault dislocation, and argue that active faults contribute to Bouguer gravity anomaly in the NE Japan arc. On the other hand, seismicity and active fault distribution tend to be located in the region with high gradient of thermal gradients or along the boundary between high and low seismic wave velocity [5-7]. Thermal gradient and seismic wave velocity reflect mechanical behaviors (viscosity and elasticity) and they are indices of crustal rheology. However, relationship between gravity anomaly and the influence of the inhomogeneity in crustal rheological structures including active fault distributions have been not unknown yet. In addition, although large positive gravity anomaly is expected along the Ou-backbone Range by its pop-up structure, negative or small positive gravity anomaly zone exists along the Ou-backbone Range. So, we study relationship between gravity anomaly and rheological properties in the NE Japan arc. First, we calculated gravity anomaly due to volumetric strain by fault dislocation model in a homogeneous elastic half space. In this case, considering compressive stress field that has continued since 3 Ma in the NE Japan arc, we give total fault displacements in the 3 million years to active faults. This model calculation generates negative gravity anomaly less than 15 mGal around active faults and these generally agree with some negative areas of short-wavelength Bouguer gravity anomaly (such as the Ou-backbone Range, Yamagata Basin and the Niigata Plain). Next, we compare short-wavelength Bouguer gravity anomaly with three available datasets in the NE Japan (thermal gradient, crustal strain rate and P-wave velocity) along the two transects created normal to the arc. This comparison reveals the correlation between negative peak in the gravity anomaly and the peaks of thermal gradient and contraction, and negative peak of P-wave velocity around the Ou-backbone Range. The comparisons suggest the relationship between gravity anomaly and crustal rheology, and that contraction along the Ou Backbone Range produces negative gravity anomaly. The result also explains the relationship between gravity anomaly and seismicity and active fault distributions since both of them distribute to transitional areas of crustal rheological structures. Hasegawa et al. [8] pointed out that reverse faults and large contraction along the Ou Backbone Range reflects the heterogeneity in rheological properties in the NE Japan arc. Therefore, those comparisons imply that reverse faults and anelastic contraction produce continuous negative gravity anomaly along the Ou-backbone Range. Finally, we propose that the gravity anomaly can be an index of the heterogeneity in crustal rheology.

References: [1] Hagiwara, Y. (1979), J. Geod. Soc. Japan, 25, 209-210. [2] Hagiwara. Y. (1980), J. Geod. Soc. Japan, 26, 132-133. [3] Kudo, K. et al. (2010), The earth monthly, 32, 373-382. [4] Yamazaki, K. and Nagahama, H. (1999), Acta Geophys. Pol., 47, 239-257. [5] Zhao, D. and Ochi, F. (2000), JGR, 105, 579-594. [6] Shibazaki, B. (2008), JGR, 113, B08415. [7] Shibazaki, B. (2016), JGR, 121, 3099-3117. [8] Hasegawa, A. (2004), Earthquake, 56, 413-424.

©2019. Japan Geoscience Union. All Right Reserved.

Keywords: gravity anomaly, crustal rheology, fault dislocation model

©2019. Japan Geoscience Union. All Right Reserved.

On the temporal decay of the localized strain rate in the Tohoku region after the Tohoku-Oki earthquake

*Youichiro Takada[1], Tomomi Inamatsu[2]

1. Faculty of Science, Hokkaido University, 2. Dept. Natural History Sciences, Hokkaido University

The 2011 Tohoku-Oki earthquake (Mw9.0) provides us the first opportunity to examine the responses of strain concentration zones and active faults to megathrust earthquakes with dense permanent GNSS network. Along the Backbone range in the Tohoku region, strain rate localization has been found before and after the Tohoku-Oki earthquake (e.g., Miura et al., 2004; Takada and Inamatsu, 2018). In this study, we focused on the post-seismic strain rate localization along the Backbone range, and examined its driving mechanism with GNSS data and simple FEM simulation.
We used daily coordinates obtained at GEONET stations operated by GSI. We estimated surface velocity field before and after the earthquake by removing annual and semi-annual perturbations. For post-seismic period, we estimated the velocity field for every two years to use linear approximation. From the velocities thus obtained, we calculated the strain rates following the method of Shen et al (1996). Next, we approximated the long wavelength components, which reflects the afterslip and/or the viscoelastic relaxation of Asthenosphere following the Tohoku-Oki earthquake, by polynomial function for each component, and removed it to extract the short wavelength component. Then, we found patchy distribution of localized contraction (negative dilatation rate) areas along the Backbone range with these amplitudes rapidly decreasing with time.
To examine the mechanism of rapidly decreasing strain rate, we conducted a simple numerical simulation with a finite element software COMSOL Multiphysics. There are thermally active regions with many calderas along the Backbone range (e.g., Yoshida, 2001; Takada and Fukushima, 2013). On the other hand, the thermal activity of surrounding area is not very high. Considering these points, we set a rectangular elastic body and located several ellipsoids in north-south direction that consist of low viscosity Maxwell viscoelastic medium. Then we applied gravitational body force to all the model region, and supported it from a lateral boundary. In addition, we also applied a step-wise 1 MPa stress change which represents coseismic stress perturbation due to the Tohoku-Oki earthquake. From the calculated results, we removed the long wave-length component. Then, we successfully extracted the short wave-length dilatation rate around the viscoelastic ellipsoids. Just after the step-wise stress change, whole medium responded as an elastic body. Soon after that, viscous flow starts in the ellipsoids. As differential stress decreases with time in the ellipsoids due to viscous relaxation, the surrounding elastic region becomes important to support the differential stress. Thus, the localized strain rates can be large only during the viscous relaxation in the ellipsoid. After the completion of viscous relaxation, all the differential stress is supported solely by elastic region, and the localized strain rates vanish. Thus, three dimensional connectivity of low viscosity regions play an important role when considering crustal response to an externally applied stress change.

Keywords: Tohoku-Oki earthquake, GNSS, Viscoelasticity

©2019. Japan Geoscience Union. All Right Reserved.

Revisiting the Coseismic Slip Distribution of the 2011 Tohoku-oki Earthquake Considering Early Postseismic Deformation, Non-linear Viscoelasticity, and Heterogeneous Structure

*Takeshi Iinuma[1], Ryoichiro Agata[1], Yusaku Ohta[2], Ryota Hino[2], Takane Hori[1]

1. Japan Agency for Marine-Earth Science and Technology (JAMSTEC), 2. Graduate School of Science, Tohoku University

The 2011 Tohoku-oki earthquake produced large coseismic displacements that were detected by terrestrial and seafloor geodetic observations, namely, global navigation satellite systems (GNSS), GNSS-Acoustic (GNSS-A), and ocean bottom pressure (OBP) measurements. Previous studies constructed coseismic slip distribution models of the Tohoku-oki earthquake using the daily GNSS site coordinate time series, seafloor GNSS-A, and/or OBP data to estimate the coseismic displacements [e.g., Ito et al., 2011; Koketsu et al., 2011; Ozawa et al., 2011; Iinuma et al., 2012]. However, studies for these several years suggested that the coseismic displacements must include early postseismic deformation due to a low-viscosity zone beneath the Pacific plate that is necessary to explain terrestrial and seafloor postseismic crustal deformations [Sun et al., 2014; Freed et al., 2017; Suito, 2017]. This low-viscosity zone may not be persistent but could result in huge changes in stress resulting from the coseismic slip with reflecting non-linear rheology [Muto et al., 2018; Agata et al., 2019]. The effect of non-linear rheology is great immediately after a main shock. Therefore, coseismic displacements based on the daily site coordinate time series and GNSS-A measurements inevitably must include early postseismic deformation.

Thus, we derived “pure” coseismic displacements based on 1-Hz site coordinate time series at GNSS sites of the Geospatial Information Authority of Japan estimated by utilizing kinematic PPP (precise point positioning) analysis and based on 1-min average seafloor level time series at OBP sites. The residual displacements were obtained by subtracting the pure coseismic displacement from that based on the daily site coordinate time series. The data showed subsidence and trenchward motions in the entire Tohoku district. These broad deformations could not be explained solely by aftershocks nor by afterslip on the plate interface. Viscoelastic deformation that occurs immediately after the main shock is required to explain the displacement field. We present the results of our investigations into coseismic slip distribution and early postseismic deformation by applying Green’s function, which is calculated by considering the shapes of surface terrain and subducting slabs as well as heterogeneous thermal structures and power-law rheology.

References

Agata, R., et al. (2019). Rapid mantle flow with power-law creep explains deformation after the 2011 Tohoku mega-quake. *Nat. Commun.*, in press.

Freed, A. M., et al. (2017). Resolving depth-dependent subduction zone viscosity and afterslip from postseismic displacements following the 2011 Tohoku-oki, Japan earthquake. *Earth Planet. Sci. Lett.*, **459**, 279-290, doi:10.1016/j.epsl.2016.11.040.

©2019. Japan Geoscience Union. All Right Reserved.

Iinuma, T., et al. (2012). Coseismic slip distribution of the 2011 off the Pacific Coast of Tohoku Earthquake (M9.0) refined by means of seafloor geodetic data. *J. Geophys. Res.*, **117**, B07409, doi:10.1029/2012JB009186.

Ito, T., et al. (2011). Slip distribution of the 2011 off the Pacific coast of Tohoku earthquake inferred from geodetic data, *Earth Planets Space*, **63**, 627-630, doi:10.5047/eps.2011.06.023.

Koketsu, K., et al. (2011). A unified source model for the 2011 Tohoku earthquake. *Earth Planet. Sci. Lett.* , **310**, 480-487, doi:10.1016/j.epsl.2011.09.009.

Muto, J., et al. (2018). Nonlinear mechanical coupling between viscoelastic relaxation and deep afterslip in the post-seismic deformation of the 2011 Tohoku-oki earthquake. Abstract SCG57-30, presented at *JpGU Meeting 2018*, Chiba, Japan, 20-24 May.

Ozawa, S., et al. (2011). Coseismic and postseismic slip of the 2011 magnitude-9 Tohoku-Oki earthquake. *Nature*, **475**, 373-376, doi:10.1038/nature10227.

Suito, H. (2017). Importance of rheological heterogeneity for interpreting viscoelastic relaxation caused by the 2011 Tohoku-Oki earthquake. *Earth Planets Space*, **69**, 1, doi:10.1186/s40623-017-0611-9.

Sun, T., et al. (2014). Prevalence of viscoelastic relaxation after the 2011 Tohoku-oki earthquake. *Nature*, **514**, 84-87, doi:10.1038/nature13778.

Keywords: The 2011 Tohoku-oki Earthquake, Postseismic deformation, Power-law rheology

©2019. Japan Geoscience Union. All Right Reserved.

[J] Poster | S (Solid Earth Sciences)：S-CG Complex & General

Tue. May 28, 2019 3:30 PM - 5:00 PM JST | Tue. May 28, 2019 6:30 AM - 8:00 AM UTC | Poster Hall International Exhibition Hall8, Makuhari Messe_21

[S-CG61] Dynamics in mobile belts

convener:Yukitoshi Fukahata(Disaster Prevention Research Institute, Kyoto University), Toru Takeshita(Department of Natural History Sciences, Graduate School of Science, Hokkaido University), Hikaru Iwamori(Geochemical Evolution Research Program, Japan Agency for Marine-Earth Science and Technology)

The dynamic behaviours of mobile belts are expressed across a wide range of time scales, from the seismic and volcanic events that impact society during our lifetimes, to orogeny and the formation of large-scale fault systems which can take place over millions of years. Deformation occurs on length scales from microscopic fracture and flow to macroscopic deformation to plate-scale tectonics. To gain a physical understanding of the dynamics of mobile belts, we must determine the relationships between deformation and the driving stresses due to plate motion and other causes, which are connected through the rheological properties of the materials. To understand the full physical system, an integration of geophysics, geomorphology, and geology is necessary, as is the integration of observational, theoretical and experimental approaches. In addition, because rheological properties are greatly affected by fluids in the crust and fluid chemical reactions, petrological and geochemical approaches are also important. After the 2011 great Tohoku-oki earthquake, large-scale changes in seismic activity and regional scale crustal deformation were observed, making present-day Japan a unique natural laboratory for the study of the dynamics of mobile belts. This session welcomes presentations from different disciplines, such as seismology, geodesy, tectonic geomorphology, structural geology, petrology, and hydrology, as well as interdisciplinary studies, that relate to the dynamic behaviours of mobile belts.

[SCG61-P01] Three-dimensional imaging of geo-fluid distribution at NE-Japan forearc using wideband magnetotelluric measurements

*Masato Fukai[1], Yasuo Ogawa[1], Kuo Hsuan Tseng[1], Masahiro Ichiki[2], Shinichi Takakura[3] (1.Tokyo Institute of Technology, 2.Tohoku University, 3.National Institute of Advanced Industrial Science and Technology)

[SCG61-P02] **Elastic wave velocity and electrical conductivity in brine-saturated rocks and microstructure of pores**

*Arina Tomioka[1], Tohru Watanabe[1] (1.University of Toyama)

[SCG61-P03] Influence of grain shape and grain size distribution on connectivity of pores in granular materials.

*Katazakai Haruka[1], Tohru Watanabe[1] (1.Toyama University)

[SCG61-P04] Change of pore connectivity in granular materials under axial compression

*MAREMICHI ABE[1], Tohru Watanabe[1] (1.Toyama University)

[SCG61-P05] **Estimation of crustal strength using residual strain of quartz in deformed conglomerate and inhomogenous strain of conglomerate layer -As an example of multiple collision zone of Izu-Bonin arc, Fujikawa valley, Central Japan-**

*Shun Suzuki[1], Kenta Kobayashi[1] (1.Graduate School of Science and Technology, Niigata University)

[SCG61-P06] **An Introduction to Ryoke Cataclastic Rocks in Tsukide, Mie Prefecture, Japan: An Approach Using 3D Reconstructions From Thin Sections**

*Thomas Jing Yi Yeo[1], Toru Takeshita[1] (1.Department of Natural History Sciences, Graduate School of Science, Hokkaido University)

[SCG61-P07] Relationships between spacing and growth or linkage of normal faults in the Miyako Island, South Ryukyu arc, Japan

*Sumire Maeda[1], Makoto Otsubo[1], Daisuke Asahina[1], Yuki Furuno [1] (1.Research Institute of Earthquake and Volcano Geology, Geological Survey of Japan/AIST)

[SCG61-P08] **3D fault architecture along the Median Tectonic Line, eastern Kii Peninsula, SW Japan**

*Norio Shigematsu[1], Takuma Katori[1,2], Jun Kameda[3], Ayumu Miyakawa[4] (1.Research Institute of Earthquake and Volcano Geology, Geological Survey of Japan, National Institute of Advanced Industrial Science and Technology, 2.Graduate School of Science and Technology, Niigata University, 3.Department of Natural History and Sciences, Hokkaido University, 4.Research Institute of Geology and Geoinformation, Geological Survey of Japan, National Institute of Advanced Industrial Science and Technology)

[SCG61-P09] Significant of thrust zone at Fuji river basin in the South Fossa Magna, Southern Yamanashi Prefecture, Central Japan
-Study of Structural geology of Minobu and Neguma fault-

*Minami Madoka[1], Kenta Kobayashi[1] (1. Niigata university department of geology science)

[SCG61-P10] Mineralogical characteristics of fault rocks in the aftershock regions of the 2000 Western Tottori earthquake and its spatial distribution

*Shunya Kaneki[1], Tetsuro Hirono[1], Hideki Mukoyoshi[2], Kenta Kobayashi[3], Toru Takeshita[4] (1.Graduate School of Science, Osaka University, 2.Graduate School of Science and Engineering, Shimane University, 3.Graduate School of Science and Technology, Niigata University, 4.Graduate School of Science, Hokkaido University)

[SCG61-P11] Relationship between seismicity of the 2016 the Central Tottori Earthquake and fault distribution in the aftershock area

*Masayuki Ichimura[1], Hideki Mukoyoshi[2] (1.Graduate School of Natural Science and Technology, Shimane University, 2.Department of Earth Science, Shimane University)

[SCG61-P12] History of fault activity considered from the brittle shear zone and the geological structure near the Cape Otachi, Kumamoto Prefecture

*Keiji Ogashiwa[1], Kenta Kobayashi[1] (1.Niigata University)

[SCG61-P13] Study on fault activity evaluation method (A new attempt to understand fault activities) No.1 - Overall plan and current situation at Shionohira Fault -

*Kazuhiro Aoki[1], Takahiro Watanabe[1], Yukumo Tanaka[1], Kazuyoshi Seshimo[1] (1.Japan Atomic Energy Agency)

[SCG61-P14] Study on fault activity evaluation method (A new attempt to understand fault activities) No.2
- Injection experiment using a SIMFIP probe at Shionohira Fault and southern fault-

*Takahiro Watanabe[1], Yukumo Tanaka[1], Kazuhiro Aoki[1], Yves Guglielmi[2], Paul Cook[2], Florian Soom[2], Wakahama Hiroshi[3], Noujou Haruka[3], Etsuo Iwasaki[3], Masao Kametaka[3], Kazuyoshi Seshimo[1] (1.Japan Atomic Energy Agency, 2.Laurence Berkley National Laboratory, 3.DIA CONSULTANTS)

[SCG61-P15] Dynamic rupture simulation of 2018, Hokkaido Eastern Iburi earthquake: Role of non-planar fault geometry

*Tatsuya Hisakawa[1], Ryosuke Ando[1] (1.The University of Tokyo)

[SCG61-P16] A New Fully-Dynamic Earthquake Cycle Simulator Applicable to Arbitrary Nonplanar Fault Geometries - A Benchmark Test

*Daisuke Sato[1], Nadia Lapusta[2], Hiroyuki Noda[1] (1.Disaster Prevention Research Institute, Kyoto University, 2.California Institute of Technology)

[SCG61-P17] Stress and displacement Green's functions to treat volumetric inelastic strain and elastic inhomogeneity in boundary integral equation method

*Daisuke Sato[1] (1.Disaster Prevention Research Institute, Kyoto University)

[SCG61-P18] Frictional properties of dolerite and granite at intermediate slip rates and controlled ambient temperatures

*Michiyo Sawai[1], Yuuki Yokoyama[1], Kyuichi Kanagawa[1] (1.Chiba University)

[SCG61-P19] Extraction of features of strata using borehole data of geothermal area by multivariate analysis

*Ojima Hiroki[1], Kazuya Ishitsuka[2], Toru Mogi[3], Tatsuya Kajiwara[4], Takeshi Sugimoto[4], Hiroshi Asanuma[5] (1.Department of Socio-Environmental Engineering Hokkaido University, 2.Division of Urban Management, Graduate School of Engineering, Kyoto University, 3.Division of sustainable Resources Engineering, Faculty of Enginieering, Hokkaido University, 4.Geothermal Engineering Co. Ltd, 5.Fukushima Renewable Energy Institute, AIST)

[SCG61-P20] Low-temperature thermochronology of Cretaceous granitoids from the northern Northeast Japan Arc: Towards reconstructing arc-parallel thermal/denudation histories

*Shoma Fukuda[1], Shigeru Sueoka[2], Barry Paul Kohn[3], Noriko Hasebe[4], Akihiro Tamura[5], Tomoaki Morishita[5], Takahiro Tagami[1] (1.Graduate School of Science, Kyoto University , 2.Japan Atomic Energy Agency, 3.School of Earth Sciences, The University of Melbourne, 4.Institute of Nature and Environmental Technology, Kanazawa University, 5.Department of Earth Sciences, Kanazawa University)

[SCG61-P21] Uplift and denudation history of the South Fossa Magna region using low-temperature thermochronometric methods

*Yumi Kobayashi[1], Shigeru Sueoka[2], Shoma Fukuda[1], Barry P. Kohn[3], Tatsunori Yokoyama[2], Noriko Hasebe[4], Akihiro Tamura[5], Tomoaki Morishita[5], Takahiro Tagami[1] (1.Graduate School of Science, Kyoto University, 2.Tono Geoscience Center, Japan Atomic Energy Agency, 3.University of Melbourne, 4.Institute of Nature of Environmental Technology, Kanazawa University, 5.Department of Earth Sciences, Kanazawa University)

[SCG61-P22] Correlation between residual uplift and recurrence interval of the Kanto earthquake based on developmental process of coastal lowland

*Haeng-Yoong Kim[1] (1.Osaka City University, Graduate School of Science, Division of Biology &Geosciences)

[SCG61-P23] Mechanics preserving co-seismic uplift and marine terraces: dissymmetric patterns of co-seismic and inter-seismic deformation

*Kyohei Suzuki[1], Junki Komori[1], Ryosuke Ando[1] (1.Graduate School of Science, University of Tokyo)

[SCG61-P24] Enhanced resolution of stress tensor inversion by using fault instability analysis
★Invited Papers

*Katsushi Sato[1] (1.Division of Earth and Planetary Sciences, Graduate School of Science, Kyoto University)

[SCG61-P25] Focal mechanisms of the aftershocks of the 2000 Western Tottori Earthquake inferred from P wave first-motion data and spatial stress pattern

*Takaki Iwata[1] (1.Tokiwa University)

[SCG61-P26] Stress tensor inversion in focal area of the 2016 Mw7.8 Kaikoura earthquake, New Zealand

*Miu Matsuno[1], Tomomi Okada[1], Satoshi Matsumoto[2], Yuta Kawamura[2], Yoshihisa Iio[3], Tadashi Sato[1], Stephen C Bannister[4], John Ristau[4], Martha K Savage[5], John Townend[5], Jarg Pettinga[6], Francesca Ghisetti[7], Richard H Sibson[8] (1.Research Center for Prediction of Earthquakes and Volcanic Eruptions Graduate School of Science, Tohoku University, 2.Institute of Seismology and Volcanology, Faculty of Sciences, Kyushu University, 3.Disater Prevention Research Institute, Kyoto University, 4.GNS Science, New Zealand, 5.Victoria University of Wellington, Wellington, New Zealand, 6.University of Canterbury, Christchurch, New Zealand, 7.TerraGeologica, Ruby Bay, New Zealand, 8.University of Otago, Dunedin, New Zealand)

[SCG61-P27] Precise hypocenter distribution in the focal area of the 2016 Mw7.8 Kaikorua Earthquake, New Zealand

*Yuta Kawamura[1], Satoshi Matsumoto[1], Tomomi Okada[2], Miu Matsuno[2], Yoshihisa Iio[3], Tadashi Sato[2], Stephen C Bannister[4], John Ristau[4], Martha K Savage[5], John Twonend[5], Jarg Pettinga[6], Francesca Ghisetti[7], Richard H Sibson[8] (1.Kyushu University, Shimabara, Japan, 2.Tohoku University, Sendai, Japan, 3.Kyoto University, Uji, Japan, 4.GNS Science, Lower Hutt, New Zealand, 5.Victoria University of Wellington, Wellington, New Zealand, 6.University of Canterbury, Christchurch, New Zealand, 7.TerraGeologica, Ruby Bay, New Zealand, 8.University of Otago, Dunedin, New Zealand)

[SCG61-P28] **3-dimensional GPS velocities in Colombia and their implications for interplate coupling**

*Sindy Carolina Lizarazo[1], Takeshi Sagiya[2], Hector Mora-Paez[3] (1.Graduate School of Environmental Studies, Nagoya University, 2.Disaster Mitigation Research Center, Nagoya University, 3.Geological Survey of Colombia)

Three-dimensional imaging of geo-fluid distribution at NE-Japan forearc using wideband magnetotelluric measurements

*Masato Fukai[1], Yasuo Ogawa[1], Kuo Hsuan Tseng[1], Masahiro Ichiki[2], Shinichi Takakura[3]

1. Tokyo Institute of Technology, 2. Tohoku University, 3. National Institute of Advanced Industrial Science and Technology

In Tohoku Japan, the Pacific plate that subducts under the Eurasian plate is old, thick, and cold. The basalt - eclogite phase transition is expected to occur at a depth of 100 km. The water released in the dehydration reaction forms serpentinite, which is transported to the deeper part. Serpentinite decomposes at a depth of about 150 km and water rises in the mantle due to buoyancy. Therefore, it is believed that there is no rise in water caused by slab mineral dehydration in the Northeast Japan forearc (Kazahaya et al., 2014). In contrast, the seismic tomography in NE Japan fore arc (Zhao et al., 2014) imaged low velocity regions in the forarc which suggests rising fluids from slabs which is called as "Water wall". In this research, we aimed to constrain the rising fluid distribution in the forearc from the 3d electric conductivity structure by magnetotelluric observations in Kitakami Mountains.
In our model, distribution of low resistivity indicating rising fluids from the deep part was not analyzed corresponding to the P wave low velocity region of Zhao et al.(2014). However, vertical low resistivity was analyzed from the volcanic front toward forarc. The conductors spread 30 km east of the volcanic front at depths of 10-40 km. This low resistivity is in good agreement with the low velocity distribution (Zhao et al., 2014; Okada et al., 2015). The low resistivity east of volcanic front is almost vertically continuous from the uppermost mantle to the middle crust. Therefore, this may indicate that the fluid on the mantle flow reaches the uppermost mantle of the forearc and releases fluids in the forearc crust.

Keywords: geofluid, NE Japan forearc, magnetotelluric method

©2019. Japan Geoscience Union. All Right Reserved.

Elastic wave velocity and electrical conductivity in brine-saturated rocks and microstructure of pores

*Arina Tomioka[1], Tohru Watanabe[1]

1. University of Toyama

Geophysical mapping of fluids is critical for understanding crustal processes. Seismic velocity and electrical resistivity structures have been studied to reveal the fluid distribution. However, the fluid distribution has been still poorly constrained. Observed velocity and resistivity should be combined to make a quantitative inference on fluid distribution. The combined interpretation requires a thorough understanding of velocity and resistivity in fluid-saturated rocks. We have made measurements of elastic wave velocities and electrical conductivity in brine-saturated rocks under confining pressures, and examined pore structures with SEM.

Measurements and microstructural observations were made on granites (Aji, Kagawa Pref., Ohshima, Ehime Pref.), granodiorite (Enzan, Yamanashi, Pref.) and tonalite (Kadohara, Fukui Pref.). Cylindrical rock samples (D=26 mm, L=30 mm) were filled with 0.1 M KCl aqueous solution, and velocity and conductivity were simultaneously measured by using a 200 MPa hydrostatic pressure vessel. The pore-fluid was electrically insulated from the metal work by using plastic devices. The confining pressure was incrementaly increased up to 150 MPa, while the pore-fluid pressure was kept at 0.1 MPa. It took 3 days or longer for the electrical conductivity to become stationary after increasing the confining pressure.

Rock samples showed moderate increase in velocity and large decrease in conductivity under confining pressures. Electrical conductivity steeply decreased at low pressures (<20 MPa) and then showed gradual decreases. Grain boundary cracks are pervasive in rock samples. The increase in velocity and decrease in conductivity at low pressures must be caused by the closure of grain boundary cracks with small aspect ratios ($<10^{-3}$). SEM images show that the aperture of a grain boundary crack varies along its width. Large aperture parts can be open even under high pressures to be conduction paths. The difference in conductivity at high pressures must reflect the difference in the amount of large aperture parts.

Keywords: Elastic wave velocity, electrical conductivity, fluid

©2019. Japan Geoscience Union. All Right Reserved.

Influence of grain shape and grain size distribution on connectivity of pores in granular materials.

*Katazakai Haruka[1], Tohru Watanabe[1]

1. Toyama University

Transport properties such as electrical conductivity and permeability are sensitive to the connectivity of pores. Pore structure in granular materials varies with the shape and size distribution of grains. In order to understand the influence of the shape and size distribution of grains, electrical conductivity and permeability were measured on granular materials saturated with 0.1 mol/L KCl aqueous solution. Spherical glass beads and oblate quartz sand of various sizes were employed. The ratio of conductivity to porosity was significantly higher in glass beads than in quartz sand. This observation suggests that a higher connectivity of pore is established in glass beads than in quartz sand. The influence of the size distribution of grains was studied on mixtures of small (D=0.2 mm) and large (D=1 mm) glass beads. The porosity deceases from 36% to 22% as the fraction of large grains increases 0% to 60%. Electrical conductivity decreases with decreasing porosity, while permeability shows a small decrease. As the fraction of large grains increases from 60% to 100%, the porosity increases from 22% to 36% and permeability increases by around 2 orders of magnitude. This change suggests that the pore size steeply increases as the fraction of large grains increases from 60%, since permeability strongly depends on the size of pores. X-ray micro CT observation was conducted to examine pore structure.

Keywords: conductivity, permeability, pore

©2019. Japan Geoscience Union. All Right Reserved.

Change of pore connectivity in granular materials under axial compression

*MAREMICHI ABE[1], Tohru Watanabe[1]

1. Toyama University

The influence of axial compression on the connectivity of pores in granular materials was studied. Electrical conductivity and compressional wave velocity were simultaneously measured on brine-saturated granular materials under uniaxial compression. Spherical glass beads and oblate quartz sand were employed. X-ray micro CT was conducted on granular materials impregnated with epoxy resin to examine microstructure of pores. Compressional wave velocity increases and electrical conductivity decreases with increasing axial stress. When the axial stress was increased from 0 to 5 MPa, compressional wave velocity increased by around 12% in both materials and electrical conductivity decreased by 0.7 and 1.7% in glass beads and quartz sand, respectively. The increase in compressional wave velocity must reflect the increase in contact area between grains, which was observed with X-ray micro CT. The decrease in conductivity must be caused by the decrease in connectivity of pores. X-ray micro CT images show that the connectivity of pores is easily lost under axial compression in quartz sand owing to its oblate shape.

Keywords: granular material, pore, electrical conductivity

©2019. Japan Geoscience Union. All Right Reserved.

Estimation of crustal strength using residual strain of quartz in deformed conglomerate and inhomogenous strain of conglomerate layer -As an example of multiple collision zone of Izu-Bonin arc, Fujikawa valley, Central Japan-

*Shun Suzuki[1], Kenta Kobayashi[1]

1. Graduate School of Science and Technology, Niigata University

South Fossa Magna is understood as a site where the Izu-Bonin arc on the Philippine Sea plate collides with Honshu arc, and it is the only arc-arc multiple collision zone in the world. Maruyama (2008) reported deformed conglomerate outcrop accompanied by cataclastic flow in the Hamaishidake Formation (late Miocene to Pliocene). Report of them in the collision zone is not limited to the Fujikawa area, but from the Ashigara Group and from the Erimo Formation in the Hidaka collision zone of Hokkaido (Uda, 1976), have been reported. In this study, various analyzes were performed on deformed conglomerates found in the Fujikawa area, and the cause (temperature / pressure condition) and the position in the collision zone were clarified, it aimed to restrict the multiple collision phenomenon and the deformation environment of trench fill sediments.

[Outcrop outline]
It is revealed that the deformed conglomerate outcrops occurred in the geologic body (Fujikawa Shear Zone) which makes a high dip zone in the direction of NW-SE, and they are modifying the initial NS system folding. The long axis direction of the gravel showing N40W trend and the shear fabric of the gravel showing sinistral sense.

[Paleo stress analysis by multiple inverse method]
The result of the MIM analysis (Yamaji et al., 2011) using the slip data of the gravel fault plane with the flow deformation mode shows ENE-WSW compression, which is not consistent with the current Philippine Sea plate motion.

[Restrictions on forming environmental condition of deformed conglomerate]
We tried to guess the maximum heat temperature of the geological body using the carbonaceous material Raman spectrum (Kouketsu et al., 2014), and examination of the differential stress level using the internal strain of the quartz (Takagi et al., 1988). As a result, it is revealed that deformed conglomerate outcrops heated only 150℃ or less, and the maximum heated temperature is rising toward the lower formation of Hamaishidake Formation. When the geothermal gradient is estimated by layer thickness conversion, the value such as 4~5℃ / 100 m is restored, and the depth at which the 150℃ heating can be recorded is about 3~4 km. That is, the deformed conglomerate is found to be a product under shallow and low temperature conditions. On the other hand, the estimated differential stress value is 50-100 MPa, which is strongly deformed despite being a shallow deformation.

[Discussion]
As for the ENE-WSW compression obtained from cataclastic flow slip data, it can not be explained with only the motion of the Philippine Sea plate. If these as deformation events after the deposition age limit (about 5 Ma) of the Hamaishidake Formation, it is necessary to consider the influence of E-W compression from around 3 Ma (Takahashi, 2006) or the ENE movement of Amur Plate (Komatsubara, 2015), and it

©2019. Japan Geoscience Union. All Right Reserved.

means that the tectonics are not only dominated by the Philippine Sea plate. Considering trench fill sediment objects in the Fujikawa Valley as accretionary bodies, since deformed conglomerate occurs near the boundary fault of the middle and upper strata of the Fujikawa Group, it may be a deformation near the Mega Splay Fault branching from the plate boundary fault at the Tanzawa block collision stage. In addition, considering the usual crustal strength (Byerlee, 1978), theoretically it is not possible to record a differential stress value of 100 MPa at 4 km underground. However, according to the data of drilling at the plate boundary Nankai Trough (Hamada et al., 2018), it is pointed out that the differential stress value rises in the Accretionary prism and reaches nearly 100 MPa. In other words, in the geological body near the plate boundary, it is predicted that the crustal strength is large and it is placed in the high differential stress state also in the subsurface shallow part, and the deformed conglomerate is considered to be a product in such a place.

Keywords: South Fossa Magna, Multiple collision zone, Deformed conglomerate, Rheology of fault rocks

©2019. Japan Geoscience Union. All Right Reserved.

An Introduction to Ryoke Cataclastic Rocks in Tsukide, Mie Prefecture, Japan: An Approach Using 3D Reconstructions From Thin Sections

*Thomas Jing Yi Yeo[1], Toru Takeshita[1]

1. Department of Natural History Sciences, Graduate School of Science, Hokkaido University

The Japan Median Tectonic Line (MTL) is the longest fault system in Japan where it spans from Kyushu Island and extends towards the north east direction up until Ibaraki Prefecture. It has been an active strike slip fault since the Mid-Cretaceous period, which was originally formed as the southern marginal shear zone in the Ryoke belt (e.g. Hara et al., 1980) leading to the formation of mylonite and superposed by cataclasite at the core region.

This study aims to identify the kinematic history of the fault plane and its effect on the cataclastic rocks from a 3D viewpoint. The fieldwork was conducted in the hanging wall section of the MTL in Mie Prefecture, Japan. The hanging wall of the MTL in the study area is characterized by Creataceous Ryoke granitic rocks which was deformed into mylonitic rocks and was later overprinted by cataclasite at the proximal region. The main objective of this project is to identify and relate the kinematics of the MTL and physical conditions during the formation of the cataclasite.

From the thin sections observations, the grain size reduction of the mylonitic clasts was observed and was related with cataclasis. The cataclasite formed at the brittle fault zone enables chemically rich fluids to penetrate. This promotes the growth of foliated phyllosilicate minerals mainly muscovite from the alteration of presumably feldspars. Microstructural features such as riedel shears with C’ -type shear band fabric assist in indicating the sense of motion. Fracture densities and distributions are also quantified in all of the three sides of the sample in order to obtain a clearer view on the brittle properties.

Also, based on the crossed cutting relationship seen in the microstructures of the sample, a schematic deformation history of the sample was constructed. The MTL begins with a sinistral shear sense which causes the mylonitisation of the Ryoke granitoids. Upon the cooling of temperature, cataclasite was formed and transpression of the shear zone causing pressure solution seams to be precipitated which resulted in the formation of phyllonite. Lastly, a late stage reactivation of the pressure solution seams caused faulting to occur.

Furthermore, using the rake angle of the C’ and S fabrics of the Riedel shears, measured from the thin sections representing the different sides of the sample, the orientations of both the C’ and S planes could be reconstructed and plotted as a stereographic projection with values of [278/ 48N] and [124/ 82SW] respectively. The XZ plane which is 90° away from the intersection point of C’ and S planes has an orientation of [031/ 67SE]. By assuming plane strain and with the assistant of the software StrainSim v3, the simple shear strain, γ=0.73, the angular shear, Ψ=36° and material internal friction angle, Φ= 56°. Similarly, the principle stress orientations are found to be at [62°→158], [23°→301] and [15°→037] for σ_1, σ_2 and σ_3 respectively. By combining all the relationships mention above, the motion sense of the fault was identified as the NE block moving NW and downwards with a more dominant dip slip component. This dominant dip slip movement of the fault could be potentially related to the normal faulting movement of the MTL during the Ichinokawa Phase at 63-58Ma.

Moreover, the electron backscatter diffraction (EBSD) analysis of the sample is currently being conducted

©2019. Japan Geoscience Union. All Right Reserved.

to analyse the distribution of the quartz’ s and calcite’ s C-axis fabric.

References

Hara, I, Shyoji, K., Sakurai, Y., Yokoyama, S., Hide, K., 1980. Origin of the Median Tectonic Line and its initial shape. *Memoirs of the Geological Society of Japan*. No. 18, 27–49.

Keywords: Median Tectonic Line (MTL), Cataclasite, Pressure Solution Seams, Shear Zone, Fractures, Kinematics

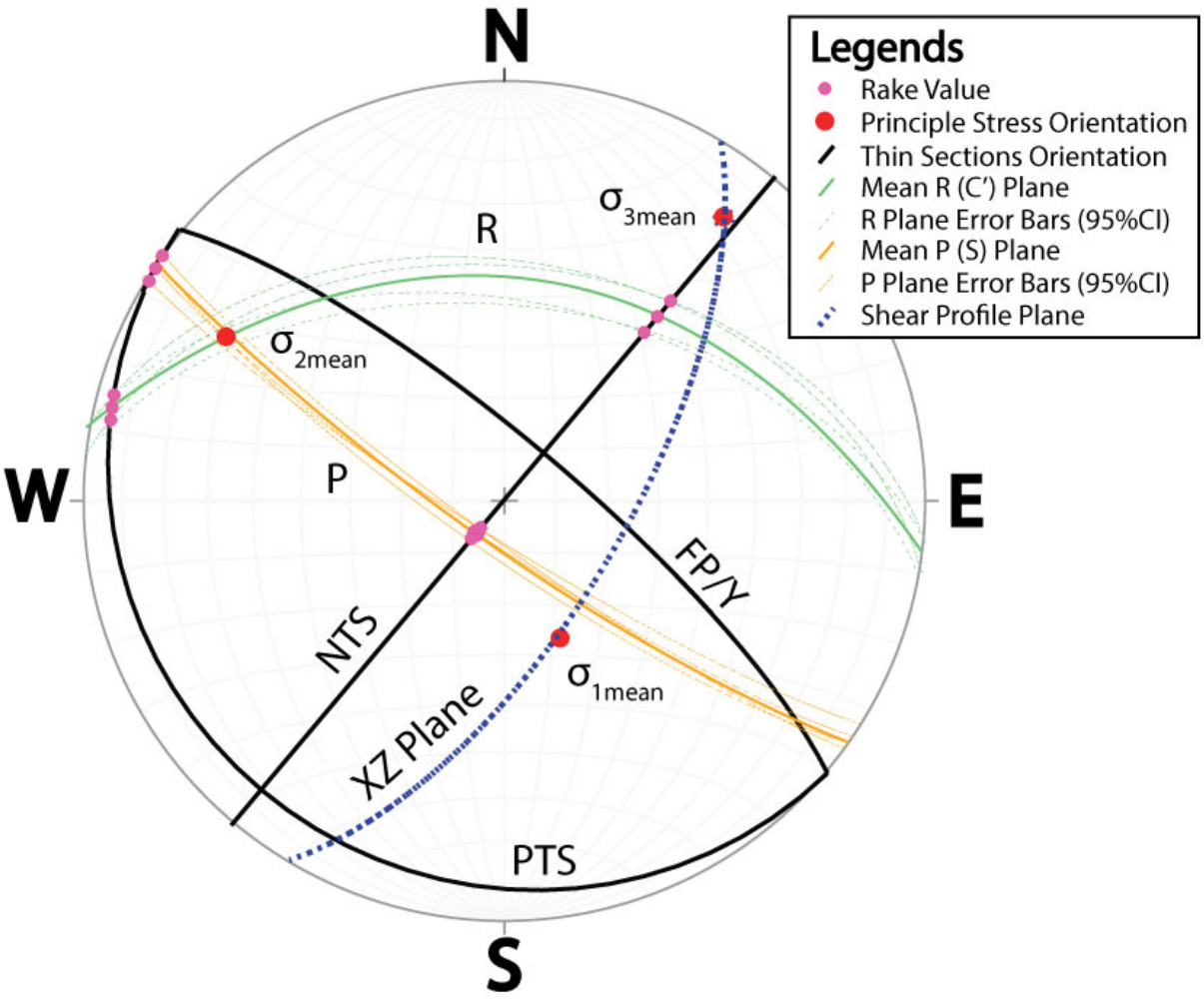

©2019. Japan Geoscience Union. All Right Reserved.

Relationships between spacing and growth or linkage of normal faults in the Miyako Island, South Ryukyu arc, Japan

*Sumire Maeda[1], Makoto Otsubo[1], Daisuke Asahina[1], Yuki Furuno [1]

1. Research Institute of Earthquake and Volcano Geology, Geological Survey of Japan/AIST

Estimating interaction and linkage of faults is one of the most important issues to evaluate the long-term activity of future earthquakes. For the long-term evaluation of the major active fault zones, Headquarters for Earthquake Research Promotion (e.g., HERP, 2010) uses so-called 5-km gap threshold (Matsuda,1990) to group and segment the fault traces. However, the fault size may change in the future, so it is necessary to introduce a multilateral index that can evaluate temporal and spatial evolution of faults.
Fault spacing, the horizontal distance between neighboring faults, has been related to stress reduction around faults (e.g., Soliva et al., 2006; Fossen and Rotevatn, 2016). Soliva et al. (2006) investigated the relationship between the fault spacing and the stress reduction area for a series of faults. Their studies show that the fault spacing is linearly related to the mechanical layer thickness. In the evolution process of normal fault, it is assumed that randomly distributed faults start to propagate and couple at the beginning, and the fault spacing becomes regularly distributed. Therefore, it may be possible to estimate the thickness of the mechanical layer in which the faults exist from the regular spacing of the saturated faults.
In this study, we investigated the normal faults in the Miyako Island, South Ryukyu arc, Japan in order to examine the possibility of fault linkage based on the fault spacing and the Coulomb shear stress perturbation. We found that the Miyako Island has three fault groups with different types of strikes, and these fault spacings are almost regularly distributed. The layer thickness of the NW-SE strike fault group can be estimated about 3,500 m based on the faults spacing. This results imply that the fault group extends only to the upper end of the seismogenic zone (3-17 km; HERP, 2012). In addition, the thickness of this fault group is close to the thickness of the Ryukyu Group and Shimajiri Group of the Miyako Island. Large-scale faults beneath the Miyako Island may be branched in the shallow soft-sedimentary rocks.

©2019. Japan Geoscience Union. All Right Reserved.

3D fault architecture along the Median Tectonic Line, eastern Kii Peninsula, SW Japan

*Norio Shigematsu[1], Takuma Katori[1,2], Jun Kameda[3], Ayumu Miyakawa[4]

1. Research Institute of Earthquake and Volcano Geology, Geological Survey of Japan, National Institute of Advanced Industrial Science and Technology, 2. Graduate School of Science and Technology, Niigata University, 3. Department of Natural History and Sciences, Hokkaido University, 4. Research Institute of Geology and Geoinformation, Geological Survey of Japan, National Institute of Advanced Industrial Science and Technology

The heterogeneous fault deformation around the brittle-plastic transition possibly affects the fault behavior significantly including the generation of earthquakes (e.g., Scholtz, 2001). To understand the effect, a detailed fault zone architecture is essential. In this study we have tried to construct a 3D fault zone architecture model based on the geological study of an exhumed fault zone, the Median Tectonic Line (MTL) in the western Kii peninsula SW Japan.

Accurate positions were determiend by applying SfM (structure from motion) and MVS (multi-view stereo) calculation (e.g., Furukawa and Hernández, 2013) to photos taken by an UAV (Unmanned Aerial Vehicles), and GNSS (Global Navigation Satellite system) surveying (e.g., Bemis et al., 2014) to reveal the 3D structures. The microstructures, chemical composition of minerals and crystallographic orientations of quartz using an electron back-scatter diffraction (EBSD) (Prior, et al., 1998) were analyzed to characterize the defomation of fault rocks. Based on these deformation features, the 3D fault zone architcture were constructed using a 3D-CAD software.

In the 3D fault zone architecture model, the fault plane of the MTL (lithological boundary) is an almost perfect plane dipping to the North. The structures can be divided into two main structures. One includes mylonite and cataclasite showing sinistral sense of shear. The other structures consist of scaly cataclasite showing dextral sense of shear and further younger structures including the lithological bonadry. The later structures cut the former structures indicating the sequence of deformation within the fault zone.

Scaly cataclasite only apper in the vicinity of the MTL, and is characterized by the strong foliation defined by the alignment of chlorite. Modal fraction chlorite is much larger than that in the surrounding Ryoke drived rocks, and pressure-solution seam is well developed. The estimated temperature based on the chlorite geothermometry is about 300 ºC (Bourdelle et al., 2013).
The deformation of the structures showing sinistral sense of shear varies from mylonite deformed at temperature of about 450 ºC (Higher-T mylonite), that deformed at about 300 ºC (Lower-T mylonite) to cataclasite deformed at about 300 ºC, suggesnting these structures record the brittle-plastic transition. One conspicuous feature in these structures is an altanation zone of black cataclasite and ultramylonite. This zone is a narrow and planar zone with width of 10 m. The cataclasite in this zone is black colored and strongly foliated. The ultramylonite in this zone show almost ramdom CPO (crstallographic preffered orientation) of quartz. We consider that this zone was the fault core when the present exhumed level experienced the brittle-plastic transiton.

Keywords: Fault Zone Architecture, Brittle–Plastic transition, the Median Tectonic Line, Mylonite, Cataclasite

©2019. Japan Geoscience Union. All Right Reserved.

Significant of thrust zone at Fuji river basin in the South Fossa Magna, Southern Yamanashi Prefecture, Central Japan
-Study of Structural geology of Minobu and Neguma fault-

*Minami Madoka[1], Kenta Kobayashi[1]

1. Niigata university department of geology science

There are Minobu fault that was certified as major active fault, Itoigawa shizuoka Tectonic Line (ISTL) and Fujikawa Kako Fault Zone (FKFZ) in the South Fossa Magna. The region is very precious to reveal formation of Japan island because the area is collision and accretion zone to Southwest Japan of Izu-Ogasawara arc. Mainly, Fujikawa group is distributed that filled trough made by past collisional block in this study area.
Minobu Fault is high probability to connect ISTL and FKFZ in the blank range of active fault. In recent years, it was shown sinistral fault sense from geomorophological point of view.(Mizumoto,2016) Howevere, nortern Minobu Fault is estimated reverse fault sense because of stratigraphy difference.
We discover and described new Minobu fault outcrops and divide Minobu fault into Segment Ⅰ and Ⅱ. We are obtained datas from stress analysis and XRD analysis in the area.
We will discuss the formation mechanism and history of geological structure deveropment of Minobu and Neguma fault in South Fossa Magna from kinematics of the faults and geological structure.

Keywords: South Fossa Magna, active faults, Itoigawa Shizuoka Tectonic Line, Fujikawa Kako Fault Zone

©2019. Japan Geoscience Union. All Right Reserved.

Mineralogical characteristics of fault rocks in the aftershock regions of the 2000 Western Tottori earthquake and its spatial distribution

*Shunya Kaneki[1], Tetsuro Hirono[1], Hideki Mukoyoshi[2], Kenta Kobayashi[3], Toru Takeshita[4]

1. Graduate School of Science, Osaka University, 2. Graduate School of Science and Engineering, Shimane University, 3. Graduate School of Science and Technology, Niigata University, 4. Graduate School of Science, Hokkaido University

A large earthquake (*Mw*6.6) occurred on 6 October 2000 in the western part of Tottori Prefecture, southwestern Japan. The main shock was considered as an almost left-lateral strike-slip event with the hypocenter located at 35.269 ˚N and 133.357 ˚E. The rupture process and slip distribution of the main shock was estimated from coseismic strong motions and geodetic data. These previous studies suggested that slip of the main shock mainly occurred in the southern part of the aftershock regions. Furthermore, Yukutake et al. (2007) estimated regional stress field before and after the main shock using aftershock focal mechanisms, and proposed that southern part of the aftershock regions may be dramatically weak in friction compared to northern and central parts. However, there are currently few researches attempting to understand regional slip behaviors of both main shock and aftershocks in association with spatial heterogeneity of physical properties of fault materials.

Mineralogical characteristics of rocks is one of the valid candidates that is likely to dominate its physical properties, and in general, increase in amount of frictionally weak minerals can reduce frictional strength of fault rocks. For understanding spatial slip behaviors in aftershock regions of the 2000 Western Tottori earthquake, we first need to investigate spatial variations in mineral composition of fault rocks. We collected more than 100 bulk rock samples from 14 fault-related outcrops, that distribute in northern, central, and southern parts of the aftershock regions. We then acquired XRD profiles of the powdered samples with internal standard (Al_2O_3) of 20 wt.%, and estimated the amount of minerals by using the RockJock software. The results clearly indicate that intact host rocks have similar mineralogical features regardless of sampling locations; they are granitic rocks composed of quartz, K-feldspar, and plagioclase. In contrast, mineral compositions of fault rocks show different characteristics by locations. In northern part of the aftershock regions, fault rocks are poor in K-feldspar and plagioclase and are rich in halloysite. In central part, fault rocks are poor in K-feldspar and plagioclase and are rich in illite. In southern part, fault rocks are poor in plagioclase and are rich in halloysite. These information tell us the representative mineralogical features of fault rocks in each part of the aftershock regions. Future friction experiments, by using representative fault rock samples under in-situ conditions, will give us a direct glimpse into the spatial variations of frictional properties in the aftershock regions of the 2000 Western Tottori earthquake, such as frictional strength and its velocity dependence. All of these information, not only seismological data but also mineral composition and physical properties of fault materials, should be incorporated for understanding the spatial heterogeneity of slip behaviors of the main shock and aftershocks of the 2000 Western Tottori earthquake.

Keywords: The 2000 Western Tottori earthquake, Fault rock, Mineral composition, XRD analysis

©2019. Japan Geoscience Union. All Right Reserved.

Relationship between seismicity of the 2016 the Central Tottori Earthquake and fault distribution in the aftershock area

*Masayuki Ichimura[1], Hideki Mukoyoshi[2]

1. Graduate School of Natural Science and Technology, Shimane University, 2. Department of Earth Science, Shimane University

The 2016 Central Tottori Earthquake (M6.6) occurred on October 21. The epicenter was Central Tottori and depth of hypocenter was 11km. Earthquake source fault was determined to be left-lateral strike fault developed NNW-SSE direction with WNW-ESE directional maximum principal stress axis. In the region, active fault related to the earthquake was not recognized. Although clarification of the occurrence of faults such strain concentration zone is important, there are no reports about detail field outcrop investigation in the area of this earthquake.
The aim of this study is to reveal relationship between seismicity of the 2016 Central Tottori Earthquake and fault distribution in the aftershock area based on field investigation and description of microstructure of the faults.

In this study area, late Cretaceous-early Paleogene medium-coarse-grained biotite granite is mainly distributed.

As a result of this study, total of 190 faults were observed in the aftershock area. Orientation of faults developed in NNW trending aftershock area were concentrated in NNW. On the other hand, faults in eastern part of aftershock area shows N-S~NE trend. Three-directional striation on the fault plane was observed in the aftershock area and only cataclasite was developed. The fault (strikes NNW) had horizontal striation was confirmed. P-foliation was observed in this fault rocks under the microscopic observation and indicated left-lateral strike slip.

The fault that had experienced strike slip, and shear sense consistent with earthquake source fault was confirmed. This result indicates that this fault had moved in the present stress field. According to previous study related to 2000 Western Tottori Earthquake, it is suggested that NNW trending fault system developed in southern part of the aftershock area was weaker than the surrounding area. With comparing these result, fault system in aftershock area of the 2016 Central Tottori Earthquake also might be weaker faults due to the orientation of faults correspond with the Y surface of the earthquake source fault.

©2019. Japan Geoscience Union. All Right Reserved.

History of fault activity considered from the brittle shear zone and the geological structure near the Cape Otachi, Kumamoto Prefecture

*Keiji Ogashiwa[1], Kenta Kobayashi[1]

1. Niigata University

[Introduction] The Hinagu fault zone is located in the western Kyushu and is an active fault zone extending 81 km roughly in the NE-SW direction. The Hinagu fault zone is a dextral slip fault with the east side uplift [URL]. The fracture zones of the Hinagu fault zone have been reported in two places in the Higo metamorphic rock distribution area and in the lower Cretaceous distribution Area near the cape Otachi (Matsumoto・Kanmera, 1964). The core of the fracture zone at Sabagami pass shows dextral slip and its outer rim shows sinistral slip (Kobayashi・Koshiwa, 2016). In addition, the geological fault parallel to the Hinagu fault is apparent sinistral slip fault (Saito et al., 2005). These facts suggest the possibility that the Hinagu fault zone was active differently from the past and the present. Analysis of the fracture zone and surface survey around the fracture zone are important for elucidating the history of fault zone activity. In addition, since Kyushu is an important area which is the meeting part of the Southwest Japan arc and the Ryukyu arc, clarifying the activity history of the Hinagu fault zone leads to the understanding of the tectonics of Kyushu. In this research, for the purpose of elucidating the history of activity of the Hinagu fault zone from the brittle shear zone and geological structure found near the Cape Otachi, Kumamoto Prefecture, the ground surface survey, the structure observation of the fault rock, the XRD analysis, the small fault Analysis and so on.

[Ground Surface Survey] As a result of the ground survey around the Cape Otachi, small faults constituting the fracture zone were observed in the lower Cretaceous Hinagu Formation, and it was roughly classified into 4 strains from the strike of the fault, the sense, and the cutting relationship. F1 is NNE-SSW trend sinistral slip fault, F2 is NNE-SSW trend dextral slip fault, F3 is NNW-SSE trend sinistral slip fault, F4 is E-W trend dextral slip fault.

F2 is a small fault group found in the brittle shear zone consisting of cataclasite. F1 is seen outside the brittle shear zone and part forms a planar cataclasite zone with a width of 5 cm. F3 and F4 are small fault groups which mutually cut. F3 deform the dike group described later. F4 cuts the brittle shear zone. Apart from the fault, we identified a folding group with a hinge in the ENE-WSW direction on the southeast side of the brittle shear zone. In addition, an andesitic dykes group with a dominant ENE-WSW strike was observed on the east side of the brittle shear zone. We confirmed the cutting and bending of the dike by F3, the injection of dike along the F3. This dike is believed to be related to the Neogene Igneous rocks in Amakusa area (Matsumoto ·Kanmera, 1964).

[Small Fault Analysis by Multiple Inverse Method (Yamaji, 1999)] Compressive Stress Field in NW-SE direction from F1, Compressive Stress Field in ENE-WSW direction from F2, Compressive Stress Field in NW-SE direction from F3 and F4 Was detected.

[Stage Segmentation] The time of formation of the fault, dike and fold observed in the vicinity of the Cape Otachi is divided into three stages, D1, D2, D3 from the stress field obtained from the cutting relation.
In D1, F1 was activated in the compressive stress field in the NNW-SSE direction. Considering the compression axis direction, fold group with fold axis in NE-SW direction is thought to be formed in D1.
In D2, F2 was activated in the compressive stress field in the ENE-WSW direction, forming a wide brittle

©2019. Japan Geoscience Union. All Right Reserved.

shear zone.
In D3, F3 and F4 were active in the compressive stress field in the NW-SE direction.
We thought that the bending and the injection of dike along F3 indicate that the dikes were deformed by F3 before consolidation. Considering the above-mentioned thing, we thought that the dike group had formed between the terminal stage of D2 and the beginning of D3.

Keywords: Hinagu fault zone

©2019. Japan Geoscience Union. All Right Reserved.

Study on fault activity evaluation method (A new attempt to understand fault activities) No.1 - Overall plan and current situation at Shionohira Fault -

*Kazuhiro Aoki[1], Takahiro Watanabe[1], Yukumo Tanaka[1], Kazuyoshi Seshimo[1]

1. Japan Atomic Energy Agency

If there is a "fault that may become active in the future" (hereinafter referred to as “inactive segment”) in the vicinity of a fault that has recently moved (hereinafter referred to as "active segment"), it appears that there is a difference in the stress state and in the "ease of activity" between the two segments. Under the current concept of nuclear regulatory standards, these segments are evaluated as part of the same series of faults due to lack of knowledge about interlocking faults.

Following the April 11, 2011 Fukushima-ken Hamadori Earthquake (4.11 earthquake), co-seismic surface ruptures trending NNW-SSE emerged over a distance of 14km between Nameishi Tabito of Iwaki city and North-west of Tsunaki Ishizumi. The surface rupture was named Shionohira fault by Ishiyama et al. (2011) and is identified to be part of the Itozawa fault (coincides to West trace of Itozawa fault by Tsutsumi and Toda, 2012). According to Imaizumi et al. (2018), the fault is said to continue extending south of the ruptured surface covering the area from Nameishi of Tabito Iwaki city to West of Sakura, Kawabe-cho and from Wakigawa, Yamadama-cho to Kobuki, Sekimoto-cho Kita Ibaraki city. In this study, the area designated as the Shionohira fault which has surfaced after the 4.11 earthquake is called the active segment and the remaining area to the south to be the inactive segment.

The authors aim to develop a fault activity evaluation method in order to clarify whether the inactive segment really moves together with the series of faults including the active section when a fault activity occurs by studying the differences between active and inactive segments in the interlocking of faults.

The authors have been conducting a series of study at the Shionohira fault and its southern extensions, reporting on the outcrop survey results (Kametaka, et al., 2015) and the frictional characteristics of fracture zones (Aoki et al., 2015, 2016). Currently, a fault slip test is carried out to assess the in-situ stress state.
In the fault slip test, a double packer is placed above and below the underground fracture to inject high pressure water from the surface and artificially trigger a slip in the fracture in order to measure the three dimensional deformation amount (micrometer to millimeter) (Guglielmi et al., 2013). This device called the Step-rate Injection Method for Fracture In-situ Properties or SIMFIP probe was designed and manufactured by Guglielmi for underground storage studies of CO2 in France and was first applied at the underground research facility (LSBB) in the south of France (Guglielmi et al., 2015). Subsequently, in-situ tests have been conducted on faults in underground research facilities such as Tournemire in France, Mont Terri in Switzerland, and the gold mine in South Dakota, USA.

This device allows to quantitatively measure the deviation of the fault by increasing the pore water pressure in the section partitioned by double packers, and to also examine the causes for leakage of groundwater, petroleum, CO2, and radioactive waste. In addition, it enables to observe fault displacement, pore pressure, and induced seismic waves at the micrometer scale, and to estimate friction and stress state of fault zones. By deepening understanding of the coupled phenomenon of hydraulics

©2019. Japan Geoscience Union. All Right Reserved.

and dynamics around the fault, the authors believe the method could be useful in elucidating the mechanism of seismic occurrence. It should be noted that this device is being applied for the first time in Japan, and the first time ever for an in-situ test of active faults.

Keywords: SIMFIP, Shionohira fault, active fault, Fukushima Hama-dori earthquake, fracuter zone characteristics, injection experiment

©2019. Japan Geoscience Union. All Right Reserved.

Study on fault activity evaluation method (A new attempt to understand fault activities) No.2
- Injection experiment using a SIMFIP probe at Shionohira Fault and southern fault-

*Takahiro Watanabe[1], Yukumo Tanaka[1], Kazuhiro Aoki[1], Yves Guglielmi[2], Paul Cook[2], Florian Soom[2], Wakahama Hiroshi[3], Noujou Haruka[3], Etsuo Iwasaki[3], Masao Kametaka[3], Kazuyoshi Seshimo[1]

1. Japan Atomic Energy Agency, 2. Laurence Berkley National Laboratory, 3. DIA CONSULTANTS

The Shionohira fault caused the April 11, 2011 Fukushima-ken Hamadori Earthquake of Mw 6.7 which occurred one month after the Tohoku-Oki earthquake of Mw 9.0. Co-seismic surface ruptures trending NNW-SSE allowed to estimate a normal slip faulting with a 2 m maximum displacement. The causes of fault activation might be related to changes in the stress state following the Tohoku-Oki earthquake. The key question is to understand why some fault segments were activated and ruptured the land surface while others remained inactive although being very close and aligned on the same fault zone, which is of importance in better assessing the risk of seismic activation of faults in Japan. This might be related to slight differences in properties between active and inactive segments. This might be related to slight differences in properties between active and inactive segments. Recent laboratory measurements on core sampled across the rupture zone show that there are differences in friction coefficients and smectite and clay mineral contents between segments (Aoki, et. al., 2016, Seshimo, et. al., 2016). These differences may condition the frictional rate and state stability of the fault. In this project, frictional stability and hydraulic permeability of the Shionohira fault are explored in situ from SIMFIP probing of borehole intervals intersecting the fault at depths of about 10-to-30m.

Surface earthquake fault caused the earthquake of April 11, 2011 coincides with the west trace of Itozawa fault (Tsutsumi and Toda, 2012). Imaizumi et. al. (2018) identified the lineament as an active fault from Wakigawa of Yamadama-machi to Obuki of Sekimoto-machi, Kitaibaraki city. No surface rupture was idenfied in this region. This study refers to the part of the fault with surface rupture as an active segment and that without surface rupture as an inactive segment.

At the Shionohira site, vertical borehole of 30 m depth was drilled and test intervals were decided based on core observations, borehole TV and caliper logging data as follows. Test 1 between depths of 7.0 and 11.5m isolated with upper and lower packers and pressurized was conducted above the recently activated fault zone in the unfaulted sandstone layers. Test 2 between depths of 12.8 and 17.3m was conducted across the recently activated fault zone.

At the Minakami-kita site, inclined borehole of 50 degrees from surface with 30 m length was drilled and fracture zones were detected at 20.40 to 23.10 m. In-situ injection experiment using a SIMFIP probe is under going, comparison results will be presented at the conference.

Keywords: SIMFIP method, active fault, Sionohira Fault, Fukushima-ken Hamadori Earthquake, fracture zone charactarizaton, injection test

©2019. Japan Geoscience Union. All Right Reserved.

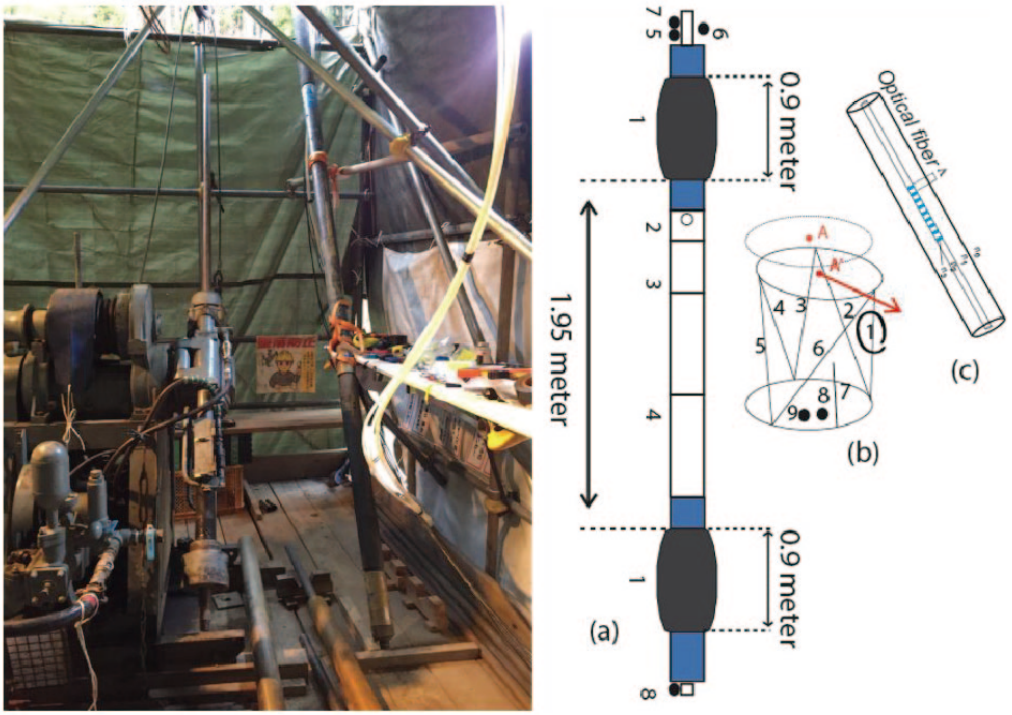

-SIMFIP probe used in Minakami-Kita tests – Left is a photo of the drill rig with the assembled SIMFIP probe set on the right -
(a) SIMFIP plan (1 packers, 2 injection sub, 3 SIMFIP cage, 4 extension subs, 5 Inclinometer, 6 Accelerometer, 7 Top pressure, 8 Bottom pressure)
(b) Principles of the sensor which is a deforming cage in 6 different directions + 1 reference (7) + 1 interval pressure (8)
(c) We build all our sensors using Bragg gages all connected on the same optical fiber.

©2019. Japan Geoscience Union. All Right Reserved.

Dynamic rupture simulation of 2018, Hokkaido Eastern Iburi earthquake: Role of non-planar fault geometry

*Tatsuya Hisakawa[1], Ryosuke Ando[1]

1. The University of Tokyo

The 2018, Hokkaido Eastern Iburi, Japan, earthquakeis an event characterized by complexity of rupture process, which may involve both reverse and strike slip depending on the locations on the fault surface. We perform dynamic rupture simulations based on simple physical laws and conditions for stressing and fault friction, taking complexity of the fault into account. The complex fault geometry is numerically treated by the boundary integral equation method accelerated by the fast domain portioning method. We search in a small number of parameter spaces for the stress ratio of the regional stress field and the frictional coefficients assumed to be the same over the fault area, rather than assigning heterogeneous distributions of the stress drop on the fault, to evaluate to what extent relatively simple forward models accounting for realistic fault geometry can explain the characteristics of coseismic observations. The fault geometry is constrained based on the aftershock distribution (NIED, 2018) and characterized primarily by the combination of three fault planes. As the result, we are able to reproduce several observed features of the event including the spatial variation of the fault slip direction, which is inferred from the seismological inversion (Okuwaki and Yagi, 2018), and the ground surface displacement observed by GEONET. The results suggest that the complex rupture event can be reproduced by a relatively simple physical model to some extent if the geometrical complexity of the faults is properly taken into account.

©2019. Japan Geoscience Union. All Right Reserved.

A New Fully-Dynamic Earthquake Cycle Simulator Applicable to Arbitrary Nonplanar Fault Geometries - A Benchmark Test

*Daisuke Sato[1], Nadia Lapusta[2], Hiroyuki Noda[1]

1. Disaster Prevention Research Institute, Kyoto University, 2. California Institute of Technology

The models and data assimilations of the real earthquake cycles are now getting on the track for providing the data beyond the classical empirical laws in the context of the seismic hazard; an example can be seen in the Third California Earthquake Rupture Forecast (UCERF3). Such large modeling is enabled by the rapid development of the earthquake simulators capable of solving the earthquake cycles in the real fault systems (Barbot et al., 2012: Richards-Dinger and Dieterich, 2012). However, there is not a fully dynamic cycle simulator applicable to wide tectonic conditions yet. The applicability of earthquake cycle simulators is thus still largely restricted.

In this research, we propose a new earthquake cycle simulator applicable to arbitrary nonplanar fault geometries. This simulator is based on the fast domain partitioning hierarchical matrices (FDP=H-matrices) (Sato and Ando, 2018), a newly developed algorithm of quasilinear time for dynamic BIEM applicable to nonplanar fault geometries. This cycle simulator thus overcomes the restriction on geometries when solving the elastodynamic fault motions in the coseismic phase, which had been the intrinsic problems for previous methods to solve the dynamic ruptures. In the presentation, after proposing the new method, we run a benchmark test of the SCEC Sequences of Earthquakes and Aseismic Slip project (SEAS) by the new simulator. Obtained results are compared with those of the previous simulators such as ByCycIE (Lapusta et al., 2000) and other simulators of volume-based methods. Simulated cycles on other nonplanar faults will be also demonstrated.

Keywords: Fully-Dynamic Earthquake Cycle Simulator, Nonplanar Fault Geometries (Subduction Zones + Ground Surfaces and Inland Faults), SCEC Sequences of Earthquakes and Aseismic Slip project (SEAS)

©2019. Japan Geoscience Union. All Right Reserved.

Stress and displacement Green's functions to treat volumetric inelastic strain and elastic inhomogeneity in boundary integral equation method

*Daisuke Sato[1]

1. Disaster Prevention Research Institute, Kyoto University

The boundary integral equation method (BIEM) is a commonly used method to simulate the fault motions accurately. Recent developments are now resolving well known problems of BIEM, such as the numerical cost problem (Sato and Ando, 2018) and the adaptabilities to elastic inhomogeneity (Kame and Kusakabe, 2012; Kusakabe and Kame, 2018). However, while it is shown to be applicable to the media other than homogeneous elastic media, obtained analytic integral kernels for simulating those media are now limited, largely due to its analytic difficulty. In this research, I obtain the the kernel expressions of those advanced BIEM in real space-time coordinate, based on the equivalent inclusion method (Eshelby, 1956; Mori and Tanaka, 1973).

First, the (volume) integral equation method (Barbot and Fialko, 2010) for the volumetric strain is shown to be reduced to BIEM of boundaries partitioning the discretized inelastic volume. Corresponding kernels are then obtained for piecewise-constant volumetric inelastic strain embedded in the three-dimensional homogeneous elastic space. The kernels are preliminarily shown to be equivalent to the part of the kernel for the inhomogeneous elastic media (Kame and Kusakabe, 2012; Kusakabe and Kame, 2018) both in static and dynamic cases.

Second, the surface integral in the representation theorem is reduced to the integral equation of the equivalent eigen-displacement. Consequently, as long as the absolute traction can be expressed with the strain and the eigen-strain, it is suggested that there can be a method to treat the inhomogeneous elastic media only by using the stress Green's function responding to the slip, already obtained analytically (Tada and Madariaga, 2001; Tada, 2006; Ando et al., 2007; Ando, 2016). By comparing the possible method with the method of Kame and Kusakabe (2012) capable of generally treating the elastic inhomogeneity in some examples, the validity of the proposal to treat inhomogeneous elastic media is investigated.

Keywords: volumetric inelastic strain, velocity structure, boundary integral equation method

©2019. Japan Geoscience Union. All Right Reserved.

Frictional properties of dolerite and granite at intermediate slip rates and controlled ambient temperatures

*Michiyo Sawai[1], Yuuki Yokoyama[1], Kyuichi Kanagawa[1]

1. Chiba University

High velocity friction experiments (up to several m/s) on many types of rocks have revealed that frictional strength decreases with increasing slip rate at seismic slip rates (e.g., Tsutsumi and Shimamoto, 1997; Di Toro et al., 2011). Coseismic weakening has been attributed to temperature rise including flash heating, melt lubrication or thermal pressurization (e.g., Rice, 2006; Hirose and Shimamoto, 2005). Although the importance of temperature during fault motion are widely recognized, the effects of temperature on frictional properties at intermediate to high slip rates remain unknown. We therefore conducted friction experiments at a wide range of temperatures and investigated the effects of temperature on the friction coefficient (μ).

Experiments were performed on dolerite (Belfast, Northern Ireland) and granite (Aji, Japan) using a rotary shear deformation apparatus at Chiba University. Samples were displaced up to 10 - 20 m at a normal stress of 1 MPa, slip rates of 1 to 300 mm/s, and ambient temperatures of 20 - 500°C in an argon atmosphere with an oxygen concentration of 0.2 %.

At 20°C and 100°C, dolerite showed velocity weakening at slip rates ranging from 1 to 30 mm/s with μ of 0.81 - 0.83 at 1 mm/s and of 0.73 at 30 mm/s. Whereas at high temperatures >300°C, friction is almost constant (μ = 0.81 - 0.85) at < 30 mm/s. At 100 mm/s, the behavior is slight velocity strengthening at 20 °C and 100°C with μ = 0.75 - 0.79 and clear velocity-weakening at more than 300°C with μ = 0.67 - 0.76. At 300 mm/s, the dolerite showed strong velocity weakening at all temperatures investigated. The amount of weakening (i.e., the drop in friction, $\Delta\mu$) increases with increasing temperature ($\Delta\mu$ = 0.1 - 0.38). Thus, the frictional properties of dolerite are affected not only by slip rate but also by ambient temperature.
Experiments using granite to decipher the effect of materials on temperature dependence are in progress. Our preliminary results are summarized as follows. At <30 mm/s, the behavior is slight velocity strengthening at room temperature and velocity-weakening at temperatures of 100-300°C. At >300°C, friction is almost constant. Friction coefficient decreases with increasing temperature of 20-300°C and increase again at >400°C. At >100 mm/s, clear velocity-weakening did not occur except at temperatures of 20°C. More results especially on granite will be reported at the meeting.

Keywords: friction, temperature dependence, dolerite, granite

©2019. Japan Geoscience Union. All Right Reserved.

Extraction of features of strata using borehole data of geothermal area by multivariate analysis

*Ojima Hiroki[1], Kazuya Ishitsuka[2], Toru Mogi[3], Tatsuya Kajiwara[4], Takeshi Sugimoto[4], Hiroshi Asanuma[5]

1. Department of Socio-Environmental Engineering Hokkaido University, 2. Division of Urban Management, Graduate School of Engineering, Kyoto University, 3. Division of sustainable Resources Engineering, Faculty of Enginieering, Hokkaido University, 4. Geothermal Engineering Co. Ltd, 5. Fukushima Renewable Energy Institute, AIST

In geothermal development, geological characteristics are often estimated qualitatively based on logging data of geothermal wells. On the other hand, the quartz index (QI) has quantitative information on minerals, and the index enables to objectively extract features of the geological formation using a statistical method. Therefore, in this study, from the QI obtained from the core cuttings in a geothermal field, we developed and examined a method to classify and extract geological features along with a well by multivariate analysis (in particular the difference in alteration degree). Specifically, we first carried out a principal component analysis to extract and emphasize the features of the data through dimensionality reduction. Then, their lithological features were classified by clustering using a Gaussian mixture model. In addition, the classification results by our method were compared with electric logs and temperature logs. In this study, we used the data obtained from wells in a geothermal area at Iwate prefecture. The geology of this area consists of andesite tuff and dacite tuff. The QI is defined as the percentage of the strongest X-ray intensity of a certain mineral in the sample from the strongest X-ray intensity of pure quartz measured under the same experimental conditions. This value means the content (weight percentage) in the sample for quartz and the relative quantitative ratio for the other minerals. In order to verify our proposed method, the principal component analysis was performed on the standardized QI data of clay minerals and compared with the results of existing geological classification based on geological interpretation. As a result of the comparison, our classification results agree with the results of existing geological classification, thus the classification of the strata by our method is valid. Next, in order to examine the effect of the dimensionality reduction by a principal component analysis, we compared the following cases: (i) clustering without dimension reduction for all QI, and (ii) clustering after applying the dimensionality reduction to all QI. In the case of dimensionality reduction, we used the principal components with a total contribution total over 95%. As a result of the comparison, the optimal classification number of the strata without the dimensionality reduction (case (i)) was 6. On the other hand, in the case of dimensional reduction (case (ii)) the optimal classification number was 10. The number of the optimal class indicates that more detailed features can be extracted using dimensionality reduction by principal component analysis. Notably, the classification in the depth range from 0 to 1000 m became detailed, highlighting the correspondence between clay, zeolite minerals and the geological formation.

Keywords: quartz index, principal component analysis, clustering

©2019. Japan Geoscience Union. All Right Reserved.

Low-temperature thermochronology of Cretaceous granitoids from the northern Northeast Japan Arc: Towards reconstructing arc-parallel thermal/denudation histories

*Shoma Fukuda[1], Shigeru Sueoka[2], Barry Paul Kohn[3], Noriko Hasebe[4], Akihiro Tamura[5], Tomoaki Morishita[5], Takahiro Tagami[1]

1. Graduate School of Science, Kyoto University , 2. Japan Atomic Energy Agency, 3. School of Earth Sciences, The University of Melbourne, 4. Institute of Nature and Environmental Technology, Kanazawa University, 5. Department of Earth Sciences, Kanazawa University

Northeast (NE) Japan Arc is categorized as an arc-trench system, where volcanism and earthquakes frequently occur. The tectonic history of the NE Japan Arc has been well-investigated based on geomorphic and geologic approaches. Furthermore, the recent multidisciplinary project (Crustal Dynamics) successfully achieved and accumulated geoscientific results by means of GPS, active faults, numerical modeling, friction experiments, etc (see also Iio et al. 2018, EPS). For estimating vertical deformation over long-term timescales (>10^6 yr.), our research group has investigated the thermal/denudation histories on every geomorphic province of the NE Japan Arc by using low-temperature thermochronology.

Thermochronology can reconstruct the time-temperature relationship of rock/mineral samples, based on radiometric ages and closure temperatures specific to the combination of radiometric dating methods and target minerals. Low-temperature thermochronology is useful for understanding upper crustal mountain building processes and has been applied to estimate the tectonic history of major orogens (e.g. European Alps: Wagner et al. 1977, Mem. Inst. Geol. Mineral., Univ. Padova; Himalayas: Blythe et al. 2007, Tectonics). However, the thermochronology approach directly measures cooling processes, rather than denudation/uplift histories. Therefore, it is noteworthy that denudation/uplift histories require some assumptions, such as appropriate geothermal gradients and dynamic equilibrium between denudation and uplift. Long-term uplift rates on >1 Myr time-scales, require estimates from such protocols, which are assumed to be equivalent to the vertical inelastic deformation of the crust (Ikeda et al. 2012, JGS).

Between 2014-2019 we collected over 100 granitic rock samples from the NE Japan Arc. Low-temperature thermochronology has been applied to many of these samples, including the apatite/zircon (U-Th)/He (namely, AHe and ZHe) (Sueoka et al. 2017, EPS) and apatite fission-track(AFT) methods (Fukuda et al. 2019, JAES:X), particularly from Cretaceous-Paleogene granites located in the southern NE Japan Arc. This research elucidated the contrast of thermal/denudation histories among the island arc provinces, i.e., Abukuma mountains, Ou Backbone Range(OBR), and Iide and Asahi mountains. In this presentation, we report results based on AHe/ZHe and AFT thermochronometry from Cretaceous granites in the northern NE Japan Arc, aimed at reconstructing arc-parallel and across-arc thermal/denudation histories.

We obtained AHe ages ranging between 88.6-0.9 Ma, AFT ages from 138.0-2.0 Ma, and ZHe ages from 83.9-7.4 Ma. The ages show contrasting thermal/denudation histories between the fore-arc side, OBR, and back-arc side, which are similar to the southern NE Japan Arc. This observation implies that arc-parallel mountains have approximately the same trend along NE Japan Arc. On the other hand, some differences were observed between the northern and southern NE Japan Arc as follows; (1) significantly

©2019. Japan Geoscience Union. All Right Reserved.

older AFT ages were obtained for Kitakami mountains (130-75 Ma) compared to the Abukuma mountains (80-40 Ma), (2) much younger AFT ages at ~2 Ma were found on the back-arc side, Taihe mountains, and (3) considering the expected relationship between expected closure temperatures, some reversal of coexisting AFT ages compared to AHe/ZHe ages (e.g., FST04, FST05) were observed.

Future work will involve thermal inverse modeling using AFT thermochronometry for estimating more rigorous constraints on thermal histories. This will also involve increasing the number of sampling localities in an attempt to extend our study area.

Keywords: Thermochronology, Northeast Japan Arc, Fission-track method, (U-Th)/He method, Island Arc

©2019. Japan Geoscience Union. All Right Reserved.

Uplift and denudation history of the South Fossa Magna region using low-temperature thermochronometric methods

*Yumi Kobayashi[1], Shigeru Sueoka[2], Shoma Fukuda[1], Barry P. Kohn[3], Tatsunori Yokoyama[2], Noriko Hasebe[4], Akihiro Tamura[5], Tomoaki Morishita[5], Takahiro Tagami[1]

1. Graduate School of Science, Kyoto University, 2. Tono Geoscience Center, Japan Atomic Energy Agency, 3. University of Melbourne, 4. Institute of Nature of Environmental Technology, Kanazawa University, 5. Department of Earth Sciences, Kanazawa University

The South Fossa Magna region is located at the junction of the Japan and Izu-Bonin arcs. Up to four crustal blocks of the Izu-Bonin arc, i.e., Kushigatayama, Misaka, Tanzawa, and Izu, collided this region and formed its crustal structures since the middle Miocene (1, 2). The timings of the collision events have been estimated by deposition ages of sediments between each block and the Japan arc. However, these questions remain unresolved.

In this study, we performed apatite fission track (AFT) and apatite (U-Th)/He (AHe) thermochronometric methods and U-Pb dating method to resolve the uplift and denudation history of the South Fossa Magna region.

The AFT ages are estimated to be 14.7 ±4.7 Ma in the Okuchichibu area (c.f., hornblende K-Ar age: 10.5 ±1.5 Ma (3)), 3.0 ±0.5 Ma, 9.2 ±2.2 Ma, and 7.6 ±0.9 Ma in the Kano Mountains (c.f., biotite K-Ar age:i.e., 10.5 ±0.4 Ma (4)), 3.6 ±2.5 Ma in the Minobu area (c.f., biotite K-Ar age: 5.4 ±0.3 Ma (5)). Also, the AFT ages are inferred at 37.0 ±5.9 Ma in Mt. Tsukuba (c.f., Rb-Sr whole rock isochron age: 61.6 ±4.3 Ma (6)), and 44.9 ±4.1 Ma in the Sori granitoid in Gumma Prefecture (c.f., biotite K-Ar age: 92.6 ±0.6 Ma (7)). The rocks which have younger AFT ages than the formation ages may reflect the uplift and denudation events since the rock formation. However, exhumation rates of the Tanzawa mountain, the closest mountain to the Izu block, did not increase before and after the collision of the Izu block (8), which may imply that the collision of the Izu block did not cause the uplift and denudation events significantly.

We also obtained the new AHe ages and U-Pb ages. The AHe ages for Okuchichibu area, Kanto mountains and Minobu area are about 3 Ma. Furthermore, according to the results of the inverse thermal analysis using the apatite FT lengths data, the granites in Okuchichibu area and the southern part of Kanto mountains cooled rapidly since about 3 Ma, and the granites in Minobu area and northern part of Kanto mountains cooled rapidly since about 1 Ma. The results of AHe ages were consistent with the results of inverse analysis. Based only on these ages, the rapid cooling ages of 3 Ma and 1 Ma are comparable to the collision ages of the Tanzawa block and the Izu block, respectively.

References

[1] Amano et al., Structural Geology 43, 11-20 (1999).
[2] Kano, Bull. Earthq. Res. Inst. Univ. Tokyo 77, 231-248 (2002).
[3] Ueno and Shibata, J. Japan. Assoc. Min. Petr. Econ. Geol. 81, 77-82 (1986).
[4] Shibata et al., Bulletin of the Geological Survey of Japan 35, 19-24 (1984).
[5] Sato et al., Gumma Mus. Natu. Hist. 19, 95-109 (2015)

©2019. Japan Geoscience Union. All Right Reserved.

[6] Arakawa and Takahashi, J.Min. Petr. Econ. Geol. 83, 232-240 (1968)
[7] Sudo, M. et al., Geochemical Journal 32, 49-58 (1998)
[8] Yamada, K. and T. Tagami, Journal of Geophysical Research 113, B03402, doi: 10.1029/2007JB005368 (2008).

Keywords: low-temperature thermochronology, South Fossa Magna, apatite fission track

©2019. Japan Geoscience Union. All Right Reserved.

Correlation between residual uplift and recurrence interval of the Kanto earthquake based on developmental process of coastal lowland

*Haeng-Yoong Kim[1]

1. Osaka City University, Graduate School of Science, Division of Biology &Geosciences

It is well known that the marine terraces are formed due to uplift of the seabed during the earthquake. The marine terrace consists of a near-flatter terrace surface emerged above sea level during the earthquake and a low terrace riser of less than several meters in height formed after the earthquake and is distributed in a staircase pattern along the coastline. In the previous research, one step of maritime terrace is often recognized as a trace of an earthquake once, and based on this premise, many previous researches were conducted to estimate the reoccurrence interval and the amount of uplift during the earthquake. However, Maemoku (1988) inferred that one step level of flat terrace surface is the topography formed by multiple repetitions of coseismic uplift and interseismic earthquake settlement occurring in the plate subduction zone of the Nankai Trough. And the stepped terrace was formed by the active fault of the land side. We got geomorphological and geological data demonstrating this previous reasoning on the Miura Peninsula located directly above the plate subduction zone of the Sagami trough.

On the rocky coast of the Miura Peninsula, two step of marine terrace surfaces formed in association with the 1923 Taisho and 1703 Genroku earthquakes are observed near 1 m and 2 m above sea level,(Matsuda et al., 1974). In the inner part of the estuary creek, which is formed many in the peninsula, the coastal lowland landfilled with sediments transported from the hinterland into the bay floor is distributed around the altitude of 2 m as similer as 1703 terrace surface. We examined the development process of coastal lowland in the inner part of estuary creek.

As a result of the detailer geomorphological interpretation, a flat coastal lowland apparently spreading as a single face is composed of multiple small maritime terraces, not one terrain. The marine terraces were divided into 5 areas with less than 2.1 m above sea level by topographical interpretation. As a result of investigating the emergent time and the distribution altitude of the marine terrace surface, the marine surface of the 1923 Taisho earthquake in the order of 1.22 m - 1.37 m in the order of younger, the wave erosion shelf surface of the 1703 Genroku earthquake by Nishihata et al. (1988): 2.3 m, the marine surface of the 1293 year pre-earthquake (after 1260-1380 cal.AD): 1.27 m, the marine surface of the earthquake (915 cal.AD to 1150 cal.AD) around the year AD is 1.63 to 1.93 m, Terraced surfaces are distributed until the earlier age.

In this way, the reasons that different formational time of terraces remain in coastal lowlands with extremely altitude is formed in Miura peninsula are as follows, because 1: the coseismic uplift due to the elastic repulsion and the interseismic subsidence accompanying the strain accumulation are repeated (Shimazaki et al., 2011; Kim and Mannen, 2018), therefore 2: a new marine surface is formed near the sea level by the next earthquake (Kim and Mannen, 2018), and 3: there is a condition that the terrace surface is preserved by the coating layer. In addition, because the height of the ground is stable in the long term due to the balance of uplift and subsidence, and it is estimated that wide coastal lowlands, which apparently appear as a continuous ground surface, develop by repetition of uplift and subsidence. Between 1293 and 1703, where the period of occurrence of the earthquake occurred long, the raised surface in 1293 returned to the original altitude, and between 1703 and 1923 in which the occurrence interval of the earthquake was short, the raised surface in 1703 The next Kanto earthquake occurred

©2019. Japan Geoscience Union. All Right Reserved.

before going back to the original altitude.

Keywords: Marine terrace, Residual uplift, Recurrence interval, Subduction type earthquake

©2019. Japan Geoscience Union. All Right Reserved.

Mechanics preserving co-seismic uplift and marine terraces: dissymmetric patterns of co-seismic and inter-seismic deformation

*Kyohei Suzuki[1], Junki Komori[1], Ryosuke Ando[1]

1. Graduate School of Science, University of Tokyo

Four large Holocene marine terraces are known in the southern part of the Boso Peninsula and called Numa I - IV. The newest one (Numa IV) was uplifted at the time of the Kanto Genroku earthquake, and from the similarity of the spatial distribution, it was considered that the Numa I-III Ire also formed from uplifts during the Genroku-type events. From this, the amount of coseismic uplift and slip amount were estimated from the height of the terraces (Matsuda et al., 1978; Nakata et al., 1980; Namegaya et al., 2011; Sato et al., 2016 etc.). However, the relationship between Holocene marine terraces and paleoseismic events was doubted in previous studies (Matsu'ura and Sato 1989, Noda et al., 2018). There is Matsu'ura and Sato (1989) model which is a mechanical model explaining the long-term surface uplift. This model expresses seismogenic region by back slip at the interseismic period and forward slip at the coseismic period and givessteady forward slip along the whole plate boundary surface. From this model, the coseismic vertical displacement pattern cancel out and the interseismic one and the uplift accumulation on the surface was attributed only to the effect of the steady-state plate motion.However, this is consequence based on a simple model expressed that slab as one plane in horizontal layered structure and assumed that the amount of back slip at the interseismic period and the amount of forward slip at the coseismic period are equal. The purpose of this study is to verify whether the coseismic uplift amount records the slip amount and remains and accumulates over earthquake cycles, and it affects coastal terrace formation process in a general mechanical model, considering the shape of the slab, the plate motion, and the coseismic fault motion.

As the calculation procedure, first, We give a constant displacement (10 m) to the edge of the oceanic plate and accumulate strain on the plate boundary. Next, We release all accumulated shear stress by coseismic fault slip,and obtain the vertical displacement pattern on the surface and the slip amount on the plate interface. Based on the fact that the principle of superposition is established in the linear elasticity theory, in this study, We separated the boundary conditions of both the interseismic period and the coseismic period,and calculated the respective vertical displacements and the residual amount by taking the sum. To verify the influence of irregularities on the actual plate boundary surface on the spatial pattern of vertical displacement, We also calculated two patterns for the case where irregularities were locally placed on the plate interface.

As a result of the calculation, we found that the interseismic slip amount in the no-cuppled area converged to 0 in the vicinity of the coupled area, and the coseismic slip amount was not uniform, and occurred across the plate boundary surface. This suggests that the slip on the plate boundary is intermittent in the seismic cycle. Next, from the vertical displacement residuals, we found that their spatial patterns at the interseismic period and the coseismic period were different.Furthermore, when local irregularities are placed on the plate boundary surface, it was found that the spatial pattern of the coseismic uplift is different corresponding to the slip amount of each model. This suggests that the height records the slip amount, and the shape of the plate boundary surface attributes actual coastal terrace formation. The consequence of this study is that the slip on the plate boundary is intermittent, and the coastal terraces depend on the coseismic slip.Therefore, the model in this study will give meaning to estimate the paleoseismic image from the height of coastal terraces.

©2019. Japan Geoscience Union. All Right Reserved.

Keywords: paleoseismic, mechanical model, Holocene marine terraces

©2019. Japan Geoscience Union. All Right Reserved.

Enhanced resolution of stress tensor inversion by using fault instability analysis

*Katsushi Sato[1]

1. Division of Earth and Planetary Sciences, Graduate School of Science, Kyoto University

Modern stress tensor inversion techniques for fault-slip analysis are based on the Wallace-Bott hypothesis which assumes that the slip directions and shear stress vectors are parallel. The hypothesis has an advantage in the applicability to high pore fluid pressure conditions and low friction faults, since the magnitudes of shear and normal stresses are not evaluated. However, the hypothesis gives only loose constraint on stress from observed faults in exchange for the wide applicability, which causes poor detectability of stresses.

This study tries to improve the detectability by introducing the fault instability (Vavrycuk et al, 2013; Sato, 2016) into the stress tensor inversion. The fault instability is defined as the nearness of the point representing shear and normal stresses on Mohr diagram to the line of Coulomb failure criteion. The fault instability is imposed on the fitness of a stress candidate to a fault-slip datum as a weight. Since the calculation of fault instability requires the friction coefficient, this study used several values of friction coefficient and compared the results.

The new method was applied to natural meso-scale fault-slip data. The faults cutting the Awa Group (Chiba Prefecture, central Japan) newly gave a reverse-faulting regime of stress in addition to normal faulting ones which can be detected by a conventioanl technique. An E-W trending tensional stress was newly detected from the faults cutting the Sekinan Group in the Beppu-Shimabara graben (Oita Prefecture, southwest Japan) where N-S trending extensional tectonism is ongoing. These resutls showed the improved resolution of stress tensor inversion by the incorporation of fault instability.

References

Sato, K., 2016, Journal of Structural Geology, 89, 44-53.
Vavrycuk, V., Bouchaala, F. and Fischer, T., 2013, Tectonophysics, 590, 189-195.

Keywords: stress tensor inversion, fault-slip analysis, fault instability

©2019. Japan Geoscience Union. All Right Reserved.

Focal mechanisms of the aftershocks of the 2000 Western Tottori Earthquake inferred from P wave first-motion data and spatial stress pattern

*Takaki Iwata[1]

1. Tokiwa University

A Bayesian approach to estimating a spatial stress pattern was developed [Iwata, 2018, JGR] (hereafter IW2018), and as an extension of this approach Iwata [2018, SSJ fall meeting] has proposed a method to infer focal mechanisms from P wave first-motion data and stress pattern estimated with the Bayesian approach. In this study, this method was applied to a real dataset taken from aftershocks of the 2000 Western Tottori earthquake.

The analyzed P wave first-motion dataset was retrieved from Kawanishi et al. [2009, JGR], which complied records from October 15 to November 30 in 2000. This dataset contains 47,570 P wave first-motions of 3592 events (for details see IW2018). The spatial pattern of stress field was taken from the result of IW2018 that also analyzed the same P wave first-motion dataset. The inferred focal mechanisms show rotation of the azimuth of P-axis around the main fault in the southern area; this feature has been seen in Yukutake and Iio [2017, EPS] and will be the reflection of the stress rotation found in the same area revealed by IW2018.

From the inferred focal mechanisms and spatial stress pattern, the normal and shear stress exerted on the fault plane was evaluated. Then, following the method of Terakawa [2010, Geology], fluid pressure for each of the events was estimated. Two datasets of the fluid pressure in the northern and southern areas of the aftershock areas were constructed and examined whether the two datasets follow the same distribution with the Kolmogorov-Smirnov test. Consequently, the test revealed that the fluid pressure in the southern area is significantly larger than that in the northern area, with a P-value of 1.6e-3.

Keywords: focal mechanism, stress field, stress rotation, P wave first-motion, spatial statistics, fluid pressure

©2019. Japan Geoscience Union. All Right Reserved.

Stress tensor inversion in focal area of the 2016 Mw7.8 Kaikoura earthquake, New Zealand

*Miu Matsuno[1], Tomomi Okada[1], Satoshi Matsumoto[2], Yuta Kawamura[2], Yoshihisa Iio[3], Tadashi Sato[1], Stephen C Bannister[4], John Ristau[4], Martha K Savage[5], John Townend[5], Jarg Pettinga[6], Francesca Ghisetti[7], Richard H Sibson[8]

1. Research Center for Prediction of Earthquakes and Volcanic Eruptions Graduate School of Science, Tohoku University, 2. Institute of Seismology and Volcanology, Faculty of Sciences, Kyushu University, 3. Disater Prevention Research Institute, Kyoto University, 4. GNS Science, New Zealand, 5. Victoria University of Wellington, Wellington, New Zealand, 6. University of Canterbury, Christchurch, New Zealand, 7. TerraGeologica, Ruby Bay, New Zealand, 8. University of Otago, Dunedin, New Zealand

We study spatio-temporal change of stress field of the 2016 Kaikoura earthquake in the northern area of South Island of New Zealand. Data from both the 51 temporary stations and 22 GEONET stations were used. Data collection was from March 2011 to December 2017. We derived focal mechanisms using HASH (Hardebeck and Shearer, 2002), By focal mechanism solutions of earthquake, we estimated stress fields of main shock of Kaikoura earthquake before and after. We used SATSI (Hardebeck and Michael, 2006] for stress tensor inversion. In our previous result (Sato, 2017 master’ s thesis in Tohoku University), there is possibility that on-fault aftershocks bias the result of stress tensor inversion. Therefore, by using Kagan angle between mainshock fault model and each focal mechanism, we remove aftershock on the faults, and perform stress tensor inversion. We use the fault model by Hamling et al. (2017). In a result, Kagan angles of many earthquakes are large, so this means that many aftershocks occurred off the fault plane. The results do not depend on threshold of Kagan angle. Obtained stress tensor inversion after main shock in areas near London Hill Fault and near Kekerengu fault are strike-slip fault type with SHmax orientation of ~N115E, which is almost same as for before the Kaikoura earthquake (e.g., Sibson et al., 2012; Townend et al., 2012), and stress tensors before and after the mainshock didn't appear to change after the earthquake beyond the estimation error. However, in the area near the hypocenter of the main shock we still cannot get a stable stress tensor. Also we plan to obtain results of a stable stress tensor for before the main shock by increasing the number of focal mechanisms of earthquakes that we examine.

©2019. Japan Geoscience Union. All Right Reserved.

Precise hypocenter distribution in the focal area of the 2016 Mw7.8 Kaikorua Earthquake, New Zealand

*Yuta Kawamura[1], Satoshi Matsumoto[1], Tomomi Okada[2], Miu Matsuno[2], Yoshihisa Iio[3], Tadashi Sato[2], Stephen C Bannister[4], John Ristau[4], Martha K Savage[5], John Twonend[5], Jarg Pettinga[6], Francesca Ghisetti[7], Richard H Sibson[8]

1. Kyushu University, Shimabara, Japan, 2. Tohoku University, Sendai, Japan, 3. Kyoto University, Uji, Japan, 4. GNS Science, Lower Hutt, New Zealand, 5. Victoria University of Wellington, Wellington, New Zealand, 6. University of Canterbury, Christchurch, New Zealand, 7. TerraGeologica, Ruby Bay, New Zealand, 8. University of Otago, Dunedin, New Zealand

The Mw7.8 Kaikoura Earthquake struck the northeastern south island, New Zealand, on November 14, 2016. A lot of researchers have tried to explain the cause of this earthquake and revealed the structure in this area. Among variety of prior researches, Clark et al. (2017) argued that this earthquake, which produced surface deformation including uplift and complex surface rupture, was caused by 21 strike-slip, reverse and oblique slip faults. Cesca et al., (2017) proposed an earthquake fault model that consists of three faults in northern, central and southern part, based on the hypocenter distribution of aftershock activity. These studies suggested in common that this earthquake was provoked by multiple faults with complex rupture process.

We had installed 75 temporary seismic stations before the earthquake in the South Island, New Zealand in addition to GEONET stations. The seismic network has successfully recorded the mainshock and the following aftershocks. Here, we relocated the hypocenters of the events associated with the Kaikoura earthquake by using data obtained from the seismic network. The hypocenters was determined by the double difference hypocenter determination algorithm (i.e. HYPODD, Waldhauser and Ellsworth, 2000). The overall distribution of the hypocenters are distinguished into two clusters, northern and southern clusters. The hypocenter distribution in vertical cross section normal to the major alignment of the aftershocks in N54W reveals that the fault in southern part dips to eastward. On the other hand, although we find out a northern cluster in terms of horizontal projection, no obvious faults are recognized in the vertical cross-section, suggesting complex fault structure in the northern cluster.

©2019. Japan Geoscience Union. All Right Reserved.

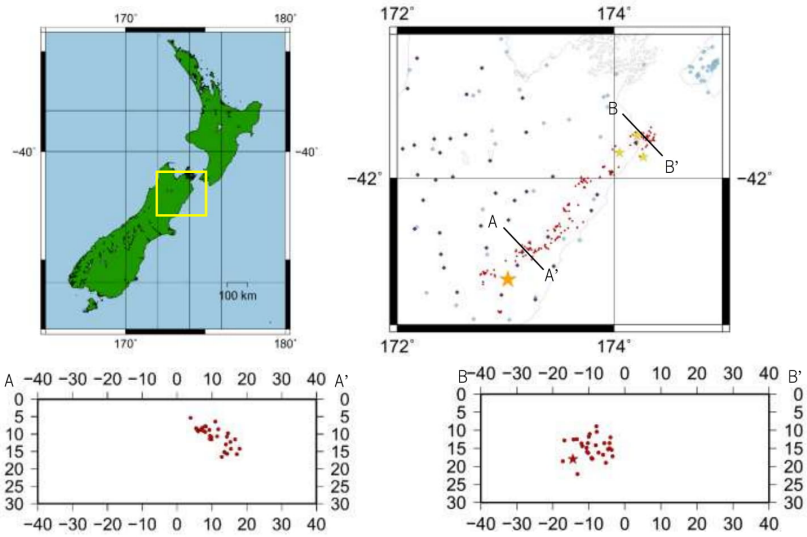

Fig. 1 Relocated hypocenter distribution in the South Island, New Zealand. Upper left) Index map of the target region. Yellow rectangle shows area displayed right map. Upper right) Map showing seismic stations and epicenters. Diamond and dot indicate location of station and event, respectively. Stars indicate epicenters for event with M > 6. Lower) Vertical cross sections along A-A' and B-B' in the upper right map. Other symbols are same as the upper right map.

©2019. Japan Geoscience Union. All Right Reserved.

3-dimensional GPS velocities in Colombia and their implications for interplate coupling

*Sindy Carolina Lizarazo[1], Takeshi Sagiya[2], Hector Mora-Paez[3]

1. Graduate School of Environmental Studies, Nagoya University, 2. Disaster Mitigation Research Center, Nagoya University, 3. Geological Survey of Colombia

Colombia is located in a region of complex interactions among the Caribbean, Nazca and South American plates, as well as the North Andean and Panama-Choco blocks. As a consequence of this tectonic setting, active faulting and intense seismicity are occurring especially in the areas of plate subduction or collision. The GeoRED project by the Geological Survey of Colombia installed a permanent GPS network in Colombia to study the regional kinematics with an intention to improve disaster mitigation activities. An initial velocity field was obtained and discussed by Mora et al. (2019) based on data from 60 sites under the ITRF2008 reference frame.

Here we present an updated result of Colombian GPS velocity field with 80 sites. The daily coordinates are calculated under the ITRF2014 reference frame with GAMIT-GLOBK software. We calculate 3-dimensional velocities with HECTOR software (Bos et al., 2013) based on the daily coordinates for the period from January 2014 to March 2016. There was no earthquake larger than magnitude 6 in Colombia, so the velocity pattern represents that of the interseismic period. For this time period, enhancement of the permanent network provides a better spatial resolution of the deformation pattern in some regions.

The results show a general consistency with the previous study, demonstrating the correctness of the current approach. In addition, vertical components show a slight of coastal uplifts at a few mm/year along the Nazca subduction zone. These signals indicate the lower limit of the plate coupling on the plate interface and we discuss the interplate coupling based on the 3-dimensional velocity data. Also, a significant margin-normal contraction is identified along a part of the Caribbean subduction zone near Colombia-Panama border. However, the vertical signal is not significant compared to the horizontal contraction, indicating that the elastic coupling model may not be applicable to this area.

Keywords: GPS velocities, Interplate coupling, Subduction, Deformation

©2019. Japan Geoscience Union. All Right Reserved.

[J] Poster | S (Solid Earth Sciences)：S-CG Complex & General

Tue. May 28, 2019 5:15 PM - 6:30 PM JST | Tue. May 28, 2019 8:15 AM - 9:30 AM UTC | Poster Hall International Exhibition Hall8, Makuhari Messe_37

[S-CG61] Dynamics in mobile belts

convener:Yukitoshi Fukahata(Disaster Prevention Research Institute, Kyoto University), Toru Takeshita(Department of Natural History Sciences, Graduate School of Science, Hokkaido University), Hikaru Iwamori(Geochemical Evolution Research Program, Japan Agency for Marine-Earth Science and Technology)

The dynamic behaviours of mobile belts are expressed across a wide range of time scales, from the seismic and volcanic events that impact society during our lifetimes, to orogeny and the formation of large-scale fault systems which can take place over millions of years. Deformation occurs on length scales from microscopic fracture and flow to macroscopic deformation to plate-scale tectonics. To gain a physical understanding of the dynamics of mobile belts, we must determine the relationships between deformation and the driving stresses due to plate motion and other causes, which are connected through the rheological properties of the materials. To understand the full physical system, an integration of geophysics, geomorphology, and geology is necessary, as is the integration of observational, theoretical and experimental approaches. In addition, because rheological properties are greatly affected by fluids in the crust and fluid chemical reactions, petrological and geochemical approaches are also important. After the 2011 great Tohoku-oki earthquake, large-scale changes in seismic activity and regional scale crustal deformation were observed, making present-day Japan a unique natural laboratory for the study of the dynamics of mobile belts. This session welcomes presentations from different disciplines, such as seismology, geodesy, tectonic geomorphology, structural geology, petrology, and hydrology, as well as interdisciplinary studies, that relate to the dynamic behaviours of mobile belts.

[SCG61-P01] Three-dimensional imaging of geo-fluid distribution at NE-Japan forearc using wideband magnetotelluric measurements

*Masato Fukai[1], Yasuo Ogawa[1], Kuo Hsuan Tseng[1], Masahiro Ichiki[2], Shinichi Takakura[3] (1.Tokyo Institute of Technology, 2.Tohoku University, 3.National Institute of Advanced Industrial Science and Technology)

[SCG61-P02] **Elastic wave velocity and electrical conductivity in brine-saturated rocks and microstructure of pores**

*Arina Tomioka[1], Tohru Watanabe[1] (1.University of Toyama)

[SCG61-P03] Influence of grain shape and grain size distribution on connectivity of pores in granular materials.

*Katazakai Haruka[1], Tohru Watanabe[1] (1.Toyama University)

[SCG61-P04] Change of pore connectivity in granular materials under axial compression

*MAREMICHI ABE[1], Tohru Watanabe[1] (1.Toyama University)

[SCG61-P05] **Estimation of crustal strength using residual strain of quartz in deformed conglomerate and inhomogenous strain of conglomerate layer -As an example of multiple collision zone of Izu-Bonin arc, Fujikawa valley, Central Japan-**

*Shun Suzuki[1], Kenta Kobayashi[1] (1.Graduate School of Science and Technology, Niigata University)

[SCG61-P06] **An Introduction to Ryoke Cataclastic Rocks in Tsukide, Mie Prefecture, Japan: An Approach Using 3D Reconstructions From Thin Sections**

*Thomas Jing Yi Yeo[1], Toru Takeshita[1] (1.Department of Natural History Sciences, Graduate School of Science, Hokkaido University)

[SCG61-P07] Relationships between spacing and growth or linkage of normal faults in the Miyako Island, South Ryukyu arc, Japan

*Sumire Maeda[1], Makoto Otsubo[1], Daisuke Asahina[1], Yuki Furuno [1] (1.Research Institute of Earthquake and Volcano Geology, Geological Survey of Japan/AIST)

[SCG61-P08] **3D fault architecture along the Median Tectonic Line, eastern Kii Peninsula, SW Japan**

*Norio Shigematsu[1], Takuma Katori[1,2], Jun Kameda[3], Ayumu Miyakawa[4] (1.Research Institute of Earthquake and Volcano Geology, Geological Survey of Japan, National Institute of Advanced Industrial Science and Technology, 2.Graduate School of Science and Technology, Niigata University, 3.Department of Natural History and Sciences, Hokkaido University, 4.Research Institute of Geology and Geoinformation, Geological Survey of Japan, National Institute of Advanced Industrial Science and Technology)

[SCG61-P09] Significant of thrust zone at Fuji river basin in the South Fossa Magna, Southern Yamanashi Prefecture, Central Japan
-Study of Structural geology of Minobu and Neguma fault-

*Minami Madoka[1], Kenta Kobayashi[1] (1. Niigata university department of geology science)

[SCG61-P10] Mineralogical characteristics of fault rocks in the aftershock regions of the 2000 Western Tottori earthquake and its spatial distribution

*Shunya Kaneki[1], Tetsuro Hirono[1], Hideki Mukoyoshi[2], Kenta Kobayashi[3], Toru Takeshita[4] (1.Graduate School of Science, Osaka University, 2.Graduate School of Science and Engineering, Shimane University, 3.Graduate School of Science and Technology, Niigata University, 4.Graduate School of Science, Hokkaido University)

[SCG61-P11] Relationship between seismicity of the 2016 the Central Tottori Earthquake and fault distribution in the aftershock area

*Masayuki Ichimura[1], Hideki Mukoyoshi[2] (1.Graduate School of Natural Science and Technology, Shimane University, 2.Department of Earth Science, Shimane University)

[SCG61-P12] History of fault activity considered from the brittle shear zone and the geological structure near the Cape Otachi, Kumamoto Prefecture

*Keiji Ogashiwa[1], Kenta Kobayashi[1] (1.Niigata University)

[SCG61-P13] Study on fault activity evaluation method (A new attempt to understand fault activities) No.1 - Overall plan and current situation at Shionohira Fault -

*Kazuhiro Aoki[1], Takahiro Watanabe[1], Yukumo Tanaka[1], Kazuyoshi Seshimo[1] (1.Japan Atomic Energy Agency)

[SCG61-P14] Study on fault activity evaluation method (A new attempt to understand fault activities) No.2
- Injection experiment using a SIMFIP probe at Shionohira Fault and southern fault-

*Takahiro Watanabe[1], Yukumo Tanaka[1], Kazuhiro Aoki[1], Yves Guglielmi[2], Paul Cook[2], Florian Soom[2], Wakahama Hiroshi[3], Noujou Haruka[3], Etsuo Iwasaki[3], Masao Kametaka[3], Kazuyoshi Seshimo[1] (1.Japan Atomic Energy Agency, 2.Laurence Berkley National Laboratory, 3.DIA CONSULTANTS)

[SCG61-P15] Dynamic rupture simulation of 2018, Hokkaido Eastern Iburi earthquake: Role of non-planar fault geometry

*Tatsuya Hisakawa[1], Ryosuke Ando[1] (1.The University of Tokyo)

[SCG61-P16] A New Fully-Dynamic Earthquake Cycle Simulator Applicable to Arbitrary Nonplanar Fault Geometries - A Benchmark Test

*Daisuke Sato[1], Nadia Lapusta[2], Hiroyuki Noda[1] (1.Disaster Prevention Research Institute, Kyoto University, 2.California Institute of Technology)

[SCG61-P17] Stress and displacement Green's functions to treat volumetric inelastic strain and elastic inhomogeneity in boundary integral equation method

*Daisuke Sato[1] (1.Disaster Prevention Research Institute, Kyoto University)

[SCG61-P18] Frictional properties of dolerite and granite at intermediate slip rates and controlled ambient temperatures

*Michiyo Sawai[1], Yuuki Yokoyama[1], Kyuichi Kanagawa[1] (1.Chiba University)

[SCG61-P19] Extraction of features of strata using borehole data of geothermal area by multivariate analysis

*Ojima Hiroki[1], Kazuya Ishitsuka[2], Toru Mogi[3], Tatsuya Kajiwara[4], Takeshi Sugimoto[4], Hiroshi Asanuma[5] (1.Department of Socio-Environmental Engineering Hokkaido University, 2.Division of Urban Management, Graduate School of Engineering, Kyoto University, 3.Division of sustainable Resources Engineering, Faculty of Enginieering, Hokkaido University, 4.Geothermal Engineering Co. Ltd, 5.Fukushima Renewable Energy Institute, AIST)

[SCG61-P20] Low-temperature thermochronology of Cretaceous granitoids from the northern Northeast Japan Arc: Towards reconstructing arc-parallel thermal/denudation histories

*Shoma Fukuda[1], Shigeru Sueoka[2], Barry Paul Kohn[3], Noriko Hasebe[4], Akihiro Tamura[5], Tomoaki Morishita[5], Takahiro Tagami[1] (1.Graduate School of Science, Kyoto University , 2.Japan Atomic Energy Agency, 3.School of Earth Sciences, The University of Melbourne, 4.Institute of Nature and Environmental Technology, Kanazawa University, 5.Department of Earth Sciences, Kanazawa University)

[SCG61-P21] Uplift and denudation history of the South Fossa Magna region using low-temperature thermochronometric methods

*Yumi Kobayashi[1], Shigeru Sueoka[2], Shoma Fukuda[1], Barry P. Kohn[3], Tatsunori Yokoyama[2], Noriko Hasebe[4], Akihiro Tamura[5], Tomoaki Morishita[5], Takahiro Tagami[1] (1.Graduate School of Science, Kyoto University, 2.Tono Geoscience Center, Japan Atomic Energy Agency, 3.University of Melbourne, 4.Institute of Nature of Environmental Technology, Kanazawa University, 5.Department of Earth Sciences, Kanazawa University)

[SCG61-P22] Correlation between residual uplift and recurrence interval of the Kanto earthquake based on developmental process of coastal lowland

*Haeng-Yoong Kim[1] (1.Osaka City University, Graduate School of Science, Division of Biology &Geosciences)

[SCG61-P23] Mechanics preserving co-seismic uplift and marine terraces: dissymmetric patterns of co-seismic and inter-seismic deformation

*Kyohei Suzuki[1], Junki Komori[1], Ryosuke Ando[1] (1.Graduate School of Science, University of Tokyo)

[SCG61-P24] Enhanced resolution of stress tensor inversion by using fault instability analysis
★Invited Papers

*Katsushi Sato[1] (1.Division of Earth and Planetary Sciences, Graduate School of Science, Kyoto University)

[SCG61-P25] Focal mechanisms of the aftershocks of the 2000 Western Tottori Earthquake inferred from P wave first-motion data and spatial stress pattern

*Takaki Iwata[1] (1.Tokiwa University)

[SCG61-P26] Stress tensor inversion in focal area of the 2016 Mw7.8 Kaikoura earthquake, New Zealand

*Miu Matsuno[1], Tomomi Okada[1], Satoshi Matsumoto[2], Yuta Kawamura[2], Yoshihisa Iio[3], Tadashi Sato[1], Stephen C Bannister[4], John Ristau[4], Martha K Savage[5], John Townend[5], Jarg Pettinga[6], Francesca Ghisetti[7], Richard H Sibson[8] (1.Research Center for Prediction of Earthquakes and Volcanic Eruptions Graduate School of Science, Tohoku University, 2.Institute of Seismology and Volcanology, Faculty of Sciences, Kyushu University, 3.Disater Prevention Research Institute, Kyoto University, 4.GNS Science, New Zealand, 5.Victoria University of Wellington, Wellington, New Zealand, 6.University of Canterbury, Christchurch, New Zealand, 7.TerraGeologica, Ruby Bay, New Zealand, 8.University of Otago, Dunedin, New Zealand)

[SCG61-P27] Precise hypocenter distribution in the focal area of the 2016 Mw7.8 Kaikorua Earthquake, New Zealand

*Yuta Kawamura[1], Satoshi Matsumoto[1], Tomomi Okada[2], Miu Matsuno[2], Yoshihisa Iio[3], Tadashi Sato[2], Stephen C Bannister[4], John Ristau[4], Martha K Savage[5], John Twonend[5], Jarg Pettinga[6], Francesca Ghisetti[7], Richard H Sibson[8] (1.Kyushu University, Shimabara, Japan, 2.Tohoku University, Sendai, Japan, 3.Kyoto University, Uji, Japan, 4.GNS Science, Lower Hutt, New Zealand, 5.Victoria University of Wellington, Wellington, New Zealand, 6.University of Canterbury, Christchurch, New Zealand, 7.TerraGeologica, Ruby Bay, New Zealand, 8.University of Otago, Dunedin, New Zealand)

[SCG61-P28] **3-dimensional GPS velocities in Colombia and their implications for interplate coupling**

*Sindy Carolina Lizarazo[1], Takeshi Sagiya[2], Hector Mora-Paez[3] (1.Graduate School of Environmental Studies, Nagoya University, 2.Disaster Mitigation Research Center, Nagoya University, 3.Geological Survey of Colombia)

Three-dimensional imaging of geo-fluid distribution at NE-Japan forearc using wideband magnetotelluric measurements

*Masato Fukai[1], Yasuo Ogawa[1], Kuo Hsuan Tseng[1], Masahiro Ichiki[2], Shinichi Takakura[3]

1. Tokyo Institute of Technology, 2. Tohoku University, 3. National Institute of Advanced Industrial Science and Technology

In Tohoku Japan, the Pacific plate that subducts under the Eurasian plate is old, thick, and cold. The basalt - eclogite phase transition is expected to occur at a depth of 100 km. The water released in the dehydration reaction forms serpentinite, which is transported to the deeper part. Serpentinite decomposes at a depth of about 150 km and water rises in the mantle due to buoyancy. Therefore, it is believed that there is no rise in water caused by slab mineral dehydration in the Northeast Japan forearc (Kazahaya et al., 2014). In contrast, the seismic tomography in NE Japan fore arc (Zhao et al., 2014) imaged low velocity regions in the forarc which suggests rising fluids from slabs which is called as "Water wall". In this research, we aimed to constrain the rising fluid distribution in the forearc from the 3d electric conductivity structure by magnetotelluric observations in Kitakami Mountains.
In our model, distribution of low resistivity indicating rising fluids from the deep part was not analyzed corresponding to the P wave low velocity region of Zhao et al.(2014). However, vertical low resistivity was analyzed from the volcanic front toward forarc. The conductors spread 30 km east of the volcanic front at depths of 10-40 km. This low resistivity is in good agreement with the low velocity distribution (Zhao et al., 2014; Okada et al., 2015). The low resistivity east of volcanic front is almost vertically continuous from the uppermost mantle to the middle crust. Therefore, this may indicate that the fluid on the mantle flow reaches the uppermost mantle of the forearc and releases fluids in the forearc crust.

Keywords: geofluid, NE Japan forearc, magnetotelluric method

©2019. Japan Geoscience Union. All Right Reserved.

Elastic wave velocity and electrical conductivity in brine-saturated rocks and microstructure of pores

*Arina Tomioka[1], Tohru Watanabe[1]

1. University of Toyama

Geophysical mapping of fluids is critical for understanding crustal processes. Seismic velocity and electrical resistivity structures have been studied to reveal the fluid distribution. However, the fluid distribution has been still poorly constrained. Observed velocity and resistivity should be combined to make a quantitative inference on fluid distribution. The combined interpretation requires a thorough understanding of velocity and resistivity in fluid-saturated rocks. We have made measurements of elastic wave velocities and electrical conductivity in brine-saturated rocks under confining pressures, and examined pore structures with SEM.

Measurements and microstructural observations were made on granites (Aji, Kagawa Pref., Ohshima, Ehime Pref.), granodiorite (Enzan, Yamanashi, Pref.) and tonalite (Kadohara, Fukui Pref.). Cylindrical rock samples (D=26 mm, L=30 mm) were filled with 0.1 M KCl aqueous solution, and velocity and conductivity were simultaneously measured by using a 200 MPa hydrostatic pressure vessel. The pore-fluid was electrically insulated from the metal work by using plastic devices. The confining pressure was incrementaly increased up to 150 MPa, while the pore-fluid pressure was kept at 0.1 MPa. It took 3 days or longer for the electrical conductivity to become stationary after increasing the confining pressure.

Rock samples showed moderate increase in velocity and large decrease in conductivity under confining pressures. Electrical conductivity steeply decreased at low pressures (<20 MPa) and then showed gradual decreases. Grain boundary cracks are pervasive in rock samples. The increase in velocity and decrease in conductivity at low pressures must be caused by the closure of grain boundary cracks with small aspect ratios ($<10^{-3}$). SEM images show that the aperture of a grain boundary crack varies along its width. Large aperture parts can be open even under high pressures to be conduction paths. The difference in conductivity at high pressures must reflect the difference in the amount of large aperture parts.

Keywords: Elastic wave velocity, electrical conductivity, fluid

©2019. Japan Geoscience Union. All Right Reserved.

Influence of grain shape and grain size distribution on connectivity of pores in granular materials.

*Katazakai Haruka[1], Tohru Watanabe[1]

1. Toyama University

Transport properties such as electrical conductivity and permeability are sensitive to the connectivity of pores. Pore structure in granular materials varies with the shape and size distribution of grains. In order to understand the influence of the shape and size distribution of grains, electrical conductivity and permeability were measured on granular materials saturated with 0.1 mol/L KCl aqueous solution. Spherical glass beads and oblate quartz sand of various sizes were employed. The ratio of conductivity to porosity was significantly higher in glass beads than in quartz sand. This observation suggests that a higher connectivity of pore is established in glass beads than in quartz sand. The influence of the size distribution of grains was studied on mixtures of small (D=0.2 mm) and large (D=1 mm) glass beads. The porosity deceases from 36% to 22% as the fraction of large grains increases 0% to 60%. Electrical conductivity decreases with decreasing porosity, while permeability shows a small decrease. As the fraction of large grains increases from 60% to 100%, the porosity increases from 22% to 36% and permeability increases by around 2 orders of magnitude. This change suggests that the pore size steeply increases as the fraction of large grains increases from 60%, since permeability strongly depends on the size of pores. X-ray micro CT observation was conducted to examine pore structure.

Keywords: conductivity, permeability, pore

©2019. Japan Geoscience Union. All Right Reserved.

Change of pore connectivity in granular materials under axial compression

*MAREMICHI ABE[1], Tohru Watanabe[1]

1. Toyama University

The influence of axial compression on the connectivity of pores in granular materials was studied. Electrical conductivity and compressional wave velocity were simultaneously measured on brine-saturated granular materials under uniaxial compression. Spherical glass beads and oblate quartz sand were employed. X-ray micro CT was conducted on granular materials impregnated with epoxy resin to examine microstructure of pores. Compressional wave velocity increases and electrical conductivity decreases with increasing axial stress. When the axial stress was increased from 0 to 5 MPa, compressional wave velocity increased by around 12% in both materials and electrical conductivity decreased by 0.7 and 1.7% in glass beads and quartz sand, respectively. The increase in compressional wave velocity must reflect the increase in contact area between grains, which was observed with X-ray micro CT. The decrease in conductivity must be caused by the decrease in connectivity of pores. X-ray micro CT images show that the connectivity of pores is easily lost under axial compression in quartz sand owing to its oblate shape.

Keywords: granular material, pore, electrical conductivity

©2019. Japan Geoscience Union. All Right Reserved.

Estimation of crustal strength using residual strain of quartz in deformed conglomerate and inhomogenous strain of conglomerate layer -As an example of multiple collision zone of Izu-Bonin arc, Fujikawa valley, Central Japan-

*Shun Suzuki[1], Kenta Kobayashi[1]

1. Graduate School of Science and Technology, Niigata University

South Fossa Magna is understood as a site where the Izu-Bonin arc on the Philippine Sea plate collides with Honshu arc, and it is the only arc-arc multiple collision zone in the world. Maruyama (2008) reported deformed conglomerate outcrop accompanied by cataclastic flow in the Hamaishidake Formation (late Miocene to Pliocene). Report of them in the collision zone is not limited to the Fujikawa area, but from the Ashigara Group and from the Erimo Formation in the Hidaka collision zone of Hokkaido (Uda, 1976), have been reported. In this study, various analyzes were performed on deformed conglomerates found in the Fujikawa area, and the cause (temperature / pressure condition) and the position in the collision zone were clarified, it aimed to restrict the multiple collision phenomenon and the deformation environment of trench fill sediments.

[Outcrop outline]
It is revealed that the deformed conglomerate outcrops occurred in the geologic body (Fujikawa Shear Zone) which makes a high dip zone in the direction of NW-SE, and they are modifying the initial NS system folding. The long axis direction of the gravel showing N40W trend and the shear fabric of the gravel showing sinistral sense.

[Paleo stress analysis by multiple inverse method]
The result of the MIM analysis (Yamaji et al., 2011) using the slip data of the gravel fault plane with the flow deformation mode shows ENE-WSW compression, which is not consistent with the current Philippine Sea plate motion.

[Restrictions on forming environmental condition of deformed conglomerate]
We tried to guess the maximum heat temperature of the geological body using the carbonaceous material Raman spectrum (Kouketsu et al., 2014), and examination of the differential stress level using the internal strain of the quartz (Takagi et al., 1988). As a result, it is revealed that deformed conglomerate outcrops heated only 150℃ or less, and the maximum heated temperature is rising toward the lower formation of Hamaishidake Formation. When the geothermal gradient is estimated by layer thickness conversion, the value such as 4~5℃ / 100 m is restored, and the depth at which the 150℃ heating can be recorded is about 3~4 km. That is, the deformed conglomerate is found to be a product under shallow and low temperature conditions. On the other hand, the estimated differential stress value is 50-100 MPa, which is strongly deformed despite being a shallow deformation.

[Discussion]
As for the ENE-WSW compression obtained from cataclastic flow slip data, it can not be explained with only the motion of the Philippine Sea plate. If these as deformation events after the deposition age limit (about 5 Ma) of the Hamaishidake Formation, it is necessary to consider the influence of E-W compression from around 3 Ma (Takahashi, 2006) or the ENE movement of Amur Plate (Komatsubara, 2015), and it

©2019. Japan Geoscience Union. All Right Reserved.

means that the tectonics are not only dominated by the Philippine Sea plate. Considering trench fill sediment objects in the Fujikawa Valley as accretionary bodies, since deformed conglomerate occurs near the boundary fault of the middle and upper strata of the Fujikawa Group, it may be a deformation near the Mega Splay Fault branching from the plate boundary fault at the Tanzawa block collision stage. In addition, considering the usual crustal strength (Byerlee, 1978), theoretically it is not possible to record a differential stress value of 100 MPa at 4 km underground. However, according to the data of drilling at the plate boundary Nankai Trough (Hamada et al., 2018), it is pointed out that the differential stress value rises in the Accretionary prism and reaches nearly 100 MPa. In other words, in the geological body near the plate boundary, it is predicted that the crustal strength is large and it is placed in the high differential stress state also in the subsurface shallow part, and the deformed conglomerate is considered to be a product in such a place.

Keywords: South Fossa Magna, Multiple collision zone, Deformed conglomerate, Rheology of fault rocks

©2019. Japan Geoscience Union. All Right Reserved.

An Introduction to Ryoke Cataclastic Rocks in Tsukide, Mie Prefecture, Japan: An Approach Using 3D Reconstructions From Thin Sections

*Thomas Jing Yi Yeo[1], Toru Takeshita[1]

1. Department of Natural History Sciences, Graduate School of Science, Hokkaido University

The Japan Median Tectonic Line (MTL) is the longest fault system in Japan where it spans from Kyushu Island and extends towards the north east direction up until Ibaraki Prefecture. It has been an active strike slip fault since the Mid-Cretaceous period, which was originally formed as the southern marginal shear zone in the Ryoke belt (e.g. Hara et al., 1980) leading to the formation of mylonite and superposed by cataclasite at the core region.

This study aims to identify the kinematic history of the fault plane and its effect on the cataclastic rocks from a 3D viewpoint. The fieldwork was conducted in the hanging wall section of the MTL in Mie Prefecture, Japan. The hanging wall of the MTL in the study area is characterized by Creataceous Ryoke granitic rocks which was deformed into mylonitic rocks and was later overprinted by cataclasite at the proximal region. The main objective of this project is to identify and relate the kinematics of the MTL and physical conditions during the formation of the cataclasite.

From the thin sections observations, the grain size reduction of the mylonitic clasts was observed and was related with cataclasis. The cataclasite formed at the brittle fault zone enables chemically rich fluids to penetrate. This promotes the growth of foliated phyllosilicate minerals mainly muscovite from the alteration of presumably feldspars. Microstructural features such as riedel shears with C’ -type shear band fabric assist in indicating the sense of motion. Fracture densities and distributions are also quantified in all of the three sides of the sample in order to obtain a clearer view on the brittle properties.

Also, based on the crossed cutting relationship seen in the microstructures of the sample, a schematic deformation history of the sample was constructed. The MTL begins with a sinistral shear sense which causes the mylonitisation of the Ryoke granitoids. Upon the cooling of temperature, cataclasite was formed and transpression of the shear zone causing pressure solution seams to be precipitated which resulted in the formation of phyllonite. Lastly, a late stage reactivation of the pressure solution seams caused faulting to occur.

Furthermore, using the rake angle of the C’ and S fabrics of the Riedel shears, measured from the thin sections representing the different sides of the sample, the orientations of both the C’ and S planes could be reconstructed and plotted as a stereographic projection with values of [278/ 48N] and [124/ 82SW] respectively. The XZ plane which is 90° away from the intersection point of C’ and S planes has an orientation of [031/ 67SE]. By assuming plane strain and with the assistant of the software StrainSim v3, the simple shear strain, γ=0.73, the angular shear, Ψ=36° and material internal friction angle, Φ= 56°. Similarly, the principle stress orientations are found to be at [62°→158], [23°→301] and [15°→037] for σ_1, σ_2 and σ_3 respectively. By combining all the relationships mention above, the motion sense of the fault was identified as the NE block moving NW and downwards with a more dominant dip slip component. This dominant dip slip movement of the fault could be potentially related to the normal faulting movement of the MTL during the Ichinokawa Phase at 63-58Ma.

Moreover, the electron backscatter diffraction (EBSD) analysis of the sample is currently being conducted

©2019. Japan Geoscience Union. All Right Reserved.

to analyse the distribution of the quartz’ s and calcite’ s C-axis fabric.

References

Hara, I, Shyoji, K., Sakurai, Y., Yokoyama, S., Hide, K., 1980. Origin of the Median Tectonic Line and its initial shape. *Memoirs of the Geological Society of Japan*. No. 18, 27–49.

Keywords: Median Tectonic Line (MTL), Cataclasite, Pressure Solution Seams, Shear Zone, Fractures, Kinematics

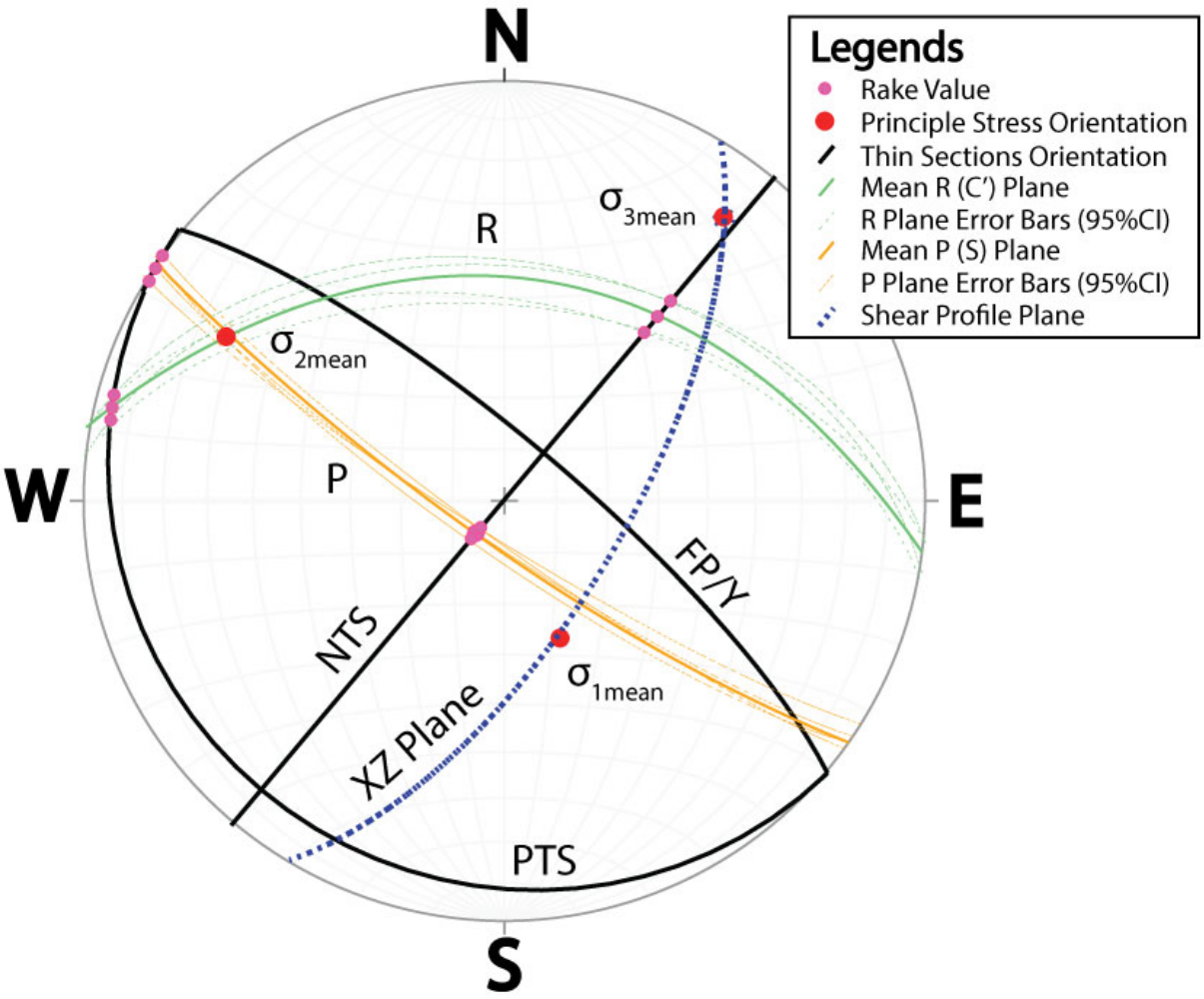

©2019. Japan Geoscience Union. All Right Reserved.

Relationships between spacing and growth or linkage of normal faults in the Miyako Island, South Ryukyu arc, Japan

*Sumire Maeda[1], Makoto Otsubo[1], Daisuke Asahina[1], Yuki Furuno [1]

1. Research Institute of Earthquake and Volcano Geology, Geological Survey of Japan/AIST

Estimating interaction and linkage of faults is one of the most important issues to evaluate the long-term activity of future earthquakes. For the long-term evaluation of the major active fault zones, Headquarters for Earthquake Research Promotion (e.g., HERP, 2010) uses so-called 5-km gap threshold (Matsuda,1990) to group and segment the fault traces. However, the fault size may change in the future, so it is necessary to introduce a multilateral index that can evaluate temporal and spatial evolution of faults.
Fault spacing, the horizontal distance between neighboring faults, has been related to stress reduction around faults (e.g., Soliva et al., 2006; Fossen and Rotevatn, 2016). Soliva et al. (2006) investigated the relationship between the fault spacing and the stress reduction area for a series of faults. Their studies show that the fault spacing is linearly related to the mechanical layer thickness. In the evolution process of normal fault, it is assumed that randomly distributed faults start to propagate and couple at the beginning, and the fault spacing becomes regularly distributed. Therefore, it may be possible to estimate the thickness of the mechanical layer in which the faults exist from the regular spacing of the saturated faults.
In this study, we investigated the normal faults in the Miyako Island, South Ryukyu arc, Japan in order to examine the possibility of fault linkage based on the fault spacing and the Coulomb shear stress perturbation. We found that the Miyako Island has three fault groups with different types of strikes, and these fault spacings are almost regularly distributed. The layer thickness of the NW-SE strike fault group can be estimated about 3,500 m based on the faults spacing. This results imply that the fault group extends only to the upper end of the seismogenic zone (3-17 km; HERP, 2012). In addition, the thickness of this fault group is close to the thickness of the Ryukyu Group and Shimajiri Group of the Miyako Island. Large-scale faults beneath the Miyako Island may be branched in the shallow soft-sedimentary rocks.

©2019. Japan Geoscience Union. All Right Reserved.

3D fault architecture along the Median Tectonic Line, eastern Kii Peninsula, SW Japan

*Norio Shigematsu[1], Takuma Katori[1,2], Jun Kameda[3], Ayumu Miyakawa[4]

1. Research Institute of Earthquake and Volcano Geology, Geological Survey of Japan, National Institute of Advanced Industrial Science and Technology, 2. Graduate School of Science and Technology, Niigata University, 3. Department of Natural History and Sciences, Hokkaido University, 4. Research Institute of Geology and Geoinformation, Geological Survey of Japan, National Institute of Advanced Industrial Science and Technology

The heterogeneous fault deformation around the brittle-plastic transition possibly affects the fault behavior significantly including the generation of earthquakes (e.g., Scholtz, 2001). To understand the effect, a detailed fault zone architecture is essential. In this study we have tried to construct a 3D fault zone architecture model based on the geological study of an exhumed fault zone, the Median Tectonic Line (MTL) in the western Kii peninsula SW Japan.

Accurate positions were determiend by applying SfM (structure from motion) and MVS (multi-view stereo) calculation (e.g., Furukawa and Hernández, 2013) to photos taken by an UAV (Unmanned Aerial Vehicles), and GNSS (Global Navigation Satellite system) surveying (e.g., Bemis et al., 2014) to reveal the 3D structures. The microstructures, chemical composition of minerals and crystallographic orientations of quartz using an electron back-scatter diffraction (EBSD) (Prior, et al., 1998) were analyzed to characterize the defomation of fault rocks. Based on these deformation features, the 3D fault zone architcture were constructed using a 3D-CAD software.

In the 3D fault zone architecture model, the fault plane of the MTL (lithological boundary) is an almost perfect plane dipping to the North. The structures can be divided into two main structures. One includes mylonite and cataclasite showing sinistral sense of shear. The other structures consist of scaly cataclasite showing dextral sense of shear and further younger structures including the lithological bonadry. The later structures cut the former structures indicating the sequence of deformation within the fault zone.

Scaly cataclasite only apper in the vicinity of the MTL, and is characterized by the strong foliation defined by the alignment of chlorite. Modal fraction chlorite is much larger than that in the surrounding Ryoke drived rocks, and pressure-solution seam is well developed. The estimated temperature based on the chlorite geothermometry is about 300 ºC (Bourdelle et al., 2013).
The deformation of the structures showing sinistral sense of shear varies from mylonite deformed at temperature of about 450 ºC (Higher-T mylonite), that deformed at about 300 ºC (Lower-T mylonite) to cataclasite deformed at about 300 ºC, suggesnting these structures record the brittle-plastic transition. One conspicuous feature in these structures is an altanation zone of black cataclasite and ultramylonite. This zone is a narrow and planar zone with width of 10 m. The cataclasite in this zone is black colored and strongly foliated. The ultramylonite in this zone show almost ramdom CPO (crstallographic preffered orientation) of quartz. We consider that this zone was the fault core when the present exhumed level experienced the brittle-plastic transiton.

Keywords: Fault Zone Architecture, Brittle–Plastic transition, the Median Tectonic Line, Mylonite, Cataclasite

©2019. Japan Geoscience Union. All Right Reserved.

Significant of thrust zone at Fuji river basin in the South Fossa Magna, Southern Yamanashi Prefecture, Central Japan
-Study of Structural geology of Minobu and Neguma fault-

*Minami Madoka[1], Kenta Kobayashi[1]

1. Niigata university department of geology science

There are Minobu fault that was certified as major active fault, Itoigawa shizuoka Tectonic Line (ISTL) and Fujikawa Kako Fault Zone (FKFZ) in the South Fossa Magna. The region is very precious to reveal formation of Japan island because the area is collision and accretion zone to Southwest Japan of Izu-Ogasawara arc. Mainly, Fujikawa group is distributed that filled trough made by past collisional block in this study area.
Minobu Fault is high probability to connect ISTL and FKFZ in the blank range of active fault. In recent years, it was shown sinistral fault sense from geomorophological point of view.(Mizumoto,2016) Howevere, nortern Minobu Fault is estimated reverse fault sense because of stratigraphy difference.
We discover and described new Minobu fault outcrops and divide Minobu fault into Segment Ⅰ and Ⅱ. We are obtained datas from stress analysis and XRD analysis in the area.
We will discuss the formation mechanism and history of geological structure deveropment of Minobu and Neguma fault in South Fossa Magna from kinematics of the faults and geological structure.

Keywords: South Fossa Magna, active faults, Itoigawa Shizuoka Tectonic Line, Fujikawa Kako Fault Zone

©2019. Japan Geoscience Union. All Right Reserved.

Mineralogical characteristics of fault rocks in the aftershock regions of the 2000 Western Tottori earthquake and its spatial distribution

*Shunya Kaneki[1], Tetsuro Hirono[1], Hideki Mukoyoshi[2], Kenta Kobayashi[3], Toru Takeshita[4]

1. Graduate School of Science, Osaka University, 2. Graduate School of Science and Engineering, Shimane University, 3. Graduate School of Science and Technology, Niigata University, 4. Graduate School of Science, Hokkaido University

A large earthquake (*Mw*6.6) occurred on 6 October 2000 in the western part of Tottori Prefecture, southwestern Japan. The main shock was considered as an almost left-lateral strike-slip event with the hypocenter located at 35.269 ˚N and 133.357 ˚E. The rupture process and slip distribution of the main shock was estimated from coseismic strong motions and geodetic data. These previous studies suggested that slip of the main shock mainly occurred in the southern part of the aftershock regions. Furthermore, Yukutake et al. (2007) estimated regional stress field before and after the main shock using aftershock focal mechanisms, and proposed that southern part of the aftershock regions may be dramatically weak in friction compared to northern and central parts. However, there are currently few researches attempting to understand regional slip behaviors of both main shock and aftershocks in association with spatial heterogeneity of physical properties of fault materials.

Mineralogical characteristics of rocks is one of the valid candidates that is likely to dominate its physical properties, and in general, increase in amount of frictionally weak minerals can reduce frictional strength of fault rocks. For understanding spatial slip behaviors in aftershock regions of the 2000 Western Tottori earthquake, we first need to investigate spatial variations in mineral composition of fault rocks. We collected more than 100 bulk rock samples from 14 fault-related outcrops, that distribute in northern, central, and southern parts of the aftershock regions. We then acquired XRD profiles of the powdered samples with internal standard (Al_2O_3) of 20 wt.%, and estimated the amount of minerals by using the RockJock software. The results clearly indicate that intact host rocks have similar mineralogical features regardless of sampling locations; they are granitic rocks composed of quartz, K-feldspar, and plagioclase. In contrast, mineral compositions of fault rocks show different characteristics by locations. In northern part of the aftershock regions, fault rocks are poor in K-feldspar and plagioclase and are rich in halloysite. In central part, fault rocks are poor in K-feldspar and plagioclase and are rich in illite. In southern part, fault rocks are poor in plagioclase and are rich in halloysite. These information tell us the representative mineralogical features of fault rocks in each part of the aftershock regions. Future friction experiments, by using representative fault rock samples under in-situ conditions, will give us a direct glimpse into the spatial variations of frictional properties in the aftershock regions of the 2000 Western Tottori earthquake, such as frictional strength and its velocity dependence. All of these information, not only seismological data but also mineral composition and physical properties of fault materials, should be incorporated for understanding the spatial heterogeneity of slip behaviors of the main shock and aftershocks of the 2000 Western Tottori earthquake.

Keywords: The 2000 Western Tottori earthquake, Fault rock, Mineral composition, XRD analysis

©2019. Japan Geoscience Union. All Right Reserved.

Relationship between seismicity of the 2016 the Central Tottori Earthquake and fault distribution in the aftershock area

*Masayuki Ichimura[1], Hideki Mukoyoshi[2]

1. Graduate School of Natural Science and Technology, Shimane University, 2. Department of Earth Science, Shimane University

The 2016 Central Tottori Earthquake (M6.6) occurred on October 21. The epicenter was Central Tottori and depth of hypocenter was 11km. Earthquake source fault was determined to be left-lateral strike fault developed NNW-SSE direction with WNW-ESE directional maximum principal stress axis. In the region, active fault related to the earthquake was not recognized. Although clarification of the occurrence of faults such strain concentration zone is important, there are no reports about detail field outcrop investigation in the area of this earthquake.
The aim of this study is to reveal relationship between seismicity of the 2016 Central Tottori Earthquake and fault distribution in the aftershock area based on field investigation and description of microstructure of the faults.

In this study area, late Cretaceous-early Paleogene medium-coarse-grained biotite granite is mainly distributed.

As a result of this study, total of 190 faults were observed in the aftershock area. Orientation of faults developed in NNW trending aftershock area were concentrated in NNW. On the other hand, faults in eastern part of aftershock area shows N-S~NE trend. Three-directional striation on the fault plane was observed in the aftershock area and only cataclasite was developed. The fault (strikes NNW) had horizontal striation was confirmed. P-foliation was observed in this fault rocks under the microscopic observation and indicated left-lateral strike slip.

The fault that had experienced strike slip, and shear sense consistent with earthquake source fault was confirmed. This result indicates that this fault had moved in the present stress field. According to previous study related to 2000 Western Tottori Earthquake, it is suggested that NNW trending fault system developed in southern part of the aftershock area was weaker than the surrounding area. With comparing these result, fault system in aftershock area of the 2016 Central Tottori Earthquake also might be weaker faults due to the orientation of faults correspond with the Y surface of the earthquake source fault.

©2019. Japan Geoscience Union. All Right Reserved.

History of fault activity considered from the brittle shear zone and the geological structure near the Cape Otachi, Kumamoto Prefecture

*Keiji Ogashiwa[1], Kenta Kobayashi[1]

1. Niigata University

[Introduction] The Hinagu fault zone is located in the western Kyushu and is an active fault zone extending 81 km roughly in the NE-SW direction. The Hinagu fault zone is a dextral slip fault with the east side uplift [URL]. The fracture zones of the Hinagu fault zone have been reported in two places in the Higo metamorphic rock distribution area and in the lower Cretaceous distribution Area near the cape Otachi (Matsumoto・Kanmera, 1964). The core of the fracture zone at Sabagami pass shows dextral slip and its outer rim shows sinistral slip (Kobayashi・Koshiwa, 2016). In addition, the geological fault parallel to the Hinagu fault is apparent sinistral slip fault (Saito et al., 2005). These facts suggest the possibility that the Hinagu fault zone was active differently from the past and the present. Analysis of the fracture zone and surface survey around the fracture zone are important for elucidating the history of fault zone activity. In addition, since Kyushu is an important area which is the meeting part of the Southwest Japan arc and the Ryukyu arc, clarifying the activity history of the Hinagu fault zone leads to the understanding of the tectonics of Kyushu. In this research, for the purpose of elucidating the history of activity of the Hinagu fault zone from the brittle shear zone and geological structure found near the Cape Otachi, Kumamoto Prefecture, the ground surface survey, the structure observation of the fault rock, the XRD analysis, the small fault Analysis and so on.

[Ground Surface Survey] As a result of the ground survey around the Cape Otachi, small faults constituting the fracture zone were observed in the lower Cretaceous Hinagu Formation, and it was roughly classified into 4 strains from the strike of the fault, the sense, and the cutting relationship. F1 is NNE-SSW trend sinistral slip fault, F2 is NNE-SSW trend dextral slip fault, F3 is NNW-SSE trend sinistral slip fault, F4 is E-W trend dextral slip fault.

F2 is a small fault group found in the brittle shear zone consisting of cataclasite. F1 is seen outside the brittle shear zone and part forms a planar cataclasite zone with a width of 5 cm. F3 and F4 are small fault groups which mutually cut. F3 deform the dike group described later. F4 cuts the brittle shear zone. Apart from the fault, we identified a folding group with a hinge in the ENE-WSW direction on the southeast side of the brittle shear zone. In addition, an andesitic dykes group with a dominant ENE-WSW strike was observed on the east side of the brittle shear zone. We confirmed the cutting and bending of the dike by F3, the injection of dike along the F3. This dike is believed to be related to the Neogene Igneous rocks in Amakusa area (Matsumoto ·Kanmera, 1964).

[Small Fault Analysis by Multiple Inverse Method (Yamaji, 1999)] Compressive Stress Field in NW-SE direction from F1, Compressive Stress Field in ENE-WSW direction from F2, Compressive Stress Field in NW-SE direction from F3 and F4 Was detected.

[Stage Segmentation] The time of formation of the fault, dike and fold observed in the vicinity of the Cape Otachi is divided into three stages, D1, D2, D3 from the stress field obtained from the cutting relation.
In D1, F1 was activated in the compressive stress field in the NNW-SSE direction. Considering the compression axis direction, fold group with fold axis in NE-SW direction is thought to be formed in D1.
In D2, F2 was activated in the compressive stress field in the ENE-WSW direction, forming a wide brittle

©2019. Japan Geoscience Union. All Right Reserved.

shear zone.
In D3, F3 and F4 were active in the compressive stress field in the NW-SE direction.
We thought that the bending and the injection of dike along F3 indicate that the dikes were deformed by F3 before consolidation. Considering the above-mentioned thing, we thought that the dike group had formed between the terminal stage of D2 and the beginning of D3.

Keywords: Hinagu fault zone

©2019. Japan Geoscience Union. All Right Reserved.

Study on fault activity evaluation method (A new attempt to understand fault activities) No.1 - Overall plan and current situation at Shionohira Fault -

*Kazuhiro Aoki[1], Takahiro Watanabe[1], Yukumo Tanaka[1], Kazuyoshi Seshimo[1]

1. Japan Atomic Energy Agency

If there is a "fault that may become active in the future" (hereinafter referred to as “inactive segment”) in the vicinity of a fault that has recently moved (hereinafter referred to as "active segment"), it appears that there is a difference in the stress state and in the "ease of activity" between the two segments. Under the current concept of nuclear regulatory standards, these segments are evaluated as part of the same series of faults due to lack of knowledge about interlocking faults.

Following the April 11, 2011 Fukushima-ken Hamadori Earthquake (4.11 earthquake), co-seismic surface ruptures trending NNW-SSE emerged over a distance of 14km between Nameishi Tabito of Iwaki city and North-west of Tsunaki Ishizumi. The surface rupture was named Shionohira fault by Ishiyama et al. (2011) and is identified to be part of the Itozawa fault (coincides to West trace of Itozawa fault by Tsutsumi and Toda, 2012). According to Imaizumi et al. (2018), the fault is said to continue extending south of the ruptured surface covering the area from Nameishi of Tabito Iwaki city to West of Sakura, Kawabe-cho and from Wakigawa, Yamadama-cho to Kobuki, Sekimoto-cho Kita Ibaraki city. In this study, the area designated as the Shionohira fault which has surfaced after the 4.11 earthquake is called the active segment and the remaining area to the south to be the inactive segment.

The authors aim to develop a fault activity evaluation method in order to clarify whether the inactive segment really moves together with the series of faults including the active section when a fault activity occurs by studying the differences between active and inactive segments in the interlocking of faults.

The authors have been conducting a series of study at the Shionohira fault and its southern extensions, reporting on the outcrop survey results (Kametaka, et al., 2015) and the frictional characteristics of fracture zones (Aoki et al., 2015, 2016). Currently, a fault slip test is carried out to assess the in-situ stress state.
In the fault slip test, a double packer is placed above and below the underground fracture to inject high pressure water from the surface and artificially trigger a slip in the fracture in order to measure the three dimensional deformation amount (micrometer to millimeter) (Guglielmi et al., 2013). This device called the Step-rate Injection Method for Fracture In-situ Properties or SIMFIP probe was designed and manufactured by Guglielmi for underground storage studies of CO2 in France and was first applied at the underground research facility (LSBB) in the south of France (Guglielmi et al., 2015). Subsequently, in-situ tests have been conducted on faults in underground research facilities such as Tournemire in France, Mont Terri in Switzerland, and the gold mine in South Dakota, USA.

This device allows to quantitatively measure the deviation of the fault by increasing the pore water pressure in the section partitioned by double packers, and to also examine the causes for leakage of groundwater, petroleum, CO2, and radioactive waste. In addition, it enables to observe fault displacement, pore pressure, and induced seismic waves at the micrometer scale, and to estimate friction and stress state of fault zones. By deepening understanding of the coupled phenomenon of hydraulics

©2019. Japan Geoscience Union. All Right Reserved.

and dynamics around the fault, the authors believe the method could be useful in elucidating the mechanism of seismic occurrence. It should be noted that this device is being applied for the first time in Japan, and the first time ever for an in-situ test of active faults.

Keywords: SIMFIP, Shionohira fault, active fault, Fukushima Hama-dori earthquake, fracuter zone characteristics, injection experiment

©2019. Japan Geoscience Union. All Right Reserved.

Study on fault activity evaluation method (A new attempt to understand fault activities) No.2
- Injection experiment using a SIMFIP probe at Shionohira Fault and southern fault-

*Takahiro Watanabe[1], Yukumo Tanaka[1], Kazuhiro Aoki[1], Yves Guglielmi[2], Paul Cook[2], Florian Soom[2], Wakahama Hiroshi[3], Noujou Haruka[3], Etsuo Iwasaki[3], Masao Kametaka[3], Kazuyoshi Seshimo[1]

1. Japan Atomic Energy Agency, 2. Laurence Berkley National Laboratory, 3. DIA CONSULTANTS

The Shionohira fault caused the April 11, 2011 Fukushima-ken Hamadori Earthquake of Mw 6.7 which occurred one month after the Tohoku-Oki earthquake of Mw 9.0. Co-seismic surface ruptures trending NNW-SSE allowed to estimate a normal slip faulting with a 2 m maximum displacement. The causes of fault activation might be related to changes in the stress state following the Tohoku-Oki earthquake. The key question is to understand why some fault segments were activated and ruptured the land surface while others remained inactive although being very close and aligned on the same fault zone, which is of importance in better assessing the risk of seismic activation of faults in Japan. This might be related to slight differences in properties between active and inactive segments. This might be related to slight differences in properties between active and inactive segments. Recent laboratory measurements on core sampled across the rupture zone show that there are differences in friction coefficients and smectite and clay mineral contents between segments (Aoki, et. al., 2016, Seshimo, et. al., 2016). These differences may condition the frictional rate and state stability of the fault. In this project, frictional stability and hydraulic permeability of the Shionohira fault are explored in situ from SIMFIP probing of borehole intervals intersecting the fault at depths of about 10-to-30m.

Surface earthquake fault caused the earthquake of April 11, 2011 coincides with the west trace of Itozawa fault (Tsutsumi and Toda, 2012). Imaizumi et. al. (2018) identified the lineament as an active fault from Wakigawa of Yamadama-machi to Obuki of Sekimoto-machi, Kitaibaraki city. No surface rupture was idenfied in this region. This study refers to the part of the fault with surface rupture as an active segment and that without surface rupture as an inactive segment.

At the Shionohira site, vertical borehole of 30 m depth was drilled and test intervals were decided based on core observations, borehole TV and caliper logging data as follows. Test 1 between depths of 7.0 and 11.5m isolated with upper and lower packers and pressurized was conducted above the recently activated fault zone in the unfaulted sandstone layers. Test 2 between depths of 12.8 and 17.3m was conducted across the recently activated fault zone.

At the Minakami-kita site, inclined borehole of 50 degrees from surface with 30 m length was drilled and fracture zones were detected at 20.40 to 23.10 m. In-situ injection experiment using a SIMFIP probe is under going, comparison results will be presented at the conference.

Keywords: SIMFIP method, active fault, Sionohira Fault, Fukushima-ken Hamadori Earthquake, fracture zone charactarizaton, injection test

©2019. Japan Geoscience Union. All Right Reserved.

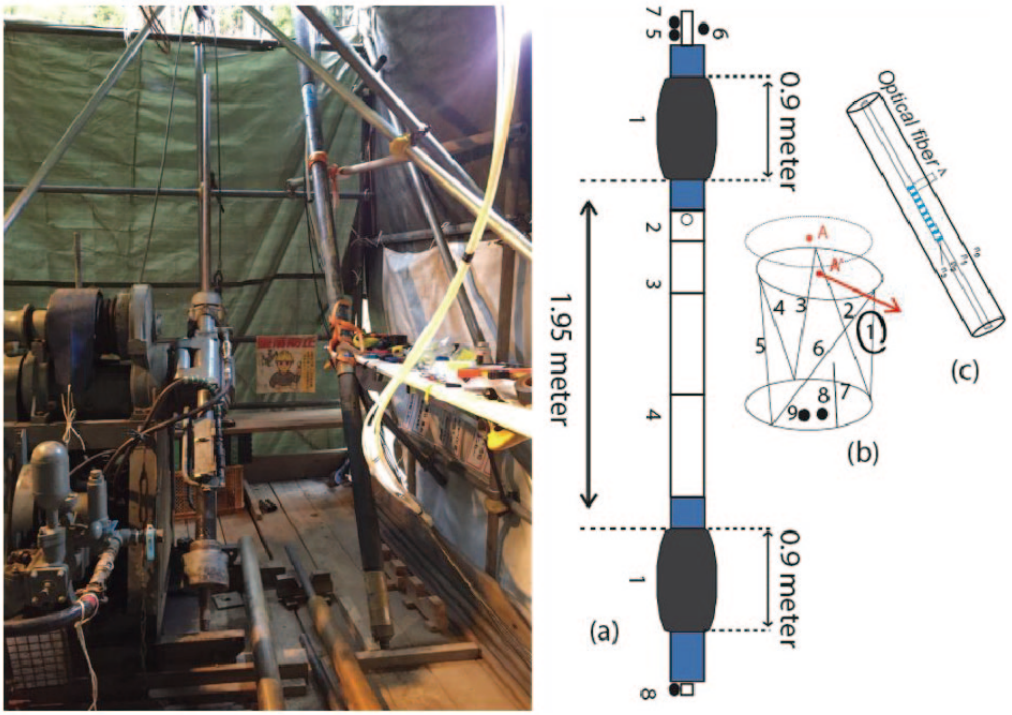

-SIMFIP probe used in Minakami-Kita tests – Left is a photo of the drill rig with the assembled SIMFIP probe set on the right -
(a) SIMFIP plan (1 packers, 2 injection sub, 3 SIMFIP cage, 4 extension subs, 5 Inclinometer, 6 Accelerometer, 7 Top pressure, 8 Bottom pressure)
(b) Principles of the sensor which is a deforming cage in 6 different directions + 1 reference (7) + 1 interval pressure (8)
(c) We build all our sensors using Bragg gages all connected on the same optical fiber.

©2019. Japan Geoscience Union. All Right Reserved.

Dynamic rupture simulation of 2018, Hokkaido Eastern Iburi earthquake: Role of non-planar fault geometry

*Tatsuya Hisakawa[1], Ryosuke Ando[1]

1. The University of Tokyo

The 2018, Hokkaido Eastern Iburi, Japan, earthquakeis an event characterized by complexity of rupture process, which may involve both reverse and strike slip depending on the locations on the fault surface. We perform dynamic rupture simulations based on simple physical laws and conditions for stressing and fault friction, taking complexity of the fault into account. The complex fault geometry is numerically treated by the boundary integral equation method accelerated by the fast domain portioning method. We search in a small number of parameter spaces for the stress ratio of the regional stress field and the frictional coefficients assumed to be the same over the fault area, rather than assigning heterogeneous distributions of the stress drop on the fault, to evaluate to what extent relatively simple forward models accounting for realistic fault geometry can explain the characteristics of coseismic observations. The fault geometry is constrained based on the aftershock distribution (NIED, 2018) and characterized primarily by the combination of three fault planes. As the result, we are able to reproduce several observed features of the event including the spatial variation of the fault slip direction, which is inferred from the seismological inversion (Okuwaki and Yagi, 2018), and the ground surface displacement observed by GEONET. The results suggest that the complex rupture event can be reproduced by a relatively simple physical model to some extent if the geometrical complexity of the faults is properly taken into account.

©2019. Japan Geoscience Union. All Right Reserved.

A New Fully-Dynamic Earthquake Cycle Simulator Applicable to Arbitrary Nonplanar Fault Geometries - A Benchmark Test

*Daisuke Sato[1], Nadia Lapusta[2], Hiroyuki Noda[1]

1. Disaster Prevention Research Institute, Kyoto University, 2. California Institute of Technology

The models and data assimilations of the real earthquake cycles are now getting on the track for providing the data beyond the classical empirical laws in the context of the seismic hazard; an example can be seen in the Third California Earthquake Rupture Forecast (UCERF3). Such large modeling is enabled by the rapid development of the earthquake simulators capable of solving the earthquake cycles in the real fault systems (Barbot et al., 2012: Richards-Dinger and Dieterich, 2012). However, there is not a fully dynamic cycle simulator applicable to wide tectonic conditions yet. The applicability of earthquake cycle simulators is thus still largely restricted.

In this research, we propose a new earthquake cycle simulator applicable to arbitrary nonplanar fault geometries. This simulator is based on the fast domain partitioning hierarchical matrices (FDP=H-matrices) (Sato and Ando, 2018), a newly developed algorithm of quasilinear time for dynamic BIEM applicable to nonplanar fault geometries. This cycle simulator thus overcomes the restriction on geometries when solving the elastodynamic fault motions in the coseismic phase, which had been the intrinsic problems for previous methods to solve the dynamic ruptures. In the presentation, after proposing the new method, we run a benchmark test of the SCEC Sequences of Earthquakes and Aseismic Slip project (SEAS) by the new simulator. Obtained results are compared with those of the previous simulators such as ByCycIE (Lapusta et al., 2000) and other simulators of volume-based methods. Simulated cycles on other nonplanar faults will be also demonstrated.

Keywords: Fully-Dynamic Earthquake Cycle Simulator, Nonplanar Fault Geometries (Subduction Zones + Ground Surfaces and Inland Faults), SCEC Sequences of Earthquakes and Aseismic Slip project (SEAS)

©2019. Japan Geoscience Union. All Right Reserved.

Stress and displacement Green's functions to treat volumetric inelastic strain and elastic inhomogeneity in boundary integral equation method

*Daisuke Sato[1]

1. Disaster Prevention Research Institute, Kyoto University

The boundary integral equation method (BIEM) is a commonly used method to simulate the fault motions accurately. Recent developments are now resolving well known problems of BIEM, such as the numerical cost problem (Sato and Ando, 2018) and the adaptabilities to elastic inhomogeneity (Kame and Kusakabe, 2012; Kusakabe and Kame, 2018). However, while it is shown to be applicable to the media other than homogeneous elastic media, obtained analytic integral kernels for simulating those media are now limited, largely due to its analytic difficulty. In this research, I obtain the the kernel expressions of those advanced BIEM in real space-time coordinate, based on the equivalent inclusion method (Eshelby, 1956; Mori and Tanaka, 1973).

First, the (volume) integral equation method (Barbot and Fialko, 2010) for the volumetric strain is shown to be reduced to BIEM of boundaries partitioning the discretized inelastic volume. Corresponding kernels are then obtained for piecewise-constant volumetric inelastic strain embedded in the three-dimensional homogeneous elastic space. The kernels are preliminarily shown to be equivalent to the part of the kernel for the inhomogeneous elastic media (Kame and Kusakabe, 2012; Kusakabe and Kame, 2018) both in static and dynamic cases.

Second, the surface integral in the representation theorem is reduced to the integral equation of the equivalent eigen-displacement. Consequently, as long as the absolute traction can be expressed with the strain and the eigen-strain, it is suggested that there can be a method to treat the inhomogeneous elastic media only by using the stress Green's function responding to the slip, already obtained analytically (Tada and Madariaga, 2001; Tada, 2006; Ando et al., 2007; Ando, 2016). By comparing the possible method with the method of Kame and Kusakabe (2012) capable of generally treating the elastic inhomogeneity in some examples, the validity of the proposal to treat inhomogeneous elastic media is investigated.

Keywords: volumetric inelastic strain, velocity structure, boundary integral equation method

©2019. Japan Geoscience Union. All Right Reserved.

Frictional properties of dolerite and granite at intermediate slip rates and controlled ambient temperatures

*Michiyo Sawai[1], Yuuki Yokoyama[1], Kyuichi Kanagawa[1]

1. Chiba University

High velocity friction experiments (up to several m/s) on many types of rocks have revealed that frictional strength decreases with increasing slip rate at seismic slip rates (e.g., Tsutsumi and Shimamoto, 1997; Di Toro et al., 2011). Coseismic weakening has been attributed to temperature rise including flash heating, melt lubrication or thermal pressurization (e.g., Rice, 2006; Hirose and Shimamoto, 2005). Although the importance of temperature during fault motion are widely recognized, the effects of temperature on frictional properties at intermediate to high slip rates remain unknown. We therefore conducted friction experiments at a wide range of temperatures and investigated the effects of temperature on the friction coefficient (μ).

Experiments were performed on dolerite (Belfast, Northern Ireland) and granite (Aji, Japan) using a rotary shear deformation apparatus at Chiba University. Samples were displaced up to 10 - 20 m at a normal stress of 1 MPa, slip rates of 1 to 300 mm/s, and ambient temperatures of 20 - 500°C in an argon atmosphere with an oxygen concentration of 0.2 %.

At 20°C and 100°C, dolerite showed velocity weakening at slip rates ranging from 1 to 30 mm/s with μ of 0.81 - 0.83 at 1 mm/s and of 0.73 at 30 mm/s. Whereas at high temperatures >300°C, friction is almost constant (μ = 0.81 - 0.85) at < 30 mm/s. At 100 mm/s, the behavior is slight velocity strengthening at 20 °C and 100°C with μ = 0.75 - 0.79 and clear velocity-weakening at more than 300°C with μ = 0.67 - 0.76. At 300 mm/s, the dolerite showed strong velocity weakening at all temperatures investigated. The amount of weakening (i.e., the drop in friction, $\Delta\mu$) increases with increasing temperature ($\Delta\mu$ = 0.1 - 0.38). Thus, the frictional properties of dolerite are affected not only by slip rate but also by ambient temperature.
Experiments using granite to decipher the effect of materials on temperature dependence are in progress. Our preliminary results are summarized as follows. At <30 mm/s, the behavior is slight velocity strengthening at room temperature and velocity-weakening at temperatures of 100-300°C. At >300°C, friction is almost constant. Friction coefficient decreases with increasing temperature of 20-300°C and increase again at >400°C. At >100 mm/s, clear velocity-weakening did not occur except at temperatures of 20°C. More results especially on granite will be reported at the meeting.

Keywords: friction, temperature dependence, dolerite, granite

©2019. Japan Geoscience Union. All Right Reserved.

Extraction of features of strata using borehole data of geothermal area by multivariate analysis

*Ojima Hiroki[1], Kazuya Ishitsuka[2], Toru Mogi[3], Tatsuya Kajiwara[4], Takeshi Sugimoto[4], Hiroshi Asanuma[5]

1. Department of Socio-Environmental Engineering Hokkaido University, 2. Division of Urban Management, Graduate School of Engineering, Kyoto University, 3. Division of sustainable Resources Engineering, Faculty of Enginieering, Hokkaido University, 4. Geothermal Engineering Co. Ltd, 5. Fukushima Renewable Energy Institute, AIST

In geothermal development, geological characteristics are often estimated qualitatively based on logging data of geothermal wells. On the other hand, the quartz index (QI) has quantitative information on minerals, and the index enables to objectively extract features of the geological formation using a statistical method. Therefore, in this study, from the QI obtained from the core cuttings in a geothermal field, we developed and examined a method to classify and extract geological features along with a well by multivariate analysis (in particular the difference in alteration degree). Specifically, we first carried out a principal component analysis to extract and emphasize the features of the data through dimensionality reduction. Then, their lithological features were classified by clustering using a Gaussian mixture model. In addition, the classification results by our method were compared with electric logs and temperature logs. In this study, we used the data obtained from wells in a geothermal area at Iwate prefecture. The geology of this area consists of andesite tuff and dacite tuff. The QI is defined as the percentage of the strongest X-ray intensity of a certain mineral in the sample from the strongest X-ray intensity of pure quartz measured under the same experimental conditions. This value means the content (weight percentage) in the sample for quartz and the relative quantitative ratio for the other minerals. In order to verify our proposed method, the principal component analysis was performed on the standardized QI data of clay minerals and compared with the results of existing geological classification based on geological interpretation. As a result of the comparison, our classification results agree with the results of existing geological classification, thus the classification of the strata by our method is valid. Next, in order to examine the effect of the dimensionality reduction by a principal component analysis, we compared the following cases: (i) clustering without dimension reduction for all QI, and (ii) clustering after applying the dimensionality reduction to all QI. In the case of dimensionality reduction, we used the principal components with a total contribution total over 95%. As a result of the comparison, the optimal classification number of the strata without the dimensionality reduction (case (i)) was 6. On the other hand, in the case of dimensional reduction (case (ii)) the optimal classification number was 10. The number of the optimal class indicates that more detailed features can be extracted using dimensionality reduction by principal component analysis. Notably, the classification in the depth range from 0 to 1000 m became detailed, highlighting the correspondence between clay, zeolite minerals and the geological formation.

Keywords: quartz index, principal component analysis, clustering

©2019. Japan Geoscience Union. All Right Reserved.

Low-temperature thermochronology of Cretaceous granitoids from the northern Northeast Japan Arc: Towards reconstructing arc-parallel thermal/denudation histories

*Shoma Fukuda[1], Shigeru Sueoka[2], Barry Paul Kohn[3], Noriko Hasebe[4], Akihiro Tamura[5], Tomoaki Morishita[5], Takahiro Tagami[1]

1. Graduate School of Science, Kyoto University , 2. Japan Atomic Energy Agency, 3. School of Earth Sciences, The University of Melbourne, 4. Institute of Nature and Environmental Technology, Kanazawa University, 5. Department of Earth Sciences, Kanazawa University

Northeast (NE) Japan Arc is categorized as an arc-trench system, where volcanism and earthquakes frequently occur. The tectonic history of the NE Japan Arc has been well-investigated based on geomorphic and geologic approaches. Furthermore, the recent multidisciplinary project (Crustal Dynamics) successfully achieved and accumulated geoscientific results by means of GPS, active faults, numerical modeling, friction experiments, etc (see also Iio et al. 2018, EPS). For estimating vertical deformation over long-term timescales (>10^6 yr.), our research group has investigated the thermal/denudation histories on every geomorphic province of the NE Japan Arc by using low-temperature thermochronology.

Thermochronology can reconstruct the time-temperature relationship of rock/mineral samples, based on radiometric ages and closure temperatures specific to the combination of radiometric dating methods and target minerals. Low-temperature thermochronology is useful for understanding upper crustal mountain building processes and has been applied to estimate the tectonic history of major orogens (e.g. European Alps: Wagner et al. 1977, Mem. Inst. Geol. Mineral., Univ. Padova; Himalayas: Blythe et al. 2007, Tectonics). However, the thermochronology approach directly measures cooling processes, rather than denudation/uplift histories. Therefore, it is noteworthy that denudation/uplift histories require some assumptions, such as appropriate geothermal gradients and dynamic equilibrium between denudation and uplift. Long-term uplift rates on >1 Myr time-scales, require estimates from such protocols, which are assumed to be equivalent to the vertical inelastic deformation of the crust (Ikeda et al. 2012, JGS).

Between 2014-2019 we collected over 100 granitic rock samples from the NE Japan Arc. Low-temperature thermochronology has been applied to many of these samples, including the apatite/zircon (U-Th)/He (namely, AHe and ZHe) (Sueoka et al. 2017, EPS) and apatite fission-track(AFT) methods (Fukuda et al. 2019, JAES:X), particularly from Cretaceous-Paleogene granites located in the southern NE Japan Arc. This research elucidated the contrast of thermal/denudation histories among the island arc provinces, i.e., Abukuma mountains, Ou Backbone Range(OBR), and Iide and Asahi mountains. In this presentation, we report results based on AHe/ZHe and AFT thermochronometry from Cretaceous granites in the northern NE Japan Arc, aimed at reconstructing arc-parallel and across-arc thermal/denudation histories.

We obtained AHe ages ranging between 88.6-0.9 Ma, AFT ages from 138.0-2.0 Ma, and ZHe ages from 83.9-7.4 Ma. The ages show contrasting thermal/denudation histories between the fore-arc side, OBR, and back-arc side, which are similar to the southern NE Japan Arc. This observation implies that arc-parallel mountains have approximately the same trend along NE Japan Arc. On the other hand, some differences were observed between the northern and southern NE Japan Arc as follows; (1) significantly

©2019. Japan Geoscience Union. All Right Reserved.

older AFT ages were obtained for Kitakami mountains (130-75 Ma) compared to the Abukuma mountains (80-40 Ma), (2) much younger AFT ages at ~2 Ma were found on the back-arc side, Taihe mountains, and (3) considering the expected relationship between expected closure temperatures, some reversal of coexisting AFT ages compared to AHe/ZHe ages (e.g., FST04, FST05) were observed.

Future work will involve thermal inverse modeling using AFT thermochronometry for estimating more rigorous constraints on thermal histories. This will also involve increasing the number of sampling localities in an attempt to extend our study area.

Keywords: Thermochronology, Northeast Japan Arc, Fission-track method, (U-Th)/He method, Island Arc

©2019. Japan Geoscience Union. All Right Reserved.

Uplift and denudation history of the South Fossa Magna region using low-temperature thermochronometric methods

*Yumi Kobayashi[1], Shigeru Sueoka[2], Shoma Fukuda[1], Barry P. Kohn[3], Tatsunori Yokoyama[2], Noriko Hasebe[4], Akihiro Tamura[5], Tomoaki Morishita[5], Takahiro Tagami[1]

1. Graduate School of Science, Kyoto University, 2. Tono Geoscience Center, Japan Atomic Energy Agency, 3. University of Melbourne, 4. Institute of Nature of Environmental Technology, Kanazawa University, 5. Department of Earth Sciences, Kanazawa University

The South Fossa Magna region is located at the junction of the Japan and Izu-Bonin arcs. Up to four crustal blocks of the Izu-Bonin arc, i.e., Kushigatayama, Misaka, Tanzawa, and Izu, collided this region and formed its crustal structures since the middle Miocene (1, 2). The timings of the collision events have been estimated by deposition ages of sediments between each block and the Japan arc. However, these questions remain unresolved.

In this study, we performed apatite fission track (AFT) and apatite (U-Th)/He (AHe) thermochronometric methods and U-Pb dating method to resolve the uplift and denudation history of the South Fossa Magna region.

The AFT ages are estimated to be 14.7 ±4.7 Ma in the Okuchichibu area (c.f., hornblende K-Ar age: 10.5 ±1.5 Ma (3)), 3.0 ±0.5 Ma, 9.2 ±2.2 Ma, and 7.6 ±0.9 Ma in the Kano Mountains (c.f., biotite K-Ar age:i.e., 10.5 ±0.4 Ma (4)), 3.6 ±2.5 Ma in the Minobu area (c.f., biotite K-Ar age: 5.4 ±0.3 Ma (5)). Also, the AFT ages are inferred at 37.0 ±5.9 Ma in Mt. Tsukuba (c.f., Rb-Sr whole rock isochron age: 61.6 ±4.3 Ma (6)), and 44.9 ±4.1 Ma in the Sori granitoid in Gumma Prefecture (c.f., biotite K-Ar age: 92.6 ±0.6 Ma (7)). The rocks which have younger AFT ages than the formation ages may reflect the uplift and denudation events since the rock formation. However, exhumation rates of the Tanzawa mountain, the closest mountain to the Izu block, did not increase before and after the collision of the Izu block (8), which may imply that the collision of the Izu block did not cause the uplift and denudation events significantly.

We also obtained the new AHe ages and U-Pb ages. The AHe ages for Okuchichibu area, Kanto mountains and Minobu area are about 3 Ma. Furthermore, according to the results of the inverse thermal analysis using the apatite FT lengths data, the granites in Okuchichibu area and the southern part of Kanto mountains cooled rapidly since about 3 Ma, and the granites in Minobu area and northern part of Kanto mountains cooled rapidly since about 1 Ma. The results of AHe ages were consistent with the results of inverse analysis. Based only on these ages, the rapid cooling ages of 3 Ma and 1 Ma are comparable to the collision ages of the Tanzawa block and the Izu block, respectively.

References

[1] Amano et al., Structural Geology 43, 11-20 (1999).
[2] Kano, Bull. Earthq. Res. Inst. Univ. Tokyo 77, 231-248 (2002).
[3] Ueno and Shibata, J. Japan. Assoc. Min. Petr. Econ. Geol. 81, 77-82 (1986).
[4] Shibata et al., Bulletin of the Geological Survey of Japan 35, 19-24 (1984).
[5] Sato et al., Gumma Mus. Natu. Hist. 19, 95-109 (2015)

©2019. Japan Geoscience Union. All Right Reserved.

[6] Arakawa and Takahashi, J.Min. Petr. Econ. Geol. 83, 232-240 (1968)
[7] Sudo, M. et al., Geochemical Journal 32, 49-58 (1998)
[8] Yamada, K. and T. Tagami, Journal of Geophysical Research 113, B03402, doi: 10.1029/2007JB005368 (2008).

Keywords: low-temperature thermochronology, South Fossa Magna, apatite fission track

©2019. Japan Geoscience Union. All Right Reserved.

Correlation between residual uplift and recurrence interval of the Kanto earthquake based on developmental process of coastal lowland

*Haeng-Yoong Kim[1]

1. Osaka City University, Graduate School of Science, Division of Biology &Geosciences

It is well known that the marine terraces are formed due to uplift of the seabed during the earthquake. The marine terrace consists of a near-flatter terrace surface emerged above sea level during the earthquake and a low terrace riser of less than several meters in height formed after the earthquake and is distributed in a staircase pattern along the coastline. In the previous research, one step of maritime terrace is often recognized as a trace of an earthquake once, and based on this premise, many previous researches were conducted to estimate the reoccurrence interval and the amount of uplift during the earthquake. However, Maemoku (1988) inferred that one step level of flat terrace surface is the topography formed by multiple repetitions of coseismic uplift and interseismic earthquake settlement occurring in the plate subduction zone of the Nankai Trough. And the stepped terrace was formed by the active fault of the land side. We got geomorphological and geological data demonstrating this previous reasoning on the Miura Peninsula located directly above the plate subduction zone of the Sagami trough.

On the rocky coast of the Miura Peninsula, two step of marine terrace surfaces formed in association with the 1923 Taisho and 1703 Genroku earthquakes are observed near 1 m and 2 m above sea level,(Matsuda et al., 1974). In the inner part of the estuary creek, which is formed many in the peninsula, the coastal lowland landfilled with sediments transported from the hinterland into the bay floor is distributed around the altitude of 2 m as similer as 1703 terrace surface. We examined the development process of coastal lowland in the inner part of estuary creek.

As a result of the detailer geomorphological interpretation, a flat coastal lowland apparently spreading as a single face is composed of multiple small maritime terraces, not one terrain. The marine terraces were divided into 5 areas with less than 2.1 m above sea level by topographical interpretation. As a result of investigating the emergent time and the distribution altitude of the marine terrace surface, the marine surface of the 1923 Taisho earthquake in the order of 1.22 m - 1.37 m in the order of younger, the wave erosion shelf surface of the 1703 Genroku earthquake by Nishihata et al. (1988): 2.3 m, the marine surface of the 1293 year pre-earthquake (after 1260-1380 cal.AD): 1.27 m, the marine surface of the earthquake (915 cal.AD to 1150 cal.AD) around the year AD is 1.63 to 1.93 m, Terraced surfaces are distributed until the earlier age.

In this way, the reasons that different formational time of terraces remain in coastal lowlands with extremely altitude is formed in Miura peninsula are as follows, because 1: the coseismic uplift due to the elastic repulsion and the interseismic subsidence accompanying the strain accumulation are repeated (Shimazaki et al., 2011; Kim and Mannen, 2018), therefore 2: a new marine surface is formed near the sea level by the next earthquake (Kim and Mannen, 2018), and 3: there is a condition that the terrace surface is preserved by the coating layer. In addition, because the height of the ground is stable in the long term due to the balance of uplift and subsidence, and it is estimated that wide coastal lowlands, which apparently appear as a continuous ground surface, develop by repetition of uplift and subsidence. Between 1293 and 1703, where the period of occurrence of the earthquake occurred long, the raised surface in 1293 returned to the original altitude, and between 1703 and 1923 in which the occurrence interval of the earthquake was short, the raised surface in 1703 The next Kanto earthquake occurred

©2019. Japan Geoscience Union. All Right Reserved.

before going back to the original altitude.

Keywords: Marine terrace, Residual uplift, Recurrence interval, Subduction type earthquake

©2019. Japan Geoscience Union. All Right Reserved.

Mechanics preserving co-seismic uplift and marine terraces: dissymmetric patterns of co-seismic and inter-seismic deformation

*Kyohei Suzuki[1], Junki Komori[1], Ryosuke Ando[1]

1. Graduate School of Science, University of Tokyo

Four large Holocene marine terraces are known in the southern part of the Boso Peninsula and called Numa I - IV. The newest one (Numa IV) was uplifted at the time of the Kanto Genroku earthquake, and from the similarity of the spatial distribution, it was considered that the Numa I-III Ire also formed from uplifts during the Genroku-type events. From this, the amount of coseismic uplift and slip amount were estimated from the height of the terraces (Matsuda et al., 1978; Nakata et al., 1980; Namegaya et al., 2011; Sato et al., 2016 etc.). However, the relationship between Holocene marine terraces and paleoseismic events was doubted in previous studies (Matsu'ura and Sato 1989, Noda et al., 2018). There is Matsu'ura and Sato (1989) model which is a mechanical model explaining the long-term surface uplift. This model expresses seismogenic region by back slip at the interseismic period and forward slip at the coseismic period and givessteady forward slip along the whole plate boundary surface. From this model, the coseismic vertical displacement pattern cancel out and the interseismic one and the uplift accumulation on the surface was attributed only to the effect of the steady-state plate motion.However, this is consequence based on a simple model expressed that slab as one plane in horizontal layered structure and assumed that the amount of back slip at the interseismic period and the amount of forward slip at the coseismic period are equal. The purpose of this study is to verify whether the coseismic uplift amount records the slip amount and remains and accumulates over earthquake cycles, and it affects coastal terrace formation process in a general mechanical model, considering the shape of the slab, the plate motion, and the coseismic fault motion.

As the calculation procedure, first, We give a constant displacement (10 m) to the edge of the oceanic plate and accumulate strain on the plate boundary. Next, We release all accumulated shear stress by coseismic fault slip,and obtain the vertical displacement pattern on the surface and the slip amount on the plate interface. Based on the fact that the principle of superposition is established in the linear elasticity theory, in this study, We separated the boundary conditions of both the interseismic period and the coseismic period,and calculated the respective vertical displacements and the residual amount by taking the sum. To verify the influence of irregularities on the actual plate boundary surface on the spatial pattern of vertical displacement, We also calculated two patterns for the case where irregularities were locally placed on the plate interface.

As a result of the calculation, we found that the interseismic slip amount in the no-cuppled area converged to 0 in the vicinity of the coupled area, and the coseismic slip amount was not uniform, and occurred across the plate boundary surface. This suggests that the slip on the plate boundary is intermittent in the seismic cycle. Next, from the vertical displacement residuals, we found that their spatial patterns at the interseismic period and the coseismic period were different.Furthermore, when local irregularities are placed on the plate boundary surface, it was found that the spatial pattern of the coseismic uplift is different corresponding to the slip amount of each model. This suggests that the height records the slip amount, and the shape of the plate boundary surface attributes actual coastal terrace formation. The consequence of this study is that the slip on the plate boundary is intermittent, and the coastal terraces depend on the coseismic slip.Therefore, the model in this study will give meaning to estimate the paleoseismic image from the height of coastal terraces.

©2019. Japan Geoscience Union. All Right Reserved.

Keywords: paleoseismic, mechanical model, Holocene marine terraces

©2019. Japan Geoscience Union. All Right Reserved.

Enhanced resolution of stress tensor inversion by using fault instability analysis

*Katsushi Sato[1]

1. Division of Earth and Planetary Sciences, Graduate School of Science, Kyoto University

Modern stress tensor inversion techniques for fault-slip analysis are based on the Wallace-Bott hypothesis which assumes that the slip directions and shear stress vectors are parallel. The hypothesis has an advantage in the applicability to high pore fluid pressure conditions and low friction faults, since the magnitudes of shear and normal stresses are not evaluated. However, the hypothesis gives only loose constraint on stress from observed faults in exchange for the wide applicability, which causes poor detectability of stresses.

This study tries to improve the detectability by introducing the fault instability (Vavrycuk et al, 2013; Sato, 2016) into the stress tensor inversion. The fault instability is defined as the nearness of the point representing shear and normal stresses on Mohr diagram to the line of Coulomb failure criteion. The fault instability is imposed on the fitness of a stress candidate to a fault-slip datum as a weight. Since the calculation of fault instability requires the friction coefficient, this study used several values of friction coefficient and compared the results.

The new method was applied to natural meso-scale fault-slip data. The faults cutting the Awa Group (Chiba Prefecture, central Japan) newly gave a reverse-faulting regime of stress in addition to normal faulting ones which can be detected by a conventioanl technique. An E-W trending tensional stress was newly detected from the faults cutting the Sekinan Group in the Beppu-Shimabara graben (Oita Prefecture, southwest Japan) where N-S trending extensional tectonism is ongoing. These resutls showed the improved resolution of stress tensor inversion by the incorporation of fault instability.

References

Sato, K., 2016, Journal of Structural Geology, 89, 44-53.
Vavrycuk, V., Bouchaala, F. and Fischer, T., 2013, Tectonophysics, 590, 189-195.

Keywords: stress tensor inversion, fault-slip analysis, fault instability

©2019. Japan Geoscience Union. All Right Reserved.

Focal mechanisms of the aftershocks of the 2000 Western Tottori Earthquake inferred from P wave first-motion data and spatial stress pattern

*Takaki Iwata[1]

1. Tokiwa University

A Bayesian approach to estimating a spatial stress pattern was developed [Iwata, 2018, JGR] (hereafter IW2018), and as an extension of this approach Iwata [2018, SSJ fall meeting] has proposed a method to infer focal mechanisms from P wave first-motion data and stress pattern estimated with the Bayesian approach. In this study, this method was applied to a real dataset taken from aftershocks of the 2000 Western Tottori earthquake.

The analyzed P wave first-motion dataset was retrieved from Kawanishi et al. [2009, JGR], which complied records from October 15 to November 30 in 2000. This dataset contains 47,570 P wave first-motions of 3592 events (for details see IW2018). The spatial pattern of stress field was taken from the result of IW2018 that also analyzed the same P wave first-motion dataset. The inferred focal mechanisms show rotation of the azimuth of P-axis around the main fault in the southern area; this feature has been seen in Yukutake and Iio [2017, EPS] and will be the reflection of the stress rotation found in the same area revealed by IW2018.

From the inferred focal mechanisms and spatial stress pattern, the normal and shear stress exerted on the fault plane was evaluated. Then, following the method of Terakawa [2010, Geology], fluid pressure for each of the events was estimated. Two datasets of the fluid pressure in the northern and southern areas of the aftershock areas were constructed and examined whether the two datasets follow the same distribution with the Kolmogorov-Smirnov test. Consequently, the test revealed that the fluid pressure in the southern area is significantly larger than that in the northern area, with a P-value of 1.6e-3.

Keywords: focal mechanism, stress field, stress rotation, P wave first-motion, spatial statistics, fluid pressure

©2019. Japan Geoscience Union. All Right Reserved.

Stress tensor inversion in focal area of the 2016 Mw7.8 Kaikoura earthquake, New Zealand

*Miu Matsuno[1], Tomomi Okada[1], Satoshi Matsumoto[2], Yuta Kawamura[2], Yoshihisa Iio[3], Tadashi Sato[1], Stephen C Bannister[4], John Ristau[4], Martha K Savage[5], John Townend[5], Jarg Pettinga[6], Francesca Ghisetti[7], Richard H Sibson[8]

1. Research Center for Prediction of Earthquakes and Volcanic Eruptions Graduate School of Science, Tohoku University, 2. Institute of Seismology and Volcanology, Faculty of Sciences, Kyushu University, 3. Disater Prevention Research Institute, Kyoto University, 4. GNS Science, New Zealand, 5. Victoria University of Wellington, Wellington, New Zealand, 6. University of Canterbury, Christchurch, New Zealand, 7. TerraGeologica, Ruby Bay, New Zealand, 8. University of Otago, Dunedin, New Zealand

We study spatio-temporal change of stress field of the 2016 Kaikoura earthquake in the northern area of South Island of New Zealand. Data from both the 51 temporary stations and 22 GEONET stations were used. Data collection was from March 2011 to December 2017. We derived focal mechanisms using HASH (Hardebeck and Shearer, 2002), By focal mechanism solutions of earthquake, we estimated stress fields of main shock of Kaikoura earthquake before and after. We used SATSI (Hardebeck and Michael, 2006] for stress tensor inversion. In our previous result (Sato, 2017 master’ s thesis in Tohoku University), there is possibility that on-fault aftershocks bias the result of stress tensor inversion. Therefore, by using Kagan angle between mainshock fault model and each focal mechanism, we remove aftershock on the faults, and perform stress tensor inversion. We use the fault model by Hamling et al. (2017). In a result, Kagan angles of many earthquakes are large, so this means that many aftershocks occurred off the fault plane. The results do not depend on threshold of Kagan angle. Obtained stress tensor inversion after main shock in areas near London Hill Fault and near Kekerengu fault are strike-slip fault type with SHmax orientation of ~N115E, which is almost same as for before the Kaikoura earthquake (e.g., Sibson et al., 2012; Townend et al., 2012), and stress tensors before and after the mainshock didn't appear to change after the earthquake beyond the estimation error. However, in the area near the hypocenter of the main shock we still cannot get a stable stress tensor. Also we plan to obtain results of a stable stress tensor for before the main shock by increasing the number of focal mechanisms of earthquakes that we examine.

©2019. Japan Geoscience Union. All Right Reserved.

Precise hypocenter distribution in the focal area of the 2016 Mw7.8 Kaikorua Earthquake, New Zealand

*Yuta Kawamura[1], Satoshi Matsumoto[1], Tomomi Okada[2], Miu Matsuno[2], Yoshihisa Iio[3], Tadashi Sato[2], Stephen C Bannister[4], John Ristau[4], Martha K Savage[5], John Twonend[5], Jarg Pettinga[6], Francesca Ghisetti[7], Richard H Sibson[8]

1. Kyushu University, Shimabara, Japan, 2. Tohoku University, Sendai, Japan, 3. Kyoto University, Uji, Japan, 4. GNS Science, Lower Hutt, New Zealand, 5. Victoria University of Wellington, Wellington, New Zealand, 6. University of Canterbury, Christchurch, New Zealand, 7. TerraGeologica, Ruby Bay, New Zealand, 8. University of Otago, Dunedin, New Zealand

The Mw7.8 Kaikoura Earthquake struck the northeastern south island, New Zealand, on November 14, 2016. A lot of researchers have tried to explain the cause of this earthquake and revealed the structure in this area. Among variety of prior researches, Clark et al. (2017) argued that this earthquake, which produced surface deformation including uplift and complex surface rupture, was caused by 21 strike-slip, reverse and oblique slip faults. Cesca et al., (2017) proposed an earthquake fault model that consists of three faults in northern, central and southern part, based on the hypocenter distribution of aftershock activity. These studies suggested in common that this earthquake was provoked by multiple faults with complex rupture process.

We had installed 75 temporary seismic stations before the earthquake in the South Island, New Zealand in addition to GEONET stations. The seismic network has successfully recorded the mainshock and the following aftershocks. Here, we relocated the hypocenters of the events associated with the Kaikoura earthquake by using data obtained from the seismic network. The hypocenters was determined by the double difference hypocenter determination algorithm (i.e. HYPODD, Waldhauser and Ellsworth, 2000). The overall distribution of the hypocenters are distinguished into two clusters, northern and southern clusters. The hypocenter distribution in vertical cross section normal to the major alignment of the aftershocks in N54W reveals that the fault in southern part dips to eastward. On the other hand, although we find out a northern cluster in terms of horizontal projection, no obvious faults are recognized in the vertical cross-section, suggesting complex fault structure in the northern cluster.

©2019. Japan Geoscience Union. All Right Reserved.

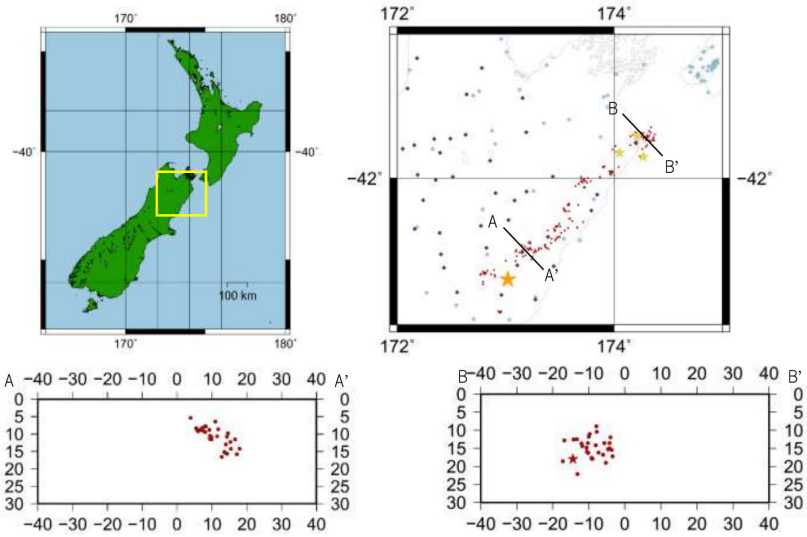

Fig. 1 Relocated hypocenter distribution in the South Island, New Zealand. Upper left) Index map of the target region. Yellow rectangle shows area displayed right map. Upper right) Map showing seismic stations and epicenters. Diamond and dot indicate location of station and event, respectively. Stars indicate epicenters for event with M > 6. Lower) Vertical cross sections along A-A' and B-B' in the upper right map. Other symbols are same as the upper right map.

©2019. Japan Geoscience Union. All Right Reserved.

3-dimensional GPS velocities in Colombia and their implications for interplate coupling

*Sindy Carolina Lizarazo[1], Takeshi Sagiya[2], Hector Mora-Paez[3]

1. Graduate School of Environmental Studies, Nagoya University, 2. Disaster Mitigation Research Center, Nagoya University, 3. Geological Survey of Colombia

Colombia is located in a region of complex interactions among the Caribbean, Nazca and South American plates, as well as the North Andean and Panama-Choco blocks. As a consequence of this tectonic setting, active faulting and intense seismicity are occurring especially in the areas of plate subduction or collision. The GeoRED project by the Geological Survey of Colombia installed a permanent GPS network in Colombia to study the regional kinematics with an intention to improve disaster mitigation activities. An initial velocity field was obtained and discussed by Mora et al. (2019) based on data from 60 sites under the ITRF2008 reference frame.

Here we present an updated result of Colombian GPS velocity field with 80 sites. The daily coordinates are calculated under the ITRF2014 reference frame with GAMIT-GLOBK software. We calculate 3-dimensional velocities with HECTOR software (Bos et al., 2013) based on the daily coordinates for the period from January 2014 to March 2016. There was no earthquake larger than magnitude 6 in Colombia, so the velocity pattern represents that of the interseismic period. For this time period, enhancement of the permanent network provides a better spatial resolution of the deformation pattern in some regions.

The results show a general consistency with the previous study, demonstrating the correctness of the current approach. In addition, vertical components show a slight of coastal uplifts at a few mm/year along the Nazca subduction zone. These signals indicate the lower limit of the plate coupling on the plate interface and we discuss the interplate coupling based on the 3-dimensional velocity data. Also, a significant margin-normal contraction is identified along a part of the Caribbean subduction zone near Colombia-Panama border. However, the vertical signal is not significant compared to the horizontal contraction, indicating that the elastic coupling model may not be applicable to this area.

Keywords: GPS velocities, Interplate coupling, Subduction, Deformation

©2019. Japan Geoscience Union. All Right Reserved.

[J] Poster | B (Biogeosciences)：B-BG Biogeosciences & Geosphere-Biosphere Interactions

Tue. May 28, 2019 1:45 PM - 3:15 PM JST | Tue. May 28, 2019 4:45 AM - 6:15 AM UTC | Poster Hall International Exhibition Hall8, Makuhari Messe_8

[B-BG02] Microbial ecology in earth and planetary sciences

convener:Michinari Sunamura(University of Tokyo Dept. of Earth & Planetary Science), Yuki Morono(Kochi Institute for Core Sample Research, Japan Agency for Marine-Earth Science and Technology), Natsuko Hamamura(Kyushu University)

Microbes have exerted the great influences on earth environments through the history of earth. Microbial ecology is a study of interaction between microbes and surrounding environments. Research target of Microbial ecology covers most of environments on the earth and planet, e.g. soil, subsurface, subseafloor, ocean, river, lake, air, space, volcano, fault and earthquake, minerals, and more. In this session , we aim to exchange informations of microbial distribution, population dynamics, function, effect on material cycles between microbial ecologist and earth&planetary scientist. We hope effective discussion from interdisciplinary approaches in this session.

[BBG02-P01] Density separation of magnetotactic bacteria *Magnetospirillum magnetotacticum* MS-1

*Kohei Masaoka[1], Yuki Morono[2], Naotaka Tomioka[2], Go-Ichiro Uramoto[1], Yuhji Yamamoto[1] (1.Kochi University, 2.Kochi Institute for Core Sample Research, Japan Agency for Marine-Earth Science and Technology)

[BBG02-P02] Exploring biogeographic patterns of marine planktonic cyanobacteria in coastal habitats- integrating uncultured and cultured approaches

*Punyasloke Bhadury[1] (1.Integrative Taxonomy and Microbial Ecology Research Group, Centre for Climate and Environmental Studies, Indian Institute of Science Education and Research Kolkata)

[BBG02-P03] The precise structure of “unsaturated” archaeol derivatives in the halophilic archaea lipid-core

*Noriaki YAMAUCHI[1] (1.Department of Earth and Planetary Sciences, Faculty of Sciences, Kyushu University)

[BBG02-P04] Estimation of microbial chemosynthesis efficiency in deep sea hydrothermal plume

*Michinari Sunamura[1] (1.University of Tokyo Dept. of Earth & Planetary Science)

Density separation of magnetotactic bacteria *Magnetospirillum magnetotacticum* MS-1

*Kohei Masaoka[1], Yuki Morono[2], Naotaka Tomioka[2], Go-Ichiro Uramoto[1], Yuhji Yamamoto[1]

1. Kochi University, 2. Kochi Institute for Core Sample Research, Japan Agency for Marine-Earth Science and Technology

Variation of the past geomagnetic field is recorded in marine sediments as a fossil magnetization, called natural remanent magnetization (NRM). NRM is carried not only by detrital and eaolian magnetic grains but also by biogenic magnetic grains originated from magnetotactic bacteria. To investigate characters of NRM carried by biogenic magnetic grains we have cultured the microaerobic bacteria *Magnetospirillum magnetotacticum* MS-1 (here under, MS-1) in laboratory and made sample using them for remanent magnetization measurements by simulating a very early process of sediment formation.

Preliminary reports on properties and characters of the remanent magnetization carried by the samples have been presented in Masaoka et al (2018JpGU; 2018SGEPSS), but MS-1 cells used for making samples rarely contain magnetite grains in these cells (3 percent of the total cells). To try to increase number of the cells containing magnetite grains, we have tested a density separation method using finer density gradients centrifugation and observed separated cells by transmission electron microscope. We will report results of observations together with those magnetic measurements.

©2019. Japan Geoscience Union. All Right Reserved.

Exploring biogeographic patterns of marine planktonic cyanobacteria in coastal habitats- integrating uncultured and cultured approaches

*Punyasloke Bhadury[1]

1. Integrative Taxonomy and Microbial Ecology Research Group, Centre for Climate and Environmental Studies, Indian Institute of Science Education and Research Kolkata

The structure of marine planktonic cyanobacterial communities in coastal habitats can strongly influence rates and fluxes of coastal carbon cycling. Biogeographic patterns of marine planktonic cyanobacterial assemblages were elucidated from four coastal habitats namely, Baltic Sea (BL), Monterey Bay (MB), South China Sea (SCS) and Sundarbans (SB) based on deep phylogeny of 16S rRNA sequences generated using next generation sequencing and Sanger sequencing approaches. Based on 16S rRNA phylogeny, four major taxonomic orders of marine planktonic cyanobacteria were recovered in varying proportions with several novel 16S rRNA sequences in each of the four targeted habitats. Members of the order Synechococcales were dominant in all the habitats (~94% sequences) while the orders Chroococcales and Oscillatoriales were only detected in SB and SCS, respectively. In the phylogenetic tree, *Synechococcus*-like sequences showed overwhelming dominance in SB and they were found in three other habitats. *Prochlorococcus*-like sequences were found in sizeable number in MB and SCS but were absent in SB and coastal BL. *Synechococcus*-like sequences were represented by three major marine clusters (5.1, 5.2, and 5.3). Three novel clades as part of *Synechococcus* cluster were detected only in SB and one novel clade in BL. These clades could have potential functional significance in coastal carbon cycling. Interestingly, cultured based approaches also revealed a new species of *Synechococcus*, *Synechococcus moorigangaii* from SB which has the ability to grow across a range of salinity and metabolize different forms of nitrogen as well as fix di-nitrogen. This reflects the potential vast unexplored functional diversity of marine planktonic cyanobacteria in coastal habitats which needs to be identified and can help towards understanding of export of carbon in coastal oceans. Overall the study has revealed that majority of the marine planktonic cyanobacterial OTUs were found to be exclusive to each habitat, whereas some were shared by two or more habitats based on beta-diversity analysis.

Keywords: Coast, marine planktonic cyanobacteria, diversity, 16S rRNA

©2019. Japan Geoscience Union. All Right Reserved.

The precise structure of “unsaturated” archaeol derivatives in the halophilic archaea lipid-core

*Noriaki YAMAUCHI[1]

1. Department of Earth and Planetary Sciences, Faculty of Sciences, Kyushu University

Archaea has a characteristic lipid-core, archaeol. Further, a characteristic diether lipid-core (C_{20}-C_{25} diether (**1**)) which is constructed from one C_{25} and one C_{20}isoprenoid is produced by halophilic archaea[1]. Recently, Dawson et al. showed the existence of several unsaturated isoprenoid diethers (such as tentative structure **2**) in the lipid-core of several halophilic archaea which was incubated with very high salt concentration[2].
Then, **2**, and the regioisomeric structure about the double bond and ether bond with a glycerol, **3**to **5** were chemically synthesized according to the reported method and the comparison of the mass spectrum of trimethylsilyl (TMS) ether were presented previously at this meeting[3].Further, **3** or **4**may be a possible structure of the real compound Dawson et al. shown at the mass spectrum.
About these unsymmetrical diether. The halophilic archaea *Haloferax sulfrifonis* was incubated and the lipid core was extracted and isolated.The analysis of the lipic core was perforemd by the GC-MS of the TMS ether. At first, **1** was detected as a main core lipid compornent. And the compound almost identical the mass specrum with the synthetic structure **2** was detected with a second minor compornent. Careful analysis of the compornent, the srtucture almost identical with **4** is also detected. This result showed the double bond in the unsaturated archaeol in *H. sulfrifonis*is the mixture of **2** and **4**. Dawson's unsaturated diether does not have a double bond at the methyl group branching position resulting from the usual isoprenoid biosynthesis (e.g. phytol), probably unsaturation is formed after the saturated isoprenoid formation with a unspecific fasion. The result of the analysis of lipid core of the archaea having unsaturated C_{20}-C_{25}diether will be presented.
[1]De Rosa *et al., J. Gen. Microbiol.*, **128**, 343 (1982).
[2] Dawson *et al. Org. Geochem.*, **48**, 1 (2012).
[3] Yamauchi (2018) *JpGU meeting 2018* BBG03-P08.

Keywords: halophilic archaea, archaeologists, ether lipid

©2019. Japan Geoscience Union. All Right Reserved.

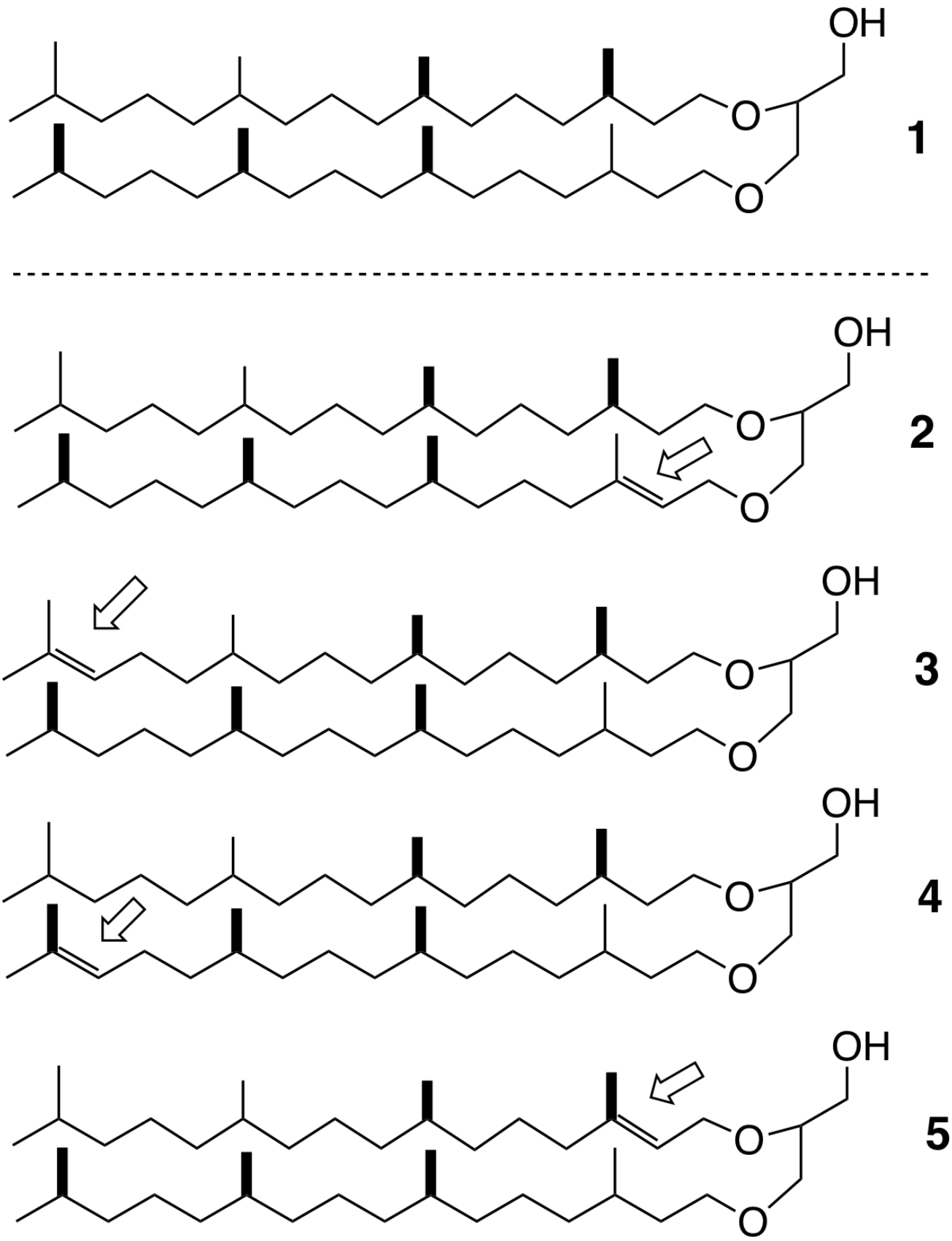

©2019. Japan Geoscience Union. All Right Reserved.

Estimation of microbial chemosynthesis efficiency in deep sea hydrothermal plume

*Michinari Sunamura[1]

1. University of Tokyo Dept. of Earth & Planetary Science

In the deep sea hydrothermal plume, chemolithotrophic microorganisms producing organic materials from inorganic carbons, such as sulfur oxidizing microorganisms, predominate. There is an estimate that in situ production of organic matter exceeds that of derived from surface photosynthesis. More than 99% of the chemical components contained in the hydrothermal fluids from the seafloor are released into deep-sea water and maximum chemical potential energy is thermodynamically calculated under low temperature condition by mixing hot hydrothermal fluid and sea water. Therefore, it is important for both deep-sea carbon dynamics and deep-sea ecosystems to estimate the microbial production in a hydrothermal plume. To estimate the primary production of microorganisms in a hydrothermal plume, it is necessary to understand the dynamics and functions of chemolitzotrophic microorganisms together with the physicochemical process of hydrothermal plume formation. We analyzed the formation process and chemical environment of hydrothermal plume and combined the dynamics of microorganisms with them to estimate the efficiency of hydrothermal energy use in microbial growth process. The formation process of the hydrothermal plume are regulated by the topography such as caldera, the stirring effect due to the deep ocean current intensity, and the density vertical structure of the water column. The composition of microbial community are known to be defined by chemical components of hydrothermal fluid. However, our result suggested that the energy efficiency and microbial total production of microorganisms is affected by these physical factors.

Keywords: microbial ecology, community structure, hydrothermal plume, deep sea

©2019. Japan Geoscience Union. All Right Reserved.

[J] Poster | B (Biogeosciences)：B-BG Biogeosciences & Geosphere-Biosphere Interactions

Tue. May 28, 2019 5:15 PM - 6:30 PM JST | Tue. May 28, 2019 8:15 AM - 9:30 AM UTC | Poster Hall International Exhibition Hall8, Makuhari Messe_38

[B-BG02] Microbial ecology in earth and planetary sciences

convener:Michinari Sunamura(University of Tokyo Dept. of Earth & Planetary Science), Yuki Morono(Kochi Institute for Core Sample Research, Japan Agency for Marine-Earth Science and Technology), Natsuko Hamamura(Kyushu University)

Microbes have exerted the great influences on earth environments through the history of earth. Microbial ecology is a study of interaction between microbes and surrounding environments. Research target of Microbial ecology covers most of environments on the earth and planet, e.g. soil, subsurface, subseafloor, ocean, river, lake, air, space, volcano, fault and earthquake, minerals, and more. In this session , we aim to exchange informations of microbial distribution, population dynamics, function, effect on material cycles between microbial ecologist and earth&planetary scientist. We hope effective discussion from interdisciplinary approaches in this session.

[BBG02-P01] Density separation of magnetotactic bacteria *Magnetospirillum magnetotacticum* MS-1

*Kohei Masaoka[1], Yuki Morono[2], Naotaka Tomioka[2], Go-Ichiro Uramoto[1], Yuhji Yamamoto[1] (1.Kochi University, 2.Kochi Institute for Core Sample Research, Japan Agency for Marine-Earth Science and Technology)

[BBG02-P02] Exploring biogeographic patterns of marine planktonic cyanobacteria in coastal habitats- integrating uncultured and cultured approaches

*Punyasloke Bhadury[1] (1.Integrative Taxonomy and Microbial Ecology Research Group, Centre for Climate and Environmental Studies, Indian Institute of Science Education and Research Kolkata)

[BBG02-P03] The precise structure of “unsaturated” archaeol derivatives in the halophilic archaea lipid-core

*Noriaki YAMAUCHI[1] (1.Department of Earth and Planetary Sciences, Faculty of Sciences, Kyushu University)

[BBG02-P04] Estimation of microbial chemosynthesis efficiency in deep sea hydrothermal plume

*Michinari Sunamura[1] (1.University of Tokyo Dept. of Earth & Planetary Science)

Density separation of magnetotactic bacteria *Magnetospirillum magnetotacticum* MS-1

*Kohei Masaoka[1], Yuki Morono[2], Naotaka Tomioka[2], Go-Ichiro Uramoto[1], Yuhji Yamamoto[1]

1. Kochi University, 2. Kochi Institute for Core Sample Research, Japan Agency for Marine-Earth Science and Technology

Variation of the past geomagnetic field is recorded in marine sediments as a fossil magnetization, called natural remanent magnetization (NRM). NRM is carried not only by detrital and eaolian magnetic grains but also by biogenic magnetic grains originated from magnetotactic bacteria. To investigate characters of NRM carried by biogenic magnetic grains we have cultured the microaerobic bacteria *Magnetospirillum magnetotacticum* MS-1 (here under, MS-1) in laboratory and made sample using them for remanent magnetization measurements by simulating a very early process of sediment formation.

Preliminary reports on properties and characters of the remanent magnetization carried by the samples have been presented in Masaoka et al (2018JpGU; 2018SGEPSS), but MS-1 cells used for making samples rarely contain magnetite grains in these cells (3 percent of the total cells). To try to increase number of the cells containing magnetite grains, we have tested a density separation method using finer density gradients centrifugation and observed separated cells by transmission electron microscope. We will report results of observations together with those magnetic measurements.

©2019. Japan Geoscience Union. All Right Reserved.

Exploring biogeographic patterns of marine planktonic cyanobacteria in coastal habitats- integrating uncultured and cultured approaches

*Punyasloke Bhadury[1]

1. Integrative Taxonomy and Microbial Ecology Research Group, Centre for Climate and Environmental Studies, Indian Institute of Science Education and Research Kolkata

The structure of marine planktonic cyanobacterial communities in coastal habitats can strongly influence rates and fluxes of coastal carbon cycling. Biogeographic patterns of marine planktonic cyanobacterial assemblages were elucidated from four coastal habitats namely, Baltic Sea (BL), Monterey Bay (MB), South China Sea (SCS) and Sundarbans (SB) based on deep phylogeny of 16S rRNA sequences generated using next generation sequencing and Sanger sequencing approaches. Based on 16S rRNA phylogeny, four major taxonomic orders of marine planktonic cyanobacteria were recovered in varying proportions with several novel 16S rRNA sequences in each of the four targeted habitats. Members of the order Synechococcales were dominant in all the habitats (~94% sequences) while the orders Chroococcales and Oscillatoriales were only detected in SB and SCS, respectively. In the phylogenetic tree, *Synechococcus*-like sequences showed overwhelming dominance in SB and they were found in three other habitats. *Prochlorococcus*-like sequences were found in sizeable number in MB and SCS but were absent in SB and coastal BL. *Synechococcus*-like sequences were represented by three major marine clusters (5.1, 5.2, and 5.3). Three novel clades as part of *Synechococcus* cluster were detected only in SB and one novel clade in BL. These clades could have potential functional significance in coastal carbon cycling. Interestingly, cultured based approaches also revealed a new species of *Synechococcus*, *Synechococcus moorigangaii* from SB which has the ability to grow across a range of salinity and metabolize different forms of nitrogen as well as fix di-nitrogen. This reflects the potential vast unexplored functional diversity of marine planktonic cyanobacteria in coastal habitats which needs to be identified and can help towards understanding of export of carbon in coastal oceans. Overall the study has revealed that majority of the marine planktonic cyanobacterial OTUs were found to be exclusive to each habitat, whereas some were shared by two or more habitats based on beta-diversity analysis.

Keywords: Coast, marine planktonic cyanobacteria, diversity, 16S rRNA

©2019. Japan Geoscience Union. All Right Reserved.

The precise structure of “unsaturated” archaeol derivatives in the halophilic archaea lipid-core

*Noriaki YAMAUCHI[1]

1. Department of Earth and Planetary Sciences, Faculty of Sciences, Kyushu University

Archaea has a characteristic lipid-core, archaeol. Further, a characteristic diether lipid-core (C_{20}-C_{25} diether (**1**)) which is constructed from one C_{25} and one C_{20}isoprenoid is produced by halophilic archaea[1]. Recently, Dawson et al. showed the existence of several unsaturated isoprenoid diethers (such as tentative structure **2**) in the lipid-core of several halophilic archaea which was incubated with very high salt concentration[2].
Then, **2**, and the regioisomeric structure about the double bond and ether bond with a glycerol, **3**to **5** were chemically synthesized according to the reported method and the comparison of the mass spectrum of trimethylsilyl (TMS) ether were presented previously at this meeting[3].Further, **3** or **4**may be a possible structure of the real compound Dawson et al. shown at the mass spectrum.
About these unsymmetrical diether. The halophilic archaea *Haloferax sulfrifonis* was incubated and the lipid core was extracted and isolated.The analysis of the lipic core was perforemd by the GC-MS of the TMS ether. At first, **1** was detected as a main core lipid compornent. And the compound almost identical the mass specrum with the synthetic structure **2** was detected with a second minor compornent. Careful analysis of the compornent, the srtucture almost identical with **4** is also detected. This result showed the double bond in the unsaturated archaeol in *H. sulfrifonis*is the mixture of **2** and **4**. Dawson's unsaturated diether does not have a double bond at the methyl group branching position resulting from the usual isoprenoid biosynthesis (e.g. phytol), probably unsaturation is formed after the saturated isoprenoid formation with a unspecific fasion. The result of the analysis of lipid core of the archaea having unsaturated C_{20}-C_{25}diether will be presented.
[1]De Rosa *et al., J. Gen. Microbiol.*, **128**, 343 (1982).
[2] Dawson *et al. Org. Geochem.*, **48**, 1 (2012).
[3] Yamauchi (2018) *JpGU meeting 2018* BBG03-P08.

Keywords: halophilic archaea, archaeologists, ether lipid

©2019. Japan Geoscience Union. All Right Reserved.

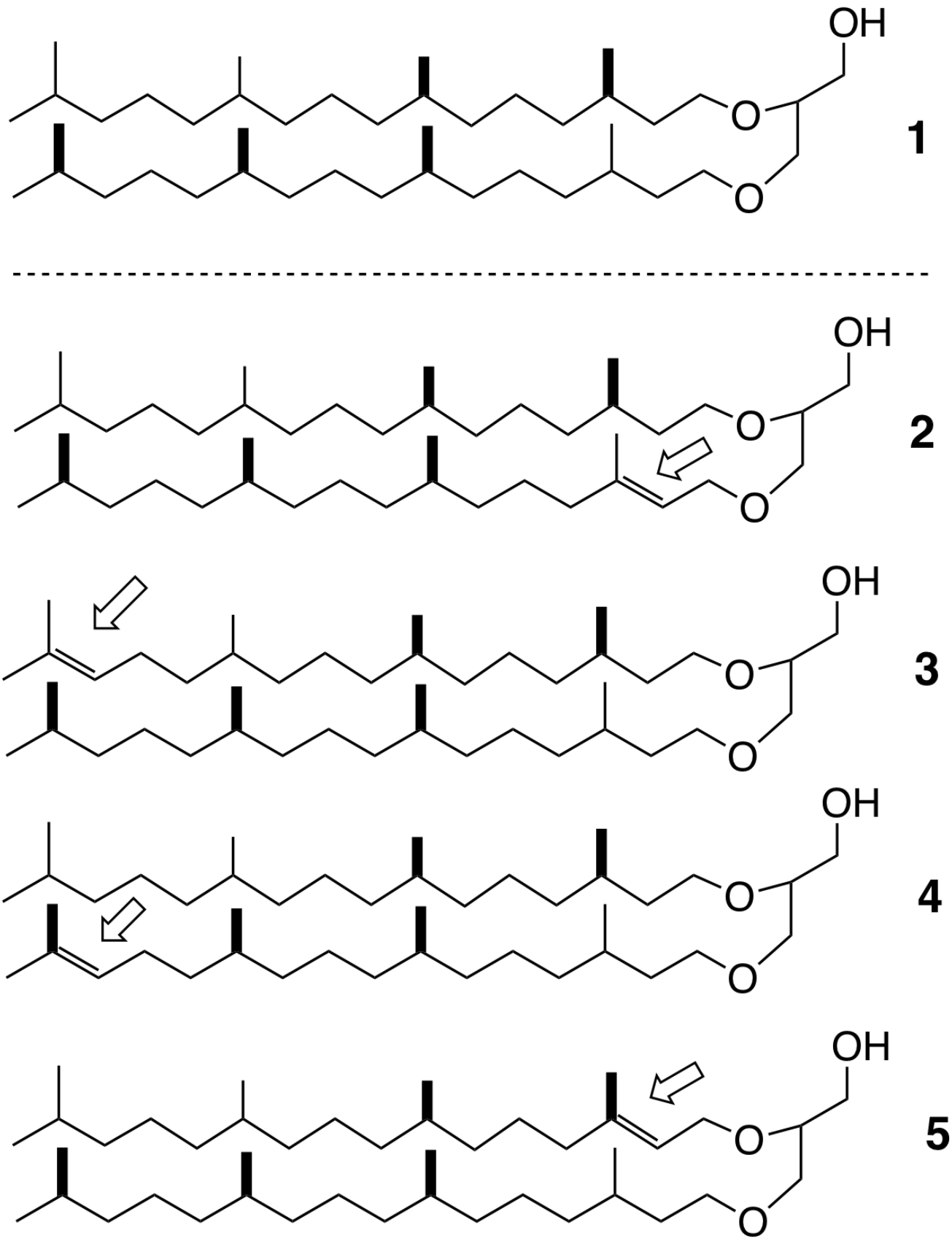

©2019. Japan Geoscience Union. All Right Reserved.

Estimation of microbial chemosynthesis efficiency in deep sea hydrothermal plume

*Michinari Sunamura[1]

1. University of Tokyo Dept. of Earth & Planetary Science

In the deep sea hydrothermal plume, chemolithotrophic microorganisms producing organic materials from inorganic carbons, such as sulfur oxidizing microorganisms, predominate. There is an estimate that in situ production of organic matter exceeds that of derived from surface photosynthesis. More than 99% of the chemical components contained in the hydrothermal fluids from the seafloor are released into deep-sea water and maximum chemical potential energy is thermodynamically calculated under low temperature condition by mixing hot hydrothermal fluid and sea water. Therefore, it is important for both deep-sea carbon dynamics and deep-sea ecosystems to estimate the microbial production in a hydrothermal plume. To estimate the primary production of microorganisms in a hydrothermal plume, it is necessary to understand the dynamics and functions of chemolitzotrophic microorganisms together with the physicochemical process of hydrothermal plume formation. We analyzed the formation process and chemical environment of hydrothermal plume and combined the dynamics of microorganisms with them to estimate the efficiency of hydrothermal energy use in microbial growth process. The formation process of the hydrothermal plume are regulated by the topography such as caldera, the stirring effect due to the deep ocean current intensity, and the density vertical structure of the water column. The composition of microbial community are known to be defined by chemical components of hydrothermal fluid. However, our result suggested that the energy efficiency and microbial total production of microorganisms is affected by these physical factors.

Keywords: microbial ecology, community structure, hydrothermal plume, deep sea

©2019. Japan Geoscience Union. All Right Reserved.

[J] Poster | B (Biogeosciences)：B-BC Biogeochemistry

Tue. May 28, 2019 10:45 AM - 12:15 PM JST | Tue. May 28, 2019 1:45 AM - 3:15 AM UTC | Poster Hall International Exhibition Hall8, Makuhari Messe_9

[B-BC03] Interrelation between Life, Water, Mineral, and Atmosphere

convener:Takeshi Kakegawa(Graduate School of Science, Tohoku University), Tadashi Yokoyama(Graduate School of Integrated Arts and Sciences, Hiroshima University), Keisuke Fukushi(Institute of Nature & Environmental Technology, Kanazawa University), Fumito Shiraishi(Department of Earth and Planetary Systems Science, Graduate School of Science, Hiroshima University)

Life on Earth is based on a diversity of physical and chemical dynamics and processes throughout the history of the Earth. It can essentially be regarded as the history of interrelation between Life, Water, Mineral (Solid Earth) and Atmosphere. To solve this kind of complex systems problems, interdisciplinary approach, a way of thinking and communication, is necessary. This session will be a cradle for such interdisciplinary researches.

[BBC03-P01] Geochemical studies for seawater/rock interaction recorded on the submarine lava flows of 12 Ma in the *Hokuroku* district in Akita, Japan and their implication to phosphorus cycle on the modern ocean floor

*Tsukasa Sai[1], Takeshi Kakegawa[1] (1.Graduate School of Science, Tohoku University)

[BBC03-P02] Detection of methylphosphonate and phosphite contained in suspended particles in spring water

*Kazuma Tsuji[1], Masahiro Maruo[3], Hajime Obata[2] (1.Graduate School of Environmental Science, The University of Shiga Prefecture, 2.Atmosphere and Ocean Research Institute, The University of Tokyo, 3.School of Environmental Science, The University of Shiga Prefecture)

[BBC03-P03] The Influence of Aerosol Optical Thickness and Mesoscale Eddies on Chlorophyll-a

*xiangguang zhang[1], Yongsheng Xu[1], Ichio Asanuma[2] (1.Institute of Oceanology, Chinese Academy of Sciences, 2.Tokyo University of Information Sciences)

[BBC03-P04] Glyoxylate from CO atmosphere via UV photochemistry

*Kenta Isoda[1], Xiaofeng Zang[1], Yuichiro Ueno[1,2] (1.Department of Earth and Planetary Sciences, Tokyo Institute of Technology, 2.Earth Life-Science Institute, Tokyo Institute of Technology)

[BBC03-P05] Carbon reservoir perturbations in the Indian subcontinent induced by the Deccan volcanism in marine and terrestrial realm

*Sohom Roy[1], Prasanta Sanyal[1], Sambit Ghosh[1] (1.Indian Institute of Science Education and Research Kolkata)

[BBC03-P06] Organic matter around Miocene Kuroko ore deposits: Implications to Archean submarine hydrothermal microbial community

*Takeshi Kakegawa[1] (1.Graduate School of Science, Tohoku University)

[BBC03-P07] Formation and solubility of hydrous carbonates formed in alkaline lakes under freezing condition

*TAKUMA KITAJIMA[1], Haruna Matsumiya[1], Keisuke Fukushi[1] (1.kanazawa university)

[BBC03-P08] Effect of difference in mineral wettability on water-mineral reaction in rock pores

*Tadashi Yokoyama[1], Naoki Nishiyama[2] (1.Graduate School of Integrated Arts and Sciences, Hiroshima University, 2.Graduate School of Life and Environmental Sciences, University of Tsukuba)

Geochemical studies for seawater/rock interaction recorded on the submarine lava flows of 12 Ma in the *Hokuroku* district in Akita, Japan and their implication to phosphorus cycle on the modern ocean floor

*Tsukasa Sai[1], Takeshi Kakegawa[1]

1. Graduate School of Science, Tohoku University

The phosphorus cycle on the modern surface environments of the Earth's is unclear. Many researchers consider that submarine basaltic rocks scavenge phosphorus by seawater/rock interaction. However, this argument is not supported by global data. In addition, uncertainties exist as to if submarine felsic rocks scavenge phosphorus during seawater/rock interaction. Thus, the purpose of this study is set to examine phosphorus behavior during seawater/rock interaction of submarine basalt and rhyolite, which ages are ca. 12 Ma. The samples are collected in the *Hokuroku* district in Akita prefecture: *Furutobe(basalt)*, *Oshigenaisawa(rhyolite)*, and *Hanaokanashizaka(basalt)*. Differences are examined in minerals and chemical compositions between outer and inner parts of basaltic pillow lava. Mineralogy and chemistry of single rhyolitic lava are examined according with different alteration patterns.
XRF analyses on bulk rock samples suggest basalt and rhyolite lost Si, Na, Ca with progress of submarine alteration. Basalt added Mg and Fe, and rhyolite added Mg and K during the same alteration. These results are consistent with combination of minerals identified by XRD and EPMA. The mobilization of elements in basalts from Furutobe is differ from others because Furutobe basalt suffered additional submarine hydrothrmal alteration.
It was found that basalt lost P, while rhyolite added P. Apatite and microcrystals of P-bearing unknown minerals are observed in basalt. In rhyolite, it is observed euhedral and anhedral crystals of 10-100 μm such as apatite, monazite, and xenotime. Primary apatite is observed in rhyolite phenocrysts, such as quartz, plagioclase, magnetite, ilmenite, and zircon. Secondary phosphate minerals are observed in vein, chalcedony developed in plagioclase pseudomorph, and Fe-bearing minerals. These clearly indicate the addition of phosphorus in altered rhyolite during seawater/rock interaction, and most likely phosphorus was supplied from seawater.
Therefore, it is suggested that basalt can supply phosphorus in ocean water as submarine alteration advanced, and rhyolite is a sink of phosphorus in the ocean floor. This knowledge is different from an established hypothesis that oceanic igneous rocks are sink of phosphorus.

Keywords: Phosphorus, Submarine alteration, Rhyolite, Basalt

©2019. Japan Geoscience Union. All Right Reserved.

Detection of methylphosphonate and phosphite contained in suspended particles in spring water

*Kazuma Tsuji[1], Masahiro Maruo[3], Hajime Obata[2]

1. Graduate School of Environmental Science, The University of Shiga Prefecture, 2. Atmosphere and Ocean Research Institute, The University of Tokyo, 3. School of Environmental Science, The University of Shiga Prefecture

Introduction

Methylphosphonate and phosphite are included in the process of constituting a biological cycle of phosphorus. Bacteria in the ocean is supposed to produce methylphosphonate and phosphite in the cell (Van Mooy et al., 2015). In freshwater system, it is strongly suggested that *Synechococcus* metabolizes methylphosphonate in subsurface layer of Lake Saiko (Yamanashi, Japan) under strong phosphorus limitation. However, methylphosphonate and phosphite in natural are considered to be dissolved in extremely low concentrations. Therefore, no reports existed that have detected these phosphorus compounds in natural waters. New analytical method for the determination of methylphosphonate and phosphite in natural was developed based on ion chromatography, and it was applied to detect them in waters of Lake Biwa (Shiga Japan) and spring nearby shore of Lake Biwa.

Methods

Ion chromatography was used to detect trace methylphosphonate and phosphite. Eluent condition was modified to separate these compounds from other major anions (chloride, nitrate, and sulfate) based on the condition for trace phosphate determination in waters of Lake Biwa (Maruo et al., 2016: Tsuji et al., in press). Water samples were obtained from Lake Biwa (Nov. 4th, 2018) and springs nearshore of Lake Biwa named “Kanabo”, in Maibara city, Shiga Prefectute (Nov. 6th, 2018). To detect methylphosphonate and phosphite in suspended matter, water samples (each 1.5 L) were filtered with a polycarbonate membrane filter (Nuclepore: Whatman, pore size of 0.2 μm). Then, the filter and MQW 25 mL were put in a glass bottle. The glass bottle was allowed to stand for 1 hour in a water bath (60˚C). After that, the extract solution contained was filtered with a disctype membrane filter (IC ACRODISC, Pall: pore size of 0.2 μm) and an all plastic syringe. The filtrate was injected in ion chromatograph system for the determination of methylphosphonate and phosphite included in suspended particles.
Immediately after collecting the sample water, the sample water was also filtered with a capsule filter (SUPOR Acropak 200 Capsule Filter, Pall: pore size 0.8 / 0.2 μm). Filtrate was used to determine methylphosphonate and phosphite dissolved in water.

Results and Discussion

Methylphosphonate (4.8 nM) and phosphite (3.6 nM) were detected in the solution extracted from suspended particles sampled in spring. Additionally, phosphite (23 nM) was detected in the solution extracted from suspended particles sampled in Lake Biwa. In dissolved fraction, both methylphosphate and phosphite were not detected at both sites. These compounds in dissolved fraction might exist in very low concentration and/or immediately utilized by biota. By ion chromatography, detection of methylphosphonate and phosphite contained in organisms sampled from other water systems is expected.

©2019. Japan Geoscience Union. All Right Reserved.

References

Tomoya Iwata (2014) Aerobic methane production in oxygenated water column of lake ecosystems. Grants-in-Aid for Scientific Research (KAKEN) 2013 Fiscal Year Final Research Report #23681003.

Tsuji K, Maruo M, Obata H (2019) Determination of trace methylphosphonate in natural waters by ion chromatography. BUNSEKI KAGAKU 68(4), in press.

Maruo M, Ishimaru M, Azumi Y, Kawasumi Y, Nagafuchi O, Obata H (2016) Comparison of soluble reactive phosphorus and orthophosphate concentrations in river waters. Limnology 17(1):7-12.

Van Mooy BAS, Krupke A, Dyhrman ST, Fredricks HF, Frischkorn KR, Ossolinski JE, Repeta DJ, Rouco M, Seewald JD, Sylva SP (2015) Major role of planktonic phosphate reduction in the marine phosphorus redox cycle. Science 348(6236): 783-785.

Keywords: Methylphosphonate, Phosphite, Ion chromatography

©2019. Japan Geoscience Union. All Right Reserved.

The Influence of Aerosol Optical Thickness and Mesoscale Eddies on Chlorophyll-a

*xiangguang zhang[1], Yongsheng Xu[1], Ichio Asanuma[2]

1. Institute of Oceanology, Chinese Academy of Sciences, 2. Tokyo University of Information Sciences

Chlorophyll-a concentration (Chl-a) has a close relationship with the nutrients and the atmospheric sedimentation is a good source for the nutrients of the sea. Moreover, the value of aerosol optical thickness (AOT) can stand for atmospheric sediment concentration. So, there should be a coupling relationship between AOT and Chl-a. The correlation analysis between AOT and Chl-a had been early assessed by previous works. For example, in South China Sea and Greenland Sea, the data analysis revealed that AOT had a big impact on the biogeochemistry of the South China Sea and there was a time-lag correlation between AOT and Chl-a in Greenland Sea.

Using 12 years' of AOT and Chl-a data from the NASA/MODIS and SeaWiFS sensors, we've studied the distributions and the coupling relationship between AOT and Chl-a all over the world. The correlation map shows some interesting areas on the earth. It is found that the highest positive correlation areas of the AOT and Chl-a time series are in the east coastal area of Africa, Baltic Sea, Caspian Sea and the band area in the Pacific between south Japan and San Francisco of USA; the highest negative correlation areas of the Chl-a and AOT time series are in The Mediterranean, west-south and east-south coastal areas of Australia.
Moreover, we analyze 10 years of measurements of SSH fields and concurrent satellite measurements of upper-ocean CHL to show that mesoscale eddies exert a strong influence on the CHL field.

Keywords: Chlorophyll-a concentration, Aerosol optical thickness, Sea surface height, Mesoscale eddy, Coupling relationship

©2019. Japan Geoscience Union. All Right Reserved.

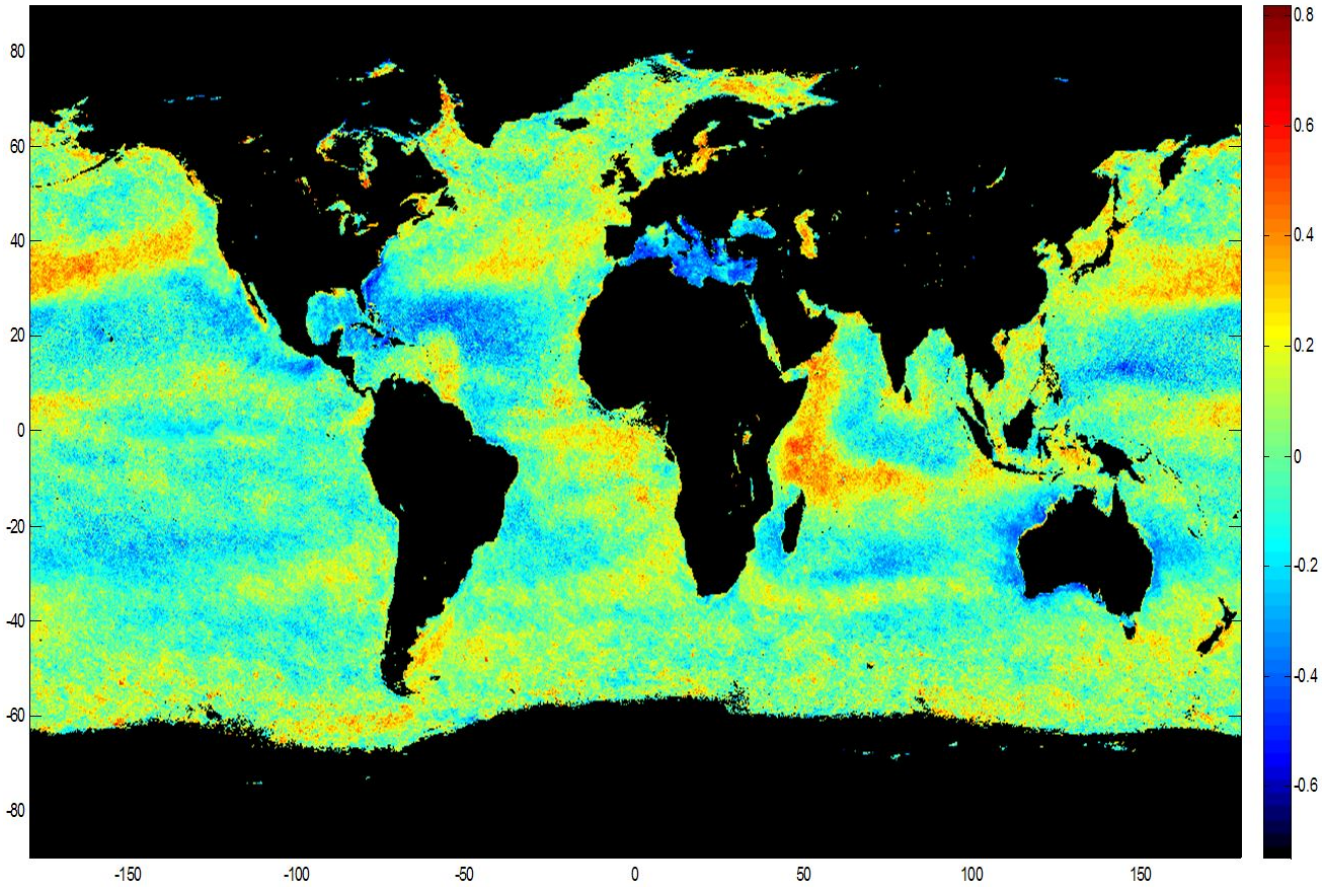

©2019. Japan Geoscience Union. All Right Reserved.

Glyoxylate from CO atmosphere via UV photochemistry

*Kenta Isoda[1], Xiaofeng Zang[1], Yuichiro Ueno[1,2]

1. Department of Earth and Planetary Sciences, Tokyo Institute of Technology, 2. Earth Life-Science Institute, Tokyo Institute of Technology

Glyoxylate could be an important compound, which can initiate a simple autocatalytic cycle and may possibly evolve to synthesize amino acids, nucleobase, pentose etc. (Eschenmoser, 2007a). However, constant supply of glyoxylate is an issue for the prebiotic environment. In this study, we aim to understand the possible condition to supply glyoxylate continuously to support such an autocatalytic cycle. First, we have performed experimental study and demonstrated that glyoxylic acid can be synthesized photochemically under carbon monoxide atmosphere. On the other hand, the UV irradiation into formaldehyde solution does not yield glyoxylic acid, except for the presence of CO in the gas phase. These results indicate that glyoxylate is not produced from formaldehyde in solution but from CO in the gas phase probably through the 3 steps: (i) HCO radical is produced from the reaction between CO and H from H_2O photolysis; (ii) The HCO radical dimerize in the gas phase, to form $(CHO)_2$(glyoxal); and (iii) The $(CHO)_2$ is oxidized into HCOCOOH (glyoxylate). An additional experiment demonstrated that UV irradiation into pure glyoxal solution can yield glyoxylate, and thus indicate that the step (iii) can proceed in the solution. Consequently, our experimental results suggests that glyoxylate can be continuously provided from atmosphere into hydrosphere if the atmosphere is rich in CO.

Keywords: atmosphere, photochemistry

©2019. Japan Geoscience Union. All Right Reserved.

Carbon reservoir perturbations in the Indian subcontinent induced by the Deccan volcanism in marine and terrestrial realm

*Sohom Roy[1], Prasanta Sanyal[1], Sambit Ghosh[1]

1. Indian Institute of Science Education and Research Kolkata

The Deccan flood basalt eruption spans across the Cretaceous-Paleogene (K/Pg) Boundary and records the largest
and the longest lava flows in the world. While the volcanism has been linked to the infamous K/Pg extinction,
however, its implications on the regional carbon budget are still not well constrained. Carbon isotope records in marine carbonates ($\delta^{13}C_{carb}$) and bulk organic matter ($\delta^{13}C_{org}$), coupled with carbon and hydrogen isotope records
of *n*-alkane ($\delta^{13}C_{alk}$ and δD_{alk} respectively) have been measured along with *n*-alkanes characterization from two
inter-trappean and one infra-trappean sedimentary sequence exposed south of the city of Rajahmundry, SE India
in order to evaluate the climatic and environmental response exacerbated by the volcanism in the marine and terrestrial realm. Overall, our data demonstrate major perturbations in the terrestrial and marine carbon cycle induced by the Deccan volcanism, with considerable environmental stress predating the K/Pg Boundary. Strong covariance between $\delta^{13}C_{org}$ and $\delta^{13}C_{carb}$ (r=-0.71) suggest that the dissolved inorganic carbon (DIC) in the shallow
marine environment was largely controlled by organic matter (OM) flux. The occurrence of large unresolved complex mixtures (UCM/n-alkane>>4) and hopanes (m/z 191) and steranes (m/z 217) in the limestones OM suggest considerable input from petroleum into the biomass. The upper part of the infra-trappean and lower parts of inter-trappean show considerable decreases in the marine $\delta^{13}C_{carb}$ values and have been inferred to occur from hydrocarbon assimilation by heterotrophs and early diagenesis of OM. Steady temporal increase in $\delta^{13}C_{carb}$ values and total organic carbon (TOC) content throughout the sequence imply increases in primary productivity, with the upper inter-trappean limestone marking the recovery phase. The $\delta^{13}C_{alk}$ values, coupled with the chain-length distribution pattern of *n*-alkanes and spore-pollen records exhibit significant turnovers in the vegetation community structure. High δD_{alk} values (~-110‰) indicate arid conditions before the deposition of mega flow episodes in Rajahmundry. Depletion in δD_{alk} values (~-150‰) observed in the middle part of the inter-trappean signifies a change to a humid condition. The increased rainfall prompted an upsurge in weathering that led to increases in freshwater influx (depletion in $\delta^{18}O_{carb}$ values) and higher terrestrial OM input (increase in long-chain *n*-alkanes). Atmospheric CO_2 concentration reconstructed from two paleosol horizons in the infra- and inter-trappean units respectively indicate major drawdown in pCO_2 across the main flow episode in Rajahmundry. It is speculated that the volcanism induced changes in pCO_2 was one of the main drivers for exacerbating changes in the carbon cycle.

Keywords: Deccan volcanism, carbon reservoir, n-alkane, stable isotope, Rajahmundry

©2019. Japan Geoscience Union. All Right Reserved.

Organic matter around Miocene Kuroko ore deposits: Implications to Archean submarine hydrothermal microbial community

*Takeshi Kakegawa[1]

1. Graduate School of Science, Tohoku University

Kuroko ore deposits were products of black smoker activities at 15 Ma paleo-Japan Sea. Kuroko is often covered by organic-rich sedimentary rocks, but details of these organic matter have not been unclear. Here I report analytical results of stable isotopes, Raman spectroscopy and bitumen compositions of organic matter around Miocene Kuroko deposits.

In general, all geochemical characteristics of organic matter were uniform in the same horizon of Kuroko deposits. On the other hand, H/C ratios and Raman spectroscopic data suggest that organic matter were extensively graphitized by thermal degradation only around Kuroko. More ^{12}C- and ^{14}N-enriched features are found in Kuroko-associated kerogen and bitumen. Such stable isotope data suggest the presence of chemoautotrophs, which utilized hydrothermal $CH_4$and NH_3. However, geochemical and geological characteristics of the examined samples suggest that hydrothermal $CH_4$and NH_3were produced by thermal degradation of sedimentary organic matter, which are mainly derived from photoautotrophs. This further suggests that chemoautotrophs at Kuroko were not independent and had strong connection to surface photoautotrophs.
Organic matter enriched in ^{12}C and ^{14}N are ubiquitous around many middle-Archean Kuroko ore deposits. Such stable isotope compositions also imply the presence of submarine hydrothermal microbial communities. However, ^{12}C- and ^{14}N-depleted organic matter, which most likely represent photoautotrophs, are also common around Archean Kuroko deposits. Such contrast stable isotope characteristics suggest that deep submarine chemoautotrophs already had linkages to surface photoautotrophs since Archean age.

Keywords: Kuroko, Chemoautotroph, stable isotope

©2019. Japan Geoscience Union. All Right Reserved.

Formation and solubility of hydrous carbonates formed in alkaline lakes under freezing condition

*TAKUMA KITAJIMA[1], Haruna Matsumiya[1], Keisuke Fukushi[1]

1. kanazawa university

Alkaline lakes have functions of absorption of atmospheric CO_2 to natural water and fixation of dissolved carbonate by mineralization. Therefore, it has been considered that alkaline lakes located in arid area inside the continents play important roles in carbon cycle on the earth surface (Finley et al., 2015; Fukushi and Matsumiya, 2018).

The common carbonate minerals are calcite and aragonite in natural environment. On the other hand, monohydrocalcite (MHC) is formed in alkaline lakes as most common carbonate minerals (Fukushi et al.2012). MHC ($CaCO_3 \cdot H_2O$) is metastable carbonate mineral with respect to calcite or aragonite (Munemoto and Fukushi, 2008). The formation of MHC requires the paragenesis of amorphous magnesium carbonate (AMC) (Nishiyama et al., 2013; Fukushi et al., 2017).

Fukushi and Matsumiya, (2018) measured the solubilities of MHC and AMC under the atmosphere at 25 ℃ and reported that MHC and AMC control the water chemistry of alkaline lakes. However, the most of surrounding environment of alkaline lakes are semiarid and cold. The lakes are covered with ice in most of the year.

During the ice forming ice, the lake water must be isolated from the atmosphere, which may lead to the decrease of low partial pressure of CO_2 in lakes. Low temperature may affect the formed mineral species and physicochemical properties of the minerals. Therefore, we can’ t discuss the water chemistry of alkaline lakes only from the knowledge obtained from the ambient condition atmosphere CO_2 pressure and 25 ℃. The purposes of this study are (1) investigation of the carbonate mineral formation from the solution simulated the alkaline lakes under low partial pressure of CO^2 at 5-50 ℃ and (2) measurements of solubilites of these carbonate minerals to estimate of water chemistry of alkaline lakes.

©2019. Japan Geoscience Union. All Right Reserved.

Effect of difference in mineral wettability on water-mineral reaction in rock pores

*Tadashi Yokoyama[1], Naoki Nishiyama[2]

1. Graduate School of Integrated Arts and Sciences, Hiroshima University, 2. Graduate School of Life and Environmental Sciences, University of Tsukuba

When water infiltrates rock pores, dissolution occurs at the contact site of water and mineral. In many cases rock pores near the ground surface are not fully saturated with water and a portion of pores is filled with air. In order to study how the presence of air in pores affects the reactivity of each rock-forming mineral, the amounts of elements leached out from the rock were compared for water-saturated condition and unsaturated condition by using a core of Berea sandstone. The sandstone consists mainly of quartz with several percentages of feldspar, carbonates, and clays. In the case of the saturated condition, initially pores were saturated with water by vacuum treatment, then water was passed through the core at a constant water head difference. In the case of the unsaturated condition, water was passed through a dry core. After the onset of the experiment under the unsaturated condition, water saturation (the fraction at which pore volume is saturated with water) became ~60% almost immediately (air 40%), and gradually increased and reached ~100% after 9 days passed. Dissolution rates of Si and Ca (amount of dissolution per unit time per whole rock) were determined by measuring the concentrations of dissolved Ca and Si in leachates. The difference in dissolution rate between unsaturated condition and saturated condition was generally greater in the case of Ca than that of Si. This appears to be due to the difference of wettability of silicates and carbonate. Probably silicates were more easily wet and many silicate surfaces dissolved even under the presence of air, while dissolution of carbonate was diminished due to the absence of water contact or the insufficient flushing of Ca in the wetting film of the carbonate surface.

©2019. Japan Geoscience Union. All Right Reserved.

[J] Poster | B (Biogeosciences)：B-BC Biogeochemistry

Tue. May 28, 2019 5:15 PM - 6:30 PM JST | Tue. May 28, 2019 8:15 AM - 9:30 AM UTC | Poster Hall International Exhibition Hall8, Makuhari Messe_39

[B-BC03] Interrelation between Life, Water, Mineral, and Atmosphere

convener:Takeshi Kakegawa(Graduate School of Science, Tohoku University), Tadashi Yokoyama(Graduate School of Integrated Arts and Sciences, Hiroshima University), Keisuke Fukushi(Institute of Nature & Environmental Technology, Kanazawa University), Fumito Shiraishi(Department of Earth and Planetary Systems Science, Graduate School of Science, Hiroshima University)

Life on Earth is based on a diversity of physical and chemical dynamics and processes throughout the history of the Earth. It can essentially be regarded as the history of interrelation between Life, Water, Mineral (Solid Earth) and Atmosphere. To solve this kind of complex systems problems, interdisciplinary approach, a way of thinking and communication, is necessary. This session will be a cradle for such interdisciplinary researches.

[BBC03-P01] Geochemical studies for seawater/rock interaction recorded on the submarine lava flows of 12 Ma in the *Hokuroku* district in Akita, Japan and their implication to phosphorus cycle on the modern ocean floor

*Tsukasa Sai[1], Takeshi Kakegawa[1] (1.Graduate School of Science, Tohoku University)

[BBC03-P02] Detection of methylphosphonate and phosphite contained in suspended particles in spring water

*Kazuma Tsuji[1], Masahiro Maruo[3], Hajime Obata[2] (1.Graduate School of Environmental Science, The University of Shiga Prefecture, 2.Atmosphere and Ocean Research Institute, The University of Tokyo, 3.School of Environmental Science, The University of Shiga Prefecture)

[BBC03-P03] The Influence of Aerosol Optical Thickness and Mesoscale Eddies on Chlorophyll-a

*xiangguang zhang[1], Yongsheng Xu[1], Ichio Asanuma[2] (1.Institute of Oceanology, Chinese Academy of Sciences, 2.Tokyo University of Information Sciences)

[BBC03-P04] Glyoxylate from CO atmosphere via UV photochemistry

*Kenta Isoda[1], Xiaofeng Zang[1], Yuichiro Ueno[1,2] (1.Department of Earth and Planetary Sciences, Tokyo Institute of Technology, 2.Earth Life-Science Institute, Tokyo Institute of Technology)

[BBC03-P05] Carbon reservoir perturbations in the Indian subcontinent induced by the Deccan volcanism in marine and terrestrial realm

*Sohom Roy[1], Prasanta Sanyal[1], Sambit Ghosh[1] (1.Indian Institute of Science Education and Research Kolkata)

[BBC03-P06] Organic matter around Miocene Kuroko ore deposits: Implications to Archean submarine hydrothermal microbial community

*Takeshi Kakegawa[1] (1.Graduate School of Science, Tohoku University)

[BBC03-P07] Formation and solubility of hydrous carbonates formed in alkaline lakes under freezing condition

*TAKUMA KITAJIMA[1], Haruna Matsumiya[1], Keisuke Fukushi[1] (1.kanazawa university)

[BBC03-P08] Effect of difference in mineral wettability on water-mineral reaction in rock pores

*Tadashi Yokoyama[1], Naoki Nishiyama[2] (1.Graduate School of Integrated Arts and Sciences, Hiroshima University, 2.Graduate School of Life and Environmental Sciences, University of Tsukuba)

Geochemical studies for seawater/rock interaction recorded on the submarine lava flows of 12 Ma in the *Hokuroku* district in Akita, Japan and their implication to phosphorus cycle on the modern ocean floor

*Tsukasa Sai[1], Takeshi Kakegawa[1]

1. Graduate School of Science, Tohoku University

The phosphorus cycle on the modern surface environments of the Earth's is unclear. Many researchers consider that submarine basaltic rocks scavenge phosphorus by seawater/rock interaction. However, this argument is not supported by global data. In addition, uncertainties exist as to if submarine felsic rocks scavenge phosphorus during seawater/rock interaction. Thus, the purpose of this study is set to examine phosphorus behavior during seawater/rock interaction of submarine basalt and rhyolite, which ages are ca. 12 Ma. The samples are collected in the *Hokuroku* district in Akita prefecture: *Furutobe(basalt)*, *Oshigenaisawa(rhyolite)*, and *Hanaokanashizaka(basalt)*. Differences are examined in minerals and chemical compositions between outer and inner parts of basaltic pillow lava. Mineralogy and chemistry of single rhyolitic lava are examined according with different alteration patterns.
XRF analyses on bulk rock samples suggest basalt and rhyolite lost Si, Na, Ca with progress of submarine alteration. Basalt added Mg and Fe, and rhyolite added Mg and K during the same alteration. These results are consistent with combination of minerals identified by XRD and EPMA. The mobilization of elements in basalts from Furutobe is differ from others because Furutobe basalt suffered additional submarine hydrothrmal alteration.
It was found that basalt lost P, while rhyolite added P. Apatite and microcrystals of P-bearing unknown minerals are observed in basalt. In rhyolite, it is observed euhedral and anhedral crystals of 10-100 μm such as apatite, monazite, and xenotime. Primary apatite is observed in rhyolite phenocrysts, such as quartz, plagioclase, magnetite, ilmenite, and zircon. Secondary phosphate minerals are observed in vein, chalcedony developed in plagioclase pseudomorph, and Fe-bearing minerals. These clearly indicate the addition of phosphorus in altered rhyolite during seawater/rock interaction, and most likely phosphorus was supplied from seawater.
Therefore, it is suggested that basalt can supply phosphorus in ocean water as submarine alteration advanced, and rhyolite is a sink of phosphorus in the ocean floor. This knowledge is different from an established hypothesis that oceanic igneous rocks are sink of phosphorus.

Keywords: Phosphorus, Submarine alteration, Rhyolite, Basalt

©2019. Japan Geoscience Union. All Right Reserved.

Detection of methylphosphonate and phosphite contained in suspended particles in spring water

*Kazuma Tsuji[1], Masahiro Maruo[3], Hajime Obata[2]

1. Graduate School of Environmental Science, The University of Shiga Prefecture, 2. Atmosphere and Ocean Research Institute, The University of Tokyo, 3. School of Environmental Science, The University of Shiga Prefecture

Introduction

Methylphosphonate and phosphite are included in the process of constituting a biological cycle of phosphorus. Bacteria in the ocean is supposed to produce methylphosphonate and phosphite in the cell (Van Mooy et al., 2015). In freshwater system, it is strongly suggested that *Synechococcus* metabolizes methylphosphonate in subsurface layer of Lake Saiko (Yamanashi, Japan) under strong phosphorus limitation. However, methylphosphonate and phosphite in natural are considered to be dissolved in extremely low concentrations. Therefore, no reports existed that have detected these phosphorus compounds in natural waters. New analytical method for the determination of methylphosphonate and phosphite in natural was developed based on ion chromatography, and it was applied to detect them in waters of Lake Biwa (Shiga Japan) and spring nearby shore of Lake Biwa.

Methods

Ion chromatography was used to detect trace methylphosphonate and phosphite. Eluent condition was modified to separate these compounds from other major anions (chloride, nitrate, and sulfate) based on the condition for trace phosphate determination in waters of Lake Biwa (Maruo et al., 2016: Tsuji et al., in press). Water samples were obtained from Lake Biwa (Nov. 4th, 2018) and springs nearshore of Lake Biwa named “Kanabo”, in Maibara city, Shiga Prefectute (Nov. 6th, 2018). To detect methylphosphonate and phosphite in suspended matter, water samples (each 1.5 L) were filtered with a polycarbonate membrane filter (Nuclepore: Whatman, pore size of 0.2 μm). Then, the filter and MQW 25 mL were put in a glass bottle. The glass bottle was allowed to stand for 1 hour in a water bath (60˚C). After that, the extract solution contained was filtered with a disctype membrane filter (IC ACRODISC, Pall: pore size of 0.2 μm) and an all plastic syringe. The filtrate was injected in ion chromatograph system for the determination of methylphosphonate and phosphite included in suspended particles.
Immediately after collecting the sample water, the sample water was also filtered with a capsule filter (SUPOR Acropak 200 Capsule Filter, Pall: pore size 0.8 / 0.2 μm). Filtrate was used to determine methylphosphonate and phosphite dissolved in water.

Results and Discussion

Methylphosphonate (4.8 nM) and phosphite (3.6 nM) were detected in the solution extracted from suspended particles sampled in spring. Additionally, phosphite (23 nM) was detected in the solution extracted from suspended particles sampled in Lake Biwa. In dissolved fraction, both methylphosphate and phosphite were not detected at both sites. These compounds in dissolved fraction might exist in very low concentration and/or immediately utilized by biota. By ion chromatography, detection of methylphosphonate and phosphite contained in organisms sampled from other water systems is expected.

©2019. Japan Geoscience Union. All Right Reserved.

References

Tomoya Iwata (2014) Aerobic methane production in oxygenated water column of lake ecosystems. Grants-in-Aid for Scientific Research (KAKEN) 2013 Fiscal Year Final Research Report #23681003.

Tsuji K, Maruo M, Obata H (2019) Determination of trace methylphosphonate in natural waters by ion chromatography. BUNSEKI KAGAKU 68(4), in press.

Maruo M, Ishimaru M, Azumi Y, Kawasumi Y, Nagafuchi O, Obata H (2016) Comparison of soluble reactive phosphorus and orthophosphate concentrations in river waters. Limnology 17(1):7-12.

Van Mooy BAS, Krupke A, Dyhrman ST, Fredricks HF, Frischkorn KR, Ossolinski JE, Repeta DJ, Rouco M, Seewald JD, Sylva SP (2015) Major role of planktonic phosphate reduction in the marine phosphorus redox cycle. Science 348(6236): 783-785.

Keywords: Methylphosphonate, Phosphite, Ion chromatography

©2019. Japan Geoscience Union. All Right Reserved.

The Influence of Aerosol Optical Thickness and Mesoscale Eddies on Chlorophyll-a

*xiangguang zhang[1], Yongsheng Xu[1], Ichio Asanuma[2]

1. Institute of Oceanology, Chinese Academy of Sciences, 2. Tokyo University of Information Sciences

Chlorophyll-a concentration (Chl-a) has a close relationship with the nutrients and the atmospheric sedimentation is a good source for the nutrients of the sea. Moreover, the value of aerosol optical thickness (AOT) can stand for atmospheric sediment concentration. So, there should be a coupling relationship between AOT and Chl-a. The correlation analysis between AOT and Chl-a had been early assessed by previous works. For example, in South China Sea and Greenland Sea, the data analysis revealed that AOT had a big impact on the biogeochemistry of the South China Sea and there was a time-lag correlation between AOT and Chl-a in Greenland Sea.

Using 12 years' of AOT and Chl-a data from the NASA/MODIS and SeaWiFS sensors, we've studied the distributions and the coupling relationship between AOT and Chl-a all over the world. The correlation map shows some interesting areas on the earth. It is found that the highest positive correlation areas of the AOT and Chl-a time series are in the east coastal area of Africa, Baltic Sea, Caspian Sea and the band area in the Pacific between south Japan and San Francisco of USA; the highest negative correlation areas of the Chl-a and AOT time series are in The Mediterranean, west-south and east-south coastal areas of Australia.
Moreover, we analyze 10 years of measurements of SSH fields and concurrent satellite measurements of upper-ocean CHL to show that mesoscale eddies exert a strong influence on the CHL field.

Keywords: Chlorophyll-a concentration, Aerosol optical thickness, Sea surface height, Mesoscale eddy, Coupling relationship

©2019. Japan Geoscience Union. All Right Reserved.

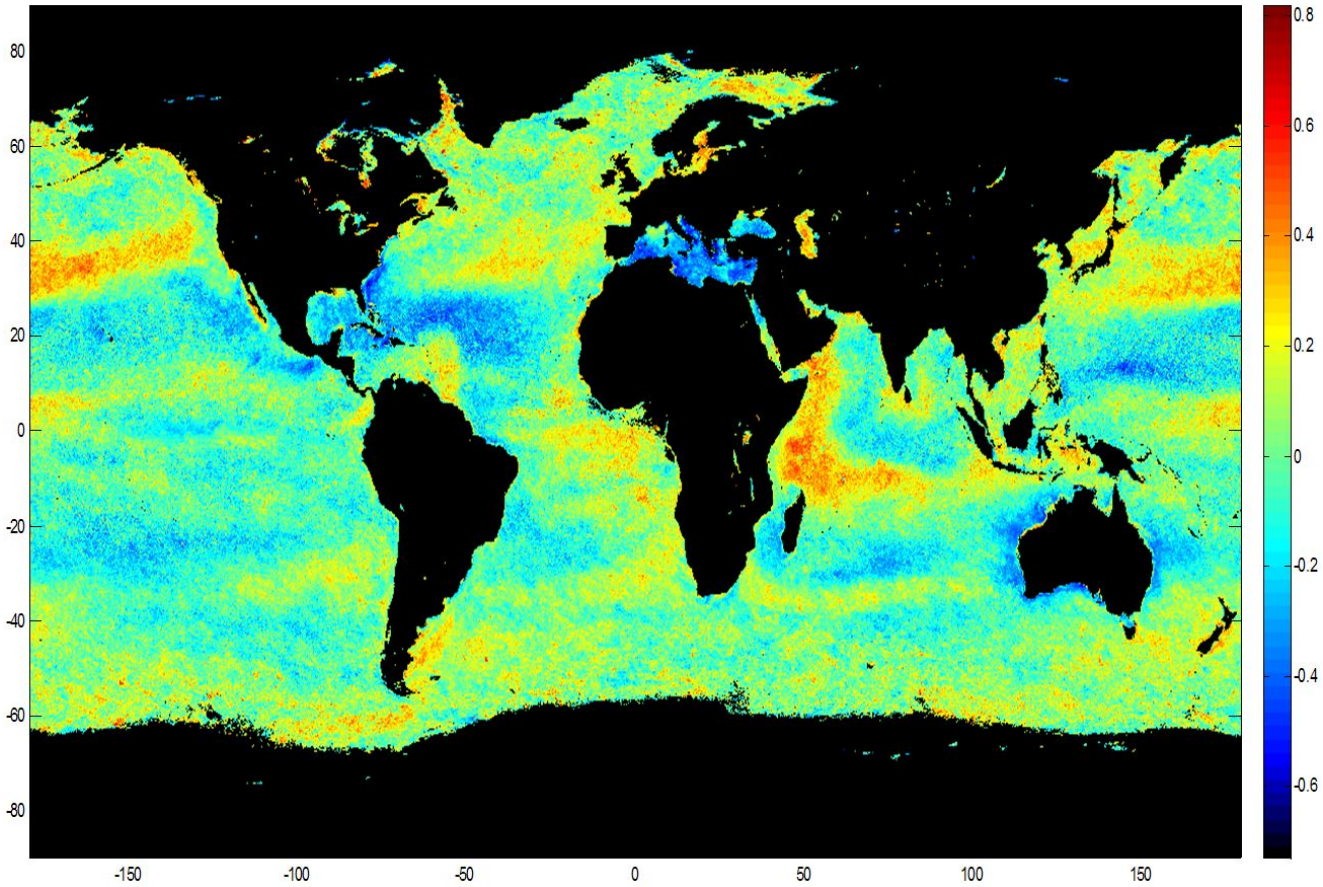

©2019. Japan Geoscience Union. All Right Reserved.

Glyoxylate from CO atmosphere via UV photochemistry

*Kenta Isoda[1], Xiaofeng Zang[1], Yuichiro Ueno[1,2]

1. Department of Earth and Planetary Sciences, Tokyo Institute of Technology, 2. Earth Life-Science Institute, Tokyo Institute of Technology

Glyoxylate could be an important compound, which can initiate a simple autocatalytic cycle and may possibly evolve to synthesize amino acids, nucleobase, pentose etc. (Eschenmoser, 2007a). However, constant supply of glyoxylate is an issue for the prebiotic environment. In this study, we aim to understand the possible condition to supply glyoxylate continuously to support such an autocatalytic cycle. First, we have performed experimental study and demonstrated that glyoxylic acid can be synthesized photochemically under carbon monoxide atmosphere. On the other hand, the UV irradiation into formaldehyde solution does not yield glyoxylic acid, except for the presence of CO in the gas phase. These results indicate that glyoxylate is not produced from formaldehyde in solution but from CO in the gas phase probably through the 3 steps: (i) HCO radical is produced from the reaction between CO and H from H_2O photolysis; (ii) The HCO radical dimerize in the gas phase, to form $(CHO)_2$(glyoxal); and (iii) The $(CHO)_2$ is oxidized into HCOCOOH (glyoxylate). An additional experiment demonstrated that UV irradiation into pure glyoxal solution can yield glyoxylate, and thus indicate that the step (iii) can proceed in the solution. Consequently, our experimental results suggests that glyoxylate can be continuously provided from atmosphere into hydrosphere if the atmosphere is rich in CO.

Keywords: atmosphere, photochemistry

©2019. Japan Geoscience Union. All Right Reserved.

Carbon reservoir perturbations in the Indian subcontinent induced by the Deccan volcanism in marine and terrestrial realm

*Sohom Roy[1], Prasanta Sanyal[1], Sambit Ghosh[1]

1. Indian Institute of Science Education and Research Kolkata

The Deccan flood basalt eruption spans across the Cretaceous-Paleogene (K/Pg) Boundary and records the largest
and the longest lava flows in the world. While the volcanism has been linked to the infamous K/Pg extinction,
however, its implications on the regional carbon budget are still not well constrained. Carbon isotope records in marine carbonates ($\delta^{13}C_{carb}$) and bulk organic matter ($\delta^{13}C_{org}$), coupled with carbon and hydrogen isotope records
of *n*-alkane ($\delta^{13}C_{alk}$ and δD_{alk} respectively) have been measured along with *n*-alkanes characterization from two
inter-trappean and one infra-trappean sedimentary sequence exposed south of the city of Rajahmundry, SE India
in order to evaluate the climatic and environmental response exacerbated by the volcanism in the marine and terrestrial realm. Overall, our data demonstrate major perturbations in the terrestrial and marine carbon cycle induced by the Deccan volcanism, with considerable environmental stress predating the K/Pg Boundary. Strong covariance between $\delta^{13}C_{org}$ and $\delta^{13}C_{carb}$ (r=-0.71) suggest that the dissolved inorganic carbon (DIC) in the shallow
marine environment was largely controlled by organic matter (OM) flux. The occurrence of large unresolved complex mixtures (UCM/n-alkane>>4) and hopanes (m/z 191) and steranes (m/z 217) in the limestones OM suggest considerable input from petroleum into the biomass. The upper part of the infra-trappean and lower parts of inter-trappean show considerable decreases in the marine $\delta^{13}C_{carb}$ values and have been inferred to occur from hydrocarbon assimilation by heterotrophs and early diagenesis of OM. Steady temporal increase in $\delta^{13}C_{carb}$ values and total organic carbon (TOC) content throughout the sequence imply increases in primary productivity, with the upper inter-trappean limestone marking the recovery phase. The $\delta^{13}C_{alk}$ values, coupled with the chain-length distribution pattern of *n*-alkanes and spore-pollen records exhibit significant turnovers in the vegetation community structure. High δD_{alk} values (~-110‰) indicate arid conditions before the deposition of mega flow episodes in Rajahmundry. Depletion in δD_{alk} values (~-150‰) observed in the middle part of the inter-trappean signifies a change to a humid condition. The increased rainfall prompted an upsurge in weathering that led to increases in freshwater influx (depletion in $\delta^{18}O_{carb}$ values) and higher terrestrial OM input (increase in long-chain *n*-alkanes). Atmospheric CO_2 concentration reconstructed from two paleosol horizons in the infra- and inter-trappean units respectively indicate major drawdown in pCO_2 across the main flow episode in Rajahmundry. It is speculated that the volcanism induced changes in pCO_2 was one of the main drivers for exacerbating changes in the carbon cycle.

Keywords: Deccan volcanism, carbon reservoir, n-alkane, stable isotope, Rajahmundry

©2019. Japan Geoscience Union. All Right Reserved.

Organic matter around Miocene Kuroko ore deposits: Implications to Archean submarine hydrothermal microbial community

*Takeshi Kakegawa[1]

1. Graduate School of Science, Tohoku University

Kuroko ore deposits were products of black smoker activities at 15 Ma paleo-Japan Sea. Kuroko is often covered by organic-rich sedimentary rocks, but details of these organic matter have not been unclear. Here I report analytical results of stable isotopes, Raman spectroscopy and bitumen compositions of organic matter around Miocene Kuroko deposits.

In general, all geochemical characteristics of organic matter were uniform in the same horizon of Kuroko deposits. On the other hand, H/C ratios and Raman spectroscopic data suggest that organic matter were extensively graphitized by thermal degradation only around Kuroko. More ^{12}C- and ^{14}N-enriched features are found in Kuroko-associated kerogen and bitumen. Such stable isotope data suggest the presence of chemoautotrophs, which utilized hydrothermal $CH_4$and NH_3. However, geochemical and geological characteristics of the examined samples suggest that hydrothermal $CH_4$and NH_3were produced by thermal degradation of sedimentary organic matter, which are mainly derived from photoautotrophs. This further suggests that chemoautotrophs at Kuroko were not independent and had strong connection to surface photoautotrophs.
Organic matter enriched in ^{12}C and ^{14}N are ubiquitous around many middle-Archean Kuroko ore deposits. Such stable isotope compositions also imply the presence of submarine hydrothermal microbial communities. However, ^{12}C- and ^{14}N-depleted organic matter, which most likely represent photoautotrophs, are also common around Archean Kuroko deposits. Such contrast stable isotope characteristics suggest that deep submarine chemoautotrophs already had linkages to surface photoautotrophs since Archean age.

Keywords: Kuroko, Chemoautotroph, stable isotope

©2019. Japan Geoscience Union. All Right Reserved.

Formation and solubility of hydrous carbonates formed in alkaline lakes under freezing condition

*TAKUMA KITAJIMA[1], Haruna Matsumiya[1], Keisuke Fukushi[1]

1. kanazawa university

Alkaline lakes have functions of absorption of atmospheric CO_2 to natural water and fixation of dissolved carbonate by mineralization. Therefore, it has been considered that alkaline lakes located in arid area inside the continents play important roles in carbon cycle on the earth surface (Finley et al., 2015; Fukushi and Matsumiya, 2018).

The common carbonate minerals are calcite and aragonite in natural environment. On the other hand, monohydrocalcite (MHC) is formed in alkaline lakes as most common carbonate minerals (Fukushi et al.2012). MHC ($CaCO_3 \cdot H_2O$) is metastable carbonate mineral with respect to calcite or aragonite (Munemoto and Fukushi, 2008). The formation of MHC requires the paragenesis of amorphous magnesium carbonate (AMC) (Nishiyama et al., 2013; Fukushi et al., 2017).

Fukushi and Matsumiya, (2018) measured the solubilities of MHC and AMC under the atmosphere at 25 ℃ and reported that MHC and AMC control the water chemistry of alkaline lakes. However, the most of surrounding environment of alkaline lakes are semiarid and cold. The lakes are covered with ice in most of the year.

During the ice forming ice, the lake water must be isolated from the atmosphere, which may lead to the decrease of low partial pressure of CO_2 in lakes. Low temperature may affect the formed mineral species and physicochemical properties of the minerals. Therefore, we can’ t discuss the water chemistry of alkaline lakes only from the knowledge obtained from the ambient condition atmosphere CO_2 pressure and 25 ℃. The purposes of this study are (1) investigation of the carbonate mineral formation from the solution simulated the alkaline lakes under low partial pressure of CO^2 at 5-50 ℃ and (2) measurements of solubilites of these carbonate minerals to estimate of water chemistry of alkaline lakes.

©2019. Japan Geoscience Union. All Right Reserved.

Effect of difference in mineral wettability on water-mineral reaction in rock pores

*Tadashi Yokoyama[1], Naoki Nishiyama[2]

1. Graduate School of Integrated Arts and Sciences, Hiroshima University, 2. Graduate School of Life and Environmental Sciences, University of Tsukuba

When water infiltrates rock pores, dissolution occurs at the contact site of water and mineral. In many cases rock pores near the ground surface are not fully saturated with water and a portion of pores is filled with air. In order to study how the presence of air in pores affects the reactivity of each rock-forming mineral, the amounts of elements leached out from the rock were compared for water-saturated condition and unsaturated condition by using a core of Berea sandstone. The sandstone consists mainly of quartz with several percentages of feldspar, carbonates, and clays. In the case of the saturated condition, initially pores were saturated with water by vacuum treatment, then water was passed through the core at a constant water head difference. In the case of the unsaturated condition, water was passed through a dry core. After the onset of the experiment under the unsaturated condition, water saturation (the fraction at which pore volume is saturated with water) became ~60% almost immediately (air 40%), and gradually increased and reached ~100% after 9 days passed. Dissolution rates of Si and Ca (amount of dissolution per unit time per whole rock) were determined by measuring the concentrations of dissolved Ca and Si in leachates. The difference in dissolution rate between unsaturated condition and saturated condition was generally greater in the case of Ca than that of Si. This appears to be due to the difference of wettability of silicates and carbonate. Probably silicates were more easily wet and many silicate surfaces dissolved even under the presence of air, while dissolution of carbonate was diminished due to the absence of water contact or the insufficient flushing of Ca in the wetting film of the carbonate surface.

©2019. Japan Geoscience Union. All Right Reserved.

[J] Oral | B (Biogeosciences)：B-BC Biogeochemistry

Tue. May 28, 2019 1:45 PM - 3:15 PM JST | Tue. May 28, 2019 4:45 AM - 6:15 AM UTC | 201A 2F

[B-BC03] Interrelation between Life, Water, Mineral, and Atmosphere

convener:Takeshi Kakegawa(Graduate School of Science, Tohoku University), Tadashi Yokoyama(Graduate School of Integrated Arts and Sciences, Hiroshima University), Keisuke Fukushi(Institute of Nature & Environmental Technology, Kanazawa University), Fumito Shiraishi(Department of Earth and Planetary Systems Science, Graduate School of Science, Hiroshima University), Chairperson:Tadashi Yokoyama, Keisuke Fukushi

Life on Earth is based on a diversity of physical and chemical dynamics and processes throughout the history of the Earth. It can essentially be regarded as the history of interrelation between Life, Water, Mineral (Solid Earth) and Atmosphere. To solve this kind of complex systems problems, interdisciplinary approach, a way of thinking and communication, is necessary. This session will be a cradle for such interdisciplinary researches.

1:45 PM - 2:00 PM JST | 4:45 AM - 5:00 AM UTC

[BBC03-01] Chemical speciation analysis of the brown and black precipitates observed in the gill chamber of the vent shrimp *Rimicaris kairei*

*Masanari Hikosaka[1], Yoshio Takahashi[2], Chong Chen[3], Robert Jenkins[1] (1.Kanazawa University, 2.Tokyo University, 3.Japan Agency for Marine-Earth Science and Technology)

2:00 PM - 2:15 PM JST | 5:00 AM - 5:15 AM UTC

[BBC03-02] Experimental study on hydrogen generation during low temperature serpentinization by using natural samples

*Shunta Higashino[1], Ryohei Kawakita[1], Tsubasa Otake[2], Tsutomu Sato[2] (1.Graduate School of Engineering, Hokkaido University, 2.Faculty of Engineering, Hokkaido University)

2:15 PM - 2:30 PM JST | 5:15 AM - 5:30 AM UTC

[BBC03-03] **Constraint on the origin of methane from Hakuba Happo serpentinite-hosted hot spring by using $^{14}CH_4$ and noble gas isotope**

*Konomi Suda[1], Takahiro AZE[2], Yosuke Miyairi[2], Yusuke Yokoyama[2], Yohei Matsui[3,2], Hisahiro Ueda[3], Takuya Saito[3], Tomohiko Sato[4], Yusuke Sawaki[2], Ryosuke Nakai[1], Hideyuki Tamaki[1], Hiroshi A Takahashi[1], Noritoshi Morikawa[1] (1.National Institute of Advanced Industrial Science and Technology, 2.The University of Tokyo, 3.Japan Agency for Marine-Earth Science and Technology, 4.Tokyo Institute of Technology)

2:30 PM - 2:45 PM JST | 5:30 AM - 5:45 AM UTC

[BBC03-04] Inhibition of calcium silicate hydrate formation by lignosulfonate and lignin

*Kanako Toda[1], Tsubasa Otake[1], Tsutomu Sato[1] (1.Laboratory of Environmental Geology, Faculty of Engineering, Hokkaido University)

2:45 PM - 3:00 PM JST | 5:45 AM - 6:00 AM UTC

[BBC03-05] Calcium carbonate formation processes on cyanobacterial surface

*Fumito Shiraishi[1], Takeru Omori[1], Naotaka Tomioka[2], Satoko Motai[2], Hiroki Suga[3], Yoshio Takahashi[3] (1.Hiroshima University, 2.JAMSTEC, 3.The University of Tokyo)

3:00 PM - 3:15 PM JST | 6:00 AM - 6:15 AM UTC

[BBC03-06] Mineralogical and geochemical study on sedimentary rock containing microfossils from 1.9 billion years ago(Ga) Gunflint Formation, Canada

*kouhei Sasaki[1], Akizumi Ishida[1], Takeshi Kakegawa[1] (1.Graduate School of Science, Tohoku University)

Chemical speciation analysis of the brown and black precipitates observed in the gill chamber of the vent shrimp *Rimicaris kairei*

*Masanari Hikosaka[1], Yoshio Takahashi[2], Chong Chen[3], Robert Jenkins[1]

1. Kanazawa University, 2. Tokyo University, 3. Japan Agency for Marine-Earth Science and Technology

The hydrothermal vent shrimp *Rimicaris* dominates the megafaunal community in many hydrothermal vent ecosystems in the globe, including Mid Atlantic Ridge, the Central Indian Ridge (CIR), and the Caribbean Mid-Cayman Rise. *Rimicaris* harbors numerous strains of episymbiotic bacteria in its gill chamber and depends on them for most of the nutrition as adults. Probably due to the metabolism of this symbiotic bacteria, the tissues in the gill chamber were found to be encrusted with brown or black iron precipitates. The precipitates are removed by molting, but in a few days after molting, *Rimicaris* will be covered with precipitates again. Although *Rimicaris* relies on episymbiotic bacteria nutritionally, it is thought that the precipitates originated from episymbiotic bacteria disturb their swimming activity, nutrient uptake by the host. Thus, the relationship between *Rimicaris* and its epibionts seems to be different from general mutualistic relationship. To understand this symbiotic relationship correctly, it is necessary to clarify the relationship among the host, episymbiotic bacteria, and the precipitates. In this study, iron chemical speciation analysis based on XAFS were performed to black and brown precipitates in the gill chamber of *Rimicaris kairei* in order to clarify the chemical environment in the gill chamber.
Specimens of *Rimicaris kairei* were collected during the YK16-E02 cruise at two hydrothermal vent site, Edmond and Kairei on the CIR. Each tissues were fixed in 99.5 % ethanol, and embedded in Epoxy resin(Epofix, Struers), and both sides polished thin section with a thickness of about 50 μm were obtained. Thin section was subjected to μ-XRF element analysis and Fe K-edge XANES analysis at KEK PF BL-4A to investigate the element distribution and the speciation of iron around the bacteria. Fitting was carried out using a software REX 2000 (Rigaku) using ferrihydrite, goethite, magnetite, $FePO_4$, pyrite, pyrrhotite as reference materials.
By observing the freeze-dried samples by scanning electron microscope (JSM-6100, JEOL) and thin section samples by polarized microscopy, it was observed that the brown precipitates forms crusts of about 50 μm in thickness and covers entirely the inside of the branchiostegite, where black precipitates occur as submicron size microparticles in organic filmy tissues around filamentous bacteria. From the XANES fitting, it was suggested that the brown precipitates contain ferrihydrite, goethite, $FePO_4$, while the black precipitates contain ferrihydrite, goethite, $FePO_4$, and pyrrhotite. It was revealed that iron exists as Fe^{3+} in the brown precipitate, but in the black precipitate, iron exist as a mixture of Fe^{2+} and Fe^{3+}. It is estimated that the brown precipitates were formed in the aerobic environment and the black precipitates were formed in the relatively anaerobic environment. Overall, our suggested that the gill chamber environment was diverse even among the same species. We will perform next-generation sequencing of microbes in the gill chamber, and we need to investigate in detail the precipitation conditions of each mineral and the environment in which the host can grow.

Keywords: hydrothermal vent, Rimicaris kairei, biomineralization, XAFS

©2019. Japan Geoscience Union. All Right Reserved.

Experimental study on hydrogen generation during low temperature serpentinization by using natural samples

*Shunta Higashino[1], Ryohei Kawakita[1], Tsubasa Otake[2], Tsutomu Sato[2]

1. Graduate School of Engineering, Hokkaido University, 2. Faculty of Engineering, Hokkaido University

Low temperature serpentinization, a reaction between ultramafic rocks and water under ambient conditions, generates hydrogen near Earth's surface environments. This reaction has been considered to play important roles in the origin of life since hydrogen may have been an important reducing gas for building blocks of life as well as early metabolisms. Furthermore, this process may be applicable for industrial hydrogen production that does not emit carbon dioxide during its production or consumption whereas the conventional method for hydrogen production essentially relies on fossil fuels. During serpentinization, hydrogen is generated by the reduction of water accompanied with oxidation of ferrous ion to ferric ion in the primary minerals of ultramafic rocks such as olivine or pyroxene. However, the amount of hydrogen produced during low temperature serpentinization is controlled by various factors, which have not been well understood, particularly, the effect of the formation of secondary minerals (Mayhew et al., 2018). Therefore, we conducted a series of experiments for hydrogen production using 10 ultramafic rock samples (dunites and harzburgites), from Japan (Horoman and Wakamatsu), Oman and Indonesia, showing various lithological features and degrees of serpentinization subjected during obduction. Mineralogical and geochemical characterizations were conducted using XRD, XRF and SEM-EDS. Experiments were then conducted by reacting the samples with water under anaerobic conditions at 90℃, for 2 weeks. After the experiments, gas, solid, and solution obtained from the experiments were analyzed by GC-RGD, XRD, and ICP-AES, respectively.

The results of experiments show that samples with lower degrees of serpentinization tend to generate larger amounts of hydrogen, and that harzburgites tend to generate more hydrogen than dunite when they are at the same degree of serpentinization. However, some highly serpentinized samples also generated large amounts of hydrogen though these results werepooly reproduced. This may have stemmed from the oxidation of trace minerals (e.g., Ni-Fe alloy) or their catalytic effects, in addition to the dissolution of Fe^{2+}-bearing primary minerals, because these minerals were heterogeneously observed by microscopy in the serpentinites. Experiments were also conducted with some additives (e.g., MgO, SiO_2, and magnetite) to investigate the effect of solution chemistry and formation of secondary minerals on hydrogen generation. The results show that hydrogen was generated the most under Si-rich conditions. Solution chemistry suggests that, olivine and pyroxene were likely dissolved more rapidly with Si-rich solutions. This is consistent with the trend that harzburgites generate hydrogen more than dunite because harzburgite contains pyroxene, which dissolved much Si compared to olivine. Moreover, thermodynamic calculations suggest that the precipitation of amorphous Mg-silicate minerals (e.g., M-S-H), which are commonly precursors of serpentine controls the solution chemistry including decreasing pH. Because the dissolution rate of the primary minerals is greater at lower pH, the precipitation of Mg-silicate minerals may have promoted the dissolution cycle of the primary minerals and therefore generation of hydrogen, especially under Si-rich conditions.

Reference

©2019. Japan Geoscience Union. All Right Reserved.

Mayhew, L. E., Ellison, E. T., Miller, H. M., Kelemen, P. B., & Templeton, A. S. (2018). Iron transformations during low temperature alteration of variably serpentinized rocks from the Samail ophiolite, Oman. *Geochimica et Cosmochimica Acta*, *222*, 704–728.

Keywords: serpentinization, serpentine, ultramafic rock, hydrogen, amorphous Mg-silicate mineral, thermodynamic calculation

©2019. Japan Geoscience Union. All Right Reserved.

Constraint on the origin of methane from Hakuba Happo serpentinite-hosted hot spring by using $^{14}CH_4$ and noble gas isotope

*Konomi Suda[1], Takahiro AZE[2], Yosuke Miyairi[2], Yusuke Yokoyama[2], Yohei Matsui[3,2], Hisahiro Ueda[3], Takuya Saito[3], Tomohiko Sato[4], Yusuke Sawaki[2], Ryosuke Nakai[1], Hideyuki Tamaki[1], Hiroshi A Takahashi[1], Noritoshi Morikawa[1]

1. National Institute of Advanced Industrial Science and Technology, 2. The University of Tokyo, 3. Japan Agency for Marine-Earth Science and Technology, 4. Tokyo Institute of Technology

Ultramafic rock-water interaction systems attract more interest from the perspective of study for origin of life since the discovery of the hyperalkaline hydrothermal system in the Atlantic Ocean in 2001 (Kelley et al., 2001). These serpentinite-hosted systems are generally characterized by high concentrations of methane (CH_4) and higher hydrocarbons (C^{2+}) regardless of seafloor or on-land (e.g., Schrenk et al., 2013; Etiope and Sherwood-Lollar, 2013). Previous stable carbon and hydrogen isotopic studies have suggested that hydrocarbons could be formed abiotically via polymerization process (Proskurowski et al., 2008; Suda et al., 2017). However, the following is still poorly constrained; when and where hydrocarbons are produced. In this study, to constrain the origin of methane, we determined the radiocarbon (^{14}C) content in CH_4 and the helium isotope obtained from serpentinite-hosted hot spring in Hakuba Happo.
Hakuba Happo hot spring lies on a serpentinized ultramafic rock body in the Shiroumadake area, which belongs to the Hida Marginal Tectonic Belt in central Japan. The hyperalkaline waters (pH>10), with temperatures of approximately 50˚C, are pumped from two borehole wells (Happo #1 and Happo #3). N_2, H_2 and CH_4 are main gas components (Homma and Tsukahara, 2008; Suda et al., 2014). Water chemistry and volatile component are controlled primarily by serpentinization reaction.
Sample collection was conducted in 2015-2018. Hot spring gas samples were collected by a displacement method in water from two borehole wells (Happo #1 and Happo #3). For radiocarbon (^{14}C) analysis of methane, firstly, CH_4 in gas samples was converted to CO_2 by using the custom-built flow-through vacuum line system (similar to Pack et al., 2015) at JAMSTEC. Secondly, the purified CO_2 gas was reduced to graphite by using the graphitization reactor with Fe powder and hydrogen gas, and then the ^{14}C content was determined by using an accelerator mass spectrometry (AMS) at AORI, the University of Tokyo. Noble gas isotope abundances were measured with a noble gas mass spectrometer at GSJ, AIST. The concentrations of CO and CO_2 in gas phase were determined by using a GC-methanizer-FID method, which was suitable for detection of trace amounts of CO and CO_2 (Kaminski et al., 2003). The concentration of dissolved inorganic carbon (DIC) in spring water was measured by using GasBench/IRMS system at GSJ, AIST.
In Hakuba Happo hot spring, CO and CO_2 were below detection limit (<0.0005 vol.%). DIC concentration was <28 μmol/L (upper values because of suspicion of air contamination during sampling), which was lower than dissolved methane concentration (124-664 μmol/L; Suda et al., 2014). Methane is the most abundant carbon compound in Hakuba Happo hot spring. If methane production occurs under on-site condition, the inorganic carbon compounds (CO, CO_2 and DIC) are not likely to be a carbon source for CH_4. The high helium isotope ratio ($^3He/^4He$) was observed in both well sites. The $^3He/^4He$ ratios for Happo #1 and Happo #3 were 4.10 R_{atm} and 4.47 R_{atm}, respectively (where R_{atm} is the atmospheric $^3He/^4He$ ratio of 1.4×10^{-6}). For Happo #1 site, relative contribution of air, mantle and crustal components are estimated to be 47%, 31% and 22%, respectively. For Happo #3 site, 69%, 24% and 8%, respectively. The result of AMS measurements on two CH_4 samples from Hakuba Happo reveals that ^{14}C contents are near the detectable limit, i.e., the ^{14}C ages of CH_4 is at least approximately 50,000 years before present. Radiocarbon evidence rules out a modern carbon compound (e.g., atmospheric CO_2, organics in surface

©2019. Japan Geoscience Union. All Right Reserved.

soil) as the carbon source of CH_4 at Hakuba Happo hot spring system. The helium isotope and $^{14}CH_4$ data could be consistent with deep-derived carbon source of the Hakuba Happo CH_4. Therefore, it will be important to consider a relation between surface reaction system and deep mantle/crustal system.

Keywords: serpentinite, hyperalkaline hot spring, methane, radiocarbon, helium isotope

©2019. Japan Geoscience Union. All Right Reserved.

Inhibition of calcium silicate hydrate formation by lignosulfonate and lignin

*Kanako Toda[1], Tsubasa Otake[1], Tsutomu Sato[1]

1. Laboratory of Environmental Geology, Faculty of Engineering, Hokkaido University

Dams and harbors have frequently dredged in order to secure the water storage capacity and shipping routes. Dredged soils are mostly treated as waste, though utilization of dredged soils for construction resources are economically and environmentally desired. Only a part of the dredged soils has been used for construction materials after mixing with steel slags due to their low physical strength. Mixture's strength development has been known to depend on utilized dredged soil. However, even under the same mixing conditions, some combinations may not be hardened. Soil composition is generally complex as it reflects the result of mineral-water-organic matter-microbe interactions occurred onto components from diverse origin. In solidification of the dredged soils to form construction materials, alkaline activators, steels slags in this case, are added, which triggers the formation of secondary phases such as calcium silicate hydrate (C-S-H). Factors affecting C-S-H formation have been reported previously (e.g., Tremblay et al., 2002; Zhu et al., 2007; Toda et al., 2018). However, inhibition mechanism of authentic organic matter in the soils and the quantitative effects of their functional groups on C-S-H formation are not fully understood.

In this context, the effects of 1) lignosulfonate and 2) lignin that contain carboxylic, sulfonic and thiol functional groups that have similar structures to soil organic matter and 3) simple organic molecule with one of carboxylic, sulfonic and thiol functional groups on C-S-H formation were investigated in this study. C-S-H was synthesized from $Ca(OH)_2$ and amorphous silica in coexistence of multiple addition ratio of lignosulfonate and lignin to expecting amount of C-S-H formed, in 100 rpm shaker at 50℃ for 10 days. After the syntheses, C-S-H were characterized by X-ray diffraction and FT-IR analysis, and chemical composition of the remaining solutions were analyzed by ICP-AES and TOC analyzer. After syntheses, solution pH were all above 12. The threshold quantity of lignosulfonate and lignin was evaluated to suppress the formation of C-S-H. Above the threshold, XRD peaks assigned to $Ca(OH)_2$ and amorphous silica could still be obtained after synthesis, without C-S-H peaks. Furthermore, below the threshold, the broad diffraction peak assigned to (001) reflection of C-S-H decreased with increasing the added amount of lignosulfonate and lignin. This suggests that lignosulfonate and lignin may suppress the dissolution of initial phases but also C-S-H crystal growth. Both of the indicated inhibition factors could occur due to the surface coverage by negatively charged functional groups in the organic matter under alkaline condition, which may be interacting with positively charged sites such as $Ca(OH)_2$ surface and CaO layer in C-S-H. C-S-H synthesis with simple organic molecule with various functional groups were also conducted to further discuss how the difference in soil organic matter structure in terms of functional group can inhibit C-S-H formation.

Keywords: dredged soils, soil organic matter, C-S-H, construction materials

©2019. Japan Geoscience Union. All Right Reserved.

Calcium carbonate formation processes on cyanobacterial surface

*Fumito Shiraishi[1], Takeru Omori[1], Naotaka Tomioka[2], Satoko Motai[2], Hiroki Suga[3], Yoshio Takahashi[3]

1. Hiroshima University, 2. JAMSTEC, 3. The University of Tokyo

Cyanobacteria is oxygenic phototroph known to calcify under optimum ambient water chemistry. Fossils of calcified cyanobacteria are widely spread especially during the Phanerozoic, and the fluctuation in their abundance is crucial for reconstructing paleo-ocean chemistry (e.g., pH). Two major mechanisms are suggested for cyanobacterial calcification: 1) the photosynthetic increase in $CaCO_3$ saturation state, and 2) the crystal nucleation sites supplied by acidic groups of extracellular polymeric substances (EPS). Previous study based on natural samples demonstrated that acidic EPS is crucial for controlling the degree and the style of calcification. However, the influence of EPS on crystal morphology, crystal arrangement, and precursor (amorphous calcium carbonate: ACC) formation are still not well understood. The present study, therefore, examined the relationship between physical/chemical characteristics of EPS and calcification styles by using cultivated cyanobacteria.
Four cyanobacteria having different EPS characteristics (*Spirulina*, *Phormidium*, *Scytonema*, and *Leptolyngbya*) were cultivated. Acid-base titrations and lectin binding analysis indicated that all investigated cyanobacteria secreted EPS containing acidic groups. These cyanobacterial cultures were incubated in an aquarium (pH = ca. 8.5, $[Ca^{2+}]$ = 2 mM, DIC = 2 mM) with light supply to cause calcification. Microelectrode measurements (pH, O_2, and Ca^{2+}) showed that all cyanobacterial cultures induced $CaCO_3$ precipitation by photosynthesis, although the degree of precipitation was different. Observations by transmission electron microscopy (TEM) and scanning transmission X-ray microscopy (STXM) revealed that the characteristics of precipitated $CaCO_3$ were significantly different among the investigated cyanobacteria. Especially, calcite formed around *Spirulina*, *Phormidium*, *Scytonema* exhibited specific features including ACC, sub-micron-sized calcite polycrystals, and superstructures, suggesting that the nucleation occurred on acidic EPS via ACC nanoparticles. In contrast, such features were rarely observed in calcite formed around *Leptolyngbya* producing only a few amounts of EPS. From these results, $CaCO_3$ formation processes on cyanobacterial surface is suggested as follows: 1) ACC nanoparticles are formed on acidic EPS, 2) crystallization takes place inside of grown ACC particles to form submicron-sized calcite polycrystals, and 3) these polycrystals grow into calcite single crystal while ACC and polycrystals remain partly.

Keywords: CaCO3, Cyanobacteria, EPS

©2019. Japan Geoscience Union. All Right Reserved.

Mineralogical and geochemical study on sedimentary rock containing microfossils from 1.9 billion years ago(Ga) Gunflint Formation, Canada

*kouhei Sasaki[1], Akizumi Ishida[1], Takeshi Kakegawa[1]

1. Graduate School of Science, Tohoku University

The ca. 1.9 Ga Gunflint microfossils are well studied by previous investigators. On the other hand, no agreements exist for primary producers indicated by microfossils, and their living environments. In this study, we performed geological, mineralogical and geochemical studies on samples from Schreiber and Mink Mountain regions. In addition, detailed morphologies of microfossils in stromatolite were observed. In Schreiber region, we discovered the novel microfossils of cyanobacteria colony, akinete, and endospore. Undiscovered microfossil type with radial wall ornamentation is found, indicating eukaryotic affinities. In particular, in situ analysis of microfossils by NanoSIMS discovered multilayered microstructure of cell wall and heterogeneous distribution of carbon, nitrogen and sulfur possibly associated with biological incorporation of those elements followed by later diagenetic modification. At Mink Mountain region, detailed observations and chemical analyses suggest that iron-oxidizing bacteria were dominant around stromatolites. Fe^{2+} and clays were supplied by local and shallow hydrothermal systems along the paleo-coastal lines. Such hydrothermal environments created local anoxic environments, allowing accumulation of Fe^{2+} followed by microbial oxidation. In summary, microbial life at the Gunflint age was more diverse and evolved than previously thought, cyanobacteria were primary producers in most places, but structure of microbial ecosystems in the Gunflint ocean dynamically changed with environments.

Keywords: Gunflint Formation, microfossils, stromatolite

©2019. Japan Geoscience Union. All Right Reserved.

[J] Oral | B (Biogeosciences)：B-BC Biogeochemistry

Tue. May 28, 2019 3:30 PM - 5:00 PM JST | Tue. May 28, 2019 6:30 AM - 8:00 AM UTC | 201A 2F

[B-BC03] Interrelation between Life, Water, Mineral, and Atmosphere

convener:Takeshi Kakegawa(Graduate School of Science, Tohoku University), Tadashi Yokoyama(Graduate School of Integrated Arts and Sciences, Hiroshima University), Keisuke Fukushi(Institute of Nature & Environmental Technology, Kanazawa University), Fumito Shiraishi(Department of Earth and Planetary Systems Science, Graduate School of Science, Hiroshima University), Chairperson:Takeshi Kakegawa, Fumito Shiraishi(Hiroshima Univ.)

Life on Earth is based on a diversity of physical and chemical dynamics and processes throughout the history of the Earth. It can essentially be regarded as the history of interrelation between Life, Water, Mineral (Solid Earth) and Atmosphere. To solve this kind of complex systems problems, interdisciplinary approach, a way of thinking and communication, is necessary. This session will be a cradle for such interdisciplinary researches.

3:30 PM - 3:45 PM JST | 6:30 AM - 6:45 AM UTC

[BBC03-07] Secular variation of multiple sulfur isotopic compositions of sulfate and sulfide during long term incubation of *Desulfovibrio desulfuricans*

*Fumihiro Matsuura[1], Hiroko Makita[2], Ken Takai[3], Yuichiro Ueno[1,3] (1.Tokyo Institute of Technology, 2.Tokyo University of Marine Science and Technology, 3.Japan Agency for Marine-Earth Science & Technology (JAMSTEC))

3:45 PM - 4:00 PM JST | 6:45 AM - 7:00 AM UTC

[BBC03-08] **Origins of volcanic SO_2 on Earth**

*Hiroshi Ohmoto[1] (1.The Pennsylvania State University)

4:00 PM - 4:15 PM JST | 7:00 AM - 7:15 AM UTC

[BBC03-09] **Volcanism, sedimentation, and development of life in a Mesoarchaean intracratonic setting: the Dominion Group, South Africa**

*Andrea Agangi[1,2], Axel Hofmann[2], Dora Paprika[2], Andrey Bekker[2,3], Frantz Ossa-Ossa[2,4] (1.Akita University, 2.University of Johannesburg, 3.University of California, 4.University of Tuebingen)

4:15 PM - 4:30 PM JST | 7:15 AM - 7:30 AM UTC

[BBC03-10] New microbial ecology results from genome centered metagenomics studies of iron carbonate and sulfidic hot springs

*Shawn E McGlynn[1], Lewis Ward[2], Takeshi Kakegawa[3], Yuichiro Ueno[1], Mayuko Nakagawa[1] (1.Earth-Life Science Institute, Tokyo Institute of Technology, 2.Harvard University, 3.Tohoku University)

4:30 PM - 4:45 PM JST | 7:30 AM - 7:45 AM UTC

[BBC03-11] Superhabitability in ultradeep rocky environments

*Yohey Suzuki[1] (1.Graduate School of Science, The University of Tokyo)

4:45 PM - 5:00 PM JST | 7:45 AM - 8:00 AM UTC

[BBC03-12] Exploring planetary habitability beneath the oceans

★Invited Papers

*Fumio Inagaki[1] (1.Japan Agency for Marine-Earth Science and Technology)

Secular variation of multiple sulfur isotopic compositions of sulfate and sulfide during long term incubation of *Desulfovibrio desulfuricans*

*Fumihiro Matsuura[1], Hiroko Makita[2], Ken Takai[3], Yuichiro Ueno[1,3]

1. Tokyo Institute of Technology, 2. Tokyo University of Marine Science and Technology, 3. Japan Agency for Marine-Earth Science & Technology (JAMSTEC)

Incubation experiments of sulfate reducing microbes have been carried out since 1950s to quantify sulfur isotope fractionation. Sulfur isotope fractionation models are constructed from the results of these experiments. These models are applicable only when steady state is accomplished in the cells; thus, most of incubation experiments targeted cells exponential growth phase. We aimed to quantify the isotope fractionation in stationary to death phase of the cells and carried out two series of incubation experiment of sulfate reducing bacteria, *Desulfovibrio desulfuricans* (DSM-642), until c.a. 2000 hours. In addition, we used glucose as electron donor to make cell specific sulfate reduction rate low. Cells grew linearly rather than exponentially until cell concentration became c.a. 2×10^7 cells/mL in the early stage of incubation. Calculated sulfur isotope fractionation increased from 13.5±3.7‰ at the earliest stage of linear growth phase to 70.5±21.0‰ at the middle of linear growth phase. The cell specific sulfate reduction rate was 1.0±0.3 fmol/cell/day when sulfur isotope fractionation became 70.5±21.0‰, consistent with the results of a previous study. In the stationary to death phase, sulfide concentration started decreasing on the contrary to our expectation. Besides, $\delta^{34}S_{sulfide}$ value increased concomitant with the decrease of $\Delta^{33}S'_{sulfide}$ value. The $\delta^{34}S'_{sulfide}$ and $\Delta^{33}S'_{sulfide}$ have good linear correlation, and that indicate a sulfide originated reaction in a closed system with a unique fractionation factor dominates sulfur cycle during stationary to death phase. The calculated enrichment factors of the reaction in the two series experiments are 10.5‰ and 30‰. These enrichment factors are large compared to those of biotic or abiotic sulfide oxidation experiments of previous studies. We checked the reaction occur without cells and infer that the reaction is caused from sulfide oxidation by oxidants containing in the medium or sulfurization of organic matter containing in the medium.

Keywords: sulfate reducing bacteria, sulfur isotope fractionation, long term incubation

©2019. Japan Geoscience Union. All Right Reserved.

Origins of volcanic SO_2 on Earth

*Hiroshi Ohmoto[1]

1. The Pennsylvania State University

SO_2 is a principal volcanic gas today. The two important questions to be addressed are: (i). the origin of S atoms in volcanic SO_2; and (ii) whether or not SO_2 was an important volcanic gas of early Earth. I have approached these questions from: (a) thermodynamic- and kinetic analyses of various reactions involving S-bearing species in silicate melts, fluids, rocks, minerals, and aqueous solutions at T = 0-1500 ˚C and P = 1-10 kb, and (b) examinations of the chemical and S-isotopic characteristics of volcanic gases and rocks in various tectonic settings on modern Earth. Here are some of the important suggestions from these investigations:

1. All of the S-bearing species from submarine volcanic eruptions have been nearly completely trapped in oceans through reactions such as: $H_2S_{(g)} = H_2S_{(aq)}$; $4SO_{2(g)} + 4H_2O = 3HSO_4^- + H_2S_{(aq)} + 3H^+$; $S_{8(g)} = 8S_{(s)}$; and $7H_2S_{(aq)} + HSO_4^- + 4Fe^{2+} = 4FeS_{2(py)} + 7H^+ + 4H_2O$. S-bearing volcanic gases have only been emitted into the atmospheres by subaerial eruptions. Therefore, on the ocean-covered planets, possibly including the pre-3.0 Ga Earth, S-bearing gases have not been emitted into the atmospheres.

2. The fluids that originated from normal-mantle-derived-magmas (i.e., $\log fO_2$ = FMQ-2 to FMQ+0.5) were initially H_2S-rich and SO_2-poor, whereas those from subduction-related arc magmas (i.e., $\log fO_2$ = FMQ+0.5 to FMQ+3) were initially SO_2- and/or H_2S-rich.

3. H_2S-rich magmatic fluids may become SO_2-rich gas, if: (i) the fluids were derived from high fO_2 magmas (i.e., $\log fO_2$ > FMQ) and ascended slowly through conduits (i.e., diffusive eruptions) and re-equilibrated with wall-rocks at P_{H2O}<10 bars, or (ii) the fluids are oxidized by reactions with an O_2-rich atmosphere, -groundwater and/or high-fO_2 wall-rocks during and/or after the ascent through conduits. In the absence of (i) and (ii), such as the Earth prior to the oxygenation of the atmosphere, H_2S-rich magmatic fluids were not transformed to SO_2 during eruptions.

4. SO_2-rich fluids from arc magmas would remain SO_2-rich during explosive or diffusive eruptions. However, if the fluids cool down to <~700˚C, SO_2 transforms to H_2S.

5. Volcanic SO_2 from arc magmas was transformed from seawater sulfate through the following processes: (i) formation of pyrite, hematite and anhydrite by reactions between SO_4^{2-}-rich seawater and hot basalts on MORs; (ii) devolatilization of H_2O- and SO_2-rich fluids from the subducting oceanic crust; (iii) formation of oxidized- and SO_4^{2-}-rich magmas by partial melting of peridotite in the mantle wedges, and (iv) degassing of SO_2-rich fluids from these magmas. If the oceans were SO_4^{2-}-poor, volcanic gases from arc magmas would be SO_2-poor.

6. Oceanic SO_4^{2-} has been produced mostly by the oxidative weathering of pyrite on land. Therefore, subaerial volcanic gases on planets with O_2-poor atmospheres would be SO_2-poor and H_2S-rich. Then, the current paradigm concerning the origin of mass-independent-fractionations of sulfur isotopes (MIF-S) in Archean-aged sedimentary rocks (i.e., the UV photolysis of volcanic SO_2 in an O_2-poor atmosphere) becomes invalid. Consequently, the MIF-S record in sedimentary rocks is not supportive evidence for the “Great Oxidation Event” at ~2.5 Ga ago. Furthermore, the current atmospheric O_2-evolution models,

©2019. Japan Geoscience Union. All Right Reserved.

which are based on the premise of SO_2-rich volcanic gases throughout geologic time, become invalid.

(7). The MIF-S in the Archean- and younger sedimentary rocks may have been created by the chemisorption isotope effects during thermochemical reductions of seawater sulfates by hydrothermally-generated, very reactive organic matter.

Keywords: volcanic SO2, evolution of the atmospheric oxygen, arc magmatism, origin of MIF-S

©2019. Japan Geoscience Union. All Right Reserved.

Volcanism, sedimentation, and development of life in a Mesoarchaean intracratonic setting: the Dominion Group, South Africa

*Andrea Agangi[1,2], Axel Hofmann[2], Dora Paprika[2], Andrey Bekker[2,3], Frantz Ossa-Ossa[2,4]

1. Akita University, 2. University of Johannesburg, 3. University of California, 4. University of Tuebingen

The ca. 3 billion-years-old Dominion Group of the Kaapvaal craton, South Africa is a >2 km-thick volcano-sedimentary succession emplaced in an intracontinental setting shortly after craton consolidation. As such, it represents one of the oldest examples of volcanism and sedimentation on stable continental crust. Deposition of the Dominion Group is interpreted to have occurred largely subaerially in a failed rift. In contrast to other Palaeo- to Mesoarchaean successions of the Kaapvaal craton, the Dominion Group is little deformed and was metamorphosed at greenschist facies grade, allowing excellent preservation of rock textures and chemical composition. The succession includes a thin basal conglomerate that marks a major, craton-scale nonconformity, and is overlain by sandstone. Volcanic rocks include intercalated massive to amygdaloidal mafic lavas of tholeiitic affinity, felsic lavas, and ignimbrites with high Fe/Mg.

In the area around the town of Ottosdal, the Dominion Group is represented by felsic volcanic rocks with intercalated, thin sedimentary layers that crop out discontinuously for several km along the strike. The presence of shallow, porphyritic intrusions that developed peperitic contacts with the sediments and the intense alteration developed in sediments underlying (but not in overlying) volcanic rocks indicate deposition of these sediments in a volcanically and hydrothermally active environment, such as volcanic lakes. These sediments are composed of carbonaceous and variably sulfidic shale and minor arenite and have a distinctive aluminium-rich composition (Al_2O_3 up to 36 wt.%) and very low contents of alkaline elements, Ca, and Fe (Na_2O content from below detection limit to 0.3 wt%; Fe_2O_3 = 0.1 to 1.6 wt%). The main mineral components of these sediments are pyrophyllite, diaspore, K-mica, rutile, and pyrite. No carbonate was found.

The total organic carbon content) is up to 1.5 wt%, and bulk-sample isotope analyses indicate strongly ^{13}C-depleted composition ($\delta^{13}C_{VPDB}$ = -45 to -29‰). These isotopic values are diagnostic of biogenic carbon fixation and the lowest, best-preserved values are indicative of methanogenesis and methanotrophy in a redox and chemically stratified shallow basin. Modern examples of volcanic environments hosting methane-producing Archaea, even under low pH and high temperature conditions, are known from Kamchatka, Russia and Argentina.

Our results indicate that restricted and ephemeral lakes that developed in Mesoarchaean volcanic environments shortly after the large-scale emergence of the Kaapvaal craton fostered life and were likely niches for life diversification. This ancient environment might be a better Mars analogue than modern caldera environments on Earth where the impact of advanced biosphere is more pronounced.

Keywords: Archaean, Terrestrial life, Alteration

©2019. Japan Geoscience Union. All Right Reserved.

New microbial ecology results from genome centered metagenomics studies of iron carbonate and sulfidic hot springs

*Shawn E McGlynn[1], Lewis Ward[2], Takeshi Kakegawa[3], Yuichiro Ueno[1], Mayuko Nakagawa[1]

1. Earth-Life Science Institute, Tokyo Institute of Technology, 2. Harvard University, 3. Tohoku University

The ability to recover microbial genomes from metagenomic datasets has revolutionized how we understand microbial inhabitants in the environment, and is a powerful way to develop detailed hypotheses of community function and evolution. In this talk, I will discuss recent genomes we have recovered from two iron rich, carbonate hot springs in Japan, and contrast these to observations in low iron, sulfidic springs. Surprisingly, despite the different chemistry, some overall trends in phylogeny and physiology are observed, however water chemistry differences such as salinity and the availability of ferrous iron does alter the observed microbial inhabitants and physiologies.
These overall results will be discussed within the context of the possible ability to recognize microbial inhabitation on Earth through time.

Keywords: metagenomics, microbial ecology, geochemistry, geobiology

©2019. Japan Geoscience Union. All Right Reserved.

Superhabitability in ultradeep rocky environments

*Yohey Suzuki[1]

1. Graduate School of Science, The University of Tokyo

It is challenging for life to proliferate in cold rocky habitats deeply isolated from photosynthetic organic matter. Although fluid circulation is previously considered to be necessary for supplying energy sources and oxidants, it is also considered that substrates available within the rocky environment are diluted by fluid circulation. As the abundance of microbial life within the rock matrix is largely unknown, I developed nanoscale analytical procedures to unveil the distributions of microbial cells, organic matters and low-temperature minerals. As a result of applying the analytical procedures to various deep-sea and subsurface rocky environments such as deep-sea hydrothermal vents, deep-sea ferromanganese crusts and deep subseafloor basaltic rocks, it is unexpectedly unveiled that the rocky habitats are superhabitalble with cell densities locally exceeding 10^{10}cells/cm^3. The superhabitablity might be explained by the coexistence of solid silicate phases such smectite clays that play roles in concentrating nutrients from the ambient fluid.In this presentation, I will introduce the analytical procedures and main results obtained from the ultradeep rocky habitats.

Keywords: deep biosphere, nanobiogeoscience, microbial ecology

©2019. Japan Geoscience Union. All Right Reserved.

Exploring planetary habitability beneath the oceans

*Fumio Inagaki[1]

1. Japan Agency for Marine-Earth Science and Technology

Since Ocean Drilling Program (ODP) Leg 201 in 2002 off Peru and eastern equatorial Pacific, numerous geochemists and microbiologists have participated in multiple expeditions of scientific ocean drilling to explore subseafloor life and the deep biosphere beneath the oceans. The discovery of diverse microbial life in marine sediments and oceanic crusts worldwide points to a notion that subseafloor microbial ecosystems may have uniquely co-evolved with Earth's dynamics and this inevitable interrelationship has shaped environemnts for more than 3 billion years. Expanding our knowledge of the comprehensive ocean-Earth-life system through scientific ocean drilling inspires new insights into the essence of "planetary habitability"—down to the Earth’s upper mantle, which with today’s drilling technology provides the deepest yet accessible limit. The deep ocean offers windows into thick piles of ocean sediment and the Earth’s interior that has vast potentials for the development of sustainable ocean-Earth-life system in the past but also into the future, yet there is still a large insufficiency in our knowledge of the habitability extent of our own planet. Such explorations towards deep frontiers will lead us to an understanding of how and why life emerged on our planet, as well as an estimation (prediction) of the possible trajectories of life on Earth, and finally, will provide hints as to whether life persists in the other celestial bodies, and which ones are the most likely to be habitable and even inhabited.

Keywords: planetary habitability, subseafloor life, mantle drilling, deep biosphere, scientific ocean drilling

©2019. Japan Geoscience Union. All Right Reserved.

[E] Oral | B (Biogeosciences)：B-CG Complex & General

Tue. May 28, 2019 9:00 AM - 10:30 AM JST | Tue. May 28, 2019 12:00 AM - 1:30 AM UTC | 201A 2F

[B-CG06] Earth and Planetary Science Frontiers for Life and Global Environment

convener:Yoshinori Takano(Japan Agency for Marine-Earth Science and Technology (JAMSTEC)), Yohey Suzuki(Graduate School of Science, The University of Tokyo), Shingo Kato(RIKEN), Keisuke Fukushi(Institute of Nature & Environmental Technology, Kanazawa University), Chairperson:Yuki Morono(JAMSTEC), Masanori Kaneko(AIST/GSJ), Shingo Kato(RIKEN)

Earth and planetary science is currently capable of sampling from four frontiers: space, polar regions, deep ocean and deep underground for the study of the origin and evolution of life. Next generation sequencing technology of nucleic acids and nanotechnology-driven innovation of solid characterizations are very powerful to expand our understanding of many fields of earth and planetary sciences. It is also important for us to be aware of global warming and climate change that dramatically affect biodiversity, biological activities and elemental cycling. The aim of this session is to cross the border of science sections to explore the frontiers of earth and planetary science.

9:00 AM - 9:15 AM JST | 12:00 AM - 12:15 AM UTC

[BCG06-01] Earth as an open system to the Universe, and five multi-layered spheres to produce a habitable planet

*Shigenori Maruyama[1] (1.Earth-Life Science Institute, Tokyo Institute of Technology)

9:15 AM - 9:30 AM JST | 12:15 AM - 12:30 AM UTC

[BCG06-02] Holocene Antarctic subglacial weathering and ice-sheet history reconstructed using the $^{10}Be/^{9}Be$ ratios of lake Maruwan Oike sediments

*Adam David Sproson[1], Yusuke Yokoyama[1,2], Yoshinori Takano[2], Yosuke Miyairi[1], Takahiro AZE[1] (1.Atmosphere and Ocean Research Institute, The University of Tokyo, 2.Department of Biogeochemistry, Japan Agency for Marine Science and Technology)

9:30 AM - 9:45 AM JST | 12:30 AM - 12:45 AM UTC

[BCG06-03] Chemical speciation and solubility of heavy elements (lead, zinc, copper, arsenic and cadmium) in contaminated soil from Kamegai mine tailing, Toyama, Japan

*Baasansuren Gankhurel[1], Keisuke Fukushi[2], Akitoshi Akehi[1], Yoshio Takahashi[3], Kazuo Kawasaki[4] (1.Graduate School of Natural Science and Technology, Kanazawa University, 2.Instutute of Nature and Environmental Technology, Kanazawa University, 3.Department of Earth and Planetary Science, The University of Tokyo, 4.Graduate School of Science and Engineering for Research, Toyama University)

9:45 AM - 10:00 AM JST | 12:45 AM - 1:00 AM UTC

[BCG06-04] High-mass resolution molecular imaging of organic compounds on the Murchison meteorite.

★Invited Papers

*Minako Hashiguchi[1], Hiroshi Naraoka[1,2] (1.Research Center for Planetary Trace Organic Compounds, Kyushu University, 2.Department of Earth and Planetary Sciences, Kyushu University)

10:00 AM - 10:15 AM JST | 1:00 AM - 1:15 AM UTC

[BCG06-05] Fe(II) oxidation processes at the surface of bacterially colonized iron deposits

★Invited Papers

*Fumito Shiraishi[1], Kohei Nakao[1], Chizuru Takashima[2], Akihiro Kano[3], TAKAAKI ITAI[3] (1.Hiroshima University, 2.Saga University, 3.The University of Tokyo)

10:15 AM - 10:30 AM JST | 1:15 AM - 1:30 AM UTC

[BCG06-06] Heme: The distribution and dynamics of a ubiquitous iron-tetrapyrrole molecule

*Yuta Isaji[1], Yoshinori Takano[1], Nanako O. Ogawa[1], Naohiko Ohkouchi[1] (1.Japan Agency for Marine-Earth Science and Technology)

Earth as an open system to the Universe, and five multi-layered spheres to produce a habitable planet

*Shigenori Maruyama[1]

1. Earth-Life Science Institute, Tokyo Institute of Technology

<Purpose>

To understand the Earth’s history including life, we need to treat the Earth as an open system within the Universe. Such an approach has not yet fully considered. Here, I demonstrate it for the first time.

<Method>

Utilizing data set derived from geological evidences that have been collected through systematic rock sampling from all the continents over 30 years, we consider the Earth system as five multi-layered spheres, 1) atmosphere-ocean, 2) biosphere, 3) crust and upper mantle inn the framework of plate tectonics, 4) lower mantle driven by plume and superplume, and 5) metallic core to cause magnetosphere which protect the life on the surface. And this Earth system is driven by the internal heat of the solid Earth and/or the solar energy for the surface. Mutual interaction between these five spheres produce the Earth’s history including life.

<Result>

The most important key factor to keep mutual interactions between spheres is the function of plate tectonics continuing over 4.4 Gyr, which has been maintaining the Earth system as the robust systematic and dynamic equilibria. Specifically, plate tectonics has circulated carbon between atmosphere-ocean, biosphere, and crust and upper mantle through carbon fixation within sediments to produce a habitable planet. Biosphere plays another significant role as a buffer of CO_2 to stabilize atmospheric temperature within habitable status (not to evolve into Venus-like planet). However, biosphere has been critically influenced by galaxy-galaxy collisions happened at 4.5-4.0 Ga (birth of Earth and Prokaryote), 2.5-2.2Ga (birth of Eukarya), 0.8-0.5 Ga (plants and metazoans) appeared in association with frequent mass extinctions.

<Discussion>

Based on the understanding of Earth’s system and its history, we are able to extend it to our future, and predict the Earth’s history including final event of disappearance of the Earth in 8 billion years. I propose the biggest 20 events of Earth’s history including future Earth.

Keywords: Earth system, Habitable planet, The biggest 20 Earth's events

©2019. Japan Geoscience Union. All Right Reserved.

Holocene Antarctic subglacial weathering and ice-sheet history reconstructed using the $^{10}Be/^{9}Be$ ratios of lake Maruwan Oike sediments

*Adam David Sproson[1], Yusuke Yokoyama[1,2], Yoshinori Takano[2], Yosuke Miyairi[1], Takahiro AZE[1]

1. Atmosphere and Ocean Research Institute, The University of Tokyo, 2. Department of Biogeochemistry, Japan Agency for Marine Science and Technology

Glaciers play an important role in the climate system via freshwater storage and the transportation of various materials from the continents to the oceans. Enhanced discharge of the former during melting events can influence global sea-level, while enhanced silicate weathering resulting from the latter can drive a reduction in atmospheric CO_2. Although these processes are known to be important through geological time, temporal changes in chemical weathering intensity and meltwater flux for the East Antarctic Ice Sheet (EAIS) are not well understood. During the last deglaciation, the EAIS retreated significantly (*1, 2*), forming isolated basins via glacio-hydro-isostatic adjustment (GIA) related crustal uplift. Sediment accumulated in these lakes provide a unique record of subglacial weathering and ice-sheet history throughout deglaciations when global temperatures and pCO_2most notably rose.

Meteoric ^{10}Be is produced in the atmosphere by cosmic rays and delivered to the Earth and ocean surface via dust and precipitation. In Antarctica, these sources of ^{10}Be become locked up in ice sheets and are subsequently released to the continental shelf during periods of melting and freshwater discharge (*3*), where they adhere to suspended particles in the water column and subsequently accumulate on the basin floor (*4, 5*). Stable ^{9}Be is present in silicate rocks and is released during subglacial weathering (*5*), with little simultaneous release of ^{10}Be (*4*), and transported to the oceans via meltwater outflow. When Be is incorporated into the authigenic phase of marine sediments, the $^{10}Be/^{9}Be$ reflects that of the overlying water column (*6*), which in turn reflects the relative dominance of freshwater flux and/or subglacial weathering.

Here, we present authigenic $^{10}Be/^{9}Be$ ratios for a sedimentary core from Lake Maruwan Oike situated at the head of the Rundvåg glacier in the Lützow-Holm Bay area of East Antarctica. Sedimentary material from L. Maruwan Oike provides an ~6,000 year record of subglacial weathering and nutrient input from the nearby glacier (*7*). Authigenic $^{10}Be/^{9}Be$ records reflect variations in freshwater flux and subglacial weathering and indicate several periods of enhanced melting of the Rundvåg glacier. This study provides further constraints on EAIS fluctuations during the Holocene and offers an insight into the behaviour of beryllium in high-latitude subglacial-marine systems.

Reference

1. M. Yamane*et al.*, The last deglacial history of Lützow-Holm Bay, East Antarctica. *Journal of Quaternary Science* **26**, 3-6 (2011).
2. A. N. Mackintosh*et al.*, Retreat history of the East Antarctic Ice Sheet since the Last Glacial Maximum. *Quaternary Science Reviews* **100**, 10-30 (2014).
3. Q. Simon*et al.*, Authigenic 10Be/9Be ratios and 10Be-fluxes (230Thxs-normalized) in central Baffin Bay sediments during the last glacial cycle: Paleoenvironmental implications. *Quaternary Science Reviews* **140**, 142-162 (2016).
4. R. P. Scherer*et al.*, Pleistocene Collapse of the West Antarctic Ice Sheet. *Science* **281**, 82 (1998).

©2019. Japan Geoscience Union. All Right Reserved.

5. C. Sjunneskog, R. Scherer, A. Aldahan, G. Possnert, 10Be in glacial marine sediment of the Ross Sea, Antarctica, a potential tracer of depositional environment and sediment chronology. *Nuclear Instruments and Methods in Physics Research Section B: Beam Interactions with Materials and Atoms* **259**, 576-583 (2007).
6. F. von Blanckenburg, J. Bouchez, River fluxes to the sea from the ocean’s 10Be/9Be ratio. *Earth and Planetary Science Letters* **387**, 34-43 (2014).
7. Y. Takano, H. Kojima, E. Takeda, Y. Yokoyama, M. Fukui, Biogeochemistry and limnology in Antarctic subglacial weathering: molecular evidence of the linkage between subglacial silica input and primary producers in a perennially ice-covered lake. *Progress in Earth and Planetary Science* **2**, 8 (2015).

Keywords: Beryllium, Holocene, Antarctica, Weathering, Glacier

©2019. Japan Geoscience Union. All Right Reserved.

Chemical speciation and solubility of heavy elements (lead, zinc, copper, arsenic and cadmium) in contaminated soil from Kamegai mine tailing, Toyama, Japan

*Baasansuren Gankhurel[1], Keisuke Fukushi[2], Akitoshi Akehi[1], Yoshio Takahashi[3], Kazuo Kawasaki[4]

1. Graduate School of Natural Science and Technology, Kanazawa University, 2. Instutute of Nature and Environmental Technology, Kanazawa University, 3. Department of Earth and Planetary Science, The University of Tokyo, 4. Graduate School of Science and Engineering for Research, Toyama University

Heavy metals such as lead, zinc, copper, arsenic and cadmium are usually found in surface soils affected by mining or smelting activities, agricultural practices and industrial areas [1,2,3]. Hara et al., [4] showed that some heavy metals including lead, arsenic and cadmium in soil surrounding the mine tailing area in Toyama Prefecture, Japan has largely exceeded the environmental standards. The total amount of trace metals in soils is generally not sufficient to assess environmental impacts of metal contamination. Therefore, chemical forms and binding types of metals enables evaluation of their behavior and bioavailability in the soil environment.The objectives of the present study were to understand the chemical speciation of As, Zn, Cu, Pb and Cd from Kamegai mine tailing area by means of sequential extraction procedure combined with synchrotron based XAFS and electron microscope.

Thirty-two soil samples were analyzed, determining the chemical fractionation of Pb, Cd, As, Zn and Cu using by the five-step sequential extraction (SEP), X-ray absorption fine structure (XAFS), X- ray diffractometer (XRD) and scanning electron microscopy. The results of SEP showed that most of the Pb was associated with non-residual fractions, mainly in crystalline iron oxides (goethite). The Cd appeared mainly associated carbonate fraction in the roots of the dried plants in the soils. The XAFS spectra of the samples showed that Pb in the soil are adsorption forms with Fe-(hydr)oxides surface. Results of XAFS analysis showed Cd in the samples are $CdCO_3$, coprecipitated with $CaCO_3$. Zn, Cu and As appeared mainly associated with the amorphous and crystalline iron oxides. Heavy metals associated with carbonates, amorphous and crystalline iron oxides, thus being potentially more mobile to the environment if conditions were more acidic or reducing.

[1] Kaasalainen, M, and Markku Y. 2003. *Environmental Pollution*126(2): 225–33. [2] Nannoni et al. 2011. *Geoderma*161(1–2): 63–73. [3] Sterckeman et al. 2000. *Environmental pollution*107(3): 377–89. [4] Junko et al. 2014. 3(7): 193–96.

Keywords: soil, heavy metals, speciation

©2019. Japan Geoscience Union. All Right Reserved.

High-mass resolution molecular imaging of organic compounds on the Murchison meteorite.

*Minako Hashiguchi[1], Hiroshi Naraoka[1,2]

1. Research Center for Planetary Trace Organic Compounds, Kyushu University, 2. Department of Earth and Planetary Sciences, Kyushu University

Introduction: Primitive meteorites contain a wide variety of organic molecules. The CHO, CHNO, CHNOS and CHN species have been identified using high-resolution mass spectroscopy for the solvent extracts of carboneceous chondrites [1-3]. These organic compounds could be synthesized and evolved via interaction of fluid with minerals [3-5]. Therefore, spatial distribution of meteoritic organic compounds is important to reveal the organic-mineral association on the parent bodies. Recently, in-situ analysis of polar organic compounds on the meteorite surface was achieved by desorption electrospray ionization/high-resolution mass spectrometry (DESI/HRMS) [7]. In this study, we further performed the DESI-HRMS imaging on the Murchison meteorite to understand the relationship between spatial distribution of polar organic compounds and minerals.

Experimental: The fragment of the Murchison meteorite (CM2) (~ a few mm) obtained by chipping was embedded in indium (In). The DESI-HRMS imaging was performed using a DESI ion source (Omni Spray 2-D, Presolia) equipped with an Orbitrap mass spectrometer (Q-Exactive Plus, Thermo Scientific) with mass resolution of ~140,000 at *m/z* 200. Methanol (LC-MS grade) was sprayed on the sample surface with a 1 or 2 μl/min flow rate. The spatial resolution was approximately 100 μm. FESEM-EDS analysis was also carried out without coating and polishing after the DESI-HRMS imaging. The surface of the Murchison meteorite fragment embedded in indium was also extracted with MeOH, and the resulting solution was applied for HPLC-HRMS to obtain chemical structural information on the organic compounds.

Results and Discussion: Alkylated homologues of $C_nH_{2n-1}N_2^+$ (n = 7–9) and $C_nH_{2n}NO^+$ (n = 9–14) were detected on the sample surface by the DESI-HRMS imaging. HPLC/HRMS analysis of MeOH extracts from the sample surface after the DESI/HRMS imaging indicated that the $C_nH_{2n-1}N_2^+$ homologues correspond to alkylimidazole, and that a few structural isomers of the $C_nH_{2n}NO^+$ homologues were present in the sample.The alkylimidazoles and $C_nH_{2n}NO^+$ homologues displayed different spatial distributions in the Murchison fragment. Moreover, the distribution pattern of compounds also different among the same homologues. These results may be due to the separation of isomers by similar chromatographic effects, or different synthetic pathways. The alkylimidazoles and $C_nH_{2n}NO^+$ homologues are mainly distributed in the matrix region of the Murchison by mineralogical observations, which is consistent with previous reports. Altered minerals (e.g., Fe-oxide, Fe-sulfide, and carbonates) occurred in this region. However, no clear relationship was found between these minerals and the organic compounds detected by DESI/HRMS imaging. Although this result might be due to scale differences between the spatial resolution of DESI-HRMS imaging and the grain size in the matrix of the Murchison, our results would indicate that alkylimidazoles and the $C_nH_{2n}NO^+$ homologues in the Murchison fragment were mainly synthesized by different processes from hydrothermal alteration on the parent body.

References: [1] Schmitt-Kopplin P. *et al.* 2010. *PNAS*, 107:2763. [2] Yamashita Y. and Naraoka H. 2014. *Geochem. J*, 48: 519. [3] Naraoka et al. 2017. *ACS,* 1, 540–550. [5] Le Guillou C. and Brearley A. 2014. *GCA*, 131, 344-367. Ito M. *et al.* 2016, *Goldschmidt Conference*, 2016. #1297. [6] Takáts Z. *et al.* 2004. *Science*, 306: 471. [7] Naraoka H. and Hashiguchi M. 2018. Rapid Commun Mass Spectrom. 32:959.

©2019. Japan Geoscience Union. All Right Reserved.

Keywords: Carbonaceous chondrite, Molecular imaging of organic compounds

©2019. Japan Geoscience Union. All Right Reserved.

Fe(II) oxidation processes at the surface of bacterially colonized iron deposits

*Fumito Shiraishi[1], Kohei Nakao[1], Chizuru Takashima[2], Akihiro Kano[3], TAKAAKI ITAI[3]

1. Hiroshima University, 2. Saga University, 3. The University of Tokyo

Fe(II) oxidation processes at the surfaces of bacterially colonized iron deposits are examined at three hot springs in Japan for which the chemical profiles of the pH, redox, and O_2 and Fe(II) concentrations at the water/deposit interface are measured via microelectrodes. The three hot springs share similar bulk chemistry with a weakly acidic pH of 5.7–6.3, a high iron concentration of 50–130 μM, and a high dissolved inorganic carbon concentration of 20–60 mM. At the Sambe and Shionoha hot springs where the bulk water O_2 concentration is ca. 80 μM, abiotic Fe(II) oxidation via autocatalysis prevails. At the Okuoku-hachikurou hot spring where the bulk water O_2 concentration is ca. 50 μM, autocatalytic Fe(II) oxidation is suppressed and biotic Fe(II) oxidation induced by cyanobacterial photosynthesis is effective. These observations indicate that an O_2 concentration of ca. 50 μM is the threshold of reversing the relative contribution of biotic and abiotic Fe(II) oxidation. Protons from Fe(II) oxidation are compensated by reactions among the dissolved inorganic carbon species, which sustain the pH condition and continuous Fe(II) oxidation at the deposit surface. The observations of this study provide implications for understanding the deposition of banded iron formations in the geological past.

©2019. Japan Geoscience Union. All Right Reserved.

Heme: The distribution and dynamics of a ubiquitous iron-tetrapyrrole molecule

*Yuta Isaji[1], Yoshinori Takano[1], Nanako O. Ogawa[1], Naohiko Ohkouchi[1]

1. Japan Agency for Marine-Earth Science and Technology

Hemes are Fe(II)-tetrapyrrole complexes that catalyze various electron transfer and redox reactions. They are essential for biological systems, and are possessed by all life forms. Because heme-iron represents as much as 40% of the iron pool in phytoplankton (Gledhill, 2007), hemes in the biomass likely comprise a major fraction in the bioavailable-iron pool which limits primary productivity in over 30% of the world oceans (Moore et al., 2013). They are also expected to be found in the sediments, either as allochthonous compounds deposited from the water column or synthesized in situ by the benthic and subsurface microorganisms. It is noteworthy that etioporphyrin III preserved in various sedimentary rocks, which is supposedly derived from heme, has a highly distinct carbon and nitrogen isotopic compositions ($\delta^{13}C$, $\delta^{15}N$) with respect to other chlorophyll-derived porphyrins in Cretaceous black shales (Ohkouchi et al., unpub. results). As such, hemes are ubiquitous in any environment where life exists, but little is known on their distribution and dynamics in natural environments.

Here, we established a new analytical method to quantify, isolate, and purify heme *b*, a major homolog of hemes, from various environmental samples. Detection of picomole levels of heme *b* is achieved with a photodiode-array detector connected to HPLC, which covers the heme *b* concentration range in particulate (> 0.7 μm; 0.15 nmol L^{-1}) and dissolved organic matter (> 3000 Da; ~0.006 nmol L^{-1}) in the coastal seawater of Tokyo Bay, as well as that in the surface sediments of the Japan Sea (~0.03 μg g^{-1} dry weight). Importantly, concentration of heme *b* in the dissolved phase was contrastingly low with respect to that in the particulate phase of the coastal seawater, which imply that hemes may constitute a major fraction of the regenerated iron in the ocean. The $\delta^{13}C$ and $\delta^{15}N$ values of heme *b* isolated and purified from various environmental samples are determined with our modified EA/IRMS (Ogawa et al., 2010). These isotopic values will be compared with those of chlorophylls and amino acids, which will reveal the sources of hemes in natural environments and the isotopic fractionation associated with their biosynthesis. Our new analytical approach will provide first detailed insights into the ubiquitous iron-tetrapyrrole molecule playing an essential role in biogeochemical cycle.

Keywords: Heme, Iron cycle, Carbon and nitrogen isotopes, HPLC

©2019. Japan Geoscience Union. All Right Reserved.

[E] Oral | B (Biogeosciences)：B-CG Complex & General

Tue. May 28, 2019 10:45 AM - 12:15 PM JST | Tue. May 28, 2019 1:45 AM - 3:15 AM UTC | 201A 2F

[B-CG06] Earth and Planetary Science Frontiers for Life and Global Environment

convener:Yoshinori Takano(Japan Agency for Marine-Earth Science and Technology (JAMSTEC)), Yohey Suzuki(Graduate School of Science, The University of Tokyo), Shingo Kato(RIKEN), Keisuke Fukushi(Institute of Nature & Environmental Technology, Kanazawa University), Chairperson:Yoshinori Takano(JAMSTEC), Keisuke Fukushi, Yohey Suzuki(Univ. Tokyo)

Earth and planetary science is currently capable of sampling from four frontiers: space, polar regions, deep ocean and deep underground for the study of the origin and evolution of life. Next generation sequencing technology of nucleic acids and nanotechnology-driven innovation of solid characterizations are very powerful to expand our understanding of many fields of earth and planetary sciences. It is also important for us to be aware of global warming and climate change that dramatically affect biodiversity, biological activities and elemental cycling. The aim of this session is to cross the border of science sections to explore the frontiers of earth and planetary science.

10:45 AM - 11:00 AM JST | 1:45 AM - 2:00 AM UTC

[BCG06-07] Diversity and evolution of biosynthetic enzymes for chlorophyll pigments

★Invited Papers

*Yusuke Tsukatani[1] (1.Japan Agency for Marine-Earth Science and Technology (JAMSTEC))

11:00 AM - 11:20 AM JST | 2:00 AM - 2:20 AM UTC

[BCG06-08] **Microdolomites are not MDACs: microbially-derived carbon source for microcrystalline dolomite found within massive gas hydrates and implications for the shallow marine carbon cycle**

★Invited Papers

*Glen Snyder[1], Ryo Matsumoto[1], Naizhong Zhang[1], Yoshihiro Kakizaki[2], Yohey Suzuki[2], Yuji Sano[3], Naoto Takahata[3], Kentaro Tanaka[3], Takumi Imajo[5], Stephen Bowden[4] (1.Gas Hydrate Research Laboratory, Meiji University, 2.University of Tokyo, 3.AORI, University of Tokyo, 4.University of Aberdeen, Scotland, 5.Tokyo University of Marine Science and Technology)

11:20 AM - 11:35 AM JST | 2:20 AM - 2:35 AM UTC

[BCG06-09] **Discriminative biogeochemical signatures of methanotrophs inhabiting different chemosynthetic fields in an active mud volcano of the Canadian Beaufort Sea**

*Dong-Hun Lee[1], Yung Mi Lee[2], Jung-Hyun Kim[2], Young Keun Jin[2], Charles Paull[3], Helge Niemann[4,5], Ji-Hoon Kim[6], Kyung-Hoon Shin[1] (1.Hanyang Univ., 2.KOPRI, 3.MBARI, 4.NIOZ and Utrecht Univ., 5.CAGE, UiT , 6.KIGAM)

11:35 AM - 11:50 AM JST | 2:35 AM - 2:50 AM UTC

[BCG06-10] Determination of the absolute stereochemistry of the hydroxyl group in 2-hydroxyarchaeol, the main lipid core of methanogenic and methanotrophic archaea

*Noriaki YAMAUCHI[1], Masanori Kaneko[2] (1.Department of Earth and Planetary Sciences, Faculty of Sciences, Kyushu University, 2.National Institute of Advanced Industrial Science and Technology)

11:50 AM - 12:10 PM JST | 2:50 AM - 3:10 AM UTC

[BCG06-11] Mineral-Microbe interaction – Identification of extracellular electron transfer mechanisms by using MetaOmics approach

★Invited Papers

*Shunichi Ishii[1], Shino Suzuki[1], Kenneth H Nealson[2] (1.Japan Agency for Marine-Earth Science and Technology (JAMSTEC), 2.University of Southern California)

12:10 PM - 12:15 PM JST | 3:10 AM - 3:15 AM UTC

[BCG06-12] Interactive discussion with the invited speakers

*Yoshinori Takano[1] (1.Japan Agency for Marine-Earth Science and Technology (JAMSTEC))

Diversity and evolution of biosynthetic enzymes for chlorophyll pigments

*Yusuke Tsukatani[1]

1. Japan Agency for Marine-Earth Science and Technology (JAMSTEC)

Photosynthesis is the process converting light energy to chemical potential energy. In phototrophic organisms, chlorophyll (Chl) and bacteriochlorophyll (BChl) pigments are essential for harvesting light energy, migrating excited energy, and transferring electrons. How photosynthesis is emerged on early earth is enigmatic, but pigments are theoretically required first in the ancient phototrophs to absorb light and start photo-induced reactions. A classic question on the evolution of pigment biosynthesis is whether Chl was evolved first or BChl first? Chl molecules mainly absorb visible light wavelength, whereas BChls absorb longer wavelength including near-infrared light region. Therefore, to know which pigment is first evolved is important to know atmospheric environment on early earth. The steps diverging to Chl or BChl in pigment biosynthetic pathways are catalyzed by enzymes similar to nitrogenase. One of the nitrogenase-like enzymes is chlorophyllide oxidoreductase which also catalyzes branching steps toward BChl-*a* and BChl-*b*. BChl-*b* absorbs longest light wavelength among naturally occurring pigments. In my talk, pigment structures and their diversified biosynthetic pathways that we recently revealed will be introduced and experimental approach to solve the evolution of chlorophyllous pigments will be presented.

Keywords: Evolution of photosynthesis, Pigment, Bacteriochlorophyll, Chlorophyll

©2019. Japan Geoscience Union. All Right Reserved.

Microdolomites are not MDACs: microbially-derived carbon source for microcrystalline dolomite found within massive gas hydrates and implications for the shallow marine carbon cycle

*Glen Snyder[1], Ryo Matsumoto[1], Naizhong Zhang[1], Yoshihiro Kakizaki[2], Yohey Suzuki[2], Yuji Sano[3], Naoto Takahata[3], Kentaro Tanaka[3], Takumi Imajo[5], Stephen Bowden[4]

1. Gas Hydrate Research Laboratory, Meiji University, 2. University of Tokyo, 3. AORI, University of Tokyo, 4. University of Aberdeen, Scotland, 5. Tokyo University of Marine Science and Technology

Methane derived authigenic carbonates (MDACs) are commonly found associated with both active and remnant submarine seeps and, under favorable conditions of pressure and temperature, are also found in close contact with marine methane hydrate. Recently, we have discovered microdolomitic aggregates inside of massive Japan Sea gas hydrates. These are fundamentally different, both in chemistry, stable isotopic composition and growth habit to the MDACs encountered outside of the hydrates. Phylogenetic analysis of microbial DNA within the dolomites reveals primarily Bacteriodetes, bacteria whose principal energy source is the degradation of complex macromolecules such as oils. Actual analysis of the oils found inside of the Sea of Japan gas hydrate confirms that they are biodegraded during burial. Previous investigations of MDACs have focused on ANME methane oxidizers (ANME) and sulfate reducing bacteria (SRB) as the primary drivers for MDAC precipitation in shallow sediment. The discovery of microbial dolomites inside saline gas-hydrate inclusions opens up a number of research avenues and applications such as: Mars-analogue studies, microbial remediation of marine oil-spills, and investigations into the role of shallow marine microbes in the conversion of organic carbon into dissolved inorganic carbon. This study was conducted under the commission from AIST as part of the methane hydrate research project funded by the Ministry of Economy, Trade and Industry, Japan. Ongoing work is being carried out thanks to a Grant-in-aid provided by the Japan Society for Promotion of Science and the Japanese Ministry of Education, Culture, Sports, and Technology (Kaken Project # 17K05712).

Keywords: Gas Hydrate, Sea of Japan, Dolomite, Biomineralization

©2019. Japan Geoscience Union. All Right Reserved.

Discriminative biogeochemical signatures of methanotrophs inhabiting different chemosynthetic fields in an active mud volcano of the Canadian Beaufort Sea

*Dong-Hun Lee[1], Yung Mi Lee[2], Jung-Hyun Kim[2], Young Keun Jin[2], Charles Paull[3], Helge Niemann[4,5], Ji-Hoon Kim[6], Kyung-Hoon Shin[1]

1. Hanyang Univ., 2. KOPRI, 3. MBARI, 4. NIOZ and Utrecht Univ., 5. CAGE, UiT , 6. KIGAM

In this study, we investigated vertical variations in methanotrophic communities in assosication with varying methane fluxes within a mud volcano (420 m water depth, MV420) of the Canadian Beaufort Sea, by analysing geochemical properties, microbial lipids, and nucleic acid signatures. Three push cores were collected from visually discriminative chemosynthetic fields that were (i) bare of organisms (BO) to the naked eye, (ii) covered with bacterial mats (BM), or (iii) siboglinid tubeworms (ST), by using a remotely operated vehicle (ROV). The methane fluxes were highest at the sites of BO (0.06 mmol cm^{-2} y^{-1}) and BM (0.04 mmol cm^{-2} y^{-1}) and substantially lower at the ST site (0.01 mmol cm^{-2} y^{-1}). All MV420 sites showed the presence of aerobic methane oxidation (MOx)- and anaerobic methane oxidation (AOM)-related lipid biomarkers (4-methyl sterols and *sn*-2-hydroxyarchaeol, respectively), which were distinctly different in comparison to the reference site where these compounds could not be detected. Our lipid biomarker results are furthermore in good agreement with 16S rRNA analyses, which revealed the presence of MOx-related bacteria (*Methlyococcales*) and AOM-related archaea (ANME-2 and ANME-3 groups) at the MV420 sites. The 4-methyl sterols derived from *Methlyococcales* were predominant in the surface layer at the BM site with a moderate methane flux, while their occurrence was limited at the BO and ST sites. Notably, the abundances of AOM-related lipid biomarkers were minor at the BO site where the methane flux was highest. However, ANME-3 and sulfate reducing bacteria (*Desulfobacteraceae* and *Desulfobulbaceae*) were abundant in the downcore sediments at the BM site. On the other hand, the abundances of the ^{13}C-depleted *sn*-2-hydroxyarchaeol potentially derived from ANME-2 and/or ANME-3 groups was predominant at the ST site, indicating their co-occurrence under a lower methane flux. Accordingly, our results suggest that a niche diversification within this MV system has shaped distinct methanotrophic communities due to the availability of electron acceptors in association with varying degree of methane fluxes and bioirrigation activity.

Keywords: Arctic, Mud volcano, chemosynthetic organism, Anaerobic methane oxidation, Aerobic methane oxidation, Methanotroph

©2019. Japan Geoscience Union. All Right Reserved.

Determination of the absolute stereochemistry of the hydroxyl group in 2-hydroxyarchaeol, the main lipid core of methanogenic and methanotrophic archaea

*Noriaki YAMAUCHI[1], Masanori Kaneko[2]

1. Department of Earth and Planetary Sciences, Faculty of Sciences, Kyushu University, 2. National Institute of Advanced Industrial Science and Technology

One of the major characteristics of archaea is the lipid core which consist of saturated isoprenoid chain and glycerol with ether bond formation. Furthermore, main lipid core of methanogenic and methanotrophic archaea is hydroxyarchaeol. The saturated isoprenoid is altered to the isoprenoid which has one hydroxyl group in the C-3 of the isoprenoid. Two regioisomeric structures, *sn*-2- and *sn* -3-hydroxyarchaeol (**1**and **2**), are existed depending on the position of the hydroxylated isoprenoid bonding to glycerol.. The distribution of the two isomer is species-dependent [1].
2-Hydroxyarchaeol (**1**) is an important biomarker indicating accumulation of methane hydrate under the seafloor, anoxic oxidation of methane, methane formation at the lake, marsh, and digestive tract of ruminant. Structure determination [1] and analysis of hydroxyarchaeol from the field samples were performed by many researchers [2][3][4], however, the absolute stereochemistry of the hydroxyl group in the ether chain, the most characteristic feature of the molecule had not been determined so far.
The previous study of the author (NY), the synthetic preparation of 2-hydroxyarchaeol equivalent by “racemic” hydroxyl groups revealed that the “racemic” 2-hydroxyarchaeols behave as two equal amounts of the compounds because of the stereochemistry of the hydroxyl group. The result was different from several analysis of field samples which descrived the 2-hydroxylarchaeol as a single compound [5].
For the determination of the stereochemistry of the hydroxyl group of 2-hydroxyarchaeol, asymmetric synthesis of the hydroxyl-group containing ether chain part was conducted and the two stereoisomers of 2-hydroxyarchaol were synthesized.
The stereochemistry of this hydroxyl group was derived from the Katsuki-Shapless epoxidation of phytol. The two isomers were regioselectivity converted to the 2-hydroxyarchaol. The analyses of “racemic” 2-hydroxylarchaeol, two isomers of synthetic 2-hydroxyarchaeol stereoisomer (**3** and **4**), and 2-hydroxyarchaeol from the lipid of *Methanosarcina barkeri* revealed the absolute stereochemistry of the aforementioned hydroxy group is 3*R* (compound **3**). The comparison of the ^{13}C NMR of synthetic 2-hydroxyarchaeol stereoisomer (**3** and **4**), and 2-hydroxyarchaeol from the methanogen culture showed slight difference because of the stereochemistry of methyl group of saturated hydrocarbon of the synthetic isomers. This result may suggest the stereochemistry of methyl group is influenced at the nature of hydroxyarchaeol-containing lipid.
[1] Sprott et al.,J Biol Chem(1990) 265: 13735.
[2] Hinrichs et al., Nature (1999) 398:802.
[3] Blumenberg et al., Science (2004) 101, 11111.
[4] Stadnitskaia et al., Org Geochem (2008) 39:1007.
[5] Yamauchi Res Org Geochem (2014) 30:33.

Keywords: methanogenic archaea, methanotrophic archaea, archaeol, structural determination

©2019. Japan Geoscience Union. All Right Reserved.

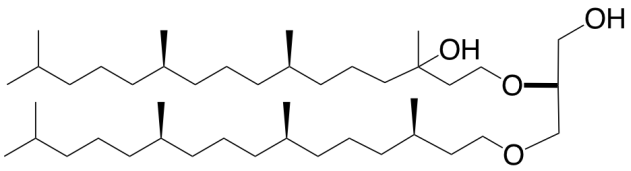

1

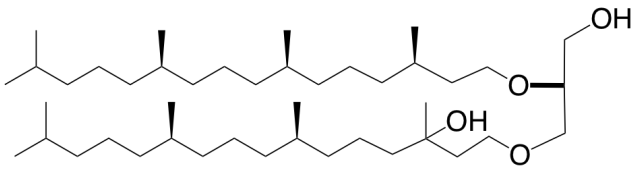

2

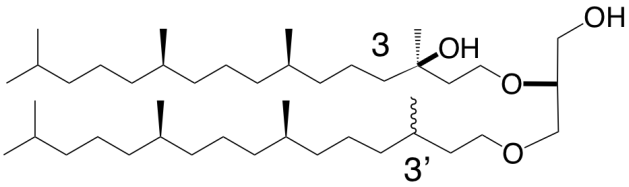

3

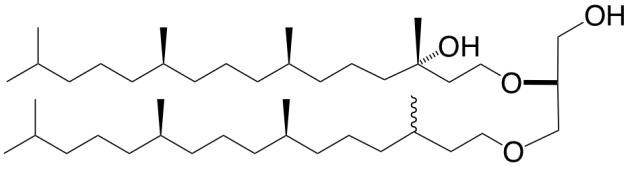

4

©2019. Japan Geoscience Union. All Right Reserved.

Mineral-Microbe interaction –Identification of extracellular electron transfer mechanisms by using MetaOmics approach

*Shunichi Ishii[1], Shino Suzuki[1], Kenneth H Nealson[2]

1. Japan Agency for Marine-Earth Science and Technology (JAMSTEC), 2. University of Southern California

Microbial reduction of solid minerals such as iron-oxides and manganese-oxides is known to occur as a result of microbial extracellular electron transfer (EET). These electron transfer activities coupled with the oxidation of organic carbon or hydrogen are considered to play important roles within complex microbial communities in soil, sediment, and the deep subsurface environments. The surface redox potentials of solid-phase oxide minerals are known to be highly variable because of variations in the crystal structure, pH, salinity, and levels of hydration, posing major challenges for EET-capable microbes to adapt in the habitats. In fact, the *in situ* redox potentials of solid-state electron acceptors have been regarded as significant geochemical variables linked to the regulation of functional genes in the EET-capable microbes. However, mechanisms that the microbes use to perform respiration of insoluble metal-oxide minerals showing different surface redox potentials are complex and are not yet well understood.

Here, we used bioelectrochemical systems to systematically evaluate the effects of surface redox potentials (e.g. +100 mV, −50 mV, −200 mV vs SHE) on EET-active microbial community development and the overall electron transfer rates. The results clearly indicate that faster biocatalytic rates were observed under electropositive electrode surface potentials than the electronegative potentials. Temporal 16S rRNA-based microbial community analyses showed that *Geobacter* phylotypes were highly diverse and apparently dependent on the surface potentials. The well-known dissimilatory metal-reducing microbes affiliated with *Geobacter metallireducens* clade were associated with lower surface potentials and less current generation, whereas *Geobacter* subsurface clades were associated with higher surface potentials and greater current generation. These results suggest that surface potentials provide a strong selective pressure, at the species and strain level, for solid mineral respirators throughout the EET-active community development.

Next, we show metabolic and transcriptional responses of the EET-active microbial communities established on the three different poised electrodes to changes in the surface redox potentials. Combination of genome-centric stimulus-induced metatranscriptomics and metabolic pathway investigation revealed that nine *Geobacter* / *Pelobacter* microbes performed EET activity differently according to their preferable surface potentials and substrates. While the *Geobacter* / *Pelobacter* microbes coded numerous numbers of multi-heme *c*-type cytochromes and conductive e-pili, wide variations in gene expression were seen in response to altering surrounding substrates and surface potentials, accelerating EET via poised electrode or limiting EET via an open circuit system. These flexible responses suggest that a wide variety of EET-active microbes utilizing diverse EET mechanisms may work together to provide such EET-active communities with an impressive ability to handle major changes in surface potential and carbon source availability.

Conclusively, these results presented here offer a new perspective on the complexity of the EET-active members in the microbial communities that were adapted to the different surface redox conditions, and some initial insights into how they may regulate community function and provide adaptability to the different minerals on the earth. Overall, these results have opened a door toward unraveling the diverse microbial life within the various geological settings especially in the mineral-rich subsurface environments.

©2019. Japan Geoscience Union. All Right Reserved.

Keywords: Metatranscriptomics, Electromicrobiology, Redox potential

©2019. Japan Geoscience Union. All Right Reserved.

Interactive discussion with the invited speakers

*Yoshinori Takano[1]

1. Japan Agency for Marine-Earth Science and Technology (JAMSTEC)

Time for interactive discussion with the invited speakers.

©2019. Japan Geoscience Union. All Right Reserved.

[E] Poster | B (Biogeosciences)：B-CG Complex & General

Tue. May 28, 2019 3:30 PM - 5:00 PM JST | Tue. May 28, 2019 6:30 AM - 8:00 AM UTC | Poster Hall International Exhibition Hall8, Makuhari Messe_22

[B-CG06] Earth and Planetary Science Frontiers for Life and Global Environment

convener:Yoshinori Takano(Japan Agency for Marine-Earth Science and Technology (JAMSTEC)), Yohey Suzuki(Graduate School of Science, The University of Tokyo), Shingo Kato(RIKEN), Keisuke Fukushi(Institute of Nature & Environmental Technology, Kanazawa University)

Earth and planetary science is currently capable of sampling from four frontiers: space, polar regions, deep ocean and deep underground for the study of the origin and evolution of life. Next generation sequencing technology of nucleic acids and nanotechnology-driven innovation of solid characterizations are very powerful to expand our understanding of many fields of earth and planetary sciences. It is also important for us to be aware of global warming and climate change that dramatically affect biodiversity, biological activities and elemental cycling. The aim of this session is to cross the border of science sections to explore the frontiers of earth and planetary science.

[BCG06-P01] Dynamisms and characteristics of dissolved organic matter (DOM) in deep aquifer: A scope for deep biosphere

*Atsushi Urai[1,2], Yoshinori Takano[2], Naohiko Ohkouchi[2] (1.Department of Science and Technology, Graduate School of Medicine, Science and Technology, Shinshu University, 2.Department of Biogeochemistry, Japan Agency for Marine-Earth Science and Technology)

[BCG06-P02] Correlations of magnetosome-related genes in Nitrospirae genomes to magnetosome geometry and redox stratification in deep-sea environments

*Shinsaku Nakano[1], Shingo Kato[2], Mariko Kouduka[1], Toshitsugu Yamazaki[3], Yohey Suzuki[1] (1.Graduate School of Science, The University of Tokyo, 2.RIKEN, 3.Atmosphere and Ocean Research Institute, The University of Tokyo)

[BCG06-P03] Reconstruction of key ecological responses leading to the most recent dead zone formations in Japan Sea through ancient DNA metabarcodring

*Mariko Kouduka[1], Yohey Suzuki[1] (1.Department of Earth and Planetary Science, The University of Tokyo, 7-3-1 Hongo, Bunkyo-ku, Tokyo, Japan.)

[BCG06-P04] Search for microbial CH_4 production processes in lake sediments and surface water associated with cyanobacterial bloom

*Makoto Matsushita[1], Yoshinori Takano[1], Hiroyuki Imachi[1], Atsushi Urai[2], Ho-Dong Park[3], Hiroki Iwata[3], Naohiko Ohkouchi[1] (1.Japan Agency for Marine-Earth Science and Technology, 2.Department of Science and Technology, Graduate School of Medicine, Science and Technology, Shinshu University, 3.Department of Environmental Sciences, Faculty of Science, Shinshu University)

[BCG06-P05] Did life emerge in a deep-sea metal sulfide chimney? New insights from an archaeal genome and a nanoscale microbe-silicate assemblage

*Hinako Takamiya[1], Hiroki Mukai[2], Mariko Kouduka[1], Shingo Kato[4], Motoo Ito[3], Yohey Suzuki[1] (1.Earth and Planetary Science Graduate School of Science, The University of Tokyo , 2.National Institute of Advanced Industrial Science and Technology, 3.Kochi Institute for Core Sample Research JAMSTEC, 4.RIKEN)

[BCG06-P06] X-ray computed nano-tomography for visualizing microbial cells and their surrounding environments

*Yuki Morono[1], Go-Ichiro Uramoto[2,1], Kentaro Uesugi[3], Nobuhisa Takeuchi[3], Masayuki Uesugi[3], Kengo Kubota[4], Tatsuhiko Hoshino[1], Fumio Inagaki[1] (1.Japan Agency for Marine-Earth Science and Technology, 2.Kochi University, 3.Japan Synchrotron Radiation Research Institute, 4.Tohoku University)

[BCG06-P07] **Carbon signatures in amino acids during deep-sea anoxic methanotrophy**

*Yoshinori Takano[1] (1.Japan Agency for Marine-Earth Science and Technology (JAMSTEC))

Dynamisms and characteristics of dissolved organic matter (DOM) in deep aquifer: A scope for deep biosphere

*Atsushi Urai[1,2], Yoshinori Takano[2], Naohiko Ohkouchi[2]

1. Department of Science and Technology, Graduate School of Medicine, Science and Technology, Shinshu University, 2. Department of Biogeochemistry, Japan Agency for Marine-Earth Science and Technology

Dissolved organic matter (DOM) is generally derived from multiple sources and affected by complicated transformation and degradation reactions. In a general geochemical description of marine environments, high-molecular-weight DOM (HMW-DOM; >1 kDa) particularly represents a unique organic carbon pool, which is accompanied by considerable difference in the molecular and stable isotopic compositions from other organic components such as particulate organic matter (POM) and low-molecular-weight DOM (LMW-DOM; <1 kDa) (e.g., Benner et al., 1997).

To date, formation of DOM fraction and potential microbial interaction in deep aquifer have been particularly poorly understood on the context of prokaryotic ecology. We investigated the molecular composition of DOM fraction including LMW and HMW by an improved method (Urai et al., 2018). The filtered samples are tentatively defined by conventional size scales; macromolecular scale (100 mm >> 40 mm), POM (40 mm >> 0.6 mm), HMW-DOM(0.6 mm>>1kDa), and total-DOM (<0.6 mm). We also have a validation to distinguish the molecular signature between phototrophic primary producers (i.e., fossil molecules) and presently living benthic prokaryotes (i.e., modern molecules; cf. biological methanogenesis, Kaneko et al., 2014). We report a preliminary result of the feasibility study and discuss a perspective from the view of deep biosphere.

References:

Benner et al. Abundance, size distribution, and stable carbon and nitrogen isotopic compositions of marine organic matter isolated by tangential-flow ultrafiltration. Marine Chemistry 57, 243-263 (1997).

Kaneko et al. Quantitative analysis of coenzyme F430 in environmental samples: a new diagnostic tool for methanogenesis and anaerobic methane oxidation. Analytical Chemistry 86, 3633-3638 (2014).

Urai et al. Algal-derived 24-ethylcholesta-5, 22-dien-3β-ol (stigmasterol) is frequently found in high-molecular-weight dissolved organic matter (HMW-DOM) during summer in freshwater and brackish lakes. Geochemical Journal 52, e15-e20 (2018).

Keywords: HMW-DOM, sterol, carbon and hydrogen isotopic compositions, deep aquifer, methanogenesis

©2019. Japan Geoscience Union. All Right Reserved.

Correlations of magnetosome-related genes in Nitrospirae genomes to magnetosome geometry and redox stratification in deep-sea environments

*Shinsaku Nakano[1], Shingo Kato[2], Mariko Kouduka[1], Toshitsugu Yamazaki[3], Yohey Suzuki[1]

1. Graduate School of Science, The University of Tokyo, 2. RIKEN, 3. Atmosphere and Ocean Research Institute, The University of Tokyo

Biogenic magnetic particles are ubiquitously found in deep-sea sediments and important carriers of rock magnetism for reconstructing the Earth’ s past regarding sediment age and geomagnetic field. However, microorganisms responsible for the formation of magnetic particles are largely unknown in the deep-sea environment, because of the difficulty in sampling, cultivation, and magnetic separation of magnetotactic cells for single-cell genomics. In this study, deep-sea sediments from Japan Sea and a metal sulfide chimney from South Mariana Trough were subjected to magnetic separation and subsequent electron microscopic observations. Although teardrop-shaped magnetite (Fe_3O_4) particles without microbial cells and 16S rRNA gene sequences related to magnetotactic Nitrospirae species were previously obtained from Japan Sea sediments with a redox zonation enriched with dissolved Fe(II) (the iron boundary), no magnetotactic cells were observed after the magnetic separation. From the metal sulfide chimney, magnetotactic cells were observed with teardrop-shaped magnetite particles. Metagenomic analysis of the chimney sample revealed that contig sequences encoding genes involved in the formation of magnetosome, membrane-bound magnetic particles, were mostly affiliated within Nitrospirae based on sequence similarity. Previous studies have reported that magnetosome-related genes are clustered together as the magnetosome island (MAI) in known magnetotactic bacteria. However, those genes were scattered in a near-complete Nitrospirae genome reconstructed from the chimney sample. Although magnetotactic bacteria are generally considered to align magnetic particles into a chain for efficiently moving in a vertical redox zonation by orienting the cell along the geomagnetic filed, Nitrospirae-affiliated genes involved in chain formation were not found in the near-complete Nitrospirae genome from the chimney with a horizontal redox zonation. Comparative analysis of near-complete Nitrospirae genomes available from public databases revealed that the chain-related genes were found in the genomes from terrestrial deep aquifers and deep-sea sediments with a vertical redox zonation. As the Nitrospirae species associated with teardrop magnetite and the iron boundary in Japan Sea was closely related to Nitrospirae species with the chain-related genes, the presence of the chain-related genes appears to be correlated with a vertical redox zonation. In addition, our results suggest that the Nitrospirae species without MAI are responsible for the production of teardrop magnetite in deep-sea environment, and that teardrop magnetite is a paleoredox indicator especially for the iron boundary.

Keywords: magnetotactic bacteria, metal sulfide chimney, magnetofossil, remnant magnetization

©2019. Japan Geoscience Union. All Right Reserved.

Reconstruction of key ecological responses leading to the most recent dead zone formations in Japan Sea through ancient DNA metabarcodring

*Mariko Kouduka[1], Yohey Suzuki[1]

1. Department of Earth and Planetary Science, The University of Tokyo, 7-3-1 Hongo, Bunkyo-ku, Tokyo, Japan.

Semi-closed ocean basins are very sensitive to climate changes as recorded in frequent formations of sediments with clearly laminated layers, which was caused by the lack of O_2 available to benthic organisms. This is so-called “dead zone formation” and caused by water stagnation after channel closure and/or nutrient inflow through upwelling and channel opening. In contrast to the hydrologic causes, it remains poorly understood about organismal causes such as enhanced primary production and heterotrophic consumption of O_2. We investigated ancient eukaryotic DNA obtained from a thinly laminated layer deposited in the Japan Sea across the most recent global warming event after Younger Dryas (TL-1). Metabarcoding of 18S rRNA gene sequences clarified that across the transition from oxygenated to anoxic bottom water conditions, dominant protist populations shifted through five stages:

Stage1: Under oxygenated bottom conditions, the most dominant taxonomic group was Marine Stramenopiles Group 9 (MAST-9). MAST-9 encompasses diverse uncharacterized planktonic species, 18S rRNA gene sequences of which were detected from both anoxic and oxic water bodies in Pacific and Atlantic Oceans, Mediterranean Sea and South China Sea.

Stage 2: Before the onset of dead zone formation, the sharp decline of MAST-9 was accompanied with the expansion of marine diatom species of the genus Skeletonema, many members of which are known to be a cause of red tide around the world.

Stage 3: The dead zone formation was synchronized with the expansion of marine radiolarians of the order Chaunacanthida, the members of which are encrusted within $SrSO_4$.

Stage 4: Stages 2 was repeated, whereas the expansion of the Chaunacanthida radiolarians was not evident.

Stage 5: The uncharacterized MAST-9 that was dominant before the dead zone formation was gradually recovered towards oxygenated bottom conditions.

From these results, it is suspected that the expansion of Radiolaria species encrusted with $SrSO_4$ triggered dead zone formation by the accelerated downward transport of dead cells and subsequent heterotrophic consumption of O_2. From bioturbated sediment samples from a maximum depth of 31 mbsf with a depositional age of 100 ka, the Chaunacanthida sequences closely related to that from the laminated sediments have been previously detected.It is therefore suggested the record of the Chaunacanthida species can be reconstructed from sediments with great depth and age.

Keywords: global warming paleo-analogue, hypoxemia expansion, molecular paleoecologcail dynamics, biogeochemical cycling

©2019. Japan Geoscience Union. All Right Reserved.

©2019. Japan Geoscience Union. All Right Reserved.

Search for microbial CH_4 production processes in lake sediments and surface water associated with cyanobacterial bloom

*Makoto Matsushita[1], Yoshinori Takano[1], Hiroyuki Imachi[1], Atsushi Urai[2], Ho-Dong Park[3], Hiroki Iwata[3], Naohiko Ohkouchi[1]

1. Japan Agency for Marine-Earth Science and Technology, 2. Department of Science and Technology, Graduate School of Medicine, Science and Technology, Shinshu University, 3. Department of Environmental Sciences, Faculty of Science, Shinshu University

Methane (CH_4) is an important greenhouse gas and contributes substantial budget to global warming. Freshwater lakes are identified as one of the main CH_4 sources, as it is estimated that they contribute to 6-16% of natural CH_4 emissions [1]. The main part of CH_4 released from lakes is considered to be produced by methanogenic archaea in anoxic sediments as terminal step in the degradation of organic matter. The microbial CH_4 production in lake sediments has been mainly investigated by microbiological studies using culture-dependent methods and molecular analysis.

Microbial CH_4 production is still regarded by many as a process limited to anoxic environments. Nevertheless, over the past few decades, increasing evidence of CH_4 accumulation in oxygen-saturated lake and marine surface water has emerged [2]. To explain the enigmatic issues, it has been proposed that CH_4 production by methanogenic archaea takes place in anoxic microenvironments such as detritus and animals' gut. Alternatively, recent studies suggest that some bacteria break down methylphosphonate (MPn) or dimethylsulfoniopropionate (DMSP) and release CH_4 as a biogenic byproduct. These novel microbial CH_4 production processes may play a potential contribution to the total atmospheric carbon cycle.

Oxic CH_4 peaks have been found to be closely associated with phytoplankton dynamics across multiple lakes. Grossart *et al*. [3] found potentially methanogenic archaea associated with cyanobacteria such as *Aphanizomenon* and *Microcystis* in oxygenated surface water. Additionally, Berg *et al*. [4] showed that hydrogen produced during nitrogen fixation by cyanobacteria can be consumed by methanogenic archaea. These studies suggest the presence of a CH_4 production process by methanogenic archaea associated with cyanobacteria in lake surface water. However, it is unclear whether the CH_4 production is taking place in actual environments.

In this study, we investigated microbial CH_4 production in sediments and surface water of Lake Suwa in Nagano Prefecture, Japan, a typical hypertrophic shallow lake, using culture-independent methods. Especially, we focused on cyanobacterial bloom and tried to identify a CH_4 production process by methanogenic archaea associated with cyanobacteria. 16S rRNA gene analyses revealed the presence of methanogenic archaea closely related to the order *Methanobacteriales*, *Methanomicrobiales*, and *Methanosarcinales* in sediment core samples from 30 cm depth. On the other hand, 16S rRNA genes and *mcrA* genes of methanogenic archaea were not detected in bulk DNA from cyanobacterial bloom sample (mainly *Microcystis*)[5]. In order to estimate the potential for methanogenic archaea, we extracted Coenzyme F430, a biomarker for methanogenic archaea, from sediment and bloom samples and determined by using HPLC [6]. F430 was detected from sediment samples, but that from bloom sample was currently below detection limit (<1 pmol).

These results suggest that methanogenic archaea actively produce CH_4 in the sediments of Lake Suwa,

©2019. Japan Geoscience Union. All Right Reserved.

however, its contribution in oxygenated surface water seems to be small. We are currently conducting a more sensitive analysis of F430 using LC-MS/MS [6] with the pre-treatment procedure [7]. The analysis may identify the CH_4 production process by methanogenic archaea associated with cyanobacteria in the surface water. Although this study did not cover other CH_4 production processes such as MPn and DMSP decomposition, our results may also be applicable to estimate the *in situ* contribution of these novel CH_4 source.

Refs.
[1] Bastviken *et al.*, *Global Biogeochem. Cycles*, 18, GB4009 (2004). [2] Tang *et al.*, *Environ. Sci. Technol. Lett.*, 3, 227-233 (2016). [3] Grossart *et al. PNAS*, 108, 19657-19661 (2011). [4] Berg *et al. World J. Microbiol. Biotechnol.*, 30, 539-545 (2014). [5] Park *et al., Environ. Toxicol. Water Qual.*, 13, 61-72 (1998). [6] Kaneko *et al.*, *Anal. Chem.*, 86, 3633-3638 (2014). [7] Kaneko *et al., Geochem. J.,* 50, 453-460 (2016).

Keywords: Microbial methane production, Methane paradox, Freshwater lake, Methanogenic archaea, Cyanobacterial bloom

©2019. Japan Geoscience Union. All Right Reserved.

Did life emerge in a deep-sea metal sulfide chimney? New insights from an archaeal genome and a nanoscale microbe-silicate assemblage

*Hinako Takamiya[1], Hiroki Mukai[2], Mariko Kouduka[1], Shingo Kato[4], Motoo Ito[3], Yohey Suzuki[1]

1. Earth and Planetary Science Graduate School of Science, The University of Tokyo , 2. National Institute of Advanced Industrial Science and Technology, 3. Kochi Institute for Core Sample Research JAMSTEC, 4. RIKEN

Deep-sea hydrothermal activities have continued for 3.8 billion years on Earth. After the formation of metal sulfide chimneys from high-temperature fluid, their low-temperature interactions with ambient seawater potentially provide the cold, stable habitat for microbial life. In such a challenging habitat with metal toxicity, 16S rRNA gene sequences formerly affiliated within Deep-Sea Hydrothermal Vent Euryarchaeota Subtype 6 (DHVE6) and recently reclassified as Pacearchaeota are dominantly detected by 16S rRNA gene sequence analysis. However, the distribution and metabolic activities of Pacearchaeota in metal sulfide chimneys are largely unknown. In this study, a metal sulfide chimney collected from a deep-sea hydrothermal field in South Mariana Trough was subjected to genome-resolved metagenomics analysis. It was revealed that a near-complete Pacearchaeota genome has carbon metabolism genes involved in glycolysis and pentose phosphate pathway linked to nucleotide salvage pathway with light-independent CO_2incorporating ribulose bisphosphate carboxylase/oxygenase (RubisCO). By comparative analysis of Pacearchaeota genomes from deep-sea metal sulfide deposits and terrestrial subsurface aquifers, the carbon metabolism was commonly found with genes annotated for Cu detoxification. Based on the NanoSIMS ion imaging analysis, we found an evidence of a dense microbial colonization inside the chimney where the surface of chalcopyrite ($CuFeS_2$) was overlayered with a silica-bearing material enriched in CN, S and P. Our results explain the geographically and physicochemically diverse distributions of Pacearchaeota indicated by 16S rRNA gene sequence analysis as well as the predominance of Pacearchaeota in the metal sulfide chimney where energy sources from photosynthesis and hydrothermal fluid are limited. The carbon metabolism operated by Pacearchaeota in one of candidate environments for the origin of life could be relevant to that operated by primitive life on early Earth.

Keywords: hydrothermal vent, metagenomic analysis, extremophile ecology, origin of life, microbial carbon metabolism, Rock life detection

©2019. Japan Geoscience Union. All Right Reserved.

X-ray computed nano-tomography for visualizing microbial cells and their surrounding environments

*Yuki Morono[1], Go-Ichiro Uramoto[2,1], Kentaro Uesugi[3], Nobuhisa Takeuchi[3], Masayuki Uesugi[3], Kengo Kubota[4], Tatsuhiko Hoshino[1], Fumio Inagaki[1]

1. Japan Agency for Marine-Earth Science and Technology, 2. Kochi University, 3. Japan Synchrotron Radiation Research Institute, 4. Tohoku University

Recent developments of the X-ray computed tomography (CT) reaches to the spatial resolution of down to few tens of nanometers scale, which is enough to visualize single microbial cells, together with those distributions as well as its surrounding environments. In this study, we tried to visualize microbial cells in the environmental samples by using nanometer-scale X-ray CT.
We used anaerobic granular sludge and subseafloor sediments for the test samples. The X-ray CT analyses were conducted at beamlines of BL20XU and BL47XU in synchrotron radiation facility of Spring-8. The soft samples were either freeze-dried or embedded in the epoxy resin for the analysis. Since the high-spatial resolution observation of the X-ray CT analysis requires a higher density of X-ray per field, the samples often deformed during the analysis, which results in the failure of the 3D reconstruction of the data. Optimization of the resin, its polymerization condition, together with the stain of the cells by osmium tetroxide to put heavy element onto the microbial cells, we could successfully visualize single microbial cells in the samples. Also, the observations of the sample at the pre- and post-edge energies of the element (such as Os) enabled specific signal enhancement of osmium-stained cells.
The investigations of subseafloor biosphere have often based on destructive measurements. Although these analyses revealed the large-scale distribution of microbes along the chemical gradients, no previous attempt explored the spatial distribution of microbial cells at their size range. The visualization of microbes with its surrounding environments will give basic but critical information to understand the microbial in-situ ecophysiology.

Keywords: X-ray Computed Tomography, Subseafloor biosphere

©2019. Japan Geoscience Union. All Right Reserved.

Carbon signatures in amino acids during deep-sea anoxic methanotrophy

*Yoshinori Takano[1]

1. Japan Agency for Marine-Earth Science and Technology (JAMSTEC)

Microorganisms play a central role in both methane production and consumption in the global carbon cycle. Oceanic methane from global deep-sea sediment is largely consumed through microbially mediated sulfate-coupled oxidation, resulting in 13C-depleted cell biomass of anaerobic methanotrophic archaea (ANME). The general ecological importance of subseafloor ANME has been well recognized in the last two decades. However, the crucial biochemical pathways for the overall anaerobic oxidation of methane (AOM) still remain enigmatic. In the present study, methanotrophic pathways were analyzed to trace 13C-depleted amino acid biosynthesis in two clades of ANME (ANME-1 and ANME-2) from the Black Sea. Compound-specific analysis of ANME-dominated microbial mats showed a significant 13C-depletion trend in association with increasing carbon numbers in protein-derived amino acid families within the pyruvate family in the order of alanine, valine, isoleucine and leucine down to -114‰. This result indicates a stepwise elongation of 13C-depleted carbon during amino acid biosynthesis. The overall results suggest that intracellular protein amino acids and the most 13C-depleted signature of leucine, which has a specific branched-chain structure, are potentially propagated as isoprenoid precursor molecules into archaeal biosynthesis, resulting in the extremely 13C- and 14C-depleted nature of ANME cells in the deep microbial oasis.

References:
Takano, Y., Chikaraishi, Y., Imachi, H., Miyairi, Y., Ogawa, N.O., Kaneko, M., Yokoyama, Y., Kruger, M. and Ohkouchi, N. (2018) Insight into anaerobic methanotrophy from 13C/12C- amino acids and 14C/12C-ANME cells in seafloor microbial ecology. Scientific Reports, 8:14070, doi: 10.1038/s41598-018-31004-5.

Supplementary Information:
https://www.nature.com/articles/s41598-018-31004-5#article-info

Acknowledgments:
We thank Dr. R. Seifert and Prof. Dr. W. Michaelis (Univ. Hamburg) and the shipboard party of the R/V Meteor cruise (M72/1: Geochemical cycling and microbial life at active gas seeps). We also thank Y. Saito, Y. Sasaki (JAMSTEC) for technical support and Dr. Y. Takaki (JAMSTEC) for the discussion of genomic sequence. The study was supported in part by the Japan Society for the Promotion of Science (JSPS) and the Submarine Resources Research Project in JAMSTEC.

Keywords: Carbon signatures in ANMEs, Organic molecules, Anoxic methanotrophy

©2019. Japan Geoscience Union. All Right Reserved.

[E] Poster | B (Biogeosciences)：B-CG Complex & General

Tue. May 28, 2019 5:15 PM - 6:30 PM JST | Tue. May 28, 2019 8:15 AM - 9:30 AM UTC | Poster Hall International Exhibition Hall8, Makuhari Messe_40

[B-CG06] Earth and Planetary Science Frontiers for Life and Global Environment

convener:Yoshinori Takano(Japan Agency for Marine-Earth Science and Technology (JAMSTEC)), Yohey Suzuki(Graduate School of Science, The University of Tokyo), Shingo Kato(RIKEN), Keisuke Fukushi(Institute of Nature & Environmental Technology, Kanazawa University)

Earth and planetary science is currently capable of sampling from four frontiers: space, polar regions, deep ocean and deep underground for the study of the origin and evolution of life. Next generation sequencing technology of nucleic acids and nanotechnology-driven innovation of solid characterizations are very powerful to expand our understanding of many fields of earth and planetary sciences. It is also important for us to be aware of global warming and climate change that dramatically affect biodiversity, biological activities and elemental cycling. The aim of this session is to cross the border of science sections to explore the frontiers of earth and planetary science.

[BCG06-P01] Dynamisms and characteristics of dissolved organic matter (DOM) in deep aquifer: A scope for deep biosphere

*Atsushi Urai[1,2], Yoshinori Takano[2], Naohiko Ohkouchi[2] (1.Department of Science and Technology, Graduate School of Medicine, Science and Technology, Shinshu University, 2.Department of Biogeochemistry, Japan Agency for Marine-Earth Science and Technology)

[BCG06-P02] Correlations of magnetosome-related genes in Nitrospirae genomes to magnetosome geometry and redox stratification in deep-sea environments

*Shinsaku Nakano[1], Shingo Kato[2], Mariko Kouduka[1], Toshitsugu Yamazaki[3], Yohey Suzuki[1] (1.Graduate School of Science, The University of Tokyo, 2.RIKEN, 3.Atmosphere and Ocean Research Institute, The University of Tokyo)

[BCG06-P03] Reconstruction of key ecological responses leading to the most recent dead zone formations in Japan Sea through ancient DNA metabarcodring

*Mariko Kouduka[1], Yohey Suzuki[1] (1.Department of Earth and Planetary Science, The University of Tokyo, 7-3-1 Hongo, Bunkyo-ku, Tokyo, Japan.)

[BCG06-P04] Search for microbial CH_4 production processes in lake sediments and surface water associated with cyanobacterial bloom

*Makoto Matsushita[1], Yoshinori Takano[1], Hiroyuki Imachi[1], Atsushi Urai[2], Ho-Dong Park[3], Hiroki Iwata[3], Naohiko Ohkouchi[1] (1.Japan Agency for Marine-Earth Science and Technology, 2.Department of Science and Technology, Graduate School of Medicine, Science and Technology, Shinshu University, 3.Department of Environmental Sciences, Faculty of Science, Shinshu University)

[BCG06-P05] Did life emerge in a deep-sea metal sulfide chimney? New insights from an archaeal genome and a nanoscale microbe-silicate assemblage

*Hinako Takamiya[1], Hiroki Mukai[2], Mariko Kouduka[1], Shingo Kato[4], Motoo Ito[3], Yohey Suzuki[1] (1.Earth and Planetary Science Graduate School of Science, The University of Tokyo , 2.National Institute of Advanced Industrial Science and Technology, 3.Kochi Institute for Core Sample Research JAMSTEC, 4.RIKEN)

[BCG06-P06] X-ray computed nano-tomography for visualizing microbial cells and their surrounding environments

*Yuki Morono[1], Go-Ichiro Uramoto[2,1], Kentaro Uesugi[3], Nobuhisa Takeuchi[3], Masayuki Uesugi[3], Kengo Kubota[4], Tatsuhiko Hoshino[1], Fumio Inagaki[1] (1.Japan Agency for Marine-Earth Science and Technology, 2.Kochi University, 3.Japan Synchrotron Radiation Research Institute, 4.Tohoku University)

[BCG06-P07] **Carbon signatures in amino acids during deep-sea anoxic methanotrophy**

*Yoshinori Takano[1] (1.Japan Agency for Marine-Earth Science and Technology (JAMSTEC))

Dynamisms and characteristics of dissolved organic matter (DOM) in deep aquifer: A scope for deep biosphere

*Atsushi Urai[1,2], Yoshinori Takano[2], Naohiko Ohkouchi[2]

1. Department of Science and Technology, Graduate School of Medicine, Science and Technology, Shinshu University, 2. Department of Biogeochemistry, Japan Agency for Marine-Earth Science and Technology

Dissolved organic matter (DOM) is generally derived from multiple sources and affected by complicated transformation and degradation reactions. In a general geochemical description of marine environments, high-molecular-weight DOM (HMW-DOM; >1 kDa) particularly represents a unique organic carbon pool, which is accompanied by considerable difference in the molecular and stable isotopic compositions from other organic components such as particulate organic matter (POM) and low-molecular-weight DOM (LMW-DOM; <1 kDa) (e.g., Benner et al., 1997).

To date, formation of DOM fraction and potential microbial interaction in deep aquifer have been particularly poorly understood on the context of prokaryotic ecology. We investigated the molecular composition of DOM fraction including LMW and HMW by an improved method (Urai et al., 2018). The filtered samples are tentatively defined by conventional size scales; macromolecular scale (100 mm >> 40 mm), POM (40 mm >> 0.6 mm), HMW-DOM(0.6 mm>>1kDa), and total-DOM (<0.6 mm). We also have a validation to distinguish the molecular signature between phototrophic primary producers (i.e., fossil molecules) and presently living benthic prokaryotes (i.e., modern molecules; cf. biological methanogenesis, Kaneko et al., 2014). We report a preliminary result of the feasibility study and discuss a perspective from the view of deep biosphere.

References:

Benner et al. Abundance, size distribution, and stable carbon and nitrogen isotopic compositions of marine organic matter isolated by tangential-flow ultrafiltration. Marine Chemistry 57, 243-263 (1997).

Kaneko et al. Quantitative analysis of coenzyme F430 in environmental samples: a new diagnostic tool for methanogenesis and anaerobic methane oxidation. Analytical Chemistry 86, 3633-3638 (2014).

Urai et al. Algal-derived 24-ethylcholesta-5, 22-dien-3β-ol (stigmasterol) is frequently found in high-molecular-weight dissolved organic matter (HMW-DOM) during summer in freshwater and brackish lakes. Geochemical Journal 52, e15-e20 (2018).

Keywords: HMW-DOM, sterol, carbon and hydrogen isotopic compositions, deep aquifer, methanogenesis

©2019. Japan Geoscience Union. All Right Reserved.

Correlations of magnetosome-related genes in Nitrospirae genomes to magnetosome geometry and redox stratification in deep-sea environments

*Shinsaku Nakano[1], Shingo Kato[2], Mariko Kouduka[1], Toshitsugu Yamazaki[3], Yohey Suzuki[1]

1. Graduate School of Science, The University of Tokyo, 2. RIKEN, 3. Atmosphere and Ocean Research Institute, The University of Tokyo

Biogenic magnetic particles are ubiquitously found in deep-sea sediments and important carriers of rock magnetism for reconstructing the Earth’ s past regarding sediment age and geomagnetic field. However, microorganisms responsible for the formation of magnetic particles are largely unknown in the deep-sea environment, because of the difficulty in sampling, cultivation, and magnetic separation of magnetotactic cells for single-cell genomics. In this study, deep-sea sediments from Japan Sea and a metal sulfide chimney from South Mariana Trough were subjected to magnetic separation and subsequent electron microscopic observations. Although teardrop-shaped magnetite (Fe_3O_4) particles without microbial cells and 16S rRNA gene sequences related to magnetotactic Nitrospirae species were previously obtained from Japan Sea sediments with a redox zonation enriched with dissolved Fe(II) (the iron boundary), no magnetotactic cells were observed after the magnetic separation. From the metal sulfide chimney, magnetotactic cells were observed with teardrop-shaped magnetite particles. Metagenomic analysis of the chimney sample revealed that contig sequences encoding genes involved in the formation of magnetosome, membrane-bound magnetic particles, were mostly affiliated within Nitrospirae based on sequence similarity. Previous studies have reported that magnetosome-related genes are clustered together as the magnetosome island (MAI) in known magnetotactic bacteria. However, those genes were scattered in a near-complete Nitrospirae genome reconstructed from the chimney sample. Although magnetotactic bacteria are generally considered to align magnetic particles into a chain for efficiently moving in a vertical redox zonation by orienting the cell along the geomagnetic filed, Nitrospirae-affiliated genes involved in chain formation were not found in the near-complete Nitrospirae genome from the chimney with a horizontal redox zonation. Comparative analysis of near-complete Nitrospirae genomes available from public databases revealed that the chain-related genes were found in the genomes from terrestrial deep aquifers and deep-sea sediments with a vertical redox zonation. As the Nitrospirae species associated with teardrop magnetite and the iron boundary in Japan Sea was closely related to Nitrospirae species with the chain-related genes, the presence of the chain-related genes appears to be correlated with a vertical redox zonation. In addition, our results suggest that the Nitrospirae species without MAI are responsible for the production of teardrop magnetite in deep-sea environment, and that teardrop magnetite is a paleoredox indicator especially for the iron boundary.

Keywords: magnetotactic bacteria, metal sulfide chimney, magnetofossil, remnant magnetization

©2019. Japan Geoscience Union. All Right Reserved.

Reconstruction of key ecological responses leading to the most recent dead zone formations in Japan Sea through ancient DNA metabarcodring

*Mariko Kouduka[1], Yohey Suzuki[1]

1. Department of Earth and Planetary Science, The University of Tokyo, 7-3-1 Hongo, Bunkyo-ku, Tokyo, Japan.

Semi-closed ocean basins are very sensitive to climate changes as recorded in frequent formations of sediments with clearly laminated layers, which was caused by the lack of O_2 available to benthic organisms. This is so-called “dead zone formation” and caused by water stagnation after channel closure and/or nutrient inflow through upwelling and channel opening. In contrast to the hydrologic causes, it remains poorly understood about organismal causes such as enhanced primary production and heterotrophic consumption of O_2. We investigated ancient eukaryotic DNA obtained from a thinly laminated layer deposited in the Japan Sea across the most recent global warming event after Younger Dryas (TL-1). Metabarcoding of 18S rRNA gene sequences clarified that across the transition from oxygenated to anoxic bottom water conditions, dominant protist populations shifted through five stages:

Stage1: Under oxygenated bottom conditions, the most dominant taxonomic group was Marine Stramenopiles Group 9 (MAST-9). MAST-9 encompasses diverse uncharacterized planktonic species, 18S rRNA gene sequences of which were detected from both anoxic and oxic water bodies in Pacific and Atlantic Oceans, Mediterranean Sea and South China Sea.

Stage 2: Before the onset of dead zone formation, the sharp decline of MAST-9 was accompanied with the expansion of marine diatom species of the genus Skeletonema, many members of which are known to be a cause of red tide around the world.

Stage 3: The dead zone formation was synchronized with the expansion of marine radiolarians of the order Chaunacanthida, the members of which are encrusted within $SrSO_4$.

Stage 4: Stages 2 was repeated, whereas the expansion of the Chaunacanthida radiolarians was not evident.

Stage 5: The uncharacterized MAST-9 that was dominant before the dead zone formation was gradually recovered towards oxygenated bottom conditions.

From these results, it is suspected that the expansion of Radiolaria species encrusted with $SrSO_4$ triggered dead zone formation by the accelerated downward transport of dead cells and subsequent heterotrophic consumption of O_2. From bioturbated sediment samples from a maximum depth of 31 mbsf with a depositional age of 100 ka, the Chaunacanthida sequences closely related to that from the laminated sediments have been previously detected.It is therefore suggested the record of the Chaunacanthida species can be reconstructed from sediments with great depth and age.

Keywords: global warming paleo-analogue, hypoxemia expansion, molecular paleoecologcail dynamics, biogeochemical cycling

©2019. Japan Geoscience Union. All Right Reserved.

©2019. Japan Geoscience Union. All Right Reserved.

Search for microbial CH_4 production processes in lake sediments and surface water associated with cyanobacterial bloom

*Makoto Matsushita[1], Yoshinori Takano[1], Hiroyuki Imachi[1], Atsushi Urai[2], Ho-Dong Park[3], Hiroki Iwata[3], Naohiko Ohkouchi[1]

1. Japan Agency for Marine-Earth Science and Technology, 2. Department of Science and Technology, Graduate School of Medicine, Science and Technology, Shinshu University, 3. Department of Environmental Sciences, Faculty of Science, Shinshu University

Methane (CH_4) is an important greenhouse gas and contributes substantial budget to global warming. Freshwater lakes are identified as one of the main CH_4 sources, as it is estimated that they contribute to 6-16% of natural CH_4 emissions [1]. The main part of CH_4 released from lakes is considered to be produced by methanogenic archaea in anoxic sediments as terminal step in the degradation of organic matter. The microbial CH_4 production in lake sediments has been mainly investigated by microbiological studies using culture-dependent methods and molecular analysis.

Microbial CH_4 production is still regarded by many as a process limited to anoxic environments. Nevertheless, over the past few decades, increasing evidence of CH_4 accumulation in oxygen-saturated lake and marine surface water has emerged [2]. To explain the enigmatic issues, it has been proposed that CH_4 production by methanogenic archaea takes place in anoxic microenvironments such as detritus and animals' gut. Alternatively, recent studies suggest that some bacteria break down methylphosphonate (MPn) or dimethylsulfoniopropionate (DMSP) and release CH_4 as a biogenic byproduct. These novel microbial CH_4 production processes may play a potential contribution to the total atmospheric carbon cycle.

Oxic CH_4 peaks have been found to be closely associated with phytoplankton dynamics across multiple lakes. Grossart *et al*. [3] found potentially methanogenic archaea associated with cyanobacteria such as *Aphanizomenon* and *Microcystis* in oxygenated surface water. Additionally, Berg *et al*. [4] showed that hydrogen produced during nitrogen fixation by cyanobacteria can be consumed by methanogenic archaea. These studies suggest the presence of a CH_4 production process by methanogenic archaea associated with cyanobacteria in lake surface water. However, it is unclear whether the CH_4 production is taking place in actual environments.

In this study, we investigated microbial CH_4 production in sediments and surface water of Lake Suwa in Nagano Prefecture, Japan, a typical hypertrophic shallow lake, using culture-independent methods. Especially, we focused on cyanobacterial bloom and tried to identify a CH_4 production process by methanogenic archaea associated with cyanobacteria. 16S rRNA gene analyses revealed the presence of methanogenic archaea closely related to the order *Methanobacteriales*, *Methanomicrobiales*, and *Methanosarcinales* in sediment core samples from 30 cm depth. On the other hand, 16S rRNA genes and *mcrA* genes of methanogenic archaea were not detected in bulk DNA from cyanobacterial bloom sample (mainly *Microcystis*)[5]. In order to estimate the potential for methanogenic archaea, we extracted Coenzyme F430, a biomarker for methanogenic archaea, from sediment and bloom samples and determined by using HPLC [6]. F430 was detected from sediment samples, but that from bloom sample was currently below detection limit (<1 pmol).

These results suggest that methanogenic archaea actively produce CH_4 in the sediments of Lake Suwa,

©2019. Japan Geoscience Union. All Right Reserved.

however, its contribution in oxygenated surface water seems to be small. We are currently conducting a more sensitive analysis of F430 using LC-MS/MS [6] with the pre-treatment procedure [7]. The analysis may identify the CH_4 production process by methanogenic archaea associated with cyanobacteria in the surface water. Although this study did not cover other CH_4 production processes such as MPn and DMSP decomposition, our results may also be applicable to estimate the *in situ* contribution of these novel CH_4 source.

Refs.
[1] Bastviken *et al.*, *Global Biogeochem. Cycles*, 18, GB4009 (2004). [2] Tang *et al.*, *Environ. Sci. Technol. Lett.*, 3, 227-233 (2016). [3] Grossart *et al. PNAS*, 108, 19657-19661 (2011). [4] Berg *et al. World J. Microbiol. Biotechnol.*, 30, 539-545 (2014). [5] Park *et al., Environ. Toxicol. Water Qual.*, 13, 61-72 (1998). [6] Kaneko *et al.*, *Anal. Chem.*, 86, 3633-3638 (2014). [7] Kaneko *et al., Geochem. J.,* 50, 453-460 (2016).

Keywords: Microbial methane production, Methane paradox, Freshwater lake, Methanogenic archaea, Cyanobacterial bloom

©2019. Japan Geoscience Union. All Right Reserved.

Did life emerge in a deep-sea metal sulfide chimney? New insights from an archaeal genome and a nanoscale microbe-silicate assemblage

*Hinako Takamiya[1], Hiroki Mukai[2], Mariko Kouduka[1], Shingo Kato[4], Motoo Ito[3], Yohey Suzuki[1]

1. Earth and Planetary Science Graduate School of Science, The University of Tokyo , 2. National Institute of Advanced Industrial Science and Technology, 3. Kochi Institute for Core Sample Research JAMSTEC, 4. RIKEN

Deep-sea hydrothermal activities have continued for 3.8 billion years on Earth. After the formation of metal sulfide chimneys from high-temperature fluid, their low-temperature interactions with ambient seawater potentially provide the cold, stable habitat for microbial life. In such a challenging habitat with metal toxicity, 16S rRNA gene sequences formerly affiliated within Deep-Sea Hydrothermal Vent Euryarchaeota Subtype 6 (DHVE6) and recently reclassified as Pacearchaeota are dominantly detected by 16S rRNA gene sequence analysis. However, the distribution and metabolic activities of Pacearchaeota in metal sulfide chimneys are largely unknown. In this study, a metal sulfide chimney collected from a deep-sea hydrothermal field in South Mariana Trough was subjected to genome-resolved metagenomics analysis. It was revealed that a near-complete Pacearchaeota genome has carbon metabolism genes involved in glycolysis and pentose phosphate pathway linked to nucleotide salvage pathway with light-independent CO_2incorporating ribulose bisphosphate carboxylase/oxygenase (RubisCO). By comparative analysis of Pacearchaeota genomes from deep-sea metal sulfide deposits and terrestrial subsurface aquifers, the carbon metabolism was commonly found with genes annotated for Cu detoxification. Based on the NanoSIMS ion imaging analysis, we found an evidence of a dense microbial colonization inside the chimney where the surface of chalcopyrite ($CuFeS_2$) was overlayered with a silica-bearing material enriched in CN, S and P. Our results explain the geographically and physicochemically diverse distributions of Pacearchaeota indicated by 16S rRNA gene sequence analysis as well as the predominance of Pacearchaeota in the metal sulfide chimney where energy sources from photosynthesis and hydrothermal fluid are limited. The carbon metabolism operated by Pacearchaeota in one of candidate environments for the origin of life could be relevant to that operated by primitive life on early Earth.

Keywords: hydrothermal vent, metagenomic analysis, extremophile ecology, origin of life, microbial carbon metabolism, Rock life detection

©2019. Japan Geoscience Union. All Right Reserved.

X-ray computed nano-tomography for visualizing microbial cells and their surrounding environments

*Yuki Morono[1], Go-Ichiro Uramoto[2,1], Kentaro Uesugi[3], Nobuhisa Takeuchi[3], Masayuki Uesugi[3], Kengo Kubota[4], Tatsuhiko Hoshino[1], Fumio Inagaki[1]

1. Japan Agency for Marine-Earth Science and Technology, 2. Kochi University, 3. Japan Synchrotron Radiation Research Institute, 4. Tohoku University

Recent developments of the X-ray computed tomography (CT) reaches to the spatial resolution of down to few tens of nanometers scale, which is enough to visualize single microbial cells, together with those distributions as well as its surrounding environments. In this study, we tried to visualize microbial cells in the environmental samples by using nanometer-scale X-ray CT.
We used anaerobic granular sludge and subseafloor sediments for the test samples. The X-ray CT analyses were conducted at beamlines of BL20XU and BL47XU in synchrotron radiation facility of Spring-8. The soft samples were either freeze-dried or embedded in the epoxy resin for the analysis. Since the high-spatial resolution observation of the X-ray CT analysis requires a higher density of X-ray per field, the samples often deformed during the analysis, which results in the failure of the 3D reconstruction of the data. Optimization of the resin, its polymerization condition, together with the stain of the cells by osmium tetroxide to put heavy element onto the microbial cells, we could successfully visualize single microbial cells in the samples. Also, the observations of the sample at the pre- and post-edge energies of the element (such as Os) enabled specific signal enhancement of osmium-stained cells.
The investigations of subseafloor biosphere have often based on destructive measurements. Although these analyses revealed the large-scale distribution of microbes along the chemical gradients, no previous attempt explored the spatial distribution of microbial cells at their size range. The visualization of microbes with its surrounding environments will give basic but critical information to understand the microbial in-situ ecophysiology.

Keywords: X-ray Computed Tomography, Subseafloor biosphere

©2019. Japan Geoscience Union. All Right Reserved.

Carbon signatures in amino acids during deep-sea anoxic methanotrophy

*Yoshinori Takano[1]

1. Japan Agency for Marine-Earth Science and Technology (JAMSTEC)

Microorganisms play a central role in both methane production and consumption in the global carbon cycle. Oceanic methane from global deep-sea sediment is largely consumed through microbially mediated sulfate-coupled oxidation, resulting in 13C-depleted cell biomass of anaerobic methanotrophic archaea (ANME). The general ecological importance of subseafloor ANME has been well recognized in the last two decades. However, the crucial biochemical pathways for the overall anaerobic oxidation of methane (AOM) still remain enigmatic. In the present study, methanotrophic pathways were analyzed to trace 13C-depleted amino acid biosynthesis in two clades of ANME (ANME-1 and ANME-2) from the Black Sea. Compound-specific analysis of ANME-dominated microbial mats showed a significant 13C-depletion trend in association with increasing carbon numbers in protein-derived amino acid families within the pyruvate family in the order of alanine, valine, isoleucine and leucine down to -114‰. This result indicates a stepwise elongation of 13C-depleted carbon during amino acid biosynthesis. The overall results suggest that intracellular protein amino acids and the most 13C-depleted signature of leucine, which has a specific branched-chain structure, are potentially propagated as isoprenoid precursor molecules into archaeal biosynthesis, resulting in the extremely 13C- and 14C-depleted nature of ANME cells in the deep microbial oasis.

References:
Takano, Y., Chikaraishi, Y., Imachi, H., Miyairi, Y., Ogawa, N.O., Kaneko, M., Yokoyama, Y., Kruger, M. and Ohkouchi, N. (2018) Insight into anaerobic methanotrophy from 13C/12C- amino acids and 14C/12C-ANME cells in seafloor microbial ecology. Scientific Reports, 8:14070, doi: 10.1038/s41598-018-31004-5.

Supplementary Information:
https://www.nature.com/articles/s41598-018-31004-5#article-info

Acknowledgments:
We thank Dr. R. Seifert and Prof. Dr. W. Michaelis (Univ. Hamburg) and the shipboard party of the R/V Meteor cruise (M72/1: Geochemical cycling and microbial life at active gas seeps). We also thank Y. Saito, Y. Sasaki (JAMSTEC) for technical support and Dr. Y. Takaki (JAMSTEC) for the discussion of genomic sequence. The study was supported in part by the Japan Society for the Promotion of Science (JSPS) and the Submarine Resources Research Project in JAMSTEC.

Keywords: Carbon signatures in ANMEs, Organic molecules, Anoxic methanotrophy

©2019. Japan Geoscience Union. All Right Reserved.

[J] Oral | B (Biogeosciences)：B-CG Complex & General

Tue. May 28, 2019 10:45 AM - 12:15 PM JST | Tue. May 28, 2019 1:45 AM - 3:15 AM UTC | 105 1F

[B-CG08] Phanerozoic biodiversity change: Extinction and diversification

convener:Yukio Isozaki(Department of Earth Science and Astronomy, Multi-disciplinary Sciences - General Systems Studies, Graduate School of Arts and Sciences, The University of Tokyo), Yusuke Sawaki(The University of Tokyo), Chairperson:Yukio Isozaki(Department of Earth Science and Astronomy, The University of Tokyo), Yusuke Sawaki(The University of Tokyo)

Phanerozoic biodiversity is the consequence of repeated extinctions and following diversifications in the past, which were caused by large-scale environmental changes, in particular, by extremely rapid and drastic forcing that changed the environments of the biosphere. Irreversible and episodic changes in material cycling on the planet and influences of severe galactic cosmic radiation enhanced by encounter with dark cloud are nominated as major driving mechanisms for the alleged rapid, large-scale environmental perturbations. The biodiversity change in the fossiliferous Phanerozoic record is characterized by 5 major mass extinctions within the long-term trend of diversity increase. Nonetheless, each extinction event has been explained rather in ad hoc manner, without any universal explanation. Therefore, ultimate triggers that caused the Phanerozoic biodiversity still remain as unsolved issues. This session discusses the ancient environmental changes related to Phanerozoic biodiversity under a new light of the recent progress in geology.

10:45 AM - 10:50 AM JST | 1:45 AM - 1:50 AM UTC

Introduction

10:50 AM - 11:10 AM JST | 1:50 AM - 2:10 AM UTC

[BCG08-01] **The Ediacaran-Cambrian transition of North China**

★Invited Papers

*Xingliang Zhang[1] (1.State Key Laboratory of Continental Dynamics, Shaanxi Key Laboratory of Early Life and Environments, and Department of Geology, Northwest University)

11:10 AM - 11:30 AM JST | 2:10 AM - 2:30 AM UTC

[BCG08-02] The Qingjiang biota – An extraordinary new Burgess Shale-type fossil Lagerstätte from the early Cambrian of South China

★Invited Papers

*Dongjing Fu[1], Xingliang Zhang[1], Robert R. Gains[2] (1.State Key Laboratory of the Continental Dynamics, Shaanxi Key Laboratory of Early Life and Environment, Department of Geology, Northwest University, Xi'an 710069, PR China, 2.Department of Geology, Pomona College, Claremont, CA 91711, USA)

11:30 AM - 11:50 AM JST | 2:30 AM - 2:50 AM UTC

[BCG08-03] Enhanced flux of extraterrestrial ^{3}He across the Permian–Triassic boundary

★Invited Papers

*Tetsuji Onoue[1], Naoto Takahata[2], Honami Sato[4], Akira Ishikawa[3], Katsuhito Soda[1], Yuji Sano[2], Yukio Isozaki[2] (1.Kumamoto Univ., 2.Univ. Tokyo, 3.Tokyo Inst. Tech., 4.Chiba Inst. Tech.)

11:50 AM - 12:10 PM JST | 2:50 AM - 3:10 AM UTC

[BCG08-04] **End-Triassic Mass Extinction: Causes and Consequences**

★Invited Papers

*Wataru Fujisaki[1] (1.Japan Agency for Marine-Earth Science and Technology)

12:10 PM - 12:15 PM JST | 3:10 AM - 3:15 AM UTC

Discussion

The Ediacaran-Cambrian transition of North China

*Xingliang Zhang[1]

1. State Key Laboratory of Continental Dynamics, Shaanxi Key Laboratory of Early Life and Environments, and Department of Geology, Northwest University

The central mountain range, known as the backbone of China, separates the country into North China and South China, which are different from each other in geology, geography, climate, and culture. The Precambrian-Cambrian transition of South China has received much attention of world scientists for beautiful sections and numerous fantastic fossil-Lagerstätten. However, the Ediacaran-Cambrian sequences of North China have some attractive points as well. The lowermost Cambrian of North China, the Xinji Formation, unconformably overlies Precambrian rocks of various ages, from Archean to late Ediacaran. The Xinji Formation is rich in SSFs of Cambrian Epoch 2 aspects and thus the Terreneuvian is absent throughout North China. The Xinji SSF assemblage is taxonomically dominated by molluscs and hyoliths, which are represented by 26 and 12 species, respectively. A number of molluscan taxa are conspecific with Australia, Antarctic and Laurentia, and thus have biostratigraphical and paleobiogeographical values. Remarkably, shell microstructures are well preserved in molluscs and hyoliths, which demonstrate how these Cambrian animals use minute mineral crystals to build their shells. Additionally, shell microstructures shed new light on the phylogenic links between the groups. Ediacaran rocks developed in marginal regions and cratonic basins. Along the south and west margins of North China, the Dongpo/Tuerkeng Shale/Slate immediately underlies the unconformity and overlies the Luoquan/Zhengmuguan Diamictite which is poorly constrained in age. The shale/slate unit above the diamictite yields a diverse form of macroscopic, soft-bodied fossils, e.g. the annulated tubular form *Shaanxilithes*, the form of a string of beads *Horodyskia*, the WiFi symbol-like form *Palaeopascichnus*, an unnamed form resembling a string of rings (which might be a segmented organism composed of many repetitive units), and small clew-like fossils of unknown affinities. Algal fossils are abundant but simple in complexity and poor in diversity. The presence of *Shaanxilithes* and *Palaeopascichnus* suggests an age of late Ediacaran. New specimens demonstrate that *Shaanxilithes* is composed of a cone-in-cone internal tube encased in a flexible external tube with irregular cross annulations. Such a morphological reconstruction is analogous to the contemporary *Cloudina* and other tubular organisms. New findings in North China would provide new insights into the biotic evolution of the Ediacaran-Cambrian transition.

Keywords: Ediacaran, Cambrian, Biodiversity, North China

©2019. Japan Geoscience Union. All Right Reserved.

The Qingjiang biota –An extraordinary new Burgess Shale-type fossil Lagerstätte from the early Cambrian of South China

*Dongjing Fu[1], Xingliang Zhang[1], Robert R. Gains[2]

1. State Key Laboratory of the Continental Dynamics, Shaanxi Key Laboratory of Early Life and Environment, Department of Geology, Northwest University, Xi' an 710069, PR China, 2. Department of Geology, Pomona College, Claremont, CA 91711, USA

Our understanding of the Cambrian explosion and of the fundamental structure of the tree of animal life rests in large part on evidence from a dramatically enhanced fossil record, characterized by the preservation of entire assemblages of soft-bodied fossils. In the one hundred years since Walcott' s original discovery of the Burgess Shale, exceptionally preserved fossil assemblages have been reported from Cambrian strata of almost every paleocontinent. Nevertheless, only the early Cambrian Chengjiang biota of Yunnan Province has matched the Burgess Shale in total diversity of soft-bodied taxa and fidelity of exceptional preservation. Here, we report the discovery of an extraordinary new early Cambrian Burgess Shale-type (BST) fossil Lagerstätte from the Changyang area of South China, which is characterized by high taxonomic diversity (101 metazoan taxa plus 8 algal forms), an unexpectedly large proportion of new taxa (53.2%), and exquisite preservation of fine aspects of labile tissue anatomy. The taxonomic richness of soft-bodied taxa (85%) approaches the top tier of BST deposits, presently occupied only by the Burgess Shale and Chengjiang biotas. Rarefaction analyses suggest that diversity may surpass all other BST biotas. Novel aspects include high abundance of cnidarians, including both medusoid and polypoid forms, new taxa resembling extant kinorhynchs, and abundant larval or juvenile forms. While approximately coeval to the Chengjiang biota, the Qingjiang biota (518 Ma) appears to have occupied a more distal environmental setting, in which a different early Cambrian ecosystem flourished. The uniqueness of the Qingjiang biota in the taxon composition and preservation quality holds special potential to provide new insights into the evolution of early metazoans and the structuring of Cambrian ecosystems across environmental gradients.

Keywords: Qingjiang Biota, Cambrian Explosion, Exceptional Preservation, South China, Burgess Shale Type

©2019. Japan Geoscience Union. All Right Reserved.

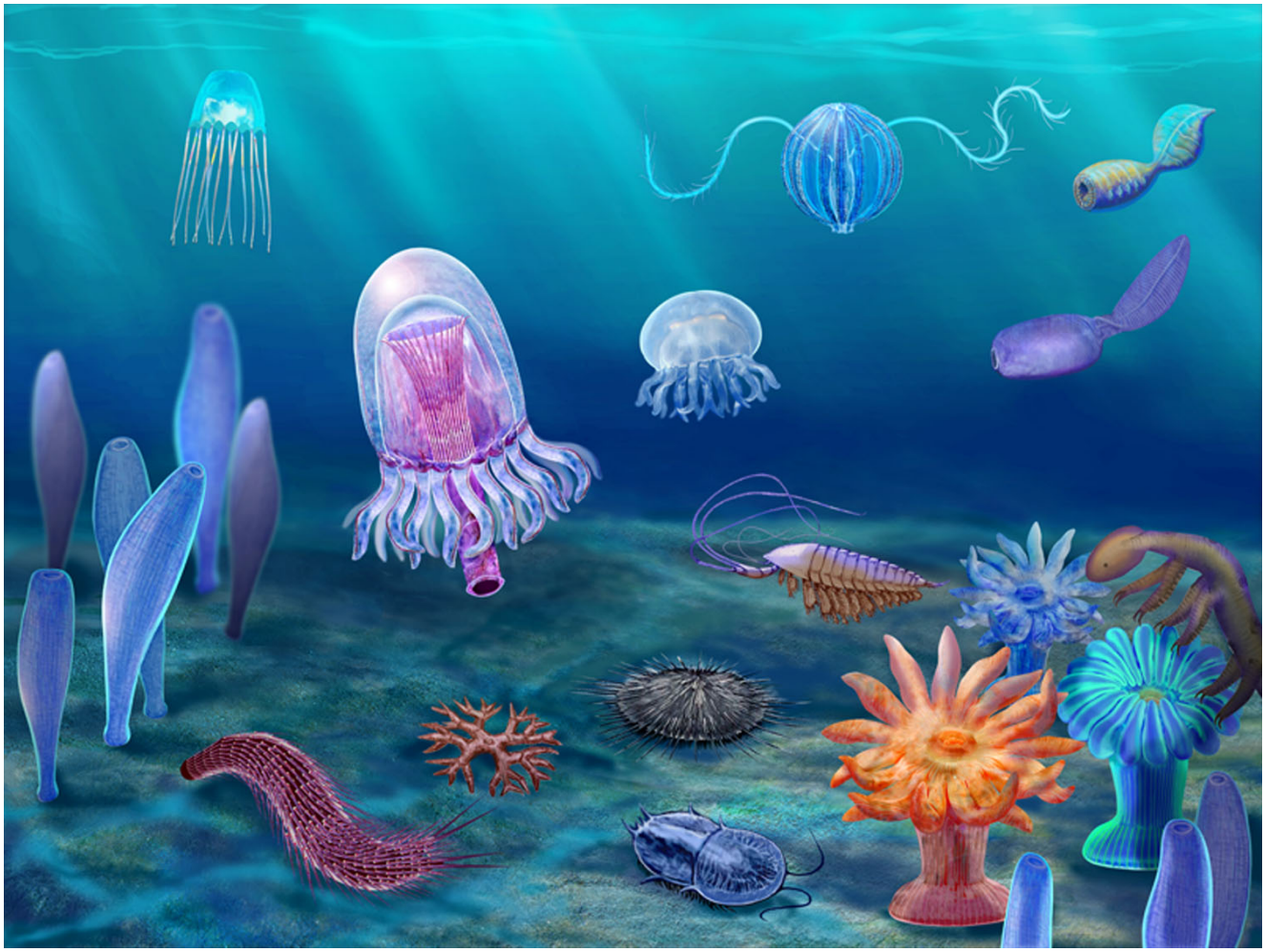

©2019. Japan Geoscience Union. All Right Reserved.

Enhanced flux of extraterrestrial ^{3}He across the Permian–Triassic boundary

*Tetsuji Onoue[1], Naoto Takahata[2], Honami Sato[4], Akira Ishikawa[3], Katsuhito Soda[1], Yuji Sano[2], Yukio Isozaki[2]

1. Kumamoto Univ., 2. Univ. Tokyo, 3. Tokyo Inst. Tech., 4. Chiba Inst. Tech.

The Solar System contains abundant submillimetre interplanetary dust particles (IDPs) that are enriched in ^{3}He. ^{3}He concentrations in ancient deep-sea sediments have been used to constrain the flux of IDPs onto the Earth for at least the last 100 Myr. However, the use of ^{3}He in detecting IDP flux is often compromised by the diffusional loss of ^{3}He in sedimentary rocks, with the exception of some Ordovician samples that record a period of unusually high extraterrestrial^{3}He ($^{3}He_{ET}$) flux. In this study, we report for the first time the preservation of extra-terrestrial ^{3}Hein deep-sea bedded chertfrom a continuous Permian-Triassic boundary (PTB) section at Waidani in Japan, which was deposited in the Panthalassa superocean.

High ^{3}He/^{4}He ratios (up to 150 Ra; 1Ra = the atmospheric ratio) were detected from acid-insoluble residues fromthe uppermost Permian deposits, which suggeststhe existence of extraterrestrial He hosted mainly in IDPs. The estimated extraterrestrial fraction of ^{3}He across the PTB revealsthat$^{3}He_{ET}$ concentrations are higher in the topmost ~1.5 m ofthe studied Permian deposits, which is 4–5 times greater than that measured in the overlying Triassic unit. Based on the $^{3}He_{ET}$ concentration and sedimentary mass accumulation rate of the PTB section at Waidani, we calculated $^{3}He_{ET}$ fluxacross the PTB.The data document the presence of an up to 4-fold increase in IDP flux for the last 500 kyr interval of the Permian.This unusual signal suggests a significant increase in the influx of interplanetary dust particles, likely related to an asteroid showerin the inner Solar System. High-resolution stratigraphy indicates that peak IDP flux occurred during the final 500 kyr of the Permian, concurrent with a pre-extinction decline in radiolarian diversity.

Keywords: Permian, Triassic, Bedded Chert, Helium, Interplanetary dust particle, Platinum group element

©2019. Japan Geoscience Union. All Right Reserved.

End-Triassic Mass Extinction: Causes and Consequences

*Wataru Fujisaki[1]

1. Japan Agency for Marine-Earth Science and Technology

The biodiversity crisis across the Triassic-Jurassic boundary (TJB; *ca.* 201 Ma) is characterized by one of the largest mass extinctions in the Phanerozoic. Significant increases in the extinction rate of marine fauna, and major turnovers in terrestrial vegetation and vertebrate groups, have been well documented across the TJB. In addition to the extinction, several unique geological episodes around the TJB were recognized; i.e., the emplacement of the Central Atlantic Magmatic Provinces (CAMP) which is associated with the breakup of Pangea, carbon cycle perturbations, and widespread ocean anoxia and associated deficits of nutrients. In the last decade, based on of the numerous data-set obtained from the shallow-marine shelf sequences around the Pangea, major advances have been made in our understanding of the TJB biotic crisis, related environmental changes, and the CAMP volcanism. However, the casual relationships between the CAMP volcanism and extinction-related environmental changes of global context still remain unclear. Therefore, the deep mid-Panthalassa, which occupied major portion of the global ocean during the Triassic-Jurassic transition, is indispensable for reconstructing the global environmental changes related to the TJB biotic crisis.

Deep-sea bedded cherts in the Mino-Tanba belt in SW Japan provide critical constraints for reconstructing paleo-environmental changes because they preserve extinction-related intervals from the Middle Permian to the Early Jurassic deposited in the deep mid-Panthalassa. Most recently, the stratigraphic $\delta^{13}C_{org}$ variation using Rhaetian (Late Triassic) to Hettangian (Early Jurassic) shales interbedded within deep-sea cherts was established in the Katsuyama section in the Mino-Tanba belt. By obtaining high-resolution Rhaetian to Hettangian $\delta^{13}C_{org}$ values, three negative carbon isotopic excursions (NCIEs) were newly detected before and across the TJB. The mid-Panthalassic NCIEs are well correlated with those in many shallow-marine regions including the base Jurassic GSSP of TJB at Kuhjoch in Austria, suggesting that three NCIEs in the Tethys and mid-Panthalassa likely reflected global perturbations of the carbon cycle, rather than local phenomena. Based on the Os isotopic records correlated with $\delta^{13}C_{org}$ stratigraphic profiles, the mid-Panthalassic NCIEs can be interpreted as the consequences of the multiple emplacements of CAMP volcanism.

On the other hand, despite the oxic deep mid-Panthalassa, widespread ocean anoxia and associated deficits of nutrients around the TJB were recently identified in the Eastern Panthalassa. Since the redox conditions were quite different between shallow-marine regions and mid-Panthalassic sites, information regarding nutrient concentrations in the mid-Panthalassa is required. Oceanic fixed nitrogen is a bio-limiting component in the modern ocean, and total nitrogen isotopic composition ($\delta^{15}N_{TN}$) of sedimentary rocks is a useful tool for the reconstruction of ancient nitrogen cycles. To advance our understanding on the global nitrogen cycle, this study for the first time provides Rhaetian to Hettangian $\delta^{15}N_{TN}$ records in combined with Mo and U concentrations from the shales in the Katsuyama section. Based on the newly obtained data-set, I comprehensively discuss relative concentrations of biologically available nitrogen compounds in the mid-Panthalassa, their possible association with the redox condition, and biodiversity during the Triassic-Jurassic transition.

Keywords: Central Atlantic Magmatic Provinces (CAMP), Panthalassic ocean, Nitrogen isotopes, Redox sensitive elements, Bedded cherts, Japan

©2019. Japan Geoscience Union. All Right Reserved.

©2019. Japan Geoscience Union. All Right Reserved.

[J] Oral | B (Biogeosciences)：B-CG Complex & General

Tue. May 28, 2019 1:45 PM - 3:15 PM JST | Tue. May 28, 2019 4:45 AM - 6:15 AM UTC | 105 1F

[B-CG08] Phanerozoic biodiversity change: Extinction and diversification

convener:Yukio Isozaki(Department of Earth Science and Astronomy, Multi-disciplinary Sciences - General Systems Studies, Graduate School of Arts and Sciences, The University of Tokyo), Yusuke Sawaki(The University of Tokyo), Chairperson:Wataru Fujisaki(Japan Agency for Marine-Earth Science and Technology)

Phanerozoic biodiversity is the consequence of repeated extinctions and following diversifications in the past, which were caused by large-scale environmental changes, in particular, by extremely rapid and drastic forcing that changed the environments of the biosphere. Irreversible and episodic changes in material cycling on the planet and influences of severe galactic cosmic radiation enhanced by encounter with dark cloud are nominated as major driving mechanisms for the alleged rapid, large-scale environmental perturbations. The biodiversity change in the fossiliferous Phanerozoic record is characterized by 5 major mass extinctions within the long-term trend of diversity increase. Nonetheless, each extinction event has been explained rather in ad hoc manner, without any universal explanation. Therefore, ultimate triggers that caused the Phanerozoic biodiversity still remain as unsolved issues. This session discusses the ancient environmental changes related to Phanerozoic biodiversity under a new light of the recent progress in geology.

1:45 PM - 2:00 PM JST | 4:45 AM - 5:00 AM UTC

[BCG08-05] Transition of biodiversity in mobile populations and the small world in local subpopulations

*Kota Imaoka[1], Kazuhito Yamasaki[1] (1.Kobe University Graduate school of Science)

2:00 PM - 2:15 PM JST | 5:00 AM - 5:15 AM UTC

[BCG08-06] Rivision of the lowermost Cambrian SSF stratigraphy

*KONO SENA[1], Yukio Isozaki[1], Tomohiko Sato[2], Xingliang Zhang[3], Wei Liu[3] (1.The University of Tokyo School of Arts &Sciences, 2.Earth-Life Science Institute, Tokyo Institute of Technology, 3.Northwest university, China)

2:15 PM - 2:30 PM JST | 5:15 AM - 5:30 AM UTC

[BCG08-07] $\delta^{88}Sr$ and $^{87}Sr/^{86}Sr$records of the Middle-Late Permian seawater: mass extinction-relevant change in ocean Sr budget

*Tomomi Kani[1], Yukio Isozaki[2], Keiji Misawa[3], Akira Ishikawa[4], Shigekazu Yoneda[5] (1.Kumamoto University, 2.The University of Tokyo, 3.National Institute of Polar Research, 4.Tokyo Tech, School of Science, 5.National Museum of Nature and Science)

2:30 PM - 2:45 PM JST | 5:30 AM - 5:45 AM UTC

[BCG08-08] Formation of stratiform manganese deposits during the Carnian (Late Triassic) “pluvial event” in the pelagic Panthalassa

*Yuki Tomimatsu[1], Tetsuji Onoue[2], Daisuke Yamashita[3], Tatsuo Nozaki[4,5,6,7], Yutaro Takaya[8] (1.Graduate school of Science and Technology, Kumamoto University, 2.Faculty of Advanced Science and Technology, Kumamoto University , 3.Satsumasendai City Office, 4.Research and Development Center for Submarine Resources, Japan Agency for Marine-Earth Science and Technology, 5.Frontier Research Center for Energy and Resources (FRC- ER), Graduate School of Engineering, Tokyo University, 6.Department of Planetology, Graduate School of Science, Kobe University, 7.Ocean Resources Research Center for Next Generation, Chiba Institute of Technology, 8.Department of Resources and Environmental Engineering School of Creative Science and Enginerring, Waseda University)

2:45 PM - 3:00 PM JST | 5:45 AM - 6:00 AM UTC

[BCG08-09] Enrichment of chalcophile elements in Cretaceous–Paleogene boundary clays

*Teruyuki Maruoka[1], Yoshiro Nishio[2] (1.Faculty of Life and Environmental Sciences, University of Tsukuba, 2.Research and Education Faculty, Kochi University)

3:00 PM - 3:15 PM JST | 6:00 AM - 6:15 AM UTC

[BCG08-10] Mass extinctions: hierarchy of causes and cosmoclimatological perspective

*Yukio Isozaki[1] (1.Department of Earth Science and Astronomy, Multi-disciplinary Sciences - General Systems Studies, Graduate School of Arts and Sciences, The University of Tokyo)

Transition of biodiversity in mobile populations and the small world in local subpopulations

*Kota Imaoka[1], Kazuhito Yamasaki[1]

1. Kobe University Graduate school of Science

Speciation is one of the factors that influences ecological biodiversity on the geological time scale (Gould 1989, Kawata, 2000). So its mechanism is the important paleontological theme that leads to learn evolution. The basic mechanism is reproductive isolation. Allopatric speciation needs geographical barriers that divide the population into two subpopulations and block the genetic flow between them of individuals (Hubbell, 2001). These isolated groups accumulate incompatible genes leading to reproductive. Sympatric speciation happens with ecological interactions in the same niche. Difference of resources and habits leads to disruptive selection and ultimately to speciation (Gavrilets, 2003). Recently, a neutral theory of speciation, without geographical barriers or ecological interactions, has been shown to predict many patterns consistent with the behaviors observed in nature, e.g. species abundance distributions and species-area relationships. This neutral speciation is driven by physical and genetic distances which are essential for assortative mating. As the condition is restricted, speciation is promoted. Such a speciation model is named 'topopatric speciation'. In addition, another factor that influences ecological biodiversity on the geological time scale is radiation (Yamasaki et al., 1999). However, many studies of topopatric speciation consider standing still populations. So we considered mobile populations and the effect of them on speciation and ecological system. Our study may show that mechanism of speciation and how populations increased their biodiversity in the past. Moreover, we considered the spatial structure of each species with networks and quantitatively showed the distribution of populations on the process of speciation. This study uses a multi agent system to simulate the neutral stochastic evolution without natural selection. We consider an initial population of diploid and genetically identical individuals. In reproduction, we extend the Dobzhansky-Muller model to the most general form contains multiple alleles. A species is defined as the concept of ring species (Irwin et al., 2001, 2005). In the simulations, we found not only the number of species in the space, but also species diversity (species abundance distributions) and genetic diversity (heterozygosity). Furthermore, we calculated average path lengths and clustering coefficients by considering individuals as nodes and linking between them which can reproduce. Our simulations showed that the number of species and species diversity, genetic diversity changed depending on the mobile speed in populations. Accordingly, the difference of mobile speed in populations influences on biodiversity. In addition, from our results we predict species abundance distributions and species-area relationships. The highest species richness was found at minimum mobile speed, then average path length is smaller and clustering coefficient is larger. So this shows that the populations have a feature of 'small world' on the network. In the small world, we can communicate quickly each other and have many strong connections. In other words, individuals can exchange genomes quickly each other and have many mates. Thus, speciation is promoted by dividing the population into local subpopulations that form the small world and accumulating genetic variation. Consequently, in mobile population, assortative mate based on isolation by physical and genetic distance without geographical barriers and ecological interactions leads to divide population and speciation.

Keywords: speciation, biodiversity, biological diffusion, Dobzhansky-Muller model, the small world

©2019. Japan Geoscience Union. All Right Reserved.

Rivision of the lowermost Cambrian SSF stratigraphy

*KONO SENA[1], Yukio Isozaki[1], Tomohiko Sato[2], Xingliang Zhang[3], Wei Liu[3]

1. The University of Tokyo School of Arts &Sciences, 2. Earth-Life Science Institute, Tokyo Institute of Technology, 3. Northwest university, China

The earliest Cambrian evolution of animals is marked by the appearance and rapid diversification of small shelly fossils (SSFs). We examined the litho- and bio stratigraphy of the lowermost Cambrian at the Xiaolantian and Hongjiachong sections in the Chengjiang area, eastern Yunnan, South China. By analyzing both outcrop and drilled core samples, we picked up many SSFs from the ca. 30 m-thick phosphorites (Zhongyicun Mb), and obtained the following results.1) the Zhongyicun Mb comprises 6 lithostratigraphic units, which include Unit 3 with characteristic black mudstone beds for a significant key for the mid-Zhongyicun Mb.2)SSFs were found from 26 horizons out of 83 in the Zhongyicun Mb and the overlying Dahai Mb. Five zones were discriminated. Interval 1 with*Acanthocasis orthocanthus, Spirellus* sp., *Protohertzina unguloformis* and*Protohertzina anabarica*(from uppermost of Unit 1 to lower part of Unit 2); Interval 2 with *Ocruranus finial, Purella*sp.and*Yunnanopleura biformis*(from upper part of Unit 2). This marks the first occurrence of cap-shaped SSFs. Interval 3 with *Helcionella*sp.and*Oelandiella korobkovi*(from Unit 3). Interval 4 with *Obtusoconus*sp.,*Conopoconis*sp. and*Erongia acculatus*(from lower part of Unit 6). Interval 5 with*Igorella* sp., *Bemella simplelx*and*Paragloborilus subglobosus*(from upper part of Unit 6). 3) In addition, at the Hongjiachong section, a unique interval with *Halkieria* sp.*,Pteromus* sp.and*Sinosachites delicatus*occurs between Interval 1 and 2.

These results from the Xiaolantian and Hongjiachong sections, the following 6 SSF zones are proposed here. Namely, 1)*Acanthocasis orthocanthus- Protohertzina anabarica*Zone, 2) *Halkieria- Pteromus*Zone, 3) *Ocruranus finial-Yunnanopleura biformis*Zone, 4)*Paracarinachites sinensis-Oelandiella korobkovi*Zone, 5) *Obtusoconus-Conopoconis*Zone, and 6) *Igorella -Bemella simplelx*Zone.Previously the Zhongyicun Mb was divided into two SSF assemblage zones (Steiner et al., 2007); however, the present study offers 6 zones. It is noteworthy that the key bed in the mid-Zhongyicun Mb, restricted within the*Paracarinachites sinensis-Oelandiella korobkovi*Zone,appears useful for regional correlation.

Keywords: Cambrain, SSF, Yunnan

©2019. Japan Geoscience Union. All Right Reserved.

δ^{88}Sr and ^{87}Sr/^{86}Srrecords of the Middle-Late Permian seawater: mass extinction-relevant change in ocean Sr budget

*Tomomi Kani[1], Yukio Isozaki[2], Keiji Misawa[3], Akira Ishikawa[4], Shigekazu Yoneda[5]

1. Kumamoto University, 2. The University of Tokyo, 3. National Institute of Polar Research, 4. Tokyo Tech, School of Science, 5. National Museum of Nature and Science

As Sr isotope compositions in seawater are globally homogeneous, these proxies are useful in checking marine Sr budget change in direct link to global calcium cycle. ^{87}Sr/^{86}Sr valueis mainlydriven by two input fluxes to seawater; riverine flux connected with weathering of time-integrated radiogenic old continent and hydrothermal input flux derived from less radiogenic mantle. δ^{88}Sr in seawaterreflects marine calcium carbonate input/output flux. The marine Sr budget changed dramatically, in particular, during the Guadalupian (Middle Pemian), with the lowest value of seawater ^{87}Sr/^{86}Sr in the Phanerozoic, i.e., “the Capitanian minimum”. This likely reflected a major global environmental change associated with the end-Guadalupian mass extinction. Likewise, the δ^{88}Sr started to decrease in the Early Permian, and reached the Phanerozoic lowest value at the end of Capitanian (late Guadalupian). We measured δ^{88}Sr values of the Middle-Upper Permian marine carbonates with detailed biostratigraphy by TRITONTIMS, with correction of isotope fractionation during mass spectrometry with ^{87}Sr-^{84}Sr double spike. Analyzed samples were from various localities in the world, e.g., the Akasaka paleo-atoll limestone (Japan), and shelf carbonates in S. China. These results confirmed that both in stable δ^{88}Sr and radiogenic ^{87}Sr/^{86}Sr ratios, low values remained throughout the Guadalupian, whereas they increased in the Wuchiapingian. The extremely low δ^{88}Sr value in seawater may reflect the increased dissolution of carbonates and/or reduced carbonate burial, i.e., enhanced carbonate weathering or suppression of reef building on shelf settings according to the coeval global sea-level drop.

Keywords: Permian, Sr isotope, carbonate

©2019. Japan Geoscience Union. All Right Reserved.

Formation of stratiform manganese deposits during the Carnian (Late Triassic) “pluvial event” in the pelagic Panthalassa

*Yuki Tomimatsu[1], Tetsuji Onoue[2], Daisuke Yamashita[3], Tatsuo Nozaki[4,5,6,7], Yutaro Takaya[8]

1. Graduate school of Science and Technology, Kumamoto University, 2. Faculty of Advanced Science and Technology, Kumamoto University , 3. Satsumasendai City Office, 4. Research and Development Center for Submarine Resources, Japan Agency for Marine-Earth Science and Technology, 5. Frontier Research Center for Energy and Resources (FRC- ER), Graduate School of Engineering, Tokyo University, 6. Department of Planetology, Graduate School of Science, Kobe University, 7. Ocean Resources Research Center for Next Generation, Chiba Institute of Technology, 8. Department of Resources and Environmental Engineering School of Creative Science and Enginerring, Waseda University

Stratiform manganese deposits have been reported from the Triassic bedded chert sequences in the Japanese accretionary complexes, which are considered to have accumulated in a mid–oceanic basin of the Panthalassa Ocean.However, their precise mineralization age and depositional environment remain poorly understood. In the present study, we investigated lithostratigraphy, conodont and radiolarian ages, and geochemistry of bedded cherts and chert-hosted manganese deposits from the Jurassic accretionary complexes (Chichibu, Mino–Tamba, and Northern Kitakami Belts) in Japan.
The studied sequences are classified into three to four lithostratigraphical units; lower bedded chert, massive chert, manganese ore (30-150 cm thick), and upper bedded chert units in ascending order. Radiolarian fossils from the lower bedded chert unit indicate the Early Carnian age, based on the occurrence of *Capnuchosphaera deweveri*and *C. triassica*, whereas the upper bedded chert unit contains Late Carnian radioralian species, including *Poulpus carcharus*and *Trialatus megacornutus*. Conodonts extracted from the upper bedded chert unit also include Late Carnian species, such as *Paragondolella praelindae*and*Metapolygnathus praecommunisti*. These occurrences of microfossils suggest that the sedimentary age of the manganese ores can be constrained from the late Early Carnian to early Late Carnian. Chemical compositions of the manganese ore are characterized by the enrichments in Mn and low concentrations of Co, Ni, and Zn. These geochemical features are similar to those in modern submarine hydrothermal manganese deposits. On the other hand, highly enrichments in V, Ni, Zn, U, and high U/Th ratio were recognized in the massive chert unit below the manganese ores, which indicate deposition under a reducing depositional environment.
Our biostratigraphic and geochemical analyses indicate that a redox state change from anoxic to oxic environments occurred in a pelagic deep seafloor in the late Early to early Late Carnian. This interval is known as a period of increased rainfall, named the Carnian Pluvial Event (CPE) in the western Tethys. CPE is characterized by the increased continental weathering which led to the increased nutrient flux and triggered the development of anoxia. It is likely that the Upper Triassic manganese deposits may have been formed during recovery from the reducing environment associated with the CPE.

Keywords: Stratiform manganese deposit, Triassic, Carnian Pluvial Event, Jurassic accretionary complex, Microfossil, Geochemistry

©2019. Japan Geoscience Union. All Right Reserved.

Enrichment of chalcophile elements in Cretaceous–Paleogene boundary clays

*Teruyuki Maruoka[1], Yoshiro Nishio[2]

1. Faculty of Life and Environmental Sciences, University of Tsukuba, 2. Research and Education Faculty, Kochi University

Cretaceous-Paleogene (K-Pg) boundary clays are enriched in chalcophile elements along with siderophile elements [1]. As elemental ratios of siderophile elements in the K-Pg boundary clays are very similar to chondritic values, the enrichment of siderophile elements in the K-Pg boundary clays results from the incorporation of meteorite condensates. On the other hand, it cannot be assumed that the chalcophile elements in the K-Pg boundary clays were supplied by meteorite condensates, because the ratios of chalcophile and siderophile elements in the K-Pg boundary clays, such as Zn/Ir, As/Ir, and Sb/Ir, are one to two orders of magnitude higher than those in chondrites. In this study, to elucidate the processes that could have contributed to the enrichment of chalcophile elements in the K-Pg boundary clays, we analyzed the chemical compositions of major and trace elements in the K-Pg boundary clays from Stevns Klint in Denmark.

The concentrations of major and trace elements in the K-Pg boundary clays varied among the collected samples even from neighboring outcrops. Cross plots of the concentrations of these elements suggested the mixing of three materials with different chemical compositions. The first component was enriched in all chalcophile elements and iron. The second component was depleted in chalcophile elements and enriched in calcium. The third component was enriched particularly in copper, silver, and lead. The first and third components included iridium that was obviously supplied at the K-Pg meteorite impact. Therefore, these two components were produced by phenomena related to the K-Pg meteorite impact. We propose that chalcophile elements were supplied to the K-Pg boundary clays by a combination of impact heating of the target rocks and intense acid rain following the impact.

Iron oxide/hydroxide grains with sizes of one to several tens of nanometers have been previously observed in the K-Pg boundary clays [2]. These likely condensed from the vapor plume that formed by impact heating at the K-Pg meteorite impact. These iron oxides/hydroxides could absorb chalcophile and siderophile elements from seawater. Such materials would have been converted to pyrites incorporating chalcophile elements under the reductive conditions on the seafloor. In addition, the correlations between the concentrations of chalcophile elements and soot have been observed in the K-Pg boundary clays [3]. This soot could have been produced by the impact heating of hydrocarbons in the target rocks. Bacterial sulfate reduction and subsequent pyrite production occur in reducing environments where hydrocarbon deposition occurs, thus resulting in the simultaneous accumulation of pyrite and hydrocarbons. Therefore, chalcophile elements accompanied by soot may have been released by impact heating of pyrite in the target rocks. Both chalcophile elements and iron, which were enriched in the first component, could have been provided by the impact heating of the target rocks.

Copper, silver, and lead, which were concentrated in the third component, are generally concentrated in acid soluble sulfides such as sphalerite and galena. Therefore, the third component was possibly supplied by intense acid rain after the K-Pg impact.

In summary, chalcophile elements in the K-Pg boundary clays comprises two components, one that is enriched in all chalcophile elements and another that is enriched particularly in copper, silver, and lead. These components were likely supplied by phenomena associated with the meteorite impact at the K-Pg boundary, such as the impact heating of the target rocks and intense acid rain.

References [1] Schmitz (1985) Geochim. Cosmochim. Acta 49, 2361-2370 [2] Belza et al. (2017)

©2019. Japan Geoscience Union. All Right Reserved.

Geochim. Cosmochim. Acta 202, 231-263 [3] Gilmour and Anders (1989) Geochim. Cosmochim. Acta 53, 503-511

Keywords: meteorite impact, impact heating, acid rain

©2019. Japan Geoscience Union. All Right Reserved.

Mass extinctions: hierarchy of causes and cosmoclimatological perspective

*Yukio Isozaki[1]

1. Department of Earth Science and Astronomy, Multi-disciplinary Sciences - General Systems Studies, Graduate School of Arts and Sciences, The University of Tokyo

This paper reviews possible causes proposed for the double-stepped extinction in regard of the current status of mass extinction studies. Causes of extinction can be grouped into four categories; from small to large scale, Caterogry 1 to Category 4. Category 1 –direct kill mechanism, Category 2 –global environmental change, Category 3 –trigger on the planet’ s surface, and Category 4 –ultimate cause. Among the Big-5 mass extinctions of the Phanerozic, two events in the Paleozoic, i.e.,the Hirnantian (Ordovician) and end-Guadalupian (Permian) events, show significant similarities in various aspects. Biological and non-biological aspects unique to these two distinct events include changes in biodiversity, isotope ratios (C, Sr *etc.*) of seawater, sea level, ocean redox state, episodic volcanism, and geomagnetism. In particular, the similar appearance of global cooling (Category 2) suggests the same cause and processes were likely responsible for the biodiversity drop. In addition to the most prevalent scenario of mantle plume-generated large igneous provinces (LIPs) (Category 3) for the end-Permian extinction, an emerging perspective of cosmoclimatology is introduced with respect to astrobiology. Galactic cosmic radiation (GCR) and solar/terrestrial responses in magnetism (Category 4) could have had a profound impact on Earth’ s climate, in particular, on extensive cloud coverage (irradiance shutdown). Furthermore, the star-burst events detected in the Milky Way Galaxy apparently coincide in timing with the cooling-associated major extinctions of the Phanerozoic and also with the Proterozoic snowball Earth episode. As an ultimate cause (Category 4) for major extinction, the episodic increase in GCR flux from the source (dark clouds derived from star-burst) against the geomagnetic shield likely determined the major climate changes, particularly global cooling in the past. The study of mass extinctions on Earth is entering a new stage with a new astrobiological perspective.

Keywords: mass extinction, global cooling, GCR, extinction cause

©2019. Japan Geoscience Union. All Right Reserved.

[J] Poster | B (Biogeosciences)：B-CG Complex & General

Tue. May 28, 2019 3:30 PM - 5:00 PM JST | Tue. May 28, 2019 6:30 AM - 8:00 AM UTC | Poster Hall International Exhibition Hall8, Makuhari Messe_23

[B-CG08] Phanerozoic biodiversity change: Extinction and diversification

convener:Yukio Isozaki(Department of Earth Science and Astronomy, Multi-disciplinary Sciences - General Systems Studies, Graduate School of Arts and Sciences, The University of Tokyo), Yusuke Sawaki(The University of Tokyo)

Phanerozoic biodiversity is the consequence of repeated extinctions and following diversifications in the past, which were caused by large-scale environmental changes, in particular, by extremely rapid and drastic forcing that changed the environments of the biosphere. Irreversible and episodic changes in material cycling on the planet and influences of severe galactic cosmic radiation enhanced by encounter with dark cloud are nominated as major driving mechanisms for the alleged rapid, large-scale environmental perturbations. The biodiversity change in the fossiliferous Phanerozoic record is characterized by 5 major mass extinctions within the long-term trend of diversity increase. Nonetheless, each extinction event has been explained rather in ad hoc manner, without any universal explanation. Therefore, ultimate triggers that caused the Phanerozoic biodiversity still remain as unsolved issues. This session discusses the ancient environmental changes related to Phanerozoic biodiversity under a new light of the recent progress in geology.

[BCG08-P01] Marine Osmium isotope record across the Aptian/Albian boundary to elucidate the relationship between the Oceanic Anoxic Event 1b and massive volcanic activities at the Southern Kerguelen Plateau

*Hironao Matsumoto[1], Junichiro Kuroda[1], Rodolfo Coccioni[2], Naohiko Ohkouchi[3], Nanako O. Ogawa[3], Saburo Sakai[3], Katsuhiko Suzuki[3], Fabrizio Frontalini[2], Andrea Mazzoli[2] (1.Department of Earth and Planetary Science, The University of Tokyo, 2.DiSPeA, University of Urbino, 3.Japan Agency for Marine-Earth Science and Technology)

[BCG08-P02] Rhaetian (Late Triassic) conodont biostratigraphy of the Panthalassa Ocean and the final extinction of conodonts at the end of the Triassic

*Kanna Yamasaki[1], Daisuke Yamashita[2], Tetsuji Onoue[1] (1.Kumamoto University, 2.Satsumasendai City Office)

[BCG08-P03] Paleoenvironmental changes across the Permian/Triassic boundary sections in the Mino Belt, central Japan

*Shinya Uemura[1], Tetsuji Onoue[1] (1.Kumamoto University)

[BCG08-P04] Geotectonic history of Mona Complex in Anglesey-Lleyn, Wales

*HISASHI ASANUMA[1], Yusuke Sawaki[1], Shigenori Maruyama[2] (1.The University of Tokyo, 2.Earth-Life Science Institute, Tokyo Institute of Technology)

[BCG08-P05] Radiogenic Sr isotope chemostratigraphy of the Ediacaran Doushantuo Formation in the Yangtze Craton, South China

*Yusuke Sawaki[1] (1.The University of Tokyo)

Marine Osmium isotope record across the Aptian/Albian boundary to elucidate the relationship between the Oceanic Anoxic Event 1b and massive volcanic activities at the Southern Kerguelen Plateau

*Hironao Matsumoto[1], Junichiro Kuroda[1], Rodolfo Coccioni[2], Naohiko Ohkouchi[3], Nanako O. Ogawa[3], Saburo Sakai[3], Katsuhiko Suzuki[3], Fabrizio Frontalini[2], Andrea Mazzoli[2]

1. Department of Earth and Planetary Science, The University of Tokyo, 2. DiSPeA, University of Urbino, 3. Japan Agency for Marine-Earth Science and Technology

Several organic-rich sediments (black shales) were deposited in the Tethys and the Atlantic Oceans from the uppermost Aptian to the lower Albian. In particular, four prominent black shale layers have been identified (i.e., Jacob, Kilian, Urbino/Paquier, and Leenhardt levels in stratigraphic order) as the sedimentary expression of Oceanic Anoxic Event (OAE) 1b. The OAE1b is characterized by a major planktic foraminiferal turnover in the Cretaceous period and its exceptionally long duration. In spite of its significant impact on the marine biological evolution, the OAE1b is one of the least studied Cretaceous OAEs. Massive volcanic activities associated with the emplacement of Southern Kerguelen Plateau were ascribed as the trigger mechanisms for the OAE1b. However, the large uncertainties in the radiometric age of Southern Kerguelen Plateau and the sedimentary sequence of OAE1b have however hampered the definition of their causal relationship. Paleo-seawater osmium isotopic record ($^{187}Os/^{188}Os$) is a powerful tool to detect the timing of volcanic pulse. Marine $^{187}Os/^{188}Os$ value mainly reflects the balance between radiogenic osmium flux from the continental crust ($^{187}Os/^{188}Os$ ~1.0-1.5) and unradiogenic osmium flux through hydrothermal activities ($^{187}Os/^{188}Os$ ~0.12). Thus, the relative contribution of hydrothermal activities (or the submarine volcanic activities) can be reconstructed from the paleo-seawater $^{187}Os/^{188}Os$ variation recorded in the sedimentary rocks. In this study, we present a new record of marine Os isotopic record from the Late Aptian to Early Albian to reveal the timing of massive volcanic activities and its relationship with OAE1b.

Pelagic sedimentary rock samples were collected from two sites; 1) Poggio le Guaine (PLG) section (Italy) that was deposited in the central-western Tethys Ocean, and 2) Deep Sea Drilling Project (DSDP) Site 463 drilled at the western Mid-Pacific Mountains in the Pacific Ocean. Based on the micropaleontological study on planktonic foraminifera and carbon isotopic analysis of bulk inorganic carbon, the stratigraphy of these two sections was precisely correlated. Indeed, the stratigraphic interval equivalent to the Jacob and Kilian levels were identified for the first time in the Pacific region. Variations of initial $^{187}Os/^{188}Os$ values were consistent between PLG section and DSDP Site 463 and summarized as follows; 1) relatively stable $^{187}Os/^{188}Os$ values in the pre-OAE1b interval, 2) decline of $^{187}Os/^{188}Os$ values at the onset of OAE1b, (3) a first sharp drop of $^{187}Os/^{188}Os$ at the extinction level, (4) a second sharp drop followed by an abrupt increase in the $^{187}Os/^{188}Os$ values at the Kilian level, and (5) fluctuation of $^{187}Os/^{188}Os$ values above the Kilian level. Combining $^{187}Os/^{188}Os$ data and other geochemical data, we interpreted that the drops of $^{187}Os/^{188}Os$ values at the extinction and Kilian levels were induced by pulses of hydrothermal activities. Massive volcanic eruptions at the Southern Kerguelen Plateau is one of the most likely candidates to have caused the decreases in isotopic composition of osmium of seawater recorded at PLG section and DSDP Site 463. The close correspondence of osmium spikes to the extinction events within the OAE1b would support a causal link between the volcanic eruptions at the Southern Kerguelen Plateau and the biotic turnover recorded across Aptian/Albian boundary.

©2019. Japan Geoscience Union. All Right Reserved.

Keywords: Oceanic Anoxic Event 1b, Osmium isotope ratio, large igneous province

©2019. Japan Geoscience Union. All Right Reserved.

Rhaetian (Late Triassic) conodont biostratigraphy of the Panthalassa Ocean and the final extinction of conodonts at the end of the Triassic

*Kanna Yamasaki[1], Daisuke Yamashita[2], Tetsuji Onoue[1]

1. Kumamoto University, 2. Satsumasendai City Office

The Rhaetian stage of the Triassic was a period characterized by intense biological, climate and environmental changes, ending with the break-up of the supercontinent Pangaea and the occurrence of the End-Triassic mass Extinction (ETE), one of the big five extinctions documented during the Phanerozoic. It is noteworthy that the ETE seems to be associated with significant $d^{13}C$ perturbations (CIEs), commonly related to the CAMP eruptive phases. The stratigraphic record of these environmental changes has been recently reported from the Upper Triassic bedded chert successions in Japan, deposited within a Paleo-Pacific (Panthalassa) deep basin. The chronology for the Rhaetian pelagic in the Panthalassa Ocean is based on the radiolarian zonation, which is well established in the Upper Triassic bedded chert successions in the Mino Belt, central Japan. Although accurate calibration for the chronostratigraphic stages and substages are established basically by means of ammonites and conodonts, most of the Japanese radiolarian zones were calibrated through correlation with zonal schemes established in other regions, and have not been calibrated conodont biostratigraphy.

Here we present Upper Norian to Rhaetian conodont biostratigraphy of an Upper Triassic bedded chert succession from the Mino belt, central Japan, where the radiolarian biostratigraphy has been investigated (Hori, 1992; Sugiyama, 1997). Based on the stratigraphic distributions of marker species, four conodont zones were defined: the *Mocina bidentata* Zone, the *Misikella hernsteini* Zone, the *M. posthernsteini* zone, and the *M. ultima* zone, in ascending order. These conodont zones are comparable to the standard Late Norian and Rhaetian conodont zones of western Tethys. The Norian/Rhaetian boundary in the study section is tentatively placed between the last occurrence of a Norian radiolarian species (*Betraccium deweveri*) and the first occurrences of Rhaetian conodont species (*M. posthernsteini*). The intercalibrated conodont—radiolarian biostratigraphy from the section accurately calibrates the radiolarian zones in Japan with standard chronostratigraphic stages and substages.

Keywords: Late Triassic, biostratigraphy, conodont, bedded chert, Mino belt, Panthalassa Ocean

©2019. Japan Geoscience Union. All Right Reserved.

Paleoenvironmental changes across the Permian/Triassic boundary sections in the Mino Belt, central Japan

*Shinya Uemura[1], Tetsuji Onoue[1]

1. Kumamoto University

The ca. 251 Ma Permian/Triassic boundary (PTB) records the largest biotic catastrophe in the Phanerozoic. A considerable amount of work for the PTB event has been done on the Tethyan platforms and peri -Pangean shelves, and some possible causes have been proposed to explain the extinction event: oceanic anoxia, meteorite impact, flood basalt volcanism and global warming. Sano et al. (2010, 2012) reported the stratigraphic variations of TOC, $\delta^{13}C_{org}$ and the number of Permian radiolarian species in the PTB siliceous rock section of the Mino Belt, central Japan, and inferred that a reducing condition in the deep Panthalassic Ocean at the PTB. In this study, we examined the geochemical and mineral compositions of the exactly the same sections of Sano et al. (2010, 2012).
The study sections, namely NF1212F and NF195, consist of Upper Permian chert (Changshingian) and Lower Triassic (Induan) black claystone intermittently with thin chert beds. A total 81 clatstone samples were obtained from the NF1212F and NF195 sections. Powder x-ray diffraction (XRD) analysis shows that the claystones below the PTB contained quartz, magnetite, illite and chlorite, while all the claystone above the boundary only contained quartz and illite. The results of XRF and ICP-MS analysis revealed that redox-sensitive trace-element (vanadium [V], chromium [Cr], molybdenum [Mo], and uranium [U]) increase in the uppermost Permian chert beds. The increasing trend in Mo/U ratio from 150 cm to 25 cm below the PTB indicates shift from anoxic to euxinic conditions. This trend suggests that strong reducing conditions developed just before the end-Permian mass extinction.

Keywords: Permian/ Triassic boundary, bedded chert, Mino belt, Panthalassic ocean, ocean anoxia

©2019. Japan Geoscience Union. All Right Reserved.

Geotectonic history of Mona Complex in Anglesey-Lleyn, Wales

*HISASHI ASANUMA[1], Yusuke Sawaki[1], Shigenori Maruyama[2]

1. The University of Tokyo, 2. Earth-Life Science Institute, Tokyo Institute of Technology

The Mona Complex in Anglesey-Lleyn records a Precambrian subduction-accretion orogeny on the Avalonian margin. It contains an accreted remnant of an oceanic crust and calc-alkaline igneous and high-pressure metamorphic rocks. Their geochronological study plays a key role in comprehension of geotectonic evolution of the Avalonian subduction system. Therefore, we have conducted U-Pb dating of detrital zircons from volcano-sedimentary rocks in the Monian Supergroup, and then K-Ar dating of white micas from pelitic and mafic schists in the Blueschist unit, the Central Shear Zone, and the New Harbour Group. Our new chronological dataset leads to re-interpretation of Anglesey-Lleyn geotectonic framework in terms of a younger analogue of comparable blueschist belts and accretionary orogens in Japan and California.

The evidences of arc-related magmatism are widely distributed in Wales and Central England, and they date back to 760 Ma. Age data of calc-alkaline granites suggest that the Avalonian subduction and its arc-related magmatism had already started by 711–677 Ma. In the period of main arc magmatism (616–555 Ma), a subduction-related accretion of the Gwna Group sediments started (by 578 Ma) on an active margin of Avalonia. Its accretion likely continued to 530 Ma. Moreover, metamorphic rocks of the Blueschist unit and the Central Shear Zone were exhumed from different crustal depths in the interval 578–530 Ma. Afterwards, sedimentation of the New Harbour and South Stack Groups occurred at < 515 ±13 Ma and < 501 ±10 Ma. Sediments of the New Harbour and South Stack Groups were finally accreted underneath the base of the Gwna Group at the accretionary wedge. The greenschist facies metamorphism of the New Harbour Group at 474 Ma constrains its minimum depositional age. In a larger perspective, our new ages are broadly contemporaneous with the calc-alkaline continental arc magmatism in NW Wales and Central England that formed by successive eastward subduction from 711 to 474 Ma.

Keywords: Avalonia, Anglesey-Lleyn, Pacific-type orogeny

©2019. Japan Geoscience Union. All Right Reserved.

Radiogenic Sr isotope chemostratigraphy of the Ediacaran Doushantuo Formation in the Yangtze Craton, South China

*Yusuke Sawaki[1]

1. The University of Tokyo

The Ediacaran period records one of the most dramatic biological episodes in Earth's history. To decipher surface environmental changes occurring in the Ediacaran, a variety of geochemical proxies have been reported by a number of studies. Ediacaran sedimentary rocks in South China figure prominently in such studies, because they are fossiliferous and accumulated at various depositional settings from shallow marine to deep basin. Recent extensive geochemical works for the Doushantuo Formation in South China demonstrate that $\delta^{13}C$ values of carbonate were variable depending on the depositional settings. In order to test whether the difference reflect spacial or temporal variation, I focus on $^{87}Sr/^{86}Sr$ ratio as a chemostratigraphic tool. However, the existing $^{87}Sr/^{86}Sr$ values are limited to shallow marine deposits, which leaves ambiguity in a variation of $^{87}Sr/^{86}Sr$ ratios in outer ocean. Our group conducted on-land drilling at Siduping and Tianping sections in South China to obtain completely continuous sedimentary rocks deposited at slope facies. We newly report stratigraphic profiles of the $^{87}Sr/^{86}Sr$ ratios at the sections. $^{87}Sr/^{86}Sr$ chemostratigraphy demonstrated some diachronous natures of $\delta^{13}C$ within the Doushantuo Formation. The enhanced continental weathering during Gaskiers glaciation likely promoted bacterial sulfate reduction and aerobic respiration of organic matter. These resulted in low $\delta^{13}C$ values of dissolved inorganic carbon and accumulations of phosphate and dissolved CO_2 species in seawater, and eventually induced the deposition of phosphorites at the shelf margin. High $^{87}Sr/^{86}Sr$ ratios during the largest negative $\delta^{13}C$ anomaly in the Ediacaran can be also recognized in the continental slope sediment. This fact supports that globally high continental weathering rate led to massive remineralization of organic matter and a consequent significant negative $\delta^{13}C_{carb}$ excursion.

©2019. Japan Geoscience Union. All Right Reserved.

[J] Poster | B (Biogeosciences)：B-CG Complex & General

Tue. May 28, 2019 5:15 PM - 6:30 PM JST | Tue. May 28, 2019 8:15 AM - 9:30 AM UTC | Poster Hall International Exhibition Hall8, Makuhari Messe_41

[B-CG08] Phanerozoic biodiversity change: Extinction and diversification

convener:Yukio Isozaki(Department of Earth Science and Astronomy, Multi-disciplinary Sciences - General Systems Studies, Graduate School of Arts and Sciences, The University of Tokyo), Yusuke Sawaki(The University of Tokyo)

Phanerozoic biodiversity is the consequence of repeated extinctions and following diversifications in the past, which were caused by large-scale environmental changes, in particular, by extremely rapid and drastic forcing that changed the environments of the biosphere. Irreversible and episodic changes in material cycling on the planet and influences of severe galactic cosmic radiation enhanced by encounter with dark cloud are nominated as major driving mechanisms for the alleged rapid, large-scale environmental perturbations. The biodiversity change in the fossiliferous Phanerozoic record is characterized by 5 major mass extinctions within the long-term trend of diversity increase. Nonetheless, each extinction event has been explained rather in ad hoc manner, without any universal explanation. Therefore, ultimate triggers that caused the Phanerozoic biodiversity still remain as unsolved issues. This session discusses the ancient environmental changes related to Phanerozoic biodiversity under a new light of the recent progress in geology.

[BCG08-P01] Marine Osmium isotope record across the Aptian/Albian boundary to elucidate the relationship between the Oceanic Anoxic Event 1b and massive volcanic activities at the Southern Kerguelen Plateau

*Hironao Matsumoto[1], Junichiro Kuroda[1], Rodolfo Coccioni[2], Naohiko Ohkouchi[3], Nanako O. Ogawa[3], Saburo Sakai[3], Katsuhiko Suzuki[3], Fabrizio Frontalini[2], Andrea Mazzoli[2] (1.Department of Earth and Planetary Science, The University of Tokyo, 2.DiSPeA, University of Urbino, 3.Japan Agency for Marine-Earth Science and Technology)

[BCG08-P02] Rhaetian (Late Triassic) conodont biostratigraphy of the Panthalassa Ocean and the final extinction of conodonts at the end of the Triassic

*Kanna Yamasaki[1], Daisuke Yamashita[2], Tetsuji Onoue[1] (1.Kumamoto University, 2.Satsumasendai City Office)

[BCG08-P03] Paleoenvironmental changes across the Permian/Triassic boundary sections in the Mino Belt, central Japan

*Shinya Uemura[1], Tetsuji Onoue[1] (1.Kumamoto University)

[BCG08-P04] Geotectonic history of Mona Complex in Anglesey-Lleyn, Wales

*HISASHI ASANUMA[1], Yusuke Sawaki[1], Shigenori Maruyama[2] (1.The University of Tokyo, 2.Earth-Life Science Institute, Tokyo Institute of Technology)

[BCG08-P05] Radiogenic Sr isotope chemostratigraphy of the Ediacaran Doushantuo Formation in the Yangtze Craton, South China

*Yusuke Sawaki[1] (1.The University of Tokyo)

Marine Osmium isotope record across the Aptian/Albian boundary to elucidate the relationship between the Oceanic Anoxic Event 1b and massive volcanic activities at the Southern Kerguelen Plateau

*Hironao Matsumoto[1], Junichiro Kuroda[1], Rodolfo Coccioni[2], Naohiko Ohkouchi[3], Nanako O. Ogawa[3], Saburo Sakai[3], Katsuhiko Suzuki[3], Fabrizio Frontalini[2], Andrea Mazzoli[2]

1. Department of Earth and Planetary Science, The University of Tokyo, 2. DiSPeA, University of Urbino, 3. Japan Agency for Marine-Earth Science and Technology

Several organic-rich sediments (black shales) were deposited in the Tethys and the Atlantic Oceans from the uppermost Aptian to the lower Albian. In particular, four prominent black shale layers have been identified (i.e., Jacob, Kilian, Urbino/Paquier, and Leenhardt levels in stratigraphic order) as the sedimentary expression of Oceanic Anoxic Event (OAE) 1b. The OAE1b is characterized by a major planktic foraminiferal turnover in the Cretaceous period and its exceptionally long duration. In spite of its significant impact on the marine biological evolution, the OAE1b is one of the least studied Cretaceous OAEs. Massive volcanic activities associated with the emplacement of Southern Kerguelen Plateau were ascribed as the trigger mechanisms for the OAE1b. However, the large uncertainties in the radiometric age of Southern Kerguelen Plateau and the sedimentary sequence of OAE1b have however hampered the definition of their causal relationship. Paleo-seawater osmium isotopic record ($^{187}Os/^{188}Os$) is a powerful tool to detect the timing of volcanic pulse. Marine $^{187}Os/^{188}Os$ value mainly reflects the balance between radiogenic osmium flux from the continental crust ($^{187}Os/^{188}Os$ ~1.0-1.5) and unradiogenic osmium flux through hydrothermal activities ($^{187}Os/^{188}Os$ ~0.12). Thus, the relative contribution of hydrothermal activities (or the submarine volcanic activities) can be reconstructed from the paleo-seawater $^{187}Os/^{188}Os$ variation recorded in the sedimentary rocks. In this study, we present a new record of marine Os isotopic record from the Late Aptian to Early Albian to reveal the timing of massive volcanic activities and its relationship with OAE1b.

Pelagic sedimentary rock samples were collected from two sites; 1) Poggio le Guaine (PLG) section (Italy) that was deposited in the central-western Tethys Ocean, and 2) Deep Sea Drilling Project (DSDP) Site 463 drilled at the western Mid-Pacific Mountains in the Pacific Ocean. Based on the micropaleontological study on planktonic foraminifera and carbon isotopic analysis of bulk inorganic carbon, the stratigraphy of these two sections was precisely correlated. Indeed, the stratigraphic interval equivalent to the Jacob and Kilian levels were identified for the first time in the Pacific region. Variations of initial $^{187}Os/^{188}Os$ values were consistent between PLG section and DSDP Site 463 and summarized as follows; 1) relatively stable $^{187}Os/^{188}Os$ values in the pre-OAE1b interval, 2) decline of $^{187}Os/^{188}Os$ values at the onset of OAE1b, (3) a first sharp drop of $^{187}Os/^{188}Os$ at the extinction level, (4) a second sharp drop followed by an abrupt increase in the $^{187}Os/^{188}Os$ values at the Kilian level, and (5) fluctuation of $^{187}Os/^{188}Os$ values above the Kilian level. Combining $^{187}Os/^{188}Os$ data and other geochemical data, we interpreted that the drops of $^{187}Os/^{188}Os$ values at the extinction and Kilian levels were induced by pulses of hydrothermal activities. Massive volcanic eruptions at the Southern Kerguelen Plateau is one of the most likely candidates to have caused the decreases in isotopic composition of osmium of seawater recorded at PLG section and DSDP Site 463. The close correspondence of osmium spikes to the extinction events within the OAE1b would support a causal link between the volcanic eruptions at the Southern Kerguelen Plateau and the biotic turnover recorded across Aptian/Albian boundary.

©2019. Japan Geoscience Union. All Right Reserved.

Keywords: Oceanic Anoxic Event 1b, Osmium isotope ratio, large igneous province

©2019. Japan Geoscience Union. All Right Reserved.

Rhaetian (Late Triassic) conodont biostratigraphy of the Panthalassa Ocean and the final extinction of conodonts at the end of the Triassic

*Kanna Yamasaki[1], Daisuke Yamashita[2], Tetsuji Onoue[1]

1. Kumamoto University, 2. Satsumasendai City Office

The Rhaetian stage of the Triassic was a period characterized by intense biological, climate and environmental changes, ending with the break-up of the supercontinent Pangaea and the occurrence of the End-Triassic mass Extinction (ETE), one of the big five extinctions documented during the Phanerozoic. It is noteworthy that the ETE seems to be associated with significant $d^{13}C$ perturbations (CIEs), commonly related to the CAMP eruptive phases. The stratigraphic record of these environmental changes has been recently reported from the Upper Triassic bedded chert successions in Japan, deposited within a Paleo-Pacific (Panthalassa) deep basin. The chronology for the Rhaetian pelagic in the Panthalassa Ocean is based on the radiolarian zonation, which is well established in the Upper Triassic bedded chert successions in the Mino Belt, central Japan. Although accurate calibration for the chronostratigraphic stages and substages are established basically by means of ammonites and conodonts, most of the Japanese radiolarian zones were calibrated through correlation with zonal schemes established in other regions, and have not been calibrated conodont biostratigraphy.

Here we present Upper Norian to Rhaetian conodont biostratigraphy of an Upper Triassic bedded chert succession from the Mino belt, central Japan, where the radiolarian biostratigraphy has been investigated (Hori, 1992; Sugiyama, 1997). Based on the stratigraphic distributions of marker species, four conodont zones were defined: the *Mocina bidentata* Zone, the *Misikella hernsteini* Zone, the *M. posthernsteini* zone, and the *M. ultima* zone, in ascending order. These conodont zones are comparable to the standard Late Norian and Rhaetian conodont zones of western Tethys. The Norian/Rhaetian boundary in the study section is tentatively placed between the last occurrence of a Norian radiolarian species (*Betraccium deweveri*) and the first occurrences of Rhaetian conodont species (*M. posthernsteini*). The intercalibrated conodont—radiolarian biostratigraphy from the section accurately calibrates the radiolarian zones in Japan with standard chronostratigraphic stages and substages.

Keywords: Late Triassic, biostratigraphy, conodont, bedded chert, Mino belt, Panthalassa Ocean

©2019. Japan Geoscience Union. All Right Reserved.

Paleoenvironmental changes across the Permian/Triassic boundary sections in the Mino Belt, central Japan

*Shinya Uemura[1], Tetsuji Onoue[1]

1. Kumamoto University

The ca. 251 Ma Permian/Triassic boundary (PTB) records the largest biotic catastrophe in the Phanerozoic. A considerable amount of work for the PTB event has been done on the Tethyan platforms and peri -Pangean shelves, and some possible causes have been proposed to explain the extinction event: oceanic anoxia, meteorite impact, flood basalt volcanism and global warming. Sano et al. (2010, 2012) reported the stratigraphic variations of TOC, $\delta^{13}C_{org}$ and the number of Permian radiolarian species in the PTB siliceous rock section of the Mino Belt, central Japan, and inferred that a reducing condition in the deep Panthalassic Ocean at the PTB. In this study, we examined the geochemical and mineral compositions of the exactly the same sections of Sano et al. (2010, 2012).
The study sections, namely NF1212F and NF195, consist of Upper Permian chert (Changshingian) and Lower Triassic (Induan) black claystone intermittently with thin chert beds. A total 81 clatstone samples were obtained from the NF1212F and NF195 sections. Powder x-ray diffraction (XRD) analysis shows that the claystones below the PTB contained quartz, magnetite, illite and chlorite, while all the claystone above the boundary only contained quartz and illite. The results of XRF and ICP-MS analysis revealed that redox-sensitive trace-element (vanadium [V], chromium [Cr], molybdenum [Mo], and uranium [U]) increase in the uppermost Permian chert beds. The increasing trend in Mo/U ratio from 150 cm to 25 cm below the PTB indicates shift from anoxic to euxinic conditions. This trend suggests that strong reducing conditions developed just before the end-Permian mass extinction.

Keywords: Permian/ Triassic boundary, bedded chert, Mino belt, Panthalassic ocean, ocean anoxia

©2019. Japan Geoscience Union. All Right Reserved.

Geotectonic history of Mona Complex in Anglesey-Lleyn, Wales

*HISASHI ASANUMA[1], Yusuke Sawaki[1], Shigenori Maruyama[2]

1. The University of Tokyo, 2. Earth-Life Science Institute, Tokyo Institute of Technology

The Mona Complex in Anglesey-Lleyn records a Precambrian subduction-accretion orogeny on the Avalonian margin. It contains an accreted remnant of an oceanic crust and calc-alkaline igneous and high-pressure metamorphic rocks. Their geochronological study plays a key role in comprehension of geotectonic evolution of the Avalonian subduction system. Therefore, we have conducted U-Pb dating of detrital zircons from volcano-sedimentary rocks in the Monian Supergroup, and then K-Ar dating of white micas from pelitic and mafic schists in the Blueschist unit, the Central Shear Zone, and the New Harbour Group. Our new chronological dataset leads to re-interpretation of Anglesey-Lleyn geotectonic framework in terms of a younger analogue of comparable blueschist belts and accretionary orogens in Japan and California.

The evidences of arc-related magmatism are widely distributed in Wales and Central England, and they date back to 760 Ma. Age data of calc-alkaline granites suggest that the Avalonian subduction and its arc-related magmatism had already started by 711–677 Ma. In the period of main arc magmatism (616–555 Ma), a subduction-related accretion of the Gwna Group sediments started (by 578 Ma) on an active margin of Avalonia. Its accretion likely continued to 530 Ma. Moreover, metamorphic rocks of the Blueschist unit and the Central Shear Zone were exhumed from different crustal depths in the interval 578–530 Ma. Afterwards, sedimentation of the New Harbour and South Stack Groups occurred at < 515 ±13 Ma and < 501 ±10 Ma. Sediments of the New Harbour and South Stack Groups were finally accreted underneath the base of the Gwna Group at the accretionary wedge. The greenschist facies metamorphism of the New Harbour Group at 474 Ma constrains its minimum depositional age. In a larger perspective, our new ages are broadly contemporaneous with the calc-alkaline continental arc magmatism in NW Wales and Central England that formed by successive eastward subduction from 711 to 474 Ma.

Keywords: Avalonia, Anglesey-Lleyn, Pacific-type orogeny

©2019. Japan Geoscience Union. All Right Reserved.

Radiogenic Sr isotope chemostratigraphy of the Ediacaran Doushantuo Formation in the Yangtze Craton, South China

*Yusuke Sawaki[1]

1. The University of Tokyo

The Ediacaran period records one of the most dramatic biological episodes in Earth's history. To decipher surface environmental changes occurring in the Ediacaran, a variety of geochemical proxies have been reported by a number of studies. Ediacaran sedimentary rocks in South China figure prominently in such studies, because they are fossiliferous and accumulated at various depositional settings from shallow marine to deep basin. Recent extensive geochemical works for the Doushantuo Formation in South China demonstrate that $\delta^{13}C$ values of carbonate were variable depending on the depositional settings. In order to test whether the difference reflect spacial or temporal variation, I focus on $^{87}Sr/^{86}Sr$ ratio as a chemostratigraphic tool. However, the existing $^{87}Sr/^{86}Sr$ values are limited to shallow marine deposits, which leaves ambiguity in a variation of $^{87}Sr/^{86}Sr$ ratios in outer ocean. Our group conducted on-land drilling at Siduping and Tianping sections in South China to obtain completely continuous sedimentary rocks deposited at slope facies. We newly report stratigraphic profiles of the $^{87}Sr/^{86}Sr$ ratios at the sections. $^{87}Sr/^{86}Sr$ chemostratigraphy demonstrated some diachronous natures of $\delta^{13}C$ within the Doushantuo Formation. The enhanced continental weathering during Gaskiers glaciation likely promoted bacterial sulfate reduction and aerobic respiration of organic matter. These resulted in low $\delta^{13}C$ values of dissolved inorganic carbon and accumulations of phosphate and dissolved CO_2 species in seawater, and eventually induced the deposition of phosphorites at the shelf margin. High $^{87}Sr/^{86}Sr$ ratios during the largest negative $\delta^{13}C$ anomaly in the Ediacaran can be also recognized in the continental slope sediment. This fact supports that globally high continental weathering rate led to massive remineralization of organic matter and a consequent significant negative $\delta^{13}C_{carb}$ excursion.

©2019. Japan Geoscience Union. All Right Reserved.

[E] Poster | M (Multidisciplinary and Interdisciplinary)：M-IS Intersection

Tue. May 28, 2019 10:45 AM - 12:15 PM JST | Tue. May 28, 2019 1:45 AM - 3:15 AM UTC | Poster Hall International Exhibition Hall8, Makuhari Messe_10

[M-IS05] New technologies to monitor thunderstorm and severe weather activities

convener:Mitsuteru Sato(Department of Cosmoscience, Hokkaido University), Yukihiro Takahashi(Department of Cosmosciences, Graduate School of Science, Hokkaido University), Hisayuki Kubota(Hokkaido University), Kozo Yamashita(Ashikaga University, Department of Engineering.)

In order to predict the intensity development of severe weather, lightning and thunderstorm are markers of severe weather, often accompanied by precipitation, hail and strong winds that can create significant natural hazards, especially in disaster-prone area. Lightning is also a strong indicator of convection, and it becomes a key parameter to predict the intensity development of tropical cyclones (typhoons and hurricanes). As the climate warms in the first decades of the 21st century, the intensity and frequency of thunderstorms is projected to increase. The need for detecting and monitoring the development of thunderstorms and lightning activities on global, local, and regional scales is therefore clear and urgent.
This session seeks topics presenting new technologies to monitor thunderstorm and severe weather activities. In addition, observational and theoretical contributions on thunderstorm microphysics and dynamics, convective systems and tropical storms are welcome. Present patterns and distributions of lightning and extreme weather events derived from the ground-based networks and satellites, as well as forecasts of future trends, are also of interest. Lightning detecting and monitoring system performance and validation, and early-warning schemes are requested, either in operational or planning phase. The session will also highlight regional and global lightning and atmospheric electricity networks and invite contributions on technological innovations in this field.

[MIS05-P01] Study on monitoring of thunderstorm activity based on multiple electrostatic measurement

*Kozo Yamashita[1], Kakeru Kanno[1], Mitsuteru Sato[2], Yukihiro Takahashi[2] (1.Ashikaga Univ., 2.Hokkaido Univ.)

[MIS05-P02] **Contribution of Rainfall and Lightning Activities to the Fair Weather Electric Field Evaluated by 3D GEC Model**

*Kittanapat Bandholnopparat[1], Mitsuteru Sato[2], Yukihiro Takahashi[2], Toru Adachi[3], Masashi Kamogawa[5], Yasuhiro Minamoto[5], Akira Kadokura[6], Tomoo Ushio[4] (1.Department of Cosmosciences, Hokkaido University, Sapporo, Japan, 2.Faculty of Science, Hokkaido University, Sapporo, Japan, 3.Meteorological Research Institute, Tsukuba, Japan, 4.Department of Aerospace Engineering, Tokyo Metropolitan University, Hino, Japan, 5.Tokyo Gakugei University, Tokyo, Japan, 6.National Institute of Polar Research, Tokyo, Japan)

[MIS05-P03] A method for locating lightning discharges using tweek atmospherics

*Masafumi Kanno[1], Hiroyo Ohya[2], Kazuo Shiokawa[3], Hiroyuki Nakata[2], Toshiaki Takano[2] (1.Graduate School of Science and Engineering, Chiba University, 2.Graduate School of Engineering, Chiba University, 3.Institute for Space-Earth Environmental Research, Nagoya University)

[MIS05-P04] Monitoring for lightning activities and thunder cloud development over the Tokyo metropolitan area during the 2018 summer

*Jun-Ichi Hamada[1], Jun Matsumoto[1], Kozo Yamashita[2], Masashi Kamogawa[3], Yukihiro Takahashi[4] (1.Faculty of Urban Environmental Sciences, Tokyo Metropolitan University, 2.Department of Engineering, Ashikaga University, 3.Department of Physics, Tokyo Gakugei University, 4.Department of Cosmosciences, Graduate School of Science, Hokkaido University)

Study on monitoring of thunderstorm activity based on multiple electrostatic measurement

*Kozo Yamashita[1], Kakeru Kanno[1], Mitsuteru Sato[2], Yukihiro Takahashi[2]

1. Ashikaga Univ., 2. Hokkaido Univ.

Quantitative evaluation of thundercloud activity is essential for early detection and short-term forecast of severe weather events such as heavy rainfall, lightning stroke, downburst, and so on. In previous researches, lightning observation based on electromagnetic measurement has been focused on as an effective tool for nowcast of thunderstorm activity. Advanced lightning sensors have high sensitivity and makes it possible to detect whole lightning activity. Lightning discharge occurs as a result of vertical atmospheric convection which causes thunderstorm. Preceding studies pointed that lighting occurrence could be an indicator of vertical deep convection in storm region and severe thunderstorm intensity.

Ground-based measurement of electrostatic field has been also considered as an efficient way to detect electrification in thundercloud and monitor development of severe storm. In preceding studies, multiple electrostatic measurement has been examined to estimate charge amount in cloud. One of the difficulties for those studies is to understand correlation between electrostatic field on ground and charges in horizontally extended thunderstorm. In this study, methodology for quantitative evaluation of charge amount in cloud is developed. We newly construct multipoint electrostatic sensor network in Tochigi, Japan. In this region, isolated thunderstorm whose horizontal scale is about 10 km occurs. By analyzing Isolated thunderstorm, we can simplify the correlation between ground-based electrostatic field and charge in cloud. In this presentation, initial result of electrostatic measurement with multiple sensors is summarized.

Keywords: thunderstorm, electrostatic field, sensor network

©2019. Japan Geoscience Union. All Right Reserved.

Contribution of Rainfall and Lightning Activities to the Fair Weather Electric Field Evaluated by 3D GEC Model

*Kittanapat Bandholnopparat[1], Mitsuteru Sato[2], Yukihiro Takahashi[2], Toru Adachi[3], Masashi Kamogawa[5], Yasuhiro Minamoto[5], Akira Kadokura[6], Tomoo Ushio[4]

1. Department of Cosmosciences, Hokkaido University, Sapporo, Japan, 2. Faculty of Science, Hokkaido University, Sapporo, Japan, 3. Meteorological Research Institute, Tsukuba, Japan, 4. Department of Aerospace Engineering, Tokyo Metropolitan University, Hino, Japan, 5. Tokyo Gakugei University, Tokyo, Japan, 6. National Institute of Polar Research, Tokyo, Japan

Lightning and precipitation are the main current sources in the global atmospheric electric circuit (GEC). The lightning and precipitation currents maintain the electrical potential gap of ~250 kV between the ionosphere and the Earth’ s surface. However, the contribution of lightning current to the GEC is not well understood due to the difficulty of estimating the global occurrence number of intracloud (IC) discharges. In addition, it is difficult to quantitatively estimate the contribution of the global precipitation current to the GEC due to the difficulty of identifying the rain volume and its global distribution. The purposes of this study are to estimate the global occurrence number of IC discharges and to investigate the contribution of lightning and precipitation currents to the GEC. Firstly, the global Z-value map obtained by the JEM-GLIMS spaced-based mission and the cloud-to-ground (CG) lightning data obtained by the WWLLN were combined to estimate the occurrence number of the global IC discharges with the time resolution of 5 minutes and with the spatial resolution of 0.2º×0.2º. Then, the estimated occurrence number of the global IC and CG discharges and the precipitation data provided by the global precipitation measurement (GPM) project were used as the input parameters in a 3-dimensional model of the GEC, which we have newly developed. In this model, the average column resistance including the influence of the cloud coverage was assumed. Using this model, we estimated the total GEC current and the fair weather electric field at the Syowa station on March 16, July 20, and September 29, 2014. It is found that the average lightning and precipitation currents in the GEC were ~70 A and ~ 670 A, respectively. It is also found that the average fair weather electric field at the Syowa station is ~ 70 V/m. The absolute value of the estimated fair weather electric field is almost consistent with the observational data. From these results, the role of lightning current in the GEC is quantitatively evaluated, and we found that the upward current from thunderclouds to the ionosphere generated by lightning discharges is only 9% while that induced by the precipitation is ~91%.

©2019. Japan Geoscience Union. All Right Reserved.

A method for locating lightning discharges using tweek atmospherics

*Masafumi Kanno[1], Hiroyo Ohya[2], Kazuo Shiokawa[3], Hiroyuki Nakata[2], Toshiaki Takano[2]

1. Graduate School of Science and Engineering, Chiba University, 2. Graduate School of Engineering, Chiba University, 3. Institute for Space-Earth Environmental Research, Nagoya University

Locating accuracy for lightning discharges of world-wide lightning location (WWLLN) is high to be less than 10 km [Rodger et al., 2005], although the accuracy of horizontal propagation distance for tweek atmospherics is low to be ~60 km [Santolik and Kolmasova, 2017]. Tweek atmospherics are very low frequency (VLF)/extremely low frequency (ELF) waves radiated from lightning discharges, and propagate between the Earth surface and the bottom of the ionosphere for a long distance (several thousand kilometers). In this study, we improve the estimation method for the tweek propagation distance, and compare between the lightning location estimated from tweek propagation distance by intersection method with those from the WWLLN data and cloud images derived by the MTSAT-2 satellite. We used two wideband VLF data observed at Kagoshima (31.48˚N, 130.72˚E) and Moshiri (44.37˚N, 142.27˚E), Japan, at 12:20-12:22 UT, on 23 August, 2013. The main point of the improvement was modification for the width of window on dynamic spectra drawn by maximum entropy method. The accuracy of the estimation became higher and the error for the propagation distance became the half of the original estimation, by using narrow window for the beginning, and wide window for the end of the tweek signals. We estimated the lightning location by both automatic and manual methods. In the manual method, the estimated location of lightning for the two-minute data was in good agreement with thick clouds observed by the MTSAT-2 satellite. However, in the automatic method, the location of the lightning was in disagreement with cloud images, because the accuracy of triggered times were not sufficient due to overlapping tweeks or noises such like short pulses just before the tweeks. In the presentation, we discuss the estimation method for the lightning location in detail.

©2019. Japan Geoscience Union. All Right Reserved.

Monitoring for lightning activities and thunder cloud development over the Tokyo metropolitan area during the 2018 summer

*Jun-Ichi Hamada[1], Jun Matsumoto[1], Kozo Yamashita[2], Masashi Kamogawa[3], Yukihiro Takahashi[4]

1. Faculty of Urban Environmental Sciences, Tokyo Metropolitan University, 2. Department of Engineering, Ashikaga University, 3. Department of Physics, Tokyo Gakugei University, 4. Department of Cosmosciences, Graduate School of Science, Hokkaido University

In order to monitor lightning activities and development of thunder cloud, we have established an observational network with electromagnetic and electrostatic field measurements over the Tokyo metropolitan area since 2016. In the summer season of 2018, we observed atmospheric electrostatic field with the electric field monitor (BOLTEK ELF-100) at Hachioji campus of Tokyo Metropolitan University and the surrounding area. Lightning activities were measured with ELV-VLF band radio observation system at a few sites in the area. We also used the worldwide lightning location network (WWLLN) data to indicate temporal and spatial variations of lightning and the climatological characteristics over the area. Lightning observations showed clear intra-seasonal variations of lightning activities over the area during the summer. Significant lightning events at around Hachioji were observed in 6th, 13th, and 27th of August as a synoptic frontal system located in the north from Kanto area. The electrostatic field measurement at Hachioji detected frequent lightning events and developing/approaching of thunder cloud near the site in these days. At the presentation, we will introduce more detail observation results on thunder cloud developments based on the XRAIN (eXtended RAdar Information Network) observation data.

This work was partly supported by Japan Science and Technology Agency (JST) and Japan International Cooperation Agency (JICA) under SATREPS.

Keywords: Lightning, Heavy rainfall

©2019. Japan Geoscience Union. All Right Reserved.

[E] Poster | M (Multidisciplinary and Interdisciplinary) : M-IS Intersection

Tue. May 28, 2019 5:15 PM - 6:30 PM JST | Tue. May 28, 2019 8:15 AM - 9:30 AM UTC | Poster Hall International Exhibition Hall8, Makuhari Messe_42

[M-IS05] New technologies to monitor thunderstorm and severe weather activities

convener:Mitsuteru Sato(Department of Cosmoscience, Hokkaido University), Yukihiro Takahashi(Department of Cosmosciences, Graduate School of Science, Hokkaido University), Hisayuki Kubota(Hokkaido University), Kozo Yamashita(Ashikaga University, Department of Engineering.)

In order to predict the intensity development of severe weather, lightning and thunderstorm are markers of severe weather, often accompanied by precipitation, hail and strong winds that can create significant natural hazards, especially in disaster-prone area. Lightning is also a strong indicator of convection, and it becomes a key parameter to predict the intensity development of tropical cyclones (typhoons and hurricanes). As the climate warms in the first decades of the 21st century, the intensity and frequency of thunderstorms is projected to increase. The need for detecting and monitoring the development of thunderstorms and lightning activities on global, local, and regional scales is therefore clear and urgent.
This session seeks topics presenting new technologies to monitor thunderstorm and severe weather activities. In addition, observational and theoretical contributions on thunderstorm microphysics and dynamics, convective systems and tropical storms are welcome. Present patterns and distributions of lightning and extreme weather events derived from the ground-based networks and satellites, as well as forecasts of future trends, are also of interest. Lightning detecting and monitoring system performance and validation, and early-warning schemes are requested, either in operational or planning phase. The session will also highlight regional and global lightning and atmospheric electricity networks and invite contributions on technological innovations in this field.

[MIS05-P01] Study on monitoring of thunderstorm activity based on multiple electrostatic measurement

*Kozo Yamashita[1], Kakeru Kanno[1], Mitsuteru Sato[2], Yukihiro Takahashi[2] (1.Ashikaga Univ., 2.Hokkaido Univ.)

[MIS05-P02] Contribution of Rainfall and Lightning Activities to the Fair Weather Electric Field Evaluated by 3D GEC Model

*Kittanapat Bandholnopparat[1], Mitsuteru Sato[2], Yukihiro Takahashi[2], Toru Adachi[3], Masashi Kamogawa[5], Yasuhiro Minamoto[5], Akira Kadokura[6], Tomoo Ushio[4] (1.Department of Cosmosciences, Hokkaido University, Sapporo, Japan, 2.Faculty of Science, Hokkaido University, Sapporo, Japan, 3.Meteorological Research Institute, Tsukuba, Japan, 4.Department of Aerospace Engineering, Tokyo Metropolitan University, Hino, Japan, 5.Tokyo Gakugei University, Tokyo, Japan, 6.National Institute of Polar Research, Tokyo, Japan)

[MIS05-P03] A method for locating lightning discharges using tweek atmospherics

*Masafumi Kanno[1], Hiroyo Ohya[2], Kazuo Shiokawa[3], Hiroyuki Nakata[2], Toshiaki Takano[2] (1.Graduate School of Science and Engineering, Chiba University, 2.Graduate School of Engineering, Chiba University, 3.Institute for Space-Earth Environmental Research, Nagoya University)

[MIS05-P04] Monitoring for lightning activities and thunder cloud development over the Tokyo metropolitan area during the 2018 summer

*Jun-Ichi Hamada[1], Jun Matsumoto[1], Kozo Yamashita[2], Masashi Kamogawa[3], Yukihiro Takahashi[4] (1.Faculty of Urban Environmental Sciences, Tokyo Metropolitan University, 2.Department of Engineering, Ashikaga University, 3.Department of Physics, Tokyo Gakugei University, 4.Department of Cosmosciences, Graduate School of Science, Hokkaido University)

Study on monitoring of thunderstorm activity based on multiple electrostatic measurement

*Kozo Yamashita[1], Kakeru Kanno[1], Mitsuteru Sato[2], Yukihiro Takahashi[2]

1. Ashikaga Univ., 2. Hokkaido Univ.

Quantitative evaluation of thundercloud activity is essential for early detection and short-term forecast of severe weather events such as heavy rainfall, lightning stroke, downburst, and so on. In previous researches, lightning observation based on electromagnetic measurement has been focused on as an effective tool for nowcast of thunderstorm activity. Advanced lightning sensors have high sensitivity and makes it possible to detect whole lightning activity. Lightning discharge occurs as a result of vertical atmospheric convection which causes thunderstorm. Preceding studies pointed that lighting occurrence could be an indicator of vertical deep convection in storm region and severe thunderstorm intensity.

Ground-based measurement of electrostatic field has been also considered as an efficient way to detect electrification in thundercloud and monitor development of severe storm. In preceding studies, multiple electrostatic measurement has been examined to estimate charge amount in cloud. One of the difficulties for those studies is to understand correlation between electrostatic field on ground and charges in horizontally extended thunderstorm. In this study, methodology for quantitative evaluation of charge amount in cloud is developed. We newly construct multipoint electrostatic sensor network in Tochigi, Japan. In this region, isolated thunderstorm whose horizontal scale is about 10 km occurs. By analyzing Isolated thunderstorm, we can simplify the correlation between ground-based electrostatic field and charge in cloud. In this presentation, initial result of electrostatic measurement with multiple sensors is summarized.

Keywords: thunderstorm, electrostatic field, sensor network

©2019. Japan Geoscience Union. All Right Reserved.

Contribution of Rainfall and Lightning Activities to the Fair Weather Electric Field Evaluated by 3D GEC Model

*Kittanapat Bandholnopparat[1], Mitsuteru Sato[2], Yukihiro Takahashi[2], Toru Adachi[3], Masashi Kamogawa[5], Yasuhiro Minamoto[5], Akira Kadokura[6], Tomoo Ushio[4]

1. Department of Cosmosciences, Hokkaido University, Sapporo, Japan, 2. Faculty of Science, Hokkaido University, Sapporo, Japan, 3. Meteorological Research Institute, Tsukuba, Japan, 4. Department of Aerospace Engineering, Tokyo Metropolitan University, Hino, Japan, 5. Tokyo Gakugei University, Tokyo, Japan, 6. National Institute of Polar Research, Tokyo, Japan

Lightning and precipitation are the main current sources in the global atmospheric electric circuit (GEC). The lightning and precipitation currents maintain the electrical potential gap of ~250 kV between the ionosphere and the Earth’ s surface. However, the contribution of lightning current to the GEC is not well understood due to the difficulty of estimating the global occurrence number of intracloud (IC) discharges. In addition, it is difficult to quantitatively estimate the contribution of the global precipitation current to the GEC due to the difficulty of identifying the rain volume and its global distribution. The purposes of this study are to estimate the global occurrence number of IC discharges and to investigate the contribution of lightning and precipitation currents to the GEC. Firstly, the global Z-value map obtained by the JEM-GLIMS spaced-based mission and the cloud-to-ground (CG) lightning data obtained by the WWLLN were combined to estimate the occurrence number of the global IC discharges with the time resolution of 5 minutes and with the spatial resolution of 0.2º×0.2º. Then, the estimated occurrence number of the global IC and CG discharges and the precipitation data provided by the global precipitation measurement (GPM) project were used as the input parameters in a 3-dimensional model of the GEC, which we have newly developed. In this model, the average column resistance including the influence of the cloud coverage was assumed. Using this model, we estimated the total GEC current and the fair weather electric field at the Syowa station on March 16, July 20, and September 29, 2014. It is found that the average lightning and precipitation currents in the GEC were ~70 A and ~ 670 A, respectively. It is also found that the average fair weather electric field at the Syowa station is ~ 70 V/m. The absolute value of the estimated fair weather electric field is almost consistent with the observational data. From these results, the role of lightning current in the GEC is quantitatively evaluated, and we found that the upward current from thunderclouds to the ionosphere generated by lightning discharges is only 9% while that induced by the precipitation is ~91%.

©2019. Japan Geoscience Union. All Right Reserved.

A method for locating lightning discharges using tweek atmospherics

*Masafumi Kanno[1], Hiroyo Ohya[2], Kazuo Shiokawa[3], Hiroyuki Nakata[2], Toshiaki Takano[2]

1. Graduate School of Science and Engineering, Chiba University, 2. Graduate School of Engineering, Chiba University, 3. Institute for Space-Earth Environmental Research, Nagoya University

Locating accuracy for lightning discharges of world-wide lightning location (WWLLN) is high to be less than 10 km [Rodger et al., 2005], although the accuracy of horizontal propagation distance for tweek atmospherics is low to be ~60 km [Santolik and Kolmasova, 2017]. Tweek atmospherics are very low frequency (VLF)/extremely low frequency (ELF) waves radiated from lightning discharges, and propagate between the Earth surface and the bottom of the ionosphere for a long distance (several thousand kilometers). In this study, we improve the estimation method for the tweek propagation distance, and compare between the lightning location estimated from tweek propagation distance by intersection method with those from the WWLLN data and cloud images derived by the MTSAT-2 satellite. We used two wideband VLF data observed at Kagoshima (31.48˚N, 130.72˚E) and Moshiri (44.37˚N, 142.27˚E), Japan, at 12:20-12:22 UT, on 23 August, 2013. The main point of the improvement was modification for the width of window on dynamic spectra drawn by maximum entropy method. The accuracy of the estimation became higher and the error for the propagation distance became the half of the original estimation, by using narrow window for the beginning, and wide window for the end of the tweek signals. We estimated the lightning location by both automatic and manual methods. In the manual method, the estimated location of lightning for the two-minute data was in good agreement with thick clouds observed by the MTSAT-2 satellite. However, in the automatic method, the location of the lightning was in disagreement with cloud images, because the accuracy of triggered times were not sufficient due to overlapping tweeks or noises such like short pulses just before the tweeks. In the presentation, we discuss the estimation method for the lightning location in detail.

©2019. Japan Geoscience Union. All Right Reserved.

Monitoring for lightning activities and thunder cloud development over the Tokyo metropolitan area during the 2018 summer

*Jun-Ichi Hamada[1], Jun Matsumoto[1], Kozo Yamashita[2], Masashi Kamogawa[3], Yukihiro Takahashi[4]

1. Faculty of Urban Environmental Sciences, Tokyo Metropolitan University, 2. Department of Engineering, Ashikaga University, 3. Department of Physics, Tokyo Gakugei University, 4. Department of Cosmosciences, Graduate School of Science, Hokkaido University

In order to monitor lightning activities and development of thunder cloud, we have established an observational network with electromagnetic and electrostatic field measurements over the Tokyo metropolitan area since 2016. In the summer season of 2018, we observed atmospheric electrostatic field with the electric field monitor (BOLTEK ELF-100) at Hachioji campus of Tokyo Metropolitan University and the surrounding area. Lightning activities were measured with ELV-VLF band radio observation system at a few sites in the area. We also used the worldwide lightning location network (WWLLN) data to indicate temporal and spatial variations of lightning and the climatological characteristics over the area. Lightning observations showed clear intra-seasonal variations of lightning activities over the area during the summer. Significant lightning events at around Hachioji were observed in 6th, 13th, and 27th of August as a synoptic frontal system located in the north from Kanto area. The electrostatic field measurement at Hachioji detected frequent lightning events and developing/approaching of thunder cloud near the site in these days. At the presentation, we will introduce more detail observation results on thunder cloud developments based on the XRAIN (eXtended RAdar Information Network) observation data.

This work was partly supported by Japan Science and Technology Agency (JST) and Japan International Cooperation Agency (JICA) under SATREPS.

Keywords: Lightning, Heavy rainfall

©2019. Japan Geoscience Union. All Right Reserved.

[E] Oral | M (Multidisciplinary and Interdisciplinary)：M-IS Intersection

Tue. May 28, 2019 1:45 PM - 3:15 PM JST | Tue. May 28, 2019 4:45 AM - 6:15 AM UTC | 101 1F

[M-IS05] New technologies to monitor thunderstorm and severe weather activities

convener:Mitsuteru Sato(Department of Cosmoscience, Hokkaido University), Yukihiro Takahashi(Department of Cosmosciences, Graduate School of Science, Hokkaido University), Hisayuki Kubota(Hokkaido University), Kozo Yamashita(Ashikaga University, Department of Engineering.), Chairperson:Mitsuteru Sato(Faculty of Science, Hokkaido University), Kozo Yamashita(Department of Technology, Ashikaga Institute of Technology)

In order to predict the intensity development of severe weather, lightning and thunderstorm are markers of severe weather, often accompanied by precipitation, hail and strong winds that can create significant natural hazards, especially in disaster-prone area. Lightning is also a strong indicator of convection, and it becomes a key parameter to predict the intensity development of tropical cyclones (typhoons and hurricanes). As the climate warms in the first decades of the 21st century, the intensity and frequency of thunderstorms is projected to increase. The need for detecting and monitoring the development of thunderstorms and lightning activities on global, local, and regional scales is therefore clear and urgent.
This session seeks topics presenting new technologies to monitor thunderstorm and severe weather activities. In addition, observational and theoretical contributions on thunderstorm microphysics and dynamics, convective systems and tropical storms are welcome. Present patterns and distributions of lightning and extreme weather events derived from the ground-based networks and satellites, as well as forecasts of future trends, are also of interest. Lightning detecting and monitoring system performance and validation, and early-warning schemes are requested, either in operational or planning phase. The session will also highlight regional and global lightning and atmospheric electricity networks and invite contributions on technological innovations in this field.

1:45 PM - 2:00 PM JST | 4:45 AM - 5:00 AM UTC

[MIS05-01] Quasi real-time observation of typhoon and thunderstorms by the system of micro-satellites and ground-based lightning sensors

*Yukihiro Takahashi[4,1], Mitsuteru Sato[1,4], Hisayuki Kubota[4], Kozo Yamashita[2], Tetsuro Ishida[4], Ellison Caparas Castro[3], Purwadi Purwadi[1], Kazuhisa Tsuboki[5], Hiroyuki Yamada[6], Taro Shinoda[5], Loren Joy De Vera Estrebillo[1], Doreena Karmina Abril Pulutan[1] (1.Graduate School of Science, Hokkaido University, 2.Department of Engineering, Ashikaga University, 3.University of the Philippines, Diliman, 4.Faculty of Science, Hokkaido University, 5.Institute for Space-Earth Environmental Research (ISEE), Nagoya University, 6.University of the Ryukyus)

2:00 PM - 2:15 PM JST | 5:00 AM - 5:15 AM UTC

[MIS05-02] **Towards the Implementation of the Understanding Lightning and Thunderstorms for Extreme Weather Monitoring and Information Sharing in the Philippines (ULAT) Project**

★Invited Papers

*Glenn Vincent C. Lopez[1] (1.Advanced Science and Technology Institute)

2:15 PM - 2:30 PM JST | 5:15 AM - 5:30 AM UTC

[MIS05-03] **Airborne observation of Super Typhoon Trami in 2018 for understanding the intensity of tropical cyclone in the Philippine Sea**

★Invited Papers

*Hisayuki Kubota[1], Kazuhisa Tsuboki[2], Hiroyuki Yamada[3], Yukihiro Takahashi[1], Taro Shinoda[2], Tadayasu Ohigashi[4], Munehiko Yamaguchi[5], Kosuke Ito[3], Tetsuo Nakazawa[5], Norio Nagahama[6], Kensaku Shimizu[6], Mitsuteru Sato[1] (1.Hokkaido University, 2.Nagoya University, 3.University of the Ryukyus, 4.National Research Institute for Earth Science and Disaster Resilience, 5.Meteorological Research Institute, 6.Meisei Electronic)

2:30 PM - 2:45 PM JST | 5:30 AM - 5:45 AM UTC

[MIS05-04] Relation between Lightning and Typhoon Activities (Typhoon LAN) in the Western Pacific Region

*Mitsuteru Sato[1], Yukihiro Takahashi[1], Hisayuki Kubota[1], Kozo Yamashita[2], Jun-Ichi Hamada[3], Joel J. Marciano[4] (1.Department of Cosmoscience, Hokkaido University, 2.Department of Engineering, Ashikaga University, 3.Graduate School of Urban Environmental Sciences, Tokyo Metropolitan University, 4.ASTI, DOST)

2:45 PM - 3:00 PM JST | 5:45 AM - 6:00 AM UTC

[MIS05-05] Infrasound multi-site observation of thunders 3: preparation process for SATREPS

★Invited Papers

*Masa-yuki Yamamoto[1] (1.Department of systems engineering, Kochi University of Technology)

3:00 PM - 3:15 PM JST | 6:00 AM - 6:15 AM UTC

[MIS05-06] Data Acquisition System for an Infrasound Network for Thunderstorm Monitoring

*Doreena Karmina Abril Pulutan[1], Yukihiro Takahashi[1], Mitsuteru Sato[1], Hisayuki Kubota[1], Kozo Yamashita[2], Masa-yuki Yamamoto[3] (1.Department of Cosmosciences, Hokkaido University, 2.Department of Engineering, Ashikaga University, 3.Department of Systems Engineering, Kochi University of Technology)

Quasi real-time observation of typhoon and thunderstorms by the system of micro-satellites and ground-based lightning sensors

*Yukihiro Takahashi[4,1], Mitsuteru Sato[1,4], Hisayuki Kubota[4], Kozo Yamashita[2], Tetsuro Ishida[4], Ellison Caparas Castro[3], Purwadi Purwadi[1], Kazuhisa Tsuboki[5], Hiroyuki Yamada[6], Taro Shinoda[5], Loren Joy De Vera Estrebillo[1], Doreena Karmina Abril Pulutan[1]

1. Graduate School of Science, Hokkaido University, 2. Department of Engineering, Ashikaga University, 3. University of the Philippines, Diliman, 4. Faculty of Science, Hokkaido University, 5. Institute for Space-Earth Environmental Research (ISEE), Nagoya University, 6. University of the Ryukyus

We are conducting a SATREPS project “ULAT” and e-ASIA project for the development of extreme weather, including typhoon and individual thunderstorm, monitoring and alert system in the Philippines in 2017-2021 under international cooperation among Japan, Philippines, Indonesia and other SE-Asian countries supported by JST, JICA, PHL-Microsat and other funds. It is well known that intensification of lightning activity is precursor of typhoon growth as well as an indicator of individual thunderstorm activity. In these projects, we apply two new technologies, that is, the lightning activity estimated by the ground-based lightning networks with 12 sites for VLF radio wave measurement in nation-wide of Philippines and with 50 sites for electrostatic field measurement in Metro Manila together with infrasound sensor and automated weather station, and the 3 dimensional capturing of thunderstorms by the on-demand operation of 50-kg micro-satellites, including the Philippine-developed DIWATA-1 and 2, RISESAT, etc. Also few more lightning stations installed in Indonesia and Japan are used. We plan to establish a new methodology to obtain very detail semi-real time information of typhoon and thunderstorm activities that cannot be achieved only with conventional observational equipment. Based on these new observations together with advanced radar measurements and drop/radio sondes campaigns, we will try to construct the cutting-edge observation system to monitor the development of typhoons and thunderstorms, which may greatly contribute to the prediction of disasters and the public alerting system.

By the end of March 2017 we started the test observation for lightning at Quezon city, Philippines, Palau and Guam, forming the network for typhoons. We also succeeded in making 3-D cloud structure with telescope and wide angle spectral camera onboard DIWATA-1, achieving high resolution of ten to several meters. Now we are establishing the real-time target pointing operation with micro-satellites based on the last-minute lightning data measured by ground networks. Adding to DIWATA-1, three more our satellites, namely, RISESAT, MicroDragon and DIWATA-2 with advanced cameras will be used in 2018-2019. In September 2018, drop sonde campaign using aircraft in the eastside of Philippines was carried out under collaboration with Nagoya University team. Here we introduce the latest results of 3-D cloud modeling using images taken by satellite and on the ground together with preliminary lightning analysis, adding to the outline of the project.

Keywords: lightning, micro-satellite, typhoon, thunderstorm

©2019. Japan Geoscience Union. All Right Reserved.

Towards the Implementation of the Understanding Lightning and Thunderstorms for Extreme Weather Monitoring and Information Sharing in the Philippines (ULAT) Project

*Glenn Vincent C. Lopez[1]

1. Advanced Science and Technology Institute

Monitoring and understanding thunderstorms are key components of mitigating the effects of torrential rainfall and typhoons. The Philippines, where year-round numerous thunderstorms are experienced, the integration of lightning data has the potential to provide short term forecasts of thunderstorms, further meteorological studies, and supplement disaster risk response strategies.

This presents the activities and updates on the Understanding Lightning and Thunderstorm for Extreme Weather Monitoring and Information Sharing in the Philippines (ULAT) Project. The ULAT Project aims to deploy a highly dense lightning detection network scattered throughout Metro Manila to gather, analyze, and archive lightning data in order to provide thunderstorm “now-casting” and supplement weather-related research and disaster response strategies.

To enable the study of the correlation between lightning activity and localized severe weather disturbances (such as thunderstorms), the Japan International Cooperation Agency (JICA) and Hokkaido University through the Science and Technology Research Partnership for Sustainable Development (SATREPS) Program has partnered with the Department of Science and Technology Institute through the Advanced Science and Technology Institute to develop local expertise and build relevant lighting monitoring infrastructure in the Philippines.

This presents the activities and updates on the Understanding Lightning and Thunderstorm for Extreme Weather Monitoring and Information Sharing in the Philippines (ULAT) Project. The ULAT Project is aimed at the following: a) establishment of a dense network of lightning and weather devices in Metro Manila and nearby municipalities to a) establish of a dense network of lightning and weather devices in the Philippines in order to provide thunderstorm “now-casting” and supplement weather-related research and disaster response studies and strategies; b) establishment of a ground receiving station for direct reception of satellite imagery and utilizing existing ground receiving facilities to develop effective observation methods by comparing to compare 3D structures of thunderclouds from satellite images with lightning/precipitation data; c) establishment of a methodology for short term forecasts; and d) development of software for sharing information on short term forecast weather to concerned agencies.

To further meet the goals of the project, there are challenges during the implementation of the project activities that needs to be addressed in the areas of equipment security, public safety, partnership agreements, site identification and selection, logistics, process, etc. The encountered challenges, alongside with their corresponding solutions, recommendations, next steps and other plans relevant to the project will be also discussed during the meeting.

Keywords: Understanding Lightning and Thunderstorms for Extreme Weather Monitoring and Information Sharing in the Philippines (ULAT) Project, Advanced Science and Technology and Institute (ASTI)

©2019. Japan Geoscience Union. All Right Reserved.

©2019. Japan Geoscience Union. All Right Reserved.

Airborne observation of Super Typhoon Trami in 2018 for understanding the intensity of tropical cyclone in the Philippine Sea

*Hisayuki Kubota[1], Kazuhisa Tsuboki[2], Hiroyuki Yamada[3], Yukihiro Takahashi[1], Taro Shinoda[2], Tadayasu Ohigashi[4], Munehiko Yamaguchi[5], Kosuke Ito[3], Tetsuo Nakazawa[5], Norio Nagahama[6], Kensaku Shimizu[6], Mitsuteru Sato[1]

1. Hokkaido University, 2. Nagoya University, 3. University of the Ryukyus, 4. National Research Institute for Earth Science and Disaster Resilience, 5. Meteorological Research Institute, 6. Meisei Electronic

Airborne observation of tropical cyclone (TC) had been conducted until 1987 over the western north Pacific region to measure the TC intensity directly. After that TC intensity was estimated by Dvorak technique using satellite data. Here we conducted dropsonde observation by the aircraft in 2018 under the two projects of T-PARCII (Tropical Cyclone-Pacific Asian Research Campaign for Improvement of Intensity estimations/forecasts) and ULAT (Understanding Lightning and Thunderstorm) of SATREPS (Science and Technology Research Partnership for Sustainable Development) in the Philippines and penetrated the eye of Super Typhoon Trami during Sep. 25 to 28. TC Trami reached its mature stage when we observed on Sep. 25. The structure of sharp eyewall and warm core in the eye were observed. On the other hand, the intensity of TC was weakened when we observed on the following day. We need to capture the signal of intensification and decay of TC by combining multiple observations for understanding the structure for a short term forecast of tropical cyclone intensity.

Keywords: Tropical cyclone, Airborne observation, Dropsonde observation

©2019. Japan Geoscience Union. All Right Reserved.

Relation between Lightning and Typhoon Activities (Typhoon LAN) in the Western Pacific Region

*Mitsuteru Sato[1], Yukihiro Takahashi[1], Hisayuki Kubota[1], Kozo Yamashita[2], Jun-Ichi Hamada[3], Joel J. Marciano[4]

1. Department of Cosmoscience, Hokkaido University, 2. Department of Engineering, Ashikaga University, 3. Graduate School of Urban Environmental Sciences, Tokyo Metropolitan University, 4. ASTI, DOST

Recent studies revealed that there is a close relation between the lightning activity and the tropical cyclone intensity, such as the maximum wind velocity and the minimum surface pressure. As many countries in the western Pacific region suffer from the attack of many tropical cyclones (typhoons) and related severe weather events, they have a strong demand to predict the intensity development of these phenomena by means of a cost-effective way. Thus, we started installing the new lightning and weather observation system, named as V-POTEKA, at Guam, Palau, and Manila in the Philippines since September 2017. The lightning observation system consists of a VLF receiver having the sensitivity in the frequency range of 1-5 kHz, an automatic data-processing unit, solar panels, and batteries. Lightning-excited pulse signals detected by the VLF receiver are automatically analyzed by the data-processing unit, and only the extracted information of the trigger time and the pulse amplitude is transmitted to the data server via the 3G data communications. From the V-POTEKA data analysis, we confirmed that there is clear relation between the lightning occurrence number in the typhoon and the maximum wind speed of Typhoon LAN, which is the category-1 weak typhoon. There is ~12-18 h time difference between the peak lightning occurrence number and peak typhoon intensity. At the presentation, we will show the results derived from these lightning observation systems and will present the relation between lightning and typhoon activities more in detail.

Keywords: lightning activity, typhoon, intensity prediction

©2019. Japan Geoscience Union. All Right Reserved.

Infrasound multi-site observation of thunders 3: preparation process for SATREPS

*Masa-yuki Yamamoto[1]

1. Department of systems engineering, Kochi University of Technology

Infrasound, low-frequency sound of 20 Hz or less, is considered as one of the remote-sensing method of lightning/thunders. Sensor network to be deployed for a SATREPS project, Philippine, is planned in Manila region in early 2019. Here, we will deploy two types of infrasound sensors. Small but impulsive pressure changes caused by the rapid expansion of the heated plasma along the path of lightning strikes can be detected by infrasound sensors with higher sensitivity range of 1 mPa. Thus, we will use multiple film type (DC type) infrasound sensor for low frequency measurements. But for the thunder infrasound signals, lower-cost microphone type (AC type) sensors can be applied for measurements. Thus, we will mainly use many microphone type infrasound sensors in Metro Manila region.
For calibrating the both sensors, in order to evaluate precise pressure level as well as detectable frequency range, we used a chamber with a pushing/pulling mechanism on it. The infrasound multi-site observation can reveal the lightning activities as close as 100 m scale when the infrasound sensors can be installed with a mesh of 10 km scale or shorter by using the speed of sound as a precise remote-sensing scale. Recently, we also checked capability of remote-sensing in Fukui area and Kanazawa area by using real thunder signals with some other methods to compare.
In this talk, we will introduce a possibility of infrasonic remote-sensing and its calibration phase, in order to realize future disaster-mitigation studies.

Keywords: Infrasound, Calibration, Remote sensing

©2019. Japan Geoscience Union. All Right Reserved.

Data Acquisition System for an Infrasound Network for Thunderstorm Monitoring

*Doreena Karmina Abril Pulutan[1], Yukihiro Takahashi[1], Mitsuteru Sato[1], Hisayuki Kubota[1], Kozo Yamashita[2], Masa-yuki Yamamoto[3]

1. Department of Cosmosciences, Hokkaido University, 2. Department of Engineering, Ashikaga University, 3. Department of Systems Engineering, Kochi University of Technology

Inside a thunderstorm, an updraft pushes ice crystals with positive charge to the top, while a downdraft pushes hailstones with negative charge to the bottom. This charge separation results in lightning. While the electric charge and peak current in lightning events have been extensively studied, they do not indicate the strength of the atmospheric convection that produces thunderstorms. Another parameter, the electrical energy from lightning, has not been thoroughly explored. We will look at the electrical energy from lightning as a possible indicator of the strength of a developing thunderstorm. Electrical energy, however, has not been clearly linked to the peak current of a lightning event. Thus, we cannot rely on peak current measurements to estimate electrical energy. Infrasound emitted by thunderstorms might be a possible way to estimate the electrical energy in lightning events. Microphones can be used to detect infrasound. This work will discuss the development of a data acquisition system that will be used to record and transmit sampled infrasonic data from microphones. This work is being undertaken under the SATREPS/ULAT Project.

Keywords: data acquisition, thunderstorm, lightning, energy

©2019. Japan Geoscience Union. All Right Reserved.

[E] Oral | M (Multidisciplinary and Interdisciplinary)：M-IS Intersection

Tue. May 28, 2019 3:30 PM - 5:00 PM JST | Tue. May 28, 2019 6:30 AM - 8:00 AM UTC | 101 1F

[M-IS05] New technologies to monitor thunderstorm and severe weather activities

convener:Mitsuteru Sato(Department of Cosmoscience, Hokkaido University), Yukihiro Takahashi(Department of Cosmosciences, Graduate School of Science, Hokkaido University), Hisayuki Kubota(Hokkaido University), Kozo Yamashita(Ashikaga University, Department of Engineering.), Chairperson:Yukihiro Takahashi(Hokkaido University), Hisayuki Kubota(Department of Cosmoscience, Hokkaido University)

In order to predict the intensity development of severe weather, lightning and thunderstorm are markers of severe weather, often accompanied by precipitation, hail and strong winds that can create significant natural hazards, especially in disaster-prone area. Lightning is also a strong indicator of convection, and it becomes a key parameter to predict the intensity development of tropical cyclones (typhoons and hurricanes). As the climate warms in the first decades of the 21st century, the intensity and frequency of thunderstorms is projected to increase. The need for detecting and monitoring the development of thunderstorms and lightning activities on global, local, and regional scales is therefore clear and urgent.
This session seeks topics presenting new technologies to monitor thunderstorm and severe weather activities. In addition, observational and theoretical contributions on thunderstorm microphysics and dynamics, convective systems and tropical storms are welcome. Present patterns and distributions of lightning and extreme weather events derived from the ground-based networks and satellites, as well as forecasts of future trends, are also of interest. Lightning detecting and monitoring system performance and validation, and early-warning schemes are requested, either in operational or planning phase. The session will also highlight regional and global lightning and atmospheric electricity networks and invite contributions on technological innovations in this field.

3:30 PM - 3:45 PM JST | 6:30 AM - 6:45 AM UTC

[MIS05-07] Estimation of Lightning Location Using V-POTEKA Lightning Observation Network

*Loren Joy De Vera Estrebillo[1], Mitsuteru Sato[2], Yukihiro Takahashi[2], Hisayuki Kubota[2], Kozo Yamashita[3], Junichi Hamada[4], Joel Marciano[5] (1.Department of Cosmosciences, Hokkaido University, 2.Faculty of Science, Hokkaido University, 3.Faculty of Engineering, Ashikaga University, 4.Graduate School of Urban Environmental Sciences, Tokyo Metropolitan University, 5.ASTI/DOST)

3:45 PM - 4:00 PM JST | 6:45 AM - 7:00 AM UTC

[MIS05-08] **Observation system for thunderstorm development using ground lightning detection network and thermal infrared camera onboard satellite LAPAN-A4 in Indonesia**

*Purwadi Purwadi[1,2], Yukihiro Takahashi[1], Mitsuteru Sato[1], Kozo Yamashita[3], M. Arif Saifudin[4] (1.Department of Cosmosciences, Hokkaido University, Sapporo 0600810, Japan, 2.Agency for Assessment and Application of Technology (BPPT), Jakarta 10340, Indonesia, 3.Department of Technology, Ashikaga Institute of Technology, Tochigi 3268558, Japan, 4.Indonesian National Institute of Aeronautics and Space (LAPAN), Jawa Barat 16310, Indonesia)

4:00 PM - 4:15 PM JST | 7:00 AM - 7:15 AM UTC

[MIS05-09] Remote Sensing Water Quality Determination using Multi-spectral Analysis

*Ahmad Shaqeer Mohamed Thaheer[1], Yukihiro Takahashi[1] (1.Hokkaido University)

4:15 PM - 4:30 PM JST | 7:15 AM - 7:30 AM UTC

[MIS05-10] Study of cloud effects on atmospheric electric field during lightning activities and snowfall using the 95-GHz cloud radar FALCON-I

★Invited Papers

*Hiroyo Ohya[1], Kota Nakamori[1], Masashi Kamogawa[2], Tomoyuki Suzuki[2], Toshiaki Takano[1], Kazuomi Morotomi[3], Hiroyuki Nakata[1], Kazuo Shiokawa[4] (1.Graduate School of Engineering, Chiba University, 2.Tokyo Gakugei University, 3.Japan Radio Co. Ltd., 4.Nagoya University)

4:30 PM - 4:45 PM JST | 7:30 AM - 7:45 AM UTC

[MIS05-11] Preferred environmental conditions of precipitation systems in and around Bangladesh observed by ground-based radars

★Invited Papers

*Fumie Murata[1], Shuhei Azuma[2], Toru Terao[3], Quamrul S.M. Hassan[4] (1.Faculty of Science and Technology, Kochi University, 2.Faculty of Science, Kochi University, 3.Faculty of Education, Kagawa University, 4.Bangladesh Meteorological Department)

4:45 PM - 5:00 PM JST | 7:45 AM - 8:00 AM UTC

[MIS05-12] Thundercloud gamma-ray observations at Kashiwazaki aiming at source altitude and beaming measurements and a new trial at Tokyo Skytree in FY2018

★Invited Papers

*Kazuhiro Nakazawa[1], Takahiro Matsumoto[2], Yuuki Wada[2], Alexia Fabiani[1], Teruaki Enoto[3], Kazufumi Okuda[2], Yoshihiro Furuta[4], Yuki Aizawa[2], Takayuki Yuasa[5], Harufumi Tsuchiya[4], Mitsuteru Sato[6], Kazuo Makishima[7] (1.Nagoya University, 2.University of Tokyo, 3.Kyoto University, 4.JAEA, 5.RIKEN, 6.Hokkaido University, 7.Kalvi IPMU, University of Tokyo)

Estimation of Lightning Location Using V-POTEKA Lightning Observation Network

*Loren Joy De Vera Estrebillo[1], Mitsuteru Sato[2], Yukihiro Takahashi[2], Hisayuki Kubota[2], Kozo Yamashita[3], Junichi Hamada[4], Joel Marciano[5]

1. Department of Cosmosciences, Hokkaido University, 2. Faculty of Science, Hokkaido University, 3. Faculty of Engineering, Ashikaga University, 4. Graduate School of Urban Environmental Sciences, Tokyo Metropolitan University, 5. ASTI/DOST

The Philippines is one of the most disaster-hit countries in the world. Its location in the western North Pacific (WNP) subjects it to numerous tropical cyclones (TC) each year that pose risk to lives, properties and infrastructures. There has been a significant development in the accuracy of TC track forecast that cross and/or make landfall within the Philippine Area of Responsibility (PAR) over the years with the use of ground-based synoptic observations, weather radars, and meteorological satellites. However, prediction of TC intensity remains a significant challenge. Lightning activity is an indicator of the dynamics and microphysics in thunderstorms, as well as severe weather phenomena, such as TCs and torrential rainfall among others. Recent studies suggest that lightning activity in tropical cyclones can give predictive information about its intensity development. Thus, a ground-based lightning observation system (V-POTEKA) has been developed, and it has been installed at three stations in the Philippines, Guam, and Palau to continuously monitor lightning activity in the WNP region since September 2017. The V-POTEKA system uses an event-trigger method that detects radio wave pulses from lightning discharges in the very low frequency (VLF) range of 1-50 kHz. It also consists of an automatic weather station (AWS), VLF sensors, and an automatic data-processing unit. The V-POTEKA system analyzes lightning data, extracts pertinent information, i.e., peak amplitude and time of the triggered waveform, and transmits data to a server through 3G communication. A geolocation software using the time-of-arrival method is being developed using the 3 sites along the WNP region. Further analysis will be conducted by incorporating data from other stations (Sapporo, Japan and Los Banos, Philippines), and an improved geolocation software will be used to investigate the relationship between the lightning activity and typhoon intensification during the dropsonde observation campaign conducted in September 2018.

Keywords: lightning location, V-POTEKA

©2019. Japan Geoscience Union. All Right Reserved.

Observation system for thunderstorm development using ground lightning detection network and thermal infrared camera onboard satellite LAPAN-A4 in Indonesia

*Purwadi Purwadi[1,2], Yukihiro Takahashi[1], Mitsuteru Sato[1], Kozo Yamashita[3], M. Arif Saifudin[4]

1. Department of Cosmosciences, Hokkaido University, Sapporo 0600810, Japan, 2. Agency for Assessment and Application of Technology (BPPT), Jakarta 10340, Indonesia, 3. Department of Technology, Ashikaga Institute of Technology, Tochigi 3268558, Japan, 4. Indonesian National Institute of Aeronautics and Space (LAPAN), Jawa Barat 16310, Indonesia

Indonesia is the tropical maritime country which has potential disaster risk caused by thunderstorm cloud. In this study, we will observe the thunderstorm development using lightning detection networks and micro-satellite. A previous study has shown that electrification process on the cloud started when the peak of the cloud reaches the threshold height and continue to growth vertical with an upward ~8 m/s (Krehbiel, 1986). With the reverse though, the lightning activity can be used to indicate the updraft presence inside the cloud. Moreover, lightning activity represents the intensity and area of precipitation and/or an updraft area. In this study, the Asia VLF lightning Observation Network (AVON) will be used to detect electromagnetic wave emitted by lightning which has been installed in Manila - Philippines, Palau, and the next will be installed in Serpong and Padang Indonesia. We will show coverage area and ambiguity of lightning geolocation created by this lightning networks. The progress in development of algorithms in the determination of the location of lightning, peak currents, and charge moment changes will also be presented. Adding to the lightning observation, cloud observation using thermal infrared camera onboard LAPAN-A4, which will be launched in 2019 FSY, will provide the temperature distribution with the surface resolution of ~180 meters and field of view of ~ 56.3 x 42.2 kilometer. Using this high resolution thermal infrared camera, the cloud top altitude can be estimated, assuming temperature profile of the ambient atmosphere. By making such observation at some time interval, the developing speed of thunderstorm can be calculated in 3D. The first lightning occurrence detected by AVON, which could be assumed as the timing that the cloud has reached the threshold height to become a thunderstorm, will initiate the micro-satellite observation with the thermal infrared camera, from which we could make a prediction of torrential rainfall.

Acknowledgement: This work was supported by Japan Society for the Promotion of Science (JSPS), Core-to-Core Program, B. Asia-Africa Science Platforms, by Japan Science and Technology Agency(JST) together with Technology and Higher Education(RISTEKDIKTI) of the of Indonesia under the e-ASIA Joint Research Program, and by Japan International Cooperation Agency (JICA) and JST, SATREPS.

Keywords: thuderstorm, lightning detection network, microsatellite, infrared thermal camera

©2019. Japan Geoscience Union. All Right Reserved.

Remote Sensing Water Quality Determination using Multi-spectral Analysis

*Ahmad Shaqeer Mohamed Thaheer[1], Yukihiro Takahashi[1]

1. Hokkaido University

Wetlands have three distinct features which are the existence of a water body, hydric soil, and specific vegetation that thrived under those conditions as mentioned. The ecosystem provides benefits to the environment and humans as one of the significant natural resources. The contamination of the waters, especially in the river, poses a serious health and environmental risk. The destruction of the catchment area will lead to the deterioration in quality and quantity of the water resource in Malaysia. The Department of Environment (DOE) under the Ministry of Water, Land and Natural Resources (NRE) has identified that the Malaysian rivers are degraded by both point and non-point sources of pollution. The major point sources of pollution in rivers are from sewage treatment plants, agro-based industries, manufacturing industries, sullage or grey water from commercial and residential premises, and pig farms. Non-point source (or diffuse) pollution is largely due to storm runoff after a downpour. Current methods using in-situ measurements are shown to be infeasible while Remote Sensing methods helps to resolve these issues such as cost, time, accessibility, and repeatability effectively. Multi-spectral Imagery has been a useful in analyzing the spectral characteristics of wetlands.

Keywords: Multi-spectral, Remote sensing, Water quality

©2019. Japan Geoscience Union. All Right Reserved.

Study of cloud effects on atmospheric electric field during lightning activities and snowfall using the 95-GHz cloud radar FALCON-I

*Hiroyo Ohya[1], Kota Nakamori[1], Masashi Kamogawa[2], Tomoyuki Suzuki[2], Toshiaki Takano[1], Kazuomi Morotomi[3], Hiroyuki Nakata[1], Kazuo Shiokawa[4]

1. Graduate School of Engineering, Chiba University, 2. Tokyo Gakugei University, 3. Japan Radio Co. Ltd., 4. Nagoya University

It is known that cloud-to-ground lightning and precipitations generated from thunderclouds are a generator of global electric circuit (e.g., Williams, 2009). In the fair weather, the atmospheric electric field at the ground is generally 100 V/m and downward (positive). The atmospheric electric field varies during not only lightning/thunderstorms, but also snowfall/blizzard (e.g., Minamoto and Kadokura, 2011). The atmospheric electric field had positive correlations with flush rate (R^2 = 0.67) and clouds of more than 30 dBZ with temperature range of -35~-5˚C (R^2 = 0.62) observed by the TRMM satellite [Lavigne et al., 2017]. However, satellite observations cannot monitor cloud internal structures in detail. In this study, we investigate the variations of the atmospheric electric field during lightning activities of 4 July, 2016, and snowfall of 23-24 November, 2016, using a field mill, the 95 GHz cloud radar, FALCON (FMCW Radar for Cloud Observations)-I, and a X-band radar (9.4 GHz). We have observed the atmospheric electric field with a Boltek field mill, and cloud reflectivity and the Doppler velocity with the FALCON-I in Chiba University, Japan, (CHB, 35.63˚N, 140.10˚E). At 16.2 km southeast from the CHB, a phased array X-band radar operated by Japan Radio Corporation observed precipitations/cloud. During lightning activities of 4 July, 2016, there were two variations in the atmospheric electric field: short pulse signals and slow variations due to passage of thunderclouds. Small increase in the atmospheric electric field in the initial phase was caused by positive charges in anvil using the FALCON-I, although the cause of the initial phase has been regarded as negative charges in the bottom of the thunderclouds so far. The duration of the short pulse signals due to lightning itself had a positive correlation with the lightning peak current (r = 0.44). During the snowfall of 23-24 November, 2016, periodic oscillations in the atmospheric electric field with periods of 70-90 minutes were observed at four observation sites; CHB, Kakioka (KAK, 36.23˚N, 140.19˚E), Tokyo Gakugei University (KGN, Kokubunji, Tokyo, 35.71˚N, 139.49˚E), and Seikei High School (MSN, Musashino, Tokyo, 35.72˚N, 139.57˚E). The distances of CHB-KAK, CHB-TGU, and CHB-SHS are 64.8 km, 55.9 km, and 49.0 km, respectively. This is the first observations of similar oscillations in the atmospheric electric field at different observation sites separated by a long distance of 50-65 km. At the end of snowfall, the periods of the oscillations became shorter to be 20-50 minutes at all sites. Based on the FALCON-I and X-band radar observations, we found that the reflectivity of the snow cloud had the same period of 80 minutes at CHB at 0-2 km heights during the snowfall. In the presentation, we will discuss the cause of the variations in the atmospheric electric field.

©2019. Japan Geoscience Union. All Right Reserved.

Preferred environmental conditions of precipitation systems in and around Bangladesh observed by ground-based radars

*Fumie Murata[1], Shuhei Azuma[2], Toru Terao[3], Quamrul S.M. Hassan[4]

1. Faculty of Science and Technology, Kochi University, 2. Faculty of Science, Kochi University, 3. Faculty of Education, Kagawa University, 4. Bangladesh Meteorological Department

Severe storms tend to occur in Bangladesh. In the pre-monsoon season (March-May) storms with intense rainfall, lightning, hails, and tornadoes are frequently observed. Precipitation systems in the monsoon season (June-September) bring large amount of rainfall and floods tend to occur. The purpose of this study is to elucidate the environmental conditions which cause severe weather. This study analyzed the ground-based radars observed during 2010-2014 with TRMM-based precipitation products and JRA55 reanalysis. The precipitation systems were classified into four types: arc-type (77 cases), line-type (59 cases), scattered-type (178 cases) and broad-type (172 cases) systems. Arc-type systems tended to occur in the pre-monsoon season, and the environmental condition had large vertical shear with dry in the mid troposphere. Line-type systems had no preferred season, and the environmental condition had weak vertical shear. The formation process seemed back building type. The scattered-type systems in the pre-monsoon season occurred in the large vertical shear, whereas that in the monsoon season occurred in the weak vertial shear. Most of the broad-type systems were occurred in the active spells of the intraseasonal variation during the monsoon season, and the scattered-type tended to appear in 1-3 days before the formation of the broad-type systems.

Keywords: Monsoon, Precipitation system, Radar

©2019. Japan Geoscience Union. All Right Reserved.

Thundercloud gamma-ray observations at Kashiwazaki aiming at source altitude and beaming measurements and a new trial at Tokyo Skytree in FY2018

*Kazuhiro Nakazawa[1], Takahiro Matsumoto[2], Yuuki Wada[2], Alexia Fabiani[1], Teruaki Enoto[3], Kazufumi Okuda[2], Yoshihiro Furuta[4], Yuki Aizawa[2], Takayuki Yuasa[5], Harufumi Tsuchiya[4], Mitsuteru Sato[6], Kazuo Makishima[7]

1. Nagoya University, 2. University of Tokyo, 3. Kyoto University, 4. JAEA, 5. RIKEN, 6. Hokkaido University, 7. Kalvi IPMU, University of Tokyo

MeV gamma rays from lightning and thundercloud reaching the groud are sometimes observed from the winter thunderstorm activities along the coastline of Japan Sea. We, the Gamma-Ray Observation of Winter Thunderclouds (GROWTH) collaboration, are observing such phenomena from 2006 at Kashiwazaki, Niigata prefecture (e.g. Tsuchiya et al. 2007), and recently increasing the number of observation sites, including Ishikawa prefecture (e.g. Wada et al. at M-IS27 session). Since FY2016, we have been operating new detectors at Kashiwazaki dedicated to measure the altitude and beaming of gamma-ray source in thundercloud. Three collimated detectors aiming at different sky regions are deployed. A minute-long gamma-ray emission (or "long-burst") was observed on Jan 26th, 2019 with the system, and we are analyzing the peaking time difference among the three detectors to perform triangulation using the wind speed. Preliminary results suggest the altitude to be lower than ~300 m, but because the emission was relatively weak and photon statistics are not enough, we are estimating the upper-limit of the source altitude and its beaming. Independently, we also started an observation campaign at the 450 m altitude of Tokyo Skytree, aiming at gamma-ray detection from lightning (so called downward TGF) of summer thunderstorm. The tower is one of the locations most frequently hit by lightning. We had three hits on May-Sep. 2018, but no TGF was observed to date, confirming the fact that not all the lightnings are observationally associated with gamma rays. Because our team is observing several downward TGFs from winter thunderstorms (e.g. Enoto et al. 2017), increasing data will enable us to compare the difference among the lightning with and without TGF. The study will be also boosted with the launch of TARANIS satellite in early 2020, dedicated for simultaneous observation of TGF, electrons, optical and radio emission from lightning.

Keywords: Thundercloud, lightning, MeV gamma rays, TGF

©2019. Japan Geoscience Union. All Right Reserved.

[J] Oral | M (Multidisciplinary and Interdisciplinary)：M-IS Intersection

Tue. May 28, 2019 9:00 AM - 10:30 AM JST | Tue. May 28, 2019 12:00 AM - 1:30 AM UTC | 303 3F

[M-IS10] Interface- and nano-phenomena on crystal growth and dissolution

convener:Yuki Kimura(Institute of Low Temperature Science, Hokkaido University), Hitoshi Miura(Graduate School of Natural Sciences, Department of Information and Basic Science, Nagoya City University), Hisao Satoh(Naka Energy Research Laboratory, Mitsubishi Materials Corporation), Katsuo Tsukamoto(Graduate School of Engineering, Osaka University), Chairperson:Yuki Kimura (Institute of Low Temperature Science, Hokkaido University)

Recent developments of observations in nano-scale opened a detail discussion concerning mechanisms of crystal growth and dissolution based on interface phenomena including dynamics. In this session, growth and dissolution mechanisms of crystals will be discussed focusing on interface phenomena of minerals in the fields of biological origin, global environment, planets and space in addition to general minerals.

9:00 AM - 9:15 AM JST | 12:00 AM - 12:15 AM UTC

[MIS10-01] Fabrication of octacalcium phosphate block through a dissolutionprecipitation reaction and its biological evaluation

*Yuki Sugiura[1], Munar L Melvin[2], Kunio Ishikawa[2] (1.National Institute of Advanced Industrial Science and Technology, 2.Kyushu University)

9:15 AM - 9:30 AM JST | 12:15 AM - 12:30 AM UTC

[MIS10-02] Development of optimized incineration process of fisheries waste for synthesizing a functional heat storage material

*Hidekazu Kobatake[1], SHinji Kirihara[1] (1.Hirosaki University Institute of Regional Innovation)

9:30 AM - 9:45 AM JST | 12:30 AM - 12:45 AM UTC

[MIS10-03] “Manipulated” Organic Crystallization and Two-step Dissolution Process Attained by Plasmonic Optical Tweezers

*Hiromasa Niinomi[1], Teruki Sugiyama[2,3,4], Miho Tagawa[5], Toru Ujihara[5], Katsuhiko Miyamoto[6,7], Takashige Omatsu[6,7], Jun Nozawa[1], Junpei Okada[1], Satoshi Uda[1] (1.Institute for Materials Research, Tohoku University, 2.Department of Applied Chemistry, National Chiao Tung University, 3.Center for Emergent Functional Matter Science, National Chiao Tung University, 4.Division of Materials Science, Nara Institute of Science and Technology, 5.Institute of Materials and Systems for Sustainability (IMaSS), Nagoya University, 6.Molecular Chirality Research Center (MCRC), Chiba University, 7.Graduate School of Engineering, Chiba University)

9:45 AM - 10:00 AM JST | 12:45 AM - 1:00 AM UTC

[MIS10-04] Investigation of liquid cell transmission electron microscopy combined with antisolvent crystallization

*Tomoya Yamazaki[1], Yuki Kimura[1] (1.Institute of Low Temperature Science Hokkkaido University)

10:00 AM - 10:30 AM JST | 1:00 AM - 1:30 AM UTC

[MIS10-05] DNA-guided crystallization of nanoparticles: optimization of crystallization conditions and structure analysis

★Invited Papers

*Miho Tagawa[1], Shoko Kojima[1], Hayato Sumi[1], Arisa Nishibu[1], Takumi Isogai[1], Maasa Yokomori[2], Shunta Harada[1], Toru Ujihara[1], Katsuo Tsukamoto[1] (1.Nagoya University, 2.The University of Tokyo)

Fabrication of octacalcium phosphate block through a dissolutionprecipitation reaction and its biological evaluation

*Yuki Sugiura[1], Munar L Melvin[2], Kunio Ishikawa[2]

1. National Institute of Advanced Industrial Science and Technology, 2. Kyushu University

Although octacalcium phosphate (OCP) powder and a collagen/gelatin composite demonstrate good potential as bone substitutes, an OCP block has not been fabricated to date. In this study, the feasibility of fabricating an OCP block was evaluated through a dissolution-precipitation reaction using a calcium sulfate hemihydrate (CSH) block as a precursor. When the block was immersed in a phosphate salt solution, its composition changed to that of OCP, while its structure was maintained. The diametral tensile strength (DTS) of the OCP block was 1.0 ±0.2 MPa. The macroporosity and microporosity of the OCP block were 33.4 ±4.5% and, 69.0 ±1.6%, respectively. New bone attached well to the OCP block, and this block was partially replaced by bone 2 weeks after implantation. Four weeks after implantation, the surface of the OCP block was nearly covered with new bone and ~30% of the block was replaced by new bone, while no replacement by bone was observed in the case of a hydroxyapatite (HAp) block used as a control. It is concluded that OCP blocks are potentially suitable for their use as artificial bone substitutes.

Keywords: Calcium phosphate, bone substitute, biomaterial

©2019. Japan Geoscience Union. All Right Reserved.

Development of optimized incineration process of fisheries waste for synthesizing a functional heat storage material

*Hidekazu Kobatake[1], SHinji Kirihara[1]

1. Hirosaki University Institute of Regional Innovation

A part of fishery waste, such as scallops or oyster shells, are utilized for fertilizer, feed, soil conditioner, or fishing ground preparations, and most of the shells from aquaculture residue are incinerated as general waste at or above 1273 K using a huge amount of fuels and cost. And the most of the incineration products are used for a landfill disposal. For the establishing the sustainable fisheries industry and local community, the reduction of the incineration cost and utilization of the incineration products are indispensable. In this research, the incineration temperature of fisheries waste was examined for lowering incineration temperature. Addition to the investigation on the incineration temperature of fisheries waste, the properties of the calcium oxide derived from the fisheries waste as heat storage material was also evaluated based on the thermal analysis.

The samples used for thermal decomposition kinetics investigation are 2 species of shells (Scallop *Mizuhopecten yessoensis*, Oyster *Crassostrea gigas*), a spines of a sea urchin *Mesocentrotus nudus*, and calcite reagent (purity 99.95%). The surface deposits on these shells and spines are removed using a wire brush or tweezers, then washed by tap water. The cleaned samples were crushed in a porcelain mortar, then dried in an oven at 383 K. The dried powder particles were allied by their size using a sieve to sort in size in the range between 63 and 125 micron meter. The thermal incineration temperature was investigated using these samples.

Calcite reagent (purity 99.95%) the sorted, shells (Scallop, Oyster, Myoida *Hiatella orietalis*, and Tube worms *Dexiospira foraminosus*), and spines of Sea urchin were thermally decomposed for 1 hour at 1273 K to be converted to calcium oxide and then reacted with distilled water to prepare $Ca(OH)_2$. The thermal decomposition temperature of the $Ca(OH)_2$ of these samples was experimentally investigated for the evaluation of the incineration product as a heat storage material.

The prepared powder samples were put in a platinum container covered with Pt disk and then installed in a Differential Scanning Calorimetry. The samples were heated up with the temperature increasing rate from 5 K /min to 40 K /min in Ar atmosphere (99.9999%).

The thermal decomposition complete temperature is depending on the temperature increasing rate. As increase of the temperature increasing rate, thermal decomposition temperature of each samples became higher. The activation energy and frequency factor of the thermal decomposition were determined from the relation between thermal decomposition complete temperature and the temperature increasing rate. However, there is only 8% difference in the activation energies of thermal decomposition among the all samples. This result implies that the thermal decomposition kinetics is mainly controlled by the frequency factor.

Meanwhile the thermal decomposition temperature of the $Ca(OH)_2$ differs each other depending on the derived specimens. There is a weak positive correlation between the thermal decomposition temperature of calcite and calcium hydroxide. The shells and spines having lower thermal decomposition temperature have lower thermal decomposition temperature of calcium hydroxide. The incineration products from shells and spines have also better reaction property than that of derived from the calcite reagent.

These differences could be caused by the microstructures of the reagent, shells and spines. The adjustment of the particle size of shells during the firing can further reduce the reaction temperature and fuels and control the reaction property as a heat storage material.

©2019. Japan Geoscience Union. All Right Reserved.

Keywords: Calcite, Shell, Thermal decomposition

©2019. Japan Geoscience Union. All Right Reserved.

“Manipulated” Organic Crystallization and Two-step Dissolution Process Attained by Plasmonic Optical Tweezers

*Hiromasa Niinomi[1], Teruki Sugiyama[2,3,4], Miho Tagawa[5], Toru Ujihara[5], Katsuhiko Miyamoto[6,7], Takashige Omatsu[6,7], Jun Nozawa[1], Junpei Okada[1], Satoshi Uda[1]

1. Institute for Materials Research, Tohoku University, 2. Department of Applied Chemistry, National Chiao Tung University, 3. Center for Emergent Functional Matter Science, National Chiao Tung University, 4. Division of Materials Science, Nara Institute of Science and Technology, 5. Institute of Materials and Systems for Sustainability (IMaSS), Nagoya University, 6. Molecular Chirality Research Center (MCRC), Chiba University, 7. Graduate School of Engineering, Chiba University

Spatiotemporal control of crystallization from a solution is often required for detailed exploration on mechanism of early stage of crystallization because the stochastic nature of nucleation process hinders us to chase its early stage. Recently, laser trapping-induced crystallization technique has received increasing attention as a possible candidate to realize spatiotemporally controllable crystallization.[1] In the technique, the crystallization is induced by trapping molecular clusters in a solution with optical tweezers, in which dielectric tiny particles are captured by electrical field gradient force generated by tightly focusing laser light by optical lens. This technique has actually demonstrated forced nucleation of various organic molecules from an unsaturated mother solution at the focal spot. Although recent progress of nanoscience including research on nucleation dynamics demands precise manipulation of nanoscopic objects, the conventional optical tweezers, electrical field gradient force of which relies on the focusing the laser by optical lens, has a limitation of diffraction limit on focusing the light. To overcome the limit, the use of near-field generated by localized surface plasmon resonance, which is collective oscillation of free electrons on surfaces of metal nanoparticles when light impinges on the nanoparticle, has been proposed. [2] Because the near-field is confined in nanoscale, the light focusing beyond the diffraction limit can be achieved consequently, allowing us to capture the smaller particles much tightly than the conventional method. However, the plasmonic optical tweezers has never been applied to crystallization. Here we applied plasmonic optical tweezers to crystallization of acetaminophen molecule from an aqueous solution.

Figure 1 shows schematic illustration of experimental setup. Periodic Au nanolattice the unit structure of which is gammadion with the size of 500 nm was fabricated on a cover glass by electron beam lithography. An aqueous solution of acetaminophen saturated at room temperature (24^{o}C) was dropped on the Au nanolattice, and then solution thin layer supported by the nanolattice was formed by capillarity. Near-infrared continuous-wave left-handed circularly polarized laser (1064 nm, 6.4×10^{9} W/m^{2}) was focused to the nanolattice supporting the solution thin layer by passing through an objective lens equipped on an inverted polarized-light optical microscope. In-situ microscopic observation for the vicinity of the focal spot was also performed simultaneous with the laser irradiation.

Figure 2 shows time-lapse micrographs of the in-situ observation in the vicinity of the focal spot. After the laser irradiation, crystals with the size of 1000 ~ 2000 nm were precipitated 19 mm away from the focal spot in annular pattern. The position of the annular pattern moved while following the change of in-plane position of the focal spot via dissolution/precipitation process, indicating that position of the crystal is manipulatable. When the plasmon excitation by laser irradiation was stopped, the crystals were disappeared via two-step dissolution process; the crystals first transformed to dense liquid droplets, and then the dense droplet disappeared through molecular diffusion.

©2019. Japan Geoscience Union. All Right Reserved.

Generally, large temperature gradient generates in the vicinity of the focal spot when localized surface plasmon resonance was excited, because of the heat generation through electron-phonon scattering. Thus, the large temperature gradient exerts thermophoretic force outward from the focal spot on acetaminophen molecules. Since the electrical field gradient force attracts the molecules towards the focal spot, the annular-patterned precipitation can be interpreted as the consequence of the balancing the electrical field gradient force as attractive force and the thermophoretic force as repulsive force. Therefore, our observation strongly suggested that plasmonic optical tweezers can precisely control crystallization.

[1] T. Sugiyama *et al.*, *Acc. Chem. Res.* **2012**, 45(11), 1946-1954.
[2] T. Shoji *et al.*, *J. Phys. Chem. Lett.* **2014**, 5(17), 2957–2967.

Keywords: Plasmonic Optical Tweezres, Crystallization of Organic Molecule, Two-step Dissolution Process

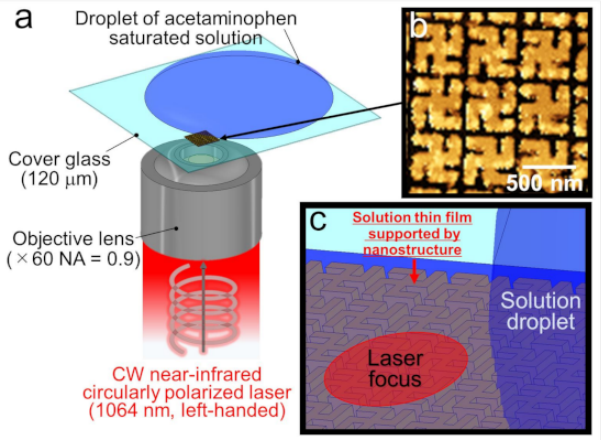

Figure 1 **a** Schematic illustration of the experimental setup **b** Atomic force microscopic image of the plasmonic Au nanolattice **c** Position of the laser focus.

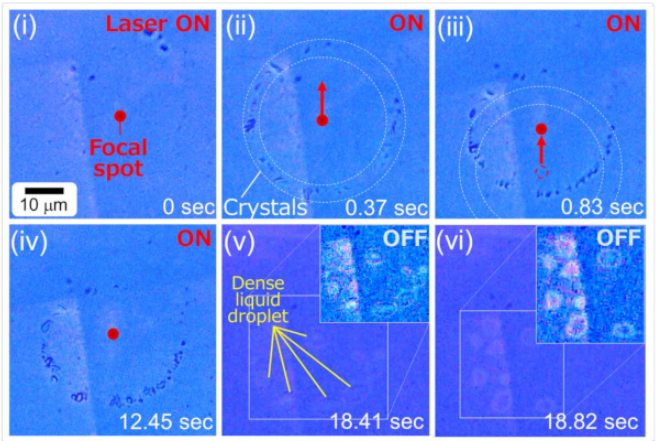

Figure 2 Time-lapse micrographs showing the dynamics of the plasmonic trapping-induced crystallization and the two-step dissolution process.

©2019. Japan Geoscience Union. All Right Reserved.

Investigation of liquid cell transmission electron microscopy combined with antisolvent crystallization

*Tomoya Yamazaki[1], Yuki Kimura[1]

1. Institute of Low Temperature Science Hokkkaido University

Crystallization of salts in solutions is a quite common phenomenon in the earth and is important not only for production of materials but also for understanding geochemical processes. However, initial stage of crystallization, called nucleation, is not fully understood and numerous studies to understand the process have been reported. Recently, multistep nucleation pathway, which formations of one or more metastable phases are required on the route to a formation of a crystalline phase, have been proposed. Liquid cell transmission electron microscopy (TEM) is a promising method for observing the nucleation process directly because the spatial resolution of this method is under nanometer scale. More recently, multistep nucleation pathways of the crystals of calcium carbonate [1] and lysozyme protein [2] have been revealed by liquid cell TEM. However, capturing a moment of a nucleation event is quite difficult because the observable area of the method is small ($< 100\ \mu m^2$) and a nucleation event is typically very rare in the tiny volume within the area. In order to observe nucleation events efficiently, a supersaturation of a sample solution should be increased with observing the solution. To create the situation, we applied the anti-solvent crystallization technique, which crystallize the solute to add the solvent with the extremely low solubility of the solute (anti-solvent), to liquid cell TEM and tried to observe the nucleation event of a salt crystal.

We used the TEM holder (Poseidon 300, Protochips Inc.) and the liquid cells of silicon chips equipped with thin silicon nitride windows. Aqueous solution of sodium chlorate under equilibrium at room temperature was enclosed in the liquid cell. The TEM holder has two injection ports of liquid, and one of the ports was filled by acetone as the anti-solvent of sodium chlorate. After starting the observation of the sample solution, acetone was injected by syringe pump for mixing the aqueous solution in the liquid cell.

Using the methods, we succeeded in observing the nucleation events of crystals. In this presentation, we will report the detailed analysis of crystals and the nucleation processes.

Acknowledgement

This work was supported partly by Grant for Basic Science Research Projects from The Sumitomo Foundation (Grant Number 170738) and JSPS KAKENHI Grant Numbers JP15H05731 and JP18J01470. T.Y. is grateful for the JSPS Research Fellowship for Young Scientists.

References

[1] M. H. Nielsen *et al.*, *Science* **345** (2014), 1158.

[2] T. Yamazaki *et al.*, *Proc. Natl. Acad. Sci.* **114** (2017), 2154.

©2019. Japan Geoscience Union. All Right Reserved.

Keywords: liquid cell transmission electron microscopy, crystal growth, solution growth, anti-solvent crystallization

©2019. Japan Geoscience Union. All Right Reserved.

DNA-guided crystallization of nanoparticles: optimization of crystallization conditions and structure analysis

*Miho Tagawa[1], Shoko Kojima[1], Hayato Sumi[1], Arisa Nishibu[1], Takumi Isogai[1], Maasa Yokomori[2], Shunta Harada[1], Toru Ujihara[1], Katsuo Tsukamoto[1]

1. Nagoya University, 2. The University of Tokyo

Due to the programmability and self-assembly characteristic, DNA is a powerful tool for guiding the assembly of nanometer-sized particles into large-scale ordered structures. Recently, DNA-guided nanoparticle crystallization has been demonstrated and many types of crystal structures have been created[1-3]. By changing particle size ratio, DNA length and complementarity, particles assemble into different types of crystals. By TEM imaging after silica encapsulations, Mirkin et al. confirmed that some of DNA-guided nanoparticle crystals assembled into wulff polyhedra in solution[3]. However, it is crucially difficult to grow large-scale wulff polyhedral single crystal of DNA-functionalized nanoparticles (DNA-NPs) with size up to several microns. Herein, we demonstrate the optimization of solution composition on DNA-NP crystal growth, specifically the effect of sodium chloride concentration and polyethylene glycol (PEG) addition into DNA-NP colloidal solution.

Au nanoparticles of diameter 7 nm were functionalized with two different sequenced thiolated-DNA strands (DNAa and DNAb), respectively. These DNA-functionalized nanoparticles, DNA-NPa and DNA-NPb, were combined with linker DNA strands, which hybridize to complementary sequences of DNAa and DNAb (Figure 1). The mixed solutions were adjusted under different sodium chloride concentration (100, 300, 500, 700 and 900 mM) and by adding PEG with different molecular weights (1000, 4000 and 8000) and subsequently heated to 65 ºC and then slowly cooled back to 25 ºC. The crystal structure of assembled DNA-NP superlattices were analyzed by small angle x-ray scattering (SAXS) and imaged by scanning electron microscope (SEM).

We confirmed the crystal structure of assembled DNA-NP aggregates was bcc by analyzing peak positions of SAXS 1D curves. The differences were seen in SAXS and SEM data with different samples under different sodium chloride concentrations. Relatively large wulff polyhedral single crystals of DNA-NP superlattices were assembled in buffer solution under 500 mM NaCl. The significant differences were seen in SAXS and SEM data with different samples by adding PEG with different molecular weights. DNA-NP superlattices assembled in the buffer solution with PEG 1000 showed a clear SAXS 1D curve which indicates bcc structure (Figure 2) and a significant increase in average crystal size were confirmed by SEM (Figure 3).

We will also present the recent progress on the formation of lattice using DNA-NPs linked by DNA polyhedral constructs. DNA polyhedron has symmetrical connecting bonds and plays a determining role in the inter-particle bonding; that allows for control of particles coordination. DNA nanostructure-directed crystallization has a power of the proposed approach for assembly of complex nanoparticle lattices[4].

[1] D. Nykypanchuk et al., *Nature* **451**, 549-552 (2008).
[2] S. Y. Park *et al.*, *Nature* **451**, 553-556 (2008).
[3] R. J. Macfarlane *et al.*, *Science* **334**, 204-208 (2011).
[4] W. Liu *et al.*, *Science* **351**, 582-586 (2016).

Keywords: DNA, Nanoparticles, SAXS, colloidal crystallization

©2019. Japan Geoscience Union. All Right Reserved.

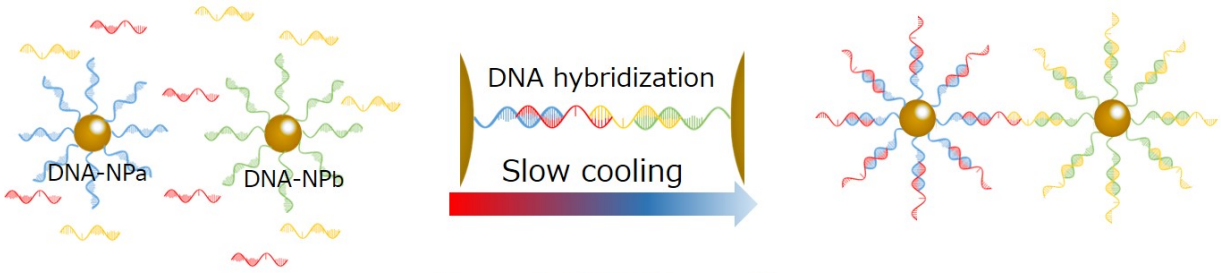

Figure 1. DNA-NP assembly

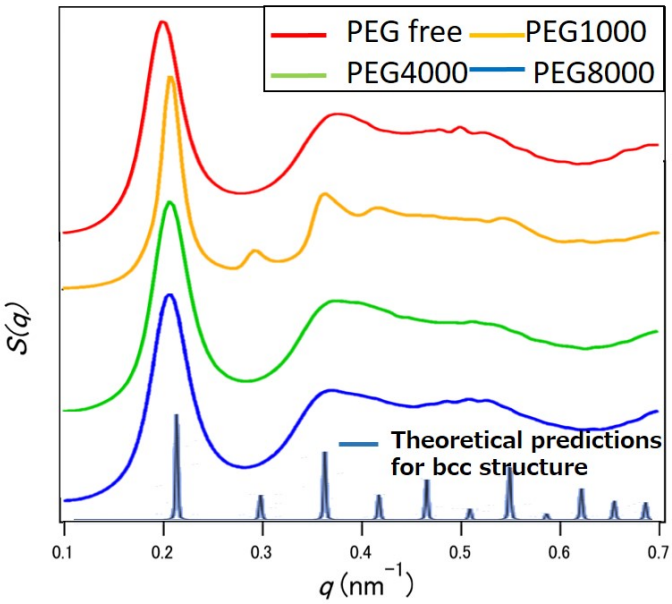

Figure 2. SAXS analysis of DNA-NP aggregates with PEG of different weights as additives

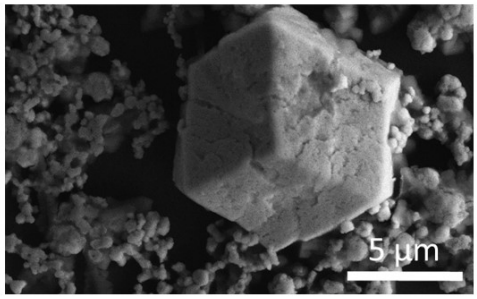

Figure 3. SEM image of DNA-NP superlattice

©2019. Japan Geoscience Union. All Right Reserved.

[J] Oral | M (Multidisciplinary and Interdisciplinary)：M-IS Intersection

Tue. May 28, 2019 10:45 AM - 12:15 PM JST | Tue. May 28, 2019 1:45 AM - 3:15 AM UTC | 303 3F

[M-IS10] Interface- and nano-phenomena on crystal growth and dissolution

convener:Yuki Kimura(Institute of Low Temperature Science, Hokkaido University), Hitoshi Miura(Graduate School of Natural Sciences, Department of Information and Basic Science, Nagoya City University), Hisao Satoh(Naka Energy Research Laboratory, Mitsubishi Materials Corporation), Katsuo Tsukamoto(Graduate School of Engineering, Osaka University), Chairperson:Hisao Satoh

Recent developments of observations in nano-scale opened a detail discussion concerning mechanisms of crystal growth and dissolution based on interface phenomena including dynamics. In this session, growth and dissolution mechanisms of crystals will be discussed focusing on interface phenomena of minerals in the fields of biological origin, global environment, planets and space in addition to general minerals.

10:45 AM - 11:00 AM JST | 1:45 AM - 2:00 AM UTC

[MIS10-06] Growth mechanism of binary colloidal crystals

*Jun Nozawa[1], Suxia Guo[1], Hiromasa Niinomi[1], Junpei Okada[1], Satoshi Uda[1] (1.Tohoku University)

11:00 AM - 11:15 AM JST | 2:00 AM - 2:15 AM UTC

[MIS10-07] Solution-Mediated-Transformation Kinetics of Norsethite

*Harutoshi Asakawa[1], Hiroshi Uneda[1], Itaru Echigo[1], Ryuichi Komatsu[1] (1.Graduate School of Sciences and Technology for Innovation Yamaguchi University)

11:15 AM - 11:30 AM JST | 2:15 AM - 2:30 AM UTC

[MIS10-08] Formation of low-crystalline magnesium silicate in natural alkaline environment and flow-through experiments

*Yuto Nishiki[1], Misato Shimbashi[1], Tsutomu Sato[2], Tsubasa Otake[2] (1.Graduate School of Engineering, Hokkaido University, 2.Faculty of Engineering, Hokkaido University)

11:30 AM - 11:45 AM JST | 2:30 AM - 2:45 AM UTC

[MIS10-09] Homogeneous Nucleation from Vapor in Al-O Binary System

*Shinnosuke Ishizuka[1], Jun Kawano[2], Tomoya Yamazaki[3], Tetsuya Hama[3], Yuki Kimura[3] (1.National Institute for Environmental Studies, 2.Faculty of Science, Hokkaido University, 3.Institute of Low Temperature Science, Hokkaido University)

11:45 AM - 12:00 PM JST | 2:45 AM - 3:00 AM UTC

[MIS10-10] Crystal growth hysteresis in birth-and-spread mechanism

*Hitoshi Miura[1] (1.Graduate School of Natural Sciences, Department of Information and Basic Science, Nagoya City University)

12:00 PM - 12:15 PM JST | 3:00 AM - 3:15 AM UTC

Discussion

Growth mechanism of binary colloidal crystals

*Jun Nozawa[1], Suxia Guo[1], Hiromasa Niinomi[1], Junpei Okada[1], Satoshi Uda[1]

1. Tohoku University

Colloidal crystals have been attracted great attention from wide application fields owing to their unique optical properties. Now, varieties structures of the colloidal crystal, e.g. non-closed packed structure, are significantly demanded for diverse applications. For this ends, to grow binary colloidal crystal is promising method since it displays rich structural diversity. However, in contrast to single component system, growth mechanism of binary system of colloidal crystals is poorly understood. Also, to grow large size of binary colloidal crystals with high crystallinity is still difficult. In this study, in-situ observation is conducted to reveal detailed growth process of binary colloidal crystals. Then, growth mechanism is discussed.
Polystyrene particles are employed in the experiment. Green fluorescent particles with 500 nm and red with 700 nm are employed. Crystallization of colloidal crystals is induced by depletion attraction.
We have found several features on the growth of binary colloidal crystals. First, it grows on substrate. The AB_2 structure (A: 700 nm, B: 500 nm) is found to be grown by utilizing crystals composed only of 700 nm particles. The AB_2 crystals also grow on crystals of 500 nm. The specific crystallographic orientations between those crystals are recognized. Combination of orientations between AB_2 and substrate are classified into four types. Heteroepitaxial growth is found to occur for growth of AB2 structure. Second, growth rate of binary colloidal crystals is quite small compare to that of single component system under the same particle concentration. We think this is attributed to complex structure of the crystals, which requires each particle incorporating to their own site. This process is not required for crystals composed of single component. Third, cluster formation at the interface is recognized. The ordered structure composed only of 500 nm is formed at growing interface. Particles of 700 nm is incorporated into the ordered structure generates AB_2 structure.
These observations provide great hints to reveal overall growth mechanism of binary colloidal crystals, which will lead to establish sophisticated growth technique to grow large and high quality crystals.

Keywords: Colloidal crystal, Crystal growth

©2019. Japan Geoscience Union. All Right Reserved.

Solution-Mediated-Transformation Kinetics of Norsethite

*Harutoshi Asakawa[1], Hiroshi Uneda[1], Itaru Echigo[1], Ryuichi Komatsu[1]

1. Graduate School of Sciences and Technology for Innovation Yamaguchi University

We investigated the induction periods of norsethie and withelite by polarized optical microscopy, X-ray diffraction measurements, pH measurements, inductively coupled plasma measurements and total organic carbon measurements. In this talk, we will show features of the solution-mediated-transformation kinetics of norsethite from the relation between nucleation rate and supersaturation.

Keywords: Norsethite, Solution-mediated transformation

©2019. Japan Geoscience Union. All Right Reserved.

Formation of low-crystalline magnesium silicate in natural alkaline environment and flow-through experiments

*Yuto Nishiki[1], Misato Shimbashi[1], Tsutomu Sato[2], Tsubasa Otake[2]

1. Graduate School of Engineering, Hokkaido University, 2. Faculty of Engineering, Hokkaido University

INTRODUCTION

Magnesium silicate formation at low temperature (25-200℃) is receiving a lot of attention in various research fields. Sepiolite and serpentine, crystalline Mg-clay minerals, are known to be formed in MgO-SiO_2-H_2O systems at low temperature. However, some studies have been suggesting that low-crystalline magnesium silicate recently should be formed in this low-temperature condition. These kinds of low-crystalline silicates have actively been studied by many reaserchers and engineers. For instance, calsium and alminium silicates are known as C-S-H (calcium silicate hydrate) and allophane/imogolite, respectively. These are studied for both natural minerals and synthesized materials. On the other hand, studies of the low-crystalline magnesium silicate are still in their infancy and little is known. Therefore, the nature of the low-crystalline magnesium silicate has not been clear yet. Since the magnesium silicate can be utilized in various engineering fields (e.g., improved oil recovery, CO_2 geological storage, geothermal power generation, concrete degradation, mineral clogging in radioactive waste disposal, treatment of environmental pollutions, etc.), the current reserch gaps in the understanding of the low-crystallline magnesium silicate formation need to be addresed so as to contribute positively to the above engineering technologies. Moreover, this study can also be applied to the field of planetary science because low-crystalline magnesium silicate should be observed even on surface of Mars and in interstellar silicate dusts.

ANALYSES OF NATURAL PRODUCTS

Firstly, this study confirmed that low-crystalline magnesium silicate forms in nature. Samples of precipitates were collected from the surface where fluid flows out from serpentinite rocks around Kamuikotan metamorphic belts, Hokkaido, Japan. Although a clear XRD pattern from the bulk samples was not observed, electron microscopy (Field emission scanning electron microscope and Transmission electron microscope; TEM) clearly identified the phase. TEM-energy dispersive X-ray spectrometry indicated that the low-crystalline phase was composed of Mg, Si, and O. Moreover, electron diffraction with TEM showed diffuse halo rings from some particles in the samples, showing the formation of low-crystalline phase. Furthermore, the fluid samples participating in formation of the precipitates were collected and analyzed. From the results, the fluid samples were alkaline ($9.50 < pH < 10.67$) and saturated with low-crystalline magnesium silicate phase (magnesium silicate hydrate reported by Lothernbach et al., 2018).

FLOW-THROUGH EXPERIMENTS

Secondly, to demonstrate the above formation, flow-through experiments in open system were conducted. Alkaline solution with 1.5 mM of dissolved silica was flowed into MgO powder in the reaction cell. TEM observation revealed the low-crystalline magnesium silicate formation as well. Moreover,

©2019. Japan Geoscience Union. All Right Reserved.

dissolution rate of Mg-bearing mineral and formation rate of magnesium silicate were obtained from dissolved silica and magnesium concentrations in the output solutions. These suggested that the magnesium silicate formation was extremely rapid under the oversaturated condition, and that the dissolution of Mg-bearing mineral is the rate-determining step during formation of the low-crystalline magnesium silicate. Although the flow-through experiments used only MgO as a Mg-bearing mineral, the above discussion can be applied to all of Mg-bearing minerals such as olivine and pyroxene because dissolution rate of MgO is greater than any other Mg-bearing minerals. Therefore, the flow-through experiments broaden the kinetical understanding of low-crystalline magnesium silicate formation not only at the Kamuikotan metamorphic belts, but also to other areas where the magnesium silicate is formed from the supply of Mg-bearing minerals in rocks/soil.

Keywords: Magnesium silicate, Transmission electron microscope, Kinetics, Kamuikotan metamorphic belts, Serpentine, Thermodynamic calculation

©2019. Japan Geoscience Union. All Right Reserved.

Homogeneous Nucleation from Vapor in Al-O Binary System

*Shinnosuke Ishizuka[1], Jun Kawano[2], Tomoya Yamazaki[3], Tetsuya Hama[3], Yuki Kimura[3]

1. National Institute for Environmental Studies, 2. Faculty of Science, Hokkaido University, 3. Institute of Low Temperature Science, Hokkaido University

A gaseous molecule can have a chemical formula that is inconsistent with its ability to act as a building block for crystals; for example, hot AlO and AlO_2 vapors cannot solidify directly to crystals. The contributions of such gases to homogeneous nucleation processes are unknown. Using in situ IR spectroscopy on nucleating nanoparticles, we show that a liquid-like behavior of nucleating nanoparticles in the Al–O system induces immiscible phase segregation. In an oxygen-deficient atmosphere, aluminum oxide nanoparticles formed with a unique shape composed of an Al metal head and an anisotropic Al_2O_3 crystalline tail. The anisotropic nanoparticles are larger than Al_2O_3 nanoparticles formed in a sufficient oxygen condition. Fewer nuclei may be available in the supersaturated gas, indicating that homogeneous nucleation is initiated by oxygen-bearing species. The nuclei grow by incorporation of Al-bearing species, changing the composition of the particle as a whole toward an Al-rich material. In situ IR measurements revealed that the degree of anisotropy continues to increase, suggesting that oxygen-bearing species also formed by oxidation on the surface of the molten Al-rich head. The scenario is supported by quantum-chemical calculations indicating that oxygen-deficient $(AlO)_n$ clusters as few as 16 molecules induce aggregation of Al atoms. Because Al metal has a significantly lower melting temperature than Al_2O_3, the immiscibility of the nucleating nanoparticles leads to vapor–liquid–solid growth. Astronomical implication will be given in the presentation.

Keywords: Homogeneous Nucleation, Cosmic Dust

©2019. Japan Geoscience Union. All Right Reserved.

Crystal growth hysteresis in birth-and-spread mechanism

*Hitoshi Miura[1]

1. Graduate School of Natural Sciences, Department of Information and Basic Science, Nagoya City University

Crystal growth hysteresis is a remarkable phenomenon induced by impurities: the crystal growth velocity when the driving force (supersaturation or supercooling) is increased is different from that when it is decreased. It has been considered that the growth hysteresis is caused by slow adsorption of impurities onto the crystal surface. On the surface, there are steps in atomic scale that advance independently due to continuous incorporations of growth units, therefore the surface is grown layer by layer (layer-by-layer growth mechanism). The step advancement is inhibited by impurities adsorbed on the surface. However, the amount of the adsorbed impurities is also affected by the step passages: frequent step passages reduce the amount of adsorbed impurities. The competition between two timescales —impurity adsorption timescale and time interval of surface-updating (terrace exposure time)— causes complex nonlinear phenomena such as crystal growth hysteresis.

The mechanism of the crystal growth hysteresis was elucidated by a mean field theory. Punin & Artamonova [1] and Miura & Tsukamoto [2] formulated the following two effects —inhibition of step advancement by adsorbed impurities (pinning effect) and removal of adsorbed impurities by step passages (impurity sweeping)— to clarify the existence of multiple steady solutions that satisfies both of two formulas at a certain range of supersaturation. In the case of constant step interval, numerical simulations based on a phase-field method demonstrated that the growth hysteresis emerges as predicted by the mean field theory even when the physical quantities are fluctuated around these averages [3]. The phase-field simulations also confirmed the emergence of hysteresis in the case that the surface is grown by a screw dislocation [4]. However, the growth hysteresis has not been investigated in the case that the surface is grown by two-dimensional nucleation (birth-and-spread mechanism), which is another mechanism to generate new steps on the surface. The birth-and-spread growth dominates the spiral growth at high supersaturation, so it is important to elucidate the impurity-induced effect for that. In this study, we theoretically investigate the growth hysteresis in the birth-and-spread growth mechanism.

At first, we formulated the interdependence between the step velocity and the amount of adsorbed impurities based on the mean field theory, in the same way in the case of the spiral growth. As the result, we found that multiple steady solutions exist at a certain range of supersaturation. This suggests that the growth hysteresis can emerge even in the birth-and-spread growth in principle. At second, we carried out the phase-field calculation with the equivalent condition of the mean field theory. We confirmed the emergence of growth hysteresis in down-and-up cycles of supersaturation. In addition, we found that the range in supersaturation at which the growth hysteresis is observed depends on the rate of supersaturation variation: slow change in supersaturation makes the hysteresis behavior unclear.

References:
[1] Y. O. Punin and O. I. Artamonova, *Kristallographiya* **32**, 1262 (1989). [2] H. Miura and K. Tsukamoto, *Cryst. Growth Des.* **13**, 3588 (2013). [3] H. Miura, *Cryst. Growth Des.* **16**, 2033 (2016). [4] H. Miura, JpGU-AGU Joint Meeting 2017, abstract MIS11-P04.

©2019. Japan Geoscience Union. All Right Reserved.

Keywords: Crystal growth, Step dynamics, Impurity effect, Phase-field method

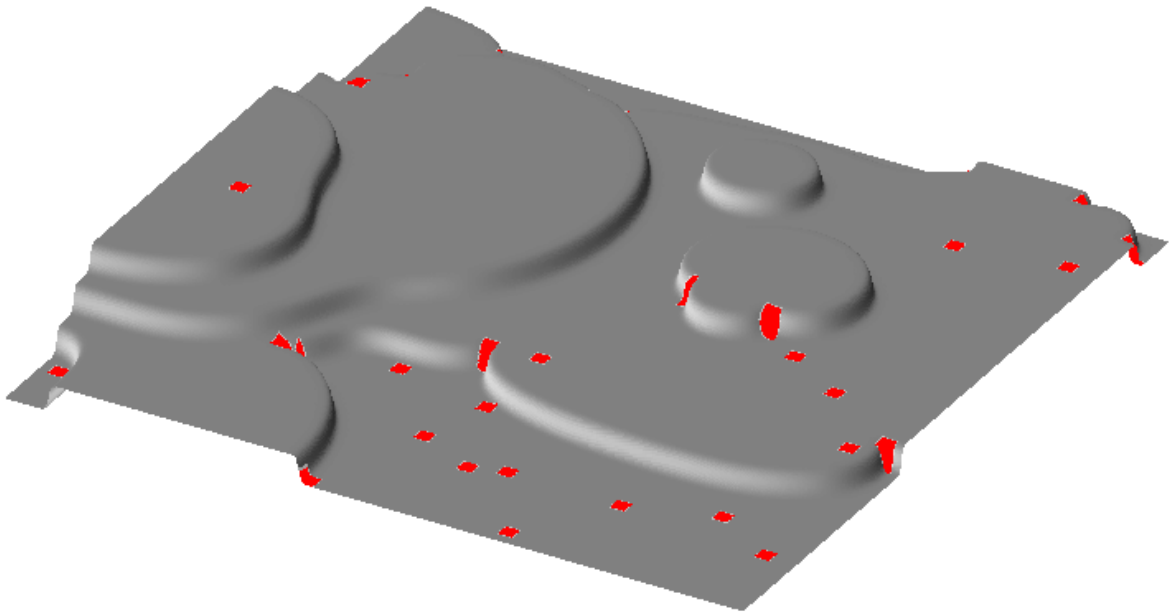

©2019. Japan Geoscience Union. All Right Reserved.

[J] Poster | M (Multidisciplinary and Interdisciplinary)：M-IS Intersection

Tue. May 28, 2019 3:30 PM - 5:00 PM JST | Tue. May 28, 2019 6:30 AM - 8:00 AM UTC | Poster Hall International Exhibition Hall8, Makuhari Messe_24

[M-IS10] Interface- and nano-phenomena on crystal growth and dissolution

convener:Yuki Kimura(Institute of Low Temperature Science, Hokkaido University), Hitoshi Miura(Graduate School of Natural Sciences, Department of Information and Basic Science, Nagoya City University), Hisao Satoh(Naka Energy Research Laboratory, Mitsubishi Materials Corporation), Katsuo Tsukamoto(Graduate School of Engineering, Osaka University)

Recent developments of observations in nano-scale opened a detail discussion concerning mechanisms of crystal growth and dissolution based on interface phenomena including dynamics. In this session, growth and dissolution mechanisms of crystals will be discussed focusing on interface phenomena of minerals in the fields of biological origin, global environment, planets and space in addition to general minerals.

[MIS10-P01] Theoretical Model of Crystallization through Homogeneous Nucleation in Water Droplets

*Kyoko Kitakami Tanaka[1], Yuki Kimura[2] (1.Tohoku University, 2.Hokkaido University, Institute of Low Temperature Science)

[MIS10-P02] Mean Height of the Self-Assembled Faceted Macrosteps: Steady Crystal Growth/Dissolution in a Reaction- (Interface-) Limited Process

*Noriko Akutsu[1] (1.Faculty of Engineering, Osaka Electro-Communication University)

[MIS10-P03] In-situ observation of natural snow crystals by optical techniques

*Yuki Kimura[1], Tomoya Yamazaki[1], Takao Maki, Yoshinori Furukawa[1] (1.Institute of Low Temperature Science, Hokkaido University)

[MIS10-P04] Visualization of local environment around forming/dissolving carbonate minerals with the fluorescent probe

*Jun Kawano[1], Kotaro Osawa[2], Takashi Toyofuku[3,4], Yukiko Nagai[4,5], Jun-ya Tanaka[6], Takaya Nagai[1] (1.Faculty of Science, Hokkaido University, 2.School of Science, Hokkaido University, 3.JAMSTEC, 4.Tokyo University of Marine Science and Technology, 5.National Museum of Nature and Science of Tokyo, 6.Graduate School of Science, Hokkaido University)

[MIS10-P05] Influence of Ammonium Nitrate on Crystallization of Norsethite from Aqueous Solution

*Itaru Echigo[1], Harutoshi Asakawa[1], Hiroshi Uneda, Ryuichi Komatsu[1] (1.Graduate School of Science and Technology for Innovation Yamaguchi University)

[MIS10-P06] Direct observation of zeolite nucleation from compacted bentonite under hyperalkaline condition

*Hisao Satoh[1], Mayumi Takazawa[2], Daisuke Hayashi[3], Masaya Ida[3] (1.Naka Energy Research Laboratory, Mitsubishi Materials Corporation, 2.Mitsubishi Materials Corporation, 3.Radioactive Waste Management Funding and Research Center)

Theoretical Model of Crystallization through Homogeneous Nucleation in Water Droplets

*Kyoko Kitakami Tanaka[1], Yuki Kimura[2]

1. Tohoku University, 2. Hokkaido University, Institute of Low Temperature Science

The crystallization process of water droplets is not only fundamentally important, but is also climate-sensitive and hence relevant to urgent problems such as climate change. However, water crystallization in environments such as cirrus clouds is difficult to explore by conventional experimental approaches. Analytical models of the crystallization process can assist our understanding of ice nucleation and predict the crystallization processes in environments that cannot be replicated in the laboratory. Experimentally, micrometer-sized droplets are known to crystallize at approximately 235 K, regardless of cooling rate and experimental method. However, the crystallization temperature of smaller (nanometer-sized) droplets suddenly drops at high cooling rates (~10^5 K/s). At very high cooling rates (10^{6-7} K/s), liquid water droplets vitrify rather than crystallize. A model that explains all of these characteristics is thus far lacking. Motivated by this knowledge gap, we construct a new model of water-droplet crystallization that evolves the homogenous nucleation and crystal growth in water droplets during cooling (Tanaka & Kimura, PCCP, 21, 2410, 2019). The crystallization process depends on the surface energy at the liquid–solid interface (which determines the liquid-to-sold nucleation rate) and the activation energy of molecular diffusion through the liquid. The model extends our previous model (Tanaka et al. J. Crystal Growth, 310, 1281, 2008) by incorporating the droplet size-dependence of the crystallization process. Especially, smaller droplets begin crystallizing later than larger droplets because they are less likely to form a nucleating center in a given time. We also try two diffusion coefficients: the diffusivity of amorphous ice (ASW) and the diffusivity of supercooled liquid (SCL) water. The model well replicated the results of previous laboratory experiments, especially, the different responses of the crystallization temperatures of the micrometer- and nanometer-sized particles as functions of cooling rate. At low cooling rates, the ASW and SCL diffusivities gave the same results for micrometer-sized particles, because these particles crystallize at temperatures around the homogenous nucleation temperature (235 K), where both diffusivities are identical. However, for nanometer-sized particles, the crystallization temperature is lower and the SCL diffusivity is more accurate than the ASW diffusivity. Calculations on small droplets also provide low-temperature information at high cooling rates, which are sparsely acquired in experiments. The critical cooling rate of vitrification was predicted as 10^{7-8} K/s with SCL diffusivity, consistent with the experimental rates.

Keywords: nucleation, crystal growth, water, vitrification

©2019. Japan Geoscience Union. All Right Reserved.

Mean Height of the Self-Assembled Faceted Macrosteps: Steady Crystal Growth/Dissolution in a Reaction- (Interface-) Limited Process

*Noriko Akutsu[1]

1. Faculty of Engineering, Osaka Electro-Communication University

Faceted macrosteps are considered to play critical roles in some reaction- (interface-) limited processes of crystal growth/dissolution [1]. For the diffusion-limited crystal growth, step dynamics of macrosteps or bunched steps with rough side surfaces has been studied theoretically and experimentally [2,3]. Whereas, for the reaction-limited crystal growth/dissolution, the step dynamics of macrosteps has not yet been studied sufficiently.

In this paper, the step dynamics of faceted macrosteps in a reaction- (interface-) limited crystal growth/dissolution is studied theoretically by using a Monte Carlo method for the non-conserved systems. The microscopic model for this Monte Carlo study is the restricted solid-on-solid model with a point-contact step-step attraction (p-RSOS model) [4]. Here, the “restricted” means the height difference between the nearest neighbor sites is restricted to {0, ±1}. The step-step attraction is assumed to be the energy gain ε_{int} by forming a bond between the neighboring steps at the meeting point. The eminent point of this p-RSOS model is that the reliable surface tension (surface free energy per unit normal area) can be calculated at equilibrium by using the density-matrix renormalization-group (DMRG) method [5]. The polar graph of the surface tension (the Wulff figure) calculated by the DMRG method is shown in Fig. 1 [6]. A faceted macrostep is self-organizing at equilibrium because of the discontinuous surface tension resulting from the microscopic step-step attraction [6].

In the non-equilibrium steady state, we found that the height of the macrostep decreases as the driving force of dissolution increases [7]. In the step-faceting zone (Fig. 1 (a)), elementary steps detach from the faceted macrostep by way of the two-dimensional (2D) nucleation at the upper edge of the faceted macrostep on the (001) and the (111) surfaces. Near equilibrium, since the kink densities of the (001) and the (111) surfaces are few, the faceted surfaces cannot move. For the large driving force, the vicinal surface roughens kinetically.

1. T. Mitani, N. Komatsu, T. Takahashi, T. Kato, S. Harada, T. Ujihara, Y. Matsumoto, K. Kurashige, and H. Okumura, J. Cryst. Growth, **423**, 45–49 (2015). A. F. Khokhryakov, Y. N. Palyanov, Y. M. Borzdov, A. S. Kozhukhov, and D. V. Shcheglov, Cryst. Growth Des. **18**, 152–158 (2018).
2. A. Pimpinelli and J. Villain, *Physics of Crystal Growth* (Cambridge University Press, Cambridge, UK, 1998). A. L. Barabasi and H. E. Stanley, *Fractal Concepts in Surface Growth* (Cambridge University Press, Cambridge, UK, 1995).
3 A. A. Chernov, Sov. Phys. USP, **4**, 116–148 (1961). T. Nishinaga, C. Sasaoka, and A. A. Chernov, Ed. I. Sunagawa, *Morphology and Growth Unit of Crystals* (Terra Scientific Publishing Company, Tokyo, 1989) pp. 139–151.
4. N. Akutsu, Applied Surface Science, **256**, 1205–1209 (2009); J. Phys. Condens. Matter, **23**, 485004 (2011).
5. N. Akutsu and T. Yamamoto, ed. T. Nishinaga, *Handbook of Crystal Growth*, Vol. I. (Elsevier, 2015) pp. 265–313.
6. N. Akutsu, “Profile of a Faceted Macrostep Caused by Anomalous Surface Tension,” Adv. Cond. Matter Physics, 2017, Article ID 2021510 (2017); AIP Adv., **6**, 035301 (2016).

©2019. Japan Geoscience Union. All Right Reserved.

7. N. Akutsu, Crystals **7**, 42 (2017); Phys. Rev. Materials **2**, 023603 (2018).

Fig. 1 Cross section of the Wulff figure and the equilibrium crystal shape (ECS). Thin solid lines: ECS. Thick solid lines and filled squares: polar graph of surface tension. (a) $k_B T/\varepsilon = 0.4$. (b) $k_B T/\varepsilon = 0.63$. Light thin solid lines: polar graph of surface tension for metastable surfaces. (c) $k_B T/\varepsilon = 0.75$. (d) $k_B T/\varepsilon = 0.4$. The original RSOS model. The figures are taken from Ref. [6].

Keywords: Monte Carlo simulation , Discontinuous surface tension of crystal, Surface free energy, Density-matrix renormalization-group method, Faceted macrosteps

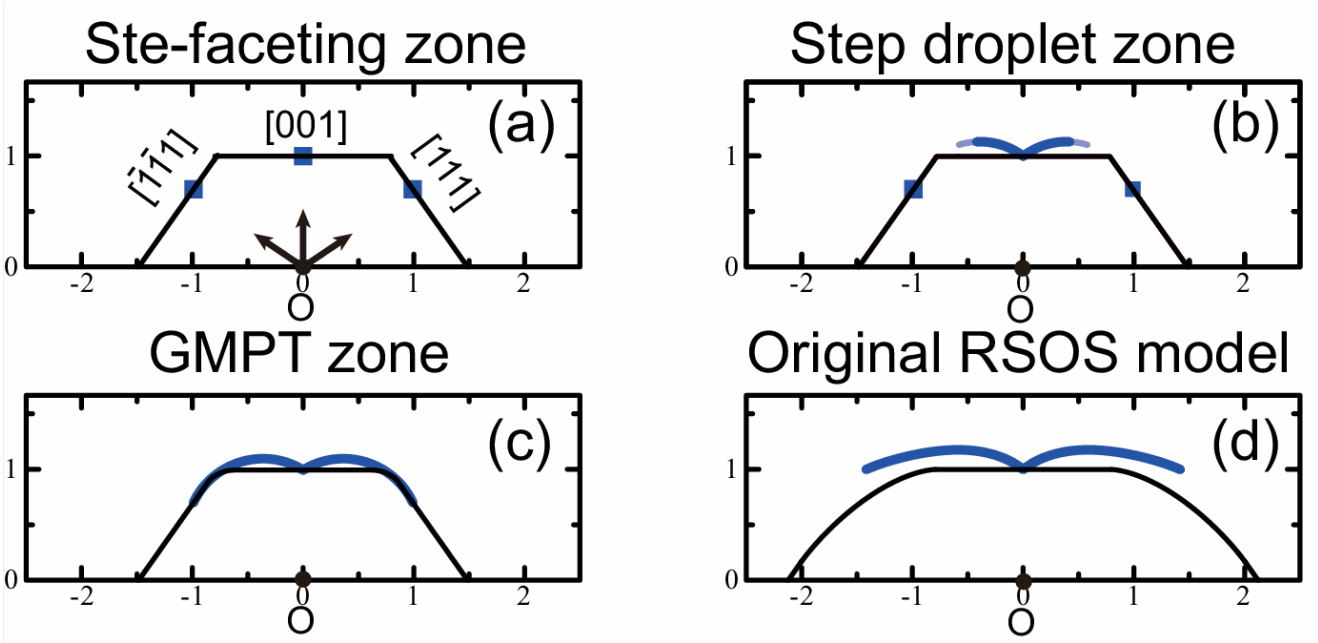

©2019. Japan Geoscience Union. All Right Reserved.

In-situ observation of natural snow crystals by optical techniques

*Yuki Kimura[1], Tomoya Yamazaki[1], Takao Maki, Yoshinori Furukawa[1]

1. Institute of Low Temperature Science, Hokkaido University

Natural snow crystals excite our interest because of several reasons such as its beautiful geometry, its symmetricity and variety. Relationship between geometry of snow crystal and its formation environment (temperature and humidity) was investigated by Ukichiro Nakaya and has been well known as Nakaya diagram. After that, the reason of why snow crystal changes their geometry, such as platy, needle and column, with slight difference of temperature and humidity, and the growth mechanisms have been studied [e.g., Sanchez et al. *PNAS* 114 (2017) 227; Brumberg et al., *PNAS* 114 (2017) 5349]. Nevertheless, there are several questions have been remained. For instance; origin of twelve-fold snow can be explained not only by a twin but by contribution of secondary prism plane; and origin of characteristic pattern can be appeared not only by intrinsic defects but also by a result of growth.

To understand snow crystals more, we have performed in-situ observation of natural snow crystals and its sublimation/regrowth experiments in an environment controllable cell under originally designed optical systems at the base of Asahi-dake in the Taisetsu area, Hokkaido, Japan for 15 nights in total for five winter seasons from 2015 to 2019. The environment controllable cell has a Peltier cooling unit, which has a water vapor source with a heater and a chromel-alumel thermocouple on top, windows for optical observation, capillary to handle a snow crystal and a platinum resistance temperature detector for temperature measurement of the cell. The optical systems consist of the modified Mach–Zehnder-type interferometer (Maki-type laser interferometer), the Michelson-type white-light interferometer microscope with a long working distance, the optimized color-filtered optical microscopes, a polarized optical microscope and so on.

We set the optical systems in a snow-lab, which is a handmade igloo-like snow room, also works as a good sound and vibration absorber. Temperature in the Taisetsu area and inside the snow-lab are around -10 to -20°C and -5 to -13°C, respectively. Higher temperature in the snow-lab than outside is due to observers and experimental systems. One advantage of the snow-lab is maintaining the humidity close to 100% because all the walls of the snow-lab have been made of snow.

We collected snow crystals directly on a black felt just outside the snow-lab and selected a snow crystal, which was put onto a glass plate for general observations of the shape and surface textures. A snow crystal is also put onto a tip of a glass rod of 1.4 mm in diameter for the Maki-type laser interferometer. Rates for sublimation and regrowth of a snow crystal were successfully measured in thickness and lateral direction simultaneously at a certain environment, where supersaturation was controlled using the environment controllable cell. In addition, surface topography of both surfaces of a snow crystal, which was put onto a Y-shaped metallic holder, could be observed using the Michelson-type white-light interferometric microscope. Here, we will summarize our attempts of these in-situ observations and the

©2019. Japan Geoscience Union. All Right Reserved.

results.

Acknowledgments: We thank Y. Sato, Y. Hirata, S. Nakatsubo, K. Fujita and S. Mori of the Technical Division in the Institute of Low Temperature Science, Hokkaido University, for their help in the development of the experimental system. This study was supported partly by the Grant for Joint Research Program of the Institute of Low Temperature Science, Hokkaido University.

Keywords: Snow, In situ observation, Interferometry, Optical microscopy

©2019. Japan Geoscience Union. All Right Reserved.

Visualization of local environment around forming/dissolving carbonate minerals with the fluorescent probe

*Jun Kawano[1], Kotaro Osawa[2], Takashi Toyofuku[3,4], Yukiko Nagai[4,5], Jun-ya Tanaka[6], Takaya Nagai[1]

1. Faculty of Science, Hokkaido University, 2. School of Science, Hokkaido University, 3. JAMSTEC, 4. Tokyo University of Marine Science and Technology, 5. National Museum of Nature and Science of Tokyo, 6. Graduate School of Science, Hokkaido University

To understand the formation or dissolution mechanism of crystal in aqueous solution, it should be important to analyze the local condition of solution just around dissolving or growing crystal. Recently, we have succeeded to visualize the distribution of pH and ionic concentration around carbonate minerals dissolving in inorganic environment, by using the fluorescent probe. In the present study, we have tried to apply this technique to the formation process of calcium carbonate.
Calcium carbonate was synthesized by the counter diffusion method, in which calcium chloride and sodium carbonate solutions were counter-diffused through an agarose gel matrix containing the fluorescent probe like 8-hydroxypyrene-1,3,6-trisul-fonic acid (HPTS). We observed under a microscope that pH in the middle part of gel first increased gradually with time and turn downward after crystals formed. The counter diffusion method with gel media for the carbonate synthesis has attracted attention as a valid tool in the study of biomineralization because the calcification sites in some organisms were recently suggested to have the features of a highly viscous sol or gel matrix. Therefore, the detail observation of the local condition around forming calcium carbonate in gel matrix could provide new insights into the knowledge of biomineralization mechanisms.

Keywords: Visulization, carbonate minerals, pH

©2019. Japan Geoscience Union. All Right Reserved.

Influence of Ammonium Nitrate on Crystallization of Norsethite from Aqueous Solution

*Itaru Echigo[1], Harutoshi Asakawa[1], Hiroshi Uneda, Ryuichi Komatsu[1]

1. Graduate School of Science and Technology for Innovation Yamaguchi University

Since norsethite $BaMg(CO_3)_2$ has birefringence higher than previous piezoelectric and optical crystals, we expect that norsethite can be used as new acousto-optics andwavelength-conversion devices. However, solubility of norsethite is low and it is difficult to control supersaturation. Hence growth of norsethite is difficult. Then, we investigated effects of ammonium nitrate NH_4NO_3 on crystallization of norsethite from aqueous solution. With increasing NH_4NO_3, solubility of norsethite increased. When concentration of NH_4NO_3 reached to 1M, solubility of norsethite became 30 times larger than without the addition of NH_4NO_3 .With further increasing NH_4NO_3, solubility of norsethite remained constant. Next, we measured induction periods of norsethite, when 1M NH_4NO_3 was added. Then, we could confirm norsethite just after mixed at 70°C by XRD measurement only in the case of the addition of 1M NH_4NO_3. Thus, we revealed that the addition of NH_4NO_3 also accelerates norsethite crystallization. This study concluded that addition of NH_4NO_3 is valid for the growth of norsethite.

Keywords: Norsethite, Aqueous Solution Growth, Ammonium Nitrate

©2019. Japan Geoscience Union. All Right Reserved.

Direct observation of zeolite nucleation from compacted bentonite under hyperalkaline condition

*Hisao Satoh[1], Mayumi Takazawa[2], Daisuke Hayashi[3], Masaya Ida[3]

1. Naka Energy Research Laboratory, Mitsubishi Materials Corporation, 2. Mitsubishi Materials Corporation, 3. Radioactive Waste Management Funding and Research Center

Since dissolution issue of smectite arose on engineered barrier system using bentonite (absorbent clay from shale consisting mostly of smectite) for radioactive waste repository for past several decades, smectite studies are focusing on (1) dissolution kinetics [1, 2], (2) hydraulic property of smectite in various states (gel to compacted [3]) and (3) alterations into the other clay and zeolites [4]. Former two issues are closely related to undersaturation of pore water and reactive surface area of smectite grains as a function of density. As the result, the pore water produced from locally dissolved smectite can gain the supersaturation with respect to potential secondary phases. The third one, the alteration, can finally lead the total thermodynamic system to the next equilibrium state consisting of secondary phases.

For understanding the alteration, we had carried out direct observation on pure montmorillonite and bentonite composed of montmorillonite, quartz and albite with or without minor amount of zeolite additive under Na, K and Ca hydroxide solution at 70 ˚C (pH 12.1) [2]. Two methods were used: (1) interferometric measurement of montmorillonite dissolution [2, 5]; (2) direct optical observation of new precipitations. The former gave the rate as a function of density, the latter provided information about nucleation. Sooner or later, the pore water likely attained to local equilibrium, as long as solution flow is limited by compaction.

Differed from previous result, dissolution of pure montmorillonite in the rates varied from 1E-9 (density < 0.01) to 1E-13 mol/m^2/s (density > 1.2) [2] did not always derive precipitation of secondary phases. However, the system, bentonite was not the case. Bentonite especially with minor amount of zeolite caused prominent nucleation of secondary zeolite after a long induction period (weeks) after solution-flow was shut-off.

This alteration behavior could be interpreted with heterogeneous nucleation model. Interfacial free energy, $\gamma_{S/L}$ between secondary phases and alkaline solution was evaluated by wetting angle measurements. There are two end-members such as low and high silica zeolite, those are analcime (ANA: $NaAlSi_2O_6$; Si/Al = 2.0) and clinoptilolite (CLP: $(NaKCa)_3Al_3Si_{15}O_{36}$; Si/Al = 5.0). Their $\gamma_{S/L}$ were measured to be and 50.54 and 71.31 mJ/m^2, respectively. Chemical equilibrium calculation predicts that CLP is the most stable phase in this reaction system. Microanalyses, however, identified the product as phillipsite (PHI: $(NaKCa)_4Al_4Si_{12}O_{32}$; Si/Al = 3.0) as intermediate composition between CLP and ANA or laumontite (LAU: $CaAl_2Si_4O_{12}$: Si/Al = 2.0). When PHI was seeded to the bentonite system, secondary zeolite was PHI. Also, the observed induction periods (Inl) mostly correlate with supersaturations ($1/S^2$). However, the I sometimes became longer than that by CLP seeding. Seed crystal with higher $g_{S/L}$ such like CLP has lower solubility and likely promotes PHI nucleation more than CLP itself. Fast PHI nucleation by CLP-seeding was an unusual. Direct observation could give us an interesting information. During the early observation in the presence of CLP seed recognized two-step process in which spherical objects were growing in ten times faster rate (5.6E-3 nm/s) than the later phase evolving to faceted (5.1E-2 nm/s). This may have contributed to shortening the induction. Such an amorphous phase is often observed especially at room temperature reaction.

©2019. Japan Geoscience Union. All Right Reserved.

This research is a part of the results of “Advancement of Processing and Disposal Technique for the Geological disposal of TRU Waste (FY2017)” under an entrustment from the Agency for Natural Resources and Energy (ANRE) in the Ministry of Economy, Trade and Industry (METI) of Japan.

[1] Cama et al. (2000) GCA, 64, 2701-2717; [2] Satoh et al. (2013) Clay Min., 48, 285-294; [3] Terada et al. (2018) Mat. Res. Exp., 6, 035514; [4] Dunkel and Putnis (2014) Eur. J. Min., 26, 61-69; [5] Ueta et al. (2016) J. Nuc. Sci, Tech., 53, 184-191.

Keywords: Montmorillonite, zeolite, nucleation, amorphous

©2019. Japan Geoscience Union. All Right Reserved.

[J] Poster | M (Multidisciplinary and Interdisciplinary)：M-IS Intersection

Tue. May 28, 2019 5:15 PM - 6:30 PM JST | Tue. May 28, 2019 8:15 AM - 9:30 AM UTC | Poster Hall International Exhibition Hall8, Makuhari Messe_43

[M-IS10] Interface- and nano-phenomena on crystal growth and dissolution

convener:Yuki Kimura(Institute of Low Temperature Science, Hokkaido University), Hitoshi Miura(Graduate School of Natural Sciences, Department of Information and Basic Science, Nagoya City University), Hisao Satoh(Naka Energy Research Laboratory, Mitsubishi Materials Corporation), Katsuo Tsukamoto(Graduate School of Engineering, Osaka University)

Recent developments of observations in nano-scale opened a detail discussion concerning mechanisms of crystal growth and dissolution based on interface phenomena including dynamics. In this session, growth and dissolution mechanisms of crystals will be discussed focusing on interface phenomena of minerals in the fields of biological origin, global environment, planets and space in addition to general minerals.

[MIS10-P01] Theoretical Model of Crystallization through Homogeneous Nucleation in Water Droplets

*Kyoko Kitakami Tanaka[1], Yuki Kimura[2] (1.Tohoku University, 2.Hokkaido University, Institute of Low Temperature Science)

[MIS10-P02] Mean Height of the Self-Assembled Faceted Macrosteps: Steady Crystal Growth/Dissolution in a Reaction- (Interface-) Limited Process

*Noriko Akutsu[1] (1.Faculty of Engineering, Osaka Electro-Communication University)

[MIS10-P03] In-situ observation of natural snow crystals by optical techniques

*Yuki Kimura[1], Tomoya Yamazaki[1], Takao Maki, Yoshinori Furukawa[1] (1.Institute of Low Temperature Science, Hokkaido University)

[MIS10-P04] Visualization of local environment around forming/dissolving carbonate minerals with the fluorescent probe

*Jun Kawano[1], Kotaro Osawa[2], Takashi Toyofuku[3,4], Yukiko Nagai[4,5], Jun-ya Tanaka[6], Takaya Nagai[1] (1.Faculty of Science, Hokkaido University, 2.School of Science, Hokkaido University, 3.JAMSTEC, 4.Tokyo University of Marine Science and Technology, 5.National Museum of Nature and Science of Tokyo, 6.Graduate School of Science, Hokkaido University)

[MIS10-P05] Influence of Ammonium Nitrate on Crystallization of Norsethite from Aqueous Solution

*Itaru Echigo[1], Harutoshi Asakawa[1], Hiroshi Uneda, Ryuichi Komatsu[1] (1.Graduate School of Science and Technology for Innovation Yamaguchi University)

[MIS10-P06] Direct observation of zeolite nucleation from compacted bentonite under hyperalkaline condition

*Hisao Satoh[1], Mayumi Takazawa[2], Daisuke Hayashi[3], Masaya Ida[3] (1.Naka Energy Research Laboratory, Mitsubishi Materials Corporation, 2.Mitsubishi Materials Corporation, 3.Radioactive Waste Management Funding and Research Center)

Theoretical Model of Crystallization through Homogeneous Nucleation in Water Droplets

*Kyoko Kitakami Tanaka[1], Yuki Kimura[2]

1. Tohoku University, 2. Hokkaido University, Institute of Low Temperature Science

The crystallization process of water droplets is not only fundamentally important, but is also climate-sensitive and hence relevant to urgent problems such as climate change. However, water crystallization in environments such as cirrus clouds is difficult to explore by conventional experimental approaches. Analytical models of the crystallization process can assist our understanding of ice nucleation and predict the crystallization processes in environments that cannot be replicated in the laboratory. Experimentally, micrometer-sized droplets are known to crystallize at approximately 235 K, regardless of cooling rate and experimental method. However, the crystallization temperature of smaller (nanometer-sized) droplets suddenly drops at high cooling rates (~10^5 K/s). At very high cooling rates (10^{6-7} K/s), liquid water droplets vitrify rather than crystallize. A model that explains all of these characteristics is thus far lacking. Motivated by this knowledge gap, we construct a new model of water-droplet crystallization that evolves the homogenous nucleation and crystal growth in water droplets during cooling (Tanaka & Kimura, PCCP, 21, 2410, 2019). The crystallization process depends on the surface energy at the liquid–solid interface (which determines the liquid-to-sold nucleation rate) and the activation energy of molecular diffusion through the liquid. The model extends our previous model (Tanaka et al. J. Crystal Growth, 310, 1281, 2008) by incorporating the droplet size-dependence of the crystallization process. Especially, smaller droplets begin crystallizing later than larger droplets because they are less likely to form a nucleating center in a given time. We also try two diffusion coefficients: the diffusivity of amorphous ice (ASW) and the diffusivity of supercooled liquid (SCL) water. The model well replicated the results of previous laboratory experiments, especially, the different responses of the crystallization temperatures of the micrometer- and nanometer-sized particles as functions of cooling rate. At low cooling rates, the ASW and SCL diffusivities gave the same results for micrometer-sized particles, because these particles crystallize at temperatures around the homogenous nucleation temperature (235 K), where both diffusivities are identical. However, for nanometer-sized particles, the crystallization temperature is lower and the SCL diffusivity is more accurate than the ASW diffusivity. Calculations on small droplets also provide low-temperature information at high cooling rates, which are sparsely acquired in experiments. The critical cooling rate of vitrification was predicted as 10^{7-8} K/s with SCL diffusivity, consistent with the experimental rates.

Keywords: nucleation, crystal growth, water, vitrification

©2019. Japan Geoscience Union. All Right Reserved.

Mean Height of the Self-Assembled Faceted Macrosteps: Steady Crystal Growth/Dissolution in a Reaction- (Interface-) Limited Process

*Noriko Akutsu[1]

1. Faculty of Engineering, Osaka Electro-Communication University

Faceted macrosteps are considered to play critical roles in some reaction- (interface-) limited processes of crystal growth/dissolution [1]. For the diffusion-limited crystal growth, step dynamics of macrosteps or bunched steps with rough side surfaces has been studied theoretically and experimentally [2,3]. Whereas, for the reaction-limited crystal growth/dissolution, the step dynamics of macrosteps has not yet been studied sufficiently.

In this paper, the step dynamics of faceted macrosteps in a reaction- (interface-) limited crystal growth/dissolution is studied theoretically by using a Monte Carlo method for the non-conserved systems. The microscopic model for this Monte Carlo study is the restricted solid-on-solid model with a point-contact step-step attraction (p-RSOS model) [4]. Here, the “restricted” means the height difference between the nearest neighbor sites is restricted to {0, ±1}. The step-step attraction is assumed to be the energy gain ε_{int} by forming a bond between the neighboring steps at the meeting point. The eminent point of this p-RSOS model is that the reliable surface tension (surface free energy per unit normal area) can be calculated at equilibrium by using the density-matrix renormalization-group (DMRG) method [5]. The polar graph of the surface tension (the Wulff figure) calculated by the DMRG method is shown in Fig. 1 [6]. A faceted macrostep is self-organizing at equilibrium because of the discontinuous surface tension resulting from the microscopic step-step attraction [6].

In the non-equilibrium steady state, we found that the height of the macrostep decreases as the driving force of dissolution increases [7]. In the step-faceting zone (Fig. 1 (a)), elementary steps detach from the faceted macrostep by way of the two-dimensional (2D) nucleation at the upper edge of the faceted macrostep on the (001) and the (111) surfaces. Near equilibrium, since the kink densities of the (001) and the (111) surfaces are few, the faceted surfaces cannot move. For the large driving force, the vicinal surface roughens kinetically.

1. T. Mitani, N. Komatsu, T. Takahashi, T. Kato, S. Harada, T. Ujihara, Y. Matsumoto, K. Kurashige, and H. Okumura, J. Cryst. Growth, **423**, 45–49 (2015). A. F. Khokhryakov, Y. N. Palyanov, Y. M. Borzdov, A. S. Kozhukhov, and D. V. Shcheglov, Cryst. Growth Des. **18**, 152–158 (2018).
2. A. Pimpinelli and J. Villain, *Physics of Crystal Growth* (Cambridge University Press, Cambridge, UK, 1998). A. L. Barabasi and H. E. Stanley, *Fractal Concepts in Surface Growth* (Cambridge University Press, Cambridge, UK, 1995).
3 A. A. Chernov, Sov. Phys. USP, **4**, 116–148 (1961). T. Nishinaga, C. Sasaoka, and A. A. Chernov, Ed. I. Sunagawa, *Morphology and Growth Unit of Crystals* (Terra Scientific Publishing Company, Tokyo, 1989) pp. 139–151.
4. N. Akutsu, Applied Surface Science, **256**, 1205–1209 (2009); J. Phys. Condens. Matter, **23**, 485004 (2011).
5. N. Akutsu and T. Yamamoto, ed. T. Nishinaga, *Handbook of Crystal Growth*, Vol. I. (Elsevier, 2015) pp. 265–313.
6. N. Akutsu, “Profile of a Faceted Macrostep Caused by Anomalous Surface Tension,” Adv. Cond. Matter Physics, 2017, Article ID 2021510 (2017); AIP Adv., **6**, 035301 (2016).

©2019. Japan Geoscience Union. All Right Reserved.

7. N. Akutsu, Crystals **7**, 42 (2017); Phys. Rev. Materials **2**, 023603 (2018).

Fig. 1 Cross section of the Wulff figure and the equilibrium crystal shape (ECS). Thin solid lines: ECS. Thick solid lines and filled squares: polar graph of surface tension. (a) $k_B T/\varepsilon = 0.4$. (b) $k_B T/\varepsilon = 0.63$. Light thin solid lines: polar graph of surface tension for metastable surfaces. (c) $k_B T/\varepsilon = 0.75$. (d) $k_B T/\varepsilon = 0.4$. The original RSOS model. The figures are taken from Ref. [6].

Keywords: Monte Carlo simulation , Discontinuous surface tension of crystal, Surface free energy, Density-matrix renormalization-group method, Faceted macrosteps

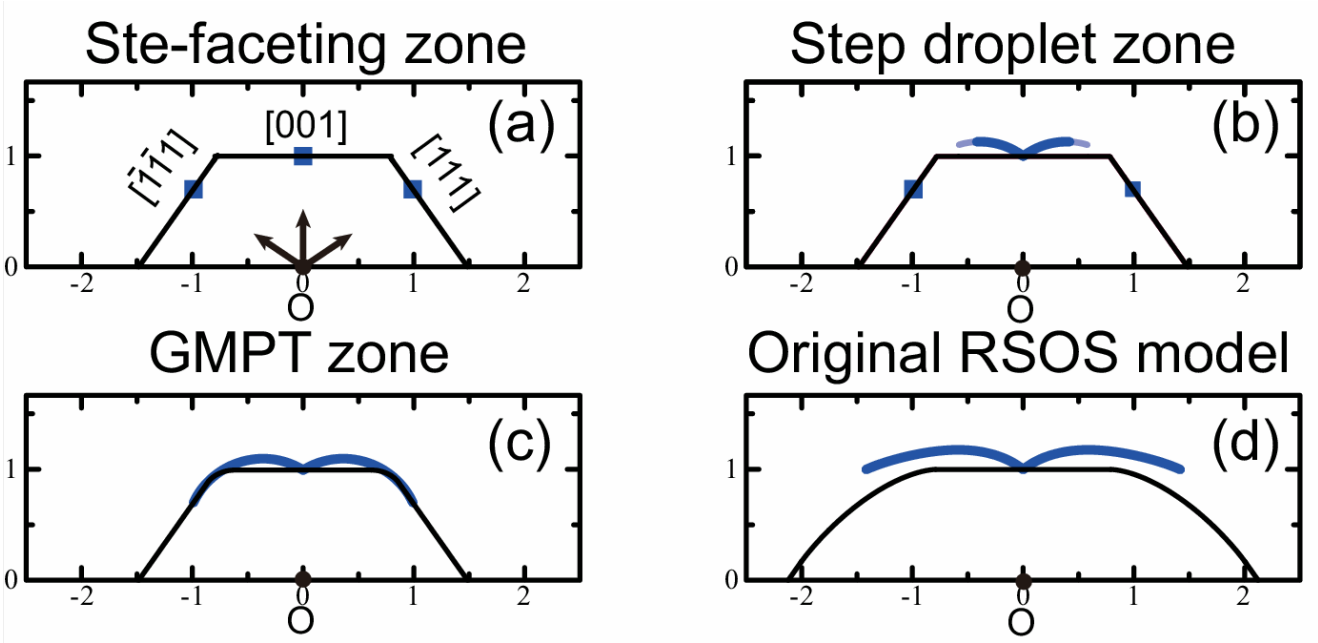

©2019. Japan Geoscience Union. All Right Reserved.

In-situ observation of natural snow crystals by optical techniques

*Yuki Kimura[1], Tomoya Yamazaki[1], Takao Maki, Yoshinori Furukawa[1]

1. Institute of Low Temperature Science, Hokkaido University

Natural snow crystals excite our interest because of several reasons such as its beautiful geometry, its symmetricity and variety. Relationship between geometry of snow crystal and its formation environment (temperature and humidity) was investigated by Ukichiro Nakaya and has been well known as Nakaya diagram. After that, the reason of why snow crystal changes their geometry, such as platy, needle and column, with slight difference of temperature and humidity, and the growth mechanisms have been studied [e.g., Sanchez et al. *PNAS* 114 (2017) 227; Brumberg et al., *PNAS* 114 (2017) 5349]. Nevertheless, there are several questions have been remained. For instance; origin of twelve-fold snow can be explained not only by a twin but by contribution of secondary prism plane; and origin of characteristic pattern can be appeared not only by intrinsic defects but also by a result of growth.

To understand snow crystals more, we have performed in-situ observation of natural snow crystals and its sublimation/regrowth experiments in an environment controllable cell under originally designed optical systems at the base of Asahi-dake in the Taisetsu area, Hokkaido, Japan for 15 nights in total for five winter seasons from 2015 to 2019. The environment controllable cell has a Peltier cooling unit, which has a water vapor source with a heater and a chromel-alumel thermocouple on top, windows for optical observation, capillary to handle a snow crystal and a platinum resistance temperature detector for temperature measurement of the cell. The optical systems consist of the modified Mach–Zehnder-type interferometer (Maki-type laser interferometer), the Michelson-type white-light interferometer microscope with a long working distance, the optimized color-filtered optical microscopes, a polarized optical microscope and so on.

We set the optical systems in a snow-lab, which is a handmade igloo-like snow room, also works as a good sound and vibration absorber. Temperature in the Taisetsu area and inside the snow-lab are around -10 to -20°C and -5 to -13°C, respectively. Higher temperature in the snow-lab than outside is due to observers and experimental systems. One advantage of the snow-lab is maintaining the humidity close to 100% because all the walls of the snow-lab have been made of snow.

We collected snow crystals directly on a black felt just outside the snow-lab and selected a snow crystal, which was put onto a glass plate for general observations of the shape and surface textures. A snow crystal is also put onto a tip of a glass rod of 1.4 mm in diameter for the Maki-type laser interferometer. Rates for sublimation and regrowth of a snow crystal were successfully measured in thickness and lateral direction simultaneously at a certain environment, where supersaturation was controlled using the environment controllable cell. In addition, surface topography of both surfaces of a snow crystal, which was put onto a Y-shaped metallic holder, could be observed using the Michelson-type white-light interferometric microscope. Here, we will summarize our attempts of these in-situ observations and the

©2019. Japan Geoscience Union. All Right Reserved.

results.

Acknowledgments: We thank Y. Sato, Y. Hirata, S. Nakatsubo, K. Fujita and S. Mori of the Technical Division in the Institute of Low Temperature Science, Hokkaido University, for their help in the development of the experimental system. This study was supported partly by the Grant for Joint Research Program of the Institute of Low Temperature Science, Hokkaido University.

Keywords: Snow, In situ observation, Interferometry, Optical microscopy

©2019. Japan Geoscience Union. All Right Reserved.

Visualization of local environment around forming/dissolving carbonate minerals with the fluorescent probe

*Jun Kawano[1], Kotaro Osawa[2], Takashi Toyofuku[3,4], Yukiko Nagai[4,5], Jun-ya Tanaka[6], Takaya Nagai[1]

1. Faculty of Science, Hokkaido University, 2. School of Science, Hokkaido University, 3. JAMSTEC, 4. Tokyo University of Marine Science and Technology, 5. National Museum of Nature and Science of Tokyo, 6. Graduate School of Science, Hokkaido University

To understand the formation or dissolution mechanism of crystal in aqueous solution, it should be important to analyze the local condition of solution just around dissolving or growing crystal. Recently, we have succeeded to visualize the distribution of pH and ionic concentration around carbonate minerals dissolving in inorganic environment, by using the fluorescent probe. In the present study, we have tried to apply this technique to the formation process of calcium carbonate.
Calcium carbonate was synthesized by the counter diffusion method, in which calcium chloride and sodium carbonate solutions were counter-diffused through an agarose gel matrix containing the fluorescent probe like 8-hydroxypyrene-1,3,6-trisul-fonic acid (HPTS). We observed under a microscope that pH in the middle part of gel first increased gradually with time and turn downward after crystals formed. The counter diffusion method with gel media for the carbonate synthesis has attracted attention as a valid tool in the study of biomineralization because the calcification sites in some organisms were recently suggested to have the features of a highly viscous sol or gel matrix. Therefore, the detail observation of the local condition around forming calcium carbonate in gel matrix could provide new insights into the knowledge of biomineralization mechanisms.

Keywords: Visulization, carbonate minerals, pH

©2019. Japan Geoscience Union. All Right Reserved.

Influence of Ammonium Nitrate on Crystallization of Norsethite from Aqueous Solution

*Itaru Echigo[1], Harutoshi Asakawa[1], Hiroshi Uneda, Ryuichi Komatsu[1]

1. Graduate School of Science and Technology for Innovation Yamaguchi University

Since norsethite $BaMg(CO_3)_2$ has birefringence higher than previous piezoelectric and optical crystals, we expect that norsethite can be used as new acousto-optics andwavelength-conversion devices. However, solubility of norsethite is low and it is difficult to control supersaturation. Hence growth of norsethite is difficult. Then, we investigated effects of ammonium nitrate NH_4NO_3 on crystallization of norsethite from aqueous solution. With increasing NH_4NO_3, solubility of norsethite increased. When concentration of NH_4NO_3 reached to 1M, solubility of norsethite became 30 times larger than without the addition of NH_4NO_3 .With further increasing NH_4NO_3, solubility of norsethite remained constant. Next, we measured induction periods of norsethite, when 1M NH_4NO_3 was added. Then, we could confirm norsethite just after mixed at 70°C by XRD measurement only in the case of the addition of 1M NH_4NO_3. Thus, we revealed that the addition of NH_4NO_3 also accelerates norsethite crystallization. This study concluded that addition of NH_4NO_3 is valid for the growth of norsethite.

Keywords: Norsethite, Aqueous Solution Growth, Ammonium Nitrate

©2019. Japan Geoscience Union. All Right Reserved.

Direct observation of zeolite nucleation from compacted bentonite under hyperalkaline condition

*Hisao Satoh[1], Mayumi Takazawa[2], Daisuke Hayashi[3], Masaya Ida[3]

1. Naka Energy Research Laboratory, Mitsubishi Materials Corporation, 2. Mitsubishi Materials Corporation, 3. Radioactive Waste Management Funding and Research Center

Since dissolution issue of smectite arose on engineered barrier system using bentonite (absorbent clay from shale consisting mostly of smectite) for radioactive waste repository for past several decades, smectite studies are focusing on (1) dissolution kinetics [1, 2], (2) hydraulic property of smectite in various states (gel to compacted [3]) and (3) alterations into the other clay and zeolites [4]. Former two issues are closely related to undersaturation of pore water and reactive surface area of smectite grains as a function of density. As the result, the pore water produced from locally dissolved smectite can gain the supersaturation with respect to potential secondary phases. The third one, the alteration, can finally lead the total thermodynamic system to the next equilibrium state consisting of secondary phases.

For understanding the alteration, we had carried out direct observation on pure montmorillonite and bentonite composed of montmorillonite, quartz and albite with or without minor amount of zeolite additive under Na, K and Ca hydroxide solution at 70 ˚C (pH 12.1) [2]. Two methods were used: (1) interferometric measurement of montmorillonite dissolution [2, 5]; (2) direct optical observation of new precipitations. The former gave the rate as a function of density, the latter provided information about nucleation. Sooner or later, the pore water likely attained to local equilibrium, as long as solution flow is limited by compaction.

Differed from previous result, dissolution of pure montmorillonite in the rates varied from 1E-9 (density < 0.01) to 1E-13 mol/m^2/s (density > 1.2) [2] did not always derive precipitation of secondary phases. However, the system, bentonite was not the case. Bentonite especially with minor amount of zeolite caused prominent nucleation of secondary zeolite after a long induction period (weeks) after solution-flow was shut-off.

This alteration behavior could be interpreted with heterogeneous nucleation model. Interfacial free energy, $\gamma_{S/L}$ between secondary phases and alkaline solution was evaluated by wetting angle measurements. There are two end-members such as low and high silica zeolite, those are analcime (ANA: $NaAlSi_2O_6$; Si/Al = 2.0) and clinoptilolite (CLP: $(NaKCa)_3Al_3Si_{15}O_{36}$; Si/Al = 5.0). Their $\gamma_{S/L}$ were measured to be and 50.54 and 71.31 mJ/m^2, respectively. Chemical equilibrium calculation predicts that CLP is the most stable phase in this reaction system. Microanalyses, however, identified the product as phillipsite (PHI: $(NaKCa)_4Al_4Si_{12}O_{32}$; Si/Al = 3.0) as intermediate composition between CLP and ANA or laumontite (LAU: $CaAl_2Si_4O_{12}$: Si/Al = 2.0). When PHI was seeded to the bentonite system, secondary zeolite was PHI. Also, the observed induction periods (Inl) mostly correlate with supersaturations ($1/S^2$). However, the I sometimes became longer than that by CLP seeding. Seed crystal with higher $g_{S/L}$ such like CLP has lower solubility and likely promotes PHI nucleation more than CLP itself. Fast PHI nucleation by CLP-seeding was an unusual. Direct observation could give us an interesting information. During the early observation in the presence of CLP seed recognized two-step process in which spherical objects were growing in ten times faster rate (5.6E-3 nm/s) than the later phase evolving to faceted (5.1E-2 nm/s). This may have contributed to shortening the induction. Such an amorphous phase is often observed especially at room temperature reaction.

©2019. Japan Geoscience Union. All Right Reserved.

This research is a part of the results of “Advancement of Processing and Disposal Technique for the Geological disposal of TRU Waste (FY2017)” under an entrustment from the Agency for Natural Resources and Energy (ANRE) in the Ministry of Economy, Trade and Industry (METI) of Japan.

[1] Cama et al. (2000) GCA, 64, 2701-2717; [2] Satoh et al. (2013) Clay Min., 48, 285-294; [3] Terada et al. (2018) Mat. Res. Exp., 6, 035514; [4] Dunkel and Putnis (2014) Eur. J. Min., 26, 61-69; [5] Ueta et al. (2016) J. Nuc. Sci, Tech., 53, 184-191.

Keywords: Montmorillonite, zeolite, nucleation, amorphous

©2019. Japan Geoscience Union. All Right Reserved.

[J] Oral | M (Multidisciplinary and Interdisciplinary) : M-IS Intersection

Tue. May 28, 2019 9:00 AM - 10:30 AM JST | Tue. May 28, 2019 12:00 AM - 1:30 AM UTC | A02 TOKYO BAY MAKUHARI HALL

[M-IS11] Aqua planetology

convener:Yasuhito Sekine(Earth-Life Science Insitute, Tokyo Institute of Technology), Tomohiro Usui(Earth-Life Science Institute, Tokyo Institute of Technology), Keisuke Fukushi(Institute of Nature & Environmental Technology, Kanazawa University), Takazo Shibuya(Japan Agency for Marine-Earth Science and Technology), Chairperson:Yasuhito Sekine(Dept. Earth & Planetary Sci., University of Tokyo), Takazo Shibuya(JAMSTEC), Tomohiro Usui

This proposed session covers a wide range of topics related to aqua planetology, including chemical reactions involving water on planetary bodies, water-rock reactions within planetesimals, distribution of water in the early Solar system and the origin of water on terrestrial planets, hydrological and biogeochemical processes on Earth, geochemical cycles and habitability on Mars and icy moons, exploration of water in the solar system, and theory to understand how to build a habitable aqua planet.

9:00 AM - 9:15 AM JST | 12:00 AM - 12:15 AM UTC

[MIS11-13] A forward modeling of infrared reflectance spectra of asteroids

*Hiroyuki Kurokawa[1], Takazo Shibuya[2], Yasuhito Sekine[1], Bethany L Ehlmann[3,4] (1.ELSI, Tokyo Tech, 2.JAMSTEC, 3.Caltech, 4.JPL)

9:15 AM - 9:30 AM JST | 12:15 AM - 12:30 AM UTC

[MIS11-14] Estimation of formation mechanism and morphological condition in calcite concretion

*Takayuki Ihara[1], Sin-iti Sirono[1] (1.Nagoya University)

9:30 AM - 9:45 AM JST | 12:30 AM - 12:45 AM UTC

[MIS11-15] Reconstructing groundwater hydrology and water-rock reactions around Gale Crater on early Mars

*Natsumi Noda[1,2], Yasuhito Sekine[1], Shuya Tan[1,2], Takazo Shibuya[3], Hidenori Genda[1] (1.Earth-Life Science Institute, Tokyo Institute of Technology, 2.Department of Earth and Planetary Science, Graduate School of Science, The University of Tokyo, 3.Department of Subsurface Geobiological Analysis and Research, Japan Agency for Marine-Earth Science and Technology)

9:45 AM - 10:00 AM JST | 12:45 AM - 1:00 AM UTC

[MIS11-16] Habitable zone for a land planet

*Takanori Kodama[1], Hidenori Genda[2], Ryouta O'ishi[3], Ayako Abe-Ouchi[3] (1.University of Bordeaux, 2.Earth-Life Science Institute, Tokyo Institute of Technology, 3.Atmosphere and Ocean Research Institute, University of Tokyo)

10:00 AM - 10:15 AM JST | 1:00 AM - 1:15 AM UTC

[MIS11-17] A study on the dependence of ocean planet climate on solar constant: influence of oceanic heat transport in the case of large absorption coefficients of gray atmosphere

*Yuta Kawai[1,2], Yoshiyuki O. Takahashi[1], Masaki Ishiwatari[5], Kensuke Nakajima[3], Shin-ichi Takehiro[4], Hiroki Kashimura[1,6], Seiya Nishizawa[2], Hirofumi Tomita[2], Yoshi-Yuki Hayashi[1,6] (1.Kobe University, 2.RIKEN Center for Computational Science, 3.Kyusyu University, 4.Kyoto University , 5.Hokkaido University, 6.Center for Planetary Science)

10:15 AM - 10:30 AM JST | 1:15 AM - 1:30 AM UTC

[MIS11-18] Water cycle and its evolution: High-speed H_2O transport to upper atmosphere on Mars

★Invited Papers

*Hiromu Nakagawa[1], Shohei Aoki[1], Nao Yoshida[1], Naoki Terada[1], Takeshi Imamura[2], Kazunori Ogohara[3], Toru Kouyama[4], Hiroki Ando[6], Katsuyuki Noguchi[5], Akiho Miyamoto[1], Kosuke Takami[1], Isao Murata[1], Yasumasa Kasaba[1], IUVS team MAVEN (1.Planetary Atmosphere Physics Laboratory, Department of Geophysics, Graduate School of Science, Tohoku University, 2.Graduate school of Frontier sciences, University of Tokyo, 3.University of Shiga prefecture, 4.The National Institute of Advanced Industrial Science and Technology, 5.Nara Women's university, 6.Kyoto Sangyo university)

A forward modeling of infrared reflectance spectra of asteroids

*Hiroyuki Kurokawa[1], Takazo Shibuya[2], Yasuhito Sekine[1], Bethany L Ehlmann[3,4]

1. ELSI, Tokyo Tech, 2. JAMSTEC, 3. Caltech, 4. JPL

The mineral assemblages on asteroids are useful to constrain the aqueous environments, the temperature (T), pressure (P), water to rock ratio (W/R), and bulk chemical composition, existed in them or in their parent bodies. Near- to mid-infrared (IR) reflectance spectroscopy of asteroids contains the information of the surficial minerals in their characteristic absorption features, spectral slopes, and overall brightness or darkness. Recent remote-sensing of asteroids by Hayabusa2, OSIRIS-Rex, and Dawn spacecrafts as well as telescopic observations by AKARI infrared space telescope provided detailed IR reflectance spectra of many types of asteroids. These observations would allow us to discuss the diversity of asteroids in their principle parameter space of paleo-aqueous environments: T, P, W/R, and the bulk chemical compositions. This study aims to connect the observed IR spectra of asteroids to the original bulk compositions and T-Pconditions of them or their parent bodies. We performed a series of chemical equilibrium calculations to obtain the mineral compositions. We computed the model IR reflectance spectra from the obtained mineral compositions. The chemical equilibrium calculations assumed the rocky bulk compositions of CV chondrites. We treated W/R as a parameter (0.2-10). We fixed the relative abundance of volatiles to water. The model IR reflectance spectra were calculated by adopting the radiative transfer theory for granular surfaces. The reflectance of a model mineral assemblage was computed from the weighted average of the single scattering albedos (SSAs) of endmembers. We found that the model reflectance spectra vary according to the equilibrium mineral compositions. Reducing W/R led to the darkening in overall reflectance as the dominant minerals change from bright carbonate to serpentine, gibbsite, and dark phases: pyrite, troilite, magnetite, and organics. The change in the dominant phase is visible in the characteristic absorption features: carbonate at 3.5 micro m and 4.0 micro m and serpentine at 2.7-2.8 micro m. We note that, though carbonate has a broad absorption from 2.7 to 3.2 micro m, the absorption feature of serpentine is sharp and distinguishable.Ammonia-bearing saponite more than a few wt.% shows its characteristic absorption feature at 3.1micro m in the reflectance of mixture. In this presentation, we discuss the implications for Haybusa2 and AKARI observation results.

Keywords: Asteroids, Near-infrared spectra

©2019. Japan Geoscience Union. All Right Reserved.

Estimation of formation mechanism and morphological condition in calcite concretion

*Takayuki Ihara[1], Sin-iti Sirono[1]

1. Nagoya University

Iron oxide concretions were discovered on Meridiani plain by Mars explorer opportunity. The concretion found on Mars is called blueberry, it is spherical and the composition is mainly iron oxide. Concretions similar to them are found on the Navajo sandstone stratum in the United States of Utah , and is Gobi Desert, Mongolia. They are called Fe-oxide concretion. Both Fe-oxide concretion and blueberry have a spherical shell structure of iron oxide. [1] performed field work and analyzed element maps to investigate the mechanism of formation of Fe-oxide concretion of Utah and Gobi. As a result, [1] showed the formation mechanism of spherical Fe-oxide concretion as follows. In an eolian layer spherical calcite concretions were formed as a precursor. Second, acidic groundwater containing iron ions flows into it and reacts with $CaCO_3$ and iron precipitates in a spherical shell shape. Furthermore, [1] indicated that the iron contraction of Mars is a similar mechanism. However, the formation mechanism of spherical calcite concretion as a precursor is not known. If we can clarify the formation mechanism, we can restrict the ancient environment of Earth and Mars.

In this study, we focused on calcite concretion produced in an eolian layer. Calcite concretion of the eolian layer is produced in three forms, spherical, plate-like, fish egg (globular gathering state). It is aimed to clarify the forming mechanism and the forming conditions in indoor experiments. We will report the current experiment status. $CaCO_3$ is precipitated by evaporation in Utah's sand. In order to increase the solubility of the $CaCO_3$ aqueous solution, CO_2 is blown into the solvent. $Ca(HCO_3)_2$ is made in the solvent. By evaporating it $CaCO_3$ is precipitated in the layer of sand to generate a concretion. Then $Ca(HCO_3)_2$ is made in the solvent. It evaporates to precipitate $CaCO_3$ in the layer of sand.Utah's sand has an average particle diameter of 150 μm (Kawakami 2015). The minimum size of calcite concretion and Fe-oxide concretion discovered on Earth is several mm in diameter [2] and experiments are conducted with the aim of creating the size. $CaCO_3$ concentration and evaporation rate are changed as parameters. X-ray CT is used to analyze $CaCO_3$ in the experimental layer. In order to investigate whether $CaCO_3$ and sand can be distinguished from X-ray CT images, a experiment was conducted when $CaCO_3$ precipitated in the sand layer. The simulated sample was prepared by mixing sand from Navajo sandstone and a few mg of $CaCO_3$. As a result of the X-ray CT experiment, it was confirmed that a $CaCO_3$ having a size of 0.50 mm can be discriminated at a resolution of 0.019mm/pixel. It was also found that $CaCO_3$ and sand are close in density, so it can not be determined that $CaCO_3$ is not sufficiently larger than the average particle diameter of sand 150μm.

In the future, we will analyze the samples prepared in the experiment and try experiments under various conditions by adding experimental parameters as well as $CaCO_3$ concentration, evaporation rate and sand filling rate. Then we will clarify the formation mechanism and the morphological condition of calcite concretion in the eolian layer.

[1] Yoshida et al.(2018) Science Advances Vol.4, no.12;[2]Sally Latham Potter.2009 Chracteization of navajo sandstone hydrous ferric oxide concretions

©2019. Japan Geoscience Union. All Right Reserved.

Keywords: Spherical calcite concretion

©2019. Japan Geoscience Union. All Right Reserved.

Reconstructing groundwater hydrology and water-rock reactions around Gale Crater on early Mars

*Natsumi Noda[1,2], Yasuhito Sekine[1], Shuya Tan[1,2], Takazo Shibuya[3], Hidenori Genda[1]

1. Earth-Life Science Institute, Tokyo Institute of Technology, 2. Department of Earth and Planetary Science, Graduate School of Science, The University of Tokyo, 3. Department of Subsurface Geobiological Analysis and Research, Japan Agency for Marine-Earth Science and Technology

NASA's Mars Science Laboratory Rover, Curiosity, has provided key information on geochemistry and mineralogy of the lacustrine sediments deposited within Gale Crater on early Mars(e.g. Grotzinger et al. 2015, Rampe et al. 2017). Gale's lacustrine mudstones of Murray Formation are characterized by authigenic depositions of high levels of silica (e.g., opal CT and amorphous silica) together with iron oxides (e.g., magnetite and hematite), suggesting inputs of dissolved SiO_2 and Fe^{2+} into the early Gale lake (Hurowitz et al. 2017). One possible source of dissolved SiO_2 and Fe^{2+} is upwelling groundwater. However, little is known about the conditions of both climate and water table capable of upwelling groundwater into Gale Crater. Additionally, the chemical compositions of groundwater on early Mars, particularly the determining factors of concentrations of dissolved SiO_2 and Fe^{2+}, have been poorly constrained.

Here, we perform both hydrological modeling and hydrothermal experiments to interpret the observations. Based on the simulation and experimental results, we discuss the climate, groundwater hydrology, and input fluxes of dissolved SiO_2 and Fe^{2+} of Gale lakes.

In the hydrological modeling, we perform three-dimensional hydrological simulations for the area surrounding Gale Crater using GETFLOWS, which deals with fully-coupled surface and subsurface flows based on the hydro-geophysical equations. We find two modes of the lake distribution and groundwater flow around Gale. One is the high-evaporation mode where multiple shallow lakes can appear at local topographic lows owing to vigorous upwelling of groundwater under (semi-)arid climate conditions. The other is the low-evaporation mode where lake(s) exists only at the lowest place(s) under relatively humid climate conditions. To explain both a closed-basin lake within Gale Crater and some lakes around Gale, the high-evaporation mode is most likely to have occurred on early Mars. Our results suggest (semi-)arid climate conditions around Gale with a shallow water table. Under the arid climate conditions, evaporation of lake water would have caused effective upwelling of groundwater. Given thermal gradient within the crust, such upwelled groundwater would have experienced hydrothermal reactions with the crustal rocks.

In the hydrothermal experiments, we simulate high-temperature water-rock reactions between groundwater and Martian crustal rocks. Hydrothermal reactions at 200ºC between a synthesized Martian rock analog and fluids are performed using a Dickson-type apparatus. Various secondary minerals, such as analcime, quartz, albite, Fe(Mg-)saponite, Fe(Mg-)serpentine, and trace carbonates are also formed via the hydrothermal reactions. We find that dissolved SiO_2 concentration (1–10 mM) is buffered by dissolution of quartz; whereas, that of Fe^{2+} (~10^{-3} mM) is likely controlled by dissolution of Fe-carbonate (siderite).

Combining these simulation and experimental results, we estimate the input fluxes of dissolved SiO_2 and Fe^{2+} contained in upwelled groundwater into Gale lakes. The flux of dissolved SiO_2 corresponds to ~0.02–0.2 mm/year of the deposition rate of silica, implying that the parallel laminae of the lacustrine

©2019. Japan Geoscience Union. All Right Reserved.

mudstone(Grotzinger et al. 2015) may be varve. This further suggests ~10^5 years of warming periods to explain the thickness of Murray Formation. Upwelling groundwater might have also provided Fe^{2+} into the lake, leading to formations of Fe oxides and H_2. Our results suggest that low-latitude deep craters, including Gale, would have played key roles in upwelling deep groundwater at arid climates in the global hydrological cycles, providing reductants and greenhouse effect gas to the surface of early Mars.

Keywords: Mars, Hydrothermal experiment, hydrologic model

©2019. Japan Geoscience Union. All Right Reserved.

Habitable zone for a land planet

*Takanori Kodama[1], Hidenori Genda[2], Ryouta O'ishi[3], Ayako Abe-Ouchi[3]

1. University of Bordeaux, 2. Earth-Life Science Institute, Tokyo Institute of Technology, 3. Atmosphere and Ocean Research Institute, University of Tokyo

Most of the studies for habitable planets have focused on Earth-like planets with globally abundant water on the planetary surface. Liquid water vaporizes entirely when planets receive the insolation above a certain critical value, which is called runaway greenhouse threshold. On the other hand, the planetary climate state lapses into a snowball state when planets receive insolation below a certain value, which is called the complete freezing threshold. The habitable zone, in which planets can maintain liquid water on their surface for a long term, is determined by these thresholds.

Abe et al. (2011) focused on so-called land planets with a very small amount of water, and investigated these thresholds using a three-dimensional general circulation model. As results, they found that land planets have a wider habitable zone than Earth-like planets have. However, it is not enough to understand the relationship between the distribution of water and the climate because their range of the amount of water is extremely narrow, leading the almost same distribution of liquid water on the planetary surface.

We assumed various types of the surface water distribution, and investigated the effect of those on both the runaway greenhouse threshold and the complete freezing threshold for Earth-sized planets using a three-dimensional general circulation model. We consider the surface water distributions as longitudinally uniform water distribution and a 1-bar atmosphere whose composition is similar to the current Earth’s atmosphere. As results, both thresholds change gradually depending on the distribution of surface water. Additionally, they are dominated by the atmospheric circulation which determines the surface condition.

Keywords: Land planet, Habitable zone

©2019. Japan Geoscience Union. All Right Reserved.

A study on the dependence of ocean planet climate on solar constant: influence of oceanic heat transport in the case of large absorption coefficients of gray atmosphere

*Yuta Kawai[1,2], Yoshiyuki O. Takahashi[1], Masaki Ishiwatari[5], Kensuke Nakajima[3], Shin-ichi Takehiro[4], Hiroki Kashimura[1,6], Seiya Nishizawa[2], Hirofumi Tomita[2], Yoshi-Yuki Hayashi[1,6]

1. Kobe University, 2. RIKEN Center for Computational Science, 3. Kyusyu University, 4. Kyoto University , 5. Hokkaido University, 6. Center for Planetary Science

1. Introduction

In order to reveal the diversity of climate realized on planets with water and climate stability, our research group has been exploring climates on idealized planets. Ishiwatari et al. (2007) (INTH07) investigated solar constant dependence of climates on swamp ocean planet using a 3-dimensional atmospheric general circulation model, although oceanic heat transport is not considered. Since oceanic heat transport also affects planetary climates, for example, Rose (2015) (R15) explored climates on a planet globally covered with ocean (referred to as “ ocean planet”, here) with a coupled atmosphere-ocean-sea ice model, and showed the importance of oceanic heat transport for the climates. Recently, as an extension of INTH07, we also have investigated solar constant dependence of ocean planet climates with our coupled model. Representing ocean general circulation obviously changes atmospheric fields. However, the displacement of ice-line is small and there is no qualitative change of climate regime diagram which represents the relation between solar constant and ice-line latitude. We imagine the reason is that the variation of temperature with solar constant in partially ice-covered states obtained from gray radiation setting of INTH07 is quite smaller than that in R15. Therefore, we perform further experiments in the case of large absorb coefficients. In this presentation, the experimental results will be shown.

2. Model and Experimental setup

The model used here is our constructing coupled atmosphere-ocean-sea ice model. The atmosphere model is DCPAM, in which the 3-dimensional primitive equations are solved. Most of the atmospheric setting is same as that in INTH07, except absorb coefficients of water vapor and dry air in the gray radiation scheme are replaced with larger values, 1×10^{-1} and 1×10^{-5} [m^2/kg], respectively. The ocean and sea-ice model are zonally averaged 2-dimensional models. In the ocean model, the hydrostatic Boussinesq equations are solved, and mixing due to mesoscale eddies and convection is parameterized. The sea-ice model is a vertically 1-dimensional thermodynamics model, and the transport is represented by horizontal diffusion. The value of surface albedo is 0.5 if surface temperature is lower than 263 K, otherwise 0, but the value on grid-point is given considered the sub-grid distribution of surface temperature. In addition to experiments with the coupled model, in order to evaluate the effect of oceanic heat transport, we also perform experiments in which dynamic ocean is replaced with slab ocean. The number of atmosphere model grid is 64x32x16. The number of grid points on the ocean and sea ice models is 64x60 and 64, respectively. For most cases, the initial condition is a rest atmosphere and ocean with 280 K, but various solutions are also used. The temporal integration for slab ocean cases is basically performed over about 300 years, and, for dynamic ocean cases, over about 30,000 years with periodically synchronous coupling.

3. Results

©2019. Japan Geoscience Union. All Right Reserved.

By specifying absorb coefficients larger than that in INTH07, features of climate regime diagram are significantly changed. In dynamic ocean experiments, partially ice-covered states are obtained over 1040 ≦ S ≦ 1055 W/m^2, where S is the solar constant. The solar constant at which partially ice-covered states are obtained becomes about 300 W/m^2 smaller and the range of solar constant becomes much narrower. We also confirm the appearance of runaway greenhouse state for S > 1070 W/m^2. The latitudinal extent where large ice-cap instability occurs is wider. Although it is not easy to obtain partially ice-covered state whose ice-line is lower than 40 degrees latitude, we can discover stable partially ice-covered state with about 30 degrees ice-line when initial state and variation of solar constant are carefully chosen. Because this behavior indicates two branches for the partially ice-covered state, similar to that in R15, and we will carefully investigate the existence of solutions with low ice-line latitude. In slab ocean experiments, there are no partially ice-covered states. Therefore, we consider partially ice-covered states in dynamic ocean experiments are maintained by oceanic heat transport. Note that the setting here produces the large variation of temperature with solar constant, as calculations in R15, and the parameter range over which partially ice-covered states are obtained is potentially very narrow. It is possible that the resolution and formulation of models strongly affect the results. To evaluate the probabilities, it is necessary to conduct further experiments using slightly different parameters.

Keywords: ocean planet, dependence of climates on solar constant, a coupled atmosphere-ocean-sea ice model

©2019. Japan Geoscience Union. All Right Reserved.

Water cycle and its evolution: High-speed H_2O transport to upper atmosphere on Mars

*Hiromu Nakagawa[1], Shohei Aoki[1], Nao Yoshida[1], Naoki Terada[1], Takeshi Imamura[2], Kazunori Ogohara[3], Toru Kouyama[4], Hiroki Ando[6], Katsuyuki Noguchi[5], Akiho Miyamoto[1], Kosuke Takami[1], Isao Murata[1], Yasumasa Kasaba[1], IUVS team MAVEN

1. Planetary Atmosphere Physics Laboratory, Department of Geophysics, Graduate School of Science, Tohoku University, 2. Graduate school of Frontier sciences, University of Tokyo, 3. University of Shiga prefecture, 4. The National Institute of Advanced Industrial Science and Technology, 5. Nara Women's university, 6. Kyoto Sangyo university

It is believed that Mars underwent drastic climate change, changing its environment from warm and wet to cold and dry. This gives rise to the idea that Mars may have hosted life in the past, and indeed, may do so even today. Atmospheric and water evolution is thus an important key to understanding the history of Martian habitability. Mars must somehow have lost most of its atmosphere and water. The evolution of the Mars environment is thought to have proceeded by some combination of atmospheric escape to space and surface-subsurface adsorption. Especially, a lack of global magnetic field on Mars must have a significant impact to the atmospheric escape. The upper atmosphere is the primary reservoir for atmospheric escape. Owing to the technical difficulties associated with observations, datasets of the upper atmosphere are limited. However, the last decade has seen a renewed interest in the upper atmosphere, thanks to the aggressive explorations by the Mars Reconnaissance Orbiter (MRO), Mars Express(MEX), and Mars Volatile Evolution (MAVEN) missions. Recent studies have highlighted various interesting facts related to the efficient of material/water transport from the lower to upper atmospheric reservoir which have an impact on the atmospheric escape or evolution.

High-altitude (above 60 km) H2O was first identified by SPICAM occultations [Maltagliati et al., 2011, 2013] in the southern summer, which happens to be a dusty season at a solar longitude of 240 degree or later. Chaffin et al. [2017] demonstrated that the high-altitude H2O can considerably increase H escape on the weekly timescale, which can potentially explain the observations. Purpose of this study is to clarify the mechanism for upward transport of H2O into the upper atmosphere and formation of the detached layer of H2O and aerosols, by using multi-spacecraft dataset in order to cover whole altitude range from lower to upper atmosphere.

Here we report the detection of an extensive layer of warm air at altitudes 70-100 km on the night side that we interpreted as the result of combinations of aerosol heating, thermal tides, and/or global circulation. Such a strong warm layer for which the current models have no explanation can maintain temperature to evaporate water ice adsorbed on the aerosols and can form the detached layer of water vapor. We also measured the mesospheric distribution sub-micron aerosols is abundant than our expectation at altitudes 70-100 km. Such a detached layer of aerosol can potentially explain the warm layer, and this implies the importance of aerosols for key processes in the Martian water cycle and climate as a whole. The remarkable heating at altitudes 70-80 km was also confirmed by our dedicated ground-based observations during global dust storm 2018. The new pathway of water loss proposed by this implies much higher loss to space, in addition to the diffuse-limited escape of H2.

Keywords: Mars, water, habitability, escape, upper atmosphere

©2019. Japan Geoscience Union. All Right Reserved.

©2019. Japan Geoscience Union. All Right Reserved.

[J] Poster | M (Multidisciplinary and Interdisciplinary)：M-IS Intersection

Tue. May 28, 2019 3:30 PM - 5:00 PM JST | Tue. May 28, 2019 6:30 AM - 8:00 AM UTC | Poster Hall International Exhibition Hall8, Makuhari Messe_25

[M-IS11] Aqua planetology

convener:Yasuhito Sekine(Earth-Life Science Insitute, Tokyo Institute of Technology), Tomohiro Usui(Earth-Life Science Institute, Tokyo Institute of Technology), Keisuke Fukushi(Institute of Nature & Environmental Technology, Kanazawa University), Takazo Shibuya(Japan Agency for Marine-Earth Science and Technology)

This proposed session covers a wide range of topics related to aqua planetology, including chemical reactions involving water on planetary bodies, water-rock reactions within planetesimals, distribution of water in the early Solar system and the origin of water on terrestrial planets, hydrological and biogeochemical processes on Earth, geochemical cycles and habitability on Mars and icy moons, exploration of water in the solar system, and theory to understand how to build a habitable aqua planet.

[MIS11-P01] Three-dimensional simulations of methane-based hydrological cycles in north-pole regions of Titan

*Takufumi Chida[1,2], Yasuhito Sekine[1], Hidenori Genda[1] (1.Earth-Life Science Institute, Tokyo Institute of Technology, 2.Department of Earth and Planetary Science, University of Tokyo)

[MIS11-P02] Inclusion of brine into icy shell of Enceladus

*Ryusuke Nishitani[1], Atsushi Tani[2], Sho Sasaki[1], Jun Kimura[1] (1.Department of Earth and Space Sciences, School of Science, Osaka University, 2.Graduate School Human Development and Environment, Kobe University)

[MIS11-P03] Electron irradiations onto ice-salt mixtures at low temperatures: Implications for chemical evolution and oxidant formation on Europa

*Shuya Tan[2,1], Yasuhito Sekine[2], Tetsuya Hama[3] (1.Department of Earth and Planetary Science, Graduate School of Science, the University of Tokyo, 2.Earth-Life Science Institute, Tokyo Institute of Technology, 3.Institute of Low Temperature Science, Hokkaido University)

[MIS11-P04] Water-rock reactions in the parent body of Ryugu

*Takazo Shibuya[1], Yasuhito Sekine[2], Sakiko Kikuchi[1], Keisuke Fukushi[3], Tomoki Nakamura[4], Sei-ichiro WATANABE[5] (1.Japan Agency for Marine-Earth Science and Technology, 2.Tokyo Institute of Technology, 3.Kanazawa University, 4.Tohoku University, 5.Nagoya University)

[MIS11-P05] Investigation of the organic matter in ALH 77307 by STXM

*Hiroki Suga[1], Motoo Ito[2], Yoko Kebukawa[3], Matthew A Marcus[4], Takuji Ohigashi[5], Yoshio Takahashi[1] (1.Graduate School of Science, The University of Tokyo, 2.Kochi Institute for Core Sample Research JAMSTEC, 3.Faculty of Engineering, Yokohama National University, 4.Advanced Light Source, Lawrence Berkeley National Laboratory, 5.UVSOR Synchrotron Facility, Institute for Molecular Science)

[MIS11-P06] The development of UV spectrometer and preliminary measurement of carbonaceous chondrites

*Akira Igarashi[1], Tomoki Nakamura[1], Shingo Kameda[2], Keiichi Moroi[2] (1.Department of Earth and Planetary Materials Sciences, Faculty of Science, Tohoku University, 2.Department of Physics, Faculty of Science, Rikkyo University)

[MIS11-P07] A coupled experimental and thermodynamic study of chondrite-water interaction under anoxic condition

*Sakiko Kikuchi[1], Takazo Shibuya[1] (1.Japan Agency for Marine-Earth Science and Technology)

[MIS11-P08] Two-dimensional numerical experiments on subduction initiation in oceanic lithosphere: Effects of rheological properties of hydrous minerals

*Miki Izumi[1], Masaki Yoshida[2], Ken-ichi Hirauchi[1] (1.Department of Geosciences, Faculty of Science, Shizuoka University, 2.Department of Deep Earth Structure and Dynamics research, Japan Agency for Marine–Earth Science and Technology –JAMSTEC–)

[MIS11-P09] Electrical energy generation at hydrothermal environments in the Solar System estimated by fuel cell model experimentations

*Hiroyuki Kashima[1], Masahiro Yamamoto[1], Ken Takai[1] (1.Japan Agency for Marine-Earth Science and Technology)

[MIS11-P10] Experimental study of abiotic nitrate reduction at a high temperature and high-pressure condition and implication for nitrogen chemistry in Hadean hydrothermal environments

*Manabu Nishizawa[1], Takuya Saito[1], Akiko Makabe[1], Takazo Shibuya[1], Ken Takai[1] (1.Japan Agency for Marine-Earth Science and Technology)

[MIS11-P11] Interaction experiments between eucritic glass and 0.1 M NaCl aqueous solution at 300-500°C and 1.5 kbar: Suggestions on water-rock interactions at the bottom of Europa's subsurface ocean

*Makoto Nagasawa[1,2], Yutaro Takaya[1] (1.Department of Resources and Environmental Engineering, School of Creative Science and Engineering, Waseda University, 2.Department of Earth and Planetary Science, Graduate School of Science, The University of Tokyo)

[MIS11-P12] **Relationship between tellurium in the Fe-Mn oxides in the ocean and ambient seawater**

*Yusuke Fukami[1], Teruhiko Kashiwabara[1], Hiroshi Amakawa[1], Takazo Shibuya[1], Akira Usui[2], Katsuhiko Suzuki[1] (1.Japan Agency for Marine-Earth Science and Technology, 2.Kochi University)

[MIS11-P13] Laboratory reproduction of earthquake faulting beneath the internal ocean of Enceladus

*Takehiro Hirose[1], Takazo Shibuya[2] (1.Kochi Institute for Core Sample Research, Japan Agency for Marine-Earth Science and Technology, 2.Japan Agency for Marine-Earth Science and Technology)

[MIS11-P14] Why does Titan have an atmosphere, and why not Ganymede?—The origin of Titan-Ganymede dichotomy

*Yasuhito Sekine[1], Yuhiko Aoyama[2], Masahiro Ikoma[2], Takayuki Tanigawa[3] (1.Earth-Life Science Insitute, Tokyo Institute of Technology, 2.Dept. of Earth and Planetary Sci., University of Tokyo, 3.Section of Liberal Arts and Sciences, National Inst. of Tech., Ichinoseki College)

[MIS11-P15] Development of observation system of gas hydrate forming in the environment simulated near the bottom of icy shell in icy bodies (2)

*Atsushi Tani[1], Kenshiro Moriyama[1] (1.Graduate School of Human Development and Environment, Kobe University)

[MIS11-P16] Rheology of non-water ices inferred from diffusion coefficients: A compilation study

*Naoki Noguchi[1] (1.Graduate School of Technology, Industrial and Social Sciences, Tokushima University)

[MIS11-P17] Swelling behavior of magnesium saturated smectites

Morida Koki, Keisuke Fukushi, Hiroshi Sakuma

*Koki Morida[1] (1.Kanazawa University)

[MIS11-P18] Possibility of hydrogen peroxide as a warming agent on early Mars with oxidized condition

*Yuichi Ito[1], George HASHIMOTO[2], Yoshiyuki O. Takahashi[3], Masaki Ishiwatari[1], Kiyoshi Kuramoto[1] (1.Department of Cosmosciences, Graduate school of Science, Hokkaido University, 2.Department of Earth Sciences, Okayama University, 3.Graduate School of Science, Kobe University)

Three-dimensional simulations of methane-based hydrological cycles in north-pole regions of Titan

*Takufumi Chida[1,2], Yasuhito Sekine[1], Hidenori Genda[1]

1. Earth-Life Science Institute, Tokyo Institute of Technology, 2. Department of Earth and Planetary Science, University of Tokyo

Observations of lakes, surface modification by fluvial activities, and cloud formation all indicate that Saturn's moon Titan has the only active hydrological cycles known besides Earth [1]. Hydrocarbons such as methane and ethane condense out of a nitrogen-rich thick atmosphere, and precipitate onto the surface [1]. Methane observed in the atmosphere is continuously destroyed and lost by processes such as photolysis and direct escape [1]. Thereby, the persistence of the methane in the atmosphere is dependent on the availability of a hidden methane reservoir, resupplying the lost methane from the surface [1]. Quantifying the volume of the potential sources of methane resupply is one of the key questions of Titan's hydrological cycles [1].

Previous studies on remote-sensing observations of Titan's surface show that the elevations of some lakes and seas located near the north pole are constant from summer to early winter (corresponding to several Earth's years) within the observational errors, implying a connection with a mutual ground-methane table [2]. The preference of clouds at mid-latitudes over high-latitudes suggests that while surface methane is only observed at high latitudes, there may be a significant subsurface methane table at mid-latitudes that is available for exchange with the atmosphere [3]. The influence of subsurface flow on the hydrological cycle has been studied using a two-dimensional (2D) hydrological model, which treats the subsurface as one box at each location [4]. Thus, the 2D models cannot determine the subsurface hydraulic connection among lakes and oceans. They also cannot quantify the total volume of the subsurface methane reservoir, therefore being unable to estimate the extent of the methane-based hydrological cycles.

Here, we calculate the methane-based hydrological cycles using a surface-subsurface coupled three-dimensional hydrological simulator "GETFLOWS". GETFLOWS calculates surface and subsurface flows in a three-dimensional corner-grid blocks using Darcy's law, law of mass conservation, and Manning's equation. The main input parameters are (1) topography, (2) precipitation and evaporation rates, (3) permeability and porosity of the subsurface, and (4) levels of ground-methane table (i.e., the total methane volume in the subsurface). The topographic data was derived by interpolating the data obtained from the Cassini RADAR using the inverse distance weighting method [5]. The precipitation and evaporation data were applied from previous calculation results using general circulation model (GCM), which show good agreements of cloud formation and distribution with the observations [3,6]. The porosity and permeability values were estimated from the observations of the size of the icy grains on Titan's surface [7]. Using this model, we constrain the ground-methane table through reproducing the size and distribution of the lakes and oceans on Titan's surface as well as seasonal changes in their elevation. We discuss (1) whether the lakes and seas in the north-pole regions are hydraulically connected to the groundwater table, (2) what volume of subsurface liquid methane is active in the hydrological cycles, and (3) whether there is a subsurface transport of methane from the high to the low latitudes.

©2019. Japan Geoscience Union. All Right Reserved.

[1] Hayes et al., (2018) Nat. Geosci., 11, 306-313

[2] Hayes et al., (2016) Annu. Rev. Earth Planet. Sci., 44, 57-83

[3] Turtle et al., (2018) Geophysical Research Letters, 45, 5320-5328

[4] Horvath et al., (2016) Icarus, 277, 103-124

[5] Corlies et al., (2017) Geophysical Research Letters, 44, 11, 754-11,761

[6] Faulk et al., (2017) Nat. Geosci., 10, 827-831

[7] Brossier et al., (2018) JGR Planets, 123, 1089-1112

Keywords: Titan, Methane-based hydrological cycle

©2019. Japan Geoscience Union. All Right Reserved.

Inclusion of brine into icy shell of Enceladus

*Ryusuke Nishitani[1], Atsushi Tani[2], Sho Sasaki[1], Jun Kimura[1]

1. Department of Earth and Space Sciences, School of Science, Osaka University, 2. Graduate School Human Development and Environment, Kobe University

Investigation of Enceladus plume by Cassini spacecraft showed not only the existence of a subsurface ocean but also ocean included some salts. On the earth, it is known that sea ice includes brine into grain boundary. Similarly, icy shell of Enceladus seems to include sea water. Inclusion of sea water could cause partial melt in icy layer and could affect the geology and thermal evolution. Cox and Weeks (1975) showed that the effective partition coefficient, the ratio of concentration of sodium chloride in formed ice to that in residual liquid, depended on ice growth velocity. While, Gross et al., (1977) reported forced convection made partition coefficient low. To quantify the amount of brine included into icy shell under various condition, we investigated a partition coefficient of sodium chloride to ice by experiment and simulation.

As an experimental apparatus, unidirectional growth method used by Muraoka et al., (2016) was applied. With this method, plate-like ice can be formed in a cell and growth velocity can be controlled by controlling temperature. Ice was formed at a speed between cm/s in 5 % sodium chloride solution. As a result, effective partition coefficient of sodium chloride to ice was 1 approximately at all ice growth velocity.

To evaluate this value, ice growth in sodium chloride solution was simulated by voronoi dynamics simulation suggested by Kawano and Ohashi (2008). When ice grew under the same condition with the experiment, effective partition coefficient was 1 approximately. Next, we introduced Sherwood number into the simulation. It was found that higher Sherwood number made the effective partition coefficient lower. These results indicate that effective partition coefficient reflects condition of convection. When ice grow velocity is faster than diffusion of sodium chloride, effective partition coefficient is near 1. Since convection was not occur in this experiment, the effective partition coefficient was near 1.
In subsurface ocean of Enceladus, effective partition coefficient might be low due to convection, but in crack like tiger stripe, effective partition coefficient might be high because ice growth velocity seems to be high.

Keywords: Enceladus, brine, effective partition coefficient

©2019. Japan Geoscience Union. All Right Reserved.

Electron irradiations onto ice-salt mixtures at low temperatures: Implications for chemical evolution and oxidant formation on Europa

*Shuya Tan[2,1], Yasuhito Sekine[2], Tetsuya Hama[3]

1. Department of Earth and Planetary Science, Graduate School of Science, the University of Tokyo, 2. Earth-Life Science Institute, Tokyo Institute of Technology, 3. Institute of Low Temperature Science, Hokkaido University

The ice-rich surface of Europa is known to be irradiated with high-energy particles, such as electron, accelerated by the Jovian strong magnetic field (e.g., Paranicas et al., 2009). The high-energy particle irradiations could have caused particular chemical reactions on the surface, possibly including dissociation of H_2O and subsequent oxidation of surface salts, such as chlorides and sulfates/sulfides (e.g., Carlson et al., 2009; Hand et al., 2011). In addition, sputtering of the surface ice and salts by high-energy particles is proposed to be a major source of the tenuous atmosphere on Europa (e.g., Johnson et al., 2009; Brown and Hill, 1999). However, the detailed chemical reactions on Europa’s surface have been poorly constrained.

Here we construct a novel experimental system for irradiation of electron onto ice and salt (e.g., chloride: NaCl and $MgCl_2$) mixtures at low temperatures. Laboratory experiments on electron irradiation onto NaCl salt have been conducted at low temperatures corresponding to Europa’s surface (e.g., Hand and Carlson, 2015). However, no experiments have been performed to simulate the irradiation of electron onto ice and salt mixtures on Europa. Upon electron irradiation onto ice and chloride mixtures, chloride may be oxidized into perchlorate salts. If the surface materials are provided into the subsurface ocean through crustal recycling (e.g., Hand et al., 2007), perchlorate would become an important oxidant to generated redox disequilibria in the ocean. We report preliminary results on the electron irradiation experiments using the newly-constructed system.

Keywords: Irradiation experiment, Europa, chemical evolution

©2019. Japan Geoscience Union. All Right Reserved.

Water-rock reactions in the parent body of Ryugu

*Takazo Shibuya[1], Yasuhito Sekine[2], Sakiko Kikuchi[1], Keisuke Fukushi[3], Tomoki Nakamura[4], Sei-ichiro WATANABE[5]

1. Japan Agency for Marine-Earth Science and Technology, 2. Tokyo Institute of Technology, 3. Kanazawa University, 4. Tohoku University, 5. Nagoya University

The recent remote-sensing observation by Hayabusa2 is providing a large amount of data to unravel the origin of Ryugu. The Near Infrared Spectrometer (NIRS3) onboard Haybusa2 revealed that the IR reflectance of the global surface of Ryugu is extremely low (~0.02) and the spectra include small but clear absorption at 2.72 μm. These findings indicate the great abundance of dark materials and the subordinate amount of hydrous minerals in the surface, respectively. These materials on Ryugu are important clues to constrain the conditions of aqueous alteration such as the temperature experienced by the parent body and the original volatile compositions during accretion stage. In this work, we conducted thermodynamic modeling of chondrite-water reactions under various conditions to establish a model explaining the aqueous alteration of the parent body. In the thermodynamic calculations, a mean composition of CV chondrites was assumed for the initial bulk rock (minor amount of carbon, nitrogen and chlorine are also included) (Pearson et al., 2006; Clay et al., 2017). For the initial fluid, four cases were assumed; CO_2 concentration is 0, 1, 3 and 10 mol% (Cases 1–4, respectively) relative to water while the latter three cases also include NH_3 (0.5%) and H_2S (0.5%) additionally (Mumma and Charnley, 2011). The equilibrium temperature and pressure were assumed to be 0, 100, 200, 300 and 350 ˚C, and vapor pressure of water. In the calculations, pyrene was considered as a representative of polycyclic aromatic hydrocarbon while C1 compounds except CH_4 were included as soluble species (Zolotov, 2012).
The calculations showed that stabilities of hydrous/anhydrous minerals, carbonate, pyrene change with temperature and W/R value. In Case 1 (CO_2-free), the altered chondrite consists of serpentine, troilite and subordinate amount of hydrous/anhydrous minerals (e.g., magnetite, saponite, gibbsite and chlorite) at 0–300 ˚C. However, with increasing temperature above 300 ˚C, olivine and clinopyroxene become major phases as the amounts of serpentine, chlorite and magnetite decrease. At 350 ˚C, olivine becomes the most abundant minerals in conjunction with disappearance of serpentine. Similar temperature dependencies of hydrous mineral stabilities were also shown at low W/R in Cases 2–4 (CO_2 =1–10%) whereas carbonate is predominant at high W/R. Although the total amount of hydrous minerals in the surface of Ryugu is still unconfirmed, the calculation results suggest that the temperature of hydrothermal reactions experienced by Ryugu is lower than approximately 300 ˚C if a certain amount of hydrous minerals are present in the surface rocks. In contrast, if the amount of hydrous minerals is relatively small, higher temperatures (>350 ˚C) may account for the observed IR spectra. In this case, the parent body may have undergone high-temperature hydrothermal reactions that could occur in relatively large body. Otherwise, it is also possible that the parent body underwent instantaneous high-temperature events such as impacts after the aqueous alteration.Regarding the discriminating darkness of Ryugu, pyrene and/or magnetite are considered as the abundant dark materials on the surface of Ryugu in the predicted alteration minerals (pyrene is not dark by itself but can be altered to dark organic matter through geologic time). Especially, pyrene can be consolidated through reduction of CO_2in Cases 2–4 because of water-chondrite reactions generate abundant H_2. These solid phases are minor or absent at high W/R where carbonate is predominant but the sum of them exceeds several % at low W/R because water-chondrite reactions at low W/R generate abundant hydrogen. Therefore, the results indicate that the altered chondrites broadly become darker with decreasing W/R. However, if the water-chondrite reactions start under H_2-rich condition, the CO_2 in the fluid would be effectively reduced to form organic

©2019. Japan Geoscience Union. All Right Reserved.

materials (Cases 2–4) even at high W/R, which also potentially contribute the low reflectance of Ryugu.

©2019. Japan Geoscience Union. All Right Reserved.

Investigation of the organic matter in ALH 77307 by STXM

*Hiroki Suga[1], Motoo Ito[2], Yoko Kebukawa[3], Matthew A Marcus[4], Takuji Ohigashi[5], Yoshio Takahashi[1]

1. Graduate School of Science, The University of Tokyo, 2. Kochi Institute for Core Sample Research JAMSTEC, 3. Faculty of Engineering, Yokohama National University, 4. Advanced Light Source, Lawrence Berkeley National Laboratory, 5. UVSOR Synchrotron Facility, Institute for Molecular Science

Organic matter (OM) is one of the most important building blocks of the solar system, it contributes to the planetary evolution and relates to the origin of life. The primitive OM is preserved in the carbonaceous chondrites (CCs), comets, and interplanetary dust particles. However, it is difficult to understand that what is the primitive OM (*e.g.,* information of it such as chemical composition and occurrence). Therefore, various candidates and formation process of OM has being discussed still. Here, we focused on the one of the most pristine CCs, ALH 77307 (petrological type 3.03: less altered). Primitive OM in its matrix and chondrule rim phases were explored using X-ray microscopic analysis. The aim of this study is to find primitive OM in the most primitive CCs.

First, matrix and chondrule rim phases were identified by SEM-EDS elemental imaging. Then, the ultra-thin section of matrix and chondrule rim were prepared using FIB system in the Kochi Institute for Core Sample Research JAMSTEC. After that, prepared ultra-thin sections were analyzed by STXM installed BL4U in IMS UVSOR and beamline 5.3.2.2 in ALS LBNL to investigate OM distributions and their functional groups composition of C, N, and O.

As a result, we found two types of OM in both matrix and chondrule rim. These OM showed the same functional groups composition (aromatic C: C=C, ketonic C: C=O, carboxylic C: C=O[-HO], and graphitic layer structure: C-C) and different functional groups ratio. OMs in the chondrule rim were surrounded the aqueous alteration related secondary minerals such as iron hydroxides and carbonates. Although it was suggested that OM in the chondrule rim have the functional groups composition which related to aqueous alteration (*e.g.,* hydroxyl and aliphatic compounds), these functional groups related peaks could not be identified. Therefore, it was suggested that OM preserved original (before the accretion of the matrix and chondrule rim) information and secondary minerals origin were also before the accretion. From these characteristics, two types of OM in matrix and chondrule rim phase may have different origins such as nanoglobules and primitive insoluble OM (or insoluble OM-like nanoglobules reported in De Gregorio et al., 2013).
In this study, we succeeded in the *in-situ* observation (occurrence-preserved OM analysis with FIB system) to clarified that the original occurrence and functional groups of tow primitive OMs in ALH77307. As for the future plan, H-, C-, N-, and O-isotopic characteristics of these two OMs and carbonates are going to be analyzed by NanoSIMS in Koch Institute for Core Sample Research JAMSTEC. After that, OMs and secondary minerals morphology will be investigated by TEM in the University of Tokyo.

Keywords: ALH77307, STXM, Primitive organic matter

©2019. Japan Geoscience Union. All Right Reserved.

The development of UV spectrometer and preliminary measurement of carbonaceous chondrites

*Akira Igarashi[1], Tomoki Nakamura[1], Shingo Kameda[2], Keiichi Moroi[2]

1. Department of Earth and Planetary Materials Sciences, Faculty of Science, Tohoku University, 2. Department of Physics, Faculty of Science, Rikkyo University

Ultraviolet (UV) reflectance spectra (200-400nm) of carbonaceous chondrites provide new information on organic matters in C-complex asteroids [e. g., 1], but interpretation of UV reflectance spectra of carbonaceous chondrites are not well established [1–3] because of very low reflectivity of the meteorites and the lack of best-suited standards in the UV region.
In this study, we developed a UV spectrometer and made selection of the best-suited standard material for calibration. High sensitivity is required for the spectrometer, because primitive meteorites such as carbonaceous chondrites are very dark in the UV wavelength region. The detector is an Ocean Optics Maya2000 PRO that has sensitivity in a range from 165 to 620 nm and spectral resolution of 0.035–0.68 nm. Light source is Hamamatsu Photonics Deuterium lamp (H2D2 light source unit) L11799 that has intensity in a range from 160 to 400 nm with atmospheric UV-radiation. We set a light source, meteorite sample, and a detector with minimum distance each other with a phase angle of 30 degrees. We tested and evaluated a wide variety of natural and artificial materials as a candidate for a reflectance standard, including $BaSO_4$, CaF_2, and Quartz, in a way similar to those described in [2]. The results of the test measurements suggest that Quartz powder is the best standard in the ultraviolet region, because it shows relatively flat spectrum compared with the other candidates.
For preliminary measurements of carbonaceous chondrites, we measured hydrated and partially- or completely dehydrated CM chondrites (Murray, Murchison, Yamato (Y-) 793321, Jbilet Winselwan, Murchison heated at 600˚C, Belgica (B-) 7904, Y86720). They are classified to heating stages I-IV (stage IV is the highest heating degree) based on mineralogical evidence [4]. They were crushed into a powder with <77 or <155 μm in size and used for spectral measurements. The results show that overall UV reflectance decreases from stage I to II, but increases with increasing heating stages from II to IV, whereas spectral slope in the 200-400nm region decreases with increasing heating degree. These changes are consistent with those observed in [1] and probably attributed to graphitization of IOM (Insoluble Organic Matter) in carbonaceous chondrites with increasing heating temperature.

References: [1] Applin, D.M. et al. (2018) Icarus, 307, 40-82. [2] Cloutis E.A. et al. (2008) Icarus, 97, 321-347. [3] Trigo-Rodriguez J.M. et al. (2014) Monthly Notices of the Royal Astronomical Society, 437, 227-240. [4] Nakamura, T. (2005). Journal of Mineralogical and Petrological Sciences, 100(6), 260-272.

Keywords: ultraviolet reflectance spectra, carbonaceous chondrite

©2019. Japan Geoscience Union. All Right Reserved.

A coupled experimental and thermodynamic study of chondrite-water interaction under anoxic condition

*Sakiko Kikuchi[1], Takazo Shibuya[1]

1. Japan Agency for Marine-Earth Science and Technology

The presence of hydrous minerals in chondrites have been considered as an important evidence for the former presence of liquid water in parent bodies. However, the detailed evolutionary history of parent bodies (e.g., temperature fluid composition and water/rock ratio) are still poorly constrained, because the alteration processes of chondritic rock are not well defined and very few relevant experimental data are available. Here we investigate alteration process of chondrites by experiments simulating reactions between synthetic chondrite (mixtures of olivine, pyroxene, glass, Fe_{metal}, and troilite) and NH_3-containing solutions at 25 and 80 ˚C under anoxic conditions. We also compared the experimental results with those predicted from thermodynamic calculations to understand the equilibrium and kinetic conditions of chondrite-water interaction.
The experiments up to 7 months showed that the water-rock reactions caused a series of mineral alterations and production of H_2(aq), especially at 80 ˚C. X-ray diffraction analysis revealed that the formation of pyrrhotite was notable during the first few days in the experiment, which was likely resulted from the dissolution of troilite. In contrast, precipitation of saponite was evident after 100 days in the experiment, which was probably caused by the dissolution of Si-rich glass in the synthetic chondrites. Transmission electron microscope observation revealed that the saponite and secondary Si-rich amorphous phases densely covered the surface of the original olivine, glass, pyroxene, and troilite. These results imply that amorphous silica precipitated after the formation of pyrrhotite, followed by the precipitation of saponite. A part of these mineral assemblages obtained from our experiment was inconsistent with those predicted from the thermodynamic equilibrium calculations, suggesting that some metastable alteration minerals occur in the chondrite-water system before the complete equilibrium is achieved.

Keywords: chondrite, saponite, pyrrhotite

©2019. Japan Geoscience Union. All Right Reserved.

Two-dimensional numerical experiments on subduction initiation in oceanic lithosphere: Effects of rheological properties of hydrous minerals

*Miki Izumi[1], Masaki Yoshida[2], Ken-ichi Hirauchi[1]

1. Department of Geosciences, Faculty of Science, Shizuoka University, 2. Department of Deep Earth Structure and Dynamics research, Japan Agency for Marine–Earth Science and Technology –JAMSTEC–

How subduction begins on the Earth remains one of major outstanding problems in plate tectonics. For plate subduction to be initiated, previous numerical studies have assumed a preexisting weak fault with the coefficient of friction (μ) of around zero. When comparing the surface environment of the Earth with other terrestrial planets where plate tectonics is not occurring, only earth has an ocean. If seawater transport deeply along faults between plates, water–rock interaction will occur to form mechanically weak hydrous minerals. Therefore, we focus on effects of rheological properties of hydrous minerals and conduct a two-dimensional numerical simulation of subduction initiation in oceanic lithosphere. We found that plate subduction occurs with an assumption of antigorite flow law (dislocation creep), talc friction (i.e., μ= 0.1), and high pore fluid pressure ratio (λ = 0.9) for the weak fault zone. We also confirm that the maximum average strength of the weak fault for subduction to be initiated must be below 5 MPa. In our models, no oceanic plates sinks deep into the mantle, suggesting that additional effects are needed for the plate to fracture and then subduct into the deep mantle.

Keywords: plate tectonics, subduction initiation, hydrous mineral, oceanic lithosphere, antigorite, talc

©2019. Japan Geoscience Union. All Right Reserved.

Electrical energy generation at hydrothermal environments in the Solar System estimated by fuel cell model experimentations

*Hiroyuki Kashima[1], Masahiro Yamamoto[1], Ken Takai[1]

1. Japan Agency for Marine-Earth Science and Technology

A prime consideration for habitability of planets and moons is to constrain available free energy provided in the environment that could support the extant life and/or could drive chemical evolution. On Earth, primary production of a biosphere have been considered to be supported by phototrophs and chemotrophs with light and chemical energy, but recent studies discovered prokaryotes defined as electrotrophs that are capable of using electrons provided by artificial electrodes as the sole energy source for cellular activities [1]. This suggests that electrical energy could support the formation and evolution of a biosphere, and requires us to consider electrical energy, in addition to light and chemical energies, provided at the environment to estimate the habitability.

Although we have not yet had direct evidence for an electrotrophic ecosystem in a natural setting, spontaneous electrical current through conductive minerals and microbial matrixes that could support a life have been observed in sea floor environments on Earth. A promising example for spontaneous electrical energy generation is the marine hydrothermal environments in which conductive mineral deposits chemically separate hydrothermal fluid and sea water. Studies demonstrated that a marine hydrothermal system being functioning as analogous to a fuel cell generating power where sulfide deposit couples electrochemical oxidation of sulfide in the hydrothermal fluid and reduction of dissolved oxygen in the sea water with its electrocatalytic activity and electrical conductance [2].

As moons in the Solar System such as Enceladus and Europa are suggested to possess oceans with hydrothermal activity, it is hypothesized that those hydrothermal systems also generate electrical energy that provide free energy capable of supporting a biosphere. The present study is to estimate potentials of electrical energy generation at hydrothermal systems in oceans of the Solar System with laboratory electrochemical model experiments reproducing hydrothermal systems. Namely, electrochemical characterizations were conducted by using electrodes covered by sulfide minerals simulating hydrothermal deposits with electrolytes simulating hydrothermal fluids and seawaters. This presentation discusses electrocatalytic properties and potential power production of simulated hydrothermal systems with results of voltammetry tests and fuel cell polarization tests.

References: [1] Kumar, A. et al., (2017) Nature Reviews Chemistry 1, 0024. [2] Yamamoto, M. et al., (2018) ChemElectroChem 5. 2162-2166.

Keywords: the Solar System, hydrothermal system, fuel cell model, habitability, electrical energy

©2019. Japan Geoscience Union. All Right Reserved.

Experimental study of abiotic nitrate reduction at a high temperature and high-pressure condition and implication for nitrogen chemistry in Hadean hydrothermal environments

*Manabu Nishizawa[1], Takuya Saito[1], Akiko Makabe[1], Takazo Shibuya[1], Ken Takai[1]

1. Japan Agency for Marine-Earth Science and Technology

Nitrogen is an essential element for life as a major component of biomolecules and electron donor/acceptor for energy metabolism. Currently, nitrogen cycle in surface environments is mainly driven by biological processes including nitrogen fixation, nitrification and denitrification. In contrast, little is known about nitrogen cycle in the pre-biotic Earth and its relation to chemical evolution. This study focuses on nitrate chemistry during water-rock interaction in deep-sea hydrothermal environments to understand the fate of atmospherically-derived nitrate in the Hadean ocean. In experiments, artificial seawater with nitrate was reacted with synthetic komatiite at 350oC and 500 bar. Our experiments show that a substantial amount of nitrate was reduced to ammonium in an experimental condition. This implies that the Hadean deep-sea hydrothermal vents may have been favorable for chemical evolution in that both electron acceptor for energy metabolism (nitrate) and reduced nitrogen for organic synthesis (ammonium) were continuously supplied to the hydrothermal fluid-seawater mixing zone.

Keywords: prebiotic chemistry, nitrogen, deep sea hydrothermal vents

©2019. Japan Geoscience Union. All Right Reserved.

Interaction experiments between eucritic glass and 0.1 M NaCl aqueous solution at 300-500℃ and 1.5 kbar: Suggestions on water-rock interactions at the bottom of Europa’s subsurface ocean

*Makoto Nagasawa[1,2], Yutaro Takaya[1]

1. Department of Resources and Environmental Engineering, School of Creative Science and Engineering, Waseda University, 2. Department of Earth and Planetary Science, Graduate School of Science, The University of Tokyo

Europa, the second satellite of Jupiter, probably has subsurface ocean under its icy crust. The yellow-brown color of its leading anti-Jovian hemisphere could be explained by endogenous substances such as sodium chloride, which suggests the presence of hydrothermal activity (water-rock interaction) [Hand and Carlson, 2015]. In this study, we conducted water-rock interaction experiments to determine the mineral assemblage of altered rock on Europa’s mantle surface and to constrain the amount of available energy for sustaining the putative chemoautotroph-based ecosystems.

In our experiments, eucritic synthesis glass and 0.1 M NaCl aqueous solution were reacted at 300-500℃ and 1.5 kbar for 8, 16 and 32 days, using cold-seal type pressure vessels. The water/rock mass ratio was fixed at 1/1 in all the experiments (50 mg of powdered glass to 50 μL of NaCl solution). Solid products were analyzed by X-ray diffractometer and SEM equipped with EDS. Water chemistry of the reacted solution were determined by ICP-MS.

The mineral assemblages observed in our experiments were as follows.
・Fe-rich smectite (saponite), epistilbite and xonotlite at 300℃ and 1.5 kbar
・Fe-rich smectite (saponite), ferroactinolite, Ca-rich plagioclase and minor amount of magnetite at 400℃ and 1.5 kbar
・Mg-rich smectite, ferroactinolite, Ca-rich plagioclase, magnetite and hydroxyapatite at 500℃ and 1.5 kbar

The formation of magnetite at 400-500℃ suggests that these high-temperature water-rock interactions may generate hydrogen and sustain chemoautotroph-based ecosystems. As a future work, we would like to evaluate the hydrogen generation potential quantitatively.

Keywords: Europa, Water-rock interaction

©2019. Japan Geoscience Union. All Right Reserved.

Relationship between tellurium in the Fe-Mn oxides in the ocean and ambient seawater

*Yusuke Fukami[1], Teruhiko Kashiwabara[1], Hiroshi Amakawa[1], Takazo Shibuya[1], Akira Usui[2], Katsuhiko Suzuki[1]

1. Japan Agency for Marine-Earth Science and Technology, 2. Kochi University

Marine ferromanganese crusts (Fe-Mn crusts) are Fe-Mn oxides widely distributed on the seafloor, and important materials for (paleo)oceanographic studies (e.g. Hein et al., 2014). Tellurium (Te) is one of the highly enriched elements in the Fe-Mn crusts by more than ten thousand times relative to that in the continental crusts (Hein et al., 2010). Variation of concentration and isotopic compositions of Te in the Fe-Mn crusts could be a potential indicator for changes in redox condition of seawater, because of two valences of Te in ocean environments (+4 and +6; Lee and Edmond, 1985). In this study, we performed the measurement for concentration and isotopic compositions of Te in the surface layer of the Fe-Mn crusts, which was in contact with ambient seawater. The results were compared with the depth profile of the dissolved oxygen in the sampling site. To investigate the relationship to ambient seawater, the Fe-Mn crusts were sampled from two seamounts located in the Northwest Pacific, which showed different dissolved oxygen profile, and analyzed for Te concentration and isotopic compositions of the surface layer.

The results show that the correlation between the Te concentration and isotopic compositions in the surface layer of the Fe-Mn crusts changes depending on water depths. With increasing depths, the Te concentration decreases more drastically at shallower water depths than at deeper water depths. Moreover, the surface samples from two seamounts show a difference in the water depths where the concentration gradient of Te in the Fe-Mn crusts changes. The changes in the concentration gradient of Te in the Fe-Mn crusts may correspond to the changes in the chemical state of Mn in conjunction with the changes in the dissolved oxygen concentration in ambient seawater. Therefore, the Te concentration in the Fe-Mn oxides potentially indicates the dissolved oxygen concentration in the marine environment. The Fe oxides and Mn oxides are observed on the surface of the Mars by recent observation of exploration vehicles (e.g. Lanza et al., 2016), and the trace elements in these oxides potentially provide the information of water environments when they are formed. In the presentation, the results of the measurement of Te in natural samples, and laboratory experiment for application to Fe-Mn oxides on Mars will be discussed.

Keywords: tellurium, Fe-Mn oxides, ocean environment, Fe-Mn crusts, stable isotope

©2019. Japan Geoscience Union. All Right Reserved.

Laboratory reproduction of earthquake faulting beneath the internal ocean of Enceladus

*Takehiro Hirose[1], Takazo Shibuya[2]

1. Kochi Institute for Core Sample Research, Japan Agency for Marine-Earth Science and Technology, 2. Japan Agency for Marine-Earth Science and Technology

The discovery of the Na-rich ice particles erupting from the surface of Enceladus indicates the presence of hydrothermal activity in Enceladus' ocean. Knowledge of water chemistry of the interior ocean is crucial for exploring planetary habitability and life. Two different processes of water-rock interaction can define the water chemistry in Enceladus' ocean: one is the static chemical interaction at the hydrothermal regions over geological timescale, and the other is the dynamic chemical interaction associated with seismogenic faulting induced by tidal force between Enceladus and Saturn or neighboring satellites. In this study, we focus on the later short-time disequilibrium interaction between water-rock during faulting. By using high-velocity friction experiment, we plan to reproduce faulting processes that are expected to occur in the interior of Enceladus, and then evaluate quantitatively the effect of the disequilibrium interaction during faulting on the water chemistry of the interior ocean. In the poster, we will present outline of the apparatus and pilot results of the experiments using San Carlos olivine and synthetic chondrite as starting materials.

Keywords: Enceladus, earthquake faulting, hydrothermal

©2019. Japan Geoscience Union. All Right Reserved.

Why does Titan have an atmosphere, and why not Ganymede?—The origin of Titan-Ganymede dichotomy

*Yasuhito Sekine[1], Yuhiko Aoyama[2], Masahiro Ikoma[2], Takayuki Tanigawa[3]

1. Earth-Life Science Insitute, Tokyo Institute of Technology, 2. Dept. of Earth and Planetary Sci., University of Tokyo, 3. Section of Liberal Arts and Sciences, National Inst. of Tech., Ichinoseki College

One of the long-standing issues in planetary science is why Saturn's moon Titan possesses a thick atmosphere and why Jupiter's moon Ganymede not. These satellites are similar in size and mass; however, only Titan has active surface environments, characterized as a thick N_2 atmosphere and liquid CH_4 cycles. Since Titan's atmospheric N_2 originates from NH_3 (Niemann et al., 2005; Sekine et al., 2011), the building materials of Titan may have contained both NH_3 and CH_4 ices in addition to H_2O ice. Previous studies hypothesized that no condensation of NH_3 and CH_4 would have occurred in the circum-Jovian disk since proto-Jupiter might have formed in a relatively warm region of the protoplanetary disk (e.g., disk temperature > 100 K) (Lunine and Stevenson, 1982). However, recent disk models show that even at a few au, the disk temperature would have become sufficiently low (i.e., < 100 K) to form NH_3 and CH_4 ices in the disk (e.g., Dodson-Robinson et al., 2009; Oka et al., 2011), thereby calling for a new explanation. Here we show that gas and solids infalling onto massive proto-Jupiter would have experienced extensive shock heating (~10^4 K) upon accretion. The shock heating is sufficient to dissociate primordial NH_3 and CH_4 to thermochemically stable N_2 and CO, which cannot condensate in the circum-Jovian disk due to their low condensation temperatures. On the other hand, dissociation of NH_3 and CH_4 proceeds only incompletely upon accretion onto less massive proto-Saturn. Accordingly, the building materials of Saturn's icy moons contain abundance of survived NH_3 and CH_4 as ices. We suggest that giant planet's mass is a critical factor to determine the chemical compositions, surface environments, and potential habitability of the icy moons.

Dodson-Robinson et al. (2009) Icarus 200, 672
Lunine and Stevenson (1982) Icarus 52, 14
Niemann et al. (2005) Nature 438, 779
Oka et al. (2011) Astrophys. J. 738, 141
Sekine et al. (2011) Nature Geosci. 4, 359

Keywords: icy satellite, planetary atmosphere, planetary formation

©2019. Japan Geoscience Union. All Right Reserved.

Development of observation system of gas hydrate forming in the environment simulated near the bottom of icy shell in icy bodies (2)

*Atsushi Tani[1], Kenshiro Moriyama[1]

1. Graduate School of Human Development and Environment, Kobe University

Gas hydrates are clathrate compounds where hydrogen-bonded water cages include a guest gas molecule. Methane hydrate is one of famous gas hydrates because it is naturally found in deep-sea and permafrost sediments on the Earth. Gas hydrates would exist in icy bodies as well. One of the candidates is Pluto where the presence of subsurface ocean is suggested. Gas hydrates may exist between the ice shell and subsurface ocean and play an important role as insulator to keep warm inside. The presence of subsurface ocean is also suggested in some icy satellites like Enceladus. INMS (Ion and Neutral Mass Spectrometer) aboard the Cassini spacecraft has investigated composition of the plumes there that includes H2O (< 90 %), CH4, CO2, NH3, and other various organic materials. These results could reflect the composition of the subsurface ocean and imply the presence of clathrate hydrates in the ocean. Density of gas hydrates depends on guest gas molecules. For example, methane hydrate is lighter than the water, whereas CO2 hydrate is heavier. If CO2 hydrate forms at the bottom of the icy shell, the average density may become large and the ice (water ice + CO2 hydrate) may start to sink locally. If the size of each gas hydrate become small and granular gas hydrates exist in subsurface ocean, heat can be transfer by not only thermal conduction but also convection. This means that icy bodies may be cooled faster. To elucidate how gas hydrates form in the subsurface ocean in icy bodies, we have developed the observation system of gas hydrate formation and dissociation below the ice sheet. In the presentation, we report the progress of the observation system.

Keywords: icy bodies, gas hydrate, crystal growth

©2019. Japan Geoscience Union. All Right Reserved.

Rheology of non-water ices inferred from diffusion coefficients: A compilation study

*Naoki Noguchi[1]

1. Graduate School of Technology, Industrial and Social Sciences, Tokushima University

Non-water ices such as solid N_2, CO, CO_2, CH_4, and clathrate hydrates are a main constituent of the surfaces and crusts of the icy bodies. Understanding rheological properties of them are essential to understanding the dynamics including thermal convection, flow of glacier, and relaxation of topography. Several researchers investigated the rheological properties of them directly by low-temperature deformation experiments: solid N_2, CH_4 (Yamashita et al. 2010), CO_2 (Yamashita and Kato 1997, Durham et al. 1999), and CH_4 clathrate hydrate (Durham et al. 2003). They revealed the viscosities and plastic deformation mechanisms with a stress exponent of $n > 2$ in the range of 0.1 −100 MPa. However, the deformation experiment at low-stress conditions below 0.1 MPa is technically very difficult. The extrapolation of the plastic-flow law under their mechanisms to the low stress conditions may give an overestimate for the viscosity, because the diffusion creep can dominate in the low stress conditions below 0.1 MPa Under the diffusion creep regime, the viscosity behaves as Newtonian fluid, and is sensitive to the grain size. Although the viscosity under the diffusion creep regime cannot be measured directly, it can be estimated from diffusion coefficients based on the theories of diffusion creep (Frost and Ashby 1982). I will discuss the rheological properties of non-water ices inferred from the diffusion coefficients. There are many non-water ices whose diffusion coefficients have not determined yet by experiments. This substance includes solid CO and clathrate hydrates. In the case of molecular solids, the diffusion enthalpy has a correlation with the sublimation enthalpy (Chadwick and Sherwood 1971). I estimated the diffusion coefficients using the correlation in order to infer the rheological property.

Keywords: Non-water ice, Rheology, Diffusion, Icy body

©2019. Japan Geoscience Union. All Right Reserved.

Swelling behavior of magnesium saturated smectites

Morida Koki, Keisuke Fukushi, Hiroshi Sakuma

*Koki Morida[1]

1. Kanazawa University

Smectite belongs to clay minerals formed in the presence of liquid water. Smectites are composed of 2:1 layer with tetrahedral sheet and octahedral sheet. Smectites are categorized to di-octahedral type (e.g., nontronite and montmorillonite) and tri-octahedral type (e.g. saponite). The interlayer between the sheets is occupied by hydrated cations. The interlayer cations are usually Na^{+}, K^{+}, Mg^{2+}, Ca^{2+}. The distances of interlayer (basal spacing) depend on type of interlayer cations and relative humidity (RH). The basal spacing can change from 9 to 15 Å as function of amount of RH. At 0% of RH, basal spacings are around 10 Å when interlayer cation is Na^{+} or K^{+}. That is 12 Å when interlayer cation is Ca^{2+}. On the other hand, the basal spacings ranges from 11 to 14 Å when interlayer cation is Mg^{2+} (Sato et al, 1992; Morodome and Kawamura 2009).

Curiosity rover sent to the Gale crater on mars examines the possibility of existence of life and habitable environment (Vaniman et al, 2014). Water is essential for life. Therefore, in order to estimate possibility of life, it is important to know water quality. Gale crater is thought to be an ancient lake. Curiosity obtained the lacustrine sediment samples and analyzed the mineralogical and geochemical characteristics of the sediments. From the CheMin-XRD analyses, smectites were discovered in JohnKlein and Cumberland sites. The smectites are presumed to be saponite (Vaniman et al, 2014; Bristow et al, 2015). The basal spacing in Cumberland’s saponite exhibited 13.2 Å at RH0%. Now it has been under debates whether the interlayer cation in Cumberland’s saponite is $MgOH^{+}$ or Mg^{2+} ion.

Suquet et al, 1975 showed that basal spacing of Mg^{2+} saturated saponite is 11.4 Å at RH0%. Therefore, Vaniman et al. 2014 and Bristow et al, 2015 presumed that the interlayer cation in Cumberland’s saponite is $MgOH^{+}$ ion. However, basal spacing of some other Mg^{2+} saturated smectites exhibited above 13.2 Å. This study experimentally assess the basal spacing of smectites including saponite under several atomospheric compositions with N_2, air or CO_2.

©2019. Japan Geoscience Union. All Right Reserved.

Possibility of hydrogen peroxide as a warming agent on early Mars with oxidized condition

*Yuichi Ito[1], George HASHIMOTO[2], Yoshiyuki O. Takahashi[3], Masaki Ishiwatari[1], Kiyoshi Kuramoto[1]

1. Department of Cosmosciences, Graduate school of Science, Hokkaido University, 2. Department of Earth Sciences, Okayama University, 3. Graduate School of Science, Kobe University

Recently, Lanza et al. (2016) reported the detection of the high Mn-oxides abundances of Martian rocks in Gale Crater, where preserves the past martian surface environment during 3–4 Ga. This observation suggests that both liquid water and a highly oxidized atmosphere existed on early Mars, since the precipitation of such a Mn-oxide-rich rock requires highly oxidizing condition in water. On the other hand, the Solar luminosity at 4 Ga would be only 75 % of the current value. Due to this, it is thought that additional greenhouse components in CO2–H2O atmospheres could have played a key role for warming on early Mars on the basis of climate models (e.g., Kasting 1991). However, no previous atmospheric models have shown that highly oxidized atmosphere can warm the mean surface temperature of early Mars above 273 K. As a gaseous material oxidizing martian surface, hydrogen peroxide, H2O2, has been received attention (e.g., Zahnle et al. 2008) On the other side, anyone does not focus on H2O2 as a greenhouse gas, owing to the extremely low abundance in the current Martian atmosphere. Although hydrogen peroxide is photo-chemically unstable, its absorption for far-infrared radiation per a molecule is very strong. Thus, hydrogen peroxide might warm early Mars, if the atmosphere was highly oxidized.
To test this idea, we use a 1-D atmospheric energy balance model with a line-by-line radiative transfer calculation. Then, by parameterizing the abundance of H2O2 in a CO2-dominant atmosphere, we estimate how much the surface temperature is warmed. We found that the temperature increased at most only 3 K, in the case of the atmosphere with the saturated abundance of H2O2. On the other hand, when the abundance of condensation nuclei in the upper atmosphere is low, H2O2 is expected to be possibly super-saturated. In the case of the atmosphere with pressure of > 2bar and 1 ppm H2O2, the surface temperature can exceed 273 K. Also, in the case for 10 ppm H2O2, at least 1 bar atmosphere is required to warm the surface temperature above 273 K. In particular, for the 2 bar atmospheres including H2O2 with a molar fraction of 1 ppm and 10 ppm, the surface temperatures increase about 40 K and 80 K from 230 K, respectively. In this presentation, we will discuss about the possibility that H2O2 concentrates to be super-saturated from the view of photochemical production and condensation processes.

Keywords: Mars, Liquid water, Atmosphere

©2019. Japan Geoscience Union. All Right Reserved.

[J] Poster | M (Multidisciplinary and Interdisciplinary)：M-IS Intersection

Tue. May 28, 2019 5:15 PM - 6:30 PM JST | Tue. May 28, 2019 8:15 AM - 9:30 AM UTC | Poster Hall International Exhibition Hall8, Makuhari Messe_44

[M-IS11] Aqua planetology

convener:Yasuhito Sekine(Earth-Life Science Insitute, Tokyo Institute of Technology), Tomohiro Usui(Earth-Life Science Institute, Tokyo Institute of Technology), Keisuke Fukushi(Institute of Nature & Environmental Technology, Kanazawa University), Takazo Shibuya(Japan Agency for Marine-Earth Science and Technology)

This proposed session covers a wide range of topics related to aqua planetology, including chemical reactions involving water on planetary bodies, water-rock reactions within planetesimals, distribution of water in the early Solar system and the origin of water on terrestrial planets, hydrological and biogeochemical processes on Earth, geochemical cycles and habitability on Mars and icy moons, exploration of water in the solar system, and theory to understand how to build a habitable aqua planet.

[MIS11-P01] Three-dimensional simulations of methane-based hydrological cycles in north-pole regions of Titan

*Takufumi Chida[1,2], Yasuhito Sekine[1], Hidenori Genda[1] (1.Earth-Life Science Institute, Tokyo Institute of Technology, 2.Department of Earth and Planetary Science, University of Tokyo)

[MIS11-P02] Inclusion of brine into icy shell of Enceladus

*Ryusuke Nishitani[1], Atsushi Tani[2], Sho Sasaki[1], Jun Kimura[1] (1.Department of Earth and Space Sciences, School of Science, Osaka University, 2.Graduate School Human Development and Environment, Kobe University)

[MIS11-P03] Electron irradiations onto ice-salt mixtures at low temperatures: Implications for chemical evolution and oxidant formation on Europa

*Shuya Tan[2,1], Yasuhito Sekine[2], Tetsuya Hama[3] (1.Department of Earth and Planetary Science, Graduate School of Science, the University of Tokyo, 2.Earth-Life Science Institute, Tokyo Institute of Technology, 3.Institute of Low Temperature Science, Hokkaido University)

[MIS11-P04] Water-rock reactions in the parent body of Ryugu

*Takazo Shibuya[1], Yasuhito Sekine[2], Sakiko Kikuchi[1], Keisuke Fukushi[3], Tomoki Nakamura[4], Sei-ichiro WATANABE[5] (1.Japan Agency for Marine-Earth Science and Technology, 2.Tokyo Institute of Technology, 3.Kanazawa University, 4.Tohoku University, 5.Nagoya University)

[MIS11-P05] Investigation of the organic matter in ALH 77307 by STXM

*Hiroki Suga[1], Motoo Ito[2], Yoko Kebukawa[3], Matthew A Marcus[4], Takuji Ohigashi[5], Yoshio Takahashi[1] (1.Graduate School of Science, The University of Tokyo, 2.Kochi Institute for Core Sample Research JAMSTEC, 3.Faculty of Engineering, Yokohama National University, 4.Advanced Light Source, Lawrence Berkeley National Laboratory, 5.UVSOR Synchrotron Facility, Institute for Molecular Science)

[MIS11-P06] The development of UV spectrometer and preliminary measurement of carbonaceous chondrites

*Akira Igarashi[1], Tomoki Nakamura[1], Shingo Kameda[2], Keiichi Moroi[2] (1.Department of Earth and Planetary Materials Sciences, Faculty of Science, Tohoku University, 2.Department of Physics, Faculty of Science, Rikkyo University)

[MIS11-P07] A coupled experimental and thermodynamic study of chondrite-water interaction under anoxic condition

*Sakiko Kikuchi[1], Takazo Shibuya[1] (1.Japan Agency for Marine-Earth Science and Technology)

[MIS11-P08] Two-dimensional numerical experiments on subduction initiation in oceanic lithosphere: Effects of rheological properties of hydrous minerals

*Miki Izumi[1], Masaki Yoshida[2], Ken-ichi Hirauchi[1] (1.Department of Geosciences, Faculty of Science, Shizuoka University, 2.Department of Deep Earth Structure and Dynamics research, Japan Agency for Marine–Earth Science and Technology –JAMSTEC–)

[MIS11-P09] Electrical energy generation at hydrothermal environments in the Solar System estimated by fuel cell model experimentations

*Hiroyuki Kashima[1], Masahiro Yamamoto[1], Ken Takai[1] (1.Japan Agency for Marine-Earth Science and Technology)

[MIS11-P10] Experimental study of abiotic nitrate reduction at a high temperature and high-pressure condition and implication for nitrogen chemistry in Hadean hydrothermal environments

*Manabu Nishizawa[1], Takuya Saito[1], Akiko Makabe[1], Takazo Shibuya[1], Ken Takai[1] (1.Japan Agency for Marine-Earth Science and Technology)

[MIS11-P11] Interaction experiments between eucritic glass and 0.1 M NaCl aqueous solution at 300-500°C and 1.5 kbar: Suggestions on water-rock interactions at the bottom of Europa's subsurface ocean

*Makoto Nagasawa[1,2], Yutaro Takaya[1] (1.Department of Resources and Environmental Engineering, School of Creative Science and Engineering, Waseda University, 2.Department of Earth and Planetary Science, Graduate School of Science, The University of Tokyo)

[MIS11-P12] **Relationship between tellurium in the Fe-Mn oxides in the ocean and ambient seawater**

*Yusuke Fukami[1], Teruhiko Kashiwabara[1], Hiroshi Amakawa[1], Takazo Shibuya[1], Akira Usui[2], Katsuhiko Suzuki[1] (1.Japan Agency for Marine-Earth Science and Technology, 2.Kochi University)

[MIS11-P13] Laboratory reproduction of earthquake faulting beneath the internal ocean of Enceladus

*Takehiro Hirose[1], Takazo Shibuya[2] (1.Kochi Institute for Core Sample Research, Japan Agency for Marine-Earth Science and Technology, 2.Japan Agency for Marine-Earth Science and Technology)

[MIS11-P14] Why does Titan have an atmosphere, and why not Ganymede?—The origin of Titan-Ganymede dichotomy

*Yasuhito Sekine[1], Yuhiko Aoyama[2], Masahiro Ikoma[2], Takayuki Tanigawa[3] (1.Earth-Life Science Insitute, Tokyo Institute of Technology, 2.Dept. of Earth and Planetary Sci., University of Tokyo, 3.Section of Liberal Arts and Sciences, National Inst. of Tech., Ichinoseki College)

[MIS11-P15] Development of observation system of gas hydrate forming in the environment simulated near the bottom of icy shell in icy bodies (2)

*Atsushi Tani[1], Kenshiro Moriyama[1] (1.Graduate School of Human Development and Environment, Kobe University)

[MIS11-P16] Rheology of non-water ices inferred from diffusion coefficients: A compilation study

*Naoki Noguchi[1] (1.Graduate School of Technology, Industrial and Social Sciences, Tokushima University)

[MIS11-P17] Swelling behavior of magnesium saturated smectites

Morida Koki, Keisuke Fukushi, Hiroshi Sakuma

*Koki Morida[1] (1.Kanazawa University)

[MIS11-P18] Possibility of hydrogen peroxide as a warming agent on early Mars with oxidized condition

*Yuichi Ito[1], George HASHIMOTO[2], Yoshiyuki O. Takahashi[3], Masaki Ishiwatari[1], Kiyoshi Kuramoto[1] (1.Department of Cosmosciences, Graduate school of Science, Hokkaido University, 2.Department of Earth Sciences, Okayama University, 3.Graduate School of Science, Kobe University)

Three-dimensional simulations of methane-based hydrological cycles in north-pole regions of Titan

*Takufumi Chida[1,2], Yasuhito Sekine[1], Hidenori Genda[1]

1. Earth-Life Science Institute, Tokyo Institute of Technology, 2. Department of Earth and Planetary Science, University of Tokyo

Observations of lakes, surface modification by fluvial activities, and cloud formation all indicate that Saturn's moon Titan has the only active hydrological cycles known besides Earth [1]. Hydrocarbons such as methane and ethane condense out of a nitrogen-rich thick atmosphere, and precipitate onto the surface [1]. Methane observed in the atmosphere is continuously destroyed and lost by processes such as photolysis and direct escape [1]. Thereby, the persistence of the methane in the atmosphere is dependent on the availability of a hidden methane reservoir, resupplying the lost methane from the surface [1]. Quantifying the volume of the potential sources of methane resupply is one of the key questions of Titan's hydrological cycles [1].

Previous studies on remote-sensing observations of Titan's surface show that the elevations of some lakes and seas located near the north pole are constant from summer to early winter (corresponding to several Earth's years) within the observational errors, implying a connection with a mutual ground-methane table [2]. The preference of clouds at mid-latitudes over high-latitudes suggests that while surface methane is only observed at high latitudes, there may be a significant subsurface methane table at mid-latitudes that is available for exchange with the atmosphere [3]. The influence of subsurface flow on the hydrological cycle has been studied using a two-dimensional (2D) hydrological model, which treats the subsurface as one box at each location [4]. Thus, the 2D models cannot determine the subsurface hydraulic connection among lakes and oceans. They also cannot quantify the total volume of the subsurface methane reservoir, therefore being unable to estimate the extent of the methane-based hydrological cycles.

Here, we calculate the methane-based hydrological cycles using a surface-subsurface coupled three-dimensional hydrological simulator "GETFLOWS". GETFLOWS calculates surface and subsurface flows in a three-dimensional corner-grid blocks using Darcy's law, law of mass conservation, and Manning's equation. The main input parameters are (1) topography, (2) precipitation and evaporation rates, (3) permeability and porosity of the subsurface, and (4) levels of ground-methane table (i.e., the total methane volume in the subsurface). The topographic data was derived by interpolating the data obtained from the Cassini RADAR using the inverse distance weighting method [5]. The precipitation and evaporation data were applied from previous calculation results using general circulation model (GCM), which show good agreements of cloud formation and distribution with the observations [3,6]. The porosity and permeability values were estimated from the observations of the size of the icy grains on Titan's surface [7]. Using this model, we constrain the ground-methane table through reproducing the size and distribution of the lakes and oceans on Titan's surface as well as seasonal changes in their elevation. We discuss (1) whether the lakes and seas in the north-pole regions are hydraulically connected to the groundwater table, (2) what volume of subsurface liquid methane is active in the hydrological cycles, and (3) whether there is a subsurface transport of methane from the high to the low latitudes.

©2019. Japan Geoscience Union. All Right Reserved.

[1] Hayes et al., (2018) Nat. Geosci., 11, 306-313

[2] Hayes et al., (2016) Annu. Rev. Earth Planet. Sci., 44, 57-83

[3] Turtle et al., (2018) Geophysical Research Letters, 45, 5320-5328

[4] Horvath et al., (2016) Icarus, 277, 103-124

[5] Corlies et al., (2017) Geophysical Research Letters, 44, 11, 754-11,761

[6] Faulk et al., (2017) Nat. Geosci., 10, 827-831

[7] Brossier et al., (2018) JGR Planets, 123, 1089-1112

Keywords: Titan, Methane-based hydrological cycle

©2019. Japan Geoscience Union. All Right Reserved.

Inclusion of brine into icy shell of Enceladus

*Ryusuke Nishitani[1], Atsushi Tani[2], Sho Sasaki[1], Jun Kimura[1]

1. Department of Earth and Space Sciences, School of Science, Osaka University, 2. Graduate School Human Development and Environment, Kobe University

Investigation of Enceladus plume by Cassini spacecraft showed not only the existence of a subsurface ocean but also ocean included some salts. On the earth, it is known that sea ice includes brine into grain boundary. Similarly, icy shell of Enceladus seems to include sea water. Inclusion of sea water could cause partial melt in icy layer and could affect the geology and thermal evolution. Cox and Weeks (1975) showed that the effective partition coefficient, the ratio of concentration of sodium chloride in formed ice to that in residual liquid, depended on ice growth velocity. While, Gross et al., (1977) reported forced convection made partition coefficient low. To quantify the amount of brine included into icy shell under various condition, we investigated a partition coefficient of sodium chloride to ice by experiment and simulation.

As an experimental apparatus, unidirectional growth method used by Muraoka et al., (2016) was applied. With this method, plate-like ice can be formed in a cell and growth velocity can be controlled by controlling temperature. Ice was formed at a speed between cm/s in 5 % sodium chloride solution. As a result, effective partition coefficient of sodium chloride to ice was 1 approximately at all ice growth velocity.

To evaluate this value, ice growth in sodium chloride solution was simulated by voronoi dynamics simulation suggested by Kawano and Ohashi (2008). When ice grew under the same condition with the experiment, effective partition coefficient was 1 approximately. Next, we introduced Sherwood number into the simulation. It was found that higher Sherwood number made the effective partition coefficient lower. These results indicate that effective partition coefficient reflects condition of convection. When ice grow velocity is faster than diffusion of sodium chloride, effective partition coefficient is near 1. Since convection was not occur in this experiment, the effective partition coefficient was near 1.
In subsurface ocean of Enceladus, effective partition coefficient might be low due to convection, but in crack like tiger stripe, effective partition coefficient might be high because ice growth velocity seems to be high.

Keywords: Enceladus, brine, effective partition coefficient

©2019. Japan Geoscience Union. All Right Reserved.

Electron irradiations onto ice-salt mixtures at low temperatures: Implications for chemical evolution and oxidant formation on Europa

*Shuya Tan[2,1], Yasuhito Sekine[2], Tetsuya Hama[3]

1. Department of Earth and Planetary Science, Graduate School of Science, the University of Tokyo, 2. Earth-Life Science Institute, Tokyo Institute of Technology, 3. Institute of Low Temperature Science, Hokkaido University

The ice-rich surface of Europa is known to be irradiated with high-energy particles, such as electron, accelerated by the Jovian strong magnetic field (e.g., Paranicas et al., 2009). The high-energy particle irradiations could have caused particular chemical reactions on the surface, possibly including dissociation of H_2O and subsequent oxidation of surface salts, such as chlorides and sulfates/sulfides (e.g., Carlson et al., 2009; Hand et al., 2011). In addition, sputtering of the surface ice and salts by high-energy particles is proposed to be a major source of the tenuous atmosphere on Europa (e.g., Johnson et al., 2009; Brown and Hill, 1999). However, the detailed chemical reactions on Europa’s surface have been poorly constrained.

Here we construct a novel experimental system for irradiation of electron onto ice and salt (e.g., chloride: NaCl and $MgCl_2$) mixtures at low temperatures. Laboratory experiments on electron irradiation onto NaCl salt have been conducted at low temperatures corresponding to Europa’s surface (e.g., Hand and Carlson, 2015). However, no experiments have been performed to simulate the irradiation of electron onto ice and salt mixtures on Europa. Upon electron irradiation onto ice and chloride mixtures, chloride may be oxidized into perchlorate salts. If the surface materials are provided into the subsurface ocean through crustal recycling (e.g., Hand et al., 2007), perchlorate would become an important oxidant to generated redox disequilibria in the ocean. We report preliminary results on the electron irradiation experiments using the newly-constructed system.

Keywords: Irradiation experiment, Europa, chemical evolution

©2019. Japan Geoscience Union. All Right Reserved.

Water-rock reactions in the parent body of Ryugu

*Takazo Shibuya[1], Yasuhito Sekine[2], Sakiko Kikuchi[1], Keisuke Fukushi[3], Tomoki Nakamura[4], Sei-ichiro WATANABE[5]

1. Japan Agency for Marine-Earth Science and Technology, 2. Tokyo Institute of Technology, 3. Kanazawa University, 4. Tohoku University, 5. Nagoya University

The recent remote-sensing observation by Hayabusa2 is providing a large amount of data to unravel the origin of Ryugu. The Near Infrared Spectrometer (NIRS3) onboard Haybusa2 revealed that the IR reflectance of the global surface of Ryugu is extremely low (~0.02) and the spectra include small but clear absorption at 2.72 μm. These findings indicate the great abundance of dark materials and the subordinate amount of hydrous minerals in the surface, respectively. These materials on Ryugu are important clues to constrain the conditions of aqueous alteration such as the temperature experienced by the parent body and the original volatile compositions during accretion stage. In this work, we conducted thermodynamic modeling of chondrite-water reactions under various conditions to establish a model explaining the aqueous alteration of the parent body. In the thermodynamic calculations, a mean composition of CV chondrites was assumed for the initial bulk rock (minor amount of carbon, nitrogen and chlorine are also included) (Pearson et al., 2006; Clay et al., 2017). For the initial fluid, four cases were assumed; CO_2 concentration is 0, 1, 3 and 10 mol% (Cases 1–4, respectively) relative to water while the latter three cases also include NH_3 (0.5%) and H_2S (0.5%) additionally (Mumma and Charnley, 2011). The equilibrium temperature and pressure were assumed to be 0, 100, 200, 300 and 350 ˚C, and vapor pressure of water. In the calculations, pyrene was considered as a representative of polycyclic aromatic hydrocarbon while C1 compounds except CH_4 were included as soluble species (Zolotov, 2012).
The calculations showed that stabilities of hydrous/anhydrous minerals, carbonate, pyrene change with temperature and W/R value. In Case 1 (CO_2-free), the altered chondrite consists of serpentine, troilite and subordinate amount of hydrous/anhydrous minerals (e.g., magnetite, saponite, gibbsite and chlorite) at 0–300 ˚C. However, with increasing temperature above 300 ˚C, olivine and clinopyroxene become major phases as the amounts of serpentine, chlorite and magnetite decrease. At 350 ˚C, olivine becomes the most abundant minerals in conjunction with disappearance of serpentine. Similar temperature dependencies of hydrous mineral stabilities were also shown at low W/R in Cases 2–4 (CO_2 =1–10%) whereas carbonate is predominant at high W/R. Although the total amount of hydrous minerals in the surface of Ryugu is still unconfirmed, the calculation results suggest that the temperature of hydrothermal reactions experienced by Ryugu is lower than approximately 300 ˚C if a certain amount of hydrous minerals are present in the surface rocks. In contrast, if the amount of hydrous minerals is relatively small, higher temperatures (>350 ˚C) may account for the observed IR spectra. In this case, the parent body may have undergone high-temperature hydrothermal reactions that could occur in relatively large body. Otherwise, it is also possible that the parent body underwent instantaneous high-temperature events such as impacts after the aqueous alteration.Regarding the discriminating darkness of Ryugu, pyrene and/or magnetite are considered as the abundant dark materials on the surface of Ryugu in the predicted alteration minerals (pyrene is not dark by itself but can be altered to dark organic matter through geologic time). Especially, pyrene can be consolidated through reduction of CO_2in Cases 2–4 because of water-chondrite reactions generate abundant H_2. These solid phases are minor or absent at high W/R where carbonate is predominant but the sum of them exceeds several % at low W/R because water-chondrite reactions at low W/R generate abundant hydrogen. Therefore, the results indicate that the altered chondrites broadly become darker with decreasing W/R. However, if the water-chondrite reactions start under H_2-rich condition, the CO_2 in the fluid would be effectively reduced to form organic

©2019. Japan Geoscience Union. All Right Reserved.

materials (Cases 2–4) even at high W/R, which also potentially contribute the low reflectance of Ryugu.

©2019. Japan Geoscience Union. All Right Reserved.

Investigation of the organic matter in ALH 77307 by STXM

*Hiroki Suga[1], Motoo Ito[2], Yoko Kebukawa[3], Matthew A Marcus[4], Takuji Ohigashi[5], Yoshio Takahashi[1]

1. Graduate School of Science, The University of Tokyo, 2. Kochi Institute for Core Sample Research JAMSTEC, 3. Faculty of Engineering, Yokohama National University, 4. Advanced Light Source, Lawrence Berkeley National Laboratory, 5. UVSOR Synchrotron Facility, Institute for Molecular Science

Organic matter (OM) is one of the most important building blocks of the solar system, it contributes to the planetary evolution and relates to the origin of life. The primitive OM is preserved in the carbonaceous chondrites (CCs), comets, and interplanetary dust particles. However, it is difficult to understand that what is the primitive OM (*e.g.,* information of it such as chemical composition and occurrence). Therefore, various candidates and formation process of OM has being discussed still. Here, we focused on the one of the most pristine CCs, ALH 77307 (petrological type 3.03: less altered). Primitive OM in its matrix and chondrule rim phases were explored using X-ray microscopic analysis. The aim of this study is to find primitive OM in the most primitive CCs.

First, matrix and chondrule rim phases were identified by SEM-EDS elemental imaging. Then, the ultra-thin section of matrix and chondrule rim were prepared using FIB system in the Kochi Institute for Core Sample Research JAMSTEC. After that, prepared ultra-thin sections were analyzed by STXM installed BL4U in IMS UVSOR and beamline 5.3.2.2 in ALS LBNL to investigate OM distributions and their functional groups composition of C, N, and O.

As a result, we found two types of OM in both matrix and chondrule rim. These OM showed the same functional groups composition (aromatic C: C=C, ketonic C: C=O, carboxylic C: C=O[-HO], and graphitic layer structure: C-C) and different functional groups ratio. OMs in the chondrule rim were surrounded the aqueous alteration related secondary minerals such as iron hydroxides and carbonates. Although it was suggested that OM in the chondrule rim have the functional groups composition which related to aqueous alteration (*e.g.,* hydroxyl and aliphatic compounds), these functional groups related peaks could not be identified. Therefore, it was suggested that OM preserved original (before the accretion of the matrix and chondrule rim) information and secondary minerals origin were also before the accretion. From these characteristics, two types of OM in matrix and chondrule rim phase may have different origins such as nanoglobules and primitive insoluble OM (or insoluble OM-like nanoglobules reported in De Gregorio et al., 2013).
In this study, we succeeded in the *in-situ* observation (occurrence-preserved OM analysis with FIB system) to clarified that the original occurrence and functional groups of tow primitive OMs in ALH77307. As for the future plan, H-, C-, N-, and O-isotopic characteristics of these two OMs and carbonates are going to be analyzed by NanoSIMS in Koch Institute for Core Sample Research JAMSTEC. After that, OMs and secondary minerals morphology will be investigated by TEM in the University of Tokyo.

Keywords: ALH77307, STXM, Primitive organic matter

©2019. Japan Geoscience Union. All Right Reserved.

The development of UV spectrometer and preliminary measurement of carbonaceous chondrites

*Akira Igarashi[1], Tomoki Nakamura[1], Shingo Kameda[2], Keiichi Moroi[2]

1. Department of Earth and Planetary Materials Sciences, Faculty of Science, Tohoku University, 2. Department of Physics, Faculty of Science, Rikkyo University

Ultraviolet (UV) reflectance spectra (200-400nm) of carbonaceous chondrites provide new information on organic matters in C-complex asteroids [e. g., 1], but interpretation of UV reflectance spectra of carbonaceous chondrites are not well established [1–3] because of very low reflectivity of the meteorites and the lack of best-suited standards in the UV region.
In this study, we developed a UV spectrometer and made selection of the best-suited standard material for calibration. High sensitivity is required for the spectrometer, because primitive meteorites such as carbonaceous chondrites are very dark in the UV wavelength region. The detector is an Ocean Optics Maya2000 PRO that has sensitivity in a range from 165 to 620 nm and spectral resolution of 0.035–0.68 nm. Light source is Hamamatsu Photonics Deuterium lamp (H2D2 light source unit) L11799 that has intensity in a range from 160 to 400 nm with atmospheric UV-radiation. We set a light source, meteorite sample, and a detector with minimum distance each other with a phase angle of 30 degrees. We tested and evaluated a wide variety of natural and artificial materials as a candidate for a reflectance standard, including $BaSO_4$, CaF_2, and Quartz, in a way similar to those described in [2]. The results of the test measurements suggest that Quartz powder is the best standard in the ultraviolet region, because it shows relatively flat spectrum compared with the other candidates.
For preliminary measurements of carbonaceous chondrites, we measured hydrated and partially- or completely dehydrated CM chondrites (Murray, Murchison, Yamato (Y-) 793321, Jbilet Winselwan, Murchison heated at 600˚C, Belgica (B-) 7904, Y86720). They are classified to heating stages I-IV (stage IV is the highest heating degree) based on mineralogical evidence [4]. They were crushed into a powder with <77 or <155 μm in size and used for spectral measurements. The results show that overall UV reflectance decreases from stage I to II, but increases with increasing heating stages from II to IV, whereas spectral slope in the 200-400nm region decreases with increasing heating degree. These changes are consistent with those observed in [1] and probably attributed to graphitization of IOM (Insoluble Organic Matter) in carbonaceous chondrites with increasing heating temperature.

References: [1] Applin, D.M. et al. (2018) Icarus, 307, 40-82. [2] Cloutis E.A. et al. (2008) Icarus, 97, 321-347. [3] Trigo-Rodriguez J.M. et al. (2014) Monthly Notices of the Royal Astronomical Society, 437, 227-240. [4] Nakamura, T. (2005). Journal of Mineralogical and Petrological Sciences, 100(6), 260-272.

Keywords: ultraviolet reflectance spectra, carbonaceous chondrite

©2019. Japan Geoscience Union. All Right Reserved.

A coupled experimental and thermodynamic study of chondrite-water interaction under anoxic condition

*Sakiko Kikuchi[1], Takazo Shibuya[1]

1. Japan Agency for Marine-Earth Science and Technology

The presence of hydrous minerals in chondrites have been considered as an important evidence for the former presence of liquid water in parent bodies. However, the detailed evolutionary history of parent bodies (e.g., temperature fluid composition and water/rock ratio) are still poorly constrained, because the alteration processes of chondritic rock are not well defined and very few relevant experimental data are available. Here we investigate alteration process of chondrites by experiments simulating reactions between synthetic chondrite (mixtures of olivine, pyroxene, glass, Fe_{metal}, and troilite) and NH_3-containing solutions at 25 and 80 ˚C under anoxic conditions. We also compared the experimental results with those predicted from thermodynamic calculations to understand the equilibrium and kinetic conditions of chondrite-water interaction.
The experiments up to 7 months showed that the water-rock reactions caused a series of mineral alterations and production of H_2(aq), especially at 80 ˚C. X-ray diffraction analysis revealed that the formation of pyrrhotite was notable during the first few days in the experiment, which was likely resulted from the dissolution of troilite. In contrast, precipitation of saponite was evident after 100 days in the experiment, which was probably caused by the dissolution of Si-rich glass in the synthetic chondrites. Transmission electron microscope observation revealed that the saponite and secondary Si-rich amorphous phases densely covered the surface of the original olivine, glass, pyroxene, and troilite. These results imply that amorphous silica precipitated after the formation of pyrrhotite, followed by the precipitation of saponite. A part of these mineral assemblages obtained from our experiment was inconsistent with those predicted from the thermodynamic equilibrium calculations, suggesting that some metastable alteration minerals occur in the chondrite-water system before the complete equilibrium is achieved.

Keywords: chondrite, saponite, pyrrhotite

©2019. Japan Geoscience Union. All Right Reserved.

Two-dimensional numerical experiments on subduction initiation in oceanic lithosphere: Effects of rheological properties of hydrous minerals

*Miki Izumi[1], Masaki Yoshida[2], Ken-ichi Hirauchi[1]

1. Department of Geosciences, Faculty of Science, Shizuoka University, 2. Department of Deep Earth Structure and Dynamics research, Japan Agency for Marine–Earth Science and Technology –JAMSTEC–

How subduction begins on the Earth remains one of major outstanding problems in plate tectonics. For plate subduction to be initiated, previous numerical studies have assumed a preexisting weak fault with the coefficient of friction (μ) of around zero. When comparing the surface environment of the Earth with other terrestrial planets where plate tectonics is not occurring, only earth has an ocean. If seawater transport deeply along faults between plates, water–rock interaction will occur to form mechanically weak hydrous minerals. Therefore, we focus on effects of rheological properties of hydrous minerals and conduct a two-dimensional numerical simulation of subduction initiation in oceanic lithosphere. We found that plate subduction occurs with an assumption of antigorite flow law (dislocation creep), talc friction (i.e., μ= 0.1), and high pore fluid pressure ratio (λ = 0.9) for the weak fault zone. We also confirm that the maximum average strength of the weak fault for subduction to be initiated must be below 5 MPa. In our models, no oceanic plates sinks deep into the mantle, suggesting that additional effects are needed for the plate to fracture and then subduct into the deep mantle.

Keywords: plate tectonics, subduction initiation, hydrous mineral, oceanic lithosphere, antigorite, talc

©2019. Japan Geoscience Union. All Right Reserved.

Electrical energy generation at hydrothermal environments in the Solar System estimated by fuel cell model experimentations

*Hiroyuki Kashima[1], Masahiro Yamamoto[1], Ken Takai[1]

1. Japan Agency for Marine-Earth Science and Technology

A prime consideration for habitability of planets and moons is to constrain available free energy provided in the environment that could support the extant life and/or could drive chemical evolution. On Earth, primary production of a biosphere have been considered to be supported by phototrophs and chemotrophs with light and chemical energy, but recent studies discovered prokaryotes defined as electrotrophs that are capable of using electrons provided by artificial electrodes as the sole energy source for cellular activities [1]. This suggests that electrical energy could support the formation and evolution of a biosphere, and requires us to consider electrical energy, in addition to light and chemical energies, provided at the environment to estimate the habitability.

Although we have not yet had direct evidence for an electrotrophic ecosystem in a natural setting, spontaneous electrical current through conductive minerals and microbial matrixes that could support a life have been observed in sea floor environments on Earth. A promising example for spontaneous electrical energy generation is the marine hydrothermal environments in which conductive mineral deposits chemically separate hydrothermal fluid and sea water. Studies demonstrated that a marine hydrothermal system being functioning as analogous to a fuel cell generating power where sulfide deposit couples electrochemical oxidation of sulfide in the hydrothermal fluid and reduction of dissolved oxygen in the sea water with its electrocatalytic activity and electrical conductance [2].

As moons in the Solar System such as Enceladus and Europa are suggested to possess oceans with hydrothermal activity, it is hypothesized that those hydrothermal systems also generate electrical energy that provide free energy capable of supporting a biosphere. The present study is to estimate potentials of electrical energy generation at hydrothermal systems in oceans of the Solar System with laboratory electrochemical model experiments reproducing hydrothermal systems. Namely, electrochemical characterizations were conducted by using electrodes covered by sulfide minerals simulating hydrothermal deposits with electrolytes simulating hydrothermal fluids and seawaters. This presentation discusses electrocatalytic properties and potential power production of simulated hydrothermal systems with results of voltammetry tests and fuel cell polarization tests.

References: [1] Kumar, A. et al., (2017) Nature Reviews Chemistry 1, 0024. [2] Yamamoto, M. et al., (2018) ChemElectroChem 5. 2162-2166.

Keywords: the Solar System, hydrothermal system, fuel cell model, habitability, electrical energy

©2019. Japan Geoscience Union. All Right Reserved.

Experimental study of abiotic nitrate reduction at a high temperature and high-pressure condition and implication for nitrogen chemistry in Hadean hydrothermal environments

*Manabu Nishizawa[1], Takuya Saito[1], Akiko Makabe[1], Takazo Shibuya[1], Ken Takai[1]

1. Japan Agency for Marine-Earth Science and Technology

Nitrogen is an essential element for life as a major component of biomolecules and electron donor/acceptor for energy metabolism. Currently, nitrogen cycle in surface environments is mainly driven by biological processes including nitrogen fixation, nitrification and denitrification. In contrast, little is known about nitrogen cycle in the pre-biotic Earth and its relation to chemical evolution. This study focuses on nitrate chemistry during water-rock interaction in deep-sea hydrothermal environments to understand the fate of atmospherically-derived nitrate in the Hadean ocean. In experiments, artificial seawater with nitrate was reacted with synthetic komatiite at 350oC and 500 bar. Our experiments show that a substantial amount of nitrate was reduced to ammonium in an experimental condition. This implies that the Hadean deep-sea hydrothermal vents may have been favorable for chemical evolution in that both electron acceptor for energy metabolism (nitrate) and reduced nitrogen for organic synthesis (ammonium) were continuously supplied to the hydrothermal fluid-seawater mixing zone.

Keywords: prebiotic chemistry, nitrogen, deep sea hydrothermal vents

©2019. Japan Geoscience Union. All Right Reserved.

Interaction experiments between eucritic glass and 0.1 M NaCl aqueous solution at 300-500℃ and 1.5 kbar: Suggestions on water-rock interactions at the bottom of Europa’s subsurface ocean

*Makoto Nagasawa[1,2], Yutaro Takaya[1]

1. Department of Resources and Environmental Engineering, School of Creative Science and Engineering, Waseda University, 2. Department of Earth and Planetary Science, Graduate School of Science, The University of Tokyo

Europa, the second satellite of Jupiter, probably has subsurface ocean under its icy crust. The yellow-brown color of its leading anti-Jovian hemisphere could be explained by endogenous substances such as sodium chloride, which suggests the presence of hydrothermal activity (water-rock interaction) [Hand and Carlson, 2015]. In this study, we conducted water-rock interaction experiments to determine the mineral assemblage of altered rock on Europa’s mantle surface and to constrain the amount of available energy for sustaining the putative chemoautotroph-based ecosystems.

In our experiments, eucritic synthesis glass and 0.1 M NaCl aqueous solution were reacted at 300-500℃ and 1.5 kbar for 8, 16 and 32 days, using cold-seal type pressure vessels. The water/rock mass ratio was fixed at 1/1 in all the experiments (50 mg of powdered glass to 50 μL of NaCl solution). Solid products were analyzed by X-ray diffractometer and SEM equipped with EDS. Water chemistry of the reacted solution were determined by ICP-MS.

The mineral assemblages observed in our experiments were as follows.
・Fe-rich smectite (saponite), epistilbite and xonotlite at 300℃ and 1.5 kbar
・Fe-rich smectite (saponite), ferroactinolite, Ca-rich plagioclase and minor amount of magnetite at 400℃ and 1.5 kbar
・Mg-rich smectite, ferroactinolite, Ca-rich plagioclase, magnetite and hydroxyapatite at 500℃ and 1.5 kbar

The formation of magnetite at 400-500℃ suggests that these high-temperature water-rock interactions may generate hydrogen and sustain chemoautotroph-based ecosystems. As a future work, we would like to evaluate the hydrogen generation potential quantitatively.

Keywords: Europa, Water-rock interaction

©2019. Japan Geoscience Union. All Right Reserved.

Relationship between tellurium in the Fe-Mn oxides in the ocean and ambient seawater

*Yusuke Fukami[1], Teruhiko Kashiwabara[1], Hiroshi Amakawa[1], Takazo Shibuya[1], Akira Usui[2], Katsuhiko Suzuki[1]

1. Japan Agency for Marine-Earth Science and Technology, 2. Kochi University

Marine ferromanganese crusts (Fe-Mn crusts) are Fe-Mn oxides widely distributed on the seafloor, and important materials for (paleo)oceanographic studies (e.g. Hein et al., 2014). Tellurium (Te) is one of the highly enriched elements in the Fe-Mn crusts by more than ten thousand times relative to that in the continental crusts (Hein et al., 2010). Variation of concentration and isotopic compositions of Te in the Fe-Mn crusts could be a potential indicator for changes in redox condition of seawater, because of two valences of Te in ocean environments (+4 and +6; Lee and Edmond, 1985). In this study, we performed the measurement for concentration and isotopic compositions of Te in the surface layer of the Fe-Mn crusts, which was in contact with ambient seawater. The results were compared with the depth profile of the dissolved oxygen in the sampling site. To investigate the relationship to ambient seawater, the Fe-Mn crusts were sampled from two seamounts located in the Northwest Pacific, which showed different dissolved oxygen profile, and analyzed for Te concentration and isotopic compositions of the surface layer.

The results show that the correlation between the Te concentration and isotopic compositions in the surface layer of the Fe-Mn crusts changes depending on water depths. With increasing depths, the Te concentration decreases more drastically at shallower water depths than at deeper water depths. Moreover, the surface samples from two seamounts show a difference in the water depths where the concentration gradient of Te in the Fe-Mn crusts changes. The changes in the concentration gradient of Te in the Fe-Mn crusts may correspond to the changes in the chemical state of Mn in conjunction with the changes in the dissolved oxygen concentration in ambient seawater. Therefore, the Te concentration in the Fe-Mn oxides potentially indicates the dissolved oxygen concentration in the marine environment. The Fe oxides and Mn oxides are observed on the surface of the Mars by recent observation of exploration vehicles (e.g. Lanza et al., 2016), and the trace elements in these oxides potentially provide the information of water environments when they are formed. In the presentation, the results of the measurement of Te in natural samples, and laboratory experiment for application to Fe-Mn oxides on Mars will be discussed.

Keywords: tellurium, Fe-Mn oxides, ocean environment, Fe-Mn crusts, stable isotope

©2019. Japan Geoscience Union. All Right Reserved.

Laboratory reproduction of earthquake faulting beneath the internal ocean of Enceladus

*Takehiro Hirose[1], Takazo Shibuya[2]

1. Kochi Institute for Core Sample Research, Japan Agency for Marine-Earth Science and Technology, 2. Japan Agency for Marine-Earth Science and Technology

The discovery of the Na-rich ice particles erupting from the surface of Enceladus indicates the presence of hydrothermal activity in Enceladus' ocean. Knowledge of water chemistry of the interior ocean is crucial for exploring planetary habitability and life. Two different processes of water-rock interaction can define the water chemistry in Enceladus' ocean: one is the static chemical interaction at the hydrothermal regions over geological timescale, and the other is the dynamic chemical interaction associated with seismogenic faulting induced by tidal force between Enceladus and Saturn or neighboring satellites. In this study, we focus on the later short-time disequilibrium interaction between water-rock during faulting. By using high-velocity friction experiment, we plan to reproduce faulting processes that are expected to occur in the interior of Enceladus, and then evaluate quantitatively the effect of the disequilibrium interaction during faulting on the water chemistry of the interior ocean. In the poster, we will present outline of the apparatus and pilot results of the experiments using San Carlos olivine and synthetic chondrite as starting materials.

Keywords: Enceladus, earthquake faulting, hydrothermal

©2019. Japan Geoscience Union. All Right Reserved.

Why does Titan have an atmosphere, and why not Ganymede?—The origin of Titan-Ganymede dichotomy

*Yasuhito Sekine[1], Yuhiko Aoyama[2], Masahiro Ikoma[2], Takayuki Tanigawa[3]

1. Earth-Life Science Insitute, Tokyo Institute of Technology, 2. Dept. of Earth and Planetary Sci., University of Tokyo, 3. Section of Liberal Arts and Sciences, National Inst. of Tech., Ichinoseki College

One of the long-standing issues in planetary science is why Saturn's moon Titan possesses a thick atmosphere and why Jupiter's moon Ganymede not. These satellites are similar in size and mass; however, only Titan has active surface environments, characterized as a thick N_2 atmosphere and liquid CH_4 cycles. Since Titan's atmospheric N_2 originates from NH_3 (Niemann et al., 2005; Sekine et al., 2011), the building materials of Titan may have contained both NH_3 and CH_4 ices in addition to H_2O ice. Previous studies hypothesized that no condensation of NH_3 and CH_4 would have occurred in the circum-Jovian disk since proto-Jupiter might have formed in a relatively warm region of the protoplanetary disk (e.g., disk temperature > 100 K) (Lunine and Stevenson, 1982). However, recent disk models show that even at a few au, the disk temperature would have become sufficiently low (i.e., < 100 K) to form NH_3 and CH_4 ices in the disk (e.g., Dodson-Robinson et al., 2009; Oka et al., 2011), thereby calling for a new explanation. Here we show that gas and solids infalling onto massive proto-Jupiter would have experienced extensive shock heating (~10^4 K) upon accretion. The shock heating is sufficient to dissociate primordial NH_3 and CH_4 to thermochemically stable N_2 and CO, which cannot condensate in the circum-Jovian disk due to their low condensation temperatures. On the other hand, dissociation of NH_3 and CH_4 proceeds only incompletely upon accretion onto less massive proto-Saturn. Accordingly, the building materials of Saturn's icy moons contain abundance of survived NH_3 and CH_4 as ices. We suggest that giant planet's mass is a critical factor to determine the chemical compositions, surface environments, and potential habitability of the icy moons.

Dodson-Robinson et al. (2009) Icarus 200, 672
Lunine and Stevenson (1982) Icarus 52, 14
Niemann et al. (2005) Nature 438, 779
Oka et al. (2011) Astrophys. J. 738, 141
Sekine et al. (2011) Nature Geosci. 4, 359

Keywords: icy satellite, planetary atmosphere, planetary formation

©2019. Japan Geoscience Union. All Right Reserved.

Development of observation system of gas hydrate forming in the environment simulated near the bottom of icy shell in icy bodies (2)

*Atsushi Tani[1], Kenshiro Moriyama[1]

1. Graduate School of Human Development and Environment, Kobe University

Gas hydrates are clathrate compounds where hydrogen-bonded water cages include a guest gas molecule. Methane hydrate is one of famous gas hydrates because it is naturally found in deep-sea and permafrost sediments on the Earth. Gas hydrates would exist in icy bodies as well. One of the candidates is Pluto where the presence of subsurface ocean is suggested. Gas hydrates may exist between the ice shell and subsurface ocean and play an important role as insulator to keep warm inside. The presence of subsurface ocean is also suggested in some icy satellites like Enceladus. INMS (Ion and Neutral Mass Spectrometer) aboard the Cassini spacecraft has investigated composition of the plumes there that includes H2O (< 90 %), CH4, CO2, NH3, and other various organic materials. These results could reflect the composition of the subsurface ocean and imply the presence of clathrate hydrates in the ocean. Density of gas hydrates depends on guest gas molecules. For example, methane hydrate is lighter than the water, whereas CO2 hydrate is heavier. If CO2 hydrate forms at the bottom of the icy shell, the average density may become large and the ice (water ice + CO2 hydrate) may start to sink locally. If the size of each gas hydrate become small and granular gas hydrates exist in subsurface ocean, heat can be transfer by not only thermal conduction but also convection. This means that icy bodies may be cooled faster. To elucidate how gas hydrates form in the subsurface ocean in icy bodies, we have developed the observation system of gas hydrate formation and dissociation below the ice sheet. In the presentation, we report the progress of the observation system.

Keywords: icy bodies, gas hydrate, crystal growth

©2019. Japan Geoscience Union. All Right Reserved.

Rheology of non-water ices inferred from diffusion coefficients: A compilation study

*Naoki Noguchi[1]

1. Graduate School of Technology, Industrial and Social Sciences, Tokushima University

Non-water ices such as solid N_2, CO, CO_2, CH_4, and clathrate hydrates are a main constituent of the surfaces and crusts of the icy bodies. Understanding rheological properties of them are essential to understanding the dynamics including thermal convection, flow of glacier, and relaxation of topography. Several researchers investigated the rheological properties of them directly by low-temperature deformation experiments: solid N_2, CH_4 (Yamashita et al. 2010), CO_2 (Yamashita and Kato 1997, Durham et al. 1999), and CH_4 clathrate hydrate (Durham et al. 2003). They revealed the viscosities and plastic deformation mechanisms with a stress exponent of $n > 2$ in the range of 0.1 −100 MPa. However, the deformation experiment at low-stress conditions below 0.1 MPa is technically very difficult. The extrapolation of the plastic-flow law under their mechanisms to the low stress conditions may give an overestimate for the viscosity, because the diffusion creep can dominate in the low stress conditions below 0.1 MPa Under the diffusion creep regime, the viscosity behaves as Newtonian fluid, and is sensitive to the grain size. Although the viscosity under the diffusion creep regime cannot be measured directly, it can be estimated from diffusion coefficients based on the theories of diffusion creep (Frost and Ashby 1982). I will discuss the rheological properties of non-water ices inferred from the diffusion coefficients. There are many non-water ices whose diffusion coefficients have not determined yet by experiments. This substance includes solid CO and clathrate hydrates. In the case of molecular solids, the diffusion enthalpy has a correlation with the sublimation enthalpy (Chadwick and Sherwood 1971). I estimated the diffusion coefficients using the correlation in order to infer the rheological property.

Keywords: Non-water ice, Rheology, Diffusion, Icy body

©2019. Japan Geoscience Union. All Right Reserved.

Swelling behavior of magnesium saturated smectites

Morida Koki, Keisuke Fukushi, Hiroshi Sakuma

*Koki Morida[1]

1. Kanazawa University

Smectite belongs to clay minerals formed in the presence of liquid water. Smectites are composed of 2:1 layer with tetrahedral sheet and octahedral sheet. Smectites are categorized to di-octahedral type (e.g., nontronite and montmorillonite) and tri-octahedral type (e.g. saponite). The interlayer between the sheets is occupied by hydrated cations. The interlayer cations are usually Na^{+}, K^{+}, Mg^{2+}, Ca^{2+}. The distances of interlayer (basal spacing) depend on type of interlayer cations and relative humidity (RH). The basal spacing can change from 9 to 15 Å as function of amount of RH. At 0% of RH, basal spacings are around 10 Å when interlayer cation is Na^{+} or K^{+}. That is 12 Å when interlayer cation is Ca^{2+}. On the other hand, the basal spacings ranges from 11 to 14 Å when interlayer cation is Mg^{2+} (Sato et al, 1992; Morodome and Kawamura 2009).

Curiosity rover sent to the Gale crater on mars examines the possibility of existence of life and habitable environment (Vaniman et al, 2014). Water is essential for life. Therefore, in order to estimate possibility of life, it is important to know water quality. Gale crater is thought to be an ancient lake. Curiosity obtained the lacustrine sediment samples and analyzed the mineralogical and geochemical characteristics of the sediments. From the CheMin-XRD analyses, smectites were discovered in JohnKlein and Cumberland sites. The smectites are presumed to be saponite (Vaniman et al, 2014; Bristow et al, 2015). The basal spacing in Cumberland’s saponite exhibited 13.2 Å at RH0%. Now it has been under debates whether the interlayer cation in Cumberland’s saponite is $MgOH^{+}$ or Mg^{2+} ion.

Suquet et al, 1975 showed that basal spacing of Mg^{2+} saturated saponite is 11.4 Å at RH0%. Therefore, Vaniman et al. 2014 and Bristow et al, 2015 presumed that the interlayer cation in Cumberland’s saponite is $MgOH^{+}$ ion. However, basal spacing of some other Mg^{2+} saturated smectites exhibited above 13.2 Å. This study experimentally assess the basal spacing of smectites including saponite under several atomospheric compositions with N_2, air or CO_2.

©2019. Japan Geoscience Union. All Right Reserved.

Possibility of hydrogen peroxide as a warming agent on early Mars with oxidized condition

*Yuichi Ito[1], George HASHIMOTO[2], Yoshiyuki O. Takahashi[3], Masaki Ishiwatari[1], Kiyoshi Kuramoto[1]

1. Department of Cosmosciences, Graduate school of Science, Hokkaido University, 2. Department of Earth Sciences, Okayama University, 3. Graduate School of Science, Kobe University

Recently, Lanza et al. (2016) reported the detection of the high Mn-oxides abundances of Martian rocks in Gale Crater, where preserves the past martian surface environment during 3–4 Ga. This observation suggests that both liquid water and a highly oxidized atmosphere existed on early Mars, since the precipitation of such a Mn-oxide-rich rock requires highly oxidizing condition in water. On the other hand, the Solar luminosity at 4 Ga would be only 75 % of the current value. Due to this, it is thought that additional greenhouse components in CO2–H2O atmospheres could have played a key role for warming on early Mars on the basis of climate models (e.g., Kasting 1991). However, no previous atmospheric models have shown that highly oxidized atmosphere can warm the mean surface temperature of early Mars above 273 K. As a gaseous material oxidizing martian surface, hydrogen peroxide, H2O2, has been received attention (e.g., Zahnle et al. 2008) On the other side, anyone does not focus on H2O2 as a greenhouse gas, owing to the extremely low abundance in the current Martian atmosphere. Although hydrogen peroxide is photo-chemically unstable, its absorption for far-infrared radiation per a molecule is very strong. Thus, hydrogen peroxide might warm early Mars, if the atmosphere was highly oxidized.
To test this idea, we use a 1-D atmospheric energy balance model with a line-by-line radiative transfer calculation. Then, by parameterizing the abundance of H2O2 in a CO2-dominant atmosphere, we estimate how much the surface temperature is warmed. We found that the temperature increased at most only 3 K, in the case of the atmosphere with the saturated abundance of H2O2. On the other hand, when the abundance of condensation nuclei in the upper atmosphere is low, H2O2 is expected to be possibly super-saturated. In the case of the atmosphere with pressure of > 2bar and 1 ppm H2O2, the surface temperature can exceed 273 K. Also, in the case for 10 ppm H2O2, at least 1 bar atmosphere is required to warm the surface temperature above 273 K. In particular, for the 2 bar atmospheres including H2O2 with a molar fraction of 1 ppm and 10 ppm, the surface temperatures increase about 40 K and 80 K from 230 K, respectively. In this presentation, we will discuss about the possibility that H2O2 concentrates to be super-saturated from the view of photochemical production and condensation processes.

Keywords: Mars, Liquid water, Atmosphere

©2019. Japan Geoscience Union. All Right Reserved.

[J] Oral | M (Multidisciplinary and Interdisciplinary)：M-IS Intersection

Tue. May 28, 2019 10:45 AM - 12:15 PM JST | Tue. May 28, 2019 1:45 AM - 3:15 AM UTC | A02 TOKYO BAY MAKUHARI HALL

[M-IS21] Gas hydrate in environmental-resource sciences

convener:Hitoshi Tomaru(Department of Earth Sciences, Chiba University), Akihiro Hachikubo(Kitami Institute of Technology), Atsushi Tani(Graduate School of Human Development and Environment, Kobe University), Shusaku Goto(Institute for Geo-Resources and Environment National Institute of Advanced Industrial Science and Technology), Chairperson:Naoto Ishida, 戸丸 仁

An increasing number of researches focusing on natural gas hydrates has recently been conducted from the environmental, material, and resource scientific viewpoints. This session aims to share and discuss the latest research results associated with natural/experimental gas hydrates to understand and examine the nature and potential of gas hydrates in the past-present-future of the Earth and the development/application for our life. Because the researches on gas hydrates are interdisciplinary, broad topics from field and experimental researches, modeling, etc. will be presented in this session.

10:45 AM - 11:00 AM JST | 1:45 AM - 2:00 AM UTC

[MIS21-01] Equilibrium pressure of clathrate hydrates encaged $^{13}CH_4$

*Yuki Kikuchi[1], Akihiro Hachikubo[1], Takahiro Ozeki[1], Satoshi Takeya[2] (1.Kitami Institute of Technology, 2.National Institute of Advanced Industrial Science and Technology (AIST))

11:00 AM - 11:15 AM JST | 2:00 AM - 2:15 AM UTC

[MIS21-02] Hydrogen isotopic fractionation of ethane encaged in different crystallographic structure

*Jumpei Matsuda[1], Akihiro Hachikubo[1], Satoshi Takeya[2] (1.Kitami Institute of Technology, 2.National Institute of Advanced Industrial Science and Technology (AIST))

11:15 AM - 11:30 AM JST | 2:15 AM - 2:30 AM UTC

[MIS21-03] Trend of effect of temperature on C–H symmetric stretching vibrational frequencies of hydrocarbon molecules in 12, 14 and 16-hedra cages of gas hydrates

*Go Fuseya[1], Satoshi Takeya[2], Akihiro Hachikubo[1] (1.Kitami Institute of Technology, 2.National Institute of Advanced Industrial Science and Technology (AIST))

11:30 AM - 11:45 AM JST | 2:30 AM - 2:45 AM UTC

[MIS21-04] The study on relations of the methane plume and atmospheric methane concentration

*Chiharu Aoyama[1] (1.Tokyo University of Marine Science and Technology)

11:45 AM - 12:00 PM JST | 2:45 AM - 3:00 AM UTC

[MIS21-05] Sampling of Methane Bubble Plumes and Solid Gas Hydrate on the Cascadia Margin, Pacific Northwest

*John E Lupton[1], Tamara Baumberger[1], Robert W. Embley[1], Susan G. Merle[1], Camilla Wilkinson[1], Conrad Young[2] (1.NOAA Pacific Marine Environmental Laboratory, Newport, Oregon, USA, 2.Young Engineering, Ramona, CA. USA)

12:00 PM - 12:15 PM JST | 3:00 AM - 3:15 AM UTC

Discussion

Equilibrium pressure of clathrate hydrates encaged $^{13}CH_4$

*Yuki Kikuchi[1], Akihiro Hachikubo[1], Takahiro Ozeki[1], Satoshi Takeya[2]

1. Kitami Institute of Technology, 2. National Institute of Advanced Industrial Science and Technology (AIST)

Methane molecule is composed of carbon and hydrogen, and three kinds of isotopologues, $^{12}CH_4$ (98.9%), $^{13}CH_4$ (1.1%), and CH_3D (0.013%) exist in nature. We often measure stable carbon isotope ($^{13}C/^{12}C$) of methane to understand its gas origin. Since their weight of isotopologues differ with each other, physicochemical properties of them are also different. Pure methane hydrate must be "mixed-gas hydrate" of their isotopologues. Ozeki *et al.* (2018) measured an equilibrium pressure of CH_3D hydrate, but that of $^{13}CH_4$ has not been studied yet. Fractionation of hydrogen isotope of methane during the formation of methane hydrate has been reported by Hachikubo *et al.* (2007) that δ D of hydrate-bound methane becomes several ‰smaller than that of residual methane. This result suggests that the equilibrium pressure of CH_3D hydrate is larger than that of CH_4 hydrate, and Ozeki *et al.* (2018) demonstrated the difference between these equilibrium pressures. Since Hachikubo *et al.* (2007) showed no isotopic fractionation in methane $\delta^{13}C$, the equilibrium pressures of $^{12}CH_4$ and $^{13}CH_4$ hydrates are thought to be almost the same. In this study, we measured the equilibrium pressures of $^{13}CH_4$ hydrate to check the difference from that of $^{12}CH_4$ hydrate.

Methane hydrate samples were synthesized in small pressure cells (volume: 5 mL). Fine ice powder (1g) was put in a pressure cell, and introduced $^{13}CH_4$ (purity: 99.5%, Taiyo-Nissan). Clathrate hydrate was formed by melting the ice powder at the temperature of 273.2K under high pressure of methane. We also prepared normal methane (purity: 99.99% for methane, but 98.9% for $^{12}CH_4$, Takachiho Chemical Industry Co. Ltd.) hydrate as a reference, using the same preparation method. These pressure cells were placed in a temperature-controlled liquid bath, and measured their equilibrium pressures from 269.5K to 277.9K.

The difference in equilibrium pressure between $^{13}CH_4$ and normal methane (mainly $^{12}CH_4$) hydrates was smaller than the measurement error. This results agree with the previous report by Hachikubo *et al.* (2007).

References

Ozeki T, Kikuchi Y, Takeya S, Hachikubo A (2018) Phase equilibrium of isotopologue methane hydrates enclathrated CH_3D and CD_4. J Chem Eng Data 63(6): 2266-2270, doi: 0.1021/acs.jced.8b00203

Hachikubo A, Kosaka T, Kida M, Krylov A, Sakagami H, Minami H, Takahashi N, Shoji H (2007) Isotopic fractionation of methane and ethane hydrates between gas and hydrate phases. Geophys Res Lett 34: L21502. doi:10.1029/2007GL030557

Keywords: gas hydrate, methane hydrate, equilibrium pressure, stable isotope

©2019. Japan Geoscience Union. All Right Reserved.

Hydrogen isotopic fractionation of ethane encaged in different crystallographic structure

*Jumpei Matsuda[1], Akihiro Hachikubo[1], Satoshi Takeya[2]

1. Kitami Institute of Technology, 2. National Institute of Advanced Industrial Science and Technology (AIST)

Methane and ethane mixed-gas hydrate forms the cubic structure II in appropriate gas composition. Hachikubo *et al.* (2009) measured isotopic compositions of Lake Baikal gas hydrates and showed that δD of hydrate-bound ethane in the structure II is smaller than that in the structure I. These results might be explained by the difference in hydrogen isotope fractionation between formation processes of the structure I and II. In the last JpGU meeting we reported that the isotopic difference between gas and hydrate phases increased to 9-12‰ in the case of the structure II, whereas the difference was 1-2‰ in the case of the structure I. However, the effect of methane on the isotopic fractionation of ethane is unknown. In this study, we choose argon instead of methane and synthesize argon and ethane mixed-gas hydrates to check the isotopic difference in ethane between gas and hydrate phases.

0.7 g of fine ice powder was introduced in a pressure cell (volume: 30 mL). Argon and ethane mixed-gas were introduced in the cell and gas hydrate sample formed at 274.2 K. Before the retrieval of gas hydrate sample, residual gas was sampled, and then gas hydrate was cooled at the temperature of liquid nitrogen and retrieved the hydrate-bound gas. We controlled the ethane composition of initial gas from 3% to 25%. We measured compositions of argon and ethane by a gas chromatograph, and hydrogen isotopic composition (δD) of ethane by a CF-IRMS. Crystallographic structure of gas hydrate was determined using a Raman spectrometer, because the Raman spectra (around 1000 cm^{-1}) of C-C stretching mode of ethane in hydrate phase provide information of the crystallographic structure.

Because ethane was concentrated into hydrate phase rather than argon, ethane compositions of hydrate-bound gas distributed from 30% to 71%. In the case of low concentration of ethane, crystallographic structure II forms due to the effect of argon (the structure II former). δD of hydrate-bound ethane was about 4-7‰ smaller than that of residual ethane in the case of structure II, where ethane composition was 30-36% in the hydrate phase. On the other hand, in the case of high concentration of ethane (around 70% in the hydrate phase) δD of hydrate-bound ethane was around 2‰ larger than that of residual ethane. In the transition zone between the structures I and II the isotopic difference between hydrate and residual gas phases seemed to be an intermediate value (1-4‰). From these results we can conclude that light ethane (C_2H_6) prefers to be encaged into the structure II clathrate hydrate, compared to heavy ethane (C_2H_5D).

Reference

Hachikubo A, Khlystov O, Manakov A, Kida M, Krylov A, Sakagami H, Minami H, Takahashi N, Shoji H, Kalmychkov G, Poort J (2009) Model of formation of double structure gas hydrates in Lake Baikal based on isotopic data. Geophys Res Lett 36: L18504. doi:10.1029/2009GL039805

Keywords: gas hydrate, ethane, hydrogen isotope ratio

©2019. Japan Geoscience Union. All Right Reserved.

©2019. Japan Geoscience Union. All Right Reserved.

Trend of effect of temperature on C–H symmetric stretching vibrational frequencies of hydrocarbon molecules in 12, 14 and 16-hedra cages of gas hydrates

*Go Fuseya[1], Satoshi Takeya[2], Akihiro Hachikubo[1]

1. Kitami Institute of Technology, 2. National Institute of Advanced Industrial Science and Technology (AIST)

Clathrate hydrates are crystalline inclusion compounds that consist of guest molecules of suitable sizes and shapes trapped in well-defined cages formed by water molecules. Clathrate hydrates with natural gases as guest molecules are commonly known as gas hydrates. Gas hydrates with enclathrated hydrocarbon gases that exist in sea or lake bottom sediments and permafrost layers have attracted considerable interest as a potential source of unconventional natural gas.

There are three common crystallographic structures of hydrates, structure I (sI), structure II (sII), and structure H (sH). The unit cell of sI hydrates are composed of two pentagonal dodecahedral (5^{12}) and six tetrakaidecahedral ($5^{12}6^2$) water cages. The unit cell of sII hydrates are composed of sixteen 512 cages and eight hexakaidecahedral ($5^{12}6^4$) water cages. Small guest molecules such as methane (CH_4) or ethane (C_2H_6) form sI hydrates and larger molecules such as propane (C_3H_8) form sII hydrates.

In this study, we observed the variations of Raman shifts of C–H symmetric stretching vibrations of various hydrocarbons encaged in $5^{12,}$ $5^{12}6^2$ and $5^{12}6^4$ cages of sI and sII hydrates. By changing temperature, we investigated variations of Raman shifts of C–H symmetric stretching vibrations of guest hydrocarbons. It was revealed that the vibrations of guest hydrocarbons in smaller sI 51262 cages were greater than those in bigger sII 51264 cages. These results are inconsistent with our prediction in earlier study (Fuseya et al. 2018), that is, the volume of host water cages increases, and the variations of the Raman shifts of C–H symmetric stretching vibrations of guest hydrocarbon molecules in host water cages due to change temperature increase. Taking into account the facts obtained in this study and in our earlier study, we conclude that the temperature change of Raman shifts of C–H symmetric stretching vibrations is affected by geometric asymmetry of host water cages.

Reference

Sloan and Koh (2008) Clathrate Hydrates of Natural Gases, 3rd ed., CRC Press: Boca Raton, FL, USA

Fuseya *et al.* (2018) Effect of temperature and large guest molecules on the C–H symmetric stretching vibrational frequencies of methane in structure H and I clathrate hydrates. *RSC Adv.* **8**: 3237-3242. doi: 10.1039/c7ra12334e

Keywords: gas hydrate, Raman spectroscopy, powder X-ray diffraction, molecular vibrations

©2019. Japan Geoscience Union. All Right Reserved.

The study on relations of the methane plume and atmospheric methane concentration

*Chiharu Aoyama[1]

1. Tokyo University of Marine Science and Technology

PurposeWhen methane seeps out to the sea from the seabed, the following need to be observed and confirmed if the water concentration remains the same. High methane concentration in the atmosphere directly above the seeping point and separation of methane hydrate into gas and water. Then, by confirming the impact on the environment, we propose a survey method for environmental impact assessment of surface methane hydrate.**Method**The experimental site of this research was Umitaka Spur in offshore Niigata prefecture where a large amount of surface methane hydrate plumes is confirmed and investigated on the DAIIICHI KAIYOMARU(KAIYO Engineering). The experimental period was two days, August 6 and August 7.Atmospheric methane concentration was measured during this experiment using LI-7700 (LI-COR) which introduced Flux measurement to measure ppm of specific substances present in the atmosphere. Methane concentration was measured by LI-7700 which was attached to the upper bridge so it will not be affected by the exhaust of the ship. We measure the concentration of methane in the atmosphere from departure to arrival and graphed the data every hour.Using a quantitative echo sounder, we also explored if methane plumes exist underwater the atmospheric methane concentration becomes higher.**Summary** Methane concentration in the atmosphere of the sea, the area near directly above, in the sea area where the methane seeps from the seabed to the sea tends to rise. **Proposal for environmental impact assessment** When extracting surface methane hydrate and at experimental stages at sea, it is effective to monitor methane concentration on the sea, not in the seawater to detect sudden seepage of methane into seawater as soon as possible. Even if methane hydrate leaks into the sea, there is no change in sodium concentration, so we do not have be concerned about the influence on the environment.

Keywords: methaneplume, methane concentration in atmosphere, Japan sea

©2019. Japan Geoscience Union. All Right Reserved.

Sampling of Methane Bubble Plumes and Solid Gas Hydrate on the Cascadia Margin, Pacific Northwest

*John E Lupton[1], Tamara Baumberger[1], Robert W. Embley[1], Susan G. Merle[1], Camilla Wilkinson[1], Conrad Young[2]

1. NOAA Pacific Marine Environmental Laboratory, Newport, Oregon, USA, 2. Young Engineering, Ramona, CA. USA

The Cascadia Margin along California, Oregon, and Washington is host to hundreds of offshore methane seeps that produce bubble streams that ascend through the water column. In addition to the bubble streams, seismic reflection studies have detected the presence of extensive methane hydrate deposits beneath the seafloor. There are also a few sites along the Cascadia Margin where hydrate deposits are exposed and visible on the seafloor. During an expedition in 2016, our group used an ROV to collect uncontaminated samples of the bubble stream gas at several Cascadia Margin sites using special gas-tight bottles. Although we have successfully obtained samples of the bubble streams, the question remains as to whether the bubble streams are produced by the dissociation of hydrate, or instead represent free gas ascending through the sediment. We have developed a new sampler in which small samples of hydrate can be hermetically sealed into a small gas-tight volume in-situ while incorporating only a small amount of ambient seawater. The hydrate is then allowed to dissociate in the sample volume without exposure to air or other contaminates. During a return expedition to the Cascadia margin in June 2018 we successfully sampled solid methane hydrate at two sites using this new sampler and also collected additional samples of the free gas bubble streams. The paper will compare the results from these hydrate collections with the composition of the free gas.

Keywords: methane, hydrate, Cascadia Margin

©2019. Japan Geoscience Union. All Right Reserved.

[J] Oral | M (Multidisciplinary and Interdisciplinary)：M-IS Intersection

Tue. May 28, 2019 1:45 PM - 3:15 PM JST | Tue. May 28, 2019 4:45 AM - 6:15 AM UTC | A02 TOKYO BAY MAKUHARI HALL

[M-IS21] Gas hydrate in environmental-resource sciences

convener:Hitoshi Tomaru(Department of Earth Sciences, Chiba University), Akihiro Hachikubo(Kitami Institute of Technology), Atsushi Tani(Graduate School of Human Development and Environment, Kobe University), Shusaku Goto(Institute for Geo-Resources and Environment National Institute of Advanced Industrial Science and Technology), Chairperson:八久保 晶弘(北見工業大学), 戸丸 仁

An increasing number of researches focusing on natural gas hydrates has recently been conducted from the environmental, material, and resource scientific viewpoints. This session aims to share and discuss the latest research results associated with natural/experimental gas hydrates to understand and examine the nature and potential of gas hydrates in the past-present-future of the Earth and the development/application for our life. Because the researches on gas hydrates are interdisciplinary, broad topics from field and experimental researches, modeling, etc. will be presented in this session.

1:45 PM - 2:00 PM JST | 4:45 AM - 5:00 AM UTC

[MIS21-06] The distribution of atmospheric CH_4 concentration and gas plume location in the sea around Japanese islands.

*Shinsuke Aoki[1], Shujiro Komiya[2], Kosuke Noborio[3], Ryo Matsumoto[4] (1.Graduate School of Agriculture, Meiji Universiy, 2.Max Planck Institute, 3.School of Agriculture, Meiji Universiy, 4.Gas Hydrate Laboratory - Meiji University Organization for the Strategic Coordination of Research and Intellectual Property)

2:00 PM - 2:15 PM JST | 5:00 AM - 5:15 AM UTC

[MIS21-07] Reaction/fixation/migration of methane within the gas chimney on the Umitaka Spur, eastern margin of the Japan Sea

*Hitoshi Tomaru[1], Ryo Matsumoto[2] (1.Department of Earth Sciences, Chiba University, 2.Gas Hydrate Research Laboratory, Meiji University)

2:15 PM - 2:30 PM JST | 5:15 AM - 5:30 AM UTC

[MIS21-08] Slope failures induced by methane hydrate dissociation: a case of submarine slide in the southwestern Oki Trough, Japan Sea

*Naoto Ishida[1], Shota Morihita[2], Takao Ebinuma[1], Hitoshi Tomaru[3], Ryo Matsumoto[4] (1.Social Systems and Civil Engineering, Graduate School of Engineering, Tottori University, 2.Department of Social Systems and Civil Engineering, Faculty of Engineering, Tottori University, 3.Department of Earth Sciences, Faculty of Science, Chiba University, 4.Gas Hydrate Research Laboratory, Organization for the Strategic Coordination of Research and Intellectual Properties, Meiji University)

2:30 PM - 2:45 PM JST | 5:30 AM - 5:45 AM UTC

[MIS21-09] Origin and evolution of H_2S-bearing methane hydrate in the Sea of Japan

*Ryo Matsumoto[1], Tomoko Fukazawa[2], Akihiro Hiruta[1], Glen Snyder[1] (1.Organization for the Strategic Laboratory of Research and Intellectual Properties, Meiji University, 2.Department of Applied Chemistry, School of Science and Technoloty, Meiji University)

2:45 PM - 3:00 PM JST | 5:45 AM - 6:00 AM UTC

[MIS21-10] Discovery of gas hydrate at the new point off Abashiri, the Sea of Okhotsk

*Akihiro Hachikubo[1], Jumpei Matsuda[1], Satoshi Yamashita[1], Hirotoshi Sakagami[1], Masaaki Konishi[1], Hirotsugu Minami[1], Kenji Nishina[2], Kenji Sakaguchi[3] (1.Kitami Institute of Technology, 2.Geological Survey of Hokkaido, Hokkaido Research Organization, 3.Kushiro Fisheries Research Institute, Hokkaido Research Organization)

3:00 PM - 3:15 PM JST | 6:00 AM - 6:15 AM UTC

[MIS21-11] All about gas hydrates and heat flow offshore Chile

*LUCIA ALEJANDRA VILLAR MUNOZ[1], IVAN VARGAS-CORDERO[2], JOAQUIM P. BENTO[3], JAN BEHRMANN[1], UMBERTA TINIVELLA[4], MICHELA GIUSTINIANI[4] (1.Helmholtz Centre for Ocean Research, 2.Universidad Andres Bello , 3.Pontificia Universidad Catolica de Valparaiso, 4.Istituto Nazionale di Oceanografia e di Geofisica Sperimentale)

The distribution of atmospheric CH_4 concentration and gas plume location in the sea around Japanese islands.

*Shinsuke Aoki[1], Shujiro Komiya[2], Kosuke Noborio[3], Ryo Matsumoto[4]

1. Graduate School of Agriculture, Meiji Universiy, 2. Max Planck Institute, 3. School of Agriculture, Meiji Universiy, 4. Gas Hydrate Laboratory - Meiji University Organization for the Strategic Coordination of Research and Intellectual Property

In previous studies, methane emissions from the seabed have been reported worldwide. The reports that methane reached the atmosphere are limited to some sea areas with shallow water depths in the Arctic Ocean. Most of the researches reported that methane does not reach the atmosphere in many other sea areas and is decomposed in the water column. However, a methane hydrate shell is formed on the surface of methane bubbles released from the seabed in the gas hydrate stability zone. The methane hydrate shell delays the dissolution of methane in the water column. Therefore, a system efficiently transports methane to a shallow location in the ocean. It is difficult to clarify the amount of methane carried by this transport system and it is pointed out that some methane may release into the atmosphere. As methane is one of the greenhouse gases like carbon dioxide, release to the atmosphere leads to an increase in atmospheric concentrations and can be a cause of climate change. On the other hand, if an increase in atmospheric concentration occurs, there is a possibility that it can help in searching the methane hydrate-bearing area from the observation with the artificial satellite. Our objectives were to investigate the influence of gas seep from the sea floor on atmospheric methane concentration. In this study, we performed continuous measurement of atmospheric methane concentration, observed gas plume and measured water temperature profile by CTD. The survey area is the Japan Sea (7 K 14 and 7 K 15 cruises) where the gas plumes were reported and the Pacific Ocean (MR 15 - 3, KH 16 - 3, KH 17 - 3 cruise) as the control area. The upper limit of the stable region of methane hydrate was estimated from the water temperature profile by CTD and the phase equilibrium curve of methane hydrate in seawater for each sea area. Atmospheric methane concentration observed in the Pacific Ocean at 1.9 ppm slightly higher than the average concentration of the whole earth. Atmospheric methane concentration observed around the Japanese islands was also the mode of 1.9 ppm, which was the highest in methane concentration (> 2.1 ppm) compared with other sea areas only in the Mogami trough and off Abashiri. As gas plume was observed in these two regions, it seems that capture the influence of the gas plume on the atmosphere. However, since the methane concentration observed in other gas plume sites (off Tokachi and off Hidaka) was almost unchanged from those in which no gas plume was observed, all gas plumes did not always influence atmospheric concentrations. A high methane concentration was observed only the surrounding of the gas plume at Mogami trough and off Abashiri. However, high concentrations are not always observed when passing through the same gas plume point, but different concentrations are observed depending on time. This is considered to be caused by the methane discharged from the sea floor is flowed by ocean currents and offshore winds, and the amount of methane discharged has changed. The upper limit of the gas hydrate stability estimated from the water temperature profile was slightly shallow in off Abashiri and Mogami trough. Heeschen et al. (2003) reported that the height of the gas plume coincided with the water depth at the upper limit of the gas hydrate stability, but the gas plume observed shallower than a depth of the upper limit off Abashiri. This results suggested that methane emitted from the seafloor reaches the atmosphere at not only the gas plume with shallow water depth but the gas plume with a shallow upper limit of the gas hydrate stability. This study was conducted under the commission from AIST as a part of the methane hydrate research project funded by METI (the Ministry of Economy, Trade, and Industry, Japan). We appreciate the support of the crew during 7K14, 7K15,

©2019. Japan Geoscience Union. All Right Reserved.

MR15-3, KH16-3, and KH17-3 cruise.

Keywords: gas hydrate, gas plume, methane (CH4)

©2019. Japan Geoscience Union. All Right Reserved.

Reaction/fixation/migration of methane within the gas chimney on the Umitaka Spur, eastern margin of the Japan Sea

*Hitoshi Tomaru[1], Ryo Matsumoto[2]

1. Department of Earth Sciences, Chiba University, 2. Gas Hydrate Research Laboratory, Meiji University

Pore water geochemistry has reported that methane is oxidized anaerobically by sulfate (anaerobic oxidation of methane: AOM) at the sulfate-methane interface (SMI), and the methane flux has been estimated using the sulfate gradient or SMI depth. The methane flux is therefore an essential factor for assessing the near-seafloor environment of high methane potential area. Gas chimney, characterized by active methane migration, often associates with methane hydrate accumulation just below the seafloor and methane plume in the overlying water column on the Umitaka Spur, eastern margin of the Japan Sea. However, the behavior of these methane cannot be examined by the change of sulfate concentration, direct measurements of the amount of methane in hydrate phase and methane seepage are required. In this research, we estimated the amount of methane that is 1) oxidized at SMI via AOM, 2) fixed in gas hydrate deposit, and 3) released into water column, using independent data sets recently obtained on the Umitaka Spur, respectively, in order to understand more practically the behavior of methane within the gas chimney.
The methane flux oxidized at the SMI was calculated to be >600 mmol/m^2/yr using the SMI depth of <1 mbsf within the gas chimney. Assuming that the methane flux has been constant and all the methane has formed hydrates of 6×10^8 m^3 within 200×250 m gas chimney in <363 ka (data from METI coring), the methane flux directly associated with hydrate was estimated to be >1500 mmol/m^2/yr. The methane flux released into the water column was calculated to be <5 mmol/m^2/yr using the methane concentration in bottom water of <1500 nM and bottom water current of <10 cm/s. These numbers are still tentative because sedimentation rate within gas chimney is rather variable among sites, gaseous methane in sediment must be accounted, a part of methane hydrate has dissolved during massive accumulation of hydrate body, etc. However, recent intensive researches on the shallow gas hydrate system have provided the better understanding of total methane behavior within the gas chimney.
This study was conducted partially under the commission from AIST as a part of the methane hydrate research project funded by METI (the Ministry of Economy, Trade and Industry, Japan).

Keywords: gas hydrate, methane flux, Japan Sea

©2019. Japan Geoscience Union. All Right Reserved.

Slope failures induced by methane hydrate dissociation: a case of submarine slide in the southwestern Oki Trough, Japan Sea

*Naoto Ishida[1], Shota Morihita[2], Takao Ebinuma[1], Hitoshi Tomaru[3], Ryo Matsumoto[4]

1. Social Systems and Civil Engineering, Graduate School of Engineering, Tottori University, 2. Department of Social Systems and Civil Engineering, Faculty of Engineering, Tottori University, 3. Department of Earth Sciences, Faculty of Science, Chiba University, 4. Gas Hydrate Research Laboratory, Organization for the Strategic Coordination of Research and Intellectual Properties, Meiji University

A huge submarine slide in the Oki Trough, Japan Sea, was examined from the viewpoint of methane hydrate dissociation due to BGHS (Base of Gas Hydrate Stability) fluctuation. The submarine slide, which occurred 34 ka, is located in the southwestern slope of the Oki Trough having a 1.6 degrees slant. Geothermal gradients were measured at the 700 m and 1000 m water depths by the side of the slide as 83.13 mK/m and 99.42 mK/m, respectively. Based on our simulation, the BGHS was situated just below the landslide masses at the time of the slope failure. The response of BGHS to the external factors, e.g. sea-level change, sedimentation, etc., is prominently involved in methane hydrate disassociation, which makes the submarine ground unstable. Relation between the slope failure and the methane hydrate disassociation is strongly suggested in the study case.

Unpublished data by surveys conducted under the commission from AIST as a part of the methane hydrate research project funded by the Ministry of Economy, Trade and Industry, Japan was used in this study.

Keywords: base of gas hydrate stability, submarine slide, shallow-type methane hydrate, Oki Trough, Japan Sea

©2019. Japan Geoscience Union. All Right Reserved.

Origin and evolution of H_2S-bearing methane hydrate in the Sea of Japan

*Ryo Matsumoto[1], Tomoko Fukazawa[2], Akihiro Hiruta[1], Glen Snyder[1]

1. Organization for the Strategic Laboratory of Research and Intellectual Properties, Meiji University, 2. Department of Applied Chemistry, School of Science and Technoloty, Meiji University

Thick massive deposits of hydrates of the Sea of Japan have accumulate in gas chimneys in two steps. The first step is related to a 25 million years' rifting of the Sea of Japan, characterized by a high heat flows, high TOC sediments and a tectonic inversion at a few million years ago. Tectonic inversion has developed deep reverse faults and tight folds with open fracture systems, which facilitated the development of gas chimney structures. Second one is a glacial-interglacial cycles for a few 100 ka. Eustatic sea level fall resulted in a shoal up the base of gas hydrate stability (BGGS), dissociation of deep-seated hydrates, and enhanced methane-flux and massive accumulation of hydrates. Shallow hydrates are characterized by high H2S contents up to a few %v/v, reflecting AOM in shallow subsurface. Shallow H2S-bearing hydrates have repeatedly and intermittently accumulated on the top of gas chimneys at glacial period, while the H2S contents rapidly decreased with depth due to recrystallization perhaps through molecular diffusion during burial diagenesis. Key conditions to develop massive deposits of shallow hydrates are strong flux of mixed-microbial and thermogenic gases and a recycling of deep-seated hydrates during the glacial-interglacial.

Keywords: shallow gas hydrates, H2S, eustatic sea level change

©2019. Japan Geoscience Union. All Right Reserved.

Discovery of gas hydrate at the new point off Abashiri, the Sea of Okhotsk

*Akihiro Hachikubo[1], Jumpei Matsuda[1], Satoshi Yamashita[1], Hirotoshi Sakagami[1], Masaaki Konishi[1], Hirotsugu Minami[1], Kenji Nishina[2], Kenji Sakaguchi[3]

1. Kitami Institute of Technology, 2. Geological Survey of Hokkaido, Hokkaido Research Organization, 3. Kushiro Fisheries Research Institute, Hokkaido Research Organization

To understand environment of near-surface gas hydrates at the sea floor, HKS16, HKS17, and HKS18 cruses were conducted using RV Hokushin-Maru (255t) of the Kushiro Fisheries Research Institute off Abashiri, the Sea of Okhotsk, in a framework of joint research between Kitami Institute of Technology and Hokkaido Research Organization. We report success in retrieval of hydrate-bound sediment cores using a research vessel belonging to Hokkaido Prefecture. In this area, natural gas hydrates have been recovered in the NT13-20 and C020 cruises using RV Natsushima and TS Oshoro-maru, respectively. We also observed gas hydrate crystals with many crabs at the seepage sites using a remotely operated vehicle (ROV, KAIYO3000) in the 1KY17 cruise. In the cruise of HKS18, we got gas hydrate samples from a gas seepage site, located 2 km south from the 1KY17 site.

In the HKS18 cruise, we used a hydrostatic corer optimally tuned for a small vessel and a transponder to know exact position of the corer. We obtained nine sediment cores, including two hydrate-bound cores. Gas hydrate crystals were preserved in liquid nitrogen, and sediment gases were obtained by a headspace gas method. Raman spectroscopic analysis was conducted to know crystallographic structure, hydration number and cage occupancies. Molecular and isotopic compositions of gas samples were measured using a gas chromatograph and an isotope ratio mass spectrometer, respectively.

Crystallographic structure of gas hydrate samples belonged to the structure I, and hydration number was estimated as 6.00±0.02. Hydrate-bound H_2S molecules were also detected in the Raman spectra. Hydrate-bound gas was mainly methane, and C_1 / (C_2 + C_3) distributed between 30,000 and 60,000. C_1 $\delta^{13}C$ and δD were -66‰ and -197‰. These molecular and isotopic compositions of hydrate-bound hydrocarbons suggested microbial origin. The depths of sulfate-methane interface (SMI) in HC1807, HC1808, and HC1810 cores were less than 30 cm, indicating high gas flux. Concentrations of H_2S in the headspace gas samples were in the same order (around 1 mM), therefore process of anaerobic oxidation of methane was active. C_1 / (C_2 + C_3) of headspace gases in the hydrate-bound cores (HC1807 and HC1808) distributed between 4,000 and 9,000, and those of other sediment cores were relatively small, indicating that they are in the oxidation layer above the SMI depth. Headspace gas in the HC1808 core contained a lot of isobutane. It is possible that thermogenic gas supplied from deeper sediment layer partly mixes with microbial gas.

Keywords: gas hydrate, Sea of Okhotsk, gas origin

©2019. Japan Geoscience Union. All Right Reserved.

All about gas hydrates and heat flow offshore Chile

*LUCIA ALEJANDRA VILLAR MUNOZ[1], IVAN VARGAS-CORDERO[2], JOAQUIM P. BENTO[3], JAN BEHRMANN[1], UMBERTA TINIVELLA[4], MICHELA GIUSTINIANI[4]

1. Helmholtz Centre for Ocean Research, 2. Universidad Andres Bello , 3. Pontificia Universidad Catolica de Valparaiso, 4. Istituto Nazionale di Oceanografia e di Geofisica Sperimentale

From a geological point of view, Chile lies in an incomparable area of the globe, which include four tectonic plates moving against (Nazca, Antarctic, South American and Scotia plates), two triple junctions (Chile and Fuegian triple junctions), numerous mega-earthquakes and tsunami-related, more than 500 active volcanoes, the Andes, and several mineral resources. One of the last natural resources where the Chilean government and institutions have focused on is in gas hydrate, which is a solid ice-like form of water that contains gas molecules highly-concentrated in methane. Since Chile import most of its gas budget, hence the discovery of this new resource open a new window for the national economy, but also for geosciences, due to methane that escapes from sediments and enter to the ocean or even reach the atmosphere could pose a great environmental threat. To identify the presence of hydrates, in this thesis it was used the bottom-simulating reflector BSR, which has the half amplitude and opposite polarity relative to the seafloor.

Moreover, fluids play a key role in the nucleation and rupture propagation of earthquakes in convergent margins, since are a major agent of advective heat transfer from depth to the Earth’ s surface. If provide enough information for the regional heat flow we will improve our knowledge of these violent shakes of plate motion. For this purpose, it is crucial to know the BSR-depth, which serves to calculate the steady-state heat flow q (mW m^{-2}), and therefore, the heat flow can be envisaged in a regional overview.

This work aims to investigate the tectonic processes of the Chilean forearc through the calculation of the regional BSR-derived heat flow, identification of fluid escape sites, description of the distribution of gas hydrates and estimation of the gas hydrate and free gas reservoirs .

One of the major results is the regional overview of the thermal regime and BSR-based gas hydrate distribution along the Chilean forearc. Here, the BSR was identified into the marine sediments mainly along the accretionary prism between 33˚-57˚S, around 2000 m water depth, and between 90-600 m below seafloor. The heat flow estimated through the forearc on the upper and middle continental slope, from Valparaiso to Chiloe (33˚-43˚S), shows common values of heat flow for the continental basement and overlying slope sediments. However, on the lower slope of the actively deforming accretionary wedge, some places show unexpected values, which indicates that advecting pore fluids from deeper may transport a considerable part of the heat there.

Southern, a second approach was made over a large area of extremely anomalous heat flow that is associated with a major tectonic feature: the Chile Triple Junction. In this unusual place, the Nazca, Antarctic and South American plate converge in a common point; while an active spreading centre (the Chile Rise) is subducting beneath the continental plate. Here, gas hydrates are located in very shallow sediments and the extreme values of heat flow estimated (<280 mW m^{-2}) indicate that the overriding South American Plate is effectively heated by subjacent zero-age oceanic plate material. In order to improve the understanding of the geological risk, in case the methane is released to the ocean/atmosphere system, it was estimated the concentration of gas hydrate in this particular region.

©2019. Japan Geoscience Union. All Right Reserved.

Finally, in the southernmost tip of the continent (offshore Patagonia), the heat flow estimated once again shows a range of values typical for subduction zones of oceanic crust older than 10 Ma. Here, a high concentration of methane hydrate is present beneath the active margin. The average thickness of the gas hydrate layer modelled is almost 300 m and the volume of methane estimated is more than $3x10^{13}$ m^3 at standard pressure-temperature conditions, concluding that the active forearc of the Chilean Patagonia is an important reservoir of methane hydrates.

Keywords: gas hydrates, heat flow, BSR, active margin, Chile, fluids flow

©2019. Japan Geoscience Union. All Right Reserved.

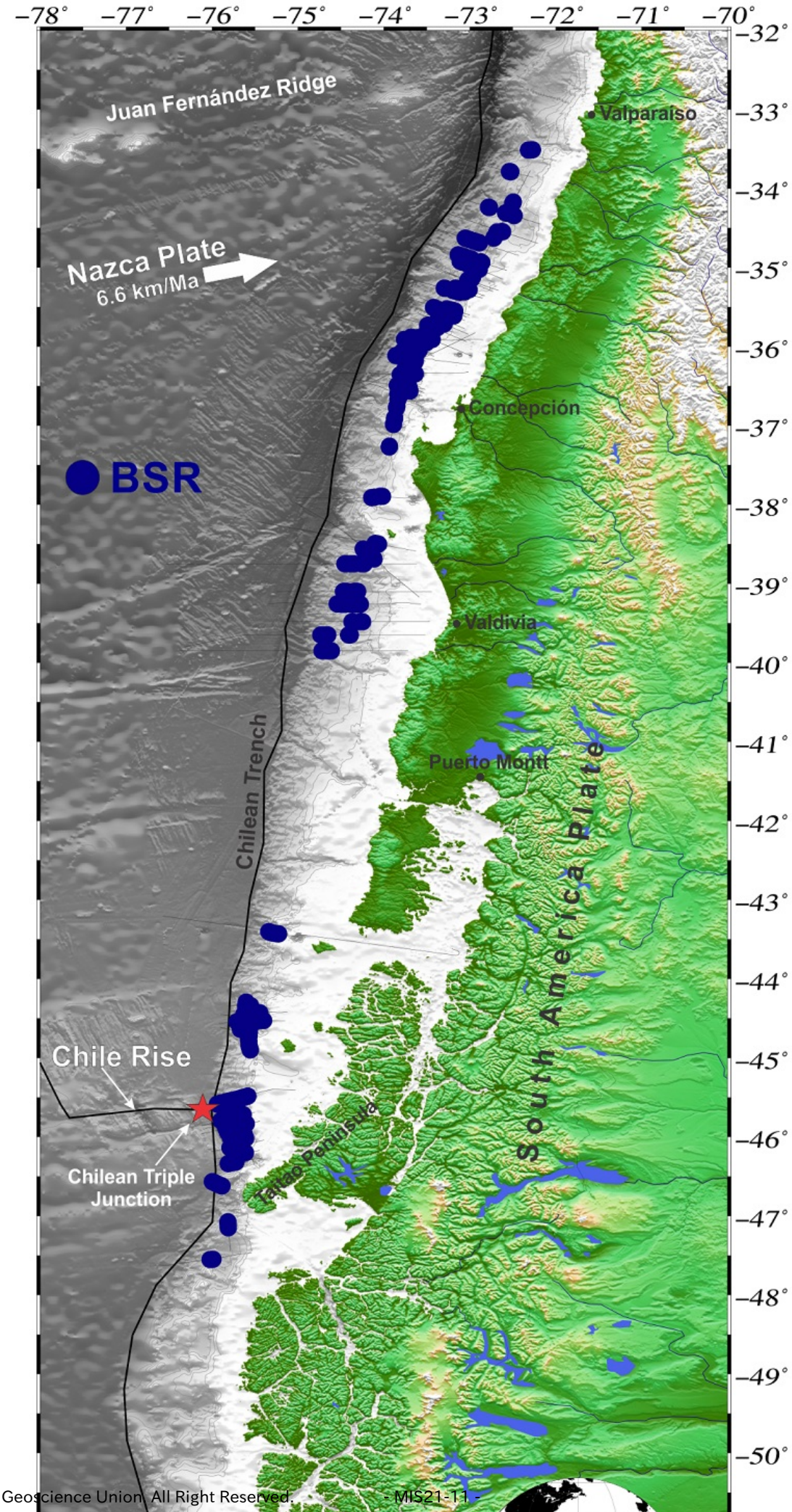

©2019. Japan Geoscience Union. All Right Reserved.

©2019. Japan Geoscience Union. All Right Reserved.

[J] Poster | M (Multidisciplinary and Interdisciplinary)：M-IS Intersection

Tue. May 28, 2019 3:30 PM - 5:00 PM JST | Tue. May 28, 2019 6:30 AM - 8:00 AM UTC | Poster Hall International Exhibition Hall8, Makuhari Messe_26

[M-IS21] Gas hydrate in environmental-resource sciences

convener:Hitoshi Tomaru(Department of Earth Sciences, Chiba University), Akihiro Hachikubo(Kitami Institute of Technology), Atsushi Tani(Graduate School of Human Development and Environment, Kobe University), Shusaku Goto(Institute for Geo-Resources and Environment National Institute of Advanced Industrial Science and Technology)

An increasing number of researches focusing on natural gas hydrates has recently been conducted from the environmental, material, and resource scientific viewpoints. This session aims to share and discuss the latest research results associated with natural/experimental gas hydrates to understand and examine the nature and potential of gas hydrates in the past-present-future of the Earth and the development/application for our life. Because the researches on gas hydrates are interdisciplinary, broad topics from field and experimental researches, modeling, etc. will be presented in this session.

[MIS21-P01] Raman spectroscopic analysis of isotopologue methane hydrates

*Yuki Kikuchi[1], Jumpei Matsuda[1], Akihiro Hachikubo[1], Satoshi Takeya[2] (1.Kitami Institute of Technology, 2.National Institute of Advanced Industrial Science and Technology (AIST))

[MIS21-P02] Gas origin of hydrate-bound gas in Lake Baikal

*Jumpei Matsuda[1], Yuki Kikuchi[1], Akihiro Hachikubo[1], Oleg Khlystov[2], Gennadiy Kalmychkov[3], Marc De Batist[4], Hirotoshi Sakagami[1], Hirotsugu Minami[1], Satoshi Yamashita[1] (1.Kitami Institute of Technology, 2.Limnological Institute, SB RAS, 3.Vinogradov Institute of Geochemistry, SB RAS, 4.Ghent University)

[MIS21-P03] Validation of self-preservation effect of methane and ethane mixed-gas hydrate by Raman spectroscopy

*Yunosuke Hase[1], Jumpei Matsuda[1], Akihiro Hachikubo[1], Satoshi Takeya[2] (1.Kitami Institute of Technology, 2.National Institute of Advanced Industrial Science and Technology (AIST))

[MIS21-P04] Experimental study on the phase equilibrium condition of CO_2 hydrate with marine sediment

*Daisuke Maki[1], Hitoshi Tomaru[1] (1.Graduate School of Science and Engineering, Chiba University)

[MIS21-P05] Raman spectroscopic analysis of structure H gas hydrates encapsulating cyclic hydrocarbons

*Go Fuseya[1], Satoshi Takeya[2], Akihiro Hachikubo[1] (1.Kitami Institute of Technology, 2.National Institute of Advanced Industrial Science and Technology (AIST))

[MIS21-P06] Investigation of self-preservation of argon hydrate by measuring specific surface area

*Yuki Ikeura[1], Daisuke Yahagi[1], Akihiro Hachikubo[1], Satoshi Takeya[2] (1.Kitami institute of technology, 2.National Institute of Advanced Industrial Science and Technology (AIST))

[MIS21-P07] Carbon isotope fractionation of CO_2 during the formation of clathrate hydrate

*Hiromi Kimura[1], Jumpei Matsuda[1], Yuki Kikuchi[1], Akihiro Hachikubo[1], Satoshi Takeya[2] (1.Kitami Institute of Technology, 2.National Institute of Advanced Industrial Science and Technology)

[MIS21-P08] Gas hydrate survey off Tokachi (the Pacific Ocean) in the framework of practical education of Kitami Institute of Technology

*Yunosuke Hase[1], Jumpei Matsuda[1], Yuki Ikeura[1], Akihiro Hachikubo[1], Masaaki Konishi[1], Hirotoshi Sakagami[1], Hirotsugu Minami[1], Satoshi Yamashita[1] (1.Kitami Institute of Technology)

[MIS21-P09] **Geochemistry of pore water and gas in shallow sediments from offshore Primorsky Krai, Russia**

*Musashi Yokoyama[1], Hitoshi Tomaru[1], Ryo Matsumoto[2], Glen Snyder[2], A.V. Yatsuk[3], D.A Shvalov[3] (1.Department Earth Sciences, Chiba University, 2.Gas Hydrate Research Laboratory, Meiji University, 3.Gas Geochemistry Laboratory, V.I.Ilichev Pacific Oceanological Institute)

[MIS21-P10] Late Quaternary Total Organic Carbon fluctuation in the eastern Japan Sea and offshore of the Russian maritime provinces

*Yuta Hirano[1], Kyousuke Sakamoto[1], Naoto Ishida[2], Takao Ebinuma[2], Koji Seto[3], Ryo Matsumoto[4] (1.Graduate School of Sustainability Science Methane Hydrate Course ,Tottori University, 2.Tottori Univ., 3.Shimane Univ., 4.Meiji Univ.)

[MIS21-P11] Geochemical behavior of carbon in shallow sediment within the gas chimney in Hidaka Trough, offshore Hokkaido

Tsuyoshi Mamata[1], *Hitoshi Tomaru[1], Ryo Matsumoto[2] (1.Department of Earth Sciences, Chiba University, 2.Gas Hydrate Research Laboratory, Meiji University)

Raman spectroscopic analysis of isotopologue methane hydrates

*Yuki Kikuchi[1], Jumpei Matsuda[1], Akihiro Hachikubo[1], Satoshi Takeya[2]

1. Kitami Institute of Technology, 2. National Institute of Advanced Industrial Science and Technology (AIST)

Raman spectroscopy is one of the useful tool to get information of gas hydrate crystals. Natural gas hydrates in submarine/sublacustrine sediment mainly encage methane. Methane molecule is composed of carbon and hydrogen, and three kinds of isotopologues, $^{12}CH_4$, $^{13}CH_4$, and CH_3D exist in nature. Ozeki *et al.* (2018) first reported Raman spectra of CH_3D and CD_4 hydrates and compared with CH_4 (mainly $^{12}CH_4$) hydrate. We report Raman spectra of $^{13}CH_4$ hydrate and summarize Raman spectra of isotopologue methane hydrates.

$^{13}CH_4$ hydrate sample was synthesized in a small pressure cell (volume: 5 mL). Fine ice powder (1g) was put in the pressure cell, and introduced appropriate amount of $^{13}CH_4$ (purity: 99.5%, Taiyo-Nissan). $^{13}CH_4$ hydrate was formed by melting the fine ice powder at the temperature of 273.2 K under high pressure of $^{13}CH_4$. We retrieved the hydrate sample at 77 K and its Raman spectra was obtained at 123 K in the range 2,500-3,300 cm^{-1} using a Raman spectrometer (RMP-210, JASCO Corporation). The Raman peaks were fitted in the range 2,800-3,000 cm^{-1} for the C-H stretching peaks of methane using a Voigt function to obtain the integrated intensities of the two peaks corresponding to methane encaged in the large and small cages of the cubic structure I.

Raman shifts for the C-H stretching and bending modes of $^{13}CH_4$ was 0.8 cm^{-1} and 14 cm^{-1} smaller than those of $^{12}CH_4$, respectively, suggesting that ^{13}C-H bonds affect its vibrational frequency. Hydration number of $^{13}CH_4$ was estimated as 6.00±0.02, almost the same as that of $^{12}CH_4$ (6.02±0.02). Therefore, Cage occupancies of $^{13}CH_4$ and $^{12}CH_4$ hydrates showed no difference between them.

Reference

Ozeki T, Kikuchi Y, Takeya S, Hachikubo A (2018) Phase equilibrium of isotopologue methane hydrates enclathrated CH_3D and CD_4. J Chem Eng Data 63(6): 2266-2270, doi: 0.1021/acs.jced.8b00203

Keywords: methane hydrate, Raman spectroscopy, isotopologues

©2019. Japan Geoscience Union. All Right Reserved.

Gas origin of hydrate-bound gas in Lake Baikal

*Jumpei Matsuda[1], Yuki Kikuchi[1], Akihiro Hachikubo[1], Oleg Khlystov[2], Gennadiy Kalmychkov[3], Marc De Batist[4], Hirotoshi Sakagami[1], Hirotsugu Minami[1], Satoshi Yamashita[1]

1. Kitami Institute of Technology, 2. Limnological Institute, SB RAS, 3. Vinogradov Institute of Geochemistry, SB RAS, 4. Ghent University

In the framework of international collaboration between Kitami Institute of Technology (Japan), Limnological Institute (Russia), and Ghent University (Belgium), natural gas hydrates have been recovered from lake-bottom sediments at Lake Baikal. Near-surface gas hydrate was first discovered at the Malenky mud volcano at the southern Baikal basin in 2000. Multi-phase Gas Hydrate Project (MHP, 2009-2018) has revealed distribution of near-surface gas hydrates at the southern and central Baikal basins. We found six new places (Enkhelook, Soukhaya, KIT, LIN, PosolCanyon1, and PosolCanyon2) during the VER18-03 cruise in 2018. The total number of places where near-surface gas hydrates were retrieved is 53. In this report, we summarize characteristics of hydrate-bound gases retrieved from all the sites since 2005.

Gas hydrate crystals were recovered from lake-bottom sediment cores, and hydrate-bound gas samples were stored in 5-mL vials. Total number of hydrate-bound gas samples was 626. Molecular and isotopic compositions of hydrate-bound gas were measured using a gas chromatograph and a stable isotope ratio mass spectrometer.

In the Bernard plot, C_1 $\delta^{13}C$ and C_1 / (C_2 + C_3) distributes from -70‰ to -44‰ and from 6 to 100,000, respectively, suggesting that the origin of hydrate-bound gas is microbial, thermogenic, and their mixed-gas. Almost all data are plotted on the mixing line between microbial and thermogenic, however, Gorevoy Utes (oil seep site) showed thermogenic C_1 with small composition of C_2 and C_3. The data concentrates in the microbial field (C_1 $\delta^{13}C$: -66‰ and C_1 / (C_2 + C_3): 1,000-10,000). C_1 δD of thermogenic C_1 increases with C_1 $\delta^{13}C$. C_2 $\delta^{13}C$ distributes from -69‰ to -23‰. 17 sites (ex. Solzan, Talanka, Turka, KIT, etc.) showed microbial C_1 and C_2. 27 sites (Malenky, Oblom, Seep13, Kukuy K6, etc.) showed microbial C_1 and thermogenic C_2, indicating that small amount of thermogenic gas is mixed with microbial gas. Other sites (Mamay, PosolBank, Gorevoy Utes, Kedr, etc.) showed thermogenic C_1 and C_2. The Milkov plot (relation between C_1 $\delta^{13}C$ and C_2 $\delta^{13}C$) can express mixing condition between microbial and thermogenic rather than the Bernard plot. C_2 δD decreased with decrease in C_2 $\delta^{13}C$, therefore microbial C_2 is both depleted in ^{13}C and D. We conclude that hydrate-bound gas at Lake Baikal is mainly microbial gas, and thermogenic gas ascends from deep layer at some areas (Kedr, PosolBank, Kukuy, and Gorevoy Utes) and forms the structure II gas hydrate.

Keywords: gas hydrate, Lake Baikal, gas origin

©2019. Japan Geoscience Union. All Right Reserved.

Validation of self-preservation effect of methane and ethane mixed-gas hydrate by Raman spectroscopy

*Yunosuke Hase[1], Jumpei Matsuda[1], Akihiro Hachikubo[1], Satoshi Takeya[2]

1. Kitami Institute of Technology, 2. National Institute of Advanced Industrial Science and Technology (AIST)

Methane hydrate can be stored long time under atmospheric pressure below 273.2K, even though their P-T conditions is unstable, namely "self-preservation effect". On the contrary, Takeya and Ripmeester (2008) reported that ethane hydrate shows no self-preservation. In natural condition, methane and ethane mixed-gas hydrates have been found at Lake Baikal, however, there is no information for the mixed-gas system. In the last JpGU meeting we report self-preservation effect for mixed-gas hydrate, but the conditions of samples are not uniform. Because the size of crystals affect rate of survival at higher temperature, we controlled the specific surface of area of gas hydrate samples in this study.

We put 0.7 g of fine ice balls (diameter: 0.108-0.180 mm) into a pressure cell (volume: 30 mL) and mixed-gas of methane and ethane was introduced. Hydrate crystals formed at 273.2 K. The gas hydrate sample was degased and recovered at the temperature of liquid nitrogen. We controlled the ethane composition of hydrate-bund gas from 0% to 100%, covering the area of methane-rich structure I, ethane-rich structure I, and their intermediate structure II. We measured compositions of methane and ethane by a gas chromatograph (GC-2014, Shimadzu Corporation). Gas hydrate samples were placed on a temperature-controlled device and kept at 80 K. Raman spectra of hydrate samples were obtained using a Raman spectrometer (RMP-210, JASCO Corporation). We checked the Raman spectra of C-H stretching mode at 83 K, and then increased the sample temperature every 10 K until complete dissociation. We calculated the Raman peak area for C-H stretching mode of methane and ethane around 2900 cm^{-1} by a peak fitting method and obtained the survival rate of gas hydrate samples with temperature.

Pure methane hydrate survived well, more than 20% of hydrate still remained at 263 K, whereas pure ethane hydrate completely dissociated at around 200 K. These results agree well with our previous report. As for mixed-gas hydrate composed of methane and ethane, the rates of survival of structure I were lower than that of pure methane hydrate, but the crystals remained till 253 K, suggesting self-preservation. That of structure II well remained at 83-183 K, but quickly disappeared at 213 K. Therefore, it is possible that the survival rate of mixed-gas hydrate composed of methane and ethane depends on not only gas composition but also crystallographic structure.

Reference

Takeya S, Ripmeester JA (2008) Dissociation behavior of clathrate hydrates to ice and dependence on guest molecules. Angew Chem Ed 47: 1276-1279

Keywords: gas hydrate, self preservation effect, methane, ethane

©2019. Japan Geoscience Union. All Right Reserved.

Experimental study on the phase equilibrium condition of CO_2 hydrate with marine sediment

*Daisuke Maki[1], Hitoshi Tomaru[1]

1. Graduate School of Science and Engineering, Chiba University

Gas hydrate accumulation has been found in the marine sediments around Japan, and has been regarded as an unconventional gas resource because it contains a huge amount of methane. The phase equilibrium condition of gas hydrate provides a key parameter to estimate the distribution and resource potential of gas hydrate. Although the influences of temperature, pressure, gas/water composition, etc. on the phase equilibrium have been studied so far, experimental studies concerning the effect of sediment particles in shallow gas hydrate deposit are not well understood. In this study, we synthesized carbon dioxide hydrate which has similar physicochemical behavior to methane hydrate and examined the phase equilibrium condition with the mud collected near the shallow gas hydrate in the Japan Sea. It was found that the equilibrium condition with mud was significantly reduced; about 0.2℃ lower and about 0.1 MPa higher compare to mud-free environment. Our results strongly indicates that the existence of mud may change the stability condition of gas hydrate in the natural environment and it is necessary to consider this effect for estimating gas hydrate distribution and stability fields.

Keywords: gas hydrate, phase equilibrium

©2019. Japan Geoscience Union. All Right Reserved.

Raman spectroscopic analysis of structure H gas hydrates encapsulating cyclic hydrocarbons

*Go Fuseya[1], Satoshi Takeya[2], Akihiro Hachikubo[1]

1. Kitami Institute of Technology, 2. National Institute of Advanced Industrial Science and Technology (AIST)

Clathrate hydrates are crystalline inclusion compounds that consist of well-defined cages formed by water molecules and guest molecules of suitable sizes and shapes trapped in the cages. Clathrate hydrates including natural gases as guest molecules are commonly known as gas hydrates. Gas hydrates in sea or lake bottom sediments and permafrost layers have attracted considerable interest as a potential source of unconventional natural gas. There are three common crystallographic structure of hydrates, structure I (sI), structure II (sII) and structure H (sH). In the case of microbially sourced gas hydrate system, the gas hydrates are generally sI CH_4 hydrates. On the other hand, sH hydrate was found at northern Cascadia margin, where thermogenic larger hydrocarbons exist [Lu et al. 2007]. For instance,, cyclohexane (CH), methylcyclopentane (MCP), methylcyclohexane (MCH) and other large hydrocarbons, which is capable of forming sH hydrate with help gas like CH_4, were detected at the area. From the above, study for sH hydrate which encapsulating these large hydrocarbons are important for further understanding of natural gas hydrates.

In this study, sH CH_4 and larger cyclic hydrocarbon (CH, MCP and MCH) mixed hydrates were prepared. We observed the variations of Raman spectra of these cyclic hydrocarbons due to enclathrated water cages of gas hydrate. C–H and C–C stretching regions of enclathrated these cyclic hydrocarbons were measured by the Raman spectroscopic method., The Raman spectra of C–C stretching region of these hydrocarbon are useful for identification of guest molecules in natural gas hydrates because the number of Raman peaks of C–C stretching region are smaller than that of C–H stretching region.

Reference

Lu *et al.* (2007) Effect of temperature and large guest molecules on the C–H symmetric stretching vibrational frequencies of methane in structure H and I clathrate hydrates. *Nature.* **8**: 303-306.

doi: 10.1038/nature0546.

Keywords: gas hydrate, Raman spectroscopy

©2019. Japan Geoscience Union. All Right Reserved.

Investigation of self-preservation of argon hydrate by measuring specific surface area

*Yuki Ikeura[1], Daisuke Yahagi[1], Akihiro Hachikubo[1], Satoshi Takeya[2]

1. Kitami institute of technology, 2. National Institute of Advanced Industrial Science and Technology (AIST)

Self-preservation occurs during the dissociation of gas hydrate and drastically decreases speed of dissociation at around 253K and under atmospheric pressure in the case of methane hydrate. Takeya and Ripmeester (2008) revealed that not only methane but also nitrogen, oxygen, argon, and CO_2 hydrates showed the same self-preservation effect. This phenomena is explained that (1) gas hydrate dissociates below the ice point, (2) ice remains on the surface of crystals, (3) ice layer forms and covers on the surface of hydrate and prevent from further dissociation. We developed a device for measuring specific surface area of snow particles (Hachikubo *et al.*, 2014), and it is also available for gas hydrate crystals. Because self-preservation phenomena depends on temperature, we investigated the change of specific surface area of argon hydrate samples in their dissociation process under various temperature conditions.

Fine ice balls (diameter: 0.108-0.180 mm) were formed in liquid nitrogen using water spray and sieved in a cold room (temperature: 255 K). 3 g of ice balls were put into a pressure cell (volume: 30 mL) and measured their specific surface area. After that, argon was introduced and hydrate crystals formed at 273.2 K. Temperature of the samples were controlled at 226K, 243K, 254K, and 263K, and then the residual gases in the pressure cell were quickly removed. The internal pressure decreased to the atmospheric pressure and the samples started to dissociate. Dissociation times were controlled as 1 minute, 10 minutes, and 100 minutes, and after that the samples were fixed at the temperature of liquid nitrogen and we measured their specific surface area. Their dissociation rate were estimated from weight data of gas and water. Specific surface area of the original fine ice balls and (pure) argon hydrate samples were also measured.

Ice balls were expected to change completely into “hydrate balls”, however, more fine and irregular grains of argon hydrate were observed using an optical microscope Specific surface area of original ice balls was 71±5 [m^2 kg^{-1}], and that of argon hydrate increased to 119 [m^2 kg^{-1}]. When the dissociation period was 1 minute, more than 90% of hydrate still remained at 226-263 K. The rate of dissociation at 254 K was fastest in the case of 10 minutes dissociation (65% of hydrate remained), but about 80% of hydrate sample remained at 263 K. The specific surface area was around 120 [m^2 kg^{-1}] after 10 minutes at 263 K, indicating that the condition of surface was not changed at 263 K. On the other hand, the specific surface area increased to 279 [m^2 kg^{-1}] at 226 K after 10 minutes. Therefore, these results indicate that the self-preservation effect appeared at 263 K and kept the surface of crystals smooth rather than the case at 226 K.

References

Takeya S, Ripmeester JA (2008) Dissociation behavior of clathrate hydrates to ice and dependence on guest molecules. Angew Chem Int Ed 47: 1276-1279

Hachikubo A, Yamaguchi S, Arakawa H, Tanikawa T, Hori M, Sugiura K, Matoba S, Niwano M, Kuchiki K,

©2019. Japan Geoscience Union. All Right Reserved.

Aoki T (2014) Effects of temperature and grain type on time variation of snow specific surface area. Bull Glaciol Res 32: 47-53

Keywords: gas hydrate, argon, self preservation effect, specific surface area

©2019. Japan Geoscience Union. All Right Reserved.

Carbon isotope fractionation of CO_2 during the formation of clathrate hydrate

*Hiromi Kimura[1], Jumpei Matsuda[1], Yuki Kikuchi[1], Akihiro Hachikubo[1], Satoshi Takeya[2]

1. Kitami Institute of Technology, 2. National Institute of Advanced Industrial Science and Technology

Hydrogen Isotope fractionation in methane during the formation of clathrate hydrate was reported by Hachikubo *et al.* (2007) that δ D of hydrate-bound methane is 4.8±0.4‰ lower than that of residual methane at 274.2K. Although natural methane hydrates distribute widely in the world, natural CO_2 hydrate was only reported at the Okinawa Trough (Sakai *et al.*, 1990). It is also possible that CO_2 hydrate exists in Mars. Isotopic fractionation of guest gas may provide useful information to understand formation processes of gas hydrate. Luzi *et al.* (2011) revealed that CO_2 $\delta^{13}C$ in hydrate-bound gas is 0.9‰ lower than that of residual gas, suggesting that light CO_2 molecules prefer to be encaged into clathrate cages. In this study, we checked the temperature effect on the isotopic difference between residual and hydrate-bound CO_2.

Samples of CO_2 hydrate (weight: 0.7 g) were experimentally prepared in a pressure cell (volume: 30 mL), and the temperature was controlled by a liquid bath (258-274 K) and cold rooms (226-254 K). Isotopic compositions of both residual and hydrate-bound CO_2 were measured by an isotope ratio mass spectrometer (IRMS). Samples were formed in the temperature range from 226 K to 274 K. The carbon isotopic differences between hydrate-bound and residual CO_2 distributed between 1.2‰ and 1.5‰, agreed fairly well with the previous report (Luzi *et al.*, 2011). The difference seemed to be large (1.5-2.0 ‰) at 226 K, indicating that the equilibrium pressure of $^{13}CO_2$ hydrate is slightly larger than that of $^{12}CO_2$ hydrate, and the difference between them becomes large in lower temperature. We will show these equilibrium data for $^{13}CO_2$ and $^{12}CO_2$ hydrates and compare with the results in stable isotope.

Reference

Hachikubo A, Kosaka T, Kida M, Krylov A, Sakagami H, Minami H, Takahashi N, Shoji H (2007) Isotopic fractionation of methane and ethane hydrates between gas and hydrate phases. Geophys Res Lett 34: L21502. doi:10.1029/2007GL030557

Sakai H, Gamo T, Kim ES, Tsutsumi M, Tanaka T, Ishibashi J, Wakita H, Yamano M, Oomori T (1990) Venting of carbon dioxide-rich fluid and hydrate formation in mid-okinawa trough backarc basin. Science: 248, 4959, 1093-1096.

Luzi M, Schicks JM, Erzinger J (2011) Carbon isotopic fractionation of synthetic methane and carbon dioxide hydrates. Proc. 7th International Conference on Gas Hydrates (ICGH2011).

Keywords: gas hydrate, stable isotope, carbon dioxide, isotopic fractionation

©2019. Japan Geoscience Union. All Right Reserved.

Gas hydrate survey off Tokachi (the Pacific Ocean) in the framework of practical education of Kitami Institute of Technology

*Yunosuke Hase[1], Jumpei Matsuda[1], Yuki Ikeura[1], Akihiro Hachikubo[1], Masaaki Konishi[1], Hirotoshi Sakagami[1], Hirotsugu Minami[1], Satoshi Yamashita[1]

1. Kitami Institute of Technology

Distribution of BSR (bottom simulating reflector) has been reported off Tokachi, the Pacific Ocean (Hayashi *et al.*, 2010). Kitami Institute of Technology started gas hydrate survey in this area on 2014, using TS Oshoro-maru of Hokkaido University. This program is conducted in the framework of practical education (name of lecture: “Practical learning about the Okhotsk Region, its history and the natural environment”), and about 40 students participate the cruise. Three cruises (C008, C046, and C061) were executed in 2014-2018. We found many gas seeps ascending from sea floor, those height exceeded 700 m from the sea floor. We recovered gas-rich sediment cores by a gravity and hydrostatic corers. Here, we report characteristics of sediment gas in this area.

Samples of sediment gas, mainly dissolved gases in pore water, were obtained by a headspace gas method. 10 mL sediment was sampled from the sediment core by a plastic syringe (volume: 5 mL) and put into a 25 mL vial. 10 mL NaCl aqueous solution was introduced into the vial by using a micropipette and sealed employing a butyl rubber septum to make a headspace (5 mL volume). To avoid any changes in the headspace, preservative (benzalkonium chloride, BKC) was added and the headspace part was flushed by helium. We roughly checked gas composition of sediment gases onboard using a portable gas chromatograph, and after that we measured the molecular and isotopic compositions of headspace gases using another gas chromatograph and CF-IRMS in our laboratory.

Concentration of C_1 increased with depth, and exceeded 1 [mM] in the bottom of some sediment cores (C008-GC1403, C046-GC1702, and C061-GC1803), indicating that their depths of SMI (sulfate-methane interface) were small and active gas seep existed at the sea floor. The minimum SMI depth was 50 [cmbsf] in C008-GC1403. C_1 / (C_2 + C_3) in these gas-rich layer was from 300 to 700. Concentration of H_2S exceeds 1 [mM] in the bottom of sediment cores. These results indicate that microbial gas is supplied from lower layer and AOM (anaerobic oxidation of methane) processes is active in beneath the sea floor. C_1 $\delta^{13}C$ profiles showed minimum values (lower than -100‰) at the SMI depth in C061-GC1803. C_2 $\delta^{13}C$ distributed between -55‰ and -30‰, suggesting that C_2 seems also microbial origin.

Reference

Hayashi M, Saeki T, Inamori T, Noguchi S (2010) The distribution of BSRs related to methane hydrates, offshore Japan. J Jpn Assoc Petrol Technol 75(1): 42-53

Keywords: gas hydrate, methane, the Pacific Ocean

©2019. Japan Geoscience Union. All Right Reserved.

Geochemistry of pore water and gas in shallow sediments from offshore Primorsky Krai, Russia

*Musashi Yokoyama[1], Hitoshi Tomaru[1], Ryo Matsumoto[2], Glen Snyder[2], A.V. Yatsuk[3], D.A Shvalov[3]

1. Department Earth Sciences, Chiba University, 2. Gas Hydrate Research Laboratory, Meiji University, 3. Gas Geochemistry Laboratory, V.I.Ilichev Pacific Oceanological Institute

Offshore region of Primorsky Krai, Russia, in the northern Japan Sea is located in the boundary area between the shallower Tatar Trough on the north and deeper Japan Basin in the south. The marginal area of the Japan Sea has been characterized by the dense distribution of gas chimneys, which are identified by columnar blanking structureon acoustic records, e.g., W-S-E Tsushima Basin, Oki Trough, Joetsu Basin, Mogami Trough, and SW Sakhalin Island. Gas chimney structure delivers hydrocarbon gas, mainly methane, significantly from deep sediment to surface sediment, which may cause gas hydrate accumulation, carbonate precipitation, gas seepage, etc. Therefore it is one of the key structures controlling near-seafloor phenomena. In this research, we analyzed chemical compositions of pore water and gas collected from shallow sediments, off Primorsky, Russia (R/V Akademik M.A. Lavrentyev, Cruise LV81, 2018), and estimated the methane flux to characterize the geochemical environment near the seafloor. The sulfate concentrations linearly decrease with depth and the methane/ethane ratios are as low as ~100 at all sites, reflecting anaerobic oxidation of methane (AOM) is active at the sulfate methane interface (SMI). Decreases in calcium and magnesium were also obvious, indicating carbonate precipitation in response to alkalinity increase due to AOM. The methane flux estimated from SMI depths are generally high in the northern research area compared to southern area, in particular, at shallow gas chimney sites (SMI at ~1.5 mbsf, <1500 mWD). At the northern-most deep gas chimney sites, methane fluxes are relatively low. These results indicate that organic matter was primarily derived along the trough (from north to south) rather than the landward slope off Primorsky, and the methane generated in the sediment of deep area of the trough migrated through the porous layers to the shallow sites where the gas chimney is active. The geochemistry of pore water and gas depicts the shallow geochemical environments associated methane migration in research area.

Keywords: gas chimney, methane

©2019. Japan Geoscience Union. All Right Reserved.

Late Quaternary Total Organic Carbon fluctuation in the eastern Japan Sea and offshore of the Russian maritime provinces

*Yuta Hirano[1], Kyousuke Sakamoto[1], Naoto Ishida[2], Takao Ebinuma[2], Koji Seto[3], Ryo Matsumoto[4]

1. Graduate School of Sustainability Science Methane Hydrate Course ,Tottori University, 2. Tottori Univ., 3. Shimane Univ., 4. Meiji Univ.

In the Sea of Japan, three cores were taken from the Oki Trough (PC1606), Mogami Trough South (PC1726), and the offshore of the Russian Primorye (Lv81-35GC). Total organic carbon (TOC), total nitrogen (TN), and total sulfur (TS) in sediments were measured from these cores, and the organic carbon concentration and the origin of organic matter were clarified. The organic carbon concentration in the sediment reflects the past primary production. All cores have high correlation between TN and TOC. The value of C/N is from 6 to 10. On the other hand, there is no correlation between TS and TOC. The value of C/S varies from 0.2 to 11. The TOC concentration of PC1726 and Lv81-35GC is almost coincide with PC1606. However, the peak around 10 ka detected in PC1606 is unclear in the other cores. In the period of the Last Glacial Maximum, primary production declined at all areas. However, the subsequent reactions were different in each area.

Keywords: Total Organic Carbon, Japan Sea, Late Quaternary, Shallow type methane hydrate

©2019. Japan Geoscience Union. All Right Reserved.

Geochemical behavior of carbon in shallow sediment within the gas chimney in Hidaka Trough, offshore Hokkaido

Tsuyoshi Mamata[1], *Hitoshi Tomaru[1], Ryo Matsumoto[2]

1. Department of Earth Sciences, Chiba University, 2. Gas Hydrate Research Laboratory, Meiji University

The Hidaka Trough, offshore Hokkaido, has recently been characterized by subsurface gas chimney structures associated with mound/pockmark topography and methane plume, which indicate an intensive gas migration from deep sediments to the surface area. In the region where remarkable gas chimneys are developed such as in offshore Joetsu, shallow marine sediments are characterized by the precipitation of authigenic carbonate, massive gas hydrates and development of chemotrophs because of high methane concentration near the seafloor. In these environments, anaerobic oxidation of methane utilizes both methane and sulfate, resulting in sulfate depleted in shallow sediment. Inorganic carbon generated by methane oxidation does not incorporate only with calcium ion to form carbonate but also is reduced by microbially-mediated methanogenic reaction. Carbon is therefore a key substance near the depth of sulfate methane interface (SMI) in high methane flux area. This study aims to figure out the chemical reaction associated with carbon, which characterizes geochemical environment in shallow sediments, by analyzing concentrations of dissolved ions and hydrocarbons, and stable isotopic composition ($\delta^{13}C$) of dissolved carbons collected from shallow sediments with gas chimney structures in the Hidaka Trough, offshore Hokkaido.
In the area of calyptogena community, the SMI locates at shallow depth and indicates reductive environment is established because of sulfate depletion. The sulfate is depleted at shallower depth in the area with carbonates near the seafloor, where the concentration of calcium ion is also lower than other areas. These results indicate carbonate formed at higher rate in the area with higher methane flux. Total organic carbon amount decrease with depth above the SMI, the residual organic matter in sediment generates methane at depth and enhances the methane flux toward the seafloor. Based on the composition of dissolved hydrocarbons and $\delta^{13}C$ of methane, although the methane is generally of biogenic origin over the research areas in the Hidaka Trough, the $\delta^{13}C$ of methane increase rapidly with depth on the mound center, indicating thermogenic methane predominantly migrate from deeper sediments at the site. Biogeochemical behavior of carbon varies not only among sampling sites but also among relative locations on the single gas chimney structure.

Keywords: SMI, gas chimney, Hidaka Trough

©2019. Japan Geoscience Union. All Right Reserved.

[J] Poster | M (Multidisciplinary and Interdisciplinary)：M-IS Intersection

Tue. May 28, 2019 5:15 PM - 6:30 PM JST | Tue. May 28, 2019 8:15 AM - 9:30 AM UTC | Poster Hall International Exhibition Hall8, Makuhari Messe_45

[M-IS21] Gas hydrate in environmental-resource sciences

convener:Hitoshi Tomaru(Department of Earth Sciences, Chiba University), Akihiro Hachikubo(Kitami Institute of Technology), Atsushi Tani(Graduate School of Human Development and Environment, Kobe University), Shusaku Goto(Institute for Geo-Resources and Environment National Institute of Advanced Industrial Science and Technology)

An increasing number of researches focusing on natural gas hydrates has recently been conducted from the environmental, material, and resource scientific viewpoints. This session aims to share and discuss the latest research results associated with natural/experimental gas hydrates to understand and examine the nature and potential of gas hydrates in the past-present-future of the Earth and the development/application for our life. Because the researches on gas hydrates are interdisciplinary, broad topics from field and experimental researches, modeling, etc. will be presented in this session.

[MIS21-P01] Raman spectroscopic analysis of isotopologue methane hydrates

*Yuki Kikuchi[1], Jumpei Matsuda[1], Akihiro Hachikubo[1], Satoshi Takeya[2] (1.Kitami Institute of Technology, 2.National Institute of Advanced Industrial Science and Technology (AIST))

[MIS21-P02] Gas origin of hydrate-bound gas in Lake Baikal

*Jumpei Matsuda[1], Yuki Kikuchi[1], Akihiro Hachikubo[1], Oleg Khlystov[2], Gennadiy Kalmychkov[3], Marc De Batist[4], Hirotoshi Sakagami[1], Hirotsugu Minami[1], Satoshi Yamashita[1] (1.Kitami Institute of Technology, 2.Limnological Institute, SB RAS, 3.Vinogradov Institute of Geochemistry, SB RAS, 4.Ghent University)

[MIS21-P03] Validation of self-preservation effect of methane and ethane mixed-gas hydrate by Raman spectroscopy

*Yunosuke Hase[1], Jumpei Matsuda[1], Akihiro Hachikubo[1], Satoshi Takeya[2] (1.Kitami Institute of Technology, 2.National Institute of Advanced Industrial Science and Technology (AIST))

[MIS21-P04] Experimental study on the phase equilibrium condition of CO_2 hydrate with marine sediment

*Daisuke Maki[1], Hitoshi Tomaru[1] (1.Graduate School of Science and Engineering, Chiba University)

[MIS21-P05] Raman spectroscopic analysis of structure H gas hydrates encapsulating cyclic hydrocarbons

*Go Fuseya[1], Satoshi Takeya[2], Akihiro Hachikubo[1] (1.Kitami Institute of Technology, 2.National Institute of Advanced Industrial Science and Technology (AIST))

[MIS21-P06] Investigation of self-preservation of argon hydrate by measuring specific surface area

*Yuki Ikeura[1], Daisuke Yahagi[1], Akihiro Hachikubo[1], Satoshi Takeya[2] (1.Kitami institute of technology, 2.National Institute of Advanced Industrial Science and Technology (AIST))

[MIS21-P07] Carbon isotope fractionation of CO_2 during the formation of clathrate hydrate

*Hiromi Kimura[1], Jumpei Matsuda[1], Yuki Kikuchi[1], Akihiro Hachikubo[1], Satoshi Takeya[2] (1.Kitami Institute of Technology, 2.National Institute of Advanced Industrial Science and Technology)

[MIS21-P08] Gas hydrate survey off Tokachi (the Pacific Ocean) in the framework of practical education of Kitami Institute of Technology

*Yunosuke Hase[1], Jumpei Matsuda[1], Yuki Ikeura[1], Akihiro Hachikubo[1], Masaaki Konishi[1], Hirotoshi Sakagami[1], Hirotsugu Minami[1], Satoshi Yamashita[1] (1.Kitami Institute of Technology)

[MIS21-P09] **Geochemistry of pore water and gas in shallow sediments from offshore Primorsky Krai, Russia**

*Musashi Yokoyama[1], Hitoshi Tomaru[1], Ryo Matsumoto[2], Glen Snyder[2], A.V. Yatsuk[3], D.A Shvalov[3] (1.Department Earth Sciences, Chiba University, 2.Gas Hydrate Research Laboratory, Meiji University, 3.Gas Geochemistry Laboratory, V.I.Ilichev Pacific Oceanological Institute)

[MIS21-P10] Late Quaternary Total Organic Carbon fluctuation in the eastern Japan Sea and offshore of the Russian maritime provinces

*Yuta Hirano[1], Kyousuke Sakamoto[1], Naoto Ishida[2], Takao Ebinuma[2], Koji Seto[3], Ryo Matsumoto[4] (1.Graduate School of Sustainability Science Methane Hydrate Course ,Tottori University, 2.Tottori Univ., 3.Shimane Univ., 4.Meiji Univ.)

[MIS21-P11] Geochemical behavior of carbon in shallow sediment within the gas chimney in Hidaka Trough, offshore Hokkaido

Tsuyoshi Mamata[1], *Hitoshi Tomaru[1], Ryo Matsumoto[2] (1.Department of Earth Sciences, Chiba University, 2.Gas Hydrate Research Laboratory, Meiji University)

Raman spectroscopic analysis of isotopologue methane hydrates

*Yuki Kikuchi[1], Jumpei Matsuda[1], Akihiro Hachikubo[1], Satoshi Takeya[2]

1. Kitami Institute of Technology, 2. National Institute of Advanced Industrial Science and Technology (AIST)

Raman spectroscopy is one of the useful tool to get information of gas hydrate crystals. Natural gas hydrates in submarine/sublacustrine sediment mainly encage methane. Methane molecule is composed of carbon and hydrogen, and three kinds of isotopologues, $^{12}CH_4$, $^{13}CH_4$, and CH_3D exist in nature. Ozeki *et al.* (2018) first reported Raman spectra of CH_3D and CD_4 hydrates and compared with CH_4 (mainly $^{12}CH_4$) hydrate. We report Raman spectra of $^{13}CH_4$ hydrate and summarize Raman spectra of isotopologue methane hydrates.

$^{13}CH_4$ hydrate sample was synthesized in a small pressure cell (volume: 5 mL). Fine ice powder (1g) was put in the pressure cell, and introduced appropriate amount of $^{13}CH_4$ (purity: 99.5%, Taiyo-Nissan). $^{13}CH_4$ hydrate was formed by melting the fine ice powder at the temperature of 273.2 K under high pressure of $^{13}CH_4$. We retrieved the hydrate sample at 77 K and its Raman spectra was obtained at 123 K in the range 2,500-3,300 cm^{-1} using a Raman spectrometer (RMP-210, JASCO Corporation). The Raman peaks were fitted in the range 2,800-3,000 cm^{-1} for the C-H stretching peaks of methane using a Voigt function to obtain the integrated intensities of the two peaks corresponding to methane encaged in the large and small cages of the cubic structure I.

Raman shifts for the C-H stretching and bending modes of $^{13}CH_4$ was 0.8 cm^{-1} and 14 cm^{-1} smaller than those of $^{12}CH_4$, respectively, suggesting that ^{13}C-H bonds affect its vibrational frequency. Hydration number of $^{13}CH_4$ was estimated as 6.00±0.02, almost the same as that of $^{12}CH_4$ (6.02±0.02). Therefore, Cage occupancies of $^{13}CH_4$ and $^{12}CH_4$ hydrates showed no difference between them.

Reference

Ozeki T, Kikuchi Y, Takeya S, Hachikubo A (2018) Phase equilibrium of isotopologue methane hydrates enclathrated CH_3D and CD_4. J Chem Eng Data 63(6): 2266-2270, doi: 0.1021/acs.jced.8b00203

Keywords: methane hydrate, Raman spectroscopy, isotopologues

©2019. Japan Geoscience Union. All Right Reserved.

Gas origin of hydrate-bound gas in Lake Baikal

*Jumpei Matsuda[1], Yuki Kikuchi[1], Akihiro Hachikubo[1], Oleg Khlystov[2], Gennadiy Kalmychkov[3], Marc De Batist[4], Hirotoshi Sakagami[1], Hirotsugu Minami[1], Satoshi Yamashita[1]

1. Kitami Institute of Technology, 2. Limnological Institute, SB RAS, 3. Vinogradov Institute of Geochemistry, SB RAS, 4. Ghent University

In the framework of international collaboration between Kitami Institute of Technology (Japan), Limnological Institute (Russia), and Ghent University (Belgium), natural gas hydrates have been recovered from lake-bottom sediments at Lake Baikal. Near-surface gas hydrate was first discovered at the Malenky mud volcano at the southern Baikal basin in 2000. Multi-phase Gas Hydrate Project (MHP, 2009-2018) has revealed distribution of near-surface gas hydrates at the southern and central Baikal basins. We found six new places (Enkhelook, Soukhaya, KIT, LIN, PosolCanyon1, and PosolCanyon2) during the VER18-03 cruise in 2018. The total number of places where near-surface gas hydrates were retrieved is 53. In this report, we summarize characteristics of hydrate-bound gases retrieved from all the sites since 2005.

Gas hydrate crystals were recovered from lake-bottom sediment cores, and hydrate-bound gas samples were stored in 5-mL vials. Total number of hydrate-bound gas samples was 626. Molecular and isotopic compositions of hydrate-bound gas were measured using a gas chromatograph and a stable isotope ratio mass spectrometer.

In the Bernard plot, C_1 $\delta^{13}C$ and C_1 / (C_2 + C_3) distributes from -70‰ to -44‰ and from 6 to 100,000, respectively, suggesting that the origin of hydrate-bound gas is microbial, thermogenic, and their mixed-gas. Almost all data are plotted on the mixing line between microbial and thermogenic, however, Gorevoy Utes (oil seep site) showed thermogenic C_1 with small composition of C_2 and C_3. The data concentrates in the microbial field (C_1 $\delta^{13}C$: -66‰ and C_1 / (C_2 + C_3): 1,000-10,000). C_1 δD of thermogenic C_1 increases with C_1 $\delta^{13}C$. C_2 $\delta^{13}C$ distributes from -69‰ to -23‰. 17 sites (ex. Solzan, Talanka, Turka, KIT, etc.) showed microbial C_1 and C_2. 27 sites (Malenky, Oblom, Seep13, Kukuy K6, etc.) showed microbial C_1 and thermogenic C_2, indicating that small amount of thermogenic gas is mixed with microbial gas. Other sites (Mamay, PosolBank, Gorevoy Utes, Kedr, etc.) showed thermogenic C_1 and C_2. The Milkov plot (relation between C_1 $\delta^{13}C$ and C_2 $\delta^{13}C$) can express mixing condition between microbial and thermogenic rather than the Bernard plot. C_2 δD decreased with decrease in C_2 $\delta^{13}C$, therefore microbial C_2 is both depleted in ^{13}C and D. We conclude that hydrate-bound gas at Lake Baikal is mainly microbial gas, and thermogenic gas ascends from deep layer at some areas (Kedr, PosolBank, Kukuy, and Gorevoy Utes) and forms the structure II gas hydrate.

Keywords: gas hydrate, Lake Baikal, gas origin

©2019. Japan Geoscience Union. All Right Reserved.

Validation of self-preservation effect of methane and ethane mixed-gas hydrate by Raman spectroscopy

*Yunosuke Hase[1], Jumpei Matsuda[1], Akihiro Hachikubo[1], Satoshi Takeya[2]

1. Kitami Institute of Technology, 2. National Institute of Advanced Industrial Science and Technology (AIST)

Methane hydrate can be stored long time under atmospheric pressure below 273.2K, even though their P-T conditions is unstable, namely "self-preservation effect". On the contrary, Takeya and Ripmeester (2008) reported that ethane hydrate shows no self-preservation. In natural condition, methane and ethane mixed-gas hydrates have been found at Lake Baikal, however, there is no information for the mixed-gas system. In the last JpGU meeting we report self-preservation effect for mixed-gas hydrate, but the conditions of samples are not uniform. Because the size of crystals affect rate of survival at higher temperature, we controlled the specific surface of area of gas hydrate samples in this study.

We put 0.7 g of fine ice balls (diameter: 0.108-0.180 mm) into a pressure cell (volume: 30 mL) and mixed-gas of methane and ethane was introduced. Hydrate crystals formed at 273.2 K. The gas hydrate sample was degased and recovered at the temperature of liquid nitrogen. We controlled the ethane composition of hydrate-bund gas from 0% to 100%, covering the area of methane-rich structure I, ethane-rich structure I, and their intermediate structure II. We measured compositions of methane and ethane by a gas chromatograph (GC-2014, Shimadzu Corporation). Gas hydrate samples were placed on a temperature-controlled device and kept at 80 K. Raman spectra of hydrate samples were obtained using a Raman spectrometer (RMP-210, JASCO Corporation). We checked the Raman spectra of C-H stretching mode at 83 K, and then increased the sample temperature every 10 K until complete dissociation. We calculated the Raman peak area for C-H stretching mode of methane and ethane around 2900 cm^{-1} by a peak fitting method and obtained the survival rate of gas hydrate samples with temperature.

Pure methane hydrate survived well, more than 20% of hydrate still remained at 263 K, whereas pure ethane hydrate completely dissociated at around 200 K. These results agree well with our previous report. As for mixed-gas hydrate composed of methane and ethane, the rates of survival of structure I were lower than that of pure methane hydrate, but the crystals remained till 253 K, suggesting self-preservation. That of structure II well remained at 83-183 K, but quickly disappeared at 213 K. Therefore, it is possible that the survival rate of mixed-gas hydrate composed of methane and ethane depends on not only gas composition but also crystallographic structure.

Reference

Takeya S, Ripmeester JA (2008) Dissociation behavior of clathrate hydrates to ice and dependence on guest molecules. Angew Chem Ed 47: 1276-1279

Keywords: gas hydrate, self preservation effect, methane, ethane

©2019. Japan Geoscience Union. All Right Reserved.

Experimental study on the phase equilibrium condition of CO_2 hydrate with marine sediment

*Daisuke Maki[1], Hitoshi Tomaru[1]

1. Graduate School of Science and Engineering, Chiba University

Gas hydrate accumulation has been found in the marine sediments around Japan, and has been regarded as an unconventional gas resource because it contains a huge amount of methane. The phase equilibrium condition of gas hydrate provides a key parameter to estimate the distribution and resource potential of gas hydrate. Although the influences of temperature, pressure, gas/water composition, etc. on the phase equilibrium have been studied so far, experimental studies concerning the effect of sediment particles in shallow gas hydrate deposit are not well understood. In this study, we synthesized carbon dioxide hydrate which has similar physicochemical behavior to methane hydrate and examined the phase equilibrium condition with the mud collected near the shallow gas hydrate in the Japan Sea. It was found that the equilibrium condition with mud was significantly reduced; about 0.2℃ lower and about 0.1 MPa higher compare to mud-free environment. Our results strongly indicates that the existence of mud may change the stability condition of gas hydrate in the natural environment and it is necessary to consider this effect for estimating gas hydrate distribution and stability fields.

Keywords: gas hydrate, phase equilibrium

©2019. Japan Geoscience Union. All Right Reserved.

Raman spectroscopic analysis of structure H gas hydrates encapsulating cyclic hydrocarbons

*Go Fuseya[1], Satoshi Takeya[2], Akihiro Hachikubo[1]

1. Kitami Institute of Technology, 2. National Institute of Advanced Industrial Science and Technology (AIST)

Clathrate hydrates are crystalline inclusion compounds that consist of well-defined cages formed by water molecules and guest molecules of suitable sizes and shapes trapped in the cages. Clathrate hydrates including natural gases as guest molecules are commonly known as gas hydrates. Gas hydrates in sea or lake bottom sediments and permafrost layers have attracted considerable interest as a potential source of unconventional natural gas. There are three common crystallographic structure of hydrates, structure I (sI), structure II (sII) and structure H (sH). In the case of microbially sourced gas hydrate system, the gas hydrates are generally sI CH_4 hydrates. On the other hand, sH hydrate was found at northern Cascadia margin, where thermogenic larger hydrocarbons exist [Lu et al. 2007]. For instance,, cyclohexane (CH), methylcyclopentane (MCP), methylcyclohexane (MCH) and other large hydrocarbons, which is capable of forming sH hydrate with help gas like CH_4, were detected at the area. From the above, study for sH hydrate which encapsulating these large hydrocarbons are important for further understanding of natural gas hydrates.

In this study, sH CH_4 and larger cyclic hydrocarbon (CH, MCP and MCH) mixed hydrates were prepared. We observed the variations of Raman spectra of these cyclic hydrocarbons due to enclathrated water cages of gas hydrate. C–H and C–C stretching regions of enclathrated these cyclic hydrocarbons were measured by the Raman spectroscopic method., The Raman spectra of C–C stretching region of these hydrocarbon are useful for identification of guest molecules in natural gas hydrates because the number of Raman peaks of C–C stretching region are smaller than that of C–H stretching region.

Reference

Lu *et al.* (2007) Effect of temperature and large guest molecules on the C–H symmetric stretching vibrational frequencies of methane in structure H and I clathrate hydrates. *Nature.* **8**: 303-306.

doi: 10.1038/nature0546.

Keywords: gas hydrate, Raman spectroscopy

©2019. Japan Geoscience Union. All Right Reserved.

Investigation of self-preservation of argon hydrate by measuring specific surface area

*Yuki Ikeura[1], Daisuke Yahagi[1], Akihiro Hachikubo[1], Satoshi Takeya[2]

1. Kitami institute of technology, 2. National Institute of Advanced Industrial Science and Technology (AIST)

Self-preservation occurs during the dissociation of gas hydrate and drastically decreases speed of dissociation at around 253K and under atmospheric pressure in the case of methane hydrate. Takeya and Ripmeester (2008) revealed that not only methane but also nitrogen, oxygen, argon, and CO_2 hydrates showed the same self-preservation effect. This phenomena is explained that (1) gas hydrate dissociates below the ice point, (2) ice remains on the surface of crystals, (3) ice layer forms and covers on the surface of hydrate and prevent from further dissociation. We developed a device for measuring specific surface area of snow particles (Hachikubo *et al.*, 2014), and it is also available for gas hydrate crystals. Because self-preservation phenomena depends on temperature, we investigated the change of specific surface area of argon hydrate samples in their dissociation process under various temperature conditions.

Fine ice balls (diameter: 0.108-0.180 mm) were formed in liquid nitrogen using water spray and sieved in a cold room (temperature: 255 K). 3 g of ice balls were put into a pressure cell (volume: 30 mL) and measured their specific surface area. After that, argon was introduced and hydrate crystals formed at 273.2 K. Temperature of the samples were controlled at 226K, 243K, 254K, and 263K, and then the residual gases in the pressure cell were quickly removed. The internal pressure decreased to the atmospheric pressure and the samples started to dissociate. Dissociation times were controlled as 1 minute, 10 minutes, and 100 minutes, and after that the samples were fixed at the temperature of liquid nitrogen and we measured their specific surface area. Their dissociation rate were estimated from weight data of gas and water. Specific surface area of the original fine ice balls and (pure) argon hydrate samples were also measured.

Ice balls were expected to change completely into “hydrate balls”, however, more fine and irregular grains of argon hydrate were observed using an optical microscope Specific surface area of original ice balls was 71±5 [m^2 kg^{-1}], and that of argon hydrate increased to 119 [m^2 kg^{-1}]. When the dissociation period was 1 minute, more than 90% of hydrate still remained at 226-263 K. The rate of dissociation at 254 K was fastest in the case of 10 minutes dissociation (65% of hydrate remained), but about 80% of hydrate sample remained at 263 K. The specific surface area was around 120 [m^2 kg^{-1}] after 10 minutes at 263 K, indicating that the condition of surface was not changed at 263 K. On the other hand, the specific surface area increased to 279 [m^2 kg^{-1}] at 226 K after 10 minutes. Therefore, these results indicate that the self-preservation effect appeared at 263 K and kept the surface of crystals smooth rather than the case at 226 K.

References

Takeya S, Ripmeester JA (2008) Dissociation behavior of clathrate hydrates to ice and dependence on guest molecules. Angew Chem Int Ed 47: 1276-1279

Hachikubo A, Yamaguchi S, Arakawa H, Tanikawa T, Hori M, Sugiura K, Matoba S, Niwano M, Kuchiki K,

©2019. Japan Geoscience Union. All Right Reserved.

Aoki T (2014) Effects of temperature and grain type on time variation of snow specific surface area. Bull Glaciol Res 32: 47-53

Keywords: gas hydrate, argon, self preservation effect, specific surface area

©2019. Japan Geoscience Union. All Right Reserved.

Carbon isotope fractionation of CO_2 during the formation of clathrate hydrate

*Hiromi Kimura[1], Jumpei Matsuda[1], Yuki Kikuchi[1], Akihiro Hachikubo[1], Satoshi Takeya[2]

1. Kitami Institute of Technology, 2. National Institute of Advanced Industrial Science and Technology

Hydrogen Isotope fractionation in methane during the formation of clathrate hydrate was reported by Hachikubo *et al.* (2007) that δ D of hydrate-bound methane is 4.8±0.4‰ lower than that of residual methane at 274.2K. Although natural methane hydrates distribute widely in the world, natural CO_2 hydrate was only reported at the Okinawa Trough (Sakai *et al.*, 1990). It is also possible that CO_2 hydrate exists in Mars. Isotopic fractionation of guest gas may provide useful information to understand formation processes of gas hydrate. Luzi *et al.* (2011) revealed that CO_2 $\delta^{13}C$ in hydrate-bound gas is 0.9‰ lower than that of residual gas, suggesting that light CO_2 molecules prefer to be encaged into clathrate cages. In this study, we checked the temperature effect on the isotopic difference between residual and hydrate-bound CO_2.

Samples of CO_2 hydrate (weight: 0.7 g) were experimentally prepared in a pressure cell (volume: 30 mL), and the temperature was controlled by a liquid bath (258-274 K) and cold rooms (226-254 K). Isotopic compositions of both residual and hydrate-bound CO_2 were measured by an isotope ratio mass spectrometer (IRMS). Samples were formed in the temperature range from 226 K to 274 K. The carbon isotopic differences between hydrate-bound and residual CO_2 distributed between 1.2‰ and 1.5‰, agreed fairly well with the previous report (Luzi *et al.*, 2011). The difference seemed to be large (1.5-2.0 ‰) at 226 K, indicating that the equilibrium pressure of $^{13}CO_2$ hydrate is slightly larger than that of $^{12}CO_2$ hydrate, and the difference between them becomes large in lower temperature. We will show these equilibrium data for $^{13}CO_2$ and $^{12}CO_2$ hydrates and compare with the results in stable isotope.

Reference

Hachikubo A, Kosaka T, Kida M, Krylov A, Sakagami H, Minami H, Takahashi N, Shoji H (2007) Isotopic fractionation of methane and ethane hydrates between gas and hydrate phases. Geophys Res Lett 34: L21502. doi:10.1029/2007GL030557

Sakai H, Gamo T, Kim ES, Tsutsumi M, Tanaka T, Ishibashi J, Wakita H, Yamano M, Oomori T (1990) Venting of carbon dioxide-rich fluid and hydrate formation in mid-okinawa trough backarc basin. Science: 248, 4959, 1093-1096.

Luzi M, Schicks JM, Erzinger J (2011) Carbon isotopic fractionation of synthetic methane and carbon dioxide hydrates. Proc. 7th International Conference on Gas Hydrates (ICGH2011).

Keywords: gas hydrate, stable isotope, carbon dioxide, isotopic fractionation

©2019. Japan Geoscience Union. All Right Reserved.

Gas hydrate survey off Tokachi (the Pacific Ocean) in the framework of practical education of Kitami Institute of Technology

*Yunosuke Hase[1], Jumpei Matsuda[1], Yuki Ikeura[1], Akihiro Hachikubo[1], Masaaki Konishi[1], Hirotoshi Sakagami[1], Hirotsugu Minami[1], Satoshi Yamashita[1]

1. Kitami Institute of Technology

Distribution of BSR (bottom simulating reflector) has been reported off Tokachi, the Pacific Ocean (Hayashi *et al.*, 2010). Kitami Institute of Technology started gas hydrate survey in this area on 2014, using TS Oshoro-maru of Hokkaido University. This program is conducted in the framework of practical education (name of lecture: “Practical learning about the Okhotsk Region, its history and the natural environment”), and about 40 students participate the cruise. Three cruises (C008, C046, and C061) were executed in 2014-2018. We found many gas seeps ascending from sea floor, those height exceeded 700 m from the sea floor. We recovered gas-rich sediment cores by a gravity and hydrostatic corers. Here, we report characteristics of sediment gas in this area.

Samples of sediment gas, mainly dissolved gases in pore water, were obtained by a headspace gas method. 10 mL sediment was sampled from the sediment core by a plastic syringe (volume: 5 mL) and put into a 25 mL vial. 10 mL NaCl aqueous solution was introduced into the vial by using a micropipette and sealed employing a butyl rubber septum to make a headspace (5 mL volume). To avoid any changes in the headspace, preservative (benzalkonium chloride, BKC) was added and the headspace part was flushed by helium. We roughly checked gas composition of sediment gases onboard using a portable gas chromatograph, and after that we measured the molecular and isotopic compositions of headspace gases using another gas chromatograph and CF-IRMS in our laboratory.

Concentration of C_1 increased with depth, and exceeded 1 [mM] in the bottom of some sediment cores (C008-GC1403, C046-GC1702, and C061-GC1803), indicating that their depths of SMI (sulfate-methane interface) were small and active gas seep existed at the sea floor. The minimum SMI depth was 50 [cmbsf] in C008-GC1403. C_1 / (C_2 + C_3) in these gas-rich layer was from 300 to 700. Concentration of H_2S exceeds 1 [mM] in the bottom of sediment cores. These results indicate that microbial gas is supplied from lower layer and AOM (anaerobic oxidation of methane) processes is active in beneath the sea floor. C_1 $\delta^{13}C$ profiles showed minimum values (lower than -100‰) at the SMI depth in C061-GC1803. C_2 $\delta^{13}C$ distributed between -55‰ and -30‰, suggesting that C_2 seems also microbial origin.

Reference

Hayashi M, Saeki T, Inamori T, Noguchi S (2010) The distribution of BSRs related to methane hydrates, offshore Japan. J Jpn Assoc Petrol Technol 75(1): 42-53

Keywords: gas hydrate, methane, the Pacific Ocean

©2019. Japan Geoscience Union. All Right Reserved.

Geochemistry of pore water and gas in shallow sediments from offshore Primorsky Krai, Russia

*Musashi Yokoyama[1], Hitoshi Tomaru[1], Ryo Matsumoto[2], Glen Snyder[2], A.V. Yatsuk[3], D.A Shvalov[3]

1. Department Earth Sciences, Chiba University, 2. Gas Hydrate Research Laboratory, Meiji University, 3. Gas Geochemistry Laboratory, V.I.Ilichev Pacific Oceanological Institute

Offshore region of Primorsky Krai, Russia, in the northern Japan Sea is located in the boundary area between the shallower Tatar Trough on the north and deeper Japan Basin in the south. The marginal area of the Japan Sea has been characterized by the dense distribution of gas chimneys, which are identified by columnar blanking structureon acoustic records, e.g., W-S-E Tsushima Basin, Oki Trough, Joetsu Basin, Mogami Trough, and SW Sakhalin Island. Gas chimney structure delivers hydrocarbon gas, mainly methane, significantly from deep sediment to surface sediment, which may cause gas hydrate accumulation, carbonate precipitation, gas seepage, etc. Therefore it is one of the key structures controlling near-seafloor phenomena. In this research, we analyzed chemical compositions of pore water and gas collected from shallow sediments, off Primorsky, Russia (R/V Akademik M.A. Lavrentyev, Cruise LV81, 2018), and estimated the methane flux to characterize the geochemical environment near the seafloor. The sulfate concentrations linearly decrease with depth and the methane/ethane ratios are as low as ~100 at all sites, reflecting anaerobic oxidation of methane (AOM) is active at the sulfate methane interface (SMI). Decreases in calcium and magnesium were also obvious, indicating carbonate precipitation in response to alkalinity increase due to AOM. The methane flux estimated from SMI depths are generally high in the northern research area compared to southern area, in particular, at shallow gas chimney sites (SMI at ~1.5 mbsf, <1500 mWD). At the northern-most deep gas chimney sites, methane fluxes are relatively low. These results indicate that organic matter was primarily derived along the trough (from north to south) rather than the landward slope off Primorsky, and the methane generated in the sediment of deep area of the trough migrated through the porous layers to the shallow sites where the gas chimney is active. The geochemistry of pore water and gas depicts the shallow geochemical environments associated methane migration in research area.

Keywords: gas chimney, methane

©2019. Japan Geoscience Union. All Right Reserved.

Late Quaternary Total Organic Carbon fluctuation in the eastern Japan Sea and offshore of the Russian maritime provinces

*Yuta Hirano[1], Kyousuke Sakamoto[1], Naoto Ishida[2], Takao Ebinuma[2], Koji Seto[3], Ryo Matsumoto[4]

1. Graduate School of Sustainability Science Methane Hydrate Course ,Tottori University, 2. Tottori Univ., 3. Shimane Univ., 4. Meiji Univ.

In the Sea of Japan, three cores were taken from the Oki Trough (PC1606), Mogami Trough South (PC1726), and the offshore of the Russian Primorye (Lv81-35GC). Total organic carbon (TOC), total nitrogen (TN), and total sulfur (TS) in sediments were measured from these cores, and the organic carbon concentration and the origin of organic matter were clarified. The organic carbon concentration in the sediment reflects the past primary production. All cores have high correlation between TN and TOC. The value of C/N is from 6 to 10. On the other hand, there is no correlation between TS and TOC. The value of C/S varies from 0.2 to 11. The TOC concentration of PC1726 and Lv81-35GC is almost coincide with PC1606. However, the peak around 10 ka detected in PC1606 is unclear in the other cores. In the period of the Last Glacial Maximum, primary production declined at all areas. However, the subsequent reactions were different in each area.

Keywords: Total Organic Carbon, Japan Sea, Late Quaternary, Shallow type methane hydrate

©2019. Japan Geoscience Union. All Right Reserved.

Geochemical behavior of carbon in shallow sediment within the gas chimney in Hidaka Trough, offshore Hokkaido

Tsuyoshi Mamata[1], *Hitoshi Tomaru[1], Ryo Matsumoto[2]

1. Department of Earth Sciences, Chiba University, 2. Gas Hydrate Research Laboratory, Meiji University

The Hidaka Trough, offshore Hokkaido, has recently been characterized by subsurface gas chimney structures associated with mound/pockmark topography and methane plume, which indicate an intensive gas migration from deep sediments to the surface area. In the region where remarkable gas chimneys are developed such as in offshore Joetsu, shallow marine sediments are characterized by the precipitation of authigenic carbonate, massive gas hydrates and development of chemotrophs because of high methane concentration near the seafloor. In these environments, anaerobic oxidation of methane utilizes both methane and sulfate, resulting in sulfate depleted in shallow sediment. Inorganic carbon generated by methane oxidation does not incorporate only with calcium ion to form carbonate but also is reduced by microbially-mediated methanogenic reaction. Carbon is therefore a key substance near the depth of sulfate methane interface (SMI) in high methane flux area. This study aims to figure out the chemical reaction associated with carbon, which characterizes geochemical environment in shallow sediments, by analyzing concentrations of dissolved ions and hydrocarbons, and stable isotopic composition ($\delta^{13}C$) of dissolved carbons collected from shallow sediments with gas chimney structures in the Hidaka Trough, offshore Hokkaido.
In the area of calyptogena community, the SMI locates at shallow depth and indicates reductive environment is established because of sulfate depletion. The sulfate is depleted at shallower depth in the area with carbonates near the seafloor, where the concentration of calcium ion is also lower than other areas. These results indicate carbonate formed at higher rate in the area with higher methane flux. Total organic carbon amount decrease with depth above the SMI, the residual organic matter in sediment generates methane at depth and enhances the methane flux toward the seafloor. Based on the composition of dissolved hydrocarbons and $\delta^{13}C$ of methane, although the methane is generally of biogenic origin over the research areas in the Hidaka Trough, the $\delta^{13}C$ of methane increase rapidly with depth on the mound center, indicating thermogenic methane predominantly migrate from deeper sediments at the site. Biogeochemical behavior of carbon varies not only among sampling sites but also among relative locations on the single gas chimney structure.

Keywords: SMI, gas chimney, Hidaka Trough

©2019. Japan Geoscience Union. All Right Reserved.

[J] Oral | M (Multidisciplinary and Interdisciplinary)：M-IS Intersection

Tue. May 28, 2019 9:00 AM - 10:30 AM JST | Tue. May 28, 2019 12:00 AM - 1:30 AM UTC | 202 2F

[M-IS27] Atmospheric electricity: Applications toward natural disaster mitigation

convener:Yasuhide Hobara(Graduate School of Information and Engineering Department of Communication Engineering and Informatics, The University of Electro-Communications), Masashi Kamogawa(Department of Physics, Tokyo Gakugei University), Chairperson:Takeshi Morimoto

In recent years, various types of natural disasters caused by climate change, earthquake, etc. occur frequently in the world. In 2018 heavy precipitation in various regions of Japan and the earthquakes in Hokkaido and Indonesiaproduced/greater human and economic/damage.

In 2019JpGU Atmospheric Electricity (AE) session, invited experts are going to introduce their scientific challenges in order to monitor, predict and mitigate natural disasters by using knowledge of the atmospheric electricity. For example, monitoring and prediction of extreme weather by the latest weather radar system and lightning observations, electromagnetic phenomena prior to earthquakes, etc. will be included. We certainly welcome contributed papers regarding all topics on atmospheric electricityincluding global circuit, ion and fair weather electricity, thunderstorm electrification, lightning physics, lightning and meteorology, electrical effects of thunderstorms on the middle and upper atmosphere such as transient luminous events and high energy phenomena, lightning protection, terrestrial electromagnetic environment and so on.

9:00 AM - 9:15 AM JST | 12:00 AM - 12:15 AM UTC

[MIS27-01] Advantage and Disadvantage of the Phased Array Weather Radar

*Tomoo Ushio[1], Tomoaki Mega[1], Hiroshi Kikuchi[2], Eiichi Yoshikawa[3] (1.Tokyo Metropolitan University, 2.University of Electro-Communications, 3.JAXA)

9:15 AM - 9:30 AM JST | 12:15 AM - 12:30 AM UTC

[MIS27-02] Initial Observations with X-band Dual Polarimetric Phased Array Weather Radar in Tokyo

*Hiroshi Kikuchi[1], Taku Suezawa[2], Yasuhide Hobara[1], Tomoo Ushio[2] (1.The University of Electro-Communications, 2.Tokyo Metropolitan University)

9:30 AM - 9:45 AM JST | 12:30 AM - 12:45 AM UTC

[MIS27-03] Three-dimensional total lightning characteristics of convective cells observed by the Tokyo LMA in the summer season in Tokyo Metropolitan area

*Namiko Sakurai[1], Paul R. Krehbiel[2], William Rison[2], Ronald J. Thomas[2], Daniel Rodeheffer[2], Shingo Shimizu[1], Koyuru Iwanami[1], Takeshi Maesaka[1], Kaori Kieda[1], Yasushi Uji[1] (1.National Research Institute For Earth Science and Disaster Resilience, 2.New Mexico Tech.)

9:45 AM - 10:00 AM JST | 12:45 AM - 1:00 AM UTC

[MIS27-04] Estimating rainfall in heavy rain events using lightning data in Japan

*Ogawa Tetsuya[1], Yasuhide Hobara[1], Hiroyuki IWASAKI[2], Stan Heckman[3], Michael Stock[3] (1.University of Electro-Communications, 2.Gunma University, 3.EarthNetworks)

10:00 AM - 10:15 AM JST | 1:00 AM - 1:15 AM UTC

[MIS27-05] The Effect of Lightning Phenomena on Lightning Protection for Objects on the Ground

★Invited Papers

*Yokoyama Shigeru[1] (1.Shizuoka University)

10:15 AM - 10:30 AM JST | 1:15 AM - 1:30 AM UTC

[MIS27-06] Lightning charge moment changes deduced from highly sensitive ELF magnetic field observations in Southeast Asia

*Yasuhide Hobara[1], Amir Izzani Mohamed[2], Chandima Gomes[3], Wan Ismail Bin Ibrahim[2], Zulkurnain Abdul-Malek[4], Syahrun Nizam[5], Michael Stock[6], Kazuo Shiokawa[7], Hiroshi Kikuchi[1], Takuo T. Tsuda[1]
(1.Graduate School of Information and Engineering Department of Communication Engineering and Informatics, The University of Electro-Communications, 2.University of Malaysia Pahang Pekan, Malaysia, 3.University of the Witwatersrand Johannesburg, South Africa, 4.Universiti Teknologi Malaysia Johor Bahru, Malaysia, 5.University Malaysia Perlis Perlis, Malaysia, 6.EarthNetworks, Inc. Germantown, USA, 7.Nagoya University, Nagoya, Japan)

Advantage and Disadvantage of the Phased Array Weather Radar

*Tomoo Ushio[1], Tomoaki Mega[1], Hiroshi Kikuchi[2], Eiichi Yoshikawa[3]

1. Tokyo Metropolitan University, 2. University of Electro-Communications, 3. JAXA

Recent progress of information and communication technologies has been enabling us to realize a rapid scanning radar system. In 2012, Toshiba Corporation and Osaka University succeeded in developing a new type of Phased Array Radar (PAR) system (Yoshikawa et al. 2013, Ushio et al. 2015, Mizutani et al. 2018) under a grant of National Institute of Communication and Information Technology (NICT), and installed in Suita Campus, Osaka University. This PAR system can scan the whole sky within 30 seconds up to 60 km in radius over 100 elevation angles with digital beam forming technique, and the initial observation results demonstrate the unique capability of the new PAR system. However, the observation is sometimes seriously contaminated by strong ground clutter through relatively high sidelobes at transmitting stage. In this study, a new clutter mitigation algorithm from adaptive beam forming technique on Minimum Mean Square Error (MMSE) formulation was investigated, and succeeded in suppressing not only the ground clutter but also ghost echo from strong precipitation echo nearby more than 20dB. And also the adaptive algorithm was applied to supress the range sidelobe and showed the sidelobe level of -60dB. In this presentation, the advantages and disadvantages of the PAR will be discussed based on the observation results.

©2019. Japan Geoscience Union. All Right Reserved.

Initial Observations with X-band Dual Polarimetric Phased Array Weather Radar in Tokyo

*Hiroshi Kikuchi[1], Taku Suezawa[2], Yasuhide Hobara[1], Tomoo Ushio[2]

1. The University of Electro-Communications, 2. Tokyo Metropolitan University

The weather radars using parabolic dish antenna generally require 5-10 minutes to mechanically rotate and to tilt upwards as they sample the atmosphere at several different elevation angles. The number of the observable elevation angles is about ten or so. The single polarization phased array weather radar (SP-PAWR), which has been developed in 2012, was designed to conduct precipitation measurement of a radar reflectivity factor, in less than 10 or 30 seconds in a range of 20 or 60 km in real-time, respectively. As a next radar development project, a dual polarimetric phased array weather radar (Multi-parameter phased array radar; MP-PAWR) is being developed. It can provide multi-parameter measurements that reveal detailed microphysics of storms in addition to accurate precipitation estimation, and can improve weather forecasts.
The first made MP-PAWR, which simultaneously transmits pulses of horizontal and vertical polarized radiation, has been developed and installed in December 2017, at Saitama University, Japan. The center of frequency is 9.4GHz (X-band). The MP-PAWR has a scanning scheme similar to the SP-PAWR, which uses the mechanical and electronic scanning in azimuth and elevation angles, respectively. The MP-PAWR provides the polarimetric precipitation measurements in three-dimensional volume scanning in less than 30 or 60 seconds in a range of 60 or 80 km in real-time, respectively.
In this presentation, we will show the initial observation results. To confirm reliability of the measurements and to evaluate the accuracy of the measurements by the MP-PAWR, the initial observation results of the MP-PAWR are compared with an optical disdrometer data.

Keywords: Precipitation Observation, Phased array radar

©2019. Japan Geoscience Union. All Right Reserved.

Three-dimensional total lightning characteristics of convective cells observed by the Tokyo LMA in the summer season in Tokyo Metropolitan area

*Namiko Sakurai[1], Paul R. Krehbiel[2], William Rison[2], Ronald J. Thomas[2], Daniel Rodeheffer[2], Shingo Shimizu[1], Koyuru Iwanami[1], Takeshi Maesaka[1], Kaori Kieda[1], Yasushi Uji[1]

1. National Research Institute For Earth Science and Disaster Resilience, 2. New Mexico Tech.

The National research Institute for Earth science and Disaster resilience, Japan (NIED) has observed three-dimensional total lightning with Lightning Mapping Array in Tokyo metropolitan area (Tokyo LMA) since 2017. In this study, we report various total lightning characteristics of convective cells observed by the Tokyo LMA in the summer season. Three convective cells developed at around 14:00 JST on 30 August 2017 in Tokyo. They were located at a short distance each other, and they merged into a multi-cell thunderstorm after a while. The total lightning characteristics of the three convective cells before they merged into the multi-cell thunderstorm are as follows: in one convective cell which was located in the middle of the cells, IC lightning flashes preceded the first CG lightning for about 20 minutes. On the other hand, a CG lightning flash firstly occurred in another convective cell. In the other convective cell, IC lightning flashes predominated. These three cells and the multi-cell thunderstorm had normal tripole structures. In addition, several bolt-from-the-blue were observed in these three cells.

Keywords: lightning

©2019. Japan Geoscience Union. All Right Reserved.

Estimating rainfall in heavy rain events using lightning data in Japan

*Ogawa Tetsuya[1], Yasuhide Hobara[1], Hiroyuki IWASAKI[2], Stan Heckman[3], Michael Stock[3]

1. University of Electro-Communications, 2. Gunma University, 3. EarthNetworks

In this study, we examined the relationship between total lightning (TL) and heavy rainfall in high spatio-time resolution by using 37 severe thunderstorms in Japan. TL is continuously monitored by the Japanese Total Lightning Network (JTLN) deployed by UEC and operated jointly by UEC and EarthNetworks, whilst high spatio-temporal precipitation data is obtained by eXtended Rader Information Network (XRAIN) operated by Ministry of Land, Infrastructure, Transport and Tourism in Japan. As a result, positive linear relation with rather high cross correlation (r2 ~ 0.54 between TL and Precipitation Volume (PV) [m3] has been obtained. The cross correlation between TL and PV is much higher than that for cloud-to-ground lightning (CG) and PV. Although the slope of linear relation (TL vs. PV) varies depending on heavy rain events, TL can be promising tool to estimate severe rainfall.

Keywords: lightning, Total lightning, severe weather

©2019. Japan Geoscience Union. All Right Reserved.

The Effect of Lightning Phenomena on Lightning Protection for Objects on the Ground

*Yokoyama Shigeru[1]

1. Shizuoka University

When lightning strikes the transmission line or the distribution line, high voltage is generated between the wire and the earth, discharge occurs in the insulator, and power failure occurs. A high voltage is generated when the peak value of the lightning current is large. Also, as the wave front length of the current is shorter, a higher voltage is generated. On the other hand, the lightning rod fails to catch the lightning discharge and destroys the roof and wall of the building even with the low peak value of the lightning current. Furthermore, damage caused by lightning arrester burnout is not much affected by the length of wave front length, and it is greatly influenced by the duration (charge amount) of the lightning current. Table 1 shows the relationship between the types of lightning damage and lightning parameters. Since lightning properties related to lightning damage of ground structures depend upon the object, it is important to fully understand the lightning phenomena to take countermeasures against lightning damages. Moreover, it is also necessary to clarify the seasonal and local characteristics of lightning from the viewpoint of risk management because there are lightning with significantly different properties from ordinary summer lightning such as the Japanese winter lightning. In this paper I will explain the lightning properties necessary for countermeasures against lightning damage and consider the issues of lightning observations in the future.

Keywords: Lightning, Lightning Protection, Power Grid, Wind Power

©2019. Japan Geoscience Union. All Right Reserved.

表１雷被害と関係する雷のパラメータ

	電流波高値	雷撃距離	波頭峻度（波頭長の逆数）	波尾長（電流継続時間）		対策法	備考
絶縁破壊(碍子など回復可能なもの)	◎		○			架空地線、避雷器、SPD	統流の影響
絶縁破壊(半導体など)	◎					SPD,光ファイバ	
通過電荷量によるエネルギー被害(避雷器焼損、架空地線素線切れ)				○		避雷器（SPD）の容量増加	
オーミックロス（エネルギー）によるエネルギー被害（風車塔体内焼損など）	○			○		引下げ導体と受雷部などの接続部強固化	
送電線架空地線遮蔽失敗		○				架空地線の２条化	
建築物損壊（コンクリート、レンガ等）		○				避雷針（受雷部）の強化	
建築物損壊、着火（藁葺き屋根、桧皮葺き屋根）		○		◎		避雷針（受雷部）の強化	消火体制
ノイズ（EMC 的影響）	○		○			離隔距離の確保、信号線の電磁シールド	雷電流の通過による回路の誤動作など

©2019. Japan Geoscience Union. All Right Reserved.

Lightning charge moment changes deduced from highly sensitive ELF magnetic field observations in Southeast Asia

*Yasuhide Hobara[1], Amir Izzani Mohamed[2], Chandima Gomes[3], Wan Ismail Bin Ibrahim[2], Zulkurnain Abdul-Malek[4], Syahrun Nizam[5], Michael Stock[6], Kazuo Shiokawa[7], Hiroshi Kikuchi[1], Takuo T. Tsuda[1]

1. Graduate School of Information and Engineering Department of Communication Engineering and Informatics, The University of Electro-Communications, 2. University of Malaysia Pahang Pekan, Malaysia, 3. University of the Witwatersrand Johannesburg, South Africa, 4. Universiti Teknologi Malaysia Johor Bahru, Malaysia, 5. University Malaysia Perlis Perlis, Malaysia, 6. EarthNetworks, Inc. Germantown, USA, 7. Nagoya University, Nagoya, Japan

In 2018 we established the new permanent observation site in Pahang, Malaysia and started continuous recording of horizontal magnetic waveforms in the Extremely Low Frequency (ELF) band by using high sensitivity search coils. We carried out test measurements at four different locations in Malay peninsula and found out that Pahang is the most electromagnetically quiet place for measurement. Initial results indicate a very good performance registering clear waveforms from lightning discharges. We successfully estimated individual lightning charge moment changes (CMCs) with a small lower bound (~few Ckm) with a lightning location data from total lightning network indicative of deducing spatial and temporal dependence of lightning with CMC over Southeast Asia region.

Keywords: Lightning, ELF (Extremely Low Frequency), Charge Moment Changes

©2019. Japan Geoscience Union. All Right Reserved.

[J] Oral | M (Multidisciplinary and Interdisciplinary)：M-IS Intersection

Tue. May 28, 2019 10:45 AM - 12:15 PM JST | Tue. May 28, 2019 1:45 AM - 3:15 AM UTC | 202 2F

[M-IS27] Atmospheric electricity: Applications toward natural disaster mitigation

convener:Yasuhide Hobara(Graduate School of Information and Engineering Department of Communication Engineering and Informatics, The University of Electro-Communications), Masashi Kamogawa(Department of Physics, Tokyo Gakugei University), Chairperson:Yasuhide Hobara

In recent years, various types of natural disasters caused by climate change, earthquake, etc. occur frequently in the world. In 2018 heavy precipitation in various regions of Japan and the earthquakes in Hokkaido and Indonesiaproduced/greater human and economic/damage.
In 2019JpGU Atmospheric Electricity (AE) session, invited experts are going to introduce their scientific challenges in order to monitor, predict and mitigate natural disasters by using knowledge of the atmospheric electricity. For example, monitoring and prediction of extreme weather by the latest weather radar system and lightning observations, electromagnetic phenomena prior to earthquakes, etc. will be included. We certainly welcome contributed papers regarding all topics on atmospheric electricityincluding global circuit, ion and fair weather electricity, thunderstorm electrification, lightning physics, lightning and meteorology, electrical effects of thunderstorms on the middle and upper atmosphere such as transient luminous events and high energy phenomena, lightning protection, terrestrial electromagnetic environment and so on.

10:45 AM - 11:00 AM JST | 1:45 AM - 2:00 AM UTC

[MIS27-07] Earthquake precursory electromagnetic phenoma : Summary and prospective

★Invited Papers

*Masashi Hayakawa[1] (1.Hayakawa Institute of Seismo Electromagnetics.Co. LTD. University of Electro-Communications venture company)

11:00 AM - 11:15 AM JST | 2:00 AM - 2:15 AM UTC

[MIS27-08] Detection of lower ionospheric anomaly preceding earthquake using nonlinear autoregressive neural network

*Kakeru Matsuki[1], Hayato Iibuchi[1], Hendy Santosa[3], Yasuhide Hobara[1], Michael A Balikhin[2] (1.The University of Electro-Communications , 2.University of Sheffield, 3.University of Bengkulu)

11:15 AM - 11:30 AM JST | 2:15 AM - 2:30 AM UTC

[MIS27-09] Analysis of multipoint measurements of plasma turbulence

*Michael A Balikhin[1], Simon N Walker[1] (1.University of Sheffield)

11:30 AM - 11:45 AM JST | 2:30 AM - 2:45 AM UTC

[MIS27-10] Progress of Observation Project for High-energy Phenomena in Winter Thunderstorms

*Yuuki Wada[1,2], Teruaki Enoto[3], Takahiro Matsumoto[1], Kazuhiro Nakazawa[4], Yoshihiro Furuta[5], Takayuki Yuasa, Harufumi Tsuchiya[5], Daisuke Yonetoku[6], Tatsuya Sawano[6], Kazuo Makishima[1,2], Masashi Kamogawa[7], Yoshitaka Nakamura[8], Takeshi Morimoto[9], Mitsuteru Sato[10], Hideo Sakai[11], Hidehito Nanto[12], Tomoo Ushio[13] (1.The University of Tokyo, 2.RIKEN, 3.Kyoto University, 4.Nagoya University, 5.Japan Atomic Energy Agency, 6.Kanazawa University, 7.Tokyo Gakugei University, 8.Kobe City College of Technology, 9.Kindai University, 10.Hokkaido University, 11.University of Toyama, 12.Kanazawa Institute of Technology, 13.Tokyo Metropolitan University)

11:45 AM - 12:00 PM JST | 2:45 AM - 3:00 AM UTC

[MIS27-11] Electromagnetic and stroke current observations on rocket-triggered lightning

*Takeshi Morimoto[1], Shinya Kurokawa[1], Yoshitaka Nakamura[2], Kazuo Yamamoto[3] (1.Kindai University, 2.Kobe City College of Technology, 3.Chubu University)

12:00 PM - 12:15 PM JST | 3:00 AM - 3:15 AM UTC

Discussion

Earthquake precursory electromagnetic phenoma : Summary and prospective

*Masashi Hayakawa[1]

1. Hayakawa Institute of Seismo Electromagnetics.Co. LTD. University of Electro-Communications venture company

This paper describes the overview of electromagnetic phenomena mainly prior to an earthquake (EQ)(so-colled Seismo Electromagnetics). Initially this paper will report on the history of seismo-electromagnetics, findings for the 1995 Kobe EQ and the 2011 Tohoku EQ, recent statistical results, latest achievement (lithosphere-atomosphere-ionosphere coupling), prospective, etc.

Keywords: Seismo-Electromagnetics

©2019. Japan Geoscience Union. All Right Reserved.

Detection of lower ionospheric anomaly preceding earthquake using nonlinear autoregressive neural network

*Kakeru Matsuki[1], Hayato Iibuchi[1], Hendy Santosa[3], Yasuhide Hobara[1], Michael A Balikhin[2]

1. The University of Electro-Communications , 2. University of Sheffield, 3. University of Bengkulu

It is possible to monitor the state of the lower ionosphere by observing the VLF (Very Low Frequency) transmitter radio waves with a frequency band of 10 to 50 kHz propagating between the Earth and the ionosphere. In recent years, NARX - NN (Nonlinear Auto Regressive with eXogenous Input - Neural Network) has been applied as a highly accurate modeling and prediction method of temporal variation of VLF band transmitter radio wave amplitude. As a result, we obtain the extremely high prediction accuracy of cross correlation coefficient 0.9 or more between predicted and observed amplitude. Meanwhile, anomalies in the VLF band transmitter radio wave amplitude have been reported indicating the disturbance of the lower ionosphere at night from a week to few days before large earthquakes. Since the accuracy of anomaly detection is not high yet, this study aims to improve the detection accuracy of the lower ionospheric disturbance by analyzing the nighttime amplitude of the VLF band transmission wave using NARX - NN. By specifying the external factors that affect the lower ionospheric disturbance preceding the earthquakes and statistically investigating the difference between observed and predicted values of the VLF amplitude, we contribute to understand occurrence mechaism of lower seismo ionospheric anomalies.

©2019. Japan Geoscience Union. All Right Reserved.

Analysis of multipoint measurements of plasma turbulence

*Michael A Balikhin[1], Simon N Walker[1]

1. University of Sheffield

The presentation is devoted to the review of advanced methods for the analysis of multipoint measurements of plasma turbulence. Both time and frequency domain methods are reviewed. Using examples of in situ spacecraft observations of plasma turbulence it is shown how the system science based approaches can be used to identify linear and nonlinear dynamical processes within the turbulence.

Keywords: Turbulence, Dynamical processes

©2019. Japan Geoscience Union. All Right Reserved.

Progress of Observation Project for High-energy Phenomena in Winter Thunderstorms

*Yuuki Wada[1,2], Teruaki Enoto[3], Takahiro Matsumoto[1], Kazuhiro Nakazawa[4], Yoshihiro Furuta[5], Takayuki Yuasa, Harufumi Tsuchiya[5], Daisuke Yonetoku[6], Tatsuya Sawano[6], Kazuo Makishima[1,2], Masashi Kamogawa[7], Yoshitaka Nakamura[8], Takeshi Morimoto[9], Mitsuteru Sato[10], Hideo Sakai[11], Hidehito Nanto[12], Tomoo Ushio[13]

1. The University of Tokyo, 2. RIKEN, 3. Kyoto University, 4. Nagoya University, 5. Japan Atomic Energy Agency, 6. Kanazawa University, 7. Tokyo Gakugei University, 8. Kobe City College of Technology, 9. Kindai University, 10. Hokkaido University, 11. University of Toyama, 12. Kanazawa Institute of Technology, 13. Tokyo Metropolitan University

In strong electric fields of thunderclouds and lightning, electrons are accelerated to relativistic energy, and emit bremsstrahlung gamma rays which are observed by space bourne, airbourne, and on-ground experiments. To reveal the mechanism and condition where the electron acceleration takes place, we have been performing the Gamma-Ray Observation of Winter Thunderclouds (GROWTH) experiments in coastal areas of Japan Sea since 2007. In 2015, we started multi-point observation campaigns with portable radiation detectors in Ishikawa and Niigata Prefectures. So far, we have revealed characteristics of long-lasting gamma-ray bursts from thunderclouds (long bursts: Tsuchiya et al. 2007), and photonuclear reacitons in the atmosphere triggered by terrestrial gamma-ray flashes coincident with lightning discharges (short bursts: Enoto et al. 2017). We are expanding the number of detectors to observe more events of such long and short bursts with multiple detectors. in the 2018-2019 winter season, we operated more than 20 radiation detectors. We are also promoting joint-observation campaigns with low-frequency radio and atmospheric electric-field measurements (Wada et al. 2018). We succeeded in the first simultaneous detection of long and short burst events in Kanazawa. Because the short-burst-triggering LF pulse took place within 1 km from the position where the long burst ceased, it is suggested that the strong electric field responsible for the long burst assisted the short burst. We will report the progress of the GROWTH project and this simultaneous detection event.

Keywords: lightning, gamma ray, radiation

©2019. Japan Geoscience Union. All Right Reserved.

Electromagnetic and stroke current observations on rocket-triggered lightning

*Takeshi Morimoto[1], Shinya Kurokawa[1], Yoshitaka Nakamura[2], Kazuo Yamamoto[3]

1. Kindai University, 2. Kobe City College of Technology, 3. Chubu University

Rocket-triggered lightning is the most effective technique for artificial triggering lightning. It involves launching a small rocket trailing a thin grounded wire toward an overhead charged cloud. This technique is incredibly favorable for various lightning observations for example earth currents, leader developments, related electromagnetic and high-energy radiations etc. because a lightning strike is induced at the desired location. In Japan, a number of rocket-triggered lightning experiments were succeeded in winter thunderstorm seasons.

During the winter of 2017-18, the authors conducted a rocket-triggered lightning experiment in Noto Peninsula, facing to the Sea of Japan in Ishikawa Prefecture. A conductive wire was connected to the rocket and launched at faster than 100 m/s. A rope was also connected to prevent the rocket from rising above an altitude of 200 m. The rod-type ground electrode with a diameter of 1 cm was buried at a depth of 1 m.

We were successful in triggering lightning stroke at 1352:28h December 29, 2017. The two types of Rogowski coils to measure lightning current, hi-speed video cameras, RF antennas in VHF and LF bands were equipped around the striking point. The corona current and e-field were measured at about the distance of 50 m from the point. The measured lightning current was reached to -12 kA and continued for 290 ms. The recorded images with high time resolutions against recoded RF radiations and the current will be demonstrated in this talk.

Keywords: Rocket-triggered lightning, Winter thunderstorm, Lightning current, EM observations

©2019. Japan Geoscience Union. All Right Reserved.

[J] Poster | M (Multidisciplinary and Interdisciplinary)：M-IS Intersection

Tue. May 28, 2019 3:30 PM - 5:00 PM JST | Tue. May 28, 2019 6:30 AM - 8:00 AM UTC | Poster Hall International Exhibition Hall8, Makuhari Messe_27

[M-IS27] Atmospheric electricity: Applications toward natural disaster mitigation

convener:Yasuhide Hobara(Graduate School of Information and Engineering Department of Communication Engineering and Informatics, The University of Electro-Communications), Masashi Kamogawa(Department of Physics, Tokyo Gakugei University)

In recent years, various types of natural disasters caused by climate change, earthquake, etc. occur frequently in the world. In 2018 heavy precipitation in various regions of Japan and the earthquakes in Hokkaido and Indonesiaproduced/greater human and economic/damage.

In 2019JpGU Atmospheric Electricity (AE) session, invited experts are going to introduce their scientific challenges in order to monitor, predict and mitigate natural disasters by using knowledge of the atmospheric electricity. For example, monitoring and prediction of extreme weather by the latest weather radar system and lightning observations, electromagnetic phenomena prior to earthquakes, etc. will be included. We certainly welcome contributed papers regarding all topics on atmospheric electricityincluding global circuit, ion and fair weather electricity, thunderstorm electrification, lightning physics, lightning and meteorology, electrical effects of thunderstorms on the middle and upper atmosphere such as transient luminous events and high energy phenomena, lightning protection, terrestrial electromagnetic environment and so on.

[MIS27-P01] Design of C-band polarimetric phased array weather radar

★Invited Papers

*Kento Nakamura[1], Hiroshi Kikuchi[2], Tomoaki Mega[1], Tomoo Ushio[1] (1.Tokyo metropolitan university, 2.The University of Electro-Communications)

[MIS27-P02] Examination of Improving the Precision of Ionospheric F-Layer Electron Density Estimation Using Thunder-origin Whistler Wave

*Shu Hirai[1], Shogo Kanazawa[1], Yasuhide Hobara[1], Jean-Louis Pincon[2] (1.The University of Electro-Communications, 2.LPC2E/CNRS)

[MIS27-P03] Rn flux anomaly and local seiemicity around Asahi station,Boso,Japan

*Haruna Kojima[1], Katsumi Hattori[2], Chie Yoshino[2], Michikuni Shimo[3], Toshiharu Konishi[4], Ryuichi Furuya[5] (1.Graduate School of Science and Engineering,Chiba University, 2.Department of Earth Sciences,Graduate School of Scince, 3.Fujita Health University, 4.OHYO KOKEN KOGYO Co.,Ltd, 5.COM SYSTEM Inc.)

[MIS27-P04] Study on electric energy derivation of lightning using optical observation of lightning from TRMM tropical rainfall observation satellite

*Hirata Kodai[1], Yasuhide Hobara[1], Hiroshi Kikuchi[1] (1.The University of Electro-Communications)

Design of C-band polarimetric phased array weather radar

*Kento Nakamura[1], Hiroshi Kikuchi[2], Tomoaki Mega[1], Tomoo Ushio[1]

1. Tokyo metropolitan university, 2. The University of Electro-Communications

Most of the severe phenomena, such as a tornado, a downburst, and microburst, are caused by locally generated cumulonimbus cloud in a short time. In order to observe the evolution of the inner structure of the rain cloud that changes on a scale of several minutes, a weather radar with higher spatiotemporal resolution is needed.
A weather radar with polarimetric observations can provide multi-parameter measurements that reveal detailed microphysics of storms in addition to accurate precipitation estimation, and improve weather forecasts. As a next radar development project, we plan to develop a polarimetric weather phased array weather radar. It is expected that the future phased array radar will achieve a polarimetric capability. The transmitted frequency of the under consideration radar is C-band (5GHz).
It is capable of measuring the 3-D rainfall distribution in less than 1 min in a range of several hundred kilometers, respectively.However, it is difficult to maintain high accuracy of observation of polarimetric phased array weather radar because of the following topics.
1) the effect of deterioration of the antenna characteristics, which are formed by the digital beam forming, in oblique direction are deteriorated. 2) the performance of the cross polarization discrimination, which is performance to distinguish between horizontal waves and vertical waves, are reduced in oblique direction. These problems caused the ununiformity of the accuracy of rainfall estimates.In this paper, we proposed the design of C-band antenna elements and array antennas. We designed the three type of the antenna array, which are a planner, a cylinder, and a semi-spherical types. And also a numerical simulation was conducted to evaluate the accuracy of rainfall estimates using three different arrays.

©2019. Japan Geoscience Union. All Right Reserved.

Examination of Improving the Precision of Ionospheric F-Layer Electron Density Estimation Using Thunder-origin Whistler Wave

*Shu Hirai[1], Shogo Kanazawa[1], Yasuhide Hobara[1], Jean-Louis Pincon[2]

1. The University of Electro-Communications, 2. LPC2E/CNRS

The ionosphere temporally and spatially fluctuates by solar activity or an atmospheric weather phenomenon. It is known that the fluctuation of the electron density which constitutes the ionosphere causes the positioning error of GPS or the instability of the communication, so it is important for engineering of investigating the spatiotemporal condition of the ionosphere over the whole world. There are various methods for measuring the electron density of the ionosphere, but it is difficult to obtain the electron density data on sea far from the land because they are almost based on ground observation. To obtain the data over the world, this study focuses on estimation method of the ionosphere F-Layer electron density using whistler wave derived from the thunder generated on both ground and sea. In the previous study, the electron density estimation above the middle latitude almost correspond to the model of the ionosphere (IRI), but the data in low latitude is largely different. As the result of underestimating real propagation distance because of assuming that lightning was generated right under the satellite, it has the possibility to overestimated the electron density estimation.
Therefore, the purpose of this study is to investigate the possibility of improving the precision of ionospheric F-Layer electron density estimation using the whistler wave. Specifically, arrival direction of the whistler wave is determined by using the data of 3 magnetic field components observed by the low altitude satellite DEMETER. We aim to improve the precision of electron density estimation, especially low latitude by considering the propagation distance in the ionosphere which is estimated from the whistler wave’s propagation course.

Keywords: whistler, electron density, ionosphere

©2019. Japan Geoscience Union. All Right Reserved.

Rn flux anomaly and local seiemicity around Asahi station,Boso,Japan

*Haruna Kojima[1], Katsumi Hattori[2], Chie Yoshino[2], Michikuni Shimo[3], Toshiharu Konishi[4], Ryuichi Furuya[5]

1. Graduate School of Science and Engineering,Chiba University, 2. Department of Earth Sciences,Graduate School of Scince, 3. Fujita Health University, 4. OHYO KOKEN KOGYO Co.,Ltd, 5. COM SYSTEM Inc.

In recent years, there are many studies reported electromagnetic phenomena preceding earthquakes such as ionospheric anomalies. Lithosphere-Atmosphere-Ionosphere Coupling (LAIC) model has been proposed to explain these phenomena. In this study, to explain the possibility of the chemical channel of LAIC, we have installed sensors for atmospheric electric field (AEF), atmospheric ion concentration (AIC), atmospheric Rn concentration (ARC), ground Rn concentration (GRC), and weather elements at Asahi station, Boso Peninsula, Japan. Because the atmospheric electricity parameters could be mainly influenced by weather factors, it is necessary to remove these influences as much as possible. In this sense, we apply the MSSA (Multi-channel Singular Spectral Analysis) to remove these influences from the GRC variation and estimate the Rn flux from the ground. Then, we investigate the correlation between the changes in the Rn flux and seismicity around the station. As a result, we found the correlation between Rn flux and regional cumulative seismic moment and/or Es index, which indicates the daily seismic energy near the station received at the station. It is highly suggestive of the effectiveness of GRC monitoring in regional seismicity around the station. Further researches such as network observations will be required for the detailed consideration on the correlation between Rn flux and seismicity such as magnitude and distance dependences.

Keywords: Lithosphere-Atmosphere-Ionosphere Coupling, atmospheric electric field, atmospheric ion concentration, ground Rn concentration

©2019. Japan Geoscience Union. All Right Reserved.

Study on electric energy derivation of lightning using optical observation of lightning from TRMM tropical rainfall observation satellite

*Hirata Kodai[1], Yasuhide Hobara[1], Hiroshi Kikuchi[1]

1. The University of Electro-Communications

Lightning is an electric phenomenon in the atmosphere that occurs on a global scale and its electrical characteristics are extremely important parameters for physically and optically understanding lightning discharge phenomena. Lightning charge moment Qds is a parameter that can represent the magnitude of lightning energy in the electrical characteristics of lightning and its magnitude is due to damage to the wind turbine at the wind power plant. It is understanding that it will affect the damage of natural disasters such as damage and mountain fires. There is a method that can remotely derive Qds by observing the electromagnetic waves radiated at the time of lightning discharge from the ground observation instruments. Especially ELF band transients are progressing to estimate Qds by observation. In recent years, researches have been conducted to estimate Qds from the optical emission intensity of lightning discharge. Using this method, it is expected that Qds can be calculated for lightning discharge occurred all over the world. In this study, therefore, the lightning observation data, which were obtaind by the lightning imaging sensor installed on tropical rain observation satellite TRMM, are used to estimate the derivation of Qds across the whole world by deriving the correlation between the data on the lightning emission intensity obtained from the equipment LIS and the lightning charge moment Qds obtained from the ELF electromagnetic wave ground measurement data. As a result, it was shown that there is a strong positive correlation between the Qds and optical lihgning emission. The correlation coefficient was about 0.9. It was shown that lightning charge moment Qds estimation can be expected from the value of lightning emission intensity. In the future, we will improve the accuracy of deriving the lightning charge moment Qds from the lightning emission intensity. The time-space distribution of lightning charge moment Qds of the world lightning characteristics will be find based on the data of optical observation of lightning by LIS over 19 years.

©2019. Japan Geoscience Union. All Right Reserved.

[J] Poster | M (Multidisciplinary and Interdisciplinary)：M-IS Intersection

Tue. May 28, 2019 5:15 PM - 6:30 PM JST | Tue. May 28, 2019 8:15 AM - 9:30 AM UTC | Poster Hall International Exhibition Hall8, Makuhari Messe_46

[M-IS27] Atmospheric electricity: Applications toward natural disaster mitigation

convener:Yasuhide Hobara(Graduate School of Information and Engineering Department of Communication Engineering and Informatics, The University of Electro-Communications), Masashi Kamogawa(Department of Physics, Tokyo Gakugei University)

In recent years, various types of natural disasters caused by climate change, earthquake, etc. occur frequently in the world. In 2018 heavy precipitation in various regions of Japan and the earthquakes in Hokkaido and Indonesiaproduced/greater human and economic/damage.

In 2019JpGU Atmospheric Electricity (AE) session, invited experts are going to introduce their scientific challenges in order to monitor, predict and mitigate natural disasters by using knowledge of the atmospheric electricity. For example, monitoring and prediction of extreme weather by the latest weather radar system and lightning observations, electromagnetic phenomena prior to earthquakes, etc. will be included. We certainly welcome contributed papers regarding all topics on atmospheric electricityincluding global circuit, ion and fair weather electricity, thunderstorm electrification, lightning physics, lightning and meteorology, electrical effects of thunderstorms on the middle and upper atmosphere such as transient luminous events and high energy phenomena, lightning protection, terrestrial electromagnetic environment and so on.

[MIS27-P01] Design of C-band polarimetric phased array weather radar

★Invited Papers

*Kento Nakamura[1], Hiroshi Kikuchi[2], Tomoaki Mega[1], Tomoo Ushio[1] (1.Tokyo metropolitan university, 2.The University of Electro-Communications)

[MIS27-P02] Examination of Improving the Precision of Ionospheric F-Layer Electron Density Estimation Using Thunder-origin Whistler Wave

*Shu Hirai[1], Shogo Kanazawa[1], Yasuhide Hobara[1], Jean-Louis Pincon[2] (1.The University of Electro-Communications, 2.LPC2E/CNRS)

[MIS27-P03] Rn flux anomaly and local seiemicity around Asahi station,Boso,Japan

*Haruna Kojima[1], Katsumi Hattori[2], Chie Yoshino[2], Michikuni Shimo[3], Toshiharu Konishi[4], Ryuichi Furuya[5] (1.Graduate School of Science and Engineering,Chiba University, 2.Department of Earth Sciences,Graduate School of Scince, 3.Fujita Health University, 4.OHYO KOKEN KOGYO Co.,Ltd, 5.COM SYSTEM Inc.)

[MIS27-P04] Study on electric energy derivation of lightning using optical observation of lightning from TRMM tropical rainfall observation satellite

*Hirata Kodai[1], Yasuhide Hobara[1], Hiroshi Kikuchi[1] (1.The University of Electro-Communications)

Design of C-band polarimetric phased array weather radar

*Kento Nakamura[1], Hiroshi Kikuchi[2], Tomoaki Mega[1], Tomoo Ushio[1]

1. Tokyo metropolitan university, 2. The University of Electro-Communications

Most of the severe phenomena, such as a tornado, a downburst, and microburst, are caused by locally generated cumulonimbus cloud in a short time. In order to observe the evolution of the inner structure of the rain cloud that changes on a scale of several minutes, a weather radar with higher spatiotemporal resolution is needed.
A weather radar with polarimetric observations can provide multi-parameter measurements that reveal detailed microphysics of storms in addition to accurate precipitation estimation, and improve weather forecasts. As a next radar development project, we plan to develop a polarimetric weather phased array weather radar. It is expected that the future phased array radar will achieve a polarimetric capability. The transmitted frequency of the under consideration radar is C-band (5GHz).
It is capable of measuring the 3-D rainfall distribution in less than 1 min in a range of several hundred kilometers, respectively.However, it is difficult to maintain high accuracy of observation of polarimetric phased array weather radar because of the following topics.
1) the effect of deterioration of the antenna characteristics, which are formed by the digital beam forming, in oblique direction are deteriorated. 2) the performance of the cross polarization discrimination, which is performance to distinguish between horizontal waves and vertical waves, are reduced in oblique direction. These problems caused the ununiformity of the accuracy of rainfall estimates.In this paper, we proposed the design of C-band antenna elements and array antennas. We designed the three type of the antenna array, which are a planner, a cylinder, and a semi-spherical types. And also a numerical simulation was conducted to evaluate the accuracy of rainfall estimates using three different arrays.

©2019. Japan Geoscience Union. All Right Reserved.

Examination of Improving the Precision of Ionospheric F-Layer Electron Density Estimation Using Thunder-origin Whistler Wave

*Shu Hirai[1], Shogo Kanazawa[1], Yasuhide Hobara[1], Jean-Louis Pincon[2]

1. The University of Electro-Communications, 2. LPC2E/CNRS

The ionosphere temporally and spatially fluctuates by solar activity or an atmospheric weather phenomenon. It is known that the fluctuation of the electron density which constitutes the ionosphere causes the positioning error of GPS or the instability of the communication, so it is important for engineering of investigating the spatiotemporal condition of the ionosphere over the whole world. There are various methods for measuring the electron density of the ionosphere, but it is difficult to obtain the electron density data on sea far from the land because they are almost based on ground observation. To obtain the data over the world, this study focuses on estimation method of the ionosphere F-Layer electron density using whistler wave derived from the thunder generated on both ground and sea. In the previous study, the electron density estimation above the middle latitude almost correspond to the model of the ionosphere (IRI), but the data in low latitude is largely different. As the result of underestimating real propagation distance because of assuming that lightning was generated right under the satellite, it has the possibility to overestimated the electron density estimation.
Therefore, the purpose of this study is to investigate the possibility of improving the precision of ionospheric F-Layer electron density estimation using the whistler wave. Specifically, arrival direction of the whistler wave is determined by using the data of 3 magnetic field components observed by the low altitude satellite DEMETER. We aim to improve the precision of electron density estimation, especially low latitude by considering the propagation distance in the ionosphere which is estimated from the whistler wave’s propagation course.

Keywords: whistler, electron density, ionosphere

©2019. Japan Geoscience Union. All Right Reserved.

Rn flux anomaly and local seiemicity around Asahi station,Boso,Japan

*Haruna Kojima[1], Katsumi Hattori[2], Chie Yoshino[2], Michikuni Shimo[3], Toshiharu Konishi[4], Ryuichi Furuya[5]

1. Graduate School of Science and Engineering,Chiba University, 2. Department of Earth Sciences,Graduate School of Scince, 3. Fujita Health University, 4. OHYO KOKEN KOGYO Co.,Ltd, 5. COM SYSTEM Inc.

In recent years, there are many studies reported electromagnetic phenomena preceding earthquakes such as ionospheric anomalies. Lithosphere-Atmosphere-Ionosphere Coupling (LAIC) model has been proposed to explain these phenomena. In this study, to explain the possibility of the chemical channel of LAIC, we have installed sensors for atmospheric electric field (AEF), atmospheric ion concentration (AIC), atmospheric Rn concentration (ARC), ground Rn concentration (GRC), and weather elements at Asahi station, Boso Peninsula, Japan. Because the atmospheric electricity parameters could be mainly influenced by weather factors, it is necessary to remove these influences as much as possible. In this sense, we apply the MSSA (Multi-channel Singular Spectral Analysis) to remove these influences from the GRC variation and estimate the Rn flux from the ground. Then, we investigate the correlation between the changes in the Rn flux and seismicity around the station. As a result, we found the correlation between Rn flux and regional cumulative seismic moment and/or Es index, which indicates the daily seismic energy near the station received at the station. It is highly suggestive of the effectiveness of GRC monitoring in regional seismicity around the station. Further researches such as network observations will be required for the detailed consideration on the correlation between Rn flux and seismicity such as magnitude and distance dependences.

Keywords: Lithosphere-Atmosphere-Ionosphere Coupling, atmospheric electric field, atmospheric ion concentration, ground Rn concentration

©2019. Japan Geoscience Union. All Right Reserved.

Study on electric energy derivation of lightning using optical observation of lightning from TRMM tropical rainfall observation satellite

*Hirata Kodai[1], Yasuhide Hobara[1], Hiroshi Kikuchi[1]

1. The University of Electro-Communications

Lightning is an electric phenomenon in the atmosphere that occurs on a global scale and its electrical characteristics are extremely important parameters for physically and optically understanding lightning discharge phenomena. Lightning charge moment Qds is a parameter that can represent the magnitude of lightning energy in the electrical characteristics of lightning and its magnitude is due to damage to the wind turbine at the wind power plant. It is understanding that it will affect the damage of natural disasters such as damage and mountain fires. There is a method that can remotely derive Qds by observing the electromagnetic waves radiated at the time of lightning discharge from the ground observation instruments. Especially ELF band transients are progressing to estimate Qds by observation. In recent years, researches have been conducted to estimate Qds from the optical emission intensity of lightning discharge. Using this method, it is expected that Qds can be calculated for lightning discharge occurred all over the world. In this study, therefore, the lightning observation data, which were obtaind by the lightning imaging sensor installed on tropical rain observation satellite TRMM, are used to estimate the derivation of Qds across the whole world by deriving the correlation between the data on the lightning emission intensity obtained from the equipment LIS and the lightning charge moment Qds obtained from the ELF electromagnetic wave ground measurement data. As a result, it was shown that there is a strong positive correlation between the Qds and optical lihgning emission. The correlation coefficient was about 0.9. It was shown that lightning charge moment Qds estimation can be expected from the value of lightning emission intensity. In the future, we will improve the accuracy of deriving the lightning charge moment Qds from the lightning emission intensity. The time-space distribution of lightning charge moment Qds of the world lightning characteristics will be find based on the data of optical observation of lightning by LIS over 19 years.

©2019. Japan Geoscience Union. All Right Reserved.

[E] Oral | M (Multidisciplinary and Interdisciplinary)：M-GI General Geosciences, Information Geosciences & Simulations

Tue. May 28, 2019 10:45 AM - 12:15 PM JST | Tue. May 28, 2019 1:45 AM - 3:15 AM UTC | 301B 3F

[M-GI29] Near Surface Investigation and Modeling for Groundwater Resources Assessment and Conservation

convener:Jui-Pin Tsai(National Cheng Kung University, Taiwan), Hwa-Lung Yu(National Taiwan University), Ching-Chung Cheng(National Chiao Tung University Taiwan), Jing-Sen Cai(China University of Geosciences), Chairperson:Jui-Pin Tsai(National Cheng Kung University, Taiwan), Hwa-Lung Yu(National Taiwan University, Taiwan)

Groundwater resources serve as a vital source for regional water supply under the climate change condition. However, improper use of the available groundwater resources leads to serious environmental disasters such as land subsidence or seawater intrusion. Therefore, groundwater management is a key issue for groundwater resources conservation. Before applying any management practice, it is essential to accurately assess the groundwater system in multi-scales. In this session, we focus on the issues associated with the application of near-surface investigation and modeling on groundwater resources assessment. We welcome studies related to numerical modeling, spatiotemporal modeling, data fusion, and field investigation using hydrogeological approaches, geophysical approaches, geochemical approaches, and remote sensing. We also welcome the studies associated with groundwater contamination transport and remediation, geothermal energy exchange, groundwater microorganisms, hot spring, volcanic hydrology, and environmental disasters evaluation and prevention. We especially encourage the pilot groundwater management studies that solve multi-scale and interdisciplinary problems.

10:45 AM - 11:00 AM JST | 1:45 AM - 2:00 AM UTC

[MGI29-01] Groundwater management for global sustainability

★Invited Papers

*Makoto Taniguchi[1] (1.Research Institute for Humanity and Nature)

11:00 AM - 11:15 AM JST | 2:00 AM - 2:15 AM UTC

[MGI29-02] **Building the large-scale specific yields over the Zhuoshui river alluvial fan and Minzhu basin with gravimetric technique**

*Ren-Jhih Yang[1], Shen Yu Hsiao[1], Yan-Jyun Lin[1], Zhen-Yu Wu[1] (1.National Chung Hsing University)

11:15 AM - 11:30 AM JST | 2:15 AM - 2:30 AM UTC

[MGI29-03] **Poro-elastic Deformation of a Heterogenous Geologic Medium due to Groundwater Withdrawal**

*Ajit Joshi[1], Masaatsu Aichi[1] (1.Department of Environment Systems, Graduate School of Frontier Sciences, The University of Tokyo)

11:30 AM - 11:45 AM JST | 2:30 AM - 2:45 AM UTC

[MGI29-04] **Analytical Solution of a Ditch Drainage System for the restoration of waterlogged site considering a Subsurface Source/Sink**

*SHUBHAM TIWARI[1], BRIJESH KUMAR YADAV[1], RATAN SARMAH[2] (1.Indian Institute of Technology Roorkee, 2.Indian Institute of Technology Ropar)

11:45 AM - 12:00 PM JST | 2:45 AM - 3:00 AM UTC

[MGI29-05] **Variable-density flow and mass transport in unsaturated-saturated aquifers under horizontal groundwater flow conditions**

*Jiaqi Liu[1], Tomochika Tokunaga[1] (1.The University of Tokyo)

12:00 PM - 12:15 PM JST | 3:00 AM - 3:15 AM UTC

[MGI29-06] A practical approach to evaluating water inflow for underground water-sealed storage cavern

*Jing-Sen Cai[1] (1.China University of Geosciences)

Groundwater management for global sustainability

*Makoto Taniguchi[1]

1. Research Institute for Humanity and Nature

Groundwater management is important for global sustainability, because of not only large groundwater footprints through global trade of agricultural/industrial materials, but also climate change impacts on groundwater resources directly and indirectly, and carbon emissions through human activities using groundwater. Interactions between groundwater-food-energy nexus and environmental/economical impacts under the conditions of climate change and urbanization, are essential for global sustainability as the center of information among nature, society and humanity. Natural and social tipping points related to groundwater such as land subsidence and saltwater intrusion, regime shifts, and resilience, are the keys for the future of hydrogeology and a sustainable society. Sustainable groundwater management has cultural dependency because of differences in hydroclimate, hydrogeology, water management, and water culture in each area. Therefore, an interaction between humanity and nature is the most important for finding solutions of groundwater management towards sustainability for the current complicated and wicked global environmental problems.

Keywords: groundwater management, global sustainability, groundwater-energy-food nexus

©2019. Japan Geoscience Union. All Right Reserved.

Building the large-scale specific yields over the Zhuoshui river alluvial fan and Minzhu basin with gravimetric technique

*Ren-Jhih Yang[1], Shen Yu Hsiao[1], Yan-Jyun Lin[1], Zhen-Yu Wu[1]

1. National Chung Hsing University

This study estimates the large-scale specific yields (S_y) of the aquifer in the Zhuoshui river alluvial fan and its upstream, Minzhu basin, by gravity data combined with groundwater level data and electrical resistivity tomography (ERT) data. The S_y results from gravimetric technique are rigorously compared with those from hydraulic technique. There are eight gravity stations over the Zhuoshui river alluvial fan, and four over the Minzhu basin.The distribution of all gravity stations is shown in the attached figure. The ERT data are only used for S_y estimation in the "SMOF" gravity station in the Minzhu basin. The strategies for modeling groundwater level changes include the terrain correction method and the Bouguer correction method. The environmental factors influencing the S_y estimation are also discussed. We expect that the groundwater resources in the Zhuoshui river alluvial fan and Minzhu basin can be accurately explored by this study and the results can provide an important reference for groundwater resource management.

Keywords: Gravimetry, Large-scale specific yield, Groundwater resource

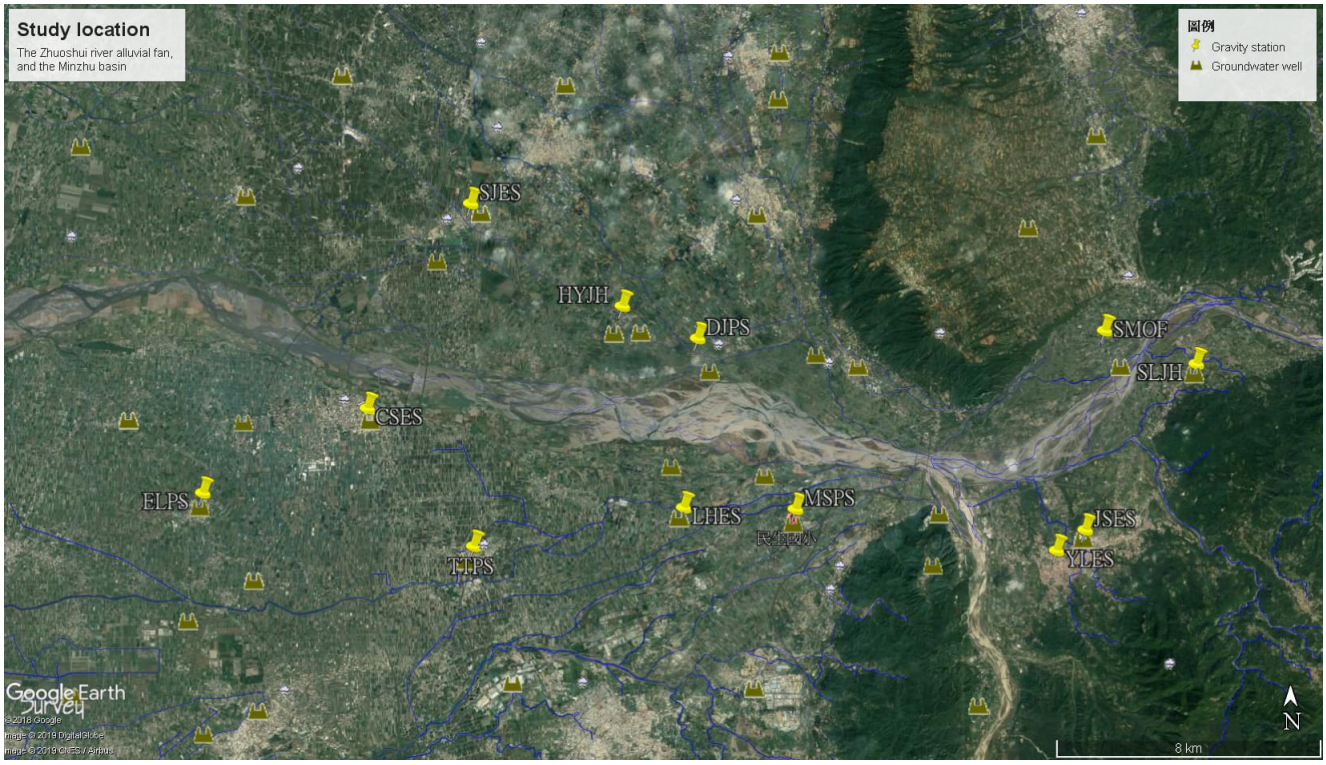

©2019. Japan Geoscience Union. All Right Reserved.

Poro-elastic Deformation of a Heterogenous Geologic Medium due to Groundwater Withdrawal

*Ajit Joshi[1], Masaatsu Aichi[1]

1. Department of Environment Systems, Graduate School of Frontier Sciences, The University of Tokyo

Land subsidence around coastal cities in the world have been recognized as a major concern due to risk of flooding from seawater. As an example, land surface near the Tokyo and surrounding regions in Chiba Prefecture in Japan have been subsiding at rates of few centimeters per year based on data from satellite observations and ground survey measurements. Such changes in land surface elevations may have caused due to subsurface fluid (water/methane) extraction from the Plio-Pleistocene sand reservoirs of the Kanto groundwater basin located in and around Tokyo and Chiba. Fluid removal from subsurface geologic medium can reduce pore fluid pressures underneath and subsequently strain the medium causing pore spaces to collapse. Stratigraphic and lithological interpretation of rocks exposed in outcrops from the Kujukuri region in Chiba showed alternations of sandstone-mudstone units and were characterized by transgressive-regressive cycles of vertical heterogeneity indicating a gradual transition of sediment size from coarse-grained sandstone to fine-grained siltstone/mudstone. The present research hypothesized that presence of local geological heterogeneities in a geologic medium can alter hydraulic properties of the medium affecting its deformation. The main purpose of this research was to determine effect of vertical heterogeneity on rock deformation and to predict land surface subsidence due to groundwater extraction. The research hypothesis was tested using a one-dimensional solution to equations for pore fluid mass conservation and Darcy’ s flow mechanics for a poro-elastic medium saturated with water. Porosity and permeability, both dependent upon clay content, were related by a modified form of Kozeny-Carman equation.

Simulations results for a hypothetical 130 m thick water-saturated porous medium under different geological conditions were compared to investigate heterogeneity effect on deformation. Results showed hydraulic strain in mudstone increased by orders of magnitude higher than less compressible and more diffusive sandstone. Simulation results also confirmed that geological heterogeneity would affect poro-elastic deformation by altering hydraulic diffusivity and bulk compressibility of a geologic medium. Moreover, model predicted land surface subsidence, using stratigraphic sections from the Kanto basin, were in good agreement with field deformation measurements from leveling survey. In addition, local heterogeneity can be more important for a geologic medium saturated with multiple fluids (methane/water) which will be addressed in future research.

Keywords: Poro-elastic modeling, Geological heterogeneity, Land subsidence

©2019. Japan Geoscience Union. All Right Reserved.

Analytical Solution of a Ditch Drainage System for the restoration of waterlogged site considering a Subsurface Source/Sink

*SHUBHAM TIWARI[1], BRIJESH KUMAR YADAV[1], RATAN SARMAH[2]

1. Indian Institute of Technology Roorkee, 2. Indian Institute of Technology Ropar

Drainage plays an important role in the field of agricultural science, as it helps in removing excess water from the soil quickly. An analytical solution is developed for the prediction of transient seepage to a fully penetrating ditch drainage system receiving water from a ponded surface with an influence of subsurface source/sink. The proposed solution is quite versatile to tackle the presence of source and sink effect in the flow domain. A subsurface flow domain of confined nature is assumed as study area which is having finite extends in horizontal and vertical directions. The hydraulic property of the soil matrix is considered as homogeneous and anisotropic in nature. The accuracy of this solution is analyzed by comparing with numerical solution obtained from finite difference method and other existing simplified case on MATLAB programming software. With the imposition of the source and sink term in the flow domain, the path line and travel time of water molecules started deviating from their original position. It was observed that discharge to the drains has a strong influence of the source/sink term. It is expected that the proposed model will help in the understanding of the flow dynamics associated with the ditch drainage system subjected to source/sink in real field conditions.

Keywords: Transient seepage, Ditch drains, Source/sink, Water logging

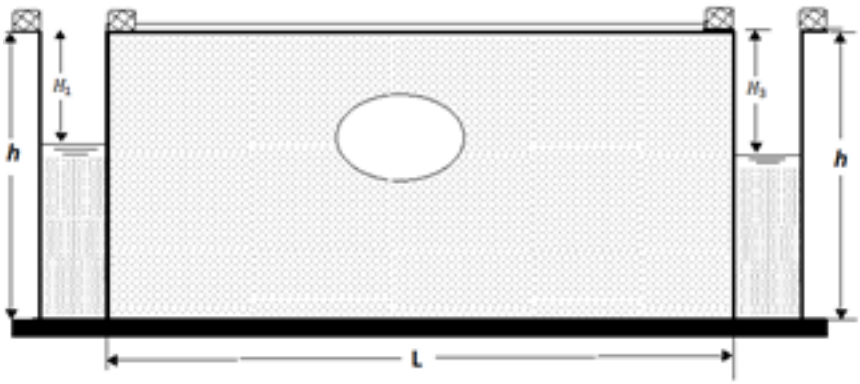

©2019. Japan Geoscience Union. All Right Reserved.

Variable-density flow and mass transport in unsaturated-saturated aquifers under horizontal groundwater flow conditions

*Jiaqi Liu[1], Tomochika Tokunaga[1]

1. The University of Tokyo

Density-induced fingering is an important mass transport process in a variety of groundwater flow settings. This study numerically investigated density-driven flow and mass transport in a 2-D vertical conceptual model of an unsaturated-saturated aquifer. The modeled domain consisted of 300 m long, with horizontal groundwater flow and vertical injection of dense solute from the top. In total, 158 numerical simulation cases were designed with various configurations of horizontal groundwater flow, the rate of solute injection, aquifer properties, and dispersivity. The numerical code FEFLOW was adopted which can solve both variable-density groundwater flow and unsaturated-saturated flow in porous media. Three dimensionless numbers, the convective ratios M_x and M_z and the Rayleigh number Ra_d, were applied to quantitively evaluate the relative magnitudes among the driving forces in the simulation cases. Three end-member flow regimes were identified that were dominated by the horizontal hydraulically-driven flow, the vertical hydraulically-driven flow, and the vertical density-driven flow, respectively. The plots of the simulation results in the M_x-M_z-Ra_d diagram enabled a clear distinction among the clusters of flow regimes and suggested the dominant driving force of each flow regime. The parameter sensitivity and regime shifts were also analyzed with the M_x-M_z-Ra_d diagram. The classification of flow regimes and the proposed M_x-M_z-Ra_d diagram provided a basic reference and a useful tool for understanding the mechanisms of variable-density flow processes under complex field situations.

Keywords: Variable-density flow, Numerical simulations, Dimensionless numbers

©2019. Japan Geoscience Union. All Right Reserved.

A practical approach to evaluating water inflow for underground water-sealed storage cavern

*Jing-Sen Cai[1]

1. China University of Geosciences

A practical approach that has been successfully applied to evaluate the water inflow for the project of underground water-sealed storage cavern in fractured granite in China are introduced. This approach consists of two steps: investigation of the distribution of groundwater flow path and modeling to evaluate the water inflow in the cavern. Firstly, field investigation methods such as geological survey and mapping, engineering drilling, borehole imaging and engineering geophysical prospecting are used to investigate the distribution of fracture zones and faults. Subsequently, the piecewise water pressure test is performed in the existing boreholes to search the seepage passage which is dictated by the section with large permeability coefficient. Based on this, models such as Hirishi Oshima empirical equation, Misaki Sato Kuniki empirical equation and the empirical analytical equation are utilized to evaluate the water inflow in the traffic tunnel, main cavern and shaft during the construction stage. Results indicate that the seepage passage determined by the piecewise water pressure test corresponds well to the location of fracture zones revealed by field investigation. The evaluation results are confirmed by the surrounding rock quality and water inflow location uncovered by the excavation afterward, which demonstrate the validity of this comprehensive approach.

Keywords: field study, underground water-sealed storage cavern, fractured granite, water inflow, borehole imaging, piecewise water pressure test

©2019. Japan Geoscience Union. All Right Reserved.

[E] Poster | M (Multidisciplinary and Interdisciplinary)：M-GI General Geosciences, Information Geosciences & Simulations

Tue. May 28, 2019 3:30 PM - 5:00 PM JST | Tue. May 28, 2019 6:30 AM - 8:00 AM UTC | Poster Hall International Exhibition Hall8, Makuhari Messe_28

[M-GI29] Near Surface Investigation and Modeling for Groundwater Resources Assessment and Conservation

convener:Jui-Pin Tsai(National Cheng Kung University, Taiwan), Hwa-Lung Yu(National Taiwan University), Ching-Chung Cheng(National Chiao Tung University Taiwan), Jing-Sen Cai(China University of Geosciences)

Groundwater resources serve as a vital source for regional water supply under the climate change condition. However, improper use of the available groundwater resources leads to serious environmental disasters such as land subsidence or seawater intrusion. Therefore, groundwater management is a key issue for groundwater resources conservation. Before applying any management practice, it is essential to accurately assess the groundwater system in multi-scales. In this session, we focus on the issues associated with the application of near-surface investigation and modeling on groundwater resources assessment. We welcome studies related to numerical modeling, spatiotemporal modeling, data fusion, and field investigation using hydrogeological approaches, geophysical approaches, geochemical approaches, and remote sensing. We also welcome the studies associated with groundwater contamination transport and remediation, geothermal energy exchange, groundwater microorganisms, hot spring, volcanic hydrology, and environmental disasters evaluation and prevention. We especially encourage the pilot groundwater management studies that solve multi-scale and interdisciplinary problems.

[MGI29-P01] Modelling of self-potential signals associated with groundwater flows

*ayaka ishikawa[1], Katsumi Hattori[1] (1.chiba university)

[MGI29-P02] Estimating the Hydraulic Conductivity and Heat Capacity of the Aquifer between the River and Well Site Using Joint Inversion Approach

*Jui-Pin Tsai[1], Chin-Tsai Hsiao[4], Liang-Cheng Chang[2], You-Cheng Chen[2], Chun-Hung Chen[3], Yun-Ta Cheng[3], Jen-Hung Yu[3] (1.National Cheng Kung University, Taiwan , 2.National Chiao Tung University, Taiwan , 3.Water Resources Planning Institute, Water Resources Agency, Taiwan, 4.Department of Information Management, Chung Chou University of Science and Technology)

[MGI29-P03] Evaluation on Soil Permeability Using Electrical Resistant Tomography

*CHIHPING KUO[1], BONIAN SHEN[1], CHIHWEI HUANG[1], YUCHIAO LEE[1], SHENXIANG HUANG[1], YENLIN CHEN[1] (1.Department and Institute of Civil Engineering and Environmental Informatics, Minghsin University of Science and Technology)

[MGI29-P04] The Potential Study of Open Loop System Geothermal Heat Pump in Gifu City, Japan

*Randa Permanda[1], Tomoyuki Ohtani[2] (1.Department of Civil and Environmental Engineering, Gifu University, 2.Department of Civil Engineering, Gifu University)

[MGI29-P05] Application of TL-CHERT Smart Characterization Method to Investigate a Groundwater Contaminated Site

*Tzu-Pin Wang[1,2,5], Yao-Tsung Chen[3], Tien-Hsing Tung[3], Chih-Hung Cheng[2], Jie Wang[4] (1.NCU TW, 2.Geophysical Technology and Engineering Co.,Ltd. R.O.C, 3.Apollo Technology Co.,Ltd. R.O.C., 4.Department of Civil Engineering, Chien Hsin University of Science and Technology, Taoyuan City, Taiwan, 5.Disaster Reduction Research Center, Chien Hsin University of Science and Technology, Taoyuan City, Taiwan)

[MGI29-P06] Data Assimilation in Hydraulic Conductivity Identification using Bayesian Statistical Method

*Shih-Yang Cheng[1], Kuo-Chin Hsu[1] (1.National Cheng Kung Univ.)

[MGI29-P07] Groundwater recharge estimation by using empirical orthogonal function method

Hua-Ting Zeng [1], *Hwa-Lung Yu[1] (1. National Taiwan University)

[MGI29-P08] The Application of Drought Early Warning Index for Regional Hydrological Circumstance Analysis

*Chih Chao Ho[1], Ta Wei Chen[2] (1.Construction and Disaster Prevention Research Center, Feng Chia Univ., 2.Taiwan Hsin-Chu Irrigation Association)

Modelling of self-potential signals associated with groundwater flows

*ayaka ishikawa[1], Katsumi Hattori[1]

1. chiba university

Landslides triggered by rainfall are one of the most dangerous natural disasters which give the loss of lives and properties. Although the importance of the short-term forecast of landslides is widely accepted, it is not achieved. In this research, we pay attention to electro-magnetic approach for monitoring ground water condition under the slope. That is, we understand the processes of the landslide and develop the system for forecast to detect precursory signal through the electromagnetic changes. In this study, we apply the self-potential approach, which is related on electro-kinetic effects or streaming potential. We have conducted several flume tests and sandbox experiments and the results showed the repeatability of the phenomena or correlation between self-potential and ground water condition. Therefore, we will report the model and numerical computation for the sandbox experiment on injection in this presentation.

SP signals measured in the sandbox during pumping experiment are considered to be due to the electro-kinetic effects. The total current density j is $j=sE-l\mathrm{d}h/\mathrm{d}x_i$, where s (in S m^{-1}) is the electrical conductivity, E (in Vm^{-1}) is the electric field, l (in A Pa^{-1} m^{-1}) is the current coupling coefficient, and h (in m) is the hydraulic head. The variation of SP signals of the sandbox gives quasi-instantaneous information on changes of the hydraulic head. Therefore we consider this problem with quasi-static limit condition i.e. div j = 0. It leads $\mathrm{div}(s\,\mathrm{grad}\,phi)=-\mathrm{div}(l\,\mathrm{grad}\,h)$.Where phi (in V) is electric potential. In addition, we assume that s and l are uniform through the sandbox because we assume saturated condition. Finally, the solved equation is $s\mathrm{d}^2phi/dx_i^2=-l\mathrm{d}^2h/dx_i^2$. We simulated distribution of hydraulic head during pumping test using finite element method. Then, we modeled the SP generation.

Consequently, the variation of SP modeled and observed are generally consistent with each other. Therefore, we found that groundwater flows control the occurrence of SP in the sandbox experiment. However, in the detail of time variation, modeled SP differ from those of observed partly. We consider that heterogeneity of soil or necessary of 3D modeling could cause these discordances. Details will be shown in our presentation.

Keywords: self-potential, ground water flow, modelling

©2019. Japan Geoscience Union. All Right Reserved.

Estimating the Hydraulic Conductivity and Heat Capacity of the Aquifer between the River and Well Site Using Joint Inversion Approach

*Jui-Pin Tsai[1], Chin-Tsai Hsiao[4], Liang-Cheng Chang[2], You-Cheng Chen[2], Chun-Hung Chen[3], Yun-Ta Cheng[3], Jen-Hung Yu[3]

1. National Cheng Kung University, Taiwan , 2. National Chiao Tung University, Taiwan , 3. Water Resources Planning Institute, Water Resources Agency, Taiwan, 4. Department of Information Management, Chung Chou University of Science and Technology

This study continued to measure the water temperature and pressure at the riverbed, agricultural waterway, and groundwater monitoring well from Oct. to Nov. 2018. These observations were then used to estimate the hydraulic conductivity (K) and flux between the river and the aquifer of the well site. The water pressure data reveal that the correlation coefficient between river and groundwater level reaches 0.9 and that between the agricultural waterway and groundwater level is almost 0. This reveals that the groundwater head variation mainly affected by the river stage of the nearby river. The temperature data show that the groundwater temperature is correlated to the temperature of the river water and is uncorrelated to the air temperature. Accordingly, the temperature and head data of the groundwater and river water were used to estimate K and heat capacity of the aquifer between the river and well site using a joint inversion approach. The results show that the estimated K and heat capacity are 67.53 m ⁄ day and 4485000 J ⁄ (m^3–℃), respectively.

Keywords: Hydraulic conductivity, Soil heat capactiy , Joint inversion, Temperature, Groundwater head , Interaction between groundwater and river water

©2019. Japan Geoscience Union. All Right Reserved.

Evaluation on Soil Permeability Using Electrical Resistant Tomography

*CHIHPING KUO[1], BONIAN SHEN[1], CHIHWEI HUANG[1], YUCHIAO LEE[1], SHENXIANG HUANG[1], YENLIN CHEN[1]

1. Department and Institute of Civil Engineering and Environmental Informatics, Minghsin University of Science and Technology

The permeability of soil is used to adapt field constant head permeability test or variable head permeability test. The former test is suitable for soil with higher permeability like sand and gravels; the later test is suitable for soil with lower permeability like silt and clays. Both tests need in-situ drilling holes. The required operating time is usually about couple of hours. A widely used geophysical method, Electrical Resistant Tomography (ERT), is adapted here to evaluate the soil permeability. Two types of soil with different permeability were performed, and the results were compared with the result of same samples using traditional permeability test. The result showed that they were very close. The operating time of ERT for one soil was only less than one hour. The idea of evaluating soil permeability using ERT is proposed in this study.

Keywords: Soil Permeability, Electrical Resistant Tomography

主機設定 (107.10.31 攝於明學樓噴水池旁)

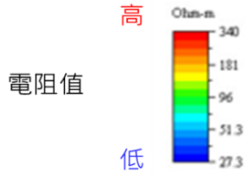

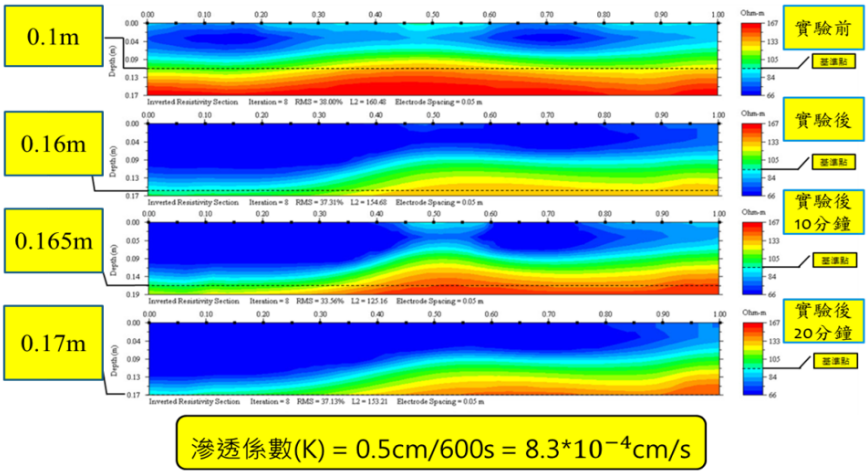

©2019. Japan Geoscience Union. All Right Reserved.

The Potential Study of Open Loop System Geothermal Heat Pump in Gifu City, Japan

*Randa Permanda[1], Tomoyuki Ohtani[2]

1. Department of Civil and Environmental Engineering, Gifu University, 2. Department of Civil Engineering, Gifu University

Geothermal heat pumps (GHPs) are considered to be one of the most energy efficient and environmentally friendly air-conditioning systems for temperate zones. In Japan, the expansive use of GHPs technology is finite, because of insufficient information on the advantages offered by the system and high installation cost. Therefore, the prediction of potential energy of GHPs at the first stage of installation is desirable. Open-loop system is one of GHPs types system which mostly depends on geological and hydrogeological parameter. This system interacts directly with ground and groundwater factor, because it uses groundwater as direct heat transfer medium through extraction and injection wells. Accordingly, groundwater flow with heat transfer is the most important factor that could affect the performance of open-loop GHPs system. Therefore groundwater flow system as well as distribution of subsurface temperature must be comprehended in detail. The aim of this study is to understand the distribution of groundwater flow and heat transport in study area from the simulation study using the program, FEFLOW. FEFLOW is a finite element code which can numerically simulate groundwater flow and heat transport. As the final result, the simulation model can be used to understand of open loop GHPs system in specified area.

The study area is an alluvial fan of the Nagara River, Gifu city, Japan. It is bounded by mountain ranges from north to northeast side and plain area remains. The Nagara River flows in the center of the plain. This alluvial fan is composed of sands and gravels and often intercalate thin fine sand and silt layers. Groundwater flow occur mainly in the Quaternary deposits, which are sand and gravel layers. Alluvial fans are recharge areas of groundwater and rapid groundwater flow are expected. The underground temperature in alluvial fan is affected by rapid groundwater flow recharged from a river. For assessment of potential energy of open loop GHPs, 3D model of groundwater flow with heat transport in Gifu city was developed using FEFLOW program. Model is constructed first by geological and hydrogeological data. The pre-existing geological columns and profile of study area were collected, which consisted of borehole and cross section data. Furthermore, pre-existing hydrogeological data which consist of groundwater table, underground temperature, and temperature of river water data in study area are also compiled to construct the simulation model. Boundary condition of groundwater flow system is defined by water table distribution. Bottom of the model is basement rock, treated as impermeable boundary and lateral sides are set as no flow boundaries. For boundary conditions of heat transport, top and bottom of the model are fixed by constant temperature boundaries, and lateral sides are as insulated. Based on constructed model, the simulation on groundwater flow with heat transport is performed. The effectiveness of heat transport and fluid flow are affected by material properties. Material properties were determined on the basis of formation types. Groundwater temperature were matched against observed temperatures, using the result of groundwater flow simulation. The observed underground temperatures in study area are fluctuated not only near surface but also in aquifer. This temperature change is resulted from lateral flow of the recharged groundwater. The calculated groundwater temperature will be adjusted until simulation result agreed with observed data from field. So that model can represent the groundwater flow system in alluvial fan of the Nagara River, Gifu city, Japan. For future plan, simulation model is used to investigate potential open loop GHPs system resulted from presence flowing groundwater in study area. This

©2019. Japan Geoscience Union. All Right Reserved.

simulation model is effective to predict the natural change of underground temperature, one main factor that affecting heat pumps efficiency.

Keywords: Geothermal heat pump, Groundwater flow, Heat transport, Open loop system, FEFLOW

©2019. Japan Geoscience Union. All Right Reserved.

Application of TL-CHERT Smart Characterization Method to Investigate a Groundwater Contaminated Site

*Tzu-Pin Wang[1,2,5], Yao-Tsung Chen[3], Tien-Hsing Tung[3], Chih-Hung Cheng[2], Jie Wang[4]

1. NCU TW, 2. Geophysical Technology and Engineering Co.,Ltd. R.O.C, 3. Apollo Technology Co.,Ltd. R.O.C., 4. Department of Civil Engineering, Chien Hsin University of Science and Technology, Taoyuan City, Taiwan, 5. Disaster Reduction Research Center, Chien Hsin University of Science and Technology, Taoyuan City, Taiwan

The Environmental Protection Administration in Taiwan effectively integrates Cross-Hole Electrical Resistivity Tomography (CHERT) into remediation planning in the anticipatory improvement project of sites with no polluter. During the reagent injection, Time-lapse Cross-Hole Electrical Resistivity (TL-CHERT) data are collected continuously. After data preprocessing and inversion algorithm, the ERT results are presented in images. 4D images could depict the main transmission range of reagent during the reagent injection, and further adjust or revise the second stage of remediation design. Therefore, CHERT could not only improve the remediation of complex groundwater contaminated sites, but also achieve the goal of precise surgical remediation. Besides, setting geophysical exploration equipment together with monitoring wells could greatly increase the use efficiency of the wells. Because groundwater contamination is usually a severe problem, a cross-professional cooperation is necessary. It is expected that this study will provide a worth case study for the survey application of similar contaminated site.

Keywords: CHERT, groundwater, pollution, resistiviy, geophysics, SCM

©2019. Japan Geoscience Union. All Right Reserved.

Data Assimilation in Hydraulic Conductivity Identification using Bayesian Statistical Method

*Shih-Yang Cheng[1], Kuo-Chin Hsu[1]

1. National Cheng Kung Univ.

Characterizing spatially heterogeneous hydraulic conductivity plays a crucial role in groundwater resources management and subsurface contaminant remediation. Since the direct measurements of hydraulic conductivity are sparse, the uncertainty is inherent in the estimated parameters. We propose decreasing the uncertainty by assimilating auxiliary data (electrical resistivity) with the direct data (hydraulic conductivity) using Bayesian statistical method. Different from classical geostatistical methods, both linear and nonlinear relations between the direct and auxiliary data can be considered in Bayesian statistical method. A synthetic example is designed to evaluate the method. Results show that the accuracy of hydraulic conductivity is improved through the Bayesian statistical method. Moreover, the effectiveness of auxiliary data in estimation error decrease is more significant when high correlation exists. However, the relation type has little influence on the accuracy. The estimation uncertainty quantified by variance is also compared. The uncertainty is inversely proportional to the amounts of auxiliary data and the correlation in both linear and nonlinear cases. The usefulness of auxiliary data in variance reduction is more obvious in linear cases. A systemic discussion of the sampling strategies of auxiliary data for improving hydraulic conductivity identification is also proposed.

Keywords: Data assimilation, Bayesian statistical method, Hydraulic conductivity, Nonlinear

©2019. Japan Geoscience Union. All Right Reserved.

Groundwater recharge estimation by using empirical orthogonal function method

Hua-Ting Zeng [1], *Hwa-Lung Yu[1]

1. National Taiwan University

Groundwater recharge estimation has been challenging due to the limited knowledge of the hyogeological heterogeneity. This issue is particularly important in the areas with high dependence on groundwater resources. This study proposed a data-driven approach along with a simple ODE model to estimate the groundwater recharge in our study area, Cho-shui river aquifer which is one of the most water-abundant aquifers in Taiwan; however, is suffered from the water overdraft. We analyzed the daily groundwater level observations during 2004-2010 from all wells across the entire study area. Based upon our proposed method, we identified two major recharge areas, i.e., proximal fan of the aquifer and Min-Chu basin at its upstream. The two areas obtained about 181.9 million and 78.8million tons of recharge water annually, resectively, in which about 131 million tons of water flowing from Min-Chu basin into Cho-shui aquifer annually. In summary, this study proposed a novel method for the groundwater recharge estimation.

Keywords: Groundwater, Recharge, EOF

©2019. Japan Geoscience Union. All Right Reserved.

The Application of Drought Early Warning Index for Regional Hydrological Circumstance Analysis

*Chih Chao Ho[1], Ta Wei Chen[2]

1. Construction and Disaster Prevention Research Center, Feng Chia Univ., 2. Taiwan Hsin-Chu Irrigation Association

Recently, rainfall become more unevenly both in special and temporal distribution caused by global climate change. The frequency of drought decrease from once every 17 years to once every 9 years. How to define warning signs of a drought and propose adaptive strategies is one of the key topic for water resources management. The drought can be divided into meteorological drought, agricultural drought and hydrological drought. The study tries to introduces difference Drought Early Warning Index, such as Standardized Precipitation Index, Standardized Groundwater Index, Normalized Difference Vegetation Index etc., to predict drought circumstance. The result can be a reference for development of drought early warning system.

Keywords: Standardized Precipitation Index, Standardized Groundwater Index, Normalized Difference Vegetation Index

©2019. Japan Geoscience Union. All Right Reserved.

[E] Poster | M (Multidisciplinary and Interdisciplinary)：M-GI General Geosciences, Information Geosciences & Simulations

Tue. May 28, 2019 5:15 PM - 6:30 PM JST | Tue. May 28, 2019 8:15 AM - 9:30 AM UTC | Poster Hall International Exhibition Hall8, Makuhari Messe_47

[M-GI29] Near Surface Investigation and Modeling for Groundwater Resources Assessment and Conservation

convener:Jui-Pin Tsai(National Cheng Kung University, Taiwan), Hwa-Lung Yu(National Taiwan University), Ching-Chung Cheng(National Chiao Tung University Taiwan), Jing-Sen Cai(China University of Geosciences)

Groundwater resources serve as a vital source for regional water supply under the climate change condition. However, improper use of the available groundwater resources leads to serious environmental disasters such as land subsidence or seawater intrusion. Therefore, groundwater management is a key issue for groundwater resources conservation. Before applying any management practice, it is essential to accurately assess the groundwater system in multi-scales. In this session, we focus on the issues associated with the application of near-surface investigation and modeling on groundwater resources assessment. We welcome studies related to numerical modeling, spatiotemporal modeling, data fusion, and field investigation using hydrogeological approaches, geophysical approaches, geochemical approaches, and remote sensing. We also welcome the studies associated with groundwater contamination transport and remediation, geothermal energy exchange, groundwater microorganisms, hot spring, volcanic hydrology, and environmental disasters evaluation and prevention. We especially encourage the pilot groundwater management studies that solve multi-scale and interdisciplinary problems.

[MGI29-P01] Modelling of self-potential signals associated with groundwater flows

*ayaka ishikawa[1], Katsumi Hattori[1] (1.chiba university)

[MGI29-P02] Estimating the Hydraulic Conductivity and Heat Capacity of the Aquifer between the River and Well Site Using Joint Inversion Approach

*Jui-Pin Tsai[1], Chin-Tsai Hsiao[4], Liang-Cheng Chang[2], You-Cheng Chen[2], Chun-Hung Chen[3], Yun-Ta Cheng[3], Jen-Hung Yu[3] (1.National Cheng Kung University, Taiwan , 2.National Chiao Tung University, Taiwan , 3.Water Resources Planning Institute, Water Resources Agency, Taiwan, 4.Department of Information Management, Chung Chou University of Science and Technology)

[MGI29-P03] Evaluation on Soil Permeability Using Electrical Resistant Tomography

*CHIHPING KUO[1], BONIAN SHEN[1], CHIHWEI HUANG[1], YUCHIAO LEE[1], SHENXIANG HUANG[1], YENLIN CHEN[1] (1.Department and Institute of Civil Engineering and Environmental Informatics, Minghsin University of Science and Technology)

[MGI29-P04] The Potential Study of Open Loop System Geothermal Heat Pump in Gifu City, Japan

*Randa Permanda[1], Tomoyuki Ohtani[2] (1.Department of Civil and Environmental Engineering, Gifu University, 2.Department of Civil Engineering, Gifu University)

[MGI29-P05] Application of TL-CHERT Smart Characterization Method to Investigate a Groundwater Contaminated Site

*Tzu-Pin Wang[1,2,5], Yao-Tsung Chen[3], Tien-Hsing Tung[3], Chih-Hung Cheng[2], Jie Wang[4] (1.NCU TW, 2.Geophysical Technology and Engineering Co.,Ltd. R.O.C, 3.Apollo Technology Co.,Ltd. R.O.C., 4.Department of Civil Engineering, Chien Hsin University of Science and Technology, Taoyuan City, Taiwan, 5.Disaster Reduction Research Center, Chien Hsin University of Science and Technology, Taoyuan City, Taiwan)

[MGI29-P06] Data Assimilation in Hydraulic Conductivity Identification using Bayesian Statistical Method

*Shih-Yang Cheng[1], Kuo-Chin Hsu[1] (1.National Cheng Kung Univ.)

[MGI29-P07] Groundwater recharge estimation by using empirical orthogonal function method

Hua-Ting Zeng [1], *Hwa-Lung Yu[1] (1. National Taiwan University)

[MGI29-P08] The Application of Drought Early Warning Index for Regional Hydrological Circumstance Analysis

*Chih Chao Ho[1], Ta Wei Chen[2] (1.Construction and Disaster Prevention Research Center, Feng Chia Univ., 2.Taiwan Hsin-Chu Irrigation Association)

Modelling of self-potential signals associated with groundwater flows

*ayaka ishikawa[1], Katsumi Hattori[1]

1. chiba university

Landslides triggered by rainfall are one of the most dangerous natural disasters which give the loss of lives and properties. Although the importance of the short-term forecast of landslides is widely accepted, it is not achieved. In this research, we pay attention to electro-magnetic approach for monitoring ground water condition under the slope. That is, we understand the processes of the landslide and develop the system for forecast to detect precursory signal through the electromagnetic changes. In this study, we apply the self-potential approach, which is related on electro-kinetic effects or streaming potential. We have conducted several flume tests and sandbox experiments and the results showed the repeatability of the phenomena or correlation between self-potential and ground water condition. Therefore, we will report the model and numerical computation for the sandbox experiment on injection in this presentation.

SP signals measured in the sandbox during pumping experiment are considered to be due to the electro-kinetic effects. The total current density j is $j=sE-l\mathrm{d}h/\mathrm{d}x_i$, where s (in S m^{-1}) is the electrical conductivity, E (in Vm^{-1}) is the electric field, l (in A Pa^{-1} m^{-1}) is the current coupling coefficient, and h (in m) is the hydraulic head. The variation of SP signals of the sandbox gives quasi-instantaneous information on changes of the hydraulic head. Therefore we consider this problem with quasi-static limit condition i.e. div j = 0. It leads $\mathrm{div}(s\,\mathrm{grad}\,phi)=-\mathrm{div}(l\,\mathrm{grad}\,h)$.Where phi (in V) is electric potential. In addition, we assume that s and l are uniform through the sandbox because we assume saturated condition. Finally, the solved equation is $s\mathrm{d}^2phi/dx_i^2=-l\mathrm{d}^2h/dx_i^2$. We simulated distribution of hydraulic head during pumping test using finite element method. Then, we modeled the SP generation.

Consequently, the variation of SP modeled and observed are generally consistent with each other. Therefore, we found that groundwater flows control the occurrence of SP in the sandbox experiment. However, in the detail of time variation, modeled SP differ from those of observed partly. We consider that heterogeneity of soil or necessary of 3D modeling could cause these discordances. Details will be shown in our presentation.

Keywords: self-potential, ground water flow, modelling

©2019. Japan Geoscience Union. All Right Reserved.

Estimating the Hydraulic Conductivity and Heat Capacity of the Aquifer between the River and Well Site Using Joint Inversion Approach

*Jui-Pin Tsai[1], Chin-Tsai Hsiao[4], Liang-Cheng Chang[2], You-Cheng Chen[2], Chun-Hung Chen[3], Yun-Ta Cheng[3], Jen-Hung Yu[3]

1. National Cheng Kung University, Taiwan , 2. National Chiao Tung University, Taiwan , 3. Water Resources Planning Institute, Water Resources Agency, Taiwan, 4. Department of Information Management, Chung Chou University of Science and Technology

This study continued to measure the water temperature and pressure at the riverbed, agricultural waterway, and groundwater monitoring well from Oct. to Nov. 2018. These observations were then used to estimate the hydraulic conductivity (K) and flux between the river and the aquifer of the well site. The water pressure data reveal that the correlation coefficient between river and groundwater level reaches 0.9 and that between the agricultural waterway and groundwater level is almost 0. This reveals that the groundwater head variation mainly affected by the river stage of the nearby river. The temperature data show that the groundwater temperature is correlated to the temperature of the river water and is uncorrelated to the air temperature. Accordingly, the temperature and head data of the groundwater and river water were used to estimate K and heat capacity of the aquifer between the river and well site using a joint inversion approach. The results show that the estimated K and heat capacity are 67.53 m ⁄ day and 4485000 J ⁄ (m^3–℃), respectively.

Keywords: Hydraulic conductivity, Soil heat capactiy , Joint inversion, Temperature, Groundwater head , Interaction between groundwater and river water

©2019. Japan Geoscience Union. All Right Reserved.

Evaluation on Soil Permeability Using Electrical Resistant Tomography

*CHIHPING KUO[1], BONIAN SHEN[1], CHIHWEI HUANG[1], YUCHIAO LEE[1], SHENXIANG HUANG[1], YENLIN CHEN[1]

1. Department and Institute of Civil Engineering and Environmental Informatics, Minghsin University of Science and Technology

The permeability of soil is used to adapt field constant head permeability test or variable head permeability test. The former test is suitable for soil with higher permeability like sand and gravels; the later test is suitable for soil with lower permeability like silt and clays. Both tests need in-situ drilling holes. The required operating time is usually about couple of hours. A widely used geophysical method, Electrical Resistant Tomography (ERT), is adapted here to evaluate the soil permeability. Two types of soil with different permeability were performed, and the results were compared with the result of same samples using traditional permeability test. The result showed that they were very close. The operating time of ERT for one soil was only less than one hour. The idea of evaluating soil permeability using ERT is proposed in this study.

Keywords: Soil Permeability, Electrical Resistant Tomography

主機設定 (107.10.31 攝於明學樓噴水池旁)

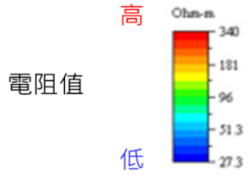

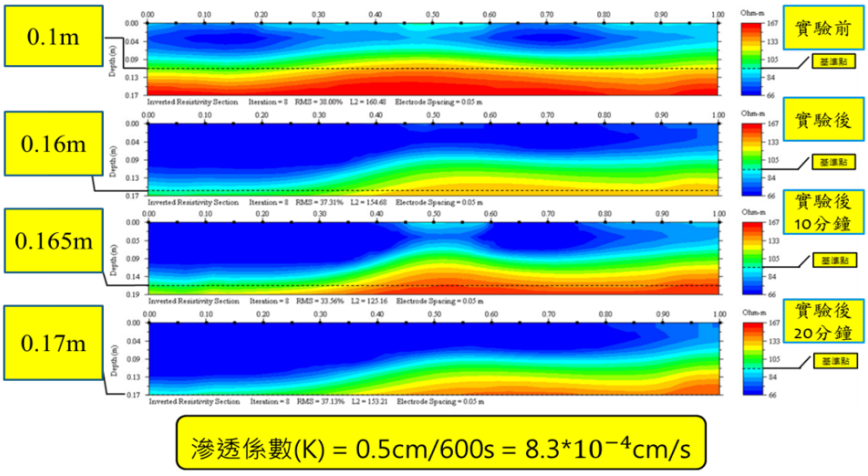

©2019. Japan Geoscience Union. All Right Reserved.

The Potential Study of Open Loop System Geothermal Heat Pump in Gifu City, Japan

*Randa Permanda[1], Tomoyuki Ohtani[2]

1. Department of Civil and Environmental Engineering, Gifu University, 2. Department of Civil Engineering, Gifu University

Geothermal heat pumps (GHPs) are considered to be one of the most energy efficient and environmentally friendly air-conditioning systems for temperate zones. In Japan, the expansive use of GHPs technology is finite, because of insufficient information on the advantages offered by the system and high installation cost. Therefore, the prediction of potential energy of GHPs at the first stage of installation is desirable. Open-loop system is one of GHPs types system which mostly depends on geological and hydrogeological parameter. This system interacts directly with ground and groundwater factor, because it uses groundwater as direct heat transfer medium through extraction and injection wells. Accordingly, groundwater flow with heat transfer is the most important factor that could affect the performance of open-loop GHPs system. Therefore groundwater flow system as well as distribution of subsurface temperature must be comprehended in detail. The aim of this study is to understand the distribution of groundwater flow and heat transport in study area from the simulation study using the program, FEFLOW. FEFLOW is a finite element code which can numerically simulate groundwater flow and heat transport. As the final result, the simulation model can be used to understand of open loop GHPs system in specified area.

The study area is an alluvial fan of the Nagara River, Gifu city, Japan. It is bounded by mountain ranges from north to northeast side and plain area remains. The Nagara River flows in the center of the plain. This alluvial fan is composed of sands and gravels and often intercalate thin fine sand and silt layers. Groundwater flow occur mainly in the Quaternary deposits, which are sand and gravel layers. Alluvial fans are recharge areas of groundwater and rapid groundwater flow are expected. The underground temperature in alluvial fan is affected by rapid groundwater flow recharged from a river. For assessment of potential energy of open loop GHPs, 3D model of groundwater flow with heat transport in Gifu city was developed using FEFLOW program. Model is constructed first by geological and hydrogeological data. The pre-existing geological columns and profile of study area were collected, which consisted of borehole and cross section data. Furthermore, pre-existing hydrogeological data which consist of groundwater table, underground temperature, and temperature of river water data in study area are also compiled to construct the simulation model. Boundary condition of groundwater flow system is defined by water table distribution. Bottom of the model is basement rock, treated as impermeable boundary and lateral sides are set as no flow boundaries. For boundary conditions of heat transport, top and bottom of the model are fixed by constant temperature boundaries, and lateral sides are as insulated. Based on constructed model, the simulation on groundwater flow with heat transport is performed. The effectiveness of heat transport and fluid flow are affected by material properties. Material properties were determined on the basis of formation types. Groundwater temperature were matched against observed temperatures, using the result of groundwater flow simulation. The observed underground temperatures in study area are fluctuated not only near surface but also in aquifer. This temperature change is resulted from lateral flow of the recharged groundwater. The calculated groundwater temperature will be adjusted until simulation result agreed with observed data from field. So that model can represent the groundwater flow system in alluvial fan of the Nagara River, Gifu city, Japan. For future plan, simulation model is used to investigate potential open loop GHPs system resulted from presence flowing groundwater in study area. This

©2019. Japan Geoscience Union. All Right Reserved.

simulation model is effective to predict the natural change of underground temperature, one main factor that affecting heat pumps efficiency.

Keywords: Geothermal heat pump, Groundwater flow, Heat transport, Open loop system, FEFLOW

©2019. Japan Geoscience Union. All Right Reserved.

Application of TL-CHERT Smart Characterization Method to Investigate a Groundwater Contaminated Site

*Tzu-Pin Wang[1,2,5], Yao-Tsung Chen[3], Tien-Hsing Tung[3], Chih-Hung Cheng[2], Jie Wang[4]

1. NCU TW, 2. Geophysical Technology and Engineering Co.,Ltd. R.O.C, 3. Apollo Technology Co.,Ltd. R.O.C., 4. Department of Civil Engineering, Chien Hsin University of Science and Technology, Taoyuan City, Taiwan, 5. Disaster Reduction Research Center, Chien Hsin University of Science and Technology, Taoyuan City, Taiwan

The Environmental Protection Administration in Taiwan effectively integrates Cross-Hole Electrical Resistivity Tomography (CHERT) into remediation planning in the anticipatory improvement project of sites with no polluter. During the reagent injection, Time-lapse Cross-Hole Electrical Resistivity (TL-CHERT) data are collected continuously. After data preprocessing and inversion algorithm, the ERT results are presented in images. 4D images could depict the main transmission range of reagent during the reagent injection, and further adjust or revise the second stage of remediation design. Therefore, CHERT could not only improve the remediation of complex groundwater contaminated sites, but also achieve the goal of precise surgical remediation. Besides, setting geophysical exploration equipment together with monitoring wells could greatly increase the use efficiency of the wells. Because groundwater contamination is usually a severe problem, a cross-professional cooperation is necessary. It is expected that this study will provide a worth case study for the survey application of similar contaminated site.

Keywords: CHERT, groundwater, pollution, resistiviy, geophysics, SCM

©2019. Japan Geoscience Union. All Right Reserved.

Data Assimilation in Hydraulic Conductivity Identification using Bayesian Statistical Method

*Shih-Yang Cheng[1], Kuo-Chin Hsu[1]

1. National Cheng Kung Univ.

Characterizing spatially heterogeneous hydraulic conductivity plays a crucial role in groundwater resources management and subsurface contaminant remediation. Since the direct measurements of hydraulic conductivity are sparse, the uncertainty is inherent in the estimated parameters. We propose decreasing the uncertainty by assimilating auxiliary data (electrical resistivity) with the direct data (hydraulic conductivity) using Bayesian statistical method. Different from classical geostatistical methods, both linear and nonlinear relations between the direct and auxiliary data can be considered in Bayesian statistical method. A synthetic example is designed to evaluate the method. Results show that the accuracy of hydraulic conductivity is improved through the Bayesian statistical method. Moreover, the effectiveness of auxiliary data in estimation error decrease is more significant when high correlation exists. However, the relation type has little influence on the accuracy. The estimation uncertainty quantified by variance is also compared. The uncertainty is inversely proportional to the amounts of auxiliary data and the correlation in both linear and nonlinear cases. The usefulness of auxiliary data in variance reduction is more obvious in linear cases. A systemic discussion of the sampling strategies of auxiliary data for improving hydraulic conductivity identification is also proposed.

Keywords: Data assimilation, Bayesian statistical method, Hydraulic conductivity, Nonlinear

©2019. Japan Geoscience Union. All Right Reserved.

Groundwater recharge estimation by using empirical orthogonal function method

Hua-Ting Zeng [1], *Hwa-Lung Yu[1]

1. National Taiwan University

Groundwater recharge estimation has been challenging due to the limited knowledge of the hyogeological heterogeneity. This issue is particularly important in the areas with high dependence on groundwater resources. This study proposed a data-driven approach along with a simple ODE model to estimate the groundwater recharge in our study area, Cho-shui river aquifer which is one of the most water-abundant aquifers in Taiwan; however, is suffered from the water overdraft. We analyzed the daily groundwater level observations during 2004-2010 from all wells across the entire study area. Based upon our proposed method, we identified two major recharge areas, i.e., proximal fan of the aquifer and Min-Chu basin at its upstream. The two areas obtained about 181.9 million and 78.8million tons of recharge water annually, resectively, in which about 131 million tons of water flowing from Min-Chu basin into Cho-shui aquifer annually. In summary, this study proposed a novel method for the groundwater recharge estimation.

Keywords: Groundwater, Recharge, EOF

©2019. Japan Geoscience Union. All Right Reserved.

The Application of Drought Early Warning Index for Regional Hydrological Circumstance Analysis

*Chih Chao Ho[1], Ta Wei Chen[2]

1. Construction and Disaster Prevention Research Center, Feng Chia Univ., 2. Taiwan Hsin-Chu Irrigation Association

Recently, rainfall become more unevenly both in special and temporal distribution caused by global climate change. The frequency of drought decrease from once every 17 years to once every 9 years. How to define warning signs of a drought and propose adaptive strategies is one of the key topic for water resources management. The drought can be divided into meteorological drought, agricultural drought and hydrological drought. The study tries to introduces difference Drought Early Warning Index, such as Standardized Precipitation Index, Standardized Groundwater Index, Normalized Difference Vegetation Index etc., to predict drought circumstance. The result can be a reference for development of drought early warning system.

Keywords: Standardized Precipitation Index, Standardized Groundwater Index, Normalized Difference Vegetation Index

©2019. Japan Geoscience Union. All Right Reserved.

[J] Poster | M (Multidisciplinary and Interdisciplinary)：M-GI General Geosciences, Information Geosciences & Simulations

Tue. May 28, 2019 1:45 PM - 3:15 PM JST | Tue. May 28, 2019 4:45 AM - 6:15 AM UTC | Poster Hall International Exhibition Hall8, Makuhari Messe_9

[M-GI34] Marine Manganese Minerals

convener:Akira Usui(Marine Core Research Center, Kochi University), Yoshio Takahashi(Department of Earth and Planetary Science, Graduate School of Science, The University of Tokyo), Katsuhiko Suzuki(Research and Development Center for Submarine Resources, Japan Agency for Marine-Earth Science and Technology), Takashi Ito(Faculty of Education, Ibaraki University)

Marine manganese deposits include nodules and crusts of massive iron-manganese oxide aggregates associated with useful metals. The deposits are known as potential resources of cobalt, copper, nickel, rare earth elements, platinum, and tellurium. However, the controlling parameters on the regional and temporal variations in chemical and mineralogical composition have not been clarified yet. In this session, various factors in the growth of manganese oxides, enrichment and circulation of metals, paleoenvironment, and formation age of manganese deposits will be discussed from viewpoints of geology, mineralogy, paleocean sciences, geochemistry, microbiology, and sea floor engineering.

[MGI34-P01] Microstratigraphy of hydrogenetic ferromanganese crusts in the Takuyo-Daisan and -Daigo seamounts

*Akira Usui[1], An-na Nagaoka[2], Michiko Kawamura[1] (1.Marine Core Research Center, Kochi University, 2.Graduate School of Science, Kochi University)

[MGI34-P02] Manganese Crusts with Super Smooth Surface (3S Manganese Crusts) observed at Takuyo No.3 Seamount, Northwest Pacific

*Masaki Saito[1], Takashi Ito[2] (1.Graduate School of Education,Ibaraki University, 2.Department of Education,Ibaraki University)

[MGI34-P03] Geochemical characteristics of the nuclei of ferromanganese nodules in the Minamitorishima EEZ

*Daiki Terauchi[1], Kentaro Nakamura[1], Ryo Shimomura[1], Koichi Horinouchi[1], Kazutaka Yasukawa[1,2], Shiki Machida[2,1], Yasuhiro Kato[1,2,3] (1.Department of Systems Innovation, School of Engineering, University of Tokyo, 2.Ocean Resources Research Center for Next Generation, Chiba Institute of Technology, 3.Frontier Research Center for Energy and Resources, School of Engineering, The University of Tokyo)

[MGI34-P04] Micro X-ray fluorescence mapping for the whole cross-section of ferromanganese nodules in the western North Pacific

*Shiki Machida[1,2], Ryo Shimomura[2], Koichi Horinouchi[2], Kentaro Nakamura[2], Tetsu Kogiso[3], Yasuhiro Kato[2,1] (1.Ocean Resources Research Center for Next Generation, Chiba Institute of Technology, 2.University of Tokyo, 3.Kyoto University)

Microstratigraphy of hydrogenetic ferromanganese crusts in the Takuyo-Daisan and -Daigo seamounts

*Akira Usui[1], An-na Nagaoka[2], Michiko Kawamura[1]

1. Marine Core Research Center, Kochi University, 2. Graduate School of Science, Kochi University

Hydrogenetic ferromanganese crusts cover almost all the rock outcrops on the slopes of the Takuyo #3 and #5 seamounts. The secular variations in physical properties are in some cases correlated with the mineral composition or chemical compositions. The youngest Pliocene Zone is enriched with tiny quartz particles with benthic foraminifers, while the older Miocene zone is characterized by coarser mineral grains of volcanic rock origin. Thus the apparent zoning and correlation patterns are overlapped both with local and regional environmental parameters.

Keywords: ferromanganese crust, microstratigraphy, seamount

©2019. Japan Geoscience Union. All Right Reserved.

Manganese Crusts with Super Smooth Surface (3S Manganese Crusts) observed at Takuyo No.3 Seamount, Northwest Pacific

*Masaki Saito[1], Takashi Ito[2]

1. Graduate School of Education,Ibaraki University, 2. Department of Education,Ibaraki University

During the research cruises, JAMSTEC KR17-07C and KR 18-11C, the detailed observations based on ROV "Kaiko" revealed that the manganese crusts with several cm order of Mn oxide layer in thickness spread over in the northern ridge of Takuyo No.3 Seamount. In addition, the crusts having super smooth surfaces (3S crusts) were also observed. In general, the surface structure of marine manganese oxide has been classified into two types, s (smooth) and r (rough). However, the smooth surface observed this time is obviously different from the common s type surface structure, and there is a possibility that a new classification in the manganese oxide surface is required.

In this study, the characteristics of the distribution of the 3S manganese crusts and the surface structure were examined preliminary. For examining the characteristics of the distribution, the image data taken with a digital still camera mounted on ROV "Kaiko" Mk - IV was used. These images were taken randomly by onboard operators during each dive. We checked the images one by one and counted the images showing the 3S crusts. Also, the distribution frequency (shots/min.) of the 3S crusts was measured.

As a result of the image analysis, it is clear that the distribution of the 3S crusts at Takuyo No.3 seamount has water depth dependence. The main distribution area of the 3S crusts is between 1400 - 1600m in water depth. The super smooth surface did not spread over the entire surface of each crust but was found on the edges of the side surface of the crusts mainly.

SEM observation of the samples showed a clear difference between the 3S crusts and common s type surfaces. The surface of the super smooth surface was literally extremely smooth even at the level of SEM observation, but it was also confirmed that there were many scratches of several tens of microns in length. This scratches appeared not only in one direction but also in random distribution. We have the plan to clarify the formation process of super smooth surface based on mineral and chemical compositions and micro CT observations in addition to further SEM observations.

Keywords: manganese crusts, Takuyo No.3 Seamount, Super Smooth Surface, 3S Manganese Crusts

©2019. Japan Geoscience Union. All Right Reserved.

Geochemical characteristics of the nuclei of ferromanganese nodules in the Minamitorishima EEZ

*Daiki Terauchi[1], Kentaro Nakamura[1], Ryo Shimomura[1], Koichi Horinouchi[1], Kazutaka Yasukawa[1,2], Shiki Machida[2,1], Yasuhiro Kato[1,2,3]

1. Department of Systems Innovation, School of Engineering, University of Tokyo, 2. Ocean Resources Research Center for Next Generation, Chiba Institute of Technology, 3. Frontier Research Center for Energy and Resources, School of Engineering, The University of Tokyo

Ferromanganese nodules are polymetallic concretion mainly composed of Mn- and Fe-oxyhydroxides with significant concentrations of valuable metals such as Ni, Cu and Co [1, 2]. The nodules can be found on deep-sea sediments worldwide, and their dense distribution has recently been discovered in the Japanese exclusive economic zone (EEZ) around Minamitorishima Island [3, 4].

It is well known that almost all ferromanganese nodules have nuclei, which clearly indicates that growth of a nodule generally starts on nucleus surface. Characterizing the nuclei of the nodules can, thus, provide important information on the conditions for the growth initiation of the nodules. Previous study [5] revealed that the nuclei of the nodules in the Minamitorishima EEZ can be classified into four types (nucleus I ~ IV), and that the majority of the nuclei is consolidated pelagic clay (nucleus I). However, detailed chemical characteristics of the nucleus I, as well as those of the other types of nuclei, have not yet been fully understood.

Here, we performed major and trace element analysis of the nuclei (especially of the nucleus I) in order to reveal their chemical features. In the presentation, we will show the results of the chemical characterization of the nuclei and then will discuss the origin of the nuclei of ferromanganese nodules in the Minamitorishima EEZ.

References

[1] Petersen et al. (2016) *Marine Policy,* **70**, 175–187, [2] Hein et al. (2013) *Ore Geology Reviews*, **51**, 1–14, [3] Machida et al. (2016) *Geochemical Journal*, **50**, 539–555, [4] JAMSTEC press release, August 26, 2016, [5] Shimomura et al. (2018) *JpGU meeting 2018.*

Keywords: ferromanganese nodules, nuclei, consolidated pelagic clay, chemical composition, Minamitorishima EEZ

©2019. Japan Geoscience Union. All Right Reserved.

Micro X-ray fluorescence mapping for the whole cross-section of ferromanganese nodules in the western North Pacific

*Shiki Machida[1,2], Ryo Shimomura[2], Koichi Horinouchi[2], Kentaro Nakamura[2], Tetsu Kogiso[3], Yasuhiro Kato[2,1]

1. Ocean Resources Research Center for Next Generation, Chiba Institute of Technology, 2. University of Tokyo, 3. Kyoto University

A dense field of hydrogenous ferromanganese nodules was discovered on a small seamount approximately 300 km east of Minamitorishima (Marcus) Island, in the western North Pacific [1]. Previous study [1] defined two fundamental features on structure and geochemistry of nodules, as follows. The large nodules generally consist of three concentric layers: the outermost mottled (sediment-filled) layer L0; the massive black layer L1; and the innermost porous (sediment-filled) layer L2. Elements including Fe, Ti, and Co are concentrated in the nodule rim rather than the center. In contrast, Mn, Al, P, Ca, Ni, and Zn are concentrated in the center, and decrease toward the rim.

To further investigate the relationship between structure of oxide layers and its geochemical features, we conducted mapping analysis for polished slab of nodules including nuclei and whole layers of oxide by a microfocus X-ray fluorescence analytical microscope (XGT-7000; HORIBA) at Kyoto University. Analysis was conducted in vacuo, and the intensity of Si, Al, P, Ca, K, Mn, Fe, Ti, Ni, Cu, and Y were determined by an energy-dispersive spectrometer at an accelerating voltage of 50 kV, 100 μm beam, and intervals of approximately 160 μm.

We identified that L2 is further sub-divided into three layers, which correspond to layers obtained by X-ray CT [2]. The most inner part of L2 (around nuclei) is characterized by high intensity of Ti and Fe. In contrast, outer part of L2 is characterized by higher intensity of Mn than that of the inner part. Many spots of high intensity of P, Ca, and Y, indicating particles of calcium phosphate including highly amount of Y (and probably rare-earth elements), are observed in the entire area of L2. We found that L1 is clearly characterized by low Si. Furthermore, we observed thin layers showing high intensity of Cu and Ni at the sediment-filled boundaries between L1 and L2, and L1 and L0. Existence of such thin layers suggests that nodules were fully covered by pelagic sediment at the intervals before formation of L1 and L0.

References: [1] Machida et al. (2016) *Geochem. J.***50**, 539-555. [2] Shimomura et al. (2018) *Goldschmidt Conference 2018*.

Keywords: ferromanganese nodule, micro X-ray analysis, Minamitorishima EEZ

©2019. Japan Geoscience Union. All Right Reserved.

[J] Poster | M (Multidisciplinary and Interdisciplinary)：M-GI General Geosciences, Information Geosciences & Simulations

Tue. May 28, 2019 5:15 PM - 6:30 PM JST | Tue. May 28, 2019 8:15 AM - 9:30 AM UTC | Poster Hall International Exhibition Hall8, Makuhari Messe_48

[M-GI34] Marine Manganese Minerals

convener:Akira Usui(Marine Core Research Center, Kochi University), Yoshio Takahashi(Department of Earth and Planetary Science, Graduate School of Science, The University of Tokyo), Katsuhiko Suzuki(Research and Development Center for Submarine Resources, Japan Agency for Marine-Earth Science and Technology), Takashi Ito(Faculty of Education, Ibaraki University)

Marine manganese deposits include nodules and crusts of massive iron-manganese oxide aggregates associated with useful metals. The deposits are known as potential resources of cobalt, copper, nickel, rare earth elements, platinum, and tellurium. However, the controlling parameters on the regional and temporal variations in chemical and mineralogical composition have not been clarified yet. In this session, various factors in the growth of manganese oxides, enrichment and circulation of metals, paleoenvironment, and formation age of manganese deposits will be discussed from viewpoints of geology, mineralogy, paleocean sciences, geochemistry, microbiology, and sea floor engineering.

[MGI34-P01] Microstratigraphy of hydrogenetic ferromanganese crusts in the Takuyo-Daisan and -Daigo seamounts

*Akira Usui[1], An-na Nagaoka[2], Michiko Kawamura[1] (1.Marine Core Research Center, Kochi University, 2.Graduate School of Science, Kochi University)

[MGI34-P02] Manganese Crusts with Super Smooth Surface (3S Manganese Crusts) observed at Takuyo No.3 Seamount, Northwest Pacific

*Masaki Saito[1], Takashi Ito[2] (1.Graduate School of Education,Ibaraki University, 2.Department of Education,Ibaraki University)

[MGI34-P03] Geochemical characteristics of the nuclei of ferromanganese nodules in the Minamitorishima EEZ

*Daiki Terauchi[1], Kentaro Nakamura[1], Ryo Shimomura[1], Koichi Horinouchi[1], Kazutaka Yasukawa[1,2], Shiki Machida[2,1], Yasuhiro Kato[1,2,3] (1.Department of Systems Innovation, School of Engineering, University of Tokyo, 2.Ocean Resources Research Center for Next Generation, Chiba Institute of Technology, 3.Frontier Research Center for Energy and Resources, School of Engineering, The University of Tokyo)

[MGI34-P04] Micro X-ray fluorescence mapping for the whole cross-section of ferromanganese nodules in the western North Pacific

*Shiki Machida[1,2], Ryo Shimomura[2], Koichi Horinouchi[2], Kentaro Nakamura[2], Tetsu Kogiso[3], Yasuhiro Kato[2,1] (1.Ocean Resources Research Center for Next Generation, Chiba Institute of Technology, 2.University of Tokyo, 3.Kyoto University)

Microstratigraphy of hydrogenetic ferromanganese crusts in the Takuyo-Daisan and -Daigo seamounts

*Akira Usui[1], An-na Nagaoka[2], Michiko Kawamura[1]

1. Marine Core Research Center, Kochi University, 2. Graduate School of Science, Kochi University

Hydrogenetic ferromanganese crusts cover almost all the rock outcrops on the slopes of the Takuyo #3 and #5 seamounts. The secular variations in physical properties are in some cases correlated with the mineral composition or chemical compositions. The youngest Pliocene Zone is enriched with tiny quartz particles with benthic foraminifers, while the older Miocene zone is characterized by coarser mineral grains of volcanic rock origin. Thus the apparent zoning and correlation patterns are overlapped both with local and regional environmental parameters.

Keywords: ferromanganese crust, microstratigraphy, seamount

©2019. Japan Geoscience Union. All Right Reserved.

Manganese Crusts with Super Smooth Surface (3S Manganese Crusts) observed at Takuyo No.3 Seamount, Northwest Pacific

*Masaki Saito[1], Takashi Ito[2]

1. Graduate School of Education,Ibaraki University, 2. Department of Education,Ibaraki University

During the research cruises, JAMSTEC KR17-07C and KR 18-11C, the detailed observations based on ROV "Kaiko" revealed that the manganese crusts with several cm order of Mn oxide layer in thickness spread over in the northern ridge of Takuyo No.3 Seamount. In addition, the crusts having super smooth surfaces (3S crusts) were also observed. In general, the surface structure of marine manganese oxide has been classified into two types, s (smooth) and r (rough). However, the smooth surface observed this time is obviously different from the common s type surface structure, and there is a possibility that a new classification in the manganese oxide surface is required.

In this study, the characteristics of the distribution of the 3S manganese crusts and the surface structure were examined preliminary. For examining the characteristics of the distribution, the image data taken with a digital still camera mounted on ROV "Kaiko" Mk - IV was used. These images were taken randomly by onboard operators during each dive. We checked the images one by one and counted the images showing the 3S crusts. Also, the distribution frequency (shots/min.) of the 3S crusts was measured.

As a result of the image analysis, it is clear that the distribution of the 3S crusts at Takuyo No.3 seamount has water depth dependence. The main distribution area of the 3S crusts is between 1400 - 1600m in water depth. The super smooth surface did not spread over the entire surface of each crust but was found on the edges of the side surface of the crusts mainly.

SEM observation of the samples showed a clear difference between the 3S crusts and common s type surfaces. The surface of the super smooth surface was literally extremely smooth even at the level of SEM observation, but it was also confirmed that there were many scratches of several tens of microns in length. This scratches appeared not only in one direction but also in random distribution. We have the plan to clarify the formation process of super smooth surface based on mineral and chemical compositions and micro CT observations in addition to further SEM observations.

Keywords: manganese crusts, Takuyo No.3 Seamount, Super Smooth Surface, 3S Manganese Crusts

©2019. Japan Geoscience Union. All Right Reserved.

Geochemical characteristics of the nuclei of ferromanganese nodules in the Minamitorishima EEZ

*Daiki Terauchi[1], Kentaro Nakamura[1], Ryo Shimomura[1], Koichi Horinouchi[1], Kazutaka Yasukawa[1,2], Shiki Machida[2,1], Yasuhiro Kato[1,2,3]

1. Department of Systems Innovation, School of Engineering, University of Tokyo, 2. Ocean Resources Research Center for Next Generation, Chiba Institute of Technology, 3. Frontier Research Center for Energy and Resources, School of Engineering, The University of Tokyo

Ferromanganese nodules are polymetallic concretion mainly composed of Mn- and Fe-oxyhydroxides with significant concentrations of valuable metals such as Ni, Cu and Co [1, 2]. The nodules can be found on deep-sea sediments worldwide, and their dense distribution has recently been discovered in the Japanese exclusive economic zone (EEZ) around Minamitorishima Island [3, 4].

It is well known that almost all ferromanganese nodules have nuclei, which clearly indicates that growth of a nodule generally starts on nucleus surface. Characterizing the nuclei of the nodules can, thus, provide important information on the conditions for the growth initiation of the nodules. Previous study [5] revealed that the nuclei of the nodules in the Minamitorishima EEZ can be classified into four types (nucleus I ~ IV), and that the majority of the nuclei is consolidated pelagic clay (nucleus I). However, detailed chemical characteristics of the nucleus I, as well as those of the other types of nuclei, have not yet been fully understood.

Here, we performed major and trace element analysis of the nuclei (especially of the nucleus I) in order to reveal their chemical features. In the presentation, we will show the results of the chemical characterization of the nuclei and then will discuss the origin of the nuclei of ferromanganese nodules in the Minamitorishima EEZ.

References

[1] Petersen et al. (2016) *Marine Policy,* **70**, 175–187, [2] Hein et al. (2013) *Ore Geology Reviews*, **51**, 1–14, [3] Machida et al. (2016) *Geochemical Journal*, **50**, 539–555, [4] JAMSTEC press release, August 26, 2016, [5] Shimomura et al. (2018) *JpGU meeting 2018.*

Keywords: ferromanganese nodules, nuclei, consolidated pelagic clay, chemical composition, Minamitorishima EEZ

©2019. Japan Geoscience Union. All Right Reserved.

Micro X-ray fluorescence mapping for the whole cross-section of ferromanganese nodules in the western North Pacific

*Shiki Machida[1,2], Ryo Shimomura[2], Koichi Horinouchi[2], Kentaro Nakamura[2], Tetsu Kogiso[3], Yasuhiro Kato[2,1]

1. Ocean Resources Research Center for Next Generation, Chiba Institute of Technology, 2. University of Tokyo, 3. Kyoto University

A dense field of hydrogenous ferromanganese nodules was discovered on a small seamount approximately 300 km east of Minamitorishima (Marcus) Island, in the western North Pacific [1]. Previous study [1] defined two fundamental features on structure and geochemistry of nodules, as follows. The large nodules generally consist of three concentric layers: the outermost mottled (sediment-filled) layer L0; the massive black layer L1; and the innermost porous (sediment-filled) layer L2. Elements including Fe, Ti, and Co are concentrated in the nodule rim rather than the center. In contrast, Mn, Al, P, Ca, Ni, and Zn are concentrated in the center, and decrease toward the rim.

To further investigate the relationship between structure of oxide layers and its geochemical features, we conducted mapping analysis for polished slab of nodules including nuclei and whole layers of oxide by a microfocus X-ray fluorescence analytical microscope (XGT-7000; HORIBA) at Kyoto University. Analysis was conducted in vacuo, and the intensity of Si, Al, P, Ca, K, Mn, Fe, Ti, Ni, Cu, and Y were determined by an energy-dispersive spectrometer at an accelerating voltage of 50 kV, 100 μm beam, and intervals of approximately 160 μm.

We identified that L2 is further sub-divided into three layers, which correspond to layers obtained by X-ray CT [2]. The most inner part of L2 (around nuclei) is characterized by high intensity of Ti and Fe. In contrast, outer part of L2 is characterized by higher intensity of Mn than that of the inner part. Many spots of high intensity of P, Ca, and Y, indicating particles of calcium phosphate including highly amount of Y (and probably rare-earth elements), are observed in the entire area of L2. We found that L1 is clearly characterized by low Si. Furthermore, we observed thin layers showing high intensity of Cu and Ni at the sediment-filled boundaries between L1 and L2, and L1 and L0. Existence of such thin layers suggests that nodules were fully covered by pelagic sediment at the intervals before formation of L1 and L0.

References: [1] Machida et al. (2016) *Geochem. J.***50**, 539-555. [2] Shimomura et al. (2018) *Goldschmidt Conference 2018*.

Keywords: ferromanganese nodule, micro X-ray analysis, Minamitorishima EEZ

©2019. Japan Geoscience Union. All Right Reserved.

[J] Oral | M (Multidisciplinary and Interdisciplinary)：M-GI General Geosciences, Information Geosciences & Simulations

Tue. May 28, 2019 3:30 PM - 5:00 PM JST | Tue. May 28, 2019 6:30 AM - 8:00 AM UTC | A09 TOKYO BAY MAKUHARI HALL

[M-GI34] Marine Manganese Minerals

convener:Akira Usui(Marine Core Research Center, Kochi University), Yoshio Takahashi(Department of Earth and Planetary Science, Graduate School of Science, The University of Tokyo), Katsuhiko Suzuki(Research and Development Center for Submarine Resources, Japan Agency for Marine-Earth Science and Technology), Takashi Ito(Faculty of Education, Ibaraki University), Chairperson:takashi ito(Ibaraki Univ.), Yoshio Takahashi(東京大学), Katsuhiko Suzuki(JAMSTEC)

Marine manganese deposits include nodules and crusts of massive iron-manganese oxide aggregates associated with useful metals. The deposits are known as potential resources of cobalt, copper, nickel, rare earth elements, platinum, and tellurium. However, the controlling parameters on the regional and temporal variations in chemical and mineralogical composition have not been clarified yet. In this session, various factors in the growth of manganese oxides, enrichment and circulation of metals, paleoenvironment, and formation age of manganese deposits will be discussed from viewpoints of geology, mineralogy, paleocean sciences, geochemistry, microbiology, and sea floor engineering.

3:30 PM - 3:45 PM JST | 6:30 AM - 6:45 AM UTC

[MGI34-01] Challenges in microstratigraphy on the hydrogenetic ferromanganese crusts: Depositional processes and environments recorded as secular variations in microstructure, chemical and mineralogical compositions.

*Akira Usui[1], Anna Nagaoka[2], Go-Ichiro Uramoto[1], Masafumi MURAYAMA[3] (1.Marine Core Research Center, Kochi University, 2.Graduate School of Science, Kochi University, 3.Fac. Agriculture and Marine Sciences, Kochi University)

3:45 PM - 4:00 PM JST | 6:45 AM - 7:00 AM UTC

[MGI34-02] Abundant ferromanganese microparticles in oxic pelagic sediments

*Go-Ichiro Uramoto[1,2], Yuki Morono[2], Naotaka Tomioka[2], Shigeyuki Wakaki[2], Ryoichi Nakada[2], Rota Wagai[3], Kentaro Uesugi[4], Akihisa Takeuchi[4], Masato Hoshino[4], Yoshio Suzuki[4,5], Satoshi Mitsunobu[6], Fumito Shiraishi[7], Hiroki Suga[5], Yasuo Takeichi[8], Yoshio Takahashi[5], Fumio Inagaki[2] (1.Kochi University, 2.Japan Agency for Marine-Earth Science and Technology, 3.National Agriculture and Food Research Organization, 4.Japan Synchrotron Radiation Research Institute, 5.University of Tokyo, 6.Ehime University, 7.Hiroshima University, 8.High Energy Accelerator Research Organization)

4:00 PM - 4:15 PM JST | 7:00 AM - 7:15 AM UTC

[MGI34-03] Fractionation of Zirconium-Hafnium in ferromanganese crusts

*Aya Sakaguchi[1], Junpei Inagaki[1], Minami Inoue[2], Akira Usui[3], Hiromitsu Haba[4], Masashi Kaneko[5], Shinya Yamasaki[1], Keisuke Sueki[1], Yoshio Takahashi[6] (1.Faculty of Pure and Applied Science, 2.Graduate School of Science, Hiroshima University, 3.Center for Advanced Marine Core Research , Kochi University, 4.Nishina Center, Riken, 5.Nuclear Science and Engineering Center, Japan Atomic Energy Agency, 6.Graduate School of Science, The University of Tokyo)

4:15 PM - 4:30 PM JST | 7:15 AM - 7:30 AM UTC

[MGI34-04] Isotope fractionation of Mo-like elements during adsorption to ferromanganese oxides

*Masato Tanaka[1], Yoshio Takahashi[1] (1.Graduate School of Science, The University of Tokyo)

4:30 PM - 4:45 PM JST | 7:30 AM - 7:45 AM UTC

[MGI34-05] **Distinct distribution trends of arsenate and molybdate in marine ferromanganese nodules**

*Shitong Yang[1], Soichiro Uesugi[1], Haibo Qin[1], Akira Usui[2], Yoshio Takahashi[1] (1.Department of Earth and Planetary Science, Graduate School of Science, The University of Tokyo, 2.Geology Department, Kochi University)

4:45 PM - 5:00 PM JST | 7:45 AM - 8:00 AM UTC

[MGI34-06] Mineralogical and geochemical characteristics of ferromanganese nodules in the Minamitorishima EEZ

*Kentaro Nakamura[1], Koichi Horinouchi[1], Ryo Shimomura[1], Shiki Machida[2], Kazutaka Yasukawa[1,2], Koichiro Fujinaga[1,2], Yasuhiro Kato[1,2] (1.Department of Systems Innovation, School of Engineering, University of Tokyo, 2.ORCeNG, Chiba Institute of Technology)

Challenges in microstratigraphy on the hydrogenetic ferromanganese crusts: Depositional processes and environments recorded as secular variations in microstructure, chemical and mineralogical compositions.

*Akira Usui[1], Anna Nagaoka[2], Go-Ichiro Uramoto[1], Masafumi MURAYAMA[3]

1. Marine Core Research Center, Kochi University, 2. Graduate School of Science, Kochi University, 3. Fac. Agriculture and Marine Sciences, Kochi University

We attempted to apply the method of Shima-Shima-gaku (lamina stratigraphy named by prof. S. Kawakami) on the secular variations in growth structure, chemical and mineralogical properties between the growth columns of the hydrogenetic ferromanganese deposit. The critera for describing each bands or zones based on the macroscopic (=physical) properties are not always consistant with chronological correlations or may not match with mineral/chemical composition. Our microscopic characterization using optical microscope, XRF mapping, XRD, acid-leach, micro-focus X-ray CT proved a possibility of separating local and regional sources of each mineral particle or element which is closely associated the environments of eposition.

Keywords: marine manganese deposit, manganese crust, microstratigraphy, Shima-Shima-gaku

©2019. Japan Geoscience Union. All Right Reserved.

Abundant ferromanganese microparticles in oxic pelagic sediments

*Go-Ichiro Uramoto[1,2], Yuki Morono[2], Naotaka Tomioka[2], Shigeyuki Wakaki[2], Ryoichi Nakada[2], Rota Wagai[3], Kentaro Uesugi[4], Akihisa Takeuchi[4], Masato Hoshino[4], Yoshio Suzuki[4,5], Satoshi Mitsunobu[6], Fumito Shiraishi[7], Hiroki Suga[5], Yasuo Takeichi[8], Yoshio Takahashi[5], Fumio Inagaki[2]

1. Kochi University, 2. Japan Agency for Marine-Earth Science and Technology, 3. National Agriculture and Food Research Organization, 4. Japan Synchrotron Radiation Research Institute, 5. University of Tokyo, 6. Ehime University, 7. Hiroshima University, 8. High Energy Accelerator Research Organization

Manganese is the third most abundant metallic element, after iron and titanium, in the Earth’ s crust, and ferromanganese minerals are sensitive to changes in redox condition. Assessing the formation and preservation of ferromanganese minerals is important for understanding the global marine cycles of manganese and numerous associated trace elements. The most extensive manganese mineral deposits occur on abyssal plains, including those below open-ocean gyres. However, the extent of ferromanganese minerals buried in subseafloor sediments remains unclear. During the Integrated Ocean Drilling Program (IODP) Expedition 329, we drilled the entire sedimentary sequence at 6 sites in the ultra-oligotrophic region of the South Pacific Gyre (SPG), where dissolved O_2 and aerobic microbial communities are present from the seafloor to the sediment-basement interface [1]. By using high-resolution imaging techniques, we found abundant (10^8-10^9 particles cm^{-3}) micrometer-scale ferromanganese mineral particles (Mn-microparticles) in the oxic pelagic clays of the South Pacific Gyre [2]. Furthermore, we established microparticle separation technique by the combined use of density concentration and flowcytometer/particles sorting techniques. Major and trace element compositional analyses revealed that iron and manganese were the major components of Mn-microparticles, while they also contained rare-earth elements. From the number of Mn-microparticles per unit volume of sediment and the global distribution of oxic pelagic clays, we estimated the number of Mn-microparticles to be 1.5-8.8 $\times 10^{28}$ particles, which accounted for 1.28-7.62 Tt of manganese. This estimate is at least 2 orders of magnitude larger than the manganese budget for manganese nodules and manganese crusts on the seafloor. Along with the examination of manganese input, formation, and preservation, this study provides new insights into the global budget of metallic elements in the abundant Mn-microparticles present in deep subseafloor environments.

[1] D’ Hondt, S., Inagaki, F., Zarikian, C. A., Abrams, L. J., Dubois, N., Engelhardt, T., Evans, H., Ferdelman, T., Gribsholt, B., Harris, R. N., Hoppie, B. W., Hyun, J.-H., Kallmeyer, J., Kim. J., Lynch, J. E., McKinley, C. C., Mitsunobu, S., Morono, Y., Murray, R. W., Pockalny, R., Sauvage, J., Shimono, T., Shiraishi, F., Smith, D. C., Smith-Duque, C., Spivack, A. J., Steinsbu, B. O., Suzuki, Y., Szpak, M., Toffin, L., Uramoto, G., Yamaguchi, T. Y., Zhang, G., Zhang, X.-H., and Ziebis, W. Presence of oxygen and aerobic communities from seafloor to basement in deep-sea sediment. *Nature Geosciences,* 8(4), 299-304, 2015.
[2] Uramoto, G.-I., Morono, Y., Tomioka, N., Wakaki, S., Wagai, R., Uesugi, K., Takeuchi, A., Hoshino, M., Suzuki, Y., Shiraishi, F., Mitsunobu, S., Suga, H., Nakada, R., Takeichi, Y., Takahashi, Y., and Inagaki, F., Significant contribution of subseafloor microparticles to the global manganese budget. *Nature Communications*. **10**, 400, https://doi.org/10.1038/s41467-019-08347-2, 2019

Keywords: Mn-microparticle, oxic pelagic clay, IODP Exp. 329

©2019. Japan Geoscience Union. All Right Reserved.

Fractionation of Zirconium-Hafnium in ferromanganese crusts

*Aya Sakaguchi[1], Junpei Inagaki[1], Minami Inoue[2], Akira Usui[3], Hiromitsu Haba[4], Masashi Kaneko[5], Shinya Yamasaki[1], Keisuke Sueki[1], Yoshio Takahashi[6]

1. Faculty of Pure and Applied Science, 2. Graduate School of Science, Hiroshima University, 3. Center for Advanced Marine Core Research , Kochi University, 4. Nishina Center, Riken, 5. Nuclear Science and Engineering Center, Japan Atomic Energy Agency, 6. Graduate School of Science, The University of Tokyo

Ferromanganese crusts (FMCs) are abyssal benthic chemical sediments that consist mainly of Fe and Mn oxide and hydroxide minerals, enriched with trace and precious metals. Due to their similar physicochemical properties, the elements zirconium (Zr) and hafnium (Hf), which are concentrated in FMCs, have a theoretically uniform ratio (Zr/Hf), which ratio is found in numerous systems. However, recent advances in analytical techniques have allowed observation of significant differences in the fractionation of these elements between seawater (Zr/Hf~45-350; Firdaus et al. 2011) and FMCs (Zr/Hf~57-88; Schmidt et al., 2014). In this study, we conducted adsorption experiments and XAFS analyses to clarify the concentrations and fractionation mechanisms of Zr-Hf in FMCs using synthesized minerals (Ferrihydrite and δ-MnO_2), radio-Zr and Hf tracers, and natural samples.

Six FMCs were collected from the Takuyo-Daigo and Ryusei seamounts, at water depths of from 950 m to 3000 m, using a ROV equipped with a live video camera and manipulators. The near surface layers (less than 1 mm) of all the FMCs were analyzed with XAFS and ICP-MS for Zr, Hf and other elements, and with XRD for mineral composition. Radiotracers were produced using the RIKEN AVF cyclotron for adsorption and co-precipitation experiments. Appropriate amounts of these tracers were added to 0.7 M NaCl solutions containing desferrioxamine B (DFOB) to obtain some Zr and Hf concentrations of solutions. The speciations of these elements in said solutions were confirmed by ESI-TOF-MS. Synthesized Ferrihydrite or δ-MnO_2 was added to the solutions and stirred for three hours at a pH of 8. In addition, Ferrihydrite or δ-MnO_2 was synthesized in said solutions. The activities of radio tracers in the filtered solutions were measured using a Ge detector. The adsorption/co-precipitation amounts to the solid phase were calculated using the differences in the radioactivity of the solution before and after filtration.

The major mineral composition of Fe and Mn in the FMCs did not vary significantly with the water depth of these seamounts. The concentrations of Zr and Hf increased with depth, and their ratios were totally fractionated from those of the seawater (Firdaus et al., 2011). Hf was more enriched in all FMCs than was Zr. The observed Zr chemical states in the FMCs were mainly coprecipitation with Ferrihydrite and coprecipitation with d-MnO2. In our adsorption experiments, the largest adsorption rate was observed in Hf to δ-MnO_2, followed in order by Zr to δ-MnO_2, Hf to Ferrihydrite and Zr to Ferrihydrite. The partition coefficients (K_D values) were calculated using the concentration ranges of Zr and Hf in seawater, where it was clear that Hf adsorbed more on both. Even though complexation rates estimated by RI-TLC were considered, there was no change in the adsorption behaviors in these experiments. For these samples, we found that the bond lengths between Zr-O and Hf-O in the first shells were shortened when they were incorporated into the oxides, with Hf-O becoming more shortened compared to Zr-O. The DFT calculations showed that Zr and Hf adsorbs on Fe and Mn oxides as bidentate-mono nuclear and bidentate-binuclear structures. The calculation results for the binding energies and bond orders of Zr and Hf to minerals gave a reasonable explanation of the fractionation mechanism for Zr-Hf pairs in FMCs.

©2019. Japan Geoscience Union. All Right Reserved.

Keywords: Ferromanganese crusts, Zirconium, Hafnium

©2019. Japan Geoscience Union. All Right Reserved.

Isotope fractionation of Mo-like elements during adsorption to ferromanganese oxides

*Masato Tanaka[1], Yoshio Takahashi[1]

1. Graduate School of Science, The University of Tokyo

A large mass-dependent isotope fractionation between seawater and ferromanganese oxides was observed, where lighter isotopes of Mo were preferentially incorporated into ferromanganese oxides. The large isotopic fractionation of molybdenum (Mo) is most likely caused by geometrical change from tetrahedral (Td) to distorted octahedral (Oh) during adsorption on manganese oxides based on X-ray absorption fine structure (XAFS) spectroscopy. The coordination number relates to its ionic radius. Thus, the elements which have similar ionic radius to Mo are expected to show the similar phenomena to Mo, i.e. the large isotope fractionation. Germanium (Ge) and Vanadium (V) can be candidate of such elements because they have similar ionic radius to Mo (Ge(IV): r= 0.53 Å, V(V): r=0.54 Å, and Mo(VI): r=0.59 Åfor 6-hold coordination). In this study, we examine the adsorption structure of Ge and V on Fe-/Mn-(oxyhydr)oxides by XAFS spectroscopy. Furthermore, the isotope fractionation during adsorption on the minerals is estimated by quantum chemical calculations.

XAFS analysis indicated that the adsorbed species of Ge on Fe- and Mn-(oxyhydr)oxides have Td geometry. On the other hand, the adsorbed structure of V on ferrihydrite is Td whereas that on δ-MnO_2 is distorted Oh. This trend of V in adsorbed species is similar to that of Mo. The geometries of hydrated species of Ge and V are Td. Thus, it is expected that a large V isotope fractionation occur during adsorption on Mn oxide, but a small fractionation in the case of Ge. In fact, a large isotope fractionation for V and a small isotope fractionation for Ge were estimated by quantum chemical calculations. This finding indicates that the requirement to show a Mo like large isotope fractionation during adsorption is not only an appropriate ionic radius. Recently, we found that two elemental properties of Mo(VI), namely d^0 electronic configuration and appropriate ionic radius, lead to the large isotope fractionation. In fact, V(V) possesses d^0 electronic configuration, but Ge(IV) does not. Tungsten (W)(VI) also satisfies the two properties and shows a large isotope fractionation during adsorption on Fe-/Mn-(oxyhydr)oxides. Thus, the elements which have the two elemental properties (Mo-like elements) can exhibit a Mo like large isotope fractionation during ferromanganese oxides.

Keywords: molybdenum, ferromanganese oxide, isotope fractionation, quantum chemical calculation, vanadium, germanium

©2019. Japan Geoscience Union. All Right Reserved.

Distinct distribution trends of arsenate and molybdate in marine ferromanganese nodules

*Shitong Yang[1], Soichiro Uesugi[1], Haibo Qin[1], Akira Usui[2], Yoshio Takahashi[1]

1. Department of Earth and Planetary Science, Graduate School of Science, The University of Tokyo, 2. Geology Department, Kochi University

Marine ferromanganese nodules or crusts with the hydrogenetic (HG), diagenetic (DG) and hydrothermal (HT) origins, are important sedimentary substrates for various elements such as lead (Pb), zinc (Zn), cobalt (Co), cerium (Ce), molybdenum (Mo), tungsten (W), arsenic (As), antimony (Sb), tellurium (Te), and etc. However, the distribution behaviors and host phases of tetrahedral arsenate (AsO_4^{3-}) and molybdate (MoO_4^{2-}) oxyanions in the ferromanganese oxides are far from understood. Herein, we combine sequential extraction approach and spectroscopic analyses to explore the mineralogical components of HG ferromanganese nodules collected from the Pacific Ocean and the speciation of arsenate and molybdate therein.

X-ray diffraction (XRD), X-ray absorption near-edge structure (XANES) and extended X-ray absorption fine structure (EXAFS) spectroscopy analyses indicate that the predominant manganese and iron phases were vernadite (δ-MnO_2) and ferrihydrite, respectively. According to the sequential extraction examination, both As and Mo are associated with the iron (oxyhydr)oxide phases. As K-edge EXAFS analyses indicate the immobilization of arsenate by ferrihydrite via forming inner-sphere complexes in double corner-shared form. This result is consistent with the sequential extraction data. However, Mo L_3-edge XANES analyses suggest the adsorption of molybdate on vernadite surfaces via the edge-shared complexation, being contrary to the conclusion derived from the sequential extraction results. This inconsistency reveals the unreliability of sequential extraction approach to verify the host phase of trace elements in complicated natural samples due to the potential occurrence of re-adsorption risk.

According to the spectroscopic analyses, chemical binding (ΔG_{chem}) rather than the previously proposed coulombic interaction (ΔG_{coul}) is the predominant driving force for the retention of arsenate and molybdate by HG ferromanganese nodules. The disparate distribution trends of arsenate and molybdate are attributed to their different intrinsic properties (e.g., averaged dissociation constants of conjugate acids) and the diverse properties (e.g., surface site densify, adsorption equilibrium constant and crystalline structure) of ferrihydrite and vernadite. These research findings will help assess the geochemical behaviors and environmental fate of trace elements in marine environment.

Keywords: Marine ferromanganese nodules, Arsenate , Molybdate, Host phases, Geochemical behaviors

©2019. Japan Geoscience Union. All Right Reserved.

Mineralogical and geochemical characteristics of ferromanganese nodules in the Minamitorishima EEZ

*Kentaro Nakamura[1], Koichi Horinouchi[1], Ryo Shimomura[1], Shiki Machida[2], Kazutaka Yasukawa[1,2], Koichiro Fujinaga[1,2], Yasuhiro Kato[1,2]

1. Department of Systems Innovation, School of Engineering, University of Tokyo, 2. ORCeNG, Chiba Institute of Technology

Ferromanganese nodules are spherical material mainly composed of manganese, iron, and other transition metal (oxyhydro)oxides, which are widely distributed on the deep seafloor around the world [1]. It has been widely accepted that ferromanganese nodules can be classified into three types: hydrogenetic, diagenetic and hydrothermal types [1]. Among them, hydrogenetic nodules are composed of Fe–Mn (oxyhydr)oxides that precipitated from seawater and thus, this type of nodules can be expected to provide proxy paleoceanographic records [2, 3, 4, 5].
In this study, we investigated mineralogy and geochemistry of ferromanganese nodules sampled from the Minamitorishima EEZ for the purpose of elucidating formation environment of the nodules. Both the ferromanganese mineral phase and bulk chemical compositions clearly show that these nodules are hydrogenetic in origin. Based on X-ray CT and micro X-ray mapping analyses, oxide layer of the nodules can be subdivided into five layers [6. 7]. Although ferromanganese mineral is common to all the oxide layers, we found that Mn/Fe and Ni content systematically changed from inner layer to outer layer. The result implies that bottom water of the Minamitorishima EEZ has gradually been oxygenated toward the present.

Keywords: ferromanganese nodules, ferromanganese mineral, bulk chemical compositions, formation environment, Minamitorishima EEZ

©2019. Japan Geoscience Union. All Right Reserved.

[J] Oral | M (Multidisciplinary and Interdisciplinary)：M-GI General Geosciences, Information Geosciences & Simulations

Tue. May 28, 2019 1:45 PM - 3:15 PM JST | Tue. May 28, 2019 4:45 AM - 6:15 AM UTC | 301B 3F

[M-GI35] Development of computational sciences on planetary formation, evolution and surface environment

convener:Yoshi-Yuki Hayashi(Department of Planetology/CPS, Graduate School of Science, Kobe University), Masaki Ogawa(Division of General Systems Studies, Graduate School of Arts and Sciences, University of Tokyo), Shigeru Ida(Earth-Life Science Institute, Tokyo Institute of Technology), Kanya Kusano(Institute for Space-Earth Environmental Research, Nagoya University), Chairperson:Hiroki Kashimura

Computer simulations have been recognized as one of the fundamental tools in understanding planetary formation, evolution and diversity of surface environment. However, is may be notified that the continuous development of computational abilities in recent years does not seem to be well utilized in improving numerical simulations in those fields; computational efficiency has been improved by 6 orders of magnitude compared from the early 90's, many of our simulations do not seem to catch up qualitatively and quantitatively such improvement. We propose here in this session to ask those who are interested in computational sciences of various fields not only of planetary formation and evolution but also of earth and planetary sciences in general to join. The aim is to discuss various scientific and technical aspects of our numerical simulations to improve our skills to fully utilize those development of computational resources that is realized or will be realized in near future as "K" to "post-K".

1:45 PM - 2:00 PM JST | 4:45 AM - 5:00 AM UTC

[MGI35-01] Simulation Studies of Solar Activities as a Cause of Solar-Terrestrial Environment Variation

*Kanya Kusano[1], Hideyuki Hotta[2] (1.Institute for Space-Earth Environmental Research, Nagoya University, 2.Faculty of Science and Engineering, Chiba University)

2:00 PM - 2:15 PM JST | 5:00 AM - 5:15 AM UTC

[MGI35-02] Development of a global non-hydrostatic Martian atmospheric model and its high-resolution simulation

*Hiroki Kashimura[1], Hisashi Yashiro[2], Seiya Nishizawa[2], Hirofumi Tomita[2], Kensuke Nakajima[3], Masaki Ishiwatari[4], Yoshiyuki O. Takahashi[1], Yoshi-Yuki Hayashi[1] (1.Kobe University/Center for Planetary Science, 2.RIKEN Center for Computational Science, 3.Kyushu University, 4.Hokkaido University)

2:15 PM - 2:30 PM JST | 5:15 AM - 5:30 AM UTC

[MGI35-03] Numerical simulations on the collision, adhesion, and growth of dust particles in turbulent gas in a protoplanetary disk

*Takashi Ishihara[1], Kohei Hamabata[2], Yoshiki Sakurai[2], Masayuki Umemura[3] (1.Graduate School of Environmental and Life Science, Okayama University, 2.Graduate School of Engineering, Nagoya University, 3.Center for Computational Sciences, University of Tsukuba)

2:30 PM - 2:45 PM JST | 5:30 AM - 5:45 AM UTC

[MGI35-04] Development of N-body Simulation Code for Planetary System Formation With Particle-Particle Particle-Tree Scheme

*Yota Ishigaki[1,4], Junko Kominami[2], Junichiro Makino[3], Masaki Fujimoto[4] (1.University of Tokyo, 2.Tokyo Institute of Technology, 3.RIKEN AICS, 4.Institite of Space and Astronautical Science, Japan Aerospace Exploration Agency)

2:45 PM - 3:00 PM JST | 5:45 AM - 6:00 AM UTC

[MGI35-05] Current status of post-K Exploratory Challenge, computational planetary science

*Junichiro Makino[1,2] (1.Kobe Univ, 2. RIKEN R-CCS)

3:00 PM - 3:15 PM JST | 6:00 AM - 6:15 AM UTC
Discussion

Simulation Studies of Solar Activities as a Cause of Solar-Terrestrial Environment Variation

*Kanya Kusano[1], Hideyuki Hotta[2]

1. Institute for Space-Earth Environmental Research, Nagoya University, 2. Faculty of Science and Engineering, Chiba University

Solar activity is the main driver of disturbance of solar-terrestrial environment, and an extreme space weather disaster caused by a giant solar eruption is a potential risk to modern society. The prediction is just a way to mitigate the space weather disaster. In this study, in order to improve our understanding and predictability of the solar-terrestrial environmental variation, we are developing the various types of simulations of solar activities. In this paper, we will report the recent progress of the following two topics. The first topic is for the comprehensive simulation of the whole solar convection zone. Since comprehensive calculation covering whole convection zone has not been carried out ever due to significant temporal and spatial differences between deep and surface layers, our understanding for connection between the solar surface and the deep solar interior has been limited. Here we succeed in carrying out such a calculation for the first time. The results show that the surface region has an unexpectedly small effect on the deep convection zone. The second topic is for the physics-based prediction of imminent giant solar flares. The results indicate that the non-linear force-free modeling based on the vector magnetic field data can be a powerful tool to predict when, where and how large giant solar flares will occur.

Keywords: solar convection zone, solar flares, space weather

©2019. Japan Geoscience Union. All Right Reserved.

Development of a global non-hydrostatic Martian atmospheric model and its high-resolution simulation

*Hiroki Kashimura[1], Hisashi Yashiro[2], Seiya Nishizawa[2], Hirofumi Tomita[2], Kensuke Nakajima[3], Masaki Ishiwatari[4], Yoshiyuki O. Takahashi[1], Yoshi-Yuki Hayashi[1]

1. Kobe University/Center for Planetary Science, 2. RIKEN Center for Computational Science, 3. Kyushu University, 4. Hokkaido University

Scales of atmospheric motions in Earth range from a few meter scale to the planetary scale, and multi-scale phenomena interact with each other. This is a reason for promoting an atmospheric simulation with higher resolution. The situation must be the same in other planets such as Mars. In the Martian atmosphere, dust storms in various scales—from dust devils of tens to hundreds of meter scales, to local dust storm of several tens of kilometer scale, and to global dust storm—have been observed. However, interactions between these scales are unknown. In addition, since Mars has a thin atmosphere and no ocean, the temperature difference between day and night is large and vertical convection should play an essential role in the Martian meteorology, but it is also unknown. To investigate these mysteries, global atmospheric simulations with horizontal resolution as high as few kilometers are required. Additionally, in order to explicitly simulate vertical convection, it is necessary to solve the governing equations without assuming the hydrostatic balance.

We are developing a non-hydrostatic global Martian atmospheric model (Martian SCALE-GM) which is suitable for large-scale parallel computation, targeting to perform high-resolution simulations described above on the post-K computer. SCALE-GM (http://scale.aics.riken.jp/) is being developed by using the dynamical core of NICAM (Tomita and Satoh, 2005; Satoh et al., 2008; Satoh et al., 2014), a non-hydrostatic model using a finite volume method in the icosahedral grid systems (Tomita et al., 2001, 2002), that has been used for simulations of Earth atmosphere and climate, and by aiming at sharing of physical process modules with the regional model (SCALE-RM) and application to other planetary atmospheres. We are developing Martian SCALE-GM by incorporating constants and physical process modules of the Martian atmosphere. The Martian physical modules are taken from DCPAM (https://www.gfd-dennou.org/library/dcpam/), an existing pan-planetary atmospheric general circulation model (GCM). DCPAM is a traditional, hydrostatic GCM using a spectral method for horizontal discretization.

In this study, we ported a Martian atmospheric radiation model (Forget et al., 1999) and a soil model from DCPAM to SCALE-GM and performed a test of temperature evolution in a vertical 1D-atmosphere and soil. The atmosphere model has 100 layers (Δz = 1 km), and distribution of dust is fixed with 0.2 optical depth. The soil model has 18 layers. Soil's heat capacity and thermal conductivity are set to 9.7×10^5 [J K^{-1} kg^{-1}] and 0.076 [W m^{-1} K^{-1}], respectively. Surface albedo is fixed at 0.2. For the calculation of surface fluxes and vertical diffusion, BH91B95 (Beljaars & Holstang, 1991; Beljaars, 1995) and MY2.5 (Mellor & Yamada, 1982) are used, respectively. The initial condition is the 200 K constant temperature atmosphere and soil. We have confirmed that both models (SCALE-GM and DCPAM) show almost the same temperature evolution.

Next, we performed 3D calculations under a Mars-like condition in 7 different horizontal resolutions and checked the dependence of the numerical solutions on the horizontal resolution. Horizontal grid intervals are $240\times(1/2)^n$ [km] (n = 0, 1, 2, 3, 4, 5, 6); i.e., 3.75 km at minimum. The horizontal diffusion

©2019. Japan Geoscience Union. All Right Reserved.

representing turbulent mixing in sub-grid scales is given in the 3rd order Laplacian with the relaxation time for the shortest scale given by $100\times(1/2)^n$ [s]. The atmosphere is divided into 36 layers, which are concentrated near the surface. To avoid wave reflections at the model top, a sponge layer represented by 1st order Laplacian is set above 40 km altitude; the relaxation time for the shortest scale is given by $3600\times(1/4)^n$ [s] except for the case of $\Delta x = 3.75$ km, in which 3 s is used. The 4th order Runge-Kutta method is used for time-integration with a time step of $360\times(1/2)^n$ [s]. The surface albedo is set to 0.5. Neither topography nor condensation processes are included.

Numerical solutions showed that vertical convections due to diurnal solar heating did not appear clearly in the cases with Δx larger than 15 km, whereas they appeared in higher resolution cases. Furthermore, it was confirmed that the horizontal scale and occurrence local-time of the vertical convection are highly dependent on the horizontal resolution at least in this range.

(Figure: Horizontal resolution dependence of vertical wind. Snapshots at 2 km altitude after 30 days from the spring equinox of the Northern hemisphere.)

Keywords: Mars, atmosphere, global, non-hydrostatic, high-resolution simulation, model development

©2019. Japan Geoscience Union. All Right Reserved.

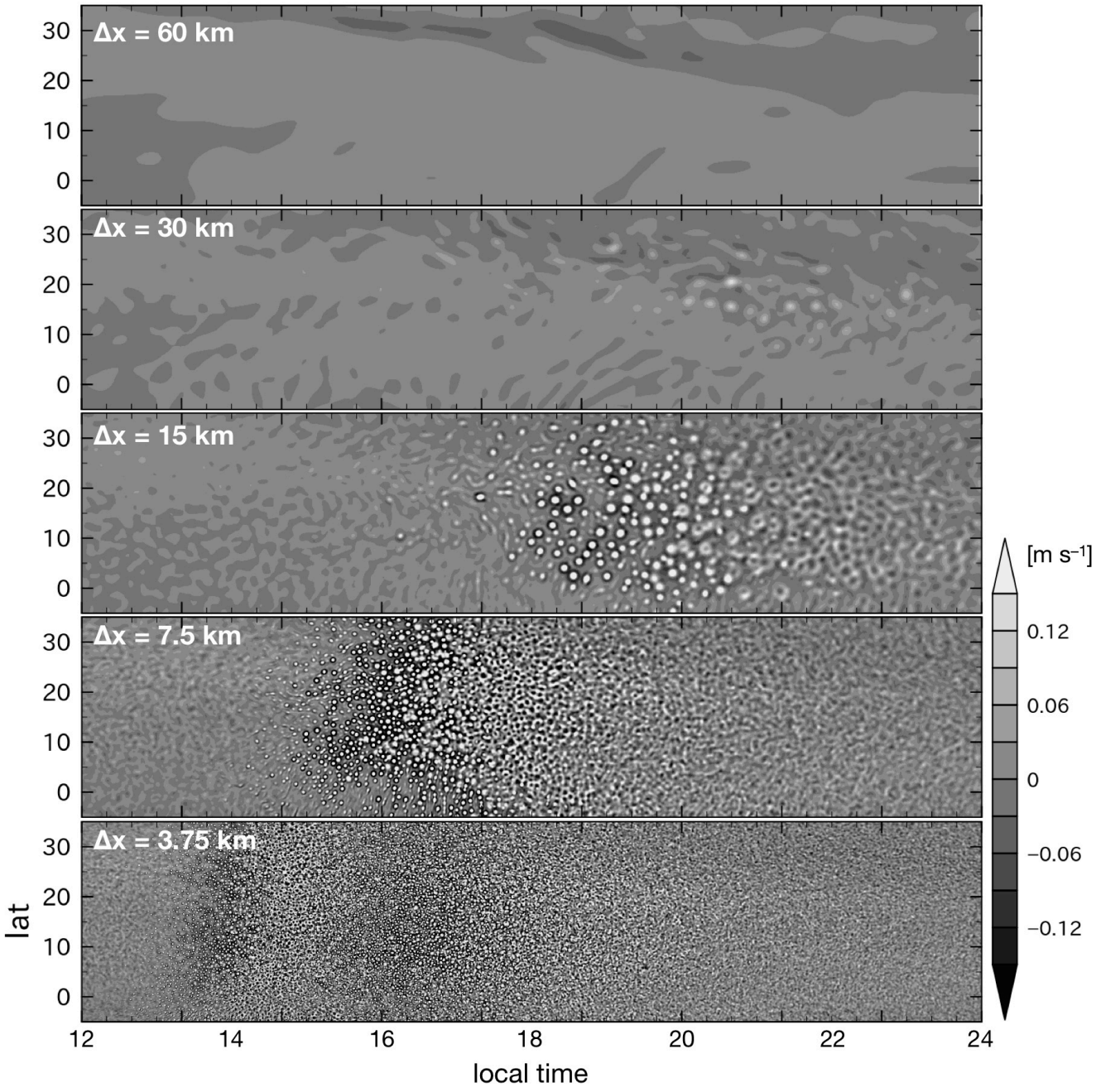

©2019. Japan Geoscience Union. All Right Reserved.

Numerical simulations on the collision, adhesion, and growth of dust particles in turbulent gas in a protoplanetary disk

*Takashi Ishihara[1], Kohei Hamabata[2], Yoshiki Sakurai[2], Masayuki Umemura[3]

1. Graduate School of Environmental and Life Science, Okayama University, 2. Graduate School of Engineering, Nagoya University, 3. Center for Computational Sciences, University of Tsukuba

In a protoplanetary disk, dust grains, which are icy or rocky microscopic particles, are present at about one percent of gas mass. The dust grains collide and adhere with each other to grow in size repeatedly in turbulent gas of a protoplanetary disk. Planetesimals are widely believed to form as a consequence of this hierarchical coagulation from submicron-size dust particles to kilometer-size bodies in a protoplanetary disk. However, it has been argued that there are several physical barriers such as bouncing and radial drift barriers in the planetesimal formation process, and these remain unresolved, especially for silicate dust. In recent years, as a possible solution to these problems, the effect of turbulent clustering of dust grains has been attracting attentions.

In previous studies, it was pointed out that the clustering of particles by turbulence promotes adhesion growth (Pan et al, ApJ2011), and the statistics such as the collision velocity of dust particles in turbulent flow were investigated by a direct numerical simulation (DNS) of turbulence, solving the Navier–Stokes equations (Pan and Padoan, ApJ 2015). Recently, a series of large-scale DNSs of turbulence was conducted to study the velocity distribution of colliding particles in the turbulent flow and the dependence on flow nonlinearity (Reynolds number) (Ishihara et al, ApJ2018). However, numerical simulations on the coagulation process of dust particles were not performed. Therefore, whether dust grains grow hierarchically has not been clarified.

In this study, we developed a parallel code (using MPI and OpenMP) to simulate the collisional adhesion process of dust particles, in which the critical collision velocity (Wada et al, A & A, 2013) is taken into account, and investigated the adhesion processes of 512^3 dust particles using a large-scale DNS of turbulence.
As a result, we have found the following by the analyses of the obtained data:
(1) Dust particles collides with each other within the critical collision velocity preferentially at positions with smaller enstrophy (intensity of vorticity), while dust particles collide with the critical or higher collision velocity at positions with larger enstrophy.
(2) Even if the average collision speed exceeds the critical collision velocity, the collisions within the critical collision velocity can occur repeatedly, and thus rapidly growing dust grains do exist.
(3) The sticking probability of dust particles directly obtained by our simulations is larger than that estimated by the previous DNS data analysis (Ishihara et al ApJ 2018).
(4) The Reynolds number dependence of the dust motion for grains with long stopping time (the response time to flow change) is very weak. Hence, even in protoplanetary disk turbulence with much larger Reynolds number, the same growth process as in this study is expected.

The reasons and implication of the above results will be discussed by conducting the additional data analysis.

Keywords: Protoplanetary disk, Planetesimal formation, Numerical simulations on the collision, adhesion, and growth of dust particles

©2019. Japan Geoscience Union. All Right Reserved.

©2019. Japan Geoscience Union. All Right Reserved.

Development of N-body Simulation Code for Planetary System Formation With Particle-Particle Particle-Tree Scheme

*Yota Ishigaki[1,4], Junko Kominami[2], Junichiro Makino[3], Masaki Fujimoto[4]

1. University of Tokyo, 2. Tokyo Institute of Technology, 3. RIKEN AICS, 4. Institite of Space and Astronautical Science, Japan Aerospace Exploration Agency

In general, the planetary system is thought to be formed from protoplanetary disks surrounding the central star. In particular, it is accepted that terrestrial planets and the cores of gas giant planets are formed by accretion of km size objects (planetesimals) in the protoplanetary disk. The accretion process of the planets has been mainly discussed using the gravitational multi-body simulations (N-body simulations) of planetesimal systems. Various unresolved problems have been pointed out in the conventional standard planetary system formation theory.In recent years, new planetary system formation models have been proposed to solve these problems.However, there is no model with no problem even in these new models. Since N-body simulations with sufficient number of particles has not been performed, the generalized planetary system formation theory has not been constructed yet.

We have developed a new N-body simulation code with particle-particle particle-tree (P^3T) scheme for planetary system formation, GPLUM. The code GPLUM uses a fourth-order Hermite scheme to calculate gravitational interactions between particles within a cut-off radius and a Barnes-Hut tree scheme for gravitational interactions from particles beyond. The conventional simulation codes with P^3T scheme has the bottleneck that the calculation speed decreases when the mass ratio among the particles becomes large. We have solved it by implementing an algorithm which determines the cut-off radius based on mass and orbital semi-major axis of particles individually for each particle. The performance of GPLUM is significantly improved for the simulations of particle systems with mass distribution.

By improving the performance of the N-body simulation code, we made it possible to carry out numerous global simulation with various parameters. GPLUM allows us to perform N-body simulations with ~10^6-10^7 particles. By using GPLUM, we will perform N-body simulations with wide range and high resolution and investigate various parameters by perform parameter studies with N-body simulations.

Keywords: N-body simulation, planetary system formation

©2019. Japan Geoscience Union. All Right Reserved.

Current status of post-K Exploratory Challenge, computational planetary science

*Junichiro Makino[1,2]

1. Kobe Univ, 2. RIKEN R-CCS

In FY 2016, as one of research project for post-K supercomputer, "Exploratory Challenge 3 Elucidation of the Birth of Exoplanets and the Environmental Variations of Planets in the Solar System" has been started. This FY is the last year for the two-year production phase, even though the post-K computer will not be ready until FY 2021. In this talk, I'll overview this project (we call this project computational planetary science project for short).

The development of post-K supercomputer was started in 2014, and its planed completion year is around 2021, with up to 100 times faster speed on real applications compared to K computer. As one of four "Exploratory Challenges", computational planetary science has been selected, and it is assigned to Kobe University, with other eight research institutes.

The computational planetary science project consists of four sub topics: planetary formation, dynamics and evolution of planets, solar activities and environmental change, and the origin of life. In this talk, I'll overview these topics, computational challenges, and products so far and future prospects.

Keywords: High Performance Computing, Computational Science

©2019. Japan Geoscience Union. All Right Reserved.

[J] Poster | M (Multidisciplinary and Interdisciplinary)：M-GI General Geosciences, Information Geosciences & Simulations

Tue. May 28, 2019 3:30 PM - 5:00 PM JST | Tue. May 28, 2019 6:30 AM - 8:00 AM UTC | Poster Hall International Exhibition Hall8, Makuhari Messe_29

[M-GI35] Development of computational sciences on planetary formation, evolution and surface environment

convener:Yoshi-Yuki Hayashi(Department of Planetology/CPS, Graduate School of Science, Kobe University), Masaki Ogawa(Division of General Systems Studies, Graduate School of Arts and Sciences, University of Tokyo), Shigeru Ida(Earth-Life Science Institute, Tokyo Institute of Technology), Kanya Kusano(Institute for Space-Earth Environmental Research, Nagoya University)

Computer simulations have been recognized as one of the fundamental tools in understanding planetary formation, evolution and diversity of surface environment. However, is may be notified that the continuous development of computational abilities in recent years does not seem to be well utilized in improving numerical simulations in those fields; computational efficiency has been improved by 6 orders of magnitude compared from the early 90's, many of our simulations do not seem to catch up qualitatively and quantitatively such improvement. We propose here in this session to ask those who are interested in computational sciences of various fields not only of planetary formation and evolution but also of earth and planetary sciences in general to join. The aim is to discuss various scientific and technical aspects of our numerical simulations to improve our skills to fully utilize those development of computational resources that is realized or will be realized in near future as "K" to "post-K".

[MGI35-P01] Global N-body Simulation from Inner Region to Outer Region

*Junko Kominami[1], Shigeru Ida[1], Junichiro Makino[2], Yota Ishigaki[5], Hiroshi Daisaka[3], Masaki Fujimoto[4] (1.Tokyo Institute of Technology, 2.Kobe University, 3.Hitotsubashi University, 4.JAXA, 5.Tokyo University)

[MGI35-P02] Attempts at numerical modeling of 3-D mantle convection with magmatism and plate tectonics

*Masanori Kameyama[1,2], Masaki Ogawa[3,2], Takehiro Miyagoshi[2], Takatoshi Yanagisawa[2] (1.Geodynamics Research Center, Ehime University, 2.Japan Agency for Marine-Earth Science and Technology, 3.University of Tokyo at Komaba)

[MGI35-P03] Surface zonal flows induced by anelastic thermal convection in a rapidly rotating spherical shell

*Youhei SASAKI[1], Shin-ichi Takehiro[2], Keiichi ISHIOKA[3], Takeshi Enomoto[4] (1.Department of Mathematics, Kyoto University, 2.Research Institute for Mathematical Sciences, Kyoto University, 3.Department of Earth and Planetary Sciences, Kyoto University, 4.Disaster Prevention Research Institute, Kyoto University)

[MGI35-P04] Protostellar flares driven by accretion in protoplanetary disks

*Shinsuke Takasao[1], Kengo Tomida[2], Shinsuke Takasao[2], Takeru Suzuki[3] (1.Nagoya University, 2.Osaka University, 3.University of Tokyo)

[MGI35-P05] Cross-reference simulations by scalable communication library for the study of wave-particle interactions in planetary magnetospheres

*Yuto Katoh[1], Keiichiro Fukazawa[2], Takeshi Nanri[3], Yohei Miyake[4] (1.Department of Geophysics, Graduate School of Science, Tohoku University, 2.Academic Center for Computing and Media Studies, Kyoto University, 3.Research Institute for Information Technology, Kyushu University, 4.Graduate School of System Informatics, Kobe University)

[MGI35-P06] Radiative transfer calculation for various planetary atmospheres: Application to a general circulation model

*Yoshi-Yuki Hayashi[1], George HASHIMOTO[2], Kiyoshi Kuramoto[3], Masaki Ishiwatari[3], Yoshiyuki O. Takahashi[1] (1.Department of Planetology/CPS, Graduate School of Science, Kobe University, 2.Department of Earth Sciences, Okayama University, 3.Department of Cosmosciences, Graduate School of Sciences, Hokkaido University)

[MGI35-P07] Effect of the compressibility of turbulent flows on dust particle collision statistics in a protoplanetary disk

*Yoshiki Sakurai[1], Hitomi Furuya[2], Naoki Kobayashi[1], Takashi Ishihara[3], Naoya Okamoto[4], Kenji Shiraishi[5], Masayuki Umemura[6] (1.Graduate School of Engineering, Nagoya University, 2.Doctoral and Master's Programs in Physics, Graduate School of Pure and Applied Sciences, University of Tsukuba, 3.Graduate School of Environmental and Life Science, Okayama University, 4.Center for Computational Science, Graduate School of Engineering, Nagoya University, 5.Institute of Materials and Systems for Sustainability, Nagoya University, 6.Center for Computational Science, University of Tsukuba)

[MGI35-P08] Algorithms to use accelerators effectively with FDPS and performance of applications

*Daisuke Namekata[1], Masaki Iwasawa[1], Keigo Nitadori[1], Kentaro Nomura[1], Long Wang[3,1], Miyuki Tsubouchi[1], Junichiro Makino[2,1,4] (1.RIKEN Center for Computational Science, 2.Department of Planetology, Graduate School of Science, Kobe University, 3.Helmholtz Institut fur Strahlen und Kernphysik, 4.Earth-Life Science Institute, Tokyo Institute of Technology)

Global N-body Simulation from Inner Region to Outer Region

*Junko Kominami[1], Shigeru Ida[1], Junichiro Makino[2], Yota Ishigaki[5], Hiroshi Daisaka[3], Masaki Fujimoto[4]

1. Tokyo Institute of Technology, 2. Kobe University, 3. Hitotsubashi University, 4. JAXA, 5. Tokyo University

Most of the past N-body simulations started from initial conditions that were limited to radially narrow disks, for the limit of the particle number. However, several senarios have been proposed to expain the formation of Solar System, which includes the migration of planets radially with tens of AU. Hence, in order to construct the general formation scenario, we need to carry out simulations which cover the whole disk (~0.5AU - 40AU). We carried out the N-body simulation starting from planetesimal disk ranging from 0.5 - 40 AU. Surface density discontinuity at the ice line and the runaway gas accretion of the gas giant planets were included in the simulation. The initial number of particles was ~570000. Further investigation carrying out more simulations using different parameters are necessary. Here we introduce the first simulation that covers wide area of the disk.

Keywords: N-body simulation, Solar System, planetesimal accretion

©2019. Japan Geoscience Union. All Right Reserved.

Attempts at numerical modeling of 3-D mantle convection with magmatism and plate tectonics

*Masanori Kameyama[1,2], Masaki Ogawa[3,2], Takehiro Miyagoshi[2], Takatoshi Yanagisawa[2]

1. Geodynamics Research Center, Ehime University, 2. Japan Agency for Marine-Earth Science and Technology, 3. University of Tokyo at Komaba

We are developing 3-D numerical models of mantle convection including the effects of mantle magmatism and plate tectonics, in order to deepen the insights into the thermo-chemical evolution of the mantles of terrestrial bodies. The mantle magmatism is modeled by the generation of liquid phase (magma) owing to the pressure-release melting induced by ascending flows of solid-state convection and the motion of the generated magma as a permeable flow through the solid matrix driven by a buoyancy due to the density difference between the solid and the liquid phases. The coherent motion of tectonic plates is, on the other hand, helped by the narrow zones of low viscosity within the highly viscous "lithosphere" along the top cold surface generated by the stress-history-dependent rheology. However, despite their crucial roles in controlling the overall flow structures, these two mechanisms are incompatible with the solid-state convection of the mantle in essence from the numerical aspects: the localized irregularities caused by them severely deteriorate the large-scale numerical solution of solid-state convection particularly by the multigrid method. In this presentation, we will show the current status and outcrops of our attempts to overcome the numerical difficulty, together with some examples of 3-D experiments running on massive (super)computers.

Keywords: rocky planets, mantle dynamics, mantle magmatism, plate tectonics

©2019. Japan Geoscience Union. All Right Reserved.

Surface zonal flows induced by anelastic thermal convection in a rapidly rotating spherical shell

*Youhei SASAKI[1], Shin-ichi Takehiro[2], Keiichi ISHIOKA[3], Takeshi Enomoto[4]

1. Department of Mathematics, Kyoto University, 2. Research Institute for Mathematical Sciences, Kyoto University, 3. Department of Earth and Planetary Sciences, Kyoto University, 4. Disaster Prevention Research Institute, Kyoto University

Banded structures and alternating zonal jets observed in the surface atmospheres of Jupiter and Saturn have attracted many researchers in planetary atmospheric sciences, however, satisfactory physical explanations and understandings are not yet obtained. In this study, we perform massive parallel numerical experiments treating both small scale convection and planetary scale flows simultaneously, solve fine structures of turbulent motions which have not yet been resolved by the previous numerical models so far, and try to illustrate dynamical origin of global scale structures of surface flows of Jovian planets.

For this purpose, we developed and parallelized an anelastic model of thermal convection in a rotating spherical shell considering basic radial density variation. The spectral transformation library used in this model was improved to introduce MPI parallelization not only in the latitude direction but also in the radial direction. As a result, we succeeded in increasing the number of parallel processes which had been limited by the number of latitudinal grid points, and more massive parallel numerical experiments became possible.

Followup and extended numerical experiments of Case 2 in Gastine et al.(2014) were performed with the developed anelastic convection model. When the time integration is as short as viscous diffusion time, the latitudinal profile of induced surface zonal flow is consistent with that of Gastine et al. (2014). However, when time integration is further extended, prograde surface zonal flows in high latitudes start to develop, and become prominent. This result suggests that surface zonal flows obtained by the previous studies may not be statistically steady states.

Keywords: Jovian planets, anelastic system

©2019. Japan Geoscience Union. All Right Reserved.

Protostellar flares driven by accretion in protoplanetary disks

*Shinsuke Takasao[1], Kengo Tomida[2], Shinsuke Takasao[2], Takeru Suzuki[3]

1. Nagoya University, 2. Osaka University, 3. University of Tokyo

X-ray observations reveal that protostars produce huge explosions frequently. There is discussions that protostellar flares may play roles in forming chondrules that are important building blocks of planets. Protostellar flares are similar to solar flares, and are considered as explosions driven by magnetic energy release. However, protostellar flares are much more energetic than solar flares. The huge energy suggests that flare size should be larger than the stellar radius, which implies that a different energy build up process is required. We investigate the mechanism of protostellar flares using 3D MHD simulations. Our simulations revealed that the energy build up is done by the accumulation of magnetic flux by accretion from the protoplanetary disk. In this paper we will discuss the physics on the basis of our simulaitons.

Keywords: protoplanetary disks, flare

©2019. Japan Geoscience Union. All Right Reserved.

Cross-reference simulations by scalable communication library for the study of wave-particle interactions in planetary magnetospheres

*Yuto Katoh[1], Keiichiro Fukazawa[2], Takeshi Nanri[3], Yohei Miyake[4]

1. Department of Geophysics, Graduate School of Science, Tohoku University, 2. Academic Center for Computing and Media Studies, Kyoto University, 3. Research Institute for Information Technology, Kyushu University, 4. Graduate School of System Informatics, Kobe University

We have been developing a cross-reference simulation code by scalable communication library for the study of wave-particle interactions in planetary magnetospheres. We use Advanced Communication Primitives (ACP; http://ace-project.kyushu-u.ac.jp/main/jp/01_overview/) library for the communication among the simulation codes, which enables us to carry out 'strong' cross-reference simulations; the data exchange among simulation codes is conducted by direct memory access, instead of file output as has been used in conventional 'weak' cross-reference simulations. By a series of electron-hybrid and MHD cross-reference simulations, we study the generation and propagation of whistler-mode chorus emissions in the planetary magnetosphere. Chorus emissions are electromagnetic plasma waves commonly observed in planetary magnetospheres and are a group of coherent wave elements changing their frequency in time. While the generation process of chorus has been reproduced by numerical experiments [e.g., Katoh and Omura, GRL 2007a] and has been explained by the nonlinear wave growth theory [Omura et al., JGR 2008, 2009], previous studies revealed similarities and differences of the spectral characteristics of chorus in planetary magnetospheres, which has not been understood yet. In the cross-reference simulations, we use the MHD code for the investigation of the range of variation of the spatial scale of the planetary magnetosphere. The electron hybrid code is used to reproduce the generation process of chorus emissions under the initial conditions provided from the MHD simulations. An electron fluid code [Katoh, 2014] is also used for the study of the propagation of chorus emissions in the meridional plane of the magnetosphere. We describe the simulation models used in the developing code and show their initial results.

Keywords: numerical experiments, cross-reference simulation, planetary magnetosphere

©2019. Japan Geoscience Union. All Right Reserved.

Radiative transfer calculation for various planetary atmospheres: Application to a general circulation model

*Yoshi-Yuki Hayashi[1], George HASHIMOTO[2], Kiyoshi Kuramoto[3], Masaki Ishiwatari[3], Yoshiyuki O. Takahashi[1]

1. Department of Planetology/CPS, Graduate School of Science, Kobe University, 2. Department of Earth Sciences, Okayama University, 3. Department of Cosmosciences, Graduate School of Sciences, Hokkaido University

A lot of exoplanets have been discovered. One of the interesting questions on those exoplanets is its surface environment and circulation structure. A first step to understand surface environments is an investigation of radiative budget of the planets. Further, now a days, several general circulation models are used to simulate surface environments of various planets. But, calculation of radiative transfer of various planets have several difficulties. One of those is huge computational cost, and another is uncertainty of radiative properties of atmospheres which is very different from Earth's atmosphere. In this study, we are developing a radiation model which can be applied to various planetary atmospheres and try to implement it into our general circulation model.

In developing a radiation model for atmospheric circulation models, a line-by-line model is developed, first. The line-by-line calculation requires huge computational cost. In our line-by-line model, we assign several atmospheric layers to each MPI process to perform parallel computation. In typical calculation conditions, number of atmospheric layers is order of 10 to 100. Our calculation scales very well if the computation is performed with this number of processors. In order to validate the model, radiative fluxes and tendencies are calculated for the Earth, Venus, present Mars, and early Mars.

After the validation of the line-by-line calculation, we develop a radiation model based on correlated k-distribution method, which require much fewer computational cost and can be implemented into a general circulation model. In the presentation, comparison of radiative fluxes and tendencies calculated by our model with those by observation and/or by other models will be presented. In addition, some examples of general circulation model simulations will be presented, too.

Keywords: planetary atmosphere, radiative transfer, Earth, Mars, Venus

©2019. Japan Geoscience Union. All Right Reserved.

Effect of the compressibility of turbulent flows on dust particle collision statistics in a protoplanetary disk

*Yoshiki Sakurai[1], Hitomi Furuya[2], Naoki Kobayashi[1], Takashi Ishihara[3], Naoya Okamoto[4], Kenji Shiraishi[5], Masayuki Umemura[6]

1. Graduate School of Engineering, Nagoya University, 2. Doctoral and Master's Programs in Physics, Graduate School of Pure and Applied Sciences, University of Tsukuba, 3. Graduate School of Environmental and Life Science, Okayama University, 4. Center for Computational Science, Graduate School of Engineering, Nagoya University, 5. Institute of Materials and Systems for Sustainability, Nagoya University, 6. Center for Computational Science, University of Tsukuba

Planetesimals are believed to form by hierarchical coagulation from submicron-size dust particles to kilometer-size bodies in turbulent flows in a protoplanetary disk. However, several barriers, e.g., radial drift, bouncing, and fragmentation barriers, in the planetesimal formation process are not completely resolved, especially for silicate dust. To resolve these barriers, it is important to accurately understand the role of turbulence in the coagulation process.

In the Minimum-mass Solar Nebula (MMSN) Model (Hayashi 1981), the Reynolds number (Re) and the Mach number (Ma) of turbulence in protoplanetary disks range Re=10^8~10^11 and Ma=0.01~0.32, respectively. Pan et al. (2011) conducted an approximate simulation of compressible turbulence (Ma~1.0) and showed that turbulent clustering may considerably enhance the particle collision rate. Pan & Padoan (2013, 2014, 2015) and Pan et al.(2014) peformed a direct numerical simulation (DNS) of the Navier–Stokes equations on weakly compressible turbulence (Re~1000 and Ma~0.1) at low Re to study the effect of turbulent clustering. Pan & Padoan (2015) found that the rms relative velocity of particle pairs is smaller by more than a factor of two compared to that by turbulent model (Ormel & Cuzzi 2007). Their studies demonstrated that the turbulent clustering should be taken into account to consider the coagulation process.

Recently, Ishihara et al (2018) performed DNSs of incompressible turbulence at high Re (up to Re=16100) to study the motion of dust particles in turbulence. They showed that the collision statistics of the dust particles with large inertia are not so sensitive to the Reynolds number and confirmed that they are consistent with those by Pan & Padoan or Pan et al at low Re. However, the effect of compressibility of turbulence on the collision statistics is not yet quantitatively investigated.

In this paper, we perform DNSs of incompressible and compressible turbulence with Ma=0.1 and 0.3 and set the ratio of dilatation component (ed) and solenoid component (es) of the mean energy dissipation rate (ed/es) to 0.01 and 0.1 to study quantitatively the effect of compressibility of the inertial particle collision statistics. The motion of inertial particles is characterized by the Stokes number (St=tp/T, where tp is the particle stopping time and T is the time-scale of largest eddies), and we track eight sets of inertial particles with from St=0 to St=0.3. Our results are as follows:

(1) The compressibility of turbulent flow is characterized by both of Ma and ed/es.

©2019. Japan Geoscience Union. All Right Reserved.

(2) In case of Ma=0.3, the local Ma can exceed unity so that shocklets can be generated in the turbulent flow.

(3) The local Mach number is high at positions with higher enstrophy.

(4) In case of Ma=0.1-0.3, relative velocity of colliding particles and collision kernel have weak Mach number dependence but may depend when the value of the ratio of ed/es is large.

Our results show that compressibility considered in protoplanetary disk turbulence has little influence on particle collision statistics.

Keywords: planetesimal formation, turbulence, inertial particle

©2019. Japan Geoscience Union. All Right Reserved.

Algorithms to use accelerators effectively with FDPS and performance of applications

*Daisuke Namekata[1], Masaki Iwasawa[1], Keigo Nitadori[1], Kentaro Nomura[1], Long Wang[3,1], Miyuki Tsubouchi[1], Junichiro Makino[2,1,4]

1. RIKEN Center for Computational Science, 2. Department of Planetology, Graduate School of Science, Kobe University, 3. Helmholtz Institut fur Strahlen und Kernphysik, 4. Earth-Life Science Institute, Tokyo Institute of Technology

Numerical simulations based on particle methods have played an important role in understanding the formation and evolution of planets and planetary systems. Along with the improvement of the computing capacity of computers, more large-scale simulations and simulations taking into consideration various physical phenomena have come to be performed, in order to understand the reality in more detail.

However, it is becoming increasingly difficult to develop a simulation code that runs efficiently on modern HPC (high-performance computing) systems. The main reason for this difficulty is that modern HPC platforms have become very complex, and thus it requires lots of efforts necessary to develop complex programs to make efficient use of such platforms. Typical modern HPC systems are actually a cluster of computing nodes connected a network with a limited communication bandwidth. The number of nodes can reach up to 100,000 in the largest systems at present. Thus, we need to develop simulation code so that it shows a good load balance and requires minimal communication. In recent years, the architecture of large-scale HPC systems have been shifting from homogeneous multi-core processors to accelerator-based systems and heterogeneous multi-core processors for economical reasons. This makes code development more difficult for the following reasons. One is that for many applications, the communication bandwidth between CPUs and accelerators becomes the bottleneck. The second one is that because CPUs and accelerators have separate memory spaces, the programming is complicated and we cannot use existing programs. Thus, the time required for code development has been increasing more and more, which causes stagnation of research.

To improve the situation, we have developed a framework called FDPS (Framework for Developing Particle Simulators), which enables researchers to develop their own high-performance parallel particle-based simulation programs easily. The basic idea of FDPS is to provide a high-performance implementation of parallel algorithms for particle-based simulations in a ``generic" form, so that researchers can define his/her own particle data structure and interparticle interaction functions and supply them to FDPS framework. FDPS framework compiled with user-supplied data type and interaction function provides all necessary functions for parallelization, and using those functions researchers can write their programs as though they are writing simple non-parallel program which runs on their laptop computers. FDPS offers very good performance on large-scale parallel systems consisting of ``homogeneous" multi-core processors, such as K computer and Cray systems based on x86 processors. In FDPS version 2, we have extended FDPS so that it can use accelerators by writing the interaction function that uses the accelerator hardware. However, the efficiency was limited by the latency and bandwidth of communication between the CPU and the accelerator and also by the mismatch between the available degree of parallelism of the interaction function and that of the hardware parallelism, and thus would be rather poor.

In order to make it possible for FDPS to use more efficiently accelerator hardware such as GPGPUs

©2019. Japan Geoscience Union. All Right Reserved.

(General-purpose computing on graphics processing units), we introduced a new interface of user-provided interaction function. We also implemented new techniques which reduce the amount of work on the side of CPU per timestep and amount of communication between CPU and accelerators. We have measured the performance of N-body simulations on a systems with NVIDIA Volta GPGPU using FDPS and the achieved performance is around 27 % of the theoretical peak limit.

Keywords: Computational Science, Software development, Accelerators

©2019. Japan Geoscience Union. All Right Reserved.

[J] Poster | M (Multidisciplinary and Interdisciplinary)：M-GI General Geosciences, Information Geosciences & Simulations

Tue. May 28, 2019 5:15 PM - 6:30 PM JST | Tue. May 28, 2019 8:15 AM - 9:30 AM UTC | Poster Hall International Exhibition Hall8, Makuhari Messe_49

[M-GI35] Development of computational sciences on planetary formation, evolution and surface environment

convener:Yoshi-Yuki Hayashi(Department of Planetology/CPS, Graduate School of Science, Kobe University), Masaki Ogawa(Division of General Systems Studies, Graduate School of Arts and Sciences, University of Tokyo), Shigeru Ida(Earth-Life Science Institute, Tokyo Institute of Technology), Kanya Kusano(Institute for Space-Earth Environmental Research, Nagoya University)

Computer simulations have been recognized as one of the fundamental tools in understanding planetary formation, evolution and diversity of surface environment. However, is may be notified that the continuous development of computational abilities in recent years does not seem to be well utilized in improving numerical simulations in those fields; computational efficiency has been improved by 6 orders of magnitude compared from the early 90's, many of our simulations do not seem to catch up qualitatively and quantitatively such improvement. We propose here in this session to ask those who are interested in computational sciences of various fields not only of planetary formation and evolution but also of earth and planetary sciences in general to join. The aim is to discuss various scientific and technical aspects of our numerical simulations to improve our skills to fully utilize those development of computational resources that is realized or will be realized in near future as "K" to "post-K".

[MGI35-P01] Global N-body Simulation from Inner Region to Outer Region

*Junko Kominami[1], Shigeru Ida[1], Junichiro Makino[2], Yota Ishigaki[5], Hiroshi Daisaka[3], Masaki Fujimoto[4] (1.Tokyo Institute of Technology, 2.Kobe University, 3.Hitotsubashi University, 4.JAXA, 5.Tokyo University)

[MGI35-P02] Attempts at numerical modeling of 3-D mantle convection with magmatism and plate tectonics

*Masanori Kameyama[1,2], Masaki Ogawa[3,2], Takehiro Miyagoshi[2], Takatoshi Yanagisawa[2] (1.Geodynamics Research Center, Ehime University, 2.Japan Agency for Marine-Earth Science and Technology, 3.University of Tokyo at Komaba)

[MGI35-P03] Surface zonal flows induced by anelastic thermal convection in a rapidly rotating spherical shell

*Youhei SASAKI[1], Shin-ichi Takehiro[2], Keiichi ISHIOKA[3], Takeshi Enomoto[4] (1.Department of Mathematics, Kyoto University, 2.Research Institute for Mathematical Sciences, Kyoto University, 3.Department of Earth and Planetary Sciences, Kyoto University, 4.Disaster Prevention Research Institute, Kyoto University)

[MGI35-P04] Protostellar flares driven by accretion in protoplanetary disks

*Shinsuke Takasao[1], Kengo Tomida[2], Shinsuke Takasao[2], Takeru Suzuki[3] (1.Nagoya University, 2.Osaka University, 3.University of Tokyo)

[MGI35-P05] Cross-reference simulations by scalable communication library for the study of wave-particle interactions in planetary magnetospheres

*Yuto Katoh[1], Keiichiro Fukazawa[2], Takeshi Nanri[3], Yohei Miyake[4] (1.Department of Geophysics, Graduate School of Science, Tohoku University, 2.Academic Center for Computing and Media Studies, Kyoto University, 3.Research Institute for Information Technology, Kyushu University, 4.Graduate School of System Informatics, Kobe University)

[MGI35-P06] Radiative transfer calculation for various planetary atmospheres: Application to a general circulation model

*Yoshi-Yuki Hayashi[1], George HASHIMOTO[2], Kiyoshi Kuramoto[3], Masaki Ishiwatari[3], Yoshiyuki O. Takahashi[1] (1.Department of Planetology/CPS, Graduate School of Science, Kobe University, 2.Department of Earth Sciences, Okayama University, 3.Department of Cosmosciences, Graduate School of Sciences, Hokkaido University)

[MGI35-P07] Effect of the compressibility of turbulent flows on dust particle collision statistics in a protoplanetary disk

*Yoshiki Sakurai[1], Hitomi Furuya[2], Naoki Kobayashi[1], Takashi Ishihara[3], Naoya Okamoto[4], Kenji Shiraishi[5], Masayuki Umemura[6] (1.Graduate School of Engineering, Nagoya University, 2.Doctoral and Master's Programs in Physics, Graduate School of Pure and Applied Sciences, University of Tsukuba, 3.Graduate School of Environmental and Life Science, Okayama University, 4.Center for Computational Science, Graduate School of Engineering, Nagoya University, 5.Institute of Materials and Systems for Sustainability, Nagoya University, 6.Center for Computational Science, University of Tsukuba)

[MGI35-P08] Algorithms to use accelerators effectively with FDPS and performance of applications

*Daisuke Namekata[1], Masaki Iwasawa[1], Keigo Nitadori[1], Kentaro Nomura[1], Long Wang[3,1], Miyuki Tsubouchi[1], Junichiro Makino[2,1,4] (1.RIKEN Center for Computational Science, 2.Department of Planetology, Graduate School of Science, Kobe University, 3.Helmholtz Institut fur Strahlen und Kernphysik, 4.Earth-Life Science Institute, Tokyo Institute of Technology)

Global N-body Simulation from Inner Region to Outer Region

*Junko Kominami[1], Shigeru Ida[1], Junichiro Makino[2], Yota Ishigaki[5], Hiroshi Daisaka[3], Masaki Fujimoto[4]

1. Tokyo Institute of Technology, 2. Kobe University, 3. Hitotsubashi University, 4. JAXA, 5. Tokyo University

Most of the past N-body simulations started from initial conditions that were limited to radially narrow disks, for the limit of the particle number. However, several senarios have been proposed to expain the formation of Solar System, which includes the migration of planets radially with tens of AU. Hence, in order to construct the general formation scenario, we need to carry out simulations which cover the whole disk (~0.5AU - 40AU). We carried out the N-body simulation starting from planetesimal disk ranging from 0.5 - 40 AU. Surface density discontinuity at the ice line and the runaway gas accretion of the gas giant planets were included in the simulation. The initial number of particles was ~570000. Further investigation carrying out more simulations using different parameters are necessary. Here we introduce the first simulation that covers wide area of the disk.

Keywords: N-body simulation, Solar System, planetesimal accretion

©2019. Japan Geoscience Union. All Right Reserved.

Attempts at numerical modeling of 3-D mantle convection with magmatism and plate tectonics

*Masanori Kameyama[1,2], Masaki Ogawa[3,2], Takehiro Miyagoshi[2], Takatoshi Yanagisawa[2]

1. Geodynamics Research Center, Ehime University, 2. Japan Agency for Marine-Earth Science and Technology, 3. University of Tokyo at Komaba

We are developing 3-D numerical models of mantle convection including the effects of mantle magmatism and plate tectonics, in order to deepen the insights into the thermo-chemical evolution of the mantles of terrestrial bodies. The mantle magmatism is modeled by the generation of liquid phase (magma) owing to the pressure-release melting induced by ascending flows of solid-state convection and the motion of the generated magma as a permeable flow through the solid matrix driven by a buoyancy due to the density difference between the solid and the liquid phases. The coherent motion of tectonic plates is, on the other hand, helped by the narrow zones of low viscosity within the highly viscous "lithosphere" along the top cold surface generated by the stress-history-dependent rheology. However, despite their crucial roles in controlling the overall flow structures, these two mechanisms are incompatible with the solid-state convection of the mantle in essence from the numerical aspects: the localized irregularities caused by them severely deteriorate the large-scale numerical solution of solid-state convection particularly by the multigrid method. In this presentation, we will show the current status and outcrops of our attempts to overcome the numerical difficulty, together with some examples of 3-D experiments running on massive (super)computers.

Keywords: rocky planets, mantle dynamics, mantle magmatism, plate tectonics

©2019. Japan Geoscience Union. All Right Reserved.

Surface zonal flows induced by anelastic thermal convection in a rapidly rotating spherical shell

*Youhei SASAKI[1], Shin-ichi Takehiro[2], Keiichi ISHIOKA[3], Takeshi Enomoto[4]

1. Department of Mathematics, Kyoto University, 2. Research Institute for Mathematical Sciences, Kyoto University, 3. Department of Earth and Planetary Sciences, Kyoto University, 4. Disaster Prevention Research Institute, Kyoto University

Banded structures and alternating zonal jets observed in the surface atmospheres of Jupiter and Saturn have attracted many researchers in planetary atmospheric sciences, however, satisfactory physical explanations and understandings are not yet obtained. In this study, we perform massive parallel numerical experiments treating both small scale convection and planetary scale flows simultaneously, solve fine structures of turbulent motions which have not yet been resolved by the previous numerical models so far, and try to illustrate dynamical origin of global scale structures of surface flows of Jovian planets.

For this purpose, we developed and parallelized an anelastic model of thermal convection in a rotating spherical shell considering basic radial density variation. The spectral transformation library used in this model was improved to introduce MPI parallelization not only in the latitude direction but also in the radial direction. As a result, we succeeded in increasing the number of parallel processes which had been limited by the number of latitudinal grid points, and more massive parallel numerical experiments became possible.

Followup and extended numerical experiments of Case 2 in Gastine et al.(2014) were performed with the developed anelastic convection model. When the time integration is as short as viscous diffusion time, the latitudinal profile of induced surface zonal flow is consistent with that of Gastine et al. (2014). However, when time integration is further extended, prograde surface zonal flows in high latitudes start to develop, and become prominent. This result suggests that surface zonal flows obtained by the previous studies may not be statistically steady states.

Keywords: Jovian planets, anelastic system

©2019. Japan Geoscience Union. All Right Reserved.

Protostellar flares driven by accretion in protoplanetary disks

*Shinsuke Takasao[1], Kengo Tomida[2], Shinsuke Takasao[2], Takeru Suzuki[3]

1. Nagoya University, 2. Osaka University, 3. University of Tokyo

X-ray observations reveal that protostars produce huge explosions frequently. There is discussions that protostellar flares may play roles in forming chondrules that are important building blocks of planets. Protostellar flares are similar to solar flares, and are considered as explosions driven by magnetic energy release. However, protostellar flares are much more energetic than solar flares. The huge energy suggests that flare size should be larger than the stellar radius, which implies that a different energy build up process is required. We investigate the mechanism of protostellar flares using 3D MHD simulations. Our simulations revealed that the energy build up is done by the accumulation of magnetic flux by accretion from the protoplanetary disk. In this paper we will discuss the physics on the basis of our simulaitons.

Keywords: protoplanetary disks, flare

©2019. Japan Geoscience Union. All Right Reserved.

Cross-reference simulations by scalable communication library for the study of wave-particle interactions in planetary magnetospheres

*Yuto Katoh[1], Keiichiro Fukazawa[2], Takeshi Nanri[3], Yohei Miyake[4]

1. Department of Geophysics, Graduate School of Science, Tohoku University, 2. Academic Center for Computing and Media Studies, Kyoto University, 3. Research Institute for Information Technology, Kyushu University, 4. Graduate School of System Informatics, Kobe University

We have been developing a cross-reference simulation code by scalable communication library for the study of wave-particle interactions in planetary magnetospheres. We use Advanced Communication Primitives (ACP; http://ace-project.kyushu-u.ac.jp/main/jp/01_overview/) library for the communication among the simulation codes, which enables us to carry out 'strong' cross-reference simulations; the data exchange among simulation codes is conducted by direct memory access, instead of file output as has been used in conventional 'weak' cross-reference simulations. By a series of electron-hybrid and MHD cross-reference simulations, we study the generation and propagation of whistler-mode chorus emissions in the planetary magnetosphere. Chorus emissions are electromagnetic plasma waves commonly observed in planetary magnetospheres and are a group of coherent wave elements changing their frequency in time. While the generation process of chorus has been reproduced by numerical experiments [e.g., Katoh and Omura, GRL 2007a] and has been explained by the nonlinear wave growth theory [Omura et al., JGR 2008, 2009], previous studies revealed similarities and differences of the spectral characteristics of chorus in planetary magnetospheres, which has not been understood yet. In the cross-reference simulations, we use the MHD code for the investigation of the range of variation of the spatial scale of the planetary magnetosphere. The electron hybrid code is used to reproduce the generation process of chorus emissions under the initial conditions provided from the MHD simulations. An electron fluid code [Katoh, 2014] is also used for the study of the propagation of chorus emissions in the meridional plane of the magnetosphere. We describe the simulation models used in the developing code and show their initial results.

Keywords: numerical experiments, cross-reference simulation, planetary magnetosphere

©2019. Japan Geoscience Union. All Right Reserved.

Radiative transfer calculation for various planetary atmospheres: Application to a general circulation model

*Yoshi-Yuki Hayashi[1], George HASHIMOTO[2], Kiyoshi Kuramoto[3], Masaki Ishiwatari[3], Yoshiyuki O. Takahashi[1]

1. Department of Planetology/CPS, Graduate School of Science, Kobe University, 2. Department of Earth Sciences, Okayama University, 3. Department of Cosmosciences, Graduate School of Sciences, Hokkaido University

A lot of exoplanets have been discovered. One of the interesting questions on those exoplanets is its surface environment and circulation structure. A first step to understand surface environments is an investigation of radiative budget of the planets. Further, now a days, several general circulation models are used to simulate surface environments of various planets. But, calculation of radiative transfer of various planets have several difficulties. One of those is huge computational cost, and another is uncertainty of radiative properties of atmospheres which is very different from Earth's atmosphere. In this study, we are developing a radiation model which can be applied to various planetary atmospheres and try to implement it into our general circulation model.

In developing a radiation model for atmospheric circulation models, a line-by-line model is developed, first. The line-by-line calculation requires huge computational cost. In our line-by-line model, we assign several atmospheric layers to each MPI process to perform parallel computation. In typical calculation conditions, number of atmospheric layers is order of 10 to 100. Our calculation scales very well if the computation is performed with this number of processors. In order to validate the model, radiative fluxes and tendencies are calculated for the Earth, Venus, present Mars, and early Mars.

After the validation of the line-by-line calculation, we develop a radiation model based on correlated k-distribution method, which require much fewer computational cost and can be implemented into a general circulation model. In the presentation, comparison of radiative fluxes and tendencies calculated by our model with those by observation and/or by other models will be presented. In addition, some examples of general circulation model simulations will be presented, too.

Keywords: planetary atmosphere, radiative transfer, Earth, Mars, Venus

©2019. Japan Geoscience Union. All Right Reserved.

Effect of the compressibility of turbulent flows on dust particle collision statistics in a protoplanetary disk

*Yoshiki Sakurai[1], Hitomi Furuya[2], Naoki Kobayashi[1], Takashi Ishihara[3], Naoya Okamoto[4], Kenji Shiraishi[5], Masayuki Umemura[6]

1. Graduate School of Engineering, Nagoya University, 2. Doctoral and Master's Programs in Physics, Graduate School of Pure and Applied Sciences, University of Tsukuba, 3. Graduate School of Environmental and Life Science, Okayama University, 4. Center for Computational Science, Graduate School of Engineering, Nagoya University, 5. Institute of Materials and Systems for Sustainability, Nagoya University, 6. Center for Computational Science, University of Tsukuba

Planetesimals are believed to form by hierarchical coagulation from submicron-size dust particles to kilometer-size bodies in turbulent flows in a protoplanetary disk. However, several barriers, e.g., radial drift, bouncing, and fragmentation barriers, in the planetesimal formation process are not completely resolved, especially for silicate dust. To resolve these barriers, it is important to accurately understand the role of turbulence in the coagulation process.

In the Minimum-mass Solar Nebula (MMSN) Model (Hayashi 1981), the Reynolds number (Re) and the Mach number (Ma) of turbulence in protoplanetary disks range Re=10^8~10^11 and Ma=0.01~0.32, respectively. Pan et al. (2011) conducted an approximate simulation of compressible turbulence (Ma~1.0) and showed that turbulent clustering may considerably enhance the particle collision rate. Pan & Padoan (2013, 2014, 2015) and Pan et al.(2014) peformed a direct numerical simulation (DNS) of the Navier–Stokes equations on weakly compressible turbulence (Re~1000 and Ma~0.1) at low Re to study the effect of turbulent clustering. Pan & Padoan (2015) found that the rms relative velocity of particle pairs is smaller by more than a factor of two compared to that by turbulent model (Ormel & Cuzzi 2007). Their studies demonstrated that the turbulent clustering should be taken into account to consider the coagulation process.

Recently, Ishihara et al (2018) performed DNSs of incompressible turbulence at high Re (up to Re=16100) to study the motion of dust particles in turbulence. They showed that the collision statistics of the dust particles with large inertia are not so sensitive to the Reynolds number and confirmed that they are consistent with those by Pan & Padoan or Pan et al at low Re. However, the effect of compressibility of turbulence on the collision statistics is not yet quantitatively investigated.

In this paper, we perform DNSs of incompressible and compressible turbulence with Ma=0.1 and 0.3 and set the ratio of dilatation component (ed) and solenoid component (es) of the mean energy dissipation rate (ed/es) to 0.01 and 0.1 to study quantitatively the effect of compressibility of the inertial particle collision statistics. The motion of inertial particles is characterized by the Stokes number (St=tp/T, where tp is the particle stopping time and T is the time-scale of largest eddies), and we track eight sets of inertial particles with from St=0 to St=0.3. Our results are as follows:

(1) The compressibility of turbulent flow is characterized by both of Ma and ed/es.

©2019. Japan Geoscience Union. All Right Reserved.

(2) In case of Ma=0.3, the local Ma can exceed unity so that shocklets can be generated in the turbulent flow.

(3) The local Mach number is high at positions with higher enstrophy.

(4) In case of Ma=0.1-0.3, relative velocity of colliding particles and collision kernel have weak Mach number dependence but may depend when the value of the ratio of ed/es is large.

Our results show that compressibility considered in protoplanetary disk turbulence has little influence on particle collision statistics.

Keywords: planetesimal formation, turbulence, inertial particle

©2019. Japan Geoscience Union. All Right Reserved.

Algorithms to use accelerators effectively with FDPS and performance of applications

*Daisuke Namekata[1], Masaki Iwasawa[1], Keigo Nitadori[1], Kentaro Nomura[1], Long Wang[3,1], Miyuki Tsubouchi[1], Junichiro Makino[2,1,4]

1. RIKEN Center for Computational Science, 2. Department of Planetology, Graduate School of Science, Kobe University, 3. Helmholtz Institut fur Strahlen und Kernphysik, 4. Earth-Life Science Institute, Tokyo Institute of Technology

Numerical simulations based on particle methods have played an important role in understanding the formation and evolution of planets and planetary systems. Along with the improvement of the computing capacity of computers, more large-scale simulations and simulations taking into consideration various physical phenomena have come to be performed, in order to understand the reality in more detail.

However, it is becoming increasingly difficult to develop a simulation code that runs efficiently on modern HPC (high-performance computing) systems. The main reason for this difficulty is that modern HPC platforms have become very complex, and thus it requires lots of efforts necessary to develop complex programs to make efficient use of such platforms. Typical modern HPC systems are actually a cluster of computing nodes connected a network with a limited communication bandwidth. The number of nodes can reach up to 100,000 in the largest systems at present. Thus, we need to develop simulation code so that it shows a good load balance and requires minimal communication. In recent years, the architecture of large-scale HPC systems have been shifting from homogeneous multi-core processors to accelerator-based systems and heterogeneous multi-core processors for economical reasons. This makes code development more difficult for the following reasons. One is that for many applications, the communication bandwidth between CPUs and accelerators becomes the bottleneck. The second one is that because CPUs and accelerators have separate memory spaces, the programming is complicated and we cannot use existing programs. Thus, the time required for code development has been increasing more and more, which causes stagnation of research.

To improve the situation, we have developed a framework called FDPS (Framework for Developing Particle Simulators), which enables researchers to develop their own high-performance parallel particle-based simulation programs easily. The basic idea of FDPS is to provide a high-performance implementation of parallel algorithms for particle-based simulations in a ``generic" form, so that researchers can define his/her own particle data structure and interparticle interaction functions and supply them to FDPS framework. FDPS framework compiled with user-supplied data type and interaction function provides all necessary functions for parallelization, and using those functions researchers can write their programs as though they are writing simple non-parallel program which runs on their laptop computers. FDPS offers very good performance on large-scale parallel systems consisting of ``homogeneous" multi-core processors, such as K computer and Cray systems based on x86 processors. In FDPS version 2, we have extended FDPS so that it can use accelerators by writing the interaction function that uses the accelerator hardware. However, the efficiency was limited by the latency and bandwidth of communication between the CPU and the accelerator and also by the mismatch between the available degree of parallelism of the interaction function and that of the hardware parallelism, and thus would be rather poor.

In order to make it possible for FDPS to use more efficiently accelerator hardware such as GPGPUs

©2019. Japan Geoscience Union. All Right Reserved.

(General-purpose computing on graphics processing units), we introduced a new interface of user-provided interaction function. We also implemented new techniques which reduce the amount of work on the side of CPU per timestep and amount of communication between CPU and accelerators. We have measured the performance of N-body simulations on a systems with NVIDIA Volta GPGPU using FDPS and the achieved performance is around 27 % of the theoretical peak limit.

Keywords: Computational Science, Software development, Accelerators

©2019. Japan Geoscience Union. All Right Reserved.

[E] Poster | M (Multidisciplinary and Interdisciplinary) : M-ZZ Others

Tue. May 28, 2019 1:45 PM - 3:15 PM JST | Tue. May 28, 2019 4:45 AM - 6:15 AM UTC | Poster Hall International Exhibition Hall8, Makuhari Messe_10

[M-ZZ50] Governance for Trans-boundary Volcanic Disaster

convener:Mayumi Sakamoto(Graduate School of Disaster Resilience and Governance, University of Hyogo), Haruhisa Nakamichi(Sakurajima Volcano Research Center, Disaster Prevention Research Institute, Kyoto University), MASARU ARAKIDA(Asian Disaster Reduction Center)

Volcanic monitoring systems are developed and managed for the purpose to observe a specific volcanic activity in each country based on its own regulation. However, the experience of Icelandic volcano Eyjafjallajokull eruption in 2010 caused huge air traffic disturbances, and left large economic and social impact to international community. In order to reduce possible financial, environmental, health or social damages caused by trans-boundary volcanic disaster, it is important to develop international cooperative system to monitor and share the information of emission, dispersion or deposition of volcanic products. In this session, we discuss trans-boundary effect of volcanic eruption, and how to establish international collaborative mechanism from different research disciplines such as disaster management, volcanology, environmental politics or international law.

[MZZ50-P01] Governance for Trans-boundary Volcanic Disaster -a case of 2010 Eyjafjallajökull Eruption-

*Mayumi Sakamoto[1] (1.Graduate School of Disaster Resilience and Governance, University of Hyogo)

[MZZ50-P02] Regional Cooperation against Cross-border Disasters

*MASARU ARAKIDA[1] (1.Asian Disaster Reduction Center)

[MZZ50-P03] Issues of Japan's volcanic disaster prevention system as viewed from overseas alert systems

*Erika Ishimizu[1], Mayumi Sakamoto[1] (1.Graduate School of Disaster Resilience and Governance University of Hyogo)

Governance for Trans-boundary Volcanic Disaster -a case of 2010 Eyjafjallajökull Eruption-

*Mayumi Sakamoto[1]

1. Graduate School of Disaster Resilience and Governance, University of Hyogo

The volcanic eruption occurred in one country can trigger different effect in other country. The experience of 2010 Icelandic volcano Eyjafjallajökull eruption demonstrated the necessity of international governance for trans-boundary effect caused by eruption. In Iceland, national disaster response was effective to evacuate people from hazardous area and there were no humanitarian damages caused by eruption. However, the estimation of volcanic ash plumes and its dispersion caused huge international air traffic disruption or airport closure, and left large international economic and industrial impact. Followings are problems found through the 2010 eruption.
First, the necessity of international collaboration for observing atmospheric dispersion of volcanic ash. As for 2010 eruption, Icelandic Meteorological Agency (IMO) informed London Volcanic Ash Advisory Center (VAAC) which observes Iceland, about the plume height, ash content and other data. Based on the provided data, London VAAC predicted ash dispersion over Europe. However, there was no detailed discussion between IMO and London VAAC when and how often they communicate prior to eruption. It is important to update forecast using satellite imagery or observation of ashfalls in other countries.
Second, the necessity of immediate information sharing with both local and international medias. During the eruption, there was a huge need for information from international medias. A communication team, composed by professional communicator from various institutions gathered at the National Crisis Coordination and Command Center (NCCCC). Press conference were held and status reports were prepared and distributed. Such an international information sharing system should be discussed prior to disaster.
Disaster management systems are generally developed to respond hazard activity in each country based on its own regulation. However, 2010 experience showed there is no international agreement or regime to respond such a trans-boundary effect. Immediate crisis communication among hazard origin country, international institute and possibly affective country is required to reduce secondary effect, which shows importance or precautionary approaches for trans-boundary volcanic disaster.

Keywords: trans-boudary disaster, volcano, governance, Eyjafjallajökull

©2019. Japan Geoscience Union. All Right Reserved.

Regional Cooperation against Cross-border Disasters

*MASARU ARAKIDA[1]

1. Asian Disaster Reduction Center

Since affected area by disasters such as floods on international scale river, haize by forest fire, and volcanic ejectaare are recognized as no boundaries, there are many benefits of working together through regional cooperation. These include the sharing of best practices for handling major disasters, responding together on search and rescue efforts, and understanding and improving DRR through early warnings, the mutual exchange of information, joint education and training exercises, and joint assistance on disaster response.

Keywords: cross-border disaster, regional cooperation

©2019. Japan Geoscience Union. All Right Reserved.

Issues of Japan's volcanic disaster prevention system as viewed from overseas alert systems

*Erika Ishimizu[1], Mayumi Sakamoto[1]

1. Graduate School of Disaster Resilience and Governance University of Hyogo

Volcanic alert levels was introduced in Japan in 2007. Thereafter, the level was raised or lowered for several volcanoes, some volcanoes erupted and residents evacuated. Among them, the problem of exploiting volcanic alert levels for evacuation has become clear. In this research, by comparing Japan's warning system with overseas (the United States, Indonesia, New Zealand), we will examine the issues of Japanese volcanic disaster prevention system and future disaster prevention system.
In Japan, several institutions, such as universities and Japan Meteorological Agency (JMA), are conducting observations of volcanic activity. In the volcano where volcanic alert levels is introduced, JMA announces five levels of volcanic alert levels according to the activity of the volcano. Each municipality carries out basic disaster response such as issuance of evacuation information.
In the United States, the United States Geological Survey (USGS) will unite from the observation of a volcano to the announcement of an alarm (4 stages). Basic disaster response is handled by municipalities and counties. If requested, the state government responds, and if it is still difficult, FEMA is asked.
In Indonesia, the Center of Volcanology and Geological Hazard Mitigation (PVMBG) classify active volcanoes into three stages, ranging from A to C class, and is conducting observations. When the volcano becomes active, they present four levels of warning level. The basic disaster response such as the issuance of evacuation information is taken by the Regional Disaster Management Agency in Indonesia (BPBD), and the National Agency for Disaster Countermeasure (BNPB) supports this. If evacuation accompanied with level rise but the eruption does not occur, BNPB bears the expenses.
In New Zealand, GNS Science Corporation conducts observation of volcanic activity and issuance of alarm (6 stages).An evacuation information issuance is made by CDEM which is a collaboration body of local public bodies.
This presentation discusses issues of volcanic disaster prevention system in Japan and future disaster prevention system by comparing systems of each country.

Keywords: volcano, volcanic disaster prevention system , volcanic alert level

©2019. Japan Geoscience Union. All Right Reserved.

[E] Poster | M (Multidisciplinary and Interdisciplinary)：M-ZZ Others

Tue. May 28, 2019 5:15 PM - 6:30 PM JST | Tue. May 28, 2019 8:15 AM - 9:30 AM UTC | Poster Hall International Exhibition Hall8, Makuhari Messe_50

[M-ZZ50] Governance for Trans-boundary Volcanic Disaster

convener:Mayumi Sakamoto(Graduate School of Disaster Resilience and Governance, University of Hyogo), Haruhisa Nakamichi(Sakurajima Volcano Research Center, Disaster Prevention Research Institute, Kyoto University), MASARU ARAKIDA(Asian Disaster Reduction Center)

Volcanic monitoring systems are developed and managed for the purpose to observe a specific volcanic activity in each country based on its own regulation. However, the experience of Icelandic volcano Eyjafjallajokull eruption in 2010 caused huge air traffic disturbances, and left large economic and social impact to international community. In order to reduce possible financial, environmental, health or social damages caused by trans-boundary volcanic disaster, it is important to develop international cooperative system to monitor and share the information of emission, dispersion or deposition of volcanic products. In this session, we discuss trans-boundary effect of volcanic eruption, and how to establish international collaborative mechanism from different research disciplines such as disaster management, volcanology, environmental politics or international law.

[MZZ50-P01] Governance for Trans-boundary Volcanic Disaster -a case of 2010 Eyjafjallajökull Eruption-

*Mayumi Sakamoto[1] (1.Graduate School of Disaster Resilience and Governance, University of Hyogo)

[MZZ50-P02] Regional Cooperation against Cross-border Disasters

*MASARU ARAKIDA[1] (1.Asian Disaster Reduction Center)

[MZZ50-P03] Issues of Japan's volcanic disaster prevention system as viewed from overseas alert systems

*Erika Ishimizu[1], Mayumi Sakamoto[1] (1.Graduate School of Disaster Resilience and Governance University of Hyogo)

Governance for Trans-boundary Volcanic Disaster -a case of 2010 Eyjafjallajökull Eruption-

*Mayumi Sakamoto[1]

1. Graduate School of Disaster Resilience and Governance, University of Hyogo

The volcanic eruption occurred in one country can trigger different effect in other country. The experience of 2010 Icelandic volcano Eyjafjallajökull eruption demonstrated the necessity of international governance for trans-boundary effect caused by eruption. In Iceland, national disaster response was effective to evacuate people from hazardous area and there were no humanitarian damages caused by eruption. However, the estimation of volcanic ash plumes and its dispersion caused huge international air traffic disruption or airport closure, and left large international economic and industrial impact. Followings are problems found through the 2010 eruption.
First, the necessity of international collaboration for observing atmospheric dispersion of volcanic ash. As for 2010 eruption, Icelandic Meteorological Agency (IMO) informed London Volcanic Ash Advisory Center (VAAC) which observes Iceland, about the plume height, ash content and other data. Based on the provided data, London VAAC predicted ash dispersion over Europe. However, there was no detailed discussion between IMO and London VAAC when and how often they communicate prior to eruption. It is important to update forecast using satellite imagery or observation of ashfalls in other countries.
Second, the necessity of immediate information sharing with both local and international medias. During the eruption, there was a huge need for information from international medias. A communication team, composed by professional communicator from various institutions gathered at the National Crisis Coordination and Command Center (NCCCC). Press conference were held and status reports were prepared and distributed. Such an international information sharing system should be discussed prior to disaster.
Disaster management systems are generally developed to respond hazard activity in each country based on its own regulation. However, 2010 experience showed there is no international agreement or regime to respond such a trans-boundary effect. Immediate crisis communication among hazard origin country, international institute and possibly affective country is required to reduce secondary effect, which shows importance or precautionary approaches for trans-boundary volcanic disaster.

Keywords: trans-boudary disaster, volcano, governance, Eyjafjallajökull

©2019. Japan Geoscience Union. All Right Reserved.

Regional Cooperation against Cross-border Disasters

*MASARU ARAKIDA[1]

1. Asian Disaster Reduction Center

Since affected area by disasters such as floods on international scale river, haize by forest fire, and volcanic ejectaare are recognized as no boundaries, there are many benefits of working together through regional cooperation. These include the sharing of best practices for handling major disasters, responding together on search and rescue efforts, and understanding and improving DRR through early warnings, the mutual exchange of information, joint education and training exercises, and joint assistance on disaster response.

Keywords: cross-border disaster, regional cooperation

©2019. Japan Geoscience Union. All Right Reserved.

Issues of Japan's volcanic disaster prevention system as viewed from overseas alert systems

*Erika Ishimizu[1], Mayumi Sakamoto[1]

1. Graduate School of Disaster Resilience and Governance University of Hyogo

Volcanic alert levels was introduced in Japan in 2007. Thereafter, the level was raised or lowered for several volcanoes, some volcanoes erupted and residents evacuated. Among them, the problem of exploiting volcanic alert levels for evacuation has become clear. In this research, by comparing Japan's warning system with overseas (the United States, Indonesia, New Zealand), we will examine the issues of Japanese volcanic disaster prevention system and future disaster prevention system.
In Japan, several institutions, such as universities and Japan Meteorological Agency (JMA), are conducting observations of volcanic activity. In the volcano where volcanic alert levels is introduced, JMA announces five levels of volcanic alert levels according to the activity of the volcano. Each municipality carries out basic disaster response such as issuance of evacuation information.
In the United States, the United States Geological Survey (USGS) will unite from the observation of a volcano to the announcement of an alarm (4 stages). Basic disaster response is handled by municipalities and counties. If requested, the state government responds, and if it is still difficult, FEMA is asked.
In Indonesia, the Center of Volcanology and Geological Hazard Mitigation (PVMBG) classify active volcanoes into three stages, ranging from A to C class, and is conducting observations. When the volcano becomes active, they present four levels of warning level. The basic disaster response such as the issuance of evacuation information is taken by the Regional Disaster Management Agency in Indonesia (BPBD), and the National Agency for Disaster Countermeasure (BNPB) supports this. If evacuation accompanied with level rise but the eruption does not occur, BNPB bears the expenses.
In New Zealand, GNS Science Corporation conducts observation of volcanic activity and issuance of alarm (6 stages).An evacuation information issuance is made by CDEM which is a collaboration body of local public bodies.
This presentation discusses issues of volcanic disaster prevention system in Japan and future disaster prevention system by comparing systems of each country.

Keywords: volcano, volcanic disaster prevention system , volcanic alert level

©2019. Japan Geoscience Union. All Right Reserved.

[E] Oral | M (Multidisciplinary and Interdisciplinary)：M-ZZ Others

Tue. May 28, 2019 3:30 PM - 5:00 PM JST | Tue. May 28, 2019 6:30 AM - 8:00 AM UTC | 304 3F

[M-ZZ50] Governance for Trans-boundary Volcanic Disaster

convener:Mayumi Sakamoto(Graduate School of Disaster Resilience and Governance, University of Hyogo), Haruhisa Nakamichi(Sakurajima Volcano Research Center, Disaster Prevention Research Institute, Kyoto University), MASARU ARAKIDA(Asian Disaster Reduction Center), Chairperson:Mayumi Sakamoto(兵庫県立大学大学院減災復興政策研究科), Haruhisa Nakamichi(京都大学防災研究所), Masaru Arakida(アジア防災センター)

Volcanic monitoring systems are developed and managed for the purpose to observe a specific volcanic activity in each country based on its own regulation. However, the experience of Icelandic volcano Eyjafjallajokull eruption in 2010 caused huge air traffic disturbances, and left large economic and social impact to international community. In order to reduce possible financial, environmental, health or social damages caused by trans-boundary volcanic disaster, it is important to develop international cooperative system to monitor and share the information of emission, dispersion or deposition of volcanic products. In this session, we discuss trans-boundary effect of volcanic eruption, and how to establish international collaborative mechanism from different research disciplines such as disaster management, volcanology, environmental politics or international law.

3:30 PM - 3:35 PM JST | 6:30 AM - 6:35 AM UTC

Introduction

3:35 PM - 3:50 PM JST | 6:35 AM - 6:50 AM UTC

[MZZ50-01] The development of the European collaborative mechanism of volcanic monitoring systems after 2010 Eyjafjallajokull eruption - from the perspective of European Union law -

*Chizu Arashima[1] (1.KOBE GAKUIN UNIVERSITY)

3:50 PM - 4:05 PM JST | 6:50 AM - 7:05 AM UTC

[MZZ50-02] Preparing for volcanic disasters: Risk communication issues when dealing with international tourists.

★Invited Papers

*Ana Maria Cruz Naranjo[1], Giuseppe Aliperti[1] (1.Kyoto University Disaster Prevention Research Institute)

4:05 PM - 4:20 PM JST | 7:05 AM - 7:20 AM UTC

[MZZ50-03] Mitigation of volcanic hazard in Sakurajima, Japan, through the coordinating committee and through communication with the public

*Haruhisa Nakamichi[1] (1.Sakurajima Volcano Research Center, Disaster Prevention Research Institute, Kyoto University)

4:20 PM - 4:35 PM JST | 7:20 AM - 7:35 AM UTC

[MZZ50-04] An experimental forecasting technique for the ash hazard from Sakurajima volcano, Japan

*Alexandros Panagiotis Poulidis[1], Tetsuya Takemi[1], Masato Iguchi[1] (1.Disaster Prevention Research Institute, Kyoto University)

4:35 PM - 4:50 PM JST | 7:35 AM - 7:50 AM UTC

[MZZ50-05] Utilization of Space Technology for Early Warning and Efficiently Response Against Transboundary Disaster

★Invited Papers

*Koji Suzuki[1] (1.Asian Disaster Reduction Center, Research Center for Urban Safety and Security Kobe University)

4:50 PM - 5:00 PM JST | 7:50 AM - 8:00 AM UTC

[MZZ50-06] Discussion -Research Framework for Trans-boudary Disaster

*Mayumi Sakamoto[1] (1.Graduate School of Disaster Resilience and Governance, University of Hyogo)

The development of the European collaborative mechanism of volcanic monitoring systems after 2010 Eyjafjallajokull eruption - from the perspective of European Union law -

*Chizu Arashima[1]

1. KOBE GAKUIN UNIVERSITY

The eruption of Icelandic volcano Eyjafjallajokull in 2010 caused huge international air traffic disturbances and left significant economic and social damages to the international society. The lesson learned from the disaster is that not only the estimates by Volcanic Ash Advisory Centre (VAAC) but also the on-going observations are needed to estimate the concentration more accurately. These observations are carried out by various volcanic observatory institutions. They play key roles in reducing/preventing possible economic, environmental, health or social damages caused by such trans-boundary volcanic disaster, by providing key scientific information and interpretation during eruption crises. To address the fragmentation of scientific data and make use of scientific information, the European collaborative mechanism of volcanic monitoring systems to share information should be established on a sufficient financial basis.
At present, European Network of Observatories and Research Infrastructures for Volcanology (EUROVOLC) is coordinated by Icelandic Meteorological Office with 16 other partners from 7 European countries. EUEOVOLC is a 3-year project from February 1 2018 and is funded by the European Commission of the European Union (EU) under “Horizon 2020” with 5 million Euros. Horizon 2020 - the Framework Programme for Research and Innovation (2014-2020) was established by REGULATION (EU) No 1291/2013. Its Article 7 provides association of third countries to Horizon 2020. Associated countries include European Free Trade Association members, including Iceland. Therefore, EUROVOLC is funded by the EU. Horizon 2020 falls under the areas of research, technological development and space where the EU has shared competence with the Member States and the EU “shall have competence to carry out activities, in particular to define and implement programmes; however, the exercise of that competence shall not result in Member States being prevented from exercising theirs” (Article 4(3) of the Treaty on the Functioning of the European Union (TFEU)).
Concerning natural disasters, the 2007 Treaty of Lisbon introduced new provisions of TFEU. They are included both in the areas of civil protection under PART THREE UNION POLICIES AND INTERNAL ACTIONS of TFEU and humanitarian aid under PART FIVE THE UNION'S EXTERNAL ACTION of TFEU. Disaster prevention is provided in the former, as Article 196(1) of TFEU provides that “(t)he Union shall encourage cooperation between Member States in order to improve the effectiveness of systems for preventing and protecting against natural or man-made disasters”. Civil protection is the area where “(t)he Union shall have competence to carry out actions to support, coordinate or supplement the actions of the Member States” (Article 6 of TFEU).
For the implementation, the Directorate-General for European Civil Protection and Humanitarian Aid Operations (ECHO) of the European Commission plays the role. Under ECHO, there is EU Civil Protection Mechanism (UCPM). It was established by DECISION No 1313/2013/EU. Iceland is a participating state of the UCPM. UCPM is not at present a forum to establish a European collaborative mechanism of volcanic monitoring systems. However, it is worthy to note that Proposal for a DECISION amending Decision No 1313/2013/EU in 2017 acknowledges that disaster prevention efforts are crucial to limit the need for crisis and emergency support. It proposes that UCPM "shall support, complement and facilitate coordination of Member States’ action" "to increase the availability and use of scientific knowledge on

©2019. Japan Geoscience Union. All Right Reserved.

disasters". It also proposes that the Commission shall "take actions to improve the knowledge base on disaster risks and facilitate the sharing of knowledge, the results of scientific research, best practices and information, including among Member States that share common risks".
At present, the European collaborative mechanism of volcanic monitoring systems is financially supported by project-based funds of Horizon 2020. However, if the Proposal is adopted and the importance of sharing scientific information in disaster prevention is recognized, more opportunity and regular financial support to develop European collaborative mechanism of volcanic monitoring systems may be given.

Keywords: European Union, EU civil protection mechanism, EUROVOLC, Eyjafjallajokull, disaster prevention, volcanic eruption

©2019. Japan Geoscience Union. All Right Reserved.

Preparing for volcanic disasters: Risk communication issues when dealing with international tourists.

*Ana Maria Cruz Naranjo[1], Giuseppe Aliperti[1]

1. Kyoto University Disaster Prevention Research Institute

This paper provides insights on the risk communication behavior of international tourists visiting Japan. The study builds on the premise that even if tourism-oriented risk communication has been strongly investigated, tourists' risk information seeking and processing has been under-investigated. We thus explore risk information seeking and processing of international tourists in Japan. Japan has been selected as a case study for several reasons. First, the level of exposure of the country to natural hazards, such as volcanic eruptions, tsunamis, earthquakes, and typhoons, is high. Second, due to the increasing presence of tourists in recent years, the number of people exposed to disaster-related risk in Japan has also drastically increased. In the case of a major volcanic eruption with disruption to air traffic, the provision of risk information to tourists already in Japan, as well as those preparing to travel is of critical importance. The overall aim of the study consists on providing cross-country evidence to inform risk-communication strategies and improve tourists' disaster preparedness. In order to investigate the tourists' perspective, we adopted the Risk Information Seeking and Processing (RISP) model.

Keywords: risk communication, tourists, disasters

©2019. Japan Geoscience Union. All Right Reserved.

Mitigation of volcanic hazard in Sakurajima, Japan, through the coordinating committee and through communication with the public

*Haruhisa Nakamichi[1]

1. Sakurajima Volcano Research Center, Disaster Prevention Research Institute, Kyoto University

The Sakurajima Volcanological Observatory, at present the Sakurajima Volcano Research Center (SVRC), was founded in 1960 as a part of the Disaster Prevention Research Institute, Kyoto University, following the request from local governments and residents of the volcanic area. The SVRC contributes to society by releasing scientific results and knowledge on volcanic hazard to the public, as well as by advising national and local governments on hazard mitigation strategies. Volcano experts are required to issue a warning when a volcanic eruption is ongoing or imminent. The SVRC evaluates volcanic activity using observational data. It communicates and interacts often with local government offices, such as the ones in Kagoshima Prefecture, Kagoshima City, Tarumizu City, local branches of ministries of the national government, the Osumi Office of Rivers and National Highways (OORNH), and the Kagoshima Local Meteorological Office (KLMO). The SVRC and these offices work in close cooperation. For example, the meeting of the Coordinating Committee for Hazard Mitigation of Sakurajima Volcano has been taking place regularly every two months since 2006. The purpose of the Coordinating Committee is to share up-to-date observational results, to cooperate and to examine special topics to respond in terms of hazard mitigation in case of volcanic eruptions of the Sakurajima. The KLMO provides information on the volcanic activity of the Sakurajima as necessary, on the basis of the continuous observation and monitoring conducted in cooperation with the SVRC, OORNH, and other relevant bodies.

The Kyoto University has research facilities located across Japan, and organizes open-doors weeks at these facilities, i.e. the “KYODAI Weeks”, every year in October and November. As a part of this event, the SVRC opens not only the observatory, but also an underground observation tunnel to the public, so that the visitors can understand the instrumentation employed to monitor volcanic phenomena. We installed a group of PC displays at the Sakurajima Visitor Center in March 2017 to show real-time seismic and ground deformation data to the general public visiting Sakurajima. In addition, we explained to “volcano guides” how to interpret these monitoring data, so that they can explain these data from the point of view of volcanology to the general public in a straightforward manner.

Keywords: Volcano Hazard, Coordinating Committee, Monitoring Data Display, Doors Open

©2019. Japan Geoscience Union. All Right Reserved.

An experimental forecasting technique for the ash hazard from Sakurajima volcano, Japan

*Alexandros Panagiotis Poulidis[1], Tetsuya Takemi[1], Masato Iguchi[1]

1. Disaster Prevention Research Institute, Kyoto University

Introduction

The long-lasting activity from Sakurajima volcano introduces hazardous amounts of volcanic ash into the atmosphere, adversely affecting the surrounding areas (e.g. Biass *et al.* (2017), Poulidis *et al.*, (2018)), making accurate localized forecasts a necessity. Here, we present initial results from an experimental forecasting methodology carried out by the Sakurajima Volcanological Observatory (SVO), Kyoto University, focusing on three points: *(i)* high resolution (333m mesh), *(ii)* use of Eruption Source Parameters (ESPs) that are derived from geophysical signals (Iguchi, 2016) and allow for a proactive forecasting approach, and *(iii)* use of dedicated models in order to properly represent the plume structure.

Forecast Methodology

A combined modelling approach is presented: Japan Meteorological Agency (JMA) forecast data are dynamically downscaled to 333m using the Weather Research and Forecasting (WRF) model (Skamarock and Klemp, 2008), while the FALL3D volcanic ash transport and deposition (VATD) model (Folch *et al.*, 2009) is used for the introduction of the plume and dispersal modelling. A quasi-online coupling approach is used here, with WRF data output every 10mins so that the resolved variablity in the wind fields is well-represented in the ash dispersal simulations. In order to study the sensitivity of results to the timing relative to eruption, a total of 5 pseudo-forecast simulations were carried out using data up to 13 hours before the eruption.

June 16, 2018 Eruption

Sakurajima erupted at 0719 JST (JST=UTC+9), June 16 2018, with a reported plume height of 4700 m above the vent. Deposition occurred west and southwest of the volcano, reaching the southern coast of the Satsuma peninsula. Ashfall locations were reported by the JMA, while the SVO carried out a post-eruption survey to collect samples. A comparison of disdrometer observations (which measure airborne ash size) and ground deposits suggest the presence of large aggregates (e.g. Bagheri *et al.*, (2016)), a fact that needs to be accounted for in order to have successful simulations.

Forecast Simulation Results and Conclusions

Initially, a control simulation was carried out using the final mass discharge rate output. Although qualitatively similar to the JMA ash forecast, it offered two key improvements: *(i)* ash deposition over the volcano occured along a narrow path, correctly reproducing the observed pattern, and *(ii)* the observed area of maximum ashfall (>1 mm deposit thickness) was reproduced correctly at a distance from the vent, over the southwestern shore of the volcano.

Forecast time sensitivity simulations showed consistent ash dispersal patterns. Simulation results using forecast data up to 10 hours before the eruption time were qualitatively similar. Up to 4 hours before the eruption, the observation to estimate ratios for the two disdrometers were constrained to factor of 4, allowing for the proposed methodology to be confidently used in forecast timescales.

©2019. Japan Geoscience Union. All Right Reserved.

References
Bagheri *et al.* (2016) *J. Volcanol. Geophys. Res.*
Biass *et al.* (2017) *Bull. Volcanol.*
Folch *et al.* (2009) *Comput. Geosci.*
Iguchi (2016) *J. Disaster. Res.*
Poulidis *et al.* (2018) *Atmos. Environ.*
Skamarock and Klemp (2008) *J. Comput. Phys.*

Keywords: Ash dispersal, Hazard forecasting, Sakurajima, FALL3D, Weather Research and Forecasting

©2019. Japan Geoscience Union. All Right Reserved.

Utilization of Space Technology for Early Warning and Efficiently Response Against Transboundary Disaster

*Koji Suzuki[1]

1. Asian Disaster Reduction Center, Research Center for Urban Safety and Security Kobe University

Space-based Technology contributes DRR field via Sentinel Asia. It provides near real-time observations from space, delivered online, can be used as early warning, as well as information to guide response and post-disaster recovery planning or operations. Eight space agencies in Asia are providing satellite data to Asian countries for emergency response, mapping, evaluation, and recovery. Furthermore, Michibiki, a kinds of GPS satellite developed by Japan has avility to disseminate early warning message through the local speakers and smartphones.

Keywords: Space-based technology, Sentinel Asia, QZSS, Early warning message platform, Transboudary disaster

©2019. Japan Geoscience Union. All Right Reserved.

Discussion -Research Framework for Trans-boudary Disaster

*Mayumi Sakamoto[1]

1. Graduate School of Disaster Resilience and Governance, University of Hyogo

Volcanic disaster occurred in one country may cause different environmental or health effect in other country. In order to mitigate direct or secondary effect caused by eruption, it is important to discuss international collaborative mechanism to share information and take necessary measures. In this session, we discuss about how to establish a research framework for trans-boudary volcanic disaster.

Keywords: governance, trans-boudary, volcano, disaster

©2019. Japan Geoscience Union. All Right Reserved.